

TS
200
I5

THE JOURNAL OF THE INSTITUTE OF METALS

VOLUME LXXXI

1952-53

EDITOR

N. B. VAUGHAN, M.Sc.

*The Right of Publication and of Translation is Reserved.
The Institute of Metals is not responsible for the statements
made or for the opinions expressed in the following pages.*



LONDON

PUBLISHED BY THE INSTITUTE OF METALS

4 GROSVENOR GARDENS, S.W.1

1953

Copyright]

[Entered at Stationers' Hall

PAST-PRESIDENTS

Sir WILLIAM HENRY WHITE, K.C.B., LL.D., D.Eng., Sc.D., F.Inst.Met., F.R.S., 1908–1910 (*deceased*).

Sir GERARD ALBERT MUNTZ, Bart., 1910–1912 (*deceased*).

Professor WILLIAM GOWLAND, A.R.S.M., F.R.S., 1912–1913 (*deceased*).

Professor ALFRED KIRBY HUNTINGTON, A.R.S.M., 1913–1914 (*deceased*).

Engineer Vice-Admiral Sir HENRY JOHN ORAM, K.C.B., F.Inst.Met., F.R.S., 1914–1916 (*deceased*).

Sir GEORGE THOMAS BEILBY, LL.D., D.Sc., F.R.S., 1916–1918 (*deceased*).

Professor Sir HENRY CORT HAROLD CARPENTER, M.A., Ph.D., D.Sc., D.Met., A.R.S.M., F.Inst.Met., F.R.S., 1918–1920 (*deceased*).

Engineer Vice-Admiral Sir GEORGE GOODWIN GOODWIN, K.C.B., LL.D., F.Inst.Met., 1920–1922 (*deceased*).

LEONARD SUMNER, O.B.E., M.Sc., J.P., F.Inst.Met., 1922–1924 (*deceased*).

Professor-Emeritus THOMAS TURNER, M.Sc., A.R.S.M., F.Inst.Met., 1924–1926 (*deceased*).

Sir JOHN DEWRANCE, G.B.E., F.Inst.Met., 1926–1928 (*deceased*).

WALTER ROSENHAIN, D.Sc., B.C.E., F.Inst.Met., F.R.S., 1928–1930 (*deceased*).

RICHARD SELIGMAN, Ph.nat.D., F.Inst.Met., 1930–1932.

Sir HENRY FOWLER, K.B.E., LL.D., D.Sc., 1932–1934 (*deceased*).

HAROLD MOORE, C.B.E., D.Sc., Ph.D., F.Inst.Met., 1934–1936.

WILLIAM ROBB BARCLAY, O.B.E., F.Inst.Met., 1936–1938 (*deceased*).

CECIL HENRY DESCH, D.Sc., LL.D., Ph.D., F.Inst.Met., F.R.S., 1938–1940.

The Hon. RICHARD MARTIN PETER PRESTON, D.S.O., 1940–1942.

Lieut.-Colonel Sir JOHN HENRY MAITLAND GREENLY, K.C.M.G., C.B.E., M.A., F.Inst.Met., 1942–1944 (*deceased*).

Sir WILLIAM THOMAS GRIFFITHS, D.Sc., 1944–1946 (*deceased*).

Colonel Sir PAUL GOTTLIEB JULIUS GUETERBOCK, K.C.B., D.S.O., M.C., T.D., D.L., J.P., M.A., A.D.C.,
F.Inst.Met., 1946–1948.

Sir ARTHUR JOHN GRIFFITHS SMOUT, J.P., F.Inst.Met., 1948–1950.

HUBERT SANDERSON TASKER, B.A., 1950–1951.

Professor ALFRED JOHN MURPHY, M.Sc., 1951–1952.

COLIN JAMES SMITHELLS, M.C., D.Sc., 1952–1953.

COUNCIL AND OFFICERS

FOR THE YEAR 1953-54

PRESIDENT

Professor F. C. THOMPSON, D.Met., M.Sc.

PAST-PRESIDENTS

Professor A. J. MURPHY, M.Sc.

C. J. SMITHELLS, M.C., D.Sc.

H. S. TASKER, B.A.

VICE-PRESIDENTS

G. L. BAILEY, C.B.E., M.Sc.

Major C. J. P. BALL, D.S.O.,
M.C.

S. F. DOREY, C.B.E., D.Sc.,
F.R.S.

A. B. GRAHAM

P. V. HUNTER, C.B.E.
Professor G. V. RAYNOR, M.A.,
D.Phil., D.Sc.

HONORARY TREASURER

E. H. JONES

ORDINARY MEMBERS OF COUNCIL

ALFRED BAER, B.A.

W. A. BAKER, D.Sc.

N. I. BOND-WILLIAMS, B.Sc.

K. W. CLARKE

J. C. COLOQUHOUN, M.B.E.

E. R. GADD

The Hon. JOHN GRIMSTON, M.P.

N. P. INGLIS, Ph.D., M.Eng.

IVOR JENKINS, D.Sc.

L. B. PFEIL, O.B.E., D.Sc.,

A.R.S.M., F.R.S.

A. G. RAMSAY, Ph.D., B.Sc.

CHRISTOPHER SMITH

H. SUTTON, C.B.E., D.Sc.

Major P. L. TEED, A.R.S.M.

W. J. THOMAS

EX-OFFICIO MEMBERS OF COUNCIL

H. H. SYMONDS

(*Birmingham Local Section*)

C. E. RANSLEY, Ph.D., M.Sc.

(*London Local Section*)

R. T. PARKER, B.Sc., Ph.D.,

A.R.S.M.

(*Oxford Local Section*)

E. A. FOWLER, B.Sc., A.R.T.C.

(*Scottish Local Section*)

W. R. MADDOCKS, B.Sc., Ph.D.

(*Sheffield Local Section*)

K. M. SPRING

(*South Wales Local Section*)

REPRESENTATIVES OF OTHER BODIES

The following, in accordance with Article 32, represent Government Departments and allied societies at Council meetings, for purposes of liaison

ADMIRALTY	Captain (E.) H. J. B. GRYLLS, R.N.
WAR OFFICE	Major-General W. A. LORD, C.B.E.
IRON AND STEEL INSTITUTE	JAMES MITCHELL, C.B.E.
INSTITUTION OF METALLURGISTS	MAURICE COOK, D.Sc., Ph.D.; E. G. WEST, B.Sc., Ph.D.

SECRETARY

Lieut.-Colonel S. C. GUILLAN, T.D.

ASSISTANT SECRETARY

Major R. E. MOORE

EDITOR OF PUBLICATIONS

N. B. VAUGHAN, M.Sc.

CHAIRMEN, HONORARY SECRETARIES AND TREASURERS OF THE LOCAL SECTIONS

at 31 December 1953

Birmingham

Chairman : H. H. SYMONDS, 77 Antrobus Road, Sutton Coldfield, Warwickshire.

Hon. Secretary : A. W. MATTHEWS, 124 Hay Green Lane, Birmingham 30.

Hon. Treasurer : R. CHADWICK, M.A., 5 Fairmead Rise, King's Norton, Birmingham 30.

London

Chairman : C. E. RANSLEY, Ph.D., M.Sc., Research Laboratories, The British Aluminium Company, Ltd., Chalfont Park, Gerrards Cross, Bucks.

Hon. Secretary : E. C. RHODES, Ph.D., B.Sc., The Mond Nickel Company, Ltd., Development and Research Department, Bashley Road, London, N.W.10.

Hon. Treasurer : E. G. V. NEWMAN, B.Sc., A.R.S.M., The Royal Mint, London, E.C.3.

Oxford

Chairman : R. T. PARKER, B.Sc., Ph.D., A.R.S.M., Aluminium Laboratories, Ltd., Banbury, Oxon.

Hon. Secretary : O. R. SMITH, B.Sc., Aluminium Laboratories, Ltd., Banbury, Oxon.

Hon. Treasurer : J. C. ARROWSMITH, M.Met., Pressed Steel Company of Great Britain, Ltd., Oxford.

Scottish

Chairman : E. A. FOWLER, B.Sc., A.R.T.C., Scotts' Shipbuilding and Engineering Company, Ltd., Greenock, Renfrewshire.

Hon. Secretary : MATTHEW HAY, A. Cohen and Co., Ltd., Craigton Industrial Estate, Barfillan Drive, Cardonald, Glasgow, S.W.2.

Hon. Treasurer : N. J. MACLEOD, Steven and Struthers, Ltd., 86 Eastvale Place, Kelvinhaugh, Glasgow, C.3.

Sheffield

Chairman : W. R. MADDOCKS, B.Sc., Ph.D., The University, St. George's Square, Sheffield 1.

Hon. Secretary and Treasurer : A. J. MACDOUGALL, M.Met., The University, St. George's Square, Sheffield 1.

South Wales

Chairman : K. M. SPRING, 36 Beechwood Road, Uplands, Swansea.

Hon. Secretary : P. W. A. CUNNIFFE, Thirlmere, Mansel Road, Bonymaen, Swansea.

Hon. Treasurer : P. J. LIPTRON, M.Eng., The National Smelting Co., Ltd., Swansea Vale Works, Llansamlet, Swansea.

CORRESPONDING MEMBERS TO THE COUNCIL

at 31 December 1953

Australia

Professor H. K. WÖRNER, D.Sc.,
Professor of Metallurgy, University of Melbourne, Carlton, N.3, Melbourne, Victoria.

Belgium

H. P. A. FÉRON,
Administrateur-Directeur, Visseries et Tréfileries Réunies, 2 Avenue Général Leman, Haren, Bruxelles.

Canada

G. S. FARNHAM, B.A., M.Sc., Ph.D.,
The International Nickel Co. of Canada, Ltd., 25 King St. W., Toronto 1, Ontario.
Professor F. A. FORWARD, B.A.Sc.,
Head of the Department of Mining and Metallurgy, University of British Columbia, Vancouver, B.C.
Professor G. LETENDRE, B.A., Ph.D.,
Professor of Metallurgy and Director, Department of Mining and Metallurgical Engineering, Faculty of Sciences,
Laval University, Boulevard de l'Entente, Quebec City, P.Q.

France

Professor P. A. J. CHEVENARD,
Administrateur et Conseiller Scientifique, Société Anonyme de Commentry-Fourchambault et Decazeville, 84 rue de Lille, Paris 7e.
JEAN MATTER,
Vice-Président et Directeur-Général, Société Centrale des Alliages Légers, Issoire, Puy-de-Dôme.

India

N. P. GANDHI, M.A., B.Sc., A.R.S.M., D.I.C.,
183 Lam Road, Devlali.

Italy

LENO MATTEOLI, Dott.chim.,
Vice-Director, Breda Istituto di Ricerche Scientifiche Applicate all' Industria, S.p.A., Sesto S. Giovanni, Milano.

Netherlands

M. HAMBURGER,
Director, N.V. Royal Nederlandsche Lood- en Zinkpletterijen voorheen A.D. Hamburger, Leidschekade 30, Utrecht.

South Africa

G. H. STANLEY, D.Sc., A.R.S.M.,
24 Duncombe Road, Forest Town, Johannesburg, Transvaal.
Professor L. TAVERNER, A.R.S.M., D.I.C.,
Professor of Metallurgy and Assaying, University of the Witwatersrand, Johannesburg, Transvaal.

Spain

Professor J. ORLAND, M.Sc., M.A., Ph.D., D.D.,
Head of the Department of Metallography and Strength of Materials, Instituto Católico de Artes e Industrias,
Alberto Aguilera 23, Madrid.

Sweden


Professor CARL BENEDICKS, Fil.Dr., Dr.-Ing.e.h., Dr.Techn.h.c.,
Drottninggatan 95 B, Stockholm.
Professor AXEL HULTGREN,
Valevågen 49, Djursholm 2.

Switzerland

O. H. C. MESSNER, Dipl.Ing., Dr.sc.techn.,
Stauffacherquai 40, Zürich 4.
Professor A. VON ZERLEDER, Dr.-Ing.,
Director, Research Laboratories, Société Anonyme pour l'Industrie de l'Aluminium Chippis, Rosenbergstrasse 25,
Neuhausen a./Rheinfall.

United States of America

Professor R. F. MEHL, Ph.D., Eng.D., Sc.D.,
Director, Metals Research Laboratory, Carnegie Institute of Technology, Pittsburgh, Pa.
Professor C. S. SMITH, Sc.D.,
Professor of Metallurgy and Director of the Institute for the Study of Metals, University of Chicago, Chicago 37, Ill.
Dr. R. A. WILKINS,
Vice-President, Revere Copper and Brass, Inc., Rome, N.Y.



Digitized by the Internet Archive
in 2024



PROFESSOR F. C. THOMPSON, D.MET., M.SC.
(*President, 1953-54*)

CONTENTS

MINUTES OF PROCEEDINGS

	PAGE
General Meeting, Birmingham, 8 January 1953	xi
Annual General Meeting, London, 23-26 March 1953	xi
Annual Autumn Meeting, Southport, 21-25 September 1953	xiii
General Meeting, London, 27 November 1953	xvi

PAPERS, NOTES, AND DISCUSSIONS

	PAGE	
	Paper	Discn.
1409. Some Friction Effects in Wire Drawing. By G. D. S. MacLellan, M.A., Ph.D.	1	713
1410. The Viscosity of Molten Tin, Lead, Zinc, Aluminium, and Some of Their Alloys. By T. P. Yao, B.Sc., Ph.D., and V. Kondic, B.Sc., Ph.D.	17	714
1411. The Constitution of Nickel-Rich Alloys of the Nickel-Titanium-Aluminium System. By A. Taylor, Ph.D., F.Inst.P., and R. W. Floyd, B.Sc., A.I.M.	25	765
1412. Relative Grain Translations in the Plastic Flow of Aluminium. By W. A. Rachinger, M.Sc.	33	715
1413. The Influence of Primary Particles on the Grain-Size of Cast Magnesium-Aluminium Alloys. By W. A. Baker, B.Sc., F.I.M., (Mrs.) Myriam D. Eborall, B.A., and A. Cibula, M.A., A.I.M.	43	
1414. The Young's Modulus, Poisson's Ratio, and Rigidity Modulus of Some Aluminium Alloys. By N. Dudzinski, Dipl.Ing.(Chem.)	49	722
1415. Distribution Equilibria in Some Ternary Systems Me_1-Me_2-B and the Relative Strength of the Transition-Metal-Boron Bond. By Professor G. Hägg, Ph.D., and R. Kiessling, Ph.D.	57	
1416. The Recovery of Polycrystalline Aluminium. By J. A. Ramsey, M.Sc.	61	715
1417. The Solid Solubility of Silver in Aluminium. By L. Rotherham, M.Sc., F.Inst.P., F.I.M., and L. W. Larke, A.F.R.Ae.S., L.I.M.	67	
1418. The Constitution of Tantalum-Titanium Alloys. By D. Summers-Smith, B.Sc., A.R.T.C.	73	426
1419. Residual Stresses in Aluminium Alloy Sand Castings. By R. A. Dodd, M.Sc., Ph.D., A.I.M., A.R.I.C.	77	
1420. The Creep/Time Relationship under Constant Tensile Stress. By S. Bhattacharya, B.Sc., Ph.D., W. K. A. Congreve, Ph.D., and Professor F. C. Thompson, D. Met., M.Sc.	83	715
1421. The Temperature Dependence of Transient and Secondary Creep of an Aluminium Alloy to British Standard 2L42 at Temperatures Between 20° and 250° C. and at Constant Stress. By A. E. Johnson, D.Sc., M.Sc.Tech., M.I.Mech.E., and N. E. Frost, B.Sc., A.M.I.Mech.E.	93	715
1422. On the Foot-Hills of the Plastic Range. Twenty-Third Autumn Lecture. By Professor H. W. Swift, M.A., D.Sc., M.I.Mech.E.	109	
1423. The Embrittlement of Copper-Antimony Alloys at Low Temperatures. By D. McLean, B.Sc.	121	
1424. The Gold-Platinum System. By A. S. Darling, B.Sc.Eng., A.M.I.Mech.E., R. A. Minter, and J. C. Chaston, Ph.D., A.R.S.M., F.I.M.	125	599
1425. Crystal Slip in Aluminium During Creep. By D. McLean, B.Sc.	133	715
1426. The Viscosity of Aluminium and Binary Aluminium Alloys. By Professor W. R. D. Jones, D.Sc., and W. L. Bartlett, B.Sc., Ph.D.	145	714
1427. Plastic Deformation of Coarse-Grained Aluminium. By (Mrs.) V. M. Urie, B.Sc., and H. L. Wain, B.Met.E.	153	715
1428. Direct Examination of Solid Surfaces Using a Commercial Electron Microscope in Reflection. By J. W. Menter, M.A., Ph.D., A.Inst.P.	163	
1429. A Study of Order-Disorder and Precipitation Phenomena in Nickel-Chromium Alloys. By A. Taylor, Ph.D., F.Inst.P., and K. G. Hinton, B.Sc.	169	765
1430. Deformation of Magnesium at Various Rates and Temperatures. By J. W. Suiter, B.Sc., and W. A. Wood, D.Sc.	181	715
1431. The Effect of Certain Solute Elements on the Recrystallization of Copper. By V. A. Phillips, A.R.S.M., B.Sc., D.Eng., A.I.M., and Professor Arthur Phillips, D.Eng.	185	662
1432. Equilibrium Relations at 460° C. in Aluminium-Rich Alloys Containing 0-7% Copper, 0-7% Magnesium, and 1-2% Silicon. By H. J. Axon, B.Met., D.Phil.	209	
1433. An Example of Strain-Relief in Powder Specimens. By J. Gordon Parr, B.Sc.	214	
1434. The Sub-Grain Structure in Aluminium Deformed at Elevated Temperatures. By J. A. Ramsey, M.Sc.	215	715
1435. The High-Temperature Oxidation of Some Cobalt-Base and Nickel-Base Alloys. By Professor A. Preece, M.Sc., F.I.M., and G. Lucas, Ph.D.	219	727
1436. High-Temperature Oxidation Characteristics of a Group of Oxidation-Resistant Copper-Base Alloys. By J. P. Dennison, Ph.D., B.Sc., and Professor A. Preece, M.Sc., F.I.M.	229	727
1437. A Method of Determining Orientations in Aluminium Single Crystals and Polycrystalline Aggregates. By G. E. G. Tucker, B.Sc., and P. C. Murphy, B.Sc., A.I.M.	235	733

		PAGE	
	Paper	Discn.	
1438. Creep at 250° and 300° C. of Some Magnesium Alloys Containing Cerium. By G. A. Mellor, M.Sc., F.I.M., and R. W. Ridley, B.Sc.		245	
1439. New Values of the Coefficients of Equivalence for Manganese, Iron, Cobalt, and Nickel in Copper-Zinc Alloys. By J. B. Haworth, D.Phil., B.Met.		254	
1440. The Effect of Minor Additions on the Age-Hardening Properties of a High-Purity Lead-Antimony Alloy. By L. M. T. Hopkin, B.Sc., A.R.S.M., A.I.M., and C. J. Thwaites, B.Sc., A.R.S.M.		255	
1441. The Effect of Cold Work on the Microstructure and Corrosion-Resistance of Aluminium-5% Magnesium Alloys Containing 0-1% Zinc. By P. Brenner, Dr. Ing., and G. J. Metcalfe, M.Sc.Tech.		261	738
1442. Atmospheric Corrosion and Stress-Corrosion of Aluminium-Copper-Magnesium and Aluminium-Magnesium-Silicon Alloys in the Fully Heat-Treated Condition. By G. J. Metcalfe, M.Sc.Tech.		269	738
1443. The Measurement of the Relative Hardnesses of Fine Powder Particles. By J. B. Matthews, B.Sc., Ph.D., F.R.I.C.		279	
1444. Crystal Fragmentation in Aluminium During Creep. By D. McLean, B.Sc.		287	715
1445. Grain-Boundary Slip During Creep of Aluminium. By D. McLean, B.Sc.		293	715
1446. Intercrystalline Corrosion in Cast Zinc-Aluminium Alloys. By C. W. Roberts, B.Sc., A.I.M.		301	680
1447. The Constitution of Chromium-Manganese Alloys Below 1000° C. By W. B. Pearson, D.F.C., M.A., D.Phil., and W. Hume-Rothery, O.B.E., F.R.S.		311	
Report of Council for the Year Ended 31 December 1952		315	
Report of the Honorary Treasurer for the Year Ended 30 June 1952		325	
SYMPOSIUM ON THE CONTROL OF QUALITY IN THE PRODUCTION OF WROUGHT NON-FERROUS METALS AND ALLOYS. I.—THE CONTROL OF QUALITY IN MELTING AND CASTING			
1448. The Principles of Technical Control in Metallurgical Manufacture. By A. R. E. Singer, B.Sc., Ph.D.		329	
1449. The Control of Quality in the Production of Brass Ingots and Billets. By Maurice Cook, D.Sc., Ph.D., F.I.M., and C. L. M. Cowley, B.Sc., A.I.M.		341	
1450. The Control of Quality in Melting and Casting Copper and High-Conductivity Copper-Base Alloys. By J. Sykes, F.I.M.		351	
1451. The Control of Quality in the Casting of Zinc and Zinc Alloy Rolling Slabs and Extrusion Billets. By C. W. Roberts, B.Sc., A.I.M., and B. Walters, M.A.		365	
1452. The Control of Quality in the Melting and Casting of Aluminium Alloys for Working. By R. T. Staples and H. J. Hurst		377	
1453. The Control of Quality in Melting and Casting Magnesium Alloys for Hot Working. By R. G. Wilkinson, B.Sc., and S. B. Hirst, B.Sc.Tech.		393	
Joint Discussion			701
<hr/>			
1454. Presidential Address. By Professor F. C. Thompson, D.Met., M.Sc.		401	
1455. The Kinetics of the Eutectoid Transformation in Zinc-Aluminium Alloys. By R. D. Garwood, M.Sc., and A. D. Hopkins, M.Sc.		407	742
1456. The Liquid Immiscibility Region in the Aluminium-Lead-Tin System at 650°, 730°, and 800° C. By Morgan H. Davies, B.Sc.		415	
1457. The Influence of Thallium on the Creep of Lead. By R. C. Gifkins, B.Sc., A.I.M.		417	
1458. Some Metallographic Observations on Aged Aluminium-Copper Alloys. By I. J. Polmear, B.Met.E., and H. K. Hardy, M.Sc., Ph.D., A.R.S.M., A.I.M.		427	
1459. The Log-Log Plot of Solubility Data in Ternary Metallic Systems. By H. K. Hardy, M.Sc., Ph.D., A.R.S.M., A.I.M.		432	
1460. Mechanical Anisotropy in Some Ductile Metals. By Professor W. A. Backofen, S.B., Sc.D., and B. B. Hundy, B.Sc., Ph.D.		433	
1461. The Formation of Intercrystalline Voids in Solution-Treated Magnesium-Aluminium Alloys. By E. Lardner, B.Sc., A.I.M.		439	742
1462. A Note on the Mathematical Analysis of Creep Curves. By L. M. T. Hopkin, B.Sc., A.R.S.M., A.I.M.		443	
1463. Equilibrium Relations at 460° C. in Aluminium-Rich Alloys Containing 0-7% Copper, 0-7% Magnesium, and 0-6% Silicon. By H. J. Axon, B.Met., D.Phil.		449	
1464. The Constitution of Nickel-Rich Alloys of the Nickel-Chromium-Aluminium System. By A. Taylor, Ph.D., F.Inst.P., and R. W. Floyd, B.Sc., A.I.M.		451	765
1465. The Present and Future Metallurgical Requirements of the Chemical Engineer. Forty-Third May Lecture. By Sir Christopher Hinton, M.A., M.I.C.E., M.I.Mech.E.		465	
1466. The Use of Diamond Abrasives for a Universal System of Metallographic Polishing. By L. E. Samuels, B.Met.E.		471	
1467. The Solubility of Indium in Copper. By Professor E. A. Owen, M.A., D.Sc., and E. A. O'Donnell Roberts, M.Sc., Ph.D.		479	

	PAGE	
	<i>Paper</i>	<i>Discn.</i>
1468. Priming Paints for Light Alloys. By J. G. Rigg, Ph.D., and E. W. Skerrey, B.Sc., A.I.M.	481	748
1469. The Continuity of Slip Lines Across a Grain Boundary. By G. J. Ogilvie, Ph.D.	491	
1470. Hydrogen Blisters in Brass Sheet. By R. Eborall, M.A., and A. J. Swain, M.A.	497	
1471. Critical-Strain Effects in Cold-Worked Wrought Aluminium and Its Alloys. By W. M. Williams, B.Sc., and R. Eborall, M.A.	501	
1472. The Application of Grain Refinement to Cast Copper-Aluminium Alloys Containing the Beta Phase. By J. P. Dennison, B.Sc., Ph.D., and E. V. Tull, B.Sc., A.I.M.	513	
1473. The Structure of Titanium-Tin Alloys in the Range 0-25 At.-% Tin. By H. W. Worner, M.Sc.	521	
1474. Some Observations on Creep and Fracture from Investigations on Lead Cable-Sheath Alloys. By A. Latin, Ph.D., M.Eng., F.I.M.	529	
1475. Simultaneous Determination of the Surface Tension of Tin and its Contact Angle with Silica by the Use of Conical Capillaries. By D. V. Atterton, M.A., Ph.D., and T. P. Hoar, M.A., Ph.D., F.I.M.	541	
1476. A Theoretical Investigation of the Deformation Textures of Titanium. By D. N. Williams, Ph.D., and Professor D. S. Eppelsheimer, D.Sc.	553	
1477. The Influence of Composition on the Incidence of Strain Markings in Aluminium Alloys. By W. H. L. Hooper, B.Sc., A.I.M.	563	751
1478. The Properties of Cast Chromium Alloys at Elevated Temperatures, I.—The Melting and Casting of Chromium-Rich Alloys. By A. H. Sully, M.Sc., Ph.D., F.Inst.P., F.I.M., E.A. Brandes, B.Sc., A.R.C.S., F.I.M., and A. G. Provan, B.Sc., A.R.T.C., A.R.I.C. II.—Some Properties of Certain Binary Chromium-Rich Alloys. By A. H. Sully and E. A. Brandes. III.—The Creep Properties of Ternary and More Complex Chromium-Base Alloys. By A. H. Sully and E. A. Brandes.	569	760
1479. The Effect of Temperature and Purity on the Ductility and Other Properties of Chromium. By A. H. Sully, Ph.D., M.Sc., F.Inst.P., F.I.M., E. A. Brandes, B.Sc., A.R.C.S., F.I.M., and K. W. Mitchell, B.Sc.(Eng.), Wh.Sch., A.M.I.Mech.E.	585	760
1480. The Stepped Stress/Strain Curve of Some Aluminium Alloys. By N. Krupnik, D.I.C., and Professor Hugh Ford, D.Sc., Ph.D.	601	751
1481. Discontinuous Flow and Strain-Ageing in a 6% Tin Phosphor-Bronze. By N. H. Polakowski, Dipl.Ing., Ph.D.	617	751
1482. Yield-Point Phenomena and Stretcher-Strain Markings in Aluminium-Magnesium Alloys. By V. A. Phillips, A.R.S.M., D.Eng., B.Sc., A.I.M., A. J. Swain, M.A., and R. Eborall, M.A.	625	751
1483. Some Methods of Measuring Surface Topography as Applied to Stretcher-Strain Markings on Metal Sheet. By W. H. L. Hooper, B.Sc., A.I.M., and J. Holden, Ph.D.	648	751
1484. Effect of Composition and Heat-Treatment on Yield-Point Phenomena in Aluminium Alloys. By V. A. Phillips, A.R.S.M., D.Eng., B.Sc., A.I.M.	649	751
1485. Growth of Sulphide Films on Copper. By T. P. Hoar, M.A., Ph.D., F.I.M., and A. J. P. Tucker, M.A., Ph.D.	665	763
1486. The Oxidation of Copper in the Temperature Range 200°-800° C. By R. F. Tylecote, M.A., M.Sc., Ph.D., F.I.M.	681	763
Name Index	766	

LIST OF PLATES

	Professor F. C. Thompson, D.Met., M.Sc., President 1953-54	frontispiece
I.	Paper by Dr. G. D. S. MacLellan	facing p. 60
II.	Discussion on paper by Mr. E. C. W. Perryman and Mr. G. B. Brook	between pp. 60 and 61
III-IV.	Paper by Dr. A. Taylor and Mr. R. W. Floyd	between pp. 60 and 61
V.	Paper by Mr. W. A. Rachinger	between pp. 60 and 61
VI.	Paper by Mr. W. A. Baker, Mrs. M. D. Eborall, and Mr. A. Cibula	between pp. 60 and 61
VII.	Paper by Mr. N. Dudzinski	between pp. 60 and 61
VIII-IX.	Paper by Mr. J. A. Ramsey	between pp. 108 and 109
X.	Paper by Mr. L. Rotherham and Mr. L. W. Larke	between pp. 108 and 109
XI.	Paper by Mr. D. Summers-Smith	facing p. 109
XII.	Lecture by Professor H. W. Swift	facing p. 168
XIII.	Paper by Mr. D. McLean	between pp. 168 and 169
XIV-XV.	Paper by Mr. A. S. Darling, Mr. R. A. Mintern, and Dr. J. C. Chaston	between pp. 168 and 169
XVI-XIX.	Paper by Mr. D. McLean	between pp. 168 and 169
XX.	Paper by Mrs. V. M. Urie and Mr. H. L. Wain	between pp. 168 and 169
XXI-XXIII.	Paper by Dr. J. W. Menter	between pp. 168 and 169
XXIV-XXV.	Paper by Mr. J. W. Suiter and Dr. W. A. Wood	between pp. 228 and 229
XXVI-XXIX.	Paper by Dr. V. A. Phillips and Professor A. Phillips	between pp. 228 and 229
XXX.	Paper by Mr. J. A. Ramsey	between pp. 228 and 229
XXXI.	Paper by Professor A. Preece and Dr. G. Lucas	facing p. 229
XXXII.	Paper by Dr. J. P. Dennison and Professor A. Preece	facing p. 268
XXXIII.	Paper by Mr. G. E. G. Tucker and Mr. P. C. Murphy	between pp. 268 and 269
XXXIV-XXXVI.	Paper by Mr. G. A. Mellor and Mr. R. W. Ridley	between pp. 268 and 269
XXXVII.	Paper by Mr. L. M. T. Hopkin and Mr. C. J. Thwaites	between pp. 268 and 269
XXXVIII.	Paper by Dr. P. Brenner and Mr. G. J. Metcalfe	between pp. 268 and 269
XXXIX-XL.	Paper by Mr. G. J. Metcalfe	between pp. 328 and 329
XLI-XLII.	Paper by Mr. D. McLean	between pp. 328 and 329
XLIII-XLIV.	Paper by Mr. C. W. Roberts	between pp. 328 and 329
XLV.	Paper by Dr. W. B. Pearson and Dr. W. Hume-Rothery	between pp. 328 and 329
XLVI-XLVII.	Paper by Dr. M. Cook and Mr. C. L. M. Cowley	between pp. 400 and 401
XLVIII-LI.	Paper by Mr. J. Sykes	between pp. 400 and 401
LII-LIHI.	Paper by Mr. C. W. Roberts and Mr. B. Walters	between pp. 400 and 401
LIV-LVII.	Paper by Mr. R. T. Staples and Mr. H. J. Hurst	between pp. 400 and 401
LVIII-LXI.	Paper by Mr. R. G. Wilkinson and Mr. S. B. Hirst	between pp. 400 and 401
LXII-LXIII.	Paper by Mr. R. D. Garwood and Mr. A. D. Hopkins	between pp. 432 and 433
LXIV-LXV.	Paper by Mr. R. C. Gifkins	between pp. 432 and 433
LXVI.	Paper by Mr. I. J. Polmear and Dr. H. K. Hardy	between pp. 432 and 433
LXVII.	Paper by Professor W. A. Backofen and Dr. B. B. Hundy	facing p. 464
LXVIII.	Paper by Mr. E. Lardner	between pp. 464 and 465
LXIX-LXXII.	Paper by Dr. A. Taylor and Mr. R. W. Floyd	between pp. 464 and 465
LXXIII-LXXIV.	Paper by Mr. L. E. Samuels	between pp. 496 and 497
LXXV-LXXVII.	Paper by Dr. J. G. Rigg and Mr. E. W. Skerrey	between pp. 496 and 497
LXXVIII.	Paper by Dr. G. J. Ogilvie	facing p. 497
LXXIX.	Paper by Mr. W. M. Williams and Mr. R. Eborall	facing p. 568
LXXX.	Paper by Dr. J. P. Dennison and Mr. E. V. Tull	between pp. 568 and 569
LXXXI.	Paper by Mr. H. W. Worner	between pp. 568 and 569
LXXXII.	Paper by Dr. A. Latin	between pp. 568 and 569
LXXXIII-LXXXIV.	Paper by Mr. W. H. L. Hooper	between pp. 568 and 569
LXXXV-LXXXVIII.	Paper by Dr. A. H. Sully, Mr. E. A. Brandes, and Mr. A. G. Provan	between pp. 712 and 713
LXXXIX.	Paper by Dr. A. H. Sully, Mr. E. A. Brandes, and Mr. K. W. Mitchell	between pp. 712 and 713
XC-XCII.	Paper by Dr. V. A. Phillips, Mr. A. J. Swain, and Mr. R. Eborall	between pp. 712 and 713
XCIII.	Paper by Dr. T. P. Hoar and Mr. A. J. P. Tucker	between pp. 712 and 713
XCIV.	Paper by Dr. R. F. Tylecote	between pp. 712 and 713
XCV-XCVI.	Discussion on Control of Quality	between pp. 712 and 713
XCVII-CVI.	Discussion on Various Papers	between pp. 744 and 745

THE INSTITUTE OF METALS

MINUTES OF PROCEEDINGS

GENERAL MEETING

8 January 1953

A GENERAL MEETING of the Institute of Metals was held in the University, Edgbaston, Birmingham, on Thursday, 8 January 1953. The Chair was taken by Mr. J. W. THOMAS, Chairman of the Metallurgical Engineering Committee.

Before the meeting members paid a visit to the Aitchison Laboratories, by invitation of Professor A. J. MURPHY.

INFORMAL DISCUSSION ON "ROLLS AND THEIR MAINTENANCE IN THE NON-FERROUS METALS INDUSTRY"

The discussion was opened by Mr. W. H. BOWMAN, Mr. S. G. TEMPLE, and Mr. L. S. D. SMITH. Numerous contributions were made, a summary of which is published in the *Bulletin*, 1951-53, vol. 1, pp. 199-202 (May 1953).

At the conclusion of the meeting, votes of thanks were passed to the University authorities for permission to use the Chemistry Lecture Theatre for the meeting, and to Professor A. J. Murphy for his invitation to members to visit the Aitchison Laboratories.

ANNUAL GENERAL MEETING

THE FORTY-FIFTH ANNUAL GENERAL MEETING of the Institute of Metals was held in London from Monday to Thursday, 23-26 March 1953.

Monday, 23 March

MAY LECTURE

The Forty-Third May Lecture was delivered by Sir CHRISTOPHER HINTON, M.A., M.I.C.E., M.I.Mech.E., Deputy Controller of Atomic Energy (Production), Ministry of Supply, on "The Present and Future Metallurgical Requirements of the Chemical Engineer," in the Lecture Theatre of the Royal Institution, Albemarle Street, London, W.1., at 6.0 p.m. The President, Dr. C. J. SMITHELLS, M.C., occupied the Chair.

At the conclusion, Dr. N. P. INGLIS, M.Eng., Member of Council, proposed a hearty vote of thanks to Sir Christopher Hinton for his lecture, which is printed on pp. 465-470 of this volume of the *Journal*.

In the evening, the Council entertained Sir Christopher Hinton to dinner at the United Service Club, Pall Mall, S.W.1.

Tuesday, 24 March

The meeting was resumed at the Park Lane Hotel, Piccadilly, W.1, at 10.30 a.m. The retiring President, Dr. C. J. SMITHELLS, M.C., occupied the Chair at the opening of the meeting.

The Chairman welcomed members and visitors attending the meeting from overseas.

The minutes of the previous General Meetings, held in London on 19 November 1952 and in Birmingham on 8 January 1953, were taken as read and signed by the Chairman.

ELECTIONS OF ORDINARY MEMBERS, JUNIOR MEMBERS, AND STUDENT MEMBERS

The SECRETARY (Lieut.-Colonel S. C. GUILLAN, T.D.) announced that since the Annual Autumn Meeting held in Oxford in September 1952, a total of 215 Ordinary Members,

Junior Members, and Student Members had been elected on 12 October, 19 November, 12 December, and 31 December 1952, and 15 January, 13 February, 25 February, and 23 March 1953, the lists of whose names are printed in the *Bulletin*, 1951-53, vol. 1, pp. 129, 136, 142, 173, 183, 184, and 194.

REPORT OF COUNCIL FOR THE YEAR ENDED 31 DECEMBER 1952

The CHAIRMAN moved, Professor HUGH FORD seconded, and there was carried unanimously, a motion for the adoption of the Report of Council for the Year Ended 31 December 1952, which is printed on pp. 315-324 of this volume of the *Journal*.

REPORT OF THE HONORARY TREASURER FOR THE FINANCIAL YEAR ENDED 30 JUNE 1952

In the absence of the Honorary Treasurer, Mr. E. A. BOLTON, M.Sc. (Member of Council), presented the Report of the Honorary Treasurer and the accounts for the financial year ended 30 June 1952, and moved their adoption. Mr. A. B. GRAHAM (Vice-President) seconded the motion, which was carried unanimously.

The Report and accounts are printed in this volume of the *Journal*, pp. 325-328.

RE-ELECTION OF AUDITORS

It was proposed, seconded, and carried unanimously that Messrs. Poppleton and Appleby be re-elected auditors to the Institute for the year 1953-54.

ELECTION OF OFFICERS FOR 1953-54

The SECRETARY announced that the following officers had been elected to fill vacancies on the Council for the year 1953-54:

President:

Professor F. C. THOMPSON, D.Met., M.Sc.

Vice-Presidents:

Major C. J. P. BALL, D.S.O., M.C.

Professor G. V. RAYNOR, M.A., D.Phil., D.Sc.

Ordinary Members of Council:

W. A. BAKER, B.Sc.

J. C. COLQUHOUN, M.B.E.

E. R. GADD

The Hon. JOHN GRIMSTON, M.P.

SENIOR VICE-PRESIDENT FOR 1953-54

The SECRETARY announced that the Council had elected Dr. S. F. DOREY, C.B.E., F.R.S., to be Senior Vice-President for 1953-54, and that he would be its next nominee for the Presidency.

VOTE OF THANKS TO RETIRING OFFICERS

Professor A. J. MURPHY, M.Sc. (Past-President) proposed, Dr. E. G. WEST seconded, and there was carried with acclamation a hearty vote of thanks to the following retiring officers for their services on the Council: Sir Arthur Smout, J.P.,

Past-President; Professor H. O'Neill, D.Sc., M.Met., Vice-President; and Mr. E. A. Bolton, M.Sc., Mr. C. H. Davy, and Professor A. G. Quarrell, D.Sc., Ph.D., A.R.C.S., D.I.C., Ordinary Members of Council.

INDUCTION OF THE NEW PRESIDENT

The CHAIRMAN (Dr. C. J. Smithells, M.C.) then introduced the new President, Professor F. C. THOMPSON, D.Met., M.Sc., and inducted him into the Chair.

VOTE OF THANKS TO THE RETIRING PRESIDENT

Dr. L. B. PFEIL, F.R.S. (Member of Council) proposed, Professor H. O'NEILL, D.Sc., M.Met., seconded, and there was carried with acclamation a hearty vote of thanks to the retiring President, Dr. C. J. Smithells, M.C. Dr. Smithells briefly responded.

PRESIDENTIAL ADDRESS

Professor F. C. THOMPSON, D.Met., M.Sc., then delivered his Presidential Address, which is printed on pp. 401-405 of this volume of the *Journal*.

A vote of thanks to the President for his Address was moved by Dr. J. W. CUTHBERTSON, seconded by Dr. IVOR JENKINS (Member of Council), and carried with acclamation.

INSTITUTE OF METALS (PLATINUM) MEDAL

The SECRETARY announced that the Institute of Metals (Platinum) Medal for 1953 had been awarded to Professor GEORG MASING, Dr.phil., Dr.Ing.e.h., of the Institut für allgemeine Metallkunde, Universität Göttingen, in recognition of his outstanding contributions in the field of metallography.

Professor Masing was unable to be present at the meeting to receive the medal.

ROSENHAIN MEDAL

The SECRETARY announced that the Rosenhain Medal for 1953 had been awarded to Dr. CHARLES ERIC RANSLEY, of the Research Laboratories, The British Aluminium Co., Ltd., Gerrards Cross, in recognition of his outstanding experimental and theoretical work on gas-metal equilibria. The President then presented the medal to Dr. Ransley.

W. H. A. ROBERTSON MEDAL

The SECRETARY announced that the W. H. A. Robertson Medal for 1952 had been awarded to Mr. JOHN FRANCIS WRIGHT, of the West Midlands Gas Board, for his paper on "Gas Equipment for the Thermal Treatment of Non-Ferrous Metals and Alloys" (*Journal*, 1951-52, vol. 80, pp. 269-285). The President then presented the medal to Mr. Wright.

STUDENTS' ESSAY PRIZES

The SECRETARY announced that as a result of the 1952 Students' Essay Competition, prizes had been awarded to Mr. R. D. STACEY, of the University of Birmingham, for an essay on "Some Experimental Evidence for Dislocations" and to Mr. G. THOMAS, B.Sc., of Cambridge University, for an essay on "Martensitic Transformations in Non-Ferrous Metals and Alloys". The President then presented the prizes.

DISCUSSION OF PAPERS

The meeting was resumed in the afternoon at the Park Lane Hotel, when the President, Professor F. C. THOMPSON, D.Met., M.Sc., occupied the Chair.

A joint discussion was held on the following two papers, which had previously been published in the *Journal*:

"The Effect of Certain Solute Elements on the Recrystallization of Copper," by V. A. Phillips, A.R.S.M., B.Sc., D.Eng., A.I.M., and Arthur Phillips, D.Eng.

"Segregation of Iron and Phosphorus at the Grain Boundaries in 70:30 Brass During Grain Growth," by H. M. Miekko-oja, Sc.D.

Young's Modulus of Alloys

A discussion then took place on the theme "Young's Modulus of Alloys", based on the following papers published in the *Journal*:

"A Study of Some Factors Influencing the Young's Modulus of Solid Solutions", by A. D. N. Smith, B.A.

"The Young's Modulus, Poisson's Ratio, and Rigidity Modulus of Some Aluminium Alloys", by N. Dudzinski, Dipl.Ing.

At the conclusion of each discussion a vote of thanks to the authors was proposed by the Chairman and carried with acclamation.

DINNER AND DANCE

In the evening a dinner and dance was held at the Park Lane Hotel.

Wednesday, 25 March

At the resumed meeting, at 10.30 a.m. at the Park Lane Hotel, Piccadilly, W.1, two concurrent scientific sessions were held: (i) an all-day Symposium on "The Control of Quality in the Production of Wrought Non-Ferrous Metals and Alloys". Part I.: "The Control of Quality in Melting and Casting" and (ii) discussions on other papers previously published in the *Journal*.

SYMPOSIUM ON "THE CONTROL OF QUALITY IN THE PRODUCTION OF WROUGHT NON-FERROUS METALS AND ALLOYS".
PART I.: "THE CONTROL OF QUALITY IN MELTING AND CASTING".

At the morning session the Chair was taken by the President, Professor F. C. THOMPSON, D.Met., M.Sc.

Mr. N. I. BOND-WILLIAMS, B.Sc. (Member of Council) as rapporteur, introduced the following six papers (see this volume, pp. 329-400) which had been contributed to the Symposium.

In the afternoon, the Chair was taken by Mr. W. J. THOMAS, Chairman of the Metallurgical Engineering Committee.

There was an all-day discussion, a report of which is printed on pp. 701-712 of this volume of the *Journal*.

"The Principles of Technical Control in Metallurgical Manufacture", by A. R. E. Singer, B.Sc., Ph.D.

"The Control of Quality in the Production of Brass Ingots and Billets", by Maurice Cook, D.Sc., Ph.D., F.I.M., and C. L. M. Cowley, B.Sc., A.I.M.

"The Control of Quality in Melting and Casting Copper and High-Conductivity Copper-Base Alloys", by J. Sykes, F.I.M.

"The Control of Quality in the Casting of Zinc and Zinc Alloy Rolling Slabs and Extrusion Billets", by C. W. Roberts, B.Sc., A.I.M., and B. Walters, M.A.

"The Control of Quality in the Melting and Casting of Aluminium Alloys for Working", by R. T. Staples and H. J. Hurst.

"The Control of Quality in Melting and Casting Magnesium Alloys for Hot Working", by R. G. Wilkinson, B.Sc., and S. B. Hirst, B.Sc.Tech.

At the conclusion of the Symposium, a vote of thanks to the authors was proposed by the Chairman and carried with acclamation.

DISCUSSION OF OTHER SCIENTIFIC PAPERS

At the morning session, the Chair was taken by Dr. L. B. PFEIL, F.R.S. (Member of Council).

Discussions took place based on two groups of papers.

Corrosion of Alloys

"The Effect of Cold Work on the Microstructure and Corrosion-Resistance of Aluminium-5% Magnesium Alloys Containing 0-1% Zinc", by P. Brenner, Dr. Ing., and G. J. Metcalfe, M.Sc.Tech.

"Atmospheric Corrosion and Stress-Corrosion of Aluminium-Copper-Magnesium and Aluminium-Magnesium-Silicon Alloys in the Fully Heat-Treated Condition", by G. J. Metcalfe, M.Sc.Tech.

"Intercrystalline Corrosion in Cast Zinc-Aluminium Alloys", by C. W. Roberts, B.Sc., A.I.M.

High-Temperature Oxidation of Alloys

"The High-Temperature Oxidation of Some Cobalt-Base and Nickel-Base Alloys", by A. Preece, M.Sc., F.I.M., and G. Lucas, Ph.D.

"High-Temperature Oxidation Characteristics of a Group of Oxidation-Resistant Copper-Base Alloys", by J. P. Dennison, Ph.D., B.Sc., and A. Preece, M.Sc., F.I.M.

At the conclusion of each discussion a vote of thanks to the authors was proposed by the Chairman and carried with acclamation.

At the afternoon session, the Chair was taken by Mr. G. L. BAILEY, C.B.E., M.Sc. (Vice-President).

Creep and Plastic Deformation

A general discussion took place based on the following 16 papers which had previously been published in the *Journal*:

"The Effect of Grain-Size on the Structural Changes Produced in Aluminium by Slow Deformation", by W. A. Rachinger, M.Sc.

"Stress-Recovery in Aluminium", by W. A. Wood, D.Sc., and J. W. Suiter, B.Sc.

"Creep Processes in Coarse-Grained Aluminium", by D. McLean, B.Sc.

"Electron-Microscopic Studies of Slip in Aluminium During Creep", by J. Trotter.

"Boundary Slip in Bicrystals of Tin", by K. E. Puttick, B.Sc., and R. King, B.Sc.

"X-Ray Diffraction Studies in Relation to Creep", by G. D. Greenough, Ph.D., (Mrs.) Catherine M. Bateman, B.Sc., and (Mrs.) Edna M. Smith, B.A.

"Relative Grain Translations in the Plastic Flow of Aluminium", by W. A. Rachinger, M.Sc.

"The Recovery of Polycrystalline Aluminium", by J. A. Ramsey, M.Sc.

"The Creep/Time Relationship under Constant Tensile Stress", by S. Bhattacharya, B.Sc., Ph.D., W. K. A. Congreve, B.A.Sc., Ph.D., and F. C. Thompson, D.Met., M.Sc.

"The Temperature-Dependence of Transient and Secondary Creep of an Aluminium Alloy to British Standard 2L42 at Temperatures Between 20° and 250° C. and at Constant Stress", by A. E. Johnson, D.Sc., M.Sc.Tech., M.I.Mech.E., and N. E. Frost, B.Sc., A.M.I.Mech.E.

"Crystal Slip in Aluminium During Creep", by D. McLean, B.Sc.

"Plastic Deformation of Coarse-Grained Aluminium", by (Mrs.) V. M. Urie, B.Sc., and H. L. Wain, B.Met.E.

"Deformation of Magnesium at Various Rates and Temperatures", by J. W. Suiter, B.Sc., and W. A. Wood, D.Sc.

"The Sub-Grain Structure in Aluminium Deformed at Elevated Temperatures", by J. A. Ramsey, M.Sc.

"Crystal Fragmentation in Aluminium During Creep", by D. McLean, B.Sc.

"Grain-Boundary Slip During Creep of Aluminium", by D. McLean, B.Sc.

At the conclusion of the discussion, a vote of thanks to the authors was proposed by the Chairman and carried with acclamation.

CONVERSAZIONE AND EXHIBITION

In the evening a conversazione and exhibition was held at the Institute's Headquarters, 4 Grosvenor Gardens, London, S.W.1.

Thursday, 26 March

INFORMAL DISCUSSION ON "LIQUID METALS"

The meeting was resumed at 10.0 a.m. at the Park Lane Hotel, Piccadilly, W.1, when the President, Professor F. C. THOMPSON, D.Met., M.Sc., occupied the Chair.

An Informal discussion took place on "Liquid Metals", introduced by Dr. V. KONDIC and Dr. B. R. T. FROST, which concluded at 12.30 p.m.

VISITS TO WORKS AND LABORATORIES

Visits were paid to the following works and laboratories: The British Non-Ferrous Metals Research Association, Euston Street, London, N.W.1.

Hoover, Ltd., Greenford.

The Pyrene Co., Ltd., Brentford.

Vickers-Armstrongs, Ltd., Weybridge.

The meeting then concluded.

ANNUAL AUTUMN MEETING

THE FORTY-FIFTH ANNUAL AUTUMN MEETING of the Institute of Metals was held in Southport from Monday to Friday, 21-25 September 1953.

Monday, 21 September

A General Meeting was held at the Town Hall, Lord Street, Southport, at 6.30 p.m., the Chair being taken by the President, Professor F. C. THOMPSON, D.Met., M.Sc.

The Chairman welcomed members, ladies, and delegates attending the meeting from overseas.

The minutes of the previous general Meeting, held in London from 23 to 26 March 1953, were taken as read and signed by the Chairman.

ELECTIONS OF ORDINARY MEMBERS, JUNIOR MEMBERS, AND STUDENT MEMBERS

The SECRETARY (Lieut.-Colonel S. C. GUILLAN, T.D.) announced that since the last General Meeting held in London in March 1953, a total of 188 Ordinary Members, Junior Members, and Student Members had been elected on 14 April, 30 April, 19 May, 12 June, 30 June, 24 August, and 8 September 1953, lists of whose names are printed in the *Bulletin*, 1951-53, vol. 1, pp. 207, 213, 222, and 223, and 1953-54, vol. 2, pp. 12 and 13.

ELECTION OF OFFICERS FOR 1954-55

The SECRETARY announced that the following members would retire from the Council at the 1954 Annual General Meeting, as required by the Articles of Association:

President:

Professor F. C. THOMPSON, D.Met., M.Sc.

Past-President:

H. S. TASKER, B.A.

Vice-Presidents:

A. B. GRAHAM

P. V. HUNTER, C.B.E.

Ordinary Member of Council:

L. B. PFEIL, O.B.E., D.Sc., A.R.S.M., F.R.S.

He stated that, in accordance with the Articles of Association, Professor F. C. THOMPSON, D.Met., M.Sc., would fill the

vacancy as Past-President and that, in accordance with Article 22, the Council had nominated the following members to fill the other vacancies :

As President :

S. F. DOREY, C.B.E., D.Sc., F.R.S.

As Vice-Presidents :

MAURICE COOK, D.Sc., Ph.D.
L. B. PFEIL, O.B.E., D.Sc., A.R.S.M., F.R.S.
Major P. LITHERLAND TEED, A.R.S.M.

As Ordinary Members of Council :

R. D. HAMER, B.Sc., Dipl. Ing.
G. P. TINKER, M.Sc.

He reminded members of their rights, under Article 22, to make other nominations, if desired, before the conclusion of the meeting.

SENIOR VICE-PRESIDENT FOR 1954-55

The SECRETARY announced that, in accordance with Article 42, the Council had elected Dr. MAURICE COOK as Senior Vice-President for 1954-55, and that he would be their nominee for the Presidency in 1955-56.

AUTUMN LECTURE

The Chairman introduced Dr. MAURICE COOK, who delivered the Twenty-Fourth Autumn Lecture on "The New Metal Titanium". At the conclusion of the lecture, a hearty vote of thanks to Dr. Cook was proposed by Mr. G. L. BAILEY, C.B.E., M.Sc. (Vice-President) and carried with acclamation. The lecture was printed in the *Journal*, 1953-54, **82**, 93-106.

Tuesday, 22 September

WELCOME TO SOUTHPORT

The meeting was resumed at 9.30 a.m. in the Town Hall, Southport, when the Chair was taken by Lieut.-Commander G. K. RYLANDS, O.B.E., J.P., R.N. (ret'd.), Chairman of the Reception Committee.

His Worship the Mayor of Southport (Alderman WILLIAM TATTERSALL, J.P.), and Lieut.-Commander RYLANDS welcomed members and their ladies to Southport on behalf of the Town and the Reception Committee, respectively. Mr. W. B. WRAGGE, B.Sc. (President of the Manchester Metallurgical Society) also welcomed members and ladies on behalf of the host Societies—the Manchester Metallurgical Society and the Liverpool Metallurgical Society. The President, Professor F. C. THOMPSON, D.Met., M.Sc., replied.

The meeting was then briefly adjourned until 9.50 a.m. when two concurrent scientific sessions took place.

DISCUSSION OF PAPERS

At Session A, Dr. C. J. SMITHELLS, M.C. (Past-President) occupied the Chair, and a general discussion was held based on the following group of papers published in the *Journal*:

Stretcher-Strain Markings

"Some Observations on the Occurrence of Stretcher-Strain Markings in an Aluminium-Magnesium Alloy", by R. Chadwick, M.A., F.R.I.C., F.I.M., and W. H. L. Hooper, B.Sc., A.I.M.

"The Influence of Composition on the Incidence of Strain Markings in Aluminium Alloys", by W. H. L. Hooper, B.Sc., A.I.M.

"The Stepped Stress/Strain Curve of Some Aluminium Alloys", by N. Krupnik, D.I.C., and H. Ford, D.Sc., Ph.D.

"Discontinuous Flow and Strain-Ageing in a 6% Tin Phosphor-Bronze", by N. H. Polakowski, Dipl. Ing., Ph.D.

"Yield-Point Phenomena and Stretcher-Strain Markings in Aluminium-Magnesium Alloys", by V. A. Phillips, A.R.S.M., D.Eng., B.Sc., A.I.M., A. J. Swain, M.A., and R. Eborall, M.A.

"Some Methods of Measuring Surface Topography as Applied to Stretcher-Strain Markings on Metal Sheet", by W. H. L. Hooper, B.Sc., A.I.M., and J. Holden, Ph.D.

"Effect of Composition and Heat-Treatment on Yield-Point Phenomena in Aluminium Alloys", by V. A. Phillips, A.R.S.M., D.Eng., B.Sc., A.I.M.

The following paper was then discussed :

"Priming Paints for Light Alloys", by J. G. Rigg, Ph.D., and E. W. Skerrey, B.Sc., A.I.M.

At the conclusion of each discussion a vote of thanks to the authors was proposed by the Chairman and carried with acclamation.

At Session B, the Chair was taken by Mr. G. L. BAILEY, C.B.E., M.Sc. (Vice-President) and two groups of papers were discussed :

Oxidation and Sulphidation of Copper

"The Oxidation of Copper in the Temperature Range 200°-800° C.", by R. F. Tylecote, M.A., M.Sc., Ph.D., F.I.M.

"Growth of Sulphide Films on Copper", by T. P. Hoar, M.A., Ph.D., F.I.M., and A. J. P. Tucker, M.A., Ph.D.

Diffusion and the Kirkendall Effect

"Micrographic Aspects of the Diffusion of Zinc and Aluminium in Copper", by H. Bückle, Dr. Ing., and J. Blin.

"The Formation of Intracrystalline Voids in Solution-Treated Magnesium-Aluminium Alloys", by E. Lardner, B.Sc., A.I.M.

At the conclusion of each discussion a vote of thanks to the authors was proposed by the Chairman and carried with acclamation.

VISITS

In the afternoon, visits were paid by members to the works of: Automatic Telephone and Electric Co., Ltd., Liverpool; British Insulated Callender's Cables, Ltd., and British Copper Refiners, Ltd., Prescott; The English Electric Co., Ltd., Liverpool; Fibreglass, Ltd., St. Helens; The Manganese Bronze and Brass Co., Ltd., Birkenhead; D. Napier and Son, Ltd., Liverpool; and Pilkington Brothers, Ltd., St. Helens. Other members and ladies paid visits to the works of Horrockses Crewdson Spinning and Manufacturing Co., Ltd., Preston; Liverpool Cathedral; and Speke Hall, Liverpool.

CIVIC RECEPTION

In the evening, members and ladies were the guests of the Mayor and Corporation of Southport at a Civic Reception in the Town Hall.

Wednesday, 23 September

VISITS

Members and ladies paid all-day visits to places distant from Southport, as follows :

(i) The Lancashire Steel Corporation, Ltd., Irlam, and Rylands Brothers, Ltd., Warrington.

(ii) Ministry of Supply, Division of Atomic Energy (Production), Metallurgical Laboratories, Culcheth, and The British Aluminium Co., Ltd., Warrington.

(iii) John Summers and Sons, Ltd., Shotton.

(iv) Metropolitan-Vickers Electrical Co., Ltd., Trafford Park, and Magnesium Elektron, Ltd., Clifton Junction.

(v) Richard Johnson and Nephew, Ltd., Manchester, and Leyland Motors, Ltd., Leyland.

(vi) Thornton Research Centre, The Shell Petroleum Co., Ltd., Thornton-le-Moors, and the Stanlow Refinery of the Shell Refining and Marketing Co., Ltd.

(vii) The City of Chester and Lever Brothers, Ltd., Port Sunlight.

BANQUET

In the evening, members and their ladies were the guests of the Reception Committee at a Banquet and Dance at the Prince of Wales Hotel, Southport.

Thursday, 24 September

The meeting was resumed in the Town Hall, Southport, at 9.45 a.m., when two concurrent scientific sessions were held.

INFORMAL DISCUSSION ON "DAMPING CAPACITY"

The President, Professor F. C. THOMPSON, D.Met., M.Sc., took the Chair at Session A. An informal discussion took place on "Damping Capacity", which was opened by Dr. K. M. ENTWISTLE, who gave a survey of the work on the subject.

DISCUSSION OF PAPERS

At Session B the Chair was taken by Dr. L. B. PFEIL, O.B.E., A.R.S.M., F.R.S. (Member of Council), and discussions took place on two groups of papers published in the *Journal*.

Structure of Nickel Alloys

"The Constitution of Nickel-Rich Alloys of the Nickel-Titanium-Aluminium System", by A. Taylor, Ph.D., F.Inst.P., and R. W. Floyd, B.Sc., A.I.M.

"A Study of Order-Disorder and Precipitation Phenomena in Nickel-Chromium Alloys", by A. Taylor, Ph.D., F.Inst.P., and K. G. Hinton, B.Sc.

"The Constitution of Nickel-Rich Alloys of the Nickel-Chromium-Aluminium System", by A. Taylor, Ph.D., F.Inst.P., and R. W. Floyd, B.Sc., A.I.M.

Properties of Chromium and Its Alloys

"The Properties of Cast Chromium Alloys at Elevated Temperatures. I.—The Melting and Casting of Chromium-Rich Alloys. II.—Some Properties of Certain Binary Chromium-Rich Alloys. III.—The Creep Properties of Ternary and More Complex Chromium-Base Alloys", by A. H. Sully, M.Sc., Ph.D., F.Inst.P., F.I.M., E. A. Brandes, B.Sc., A.R.C.S., F.I.M., and A. G. Provan, B.Sc., A.R.T.C., A.R.I.C.

"The Effect of Temperature and Purity on the Ductility and Other Properties of Chromium", by A. H. Sully, M.Sc., Ph.D., F.Inst.P., F.I.M., E. A. Brandes, B.Sc., A.R.C.S., F.I.M., and K. W. Mitchell, B.Sc.(Eng.), Wh.Sch., A.M.I. Mech.E.

In each case a vote of thanks to the authors was proposed by the Chairman and carried with acclamation.

VOTES OF THANKS

At 12.10 p.m. the President, Professor F. C. THOMPSON, D.Met., M.Sc., took the Chair at a General Meeting.

Dr. S. F. DOREY, C.B.E., F.R.S., Senior Vice-President, moved:

"That the best thanks of the Institute of Metals be, and are hereby, extended to:

(i) The Presidents and Councils of the Manchester Metallurgical Society and the Liverpool Metallurgical Society for their kind invitation to the Institute to hold this Autumn Meeting in Southport.

(ii) The Chairman, Lieut.-Commander G. K. Rylands, O.B.E., R.N. (Retd.), J.P., the Honorary Secretary, Mr. S. V. Radcliffe, and the members of the Reception Committee, for the excellent arrangements made for this meeting.

(iii) The companies and individuals who so generously subscribed to the Hospitality Fund in connection with this meeting.

(iv) His Worship the Mayor of Southport (Alderman William Tattersall, A.M.I.Mech.E., J.P.) for his welcome and for his hospitality.

(v) The Corporation of Southport for kindly placing accommodation for this meeting at the disposal of the Institute and for their hospitality.

(vi) The Directors of the following establishments and companies for their invitations to members and guests to visit their works and laboratories and for their hospitality: Automatic Telephone and Electric Co., Ltd., Liverpool; The British Aluminium Co., Ltd., Warrington; British Insulated Callender's Cables, Ltd., and British Copper Refiners, Ltd., Prescott; Division of Atomic Energy (Production), Ministry of Supply, Culcheth; The English Electric Co., Ltd., Liverpool; Fibreglass Ltd., St. Helens; Horrockses Crewdson Spinning and Manufacturing Co., Ltd., Preston; W. and R. Jacob and Co. (Liverpool), Ltd., Aintree; Richard Johnson and Nephew, Ltd., Manchester; The Lancashire Steel Corporation, Ltd., Irlam; Arthur H. Lee and Sons, Ltd., Birkenhead; Lever Brothers, Port Sunlight, Ltd., Port Sunlight; Leyland Motors Ltd., Leyland; Magnesium Elektron, Ltd., Clifton Junction; Manganese Bronze and Brass Co., Ltd., Birkenhead; Metropolitan-Vickers Electrical Co., Ltd., Trafford Park; D. Napier and Son, Ltd., Liverpool; Pilkington Brothers, Ltd., St. Helens; Rylands Brothers, Ltd., Warrington; The Shell Petroleum Co., Ltd., Thornton-le-Moors; The Shell Refining and Marketing Co., Ltd., Stanlow; John Summers and Sons, Ltd., Shotton; and Williams, Harvey and Co., Ltd., Bootle.

(vii) All others who have contributed in any way to the success of this meeting."

Dr. L. B. PFEIL, O.B.E., A.R.S.M., F.R.S., Member of Council, seconded the motion, which was put to the meeting by the President and carried with acclamation.

Mr. H. J. MILLER, M.Sc. (President of the Liverpool Metallurgical Society) replied on behalf of the hosts.

The business meeting then terminated.

VISITS

In the afternoon members visited the works of: British Insulated Callender's Cables, Ltd., and British Copper Refiners, Ltd., Prescott; The Manganese Bronze and Brass Co., Ltd., Birkenhead; and Williams, Harvey and Co., Ltd., Bootle. Other members and ladies visited the tapestry works of Arthur H. Lee and Sons, Ltd., Birkenhead, the biscuit factory of W. and R. Jacob and Co. (Liverpool), Ltd., Aintree, and Knowsley Hall, Prescott.

Friday, 25 September

TOUR IN NORTH WALES

A party of members and ladies took part in an all-day tour in North Wales.

The meeting then concluded.

RECEPTION COMMITTEE

The arrangements for the meeting were made with the assistance and advice of a Reception Committee constituted as follows:

Lieut.-Commander G. K. RYLANDS, *Chairman* (Rylands Brothers, Ltd., Warrington).

Dr. W. E. ALKINS (Thomas Bolton and Sons, Ltd., Stoke-on-Trent).

Mr. H. ALLISON (Metropolitan-Vickers Electrical Co., Ltd., Manchester; President, Manchester Metallurgical Society, 1952-53).

Dr. S. F. BARCLAY (Mather and Platt, Ltd., Manchester).

Mr. E. BOWYER (British Insulated Callender's Cables, Ltd., Prescott).

Mr. C. F. BRERETON (Richard Johnson and Nephew, Ltd., Manchester).

Mr. R. S. BROWN (Rylands Brothers, Ltd., Warrington; President, Liverpool Metallurgical Society, 1952-53).
 Mr. G. T. CALLIS (Manganese Bronze and Brass Co., Ltd., Birkenhead).
 Mr. B. G. CHURCHER (Metropolitan-Vickers Electrical Co., Ltd., Manchester).
 Mr. C. F. DAVEY (Thomas Bolton and Sons, Ltd., Widnes).
 Sir ROY H. DOBSON (A. V. Roe and Co., Ltd., Middleton).
 Mr. I. W. F. FAIRHOLME (Richard Johnson and Nephew, Ltd., Manchester).
 Mr. W. L. GOVIER (Imperial Chemical Industries, Ltd., Metals Division, Kirkby).
 Capt. A. C. JESSUP (Magnesium Elektron, Ltd., Clifton Junction).
 Dr. W. L. KENT (The British Aluminium Co., Ltd., Warrington).
 Mr. S. KERR (The Lancashire Steel Corporation, Ltd., Irlam).
 Mr. H. J. MILLER (President, Liverpool Metallurgical Society).
 Professor E. C. ROLLASON (University of Liverpool).
 Mr. L. ROTHERHAM (Ministry of Supply, Division of Atomic Energy (Production), Risley).
 Mr. F. R. SMITH (The English Electric Co., Ltd., and D. Napier and Son, Ltd., Liverpool).
 Professor F. C. THOMPSON (University of Manchester).
 Mr. W. T. T. WILCOX (The Shell Petroleum Co., Ltd.).

Mr. W. B. WRAGGE (President, Manchester Metallurgical Society).
 Mr. S. V. RADCLIFFE, *Honorary Secretary* (Rylands Brothers, Ltd., Warrington).

GENERAL MEETING

27 November 1953

A GENERAL MEETING of the Institute of Metals was held, jointly with the Institution of Metallurgists, at the Royal Institution, Albemarle Street, London, W.1, on Friday, 27 November 1953, from 10.30 a.m. to 4.30 p.m. The Chair was taken by the President of the Institute of Metals, Professor F. C. THOMPSON, D.Met., M.Sc.

INFORMAL DISCUSSION ON "THE TRAINING OF METALLURGISTS FOR INDUSTRY"

An informal discussion was held, which was opened at the morning session by Professor A. G. QUARRELL, D.Sc., Ph.D., A.R.C.S., D.I.C., Professor of Metallurgy, University of Sheffield, and at the afternoon session by Mr. JAMES MITCHELL, C.B.E., Director of Stewarts and Lloyds, Ltd., Corby, and President of the Iron and Steel Institute. A condensed account of the discussion is printed in the *Bulletin*, 1953-54, vol. 2, pp. 88-89 (March 1954).

SOME FRICTION EFFECTS IN WIRE DRAWING * 1409

By G. D. S. MacLELLAN,† M.A., Ph.D.

SYNOPSIS

The paper develops a generalized version of Sachs's theory, to allow for the effect of a cylindrical extension to a conical die channel, commonly called a "parallel". Previously published results are re-examined in the light of this analysis, and results from further experimental investigations are given. It is concluded that "parallels" have an appreciable effect on the drawing force, and that allowance must be made for their effect in the derivation of coefficients of friction from back-pull experiments.

An attempt to determine coefficients of friction from experiments with "split" dies was also made. Such a method, if successful, would give results independent of plasticity theory, but the results obtained were inconclusive. This was probably due to the penetration of lubricant between the halves of the split dies, which gave rise to additional forces of unknown magnitude.

SYMBOLS USED IN THE PAPER

A	.	Cross-sectional area of wire at any section (in. ²).
D	.	Diameter of wire at any section (in.).
F	.	Resultant axial load on the die (lb.).
F_s	.	Resultant force on one half of the die, in a plane perpendicular to the wire axis (lb.).
P	.	Drawing force (lb.).
Q	.	Back-pull (lb.).
Y	.	Yield stress of wire at any section (lb./in. ²).
b	.	Back-pull factor $(P_0 - F)/Q$. (N.B. $P_0 = F_0$.)
l	.	Length of "parallel", expressed as a fraction of D_2 .
p (subscript)	.	"Parallel."
r	.	Fractional reduction of area $(A_1 - A_2)/A_1$.
t (subscript)	.	Used occasionally to distinguish total force on die from that on conical part of die alone.
0 (subscript)	.	Value of parameter in the absence of back-pull.
1 (subscript)	.	Value of parameter at entry to die.
2 (subscript)	.	Value of parameter at exit from die.
α	.	Die semi-angle.
ϵ	.	Natural strain $\log_e (A_1/A_2)$.
λ	.	$\mu \cot \alpha$ (abbreviation).
μ	.	Coefficient of friction.
σ	.	Stress.

I.—INTRODUCTION

THE paper consists largely of a condensation of parts of a Dissertation submitted by the author at Cambridge University in 1948. Since then Baron and Thompson have published an account of a similar investigation.¹ Consequently, a comparative discussion of their results and conclusions has been incorporated here.

The object of the original work was to develop a theoretical analysis which would account for certain experimentally observed features of the wire-drawing process resulting from friction effects. The conclusions reached are in essential agreement with those of Baron and Thompson, with certain additions and minor changes summarized in Section VI.

The extension of the theory of the wire-drawing process advanced has been tested on all known published experimental results which provide sufficient data, as well as on some previously unpublished

results obtained at Cambridge and elsewhere, and it appears to go further towards explaining and correlating these results than previous theories. There is still a need, however, for a much more elaborate investigation to secure complete and reliable data over a wider range of materials and conditions. The present paper attempts to indicate the significant variables for such a project.

II.—WIRE-DRAWING THEORY

1. GENERAL REMARKS

The theory developed in the next section was originated by Sachs,² and has been subsequently discussed and generalized by Davis and Dokos,³ Lunt and MacLellan,⁴ and MacLellan.⁵ The only additional comment appropriate here is that D. G. Christopherson has pointed out in a private communication that the equivalence of the von Mises and the maximum-shear-stress yield criteria in wire drawing, proved by Lunt and MacLellan⁴ for small values of μ , is true for any magnitude and distribution of the surface frictional shear stress; that is, it follows merely from the axial symmetry of the stress distribution and the coincidence of the principal axes of strain increment and stress.

With the assumptions described in the above papers, and for a conical die channel, the following relation results:

$$P = (1 + \mu \cot \alpha) \cdot A_2^{1 + \mu \cot \alpha} \int_{A_2}^{A_1} \frac{Y}{A^{1 + \mu \cot \alpha}} \cdot dA + \left(\frac{A_2}{A_1} \right)^{1 + \mu \cot \alpha} \cdot Q. \quad (1)$$

where Y is a function of A only, i.e. variation of yield stress across the section of the wire is neglected. In many cases Y is best expressed as a function of the natural strain $\epsilon \left(= \log_e \frac{A_1}{A_2} \right)$, cf. Baron and Thompson,¹

* Manuscript received 26 October 1951.

† Engineering Laboratory, Cambridge University.

and with this change of the independent variable and the substitution of $\lambda = \mu \cot \alpha$, we get:

$$\frac{P}{A_2} = (1 + \lambda) e^{-\lambda \epsilon} \int_0^\epsilon Y \cdot e^{\lambda \epsilon} \cdot d\epsilon + e^{-\lambda \epsilon} \cdot \frac{Q}{A_1} \quad (2)$$

Sachs's original solution, for $Y = \text{constant}$ and $Q = 0$, expressed in these terms, becomes:

$$\frac{P}{A_2} = \left(1 + \frac{1}{\lambda}\right) \cdot Y_m \cdot (1 - e^{-\lambda \epsilon}) \quad (3)$$

The integrals in equations (1) and (2) can be evaluated graphically or analytically if μ , and hence λ , is known. In experimental work it is usually required to find μ . It is then essential to assume an analytical approximation for the variation of Y with ϵ (or A), if an explicit relation for λ , and hence for μ , is to be obtained.

Hill and Tupper's solution⁶ of the wire-drawing problem from considerations of the strain configuration and the associated stress distribution has not been adopted, because in its present form it reveals two major inconsistencies. The first, concerned with the failure of the analogy between the two- and three-dimensional patterns, has been mentioned in the discussion⁷ of Baron and Thompson's paper. Secondly, their solution appears to imply maximum shear stresses in the wire at the exit end of the die considerably greater than the yield stress; specifically, the sum of the last two columns of their Table I gives the ratio of the sum of the theoretical longitudinal tensile and lateral compressive stresses to the yield stress in the exit plane, and its value ranges from 1.087 to 1.668 for the various conditions represented. Baron and Thompson adduce a number of other arguments for not accepting Hill and Tupper's solution in its present form.

2. DEVELOPMENT OF THEORY TO ALLOW FOR A PARALLEL EXTENSION

Difficulty was found in accounting for a number of experimental observations until allowance was made for the effect of a parallel extension. Many dies are still produced with an appreciable length of "parallel", or at least with a relief taper of only 1° or 2° , with the object of increasing their strength and resistance to abrasion. Even those which are nominally conical are almost certainly rounded off at the throat in the processes of manufacture and polishing.

To provide a basis for the extension of the theoretical analysis, certain assumptions concerning the behaviour of the wire in the parallel must be made. The chief of these are:

(i) The mean coefficient of friction μ at the wire/die interface is the same in the parallel as in the conical part of the die channel.

(ii) The wire does not neck-down in the parallel, i.e. it remains everywhere in contact with the die channel.

(iii) Although there can be little or no further plastic deformation in the parallel, the maximum shear stress in the wire remains everywhere in the

parallel equal to the yield stress Y_2 of the wire as it leaves the conical section of the die channel.

In justification of assumption (ii), it is only necessary to point out that if necking-down takes place, the longitudinal drawing stress must be equal to the yield stress for the strain-hardened wire. Such a state of stress in strain-hardened wire implies little margin of safety against the wire breaking, and is therefore unlikely to be of much practical importance. A smaller reduction, and consequently a smaller drawing stress, would be used. On the other hand, the wire leaves the conical deformation zone in a state of limiting stress. Owing to friction in the parallel, the longitudinal tensile stress will increase, and consequently the lateral compressive stress must decrease. Thus, just sufficient plastic flow will take place at each section of the parallel to relieve the pressure at that section to the value which, together with the longitudinal tensile stress, will satisfy the plastic-stress condition of assumption (iii). The amount of additional plastic deformation required will be very small, and little error will be introduced by assuming that the yield stress remains constant at Y_2 .

Consider a cylindrical parallel extension to the conical die channel, of diameter D_2 and length l . D_2 . The condition for statical equilibrium of the metal in the parallel, assuming as usual a stress distribution uniform across the wire section, is:

$$\frac{\pi}{4} \cdot D_2^2 \cdot \frac{d\sigma_z}{dz} = \mu \cdot \pi D_2 \cdot \sigma_h \quad (4)$$

where z is the co-ordinate in the direction of drawing, σ_z and σ_h are the axial tensile and lateral compressive stresses, respectively, and μ is the coefficient of friction at the interface. In combination with the plastic stress condition:

$$\sigma_h + \sigma_z = Y_2 \quad (5)$$

we get by integration:

$$P_t = A_2 Y_2 (1 - e^{-4\mu l}) + P \cdot e^{-4\mu l} \quad (6)$$

where P_t is the total drawing force and P is the drawing force in the absence of parallel. Thus the additional drag P_p due to the parallel is:

$$P_p = P_t - P = (A_2 Y_2 - P)(1 - e^{-4\mu l}) \quad (7)$$

which can sometimes be written with sufficient accuracy (10% error for $\mu l = 0.05$):

$$P_p = 4\mu l (A_2 Y_2 - P) \quad (8)$$

Neglecting the effect of back-pull on μ and Y_2 , and using equation (1) to express P in terms of the drawing force without back-pull P_0 , and the back-pull Q , for a simple conical die channel:

$$P = P_0 + Q \cdot \left(\frac{A_2}{A_1}\right)^{1+\mu \cot \alpha} \quad (9)$$

we obtain:

$$P_t = P_{0,t} + Q \cdot e^{-4\mu l} \cdot \left(\frac{A_2}{A_1}\right)^{1+\mu \cot \alpha} \quad (10)$$

where the suffix 0 signifies drawing force without

back-pull. The slope of the F/Q curve, or back-pull factor b , for a die with parallel is thus given by:

$$b = 1 - e^{-4\mu l}(1 - r)^{1 + \mu \cot \alpha} \quad (11)$$

where r is the fractional reduction of area $(A_1 - A_2)/A_1$.

The variation of b with r for different values of μ , l , and $\cot \alpha$ is shown in Fig. 1.

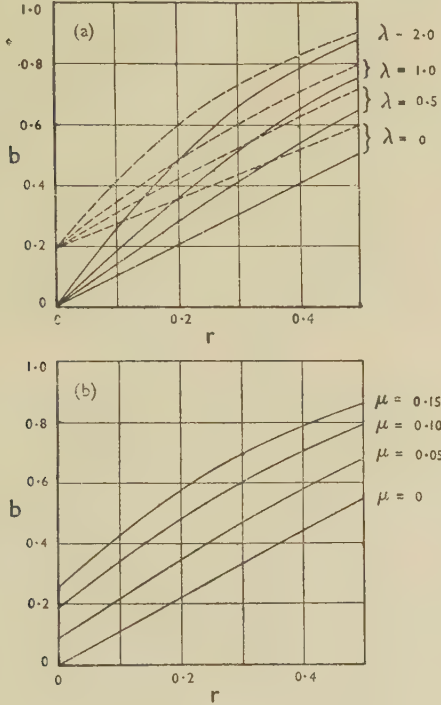


FIG. 1.—Theoretical Variation of Back-Pull Factor (a) for Two Values of μl and (b) for Particular Values of α and l .

(a) $\mu l = 0$ (—); $\mu l = 0.05$ (---); $\mu \cot \alpha = \lambda$.
(b) $\cot \alpha = 10$; $l = 0.5$.

Fig. 1 (a) shows clearly that, even for $\mu l = 0.05$, with $r = 0.3$ and $b = 0.5$, neglect of the effect of parallel would lead to an estimate of μ about twice too large. When $l = 0$, equation (11) reduces to:

$$b = 1 - (1 - r)^{1 + \mu \cot \alpha} \quad (12)$$

the relation previously given by MacLellan.⁵

It is of interest to note that equations (6) and (11) imply non-zero values of $P_{0,t}$ and b , respectively, for $r = 0$. Equation (6) leads to:

$$\begin{aligned} P_{0,t}(r=0) &= A_2 Y_2 (1 - e^{-4\mu l}) \\ &= A_1 Y_1 (1 - e^{-4\mu l}) \end{aligned} \quad (13)$$

since $A_1 = A_2$ and $Y_1 = Y_2$ for $r = 0$; and equation (11) leads to:

$$b_{(r=0)} = 1 - e^{-4\mu l} \quad (14)$$

Neither of these results is likely to be accurate, because the assumption that the wire will be just plastic at entry to the parallel is not fulfilled for $r = 0$, but the existence of any such intercepts on the ordinate axes of the $P_{0,t}/r$ and b/r graphs may be explainable thus.

Francis and Thompson⁸ and Davis and Dokos³ have noted the existence of intercepts on some $P_{0,t}/r$ curves, and have discussed their significance. The former workers suggest that the explanation is due to friction loss in some form; the magnitudes of their intercepts can now be accounted for not unreasonably in terms of the present theory of the effect of parallel. The latter suggest that the effect is due to an elasticity effect of some sort, but their reasoning is far from convincing, cf. MacLellan⁵ and Baron and Thompson,¹ and the present analysis offers a more plausible explanation. Insufficient details are given about their dies for any calculations to be made. Some results obtained by the present author, revealing intercepts, are reported below.

III.—THE APPLICATION OF THE THEORY

The object of this section is to establish the validity of the more complete theoretical analysis which allows for the effect of parallel, and which has been presented above. It is not possible to review all the available data as fully as was done in the original Dissertation, but the sources and the relative value of those employed for the present analysis will be briefly discussed. The collected results are summarized in Table III (p. 11).

1. EXPERIMENTS WITHOUT BACK-PULL

The only published results concerning the magnitude of the drag due to the parallel, P_p , are those of Linicus and Sachs⁹ and of Baron and Thompson.¹ The former compared the forces required to draw 63:37 brass through 3-mm. steel dies ($\alpha = 8^\circ$), with and

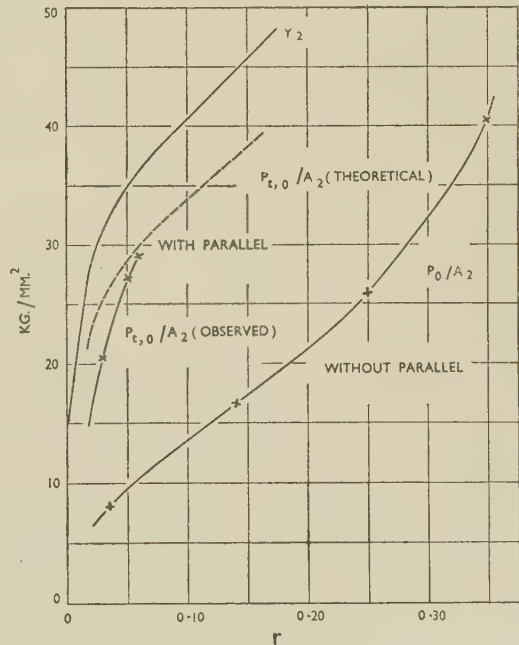


FIG. 2.—Effect of Parallel on Drawing Stress. $Q = 0$.
(According to Linicus and Sachs,⁹ Fig. 31.)

without a 10-mm. cylindrical extension. Their results are reproduced in Fig. 2, together with the curve for Y_2 obtained from tests on the wire when drawn through a plain conical tungsten carbide die ($\alpha = 8^\circ$).

Using Linicus and Sachs's estimate of $\mu = 0.1$ for brass on hardened steel, with rapeseed oil as lubricant, $e^{-4\mu l} = 0.26$, and the corresponding theoretical curve obtained by the use of equation (6) is shown dotted in Fig. 2. The curve "without parallel", incidentally, tends towards an intercept on the P/A_2 axis, which suggests either that it was not in fact "without parallel" or that other effects contribute to the behaviour of the curve for $r \rightarrow 0$.

Corresponding calculations have been made for the published data provided by Baron and Thompson in their Fig. 9. The results have been given in a contribution to the discussion of their paper,⁷ and the general conclusion is that the present theory overestimates the magnitude of P_p by a factor of 2. No satisfactory explanation of this is known.

2. PREVIOUS EXPERIMENTS WITH BACK-PULL

Howden and Lunt,¹⁰ Wistreich,¹¹ and Baron and Thompson¹ have provided the only published discussions of the variation of back-pull factor b with the experimental variables. Lewis,¹² Simons,¹³ and Thompson¹⁴ have furnished isolated data, which it is, however, of interest to analyse and fit into the general picture. Lueg and Pomp¹⁵ carried out a more extensive investigation, but were primarily interested in the immediate practical results of drawing with back-pull, such as the saving of power and changes in the diameter and temperature of the wire as it leaves the die. W. C. Heselwood has also made some experiments, quoted by Wistreich,¹¹ and described in an unpublished report. R. W. Lunt and his fellow workers have made a large number of back-pull measurements (so far unpublished) in connection with die wear and lubrication experiments, and sets of their results relevant to the present discussion have been analysed in detail.

(a) *Howden and Lunt*.¹⁰—Values of μ were derived from values of b by means of the form of the back-pull theory given by Lunt and MacLellan,⁴ but the authors did not attempt to consider the effect of parallel, although this is stated to have been in some cases as much as $l = 0.5$. Their data have now been re-analysed, and are considered further below.

(b) *Wistreich*.¹¹—This paper contains a fairly complete review of the experimental observations of the variation of b , but without any attempt to explain the results.

(c) *Baron and Thompson*.¹—Their investigation provides considerable new data on the variation of b , and corresponding values of μ evaluated by means of equation (12), for a wide range of dies, lubricants, and reductions of area. It appears from their results that any effect of parallel, even if due only to a small radius at the throat of the die, was negligible, except possibly for very small reductions of area. Anomalous results

for such reductions are explained in terms of "redundant strain", but curvature of the die channel may have been a contributing factor.

An important conclusion from their investigation is that μ is independent of r . Variation of r was achieved by drawing wire from one coil through one of a series of dies, i.e. A_1 was kept constant and A_2 varied. It will be seen that the same conclusion is reached by the present author by the method of drawing different sizes of wire through one die, i.e. A_2 kept constant and A_1 varied. Data from Baron and Thompson's Table IV and Fig. 16 are included in Table III as typical of their results, the values of μ tabulated being the average derived from their curves 1, 2, and 3, for which μ is more nearly constant.

(d) *Lewis*.¹²—Slightly strain-hardened basic mild steel ($D_1 = 0.025$ in.) was drawn at 30 ft./min. through a tungsten carbide die ($\alpha = 5^\circ$, $l = 0.5$) with soap as lubricant and $r = 0.228$. The data give $b = 0.50$, and consequently $\mu = 0.087$ from equation (11); neglect of the effect of parallel would give $\mu = 0.145$.

(e) *Simons*.¹³—As Baron and Thompson¹ point out, the back-pull curve published by Simons shows an appreciable departure from linearity, due, they suggest, to variations of μ with interfacial pressure. The data relate to 0.44% carbon patented steel wire ($D_1 = 0.098$ in.), drawn "at very slow speed" with dry soap as lubricant through a tungsten carbide die ($\alpha = 7^\circ$, $l = 0.5$, $r = 0.333$). Approximating to the curve by the best straight line, determined by the method of least squares, its slope gives $b = 0.55$; correspondingly, $\mu = 0.075$, which agrees well with Lewis's result, while neglecting the effect of parallel would give $\mu = 0.120$.

(f) *Thompson*.¹⁴—One set of results is directly comparable with those of Simons. Mild-steel wire ($D_1 = 0.0715$ in.) was drawn with a "very good" soap lubricant (No. 3535) at a speed of 0.06 in./min. through a tungsten carbide die ($\alpha = 5.5^\circ$, $l = 0$, $r = 0.191$). The back-pull curve gives $b = 0.315$, and consequently $\mu = 0.074$. However, when the speed was raised to 3.22 in./min., b fell to 0.20, and correspondingly $\mu = 0.004$. This is the opposite of a speed effect noted by Baron and Thompson,¹ who found that μ increased with speed (cf. their Fig. 21), and also contrary to the effect Thompson himself obtained with 7% nickel silver drawn through the same die as the mild steel; for this μ rose from 0.039 to 0.075 for a speed increase from 0.06 to 3.22 in./min.

A further point, of somewhat academic interest, is that back-pull experiments carried out with the die rotating led in several instances to values of b less than r —implying effectively negative values of μ , according to the present theory.

(g) *Lueg and Pomp*.¹⁵—Because of their more practical interests, little information is given in the published account of the work of Lueg and Pomp about the shapes of the die channels or the mechanical properties of the wire. In a private communication A. Pomp has stated: "The dies were of the same

nature as those used in commerce. The die channel has not been examined more closely. It is to be assumed that a short piece of cylindrical shape is attached to the cone-shaped part, as this is generally used for wire-drawing dies. The die angle has not been tested. It is to be assumed that variations are less than 1% from the angle stated (11° total)."

Their results relate to a 0.58% carbon steel wire ($D_1 = 4.0$ mm. = 0.157 in.) and to a low-carbon rolled steel wire ($D_1 = 5.0$ mm.), the drawing being through tungsten carbide dies with drawing oil as lubricant. The unspecified amount of parallel limits the value of the results for the present purpose. However, whereas Wistreich¹¹ concludes that for the

one of the drafts is anomalous owing to the rusty and scarred surface of the wire; this subsequently became burnished by the reduction, and the other results form a consistent series. Wistreich concludes that b increased by about 30% with cold work. This implies an increase in μ , but the fact that the variation of b with tensile strength is discontinuous for the two steels tested, suggests that μ is not a function specifically of the mean interfacial pressure, but rather of the variation of the state of the wire and its surface as a result of cold-work.

(h) *Heselwood*.—Wistreich¹¹ quotes Heselwood's results to suggest that, for steels drawn through tungsten carbide dies with soap as lubricant, b increases with increasing α , the reverse of the variation suggested by equation (12). Re-examination of the die-channel profiles by Howden and Lunt,* by means of Wood's metal casts, revealed that the dies had curved profiles, and that instead of the 6° and 8° quoted for the two dies by Heselwood, the actual die angle α was approximately 5° (average) for both dies for the relevant reduction of area ($r = 0.20$). The converging parts were followed by virtually parallel extensions which Heselwood described as having a "bearing relief of 1° ", but which in the light of the present theory appear to have acted as parallels of length $l = 1.2$ and 2.0 , respectively (the values of l being obtained from Heselwood's figures for "length of bearing"). The corresponding values of μ , calculated from equation (11), range between 0.052 and 0.093, being approximately the same for the same steel in each die; thus the coefficient of friction appears to depend more on the surface of the wire than on the surface of the die. (If the effect of parallel is neglected, the apparent coefficients of friction, obtained by the use of equation (12), range from 0.21 to 0.35.)

(i) *Lunt and Fellow Workers*.—Experiments were made on a specially constructed drawbench, incorporating a spring-mounted die-holder by means of which the force on the die could be determined. Copper wire was drawn through tungsten carbide and diamond dies, the die sizes being in the range 0.035–0.040 in. dia., and the usual drawing speed 1.5 ft./min. Various lubricants were used, these normally being brushed on to wire which had previously been degreased in ethylene trichloride, washed in 5% nitric acid solution, rinsed in water, and dried. The mechanical properties of the wire unfortunately were not measured, so there can be no quantitative discussion of the effect of parallel on the magnitude of the observed drawing forces.

The detailed review given in the present author's Dissertation will not be repeated here, but the general conclusions, from those of Lunt's results sufficiently related to reveal a dependency of b on r , with other conditions kept nearly constant, is that they can all be reasonably explained in terms of equation (11). In particular, although a parallel must be stipulated for much of the data for which the exact profile of the

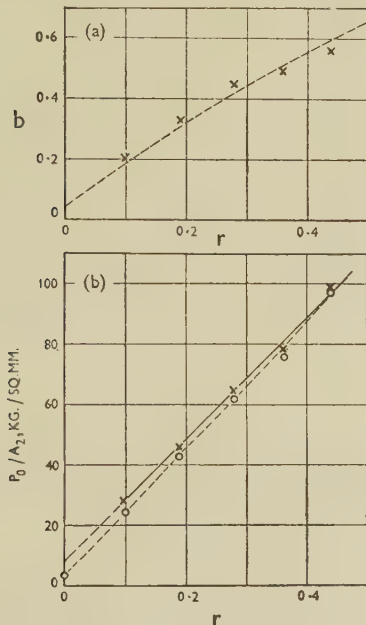


FIG. 3.—Variation of (a) Back-Pull Factor and (b) Drawing Stress with Reduction of Area. (According to Lueg and Pomp.¹⁵) 0.58% C patented steel wire; tungsten carbide ($5\frac{1}{2}^\circ$) series of dies; Lubricant: drawing oil. Theoretical curve: $\mu l = 0.0125$; $\mu \cot \alpha = 0.5$ ($\alpha = 5\frac{1}{2}^\circ$, $\mu = 0.05$, $l = 0.25$). Ringed points in Fig. 3 (b) obtained after allowance for parallel.

first of Lueg and Pomp's data $b = 0.14 + 1.03r$, and, implicitly, therefore that it does not satisfy equation (12) which applies to dies without parallel, Fig. 3 (a) shows that the results are adequately explained on the supposition of $\mu = 0.05$ and parallels of magnitude $l = 0.25$. Values of yield stress Y are not given in the paper, but from data for the breaking load after drawing (*Brucklast*), an upper limit to Y_2 , and hence to P_p/A_2 according to equation (7), can be calculated. With this allowance for the effect of parallel, the intercept of the P_0/A_2 against r curve on the ordinate axis is reduced, but does not vanish, as shown in Fig. 3 (b).

Lueg and Pomp's other results are for wire drawn successively through a series of dies, each draft having $r = 0.30$, approx. These have been discussed by Wistreich,¹¹ and Pomp, in his private communication, has confirmed Wistreich's conclusion that the result for

* Private communication.

die channel has not been known, in all five instances of diamond dies where the profiles were examined under a microscope through flat "windows" in the sides of the crystals, before they were mounted in their metal cases, the results are explainable on the present theory. In four of them, no appreciable parallel could be detected and correspondingly the observed b/r relationship can be explained within the probable experimental error on the assumption that $l = 0$, as shown for example in Fig. 4 (a), curve B. In the other, the channel profile was curved (α ranged from a mean effective value of about 2° at $r = 0.025$ to about 10° at $r = 0.25$, followed by a parallel of effective length about $l = 0.25$), and the corresponding b/r curves obtained with different lubricants reveal

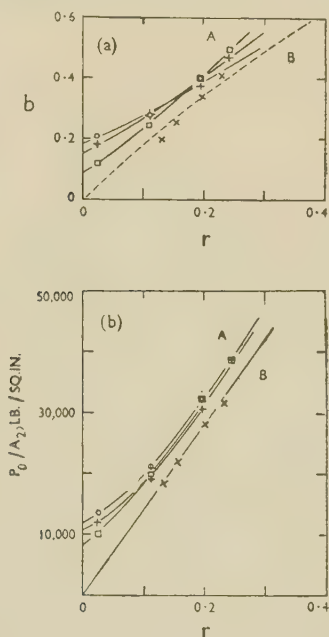


FIG. 4.—Variation of (a) Back-Pull Factor and (b) Drawing Stress with Reduction of Area, for (A) Non-Conical and (B) Conical Diamond Dies. (According to Lunt.)

A. Non-conical die (0.0367 in. dia.). Lubricant: \square Colza oil; \circ D.T.D. 417A; + brown soap.

B. 5° conical die (0.350 in. dia.). Lubricant: \times Ethyl palmitate.

The broken curve in Fig. 4 (a) is a theoretical one derived from equation (11) with $l = 0$, $\alpha = 5^\circ$, and $\mu = 0.075$.

large intercepts on the b axis, as shown in Fig. 4 (a), curves A. The presence and absence of intercepts in the P_0/r curves similarly correspond, although no quantitative comparison with the theory can be made without knowledge of the mechanical properties of the wire. All the results for the non-curved die profiles are summarized in Table III, the two tungsten carbide dies being the same as those used by Heselwood and thus providing an independent check on the absence of any specific die effect.

3. CONCLUSIONS

The results reviewed are generally consistent with the present author's extended theory, but as none of

the work, except that of Baron and Thompson, was designed with the object of assessing the validity of a theoretical analysis, it was desirable, as previously mentioned, to obtain additional confirmation, and the experiments described in the next Section were accordingly undertaken.

Amongst the data quoted above, there are a few anomalous results, such as the large variation of μ with speed noted by Thompson¹⁴ and the apparent increase of μ noted by Baron and Thompson¹ for small reductions. These serve to emphasize the fact that there are many variable factors in the wire-drawing process, and the best that a theory such as that advanced in the present paper can do is to account for the major trends in the observed phenomena, without too much complexity and over the range of the variables of practical importance.

IV.—EXPERIMENTAL INVESTIGATION

The objects of the experimental work were:

(i) To obtain additional data concerning the variation of the back-pull factor.

(ii) To investigate the possibilities of using a split die to deduce values of the coefficient of friction μ in wire drawing, without reference to plasticity theory, as suggested by MacLellan⁵; specifically, for a simple conical die channel:

$$\mu = \frac{F \cot \alpha - \pi F_s^*}{F + \pi F_s^* \cot \alpha} \quad (15)$$

where F is the axial force and F_s the splitting force on the die, that is, the transverse component of the reaction between the wire and one half of the die.

1. APPARATUS

To simplify the attempted measurement of the splitting force F_s , it was decided to measure P and Q directly, rather than the axial force on the die ($F = P - Q$). The drawing force P has been measured directly by Becker,¹⁶ and by Rosenhain and Stott,¹⁷ in each case by turning the wire, after it left the die, through 180° round a spring-supported pulley, whose deflection could be measured. This was the method now adopted.

A general view of the apparatus is shown in Fig. 5 (Plate I) and a close-up view in Fig. 6 (Plate I). The dies used all had throat dia. of about 0.040 in., which represented a compromise between the desirability of a small size of wire (to avoid the necessity for handling large weights of wire and for providing large drawing power), and of a large size of die (to reduce the effect of slight errors in manufacture and to ease the die-makers' problem in the production of split dies). In addition, if the pulley method of measuring P was to be satisfactory, it was necessary that the drawn wire should be sufficiently flexible not to affect the measurements; this was confirmed by comparing calibration tests made with string and with samples of the wire, when no effect could be detected.

* A misprint occurred in the original statement of the equation.

The wire was fed to the die over a 4-in.-dia. guiding pulley, mounted on a ball-race, and on leaving the die it was turned through 180° round an identical pulley and thence passed to a 4.15-in.-dia. steel drawing-capstan or "block". This block was driven through two gear-boxes by means of belt-and-chain drives from a $\frac{1}{2}$ h.p. D.C. electric motor, the range of drawing speed being 0.5–5.0 ft./min. (0.25–2.5 cm./sec.). A reversing switch was fitted, so that the tension in the drawn wire could be reduced smoothly.

The second pulley, on the exit side of the die, was freely supported by a length of chain, which passed round a small ball-race guide to one end of a pivoted lever. The other end of the lever was linked to the base of the draw-bench frame by a spring, selected to give a suitable range of movement for the range of loads of interest at any particular time. The movement of the spring operated a 12-in. radius pointer giving approximately 10:1 magnification. Calibration was carried out with the appropriate spring in position, the die removed, and a dead load applied by the ordinary back-pull loading system. Friction losses at the various guide pulleys were negligible, to the accuracy to which the drawing force could be measured; this was confirmed by replacing the spring by a weight-pan, when the change of load required just to maintain motion in one direction rather than the other was less than 0.2 lb.

The die support was such that either ordinary tungsten carbide and diamond dies could be used, or one of two special "split" dies, one steel and the other tungsten carbide; the lower half of the latter is shown in Fig. 6 (Plate I). Each of the halves of the split dies was supported behind against the drawing force by three $\frac{1}{8}$ -in.-dia. steel balls, two of which were guided by triangular grooves in both dies and back-plate, and one by a groove in the back-plate alone. This gave the kinematically correct design of line-and-point support, and at the same time kept friction opposing vertical movement of the upper half of the die to a minimum. The steel balls were held approximately in position by pins projecting from the bottom of the grooves in the die. The tungsten carbide split die was so made that wire could be drawn through it in either direction, the effective die angle in one direction being approximately twice that in the other direction; the groove in the lower half of the die for use when the die is reversed is visible in Fig. 6.

Contact between the two halves of the split dies took place only in the neighbourhood of the die channel itself, over a nominal area of approximately $\frac{1}{2}$ -in. square. For the correct relative positioning of the two halves reliance was placed on the three-ball supports, the grooves and flat surfaces of which were machined with the halves still pinned together by the tightly fitting pegs which were in place when the die channels were drilled and polished. The holes from which the pegs have been withdrawn are visible in Fig. 6.

The upper half of the die was pressed on to the lower by means of an open-coiled helical compression

spring, shown in Fig. 5. The force in the spring was transmitted to the die by a $\frac{5}{8}$ -in.-dia. steel ball; this was centred on the die by a 0.1 in.-dia. recess in its top surface vertically above the throat of the die channel. Since the resultant vertical force on the top half of the die due to the wire acted within about 0.02 in. of the die throat, and the half-die was 1.3 in. thick, the two main vertical forces were collinear and caused no couple. The compression spring, chosen to suit the range of forces involved, was separately calibrated in a compression-testing machine, the compressed length of the spring being measured by means of a pair of external calipers. The force exerted by the spring on the die was varied by means of the screw head visible at the top of Fig. 5.

Two dial gauges, reading directly to 0.0005 in., were so mounted as to detect relative vertical movement of the two halves of the die. They were supported by means of brackets welded to the back of the die-holder, so that elastic displacements of the gauges relative to the bottom half of the die, due to the compression spring loading, were kept very small.

2. WIRE

In the early stages of the investigation soft iron wire was used, but copper wire proved easier to handle, gave smoother drawing with a more nearly constant value for the drawing force under any given drawing conditions, and yielded more reproducible results; it was therefore employed for all the later readings.

Owing to the difficulty of producing a series of geometrically similar dies, particularly of the split variety used in some of the experiments, it was more convenient to obtain a range of r by drawing different sizes of wire through one die. For this purpose, four coils of copper wire were obtained which, for ease of working, had been prepared in a slightly hardened state by giving them a 10% reduction of area after the last anneal down to the sizes as delivered, namely 0.0419, 0.0449, 0.0477, and 0.0508 in. dia.

Before and after drawing, the wire diameters were measured with a Zeiss micrometer, reading to 0.0001 in., and samples of the wires were tested on a Hounsfield tensometer. Load/extension curves can easily be recorded on this instrument, but it is a lengthy procedure to correct the extension observations with allowances for initial kinks in the wire. Consequently, these curves were used only to determine the yield stress and ultimate tensile stress of the various wires. The careful work of Ford on strip-rolling of copper¹⁸ has shown that the value of the stress at which the load/extension curve bends over into the plastic-deformation region is a suitable measure of the yield stress for roll-torque calculations, and therefore the same assumption has been made for wire drawing. The ultimate tensile stress is the breaking load of the wire divided by its area before testing.

Typical results are shown in Table I, the various reductions of area being obtained by drawing the different sizes of wire through a tungsten carbide die ($D_2 = 0.0395$ in., $\alpha = 6\frac{1}{2}^\circ$). The yield stress of the

wires before drawing ranged within $\pm 7\%$ of the mean of 40,000 lb./in.², and the ultimate tensile strength within $\pm 5\%$ of 42,000 lb./in.², but the results

TABLE I.—*Mechanical Properties of Copper Wire Used in Drawing Experiments.*

D_1 , in.	D_2 , in.	r	Yield Stress, lb./in. ²		U.T.S., lb./in. ²	
			Before Drawing	After Drawing	Before Drawing	After Drawing
0.0419	0.0395	0.112	39,000	45,000	40,000	46,000
0.0449	0.0395	0.225	36,700	49,000	41,000	50,500
0.0477	0.0395	0.315	43,500	54,000	44,200	55,000
0.0508	0.0393	0.400	40,500	56,500	41,500	57,000

after drawing lie within about 2% of smooth curves when plotted as functions of r , each point plotted representing the result of two or three tests which were in close agreement.

3. DIES

In the first series of experiments, ordinary industrial tungsten carbide and diamond dies in a newly polished state were used. The die-channel shapes were determined as far as possible by inspecting the profile of wire, partially drawn and then withdrawn from each die, on a Hilger projection microscope at a magnification of $\times 50$. This procedure gives no indication of the length of parallel, if any, but from a comparison of corresponding results obtained for the split dies with their channel shapes observed directly, the method appears to give an indication of the shape of the converging part of the channel accurate within $\frac{1}{2}^\circ$.

Figs. 7 and 8 (Plate I) are photographs of one half of the steel and the tungsten carbide split dies, respectively, taken by means of a Vickers projection microscope. The edges of the channels are not sharply defined because during polishing, for which process the two halves of the dies were tightly clamped together, the polishing powder tended to work its way between the halves, and in so doing, rounded off the edges of the semicircular channels. Consequently wire drawn through these dies always revealed slight "fins". Their height was less than 1% of the wire diameter, so that they exercised a negligible effect on the flow of the metal. Again, on account of manufacturing difficulties the complete die channels were not truly circular. The carbide die was 0.004 in. out-of-round, and the steel die was initially about the same, though it wore to appreciably more. Mean diameters have been used in calculations.

There is considerable rounding of the die-channel profile of the steel die over the length for which the wire makes contact with it (for $r = 0.40$, this is about 0.065 in., or 0.65 in. in the photograph). The mean effective semi-angle for the converging part of the channel has been taken as $5\frac{3}{4}^\circ$.

As mentioned, the carbide die can be used for drawing in either direction, and it has much more nearly

conical converging channels. The semi-angles have been taken as 6° and $11\frac{1}{2}^\circ$. The apparent rounding at the throat is much less than for the steel die, but is greater at one edge than the other.

4. LUBRICATION

After some preliminary tests, the observations were all made with castor oil as lubricant. This gives smooth drawing and is commonly used industrially. It was applied by means of a paint brush after the wire had been cleaned with acetone, just before drawing.

V.—EXPERIMENTAL RESULTS

1. BACK-PULL EXPERIMENTS

No effect of drawing speed on the drawing force has been detected in the range 0.5–5.0 ft./min., so that all the results recorded are for a drawing speed of 1.0 ft./min. The usual closely linear relation between drawing force and back-pull has always been obtained, except for slight departures at the extremes of the range of Q . Some typical results are shown in Fig. 9,

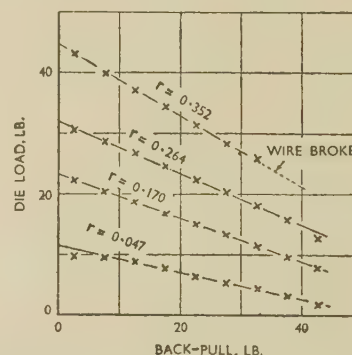


FIG. 9.—Typical Back-Pull Curves Obtained with Tungsten Carbide Split Die ($a = 11\frac{1}{2}^\circ$).

and others were given in the discussion of Baron and Thompson's paper.⁷ For $Q = 0$, it is difficult to ensure that the wire enters the die axially, and reproducible results are not easily obtained. Consequently, observations were not normally recorded with Q less than 2.6 lb. (the weight of the wedge grip and weight pan alone), and the values of P_0 referred to later have been determined by extrapolation. For high values of Q , when the wire was almost at breaking point on the drawn side, the results also tended to be erratic.

The curvature of back-pull curves noted by Baron and Thompson in their experimental results,¹ and explained in terms of a decrease of μ with increasing Q , has not been found in the experiments described here.

Each point on the curves of Fig. 9 represents the mean of three observations, between which the wire was partially slacked off by reversing the motor. In making any single observation wire was drawn for 15–20 sec. From a few observations made over a longer period this was found to give a result usually

within $\pm 1\%$ of the longer-period average. Reproducibility of back-pull curves between one day and another a week or two later, was not so good, changes of 3 or 4% occurring in the value of the back-pull factor. This may be due to variations in the surfaces of the wires or dies, in the lubricant, and in the atmospheric conditions of temperature and humidity. Where such reproducibility tests have been made, the average of the values of b has been taken.

TABLE II.—Data for Copper Wire Drawn Through Tungsten Carbide "Ardoloy" Die ($\alpha = 6^\circ$, $l = 0.31$).

D_1 , in.	D_2 , in.	r	b	P_0 , lb.	Y_2 , lb./in. ²	$\frac{P_0}{\mu l} = \frac{P_0}{0.05}$, lb.	$\frac{P_0}{A_0}$, lb./in. ²	$\frac{(P_0 - P_2)}{A_2}$, lb./in. ²
0.0419	0.0395	0.112	0.38	20.8	46,000	7.9	17,000	10,500
0.0449	0.0395	0.226	0.59	34.3	49,000	5.7	28,000	23,300
0.0477	0.0395	0.314	0.69	46.6	54,000	4.3	38,000	34,500
0.0508	0.0393	0.401	0.77	62.0	57,000	1.5	51,000	50,000

The diameter of the drawn wire D_2 shows a slight decrease for the greatest reduction of area. This suggests continued plastic flow of the metal after leaving the conical part of the die, under the influence of the correspondingly large drawing stresses. The effect is apparently sufficiently small not to have upset the agreement of the experimental results with the theoretical analysis.

The relation between b and r revealed in Fig. 10 (a) is far from the simple proportionality predicted by Hill's theory,¹⁹ as quoted by Baron and Thompson, on the assumption that μ is independent of r . In this theory, effects of parallel were not considered, and the following relation was obtained:

$$b = r(1 + \mu \cot \alpha) \quad (16)$$

If it is supposed that the absence of proportionality in these results is due to a variation of μ , the corresponding range of μ is from 0.25, at small reductions, to 0.097, at the largest, a result which is most improbable when compared with other better-known friction phenomena.

If, however, the theoretical relation of equation (11) is used, allowing for the effect of parallel, a theoretical curve can be fitted with good agreement to the results now observed, just as for the previously published results reviewed in Section III, 2. The values of the parameter $\mu \cot \alpha$ and μl for this fitted curve presuppose the existence of a parallel for which $l = 0.31$, and a corresponding value of $\mu = 0.16$. This figure is roughly the mean of the μ values calculated from equation (16), but it provides a more acceptable explanation of the observed variation of b with r . As has been mentioned, l could not be determined from the profile of partly-drawn wire, but confirmation of the estimate is provided by Fig. 10 (b).

The curve of P_0/A_2 against r shown in curve C of Fig. 10 (b) is, in this instance, identical in shape with that which would be obtained by plotting P_0 against r , because A_2 is kept constant. Since stress is a more fundamental quantity than force in the deformation of metals, it has seemed more appropriate to consider the former as the dependent variable.*

FIG. 10.—Variation of (a) Back-Pull Factor and (b) Drawing Stress with Reduction of Area, for Various Conical Dies with Parallel.

The curves in Fig. 10 (a) are theoretical ones, corresponding to equation (11), with the values of the parameters μ and $\mu \cot \alpha$ shown below. In Fig. 10 (b) the ringed points represent the values of the drawing stress after allowance has been made for the effect of parallel according to equation (17), using the same values for the two parameters.

- A. 12° diamond dies (\times 0.0383 in. dia., $12\frac{1}{2}^\circ$ die; $+$ 0.0406 in. dia., $11\frac{1}{2}^\circ$ die; \bullet 0.0424 in. dia., $11\frac{1}{2}^\circ$ die). $\mu l = 0.04$; $\mu \cot \alpha = 1.0$ ($\mu = 0.021$, $l = 0.19$, $\alpha = 12^\circ$).
- B. $5\frac{1}{2}^\circ$ diamond die (0.0449 in. dia.). $\mu l = 0.04$; $\mu \cot \alpha = 1.0$ ($\mu = 0.1$, $l = 0.4$, $\alpha = 5\frac{1}{2}^\circ$).
- C. 6° tungsten carbide die (0.0395 in. dia.). $\mu l = 0.05$; $\mu \cot \alpha = 1.5$ ($\mu = 0.16$, $l = 0.31$, $\alpha = 6^\circ$).

Firstly, results obtained with a tungsten carbide "Ardoloy" die are summarized in Table II, and the corresponding curves for b and P_0/A_2 as functions of r are plotted in Fig. 10, curve C. The results are typical, so that it is convenient to discuss them immediately.

* There has been some confusion as to the results of the two methods of plotting in the past, owing to the fact that if r is achieved by using a series of dies rather than a series of wires, A_2 varies, and curves of P_0/A_2 against r differ in shape from those of P_0 against r . An example of this confusion is to be found in a comparison of Fig. 7 of Francis and Thompson⁸ with Fig. 15 of Thompson and Francis,²⁰ the results of which are claimed to be "in complete agreement". The former in fact shows a linear dependence of P_0 on r with A_1

constant, but consequently a curved relationship between P_0/A_2 and r ; the latter also shows a linear dependence of P_0 on r , in this case with A_2 kept constant, and therefore a linear dependence of P_0/A_2 on r . The exact shape of the curves in either case, however, must depend on the work-hardening characteristics of the metal being drawn, and the occurrence of a linear relationship in any particular instance must be largely fortuitous. The results are therefore not considered further from this point of view.

The significant feature is the tendency in these and in many other results for the curves to lead to a positive intercept on the P_0/A_2 axis, as was mentioned at the end of Section II, 2. From equations (6) and (7) we obtain the following equation which expresses the drag due to the parallel in terms of the observed total drawing force:

$$P_p = (A_2 Y_2 - P_t)(e^{4\mu l} - 1). \quad (17)$$

In Table II, P_p calculated from this equation is tabulated, using the value of μl (0.05) corresponding to the theoretical curve *c* of Fig. 10 (a). With this allowance for the effect of parallel, the equivalent tensile stress on the reduced section for a die without parallel, $(P_0 - P_p)/A_2$, has also been plotted in Fig. 10 (b). The points lie on a smooth curve passing through the origin.

Confirmation of all these characteristics of the results is provided by corresponding sets of data obtained with four diamond dies. The results are summarized in curves *A* and *B* of Fig. 10, those represented by curves *A* being for three dies all of which had approximately the same die angle, and those represented by curves *B* for the fourth die, which had a die angle roughly half that of the others. The b/r results are again satisfactorily co-ordinated by theoretical curves satisfying equation (11), but surprisingly the same theoretical curve is involved in each case. This implies that $\mu = 0.1$ for the $5\frac{1}{2}^\circ$ die, compared with $\mu = 0.2$ for the other three, of twice the die angle. There is similar evidence of such an effect of die angle, though less marked, from tests on the carbide split die, described below, and Baron and Thompson¹ record a similar result in Table IV of their paper. A comparison with the series of theoretical curves shown in Fig. 1 shows that the shift of the theoretical curve corresponding to halving the die angle for constant μ (whatever the value of l) would be considerably greater than any probable experimental error in the results. There were no obvious roughnesses of the die-channel surfaces to account for the high value of μ .

Finally, Fig. 11 summarizes the data obtained from experiments on the steel and the tungsten carbide dies, when used as ordinary dies with the two halves clamped together.

The data for the steel die, shown in curves *A*, are scattered, partly owing to the difficulty of reproducing results on account of the high rate of wear of the die channel. The results, however, exhibit the same trends, and allowance for the effect of parallel has the usual effect of correlating the b/r results and accounting for the P_0/r intercept. The surprising feature of the results is the value of l , namely 0.33, which has to be adopted to account for the intercepts on both curves. Direct inspection of the die-channel shape, Fig. 7 (Plate I), indicates a slightly curved contour at the throat, with a length of channel in which the sides are approximately parallel, of about $l = 0.12$.

The results for the tungsten carbide split die are similar. A direct estimate of the length of parallel is $l = 0.1$, but the apparent effective value is about 0.4.

The larger die angle causes a slight increase in μ , as remarked above, and the intercept on the P_0/A_2 axis for the 6° die is not wholly accounted for by the assumed values for μ and l , see Fig. 11 (b), curve *B*.

The data as a whole for l and μ as a function of the die, from both this and previously published investigations, are summarized in Table III. The values of both quantities fall within reasonable ranges, although some individual results are unexpected. Firstly, the values of μ range from 0.05 to 0.21, but are mostly between 0.06 and 0.10. These are of a magnitude to

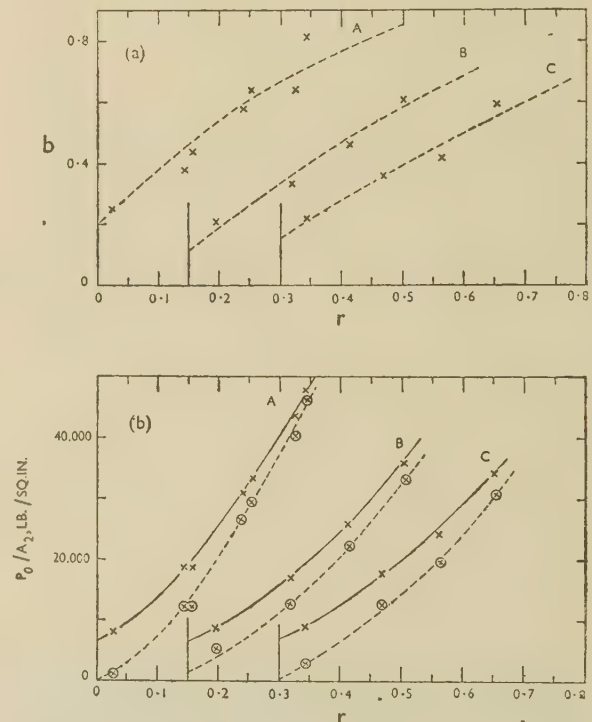


Fig. 11.—Variation of (a) Back-Pull Factor and (b) Drawing Stress with Reduction of Area for Steel and Carbide Split Dies.

The curves shown have the equivalent significance to those in Fig. 10.

- A. $5\frac{1}{2}^\circ$ steel split die (0.0412–0.0417 in. dia.). $\mu l = 0.06$; $\mu \cot \alpha = 1.5$ ($\mu = 0.16$, $l = 0.33$, $\alpha = 5\frac{1}{2}^\circ$).
- B. 6° tungsten carbide split die (0.0409 in. dia.). $\mu l = 0.032$; $\mu \cot \alpha = 0.75$ ($\mu = 0.08$, $l = 0.40$, $\alpha = 6^\circ$).
- C. $11\frac{1}{2}^\circ$ tungsten carbide split die (0.0409 in. dia.). $\mu l = 0.04$; $\mu \cot \alpha = 0.5$ ($\mu = 0.10$, $l = 0.40$, $\alpha = 11\frac{1}{2}^\circ$).

be expected for boundary lubrication, and their total range is considerably reduced by the allowance for parallel. This has been mentioned earlier in the discussion of previously published data, but the same conclusion follows from the fact that without allowance for parallel many of the series of b/r data could only be related by supposing a large variation in μ .

Secondly, those data which do not reveal an intercept on the b/r graphs do not show one in the P_0/A_2 against r graphs. This applies to the diamond-die results of Lunt and his fellow workers, and to Baron and Thompson's results. The latter are not conclusive, however, because in achieving a range of r between 0.185 and 0.42 with a series of three dies,

TABLE III.—Summary of Back-Pull Data.

Fig. No.	Source	Wire	Die Material	Lubricant	α	l	μ
	Baron and Thompson ¹	63 : 37 Brass	WC	Soap	5°	0	0.06
		" "	"	Castor oil	5°	0	0.12
	Lewis ¹²	Mild Steel	WC	Soap	5°	0.5	0.087
	Simons ¹³	0.44% C Steel	WC	Dry soap	7°	0.5	0.075
	Thompson ¹⁴	Mild Steel	WC	Soap	5½°	0 "	0.074
3	Lueg and Pomp ¹⁵	0.58% C Patented Steel	WC (5 dies)	Drawing oil	5½°	0.25	0.05
	Heselwood	Mild Steel	WC	Soap	5°	2.0	0.058
		18 : 8 Stainless	"	"	5°	1.2	0.052
		" "	"	"	5°	2.0	0.093
		High-C Steel	"	"	5°	1.2	0.083
		Red Fox 135	"	"	5°	2.0	0.093
			"	"	5°	2.0	0.058
	Lunt <i>et al.</i>	Copper	WC	D.T.D. 417A	5°	2.0	0.06
		"	"	"	5°	1.2	0.06
		"	"	Colza oil	6½°	0.2	0.16
		"	"	Brown soap	6½°	0.2	0.12
4		"	Diamond	Ethyl palmitate	5°	0	0.075
		"	Diamond (3 dies)	Ethyl stearate	8½°	0	0.075
10	MacLellan	Copper	WC	Castor oil	6°	0.3	0.16
10		"	Diamond (3 dies)	"	12°	0.2	0.21
10		"	Diamond	"	5½°	0.4	0.10
11		"	Steel (split)	"	5½°	0.3	0.15
11		"	WC (split)	"	6°	0.4	0.08
11		"	"	"	11½°	0.4	0.10

α also ranged from 4.7° to 5.8°; in terms of the cotangent of the angle, this is a range from 12.1 to 9.8.

Thirdly, the effective values of l for all the data except those from the split dies are consistent with

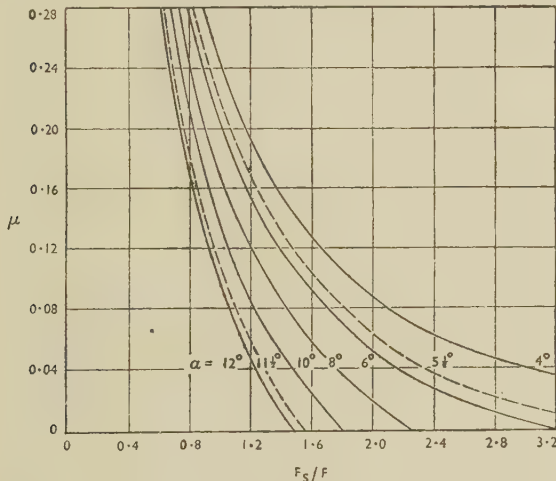


FIG. 12.—Theoretical Variation of μ with F_s/F for a Conical Die Channel.

what might be expected from the other limited evidence available. The split dies give results implying unexpectedly large values of l . The cause of this is not known but the fact remains that the shapes of the b/r and P_0/A_2 against r curves can be satisfactorily correlated for particular values of l .

2. SPLIT-DIE EXPERIMENTS

For a conical die channel, the coefficient of friction is given by equation (15). From the preceding section, and from the results that follow, it appears necessary once again to consider the effect of parallel. The magnitude of the splitting force F_s is affected by the pressure distribution on the wall of the parallel, and thus it is impossible to arrive at a value of μ without reference to the stress distribution in the part of the wire within the parallel zone. Making the same assumptions as in Section II, 2, a very lengthy expression is obtained relating the total splitting force $F_{s,t}$, including the effect of parallel, to the total axial die reaction F_t . With the approximations $\mu^2 \ll 1$, $\mu \ll \cot \alpha$, and $2\mu l \ll 1$ (the last only when it occurs in terms of small order), we obtain :

$$F_{s,t} = \frac{4l \left(A_2 Y_2 - \frac{P_{0,t}}{b} \right)}{\pi(1 + \mu \cot \alpha)} + \frac{\cot \alpha + 4l \left(\frac{1}{b} - 1 - \mu \cot \alpha \right)}{\pi(1 + \mu \cot \alpha)(1 - 4\mu l)} \cdot F_t \quad (17)$$

in which b can be replaced by a function of r as given by equation (11).

For $l = 0$ equation (17) reduces, as it should, to equation (15), with the approximation $\mu \ll \cot \alpha$. Fig. 12 shows μ as a function of F_s/F for different values of α with $l = 0$. It will be observed that for each value of α , F_s/F has its maximum value, $\cot \alpha / \pi$, when $\mu = 0$.

To determine F_s , the two halves of the die were initially pressed together by means of the calibrated spring with a force much greater than that which the wire could exert in the opposite direction. With drawing in progress at 1 ft./min., the force in the spring was gradually reduced by slow and steady rotation of the screw head, using a box spanner. When both dial gauges indicated relative movement of at least 0.00025 in. between the halves of the die, the corresponding compressive force was deduced from the length of the compressed spring. This measurement was made a sufficient number of times (usually three) for a consistent reading to be obtained with each value of the back-pull.

It had been intended to obtain a check on this measurement by recording also the compressive force for which the drawing force began to drop as a result of the separation of the die halves. This proved to be less sensitive, however, and the drawing force showed no consistent drop until the separation exceeded about 0.001 in. Throughout the experiments, the dead-weight of the upper half-die, the ball, and the spring was allowed for.

Results for the carbide die are shown in Figs. 13 and 14. They are more scattered than those for the simple back-pull experiments, because an average value of F_s over a length of wire cannot be obtained; once the position of limiting equilibrium of the upper half of the die has been reached by loosening the compression spring, any further slight increase in F causes the die halves to separate further and conditions change permanently. On each diagram are

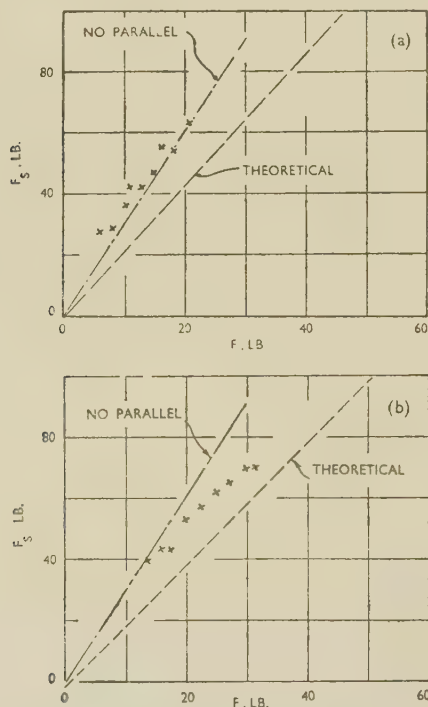


FIG. 13.—Variation of Splitting Force with Axial Die Reaction for a 6° Tungsten Carbide Split Die.

(a) $r = 0.170$; (b) $r = 0.264$.

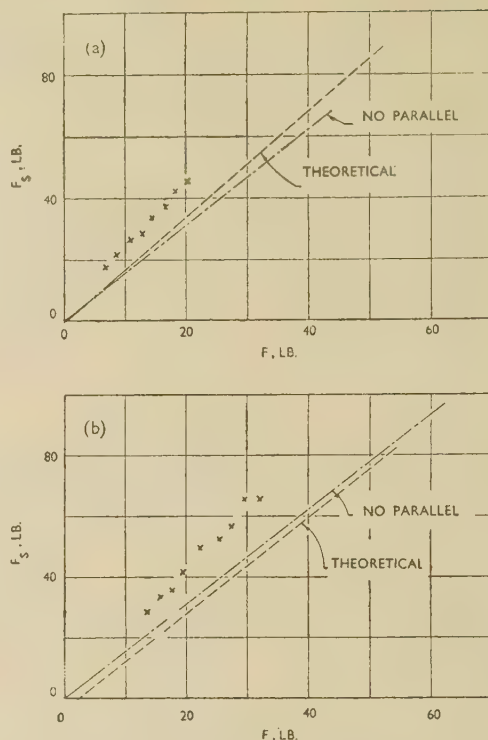


FIG. 14.—Variation of Splitting Force with Axial Die Reaction for a 11½° Tungsten Carbide Split Die.

(a) $r = 0.170$; (b) $r = 0.264$.

shown two straight lines: one represents the line of greatest possible slope, corresponding to no parallel and no friction, the other the theoretical straight line corresponding to equation (17), with the values of μ and l obtained in the back-pull experiments.

Although each set of results indicates an approximately linear relation between F_s and F as the back-pull Q is varied, none is adequately represented by a straight line through the origin, and each is above the theoretical line derived from the experimentally determined back-pull factor. From their differing positions relative to the no parallel, no friction lines, it seems that no consistent explanation can be found which neglects parallel. The fact that all indicate a higher splitting force than would be expected from back-pull results, suggests that some further factor contributes to the total effective splitting force. Hydrostatic pressure developed in the lubricating oil which penetrates between the halves of the die provides a possible explanation.

This oil penetration occurred even when the halves of the die were first cleaned, and then kept tightly clamped by the spring during the whole of a drawing operation, and was apparent as an easily visible film of oil. Attempts to draw unlubricated wire were unsuccessful because the drawing force fluctuated wildly. No theoretical estimate of the magnitude of the possible effect has been obtained, and the investigation had to be concluded before the effect of lubricants of

different viscosity or surface tension could be investigated.

The observations were concerned only with static balance of the forces on the upper half-die, so forces due to dynamic effects, such as the rate of separation of the die halves in the presence of an intervening oil film, need not be considered.

The steel split die gave generally similar, but less reproducible results.

VI.—CONCLUSIONS

(1) The results of the investigation are in general agreement with those of Baron and Thompson.¹

(2) A theory of wire drawing which does not allow for the effect of cylindrical extensions to the conical die channel is frequently inadequate. Such an extension of Sachs's theory has been made, and accounts for many observed effects.

(3) The variation of coefficient of friction with interfacial pressure, noted by Baron and Thompson, is not of sufficient magnitude to influence the usefulness of a theoretical analysis which neglects the variation.

(4) The values of μ which result from the theoretical analysis of the back-pull results are mostly in the range 0.06–0.10, and without the allowance made for the effect of parallel, this range would be considerably greater.

(5) Allowance for parallel also provides an explanation of the presence of intercepts on curves of drawing force (or stress) as a function of reduction of area.

(6) The magnitudes of the parallels implied by the theory are not unreasonable, except for the split dies, though few direct checks are available. For the split dies, the magnitudes are unexpectedly large, but the use of such dies may have affected the deformation process more than is apparent from an examination of the external surface of the wire.

(7) The split-die method of determining μ independently of plasticity theory has not proved satisfactory in this investigation, although time was a limiting factor in the experimental work. It is believed

that penetration of lubricant between the halves of the die was the cause of the inconclusive results.

(8) In any further investigations of friction and lubrication effects in wire drawing, the need for a full record of the mechanical properties of the wire and of the die profiles is stressed. Measurement of the latter is now a practical possibility as a result of the development of a die profilometer by the British Iron and Steel Research Association, as described by Withers.²¹ The back-pull experimental procedure appears to lead to a reliable estimate of the effect of parallels on stress distribution, and although the need for any appreciable length of parallel disappeared many years ago with the introduction of carbide instead of steel dies, some present manufacturing methods appear to lead to their creation. Their presence causes an increase in drawing force, with no compensating advantage, at least as far as the wire is concerned. A fuller investigation of this problem would, however, be of interest.

(9) The conclusions reached as a result of this investigation are necessarily still to some extent tentative, owing to insufficient data, but it has been felt desirable to present the work as far as it has been carried in the hope that it will provide a useful basis and pointer for further investigations.

ACKNOWLEDGEMENTS

The author is indebted to Professor E. K. Rideal, F.R.S., Dr. R. W. Lunt, and Professor D. G. Christopherson for encouragement and discussions at different stages of this investigation; to Thomas Bolton and Sons, Ltd., for permission to make use of results obtained by Dr. Lunt in one of their research projects, and for the supply of wire and dies used in the work at Cambridge; to Bruntons (Musselburgh), Ltd., and British Ropes, Ltd., Doncaster, for the special manufacture of split dies; to Mr. D. Searle and other members of the Engineering Laboratory staff for assistance with apparatus; and to the British Iron and Steel Research Association for a grant for equipment.

REFERENCES

1. H. G. Baron and F. C. Thompson, *J. Inst. Metals*, 1950–51, **78**, 415.
2. G. Sachs, *Z. angew. Math. u. Mech.*, 1927, **7**, 235.
3. E. A. Davis and S. J. Dokos, *J. Appl. Mechanics*, 1944, **11**, A193.
4. R. W. Lunt and G. D. S. MacLellan, *J. Inst. Metals*, 1946, **72**, 65.
5. G. D. S. MacLellan, *J. Iron Steel Inst.*, 1948, **158**, 347.
6. R. Hill and S. J. Tupper, *J. Iron Steel Inst.*, 1948, **159**, 353.
7. G. D. S. MacLellan, *J. Inst. Metals*, 1951, **79**, 501 (discussion).
8. E. L. Francis and F. C. Thompson, *J. Inst. Metals*, 1931, **46**, 313.
9. W. Linicus and G. Sachs, *Mitt. Material., Sonderheft*, 1931, (16), 38.
10. J. M. Howden and R. W. Lunt, *Wire Ind.*, 1945, **12**, 411, 641.
11. J. G. Wistreich, *J. Iron Steel Inst.*, 1947, **157**, 417.
12. K. B. Lewis, *Wire and Wire Products*, 1933, **8**, 197, 234, 266, 331.
13. L. Simons, *ibid.*, 1938, **13**, 229.
14. F. C. Thompson, *J. Iron Steel Inst.*, 1933, **128**, 369F.
15. W. Lueg and A. Pomp, *Stahl u. Eisen*, 1943, **63**, 229.
16. R. Becker, *Z. techn. Physik*, 1925, **6**, 298.
17. W. Rosenhain and V. H. Stott, *Proc. Roy. Soc.*, 1933, [A], **140**, 9.
18. H. Ford, *Proc. Inst. Mech. Eng.*, 1948, **159**, 115.
19. R. Hill, Confidential report of the British Iron and Steel Research Association, 1948.
20. F. C. Thompson and E. L. Francis, *Carnegie Schol. Mem., Iron Steel Inst.*, 1931, **20**, 87.
21. J. M. Withers, *J. Iron Steel Inst.*, 1950, **164**, 63.

Mechanism of Precipitation in Aluminium-Magnesium Alloys

By E. C. W. PERRYMAN and G. B. BROOK

(*J. Inst. Metals*, 1951, **79**, 19.)

Dr. C. EDELEANU,* M.A. (Member): I should like to ask the authors to clarify two points. I cannot fully understand why they insist that the precipitate particles found after certain ageing treatments are rods and not plates. Although I agree with them that rods could sometimes look like lines in a random section, the chances are small. The chances of two systems being parallel to the polished surface would be even smaller; whilst the appearance of three systems in one of the grains in Fig. 4 (Plate I of the paper) suggests the presence of more than three rod directions if, in fact, these particles are rods.

I am sure that the authors realize that the energies of activation as calculated in the present case are not easy to interpret, and I feel that the value of Fig. 20 (p. 26) is more practical than theoretical. I would therefore like to ask what accuracy they claim for this figure, and whether it is based on data other than it was possible to give in Figs. 17 and 18 (Plate VI of the paper).

Professor P. LACOMBE,† Dr.-ès-Sci. (Member) and M. A. BERGHÉZAN ‡: The particular interest of the work by Perryman and Brook lies in their attempt to study systematically the decomposition of aluminium-magnesium solid solutions by comparison and combination of various experimental methods, such as hardness measurements, and metallographic and X-ray examination. However, the degree of agreement between the different methods, and the comparison of certain micrographic features, does not always seem very decisive. We should welcome further information on the following points.

(1) The distinction between continuous and discontinuous precipitation seems somewhat arbitrary, if one takes as sole criterion the character of the X-ray lines at large angles of diffraction. To assume the existence of discontinuous precipitation from the simultaneous occurrence of lines corresponding to the initial quenched and the final equilibrium solid solutions, does not appear to take sufficient account of the fact that X-ray diagrams can give only an average result. The volume of metal irradiated by the X-ray beam includes a large number of grains whose dimensions, structural condition, and uniformity of magnesium content may be very different. It follows that the rate of decomposition may vary greatly, not only from one grain to another, but even within a single grain, as we have shown elsewhere.§ In particular, the existence of intragranular boundaries, due to polygonization in solid-solution grains, leads to a considerable lack of uniformity of precipitation even within a single grain (see Figs. A and B, Plate II). The micrograph shown in Fig. 11 (Plate III of the paper), not interpreted by the authors, strongly resembles the intragranular networks which we have shown to

exist in the aluminium-zinc and aluminium-copper solid solutions.

There is no need even to introduce the phenomenon of polygonization to provide evidence for the occurrence of these important differences in rate of decomposition of the solid solution. One of us (P. L.),|| when investigating aluminium-magnesium alloys high in magnesium (>9%), experienced considerable difficulty in homogenizing a polycrystalline aggregate in the as-cast condition. In alloys of high magnesium content, such as those used by Perryman and Brook, it is frequently possible to distinguish by simple micro-examination after anodic oxidation, considerable variations of magnesium concentration on a scale larger than that of the grain-size.¶ This represents a persistence of the concentration differences associated with solidification. In the study of the decomposition of solid solutions, it is thus extremely important to ensure that all the constituent crystals are in a state of complete homogeneity. The uniformity and definition of the K_{α_1, α_2} doublet for large diffraction angles provide a criterion of this initial homogeneity in a quenched solid solution. This condition does not seem to have been fulfilled in the alloy shown in Fig. 14 (Plate IV of the paper).

(2) The authors state that the rate of precipitation at the grain boundaries varies from one boundary to another, depending on the relative orientation of the neighbouring grains, large differences of orientation giving rise to the highest rates of precipitation. Experimental evidence of this very important fact, associated with the internal energy and the specific structure of the grain boundaries, was first given by Chalmers and his co-workers** in connection with this same alloy and also with copper-beryllium alloy. We have drawn attention to the same fact in respect of aluminium-zinc and aluminium-copper alloys.†† Fig. C (Plate II) shows two twinned crystals in aluminium-12% zinc solid solution after prolonged ageing at room temperature. Precipitation is restricted to the discontinuities of the twin boundary, the straight portion of the boundary, corresponding to the trace of the twin plane (111), being completely devoid of such precipitation. This result agrees with the concept of energy minima of twin boundaries, due to Read and Shockley.‡‡ Finally, the authors state that an increasing zinc content retards the rate of precipitation at boundaries. This very important conclusion does not, however, seem to be supported by a comparison of Figs. 7 and 8 (Plate II of the paper).

(3) The hypothesis of the existence of two intermediate precipitated phases, β_1 and β_2 , based on differences of sharpness (definition) of the X-ray lines, seems a little arbitrary, all the more so as the authors state that the lattice spacings corresponding to the diffuse rays of β_2 are the same as those for certain β_1 lines.

* Brown-Firth Research Laboratories, Sheffield; formerly Metallurgy Department, Cambridge University.

† Laboratoire de Chimie Appliquée, Ecole Nationale Supérieure de Chimie, Paris; formerly Laboratoire de Professeur Chaudron, Vitry-sur-Seine.

‡ Centre de Recherches des Tréfileries et Laminiers du Havre, Antony (Seine); formerly Laboratoire de Vitry-sur-Seine du Centre National de la Recherche Scientifique.

§ P. Lacombe and A. Berghézan, *Compt. rend.*, 1949, **228**,

1733; **229**, 365; *Aluminium*, 1949, **18**, 365.

|| P. Lacombe, Thesis, Université de Paris, 1943.

¶ P. Lacombe and P. Morize, *Métaux et Corrosion*, 1944, **19**, 30.

** P. J. E. Forsyth, R. King, G. J. Metcalfe, and B. Chalmers, *Nature*, 1946, **158**, 875.

†† A. Berghézan, (in the press).

‡‡ W. T. Read and W. Shockley, *Phys. Rev.*, 1950, [ii] **78**, 275.

The AUTHORS (*in reply*): While we agree with Professor Lacombe that the rate of precipitation may vary from one grain to another, we do not think that this can explain the simultaneous occurrence of X-ray-diffraction lines corresponding to the initial quenched and the final equilibrium solid solutions. If discontinuous precipitation did not occur and there was a variation in rate of precipitation from one grain to another, then by X-ray examination we should observe lines which increased in breadth with time of ageing; we would not expect to see the sudden appearance of new lines corresponding to the equilibrium solid solution. One of us (E. C. W. P.) has also experienced great difficulty in homogenizing as-cast aluminium-magnesium alloys. Even after a long homogenizing treatment the segregation of magnesium is clearly shown by large variations in rate of precipitation from one area to another. The wrought material which was used for this work did not, however, show any variation in rate of precipitation similar to that observed in cast material. Professor Lacombe suggests that the structure shown in Fig. 11 (Plate III of the paper) may be polygonized. This type of structure was not, however, observed in the commercial-purity 7% magnesium alloy. It may be that the impurities present in the 7% magnesium alloy prevented polygonization from occurring. The fact that discontinuous precipitation was observed both in the super-purity 10% magnesium alloy and in the commercial-purity 7% magnesium alloy suggests that even if polygonization had occurred it was not responsible for the observed X-ray-diffraction effects.

Professor Lacombe suggests that Fig. 14 shows that our initial solid solution was not uniform. This photograph has, unfortunately, not reproduced very well. On the

original film each streak could be seen to be made up of four spots, corresponding to the $K_{\alpha 1}$ and $K_{\alpha 2}$ reflections from the old and new solid solutions. The spots were not sharp because the specimen had been aged almost to maximum hardness. The X-ray-diffraction rings from the as-quenched solid solution, moreover, were always very sharp.

Professor Lacombe claims that Figs. 7 and 8 do not support our contention that zinc decreases the rate of precipitation at grain boundaries. We would like to refer him to some photographs showing the same feature in a paper by Perryman and Hadden.* This effect of zinc is shown in a striking manner by carrying out stress-corrosion tests. For short ageing times the effect of zinc is to decrease the stress-corrosion susceptibility, because of the less-continuous nature of the grain-boundary precipitate in the zinc-bearing alloys. When, however, the ageing time is such that a continuous grain-boundary network has been formed in both the zinc-free and zinc-bearing alloys there is no difference in stress-corrosion susceptibility.

Regarding Dr. Edeleanu's remarks, we do not think the precipitate is in plate form because we never saw anything which resembled the flat section of a plate. We do not insist that the precipitate is in the form of rods, but only suggest that this is a possibility. While we agree that the probability of a rod appearing as a line in a random section is small, we would like to point out that if there is some preferred orientation then the probability would be increased. The values of the activation energy given on p. 26 were based on age-hardening curves only. We do not claim any high accuracy for these figures, since, as can be seen from the age-hardening curves, the time for maximum hardness cannot be determined very accurately.

* E. C. W. Perryman and S. E. Hadden, *J. Inst. Metals*, 1950, **77**, 207.

THE VISCOSITY OF MOLTEN TIN, LEAD, ZINC, ALUMINIUM, AND SOME OF THEIR ALLOYS*

1410

By T. P. YAO,† B.Sc., Ph.D., STUDENT MEMBER, and V. KONDIC,‡
B.Sc., Ph.D, MEMBER

SYNOPSIS

An oscillating-pendulum method has been used to determine the viscosity of molten tin, lead, zinc, and aluminium as a function of temperature. The binary tin-zinc and tin-lead systems were also investigated, as well as the effect of titanium on the viscosity of aluminium, and of furnace atmosphere and holding time on the viscosity of zinc. Viscosity values for the pure metals agreed very closely with those generally accepted, except near the freezing point. In this region the viscosity of some metals and alloys proved greater than predicted by the logarithmic law. When plotted against composition, at a constant degree of superheat, the viscosity of tin-zinc alloys showed maxima in the region of the pure metals and a minimum corresponding to the eutectic. Small additions of titanium appreciably increased the viscosity of aluminium, and the viscosity of zinc increased with time of exposure to the atmosphere.

The viscosities of metals and alloys near the freezing point appear to undergo certain changes that may account for the anomalous behaviour of the metals during fluid flow. It is not possible at present to say whether these changes are due to the presence of undissolved phases in the molten metals, or are a result of other factors affecting the liquid state.

I.—INTRODUCTION AND EARLIER WORK

DATA on the physical properties of molten alloys are still comparatively scarce. It is indeed only recently that any marked interest in the subject has been aroused, following the realization that some aspects and phenomena of the solid state cannot be adequately studied or understood without a greater knowledge of the liquid state. Viscosity, in particular, has proved a useful property, both as a means of checking the various theories of the liquid state and in throwing light on such practical problems connected with molten metals as casting fluidity, shrinkage porosity, exudations, and removal of impurities during refining.

Two points regarding viscosity are of major interest: its variation with temperature near the melting point, and its relation to alloy constitution. No definite conclusions could be reached on these points from existing data.

The relationship of viscosity to temperature has been studied experimentally by Fawsitt,¹ Sauerwald,² Stott,³ and others, and theoretically and experimentally by Andrade.⁴ Most of the data available, however, do not cover the temperature range very close to the melting point; for example, Fawsitt's measurements start at temperatures 2° C. or more above the melting point, those of Sauerwald at 20° C., and those of Stott at 6° C. Chiong,⁵ on the other hand, measured the viscosity right down to the freezing point. Andrade⁴ concluded that viscosity is related to temperature by a general relationship of the type:

$$\ln \eta = A + B/T$$

and this has been confirmed by numerous workers in the temperature ranges investigated.

Work on the viscosity of binary alloys has been carried out by Fawsitt,¹ Plüss,⁶ Sauerwald,² Gebhardt and Becker,⁷ Erwing, Grand, and Miller,⁸ and others, the main point of interest being the possible existence of a deviation of the viscosity/composition relationship from the simple law of mixtures. Plüss observed definite minima in the viscosity/composition curves of tin-lead and tin-bismuth alloys in the eutectic range. This finding has been disputed by Sauerwald, and quite recently Erwing and his associates have reported that the viscosity of sodium-potassium alloys complies with the law of mixtures. One important point in this controversy, however, still requires further experimental evidence, namely, the effect of the molten-metal temperature. The law may be obeyed at high degrees of superheat, but there is no justification for assuming *a priori* that it holds down to the liquidus temperature. Moreover, quite different viscosity/constitution/temperature relationships are obtained when absolute temperatures are plotted, and when a constant temperature above the liquidus is used. This point is discussed in later sections.

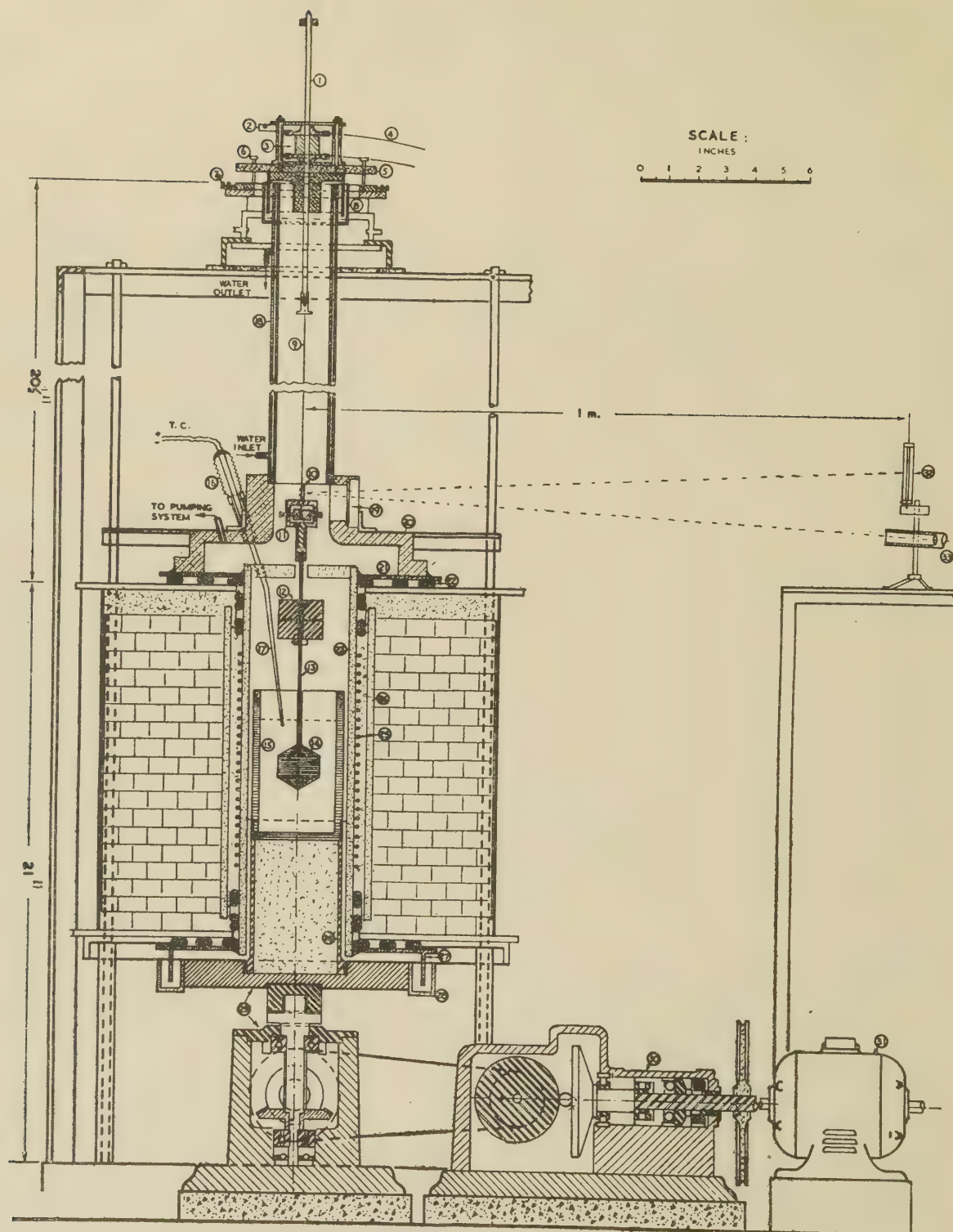
II.—EXPERIMENTAL METHOD AND RESULTS

As in this case it was desired to obtain viscosity values close to the freezing point, as well as to extend the research eventually to high-melting-point metals, the capillary method of viscosity measurement was unsuitable, and the choice lay between the rotation

* Manuscript received 19 November 1951.

† Royal School of Mines, London; formerly Birmingham University.

‡ Lecturer in Metallurgy, Department of Industrial Metallurgy, Birmingham University.



method and one of the oscillation methods. The apparatus finally adopted was such that both the rotating-crucible and oscillating-pendulum methods could be employed (Fig. 1).

A cylindrical crucible, 7 cm. in dia. and 12 cm. high (15) was held in the closed system of a resistance furnace (24), the oscillation system consisting of a solid graphite torsion pendulum (14), an inertia weight (12), a concave mirror (10), a bifilar tungsten suspension wire (9), and a torsion head. The torsion pendulum was 4 cm. in dia. and had a cylindrical portion 2 cm. long, with conical ends having an apex at 120°. This shape was selected on the ground that it reduced end-effects, while possessing a sufficiently large surface area. The hard-drawn tungsten suspension wire, 0.004 in. in dia. and 20 cm. long, had its upper ends firmly soldered to a steel suspension rod (1) and its lower end loop passing over a grooved pulley (11). In this way an automatic adjustment could be made to equalize tension in the two wires. The torsion head comprised two remote-controlled pulleys (3), with the suspension rod (1) passing through their centres. The whole suspension system could be twisted through a given angle by means of a pair of flexible wires (4) and a pair of pulleys, outside the closed system.

In the rotating-crucible method, a ball-and-disc continuously-variable-speed transmitter was used. The top of the furnace and the space surrounding the suspension system were water-cooled. The whole apparatus could be evacuated through a pumping system, and then filled with an inert gas. The angle of oscillation or deflection was recorded either by direct reading on a scale, or photographically.

The temperature of the furnace was regulated by means of a potentiometric controller in conjunction with a variable-voltage transformer. During a single measurement the temperature was held within $\pm \frac{1}{2}^{\circ}\text{C}$. and measured potentiometrically. With the thermocouple situated as shown in Fig. 1, no temperature gradients were detected in the molten metal at a given temperature.

In calibrating the apparatus, both rotation and oscillation methods of measuring viscosity were used. The latter was found preferable, as it gave higher

the crucible and collect round the pendulum wire. The oscillation method was consequently adopted throughout.

Most workers who have used this method of viscosity measurement agree that a fully mathematical treat-

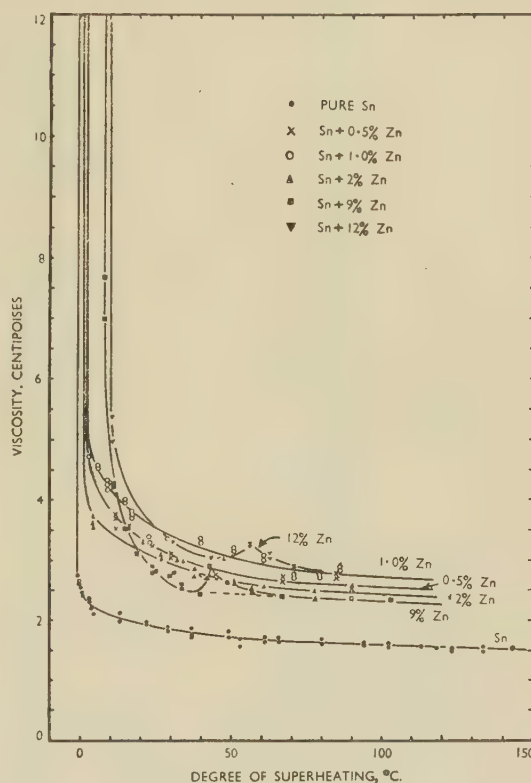


FIG. 3.—Viscosity of Tin and Tin-Rich Zinc Alloys.

ment is too complex. The empirical method of calibrating the apparatus against liquids of known viscosity was therefore employed and gave satisfactory results. After calibrating with water, with 20% sugar solution, and with pure metals at different temperatures, the following empirical relationship was found :

$$\lambda - \lambda_0 = C_1 \sqrt{\eta \rho T} + C_2 \eta T + C_3 \eta \rho T$$

where λ is the logarithmic decrement of the amplitude of oscillation in the liquid used and λ_0 that in air, η is the coefficient of viscosity, ρ the density of the liquid, T the period of oscillation, and C_1 , C_2 , and C_3 the apparatus constants, which in the present case were found to be 0.0778, 0.002825, and 0.002796, respectively. In a single test the value of the log decrement was either obtained by direct reading from the scale, or calculated from the photographic record, as shown, for tin, in Fig. 2 (a) and (b).

Tin of 99.9885%, lead of 99.9962%, and aluminium of 99.9935% purity were used and are referred to as "super-pure" metals; these materials were also used for making up the various alloys. In addition, commercially pure tin (99.23%), zinc (99.9962%), and aluminium (99.55%) were used. Before melting, the

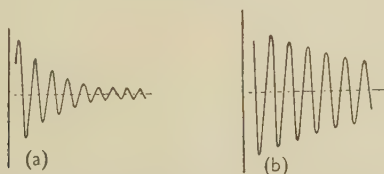


FIG. 2.—Oscillation Graphs of Commercially Pure Tin : (a) Near the Melting Point (log dec. 0.127); (b) at 400°C. (log dec. 0.0627).

accuracy and fewer experimental difficulties in the type of work described. The chief drawbacks to the rotation method arose from eccentricity and external-vibration effects, and above all, from the tendency for the accumulated oxide skin to move to the centre of

TABLE I.—Viscosity of Super-Pure and Commercially Pure Metals.

Metal	Temp., °C.	Viscosity,* poises	Metal	Temp., °C.	Viscosity,* poises
Tin (99.9885%)	231	0.0275	Crown Zinc (99.9962%)	419.5	0.0597
		0.0267			0.0576
	232	0.0268		422.5	0.0504
		0.0263			0.0498
	232.5	0.0256		426	0.0469
		0.0254			0.0459
	233	0.0246		431	0.0430
		0.0244			0.0403
	235	0.0238		444	0.0432
		0.0235			0.0420
	235.5	0.0226		448.5	0.0435
		0.0220			0.0402
	236.5	0.0222		451	0.0412
		0.0211			0.0402
	245	0.0210		454	0.0410
		0.0199			0.0401
	254	0.0197		462	0.0393
		0.0194			0.0371
	258	0.0192		473	0.0394
		0.0189			0.0390
	261	0.0189		478	0.0386
		0.0182			0.0366
	269	0.0186		483	0.0374
		0.0176			0.0365
	281	0.0174		506	0.0369
		0.0173			0.0365
	285	0.0169		511	0.0353
		0.0156			0.0347
	293	0.0170		524	0.0370
		0.0164			0.0340
	298.5	0.0170		535	0.0370
		0.0165			0.0340
	312	0.0169		555	0.0353
		0.0160			0.0340
	326	0.0163		560	0.0345
		0.0158			0.0343
	334	0.0161		600	0.0331
		0.0156			0.0328
	345	0.0153			
		0.0151	Aluminium (99.9935%)	659	0.0441
	349	0.0154			0.0427
		0.0152		659.5	0.0418
	355	0.0153			0.0416
		0.0149		662	0.0357
	365.5	0.0150			0.0353
		0.0148		665	0.0325
	375.5	0.0151			0.0325
		0.0150		672	0.0330
	384	0.0152			0.0325
		0.0148		685	0.0317
	387	0.0152			0.0302
Tin (99.23%)	240	0.0274		690	0.0320
		0.0268			0.0302
	243	0.0258		700	0.0296
		0.0252			0.0295
	245	0.0252		727	0.0270
		0.0248			0.0267
	252	0.0230		738	0.0274
		0.0228			0.0267
	265	0.0228		745	0.0262
		0.0227			0.0253
	275	0.0224		781	0.0254
		0.0222			0.0240
Tin (99.23%)	292	0.0221		783	0.0258
		*0.0220			0.0234
	310	0.0219		797	0.0268
		0.0218			0.0268
	318	0.0214	Aluminium (99.55%)	662.5	0.295
		0.0208			0.257
	329	0.0205		663	0.1519
		0.0204			0.1480
	345	0.0203		663.5	0.1210
		0.0202			0.1195

Metal	Temp., °C.	Viscosity,* poises	Metal	Temp., °C.	Viscosity,* poises
Aluminium (99.55%)	665	0.1192	Aluminium (99.55%)	750.5	0.0690
		0.1140			0.0671
	671	0.1140		756	0.0655
		0.1122			0.0643
	675	0.1102		766.5	0.0593
		0.1096			0.0578
	680	0.1110	Lead (99.9962%)	343	0.0273
		0.1035		349	0.0268
	689	0.1001		353	0.0260
		0.0995		360	0.0248
	706	0.0750		380	0.0241
		0.0743		431	0.0221
	716	0.0740		443	0.0199
		0.0739		463	0.0196
	723	0.0721		480	0.0193
		0.0710		490	0.0190
Aluminium (99.55%)	740.5	0.0688		500	0.0187
		0.0671			

* Most of the results were obtained by repeated direct-reading measurements.

furnace system was evacuated to 0.05 mm. mercury and then refilled with nitrogen or argon to a pressure slightly above 1 atm.

Viscosity values for the super-pure and commercially pure metals, obtained at different temperatures, are given in Table I. Values for the tin-zinc alloys are plotted in Figs. 3 and 4, while Fig. 5 shows viscosity plotted against composition for these alloys at 20°, 30°, and 40° C. superheat. The tin-lead system was studied at the tin-rich end only, and the results

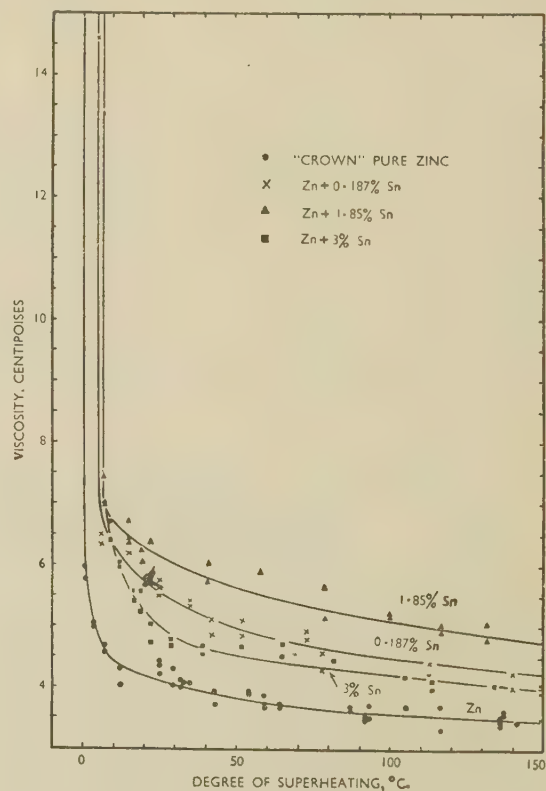


FIG. 4.—Viscosity of Zinc and Zinc-Rich Tin Alloys.

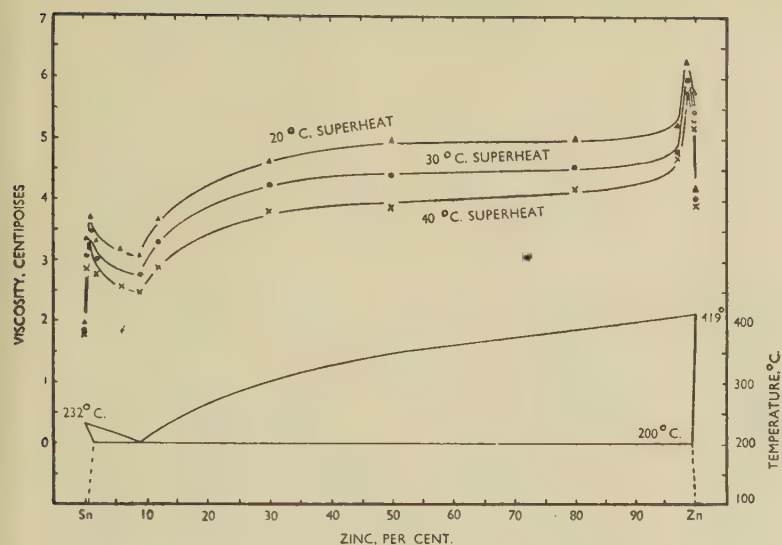


FIG. 5.—Viscosity/Constitution Relationship in Tin-Zinc Binary System.

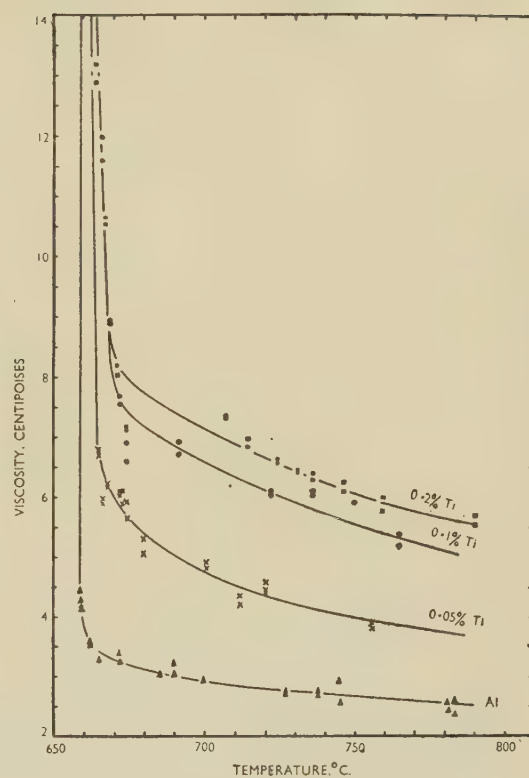


FIG. 6.—Effect of Small Additions of Titanium on the Viscosity of Aluminium.

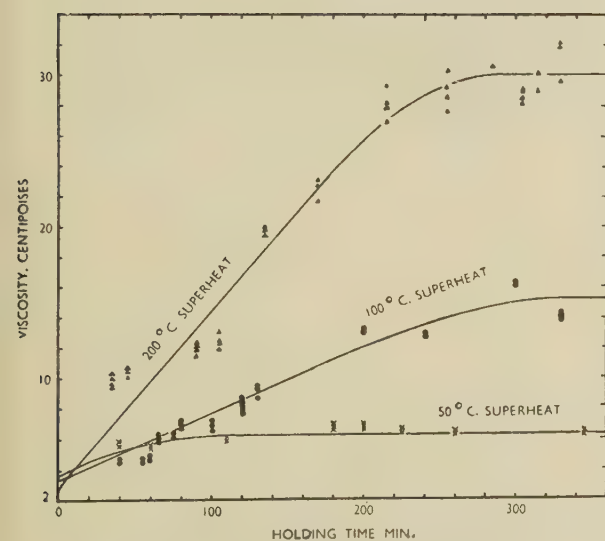


FIG. 7.—Effect of Holding Time on the Viscosity of Zinc Melted in Air.

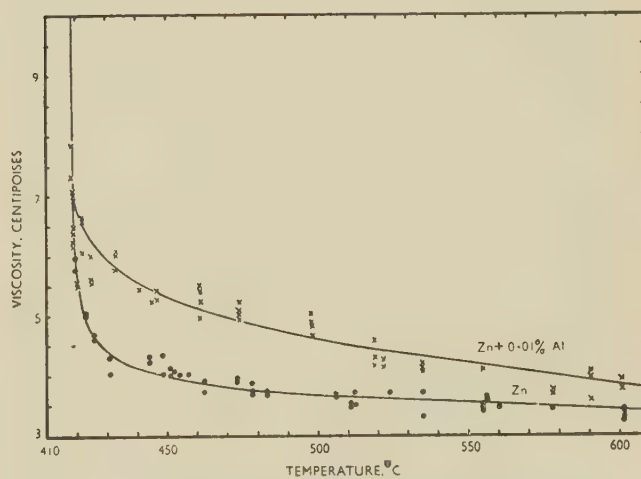


FIG. 8.—Viscosity of Zinc (Melted in Argon Atmosphere) and of Zinc with 0.01% Aluminium (Melted in Air).

are contained in Table II. The effect of small additions of titanium on the viscosity of aluminium is shown in Fig. 6, and Fig. 7 shows the changes in

TABLE II.—*Viscosity of Tin-Rich Binary Tin-Lead Alloys*

Lead Content, %	Temp., °C.	Viscosity,* poises	Lead Content, %	Temp., °C.	Viscosity,* poises
2.5	229	Liquidus	30	367	0.0196
	230	0.0854		396.5	0.0188
	240	0.0205		446	0.0179
	242	0.0198	38.2 (eutectic)	186	Liquidus
	252.5	0.0178		187	0.0375
	267	0.0174		188	0.0310
	276	0.0165		194	0.0277
	293	0.0163		200.5	0.0266
	299	0.0157		211.5	0.0221
	351	0.0151		221.5	0.0206
	393	0.0144		234	0.0199
30	190.5	Liquidus		251.5	0.0206
	200	0.0397		268.5	0.0202
	215	0.0253		277.5	0.0241
	230.5	0.0247		299	0.0228
	250.5	0.0224		318	0.0232
	276	0.0213		357.5	0.0226
	301	0.0211		446	0.0214
	335	0.0205		452.5	0.0212

* The results were obtained by the photographic-recording method.

viscosity of molten zinc after exposure to the atmosphere for various times. The alteration in the viscosity of zinc due to small additions of aluminium is illustrated in Fig. 8.

III.—DISCUSSION OF RESULTS

1. VISCOSITY/TEMPERATURE RELATIONSHIP

Most of the published data on the viscosity of pure metals, when plotted in a $\ln \eta - 1/T$ graph give a straight-line relationship, as anticipated by Andrade's equation, quoted above. It appears, however, that this relationship breaks down when the freezing point of some metals is approached, as shown for tin in Fig. 9. Similar results were obtained with lead, zinc, and aluminium. One of the major effects of alloying additions or impurities is to cause this steep rise in viscosity to occur at a higher temperature than in the pure metal. Fig. 10 shows the effect in the aluminium-titanium system, similar results, though of different orders of magnitude, being observed with other alloying additions.

The only other published examples of this type of viscosity/temperature relationship are those of Polyak and Sergeev⁹ and of Chiong.⁵ Polyak and Sergeev found a relationship of the type described in aluminium-silicon alloys, and Chiong in alloys of sodium and potassium.

These results give rise to the question whether the deviation from the logarithmic straight-line relationship represents the true viscosity change with temperature of pure metals, or is attributable to some cause inherent in the method of measurement used.

That the former is more likely is supported by the fact that: (i) the deviations observed become apparent before the normal thermal arrest, characterized by the liberation of the heat of solidification, takes place;

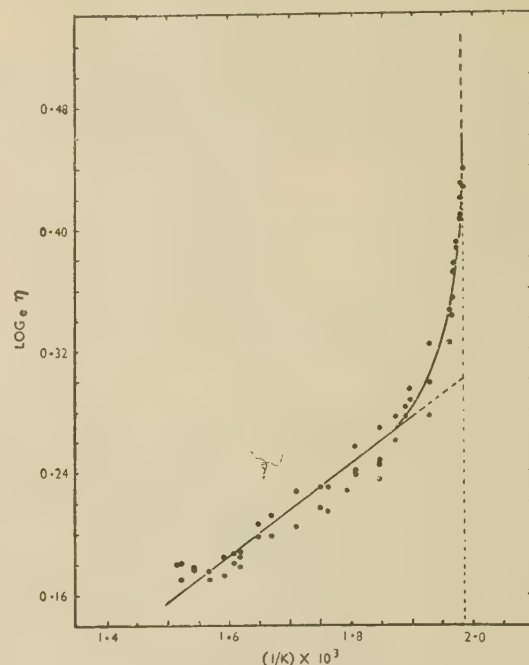


FIG. 9.— Log_e Viscosity of Tin Plotted Against the Inverse Absolute Temperature.

and (ii) the data available on the variation of surface tension with temperature or with composition of the alloys, do not exhibit any changes that could account for the observed viscosity relationships; nor, for that matter, could the results be explained by assuming a change in any other property of the liquid metal during the free oscillation of the pendulum.

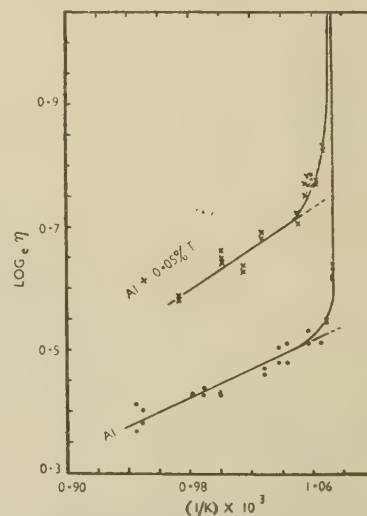


FIG. 10.— Log_e Viscosity of Aluminium and of Aluminium with 0.05% Titanium Plotted Against the Inverse Absolute Temperature.

A further interesting point is the supporting evidence to be derived from determinations of the casting fluidity, or spiral fluidity, of alloys. In this test, as described in earlier papers,^{10, 11} the metal is allowed to run along a channel in such a manner that any viscosity changes in the molten metal will affect the length of the cast spiral. That the two phenomena are related can be seen from a comparison of curves showing the relationships, respectively, between viscosity and temperature and spiral fluidity and temperature (see Fig. 11 (pure tin) and Fig. 12 (the tin-lead eutectic)).

On the evidence available, we are therefore led to the conclusion that, with some metals and alloys, the viscosity may increase on approaching the freezing point, to an extent not predicted by the logarithmic straight-line relationship. At this stage, any explanation of the phenomenon can be only conjectural, but one possible cause is suggested. Homogeneous metallic liquids may contain, just above the melting point, a sufficient number of other phases (impurities, which may act as foreign nuclei) to increase the viscosity of the pure molten metal. A true solution or ideal metallic liquid may thus fully obey Andrade's equation right down to the freezing point; but just above it enough seeds of nucleation may be present to raise the apparent viscosity without any temperature effects in the liquid being detectable. That some such mechanism may operate can be seen, for example, from the very widely established experimental observation that liquid metals do not undercool unless first heated to a

2. VISCOSITY/CONSTITUTION RELATIONSHIP

In plotting the curve of viscosity against composition for a binary alloy there are two ways of selecting the temperature variable: (i) the absolute tempera-

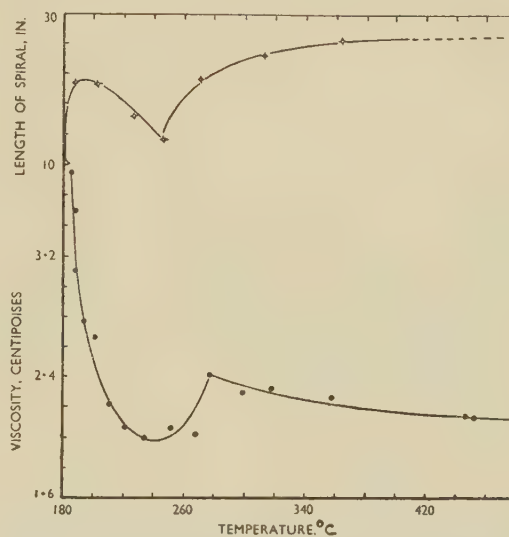


FIG. 12.—Viscosity and Casting Fluidity of the Tin-Lead Eutectic Plotted Against Temperature.

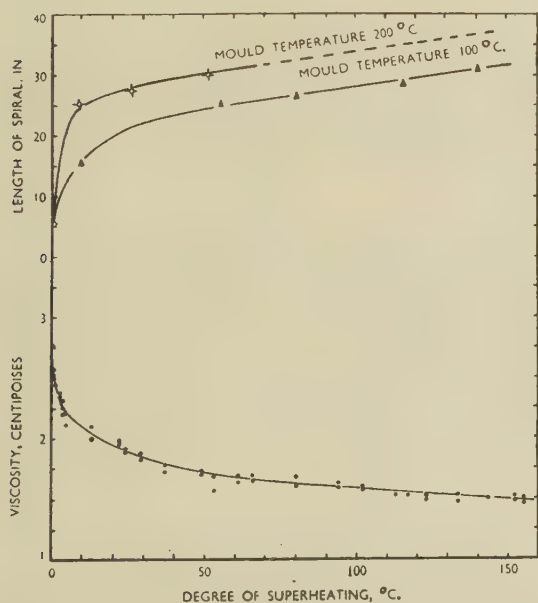


FIG. 11.—Viscosity and Casting Fluidity of Pure Tin Plotted Against Temperature.

few degrees above the melting point. The self-nucleating effect might easily prove to be reversible, especially under slow-cooling conditions, such as were used in the present investigation.

ture can be taken as constant, the type of graph then obtained being that shown in Fig. 13, full line (e.g. Gebhardt and Becker⁷ for the gold-silver system, Erwing *et al.*⁸ for the sodium-potassium system, and similar examples given by Sauerwald); or (ii) a constant temperature above the liquidus (or the superheating temperature) can be chosen, in which case a graph of the type shown in Fig. 5 (upper half) is obtained. The method of plotting selected depends on the degree of emphasis which it is desired to place on the effect of a particular variable, (i) being better suited to a purely thermodynamic study of viscosity, while (ii) would be chosen for an investigation of the effect of solute atoms on the viscosity of the solvent. In some metallurgical applications of the viscosity data of alloys, it is necessary to compare the relative viscosity at different alloy compositions against the same standard, that of maximum viscosity (which is, experimentally, the liquidus temperature). For example, when Erwing, Grant, and Miller's data on the viscosity of sodium-potassium alloys are plotted at constant absolute temperature and at constant superheat, the result is as shown dotted in Fig. 13. The constant-superheat curve in this figure is similar to that shown in Fig. 5 for the tin-zinc system. The fact that the addition of solute atoms appreciably increases the viscosity of the solvent is clearly brought out by this method of plotting, whereas it is completely masked in the constant-temperature method. Thus, while the latter method of plotting is advantageous for a theoretical discussion, the former method has distinct advantages in certain metallurgical applications, as is shown by the following example.

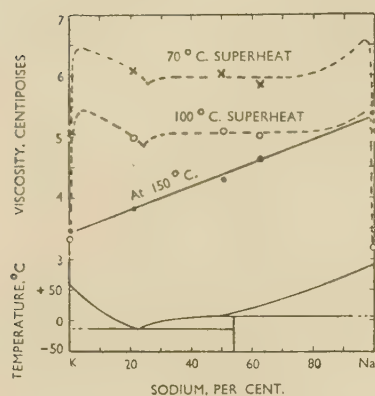


FIG. 13.—Viscosity/Constitution Relationship in Sodium-Potassium Binary System.

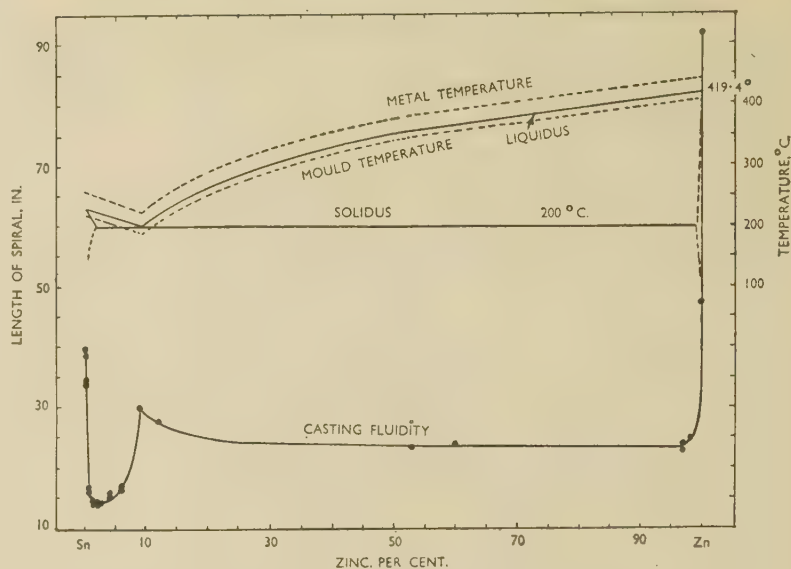


FIG. 14.—Casting Fluidity of Tin-Zinc Binary Alloys.

The casting fluidity of an alloy, obtained in the manner indicated, when plotted against composition, gives a graph such as that shown in Fig. 14. Constant absolute temperature is here rarely used, as it does not distinguish the relative casting fluidity of various alloys for foundry applications. It has frequently been suggested that the fluidity/composition relationship is not affected by viscosity variations in the same composition range. When, however, both properties are plotted at constant superheat, the curves (Figs. 5 and 14) exhibit maxima and minima in the same composition range. Similar examples of the inter-relationship between fluidity and viscosity are apparent in Figs. 7 and 15, which show the changes in the fluidity and viscosity of zinc as a function of time of holding at the superheating temperature, and in Fig. 12 in connection with the tin-lead eutectic. On the basis of the above evidence, it cannot be accepted that the solidification interval of an alloy is the directly important factor controlling the casting fluidity.

The main conclusion to be drawn from the data available on the effect of solute atoms on the viscosity of the solvent metal, is that insoluble or sparingly soluble elements may introduce larger viscosity changes in the solvent than are produced by more

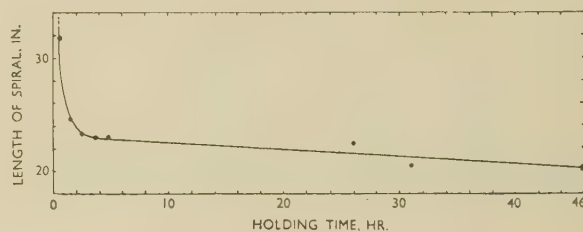


FIG. 15.—Effect of Holding Time on the Casting Fluidity of Zinc.

soluble elements. Further experimental evidence is required before any theoretical analysis can be undertaken or generalization of the results to cover binary alloy systems.

ACKNOWLEDGEMENTS

The authors wish to express their thanks to Professor A. J. Murphy, of the Industrial Metallurgy Department, Birmingham University, for his helpful interest and support, to the University Grants Committee for financial aid, and to the Tin Research Institute, the Imperial Smelting Corporation, Ltd., and Goodlass Wall and Lead Industries, Ltd., for the supply of pure metals.

REFERENCES

1. C. E. Fawsitt, *J. Chem. Soc.*, 1908, **93**, 1299.
2. F. Sauerwald and K. Topler, *Z. anorg. Chem.*, 1926, **157**, 117.
3. V. H. Stott, *Proc. Phys. Soc.*, 1933, **45**, 530.
4. E. N. da C. Andrade, *Phil. Mag.*, 1934, [vii], **17**, 497, 698.
5. Y. S. Chiong, *Proc. Roy. Soc.*, 1936, [A], **157**, 264.
6. M. Plüss, *Z. anorg. Chem.*, 1915, **93**, 1.
7. E. Gebhardt and M. Becker, *Z. Metallkunde*, 1951, **42**, (4), 111.
8. C. T. Erwing, J. A. Grand, and R. R. Miller, *J. Amer. Chem. Soc.*, 1951, **73**, (3), 1168.
9. E. V. Polyak and S. V. Sergeev, *Compt. rend. (Doklady) Acad. Sci. U.R.S.S.*, 1941, **33**, 244.
10. V. Kondic and H. J. Kozlowski, *J. Inst. Metals*, 1949, **75**, 665.
11. T. P. Yao and V. Kondic, *Metal Ind.*, 1951, **79**, (21), 435.

THE CONSTITUTION OF NICKEL-RICH ALLOYS OF THE NICKEL-TITANIUM-ALUMINIUM SYSTEM *

1411

By A. TAYLOR,† Ph.D., F.Inst.P., MEMBER, and R. W. FLOYD,‡
B.Sc., A.I.M., MEMBER

SYNOPSIS

The equilibrium relationships of the phases in nickel-rich alloys of the nickel-titanium-aluminium system over the range 750°–1150° C. have been determined by a combination of micrographic and X-ray-diffraction techniques. At 750° C. the face-centred cubic primary nickel solid solution, γ , holds more than 12 at.-% titanium and aluminium in solution. The γ phase is in equilibrium with the intermetallic compound η -Ni₃Ti and the extensive face-centred cubic ordered phase, γ' , based on Ni₃Al. A brief survey of alloys with 50 at.-% nickel has revealed a ternary Ni₂TiAl phase, β_3 , with a Cu₂ZnAl type of structure, in equilibrium with the β_1 -NiAl and β_2 -NiTi phases, which have CsCl-type structures. In the course of the work the boundaries of the γ and γ' phase fields in the nickel-aluminium system have been revised.

I.—INTRODUCTION

THE investigation of the structure of nickel-rich alloys containing titanium and aluminium was undertaken as part of a general study of complex alloys having nickel as the main component. It involves the study by micro-examination and X-ray analysis of the phase relationships in alloys with more than 50 at.-% nickel over the temperature range 750°–1150° C. Recent work on the nickel-titanium binary system has been described elsewhere,¹ and in the present paper an account is given of a study of the nickel end of the nickel-aluminium phase diagram that was carried out because of lack of agreement between the several published diagrams, none of which could satisfactorily be linked with the results for the ternary system. As far as is known, no description of any part of the ternary nickel-titanium-aluminium system has appeared in the literature.

II.—EXPERIMENTAL PROCEDURE

The alloys were synthesized by melting together selected Mond nickel pellet, Kroll titanium from Metal Hydrides, Ltd., and high-purity aluminium from The

annealed *in vacuo* at about 1200° C. for 4 days to promote homogeneity. Samples for chemical and X-ray analysis and micro-examination were then obtained.

In the first instance the general layout of the ternary system was determined by the X-ray examination of powder samples slowly cooled from 900° C. over 2 weeks. Subsequently, although some information was obtained from X-ray analysis of quenched powders, the greater part of the investigation was carried out by micro-examination. The micro- and X-ray specimens were heat-treated according to the same schedule of times and temperatures as given below:

Temperature, °C.	Annealing Time
1150	2 hr.
1000	1 day
850	10 days
750	3 weeks

Various etching reagents were used to reveal the microstructures, the choice depending mainly on the composition of the alloy. For most of the ternary alloys, an aqueous solution of 5% hydrochloric acid and 10% glycerine, used electrolytically, was found suitable; some of the high-titanium alloys etched more clearly if 5% nitric acid was added to the mixture. The X-ray-diffraction patterns were obtained in a 9-cm. Debye-Scherrer camera, using manganese or copper K_α radiation, and for the accurate determination of lattice parameters² the spacings were extrapolated against the function $\frac{1}{2}(\cos^2\theta/\sin\theta + \cos^2\theta/\theta)$.

TABLE I.—Analyses of Raw Materials (Wt.-%)

	Ni	Ti	Al	Cu	Fe	Mn	Mg	Si	C
Nickel	Bal.	0.002	0.018	0.002	0.034
Titanium	...	Bal.	0.015	0.05	0.015	...	0.04	0.035	...
Aluminium	Bal.	0.005	0.005	...	0.001

British Aluminium Co., Ltd. The analyses of these metals, mainly estimated spectrographically, are given in Table I. Most of the alloys were melted in magnesia-lined crucibles in a 4-kVA. high-frequency induction furnace under a low pressure of hydrogen, while a few alloys of low nickel content were melted in argon in a Kroll-type arc furnace. All the ingots were

III.—THE NICKEL-TITANIUM SYSTEM

The nickel-titanium system has been described in a recent paper on the nickel-chromium-titanium system.¹ The phases of the nickel-titanium system which occur in the part of the nickel-titanium-aluminium system described below are the face-

* Manuscript received 10 April 1952.

† Horizons Inc., Cleveland, O., U.S.A.; formerly with

The Mond Nickel Co., Ltd., Birmingham.

‡ The Mond Nickel Co., Ltd., Birmingham.

centred cubic primary solid solution of titanium in nickel (γ), the hexagonal intermetallic compound of stoichiometric composition Ni_3Ti (η), and the body-centred cubic phase (β) based on NiTi . The solubility of titanium in the γ solid solution at 1150°C . is 13

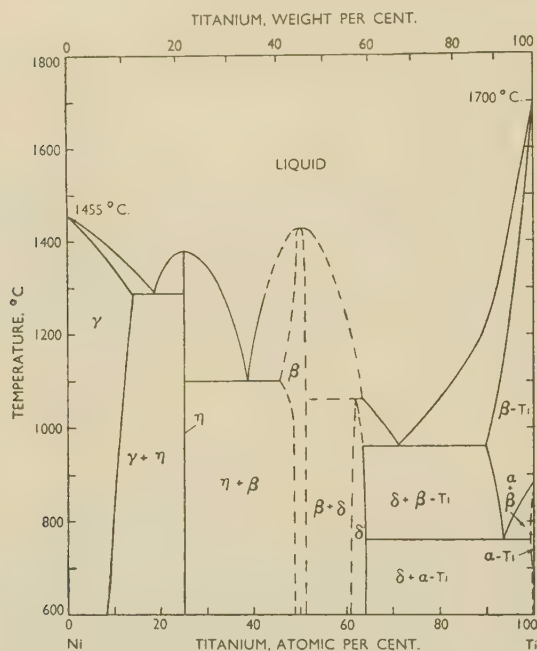


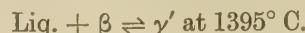
FIG. 1.—Tentative Nickel-Titanium Phase Diagram.

at.-%, decreasing steadily to 9.4 at.-% at 750°C . In alloys with higher titanium contents, γ is in equilibrium with η , which, when present in small amounts, occurs in the form of thin plates, so that the microstructures have a Widmannstätten pattern. Beyond 25 at.-% titanium, the η phase is in equilibrium with β . A composite nickel-titanium phase diagram based on the most recent data available is given in Fig. 1.

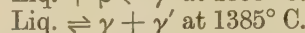
IV.—THE NICKEL-ALUMINIUM SYSTEM

The first phase diagram for the nickel-aluminium system was that of Gwyer,³ who established a maximum in the liquidus at NiAl , and the three intermediate phases NiAl (β), NiAl_2 , and NiAl_3 . Itaka,⁴ when investigating nickel-rich alloys, found phases of compositions Ni_3Al and Ni_5Al , but his phase diagram appears highly improbable, as does that of Nishimura and Watanabe,⁵ who concluded that the Ni_5Al phase was, in fact, Ni_4Al and that the Ni_3Al phase did not exist. Meanwhile a survey of the whole system by Bradley and Taylor,⁶ based on an X-ray analysis of slowly cooled powders, established beyond doubt the existence of the Ni_3Al phase (γ') and Ni_2Al_3 (δ), which corresponded with Gwyer's NiAl_2 . Their diagram incorporated the thermal-arrest results of Gwyer and showed the ordered face-centred cubic Ni_3Al phase merging with the random face-centred cubic nickel solid solution (γ) at temperatures above 1100°C . Alexander and Vaughan⁷ explored the system by the

methods of thermal and micrographic analysis and observed the same sequence of phases as Bradley and Taylor. However, the Ni_3Al phase was shown to exist quite separately from the nickel solid solution at all temperatures up to the solidus. Their liquidus and solidus curves follow those obtained by Gwyer, except in the neighbourhood of Ni_3Al , where the following peritectic and eutectic reactions were found:



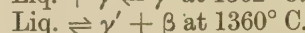
and



Later, Schramm⁸ investigated nickel-base alloys up to 50 at.-% Al mainly by thermal analysis, and concluded that the reactions occurring at the solidus were:



and



By a comparison of the cast structures of nickel-aluminium alloys around Ni_3Al with a corresponding series containing a small addition of chromium, one of the present authors⁹ has demonstrated that Ni_3Al is in fact formed by the reaction between the liquid and β phase as determined by Alexander and Vaughan, thus invalidating Schramm's conclusions.

Apart from this difference between the phase diagrams given by Alexander and Vaughan and by Schramm, there is considerable lack of agreement as to the positions of the boundaries of the γ and γ' phase fields. Further, the boundaries for the binary nickel-aluminium system deduced from the recent metallographic study of the iron-nickel-aluminium system by Bradley¹⁰ did not correspond with any of those

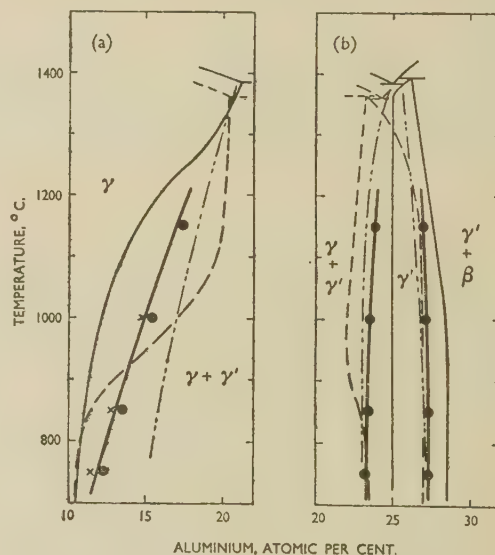


FIG. 2.—The Boundaries of the γ and γ' Phase Fields in the Nickel-Aluminium System.

KEY.
 — Alexander and Vaughan.⁷
 - - - Schramm.⁸
 x X-ray.
 . . . Bradley.¹⁰
 ● Micrographic.
 — Present work.

published earlier, except the γ' boundaries below 800°C . as determined by Schramm and Bradley and Taylor. These differences are clearly brought out in

TABLE II.—Compositions, Structures, and Lattice Parameters of Nickel-Aluminium Alloys

Alloy Number	Aluminium, at.-%	Observed Microstructure				Lattice Parameter, kX			
		1150° C.	1000° C.	850° C.	750° C.	1150° C.	1000° C.	850° C.	750° C.
		γ Phase							
278	4.9	3.5257
279	7.5	3.5309
280	11.1	γ	γ	3.5367
281	12.1	...	γ	γ	γ	3.5383
282	12.4	γ	γ	γ	$\gamma + \gamma'$...	3.5405	...	3.5384
γ' Phase									
283	14.0	γ	γ	$\gamma + \gamma'$	$\gamma + \gamma'$...	3.5433	3.5409	3.5483
284	15.4	γ	γ	$\gamma + \gamma'$	3.5385	3.5407	3.5385
285	16.1	γ	$\gamma + \gamma'$	$\gamma + \gamma'$	3.5439	3.5402	...
263	17.3	γ	$\gamma + \gamma'$	3.5448
265	18.3	$\gamma + \gamma'$	$\gamma + \gamma'$	3.5410	...
266	19.8	$\gamma + \gamma'$	$\gamma + \gamma'$	3.5436	3.5406	...
γ' Phase									
200	21.1	$\gamma + \gamma'$	$\gamma + \gamma'$	$\gamma + \gamma'$	$\gamma + \gamma'$	3.5554	3.5580	3.5570	...
201	23.2	$\gamma + \gamma'$	$\gamma + \gamma'$	$\gamma + \gamma'$	$\gamma + \gamma'$	3.5560	3.5587	3.5574	...
202	25.1	γ'	γ'	γ'	γ'	3.5588	3.5592	3.5602	3.5603
22	25.9	...	γ'	γ'	3.5599
203	26.4	γ'	γ'	γ'	γ'	3.5630	3.5631	3.5627	3.5624
204	27.8	$\gamma' + \beta$	$\gamma' + \beta$	$\gamma' + \beta$	$\gamma' + \beta$	3.5674	3.5662	3.5650	3.5654

Fig. 2, in which the various limits of the γ and γ' phase fields are superimposed. Since the γ phase in the ternary nickel-titanium-aluminium system determined in the present investigation could not satisfactorily be extrapolated to any of the published boundary positions on the binary system, it was found necessary to redetermine the solubility of aluminium in nickel over the range 750°–1150° C. and to check the extent of the γ' phase in the binary system.

The chemical compositions, structures, and lattice parameters of the nickel-aluminium alloys which have been examined are given in Table II. The $\gamma/(\gamma + \gamma')$ boundary was explored by microscopic examination of quenched lumps and by lattice-parameter measurements of the γ phase in quenched filings. Because of the possibility of contamination of the filings by silica or of loss of aluminium due to volatilization, no filings were heat-treated above 1000° C. The lattice-parameter/composition relationship for the γ phase is shown in Fig. 3, and typical microstructures of alloys lying near the $\gamma/(\gamma + \gamma')$ boundary are shown in Figs. 8 and 9 (Plate III). Both X-ray and micrographic examinations gave results which were self-consistent over the temperature range investigated, but, as shown in Fig. 2, the X-ray results are consistently lower by 0.4% aluminium. This difference may be attributed to two factors: (a) the faster rate of attainment of equilibrium in cold-worked filings as compared with lump specimens which have undergone no deformation, and (b) the sensitivity of spacing measurements to the formation of sub-microscopic nuclei of the precipitating phase γ' .

Nevertheless, the difference in boundary position obtained by the two methods in the present investigation is very much smaller than the difference between the positions determined by previous investigators.

Extrapolated above 1250° C., the boundary is in

good agreement with those of Alexander and Vaughan and of Bradley,¹⁰ whereas in the range 700°–900° C. it is in agreement with the early boundary of Bradley and Taylor based on X-ray work. In this temperature range the boundary positions fixed by Alexander and Vaughan⁷ and by Schramm⁸ are closer to the

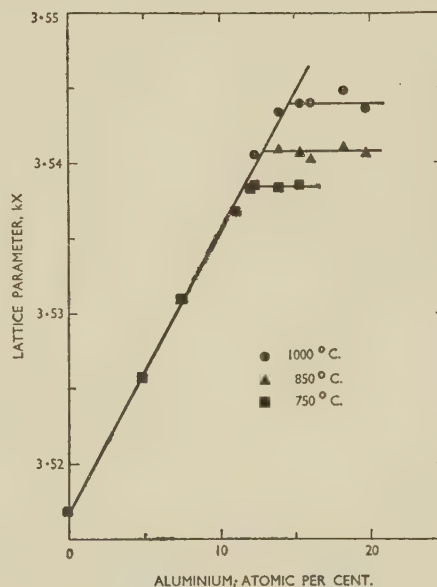


FIG. 3.—Lattice Parameters of the γ Phase in Nickel-Aluminium Alloys.

new boundary than that obtained by Bradley in his recent publication. Both the present boundary and Bradley's run smoothly to the eutectic temperature without any inflections such as are shown by Alexander and Vaughan and Schramm. The present results are to be preferred to those of Bradley, since his boundary position arises by extrapolation from an

attempt to smooth out the γ boundary within the ternary iron-nickel-aluminium system.

Data were also obtained on the lattice spacing of the γ' phase at the $(\gamma + \gamma')/\gamma'$ boundary. However, the results were inconsistent, and before proceeding to an exploration of the γ' phase field it was decided to investigate the cause of this variability. It was observed that the diffraction pattern of the γ' phase in X-ray photographs of two-phase alloys was often diffuse, and that the lattice parameter fell anywhere in the range 3.56–3.58 kX. This was in accordance with the early results given by Bradley and Taylor, who thought that the correct spacing was around 3.58 kX. The lower spacings could be attributed to the impoverishment of the filed specimens by evaporation of aluminium in the evacuated silica capsules used for heat-treatment or to replacement of some of the aluminium atoms by silicon. In order to determine how the atmosphere and container in which the specimens were heat-treated influenced the lattice parameter of Ni_3Al , a large batch of filings from a single alloy was prepared and divided into eight samples, which were heat-treated under the conditions given in Table III. All eight specimens were heat-treated simultaneously in the same furnace for 16 hr. at 1000°C . and all were water-quenched at the same instant.

The diffraction patterns obtained from this series of treatments showed surprising differences and could be divided into two groups, those of a single phase (γ'), with a lattice parameter of 3.56 kX, and those showing two phases (γ and γ'), with parameters of about 3.545 and 3.58 kX respectively, the intensities of the two patterns varying from specimen to specimen. The lattice parameter of 3.56 kX was obtained for both the samples contained within silica capsules as well as for the sample heat-treated in a nickel-4½% aluminium alloy capsule in an argon atmosphere. All the other samples gave two-phase patterns. To determine whether the variation was due to pick-up of silicon or other impurities, each of the samples and the metal containers were examined spectrographically, but the only variations that could be detected were insignificant. Because of the very small amount of sample available, it was not possible to determine the aluminium content in each powder specimen after heat-treatment.

Whenever the patterns of two phases could be seen in the X-ray photographs, that with the lower spacing corresponded to the saturated γ phase at the $\gamma/(\gamma + \gamma')$ boundary. This suggested that the filings had lost enough aluminium by evaporation to lie in the $(\gamma + \gamma')$ field, in which case the γ' phase present would have the composition of the phase boundary at the quenching temperature. It would therefore be expected that such two-phase alloys would yield the lowest γ' parameter, yet the observed γ' lattice spacing was, in fact, higher than that of single-phase γ' samples, which showed no sign of having lost aluminium.

To explore the possibility of a transformation in the

γ' phase occurring fairly rapidly at about room temperature, as suggested by Bradley and Taylor,⁶ a test-piece from a 5-kg. melt of Ni_3Al was heated in a Leitz dilatometer to 1000°C . at a rate of 3°C./min. and

TABLE III.—Heat-Treatment of X-ray Samples of Alloy 212 (Ni_3Al)

Heat Treatment	Container	Apparent Structure	Lattice Parameter of γ' Phase, kX
16 hr. at 1000°C . W.Q.	Sealed, evacuated silica capsule.	γ'	...
	Alumina tube in sealed evacuated silica capsule.	γ'	3.5614
	Alumina tube in continuously evacuated nickel tube.	$\gamma + \gamma'$...
	Nickel capsule in continuously evacuated nickel tube.	$\gamma + \gamma'$...
	Ni-4½% Al alloy capsule in continuously evacuated nickel tube.	$\gamma + \gamma'$...
	Alumina tube in argon-filled nickel tube.	$\gamma + \gamma'$	3.5785 ($\gamma = 3.5431$)
	Nickel capsule in argon-filled nickel tube.	$\gamma + \gamma'$...
	Ni-4½% Al alloy capsule in argon-filled nickel tube.	γ'	3.5610
As filed ½ hr. at 500°C .	Sealed evacuated silica capsule.	γ'	3.5591

subsequently cooled slowly to room temperature overnight. An almost perfectly smooth dilatation/temperature curve was obtained, both on heating and cooling, the final length of the bar being exactly the same as the initial length. Later the same bar was cooled in liquid nitrogen to -196°C ., and again no anomalous expansion or contraction was observed. Combining the results, a smooth expansion curve

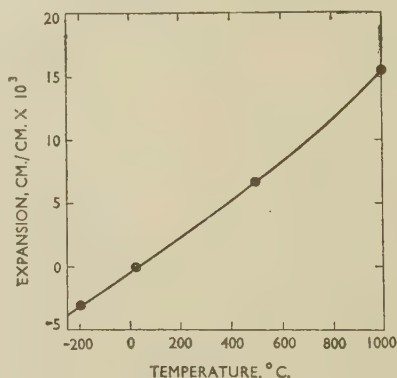


Fig. 4.—Thermal Expansion of Ni_3Al .

could be drawn from -196° to 1000°C . (Fig. 4), so that the possibility of a transformation seems remote.

In the absence of any other explanation of the peculiar behaviour of filed X-ray samples of Ni_3Al , it was concluded that the cause of the variability was in some way associated with the heat-treatment of the filings. Because of this, a new technique was adopted for the X-ray examination of alloys used for establishing the extent of the γ' phase field. The

heat-treated specimens used for micro-examination were carefully ground to remove any impoverished layers from the surface, and filings were obtained from the clean faces. These filings were sealed in evacuated silica capsules and given the shortest low-temperature heat-treatment that would permit crystal recovery without diffusion and yield sharp diffraction lines

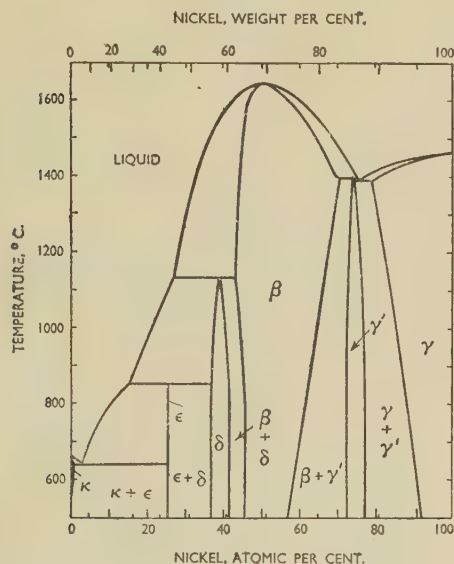


FIG. 5.—The Nickel-Aluminium Phase Diagram.

capable of being accurately measured. By trial and error, heat-treatment for 10 min. at 600° C. was found to be satisfactory, and in alloys consisting of ($\gamma + \gamma'$), γ' , and ($\gamma' + \beta$) the lattice parameter of the γ' phase lay consistently low and within the range 3.556–3.567 kX, the alloy of composition Ni_3Al having a range of 3.5588–3.5603 kX (see Table II). From these figures it would appear that it is the occasional high parameter for Ni_3Al of up to 3.58 kX which is anomalous and not the low value. Assuming a linear relationship between parameter and composition, a parameter of 3.58 kX would correspond to a composition near Ni_2Al . Such an increase in aluminium content at the surface of the filings during heat-treatment would be most unlikely, and were it to occur one would expect the resulting alloy to consist entirely of β phase.

The unpredictable occurrence of the anomalously high lattice spacings of the Ni_3Al phase would seem to constitute an important problem, since, in the binary system, the determination of the extent of the phase by conventional X-ray methods is rendered very difficult. Fortunately γ' -phase alloys containing a third element such as titanium do not appear to be susceptible to this behaviour and give much more consistent spacings without resort to special treatment. It was evident that to explain satisfactorily the phenomenon of the lattice-parameter variations a considerable amount of additional work would be required, but this was considered to lie beyond the

scope of the present investigation and was not undertaken.

Although the technique of using filings from samples heat-treated in lump form gave results better than those previously obtained, they were still not good enough for the determination of the γ' -phase boundaries. These were located with sufficient accuracy by micro-examination of the lump samples (Figs. 10–13, Plate III), which showed that the γ' phase is stable over a range of 3 at.-% aluminium about the stoichiometric composition Ni_3Al at 1150° C., taking into solution a little nickel and aluminium as the temperature falls, so that at 750° C. the range of composition is 23.3–27.3 at.-% aluminium, as shown in Fig. 2 (b). The position of the phase boundaries and the slight broadening of the phase field with decreasing temperature are in good agreement with the metallographic work of Bradley.¹⁰

No attempt has been made to establish any of the other phase boundaries in the nickel-aluminium system. A complete phase diagram for this system, incorporating the new boundaries and the latest data available in the literature, is given in Fig. 5.

V.—THE NICKEL-TITANIUM-ALUMINIUM SYSTEM

The structures of the alloys of the ternary system after heat-treatment are summarized in Table IV, and isothermal sections of the system derived from these results are presented in Fig. 6 (a)–(d).

The inter-relationships between the primary nickel solid solution (γ) and the two neighbouring phases, η (Ni_3Ti) and γ' (Ni_3Al), in the ternary system nickel-titanium-aluminium have been studied in detail, and the work extended to include data on alloys down to 50 at.-% nickel. As shown in Fig. 6 (a)–(d), the γ phase field remains roughly triangular in shape, shrinking towards the nickel corner as the temperature falls, while the γ apex of the ($\gamma + \gamma' + \eta$) three-phase field closely approaches the nickel-titanium side of the composition triangle. If the aluminium content is kept low, increase in the titanium content results in the occurrence of η -phase needles in the γ -phase matrix, as shown in Fig. 14 (Plate IV). The two-phase ($\gamma + \eta$) field takes the form of a narrow wedge with its apex at Ni_3Ti . The change in position with temperature of the aluminium-rich side of this phase field is indicated by the photomicrographs in Figs. 15–17 (Plate IV).

The ($\gamma + \gamma'$) two-phase field is extensive, reaching at 750° C. almost to the nickel-titanium side of the system at the γ end, and to about 16 at.-% titanium at the γ' end. The γ' phase, when it occurs in a matrix of γ , can be readily distinguished microscopically from the η phase by its globular form, which is in marked contrast to the acicular or lamellar form of the Ni_3Ti crystals. The structure shown in Fig. 18 (Plate IV) illustrates an alloy lying near the $\gamma/(\gamma + \gamma')$ boundary. As the proportion of γ' phase increases so the globules become coarser (Fig. 19,

TABLE IV.—Compositions and Structures of Nickel-Titanium-Aluminium Alloys

Alloy No.	Analysed Composition, at.-%			Observed Structure			
	Ni	Ti	Al	1150° C.	1000° C.	850° C.	750° C.
155	90.5	9.5	0	γ	γ	γ	$\gamma + \eta$
248	90.4	7.4	2.2	γ	γ	γ	γ
249	89.7	2.6	7.6	γ	γ	γ	γ
19	89.4	5.6	5.0	γ	γ	$\gamma + \gamma'$	$\gamma + \gamma'$
246	89.0	5.3	5.7	γ	γ	$\gamma + \gamma'$	$\gamma + \gamma'$
156	88.6	11.4	0	γ	γ	$\gamma + \eta$	$\gamma + \eta$
244	88.4	9.2	2.4	γ	γ	$\gamma + \gamma'$	$\gamma + \gamma'$
238	88.2	5.2	6.6	γ	γ	$\gamma + \gamma'$	$\gamma + \gamma'$
245	87.9	7.5	4.6	γ	$\gamma + \gamma'$	$\gamma + \gamma'$	$\gamma + \gamma'$
247	87.4	2.6	10.0	γ	γ	$\gamma + \gamma'$	$\gamma + \gamma'$
157	86.8	30.2	0	$\gamma + \eta$	$\gamma + \eta$	$\gamma + \eta$	$\gamma + \eta$
240	86.4	11.1	2.5	$\gamma + \eta$	$\gamma + \gamma' + \eta$	$\gamma + \gamma' + \eta$...
242	86.1	7.5	6.4	$\gamma + \gamma'$	$\gamma + \gamma'$	$\gamma + \gamma'$	$\gamma + \gamma'$
45	85.8	10.2	4.0	$\gamma + \gamma'$	$\gamma + \gamma'$	$\gamma + \gamma'$	$\gamma + \gamma'$
235	85.7	13.3	1.0	$\gamma + \eta$	$\gamma + \eta$	$\gamma + \gamma' + \eta$	$\gamma + \gamma' + \eta$
236	85.6	12.2	2.2	$\gamma + \eta$	$\gamma + \eta$	$\gamma + \gamma' + \eta$...
237	85.4	11.6	3.0	$\gamma + \gamma' + \eta$	$\gamma + \gamma' + \eta$	$\gamma + \gamma' + \eta$...
243	85.6	2.9	11.6	$\gamma + \gamma'$	$\gamma + \gamma'$	$\gamma + \gamma'$	$\gamma + \gamma'$
241	84.8	10.6	4.6	$\gamma + \gamma'$	$\gamma + \gamma'$	$\gamma + \gamma'$...
20	84.3	5.2	10.5	$\gamma + \gamma'$	$\gamma + \gamma'$	$\gamma + \gamma'$	$\gamma + \gamma'$
239	82.8	2.5	14.7	$\gamma + \gamma'$	$\gamma + \gamma'$	$\gamma + \gamma'$	$\gamma + \gamma'$
234	81.0	13.8	5.2	$\gamma + \gamma' + \eta$	$\gamma + \gamma' + \eta$	$\gamma + \gamma' + \eta$...
46	78.7	12.7	8.6	$\gamma + \gamma'$	$\gamma + \gamma'$	$\gamma + \gamma'$	$\gamma + \gamma'$
47	78.5	18.3	3.2	$\gamma + \gamma' + \eta$	$\gamma + \gamma' + \eta$	$\gamma + \gamma' + \eta$	$\gamma + \gamma' + \eta$
195	78.1	8.5	13.4	$\gamma + \gamma'$	$\gamma + \gamma'$	$\gamma + \gamma'$...
233	77.6	4.7	17.7	$\gamma + \gamma'$	$\gamma + \gamma'$	$\gamma + \gamma'$...
254	76.6	10.0	13.4	γ'	γ'	γ'	γ'
252	76.6	4.6	18.8	γ'	γ'	γ'	γ'
253	76.3	7.5	16.2	γ'	γ'	γ'	γ'
258	75.8	19.2	5.0	$\gamma' + \eta$	$\gamma' + \eta$	$\gamma' + \eta$	$\gamma' + \eta$
255	75.7	12.4	11.9	γ'	γ'	γ'	γ'
256	75.6	14.8	9.6	γ'	γ'	γ'	γ'
21	74.8	5.8	19.4	γ'	γ'	γ'	γ'
257	74.8	18.0	7.2	$\gamma' + \eta$	$\gamma' + \eta$	$\gamma' + \eta$	$\gamma' + \eta$
28	74.7	25.3	0	η	η	η	η
27	74.6	22.0	3.4	$\gamma' + \eta$	$\gamma' + \eta$
24	74.6	9.9	15.5	γ'	γ'	γ'	γ'
25	74.4	15.0	10.6	γ'	γ'	γ'	γ'
26	74.4	20.0	5.6	$\gamma' + \eta$	$\gamma' + \eta$	$\gamma' + \eta$	$\gamma' + \eta$
49	73.7	13.2	13.1	$\gamma + \gamma'$
75	72.5	10.9	16.6	$\gamma' + \beta$	$\gamma' + \beta$	$\gamma' + \beta$	$\gamma' + \beta$
197	72.0	13.9	14.1	$\gamma' + \beta$	$\gamma' + \beta$	$\gamma' + \beta$...
23	69.9	4.6	25.5	$\gamma' + \beta$	$\gamma' + \beta$	$\gamma' + \beta$	$\gamma' + \beta$
232	69.8	9.4	20.8	$\gamma' + \beta$	$\gamma' + \beta$	$\gamma' + \beta$...
230	61.4	18.3	20.3	...	$\gamma' + \beta$
290 *	50	50	0	...	β_2
289 *	50	37.5	12.5	...	$\beta_2 + \beta_3$
288 *	50	25	25	...	β_3
287 *	50	12.5	37.5	...	$\beta_1 + \beta_3$
286 *	50	0	50	...	β_1

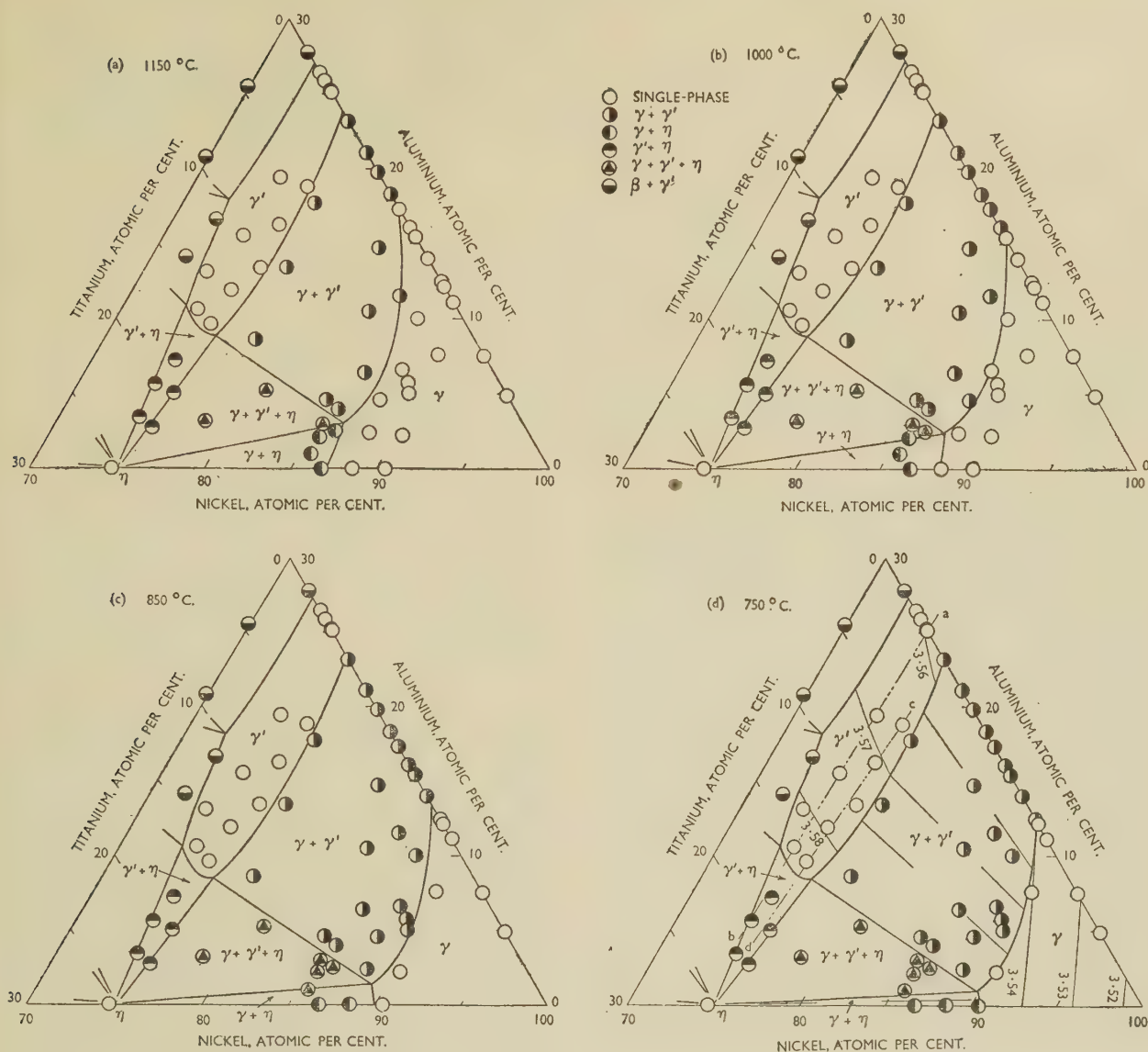
* Compositions nominal.

Plate IV) until the residual γ phase is present only as a fine network around the γ' grains (Fig. 20, Plate IV).

The γ' phase, in contrast to the η phase, exists over a considerable range of composition. The range of solubility of aluminium in the ternary γ' phase is much the same as in the binary nickel-aluminium system, but it is possible to dissolve titanium until three out of every five aluminium atoms are replaced by titanium. Since the atomic radii decrease in the order

titanium, aluminium, nickel, the titanium atoms preferentially replace the aluminium atoms which occupy the cube corners of the face-centred unit cell of Ni_3Al , leaving the nickel atoms in the cube faces.

The replacement of aluminium by titanium results in an increase in lattice parameter from 3.560 kX at 0% titanium to 3.583 kX at about 15 at.-% titanium. There was no evidence of abnormally high lattice parameters in the ternary alloys corresponding with those



FIGS. 6.—The Nickel-Titanium-Aluminium Phase Diagram—Isothermal Sections for (a) 1150° C., (b) 1000° C., (c) 850° C., and (d) 750° C.

observed in the binary nickel-aluminium alloys, all the spacings indicating that the true value for Ni_3Al is about 3.560 kX. The interatomic distance in the γ' phase at the $\gamma'/(\gamma' + \eta)$ boundary is 2.535 kX, which is within $\frac{1}{2}\%$ of the interatomic distance in the basal planes of Ni_3Ti 2.545 kX. Together with the similarity of the two structures on the equivalent planes (111) cubic and (0001) hexagonal, this factor seems to have a powerful effect on the equilibrium between the two phases, for over the range of temperature from 750° to 1150° C. the solubility of titanium in γ' remains almost constant at 15.6–15.9 at.-%. This position of the boundary has been arrived at from consideration of the X-ray data, given in Table V, from two series of alloys along the lines marked *ab* and *cd* in Fig. 6 (d), which gave the same boundary

position. On the other hand, microscopical examination of alloys in the series along *cd* indicated that the boundary should lie at about 14 at.-% titanium. The appearance under the microscope of a typical $(\gamma' + \eta)$ alloy is shown in Fig. 21 (Plate IV).

The discrepancy between the X-ray and micrographic results probably lies in the mode of specimen preparation. When the crystal structures of the two phases coexisting in equilibrium with each other are as closely related as are those of the γ' and η phases, it would be anticipated that approach to equilibrium would be very slow indeed, unless the specimen was heavily strained by mechanical work in order to accelerate the diffusion processes. The filings used for X-ray examination have received a considerable amount of cold work in their preparation,

TABLE V.—*Lattice Parameters of the γ' Phase in the Nickel-Titanium-Aluminium System*

Alloy No.	Composition, at.-%			Lattice Parameter, kX		
	Ni	Ti	Al			
Series <i>ab</i>				Slowly cooled from 900° C.		
22	74.1	0	25.9	3.5599		
21	74.8	5.8	19.4	3.5700		
24	74.6	9.9	15.5	3.5760		
25	74.4	15.0	10.6	3.5819		
26	74.4	20.0	5.6	3.5827		
Series <i>cd</i>				1150° C.	1000° C.	750° C.
252	76.6	4.6	18.8	...	3.5657	...
254	76.6	10.0	13.4	...	3.5750	...
255	75.7	12.4	11.9	3.5789
256	75.6	14.8	9.6	3.5835	3.5836	3.5834
257	74.8	18.0	7.2	3.5846	3.5846	3.5853

and in these the approach to equilibrium should be rapid. To give a corresponding amount of strain to a lump specimen of an alloy consisting mainly of γ' phase is impossible owing to the susceptibility to intergranular cracking which is characteristic of γ' . In an attempt to pre-stress the 75.6/14.8/9.6 at.-% nickel-titanium-aluminium alloy, a small lump was hammered until it showed signs of cracking and was then annealed at 1000° C. The recrystallized areas of the cold-worked specimen indicated a reduction in the amount of η phase. This was in accord with the X-ray findings, but owing to difficulties in preparation of microspecimens consisting of the two phases γ' and η , it was not easy to be certain on this point. It was decided that in this case the position of the $\gamma'/(\gamma' + \eta)$ boundary was more accurately determined by the X-ray method. The width of the γ' phase field was estimated from the microstructures.

In addition to the detailed study of the γ , γ' , and η phases of the system, a cursory examination of the system to 50 at.-% nickel has been made. A series of five alloys equally spaced from NiTi to NiAl were studied and provided rather unexpected results. It was known that both phases had ordered body-centred cubic structures of the CsCl type and that in some systems, such as iron-nickel-aluminium¹⁰ and copper-nickel-aluminium,¹¹ the β -NiAl phase was stable over very wide ranges of composition. In addition, there was the evidence of the replaceability of aluminium by titanium in the Ni_3Al structure. From this it was expected that a continuous series of solid solutions would extend as a single β -phase field from NiAl to NiTi. X-ray photographs showed that the lattice parameter of the alloy Ni_2TiAl (2.93 kX) lay midway between those of NiTi (3.005 kX) and NiAl (2.882 kX), suggesting a continuous series, but the other two alloys $\text{Ni}_4\text{Ti}_3\text{Al}$ and Ni_4TiAl_3 both gave diffraction patterns of two body-centred cubic phases. The two-phase structure of these alloys was confirmed by micro-examination. Thus there must be three separate single-phase regions based on NiTi, Ni_2TiAl , and NiAl, linked by two-phase regions. How these

link with the η and γ' phase fields has not been determined in this brief survey, but the most probable way is shown in Fig. 7. The Ni_2TiAl phase is of interest, as it shows not just the simple ordering of the CsCl type with the nickel atoms at the cube corners, but also ordering of the titanium and aluminium

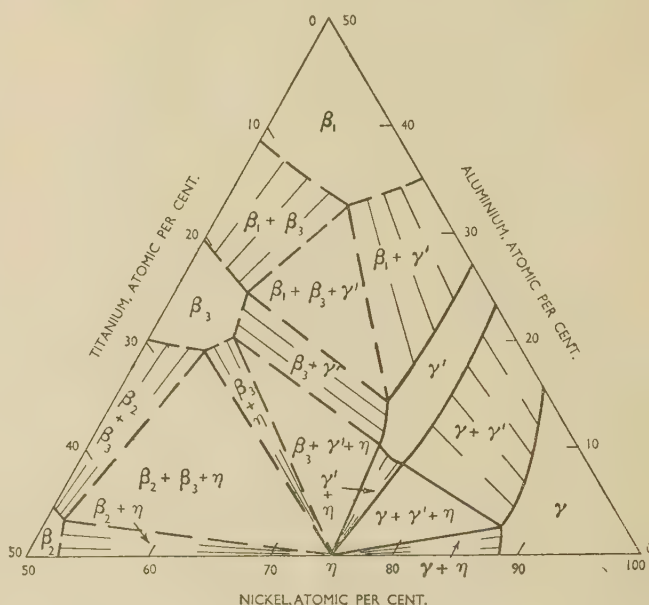


Fig. 7.—A Possible Form of the Nickel-Titanium-Aluminium Phase Diagram for Alloys Containing more than 50 at.-% Nickel.

atoms in alternate cube-centre positions, giving a superlattice of the Cu_2MnAl type. From the strength of the superlattice lines given by samples of Ni_2TiAl quenched from 1000° and 1200° C., it appears likely that the alloy is fully ordered from the temperature of its formation. A notable characteristic of this phase is its extreme brittleness, which necessitates the greatest care in the preparation of microspecimens.

ACKNOWLEDGEMENTS

The authors wish to thank The Mond Nickel Co., Ltd., for permission to publish this paper, and Mr. H. W. G. Hignett for his very helpful interest.

REFERENCES

1. A. Taylor and R. W. Floyd, *J. Inst. Metals*, 1951-52, **80**, 577.
2. A. Taylor and H. Sinclair, *Proc. Phys. Soc.*, 1945, **57**, 126.
3. A. G. C. Gwyer, *Z. anorg. Chem.*, 1908, **57**, 133.
4. I. Iitaka, *Tetsu to Hagane*, 1924, **10**, 1.
5. H. Nishimura and S. Watanabe, *Japan Nickel Rev.*, 1937, **5**, 552.
6. A. J. Bradley and A. Taylor, *Proc. Roy. Soc.*, 1937, [A], **159**, 56.
7. W. O. Alexander and N. B. Vaughan, *J. Inst. Metals*, 1937, **61**, 247.
8. J. Schramm, *Z. Metallkunde*, 1941, **33**, 347.
9. R. W. Floyd, *J. Inst. Metals*, 1951-52, **80**, 551.
10. A. J. Bradley, *J. Iron Steel Inst.*, 1949, **163**, 19.
11. W. Köster, U. Zwicker, and K. Moeller, *Z. Metallkunde*, 1948, **39**, 225.

RELATIVE GRAIN TRANSLATIONS IN THE PLASTIC FLOW OF ALUMINIUM *

1412

By W. A. RACHINGER,† M.Sc., JUNIOR MEMBER

SYNOPSIS

The geometry of plastic deformation in the interior of a polycrystalline aggregate has been investigated by means of a grain-counting technique. The respective contributions of grain elongation and relative grain movements to the deformation have been determined for various conditions of temperature and strain rate. At higher temperatures and lower rates of deformation the grains do not elongate in conformity with the aggregate, but tend to remain equiaxed, the external deformation being due to the relative movements of the grains.

In addition, the behaviour of the surface regions of a polycrystal subjected to high-temperature creep conditions has been studied. The mechanism of plastic flow at the surface is found to be quite different from that in the interior, the transition taking place in a region of only 0.010 in. thickness.

I.—INTRODUCTION

GEOMETRICAL considerations alone indicate that the deformation of a polycrystalline aggregate is due to two factors at most, namely, a change in shape of each individual grain and a relative movement of each grain as a whole past its neighbours. Change in shape of the grains during deformation has long been recognized, e.g. in the elongation of grains in rolled sheet. However, the role of relative translatory grain movements, or grain-boundary flow, as it is sometimes called, is not so well known. It has often been suggested that grain-boundary flow is an important factor in the creep of metals at high temperatures, but comparatively little direct experimental evidence is available to support this hypothesis.

Rosenhain¹ was possibly the first to produce evidence of relative grain movements. He observed that when pure iron was strained at 900° C., differences in level of the grains occurred on the originally flat polished surface, thus indicating that relative translations of the grains had taken place. Hanson and Wheeler² made similar observations on aluminium subjected to creep deformation at 250° C. They also saw indirect evidence for relative grain movements in the phenomenon of intercrystalline failure and in the non-appearance of slip bands at high temperatures, the latter indicating that some other mechanism of deformation might be operative.

In recent years further evidence of a more quantitative nature has been forthcoming. Moore, Betty, and Dollins³ demonstrated that during creep the grains of a lead-tin alloy move relative to each other. After deformation, a set of fine scratches, originally present on the specimen surface, were found to exhibit steps and changes of direction at the boundaries. King, Cahn, and Chalmers⁴ investigated the displacements at the boundary of a bicrystal of tin deformed at 222° C. A scratch drawn across the boundary became

broken into two parts which moved relative to each other during the deformation, thus indicating that relative translation of the two crystals had taken place at the boundary. Betteridge and Franklin⁵ have shown that such movements occur at the boundaries of an antimony-tin alloy and have indicated how the relative translation of two grains may be accommodated by shear in a neighbouring grain. Servi and Grant⁶ have found that creep in aluminium is accompanied by both relative grain movements and grain-boundary migration. Kê⁷ demonstrated the viscous behaviour of grain boundaries in aluminium by internal-friction measurements and further suggested⁸ that the relative movement of the grains occurs by shear processes within small disordered groups of atoms in the grain-boundary region. It has often been suggested⁹ that the quasi-viscous component of the Andrade creep equation is due in part at least to the sliding of grains, one past the other, at "viscous" grain boundaries. One further piece of evidence for relative grain movements has been produced by Gifkins.¹⁰ Two specimens of a lead-thallium alloy were extended, one rapidly and one slowly, by 50%. The microstructure of the rapidly deformed specimen showed elongated grains exhibiting heavy slip markings, whereas the grains of the slowly extended specimen remained essentially equiaxed and undistorted. This suggests that during the slow deformation the grains moved past each other without suffering any large strains.

The object of the work to be described in Section II was to investigate phenomena of this type and to produce evidence of a quantitative nature for the occurrence of relative grain movements. In particular, it was desired to determine the effect of both temperature and rate of deformation on the parts played by the two possible mechanisms, viz. change in shape of the grains and relative movement of the grains, in the plastic flow of polycrystalline aluminium.

* Manuscript received 18 February 1952.

† Aeronautical Research Laboratories, Department of Supply, Melbourne, Australia.

II.—EFFECT OF TEMPERATURE AND RATE OF STRAINING ON THE DEFORMATION PROCESSES IN THE INTERIOR OF A POLYCRYSTAL

Essentially, the experimental method consisted of measuring the average strain produced in the grains of a polycrystalline aggregate which had been subjected to a known overall deformation. Tensile specimens whose grains were originally equiaxed were deformed under various conditions of temperature and strain rate. By making grain counts on the deformed specimens, the average "length" and "width" of the grains were found, and hence the average strain suffered by them could be determined. If this average strain in the grains was found to be less than the overall strain in the aggregate, the difference could be attributed to relative grain movements.

1. EXPERIMENTAL

Aluminium (99.95%) tensile specimens of 2 in. gauge-length and cross-section 1×0.06 in. were recrystallized to a fine grain-size and stabilized by annealing for 15 hr. at 400°C . In order to check that the grains were equiaxed, two of the specimens were sectioned to half thickness, electropolished, and etched, and grain counts made in directions parallel and perpendicular to the specimen axis. These longitudinal and transverse counts were compared by a statistical method, namely, a *t*-test, and it was found that the grains were equiaxed, having an average linear size corresponding to 10.12 grains/mm. These two specimens were assumed to be representative of the batch in their linear grain dimensions in the two directions. The remaining specimens were extended approximately 50% in a tensile test, each at a particular temperature in the range 20 – 350°C ., and at either the high rate of 10% elongation/min. or the low rate of 0.1% elongation/hr. During the test the temperature at the centre of the specimen was controlled to within $\pm 1^\circ\text{C}$., and the temperature variation along the gauge-length was never greater than 4°C .

To ensure that the results obtained were not in any way due to surface phenomena, the observations were made on an internal section of the specimens. The deformation processes at the surface are considered separately in Section III. After deformation each specimen was sectioned to half thickness by taking light cuts with a surface grinder, then ground on successively finer grades of abrasive, and finally electropolished and etched with a grain-boundary etching reagent.

Grain counts were then made in directions parallel and perpendicular to the axis of tensile stressing. A low-power travelling microscope was traversed across 200 grains of the specimen, and the length of traverse measured. Six such traverses were made in the longitudinal direction and six in the transverse

direction, involving the counting of 2400 grains for each specimen. Since no intercrystalline fissures appeared in the plane of section, it was not necessary to measure the dimensions of each individual grain. An average value of the grain dimensions could be obtained merely by measuring the length of traverse containing a given number of grains. From the longitudinal and transverse counts it is possible to determine N_L and N_T , the mean number of grains/mm. in the longitudinal and transverse directions, respectively, together with other statistical quantities required for the error calculation mentioned below.

2. MEASUREMENT OF THE STRAIN IN THE GRAINS

The average grain-sizes N_L and N_T are essentially the reciprocals of the final "length" and "width" of the grains, and since it is known that the latter were equiaxed originally it is possible to determine the average strain in the grains by the following method.

If the specimen suffers an overall longitudinal strain e_s , the final configuration of the grains may be considered as arising from the operation of three separate processes:

- (a) A non-directional growth of the grains by a linear factor K .
- (b) A longitudinal tensile strain of average amount e_g in the grains.
- (c) Relative translatory movements of the grains which account for the difference between the specimen elongation e_s and the average grain elongation e_g .

It is to be noted that the possible complicating factors of directional grain growth, recrystallization, or any other process which involves a wholesale redistribution of the positions of grain boundaries, have been ignored. The possible existence and influence of these factors will be discussed in Section V.

Because of the additive nature of the three processes (a), (b), and (c), and also because it is only the end result of deformation which is observed in the grain counts, it is immaterial whether these processes are considered to operate concurrently or separately in any particular order. For simplicity of analysis, it will be assumed that the three processes take place separately in the order indicated above.

In the original material:

- the number of grains/mm. in the longitudinal direction
- = the number of grains/mm. in the transverse direction
- = n (which from the grain counts on the original material was found to be equal to 10.12).

$1/n$ is therefore equal to the mean chord length of the grains, since the traverse line along which the count is made is the sum of 200 intercepts, each intercept being a randomly chosen chord of a grain.

After a non-directional grain growth by a linear factor K :

$$\begin{aligned} & \text{the number of grains/mm. in the longitudinal direction} \\ &= \text{the number of grains/mm. in the transverse direction} \\ &= n/K. \end{aligned}$$

If each grain now suffers a longitudinal tensile strain of amount e_G , then all chords parallel to the axis of tension will increase in length by a factor of $(1 + e_G)$, and hence the mean chord length in this direction will also increase by this factor. Similarly, all chords, and hence the mean chord length, in the transverse direction will be reduced by a factor $(1 + e_G)^{-\frac{1}{2}}$. Thus at this stage:

the number of grains/mm. in the longitudinal direction

$$= \frac{n}{K} \cdot \frac{1}{1 + e_G}$$

the number of grains/mm. in the transverse direction

$$= \frac{n}{K} (1 + e_G)^{\frac{1}{2}}.$$

Relative translatory movements of the grains now take place to increase the strain in the specimen to its final value e_S . On completion of this process the average grain dimensions are unchanged, the grains having moved relative to each other without, on the average, having changed either their size or shape.

Thus, the measured grain dimensions in the longitudinal and transverse directions, N_L and N_T , may be related to the strain in the grains e_G and the grain-growth factor K as follows:

$$N_L = \frac{n}{K} \cdot \frac{1}{1 + e_G}$$

$$N_T = \frac{n}{K} (1 + e_G)^{\frac{1}{2}}$$

from which:

$$e_G = (N_T/N_L)^2 - 1 \quad (1)$$

and

$$K = n(N_L N_T^2)^{-\frac{1}{3}} \quad (2)$$

Equation (1) allows the strain in the grains to be determined from the longitudinal and transverse counts, the only requirement being that the grains are initially equiaxed; whilst equation (2) allows the evaluation of the growth factor K if, in addition, the original grain-size is known.

3. RESULTS

The results of the grain counting and subsequent calculations are shown in Table I. The values of grain dimensions and the derived quantities are shown for all combinations of temperature and strain rate. The low rate of elongation of 0.1%/hr. is referred to as "slow", whilst "rapid" refers to the high rate of 10% elongation/min. Because of the statistical

nature of the experiment it is not possible to quote precise values of e_G and K . It was therefore desirable to give some indication of the experimental error in these quantities. For this reason the 95% confidence ranges for both e_G and K were determined by standard statistical methods. There is a 95% probability that the true values of e_G and K lie within the ranges indicated.

The corresponding confidence range of e_G/e_S is also shown. This parameter is a convenient measure of

TABLE I.—Values Derived from Grain-Counting Calculations for Interior of Polycrystal.

Temp., °C.	Strain Rate	N_T	N_L	e_S	e_G	e_G/e_S	K
20	Slow	12.70	6.65	0.52	0.54 ± 0.06	1.04 ± 0.12	0.99 ± 0.05
100	"	11.81	6.63	0.53	0.47 ± 0.06	0.89 ± 0.11	1.04 ± 0.04
200	"	10.63	6.65	0.42	0.37 ± 0.06	0.88 ± 0.14	1.11 ± 0.06
250	"	9.42	8.79	0.48	0.05 ± 0.06	0.10 ± 0.13	1.10 ± 0.07
300	"	9.00	8.21	0.47	0.06 ± 0.06	0.13 ± 0.13	1.16 ± 0.06
350	"	6.92	6.09	0.51	0.08 ± 0.06	0.16 ± 0.12	1.52 ± 0.08
20	Rapid	11.58	5.98	0.49	0.55 ± 0.06	1.12 ± 0.12	1.08 ± 0.06
350	"	11.41	6.16	0.59	0.51 ± 0.06	0.86 ± 0.10	1.09 ± 0.05

the relative contributions of the two processes (b) and (c) to the deformation. If the deformation is due only to straining of the grains, then $e_G/e_S = 1$, but if, at the other extreme, the deformation is due only to relative translatory movements of the grains, no change in the average shape of the grains having taken place, then e_G/e_S is zero. The parameter will vary between zero and unity according to the relative contributions of the two processes.

The numerical values of K indicate that, with the exception of the 350° C. deformation, grain growth has not occurred. The implications of this will be discussed later. With slow deformation at 200° C. or below, the main contribution to the deformation is the change in shape of the grains, e_G being approximately equal to e_S , i.e. e_G/e_S being of the order of unity. However, at 250° C. or above, e_G/e_S assumes a value of the order of 0.15, indicating that relative translatory grain movements account for the greater part of the deformation. The results are quite striking, when it is considered that, say, in the 300° C. case, the specimen has elongated 47% whilst the grains have suffered only approximately 6% elongation. Thus, it appears that with slow deformation there is a relatively small temperature range over which the mechanism of deformation markedly changes. With rapid straining the change in shape of the grains is the predominant factor in the deformation from 20° to 350° C. Since the upper limit of e_G/e_S is less than unity for the case of rapid deformation at 350° C., it is likely that relative grain movements account for a small part of the overall strain.

Summarizing, it would seem that the interior grains of a polycrystal suffer approximately the same strain as the aggregate, if the specimen is deformed at the rapid rate in the range 20°–350° C. or at the slow rate within the range 20°–200° C. If, however, an aggregate is deformed slowly within the range 200°–350° C., the grains undergo changes in shape which are slight

in comparison with the change in shape of the specimen. In fact, they depart only very slightly from their original equiaxed shape, even though the specimen has suffered a large deformation. If, for the moment, one neglects the effect of recrystallization or any other process of grain-boundary rearrangement which could alter the average shape of the grains and yet make no contribution to the deformation of the aggregate, then this slow-rate high-temperature deformation may be attributed to relative translatory grain movements, the grains sliding past each other without changing their shape to any large extent. The complicating effects of recrystallization and grain-boundary rearrangement will be discussed later.

III.—DEFORMATION PROCESSES AT THE SURFACE OF A POLYCRYSTAL

The results of the preceding section apply to the behaviour of grains surrounded on all sides by other grains, the grain counts being made on a central-section plane of the specimen. It became of interest to study the behaviour of grains at the surface of the specimen, and in particular, to determine whether the mechanism of relative grain movement is inhibited at a free surface.

Because of the surface rumpling and grain-boundary migration produced by slow deformation at elevated temperatures, it is not practicable to make grain counts at the surface of a specimen deformed under these conditions. However, it is possible to obtain, by indirect methods, some idea of the contribution of relative grain movements to the overall deformation of the surface layer. The appearance of new grains at the surface, the displacement of grid lines ruled on the surface, and the contour of the deformed surface are all useful in this respect.

1. METHODS OF INVESTIGATING SURFACE DEFORMATION

If it is assumed that the two mechanisms of grain elongation and relative grain movements are contributing to the macroscopic strain and that no large-scale grain boundary rearrangements are taking place, then a simple calculation serves to indicate how the surface grains would behave. There is no need for a detailed analysis of the behaviour of the aggregate during deformation. Only the end result need be considered. The effects of the two mechanisms are additive, and it is immaterial whether they operate consecutively or concurrently. The notation used is the same as that of the previous section, e_g being the strain suffered by the grains, whilst the specimen is strained by an amount e_s .

(a) *The Appearance of New Grains at the Surface*

Consider a particular region of the surface having area A and containing n^2A grains, n being the number of grains per unit length. After an overall tensile strain e_s this region will have an area of $A(1 + e_s)^{\frac{1}{2}}$.

However, in the course of this deformation the grain dimensions will have changed owing to the strain e_g , and the average area of a grain section will be $(1 + e_g)^{\frac{1}{2}}/n^2$. Thus, the number of grains within this region will now be $n^2A\left(\frac{1 + e_s}{1 + e_g}\right)^{\frac{1}{2}}$. Therefore the number of grains within a given region will be increased by a factor $\left(\frac{1 + e_s}{1 + e_g}\right)^{\frac{1}{2}}$.

It is of interest to consider the extreme cases. If the overall strain is due entirely to deformation of the grains, then $e_s = e_g$ and the factor is unity. If, however, the overall strain is due to relative grain movements, then $e_g = 0$ and the factor is $(1 + e_s)^{\frac{1}{2}}$. This would equal 1.22 for a 50% elongation. Thus, under these conditions, one would expect a 22% increase in the number of surface grains, these grains having forced their way into the surface from the underlying layers.

(b) *The Displacement of Grid Lines*

The final configuration of a set of longitudinal and transverse grid lines ruled on the surface should also indicate the nature of the deformation process at the surface. The portions of the grid contained within each grain should behave in the same way as the immediate surface layer of the grain itself. Thus, if the grain deforms, then the grid should deform in a like manner, and if the grains move relatively to each other, then the portions of the grid contained within the grains should also move relatively. The rulings would therefore become discontinuous at grain boundaries, and the line segments so defined would suffer the same strains as the grains which contain them. It is a simple matter to calculate the average magnitude of the discontinuities that occur at grain boundaries. The analysis is essentially as follows:

A longitudinal line of unit length will, after deformation, assume the appearance of a set of line segments of total length $(1 + e_g)$. These will be distributed over a length $(1 + e_s)$, and thus the total length of longitudinal gaps will be $(e_s - e_g)$. Now, there will be n such gaps, since the original unit line crossed n grain boundaries. Hence the average longitudinal gap occurring at the boundaries will be of length $(e_s - e_g)/n$.

The average length of the discontinuities occurring in transverse rulings may be derived in a similar manner. A transverse line of unit length will break up into line segments which will be contracted so that their total length is $(1 + e_g)^{-\frac{1}{2}}$. These lines will be contained within a region of length $(1 + e_s)^{-\frac{1}{2}}$, and thus overlapping will occur, the average length of overlap at each grain boundary being $\{(1 + e_g)^{-\frac{1}{2}} - (1 + e_s)^{-\frac{1}{2}}\}/n$. The final configuration of the lines and the sizes of the discontinuities are shown in Figs. 1 (a) and (b).

In practice, it is found that conditions are not quite as simple as are assumed in this calculation. Here it was considered that the grain boundary remained

essentially "fixed" in position and that a single gap appeared in the grid line, due to the relative movement of the grains, one on either side of the boundary. However, in actual fact, grain-boundary migration takes place during deformation. If the migration occurs in a discontinuous fashion, it would be expected that instead of a single discontinuity there would be a series of discontinuities, one at each position of the grain boundary. If, however, the grain boundary were to migrate continuously, or nearly so, whilst relative grain movements were taking place, then the grid line would appear to be bent in the region traversed by the grain boundary. The two extremes in this type of discontinuity are shown in Fig. 2 (Plate V), a photomicrograph of aluminium slowly deformed at 300° C. The heavy scratch line in the

exhibit a gradual change throughout the region traversed by the grain boundary.

It can be seen that measurements of the surface contour in the region of grain boundaries will, in the same way as grid-ruling measurements, give some idea of the nature of the deformation process. The relevant experimental details and results are given below.

2. MEASUREMENTS AT THE SPECIMEN SURFACE

In order to determine the contribution of relative grain movements to the deformation at the surface, it was necessary to deform under conditions known to be favourable to this process. Therefore, tensile test-pieces of similar shape and of the same grain-size as those described in Section II were elongated at the constant rate of 0.1%/hr. at 300° C., the final elongation reached being 50%. The observed effects of deformation are as follow.

(a) The Appearance of New Grains

Microscopic examination of the surface after deformation afforded little evidence of new grains being forced up from the underlying layers. Photomicrographs of the same region taken both before and after deformation showed essentially the same set of grains. It is, however, possible that some small sections of new grains appeared in the broadened grain-boundary regions. After removal of the surface by electropolishing, a few fissures were evident at boundaries where neighbouring grains had parted. It was as though the surface behaves as a thin skin, which retains its continuity even though small fissures appear beneath it. These fissures were not very deep, being no greater than 0.006 in.

These observations indicate that the number of grains within a given surface region remain roughly constant during deformation. Thus, it may be concluded that e_g is approximately equal to e_s , i.e. the grains at the surface are suffering approximately the same deformation as the specimen. The appearance of fissures just below the surface, however, indicates that some relative grain movement is taking place in this region. This is discussed further in Section IV.

(b) The Displacement of Grid Lines

The lateral displacements of both longitudinal and transverse grid lines at grain boundaries were measured by means of a microscope fitted with a measuring eyepiece. The average displacement of the transverse grid lines was 0.008 mm., which, according to the previous analysis, is equal to $(e_s - e_g)/n$, where $n = 10.1$ grains/mm. and $e_s = 0.50$. Thus, the assessed value of strain in the grains is $e_g = 0.42$. The longitudinal lines were found to suffer lateral displacements of average value 0.004 mm. This, on substitution in the relevant formula, yields a value of $e_g = 0.37$. The measurements of grid-line displacements would therefore indicate that, at the surface, the grains are suffering strains of approximately 40%, whereas the aggregate has elongated by 50%.

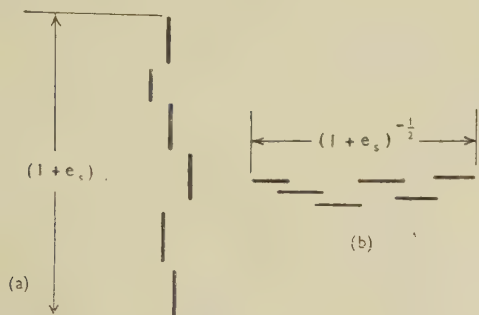


FIG. 1.—(a) Final Configuration of a Longitudinal Grid Line.

Average length of gap = $(e_s - e_g)/n$.

Average lateral displacement = $\{(1 + e_g)^{-1/2} - (1 + e_s)^{-1/2}\}/n$.

(b) Final Configuration of a Transverse Grid Line.

Average length of overlap = $\{(1 + e_g)^{-1/2} - (1 + e_s)^{-1/2}\}/n$.

Average lateral displacement = $(e_s - e_g)/n$.

centre exhibits a single discontinuity at the upper boundary of the grain, while it is bent in the region over which the lower boundary has migrated.

In cases where the grid lines are either bent or exhibit a series of minute gaps or overlaps in the region over which the boundary has migrated, it is, of course, not practicable to measure the total length of gap or overlap. However it is still possible to measure the lateral displacements of the lines and to obtain, by the formulæ shown above, a rough idea, at least, of the relative contributions of the two mechanisms to the deformation of the surface.

(c) The Surface Contour

If relative grain movements are contributing to the deformation, an originally flat specimen surface should become rumpled, changes in level occurring at grain boundaries. The magnitude of these displacements will be just the same as the lateral displacement of longitudinal grid lines. Thus, at each grain boundary one would expect a change in level of average magnitude $\{(1 + e_g)^{-1/2} - (1 + e_s)^{-1/2}\}/n$. If the grain boundary migrates during deformation, the surface level would not change sharply but would

(c) *Measurements of Surface Contour*

The displacements having components perpendicular to the specimen surface were measured with a Talysurf surface analyser. Longitudinal traverses were made between two scribed lines. The traverse line is permanently marked on the specimen surface, since the stylus leaves a fine scratch in its path. This scratch line was later traversed with a travelling microscope, and, using the scribed lines as reference marks, the positions of grain boundaries and any other features of interest were plotted on the pen record. In this way it was possible to measure the relative displacements at grain boundaries. The average value of this quantity was found to be approximately 0.003 mm., which when equated to $\{(1 + e_g)^{-1} - (1 + e_s)^{-1}\}/n$ yields a value of e_g of 0.40, again indicating a grain elongation of roughly 40% in comparison with a specimen elongation of 50%.

Summarizing, it would appear from all three methods of measurement that, at the surface, the deformation is predominantly grain elongation, only a small amount of the macroscopic strain being due to relative grain movements. In fact, the quantitative measurement indicates that an overall specimen elongation of 50% is accompanied by a tensile strain in the grain-sections at the surface of approximately 40%.

IV.—THE DEPTH EFFECT

It is of interest to compare the results of Sections II and III and to observe the marked difference in behaviour of the surface grains and those in the interior. Table I shows that the grains in the interior of an aggregate slowly strained to 47% elongation at 300° C. have suffered only 6% strain, most of the macroscopic strain being due to relative grain movements. On the other hand, the surface grains of an aggregate deformed to 50% elongation under identical conditions exhibit a 40% strain, only a small amount of the external deformation being due to relative movement of grains. Naturally the nature and the extent of the transition from one mechanism to the other became of great interest and was accordingly investigated.

The grain-counting procedure described in Section II was utilized. By making grain counts at various depths below the surface, it should be possible to define the region over which the deformation mechanism changes, provided that this region is not too narrow. A specimen was elongated by 50% at 300° C. at the rate of 0.1%/hr. Grain counts were made at distances of 0.001, 0.004, 0.006, and 0.010 in. below the surface, the excess material being removed by abrasion and electropolishing. The results are shown in Table II, in which the 95% confidence ranges for both e_g and K are quoted.

The experimental results show quite clearly that the deformation mechanism changes markedly over a narrow region, the grain elongation decreasing rapidly

with increasing depth below the surface. In fact, for an overall specimen elongation of 50%, the grain elongation changes from approximately 40% at the surface to 5% at a depth of 0.010 in., this strain being characteristic of the grains in the interior of the

TABLE II.—*Values Showing Region of Change in Mechanism of Deformation.*

Depth Below Surface, in.	N_T	N_L	e_g	K
0.001	12.32	8.24	0.31 ± 0.06	1.08 ± 0.06
0.004	10.66	8.64	0.15 ± 0.05	1.02 ± 0.06
0.006	10.75	9.07	0.12 ± 0.03	1.00 ± 0.05
0.010	9.93	9.22	0.05 ± 0.03	1.05 ± 0.05

specimen. The smallness of this region is probably best realized from the fact that it is only two grains in depth. Thus, it is likely that large strain gradients exist within the grains in this region.

The tendency for the grains to elongate in the vicinity of the surface may possibly be explained by the influence of the surface oxide film or by energy considerations. Large-scale movements of grains at the surface would cause severe rumpling and a correspondingly large increase in both the area and the energy of the surface. The marked differences found in the deformation processes at the surface and in the interior may explain the differences in creep behaviour of specimens of different sizes. Andrade¹¹ has observed differences of this type in a lead-tellurium alloy subjected to rapid (1% elongation/min.) creep conditions and has shown the existence of surface effects sufficient to account for them.

Incidentally, the existence of a depth effect emphasizes the danger of interpreting observations made at a surface as representative of the specimen as a whole.

V.—THE MECHANISM OF DEFORMATION

The results described in the previous Sections indicate three main features:

(a) With rapid deformation of aluminium in the range 20°–350° C. or slow deformation between 20° and 200° C., the strain in the specimen is due, for the most part, to strains suffered by each grain of the aggregate.

(b) On slow deformation at 250° C. or above, the grains in the interior of an aggregate appear to elongate only by amounts that are small in comparison with the overall strain.

(c) On slow deformation at 300° C., the grain sections at the surface suffer considerable elongation, but with increasing depth below the surface the tendency for the grains to remain equiaxed becomes more marked.

The mechanism of grain elongation has been studied by many investigators, who have interpreted this phenomenon in terms of slip, deformation banding,

cell movements, &c. Any of these mechanisms, or a combination of them, is possible, although slip, if it occurs in the surface grains of an aggregate slowly deformed at 300° C., must be very uniformly distributed, since slip bands are not observed under these conditions.¹² Honeycombe¹³ has observed structures suggestive of kinking in aluminium single crystals deformed at room temperature. It is likely that such a process may take place at the surface of polycrystals deformed slowly at elevated temperatures, since structures similar to those found by Honeycombe have been observed under these conditions.¹⁴ Another possible mechanism of grain elongation at the higher temperatures is that of relative movements of the sub-structure elements, as suggested by Wilms and Wood.¹⁵ Their observations indicate that, on high-temperature deformation, the grains break down into a set of small elements or "cells" of slightly different orientation. Now it is likely that these cells may move relatively to each other and give rise to an elongation of the grains, in the same way as the relative movements of grains may give rise to the deformation of an aggregate. However, since the orientation differences between the cells are in general much smaller than those between the grains of an aggregate, the cell boundaries would be much more resistant to flow than the grain boundaries, and one might therefore expect the contribution of cell movements to grain elongation to be rather small.

Grain elongation alone does not account for all the observed facts, however. It plays only a minor role at high temperatures and low strain rates. The main interest of this investigation was the other mechanism, by means of which the grains were able to remain equiaxed, or nearly so, while the aggregate as a whole suffered considerable deformation. It has been suggested that relative movement of grains is the operative mechanism. However, there is another possibility, namely, grain elongation followed by a rearrangement of grain boundaries causing the grains to re-assume their equiaxed shape. The return to the equiaxed state could be due either to recrystallization or to a migration of the grain boundaries under the influence of their tension forces.

It is rather difficult to distinguish between these two deformation mechanisms, although there is some evidence in favour of relative grain movements. Recrystallization certainly did not occur in the surface grains, since the grain-boundary network suffered little change during deformation except in the case of slow deformation at 350° C. Here, the difficulty of identifying a given set of grains may have been due either to recrystallization or to high mobility of grain boundaries. It is also unlikely that recrystallization occurred in the interior of the specimen, since the results of Tables I and II indicate that, with the exception of the 350° C. slow deformation, the average grain volume remained essentially unchanged after deformation, K being approximately equal to unity. In most cases there appears to be a slight increase in

grain-size, but this may be due merely to experimental technique. It was found that the grain boundaries of the deformed material did not etch as clearly as those of the annealed metal, and as a consequence some grains were probably missed in the counts on the former, thus giving rise to an apparent increase in grain-size. The large increase in grain-size during the slow deformation at 350° C. may have been due to either grain growth or recrystallization. It therefore seems clear that, with the possible exception of the case of slow deformation at 350° C., the equiaxed condition of the grains in the deformed aggregates is not due to the co-operative action of grain elongation and recrystallization.

The possibility of a rearrangement of grain boundaries under the action of their tension forces seems somewhat remote. The boundaries of the interior grains have a rather ragged appearance, and, if their tension forces are insufficient to reduce these short-range curvatures, it seems unlikely that they could cause a wholesale rearrangement of the boundaries to produce equiaxed grains.

These observations indicate that grain elongation and boundary rearrangement is not likely to be the operative mechanism. There is also some positive evidence in favour of the alternative mechanism of relative grain movements. The displacement of grid lines at the upper boundary in Fig. 2 (Plate V) indicates quite clearly that relative movement of the grains has taken place. If the other mechanism had been operative, the grid line would have remained continuous. This type of observation is, of course, confined to the surface, and for reasons stated in Section IV it was thought preferable to design an experiment capable of showing that relative grain movements take place in the interior of a polycrystal. The problem is essentially one of forming a grid line or marker of some description in the interior of the specimen. The most satisfactory procedure was found to be as follows.

Two bars of aluminium, whose mating faces had previously been cleaned with a rotating wire brush, were pressure-welded at room temperature by compressive loading sufficient to cause 80% reduction in thickness. The welded bar was then rolled into sheet of 0.10 in. thickness. Fig. 3 (Plate V) is a photomicrograph of a section of this sheet after recrystallization. The presence of an oxide film AB at the weld junction is obvious. This oxide film, which is in the form of a plane parallel to the rolling plane, may be used to illustrate the deformation mechanism in the interior in the same way as grid lines were utilized at the surface. The line of oxide exhibits no irregularities, and so any deflections of the line caused by the deformation may be interpreted in terms of the deformation mechanisms.

A specimen cut from this sheet was recrystallized and slowly extended by 50% at 300° C. After this the specimen was sectioned transversely, polished, and heavily etched. Fig. 4 (Plate V) is a photomicrograph from this section. The change in shape of the oxide

film is obvious. It now exhibits fairly sharp bends and also a lateral displacement at the grain boundary. This displacement is definite evidence of relative translatory movement at the grain boundary. The curvatures exhibited by the film, however, cannot be uniquely interpreted. They may be due to relative grain movements at a mobile boundary (cf. the bending of the scratch line at the lower boundary in Fig. 2), or, alternatively, they may be the result of inhomogeneous deformation within the grain.

The only direct evidence for relative grain movements in the interior of a polycrystal is the lateral displacement of the oxide film at the boundary. This, however, provides only qualitative evidence, and cannot be interpreted quantitatively, since the presence of the film will no doubt have an effect on the deformation processes. It certainly seems likely that it would inhibit the relative movement of those grains whose boundaries it intersects.

Although the possibility of grain elongation accompanied by a rearrangement of boundaries cannot be completely rejected, the evidence cited in this Section suggests that the deformation is due to relative grain movements.

If the deformation is to proceed by this mechanism without the formation of voids, then it is necessary that the grains should be continually adjusting their shape as they slide past each other. These minor adjustments of shape could be due to the operation of any of the mechanisms suggested to account for grain elongation. However, in this case it is necessary that the mechanism should be operative only within small regions of the grains.

Another process by means of which the grains could adjust their shape is grain-boundary migration. Fig. 2 certainly indicates that this process has been operative during the deformation. Since localized plastic deformation is restricted, in that the individual grain volumes must remain constant, it seems that the more flexible process of grain-boundary migration would be that most likely to cause the minor adjustments of shape.

The deformation of a polycrystalline aggregate would, therefore, appear to be due to the operation of at least three processes, namely :

- (i) A relative movement of the grains due to sliding at their boundaries.
- (ii) A deformation of the grains due to slip, cell movements, &c.
- (iii) A continual adjustment of the shape of the grains, which allows relative movements to take place without the creation of voids at the boundaries.

These processes may be illustrated by a soap-film model described in the Appendix.

The contribution of processes (i) and (ii) to the overall deformation has been determined and found to be sensitive to the temperature and rate of deformation and also to the depth below the surface. Since it was only the end result of deformation that

was observed, it is not possible to draw any conclusions as to the relative roles played by the two processes at any stage of the test. However, if the rate of deformation is considered to be a factor in determining which of the two processes predominates, then it is possible to infer something of the changes in the mechanism of deformation under certain creep conditions. In the primary stage the rate of elongation is relatively high, and the grain-elongation mechanism would be expected to be more predominant than during the secondary stage, when the creep rate is somewhat reduced. It has often been suggested⁹ that such a change in the deformation mechanism occurs on passing from the primary to the secondary stage of creep.

Although the work described above gives an overall picture of the geometry of the deformation, it provides no insight into the atomic processes involved in relative grain movements. Elucidation of these processes must await the development of techniques that will allow the study of dynamic conditions at grain boundaries.

ACKNOWLEDGEMENTS

This work forms part of a joint research programme on the deformation of metals under the general direction of Mr. H. A. Wills, of the Department of Supply, and Professor J. Neill Greenwood and Dr. W. A. Wood of the Baillieu Laboratory, University of Melbourne, to whom the author wishes to express his thanks. The helpful discussions with his colleagues at the Aeronautical Research Laboratories and the Baillieu Laboratory, are also gratefully acknowledged.

APPENDIX

A Soap-Film Model Illustrating the Deformation Processes

It is possible to illustrate the grain-elongation and grain-movement mechanisms by means of a simple

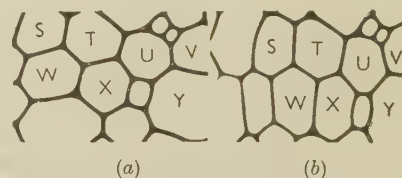


FIG. 5.—Thin-Walled Bubble Array : (a) Before Deformation ; (b) After Deformation.

model. A glass plate was suspended a few millimetres above the surface of a soap solution, and bubbles were blown in the solution with the aid of a fine-bore tube. The bubbles form into a honeycomb-like network, the soap films constituting vertical walls stretching from the liquid surface to the glass plate. The array, as shown in Fig. 5 (a), resembles the microstructure of a metal, the soap films forming the "grain" boundaries. By adjusting the height of

the glass plate above the liquid surface, the thicknesses of the "grain" boundaries may be varied. A structure having thin boundaries deforms by "grain" elongation, whereas one with thick boundaries deforms by relative "grain" movements. An alternative

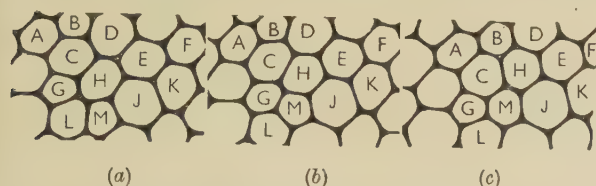


FIG. 6.—Thick-Walled Bubble Array: (a) Before Deformation; (b) After Deformation; (c) After Further Deformation.

method of reducing the thickness of the boundary films is to collect the bubbles between two parallel glass plates and allow the excess liquid to drain off.

Fig. 5 (a) is a photograph of a structure having thin "grain boundaries". On subjecting this array to an external strain, the "grains" elongate considerably

(Fig. 5 (b)). A structure with relatively thicker boundaries is shown in Fig. 6 (a). Owing to the spreading of the films at the glass surface, the difference in thickness is not truly reproduced in the photographs. Application of an external strain causes relative "grain" movements to take place. Figs. 6 (b) and (c) illustrate successive stages in the deformation. Note how "grain" *M* becomes contiguous first with "grain" *G* and then with "grain" *C*, and also how "grains" *B* and *H* become contiguous, causing the separation of "grains" *C* and *D*. In this case the "grains" remain, on the average, equiaxed after deformation. The minor changes in the shape of the grains, which are geometrically necessary if voids are not to be created, are also illustrated by the model, indicating that the necessary deviation of the grain boundary from its original position is rather small.

The model, although it does not give an ideal representation of the deformation processes in a metal, serves quite a useful purpose in demonstrating the possible geometry of relative grain movements.

REFERENCES

1. W. Rosenhain, "An Introduction to the Study of Physical Metallurgy", p. 259. 1914: London (Constable & Co.).
2. D. Hanson and M. A. Wheeler, *J. Inst. Metals*, 1931, **45**, 229.
3. H. F. Moore, B. B. Betty, and C. W. Dollins, *Univ. Illinois Bull.*, 1935, **32**, (23).
4. R. King, R. W. Cahn, and B. Chalmers, *Nature*, 1948, **161**, 682.
5. W. Betteridge and A. W. Franklin, *J. Inst. Metals*, 1951-52, **80**, 147.
6. I. S. Servi and N. J. Grant, *Trans. Amer. Inst. Min. Met. Eng.*, 1951, **191**, 917.
7. T.-S. Kê, *Phys. Rev.*, 1947, [ii], **71**, 533.
8. T.-S. Kê, *J. Appl. Physics*, 1949, **20**, 274.
9. E. Orowan, *J. West Scotland Iron Steel Inst.*, 1946-47, **54**, 57.
10. R. C. Gifkins, *J. Inst. Metals*, 1951, **79**, 233.
11. E. N. da C. Andrade and A. J. Kennedy, *Proc. Phys. Soc.*, 1951, [B], **64**, 363.
12. W. A. Wood and W. A. Rachinger, *J. Inst. Metals*, 1949-50, **76**, 237.
13. R. W. K. Honeycombe, *Proc. Phys. Soc.*, 1950, [A], **63**, 672.
14. W. A. Rachinger, *J. Inst. Metals*, 1951-52, **80**, 415.
15. G. R. Wilms and W. A. Wood, *ibid.*, 1948-49, **75**, 693.

THE INFLUENCE OF PRIMARY PARTICLES ON THE 1413 GRAIN-SIZE OF CAST MAGNESIUM-ALUMINIUM ALLOYS*

By W. A. BAKER,† B.Sc., F.I.M., MEMBER, MYRIAM D. EBORALL,‡ B.A., and A. CIBULA,‡ M.A., A.I.M., MEMBER

(Contribution from the British Non-Ferrous Metals Research Association.)

SYNOPSIS

Although the superheating and carbon processes for the grain-refinement of magnesium-aluminium alloys have now been in use for several years, their *modus operandi* remains obscure. The work described was directed towards determining whether the processes were basically similar or dissimilar, and whether a nucleating substance was responsible for both, or either, of them. Accordingly, the occurrence of primary particles in alloys of commercial and high purity, and their relation to changes in grain-size, brought about in various ways, have been studied. Two types of primary particle were found, one an iron-rich phase, and the other of unknown identity. It is concluded that neither of these types of particle is primarily responsible for grain refinement, but that a nuclear mechanism does operate during both processes. The evidence obtained, although incomplete, is consistent with aluminium carbide being the grain refiner.

I.—SCOPE OF WORK

For many years the cast magnesium-aluminium alloys of commercial interest were grain refined by superheating the melts to temperatures in the region of 800°–900° C. before casting at lower temperatures. More recently, refinement has been effected by adding carbon to the molten alloys at somewhat lower temperatures. The mechanisms responsible for the grain refinement resulting from these two treatments are not established, although several writers¹⁻³ have suggested that both treatments introduce into the molten alloys substances which form primary particles capable of nucleating the crystals of the magnesium-rich solid solution. There is experimental evidence supporting this view; e.g. Achenbach, Nipper, and Piwowarsky² found that, in the absence of superheating, melts of these alloys undercooled about 1° C. before solidification began, whereas superheated melts showed much less undercooling. Tiner⁴ confirmed this difference in behaviour.

Although no assumption was made about the grain-refining mechanism, all the work described below was directed towards determining what primary particles were present in magnesium-aluminium melts, how they influenced the grain-size of the casting, and their identity. Two types of particle were found in superheated alloys; one type was iron-bearing, and it has been shown that these particles are not responsible for grain refinement. It was thought possible that the other particles caused grain refinement, but

unfortunately their identity could not be established.

During the course of the work, which was originally concerned with grain refinement by superheating, two further contributions to the knowledge and technique of grain refining were made; the carbon process was introduced by American workers and the mechanism of grain refinement of aluminium-base alloys was established by Cibula.⁵ As a result of this, further experiments, also described below, were carried out, firstly, to determine whether carbon had been a significant variable in the earlier work on superheated material, and secondly, to find out whether the grain refinement of magnesium-base alloys was analogous to that of aluminium-base alloys.

The results, although not entirely conclusive, suggest that the same grain-refining mechanism operates in magnesium-aluminium alloys whether refinement is brought about by superheating or by carbon additions, and that the process is one of nucleation, similar to that causing grain refinement of aluminium-base alloys. The identity of the nucleating substance, or substances, has not been established, however.

II.—FACTORS AFFECTING GRAIN REFINEMENT BY SUPERHEATING

The degree of refinement achieved depends upon the time taken to superheat, the temperature attained, the time at this temperature, the time taken to cool

* Manuscript received 15 February 1952. The work described in this paper was made available to members of the B.N.F.M.R.A. in three confidential research reports issued in 1945, 1947, and 1950.

† Research Manager, British Non-Ferrous Metals Research Association, London.

‡ Investigator, British Non-Ferrous Metals Research Association, London.

to casting temperature, and the time of holding at relatively low temperatures before casting. The effects of some of these variables were investigated as a preliminary to the study of primary particles, and the results were in keeping with Fox and Lardner's observations.¹

The effect of aluminium content was also studied; the composition of the melts varied from 0.5 to 9% aluminium, and it was found that, in general, alloys of low aluminium content required a greater degree of superheating than alloys of high aluminium content, if maximum refinement were to be obtained. The changes in grain-size were usually more marked in alloys of low aluminium content (e.g. 3%), than in the alloys of commercial interest (8–10%).

III.—PRIMARY PARTICLES IN MAGNESIUM-ALUMINIUM ALLOYS

1. IRON-BEARING CONSTITUENTS

Fox and Lardner¹ refer, *inter alia*, to the well-known fact that holding the molten magnesium-aluminium alloys at relatively low temperatures (e.g. 50° C. above the liquidus) promotes coarse grain in the cast materials. Very marked effects were obtained in this way in the present work, and were found to be linked with the sedimentation of primary particles. In a typical experiment, a 1-kg. melt of a commercial-purity magnesium-3% aluminium alloy was held for 1 hr. at 680° C. in an iron crucible, under a proprietary carnallite-base flux, and the metal was then carefully decanted into a series of sand moulds to give specimens 1½ in. in dia. Of the four bars poured, the first three were very coarse grained (3–4 mm. grain dia.), whereas the last was fine grained (0.1 mm.) (Fig. 1, Plate VI). Samples from the first- and last-poured bars were quickly remelted in carbon crucibles and centrifuged while molten (in an apparatus described elsewhere⁶) at about 680° C. It was found that the fine-grained specimens then yielded substantial segregates, whereas the very coarse-grained specimens yielded no segregates; where prolonged holding had failed to cause marked grain coarsening, some segregate was found in all the bars. Figs. 4 and 5 (Plate VI) are typical microsections through the outer ends of the centrifuged specimens.

Before centrifuging, the coarse-grained specimens of Fig. 1 contained 0.01% iron and 0.02% manganese, and the fine-grained specimens 0.07% iron and 0.025% manganese. That this difference in iron content was mainly due to segregation of iron-rich primaries, while the melt was held at 680° C., was shown by the results of the following experiments. Segregates obtained on centrifuging, similar to those shown in

Fig. 4, were isolated from alloys containing 2, 7, and 33% aluminium by machining from the surfaces of centrifuged samples the layers containing the segregates and dissolving the matrix in 5% nitric acid in alcohol. Powder X-ray photographs of the residues gave patterns corresponding to the compounds FeAl, Fe₂Al₅, and FeAl₃, respectively.

The mode of occurrence of the iron-bearing primaries was affected by the history of the melt; in alloys which had been held molten at relatively low temperatures (*ca.* 680° C.) for some time and then sand cast, they appeared as clusters of rounded particles, whereas in alloys superheated before casting they were fairly uniformly dispersed and of well-defined cubic shape (Fig. 2, Plate VI).

These results suggested that iron-rich particles were functioning as centres of crystallization, and it was supposed that superheating caused solution of the iron and that, during subsequent cooling to the casting temperature, a fine dispersion of iron-rich particles was precipitated and favoured a fine grain. That this precipitation could occur was proved by some work on the solubility of iron in the molten alloys⁷ which showed that the solubility increases greatly as the melt is superheated.

However, further experiments, an example of which follows, showed that primary iron-bearing particles were not responsible for grain refinement. High-purity magnesium-3% aluminium melts, containing only 0.002–0.003% iron (which should be retained in solution at the liquidus temperature⁷), were made from super-pure aluminium (99.99%) and magnesium (ferrosilicon process, 0.001% Fe, <0.01% Si); they were held molten for long periods at 680° C. in graphite crucibles under a flux made from high-purity chemicals and then sand cast into 1½-in.-dia. bars. The bars first poured had grain-sizes in the range 0.2–0.3 mm., and the bars poured last were only a little finer grained (0.1 mm.), i.e. no marked grain coarsening was obtained; moreover, none of the castings yielded any trace of primary iron-bearing particles on centrifuging. It was also found that, if certain fluxes* were used, superheating had no grain-refining effect, even on commercial-purity 3% aluminium alloys melted in iron crucibles, in which the effect is normally most marked; nevertheless, these alloys yielded large precipitates of the iron-rich phase on centrifuging. Moreover, superheating high-purity alloys of this aluminium content, under these fluxes but in graphite crucibles, caused marked grain coarsening. These effects were less pronounced, or not apparent at all, with alloys of higher aluminium content, e.g. 6–9%, but at 3% aluminium they were reproduced repeatedly. The significance of flux composition remains obscure, but the fact that both coarse and fine grain-sizes can

* The fluxes in question included] very high-purity magnesium chloride/potassium chloride and magnesium chloride/magnesium fluoride mixtures. The grain-sizes of the castings were of the order of 0.5–1 mm. dia., compared with 0.1–0.2 mm. after superheating under the usual carnallite-base

proprietary fluxes. The latter fluxes contain sodium and calcium salts and, when chlorides of these metals were added to the above-mentioned fluxes, the 3% aluminium alloy responded to superheating in the usual way.

be obtained whether iron-bearing particles are present or not, leaves little room for doubt that these particles are not alone responsible for the grain refinement usually resulting from superheating.

2. NEEDLE-SHAPED CONSTITUENT

On centrifuging samples of the high-purity alloys a segregate of another primary constituent was observed (Fig. 3, Plate VI). More concentrated segregates (Fig. 6, Plate VI) were obtained by cutting a thin slice from the outer layer of the centrifuged sample, remelting it in a suitably shaped steel crucible, and centrifuging again in a direction normal to the original one.

The particles, which were slate-grey in colour, and needle-shaped, were normally very small indeed and could be resolved only under an oil-immersion lens. They could be found, but only after tedious search, in the structure of the as-cast material.

(a) Incidence

Except where otherwise stated, the following observations regarding the incidence of these particles were made on 3% aluminium alloy melted in graphite crucibles.

(i) Segregates of the particles were first observed in high-purity magnesium-aluminium alloys which had been superheated, but subsequently they were also found intimately (but apparently mechanically) associated with iron-rich segregates centrifuged from commercial-purity magnesium-aluminium alloys which had been similarly treated. Where both types of particle were present, the needles were not easily revealed, because they were not much harder than the matrix, whereas the hard iron-rich phase tended to stand in relief. Samples of commercial-purity alloys which had been made coarse grained by holding at low temperatures were free from the needle-shaped particles, presumably because they had been carried down with the iron-rich particles which segregated under gravity when the melt was held at fairly low temperatures.

(ii) The size and number of the particles observed in super-pure magnesium-aluminium alloys varied with the aluminium content of the alloy, with the composition of the flux used, with superheating temperature, and with the rate of cooling of the melt after superheating. Other factors being constant, the particles were larger and more numerous the lower the aluminium content in the range 9–3% aluminium.

The effects of superheating temperature and of flux composition were carefully examined in the 3% aluminium alloy only. It was found that the number and size of the particles increased with increasing superheating temperature with any given flux. Practically none were seen in specimens which had not been heated above 700° C., but the constituent increased in particle size and amount in specimens superheated to 850°, 900°, and 950° C., respectively.

Varying the flux composition had the following effects: metal treated with the high-purity 60:40

magnesium chloride/potassium chloride flux in carbon crucibles became coarse grained on superheating and yielded relatively large and numerous particles; metal treated with the magnesium chloride/potassium chloride fluxes containing additions of sodium or calcium chloride was fine grained after superheating and yielded somewhat smaller and fewer particles; metal treated with the 60:40 magnesium chloride/magnesium fluoride flux was fairly coarse grained after superheating and yielded very small traces of minute particles.

(iii) The particles were not found in super-pure magnesium-aluminium alloys containing small amounts (0.005–0.01%) of beryllium, whether the beryllium was added before or after superheating; nor was any reaction product observed in material to which the beryllium was added at the superheating temperature, there being little or no segregate in centrifuged samples of such material. Similarly, no gravity segregate was found in a super-purity alloy with a beryllium addition when it was allowed to freeze in the graphite crucible. The beryllium additions invariably caused marked grain coarsening (e.g. 3 mm. or larger grain dia. in 3% aluminium alloys).

(iv) The particles were not seen in centrifuged samples of magnesium-zinc, magnesium-tin, or magnesium-manganese alloys. None of these alloys was markedly grain refined by superheating. (A different primary particle was detected in magnesium-tin alloys; these particles were rosette-shaped and apparently of duplex structure.)

(v) Centrifuged samples of as-received super-pure and commercial-purity aluminium and magnesium, from which the alloys under investigation were made, were examined. A very few minute needles were found in the super-pure aluminium, and these appeared to be identical with the constituent seen in magnesium-aluminium alloys. The commercial-purity aluminium contained many larger needle-shaped particles, but these were of a different colour, and were almost certainly particles of the Al-Fe-Si β phase; they were distributed widely in the sample and were not segregated by centrifuging.

Centrifuged samples of super-pure aluminium previously superheated to 900° C. in a graphite crucible under a high-purity carnallite-base flux, yielded a moderate number of fairly large and thick needle-shaped particles, similar to those seen in magnesium-aluminium alloys. Super-pure magnesium treated in the same way also yielded a segregate of fairly large particles of similar colour, but the particles were of irregular shape, probably thin plates, and differed significantly in appearance from those in aluminium and magnesium-aluminium alloys.

(b) Separation by Centrifuging and Its Effect on the Grain-Size of the Metal

In the course of the experiments outlined in (ii) above, the grain-sizes of samples containing the needle-shaped particles were measured before and after

segregating the particles by centrifuging. The specimens were allowed to cool in the furnace after centrifuging, and control specimens were put through the same cycle of heating and cooling but without centrifuging.

No change occurred in the grain-size of alloys containing 6 or 9% aluminium in either the control or the centrifuged samples, but in the 3% aluminium alloys centrifuging caused grain coarsening, which was most pronounced when the temperature of centrifuging was near to the liquidus temperature (e.g. 10°–20° C. above the liquidus). For example, material superheated under 50:30:20 magnesium chloride/potassium chloride/sodium chloride flux and having an initial grain-size of 0.1 mm., yielded control specimens with a grain-size of 0.3–0.4 mm., whereas centrifuged samples had grain-sizes ranging from 0.6 to 1.5 mm.

The failure to produce grain coarsening by centrifuging at higher temperatures could be accounted for if the nucleating particles continued to separate as the temperature fell to the liquidus after centrifuging had ceased.

(c) *Attempts at Identification*

The correlation between the behaviour of the needle-shaped constituent and grain-size seemed good enough to warrant attempts to identify the compound.

Accordingly, gravity segregates of very large needles (Fig. 7, Plate VI) were obtained by superheating melts of the 3% aluminium alloy to 950° C., under 60:40 magnesium chloride/potassium chloride flux and cooling in the furnace (cooling time to usual casting temperature 25–40 min.). Both gravity and centrifuged segregates were examined.

Spectrographic comparison of regions to which the material had been segregated by centrifuging and of the regions freed from the constituent in the same way, revealed no significant differences in composition. Polarographic examination of solutions of the corresponding materials gave the same results. It may be concluded with confidence that none of the following metallic elements is present in significant amounts in the primary constituent: copper, bismuth, antimony, molybdenum, arsenic, lead, thallium, tin, indium, cadmium, europium, niobium, chromium, titanium, zinc, nickel, cobalt, ytterbium, tellurium, and vanadium.

This evidence suggested that the constituent was a compound of aluminium and/or magnesium with a non-metallic element or elements, and attempts were next made to identify this non-metallic element.

Vacuum fusion at 1800° C. in carbon crucibles* revealed a little more oxygen in the segregated than in "blank" samples, but this was accounted for by a small content of silica (ca. 0.04%) in the former sample. It was estimated that the segregated samples contained ca. 4% by volume of the unknown constituent, and the silica therefore evidently represented only a small fraction of it. Similar amounts of hydrogen

and nitrogen were found in the "segregated" and "blank" samples; the amounts were a very small fraction of what would be expected if the primary particles were a hydride or nitride. The possibility that the non-metallic was carbon was therefore next explored.

A sample containing a concentrate of the primary particles was "burnt" in excess oxygen in a closed system, but no carbon dioxide was detected. This was thought to signify that the particles were not a carbide, but it is possible that they became enveloped in films of aluminium as the magnesium was oxidized, and that the conditions of combustion did not ensure access of oxygen to the particles. Accordingly the influence of carbon was examined indirectly by means of the experiments next described.

IV.—THE POSSIBLE SIGNIFICANCE OF CARBON

As stated earlier, most of the above observations were made on materials which had been melted and otherwise treated in carbon crucibles; the significance of the observations consequently became uncertain when the carbon grain-refining process was subsequently discovered. Accordingly, a few of the tests were later repeated, this time using pure recrystallized alumina (Δ RR) crucibles; the fluxes were mixtures of high-purity magnesium, potassium, and sodium chlorides, prefused in alumina crucibles.

The grain of the 3% and 8% aluminium alloys superheated to 850°–900° C. for 15 min. under these conditions was coarse; alloys containing 3% aluminium had a grain dia. of 1.5 mm. after the superheating treatment, and alloys containing 8% aluminium a grain dia. of 0.3 mm. (Similar alloys treated in the same way, but in graphite (or iron) crucibles, would have had grain-sizes of the order of 0.1–0.2 mm. and <0.1 mm., respectively.) Melts of these materials heated to 770°–800° C., in the same crucibles and under the same fluxes but treated by stirring-in powdered carbon (0.5% of the charge weight), gave fine-grained castings (0.13 mm. grain dia. at 3% aluminium and 0.08 mm. grain dia. at 8% aluminium).

Samples of the alloys were remelted and centrifuged as before, but stainless-steel crucibles were used instead of the carbon crucibles employed in earlier work. A very small amount of the needle-like constituent referred to earlier was detected in materials which had been superheated, but none was found in the carbon-treated alloys.

It was deduced from these experiments that carbon plays an important part in grain refinement, whether effected by superheating or by carbon treatment.

V.—DISCUSSION AND CONCLUSIONS

It is clear from the foregoing evidence that two types of primary particles are present in molten magnesium–aluminium alloys after superheating under

* The authors are indebted to Mr. H. A. Sloman, National Physical Laboratory, Teddington, for carrying out this work.

certain conditions. It has been established that the iron-bearing primary particles are not responsible for grain refinement. There is some correlation, however, between the presence of the unidentified primary constituent and grain refinement. This correlation is not entirely satisfactory; for example, the effects of varying the flux composition and of carbon grain refinement cannot be adequately explained by the observed behaviour of the needle-shaped constituent during these processes. Therefore, it cannot definitely be concluded that the constituent provides nuclei for the crystallization of the magnesium-base solid solution.

The fact that the grain-coarsening effect of holding at temperatures just above the liquidus is more marked^{8,9} in materials grain refined by superheating than in materials refined by carbon additions might indicate that the two grain-refining processes differ in kind. The present work suggests, however, that a single mechanism may be responsible because superheating under conditions designed to exclude carbon did not cause grain refinement. Moreover, the observations on some primary constituents in the alloys offer a simple explanation of the effect mentioned above, namely, that the iron dissolved during the superheating process precipitates during holding, and the precipitate, settling under gravity, carries with it other particles which would otherwise remain suspended and act as nuclei during solidification.

This view is supported by the fact that, in several other important respects, the two processes have common features. In particular, both appear to work well only with magnesium-aluminium alloys; magnesium, magnesium-zinc, magnesium-manganese, and magnesium-tin alloys do not respond to superheating, and it is reported¹⁰ that the carbon process does not grain refine the first three alloys.

Additions of beryllium and titanium destroy or prevent the effect of superheating; at least one of these elements forms a very stable carbide, and their effect suggested the possibility that a less stable carbide, the formation of which would be prevented by titanium or beryllium additions, was normally responsible for grain refinement.

It has been suggested^{8,10} that aluminium forms a carbide which could provide nuclei for the crystallization of the magnesium-base solid solution.

A near equality of lattice dimensions has been

observed in the great majority of cases of nucleation and formation of oriented overgrowths. The closeness of fit required, however, varies in different cases and, although a similarity of lattice dimensions is usually essential, it is not always sufficient; in particular, the nature of the interatomic bondings, in the substrate and the deposit, exerts a considerable influence,¹¹⁻¹³ and the presence of strong adsorption bonds between these substances favours oriented overgrowth.

Aluminium carbide appears to fulfil the necessary conditions; this compound has a layer structure in which the aluminium ions occur in hexagonally packed sheets; the closest distance of approach of the aluminium ions is 3.33 Å.¹⁴ (at room temperature), which is only 4% greater than the corresponding distance in the close-packed planes of metallic magnesium (3.20 Å.). Also, as magnesium and aluminium form stable compounds, strong adsorption might be expected between the aluminium atoms of the carbide and the magnesium atoms of the magnesium-rich solution. Since titanium does not form stable compounds with magnesium, it may be assumed that atoms of this metal, when present in the carbides, do not form strong adsorption bonds with magnesium atoms in the melt. This may explain why, although the structure of titanium carbide is otherwise suitable for nucleating magnesium overgrowth, no grain refinement occurs.

The authors realize that this work is inconclusive and that their understanding of grain refinement remains incomplete. It can only be said that the needle-shaped constituent has some influence on grain-size and that aluminium carbide could theoretically be the grain refiner. It cannot be concluded, however, that the needle-shaped constituent is aluminium carbide, for it was not detected in materials refined by carbon additions. Indeed, it is possible that the grain-refining nuclei, whether consisting of carbide particles or not, are so very small that the methods used did not reveal them.

ACKNOWLEDGEMENTS

The authors' thanks are due to the Director and Council of the British Non-Ferrous Metals Research Association for permission to publish this work.

REFERENCES

1. F. A. Fox and E. Lardner, *J. Inst. Metals*, 1945, **71**, 1.
2. K. Achenbach, H. A. Nipper, and E. Piwowarsky, *Giesserei*, 1939, **26**, 597, 621.
3. C. E. Nelson, *Trans. Amer. Found. Soc.*, 1948, **56**, 1.
4. N. Tiner, *Trans. Amer. Inst. Min. Met. Eng.*, 1946, **166**, 242.
5. A. Cibula, *J. Inst. Metals*, 1949-50, **76**, 321.
6. W. A. Baker and M. D. Smith, *B.N.F.M.R.A. Research Rep. A.694*, 1945. (Available for inspection at the Patent Office.)
7. W. A. Baker and M. D. Eborall, *Metallurgia*, 1951, **44**, 145.
8. J. A. Davis, L. W. Eastwood, and J. De Haven, *Amer. Foundryman*, 1945, **8**, (1), 34.
9. B.N.F.M.R.A., unpublished work.
10. C. H. Mahoney, A. L. Tarr, and P. E. Le Grand, *Trans. Amer. Inst. Min. Met. Eng.*, 1945, **161**, 328.
11. J. H. van der Merwe, *Discussions Faraday Soc.*, 1949, (5), 201.
12. G. W. Johnson, *Nature*, 1950, **166**, 189.
13. G. P. Thomson, *Proc. Phys. Soc.*, 1948, **61**, 403.
14. M. v. Stackelberg and E. Schnorrenberg, *Z. physikal. Chem.*, 1934, [B], **27**, 37.

THE YOUNG'S MODULUS, POISSON'S RATIO, AND RIGIDITY MODULUS OF SOME ALUMINIUM ALLOYS *

1414

By N. DUDZINSKI,† Dipl.Ing.(Chem.), MEMBER

SYNOPSIS

The elastic properties of various binary and ternary aluminium-base alloys have been examined. With the exception of calcium, strontium, and magnesium, all the alloying elements investigated were found to enhance the value of Young's modulus (E) of the binary alloys, chromium having the greatest effect (about 0.47×10^6 lb./in.² for 1 wt.-%) and titanium, vanadium, molybdenum, iron, tungsten, copper, and silver having a diminishing influence in the order named. The specific Young's modulus, i.e. the ratio of E to density, of binary alloys was substantially increased by the addition of manganese and chromium.

In the ternary systems, aluminium-manganese-chromium alloys showed the highest increment in E (about 0.5×10^6 lb./in.² per 1 wt.-% of manganese + chromium); there was no improvement, however, in the presence of copper or silicon. A substantial gain in E was observed in aluminium-copper-vanadium and aluminium-manganese-nickel alloys.

The rigidity modulus was found to increase linearly with concentration of the alloying element.

I.—INTRODUCTION

IN the course of an investigation ¹ into the mechanical properties of aluminium alloys, it was observed that their Young's modulus values were improved by the addition of certain elements, and that a linear relationship existed between the Young's modulus of the alloy (E) and the concentration of the added element. This improvement was attributed to the relatively high elastic properties of the intermetallic compounds present in the alloys concerned.

The work now described was undertaken to provide information on the effect of a number of elements not previously investigated, in connection with the development of an aluminium alloy having a high Young's modulus, for use in aircraft structures. The alloys studied were the binary alloys of aluminium with calcium, strontium, magnesium, copper, silver, chromium, iron, tungsten, molybdenum, vanadium, and titanium, all of which form intermetallic compounds with aluminium. A number of ternary alloys in which ternary compounds are believed to exist, together with two quaternary alloys, were also included. In view of the importance of the rigidity modulus in aircraft design, this property was also determined for a number of the alloys, as it was not known whether an improvement in Young's modulus was accompanied by an equivalent improvement in the rigidity modulus.

II.—EXPERIMENTAL PROCEDURE

1. CHILL-CAST BARS

Melts of about 3 lb. each, in alloys of the following nominal compositions, were prepared in a Salamander crucible heated in an electric furnace :

Binary Alloys

- (a) Ca 0.5 and 6%.
- (b) Sr 1, 1.5, 2, and 2.5%.
- (c) Mg 3, 6, 10, 12.5, and 15%.
- (d) Cu 3, 5, 8, 10, 15, and 33%.
- (e) Ag 0.5, 2, 4, 6, 8, and 10%.
- (f) Cr 0.5, 1, 3, 4, 5, and 6%.
- (g) Fe 1, 2, 4, 7, and 9%.
- (h) W 1, 2, 3.5, and 5%.
- (i) Mo 1, 1.5, and 2%.
- (j) V 0.5, 1, 1.5, 2, 2.5, 3, 3.5, and 4%.
- (k) Ti 1, 1.5, 2, 2.5, and 3%.

Ternary Alloys

- (l) Si 12 + Mg 2.5, 5, 7.5, and 10%.
- (m) Si 12 + Cr 0.5, 1, 1.5, and 2.5%.
- (n) (i) Mn 1 + Cr 4, 3, and 2%.
- (ii) Mn 2 + Cr 2, 1, and 0.5%.
- (iii) Cr 1 + Mn 4 and 3%.
- (o) (i) V 1 + Cu 8, 7, 6, and 4%.
- (ii) V 1.5 + Cu 4 and 2%.
- (iii) Cu 1 + V 2, 3, and 3.5%.
- (p) (i) Ni 1 + Mn, 10, 7, and 4%.
- (ii) Ni 2 + Mn 5%.
- (iii) Mn 2 + Ni 2, 4, and 6%.
- (iv) Mn 1 + Ni 4, 6, and 8%.

Quaternary Alloys

- (q) Si 12 + Mn 4 + Cr 1%.
- (r) Cu 4 + Mn 4 + Cr 1%.

The alloys were degassed by passing chlorine through the melt before pouring. The vertical iron mould previously used was found to be unsatisfactory for the more sluggish high-melting-point alloys prepared

* Manuscript received 22 December 1950 (in revised form 23 February 1952).

† Royal Aircraft Establishment, Farnborough, Hants.

For the determination of Poisson's ratio, which was used in one of the methods of obtaining the rigidity-modulus value, the lateral contraction of the test-piece when strained in tension was measured with a lateral Lamb roller extensometer (type T.72) and the stress/strain curve was plotted. Reasonably consistent values were obtained, and it is believed that the accuracy is within $\pm 2\%$.

Rigidity-modulus values were also determined directly by making torsion tests on a 0.564-in.-dia. test-piece. The R.A.E. 2-in. optical torsometer was used, precautions being taken to eliminate tension, compression, or bending forces in the test-piece when the torque was applied.

III.—EXPERIMENTAL RESULTS

1. YOUNG'S MODULUS VALUES

- (a) Ca 1.5, 3, and 4%.
(b) W 0.5%.
(c) Mo 1.5%.
(d) V 1 and 2%.

(a) Binary Alloys

The effect on Young's modulus of increasing concentrations of the elements in the binary alloys is shown in the curves plotted in Figs. 1, 2, and 3. It will be seen that, with the exception of the aluminium-silver alloys, a linear relation exists between the modulus and the concentration of the alloying element. The change in the modulus values for 1 wt.-% of each of the addition elements is given in Table I.

The Young's modulus values of the aluminium-calcium alloys were substantially lower than that of aluminium, in spite of the presence of the CaAl_4 compound which is in equilibrium with the aluminium

The alloys were stabilized by heat-treatment, since the rapid cooling of the alloys during solidification had suppressed the peritectic transformation which occurs in several of the alloy systems investigated.

The ternary aluminium-manganese-chromium alloys were annealed at 550° C. for increasing periods of time, until no further increase in their Young's modulus value was observed after quenching the alloys in cold water to retain the metastable *G* phase.

The graph plots Young's Modulus (lb./sq. in. $\times 10^6$) on the y-axis against Alloying Element (per cent.) on the x-axis. The y-axis ranges from 7 to 10, and the x-axis ranges from 0 to 15. Four data series are shown:

- MAGNESIUM + 12% Si:** Represented by open circles, showing a slight increase in modulus from approximately 10.2 at 0% to 10.4 at 11%.
- MAGNESIUM:** Represented by open circles, showing a decrease in modulus from approximately 9.2 at 0% to 8.2 at 15%.
- STRO. ALUM.:** Represented by solid squares, showing a decrease in modulus from approximately 9.4 at 1% to 9.1 at 4%.
- CALCIUM:** Represented by solid triangles, showing a decrease in modulus from approximately 8.5 at 1% to 7.3 at 4%.

Alloying Element (per cent.)	MAGNESIUM + 12% Si (lb./sq. in. $\times 10^6$)	MAGNESIUM (lb./sq. in. $\times 10^6$)	STRO. ALUM. (lb./sq. in. $\times 10^6$)	CALCIUM (lb./sq. in. $\times 10^6$)
0	10.2	9.2	-	-
1	10.3	8.9	9.4	8.5
2	10.35	8.8	9.2	8.2
3	10.4	8.7	9.1	-
4	-	8.6	9.1	7.3
5	-	8.5	-	-
6	-	8.4	-	-
7	-	8.3	-	-
8	-	8.2	-	-
10	-	8.1	-	-
11	10.4	-	-	-
12	-	8.0	-	-
13	-	7.9	-	-
15	-	7.8	-	-

FIGS. 1-3.—Variation of Young's Modulus with Percentage of Alloying Element.

KEY TO FIG. 1.

- | | | | |
|---|----------|---|---|
| ○ | As cast. | + | Annealed 1½ hr. at 550° C., and quenched in cold water. |
| ■ | | ▲ | " " " slowly cooled. |

As in the previous experiments, the Young's modulus was determined from the stress/strain curve obtained on a British Standard No. 3A.4 test-piece, using a Lamb extensometer. The average reading for four loadings was taken, and it is believed that the modulus values so obtained are accurate to within $\pm 0.5\%$.

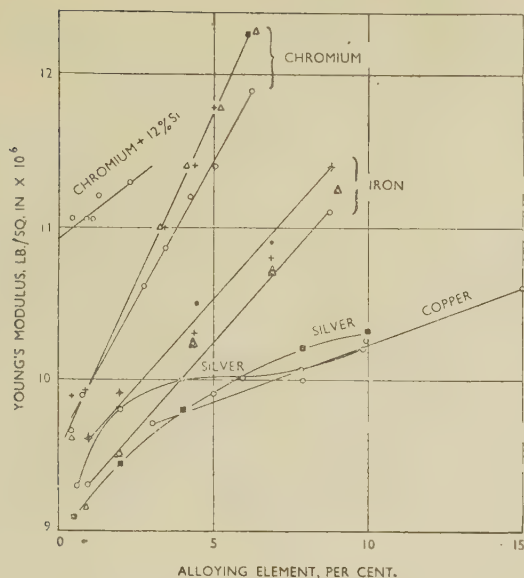


Fig. 2.

KEY.

- As cast.
 + Annealed 5 hr. at 625° C., and quenched in cold water.
 △ " " " 530° C., " " "
 ● " " " 625° C., and slowly cooled.
 ■ " " " 540° C., and quenched in cold water; 48 hr. at 250° C.

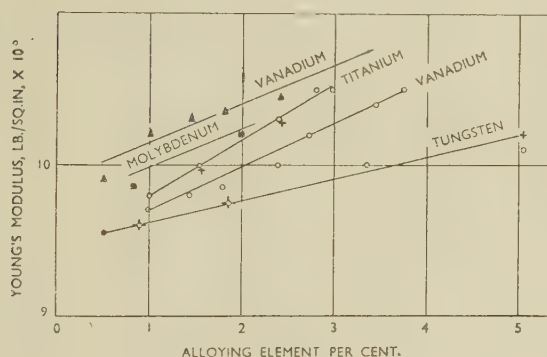


Fig. 3.

KEY.

- As cast.
 + Annealed 16 hr. at 550° C., and quenched in cold water.
 △ " " " 5 " 630° C., " " "
 ● Forged Al-W alloy, annealed 1 hr. at 550° C., and quenched in cold water.
 ■ " Al-V alloys, " " " " " "

solid solution. Köster and Rauscher² found that the addition of calcium to aluminium rapidly reduced the elastic modulus and attributed the reduction to the low modulus of CaAl_4 due to its possessing a structure of relatively high symmetry. It is also possible that the low modulus of the compound is connected with the low modulus value of calcium itself, which the author determined and found to be 2.65×10^6 lb./in.².

Strontium forms a compound, SrAl_4 , and also lowers the Young's modulus of aluminium, though its effect, weight for weight, is less detrimental. This can be explained by the fact that, although calcium and

strontium form aluminium compounds of similar structure, the higher atomic weight of strontium gives a smaller volume of compound for the same weight of the element.

The effect of adding magnesium is to lower the Young's modulus of aluminium, but to a much smaller degree than with either calcium or strontium.

Silver differs from the other elements investigated in that the relation between the modulus value of the alloy and the concentration of silver is not linear. A small improvement in the modulus value is obtained by the addition of up to 4% silver, but the value remains more or less constant in the range 4–10%. It is to be expected that the high atomic weight of silver and the close-packed hexagonal structure of the phase in equilibrium with the aluminium solid solution would tend to reduce the effectiveness of silver in increasing the modulus of aluminium.

Copper is an important alloying element in commercial aluminium alloys, but unfortunately it has only a slightly beneficial effect on the modulus value. The

TABLE I.—Increment in Young's Modulus for 1 Wt.-% of Added Element.

Element	Lb./in ² . $\times 10^6$	Element	Lb./in ² . $\times 10^6$
Chromium .	0.470 *	Nickel .	0.164
Chromium .	0.370 †	Tungsten .	0.125
Titanium .	0.375	Silicon .	0.104
Manganese .	0.340	Copper .	0.080
Vanadium .	0.320	Silver .	0.075
Molybdenum .	0.300	Magnesium .	−0.082
Iron .	0.230	Strontium .	−0.200
Beryllium .	0.188	Calcium .	−0.304
Cobalt .	0.186		

* Annealed alloys.

† As-cast alloys.

values obtained in the present work are in agreement with those given by Guillet.³

Chromium was found to be a very useful alloying element for increasing the modulus of aluminium. The high elastic properties of the annealed aluminium-chromium alloys can be explained by the presence of the compound CrAl_7 , which contains a large proportion of aluminium atoms, and therefore for a given weight of the alloying element occupies a large volume as compared with that of the compounds which aluminium forms with many of the other elements. These alloys, which were tested in the chill-cast condition, have somewhat lower E values, due, no doubt, to the presence of $\text{Cr}_2\text{Al}_{11}$ as the result of suppressing the peritectic reaction: $\text{Cr}_2\text{Al}_{11} + \text{liquid} \rightarrow \text{CrAl}_7$. The $\text{Cr}_2\text{Al}_{11}$ compound contains a lower proportion of aluminium than the CrAl_7 and has a more symmetrical structure, both these factors being unfavourable to an increase in the Young's modulus.

The structure of an alloy with 6.37% chromium is illustrated in Fig. 4 (Plate VII), in which the phase $\text{Cr}_2\text{Al}_{11}$ is seen in a shell of CrAl_7 .

It was found that aluminium-iron alloys have Young's modulus values higher than those of alu-

minium-cobalt alloys. Microscopical examination of the aluminium-iron alloys as shown in Fig. 5 (Plate VII), revealed the presence of both FeAl_3 and Fe_2Al_7 , and it is probably the latter compound which is the more effective in raising the modulus. Annealing just below the eutectic temperature to bring about the transformation $\text{FeAl}_3 \rightarrow \text{Fe}_2\text{Al}_7$ resulted, however, in only a slight improvement in E , owing to the low rate of diffusion of iron in aluminium.

Titanium is second only to chromium for its effectiveness in raising the Young's modulus of aluminium. This is due to the high elastic modulus of the compound TiAl_3 which titanium forms with aluminium, and the relatively low density of titanium.

Tungsten forms two compounds^{4, 5} with aluminium, which contain a large proportion of aluminium atoms, but this favourable factor is offset by the high atomic weight of the element, and therefore the increase in modulus value is only small when the tungsten content

gave values for the heat of formation of the following intermetallic compounds:

Compound	Heat of Formation, kg.cal./g.-atom
CuAl_2	3.2
FeAl_3	6.1
Co_2Al_9	7.7
NiAl_3	9.5
CaAl_4	13.0

The Young's modulus values for the alloys in which the above compounds are formed should have increased in the same order as the heats of formation of the compounds. The experiments have shown, however, that the presence of CaAl_4 in aluminium considerably reduces the elastic modulus, and that the elastic-modulus values for aluminium-iron alloys are higher than for the alloys containing either cobalt or nickel. The values for the heats of formation of the other intermetallic compounds investigated are not known.

TABLE II.—Values of Young's Modulus for Ternary Aluminium-Manganese-Chromium Alloys in the Chill-Cast Condition, and After Heat-Treatment.

Heat-treatment: annealed at 550° C. for various periods and quenched in cold water.

Chemical Composition		Young's Modulus, lb./in. ² × 10 ⁶									Increase in <i>E</i> , %
		As cast		Heat-Treated							
				<i>E</i> ₀ †	<i>E</i> ₁	<i>E</i> ₂	<i>E</i> ₃	<i>E</i> ₄	<i>E</i> ₅	Δ <i>E</i> Max.	
Mn, %	Cr, %	Obs.	Calc.								
1.69 *	0.41 *	10.15	10.3	10.15	10.4	10.35	10.45	10.5	10.3	0.35	3.5
4.03 *	0.82 *	10.8	11.2	10.8	11.15	11.5	11.95	11.75	11.6	1.15	10.6
2.0	0.5	10.8	10.4	10.8	10.9	11.0	10.9	10.9	...	0.2	1.8
4.0	1.0	11.35	11.2	11.35	11.35	12.35	12.1	12.1	...	1.0	8.8
3.0	1.0	10.85	10.9	10.85	11.0	11.15	11.3	0.45	4.2
2.0	1.0	10.7	10.5	10.7	10.55	10.55	10.65	0	...
2.0	2.0	11.3	10.9	11.3	10.85	11.0	11.0	−0.3	...
1.0	2.0	10.65	10.6	10.65	10.3	10.4	10.5	−0.15	...
1.0	3.0	10.75	10.9	10.75	10.9	10.55	10.6	0.15	1.4
1.0	3.0	10.7	11.2	10.7	10.9	10.5	10.4	−0.2	...

* Compositions nominal except for alloys marked.

† E_0 , E_1 , E_2 , E_3 , E_4 , E_5 = elastic moduli after annealing for 0, 21, 53, 73, 93, 123 days, respectively.

is expressed on a percentage-weight basis. An alloy with 3.44% tungsten had the structure shown in Fig. 6 (Plate VII), in which two constituents separated, W_2Al_9 , in the form of needles or plates, and WAl_{12} , often assuming the shape of a deformed cross; some particles are seen in a transitional state.

Vanadium is quite effective in raising the modulus of aluminium, particularly when the alloy is annealed to promote the transformation: $\text{VAl}_3 + \text{liquid} \rightarrow \text{VAl}_4$. The structure of a binary aluminium-2.4% vanadium alloy, shown in Fig. 7 (Plate VII), is composed of the α solid-solution matrix and the VAl_3 and VAl_4 constituents.

It was suggested in the previous paper¹ that the heat of formation of a compound should be correlated with the elastic modulus. This suggestion was based on the fact that the compounds with high heat of formation have tight bonding between atoms, and that therefore their elastic modulus should be high.

Oelsen and Middel,⁶ and Kubaschewski and Walter⁷

(b) Ternary Alloys

On adding magnesium to an aluminium-12% silicon alloy, the Young's modulus is not changed by the formation of Mg_2Si . This compound has a modulus of about the same value as aluminium, and is therefore a useful constituent in the aluminium-silicon alloys since it increases their strength without reducing the elastic modulus.

The formation of ternary phases⁸ in the aluminium-silicon-chromium alloys was found to lower their elastic properties as compared with the corresponding binary aluminium-chromium alloys.

The Young's modulus values obtained for aluminium-manganese-chromium alloys in the chill-cast condition are shown in Table II.

In the chill-cast condition no ternary compound was found in the alloys containing manganese and chromium, and the Young's modulus values obtained on these alloys were generally close to those which would

be expected from calculation based on the individual effects of the two elements. An interesting feature of the aluminium–chromium–manganese system, according to Raynor and Little,⁹ is that on annealing below 590° C. a ternary compound makes its appearance. This phase, denoted *G*, is in equilibrium with the solid solution when the manganese content is roughly four times the chromium content. With the object of forming the *G* phase, the alloys were annealed at 550° C. for periods of up to 123 days. At intervals during these annealing treatments the alloys were quenched in water, their microstructures examined, and their elastic properties determined. The maximum modulus values obtained, together with the percentage increases, are also recorded in Table II.

The greatest increase in *E*, as a result of the annealing treatment, was observed in the alloys containing 4.03% manganese and 0.82% chromium, and 4.0% manganese and 1.0% chromium, in which the modulus values were raised by 10.6% and 8.8%, respectively. This is equivalent to an increase in modulus of the order of 0.5×10^6 lb./in.² for each 1 wt.-% of (manganese + chromium). In Fig. 8 (Plate VII) is shown the structure of a ternary aluminium alloy containing

TABLE III.—*Values of Young's Modulus for Ternary Aluminium–Copper–Vanadium Alloys in the Chill-Cast Condition, and After Heat-Treatment.*

Heat-treatment: 20 days at 500° C. and quenched in cold water.

Chemical Composition		Young's Modulus, lb./in. ² × 10 ⁶		
		Calculated	Observed	
Cu, %	V, %		As Cast	Heat-Treated
8.43	0.88	10.45	10.55	10.7
6.36	0.82	10.3	10.5	10.7
4.17	0.87	10.15	10.45	10.5
6.72	1.06	10.6	10.95	11.2
4.29	1.31	10.45	10.6	10.8
2.15	1.72	10.3	10.65	10.9
1.08	1.86	10.2	10.5	10.85
1.06	2.84	10.55	10.6	...
1.06	3.49	10.85	10.5	10.8

4.03% manganese and 0.82% chromium, after a long annealing treatment. The dark *θ* phase, which is CrAl₇ containing manganese in solid solution, is seen surrounded by the light *G* phase.

The aluminium–copper–vanadium alloys listed in Table III show higher Young's modulus values than would be expected from the contribution made by the individual components in the binary alloys. This is particularly marked in the alloys in which the ratio of copper to vanadium is about 6:1 or 1:1. Prolonged annealing of the alloys effects a further improvement in *E*, probably owing to the formation of a ternary compound. The structure of a ternary aluminium alloy containing 6.72% copper and 1.06% vanadium is shown in Fig. 9 (Plate VII). The dark VAl₃ compound is seen embedded in VAl₄. The CuAl₂ phase separated in association with a new

TABLE IV.—*Values of Young's Modulus for Ternary Aluminium–Manganese–Nickel Alloys in the Chill-Cast Condition, and After Heat-Treatment.*

Heat-treatment *A*: 20 days at 500° C., and quenched in cold water.

B: An additional period of 20 days at 500° C., cooled in the furnace.

Chemical Composition		Young's Modulus, lb./in. ² × 10 ⁶			
		Calculated	Observed		
			As Cast	Heat-Treated	
Mn, %	Ni, %			<i>A</i>	<i>B</i>
9.45	1.12	12.8	12.5	12.4	12.6
6.55	1.01	11.9	11.5	11.2	11.2
4.73	0.86	11.45	11.45	11.0	11.15
4.40	1.90	11.3	11.45	10.9	11.0
2.01	2.04	10.5	10.65	10.3	10.4
2.03	4.04	10.8	11.2	10.6	10.9
2.03	5.76	11.15	11.6	11.2	11.35
1.03	4.42	10.55	11.2	10.9	10.9
1.06	6.38	10.9	11.25	11.05	11.1
1.01	8.36	11.05	11.75	11.5	11.5

constituent in the form of short needles, denoted *T*, which is probably a ternary compound. Both constituents etched black in 25% nitric acid, the acicular phase etching a little deeper than CuAl₂.

The results obtained on the aluminium–manganese–nickel alloys are given in Table IV.

The Young's modulus values of a number of the alloys were higher than the calculated values. This is particularly marked in the alloy containing about 1% manganese and 8.4% nickel. This suggests the formation of a ternary compound, although one was not detected in the metallographic examination of the alloys. Prolonged annealing of these alloys, followed by quenching in cold water, resulted in a decrease in *E* due, it is believed, to the presence of minute quenching cracks in the intermetallic compounds. Similar phenomena have been observed by Guillet and Portevin¹⁰ in copper alloys. When the quenched

TABLE V.—*Values of Young's Modulus for Quaternary Aluminium–Silicon–Manganese–Chromium, and Aluminium–Copper–Manganese–Chromium Alloys in the Chill-Cast Condition, and After Heat-Treatment.*

Heat-treatment *A*: 20 days at 500° C., and quenched in cold water.

B: An additional period of 20 days at 500° C., cooled in the furnace.

Chemical Composition				Young's Modulus, lb./in. ² × 10 ⁶			
				Calculated	Observed		
					As Cast	Heat-Treated	
Si, %	Cu, %	Mn, %	Cr, %			<i>A</i>	<i>B</i>
12.7	...	4.16	1.07	12.60	12.55	12.35	12.5
...	4.64	3.76	0.90	11.5	11.40	11.05	11.25

TABLE VI.—Values of Specific Gravity and Specific Young's Modulus for Binary Aluminium Alloys.

Chemical Composition						Sp. Gr., <i>D</i>	E/D , lb./in. ² × 10 ⁶
Cu, %	Ni, %	Co, %	Fe, %	Mn, %	Cr, %		
3.01	2.79	3.45
4.98	2.81	3.5
7.86	2.87	3.5
9.9	2.92	3.5
15.0	2.97	3.55
32.7	3.6	3.35
...	0.99	2.77	3.6
...	2.89	2.81	3.65
...	5.0	2.85	3.7
...	7.56	2.93	3.75
...	10.0	2.95	3.8
...	14.65	3.08	3.95
...	...	1.2	2.74	3.7
...	...	2.08	2.75	3.7
...	...	3.1	2.78	3.8
...	...	4.01	2.79	3.8
...	...	6.57	2.85	3.9
...	1.03	2.74	3.4
...	1.96	2.75	3.45
...	4.4	2.81	3.65
...	6.93	2.85	3.75
...	8.83	2.88	3.85
...	1.67	...	2.75	3.7
...	3.45	...	2.79	3.8
...	5.16	...	2.86	3.9
...	8.4	...	2.93	4.2
...	10.0	...	2.96	4.4
...	14.56	...	3.06	4.65
...	0.46	2.72	3.5
...	0.83	2.73	3.6
...	3.43	2.79	3.9
...	4.25	2.84	3.95
...	6.37	2.88	4.15

aluminium-manganese-nickel alloys were further annealed and slowly cooled in the furnace, the slight improvement observed in their modulus values was probably attributable to the relief of internal stresses induced during the quenching operation. When the ratio of manganese to nickel was 9:1 or 6:1, the values of Young's modulus were lower than the calculated values. The reason for this is not known.

(c) Quaternary Alloys

The Young's modulus values obtained for alloys of aluminium-silicon-manganese-chromium and aluminium-copper-manganese-chromium in the chill-cast condition agreed with the values calculated from the observed effect of the individual elements in the respective binary alloys, as shown in Table V. Prolonged annealing of the alloys at 500° C., followed by quenching in cold water, reduced their *E* value; further heat-treatment at the same temperature followed by furnace cooling resulted in an almost complete recovery of the Young's modulus value of the aluminium-silicon-manganese-chromium alloy, but only a partial recovery in the other alloy. This is no doubt due to the presence of internal cracks in the

aluminium-copper-manganese-chromium alloy. It is disappointing to find that the ternary MnCrAl₁₃ compound, which exists under certain conditions in the aluminium-manganese-chromium alloys, is not formed in the presence of silicon or copper, as these two elements would have been useful additions from the standpoint of improving the other mechanical properties.

(d) Specific Young's Modulus Values

The specific Young's modulus value is of importance to the structural designer, and in Table VI are given the values for a number of the alloys investigated. It will be seen that, in general, the specific modulus of the alloy increases with the concentration of the alloying element.

2. POISSON'S RATIO AND RIGIDITY MODULUS VALUES

Tables VII and VIII give the values obtained on a series of binary alloys for Poisson's ratio and the rigidity modulus as calculated from the formula

TABLE VII.—Values of Poisson's Ratio and Rigidity Modulus for Binary Aluminium-Silicon Alloys in the Chill-Cast Condition, and for Binary Aluminium Alloys with Nickel, Cobalt, Beryllium, and Iron After Heat-Treatment.

Heat-treatment: 3 hr. at 500° C., and quenched in cold water; 16 hr. at 175° C.

Al-Fe: 5 hr. at 520° C., and quenched in cold water.

Chemical Composition						Poisson's Ratio, σ	Rigidity Modulus, lb./in. ² × 10 ⁶	
Si, %	Ni, %	Co, %	Be, %	Fe, %			Indirect	Direct (Torsion)
5.3	0.335	3.85
10.6	0.32	4.05
15.2	0.315	4.3
19.0	0.315	4.35
26.4	0.305	4.6
31.0	0.295	4.85
...	0.99	0.355	3.75	3.8	...
...	2.89	0.365	3.95
...	5.0	0.355	4.0	3.9	...
...	7.56	0.325	4.15
...	10.0	0.325	4.3	4.25	...
...	14.65	0.32	4.65	4.7	...
...	...	1.2	0.325	3.6
...	...	2.08	0.31	3.7
...	...	3.1	0.315	3.85
...	...	4.01	0.31	3.9
...	...	6.57	0.31	4.35
...	1.21	...	0.325	3.65
...	2.37	...	0.335	3.7
...	2.97	...	0.335	3.75
...	4.25	...	0.305	3.95
...	5.6	...	0.32	4.0
...	1.03	0.335	3.4	3.65	...
...	1.96	0.34	3.55	3.8	...
...	4.4	0.315	3.85	4.05	...
...	6.93	0.31	4.1	4.25	...
...	8.83	0.315	4.25

$G = \frac{1}{2}E/(1 + \sigma)$, where G is the rigidity modulus, E the Young's modulus, and σ Poisson's ratio of the alloy. For comparison, the rigidity modulus was also determined directly by torsion tests on a number of

TABLE VIII.—Values of Poisson's Ratio and Rigidity Modulus for Ternary Aluminium-Nickel (Cobalt, or Beryllium)-12% Silicon Alloys After Heat-Treatment.

Heat-treatment: 3 hr. at 500° C., quenched in cold water; 16 hr. at 175° C.

Chemical Composition				Poisson's Ratio, σ	Rigidity Modulus, lb./in. ² $\times 10^3$	
Ni, %	Co, %	Be, %	Si, %		Indirect	Direct (Torsion)
1.03	12.8	0.33	4.25	4.2
3.0	12.33	0.32	4.35	4.45
4.9	10.4	0.315	4.55	4.5
8.85	14.8	0.29	4.85	4.9
10.1	12.6	0.295	5.0	...
15.8	13.4	0.255	5.2	...
...	1.17	...	11.55	0.315	4.4	...
...	2.15	...	10.0	0.315	4.5	...
...	3.13	...	12.10	0.31	4.6	...
...	8.0	...	13.15	0.30	4.75	...
...	...	1.05	11.6	0.315	4.2	...
...	...	1.95	11.5	0.32	4.3	...
...	...	2.91	10.5	0.32	4.5	...
...	...	3.22	10.6	0.31	4.6	...

TABLE IX.—Effect of Alloying Elements on Rigidity Modulus and Young's Modulus.

Element	Increment in G for 1 wt.-% of Element, lb./in. ² $\times 10^3$		Percentage Increase in G for 1 wt.-% of Element		Percentage Increase in E for 1 wt.-% of Element	
	Binary Alloys	Ternary Alloys with 12% Si	Binary Alloys	Ternary Alloys with 12% Si	Binary Alloys	Ternary Alloys with 12% Si
Cobalt	0.145	0.036	4.0	0.85	1.95	2.3
Iron	0.105	...	2.95	...	2.4	...
Beryllium	0.074	0.11	1.35	2.55	2.0	2.75
Nickel	0.063	0.068	1.75	1.45	1.7	1.45
Silicon	0.044	...	1.25	...	1.1	...

the alloys. It will be seen that good agreement was obtained between the values calculated from the formula and those determined by direct measurement.

When the rigidity modulus is plotted against the

weight per cent of the alloy content in each of the binary systems investigated, it is found that a linear relationship exists, as was noted in the Young's modulus/composition curves. The effect of 1 wt.-% of each of the alloying elements investigated on the Young's modulus and rigidity modulus values is given in Table IX. It will be observed that, with the exception of beryllium, all the alloying elements investigated have a greater effect on the rigidity modulus of aluminium than on the Young's modulus.

IV.—CONCLUSIONS

With the exception of calcium, strontium, and magnesium, all the elements investigated improve the Young's modulus of aluminium. In all cases but that of silver, this improvement is proportional to the concentration of the alloying element, and is particularly marked with chromium. The improvement depends on the structure of the intermetallic compound which the alloying element forms with aluminium. Thus, for a given alloy content it will be greater the more aluminium atoms there are in the compound.

In ternary alloys, the presence of ternary compound is reflected in the Young's modulus value, and a useful increase in modulus is obtained in aluminium-manganese-chromium alloys with a manganese : chromium ratio of 4 : 1. The specific modulus of this alloy is also high.

The assumption that intermetallic compounds of high heat of formation have high elastic properties does not hold for all alloys.

The rigidity modulus is proportional to the concentration of the alloying element, and, with the exception of aluminium-beryllium alloys, is improved to a greater extent by a given alloying addition than the Young's modulus.

It is considered that the work described in this and previous papers provides sufficient information on which to base the development of a commercial alloy having elastic properties about 20% higher than those of the aluminium alloys at present in use.

ACKNOWLEDGEMENTS

The author wishes to thank the Ministry of Supply for permission to publish this work, and is indebted to Mr. H. C. Davies, B.Sc., B.Sc.(Eng.) and Mr. A. Bacon, Assoc. Met., for carrying out the chemical analysis.

REFERENCES

1. N. Dudzinski, J. R. Murray, B. W. Mott, and B. Chalmers, *J. Inst. Metals*, 1948, **74**, 291.
2. W. Köster and W. Rauscher, *Z. Metallkunde*, 1948, **39**, 110.
3. L. Guillet, Jr., *Thesis: Univ. Paris*, 1939; also *Rev. Mét.*, 1939, **36**, 497.
4. W. D. Clark, *J. Inst. Metals*, 1940, **66**, 271.
5. L. F. Mondolfo, "Metallography of Aluminium Alloys", p. 49. 1943: New York (John Wiley and Sons).
6. W. Oelsen and W. Middel, *Mitt. K.-W. Inst. Eisenforschung*, 1937, **19**, 1.
7. O. Kubaschewski and A. Walter, *Z. Elektrochem.*, 1939, **45**, 630.
8. L. F. Mondolfo, *loc. cit.*, p. 74.
9. G. V. Raynor and K. Little, *J. Inst. Metals*, 1945, **71**, 493.
10. L. Guillet, Jr., and A. Portevin, *Compt. rend.*, 1940, **210**, 335.

NOTICE TO AUTHORS OF PAPERS FOR THE "JOURNAL" AND CONTRIBUTORS TO DISCUSSIONS

1. Papers will be considered for publication from non-members as well as members of the Institute. They are accepted for publication in the *Journal* and not necessarily for presentation at any meeting of the Institute. MSS. should be addressed to The Editor of Publications, The Institute of Metals, 4 Grosvenor Gardens, London, S.W.1.

2. Papers suitable for publication may be classified as:

(a) Papers recording the results of original research.
(b) First-class reviews of, or accounts of progress in, a particular field.

(c) Papers descriptive of works methods, or recent developments in metallurgical plant and practice.

(d) Papers in classes (a), (b), and (c) above, previously published in languages other than English, French, German, or Italian, if of sufficient merit.

3. **Manuscripts and illustrations** should be submitted in duplicate. MSS. must be typewritten (*double-line spacing*) on one side of the paper only, and authors are requested to sign a declaration that neither the paper nor a substantial part thereof has been published elsewhere. Exceptions may be made in certain cases where a paper has been published in a language other than English, French, German, or Italian (see 2(d) above). MSS. not accepted are normally returned within 6 months of receipt.

In the interests of economy, all papers must be written as concisely as possible; in general, internal research reports are not in suitable form for publication as papers in the *Journal*. All but the simplest mathematical expressions should be written by hand, with capital and small letters clearly distinguished. Superscript and subscript letters should also be plainly indicated. Greek letters and special signs should be identified in the margin. For style, spelling, and abbreviations used, any recent issue of the *Journal* may be consulted.

4. **Synopsis.** Every paper must have a synopsis (not exceeding 250 words in length) which, in the case of a paper reporting original research, should state its objects, the ground covered, and the nature of the results. The synopsis will appear at the beginning of the paper, and should be in a form suitable for use by abstracting organizations. Extracts from a "Guide for the Preparation of Synopses" drawn up by the Abstracting Services Consultative Committee are reproduced below.

5. **References** must be collected at the end of the paper and must be numbered in the order in which they occur in the MS. Initials of authors must be given, and the Institute's official abbreviations for periodical titles (as used in *Metallurgical Abstracts*) should be employed, where known. References to papers should be set out in the style:

A. L. Dighton and H. A. Miley, *Trans. Electrochem. Soc.*, 1942, 81, 321 (i.e. year, volume, page).

References to books should be in the following style:

C. Zener, "Elasticity and Anelasticity of Metals". Chicago: 1948 (University of Chicago Press).

6. **Illustrations.** Each illustration must have a number and description; only one set of numbers must be used in one paper, and it is desirable to number the half-tone illustrations consecutively, rather than to intersperse them with the line figures. The captions should be typed on a separate sheet.

The set of **line figures** sent for reproduction must be drawn (about twice the size to appear in the *Journal*) in Indian ink on smooth white Bristol board, good-quality drawing paper, co-ordinate paper, or tracing cloth, which are preferred in the order given. Co-ordinate paper, if used, must be blue-lined, with the co-ordinates to be reproduced finely drawn in Indian ink. Curves should be drawn boldly (i.e. at least twice the thickness of the frame). Experimental points should be indicated by open or closed circles, triangles, squares, &c. (preferably not crosses). Curves should be broken on each side of such symbols and plenty of allowance should be made for closing up in blockmaking. All lettering and numerals, &c., should preferably be in *pencil*, so that the Institute's standard lettering may be affixed, and ample margins must be left outside the framework of the figures to enable this to be done. The second set of line illustrations may be photostat copies.

Photographs must be restricted in number, owing to the expense of reproduction, and photomicrographs should be trimmed to the smallest possible of the following sizes consistent with adequate representation of the subject: 4 in. deep by 3 in. wide: 2 in. deep by 3 in. wide: 2 in. square. Magnifications of photomicrographs must be given in each case. Photographs for reproduction should be loose, not pasted down (and not fastened together with a clip, which damages them), and the figure number and author's name should be written on the back of each. Captions should be given to the photomicrographs, but these should be kept as brief as possible.

Because of the present high cost of printing and paper it is imperative that authors restrict illustrations (particularly photographs) to the absolute minimum deemed necessary to support their argument. Only in exceptional cases will illustrations be reproduced if already printed and readily available elsewhere.

7. **Tables or Diagrams.** Results of experiments, &c., may be given in the form of tables or figures, *but* (unless there are exceptional reasons) *not both*. Tables should bear Roman numbers, and each should have a heading that will make the data intelligible without reference to the text.

8. **Corrections.** A certain number of corrections in proof are inevitable, but any modification of the original text is to be avoided. Since corrections are very expensive, the Institute reserves the right to require authors to contribute towards their cost if the Editor deems them to be excessive. The Institute also reserves the right to require a contribution to the cost of remaking any block where this is necessitated by an error on the author's part.

9. **Reprints.** Individual authors are presented with a maximum of 25, and two or more authors with a maximum of 50 reprints from the *Journal*, without covers. Limited numbers of additional reprints can be supplied at the author's expense, if ordered before proofs are passed for press. (Orders should preferably be placed when submitting MSS.)

10. **Discussion.** Except in the case of special symposia, shorthand records of discussions are not taken at meetings. Written discussion may be submitted on any paper, preferably typewritten (*double-line spacing*). References should be given in the form of footnotes. Paragraphs 6 and 7 above are also applicable to such contributions. Reprints of discussion cannot be supplied to contributors.

GUIDE FOR THE PREPARATION OF SYNOPSSES

(As recommended by the Abstracting Services Consultative Committee)

1. **Purpose.** The synopsis is not part of the paper; it is intended to convey briefly the content of the paper, to draw attention to all new information, and to the main conclusions. It should be factual.

2. **Style of writing.** The synopsis should be written concisely and in normal rather than abbreviated English. It is preferable to use the third person. Where possible use standard rather than proprietary terms, and avoid unnecessary contracting.

It should be presumed that the reader has some knowledge of the subject, but has not read the paper. The synopsis should therefore be intelligible in itself without reference to the paper; for example, it should not cite sections or illustrations by their numerical references in the text.

3. **Content.** The title of the paper is usually read as part of the synopsis. The opening sentence should be framed accordingly and repetition of the title avoided. If the title is insufficiently comprehensive, the opening should indicate the subjects covered. Usually the beginning of a synopsis should state the objective of the investigation.

It is sometimes valuable to indicate the treatment of the subject by such words as: brief, exhaustive, theoretical, &c.

The synopsis should indicate newly observed facts, conclusions of an

experiment or argument and, if possible, the essential parts of any new theory, treatment, apparatus, technique, &c.

It should contain the names of any new compound, mineral species, &c., and any new numerical data, such as physical constants; if this is not possible, it should draw attention to them. It is important to refer to new items and observations, even though some are incidental to the main purpose of the paper; such information may otherwise be hidden, though it is often very useful.

When giving experimental results the synopsis should indicate the methods used; for new methods the basic principle, range of operation, and degree of accuracy should be given.

4. **References.** If it is necessary to refer to earlier work in the summary, the reference should always be given in full and not by number. Otherwise references should be left out.

When a synopsis is completed, the author is urged to revise it carefully, removing redundant words, clarifying obscurities, and rectifying errors in copying from the paper. Particular attention should be paid by him to scientific and proper names, numerical data, and chemical and mathematical formulae.

DISTRIBUTION EQUILIBRIA IN SOME TERNARY SYSTEMS $\text{Me}_1\text{--Me}_2\text{--B}$ AND THE RELATIVE STRENGTH OF THE TRANSITION-METAL-BORON BOND*

1415

By PROFESSOR G. HÄGG,† Ph.D., MEMBER, and R. KIESSLING,‡ Ph.D., MEMBER

SYNOPSIS

In ternary systems $\text{Me}_1\text{--Me}_2\text{--B}$, where Me_1 and Me_2 both belong to the first series of transition metals, the distribution of the metals between the two phases $(\text{Me}_1, \text{Me}_2)_2\text{B}$ and $(\text{Me}_1, \text{Me}_2)\text{B}$ in equilibrium with each other has been determined by X-ray methods. The results show that the metal with the lower atomic number is always concentrated in the phase richest in boron. This is taken to indicate that the transition metals in the first series are more strongly bound to boron the lower their atomic number.

I.—INTRODUCTION

It is now generally supposed that the strength of the transition-metal-non-metal bond in metallic hydrides, carbides, and nitrides decreases with increasing atomic number of the metal, within a transition-metal series.¹⁻⁴ There is evidence that this rule also holds for the corresponding bonds in the metallic borides,^{5,6} and the present investigation was undertaken to throw more light upon this question.

Consider two boride phases, p' and p'' , of the same metal Me_1 , the phase p' being assumed to contain less boron than p'' . Both p' and p'' are supposed to be capable of dissolving a second metal, Me_2 , by replacement of Me_1 . It must be regarded as highly probable that Me_1 and Me_2 will be distributed between the two phases in such a way that the metal most strongly bound to boron is concentrated in the phase richest in boron.

Distribution equilibria of this kind have been studied in the systems Mn–Cr–B, Fe–Mn–B, Co–Mn–B, Ni–Mn–B, and Co–Fe–B in the range 33–50 at.-% boron, the study being limited to the isothermal sections at 1100°C. In the range investigated, the systems Fe–Mn–B, Co–Mn–B, and Co–Fe–B contain the phase $(\text{Me}_1, \text{Me}_2)_2\text{B}$ of the CuAl_2 type in equilibrium with the phase $(\text{Me}_1, \text{Me}_2)\text{B}$ of the FeB type. In both phases all ratios of Me_1 to Me_2 are possible, i.e. there is complete mutual solubility between corresponding phases in the two binary systems $\text{Me}_1\text{--B}$ and $\text{Me}_2\text{--B}$. Equilibria between phases of the same types have also been studied in the systems Ni–Mn–B and Mn–Cr–B, but owing to the appearance of other phases these equilibria exist only near the manganese side. Only a few observations have been made on the system Mn–Cr–B.

II.—PRESENTATION OF THE EQUILIBRIUM DATA

The compositions of the two phases in equilibrium can be represented by tie-lines in a triangular diagram. Fig. 1 shows a section at 1100°C. of the system Co–Mn–B with experimentally determined tie-lines connecting the phases $(\text{Co}, \text{Mn})_2\text{B}$ and $(\text{Co}, \text{Mn})\text{B}$.

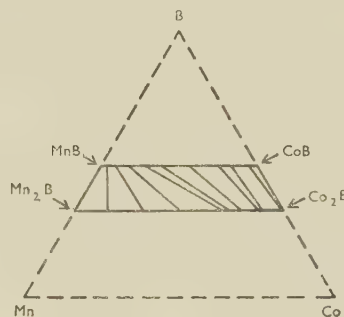


FIG. 1.—Co–Mn–B System. Isothermal section at 1100°C. of the two-phase field $(\text{Co}, \text{Mn})_2\text{B} + (\text{Co}, \text{Mn})\text{B}$. The directions of some tie-lines are shown.

Although the tie-lines plainly show that in this case manganese is concentrated in the latter phase, the limitations of the triangular diagram do not permit of a closer discussion. Two other methods of presentation, have therefore been used and are described below.

Let n_1' and n_1'' represent the total numbers of atoms Me_1 in the phases p' and p'' , respectively, and n_2' and n_2'' similarly the total numbers of atoms Me_2 in the two phases. Then the fraction of the metal atoms which are Me_1 atoms in phase p' is denoted by :

$$x_1' = n_1' / (n_1' + n_2')$$

and similarly for x_2' , x_1'' , and x_2'' .

* Manuscript received 17 December 1951.

† Professor of General and Inorganic Chemistry, University of Uppsala, Sweden.

‡ Lecturer in Inorganic Chemistry, University of Uppsala, Sweden.

The distribution ratios α are then defined as quotients of x values for the same metal in the two phases. Since, in the systems under discussion a given metal is concentrated in one phase at all compositions of a specific ternary system, the representation is facilitated by defining the ratios α_1 and α_2 so that they are less than unity for both metals. If $x_1' > x_1''$, it follows that $x_2'' > x_2'$, and hence:

$$\alpha_1 = x_1''/x_1'; \quad \alpha_2 = x_2'/x_2''$$

As long as the solid solutions are sufficiently dilute, they possess the properties of ideal solutions. Thus, α_1 is constant if the solutions contain only small amounts of Me_1 , and α_2 is constant if the solutions contain only small amounts of Me_2 . The more alike are the two metals, Me_1 and Me_2 , the more closely do the α values approach unity.

One way of representing the distribution of Me_1 and Me_2 between the two phases is to plot x_1' against x_1'' or x_2' against x_2'' . Examples of diagrams of this type are shown in Fig. 3 (a) and (b). If, as in these figures, x_1' is plotted against x_1'' , the tangents to the curve at its terminal points $x_1' = x_1'' = 0$ and 1 have the slopes $1/\alpha_1$ and α_2 , respectively. As long as the α value in question is constant, which implies that the solution is ideal, the curve is linear and coincides with the tangent.

The second method of representation gives the variation of α as a function of $(x_1' + x_1'')/2$ or $(x_2' + x_2'')/2$, i.e. the mean fraction of each metal in the two phases. Examples are given in Fig. 4 (a-d). Each figure shows both α_1 and α_2 (defined as above), but these two variables are interdependent. A curve for α_1 must start with a horizontal part (ideal solution) from the end where $(x_1' + x_1'')/2 = 0$. It then rises and reaches the value $\alpha_1 = 1$ at the other end of the diagram. The course of the α_2 curve is analogous. The two curves always intersect at $(x_1' + x_1'')/2 = (x_2' + x_2'')/2 = 0.5$.

III.—EXPERIMENTAL METHODS

The materials used were manganese, distilled in high vacuum (99.9%), iron (Baker's CP, 99.9%), cobalt (Ferrolegeringar "Extra fine", 99.12%), nickel (E. Merck, puriss. cobalt-free), chromium (electrolytic, 99.9%), and boron. Part of the boron used was prepared by the reduction of boron tribromide with hydrogen (purity 98.5%) and part was obtained commercially (Fairmount, electrolytic boron 99%+). The two metals concerned and boron were carefully mixed, pressed into pellets and melted once or twice in a high-frequency vacuum furnace at about 1500°C. under a pressure of 10^{-4} - 10^{-3} mm. mercury. The weight of the specimens was about 1-2 g., and zirconia or magnesia crucibles were used. No reaction was noted between the crucible and the melt. The alloys were annealed at 1100°C. in evacuated silica tubes (in contact with the walls) for 10-24 hr. and quenched.

The metal content of the alloys (all of which could be dissolved in nitric acid) was determined by the usual methods, e.g. manganese volumetrically by the persulphate-arsenite method, iron by titration with permanganate, and cobalt and nickel by electro-deposition. No analyses of the chromium alloys were carried out, the composition of the few alloys investigated being assumed to be the same as the nominal composition.

The partition of the two metals between the $(Me_1, Me_2)_2B$ and the $(Me_1, Me_2)B$ phases could be directly determined by X-ray methods without any separation of the two phases. The lengths of the axes of the unit cells of both phases depend only on the ratio Me_1/Me_2 , varying between the values for the single-metal phases. Several alloys of both $(Me_1, Me_2)_2B$ and $(Me_1, Me_2)B$ were prepared with different Me_1/Me_2 ratios, in order to study the variation of the axes. Owing to the somewhat slight variations in the dimensions with changes in composition, this

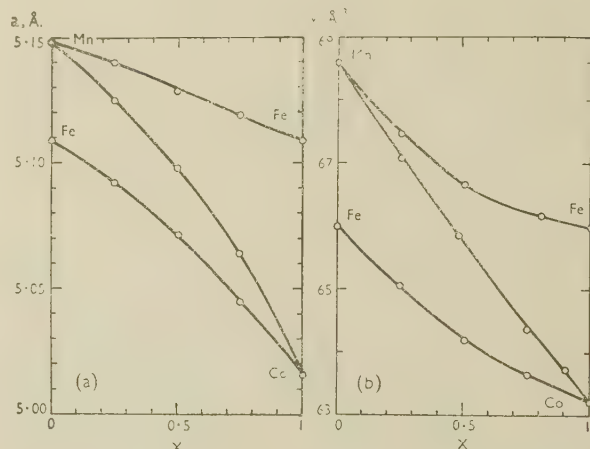


FIG. 2.—(a) $(Me_1, Me_2)_2B$ Phases. Variation of the a -axis of the tetragonal unit cell with metal content. (b) $(Me_1, Me_2)B$ Phases. Variation of the volume V of the orthorhombic unit cell with metal content.

method does not permit of any high accuracy, but is the only method possible in the present case.

For the $(Me_1, Me_2)_2B$ phases the ratio Me_1/Me_2 was determined from the length of the a -axis of the tetragonal unit cell, the variation of the c -axis in most systems being too small to give accurate results. The variation of the a -axis with the metal content is shown in Fig. 2 (a).

For the $(Me_1, Me_2)B$ phases the ratio Me_1/Me_2 was determined from the volume of the orthorhombic unit cell. For these phases the variations of all the three axes were large enough to make a determination possible. The volume was considered to represent a suitable mean value, and its variation with the metal content is given in Fig. 2 (b).

The X-ray photographs were taken with CrK_{α} radiation in a camera of the Guinier type, using a curved quartz monochromator.

IV.—EXPERIMENTAL RESULTS

The three systems Fe-Mn-B, Co-Mn-B, and Co-Fe-B were found to be closely related in the range between 33 and 50 at.-% boron. A two-phase field exists with a $(\text{Me}_1, \text{Me}_2)_2\text{B}$ phase of the CuAl_2 type and a $(\text{Me}_1, \text{Me}_2)\text{B}$ phase of the FeB type in equilibrium. This result was to be expected in view of the close relation between the binary Me-B systems in the range concerned. Fig. 1 shows the isothermal section of the Co-Mn-B system for a boron content between 33 and 50 at.-%. The directions of several tie-lines are given, which show that manganese is always present in greater amount in the $(\text{Co}, \text{Mn})\text{B}$ phase, i.e. the phase richest in boron, than in the $(\text{Co}, \text{Mn})_2\text{B}$ phase. The systems Fe-Mn-B and Co-Fe-B exhibit similar features. In these systems also, the metal with the lower atomic number is present in greater amount in the $(\text{Me}_1, \text{Me}_2)\text{B}$ phase than in the $(\text{Me}_1, \text{Me}_2)_2\text{B}$ phase. The difference in concentration in the two phases, however, which is nearly the same for the systems Fe-Mn-B and Co-Fe-B, is larger for the system Co-Mn-B.

The system Ni-Mn-B is more complicated than the preceding systems in the range investigated. The $(\text{Ni}, \text{Mn})_2\text{B}$ phase exists for all Mn/Ni ratios, but the $(\text{Ni}, \text{Mn})\text{B}$ phase of the FeB type exists only at nickel contents up to about 12 at.-% (of the total metal content). At higher nickel contents, lines of other phases appear in the X-ray powder photographs. The system was investigated only over the range of nickel contents where there is equilibrium between the two phases $(\text{Ni}, \text{Mn})_2\text{B}$ and $(\text{Ni}, \text{Mn})\text{B}$. Within this range the ternary system is similar to the preceding systems, but shows a greater difference in the distribution of the metals between the two phases.

The results for these four systems are represented in Figs. 3 and 4, using the methods described above.

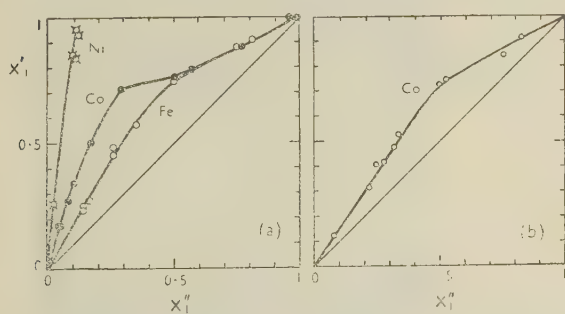


Fig. 3.—Relation Between the Fractions of the Metal Atoms which are Me_1 Atoms in the Phases $p' = (\text{Me}_1, \text{Me}_2)_2\text{B}$ and $p'' = (\text{Me}_1, \text{Me}_2)\text{B}$.

(a) $\text{Me}_1 = \text{Fe}, \text{Co}, \text{Ni}$.
 $\text{Me}_2 = \text{Mn}$.

(b) $\text{Me}_1 = \text{Co}$.
 $\text{Me}_2 = \text{Fe}$.

Fig. 3 (a) and (b) shows that the metal with the lower atomic number is present in the boron-rich phase p'' (i.e. $(\text{Me}_1, \text{Me}_2)\text{B}$) to a greater extent than in the boron-poor phase p' (i.e. $(\text{Me}_1, \text{Me}_2)_2\text{B}$). It is also evident that the difference in composition between the

two phases, p' and p'' , in equilibrium increases as the difference in atomic number between the two metals increases. The curves for the metal pairs Fe-Mn and Co-Fe are very similar, the difference in atomic number being unity in both cases.

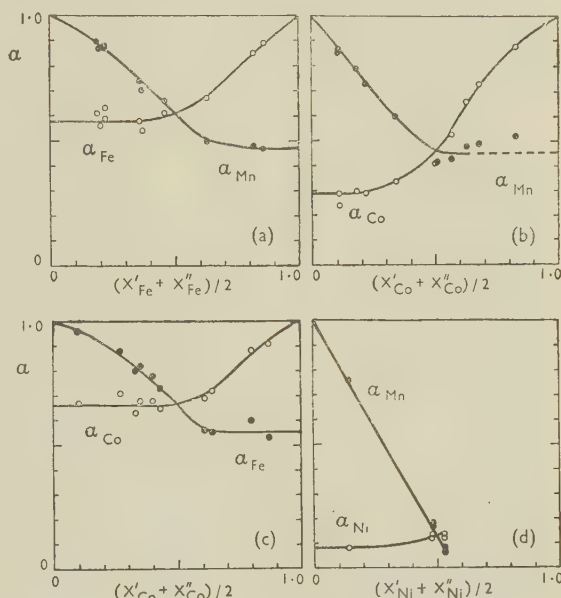


FIG. 4.—Variation of the Distribution Ratios α .

(a) Fe-Mn-B system.

(c) Co-Fe-B system.

(b) Co-Mn-B system.

(d) Ni-Mn-B system.

Fig. 4 (a-d) shows the variation of the distribution ratios α . Allowing for the uncertainty of the values, it can be seen that the α values for both metals are fairly constant over a considerable composition range of the dilute solid solutions; consequently the solutions can be considered almost ideal within this range. These constant α values have been collected in Table I. If it were possible to use labelled man-

TABLE I.—Distribution Ratios in Almost Ideal Solutions.

Metal and Atomic Number		$\alpha_1 = x_3''/x_1'$	$\alpha_2 = x_3'/x_2''$
Me_1	Me_2		
25 Mn	25 Mn	1.00	1.00
26 Fe	25 Mn	0.60	0.45
27 Co	25 Mn	0.30	0.45
28 Ni	25 Mn	0.10	(<0.10)
26 Fe	26 Fe	1.00	1.00
27 Co	26 Fe	0.65	0.55

ganese and iron atoms, Mn^* and Fe^* , and to study the systems $\text{Mn}^*-\text{Mn}-\text{B}$ and $\text{Fe}^*-\text{Fe}-\text{B}$, constant α values = 1 would be found throughout the whole composition range. These values have been added to the table for comparison. It has not been possible to determine the α_2 value for the pair Ni-Mn, but Fig. 4 (d) shows that if equilibrium between the phases

(Ni, Mn) $_2$ B and (Ni, Mn)B had existed up to the nickel-free phases, α_2 at this limit would have been less than 0.10.

The α_1 values from Table I have been plotted in Fig. 5 against the atomic number of the metal Me_1 . For the series Me_1 -Mn-B and Me_1 -Fe-B, the α_1 values decrease with increasing atomic number of Me_1 . This is perhaps the best way of showing that the metal Me_2 , having the lower atomic number of the pair

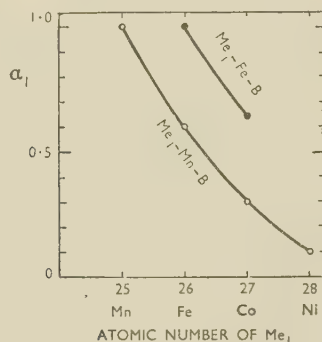


FIG. 5.—Variation of $\alpha_1 = x_1''/x_1'$ with the Atomic Number of the Metal Me_1 .

Me_1 - Me_2 , always concentrates in the boron-rich phase and that the difference in composition between the two phases in equilibrium increases with increasing difference between the atomic numbers of Me_1 and Me_2 . For the reasons given in the introduction, these results may be regarded as affording a way of representing the decrease in the strength of the metal-boron bond with increasing atomic number of the metal in the first transition-metal series.

The α_2 values vary in much the same way, although less regularly.

In the Mn-Cr-B system equilibrium between the phases (Mn, Cr) $_2$ B (CuAl $_2$ type) and (Mn, Cr)B (FeB type) exists only near the manganese side of the system. In this respect this system is analogous to the Ni-Mn-B system described above. Neither the limits of the two-phase field nor the compositions of

the phases in equilibrium were determined, but a preliminary study showed that more chromium is present in the (Mn, Cr)B phase than in the (Mn, Cr) $_2$ B phase. In the alloy richest in chromium (Cr 12, Mn 50, B 38 at.-%) the unit volume of the (Mn, Cr) $_2$ B phase was 0.1% less than that for Mn $_2$ B, while the unit volume of the (Mn, Cr)B phase was 0.6% greater than that for MnB. Evidently chromium, with a smaller atomic number than manganese, is present in greater amount in the boron-rich phase than in the boron-poor phase.

V.—CONCLUSIONS

All distribution ratios which have been determined for the two-phase equilibria studied in the four ternary systems Me_1 - Me_2 -B show that that one of the two metals which has the lower atomic number in the transition series always concentrates in the phase richest in boron. The inequality in distribution of the two metals increases with increasing difference between their atomic numbers. These facts seem to be consistent with the assumption that a metal within a particular transition series is the more strongly bound to boron the lower its atomic number.

ACKNOWLEDGEMENTS

The authors wish to thank Miss U. Nyberg for valuable help with the preparation of specimens and analyses, and Mr. S. Wahlgren for technical assistance. This investigation has been aided by a grant from the Swedish State Council for Technical Research, which is gratefully acknowledged.

REFERENCES

1. P. Ehrlich, *Z. anorg. Chem.*, 1949, **259**, 1.
2. A. Hultgren, *Jernkontorets Ann.*, 1951, **135**, 403.
3. G. Hägg, *ibid.*, 1951, **135**, 493 (discussion).
4. G. Hägg, *Värmländska Bergsmannaföreningens Ann.*, 1951, 17.
5. R. Kiessling, *Acta Chem. Scand.*, 1950, **4**, 209.
6. R. Kiessling and Y. H. Liu, *Trans. Amer. Inst. Min. Met. Eng.*, 1951, **191**, 639.

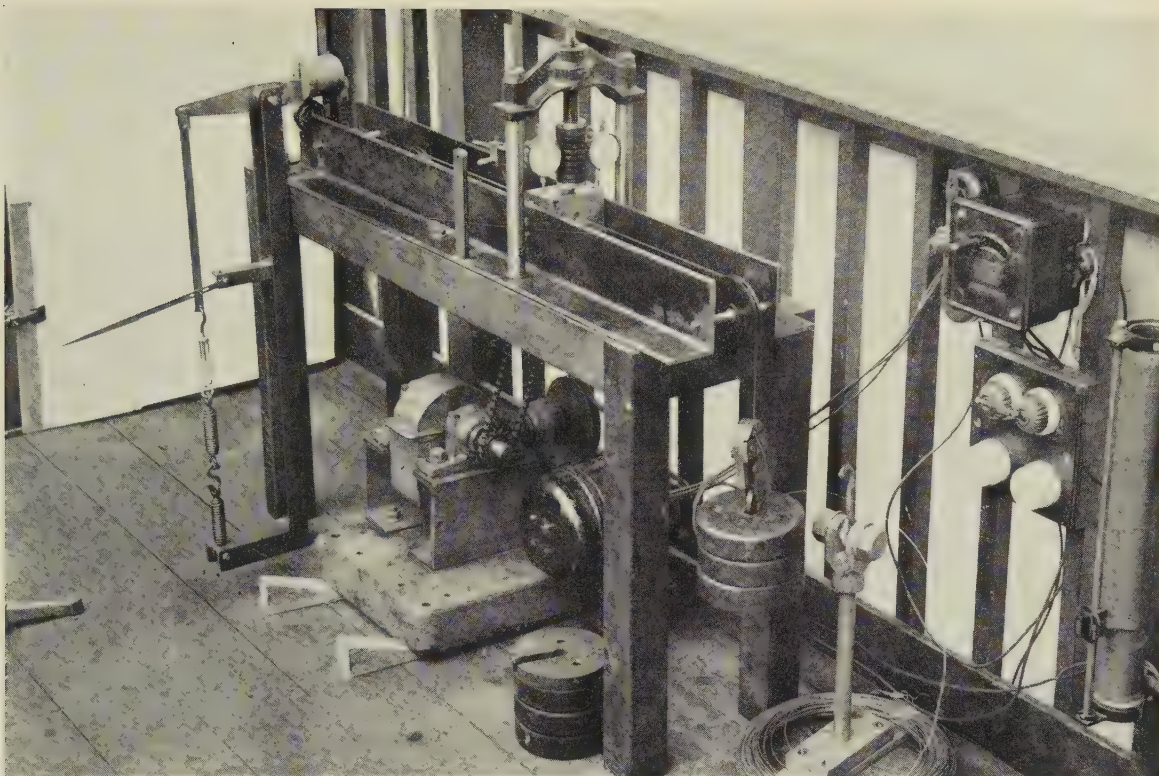


FIG. 5.—General View of Experimental Draw Bench.

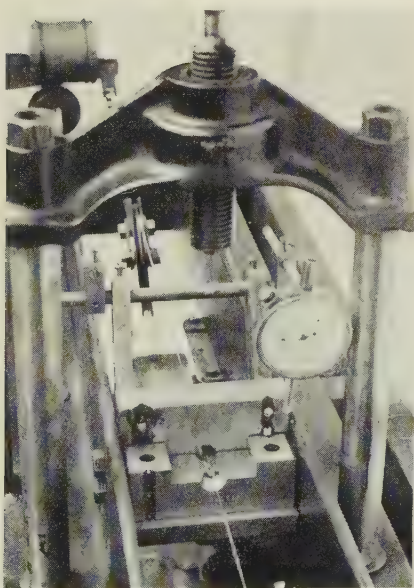


FIG. 6.—Close-Up View of Split-Die Arrangement.

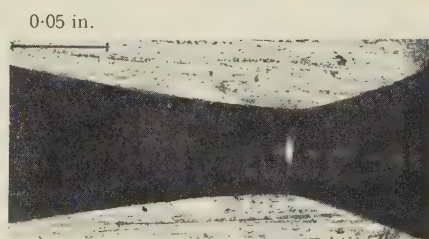


FIG. 7.—Showing Shape of Steel Split-Die Channel. $\times 10$.

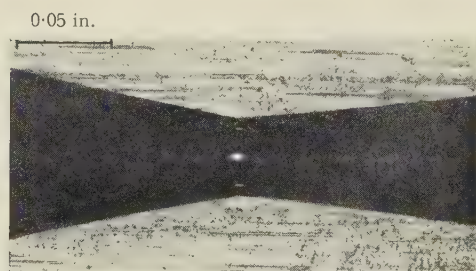


FIG. 8.—Showing Shape of Tungsten Carbide Split-Die Channel. $\times 10$.

[To face p. 60.]

FIG. A.—Intragranular Boundaries in Aluminium-4% Copper Alloy after Ageing for 5 Days at 200° C. Heterogeneous precipitation from one block to another of the macromosaic structure within one grain. JJ' is an *intergranular* boundary; Ia are *intragranular* boundaries. $\times 1500$.



FIG. B.—“ Insular ” Crystal in Aluminium-12% Zinc Alloy, Having Macromosaic or Polygonized Structure. The intragranular boundaries are revealed as a result of a difference in rate of dissolution in the electrolytic polishing bath, indicating great heterogeneity of structure and composition within one grain of an aluminium solid solution. $\times 300$.

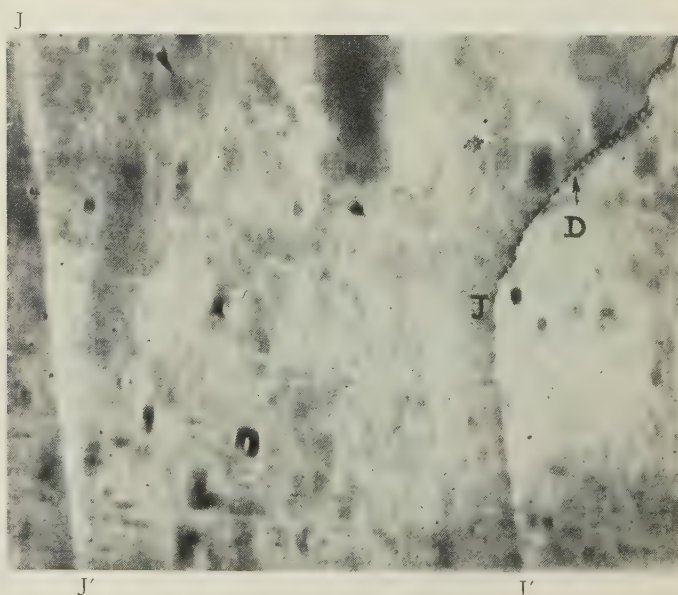


FIG. C.—Twin Crystals in Aluminium-12% Zinc Solid Solution. Precipitation occurs only in the discontinuities (D) of the twin boundary; it does not occur on the twin boundary itself JJ' . $\times 500$.

MICROSTRUCTURES OF NICKEL-ALUMINIUM ALLOYS.

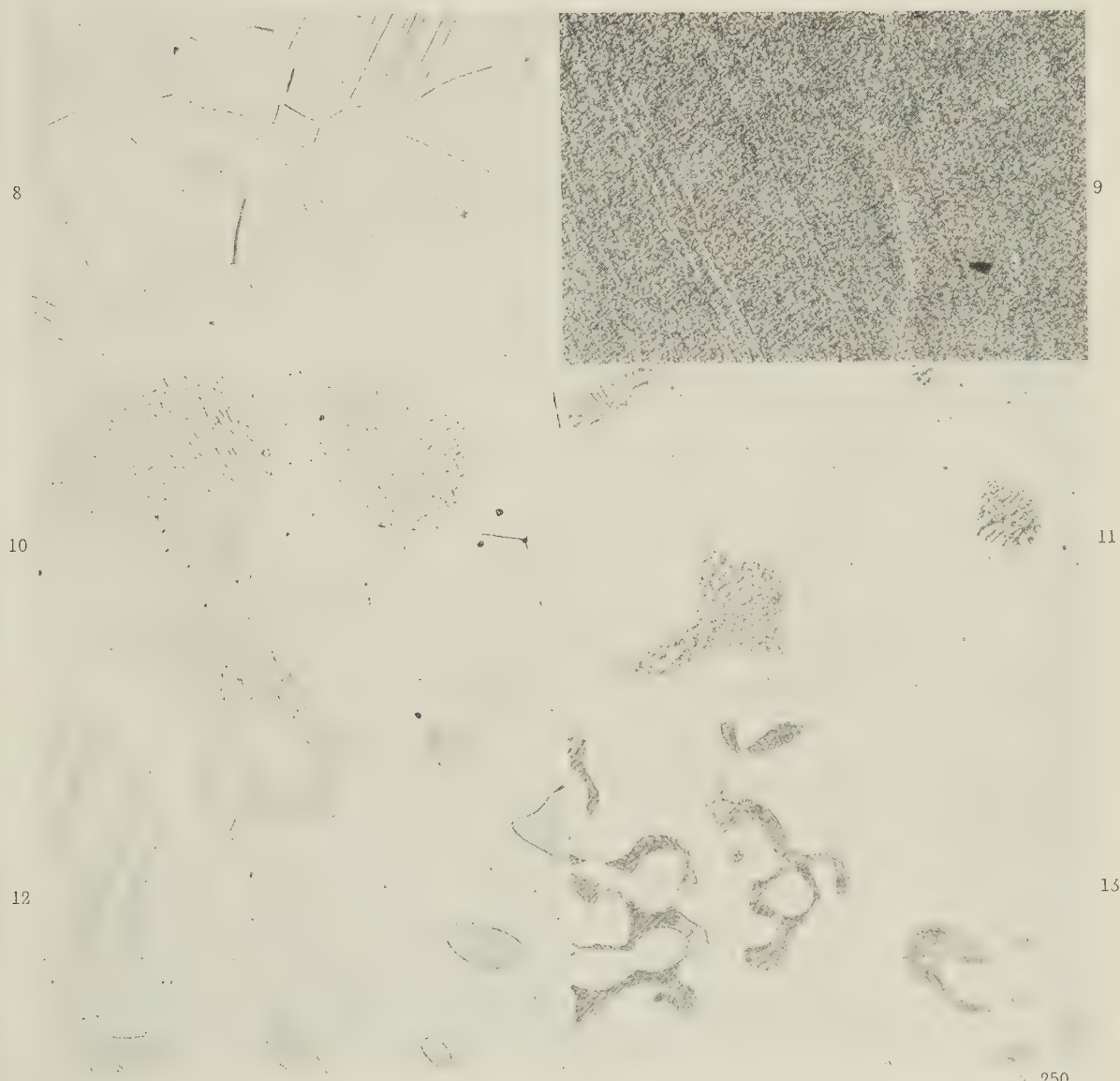


FIG. 8.—No. 263. 82.7/17.3 at.-%. 1150° C. γ .
 FIG. 9.—No. 265. 81.7/18.3 at.-%. 1150° C. $\gamma + \gamma'$.
 FIG. 10.—No. 201. 76.8/23.2 at.-%. 1150° C. $\gamma + \gamma'$.
 FIG. 11.—As Fig. 10. 750° C. $\gamma + \gamma'$.
 FIG. 12.—No. 204. 72.2/27.8 at.-%. 1150° C. $\beta + \gamma'$.
 FIG. 13.—As Fig. 12. 750° C. $\beta + \gamma'$.

MICROSTRUCTURES OF NICKEL-TITANIUM-ALUMINIUM ALLOYS.

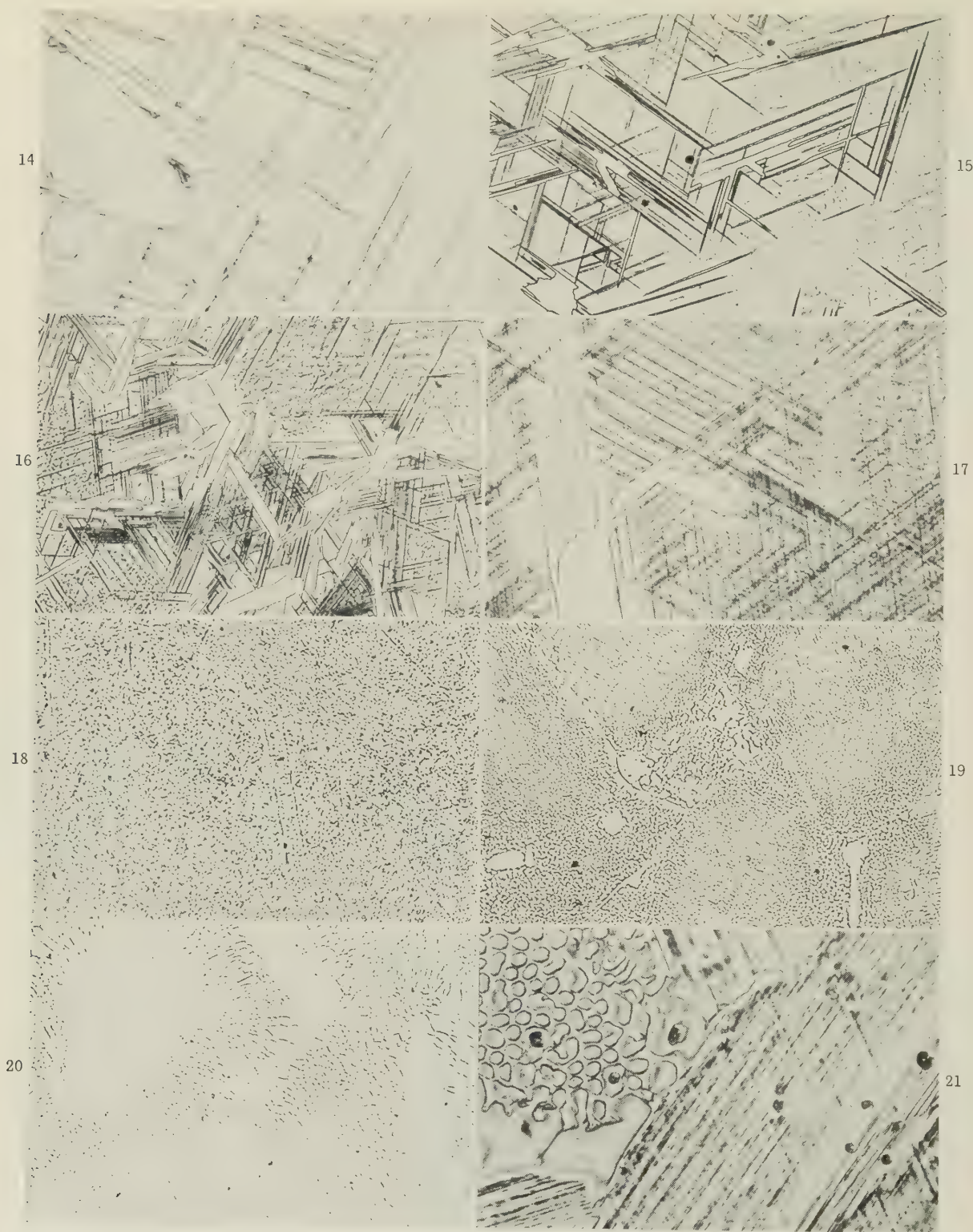


FIG. 14.—No. 235. 85.7/13.3/1.0 at.-%. 1150° C. $\gamma + \eta$. $\times 1500$.
 FIG. 15.—No. 237. 85.4/11.6/3.0 at.-%. 1150° C. $\gamma + \gamma' + \eta$. $\times 250$.
 FIG. 16.—No. 236. 85.6/12.2/2.2 at.-%. 850° C. $\gamma + \gamma' + \eta$. $\times 250$.
 FIG. 17.—As Fig. 14. 750° C. $\gamma + \gamma' + \eta$. $\times 1000$.
 FIG. 18.—No. 244. 88.4/9.2/2.4 at.-%. 850° C. $\gamma + \gamma'$. $\times 250$.
 FIG. 19.—No. 239. 82.8/2.5/14.7 at.-%. 1000° C. $\gamma + \gamma'$. $\times 250$.
 FIG. 20.—No. 233. 77.6/4.7/17.7 at.-%. 1000° C. $\gamma + \gamma'$. $\times 250$.
 FIG. 21.—No. 257. 74.8/18.0/7.2 at.-%. 1150° C. $\gamma' + \eta$. $\times 200$. (Phase-contrast illumination.)

DISPLACEMENTS AT GRAIN BOUNDARIES.

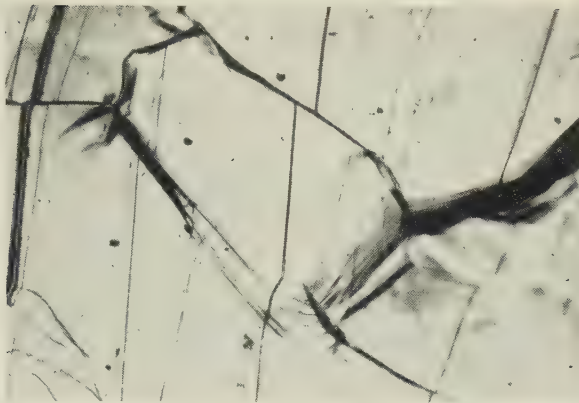


FIG. 2.—Surface of Aluminium After Slow Deformation at 300° C. $\times 250$.

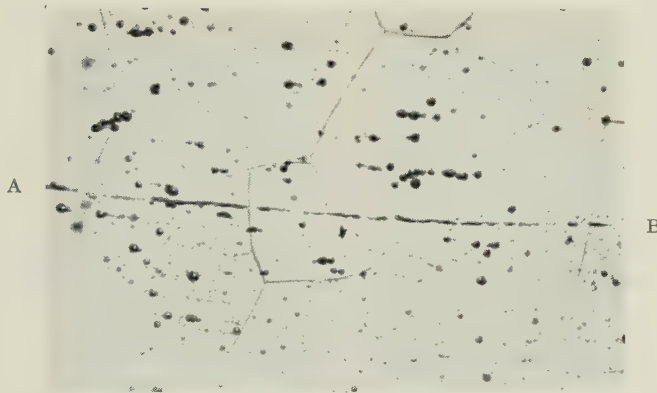


FIG. 3.—Oxide Film at Weld Junction in Interior of Aluminium Sheet. $\times 200$.

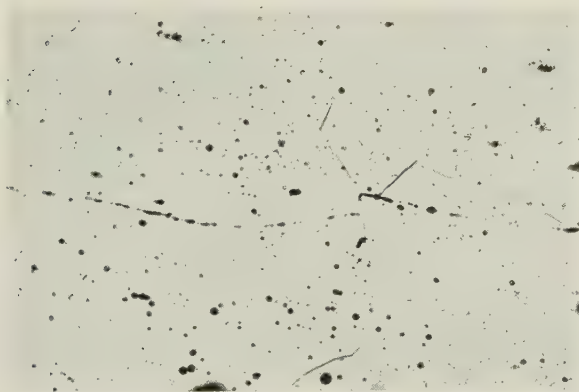


FIG. 4.—Oxide Film After Slow Deformation at 300° C. $\times 200$.

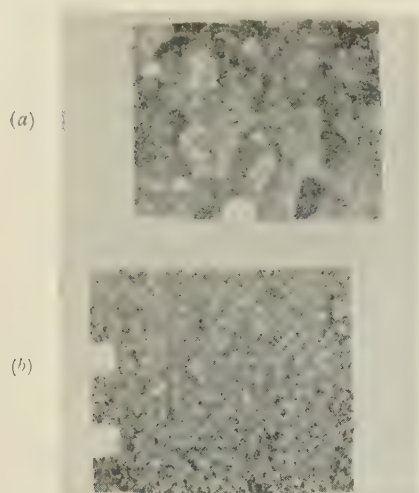


FIG. 1.—Macrostructure of Commercial-Purity Magnesium-3% Aluminium Alloy After Holding for 1 Hr. at 680° C.

(a) First-poured metal.
(b) Last-poured metal.

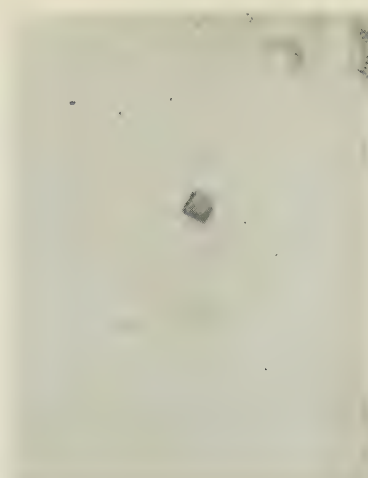


FIG. 2.—Cubic Iron Inclusion in Superheated Magnesium-3% Aluminium Alloy. $\times 2000$.

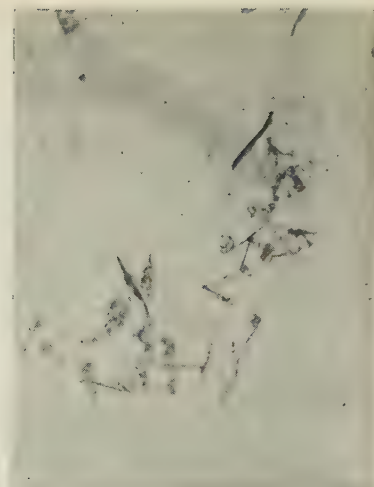


FIG. 3.—Small Needles in Centrifuged Segregate from High-Purity Magnesium-3% Aluminium Alloy Superheated to 900° C. $\times 1500$.

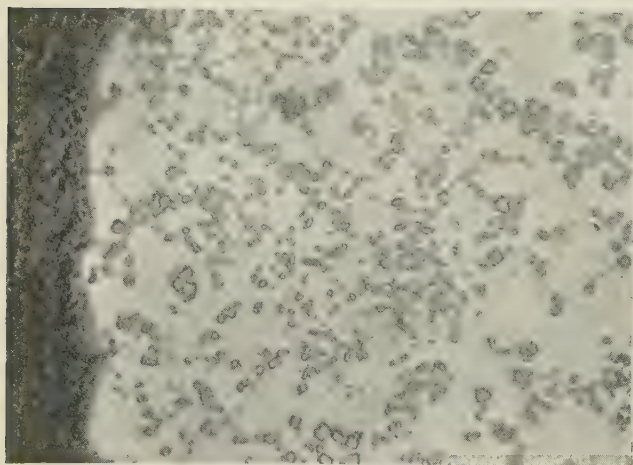


FIG. 4.—Large Iron Segregate Obtained on Centrifuging Fine-Grained Material Shown in Fig. 1 (b). $\times 500$.

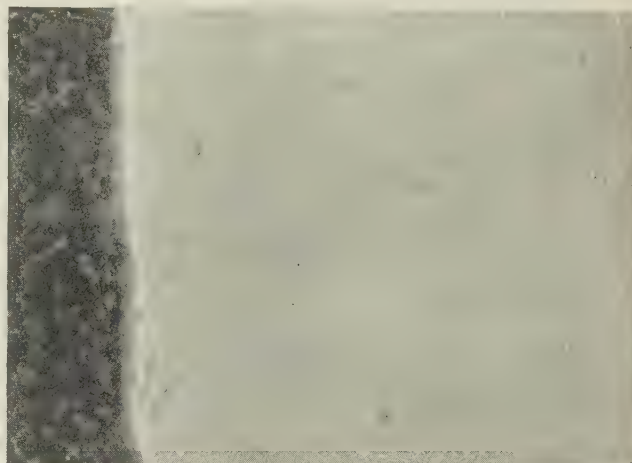


FIG. 5.—Showing Absence of Iron Segregate on Centrifuging Coarse-Grained Material Shown in Fig. 1 (a). $\times 500$.

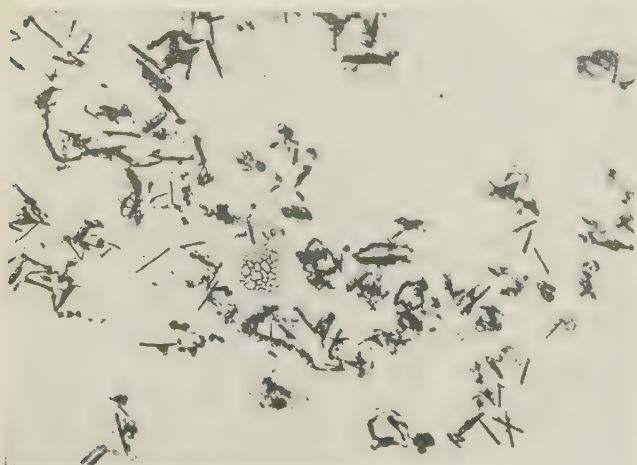


FIG. 6.—Showing Degree of Concentration of Needle-Like Constituent in High-Purity Magnesium-3% Aluminium Alloy After Centrifuging in Two Directions at Right Angles, in Succession. $\times 500$.

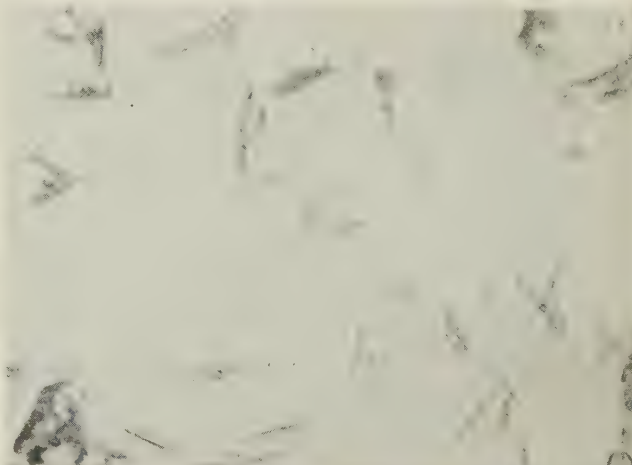


FIG. 7.—Gravity Segregate of Large Needles Obtained from High-Purity Magnesium-3% Aluminium Alloy, Superheated in a Graphite Pot and Furnace-Cooled. $\times 300$.

INTERMETALLIC COMPOUNDS IN ALUMINIUM ALLOYS.

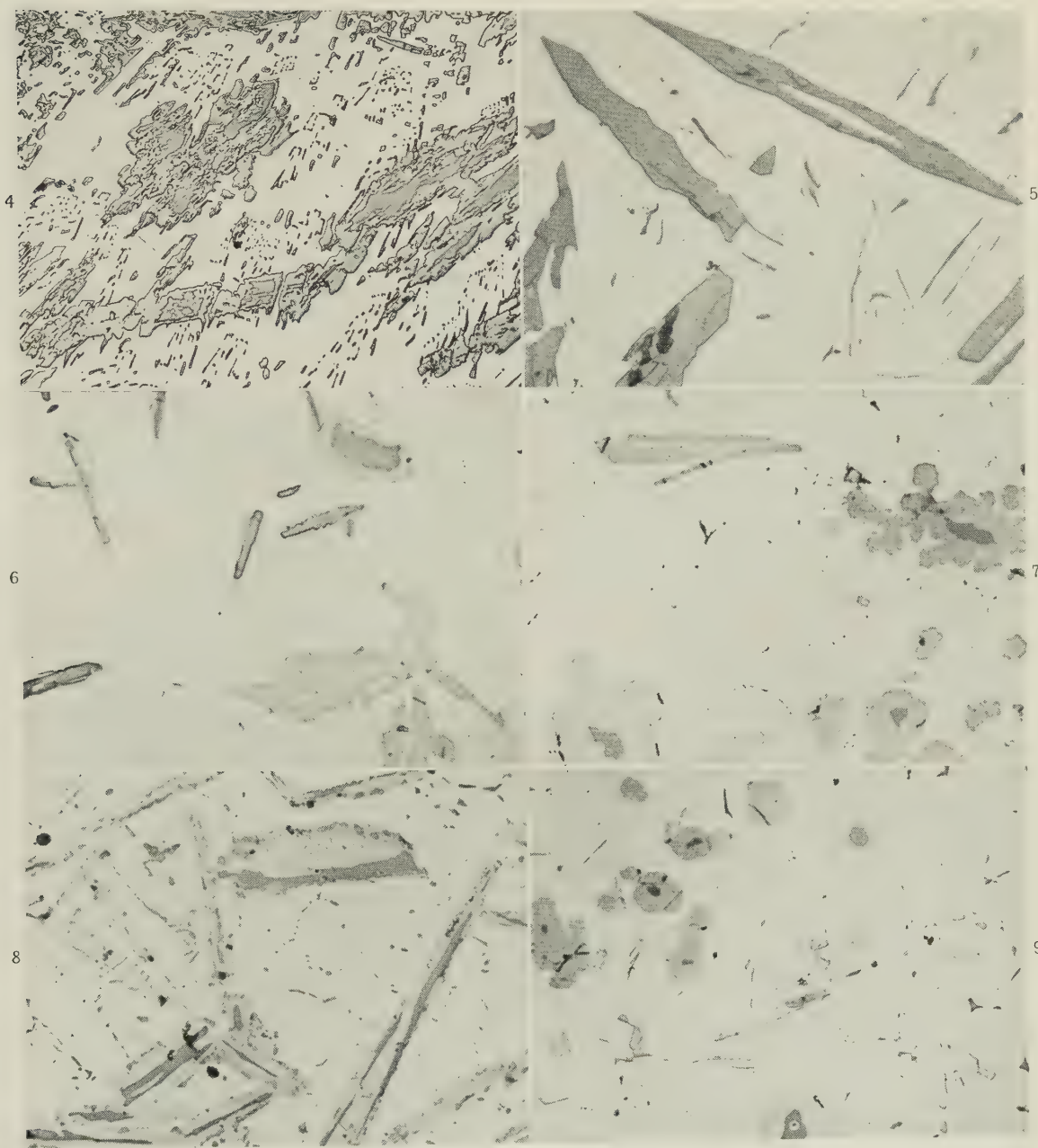


FIG. 4.—Al-Cr. α + CrAl_7 + $\text{Cr}_2\text{Al}_{11}$ (dark). Etched in 0.5% HF. $\times 250$.

FIG. 5.—Al-Fe. α + FeAl_3 (plates) + Fe_2Al_7 (needles). $\times 500$.

FIG. 6.—Al-W. α + W_2Al_3 (dark) + WAl_{12} (light). $\times 500$.

FIG. 7.—Al-V. α + VAl_3 (dark) + VAl_4 (light). $\times 250$.

FIG. 8.—Al-Mn-Cr. α + θ (dark) + G (light). $\times 250$.

FIG. 9.—Al-Cu-V. α + VAl_3 (dark) + VAl_4 (medium) + CuAl_2 (light) + T (acicular). $\times 250$.

THE RECOVERY OF POLYCRYSTALLINE ALUMINIUM*

1416

By J. A. RAMSEY,† M.Sc.

SYNOPSIS

The recovery of polycrystalline aluminium has been studied both by X-rays and microscopically. X-ray examination showed that only a few grains in a polycrystalline specimen recovered to a great extent; the majority recovered only partially. Microscopic examination revealed that recovery depended on the presence of kink bands, the degree of recovery in a given grain being contingent on the closeness of packing of the kink bands. If the bands were sufficiently closely packed, the interband material as well as the bands themselves recovered.

An interpretation of the results is given in terms of the dislocation hypothesis. On the basis of the results obtained, some criticisms are made of Cahn's theory of polygonization.

I.—INTRODUCTION

THE observation of the breakdown of the X-ray patterns on annealing a deformed metal has been elaborated by a number of workers¹⁻⁴ in recent years. The most detailed study of the phenomenon has been made by Cahn,¹ who found that annealing bent single crystals caused a fragmentation of the asterism streaks, and that, concomitantly, boundaries were developed in the crystal at right angles to the slip. This suggested that the crystal had broken down into lamellæ tilted relatively to each other. Cahn has called this process "polygonization". More recently Cahn⁵ has extended the same ideas to explain similar phenomena occurring in bent sections of a deformed crystal or kink bands.

During the same period, Wood and his colleagues^{6,7} and the present author⁸ have drawn attention to the breaking up of the grains of polycrystalline aluminium and zinc under conditions of deformation at low rates and elevated temperature. This phenomenon has been referred to as "cell formation".

In discussions on papers by these workers a number of contributors have suggested that the mechanisms of cell formation and polygonization are identical. However, marked differences in the microscopical appearance in the two cases make this view untenable in its simple form.

In the first place, cell boundaries do not bear any regular relation to the direction of the slip trace, as do the boundaries resulting from polygonization. Secondly, the absence of visible slip in many grains showing a cell structure suggested that the latter resulted directly from the deformation and is not the end product of a two-stage process. Thirdly, the cell boundaries etch as continuous lines in a similar way to grain boundaries, except that etching is not so deep as might be expected, owing to the smaller orientation differences between neighbouring cells.

It was felt that these differences might have resulted from the use of polycrystalline material in one case and single crystals deformed in a special way in the other. For this reason the experiments reported in the present paper have been performed with polycrystalline material and therefore can be compared with the findings of Wood and his colleagues. This paper deals with the effect of recovery on polycrystalline aluminium, and a further paper will deal with the relation between recovery and cell formation.

The use of the term "recovery" perhaps requires some explanation. By recovery is meant a reversion of the physical properties of a deformed metal, on heating, towards those of the fully recrystallized state, though without the formation and growth of new grains. Until recently, no structural changes had been observed during this process, and the causes of the change in physical properties were a matter of speculation. However, the work cited¹⁻⁵ has provided some X-ray and microscopic evidence of structural changes taking place before recrystallization, and it seems appropriate that they should be called "recovery". That these observations do not give a complete picture of the recovery process is undoubtedly true, for changes in physical properties occur without any structural changes being observed. This may be due to the insensitivity of our techniques or to the occurrence of changes on a smaller, perhaps atomic, scale that do not manifest themselves as phenomena which can be detected at present, or to both. Further, it was decided not to class the phenomena discussed in the present paper as "polygonization" for two reasons. Firstly, there has been a tendency to call any substructure, no matter how it was produced, polygonization and, secondly, the term polygonization suggests a definite mechanism of the formation of the substructure which, at best, is probably only partially true in polycrystalline material.

* Manuscript received 22 February 1952.

† The Baillieu Laboratory, University of Melbourne, Australia.

II.—EXPERIMENTAL PROCEDURE

Flat tensile specimens were made from strips of aluminium prepared by rolling cast ingots of purity 99.992%. Large grains, 3–5 mm. in size, were obtained by straining the specimens 2.5% and annealing at 500° C. for 1 hr. The grains were large compared with the specimen thickness, 1 mm. Under these conditions the formation of kink bands appeared to take place more easily than with finer grain-sizes. The grain-size used was also convenient because it was desired that the Debye arcs from individual grains after deformation should not overlap, in order to facilitate the study of each separate grain by X-ray methods. Some experiments were performed with specimens of a moderate grain-size of about 1 mm.

Electrolytic polishing was carried out with a solution of 70% orthophosphoric acid, 15% ethylene glycol, 5% ethylene glycol monomethyl ether, and 10% water. An interesting effect was noted in the type of polish obtained with specimens that had been subjected to strain-annealing to produce large grains, as compared with those which had not. In the former pitting to a greater or lesser extent was unavoidable, whereas in the latter excellent polishes, almost completely free from pits, were obtained. Even in a given specimen, the ends which had been held in the grips were virtually free from pits, whereas the gauge-length in which large grains had been grown was rather badly pitted. There was no apparent reason for this, though in a grain growing to a fairly large size dislocations may perhaps tend to cluster and so provide sites for the nucleation of pits.

The specimens were etched with the standard 25% nitric acid, 2% hydrofluoric acid, and 73% water solution. To reveal the structure obtained by recovery, it was necessary to warm the solution to about 50° C. and etch until the specimen showed signs of being slightly macro-etched. This took about 5–7 min. A rather better method was to etch for $\frac{1}{2}$ -min. intervals with intermediate washings for a total etching time of 5 min. This tended to limit the attack largely to the boundaries.

X-ray examination was carried out by the normal back-reflection technique and by a modification of it in which the specimen and film were oscillated through 10° in synchronism. The latter method enabled a large number of orientations in a grain to be recorded, since, instead of giving a single Debye arc, it gave a cloud consisting of contiguous arcs.

Multiple-beam interference fringes were employed to study the topography of the deformed grains. This is possible since a given fringe follows a path through points of equal "height" in the same way as contour lines on a map. Phase-contrast microscopy was also occasionally used in the examination. In all cases deformation was carried out in tension.

III.—X-RAY OBSERVATIONS

Figs. 1 and 2 (Plate VIII) illustrate typical diffraction patterns obtained from coarse-grained aluminium, after deformation, by the two techniques mentioned in Section II.

Heating specimens, that had been extended 5–20%, at 350° C. or above tended to produce a noticeable breakdown of the X-ray patterns. A grain which manifested complete breakdown with no trace of diffuseness will be called completely recovered, and one which exhibited a mixture of spots and diffuseness will be said to be partially recovered.

Fig. 3 (Plate VIII) is a diffraction pattern from a specimen stretched 16% at 21° C., annealed for 10 hr. at 350° C., then for a similar time at temperature intervals of 50° C. up to 600° C., and finally for $1\frac{3}{4}$ hr. at 630° C. A further 2 hours' heating at this temperature resulted in completed recrystallization. It may be seen in this photograph that the lower arc displays almost complete recovery. Although it was not until such a high temperature was reached that a high degree of recovery was obtained, the beginnings of breakdown of the arcs were observed within the first 2 hours' heating at 350° C.

During annealing it was found that only a few grains in a polycrystalline specimen manifested a very high degree of recovery, whereas the vast majority gave diffraction patterns consisting of a diffuse background upon which discrete spots were superimposed. In no instance was complete recovery observed in polycrystalline material, although this may have been in part due to a lack in resolving power of the technique.

However, it was thought that the important factor was probably that certain regions within the grains had recovered much more readily than the rest of the grain. The intensity variations in the diffraction pattern in Fig. 2 suggest that inhomogeneities exist within the deformed grains, as implied in the work of Calnan and Burns.*⁹ It was also found that individual grains in a fairly fine-grained aggregate showed a lesser tendency to develop spotty Debye arcs, and it is reasonable to assume that the deformation was more homogeneous in such cases.

Finally, Fig. 4 (Plate VIII) shows a diffraction pattern from a specimen stretched 10% at 500° C. The sharpness of the spots and the relative lack of continuous background suggests that the grains consist mainly of a large number of perfect crystallites. Fig. 5 (Plate VIII) is a diffraction pattern from a similar specimen elongated 10% at 21° C. and heated for 36 hr. at 500° C.

A comparison of the last two patterns underlines one of the basic differences between substructures obtained by annealing a metal deformed at low temperature and those obtained by deformation at elevated temperature. This lies in the fact that in

* A more complete study of inhomogeneities on deformation is given in a recent paper by Honeycombe.¹⁰

the latter case the grains appeared to consist almost wholly of perfect elements if the temperature was sufficiently high, whereas, in the former, such a condition was only rarely obtained.

IV.—METALLOGRAPHIC OBSERVATIONS OF RECOVERY

Two different types of substructure were obtained within the grains after recovery. Fig. 6 (Plate VIII) illustrates one type and is the result of heating a specimen extended 10% at 21° C. for 3 days at 420° C. It will be noted that recovery has modified long, narrow sections of the lattice in such a way as to enable them to be differentiated from the surrounding material by etching. Very faint areas joining up the recovered zones in the direction of their long axis were also observed. These latter regions were so faint that it was necessary to throw the microscope out of focus to produce a diffraction effect before they could be photographed. The slip lines shown in the photograph were produced after recovery by extending the specimen slightly in order to show the relation between the slip trace direction and the recovered areas. A photograph of another recovered zone is reproduced in Fig. 7 (Plate VIII). As in the previous case, the slip was the result of straining after recovery and manifests a marked deviation as it enters and leaves the recovered island. Moreover, the straightness of the slip traces across the island and the sharpness of their direction change at the boundary underline the lack of bending of the lattice within the band and the very sharp change of orientation at its boundary.

The other form of substructure developed by recovery is illustrated in Fig. 8 (Plate VIII) and consists of more or less equiaxed units in which the pattern is produced by the intersection of a marked set of boundaries running in one direction and a less conspicuous set crossing them.

In certain grains similar substructures occurred, the boundaries of which ran in different directions in different sections of the grain. The annealed, re-polished, and re-etched specimens were then subjected to a small elongation to produce slip lines. A typical result is shown in Fig. 9 (Plate VIII), in which the slip traces occur in such a way as to maintain a high angle to the direction of the sub-boundaries.

The narrowness of the majority of the recovered zones and the high-angle relation to the slip, together with the inhomogeneities in the X-ray patterns, suggested that the zones were intimately connected with deformation bands. A prediction to this effect has been made by Cahn⁵ and subsequently confirmed by him in single crystals and bicrystals.

V.—DEFORMATION BANDS AND THEIR RESPONSE TO ANNEALING

Three types of deformation band were distinguished in the deformed grains. Two ran transversely across

the slip and the third parallel to the slip. This last type has been referred to by Honeycombe¹⁰ as bands of secondary slip, and since they did not manifest any changes on heating they will not be discussed further.

The first two types of bands are illustrated in Figs. 10 and 11 (Plate VIII). The bands shown in Fig. 10 appear to consist of two lattice curvatures in opposite senses lying side by side, as is evident from the bending of the slip in their vicinity. As the photograph shows—and it was generally observed to be the case—bands of this type were found only in grains in which slip occurred predominantly on one plane. However, if a given grain had slipped on one set of planes in one part, and on another set in another part, the bands were formed so as to maintain a high angle to the slip. If duplex slip occurred, no bands were formed, so confirming the observations of Laloeuf and Crussard¹¹ and of Honeycombe.¹⁰ Fine-grained material manifested slip on more than one plane to a much greater degree, and hence fewer grains contained bands. Cahn's argument for calling these bands "kink" bands appears to be very reasonable, and they will be referred to by this name.

It was thought that the topography of the grain surface in the region of a kink band would throw additional light on their nature, and for this reason a number of bands were studied with multiple-beam interference fringes. Fig. 12 (Plate VIII) is a photograph of the fringe pattern from the bands in Fig. 10. The fringes indicate that the general slope of the grain surface is from top to bottom of the photograph. At the boundaries of the kink bands the fringe direction changes abruptly through a right angle and after crossing the band changes through another right angle back to the original direction. This indicates that a change in direction of slope of the surface has occurred along the length of the kink-band. The S-bend in the fringes across the band indicates a valley and a ridge running parallel along the band. The decrease in sharpness of the S-bend from left to right in the photograph suggests that the valley becomes shallower and the ridge lower in this direction.

The surface rumple must be related to the rotation of the lattice within the kink band, and its existence is consistent with the usual interpretation of a band. One effect present in Fig. 12 was a common feature of the bands observed by the interference method, viz. the lattice rotation was much sharper on one side of the band than the other. Note the much sharper direction changes in the fringes entering the bands from the top than those leaving from the bottom. Another frequently observed phenomenon was that the degree of lattice rotation changed along the kink bands, as shown in Fig. 12. Thus the S-bend tends to straighten out along the band from left to right in the photograph. The use of fringes confirmed what appeared to be the case from the examination of the slip traces in the band region and also indicated that the apparent curvature of the slip was, in most cases,

due both to an actual curvature in the lattice and to the surface being rumpled.

In a number of instances kink bands in one grain were connected across a grain boundary with kink bands in a neighbouring grain (see Fig. 13, Plate IX). Since no orientation relationships were measured, it is not possible to give any detail of this observation, but it seems probable that a lattice rotation in a grain near a boundary could be transferred through the boundary, and assist in developing bands in the second grain, if the orientations of the grains were similar.

Bands of the type illustrated in Fig. 11 (Plate VIII) are similar to kink bands in their relation to the main slip, but they contain within themselves slip on a second set of planes, the reason apparently being that the lattice rotation is somewhat greater within such bands. A further difference is that they are usually considerably broader than the kink bands, cf. the two bands in Fig. 11.

It was found that by polishing and etching specimens containing bands, it was quite often possible to reveal the kink bands by the etch, if this was sufficiently heavy. The etching of the kink bands occurred in two ways. On the one hand the boundary zones of the bands etched as a continuous line in a similar way to a grain boundary but less markedly. Fig. 15 (Plate IX) is the same area as Fig. 14 (Plate IX) after repolishing and etching. On the other hand, the etching often took place discontinuously by preferential attack on lines running across the bands as shown in Fig. 16 (Plate IX). The lines of preferential attack corresponded in both spacing and direction with the original slip traces. It was usually observed that the discontinuous slip-line etch tended to occur in more heavily deformed specimens or those of a relatively small grain-size and generally in the isolated bands. This observation resulted from a general survey of the deformed specimens before repolishing and could not be checked in every specific instance, and, hence, may not be very reliable. If, however, it were true, an explanation is possible by supposing that the initial stages of band formation involve the build-up of a zone of dislocations at the band boundaries and that, with further deformation, dislocations arriving at the kink band would force a penetration of the bands and build up along the slip planes.

In contrast to the etching kink bands, the bands containing slip on a second plane did not respond to etching.

Annealing affected different grains in different ways, depending on whether the kink bands were spaced widely apart or close together. The grain shown in Fig. 14 contains both the closely packed (lower right) and widely spaced (upper left) kink bands. The result of heating the specimen for 6 days at 420° C., repolishing, and re-etching is shown in Fig. 17 (Plate IX). From the photograph it is clear that the widely spaced bands have given rise to long zones of the type shown in Figs. 6 and 7 (Plate VIII).

These long zones showed occasional evidence of a boundary across them. The material between them bore no trace of a substructure. In the region of the closely packed bands, on the other hand, there was considerable evidence of breakdown of both the bands and the interband material. The length of the substructural units was small, being comparable with the width of the bands. The net result was a substructure of the type shown in the lower right-hand corner of Fig. 17, which is similar to that in Fig. 8 (Plate VIII) and corresponds to a considerable degree of recovery. In the specimens studied such complete recovery was observed only rarely, the isolated islands or incomplete recovery being the more common. This explains the observation referred to in Section III that complete dissociation of the Debye arcs into spots rarely occurred in the recovery of polycrystalline aluminium.

One further feature of the substructures observed was their relative stability on annealing. The units of the substructure, once formed, did not grow substantially at the expense of each other, nor did major changes in shape occur. The width of the units was determined by the width of the bands and their length by the degree of close packing. Fig. 18 (Plate IX) shows the effect of recovery on very narrow bands.

Phase-contrast microscopy showed an interesting feature of the recovered islands. Fig. 19 (Plate IX) is a photograph of part of the island shown in Fig. 7, and it will be noted that the boundaries of the island have a considerable width.

The failure to observe any marked degree of recovery in fine-grained material (see Section III) was no doubt due to the fact noted earlier in this section, that the deformation occurred generally by slip on more than one plane. It was found that bands of the type shown in Fig. 11 (Plate VIII) did not develop into islands during annealing.

VI.—DISCUSSION

1. POLYGONIZATION AND RECOVERY OF POLYCRYSTALLINE ALUMINIUM

The mechanism of the polygonization of bent single crystals suggested by Cahn,¹² though generally satisfactory, appears to be defective in a number of respects. When it is applied to the phenomena discussed in the preceding sections the simple dislocation model runs into serious difficulties.

In the first place, confining attention to bent single crystals, the chief deficiency of the theory appears to lie in failing to explain why, during heating, dislocations of one sign should form in more or less equally spaced lines at right angles to the slip if the crystal had been uniformly bent, i.e. if there had been a perfectly random distribution of dislocations of one sign. Cahn explains this by saying "The direction of movement of dislocations would vary at different points. . . . Dislocations would build

up along surfaces separating regions in which the movement was opposite." No reason is given as to why the movement should be opposite at different points or why the movement should result in the boundaries being more or less equally spaced.

In order to overcome this difficulty, it is necessary to postulate that pure bending did not occur, i.e. the dislocation distribution was non-random, but that the crystals were more or less sharply bent along restricted regions at right angles to the slip. This may be expected in crystals bent around a mandrel, as was the case in Cahn's experiments, since it would be expected that, as bending proceeded, the region nearer the fixed end of the crystal would be slipped and would be continually in contact with unslipped lattice, until the deformation was complete. In the ideal case of pure bending this front would move forward continuously. However in real cases, one might expect a series of relatively sharp lattice curvatures. During annealing, these regions of dislocations would act to stop dislocations moving from the zones between them and, in addition, the dislocations would tend to arrange themselves in lines, the net effect, being the result observed by Cahn. It would be interesting to know whether very uniformly bent single crystals would in fact polygonize on annealing.

Turning now to the results of annealing polycrystalline material, two effects must be explained, the one resulting in the island substructure and the other giving the more or less equiaxed type.

The former kind is relatively simple to explain. Since a kink band consists of lattice curvatures of opposite kinds, it would be made up of zones having an excess of positive and negative dislocations running parallel to each other. The dislocation distribution would not in general be uniform, but would tend to be more concentrated at the boundaries of the kink band, as evidenced by the ability to etch some band boundaries before heating. On heating, dislocation movement would take place along the slip planes; those moving inwards to the centre of the bands would meet dislocations of opposite sign moving from the other side, and annihilation would take place or a stable array would form; whereas those moving outwards would be stopped at the band boundaries, collect there, and tend to line up end to end, so removing the lattice bending and producing a sharp boundary.

In the island type of substructure there was an occasional boundary running across the islands, as shown in the recovered zone in the upper left-hand section of Fig. 17. Now, from the appearance of the interference patterns before recovery there seemed to be a change in orientation along the length of the bands. It is suggested that occasionally this orientation change occurred quite sharply. This would result in a narrow zone of dislocations of predominantly one sign which would act as a dislocation trap in a similar fashion to the band boundaries.

The major difference between widely spaced and closely packed kink bands lies in the fact that, in the

latter type, the bands were sufficiently close together for the material in the interband region to be also kinked in order to maintain the continuity of the lattice. In effect, therefore, a grain containing closely packed kink bands consists of contiguous kink bands of opposite kinds. The annealing thus resulted in the recovery of both the bands and the interband lamellæ, i.e. of the whole grain. It would be expected that as a result of the closer packing and the consequent mutual interference of the bands, the lattice rotation in a particular band would not be so uniform along its length as in the case of widely separated bands. It is suggested that this is the reason why the closely packed bands break into shorter lengths on annealing.

It seems reasonable that the stability of the substructure, once it has been formed, is due to its pattern being set by the original deformation. Dunn and Daniels¹³ have shown that growth of units of a recovery substructure at the expense of each other occurred to a very marked degree in slightly bent crystals of silicon ferrite, whereas the more heavily bent crystals showed the effect to a much lesser degree. In other words the heavier deformation produced a much greater relative tilting of neighbouring parts of the crystal and inhibited their mutual absorption after recovery. The remarkable growth of the substructure shown by Guinier and Tennevin¹⁴ is probably related to the fact that these workers used very slightly deformed crystals.

The inability of the bands showing slip on a second plane to develop into islands on annealing suggests that the occurrence of slip on another plane serves to remove the lattice curvatures which would be present in the early stages of the development of such bands.

In conclusion it may be said that the phenomenon of polygonization as generally interpreted does not lay sufficient stress on the probable role of the original deformation in fragmenting the grains. For this reason the phenomena discussed in the present paper have been referred to as recovery rather than polygonization, though it is realized that this term also is unsatisfactory because it has too broad a significance. It is for the same reason that the use of the term polygonization for phenomena involved in cell formation is considered inadequate and confusing.

2. CELL FORMATION AND RECOVERY

The similarity of the recovery substructure in some samples, e.g. Fig. 8 (Plate VIII), to cell structures obtained by Rachinger¹⁵ raised the question of there being an intimate connection between the recovery of kink bands and cell formation. This point will be discussed fully in a further paper.

ACKNOWLEDGEMENTS

The author wishes to thank Professor J. Neill Greenwood and Dr. W. A. Wood of the Baillieu

Laboratory, University of Melbourne, and his colleagues at both the Baillieu Laboratory and the Aeronautical Research Laboratories, Department of Supply, for helpful discussions during the course of the work. Especial thanks are due to Mr. R. C. Gifkins, of the Baillieu Laboratory, for his assistance in the

use of multiple-beam interferometry and phase-contrast microscopy. The author would also like to express his gratitude to Professor J. Neill Greenwood, Professor of Metallurgical Research at the University of Melbourne, for his kindness in making the facilities of his laboratory available.

REFERENCES

1. R. W. Cahn, *J. Inst. Metals*, 1949-50, **76**, 121.
2. A. Guinier and J. Tennevin, *Compt. rend.*, 1948, **226**, 1530.
3. C. Crussard, *Rev. Mét.*, 1944, **41**, 114.
4. C. G. Dunn, *Trans. Amer. Inst. Min. Met. Eng.*, 1946, **167**, 373.
5. R. W. Cahn, *J. Inst. Metals*, 1951, **79**, 129.
6. G. R. Wilms and W. A. Wood, *ibid.*, 1948-49, **75**, 693.
7. W. A. Wood and W. A. Rachinger, *ibid.*, 1949-50, **76**, 237.
8. J. A. Ramsey, *ibid.*, 1951-52, **80**, 167.
9. E. A. Calnan and B. D. Burns, *ibid.*, 1950, **77**, 445.
10. R. W. K. Honeycombe, *ibid.*, 1951-52, **80**, 39.
11. A. Laloeuf and C. Crussard, *Rev. Mét.*, 1951, **48**, 462.
12. R. W. Cahn, "Progress in Metal Physics", Vol. II, p. 151. London: 1950 (Butterworth).
13. C. G. Dunn and F. W. Daniels, *Trans. Amer. Inst. Min. Met. Eng.*, 1951, **191**, 147.
14. A. Guinier and J. Tennevin, "Progress in Metal Physics", Vol. II, p. 177. London: 1950 (Butterworth).
15. W. A. Rachinger, *J. Inst. Metals*, 1951-52, **80**, 415.

THE SOLID SOLUBILITY OF SILVER IN ALUMINIUM*

1417

By L. ROTHERHAM,† M.Sc., F.Inst.P., F.I.M., MEMBER, and
L. W. LARKE,‡ A.F.R.Ae.S., L.I.M.

SYNOPSIS

The solid-solubility curve of pure silver in super-pure aluminium up to 8 wt.-% silver has been determined by microscopical examination and electrical-resistance measurements. There is substantial agreement between the two methods over the range investigated. The resistance measurements provide a very sensitive means of detecting small structural changes. The present work may be linked with that of Raynor and Wakeman (*Phil. Mag.*, 1949, [vii], 40, 404), thus completing an accurate redetermination of the whole of the solubility curve of the aluminium-silver system.

I.—INTRODUCTION

It was desired to investigate the effect on creep properties of changes in the composition, within the solid-solution range, of binary aluminium-silver alloys. The programme envisaged the creep testing of alloys containing 0.5-8 wt.-% pure silver in super-pure aluminium. To carry out the experiments in the solid-solution state, it was necessary to know accurately the limits of solubility of silver in aluminium over the range 100°-400° C.

Previous investigations showed wide divergencies, which the recent work of Raynor and Wakeman¹ attributed to the impure nature of the materials employed. These authors further suggested that the progressive improvement in purity of available materials probably tends to a greater solubility at higher temperatures and a smaller solubility at lower temperatures than formerly reported. Their own solubility curve ends at about 400° C. and 10 wt.-%.

In designing the experiments to obtain data for the construction of the solubility curve, it was realized that the extended heat-treatment times necessary at low temperatures to produce microscopically visible structural changes would present difficulties. It was decided, therefore, to try to develop a technique capable of indicating changes in electrical resistivity on crossing a phase boundary. It was hoped that this method might be sensitive to the small structural changes which occur before any change is microscopically visible and which take place in a relatively short heat-treatment time. These two approaches, viz. microscopical examination of suitably heat-treated samples and measurements of electrical resistivity, have been used throughout the investigation.

II.—EXPERIMENTAL METHODS

1. MATERIALS USED

Nine binary aluminium-silver alloys were produced, of nominal composition 0.5, 1.0, 1.25, 1.5, 2.0, 3.0, 4.0, 6.0, and 8.0 wt.-% silver, respectively. The

0.5, 2.0, 4.0, and 8.0% alloys were made by The British Aluminium Co., Ltd., from 99.998 and 99.999% aluminium and silver of 99.98% guaranteed minimum purity; the 1.0, 1.25, 1.5, 3.0, and 6.0% alloys were prepared in the Metallurgy Department of the Royal Aircraft Establishment, from aluminium of 99.99% and silver of 99.98% purity. Later, a second batch of alloys were received from The British Aluminium Co., consisting of 0.5, 1.0, 3.0, 6.0, and 8% silver in aluminium.

TABLE I.—*Composition of Aluminium-Silver Alloys.*

Nomina Silver, %	As Analysed				
	Ag, %	Si, %	Fe, %	Cu, %	Mn, %
A	0.5	0.0075	0.0090	0.0010	Nil
	2.0	0.0025	0.0020	0.0010	"
	4.0	0.0030	0.0020	0.0015	"
	8.0	0.0025	0.0010	0.0015	"
B	0.5	0.003	0.0025	0.0015	0.0005
	1.0	0.003	0.005	0.0025	0.0005
	3.0	0.004	0.002	0.0025	Nil
	6.0	0.002	0.002	0.003	0.0005
	8.0	0.0025	0.0015	0.0035	Nil
C	1.0	0.020	0.025	0.010	Nil
	1.25	0.030	0.015	0.015	0.01
	1.50	0.030	0.015	0.015	Nil
	3.0	0.030	0.015	0.015	"
	6.0	0.040	0.015	0.015	0.01

Titanium content nil in all cases.

A = British Aluminium Company: first batch of material.

$B =$ „ „ „ second „ „

$C = \text{R.A.E.}$: cast material.

The British Aluminium Co. alloys were produced in an oil-fired crucible furnace, the 8% alloy being used as a basis material for the alloys of lower silver content. Billets 6 in. in dia. \times 24 in. long were cast and extruded to $1\frac{1}{8}$ -in.-dia. bar. Immediately before extrusion the billets were soaked for 10 hr. at 525° C. The $1\frac{1}{8}$ -in.-dia. bar was annealed at 425° C. and

* Manuscript received 14 May 1952.

† Division of Atomic Energy, Risley, Warrington, Lancs.;

formerly Royal Aircraft Establishment, Farnborough, Hants.

† Royal Aircraft Establishment, Farnborough, Hants.

quenched in cold water, before cold drawing to $\frac{7}{8}$ in. dia. The cold drawing was carried out in stages, the bar being reduced by $\frac{1}{16}$ in. at the first pass and by $\frac{1}{32}$ in. at each subsequent pass.

The R.A.E. method was as follows. Aluminium of 99.99% purity was melted in an electric-resistance furnace and the silver (99.98% minimum purity) in a gas-fired muffle furnace. The silver was added to the aluminium, and, after stirring, the melt was degassed with sodium borofluoride, skimmed, and poured at temperatures ranging from 710° to 730° C. into 1-in.-dia. chill moulds at 200° C. Approximately $\frac{1}{32}$ in. of material was removed from the surfaces of the chill-cast bars by turning before cold forging to $\frac{1}{2}$ in. square section.

The analyses of all the materials are given in Table I.

2. HEAT-TREATMENT

The methods employed necessitated the accurate control of heat-treatment temperatures over long periods. At the higher temperatures, heat-treatments were carried out in a vertical Catterson Smith air-circulating electric-resistance furnace controlled to $\pm 1^\circ$ C. For temperatures below 200° C., a Hearson-type oven, used in conjunction with an energy regulator, provided a similar accuracy of control.

The temperatures of the test-pieces undergoing heat-treatment were measured with calibrated Chromel/Alumel thermocouples, using a Cambridge potentiometer capable of reading to 2×10^{-6} V. The smaller test-pieces were placed in a large block of aluminium-silver alloy to ensure uniformity of heat-treatment. A large volume of water (50 gal.) at room temperature (20° C.) was used in quenching all test-pieces.

3. MICROGRAPHICAL EXAMINATION

Some early experiments on the preparation of surfaces for microscopical examination had indicated that the aluminium-silver alloys were not amenable to the normal mechanical polishing and etching methods. In view of these difficulties and of the large number of examinations to be made, it was decided to develop an electrolytic polishing and etching technique. The electropolishing method² finally adopted employed an electrolyte consisting of phosphoric acid, alcohol, and distilled water. The optimum conditions of current density, temperature, time, &c., were determined, and to facilitate polishing a standard test-piece of 1 cm. square section \times 2 cm. long, giving a total surface area of 10 cm.², was used. Batches of standard test-pieces were prepared from the series of alloys and initially solution heat-treated at 450° C. and quenched in cold water (20° C.). A sample from each batch was then analysed for silver.

A series of experiments, in which test-pieces from each alloy were aged at various temperatures and quenched in cold water after the requisite times, were then made. A temperature bracket was thus obtained in which, on microscopical examination, one

test-piece was observed to be in the solid-solution state, whereas the other showed a precipitated phase. This bracket was then progressively narrowed until the solubility limit was ascertained. As the determination neared the limit of solubility for any given alloy, the individual test-pieces were analysed for silver, thus ensuring accurately the position of the points obtained.

4. RESISTIVITY DETERMINATIONS

Observations on the changes in electrical resistance in both the solution heat-treated and aged conditions were made on test-pieces 0.357 in. in dia. \times 9 in. long over a test length of 5.00 in.

The apparatus consisted of a device for clamping the test-piece in series with a standard resistance of 0.0001 ohm. Owing to short-period variations, two vernier potentiometers, were necessary, each capable of measurement to an accuracy of 1×10^{-6} V., one to measure the fall in potential across the standard resistance, the other to measure the potential at the "pick-off" points on the test-piece. The power supply to the apparatus was 12 V., D.C., and the current in the circuit was maintained at 10–15 amp. by means of a variable 15-amp., 7-ohms resistance.

The experimental technique was as follows. The test-pieces were thoroughly cleaned with carbon tetrachloride, placed in the rig, and the current-input clamps tightened. The potential "pick-off" clamps were then adjusted, care being taken to tighten them sufficiently just to penetrate any oxide film present. Current was then permitted to flow in the circuit for a standard time of 1 min. to equalize the heating effect. The amount of heat dissipated was very small, of the order of 1×10^{-2} W. Simultaneous readings were then taken on the two potentiometers, and the temperature adjacent to the test-piece recorded. The potential drop across the standard resistance gave an accurate estimation of the current in the circuit, and from the known potential difference across the gauge-length the resistance of the bar was obtained from Ohm's law.

III.—EXPERIMENTAL RESULTS

1. MICROSCOPICAL EXAMINATION

Microscopical examination after electrolytic polishing and etching of the various alloys in the solid-solution state showed bright surfaces with the grain boundaries etched (Fig. 1, Plate X). The definition of the grain-boundary etch appeared to vary from one alloy to another, but no orderly relationship has been established for these changes.

Examination of the materials containing a precipitated phase (Figs. 2, 3, and 4, Plate X) showed a well-defined Widmanstätten figure which was less prominent in the immediate vicinity of grain boundaries. The grain-boundary etch revealed in general a discontinuous line of globules. This form of attack gives the first indication of departure from

the solid-solution state. The series of photomicrographs (Figs. 5-8, Plate X) for the 4% silver alloy shows the effect on the structure of increasing ageing times at 250° C.

The data obtained from the examination of the various alloys are shown graphically in Fig. 9. The points for the 10% silver alloy are from the work of Raynor and Wakeman.¹

experiment, made on Series 1 test-pieces. The bars were solution heat-treated at 450° C. for 72 hr., aged, and re-solution treated. A graphical representation of the results is shown in Fig. 10, in which the changes in resistivity plotted against wt.-% silver indicate that no significant changes occur on re-solution treatment. The resistivities of the Series 2 bars in the solid-solution state are also shown in the figure, and it is

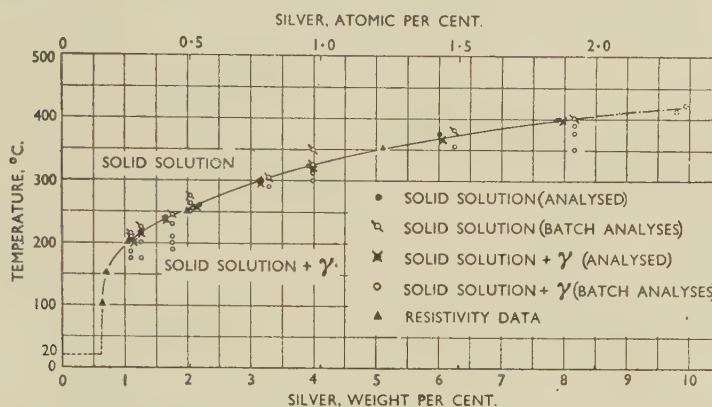


FIG. 9.—Experimental Data for Solid Solubility of Silver in Aluminium. The chain-dotted line indicates that the present determinations may be linked by a smooth curve with the work of Raynor and Wakeman.¹

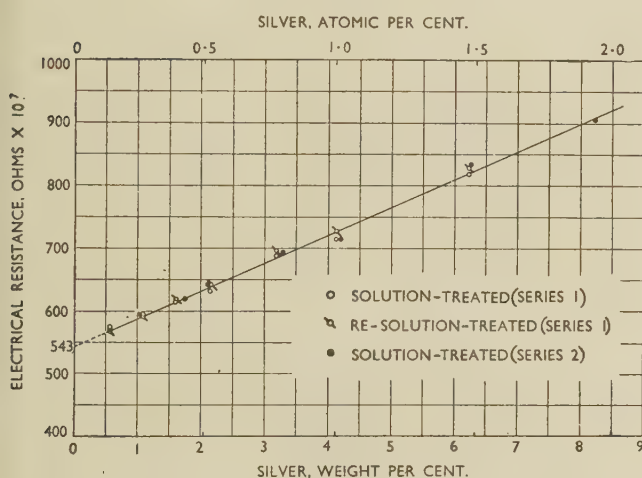


FIG. 10.—Change of Electrical Resistance with Silver Content.

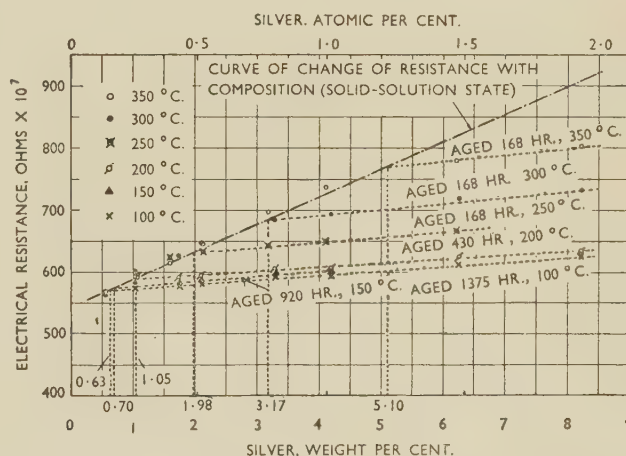


FIG. 11.—Effect of Various Ageing Treatments on Electrical Resistivity.

2. CHANGES IN ELECTRICAL RESISTIVITY

Measurements of changes in resistivity on crossing the solid-solubility boundary were made in a temperature-controlled laboratory ($20^\circ \pm 0.5^\circ \text{C.}$). Two series of test-pieces were used and are referred to as Series 1 and 2. Series 1 consisted of bars having the following silver contents: 0.56, 1.07, 1.60, 2.14, 3.17, 4.11, and 6.22 wt.-%. Series 2 included bars with 0.56, 1.03, 1.21, 1.74, 2.10, 3.28, 4.18, 6.25, and 8.22 wt.-% silver.

It was first necessary to confirm that no changes in resistivity would result from re-solution treatment after ageing. This was demonstrated by the following

apparent that there is an approximately linear relationship between the resistivity and the amount of silver in solution. This curve was used as a reference line for a series of ageing experiments.

In the ageing experiments a complete series of test-pieces were solution heat-treated and then aged at one of a number of temperatures between 100° and 350° C. Resistivity measurements were made, and the data obtained are plotted in Fig. 11. The intersections of the curves constructed from these data on the solid-solution datum line (Fig. 10) indicate the limits of solubility of silver at the various temperatures. These intersection points are included in the experimental-data curve (Fig. 9).

IV.—CONCLUSIONS AND DISCUSSION

The solubility curve of silver in aluminium has been determined by two methods. The micrographical data extend over the range 200°–400° C., that is from approximately 1 to 8 wt.-% silver, and changes in resistivity have been observed over the range 0.63–5.10% silver, that is, from 100° to 350° C. Substantial agreement is apparent between the two methods over the range of the investigation. The

a smooth curve. The limit of solubility of silver at room temperature is indicated (by extrapolation) as being approximately 0.6 wt.-%.

Microscopical examination of the precipitated phase shows a well-defined Widmanstätten figure. This type of precipitate persists throughout all the alloys examined. The precipitate, which is not an intermetallic compound but an intermediate solid solution, is deposited in the form of plates on the (111) planes.⁴ When the alloys are etched with a suitable reagent,

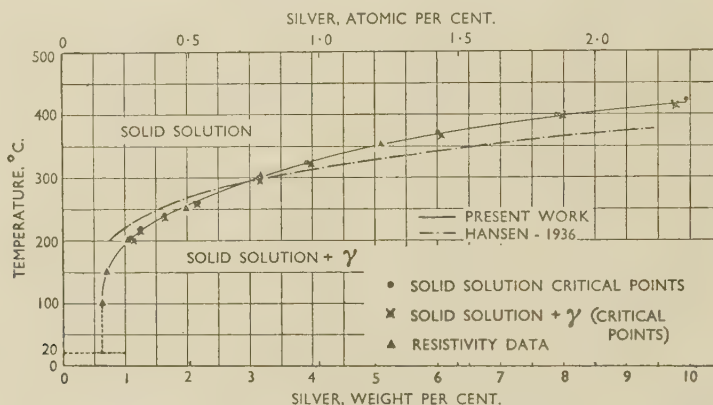


FIG. 12.—Comparison of Present Results with Those Given by Hansen.³

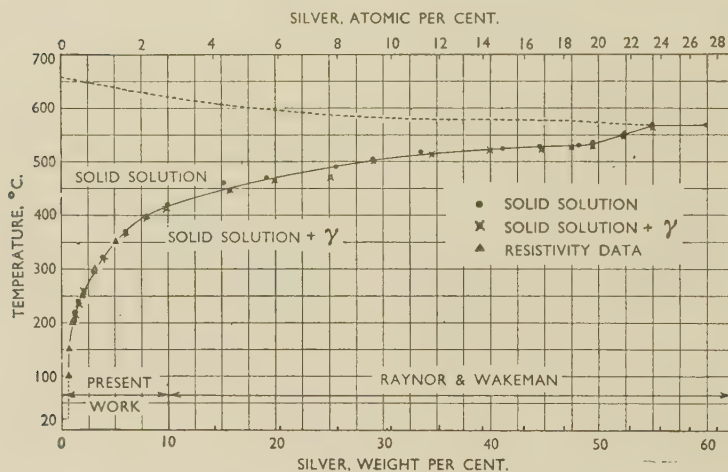


FIG. 13.—Solid Solubility of Silver in Aluminium.

solid solubility of silver in aluminium is greater at higher temperatures and less at lower temperatures than previously reported. The curve determined by the present workers crosses the curve plotted from the experimental points of Hansen³ at approximately 308° C. and 3.5 wt.-% silver (Fig. 12). Hansen's curve again crosses that determined by Raynor and Wakeman¹ at approximately 520° C. and 38 wt.-% silver. The complete solubility curve of pure silver in super-pure aluminium is shown in Fig. 13, from which it can be seen that the present determination may be linked with that of Raynor and Wakeman by

attack in the grain boundaries in the form of a discontinuous line of globules is the initial microscopical evidence of departure from the solid-solution state.

In the nominal 1% alloy, the grain-boundary precipitate after ageing for 450 hr. at 200° C. was not microscopically visible, although the resistivity technique indicated that a change had taken place. Electron micrographs, taken after electrolytic polishing in a perchloric acid electrolyte, revealed the presence of a precipitate which became microscopically visible after further ageing.

In the solid-solution state, the change in electrical

resistivity plotted against wt.-% silver gives a straight-line relationship. No significant alterations in resistivity have been observed in the materials on resolution treatment after ageing. With the alloys of lower silver content, changes in resistivity on ageing occurred before there was any visible microscopical evidence of a second phase.

The sensitivity of the resistivity technique may be established by the following experiment. If the curve (Fig. 10) is produced to zero silver content, calculation indicates the specific resistance of pure aluminium to be 2.76×10^{-6} ohm-cm. This result compares with the figure of 2.6548×10^{-6} ohm-cm. at 20° C. for super-pure aluminium (99.996%) given in the "Metals Handbook".⁵ A spot check on super-pure aluminium (99.995%) at 20° C. gives a specific resistance of 2.65×10^{-6} ohm-cm.

ACKNOWLEDGEMENTS

Thanks are due to Miss E. B. Wicks for assistance with the experimental work. Mr. H. W. L. Phillips of The British Aluminium Co., Ltd., was particularly helpful in arranging for the supply of alloys.

Publication is with the permission of the Chief Scientist, Ministry of Supply, and the Controller of H.M. Stationery Office.

REFERENCES

1. G. V. Raynor and D. W. Wakeman, *Phil. Mag.*, 1949, [vii], 40, 404.
2. L. W. Larke and E. B. Wicks, *Metallurgia*, 1950, 41, 172.
3. M. Hansen, "Der Aufbau der Zweistofflegierungen". 1936: Berlin (Julius Springer).
4. R. F. Mehl and C. S. Barrett, *Trans. Amer. Inst. Min. Met. Eng., Inst. Metals Div.*, 1931, 78.
5. —, *Metals Handbook* (Amer. Soc. Metals), 1948, 810.

THE CONSTITUTION OF TANTALUM-TITANIUM ALLOYS*

1418

By D. SUMMERS-SMITH,† B.Sc., A.R.T.C., MEMBER

SYNOPSIS

The tantalum-titanium system has been investigated by metallographic and X-ray methods, using alloys prepared from van Arkel titanium and spectrographic-standard tantalum. A continuous series of solid solutions is formed between tantalum and β -titanium above 885° C.; at 650° C. the solid solution is limited to 70 at.-% titanium. The solubility of tantalum in α -titanium is estimated as less than 0.5 at.-% at 700° C. The lattice parameters of the β solid solution show a negative deviation from Vegard's law, and yield an extrapolated value of $a = 3.288$ kX for β -titanium at room temperature.

I.—INTRODUCTION

No detailed investigation of the tantalum-titanium system has been published, though Gonser¹ has reported that tantalum and β -titanium form a continuous series of solid solutions. This continuous solid solubility is to be expected, since both tantalum and β -titanium have a body-centred cubic structure and their atomic diameters differ by less than 5%.

II.—EXPERIMENTAL METHODS

1. MATERIALS USED

As titanium is very readily contaminated with oxygen and nitrogen, strict precautions are necessary to avoid the introduction of impurities. The titanium used was prepared in the A.E.I. Laboratory by the van Arkel method, in a sealed-off glass bulb. That employed for the titanium-rich alloys contained a trace of tungsten, having been deposited on a titanium wire produced by drawing down a rod of titanium deposited on a fine tungsten wire. A typical analysis gave Si 0.03, W 0.02%, Fe not detected. No analysis was made for oxygen or nitrogen, but it is believed that they did not exceed 0.01%. Some of the original raw material used in the preparation of the pure titanium contained small quantities of iron, a certain amount of which may have been deposited with the titanium; in no case, however, was the iron content higher than 0.005%. Spectrographic analysis revealed, in addition to the above-mentioned elements, traces of boron, copper, magnesium, tin, and zinc. The transformation temperature of the titanium, determined by dilatometric means, was 885° \pm 5° C., which lies within the quoted uncertainty of the most recent value of 882.5° \pm 1° C. derived by A. D. McQuillan,² and constitutes a further confirmation of its purity, since McQuillan has shown that the transformation temperature is very sensitive to the presence of impurities.

In all other cases the titanium was deposited on tantalum wire, the rod thus formed being subsequently melted and used as a master alloy. The analytical results for the titanium so deposited were similar to those quoted above, except that tungsten was absent.

The tantalum used was in the form of H. S. Spectrographic Standard rods supplied by Johnson, Matthey and Co., Ltd., who claim a purity greater than 99.98% for this material; their spectrographic analysis indicates traces of calcium, copper, iron, nickel, niobium, silicon, and tungsten.

2. PREPARATION OF THE ALLOYS

The alloys were prepared, in the form of 5–10-g. buttons, by melting on a copper hearth in an arc furnace under an atmosphere of purified argon at reduced pressure. Previous experience had shown that there was no pick-up of metallic or gaseous impurities in this furnace, which has been described elsewhere.³ To ensure homogeneity, each alloy was melted three times, being turned over between each melting operation, and then annealed in the furnace by reducing the current in the arc until the alloy just solidified and maintaining these conditions for 20 min. Subsequent examination revealed no macroscopic segregation. Micro-segregation was removed by a further anneal of 24 hr. at 1000° C. Owing to the marked differences in the melting points of the constituents, there was some loss of titanium during melting owing to volatilization, particularly in the high-melting-point tantalum-rich alloys. No significant change in composition was found in alloys after subsequent heat-treatments, which were all at or below 1000° C.

The alloys were analysed by Johnson, Matthey and Co., Ltd., both tantalum and titanium being determined, and the analytical totals all lying between 99.41 and 100.06%.

The approximate melting points of a few of the

* Manuscript received 28 May 1952.

† Research Metallurgist, Associated Electrical Industries Research Laboratory, Aldermaston, Berkshire.

alloys were annealed in recrystallized alumina tubes in evacuated silica capsules. The capsules containing quenched specimens were not broken under water, because it was found that the hot titanium-rich

TABLE I.—X-Ray Analysis of Titanium-Rich Alloys Quenched from 900° C.

Titanium, at.-%	Intensity *	
	β Pattern	α Pattern
86.1	s	Not observed
90.0	s	w and d
90.6	w	d
91.1	Not observed	d
92.7	"	d

* s = strong, w = weak, d = diffuse.

powders reacted with the water. No difference in pattern was visible when the powders were reheated for 5 min. in very small thin-walled silica capsules, without the protective alumina tube, and re-quenched; it was therefore assumed that the quenching rates obtained with the powders in the alumina tubes were satisfactory. The results for the titanium-rich alloys quenched from 900° C. are given in Table I.

These indicate that, within the limits of detection, the β phase has transformed to α in the alloys containing 91.1 at.-% titanium and above. In the 90.0 and 90.6% titanium alloys it would appear that the transformation of β has been partly suppressed. In the 86.1% alloy no α was detected, although the lump alloy when quenched from this temperature had undergone at least a partial transformation (see Fig. 6, Plate XI).

The diffraction patterns of the α phase were rather diffuse, and it could not be determined whether it had the same parameters as α -titanium or expanded parameters, as might be expected in the super-

an accurate value for the lattice parameter of the β phase. The X-ray photographs of filings annealed and quenched from temperatures between 850° and 650° C. support the metallographic evidence for the drawing of the $(\alpha + \beta)/\beta$ boundary.

Accurate parameter measurements of the β solid solution at room temperature were made on alloys containing up to 90 at.-% titanium. Nelson and Riley's ⁵ function was used to obtain parameter values extrapolated to $\theta = 90^\circ$. For alloys containing more than 52.7% titanium the filings were annealed and quenched from temperatures above the $(\alpha + \beta)/\beta$ boundary; filings of the remaining alloys were slowly cooled to room temperature. The values obtained are given in Table II.

It was possible to obtain accurate parameter measurements by the use of copper K_α and chromium K_α radiation. With copper the (330) reflection occurs

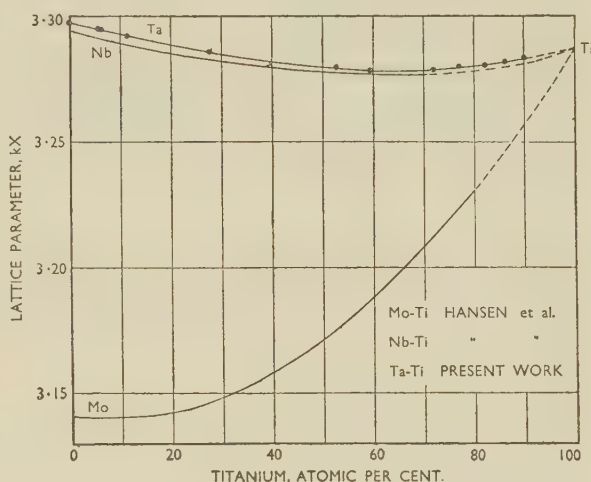


FIG. 8.—The Lattice Parameters of β -Titanium Solid Solutions.

at 83°–84° for $a = 3.297$ – 3.280 kX; for the intermediate alloys with parameters less than 3.280 kX, the (220) reflection with chromium radiation occurs at a Bragg angle of about 80°.

The parameter/composition curve is given in Fig. 8. In spite of the fact that the 82.2, 86.1, and 90 at.-% titanium alloys had partly transformed to α , the parameter values lie on a smooth curve through the other points. It would thus appear that the composition of the untransformed β had not changed during the quench. There is a negative deviation from Vegard's law.

IV.—DISCUSSION

The constitution of the binary alloys of titanium with the metals of groups VA and VIA is very similar; in all these systems, except possibly titanium-vanadium, which has not been investigated, the group V or VI component forms a continuous series of solid solutions with β -titanium. In the chromium-titanium system, M. K. McQuillan ⁶ has shown that

TABLE II.—Lattice Parameters of β -Phase Alloys at 20° C.

Titanium, at.-%	Lattice Spacing, kX	Titanium, at.-%	Lattice Spacing, kX
0	3.2912	59.5	3.2788
			3.2785 *
5.7	3.2950	72.0	3.2790
			3.2789 *
6.2	3.2948	77.0	3.2801
12.3	3.2920	82.2	3.2806
27.6	3.2857	86.1	3.2821
52.7	3.2799	90.0	3.2837

* Values obtained using CrK_α radiation; all other values obtained with CuK_α radiation.

saturated α solution formed by the martensitic transformation on quenching. The strain in this supersaturated solution is probably responsible for the diffuseness of the patterns, as the lines of the β pattern in the 86.1 and 90.0 at.-% alloys were much sharper than the α lines, and it was possible to obtain

the region of complete mutual solubility has a very restricted temperature range, a new phase being formed from the solid solution at intermediate compositions. In the other systems no intermediate phase is formed. However, the titanium-chromium system is on the border line of favourable size-difference between the components (14%) for extensive solubility, whereas in the other systems the atomic-size difference is less than 5%.

The body-centred cubic solid solution at 700° C. is limited to about 82 at.-% in the titanium-niobium system,⁷ and to about 90-92% titanium in titanium-molybdenum^{4,7}; in the present case it is limited to 73%. No data are available for titanium-tungsten alloys, though a continuous body-centred cubic solid solution has been stated to exist.¹ The solubility of all these metals in α -titanium is very restricted. The lattice parameters of the β phase have been determined by Hansen *et al.*⁷ for niobium-titanium alloys up to 70 at.-% titanium, and for molybdenum-titanium alloys up to 80 at.-% titanium. Their results are included in Fig. 8; on extrapolation, these curves coincide with the extrapolated curve for the tantalum-titanium alloys at 100%, giving a hypothetical lattice parameter for β -titanium at room temperature of $a = 3.288$ kX.

Note Added in Proof

Since the above was written, Pietrokowsky and Duwez⁸ have published a partial diagram for the

system titanium-vanadium. This indicates a continuous series of solid solutions between vanadium and β -titanium above 885° C.; at 700° C. this is restricted to 86 at.-% titanium. A value of 3.28 kX was derived for the lattice parameter of β -titanium at room temperature; this agrees well with that presented above.

ACKNOWLEDGEMENTS

The author expresses his thanks to Dr. G. A. Geach, who suggested the work; to Mr. R. A. J. Shelton, who prepared the van Arkel titanium for the alloys; and to Dr. T. E. Allibone, F.R.S., for permission to publish this paper.

REFERENCES

1. B. W. Gonser, *Indust. and Eng. Chem.*, 1950, **42**, 222.
2. A. D. McQuillan, *J. Inst. Metals*, 1950-51, **78**, 249.
3. G. A. Geach and D. Summers-Smith, *Metallurgia*, 1950, **42**, 153.
4. P. Duwez, *Trans. Amer. Inst. Min. Met. Eng.*, 1951, **191**, 765.
5. J. B. Nelson and D. P. Riley, *Proc. Phys. Soc.*, 1945, **57**, 160.
6. M. K. McQuillan, *J. Inst. Metals*, 1951, **79**, 379.
7. M. Hansen, E. L. Kamen, H. D. Kessler, and D. J. McPherson, *Trans. Amer. Inst. Min. Met. Eng.*, 1951, **191**, 881.
8. P. Pietrokowsky and P. Duwez, *Trans. Amer. Inst. Min. Met. Eng.* (in *J. Metals*), 1952, **194**, 627.

RESIDUAL STRESSES IN ALUMINIUM ALLOY SAND CASTINGS*

1419

By R. A. DODD,† M.Sc., Ph.D., A.I.M., A.R.I.C., MEMBER

SYNOPSIS

A study has been made of the extent to which the residual stresses in aluminium alloy sand castings to British Standard 2L42 (R.R.59), of a design known to induce residual stresses, are determined by the following variables: (a) percentage water in the mould, (b) pouring temperature, (c) time elapsing between pouring and stripping the casting, and (d) mould strength (green and dry sand). These variables were chosen as being likely to affect the relative cooling rates of parts of the casting of different cross-section, mould strength being the exception.

The strain consequent on sectioning the casting was measured by means of electrical-resistance strain gauges in a part of the casting subjected to a uniaxial tensile stress, the stress being determined by the relationship: $\text{Stress} = \text{Strain} \times \text{Young's Modulus}$.

It is shown that only in the case of certain designs is it theoretically possible for the stresses to vary with the moulding and casting practice, and that in such cases they are related to the variables investigated as follows: (a) The stress increases approximately linearly with increase in percentage water in the moulding sand. Over the practical range of water content (5–6.5%) for the naturally bonded sand used the stress increase is not considerable. (b) The stress increases rapidly with increase in stripping time up to the order of 10 min. Beyond this time, the rate diminishes considerably, maximum stress being attained in 1 hr. (c) A very slight increase in stress is observed with increase in pouring temperature. (d) Mould strength exerts no effect on the stress magnitude.

I.—INTRODUCTION

FROM the point of view of residual-stress formation, sand castings can conveniently be divided into two groups: (i) those in which the stresses are determined by the temperature gradients existing from the surface to the centre of the casting during cooling, and (ii) those in which the stresses (and the accompanying distortion) are determined by the different rates of cooling of members of different cross-section.

In (i), the stresses are related to the overall rate of cooling of the casting and attain appreciable magnitude only under conditions of rapid cooling. The stresses would clearly be of negligible magnitude (assuming absence of phase changes) in the case of, say, a sand-cast cylindrical billet. In (ii), the design is frequently such that stresses approaching the ultimate strength of the alloy may be set up in castings which have a slow overall rate of cooling, but different rates of cooling in components of different cross-section. Consider the simple framework design of Fig. 1 (a), comprising three parallel members connected at their extremities by yokes. This design gives rise to a simple uniaxial tensile stress in the centre member, which has a greater cross-section than the two side members. The members, X, of smaller section, solidify and contract at a greater rate than does the member, Y, of larger section, resulting in plastic deformation of the latter. The subsequent contraction of Y is hindered by the now

comparatively rigid lighter members, and it is therefore left in a state of residual tension, balanced by compressive and bending stresses in the remainder of the framework (Fig. 1 (b)).

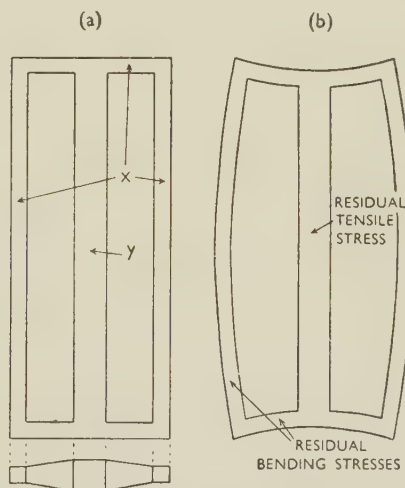


FIG. 1.—Distribution of Residual Stresses in a Framework-Type Casting. (a) Stress-free. (b) Showing residual casting stresses.

The susceptibility to cracking and distortion due to internal-stress formation in certain designs of casting has long been recognized, one of the earliest papers of importance being that of Schumann,¹ who discussed

* Manuscript received 20 March 1952.

† Department of Metallurgy, University of the Witwaters-

rand, Johannesburg, South Africa; formerly Research Fellow in Industrial Metallurgy, University of Birmingham.

stresses in iron castings in relation to design, and attempted to calculate the deformation that would result in certain simple casting shapes. In none of the extensive literature published subsequently has the effect of the moulding and metal-casting processes been considered, and it had therefore little bearing on the present work except as an aid in the selection of a suitable casting design.

A framework based on that shown in Fig. 1 (a) was originally designed by Heyn² and later used in its original or modified forms by other investigators,³⁻⁷ to study the effect of alloy composition and stress-relieving heat-treatments, &c., on the residual stresses in various cast irons and aluminium alloys. Slightly simpler designs have also been employed,^{8,9}

give greater resistance to bending. For instance, considerable rigidity can be obtained by using a raised yoke chilled to ensure a rapid rate of solidification, and the design adopted in the present research (Fig. 2) was based on this principle. The split mahogany pattern was equipped with six interchangeable centre pieces of different cross-section, so that the most suitable section for use in the investigation could be determined.

2. PREPARATION OF THE CASTINGS

Although use of the heat-treatable, high-strength wrought aluminium alloy to British Standard 2L42 (R.R.59)* was mainly dictated by its availability,

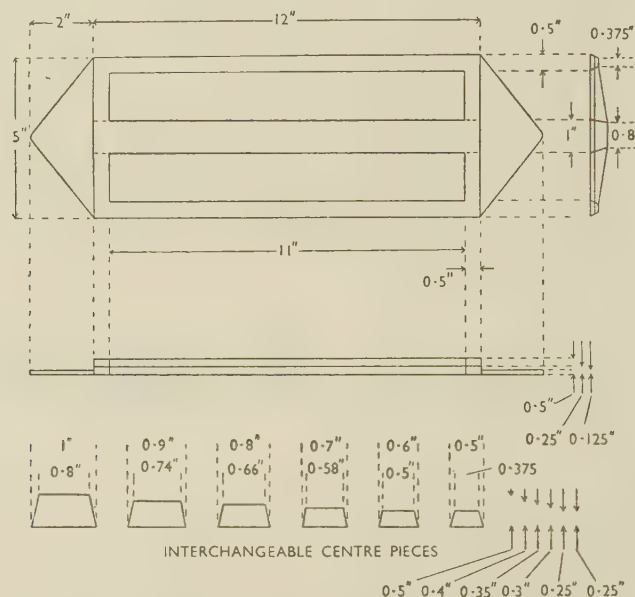


FIG. 2.—One Half of Split Pattern of Framework-Type Casting Used in the Present Research, Showing also Interchangeable Centre Pieces.

and in one case¹⁰ a pulley-wheel design was utilized for similar purposes.

II.—EXPERIMENTAL PROCEDURE

1. CASTING DESIGN

The purpose of the research required high stresses to be set up in the castings in order that the effect of the investigated variables might be easily observed. As the stresses are determined in part by the rigidity of the casting, the distortion to which this type of casting is subject (Fig. 1 (b)) causes a partial relief of the stress in the centre member, and as the stress measurement was to be confined to this member, a modified design giving greater rigidity was required. Roth and Seumel⁷ have dealt in detail with the rigidity of these framework castings, and in particular have shown how modification of the yoke (cross-piece) design can

preliminary tests indicated its suitability for simple castings of the type used, and its yield strength in the sand-cast condition made possible the formation of higher residual stresses than could have been obtained in the case of the commonly used aluminium casting alloys.

Naturally bonded Bromsgrove Red sand was used throughout the research, this being preferred to a synthetic (Southport + Bentonite) mixture on account of its ability to be moulded over a wider range of moisture contents.

An automatic ramming machine was not available, but care was taken to ensure that the density of the rammed mould was as constant as possible under conditions of hand moulding. The mould hardness was checked (cope and drag) for each green-sand mould, and through the whole series of tests (except where green strength was the variable investigated) it

* Nominal composition : copper 2.2, magnesium 1.5, silicon 0.85, iron 1.0, nickel 1.2, titanium 0.1%, remainder aluminium.

ranged from 25 to 35 degrees of hardness. For the investigation of the effect of mould strength (dry sand), green-sand moulds ranging in water content from $3\frac{1}{2}$ to $7\frac{1}{2}$ % were dried out, the compressive dry strengths varying from around 130 lb./in.² at the lower original water content to approximately 300 lb./in.² at the upper limit.

It was anticipated that running the casting via the heavy centre member would result in a considerable reduction in the cooling rate of that member, and hence some increase in internal stress. This was in itself undesirable, and, furthermore, as the mass of metal constituting the individual runners and feeding heads would vary, the effect would not be constant from one casting to another. Moreover, as the

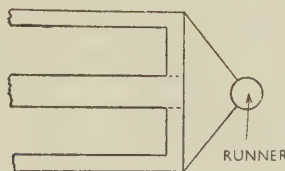


FIG. 3.—Illustrating Method of Running the Castings.

development of the stresses depended on the slower rate of solidification and cooling of the centre member as compared with the outer members and yokes, it was not possible to run the castings via the yoke. The requirements of the research could therefore only be met by running the castings through the web (Fig. 3), and satisfactory castings were found to result from this technique, using a 1-in.-dia. runner. Some shrinkage in the centre member occurred at the greater cross-sections, but this was not appreciable even in the extreme case and did not approach dimensions which seriously affected the nominal cross-sectional areas.

The pattern design, i.e. the fact that it was equipped with various sizes of centre pieces, was such that in the case of those members of smallest section and under normal conditions of cooling, the yokes would be the last components to solidify. This difficulty was overcome by chilling the yokes.

The charge, consisting of pre-alloyed ingot metal, was melted in a gas-fired furnace, being subsequently treated with a grain-refining (boron-containing) degassing agent and fluxed before pouring.

3. STRESS MEASUREMENT

Previous workers had adopted a technique involving machining through the centre member until fracture occurred, and determining the stress from the equation:

$$S = P \times A_f/A_t$$

P being the ultimate tensile strength of the alloy and A_f and A_t the areas of the fractured surface and total cross-section, respectively. There is evidence⁶ that this method tends to give low results owing to some

relief of the stress occurring before fracture, although this effect may to a certain extent be counterbalanced by stress concentrations in the machined area (due to notch effects during machining) giving rise to premature fracture.

In the present case these errors were obviated by the use of electrical-resistance strain-gauges. Two gauges were cemented longitudinally on to the centre member of the framework, and the average strain readings of the two gauges consequent on sawing through the centre piece were related to the residual stress by:

$$\text{Stress} = \text{Strain} \times \text{Young's Modulus.}$$

Details of the strain-gauge method have been described elsewhere.¹¹

III.—EXPERIMENTAL RESULTS

1. PRELIMINARY

In Fig. 4 are shown the stresses obtained by using the interchangeable centre pieces to give various cross-section ratios, A/A_0 , of the centre and outer members. Similar results have previously been reported,^{3, 5, 7} the general form of the curve OXY in Fig. 4 being independent of detailed casting design and interpreted as follows. The horizontal portion, XY , which occurs at high values of A/A_0 corresponds to the formation of a rigid outer framework, while the centre member is still in a wholly plastic condition. This portion of the curve corresponds, then, to a process of casting the centre member into a rigid outer framework which is not subjected to plastic deformation, and the stress in this member is always

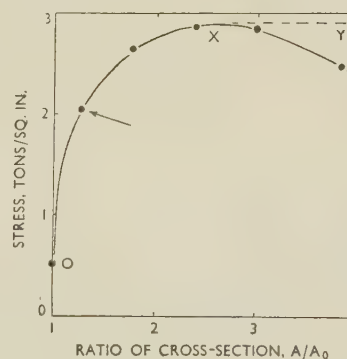


FIG. 4.—Relationship Between Stress in Centre Framework Member and Ratio of Cross-Section of Centre and Outer Members (A/A_0).

a maximum which is independent of cross-section, rate of cooling, &c., being purely a function of alloy composition. The departure from linearity of that portion of the experimental curve corresponding to XY is explained by the lack of complete rigidity of the framework. As A increases, the load on the yoke increases, and the resultant increasing distortion leads to a reduction in stress at the highest A/A_0 .

values. In the portion of the curve *OX*, the relative rates of cooling are such that some plastic deformation can take place in both the centre and the outer members, and the residual stresses would therefore be expected to exhibit some variation with factors capable of effecting alterations in the relative cooling rates of the different members. On this basis, the purpose of the research clearly necessitated the use of that centre piece (marked with an arrow in Fig. 4) giving a cross-section ratio of 1.25 : 1, and the following results apply to this particular design.

(b) *Time Between Pouring and Stripping the Casting (Fig. 5 (b))*

A rapid increase in stress is obtained with increase in stripping time up to the order of 10 min. The rate subsequently diminishes and the stress reaches a maximum for times in excess of 1 hr. Thus, although the overall rate of cooling of the casting is increased by stripping from the mould at high temperatures, the temperature difference of the members of different cross-section within the stress-formation temperature

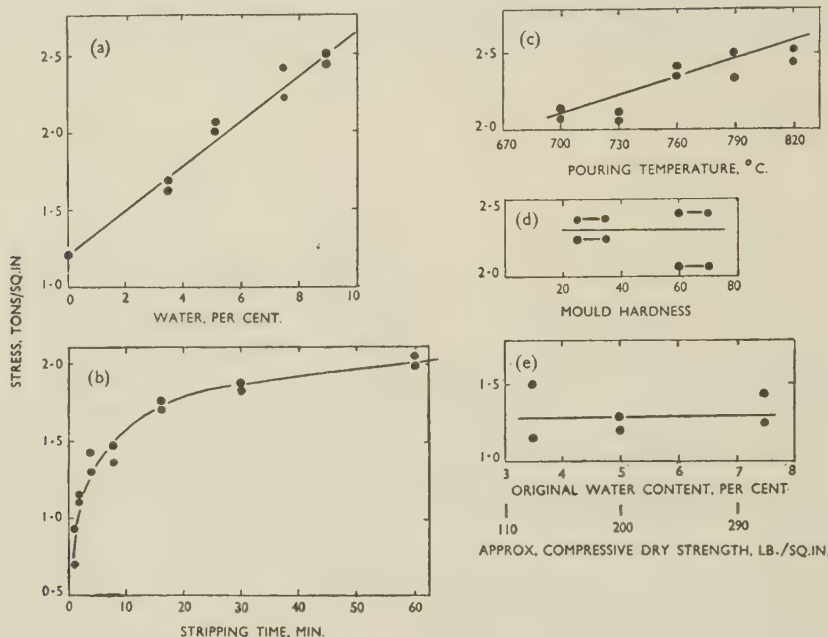


FIG. 5.—Influence on Residual Stresses of: (a) Water Content of Sand; (b) Stripping Time; (c) Pouring Temperature; (d) Mould Strength (Hardness) (Green Sand); (e) Mould Strength (Dry Sand).

- (a) Pouring temp. 730° C.; stripping time 1 hr.; mould hardness 25/35.
 (b) Pouring temp. 730° C.; green sand, 5% water; mould hardness 25/35.
 (c) Stripping time 1 hr.; green sand, 5% water; mould hardness 25/35.
 (d) Pouring temp. 730° C.; stripping time 1 hr.; green sand, 5% water.
 (e) Pouring temp. 730° C., stripping time 24 hr.

2. EFFECT OF VARIABLES

(a) *Water Content in the Sand Mould (Fig. 5 (a))*

The relationship between the percentage of water in the sand mould and the internal stress is approximately linear, the stress increasing with increasing water content. It was doubted whether an explanation of this observation could be based on the reduced green strength of the mould at the higher water contents (14 and 8 lb./in.² at 4% and 8% water, respectively), and in fact subsequent work (see Section 2 (d)) showed the internal stress to be independent of green strength (constant percentage water). It must therefore be concluded that increasing water content renders greater the difference in the cooling rates of members of different cross-section within the stress-formation temperature range, so giving an increase in stress.

range is reduced, with a consequent reduction in stress.

(c) *Pouring Temperature (Fig. 5 (c))*

A slight increase in stress with increase in pouring temperature was obtained, this observation being explained on identical lines with Section 2 (a).

(d) *Mould Strength (Green Sand) (Fig. 5 (d))*

It is evident that for green-sand moulds the stress is independent of the mould hardness (strength). It appears then, that within the relevant temperature range the mould strength is less than the hot strength of the alloy, and that the sand mould collapses under the contractile forces of the cooling casting. This collapse of the sand mould (evidenced by cracking) was in fact observed, and although it would be possible for it to occur at a comparatively late stage

in the cooling of the casting, by which time the stresses would have attained their maximum value, the results necessitate the assumption that the mould cracking occurred at some earlier stage, and that at no time was the restraining effect of the mould sufficient to affect the final stress magnitude. It is also evident that the change in the relative cooling rates brought about by the different densities of ramming of the sand mould were too small to affect the stresses appreciably.

(e) *Mould Strength (Dry Sand) (Fig. 5 (e))*

The slower rate of cooling in dry-sand moulds necessitated an increase in the stripping time, to ensure that the results could be referred to the horizontal section of the stress/stripping-time curve, and to enable the results to be compared with those obtained from the green-sand experiments. The stripping time was accordingly increased to 24 hr. The results show considerable scatter, but the stresses nevertheless appear to be independent of mould strength. Averaging the results obtained from these tests gives a mean value which lies on the extrapolated curve of Fig. 5 (a), suggesting that the stress may perhaps be dependent only on cooling rates and unrelated to the mould strength within the limits investigated. No information is available on the high-temperature mechanical properties of the alloy in the as-cast condition, and it is therefore impossible to compare the hot strength of the alloy and the dry compressive strength of the mould (maximum 310 lb./in.²). Account must also be taken of the effect of the solidification contraction of the metal in forming an air-gap round the casting. This must at least result in some initial freedom from the restraining effect of the mould during subsequent solid contraction of the casting.

IV.—DISCUSSION

It is doubtful whether the results of the research are of any practical value, except in so far as the observations on the effect of stripping time are concerned. In this respect it is clear that with a suitable casting design, very substantial reductions in stress (and distortion) can be obtained by stripping the casting from the mould in the shortest practicable

time after casting. With regard to the remaining variables, although the effect of the percentage of water in the sand is quite considerable, the change in stress within the practical limit of water content (5–61½%, assessed from the point of view of mouldability, gas evolution, &c.) is too small to be of any importance. Neither pouring temperature nor mould strength exerts any influence on the stresses.

It may be pointed out that the stresses quoted refer only to one section of the casting, and that in other more highly stressed parts the reduction in stress effected by modification of the moulding practice may be of greater significance. Although attempts have been made⁶ to obtain a more detailed picture of the stresses in simple framework castings by means of calculations based on measurements of casting distortion, the present design did not allow of any simple, complete stress evaluation. On the other hand, with castings of more massive section-size, in no circumstances could the cooling rates of the individual parts of the casting be so altered by modification of the moulding and casting practice as to result in any noticeable reduction in the stresses.

The fact that the averaged result pertaining to those castings prepared in dry-sand moulds lies on the extrapolated curve of stress against percentage water content, suggests on first consideration that the effect of the dry-sand mould is merely to alter the rate of cooling of the casting. No cracking of any dry mould was, however, observed, and it is far more likely that the restraining effect of the mould causes plastic deformation in both centre and outer members of the casting, resulting in relatively low stresses, the above-mentioned coincidence of the averaged result with the zero water content of the stress/percentage-water curve being purely fortuitous. Weight is lent to this possibility by the high resistance to hot tearing of the alloy used in the research.

ACKNOWLEDGEMENTS

The research described was carried out in the Department of Industrial Metallurgy, University of Birmingham, under the general direction of Professor A. J. Murphy, to whom the author's thanks are due for his interest and encouragement. Grateful acknowledgement is also made of the many helpful suggestions submitted by Dr. V. Kondic.

REFERENCES

1. F. Schumann, *Trans. Amer. Inst. Mech. Eng.*, 1897, **18**, 394.
2. E. Heyn, "Handbuch der Materialkunde für den Maschinenbau", Part IIA, p. 280. 1912: Berlin (Julius Springer).
3. R. v. Steiger, *Thesis, Zürich*: 1913; see *Stahl u. Eisen*, 1913, **33**, 1442.
4. O. Bauer and K. Sipp, *Giesserei*, 1936, **23**, 253.
5. R. Schneider, *Aluminium*, 1938, **20**, 188.
6. K. Grassmann and H. Lege, *Giesserei*, 1941, **28**, 342.
7. A. Roth and G. Seumel, *ibid.*, 1943, **30**, 153.
8. O. Banse, *Stahl u. Eisen*, 1919, **39**, 313.
9. P. A. Russell, *Proc. Inst. Brit. Found.*, 1945–46, **39**, A185.
10. W. Machin and M. C. Oldham, *ibid.*, 1935–36, **29**, 650.
11. R. A. Dodd, *Metallurgia*, 1952, **45**, (269), 109.

THE CREEP/TIME RELATIONSHIP UNDER CONSTANT TENSILE STRESS *

1420

By S. BHATTACHARYA,† B.Sc., Ph.D., W. K. A. CONGREVE,†
B.A.Sc., Ph.D., and PROFESSOR F. C. THOMPSON,† D.Met.,
VICE-PRESIDENT

SYNOPSIS

Work has been carried out at constant stress on copper, zinc, tin, cadmium, lead, aluminium, and the lead-tin eutectic. All the results are consistent with the equation: $\sigma_t = \sigma_0 + at^k$, where σ_t and σ_0 are, respectively, the total and the initial strain, t is the time, and a and k are constants. Creep during the primary stage may also be expressed by a corresponding equation $\sigma_p = a't'^k$, where σ_p is this primary extension. Once the primary stage is completed, the creep strain $\sigma_c = at^k$, a relationship which is not affected by the space lattice in which the metal crystallizes, temperature, applied stress, nor pre-strain. The results are in accord with the constant-temperature relationship $\sigma = bS^\alpha$, where S is the stress and b and α are constants. Combining the two relationships, it would appear that metals obey the Nutting-Scott Blair equation: $\sigma = At^kS^\alpha$, which also describes the flow of many non-metallic substances.

If $\sigma_c = at^k$, then the creep rate \times time, i.e. $\frac{d\sigma_c}{dt} \cdot t = akt^k$, gives, when plotted against time on a double log scale, a straight line parallel to that obtained for the creep/time relationship itself when similarly plotted. This prediction of the power-law equation is confirmed. The technique is important, in that it obviates the necessity of deriving σ_0 .

Since, over the range examined in this work, the use of direct elongation or of natural strain gives curves in close agreement, the creep equation may, if desired, be expressed as:

$$l_t = l_0 \exp C \left(\frac{t}{t_0} \right)^k \left(\frac{S}{S_0} \right)^\alpha + \sigma_0,$$

where l_0 and l_t are, respectively, the original length and that after time t , and t_0 and S_0 are some standard time and stress. Such an equation satisfies all dimensional requirements.

I.—INTRODUCTION

SINCE Thurston¹ and Howe² published their pioneer results on the "patience" of metals, more than thirty different equations have been put forward as representing the creep/time relationship. Some of these refer to constant load, others to constant stress; some are purely empirical, whilst others have a background which is largely philosophical. Apart from the importance of this relationship in enabling extrapolation to be effected with reasonable accuracy, any theoretical discussion of its physical significance cannot be valid unless the equation itself is soundly based. Of these equations two have received particular acceptance. In this country, and so far as fundamental physical metallurgists are concerned, that of Andrade³ has gradually become accepted almost as a physical law, and abundant evidence is available that by an appropriate choice of constants, a close fit with experimental data can be obtained over a wide range of experimental conditions. Elsewhere, and even, it is believed, among engineers here, the relationship generally employed is of a power-law type, and the main object of the present contribution

to the subject is to offer some critical comparison between the two approaches. The results recorded here represent less than 10% of those obtained, but they are in all respects typical.

II.—SHORT-TIME HIGH-STRESS TESTS

1. TESTS AT ROOM TEMPERATURE

Regarding the experimental technique adopted little need be said, since it was essentially that employed by Andrade and Chalmers.⁴ The apparatus was designed for a test-length of 10 in. and an extension of 40%, and after various trials the strain was measured by two cathetometers, reading on light gauge marks affixed near the upper and lower grips, respectively. This method of measurement, being carried out entirely on the specimen, completely eliminates any inaccuracy due to slipping at the grips or to strain of the apparatus itself. The sensitivity of the strain measurement was of the order of 2×10^{-5} , which, in view of the relatively high stresses employed, seemed adequate. Before use, the apparatus was calibrated over the whole range of extension, the maximum variation of stress being less than 1%.

* Manuscript received 21 February 1950; in revised form 28 February 1952.

† Department of Metallurgy, The University of Manchester.

The satisfactory gripping of wire specimens is never a particularly easy task since soldering of the wire to the grips is regarded as highly undesirable. In these experiments the specimen was guided centrally through holes in two clamping screws, the grips being of ebonite, to the surface of which sand-paper was attached; a length forty times the diameter of the wire was so held. This method of gripping proved entirely satisfactory.

The main work was carried out on wires of high-purity lead (99.99%), specially pure, high-conductivity copper (99.99%), and aluminium (99.8%) (representing the face-centred cubic structure); high-purity zinc (99.99%) and cadmium (99.95%) (hexagonal); "pure" tin (tetragonal), and, to a limited extent, the lead-tin eutectic.

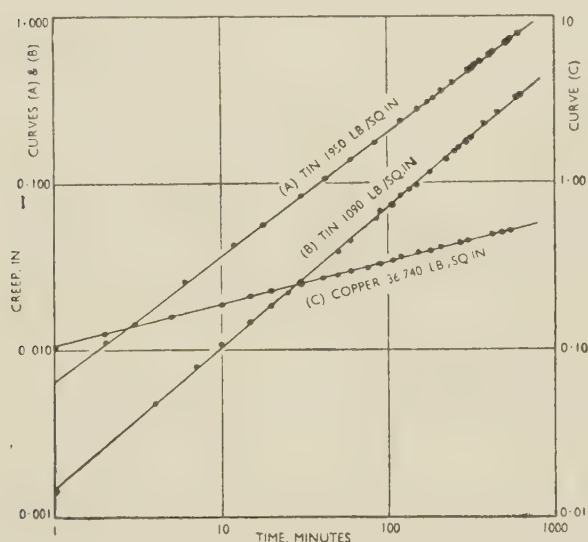


FIG. 1.—Short-Time Tests on Tin and Copper.

To eliminate inaccuracies due to bending or kinking, the specimens were strained 5% in tension and then annealed in glass tubes to obtain very straight lengths, or, later, annealed after they had been mounted in the testing machine itself. The room-temperature tests were carried out in a centrally heated room, free from draughts, the temperature fluctuation in the course of any individual experiment not exceeding about $\pm 1^\circ \text{C}$.

A considerable number of methods were tried in plotting the results, and it was soon evident that, with the exception of short-time measurements, a double-logarithmic plot (log extension against log time) could give a strictly linear relationship. For this, a choice of the "initial extension" had to be made somewhat arbitrarily. From an original plot of log extension against log time, an estimate of the "initial" extension (σ_0) was obtained by extrapolation to unit time. This value of σ_0 was then subtracted from all the experimental readings, which, on being again plotted on a double log scale, gave a curve that

normally bent away from the straight line at low values of time. To correct this, σ_0 was again adjusted, until, finally, a straight line was found which extended downwards to some, usually quite small, initial time interval. A similar result may be obtained by an algebraical method,⁵ but appears to possess no advantage over the simple, direct way here used. This procedure may seem over-arbitrary, but complete justification for it will be adduced later.

In Fig. 1 are shown typical results for tin and copper for times up to 600 min., and, in the case of tin, at different stresses. The results for zinc, lead, aluminium, and cadmium followed exactly the same lines, and typical curves are shown later.

These results, so far as they go, are completely consistent with the view that (again excluding the

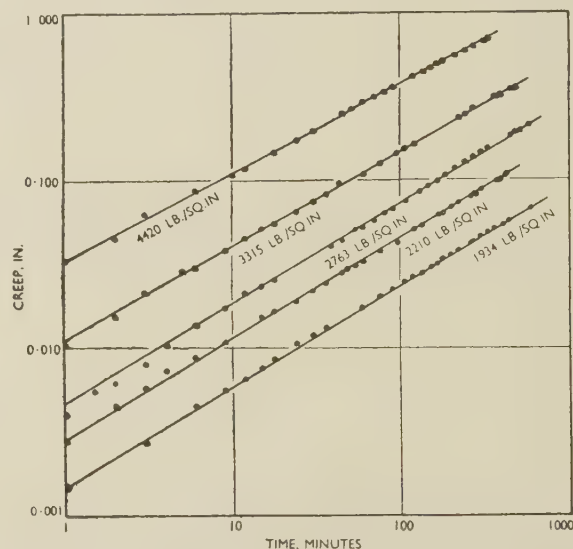


FIG. 2.—Short-Time Tests on Zinc at Various Stresses.

behaviour of the metals on, and soon after, the initial loading) the creep/time relationship under constant stress may be expressed with great exactitude by the equation :

$$\sigma_c = at^k,$$

where σ_c is the extension due to the creep, t the time, and a and k are constants; or that the total extension may be represented by an equation of the type :

$$\sigma_t = \sigma_0 + at^k,$$

where σ_t is the total and σ_0 the initial extension, σ_0 itself being the sum of the elastic strain and of an additional plastic element.

The effect of stress was investigated in more detail for zinc and cadmium, the results for zinc, which are typical of both metals, being shown in Fig. 2. Over the whole stress range, the double log plot fits the data very closely, and it is significant that these curves are essentially parallel.

In Fig. 3 are shown the results obtained by following

the procedure outlined with an annealed copper wire, obtaining from the double log plot the constants of the power-law equation, and then using these constants to derive afresh the normal, creep/time curve. The excellent agreement between the experimental curve and that calculated from the power-law relationship needs no stressing, save for the shorter-time determinations where the experimental points fall consistently above the power-law curve. This was found to be the case in all these determinations, though the effect rarely continued for so long as in this particular test. Fig. 3 is of some further importance in justifying the view that the accord between experiment and the power-law relationship

elements. The longitudinal opening permitted its being placed in position around the sample after the latter had been mounted ready for test. A second heating coil was placed on the bottom of the furnace below the lower grip. The front of the furnace, carrying two subsidiary elements wound on mica, was then screwed on, the specimen being protected from direct radiation from all these elements by aluminium sheet. The whole apparatus was then lagged with asbestos wool except for the opening closed by the door. A Cambridge controller, actuated by a thermocouple placed near the centre of the wire, maintained the temperature during the tests to within, at most, $\pm 2^\circ \text{C}$. Through two double-glass

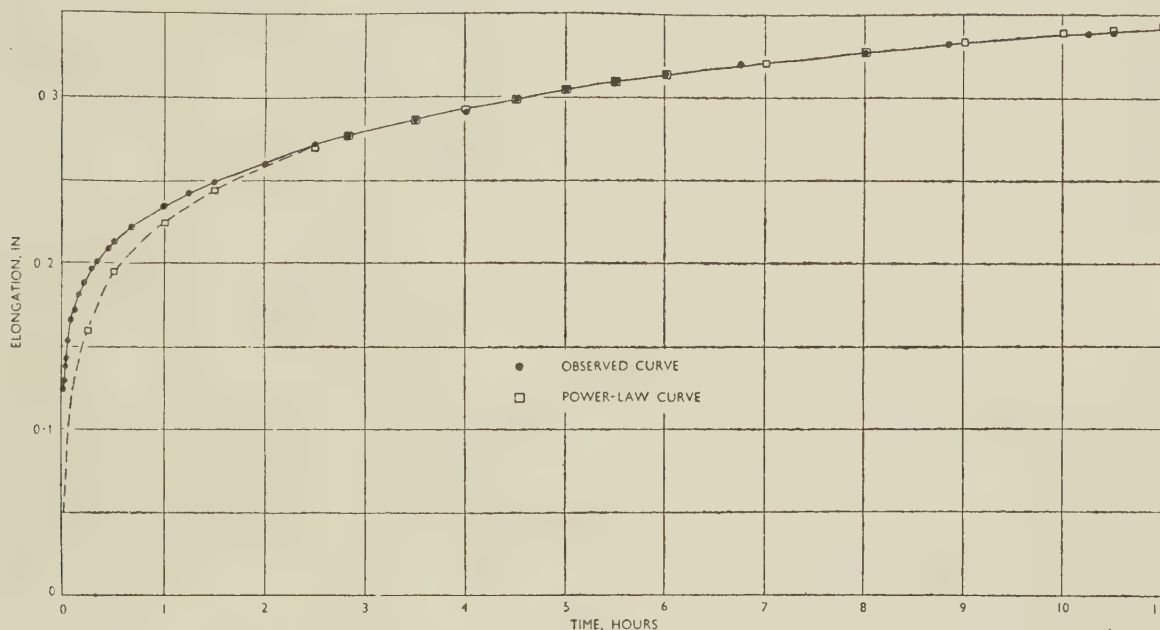


FIG. 3.—Comparison of Observed and Power-Law Curves for Annealed Copper Wire, 0.0228 in. dia. Load 13 lb.; temperature of test 20°C .

is in fact real, and is not merely the result of the plotting technique adopted. To the short-time abnormality we shall return later.

2. TESTS AT HIGHER TEMPERATURES

The foregoing results were all obtained at room temperature, and it was clearly desirable to see how far the same result was obtained at higher temperatures, though in view of the range covered by these tests it would appear improbable that the power-law relationship, if accidental, should be found to hold in all cases.

The straining apparatus was the same as that previously described, but a thermostatically controlled enclosure was provided, the temperature of which could be varied over a wide range.

This furnace consisted of an asbestos horse-shoe, 14 in. high, which supported the main heating

windows the gauge marks could be viewed by means of the cathetometers and followed through an extension of some 30%.

In the tests on wires in the fully annealed condition, in order to eliminate any localized work-hardened zones, the specimens, initially $9\frac{1}{2}$ in. long, were mounted in the grips and the gauge marks lightly attached. The furnace was placed in position, the wires annealed therein and then strained to the 10 in. required by the geometry of the machine. In the absence of this preliminary annealing, irregular extension of the specimens frequently occurred. The sample was then fully annealed *in situ*, and thereafter remained undisturbed until tested.

In Fig. 4 typical results are shown for lead at 55°C . and for aluminium at 150° and 250°C . Again, the double log plot leads to a straight line.

The tests so far reported were all carried out on fully annealed wires. The effect of pre-strain was

investigated for aluminium at 150° C., and the results are shown in Fig. 5. Curves (A), (C), and (D) are for wires with amounts of pre-strain of nil, 0.015, and 0.12, respectively, whilst in curve (B) is shown the

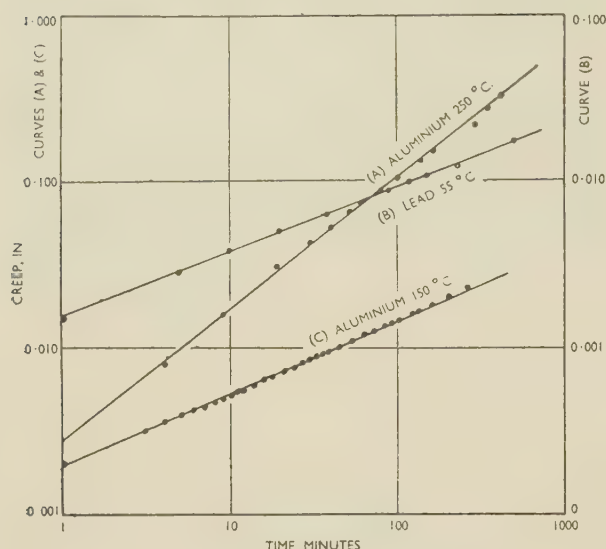


FIG. 4.—High-Temperature Tests on Aluminium and Lead.

effect of a 2-hr. period of recovery under no load, after test (C). Since the stress applied varied from test to test, the effect of the pre-strain on the constants a and k was later re-examined in detail; the significant feature of Fig. 5 is that again the data correspond throughout with a power-law relationship.

The effect of pre-strain on the material was examined for aluminium at 150° C., and the variation of the constants a and k is shown in Fig. 6.* Up to a strain of about 6% both of these vary considerably— k increasing and a falling—but thereafter little further change is to be observed. If these results may be regarded as typical, an explanation is provided of the well-known fact that with pure metals the reproducibility of tests is far from satisfactory, even the slight amount of strain involved in taking a specimen from a coil of wire and mounting it in the apparatus bringing about marked changes in the constants and hence in creep behaviour. It is, we believe, only the fact that in all these tests the specimens were annealed after being fixed in the testing machine, that enabled such unusually consistent results to be obtained.

To sum up, the net result of the data recorded in this section is that, so far as they go, they are completely in agreement with the hypothesis that creep, i.e. the total extension minus the initial elongation can be accurately represented—under constant stress—by a power-law equation.

* Since as the degree of pre-strain increased the test stress had to be raised to obtain similar rates of creep, the relationship plotted in Fig. 6 is a/S^7 , S being this applied stress.

III.—LONGER-TIME TESTS

Suggestive as the foregoing results are of the validity of the power-law relationship, the weight

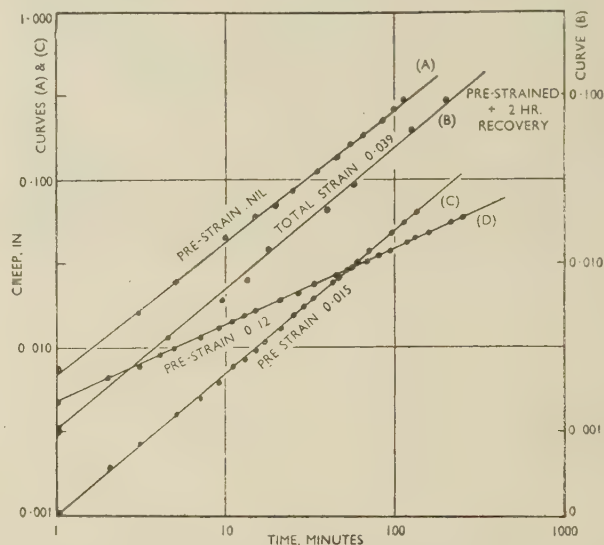


FIG. 5.—Effect of Pre-Strain on Aluminium at 150° C. Specimen B was rested 2 hr. after test (C) and then retested.

of the evidence may be regarded as inadequate owing to the relatively short times for which tests were carried out.

The results of some typical runs of longer duration are collected in Figs. 7 and 8. In Fig. 7 are recorded the results for tin up to 400 hr., for aluminium at

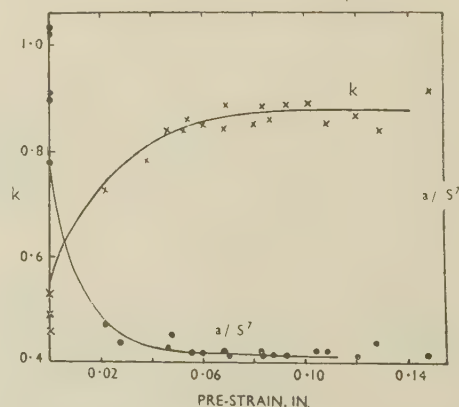


FIG. 6.—Effect of Pre-Strain on Constants a and k for Aluminium at 150° C.

150° C. up to about 600 hr., and for lead to 930 hr. In the cases of tin and lead, these tests extended beyond the onset of tertiary creep, and it will be seen that the linearity of the double log plot persists right

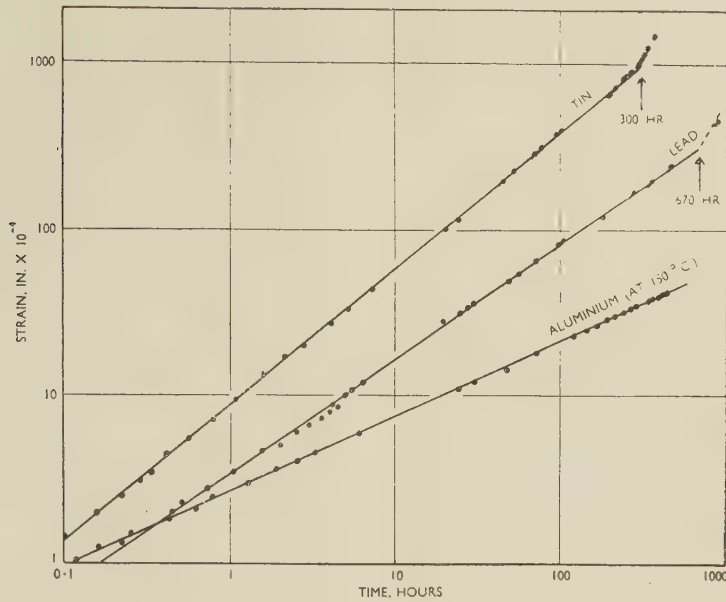


FIG. 7.—Long-Time Tests on Lead, Tin, and Aluminium. Arrows indicate onset of tertiary creep.

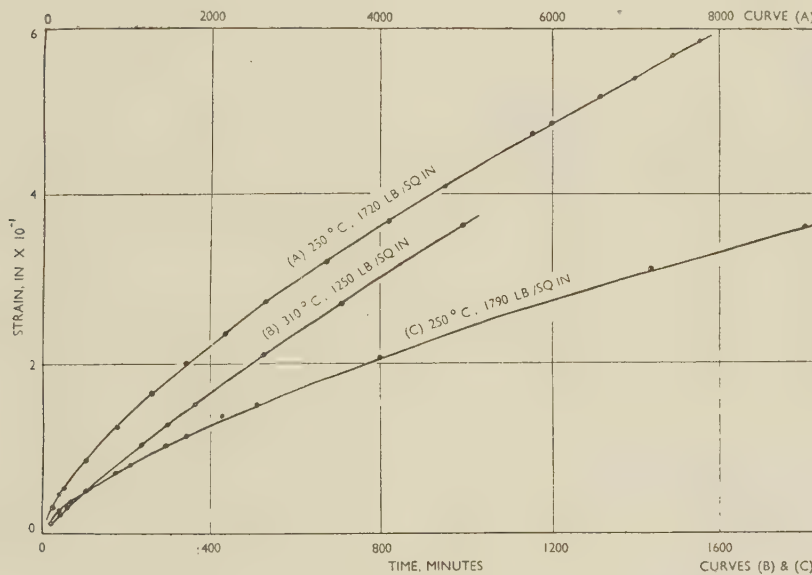


FIG. 8.—Creep/Time Curves for Aluminium Derived from Power-Law Relation. Experimental points are superimposed.

up to the time at which such creep, due to necking, sets in.

In Fig. 8 have been plotted creep/time curves for aluminium derived from the power-law equation, on which the experimental points themselves have been superimposed. A more perfect correspondence between the results and the derived curve could hardly be desired.

IV.—CREEP RATE

It has so far been assumed that the procedure of choosing a value of the initial extension such that a straight-line, double log plot is obtained, is justifiable.

We may now proceed to discuss a modified technique in which no such assumption is required.

If, in the power-law relationship, instead of the total creep, the creep rates—which are independent of the initial extension—are considered, then from the equation :

$$\sigma = at^k \quad . \quad . \quad . \quad . \quad . \quad (1)$$

$$\dot{\sigma} = \frac{d\sigma}{dt} = kat^{k-1}, \quad . \quad . \quad . \quad . \quad (2)$$

or,

$$\dot{\sigma}t = kat^k \quad . \quad . \quad . \quad . \quad . \quad (3)$$

Equation (2) requires that when plotted on a double log scale the creep-rate/time curve should be a

straight line, whilst equation (3), when plotted similarly, gives a straight line of the same slope k as that of the creep/time curve itself, i.e. if the power law be

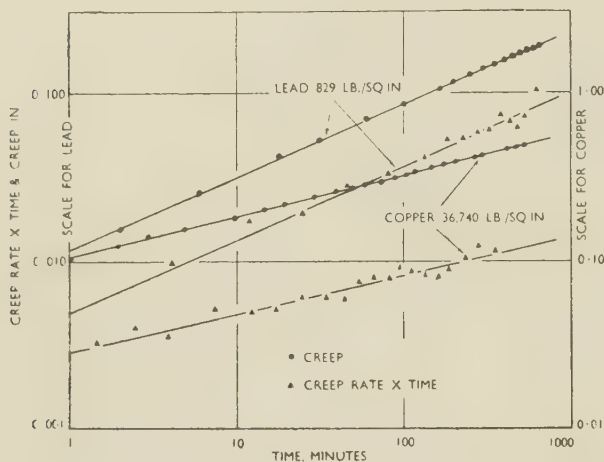


FIG. 9.—Creep/Time and Creep-Rate \times Time/Time Curves for Lead and Copper.

valid, then these two curves must be parallel to each other.

In Figs. 9 and 10 are recorded results for lead and copper, and for tin and cadmium, respectively. In each case the creep and creep-rate \times time values are plotted double logarithmically against time, and both the linearity and parallelism of the respective curves need no stressing.

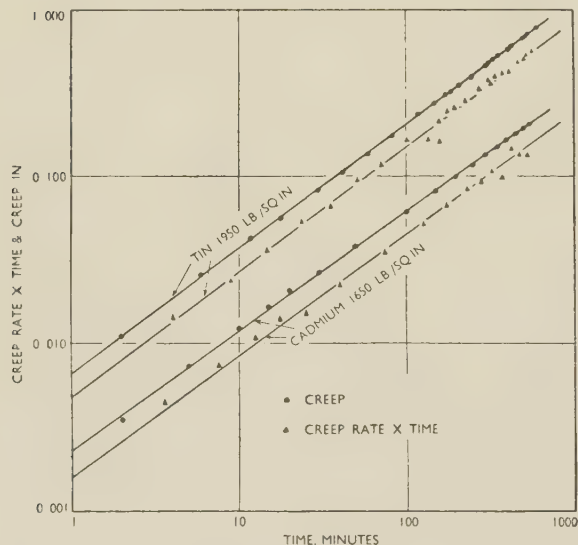


FIG. 10.—Creep/Time and Creep-Rate \times Time/Time Curves for Tin and Cadmium.

A comparison of these results with those deriving from the Andrade equation is provided in Fig. 11. In curve (A) is shown the creep/time relationship,

plotted on a double log basis, for aluminium at 250° C. and a load of 1790 lb./in.². Curve (B) is the creep-rate \times time/time curve plotted in a similar manner, whilst the broken curve is the creep-rate \times time/time curve given by the Andrade equation, the constants for which were determined with the greatest care. It is immediately evident that this latter curve bears little relationship to the experimental results, whilst that derived from the power law is, as that relationship requires, both linear and parallel to the creep/time curve (A). Exactly similar results were found for tin, lead, and cadmium.

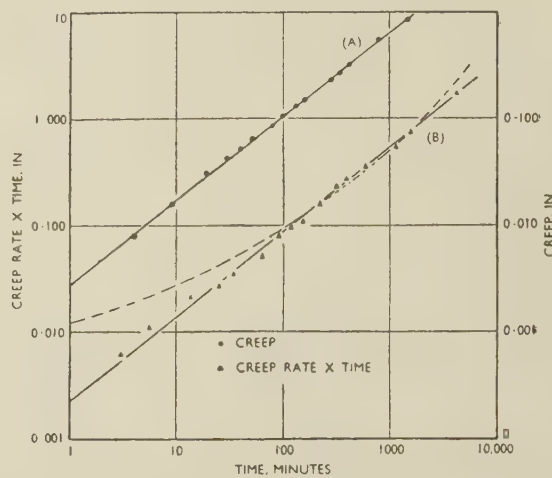


FIG. 11.—Creep/Time Curve (A) and Creep-Rate \times Time/Time Curve (B) Calculated from Power-Law Equation (full line) and Andrade Equation (broken line), for Aluminium at 250° C. and 1790 lb./in.².

Through the great kindness of Mr. E. R. W. Jones, M.A., who has had special experience in such work, two typical sets of results, one for lead at room temperature and one for aluminium at 250° C., were submitted to statistical analysis. The results for

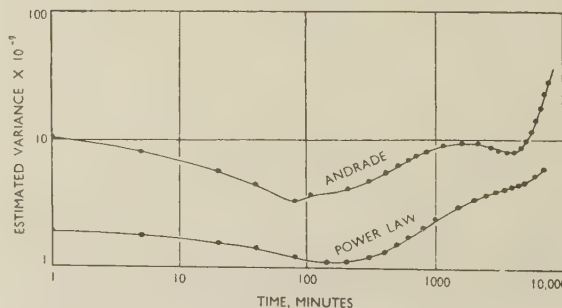


FIG. 12.—Statistical Analysis of Results for Aluminium.

aluminium are shown in Fig. 12. In both cases the power-law relationship shows a significantly smaller variance; moreover, there is a suggestion that this variance is becoming rapidly greater for the Andrade equation as the time of the test is increased.

V.—CREEP AT VERY SHORT TIMES

For small values of time, as is known, a modified relationship holds. When the load is first applied, although the elastic extension may be taken up more or less instantaneously, the plastic adjustment occurs more slowly. This state of affairs is, in fact, to be expected, as Bailey and Roberts,⁶ Gillett,⁷ Moore, Betty, and Dollins⁸ have already suggested, since the initial slip will occur in those crystals with the appropriate plane disposed as nearly as possible at 45° to the applied stress. As a result of such slipping, necessarily accompanied by reorientation, deformation will take place in other crystals, the plastic adjustment to the stress being of necessity gradual. During this stage of the deformation, the strain, and therefore the strain-hardening, cannot be uniform. Further, it must also be remembered that the stress is not imposed instantaneously and, at the beginning of the test, rises from zero to the maximum at a finite, even if rapid, rate, and a continual reshuffling of strain may be envisaged. Gradually the whole crystalline aggregate will assume a more or less uniformly strained condition, and then, and not until then, can the normal creep/time relationship, whatever it may be, be expected to become operative. It is clear then that the total extension must consist of two parts: one concerned solely with some short initial period, the other increasing continuously with the duration of the test.

Although this section of the work has not yet progressed far, it already seems possible to outline the conditions which obtain in the first few minutes of the test.

A small thin piece of glass, carrying a 1-mm. scale, graduated into hundredths, was attached to the wire near the top end by rubber solution, "Bostick", or fire-cement. A source of high-intensity light, produced by a mercury arc, was focused on the specimen by a lens of short focal length, and an image of the scale projected by means of a vertical travelling microscope on to a screen placed about 4 m. away from the apparatus, a magnification of about 100 times being obtained. A horizontal reference line was drawn on the screen, and as the load was gently applied, the extension could be measured both easily and accurately from the relative movement of the image of the scale attached to the specimen and the reference line.

Some tests were also carried out with a scale fixed near one end of the specimen and a horizontal reference line at the other. The images of these scales were projected on to a plain screen and superimposed. When the load was applied, the relative motion between the scales measured the creep, but the results obtained were similar to those with the one scale only.

In Fig. 13 are shown curves obtained for lead and tin, typical of many others determined. It will be seen that when the creep, or the product of creep rate and time, is plotted double logarithmically against time, two straight lines are obtained, which intersect

fairly abruptly; the first of these is concerned with the primary creep, which is apparently related to time by an equation of the same type as that in the secondary stage, i.e. $\sigma_p = a't^k$. This result is in accord with those obtained by Cottrell and Aytakin⁹ for "transient" creep of zinc in torsion. The results show that this stage of the creep finally disappears, and in this respect our results are not in agreement with an equation of the Andrade type in which the influence of primary creep operates, though at a progressively diminishing rate, throughout the whole of the test. These results have been obtained with measurements made down to 10 sec. after the imposition of the load, but too much importance should not at present be attached to the shortest-time tests.

Some of these tests also suggest that the initial stage of creep continues for a longer and longer period as the applied stress is raised.

From these results, it would appear reasonable to suggest that the mechanism of creep is not dissimilar

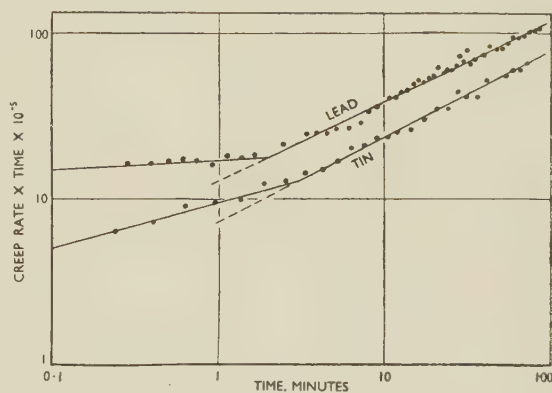


FIG. 13.—Very Short-Time Tests on Lead and Tin.

in the primary and secondary stages. The differences which do exist may well lie merely in the fact that in the former, marked inhomogeneities exist in the distribution of the strain in different crystals.

VI.—THE EFFECT OF STRESS

Although the object of this work was to examine the creep/time relationship under constant stress, a considerable amount of evidence concerning the effect of the stress has been obtained. For pure, soft metals it is by no means easy to obtain reproducible results, and no high degree of exactitude can be claimed, but a general picture does emerge.

From the general parallelism of the curves in Fig. 2, for instance, it will be at once apparent that the constant k is not greatly affected by stress, as Smith¹⁰ has already observed, though it would be unwise to say that it is unaffected. The constant a , on the other hand, changes considerably and consistently. For aluminium at 150°C ., the specimens all having received a uniform annealing treatment

of $\frac{3}{4}$ hr. at 420° C. in the machine before being tested, a relationship of the type:

$$\sigma \propto S^{\alpha},$$

is suggested.

This is in accord with the Nutting-Scott Blair¹¹ equation $\sigma = bS^{\alpha}t^k$, which has proved successful in describing the creep of many non-metallic materials.¹² The dimensional difficulties associated with this relationship have, incidentally, been overcome by Dingle.¹³ Graham's general equation¹⁴ reduces at constant temperature to a similar form, whilst the work of Carreker, quoted by Fisher and Hollomon,¹⁵ on steel is again in accord with the same formula.

Similar results, but based on fewer experimental data, are shown in Fig. 14 for copper, zinc, tin, and

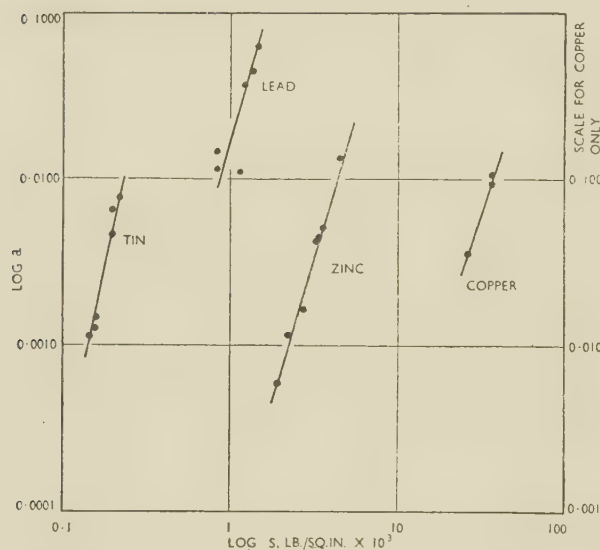


FIG. 14.—Log a /Log S Curves for Tin, Lead, Zinc, and Copper.

lead. An interesting feature of these results is the suggestion that the relationship of stress and a follows a very similar course in each of these metals.

VII.—DISCUSSION

This work has been concerned with “pure” metals under constant stress. If the authors’ belief that tertiary creep is an indication of internal failure or of necking is well-founded, this stage of the creep test must necessarily be excluded.

It has been shown that the results, except at quite short times, can be expressed with great accuracy by a straight line when the log of the creep extension is plotted against log time. From this there follows a creep/time relationship at constant stress of the form:

$$\sigma_c = at^k.$$

This result holds for metals which crystallize in face-centred cubic, hexagonal, and tetragonal lattices, and which have a wide variation in their inherent strengths, valencies, and recrystallization temperatures. It is further unaffected by temperature,

applied stress, or pre-strain, at all events over wide limits. It would, we suggest, be somewhat remarkable if this were the result of mere coincidence.

To obtain such a strictly linear relationship between log creep and log time, a value for the initial extension had to be somewhat arbitrarily chosen. The need for this disappears when creep rates are examined. From the equation $\sigma_c = at^k$, it will be seen that the logarithm of the creep rate should again give a straight-line plot against log time, and evidence has been provided that this is so. Further, if the product of the creep rate multiplied by time is plotted double logarithmically against the time, a third straight line should be obtained, which is itself parallel to the creep/time plot. Evidence has also been adduced to justify this requirement of the equation. Wherever it can be tested, the power-law equation has met the demands made upon it and met them with a degree of accuracy which is believed to be beyond the limits of mere chance.

The Andrade equation is a mathematical relationship of great flexibility. It is not surprising, therefore, that it can provide a fit—and in the majority of cases a good fit—with normal experimental data. When creep rates are used, however, and in particular the product of creep rate and time, this flexibility may be reduced. In these circumstances it has been shown that the fit based on the power law is definitely and consistently superior to that based on the Andrade relationship. The latter gives a curve when log creep rate \times time is plotted against log time; the experimental results fall on a straight line.

That the creep/time relationship is governed by an equation of a power-law type is far from novel. In what still remains the classical paper on creep testing from the point of view of engineering design, Bailey¹⁶ has reported data on the creep of steels which follow closely an equation of the type $\sigma = at^k$, so long as structural changes in the material are not taking place. Numerous other researches which support the same equation have been published by Soderberg,¹⁷ Crussard,¹⁸ and, for pure metals, by Sturm, Dumont, and Howell,⁵ Davis,¹⁹ Tyndall,²⁰ and Fisher and Hollomon.¹⁵ Tyndall incidentally worked with single crystals of zinc, and with the exception of a few which behaved in an irregular manner (which Cottrell in the discussion has ascribed to the presence of nitrogen) all his data were consistent with the power-law equation. Fisher and Hollomon,¹⁵ reporting unpublished work of Lubeck and Carreker, mentioned that this work showed that the value of the constant initial strain, σ_0 , under the conditions of the test, was greater by a factor of 10–15 than the mere elastic strain.

More recently, Graham¹⁴ has examined published data on several high-temperature alloys and on pure lead, and obtained good agreement with a more general equation, which reduces to the power law under the conditions of constant stress and temperature. Finally, it may be noted that Zener’s equation,

of similar form, $e = ct^{\frac{n}{n+m}}$, where c , n , and m are

constants, was derived on the basis of theoretical considerations.

It has been pointed out more than once that if β or k of the Andrade equation becomes zero, the equation may assume apparently different forms, and may even simulate the power-law relationship. Such arguments appear to us to be mere sophistry. Neither β nor k ever is zero. In the case of β this would involve no period of "primary" creep, which is contrary to the most convincing experimental evidence, whilst in the case of a zero k , creep would not occur at all once any initial extension had occurred.

Throughout this work the elongation of the specimen has been taken as a measure of the creep. In Fig. 15 is shown the curve obtained if results of a typical run

and where σ_0 is the initial extension, i.e. the sum of the elastic strain plus a much more considerable plastic component.

A not inconsiderable amount of work has been carried out on this primary stage of creep. The results so far as they go are again consistent with a power-law equation, $\sigma_p = at^k$. It is perhaps also significant that, although as yet very little research has been carried out on tertiary creep, it has been suggested by Graham¹⁴ that this again may be represented by the equation $\sigma = at^k$, where t is the time from the onset of the tertiary stage and σ is the creep from this time. If this be so, the whole creep curve, from beginning to end, may be governed by a single mechanism, as Zener²¹ has insisted.

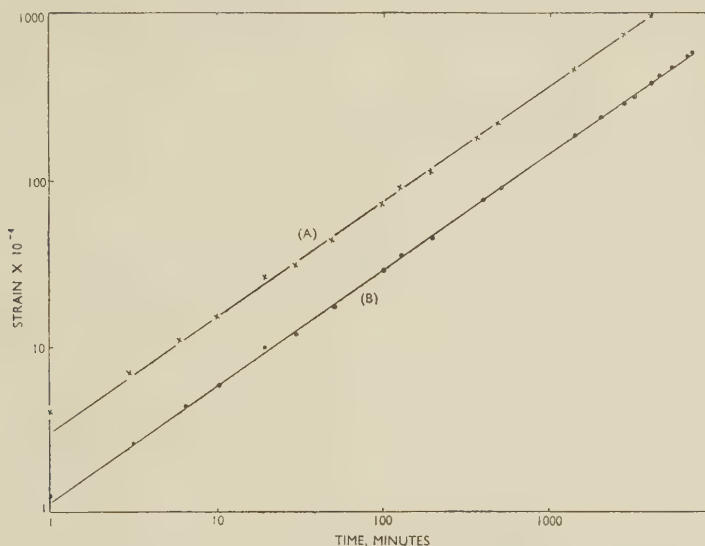


FIG. 15.—Comparison of Creep/Time Curves for Aluminium at 150° C.
(A) Increase of length/time. (B) Natural strains (to base 10)/time.

on aluminium at 150° C. are plotted as natural strains (but to base 10) and also as simple elongations. It is clear that both give the same results so far as the fundamental law is concerned.

After the initial extension, therefore, if it be so desired, the equation may be modified to :

$$l_t = l_0 \cdot \exp at^k.$$

The results of tests under different stresses have been shown to be consistent with an equation of the form : $\sigma = bS^\alpha$, which accords with other work, and which may be incorporated with the relationship $\sigma = at^k$ to give the more general equation :

$$\sigma = At^k S^\alpha.$$

Expressed in terms of natural strain, and to meet dimensional requirements, this may be modified to :

$$l_t = l_0 \exp C \left(\frac{t}{t_0} \right)^k \left(\frac{S}{S_0} \right)^\alpha + \sigma_0,$$

where, t_0 and S_0 are some standard time and stress,

We have purposely refrained from any discussion of the repercussions of our belief in the validity of the power-law equation on metallographic theory. At the moment the only real "known" is the mathematical expression for the creep process, and all else is to some extent speculative.

ACKNOWLEDGEMENTS

The authors express their thanks to The British Non-Ferrous Metals Research Association, The Aluminium Wire and Cable Co., Ltd., Charles Clifford and Sons, Ltd., Mellows and Co. Ltd., and The London Electric Wire Co. and Smith's, Ltd., who supplied the wires on which this work was carried out.

Our special thanks are due to Mr. E. R. W. Jones, M.A., for his help with the statistical analysis; Mr. A. H. Smith, M.Sc., who prepared the drawings; and to Mr. W. Ashelby, A.I.M., for help in many directions throughout the whole course of the research.

REFERENCES

1. R. H. Thurston, *Science*, 1883, **1**, 418.
2. H. M. Howe, *Trans. Amer. Inst. Min. Met. Eng.*, 1884, **13**, 646.
3. E. N. da C. Andrade, *Proc. Roy. Soc.*, 1910, [A], **84**, 1; 1914, [A], **90**, 329.
4. E. N. da C. Andrade and B. Chalmers, *ibid.*, 1932, [A], **138**, 348.
5. R. G. Sturm, C. Dumont, and F. M. Howell, *J. Appl. Mechanics*, 1936, **2**, A62.
6. R. W. Bailey and A. M. Roberts, *Proc. Inst. Mech. Eng.*, 1932, **122**, 209.
7. H. W. Gillett, *Trans. Amer. Inst. Min. Met. Eng.*, 1939, **135**, 15.
8. H. F. Moore, B. B. Betty, and C. W. Dollins, *Univ. Illinois Bull.*, 1935, **32**, (23) (*Eng. Exper. Sta. Bull.* No. 272).
9. A. H. Cottrell and V. Aytakin, *J. Inst. Metals*, 1950, **77**, 389.
10. G. V. Smith, "Properties of Metals at Elevated Temperatures", p. 111. 1950: New York and London (McGraw-Hill).
11. G. W. Scott Blair, "A Survey of General and Applied Rheology". 1949: London (Sir Isaac Pitman and Sons, Ltd.).
12. G. W. Scott Blair and P. Caffyn, *Phil. Mag.*, 1949, [vii], **40**, 80.
13. H. Dingle, *ibid.*, 1949, [vii], **40**, 94.
14. A. Graham, *Nat. Gas Turbine Estab. Rep. R.68*, 1950; see *Engineer*, 1952, **193**, (5011), 198; (5012), 234; and private communication.
15. J. C. Fisher and J. H. Hollomon, *Rep. Symposium on Plastic Deformation of Crystalline Solids, Pittsburgh, 1950*, 199.
16. R. W. Bailey, *Proc. Inst. Mech. Eng.*, 1935, **131**, 131.
17. C. R. Soderberg, *Trans. Amer. Soc. Mech. Eng.*, 1936, **58**, 733.
18. C. Crussard, *Rev. Mét.*, 1946, **43**, 307.
19. E. A. Davis, *J. Appl. Mechanics*, 1943, **10**, A101.
20. E. P. T. Tyndall, *Rep. Symposium on Plastic Deformation of Crystalline Solids, Pittsburgh, 1950*, 49.
21. C. Zener, "Elasticity and Anelasticity of Metals", p. 141, 1949: Chicago (Univ. of Chicago Press).

THE TEMPERATURE DEPENDENCE OF TRANSIENT AND SECONDARY CREEP OF AN ALUMINIUM ALLOY TO BRITISH STANDARD 2L42 AT TEMPERATURES BETWEEN 20° AND 250° C. AND AT CONSTANT STRESS *

1421

By A. E. JOHNSON,† D.Sc., M.Sc.Tech., M.I.Mech.E., MEMBER,
and N. E. FROST,† B.Sc., A.M.I.Mech.E.

(Communication from the Mechanical Engineering Research Laboratory.)

SYNOPSIS

The effects of temperature on the various phases (transient and steady-state creep) of forward creep and on creep recovery have been investigated for an aluminium alloy to British Standard 2L42 (R.R.59), by means of creep tests in pure torsion on thin-walled tubular specimens at a constant stress of 2 tons/in.², and at 50° C. intervals over the range 20°–250° C. The tests were of moderately long duration.

It is concluded that for this alloy no current fundamental theory adequately describes the transient creep between 20° and 250° C., although up to 200° C. the secondary creep rates agree quite well with theories based on the Eyring process rate conception. Superposition theories do not represent the recoverable creep measured. The total forward creep is well represented at all temperatures by an equation :

$$\gamma = K_1 t^{1/m_1} + K_2 t^{1/m_2}$$

where K_1 and $1/m_1$ refer to the non-recoverable portion of the forward creep strain, and K_2 and $1/m_2$ refer to the recoverable portion of the creep. K_1 , K_2 , and $1/m_1$ vary with temperature; $1/m_2$ is effectively constant.

I.—INTRODUCTION

IN the course of a programme of combined-stress creep, plastic strain, and relaxation tests which is being carried out, using a selected 0.17% C steel, 2L42 aluminium alloy, a magnesium alloy, and copper, it is intended to examine the effects of temperature on the various phases (transient and steady-state creep) of forward creep and on creep recovery. To this end tests in pure torsion on thin-walled tubular specimens are to be made at a constant chosen stress for each material, and at relatively close intervals of temperature over the working temperature range for the material in question.

It has been found convenient to begin work on the aluminium alloy, and the present paper gives an analysis of the results of moderately long tests at a stress of 2 tons/in.² and at 50° C. intervals over the range 20°–250° C.

An appreciable amount of theory has been formulated on transient creep, steady-state creep, and recoverable creep. Theories have been advanced by Mott and Nabarro,¹ Orowan,² and C. L. Smith³ in the

case of transient creep; and by Kauzman,⁴ Nowick and Machlin,⁵ and Feltham⁶ in the case of steady-state or secondary creep. These steady-state theories all derive from the work of Eyring⁷ on chemical process rate theory. In addition, a considerable number of semi- or wholly-empirical equations have been put forward linking creep strain or rate, time, stress, and temperature, notable among them the Andrade equation.⁸

With regard to creep recovery, two views have been taken of this (anelastic) phenomenon in the past. Firstly, the superposition or memory theory of Boltzman,⁹ with its modifications by Bennewitz¹⁰ and Becker,¹¹ has been applied; and secondly the anelastic recovery and recovery rate have been connected with the applied stress and stress rate in varieties of more or less complex equations, two examples of which are :

$$(i) \quad a_1 \sigma + a_2 D\sigma + a_3 D^2 \sigma + \&c. = b_1 \gamma + b_2 D\gamma + b_3 D^2 \gamma + \&c.$$

where a_1 , a_2 , . . . &c., b_1 , b_2 , . . . &c., are constants, the D 's are progressive differentials (with

* Manuscript received 20 February 1952.

† Mechanical Engineering Research Laboratory (D.S.I.R.),

East Kilbride, Scotland; formerly Engineering Division, National Physical Laboratory, Teddington, Middlesex.

respect to time), and σ and γ are stress and recovery strain, respectively, and

$$(ii) a_1(F_1\sigma) + a_2D(F_2\sigma) + a_3D^2(F_3\sigma) + \&c. = b_1(f_1\gamma) + b_2D(f_2\gamma) + b_3D^2(f_3\gamma) + \&c.$$

where a , b , and D have the same significance as before, and $F_1, F_2, \&c.$, and $f_1, f_2, \&c.$, denote various functions of σ and γ respectively.

Actually, where these equations have been applied, considerably simplified versions have been used.

Finally, possibly some mention should be made of the so-called "phenomenological" theories of Hollomon and Lubahn¹² and others. These theories postulate the existence of a virtual equation of state for metals, i.e. a relation between the variables of strain, strain rate (or time), stress, stress rate, and temperature, from which the behaviour of the material in any variety of test, e.g. creep, relaxation, constant stress rate, constant strain rate, $\&c.$, may be estimated. There are a number of arguments against the existence of such an equation, and Orowan and other workers have shown what appears to be evidence against such an equation by establishing that in tests in which all variables but one are retained constant, the value of the remaining variable depends on the precise experimental procedure followed in reaching the value.

A further argument against the likelihood of a reasonably simple equation of state existing is the fact that most experimental evidence indicates that processes like creep, plastic strain, and relaxation are complex affairs, being compounds of several coexisting mechanisms and, therefore, not easily represented by mathematical equations that are readily moulded into a simple equation of state.

However, quite recently attempts have been made to extend the universality of equations of state by the use, for example, of the Boltzman⁹ superposition theory and incremental- rather than total-strain equations. It may be that such devices will extend the range of validity of these equations to a point where they are of real practical use in forecasting the results of any given experiment. In the present paper such experimental facts as may indicate the possibility of the existence of equations of this type will be noted, but this will not be taken necessarily to indicate the authors' belief in their existence.

II.—EXPERIMENTAL WORK

1. MATERIAL

The material was an aluminium alloy to British Standard Specification 2L42.* Two continuously cast billets, 18 in. long and 12 in. in dia., were used and given the following heat-treatment: heated to $525^\circ \pm 5^\circ$ C. for 8 hr., quenched in boiling water, allowed to remain for 24 hr. at room temperature, then heated to 170° C. for 16 hr., and finally air cooled.

* Specification limits: Cu 1.5-3.0, Ni 0.5-1.5, Mg 1.2-1.8, Fe 1.0-1.5, Ti >0.2 , Si $>1.3\%$, Al remainder. Known commercially as R.R.59 alloy.

2. RANGE OF EXPERIMENTS

All the torsion creep tests were conducted in the N.P.L.-type combined-stress creep units, using a thin-walled test-piece of internal dia. 0.5 in., and wall thickness 0.03 in. and with a gauge-length of 2 in. The stress in all cases was 2 tons/in.², and in loading all tests particular care was taken to avoid inertia effects in applying loads to torsion scale pans. The choice of this stress enabled tests of appreciable period (400-2000 hr.), and including the phases of transient and secondary creep, to be conducted at 20° , 50° , 100° , 150° , 200° , and 250° C. A further test was made at 300° C., but as this was virtually at the point of fracture after less than 3 hr., the nature of the creep was probably what is normally regarded as tertiary creep and was almost certainly of a different mechanism from that prevailing at 250° C. and below. Other tests outside the scope of the present paper have in-

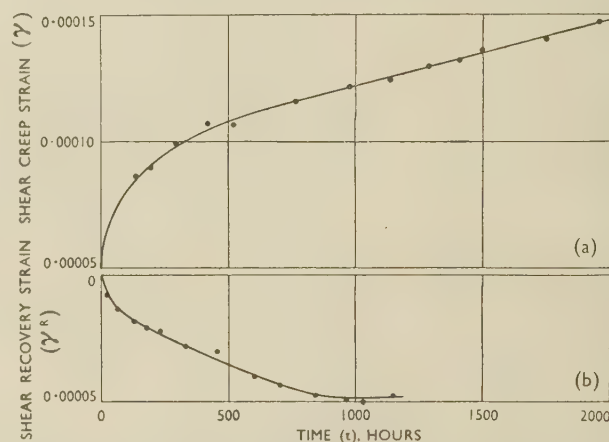


FIG. 1.—Creep and Recovery Curves at 100° C. and 2 Tons/in.² Stress.

indicated the high probability that the alloy is metallurgically unstable above 250° C. Accordingly, the test at 300° C. is not included in the data presented and analysed, although an occasional reference to it is made in the text.

Unloading of the test-pieces was carried out at a time when several of them, although perhaps not having reached their final constant rate, were little short of that rate, while in some cases the constant rate had actually been reached.

The recovery in all cases had, therefore, at the end of these tests reached an effectively maximum value (judging from previous work at the National Physical Laboratory) and the recovery curves were, therefore, strictly comparable.† The recovery tests were carried to effective completion in all cases. In the test at 20° C., the forward creep and recovery tests were precise replicas of each other.

† Some amplifying remarks are made later concerning this matter (see p. 102).

3. RESULTS

The numerical results of the creep tests are given in Table I and typical forward creep and recovery curves

are shown in Fig. 1. The remaining figures and tables relate to the analysis of the results given in the above table.

TABLE I.—*Magnitude of Creep and Creep Recovery in Tests at 2 tons/in.² Stress.*

Time, hr.	Creep Strain	Creep Recovery Strain Exclud- ing Initial Elastic Strain	Creep Strain — Recovery Strain	Creep Rate/hr. × 10 ⁻⁶
(a) 20° C. (Initial plastic strain = 0).				
10	0.0000067	Recovery curve at this temperature identical with forward creep curve.	0	0.23 ₅
20	0.0000084		0	0.13
50	0.0000108		0	0.03 ₅
100	0.0000117		0	0.01
150	0.0000121		0	0.007
200	0.0000123		0	0.003
300	0.0000125		0	0.002
400	0.0000127		0	0.002
(b) 50° C. (Initial plastic strain = 0).				
10	0.000049	0.000006 ₅	0.000042 ₅	0.49
50	0.000060	0.000012	0.000048	0.15 ₅
100	0.000065	0.000016	0.000049	0.075
200	0.000070	0.000018 ₅	0.000051 ₅	0.031
500	0.000072 ₅	0.000018 ₅	0.000054	0.005
600	0.000073	0.000018 ₅	0.000054	0.005
(c) 100° C. (Initial plastic strain = 0).				
10	0.00006	0.000007	0.000053	1.09
20	0.000066	0.000009	0.000057	0.94
50	0.000072	0.000012	0.000060	0.56
100	0.000080	0.000016	0.000064	0.31 ₅
200	0.000090 ₅	0.000021	0.000069 ₅	0.12
500	0.000108	0.000035	0.000073	0.034
1000	0.000122	0.000048 ₅	0.000073 ₅	0.027
1500	0.000135	0.000048 ₅	0.000086 ₅	0.027
2000	0.000148	0.000048 ₅	0.000100 ₅	0.027
(d) 150° C. (Initial plastic strain = 0.000052).				
10	0.000064	0.000011	0.000053	1.16
20	0.000072	0.000018	0.000054	0.72
50	0.000087	0.000026	0.000061	0.34
100	0.000102	0.000033	0.000069	0.21 ₅
150	0.000111	0.000037	0.000074	0.16 ₅
200	0.000118	0.000040	0.000078	0.10 ₅
500	0.000133	0.000043	0.000090	0.036
750	0.000141	0.000043	0.000098	0.032
1000	0.000149	0.000043	0.000106	0.032
1300	0.000158	0.000043	0.000115	0.032
(e) 200° C. (Initial plastic strain = 0.000073).				
10	0.000062	0.00004	0.000022	5.0
50	0.000136	0.000063	0.000072	1.47
100	0.000200	0.000072	0.000128	1.20
200	0.000292	0.000086	0.000206	0.62
500	0.000405	0.00010	0.000305	0.26
750	0.000465	0.00010	0.000365	0.22
1000	0.000518	0.00010	0.000418	0.20
1500	0.000606	0.00010	0.000506	0.14
2000	0.000666	0.00010	0.000566	0.09
2300	0.000688	0.00010	0.000588	0.06 ₅
(f) 250° C. (Initial plastic strain = 0).				
10	0.000195	0.00009	0.000105	5.03
20	0.000238	0.000103	0.000135	3.29
40	0.000281	0.000120	0.000161	1.75
60	0.000315	0.000131	0.000184	1.53
100	0.000377	0.000143	0.000234	1.53
150	0.000452	0.000156	0.000296	1.53
200	0.000528	0.000165	0.000363	1.53
250	0.000606	0.000172	0.000434	1.53
500	0.000988	0.000175	0.000813	1.53
750	0.001373	0.000175	0.001198	1.53

III.—DISCUSSION OF RESULTS

1. TRANSIENT CREEP AT A TORSION STRESS OF 2 TONS/IN.²

Under this heading, the application of the theories of Mott and Nabarro,¹ Orowan,² and C. L. Smith³ to the transient creep (i.e. total forward creep less secondary creep or less the product of secondary creep rate and time measured in the tests) is considered for the set of torsion tests at 2 tons/in.². A short account is first given of the bases of each theory.

(a) *The Mott and Nabarro Theory*¹

This theory is based on the idea of the gradual exhaustion of a supply of dislocations already present in a metal crystal at the beginning of a test. It is in fact designed to be more applicable to a particular type of material (a "hard" alloy under small stresses), than to the general run of materials, and was not, therefore, *a priori* expected to give any general description of the results for the present, fairly normal, material.

A fundamental assumption is that in any real metal crystal a large number of dislocations are present in the lattice, and that the movement of these under the action of applied stresses, constitutes plastic deformation. The motion of any dislocation or loop of a dislocation is impeded by a complex system of internal stresses arising from impurity atoms, precipitates, other dislocations, grain, and mosaic boundaries, &c. It is supposed that any one dislocation loop moves only when the force on it, due to externally applied stress, becomes greater than that due to the system of internal stresses, each loop accordingly having a stress σ which just gives rise to motion. The system of internal stresses may thus be characterized by a distribution function $N(\sigma)$, such that $N(\sigma)d\sigma$ specifies the number of dislocations/unit vol. which can only just be set in motion by an applied stress between σ and $(\sigma + d\sigma)$. The application of a certain stress, σ_0 , causes the immediate movement of all dislocations of characteristic stresses $\sigma \leq \sigma_0$. This immediate movement constitutes instantaneous plastic deformation. Dislocations which require an applied stress somewhat larger than σ_0 may move in the course of time with the aid of thermal-energy fluctuations, this constituting transient creep. Mott and Nabarro give the following expression for the activation energy of motion of a loop of a dislocation of length $\frac{1}{2}\lambda$:

$$U_{(c)} = 0.15 \sigma a \lambda^2 (1 - \sigma_0/\sigma)^{3/2} \quad (1)$$

where a is the lattice parameter, σ_0 the applied stress, and σ the stress under which the loop would just move immediately. Dislocations in the lattice will vibrate

about their equilibrium positions with frequency, ν , which is estimated theoretically to be of the order of 10^8 or 10^9 /sec. The chance, αdt , that the dislocation loop moves forward in time dt is given by:

$$\alpha = \nu \exp [-U(\sigma)/kT] \quad (2)$$

From (1) and (2)

$$\alpha = \nu \exp \left[-\frac{B}{kT} \left(1 - \frac{\sigma_0}{\sigma} \right)^{3/2} \right] \quad (3)$$

where $B = 0.15\sigma a\lambda^2$.

The chances of a dislocation moving backwards are taken as negligible. It is assumed that a dislocation moving forward in this manner acquires a new value of U which is large enough to prohibit further motion.

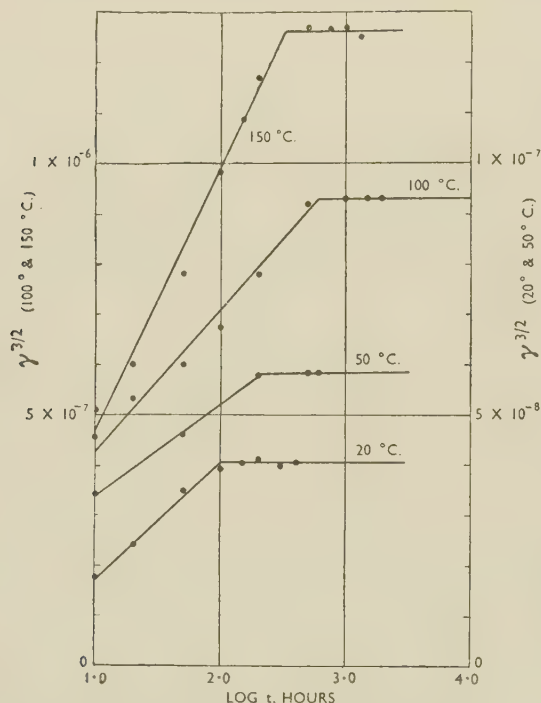


FIG. 2.—Application of Mott and Nabarro's Theory to Transient Creep in the Range 20°–150° C.

Plotted transient creep = Total creep – Secondary creep.

The number of movable dislocations in the stress range σ to $(\sigma + d\sigma)$ will decay according to the law $N(\sigma, t) = N(\sigma, 0) e^{-\alpha t}$. This gives the distribution function at any instant t . The function $e^{-\alpha t}$ probably changes from a very small value to unity over a short range of σ , and may without serious error be replaced by a sudden step which advances along the axis of σ at a rate given by setting $\alpha = 1/t$ in (3). If the step advances to stress σ_1 in time t , we obtain:

$$\left(\frac{kT \log \nu t}{B} \right)^{2/3} = \frac{\sigma_1 - \sigma_0}{\sigma_1} \approx \frac{\sigma_1 - \sigma_0}{\sigma_0}$$

The creep strain is the product of the number of dislocations moved and the average strain given rise to by each movement. If this average strain be v/V

where V is the volume of the crystal, and v is the virtual volume associated with this group of dislocations, then the total creep strain is:

$$\gamma = v \int_{\sigma_0}^{\sigma_1} N(\sigma, 0) d\sigma$$

If, over the limited range of σ concerned, the original distribution function $N(\sigma, 0)$ be taken as independent of σ , and equal to N_0 , then:

$$\gamma = v N_0 (\sigma_1 - \sigma_0) = v N_0 \sigma_0 \left(\frac{kT \log \nu t}{B} \right)^{2/3}$$

or re-arranging: $\gamma^{3/2} = [v N_0 \sigma_0]^{3/2} \left[\frac{k}{B} \right] T \log \nu t$

$$= [v N_0 \sigma_0]^{3/2} \frac{kT}{B} [\log \nu + \log t]$$

$$= A [\log \nu + \log t], \text{ say.}$$

With greater generality, a corresponding expression:

$$\gamma^c = [v N_0 \sigma_0]^c \frac{k}{B} [\log \nu + \log t] T$$

may be written.

If $\gamma^{3/2}$ be plotted against $\log t$ for each temperature, values of $A/T = [v N_0 \sigma_0]^{3/2} k/B$, and of the frequency ν may be obtained. If the theory is applied simply, these sets of values should be equal, and ν should approach the theoretical value of 10^8 or 10^9 /sec. In Fig. 2, $\gamma^{3/2}$ is plotted against $\log t$ for temperatures

TABLE II.—Creep Tests at 20°–250° C. and 2 tons/in.² Stress.

Application of equations of type $\gamma = v N_0 \sigma_0 \left(\frac{kT \log \nu t}{B} \right)^{2/3}$ in the Mott and Nabarro Theory.

Temp., °C.	In the Relation $\gamma = v N_0 \sigma_0 \left(\frac{kT \log \nu t}{B} \right)^{2/3}$		Best Value of c in Possible Generalized Relationship $\gamma^c = [v N_0 \sigma_0]^c \frac{kT}{B} [\log \nu + \log t]^*$
	Value of Constant A/T where $A/T = [v N_0 \sigma_0]^{3/2} \frac{k}{B}$	Value of Frequency, ν /hr.	
20	7.9×10^{-11}	0.57	1.47
50	5.6×10^{-10}	7.8	2.25
100	7.5×10^{-10}	3.4	2.1
150	1.22×10^{-9}	0.81	1.47
200	1.37×10^{-8}	0.03	0.52
250	2.26×10^{-9}	14.1	3

In the above relations the following definitions hold: v = volumetric change of crystals, N_0 = distribution function, σ_0 = stress, T = absolute temp., ν = frequency, t = time, B = constant.

* Obtained from plots of $\log \gamma$ against $\log \log t$.

20°, 50°, 100°, and 150° C.; similar plots were made for 200° and 250° C. It will be noted that a reasonably linear relation is obtained in each case. However, the values A/T and ν are shown in Table II, and it is seen that both sets of values vary considerably over the range of temperature chosen and that the average value of ν is 3.9/hr., which is very remote

from 10^8 or 10^9 /sec. Thus the Mott and Nabarro theory in its simple form does not appear to have any application to the present results. To see whether a better fit could be obtained with the generalized equation, plots were made of $\log \gamma$ against $\log \log t$, and the slope measured to give the value of the exponent of γ , in the generalized equation, which gave the most nearly linear plot of γ^n against $\log t$. The values are given in the last column of Table II. It will be seen that reasonably consistent values arise only at 20°, 50°, 100°, and 150° C., and that the average of these is not greatly different from 1.5, being 1.83. Above 150° C. the values change rapidly. Plotting $\gamma^{1.83}$ against $\log t$ does not, however, produce any significant change in the nature and the order of the values of A/T and ν . Evidently, therefore, the application of the Mott and Nabarro theory to the results is not appreciably improved by generalization.

(b) The Orowan Theory²

The Orowan theory of transient creep, like the older Becker¹¹ theory, is based on the idea that creep is due to thermal stress fluctuations. Orowan considered that the basic law of plastic deformations is expressed by the stress/strain relationship. As ordinarily observed the stress/strain curve, which requires some appreciable time for its determination, includes in the measured strain a proportion of transient creep strain. An ideal stress/strain curve can be described, however, in which loading is so rapid that thermal movement makes no contribution to the strain. If the final applied stress is maintained, creep occurs, since thermal agitation causes local increases of stress and, therefore, some strain. After an element of creep strain, hardening will have increased the yield stress beyond the value of the constant applied stress, and for further creep this increment of yield stress $\Delta\sigma$ must be provided by thermal agitation. The energy of activation involved is $(\Delta\sigma)^2 V / 2G$, where G is the shear modulus and V a volume. The frequency of a stress fluctuation of sufficient magnitude arising is

$$F = \text{constant} \times \exp [-(\Delta\sigma)^2 V / 2GkT].$$

Now $\Delta\sigma$ is not of constant value. When the load has just been applied, there will be a range of activation energies from zero upwards. The points of low activation energy are first used up. $\Delta\sigma$ subsequently varies by virtue of the fact that strain-hardening in creep is dependent on the rate of straining.

In order to establish the equation of transient creep, consideration must be given to the amount of glide which will result from a single successful thermal stress fluctuation. It is likely that a chain of glide processes arising from a single successful stress fluctuation is long at the beginning of transient creep, but decreases as the strain increases, and that as extension proceeds the effect of a glide process initiated by a single thermal stress fluctuation will be less considerable, as there will be fewer regions of low activation energy.

Orowan suggested that the effect of a single success-

ful thermal stress fluctuation will be dependent in some way on the total creep strain γ . The most simple assumption is that the effect is proportional to $1/\gamma$ or to $1/\gamma^2$. The creep rate is the product of the contribution to strain γ , and the number of successful fluctuations in unit time.

If λ is the slope of the stress/strain curve at a point corresponding to the applied stress, so that $\Delta\sigma = \lambda\gamma$, and if $B = V/2Gk$, we have:

$$\frac{d\gamma}{dt} = \frac{A}{\lambda\gamma} \exp(-B\lambda^2\gamma^2/T)$$

$$\text{or} \quad \frac{d\gamma}{dt} = \frac{A}{\lambda^2\gamma^2} \exp(-B\lambda^2\gamma^2/T),$$

according as the proportionality to $1/\gamma$ or $1/\gamma^2$ is assumed. It must, however, be remarked here that it is difficult to see that this formula is rigidly correct for

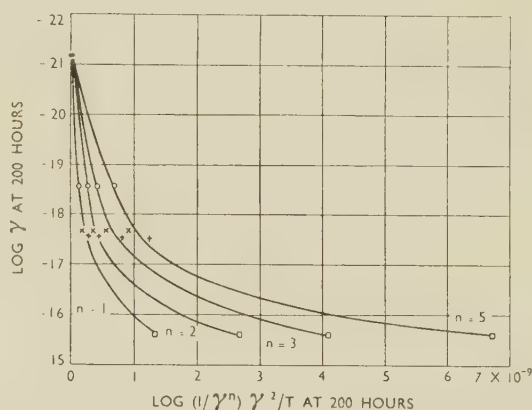


Fig. 3.—Application of Orowan's Theory to Transient Creep in the Range 20°–250° C. At 250° C. transient creep continued only for a few hours.

Plotted transient creep = Total creep — Secondary creep.

KEY.
● 20° C. × 100° C. □ 200° C.
○ 50° C. + 150° C.

a series of tests at various temperatures. If, for example, as in the present tests, the same initial stress is applied, it is very hard to believe that for an element of creep strain γ at all temperatures strain-hardening raises the yield by the same increment $\Delta\sigma$, thus giving the same value of λ for all temperatures as is implied in the formula. However, in the interests of examining the application of the formula, it has been assumed that λ is constant. Now Orowan has assumed proportionality of the effect of a successful fluctuation to γ or γ^2 , but to generalize proportionality to further powers of γ might be tentatively assumed. Thus in Fig. 3 plots of γ against $[\log (1/\gamma^n)]\gamma^2/T$ are made for values of $n = 1, 2, 3$, and 5. The result is evidently a family of somewhat similar curves which are certainly not linear. Accordingly, it appears that the present set of results cannot be represented by the Orowan equations as at present set forth, though it is understood that he contemplates some modification in the near future.

(c) The Smith Theory³

C. L. Smith has proposed a theory to eliminate the empirical terms from Orowan's formula. He assumes that after the instantaneous elongation there exists in the specimen a large number of spots of stress concentration where the local stress exceeds the mean applied stress, but is lower than the local yield stress. Each such spot would have a characteristic activation energy, E , such that thermal agitation might cause an increase in stress to the yield stress locally, and thereby initiate glide. The value of E will depend on the local conditions, and the number of spots with activa-

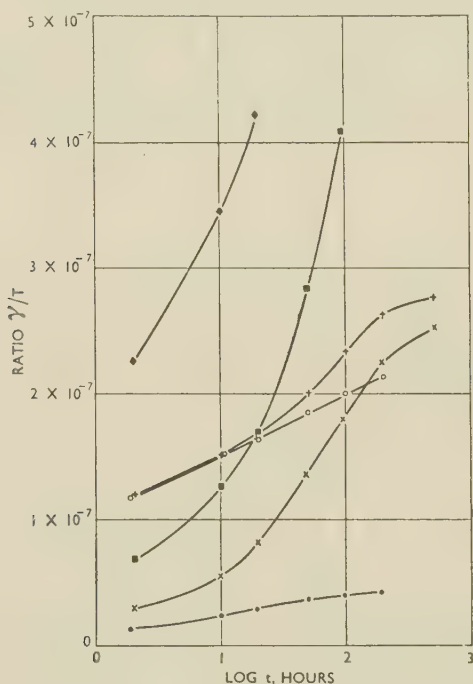
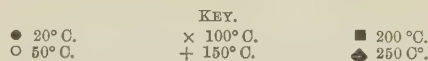


Fig. 4.—Application of Smith's Theory to Transient Creep in the Range 20°–250° C.

Plotted transient creep = Total creep — Secondary creep.



tion energies between E and $(E + dE)$ will be some function $f(E)dE$.

Some of these spots will be lost by glide, so that the distribution function changes with time. At time t the number dN lost by thermal agitation in the next short interval of time dt will be :

$$dN = -\text{constant} \times [f(E, t)dE] \exp\left(\frac{-E/kT}{dt}\right),$$

k being Boltzman's constant and T the absolute temperature.

Neglecting the possible formation of new spots in the range E to $E + dE$, the solution of this equation has the form :

$$f(E, t) = f(E, 0)e^{-\lambda t} \text{ where } \lambda = Ce^{-E/kT}$$

Taking the average amount of glide resulting from the activation of a single spot as a , then the glide in time

dt from spots with activation energies between E and $E + dE$ will be :

$$aC[f(E, 0)e^{-\lambda t}]e^{-E/kT}dEdt$$

and by integrating for all values of E the creep rate $\frac{d\gamma}{dt}$ will be given by :

$$\frac{d\gamma}{dt} = aC \int_0^{\infty} [f(E, 0)e^{-\lambda t}]e^{-E/kT}dE.$$

The form of $f(E, 0)$ is not known, but integration of the expression can be effected by taking $f(E, 0) = p = \text{a constant}$, so that the number of spots in equal energy intervals dE is the same for all values of E . Making this assumption, the rate of glide at time t is given by the expression :

$$\frac{d\gamma}{dt} = apkT \left(\frac{1 - e^{-\lambda t}}{t} \right).$$

If λt approaches >1 this approximates to $\gamma = \text{constant } T \log t$.

Thus a plot of γ/T against $\log t$ will indicate the applicability of this relation. Further generalization of the relation does not appear possible without any information as to the nature of $f(E, 0)$.

In Fig. 4 the above critical plot is made. It will be noted that there is some bunching together of the curves for 50°, 100°, 150°, and 200° C. over the range 0–100 hr., suggesting that in this range the relation may not be too wide of the mark; but the curves for 20° and 250° C. are sufficiently remote from the remainder to discountenance any possibility of general applicability.

It is evident, therefore, that the transient creep theories so far advanced do not adequately describe the creep of the aluminium alloy under investigation.

In Section III consideration of the composite (transient and steady-state) Andrade empirical equation is made, and an independent analysis of the experimental creep curves carried out.

2. STEADY-STATE OR SECONDARY CREEP AT A TORSION STRESS OF 2 TONS/IN.²

Under this heading the application of the theories of Kauzman,⁴ Nowick and Machlin,⁵ and Feltham⁶ to the secondary creep rates measured in the current set of tests at 2 tons/in.² in torsion is considered. As in the case of the transient-creep theories, some account is given of the bases of the theories.

(a) The Kauzman Theory⁴

There has been considerable speculation as to the source of quasi-viscous or steady-state creep flow, and it has been suggested that such flow is most likely to occur at points in the metal where the atomic arrangement lacks the regularity of the metallic lattice. Regions which approximate to an amorphous condition may be found in a polycrystalline metal at the grain boundaries. The grain boundaries may be considered as a region only a few atoms thick in which

the lattice undergoes a transition from the orientation of one crystal to that of its neighbour. However, no theory based on glide due to defects in amorphous regions of the metal structure has succeeded in predicting other than a linearly viscous type of flow, whereas experiment has shown that steady-state creep is, in general, not linearly dependent upon stress. There has accordingly been considerable speculation as to whether steady-state creep does not in some degree involve the motion of dislocations. Nowick and Machlin, and lately Feltham, have attempted to apply to the dislocation theory of steady-state creep the theory of rate processes which Eyring applied with success in physical chemistry,⁷ while Kauzman has followed Eyring directly in applying the process to units of flow.

Kauzman considered the total shear to be composed of a number of shear processes. A unit shear process arises when one unit of flow moves past another. If λ is the average distance moved in the direction of shear by the unit of flow and L is the average distance between layers of units of flow, the shear rate is $S = \lambda\nu/L$, where ν is the number of jumps of the kind occurring per sec.

From the activation energy, Q , the term ν can be calculated, and is given by the expression :

$$\nu = kT/h \exp (\Delta S/R) \exp (-Q/RT),$$

where k , T , and R have their usual meaning and ΔS is the increase in entropy in the process; h is Planck's constant.

In the absence of an applied stress, the jumps in one direction will be equal to those in the opposite direction and the net shear will be zero. In the presence of an applied shear stress, Kauzman takes the activation energy to be decreased in the positive direction by an amount $\tau Al/\text{mol.}$, where A is the area of the unit of flow projected in the plane of shear, l the distance moved in carrying the unit of flow from the normal to the activated state, and τ is the shear stress. There is a corresponding increase in the activation energy in the negative direction, so that the effective value of ν contributing to shear in the direction of the applied stress is the difference in the two values corresponding to the two values of the activation energy.

To estimate the shear, therefore, ν may be written :

$$\nu = 2kT/h \exp (\Delta S/R) \exp (-Q/RT) \sinh (Al\tau/kT)$$

and the rate of shear becomes :

$$\left(\frac{2\lambda}{L}\right) \left(\frac{kT}{h}\right) \exp (\Delta S/R) \exp (-Q/RT) \sinh (Al\tau/kT).$$

Where $Al\tau > kT$, as it probably is in metals, and if σ is the microscopic shear stress corresponding to the sum of the effects of the individual units of flow the equation for $\dot{\gamma}$, the microscopic shear rate becomes :

$$\dot{\gamma} = DTe^{-\Delta/T} e^{B\sigma/T}$$

or $\log_e \dot{\gamma} = C + \log_e T - A/T + B\sigma/T.$

(b) *The Nowick and Machlin Theory*⁵

The theory developed by Nowick and Machlin takes into account the work-hardening of the lattice which has already occurred before the steady-state stage of creep.

The internal stress fields resulting from such hardening reduce the effective shear stress and also reduce the rate of generation of dislocations. The expression these workers derive from the generation of positive and negative dislocations is

$$R_g = \frac{2kT}{h} \exp \left[\frac{-(vGx^2f^2 + P'\tau)}{kT} \right] \sinh \left[\frac{2qvxf(\tau_e - \tau_b)}{kT} \right]$$

in which v is the volume associated with one atom, G is the modulus of rigidity at temperature T , x is the ratio of atomic distance in the slip direction to the interplanar spacing, f is a numerical factor approximately $= \frac{1}{2}$, P' is a factor dependent on the probability of atomic oscillation in the slip direction, q is a stress-concentration factor due to the intensification of local stress round a dislocation, τ_e is the externally applied shear stress, and τ_b a back stress due to work-hardening. If the generation and movement of each dislocation is accompanied by a strain of dl/L , where dl is the spacing between atoms in the slip direction and L is the dimension of the block within which slip occurs, the creep rate is given by :

$$\dot{\gamma} = R_g \frac{dl}{L} = 2 \frac{dl}{L} \frac{kT}{h} \exp \left[\frac{-(vGx^2f^2 + P'\tau)}{kT} \right] \sinh \left[\frac{qvxf(\sigma - 2T_b)}{kT} \right].$$

If σ is reasonably large, this can be arranged to give :

$$\log_e \dot{\gamma} = C + \log_e T - A/T + B\sigma/T,$$

which is really the same form as that derived by Kauzman.

(c) *The Feltham Theory*⁶

Feltham has lately carried out creep tests on a 0.06% C steel over the range 950°–1400°C., the results of which he found to be in very good agreement with an equation :

$$\dot{\gamma} = ATe^{(-H/kT)} \sinh (q\sigma/kT)$$

where σ is the applied tensile stress, T the absolute temperature, q a constant which can be regarded as the product of a dimensionless stress-concentration factor, and a constant having the dimensions of a volume. The parameter A , which also embodies the entropy of activation of the process by which dislocations are assumed to be generated, would be dependent upon the specific mode of slip that is operative. It has been regarded as constant, particularly as any variations in its magnitude at the temperature considered would largely be concealed even by small errors in the exponential term of the above equation.

The application of these three theories to the present test results is illustrated in Figs. 5 and 6.

In addition to the tests at 2 tons/in.² at various

temperatures which have been the basis of the present work, a group of further torsion test results at 150° C. and various stresses was available. In Fig. 5 a plot of the stress σ against the creep rate U is made for these results. If the Kauzman or Nowick and Machlin type of theory holds for the aluminium alloy, a linear plot of an equation of the type $\log_e U = A + B\sigma$ would occur. The figure illustrates that this is quite clearly the case. Using the value of the absolute temperature $T = 423$, the equation can be transposed to:

$$\log_e U/T = -25.35 + 2.44\sigma/T,$$

and the numerical constants in this equation will indicate the order of the constants in the Kauzman and Nowick and Machlin equations, and also in a more indirect manner those in the Feltham equation.

In Fig. 6 the plot is made for the experimental results of $\log_e U/T$ against $-1/T$, and it is seen that with the exception of the point corresponding to 250° C., the points lie well about a straight line. This straight line corresponds to the form of the equations of Kauzman, and of Nowick and Machlin:

$$U = e^C T e^{-A/T} e^{B\sigma/T},$$

whence $C = 17.45$, $A = 3160$, and $B = 2.44$.

It has previously been emphasized that in several cases the rates measured are probably somewhat above the true secondary values, and this may account for some scatter about the mean line shown. However, in general, it appears that up to 200° C., the equations

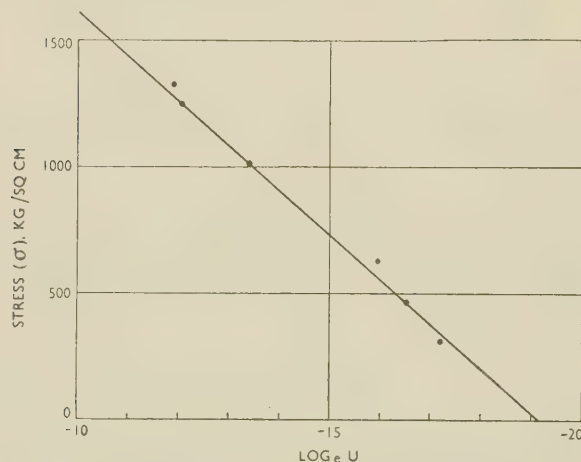


FIG. 5.—Application of Various Theories to Secondary Creep in the Range 20°–250° C. Relation between creep rate and stress at 150° C.

$$\begin{aligned}\log_e U &= -19.2 + 0.00577\sigma. \\ \log_e (U/T) &= -25.35 + 0.00577\sigma. \\ &= -25.35 + 2.44\sigma/T.\end{aligned}$$

of Kauzman and of Nowick and Machlin represent the steady-state creep of the aluminium alloy quite well.

The points corresponding to Feltham's equation are also plotted in Fig. 6:

$$U = A'T \exp(-B'/kT) \sinh(C'q'/kT)\sigma,$$

where $A' = 6.6 \times 10^{-8}$, $B'/k = 3160$, and $C'q'/k = 2.44$.

The points are quite close to the mean linear curve, but some indication is given that the order of fit might be less satisfactory outside the range shown. It appears, therefore, that the Feltham equation does not represent the results quite so well as the other two.

With regard to the divergence of the point corresponding to the test at 250° C. from the mean line, it

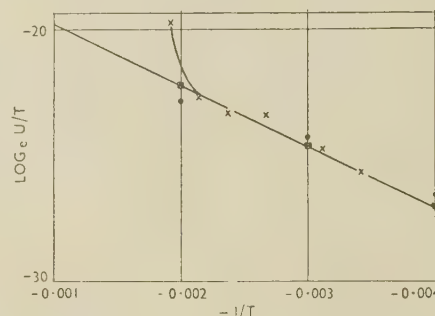


FIG. 6.—Application of Various Theories to Secondary Creep in the Range 20°–250° C.

KEY.

- × Experimental points for 2 tons/in.² stress.
- Points corresponding to reduced Nowick and Machlin theory, and also to Kauzman theory of equation $U = e^C T e^{-A/T} e^{B\sigma/T}$, where $C = -17.45$, $A = 3160$, and $B = 2.44$.
- Points corresponding to Feltham's equation $U = A' T e^{-B'/kT} \sinh(C'q'/kT)\sigma$ where $A' = 6.6 \times 10^{-8}$, $B'/k = 3160$, and $C'q'/k = 2.44$.

appears possible that this temperature represents the beginning of a range of creep in which the mechanism is rather different from that at lower temperatures. Were other points available in this range, it is possible that they might be well disposed about another straight line corresponding to a further equation of the above types. This, however, is pure conjecture.

3. RECOVERABLE CREEP FROM A TORSION STRESS OF 2 TONS/IN.²

In the matter of recoverable creep or anelastic strain, two approaches have been made. In the first the anelastic strain and the progressive differentials of the anelastic strain were through the medium of suitable constants equated to stress and differentials of stress. Two main general equations have been used. The first of these has the form:

$$\begin{aligned}a_1\sigma + a_2D\sigma + a_3D^2\sigma + \dots \\ = b_1\gamma + b_2D\gamma + b_3D^2\gamma + \dots\end{aligned}$$

where a_1, a_2 , &c., are constants, as are b_1, b_2 , &c., and the D 's are progressive differentials of the order indicated with respect to time. The most commonly used form of this equation in rheology has been the one in which a_2, a_3 , &c., and b_3, b_4 , &c., are all zero, and the equation reduces to:

$$\sigma = A(\gamma + B\dot{\gamma})$$

which has a solution of the type:

$$\gamma(t) = \frac{\sigma_0}{A} + \left(\gamma_0 - \frac{\sigma_0}{A}\right)e^{-t/B},$$

where σ_0 and γ_0 refer to zero time, and A and B are constants. In this case forward anelastic creep is the exact replica of recovery creep on removal of load.

The above equation has proved too simple for many cases of anelastic strain, and in such cases the more complex equation :

$$a_1(F_1\sigma) + a_2D(F_2\sigma) + a_3D^2(F_3\sigma) + \&c. \dots \\ = b_1(f_1\gamma) + b_2D(f_2\gamma) + b_3D^2(f_3\gamma) + \&c.,$$

may be taken, where $F_1, F_2, \&c.$, are chosen functions of stress, and $f_1, f_2, \&c.$, functions of strain. The D 's have the same significance as before.

A simple case of this equation arises when $a_2, a_3, \&c. = 0$, and $b_1, b_3, b_4, \&c. = 0$, f_2 is of the form γ^m , and F_1 of the form σ^m ; upon integration the equation then becomes $a_1\sigma t^{1/m} = b_2\gamma$, i.e. a simple power relation.

On the other hand, the approach may be made in which the Boltzman superposition or memory theory⁹ is applied. In this case each loading and unloading of the test-piece is considered to have an effect which continues throughout the whole sequence of such actions, and until the completion of recovery after the final unloading. It will be noted that theories of this type do not indicate any maximum value of recovery occurring after the onset of secondary creep, although this is now a well-recognized experimental fact. This naturally casts doubt on the suitability of theories of the Boltzman type to meet the case of creep recovery.

Mathematically, the Boltzman theory states that if, for a simple loading and recovery test (i.e. one loading and one unloading only), W is the applied load, t_1 the period of creep test, and t the current period of recovery, then the strain y_t at time t is :

$$Wa [\log (t + t_1) - \log t].$$

At $t = 0$, $y_0 = Wa \log t$, where a is a constant. Thus the recovery (as measured in the tests) is given by :

$$Wa [\log (t + t_1) - \log t - \log t_1] \\ = Wa \log (1/t_1 + 1/t).$$

The logarithmic form is, of course, a perfectly arbitrary form chosen by Boltzman, and might in general be replaced by $F(t + t_1)$ or $F(t)$, where F is a function of any type. A critical plot for this theory is obviously recovery against $\log (1/t_1 + 1/t)$. A modification of the Boltzman theory was proposed by Bennewitz,¹⁰ who considered that whereas in an amorphous body, recovery or afterworking occurred freely, it would not occur at all in a single crystal. This fact has been substantiated by several workers. Bennewitz further considered that the ordinary crystalline aggregate, consisting of regular crystals welded together at diffusion points, would exhibit the characteristics of both the above forms; recovery would occur only at places of diffusion and would be very complicated, since it would obey the superposition laws of amorphous bodies only approximately, and would be dependent upon the size and form of the crystals. In other words, Bennewitz tentatively accepted the superposition theory, but did not expect it to apply

rigidly in its simple form. To express his modification of Boltzman's theory, he suggested the formula :

$$y_t = Wa \left[\log \left(\frac{t + t_1}{\tau} + 1 \right) - \log (t/\tau + 1) \right]$$

for strain in recovery tests. When τ is a parameter of the dimensions of time at $t = 0$:

$$y_0 = Wa \log \left(\frac{t_1}{\tau} + 1 \right).$$

Recovery is then given by the expression :

$$Wa \left[\log \frac{(t + t_1 + \tau)}{(t + \tau)(t_1 + \tau)} + \log \tau \right].$$

In order to present this theory in its most favourable light, the relation :

$$\left[\log \frac{(t + t_1 + \tau)}{(t + \tau)(t_1 + \tau)} + \log \tau \right]$$

may be plotted against recovery, using the value of τ at each temperature that gives the best approach to linearity. The theory has the defect of the Boltzman theory of not indicating any maximum value for recovery.

A further modification of Boltzman's theory was proposed by Becker,¹¹ who purported to show that the Boltzman theory of elastic after-effect in its general form can be derived from the assumption of a plastic inhomogeneity of the material, if it is assumed that the plasticity takes a velocity of flow proportional to the force. If, however, the plasticity of the metal does not follow this rule, a modification of the Boltzman theory is necessary. This alteration is carried out on the assumption that the flow of the metal follows in discrete jumps regulated by a probability relationship. Becker derives the formula :

$$y_t = Wa [0.5772 + \log R + \log (t + t_1)] \\ - Wa [0.5772 + \log R + \log t]$$

and $y_0 = Wa [0.5772 + \log R + \log t_1]$

where R is the period of total relaxation. Thus the recovery is given by the expression :

$$Wa \left[\log \frac{t + t_1}{tt_1} - 0.5772 - \log R \right] \\ = Wa [\log (1/t_1 + 1/t) - 0.5772 - \log R]$$

The critical plot is obviously the recovery against the above expression.

In considering the applications of the above theories and equations to the experimental recovery results, it is as well to deal with the superposition theories first, for a reason which will become apparent.

Consideration of the test at 20° C. indicates that the recovery curve was here an exact replica of the forward creep curve. Although this is only one temperature out of several, the information indicates immediately that there is less likelihood of the experimental results being fitted by superposition theory than by equations

of the type put forward in the early paragraphs of this section.

Fig. 7 shows the plots of recovery strain against $\log(1/t + 1/t_1)$ corresponding to the Boltzman equation. It is evident that in general these plots are of the nature of a curve of double inflection, various portions of which are exhibited at the different temperatures. Therefore, a Boltzman equation using a logarithmic function has no reasonable application to the experimental results. Several other forms of function were tried within the framework of this equation, but with no greater degree of success, and in the interests of brevity the corresponding plots are not shown.

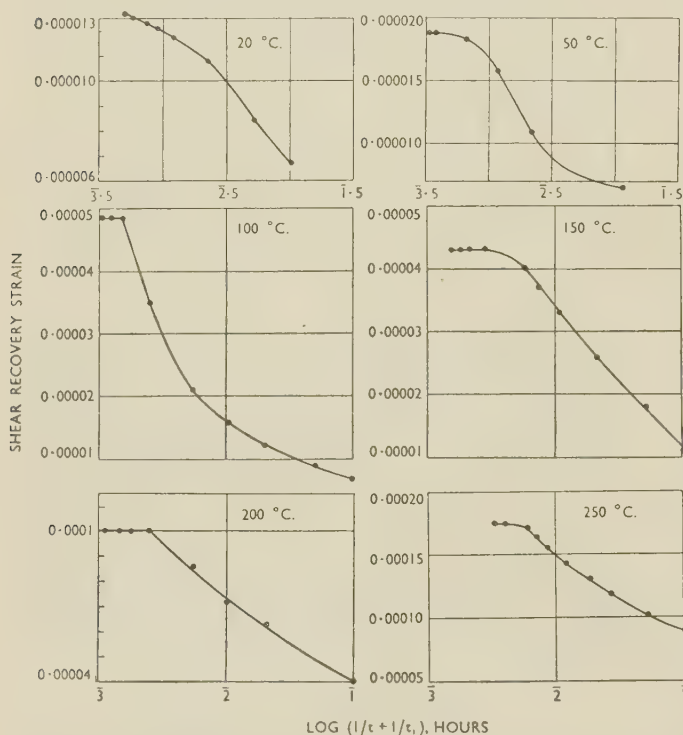


FIG. 7.—Application of Boltzman Theory to Creep Recovery at 20°–250° C. and 2 Tons/in.² Stress.

t = time in recovery test, t_1 = duration of creep test.

With regard to the Bennewitz theory,¹⁰ several plots at each temperature were made, using various possible values of τ ; but it was found that no better approach to linearity in the plots:

$$y_t = Wa \left[\log \left(\frac{t + t_1}{\tau} + 1 \right) - \log (t/\tau + 1) \right]$$

was given for any value of τ than that of $\tau = 1$, which, of course, is simply the Boltzman plot.

Plots were made corresponding to the Becker theory. Again a curve of double inflection appeared to be the basic relation, and the introduction of the relaxation term R into the equation did not appear to effect any improvement in linearity over the original Boltzman plot.

Obviously, therefore, the experimental results can-

not be explained on the basis of superposition and memory theories.

Consider now the application of the equation:

$$\gamma(t) = \frac{\sigma_0}{A} + \left(\gamma_0 - \frac{\sigma_0}{A} \right) e^{-t/B}$$

This equation may be transposed to the form $\log \dot{\gamma} = C - Dt$ for fixed values of σ_0 and γ_0 , and plots such as Fig. 8 in which $\log \dot{\gamma}$ is plotted against t constitute a check on the validity of this equation. However, in these figures the curves are decidedly non-linear, and it is evident that this equation does not describe well the experimental results.

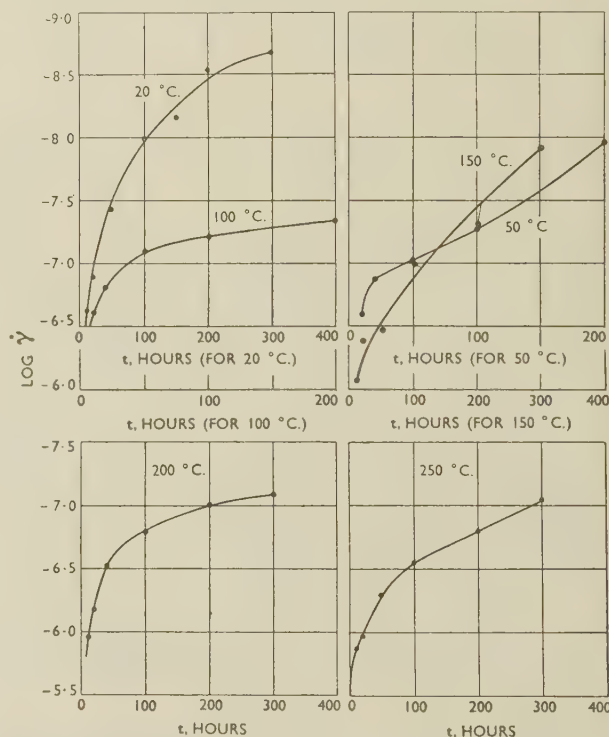


FIG. 8.—Application of Relation $\log \dot{\gamma} = C - Dt$ to Recovery at 20°–250° C. and 2 Tons/in.² Stress.

Before turning to the more general equation:

$$a_1(F_1\sigma) + a_2D(F_2\sigma) + a_3D^2(F_3\sigma) + \dots \&c. \\ = b_1(f_1\gamma) + b_2D(f_2\gamma) + b_3D^2(f_3\gamma) + \dots \&c.$$

it is worth while noting one or two points of interest arising out of previous work on creep recovery of a 0.17% C steel at the National Physical Laboratory. For this material it was found that the recovery could be represented by an expression $nf(t)$, where t was the period of recovery and n depended upon the temperature of test and also on the period of forward creep from which recovery took place. For a given period of unloading, n increased in value with temperature, while at a given temperature n tended to reach a maximum value at the beginning of secondary and the end of transient creep. Actually the change in the

value of n from about 20 hr. onwards to the end of transient creep was slight at most temperatures. Now in the case of the aluminium alloy all tests were unloaded at a time when secondary creep was virtually established, so that no direct measurement of the variation of any term such as n was made.

However, information of an indirect type is available from the test at 20° C. in which the recovery curve was an exact replica of the forward creep curve. This means that the recovery was the same $f(t)$ of time at each period of the forward creep test and that n , therefore, had the same value throughout. In what

by other tests at 150° and 50° C. for this material), and suggests a power relation between recovery and time. This type of equation was accordingly investigated by means of the $\log \gamma / \log t$ plots shown in Fig. 9. In all cases a good linear plot was obtained up to a period (which over the temperature range considered did not differ widely for the various temperatures) when recovery appeared to be virtually complete. The transition from the linear log-log relation to the sustained maximum value of recovery is in all cases very abrupt, and any transition curve is certainly not well marked. The linear log-log plot indicates a relation to hold of type $\gamma^R = K\sigma_1 t^{1/m}$. In Table III the values of K and

TABLE III.—Equations for Creep and Recovery Tests at 20°–250° C.

(t represents time in hr. from the start of the creep and recovery tests.)

Temp., °C.	Equation of Curve of Total Forward Creep Less Recoverable Creep	Equation of Creep Recovery Curve (Excluding Initial Elastic Strain)*	Equation of Total Forward Creep Curve.
20	All creep recoverable	0-0000038 $t^{0.26}$	0-0000038 $t^{0.26}$
50	0-000038 $t^{0.36}$	0-0000029 $t^{0.36}$	0-000038 $t^{0.36}$ + 0-0000029 $t^{0.36}$
100	0-000041 $t^{0.30}$	0-0000029 $t^{0.36}$	0-000041 $t^{0.30}$ + 0-0000029 $t^{0.36}$
150	0-000031 $t^{0.175}$	0-0000061 $t^{0.36}$	0-000031 $t^{0.175}$ + 0-0000061 $t^{0.36}$
200	0-00001 $t^{0.64}$	0-000021 $t^{0.27}$	0-00001 $t^{0.64}$ + 0-000021 $t^{0.27}$
250	0-000083 $t^{0.75}$	0-000052 $t^{0.22}$	0-000083 $t^{0.75}$ + 0-000052 $t^{0.22}$

* These terms acquire maximum values at the end of transient creep.

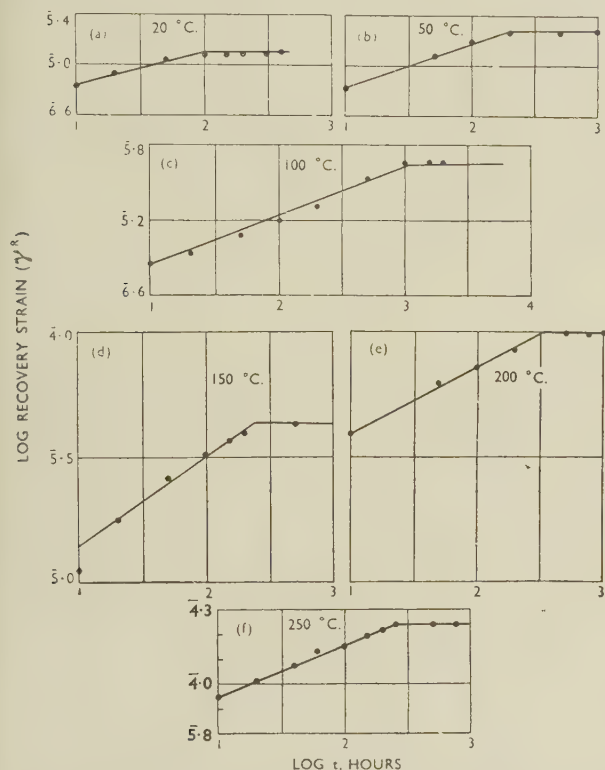


FIG. 9.—Recovery Curves at Various Temperatures and 2 Tons/in.² Stress. (Recovery excluding initial elastic strain.)

- (a) $\gamma^R = 0.0000038t^{0.26}$, (d) $\gamma^R = 0.0000061t^{0.36}$,
 (b) $\gamma^R = 0.0000029t^{0.36}$, (e) $\gamma^R = 0.000021t^{0.27}$,
 (c) $\gamma^R = 0.0000029t^{0.385}$, (f) $\gamma^R = 0.000052t^{0.22}$.

follows the assumption is made that similar conditions prevailed in the tests at other temperatures. This assumption is almost certainly justified, since in the tests on 0.17% C steel the nature of the variation of n with period of test was closely the same at all temperatures.

Considering the present material and referring to the second general equation mentioned, we may try, as an initial simplification, making all a 's except a_1 and all b 's except b_2 zero, and further letting F_1 and f_2 be simple power functions of a similar nature.

Then, by a suitable choice of the power-function exponents, and by integration a relation of the form $A\sigma t^{1/m} = \gamma$ may be obtained. This exhibits the linear stress dependence of recovery (which has been checked

$1/m$ are indicated. It will be noted that the magnitude of K increases with temperature, whereas $1/m$ does not vary greatly, all values being in the region of 0.3. Although results of the short test at 300° C. are not shown, it is interesting to note that the trend of the exponents for this temperature was of a similar nature, $1/m$ being 0.35.

It appears, therefore, that the time exponent in these relations is more or less independent of temperature in this material, the increasing recovery from a fixed stress as the temperature rises being reflected mainly in the increase in value of the arithmetical constants. Further, in view of the identity of the forward creep and recovery curves at 20° C., there seems little doubt that the recoverable creep taking place in each of the forward creep tests concerned is identical with the creep measured in the recovery tests. It should also be noted that in all cases the recovery measured corresponds to a period after what is generally taken to be the end of transient creep and the onset of secondary creep. On the evidence of previous work at the National Physical Laboratory, the recovery values are a maximum in all cases and are, therefore, quite rationally comparable.

There is, however, the point of view to be considered of those who maintain that transient creep does not end spontaneously, but merely becomes a relatively small factor in the total creep as time progresses. From this point of view, if recovery be intimately associated with transient creep, it would hardly be expected to stop in a spontaneous manner, but would probably become gradually too small to

measure. This type of decay could be simulated by an equation of the general type:

$$t = C_1 \gamma^{R_{M_1}} + C_2 \gamma^{R_{M_2}} + C_3 \gamma^{R_{M_3}} + \&c.$$

where t is the period of recovery, γ^R the recovery, and the C 's and M 's are whole-number constants. The abruptness or otherwise of the decay could then be simulated by giving appropriate values of the C 's and M 's. However, in the present case, the $C_1 M_1$ term is overwhelmingly dominant.

4. EMPIRICAL EQUATION OF THE CREEP CURVES

We have noted above that (i) no theory so far put forward gives any reasonable representation of the experimental results in the case of transient creep; (ii) the values of the secondary creep rates in themselves are well represented up to 200° C. by theories based on the application of the Eyring chemical-rate theory to the problem of viscous flow; and (iii) the recoverable portion of forward creep bears a simple power relation to time up to a period when a maximum value is reached.

Obviously the above information does not in itself enable us to formulate a complete equation of forward creep rate based entirely on theory. We have accordingly to adopt the reverse process of formulating (if this be possible) an empirical equation, in the hope that the form derived may suggest to the physicists new or modified theoretical approaches which are in line with the experimental results. Many possible forms of empirical equations have been suggested in the past, and the applicability of such forms to the current results has been considered. However, one empirical equation (the Andrade equation) has been regarded in recent years as being somewhat more than purely empirical in significance, since two individual functions in the equation have been regarded as describing transient and steady-state creep, respectively.

In work on lead, Andrade⁸ found that his curves could be well represented by an equation:

$$l = l_0(1 + Bt^{1/3})e^{kt}$$

where l is the length of the specimen at time t , B and k are constants, and l_0 is a third constant approximating to the length of the specimen at the moment when the sudden extension on loading has ceased. A close approximation to the above equation is obtained by the relation:

$$\gamma = At + Bt^{1/3}$$

and applies to the case of the present material where zero or virtually trivial plastic strain occurs initially, and l_0 becomes simply the length of specimen at zero time, enabling the equation to be reformulated as above. The application of this type of equation to the experimental results was examined both in regard to plots of total forward creep strain against time, and of forward creep strain less recoverable strain against time. The results were of the same nature in both cases. Those for the latter of the two cases are shown

in Fig. 10. In view of the fact that creep at 20° C. was completely recoverable, the plot at this temperature is not shown. Briefly, it is seen that at 250° and 200°

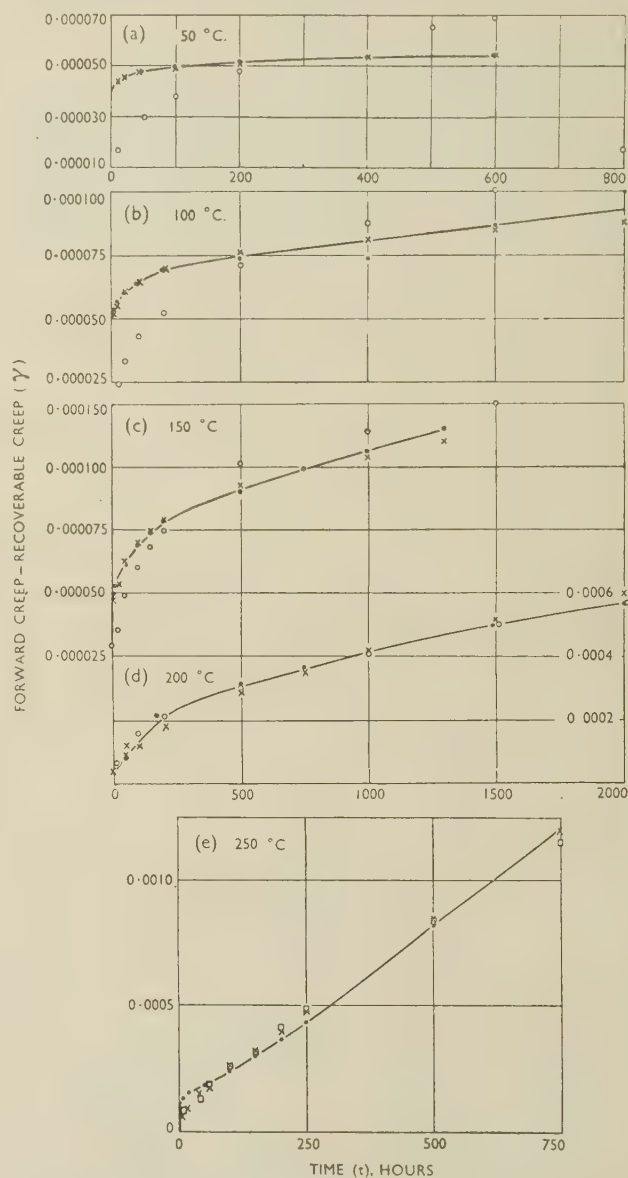


Fig. 10.—Creep Curves at Various Temperatures and 2 Tons/in. Stress. Application of Andrade's and other equations.

KEY.

- Points from experimental data.
- × Points correspond to (a) $\gamma = 0.000038t^{0.955}$, (b) $\gamma = 0.000041t^{0.10}$, (c) $\gamma = 0.000031t^{0.175}$, (d) $\gamma = 0.000012t^{0.54}$, (e) $\gamma = 0.0000083t^{0.75}$.
- Points correspond to (a) $\gamma = 0.000008t^{1/3}$, (b) $\gamma = 0.000009t^{1/3}$, (c) $\gamma = 0.0000125t^{1/3}$, (d) $\gamma = 0.00000093t + 0.000038t^{1/3}$, (e) $\gamma = 0.0000013t + 0.000025t^{1/3}$ which are the Andrade equations most nearly fitting the experimental data.

C. a good fit of experimental results is obtained by the respective equations:

$$\gamma = 0.0000013t + 0.000025t^{1/3}$$

and

$$\gamma = 0.00000093t + 0.000038t^{1/3}.$$

Obviously the unit time term is of increasing importance as the temperature rises, thus justifying in some

degree the supposition that the t term is allied to secondary creep, and the $t^{1/3}$ term to transient creep.

However, at lower temperatures, the fit of experimental results becomes much worse. The t term has to be discarded or becomes negligible, according to the point of view taken, and corresponding to the increasing importance of the transient creep portion of the forward creep strain. Unfortunately, however, the $t^{1/3}$ term proved increasingly inadequate to describe the forward creep, and, as indicated previously, this is in no sense due to effects concerned with varying initial plastic strain, since this strain is actually zero at these temperatures. It has, therefore, to be concluded that the current set of empirical results cannot be described by the Andrade equation.

Analysis was continued on the basis that the recovery strain found was an integral part of the forward creep expressible by the equations already derived for creep recovery, and an attempt was made to find an equation for the relation between forward creep less recoverable creep and time. The results shown in Fig. 10 and Table III (p. 103) were very satisfactory. At all temperatures the curves conformed with a simple power relation :

$$\gamma = K_1 t^{1/m_1},$$

in which the arithmetical constant fell in magnitude as temperature rose, while the exponent rose from a value tending to zero at 50° C. to 0.75 at 250° C. This was in agreement with the fact that all creep was recoverable at 20° C. since taking the total forward creep to be represented by a composite relation $\gamma = K_1 t^{1/m_1} + K_2 t^{1/m_2}$, the latter term being recoverable creep, the exponent $1/m_1$ would be zero at 20° C., which is precisely what does occur.

Thus, a complete equation consisting of two power terms in time has been found to represent well the total forward creep curve from temperature 20° to 250° C., and the characteristic details of this equation at each temperature are given in Table III.

It is worth noting that at 300° C., a similar type of representation was possible, but the characteristics in this case were of a different order from those represented in the range 20°–250° C., and quite definitely represented some type of discontinuity in the mechanism of distortion occurring between 250° and 300° C. as would indeed be expected in a test lasting 2–3 hr., as opposed to 400–2000 hr. in the other tests.

A mathematical shortcoming of the above equation is that the term $K_2 t^{1/m_2}$ assumes a maximum value at the end of transient creep, and subsequently retains this value. From a practical point of view this is undoubtedly the case, but, as indicated in a previous paragraph, in reality t and recovery strain γ_R may be related by a suitably framed equation of the type :

$$t = C_1 \gamma_R^{M_1} + C_2 \gamma_R^{M_2}, \text{ giving continuity} \\ + C_3 \gamma_R^{M_3} + \dots$$

Unfortunately this cannot easily be solved for γ_R in general and therefore does not lend itself to inclusion in the equation of total creep given above. Neverthe-

less, from a purist point of view it may represent the answer to the discontinuity of $K_2 t^{1/m_2}$.

IV.—PHENOMENOLOGICAL THEORIES

In the introduction mention was made of the phenomenological theories of Hollomon and Lubahn,¹² Graham,¹³ and others, and it was stated that while the present authors did not necessarily subscribe to the idea of the existence of an equation of state for metals, the present data would nevertheless be examined to see whether any indication was given that such an equation might be valid over the whole or part of the temperature range investigated.

The starting point of such an examination is obviously the equation given in the previous paragraph :

$$\gamma = K_1 t^{1/m_1} + K_2 t^{1/m_2},$$

where, if the "equation of state" were of a reasonably normal type, the constants K_1 and K_2 would be expected to be functions of stress, and the exponents $1/m_1$ and $1/m_2$ functions of temperature, or in the case of $1/m_2$ a true constant. One of the most frequently suggested equations is of the form :

$$D\sigma^A = E\gamma^B t^{CT},$$

where σ is the stress, T the absolute temperature, and D , E , A , B , and C are constants. The form t^{CT} has some support on fundamental grounds.

Now K_1 and K_2 are presumably stress-dependent, and it is clear from plots against T that this stress-dependence may be complex above, but probably relatively simple below 150° C. K_1 disappears at 20° C., where all creep is recoverable, and from 50° to 150° C. has much the same order of value, thereafter decreasing considerably. K_2 has the same order of value up to 150° C., and then increases rapidly. Since $K_2 t^{1/m_2}$ represents recoverable creep, K_2 must be linearly dependent upon stress at all temperatures. Thus, since K_2 increases with temperature above 150° C., it is presumably also a function of temperature. The chances of a reasonably simple equation of state existing above 150° C. are thus diminished.

Turning now to the exponents $1/m_1$ and $1/m_2$, in Fig. 11 a plot is made of the recovery exponent $1/m_2$ against absolute temperature, the value of this exponent at 300° C. being also included since it represents no marked change of magnitude. It is apparent that the value of $1/m_2$ varies more or less uniformly about a mean value of about 0.32, and may thus be effectively regarded as constant, say N_2 .

In Fig. 11 (a) and (b) the creep exponent $1/m_1$ is plotted linearly, and doubly logarithmically against absolute temperature. In the logarithmic plot, the points are disposed reasonably well about a mean straight line, but on the other hand there is a hint in the disposition of the points that a curve of double inflection might be the real relation between them, and of course $1/m_1$ ceases to have any significance at 20° C., where creep is completely recoverable. If the above linear log-log relation were regarded as valid,

and therefore $1/m_1 = KT^{N_1}$, say, the expression for γ would become of the form:

$$\gamma = K_1 t^{KT^{N_1}} + K_2 t^{N_2}$$

The dependence of t upon temperature in the above equation is more complex than in previous equations of state. This fact appears to confirm that any equation of state that is of reasonable simplicity is very unlikely to hold for a temperature range extending above 150°C .

Accordingly, it may be worth while to examine whether apart from the reasonably constant values of K_1 and K_2 , any other simplification arises if the temperature range be restricted to 150°C . In Fig. 11 (c)

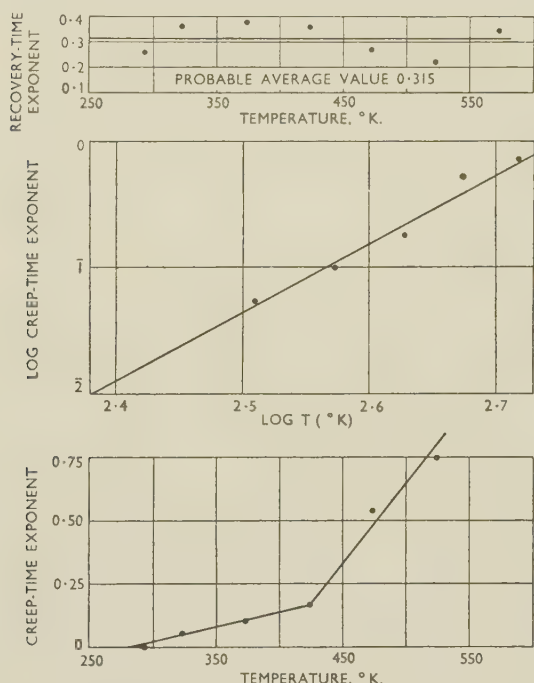


FIG. 11.—Temperature-Dependence of Time Exponents in Creep and Recovery from 20° to 250°C .

the relation between the creep-time exponent and absolute temperature is seen to be a straight line up to 423°K . (150°C .), and then a possible further linear relation at temperatures above 150°C . Neglecting the latter portion, the linear relation at lower temperatures is found to be such that the exponent $= 0.00113T - 0.32$ or is of the form $K_3T - K_4$. This is a distinct simplification compared with the relation apparently arising for the whole temperature range.

Now data obtained in the complex stress tests on this material at low and moderate stresses (2 tons/in.² torsion comes within this category at 150°C . and below) indicated that the relation held $\gamma \propto \sigma$ or in terms of combined stresses $\gamma \propto [(\sigma_1 - \sigma_2) - (\sigma_3 - \sigma_1)]$, σ_1 , σ_2 , and σ_3 , being principal stresses. The values of K_1 shown in Table III are in general accordance with this fact. So it may reasonably be suggested that for temperatures up to 150°C . the following

tentative equation of state might conceivably hold at low and moderate stresses:

$$\gamma = A\sigma[t^{(BT-C)} + Dt^N]$$

for torsion and tension tests,

$$\text{or } \gamma_1 = A[(\sigma_1 - \sigma_2) - (\sigma_3 - \sigma_1)][t^{(BT-C)} + Dt^N]$$

for general combined stresses.

Over the same temperature range, and at higher stresses, the equations might become (judging from the nature of the stress-dependence in combined-stress tests):

$$\gamma = A\sigma[t^{(BT-C)} + Dt^N] + [A_1\sigma^{n_1} + A_2\sigma^{n_2}][t^{(BT-C)}]$$

for torsion and tension tests,

$$\begin{aligned} \text{and } \gamma_1 = & A[(\sigma_1 - \sigma_2) - (\sigma_3 - \sigma_1)][t^{(BT-C)} + Dt^N] \\ & + [A_1[\Sigma(\sigma_1 - \sigma_2)^2]^{n_1} + A_2[\Sigma(\sigma_1 - \sigma_2)^2]^{n_2}] \\ & [(\sigma_1 - \sigma_2) - (\sigma_3 - \sigma_1)][t^{(BT-C)}] \end{aligned}$$

in general combined-stress tests.

The authors merely regard the above equations as a possible form, but further details on them should arise from the creep, relaxation, and recovery tests at low stresses being conducted on this material in the N.P.L.-type high-sensitivity torsion-creep unit. These tests may also settle the question of the discontinuous nature or otherwise of creep recovery.

It must not be forgotten that the recoverable term, Dt^N , in the above equation reaches a maximum value approximately at the end of transient creep and becomes effectively a constant. The validity of the above equations, therefore, depends upon the assumption that the end of transient creep occurs in much the same time within the temperature range 20° – 150°C . This is a reasonable approximation for this range, but would certainly not be valid outside it. Accordingly, to remove this shortcoming it may be that replacement of the terms involving Dt^N by a term γ_R which is the solution of an equation of the type:

$$t = [C_1\gamma^{R^{1/N_1}} + C_2\gamma^{R^{1/N_2}} + \&c.]$$

where the arithmetical constants are dependent upon unit power of stress, and all constants are chosen to make the term $C_1\gamma^{R^{1/N_1}}$ preponderantly dominant, will be a satisfactory measure. Nevertheless, the discontinuity is so abrupt in all tests as to make the previously stated equations a very good approximation from a practical point of view, purely mathematical considerations apart.

V.—CONCLUSIONS

The following conclusions appear to be justified for the set of tests at a torsion stress of 2 tons/in.²:

(1) No current fundamental theory describes the transient creep of the 2L42 alloy between 20° and 250°C .

(2) Over the range 20° – 200°C . the secondary creep rates measured agree well with the theories of Kauzmann and of Nowick and Machlin, and to a somewhat

lesser degree with those of Feltham. However, this agreement ceases to exist at 250° C.

(3) The superposition or memory theories of Boltzman, Bennowitz, and Becker, do not adequately represent the recoverable creep measured in the tests.

(4) The forward creep curve cannot be represented by an Andrade equation, except at temperatures of 200° and 250° C.

(5) The total forward creep curve is well represented at all temperatures by the equation :

$$\gamma = K_1 t^{1/m_1} + K_2 t^{1/m_2},$$

where K_1 and $1/m_1$ refer to the non-recoverable portion of the forward creep curve, and K_2 and $1/m_2$ refer to the recoverable portion of the creep. K_1 , K_2 , and $1/m_1$ vary with temperature, whereas $1/m_2$ is effectively constant. The term $K_2 t^{1/m_2}$ becomes virtually a constant at the onset of secondary creep.

(6) It seems possible that up to 150° C., and at low and moderate stresses, an approximate phenomenological equation might be expressed for this material in the form :

$$\gamma_1, \text{ \&c.} = A[(\sigma_1 - \sigma_2) - (\sigma_3 - \sigma_1)] [t^{(BT-C)} + Dt^N],$$

where σ_1 , σ_2 , and σ_3 are the principal stresses and T the absolute temperature. At higher stresses the stress function becomes more complex, and above 150° C., no reasonable phenomenological equation seems likely to hold.

ACKNOWLEDGEMENTS

The work described was carried out in the High-Temperature Mechanical Properties Section of the National Physical Laboratory as part of the programme of the Mechanical Engineering Research Board, and this paper is published by permission of the Director of the National Physical Laboratory and the Director of the Mechanical Engineering Research Organization of the Department of Scientific and Industrial Research.

REFERENCES

1. N. F. Mott and F. R. N. Nabarro, *Proc. Phys. Soc.*, 1940, [B], **52**, 86.
2. E. Orowan, *J. West Scotland Iron Steel Inst.*, 1946-47, **54**, 45.
3. C. L. Smith, *Proc. Phys. Soc.*, 1948, [B], **61**, 201.
4. W. Kauzman, *Trans. Amer. Inst. Min. Met. Eng.*, 1941, **143**, 57.
5. A. S. Nowick and E. S. Machlin, *J. Appl. Physics*, 1947, **18**, 79.
6. P. Feltham, *Iron Coal Trades Rev.*, 1950, **161**, 305.
7. H. Eyring, *J. Chem. Physics*, 1936, **4**, 283.
8. E. N. da C. Andrade, *Proc. Roy. Soc.*, 1910-11, [A], **84**, 1; 1914, [A], **90**, 329.
9. L. Boltzman, *Pogg. Ann. Physik u. Chem.*, 1876, **7**, 624.
10. K. Bennowitz, *Physikal. Z.*, 1920, **21**, 703; 1924, **25**, 417.
11. R. Becker, *Z. Physik*, 1925, **33**, 185; *Physikal. Z.*, 1925, **26**, 919.
12. J. H. Hollomon and J. D. Lubahn, *Gen. Elect. Rev.*, 1947, **50**, (2), 28; (4), 44.
13. A. Graham, *Engineer*, 1952, **193**, (5011), 198; (5012), 234.

NOTICE TO AUTHORS OF PAPERS FOR THE "JOURNAL" AND CONTRIBUTORS TO DISCUSSIONS

1. Papers will be considered for publication from non-members as well as members of the Institute. They are accepted for publication in the *Journal* and not necessarily for presentation at any meeting of the Institute. MSS. should be addressed to The Editor of Publications, The Institute of Metals, 4 Grosvenor Gardens, London, S.W.1.

2. Papers suitable for publication may be classified as:

- (a) Papers recording the results of original research.
- (b) First-class reviews of, or accounts of progress in, a particular field.
- (c) Papers descriptive of works methods, or recent developments in metallurgical plant and practice.
- (d) Papers in classes (a), (b), and (c) above, previously published in languages other than English, French, German, or Italian, if of sufficient merit.

3. Manuscripts and illustrations should be submitted in duplicate. MSS. must be typewritten (*double-line spacing*) on one side of the paper only, and authors are requested to sign a declaration that neither the paper nor a substantial part thereof has been published elsewhere. Exceptions may be made in certain cases where a paper has been published in a language other than English, French, German, or Italian (see 2(d) above). MSS. not accepted are normally returned within 6 months of receipt.

In the interests of economy, all papers must be written as concisely as possible; in general, internal research reports are not in suitable form for publication as papers in the *Journal*. All but the simplest mathematical expressions should be written by hand, with capital and small letters clearly distinguished. Superscript and subscript letters should also be plainly indicated. Greek letters and special signs should be identified in the margin. For style, spelling, and abbreviations used, any recent issue of the *Journal* may be consulted.

4. **Synopsis.** Every paper must have a synopsis (not exceeding 250 words in length) which, in the case of a paper reporting original research, should state its objects, the ground covered, and the nature of the results. The synopsis will appear at the beginning of the paper, and should be in a form suitable for use by abstracting organizations. Extracts from a "Guide for the Preparation of Synopses" drawn up by the Abstracting Services Consultative Committee are reproduced below.

5. **References** must be collected at the end of the paper and must be numbered in the order in which they occur in the MS. Initials of authors must be given, and the Institute's official abbreviations for periodical titles (as used in *Metallurgical Abstracts*) should be employed, where known. References to papers should be set out in the style:

A. L. Dighton and H. A. Miley, *Trans. Electrochem. Soc.*, 1942, 81, 321 (i.e. year, volume, page).

References to books should be in the following style:

C. Zener, "Elasticity and Anelasticity of Metals". Chicago: 1948 (University of Chicago Press).

6. **Illustrations.** Each illustration must have a number and description; only one set of numbers must be used in one paper, and it is desirable to number the half-tone illustrations consecutively, rather than to intersperse them with the line figures. The captions should be typed on a separate sheet.

The set of line figures sent for reproduction must be drawn (about twice the size to appear in the *Journal*) in Indian ink on smooth white Bristol board, good-quality drawing paper, co-ordinate paper, or tracing cloth, which are preferred in the order given. Co-ordinate paper, if used, must be blue-lined, with the co-ordinates to be reproduced finely drawn in Indian ink. Curves should be drawn boldly (i.e. at least twice the thickness of the frame). Experimental points should be indicated by open or closed circles, triangles, squares, &c. (preferably not crosses). Curves should be broken on each side of such symbols and plenty of allowance should be made for closing up in blockmaking. All lettering and numerals, &c., should preferably be in pencil, so that the Institute's standard lettering may be affixed, and ample margins must be left outside the framework of the figures to enable this to be done. The second set of line illustrations may be photostat copies.

Photographs must be restricted in number, owing to the expense of reproduction, and photomicrographs should be trimmed to the smallest possible of the following sizes consistent with adequate representation of the subject: 4 in. deep by 3 in. wide; 2 in. deep by 3 in. wide; 2 in. square. Magnifications of photomicrographs must be given in each case. Photographs for reproduction should be loose, not pasted down (and not fastened together with a clip, which damages them), and the figure number and author's name should be written on the back of each. Captions should be given to the photomicrographs, but these should be kept as brief as possible.

Because of the present high cost of printing and paper it is imperative that authors restrict illustrations (particularly photographs) to the absolute minimum deemed necessary to support their argument. Only in exceptional cases will illustrations be reproduced if already printed and readily available elsewhere.

7. **Tables or Diagrams.** Results of experiments, &c., may be given in the form of tables or figures, but (unless there are exceptional reasons) not both. Tables should bear Roman numbers, and each should have a heading that will make the data intelligible without reference to the text.

8. **Corrections.** A certain number of corrections in proof are inevitable, but any modification of the original text is to be avoided. Since corrections are very expensive, the Institute reserves the right to require authors to contribute towards their cost if the Editor deems them to be excessive. The Institute also reserves the right to require a contribution to the cost of remaking any block where this is necessitated by an error on the author's part.

9. **Reprints.** Individual authors are presented with a maximum of 25, and two or more authors with a maximum of 50 reprints from the *Journal*, without covers. Limited numbers of additional reprints can be supplied at the author's expense, if ordered before proofs are passed for press. (Orders should preferably be placed when submitting MSS.)

10. **Discussion.** Except in the case of special symposia, shorthand records of discussions are not taken at meetings. Written discussion may be submitted on any paper, preferably typewritten (*double-line spacing*). References should be given in the form of footnotes. Paragraphs 6 and 7 above are also applicable to such contributions. Reprints of discussion cannot be supplied to contributors.

GUIDE FOR THE PREPARATION OF SYNOPSES

(As recommended by the Abstracting Services Consultative Committee)

1. **Purpose.** The synopsis is not part of the paper; it is intended to convey briefly the content of the paper, to draw attention to all new information, and to the main conclusions. It should be factual.

2. **Style of writing.** The synopsis should be written concisely and in normal rather than abbreviated English. It is preferable to use the third person. Where possible use standard rather than proprietary terms, and avoid unnecessary contracting.

It should be presumed that the reader has some knowledge of the subject, but has not read the paper. The synopsis should therefore be intelligible in itself without reference to the paper; for example, it should not cite sections or illustrations by their numerical references in the text.

3. **Content.** The title of the paper is usually read as part of the synopsis. The opening sentence should be framed accordingly and repetition of the title avoided. If the title is insufficiently comprehensive, the opening should indicate the subjects covered. Usually the beginning of a synopsis should state the objective of the investigation.

It is sometimes valuable to indicate the treatment of the subject by such words as: brief, exhaustive, theoretical, &c.

The synopsis should indicate newly observed facts, conclusions of an

experiment or argument and, if possible, the essential parts of any new theory, treatment, apparatus, technique, &c.

It should contain the names of any new compound, mineral species, &c., and any new numerical data, such as physical constants; if this is not possible, it should draw attention to them. It is important to refer to new items and observations, even though some are incidental to the main purpose of the paper; such information may otherwise be hidden, though it is often very useful.

When giving experimental results the synopsis should indicate the methods used; for new methods the basic principle, range of operation, and degree of accuracy should be given.

4. **References.** If it is necessary to refer to earlier work in the summary, the reference should always be given in full and not by number. Otherwise references should be left out.

When a synopsis is completed, the author is urged to revise it carefully, removing redundant words, clarifying obscurities, and rectifying errors in copying from the paper. Particular attention should be paid by him to scientific and proper names, numerical data, and chemical and mathematical formulae.

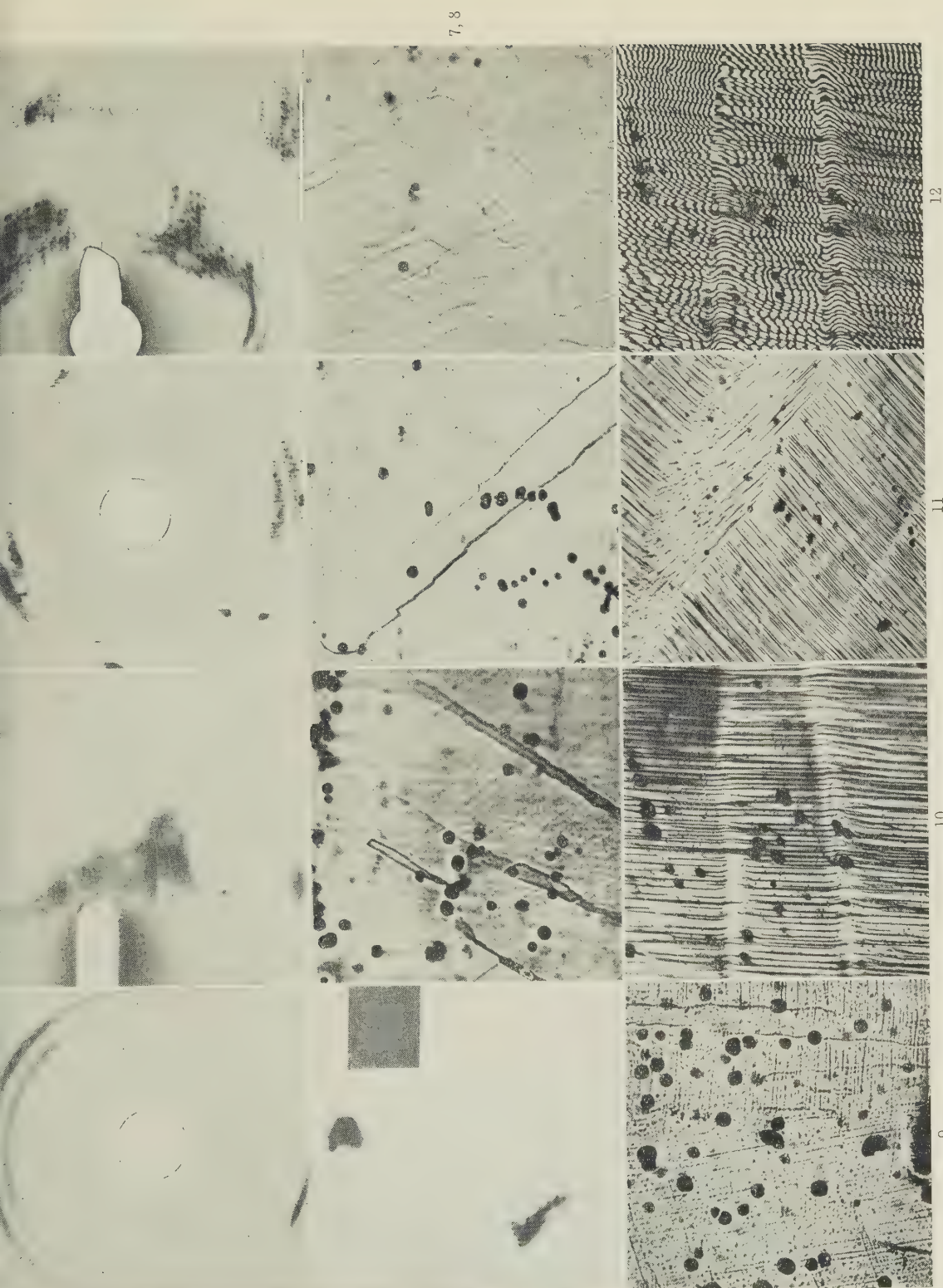


FIG. 1.—Normal Back-Reflection Pattern of Coarse-Grained Al Extended 16% at 21° C.

FIG. 2.—Back-Reflection Pattern of Coarse-Grained Al Extended 10% at 21° C. Specimen and film oscillated through 10° in synchronism.

FIG. 3.—Diffraction Pattern of Same Area as Fig. 1 After Recovery.

FIG. 4.—Diffraction Pattern of Al Extended 10% at 500° C.

FIG. 5.—Diffraction Pattern of Al Extended 10% at 21° C. and Heated for 36 Hr. at 500° C.

FIG. 6.—Islands in Al Extended 10% at 21° C. and Heated for 3 Days at 420° C. Slip produced after heating. $\times 100$.

FIG. 7.—As for Fig. 6. $\times 100$.

FIG. 8.—Substructure of Al Extended 12% at 21° C. and Heated for 3 Days at 420° C. $\times 100$.

FIG. 9.—As for Fig. 6. $\times 100$.

FIG. 10.—Kink Bands in a Specimen Extended 10% at 21° C. $\times 100$.

FIG. 11.—A Kink Band (*upper right*) and a Band Containing Slip on a Second Plane (*lower left*). $\times 100$.

FIG. 12.—Interference Fringes from Area Shown in Fig. 10. $\times 100$.

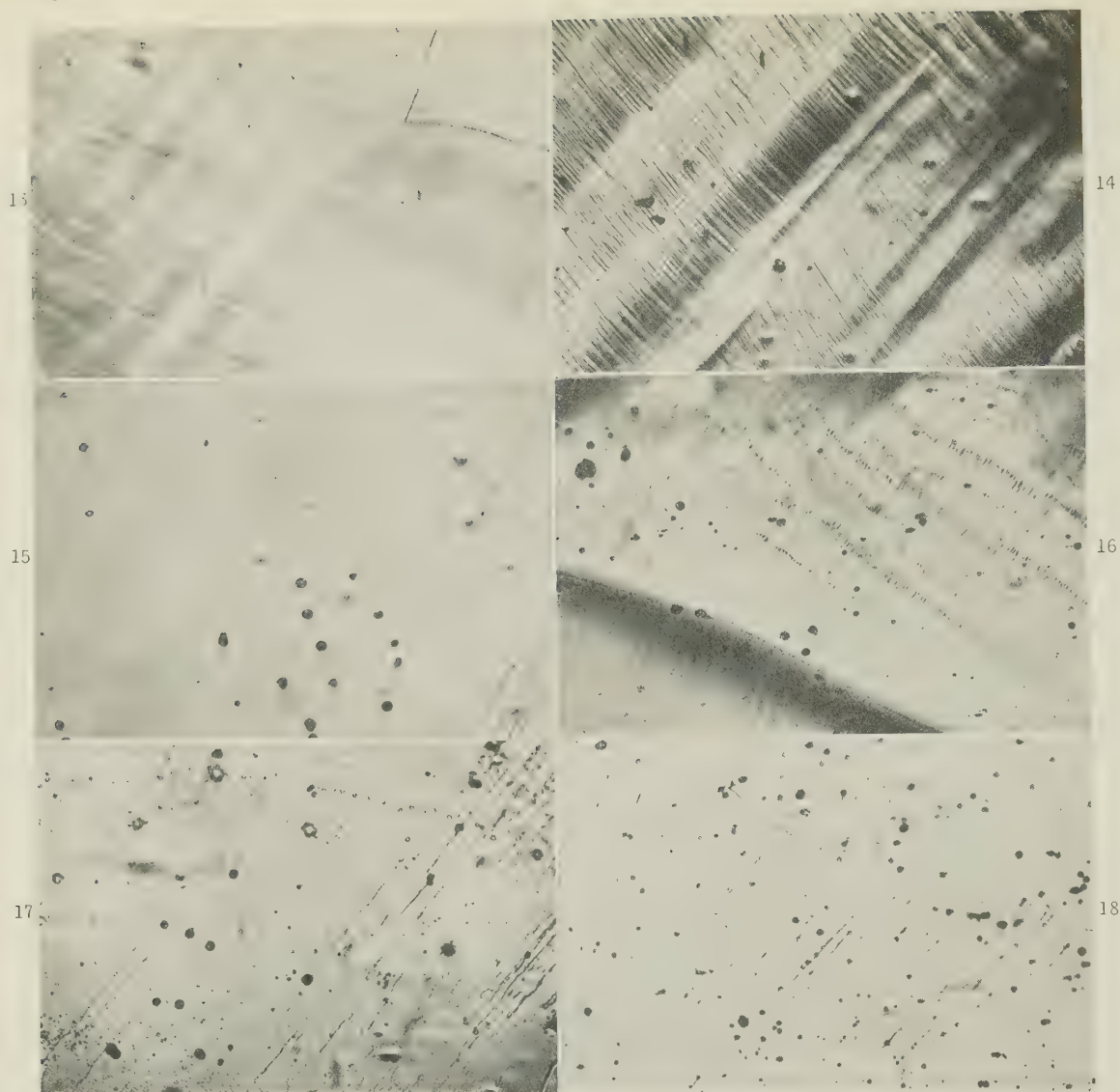


FIG. 13.—Kink Bands Crossing Grain Boundaries in a Specimen Extended 12% at 21° C., Repolished, and Etched. $\times 100$.

FIG. 14.—A Grain Containing both Closely Packed and Widely Spaced Bands. Specimen extended 10% at 21° C. $\times 100$.

FIG. 15.—Same Area as Fig. 14, after Repolishing and Etching. $\times 100$.

FIG. 16.—Specimen Extended 12% at 21° C., Repolished, and Etched. $\times 100$.

FIG. 17.—Same Area as Fig. 14, after Heating for 6 Days at 420° C., Repolished and Etched. $\times 100$.

FIG. 18.—Specimen Extended 12% at 21° C. and Heated for 3 Days at 420° C. $\times 100$.



FIG. 19.—Part of the Recovered Band in Fig. 7 Taken with Phase Contrast. $\times 400$.

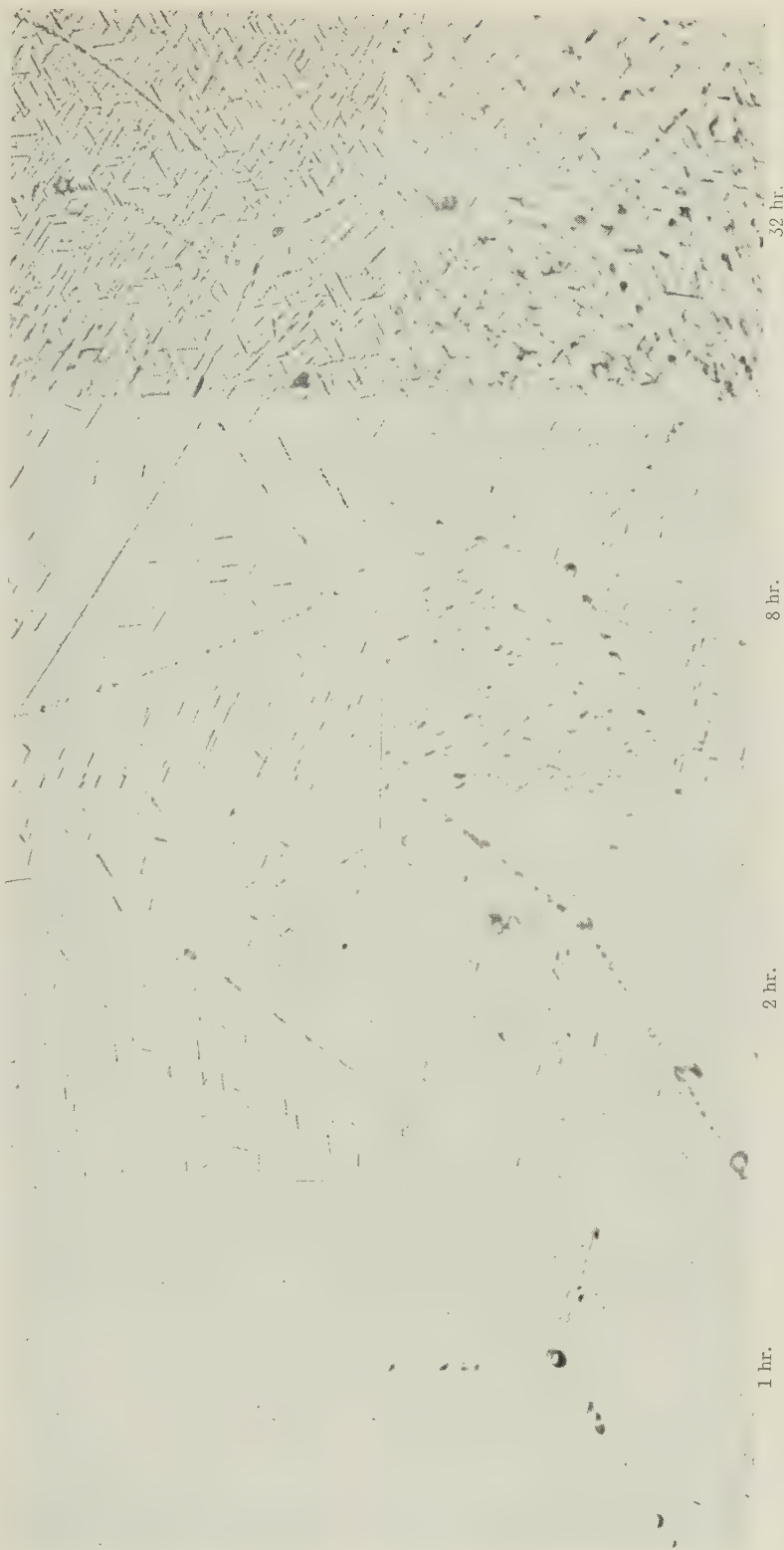
ALUMINIUM-SILVER ALLOYS.

FIG. 1.—8% Ag. Solid solution.
× 500.

FIG. 2.—2% Ag. Solution-treated, aged
168 hr. at 250° C. × 500.

FIG. 3.—4% Ag. Solution-treated, aged
72 hr. at 320° C. × 500.

FIG. 4.—8% Ag. Solution-treated, aged
72 hr. at 300° C. × 1000.



1 hr.

2 hr.

8 hr.

32 hr.

FIGS. 5-8.—4% Ag. Aged for increasing times at 250° C. × 2000.

MICROSTRUCTURES OF TANTALUM-TITANIUM ALLOYS.

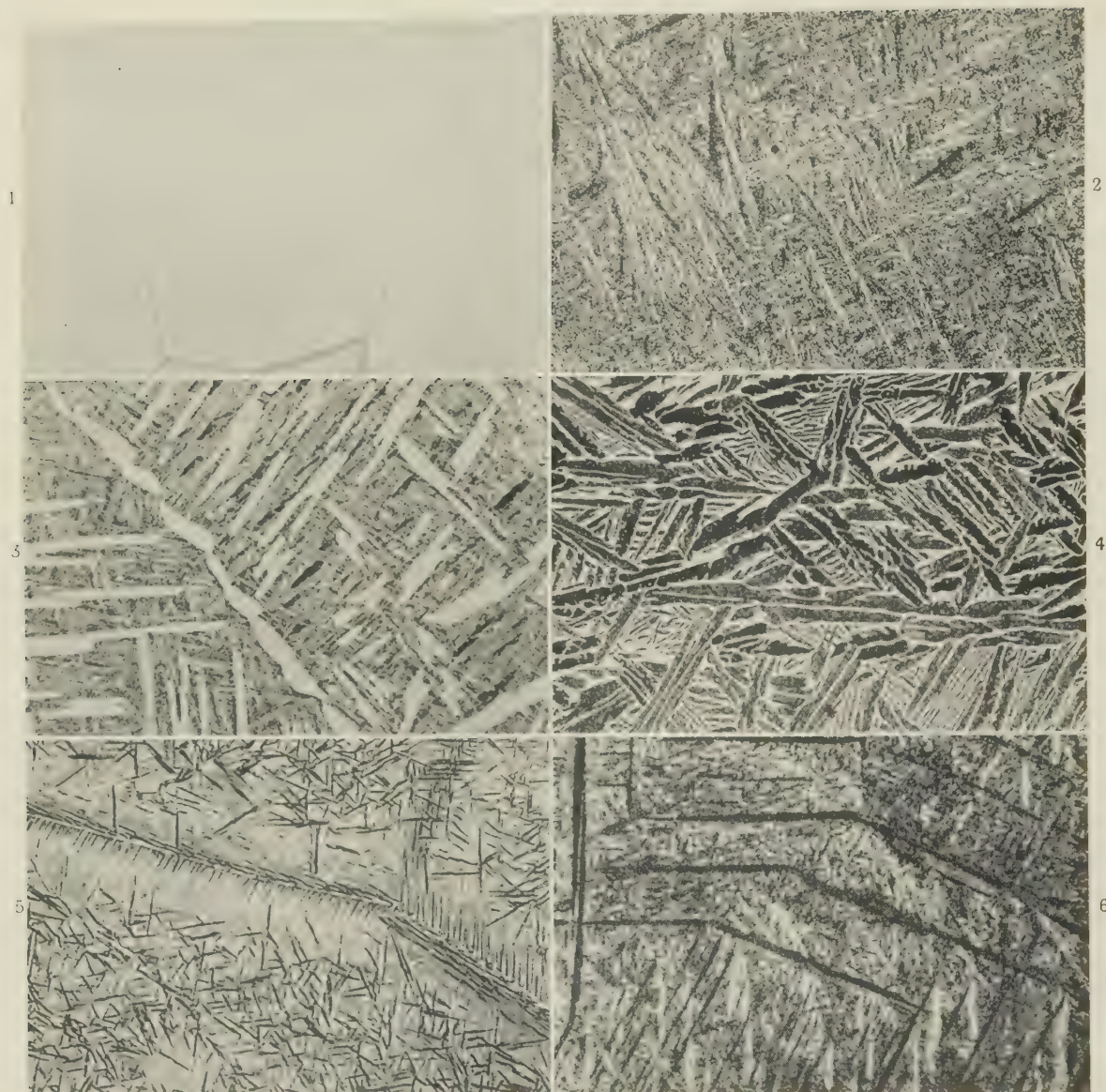


FIG. 1.—82.2 At.-% Ti, Quenched from 900° C. $\times 100$.
FIG. 2.—92.7 At.-% Ti, Quenched from 900° C. $\times 300$.
FIG. 3.—95.5 At.-% Ti, Quenched from 850° C. $\times 300$.
FIG. 4.—Same as Fig. 2, Quenched from 800° C. $\times 300$.
FIG. 5.—77.0 At.-% Ti, Quenched from 650° C. $\times 300$.
FIG. 6.—86.1 At.-% Ti, Quenched from 900° C. $\times 500$.

ON THE FOOT-HILLS OF THE PLASTIC RANGE*

1422

By PROFESSOR H. W. SWIFT,† M.A., D.Sc., M.I.Mech.E.

SYNOPSIS

In this lecture the author attempts a survey of the activities of the several classes of pure and applied scientists engaged in the general field of metal plasticity. He discusses the present state of knowledge and the extent to which research is at present able to make its contribution to the various technological processes involving plastic deformation. A classification is suggested of the most profitable directions of inquiry appropriate to the mathematician, the metal physicist, and the engineering scientist, and an appeal is made for the co-ordination of programmes and for the presentation of reports and results in a form intelligible to other scientific workers and to those more directly concerned with plastic processes in industry. The methods of mathematical plasticity are illustrated by simple examples of shear-line fields and flow grids. The limited success of more elementary methods of analysis by engineering investigators is illustrated by the deep-drawing of a cylindrical shell. An appeal is made to the metal physicist for a more realistic model of lattice structure, and for a systematic study of stress/strain relations on a wider front than heretofore.

I.—INTRODUCTION

PLASTIC deformation forms the basis of one of the oldest of the industrial arts and one of the youngest of the applied sciences. From the earliest historical times man has applied to malleable metals the group of compressive operations which include forging, coining, and hammering, for over a thousand years he has been drawing wire, and for over a century he has been drawing tubes and sheet metal. Yet little attempt had been made before the present century to formulate the principles of plastic deformation or to correlate them with the properties of metals. It is true that the basic equations of theoretical plasticity were laid down by Lévy in 1871, but so little attention did they attract that they are generally credited to von Mises, who re-enunciated them over 40 years later. And although Tresca introduced the shear-stress criterion for plastic flow in 1868, this is still commonly attributed to Guest in 1900, though he subsequently did his best to live it down.

Von Mises, of course, made other notable contributions to the theory of plasticity, and was one of the leaders of the German school which was mainly responsible for experimental and theoretical developments up to the beginning of the last war. The transfer of Continental workers to America—by cold extrusion before the war and by wire-pulling since—carried the initiative across the Atlantic for a time, but the emergence of a theoretical group at Fort Halstead during the war and the development of experimental groups under the energetic leadership of certain of the British industrial research organiza-

tions have done much to restore the balance, and in so far as results are to be judged by weight rather than volume, there is probably at the present time a greater potential of applicable theory and experiment in this country than anywhere else. Whether the appetite of industry in this country as a whole is as keen, or its digestive organs as efficient, as elsewhere is perhaps another question.

But this question must not be held to imply any doubt as to the technological skill of those engaged in the metal-forming industries in this country. There can be no doubt on this score in the mind of anyone who has visited an automobile press shop and witnessed the transformation of a flat sheet into a motor-car wing in a single stroke. Neither the man who casually presses the button nor his mate who idly applies an oily rag at the right spot on the sheet has anything to learn from Charlie Chaplin in the matter of masterly nonchalance. And it is no less impressive in an anonymous back-street works to follow the fortunes of an aluminium slug which within ten minutes of entering the shop is extruded, screwed, capped, twice enamelled and stoved, and despatched with a colourful tribute to a wonderful shaving cream, but no clue to the identity of those who produced its still more wonderful container.

Such examples are a tribute to the enterprise, courage, resourcefulness, and intuitive skill of those engaged in the metal-forming industries, but they do not prove either that industrial development has reached finality or that the principles underlying it are so well understood that they can be applied with confidence to fresh types of problems as they arise.

* Delivered at the Annual Autumn Meeting, Oxford, 15 September 1952.

† Professor of Engineering, University of Sheffield.

In fact, of course, much expense is involved in processes of trial-and-error and in the use of materials capable of withstanding plastic maltreatment, and there are still many products which have to be produced by slower operations or more expensive machinery than would be necessary if the plastic properties of materials were fully understood. There is therefore still much scope for development in technical plasticity, and this involves on the one hand the study of plastic deformation in its physical and mechanical aspects, and on the other the application of the results of this study to industrial problems. And between these there is the need for an important link; scientific results become useful only when they are interpreted in such a way that they can be understood and applied by those concerned with industrial production.

In this broad field of development there is work for many hands; for the pure scientist and the applied scientist, for the mathematician, the metallurgist, and the mere engineer. Indeed, since he is directly concerned with the finished product, the engineer is probably most conscious of the need for further knowledge over a wide front.

He realizes that almost every manufacturing operation from the ingot to the finished product is essentially related to the plastic properties of the material; rolling, forging, pressing, drawing, extrusion, and even machining. He realizes, moreover, that the plastic properties of materials are becoming increasingly significant in modern engineering design. Apart from such established processes as shrinking, over-speeding, and auto-fretage, he is beginning to take advantage of the economies made possible by considerations of plastic strain in the limit design of structures. And he is just beginning to realize that in his innocence he has in fact for many years been basing his designs on the plastic properties of ductile metals, for the "ultimate tensile strength", to which he has traditionally applied his factor of safety, is itself nothing but a function of the plastic stress/strain curve.

For his own purposes the engineer needs to be able to assess the possibilities of various processes of formation and fabrication in relation to materials which are economically available. He needs to devise these processes so as to produce results with the minimum demand on these materials and the minimum expense; he needs to design machines and equipment to carry out these processes; and he needs to be able to specify and therefore to test material suitable for these processes. And at all stages he is concerned as far as possible to eliminate the expense and delay involved in trial-and-error methods.

In this field, if in no other, and however reluctantly, the metallurgist has to accept a role complementary to the engineer. It is his concern to provide material with properties suitable for the engineer to fabricate and process, and to advise him on the specification and treatment of this material. For this purpose he needs to know—and preferably to understand—how

suitable plastic properties can be obtained, and he is continually seeking to develop new materials to circumvent the engineer's ingenuity in maltreatment. He also needs to have at his disposal means for the testing of materials, which shall be relevant to their application and acceptable to the engineer.

If they were left to their own devices, the metallurgist and the engineer would be compelled in the main to have recourse to empirical or trial-and-error methods, methods which are tedious and uneconomical, and uncongenial to the scientific mind. They are therefore gratified to realize that applied mathematicians and such physicists as are prepared to regard the atom as a unit rather than a universe, have been increasingly finding in the field of plasticity material worthy of fundamental inquiry.

The metal physicist is concerned to understand the nature and mechanism of plastic deformation in relation to atomic and crystal structure, and so to be able to correlate physical and mechanical properties with the structure and treatment of metals. In this way he should be in a position to point directions in which desirable plastic properties are likely to be found, and to guide the metallurgist in the development of materials possessing these properties. It is perhaps too much to hope that any metal physicists in the audience can see themselves in this role at present.

The mathematician's interest in plasticity can cover a considerable range. He can apply his techniques in the field of metal physics to explain plastic deformation at the atomic level and seek correlation between single-crystal and polycrystalline properties. Or, closer to the field of the engineer, he can study the distribution of stresses and strains in a material of specified properties under a given type of deformation, and he can seek to prescribe the limiting range of this deformation in relation to the intrinsic strength of the material. Engineers in their less generous moments suspect that some mathematicians are also attracted to the subject of plasticity because of the opportunity it provides for analytical virtuosity.

And so we have four distinct parties each concerned from its own point of approach, by its own route, with its own resources and its own objective, to explore the secrets and exploit the resources of the plastic range. The engineer is all too conscious that his own equipment is quite unequal to the task of scaling the real heights, so he must limit his pedestrian efforts to the foot-hills of the range. Here he can watch and admire the skill of those whose special scientific equipment enables them to climb to greater heights and perhaps even to aspire to the peaks of the range. Nor need he be entirely an onlooker, for he can make himself useful as base-porter for the pioneers, supplying them with material needs, and at the same time he can do some exploring on his own account at lower levels.

From his vantage ground on the foot-hills, he is, of course, in a good position, albeit at a respectful distance, to follow the manoeuvres and progress of

those who are struggling on the glaciers and ledges above the snowline. As he sees it, the plastic range is divided into two main massifs, between which at present there appears to be "a great gulf fixed". On one side is the massif which the mathematicians like Hill in this country and Prager in America are exploring. At its higher levels this seems to be wrapped in perpetual cloud, but it is surmounted by a noble peak which may perhaps be called the *Mathahorn*. The other massif, on which the metal physicists are busy, culminates in another peak, which members of this Institute will recognize as the *Metahorn*.

It is a little presumptuous for the engineer to attempt to define the position of the more traditional metallurgist in this terrain, but I hope I shall not be accused of abusing a privileged occasion if I suggest that the main body of this Institute is established on the foot-hills below the Metahorn at much the same level as the engineer at the foot of the Mathahorn. Our general perspectives are therefore much the same, but since the engineer is more directly on the lines of communication with the mathematicians, he feels that his views on their progress are more likely to be acceptable to metallurgists than his occasional side-long glimpses of incidents on the glide planes and edge dislocations of the Metahorn.

In this lecture, therefore, I would venture with due deference to give you a brief outline of activities on the Mathahorn as they appear to an engineer on the foot-hills, an outsider's glance at the Metahorn, and some idea of the kind of modest progress which engineers have been able to make at lower levels. First, then with your permission, as an engineer, "I will lift up mine eyes unto the Hills (and Pragers) from whence cometh my help".

II.—THE MATHEMATICIAN'S APPROACH

In so far as mathematicians are generally concerned with matter on an effectively macroscopic scale, the engineer feels competent to express an opinion on the physical premises on which their analysis is based. If these are acceptable, he has no doubt that the analysis itself is sound and he is therefore prepared to accept the results. All that he asks the mathematician, therefore, is that: (a) he should make reasonable assumptions and state them clearly, whether they occur as premises or as limitations or approximations during his analysis, and (b) he should express his results in intelligible terms and in a form in which they are safe and reasonably convenient to handle.

For the most part mathematical theory is at present confined to what is called a perfectly plastic body. Members of this Institute, in a state of post-prandial resignation, who are constrained to listen to an evening discourse in such surroundings without any hope of discussion, will not need to look far for a definition of a perfectly plastic body, but for the sake of the less introspective it is embodied quite simply in either of the cyclic stress/strain diagrams in Fig. 1. Such a body is isotropic and is characterized by the

absence of strain-hardening or creep or Bauschinger effect.

For analysis involving compound stress it is also necessary to adopt some stress criterion for yield in the material. In the study of materials, and particularly in the plastic range, it is important to recognize that any system of stress can be, and physically

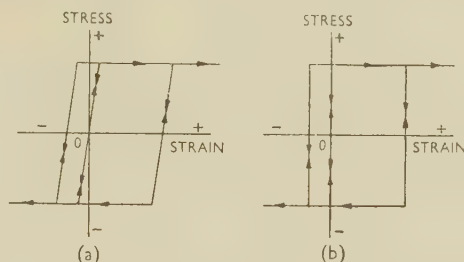


FIG. 1.—Cyclic Stress/Strain Diagrams for a Perfectly Plastic Body. (a) Elastic-plastic (Prandtl-Reuss); (b) Rigid-plastic (Lévy-v. Mises).

should be, divided into a volumetric system which tends to change the volume of the material, and a distortional or "reduced" system which tends to change its shape. This is shown diagrammatically in Fig. 2. It has been established that the volumetric stress has no significant effect on the conditions of yield, so that these can be expressed in terms of the reduced stresses s_1, s_2, s_3 in Fig. 2. For isotropic material, it can be shown mathematically that the yield criterion must be expressible as a symmetrical function of these three stresses and in particular as a

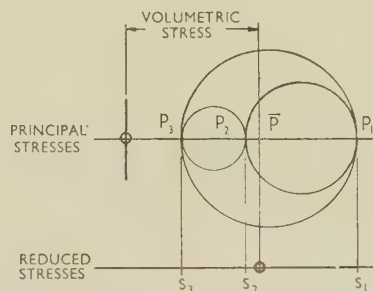


FIG. 2.—Yield Criteria for Compound Stress Analysis.

$$J_1 = s_1 + s_2 + s_3 = 0, \quad J_2 = \frac{1}{2}(s_1^2 + s_2^2 + s_3^2),$$

$$J_3 = \frac{1}{3}(s_1^3 + s_2^3 + s_3^3),$$

$$v. \text{ Mises-Hencky: } J_2 = k^2$$

$$\text{Tresca: } s_1 - s_3 = 2k$$

$$4J_2^3 - 27J_3^2 - 36k^2J_2^2 + 96k^4J_2 - 64k^6 = 0$$

function of the three so-called invariants J_1, J_2, J_3 as defined in Fig. 2. Of these J_1 is zero by definition, so the mathematician is left with J_2 and J_3 . On grounds of academic simplicity von Mises in 1913 adopted the second invariant, J_2 , as a criterion for plastic flow. The same criterion was proposed by Hencky in 1924 from the standpoint of shear-strain energy, and it has been found empirically to be serviceable for non-ferrous metals generally. So whether the particles in the metal make a calculation of the second invariant of the reduced stresses before

deciding to slide off, or whether they respond to some simpler physical urge is of no practical consequence. For the peace of mind of those ferrous metallurgists who prefer the physically simpler shear-stress yield criterion introduced by Tresca, which appears quite unsymmetrical to the normal eye, a mathematician has discovered that even this can be expressed in terms of the invariants; but at a prohibitive cost, as shown in the caption to Fig. 2.

In a perfectly plastic body the stress system will conform to the same yield condition, however much flow has occurred. In contrast to this, any ordinary metal not only hardens but also becomes anisotropic under plastic strain; so that the yield condition is not only altered in scale, but it ceases to be symmetrical and it is not uniquely determined by the resultant strain. In its present stage, the mathematical theory of plasticity has only been applied to strain-hardening materials in a few cases, and in these only as a rule on the assumption of continued isotropy.

In order to study the plastic flow of a material, it is necessary to know not only the stress conditions for

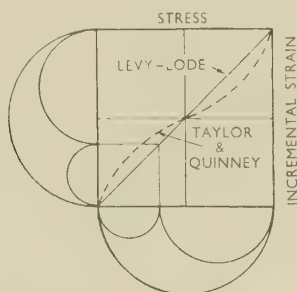


FIG. 3.—Geometry of Plastic Flow in Relation to Stress System.

flow to commence, but also the geometry of this flow in relation to the stress system. In isotropic material the principle of symmetry can be invoked to show that the principal directions of stress and strain are identical, and in a material which conforms to the von Mises yield criterion it seems justifiable to assume that at any stage the geometry of distortional strain-rates is the same as the geometry of distortional stress, as suggested by the Lévy-Lode line in Fig. 3. In fact, the present mathematical theory of plasticity is built on both these assumptions, although it is known that in metals after considerable overstrain the stress and strain systems may not be coaxial, and that in metals in ordinary commercial condition the systems of distortional stress and strain are by no means identical, as shown by the Taylor and Quinney line in Fig. 3.

The problems to which the theory of plasticity is applied are of two types:

(1) Those concerned with "contained plastic deformation" in which the total strain is small, so that the elastic strain is not negligible in comparison with the plastic. These include such problems as the auto-fretting of thick tubes and the limit design of structures.

(2) Those involving "unrestricted plastic flow", in which the plastic deformation is so great that the elastic strain is negligible. These problems include most of the technological forming processes. In most problems of this type the conditions are complex; one region may be purely elastic, another may be subject to contained plastic deformation, and another to unrestricted plastic flow. To solve such problems completely it would be necessary not only to investigate the stress and strain conditions in each region, but also to determine the boundaries between the regions. The difficulties of mapping the elastic-plastic boundary are such that very few problems involving contained plastic deformation have as yet yielded to the patience of the mathematical computer, and the boundary between the regions of contained and unrestricted flow may well be found to depend on the history of the stress/strain development. But with the simplifying assumptions discussed above, it has been found possible to map the region of unrestricted flow in a number of cases of practical interest, on the assumption that the material is rigid/plastic, so that no strain occurs except in the regions of actual plastic flow. Fig. 4 (a) (Plate XII) shows plots of this kind obtained by Green¹ for two cases of extrusion.

It should be pointed out that these solutions apply only to two-dimensional flow, or "plane strain" as the mathematicians call it. Under plane strain the conditions at every point are essentially those of simple shear, which are, of course, by no means representative of most technological processes. But comparisons made with two-dimensional models have given encouraging results, and descriptive agreement has even been obtained with models having radial symmetry.

In spite of these simplifying assumptions, the methods applied to these problems at present have two drawbacks:

(1) They are based essentially on a process of trial and error, in that they start with a guessed solution and deduce the conditions which it satisfies, which may or may not be those prescribed.

(2) There is no guarantee that the solution so achieved is unique; it merely stands until a better one is found or until it is disproved by experiment. This lack of uniqueness may prove to be an inherent feature of the hypothetical perfectly plastic body, and may disappear when it becomes possible to take strain-hardening into account.

It is clearly impossible to give any reasoned account of the plane-strain technique in this lecture, but solutions to technological problems are becoming increasingly available, and the engineer and metallurgist should be in a position at least to interpret a solution in the form in which it is usually represented and to satisfy himself that it is physically satisfactory. It may therefore be helpful to glance at the solution of an apparently simple case which nevertheless illustrates the procedure and the physical principles involved.

Fig. 5 refers to the action of a cutting tool taking a

continuous cut of depth t_0 from material capable of plastic flow.

Firstly we draw as far as possible the geometrical framework into which the plastic field has to be fitted. Next we make a guess as to a likely mode of deformation, and we draw an orthogonal mesh of lines to represent the corresponding directions of maximum shear stress. These are appropriately called "shear lines" or, less appropriately, "slip lines". These lines must obey certain rules of direction at the boundaries, depending on frictional and other conditions, and internally, depending on changes in the

and a compatible velocity diagram, we have the form of a possible solution to our problem, and we complete this by computing the impressed force system necessary to produce the flow pattern we have predicted.

If we are cautious, we then try to devise some different flow pattern which will also satisfy the prescribed conditions, but requires a smaller impressed force. If we are less cautious, we publish our first solution, and a competitor will no doubt discover the second. In either case this supersedes the first solution and stands until it is either superseded in turn or submitted to experimental test. If this

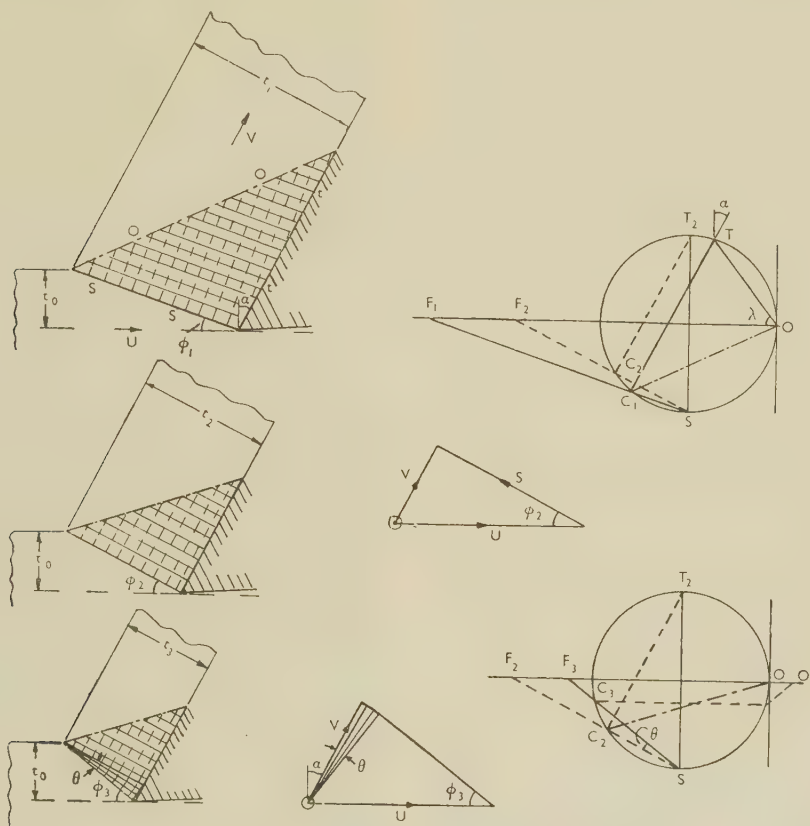


FIG. 5.—Continuous Cutting of Plastic Material.

volumetric stress. Along a straight shear line the volumetric stress is constant, along a curved line it changes in a particular way. A rectilinear mesh defines a region in which the stress system is uniform. Examples of this will be found in Fig. 4 (a) (lower diagram) and, more particularly, in Fig. 5.

When we have completed the mesh of shear lines, which is frequently composed of zones of different patterns, we draw a velocity diagram to show the direction and rate of flow at all relevant parts of the plastic field. This velocity distribution must fulfil the various boundary conditions and must be compatible with the shear-line mesh. There must be no loss or accumulation of material in any zone, and no elongation must be involved along any shear line.

When we have produced a consistent shear-line mesh

test gives qualitative agreement, we have reason to be gratified; if it gives quantitative agreement, we are outwardly jubilant, but inwardly disturbed; because we know that no real material and apparatus can fully reproduce the artificial conditions on which our solution has been based.

In Fig. 5 the essential cutting forces according to the successive solution are represented by OF_1 , OF_2 , O_3F_3 , so that the third solution is the most eligible.

A useful means of checking, or even inspiring, the shear-line field is afforded by the simulative distortion of scribed gratings on sectioned specimens. Fig. 4 (b) shows such gratings as computed by Green,¹ compared with Plasticine models prepared by him. Fig. 4 (c) shows grids obtained in the extrusion of circular lead rod, under generally comparable conditions. These

gratings show the lines of flow and the integrated distortion and reveal any surfaces of discontinuity. But the lines on these gratings must not be confused with the shear lines; they are quite different and can in general be predicted from them only by a further process of step-by-step computation.

We must now take leave of the Mathahorn, but we cannot do so without noticing again that its higher slopes are invisible in the clouds. There too, no doubt, mathematicians are hard at work, but they will need to come down below the cloud line before we shall know whether their explorations have yielded anything of material value.

And now may the engineer be allowed to take a side-long and perhaps obtrusive glance at the Metahorn?

III.—THE METAL PHYSICIST'S APPROACH

Broadly, the terms of reference of the metal physicist in the field of plasticity are to explain and ultimately to predict the plastic properties of materials in terms of their atomic arrangement and structure. Within this reference the objectives which appear most significant to the engineering scientist are:

- (1) To enable the search for new metals for plastic processes to be pursued by less empirical and fortuitous methods than prevail at the present time.
- (2) To rationalize the prediction of the effect on plastic properties of various mechanical and heat-treatments and of various alloying additions.
- (3) To enable test procedure for the plastic properties used in technological processes to be planned on fundamental lines.

These objectives suggest three main fields of scientific inquiry:

- (i) To explain the properties of a single crystal in terms of its atomic arrangement and structure.
- (ii) Knowing the plastic properties of a single crystal, to predict the properties of a polycrystalline aggregate. This inquiry must, of course, extend to aggregates in which the crystals are of various shapes, sizes, and orientations, and of different constitutions.
- (iii) To study plastic stress/strain relations in the broadest sense. This would involve separate investigations of: (a) yield conditions for material in any given state, (b) the causes, mechanism, and effects of strain-hardening, and (c) the effects of anisotropy, whether intrinsic to the method of formation or induced by work-hardening processes.

The engineer is conscious that each of these fields of inquiry is extensive, and beset by difficulties both of experiment and theory. He also realizes that they have attracted the attention of physicists and mathematicians of the first rank and that real progress is being made. Yet he cannot help feeling that a great

deal more time and effort will need to be expended before the metal physicist can hope to produce results of a kind suitable for practical application.

It is accepted that the properties of a polycrystalline body must depend on the properties of its constituent crystals, but attempts to derive the yield criterion for an aggregate whose individual crystals conform to the Schmidt law have for the most part been based on simplifying assumptions and unrealistic statistical methods, and the treatments have been one-eyed, in the sense that they have either considered stress distribution and turned a blind eye to the need for conformity of strains, or they have prescribed equality of strain and neglected the need for stress continuity. A recent treatment by Bishop and Hill,² based on certain extremum principles and applied to an aggregate of face-centred cubic crystals, does, however, seem to be more physically tenable and is likely to survive. It is interesting to find that the yield surface derived by Bishop and Hill lies quite close to that proposed by von Mises, which in its Hencky form appeals to the instincts of the engineer as a rational criterion for statistically isotropic material.

But even when the problem of the yield criterion has been solved for the various space lattices and their combinations, and when the nature and influence of marginal conditions have been finally determined, there will still lie ahead the problems associated with the geometry of plastic strain development, with the polycrystalline features of strain-hardening, and with the growth of macroscopic anisotropy, problems to which the present field of inquiry seems to be little more than an elementary introduction.

In the second general field of inquiry, that which is confined within crystal boundaries and is concerned with internal crystal structure, the engineer finds it difficult even to form his own opinion of the present state of knowledge or the direction and rate of progress. He feels confident that the science of crystal plasticity must ultimately be built up on the mechanics of a relatively simple lattice structure, yet he is presented with clear evidence that an intermediate mosaic structure can exist whose unit lies somewhere between the unit cell and the metal crystal, and which affects the intracrystalline processes of deformation and strain-hardening. At the present time this rather ill-defined structure can be used as a convenient means for explaining discrepancies between results at the crystal and atomic levels, but in due course it must further extend the field of inquiry of the metal physicist and lead to a critical study of the mosaic law.

At the atomic level the engineer realizes that he needs to tread very carefully; because he is not accustomed to deal in astronomic reciprocals, and the micro-geometry of the space lattice is based on techniques which have to be seen to be disbelieved. But he feels none the less that the traditional model of the space lattice, with which he is entertained at metallurgical lectures, would form an imperfect basis for any realistic mechanical theory. The space

lattice ostensibly consists of an array of unit cells which in nearly all metals conform to one of three simple types, and are shown as in the lower diagrams of Figs. 6 and 7, consisting of a nice round black atom

of convention, and that in fact every atom in a pure metal lattice is similar to every other atom and similarly disposed to its neighbours. But he is not so forthcoming if he is asked why his atoms are spherical and why some tolerate close packing while others, even of the same metal, need elbow-room and yet occupy only the same space. Nor is he convincing when he uses his model to demonstrate the difference between elastic and plastic strain or the doctrine of preferential slip on close-packed planes in close-packed directions.

To the simple-minded engineer, who has a weakness for working models, it seems that if every atom is the same as every other, the logical unit for a crystal lattice is a single atom, and one whose effective shape and size are such that an aggregation of identical atoms will pack into the particular array which is revealed by X-ray and similar methods. An aggregate of units of the shape shown in Fig. 6 (a), for instance, will pack together in three-dimensional space without voids, and when so packed will necessarily form a face-centred cubic lattice. If one-half of the unit were rotated through 180° relative to the other, as in Fig. 6 (b), the result would automatically build into a close-packed hexagonal lattice. The corresponding unit for a body-centred cubic lattice of identical

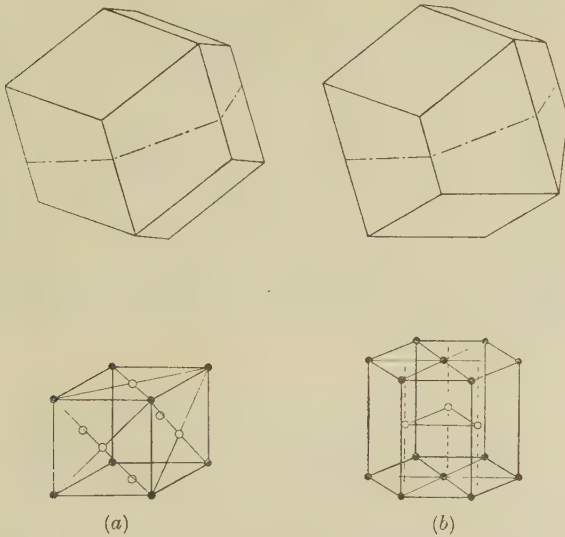


FIG. 6.—Unit Blocks for (a) Face-centred cubic lattice, and (b) Close-packed hexagonal lattice.

at each corner of the cell, together with attendant white atoms disposed in or around the cell according to its type. To the simple mind of the engineer such a cell is not a unit at all, for an aggregation of such cells would produce a crystal overpopulated to the extent of some hundreds per cent. If taxed on this point the metal physicist concedes that the real unit, in the case of a face-centred cubic lattice for example, consists of one (black) corner atom with three (white) face-centres. And when he is further pressed to explain the difference between the black atom and the white ones, he admits that this is merely a matter

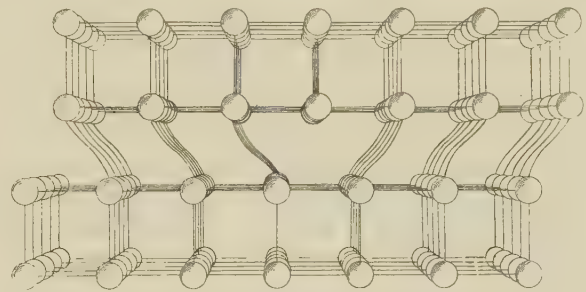


FIG. 8.—Model of Simple Cubic Lattice, Showing Dislocation.

atoms is shown in Fig. 7 (a), while the compound unit for a body-centred cubic lattice of two dissimilar elements in equal atomic proportions might be of the form shown in Fig. 7 (b). The engineer does not suggest, of course, that these solid figures are the actual shapes of the atoms, any more than are the black and white balls with vacuous interstices, but he does suggest that they represent the effective shapes in so far as resistance to interpenetration and deformation is concerned, that they show a clear distinction between elastic and plastic strain, and that they provide a more informative model of the processes of slip and dislocation than the nodulous networks of knock-kneed knobs (Fig. 8) in which the metal physicist is apt to enmesh his students.

The third field of inquiry suggested for the metal physicist, which is in effect the mapping and contouring of the plastic range so that stress/strain relationships can be fully understood in the most general sense, is a field which cannot be fully harvested until intra- and inter-crystalline mechanics is properly understood. But there seems to be a great need and

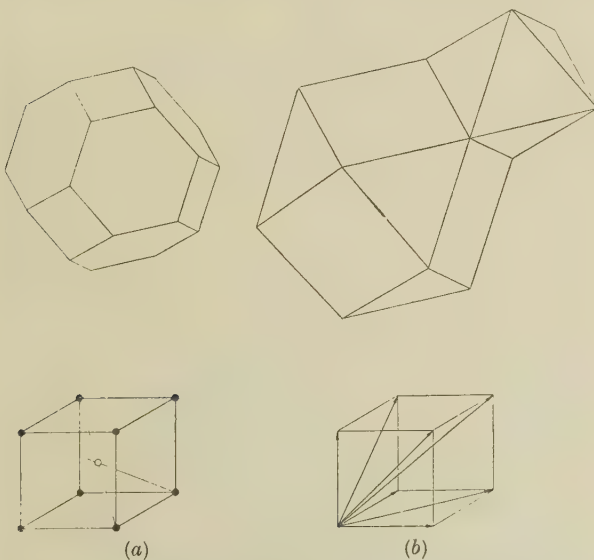


FIG. 7.—Unit Blocks for Body-Centred Cubic Lattice: (a) Identical atoms; (b) Dissimilar atoms.

great opportunity for work in this field at a more empirical level, so that the mathematician and the engineer can be provided with at least a serviceable code of practice which they can apply to problems involving strain-hardening in its more general form as affected by anisotropy and strain history. It might be claimed that a great deal is already known about stress/strain relationships in the plastic range, and it is true that a large volume of empirical data on tensile and torsional properties has been accumulated. But, as Prager has recently pointed out, these data are very largely iterative and are concentrated on a very restricted corner of the field. A good deal is known about the initial "yield surface" for annealed materials, but comparatively little about the geometry of strain which follows yield under various stress systems, or about the effect of overstrain on the enlargement, displacement, and distortion of the yield surface. And next to nothing is known of the effects of a stress system which changes during the straining process. There are, of course, certain experimental difficulties which must attend the widening of this field of inquiry; in particular, it is almost essential to have available a combined torsion and tension testing machine in which the two straining systems can be varied independently, and some means for producing thin-walled tubular specimens from intrinsically isotropic and equi-axed material. And difficulties are likely to arise in defining the inception of plastic flow in material whose yield point has become blurred by the Bauschinger or cognate effects. But this field provides scope for valuable work which, although primarily empirical, might well lead to important generalizations in the mathematical theory and might even assist investigations in the sphere of crystal plasticity.

IV.—THE ENGINEER'S APPROACH

And now, having given you an engineer's viewpoint of activities and prospects on the Mathahorn and the Metahorn, I must do my best to satisfy you that engineers on the foot-hills have not been entirely spectators. So I would like to show you something of the methods we have to adopt and the results we have obtained in our own pedestrian explorations.

In the time available it would be useless to attempt even a summary of the work which has been done in recent years on the various technological applications of plasticity, such as rolling, forging, extrusion, drawing, and forming. So I propose to invite your attention to one corner only of this field and to use the deep-drawing of a cylindrical shell (Fig. 9) as an example to illustrate the methods we have been able—one might almost say forced—to develop and the kind of results we have been able to obtain. This example has the advantage that reliable experimental data are available to check analytical results over an extended range.

In its general form this problem is at present well beyond the range of the theoretical plastician. The

conditions approximate to those of plane stress and are therefore intrinsically more difficult to handle than those of plane strain. On the other hand, it has certain simplifying features which make approximate solutions worth attempting, particularly when they can be checked from stage to stage by empirical data. The stress system is symmetrical, and its axes remain unchanged in the material throughout the drawing process. Stress and strain vary only in the direction of principal flow and, apart from bending over the die profile, there is no significant reversal of strain.

On the other hand, the conditions are more complex than in tube drawing, for example, because the stress and strain in a particle are functions of its initial position as well as its current location, so that the solution involves step-by-step computation. And the problem is further complicated by the fact that the

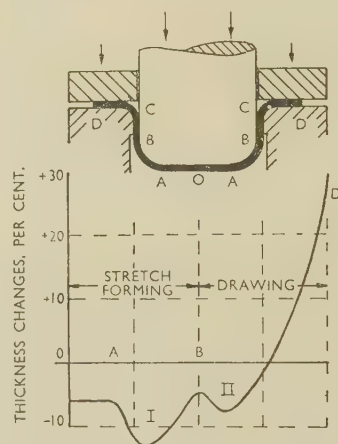


FIG. 9.—Deep Drawing of Cylindrical Shell.

strain development and plastic requirements of one part of the metal blank are fundamentally different from those of the other part.

In order to determine the punch load at various stages of the drawing process and the changes in thickness which are induced, both matters of evident importance to the press-tool engineer, it is necessary to follow the changes in stress and strain which develop as material is drawn radially inwards in the flat blank and over the lip of the die into the cylindrical walls of the cup. This process has at least three functional constituents: plane radial drawing, plastic bending and un-bending over the die, and the frictional implications of the blank-holder and die profile. In the most complete analytical treatment which is so far available,³ these three constituents are treated separately, and later superposed on the assumption that their effects on one another are small.

Several other important assumptions are made in this treatment. It is assumed that the whole of any blank-holding force is transmitted at the outer rim of the blank; it is assumed that although changes develop in the flange thickness from stage to stage, this thickness is effectively uniform at any instant, and it is

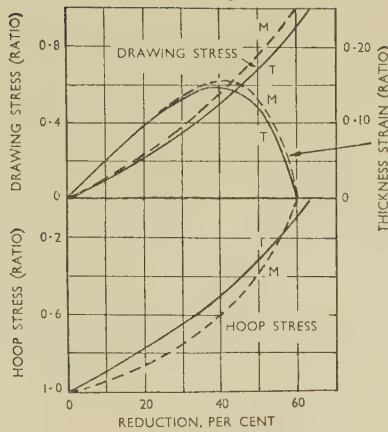


FIG. 10.—Stress and Strain in Tube Sinking. Comparison of yield hypotheses. M = v. Mises, T = Tresca.

assumed that the rate of straining is so slow that stress/strain equilibrium is maintained throughout the operation. In the bending analysis no account is taken of the Bauschinger effect. Throughout the treatment the Tresca shear-stress yield criterion and the Lévy-Lode stress/strain relation are adopted, and empirical strain-hardening characteristics are simulated by a power law, modified to allow for initial hardness, and simplified to a linear relationship over the relatively small strain interval covered by bending and unbending. In the treatment of die profile

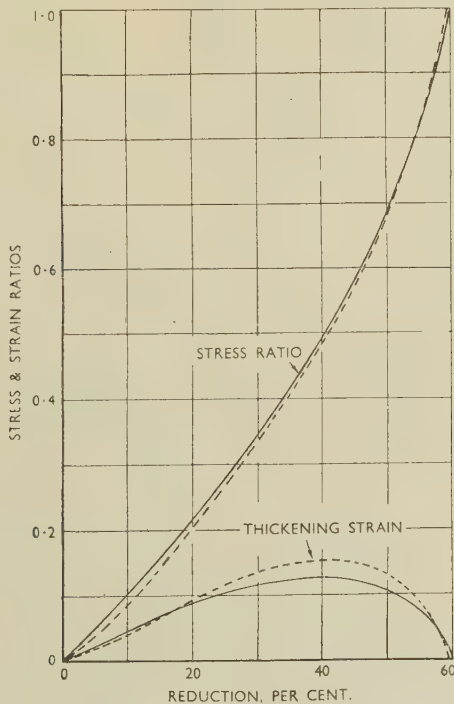


FIG. 11.—Stress and Strain in Tube Sinking. Effect of stress/strain geometry.

— — — Lévy-Lode curve $\nu = \mu$
 ————— Empirical curve $\nu = \mu^3/2$,
 based on Taylor and Quinney's measurements.⁵

friction, consideration is given to hoop compression in relation to the cup radius as well as radial tension in relation to the die profile, but these effects are superposed. The analysis leads at several points to implicit equations soluble only by processes of successive approximation; and the distribution of strains in particular can be determined only by step-by-step computation from the outer rim.

This list of articles of faith need not be accepted altogether blindly. It is possible to examine the implications of certain of the assumptions in the case of tube sinking,⁴ which is physically similar but

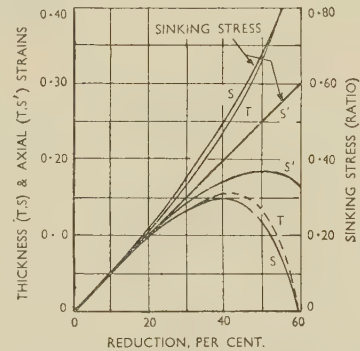


FIG. 12.—Stress and Strain in Tube Sinking. Effect of neglecting thickness changes.

T = thickening considered.
 S = " " neglected.
 S' = " " (pressure-sinking).

analytically simpler, and Figs. 10–12 show the degree of error likely to be introduced by :

- (1) The use of the Tresca in place of the von Mises criterion for yield (Fig. 10).
- (2) The use of the Lévy-Lode line (Fig. 11), in comparison with an empirical curve based on Taylor and Quinney's measurements.⁵
- (3) Neglecting thickness changes in the stress calculations (Fig. 12).

By taking reasonable conditions, it is possible also to estimate the relative importance of bending and friction in tube sinking.⁶ These are shown in Table I.

TABLE I.—Constituents of Total Sinking Stress.

Constituent	Wall thickness 0.0635 in.		Wall thickness 0.1305 in.	
	lb./in. ²	%	lb./in. ²	%
Pure radial deformation . . .	24,800	75.6	27,320	68.2
Bending and unbending . . .	3,920	11.9	8,280	20.7
Surface friction . . .	5,530	16.8	5,970	15.0
Thickness variation . . .	—1,400	—4.3	—1,560	—3.9
Total . . .	32,850	100	39,990	100

When the assumptions enumerated above are applied to the drawing of a cylindrical shell, and when values are applied for coefficients of friction based on

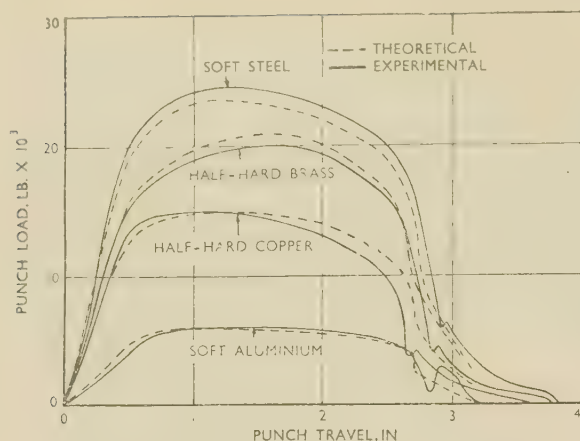


FIG. 13.—Load/Penetration Relations for Drawing of a Cylindrical Shell.

previous experience, the relationships between punch load and travel computed for certain specified dimensions and four different metals are as shown³ in Fig. 13. Autographic diagrams obtained experimentally under the same conditions are also shown, and apart from mild steel, for which the assumed coefficient of friction was probably low, comparisons show an encouraging conformity in the shapes of the diagrams as well as in maximum punch loads.

A corresponding comparison between theoretical and measured values of the thickness strain (Fig. 14) shows good agreement for all the metals examined. Radial strains (Fig. 15) agree well for aluminium and copper, but not so well for half-hard brass and mild steel. This may well be due to anisotropy, which was in fact revealed by a tendency to form ears.

The generally satisfactory outcome of this particular analysis is due in some measure, of course, to the

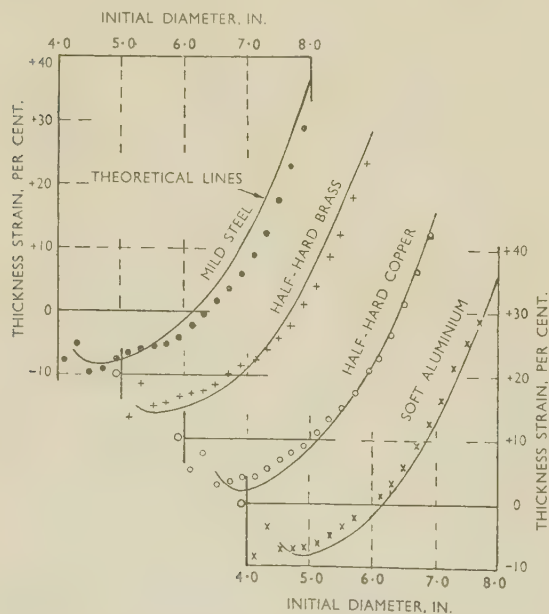


FIG. 14.—Thickness Strains in Cup Drawing.

mutual balancing of errors, but it does suggest: (a) that no physical principles or significant factors involved in the drawing operation have been overlooked, and (b) that provided reasonable assumptions and approximations are made in conformity with these principles, it is possible without recourse to exact theory, to obtain results which the press-tool engineer can apply with reasonable confidence and sufficient accuracy, albeit at present by a rather laborious procedure.

As a matter of interest, Table II gives an analysis of the press work involved in a typical cup-drawing operation, and shows in particular the contributions required by plastic bending and by friction.

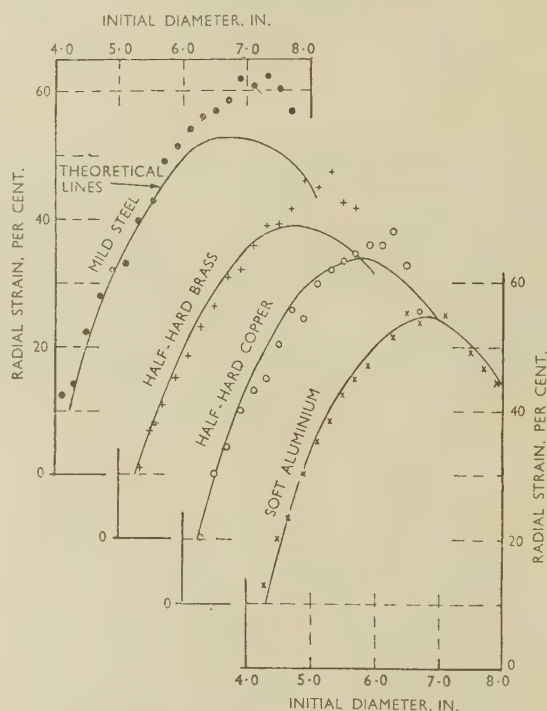


FIG. 15.—Radial Strains in Cup Drawing.

So far, so good. For given conditions we can predict the drawing load and the thickness changes from point to point. But can we predict whether the drawing operation will be successful or not? The answer is that at present we cannot. Our treatment has in fact covered only those outer parts of the blank which are drawn in and over the die-profile. The conditions of stress and strain in those inner parts which have not come under the direct influence of the die, but have been stretch-formed over the head of the punch during the drawing process, are quite different and need separate treatment. Moreover, when fracture occurs during drawing, it generally occurs in this stretch-formed zone.

If we consider the drawing operation as a whole, we shall realize that although the drawing load required is determined by conditions in the outer drawing zone, the capacity of the cup to sustain this load is deter-

mined by conditions in the inner, stretch-formed zone. It follows that a knowledge of the process of stretch-forming is essential to a full practical understanding of the deep-drawing operation.

The conditions which control stretch-forming are no less complex than those which control true drawing, for even in a simple symmetrical draw they include the profile geometry of the punch-head, the degree of lubrication over the punch-head, and the stretch-forming tension imposed by the conditions in the drawing zone. The stress system in the stretch-forming zone is essentially biaxial tension, varying in ratio and intensity from point to point and from

proportions, and in particular of the conditions under which this strain will reach locally the critical conditions for necking and consequent rupture. Some progress has been made in the study of stretch-forming under the simplified conditions when the solid punch is replaced by unilateral fluid pressure. Hill has been able to predict strain development during the earlier stages of "bulging", and at Sheffield it has been found possible to predict the critical degree of thinning at which instability occurs and failure becomes imminent. The extent of general thinning before the point of instability is so much greater than in simple tension that the "bulge test", as it is called, can be

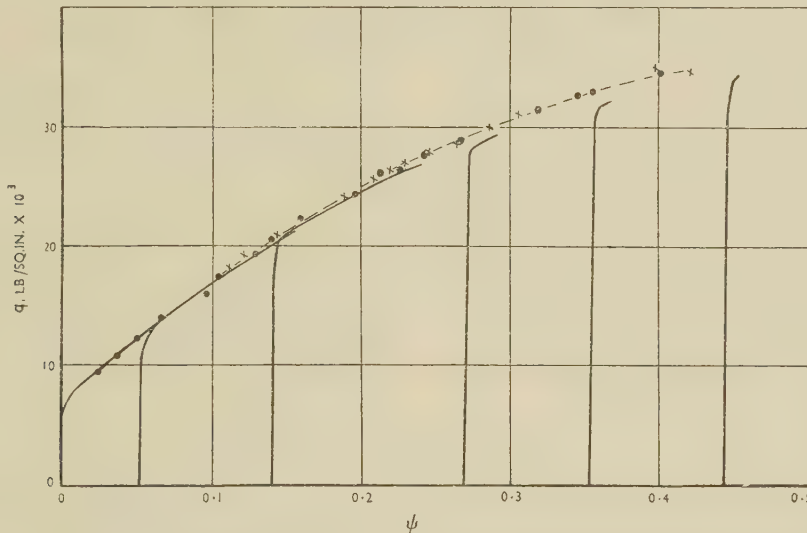


FIG. 16.—Representative Stress/Strain Curves for Brass. (P. B. Mellor.)

KEY.
 ● Soft 70:30 brass
 × Half-hard 70:30 brass } from bulge test.
 Full-line curves obtained by rolling and testing in tension.

stage to stage. The effect of this biaxial tension is to thin the metal everywhere, and locally this thinning is generally more severe than any produced in the drawing zone and more likely to lead to fracture.

For this reason a full study of the stretch-formed zone must include, and indeed be based upon, a study of strain under biaxial tension of various and varying

TABLE II.—Punch Work in a Typical Cup-Drawing Operation.

Blank dia.	8.0 in.	Punch dia.	4.0 in.
Blank thickness . . .	0.039 in.	Punch head radius . .	0.25 in.
Blank-holding	15,500 lb.	Profile radius	0.25 in.

Material: 0.08% carbon rimming steel

	In.-lb.	%
Strain work in radial drawing	41,000	70
Strain work in bending . .	4,660	
Strain work in un-bending . .	5,610	10,300
Frictional work :		
Blank-holder	3,150	
Die-profile	4,460	7,600
		100

used (Fig. 16) to obtain a strain-hardening characteristic covering a much wider range than the tensile test, and therefore more useful under conditions of severe plastic deformation, although it is more tedious to measure and compute. The results plotted in Fig. 16 are due to P. B. Mellor.

But the hydrostatic bulge is merely an elementary introduction to the more general problems of stretch-forming. Attention is now becoming focused on these problems, but a great deal of experimental and theoretical work will be required before the limiting conditions of successful drawing can be predicted with any confidence. In the meantime we must continue to rely on purely simulative tests for this purpose.

So it is clear that we are still a long way from a full understanding of the deep-drawing of even a cylindrical shell. And this is the simplest technological form of the deep-drawing process. Other problems which assume importance in unsymmetrical drawing operations, such as buckling, internal-stress distribution, spring-back, and the effect of locally applied restraints, have as yet scarcely even been formulated.

The deep-drawing process, although its problems are perhaps more obvious in their complexity than those of some other processes such as rolling and forging, is not exceptional as regards the present state of knowledge or the prospects of technological understanding. None of these processes is confined to a single problem; on the contrary, each provides a whole matrix of problems, mutually reactive and often mutually reproductive, for the study of one is liable at any time to produce a progeny of still more intractable problems calling for new methods of analysis and experiment.

In this technological field the engineer finds it difficult to believe that the theoretical plastician can ever do more than provide him with guidance and weapons, and he sometimes becomes appalled at the thought of the range of weapons of which he stands in need.

He does, however, find it instructive on occasion to sit back, as it were, and take a perspective view of a typical plastic process, such as deep-drawing. When he does this he realizes that, in spite of the technical complexity of such a process, the functional behaviour of the material in every phase and respect is basically determined by its characteristic stress/strain relationship, even up to the conditions of its ultimate rupture. It therefore seems an inevitable conclusion that, in some way as yet to be discovered, every one of the

properties which contribute to the so-called drawability of a metal is embodied in its strain-hardening characteristics. And there is little room for doubt that these characteristics in their turn are embodied in its crystalline structure, which is itself a function of its lattice arrangement, as modified by crystal-boundary conditions. So it would seem, in short, that the essential secrets of technical plasticity are somehow locked up in the lattice cell.

In spite of his assumed unconcern about happenings on the atomic scale, the engineer cannot therefore really afford to be indifferent to the activities of the metal physicist, and no-one will be more grateful if the study of crystal plasticity does bring the technical assessment of plastic properties within the ambit of a few basic principles expressible in terms of atomic structure and array.

Then, indeed, will there be flags on the Metahorn, and jubilation among the harassed mortals, whether metallurgists or engineers, on the foot-hills of the plastic range.

ACKNOWLEDGEMENT

In the preparation of diagrams and lantern slides for this lecture, the author has received valuable help from his colleagues Messrs. E. M. Loxley, M.Eng., and S. G. Harris.

REFERENCES

1. A. P. Green, *Phil. Mag.*, 1951, [vii], **42**, 365; and private communication.
2. J. F. W. Bishop and R. Hill, *ibid.*, 1951, [vii], **42**, 1298.
3. S. Y. Chung and H. W. Swift, *Inst. Mech. Eng., War Emergency Proc.*, 1952, (**68**), 1.
4. H. W. Swift, *Phil. Mag.*, 1949, [vii], **40**, 883.
5. G. I. Taylor and H. Quinney, *Phil. Trans. Roy. Soc.*, 1931, [A], **230**, 323.
6. S. Y. Chung and H. W. Swift, *J. Iron Steel Inst.*, 1952, **170**, 29.

THE EMBRITTLEMENT OF COPPER-ANTIMONY ALLOYS AT LOW TEMPERATURES*

1423

By D. McLEAN,† B.Sc., MEMBER

(Communication from the National Physical Laboratory.)

SYNOPSIS

Charpy tests on bars with an Izod V-notch have been carried out from +100° to -253° C. on slowly cooled copper alloys containing up to 1.3% antimony. In these alloys the antimony is thought to have been entirely in solid solution. Alloys containing between 0.14 and 0.56% antimony became brittle at low temperatures, the embrittlement being reversible and generally similar to that of ferritic steels at low temperature.

I.—INTRODUCTION

IN 1946 McLean and Northcott¹ showed that 70:30 brasses containing small quantities of antimony were brittle when slowly cooled from the annealing temperature, although tough when quenched. A study of the solubility of antimony in brass at 200°–400° C., showed the presence of a precipitate, whose solubility in the matrix fell from about 0.3% antimony at 400° C. to less than 0.015% at 200° C. Microscopic examination of the embrittled alloys failed, however, to reveal the presence of this phase. Instead, a faint grain-boundary film, having distinctly different characteristics, was detected. This film occurred in alloys containing upwards of 0.1% antimony.

The view was developed that the film was not a precipitate, but was due to the concentration of antimony atoms along the grain boundary. It was thought that at the annealing temperature the antimony atoms would be uniformly distributed throughout the crystals, but that as the temperature fell some of them would segregate to the grain boundary, without actually coming out of solution, and there cause embrittlement. This type of segregation was termed "equilibrium segregation", and it was regarded as a consequence of the difference in size between the atoms of the solvent and those of the solute. Atoms differing much in size from those of the solvent would be expected to segregate at regions of irregular structure, such as grain boundaries, where they could be accommodated without excessive strain.

If this is the true explanation, it should be possible to produce brittleness in solid solutions in which there is no question of the precipitation of a second phase, and the experiments described in the present paper were an attempt to produce such an embrittlement.

Antimony is very much more soluble in pure copper than in 70:30 brass. According to Mertz and Mathewson,² who made very careful observations, the solubility of antimony in copper is 2.1% at 200° C., and precipitation is so slow that 1000 hr. are required

to attain equilibrium. Copper-antimony alloys containing 1–2% antimony are, like the antimonial brasses, more brittle when furnace-cooled from the annealing temperature than when quenched. A series of pure copper-antimony alloys containing up to 1.6% antimony were therefore prepared, and their toughness was studied by means of standard V-notch Charpy tests made over a range of temperatures.

II.—EXPERIMENTAL PROCEDURE

1. PREPARATION OF SAMPLES

Seven alloys were made in 1.2-kg. lots from electrolytic copper and antimony of 99.93% purity. The copper was melted in a closed cylindrical graphite crucible, and the antimony then added. After mixing, the alloy was cooled by placing the crucible on a water-cooled metal plate, in such a way that the alloy solidified from the bottom to produce a pipe-free round ingot, 13 cm. long by 3 cm. dia., low in oxygen and without porosity. Analyses made at the top and bottom of the ingots gave the following antimony contents:

	CSB0	CSB1	CSB2	CSB3	CSB9	CSB7	CSB5
Top	0	0.08	0.14	0.25	0.58	1.31	1.68%
Bottom	0	0.08	0.14	0.24	0.55	1.28	1.53%

The ingots were annealed for 36 hr. at 675° C. and cold rolled to $\frac{5}{8}$ -in.-dia. bar. The 1.6% antimony alloy cracked too badly during rolling to be used; the 1.3% antimony alloy cracked, but could be used; and the other alloys cracked little or not at all.

Charpy impact test-pieces with an Izod V-notch were prepared, and annealed for 1 hr. at 650° C. They were cooled from the annealing temperature in the furnace, at a mean rate of 10° C./hr. from 600° to 100° C., in order to give the antimony an opportunity to segregate to the grain boundaries. Microscopic examination of the alloys after this treatment showed them to consist of uniform grains of solid solution, with no trace of the compound Cu₂Sb. There were,

* Manuscript received 12 May 1952.

† Metallurgy Division, National Physical Laboratory, Teddington, Middlesex.

however, a few rounded dark particles of a non-metallic inclusion, the number of which increased with the antimony content. The average grain diameter was from 0.03 to 0.1 mm., the antimony-rich alloys having the finer grain-size.

2. NOTCHED-BAR IMPACT TESTS

Impact tests on the alloys were made at 100°, 18°, 14°, 0°, -78°, -196°, and -253° C. The specimens were immersed in liquid baths at these temperatures, and after being allowed to reach equilibrium, were quickly removed and tested within 5-10 sec. The rise in temperature during testing would probably not have exceeded 10° C., but to minimize the rise the specimens cooled in liquid hydrogen were wrapped in thin paper cartons. The results of the tests are given in Fig. 1.

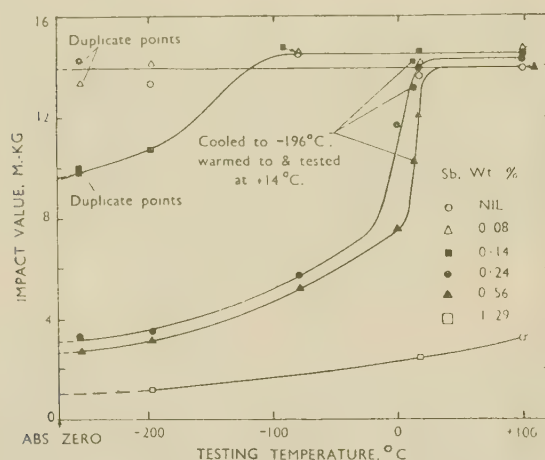


Fig. 1.—Impact Tests on Copper-Antimony Alloys.

Pure copper and the alloy containing 0.08% antimony were tough at all temperatures, the energy absorption at -253° C. being the same as at room temperature within the limits of experimental error. The 0.14% antimony alloy remained tough to -78° C. and at lower temperatures showed some sign of embrittlement. In the alloys containing 0.24 and 0.56% antimony, a clearly marked change from a tough state at high temperatures to a brittle state at low temperatures occurred. This change strongly resembled the tough-to-brittle transition observed in ferritic steels. The alloy containing 1.29% antimony behaved as though its tough-to-brittle transition might have been above 100° C., being brittle in the notched-bar test at this and all lower temperatures.

These changes were reversible. Specimens of the alloys that underwent pronounced embrittlement were tested after being cooled to -196° C. and allowed to warm again to room temperature. After this treatment their energy absorption at room temperature (as shown by the marked points in Fig. 1) was not significantly altered; consequently, no permanent constitutional change had been produced.

The fractures of the embrittled alloys at low

temperatures were in every case intercrystalline. The grain boundaries of the alloys showed no intergranular precipitate, but the alloys containing 1.29 and 0.56% antimony, when electrolytically polished and examined with the phase-contrast microscope, showed "ridge and trough" boundaries of the kind previously observed in brittle copper-bismuth alloys,³⁻⁵ and associated with a grain-boundary concentration of bismuth equivalent to a layer probably no more than one or two atoms thick (Fig. 2 (a) and (b), Plate XIII). It seems likely, therefore, that a very thin antimony-rich film may have existed around the grains of the embrittled alloys.

III.—DISCUSSION

Since no grain-boundary precipitate was seen in the alloys of highest antimony content, the explanation of the observed brittleness which best fits the experimental facts is that it was due to grain-boundary segregation of antimony without precipitation. A similar reason has been put forward to explain temper-brittleness in alloy steels.⁶

It is noteworthy that the present face-centred cubic copper alloys show a transition from tough to brittle behaviour as the test temperature decreases. It is often suggested that this transition is a function of lattice type, probably because such a transition is invariably observed with ferritic (body-centred cubic) steel when the appropriate tests are made, but neither with austenitic (face-centred cubic) steel nor with the common non-ferrous face-centred cubic metals; the transition has therefore been sometimes thought to be a property of the body-centred cubic lattice. But as it does not occur in all body-centred cubic metals and it does occur in the hexagonal metal zinc,⁷ and as, according to the present work, it can occur in a face-centred cubic metal, its incidence cannot be directly a question of lattice type.

There is, however, a feature common to all the metals having a tough-brittle transition, namely the actual or probable presence of impurity atoms which severely distort the parent lattice if relative size is any criterion, and it is reasonable to suppose that such a situation should cause a tough-to-brittle transition. It is appropriate to indicate briefly the lines of the explanation. Such solute atoms should segregate to distorted regions of the lattice, thus replacing the randomly distributed strained spots by fewer but relatively large stressed areas, such as grain-boundary interfaces. That these areas are large compared with an atom means that macroscopic fracture behaviour applies, and they will therefore embrittle the material. Furthermore, there is reason to expect distorting solute atoms to cause the yield stress to rise quickly with falling temperature.⁸ These two effects combine to make it likely that, as the test temperature is reduced, there comes a point at which the yield stress exceeds the fracture stress and brittle behaviour supervenes. The necessary conditions for brittle behaviour are more easily attained in notched

specimens, in which the triaxial stress at the root of the notch raises the effective yield stress. The body-centred cubic and hexagonal metals often fracture along cleavage planes instead of along grain boundaries. It has been pointed out by Zener⁹ that interstitial atoms present in body-centred cubic lattices may tend to aggregate on cleavage planes because the total strain energy may thereby be reduced. Consideration of the matter indicates that similar aggregation is likely in hexagonal metals, but unlikely in face-centred cubic metals. These aggregates will inevitably embrittle along the cleavage planes, and so may cause cleavage fracture. Such fracture should, however, be improbable in face-centred cubic metals.

The foregoing argument was the reason for carrying out the present experiments. The agreement between prediction and experiment in regard to the occurrence of embrittlement, the existence of a tough-to-brittle transition, and the intergranular character of the fracture offer some support for its validity.

ACKNOWLEDGEMENTS

The work described was carried out under the General Research Programme of the National Physical Laboratory and is published by permission of the Director of the Laboratory. The liquid hydrogen used was made in the Physics Division of the Laboratory.

REFERENCES

1. D. McLean and L. Northcott, *J. Inst. Metals*, 1946, **72**, 583.
2. J. C. Mertz and C. H. Mathewson, *Trans. Amer. Inst. Min. Met. Eng.*, 1937, **124**, 59.
3. E. Voce and A. P. C. Hallows, *J. Inst. Metals*, 1947, **73**, 323.
4. T. H. Schofield and F. W. Cuckow, *ibid.*, 1947, **73**, 377.
5. L. E. Samuels, *ibid.*, 1949-50, **76**, 91.
6. D. McLean and L. Northcott, *J. Iron Steel Inst.*, 1948, **158**, 169.
7. P. L. Teed, "The Properties of Metallic Materials at Low Temperatures", p. 195. London: 1950 (Chapman and Hall).
8. A. H. Cottrell, *Symposium on Plastic Deformation of Crystalline Solids, Pittsburgh*, 1950, 60.
9. C. Zener, *Phys. Rev.*, 1948, [ii], **74**, 639.

NOTICE TO AUTHORS OF PAPERS FOR THE "JOURNAL" AND CONTRIBUTORS TO DISCUSSIONS

1. **Papers will be considered for publication from non-members as well as members of the Institute.** They are accepted for publication in the *Journal* and not necessarily for presentation at any meeting of the Institute. MSS. should be addressed to The Editor of Publications, The Institute of Metals, 4 Grosvenor Gardens, London, S.W.1.

2. **Papers suitable for publication** may be classified as:

(a) Papers recording the results of original research.

(b) First-class reviews of, or accounts of progress in, a particular field.

(c) Papers descriptive of works methods, or recent developments in metallurgical plant and practice.

(d) Papers in classes (a), (b), and (c) above, previously published in languages other than English, French, German, or Italian, if of sufficient merit.

3. **Manuscripts and illustrations** should be submitted in duplicate. MSS. must be typewritten (*double-line spacing*) on one side of the paper only, and authors are requested to sign a declaration that neither the paper nor a substantial part thereof has been published elsewhere. Exceptions may be made in certain cases where a paper has been published in a language other than English, French, German, or Italian (see 2(d) above). MSS. not accepted are normally returned within 6 months of receipt.

In the interests of economy, all papers must be written as concisely as possible; in general, internal research reports are not in suitable form for publication as papers in the *Journal*. All but the simplest mathematical expressions should be written by hand, with capital and small letters clearly distinguished. Superscript and subscript letters should also be plainly indicated. Greek letters and special signs should be identified in the margin. For style, spelling, and abbreviations used, any recent issue of the *Journal* may be consulted.

4. **Synopsis.** Every paper must have a synopsis (not exceeding 250 words in length) which, in the case of a paper reporting original research, should state its objects, the ground covered, and the nature of the results. The synopsis will appear at the beginning of the paper, and should be in a form suitable for use by abstracting organizations. Extracts from a "Guide for the Preparation of Synopses" drawn up by the Abstracting Services Consultative Committee are reproduced below.

5. **References** must be collected at the end of the paper and must be numbered in the order in which they occur in the MS. Initials of authors must be given, and the Institute's official abbreviations for periodical titles (as used in *Metallurgical Abstracts*) should be employed, where known. References to papers should be set out in the style:

A. L. Dighton and H. A. Miley, *Trans. Electrochem. Soc.*, 1942, 81, 321 (i.e. year, volume, page).

References to books should be in the following style:

C. Zener, "Elasticity and Anelasticity of Metals". Chicago: 1948 (University of Chicago Press).

6. **Illustrations.** Each illustration must have a number and description; only one set of numbers must be used in one paper, and it is desirable to number the half-tone illustrations consecutively, rather than to intersperse them with the line figures. The captions should be typed on a separate sheet.

The set of **line figures** sent for reproduction must be drawn (about twice the size to appear in the *Journal*) in Indian ink on smooth white Bristol board, good-quality drawing paper, co-ordinate paper, or tracing cloth, which are preferred in the order given. Co-ordinate paper, if used, must be blue-lined, with the co-ordinates to be reproduced finely drawn in Indian ink. Curves should be drawn boldly (i.e. at least twice the thickness of the frame). Experimental points should be indicated by open or closed circles, triangles, squares, &c. (preferably not crosses). Curves should be broken on each side of such symbols and plenty of allowance should be made for closing up in blockmaking. All lettering and numerals, &c., should preferably be in *pencil*, so that the Institute's standard lettering may be affixed, and ample margins must be left outside the framework of the figures to enable this to be done. The second set of line illustrations may be photostat copies.

Photographs must be restricted in number, owing to the expense of reproduction, and photomicrographs should be trimmed to the smallest possible of the following sizes consistent with adequate representation of the subject: 4 in. deep by 3 in. wide: 2 in. deep by 3 in. wide: 2 in. square. Magnifications of photomicrographs must be given in each case. Photographs for reproduction should be loose, not pasted down (and not fastened together with a clip, which damages them), and the figure number and author's name should be written on the back of each. Captions should be given to the photomicrographs, but these should be kept as brief as possible.

Because of the present high cost of printing and paper it is imperative that authors restrict illustrations (particularly photographs) to the absolute minimum deemed necessary to support their argument. Only in exceptional cases will illustrations be reproduced if already printed and readily available elsewhere.

7. **Tables or Diagrams.** Results of experiments, &c., may be given in the form of tables or figures, *but* (unless there are exceptional reasons) *not both*. Tables should bear Roman numbers, and each should have a heading that will make the data intelligible without reference to the text.

8. **Corrections.** A certain number of corrections in proof are inevitable, but any modification of the original text is to be avoided. Since corrections are very expensive, the Institute reserves the right to require authors to contribute towards their cost if the Editor deems them to be excessive. The Institute also reserves the right to require a contribution to the cost of remaking any block where this is necessitated by an error on the author's part.

9. **Reprints.** Individual authors are presented with a maximum of 25, and two or more authors with a maximum of 50 reprints from the *Journal*, without covers. Limited numbers of additional reprints can be supplied at the author's expense, if ordered before proofs are passed for press. (Orders should preferably be placed when submitting MSS.)

10. **Discussion.** Except in the case of special symposia, shorthand records of discussions are not taken at meetings. Written discussion may be submitted on any paper, preferably typewritten (*double-line spacing*). References should be given in the form of footnotes. Paragraphs 6 and 7 above are also applicable to such contributions. Reprints of discussion cannot be supplied to contributors.

GUIDE FOR THE PREPARATION OF SYNOPSES

(As recommended by the Abstracting Services Consultative Committee)

1. **Purpose.** The synopsis is not part of the paper; it is intended to convey briefly the content of the paper, to draw attention to all new information, and to the main conclusions. It should be factual.

2. **Style of writing.** The synopsis should be written concisely and in normal rather than abbreviated English. It is preferable to use the third person. Where possible use standard rather than proprietary terms, and avoid unnecessary contracting.

It should be presumed that the reader has some knowledge of the subject, but has not read the paper. The synopsis should therefore be intelligible in itself without reference to the paper; for example, it should not cite sections or illustrations by their numerical references in the text.

3. **Content.** The title of the paper is usually read as part of the synopsis. The opening sentence should be framed accordingly and repetition of the title avoided. If the title is insufficiently comprehensive, the opening should indicate the subjects covered. Usually the beginning of a synopsis should state the objective of the investigation.

It is sometimes valuable to indicate the treatment of the subject by such words as: brief, exhaustive, theoretical, &c.

The synopsis should indicate newly observed facts, conclusions of an

experiment or argument and, if possible, the essential parts of any new theory, treatment, apparatus, technique, &c.

It should contain the names of any new compound, mineral species, &c., and any new numerical data, such as physical constants; if this is not possible, it should draw attention to them. It is important to refer to new items and observations, even though some are incidental to the main purpose of the paper; such information may otherwise be hidden, though it is often very useful.

When giving experimental results the synopsis should indicate the methods used; for new methods the basic principle, range of operation, and degree of accuracy should be given.

4. **References.** If it is necessary to refer to earlier work in the summary, the reference should always be given in full and not by number. Otherwise references should be left out.

When a synopsis is completed, the author is urged to revise it carefully, removing redundant words, clarifying obscurities, and rectifying errors in copying from the paper. Particular attention should be paid by him to scientific and proper names, numerical data, and chemical and mathematical formulae.

By A. S. DARLING,† B.Sc.Eng., A.M.I.Mech.E., MEMBER,
R. A. MINTERN,† MEMBER, and J. C. CHASTON,† Ph.D.,
A.R.S.M., F.I.M., MEMBER

SYNOPSIS

A re-investigation of the equilibrium diagram of the gold-platinum system has confirmed that a continuous series of solid solutions exists below the solidus, as suggested by Johansson and Linde (*Ann. Physik*, 1930, [v], 5, 762). The upper level of the miscibility gap has, however, been shown to lie at 1258° C. (instead of 1150° C.), and accurate determinations of the solidus have shown that an almost horizontal portion exists at 1300° C. Transformations in the solid state below 1000° C. have not been studied.

I.—INTRODUCTION

THE gold-platinum equilibrium diagram has been investigated by several workers since it was first studied by Doerinckel in 1907,¹ but no real agreement has been reached on the fundamental nature of the system, opinion being nearly equally divided between the view that the alloys form a continuous series of solid solutions and the view that a peritectic is formed.

Doerinckel, who examined only six gold-rich alloys by thermal analysis, concluded that they formed a continuous series of solid solutions. In 1928, Grigoriev,² from cooling curves of 18 alloys containing up to 61% ‡ platinum, put forward a diagram showing a peritectic reaction at about 1290° C. in alloys with between 20 and 61% platinum. The results of hardness tests at lower temperatures seemed to support this view. On the other hand, when Johansson and Linde,³ in 1930, established by X-ray diffraction and other physical methods the existence of a two-phase region of immiscibility in the solid solutions below about 1150° C., they favoured a simple single solid solution diagram of the type sketched by Doerinckel, although they made no direct observations on the position of the solidus. Their diagram has, until quite recently, been widely accepted. However, in 1951, Grube, Schneider, and Esch⁴ published an account of an investigation made in 1944–48 which, although admittedly not brought to a final conclusion, led them to propose a new diagram showing a peritectic between about 58 and 62% platinum. The evidence which probably especially swayed these workers was their confirmation of an arrest point between 1295° and 1301° C. (above the solidus arrest) in all alloys containing 21–59% platinum.

The present investigation was undertaken to attempt to establish which of these two conflicting views is correct. It appeared that previous workers had neglected (a) accurate determinations of the solidus by microscopic methods (cooling curves are

notoriously unreliable for solidus determinations in alloys with a wide melting range) and (b) determinations of the phase boundaries by observations on samples held at high temperatures.

All the early determinations of phase boundaries in the solid state were made on quenched samples, although, if the diagram was of the form suggested by Johansson and Linde, it is improbable that the high-temperature state can be retained by quenching. More recently Victorin⁵ and Grube, Schneider, and Esch⁴ have published results of high-temperature resistance measurements that are, on the whole, in good agreement with those here presented.

II.—EXPERIMENTAL DETAILS

1. PREPARATION OF ALLOYS

Platinum sponge and gold grain, both of at least 99.98% purity, were melted together in a zircon crucible in a high-frequency furnace, 100 g. ingots, $\frac{1}{2}$ -in. square, being cast in a heavy copper mould. No flux, protective atmosphere, or deoxidant was employed.

The cast ingots were soaked for 1 hr. at 850° C. and then quenched. After this treatment all alloys could be cold-worked, provided that intermediate anneals were made at 850° C. and followed by quenching. The 80% platinum alloy was the most difficult to work, but after 50% reduction could be cold-rolled with ease. All samples were rolled to sheet 0.1 in. thick, and portions were slit and drawn to wire for resistance measurements.

2. SOLIDUS DETERMINATIONS

Solidus determinations were carried out by microscopic methods. A vertical quenching furnace was constructed in which the specimens, in a platinum container, could be heated directly in contact with a

* Manuscript received 18 April 1952.

† Research Laboratories, Johnson, Matthey and Co., Ltd., Wembley, Middlesex.

‡ All compositions are quoted in weight per cent.

thermocouple at any desired rate. Upon release of a trigger, a door at the bottom of the furnace opened and the container dropped into the quenching tank.

Samples of hard-rolled sheet were heated rapidly to about 10° C. below their estimated melting point, held at this temperature for approximately 2 hr., and then heated at 20° C./hr. to the quenching temperature, which was increased by 5° C. increments until signs of fusion were observed in polished and etched microsections. Sections were mounted in Bakelite, ground down in the usual way, and polished first with "Bluebell" metal polish and then with magnesia or alumina. Magnesia was better for the final polishing of alloys at the gold-rich end, and alumina for the hard platinum-rich alloys. *Aqua regia* diluted with an equal volume of water was the best etchant for alloys containing up to 50% platinum, but for those at the platinum-rich end an electrolytic etch, using alternating current and a cyanide electrolyte, was better than hot *aqua regia*, since it did not decompose the Bakelite mounting nor pit or stain the alloys.

Signs of fusion in these alloys were very easy to detect. Typical examples are shown in Figs. 10 and 13 (Plate XV).

Table I gives the solidus limits over the range 20–

TABLE. I.—*Liquidus and Solidus Determinations.*

Gold, %		Liquidus, °C.	Solidus Limits, °C.
Nominal	Actual		
20	...	1655	1408 –1412
22.5	22.14	...	1367 –1372
25	25.46	...	1330 –1335
30	30.26	1617	1310 –1315
35	1305 –1310
40	...	1584	1305 –1310
42	1300 –1305
45	1300 –1305
50	50.29	1550	1285 –1290
55	54.77	1529	1277.5 –1282.5
60	1262.5 –1267.5
65	...	1483	1247 –1252
70	69.98	...	1233 –1237
75	...	1408	...
80	79.94	1355	1178 –1183
85	...	1274	...
92.5	...	1155	...

80% gold. The chemical analyses quoted were carried out on the actual microsections employed for the determinations, the percentage of gold being determined by precipitation twice with SO₂. Thermocouples were calibrated after each run.

These results are plotted in Fig. 1. It will be observed that between 30 and 45% gold the solidus is a gently sloping line having upper limits of 1315° C. at 30% and 1305° at 45% gold. The existence of a line so very nearly horizontal over such a wide range of composition suggested the possibility of slight errors in temperature measurement and the existence of a peritectic reaction over this range. The evidence which led us to reject the possibility of such a reaction

is described in the sections on microstructure and X-ray measurements.

3. LIQUIDUS DETERMINATIONS

For the liquidus determinations, a high-temperature resistance furnace wound with platinum-30% rhodium wire was constructed, which was capable of melting pure platinum and so had ample reserve for all the alloys. Ingots (100-g.) of the desired composition were made in a high-frequency furnace and remelted in the resistance furnace in magnesia crucibles, zircon crucibles having shown a tendency to collapse when unsupported round the walls. Cooling curves were taken with a platinum/platinum-13% rhodium thermocouple, which was calibrated after each run. With a cooling rate of about 5° C./min., well-defined arrests were obtained. At the platinum-rich end, the alloys showed a slight degree of supercooling. The duration of the arrest decreased with increase in gold content to a minimum at 75%, after which it increased.

Values of the liquidus points obtained are given in Table I.

4. DETERMINATION OF BOUNDARY OF TWO-PHASE REGION BELOW THE SOLIDUS

(a) Resistance Measurements (27.5–51% Gold)

The most satisfactory determinations of the two-phase boundaries in this region were obtained by resistance measurements on wire samples. For this work, a Tinsley potentiometer with a sensitivity of 1 μ V. was employed to compare the resistance of the specimen as it was heated with the resistance of a standard by the drop-in-volt method. For the preliminary work, a 2-in. length of wire was bent into a hairpin and potential leads of the same composition were welded to it. The current and potential leads were welded to platinum leads which led out of the furnace. By this method it was hoped to avoid alterations in composition of the piece of wire under test, since at temperatures above 1200° C., rapid diffusion of gold into platinum occurs. It was found, however, that welds made between two pieces of gold-platinum wire were very weak mechanically, and that the joint broke as soon as a temperature of about 1250° C. was reached. It was found simpler and more satisfactory to form a bead of appreciable size by fusion at one end of the sample wire and to fuse into this the two platinum lead-in wires. With this construction, any diffusion of gold into the pure platinum wires takes place merely at the expense of the large bead, without influencing the composition of the test length.

For the resistance measurements, 0.015-in.-dia. wires of twelve compositions covering the range 27.5–51% gold were drawn from slices of sheet which had been soaked at 1270° C. in the single-phase region for 17 hr. to ensure thorough homogenization, cooled to 850° C., held there for $\frac{1}{2}$ hr., and then quenched.

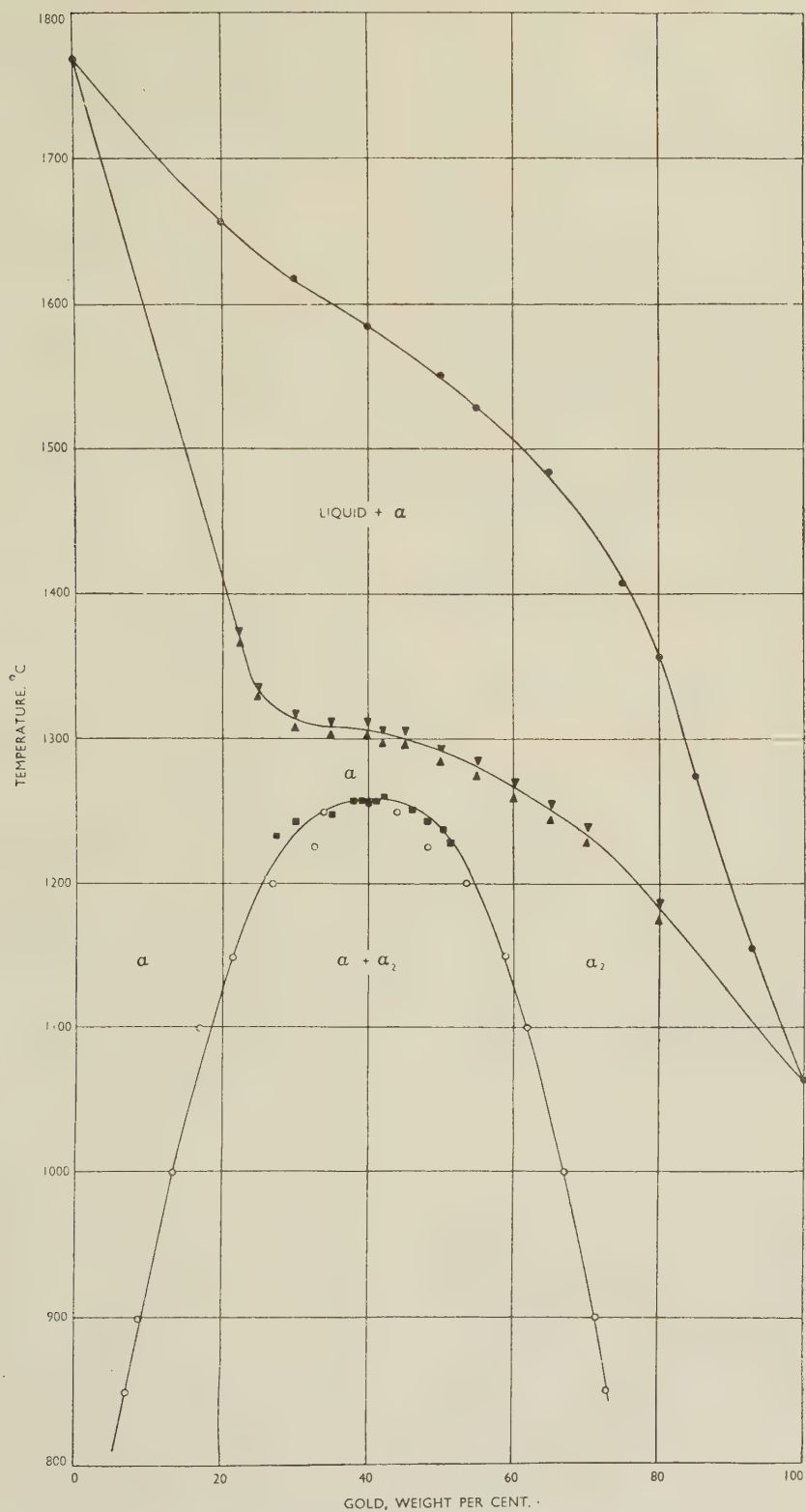


FIG. 1.—Proposed Equilibrium Diagram for the Gold-Platinum System.

KEY.

■ Resistance measurements. ● Cooling curves. ▴ Microscopic work. ○ X-ray data.

Samples of hard-drawn wire were mounted as described and heated rapidly up to 1100° C. The furnace was steadied at this temperature for $\frac{1}{2}$ hr. before resistance measurements were started. The temperature was then increased at a rate of 20°–30° C./hr., resistance readings being taken at 3° C. intervals up to about 1280°. Initial results gave rise to a suspicion that all parts of the wire were not going through the transition point at the same time, and it was therefore necessary to shorten the specimen in order to reduce any possible temperature variation throughout its length. To obtain a resistance high enough for the degree of accuracy required, the wire was drawn down to 0.008 in. The specimen finally adopted had a free length of about $\frac{3}{4}$ in., and the length in the furnace did not exceed $\frac{3}{8}$ in. It is estimated that the temperature uncertainty did not exceed 1° C.

In these measurements, parasitic and other spurious E.M.F.s (shown when the reversing switch was brought into operation) were small if the sample was suspended well away from the furnace wall. No attempt was made to calculate the resistivity of the

1280° C. The descending curves, when obtained, were all much higher than the ascending ones. This change in resistance was attributed to plastic flow of the wire under its own weight just below the solidus. It was very rare for a wire to survive its initial heating, as the welds usually broke at about 1280° C.

Table II gives the phase boundaries obtained from resistance curves, the maximum being at 1258° C.

TABLE II.—*Phase Boundaries Determined from Resistance Measurements.*

Gold, %	Location of Phase Boundary. Temp., °C.	Gold, %	Location of Phase Boundary. Temp., °C.
27.5	1233	42	1260
30	1243	46	1252
35	1248	48	1244
38	1258	50	1238
40	1257	51	1229
41	1258		

(b) X-Ray Methods

A systematic examination of the system was carried out by X-ray work in parallel with the microscopic and resistance studies. Lattice-parameter measurements were determined with a 19-cm. Debye camera, using CuK_α radiation. Back-reflection photographs were also taken from polished and etched microsections and from specimens heated electrically to a high temperature.

The lower boundaries of the two-phase region were determined by X-ray methods. Much of the preliminary work was carried out using powder specimens. Filings were taken from hard-rolled sheet and annealed at the appropriate temperature in silica quills for 4 hr. before being quenched. Specimens which were to be quenched from below 1100° C. were taken from sheet which had been soaked at that temperature for 20 hr. The filings were mounted in the silica quill and heat-treated for 4 hr. before quenching. At a later stage in the investigation it was found more convenient to employ 0.015-in. wires. These were easy to prepare, heat-treat, and quench, and gave diffraction patterns equal in quality to those from powder specimens. Lattice parameters of both phases, which were face-centred cubic, were calculated by the standard method. The accuracy of the lattice-parameter determinations was checked at intervals during the investigation by measuring the parameters of pure gold and platinum wires. The absolute values of the figures quoted are estimated to be accurate to within 1 part in 8000.

Table III summarizes the results of lattice-parameter determinations. These results are plotted in Fig. 3 to obtain the boundaries of the two-phase region, which are given in Table IV. It will be seen that parameters of the single-phase alloys fall on a smooth curve not far from the straight line predicted by Vegard's law. Specimens quenched from above 1220° C. in the range 30–50% gold gave some-

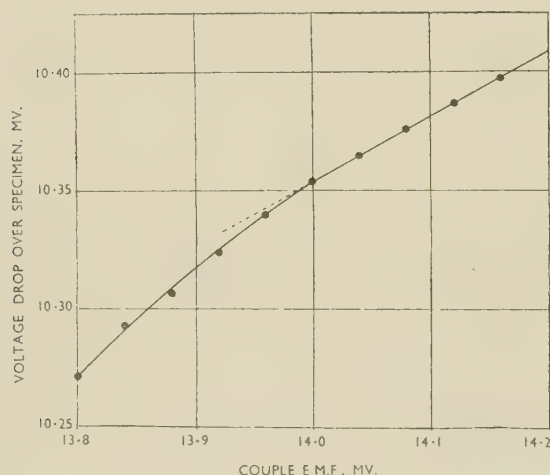


FIG. 2.—Typical Resistance Curve for 40% Gold Alloy.

sample, since it was impossible to measure the test length accurately.

Fig. 2 shows a typical resistance curve for the 40% gold alloy. The shape of the curve is in agreement with the assumption of a two-phase region up to 1256° C. In such a region the composition and relative proportions of the two phases are functions of the temperature, and change rapidly as the boundary is approached. This region corresponds with the curved portion of the line. Above 1256° C. a straight line is obtained indicating a single-phase region in which composition is independent of temperature. Many attempts were made to take resistance measurements as the wire cooled, in order to confirm the transformation point obtained on the upward run, but, in general, these were unsuccessful owing to the serious weakening of the wire at temperatures near

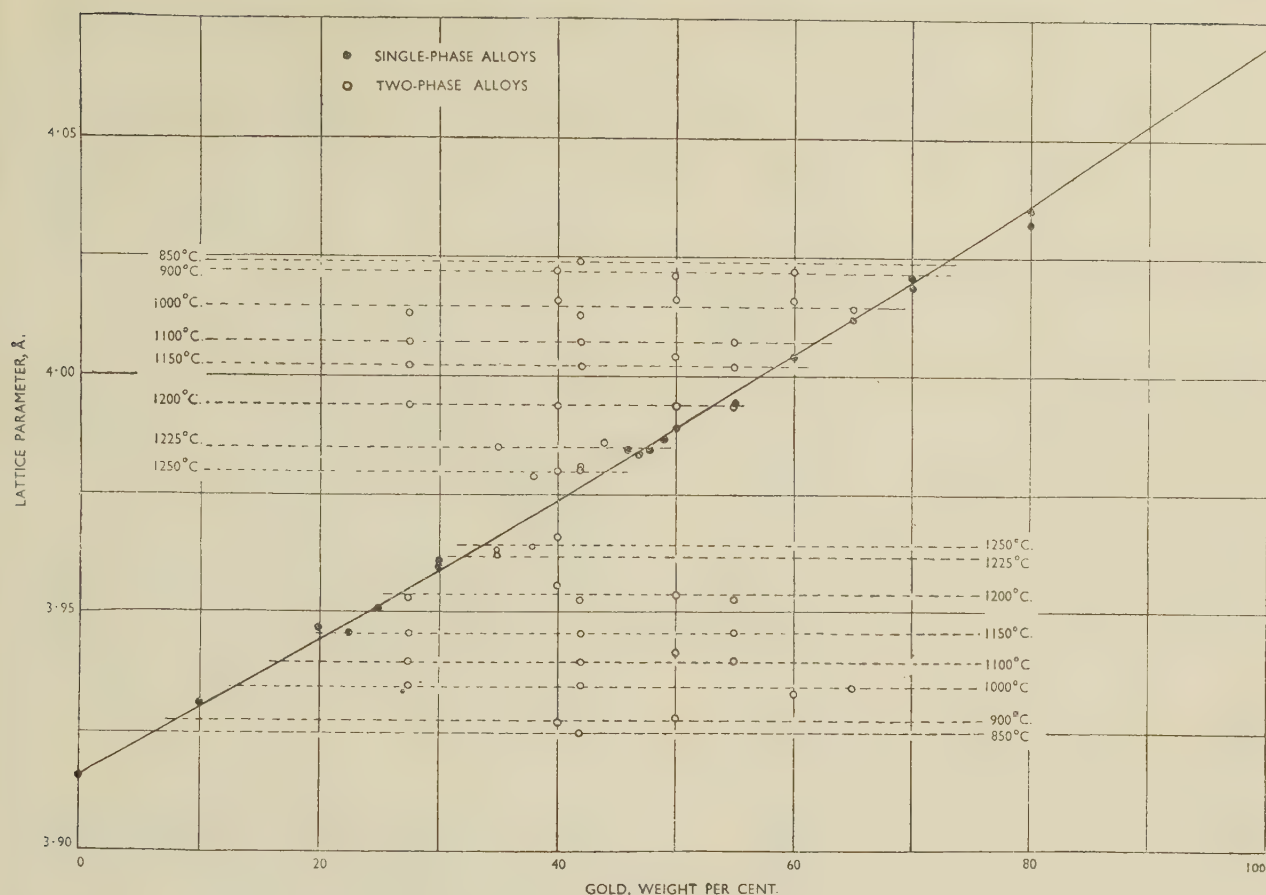


FIG. 3.—Lattice-Parameter Measurements of Gold-Platinum Alloys.

what diffuse lines which made it impossible to attain the highest precision in the determination of lattice parameters. The errors involved, however, were not considerable, as shown by the comparative sharpness of the lines in Fig. 6 (Plate XIV) which shows diffraction patterns obtained on the 42% gold alloy quenched from 1200°, 1250°, and 1280° C. At 1200° C. a well-defined two-phase structure exists. At 1250° C.

traces of a second phase are still present, but these are entirely absent at 1280° C.

To attempt to confirm the structure just below the solidus, back-reflection photographs were taken from specimens heated by the passage of a heavy electric current using the apparatus shown diagrammatically in Fig. 4; in this work small sheet tensile test-pieces were used, having a parallel portion 0.040 in. thick and 0.10 in. wide. The specimen was oscillated about an axis intersecting the X-ray beam, and temperature was measured by a thermocouple spot-welded to the rear surface of the sample. Owing to limitations in the apparatus, it was impossible to measure the specimen-to-film distance accurately, so that the results obtained were purely qualitative.

The results of tests on alloys containing 30–50% gold indicated that the second phase, present at 1220° C., disappeared below 1270° C. Fig. 7 (a) and (b) (Plate XIV) show results obtained on the 42% gold alloy photographed at 1170° C. and 1260° C. At 1170° the evidence for the existence of two phases is unmistakable; at 1260° no trace of the second phase is visible.

The results of the X-ray work thus confirm the upper boundary of the two-phase region determined by resistance measurements.

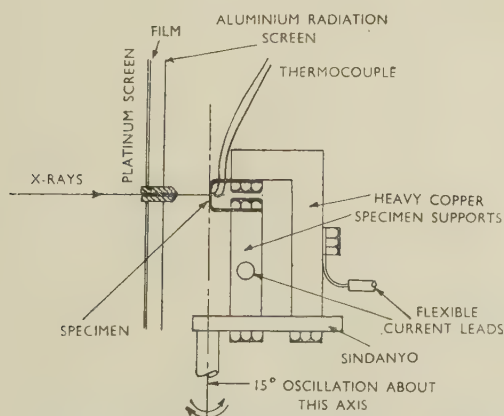


FIG. 4.—Diagram of High-Temperature X-Ray Camera.

TABLE III.—*Lattice-Parameter Measurements*

Gold, %	Quenching Temp., °C.	Form of Specimen	Lattice Parameters, kX	
10	1150	Powder	3-931 ₀	
	1250	"	3-931 ₀	
20	1280	"	3-954	
	1200	"	3-947	
22.5	1250	"	3-946 _s	
25	1200	"	3-951	
	1250	"	3-950 _s	
27.5	1280	"	3-951	
	1000	Wire	3-935	4-013
	1100	"	3-940	4-007
	1150	"	3-946	4-002
30	1200	"	3-953	3-994
	1250	"	3-960	
35	1280	Powder	3-961	
	1225	"	3-961 _s	3-985
40	1240	"	3-963	
	1250	Wire	3-962	
	1260	Powder	3-962 _s	
	1270	"	3-962	
42	1280	"	3-960	
	1250	"	3-963 _s	3-978 _s
44	900	Wire	3-927	4-022
	1000	"	3-932	4-016
46	1200	"	3-959	3-994
	1250	"	3-966 _s	3-979 _s
	850	"	3-925	4-024
	1000	"	3-935	4-013
47	1100	"	3-940	4-007
	1150	"	3-946	4-002
48	1200	"	3-953	3-994
	1250	"	3-980 _s	
49	1280	Powder	3-979 _s	
	1250	Wire		3-986
50	1250	"	3-984 _s	
	1250	Powder	3-983 _s	
51	1250	Wire	3-984 _s	
	1250	Powder	3-986 _s	
52	900	Wire	3-928	4-021
	1100	"	3-942	4-004
53	1200	"	3-954	3-994
	1250	Powder		3-988 _s
54	1100	Wire	3-940	4-007
	1150	"	3-946	4-002
55	1200	"	3-953	3-994
	1270	Powder		3-994 _s
56	1000	"	3-933	
	1250	"		4-016
57	1270	"		4-004
	1250	"		4-003 _s
58	1000	"	3-934	4-014
	1150	"		4-012
59	1000	"		4-018 _s
	1100	"		4-021
60	900	"		4-032
	1100	"		4-035

TABLE IV.—*Boundaries of Two-Phase Regions.*

Temp., °C.	Boundaries of Two-Phase Region. Gold, %		Temp., °C.	Boundaries of Two-Phase Region. Gold, %	
850	6.3	72.3	1150	21.1	58.4
900	8.2	71.1	1200	26.8	53.2
1000	13.0	66.6	1225	32.3	47.4
1100	16.8	61.7	1250	33.8	43.9

5. THE MICROSTRUCTURE OF THE ALLOYS

Much effort was expended in attempts to establish the structure of alloys with 25–65% gold after quenching from just below the solidus. It was

eventually found possible to obtain clear and reproducible structures by etching alloys with up to about 48% gold electrolytically in 10% sodium cyanide solution, using alternating current. Figs. 8–13 (Plate XV) show the microstructures of alloys with 40 and 42% gold after quenching from temperatures between 1280° and 1310° C. All these structures are unmistakably those of a single-phase solid solution. Figs. 9 and 12 exhibit intercrystalline cracks, due to quenching stresses, and in Figs. 10 and 13 signs of incipient melting can be detected.

Specimens in the middle range of composition quenched from above the two-phase region were always very hard and frequently cracked as a result of quenching stresses; the cracks were always intercrystalline and occasionally, when a polished sample was etched, a complete grain would become detached from the surface, leaving a cavity with well-defined facets in the polished surface.

There were no difficulties in preparing etched microsections of specimens quenched at temperatures below 1200° C., and the microstructure was invariably that which would be expected from Fig. 1. Typical examples of the two-phase structure in the 40 and 50% gold alloys after quenching from 1200° C. are shown in Figs. 14 and 15 (Plate XV), respectively.

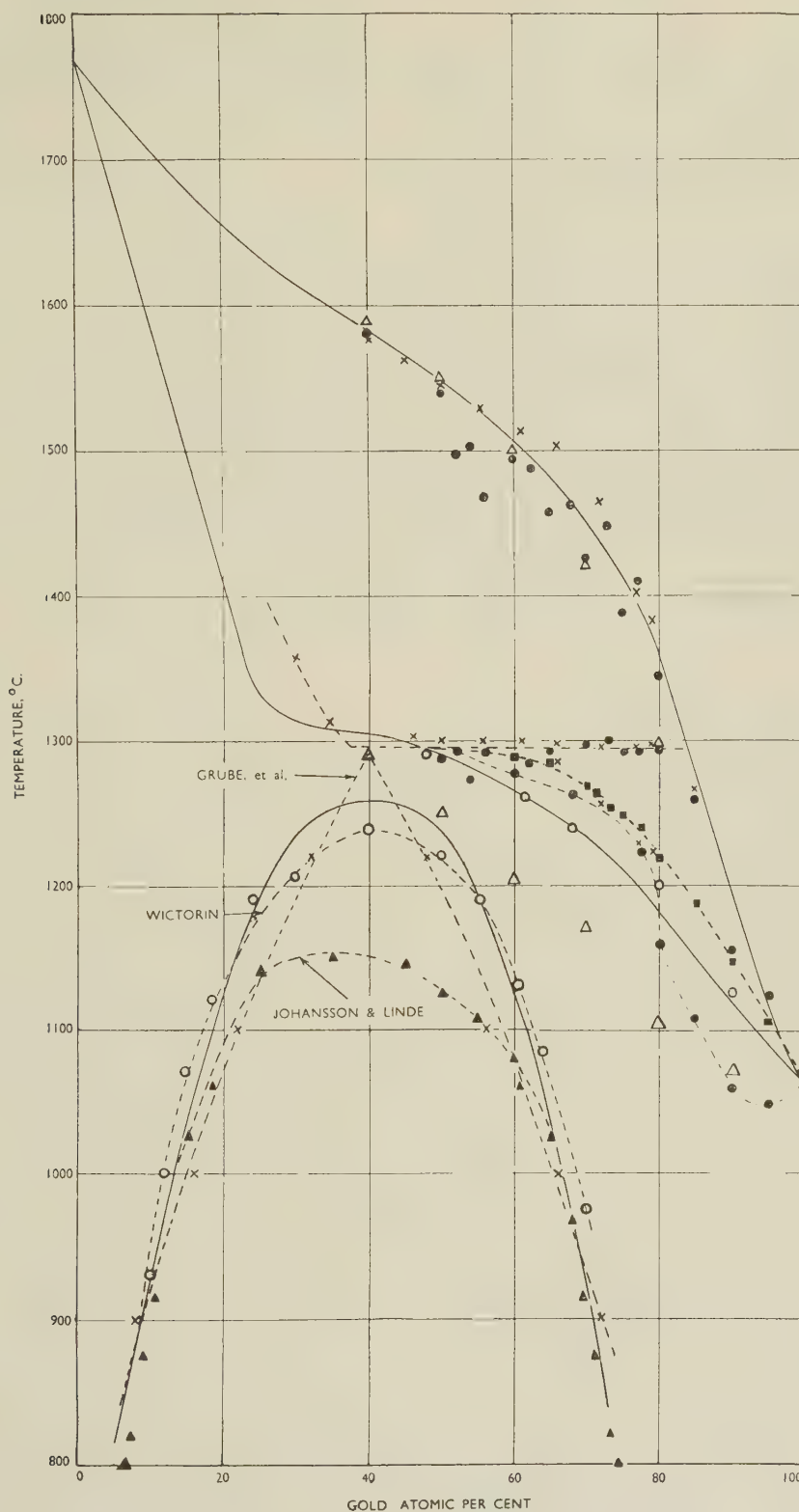
III.—DISCUSSION

The results of this investigation have been plotted to give the diagram shown in Fig. 1, and in Fig. 5 the new diagram is superimposed on plots of the experimental results of earlier investigators.

The liquidus now proposed falls very fairly midway between all the earlier points in the region for which data are available (for alloys with more than 40% gold) and does not appear to be controversial.

The solidus, which is drawn through the points determined from microscopical observation on quenched specimens containing 22–80% gold, falls in general below the arrest points found in earlier studies by thermal analysis. On the other hand, values found by Wictorin by high-temperature resistance measurements (unfortunately restricted to alloys with less than about 48% gold) all fall closely on the curve. The main point of interest in the solidus curve here presented is the inflection which causes it to become nearly horizontal between 30 and 40% gold. The existence of such a horizontal region will, of course, be reflected in the cooling curves of all alloys containing more than 40% gold and these, as has been recorded by nearly all previous investigators, accordingly show an arrest at just below 1300° C. Such an arrest is not of itself conclusive evidence for the existence of a peritectic reaction, as has often been assumed; and all the observations recorded in the present paper support the view that one continuous series of solid solutions exist below the solidus in this system.

The region of limited solubility in the solid solution certainly extends to much higher temperatures than



Doerinckel ¹ (thermal analysis)	. . .
Grigoriev ² (thermal analysis)	. . .
Johansson and Linde ³ (resistance methods)	. . .
Wictorin ⁵ (resistance methods)	. . .

KEY.

Grube, <i>et al.</i> ⁴	{(thermal analysis)	×
	{(resistance methods)	■
	{(X-ray diffraction)	×

those shown by Johansson and Linde, and the curve here drawn is in fair agreement with the more recent results of Wictorin and of Grube and his collaborators. The nomenclature which has been adopted was first proposed, it is believed, by Marsh, and has the advantage that it suggests clearly that the solid solution at first formed is continuous over the whole range of possible compositions, but that at lower temperatures the mutual solubility becomes limited; so that alloys in the central range of composition split up into gold-rich and platinum-rich members (α_2 and α_1) of the same phase (α). The more common nomenclature, suggesting that the original α phase breaks up into two phases ($\alpha + \beta$), implies that a new phase β has appeared, which is not in accordance with the facts.

The system is of some theoretical interest as an illustration of threshold behaviour in the transition from the type having one continuous solid solution to the type with two solid solutions and a peritectic. If the solid solubilities of gold and platinum at the

solidus temperature were only slightly less, a peritectic would be formed. As it is, the solidus is distorted to the unusual form here shown. Attention may be drawn to the similarities between this and the aluminium-zinc system.

ACKNOWLEDGEMENT

The authors' thanks are due to the directors of Johnson, Matthey and Co., Ltd. for permission to publish this paper.

REFERENCES

1. F. Doerinckel, *Z. anorg. Chem.*, 1907, **34**, 345.
2. A. T. Grigoriev, *Izvest. Inst. Platiny*, 1928, **6**, 184; and *Z. anorg. Chem.*, 1929, **178**, 97.
3. C. H. Johansson and J. O. Linde, *Ann. Physik*, 1930, [v], **5**, 762.
4. G. Grube, A. Schneider, and U. Esch, *Heraeus Festschrift*, **1951**, 20.
5. C. G. Wictorin, *Arkiv Mat., Astron. Fysik*, 1949, [B], **36**, (9).

By D. McLEAN,† B.Sc., MEMBER

(Communication from the National Physical Laboratory.)

SYNOPSIS

A study has been made of the types of slip band formed in pure polycrystalline aluminium undergoing creep strain at 200° C. in order to ascertain how much of the total strain was due to each type of slip and to determine the influence of grain-size and stress upon the phenomena. Two types of slip band were observed: (i) prominent slip bands of about $\frac{3}{4}$ μ displacement spaced about 30 μ apart on average, and (ii) fine slip lines of about 50–500 Å. displacement and spaced less than 1 μ apart. The former are the slip bands reported by Hanson and Wheeler (*J. Inst. Metals*, 1931, 45, 229) and others. The fine slip lines filled the interspaces between the former. Close examination showed that the prominent bands were simply lamellar regions where this general fine slip had occurred to an unusually large extent, thus producing a prominent step in the surface. Broadly speaking, the number of prominent slip bands and the mean displacement at these bands increased with increasing grain-size and stress. As a result, the strain due to these bands increased considerably with increasing grain-size and perhaps slightly with stress. In no case, however, was it more than half the total strain, and it was usually much less. The greater part of the strain was attributable to the fine slip lines.

The results are discussed in terms of dislocation theory; the general fine slip accords with the idea of a network of Frank–Read dislocation sources, and the prominent slip bands may be produced by sources, dislocations from which encounter no important obstacles before reaching the grain boundary, for such sources should emit many dislocations.

I.—INTRODUCTION

If coarse-grained aluminium is stretched fairly slowly at an elevated temperature, very prominent slip bands form. Displacement on them continues during steady extension—secondary-stage flow, to use the terminology of creep. However, if the grain-size is small enough, no slip bands can be seen unless the load, and therefore the rate of stretch, is increased. These facts were first demonstrated by Hanson and Wheeler¹ for aluminium over a limited range of conditions. Recently, Wood and his co-workers² have given very clear and explicit evidence over a range of conditions sufficiently wide for there to be no doubt of the correctness of these conclusions, at least for aluminium. Some further confirmation has been provided by Wyon and Crussard.³

Because slip bands were not observed in fine-grained aluminium stretched slowly, although the specimen certainly extended and individual grains unquestionably changed their shapes, Hanson and Wheeler have surmised that perhaps very small amounts of slip, too small to be detected, occurred on very numerous closely spaced planes. However, none of the workers mentioned have observed this fine slip.

In a previous paper⁴ some work was reported in which such fine slip was observed. In that paper the extension directly due to the prominent slip bands was determined, being derived from measurements of the slip displacements and the number of slip bands. The proportion of the total extension due to the prominent slip bands was less than half. Most of the

remainder was ascribed to the fine slip. In the present paper further work along the same lines is described, in which the effect of grain-size and applied stress on the appearance of slip phenomena under the microscope and on the proportion of the extension due to the prominent slip bands was investigated. The metal used was again super-pure aluminium.

It is deduced that in practically all the circumstances examined the fine slip lines contributed more extension than did the prominent slip bands. The number of prominent slip bands and the displacement they underwent increased on the whole with increase in grain-size or stress, which is quantitative confirmation of the observations of Hanson and Wheeler. The fraction of the total extension contributed by the prominent slip bands also increased with increase in grain-size and appeared to increase slightly with increase in stress. A connection between the prominent slip bands and the fine slip lines is emphasized; the former were simply those places where fine slip occurred in intensified fashion.

Displacements at the grain boundary were observed in addition to those at slip bands; in all cases these made a very minor contribution to the total extension, amounting to a few per cent only.

II.—EXPERIMENTAL DETAILS

1. MATERIAL

Eight specimens of two types, parallel-sided and tapered, were used. They were cut from cold-rolled super-pure aluminium strip, the chief impurities of which were 0.002–0.003% iron, 0.003% silicon, and

* Manuscript received 17 February 1952.

† Metallurgy Division, National Physical Laboratory, Teddington.

0.003% copper. The specimens were polished in the cold-rolled condition, finished by electrolytic polishing, annealed, and re-polished electrolytically. They were then lightly etched to remove the oxide film left by the electrolytic polish.

The crystal structure after annealing appeared equi-axed to qualitative observation, and the subsequent deformation behaviour indicated no obvious departure from random orientation.

2. SPECIMENS

(a) Parallel-Sided Specimens

Three specimens were parallel-sided, of section 0.25 in. \times 0.375 in. One of these was annealed at 500° C. to acquire a comparatively coarse grain-size of 1 grain/mm., as measured by the linear-intercept method. The other two were annealed at 325° C. to acquire a grain-size of $9\frac{1}{2}$ grains/mm. The coarse-

not reloaded, the changes measured were due to uninterrupted creep.

Since the specimens were tapered, so that the operative stress varied along the length, it is desirable to describe briefly how curves relating to a definite initial load were obtained. To measure the elongation, fine lines were scribed with a diamond tool across the width of the test-piece at 1-cm. intervals, and the distances between them were accurately measured before and after test, the changes being measured to ± 0.0005 cm., i.e. 0.05% of the initial distance. These changes related to the overall effect of the steadily changing load along a 1-cm. length of the taper. They were plotted as in Fig. 1 to give a curve of load against extension for each specimen, using a logarithmic abscissa to relieve the congestion at low extensions. From these curves the extension/time curves for the particular loads $\frac{1}{3}$, $\frac{1}{2}$, and $\frac{3}{4}$ ton/in.² were derived and are given in Fig. 3 (p. 137).

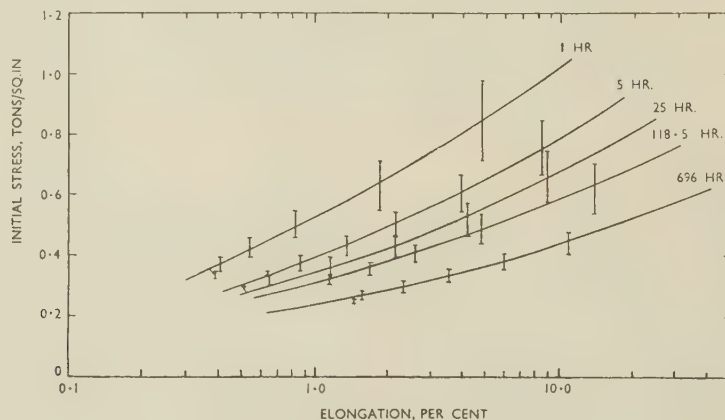


FIG. 1.—Initial Stress Plotted Against Elongation for Tapered Specimens. All tests were at constant load, so that the applied stress increased as the test progressed.

grained specimen and one of the fine-grained ones were then stretched at 200° C. under a load of $\frac{1}{2}$ ton/in.² until fracture occurred, which took about 1000 hr. They were not stretched uninterruptedly, but were periodically removed from the creep machine for examination and measurement. The other fine-grained specimen was given one stretch of 6 hr. under the same conditions and then measured; the results for this specimen, which thus duplicated those from the first fine-grained specimen, are recorded on the appropriate curves given later. Good agreement was obtained, as shown for example by Fig. 3 (d) (p. 137).

(b) Tapered Specimens

The other five specimens were of the same thickness but tapered in width. This was a convenient way of obtaining a range of stress from about $\frac{1}{3}$ to $\frac{3}{4}$ ton/in.² They were annealed at 425° C. to acquire a grain-size of $4\frac{1}{2}$ grains/mm., intermediate between the coarse- and fine-grained parallel-sided specimens. Each specimen was stretched, also at 200° C., for a certain time—1, 5, 25, 118 $\frac{1}{2}$, and 696 hr.—removed from the machine and measured. As these specimens were

A somewhat similar procedure was adopted for the determination of slip-band displacements and numbers of slip bands, a difference being, however, that the displacement and number could be determined corresponding to a particular stress. Fifty measurements were made in a line across the width of the specimen at seven positions along the length of each specimen. The results for the displacements are plotted in Fig. 6 (p. 140) and those for the number of prominent slip bands in Fig. 7 (p. 140). Curves relating to the particular stresses above were derived from these.

Since the stress at any point along the length of the tapered specimens was determined by simple calculation from the cross-sectional area at that point, a test was made to see whether this was accurate, for the lengthwise taper was bound to introduce some error, albeit a small one. The true stress distribution was determined photoelastically in a similarly shaped specimen cut from suitable Bakelite sheet. The calculated shear stress was found to lie between 98 and 99% of the true shear stress from the wide end of the taper to within $\frac{1}{4}$ in. of the waist, where it fell to 94% of the true stress. The correction was judged

small enough to ignore; consequently the calculated stresses have been used throughout.

3. MICROSCOPICAL METHODS USED

Five types of microscope were used:

- (i) Linnik-Zeiss two-beam interference microscope.
- (ii) Multiple-beam interference microscope.
- (iii) Normal microscope.
- (iv) Phase-contrast microscope.
- (v) Polarizing microscope.

The first two were used for making measurements of vertical slip displacement. The Linnik-Zeiss microscope works at a fairly high power and so views a relatively small field. It has a sensitivity of 250–500 Å. for vertical displacement. The type of interference image sometimes obtained with slip bands of small displacement at low extension of the specimen is shown in Fig. 12 (Plate XVI); the fringes were abruptly displaced where they crossed a slip band. The displacements in Fig. 12 ranged from about $\frac{1}{2}$ to about $\frac{1}{2}$ a fringe spacing, i.e. from about 500 to 1500 Å.* At other times the fringe displacement was not abrupt, but gradual, as shown in Fig. 13 (Plate XVI), denoting a slip displacement more gently sloping with respect to the specimen surface. In fields such as those shown in Fig. 12 or 13, it was a straightforward matter to measure the slip displacements. At larger specimen extensions the interference images were more complex; a typical one is shown in Fig. 14 (Plate XVI). However, examination will show that it is possible here to measure the slip displacements without much arbitrariness.

In the fine-grained specimen at large extensions, the interference images denoted a surface that was too uniformly undulating to permit anything approaching an objective measurement, e.g. Fig. 23 (Plate XVII). Where measurements were possible, 50 or 100 were made (50 on the tapered specimens, 100 on the parallel-sided specimens) to obtain a mean value. As may be seen from the graphs, such as Fig. 6 or 9, mean values did not as a rule deviate by more than $\pm 10\%$ from a smooth curve of best fit.

The multiple-beam microscope is more sensitive than the Linnik-Zeiss; it has a sensitivity of about 100 Å., it uses a lower power, and views a larger field. It was used in this work for measurements on the fine-grained specimen at low extension. The type of image obtained with it is illustrated by Figs. 29–31 (Plate XIX), which show the same field before test, after 0.8% extension, and after 1.7% extension, respectively. (The faint extra set of interference lines in Fig. 29 were formed inside the microscope and were eliminated before the subsequent micrographs were taken.) These micrographs well illustrate how quickly practically every part of the specimen surface became rumpled and bent. The fringes were finer than those formed in the two-beam microscope, whence the

higher sensitivity of the multiple-beam arrangement. To determine a mean value of slip displacement, each displacement along every other fringe was measured until 100 measurements had been made. Since the spacing between the fringes varied considerably after the specimen had been stretched, the spacing value used to convert the actual measurements in millimetres of fringe shift into corresponding variations of surface level was the mean spacing of the two fringes on either side of the one along which measurements were being made. This mean spacing was determined separately at each point where a measurement of fringe shift was made.

The results obtained with the two-beam and multiple-beam microscopes were consistent. In Fig. 8 the first three points for slip displacement in the fine-grained specimen were determined with the multiple-beam microscope; the remainder (including the duplicate point) were determined with the two-beam. The two sets fall on the same smooth curve. An indication of the overall reproducibility of the interference measurements is given by the point for the duplicate fine-grained specimen. It lies close to the same smooth curve.

The normal and phase-contrast microscopes were used for general examination, the latter being used because of its high sensitivity to surface steps. Since one purpose of this work was to make a quantitative examination of slip movements, it was useful to have a definite value for the sensitivity of these microscopes. This was obtained by comparing fields as registered by these and by the interference microscope. The normal micrograph, Fig. 32 (Plate XIX), is of a portion of the field shown in the multiple-beam interference micrograph, Fig. 30 (Plate XIX). Fig. 33 (Plate XIX) shows the same portion as seen by the phase-contrast microscope. All were taken at the same specimen extension (0.8%). Four slip bands are indicated by the arrows *A*, *B*, *C*, and *D*; the arrow-heads lie at the same points of the slip bands in all three micrographs. From the interference micrograph it can be seen that the vertical displacement was about 400 Å. for slip band *A* and about 200 Å. for slip band *D*. These slip bands are easily visible in the normal and phase-contrast micrographs. Between slip bands *C* and *D* is another, easily visible in the phase-contrast micrograph, faintly visible in the normal micrograph, and weakly perceptible in the interference micrograph with a displacement of about 100 Å. Hence the normal microscope was sensitive to vertical displacements of about 100 Å. and the phase-contrast microscope appreciably more sensitive, probably to about 50 Å. This superiority of the phase-contrast over the normal microscope is confirmed by comparing the crystal marked *X* in Figs. 33 and 32; the former reveals slip bands within it, but the latter does not. The normal micrograph was taken with a 32-mm., 0.15-N.A. bloomed objective; the sensitivity would, of course,

* One fringe spacing represents 2730 Å. (= 0.273 μ) difference in surface elevation.

decrease for objectives of higher numerical aperture. The phase-contrast micrograph was taken with a 16-mm., 0.28-N.A. objective; the sensitivity appeared much the same for all the phase-contrast objectives available for this work (16 mm., 0.28 N.A. to 1.8 mm., 1.3 N.A., all positive phase-contrast with phase rings of nominally 15% transmission). Hence the superiority of phase contrast over normal examination for detecting small changes in level was greater the higher the power of objective used. This was a particularly useful feature of phase contrast, since it gave high sensitivity at the highest optical power, where the normal and interference microscope failed.

III.—DERIVATION OF TOTAL SLIP DISPLACEMENT \bar{p} FROM VERTICAL COMPONENT \bar{v}

The interference measurements gave only the mean vertical component of slip displacement \bar{v} ,* whereas to calculate the extension due to slip it was necessary to know the total displacement in the slip direction, \bar{p} .

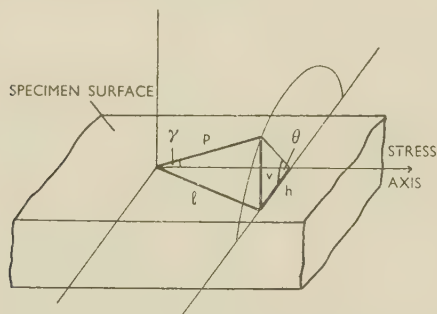


FIG. 2.—Relation Between Slip Components.

In the previous work \bar{p} was ascertained by measuring also \bar{l} (see Fig. 2 for explanation of p , l , &c.), since $\bar{p} = \sqrt{\bar{v}^2 + \bar{l}^2}$.

This was the only permissible method in that work because the specimen used had a preferred orientation. However, measurements of l were neither as sensitive nor as accurate as those of v , and it was judged desirable to dispense with them if possible. The randomness of crystal orientation of the present specimens made an alternative procedure seem possible, since it eliminated anisotropy due to preferred orientation. If it could also be assumed that no surface effect intruded to produce anisotropy, it was possible to calculate \bar{p} from \bar{v} by the averaging procedure given in the Appendix (p. 144), according to which:

$$\bar{p} = 2\frac{1}{4} \bar{v} \sqrt{1 + E} \quad (1)$$

In this formula $2\frac{1}{4}$ is an averaging factor; E is the fractional extension, and the factor $\sqrt{1 + E}$ allows for the diminution of distances parallel to the specimen thickness as the specimen extends. To ascertain if

anisotropy occurred, lines parallel to the specimen length were scribed, and the components of displacement normal to these, \bar{h} (see Fig. 2), were measured. In the absence of anisotropy, it can be seen from Fig. 2 that \bar{v} and \bar{h} were equivalent and so should have been equal. Even where the scribed lines were of good quality, the sensitivity for the measurements of \bar{h} was comparatively poor, about 0.5μ (5000 Å.), and consequently measurements of \bar{h} could be made only after the specimen had undergone creep for some time. This limited the number of reliable comparisons of \bar{v} and \bar{h} to one. However, in these same specimens values of \bar{v} and \bar{h} for grain boundaries were also measured. These will be reported in detail elsewhere, but as more \bar{h} values were large enough to be measured and the accuracy was therefore higher, some of the corresponding values of \bar{v} and \bar{h} for grain-boundary displacement are given here. The data are presented in Table I.

TABLE I.—Values of \bar{v} and \bar{h} and Ratio \bar{h}/\bar{v} .

Each figure is the mean of 50 or 100 separate readings, each reading being taken at a separate slip band or grain boundary.

Grains/mm.	Load, ton/in. ²	Time of Creep, hr.	\bar{v} , microns	\bar{h} , microns	\bar{h}/\bar{v}	Mean \bar{h}/\bar{v}
<i>Slip Bands</i>						
1	0.5	132½	0.475	0.70	1.47	1.47
<i>Grain Boundaries</i>						
1	0.5	35½	0.92	1.28	1.39	1.35
	...	132½	1.14	1.49	1.31	
4½	0.615	5	0.36	0.345	0.96	0.96
	0.77	5	0.56	0.54	0.96	
9¼	0.5	392	1.77	1.96	1.11	1.02
	0.5	860	3.77	3.42	0.91	
	0.5	901	4.1	4.3	1.05	

For the one specimen—the coarse-grained—where the ratio \bar{h}/\bar{v} is available for both slip bands and grain boundaries, there is reasonable agreement in the two cases. For the two smaller grain-sizes the ratio of \bar{h}/\bar{v} was quite close to unity, but for the coarse-grained specimen it was distinctly larger. This suggests that the direction of displacement with respect to the surface does influence its magnitude, but that this influence becomes apparent only when the obstruction to slip bands by grain boundaries, or to grain boundaries at grain corners, of both of which there are fewer the larger the grain-size, ceases to mask it. However, in view of the closeness of the ratio to unity, it seemed reasonable to use equation (1) unchanged to determine \bar{p} , but to employ for the coarse-grained specimen a corrected value of $\bar{v} = \sqrt{\bar{h}\bar{v}} = 1.17 \bar{v}$ (the mean of the three values of \bar{h}/\bar{v} given for this specimen is 1.37; $\sqrt{1.37} = 1.17$).

In determining \bar{p} from the experimentally measured quantity \bar{v} , there intervene only a constant factor of $2\frac{1}{4}$ or $2\frac{1}{4} \times 1.17$ and the elongation, which was determined fairly accurately. Consequently, to give

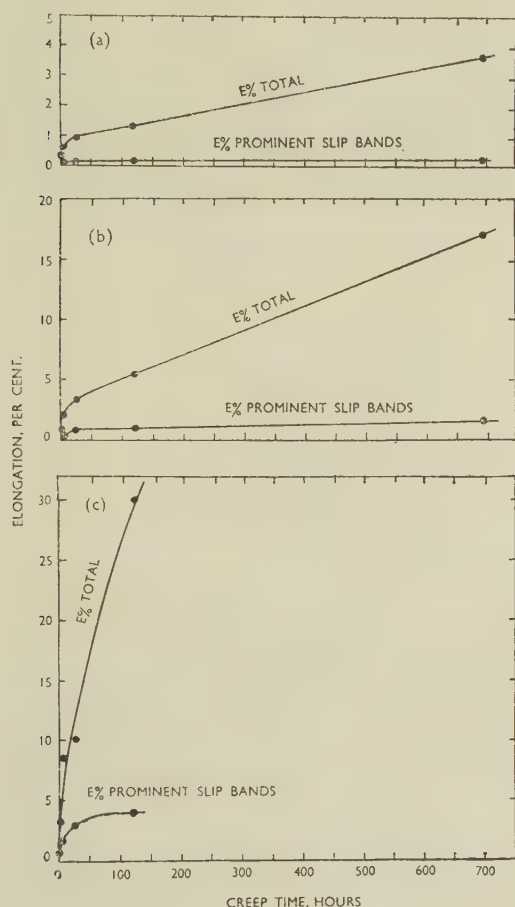
* The bar over a symbol is used to denote a mean value.

values of \bar{p} instead of \bar{v} does not obscure experimental errors in measuring \bar{v} . As \bar{p} is a more significant quantity than \bar{v} and is the quantity required for calculation of extension, results have been presented in terms of \bar{p} .

The values of \bar{p} were used to determine the extension due to prominent slip bands from the equation ⁴:

$$E\% \text{ slip} = 100(\sqrt{1 + \sqrt{2np + n^2p^2}} - 1) \quad (2)$$

in which n is the number of slip bands/cm. of unstretched specimen length.



coarse-grained, and eventually the extension/time curves crossed.

The curve for $\frac{1}{2}$ ton/in.² in Fig. 3 (b) for a grain-size of $4\frac{1}{2}$ grains/mm. lies out of sequence compared with the curves for the coarse- (1 grain/mm.) and fine- ($9\frac{1}{4}$ grains/mm.) grained specimens, the extensions being too small in the early stages. This was ascribed to the reduced opportunity for recovery presented by continuous compared with interrupted loading.

The extension at any given time increased rapidly with stress; after 1 hr., for example, the extensions

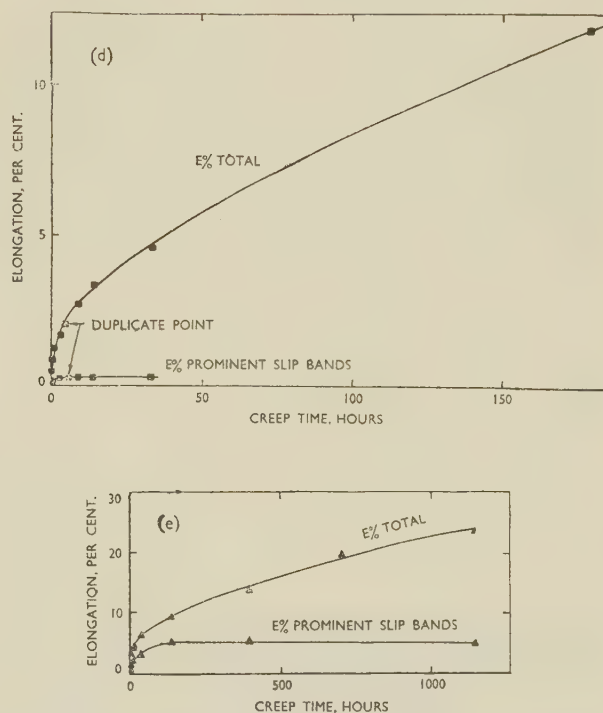


FIG. 3.—Curves Against Time of Total Extension and of Extension Due to Prominent Slip Bands for Various Grain-Sizes and Stresses.

- (a) 0.33 ton/in.², 4.5 grains/mm.
- (b) 0.5 ton/in.², 4.5 grains/mm.
- (c) 0.75 ton/in.², 4.5 grains/mm.
- (d) 0.5 ton/in.², 9.25 grains/mm.
- (e) 0.5 ton/in.², 1 grain/mm.

IV.—THE CREEP EXTENSION

The creep extension/time curves corresponding to initial stresses of $\frac{1}{3}$, $\frac{1}{2}$, and $\frac{3}{4}$ ton/in.² derived from the measurements on tapered specimens are given in Fig. 3. The curves for the fine- and coarse-grained specimens are given in Fig. 3 (d) and (e), the former showing on an enlarged scale the region where the slip bands could be measured.

The coarse-grained specimen gave faster transient creep than the fine-grained specimen; after 1 hr., for example, the extensions were 2.3% and 1.1% respectively. However, beyond about 50 hr. the fine-grained specimen extended more rapidly than the

were 0.3, 0.9, and 3.1% for initial stresses of $\frac{1}{3}$, $\frac{1}{2}$, and $\frac{3}{4}$ ton/in.², respectively.

V.—QUALITATIVE OBSERVATIONS ON SLIP BANDS

As in the previous work, two main types of slip were observed, prominent slip bands and fine slip lines. It transpired that the whole surface was covered with fine slip lines, and that the prominent bands were simply places where local intensification of this general fine slip had occurred.

The different types of prominent slip band observed previously—serrated ⁴ (corded ⁵), single, and multiple

slip bands—were not observed in the present specimens. All the prominent slip bands were of the type described previously as “wide”. The reason for this is thought to lie in the preparation of the specimen.

The most obvious slip markings to be seen on a specimen after test were the prominent slip bands. Examples are shown in Figs. 15 and 16 (Plate XVI) at $\times 100$. At this relatively low magnification they appeared as black lines or bands, some of which were straight, some curved, and some of which crossed crystal boundaries. Usually only one set of prominent bands occurred in each crystal.

More detailed examination revealed the presence of fine slip lines filling the interspaces between the prominent bands. They occurred in the fields shown in Figs. 15 and 16, but cannot be detected at this magnification. As before, they could be detected at high power with the phase-contrast microscope at an early stage (Fig. 17, Plate XVI) and with the normal microscope at a later stage (Fig. 18, Plate XVI). Two

ent slip bands. Intermediate types could certainly be found, but were comparatively infrequent. On very many slip planes or groups of slip planes, either little slip or much slip occurred. There was thus a rather marked tendency, which varied with conditions in the way described below, for fine slip to occur either uniformly over the surface or to be heavily concentrated in particular places, but not for intermediate degrees of concentration to occur. The following figures for the coarse-grained specimen give a quantitative impression of the difference in the two cases: the prominent slip bands (the heavy concentration) were about 30μ apart and represented steps in the surface about $\frac{3}{4}\mu$ (7500 \AA .) high; the fine slip lines (the uniform distribution) were spaced less than 1μ apart and represented steps in the surface of tens to hundreds of \AA high. This was why it was reasonable to classify the slip phenomena quite sharply into two types.

The fact that the prominent slip bands consisted of

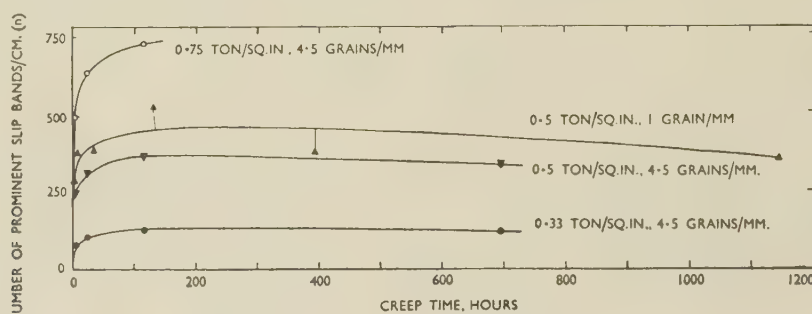


FIG. 4.—Density of Prominent Slip Bands Plotted Against Time.

or three sets of fine slip lines occurred over most of the surface of practically every crystal.

Detailed examination of the prominent slip bands revealed that they each consisted of a group of fine slip lines. This structure is shown in Fig. 19 (Plate XVII), which illustrates portions of four prominent slip bands. It required that the straight parts of the prominent slip bands should have been parallel to one set of fine slip lines, and this was observed to be so. The prominent slip bands thus resembled those observed by Treuting and Brick,⁶ Heidenreich and Shockley,⁷ and Brown.⁸ For the prominent slip bands to be visible as such, either more displacement than usual must have occurred on each fine slip line or the fine slip lines were closer together than usual, or both these things had happened, so that there existed a step in the surface that could easily be seen at low power. Although the prominent slip bands were so strikingly evident to low-power examination, they were thus really a secondary phenomenon. The more fundamental phenomenon was the general fine slip, which constituted the bricks from which other slip appearances were built.

It might therefore be expected that a whole range of types of slip band would form, from single fine slip lines through groups of a few fine slip lines to promi-

locally intensified fine slip explained why they did not have to follow crystallographic planes on a macroscopic scale. Fig. 20 (Plate XVII) shows at high magnification bends in two prominent slip bands such as the bend circled in Fig. 15 (Plate XVI), and illustrates how locally intensified fine slip combined to produce the bend. Formed in this way, the prominent bands could bend or cross crystal boundaries although the true slip direction was everywhere preserved. The initiation of prominent slip bands at grain corners, which was sometimes observed, is presumably to be explained in the same way. Occasionally slip bands initiated at adjacent corners joined up to produce movement of a triangular-shaped area, such as that marked WWW in Fig. 21 (Plate XVII).

Bent slip bands have usually been accounted for by cross-slip, e.g. Blewitt and Koehler.⁹ Some cross-slip almost necessarily occurred in the present work, since two or three directions of fine slip were the rule (cross-slip can be seen in Fig. 20, for example), but most of the bending seemed to be due to locally intensified fine slip on planes parallel to the straight parts of the prominent slip bands, as in Fig. 20. This arrangement would require that the bent parts of prominent slip bands contained a high density of screw dislocations.

The prominent slip bands in particular were influenced by the specimen grain-size and by the applied stress. They were observed to be more prevalent the coarser the grain-size and the higher the stress, a similar observation to that of Hanson and Wheeler¹ and Wood and his co-workers.² The magnitude of the influence of stress is indicated in Figs. 4 and 5. In the former the density of prominent slip bands, i.e. the number intersecting a line that, before extension, was 1 cm. long, is plotted against time, and in the latter against elongation. (The density for the fine-grained specimen is not given, as no density measurements were made on it for the reason mentioned below.) For both a given time and a given elongation the density increased with stress.

During extension, the prominent slip bands underwent a change that appeared to be due to the changing incidence of fine slip and which emphasized the secondary character of the former. They tended to become wider and their profiles more rounded, stand-

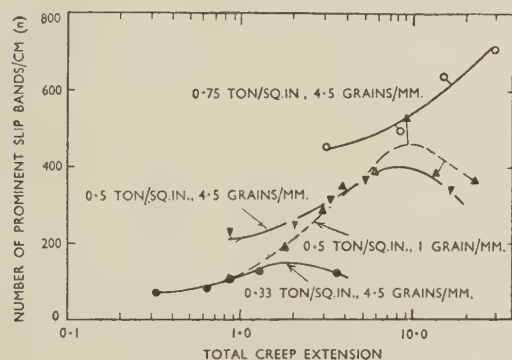


FIG. 5.—Density of Prominent Slip Bands Plotted Against Extension.

ing out less prominently from the increasingly rumpled surface. This is similar to Brown's observation⁸ that with increasing extension the number of lamellae in each slip band increased, but the displacement on each lamella remained unchanged. Fig. 22 (Plate XVII) shows the appearance under the interference microscope of prominent slip bands (SS) at 2% extension. Fig. 23 (Plate XVII) shows the appearance at 19.8% extension of what originally had been a similar area. The prominent slip bands could not then be distinguished from the generally undulating surface. This implies that, as extension progressed, fine slip became less and less concentrated in the original places of concentration—the prominent slip bands—which would be a consequence of greater resistance to further slip developing where a greater amount of slip had already occurred. In the fine-grained specimen this process went so far that eventually very few prominent slip bands could be distinguished. For this reason measurements of density of prominent slip bands could not be made on the fine-grained specimen. The process did not go so far with a coarser grain-size, although many bands became less prominent as extension progressed, as may be seen by

comparing the slip band AA in Fig. 19 (Plate XVII) with the same slip band in Fig. 24 (Plate XVII) which shows the same field at a later stage. On the other hand in this specimen a few slip bands were observed that became more prominent as extension progressed, showing that slip continued to occur along them in concentrated fashion for a long time (compare the slip band BB in Figs. 19 and 24). No effect of stress on the change in prominent slip bands with extension was observed in the range investigated.

It follows that the influence already referred to of specimen grain-size on the density of prominent slip bands changed somewhat with extension. At a low extension the prominent slip bands were more apparent the larger the grain-size, because they formed in greater numbers and more distinctly in large grains, being sharper and bigger surface steps; in other words, more fine slip was concentrated into narrower bands in large grains. At a large extension the prominent slip bands were more marked the larger the grain-size for the additional reason that they disappeared from large grains less rapidly, implying that fine slip remained more concentrated in large grains.

The appearance of the fine slip lines changed during elongation in the way observed previously. However, whereas in the coarse-grained specimen the fine slip lines could be seen neither with the phase-contrast nor with the normal microscope at extensions of about 4–10%, in the other specimens the lines merely became less distinct within this range of elongation. This suggests that at these intermediate elongations fine slip was more uniform in the coarse-grained specimen.

A very irregular type of slip seen at low stress was also ascribed to local intensification of the general fine slip. After a small extension a general fine-scale rumpling of the surface could be seen in some crystals, having a maximum amplitude of 100–200 Å., as estimated with the phase-contrast microscope. An example is shown in the phase-contrast micrograph Fig. 25 (Plate XVIII) (0.3% extension in 1 hr. at $\frac{1}{3}$ ton/in.²). At a larger extension this sort of appearance had apparently developed into an extremely irregular type of slip band of amplitude about 500 Å. which is illustrated by Fig. 26 (Plate XVIII) (1.3% extension in 118½ hr. at $\frac{1}{3}$ ton/in.²). Such appearances could clearly result from slip on short lengths of neighbouring planes.

All the observations so far referred to were made on the specimen surfaces, and it is natural to question whether they represented the processes going on in the interior of the specimen. Some qualitative reassurance on this point was given by an examination of the grain shown in Fig. 27 (Plate XVIII), which contains groups of straight prominent slip bands joined by curved, rather irregular ones; such appearances were observed only in the coarse-grained specimen. This field, when polished flat and oxidized anodically, gave the structure shown in Fig. 28 (Plate XVIII). The broad dark bands in the latter photograph indicate in-

creased disorientation of the sub-crystals and appear to correspond to the groups of prominent slip bands. Weaker, narrower bands following the general direction of the curved prominent slip bands can also be seen. These observations seem to mean that the locally intensified fine slip observed on the surface as

that Yamaguchi found a linear increase in n for aluminium specimens extended rapidly.¹⁰

The curves in Fig. 7 extrapolate backwards to a stress of about $\frac{1}{4}$ ton/in.² at $n = 0$, apparently suggesting that no prominent slip bands were formed at lower stresses. This is elucidated by extrapolating

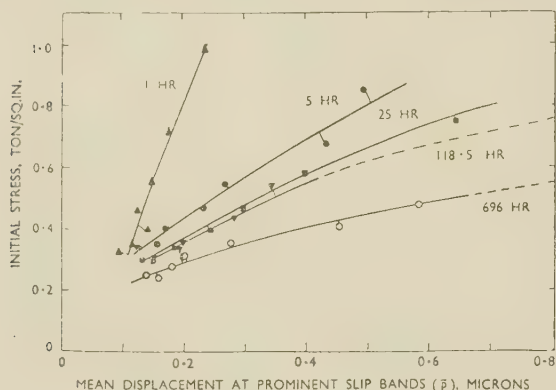


FIG. 6.—Mean Displacement at Prominent Slip Bands (\bar{p}) Plotted Against Initial Stress.

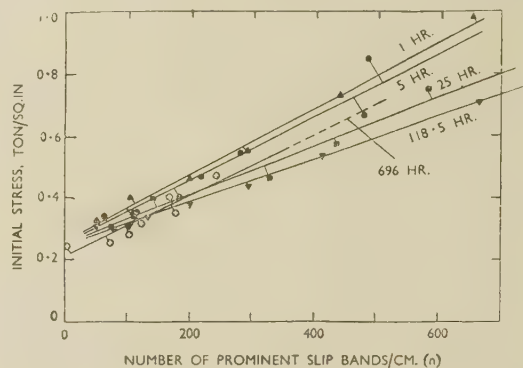


FIG. 7.—Density of Prominent Slip Bands (number intercepted by a line that, before extension, was 1 cm. long) Plotted Against Initial Stress.

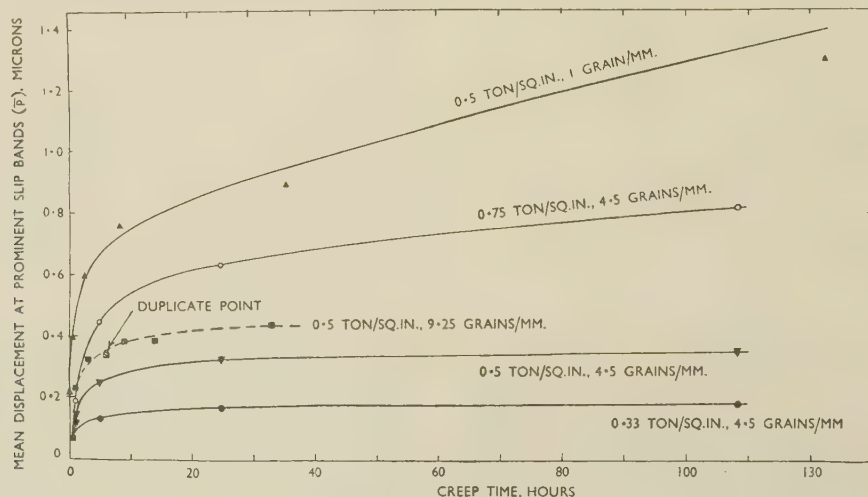


FIG. 8.—Mean Displacement at Prominent Slip Bands (\bar{p}) Plotted Against Time. The curve for the fine-grained specimen (---■---) relates to the mean slip displacement per crystal, not per slip band, and is therefore not comparable quantitatively with the others.

prominent bands had occurred also in the crystal interior.

VI.—EXTENSION DUE TO PROMINENT SLIP BANDS

The observations just described show that structurally the prominent slip bands were secondary to the fine slip lines. The work described in this section aimed at determining the extension due to the prominent slip bands to see how important they were quantitatively.

In Fig. 6 are plotted the curves of mean displacement at prominent slip bands (\bar{p}) against stress for the tapered (medium grain-sized) specimens. In Fig. 7 are plotted the curves of density of prominent slip bands (n) against stress. Both \bar{p} and n increased approximately linearly with stress. It may be noted

backwards the curves of \bar{p} against stress (Fig. 6), which meet approximately at the point stress = $\frac{1}{4}$ ton/in.², $\bar{p} = 800 \text{ \AA}$. A value of \bar{p} of 800 \AA . corresponds to a value of \bar{v} of 350 \AA ., which is about the limit of sensitivity of the Linnik-Zeiss microscope. Naturally, no values of \bar{p} below this would be recorded, and this value counts as the arbitrary smallest size of prominent slip band measured.

The curve of slip-band density at 696 hr. crosses the other curves (Fig. 7), there being more slip bands at 696 hr. than at earlier times for a low stress but fewer for a high stress. If this is not due to experimental error, it is presumably a consequence of the increasing uniformity of slip with increasing extension already referred to.

In Figs. 8 and 9 are given the curves of \bar{p} against time derived from these specimens for stresses of $\frac{1}{3}$, $\frac{1}{2}$,

and $\frac{3}{4}$ ton/in.², together with the \bar{p} /time curve for the coarse-grained specimen. Fig. 8 shows the early parts of the curves on an open time scale, and Fig. 9 shows the whole curves to fracture. The curve of mean slip displacement/crystal against time for the fine-grained specimen is also included in Fig. 8. As previously

slip displacements being larger the higher the stress if the curves are extrapolated until they cross. But at low extensions this plot shows that there were smaller slip displacements the higher the stress. To understand this apparently paradoxical result it must be remembered that the slip displacements plotted

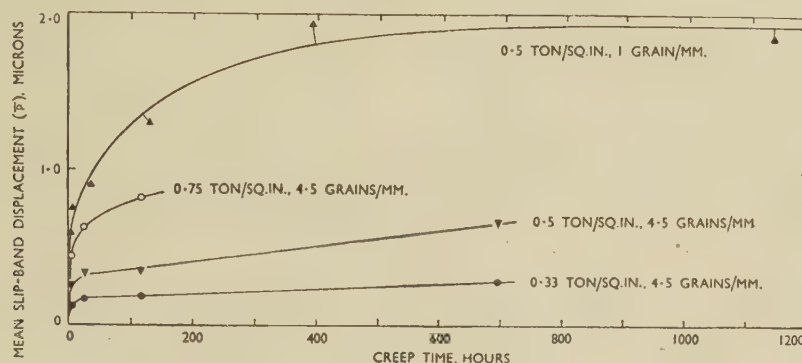


FIG. 9.—Mean Displacement at Prominent Slip Bands Plotted Against Time.

mentioned, individual prominent slip bands could not be separated in this specimen, but it was possible to measure the total prominent slip displacement/crystal in the early stages. This curve does not, of course, compare directly with the others in a quantitative way. In Fig. 4 are given the curves of n against time for the same specimens, excluding of course the fine-grained specimen. The density n appears to fall in the later stages because of the increasingly rounded profile of the prominent slip bands, as mentioned in the previous section. All the curves in Figs. 4, 8, and 9, resemble creep extension/time curves, having a rapid initial rise and then tending to level off. For the n /time curves, however, the initial rise was the more rapid and the levelling off the more abrupt. The difference between the \bar{p} /time curves (Fig. 9) for the coarse-grained specimen (1 grain/mm., $\frac{1}{2}$ ton/in.²) and the curve for the tapered specimen ($4\frac{1}{2}$ grains/mm.) relating to $\frac{1}{2}$ ton/in.² is sufficiently great, even though the former relates to interrupted and the latter to continuous loading, for it to appear permissible to conclude that larger slip displacements occur with a coarser grain-size. This is also clear, of course, from the fact that prominent slip bands were not prominent enough to be separated in the fine-grained specimen.

The curves of \bar{p} and n against time make clear the facts that, at any given time, there were more prominent slip bands the higher the stress and that the mean displacement undergone by these slip bands was larger the higher the stress or the bigger the grain-size. They do not make clear, however, the situation at a given extension. The same quantities are therefore plotted against extension in Figs. 5 and 10 (actually against log $E\%$ in order to spread out the low-extension region). Fig. 5 shows the expected result that, at any given extension, there were more prominent slip bands the higher the stress. At large extensions, Fig. 10 indicates a similar result, the mean

were mean values; evidently the extra slip bands brought into action by a higher stress cannot have immediately undergone as much displacement as the "easy" slip bands which operated for a lower stress.

The curves, against time, of extension calculated from these data as being due to the prominent slip bands are given in Fig. 3, which also includes the curves of total extension against time. The former curves are also similar in shape to the latter. It is clear from Fig. 3 (d) and (e) that the fraction of the total extension that was due to prominent slip bands increased with grain-size.

Finally, this fraction is plotted in Fig. 11 against log extension for each of the five combinations of grain-size and stress referred to in this work. The

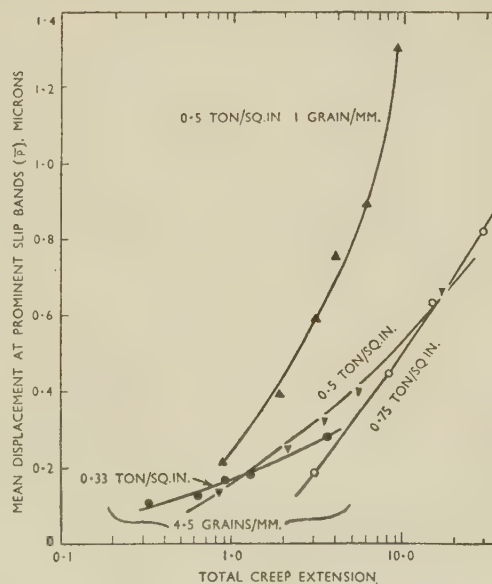


FIG. 10.—Mean Displacement at Prominent Slip Bands Plotted Against Extension.

curves have larger maximum ordinates the bigger the grain-size and, to a smaller extent, the bigger the stress.*

All the curves in Fig. 11 have similar shapes, rising from a low value at an early stage of creep to a maximum, that occurs at a lower extension the smaller the grain-size, and then falling. The decline in the later stages of creep was obviously due to the decreasing prominence of the slip bands referred to earlier that took place during second-stage creep. The rise in the early stage seems to mean that most of the very early rapid extension was the result of uniform fine slip, and that the concentration of fine slip in particular places which produced the prominent bands was a

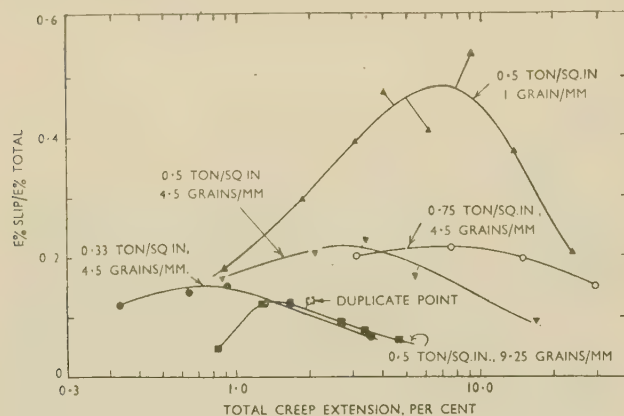


FIG. 11.—Fraction of Total Creep Due to Prominent Slip Bands.

subsequent development. The following sequence of events therefore seems to have occurred: (1) uniform fine slip; (2) concentration of fine slip in particular places; and (3) the gradual increase in width of the concentrated regions until, in the limit, a fair degree of uniformity was once again achieved.

The fraction of the total extension due to prominent slip bands was largest for the coarse-grained specimen, in which these bands were strikingly evident. Even in this specimen, however, the fraction of slip due to them never exceeded $\frac{1}{2}$, and at an early or at a late stage was only about $\frac{1}{5}$. Consequently, from the point of view of extension contributed, the prominent slip bands were secondary to the fine slip lines in all the specimens examined.

VII.—DISCUSSION

1. VALIDITY OF THE MEASUREMENTS

It may be argued that the assumptions made in calculating the extension due to prominent slip bands from the measured displacement may invalidate Fig. 11, since they may make the calculated slip extension substantially in error. They could render incorrect only the chief conclusion drawn from Fig. 11, namely that in most conditions examined the promi-

ent slip bands contributed less extension than the fine slip lines, only if this error were a substantial underestimate. However, the calculated extension cannot underestimate the true extension due to prominent slip bands by more than a factor of 2, since a larger factor would make the maximum of the curve in Fig. 11 for the coarse-grained specimen exceed unity. The factor must in fact be appreciably less than 2, since some fine slip undoubtedly occurred and a certain amount of extension occurred owing to the displacement at grain boundaries. If all the curves in Fig. 11 were raised by a factor somewhat less than 2, the conclusion would still stand that during most of the duration of creep under the conditions examined the prominent slip bands contributed less than half the extension.

There was in addition direct evidence as in the previous work that fine slip contributed appreciably to the extension. At about 1% total extension a rough estimate of the extension due to fine slip made from the fine slip displacements as gauged with the phase-contrast microscope gave the approximate result 1%, so that a substantial part of the extension at this stage must have been the result of fine slip. Further, the interference microscope gave direct, though qualitative, proof. For example, the fringes in Fig. 12 (Plate XVI) sometimes change direction on crossing a prominent slip band; a portion *AB* of one fringe has been continued along *BC* to show the deviation. And, unless it is assumed that a viscous, Plasticene type of deformation occurred, complex surface undulations such as are shown in Fig. 14 (Plate XVI) could not be produced except by a great deal of fine slip in between the prominent slip bands.

2. THEORETICAL

It seems to be generally thought that slip is confined to relatively narrow bands separated by relatively wide, undeformed interspaces, especially as far as rapid deformation is concerned. For example, Carpenter and Robertson¹¹ write that "a relatively large amount of movement takes place in closely spaced groups of planes, while the intervening portions of the crystal are not affected". However, Brown and Honeycombe¹² have shown that extremely finely spaced slip occurs in super-pure aluminium deformed at room temperature (apparently at the rate of a tensile test). As it has also been observed in the present work during creep, it is at least possible that fine slip is common.

Such a situation would be consistent with dislocation theory, which envisages that under suitable circumstances only portions of dislocations may move. It would in fact reduce the quantitative, though not the qualitative, importance of one of the main problems of the dislocation theory, namely that of accounting for large slip displacements.

The very large number of slip lines observed by Brown

* There is a degree of smoothing in the curves for the medium-grained specimens, as the fractions were calculated from the smoothed curves of *E*% slip against time.

and Honeycombe and in the present work supports the theory of a network of dislocation sources covering the whole volume of each crystal, such as the network of Frank-Read¹³ sources described by Mott.¹⁴ These sources have the characteristic that after emitting a dislocation the source reverts to its initial state and will emit successive dislocations until prevented by the reaction of dislocations generated. A network of such sources would respond to local variations in stress, producing more dislocations and larger slip displacements where the stress was locally high. They could thus explain in a general way the irregular slip and the bending of prominent slip bands, the latter of which occurred mainly near grain boundaries and corners, i.e. places where local variations in stress might be expected.

The problem is to explain why slip displacement was concentrated in bands and not distributed more generally. It is clear that the concentration was considerably less than low-power micrographs indicated, and thus that the effect to be explained was less than might have been supposed. Nevertheless, some effect existed. The concentration was more pronounced the coarser the grain-size, and it is natural to connect any differences in slip behaviour that depends on grain-size with the differences in spacing between grain boundaries, which constitute important obstacles to slip. If no other obstacles exist, or until they are set up, dislocations arising from any particular source will travel to the grain boundary. Eshelby, Frank, and Nabarro¹⁵ have shown that the number of dislocations emitted from a source is linearly proportional to the distance in which they are packed. Assuming a source situated in the centre of a grain, which would therefore emit the largest number of dislocations, and inserting appropriate values into equations (17) and (20) of their paper (see Appendix, p. 144), we find that in the coarse-grained specimen 500 dislocations should have been emitted and the maximum slip displacement should have been 1400 Å., and that corresponding values for the fine-grained specimen should have been 50 dislocations and 140 Å. According to equation (20) the slip-band displacement should not be uniform over the whole length of the slip band, but should be zero at the boundary and should rise at positions away from the boundary according to the square root of the distance. A variation of displacement of this general character was actually observed, but it hardly obeyed the square-root law; the displacement at first increased rapidly at positions away from the boundary, but soon reached a value that remained uniform, apart from minor irregularities, across most of the crystal. Some deviation from the behaviour predicted by the equation doubtless occurred because of the enormous stress concentration that would be produced by such a large number of dislocations as 500, which would take the effective stress outside the elastic domain assumed in deriving the equation. Nevertheless, this effect of a larger grain-size of permitting more dislocations to be produced from a favourably situated source does appear to provide a

basic reason for the larger slip-band displacements observed with coarser grain-size, and as the shear or extension caused by the movement of dislocations is proportional to the distance moved, the increase in transient creep observed with increase in grain-size is explained on two counts. Unlike the prominent slip bands, the fine slip lines were similar in all specimens. From this it is concluded that they were produced by dislocations having a relatively short "free path" because of barriers encountered in the grain interior, so that grain-size had little effect. Hence it is concluded that the prominent slip bands were due to the chance distribution of these barriers, which offered a sufficiently unimpeded path to dislocations emitted by certain favourably placed sources for the latter to emit a large number of dislocations.

To explain why the prominent slip bands were each composed of a number of slip lines instead of being single, it must be supposed either that dislocations emitted by one source were deflected on to adjacent planes, or that they could increase the stress on sources located in neighbouring planes and make these emit dislocations. It appears that temperature activation plays some part in this, since the prominent bands developed over a period of time and since Brown⁸ has shown that, for approximately constant rate of strain, there are more slip lines in each band the higher the temperature.

In equations (17) and (20) of the paper referred to,¹⁵ stress plays a similar role to distance. Consequently the influence of stress on slip displacement and on transient creep extension is to be explained in the same way as the influence of grain-size.

Note Added in Proof

Since this paper was written, the author has seen one by Kurnosov, Tronina, and Yakutovich¹⁶ describing similar work on zinc and iron, the specimens apparently being deformed fairly rapidly. These workers also have come to the conclusion that under their conditions of deformation much of the deformation was not localized in the prominent slip bands. They observed that the interference fringes did not always maintain the same direction in the spaces between prominent slip bands, and they report that the proportion of extension due to the prominent slip bands diminished when the temperature of test was lowered. They calculate the proportions in two specimens, strained at room temperature and at -196°C . as about 1/10th and 1/30th respectively, but from the figures given it appears that this is a miscalculation and that the correct proportions were about $\frac{1}{2}$ and $\frac{1}{4}$.

Wilsdorf and Kuhlmann-Wilsdorf¹⁷ and Kuhlmann-Wilsdorf *et al*¹⁸ have also recently reported fine slip lines some hundreds of Ångströms apart and some tens of Ångströms high, which they observed in the spaces between the prominent slip bands on strained high-purity aluminium. The rate of straining is not given, and was therefore probably similar to that employed in tensile testing.

ACKNOWLEDGEMENTS

The author desires to acknowledge the assistance given by Mr. M. H. Farmer, who took many of the measurements and photographs, helpful advice from Dr. N. P. Allen, and the supply of some multiple-beam reflectors by Professor S. Tolansky. The creep straining and the photo-elastic measurements were carried out in the Engineering Division of the National Physical Laboratory, and the scribing and length measurements on the tapered specimens in the Metrology Division of the National Physical Laboratory. Apart from this, the work was carried out in the Metallurgy Division as part of the General Research Programme, and is published by permission of the Director of the Laboratory.

REFERENCES

1. D. Hanson and M. A. Wheeler, *J. Inst. Metals*, 1931, **45**, 229.
2. G. R. Wilms and W. A. Wood, *ibid.*, 1948-49, **75**, 693.
3. W. A. Wood and W. A. Rachinger, *ibid.*, 1949-50, **76**, 237.
4. W. A. Wood and R. F. Scrutton, *ibid.*, 1950, **77**, 423.
5. G. Wyon and C. Crussard, *Rev. Mét.*, 1951, **48**, 121.
6. D. McLean, *J. Inst. Metals*, 1951-52, **80**, 507.
7. J. Trotter, *ibid.*, p. 521.
8. R. G. Treuting and R. M. Brick, *Trans. Amer. Inst. Min. Met. Eng.*, 1942, **147**, 128.
9. R. D. Heidenreich and W. Shockley, *J. Appl. Physics*, 1947, **18**, 1029.
10. A. F. Brown, "Metallurgical Applications of the Electron Microscope", (*Inst. Metals Monograph and Rep. Series*, No. 8), 1950, 103.
11. T. H. Blewitt and J. S. Koehler, *Symposium on Plastic Deformation of Crystalline Solids (Pittsburgh)*, 1950, p. 77.
12. K. Yamaguchi, *Sci. Papers Inst. Phys. Chem. Research*, (Tokyo), 1928, **8**, 289.
13. H. C. H. Carpenter and J. M. Robertson, "Metals", p. 104. London: 1939 (Oxford University Press).
14. A. F. Brown and R. W. K. Honeycombe, *Phil. Mag.*, 1951, [vii], **42**, 1146.
15. F. C. Frank and W. T. Read, *Symposium on Plastic Deformation of Crystalline Solids (Pittsburgh)*, 1950, p. 44.
16. N. F. Mott, *Proc. Phys. Soc.*, 1951, [B], **64**, 729.
17. J. D. Eshelby, F. C. Frank, and F. R. N. Nabarro, *Phil. Mag.*, 1951, [vii], **42**, 351.
18. D. G. Kurnosov, N. M. Tronina, and M. V. Yakutovich, *Zhur. Tekhn. Fiziki*, 1948, **18**, 197.
19. H. Wilsdorf and D. Kuhlmann-Wilsdorf, *Naturwiss.*, 1951, **38**, 502.
20. D. Kuhlmann-Wilsdorf, J. H. van der Merwe, and H. Wilsdorf, *Phil. Mag.*, 1952, [vii], **43**, 632.

APPENDIX

Calculation of Mean Total Slip Displacement \bar{p} from Interference Measurements of Mean Vertical Displacement \bar{v}

Case 1.— $\gamma = 45^\circ$ (see Fig. 2, p. 136)

This is approximately true for slip bands.

$$\bar{v} = \frac{2}{\pi} \cdot \bar{p} \sin \gamma \int_0^{\pi/2} \sin \theta d\theta = \frac{2}{\pi} \frac{\bar{p}}{\sqrt{2}}$$

$$\therefore \frac{\bar{p}}{\bar{v}} = \frac{\pi}{\sqrt{2}} = 2.24$$

$$\frac{\bar{v}}{\bar{p}} = 0.45$$

Case 2.— γ Can Take All Values

This is the more general case, in which it is necessary to assume some relation between displacement p and resolved shear stress in the direction of p . According to Fig. 6 (p. 140) it is not far wrong to assume a linear relation, i.e.

$$p = \frac{F}{a} \sin 2\gamma \quad (3)$$

where F is the applied tensile stress and a is some constant.

$$\begin{aligned} \text{Then} \quad &= \frac{2F}{a\pi} \int_0^{\pi/2} \sin 2\gamma d\gamma \\ &= \frac{2F}{\pi a} \end{aligned}$$

$$\begin{aligned} \text{and } \bar{v} &= \left(\frac{2}{\pi}\right)^2 \frac{F}{a} \int_0^{\pi/2} \int_0^{\pi/2} \sin 2\gamma \sin \gamma \sin \theta d\theta d\gamma \\ &= \frac{4F}{\pi^2 a} \int_0^{\pi/2} 2 \sin^2 \gamma \cos \gamma d\gamma \\ &= \frac{8F}{3\pi^2 a} \left| \cos^3 \gamma \right|_0^{\pi/2} \\ v &= \frac{8F}{3\pi^2 a} \\ \therefore \frac{\bar{p}}{\bar{v}} &= \frac{3\pi}{4} = 2.35 \quad \text{or} \quad \frac{\bar{v}}{\bar{p}} = 0.425 \end{aligned}$$

The ratios come out much the same in both cases. The ratio $\bar{p}/\bar{v} = 2\frac{1}{4}$ has been used.

One further point has to be considered. The measurement of v was made normal to the surface as this existed at elongation E , and not normal to the original surface. The effect of the rotation of gliding surfaces that occurs as extension proceeds would be to reduce the angle γ and thus decrease the measured \bar{v} , and so increase the ratio \bar{p}/\bar{v} . The reduction in \bar{v} must on average occur to the same extent as the reduction in specimen thickness, i.e.

true \bar{v} at elongation E = measured $\bar{v} \times \sqrt{1+E}$.

Hence,

$$\text{true } \bar{p} = 2\frac{1}{4} \times \text{measured } \bar{v} \times \sqrt{1+E}. \quad (1)$$

The equations (17) and (20) in the paper by Eshelby, Frank, and Nabarro¹⁵ are:

$$\text{Equation (17): } L = 2nA/\tau_0,$$

where L is the length of the slip plane occupied by dislocations, n is the number of dislocations, τ_0 is the applied stress, and $A = \mu\lambda/2\pi(1-\sigma)$ for an edge dislocation. Here, μ is the shear modulus, λ is the slip distance, and σ is Poisson's ratio.

$$\text{Equation (20): } \Delta = \frac{2\lambda\tau_0}{\pi A} \sqrt{Lx},$$

where Δ is the relative displacement above and below the slip plane at the point x . Strictly, Δ is stepped, increasing by λ each time a dislocation is passed. This equation gives the smoothed representation of Δ when there are enough dislocations for Δ to approximate to a smooth curve.

THE VISCOSITY OF ALUMINIUM AND BINARY ALUMINIUM ALLOYS*

1426

By PROFESSOR W. R. D. JONES,† D.Sc., MEMBER, and W. L. BARTLETT,‡ B.Sc., Ph.D., JUNIOR MEMBER

SYNOPSIS

An apparatus, based upon the outer-rotating-cylinder method, has been constructed to study the variation of viscosity with temperature for pure aluminium and its variation with temperature and composition for a number of binary aluminium alloys. The results show that aluminium and its alloys exhibit a characteristic change point on their viscosity/temperature curves at 760°–770° C., which appears to be due to some change of state in the liquid. For the binary alloys, the viscosity varies in accordance with the equilibrium diagram, there being a maximum at the limit of solid solubility and a minimum at the eutectic. Modification increases the viscosity of the eutectic aluminium–silicon alloy by about 30% and either eliminates, or raises the temperature of, the change point on the viscosity/temperature curve.

I.—INTRODUCTION

"FLUIDITY" is generally considered to be synonymous with "castability," i.e. the ability of a molten metal in a given condition to fill a mould prepared under definite conditions. It should not be confused with "fluidity" as understood by the physicist, which is the reciprocal of "viscosity". There must be some correlation between the two interpretations. One of the controlling factors in obtaining a sound casting in the foundry is the variation in viscosity of the liquid with temperature and constitution, as indicated by Kondic and Kozlowski.¹ The fluidity of metals and alloys has been measured in many foundries, but, as such tests are empirical, a knowledge of the actual casting characteristics of a metal or alloy is a matter of experience. There are relatively few data available on the effect of temperature and constitution on viscosity.

Many methods for the determination of viscosity have been developed, most of them open to objection on the grounds of the need for empirical calibration. Among previous investigations of the viscosity of aluminium and its alloys are those carried out by Saito and Matsukawa,² using an inner-rotating-cylinder type of viscometer, and by Polyak and Sergeev³ using an oscillating-sphere apparatus. The results of the two series of experiments do not agree. Saito and Matsukawa observed the viscosity/temperature curves for aluminium and its alloys to be similar, all exhibiting a change point at 765° C., above which the viscosity was practically constant; below this temperature the value rose gradually to the solidification temperature, with an almost vertical rise over a small temperature range near this point. These results do not indicate any relationship between viscosity and constitution. For aluminium (99.8%)

the values recorded were 0.03043 poise at 773° C., and 0.03282, 0.03339, 0.03965, and 0.05082 poise at 659° C. Polyak and Sergeev recorded for pure aluminium lower values above 700° C. and higher values below, e.g. 0.06350 poise at 670° C., and 0.01880 at 765° C. No change point at 765° C. was recorded, but a correlation between viscosity and composition was observed.⁴ Both sets of results were obtained with viscometers which were calibrated empirically, and neither group of workers apparently paid much attention to one of the controlling factors in the determination of viscosity, viz. the presence of "non-slip" between the moving components and the liquid being tested.

II.—DESIGN OF VISCOMETER

It was decided to develop a viscometer based on the principle of an outer rotating cylinder. The underlying theory of this method has been given by Poynting and Thomson,⁵ who state that:

$$\eta = Tt/2\pi \left(\frac{4\pi r_2^2 r_1^2}{r_2^2 - r_1^2} \right) L \quad (1)$$

where η = viscosity (poises), T = torque exerted on inner cylinder (dyne-cm.), t = time of 1 revolution (sec.), r_1 = radius of inner cylinder (cm.), r_2 = radius of outer cylinder (cm.), and L = height of inner cylinder (cm.).

The torque T , measured by the angle of twist (θ radians) in a calibrated suspension, $=K_1\theta$, where K_1 is the torsion constant of the suspension.

$$\therefore \eta = K\theta t \quad (2)$$

If K is the apparatus constant:

$$K = K_1/2\pi \left(\frac{4\pi r_2^2 r_1^2}{r_2^2 - r_1^2} \right) L \quad (3)$$

* Manuscript received 9 May 1952.

† Professor of Metallurgy, University College, Cardiff.

‡ Research Assistant, University College, Cardiff.

The theoretical derivation of K in equation (1) assumes that the cylinders are of infinite length and, therefore, in practice the effect of the ends of the cylinders must be taken into consideration. These "end effects" give rise to an apparent lengthening of the inner cylinder, and the "effective length" must be substituted in the expression for K . The end

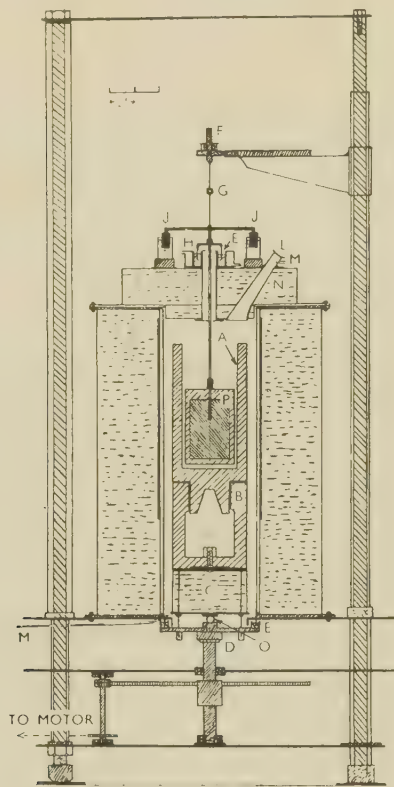


FIG. 1.—The Viscometer.

- | | | | |
|---|----------------------------|----|-------------------------------------|
| A | Graphite crucible. | H | Steel bell. |
| B | Graphite stand. | JJ | Damping vanes. |
| C | Heat-insulated base. | L | Window. |
| D | Turntable. | M | Gas inlet. |
| E | Water-cooled mercury seal. | N | Insulated lid. |
| F | Suspension head. | O | Ball-and-socket pivot. |
| G | Mirror. | P | Inner graphite cylinder (weighted). |

effects can be found experimentally by immersing the inner cylinder to different depths in the liquid, giving:

$$\eta = K_2 \frac{\theta_1 t}{L_1 + l_1} = K_2 \frac{\theta_2 t}{L_2 + l_1} = K_2 \frac{\theta_3 t}{L_3 + (l_1 + l_2)}$$

The effective length is then $L + (l_1 + l_2)$, where l_1 = end effect due to bottom and l_2 = end effect due to top, i.e. effective when the cylinder is completely immersed, and will take into account any effect due to the connecting-rod of the inner cylinder.

The apparatus designed is illustrated in Fig. 1. The rotating system consisted of a machined graphite cylindrical crucible (A), 12 cm. in internal dia., surrounded by the furnace and supported on a graphite stand (B) carried on a heat-insulated base (C) attached

to a turntable (D). The level of the turntable was so adjusted that a water-cooled mercury gas seal (E) could be placed between it and the top plate of the stand to which was bolted the base-plate of the furnace. Transmission from a $\frac{1}{2}$ -H.P., D.C. motor to the turntable was effected by a worm-and-gear system (with suitably placed ball races), carried underneath the stand. The gears gave a reduction of 90 : 1, the speed of the motor being controlled by external series resistances to give a suitable speed to the turntable. A constant speed of revolution was obtained by using a D.C. battery to supply the current. The suspension system was made up of a fine cold-drawn calibrated phosphor-bronze wire held in the suspension head (F), supporting from its bottom end a stainless-steel rod which carried a stainless-steel mirror (G) (focal length 100 cm.) and a steel bell (H) which formed part of the mercury seal (E) at the lid. The lower end of this rod was joined to the steel rod carrying the main cylinder. The inner cylinder (P) (11 cm. dia. \times 15 cm. long) was machined from graphite and was capable of being weighted internally to overcome any buoyancy effects. The suspension head consisted of a draw-collet chuck mounted on a stage capable of very fine adjustment horizontally in any direction. The suspension wire was independently calibrated by a moment-of-inertia method. Measurement of the angular displacement of the wire was made by means of a lamp-and-scale unit working in conjunction with the mirror (G). A purification train, for removal of oxygen from the inert gas—usually nitrogen—consisted of the usual pyrogallol scrubbers, reduced copper oxide in a furnace at 600° C., and a molten-metal (aluminium and/or sodium) scrubber to ensure maximum removal of oxygen. The apparatus was rendered gas-tight by making all bolted joints on suitable gaskets and incorporating gas seals between the stand and turntable and between the suspension mechanism and the furnace top.

Tests were carried out on water and rape oil at room temperature in order to determine the end effects and hence the apparatus constant K . The effect of varying conditions in the coaxial-cylinder system upon the apparatus constant was also studied. The results showed the accuracy of the apparatus to be within $\pm 0.5\%$, by comparison with values quoted in the International Critical Tables. The end effects were independent of the liquid medium and were constant if (a) the height of fluid above the inner cylinder, and (b) the bottom clearance between the two cylinders, were maintained between 5 and 15 mm. Eccentricity between the cylinders of up to 0.5 mm. had no appreciable effect upon the final value; the mercury seal on the suspension, although increasing the damping of any oscillations, did not affect the actual angular displacement.

An assumption in the derivation of equation (1) is that there shall be no slip between the liquid medium and the cylinder material. In the cases of water and of rape oil, with graphite as the cylinder material, this condition was fulfilled, and it was observed that,

in accordance with equation (2), with constant η , θ was inversely proportional to t , the graph of θ against $1/t$ being linear and passing through the origin (Fig. 2). If, however, the surface of the graphite was treated by impregnation with wax so as to promote slip, then the

all determinations. Sufficient time was allowed for both motor-speed and temperature to become stable. Temperature measurements were made by means of a dip thermocouple, the hot junction of which was in contact with the surface of the inner cylinder.

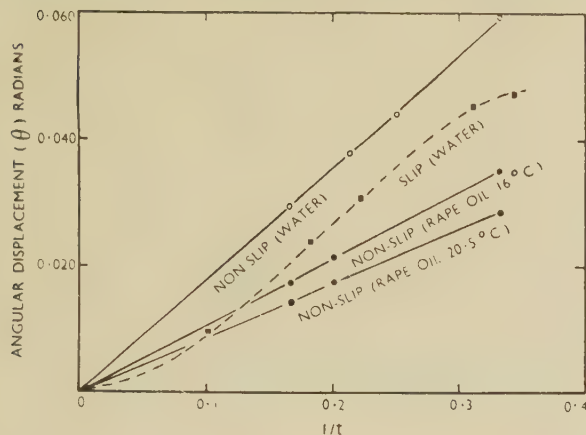


FIG. 2.—Relation between Angular Displacement θ , and Speed, $1/t$, for Conditions of Non-Slip and Slip. (Water at room temp., rape oil at 16° and 20.5° C.)

straight portion of the graph did not extrapolate back to the origin. It is to be expected, then, that the complete form of the curve will be as also shown in Fig. 2. This can be of use in determining whether or not there is slip between molten aluminium and the graphite-cylinder wall. Application of the apparatus constant K , as determined at room temperature, to results obtained at elevated temperatures might incur errors arising from two sources: (i) thermal expansion of the cylinders, and (ii) alteration of the torsion characteristics of the suspension wire due to temperature changes.

Experiments proved that the thermal expansion of the graphite up to the maximum temperature of test was negligible and also that, as a result of the water-cooling system on the lid, there was no appreciable change in the torsion characteristics of the wire. It may be assumed, therefore, that the apparatus constant as determined at room temperature can be used for values obtained at elevated temperatures.

After preliminary tests with pure aluminium, the following technique was adopted: Melting and alloying was conducted in an inert atmosphere and, as an added precaution to ensure the absence of any oxide skin during a determination, the surface of the melt was lightly skimmed immediately before a reading was taken. Viscosity determinations were carried out at turntable speeds of 10, 15, and 20 r.p.m. and between the melting point and 800°–850° C., at the same temperature during heating and cooling. At each temperature of test, the concentricity of the cylinders was checked and any eccentricity exceeding 0.5 mm. was corrected. The height of fluid above the inner cylinder and the bottom clearance were maintained between 5 and 15 mm. for

III.—RESULTS OF EXPERIMENTS

1. THE VISCOSITY OF HIGH-PURITY ALUMINIUM

A preliminary series of tests were carried out on aluminium over the range 660°–850° C., using an atmosphere of oxygen-free nitrogen. The results showed that the graph of θ against $1/t$ was linear and passed through the origin. It may therefore be assumed that there was no slip between the molten aluminium and the cylinders. Since the temperatures of test were chosen at random, it may further be assumed that this condition prevailed over the entire temperature range. The results confirmed that variation of the bottom clearance and of the height of fluid above the inner cylinder between 5 and 15 mm. did not affect the calculated value of η .

Determinations were then carried out to obtain a full viscosity/temperature curve up to 850° C. This curve is shown in Fig. 3. Each value obtained was

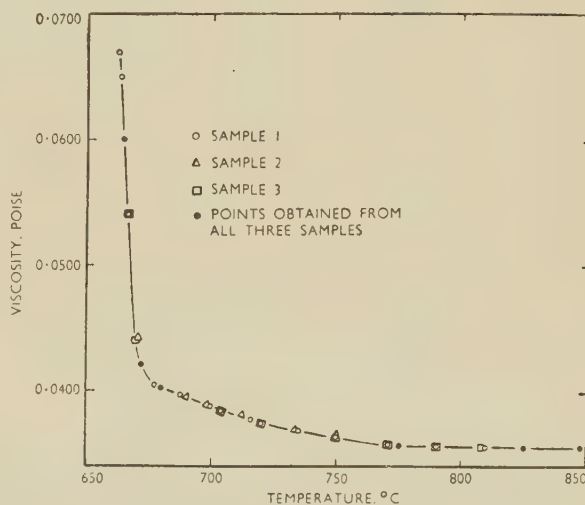


FIG. 3.—Viscosity/Temperature Curves for High-Purity Aluminium.

reproducible to the third digit and to within ± 3 on the fourth, e.g.:

		η , poise	
700° C.	Temp. increasing	.	0.03862
	" decreasing	.	0.03858
	Mean	.	0.03860
750° C.	Temp. increasing	.	0.03625
	" decreasing	.	0.03623
	Mean	.	0.03624

The mean values so obtained are given in Fig. 3. It can be seen that the curve has two inflections, and is divisible, therefore, into three parts. Above approximately 765° C. the viscosity is almost constant, whereas below this point there is a gradual

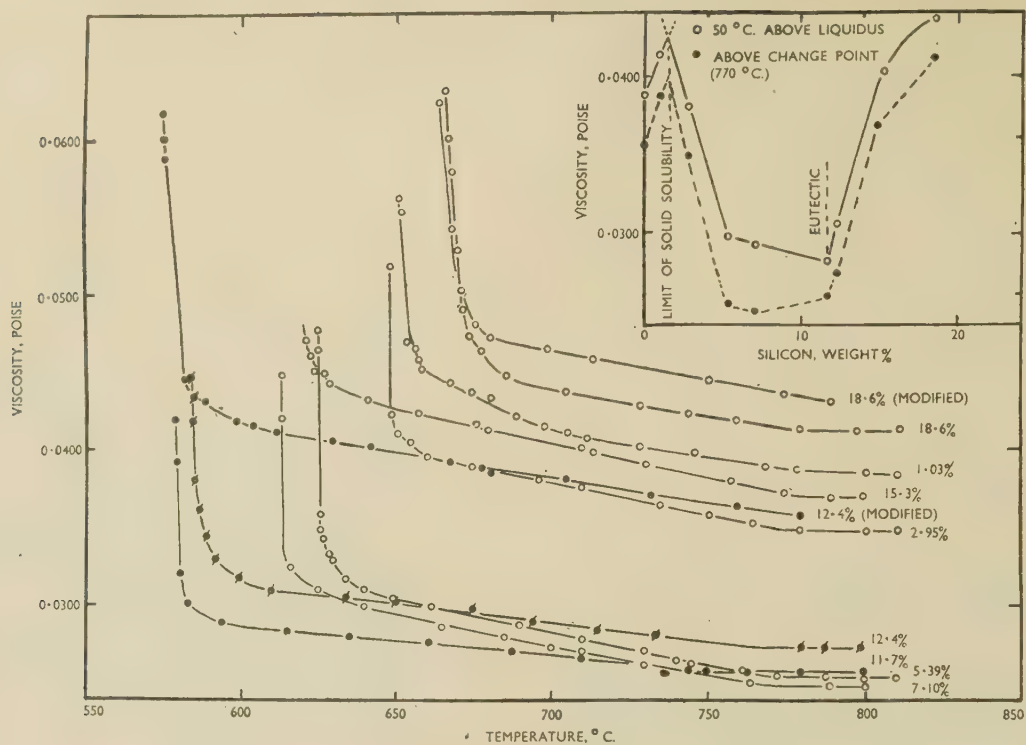


FIG. 4.—Viscosity/Temperature Curves for Aluminium-Silicon Alloys.

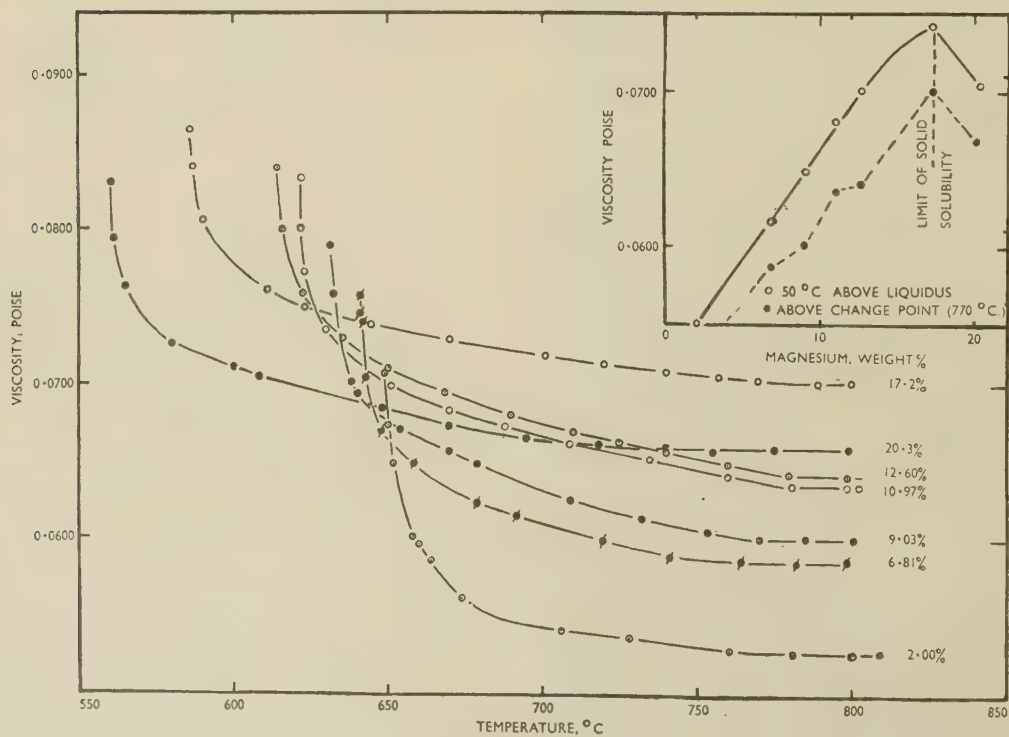


FIG. 5.—Viscosity/Temperature Curves for Aluminium-Magnesium Alloys.

increase with decrease in temperature. The relationship between viscosity and temperature in this range is not, however, linear. Below about 675° C. the viscosity increases rapidly with small changes in temperature, the curve becoming linear and almost vertical. Between 662° C. and the freezing point

The materials used were: electrolytic copper, high-purity magnesium of Canadian origin (99.95–99.97%), “Mond” nickel, silicon of 95–96% purity, “Severn” zinc (99.99%), and high-purity aluminium (99.9%). Samples for chemical analysis were taken from the top and bottom of the melt by means of a

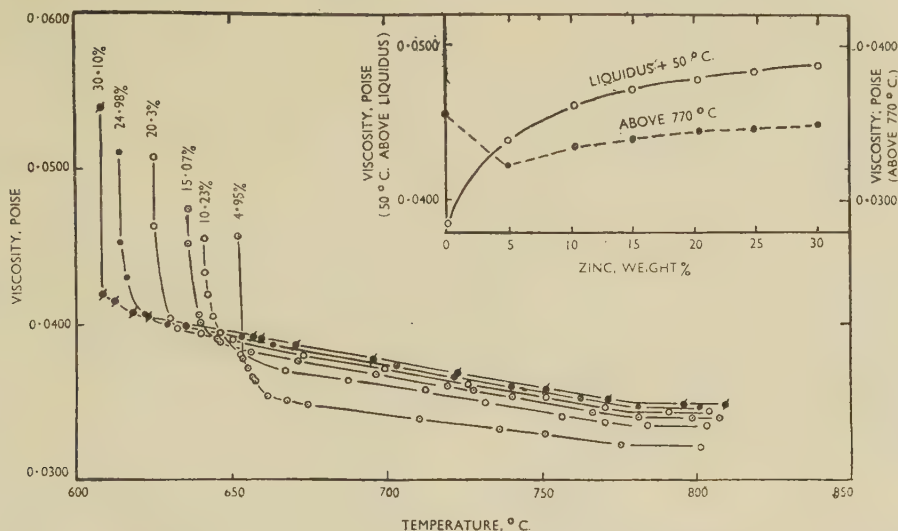


Fig. 6.—Viscosity/Temperature Curves for Aluminium-Zinc Alloys.

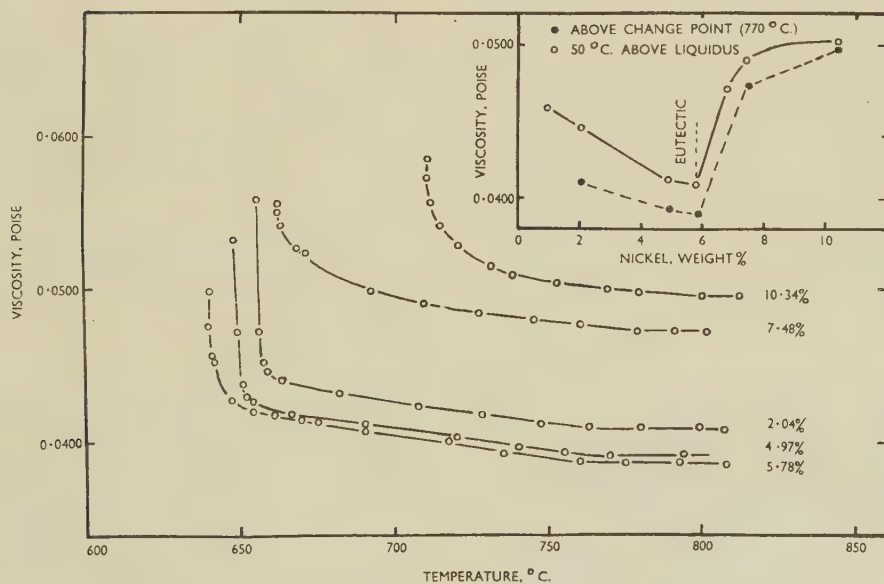


Fig. 7.—Viscosity/Temperature Curves for Aluminium-Nickel Alloys.

(658°–659° C.) no satisfactory results could be obtained owing to the high and rapidly varying viscosity of the melt.

2. THE VISCOSITY OF BINARY ALUMINIUM ALLOYS

Binary alloys of the following compositions were tested: copper 0–33%; silicon 0–20%; zinc 0–30%; nickel 0–10%; magnesium 0–20%.

specialty made graphite-coated “thief”. Alloying was carried out in the apparatus under the inert atmosphere by means of hardener alloys, the level of the melt being suitably adjusted to conform with the conditions for a constant value of K . Sampling was carried out at the beginning and at the end of the determination of the viscosity/temperature curve. There was no appreciable segregation in any alloy and no variation in composition during the test. The

determinations were carried out in an atmosphere of nitrogen, except in the case of the magnesium alloys, for which argon was used. The results are shown in Figs. 4-8.*

IV.—DISCUSSION

1. EXISTENCE OF A CHANGE POINT

Aluminium and its alloys all exhibit a change point at about $770^{\circ}\text{C}.$, above which, up to the maximum temperature of test, there is little variation of viscosity with temperature. Spells⁶ observed that between

experiments), the presence of which they confirmed by thermal analysis and electrical-resistance experiments. It would appear, therefore, as they suggest, that the change point indicates some change of state in the molten aluminium (or alloy). These authors state that the change point at $765^{\circ}\text{C}.$ is independent of composition, whereas the results now obtained show that the change point ($765^{\circ}\text{C}.$) for high-purity aluminium, tends to vary slightly with alloy content in accordance with the equilibrium diagram. The temperature of the change tends to increase with increase of alloying metal up to the limit of solid solubility. With further increase, the temperature

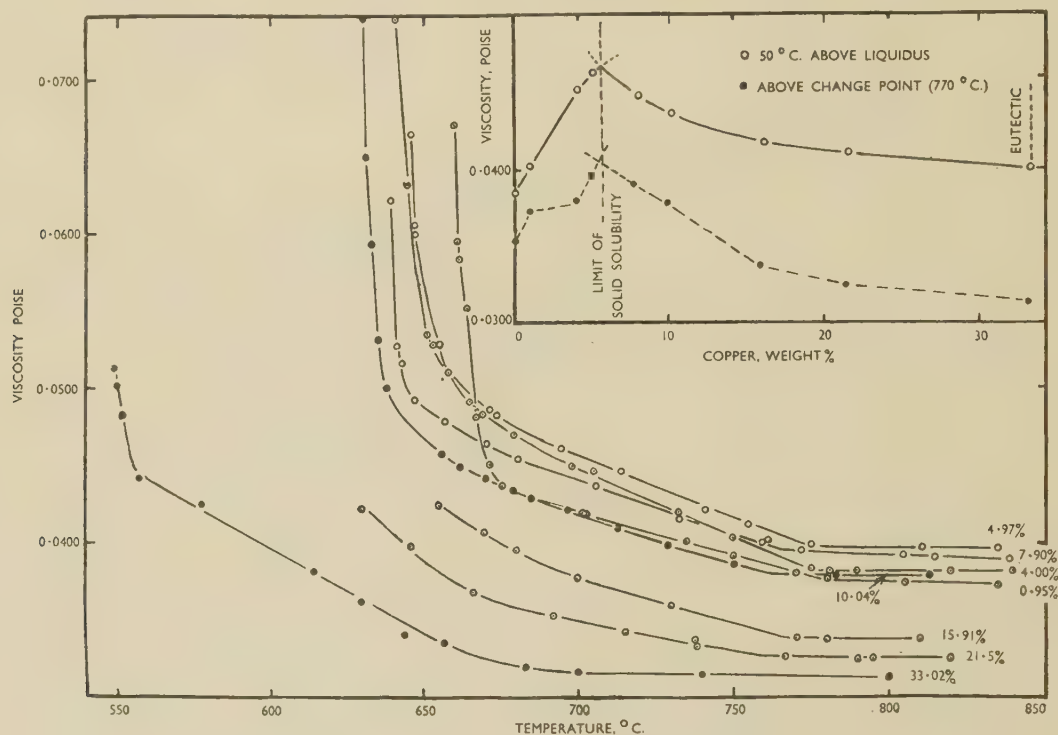


FIG. 8.—Viscosity/Temperature Curves for Aluminium-Copper Alloys.

1000° and $1100^{\circ}\text{C}.$, the viscosity of molten gallium varied by only 2%, i.e. it was nearly constant. His work was intended to demonstrate the probability that, for any molten metal, there is a temperature above which the viscosity is almost constant. It is to be expected, however, that this temperature will be considerably higher than the melting point, as was found by Spells in the case of gallium (melting point about $30^{\circ}\text{C}.$, constancy in viscosity attained at $1000^{\circ}\text{C}.$). It is unlikely, therefore, that the change point observed with aluminium, at about $100^{\circ}\text{C}.$ above the melting point, corresponds to such a temperature.

A more probable explanation is that put forward by Saito and Matsukawa.² Their curves show a change point (similar to that observed in the present

of the change is reduced until the eutectic composition is reached; beyond this it again increases, eventually becoming almost constant.

2. VARIATION OF THE VISCOSITY/TEMPERATURE CURVE WITH COMPOSITION

The viscosity/temperature curve for the pure metal, the basic form of which is unaltered by the addition of a second element, shows below the change point a gradual and almost linear increase in viscosity with decrease in temperature to some 10° – $20^{\circ}\text{C}.$ above the freezing point. At this point the general slope of the curve increases rapidly until it becomes almost vertical just before solidification.

The effect of an alloying element is to alter (a) the general slope of the curve below the change point, i.e.

* In some cases, incomplete curves are shown, some of the results being rejected owing to contamination of the melt.

the rate of increase of viscosity with decrease of temperature, and (b) the rate at which the slope increases as the liquidus is approached.

In all cases the low-percentage alloy curve is similar to the curve for the pure metal, but with a higher alloy content each element exerts a characteristic effect, that of copper being to increase the rate of increase of viscosity with decrease of temperature. The rate of increase of the slope of the curve on approaching the liquidus is slower than that for the pure metal, over a range of some 30° C. above the liquidus.

The slope of the silicon-alloy curves below the change point is decreased, the curves being linear. The rate of change of slope is less than that for the pure metal, but greater than that for the copper alloys, and extends over 20° C. The slope of the magnesium-alloy curves, as for the copper alloys, is increased, being intermediate between that for the copper alloys and that for the pure metal. The rate of change of slope is small, extending over 35°–40° C. The slope of the zinc-alloy curves is intermediate between that for the pure metal and that for the silicon alloys. The curves are again linear. The rate of change near the liquidus is similar to that for the silicon alloys. The curve for the nickel alloys is linear, the slope being the smallest observed. For alloys below the eutectic composition, the rate of change of the slope near the liquidus is fairly high. Above the eutectic composition, the rate is smaller.

Variation of the percentage of element present in any particular binary series, does not appear to have an appreciable effect upon the slope of the viscosity/temperature curve below the change point at about 770° C., although alloys of eutectic composition show a rapid change of slope near the liquidus which is independent of the general rate of change of slope of the system. It would appear, therefore, that where there is no freezing range, the rate of change of slope will be rapid.

The effect of alloying additions upon the viscosity appears to be dependent upon the equilibrium diagram of the particular alloy system. There is an initial rapid rise in viscosity with small additions of alloying element, after which the viscosity increases less rapidly up to the limit of solid solubility. Between this composition and the eutectic point, the viscosity decreases. Small additions beyond the eutectic composition cause a second rapid increase in viscosity, but further alloying additions give only slight increases, and the viscosity eventually becomes almost constant. Hence viscosity/composition diagrams can be plotted showing a maximum at the limit of solid solubility and a minimum at the eutectic composition. The structure of the alloys appears, therefore, to affect the viscosity; this, however, persists only up to the change point, above which the viscosity is independent of the composition of the alloy. Viscosity/composition diagrams at 50° C. above the liquidus, and also above the change point at 770° C., for the alloy systems under examination are shown

inset in Figs. 4–8. Similar diagrams can be plotted at constant temperature, e.g. 700° C.^{3, 4}

Examination of these diagrams shows that:

(a) When the solubility range is small (silicon and copper, Figs. 4 and 8), the initial increase in viscosity with increase in alloying content is rapid; whereas if the range is large, (magnesium and zinc, Figs. 5 and 6) the increase is more gradual.

(b) With a small range between the limit of solid solubility and the eutectic, as e.g. in the aluminium-silicon system, there is an initial fairly rapid decrease in viscosity (Fig. 4), followed by a gradual decrease up to the eutectic composition. If this range is comparatively large, as in the aluminium-copper system, the decrease in viscosity is much smaller (Fig. 8).

In the case of the aluminium-nickel alloys, the limit of solid solubility is about 0.05% nickel. Determinations were not carried out in this range owing to difficulties in accurate chemical analysis, but the trend of the diagram, confirmed by single spot determinations on low-alloy contents (not less than 1%), indicates that a very rapid increase in viscosity would occur between 0% and the limit of solid solubility.

3. THE EFFECT OF MODIFICATION ON THE VISCOSITY OF ALUMINIUM-SILICON ALLOYS

Fig. 4 shows, together with the normal viscosity/temperature curve for a 12.4% silicon alloy, the curve obtained with the modified alloy. It was found impracticable to add an accurately known amount of sodium to the melt or to analyse accurately the sodium content (of the order of 0.05%). Accordingly, an excess of sodium was added in an aluminium capsule and the surplus allowed to burn off slowly by creating a slow air leak in the apparatus. The progress of the burning-off was followed by means of specimens taken from the melt and examined under the microscope to detect over-modification, modification, or reversion. Since the tests were carried out under an inert atmosphere, the alloy, having reached the modified state, retained its modified structure over a period of time sufficient to enable a viscosity/temperature curve to be obtained. A similar series of tests was carried out upon an 18.6% silicon alloy (Fig. 4).

The results show that:

(a) The effect of modification upon the 12.4% silicon alloy was to cause an increase in viscosity of the order of 30%. In the case of the 18.6% alloy, the increase was much less, of the order of 5%.

(b) For both alloys, depression of the liquidus occurred, to the extent of 7°–10° C. for the 12.4% alloy and about 2° C. for the 18.6% alloy.

(c) The temperature of the characteristic change point, shown by aluminium and by all the alloys examined, was either raised or eliminated by modification, indicating some form of structural change in the liquid metal.

It was observed that over-modification and partial reversion gave viscosity values intermediate between those of the modified and normal alloys. Modification appears, therefore, to occur at a maximum viscosity value as compared with the normal, over-modified, and partially reverted states. By analogy with the viscosity/composition diagrams given by the alloy system generally, it is possible that this maximum may indicate a limit of solid solubility of sodium in the eutectic aluminium-silicon alloy or one of its constituents. Unfortunately, viscosity/composition diagrams of sodium in this alloy and in aluminium could not be obtained to confirm this, since there was no means available of determining sodium with sufficient accuracy. Further work upon these lines, however, may possibly aid in the development of a satisfactory theory of modification.

V.—CONCLUSIONS

Aluminium and some of its binary alloys exhibit a characteristic change point in their viscosity/temperature curves in the region of 760°–770° C., which would appear to be due to some change of state in the liquid metal. In the case of binary alloys, the temperature at which the change takes place is not constant, and tends to vary slightly in accordance with the equilibrium diagram, a maximum occurring at the limit of solid solubility and a minimum at the eutectic. Above this temperature the viscosity is almost constant. Near the liquidus temperature a second change point occurs in the viscosity/temperature curves, the slope of the curves altering over a range of temperature until it is almost vertical. The rate of

change of slope with temperature at this point depends on the alloying element. It is most rapid when there is no freezing range, i.e. with eutectic alloys and pure aluminium. It is possible that this change point may indicate a transition zone between the close-packed structure of the solid state and a close-packed "grouping" of the liquid state. Modification causes an increase in the viscosity of aluminium-silicon alloys, with the elimination of the characteristic change point and a lowering of the liquidus. Comparison with the viscosity of the over-modified and partially reverted alloy indicates that modification takes place at a maximum viscosity. This may mean that modification occurs at a limit of solid solubility of sodium in aluminium-silicon alloy or one of its constituents, and further work in this direction should yield useful information.

ACKNOWLEDGEMENT

One of the authors (W. L. B.) acknowledges gratefully financial assistance from the Department of Scientific and Industrial Research.

REFERENCES

1. V. Kondic and H. J. Kozlowski, *J. Inst. Metals*, 1948–49, **75**, 665.
2. D. Saito and T. Matsukawa, *Mem. Coll. Eng. Kyoto Imp. Univ.*, 1932, **7**, 49.
3. E. V. Polyak and S. V. Sergeev, *Comp. Rend. (Doklady) Acad. Sci. U.R.S.S.*, 1941, **30**, 137.
4. E. V. Polyak and S. V. Sergeev, *ibid.*, 1941, **33**, 244.
5. J. H. Poynting and J. J. Thomson, "Properties of Matter", (14th edn.). 1947: London (Charles Griffin & Co.).
6. K. E. Spells, *Proc. Phys. Soc.*, 1936, **48**, 299.

PLASTIC DEFORMATION OF COARSE-GRAINED ALUMINIUM *

1427

By (Mrs.) V. M. URIE,† B.Sc., and H. L. WAIN,† B.Met E.,
MEMBER

SYNOPSIS

A fine grid, photographically reproduced on the specimen surface, has been used to measure local elongations in the individual grains of deformed specimens of coarse-grained aluminium. In agreement with previous workers, it has been found that the elongation varied from grain to grain and within the individual grains of the aggregate. The elongation was generally restricted in the vicinity of grain boundaries, and the form of the restriction appeared to depend on the orientation relationships between neighbouring grains. The occurrence of deformation bands in the specimen during elongation produced corresponding fluctuations in the elongation curves which increased in magnitude with the overall elongation of the specimen.

I.—INTRODUCTION

SINCE the elastic limit of polycrystalline materials is generally greater than that of corresponding single crystals; it follows that the crystals of an aggregate do not deform as if they were in the free state. The reason for this difference in behaviour has been the subject of much investigation.

It is generally agreed that the amount of deformation and work-hardening varies widely from grain to grain and also within any particular grain of an aggregate, but opinion differs as to the precise behaviour in the neighbourhood of a grain boundary. Carpenter and Elam¹ have observed that less deformation occurs near the boundary during the deformation of coarse-grained aluminium, and that this effect can extend into the grain to a distance of 2.5 mm. from the boundary. X-ray measurements by Aston² have shown that a smaller change in crystal orientation occurs in the boundary regions than in the body of the crystal; this, he stated, indicates less deformation near the boundary. Similar results have been obtained by Hibbard³ for coarse-grained copper specimens. Yamaguchi's measurements⁴ of the local elongations in the grains of aluminium specimens deformed in tension confirmed the inhomogeneity of deformation, as did also the work of Barrett and Levenson⁵ on aluminium tested in compression. In addition, the former investigation indicated that elongation is always less near the boundary than in the adjacent crystals.

The strengthening effect of grain boundaries observed by all these investigators has been studied in more detail by Chalmers,⁶ who has shown that the elastic limit of bicrystalline specimens of tin increases linearly with the angle between the tetragonal axes of the two crystals, this increase being independent of the grain-boundary area. Chalmers regards the

boundary as a transition zone between the lattices of the neighbouring grains, and as the angle between the grains is increased, this zone becomes more effective in preventing slip, with a resultant increase in elastic limit. Further interesting results on the inhomogeneity of deformation within a grain have been obtained by Miller⁷ from tensile tests on specimens consisting of a single crystal bounded at one end by a polycrystalline region. These specimens were examined after the stress had been raised to a level which produced plastic deformation in the single crystal, but none in the polycrystal. It was found that a transition zone was induced in the single crystal, immediately adjacent to the polycrystalline part of the specimen, in which the deformation varied from zero to that of the bulk of the single crystal.

In a more recent investigation of large-grained specimens of commercially pure aluminium, Boas and Hargreaves⁸ have confirmed the inhomogeneity of deformation of the grains of an aggregate, and have found that the deformation varies within each grain in such a way that for any particular grain the deformation near the boundary is greater or smaller than that at the centre, according to whether the adjacent grain is more or less deformed. There was no evidence in this work of any restriction in deformation at grain boundaries.

In the present investigation, the local elongations in the individual grains of polycrystalline aluminium were measured on a finer scale than that used previously. The method adopted was to reproduce a fine grid photographically on to the specimen surface and to measure local elongations over 0.5-mm. gauge-lengths along traverses parallel to the direction of the applied tensile load. This photo-grid technique has been used to determine the strain distribution produced by metal-working processes such as deep drawing, drop-hammer forging, dimpling, and bend-

* Manuscript received 25 February 1952.

† Aeronautical Research Laboratories, Department of Supply, Melbourne, Australia.

ing,⁹⁻¹⁴ and these experiments have shown that the grid deforms with the specimen and does not flake or crack even after very considerable deformation. High-purity aluminium was used to overcome complications due to the presence of intermetallic compounds in commercial aluminium, whilst the photo-grid method eliminated the surface distortion which would be produced by scratches or hardness impressions used by previous investigators as gauge-marks for elongation measurements.

II.—EXPERIMENTAL TECHNIQUE

1. PREPARATION OF SPECIMENS

The material used was Alcoa high-purity aluminium (99.99+%). Tensile specimens having a gauge-length of 2.5 in. and a width of 0.5 in. were cut from $\frac{1}{8}$ -in.-thick sheet produced by cold rolling the original ingot without intermediate annealing. The faces of the specimens were ground flat and a grain-refining anneal was given. A very coarse grain-size (5–15 mm.) was produced by the method of critical straining and annealing (2.4% elongation followed by heating to 600° C. over a period of several days). These specimens were then polished on fine emery paper, annealed at 200° C. to relieve the surface strains, and electropolished in a bath consisting of 70% orthophosphoric acid, 15% water, 10% ethylene glycol, and 5% ethylene glycol monomethyl ether at a current density of approximately 1.5 amp./in.². This gave a highly polished, strain-free surface on which the grain boundaries could be detected as fine lines. Etch-pits for subsequent orientation measurements were developed by a light etch in Tucker's reagent.

2. ORIENTATION MEASUREMENTS

The orientations of the individual grains in the specimens were determined by goniometric measurements of etch-pit reflections, which gave the angles between the (100) planes and the specimen axis. These reflections were plotted stereographically, and the method of Carpenter and Elam¹⁵ was used to determine the operative (111) slip plane and $[10\bar{1}]$ direction for each grain. The angles χ and λ between the specimen axis and the operative slip plane and slip direction, respectively, were then measured for each crystal.

3. PHOTO-GRID TECHNIQUE

The surface of the specimen was sensitized with a solution of photo-engraving glue containing ammonium dichromate, and, when completely dry, it was exposed to ultra-violet light through a suitable grid negative.

Washing in lukewarm water for 10 sec. dissolved the unexposed portion of the sensitized surface, and the grid was finally dyed in a solution of nigrosin to give the required network of fine blue-black lines.

The negative used contained 6 lines/mm. and was printed on to the specimen so that the lines were longitudinal and transverse. The grid was measured along longitudinal traverses, using a toolmaker's microscope reading to 0.0001 in., and, by measuring every third transverse line of the grid, gauge-lengths of approximately 0.5 mm. along the length of the specimen were obtained. The beginning of each traverse was fixed by a fine needle indentation, and, by measuring the grid along the same traverse before and after deformation, local elongations could be calculated. Sufficient accuracy could be obtained only by measuring to a particular feature of a grid line which was noted and to which return could subsequently be made. This involved measuring the grid at a magnification of $\times 250$. The possible error in the elongation determinations over 0.5-mm. gauge-lengths was calculated to be $\pm 1\%$.

III.—EXPERIMENTAL RESULTS

Typical local-elongation curves for a coarse-grained aluminium specimen (S5) after 5 and 10% total elongation in tension are shown in Figs. 1 and 2. Elongations are plotted against position along two different traverses on the specimen surface, which are shown in relation to the grain structure of the specimen. The density and direction of slip lines along the respective traverses after 10% total elongation have been diagrammatically represented.

It can be seen at once from Figs. 1 and 2 that, as other workers have found, there is a variation in elongation from grain to grain and also within each individual grain of the aggregate. A further important point is that the elongation is generally restricted in the vicinity of a grain boundary. In some cases the maximum restriction in elongation occurs at the exact position of the boundary, but this is not generally the case. Where the two neighbouring grains had very different average elongations, as frequently happened, it was found that the maximum restriction occurred just inside that grain for which the average elongation was less. Moreover, a comparison of the elongation curves of grains 3 and 4 in Figs. 1 and 2, respectively, illustrates that the same grain may deform by different amounts when surrounded by different grains.

Exceptions to this general rule of restricted elongation near grain boundaries occasionally occurred, an example being provided by the boundary between grains 4 and 5 (Fig. 1). In this case the elongation of both neighbouring grains increases progressively towards the boundary, and although the elongation is slightly less in the immediate vicinity of the boundary, this restriction is not more marked than the normal fluctuations which occur in each grain.

Thus the behaviour of the elongation curves at grain boundaries seems to fall into three categories, which are illustrated schematically by the full curves of Fig. 5. The most common type of behaviour,

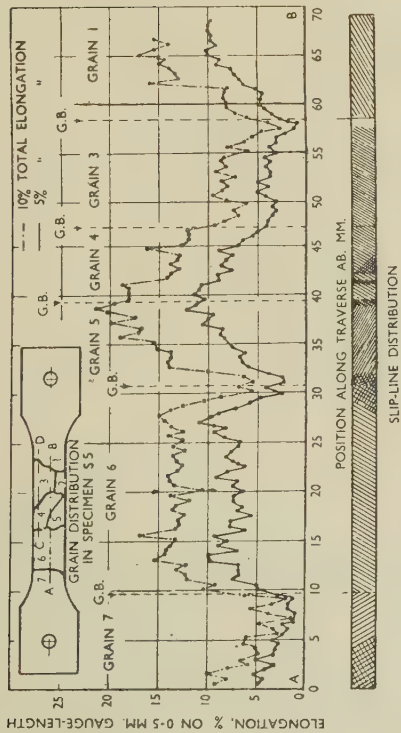


Fig. 1.—Local Elongations Along Traverse *AB* of Coarse-Grained Aluminium Specimen (*S5*) After 5 and 10% Total Elongation in Tension.

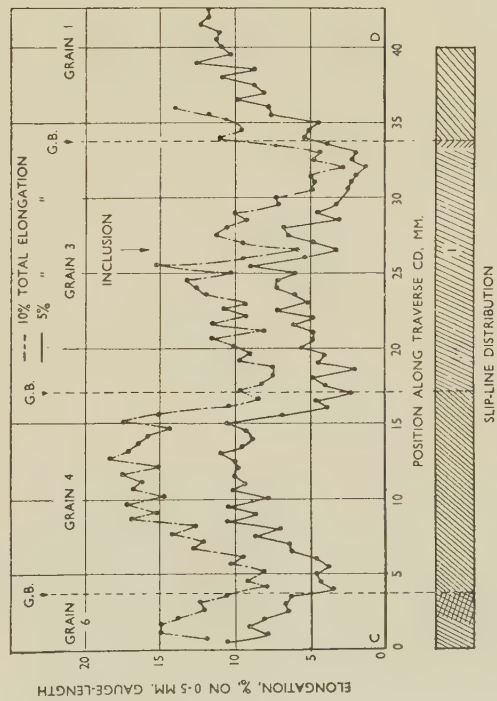


Fig. 2.—Local Elongations Along Traverse *CD* of Coarse-Grained Aluminium Specimen (*S5*) After 5 and 10% Total Elongation in Tension.

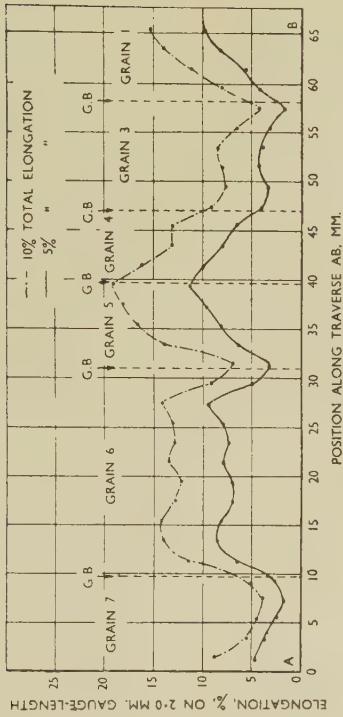


Fig. 3.—Averaged Local Elongations Along Traverse *AB* of Specimen *S5* After 5 and 10% Total Elongation in Tension.

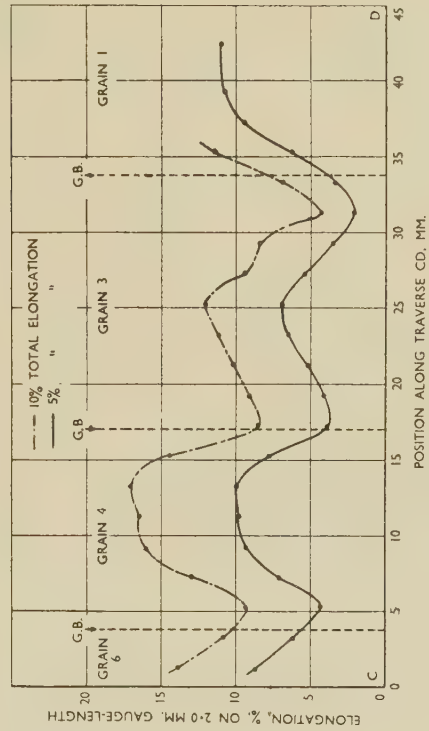


Fig. 4.—Averaged Local Elongations Along Traverse *CD* of Specimen *S5* After 5 and 10% Total Elongation in Tension.

illustrated in Fig. 5 (a), was found when the average deformation in the crystals on either side of the boundary was considerably different. In such cases

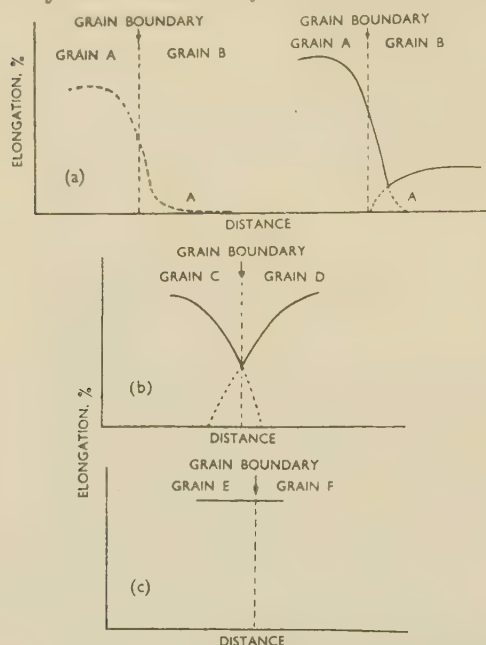


FIG. 5.—Diagrammatic Representation of the Three Types of Elongation Curve Obtained near Grain Boundaries.

there was a very marked restriction in elongation just inside that grain in which the average elongation was less. The other two types of curve occurred at the

apparent change in the slip characteristics of the softer grain as the boundary was approached, though such a change did, in general, occur in the harder grain. For example, in some cases double slip occurring across the harder grain changed to single slip near the position of the minimum in the elongation curve and continued to the grain boundary. In other cases the slip lines became weaker, or sometimes disappeared, between the minimum in the elongation curve and the grain boundary, and in one instance a completely different set of slip lines near the boundary followed a region of no slip. There was one example of a deformation band occurring at the position of the minimum in the elongation curve. At a boundary where the elongation curve corresponded to the second type (Fig. 5 (b)), single slip occurred across each grain, except for a small amount of double slip on either side of the grain boundary. In one grain the slip traces became weak near the grain boundary. In an example of the third type of curve (Fig. 5 (c)), the slip occurring throughout each grain extended right to the boundary, and there was some evidence of the continuation of one set of slip lines into the neighbouring grain.

Referring again to Figs. 1 and 2, it can be seen that, in addition to the general restriction in elongation near grain boundaries, there are superimposed short-term fluctuations in elongation values across each grain. These have a period of the order of 1 mm. and become more marked as the total elongation of the specimen is increased. Although these short-term fluctuations are believed to be real effects, as will be

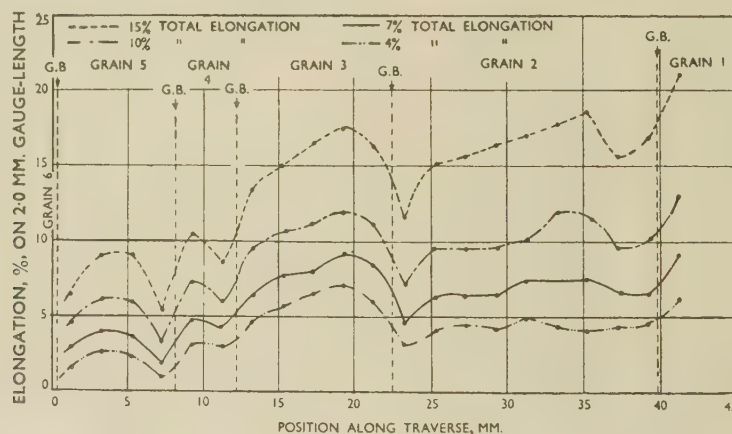


FIG. 6.—Averaged Local Elongations of the Grains of Specimen S6 After Various Total Elongations in Tension.

boundaries between grains whose average elongations were approximately equal. In one instance (Fig. 5 (b)) there was a marked restriction in elongation at the position of the grain boundary, whereas in the other (Fig. 5 (c)) the boundary had little influence on elongation.

Under microscopic examination the distribution of slip lines near grain boundaries appeared to vary with the type of elongation curve obtained. Thus, with curves of the first type (Fig. 5 (a)), there was no

discussed later, they somewhat confuse the main trends of the curves, and accordingly "averaged" curves were produced by plotting the mean of each four successive readings against position in the traverse. These curves, presented in Figs. 3 and 4, are interesting in that, although short-term fluctuations and even effects due to inclusions are smoothed out, the important points noted before of inhomogeneity of deformation and general restriction of elongation near grain boundaries are quite clearly apparent.

The sensitivity of the grid method of measuring local elongations is illustrated by the large fall in elongation which occurred in both curves near the middle of grain 3 (Fig. 2). Microscopic inspection showed that this drop coincided with an inclusion, probably Al_2O_3 , which was clearly visible on the surface and around which very few slip lines were present.

The "averaged" local elongations obtained on another specimen (S6) after 4, 7, 10, and 15% total elongation are presented in Fig. 6 and illustrate that the variation of elongation from grain to grain and within each grain, and the general restriction near grain boundaries, became more pronounced as deformation proceeded. Another effect of increasing

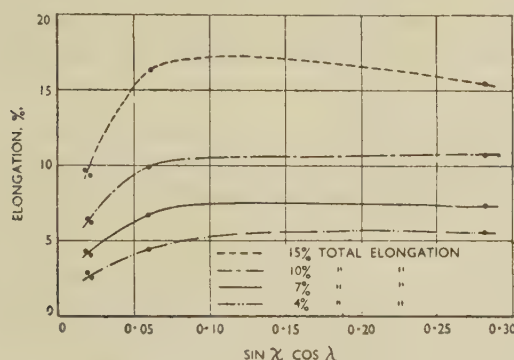


FIG. 7.—Averaged Elongations of the Grains of Specimen S6 Plotted Against the Value of $\sin \chi \cos \lambda$ Calculated for Each Grain.

deformation was the formation of a series of shallow "waves" on the originally flat surface of the specimen. These "waves" crossed each grain, changed direction at grain boundaries, and had the appearance of deformation bands as illustrated in Fig. 8 (Plate XX). Closer examination of the surface revealed that each deformation band seemed to occur at the position of a peak in the elongation curve, although the complexity of the bands, and the fact that the distance between them was of the same order as the gauge-lengths over which the elongation measurements were taken, made precise correlation difficult. Microscopic examination showed that very little change, if any, occurred in the direction of the slip lines on crossing a deformation band (see Fig. 9, Plate XX).

The average elongations of the grains in this specimen were estimated from Fig. 6, neglecting as far as possible effects due to grain boundaries and inclusions. These average elongations are plotted in Fig. 7 against the values of the function $\sin \chi \cos \lambda$, which is a measure of the shear stress in the slip system of each grain.

IV.—DISCUSSION

The facts that in a large-grained aggregate some grains deform more than others and that the deformation within a grain is inhomogeneous are well estab-

lished and are confirmed in the present work. This inhomogeneity is quite spectacular; for example, in a specimen which has been elongated 10%, the local elongations over 0.5-mm. gauge-lengths may vary from 2 to 22%. The average elongation of the grains at any stage of deformation depends on the shear stress in the grain, i.e. on the appropriate value of $\sin \chi \cos \lambda$. This elongation/resolved-shear-stress relationship is not linear, but this is to be expected in view of the restrictions in elongation at grain boundaries and the variation in the rate of work-hardening with orientation.

Probably the most interesting feature of this work is the pronounced restriction which occurs in the elongation values near grain boundaries and which may persist to distances up to 4 mm. from the boundary. This is in agreement with some previous workers, particularly Yamaguchi,⁴ but in contrast to the results of Boas and Hargreaves.⁸ It has been found that the behaviour of the elongation curves at grain boundaries appears to belong to one of three types, which are illustrated schematically in Fig. 5, and a qualitative attempt can be made to explain the nature of these curves in the following way.

It is considered that the grain-boundary regions in a polycrystalline aggregate can act as barriers to deformation and that their effectiveness in this respect will vary with the difference in orientation of the crystals on each side of the boundary. Supporting evidence for this point of view is, firstly, that Miller⁷ has shown that a rigid boundary produces a restriction in the deformation of a single crystal of zinc immediately adjacent to the boundary; secondly, Chalmers⁶ evidence of an approximately linear relationship between the elastic limits of bicrystals of tin and the angle between the tetragonal axes of the two crystals can be interpreted as an increase in the effectiveness of the grain boundary in preventing slip as the angle between the grains is increased; and thirdly, Lacombe and Beaujard¹⁶ have shown that, although slip lines normally stop at grain boundaries, they may be propagated across them when the orientations of the neighbouring grains are similar.

The most common type of elongation curve that was obtained occurred when the average deformation of neighbouring grains was considerably different, and showed a minimum in the hard-grain side of the grain boundary. Consider the deformation of such a combination on the assumption that the grain-boundary region provides an efficient bar to deformation as described above. At low stresses the softer grain will be deformed, but no general deformation will occur in the harder one, and the deformation of the softer crystal will be reduced near the boundary, as in Miller's experiments. Moreover, it is reasonable to suppose that there will be some induced deformation in the harder grain near the boundary, owing to the fact that continuity of deformation must be maintained and a grain boundary in a pure metal is unlikely to inhibit slip completely. At this stage the elongation curve will be as shown on the left in Fig. 5 (a).

As the external stress on the specimen is increased, general deformation of the harder grain will begin. The portion of this grain between point *A* (Fig. 5 (*a*)) and the grain boundary will already have been deformed and work-hardened under the influence of the deformation of the softer grain, and this will, in turn, produce a restriction in the deformation of the harder grain near the boundary. Thus, the final elongation curve will be as indicated in the right-hand curve in Fig. 5 (*a*) and will show a minimum on the hard-grain side of the grain boundary. Some support for this explanation is provided by the distribution of slip lines in such cases, although further information is necessary before any real conclusions can be drawn. It was generally found that, in the softer grain, the slip characteristic of the grain extended right to the boundary. In the harder grain, on the other hand, characteristic slip extended across the grain to the position corresponding approximately to the minimum in the elongation curve. Between this position and the grain boundary, the nature of the slip changed in ways which indicated a confused type of deformation, which is consistent with the supposition that deformation was induced in this part of the grain by the deformation of its softer neighbour.

The types of elongation curve represented by Figs. 5 (*b*) and (*c*) were obtained when the average deformation in grains on either side of the boundary was approximately the same. If the grain-boundary region constitutes an efficient bar to deformation, restrictions will occur in each grain near the boundary and a roughly symmetrical curve will be obtained with a restriction in elongation at the grain boundary (Fig. 5 (*b*)). As the effectiveness of the grain-boundary region as a bar to deformation decreases, the elongation restriction at the grain boundary will decrease and may ultimately become zero, and the crystals will deform as though no boundary were present (Fig. 5 (*c*)). The evidence available from the distribution of slip lines again supports these explanations. For example, at a boundary where the elongation curve corresponded to Fig. 5 (*b*), the characteristic single slip occurring across each grain changed to double slip in the immediate vicinity of the grain boundary. This indicates that the deformation conditions become more complicated near the boundary, owing to the induced deformation in each grain from movement of the other, which agrees with the assumption that the boundary area in this case constituted an efficient bar to slip transference. On the other hand, for the type of curve represented by Fig. 5 (*c*), the assumption that the boundary region was not effective in interfering with slip transference is supported by the fact that examples were found of slip lines in one grain crossing the boundary into its neighbour.

Another point of interest in this work is the short-term fluctuations that occur in the elongation curves (see Figs. 1 and 2). These are believed to represent a real effect since (*a*) the variation in elongation values is much greater than the experimental errors in-

volved in the gauge-length measurements, (*b*) the peaks and valleys in the curves generally occur in the same position and become more marked as deformation proceeds, and (*c*) the peaks and valleys are associated with macroscopic features of the surface of the deformed specimen. These surface features are most probably deformation bands which have been observed in aluminium by several workers.^{5, 17-19} The present work shows that the local fluctuations in elongation may be as much as 5% when the overall elongation of the specimen is 15%, and that they increase in magnitude as the overall elongation increases. This is in agreement with the description of the development of a deformation band which has been given by Cahn.¹⁷ In addition, as far as could be determined, the position of a deformation band coincided with a maximum in the elongation curve, so it appears that deformation bands play an increasingly important part in deformation as it proceeds.

It is difficult to reconcile the results of Yamaguchi⁴ and the present authors, both of which showed frequent restrictions in elongation near grain boundaries, with the conclusion of Boas and Hargreaves⁸ that the deformation of a grain near a boundary depends only on the deformation of the neighbouring grain. It is not to be expected that the elongation curves obtained by Boas and Hargreaves would show grain-boundary restrictions, since the points on these curves were spaced about 10 mm. apart, which is greater than the distance over which the grain-boundary restriction generally influenced the elongation curves. However, hardness changes were determined at approximately 1-mm. intervals, which should have been close enough to reveal such effects. There were, in fact, some indications in Boas and Hargreaves' results that hardness changes were less near grain boundaries than in the body of the adjacent crystals, notably at the boundaries between grains 1 and 2 (Fig. 1 (*a*)) and between grains 4 and 5 (Fig. 1 (*b*)) of their paper.⁸ However, there was nothing as marked as occurred in the elongation curves of Yamaguchi and the present authors.

Finally, there is some evidence both in the present work and that of Yamaguchi to indicate that, as deformation proceeds, the restriction in elongation near grain boundaries becomes more pronounced, and also that the smaller the grain-size the greater is the area over which the grain-boundary influence is effective. This would probably be even more marked if the crystal were completely surrounded by other crystals instead of having two free surfaces, as in the present experiments. Thus, for an ordinary fine-grained specimen, it would appear that the deformation would be controlled largely by the interactions of grains at boundaries and that the orientation of the grains would be of importance only in so far as it affected the behaviour at grain boundaries. This may provide a basis for the explanation of the well-known increase in the strength of metals with decreasing grain-size.

V.—CONCLUSIONS

(1) There is a variation in the amount of elongation between the grains, and also within the individual grains of a polycrystalline aluminium aggregate deformed in tension. The elongation of the grains depends to a certain extent on the resolved shear stress in the slip system, but the relationship is not linear.

(2) Elongation curves generally show restrictions in the neighbourhood of grain boundaries, and the form of the restriction appears to depend on the orientation relationships of adjacent grains.

(3) The production of deformation bands during

elongation causes corresponding fluctuations in the elongation curves which increase as the overall elongation of the specimen is increased.

ACKNOWLEDGEMENTS

The work described forms part of the general programme of the Aeronautical Research Laboratories, Department of Supply, Melbourne, Australia, and thanks are due to the Chief Scientist, Department of Supply, for permission to publish. The authors also wish to thank Dr. W. Boas, Chief of the Division of Tribophysics, C.S.I.R.O., and Mr. J. B. Dance of these Laboratories for helpful discussions during the progress of the investigation.

REFERENCES

1. H. C. H. Carpenter and C. F. Elam, *Proc. Roy. Soc.*, 1921, [A], **100**, 329.
2. R. L. Aston, *Proc. Camb. Phil. Soc.*, 1927, **23**, 549.
3. W. R. Hibbard, *Trans. Amer. Inst. Min. Met. Eng.*, 1949, **180**, 52.
4. K. Yamaguchi, *Sci. Papers Inst. Phys. Chem. Research (Tokyo)*, 1927, **6**, 271.
5. C. S. Barrett and L. H. Levenson, *Trans. Amer. Inst. Min. Met. Eng.*, 1940, **137**, 112.
6. B. Chalmers, *Proc. Roy. Soc.*, 1937, [A], **162**, 120.
7. R. F. Miller, *Trans. Amer. Inst. Min. Met. Eng.*, 1934, **111**, 135.
8. W. Boas and M. E. Hargreaves, *Proc. Roy. Soc.*, 1948, [A], **193**, 89.
9. G. A. Brewer and R. B. Glassco, *J. Aeronaut. Sci.*, 1941, **9**, (1), 1.
10. K. Cornell, *Amer. Photography*, 1942, **36**, (11), 16.
11. C. P. O'Haven and J. F. Harding, *Proc. Soc. Exper. Stress Analysis*, 1944, **2**, (2), 59.
12. — *Iron Age*, 1945, **156**, (19), 78.
13. — *Nat. Bur. Stand. Tech. News Bull.*, 1949, **33**, (11), 125.
14. — *J. Franklin Inst.*, 1950, **249**, 238.
15. H. C. H. Carpenter and C. F. Elam, *Proc. Roy. Soc.*, 1925, [A], **107**, 171.
16. P. Lacombe and L. Beaujard, *J. Inst. Metals*, 1948, **74**, 1.
17. R. W. Cahn, *ibid.*, 1951, **79**, 129.
18. R. W. K. Honeycombe, *Proc. Phys. Soc.*, 1950, [A], **63**, 672.
19. N. K. Chen and C. H. Mathewson, *Trans. Amer. Inst. Min. Met. Eng.*, 1951, **191**, 653.

The Ageing Characteristics of Binary Aluminium-Copper Alloys

By H. K. HARDY

(*Journal*, 1951, 79, 321.)

Mr. T. J. HEAL,* B.Sc., A.Inst.P., and Miss J. M. SILCOCK,* B.Sc.: It may be of interest to record briefly some of the structures we have found by X-ray methods in crystals cut from Dr. Hardy's hardness specimens. The alloy with 4% copper shows G.P. zones [1] for ageing times at 130° C. corresponding to half the flat on the hardness curves. G.P. zones [2] were present at peak hardness, together with about one-tenth of the possible quantity of θ' . Peak hardness at 190° C. corresponds to G.P. zones [2], with about one-third of the possible amount of θ' present. At 220° C. a little θ' was present in the 4% alloy after a few minutes, but only about 60% of the possible θ' was found at the peak hardness. The 3% alloy shows θ' only at the peak hardness at 190° C., but in this case the total possible quantity of θ' is present.

Full details of the work will be published later.

Mr. T. L. JOHNSTON,† B.Eng. (Student Member): Of the numerous investigators of ageing phenomena too many have sought to deduce general conclusions and theories from limited observations on a particular alloy system, largely ignoring the work of others. This has resulted in conflicting conclusions, often arising from failure to realize the full significance of such factors as:

(1) Nature of the alloy system (e.g. valency, electrochemical, strain-energy, solubility limit, and structural relationships).

(2) Effects of varying composition, ageing temperature, and cooling rate from the solution temperature within a given system.

(3) The property selected as a criterion of ageing and the particular experimental technique adopted.

It follows that the expectation of establishing a comprehensive theory in descriptive terms is a mistaken one. Dr. Hardy, in his interpretation of experimental results obtained by himself and others, has demonstrated the power of the thermodynamic approach. The experimental results given in the most recent of his papers are of interest to us in view of the work proceeding at Liverpool. A study is being made of the influence of progressive stages of ageing on the response to uniaxial constant stress of a high-purity aluminium-4.25% copper alloy. Our requirements led to the adoption of specimens over 20 cm. long, having a cross-section 6×1 mm. In order to establish a direct comparison with Gayler's‡ work, the microscopic changes and hardness/time relationships for this particular alloy have been determined, and it is hoped to publish full details shortly.

Besides confirming the general qualitative features of the curves obtained by Gayler and by Hardy, the most important result of these hardness measurements has been the realization that the rate of cooling from the solution heat-treatment temperature has a profound influence on the subsequent

ageing behaviour, much more even than that reported by Gayler. The relatively small cross-section of the specimens used in our work resulted in cooling rates, and hence stress distributions, more sensitive to variations in the quenching conditions than with the form of specimen used by Gayler. The curves for specimens cooled in still air and water, respectively, at room temperature, and aged at 150° C. suffice to illustrate this point (see Fig. A).

The most important departure from the microstructural changes reported by Gayler is that whereas θ'' (G.P. zones [2]) formed during the final rise to peak hardness in specimens that have been air-cooled, has a quasi-random distribution, that formed in water-cooled specimens possesses a definite Widmanstätten distribution; this is contrary to Gayler's opinion that a Widmanstätten type of precipitate is formed only after the maximum hardness has been reached.

With regard to Appendix II (p. 359) of Dr. Hardy's paper, the analysis of the growth of G.P. zones during the initial rise rests on the assumption that the ratio of the hardness increment to the total change in hardness may be taken as giving the fraction to which the process has proceeded, and that this is a simple function of the depletion of solute. As far as I am aware, there is no evidence to show that this assumption is justified. Indeed, any analysis of hardness results calls for extreme caution; for not only is the relationship between structure and the properties measured in a hardness test very complex, but changes in hardness depend in part on the state and distribution of the solute and not solely upon the proportion remaining in solution.

Scheil's analysis of the case where the heat of solution is negative, which Dr. Hardy has discussed, involves a difficulty which is not easy to resolve. In a terminal solid solution, the variation of the limit of solubility c of a solute with temperature can, for small values of c , be expressed by the equation:

$$c = \text{const. exp } (-\Delta H/RT) \S$$

where ΔH is the heat absorbed when one g. molecule of solute goes into solution, i.e. ΔH is positive. This equation has also been derived by Cottrell || by making a series of simplifying assumptions for the state of affairs where $V_{AB} - \frac{1}{2}(V_{AA} + V_{BB})$ is positive (see p. 355 of the paper). This equation not only applies to the systems copper-silver and lead-tin, but also proves to be applicable to the aluminium-copper, aluminium-magnesium, and magnesium-zinc systems, in which the occurrence of intermediate constituents suggests that the interaction energy between like atoms is greater than that between unlike atoms and hence, assuming that the strain-energy factor may be ignored, ΔH will be negative. But if this be so, not only would the above equation be inapplicable, but, in accordance with Le Chatelier's principle, the solubility would decrease with increasing temperature.

* Fulmer Research Institute, Ltd., Stoke Poges, Bucks.

† Department of Metallurgy, University of Liverpool.

‡ M. L. V. Gayler and R. Parkhouse, *J. Inst. Metals*, 1940, 66, 67.

M. L. V. Gayler, *ibid.*, 1946, 72, 243.

§ Cited by C. Zener, *Thermodynamics in Physical Metallurgy* (Amer. Soc. Metals), 1950, p. 18.

|| A. H. Cottrell, "Theoretical Structural Metallurgy", p. 170. 1948. London (Edward Arnold and Co.).

The equation for the heat of solution (in solid alloys) may be written in the form :

$$\Delta H = [(L-M)c + M + V]c(1-c)$$

where $V = zN[V_{AB} - \frac{1}{2}(V_{AA} + V_{BB})]$, and L and M are strain energies associated with the replacement of a B atom in a B lattice by an A atom and vice versa.* Now even if V is negative, it may be possible for ΔH to be positive, provided that the strain-energy factors are favourable.

We feel, therefore, that although in liquid alloys negative heats of solution are associated with systems in which there

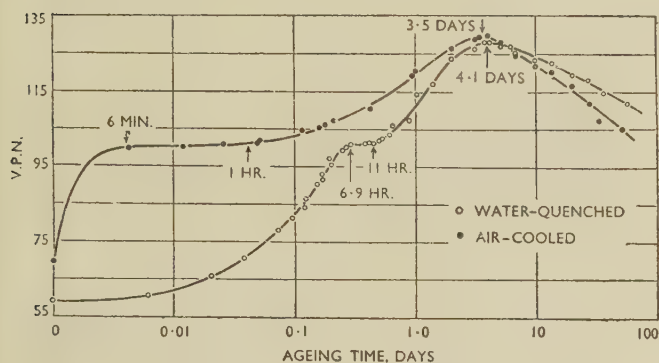


FIG. A.—Time/Hardness Curve for Aluminium-4.25% Copper Alloy Aged at 150° C. Solution-treatment temp. 540° C. (Johnston.)

is a tendency for intermediate constituents to be formed and order-disorder changes to take place, it may not be possible to extend this generalization to solid alloys. Clearly there is a need for more thermodynamic data concerning solid solutions.

Dr. J. L. MEIJERING †: Although a normal (more or less symmetrical) negative heat-of-mixing curve permits precipitation of superstructures, as in the gold-copper system, it seems difficult to give a satisfactory quantitative picture of segregation at concentrations as low as 2 at.-%. It can be shown, however, that the disordered face-centred cubic phase in the aluminium-copper system has an inflected heat-of-mixing curve. According to Oelsen and Middel's calorimetric measurements, ‡ 9.5 kg.cal. is evolved when one mole of copper and two moles of aluminium (both f.c.c.) combine to form θ . The energy necessary to dissolve this amount of θ in aluminium is given by the temperature dependence of the solubility of copper in aluminium, θ being the coexisting phase. The coefficient B , in the well-known formula $\log x = A - B/T$ yields 9.8 or 12.1 kg.cal., depending on the solubility curve taken. Consequently, an energy of 0.3–2.6 kg.cal. is needed to dissolve one mole of pure copper in a large amount of aluminium, which means that the integral heat-of-mixing curve of the face-centred cubic phase is positive at the aluminium-rich side, while it is strongly negative at the copper-rich side (type I, Fig. B). (Oelsen and Middel's curve reached -3.1 kg.cal./mole at 19 at.-% aluminium, the terminal α -aluminium bronze.) It is not essential that the heat of mixing should be just positive at the aluminium-rich side; a curve of type II (Fig. B) is also inflected and also results in a miscibility gap in the face-centred cubic phase. Calculations of the extent of this gap are somewhat uncertain,

but they suffice to show that, even at 230° C., the metastable solubility is still low, probably less than 1 wt.-% copper.§ The concentration of the coexisting disordered f.c.c. copper-rich phase is found to be (quite roughly) about 50 at.-%. As the heat of mixing in this central region of the diagram is strongly negative, the formation of superstructures is natural. Thus, there appears to be no objection to assuming that the G.P. zones [1] are disordered and the G.P. zones [2] ordered, which, I think, makes Dr. Hardy's beautiful scheme still more convincing.

It is worth noting that a miscibility gap in the disordered face-centred cubic phase, as well as superstructures based on that lattice, is found under stable conditions in the platinum-silver system. An approximate calculation yields an energy curve that is positive at the platinum-rich side and negative at the silver-rich side. The same is found to apply to the aluminium-silver system. According to activity measurements by Schmahl,|| the curve of the energy (or at least the non-ideal part of the free energy) of mixing in the face-centred cubic palladium-silver and palladium-gold phases must also be inflected. Apparently these very asymmetrical cases are not exceptional.

Mr. E. C. W. PERRYMAN, ¶ M.A., A.I.M. (Member): According to Dr. Hardy's interpretation (p. 352), the "light phenomenon" is due to the lower solute content of the solid solution, which will be in equilibrium with G.P. zones [2] formed either from the matrix or from G.P. zones [1]. Now in either case downhill diffusion will take place, and so one would expect the G.P. zone [2] to be situated within a region whose orientation is the same as that of the matrix and whose concentration increases from the edge of the G.P. zone [2] to the edge of the new solid-solution zone in equilibrium with the G.P. zone [2]. This hypothesis does not seem to fit in with the fact that sharp boundaries to the "light phenomenon" are observed both in aluminium-copper and aluminium-zinc alloys.** In the case of aluminium-zinc alloys, the first change in microstructure that we observed on ageing at room temperature was the formation of pits, which were thought to be due to clusters of zinc atoms at the grain boundaries. Shortly after the formation of pits, the light phenomenon first

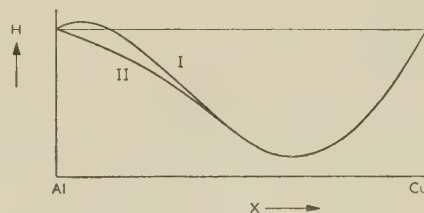


FIG. B.—Inflected Energy Curves.

I, Mainly negative; II, completely negative. (Meijering.)

appeared; this was, however, long before the equilibrium precipitate was apparent. In fact, it appeared to be the equilibrium precipitate which stopped the growth of the "light phenomenon".

It might be argued that in the aluminium-zinc system, as in the aluminium-copper system, two types of G.P. zones are formed. On the basis of Dr. Hardy's theory of age-hardening, this seems to be unlikely, because the age-hardening curve at room temperature is single-stage, the hardness increasing to a constant value. As mentioned above, if the "light

* A. W. Lawson, *Thermodynamics in Physical Metallurgy* (Amer. Soc. Metals), 1950, p. 94.

† Research Laboratories, N.V. Philips' Gloeilampenfabrieken, Eindhoven, Netherlands.

‡ W. Oelsen and W. Middel, *Mitt. K. W. Inst. Eisenforsch.*, 1937, 19, 1.

§ J. L. Meijering, *Rev. Mét.*, (in the press).

|| N. G. Schmahl, *Z. anorg. Chem.*, 1951, 266, 1.

¶ Research Investigator, Aluminium Laboratories Ltd., Kingston, Ont., Canada; formerly British Non-Ferrous Metals Research Association, London.

** E. C. W. Perryman and J. C. Blade, *J. Inst. Metals*, 1950, 77, 263 (see Fig. 19, Plate XXI).

phenomenon" is formed according to Dr. Hardy's hypothesis, then its orientation would be expected to be the same as the supersaturated matrix in which it is formed. With the aluminium-zinc alloys we found that the pits representing clusters of zinc atoms were always formed at the advancing boundary of the "light phenomenon" and not at the straight boundary. This is shown in Fig. C, which is an electron micrograph prepared from a Formvar replica of an electrolytically polished surface of an aluminium-10% zinc alloy aged at room temperature for 198 days. Such clusters of zinc atoms will form more easily at boundaries where the lattice misfit is greatest, and thus it would appear

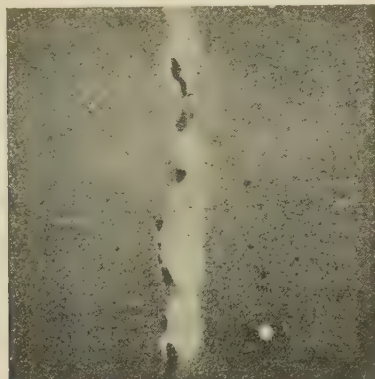


FIG. C.—Aluminium-Zinc Alloy, Solution-Treated and Aged 198 Days at Room Temperature. Electron micrograph from plain Formvar replica. $\times 10,000$ approx. (Perryman.)

that the orientation of the "light phenomenon" is different from that of the grain into which it grows. Further support for this is found in the fact that, when nitric acid was used for etching, some grain boundaries at which no change in structure had occurred were revealed, together with the advancing boundary of the "light phenomenon". The straight boundary of the light phenomenon, however, was not shown up with nitric acid and not until the specimen was further etched with Wassermann's reagent* was this revealed.

I agree with Dr. Hardy that the "light phenomenon" cannot be the solid solution in equilibrium at the temperature of ageing unless it is formed together with the equilibrium precipitate, which does not seem to be the case with either aluminium-zinc or aluminium-copper alloys. I would, however, like to ask Dr. Hardy whether he could hazard a guess as to the composition of the solid solution which he thinks is formed around the G.P. zones [2]. The tests we carried out showed that the delayed intercrystalline cracking in

aluminium-zinc alloys was probably due to the presence of the "light phenomenon" at the grain boundaries, and this result suggests that the difference in solute concentration between the supersaturated matrix and the areas showing the light phenomenon is quite appreciable.

The AUTHOR (*in reply*): Mr. Johnston is quite correct in pointing out that care must be taken to avoid drawing a detailed picture of the precipitation process from a very small range of experimental evidence. It is also a wise precaution to remember that, although disagreement between theory and experiment disproves the theory, agreement between theory and experiment does not prove the theory but only shows that it may be correct. Scheil's analysis of the precipitation process as an ordering reaction was described because it was the most satisfactory formal basis when the paper was written. It was realized that a more rigorous application of statistical mechanics might indicate difficulties in the formation of the G.P. zones [1], since these require a second-order transformation on Scheil's analysis. Dr. Meijering's calculations are all the more welcome, since they suggest an alternative form for the free-energy/compositional relationship which predicts disordered G.P. zones [1] but does not preclude ordering of the G.P. zones [2].

The difficulties which Mr. Johnston has had with the equation for the solubility curve of a terminal solid solution in equilibrium with a phase whose composition is independent of temperature are easily cleared up. ΔH is the heat required to transfer one g.-atom of the solute from the intermetallic compound to the solid solution. A negative heat of solution of the solid solution does not preclude a positive value of ΔH , provided that the intermetallic compound has a sufficiently negative heat of formation.

It is agreed that there is no evidence to show that the ratio hardness increment/total change in hardness is a simple function of the solute depletion. But it is the simplest assumption on which to make an analysis of the growth of the G.P. zones.

I entirely agree with Mr. Perryman that the orientation of the "light phenomenon" differs from that of the grain into which it is growing. It probably has the orientation of the grain from which it has grown. Although I have seen particles of precipitate at the new interface, as shown in Fig. C, I have also observed many examples in which the particles were irregularly distributed throughout the "light phenomenon," but I agree that these particles will tend to anchor the moving grain boundary. I do not find it surprising that the old interface remains sharp, because the rate of diffusion at room temperature is very low. It is probable that the grain-boundary migration, as it sweeps out a small volume of metal, provides the path by which the diffusion process can occur more rapidly. However, as soon as a more stable precipitate has been formed, the less stable compounds in its immediate vicinity will be forced to redissolve.

* E. C. W. Perryman and J. C. Blade, *J. Inst. Metals*, 1950, 77, 263.

DIRECT EXAMINATION OF SOLID SURFACES USING A COMMERCIAL ELECTRON MICROSCOPE IN REFLECTION*

1428

By J. W. MENTER,† M.A., Ph.D., A.Inst.P.

SYNOPSIS

The modifications necessary for the conversion of the Metropolitan-Vickers EM3 electron microscope for use in the direct examination of solid surfaces by reflection, are described. The geometry, resolution, and depth of focus of the image are discussed. A range of specimens with widely varying surface topography have been examined in order to illustrate the value of the technique and to determine the effect on the image of varying the angle of inclination of the specimen.

I.—INTRODUCTION

It has long been recognized that the need to make replicas imposes a severe limitation on the use of the transmission electron microscope for the examination of solid surfaces. A number of workers have shown, however, that direct examination of a metallic surface is possible by converting the transmission electron microscope for use in reflection. For this purpose the electron gun and condenser lens are inclined at a small angle to the vertical, and the specimen also is so inclined that the electron beam strikes its surface at a small glancing angle. The image is formed by the electrons scattered from the surface in the direction of the axis of the objective and projector lenses. The early work of Ruska and Müller^{1,2} showed that to achieve high resolution it was necessary for both the glancing angle of the electron beam on to the specimen surface and the angle of inclination of the surface to the optical axis of the microscope to be small. The first useful results obtained by this method were those of von Borries and others, using a modified Siemens instrument.³⁻⁶ Raether^{7,8} has published a number of reflection photographs of mechanically and electrolytically polished surfaces, and more recently a renewed interest in the technique has been shown by Soviet workers,^{9,10} by French workers at Toulouse, and in this country, where an electron microscope specially designed for reflection has been built in the Cavendish Laboratory (B.I.S.R.A. project).

The purpose of the present paper is to describe how the modifications necessary for reflection work may be made to the standard EM3 model Metropolitan-Vickers electron microscope and to indicate the type of information that can be obtained.

II.—CONSTRUCTIONAL DETAILS

Following the method of von Borries, the electron gun and condenser lens are inclined at 8° to the

optical axis in a vertical plane containing the traverse direction of the mechanism (*a*) for tilting the specimen (Fig. 8, Plate XXII). (This is provided in the standard transmission instrument for taking stereophotographs.) The tilt of the gun is obtained by inserting a brass wedge-shaped collar (*b*) between the base of the condenser lens and the top of the specimen chamber. In the upper surface of the collar, which is inclined at 8° to the horizontal, there is a groove which contains a rubber ring for maintaining the vacuum. The gun and condenser lens assembly is mounted on the upper surface of the collar with a sideways displacement such that the illuminating beam crosses the axis of the microscope near the normal (i.e. transmission) specimen plane.

The specimen, in the form of a rectangular block, 1 × 0.5 × 0.1 cm., is mounted in a modified specimen holder in the usual specimen stage. The lower end of the specimen is located approximately in the normal specimen plane. By using the stereocontrol, the specimen may thus be tilted to any angle between 0° and 8° from the axis of the microscope, about an axis perpendicular to the plane of incidence. The normal stage-traversing controls are conveniently situated so that the specimen may be traversed in two mutually perpendicular horizontal directions, respectively in and perpendicular to the plane of incidence of the electron beam. The point of observation of the specimen may also be changed in a vertical direction, but to achieve this it is necessary to displace the gun assembly sideways by means of the gun lateral controls, in order to maintain the reflected beam coincident with the axis of the microscope. In addition, the focus of the objective lens must be readjusted when the point of observation moves along the axis. Since in this microscope the normal specimen plane is outside the pole pieces of the objective lens, no limitations are imposed on the area of specimen surface that can be investigated, other

* Manuscript received 21 July 1952.

† I.C.I. Fellow, Research Laboratory for the Physics and

Chemistry of Surfaces, Department of Physical Chemistry, University of Cambridge.

than those arising from the extent of the stage-traverse controls and the inevitable reduction in magnification and resolving power as the object point moves away from the lens.

III.—ELECTRON-OPTICAL CONSIDERATIONS

1. MAGNIFICATION RELATIONS *

The relation between the object and the image formed by the objective lens is shown in Fig. 1. The plane of the specimen $ABCD$ is inclined at an angle θ to the optical axis of the microscope HH' , intersecting it at O . PO , inclined at an angle β to HH' in the plane of incidence POQ , is the direction of the incident beam from the gun. OY and OX are perpendicular axes lying in the plane of the specimen surface and are, respectively, in and perpendicular to the plane of incidence. The image plane $KLMN$ is perpendicular to the optical axis HH' .

Owing to the inclination of the specimen, the magnification of the final image varies with the azimuthal angle ϕ measured in the plane of the specimen from the plane of incidence. Thus if m_1^0 is the magnification of the objective in a direction perpendicular to the plane of incidence, the magnification m_{11}^0 in a direction in the plane of incidence ($\phi = 0^\circ$), is given by:

$$m_{11}^0 = m_1^0 \sin \theta \quad . \quad . \quad . \quad (1)$$

The projector lens (magnification m^p) enlarges the first image in the usual way. Thus we may write for the total magnifications $m_{11} = m^p m_{11}^0$, $m_1 = m^p m_1^0$:

$$m_{11} = m_1 \sin \theta \quad . \quad . \quad . \quad (2)$$

Furthermore, apart from the rotation of the image as a whole which always occurs in an electron lens, a

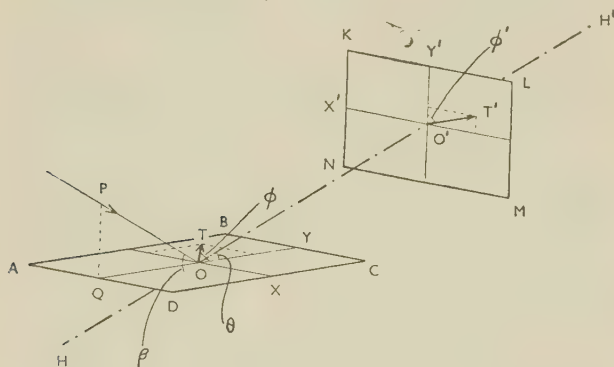


FIG. 1.—Relation Between Object and Image in Objective Lens.

line OT at azimuth ϕ in the specimen will be rotated to an azimuth ϕ' in the image owing to the inclination of the specimen, where:

$$\tan \phi' = \tan \phi / \sin \theta \quad . \quad . \quad . \quad (3)$$

The magnification $m_{\phi'}$, along the line $O'T'$ in the final image, will then be:

$$m_{\phi'} = m_1 \sin \theta \sec \phi' (1 + \tan^2 \phi' \sin^2 \theta)^{-\frac{1}{2}} \quad (4)$$

Thus, a circle in the plane of the specimen will be imaged as an ellipse in which the ratio of the minor and major axes is equal to $\sin \theta$. Relation (3) is illustrated in Fig. 2 for values of $\theta = 2^\circ, 4^\circ, 8^\circ, 16^\circ$, and 90° . It is clear that the distortion of the image due to the inclination of the specimen becomes less marked as θ increases. A scratch on the surface making an angle of 30° with the direction OY would

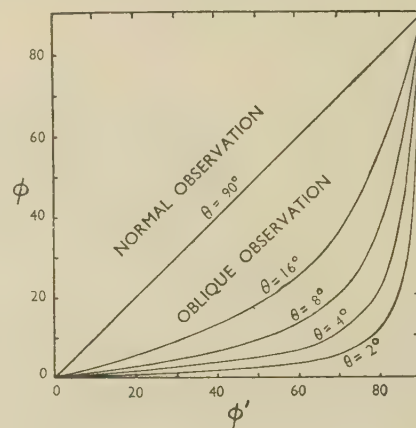


FIG. 2.—Rotation in Image Caused by Inclination of Specimen.

appear on the image at an angle to OX' of approximately $3\frac{1}{2}^\circ$ with $\theta = 2^\circ$, and at $13\frac{1}{2}^\circ$ with $\theta = 8^\circ$.

An asperity on the surface under observation, if sufficiently thick, will interrupt the electron beam and cast a shadow on the surface behind it. It may easily be shown that the height of the asperity is related to the length l of the shadow measured in the final image by the expression:

$$h = \frac{l}{m_1 \sin \theta} \tan (\beta - \theta) \quad . \quad . \quad (5)$$

θ being the angle of inclination of the surface on which the shadow falls.

2. RESOLUTION

The resolution achievable with the electron microscope is determined mainly by spherical and chromatic aberrations, astigmatism, and the diffraction error. On account of the relatively large amount of inelastic scattering suffered by an electron beam directed on to a surface at glancing incidence, the chromatic aberration is comparatively great, and it is this which is mainly responsible for limiting the resolution obtainable in the reflection microscope. Furthermore, owing to the wide angle of scattering of the electron beam, the angular aperture of the electrons forming the image will be determined by the limiting rays accepted by the physical aperture of the objective lens, and in general this will be considerably greater than the angular aperture of the beam emerging from the electron gun. This implies that no advantage is to be gained by defocusing the condenser lens for

* Acknowledgement is made to the paper by Kushnir *et al.*¹⁰ for some of the results quoted in this section.

photography, as in standard transmission practice. One can therefore work with the condenser lens at critical focus, i.e. with maximum illumination. This is desirable in any case, as the absolute intensity of the image is much lower than in transmission. The aberration coefficients of the objective lens increase with increasing focal length, so that it is advisable to work as near the objective lens as possible.

It is possible to determine the order of magnitude of the resolution to be expected in a direction perpendicular to the plane of incidence in the image of a point near the lower extremity of the specimen. Neglecting all aberrations except chromatic, we may write :

$$\delta_1 = \alpha f \Delta V / V \quad . \quad . \quad . \quad (6)$$

where δ_1 is the radius of the disc of confusion in a plane perpendicular to the plane of incidence, due to chromatic aberration, α the semi-angular aperture of the illumination (including scattering by the specimen), f the focal length of the objective lens, V the accelerating voltage, and ΔV the average loss of energy by the electrons in scattering from the specimen.

Relation (6) ignores the effect of variations in the H.T. supply voltage and excitation current in the objective lens, these being negligible in comparison with energy losses due to scattering at the specimen.

According to Kushnir *et al.*,¹⁰ the value of ΔV at 80 kV. is 100 V. (the so-called "half-width" of the energy-distribution curve of the scattered electrons). Thus, $\Delta V/V = 1/800$.

Taking a reasonable value of $\alpha \cong 3 \times 10^{-3}$ radians and putting $f \cong 5$ mm., with an accelerating potential of 80 kV., we find that :

$$\delta_1 \cong 190 \text{ \AA}.$$

The resolution in a direction in the plane of incidence will be worse by a factor $1/\sin \theta$, i.e. for $\theta = 6^\circ$, $\delta_{||} \cong 2000 \text{ \AA}.$

Some improvement in δ_1 could be obtained by reducing α , i.e. by decreasing the diameter of the objective aperture. To obtain a resolution better than $100 \text{ \AA}.$, it is estimated that an aperture size of the order of 10μ would be required. It is doubtful whether the intensity of the image would be adequate for precise focusing at the necessary magnification.

Good results have been obtained using a 30μ aperture situated in the normal position for transmission work, and with careful alignment a resolution better than $400 \text{ \AA}.$ has been achieved, with a focal length somewhat greater than that used in the above calculation. The vertical adjustment of the objective aperture holder provided in the EM3 microscope is particularly useful for obtaining high-resolution images. The image may be focused with the aperture fully raised, when it admits a maximum aperture of rays. If it is well aligned, it may then be lowered for photography, so obtaining the advantage of a low aperture and high resolution in the recorded image, even though the image may be too faint for focusing

with the aperture in this position. Under these conditions of small aperture, satisfactory images may be recorded on Ilford Contrasty Lantern Plates at a magnification (m_1) of several thousand with exposure times of the order of 20 sec.

3. DEPTH OF FOCUS

If α is the semi-angular aperture of the beam and δ the resolving power, the depth of focus is given by :

$$\pm d = \delta / \alpha ;$$

with $\delta = 200 \text{ \AA}.$ and $\alpha = 3 \times 10^{-3}$ radians, we have $2d = 13 \mu$.

Thus, the depth of focus in the plane of incidence is very high. Moreover, owing to the small angle of inclination of the specimen, the depth of focus in a direction perpendicular to the plane of the surface is also very great. Theoretically, a vertical feature in a plane through the centre of the "in-focus" region of the specimen will also be in focus up to a distance $d/\sin \theta$ from the surface, i.e. up to 65μ for $\theta = 6^\circ$. In general, a surface showing features of this size would not be examined by this technique, as most of the details of the image would be obscured by the shadows cast by the asperities. The high depth of focus in this direction does mean, however, that it is possible to obtain focused images of features considerably displaced from the mean level of the surface. In this respect the reflection electron microscope has a distinct advantage over both the optical microscope, in which the depth of focus is very small at high magnifications, and the plastic-replica technique in transmission. Artefacts are very common in plastic replicas of large surface features owing to the strains set up in the mechanically weak plastic film.

IV.—EXPERIMENTAL RESULTS

A range of specimens of widely varying surface topography have been investigated in order to study the effect of various parameters on the image. The operating voltage in all cases was 75 kV. (In Fig. 4 (Plate XXI) are shown electron micrographs of the surface of a standard electron-microscope square specimen grid, made by electrodeposition of copper, together with optical micrographs, taken with vertical illumination, for comparison (Fig. 3, Plate XXI). The plane of incidence may be approximately determined by observing the direction of the shadows on the surface. The foreshortening of the image in a direction in the plane of incidence is clearly shown. One side of the grid has a high optical reflectivity (Fig. 3(a)). The electron micrograph of this side (Fig. 4(a)) shows that it is indeed quite flat, except for the long straight ridges which are in fact replicas of the scratches on the surface on to which the grid was electrodeposited. Fig. 4(b) shows that the other surface, which has a matt appearance optically (see Fig. 3(b)), is strikingly different. The rounded asperities are typical of an electrodeposited layer. The width of the grid bars is nominally 40μ , but the measured width of the

illuminated surface on the shiny side of the grid is only $20\ \mu$ on account of the marked curvature of the sides of the bars. It can be seen from the enlarged photograph of the shiny side (Fig. 4 (c)) how the image of the side of a "vertical" bar is lost in the shadow cast by a "horizontal" bar. This photograph also shows the detailed structure of the ridges on the surface and illustrates how these are continued down the curved sides of the grid bars. It is at once clear that the shadows cast by the asperities on the surface are an important source of contrast in reflection images. Thus, with a fixed angle of tilt of the illuminating system to the optical axis of the microscope, the most suitable angle of inclination is a function of the ratio of the mean height and mean distance between asperities on the surface. If the asperities are high and densely packed, as in the image of the matt side of the grid, only their uppermost parts are illuminated and the lower regions of the surface are engulfed in shadow. The effect is particularly well illustrated by the series of micrographs shown in Plate XXII (Fig. 6 (a)–(c)). These were taken from a mica cleavage face onto which a thick layer of silver had been previously evaporated at normal incidence in order to make the surface conducting. With a large angle of inclination of the specimen (7°) only the front steps of the cleavage edge are resolved, the back steps being obscured by shadow (Fig. 6 (a)). Moreover, in this particular case the scattering of electrons from the front edge is so great that the photographic plate has suffered halation and the definition of the edges is seriously impaired. At an intermediate angle ($5\frac{1}{2}^\circ$) (Fig. 6 (b)) some detail can be seen on both sides of the terrace. With a yet smaller angle (4°) (Fig. 6 (c)) the contrast is changed markedly, so that the back edge of the terrace is shown to best advantage. Again, it is instructive to compare these photographs with the optical micrograph of the same region taken with vertical illumination (Fig. 7, Plate XXII). The marked foreshortening of the image due to the inclination of the specimens is clearly seen.

The optical micrograph of this surface feature was taken after the specimen had been irradiated by the electron beam in the microscope. Within the dark band across the photograph where the electron beam has fallen, the silver has become discoloured. Furthermore, behind the asperities on the surface, where the beam has not fallen, can be seen "shadows" where the surface is not discoloured and the silver retains its high optical reflectivity. The origin of this discoloration is not clear, but it is probably carbonaceous contamination similar to that observed to build up on transmission specimens. It occurs on all metals so far studied, and may be used to advantage as an indirect method of measuring the heights of very small surface features. Thus, with a glancing angle of 2° of the beam on the surface, the length of the shadow formed by an asperity measured on the specimen will be approximately thirty times the height of the asperity. If the optical magnification is say, $1000\times$, a vertical magnification of surface asperities of

$30,000\times$ can thus be obtained. It is possible in this way to reveal extremely small vertical features on a surface and to obtain an approximate estimate of their height. The accuracy of this method of determining heights is limited on account of the divergence of the electron beam, which is comparable with the angle of illumination at very small glancing angles. Furthermore, some electrons will be scattered by the asperity into the true geometrical shadow, thus reducing further the definition of the edge of the shadow.

It may be noted in passing that the discoloration of the surface is a useful guide in identifying a particular region of the specimen when making direct comparisons between optical and electron micrographs from the same area.

The study of elementary slip processes in metals by electron microscopy has hitherto been limited mainly to aluminium, where the anodically formed oxide film may be used as a faithful high-resolution replica of the deformation on the surface (Brown,¹¹ Heidenreich and Shockley,¹² Yakutovich, *et al.*¹³). More recently Brown¹⁴ has used the methyl methacrylate replica for studying slip in cadmium. However, there are obvious advantages in avoiding the use of replicas, and it therefore seemed desirable to employ the reflection technique for the direct examination of slip phenomena in metals. A preliminary study has been made of slip in cadmium. Dr. R. W. K. Honeycombe of the Metallurgy Department, University of Sheffield, kindly prepared spectroscopically pure polycrystalline specimens which had been electropolished and then deformed in tension. In Fig. 9 (a)–(c) (Plate XXIII) are shown electron micrographs from different areas of a specimen which had been deformed by 1%. Fig. 9 (a) and (b) are from adjacent areas and Fig. 10 (Plate XXIII) is an optical micrograph covering these areas, taken after the specimen had been examined in the microscope. It will be seen that in grain *A*, where the surface has been not too heavily discoloured, the contrast of the slip markings in the optical micrograph is considerably enhanced by the discoloration. The electron micrographs show a number of interesting features. The grain boundaries are particularly well defined, probably on account of differential attack on the individual grains during polishing and possibly further enhanced by grain-boundary movement during deformation. The line *XY* in grain *A* marks a small change in slope of the surface, which is barely perceptible in the optical micrograph. Thus, an additional source of contrast in reflection images is provided by the changes in slope of the surface. Examination of twins in the surface of cleaved single crystals of zinc has shown that changes of slope about an axis parallel to the plane of incidence are also contrasted in the image, although not so strikingly as those about an axis perpendicular to the plane of incidence. The slip lamellae shown here appear with good contrast, particularly when their angle of inclination to the plane of incidence is fairly high, as on grains *A* and

B. The contrast is best when the slip lines are perpendicular to the plane of incidence, which is, of course, the direction of least resolution. However, there will be some intermediate direction where the best compromise between contrast and resolution can be achieved. This will depend on the orientation of the slip plane with respect to the free surface, the amount of slip on each plane, the spacing of the planes on which slip occurs, and the angle of illumination. It is therefore advantageous to use a specimen holder in which it is possible to rotate the specimen about an axis perpendicular to its surface. Fig. 9 (c) (Plate XXIII) shows some widely spaced slip lines (direction indicated by arrow) at an early stage of deformation. Fig. 5 (Plate XXI) illustrates an area of a specimen which had undergone 10% deformation. Here the structure of the slip markings is much coarser and the amount of slip on individual lamellæ much greater, as shown by the longer shadows. Again, the maximum amount of detail visible will depend on the parameters mentioned above, the angle of illumination becoming particularly important.

Another field in which the application of the electron microscope has been severely limited by the need to make plastic replicas, is that concerned with the study of surface damage after sliding between two surfaces. The reflection technique should prove useful here on account of the great depth of focus in a direction perpendicular to the surface. Fig. 11 (a) and (b) (Plate XXIII) are electron micrographs of scratches made by a hemispherical steel slider on a mechanically polished copper surface with loads of 0.5 and 20 g.,

respectively. At the lighter load the traces of the polishing scratches can be seen in the bottom of the track made by the slider. In both cases the pile-up of deformed copper at the sides of the track is clearly visible. In Fig. 11 (b) very small undulations appear along the direction of the track. These were probably a result of some mechanical imperfection in the machine producing the scratches. Their visibility has been enhanced by the foreshortening of the image in a direction parallel to the plane of incidence. It is doubtful whether such a feature would be readily seen in the light microscope. The direction of the track must be close to the plane of incidence, otherwise this piled-up material obscures the detail within the track.

ACKNOWLEDGEMENTS

The author wishes to thank Dr. F. P. Bowden for his encouragement, the many workers in the Laboratory and the Department of Metallurgy for assistance with the preparation of specimens, and in particular Dr. A. J. W. Moore for his advice on metallurgical problems and for taking the optical photomicrographs. He is indebted to Dr. V. E. Cosslett and Mr. D. Jones of the Cavendish Laboratory for many useful discussions.

Grateful acknowledgement is made to the Managers of the I.C.I. Fellowship Fund for the award of a Fellowship and to Imperial Chemical Industries, Ltd., and the Anglo-Iranian Oil Co., Ltd., for grants for equipment.

REFERENCES

1. E. Ruska, *Z. Physik*, 1933, **83**, 492.
2. E. Ruska and H. O. Müller, *ibid.*, 1940, **116**, 366.
3. B. v. Borries, *ibid.*, 1940, **116**, 370.
4. B. v. Borries and W. Ruttman, *Wiss. Veröff. Siemens-Werken, Werkstoff-Sonderheft*, 1940, 342.
5. L. Koch and A. Lehmann, *ibid.*, 363; also *Aluminium*, 1941, **23**, 304.
6. E. Semmler-Alter and I. Ziesecke, *Z. Metallkunde*, 1944, **36**, 115.
7. H. Raether, *Optik*, 1946, **1**, 296.
8. H. Raether, *Métaux et Corrosion*, 1947, **22**, 2.
9. N. G. Sushkin, A. G. Plakhov, U. M. Kushnir, P. V. Zeitzev, A. R. Bertin, and N. P. Levkin, *Izvest. Akad. Nauk S.S.S.R.*, 1951, [Fiz.], **15**, 285.
10. U. M. Kushnir, L. M. Biberman, and N. P. Levkin, *ibid.* 1951, [Fiz.], **15**, 306.
11. A. F. Brown, "Metallurgical Applications of the Electron Microscope" (*Inst. Metals Monograph and Report Series*, No. 8), 1950, p. 103.
12. R. D. Heidenreich and W. Shockley, *J. Appl. Physics*, 1947, **18**, 1029.
13. M. V. Yakutovich, E. S. Yakovleva, R. M. Lerinman, and N. N. Buinov, *Izvest. Akad. Nauk S.S.S.R.*, 1951, [Fiz.], **15**, 383.
14. A. F. Brown, *Advances in Physics*, 1952, **1**, (in the press).

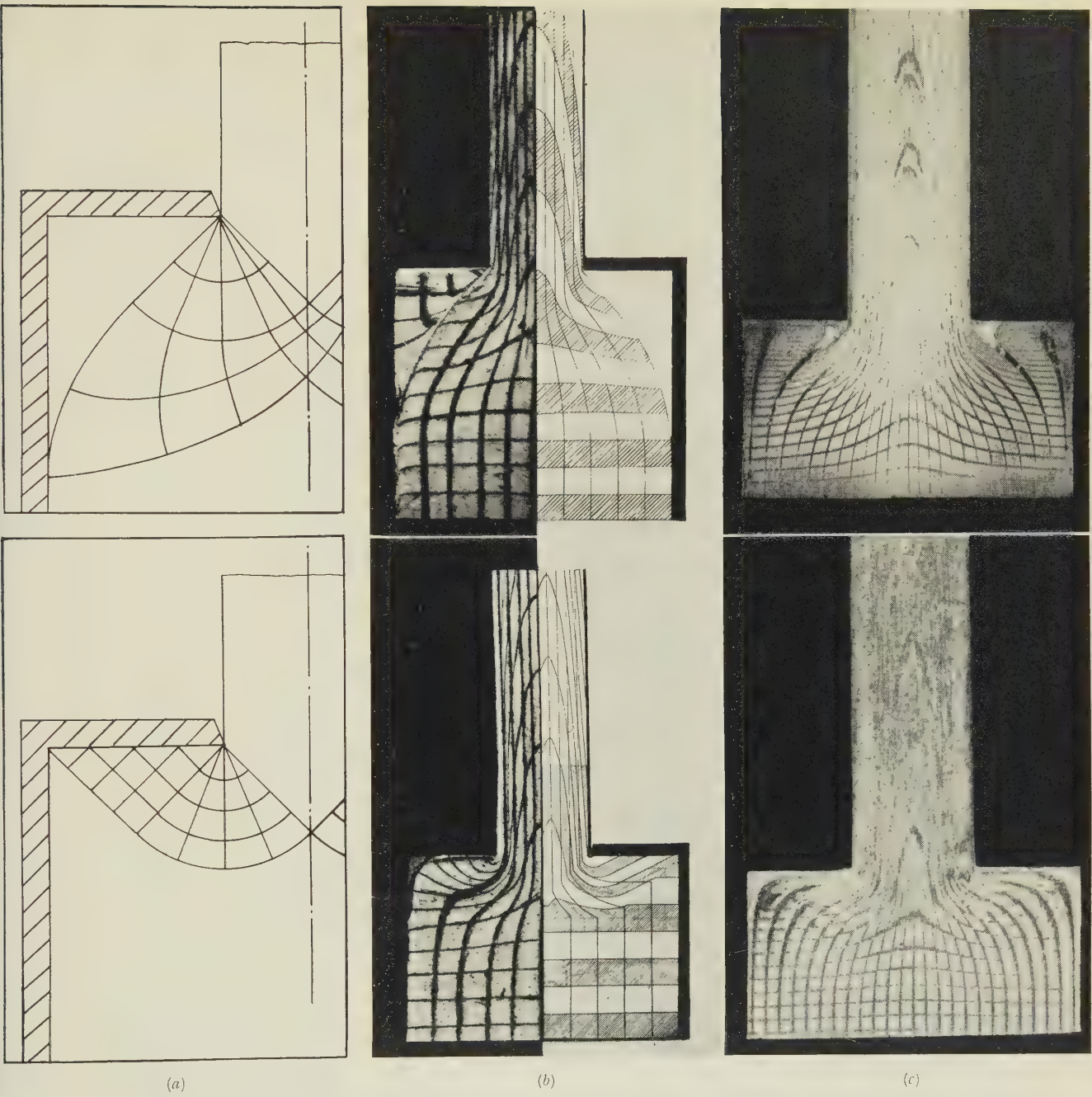


FIG. 4.—Plastic Flow in Extrusion.

- (a) Theoretical shear-line fields with and without friction. (*Green.*)
- (b) Flow grids, Plasticine and theoretical. (*Green.*)
- (c) Flow grids, lead rod extrusion.

(b) Courtesy *Philosophical Magazine*.

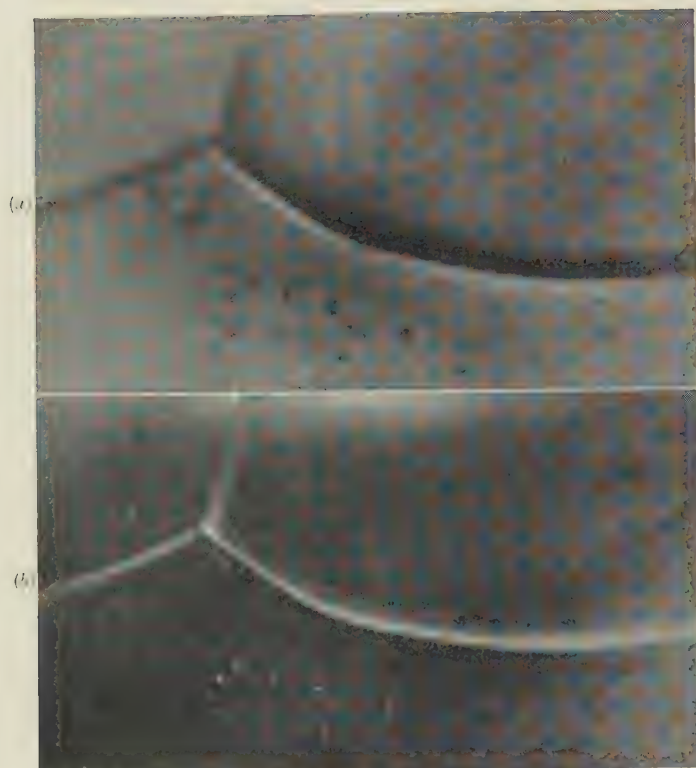


FIG. 2.—Ridge and Trough Boundaries in Copper-1.29% Antimony Alloy. (a) Positive phase contrast. (b) Negative phase contrast. The former renders elevations bright and depressions dark; the latter has the reverse effect. $\times 3000$.

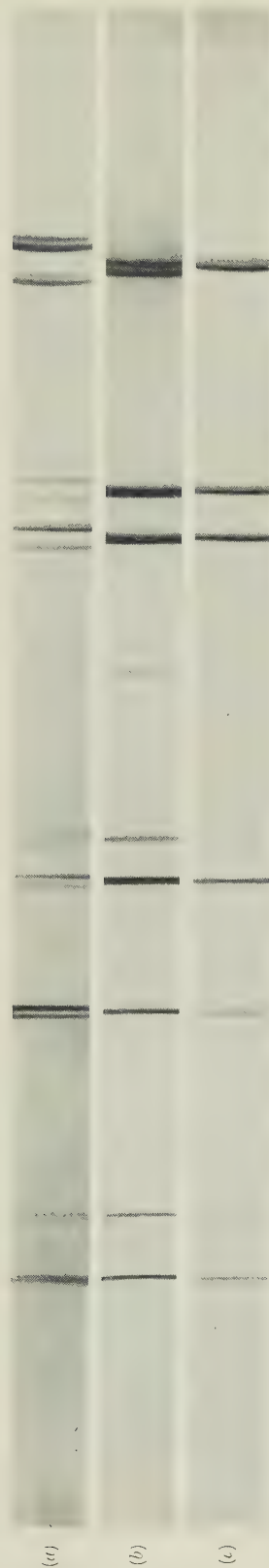


FIG. 6.—X-Ray Powder Patterns of 42% Gold Alloy Quenched from (a) 1200°, (b) 1250°, and (c) 1280° C.

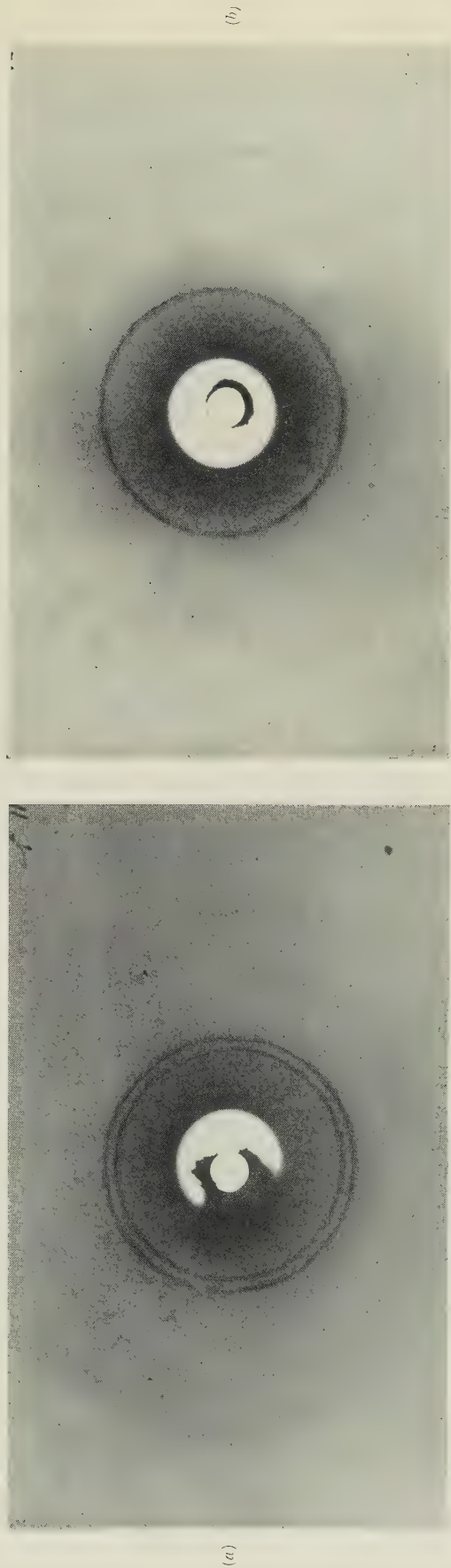


FIG. 7.—Diffraction Patterns of 42% Gold Alloy at (a) 1170° C. and (b) 1260° C.

MICROSTRUCTURES OF GOLD-PLATINUM ALLOYS. $\times 250$.

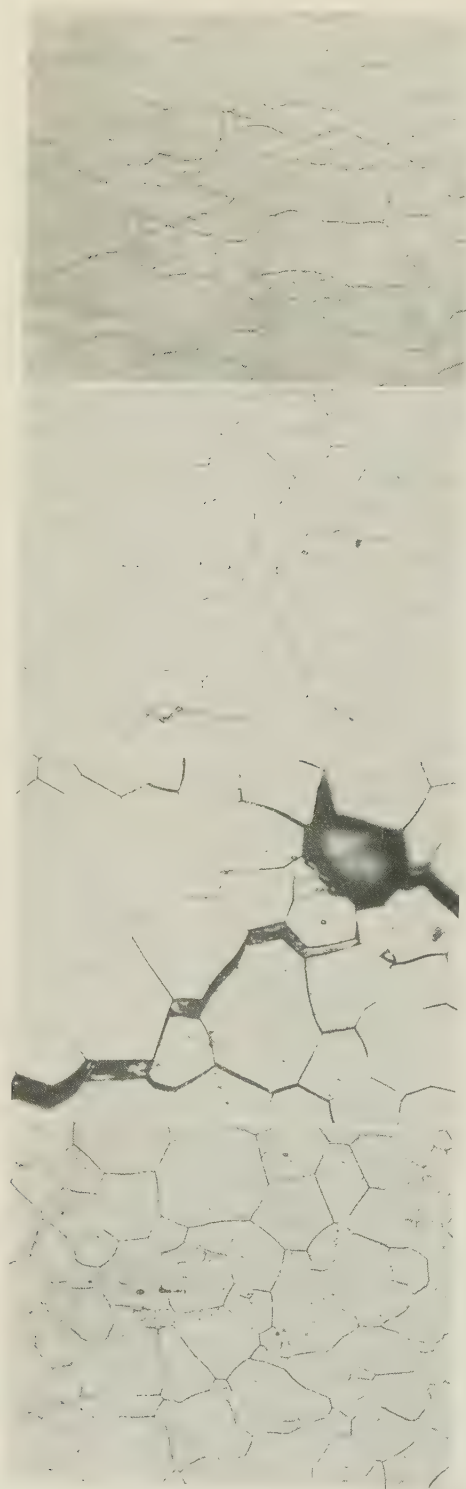


FIG. 8.—40% Gold. Quenched from 1280° C. FIG. 9.—40% Gold. Quenched from 1300° C. FIG. 10.—40% Gold. Quenched from 1310° C. FIG. 11.—42% Gold. Quenched from 1295° C.

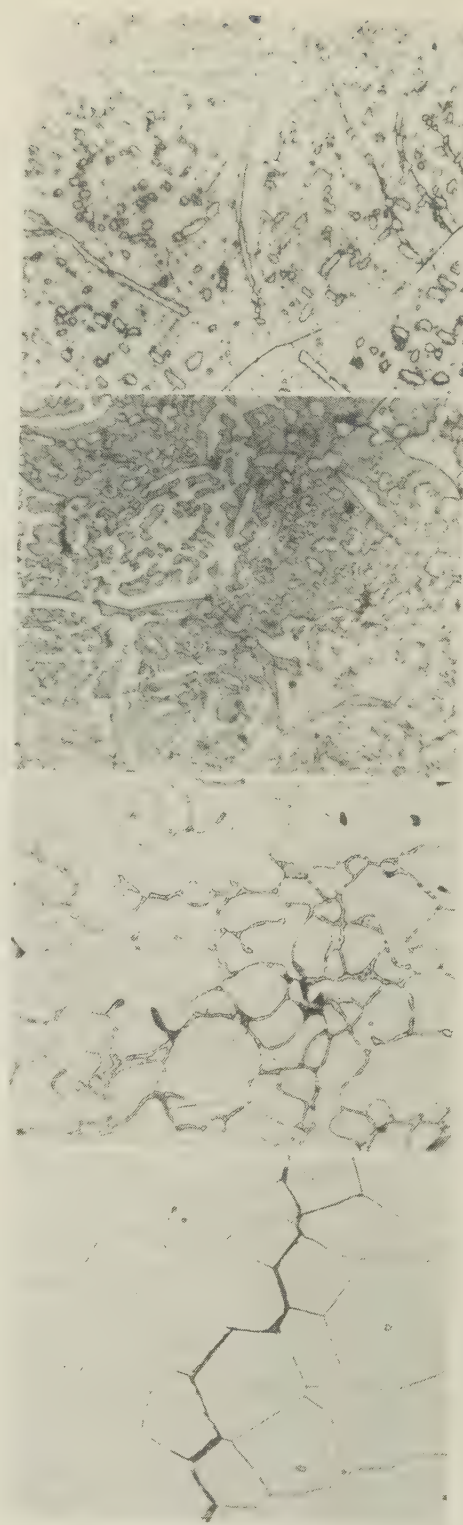
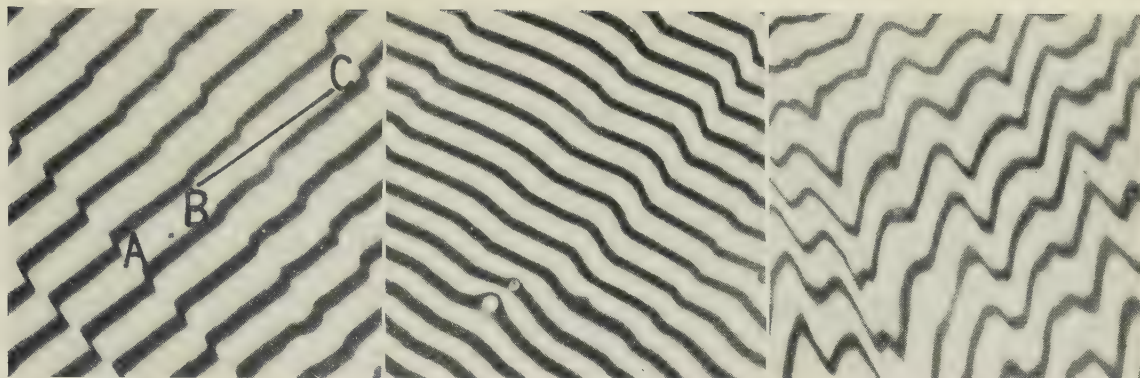


FIG. 12.—42% Gold. Quenched from 1300° C. FIG. 13.—42% Gold. Quenched from 1310° C. FIG. 14.—40% Gold. Quenched after 20 hr. at 1200° C. FIG. 15.—50% Gold. Quenched after 20 hr. at 1200° C.

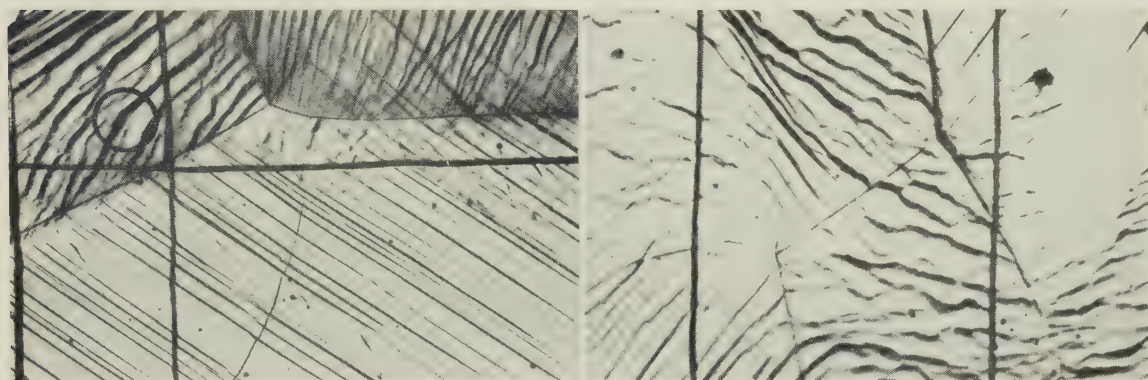


LINNIK-ZEISS INTERFERENCE MICROGRAPHS OF MEDIUM-GRAINED SPECIMENS. $\times 500$.

FIG. 12.—Slip Displacement at an Angle to the Surface. $\frac{1}{2}\%$ Extension, 0.4 ton/in.², 1 hr.

FIG. 13.—Slip Displacement Nearly Parallel to the Surface. 1.3% Extension, $\frac{1}{3}$ ton/in.², 118 $\frac{1}{2}$ hr.

FIG. 14.—More Complex Surface Distortion. 5% Extension, $\frac{1}{2}$ ton/in.², 118 $\frac{1}{2}$ hr.



FIGS. 15 and 16. Prominent Slip Bands in Coarse-Grained Specimen at 4% Extension. $\times 100$.

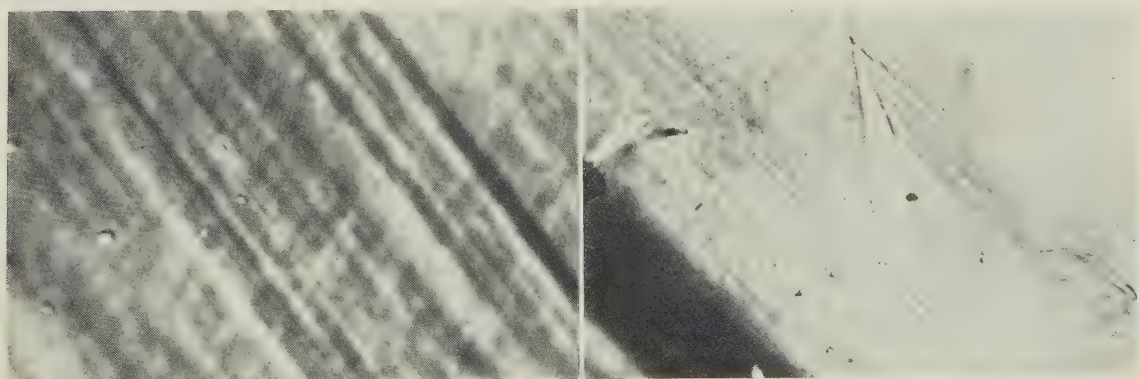


FIG. 17.—Phase-Contrast Micrograph, Showing Fine Slip Lines at Low Extension. Fine-grained specimen at 2.7% extension. $\times 1500$.

FIG. 18.—Normal Micrograph, Showing Fine Slip Lines at Large Extension. At bottom left is a prominent slip band. Coarse-grained specimen at 23.6% extension. $\times 1000$.

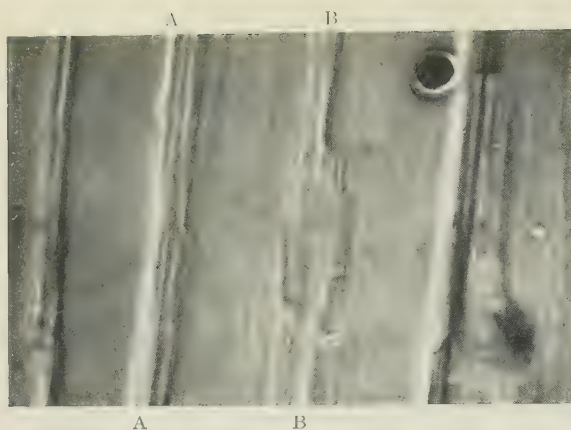


FIG. 19.—Prominent Slip Bands in Coarse-Grained Specimen at 4% Extension. $\times 750$.

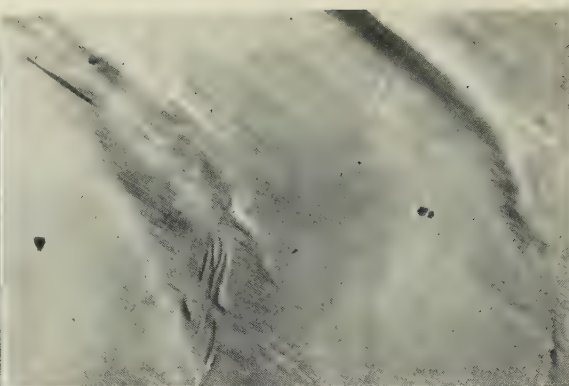


FIG. 20.—Bends in Prominent Slip Bands Similar to Region Circled in Fig. 15. Coarse-grained specimen at 13.8% extension. $\times 750$.

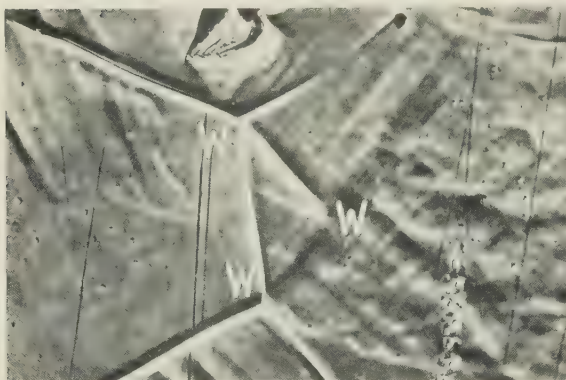


FIG. 21.—Phase-Contrast Micrograph, Showing Movement of Wedge WWW Due to Slip Induced at Neighbouring Grain Corners by Grain-Boundary Movement. Fine-grained specimen at 1.67% extension. $\times 500$.

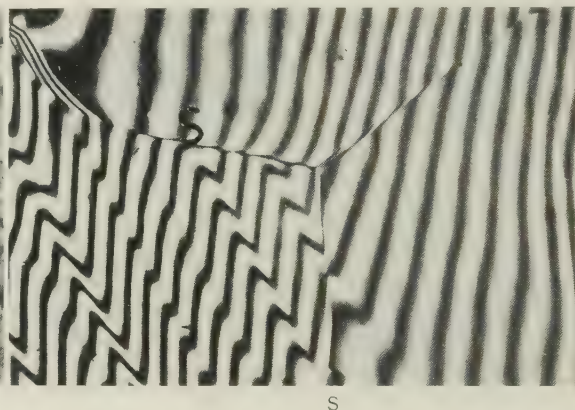


FIG. 22.—Interference Micrograph, Showing Prominent Slip Bands (SS) at Low Extension. Fine-grained specimen at 1.95% extension. $\times 500$.

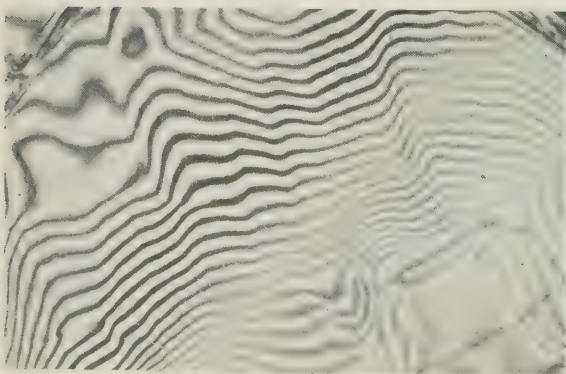


FIG. 23.—Interference Micrograph, Showing Appearance at Large Extension. Fine-grained specimen at 19.8% extension. $\times 500$.

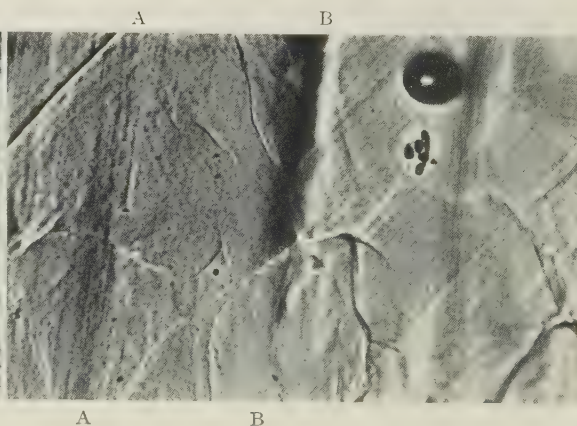


FIG. 24.—Same Field as Fig. 19 at 23.6% Extension. $\times 750$.

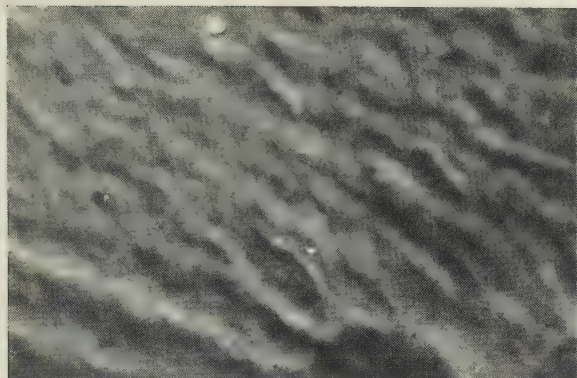


FIG. 25.—Phase-Contrast Micrograph, Showing Fine-Scale Rumpling Due to Irregular Slip. Medium-grained specimen, extension 0.3%, $\frac{1}{3}$ ton/in.², 1 hr. $\times 1500$.

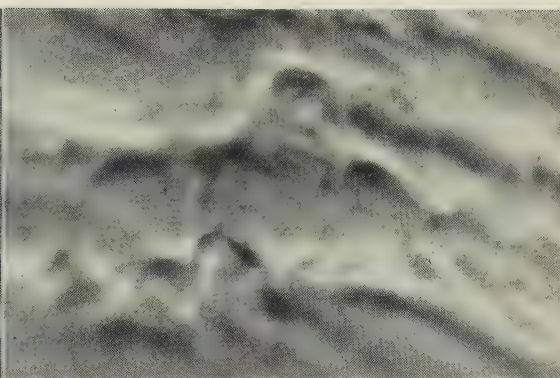


FIG. 26.—Phase-Contrast Micrograph Showing Irregular Slip. Medium-grained specimen, extension 1.3%, $\frac{1}{3}$ ton/in.², 118½ hr. $\times 1500$.

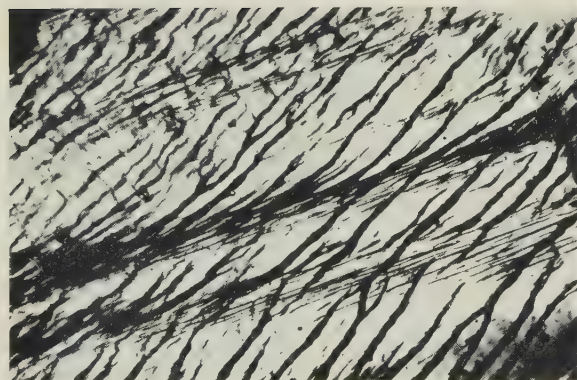


FIG. 27.—Coarse-Grained Specimen, Extension 23.6%. $\times 50$.

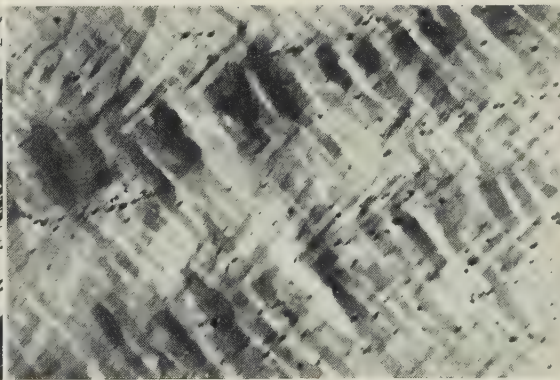


FIG. 28.—Same Field as Fig. 27, Polished and Anodized. Photographed in polarized light. $\times 50$.

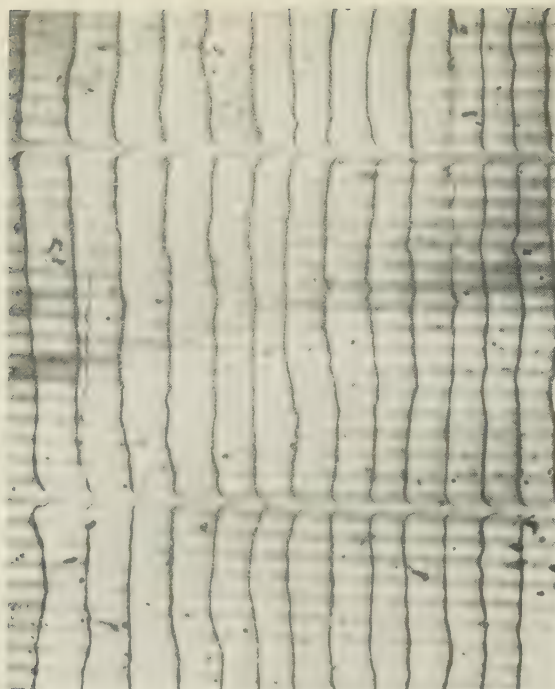


FIG. 29.—Multiple-Beam Interference Micrograph Before Extension. $\times 100$.

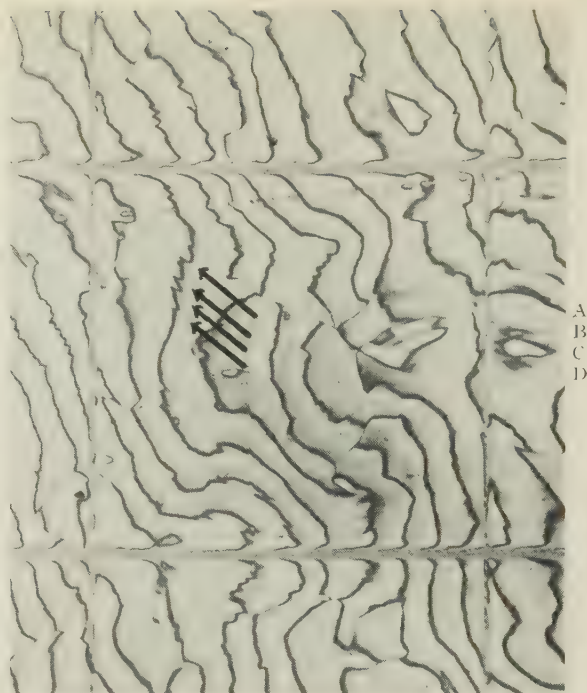


FIG. 30.—The Same Area as Fig. 29 After 0.8% Extension. $\times 100$.



FIG. 31.—The Same Area as Fig. 29 After 1.7% Extension. $\times 100$.

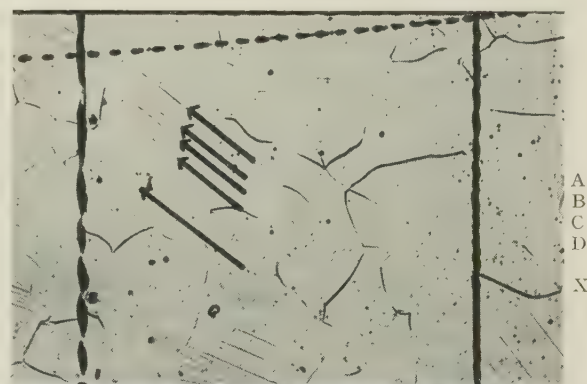


FIG. 32.—Normal Micrograph of the Field Shown in Fig. 30. $\times 100$.



FIG. 33.—Phase-Contrast Micrograph of Field Shown in Fig. 30. $\times 100$.

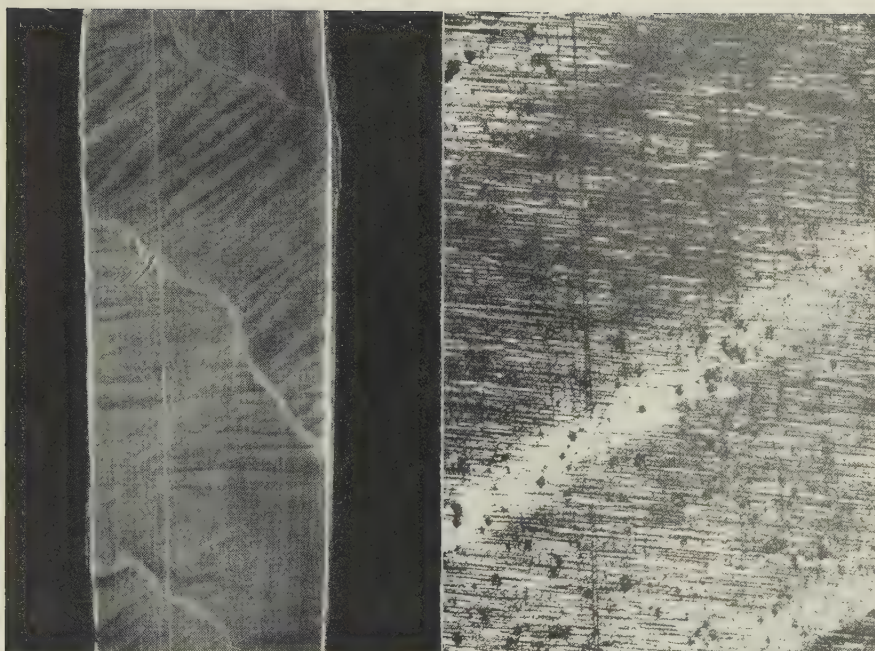


FIG. 8.—Specimen S6 After 15% Elongation, Showing Surface “Waviness” Due to the Formation of Deformation Bands. $\times 2$ (approx.).

FIG. 9.—Photomicrograph of Grain 3 of Specimen S6, Showing Deformation Bands (Light Areas) on the Surface. $\times 80$.

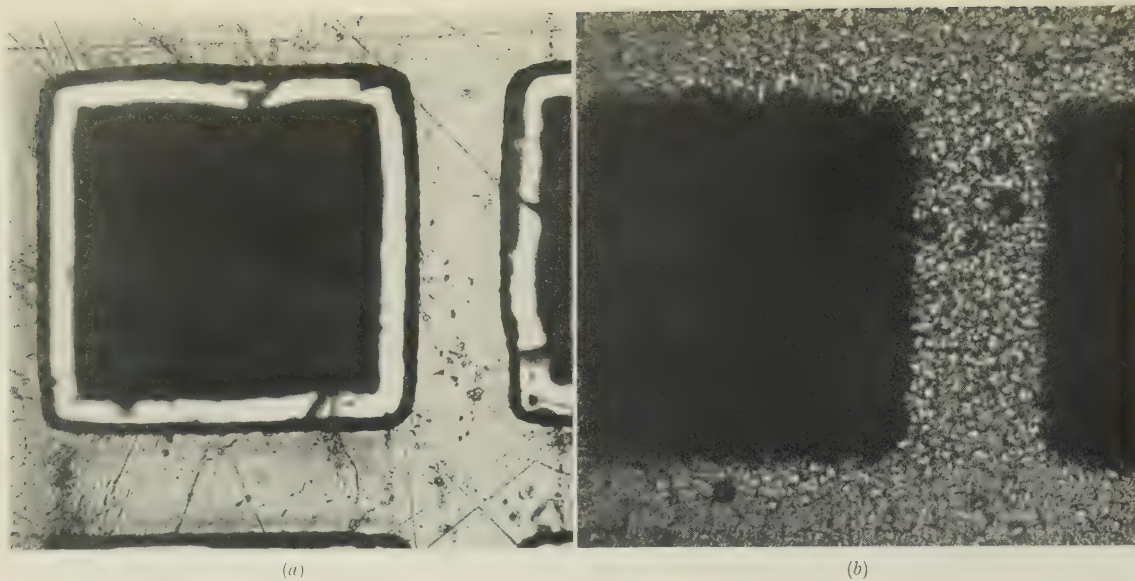


FIG. 3.—Optical Micrographs of (a) Shiny and (b) Matt Side of Electron-Microscope Specimen Grid Made by Electrodeposition of Copper. Vertical illumination. $\times 500$.

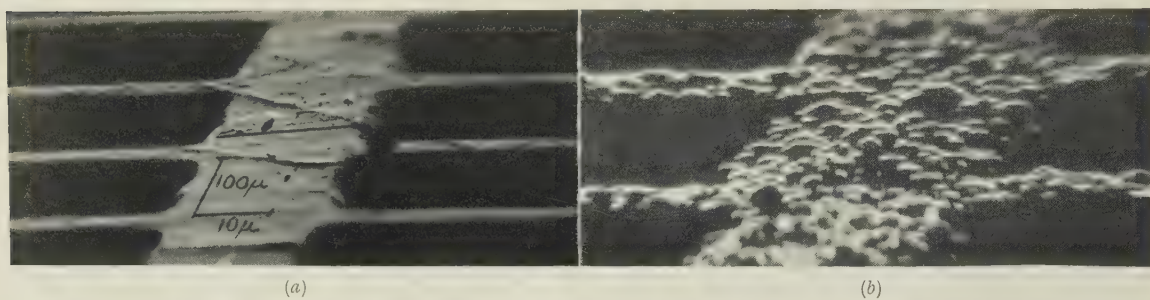


FIG. 4.—Electron Micrographs of (a) Shiny and (b) Matt Side of Electron-Microscope Specimen Grid.

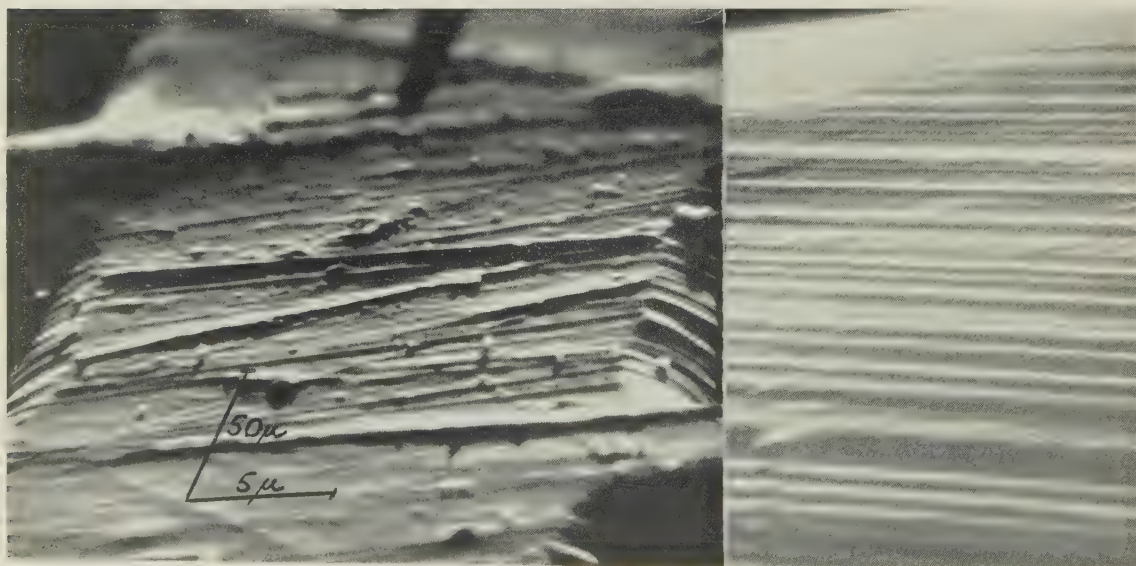


FIG. 4 (c).—An Enlarged Photograph of the Shiny Side of the Grid Shown in Fig. 4 (a).

FIG. 5.—Electron Micrograph of Electro-polished Cadmium Surface After 10% Deformation. $m_{\perp} \times 5000$; $m_{\parallel} \times 500$.

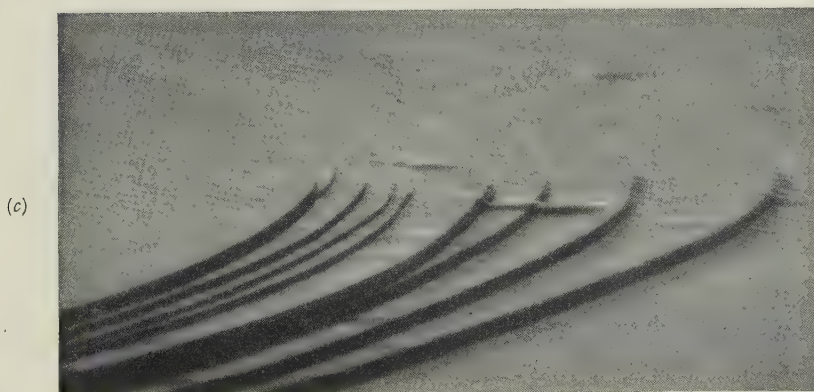
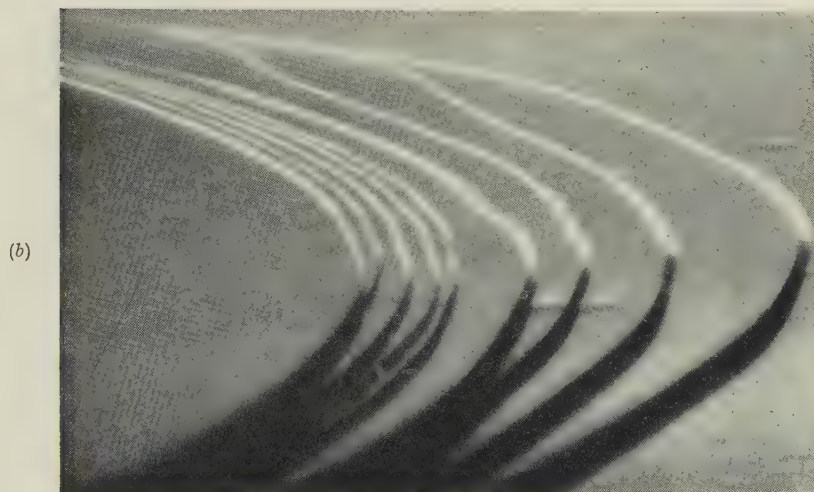
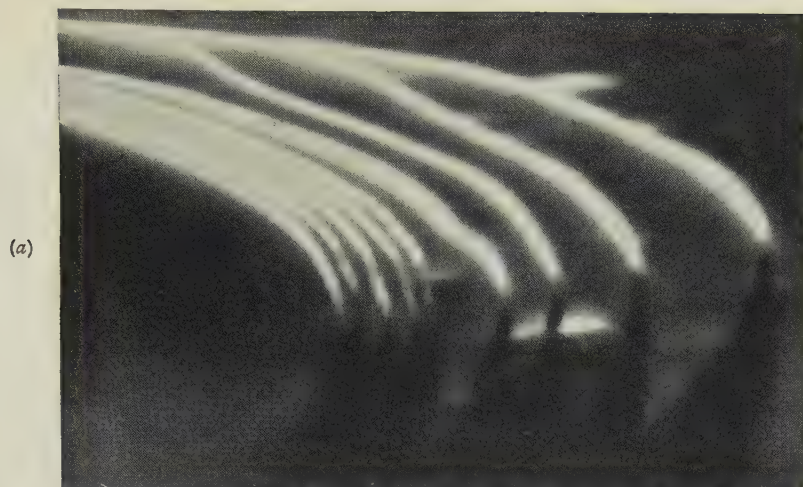


FIG. 6.—Electron Micrographs of Cleavage Steps on Mica.

- (a) $m_{\perp} \times 8000$; $m_{\parallel} \times 1000$; $\theta = 7^{\circ}$.
 (b) $m_{\perp} \times 8000$; $m_{\parallel} \times 750$; $\theta = 5\frac{1}{2}^{\circ}$.
 (c) $m_{\perp} \times 8000$; $m_{\parallel} \times 560$; $\theta = 4^{\circ}$.

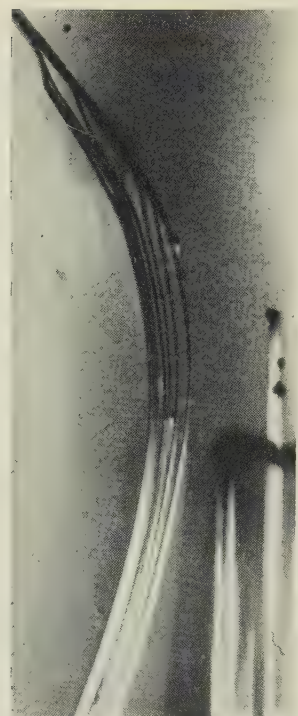


FIG. 7.—Optical Micrograph of Same Area as Shown in Fig. 6 (a)–(c). Vertical illumination. $\times 750$.

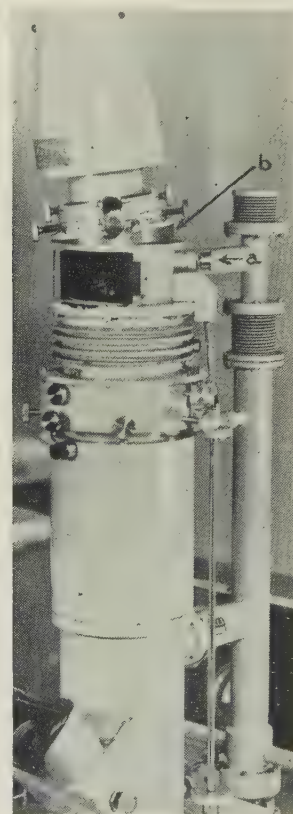


FIG. 8.—View of Microscope Arranged for Reflection, Showing (a) Control for Tilting Specimen, and (b) Wedge-Shaped Collar for Tilting Electron Gun.

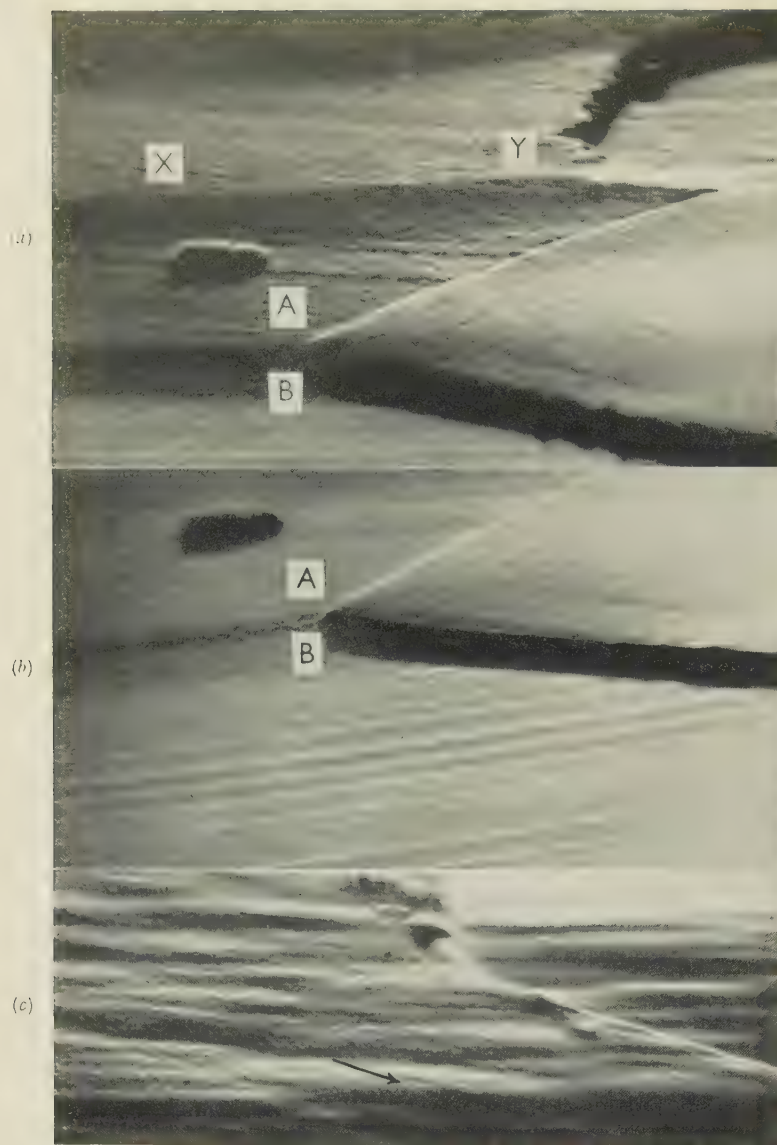


FIG. 9 (a) (c).—Electron Micrographs from Different Areas of Electropolished Cadmium Surface After 1% Deformation.

$m_{\perp} \times 4500$; $m_{\parallel} \times 400$.

Arrow indicates direction of slip lines (best seen by tilting the page).

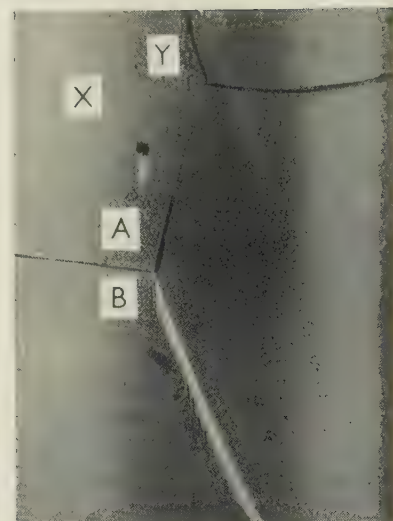


FIG. 10.—Optical Micrograph of Areas Shown in Fig. 9 (a) and (b). Vertical illumination. $\times 500$.

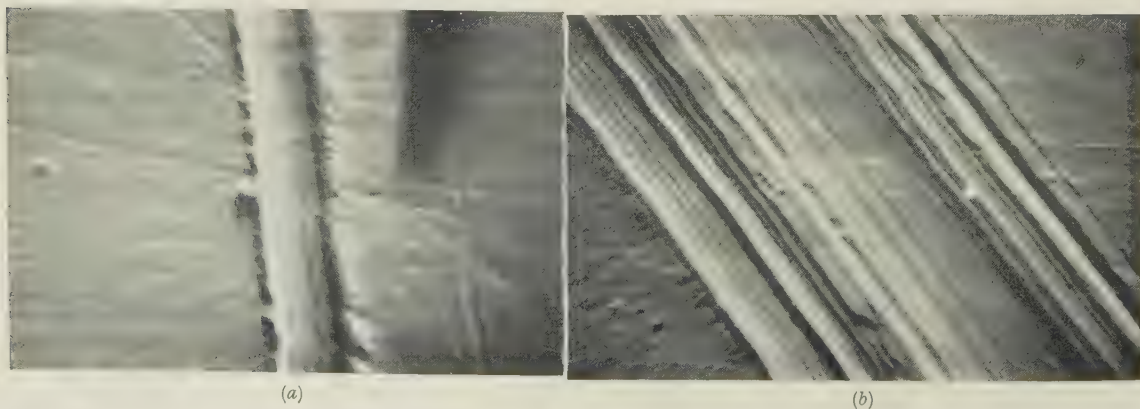


FIG. 11.—Electron Micrographs of Scratch on Mechanically Polished Copper Made by Steel Slider under Load of (a) 0.5 g.; (b) 20 g.

(a) $m_{\perp} \times 4300$; (b) $m_{\perp} \times 2000$.

A STUDY OF ORDER-DISORDER AND PRECIPITATION PHENOMENA IN NICKEL-CHROMIUM ALLOYS*

1429

By A. TAYLOR,† Ph.D., F.Inst.P., MEMBER, and K. G. HINTON,‡ B.Sc.

SYNOPSIS

Electrical resistivity, specific heat, and X-ray measurements have been made on Ni_3Cr and $\text{Ni}_{15}\text{Cr}_4\text{Al}$. It has been shown that both these alloys undergo an order-disorder type of transformation at approximately the same temperature and that an additional high-temperature transformation occurs in the ternary alloy, consistent with the precipitation and the re-solution of a second phase.

I.—INTRODUCTION

THE face-centred cubic γ -phase of the binary nickel-chromium system has a composition range extending from approximately 50 at.-% chromium to pure nickel.¹ Within this range, and particularly in the region of Ni_3Cr , are to be found non-magnetic alloys of high electrical resistivity. This, coupled with their excellent mechanical properties and resistance to oxidation and corrosion at elevated temperatures, gives them considerable importance as commercial electrical-heating and engineering materials.

It has been known for some time that alloys based on Ni_3Cr display a marked anomaly in their electrical resistance/temperature curves,²⁻⁵ which on the basis of differential cooling curves and specific-heat measurements, has been tentatively ascribed, among other things, to an order-disorder type of transformation. However, the shape of the resistivity curve is not of the type normally associated with an order-disorder type of transformation, and early X-ray-diffraction studies^{3,6} failed to reveal superlattice lines consistent with an ordering process in the crystal lattice.

The experiments described in the present paper form part of a wider series of X-ray, electrical-resistivity, and specific-heat studies that have been made on nickel-chromium and nickel-chromium-aluminium alloys. In general, these experiments confirm the view that the anomalous variations in electrical resistance of Ni_3Cr are associated with an order-disorder type of transformation if, as will be shown, these are due to the mean free path of the conduction electrons in the lattice being equal in magnitude to a few interatomic distances. By replacing one atom of chromium in five by an atom of aluminium, thus changing the composition from Ni_3Cr to $\text{Ni}_{15}\text{Cr}_4\text{Al}$, the difference in X-ray atomic scattering factor between nickel atoms and the remainder was increased sufficiently to permit direct observation of the superlattice reflections in the

Debye-Scherrer spectra. This confirmed that the change inferred from the specific-heat observations was a genuine order-disorder transformation.

In the low-temperature equilibrium condition, the alloy $\text{Ni}_{15}\text{Cr}_4\text{Al}$ lies just beyond the solubility limit of the γ nickel-rich primary solid solution⁷ and consists of two phases, γ and γ' , the latter being based on the Ni_3Al phase of the nickel-aluminium binary system.⁸ By means of resistivity and specific-heat measurements, it has been possible to follow the processes of precipitation and re-solution of the γ' phase and to separate their effects from those produced by the order-disorder transformation.

II.—MATERIALS USED

The alloys Ni_3Cr and $\text{Ni}_{15}\text{Cr}_4\text{Al}$ were melted in sillimanite crucibles in a high-frequency induction furnace under a sodium silicate slag. Selected high-purity Mond nickel pellet was employed with high-grade chromium and aluminium, the furnace charge weighing approximately 14 lb. The final analyses of the alloys were as shown in Table I.

TABLE I.—Composition of the Alloys.

Alloy	Specimen	Chemical Composition, wt.-%							
		Ni	Cr	Al	Ti	Fe	Si	C	Mn
Ni_3Cr	Specific Heat Resistivity	Bal.	23.46	0.04	0.2	0.04	0.29	0.03	0.08
		Bal.	23.2	0.04	0.01	0.04	0.07	...	0.07
$\text{Ni}_{15}\text{Cr}_4\text{Al}$	Specific Heat Resistivity	Bal.	19.7	2.52	...	0.27	0.37	0.09	trace
		Bal.	18.1	2.65	...	0.27	0.32	0.01	trace

For specific-heat measurements, the ingots were forged after a prolonged homogenizing treatment at 1200°C. to approximately $1\frac{3}{8}$ in. square bars from which the specimens were machined. For resistivity measurements bars were drawn into two batches of wire, one 0.036 in. and the other 0.020 in. in dia., with several intermediate anneals.

* Manuscript received 8 May 1952.

† Horizons Inc., Cleveland, O., U.S.A.; formerly with

The Mond Nickel Co., Ltd., Birmingham.

‡ The Mond Nickel Co., Ltd., Birmingham.

III.—EXPERIMENTAL PROCEDURE

1. RESISTIVITY MEASUREMENTS

Several sets of resistivity measurements were made with wire 0.020 and 0.036 in. in dia. Before winding any specimens, the 0.020-in.-dia. wire was stretched horizontally between terminals and heated electrically to 1000°–1050° C. in about 5 sec., maintained at this temperature for approximately 15 sec., and then air-quenched by switching off the current. About 2 m. of wire were wound on a porcelain former and the assembly, together with a platinum–10% rhodium/platinum thermocouple, was coated with a sillimanite spray before being surrounded with fine alumina powder in a pure graphite crucible that was heated by a furnace having a uniform temperature distribution. Resistance measurements to an accuracy of 1 part in 2000 were made with a Post Office box, connection to the specimen being made through 0.036-in.-dia. wires. When rapid temperature rises were required to attain a maximum temperature not exceeding 550° C., the alumina packing and graphite crucibles were dispensed with.

In normal runs, in which the specimen was raised to 1000° or 1050° C., the heating rate was relatively slow, 6 hr. being taken to reach the maximum temperature. Specimens were maintained at 1000° C. overnight and then cooled during the following day. All experiments were started with the specimens initially in the quenched condition and several runs up to and down from 1000° C. were made in order to test reproducibility. Measurements of the diameter of the specimens after the completion of each experiment indicated that any error due to decrease in cross-section by oxidation was not serious.

A second series of resistivity specimens was made from the 0.036-in.-dia. wire in the form of a long hair-pin bent back on itself three times, and the resistance was compared with that of a standard resistance by means of a vernier potentiometer. These specimens could, on the attainment of equilibrium after a suitably prolonged anneal, be pushed through the furnace and quenched in liquid nitrogen, at which temperature resistivity measurements were also made. In general, the results obtained from the 0.020- and 0.036-in.-dia. wires were in excellent agreement.

2. SPECIFIC-HEAT MEASUREMENTS

Several types of apparatus were considered, but because of the errors involved if the whole of the specimen is not at a uniform temperature, it was finally decided to use a form of apparatus developed by Sykes⁹ and Sykes and Jones.¹⁰ In this apparatus the specimen, in the form of a hollow cylinder, is mounted inside another cylinder in such a manner that the electrical and thermal conductivity between the two is kept very low. The temperature of the outer cylinder is increased at a reasonably uniform rate by means of a surrounding furnace, and a small heating coil inside the specimen is used to keep the

test material at the same temperature as its surroundings. A thermocouple indicates the temperature of the outer cylinder, and differences between the temperatures of the specimen and the isothermal enclosure are shown by a galvanometer connected to a differential thermocouple. Since the outer cylinder is at the same temperature as the specimen, heat losses from the latter are eliminated, and the specific heat can be calculated from a knowledge of the mass of the specimen, the rate of rise of temperature, and the energy input.

In the experiments on Ni₃Cr the specimen was 3.6 cm. long, 3.0 cm. outside dia., and had a wall thickness of 0.8 cm. The mass was about 250 g. The outer cylinder was made of Monel metal because of its fairly high thermal conductivity and its smooth specific heat/temperature curve in the temperature range under consideration. In view of a suggestion by Sykes that noble-metal thermocouples would probably be an improvement on the base-metal thermocouples employed in his experiments, platinum–10% rhodium/platinum couples were used, calibrated in accordance with the 1927 International Temperature Scale and accurate to $\pm 1^\circ$ C. Errors due to variations along the differential thermocouple were kept to a minimum by using for the hot junctions of the long sections the ends of two wires which were originally adjacent in a single length of platinum, and by keeping down the length of the platinum–10% rhodium wire to 20 cm.

The use of platinum-metal couples and the care taken in their construction considerably reduced errors due to variations along the thermocouple wires, but because of their comparatively low sensitivity other sources of spurious voltages became more important than in the original apparatus of Sykes. Thus, it was found necessary to modify the original method of bringing the ends of the differential thermocouple out of the vacuum enclosure through glass-metal seals because it was not possible to reduce completely the effects of radiation from the furnace. The method adopted for both thermocouples was to bring them out through a rubber stopper, and to have the junctions with the leads from the measuring apparatus at the temperature of melting ice. Precautions taken in the selection of these external leads were similar to those taken with the platinum wires of the differential thermocouple, and the junctions of the leads from this couple to the galvanometer were shielded from draughts.

The method of attaching the thermocouples was also different from that used by Sykes, who clamped the ends of the wires forming the hot junctions in holes spaced across the specimen and across the outer cylinder. Because the sensitivity of a base metal/platinum couple may be quite large compared with that of a platinum–10% rhodium/platinum thermocouple, slight variations of temperature across the specimen or Monel cylinder may give rise to serious errors in the values of specific heat, and it was therefore decided that it would be safer to compare the

temperatures of the specimen and its enclosure at only one point in each rather than to use the split-couple method of Sykes.

To determine whether serious errors were caused by a spurious deflection of the galvanometer when the specimen and its surroundings were at the same temperature, the furnace was allowed to stabilize at about 600° C. after a specific-heat determination, and the differential thermocouple voltage was noted several times during a period of about 6 hr. It was not possible to hold the furnace temperature absolutely constant, but the mean of the readings always gave less than 0.05° C. difference between the specimen and the Monel cylinder.

As had been found by Sykes, electrical leakage

the energy input to the specimen were calibrated against standard resistances and a high-accuracy vernier potentiometer.

IV.—RESULTS ON Ni₃Cr

1. RESISTIVITY

Fig. 1 illustrates a typical set of resistivity results for Ni₃Cr, having a room-temperature specific resistance of 106.0 $\mu\Omega$ -cm. in the initial quenched condition.

Curve (a) shows the manner in which the resistance of the quenched wire increased with temperature up to 1000° C. with a rate of heating of approximately 150° C./hr. On standing overnight for 18 hr. at 1000° C., no appreciable change in resistance was

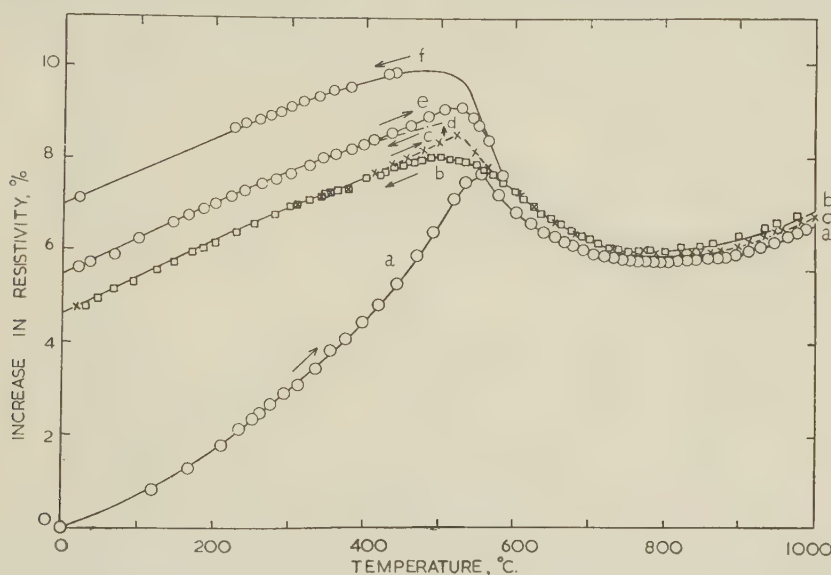


FIG. 1.—Percentage Increase in Resistivity with Temperature of Ni₃Cr ($R_0 = 106 \mu\Omega$ -cm.).

- (a) Heating curve for Ni₃Cr quenched from 1000° C.
- (b) Cooling curve.
- (c) Heating curve.

- (d) Cooling curve after soaking at 510° C. for 21 hr.
- (e) Heating curve after (d).
- (f) Cooling curve after soaking at 440° C. for 360 hr.

from the specimen heater circuit to the differential thermocouple made results unreliable at temperatures above 600° C. when direct current was used for heating the specimen, and so alternating current was used in these experiments. It was possible to obtain results at temperatures up to 950° C. and sometimes higher before a spurious deflection of the galvanometer connected to the differential thermocouple made it impossible to determine when the temperatures of the specimen and the enclosure were equal. For spurious currents of small magnitude, the effective zero position of the galvanometer was determined by opening the heater circuit for a short time at intervals of a few minutes, but because of the erratic nature of the leakage, results obtained with a zero correction greater than the equivalent of 0.1° C. are not considered reliable and are not included here.

All the electrical instruments used in determining

observed, and it could therefore be assumed that the wire was in an equilibrium condition. On cooling down at a similar rate, curve (b) was followed. At room temperature the permanent increase in resistivity was 4.8%. Reheating made the resistance follow curve (c), which showed a rather higher maximum than (b) at 520° C., the two curves coinciding again in the neighbourhood of 600° C. Further cooling and heating carried out at the same rate reproduced curves (b) and (c) almost exactly. If the wire was cooled very slowly, the cooling curve below 510° C. showed appreciably higher resistivity values, by an amount dependent on the rate of cooling over the range 560° to about 350° C. For example, after heating the wire to 510° C. and maintaining it there for 21 hr., the resistance rose appreciably, and the subsequent cooling curve (d) was obtained, followed by the heating curve (e). The change in resistance on

cooling from 440° C., after soaking at that temperature for 360 hr. to promote equilibrium, is shown by the uppermost curve (f). These results are in close conformity with those of Yano.³

It was quite clear from these curves that the precise value of the resistance in the region immediately below 560° C. was strongly susceptible to the soaking time at any particular temperature. Accordingly, a second series of resistivity measurements was made, using 0.036-in.-dia. wire in the form of hairpin specimens, which were soaked until equilibrium was obtained and then pushed straight through the furnace into liquid nitrogen to obtain a rapid quench and a sub-zero value of the resistivity. The series of curves shown in Fig. 2, covering the temperature range from -190° to 1350° C., shows the course of the resistivity changes under equilibrium conditions. The broken curve was obtained by an extrapolation

which it remained constant up to 800° C., and then fell to 1.5° C./min. at 1000° C.

An analysis of the accuracy of the results shows that the errors involved are much the same as those experienced by Sykes, except in the case of the power input to the specimen, where the accuracy of measurement is somewhat lower than is possible when direct current is used. When all the known sources of error are taken into account, it is found that the probable error in the specific heat is $\pm 2.5\%$ at temperatures up to 750° C., rising to $\pm 3.5\%$ at 1000° C.

A check on the accuracy of specific-heat values obtained in this apparatus was made by determining the specific heat of nickel and comparing the results with the most probable values given by Sykes and Wilkinson.¹¹ Agreement between the two sets of values is excellent throughout the range of temperatures considered by these authors (up to 580° C.),

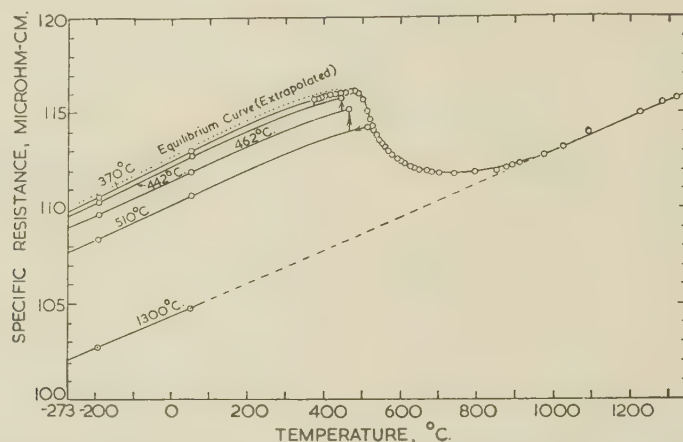


Fig. 2.—Resistivity of Ni_3Cr Under Equilibrium Conditions. Ni_3Cr quenched in liquid nitrogen from temperatures indicated.

method and indicates the highest attainable value of resistance under equilibrium conditions.

These changes in resistivity are clearly time- and temperature-dependent. They are anomalous in that the alloy Ni_3Cr has a homogeneous single-phase structure which is subject neither to magnetic transformations nor to the precipitation or re-solution of a second phase. Moreover, at first sight it is difficult to reconcile the change with an order-disorder type of transformation, since, in a normal alloy such as Cu_3Au or CuZn , the resistivity falls sharply on cooling through the critical temperature and continues to fall as the degree of order increases. In the case of Ni_3Cr , on the other hand, it rises and continues to rise until it attains the equilibrium maximum.

2. SPECIFIC HEAT

Specific heat/temperature curves for a specimen with various initial heat-treatments are shown in Fig. 3. The heating rate was constant for any particular temperature throughout the series, but it did vary over the temperature range, starting at 1.6° C./min. at 100° C., rising to 2° C./min. at 300° C., at

except over about 20° C. just above the Curie point, where the present results are up to 3% higher than the probable values given by Sykes and Wilkinson.

Fig. 3 shows that the specific heat/temperature curves for Ni_3Cr follow the general trend of such curves, but certain anomalous features present themselves at intervals between 200° and 900° C. The first of these lies between 200° and 320° C.; its magnitude is only of the same order as the probable error of the results, but it was obtained consistently for specimens water-quenched from 1150° C. and was absent for slowly cooled specimens, so that it appears to be a genuine anomaly in the specific heat of quenched Ni_3Cr . The second of the variations is again a decrease in specific heat, and occurs in the temperature range 380°–540° C., and again for the specimen quenched from 1150° C., but not when in the slowly cooled condition. This is immediately followed at higher temperatures by an anomalously high specific heat, the values being higher in the case of the specimen after annealing than when it was quenched from 1150° C. After the specimen had been cooled at an intermediate rate, the shape of the specific heat/

temperature curve was similar to that for the more slowly cooled condition, but the maximum specific-heat value was about 10% lower. Thus, as in the case of the resistivity changes which occur in the neighbourhood of 500° C., these anomalous variations are time- and temperature-dependent.

The last of the unusual features presented by the specific-heat curves below 1000° C. is the difference between the results for the quenched and slowly cooled specimens. Whereas the specific heat of the quenched specimen increases uniformly with temperature above 640° C., that for the specimen in the annealed condition appears to remain almost constant up to 840° C. before rising to coincide with the values for the former condition at about 980° C. There appears to be a tendency for the curves for the specimen in each of the slowly cooled conditions to follow

the visibility level against the general background fog. On the other hand, replacing one chromium atom in five by an atom of aluminium was sufficient to produce, in well-annealed specimens, a clearly defined set of superlattice reflections consistent with a high degree of long-range order. Now that the neutron-scattering powers of chromium and nickel are known,¹² it is probable that a much better indication of the degree of order in the lattice and the size of the ordered nuclei can be obtained by neutron diffraction than by X-rays.

In general, an alloy with a high degree of order has an appreciably lower lattice parameter than when in the disordered condition.^{13, 14} In the case of Ni_3Cr , quenching a powder specimen from above 750° C. yields a lattice parameter of 3.5446 kX, whereas a specimen slowly cooled from 900° C. to room tempera-

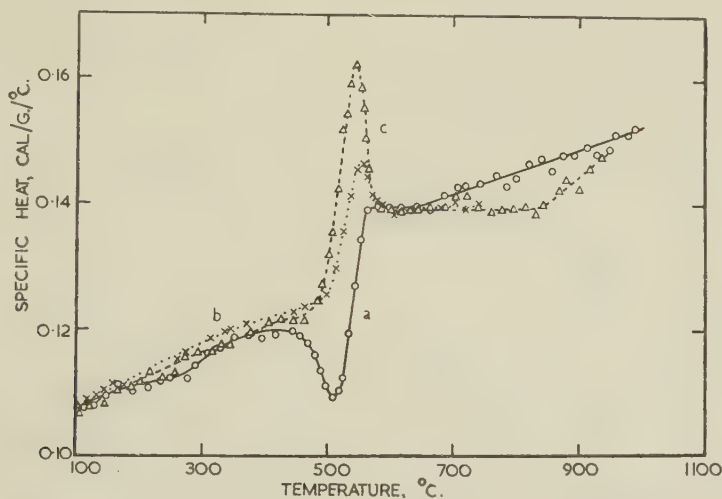


FIG. 3.—Specific Heats of Ni_3Cr at Various Temperatures at Constant Pressure. Specimen (a) water-quenched after 8 hr. at 1150° C.; (b) furnace-cooled in 16½ hr. from 770° to 200° C., and (c) water-quenched after 8 hr. at 1150° C., and furnace cooled in 15 hr. from 670° to 540° C., at 20° C./day to 480° C., 10° C./day to 430° C., and 5° C./day to 370° C.

that for the quenched specimen in the region of 710° C., but the increase does not continue over a wide enough temperature range to give a reliable indication that it is not due to experimental error.

3. X-RAY EXAMINATION

On account of the closeness of the atomic scattering factors of nickel and chromium, the superlattice lines in the Debye-Scherrer spectrum of Ni_3Cr would be expected to be extremely faint even under the most favourable conditions when MnK_α radiation is employed. Annealed filings and wire specimens of Ni_3Cr gave unsatisfactory results, and in only one case, namely in a glancing-angle photograph from an actual specific-heat specimen, could the superlattice lines be confidently identified. Since the breadths of the superlattice reflections are dependent on the size of the ordered regions, the specimens might have consisted of highly ordered, but relatively small, anti-phase domains, and this would tend to broaden the already weak superlattice lines until they were below

ture over a period of 6 days gives the appreciably lower parameter of 3.5440 kX. This parameter change, though small, is in the direction to be expected for an ordered lattice.

V.—INTERPRETATION OF THE RESULTS ON Ni_3Cr

1. SPECIFIC HEAT

In general, the lattice-parameter data and the observation of superlattice reflections in favourable cases, when some of the chromium atoms are replaced by atoms of aluminium, are sufficient evidence to indicate that Ni_3Cr itself undergoes a genuine order-disorder type of transformation. This is further supported by the specific-heat data.

An attempt to calculate the specific heat/temperature curve for Ni_3Cr , assuming no anomalies, has been made, using the Debye formula to obtain the specific heats at constant volume and correcting for thermal expansion. The curve so obtained is about 5% below

the experimental value at 100° C. and the difference increases as the temperature rises. A calculation for temperatures above 500° C., where the specific heat of nickel is little affected by the disordering (short range) of the electron spins, has been made, using the experimental values of the specific heat of nickel obtained in this investigation and values for chromium given by Armstrong and Grayson-Smith.¹⁵ The calculated curve, which is in good agreement with the extrapolation of the lower-temperature portion of the experimental curves, lies about 5% below the actual experimental curve at 700° C. and approaches it more closely at higher temperatures, thus forming a useful baseline to the experimental curve.

The possible causes of the variations of the experimental curve from the type of curve obtained for materials having no transformations in the relevant temperature range will now be discussed. As has already been mentioned, the small anomaly occurring in the quenched alloy in the neighbourhood of 270° C. may be due to experimental error, and so further consideration of it will be delayed until the reasons for the larger variations in the region of 500° C. have been examined. From the great length of time required for slowly cooling the specimen (about 3 weeks) in order to obtain the highest value of the maximum specific heat at 540° C., it seems certain that the energy changes are due to atomic diffusion which results in a phase change or a transformation of the order-disorder type.

Although Ni₃Cr has a homogeneous single-phase structure, there was present in the specific-heat specimen a certain amount of impurity, and microscopical examination showed the presence of a small amount of a grain-boundary precipitate, probably a carbide phase. Precipitation of a phase from solid solution is known to give specific-heat anomalies similar to those under consideration, and it may be that they were due to this cause, though the explanation does not seem reasonable when the curves are examined more closely. In the case of the specimen in the very slowly cooled condition, it would be expected that considerable growth of the precipitate nuclei would take place during the three weeks of slow cooling, the re-solution of the nuclei then giving rise to a much broader maximum than that which was obtained near 540° C., or perhaps to two maxima as is often observed in such circumstances. Only one maximum may have been obtained because of a steep limit of solubility/temperature curve, or because the lower-temperature maximum is suppressed by low atomic mobility; but in this case it would not be expected that the curves for the specimen in the very slowly cooled and comparatively rapidly cooled conditions would coincide along the higher-temperature region of the anomaly, as was found in this series of experiments.

The other explanation is that ordering of the lattice gave rise to the specific-heat minimum in the region of 510° C. and that the destruction of the superlattice was accompanied by the specific-heat maximum near

540° C. A fact which supports this supposition is that the curves obtained resemble closely those for other alloys which are known to order, including that given in Fig. 8 (p. 179) for Ni₁₅Cr₄Al, which shows distinct superlattice lines on X-ray-diffraction photographs after being annealed at about 500° C. There are, however, some differences between these specific heat/temperature curves and curves for other materials which require an explanation. In the case of Cu₃Au, for example, the decrease in the specific heat from the maximum value is much more rapid than for Ni₃Cr. The lag in these experiments may have been due to variations of temperature across the specimen, but this does not seem likely when the rapid decrease from the maximum value above the Curie point of nickel is considered. It is more probable that the rate of rise of temperature of 2° C./min. was too fast for equilibrium to be attained at any particular temperature, the sluggishness perhaps being accentuated by impurities which, according to Haughton and Payne,¹⁶ give rise to a similar effect in copper-gold alloys.

There are two possible reasons for the absence of the very high (theoretically infinite) value of specific heat which would be expected from the latent-heat absorption predicted by the theories of Bragg and Williams¹⁷ and of Peierls¹⁸ for alloys of the type A₃B at the critical temperature. The specific heats obtained are mean values over time intervals of 1 min., and so abnormalities of short duration tend to become smoothed out, though the absorption or liberation of latent heat should be shown by irregularities in the movement of the spot from the galvanometer indicating the differential thermocouple voltage. No large irregularities in galvanometer deflection have been observed, so it is probable that much of the rounding of the curve at the critical temperature is due to incomplete ordering in the specimen, since it has been shown by Sykes and Jones¹⁹ that no latent heat is observed in the case of Cu₃Au if antiphase nuclei are present.

The difficulty of observing the additional X-ray-diffraction lines from the superlattice is presumably also due to the formation of antiphase nuclei that do not readily coalesce, because, as has been shown theoretically by Bethe,²⁰ most of the energy given out during the formation of a superlattice comes from short-range ordering. By employing the Sykes and Jones method of continuing the actual specific heat/temperature curve above the maximum along the line of steepest slope to meet the curve calculated from the specific heats of nickel and chromium, it is found that the total energy of ordering available below the critical temperature is about 1.75 cal./g., compared with 5.5 cal./g. for Cu₃Au.

An explanation of the small difference at 280° C. between the specific heat/temperature curves for the alloy in the quenched and slowly cooled conditions will now be considered. A similar anomaly was found by Sykes and Jones for Cu₃Au, and, because in their case the change in energy was as large as the

energy released on ordering in the experiments on Ni_3Cr , they were able to carry out experiments to determine its cause. Their view that the anomaly occurring at the lower temperature was due to ordering has been supported by Germer and Haworth,²¹ who obtained superlattice lines on electron-diffraction photographs after heating the specimen at 196°C . "for a few hours". To explain the decrease in the rate of ordering that occurred with two of their specimens which had received different heat-treatments, Sykes and Jones assumed that two processes were involved. In the case of a specimen water-quenched from above the Curie point for order, they assumed that the decrease occurred when the antiphase domains came into contact with one another, and that the decrease in the case of a specimen water-quenched from just below the critical temperature was due to local sub-microscopic fluctuations in chemical composition.

When the first part of the theory is used to try to explain the anomaly in the case of Ni_3Cr , it is seen that the number of atoms in the domains must be very much smaller than the number in the domain boundary surfaces, because the amount of energy released in the first stage is very small compared with that released just below the critical temperature. With such a large proportion of the energy available in the boundaries, the specimen should be able to continue ordering, and the fact that it does not suggests that this part of the theory may not be important in the case of Ni_3Cr . In the second process, put forward independently by the authors to account for the two specific-heat minima in Ni_3Cr , it is supposed that the rate of ordering is small at temperatures between the two minima because local variations from the optimum composition in areas outside the ordered nuclei are increased by the growth of the nuclei, and that the rate increases again when the temperature is high enough for appreciable diffusion to take place between areas of dissimilar composition. It appears to be a weakness of the Sykes and Jones theory that two mechanisms are used to explain the almost complete cessation of ordering which occurs at the same temperature for two different heat-treatments of the Cu_3Au specimen, and it may be that, as in the case of Ni_3Cr , the second process is the dominant factor in reducing the rate of ordering in this alloy, although contacts between antiphase domains may modify the rate and may even be predominant at different heating rates during the specific-heat determinations, or for different alloys.

At temperatures above 570°C ., the point at which long-range order disappears, the specific heats for the specimen in the quenched and slowly cooled conditions become coincident. The values which would be obtained by extrapolating the anomaly-free low-temperature part of the curves in Fig. 3 (p. 173) are rather lower than the experimental ones, a state of affairs to be expected above the critical point for long-range order, because of the energy absorption during the reduction of local order which continues above the

critical temperature.^{18, 20} Above 700°C . there occurs the fourth of the specific-heat anomalies already mentioned. No satisfactory explanation of the difference between the curves for the specimen in the quenched and slowly cooled conditions has been found; it is unlikely to be due to experimental error, since the curve for the quenched condition has been confirmed by a second set of measurements, and curve (b) in Fig. 3 shows that the specimen cooled from 770° to 200°C . in $16\frac{1}{2}$ hr. behaves like the more slowly cooled one at temperatures up to 740°C . It is possible that the heating and cooling cycle applied after the specific-heat determinations had been made on the quenched specimen brought it into a condition which was not fully eliminated by the subsequent annealing treatment. Circumstances have precluded additional experiments to check this.

2. THE ANOMALOUS RESISTIVITY

In the absence of phase changes, precipitation phenomena, or magnetic transformations, there remain two other possible explanations for the anomalous resistivity changes in Ni_3Cr . The first requires some form of valency change which could be associated with a liberation of electrons from the inner orbitals of nickel. This explanation seems most improbable on account of the time factor involved in attaining equilibrium conditions. The second explanation is based on the order-disorder transformation indicated by the X-ray data and in particular by the specific heat results, the anomalously high values of which above the critical temperature imply the persistence of some degree of short-range order. As stated previously, the change in resistance seems to be in the wrong direction, because it rises by about 7% on cooling slowly through the critical temperature, whereas for a normal change, such as occurs in Cu_3Au , there is a fall in resistivity of more than 50%.²² The rise in Ni_3Cr is clearly not due to any impurities, since with slow rates of cooling or prolonged annealing such impurities would tend to aggregate and the resistivity would fall.

In the general case typified by Cu_3Au , order occurs in small antiphase nuclei, the boundaries of which scatter the conductivity electrons and contribute thereby to the resistivity of the alloy.¹⁹ As annealing proceeds, not only does the degree of order increase, thereby reducing the resistance, but some of the contiguous antiphase domains also increase in size, thus reducing the effective boundary surface and, consequently, the degree of electron scattering at the domain boundaries, and, with it, the resistivity. On the other hand, in Ni_3Cr , prolonged annealing below the critical temperature carried out to increase the degree of long-range order causes the resistivity to rise to an equilibrium value.

It would seem, then, that the influence of the boundary walls between the antiphase domains is very small in the case of Ni_3Cr . This is presumably due to the very small mean free path of the electrons, which reveals itself in the very high resistivity, namely

106.0 $\mu\Omega\text{-cm.}$ On the other hand, the low resistivity of Cu_3Au , which falls to less than 6.0 $\mu\Omega\text{-cm.}$ at room temperature for the fully ordered state, indicates a very long mean free path, and consequently scattering by the antiphase domain boundaries becomes of considerable importance.²²

It can be shown from the wave-mechanical theory of the scattering of electrons in a metal lattice²³ that the resistivity ρ is related to the mean free path $\bar{\lambda}$ of the conductivity electrons by the equation:

$$\bar{\lambda} = h/\rho e^2 (\pi/3N)^{1/3}$$

where e is the electronic charge = 1.59×10^{-20} abs. e.m.u., h is Planck's constant = 6.549×10^{-27} erg sec., ρ is the specific resistance = 106.0×10^{-6} $\Omega\text{-cm.}$ for quenched Ni_3Cr , N is the number of atoms/c.c. = $4/(a_w)^3 = 4/(3.55 \times 10^{-8})^3$ and a_w is the lattice parameter of the unit cell of Ni_3Cr . Hence $\bar{\lambda} = 12.6 \text{ \AA.}$, which is of the same order as 3-4 unit cells. Thus only the degree of order and not the size of the antiphase domains can have any effect on the electrical resistivity, because the electrons would be scattered long before they approached the boundaries of the domains.

When the face-centred cubic lattice of Ni_3Cr is fully disordered, X-rays can be strongly reflected only from planes such as (111), (200), (220), &c., and these planes must also be strong electron-wave reflectors.

When the lattice is fully ordered, planes (100), (110), (210), &c., also become X-ray reflectors, albeit very weak ones, and they will consequently become electron reflectors provided that twice the spacing of the planes is of the same order and slightly larger than the wavelength of the conductivity electrons. The wavelength of the conductivity electrons can be readily computed from Brillouin-zone theory, provided it is known just how many valency electrons each atom supplies to the lattice. This is difficult for such transition elements as nickel and chromium, but serious error in the estimation is not likely to arise if a value of 0.6 valency electron is assumed to be contributed by each nickel atom and 1.0 valency electron by each atom of chromium.

The minimum wave-length ($\lambda_{\min.}$) of the valency electrons is given by $\lambda_{\min.}^3 = 8\pi/3n$, where n is the number of free electrons/unit volume of the crystal, and is equal to $(3 \times 0.6 + 1)/3.55^3$. Substituting this in the equation gives $\lambda_{\min.} = 5.12 \text{ \AA.}$ This is just small enough to satisfy the Bragg relation $2d\sin\theta = \lambda$ for the (100) planes, which are 3.55 \AA. apart, and although λ is just too big for planes (110), which are 2.52 \AA. apart, some reflection from these planes can nevertheless be shown to occur if the well-known reciprocal-lattice construction is applied, since the sphere of reflection will cut through the smeared-out reciprocal-lattice points representing lattice regions having the same order of size as the mean free paths of the electrons. As the electrons will be reflected back at almost normal incidence from these two sets of planes, it would seem, on account of their very short mean free path, that any increase in the degree of

order should increase the resistivity of the material, irrespective of whether long-range or short-range order exists in the lattice, since the reflecting power of the planes increases with the degree of order. Furthermore, as the amount of electron scattering is already very high in the disordered material, it would be anticipated that the net increase in resistance would only be relatively small. This is indeed the case.

Assuming that the increase in resistivity is, in fact, due to the creation of a fresh Brillouin zone by the increase in the degree of order obtaining in the lattice, it becomes possible to express in a semi-quantitative way the dependence of resistivity upon temperature.

In a normal alloy like Cu_3Au , where the mean free path of the valency electrons is very large and there are no complications due to the presence of transition elements, it can safely be assumed that the superlattice has a resistance similar to that of a pure metal and falls to zero at the absolute zero of temperature. Thus, according to Bragg and Williams,¹⁷ for a fully ordered lattice when the degree of order $S = 1$,

$$\rho_1 = \alpha_1 T \quad (1)$$

where ρ_1 is the resistivity in $\mu\Omega\text{-cm.}$ for the fully ordered lattice at temperature T° absolute and α_1 is the temperature coefficient. Also for $S = 0$,

$$\rho_0 = \rho_d + \alpha_0 T \quad (2)$$

where ρ_0 is the resistivity at temperature T of the fully disordered alloy having a residual resistivity ρ_d at the absolute zero and temperature coefficient α_0 .

Thus, for any intermediate value of long-range order S , the resistivity ρ_s is given by:

$$\begin{aligned} \rho_s &= S\rho_1 + (1 - S)\rho_0 \\ &= \rho_d(1 - S) + T\{\alpha_1 S + \alpha_0(1 - S)\} \quad (3) \end{aligned}$$

In the case of Ni_3Cr , the experimental results on quenched and annealed specimens indicate that even at the absolute zero there is a very high value of the residual resistivity. If the equilibrium case is considered, as shown by the dotted curve in Fig. 2 (p. 172), the lattice may be considered to be long-range ordered below the critical temperature T_c and short-range ordered above T_c . At $T = 0^\circ \text{K.}$ and $S = 1$, let ρ_ω be the amount of residual resistivity for complete long-range order and α_1 the resistivity temperature coefficient. Then for temperatures below T_c , to a first approximation:

$$\rho_1 = \rho_\omega(1 + \alpha_1 T) \quad (4)$$

Also, if ρ_0 , ρ_d , and α_0 are respectively the resistivity at $T^\circ \text{K.}$, the residual resistivity, and temperature coefficient for the hypothetical fully disordered stage:

$$\rho_0 = \rho_d(1 + \alpha_0 T) \quad (5)$$

For the intermediate state with degree of order S , using the simple additive law of Bragg and Williams:¹⁷

$$\begin{aligned} \rho_s &= S\rho_1 + (1 - S)\rho_0 \\ &= S\rho_\omega(1 + \alpha_1 T) + (1 - S)\rho_d(1 + \alpha_0 T) \end{aligned} \quad (6)$$

$$\text{Hence } \rho_s = \rho_d + (\rho_\omega - \rho_d)S + \alpha_0 \rho_d T + (\alpha_1 \rho_\omega - \rho_d \alpha_0)ST \quad (7)$$

The values of S as a function of T/T_c have been computed by Peierls¹⁸ and by Nix and Shockley.²⁴ From the specific-heat results $T_c = 544^\circ \pm 4^\circ \text{C.} = 817^\circ \pm 4^\circ \text{K.}$, and therefore S for any temperature may be computed, using the Peierls curve.

Before equation (7) can be used, it is necessary to obtain values of the temperature coefficients of resistivity α_0 and α_1 , for the disordered and ordered conditions and also values of ρ_d and ρ_ω for complete disorder and complete order, respectively, for $T = 0^\circ \text{K.}$ The temperature coefficients may easily be obtained to a sufficient degree of accuracy from the upper and lower branches of the resistivity curves in Fig. 2 (p. 172). By extrapolating back to absolute zero the equilibrium curves corresponding to various annealing temperatures, as shown in Fig. 2, a series of values of

would presumably contain a mixture of highly ordered and partially ordered regions at the critical temperature, so that the resistivity would be somewhere between the two extremes and the peak of the curve would become rounded, as found experimentally. On cooling down, the alloy tends to order at the critical temperature, but on account of the slowing down of atomic mobility, the equilibrium degree of order cannot be approached as closely as on the heating cycle, unless sufficient time is given. Consequently, the resistivity peak of the curve for a cooling alloy lies appreciably below the peak value for the heating curve, as is clearly shown in Fig. 1 (p. 171). Thus, allowing for the approximations made, it would seem that the order-disorder theory can give a semi-quantitative explanation for the shape of the resistivity curves of Ni_3Cr .

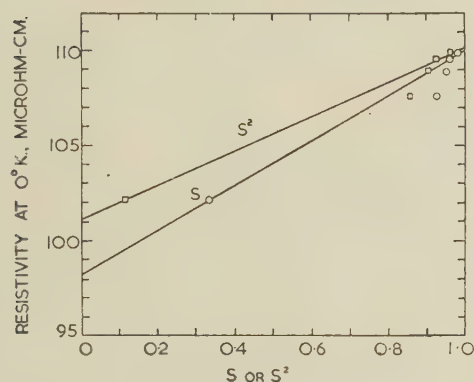


FIG. 4.—Plots of Resistivity (ρ_s) Against Degree of Order (S) and (S^2).

ρ_s at $T = 0^\circ \text{K.}$ is obtained for which a series of S values from the Peierls curve of S versus T/T_c may be derived. According to equation (6), $\rho_{s(T=0)}$ is a linear function of S . Hence by plotting $\rho_{s(T=0)}$ against S and extrapolating to $S = 0$ and $S = 1$, the values of ρ_ω and ρ_d may be derived as shown in Fig. 4.

The extrapolated values $\rho_d = 98.2 \mu\Omega\text{-cm.}$ and $\rho_\omega = 110.1 \mu\Omega\text{-cm.}$ inserted into equation (7) along with $\alpha_0 = 0.881 \times 10^{-4}$ and $\alpha_1 = 0.979 \times 10^{-4} \Omega/^\circ\text{K.}$, lead to a resistivity value:

$$\rho_s = 98.2 + 11.9 S + 0.875 \times 10^{-2} T + 0.215 \times 10^{-2} ST \quad (8)$$

Fig. 5 shows the comparison between the equilibrium curve based on the experimental data and the curve obtained with the aid of equation (8). A theoretical curve for complete disorder is also included, but can never be realized in practice because even at the melting point some degree of short-range order must persist. In the region of the critical temperature there is a sharp discontinuity in the theoretical value of the resistivity, owing to the sharp fall in the degree of order. In heating up, the alloy

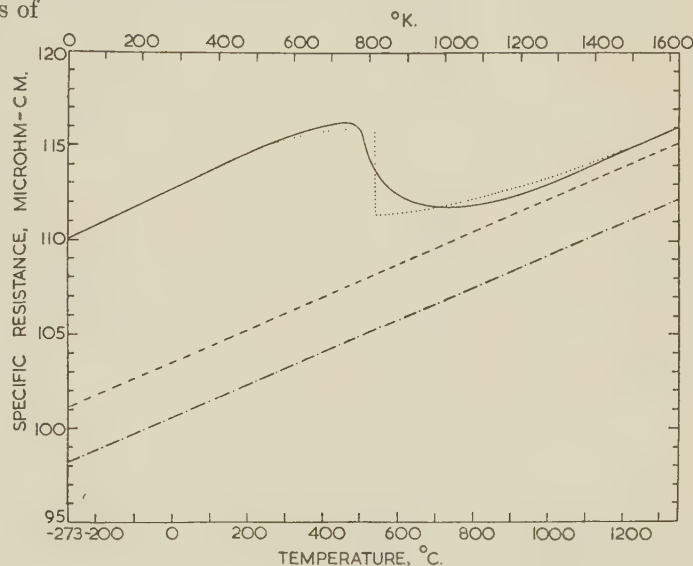


FIG. 5.—Equilibrium Resistivity of Ni_3Cr Compared with Theory.

KEY.
 ————— Equilibrium Curve, $S = 1$ at $T = 0^\circ \text{K.}$
 Peierls' Theory.
 - - - - - Complete Disorder. $R = f(S)$.
 - - - - - Complete Disorder. $R = f(S^2)$.

The above treatment followed that of Bragg and Williams in assuming a linear relationship between the resistivity ρ_s and the degree of order S . Now in X-ray diffraction, for mosaic crystals, the intensity of a given reflection is a function of the square of the structure amplitude F . Thus, in Ni_3Cr , the reflected intensity I_m for the main lattice lines would be proportional to $(3f_{\text{Ni}} + f_{\text{Cr}})^2$, and the reflected intensity I_s for the superlattice lines would be proportional to $(f_{\text{Ni}} - f_{\text{Cr}})^2 S^2$, where f is the atomic scattering factor.²⁵ It would similarly be expected that the intensity of electron reflection and hence the change in resistivity, would also be proportional to S^2 , the assumption that it is proportional to S being equivalent to the case of a perfect crystal subject to primary extinction. For mosaic crystals, the simple linear

additive law of Bragg and Williams expressed by equation (6) must be modified to:

$$\rho_s = S^2\rho_1 + (1 - S^2)\rho_0 = S^2\rho_\omega(1 + \alpha_1 T) + (1 - S^2)\rho_d(1 + \alpha_0 T) \quad (9)$$

and the values of $\rho_{s(T=0)}$ must now be plotted against S^2 instead of S as shown in Fig. 4. For $T = 0$, equation (9) may be written in the form $(\rho_s - \rho_\omega)/(\rho_d - \rho_\omega) = 1 - S^2$, an expression obtained by Dienes,²⁶ using a different method of approach.

The value of ρ_ω obtained by extrapolating to $S^2 = 1$ is almost exactly the same as before, namely 110.1 $\mu\Omega\text{-cm.}$, so that the position of the equilibrium curve is substantially unchanged. As shown in Fig. 5 (p. 177), however, there is rather closer agreement between the theoretical curve from equation (9) and the equilibrium curve. The theoretical resistivity curve corresponding to the hypothetical case of com-

position lay just within the $(\gamma + \gamma')$ two-phase field. Its primary interest lay in the fact that with long soaking at 480° C. the alloy yielded X-ray spectra with sharp superlattice lines indicative of long-range ordering. Fig. 6 illustrates the resistivity changes in the alloy. Before making the specimens, the hard, cold-drawn wire was softened by raising its temperature in a few seconds to 1000° C., maintaining it there for 15 sec., and switching the current off. In this air-quenched condition, not all the γ' phase was in solution, and the alloy was substantially disordered. The maximum in the region of 530° C., shown by curves (a), (b), and (c) for all thermal histories, are clearly associated with the order-disorder transformation, as in the case of Ni_3Cr . Curve (a) for the quenched specimen is seen to have a well-defined inflection at 650° C., associated with the precipitation of γ' phase, which is taken back into solution at 1050° C. with the

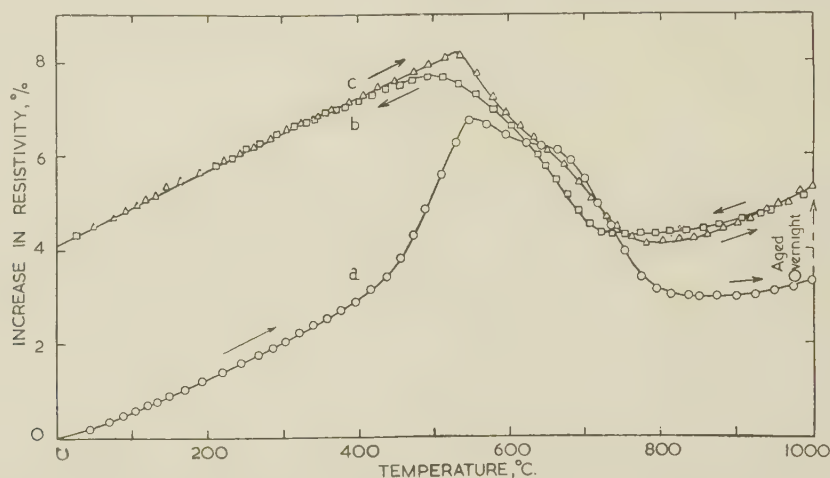


FIG. 6.—Percentage Increase in Resistivity of $\text{Ni}_{15}\text{Cr}_4\text{Al}$ with Temperature.

(a) Heating curve after quenching from 1000° C. (b) Cooling curve from 1080° C. (c) Reheating curve from 20° C.

plete disorder also tends to lie closer to the line corresponding to the course of the quench from 975° C.

If the Peierls curve σ for short-range order below $T/T_c = 1$ had been taken, an even greater degree of agreement between the theoretical and equilibrium curves could have been obtained. However, such a choice would have been unjustified because the rate of cooling through the critical temperature should have been slow enough to ensure long-range order. In any event, the smallness of the resistivity change in Ni_3Cr and the approximations made in the calculations of S and σ do not enable a clear-cut decision to be made as to the precise order function to be chosen.

VI.—ORDER-DISORDER AND PRECIPITATION PHENOMENA IN $\text{Ni}_{15}\text{Cr}_4\text{Al}$

1. RESISTIVITY

This alloy was intended to have a composition just within the γ -phase field of the nickel-chromium-aluminium system, but when analysed it was found to contain a slight excess of aluminium and the com-

consequent rise in resistivity. Parallel changes in the specific heat of the alloy also occur and will be described in the next section.

In Fig. 7, an attempt is made to analyse curves (a) and (b) of Fig. 6. Before discussing the resistivity curves for the quenched specimen on reheating, it will be convenient to analyse the resistivity curve of the specimen during cooling from an 18-hr. solution-treatment at 1050° C., at which temperature equilibrium had been reached. Reducing the temperature causes the resistivity of the homogeneous solid solution to fall from its value at 1050° C., and then to increase again, as shown in curve (b); but the increase is partly composed of the normal increase due to the increase in order and partly due to the precipitation of the γ' phase. The broken line, curve (c), represents the probable course of the resistivity curve if the order-disorder transformation alone had progressed without any appreciable precipitation near the critical temperature. Curve (e), representing the difference between (b) and (c), indicates the formation of coherent zones which become "frozen in" at the lower tempera-

tures without being given the opportunity to grow at the adopted rate of cooling.

Consider now curve (a), obtained by heating the specimen originally quenched from 1000° C. At 560° C. the alloy is substantially disordered, but the resistivity rises to a secondary maximum as a result of the effects of precipitation which are superimposed upon the normal curve. It seems that at approxi-

taken back into solution before this stage has occurred. This is in complete agreement with the shape of the specific-heat curve. These changes can best be followed by curve (d), which represents the difference between curve (a) and curve (c).

Above 700° C., curves (b) and (c) are coincident, so that the difference between (c) and (a) is now negative. This is interpreted as being due simply to the rate of

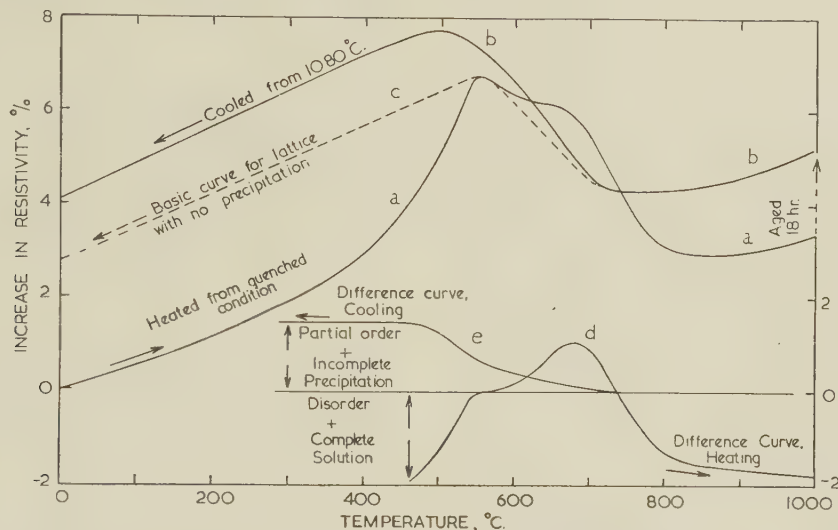


FIG. 7.—Analysis of Resistivity Curves of $\text{Ni}_{15}\text{Cr}_4\text{Al}$.

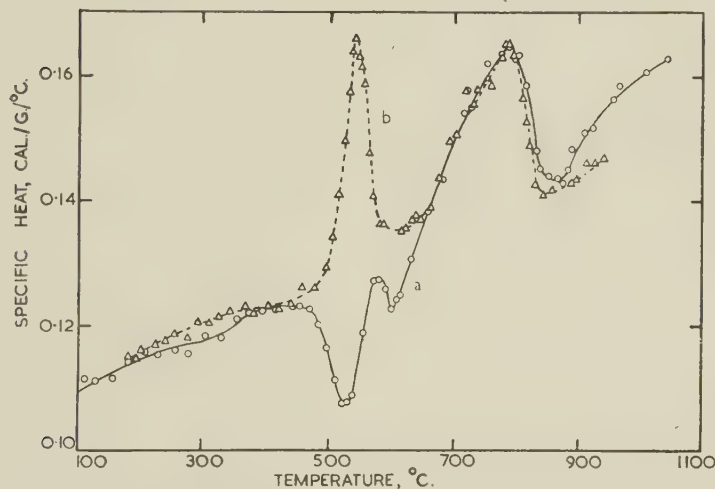


FIG. 8.—Specific Heat of $\text{Ni}_{15}\text{Cr}_4\text{Al}$ at Various Temperatures and at Constant Pressure. Specimen (a) water-quenched after 8 hr. at 1130° C., and (b) water-quenched after 8 hr. at 1130° C., and then cooled at 4° C./day from 480° to 370° C.

mately 530° C., when atomic mobility becomes sufficiently high for the order-disorder transformation to proceed at a substantial rate, the rate of diffusion is also sufficient to enable coherent zones of sub-microscopic size to form in the lattice. As these zones grow in size and number, they distort the lattice, both processes increasing the scatter of electrons and causing the resistance to increase. Above 680° C. the resistivity curve reverts towards the Ni_3Cr type, presumably because the zones have grown beyond a critical size or because they have been

heating. The γ' phase which was originally present in the quenched specimen plus that precipitated above 530° C. has not had the opportunity of being taken back into solution, and thus the impoverished γ solid solution has an exceptionally low resistivity. This now rises quite rapidly to its full equilibrium value on soaking at 1050° C.

2. SPECIFIC HEAT

Two specific heat/temperature curves, obtained under conditions as far as possible the same as in the

case of Ni_3Cr , are given in Fig. 8; one for a specimen water-quenched after soaking for 8 hr. at 1130°C ., and one for a specimen slowly cooled from 480°C . Between 100° and 570°C . they are similar in shape to the equivalent curves for Ni_3Cr . Since X-ray data show clearly that $\text{Ni}_{15}\text{Cr}_4\text{Al}$ develops an ordered structure when annealed at about 500°C ., this similarity, as has already been pointed out, supports the ordering theory in the case of Ni_3Cr .

When allowances are made for the specific heat of aluminium, the results for the two alloys in the slowly cooled condition closely follow the same curve, thus indicating that the energy changes associated with the order-disorder transformation in the two cases are the same within the limit of experimental error. The temperature at which the maximum value of the specific heat occurs is also about the same for the two alloys, being 544°C . for Ni_3Cr and 540°C . for $\text{Ni}_{15}\text{Cr}_4\text{Al}$, though ordering appears to take place at lower temperatures for the binary alloy. Thus the first stage of ordering takes place in the temperature range 220° – 320°C . for Ni_3Cr and in the range 260° – 380°C . for $\text{Ni}_{15}\text{Cr}_4\text{Al}$, and the temperatures for the minimum specific heat in the second stage are 510° and 530°C ., respectively.

Above the temperature of the order-disorder transformation, the curves for $\text{Ni}_{15}\text{Cr}_4\text{Al}$ differ considerably from those for Ni_3Cr , a sharp minimum in the case of the water-quenched ternary alloy occurring at 600°C . and a maximum at 790°C . In the case of the specimen in the slowly cooled condition, the minimum is considerably smaller than that for the quenched specimen, but the maximum value is unaltered, which suggests that the release of energy was almost complete at about 640°C . in the case of the quenched specimen, and that very little more would have been given out if the rate of rise of temperature had been smaller. As with the resistance anomalies at temperatures above that for long-range order, the specific-heat variations can be explained by the precipitation of nuclei of the γ' phase at about 600°C ., followed at higher temperatures by re-resolution of the precipitate, which the sharpness of the maximum suggests takes place before there is any appreciable growth of the nuclei. Above 680°C . the alloy becomes single phase (if impurities are neglected), but the shape of the curve for the quenched specimen appears to be different from that for the equivalent Ni_3Cr curve and possibly different from that for the slowly cooled specimen. The difference between the curves for the ternary alloy in the two conditions of heat-treatment may be due to experimental error, since serious electrical leakage started at an unusually low temperature for the slowly cooled specimen, but the difference between this alloy and Ni_3Cr in the quenched condition has been confirmed by a second experiment. Circumstances have prevented the carrying out of further work to resolve the difficulties.

VII.—CONCLUSIONS

The chief evidence for the formation of a highly ordered structure in the binary alloy Ni_3Cr is supplied

by specific-heat measurements. Confirmatory specific-heat and X-ray evidence is derived from the ternary alloy $\text{Ni}_{15}\text{Cr}_4\text{Al}$, which gives superlattice reflections of appreciable intensity in its Debye-Scherrer X-ray-diffraction pattern. The anomalous resistivity changes in Ni_3Cr and $\text{Ni}_{15}\text{Cr}_4\text{Al}$ are interpreted on the basis of an order-disorder transformation, and it is shown how the creation of new sets of reflecting planes by the ordering process may lead to a small increase in resistivity if the mean free path of the conductivity electrons is of the order of a few interatomic distances. Above the critical temperature for ordering, the resistivity and specific-heat curves of $\text{Ni}_{15}\text{Cr}_4\text{Al}$ display a number of inflections which are not revealed by Ni_3Cr . These inflections have been shown to be associated with the precipitation, crystal growth, and re-resolution of a fully ordered face-centred cubic structure based upon the Ni_3Al phase of the nickel-aluminium binary system.

ACKNOWLEDGEMENT

The authors wish to express their sincere thanks to The Mond Nickel Co., Ltd., for permission to publish this paper.

REFERENCES

1. C. H. M. Jenkins, E. H. Bucknall, C. R. Austin, and G. A. Mellor, *J. Iron Steel Inst.*, 1937, **136**, 195p.
2. J. H. Thomas and R. M. Davies, *Phil. Mag.*, 1936, [vii], **22**, 681.
3. Z. Yano, *Japan Nickel Rev.*, 1941, **9**, 17.
4. J. M. Hinkle, *Dissert. Univ. Michigan*, 1948.
5. H. Grover and J. Hutzenlaub, *Phys. Rev.*, 1939, [ii], **56**, 212.
6. E. R. Jette, V. H. Nordstrom, B. Queneau, and F. Foote, *Trans. Amer. Inst. Min. Met. Eng.*, 1934, **111**, 361.
7. A. Taylor and R. W. Floyd. To be published.
8. A. J. Bradley and A. Taylor, *Proc. Roy. Soc.*, 1937, [A], **159**, 56.
9. C. Sykes, *ibid.*, 1935, [A], **148**, 422.
10. C. Sykes and F. W. Jones, *J. Inst. Metals*, 1936, **59**, 257.
11. C. Sykes and H. Wilkinson, *Proc. Phys. Soc.*, 1938, **50**, 834.
12. C. G. Shull and E. O. Wollan, *Phys. Rev.*, 1951, [ii], **81**, 527.
13. A. J. Bradley and A. H. Jay, *J. Iron Steel Inst.*, 1932, **125**, 339p.
14. W. Betteridge, *J. Inst. Metals*, 1948–49, **75**, 559.
15. L. D. Armstrong and H. Grayson-Smith, *Canad. J. Research*, 1950, [A], **28**, 51.
16. J. L. Houghton and R. J. M. Payne, *J. Inst. Metals*, 1931, **46**, 457.
17. W. L. Bragg and E. J. Williams, *Proc. Roy. Soc.*, 1934, [A], **145**, 699.
18. R. Peierls, *ibid.*, 1936, [A], **154**, 207.
19. C. Sykes and F. W. Jones, *ibid.*, 1936, [A], **157**, 213.
20. H. A. Bethe, *ibid.*, 1935, [A], **150**, 552.
21. L. H. Germer and F. E. Haworth, *Phys. Rev.*, 1939, [ii], **56**, 212.
22. C. Sykes and H. Evans, *J. Inst. Metals*, 1936, **58**, 255.
23. N. F. Mott and H. Jones, "The Theory of the Properties of Metals and Alloys". Oxford: 1936 (Clarendon Press).
24. F. C. Nix and W. Shockley, *Rev. Modern Physics*, 1938, **10**, 1.
25. A. Taylor, "An Introduction to X-Ray Metallography", p. 176. London: 1945 (Chapman and Hall).
26. G. J. Dienes, *J. Appl. Physics*, 1951, **22**, 1020.

DEFORMATION OF MAGNESIUM AT VARIOUS RATES AND TEMPERATURES *

1430

By J. W. SUITER,† B.Sc., STUDENT MEMBER, and W. A. WOOD,†
D.Sc., MEMBER

SYNOPSIS

It is shown by X-ray and metallographic studies that polycrystalline magnesium, when deformed, behaves in a similar way to aluminium and zinc in that, at both elevated temperatures and slow strain rates, a sub-grain or cell structure is formed within the grains. The work, however, brings out a new feature, namely that it appears necessary to postulate the formation of crystallite "debris" at the grain boundaries in order to correlate the X-ray and metallographic observations.

I.—INTRODUCTION

THE change in the mechanism of deformation of metals with change in the conditions of deformation has been the subject of a number of investigations. In work on aluminium it has been shown that as the temperature of deformation is increased or the rate of deformation decreased, the operative mechanism changes from the customary slip process to relative grain movements. At intermediate temperatures or rates of strain, it has been found that the metallic grains break down into cells during the deformation. The formation and behaviour of these cells have been studied extensively.¹⁻³ However, such cells have not been found to be as well marked in lead or lead alloys deformed under a wide range of conditions.^{2,4} Studies of the deformation characteristics of zinc,^{5,6} and more recently of a tin-antimony alloy,⁷ have shown that under suitable conditions of deformation, cells are formed in these metals.

Though the size of the cells in general varies systematically with the conditions of deformation, Calnan and Burns³ and Ramsey⁶ noticed in the case of coarse-grained aluminium and of zinc, respectively, that the breakdown of the grains into cells was most marked in the grain-boundary regions. The present paper describes experiments with magnesium deformed over a range of conditions. They show that with this less-ductile metal the breakdown of the grains takes a less regular form than with aluminium and introduces interesting new features into the X-ray and metallographic observations.

II.—EXPERIMENTAL METHODS

The test material was magnesium of 99.75% purity, 0.2% lead and 0.02% iron being the main impurities. From hot-rolled sheet, flat tensile specimens were produced with a parallel-sided gauge-length of 2 in. and a cross-section of 0.30 × 0.06 in. These specimens were annealed in air for 1 hr. at 530° C. to

produce strain-free grains approximately 2×10^{-2} cm. in size.

The specimens were prepared for metallographic examination by electropolishing in the Jacquet solution⁸ containing 37.5% orthophosphoric acid (sp. gr. 1.71) and 62.5% ethyl alcohol. A 5% solution of nitric acid in alcohol was used to etch the specimens.

The specimens were deformed in a constant-strain-rate machine which has been described in a previous paper.⁹ Strain rates of the order of 10%/min. and 0.15%/hr. were employed. For deformation at elevated temperatures the specimen was surrounded by a furnace with the temperature controlled to $\pm 2^\circ$ C. and with the temperature gradient along the gauge-length of the specimen not exceeding $\pm 2^\circ$ C.

The structure of the specimens was examined, both before and after deformation, by metallographic and X-ray methods. The X-ray-diffraction patterns were the usual back-reflection type, obtained from a stationary specimen, using FeK_α radiation and a specimen-film distance of 10 cm.

III.—EXPERIMENTAL OBSERVATIONS

1. AFTER RAPID DEFORMATION AT VARIOUS TEMPERATURES

The standard initial condition of the specimens before deformation is illustrated in Figs. 1 and 2 (Plate XXIV). The sharp and discrete spots of the diffraction pattern in Fig. 1 indicate that the corresponding grains are relatively perfect and of homogeneous orientation. It should be noted that the boundaries of the annealed grains (Fig. 2) are quite smooth.

Rapid deformation at 22° C. appears to take place mainly by mechanical twinning, as shown in Fig. 4 (Plate XXIV). This photomicrograph also shows the presence of some slip, but it is a relatively rare occurrence and, in general, an area showing any signs of slip is fairly difficult to find. The irregular nature of the deformation twins is an interesting feature.

* Manuscript received 7 July 1952.

† Baillieu Laboratory, University of Melbourne, Australia.

However, it can be seen that the twins have the same general direction within a given grain. The rumpling of the surface of the specimen indicates that the structure of the specimen after 5.3% strain has become disoriented. This is confirmed by the X-ray pattern (Fig. 3, Plate XXIV). The disorientation of the structure is so marked that the Debye circles become continuous, under the present experimental conditions, after strains as low as 1–2%.

The metallographic signs of rapid deformation at 300° C. (Fig. 6, Plate XXIV), are quite different from those of deformation at room temperature. The most noticeable feature is the absence of mechanical twinning. This is in agreement with the observations of Barrett and Haller,¹⁰ who found that the amount of twinning in magnesium decreased as the temperature of deformation was raised. Occasional grains have deformed by slip. In other metals, e.g. aluminium, it has been found that slip formed at higher temperatures was broader and more widely spaced than slip formed at room temperature. This does not appear to be the case in magnesium, however, for the slip formed at 300° C. is almost identical with that formed at 22° C.

As is shown by the formation of facets on the surface of the grains (Fig. 6), most grains have broken up into several blocks. At first sight it may be thought that these facets are related to the formation of mechanical twins. Such twins, however, would have to be rather different from those formed at room temperature, because if a specimen after straining at 300° C. is further strained at room temperature, it can be seen that the sub-boundaries formed at 300° C. bear no relation to the twins formed at room temperature. The blocks shown in the grains in Fig. 6 have been identified with the cells previously found by other workers in aluminium and zinc. As will be shown later, these cells are discrete blocks, each slightly disoriented with respect to its neighbours.

With all these marked changes in the metallographical features of deformation, it might be expected that there would be accompanying changes in the X-ray-diffraction patterns. Fig. 5 (Plate XXIV) shows, however, that this is not the case. The diffraction circles obtained from the specimen rapidly strained at 300° C. are a little sharper than those obtained from the specimen strained at 22° C. The discrete spots found to be characteristic of cells in aluminium do not appear to be present. It is suggested that the continuous diffraction circles arise from a fine debris in the grain-boundary regions and that this masks the discrete spots arising from the cells. This is fully discussed in the next section.

The diffraction pattern obtained from a specimen rapidly strained at 400° C. shows some changes. The pattern (Fig. 7, Plate XXIV), consists of a number of relatively sharp spots superimposed on the continuous circles. The metallographic features shown in Fig. 8 (Plate XXIV), appear to be rather similar to those of rapid deformation at 300° C. Firstly, there is a decrease in the number of grains which deform by slip the higher the temperature of deformation; secondly, the

debris around the grain boundaries is clearly shown in some boundaries, and it can be seen that this debris is on a coarser scale than that formed at 300° C. This decrease in fragmentation in the grain-boundary regions can be used to explain the changes in the X-ray patterns. These points on grain-boundary debris are more fully discussed in the next section on the slow deformation of magnesium at various temperatures.

2. AFTER SLOW DEFORMATION AT VARIOUS TEMPERATURES

At temperatures of the order of 100°–150° C. slow deformation (0.15% strain/hr.) takes place mainly by slip, with very little activity at the grain boundaries. Above 200° C., the grains break down into cells, and some activity occurs at the grain boundaries. The results of slow straining at 200° C. are shown in Figs. 9 and 10 (Plate XXIV). The micrograph (Fig. 10) shows by the facets on the surface that the grains have broken down into cells, although some grains have deformed by slip.

The cell structure and the grain-boundary regions are perhaps more readily visible in Fig. 12 (Plate XXV), which is at a higher magnification. There are several points of interest in this figure. Firstly, it can be seen that some grains break down into cells more readily than others. This may be due to two causes. The breakdown of a grain into cells may be influenced by the orientation of the grain with respect to the stress axis, or the breakdown may be influenced by the constraints which the neighbouring grains impose on any particular grain.

The second point of interest in Fig. 12 is the distribution of cell sizes within a given grain. It appears that not only is the cell structure more marked near the grain boundaries, but also that the cells are rather smaller in size in these regions. Although this is not the case with every grain boundary, the occurrence of the phenomenon is by no means uncommon.

Apart from the tendency towards smaller cells in the grain-boundary regions, Fig. 12 also shows that there is a very finely rumpled region adjacent to the grain boundaries. Much of this fine rumpling is not revealed at low magnifications (see Fig. 10). The apparently very disturbed nature of the grain boundary may be due to irregular grain-boundary migrations. This would be the case if the boundaries were revealed at intermediate stages in their migration across a narrow region. Some of the disturbed region is probably due to this cause, but some of it is probably the result of fine fragmentation of the grains in the boundary regions. Some support for the fragmentation idea can be gained from Fig. 13 (Plate XXV), which shows the same area as that in Fig. 12 after repolishing and etching.

Fig. 13 reveals several important points. In the repolished and etched specimen two series of boundaries can be seen. One set is very marked, and appears as definite black lines. Within these marked boundaries are fine networks of lines which are not as marked as the first set. By comparison of Figs. 12

and 13 it can be seen that the more heavily marked boundaries coincide fairly closely with the original grain boundaries. The small misfits could easily be accounted for by boundary migrations. Moreover, the less-marked boundaries of Fig. 13 coincide with the cell boundaries of Fig. 12. This explains the difference between the two boundaries. The etching of a boundary depends on the disorientation across it. Thus the grain boundaries with a large disorientation across them are heavily etched, whereas the cell boundaries across which only a small disorientation exists, are only lightly etched. Two points can be learned from these observations. Firstly, recrystallization in the usual sense has not occurred, because the original grain boundaries can still be revealed by repolishing and etching and no new grain-boundary networks appear. This can perhaps be seen more clearly at a lower magnification (Figs. 10 and 11). Secondly, the fact that cells can be revealed by repolishing and etching indicates that they are discrete blocks of crystal lattice with a small but clear-cut disorientation at their boundaries. The slopes seen on the surface of the deformed specimen then correspond to the disorientation of definite blocks and not to a general distortion of the grains.

From the difference between grain and cell boundaries it is now possible to get some further information from Fig. 13 concerning the regions adjacent to the grain boundaries. In the annealed condition (Fig. 2, Plate XXIV), the grain boundaries are quite smooth but repolishing and etching shows that the boundaries have become very ragged after deformation. The ragged nature of the boundaries fits in with the small cells in the boundary regions. Very small blocks or plates can also be seen lying close to the grain boundaries. From the fairly heavy etching of these blocks, it appears that there is a somewhat greater disorientation between them than is generally found between cells. This supports the view that a debris of fine blocks is formed in the grain-boundary regions. Such a debris could result from the relative movements of grains under such conditions that the grain-boundary flow occurs only with some difficulty.

The idea of a debris of fine crystallites in the grain boundaries can be used to explain the X-ray-diffraction pattern given by the deformed specimen. Continuous diffraction circles might be expected to arise from such a debris of fine crystallites and mask any discrete diffraction spots due to the larger cells within the grains. This is the result obtained after slow deformation at 200° C. The diffraction pattern shown in Fig. 9 consists of continuous circles in which a few weak intensity maxima can be seen. The pattern obtained does not change with continued deformation after the specimen has been strained more than about 5%.

In general, it has been found that grain-boundary flow occurs more readily the higher the temperature of deformation. On this basis, it might be expected that less debris would be formed in the grain-boundary regions during deformation at higher temperatures.

This indeed appears to be the case. Fig. 14 (Plate XXV) shows the diffraction pattern from a specimen slowly strained at 250° C. The continuous circles of the pattern are much weaker than those of the pattern obtained from a specimen strained at 200° C. (Fig. 9, Plate XXIV) and the discrete spots are much more apparent, indicating that the amount of fine crystallite debris, which gives rise to the continuous circles, has been reduced. This view is confirmed by the microstructure obtained by repolishing and etching the specimen (Fig. 15, Plate XXV). The grain boundaries are seen to be much less ragged than in the previous case, indicating that the number of small cells and crystallite debris is greatly reduced in the boundary region.

The amount of debris in the grain boundaries decreases further as the temperature of deformation is raised until at 350° C. almost no debris is formed. This is shown by the X-ray pattern (Fig. 16, Plate XXV), which consists almost entirely of discrete spots with only very faint continuous circles. The microstructure after repolishing and etching the specimen (Fig. 17, Plate XXV), reveals that the grain boundaries after deformation are almost as smooth as the original annealed grain boundaries seen in Fig. 2 (Plate XXIV).

3. STRESS/STRAIN CURVES AT VARIOUS TEMPERATURES

The stress/strain curves for specimens slowly strained at various temperatures are shown in Fig. 18. The

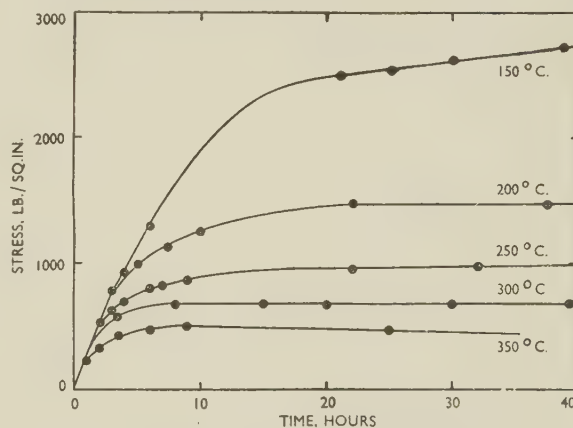


FIG. 18.—Stress/Strain Curves for Specimens Strained at 0.15%/hr. at Various Temperatures.

stress is that required to maintain the constant slow rate of strain. It is interesting to compare the shapes of these curves with the metallographical aspects of deformation. In the curves a horizontal portion indicates that continued strain-hardening is absent. Comparison shows that it is when slip ceases to be an operative mechanism that strain-hardening is almost entirely absent. This occurs at temperatures of about 200° C. At higher temperatures deformation takes place almost entirely by relative grain movements

and cell formation, and strain-hardening is absent, as was previously found by Wood and Rachinger¹¹ for aluminium.

IV.—DISCUSSION

The present work differs from the preceding researches on aluminium, already mentioned, in that it introduces the concept of what has been described as debris at the grain boundaries. It appears that the zone between neighbouring grains is broken down during slow deformation into much smaller cells than those in the body of the grain. This is due presumably to the mechanical anisotropy of the hexagonal magnesium, which renders it less ductile in a polycrystalline aggregate than the cubic aluminium. As viewed by the authors, the relative movement of the grains at the boundaries causes localized rumpling and twisting of the structure, and thus produces lines of high elastic strain where the atomic separation is momentarily larger than normal. Dislocations then drift to these regions, relieving the strain and forming sub-boundaries between what then become small cells or crystallites of slightly different orientation. This, in a

sense, is what other workers have termed polygonization in the case of deformation by slip. However, it can occur in magnesium, as in aluminium, when there is no slip. Moreover, the larger cells, whose shape can clearly be seen both before and after etching the deformed surfaces, have not the regular appearance predicted by the slip-polygonization theories. Therefore the authors prefer the more general interpretation of the "fragmentation" of the grains.

There is nothing in the observations to show how stable the sub-boundaries may be in the boundary zone. Presumably fresh distortions of the structure take place as more relative grain movements occur, and so give rise to further sub-boundaries. As a result there will be a tendency to decrease the average size of the resulting cells. This would explain the continuous ring which forms the background to the reflection spots from the larger cells.

ACKNOWLEDGEMENTS

The authors wish to express their thanks to Professor J. N. Greenwood for encouragement and advice, and to their colleagues at the Baillieu Laboratory with whom many points were discussed.

REFERENCES

1. W. A. Wood, G. R. Wilms, and W. A. Rachinger, *J. Inst. Metals*, 1951, **79**, 159.
2. G. B. Greenough and E. M. Smith, *ibid.*, 1950, **77**, 435.
3. E. A. Calnan and B. D. Burns, *ibid.*, 1950, **77**, 445.
4. R. C. Gifkins, *ibid.*, 1951, **79**, 233.
5. A. H. Cottrell and V. Aytakin, *ibid.*, 1950, **77**, 389.
6. J. A. Ramsey, *ibid.*, 1951-52, **80**, 167.
7. W. Betteridge and A. W. Franklin, *ibid.*, 1951-52, **80**, 147.
8. P. A. Jacquet, *Métaux, Corrosion-Usure*, 1944, **19**, 71.
9. W. A. Wood and J. W. Suiter, *J. Inst. Metals*, 1951-52, **80**, 501.
10. C. S. Barrett and C. T. Haller, Jr., *Trans. Amer. Inst. Min. Met. Eng.*, 1947, **171**, 246.
11. W. A. Wood and W. A. Rachinger, *J. Inst. Metals*, 1949-50, **76**, 237.

THE EFFECT OF CERTAIN SOLUTE ELEMENTS ON THE RECRYSTALLIZATION OF COPPER *

1431

By V. A. PHILLIPS,† A.R.S.M., B.Sc., D.Eng., A.I.M., MEMBER,
and PROFESSOR ARTHUR PHILLIPS,‡ D.Eng.

SYNOPSIS

Using the method developed by Thorley (*J. Inst. Metals*, 1950, **77**, 141), activation energies were calculated for the two stages postulated in Cook and Richards' theory of recrystallization (*ibid.*, 1947, **73**, 1) from hardness results on pure copper and binary alloys containing small amounts of phosphorus, silver, cadmium, arsenic, tellurium, and oxygen. The materials, of 0.010–0.018 mm. initial grain-size, were cold-rolled to 95% reduction and annealed isothermally at 35.6°–400° C. The two activation energies, although nearly equal for pure copper and some alloys, differed considerably in, for example, alloys containing 0.01 at.-% arsenic or less.

A variation with temperature of the slope of x (fraction recrystallized) versus $\log t$ (t = annealing time) plots and of $1/T$ (reciprocal absolute annealing temperature) versus $\log t_{\frac{1}{2}}$ (time for 50% recrystallization) plots, was found for certain alloys, as predicted from the theory.

Approximate measurements were made of growth and nucleation rates; they varied exponentially with temperature for pure copper. The growth rate, G , was constant with t for pure copper and three alloys. The rate of nucleation N at 215.8° C. decreased with increase in t for a 0.021 at.-% phosphorus alloy. $\log G$ and $\log N$ were approximately inversely proportional to $\log t_{\frac{1}{2}}$ for all the materials.

Structures were studied micrographically and by X-rays, and pole figures determined on alloys containing 0.021 at.-% phosphorus, 0.0271 at.-% silver, 0.018 at.-% cadmium, and 0.047 at.-% arsenic, annealed at 350° C. The effect of grain-size and of rolling reduction from 90 to 97.5% was explored for pure copper and two alloys with phosphorus.

I.—INTRODUCTION

Cook and Richards¹ have established that severely cold-rolled copper strip will, under suitable conditions, recrystallize at temperatures as low as the ambient temperature. They concluded that the phenomenon was closely linked with the formation of a highly-preferred cubically oriented recrystallization texture. It has long been known that even minute amounts of certain solutes greatly raise the temperature at which pure copper will soften or recrystallize after cold working. It is also known² that quite small amounts of certain solutes have little effect on the texture developed by cold working, but greatly influence the recrystallization texture.

The object of the present work was to study the effect of a number of solutes on the low-temperature recrystallization of high-purity copper after severe cold-rolling. By using 99.999+ % purity copper as a basis material and making up oxygen-free alloys, it has proved possible to study the effect of adding as little as 0.001% of another element. With the exception of tellurium and oxygen, the additions were within the solid-solubility limits at room temperature.^{3, 4} The tellurium alloys were solution-treated to retain all the tellurium in solution. Because oxygen is almost always present in copper and little is known of its effect on recrystallization, an oxygen alloy was

included, in spite of the fact that this would contain a second constituent, namely cuprous oxide.

The slow rate of the annealing process at low temperatures enabled the changes in structure to be examined in detail; the velocity of recrystallization was determined from measurements of the diamond pyramid hardness, as in the work of Cook and Richards.⁵ Since recrystallization follows the general exponential law of change, the measurement of the time to recrystallize to a given extent at constant temperature provides a more sensitive method of studying the influence of composition than isochronous short-time tests. Furthermore, the isothermal data lend themselves more readily to mathematical treatment than isochronous data and enable activation energies to be derived. Accordingly, after a number of preliminary tests in which the effect of such factors as the initial grain-size of the strip, the degree of cold rolling, and the annealing temperature were explored, the rates of recrystallization were determined on strips of 16 alloys of a controlled grain-size, cold-rolled to approximately 95% reduction, and annealed isothermally for various times at 35.6°–400° C.

II.—THEORETICAL

Thorley⁶ has shown how separate activation energies can be calculated for the two stages postulated in the Cook and Richards⁵ theory of the recrystalliza-

* Manuscript received 4 June 1951; in revised form 18 August 1952.

† Investigator, British Non-Ferrous Metals Research

Association, London; formerly at Yale University, New Haven, Conn., U.S.A.

‡ Professor of Metallurgy, Yale University, New Haven, Conn., U.S.A.

tion of heavily cold-rolled copper. Since these activation energies were similar if not identical for the high-purity tough-pitch copper studied, some of the more interesting consequences of the theory were not revealed.

1. CALCULATION OF ACTIVATION ENERGIES P AND Q

The derivation from the Cook and Richards' theory of the accurate equation for the variation of the fraction recrystallized with annealing time has been given by Thorley.⁶ He showed that:

$$\ln \frac{1}{1-x} = A \left\{ t + \frac{1}{\beta} (e^{-\beta t} - 1) \right\} \quad (1)$$

which contains no approximations for β , and in which x is the fraction recrystallized after annealing time t (hr.).

$$A = ae^{-Q/RT} \quad (2)$$

where a is a constant independent of time, R is the gas constant, T is the absolute annealing temperature, and Q is an activation energy for the second stage of recrystallization.

$$\beta = be^{-P/RT} \quad (3)$$

where β is a constant varying with temperature, b a constant independent of time, and P an activation energy for the first stage of recrystallization.

If t is very small in equation (1), so that $e^{-\beta t} \rightarrow 1 - \beta t$, then $x = 0$, and Thorley points out that there will be a short initial period in which the amount of recrystallized material is almost zero and the rate of increase of x is small. For large values of t , $e^{-\beta t} \rightarrow 0$ and equation (1) becomes:

$$\ln \frac{1}{1-x} = A(t - t_0) \quad (4)$$

where $t_0 = \frac{1}{\beta}$, i.e. $\ln \frac{1}{1-x}$ is linear with t for high values of t and has a slope A and an intercept t_0 on the t axis.

Since from (2)

$$\ln A = \ln a - Q/RT \quad (5)$$

and from (3)

$$\ln \beta = \ln b - P/RT \quad (6)$$

by plotting $\ln A$ and $\ln t_0$ against $1/T$ for various annealing temperatures from Cook and Richards' data, Thorley obtained linear curves whose slopes yielded P and Q .

2. VARIATION OF SLOPE OF x VERSUS $\ln t$ PLOT WITH TEMPERATURE

As pointed out previously,⁷ the slope of the x versus $\ln t$ plot should be independent of temperature if and only if $P = Q$.

Thus from (1) consider conditions at $x = \frac{1}{2}$, where $e^{-\beta t}$ is small compared with 1, i.e. $t_{\frac{1}{2}}$ (half-recrystallization time) is within the straight portion of the $\ln \frac{1}{1-x}$ versus t plot.

$$\text{Then } \ln 2 = A \left(t_{\frac{1}{2}} - \frac{1}{\beta} \right)$$

$$\text{or } t_{\frac{1}{2}} = \frac{1}{\beta} + \frac{\ln 2}{a}$$

$$t_{\frac{1}{2}} = \frac{1}{b} \cdot e^{P/RT} + \frac{\ln 2}{a} \cdot e^{Q/RT} \quad (7)$$

Differentiating (1):

$$\frac{1}{1-x} \cdot \frac{dx}{dt} = A(1 - e^{-\beta t}) \quad (8)$$

or, at $x = \frac{1}{2}$, neglecting $e^{-\beta t}$

$$\left(\frac{dx}{dt} \right)_{x=\frac{1}{2}} = \frac{1}{2} A \quad (9)$$

$$\begin{aligned} \left(\frac{dx}{d(\ln t)} \right)_{x=\frac{1}{2}} &= \frac{1}{2} A t_{\frac{1}{2}} \\ &= \frac{1}{2} \left(\ln 2 + \frac{a}{b} \cdot e^{\frac{P-Q}{RT}} \right) \text{ from (2) and (7)} \end{aligned} \quad (10)$$

Thus the slope of the x versus $\ln t$ plot is dependent on temperature except when $P = Q$. Consequently, when the rate of recrystallization is measured for a particular material at different temperatures and the fraction recrystallized is plotted against the logarithm of the annealing time, the family of curves obtained do not superimpose according to the theory when displaced along the $\ln t$ axis, except as a special case when $P = Q$. It is clear from equation (10) that the effect of temperature on the slope is dependent on the values of the temperature-independent constants a and b as well as on P and Q .

3. VARIATION OF THE SLOPE OF $1/T$ VERSUS $\ln t_{\frac{1}{2}}$ PLOT WITH TEMPERATURE

As shown previously,⁷ the Cook and Richards' theory further predicts that the slope of the $\ln t_{\frac{1}{2}}$ versus $1/T$ plot should not be linear except as an approximation when $1/T \rightarrow \infty$, i.e. when T diminishes. Thus putting $1/T = \phi$ in equation (7) and differentiating:

$$\begin{aligned} \frac{d}{d\phi} (\ln t_{\frac{1}{2}}) &= \frac{\frac{Q}{R} \cdot \frac{\ln 2}{a} \cdot e^{\frac{Q}{R} \cdot \phi} + \frac{P}{R} \cdot \frac{1}{b} \cdot e^{\frac{P}{R} \cdot \phi}}{\frac{\ln 2}{a} \cdot e^{\frac{Q}{R} \cdot \phi} + \frac{1}{b} \cdot e^{\frac{P}{R} \cdot \phi}} \\ &= \frac{Q}{R} - \left(\frac{Q-P}{R} \cdot \frac{1}{1 + \frac{b \ln 2}{a} \cdot e^{\frac{Q-P}{R} \cdot \phi}} \right) \end{aligned} \quad (11)$$

Therefore if $Q > P$, as $\phi \rightarrow \infty$, the slope of the $\ln t_{\frac{1}{2}}$ versus $1/T$ plot $\rightarrow Q/R$ and increases to this value. Alternatively, since:

$$\begin{aligned} \frac{d}{d\phi} (\ln t_{\frac{1}{2}}) &= \frac{P}{R} - \left(\frac{P-Q}{R} \cdot \frac{1}{1 + \frac{a}{b \ln 2} \cdot e^{\left(\frac{P-Q}{R}\right) \cdot \phi}} \right) \end{aligned} \quad (12)$$

if $P > Q$, as $\phi \rightarrow \infty$, the slope $\rightarrow P/R$ and increases to this value.

If $P = Q$, the second term in equations (11) and (12) is zero and the slope is constant and equal to P/R (or Q/R). However, if $P \neq Q$, it is necessary to evaluate the second term in order to decide whether it can be neglected in a given case.

III.—EXPERIMENTAL PROCEDURE

1. PREPARATION OF MATERIALS

The copper used was of 99.999+ % purity and details of its manufacture have been reported pre-

The alloys were melted in closed high-purity graphite crucibles in a high-frequency induction furnace and solidified in the crucible. Phosphorus, cadmium, arsenic, and tellurium additions were made in the form of hardener alloys containing 15.0, 0.24, 0.12, and 0.195 % alloying element, respectively, in order to minimize melting losses. The hardener alloys were prepared from 99.999+ % purity copper, except the phosphorus-containing alloy, for which commercial high-purity copper was used. Silver was added directly as 99.99 % purity foil. In each case the copper was held molten for about 5 min. in order to permit thorough deoxidation by the graphite of the

TABLE I.—Analyses and Annealing Treatments Used in the Preparation of Starting Strips.

Alloy No.	Calculated Addition, Wt.-%	Homogenization		Addition by Analysis		Annealing Temperatures, °C.				Average Grain-Size, mm.
		Time, hr.	Temp., °C.	Wt.-%	At.-%	After First 3-Way Compression	After Second 3-Way Compression	After Compression to Strips		
								First Anneal	Re-Anneal	
Strips for Exploratory Tests (0.300 in. Thick)										
Cu(3) <i>S</i> * Cu(3) <i>L</i> *	} none	none	none	460	350	{ 270 + 310	310 850	0.023 1.2-1.5
P-L(4) <i>S</i> P-L(4) <i>L</i>	} 0.0010 P	40	860	0.00086	0.00175	480	380	{ 410 410	... 850	0.042 0.3 (some 1.0-4.0)
P-H(7) <i>S</i> P-H(7) <i>L</i>	} 0.010 P	40	860	0.0102	0.0208	500	380	{ 460 460	... 850	0.055 0.9-1.2
Strips for Main Tests (0.400 in. Thick)										
Cu(1) Cu(21) <i>t</i> † Cu(21) <i>b</i> †	} none	{ ... 40	{ ... 850	} none	none	400	220	280	...	0.010
P-L(5) P-M(6) P-H(20)	0.0010 P 0.0050 P 0.010 P	40	850	{ 0.0012 0.0056 0.0103	0.0025 0.0114 0.0210	510 490 500	300 320 340	280	300	{ 0.012 0.013 0.012
Ag-L(9) Ag-M(10) Ag-H(11)	0.0050 Ag 0.010 Ag 0.050 Ag	40 43 40	850 850 850	0.0050 0.0088 0.0453	0.0030 0.0053 0.0271	500 450 570	270 270 350	280 280 330 350	0.014 0.014 0.017
Cd-L(12) Cd-M(13) Cd-H(14)	0.0050 Cd 0.010 Cd 0.050 Cd 12 650	... 0.0085 0.032	... 0.0049 0.018	560 570 650	340 370 395	280 330 380	300 350 ...	0.018 0.016 0.016
As-L(15) As-M(16) As-H(17)	0.0050 As 0.010 As 0.050 As	40	800	{ 0.0055 0.011 0.055	0.0047 0.0094 0.047	430 480 480	245 265 275	280	...	{ 0.013 0.018 0.014
Te-L(18) Te-M(19)	0.00050 Te 0.00150 Te	1.3 3	790 † 850 †	... 0.0015	... 0.00075	400 560	240 395	280 280	... 300	0.014 0.013
O(8)	... O	0.032	0.126	280	0.013

* *S* and *L* refer to small and large initial grain-size in the strip, respectively.

† Bottom half *b* of the ingot was homogenized for comparison with untreated top half *t*.

‡ Solution treatment. Ingots were water-quenched after this treatment.

viously.⁸ A quantity of this copper was remelted for the pure copper ingots and a further supply was used to make up 15 alloys having compositions shown in Table I. The notation in the first column of Table I was employed to identify the alloys: -L, -M, and -H signify the lowest, medium, and highest alloying addition in each case.

crucible before the hardener was added. After the charge had been held molten for a further 15 min. the crucible was lowered out of the furnace at approximately 1 in./min. with the power still on. In this way oxygen-free, pipeless ingots were obtained, approximately 1.1 in. square by 3 in. long and weighing about 1½ lb. The one alloy with oxygen was

prepared by pouring an oxygen-free melt of copper through the air into an open graphite mould, the piped portion of the ingot being discarded.

Every precaution was taken throughout the work to maintain the purity of the materials. Thus the copper in the charge was cleaned by pickling in 1:1 nitric acid, washing, pickling in warm 1:1 hydrochloric acid, washing in tap and distilled water, and drying in a hot-air oven. Iron contamination from the tool was removed after every machining operation by similar pickling.

The composition of the alloys was checked by analysis, except where the additions were too small to permit this (Table I). Samples for analysis were taken from the homogenized material (from the cast ingot in the case of the oxygen alloy). Samples from both the top and bottom of the cast ingot P-H(7) were analysed, but showed no significant difference. Spectrographic analysis of the strips prepared from the pure copper ingots Cu(1), Cu(3), and Cu(21)*t* showed faint traces of calcium, possibly due to handling with the fingers; traces of lead estimated to be less than 0.0005%; traces of silver of the order of 0.00001%; and, in Cu(1) only, a trace of zinc too small to be estimated. No other impurities were detected.

Dendritic markings spaced about 0.01 in. apart appeared on the surface when the ingots were etched in dilute nitric acid. A light etch revealed them clearly in the phosphorus and arsenic series of alloys, but a heavy etch was required to reveal them in the silver and cadmium series. Even in the copper of 99.999+ % purity it was possible to reveal dendrites after careful surface preparation and prolonged etching. For a particular solute the markings produced by etching for the same time were clearer the higher the solute content. Fig. 1 (Plate XXVI) shows markings on the alloy P-H(20) that are typical of those obtained, and resemble markings observed previously on cast copper-base alloys.⁹ Since the markings were presumably due to segregation of the solute, the ingots that showed pronounced markings on etching were homogenized (Table I). After these treatments the markings revealed by etching were scarcely perceptible in any of the materials. All the homogenization and annealing treatments (Table I), with the exception of the annealing of O(8), were carried out in an atmosphere of nitrogen ($7 \pm 1\%$) hydrogen mixture in order to avoid oxidation.

All the ingots except O(8) were cut into two roughly cube-shaped pieces, which were compressed alternately between the three pairs of faces in order to cold work the material severely without changing its shape or producing a marked texture. The compression was carried out between polished and greased steel plates, and the direction of compression was changed after compressing 10%, or in some cases 20%, in order to avoid barrelling. The first three-way compression consisted of six 10% stages (three 20% stages for Cu(3), P-L(4), and P-H(7)), after which the materials were annealed for 1 hr. They were then subjected to a further compression consisting of nine

10% stages (six for Cu(3), P-L(4), and P-H(7)), and again annealed (Table I).

The roughly cube-shaped pieces of Cu(3), P-L(4), and P-H(7) were now compressed by about 60% reduction, one half of the material to 0.300 in. and the other half to 0.320 in. The 0.300-in. thick materials were annealed to a fine grain-size, while the 0.320-in.-thick materials were annealed, compressed to 0.300 in., and finally annealed at 850° C., giving a coarse grain-size (Table I). The cube-shaped pieces of the remaining materials were compressed (and cold-rolled in some cases) to a thickness of 0.400 in. and then annealed. Samples which appeared to be incompletely annealed, as judged from the microstructure and hardness, were re-annealed at a higher temperature.

Grain-sizes were measured on all the materials. Estimates were made on cross-sections using a lineal-analysis method ($\pm 5\%$ accuracy), except on Cu(3)*L*, P-L(4)*L*, and P-H(7)*L*, where measurements were made on the surface of the strips by comparison with standard charts. The grain-sizes of all the 0.400-in.-thick strips were within the range 0.010–0.018 mm. A number of these strips were examined by means of a glancing X-ray technique and found to be random in orientation.

The oxygen alloy ingot O(8) was heated to 850° C. and forged alternately between the three pairs of faces in order to break up the network of cuprous oxide. It was then heated to 850° C., hot rolled to 0.58 in. thickness, and, when cold, compressed alternately in two directions to a final thickness of 0.400 in. Annealing gave a grain-size of 0.013 mm.

2. COLD ROLLING AND ANNEALING

The Cu(3), P-L(4), and P-H(7) *S* and *L* strips were each cold-rolled to three final thicknesses, namely 0.030, 0.015, and 0.0075 in., corresponding to reductions of 90, 95, and 97.5% respectively. These materials were stored at room temperature. The 0.400-in.-thick strips of all the remaining alloys were cold-rolled 95% to 0.020 in. thickness, except one batch comprising Cu(21) and O(8), which were rolled (in error) 93.8% to 0.025 in. thickness. Undue heating during rolling was avoided by using small passes and immersing the strips in cold water between passes. The 0.400-in.-thick strips were rolled in 6 batches at 2- or 3-day intervals, the batches comprising: (i) phosphorus alloys, (ii) cadmium alloys, (iii) silver alloys, (iv) arsenic and tellurium alloys, (v) Cu(21) *t* and *b* and O(8), and (vi) Cu(1). The alloys in any one batch were passed through the rolls in sequence, and put into the annealing baths at about the same time; thus the beginning of the annealing of the six batches was staggered. The 0.020 in.-thick materials were stored in a cold box below -30° C. when they were not in the annealing baths or undergoing tests. However, in the case of some of the most stable materials, supplementary tests involving anneals at temperatures above 215.8° C. were carried out later on material which had been stored at room temperature for about 4 months.

Annealing was carried out in five oil baths ranging in temperature from 36° to 216° C. (Table II). For additional short-time anneals, a silicone fluid bath was used for temperatures up to 380° C., controlled to

TABLE II.—Annealing Bath Temperatures.

Bath No.	Cu(3), P-L(4), and P-H(7)		All Other Alloys	
	Mean Temp., °C.	Standard Deviation, °C.	Mean Temp., °C.	Standard Deviation, °C.
1	35.5	0.5	35.6	0.4
2	71.4	1.2	82.8	2.8
3	101.4	1.6	117.0	2.1
4	132.8	1.4	169.4	2.3
5	165.8	2.3	215.8	4.2

$\pm 2^\circ$ C., and a lead bath was used for anneals at 400° C., controlled to $\pm 5^\circ$ C. Separate specimens were obtained for each annealing time for all the strips which had been rolled 95% or 93.8%. It was necessary, however, to quench a whole strip to room temperature in order to cut off a specimen and replace the remainder in the bath. This procedure was found to be satisfactory.

3. TESTING

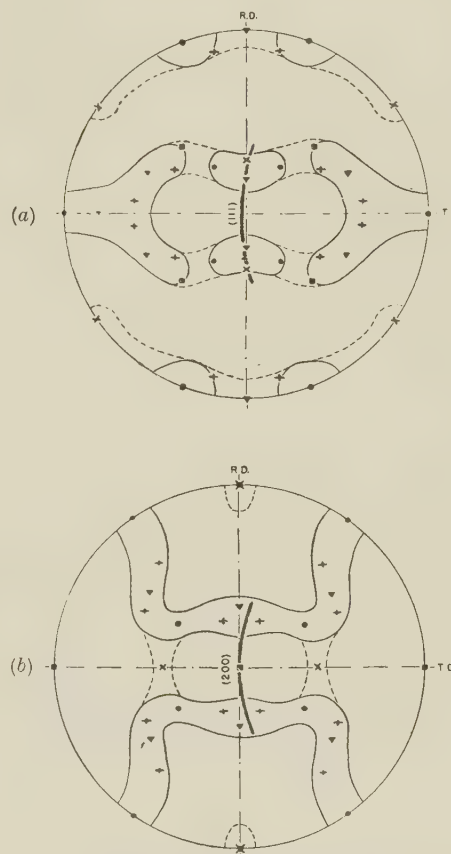
The microstructure was examined in sections parallel to the surface of the strip or in longitudinal or transverse cross-sections. Care was taken in the preparation and testing of all specimens to ensure no appreciable temperature rise. All specimens were polished by an electrolytic method described by Jacquet,¹⁰ and an electrolytic "sulphide filming" etch, previously employed on brasses,¹¹ was used. After etching, the worked material appeared dark and rough under vertical illumination, while the cubically aligned grains appeared bright.

The structure was also examined by a glancing-angle X-ray method developed by Yen.¹² The specimen was mounted with its surface inclined at 25° to the X-ray beam about an axis transverse to the rolling direction, and photographed using copper radiation. It was not considered necessary to etch away the surface before examination, since photographs taken on the surface of a number of strips were identical with further photographs taken after etching to expose the middle of the strips. The portions of the 111 and 200 Debye-Scherrer rings recorded in the glancing-angle photographs, superimposed on the (111) and (100) pole figures of cold-rolled copper,^{2, 13} are shown in Fig. 21 (a) and (b), due to Yen.¹²

The method used for the pole-figure determinations was as follows: Samples were dissolved to 0.003 in. thickness in dilute nitric acid, and transmission photographs were taken, using copper radiation. Photographs were taken at approximately 10° intervals, one series with the incident beam in the plane containing the rolling direction and the normal to the rolling plane, and a second series with the beam in the

plane containing the transverse direction and the normal to the rolling plane. Intensities were judged visually from the photographs and classified into four groups, according to the degree of blackening. No correction was made for the varying absorption at different angles of incidence.

Hardness tests were made on the as-rolled surface of the strips, using the Tukon tester fitted with a Vickers diamond pyramid indenter. Experience showed that more representative hardness values were obtained using a 3.5-kg. load than with smaller loads, although there may have been slight errors in determining the hardness of the almost completely annealed strips,



[Courtesy American Institute of Mining and Metallurgical Engineers.]

FIG. 21.—Ideal Orientations Superimposed upon Outline of the (a) (111) and (b) (100) Pole Figures of Cold-Rolled Copper. The shaded arc at vertical position represents the portion of 111 and 200 Debye-Scherrer rings produced in glancing photographs. Orientations indicated: ● (110) [112], ▼ (112) [111], + (124) [533], ■ (100) [001], × (110) [001]. (Yen.)

owing to the anvil effect. In general, the average of four tests, two on each surface of the strip, was used; if the scatter was more than a few hardness numbers, further tests were made.

It was found possible micrographically to identify the recrystallized grains when they were about 0.001 mm. in dia., but no changes were apparent in glancing-angle X-ray photographs before the appearance of discrete spots due to the recrystallized grains. The

spots did not appear until a later stage corresponding to a substantial decrease in hardness. On the other hand, glancing-angle photographs provided a more sensitive indication of the presence of small amounts of residual worked material than either hardness tests or micrographic examination.

IV.—EXPERIMENTAL RESULTS

1. STRUCTURE OF COLD-ROLLED STRIPS

Micro-examination of the rolled strips showed that the initial annealed crystals were elongated in the rolling direction and reduced in thickness. The rolling texture was consistent with the usual (110) $[\bar{1}12]$ plus (112) $[11\bar{1}]$ ideal orientations,² but in addition the less frequently reported^{13, 14} minor texture (100) [001] was always present, resulting in an intensity maximum at the centre of the 200 arc in the glancing-angle photographs, as shown in Fig. 7 (Plate XXVI). The rolling texture appeared to be independent of composition, and the tests on the Cu(3), P-L(4), and P-H(7) alloy strips of two widely different initial grain-sizes, showed that it was also independent of variation in rolling reduction from 90 to 97.5% and of grain-size in the range studied. The independence of initial grain-size agrees with previous work.¹⁵

Deformation markings were observed in the etched condition on cold-rolled strips of, for example, Cu(3), P-L(4), and P-H(7). The common type consisted of fairly continuous and fairly straight bands running across a grain and varying in direction from grain to grain. As many as three sets of different directions were observed inside one grain, but generally only one set was visible and sometimes none. Two sets are visible in one of the grains shown in Fig. 2 (Plate XXVI). In two specimens only a wavy type of marking was observed, as illustrated in Fig. 3 (Plate XXVI), closely resembling deformation markings previously reported in compressed iron.² The specimen of P-L(4)*L* shown in Fig. 3 was partially recrystallized, and several new grains can be seen.

2. STRUCTURE OF ANNEALED STRIPS

The early stages of recrystallization were studied in rolling-plane sections of strips of Cu(3)*S*, Cu(3)*L*, P-L(4)*S*, and P-L(4)*L*. It was observed that recrystallization almost invariably began at the deformation markings and only rarely at grain boundaries, and it reached an advanced state in some of the deformed grains before it had begun in others. This is shown in Fig. 4 (Plate XXVI), where the field covers a part of about ten of the original grains, whose boundaries are visible approximately parallel to the rolling direction. Owing to the low magnification, the tiny recrystallized grains appear as dark specks, clearly revealing the deformation markings along which they have formed. Adcock¹⁶ similarly found that recrystallization began along the deformation markings in copper-nickel alloys.

The pure copper Cu(3)*S* with an average original grain-size of 0.023 mm. gave a predominantly cube recrystallization texture after rolling to 90, 95, or 97.5% reduction and annealing in the range 35.5°–165.8° C. (Figs. 5 and 8, Plate XXVI). When the initial grain-size of Cu(3) was increased to 1.4 mm., the amount of cube texture formed was greatly decreased (Figs. 5 and 6, Plate XXVI). In contrast to the behaviour of Cu(3), variation of the initial grain-size of P-L(4) from 0.042 to 0.3 mm. had little effect on the texture, which was fairly random and contained only a small proportion of cube texture (Figs. 9 and 10, Plate XXVI). P-H(7)*L* and *S* rolled 97.5% did not recrystallize during an anneal of 772 hr. at 165.8° C., but the textures after a 1-hr. anneal at 500° C. were almost completely random (Figs. 11 and 12, Plate XXVI).

In Cu(3)*S* and *L* and P-L(4)*S* and *L*, the amount of cube texture tended to increase as the rolling reduction was increased from 90 to 95 to 97.5% as shown for Cu(3)*S* by Figs. 5 and 8 (Plate XXVI). A glancing X-ray photograph of Cu(3)*S* rolled to 90% reduction and annealed (Fig. 8, Plate XXVI) shows the presence of the cube texture, a secondary texture indicated by the subsidiary maxima to either side of centre of the (111) arc, and also some grains of random orientations. Fig. 5 (Plate XXVI) shows that both the subsidiary texture and the random grains were less evident after 97.5% reduction. The secondary texture corresponded fairly well to the (112) $[11\bar{1}]$ ideal orientation, but could also correspond approximately to a first-order twin of the cubically aligned material. A comparison of Figs. 7 and 8 (Plate XXVI) shows that the subsidiary maxima do not coincide exactly with the intensity maxima in the rolling texture, so that the formation of this secondary texture must involve some reorientation of the worked material.

The recrystallization textures of samples of Ag-H(11), P-H(20), Cd-H(14), and As-H(17), cold-rolled to 95% reduction and annealed for 1 hr. at 350° C., were completely determined by means of pole figures (Fig. 22 (a)–(d)). The annealing temperature of 350° C. was low enough to avoid much grain growth.

The pole figure of Ag-H(11) showed that all the grains had orientations within 12° of the ideal orientation (100) [001], and most were within 10° of this orientation (Fig. 22 (a)). By contrast, the texture of P-H(20) was quite random, and no maxima of the highest intensity were present (Fig. 22 (b)) as in the other pole figures (Fig. 22 (a), (c), and (d)). The main orientations present in P-H(20) could be described as a mixture of (110) $[\bar{1}12]$, (112) $[11\bar{1}]$, and (110) [001]; thus the addition of 0.021 at.-% phosphorus suppressed the cube texture. Previous workers¹⁷ had found that 0.05 wt.-% phosphorus suppressed the cube texture. Fig. 22 (b) closely resembles the pole figure determined by Yen.¹²

The texture of Cd-H(14) (Fig. 22 (c)) was more complex than the textures of Ag-H(11) and P-H(20).

Thus, whereas some of the main intensity maxima could be described as (100) [001], others could best be described as a mixture of (110) $[\bar{1}12]$ and (124) $[53\bar{3}]$, with some (112) $[11\bar{1}]$. A similarity may be noted between this pole figure and that characteristic of 70 : 30 brass,² in which all the main maxima are close to the (113) $[2\bar{1}1]$ orientation. However, the maxima in the Cd-H(14) pole figure are not

to the first-order twins of (100) [001] fall within second-order intensity regions in the Cd-H(14) pole figure, and twins were observed inside the cubically oriented grains in the microstructure of a specimen annealed for 1 hr. at 350° C. However, the second-order intensity regions could not be described adequately in terms of the first-order twin orientations alone.

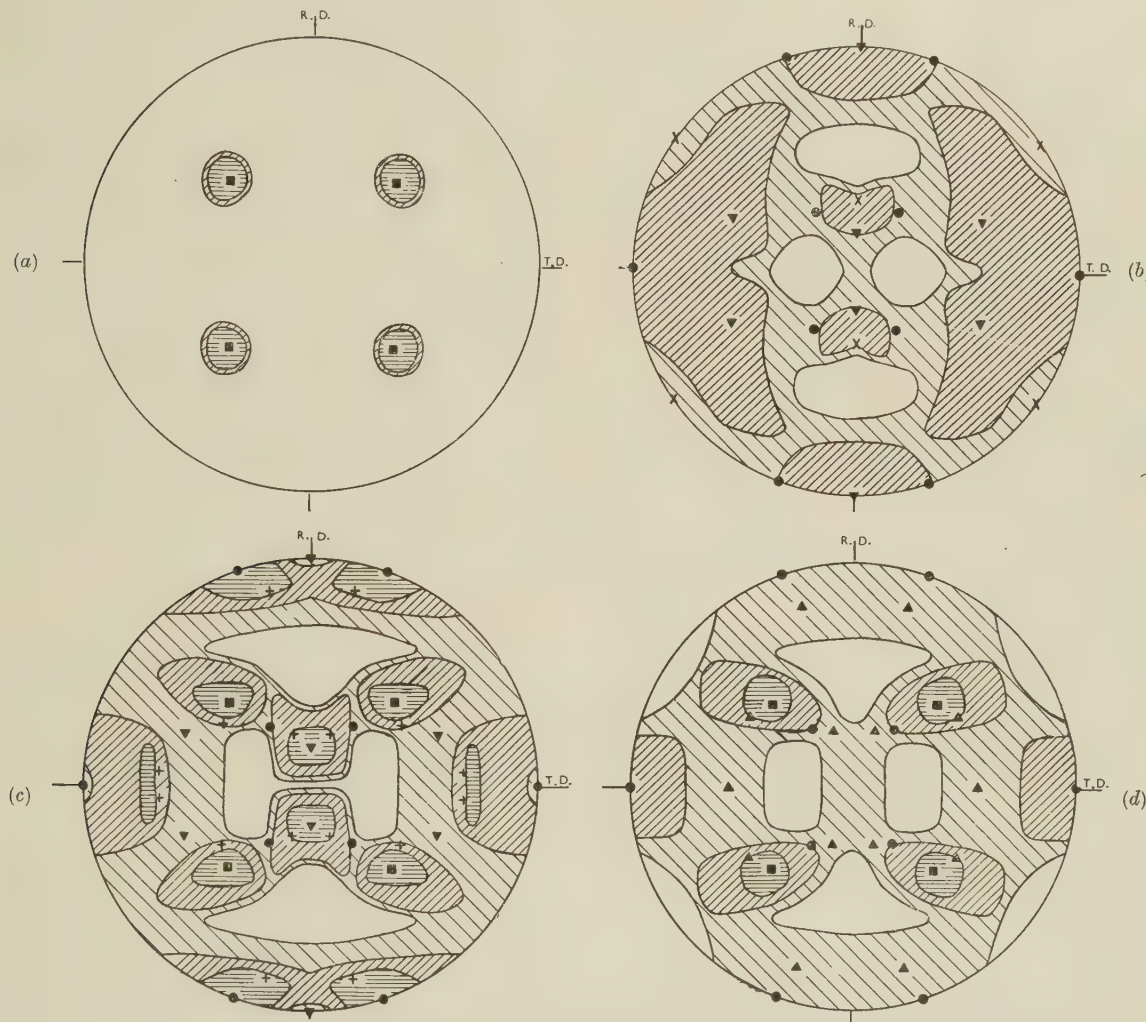


FIG. 22.—(111) Pole Figures. Alloy annealed at 350° C. for 1 hr. (a) Ag-H(11). (b) P-H(20). (c) Cd-H(14). (d) As-H(17).

KEY.
 ■ (100) [001] ▼ (112) $[11\bar{1}]$ + (124) $[53\bar{3}]$ ● (110) $[\bar{1}12]$ ▲ (113) $[2\bar{1}1]$ × (110) [001]

adequately accounted for by the (113) $[2\bar{1}1]$ orientation. Since the pure copper gave a nearly perfect cube texture, the cadmium addition may be regarded as tending to suppress the cube texture and helping to retain the rolling texture. However, some re-orientation occurred during recrystallization, since the maxima on the (111) arcs in the glancing-angle X-ray photograph of Cd-H(14) annealed at 350° C. do not coincide exactly with the maxima on the (111) arcs in the photograph of the rolling texture as shown in Fig. 14 (Plate XXVIII). The ideal orientations corresponding

The pole figure of As-H(17) (Fig. 22 (d)) showed that the orientation of the majority of the grains was close to the (100) [001] ideal orientation, whereas the orientations of the other grains covered a wide range which could best be described as a mixture of (110) $[\bar{1}12]$ and (113) $[2\bar{1}1]$. Arsenic thus tended to suppress the cube texture, but per atom added was much less effective than either phosphorus or cadmium. Previous workers also had found that arsenic tended to suppress the cube texture in copper.¹⁸

After annealing at 350° C. for 1 hr. Cu(1), Cu(21)t,

Cu(21)b, Ag-L(9), Ag-M(10), Ag-H(11), Cd-L(12), Cd-M(13), As-L(15), As-M(16), Te-L(18), Te-M(19), and O(8) all gave a nearly perfect cube texture (Figs. 13 and 14, Plates XXVII and XXVIII). On the other hand, P-L(5), Cd-H(14), and As-H(17) gave a mixed texture containing cubically aligned material. Increase of phosphorus content tended to suppress the cube texture; thus the texture of P-M(6) and P-H(20) was fairly random.

As shown by Figs. 13 and 14, in instances where alloys recrystallized at more than one temperature during annealing in the range 35.6°–215.8° C., increase of temperature caused no change in recrystallization texture which could be generalized. Usually, however, when the cube texture was formed, some grains of other orientations were present after annealing in this range, but were absent after annealing at 350° C. Previous workers⁵ had similarly found an increase in the amount of cube texture in copper with increase in annealing temperature over the range 100°–900° C. There was no evidence that increase of temperature led to a greater degree of perfection of the cube texture.

Figs. 15 and 16 (Plate XXIX) show microstructures which are typical of longitudinal and rolling-plane sections, respectively, of strips which had recrystallized readily at 35.6° or 82.8° C. and possessed the cube recrystallization texture. One or two grain boundaries are visible inside the largest white area in Fig. 15, and in places in Fig. 16 the original grain boundaries are still visible together with deformation markings. It will be noted that in both sections the recrystallized grains tend to be elongated in the rolling direction. The tiny round spots inside the white grains are etch pits which appeared to have no regular shape related to the structure. Although occurring only in the strips that recrystallized readily at low temperatures, this coarse elongated structure is not peculiar to recrystallization carried out at a particularly low temperature, since the same structure was observed in Cu(21)t whether recrystallized at 82.8° or 215.8° C.

The grains in P-H(20) as shown in Fig. 19 (Plate XXIX), and, as in the other strips which tended to give a random texture on recrystallization, revealed no tendency to elongation in the rolling direction. The structure in P-H(20) was some ten times finer than that of the pure coppers. Whereas the addition of 0.021 at.-% phosphorus to pure copper in P-H(20) greatly retarded recrystallization and changed the recrystallization texture, the addition of 0.0271 at.-% silver in Ag-H(11) greatly retarded recrystallization without changing the texture. The latter alloy showed very little elongation of the growing cubically oriented grains in the rolling direction, and the structure was much finer than in the pure coppers, as can be seen in Fig. 20 (Plate XXIX).

It was noted in partially recrystallized samples that in places the boundaries between the new grains and residual deformed material were inclined at approximately 45° to the rolling direction, although in general

the boundaries were ragged or irregularly rounded. Figs. 16 and 17 (Plate XXIX) show examples of this phenomenon in a rolling-plane section of Cu(21)t partially recrystallized by annealing in boiling water. In Fig. 16 one or two of the original grains elongated as a result of the rolling are almost completely surrounded by recrystallized cubically oriented material. The latter appears to have grown into an isolated grain at a number of points along its boundary, and it is easy to envisage how in time a worked grain might be split up into small islands of worked material. Such observations suggest that the twin-like inclusions inside the cubically oriented grains in Figs. 16 and 17 (Plate XXIX), whose boundaries make angles of about 45° to the rolling direction, are residual islands of deformed material. The fact that they appeared brown and rough after etching confirms this view.

The boundaries of the cubically aligned grains in Cu(21)t appeared dark after etching and were often irregular in thickness, as in Fig. 18 (Plate XXIX), where they may be seen linking "islands" of worked material. They were not observed to be discontinuous. A few grains of orientations differing from the cubic are visible in both Figs. 17 and 18. These appeared brown and smooth after etching, and showed distinct boundaries with both worked and cubically aligned recrystallized grains. Some contained twins making angles other than 45° to the rolling direction.

3. RECRYSTALLIZED GRAIN-SIZE

The grain-sizes of a number of the alloys were determined by means of lineal analysis on longitudinal

TABLE III.—*Effect of Annealing Time and Temperature and of Composition on the Grain-Size of Strips Rolled to 95% Reduction.*

Alloy No.	Original Average Grain-Size, mm.	Annealing Time, hr.	Annealing Temp., °C.	Average Grain-Size, mm.
P-L(5) As-H(17)	0.012 0.014	1538 1538	} 169.4 {	0.007 0.014
P-L(5) { P-M(6) P-H(20) As-H(17) {	0.012 0.012 0.013 0.012 0.014 0.014	96 1538 1538 1538 24 1538		0.007 0.007 0.009 0.010 0.010 0.013
P-L(5) P-M(6) P-H(20) Cd-H(14) As-H(17)	0.012 0.013 0.012 0.016 0.014	} 1	350	0.015–0.090 * 0.014 0.016 0.008 0.015

* The structure was a mixture of these two average grain-sizes, as estimated by comparison with the A.S.T.M. Standard Grain-Size Charts.

or cross-sections (Table III). In all cases the times of annealing were sufficient to permit complete recrystallization.

The grain-size of P-L(5) was the same after 96 hr. as after 1538 hr. at 215.8°C ., whereas that of As-H(17) was only slightly greater after 1538 hr. than after 24 hr. at 215.8°C . (Table III). Owing to the low boundary energy between grains of similar orientation, the grain-sizes of the wholly cubically aligned specimens would be expected to be even more stable. No change in texture should therefore have occurred in specimens that were kept in the annealing baths for a longer time than that necessary for complete recrystallization, before taking glancing-angle X-ray photographs, as shown by Figs. 13 and 14 (Plates XXVII and XXVIII).

With the exception of that of P-L(5) annealed at 350°C ., all the grain-sizes of the strips containing non-cubically aligned material (Table III), were very fine, unlike those of the totally cubically aligned strips, which were of the order of 0.1 mm. Increase of annealing temperature from 169.4°C to 215.8°C caused no significant change in the grain-sizes of P-L(5) and As-H(17). Further increase of annealing temperature to 350°C caused no significant change in the grain-size of As-H(17), though it presumably resulted in considerable grain growth in P-L(5) because the microstructures consisted of a mixture of small and large grains.

4. RATES OF RECRYSTALLIZATION

(a) From Hardness Measurements

Following Cook and Richards,⁵ the rate of recrystallization was determined from diamond pyramid

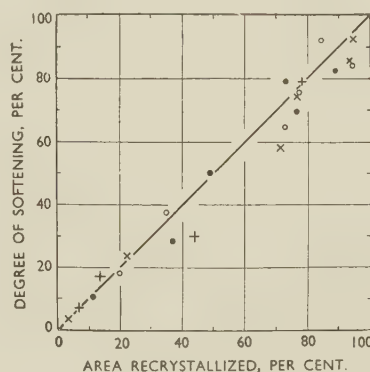


FIG. 23.—Correlation of Degree of Recrystallization with Degree of Softening.

KEY.
 ● Cu(1), 82.8°C . × Ag-M(10), 117.0°C .
 ○ Ag-L(9), 82.8°C . + Ag-H(11), 215.8°C .

hardness measurements, the relation between hardness and degree of recrystallization being first established.

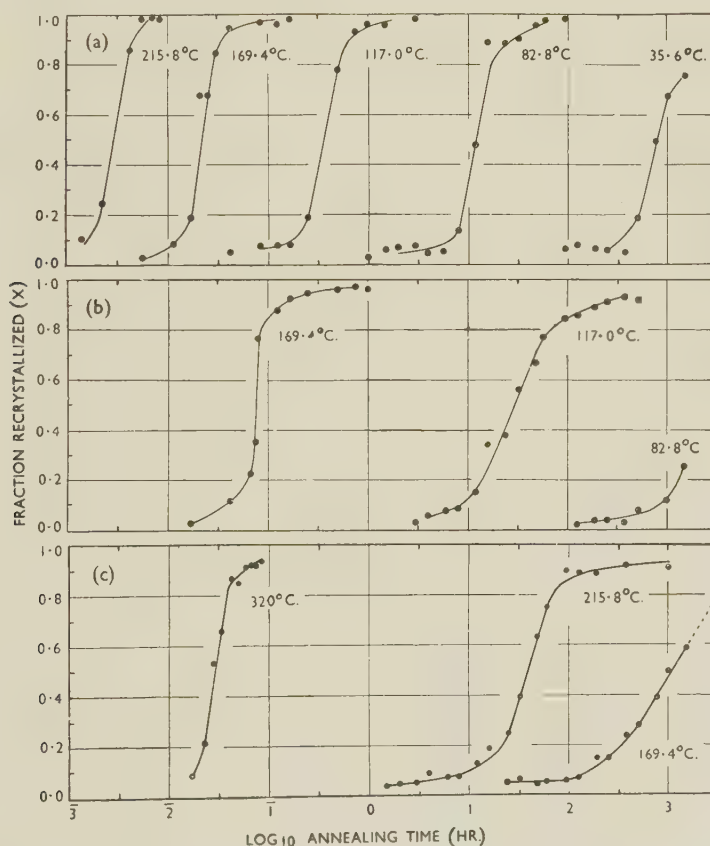


FIG. 24.—Variation of the Fraction Recrystallized, Calculated from the Hardness, with Annealing Time.

(a) Cd-M(13). (b) As-L(15). (c) P-M(6).

Microsections of strips of Cu(1), Ag-L(9), Ag-M(10), and Ag-H(11) annealed to various stages of recrystallization were prepared in a pack. Usually two areas on a longitudinal section and two on a cross section were examined at a magnification of $\times 150$.

The percentage of the area occupied by the white recrystallized regions was determined by making a tracing (4×3 in.) from the image projected on the ground-glass screen of the projection microscope. The tracing was afterwards placed over a sheet of

TABLE IV.—*Estimated Degree of Recrystallization and Corresponding Hardness Values (3.5 kg. Load).*

Cu(1) 82-8° C.			Ag-L(9) 82-8° C.			Ag-M(10) 117-0° C.			Ag-H(11) 215-8° C.		
Area Re-crystallized, %	D.P.H. No.	Softening, %	Area Re-crystallized, %	D.P.H. No.	Softening, %	Area Re-crystallized, %	D.P.H. No.	Softening, %	Area Re-crystallized, %	D.P.H. No.	Softening, %
0	114.5	0	0	116.5	0	0	113.5	0	0	118.5	0
11.5	107	10.5	20	103	18	3.5	111	3.5	7	113	7
37	94	28.5	35	88	37.5	22.5	96.5	23.5	13.5	105.5	17
49	78.5	50	73	67.5	64.5	71	71.5	58	44	95.5	30
76.5	64.5	69.5	77.5	59	75.5	76.5	60	74	78.5	58.5	79
73	57.5	79	94.5	52.5	84	93.5	51.5	85.5
89	55	82.5	84.5	46.5	92	94.5	46.5	92.5
100	42.5	100	100	40.5	100	100	41	100	100	42.5	100

TABLE V.—*The Effect of Annealing Time and Temperature on Diamond Pyramid Hardness Values (1).*

Time of Anneal	Cu(1) 215-8° C.	Cu(1) 169-4° C.	O(8) 215-8° C.	O(8) 169-4° C.	Cu(21)† 215-8° C.	Cu(21)† 169-4° C.	Cu(21)‡ 215-8° C.	Cu(21)‡ 169-4° C.	Te-L(18) 215-8° C.	Te-L(18) 169-4° C.	Te-M(19) 169-4° C.	Ag-L(9) 215-8° C.	Ag-L(9) 169-4° C.
0 sec.	114.5	114.5	120.5	120.5	115	115	115.5	115.5	119	119	116	116.5	116.5
5 "	115.5	...	117	...	113	...	110.5	116	117.5
10 "	87.5	...	114	...	82.5	112	90	111.5	...	115.5	113.5
15 "	49	115.5	93	115.5	51	...	57	113.5
20 "	50	...	60	...	47.5	114.5	51.5	105	...	106.5	111.5
25 "	46.5	...	48
30 "	...	112.5	49	115.5	47	110.5	49	100.5	...	80.5	81.5	...	117
40 "	49	...	47.5	101	47	87	...	48	69
45 "	...	93	...	114	46.5	119
50 "	43	...	47	88	45	48.5	48
1 min.	43	54.5	49	86	47	49	47	69.5	43	46	43.5	45.5	71.5
1.5 "	69	73.5
2 "	62	44
2.5 "	...	50	50	53.5	47	48.5	46	51.5	43	43.5	45	43.5	46
5 "	...	47	47	50.5	...	48	...	49.5	41.5	41	44	43.5	44.5
7.5 "	...	44.5	...	51	...	47	...	50.5	41
10 "	48.5	47.5	42.5
15 "	49	47
30 "	50
16 hr.	42.5	42.5	...	43	41.5	40.5	...
24 "	41

Time of Anneal	Ag-M(10) 215-8° C.	Ag-M(10) 169-4° C.	Ag-H(11) 320° C.	Cd-L(12) 215-8° C.	Cd-L(12) 169-4° C.	Cd-M(13) 215-8° C.	Cd-M(13) 169-4° C.	Cd-H(14) 400° C.	Cd-H(14) 380° C.	As-L(15) 215-8° C.	As-H(17) 270° C.	P-L(5) 280° C.	P-M(6) 320° C.
0 sec.	116	116	121	117.5	117.5	118	118	119	119	116	127	113.5	122
5 "	113	115	110.5	116
10 "	96.5	112.5	99.5	113	...	118	...
15 "	52.5	112.5	122.5	53.5	...	116	...	108.5
20 "	48	112	44	116	55	...	114	...
25 "	43.5
30 "	47	113.5	80	...	115	44	...	114	...	43.5	124	108	...
40 "	44	96.5	43.5	112	44.5	...	99	...
45 "	...	110	61.5	116
50 "	44.5	71	42.5	43.5	...	90.5	...
60 "	46.5	105	57.5	45.5	48	45	104	105.5	111	47.5	120	76	115.5
70 "	70	...
75 "	49	67	103
80 "	59	105
90 "	...	81.5	45.5
100 "	67	92	116.5
105 "	43	96	54.5	80
110 "	54.5
2 min.	...	50.5	42.5	94	...	95	52.5	70
2.5 "	43.5	49	...	45.5	45.5	45.5	47	69.5	...	43.5	68.5	48.5	53.5
3 "	40.5	60.5	94.5	...	54.5	...	54
3.5 "	60	52.5	...	50
4 "	66.5	...	48	...	49.5
4.5 "	49.5
5 "	44.5	43.5	...	44	45	44	45.5	49.5	63	42.5	47	...	48
6 "	48
7 "
7.5 "	...	45	43.5	...	46	47	48
10 "	...	44.5	44.5
15 "	...	44
1 hr.
16 "	41	42.5	42

abscissa and fraction recrystallized equal to the percentage softening as ordinate.

The growth rates of Cu(1) at 35.6° C., P-H(20) at 215.8° C., Ag-L(9) at 82.8° C., and Ag-H(11) at 215.8° C. were determined by plotting the largest dimension of the largest grain visible in a section against the annealing time as shown in Figs. 25 and

Time of Anneal	P-H(20) 340° C.	P-H(20) 290° C.	Cu(1) 117-0° C.	Cu(1) 82-8° C.	O(8) 117-0° C.	Cu(21) 117-0° C.	Cu(21) 82-8° C.	Cu(21) 117-0° C.	Cu(21) 82-8° C.	Te-L(18) 117-0° C.	Te-L(18) 82-8° C.	Te-M(19) 215-8° C.	Te-M(19) 117-0° C.	Te-M(19) 82-8° C.
0 sec.	129	129	114-5	114-5	120-5	115	115	115-5	115-5	119	119	116	116	116
20 "	115
40 "	106
60 "	78
80 "	61-5	...	115	...	118	115-5	...	115	...	114	116	44	116	...
100 "	50-5
2 min.	46
2-5 "	...	120	114-5	...	119-5	115	...	115	...	113	114-5	44	114-5	...
5 "	...	115	114-5	...	118	114	...	114-5	...	78-5	115	...	109-5	...
7-5 "	...	115	114-5	...	119-5	114-5	...	108	...	53-5	114	...	82-5	...
9 "	...	111
10 "	...	102	111	...	118-5	113	...	100-5	...	48-5	113-5	...	61	...
12-5 "	...	91-5
13-5 "	...	87-5
15 "	...	69-5	102	...	114	99	...	80-5	...	43-5	115-5	...	49	...
17-5 "	...	60-5
20 "	...	60-5	79	...	109	87-5
22-5 "	...	55	73
25 "	...	53-5	66	...	100
27-5 "	63
30 "	...	47-5	57-5	117-5	83	63	116-5	58	115	43-5	114	...	40	114-5
45 "	51	...	68-5	50-5	...	53-5	109	...	43	...
1 hr.	47	118	56-5	46	119	47-5	118	43	103	42	43	114
1-5 "	47-5	116-5	61	...	117	45	114-5	...	80-5	111
2 "	43-5	116	57	...	116-5	45-5	114	...	62-5	100
3 "	115	53-5	...	116-5	46-5	113-5	...	48	61-5
4 "	107	53-5	...	111-5	...	100	...	42-5	48
6 "	94	50-5	...	81-5	...	77	...	42-5	43-5
8 "	76-5	50	...	83	...	68	42
12 "	64-5	49	...	63-5	...	50-5
16 "	57-5	48-5	...	60-5	...	48	41-5
24 "	52-5	47-5	...	51-5	...	45	...	42-5	42-5
32 "	55	48-5
48 "	46-5	46-5	...	46-5
59 "	47	45-5
96 "	46-5	47-5

Time of Anneal	Ag-L(9) 117-0° C.	Ag-L(9) 82-8° C.	Ag-M(10) 117-0° C.	Ag-H(11) 290° C.	Cd-L(12) 117-0° C.	Cd-L(12) 82-8° C.	Cd-M(13) 117-0° C.	Cd-M(13) 82-8° C.	Cd-H(14) 360° C.	As-L(15) 169-4° C.	As-M(16) 215-8° C.</
----------------	----------------------	---------------------	-----------------------	---------------------	-----------------------	----------------------	-----------------------	----------------------	---------------------	-----------------------	-------------------------

TABLE VII.—The Effect of Annealing Time and Temperature on Diamond Pyramid Hardness Values (3).

Time of Anneal	Cu(1) 35-6° C.	O(8) 82-8° C.	O(8) 35-6° C.	Cu(21) 35-6° C.	Cu(21) 35-6° C.	Te-M(18) 35-6° C.	Te-M(19) 35-6° C.	Ag-L(9) 35-6° C.	Ag-M(10) 82-8° C.	Ag-M(10) 35-6° C.	Ag-H(11) 215-8° C.	Ag-H(11) 169-4° C.	Ag-H(11) 117-0° C.	Ag-H(11) 82-8° C.
0 hr.	114.5	120.5	120.5	115	115.5	119	116	116.5	116	116	118	118	118	118
0.5 "	...	116
1 "	...	117.5	115
1.5 "	111.5
2 "	112.5
3 "	...	118.5	115
4 "	...	119	114
6 "	...	116	114	118.5	...
8 "	...	107.5	107.5
12 "	...	94.5	104.5	119	118
16 "	...	92.5	91.5
24 "	115	79	117	115	114	70.5	...	118	117.5	117.5	120.5
32 "	115	74.5	115.5	114.5	115.5	53
48 "	115.5	67.5	117.5	116	115.5	53	...	118.5	119.5	117	118
59 "	116.5	61	116.5	114.5	116	50.5
96 "	115	55.5	117	114	113	64.5	109.5	112	50	115	118	119.5	116	116
128 "	114.5	49	118.5	114	112	49.5	90	111.5	52.5	114	115.5
192 "	117	49.5	119	117	111	45.5	61.5	109.5	51	113	113	118.5	118	120
250 "	117.5	46.5	118.5	115	108	44	53.5	110.5	49.5	117	113
384 "	117	...	117.5	112.5	85	44.5	46.5	106	51	116	105.5	119	117.5	118
512 "	112.5	...	117	100	68	43	46	96.5	51	113	95.5
768 "	98	...	113	82.5	59.5	70.5	...	112.5	75	119	120.5	118
1019 "	95	...	110	69.5	57.5	60	47	113	58.5	117.5	120.5	118.5
1272 "	85.5
1468 "	101	51.5	52
1538 "	117	52	122	121	120

Time of Anneal	Cd-L(12) 35-6° C.	Cd-M(13) 35-6° C.	Cd-H(14) 215-8° C.	Cd-H(14) 169-4° C.	Cd-H(14) 117-0° C.	As-L(15) 117-0° C.	As-L(15) 82-8° C.	As-L(15) 35-6° C.	As-M(16) 117-0° C.	As-M(16) 82-8° C.	As-M(16) 35-6° C.	As-H(17) 169-4° C.	As-H(17) 117-0° C.	As-H(17) 82-8° C.
0 hr.	117.5	118	119	119	119	116	116	116	120	120	120	127	127	127
0.5 "	113.5
1 "	118	116	120	127
1.5 "	112.5
2 "	112
3 "	114	115
4 "	112	129
6 "	110.5
8 "	110	116.5
12 "	105	117.5	120.5	124.5	129.5
16 "	91	114.5
24 "	119	118	...	88	115.5	...	117	118	...	124.5	128.5	129.5
32 "	120.5	121	118.5	74.5	116	...	115	120
48 "	120	121	118.5	66.5	114.5	...	115	118.5
59 "	115	112	120.5	121.5	119	59	115	...	112.5	116.5	...	119	128	129
96 "	113.5	113.5	...	121.5	117	53.5	113	...	115	116
128 "	110.5	112.5	120.5	120.5	118	52.5	114.5	114	110.5	118.5	117.5	107.5	127	130
192 "	113.5	113.5	119.5	121.5	117	50	113	...	111	89
250 "	81.5	114	117	119.5	117.5	48.5	113	114	107	115.5	120	74.5	126.5	129
384 "	83.5	114.5	119.5	120	119	47	114	...	101	58	125	...
512 "	52.5	104	116	117	116.5	48	110.5	115	94.5	118	117	51	123.5	130
768 "	66.5	81	115	121	118	115.5	90	...	116	50.5	126	...
1019 "	46.5	67	109.5	121	117	...	107.5	117	83.5	116	119	47.5	126.5	130.5
1538 "	...	61	101	97.5	119	75.5	45.5	...	130.5

TABLE VIII.—The Effect of Annealing Time and Temperature on Diamond Pyramid Hardness Values (4).

Time of Anneal	As-H(17) 35-6° C.	P-L(5) 169-4° C.	P-L(5) 117-0° C.	P-L(5) 82-8° C.	P-L(5) 35-6° C.	P-M(6) 215-8° C.	P-M(6) 169-4° C.	P-M(6) 117-0° C.	P-M(6) 82-8° C.	P-M(6) 35-6° C.	P-H(20) 215-8° C.	P-H(20) 169-4° C.	P-H(20) 117-0° C.
0 min.	127	113.5	113.5	113.5	113.5	122	122	122	122	122	129	129	129
5 "	...	112	124.5
10 "	...	113
15 "	...	114
30 "	...	111.5	120.5
45 "	...	111
1 hr.	...	110.5	119	124	126	...
1.5 "	...	110	111	119
2 "	...	108.5	118.5	123.5
3 "	...	107.5	118	122
4 "	...	105.5	115	122.5	126.5	...
6 "	...	104	111.5	116.5	120
8 "	...	98	116	119
12 "	...	89	115.5	112	120.5	124.5	...
16 "	...	76.5	107.5	...	122	118.5
24 "	...	73	111.5	114	...	102.5	118	...	125.5	...	116.5	...	126.5
32 "	...	64.5	113.5	90	117	122.5	114	124.5	...
48 "	...	63	112	72	118.5	109
59 "	...	59.5	111	114.5	...	62.5	118	121	122	...	100.5	124.5	127.5
96 "	...	55.5	112	51	117.5	67.5
128 "	126	57	110.5	114.5	112.5	51.5	116.5	120	123	119.5	58.5
192 "	...	54.5	111.5	52	111	54	122	128
250 "	127	52	111	114.5	113	...	110.5	118	122.5	120	52.5	121	127
384 "	...	54	105.5	49	103.5	52	119.5	...
512 "	126.5	...	104.5	114.5	112	...	100	125	123.5	120	51	118.5	126
768 "	125.5	...	95.5	112	91.5	51	118.5	125
1019 "	130.5	50.5	91.5	111.5	112.5	50	83	121.5	123	121.5	48.5	114.5	124.5
1538 "	130	54	83	42	75.5	124	123.5	...	47.5	115.5	...

26 and measuring the slope (Table IX). Where more than one microsection was examined, the figure quoted for the size of the largest grain in Table IX is an average value. The results, which refer to the

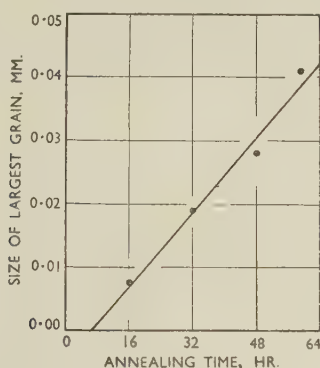


FIG. 25.—Variation of Size of Largest Grain with Annealing Time at 215.8° C. for P-H(20).

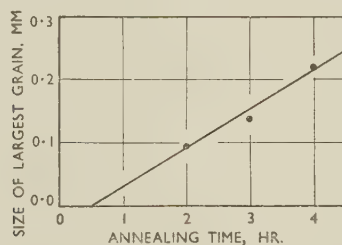


FIG. 26.—Variation of Size of Largest Grain with Annealing Time at 82.8° C. for Ag-L(9).

early stages of recrystallization before impingement of the growing grains occurred, show that the growth rate remained constant with annealing time. On extrapolation the curves intersected the time axis at a positive value. This "incubation period" was found to be small compared with the time required for complete recrystallization. It should be noted that the growth rates here are twice the more usual "radial growth rates".

TABLE IX.—Variation of Size of Largest Grain with Annealing Time.

Alloy No.	Annealing		No. of Sections Examined			Size of Largest Grain, mm. $\times 10^{-2}$	Growth Rate Determined Graphically, mm./sec.	Half-Softening Time, hr.
	Time, hr.	Temp., °C.	C*	L*	R*			
Cu(1)	250	35.6	1	5.5	5.62×10^{-8}	1900
	768		...	1	...	14.5		
P-H(20)	16	215.8	1	1	...	0.75	2.06×10^{-7}	80
	32		1	1	...	1.9		
	48		1	1	...	2.8		
	59		1	1	...	4.1		
Ag-L(9)	2	82.8	2	2	...	9.5	1.69×10^{-6}	4.83
	3		1	1	...	14.0		
	4		2	1	...	22.0		
Ag-H(11)	250	215.8	2	2	...	3.0	3.13×10^{-8}	700
	384		3	3	...	4.8		
	512		1	1	...	5.5		

* C = Cross section; L = Longitudinal section; R = Rolling-plane section.

An approximate method was used to measure the growth rates of other materials (Table X), using in each case only one annealing time. The largest dimension of the largest grain in a photomicrograph generally at $\times 200$ magnification was measured. This figure divided by the annealing time gave the approximate growth rate. Where more than one microsection was examined the figure quoted for the growth rate in Table X is an average value. Specimens were selected at an early stage in recrystallization so that effects due to impingement of the growing

TABLE X.—Effect of Composition and Temperature on the Growth Rate.

Alloy No.	Annealing Temp., °C.	Annealing Time	No. of Observations of \bar{G} Averaged		Growth Rate (\bar{G}), mm./sec.	$\log_{10} \bar{G}$	$\log_{10} t_{\frac{1}{2}}$
			C*	L*			
Cu(1) Cd-L(12)	35.6	† 192 hr.	1	1	5.62×10^{-8}	8.75	3.28
			1	1	4.15×10^{-7}	7.62	2.53
Cu(1) Cu(21)t Cu(21)b Ag-L(9) Ag-M(10) Cd-L(12) Cd-M(13) Te-L(18) Te-M(19) O(8)	82.8	4, 6, 8 hr.	2	3	7.35×10^{-6}	6.87	0.86
		6 hr.	1	...	5.55×10^{-6}	6.75	0.88
		4 hr.	1	1	1.28×10^{-5}	5.11	0.76
		†	5	4	1.69×10^{-5}	5.23	0.68
		12 hr.	1	...	6.41×10^{-6}	6.81	1.32
		3 hr.	1	...	2.38×10^{-5}	5.38	0.60
		8 hr.	1	...	1.39×10^{-5}	5.14	1.08
		1 hr.	1	1	6.25×10^{-5}	5.50	0.18
		2 hr.	1	1	3.13×10^{-5}	5.80	0.39
		8 hr.	1	1	4.90×10^{-6}	6.69	1.32
	100.0	1.5 hr.	3R†	...	5.55×10^{-5}	5.74	...
	117.0	15 min.	2	2	1.67×10^{-4}	4.22	1.82
Te-L(18)	169.4	20 sec.	1	...	4.0×10^{-3}	3.60	3.92
Cu(21)t P-L(5) P-M(6) P-H(20) Ag-M(10) Ag-H(11) Cd-H(14) As-L(15) As-M(16) As-H(17)	215.8	10 sec.	1	...	2.0×10^{-2}	2.30	3.44
		30 min.	1	...	9.70×10^{-6}	6.99	0.08
		24 hr.	1	...	2.01×10^{-7}	7.30	1.57
		†	4	4	2.06×10^{-7}	7.32	1.90
		10 sec.	1	...	2.0×10^{-2}	2.30	3.52
		†	6	6	3.13×10^{-8}	8.50	2.84
		1538 hr.	1	...	3.15×10^{-9}	9.50	3.31
		15 sec.	1	...	3.70×10^{-3}	3.57	3.71
		2.5 min.	1	...	1.16×10^{-3}	3.06	2.74
		2 hr.	1	...	5.95×10^{-6}	6.77	0.56

* C = Cross section; L = Longitudinal section; † R = Rolling-plane section. ‡ See Table IX.

grains were avoided. The method involves the assumption that the growth rate is constant with annealing time, and the incubation period is neglected.

(c) From Nucleation-Rate Measurements

The average number of new grains/unit area was determined on a number of materials at an early stage in recrystallization. Photomicrographs of etched cross and/or longitudinal sections were prepared, generally at $\times 400$, and the number of grains was counted in 18 squares of side 1 cm. picked at random from a larger area. These are recorded in Table XI. On materials Cu(1) at 82.8° C., P-H(20) at 215.8° C., and Ag-H(11) at 215.8° C. samples recrystallized to varying degrees were examined in this way, but on

other materials only a single sample was examined (Table XI).

The method described by Johnson¹⁹ was used to calculate the number of grains/unit volume in P-H(20) and Ag-H(11) annealed for varying times to different degrees of recrystallization. The grains in each planar area group ($2^{2\frac{1}{2}-W}$ to $2^{1\frac{1}{2}-W}$ in.², where $W = 1, 2, 3 \dots$) were counted on photographs at $\times 400$ magnification

in a square of side 4 in. (a rectangle 6 in. \times 4 in. in the case of Cu(1) annealed for 4 hr. at 82.8° C.). The counts were made on a single cross section, except on Ag-H(11) annealed for 768 hr. at 215.8° C., where a single longitudinal section was used. The proportion of the volume occupied by each size group was computed from the planar size distribution and the fraction recrystallized was calculated from the

TABLE XI.—Effect of Time, Temperature, and Composition on the Number of Grains/Unit Area in Planar Sections.

Alloy	Annealing		Sections Examined		Average No. of Grains/cm. ² $\times 10^{-5}$	Calculated Fraction Non-Re-crystallized	$n = \frac{n \times 10^{-5} \text{ Av. No. of Grains/cm.}^2}{\text{Fraction Non-Re-crystallized}}$	$N' = \frac{n}{\text{time (sec.)}}$	$\text{Log}_{10} N'$	$\text{Log}_{10} t_{\frac{1}{2}} \text{ (t in hr.)}$
	Time, hr.	Temp., °C.	C *	L *						
Cu(1)	768	35.6	1	1	6.8	0.77	8.8	0.32	1.51	3.28
Cd-L(12)	192		1	1	4.3	0.97	4.5	0.65	1.81	2.53
Cu(1)	4		1	1	3.8	0.90	4.2	29	1.46	0.86
Cu(21)t	6		2	1	4.7	0.71	6.5	30	1.48	
	8		1	...	5.9	0.38	15.6	54	1.73	
Cu(21)t	6		1	2	4.7	0.54	7.7	36	1.56	0.88
O(8)	8	82.8	1	...	5.1	0.79	6.4	22	1.34	1.32
Ag-L(9)	3		1	1	7.3	0.82	8.9	82	1.91	0.68
Cd-L(12)	3		1	...	4.0	0.89	4.5	42	1.62	0.60
Cd-M(13)	8		1	...	12.2	0.87	14.0	49	1.69	1.08
Te-L(18)	1		1	...	7.0	0.79	8.8	245	2.39	0.18
Te-M(19)	2		1	...	5.5	0.78	7.0	97	1.99	0.39
Te-L(18)	0.0055	169.4	1	...	8.0	0.85	9.5	48,000	4.68	3.92
Cu(21)t	0.0028	215.8	1	...	7.0	0.56	12.6	125,000	5.10	3.44
P-L(5)	0.5		1	...	8.6	0.84	10.2	567	2.75	0.08
P-M(6)	24		1	...	18.4	0.77	23.9	28	1.45	1.57
P-H(20)	48		1	1	19.6	0.81	24.2	14	1.15	1.90
Ag-M(10)	0.0028		1	...	5.0	0.73	6.8	67,400	4.83	3.52
Ag-H(11)	384		1	1	6.1	0.84	7.3	0.53	1.72	2.85
Cd-H(14)	1538		1	...	19.2	0.75	25.6	0.46	1.66	3.31
As-L(15)	0.0042		1	...	9.3	0.81	10.3	68,100	4.83	3.71
As-M(16)	0.042		1	...	7.8	0.68	11.6	7,670	3.88	2.74
As-H(17)	2		1	...	19.5	0.83	23.5	327	2.51	0.56

* C = Cross section; L = Longitudinal section.

TABLE XII.—Number of Grains/Unit Area and Unit Volume Computed from Planar Size Distribution.

Alloy	Annealing		Fraction Non-Re-crystallized Calculated from Hardness (f)	$D \times 10^{-5}$ $D = \text{No. of Grains/cm.}^2$	$N' = \frac{D}{ft \text{ (sec.)}}$	$B \times 10^{-7\frac{1}{2}}$ $B = \text{No. of (Spherical) Grains/c.c.}$	$N \times 10^{-3}$ $N = \frac{B}{ft \text{ (sec.)}}$	$\frac{B}{D} \times 10^{-3}$	$\frac{B}{f} \times 10^{-9}$	$\text{Log}_{10} \frac{B}{f}$
	Time t , hr.	Temp., °C.								
P-H(20)	16	215.8	0.93	14.6	27.2	271	160	13.0	9.19	9.963
	32		0.87	11.8	11.8	180	56.7	10.7	6.54	9.816
	48		0.81	22.6	16.2	458	104	14.2	17.93	10.254
	59		0.71	20.3	13.5	388	81.3	13.4	17.30	10.238
	96		0.31	31.0	28.9	538	159	12.2	54.80	10.739
	128		0.19	31.0	35.5	497	180	11.2	82.75	10.918
Ag-H(11)	384	215.8	0.84	10.9	0.94	216	5.88	13.9	8.12	9.910
	512		0.70	12.9	1.0	191	4.68	10.4	8.63	9.936
	768		0.43	16.6	1.4	208	5.52	8.74	15.30	10.185
Cu(1)	4	82.8	0.90	1.51	11.7	29	70.7	13.4	1.02	9.009

hardness. From these figures the number of grains (assumed spherical) of each size group/unit volume was calculated. Summation gave the number of spherical grains/unit volume shown in Table XII. The number of grains/unit area shown in Table XII was computed in a similar manner from the planar size distribution and the fraction recrystallized.

V.—DISCUSSION OF RESULTS

1. RELATION BETWEEN DIAMOND PYRAMID HARDNESS AND PERCENTAGE OF METAL RECRYSTALLIZED

The results given in Table IV and plotted in Fig. 23 (p. 193) indicate that the percentage softening calculated from the diamond pyramid hardness is approximately equal to the percentage of metal recrystallized. Cook and Richards⁵ reached a similar conclusion in the case of commercial high-conductivity copper.

2. THE ACTIVATION ENERGIES P AND Q

As established in the last section, the percentage softening is approximately equal to the percentage of the metal recrystallized in the case of Cu(1) and Ag-L(9) annealed at 82.8° C., Ag-M(10) annealed at 117.0° C., and Ag-H(11) annealed at 215.8° C. On the assumption that this relation was valid for all the alloys examined and for all the annealing temperatures employed, values of x were calculated from the hardness data. If H_h and H_0 are the initial and final hardness values and H_t the hardness after annealing time t (hr.) when a proportion x of the material is recrystallized, then :

$$x = \frac{H_h - H_t}{H_h - H_0} \quad (13)$$

Curves of $\ln \frac{1}{1-x}$ against t were plotted for all the alloys annealed at various temperatures giving curves similar to that shown in Fig. 27. In the vast majority of these curves $t_{\frac{1}{2}}$, the half-softening time, fell within the linear portion. Accordingly, it was considered

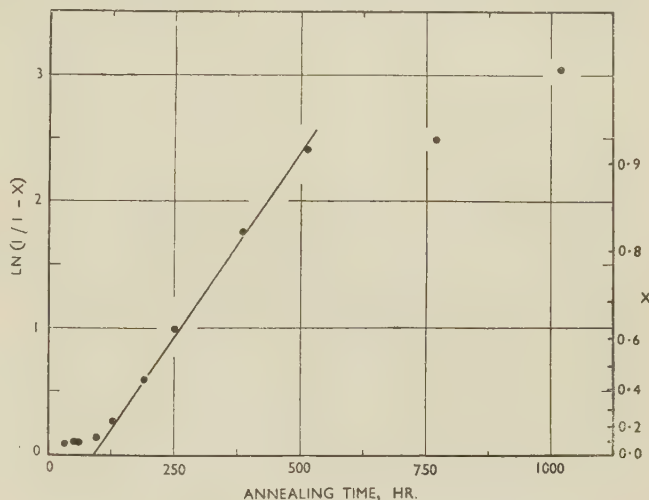


FIG. 27.—Variation of $\ln \frac{1}{1-x}$ with Time at 169.4° C. for As-H(17).

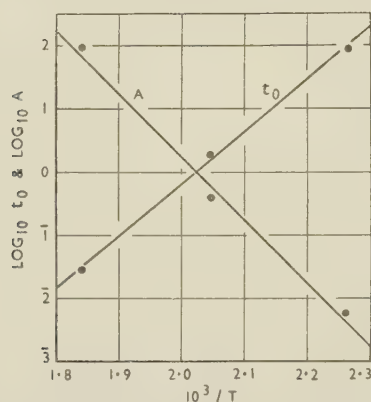
more satisfactory to derive A and B (see Section II, 1) from the straight-line portion of the curve rather than from the earlier part where $t < t_{\frac{1}{2}}$ or frequently $\ll t_{\frac{1}{2}}$ and the errors in determining x become large compared with x . The straight-line portion of the $\ln \frac{1}{1-x}/t$ curves was produced to cut the time axis and its slope

TABLE XIII.—Slope A and Intercept t_0 Measured from Plots of $\log_{10} t_0$ and $\log_{10} A$ Against $1/T$.

Alloy	35.6° C.		82.8° C.		117.0° C.		169.4° C.		215.8° C.	
	$\log_{10} A$ (hr. ⁻¹)	$\log_{10} t_0$ (hr.)	$\log_{10} A$ (hr. ⁻¹)	$\log_{10} t_0$ (hr.)	$\log_{10} A$ (hr. ⁻¹)	$\log_{10} t_0$ (hr.)	$\log_{10} A$ (hr. ⁻¹)	$\log_{10} t_0$ (hr.)	$\log_{10} A$ (hr. ⁻¹)	$\log_{10} t_0$ (hr.)
Cu(1)	4.69	2.48	1.03	0.44	0.73	1.33	2.16	3.99	2.98	3.36
Cu(21) ^t	3.25	2.60	1.23	0.58	0.70	1.34	1.84	3.88	3.04	3.34
Cu(21) ^b	3.55	2.35	1.31	0.46	0.61	1.04	1.96	3.77	2.94	3.36
P-L(5)	4.60	2.11	2.60	0.40	1.84	1.26
P-M(6)	4.83	1.11	2.50	1.05
P-H(20)	2.37	1.62
Ag-L(9)	3.30	2.50	1.40	0.36	0.73	1.26	1.84	3.56
Ag-M(10)	2.89	1.02	0.32	1.57	1.97	2.18	3.05	3.40
Ag-H(11)	3.31	2.50
Cd-L(12)	3.81	2.28	1.61	0.43	1.08	1.06	3.35	2.01
Cd-M(13)	3.23	2.54	1.40	0.91	0.68	1.32	2.01	2.14	3.11	3.41
Cd-H(14)	4.46	2.72
As-L(15)	4.49	2.79	2.44	0.70	1.55	2.78	3.07	3.60
As-M(16)	4.92	1.48	1.73	1.48	1.48	2.43
As-H(17)	3.76	1.95	1.59	0.27
Te-L(18)	2.40	1.70	0.04	1.91	1.33	2.62	2.38	3.68
Te-M(19)	2.08	1.95	0.04	0.26	1.15	2.90	2.32	3.72
O(8)	4.73	2.54	2.62	0.70	0.24	1.00	1.83	3.90	2.52	3.43

TABLE XIV.—Slope A and Intercept t_0 Measured from Plots of $\log_{10} t_0$ and $\log_{10} A$ Against $1/T$.

Temp., °C.	P-L(5)		P-M(6)		P-H(20)		Ag-H(11)		Cd-H(14)		As-H(17)	
	$\log_{10} A$ (hr. ⁻¹)	$\log_{10} t_0$ (hr.)	$\log_{10} A$ (hr. ⁻¹)	$\log_{10} t_0$ (hr.)	$\log_{10} A$ (hr. ⁻¹)	$\log_{10} t_0$ (hr.)	$\log_{10} A$ (hr. ⁻¹)	$\log_{10} t_0$ (hr.)	$\log_{10} A$ (hr. ⁻¹)	$\log_{10} t_0$ (hr.)	$\log_{10} A$ (hr. ⁻¹)	$\log_{10} t_0$ (hr.)
270	1.97	2.46
280	1.99	3.95
290	0.98	1.13	1.15	2.89
320	1.76	2.20	2.09	3.44
340	2.12	3.96
360	0.87	2.90
380	1.32	2.06
400	1.64	2.17

FIG. 28.—Relation Between $\log_{10} t_0$, $\log_{10} A$, and $1/T$ for As-H(17).TABLE XV.—Effect of Alloying on Q_R , P , and Q for Pure Copper (95% Reduction* by Cold Rolling, Original Grain-Size 0.010–0.018 mm.).

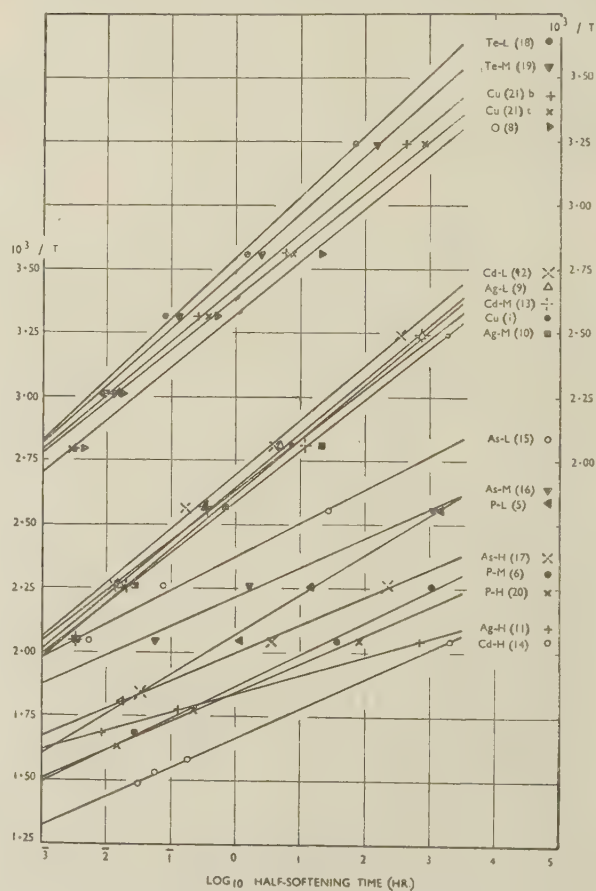
Alloy	Addition by Analysis, at.-%	Activation Energies, kg.cal./mol.		
		Q_R	P	Q
Cu(1)	...	23	20 ± 0.5	25.5 ± 1.5
Cu(21)t	...	22.5	20.5 ± 0.5	22 ± 0.5
Cu(21)b	...	21.5	20 ± 1	20.5 ± 0.5
P-L(5)	0.0025 P	29	25.5 ± 0.5	31 ± 0.5
P-M(6)	0.0114 P	36.5	29.5 ± 6.5	43 ± 1.5
P-H(20)	0.0210 P	41	40.5 ± 0.5	42 ± 0.5
Ag-L(9)	0.0030 Ag	21.5	22.5 ± 0.5	22.5 ± 0.5
Ag-M(10)	0.0053 Ag	22.5	22 ± 1	25 ± 0.5
Ag-H(11)	0.0271 Ag	63	64.5 ± 0.5	63.5 ± 0.5
Cd-L(12)	0.0029 Cd †	21.5	20.5 ± 0.5	26 ± 1.5
Cd-M(13)	0.0049 Cd	21.5	20.5 ± 0.5	22.5 ± 0.5
Cd-H(14)	0.018 Cd	40	39.5 ± 2.5	43 ± 0.5
As-L(15)	0.0047 As	35	26 ± 2	42 ± 0.5
As-M(16)	0.0094 As	40	25 ± 3	40.5 ± 0.5
As-H(17)	0.047 As	42	38 ± 0.5	46 ± 0.5
Te-L(18)	0.00025 Te †	19	20 ± 0.5	19 ± 0.5
Te-M(19)	0.00075 Te	20	20 ± 0.5	20.5 ± 0.5
O(8)	0.126 O	20.5	22 ± 1.5	24 ± 0.5

* Except Cu(21)t and b and O(8), which were rolled to 93.8% reduction.

† By synthesis, not by analysis.

A and intercept t_0 measured. The results are recorded in Tables XIII and XIV.

By plotting $\log_{10} t_0$ and $\log_{10} A$ against $1/T$ (T = absolute annealing temperature), straight lines were obtained, in accordance with expressions (5) and (6), the slopes of which gave activation energies P and Q , respectively. Fig. 28 shows an example of the curves obtained. Values of P and Q are given in Table XV, together with values of Q_R which are activation energies for overall recrystallization. Q_R was derived from a plot of $\log t_{\frac{1}{2}}$ against $1/T$ (Fig. 29) by drawing

FIG. 29.—Variation of $\log t_{\frac{1}{2}}$ with $1/T$.

the best straight lines through the data for each alloy and using the relation

$$\ln t_{\frac{1}{2}} = \frac{Q_R}{R} \cdot \frac{1}{T} + k \quad (14)$$

The values of $t_{\frac{1}{2}}$ employed, derived from plots of hardness versus annealing time, are shown in Tables XVI and XVII.

TABLE XVI.—*Half-Softening Times Derived from Isothermal Softening Curves.*

Alloy	Half-Softening Time, hr.				
	35-6° C.	82-8° C.	117-0° C.	169-4° C.	215-8° C.
Cu(1)	1900	7-2	0-333	0-0139	0-0033
Cu(21) ^a	825	7-6	0-37	0-0144	0-00277
Cu(21) ^b	417	5-75	0-25	0-0131	0-00311
P-L(5)	1500	15-0	1-20
P-M(6)	1070	37
P-H(20)	80
Ag-L(9)	705	4-83	0-333	0-0161	...
Ag-M(10)	...	21-0	0-666	0-0264	0-0033
Ag-H(11)	700
Cd-L(12)	340	4-0	0-166	0-0125	...
Cd-M(13)	780	12-0	0-366	0-020	0-0033
Cd-H(14)	2040
As-L(15)	28-0	0-0783	0-00514
As-M(16)	1140	1-633	0-055
As-H(17)	225	3-633
Te-L(18)	70-0	1-50	0-080	0-0083	...
Te-M(19)	150	2-45	0-132	0-0090	...
O(8)	...	21-0	0-50	0-0175	0-00445

TABLE XVII.—*Half-Softening Times from Supplementary Softening Curves.*

Temp., °C.	Half-Softening Time, hr.					
	P-L(5)	P-M(6)	P-H(20)	Ag-H(11)	Cd-H(14)	As-H(17)
270	0-0333
280	0-0167
290	0-2283	0-1283
320	...	0-0272	...	0-0083
340	0-015
360	0-1867	...
380	0-0556	...
400	0-0306	...

The description of the rates of recrystallization in terms of a single activation energy, Q_R , and a single constant k , has the merit of simplicity, but provides an adequate interpretation of the results only when P and Q are approximately equal. Therefore it does not provide an adequate basis for a general theory of recrystallization, but is to be regarded as an approximate analysis ignoring the variation of the slopes of x versus $\ln t$ and $1/T$ versus $\ln t_{\frac{1}{2}}$ plots with temperature.

For two materials $P > Q$ and for twelve materials Q_R is significantly $> P$ (Table XV). The differences are biggest in the case of the arsenic and phosphorus alloys, less in the case of the cadmium alloys, and small or insignificant in the silver, tellurium, and oxygen alloys and in the pure coppers. When P and Q are

very different, the value of Q_R falls somewhere between them; when P and Q are almost equal, Q_R has about the same value. For both arsenic and phosphorus, Q is much larger than P for the smallest solute addition, but P increases with increase in solute concentration faster than Q . This suggests that recrystallization proceeds in two stages, the second of which is impeded more than the first by a small amount of solute.

3. VARIATION OF SLOPE OF x VERSUS $\ln t$ PLOT WITH TEMPERATURE

Plots of x versus $\log_{10} t$ were prepared for each alloy for the various annealing temperatures (see, for example, Fig. 24 (a)–(c), p. 193). For some of the materials, such as Cd-M(13) (Fig. 24 (a)), the curves were of the same form and could be superimposed more or less exactly by displacement along the time axis. For other materials, such as As-L(15) (Fig. 24 (b)) and P-M(6) (Fig. 24 (c)), this was not so. On considering the portions of the curves between $x = 0.2$ and $x = 0.8$, it will be seen that whereas for Cd-M(13) the slope shows little change with temperature, for As-L(15) and P-M(6) the slope increases with temperature.

The slopes of the $x/\log_{10} t$ curves were measured at $x = 0.5$ by drawing the best straight line through points between $x = 0.2$ and 0.8 or, where necessary, over a shorter range $x = 0.4$ to 0.6 . The slope at $x = 0.5$ was also calculated from equation (10) for the corresponding temperatures, using values of a and b determined from the Thorley-type plots of $\ln t_0$ and $\ln A$ against $1/T$, using equations (5) and (6), viz. :

$$\ln A = \ln a - Q/RT$$

$$\text{and} \quad \ln \beta = \ln b - P/RT, \text{ where } \beta = 1/t_0$$

Thus $\ln a = Q/RT$, when $A = 1$ or $\ln A = 0$ and the value of $1/T$ when $\ln A = 0$ can be read from the graph.

Similarly, $\ln(1/b) = -P/RT$ when $\ln t_0 = 0$ and the value of $1/T$ when $\ln t_0 = 0$ can be read from the graph. The values of P and Q have already been determined (Table XV).

Values of a and b , values of the calculated slopes of the x versus $\ln t$ plots and the measured slopes of x versus $\log_{10} t$ plots converted to refer to $\ln t$ are shown in Table XVIII. Where the data do not permit reliable figures to be obtained, the values are omitted. It will be seen that, considering the limitations of the data, the measured and calculated values of the slope agree remarkably well. The theory thus accounts for the increase in slope with increase in temperature, as for example, the slope of the curves for Ag-M(10) and As-H(17).

4. VARIATION OF THE SLOPE OF $1/T$ VERSUS $\ln t_{\frac{1}{2}}$ PLOTS WITH TEMPERATURE

As shown in Table XV, P and Q differed considerably in some cases. The magnitude of the second (bracketed) term in equation (11) or (12) (p. 186) has

TABLE XVIII.—Values of Constants a and b and Variation of Calculated and Measured Slopes of x versus $\ln t$ Plots with Temperature.

Alloy	a	b	Temp., °C.	Slope of $x/\ln t$ Plot at $x = 0.5$	
				Calculated	Measured
Cu(1)	6×10^{14}	8×10^{11}	82.8	0.5	0.5
			117.0	0.6	0.9
Cu(21) t	8×10^{12}	1×10^{12}	35.6	0.7	0.5
			117.0	0.9	1.1
Cu(21) b	1×10^{12}	1×10^{12}	35.6	0.6	0.5
			82.8	0.6	0.7
			117.0	0.7	0.5
P-L(5)	1×10^{14}	2×10^{12}	169.4	0.4	0.3
P-M(6)	5×10^{17}	...	169.4	...	0.3
			215.8	...	0.5
			320	...	1.1
P-H(20)	1.5×10^{17}	3×10^{16}	215.8	0.9	0.8
			290	1.1	0.8
			340	1.1	0.7
Ag-L(9)	2×10^{13}	3×10^{13}	35.6	0.7	0.7
			82.8	0.7	0.6
			117.0	0.7	0.7
			169.4	0.7	0.7
Ag-M(10)	2×10^{14}	4×10^{12}	82.8	0.7	0.7
			117.0	0.9	0.7
			169.4	1.2	1.2
			215.8	1.5	1.4
Ag-H(11)	5×10^{25}	2×10^{26}	215.8	0.7	0.7
			290	0.7	0.9
Cd-L(12)	8×10^{15}	2×10^{12}	82.8	1.1	0.9
			117.0	1.9	0.9
			169.4	3.9	1.5
Cd-M(13)	2×10^{13}	8×10^{11}	35.6	0.8	0.7
			82.8	1.1	0.9
			117.0	1.3	0.9
			169.4	1.7	1.2
Cd-H(14)	5×10^{15}	8×10^{14}	360	0.6	0.6
			380	0.6	0.6
			400	0.6	0.6
As-L(15)	1.5×10^{22}	1×10^{14}	117.0	0.4	0.4
			169.4	1.4	3.3
As-M(16)	5×10^{19}	8×10^{12}	117.0	0.4	0.2
			169.4	0.4	0.5
			215.8	0.7	0.7
As-H(17)	2×10^{20}	8×10^{16}	169.4	0.5	0.6
			215.8	0.7	0.6
			270	1.1	1.5
Te-L(18)	9×10^{11}	3×10^{12}	82.8	1.0	0.8
			117.0	0.9	0.8
			169.4	0.8	0.9
Te-M(19)	4×10^{12}	1.5×10^{12}	35.6	0.8	0.9
			82.8	0.9	0.9
			117.0	1.0	1.0
			169.4	1.0	0.9
O(8)	5×10^{13}	1×10^{13}	82.8	0.5	0.3
			117.0	0.5	0.5
			169.4	0.6	0.7

been calculated from these figures, using the values of a and b given in Table XVIII, for the lowest and highest temperatures for which values of $t_{\frac{1}{2}}$ were obtained experimentally in the case of each material (Table XIX). The calculated slope has been obtained

TABLE XIX.—Variation of the Calculated and Measured Slopes of $1/T$ versus $\ln t_{\frac{1}{2}}$ Plots with Temperature.

Alloy	$P/R \times 10^{-3}$	$Q/R \times 10^{-3}$	Temp., °C.	2nd Term in Equation (11) or (12) $\times 10^{-3}$	Calculated Slope, $\frac{d(\ln t_{\frac{1}{2}})}{d\phi}$	$Q_R/R \times 10^{-3}$	$Q'_R/R \times 10^{-3}$
Cu(1)	10.1	12.9	35.6	0.3	12.6	11.6	{13.0 10.6 ...
			59.2	0.6	12.3		
			143.2	1.6	11.3		
			215.8	2.2	10.7		
Cu(21) t	10.3	11.1	35.6	0.4	10.7	11.3	...
			215.8	0.6	10.5		
Cu(21) b	10.1	10.3	35.6	0	10.2	10.8	...
			215.8	0	...		
P-L(5)	12.9	15.6	117.0	0.2	15.4	14.6	...
			280	1.0	14.6		
P-H(20)	20.4	21.1	215.8	0.4	20.7	20.7	...
			340	0.5	20.6		
Ag-L(9)	11.4	11.4	35.6	0	11.4	10.8	...
			169.4	0	11.4		
Ag-M(10)	11.1	12.6	82.8	0.8	11.8	11.3	...
			215.8	1.2	11.4		
Ag-H(11)	32.5	32.0	215.8	0	32.3	31.7	...
			320	0	32.3		
Cd-L(12)	10.3	13.1	35.6	1.2	11.9	10.8	...
			169.4	2.6	10.5		
Cd-M(13)	10.3	11.4	82.8	0.7	10.7	10.8	...
			215.8	0.9	10.5		
Cd-H(14)	20.0	21.7	215.8	0.4	21.3	20.1	...
			400	0.7	21.0		
As-L(15)	13.1	21.2	117.0	1.5	19.7	17.6	{19.2 12.8 ...
			143.2	3.5	17.7		
			192.6	6.9	14.3		
			215.8	7.6	13.6		
As-M(16)	12.6	20.4	117.0	0.2	20.2	20.1	{21.7 16.1 ...
			143.2	0.5	19.9		
			192.6	2.4	18.0		
			215.8	3.9	16.5		
As-H(17)	19.2	23.2	169.4	1.2	22.0	21.1	...
			270	2.8	20.4		
Te-L(18)	0.1	9.6	35.6	0	9.9	9.6	...
			169.4	0	9.9		
Te-M(19)	10.1	10.3	35.6	0	10.2	10.1	...
			169.4	0	10.2		
O(8)	11.1	12.1	35.6	0	11.6	10.3	...
			215.8	0	11.6		

by subtracting the calculated second term from P/R or Q/R , whichever is the larger. Where the second term was zero, the average of P/R and Q/R has been taken. The measured slope obtained from Fig. 29 is given in column 7 of Table XIX. This would be expected to lie somewhere between the calculated values for the lowest and higher temperatures (column 6), and this is so in some cases.

In three instances, namely Cu(1), As-L(15), and As-M(16), a measurement has been made of the slope at the two ends of the temperature range. Thus, for Cu(1) a straight line was drawn through the $1/T$ versus

In $t_{\frac{1}{2}}$ points obtained experimentally for 35.6° and 82.8° C. and the slope $Q'_R/R = 13.0$ measured. This corresponds to the value 12.3 calculated for 59.2° C., which is the temperature midway between 35.6° and 82.8° C. Similarly, the slope measured from the 117.0° and 169.4° C. points was 10.6 and that calculated for 143.2° C. was 11.3. The 215.8° C. experimental point was not used, since the recrystallization time was so short that the experimental error became, rather large in proportion. In the case of As-L(15), the theory predicts that the slope should decrease from 17.7 at 143.2° C. to 14.3 at 192.6° C., whereas the measured slope between 117.0° and 169.4° C. was 19.2, and between 169.4° and 215.8° C., 12.8. The agreement is thus qualitative but not quantitative, which is all that can be expected in view of the small number of temperatures employed. Results for the As-M(16) alloy are similar (Table XIX).

In some instances the results, e.g. those for Cd-M(13), show that the second term may be appreciable, although its variation with temperature is insignificant. In such a case the curve would still be linear, though of a different slope from that expected from single-stage theory. In other instances, e.g. the results for Cu(21)*b*, Ag-H(11), and Te-L(18), the second term is negligible, and no variation of the slope of the $1/T$ versus $\ln t_{\frac{1}{2}}$ plots with temperature would be expected.

The results indicate that there is a significant temperature dependence of the slope of $1/T$ versus $\ln t_{\frac{1}{2}}$ plots in the case of the alloys containing 0.0047 or 0.0094 at.-% arsenic and possibly in pure copper. The two arsenic alloys would be particularly suitable for further investigation using more precise temperature control and annealing temperatures at, say, 10° C. intervals over the range 117°–216° C.

5. GROWTH RATES

The results given in Table IX (p. 197) and plotted in Figs. 25 and 26 (p. 197) indicate that the growth rate is constant with annealing time at a particular temperature, in conformity with previous work on a variety of materials.²⁰⁻²² This is true both for the materials Cu(1), Ag-L(9), and Ag-H(11) which recrystallized to the cube texture and for P-H(20) which gave a rather random texture. The curves when extrapolated intercept the time axis at a positive value. This may be interpreted either as indicating that growth started at zero annealing time but was slower than at the later stage when the grains became large enough to measure, or that growth occurred at a constant rate from the earliest stage, but that some time elapsed before a stable nucleus was formed which could grow freely.

Fig. 30, in which the logarithm of the growth rate (Table X, p. 197) has been plotted against the reciprocal of the absolute annealing temperature for the combined data on Cu(1) and Cu(21)*t* and *b*, shows that the growth rate varies exponentially with temperature. This result is to be expected from the work on aluminium, silicon ferrite, and other materials.^{20, 21, 23}

The curve in Fig. 30 can be represented by an equation:

$$\ln G = -\frac{Q_G}{R} \cdot \frac{1}{T} + w \quad (15)$$

where Q_G is an activation energy for growth, w a constant, and the other symbols have their usual meaning. From the slope of the curve (Fig. 30), Q_G was found to be 21.5 kg.cal./mol., which is similar to the values of P , Q , and Q_R for the three pure coppers (Table XV, p. 200).

A similar relation was obtained for Ag-M(10) by plotting the results from Table X, which gave $Q_G = 21$ kg.cal./mol., a value similar to those of Q_R and P (Table XV).

The results in Table X show the effect of composition on the growth rate. All the alloys that recrystallized to the cube texture, with the exception of

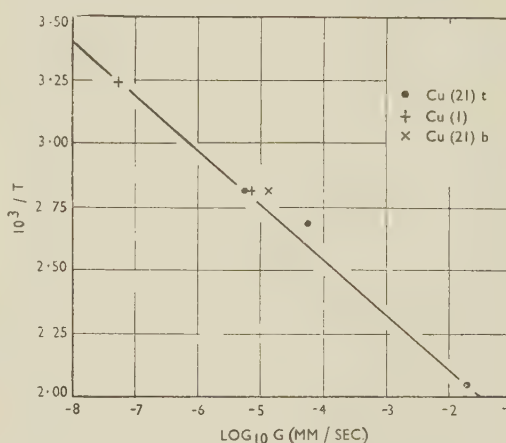


Fig. 30.—Variation of Log Growth Rate with $1/T$.

Ag-H(11), had growth rates similar to that of pure copper at the same temperature. On the other hand, the alloys that tended to have a more random recrystallization texture than pure copper, had much smaller growth rates than the latter. The 0.0271 at.-% silver alloy Ag-H(11) was exceptional in that the alloying addition greatly reduced the growth rate but did not significantly alter the texture.

In some cases variation of composition had an effect on the growth rate great even in comparison with the enormous effect of temperature. A comparison of the rates of recrystallization calculated from the hardness, and the growth rates, shows that the effect of certain solutes in retarding or accelerating recrystallization is independently reflected in the measured rates of growth. It appears that the logarithm of the growth rate varies linearly with the logarithm of the half-softening time as shown by Fig. 31.

Thus

$$\log_{10} G = m' \log_{10} t_{\frac{1}{2}} + k' \quad (16)$$

where k' from Fig. 31 = 5.70 for $m' = -1$ and m' lies between -0.95 and -1.05 , which are the slopes of the dotted curves *A* and *C*, respectively, in Fig. 31, and may well be -1.00 corresponding to curve *B*.

Combining equations (15) and (16) :

$$-\frac{Q_G}{R} \cdot \frac{1}{T} + w = m' \ln t_{\frac{1}{2}} + 2.303 k'. \quad (17)$$

On comparing relations (17) and (14), it will be seen that when $m' = -1$, $Q_G = Q_R$. This suggests, and consideration confirms, that relation (16) is in fact a good approximation only when P and Q are approximately equal. The points which deviate from the full-line curve ($m' = -1$) in Fig. 31 are in general those for materials for which P and Q differ appreciably.

Although deviations from relation (16) occur when P and Q differ, the general effect of composition on the growth rate is clearly reflected by the curves showing the variation of the logarithm of the half-softening time with atomic per cent. of solute, as shown in

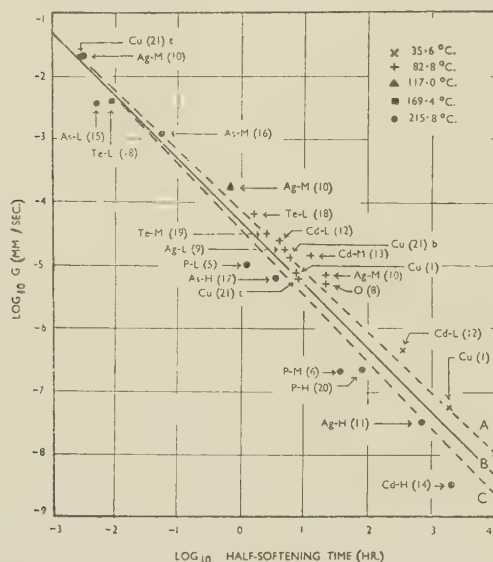


FIG. 31.—Relation Between the Log Growth Rate and $\log t_{\frac{1}{2}}$.

Fig. 32, in which values of $t_{\frac{1}{2}}$ at 215.8° C. recorded in Table XVI have been plotted. The first small addition of phosphorus, unlike that of cadmium, silver, or arsenic, produced a large increase in the half-softening time and a corresponding big decrease in the growth rate (Table X, p. 197); whereas the maximum increase in half-softening time seems to be largely realized by the addition of 0.015–0.025 at.-% phosphorus, the curves for cadmium and silver are still rising steeply in this region. The addition of about 0.05 at.-% arsenic produced a smaller increase in half-softening time than the addition of rather less than 0.03 at.-% phosphorus, cadmium, or silver.

Cook and Richards⁵ found for commercial high-purity oxygen-bearing copper of two original grain-sizes that

$$\log_{10} t_{\frac{1}{2}} = dS + q \quad (18)$$

where S is the rolling reduction (80–98.75%), d a constant dependent only on temperature, and q a constant.

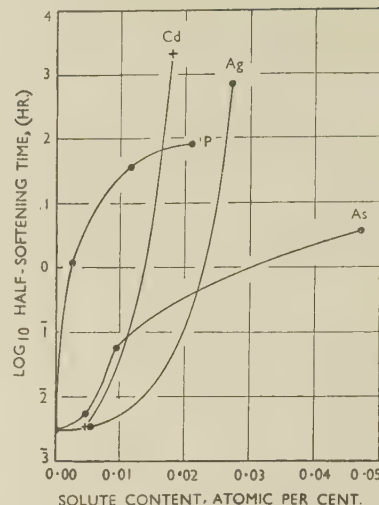


FIG. 32.—Variation of $\log t_{\frac{1}{2}}$ at 215.8° C. with Solute Content.

It follows from (16) that :

$$\log_{10} G \propto S \quad (19)$$

Thus when P and Q are approximately equal, it is probable that the logarithm of the growth rate is directly proportional to the rolling reduction, at any rate in the range 80–98.75% reduction.

6. NUCLEATION RATES

The number of spherical grains/c.c. recorded in Table XII (p. 198) is plotted against time for P-H(20) annealed at 215.8° C. in Fig. 33. The rate of nucleation N , defined as the number of grains appearing/c.c./sec., was obtained from Fig. 33 by measuring the slope of the graph at various points and dividing by the fraction non-recrystallized as calculated from the hardness. The rate of nucleation was initially rapid, but decreased rapidly with increase in annealing time and appeared to approach a constant rate at longer annealing times (Fig. 34).

It will be seen from Table XII (p. 198) that the ratio (B/D) of the number of spherical grains/c.c. to the

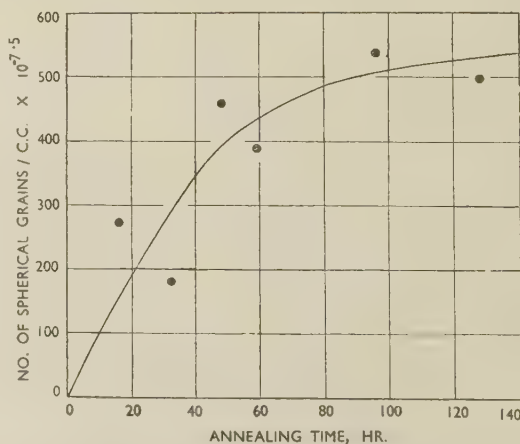


FIG. 33.—Relation Between Number of (Spherical) Grains/Unit Volume and Time of Annealing at 215.8° C. for P-H(20).

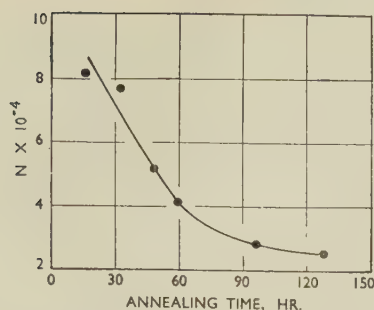


FIG. 34.—Variation of the Spatial Rate of Nucleation with Time of Annealing at 215.8° C. for P-H(20).

number of grains/cm.² was fairly constant for all the materials examined, whatever the stage of recrystallization. Thus the “planar” nucleation rate or number of grains appearing/cm.²/sec. is directly proportional to the “spatial” nucleation rate. If the number of grains/unit vol. (or area) varies linearly with the time of annealing, as in the case of P-H(20) annealed at 215.8° C. up to about 15–20% complete recrystallization (Fig. 33), then the slope of the curve can be calculated from a single grain count on a specimen recrystallized ≥ 15 –20%, and the rate of nucleation is given by :

$$N_{(\text{spatial})} = B/ft \quad (20)$$

where f is the fraction non-recrystallized and t is the annealing time in seconds. Similarly

$$N'_{(\text{planar})} = D/ft \quad (21)$$

Thus the spatial rates of nucleation can be obtained from the values of N' in Table XI (p. 198) by multiplying by B/D to a good approximation in the cases where the specimens were at an early stage in recrystallization.

Fig. 35, in which data for the two pure coppers Cu(1) and Cu(21) t have been combined, shows that the logarithm of the planar rate of nucleation, N' , varies

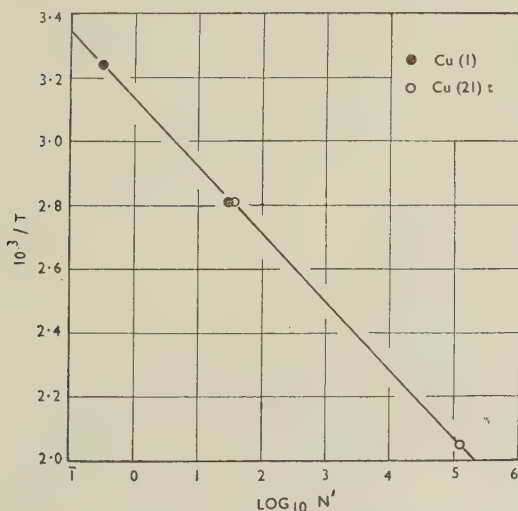


FIG. 35.—Variation of $\log N'$, the “Planar” Rate of Nucleation, with $1/T$ for Cu(1) and Cu(21) t .

linearly with the reciprocal absolute annealing temperature.

Thus

$$\ln N' = -\frac{Q_N}{R} \cdot \frac{1}{T} + l' \quad (22)$$

where Q_N is an activation energy for nucleation, l' a constant, and the other symbols have their usual meaning.

Similarly

$$\ln N = -\frac{Q_N}{R} \cdot \frac{1}{T} + l \quad (23)$$

because the slope of Fig. 35 is unaffected if $\log_{10} N' \cdot \frac{B}{D}$ ($= \log_{10} N$) is plotted in place of $\log_{10} N'$.

This exponential relation agrees with published work on aluminium.²⁰

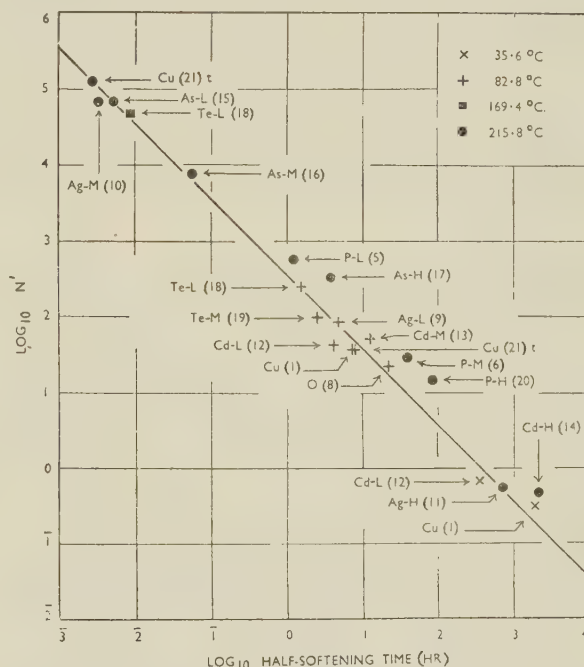


FIG. 36.—Relation Between $\log N'$, the “Planar” Rate of Nucleation, and $\log t_{1/2}$.

The slope of Fig. 35 gave $Q_N = 21$ kg.cal./mol., which is similar to the values of the activation energy P for Cu(1) and Cu(21) t (Table XV, p. 200). If it is assumed that the exponential relation is valid, values of Q_N of 19 kg.cal./mol. may be calculated from the results obtained at two temperatures for both Cd-L(12) and Te-L(18) (Table XI, p. 198). This figure is similar to the values of the activation energies Q_R and P in the case of Cd-L(12) and Q_R , P , and Q in the case of Te-L(18) (Table XV).

The logarithm of the planar rate of nucleation, N' (Table XI), was found to vary inversely as the logarithm of the half-softening time (Fig. 36), just as in the case of the growth rate (Fig. 31 (p. 204) and expression (16)).

Thus

$$\log_{10} N' = m'' \log_{10} t_{1/2} + k'' \quad (24)$$

where k'' from Fig. 36 = 2.55 for $m'' = -1$, corresponding to the curve drawn.

Combining equations (22) and (24):

$$-\frac{Q_N}{R} \cdot \frac{1}{T} + l' = m'' \log_{10} t_{\frac{1}{2}} + k'' \quad (25)$$

By comparing equations (25) and (14), it will be seen that when $m'' = -1$, $Q_N = Q_R$. This suggests that relation (24) is in fact only strictly valid when P and Q are approximately equal, as in the case of relation (16). Relation (26) may be derived in the same way as (19):

$$\log_{10} N \propto S \quad (26)$$

Thus when P and Q are approximately equal, it is probable that the logarithm of the nucleation rate is directly proportional to the rolling reduction S at least in the range 80–98.75% reduction.

As in the case of the growth rate, the effect of composition on the rate of nucleation at, for example,

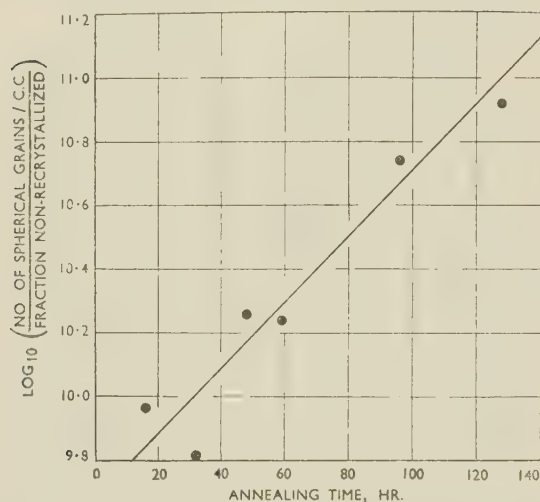


FIG. 37.—Relation Between \log_{10} No. of (Spherical) Grains/c.c. Fraction Non-Recrystallized and the Time of Annealing at 215.8° C. for P-H(20).

215.8° C. may be judged from the variation of the logarithm of the half-softening time with composition as shown in Fig. 32, in as far as relation (24) is valid.

One further relation is of interest. As shown in Fig. 37 the logarithm of the number of (spherical) grains/unit vol. divided by the fraction still non-recrystallized (Table XII, p. 198) was found to vary in an approximately linear fashion with annealing time for P-H(20) annealed at 215.8° C. The number of grains/unit area varies with annealing time in a similar manner.

VII.—SUMMARY

Small additions of certain elements were found to have a remarkable effect on the recrystallization of 99.999+ % purity copper cold rolled to about 95% reduction and annealed isothermally at temperatures in the range 35.6°–400° C. The alloying elements studied were phosphorus, silver, cadmium, arsenic, tellurium, and oxygen. With the exception of the

last two, the various additions were within the known solid-solubility limits. The oxygen alloy contained an amount of oxygen similar to that in tough-pitch commercial copper. The two tellurium alloys were solution-treated, but it seems probable that a part of the tellurium was precipitated during subsequent annealing operations. The main effects of these additions are summarized below, and unless otherwise stated all observations refer to material with an initial grain-size of 0.010–0.018 mm. dia.

None of the additions had any apparent effect on the texture produced by cold rolling which, although not determined fully, was consistent with the (110) $[\bar{1}12]$ plus (112) $[11\bar{1}]$ ideal orientations reported previously, but which, in addition, always contained the less frequently reported minor texture (100) $[001]$.

Recrystallization was observed to begin at deformation markings both in strips of pure copper, whether of 0.023 or of 1.2–1.5 mm. original grain-size, and in strips of an alloy containing 0.00175 at.-% phosphorus, whether of 0.042 or of 0.3 mm. original grain-size. Recrystallization proceeded at different rates in different grains.

After annealing for various times, the percentage softening calculated from the diamond pyramid hardness was found to be approximately equal to the percentage of metal recrystallized both for pure copper and for alloys containing 0.0030, 0.0053, and 0.0271 at.-% silver. On the assumption that this relation was valid for the other materials, analysis of the hardness data showed that they supported the recrystallization theory proposed by Cook and Richards and extended by Thorley. This theory postulates two separate stages of recrystallization governed by activation energies P and Q , respectively.

The theory predicts that the slope of α (fraction recrystallized) versus $\log t$ (t = annealing time) plots should vary with temperature when P and Q differ. In alloys containing 0.0053 at.-% silver, 0.0049 at.-% cadmium, 0.0047 or 0.047 at.-% arsenic, the slope increased with increase in temperature as predicted, and there was reasonable agreement between the calculated and measured values of the slope. The theory also predicts that for some of the alloys the slope of $1/T$ (T = absolute annealing temperature) versus $\log t_{\frac{1}{2}}$ ($t_{\frac{1}{2}}$ = time for 50% recrystallization) plots should vary with temperature. The results on a pure copper and on alloys containing 0.0047 and 0.0094 at.-% arsenic indicate that the slope decreases with increase in temperature, in qualitative agreement with the predicted trend.

Activation energies P and Q for the first and second stages of recrystallization, respectively, were determined for all the materials. The average values of P and Q obtained for the three pure coppers were 20 (range 20–20.5) and 22.5 (range 20.5–25.5) kg.cal./mol. respectively. In the alloys the values of P obtained ranged from 20 to 64.5 and those of Q from 19 to 63.5 kg.cal./mol. All alloying additions with the exception of tellurium tended to increase P and Q , which in general increased progressively with further additions of

solite. The highest values of P and Q (64.5 and 63.5 kg.cal./mol., respectively) were realized by the addition of 0.0271 at.-% silver. The addition of 0.00025 at.-% tellurium had no effect on P , but decreased Q to 19 kg.cal./mol. The alloy containing 0.126 at.-% oxygen gave values of P and Q of 22 and 24 kg.cal./mol., respectively. The progressive addition of silver appeared to increase P and Q by similar amounts, whereas the progressive addition of phosphorus or arsenic increased Q more than P , although the values of P and Q converged at higher additions.

The addition of 0.126 at.-% oxygen to pure copper slightly increased the half-softening time and possibly P and Q , but otherwise had little effect on recrystallization. The effects of additions of 0.00025 and 0.00075 at.-% tellurium were also small, but in the reverse direction. Thus tellurium appreciably decreased the half-softening time, increased the rates of nucleation and growth, and slightly decreased the activation energy for the second stage of recrystallization. The effect of tellurium in accelerating recrystallization was greater for a 0.00025 at.-% addition than for a 0.00075 at.-% addition. The fact that tellurium accelerates recrystallization disagrees with previous work.⁴

As in the case of the pure coppers, the recrystallization texture of the oxygen, and tellurium alloys was almost completely cubic. The effects of the addition of one atom of the other elements on the recrystallization texture increased in the order: silver, arsenic, cadmium, phosphorus. Whereas the addition of 0.0271 at.-% silver to pure copper had no apparent effect on the texture, as little as 0.0025 at.-% phosphorus to a large extent suppressed the cube texture and gave instead a fairly random texture. The addition of 0.047 at.-% arsenic also partially suppressed the cube texture. Although the addition of 0.0049 at.-% cadmium had little effect, a larger addition of 0.018 at.-% partially suppressed the cube texture and tended to retain the rolling texture. The change in texture was accompanied by a change in grain structure. Thus, irrespective of annealing temperature, the grains in the highly preferred cubically oriented strips tended to be coarse and plate-like in shape and elongated in the rolling direction. On the other hand, the strips which tended to have a random texture showed fine-grained equi-axed structures.

Phosphorus was outstanding in that a very small addition produced very large effects. Thus 0.0025 at.-%, i.e. 1 atom/40,000, besides suppressing the cube texture to a considerable extent, also increased the half-softening time at 215.8° C. from about 12 sec. to 1.20 hr. and reduced the nucleation and growth rates by factors of about 20 and 2000, respectively. Larger additions produced greater effects, but it appears that little further increase in half-softening time could be produced by adding more than 0.015–0.025 at.-% phosphorus.

Silver was exceptional in that the largest addition of 0.0271 at.-% had an enormous retarding effect on

recrystallization, though, unlike phosphorus, cadmium, and arsenic, it did not change the recrystallization texture. Thus, the addition of 0.0271 at.-% silver to copper increased the half-softening time at 215.8° C. from about 12 sec. to 700 hr., decreased the rate of (planar) nucleation by a factor of about 2×10^6 , and decreased the growth rate by a factor of about 6×10^5 . It also increased the activation energy P from 20 to 64.5 and Q from 22.5 to 63.5 kg.cal./mol.

In the range 0–0.005 at.-% the effect of silver, cadmium, and arsenic/atom added on the half-softening time at 215.8° C. was very much less than that of phosphorus. In the range 0.018–0.025 at.-% the effect of silver and cadmium was greater than that of phosphorus or arsenic. Thus the first small addition of phosphorus to copper produced a much greater effect than silver, cadmium, or arsenic, but larger additions of silver and cadmium produced a greater effect than phosphorus.

The logarithm of the rate of (planar) nucleation, and similarly the logarithm of the growth rate, were found to vary approximately inversely as the logarithm of the half-softening time. Thus additions which increased the half-softening time generally decreased both the rate of nucleation and the rate of growth.

The growth rate was found to be constant with annealing time for pure copper and for alloys containing 0.0210 at.-% phosphorus, 0.0030 and 0.0271 at.-% silver, respectively. The combined data for the pure coppers indicated that the growth rate varied exponentially with annealing temperature and yielded an activation energy for growth of 21.5 kg.cal./mol. This figure is similar to the average values of P and Q for the pure coppers. All the alloys which recrystallized to the cube texture, except the 0.0271 at.-% silver alloy, had growth rates similar to that of pure copper at the same temperature, whereas the alloys which tended to have a more random recrystallization texture had smaller growth rates than pure copper.

The ratio of the number of grains (assumed spherical)/c.c. to the number of grains/cm.² in a planar section was fairly constant for all the materials examined, whatever the stage of recrystallization. Thus the "planar" nucleation rate or number of grains appearing/cm.²/sec. is directly proportional to the "spatial" nucleation rate (No./c.c./sec.). The rate of nucleation was found to decrease rapidly with increase in annealing time for a 0.0210 at.-% phosphorus alloy, but appeared to approach a constant rate at longer annealing times. The combined data for two pure coppers indicated that the rate of nucleation varied exponentially with annealing temperature and gave an activation energy of 21 kg.cal./mol. This value is similar to the activation energy for growth.

For materials for which the activation energies P and Q were approximately equal, it appeared probable that the logarithm of the rate of nucleation and similarly the logarithm of the growth rate were each directly proportional to the rolling reduction, at least in the range 80–98.75% reduction.

ACKNOWLEDGEMENTS

The authors wish to thank Dr. A. J. Phillips of the American Smelting and Refining Company for supplying materials and arranging chemical analyses. One of the authors (V.A.P.) would like to thank Yale University, London University, and the Department of Scientific and Industrial Research for financial help which made this work possible.

REFERENCES

1. M. Cook and T. Ll. Richards, *J. Inst. Metals*, 1944, **70**, 159.
2. C. S. Barrett, "The Structure of Metals". 1943: New York (McGraw-Hill).
3. J. S. Smart, Jr., and A. A. Smith, Jr., *Trans. Amer. Inst. Min. Met. Eng.*, 1943, **152**, 103.
4. J. S. Smart, Jr., and A. A. Smith, Jr., *ibid.*, 1946, **166**, 144.
5. M. Cook and T. Ll. Richards, *J. Inst. Metals*, 1947, **73**, 1.
6. N. Thorley, *ibid.*, 1950, **77**, 141.
7. V. A. Phillips, *ibid.*, 1950, **77**, 611 (discussion).
8. J. S. Smart, Jr., A. A. Smith, Jr., and A. J. Phillips, *Trans. Amer. Inst. Min. Met. Eng.*, 1941, **143**, 272.
9. L. Northcott and D. E. Thomas, *J. Inst. Metals*, 1939, **65**, 205.
10. P. A. Jacquet, *Compt. rend.*, 1949, **228**, 1027.
11. G. C. Williams and G. Rieger, *Trans. Electrochem. Soc.*, 1940, **77**, 261.
12. M.-K. Yen, *Trans. Amer. Inst. Min. Met. Eng.*, 1949, **185**, 59.
13. G. S. Zhdanov and V. I. Iveronova, *Zhur. Tekhn. Fiziki*, 1934, **4**, 911; and *Tech. Physics U.S.S.R.*, 1934, **1**, 64.
14. R. M. Brick and M. A. Williamson, *Trans. Amer. Inst. Min. Met. Eng.*, 1941, **143**, 84.
15. M. Cook and T. Ll. Richards, *J. Inst. Metals*, 1941, **67**, 203.
16. F. Adcock, *ibid.*, 1922, **27**, 73.
17. O. Dahl and F. Pawlek, *Z. Metallkunde*, 1936, **28**, 266.
18. Frhr. v. Göler and G. Sachs, *Z. Physik*, 1929, **56**, 485.
19. W. A. Johnson, *Metal Progress*, 1946, **49**, 87.
20. W. A. Anderson and R. F. Mehl, *Trans. Amer. Inst. Min. Met. Eng.*, 1945, **161**, 140.
21. W. G. Burgers, "Rekristallisation, verformter Zustand und Erholung" (Handbuch der Metallphysik, Band 3, Teil 2. Edited by G. Masing). 1941: Leipzig (Akademische Verlagsgesellschaft Becker und Erler Komm.-Ges.).
22. J. K. Stanley and R. F. Mehl, *Trans. Amer. Inst. Min. Met. Eng.*, 1942, **150**, 260.
23. J. K. Stanley, *ibid.*, 1945, **162**, 116.

EQUILIBRIUM RELATIONS AT 460° C. IN ALUMINIUM-RICH ALLOYS CONTAINING 0-7% COPPER, 0-7% MAGNESIUM, AND 1.2% SILICON *

1432

By H. J. AXON,† B.Met., D.Phil., JUNIOR MEMBER

SYNOPSIS

The equilibrium isothermal at 460° C. is given for quaternary alloys rich in aluminium and containing 0-7% magnesium, 0-7% copper, and constant silicon (1.2%). The phases encountered are the aluminium-rich solid solution, CuAl_2 , Mg_2Si , Si, the ternary phase Al_2CuMg , and a quaternary phase which probably has the composition $\text{Al}_5\text{Cu}_2\text{Mg}_3\text{Si}_6$. These phases give rise to fourteen separate phase fields. A new 460° C. isothermal for the aluminium-rich region of the aluminium-copper-silicon system is also given.

I.—INTRODUCTION

THE present paper is intended as the first of a series on the constitution of complex aluminium-rich alloys containing copper in the range 0-7%, magnesium 0-7%, and silicon 0-2%, all compositions being in weight-%. The system is to be investigated at various temperatures.

In view of the long-term nature of the investigation, it is proposed to discuss the results of previous investigators in the present paper, together with the experimental methods used in the present work, and the results so far obtained. It is hoped to publish the results of further investigation as a series of short communications which will extend the scope of the present paper. Those results of previous investigators which have a close bearing upon the present work are reported in Section II; an account of experimental methods and materials used is given in Section III; Section IV contains an account of the equilibrium relations at 460° C. for aluminium-rich alloys, containing a constant 1.2% silicon, with magnesium in the range 0-7% and copper in the range 0-7%. In view of the restricted composition range, it has been considered justifiable to plot the results using rectangular co-ordinates.

II.—PREVIOUS INVESTIGATIONS

The understanding of equilibrium relations in the quaternary system requires a knowledge of the ternary alloy systems of aluminium-copper-magnesium, aluminium-magnesium-silicon, and aluminium-copper-silicon. It is fortunate that reliable isothermals at 460° C. are available for the first two systems,^{1,2} and that the general form of the alu-

minium-copper-silicon system⁶ is known near to this temperature. It was the availability of this information which determined that the present work should start with an investigation of the quaternary system at 460° C.

1. THE SYSTEM ALUMINIUM-COPPER-MAGNESIUM

The aluminium-rich portion of this system has been studied at 460° and 375° C. by Little, Hume-Rothery, and Raynor,¹ who also considered the complicated equilibrium relations between the various ternary compounds. This work was confirmed and extended by Strawbridge, Hume-Rothery, and Little,³ who found that in the composition range 0-7% magnesium, 0-7% copper of the 460° C. isothermal there were four separate phase fields, as shown in Fig. 1, which is redrawn from the original paper.³ The phases encountered in this composition range are the solid solution of copper and magnesium in aluminium, the θ phase, which exists in the binary aluminium-copper system and which is sometimes designated CuAl_2 , and the S phase, which is a ternary compound of aluminium, copper, and magnesium. The ternary S phase exists over a small range of composition,³ but has been given the idealized formula Al_2CuMg . It has orthorhombic symmetry, and the unit cell contains 8 atoms of aluminium, 4 of copper, and 4 of magnesium, thus confirming the idealized formula.⁴

2. THE SYSTEM ALUMINIUM-MAGNESIUM-SILICON

The previous work on this system has been reviewed by Phillips,⁵ who obtained accurate boundaries for some of the phase fields at 500° and 200° C. A later study by Axon and Hume-Rothery² has given an isothermal for 460° C. which interpolates well between

* Manuscript received 12 July 1952.

† Lecturer in Electrometallurgy, The University of Manchester.

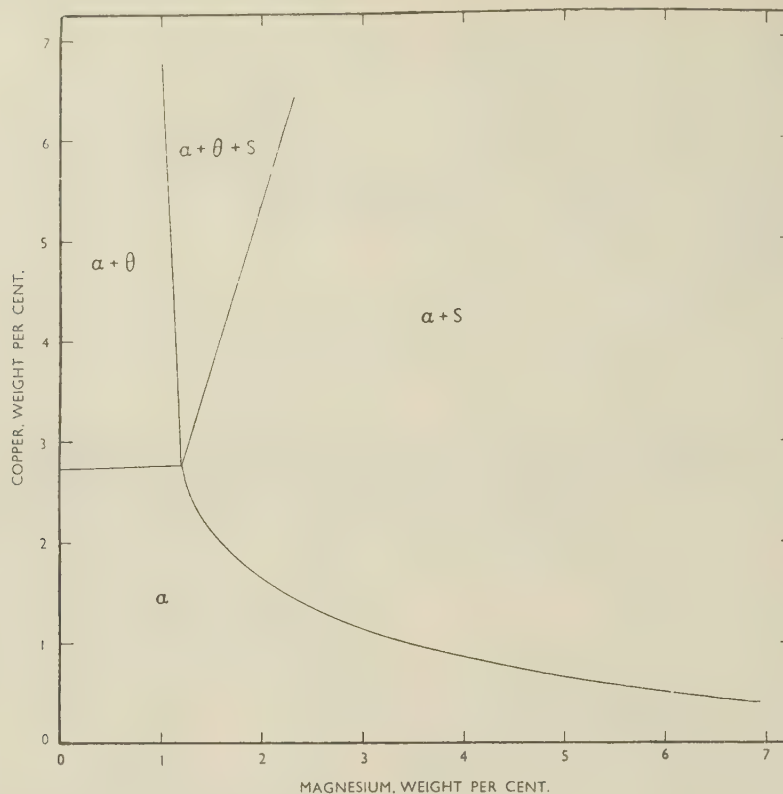


FIG. 1.—The 460° C. Isothermal for the System Aluminium-Copper-Magnesium. (Strawbridge, Hume-Rothery, and Little.³)

the results of Phillips at 500° and 200° C. This 460° C. isothermal is reproduced in Fig. 2, from which

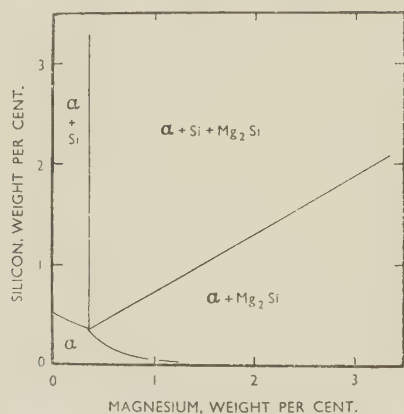


FIG. 2.—The 460° C. Isothermal for the System Aluminium-Magnesium-Silicon. (Axon and Hume-Rothery.²)

it can be seen that four separate phase fields exist in the composition range of the present investigation. The phases encountered are the aluminium-rich α solid solution, silicon, and the binary compound Mg_2Si , which forms a pseudo-binary system with aluminium.

3. THE SYSTEM ALUMINIUM-COPPER-SILICON

The general form of the liquidus and 500° C. isothermal for the aluminium-rich corner of this system

has been reviewed in the "Metals Reference Book",⁶ and agrees with the work of Gwyer, Phillips, and Mann,⁷ Matsuyama,⁸ and Hisatsune.⁹ No isothermal at 460° C. has been reported so far, and Fig. 3 shows the equilibrium relations at 460° C. as determined in the course of the present investigation. Fig. 3 agrees in form and disposition with the previously published isothermals for 400° and 500° C.,^{9, 6} there being four separate phase fields at the aluminium-rich corner of

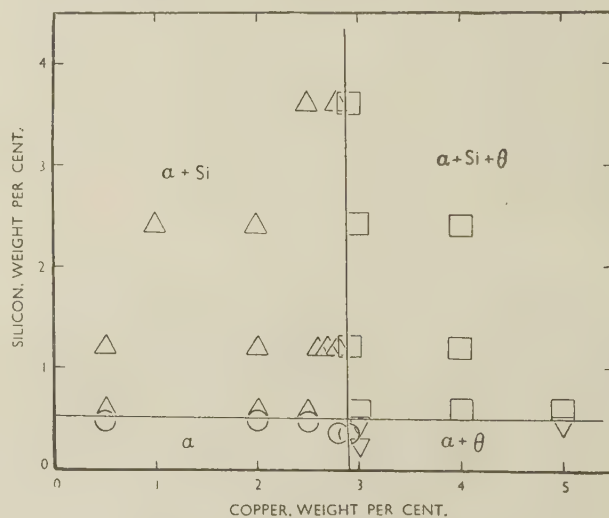


FIG. 3.—The 460° C. Isothermal for the System Aluminium-Copper-Silicon. (Present Investigation.)

the diagram. The phases are α , Si, and θ , with no ternary compound.

4. THE SYSTEM ALUMINIUM-COPPER-MAGNESIUM-SILICON

In the present work it is proposed to use the three ternary isothermals, reported above, as the bounding planes for a model of the aluminium-rich corner of the quaternary system. The model is drawn in rectangular co-ordinates so that the ternary aluminium-copper-magnesium isothermal forms the base plane, with the silicon composition axis vertical. Within the composition limits 0-7% magnesium, 0-7% copper, and 0-2% silicon, one may therefore expect the following phases from the ternary systems: α , Mg_2Si , θ , S ($=\text{Al}_2\text{CuMg}$), and Si. In addition to these, a quaternary compound has been reported by Dix, Sager, and Sager.¹⁰ This compound, which in the present work will be designated Q , has been given the idealized formula $\text{Al}_4\text{CuMg}_5\text{Si}_4$ or $\text{Al}_4\text{CuMg}_4\text{Si}_4$ by Petrov,¹¹ although Phragmén,¹² who analysed crystals of the quaternary compound, suggests that a more satisfactory formula is $\text{Al}_5\text{Cu}_2\text{Mg}_8\text{Si}_6$. Phragmén also reports that the quaternary compound has a hexagonal structure. His investigation was concerned chiefly with behaviour at the liquidus of the system, and he gives no information about equilibrium relations in the solid state. The presence of the quaternary phase, Q , is also confirmed by Töllner,¹³ and equilibrium relations in the solid state have been reported by Crowther¹⁴ and by Schrader.¹⁵

The work of Crowther was concerned chiefly with the investigation of solidus temperatures, but he suggests that in a series of alloys containing 4% copper, 1.2% silicon, and amounts of magnesium between 0% and 5% the sequence of phase fields, with increasing amounts of magnesium, is: ($\alpha + \theta + \text{Si}$); ($\alpha + \theta + \text{Si} + Q$); ($\alpha + \theta + Q$); ($\alpha + \text{Mg}_2\text{Si} + \theta + Q$); ($\alpha + \text{Mg}_2\text{Si} + \theta$), ($\alpha + \text{Mg}_2\text{Si} + \theta + S$), ($\alpha + \text{Mg}_2\text{Si} + S$) at a temperature of approximately 510° C. This sequence of phase fields is confirmed by the present work at 460° C. The same sequence of phase fields, with the addition of an ($\alpha + \text{Mg}_2\text{Si}$) field as the end member of the sequence, is reported by Schrader¹⁵ at 490° C. for alloys which contain 1.2% silicon and which lie on the line joining 6.8% copper to 6.8% magnesium.

III.—EXPERIMENTAL METHODS

The equilibrium relations were investigated by the microscopic examination of small pieces of alloy which had been chill cast and subsequently annealed in evacuated glass capsules for a period of four weeks at 460° C.

The alloys were made as ingots weighing 16 g. each by melting the aluminium in an alumina-lined crucible in an electric resistance furnace and adding the desired amounts of copper and silicon in the form of master alloys. When the aluminium-copper-silicon ternary

alloy was completely liquid, it was stirred with an alumina rod. The magnesium was then added as magnesium metal, which melted almost immediately, and the whole melt was vigorously stirred and immediately cast into a heavy iron mould; a fine-grained, chill-cast, ingot, $\frac{1}{4}$ in. in dia. was obtained in this way. A portion of each ingot was enclosed in a sealed evacuated capsule of hard glass, and the capsules were annealed for four weeks, at a temperature of $460 \pm 2^\circ \text{C}$., in tubular resistance furnaces controlled by Electroflo temperature regulators. At the end of the annealing period the capsules were quenched into cold water.

The aluminium used in the present work was supplied by The British Aluminium Co., Ltd., the magnesium by Magnesium Elektron, Ltd., and the aluminium-silicon master alloy by Blackwell's Metallurgical Works, Ltd. The aluminium-copper master alloy was prepared by melting aluminium and copper together in an alumina crucible. The purity of the materials was as follows: aluminium 99.991%, magnesium 99.95%, copper 99.99%, the aluminium-silicon master alloy contained 13.01% silicon, 0.25% iron, and 86.78% aluminium, giving a total metal content of 100.04%. This indicates that iron was the only impurity present in large amounts, a point which was confirmed by spectrographic analysis of the master alloy. The presence of 0.25% iron in the aluminium-silicon master alloy results in the addition of 0.023% iron to all specimens containing 1.2% silicon. No micrographic evidence of iron-bearing compounds was obtained in the 1.2% silicon isothermal, but the presence of iron must be remembered when considering the exact location of the phase fields.

Specimens were prepared for microscopic examination by the usual methods, using a metal polish of the "Brasso" type. Large crystals of Mg_2Si , Si, θ , Q , and S were easily identifiable without etching, but difficulty was often encountered when only minute amounts of a particular phase were suspected. Mg_2Si and Si were easily detected without etching, even when the crystals were small. Small crystals of θ , Q , and S were sometimes difficult to distinguish, particularly when the presence of more than one of these phases was suspected, and under these circumstances it was found useful to etch the specimen in cold 20% H_2SO_4 for 20 sec. This distinguished between S , which was attacked and turned brown, and θ or Q , which were not etched. The most satisfactory way of distinguishing between θ and Q was by careful examination of the unetched section, Q being harder, more definitely coloured, and less watery in appearance than θ .

The normal procedure was to examine each specimen twice, using two different cross-sections of the ingot spaced about $\frac{1}{2}$ in. apart, the intervening portion of the ingot being analysed if necessary. This was done as a check on longitudinal segregation. The critical alloys, which contained only a minute amount of θ , Q , or S , were examined at much greater length,

in some cases as many as ten new preparations were examined to confirm the presence or absence of a particular phase.

The chemical analyses were performed by Johnson, Matthey and Co., Ltd., and the author's thanks are due to Mr. A. R. Powell for his care and attention to this aspect of the work. The surface layer of each specimen was removed to a depth of about 0.5 mm. before the samples were sent for chemical analysis. This was to remove the region from which magnesium volatilized during the annealing process. In Fig. 4

four weeks at 460° C. Fourteen separate phase fields are found in the range 0–7% magnesium, 0–7% copper, in contrast with the four different phase fields which exist in the ternary system aluminium–copper–magnesium at the same temperature and over the same composition range. In Fig. 4 the point X on the vertical axis is taken from the ternary aluminium–copper–silicon system and corresponds to the $(\alpha + \text{Si})/(\alpha + \text{Si} + \theta)$ phase boundary for alloys containing 1.2% silicon. Points Y and Z on the horizontal axis are taken from the ternary aluminium–magnesium–

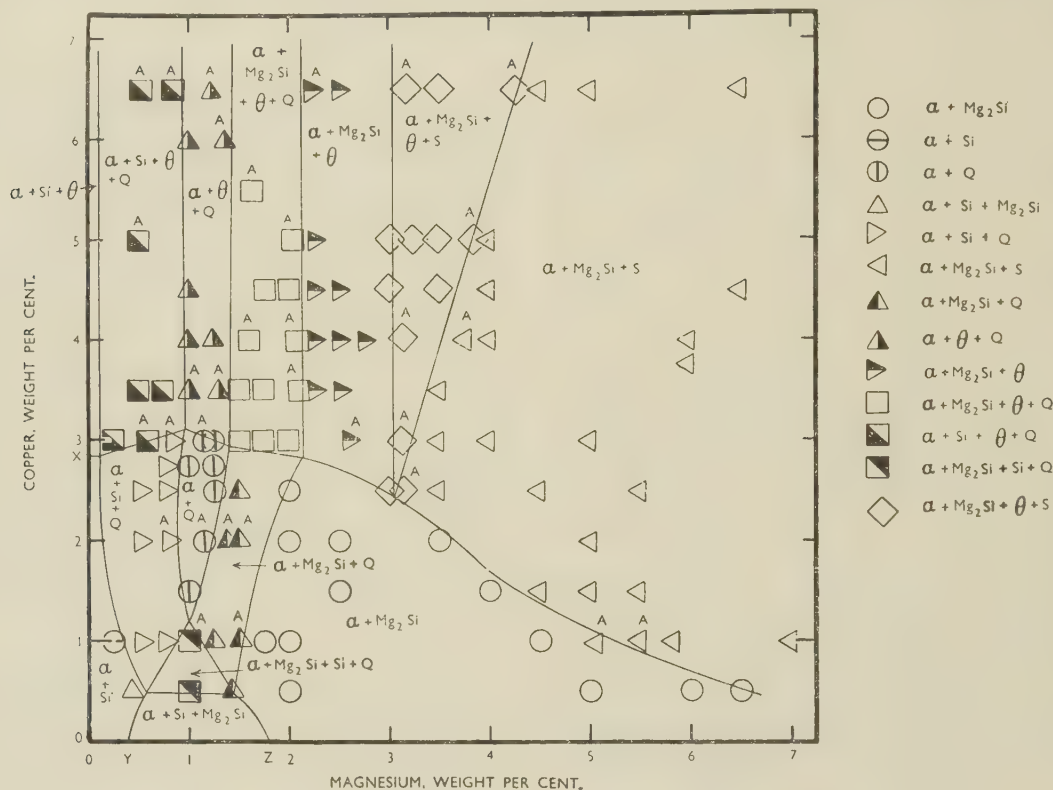


FIG. 4.—The 460° C. Isothermal for the System Aluminium–Copper–Magnesium–Silicon. All alloys in this figure contain 1.2% silicon.

the points corresponding to alloys which have been analysed are denoted by the letter *A* placed above the point. Most of these alloys were analysed for magnesium only, since previous work in this type of system^{2, 16} had shown that the desired synthetic composition with respect to copper and silicon could be obtained with very little error. Seven specimens were, however, analysed for silicon, and the analysed compositions all lay within $\pm 0.03\%$ of the desired composition (1.2% silicon). Thus the limits of accuracy of Fig. 4 are: as regards temperature $460 \pm 2^\circ \text{C.}$, and as regards composition silicon $1.2 \pm 0.03\%$ with 0.023% iron.

IV.—EXPERIMENTAL RESULTS

Fig. 4 shows the phase fields which occur on annealing aluminium-rich alloys containing 1.2% silicon for

silicon system, and correspond respectively to the $(\alpha + \text{Si})/(\alpha + \text{Si} + \text{Mg}_2\text{Si})$ and to the $(\alpha + \text{Si} + \text{Mg}_2\text{Si})/(\alpha + \text{Mg}_2\text{Si})$ phase boundaries for alloys containing 1.2% silicon.

The phase boundaries in Fig. 4 have been drawn after careful consideration of the amounts of the various phases present, and most of the experimental points lie in self-consistent areas. A small number of points lie on what appears to be the wrong side of the phase boundary, and it is necessary to discuss this apparent discrepancy. For this purpose individual points in Fig. 4 will be designated by the following notation: (x, y) , meaning an alloy containing 1.2% silicon with x wt.-% copper and y wt.-% magnesium, the compositions being synthetic (not analysed) compositions; and $(x, y)A$, meaning that the alloy was analysed for magnesium and the analysis result is used in designating the alloy.

Point (1.0, 5.04)*A* is plotted with the symbol for an ($\alpha + \text{Mg}_2\text{Si} + S$) alloy, but lies just within the ($\alpha + \text{Mg}_2\text{Si}$) phase field; of the two sections examined for this alloy, one contained only one small crystal of *S*, while the other contained three crystals of *S* grouped together, all the crystals being near the centre of the ingot. A slight degree of segregation was therefore suspected, and this point is regarded as being on or near to the ($\alpha + \text{Mg}_2\text{Si}$)/($\alpha + \text{Mg}_2\text{Si} + S$) phase boundary.

Points (2.5, 3.0) and (2.5, 3.14)*A* are of particular importance in helping to fix the position at which the four-phase region ($\alpha + \text{Mg}_2\text{Si} + \theta + S$) meets the two-phase region ($\alpha + \text{Mg}_2\text{Si}$). The two points are due to completely different specimens taken from the same casting; both specimens were repolished and examined many times, and both specimens were finally identified as containing α and Mg_2Si , together with very minute amounts of both θ and *S*. One specimen was analysed and the other was not, and the corner of the four-phase region ($\alpha + \text{Mg}_2\text{Si} + \theta + S$) has been placed between the analysed and unanalysed compositions. It should be noted that the difference between the analysed and synthetic compositions is 0.14% and that the synthetic composition is lower than the analysed composition. This is because a small extra addition of magnesium metal, over and above the synthetic composition, was made to all alloys at the time of casting. It was hoped that this extra magnesium would compensate for that which was lost by oxidation and volatilization. In practice it has been found that all the alloys which have been analysed were overcompensated, the analysed compositions being higher than synthetic compositions by 0.1-0.2% magnesium. Thus the two points (5.0, 3.0) and (4.5, 3.0) which lie just on the wrong side of the ($\alpha + \text{Mg}_2\text{Si} + \theta$)/($\alpha + \text{Mg}_2\text{Si} + \theta +$

S) boundary would be moved into the four-phase field if they were analysed. The two straight boundaries of the four-phase region ($\alpha + \text{Mg}_2\text{Si} + \theta + S$) have been drawn in terms of the analysed points only, and it is satisfactory to note that the lines drawn in this manner extrapolate to a point midway between the points (2.5, 3.0) and (2.5, 3.14)*A* mentioned above.

ACKNOWLEDGEMENTS

The author thanks Professor F. C. Thompson for research facilities and encouragement, and The Royal Society for a grant in aid of the research.

REFERENCES

1. A. T. Little, W. Hume-Rothery, and G. V. Raynor, *J. Inst. Metals*, 1944, **70**, 491.
2. H. J. Axon and W. Hume-Rothery, *J. Inst. Metals*, 1948, **74**, 315.
3. D. J. Strawbridge, W. Hume-Rothery, and A. T. Little, *J. Inst. Metals*, 1947, **74**, 191.
4. H. Perlitz and A. Westgren, *Arkiv Kemi, Mineral. Geol.*, 1943, [B], **16**, (13).
5. H. W. L. Phillips, *J. Inst. Metals*, 1946, **72**, 151.
6. C. J. Smithells (Editor), "Metals Reference Book", p. 352. London: 1949 (Butterworth's Scientific Publications).
7. A. G. C. Gwyer, H. W. L. Phillips, and L. Mann, *J. Inst. Metals*, 1928, **40**, 302.
8. K. Matsuyama, *Kinzoku no Kenkyu*, 1934, **11**, 461.
9. C. Hisatsune, *Tetsu to Hagane*, 1936, **22**, 597.
10. E. H. Dix, Jr., G. F. Sager, and B. P. Sager, *Trans. Amer. Inst. Min. Met. Eng.*, 1932, **99**, 119.
11. D. A. Petrov, *Zhur. Fiz. Khim.*, 1937, **9**, 522; and *Acta Physicochim. U.R.S.S.*, 1937, **6**, 505.
12. G. Phragmén, *J. Inst. Metals*, 1950, **77**, 489.
13. H. Töllner, *Aluminium-Archiv*, 1940, (34).
14. J. Crowther, *J. Inst. Metals*, 1949-50, **76**, 201.
15. A. Schrader, *Metall*, 1949, **3**, 111.
16. D. M. Poole and H. J. Axon, *J. Inst. Metals*, 1951-52, **80**, 599.

An Example of Strain-Relief in Powder Specimens *

14

By J. GORDON PARR,† B.Sc.

SYNOPSIS

The more complete strain-relief in powder than in solid specimens of an iron-manganese alloy is demonstrated by the lower hardness value of quenched powders, and their more rapid attainment of equilibrium on tempering.

THE ϵ phase (a close-packed hexagonal structure) is produced in iron-manganese alloys containing 10–30% manganese by a martensite reaction of nucleation and shear.^{1,2} It is formed together with either α' (body-centred cubic, supersaturated with iron) or γ (face-centred cubic) phases, or with both, depending upon the composition of the alloy.^{3,4} Although the microstructures of alloys within the range 10–30% manganese do not allow a distinction to be made between the individual phases, the ϵ phase (in the customary metallographic specimen) is always associated with a Widmanstätten pattern³ attributable to strain lines.

Needle specimens (1 cm. long, 0.5 mm. dia.) assaying 18.5% manganese, when quenched from 1250° C., exhibit an unmistakable Widmanstätten pattern. Their constitution, determined by an X-ray method,⁵ is 12% α' , 25% γ , and 63% ϵ .

Powder specimens undergo the same transformations as do the needles on quenching. Filings of an 18.5% manganese alloy (to pass through a 200-mesh screen), quenched from 1250° C., contain 15% α' , 30% γ , and 55% ϵ . Microspecimens of the powder are extremely difficult to prepare, but, so far as can be seen, they exhibit no strain lines.

If the powder is in a less strained condition, as its appearance under the microscope implies, one would expect it to have a lower hardness than the needle specimen. Microhardness measurements were made on needle and powder, with the following results:

Hardness of needle (30 g. load)	500 \pm 25 V.P.N.
Hardness of powder (10 g. load)	225 \pm 25 V.P.N.

(A 10-g. load applied to the needle produces so small an indentation that hardness values cannot be more

accurately computed than ± 50 V.P.N. Within these limits of error, hardness values determined with 10- and 30-g. loads are in agreement.) The microhardness figures therefore confirm a greater state of strain within the quenched needle specimen than within the similarly treated powder.

Tempering powder and needle in the ($\alpha + \gamma$) phase field causes the α' and ϵ phases to transform (by diffusion processes) to α (of equilibrium composition) and γ phases in an effort to achieve an equilibrium ratio. On tempering under conditions that produce α , the precipitation of this phase, which involves a volume expansion of 4%, is much longer delayed in solid than in powder samples. The 18.5% manganese specimens tempered at 450° C. produce (after the initial disappearance of α') 25% of α in powder and needle after 5 and 5000 hr., respectively. This difference in the rate of precipitation of α is explicable in terms of the greater strain energy associated with the needle specimen against which the precipitating phase must do work.

The evidence offered by hardness figures and by the precipitation rate of α , confirms the generally accepted belief of more complete strain-relief in powder than in solid specimens.

REFERENCES

1. A. R. Troiano and F. T. McGuire, *Trans. Amer. Soc. Metals*, 1943, **31**, 340.
2. J. G. Parr, *Acta Cryst.* (to be published).
3. F. M. Walters, Jr., and C. Wells, *Trans. Amer. Soc. Metals*, 1936, **24**, 359.
4. J. G. Parr, *Metal Treatment* (to be published).
5. J. G. Parr, *J. Iron Steel Inst.*, 1952, **171**, 137.

* Manuscript received 30 July 1952.

† Lecturer in Metallurgy, Liverpool University.

THE SUB-GRAIN STRUCTURE IN ALUMINIUM DEFORMED AT ELEVATED TEMPERATURES *

1434

By J. A. RAMSEY,† M.Sc.

SYNOPSIS

Sub-grain structures in coarse-grained aluminium deformed at elevated temperatures are shown by metallographic and X-ray examination to be associated with bands similar to kink bands. A marked resemblance thus exists between these sub-grain structures and those resulting from heating after straining at room temperature.

I.—INTRODUCTION

THE grains of aluminium deformed at elevated temperatures manifest a sub-grain structure of relatively perfect elements, tilted slightly with respect to each other.¹ The microstructure changes with increasing temperature of straining, or decreasing rate of deformation, the slip becoming coarse and widely spaced and finally "disappearing".[‡] The size of the elements of the sub-grain structure increases under the same conditions. These processes are accompanied in X-ray-diffraction photographs by a sharpening of the spots and a diminution in the amount of diffuse background.

X-ray-diffraction methods have also revealed that the grains of aluminium deformed at room temperature and subsequently heated develop, under certain conditions, a sub-grain structure. These X-ray changes are associated with the relief of stresses in restricted regions in which the lattice is bent. Kink bands have been found to provide favourable sites for this process.⁵ In some cases, where the kink bands lie very close together, the microstructure of the sub-grains resembles closely that obtained by deformation at elevated temperatures and termed a cell structure.⁶

The work described in the present note shows that the sub-grain structures resulting from high-temperature deformation are also intimately associated with kink banding.

II.—EXPERIMENTAL TECHNIQUE AND RESULTS

The grain-sizes studied and the polishing and etching techniques employed were similar to those reported in a recent paper.⁶ The large grain-size selected (3–5 mm.) proved particularly useful, because widely separated bands could readily be produced at

the lower deformation temperatures used. Observations were made primarily on specimens deformed at temperatures and strain rates falling within a range in which it was known that sub-grain structures could readily be produced, i.e. from 500° up to 620° C. for rapid straining, and somewhat lower temperatures for slow (0.15%/hr.) straining. A metallographic examination was also made of specimens which had been used in other work and which X-ray-diffraction photographs showed to contain well-developed sub-grain structures.

Fig. 1 (Plate XXX) shows a typical grain in a specimen extended rapidly to 8% at 500° C.; the slip was coarse and widely spaced compared with that occurring under similar conditions at room temperature. In addition, banded zones were visible running across the main slip direction. The behaviour of slip traces in these zones was like that of the traces found in the vicinity of kink bands at room temperature. The bands formed at 500° C. were, however, in general much broader than their room-temperature analogues. As illustrated in Fig. 2 (Plate XXX), repolishing and etching the specimens revealed a sub-structure within the bands. X-ray-diffraction examination showed that the Debye arcs from individual grains consisted of a mixture of relatively sharp spots and continuous, diffuse background.

Higher temperatures of deformation in general gave rise to still broader bands of the type illustrated, the slip becoming coarser and more widely spaced. The size of the sub-grains tended to increase, while grains exhibiting the sub-structure not only in the bands but also, though more faintly, in the regions between them, became more numerous. At 620° C. the majority of the grains showed sub-structure in the inter-band material.

The microstructure at this temperature, after repolishing and etching, is illustrated in Fig. 3 (Plate

the electron microscope³ and phase-contrast illumination⁴ have failed to reveal any evidence of slip, this may mean only that the surface manifestation of slip as "steps" has been removed.

* Manuscript received 20 May 1952.

† The Baillieu Laboratory, University of Melbourne, Australia.

‡ This term refers specifically to the disappearance of the coarse, high-temperature slip. Although experiments using

XXX). The diffraction pattern was characterized by a greater degree of spottiness and a less continuous background.

It was desired to compare the sub-grain structure in specimens manifesting slip and in slip-free specimens. The temperature at which slip "disappears" depends on the grain-size and the strain rate; e.g. with a grain-size of 8–10 grains/mm. and with rapid straining the critical temperature is about 400° C. With the grain-size employed and with rapid straining, it was probable that slip would vanish only close to the melting point; deformation was therefore carried out at a slow rate of 0.15%/hr. at 350° C.

Both types of sub-structure noted above⁶ were present, but most of the grains were in the "slipless" condition. The microstructure is illustrated in Figs. 4 and 5 (Plate XXX). In Fig. 4, which shows the condition after deformation, no trace is visible of the coarse slip found in the earlier specimens. Fig. 5 is a photograph of the same area after repolishing and etching. The sub-grain structure did not appear to occur preferentially in bands.* This observation was confirmed by the re-examination of similar grains in a number of specimens used in earlier work. The sub-grain structure proved much more difficult to etch than when it occurred in kink bands. It was associated with X-ray-diffraction patterns in which the arcs from individual grains consisted almost entirely of sharp spots.

In conclusion, it may be stated that the sub-grain structure in aluminium deformed at elevated temperatures frequently tends to exhibit bands closely

resembling kink bands. This suggests that it is similar in nature to the sub-grain structure obtained by heating after deformation at room temperature. "Slipless" grains, which are characteristic of deformation at very slow rates or very high temperatures, do not appear to be associated with kink bands, but this may be due to limitations of the technique, as recent investigation has revealed some banding of the sub-grain structure.

It seems likely that sub-grains found after deformation at elevated temperatures are due to the almost simultaneous formation and recovery of kink bands, and that, if the bands are sufficiently close together, the result will be a sub-grain structure covering the whole grain, very similar to the cell structure proposed by Wood and his co-workers.

ACKNOWLEDGEMENTS

The author wishes to thank Professor J. Neill Greenwood, Dr. W. A. Wood, and his colleagues at the Baillieu Laboratory, University of Melbourne, for useful discussions during the course of the work.

REFERENCES

1. G. R. Wilms and W. A. Wood, *J. Inst. Metals*, 1948–49, **75**, 693.
2. W. A. Wood and W. A. Rachinger, *ibid.*, 1949–50, **76**, 237.
3. R. I. Garrod, J. W. Suiter, and W. A. Wood, *Phil. Mag.*, 1952, [vii], **43**, 677.
4. J. W. Kelly and R. C. Gifkins, private communication.
5. R. W. Cahn, *J. Inst. Metals*, 1951, **79**, 129.
6. J. A. Ramsey, *ibid.*, 1952–53, **81**, 61.

* Some recent results, using polarized light, indicate that there is a tendency for sub-grains of like orientation to occur

in bands in similar "slipless" grains.⁴ It is not yet known whether these correspond with kink bands.

Fatigue of Metals *

Mr. D. McLEAN,† B.Sc. (Member): The natural interest of these papers is augmented by their seeming mutual inconsistency. Mr. Forsyth considers that his aluminium specimens develop a sub-crystal structure during fatigue, and his Figs. 16–18 (Plate XXXII) appear to provide conclusive evidence that this is so. He mentions tilts of orientation between adjacent sub-crystals of as much as 30°, and Fig. 18 supports this. Now, the X-ray technique used by Dr. Wood and Mr. Head, applied to material containing sub-crystals having such large differences in orientation, should show the single spots corresponding to the original grains each to be replaced by a long arc of small spots, perhaps blurred into one another to appear continuous if the sub-crystals are sufficiently strained. But this is precisely what Dr. Wood and Mr. Head do not find in their fatigued specimens. The main point of their paper is that alternating stress above a moderate frequency leaves the X-ray pattern of the specimens almost unchanged, still showing the well-separated spots of the original crystals. The evidence for this also seems conclusive—for example, their Figs. 15 and 16 (Plate XIII). Thus, the two papers lead to opposite conclusions, and each contains evidence that its own conclusion is right. Since Mr. Forsyth applied alternating stress to his specimens at the rate of 50 cycles/sec.—about ten times faster than the critical frequency in the work of Dr. Wood and Mr. Head—it is unlikely that the inconsistency is to be explained by his having operated at too low a frequency. It must be due to some of the other experimental conditions.

This main observation of Dr. Wood and Mr. Head is also of considerable interest in connection with the theory of strain-hardening. It has been usual to associate strain-hardening with X-ray line-broadening and hence with the structure deduced to cause the broadening. However, since the fatigue specimens used by Dr. Wood and Mr. Head must have been strain-hardened enough to bear the applied load, but nevertheless gave sharp or broad X-ray spots according only to the frequency at which the stress cycles were applied, there seem to be no unique connection between strain-hardening and X-ray line-broadening (and, presumably, asterism in Laue patterns).

Mr. N. H. POLAKOWSKI,‡ Dipl.-Ing.: Dr. Wood and Mr. Head set out to explain why cyclic stressing results in “brittle” fracture of a ductile metal. They suggest that this should be connected with the different degrees of disorientation produced in the crystalline structure by static or slow cyclic stressing on the one hand, and by rapid repetitions of stress on the other. In the case of annealed copper, the “critical rate of cyclic stressing” should lie between 300 and 400 cycles/min., as may be seen by comparing their Figs. 14, 17, 19, 21, 23 (Plates XIII and XIV) with Figs. 15, 18, 20, 22, 24, and from Fig. 25 (b) (p. 99). Consequently, 300 cycles/min. is still a slow speed, whereas 400 is already high.

* Joint discussion on the papers by W. A. Wood and A. K. Head (*Journal*, 1951, 79, 89) and P. J. E. Forsyth (*Journal*, 1951–52, 80, 181).

† Metallurgy Division National Physical Laboratory, Teddington.

‡ Research Student, University College, Swansea.

§ In an unsafe range of stress the progressive hardening of the specimen proceeds in much the same way, but eventually the hysteresis loop starts to increase until fracture occurs. If the test is interrupted at a stage where the fatigue crack is only beginning to develop, and the specimen is tested in ten-

The question arises whether there is any marked difference in the appearance of the fatigue fractures obtained at 400 and 300 cycles/min., corresponding to the differences between the two groups of X-ray diagrams. According to the authors' argument, I should expect the fracture to be “brittle” (i.e. a typical fatigue fracture) in the first case, but very noticeably different in the second. Could this point be clarified? An explanation would be all the more valuable, since the same kind of difference exists between Figs. 17 and 18, where the applied stress (± 3 tons/in.²) is well within the safe range, so that fracture would not be anticipated even after many millions of repetitions.

The interpretation of “dynamic overstrain” given on p. 99 tends to oversimplify the issue. Large cyclic permanent sets are produced on repeated application of reversed stress cycles, characterized by wide hysteresis loops. If the applied stress is within the safe range,§ the value of the cyclic permanent set will decrease continuously until an equilibrium between external stress and the degree of work-hardening of the specimen is reached. This condition is characterized by a very narrow steady loop “elastic hysteresis”. When all the cyclic permanent sets found in each consecutive cycle, $\pm S$, are added together, without regard to sign, the cumulative linear strain will greatly exceed the unidirectional static overstrain resulting from a static stress S . This is, of course, just what one would expect as a result of the Bauschinger effect acting on each reversal and partly offsetting the results of the overstrain induced by the preceding half-cycle.

The observations illustrated in Figs. 1–4 (Plate XI) and discussed in Section III, 1 (p. 93) of the paper represent another manifestation of the Bauschinger effect, and it is not difficult to see that the reorientation effect on reversed deformation (Figs. 1–4) is intimately connected with the relevant changes in lattice spacing found by Dr. Wood himself in a previous research.||

The introduction of the word “new” into the title of the paper tends somewhat to obscure the merits of earlier work. In particular, the results reproduced in Figs. 1–4 represent virtually a repetition of experiments carried out over 25 years ago by Czocharlski¶ and repeated in 1926 by Sachs.** A number of researches on similar lines, using various techniques (not exclusively X-ray) are reviewed by Burgers.††

It is stated on p. 99 that “as shown by measurements made by Wood and Thorpe, after a sufficient number of cycles the dynamic stress/strain curve tends to become an extension of the static elastic range”. I hold that after a sufficient number of cycles, i.e. when a state of equilibrium between stress and work-hardening is reached, the actual static stress/strain curve as measured on the specimen after removing it from the fatigue machine, will roughly form an extension of the “primitive” elastic range (OY, Fig. 25 (a)). This was actually shown to be the case by the tests of Wood and Thorpe

sion, the yield point will be raised approximately to the value of the applied stress, as shown in Fig. 25 (a) (p. 99).

|| S. L. Smith and W. A. Wood, *Proc. Roy. Soc.*, 1944, [A], 182, 409.

¶ J. Czocharlski, *Z. Metallkunde*, 1925, 17, 1 and Figs. 30, 31, 34.

** G. Sachs, *ibid.*, 1926, 18, 209 and Figs. 9, 10, 11.

†† W. G. Burgers, “Handbuch der Metallphysik” (edited by G. Masing). Band 3, Teil 2: “Rekristallisation, verformter Zustand und Erholung”, pp. 492–501. 1941: Leipzig (Akad. Verlag. Becker u. Erler).

to which reference is made, and much earlier by Memmler and Laute,* in their comprehensive experiments on the Schenck machine. The dynamic stress/strain curve for high-speed cyclic straining practically always at first sight forms an extension of the primitive elastic range, if the finite width of the hysteresis loop is neglected.

Mr. FORSYTH (*in reply*): In reply to Mr. McLean, I should like to point out that in my experiments the existence of a polygonized structure was checked by examining small regions near the fracture with the X-ray micro-beam technique. In a specimen which has been fatigued, the bulk of polygonized material in any randomly chosen region is likely to be small, and prior microscopic examination is essential in order to find the regions of marked polygonization. In this respect the detection is more difficult than might be experienced in creep, where the deformation is distributed over a larger volume of material. As might be expected, more widespread disorientation will occur per cycle at the lower frequencies, but I believe it is the regions of localized deformation that are important in fatigue, and these may occur even in the absence of this widespread disorientation.

Dr. WOOD and Mr. HEAD (*in reply*): We do not think the X-ray effect Mr. Polakowski quotes is necessarily the "re-orientation" effect to which we draw attention. The effect

shown by his Laue pictures has been interpreted as due to internal stresses and to the partial reversibility of those stresses, as he points out. It is possible that such stresses do occur, and are reversed during a stress cycle. However, the effect we are concerned with is a change in the elongation of the X-ray reflections *along the circumference* of the diffraction rings, not radially. And the observation of a partial reversibility of this elongation in a back-reflection photograph points to a reversibility in the disorientation of the broken-down grains. Moreover, the back-reflection method permits of no other interpretation. To our knowledge this observation is new. It has nothing to do with internal stresses or the Bauschinger effect. We were aware of the Laue asterism pictures, but have always regarded the changes they show as ambiguous. The further question regarding possible differences in the fracture above and below the critical rate of stressing is of great interest, but difficult to answer briefly. We are finding differences. At slow rates we can even produce intergranular fractures. But it is too early to say whether these differences are due entirely to the period of the stress cycle. The "shape" of the cycle may be important.

The basis of the inconsistency between our work and that of Mr. Forsyth, as pointed out by Mr. McLean, is not obvious. One difference, of course, is in the metals used, but there are many other possible factors, and at this stage it is not possible to offer an explanation for the difference in observations.

* K. Memmler and K. Laute, *Forsch. Ingenieurwesens*, 1930, (329); also reproduced in W. Herold, "Die Wechselfestigkeit

metallischer Werkstoffe", pp. 84-85 and Figs. 37-39. 1934: Wien (Julius Springer).

THE HIGH-TEMPERATURE OXIDATION OF SOME COBALT-BASE AND NICKEL-BASE ALLOYS *

1435

By PROFESSOR A. PREECE,† M.Sc., F.I.M., MEMBER, and
G. LUCAS,‡ Ph.D., STUDENT MEMBER

SYNOPSIS

A description is given of the oxidation characteristics of cobalt and nickel, and of a number of alloys based on these metals, in the temperature range 800°–1200° C. A simple apparatus was designed to supply an atmosphere similar in composition to that produced in gas turbines, paraffin containing 2% sulphur being used as fuel. Reactions occurring within the scales are compared with those that take place when mixtures of oxides are heated at similar temperatures. Of the reactions noted, spinel formation is shown to be detrimental to the formation of a protective oxide layer.

The effects of a number of minor alloying elements, viz. V, B, Nb, Be, Ti, Zr, Ca, Ta, Al, Ce, Si, and Th, on the oxidation of a cobalt–32% chromium alloy are described. Several elements increased the resistance to oxidation, in particular thorium and silicon; vanadium and boron, however, were highly deleterious, owing to the formation of low-melting-point oxides.

The rate of oxidation of cobalt shows a sharp decrease in the region of 950° C., and this coincides with the upper limit of stability of Co_3O_4 . It appears that the presence of this oxide at the outer surface of the scale increases the rate of oxygen transfer to the underlying CoO . From a consideration of scale structure and the occurrence of internal oxidation in a number of the alloys, it is suggested that oxygen diffusion through the scale occurs to a considerable extent.

I.—INTRODUCTION

THE experimental results described in the present paper were obtained during a general survey of the high-temperature oxidation of a number of binary alloys based on cobalt and nickel, respectively, and a more detailed examination of a cobalt–chromium alloy containing additions of a third element. The results may provide guidance, in respect of oxidation behaviour, for those working on the development of creep-resisting alloys.

II.—PREPARATION AND TESTING

1. ALLOYS USED

The metals used in the preparation of the alloys were of ordinary commercial purity, but the cobalt roundels were first melted under a stream of hydrogen to reduce the oxide present. The following binary alloys have been studied :

Cobalt + 10, 20, 25, 32, and 40% Cr
 + 5, 10, and 15% W
 + 5, 10, and 15% Mo
 + 5% Al
 + 40% Ni
Nickel + 5, 10, and 15% W
 + 5, 10, and 15% Mo
 + 5% Al.

Nickel–chromium alloys were omitted, since their properties had already been the subject of much research. All the alloys listed above were single-phase, with the exception of the cobalt–40% chromium alloy.

The cobalt–tungsten, nickel–tungsten, and nickel–molybdenum alloys were prepared by normal powder-metallurgy techniques. The metals, in the form of –200-mesh powders, were milled for 8 hr. to ensure thorough mixing and then pressed into small bars 6 in. long by $\frac{1}{2}$ in. square at 35 tons/in.² pressure. The bars were sintered *in vacuo* at a temperature approximately 20° C. below the melting point of the alloy, after which they were forged and rolled to sheet 0.05 in. thick.

The remainder of the alloys were vacuum-melted, and specimens cut from the ingots without further treatment.

2. DESCRIPTION OF THE APPARATUS

The apparatus used for oxidizing the specimens was designed to simulate the gas-turbine atmosphere, and is shown in Fig. 1. Paraffin was used as the fuel, and was allowed to flow into a controlled stream of air supplied from a small compressor. The mixture was burned in the combustion furnace, maintained at 950° C., before being led to the furnaces containing the specimens. It was necessary to equalize the pressure in the fuel reservoir with that in the combustion chamber in order to ensure a constant flow of fuel.

* Manuscript received 26 May 1952.

† Professor of Metallurgy, King's College, University of Durham.

‡ Research Assistant, Metallurgy Department, King's College, University of Durham.

The rate of paraffin injection was controlled to give an air-to-fuel ratio of 60 : 1, since this would be more corrosive than the weaker mixtures (up to 150 : 1) used in practice. An addition of carbon disulphide was made to bring the sulphur content of the fuel to 2%

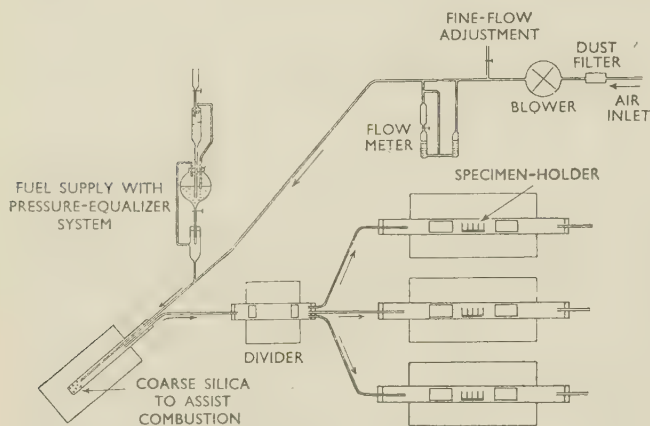


FIG. 1.—Diagram of Apparatus.

by weight. The composition by volume of the atmosphere produced was: 3.5% CO_2 , 3.3% H_2O , and 0.06% SO_2 , the remainder being air slightly enriched in nitrogen content. Throughout the text this is referred to as the "60:1 mixture", and it was found that oxidation results in this atmosphere showed no appreciable difference from those obtained in air, in spite of the high sulphur content of the fuel.

The rate of flow of the oxidizing atmosphere over the specimens was well above the critical speed. The three testing furnaces were designed to operate over the temperature range 800°–1200° C., and were controlled to $\pm 5^\circ \text{C}$.

The specimens used in the oxidation tests had a surface area from 3 to 5 cm.². Preliminary tests showed that, at the temperatures concerned, the effect of surface finish was slight and that a 1/0 emery finish was satisfactory.

The specimens were suspended by platinum wire from hooks of silica rod set in an alumina block. On removal from the furnace, the specimens were rapidly transferred to porcelain crucibles and covered to prevent loss of scale should exfoliation occur. The degree of oxidation was measured by the increase in weight.

The structure of the scale and the nature of the scale/metal interface were examined by metallographic methods. The constitution of the scale substance was determined by X-ray analysis and, as secondary reactions frequently occurred between the oxides formed, this method of examination proved most valuable. The scales, or individual layers when separation was possible, were usually examined in the powder camera, but in some cases back-reflection photographs were taken of the scale *in situ* to establish the constitution of the outer layer.

3. SINTERED OXIDE MIXTURES

For the work carried out on oxide reactions, a small die and ram were made for compressing oxide mixtures into pellets. The oxides used were of the chemically pure type. After treatment at the desired temperature for 50 hr., the pellets were re-powdered and examined in the X-ray powder camera.

III.—EXPERIMENTAL RESULTS

1. PURE COBALT AND PURE NICKEL

The rates of oxidation of cobalt and nickel were examined in oxygen, as well as in the "60:1 atmosphere". Fig. 2 shows that the mechanism of oxidation of cobalt changes at approximately 950° C.; back-reflection X-ray studies indicated that above this temperature the thin Co_3O_4 surface layer was no longer formed. Apart from this Co_3O_4 , the scales consisted of two clearly defined layers: a hard, coherent, outer layer and an inner layer of a friable nature, both of which were identified as CoO . At 800° C. the outer layer had a matt grey appearance and tended to spall on cooling, but above this temperature it remained adherent and acquired a macro-crystalline appearance.

The interface between the two layers was coincident with the original metal surface, and the continued existence of such a demarcation indicates that, from the beginning of oxidation, there is a fundamental difference in the methods of growth of the two layers. The outer layer is formed by the diffusion of metal ions into an oxygen-rich environment, and it is

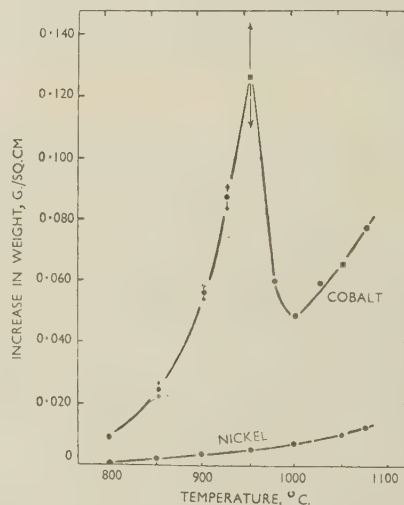


FIG. 2.—Effect of Temperature on the Oxidation After 24 Hr. of Pure Nickel and Pure Cobalt in Oxygen.

thought probable that oxygen is dissolved by this layer as it grows, giving an oxygen concentration in excess of stoichiometric requirements. The oxygen content of the inner layer, however, has to be supplied by a diffusion process from the outer layer, and the

pressure will not greatly exceed the dissociation pressure of the oxide.

The greater oxygen content of the outer layer would account for its pronounced crystallinity. Confirmation of this was found when Co_3O_4 was heated at 1000°C . and weighed at intervals. The oxide first reverted to CoO and then gradually increased in weight, becoming crystalline in appearance, and finally contained about 3 wt.-% of excess oxygen.

The thicknesses of the inner and outer layers formed after 24 hr. in oxygen at various temperatures are plotted in Fig. 3, which shows that (a) the rate of

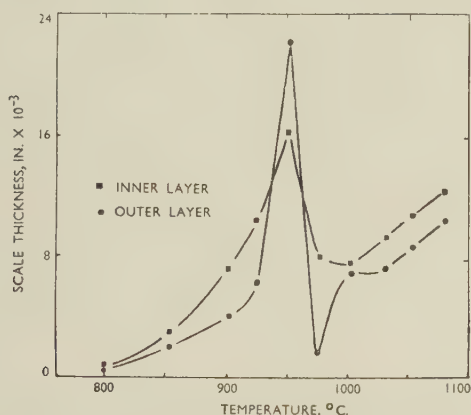


FIG. 3.—Variation with Temperature of Thicknesses of the Inner and Outer CoO Layers on Pure Cobalt After Heating for 24 Hr. in Oxygen.

formation of both layers is affected by the disappearance of the thin layer of Co_3O_4 at approximately 950°C ., and (b) the curve representing the thickness of the inner layer is the predominating one up to this temperature. This suggests that the effect of the layer of Co_3O_4 is to make the passage of the oxygen into the scale easier, possibly by increasing the rate of transfer of oxygen into the CoO layer.

It is convenient to mention here that this thin layer of Co_3O_4 was found only in the oxidation of cobalt itself, and was completely absent from the oxidation of the cobalt alloys to be discussed later.

A scale consisting of two separable layers of identical composition was also observed in the oxidation of nickel, and comprised a dark-green, coherent, outer layer and a light-green, powdery, inner layer, both NiO . If nickel oxide is heated alone it absorbs extra oxygen and acquires a dark-green colour comparable with that of the outer scale layer. As the dividing line between the two layers again coincided with the original metal surface, it appears that, in this respect, nickel oxidizes in a similar manner to cobalt.

It is interesting to note that, as mentioned by Dunn¹ the oxidation of nickel proceeds preferentially along the grain boundaries.

2. COBALT-NICKEL ALLOYS

Preliminary experiments showed that with additions of up to 40% nickel the rate of oxidation of cobalt

decreased almost linearly and the results obtained with a Co-40% Ni alloy are given in Table I.

TABLE I.—Average Oxidation Results for Cobalt and the Cobalt-40% Nickel Alloy.

Temp., $^\circ\text{C}$.	Increase in Weight, g./cm. ²	
	Co	Co-40% Ni
800	0.020	0.0008
900	0.042	0.0096
1000	0.045	0.0214
1100	0.148	0.0458

The scales formed were adherent, and in external appearance closely resembled those formed on cobalt. No signs of internal oxidation were found below 1000°C ., and only a small amount was observed at the higher temperatures.

An X-ray examination of the scales showed that both layers consisted of a solid solution of nickel oxide in cobalt oxide and that the amount of nickel oxide present in the inner layer was greater than that in the outer layer.

3. COBALT-MOLYBDENUM ALLOYS

The results of the oxidation tests on these alloys are shown in Table II.

TABLE II.—Average Oxidation Results for the Cobalt-Molybdenum Alloys.

Temp., $^\circ\text{C}$.	Increase in Weight, g./cm. ²		
	Co	Co-5% Mo	Co-10% Mo
800	0.020	0.011	0.011
900	0.042	0.023	0.022
1000	0.045	0.049	0.045
1100	0.148	0.090	0.064
1200	0.165

The addition of molybdenum to cobalt caused no significant alteration in the rate of oxidation at temperatures up to 1000°C . At 1100°C . there was a noticeable decrease in the amount of oxide formed as the molybdenum content increased. Oxidation rates at 1200°C . could not be determined accurately owing to the very rapid conversion of the metal to oxide. Pale yellow deposits of molybdic oxide were noticed on the furnace walls at this temperature, indicating that any increase-in-weight measurements made would have been subject to serious error.

When the specimens were cooled from the testing temperature, the scale usually spalled off, revealing a powdery inner layer which was brown in colour and very bulky. The outer layer appeared to be a typical CoO layer. At 1200°C . the scales were extremely porous, owing to the volatilization of MoO_3 .

X-ray examination showed that in all cases the outer layer consisted of CoO , with a small amount of

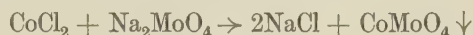
cobalt molybdate, CoMoO_4 , whereas the inner layer was chiefly cobalt molybdate with some CoO .

Cobalt Molybdate

Cobalt molybdate forms readily at the temperatures used in these tests, i.e. between 800° and 1200°C. , on heating mixtures of cobalt oxide and molybdic oxide. It was noted that, in the presence of MoO_3 , the Co_3O_4 reverted to CoO at a lower temperature than normal. This increased instability of Co_3O_4 may explain the absence of the thin layer of Co_3O_4 in the oxidation products of the cobalt-molybdenum alloys. This was found to apply to all the alloy systems investigated in this work.

When pellets originally containing cobalt oxide and molybdic oxide were removed from the furnace after the 50-hr. treatment, a curious violent disintegration occurred, with the production of a fine, bulky powder. The molybdate was therefore studied in greater detail.

Cobalt molybdate was prepared in the following manner: equivalent weights of sodium molybdate and cobalt chloride were fused together with an amount of sodium chloride equal to their combined weight, the reaction being:



The melt was cast into sticks and placed in boiling water. The soluble components were dissolved away, leaving a very finely divided precipitate of the molybdate.

It was found that the molybdate disintegrated on cooling from temperatures above 600°C. in a similar, but more rapid, manner to the mixed oxide pellets, and that it did so whether in pellet form or otherwise. The disruption, therefore, seemed to be due to some structural change on heating and cooling. X-ray examination in a high-temperature camera showed that the substance possessed a different structure at 600°C. from that at room temperature and also that the structure of the cooled molybdate was the same as that before heating. It seems, therefore, that a reversible change of structure occurs at some temperature below 600°C. The literature on sodium and potassium molybdates² shows that these compounds possess several modifications between 400° and 600°C. , and it is reasonable to attribute the disruptive effect to similar changes in cobalt molybdate. It has been noted above that the scales on the cobalt-molybdenum alloys readily exfoliated on cooling, and that the inner layer, containing the molybdate, was extremely powdery. These observations are to be expected as a result of the changes taking place in the molybdate.

No signs of fusion were observed in the scales formed on the cobalt-molybdenum alloys, although the melting point of molybdenum trioxide is approximately 760°C. This seems to suggest that the latter combines with the cobalt oxide immediately on formation, and is thus prevented from fluxing the scale. At 1200°C. the molybdate is probably unstable and decomposes soon after formation, with the rapid volatilization of molybdic oxide.

4. COBALT-TUNGSTEN ALLOYS

The oxidation results for these alloys are given in Table III.

TABLE III.—Average Oxidation Results for the Cobalt-Tungsten Alloys.

Temp., $^\circ\text{C.}$	Increase in Weight, g./cm. ²			
	Co	Co-5% W	Co-10% W	Co-15% W
800	0.020	0.031	0.037	0.023
900	0.042	0.046	0.041	0.030
1000	0.045	0.078	0.062	0.059
1100	0.148	0.119	0.111	0.104
1200	0.165	0.162	0.158	0.142

The general effect of the addition of tungsten to cobalt was to decrease the oxidation rate slightly, the decrease being proportional to the amount of tungsten present.

In general appearance the scales on these alloys resembled those on cobalt itself. X-ray examination showed that the outer layer consisted of CoO with a little cobalt tungstate, CoWO_4 , and the inner powdery layer mainly of cobalt tungstate together with a little CoO .

Some internal oxidation occurred in the 5% alloy at 900°C. , and at higher temperatures it penetrated to a considerable depth. Internal oxidation in the 10 and 15% alloys did not begin until 1100°C. , and a comparison of the three alloys oxidized at 1200°C. showed that the depth of internal oxidation decreased as the tungsten content increased, as would be expected.

5. COBALT-ALUMINIUM ALLOY

Reference to the equilibrium diagram for the cobalt-aluminium system shows that the limit of the α solid solubility is in the region of 7% aluminium, and 5% was chosen as a suitable composition in order to maintain a single-phase alloy. This amount of aluminium had little effect on the scaling rate of cobalt, except at 800° – 900°C. , as indicated by Table IV. Higher contents of aluminium were not

TABLE IV.—Average Oxidation Results for the Cobalt-5% Aluminium Alloy.

Temp., $^\circ\text{C.}$	Increase in Weight, g./cm. ²	
	Co	Co-5% Al
800	0.020	0.0008
900	0.042	0.019
1000	0.045	0.054
1100	0.148	0.105
1200	0.165	0.212

investigated, however, as the second phase in this system makes the alloy very brittle.

At all temperatures from 800° to 1200°C. , the scales formed consisted of an outer layer of CoO and

an inner layer which was a mixture of CoO and the bright blue spinel, cobalt aluminate CoAl_2O_4 . These scales spalled on cooling when formed below 1000°C ., but above this temperature they were adherent. Internal oxidation began at 900°C . and became more intense at the higher temperatures.

6. COBALT-CHROMIUM ALLOYS

The scaling properties of the cobalt-chromium alloys are indicated in Fig. 4. The higher rates of oxidation at 1200°C . for alloys with less than 25% chromium were found to be associated with the presence of a spinel, cobalt chromite, in the oxide layers. The scales formed on the alloys with higher chromium contents consisted of chromic oxide only, the spinel being completely absent, and it will be

The results obtained from X-ray examination of heated mixtures of cobalt and chromium oxides confirmed that no reactions occur below 1100°C . and that the spinel formation does not take place until this temperature is reached.

7. NICKEL-MOLYBDENUM ALLOYS

As indicated in Table V, the addition of up to 15% molybdenum had little effect on the oxidation rate of

TABLE V.—Average Oxidation Results for the Nickel-Molybdenum Alloys.

Temp., $^\circ\text{C}$.	Increase in Weight, g./cm. ²			
	Ni	Ni-5% Mo	Ni-10% Mo	Ni-15% Mo
800	0.002	0.002	0.003	0.003
900	0.005	0.006	0.007	0.007
1000	0.009	0.014	0.014	0.014
1100	0.014	0.018	0.021	0.021
1200	0.018	0.027	0.029	0.025

nickel at $800^\circ\text{--}900^\circ\text{C}$., though at higher temperatures 5% molybdenum caused a slight increase. Additions beyond 5% did not sustain this initial increase, however, and at 1200°C . a maximum was attained at approximately 10% molybdenum. No volatilization of MoO_3 was noticed with these alloys.

The scales formed at all temperatures consisted of two layers: a dark-green, coherent, outer layer of NiO and a bright-green, powdery, inner layer which was a mixture of NiO and nickel molybdate, NiMoO_4 . On cooling, the outer layer broke off with some force. This was found to be caused by a disintegration of the nickel molybdate similar to that discussed for the cobalt molybdate.

With these alloys, a small amount of internal oxidation was observed at the higher temperatures.

8. NICKEL-TUNGSTEN ALLOYS

The presence of up to 15% tungsten in nickel effected little alteration in the rate of oxidation at temperatures below 1000°C ., but at 1100° and 1200°C . it caused a moderate increase, as shown in Table VI.

TABLE VI.—Average Oxidation Results for the Nickel-Tungsten Alloys.

Temp., $^\circ\text{C}$.	Increase in Weight, g./cm. ²			
	Ni	Ni-5% W	Ni-10% W	Ni-15% W
800	0.002	0.002	0.002	0.004
900	0.005	0.006	0.006	0.008
1000	0.009	0.012	0.012	0.014
1100	0.014	0.019	0.019	0.023
1200	0.018	0.031	0.036	0.039

The oxide layers formed on these alloys were similar in appearance to those formed on nickel, and were adherent at all temperatures. The outer layer consisted chiefly of NiO with traces of nickel tungstate,

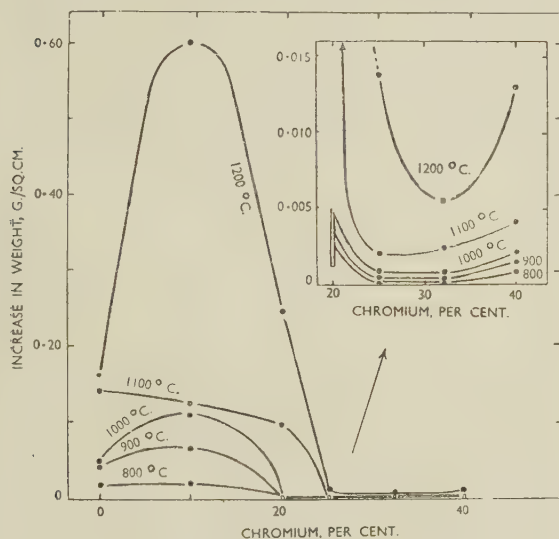


FIG. 4.—Effect of Chromium Content on the Oxidation After 50 Hr. of Cobalt-Chromium Alloys.

noticed that such alloys possess a high degree of oxidation-resistance. It would appear that immediate formation of a layer of chromic oxide suppresses the oxidation of the cobalt, thereby preventing spinel formation.

It can be seen from the results that, for temperatures up to 1100°C ., at least 25% chromium is required to provide a high degree of oxidation-resistance, while at 1200°C . a greater amount is necessary. The chromium content should not, however, exceed 37%, i.e. the solubility limit of the α phase,³ since it has been found that the rate of oxidation again increases when this limit is exceeded, as shown in Fig. 4.

The structures of the scales formed on typical alloys in this series are shown in Figs. 7 and 8 (Plate XXXI). In Fig. 7 the chromic oxide will be seen as isolated areas in the inner layer of cobalt oxide. The interface clearly visible between the two oxide layers marks the original metal surface. The latter is also clearly shown in Fig. 8. In this scale the inner layer consists of a mixture of CoO and cobalt chromite.

NiWO_4 , and the inner layer of nickel tungstate with some NiO .

Internal oxidation occurred to a considerable extent over the temperature range $900^\circ\text{--}1200^\circ\text{C}$., and its severity was a function of the temperature and the amount of tungsten present. The effect of the tungsten content on the depth and form of the internal oxidation is illustrated in Fig. 9 (a) and (b) (Plate XXXI).

9. NICKEL-ALUMINIUM ALLOY

The results obtained with the nickel-5% aluminium alloy were unusual in that a maximum occurred in the oxidation curve at 1100°C ., as shown in Fig. 5. The

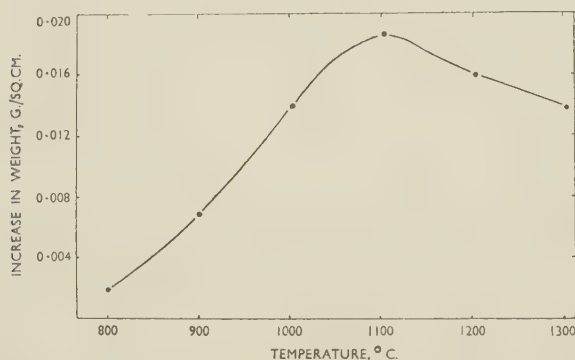


FIG. 5.—Effect of Temperature on the Oxidation After 50 Hr. of Nickel-5% Aluminium Alloy.

alloy was very resistant to oxidation at 800°C . owing to the formation of a protective film of alumina. At higher temperatures, however, the protective action of the alumina was lost, and up to 1100°C . the rate of oxidation was greater than that for nickel. Beyond 1100°C . it will be noted that the aluminium again becomes effective and the rate of oxidation is appreciably lower.

The scales formed at 900°C . and 1000°C . were duplex in character, and consisted of NiO with some alumina in the inner layer. Internal oxidation began at 900°C ., and was more intense at 1000°C . At temperatures from 1100° to 1300°C ., however, there was no internal oxidation and the scale layers consisted of (a) an outer layer of NiO , (b) a thin, powdery layer of nickel aluminate and NiO , and (c) a greyish layer of alumina on the metal surface. On cooling the specimens, the two outermost layers spalled off. It was noted that as the temperature increased, the volume of nickel oxide, and also the amount of spinel, decreased, while the alumina film provided more complete coverage. The onset of these changes in scale formation coincided with the change in direction of the curve shown in Fig. 5.

Experiments with mixtures of nickel oxide and aluminium oxide confirmed the fact that no spinel formation occurred until the mixture was heated to temperatures above 1000°C .

It is evident that in this alloy, 5% aluminium was insufficient to prevent oxidation of the base metal,

except at 800°C . The change in the mechanism of oxidation at about 1050°C . is unusual. It appears that the rate of diffusion of aluminium through nickel and the subsequent formation of aluminium oxide at the surface of the alloy is favourably influenced by rise of temperature. It seems probable that, at the higher temperatures, the rapid formation of a surface layer of aluminium oxide restricts the further oxidation of nickel. The spinel formed at high temperatures does not appear to have any serious effect on the rate of oxidation.

10. FURTHER EXPERIMENTS WITH THE COBALT-CHROMIUM ALLOYS

Although the cobalt-32% chromium alloy has extremely good oxidation-resisting properties, it suffers from one serious defect, namely that the protective chromic oxide film exfoliates rapidly on cooling from temperatures higher than $800^\circ\text{--}900^\circ\text{C}$. It was thought that the presence of small amounts of other elements in the alloy might affect the composition of the scale in such a way as to increase its adherence. Accordingly, the following additions were made to a cobalt-32% chromium alloy:

Be	0.39%	V	0.64%
B (not analysed) approx.	0.5%	Zr	0.33%
Al	0.41%	Nb	0.64%
Si	0.87%	Ce	0.33%
Ca	0.016%	Ta	0.64%
Ti	0.65%	Th	0.28%

Although the additions were intended to be of the same amount in each case, it will be seen that this was not achieved because of melting losses.

The alloys were tested in a manner similar to that described for the binary alloys, the testing time being kept constant at 50 hr. A certain amount of scatter in the increase-in-weight measurements was found with some of the alloys, and the results shown in Fig. 6 are average results. To simplify the diagram, the extent of the scatter has been omitted, but it was not sufficient to affect the positions of the curves. A considerable amount of second phase was found in the alloys containing boron and beryllium, and a small amount was also perceptible in the vanadium, titanium, and aluminium alloys. This is not regarded as being of any significance, since their mechanical properties were not under consideration.

It can be seen from the results (Fig. 6) that these small additions had a considerable influence on the rate of oxidation. They may be classified into three groups:

- (i) Elements causing a serious loss of oxidation-resistance: V, B, Nb, and Be.
- (ii) Elements having only a small beneficial effect on the oxidation-resistance: Ti, Zr, and Ca.
- (iii) Elements which markedly improve the oxidation-resistance: (a) Ta, Al, and Ce; (b) Si and Th.

Group (i): V, B, Nb, and Be

Vanadium.—It is clear that the addition of 0.64% vanadium to the alloy resulted in very severe oxida-

tion at temperatures above 900° C. At such temperatures the chromic oxide was replaced by a glossy, non-adherent, dark-green scale, which appeared to have been molten during the test, and internal oxidation occurred to a considerable extent.

Boron.—As with vanadium, the alloy containing boron formed green, adherent films of chromic oxide at 800°–900° C., but above these temperatures the scale had a glazed appearance and spalled rapidly on cooling. Internal oxidation also began at these higher temperatures, and was very severe at 1100°–1200° C.

Niobium.—The scales formed on this alloy were non-adherent throughout the temperature range con-

Group (ii): Ti, Zr, and Ca

These three alloys showed scaling characteristics similar to those of the binary cobalt–chromium alloy, i.e. a green adherent film at 800° C., slight spalling at 900° C., and at higher temperatures a dark-green, slightly macro-crystalline scale which exfoliated rapidly on cooling. No internal oxidation could be detected at temperatures up to 1100° C., but the titanium and zirconium alloys developed a small amount at 1200° C.

On examination of the scales from the titanium alloy after oxidation at 1200° C., the X-ray films showed that a compound was formed, though it was

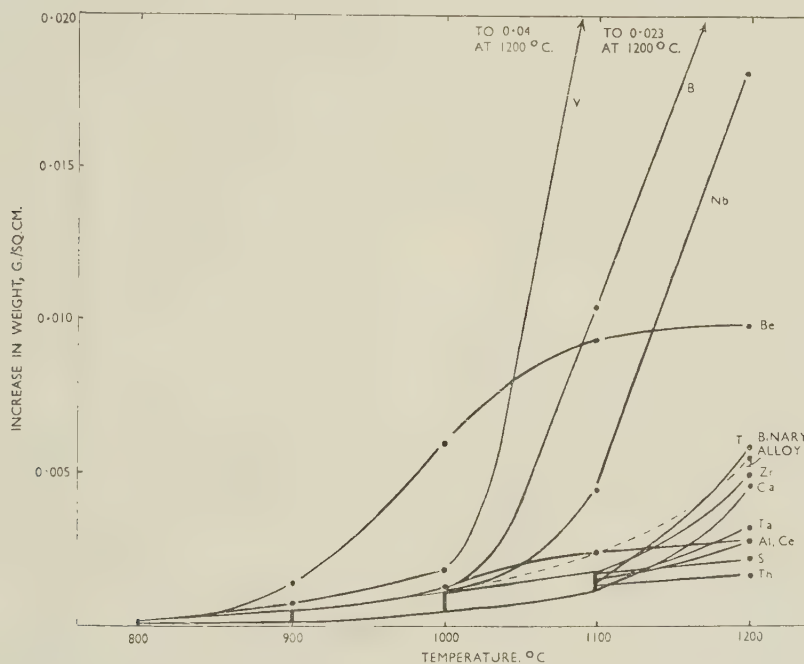


Fig. 6.—Comparison of the Extent of Oxidation of the Ternary Alloys After Heating Between 800° and 1200° C. for 50 Hr.

sidered. Signs of internal oxidation appeared at 900° C., and became more intense as the temperature increased. At 1200° C. a glaze developed on the surface of the specimen. X-ray examination of the scale showed evidence of compound formation, probably a niobate, but identification was not possible.

Beryllium.—The results obtained with the alloy containing beryllium were rather scattered, but it is clear that this element is an unsatisfactory addition. No improvement in the scale adherence was noted. Internal oxidation was evident at 900° C., and considerable penetration occurred at higher temperatures. The formation of a film of beryllium oxide round the crystal boundaries would account for the peculiar shape of the curve, since such a network would restrict further oxidation and result in an almost constant rate of oxidation whatever the temperature. The presence of a compound, believed to be beryllium chromite, was detected by X-ray analysis in the scale formed at 1200° C.

not the same as that found on heating mixtures of Cr_2O_3 and TiO_2 . It was probably a titanate containing more chromic oxide than the latter.

Calcium chromite was not detected in the scales formed on the alloy containing calcium, but this may have been due to the limitations of X-ray analysis. The oxide-pellet investigation indicated that mixtures of chromium and calcium oxides are molten above about 1000° C., and hence it would appear that the formation of calcium chromite in the scales in large amounts would be undesirable.

Similarly, zirconium oxide does not occur in the scales to an extent detectable by X-ray analysis. No compound formation, however, takes place between chromic oxide and zirconium oxide when the two are heated at temperatures up to 1200° C.

Group (iii), a): Ta, Al, and Ce

The scales formed on the alloy containing tantalum were non-adherent on cooling from temperatures

above 900° C. Internal oxidation was present at 1100° and 1200° C. to a small extent. Unlike the similar metal niobium, neither compound formation nor tantalum pentoxide could be detected by X-ray examination of the scales. Heated mixtures of tantalum pentoxide and chromic oxide, however, combine at temperatures above 1000° C., with the formation of a tantalate.

The aluminium alloy formed scales which were adherent up to 1000° C., but exfoliated on cooling from the higher temperatures. Internal oxidation was clearly visible at 900° C., and became deeper and coarser with increasing temperature.

With the addition of cerium, exfoliation still occurred from temperatures above 900° C., but internal oxidation was completely absent apart from a few isolated areas at 1200° C.

Chromic oxide was the only substance shown by X-ray examination of the scales formed on those alloys containing aluminium and cerium, indicating that the amount of aluminium oxide and cerium formed was extremely small. No reactions were noted when these two oxides were heated with chromic oxide at temperatures up to 1200° C.

Group (iii, b): Si and Th

The beneficial effect of silicon on the oxidation-resistance of alloys containing chromium has been noted by previous workers, and has been confirmed here. No improvement in the scale adherence was noted, however.

Thorium was the outstanding addition for improving the resistance to oxidation, the rate of attack at 1200° C. being only one-third that of the binary alloy. Again, however, the scales were non-adherent above 900° C. No internal oxidation was noted at any temperature in the range 800°–1200° C.

The X-ray examination of the scales formed on these two alloys showed the presence of Cr_2O_3 only, but as this method cannot detect very small amounts, it does not imply the complete absence of silicon and thorium oxides. No compound formation occurred, however, when these two oxides were heated with chromic oxide at temperatures up to 1200° C.

Figs. 11, 12, and 13 (Plate XXXI) illustrate the different types of internal oxidation found with some of the alloys mentioned in this section.

IV.—DISCUSSION OF RESULTS

1. BINARY ALLOYS

From an examination of the oxidation rates of a series of cobalt-chromium alloys, it has been shown that the amount of chromium necessary to ensure the production of a protective film of chromic oxide increases with temperature. Should cobalt oxide be formed in appreciable amounts at temperatures above 1100° C., the cobalt chromite spinel will be produced and the oxidation-resistance seriously impaired. It was also shown that, in the oxidation of pure cobalt

itself, the existence of a thin layer of the spinel Co_3O_4 resulted in a more rapid rate of oxidation than was found when such a layer was absent. It is clear, therefore, that a spinel structure is undesirable where a high degree of oxidation-resistance is required, and this conclusion is in agreement with the work of Hickman and Gulbransen⁴ on nickel-chromium alloys.

It is of interest here to record that, while examining the oxidation-resistance of a Vitallium alloy, it was noted that at 1200° C. curious surface defects occurred which caused serious local attack. Fig. 10 (Plate XXXI) shows three such areas, together with two cavities where the crystallites have been removed. It was found that very deep internal oxidation occurred at these points, and X-ray examination of the crystallites revealed that they consisted of the cobalt chromite spinel, while the ordinary scale was the normal chromic oxide.

Of the other types of compound formation noted, the disruptive properties of the molybdates make these substances highly undesirable, since scale adherence is seriously affected.

In view of statements expressed by previous workers that diffusion of oxygen through an oxide layer would be prevented by the large size of the oxygen ion, attention is drawn to the mode of oxidation found with cobalt, nickel, and some of the alloys included in the present investigation. With cobalt, it is difficult to explain the formation of the inner oxide layer inside the original surface of the specimen without assuming appreciable movement of oxygen inwards through the scale. In like manner the internal oxidation noted in certain of the alloys also supports this assumption of oxygen movement.

2. TERNARY ALLOYS

The results obtained with the ternary alloys also show that compound formation in the chromic oxide layer is an undesirable factor and that low-melting-point oxides in particular should be avoided.

The reason for the remarkable improvement resulting from small additions of thorium, silicon, and cerium is not clear. Horn⁵ has shown that, with a nickel-20% chromium alloy containing similar small additions, the change in the parabolic rate constant/at.-% added element seems to be dependent on the atomic size of that element. Such calculations, however, involve the assumption that the effect of an element on the rate of oxidation is directly proportional to the amount present, a relationship rarely found in oxidation studies. Similar calculations have shown that no correlation exists in this work between the atomic size of the element and the change in the rate constant.

Since the deterioration in the resistance to oxidation of the cobalt-chromium alloy brought about by vanadium, boron, niobium, and beryllium results from the presence of their oxides in the chromic oxide layer, it is reasonable to assume that the beneficial effect of

other elements may also be due to a modification of the protective film. Hauffe⁶ has shown that very small amounts of foreign oxides may appreciably alter the electrical conductivity of the base oxide, and consequently may explain the beneficial effects brought about by these very small amounts of addition elements.

V.—CONCLUSIONS

The main conclusions to be drawn from the results obtained in this work are:

1. The rates of oxidation of the alloys used were found to be the same in the 60 : 1 turbine atmosphere as in air, even when using paraffin with a high sulphur content as fuel.

2. The reactions observed in oxide mixtures pressed into pellet form and heated at the scaling temperatures, can be correlated with the reactions observed during scale formation on the appropriate alloy, and this has proved a valuable aid in studying scale constitution.

3. In the oxidation of pure cobalt in the range 800°–1100° C., an alteration in the mechanism was found at the upper limit of stability of Co_3O_4 , 950° C. It is suggested that the presence of a thin layer of this oxide at the outer surface of the scale increases the rate of solution of oxygen by the underlying CoO layer.

4. The most satisfactory addition for securing oxidation-resistance in cobalt-base alloys over the range 800°–1200° C. is chromium. At least 25% is desirable for temperatures up to 1000° C., and about 30% for 1200° C. The formation of a second phase is detrimental to oxidation-resistance.

5. The addition of aluminium to cobalt increases its resistance to oxidation, but has no practical application for high-temperature service, as the necessary aluminium content would produce an alloy containing a second phase, which seriously interferes with the mechanical properties of the alloy.

6. The occurrence of more than one oxide in the scale is undesirable, particularly if one of the oxides is molten at the temperature of formation, or if compound formation is possible.

7. The most deleterious type of compound found

was that which had a spinel structure. This type of structure greatly accelerated the oxidation process.

8. Of twelve minor additions made to a cobalt–32% chromium alloy, the most suitable for increasing the oxidation-resistance were, in decreasing order of merit, thorium, silicon, and cerium. It is suggested that the oxides of these elements decrease the electrical conductivity of chromic oxide, i.e. they lower the rate of diffusion of ions and electrons through the film.

9. No increase in scale adherence was noted when about $\frac{1}{2}\%$ of the following elements was added to the cobalt–32% chromium alloy: Be, Ca, Nb, B, Ti, Ce, Al, V, Ta, Si, Zr, and Th. The occurrence of internal oxidation does not seem to have any beneficial effect on the adherence of the chromic oxide film, as is sometimes suggested.

10. It is thought that, at the high temperatures used in this work, the diffusion of oxygen ions through the scale is possible and does, in fact, occur to a considerable extent.

ACKNOWLEDGEMENTS

The investigation described forms part of a research programme carried out in the Department of Metallurgy, King's College, University of Durham, and supported by the Ministry of Supply. The authors are indebted to Dr. T. Raine of the Metropolitan-Vickers Electrical Co., Ltd., and members of his staff for assistance in the preparation of the alloys and the X-ray analysis; to Dr. H. Sutton, C.B.E., of the Ministry of Supply; and to their colleagues in the University.

REFERENCES

1. J. Dunn, "Review of Oxidation and Scaling of Heated Solid Metals", p. 67. 1935: London (H.M. Stationery Office).
2. J. W. Mellor, "A Comprehensive Treatise on Inorganic and Theoretical Chemistry", Vol. XI, p. 553. 1931: London (Longmans, Green and Co.).
3. R. Edwards, Private communication.
4. J. W. Hickman and E. A. Gulbransen, *Trans. Amer. Inst. Min. Met. Eng.*, 1949, **180**, 519.
5. L. Horn, *Z. Metallkunde*, 1949, **40**, 73.
6. K. Hauffe, *Ann. Physik*, 1950, [vi], **8**, 201.

NOTICE TO AUTHORS OF PAPERS FOR THE "JOURNAL" AND CONTRIBUTORS TO DISCUSSIONS

1. Papers will be considered for publication from non-members as well as members of the Institute. They are accepted for publication in the *Journal* and not necessarily for presentation at any meeting of the Institute. MSS. should be addressed to The Editor of Publications, The Institute of Metals, 4 Grosvenor Gardens, London, S.W.1.

2. Papers suitable for publication may be classified as:

(a) Papers recording the results of original research.
(b) First-class reviews of, or accounts of progress in, a particular field.

(c) Papers descriptive of works methods, or recent developments in metallurgical plant and practice.

(d) Papers in classes (a), (b), and (c) above, previously published in languages other than English, French, German, or Italian, if of sufficient merit.

3. Manuscripts and illustrations should be submitted in duplicate. MSS. must be typewritten (*double-line spacing*) on one side of the paper only, and authors are requested to sign a declaration that neither the paper nor a substantial part thereof has been published elsewhere. Exceptions may be made in certain cases where a paper has been published in a language other than English, French, German, or Italian (see 2(d) above). MSS. not accepted are normally returned within 6 months of receipt.

In the interests of economy, all papers must be written as concisely as possible; in general, internal research reports are not in suitable form for publication as papers in the *Journal*. All but the simplest mathematical expressions should be written by hand, with capital and small letters clearly distinguished. Superscript and subscript letters should also be plainly indicated. Greek letters and special signs should be identified in the margin. For style, spelling, and abbreviations used, any recent issue of the *Journal* may be consulted.

4. **Synopsis.** Every paper must have a synopsis (not exceeding 250 words in length) which, in the case of a paper reporting original research, should state its objects, the ground covered, and the nature of the results. The synopsis will appear at the beginning of the paper, and should be in a form suitable for use by abstracting organizations. Extracts from a "Guide for the Preparation of Synopses" drawn up by the Abstracting Services Consultative Committee are reproduced below.

5. **References** must be collected at the end of the paper and must be numbered in the order in which they occur in the MS. Initials of authors must be given, and the Institute's official abbreviations for periodical titles (as used in *Metallurgical Abstracts*) should be employed, where known. References to papers should be set out in the style:

A. L. Dighton and H. A. Miley, *Trans. Electrochem. Soc.*, 1942, **81**, 321 (i.e. year, volume, page).

References to books should be in the following style:

C. Zener, "Elasticity and Anelasticity of Metals". Chicago: 1948 (University of Chicago Press).

6. **Illustrations.** Each illustration must have a number and description; only one set of numbers must be used in one paper, and it is desirable to number the half-tone illustrations consecutively, rather than to intersperse them with the line figures. The captions should be typed on a separate sheet.

The set of **line figures** sent for reproduction must be drawn (about twice the size to appear in the *Journal*) in Indian ink on smooth white Bristol board, good-quality drawing paper, co-ordinate paper, or tracing cloth, which are preferred in the order given. Co-ordinate paper, if used, must be blue-lined, with the co-ordinates to be reproduced finely drawn in Indian ink. Curves should be drawn boldly (i.e. at least twice the thickness of the frame). Experimental points should be indicated by open or closed circles, triangles, squares, &c. (preferably not crosses). Curves should be broken on each side of such symbols and plenty of allowance should be made for closing up in blockmaking. All lettering and numerals, &c., should preferably be in *pencil*, so that the Institute's standard lettering may be affixed, and ample margins must be left outside the framework of the figures to enable this to be done. The second set of line illustrations may be photostat copies.

Photographs must be restricted in number, owing to the expense of reproduction, and photomicrographs should be trimmed to the smallest possible of the following sizes consistent with adequate representation of the subject: 4 in. deep by 3 in. wide: 2 in. deep by 3 in. wide: 2 in. square. Magnifications of photomicrographs must be given in each case. Photographs for reproduction should be loose, not pasted down (and not fastened together with a clip, which damages them), and the figure number and author's name should be written on the back of each. Captions should be given to the photomicrographs, but these should be kept as brief as possible.

Because of the present high cost of printing and paper it is imperative that authors restrict illustrations (particularly photographs) to the absolute minimum deemed necessary to support their argument. Only in exceptional cases will illustrations be reproduced if already printed and readily available elsewhere.

7. **Tables or Diagrams.** Results of experiments, &c., may be given in the form of tables or figures, *but* (unless there are exceptional reasons) *not both*. Tables should bear Roman numbers, and each should have a heading that will make the data intelligible without reference to the text.

8. **Corrections.** A certain number of corrections in proof are inevitable, but any modification of the original text is to be avoided. Since corrections are very expensive, the Institute reserves the right to require authors to contribute towards their cost if the Editor deems them to be excessive. The Institute also reserves the right to require a contribution to the cost of remaking any block where this is necessitated by an error on the author's part.

9. **Reprints.** Individual authors are presented with a maximum of 25, and two or more authors with a maximum of 50 reprints from the *Journal*, without covers. Limited numbers of additional reprints can be supplied at the author's expense, if ordered before proofs are passed for press. (Orders should preferably be placed when submitting MSS.)

10. **Discussion.** Except in the case of special symposia, shorthand records of discussions are not taken at meetings. Written discussion may be submitted on any paper, preferably typewritten (*double-line spacing*). References should be given in the form of footnotes. Paragraphs 6 and 7 above are also applicable to such contributions. Reprints of discussion cannot be supplied to contributors.

GUIDE FOR THE PREPARATION OF SYNOPSES

(As recommended by the Abstracting Services Consultative Committee)

1. **Purpose.** The synopsis is not part of the paper; it is intended to convey briefly the content of the paper, to draw attention to all new information, and to the main conclusions. It should be factual.

2. **Style of writing.** The synopsis should be written concisely and in normal rather than abbreviated English. It is preferable to use the third person. Where possible use standard rather than proprietary terms, and avoid unnecessary contracting.

It should be presumed that the reader has some knowledge of the subject, but has not read the paper. The synopsis should therefore be intelligible in itself without reference to the paper; for example, it should not cite sections or illustrations by their numerical references in the text.

3. **Content.** The title of the paper is usually read as part of the synopsis. The opening sentence should be framed accordingly and repetition of the title avoided. If the title is insufficiently comprehensive, the opening should indicate the subjects covered. Usually the beginning of a synopsis should state the objective of the investigation.

It is sometimes valuable to indicate the treatment of the subject by such words as: brief, exhaustive, theoretical, &c.

The synopsis should indicate newly observed facts, conclusions of an

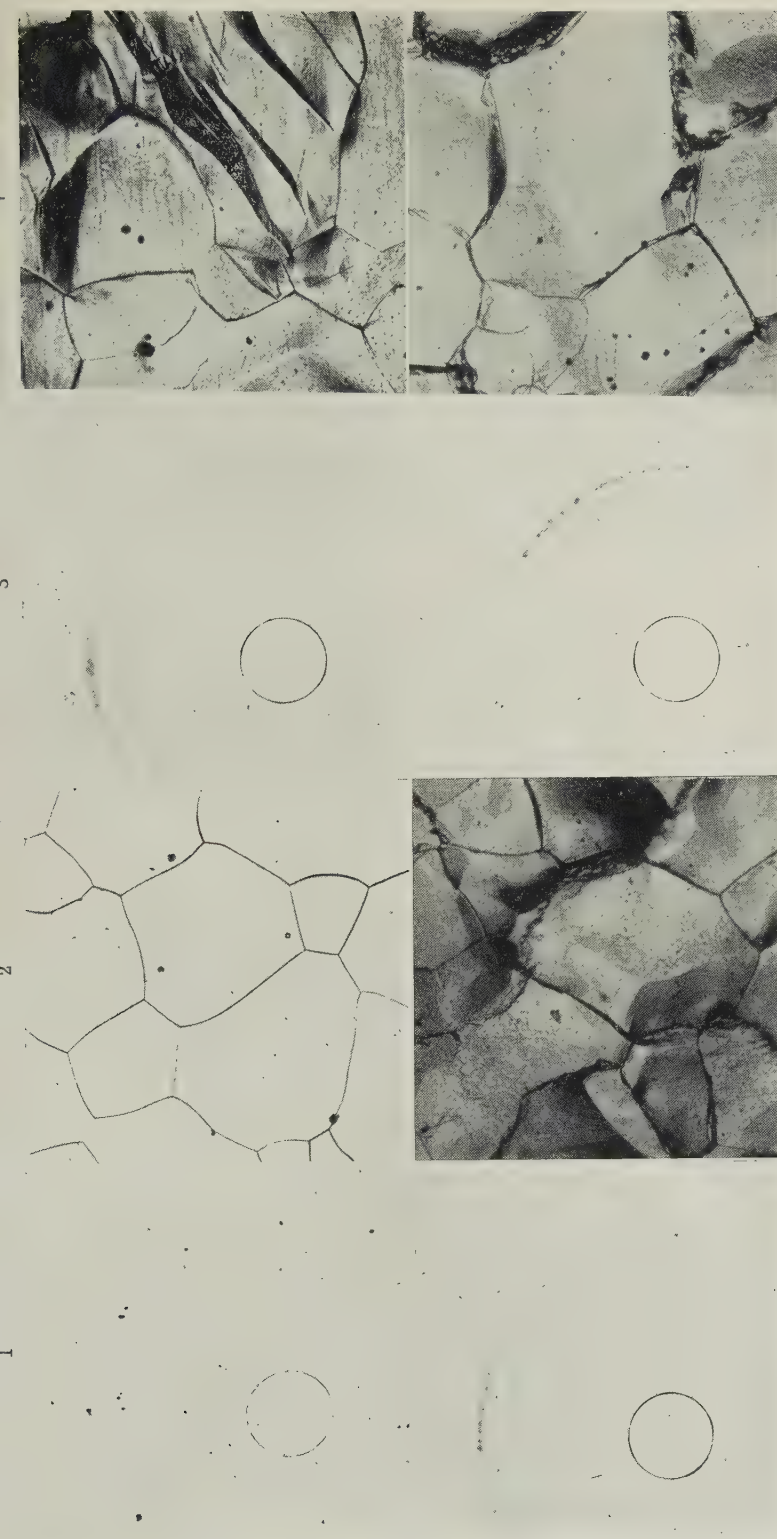
experiment or argument and, if possible, the essential parts of any new theory, treatment, apparatus, technique, &c.

It should contain the names of any new compound, mineral species, &c., and any new numerical data, such as physical constants; if this is not possible, it should draw attention to them. It is important to refer to new items and observations, even though some are incidental to the main purpose of the paper; such information may otherwise be hidden, though it is often very useful.

When giving experimental results the synopsis should indicate the methods used; for new methods the basic principle, range of operation, and degree of accuracy should be given.

4. **References.** If it is necessary to refer to earlier work in the summary, the reference should always be given in full and not by number. Otherwise references should be left out.

When a synopsis is completed, the author is urged to revise it carefully, removing redundant words, clarifying obscurities, and rectifying errors in copying from the paper. Particular attention should be paid by him to scientific and proper names, numerical data, and chemical and mathematical formulæ.

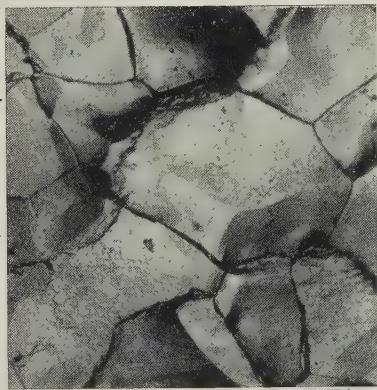


5

FIGS. 1 AND 2.—After Annealing.

FIGS. 5 AND 6.—After 7.4% Rapid Strain at 300° C.

6

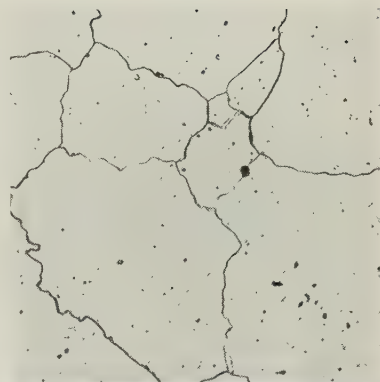
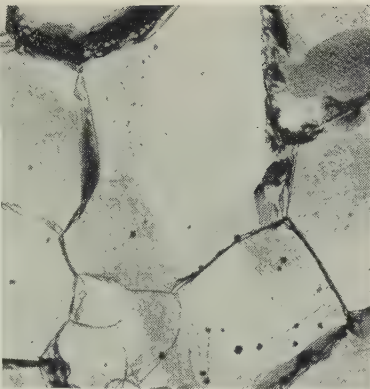


7

FIGS. 3 AND 4.—After 5.3% Rapid Strain at 22° C.

FIGS. 7 AND 8.—After 8.3% Rapid Strain at 400° C.

8



9

FIGS. 9 AND 10.—After 9.5% Slow Strain at 200° C.

FIG. 11.—As in Fig. 10 After Repolishing and Etching.

10

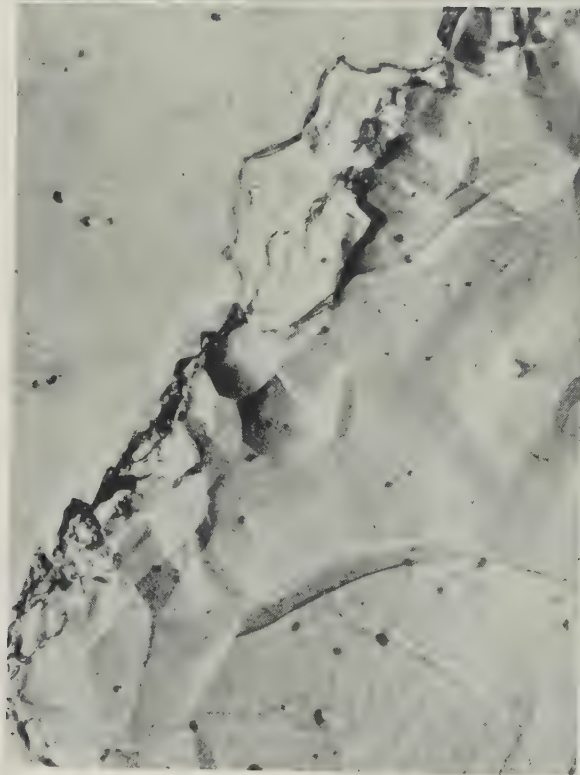


11

Photomicrographs $\times 100$.

MICROSTRUCTURES AND X-RAY PATTERNS OF MAGNESIUM.

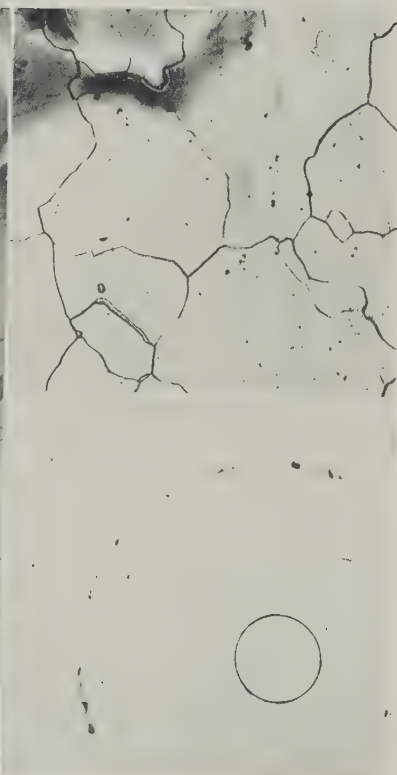
12



13



14



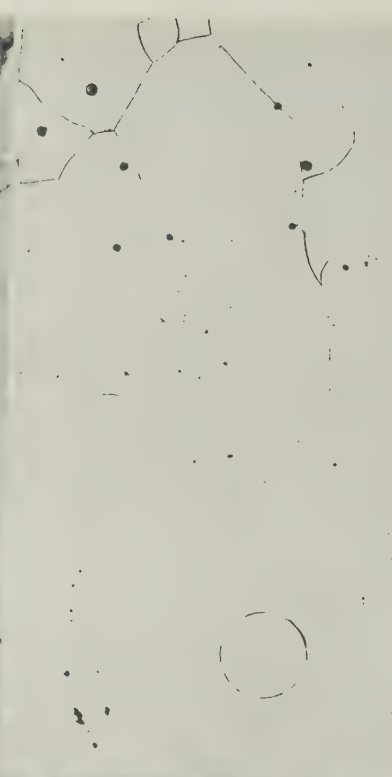
15

FIG. 12.—After 9.5% Slow Strain at 200° C. $\times 400$.

FIG. 14.—After 10.5% Slow Strain at 250° C.

FIG. 15.—Repolished and Etched After 10.5% Slow Strain at 250° C. $\times 100$.

16



17

FIG. 13.—As in Fig. 12 After Repolishing and Etching. $\times 400$.

FIG. 16.—After 7.1% Slow Strain at 350° C.

FIG. 17.—Repolished and Etched After 7.1% Slow Strain at 350° C. $\times 100$.

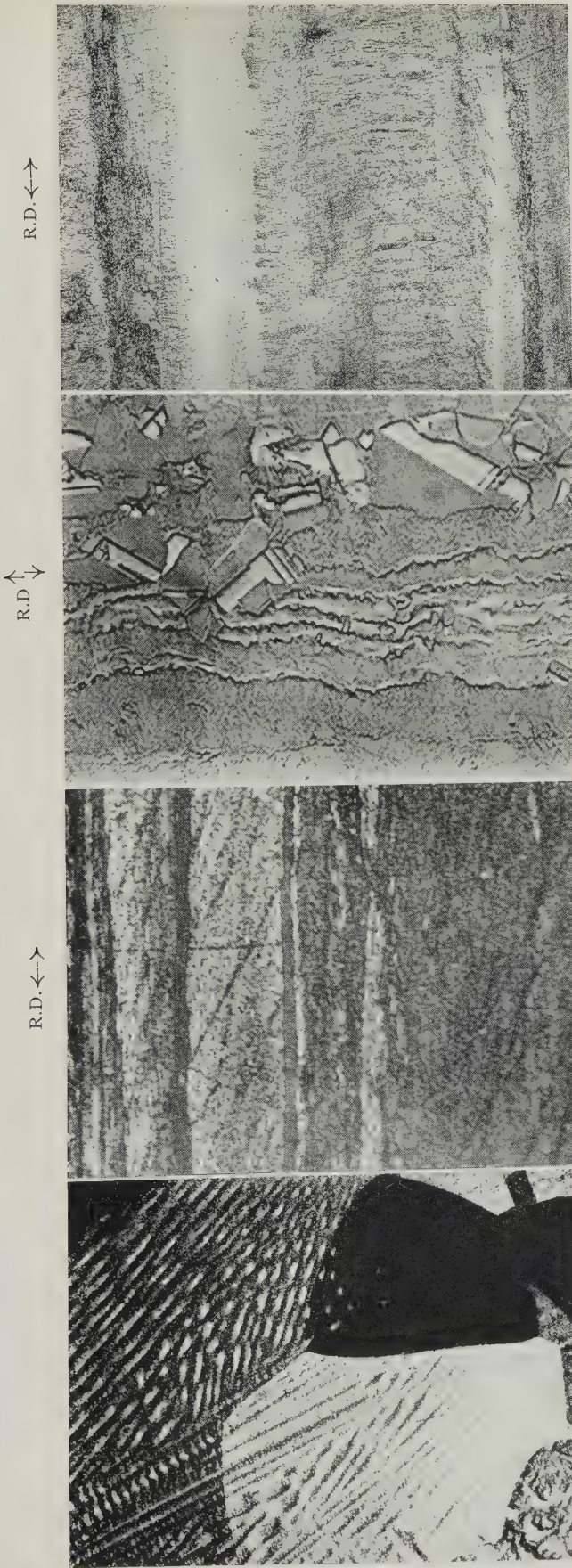


FIG. 1.—Dendritic Structure in Cast Alloy P-H(20). $\times 10$.
FIG. 2.—Deformation Markings in Cu(3)L Rolled 95% and Annealed 40 Hr. at 71.4° C. Longitudinal section. $\times 400$.
FIG. 3.—Deformation Markings in P-L(4)L Rolled 95% and Annealed 27 Hr. at 165.8° C. Rolling-plane section. $\times 800$.
FIG. 4.—Partial Recrystallization in Cu(3)L Rolled 95% and Annealed 19 Hr. at 101.4° C. Rolling-plane section. $\times 20$.

GLANCING-ANGLE X-RAY PHOTOGRAPHS.



FIG. 5.—Cu(3)S. Rolled 97.5% and Annealed 29 Hr. at 165.8° C.
FIG. 6.—Cu(3)L. Rolled 97.5% and Annealed 29 Hr. at 165.8° C.
FIG. 7.—Cu(3)S. Rolled 90%.
FIG. 8.—As Fig. 7 After Annealing for 197 Hr. at 165.8° C.
FIG. 9.—P-L(4)S. Rolled 97.5% and Annealed 231 Hr. at 165.8° C.
FIG. 10.—P-L(4)L. Rolled 97.5% and Annealed 231 Hr. at 165.8° C.
FIG. 11.—P-H(7)S. Rolled 97.5% and Annealed 1 Hr. at 500° C.
FIG. 12.—P-H(7)L. Rolled 97.5% and Annealed 1 Hr. at 500° C.

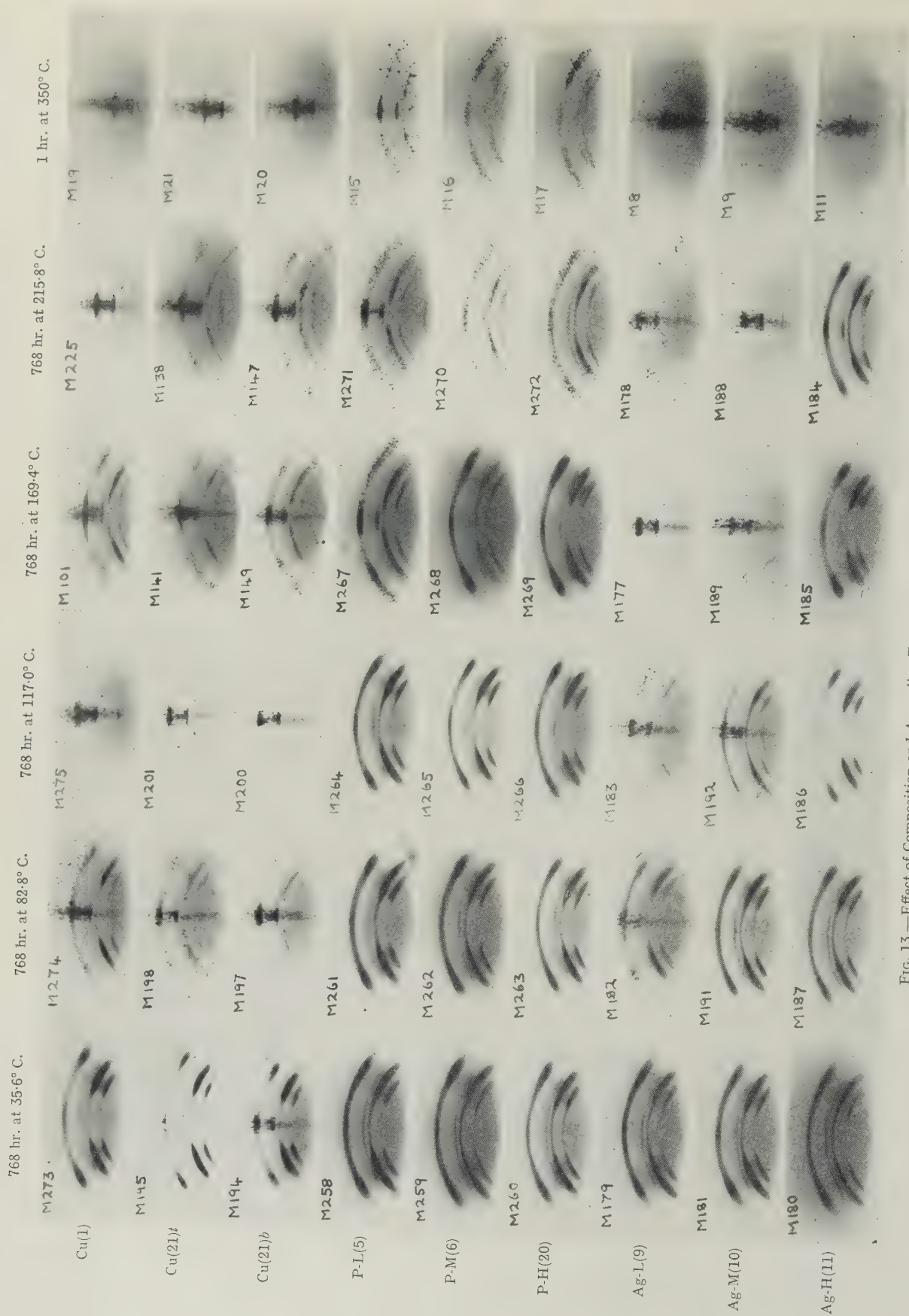
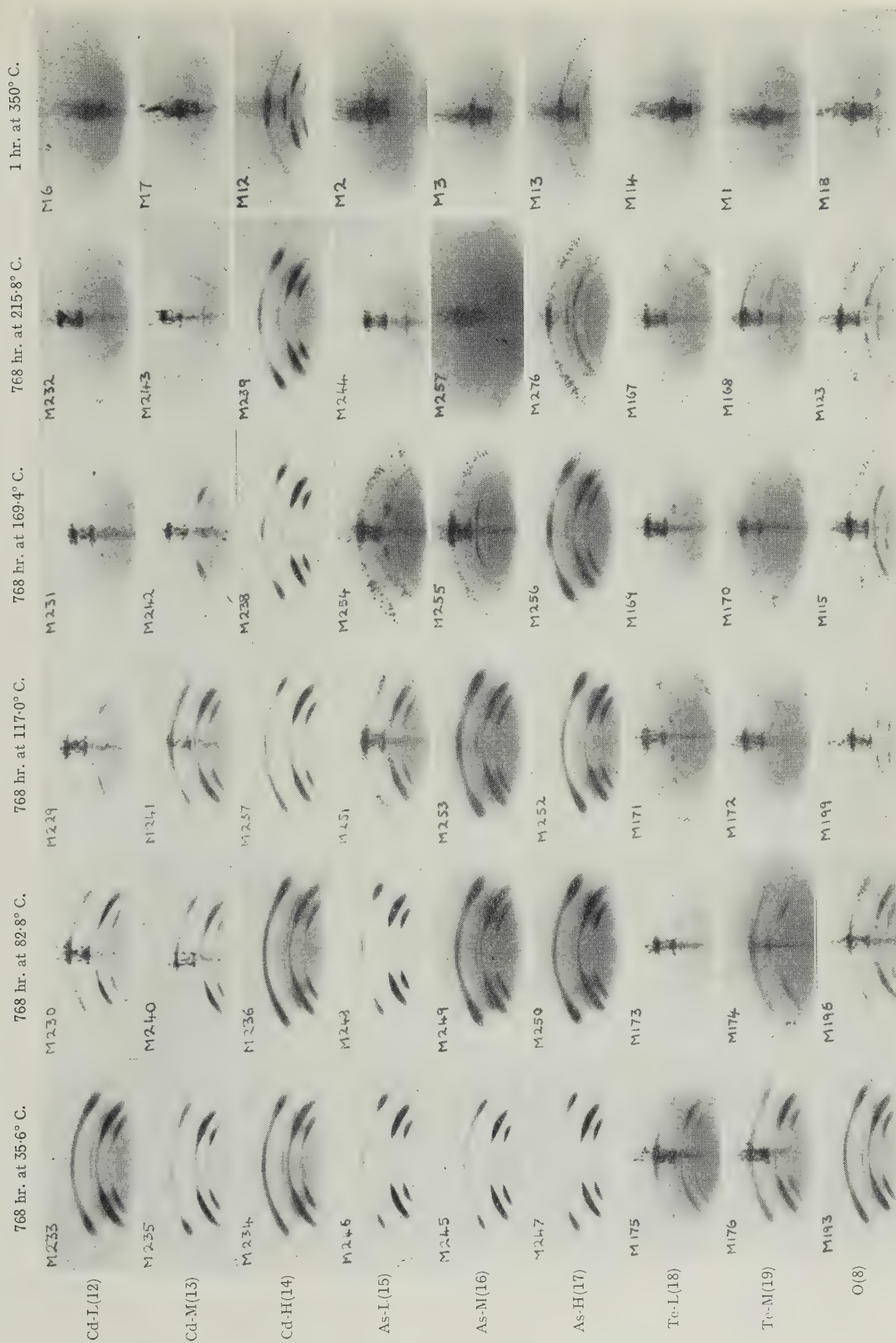


Fig. 13.—Effect of Composition and Annealing Temperature on Texture. Reproduced approx. $\times \frac{1}{2}$.

Fig. 14.—Effect of Composition and Annealing Temperature on Texture. Reproduced approx. $\times \frac{1}{2}$.

MICROSTRUCTURES SHOWING PARTIAL RECRYSTALLIZATION

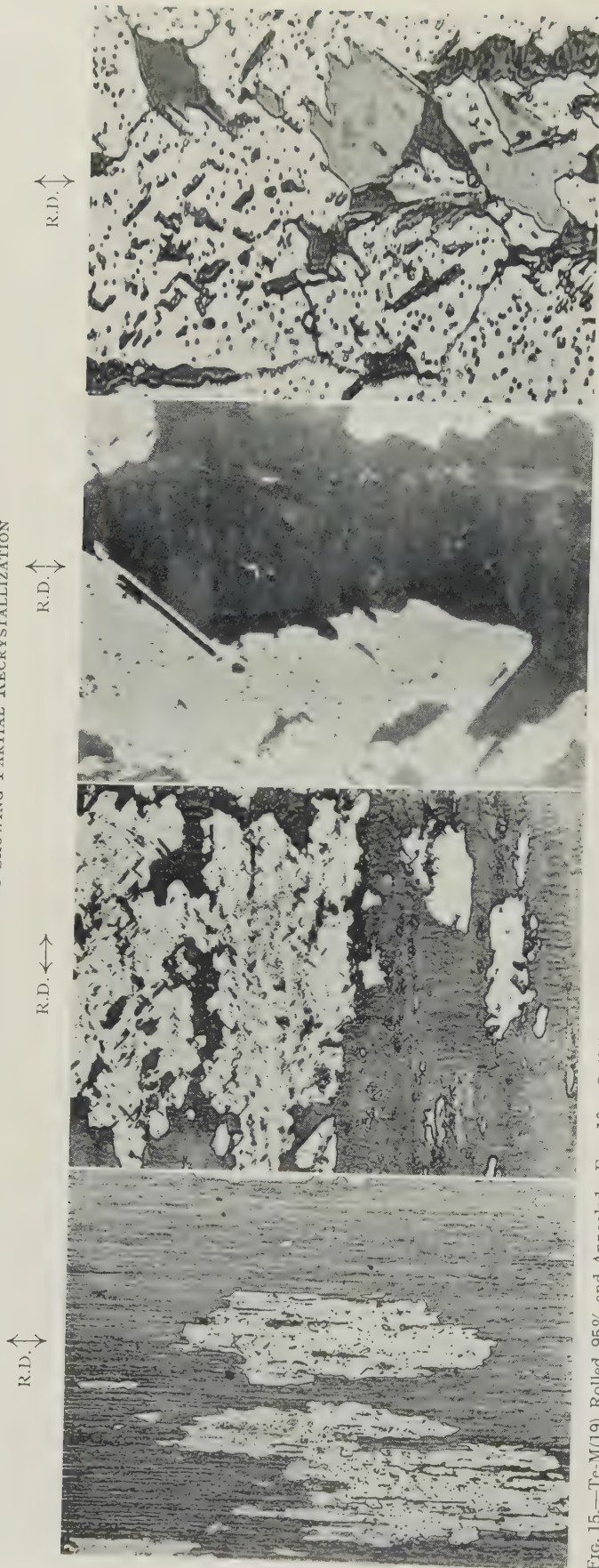


FIG. 15.—Te-M(19) Rolled 95% and Annealed 2 Hr. at 82.8° C. Longitudinal section. $\times 200$.

FIG. 16.—Cu(21)½ Rolled 95% and Annealed 1.5 Hr. at 100° C. Rolling-plane section. $\times 200$.

FIG. 17.—As Fig. 16. Different field. $\times 800$.

FIG. 18.—As Fig. 16. Different field. $\times 1000$.

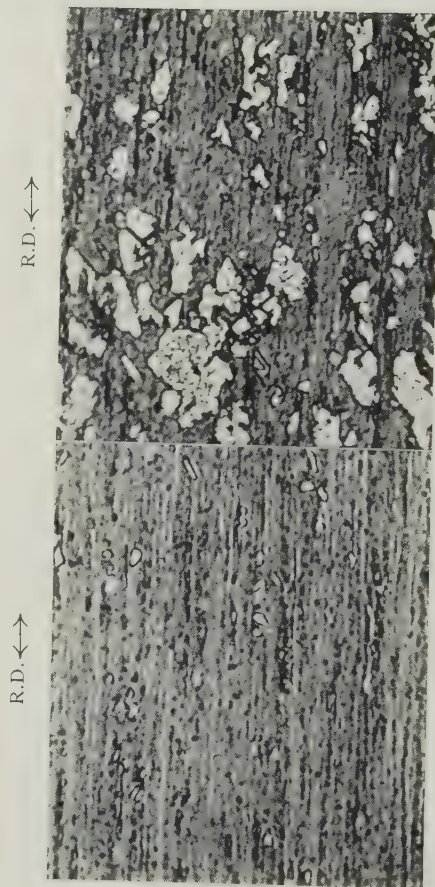


FIG. 19.—P-H(20) Rolled 95% and Annealed 16 Hr. at 165.8° C. Longitudinal section. $\times 400$.

FIG. 20.—Ag-H(11) Rolled 95% and Annealed 768 Hr. at 215.8° C. Longitudinal section. $\times 400$.

SUB-GRAIN STRUCTURE IN COARSE-GRAINED ALUMINIUM.

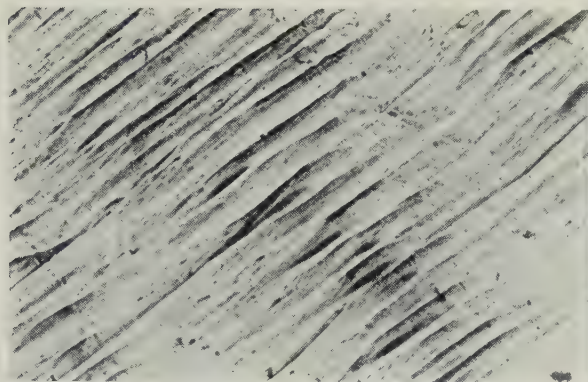


FIG. 1.—Kink Bands in a Specimen Extended Rapidly to 8% at 500° C. $\times 100$.

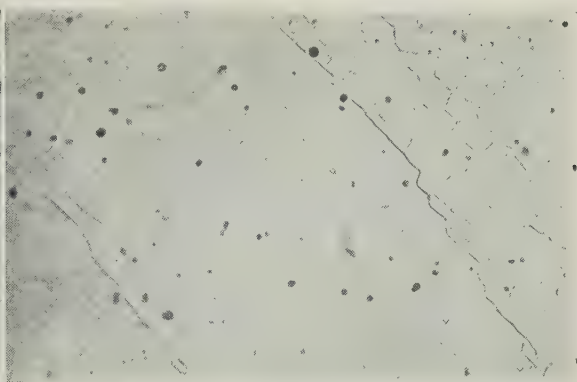


FIG. 2.—Same Area as Fig. 1 After Repolishing and Etching, Showing Substructure within the Bands. $\times 100$.

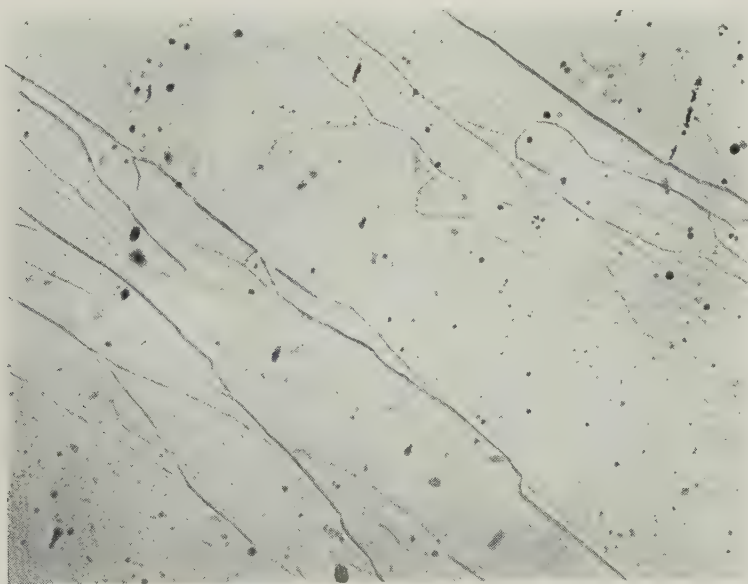


FIG. 3.—Kink Bands in a Specimen Extended Rapidly to 8% at 620° C., After Repolishing and Etching. $\times 100$.

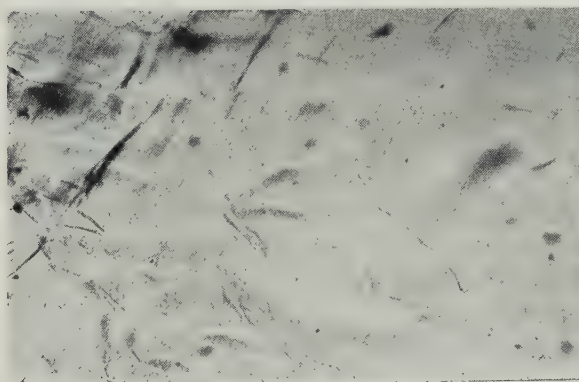


FIG. 4.—Substructure in a "Slip-Free" Grain in a Specimen Extended Slowly to 8% at 350° C. $\times 100$.

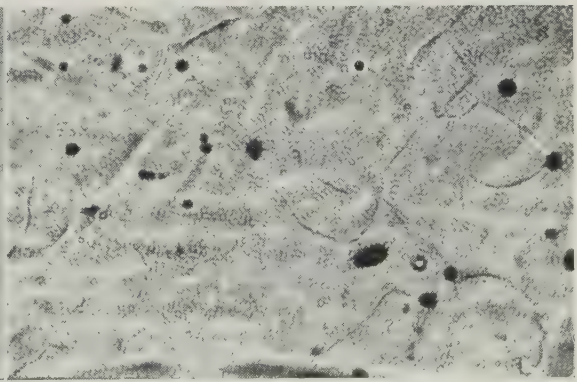


FIG. 5.—Same Area as Fig. 4 After Repolishing and Etching. $\times 100$.

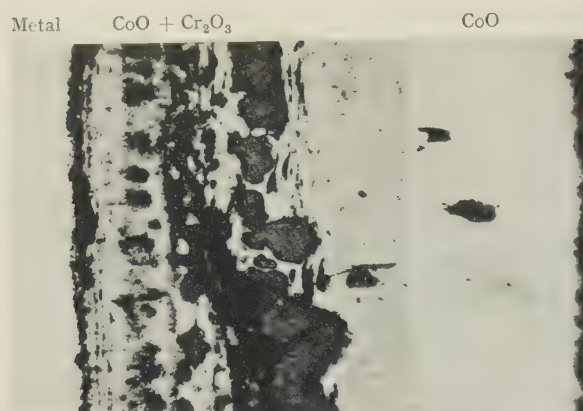


FIG. 7.—Scale on Co-10% Cr Alloy After 70 Hr. at 800° C. $\times 260$.

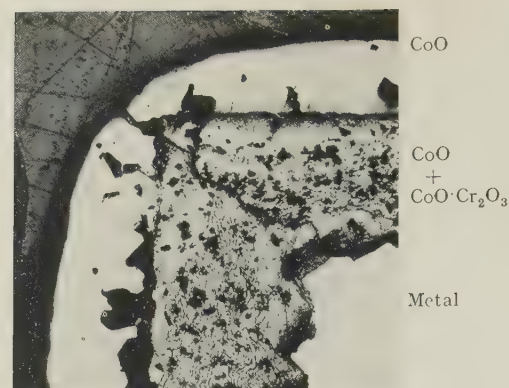
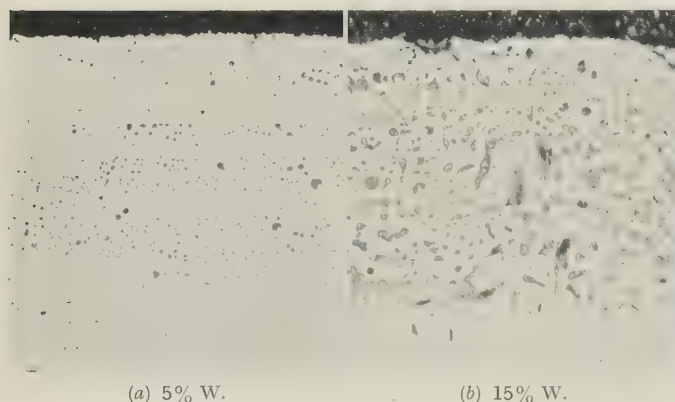


FIG. 8.—Scale on Co-10% Cr Alloy After 40 Hr. at 1100° C. $\times 45$.



(a) 5% W.



(b) 15% W.

FIG. 9.—Internal Oxidation in Ni-W Alloys After 50 Hr. at 1200° C. $\times 120$.

FIG. 10.—Crystallites of Cobalt Chromite Spinel Formed on Vitallium After 24 Hr. at 1200° C. $\times 7$.

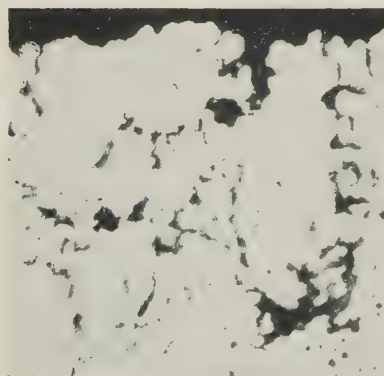


FIG. 11.—Co-32% Cr-0.5% B.



FIG. 12.—Co-32% Cr-0.64% Nb.

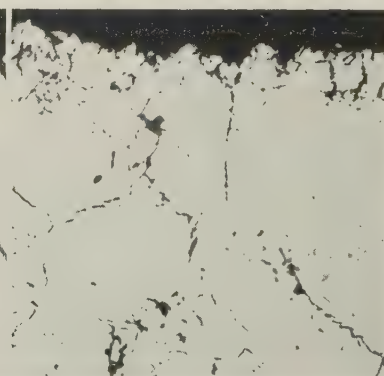


FIG. 13.—Co-32% Cr-0.39% Be.

FIGS. 11-13.—Internal Oxidation in Various Co-Cr Alloys After 50 Hr. at 1200° C. $\times 250$.

HIGH-TEMPERATURE OXIDATION CHARACTERISTICS 1436 OF A GROUP OF OXIDATION-RESISTANT COPPER-BASE ALLOYS *

By J. P. DENNISON,† Ph.D., B.Sc., JUNIOR MEMBER, and
PROFESSOR A. PREECE,‡ M.Sc., F.I.M., MEMBER

SYNOPSIS

The influence of small separate additions of aluminium, beryllium, chromium, magnesium, and silicon on the high-temperature oxidation of copper has been examined, these alloying elements having been chosen because their oxides have a high electrical resistivity. The composition and microstructure of the scales formed were studied and correlated with the rates of oxidation.

The effectiveness of the additions in conferring oxidation-resistance was in the decreasing order: beryllium, aluminium, magnesium, silicon, chromium.

Alloys having rates of oxidation less than that of copper showed divergences from the established parabolic and exponential laws. These divergences may be accounted for by a consideration of the relative rates of diffusion of copper and of the alloying element through the oxide layers.

I.—INTRODUCTION

THE results described in the present paper were obtained in a general investigation of the high-temperature oxidation characteristics of a selection of binary copper-base alloys. The alloying elements chosen were aluminium, beryllium, chromium, magnesium, and silicon.

Earlier investigations by Wagner¹ and by Price and Thomas² have demonstrated the importance, among other things, of a high electrical resistivity in the oxide film if protection against continued oxidation is desired. The elements chosen have a much higher affinity for oxygen than that of copper; their oxides are refractory, and with the exception of that of chromium, possess high electrical resistivity.

Relatively little detailed information is available concerning the exact nature of the oxide/metal interface or the constitution of the oxides formed on these alloys, especially in the temperature range 400°–700° C. It was decided therefore to begin with the simple binary alloys before proceeding to the more complex compositions.

In view of the recent publication of a comprehensive review of the literature on the oxidation of copper by Tylecote,³ only references directly connected with the present work are included.

II.—EXPERIMENTAL WORK

1. MATERIAL AND PROCEDURE

The alloys listed in Table I were prepared by melting electrolytic copper under charcoal and adding the alloying element in the form of a master alloy. Bars

of 1-in. dia. were cast by the Durville process, hot rolled to $\frac{1}{2}$ -in. dia., and machined to a smooth finish.

TABLE I.—*Compositions of Alloys Used.*

Element	Alloy Content		Copper, %	Remainder, by Difference, %
	Nominal, %	Actual, %		
Aluminium	2	2.05	97.90	0.05
	4	4.03	95.91	0.06
	6	5.96	94.00	0.04
	8	8.08	91.87	0.05
	10	9.90	90.04	0.06
Beryllium	1	1.05	98.92	0.03
	2	2.00	97.96	0.04
Chromium	0.5	0.50	99.46	0.04
	1.5	1.20	98.77	0.03
Magnesium	1	0.90	99.07	0.03
Silicon	2	2.03	97.93	0.04
	3.5	3.55	96.40	0.05

Specimens cut from these bars were exposed at the required temperatures to ordinary air and, in the preliminary part of the investigation, to the products of combustion of paraffin containing 2% sulphur burnt with a 60 : 1 air-to-fuel ratio to give an atmosphere of the following composition: N₂ 78, O₂ 17, H₂O 3, CO₂ 2, and SO₂ 0.11%.

It was found that only when the fuel contained sulphur was there any difference in the rate of oxidation. This difference, which was slight, was directly proportional to the sulphur content of the combustion atmosphere, and was apparent only at temperatures

* Manuscript received 24 June 1952.

† Lecturer in Metallurgy, University College, Swansea.

‡ Metallurgy Department, King's College, Newcastle-on-Tyne.

below 700° C. All the results reported below relate to exposure in air.

After exposure the specimens were cooled in a desiccator. The rate of oxidation was expressed as weight increase/unit of original surface area.

In most cases the scale produced was non-adherent; small particles of any scale adhering were removed by compressing the specimens in a confined space. The latter method was also adopted for removing adherent scales.

Before being sampled for analysis, the scales were powdered and thoroughly mixed. Analysis was carried out on approximately 0.5-g. samples. Copper was estimated electrolytically and the remaining solution analysed for the alloying element by standard gravimetric methods. Assuming the formula for the oxide of the alloying element, the percentage of copper in the copper oxide was used to calculate the amount of cupric oxide formed.

In microscopic examination polarized light was extremely useful in differentiating between cuprous and cupric oxides, the former appearing ruby red and the latter jet black. The crystalline appearance of cupric oxide was accentuated by partial rotation of the polarizer.

2. RESULTS

(a) Copper-Aluminium Alloys

Oxidation rates for the copper-aluminium alloys at temperatures between 400° and 1000° C. are shown in Fig. 1. The double inflection in the curves for the

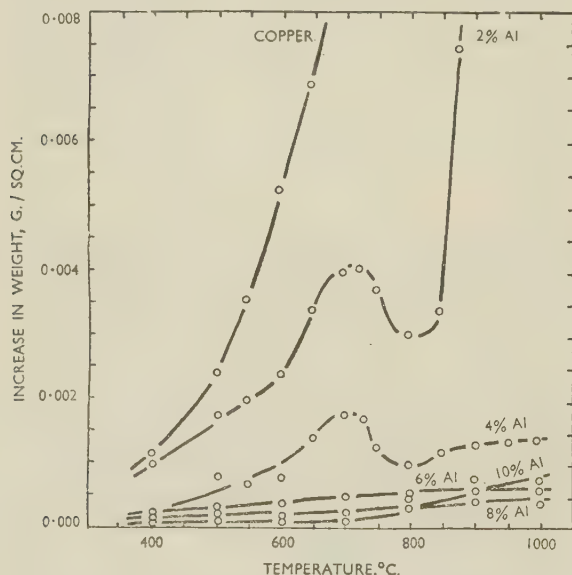


Fig. 1.—Oxidation of Copper and Copper-Aluminium Alloys After 24 Hr. at 400°–1000° C.

2 and 4% aluminium alloys in the range 700°–800° C. will be noted. The rate of oxidation does not follow the parabolic law, as shown by Figs. 2 and 3.

It seems that oxidation proceeds rapidly until a protective film of alumina is built up at the oxide/

metal interface, and then oxidation practically ceases. Fröhlich⁴ reported a similar result with additions of 1–3% aluminium at 800° C.

In the following discussion the scaling properties

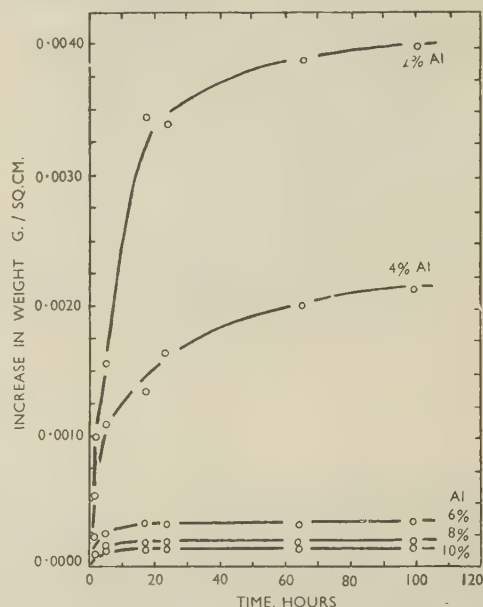


Fig. 2.—Oxidation of Copper-Aluminium Alloys After Different Times at 650° C.

of a 2% aluminium alloy are dealt with in some detail, and those of higher aluminium content are referred to only in so far as they differ from the behaviour of the 2% aluminium alloy. In all cases the rates of attack are considerably less than those for pure copper (Fig. 1).

It is interesting to note that an inflection similar to that in the rate curve at 750°–850° C. (Fig. 1) is found in Fig. 4, which shows the proportion of cupric oxide in the scale formed during a 24-hr. exposure. The curve for copper in Fig. 4 also shows a similar inflection. With the 2% aluminium alloy the minimum in the rate curve at about 850° C. corresponds to a more adherent type of scale and to the presence of a more continuous and compact film of alumina at the scale/metal interface.

In the temperature range 400° to approximately 800° C. the scale consists of cuprous oxide containing alumina particles in the initial stages; during further oxidation cupric oxide also forms, and with prolonged periods of exposure the proportion of cuprous oxide diminishes until finally the scale consists only of cupric oxide and alumina (Fig. 5). Above 875° C. cupric oxide becomes unstable and is not found in the scale. This scale is non-adherent, and consists of an outer layer of cuprous oxide and an inner duplex layer of cuprous oxide containing alumina particles distributed along definite boundaries, which probably correspond to the grain boundaries of the original metal (Fig. 11, Plate XXXII). In a thin, uneven subscale, in which alumina particles are found mainly at the

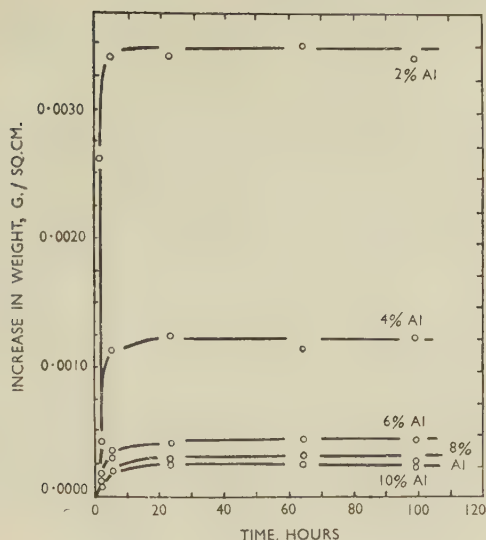


FIG. 3.—Oxidation of Copper-Aluminium Alloys After Different Times at 850° C.

grain boundaries, the impoverished metal appears to consist of pure copper. The structure of this subscale indicates that aluminium diffuses to the crystal boundary and is oxidized ahead of the advancing metal/oxide interface. The junction between the outer layer of cuprous oxide and the inner duplex layer corresponds with the original surface of the specimen.

No subscale is apparent between 750° and 850° C., and in this temperature range the proportion of alumina in the scale is greater than would correspond with the aluminium content of the alloy (Table II). (Below this temperature range there is appreciable subscale formation.) The adherent scales formed between 750° and 850° C. exhibit a continuous white film of alumina adhering to the underlying metal.

Apart from an increase in protection to be expected from a greater concentration of the alloying element, the only notable result obtained with the 4% aluminium alloy is the very considerable protection afforded

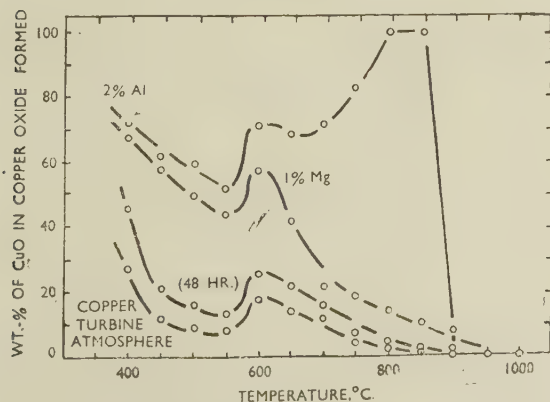


FIG. 4.—Percentage CuO in Scale Formed on Cu, 2% Al Alloy, and 1% Mg Alloy Heated for 24 Hr. at 400°–1000° C.

above 850° C. There is also a much greater proportion of cupric oxide in the scale produced on this alloy owing to the more rapid formation of a protective film of alumina at the scale/metal interface. A corresponding improvement in the adherence of the

TABLE II.—Percentage of Alloying Element Converted into Scale During 24 Hours' Oxidation in Air.

Alloy	Oxidation Temperature, °C.									
	400	500	600	650	700	750	800	850	900	1000
2% Al	1.9	2.1	2.0	1.9	1.9	2.5	3.1	2.4	2.0	1.9
1.2% Cr	1.5	1.6	1.3	1.3	1.1	...	1.2	1.3
1% Mg	0.9	...	0.9	...	1.0	1.2	1.7	1.9	2.0	...
2% Si	2.0	1.8	2.1	2.0	2.2	2.3	2.7	1.8	0.4	0
3.5% Si	...	3.2	...	4.1	...	2.8	0.8	0

scale takes place, especially at temperatures above 750° C.

The scales produced on the higher-aluminium alloys were adherent, and consisted very largely of alumina over most of the temperature range, and above 750° C. were almost entirely of alumina.

The interesting feature in the oxidation of the 2% aluminium alloy is its unusual behaviour in the

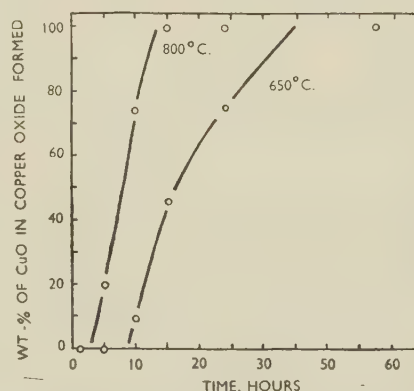


FIG. 5.—Percentage CuO in Scale Formed on 2% Al Alloy After Various Times at 650° and 800° C.

range 700°–850° C. Below this range oxidation follows the usual pattern, in which preferential oxidation of aluminium occurs in advance of the oxide/metal interface, giving rise to a subscale. The alumina particles give only partial protection, since they are located very largely at the pre-existing crystal boundaries of the alloy and do not form a continuous film at the oxide/metal interface.

It is evident that some change occurs in the mechanism of oxidation at 700° C., since the aluminium is not preferentially oxidized in advance of the oxide/metal interface as at lower temperatures; there is, consequently, no subscale formation, and the alumina forms as a compact film between the oxide and the metal. This change in the disposition of alumina in the scale gives a higher degree of protection and results in the double inflection of the rate curve in the range 700°–850° C., as shown in Fig. 1.

As the copper oxide portion of the scale in this

temperature range eventually consists entirely of cupric oxide, either oxygen must diffuse inwards to the cuprous oxide/cupric oxide interface, or cuprous oxide must dissociate into cupric oxide and copper at

continuous, it prevents further movement of copper from the underlying metal and oxidation ceases.

(b) Copper-Beryllium Alloys

The behaviour of the copper-beryllium alloys in air is shown in Figs. 6, 7, and 8. The scatter in the results obtained with the 1% beryllium alloy below 800° C. will be noted. It appears that the increased rate of diffusion of the alloying element at the higher temperatures facilitates the formation of a continuous protective film. Further evidence of this is afforded by comparing Figs. 7 and 8; the curves become asymptotic in a shorter time at 850° C. than they do at 650° C.

The addition of 2% beryllium is sufficient to give a stable protective film of beryllia over the entire temperature range. Below 600° C. it appeared as a slight tarnish layer which changed to a microcrystalline film at higher temperatures.

(c) Copper-Chromium Alloys

The addition of 1.2% chromium to copper confers no resistance to oxidation (Fig. 9). The structure of the oxide layer is similar to that formed on pure copper, except that the inner layer of cuprous oxide contains particles of Cr_2O_3 . This alloy possesses a high susceptibility to internal oxidation of a peculiar form at high temperatures, as illustrated in Fig. 12 (Plate XXXII). The tendency for Cr_2O_3 to give a Nessler-ring effect is interesting.

The lack of protection is presumably due to the low solid solubility of chromium, coupled with a low rate

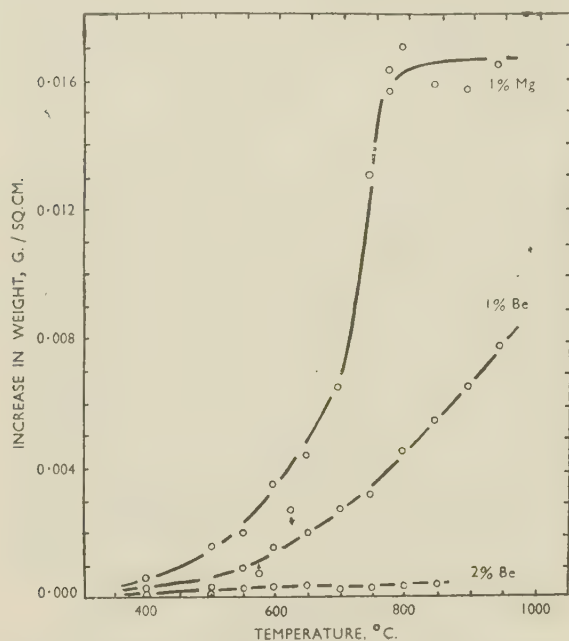


FIG. 6.—Oxidation of 1% Mg, 1% Be, and 2% Be Alloys After 24 Hr. at Different Temperatures.

that interface, copper diffusing to the outer surface. Wagner and Grünwald⁵ postulated the diffusion of cuprous ions and electrons as being responsible for the oxidation taking place by diffusion through cuprous oxide, though they also indicated the possibility of diffusion of anions through the lattice of an oxide of a metal showing its highest valency.

At temperatures above 850° C. oxide formation becomes far more rapid, and the scale that forms consists only of cuprous oxide and alumina; a thin, irregular subscale in which the alumina particles appear as a network in the inner layer of cuprous oxide, also forms.

From the results obtained it is clear that complete protection against continued oxidation is obtained by the formation of a continuous film of alumina. Under present conditions 4% aluminium is not sufficient to provide such a film, though the irregular manner in which the 4% aluminium alloy oxidizes appears to indicate that this content is near to that required to give the almost complete protection conferred by a slightly higher aluminium content.

The progress of oxide formation with these alloys would seem to be in accord with the mechanism postulated by Mott,⁶ in that the duplex layer of alumina and cuprous oxide formed in the initial stages of oxidation is transformed into an alumina film as a result of the replacement of cuprous ions by those of aluminium, the replaced copper ions diffusing outward to the oxide/gas interface. As the alumina film becomes

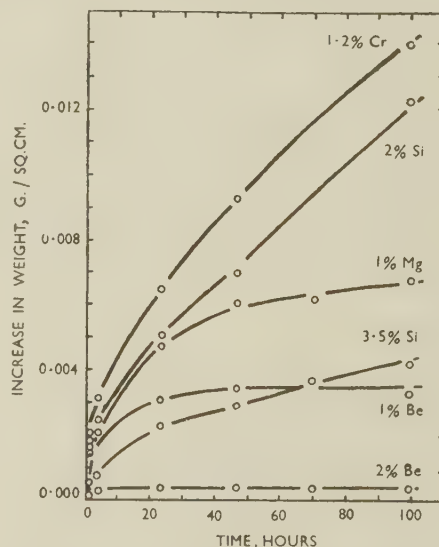


FIG. 7.—Oxidation of 1% Mg, 1.2% Cr, 1% Be, 2% Be, 2% Si, and 3.5% Si Alloys After Various Times at 650° C.

of diffusion in the copper. The maximum solubility at the solidus is near 1.2%, but decreases rapidly at lower temperatures so that at no temperature is there sufficient in solution to form a continuous protective film of chromic oxide when heated.

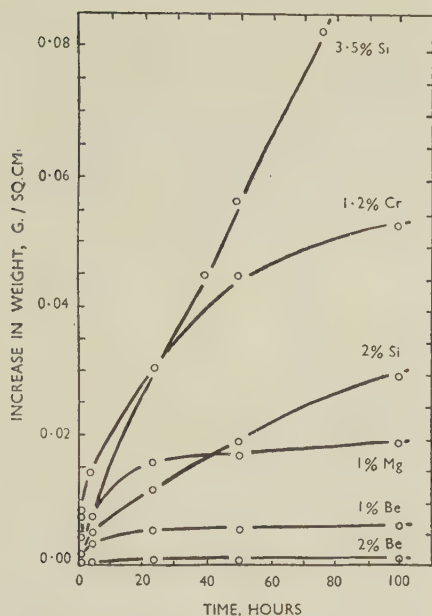


Fig. 8.—Oxidation of 1% Mg, 1.2% Cr, 1% Be, 2% Be, 2% Si, and 3.5% Si Alloys After Various Times at 850° C.

(d) Copper-Magnesium Alloys

Only the alloy containing 1.0% magnesium was examined in this system. Although this addition does not give a high degree of resistance, the change in direction in the oxidation curve shown in Fig. 6 at 750° C. is interesting. Apart from occurring at a higher temperature, it is similar to that found in the copper-aluminium and copper-silicon alloys.

Extensive subscale formation occurs at all temperatures up to approximately 750° C., but above this temperature it is slight and irregular (Fig. 13, Plate XXXII). The scales formed were non-adherent at all temperatures below 750° C.

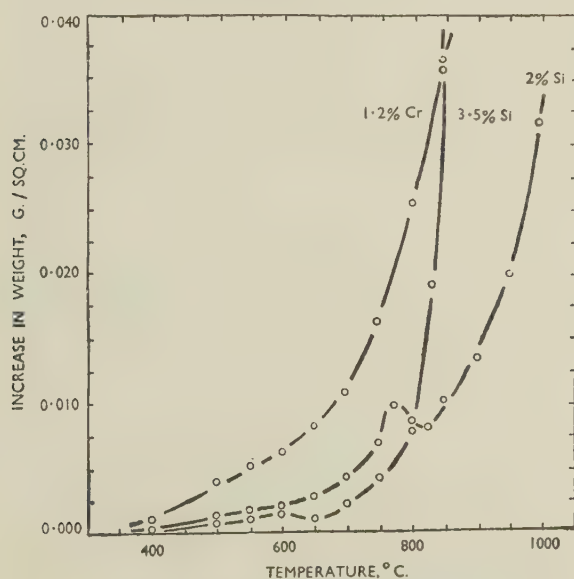


Fig. 9.—Oxidation of 1.2% Cr, 2% Si, and 3.5% Si Alloys After 24 Hr. at Different Temperatures.

(e) Copper-Silicon Alloys

The oxidation properties of copper-silicon exhibit some interesting features. As with the 2% aluminium alloy, the rate curve for the 2% silicon alloy (Fig. 9) shows a double inflection in the range 775°–825° C. At temperatures near 800° C. and below, a film of silica was found at the scale/metal interface that could be easily separated from the cuprous and cupric oxides by dissolving away the latter in hydrochloric acid. Above 825° C. this film of silica was no longer evident, and the inflections became more marked with increased time of exposure. Above 900° C. there is evidence of partial melting at the surface of the metal, although the melting point of the 2% silicon alloy is given in the literature as 1010° C.

Analyses of the scales formed on the 2% silicon alloy showed that cuprous and cupric oxides and silica were present in scales formed below 850° C., but that at higher temperatures the silica and cupric oxide are absent.

The changes occurring in the composition of the oxide layer formed on this 2% silicon alloy over the

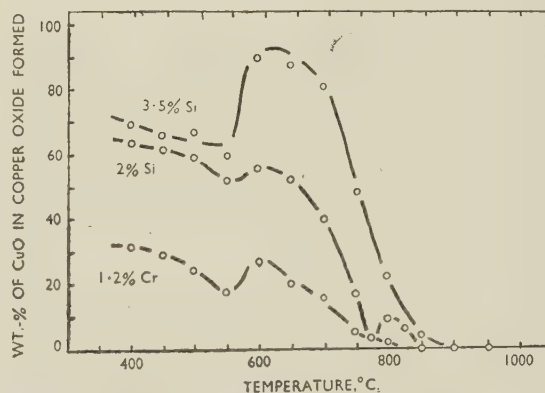


Fig. 10.—Percentage of CuO in Scale Formed on 1.2% Cr, 2% Si and 3.5% Si Alloys After 24 Hr. at Different Temperatures.

temperature range from 400° to 900° C. are shown in Fig. 10. The curve has two minima, one at 550° C., similar to that found in the oxidation of pure copper, and a second at 775° C., which corresponds with the maximum in the oxidation-rate curve shown in Fig. 9.

It is only in the limited temperature range 750°–850° C. that appreciable preferential oxidation of silicon occurs (Table II, p. 231), and this is at a maximum between 800° and 825° C. These observations are in agreement with those of Dunn,⁷ who showed that at 725° C. a film of silica could be detected at the oxide/metal interface, but that scales formed at 827° C. contained practically no silica.

At temperatures up to 750° C. subscale formation occurs, mainly along grain boundaries, and is extensive even at 550° C. (Fig. 14, Plate XXXII). Between 750° and 775° C. no subscale was observed, but the scale/metal interface was very irregular, with deep

localized penetration of scale consisting of cuprous oxide and silica (Fig. 15, Plate XXXII).

The scale/metal interface is comparatively even at 800° C. and corresponds with the minimum in the rate curve in Fig. 9 (p. 233). This even attack is presumably due to the build-up of the interface film of silica between the metal and the copper oxide layer and, as would be expected, this was associated with a much greater proportion of cupric oxide (Fig. 16, Plate XXXII). At 850° C. very little cupric oxide occurs in the scale, and the scale/metal interface again becomes irregular and the extent of the duplex zone is much diminished.

With the absence of silica in scale formed at 900° and 950° C., there is an increase in the concentration of silicon in the metal at the scale/metal interface which results eventually in the formation of a two-phase zone in the underlying metal (Fig. 17, Plate XXXII). The hard, bluish constituent in this zone appears to consist of the γ phase. Analysis of the metal in the surface layers shows a large increase in the proportion of silicon present, and also that only copper and silicon are present, thus ruling out the possibility of melting being due to either formation of copper silicate or some kind of subscale.

At 970° C. the grain boundaries in the surface layers of metal show evident incipient fusion and the formation of the γ phase. At a slightly higher temperature complete fusion eventually occurs inside an initially formed oxide jacket consisting of cuprous oxide only.

An increase in the concentration of silicon to 3.5% affords a greater degree of protection (Fig. 9), the general form of the curves bearing a close resemblance to those for the 2% silicon alloy.

It is noteworthy that the cupric oxide layer formed at 650° C. advances inwards to such an extent that the cuprous oxide in the initial duplex zone becomes partly converted to cupric oxide (Fig. 18, Plate XXXII). This may be regarded as further evidence of film growth continuing by inward diffusion of oxygen through cupric oxide.

There is a general similarity in the oxidation behaviour of the copper-aluminium and copper-silicon alloys, especially in the occurrence of maxima and minima in the rate curves. One important difference, however, is the more extensive subscale formation in the copper-silicon series at lower temperatures, which results in a higher scaling rate than that found with the copper-aluminium alloys.

III.—CONCLUSIONS

The results obtained in the present investigation demonstrate certain features in the oxidation of copper-rich alloys containing small additions of beryllium, aluminium, magnesium, silicon, and chromium. The effectiveness of these additions in conferring resistance to oxidation decreases in the order given. Chromium affords no protection whatsoever, the solid solubility of chromium in copper being

too low to permit the formation of a continuous layer of the protective oxide that is an essential requirement. The ability of an alloying element to reduce the rate of oxidation depends on the formation of a separate and continuous layer of its oxide at the scale/metal interface, which can prevent outward diffusion of copper by virtue of a high electrical resistivity and a low transport number for cuprous ions. This continuous protective film can occur only in the absence of subscale formation, and is dependent on a process of replacement in the initially duplex film of cuprous oxide and oxide of the alloying element. The existence of such a layer is generally accompanied by preferential oxidation of the alloying element.

Where the addition of the alloying element is not quite sufficient for the formation of a protective film, oxidation proceeds by the formation of a scale consisting of separate particles of cuprous oxide and the oxide of the alloying element underneath the outer layer of copper oxide. As the alloying addition is further decreased, this inner layer diminishes and may be replaced by a zone of internal oxidation in which preferential oxidation of the added element occurs at the grain boundaries of the alloy.

The behaviour of the copper-silicon is most remarkable in that at 900° C. and above the silicon diffuses into the metal away from the oxide/metal interface, whereas at lower temperatures, e.g. 800° C., the silicon diffuses towards the surface of the oxidizing metal to form a layer of silica at the oxide/metal interface.

In considering the results obtained with these alloys reference must be made also to the inflections found in the oxidation-rate and oxide-composition curves with increasing temperature. It is considered that these inflections result from an interplay of temperature-sensitive properties such as diffusion of silicon in copper and ionic transfer through copper oxide.

The conversion of an oxide layer which forms as cuprous oxide and silica to one of cupric oxide and silica during prolonged oxidation provides evidence for the inward diffusion of oxygen through cupric oxide.

ACKNOWLEDGEMENTS

Thanks are due to the Yorkshire Copper Works, Ltd., and to the British Non-Ferrous Metals Research Association for materials provided and for facilities to discuss the work during progress.

REFERENCES

1. C. Wagner, *Arch. Eisenhüttenwesen*, 1937-38, **11**, 449.
2. L. E. Price and G. J. Thomas, *J. Inst. Metals*, 1938, **63**, 21.
3. R. F. Tylecote, *ibid.*, 1950-51, **78**, 259.
4. K. W. Fröhlich, *Z. Metallkunde*, 1936, **28**, 368.
5. C. Wagner and K. Grünewald, *Z. physikal. Chem.*, 1938, [B], **40**, 445.
6. N. F. Mott, *Nature*, 1940, **145**, 996.
7. J. S. Dunn, *J. Inst. Metals*, 1931, **46**, 25.

A METHOD OF DETERMINING ORIENTATIONS IN ALUMINIUM SINGLE CRYSTALS AND POLYCRYSTALLINE AGGREGATES

1437

By G. E. G. TUCKER,† B.Sc., STUDENT MEMBER, and P. C. MURPHY,† B.Sc., A.I.M., MEMBER

SYNOPSIS

A method is described for constructing (100) pole figures from angular measurements of the etch-pits that are developed in micrographically prepared commercial and super-purity aluminium. Suitable etching reagents are indicated, and the technique of angular measurement using a metallurgical microscope is discussed in detail.

A table of angular values which reduces the calculation necessary in plotting the stereographic projections from the etch-pit data has been constructed, and is reproduced.

It has been found that the pole figures prepared by this method agree well with those produced from data obtained by X-ray-diffraction techniques.

I.—INTRODUCTION

It has been known for many years that when metals and alloys are etched with certain reagents, attack takes place at isolated points within the grains rather than by general surface etching. This localized etching produces pits whose traces on the etched surface are rectilinear figures, commonly known as etch-pits. It has also been shown that in most cases these pits are formed by attack along definite crystallographic planes; for instance, in most face-centred cubic metals etching is along {100} planes. It will therefore be seen that the positions of the sides or faces of etch-pits are related to the orientations of the grains on which they are formed.

This property has been used by many investigators to determine crystal orientations. For instance, Barrett¹ has described a method in which the reflection of light from the faces of etch-pits is employed to determine the orientation by using a two-circle goniometer. Lacombe and Beaujard² have derived certain simple orientations from the shape of the etch-pits by visual inspection, and Kostron³ has prepared graphs by means of which orientations may be estimated by using evidence obtained from etch-pits and slip lines. In another method, due to Smith and Mehl,⁴ the angles between the etch-pit sides and the sectioning plane are estimated by eye and used in plotting the poles approximately, the positions being then corrected by rotation of a standard projection.

The present paper deals with a method of plotting pole figures from data obtained by measurement of the angles of the figures formed when micrographically prepared sections of aluminium of super and commercial purity are attacked with reagents such as that

of Tucker.⁵ The measurements may be carried out on any ordinary metallurgical microscope.

II.—FORMATION OF ETCH-PITS

Etch-pits are formed in a grain when localized attack by an etching reagent takes place. Cahn⁶ states that they are likely to form at regions of high dislocation density. Mahl and Stranski⁷ believe that the pits are not formed by reaction of the aluminium crystal itself, but through the dissolution of a reaction product which they associate with a surface oxide layer.

Several techniques for the production of etch-pits have been proposed. The classical method for aluminium involves immersion in strong acid mixtures, such as Tucker's reagent, or the etch proposed by Lacombe and Beaujard.² Other methods are the electrolytic etch of Jacquesson and Manenc⁸ and the gaseous etch used by Mahl and Stranski.⁹

If the faces of the etch-pits are in fact cube planes, the pits will appear as simple rectilinear figures; Mahl and Stranski, however, consider that in some cases the true cube planes are not revealed, but instead "vicinal surfaces", which may vary by as much as 10° from the cube planes, and Kostron³ shows photographs of etch-pits with curved sides. In such cases orientation determinations based on the assumption that cube planes are revealed could not be made.

It has been found that these objections can be avoided by the use of suitable etching reagents on materials of fairly high purity such as commercial and superpure aluminium; any appreciable quantity of alloying elements gives many pits that are bounded by curved surfaces.

* Manuscript received 14 August 1952.

† Research Metallurgist, Aluminium Laboratories Limited, Banbury.

Assuming that the etching reagent attacks along the $\{100\}$ planes of the lattice, it can be seen that the etch-pits must be sections of cubes. If two of the crystallographic axes lie parallel to the sectioning plane then the etch-pit will be square or rectangular, depending upon the relative rates of attack parallel to these axes; in any case the pit formed will have a flat base parallel to the sectioning plane. If only one of the crystallographic axes is parallel to the sectioning plane, the etch-pit will be rectangular in form but will have a bottom edge, i.e. two of the faces of the pit will slope down to the base and meet in a line parallel to two of the sides of the rectangle and normal to the other two. If none of the three axes is parallel to the sectioning plane (the most general case), the etch-pit will have the form of a triangle with the three faces running down to meet in a point. The three types of ideal pits and their formation are illustrated diagrammatically in Fig. 1 (a), (b), and (c) and photographs are shown in Figs. 9, 10, and 11 (Plate XXXIII). Fig. 9 shows (001)-type pits under dark-field illumination, Fig. 10 (011)-type pits (the microscope being focused on the "bottom edge" of the pits), and Fig. 11 (111)-type pits. These pit shapes are, of course, formed only under ideal conditions; in practice less perfect shapes are frequently observed, especially in aluminium of low purity. The greatest divergence from the ideal shapes occurs in triangular etch-pits, which are frequently truncated at one or more of the apices producing 4-, 5-, or 6-sided figures.

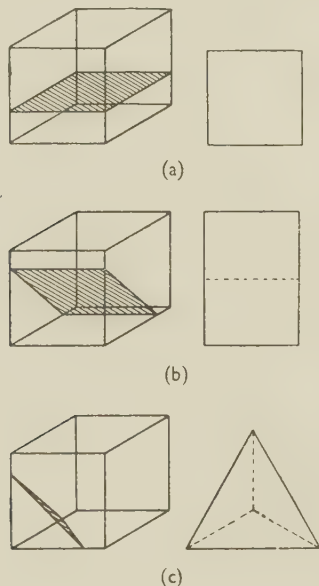


FIG. 1.—Formation of Simple Etch-Pits by Intersection of Sectioning Plane (shaded) with Lattice Cube, and Shape of Etch-Pit as seen under a Microscope. Broken lines indicate bottom edges. (a) Two axes in sectioning plane—(001) type. (b) One axis in sectioning plane—(011) type. (c) No axis in sectioning plane—(111) type.

These truncations are, however, always parallel to the sides opposite to them and obviously occur by simultaneous attack on parallel $\{100\}$ planes. The formation of such truncated pits on an equilateral

triangle is shown diagrammatically in Fig. 2 (a), and some truncated pits found in practice are illustrated in Fig. 12 (Plate XXXIII). A rather less obvious case is illustrated in Fig. 2 (b), which shows a truncation of

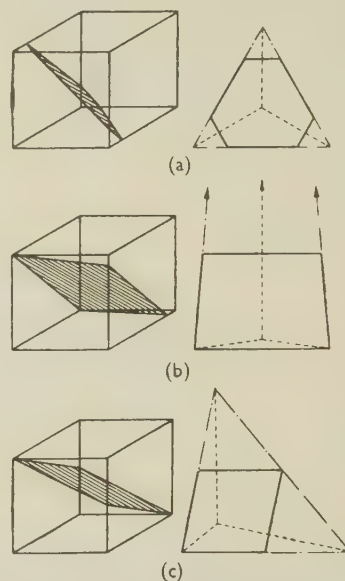


FIG. 2.—Formation of Truncated Etch-Pits by Intersection of Sectioning Plane (shaded) with Lattice Cubes, and Shape of Etch-Pits (full lines) as seen under a Microscope. Dashed lines indicate ideal triangles; dotted lines indicate bottom edges. (a) Truncated (111) type. (b) Truncated "near (011)" type. (c) Rhombic-truncated (112) type.

a very acute triangle. The etch-pit produced in this way may appear to be rectangular, but careful angular measurement (as described later) will distinguish between the two. A still more misleading case occurs when attack along one of the $\{100\}$ planes fails to reach the surface of the specimen, the etch-pit then having a rhombic instead of a triangular form. This is illustrated in Fig. 2 (c), and is shown on some of the pits in Fig. 12 (Plate XXXIII), where the truncations have resulted in the almost complete disappearance of the third side. It is not possible to measure such pits with great accuracy, but it has been found in practice that an assumption that the triangle is isosceles is rarely in great error. It is advisable to carry out a diligent search of any grain in which rhombic etch-pits occur in case there are some isolated instances of incomplete truncation which reveal the ideal triangle.

III.—TECHNIQUE OF MEASURING ANGLES OF ETCH-PITS

1. PREPARATION OF SPECIMENS

In order to obtain reliable data it is essential that the pits should be straight sided, as large as possible, and well spaced on any grain. These requirements are met only by specialized polishing and etching techniques. Each sample to be examined presents a different problem, and only the simpler cases can be prepared by any general technique.

The easiest samples to prepare satisfactorily are those with a relatively large grain-size, e.g. as-cast aluminium of commercial- or super-purity. These can be given a good metallographic polish either electrolytically or mechanically and etched in strong acid mixtures such as the etch proposed by Lacombe and Beaujard,² which contains 47% fuming nitric acid, 50% chemically pure hydrochloric acid, and 3% pure hydrofluoric acid, or a similar etch used by the present authors consisting of 35% nitric acid, 61% hydrochloric acid, and 4% hydrofluoric acid (all of Analar quality).

It is generally advisable to use electrolytic polishing, but reasonably good results can be obtained from a mechanically polished specimen if care is taken to avoid undue cold working of the surface. The time of etching depends mainly on the method of preparation and the temperature of the reagent. It is advisable to use a container made of a relatively inert substance such as polythene to avoid possible contamination of the etch. It has also been found desirable to cool the reagent to a temperature of 0°–8° C. in order to increase the etching time to 5–15 sec.

A more difficult problem is presented by relatively fine-grained polycrystalline aggregates, such as cold-rolled or annealed commercial-purity aluminium sheet. In these the etch-pits developed by the above reagents are often of very poor shape, especially if the sample has been mechanically polished. For such materials it has been found advisable to use an electrolytic polish such as that developed by Hone and Pearson¹⁰ and to etch, after washing thoroughly in cold water, in a reagent such as 71% hydrochloric acid, 4% hydrofluoric acid, and 25% ethyl or methyl alcohol, or 42% hydrochloric acid, 41% glycerol, 15% nitric acid, and 2% hydrofluoric acid (all of Analar quality). With the latter etching solution, the reagents should be mixed in the order given, to avoid undue rise in temperature.

These reagents are also used at 0°–8° C., and the time of etching for commercial-purity sheet is about 7–10 sec. For super-purity sheet the reagents recommended for large-grained specimens are more suitable, as those containing organic additions are too slow.

The section examined should be related to some logical reference directions, as is usual in X-ray work. For example, in investigating fibre textures in rods and wires, a transverse section is desirable; in sheet, a section in the rolling plane and related to the rolling direction is most useful. The polished section can be marked with a scribed line parallel to a reference direction.

2. MEASUREMENT OF ETCH-PITS

As described in Section II, etch-pits in aluminium fall broadly into two classes: rectangular pits and those based on triangles. In the latter type, the internal angles of the ideal triangle must be measured, whereas in the former type it is necessary to measure the relative distances of the bottom edge from the two

sides of the etch-pit parallel to it. In addition, with both types some measurement must be made to distinguish between geometrically similar pits differing only by a rotation about an axis perpendicular to the sectioning plane.

Consider first a rectangular pit. In this case it is necessary to measure the relative lengths QU and UT (Fig. 3). The ratio QU/UT will for the time being be arbitrarily referred to as the ratio l^2/k^2 , for reasons which will be given in the next section. In large pits it may be possible to measure the lengths directly by means of an eye-piece graticule, but this is frequently impracticable and it is necessary to estimate the ratio by eye. This can be done fairly accurately for values of the ratio near to unity, and since the error in pole position decreases with increasing values of the ratio, estimation is generally satisfactory. The ratio l^2/k^2 is sufficient to determine the crystallographic indices of the sectioning plane, and the actual orientation is then defined uniquely by the angle between the reference direction and the bottom edge.

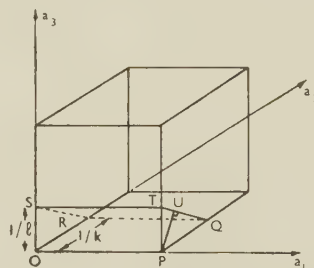


FIG. 3.—Intersection of Sectioning Plane $QRST$ of Indices $(0kl)$ with Lattice Cube.

Consider next the triangular pits. In this case it is necessary and sufficient to measure two angles of the triangle (the ideal triangle if the etch-pit is truncated) to determine the crystallographic indices of the sectioning plane, and the actual orientation may be specified with the knowledge of the angle between the reference direction and one of the etch-pit sides.

The actual process of measuring and recording for a particular sample may now be described in general terms, and may be adapted to suit individual circumstances. First, the reference direction must be marked on the polished and etched sample. This is best accomplished by scribing a fine line on the specimen. The specimen is then mounted on the stage of the microscope so that the reference direction lies parallel to a vertical cross-hair in the eye-piece or on the projection screen. Measurements may then be made at the desired number of points on the specimen, but in moving from one point to another the specimen must not be rotated relative to the stage. At each point, the specimen is rotated until one side of the etch-pit being measured is parallel to the cross-hair and the angle of rotation is recorded. Throughout this description it is assumed that the specimen is rotated in such a way that the field of

view rotates clockwise relative to the cross-hair. In rectangular pits this is the only measurement required (other than the ratio l^2/k^2) and is made such that the rotation brings the bottom edge parallel to the cross-hair, so that the ratio l^2/k^2 when taken from left to right is greater than unity. For example, in Fig. 3 the rotation would bring OP vertical rather than PO since $QU/UT > 1$. In rectangular (square) pits with no bottom edge $l^2/k^2 = \infty$, and any side may be taken as the bottom edge. In triangular pits, the vertex opposite to the side brought parallel to the cross-hair must be to the left of this side. In all cases the angle of rotation is measured and will be denoted here by θ .

Since all measurements necessary for a rectangular pit have been taken at this stage, no further rotation of the specimen is necessary. The specimen is returned to its original position (zero rotation) and moved to the next pit to be measured.

For triangular pits further rotation is necessary. In this case, after the angle θ has been noted, the specimen is rotated farther until the next side of the etch-pit, in order, is parallel to the cross-hair, but in this case the opposite vertex of the triangle will be to the right of the side. The total rotation from the original zero position is now noted, and will be referred to as $\theta + A$, since it is obviously made up of the initial rotation θ and one angle (A) of the triangle. A further rotation to the next side of the triangle (the vertex being to the left of this side) gives the reading $\theta + A + B$ for the total rotation so far, while one more rotation gives $\theta + A + B + C$, which should equal $\theta + 180^\circ$ and serves as a check on the accuracy of the measurements. The angles A , B , and C of the triangle may be obtained by subtraction. The transformation necessary to plot poles on a stereographic projection is described in the next section.

It is necessary to measure the angles as accurately as possible, particularly for triangles which have angles near to 0° or 90° , since in these regions the error in pole position may be up to ten times the error in measurement. If, however, the pits are bounded by perfectly straight sides, it is found that measurements can be reproduced to within $\frac{1}{4}^\circ$.

IV.—RELATIONSHIPS BETWEEN ETCH-PIT SHAPES AND ORIENTATION

It is proposed to demonstrate that the positions in space of the cube axes of the lattice of any grain are unambiguously related to the angles of triangular pits and the ratio l^2/k^2 in rectangular pits as discussed above.

1. TRIANGULAR ETCH-PITS

If the indices of the sectioning plane are (hkl) , then the intercepts made by that plane on the three crystallographic axes will be proportional to $\frac{1}{h}$, $\frac{1}{k}$, $\frac{1}{l}$, respectively (Fig. 4). The directions AB , BC , CA

are thus $[\bar{k}h0]$, $[0\bar{l}k]$, $[l0\bar{h}]$ respectively, leading to the relations:

$$\left. \begin{aligned} \cos \widehat{CAB} &= \frac{kl}{\sqrt{(k^2 + h^2)(l^2 + h^2)}} \\ \cos \widehat{ABC} &= \frac{hl}{\sqrt{(h^2 + k^2)(l^2 + k^2)}} \\ \cos \widehat{BCA} &= \frac{hk}{\sqrt{(k^2 + l^2)(h^2 + l^2)}} \end{aligned} \right\} \quad (1)$$

These three angles will be denoted by A , B , and C , respectively. From equations (1) the following relation, which is explicit in h , k , and l , is found:

$$\frac{h^2}{\tan A} = \frac{k^2}{\tan B} = \frac{l^2}{\tan C} \quad (2)$$

Relation (2) makes it possible to calculate the values of $\left| \frac{k}{h} \right|$ and $\left| \frac{l}{h} \right|$ from the measured values of A , B , and C .

The impossibility of assigning either sign or absolute magnitude to h , k , or l other than by definition is to be expected. Consequently, h may be assigned any

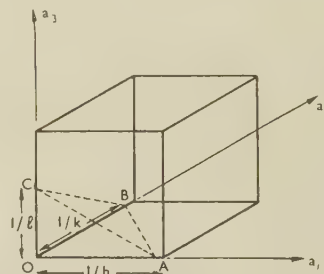


Fig. 4.—Intersection of Sectioning Plane ABC of Indices (hkl) with Lattice Cube.

convenient value, preferably chosen so that h , k , and l are integral or nearly so.

Thus, from the measurement of its etch-pit angles, the texture in any grain exhibiting triangular pits may be described as possessing an (hkl) plane in the sectioning plane. In order to specify the texture more precisely, information is required on the rotation from some standard position of this (hkl) plane about the normal to the sectioning plane. This information is usually given by stating which crystallographic direction $[uvw]$ is parallel with some reference direction. In the case of etch-pits, the angle θ between the reference direction and one side of the etch-pit is known. Suppose that this side is AB . Then, if the reference direction is $[uvw]$,

$$\left. \begin{aligned} \cos \theta &= \frac{-uk + vh}{\sqrt{(u^2 + v^2 + w^2)(k^2 + h^2)}} \\ 0 &= uh + vk + wl \end{aligned} \right\} \quad (3)$$

Solution of equations (3) leads to $\frac{v}{u}$ and $\frac{w}{u}$. Two solutions will generally be obtained for $[uvw]$. The correct one may be discovered by inspection, or more

rigorously by taking that solution which satisfies the relation :

$$\cos(\theta + A) = \frac{-ul + wh}{\sqrt{(u^2 + v^2 + w^2)(l^2 + \bar{h}^2)}} \quad (4)$$

Thus it is possible to represent the orientation of each grain by a code similar to that used for quoting rolling textures, i.e. $(hkl)[uvw]$, where the plane (hkl) lies parallel to the sectioning plane and the direction $[uvw]$ lies parallel with the reference direction, which lies in the sectioning plane.

It is often convenient to present the results in the form of a pole figure, preferably without first having to calculate (hkl) and $[uvw]$ and then rotating a standard projection. This may be done by consideration of the geometry of the etch-pits and pole figures. It is most convenient to plot (100) pole figures projected on to the sectioning plane of the specimen, since the traces of the $\{100\}$ planes in the

procedure is, of course, not permissible with single crystals, or groups of only a few crystals.

It remains to determine the angles that define the positions of the poles along the radii. Since these angles are in fact the angles between the sectioning plane and the three cube planes, they may be determined from h , k , and l , and since h , k , and l are known in terms of the original angular measurements of A , B , and C , it follows that the required angles may be expressed in terms of A , B , and C . The precise relations are :

$$\left. \begin{aligned} \sec^2 \alpha &= \tan B \cdot \tan C \\ \sec^2 \beta &= \tan A \cdot \tan C \\ \sec^2 \gamma &= \tan A \cdot \tan B \end{aligned} \right\} \quad (5)$$

where α , β , and γ are the angles between the sectioning plane and the cube planes whose traces lie opposite angles A , B , and C , respectively. Hence the three cube poles plot at angles α , β , and γ from the centre of the pole figure along the radii $450 - (\theta + A + B)$, $90 - \theta$, $270 - (\theta + A)$, respectively, measured clockwise from the reference direction.

2. RECTANGULAR ETCH-PITS

If an etch-pit is rectangular, at least one of the crystallographic axes must lie parallel to the sectioning plane. Consider such an arrangement, which is illustrated in Fig. 3 (p. 237), where the sectioning plane is $QRST$ with crystallographic indices $(0kl)$ and the three axes are $a_1a_2a_3$. The axis a_1 is parallel to the plane $QRST$. Now the true etch-pit shape, in three dimensions, is the right triangular prism $ORSPQT$, and as shown earlier, when viewed from a direction perpendicular to the plane $QRST$, the bottom edge OP appears as a line, parallel to ST and RQ , cutting TQ at U , where PU is perpendicular to TQ . Since triangles PQT , UQP , and UPT are all similar, it follows that :

$$\frac{QU}{UT} = \left(\frac{PQ}{PT}\right)^2 \quad (6)$$

i.e.

$$\frac{k^2}{UT} = \frac{l^2}{QU} \quad (7)$$

Since the ratio QU/UT may be determined it follows that the value of $\left|\frac{l}{k}\right|$ may also be determined. In this case $h = 0$, and k may be taken as any convenient value. The texture may then be quoted as $(0kl)[uvw]$ in a manner similar to that employed for triangular etch-pits. In this case :

$$\left. \begin{aligned} \cos \theta &= \frac{+u}{\sqrt{u^2 + v^2 + w^2}} \\ 0 &= vk + wl \end{aligned} \right\} \quad (8)$$

the complementary relation being :

$$\sin \theta = \frac{-vl + wk}{\sqrt{(u^2 + v^2 + w^2)(l^2 + k^2)}} \quad (9)$$

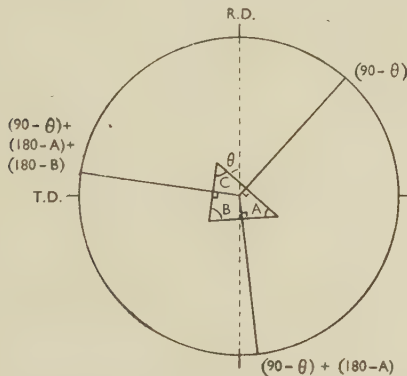


FIG. 5.—Positions of Radii Perpendicular to Sides of Etch-Pit.

sectioning plane are already known as the sides of the etch-pit. The pole of any $\{100\}$ plane lies on that great circle of the reference sphere which projects stereographically as a diameter of the pole figure perpendicular to the appropriate etch-pit side, its position along that diameter being determined by the angle between the sectioning plane and the particular $\{100\}$ plane concerned. The direction to be taken from the centre along the appropriate diameter has yet to be fixed, and this may be accomplished by arbitrary rules. It is convenient to proceed by imagining a drawing of the etch-pit to be superimposed on the pole figure in such a position that the circumcentre of the triangle is coincident with the centre of the basic circle, as illustrated in Fig. 5; the diameters may then be replaced by radii which are perpendicular bisectors of the sides of the etch-pit, there now being only one position on each radius which lies at any given angle from the centre of the pole figure. The opposite set of directions is equally correct, the two corresponding to plotting from alternative hemispheres of the original reference sphere. In addition, the two may be taken together to give a plot corresponding to that of both hemispheres superimposed, as is common in X-ray pole-figure determinations. The latter

$$\left. \begin{aligned} \cos \theta &= \frac{+u}{\sqrt{u^2 + v^2}} \\ 0 &= w \end{aligned} \right\} \dots \dots (10)$$
[illegible]

and

$$\sin \theta = \frac{-v}{\sqrt{u^2 + v^2}} \quad (11)$$

enabling the sign of v/u to be determined. For the purpose of plotting the orientation on a pole figure, k may again be put equal to 0, in which case $UT/QU = 0$, i.e. no bottom edge is visible. The angles \widehat{UTP} and \widehat{UQP} become 90° and 0° , respectively. The poles in this case then plot at the centre and at 90° from the centre on each of the radii $90 - \theta$, $180 - \theta$, $270 - \theta$, and $360 - \theta$.

V.—CALCULATION OF ANGULAR CO-ORDINATES OF {100} POLES

As shown in the previous section, the angular co-ordinates of the {100} poles may be calculated directly from the measurements made of the original etch-pit angles. The first operation is to obtain the positions of the radii of the pole figure on which the poles lie by simple subtractions from multiples of 90° . Thus the radii for triangular pits lie at angles $450 - (\theta + A + B)$, $90 - \theta$, and $270 - (\theta + A)$ to the reference direction. In rectangular and square pits the radii lie at angles $90 - \theta$, $180 - \theta$, $270 - \theta$, and $360 - \theta$.

Sectioning Plane for Various Etch-Pit Angles.

Largest Etch-Pit Angle (C)

	75	76	77	78	79	80	81	82	83	84	85	86	87	88	89
1															
2															
3															89 45 45
4														88 45 45	89 55 35
5														88 51 39	88 60 30
6															88 63 27
7													87 45 45	87 55 35	88 66 24
8													87 49 41	87 58 32	88 68 22
9												86 45 45	86 52 38	87 60 30	87 69 21
10											85 45 45	86 48 42	86 55 35	86 62 28	87 71 20
11												85 50 39	85 57 33	86 64 27	87 72 19
12										84 45 45	85 48 43	85 53 37	85 59 32	86 65 26	87 73 18
13										84 48 43	84 50 41	84 55 36	85 60 30	86 66 24	87 73 17
14										83 45 45	84 52 39	84 57 34	84 62 29	85 67 23	87 74 16
15									83 47 44	83 50 41	83 54 37	84 58 33	84 63 28	85 68 23	86 75 16
16									83 51 40	83 55 36	83 59 32	84 64 27	85 69 22	86 75 15	
17								82 46 46	82 49 42	82 53 39	83 56 35	83 60 31	84 65 26	85 70 21	86 76 15
18								81 47 44	82 51 41	82 54 37	82 58 34	83 61 30	83 66 25	84 70 21	86 76 14
19							81 49 43	81 52 39	81 55 36	82 59 33	82 62 29	83 66 25	84 71 20	86 77 14	
20						80 46 46	80 47 44	81 50 41	81 53 38	81 56 35	82 60 32	82 63 28	83 67 24	84 71 20	86 77 14
21							80 49 43	80 52 40	80 55 37	81 57 34	81 61 31	82 64 27	83 68 23	84 72 19	86 77 13
22					79 46 46	79 47 45	79 50 42	80 53 39	80 56 37	80 59 33	81 62 30	82 65 27	83 68 23	84 72 19	86 78 13
23					78 47 45	79 49 44	79 51 41	79 54 38	80 57 35	80 59 33	81 62 30	81 65 26	82 69 23	84 73 18	86 78 13
24					78 49 44	79 52 40	79 55 37	79 58 34	80 60 32	80 63 29	81 66 26	82 69 23	83 73 18	86 78 13	
25				77 48 45	77 50 43	78 51 42	78 53 39	78 56 37	79 58 34	79 61 31	80 64 28	81 67 25	82 70 22	83 74 18	86 79 12
26															
27			77 47 47	77 49 44	77 51 42	77 53 40	77 55 38	78 58 35	78 60 33	79 62 30	79 65 28	80 68 24	81 71 21	83 75 17	85 79 12
28			76 48 46	76 50 43	76 52 41	77 54 39	77 56 37	77 58 35	78 61 32	78 63 30	79 66 27	80 69 24	81 71 21	83 75 17	85 79 12
29		76 47 47	76 49 45	76 51 43	76 53 41	76 55 39	77 57 36	77 59 34	77 61 32	78 64 29	79 66 27	80 69 24	81 72 21	83 75 17	85 80 12
30	74 47 47	74 49 45	75 51 43	75 53 42	75 55 40	76 56 38	76 58 36	77 60 34	77 62 31	78 64 29	79 67 26	80 69 24	81 72 20	82 75 17	84 80 12
31															
32	74 48 46	74 50 44	74 52 43	74 54 41	75 55 39	75 57 37	75 59 35	76 61 33	76 63 31	77 65 28	78 68 26	79 70 23	80 73 20	82 76 16	84 80 11
33	73 49 46	73 51 43	73 53 42	74 54 40	74 56 38	75 58 36	75 60 34	76 62 32	76 64 30	77 66 28	78 68 26	79 70 23	80 73 20	82 76 16	84 80 11
34	73 50 45	73 52 43	73 54 42	73 55 40	74 57 38	74 59 36	75 60 34	75 62 32	76 64 30	77 66 28	78 68 26	79 71 23	80 74 19	82 77 16	84 81 11
35	72 51 44	72 53 43	73 54 41	73 55 39	74 56 37	74 58 35	75 59 33	76 61 31	76 63 29	77 65 27	78 67 25	79 71 23	80 74 19	82 77 16	84 81 11
36	72 52 44	72 54 42	72 56 41	73 57 39	73 58 37	73 60 35	74 62 33	75 63 31	75 65 29	76 67 27	77 69 25	78 72 22	80 74 19	81 77 16	84 81 11
37															
38	71 53 43	72 54 42	72 56 40	72 57 38	73 59 37	73 61 35	73 62 33	74 64 31	75 66 29	76 68 27	77 70 25	78 72 22	79 74 19	81 77 15	84 81 11
39	71 54 42	71 56 41	71 58 40	72 59 38	72 60 36	72 62 34	73 63 33	74 65 31	75 67 29	76 69 27	77 71 24	78 73 22	79 75 19	81 78 15	83 81 11
40	70 55 42	70 56 41	70 58 39	71 59 37	71 60 35	72 62 33	72 64 32	73 65 31	74 67 29	75 69 27	76 71 24	77 73 22	79 75 19	81 78 15	83 82 11
41	69 56 42	70 57 40	70 58 39	70 60 37	71 61 36	71 63 34	72 64 32	73 66 30	74 68 28	75 69 26	76 71 24	77 73 22	79 76 19	81 78 15	83 82 11
42	69 56 41	69 58 40	70 59 39	70 60 37	70 62 35	71 63 34	72 65 32	72 66 30	73 68 28	74 70 26	75 72 24	77 74 21	78 76 19	80 78 15	83 82 11
43	68 57 41	69 58 40	69 60 38	70 61 37	70 62 35	71 64 34	71 65 32	72 67 30	73 69 28	74 70 26	75 72 24	77 74 21	78 76 19	80 79 15	83 82 11
44	68 58 41	68 59 40	69 60 38	69 62 37	70 63 35	70 64 34	71 66 32	72 67 30	73 69 28	74 70 26	75 72 24	76 74 21	78 77 18	80 79 15	83 82 11
45	67 58 41	68 59 39	68 61 38	69 62 36	69 63 35	70 65 33	71 66 32	71 68 30	72 69 28	73 71 26	74 73 24	75 75 21	77 77 18	80 79 15	83 82 11
46	67 59 41	67 60 39	68 61 38	68 63 36	69 64 35	69 65 33	70 67 32	71 68 30	72 70 28	73 71 26	74 73 24	75 75 21	77 77 18	79 79 15	83 82 11
47	66 59 40	67 61 39	67 62 38	68 63 36	68 64 35	69 65 33	70 67 32	71 68 30	72 70 28	73 71 26	74 73 24	75 75 21			
48	66 60 40	66 61 39	67 62 37	67 64 36	68 65 35	69 66 33	69 67 31	70 69 30	71 70 28	72 72 26	73 74 24	74 76 22			
49	65 61 40	66 62 39	66 63 37	67 64 36	68 65 35	68 66 33	69 68 31	70 69 30	71 71 28	72 72 26					
50	65 61 40	65 62 39	66 63 37	66 65 36	67 66 35	68 67 33	69 68 31	70 70 30							
51	64 62 40	65 63 39	65 64 37	66 65 36	67 66 34	67 67 33									
52	64 62 40	64 63 39	65 64 37	65 65 36											
53	63 63 40	64 64 39													
54															
55															
56															
57															
58															
59															
60															

Smallest Etch-Pit Angle (A)

The other co-ordinate of each pole (i.e. the angle between the appropriate etch-pit face and the sectioning plane) is given for triangular pits by the relations (5). Calculation of the angles α , β , and γ for each pit has been obviated by the construction of a table, in which the values of α , β , and γ are given for all values of angles A and C at one-degree intervals. Table I gives that part of the table corresponding to the restriction that A is the smallest etch-pit angle and C the largest; α , β , and γ are given in that order. The range of values covered by Table I is sufficient for practical application of the method, since it is obvious that the nomenclature of the etch-pit angles is purely arbitrary. The use of Table I is simplified considerably by the fact that the angles α , β , and γ are in reverse order of magnitude from angles A , B , and C .

This will be illustrated by a numerical example. Suppose that the measured angles, A , B , and C are 73° , 39° , and 68° , respectively. If the angles had been in the order 39° , 68° , 73° , direct reference to Table I would have given $\alpha = 69^\circ$, $\beta = 52^\circ$, $\gamma = 45^\circ$. To obtain α , β , and γ for the actual measurements $A = 73^\circ$, $B = 39^\circ$, $C = 68^\circ$, the values obtained from the table must be re-arranged in the same way as the set 39° , 68° , and 73° must be re-arranged to give the set 73° , 39° , and 68° . This gives $\alpha = 45^\circ$, $\beta = 69^\circ$, and $\gamma = 52^\circ$. It can be seen that α , β , and γ are then in reverse order of magnitude from A , B , and C , the direct use of this property being a quicker way of obtaining the above result. The poles are then plotted at angles α , β , and γ along the appropriate radii.

For rectangular pits the angles between the etch-pit faces and the sectioning plane are 90° for two faces, $\tan^{-1} \frac{l}{k}$ for the third face, and $\tan^{-1} \frac{k}{l}$ for the fourth face. Table II gives values of $\tan^{-1} \frac{l}{k}$ for various values of l^2/k^2 ; it will be noted that $\tan^{-1} \frac{k}{l} = 90^\circ - \tan^{-1} \frac{l}{k}$.

TABLE II.—Angle Between (0kl) Plane and (010) Plane for Various Values of l^2/k^2 .

l^2/k^2	$\tan^{-1} \frac{l}{k}$	l^2/k^2	$\tan^{-1} \frac{l}{k}$
1/1	45°	11/2	$66^\circ 54'$
5/4	$48^\circ 28'$	6/1	$67^\circ 48'$
4/3	$49^\circ 6'$	7/1	$69^\circ 18'$
3/2	$50^\circ 46'$	8/1	$70^\circ 32'$
2/1	$54^\circ 44'$	9/1	$71^\circ 34'$
5/2	$57^\circ 41'$	10/1	$72^\circ 27'$
3/1	60°	15/1	$75^\circ 31'$
7/2	$61^\circ 53'$	20/1	$77^\circ 24'$
4/1	$63^\circ 26'$	25/1	$78^\circ 42'$
9/2	$64^\circ 46'$	30/1	$79^\circ 39'$
5/1	$65^\circ 54'$	$\infty/1$	90°

These angles are again plotted along the appropriate radii.

In the case of square pits the angles between the etch-pit faces and the sectioning plane are 90° for

four of the faces and 0° for the fifth. Thus the poles are plotted at the centre and at 90° along the four radii.

VI.—CONSTRUCTION OF POLE FIGURES FOR POLYCRYSTALLINE AGGREGATES

In Section IV it was shown that data obtained from an etch-pit enabled the orientation of the grain in which it was formed to be plotted on a stereographic projection. A simple extension of this procedure enables pole figures to be plotted for polycrystalline aggregates, provided that the reference direction is maintained constant throughout all the readings. In applying the method for this purpose the problem is essentially one of sampling.

If a large number of etch-pits distributed over the sectioning plane is measured and the {100} poles for each one plotted on a stereographic projection, the resulting array of points is a true pole figure and may be simplified in the conventional manner by drawing contour lines to enclose areas of equal pole density. It is merely necessary to estimate how many etch-pits must be measured and how they should be distributed in order to obtain a reliable pole figure. With regard to distribution, the most satisfactory way of distributing the points at which readings are taken is probably a triangular array such that each point has six equidistant nearest neighbours at the corners of a regular hexagon. However, a square array is probably almost as good, and when the practical details of ease of location of the specimen are taken into consideration the square array has much to commend it.

It is obviously desirable that the array shall cover as much of the area of the sectioning plane as possible, and so, for any particular specimen, the total number of readings to be taken depends on the shortest distance between two points in the array. It can be seen that an almost perfect sample should be obtained when this distance is less than the average apparent grain diameter (on the sectioning plane), but for small grain-sizes this would require a very large number of readings.

The number of pits which must be measured is determined in practice so as to achieve an economic balance between the desirability of obtaining at least one measurement on each grain of the specimen and the time and labour spent in obtaining the measurements and plotting the poles. It is obvious that the fewer measurements are required the more highly preferred the texture of the sample.

Care must be taken in drawing contour lines on the pole figure, particularly when the orientation of the sample is almost random. This arises from geometrical considerations of the stereographic projection, since equal areas on the ideal projection sphere do not plot as equal areas on the pole figures, unless they are geometrically similar and lie at the same latitude. The effect of this inequality is to make the pole density at the centre of the pole figure apparently

four times as great as that at the circumference for a perfectly random orientation. A convenient means of overcoming this difficulty is by plotting the poles initially on a specially prepared chart instead of a stereographic projection, the scales of the co-ordinates being such that equal areas on the chart correspond to equal areas on the projection sphere. Contour lines may then be drawn on the chart and subsequently transferred to a normal pole figure without replotting individual poles. The chart may conveniently be in the form of a rectangle with a linear scale (from 0° to 360°) in one direction. (This scale corresponds to the radius co-ordinate of the pole.) The other axis may then be divided into n equal ranges and the values of ω (the co-ordinate of the pole representing the angle between itself and the centre of the pole figure) at the origin, and at the end point of each of the n ranges taken to be :

$$0, \cos^{-1}\left(1 - \frac{1}{n}\right), \\ \cos^{-1}\left(1 - \frac{2}{n}\right), \dots \cos^{-1}\left(1 - \frac{n-1}{n}\right), 90^\circ$$

It can be proved that the areas formed by intersection of perpendiculars at the ends of these ranges and a set of equally spaced lines parallel to the axis of ω will plot as equal areas on the projection sphere.

It has been found convenient to take n as 10, and in this case the angles, 0° , $25^\circ 50'$, $36^\circ 52'$, $45^\circ 34'$, $53^\circ 8'$, 60° , $66^\circ 25'$, $72^\circ 32'$, $78^\circ 28'$, $84^\circ 16'$, and 90° are marked at equal intervals along the ω axis, the radius co-ordinate axis being divided into 36 equal intervals of 10° each. Thus the pole figure is effectively divided into 360 areas which appear as equal areas on the chart and correspond to equal areas on the projection sphere. Each pole may then be plotted on the chart using its two co-ordinates at their face values. Pole densities on the chart are proportional to true pole densities on the projection sphere. Contour lines drawn on the chart may then be transferred directly to the normal pole figure using a polar net.

It will be noted that since this method determines pole density directly, rather than by indirect measurements of physical quantities such as darkening of a photographic emulsion and its numerous corrections and uncontrollable variations, it is possible to give reliable quantitative estimates of the proportions of any actual orientations present in any specimen, within the limits of sampling errors.

VII.—EXAMPLES OF USE OF THE METHOD

Two examples of the use of the method described in this paper are given.

The first of these is taken from Fig. 10 (Plate III) of Lacombe and Beaujard's paper,² in which etch-pits and slip lines are visible on a single grain. Angular measurements were made on this illustration using the vertical as reference direction and the method described in the present paper applied to plot

the $\{100\}$ poles, these being shown in Fig. 6. The $\{111\}$ poles were then obtained from the $\{100\}$ poles by geometrical construction, and the observed positions of the normals to the slip lines compared with

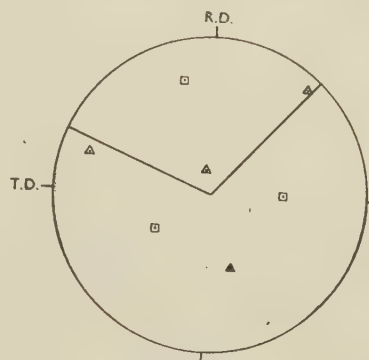


FIG. 6.—Stereographic Projection of Grain Showing Etch-Pits and Slip Lines. (Data taken from Fig. 10 (Plate III) of Lacombe and Beaujard's paper.²) Normals to slip lines shown as radii.

□ $\{100\}$ poles plotted from measurement of etch-pits.
△ $\{111\}$ poles obtained by geometrical construction from $\{100\}$ poles.

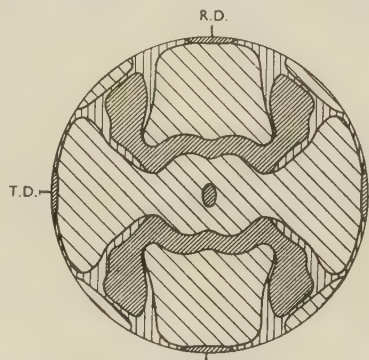


FIG. 7.—(100) Pole Figure Plotted from Measurements of Etch-Pits on Super-Purity Aluminium Cold Rolled 60% After Annealing.

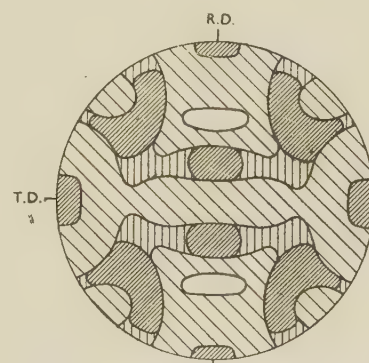


FIG. 8.—As Fig. 7, but Plotted from X-Ray Diffraction Photographs.

the calculated positions of the $\{111\}$ poles. (There is, of course, no means of determining from the photograph at what angle the slip planes are situated to the sectioning plane.) It can be seen from Fig. 6 that the agreement is good, particularly when the difficulty

of making accurate measurements on a photograph is taken into account.

The plotting of the orientation of a single crystal in this way offers considerable advantages over any X-ray technique, since the whole process, including specimen preparation, may occupy only 15 min., whereas the X-ray methods would take 2 hr. or more, particularly when the orientation is one which renders solution of the diffraction pattern difficult. The method that has been described in this paper gives a direct solution whatever the orientation.

The second example is that of a pole figure of super-purity aluminium cold rolled 60% after an intermediate anneal. The pole figure obtained by the etch-pit method using only 100 measurements is given in Fig. 7, and that obtained by X-ray means is shown in Fig. 8. In each case the pole figure was projected on to the rolling plane. The contours in each case were fixed independently by dividing the total pole density range, from zero to the maximum observed, into four approximately equally spaced ranges. The agreement is good and, furthermore, the etch-pit pole figure was produced in approximately half the time required for producing the X-ray pole figure.

VIII.—CONCLUSIONS

A method of determining orientation of individual crystals from etch-pits has been developed which is suitable for plotting pole figures for polycrystalline aggregates and does not require any apparatus additional to that normally found in a metallurgical laboratory. It yields results that agree well with X-ray means of determining orientations, and is usually faster than X-ray methods, particularly for single crystals or samples possessing highly preferred orientations. The method is particularly useful for determining the pole figures of materials whose grain-sizes are too large for X-ray-scanning methods, and it may be used to give quantitative estimates of proportions of various orientations present in any sample.

ACKNOWLEDGEMENTS

The authors wish to thank Aluminium Laboratories Limited for permission to publish this paper, and their colleagues for helpful discussions and assistance with the development and practical application of the method.

REFERENCES

1. C. S. Barrett, "Structure of Metals", New York: 1943 (McGraw-Hill).
2. P. Lacombe and L. Beaujard, *J. Inst. Metals*, 1948, **74**, 1.
3. H. Kostron, *Z. Metallkunde*, 1950, **41**, 370.
4. D. W. Smith and R. F. Mehl, *Metals and Alloys*, 1933, **4**, 31.
5. C. M. Tucker, *ibid.*, 1930, **1**, 655.
6. R. W. Cahn, *J. Inst. Metals*, 1951, **79**, 144.
7. H. Mahl and I. N. Stranski, *Z. physikal. Chem.*, 1942, [B], **51**, 319.
8. R. Jacquesson and J. Manenc, *Compt. rend.*, 1950, **230**, 959.
9. H. Mahl and I. N. Stranski, *Z. physikal. Chem.*, 1942, [B], **52**, 257.
10. A. Hone and E. C. Pearson, *Metal Progress*, 1948, **53**, 363.

CREEP AT 250° AND 300° C. OF SOME MAGNESIUM ALLOYS CONTAINING CERIUM*

1438

By G. A. MELLOR,† M.Sc., F.I.M., MEMBER and R. W. RIDLEY,‡ B.Sc.

(Communication from the National Physical Laboratory.)

SYNOPSIS

Following on an investigation (*J. Inst. Metals*, 1949, **75**, 679) of the creep strength of magnesium-cerium alloys at 200° C., tests have now been made at 250°, 300°, and 316° C., with and without addition of a third element. At 250° C. slight benefit results from additions of silicon and zirconium; silver, lithium, zinc, and cobalt have little influence on creep behaviour; and cadmium and aluminium are harmful. The best results at 300° and 316° C. were obtained with as-cast alloys containing about 2% cerium or rare earths, and 1% manganese. Both rolled and cast alloys of low manganese content can be improved by heat-treatment, but cast magnesium-cerium-manganese alloys remain the most creep-resistant.

Examination with the optical and electron microscopes showed improvement in creep-resistance to be due mainly to the presence of fine precipitates, manganese apparently restraining the coarsening of the Mg₂Ce particles.

I.—INTRODUCTION

In previous work¹ on the creep strength of magnesium-cerium alloys, it had been established that creep-resistance both in cast and in rolled bars at 200° C. was due principally to the cerium taken into solution and precipitated in a fine form at the temperature of test. Solution-treatment and ageing at 350° C. resulted in a coarser precipitate and in poor creep behaviour at 200° C. It was apparent therefore that industrial requirements for alloys maintaining their strength at 250°–300° C. were unlikely to be met by binary magnesium-cerium alloys. It was accordingly decided to explore the creep behaviour at temperatures higher than 200° C. and to see what improvement could be obtained by the addition of a third element.

The test period was extended to 1000 hr., or to 1% strain, in order to establish the long-time behaviour of the alloys. In one or two cases of particular interest tests were continued for 3000–4000 hr., and improvements due to metallurgical changes taking place during test became clearly apparent.

Reference to other published work on the effect of additions to magnesium-cerium alloys did not reveal any outstanding improvement in creep-resistance. Leontis² tested at 149° and 204° C. some 50 magnesium alloys containing zinc, together with various third elements, but no materials better in creep than binary magnesium-cerium alloys were discovered. The work of Leontis and Murphy,³ of Grube and Eastwood,⁴ and of Grube, Davis, and Eastwood⁵ in America has shown the effectiveness of manganese additions to magnesium-cerium alloys. For high

creep-resistance in the wrought state Grube and Eastwood recommend an alloy containing rare earths 2, manganese 1.5, and nickel 0.2%, and in the cast state rare earths 6, manganese 0.8, nickel 0.2, and tungsten 0.02%. In Great Britain cast alloys containing rare earths 3, zirconium 0.6% (Elektron MCZ) and rare earths 2.5, zirconium 0.6, and zinc 2.5% (Elektron ZRE 1) are widely used for elevated-temperature service.^{6,7} Zirconium and zinc contribute to grain refinement, ease of casting, and good room-temperature properties.

II.—EXPERIMENTAL METHOD

1. PREPARATION OF ALLOYS

The preparation of the alloys and metallographic examination were carried out in the Metallurgy Division of the National Physical Laboratory. Most of the alloys were made by the addition of cerium to the following analysis: cerium 98.22, silicon 0.04, iron 0.77%, remainder oxygen. Where "Mischmetall" (a mixture of cerium, lanthanum, neodymium, praseodymium, &c.) was used, the alloys are termed magnesium-rare earth alloys. As will be shown later, cerium and "Mischmetall" are very similar in their behaviour. Some alloys contained zirconium, added by means of a master alloy or "master salt" obtained from Magnesium Elektron, Ltd.

Test-pieces 8½ in. long were cast horizontally in pairs in sand moulds. For testing in the rolled condition 2¼-in.-square billets were chill cast and preheated to 500° C. for rolling to 1½ in. dia. Alloys containing lithium were rolled from 450° C.

* Manuscript received 23 May 1952.

† Metallurgy Division, National Physical Laboratory, Teddington, Middlesex.

‡ High-Temperature Mechanical Properties Section, National Physical Laboratory, Teddington, Middlesex.

2. CREEP-TEST PROCEDURE

The creep tests were carried out in the High-Temperature Mechanical Properties Section of the National Physical Laboratory.

The majority of the tests were made in a 5-ton-capacity creep machine, using specimens with a gauge-length of 5 in. and a dia. of 0.564 in. The creep strain was measured by means of a modified Martens-type mirror extensometer capable of measuring strain of the order of 1×10^{-6} . For certain tests on the rolled alloys 2-ton-capacity creep machines were used, with a smaller specimen of 2 in. gauge-length and 0.357 in. dia. These machines were equipped with a mirror-type extensometer sensitive to 1×10^{-5} strain.

The period of soaking at the test temperature before the load was applied was approximately 16 hr., the test temperature being reached in about 5 hr. The temperature of the furnace was electronically controlled and did not depart at any part of the gauge-length by more than $\pm 1^\circ \text{C.}$ from the required temperature throughout the test.

III.—EXPERIMENTAL RESULTS

1. EFFECT OF ADDITIONS TO MAGNESIUM-CERIUM ALLOYS

In choosing the third elements to be added the desirability was considered of:

- (a) Increasing the amount of cerium in solution at the solution-treatment temperature.
- (b) Preventing the formation of a coarse precipitate of Mg_2Ce at 300°C.
- (c) Producing alloys with a high solidus temperature.

Additions of manganese, aluminium, zirconium, and zinc were selected, because these elements were already employed in commercial alloys. Silver,

TABLE I.—Solidus Temperatures of Ternary Alloys.

Alloy No.	Composition		No Indication of Liquid *	Indication of Liquid *
	Ce, %	Addition Element, %		
X67	3.8	Nil	585° C.	590° C.
X88	0.81	0.38 Si	620° C.	...
X93	1.05	0.16 "	"	...
X80	1.4	0.19 "	"	...
X99	2.74	0.11 "	580° C.	600° C.
X78	0.58	1.52 Mn	610° C.	620° C.
X71	1.82	1.28 "	580° C.	600° C.
X70	4.35	1.19 "	585° C.	590° C.
X83	1.86	0.60 Zr	600° C.	610° C.
X115	2.05	0.54 "	590° C.	603° C.
X85	2.12	1.51 Ag	580° C.	600° C.
X81	2.01	1.47 Li	550° C.	580° C.
X84	2.09	1.68 Al	620° C.	...
X82	1.91	2.15 Cd	580° C.	600° C.

* Specimens water-quenched after 15 min. at temperature.

cadmium, or lithium forms an extensive solid solution in magnesium, and might therefore modify the behaviour of dissolved cerium. Cobalt had given promising results in some previous work by Haughton,⁸ and silicon was added in order to produce fine particles in the structure.

The tests at 200°C. had shown that higher creep-resistance was often obtained by increasing the

TABLE II.—Effect of Additions to Rolled and Solution-Treated Alloys Tested at 250°C. and 1 Ton./In.².

Alloy No.	Composition		Solution-Treatment Temp., °C.	At 120 Hr.		At 300 Hr.		At 1000 Hr.		Time to Reach 1% Strain, hr.
	Ce, %	Addition Element, %		Strain, %	Creep Rate, Strain/hr. $\times 10^6$	Strain, %	Creep Rate, Strain/hr. $\times 10^6$	Strain, %	Creep Rate, Strain/hr. $\times 10^6$	
X61D1	1.45	Nil	580	0.0245	0.86	0.037	0.65
X80B2	} 1.50	0.13 Si {	600	0.020	0.35	0.023	0.18
X80B3			600	0.0153	0.825	0.0274	0.55	0.0616	0.481	...
X72C7	1.71	0.25 Mn	580	0.0098	0.414
X71B1	1.82	1.28 "	580	0.0280	0.48	0.0375	0.296	0.048	0.083	...
X83B1	} 1.86	0.60 Zr {	550	0.0260	1.05
X83B2			550	0.0276	0.72	0.0367	0.336
X83B4			600	0.0162	0.744	0.0257	0.406	0.039	0.115	...
X85B1	} 2.12	1.51 Ag {	580	0.017	0.55	0.027	0.595
X85B4			550	0.0202	1.04	0.0371	0.89
X81B1	} 2.01	1.47 Li {	550	0.022	1.00	0.041	1.2
X81B2			550	0.0234	1.235
X84B1	2.09	1.68 Al	550	1.2	117	100
X82B1	1.91	2.15 Cd	550	0.0268	2.3 *

* Minimum rate at 50 hr.

amount of cerium in solution as a result of heat-treatment at a higher temperature. Specimens of a number of alloys were therefore heat-treated at temperatures from 550° to 620° C., with subsequent microscopical examination to establish the highest possible temperature which could be used for solution-

cerium in magnesium, but this point was not investigated in the present work.

The compositions of the alloys tested in the rolled, solution-treated, and water-quenched condition, and the results of creep tests, under a stress of 1 ton/in.², at 250° and 300° C. respectively, are given in Tables II

TABLE III.—*Effect of Additions to Rolled and Solution-Treated Alloys Tested at 300° C. and 1 Ton/In.²*

Alloy No.	Composition			Solution-Treatment Temp., °C.	At 120 Hr.		At 300 Hr.		At 1000 Hr.		Time to Reach 1% Strain, hr.
	Ce, %	R.E.,* %	Addition Element, %		Strain, %	Creep Rate, Strain/hr. × 10 ⁶	Strain, %	Creep Rate, Strain/hr. × 10 ⁶	Strain, %	Creep Rate, Strain/hr. × 10 ⁶	
X61D3	1.45	...	Nil	580	0.20	15.0	0.66	33.2
X83B3 X83C1	1.86	...	0.6 Zr {	600	0.102	6.9	0.24	8.5	0.89	10.6	1100
				600	0.083	5.52	0.185	5.52	0.60	5.52	>1000
X74B1	...	1.76	0.46 Mn	580	0.067	4.57	0.182	9.44
X101C1	2.7	...	1.4 „	580	0.113	5.3	0.268	14.3	2.02	27.0	620
X80B5 X80C1	1.5	...	0.13 Si {	610	0.70	158	136
				600	0.38	60.6	181
X85B2	2.12	...	1.51 Ag	580	0.31	31.5	270
X100B1 X100B2	1.83	...	1.66 Li {	580	Fractured in 73 hr.		28
				580	,, 17½,,	

* R.E. = rare earths.

TABLE IV.—*Effect of Additions to Cast Alloys Tested at 300° C. and 1 Ton/In.²*

Alloy No.	Composition			At 120 Hr.		At 300 Hr.		At 1000 Hr.		Time to Reach 1% Strain, hr.
	Ce, %	R.E., %	Addition Element, %	Strain, %	Creep Rate, Strain/hr. × 10 ⁶	Strain, %	Creep Rate, Strain/hr. × 10 ⁶	Strain, %	Creep Rate, Strain/hr. × 10 ⁶	
X33A1	5.52	...	Nil	0.44	34	230
X109A1	...	3.07	0.43 Zr	1.39	128.5	90
X115A2	2.05	...	0.54 „	53
X102A1	2.28	...	0.6 Mn	0.055	3.05	0.11	3.07	0.48	9.7	1400
X101A1	2.7	...	1.4 „ {	0.0426	2.60	0.071	1.57	0.204	2.33	>1000
X101B1				0.0450	1.76	0.078	1.78	0.242	2.16	>1000
X12A1	...	3.19	2.86 Zn	0.58	75.7	170
X104A1	3.0	...	1.57 Co	0.76	75.0	153
X99D1	2.7	...	0.11 Si	1.13	171	110
X111A1	...	2.93	2.83 Zn 0.48 Zr	0.33	25	0.78	25	380
X113A1	...	3.37	2.89 Zn 0.55 Mn	0.082	3.6	0.134	2.5	0.298	2.55	>1000

treatment without formation of liquid. The results are shown in Table I. Silicon seems to raise the sloping solidus of the magnesium-cerium diagram but not the eutectic temperature of 590° C. Zirconium appears to raise slightly the temperature of the magnesium-Mg₉Ce eutectic. Manganese additions up to 1.5% make little difference to the magnesium-cerium solidus. Leontis and Murphy³ have stated that manganese increases the solid solubility of

and III. The solution-treatment temperature was in many cases close to the maximum, but in other cases a rather lower temperature of 550° C. was used. Table IV contains the results of creep tests at 1 ton/in.² and 300° C. on a similar range of as-cast alloys. Creep curves showing some 250° C. tests extended to 1000 hr. are reproduced in Fig. 1.

Whereas silicon, zirconium, and manganese proved beneficial to rolled and solution-treated alloys at

250° C., silver and lithium made little difference to creep behaviour, and cadmium and aluminium were harmful. It is interesting to note that Mäder and Laves⁹ found that Al_2Ce is formed in preference to Mg_9Ce when aluminium is added to magnesium-cerium alloys, so that no cerium would remain in solution and the creep-resistance would be diminished. The increased resistance to creep at 250° C. resulting from the addition of silicon (see Table II) may be due

greater creep-resistance than zirconium. The use of zinc in the commercial cast alloy ZRE 1 (rare earths 2.5, zirconium 0.6, zinc 2.5%) suggested tests on alloys containing zinc, and Fig. 2 gives creep curves of cast alloys with additions of zinc plus zirconium, of manganese, and of zinc plus manganese. These all showed improvement on the binary magnesium-cerium alloys, but the general trend of the curves emphasizes the importance of manganese. Zinc or

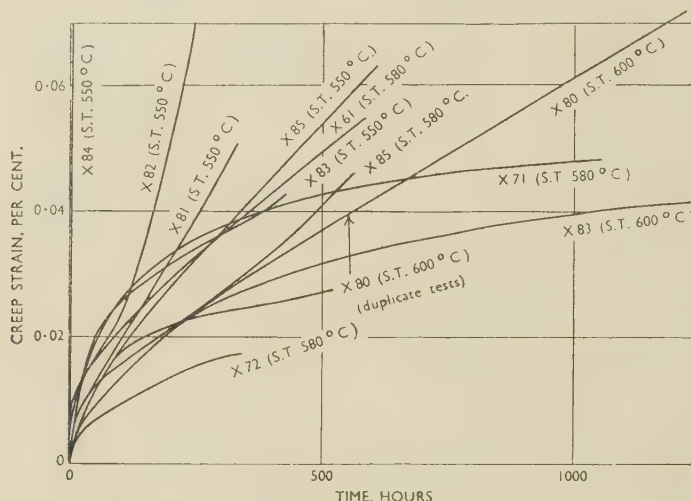


FIG. 1.—Creep Tests on Magnesium-Cerium Alloys at 250° C. and 1 Ton/In.², Showing Effect of Additions. All alloys in the rolled and solution-treated condition. For compositions see Table II.

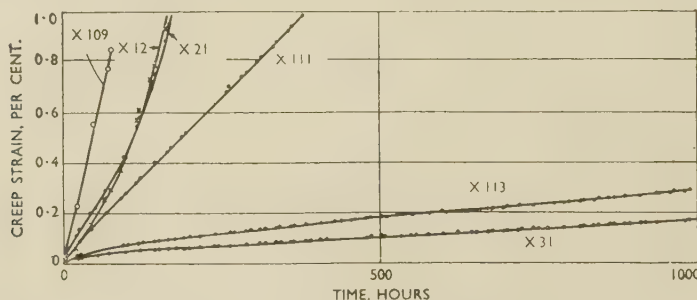


FIG. 2.—Comparison of Creep Properties of Cast Alloys Containing Rare Earths, Zinc, Manganese, and Zirconium, at 300° C. and 1 Ton/In.².

KEY.

X 12 3.19% rare earths, 2.86% Zn.
X 21 2.67% rare earths.
X 31 4.83% rare earths, 1.22% Mn.

X 109 3.07% rare earths, 0.43% Zr.
X 111 2.93% rare earths, 2.83% Zn, 0.48% Zr.
X 113 3.37% rare earths, 0.55% Mn, 2.89% Zn.

to the higher solution temperature that can be used and not to the presence of silicon particles. Silicon was found to have no useful effect in the absence of cerium.

In view of the poor results obtained at 250° C. with alloys containing cadmium or aluminium, they were not tested at 300° C. In the rolled and solution-treated state at 300° C. additions of manganese or zirconium were found to be advantageous, but lithium, silver, and silicon were harmful to the creep properties.

With alloys in the cast condition, manganese gave

zirconium alone brought about little improvement, nor did cobalt or silicon (Table IV).

Further experiments were therefore confined to the effect of manganese on alloys containing cerium or rare earths.

2. CREEP BEHAVIOUR OF MAGNESIUM-CERIUM AND MAGNESIUM-CERIUM-MANGANESE ALLOYS

(a) Tests at 250° and 300° C.

The results of a few tests of binary magnesium-cerium alloys at 250° C., with a stress of 1 ton/in.²,

TABLE V.—*Magnesium-Cerium Alloys Tested at 250° C. and 1 Ton/in.².*

Alloy No.	Ce, %	Treatment	At 120 Hr.		At 300 Hr.	
			Strain, %	Creep Rate, Strain/hr. $\times 10^6$	Strain, %	Creep Rate, Strain/hr. $\times 10^6$
X61D1	1.45	Rolled, 24 hr. at 580° C.; water-quenched.	0.0245	0.86	0.037	0.65
X69E5	2.55	Rolled, 24 hr. at 550° C.; water-quenched.	0.0232	1.35	0.046	1.375 *
X46A1 X46C1	3.5	As cast.	0.0345 0.082	1.67 3.85	0.136	2.71
X67B4	3.8	Rolled, 24 hr. at 550° C.; water-quenched.	0.029	1.50 *
X67C4 X67C3	3.8	Rolled, 24 hr. at 580° C.; water-quenched.	0.0266 0.0184	0.845 0.56	0.0368	0.39
X59B3 X59B5 X55B3	4.1 6.0	As cast. "	0.0577 0.08 0.059	2.67 3.62 1.20	0.113	2.43

* Minimum rate.

are set out in Table V. They indicate: (i) that cast material is somewhat inferior to that rolled and solution-treated, (ii) that a higher solution-treatment temperature confers some small benefit, (iii) that cerium in excess of about 1.6% gives no further

increase in strength to the rolled and solution-treated alloys, and (iv) that additions of cerium beyond 3.5% are of no advantage in cast material. The behaviour is thus very similar to that at 200° C. with a stress of 2 tons/in.².

Testing at 250° C. was not carried any further, as it was considered of greater practical importance to investigate the behaviour of magnesium-cerium alloys at 300° C. A number of tests were therefore made at that temperature, at a stress of 1 ton/in.², on alloys of varying cerium or rare-earth contents and containing additions of manganese from 0 to 1.54%.

Whereas at 200° C. such additions seemed of little value, at 300° C. the ternary magnesium-cerium-manganese alloys proved markedly superior to corresponding binary magnesium-cerium alloys. From the results given in Table VI it is possible to compare cerium with the rare earths and to assess the comparative values of cerium and manganese additions. The differences between alloys made with cerium and with rare earths are small, and although the best results were obtained with the latter, it cannot be said that the superiority was significant. The poor results on alloy X70 probably represent a failure of this particular material to respond to heat-treatment. In this connection it may be noted that Leontis¹⁰ found little difference between alloys made with cerium and with "Mischmetall" in tests at 316° C.

TABLE VI.—*Creep Tests at 300° C. and 1 Ton/in.² on Magnesium-Cerium and Magnesium-Rare Earths Alloys, with and without Manganese.*

		Alloy No.	Composition			At 120 Hr.		At 300 Hr.		At 1000 Hr.		Time to Reach 1% Strain, hr.	
			Ce, %	R.E., %	Mn, %	Strain, %	Creep Rate, Strain/hr. × 10 ⁶	Strain, %	Creep Rate, Strain/hr. × 10 ⁶	Strain, %	Creep Rate, Strain/hr. × 10 ⁶		
Rolled and solution- treated at 580° C.	Without manganese	X61D2	1.45	0.26	33.5	260	
		X61D3	1.45	0.20	15	0.66	33.2	
		X62B3	4.33	48	
		X63D1	5.95	0.82	112.6	135	
		X73C6	...	1.76	...	0.24	23.8	0.96	53.5	310	
		X103C1	...	5.4	...	0.92	120	130	
	With manganese	X78A3	0.58	...	1.52	0.114	5.08	0.242	9.5	1.72	31.5	770	
		X102C1	2.28	...	0.6	0.0735	5.95	0.198	7.6	1.23	10.0	880	
		X101C1	2.7	...	1.4	0.113	5.3	0.268	14.3	2.02	27.0	650	
		X70B1	4.35	...	1.19	1.12	330	117	
		X70B2	4.35	...	1.19	0.70	148	139	
		X74B1	...	1.76	0.46	0.067	4.57	0.182	9.44	
		X64C5	...	6.14	1.54	0.055	2.7	0.104	3.42	0.376	2.13	>1000	
	Cast alloys	Without manganese	X45B2	1.3	1.56	285	100
			X46C2	3.5	0.90	85.5	134
			X33A1	5.52	0.44	34	1.64	116	230
			X21A1	...	2.7	...	0.57	60	176
			X103A1	...	5.4	...	0.50	42	1.74	94	210
With manganese		X102A2	2.28	...	0.6	0.041	1.77	
		X102B1	2.28	...	0.6	0.0326	1.37	0.054	1.41	0.27	6.5	>1000	
		X101A1	2.7	...	1.4	0.0426	2.61	0.071	1.57	0.204	2.33	>1000	
		X101B1	2.7	...	1.4	0.045	1.76	0.078	1.78	0.242	2.16	>1000	
		X116A1	...	1.99	0.95	0.022	0.648	0.0310	0.69	0.065	0.69	>1000	
		X31A2	...	4.8	1.2	0.052	1.68	0.075	1.02	0.14	0.985	>1000	
		X31B1	...	4.8	1.2	0.054	1.46	0.08	1.45	0.178	1.49	>1000	
		X64F	...	6.14	1.54	0.098	2.32	0.16	3.0	0.35	3.55	>1000	
		X64G	...	6.14	1.54	0.099	2.32	0.127	1.10	

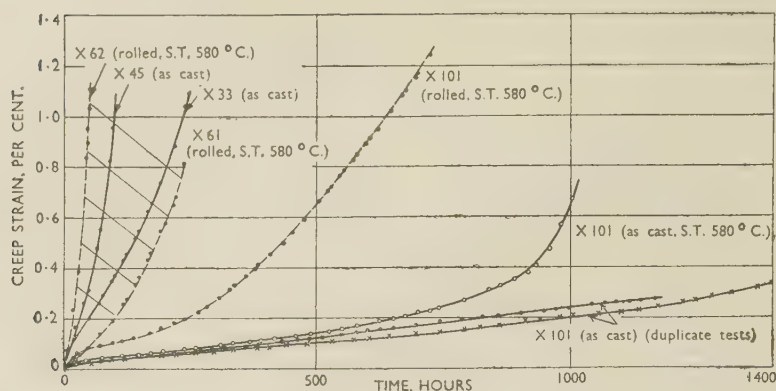


FIG. 3.—Improvement in Creep Properties of Magnesium-Cerium Alloys at 300° C. and 1 Ton/In.², Due to Addition of Manganese. The shaded area covers tests on alloys containing cerium only, in varying amounts. For compositions see Table VI.

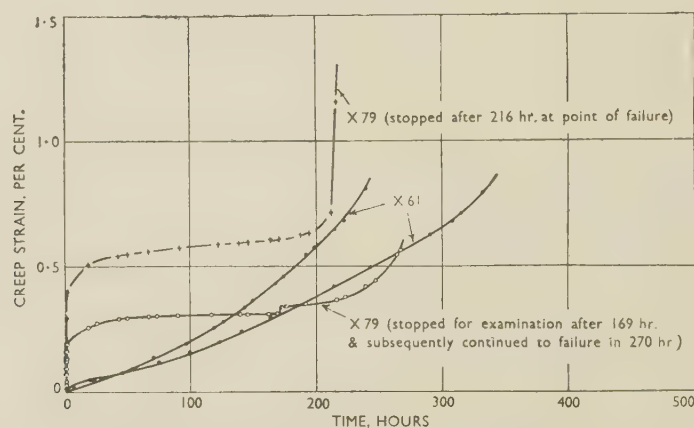


FIG. 4.—Comparison of Creep Properties of Magnesium-Manganese (X 79) and Magnesium-Cerium (X 61) Alloys, Rolled and Solution-Treated at 580° C. and Tested at 300° C. and 1 Ton/In.².

TABLE VII.—Effect of Heat-Treatment on Cast Alloys as Shown by Creep Tests at 300° C. and 1 Ton/In.².

Alloy No.	Composition			Treatment	At 120 Hr.		At 300 Hr.		At 1000 Hr.		Time to Reach 1% Strain, hr.
	Ce, %	R.E., %	Mn, %		Strain, %	Creep Rate, Strain/hr. $\times 10^4$	Strain, %	Creep Rate, Strain/hr. $\times 10^4$	Strain, %	Creep Rate, Strain/hr. $\times 10^4$	
X116A1	...	1.99	0.95	As cast.	0.022	0.648	0.031	0.69	0.064	0.69	...
X116B1				Cast, 24 hr. at 580° C., water-quenched.	0.0352	0.96	0.048	0.615	0.113	1.53	...
X116C1				Cast, 24 hr. at 580° C., water-quenched, aged 16 hr. at 350° C.	0.0083	0.456	0.0164	0.48	0.063	0.79	...
X116C2				" " "	0.0118	0.665	0.019	0.281
X102B1	2.28	...	0.6	As cast.	0.0326	1.37	0.054	1.41	0.27	6.5	...
X102B2				Cast, 24 hr. at 580° C., water-quenched.	0.0142	0.88	0.036	0.99	0.128	2.1	...
X101B1	2.7	...	1.4	As cast.	0.045	1.76	0.078	1.78	0.242	2.16	...
X101B2				Cast, 24 hr. at 580° C., water-quenched.	0.051	2.32	0.086	2.2	0.60	66.4	...
X31A2	...	4.8	1.2	As cast.	0.052	1.68	0.075	1.02	0.14	0.985	...
X31C2				Cast, 24 hr. at 580° C., water-quenched.	0.042	1.125	0.058	0.82	0.118	0.82	...
X33A1	5.52	As cast.	0.44	34	1.64	116	230
X33A2				Cast, 24 hr. at 580° C., water-quenched.	0.094	5.4	0.208	7.22	780

Both at 200° and 250° C. it had been found that no advantage was derived from cerium in excess of 1.6% in rolled and solution-treated binary magnesium-cerium alloys, and in excess of about 3% in cast alloys. There is no indication in Table VI that this conclusion cannot also be applied to the binary alloys tested at 300° C., although the number of results is limited. When manganese is present, less cerium is needed, e.g. the manganese-containing alloy X78A3 with only 0.58% cerium is stronger than any of the rolled and solution-treated alloys without manganese, and alloy X116A1 with only 1.99% rare earths is much stronger than any of the cast alloys without manganese addition.

Fig. 3 illustrates the typical improvement due to manganese. Creep curves for alloy X101 (cerium 2.7, manganese 1.4%) in the as-cast, cast and solution-treated, and rolled and solution-treated conditions are compared with curves for alloys containing cerium only (shaded area). The improvement shown by the as-cast alloy compared with those rolled and solution-treated, is typical of alloys of similar composition, and the results for duplicate creep tests give a good idea of the reproducibility obtained with cast alloys. The advantage of the longer-time tests is also well illustrated here, the effect of solution-treatment of the cast alloys becoming apparent only after 500 hr.

Grube, Davis, and Eastwood,⁵ who tested wrought magnesium-rare earths alloys with various additions, concluded that cerium (or rare earths) was responsible for the tensile properties at 316° C., while manganese was responsible for the creep properties. They found the highest resistance to creep in a 1.8% manganese alloy containing no rare earths, extruded and quenched from 560° C. and tested at 316° C. under a stress of 2000 lb./in.². The total strain at 120 hr. was 0.09% and at 607 hr. 0.281%. While the importance of manganese is confirmed in the present work, it is not considered as effective in conferring creep-resistance as cerium or rare earths. For example, an alloy containing no cerium and 1.48% manganese, rolled and solution-treated at 580° C., was tested at 300° C. and 1 ton/in.². Fig. 4 gives the results compared with those of a magnesium-cerium alloy tested under the same conditions. Although the creep rate of the manganese-containing alloy was low at 120 hr., there was early failure with intercrystalline fracture.

A limited number of cast alloys were solution-treated and tested at 300° C., and the results are set out in Table VII. Solution-treatment seems to improve the cast material where there is a high cerium or low manganese content, as in alloys X102, X33, and X31. In the case of alloys X101 and X116 solution-treatment resulted in a deterioration in creep-resistance which set in at 1000–1100 hr.

The effect of ageing at 350° C. had been found harmful both to cast and rolled binary alloys tested at 200° C. The properties of a rolled and solution-treated binary alloy (X61), tested at 300° C., were rendered much worse by ageing at 350° C., whereas a cast and solution-treated alloy containing

manganese (X116) was slightly improved by the same treatment.

It appears, then, that for the best creep-resistance at 300° C., under a stress of 1 ton/in.², cast magnesium-cerium-manganese or magnesium-rare earths-manganese alloys are to be preferred. Heat-treatment effects little improvement unless the manganese content is low, and cases exist in which the heat-treatment has resulted in a sharp deterioration.

(b) Tests at 316° C. (600° F.)

Creep tests in other laboratories are often made at 316° C. (600° F.), and it was thought desirable to determine what difference in creep strain could be expected from the rise of 16° C. Three cast alloys, X116 (rare earths 1.99, manganese 0.95%), X120 (rare earths 4.69, manganese 1.50%), and X121

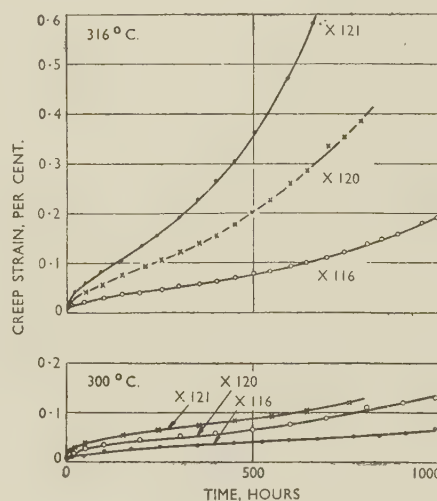


FIG. 5.—Comparison of Creep Properties of Cast Alloys Containing Manganese, at 300° and 316° C. and 1 Ton/In.².

(cerium 4.21, manganese 1.61%) were therefore tested at 1 ton/in.² at both 300° and 316° C. The creep curves reproduced in Fig. 5 show that the strain at 1000 hr. of the best alloy (X116) was 0.065% at 300° C., and 0.195% at 316° C.

Similarly, stresses applied in creep tests reported by other workers are often in multiples of 1000 lb./in.² and a direct comparison cannot be made. By extrapolation from design curves of Grube and Eastwood,⁴ it is estimated that two experimental alloys of optimum composition stressed at 2240 lb./in.² at 316° C. would extend 0.1% in 100 hr. and 130 hr., respectively. Reference to Fig. 5 shows that the alloys here included reached 0.1% strain in 130, 235, and 660 hr., respectively.

3. MICROSTRUCTURE

Cast magnesium-cerium alloys are coarse-grained, as shown in Fig. 7 (Plate XXXIV). With large amounts of cerium a continuous network of eutectic is found within the larger grain-boundary system (see Fig. 8, Plate XXXIV), and when "Mischmetall"

is added instead a eutectic of the divorced type is found, as shown in Fig. 9 (Plate XXXIV). In an alloy containing zirconium (Fig. 10, Plate XXXIV), there is some coring due to the zirconium, and divorce of the eutectic is prevented. There is nothing in the creep results obtained to suggest that the form of the eutectic has any significance.

In the binary magnesium-cerium (or magnesium-rare earths) alloys no precipitate is visible in the magnesium-rich matrix (Fig. 11, Plate XXXV), and the fact that the cast alloys show as good behaviour in creep at 300° C. as the rolled and solution-treated ones suggests that the rate of cooling of the sand-cast bar is sufficiently rapid to retain a considerable amount of cerium in solution. Addition of about 1% of manganese, however, results in a characteristic precipitate in the cast alloy, as shown in Fig. 12 (Plate XXXV).

Sand-cast magnesium-cerium alloys and magnesium-cerium-manganese alloys remain coarse-grained on solution-treatment, and the undissolved Mg_2Ce agglomerates into separate areas (Fig. 13, Plate XXXV). Alloys cast, solution-treated, and aged at 300° and 350° C. exhibit the beginnings of a new and smaller grain-boundary system linking up the areas of Mg_2Ce as illustrated in Fig. 14 (Plate XXXV).

Figs. 15 and 16 (Plate XXXV) are photomicrographs of an alloy without manganese, solution-treated and aged at 300° and 350° C., respectively, showing the increase in particle size at the higher ageing temperature. An alloy with 1.4% manganese exhibits very little increase in particle size, as may be seen from Figs. 17 and 18 (Plate XXXV). Electron micrographs of the same two alloys solution-treated and aged at 350° C. are reproduced in Figs. 19 and 20 (Plate XXXVI) at a magnification of 2500. The finer particles in the manganese-containing alloy appear as white dots in Fig. 20.

4. RELATION OF MICROSTRUCTURE TO CREEP BEHAVIOUR

In magnesium-cerium and magnesium-cerium-manganese alloys resistance to creep might be due to: (a) the eutectic network, (b) a strengthening of the matrix by dissolved cerium or manganese, or (c) precipitation before or during creep.

As a result of the earlier tests at 200° C. it was concluded that removal of the eutectic network by solution-treatment had little effect on creep behaviour. When testing at 300° C. it was found that high-cerium alloys (see alloys X33 and X102 in Table VII) were improved by solution-treatment, suggesting that a complete network of eutectic is undesirable. When the network is complete, the alloy may behave like fine-grained material which would be expected to be weaker in creep at the higher testing temperature, or the eutectic itself may be weaker than the matrix. The slight weakening of the manganese-containing alloys X101 and X116 (Table VII) by solution-treatment is probably connected not with the

agglomeration of the eutectic, but with the re-solution of the manganese precipitate. The specimen as cast begins its test with a precipitate already present, as shown in Fig. 12.

Haughton and Schofield¹¹ reported the solid solubility of cerium in magnesium to be about 1.3% at 580° C., falling to about 0.1% at 350° C. Previous work of the present authors has shown that there is coarse precipitation of Mg_2Ce on ageing at 350° C. with low resistance to creep; while, when a fine precipitate was formed at 200° C., the creep-resistance was high. If creep-resistance were due to the cerium in solution at the temperature of test, it would be expected that: (i) alloys with 0.1–0.2% cerium would be as creep-resistant as those with 1.6%, and (ii) an alloy with 1.6% cerium, solution-treated and aged at 350° C., would be more creep-resistant than one aged

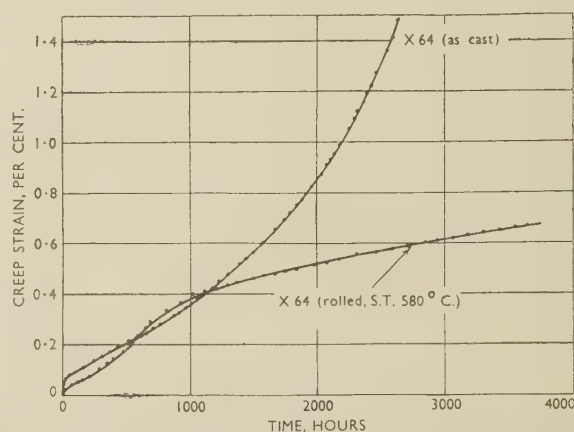


FIG. 6.—Long-Time Creep Behaviour of Alloy X64 (Rare Earths 6.14, Manganese 1.54%) in the As-Cast and the Rolled and Solution-Treated Condition, Tested at 300° C. and 1 Ton/In.²

at 200° C. In fact, neither is the case, and creep-resistance must be due mainly to a fine precipitation.

A sloping solid-solubility line is also found in the magnesium-manganese system according to Schmid and Siebel,¹² the solubility being 3.4% manganese at 600° C. and less than 0.1% at 200° C. In solution-treated and aged magnesium-cerium-manganese alloys, both Mg_2Ce and, presumably, α -manganese are precipitated.

The superiority of cast magnesium-cerium-manganese alloys in creep seems to be the result of: (a) the presence of a fine precipitate in the cast material, so that the creep specimen is strengthened before test, (b) the influence of manganese in restraining the growth of Mg_2Ce particles on ageing (see Figs. 16 and 18), and (c) possibly, of a slight increase in the solid solubility of cerium in magnesium when manganese is present. The behaviour of alloy X64 (see Table VI and Fig. 6) is of interest in that as rolled and solution-treated it is more resistant to creep than as cast. The structure of the cast alloy contains a large amount of eutectic, and may therefore be expected to be weak in creep, while in the rolled and solution-treated condition the eutectic

network has been removed. The improvement, however, is not sufficient to make the alloy as good as other cast alloys. The creep curve (Fig. 6) for the rolled and solution-treated alloy shows a double inflection after about 700 hr., followed by a decreasing creep rate, indicating a delayed precipitation during the test. Its microstructure (Fig. 21, Plate XXXVI) exhibits some grain-boundary precipitation, which is probably responsible for the decrease in the creep rate. When delayed precipitation of this kind takes place, it is important to relate the testing time to the service life of the component. The conclusions reached in Section IV relate to a service life of about 1000 hr., and may have to be modified for materials intended to last appreciably longer.

In the absence of manganese, solution-treatment and ageing at 350° C. of both cast and rolled alloys result in poor creep properties by reason of the coarse precipitate of Mg_2Ce . When sufficient manganese is present, finer particles are precipitated, as shown in Fig. 18, and the alloy resists creep.

The inferiority of rolled and solution-treated alloys in comparison with cast material, when tested at 300° C., may be due to their small grain-size and to the absence of a fine manganese precipitate at the beginning of the test.

IV.—CONCLUSIONS

Various third elements have been added to magnesium-cerium alloys, and their effect on the creep-resistance at 250° and 300° C. examined. Aluminium and cadmium decreased the creep-resistance. Little or no improvement resulted from the addition of silver, lithium, or silicon to wrought alloys, or of cobalt, silicon, or zinc to cast alloys. Zirconium and combined additions of zinc and zirconium had a favourable effect under certain conditions, but the greatest improvement was obtained with manganese. This was marked only when the test temperature was raised to 250°–300° C.; in previous work at 200° C. little effect had been observed.

The good creep-resistance of magnesium-cerium-manganese alloys is well known,³⁻⁵ but the high cerium contents often recommended appear unnecessary. In the present work the best creep-resistance was found in a cast alloy containing 2% rare earths and 1% manganese. The composition range has not been sufficiently explored to enable the limits of cerium and manganese contents for optimum creep-resistance to be defined, but it is thought unlikely that they could be appreciably reduced. The addition of "Mischmetall" has much the same effect as that of cerium.

The effect of heat-treatment varied with different compositions, but as a rule the heat-treatment of cast alloys is not justified. Creep tests of short duration may be misleading, and should be followed up by tests covering the full service life to which the alloys are to be subjected.

Cerium is effective in promoting creep-resistance by reason of a fine precipitate which forms during test at 200°–300° C. Manganese appears to modify the precipitation phenomenon, delaying the coarsening of the Mg_2Ce precipitate and possibly altering the quantity and nature of the precipitated particles. Leontis and Murphy³ noted that manganese delayed the changes in electrical conductivity on ageing these alloys. Manganese probably enters into the constitution of the Mg_2Ce precipitate in some way, since if manganese and cerium in the alloy were without action upon each other, it is unlikely that the rate of coarsening of the Mg_2Ce precipitate would be affected.

ACKNOWLEDGEMENTS

The authors desire to acknowledge the assistance rendered by Mr. L. J. V. Mackay in making up the alloys and by Miss L. V. Game in carrying out the creep tests.

The work described forms part of the research programme of the National Physical Laboratory, and the paper is published by permission of the Director of the Laboratory.

REFERENCES

1. G. A. Mellor and R. W. Ridley, *J. Inst. Metals*, 1949, **75**, 679.
2. T. E. Leontis, *Trans. Amer. Inst. Min. Met. Eng.*, 1949, **180**, 287.
3. T. E. Leontis and J. P. Murphy, *ibid.*, 1946, **166**, 295.
4. K. Grube and L. W. Eastwood, *Proc. Amer. Soc. Test. Mat.*, 1950, **50**, 989.
5. K. Grube, J. A. Davis, and L. W. Eastwood, *ibid.*, 1950, **50**, 965.
6. A. J. Murphy and R. J. M. Payne, *J. Inst. Metals*, 1947, **73**, 105.
7. R. G. Wilkinson, *Metallurgia*, 1949, **41**, 91.
8. J. L. Haughton, "Magnesium and Its Alloys". 1940: London (H.M. Stationery Office).
9. H. Mäder and F. Laves, *Aluminium*, 1943, **25**, 157.
10. T. E. Leontis, *Trans. Amer. Inst. Min. Met. Eng.*, 1949, **185**, 968.
11. J. L. Haughton and T. H. Schofield, *J. Inst. Metals*, 1937, **60**, 339.
12. E. Schmid and G. Siebel, *Metallwirtschaft*, 1931, **10**, 923.

1439 New Values of the Coefficients of Equivalence for Manganese, Iron, Cobalt, and Nickel in Copper-Zinc Alloys *

By J. B. HAWORTH,† D.Phil., B.Met., JUNIOR MEMBER

SYNOPSIS

Recent experimental work, described elsewhere (*Phil. Mag.*, 1952, [vii], 43, 613), has shown that the values ascribed by Guillet to the "coefficients of equivalence" of manganese, iron, and nickel are in error, and has enabled a hitherto undetermined coefficient to be stated for cobalt.

THE industrial alloy manufacturer has frequently made use of a system of "coefficients of equivalence" when making complex brasses. These coefficients were determined empirically by Guillet¹ for a number of metals which form solid solutions with copper-zinc alloys, and exert effects on the properties similar to changes in the zinc content. They enable proportions of these metals to be expressed in terms of zinc or copper, so that in complex alloys the nature and amounts of the additions subject to the retention of the α , $\alpha + \beta$, or β structure desired may be ascertained. Work at Oxford on the constitution of ternary alloys of copper-zinc and copper-aluminium with manganese, iron, cobalt, and nickel produced results which proved to be of particular interest with regard to the theory of the transition metals, and it was from the theoretical rather than the practical aspect that the paper was published recently.² However, the experimental work which was carried out on the copper-zinc ternary alloys is of practical significance also, as new values for several coefficients of equivalence may be derived from the results.

In the above work the effect on the solubility relationships of the α and β phases in copper-zinc and copper-aluminium alloys of small additions of manganese, iron, cobalt, and nickel was studied at a standard temperature of 672° C. by the method of annealing and microscopical examination. In this way isothermal sections were plotted in the α/β regions for the eight ternary systems. In the copper-zinc series the $\alpha/\alpha + \beta$ and $\alpha + \beta/\beta$ boundaries proved to be straight and parallel lines for small additions of the third metal, but the directions of the boundaries relative to the copper-zinc side of the ternary diagram were found to be different in each system. Furthermore, the angle between this axis and each boundary was found to increase progressively, in congruence with the series Mn-Fe-Co-Ni in the Periodic Table.

It is well known that in alloy systems such as these, where the atomic-size factors are favourable and the electrochemical factors are small, the α/β -brass type

of equilibrium is determined mainly by electron concentration. If it is assumed, therefore, that the $\alpha/\alpha + \beta$ and $\alpha + \beta/\beta$ solubility curves in the isothermal sections are lines of constant electron concentration, the slopes of the boundaries determined experimentally show that manganese, iron, cobalt, and nickel act in copper-zinc alloys as though they possessed valencies of 1.83, 1.0, 0.8, and 0.61 respectively. Thus, if one atom of copper (1 valency electron) in a copper-zinc alloy is replaced by one atom of manganese (1.83 valency electrons), there is a net increase of 0.83 electrons. In other words, one atom of manganese added to a copper-zinc alloy produces a change equivalent to the addition of 0.83 atoms of zinc. Similarly, if one atom of zinc (2 valency electrons) is replaced in a copper-zinc alloy by one atom of iron (1 valency electron), one atom of cobalt (0.8 valency electron), or one atom of nickel (0.61 valency electron), there are net changes in the number of electrons in each case of -1.0, -1.2, and -1.39, respectively. We thus arrive at the following values for the coefficients of equivalence:

Mn	- 0.83	(i.e. 1 at.-% Mn is equivalent to 0.83 at.-% Zn)
Fe	- 1.0	(,, ,, ,, Fe ,, ,, ,, 1.0 at.-% Cu)
Co	- 1.2	(,, ,, ,, Co ,, ,, ,, 1.2 at.-% Cu)
Ni	- 1.39	(,, ,, ,, Ni ,, ,, ,, 1.39 at.-% Cu)

The values for manganese, iron, and nickel may be compared with Guillet's values of +0.5, +0.9, and -1.2, respectively.¹ These latter values would be in weight per cent., but conversion to atoms per cent. would make only a slight difference in the figures.

REFERENCES

1. See, e.g., H. C. H. Carpenter and J. M. Robertson, "Metals". Vol. II, p. 1305. Oxford: 1939 (Oxford University Press).
2. J. B. Haworth and W. Hume-Rothery, *Phil. Mag.*, 1952, [vii], 43, (6), 613.

* Manuscript received 12 September 1952.

† Late Inorganic Chemistry Laboratory, Oxford; now with Sheepbridge Engineering, Ltd., Chesterfield.

THE EFFECT OF MINOR ADDITIONS ON THE AGE-HARDENING PROPERTIES OF A HIGH-PURITY LEAD-ANTIMONY ALLOY*

1440

By L. M. T. HOPKIN,† B.Sc., A.R.S.M., A.I.M., MEMBER, and
C. J. THWAITES,‡ B.Sc., A.R.S.M., JUNIOR MEMBER

(Communication from the British Non-Ferrous Metals Research Association.)

SYNOPSIS

It was found that little or no age-hardening occurred, after suitable treatments, in a lead-0.85% antimony alloy of extreme purity, although the alloy of commercial purity is known to age-harden extensively. Minor additions of various elements whose solid solubility in lead varied with temperature caused marked age-hardening of the alloy and increased the dispersion of the precipitated antimony. As little as 0.001% arsenic promoted marked hardening. Addition elements either completely or negligibly soluble at all temperatures had no effect. A possible mechanism is suggested which is similar to that offered by Hardy (*J. Inst. Metals*, 1950-51, **78**, 169) to explain the effect of minor additions on the age-hardening characteristics of an aluminium-4% copper-0.15% titanium alloy.

I.—INTRODUCTION

THE British Non-Ferrous Metals Research Association's current investigation of the creep and fatigue properties of lead and its alloys includes tests on a specially refined lead of the highest purity and on alloys of this material in which the addition element (i) is in solid solution, (ii) is insoluble, and (iii) causes age-hardening. Antimony was selected as the alloying element causing age-hardening, but it was found that a high-purity alloy containing 0.85% antimony would not age-harden in the manner characteristic of the commercial alloy. The present paper shows that the addition of small amounts of other elements to the high-purity alloy causes marked age-hardening.

II.—PREVIOUS WORK

Examination of the literature revealed that Hofmann, Schrader, and Hanemann¹ obtained no age-hardening with a 1% antimony alloy based on a lead of 99.994% purity, whereas the same alloy based on a lead of 99.960% purity age-hardened rapidly under similar conditions. Several papers were found which described how minor additions increase the rate of hardening of lead-antimony alloys. Seljesater² showed that the addition of 0.01% arsenic to a 1% antimony alloy increased the hardness, after ageing at room temperature for 28 days, by about 70%. According to Bluth and Hanemann,³ small additions of both copper and arsenic increased the rate of age-

hardening of a 1% antimony alloy. Schumacher, Bouton, and Ferguson⁴ found that the resistivity of a 1% antimony alloy decreased more rapidly with time, indicating an increased rate of precipitation, when small additions of a third element were made to the alloy. Additions of arsenic, copper, silver, nickel, and manganese were investigated by these workers, and arsenic was found to be the element with the greatest effect. Considerable effects were also obtained with 0.002% copper or with 0.005% silver. Schumacher⁵ observed that the tensile strength of a lead + 1% antimony + 0.005% arsenic alloy increased more rapidly, during ageing, than that of a binary lead-1% antimony alloy. Hofmann and Hanemann⁶ found that the resistivity of a 2% antimony alloy decreased more rapidly with time when 0.05% arsenic was present in the alloy.

From the above it is clear that minor additions of various third elements markedly increase the rate of age-hardening and precipitation in lead-antimony alloys. The present paper describes tests on the effects of small additions of arsenic, tin, copper, and silver on the age-hardening properties, after heat-treatment, of a lead-0.85% antimony alloy of high purity.

III.—EXPERIMENTAL DETAILS

It was originally expected that the high-purity binary lead-0.85% antimony alloy would age-harden, and it was extruded into rods suitable for creep and

* Manuscript received 28 August 1952. The work described in this paper was made available to members of the B.N.F.M.R.A. in a confidential research report issued in October 1951.

† Formerly Investigator, B.N.F.M.R.A.; now at Metallurgy Division, National Physical Laboratory, Teddington.

‡ Formerly Investigator, B.N.F.M.R.A.; now with the Tin Research Institute, Greenford, Middlesex.

fatigue testing. When it was found that this material did not age-harden, trial experiments were carried out on cast alloys with minor additions of the elements already mentioned.

1. MATERIALS

The analyses of the specially refined Tadanac lead and the high-purity antimony were:

Specially Refined Tadanac Lead

Element	%	Element	%	Element	%
Ag	0.00003	Tl	0.0002	Au	trace
Cu	0.0001	Sb	0.0001	In	"
Zn	0.0001	Cd	<0.0001	Ni	nil
Fe	0.0001	As	trace	Co	"
Bi	0.0001	Se + Te	"	Sn	"

High-Purity Antimony

Element	%	Element	%
Pb	0.006	As	0.006
S	<0.001	Na	0.005
Cu	<0.001	Fe	0.005
Ni	<0.001	Sb (by difference)	99.975

Chemical analysis of the binary lead-0.85% antimony alloy showed that it conformed to its nominal composition.

The ternary alloys investigated contained 0.85% antimony with separate additions of 0.01% silver, copper, and tin, and 0.001, 0.002, 0.005, 0.01, and 0.02% arsenic. Tests were also carried out on binary lead-arsenic alloys containing the same amounts of arsenic as in the ternary lead-antimony-arsenic alloys. Spectrographic analysis for these minor additions showed that the nominal and actual amounts present were almost identical.

2. PREPARATION OF THE ALLOYS

(a) *The Binary Lead-0.85% Antimony Alloy, Extruded as Rod*

The basis lead was melted in a steel pot held at 400° C. in a thermostatically controlled furnace. The required amount of antimony was dissolved in a small quantity of the lead at 450° C., which was then added to the main melt at 400° C. The metal was chill cast from a bottom-pouring crucible. The cast billets were homogenized for one week at 300° C., machined, and then extruded in a laboratory extrusion press as straight lengths of rod, $\frac{7}{16}$ in. in dia.

(b) *The Binary and Ternary Alloys Cast as Sticks*

Small charges of the extruded binary lead-0.85% antimony alloy rods were remelted in Salamander crucibles, coated on the inside with a wash of alumina. The minor additions of tin and silver were made directly to the melts, and copper and arsenic were added as 1% and 1.5% master alloys, respectively. The ternary alloys were chill cast into cylindrical sticks, which were homogenized for 4 days at 300° C. and then quenched in water. The binary lead-arsenic alloys were made up in a similar way.

3. HARDNESS DETERMINATIONS

Hardness determinations were made on metallographically polished specimens with a Vickers pyramid hardness testing machine, a load of 1 kg. being applied for 30 sec. The hardness of a material was taken as the average of the values obtained from six impressions.

IV.—RESULTS OF HARDNESS DETERMINATIONS

1. THE BINARY LEAD-0.85% ANTIMONY ALLOY

The lead-0.85% antimony alloy was extruded at each of the temperatures 160°, 200°, 250°, and 300° C. and the product air-cooled. Metallographic examination showed that the alloy was single-phase at 150° C. and higher temperatures, in accordance with the results of Obinata and Schmid.⁷

The hardness of the four rods determined immediately after extrusion was independent of grain-size, which differed as a result of the various temperatures of extrusion. The average hardness of the materials was 5.1. The four rods were aged at 20° C., but did not age-harden even after 12,000 hr. The rod extruded at 300° C. was solution-treated for 24 hr. at 175° C. and water-quenched. This material was aged at 50° and 100° C., but did not age-harden even after 2800 and 770 hr., respectively, when the tests were discontinued.

Since prestraining is known to increase the rate of age-hardening, the effect of this variable was examined. The rod extruded at 300° C. was solution-treated for 24 hr. at 175° C. and then prestrained 5 and 10% in tension; the initial hardnesses increased from 5.1 to 6.6 and 7.2, respectively. Only slight further hardening occurred in 5800 hours' ageing at 20° C., hardnesses of 7.5 and 8.5, respectively, being reached.

To examine the effect of a different temperature of solution-treatment, the as-extruded rod was heated at 300° C. for 2 hr. and water-quenched. Slow hardening took place during ageing at 50° C., the hardness increasing from 5.4 to 9.0 in about 1800 hr.

2. EFFECT OF VARIOUS MINOR ADDITIONS ON CAST LEAD-0.85% ANTIMONY ALLOY

Ternary alloys containing separate 0.01% additions of arsenic, copper, tin, and silver were homogenized for four days at 300° C., water-quenched, and aged at 20° C. The ternary alloys containing tin and copper did not harden during 1400 hr. at 20° C., whereas after a similar time the hardness of the arsenic-bearing material had increased from 7.5 to 13.8. The silver-bearing alloy aged more slowly than that containing arsenic, the hardness increasing from 6.7 to 7.7 in 1400 hr. at 20° C.

3. EFFECT OF VARIOUS ADDITIONS OF ARSENIC ON CAST BASIS LEAD AND LEAD-0.85% ANTIMONY ALLOY

Since arsenic had the greatest effect of the addition elements examined, a more extensive investigation was made of ternary alloys with a range of arsenic contents. It was also desirable that the effect of various arsenic additions to the basis lead should be

ing and hardness testing (see later paragraphs and Fig. 2). The hardness values are linearly related to the arsenic contents of the alloys, although the lines corresponding to the two heat-treatment temperatures differ markedly in slope. This indicates that the arsenic was in solid solution and mainly out of solid solution, respectively, after heat-treatment at 300° and 160° C. On this interpretation, the intersections of the straight lines for the materials heat-

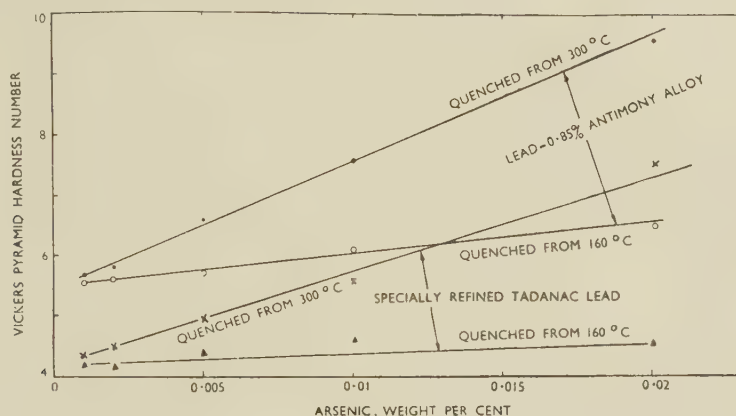


Fig. 1.—Effect of Arsenic Content and Quenching Temperature on the Initial Hardness of the Basis Lead and the Lead-0.85% Antimony Alloy.

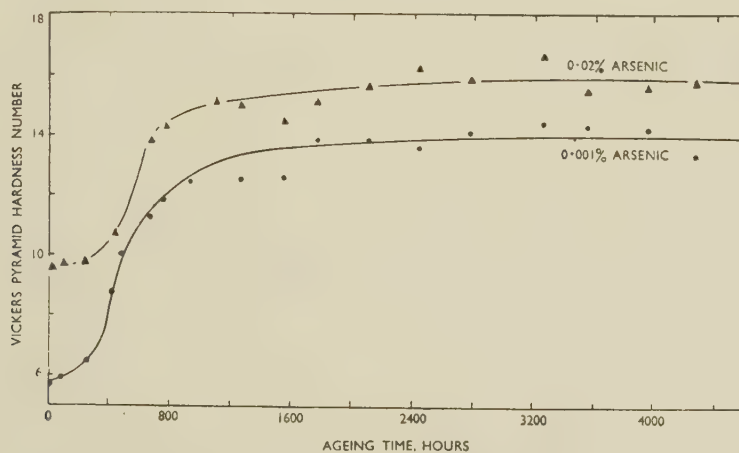


Fig. 2.—Age-Hardening Curves for Lead-0.85% Antimony Alloy Containing Various Amounts of Arsenic. Water-quenched from 300° C. and aged at 20° C.

examined. Ternary alloys containing 0.001, 0.002, 0.005, 0.01, and 0.02% arsenic, and binary lead-arsenic alloys containing the same amounts of arsenic were made up and homogenized for four days at 300° C.

(a) The Solubility of Arsenic in the Basis Lead and the Lead-0.85% Antimony Alloy

The hardnesses of the lead-arsenic and lead-0.85% antimony-arsenic alloys immediately after water-quenching from 300° and 160° C. are shown in Fig. 1. These hardness values are characteristic of the respective solution-treated alloys, because no significant change in hardness can have occurred between quench-

treated at 160° and 300° C. indicate the approximate solid solubility of arsenic at 160° C. It appears that in both the binary and ternary alloys the solid solubility of arsenic at 160° C. is less, possibly much less, than 0.001%.

(b) The Effect of Ageing

Each ternary alloy, water-quenched from 300° C., was aged at 20° and 50° C., and the age-hardening curves obtained are shown in Figs. 2 and 3. For the sake of clarity the curves of the alloys containing 0.001 and 0.02% arsenic, only, are plotted for each temperature. The curves for all the other materials

lay between these two extremes. Although the initial hardness increased markedly with arsenic content, the rate of hardening at both temperatures was independent of the arsenic content, as shown by the parallelism of the curves.

Ageing tests at 20° C. on the binary lead-arsenic alloys after water-quenching from 300° C. showed that these materials did not age-harden.

The rate of hardening, at 50° C., of the ternary alloys water-quenched after 2 hr. at 160° C. was again independent of the arsenic content, but was much

Extensive continuous precipitation occurred, during ageing at 20° C., along the slip planes in the alloy extruded at 300° C., solution-treated, and overstrained by both 5 and 10%. Only a slight increase in discontinuous precipitation occurred after the first few hours, and there was no further change.

The presence of arsenic in the lead-0.85% antimony alloy increased the dispersion, and possibly the rate, of continuous precipitation, although there was no effect on discontinuous precipitation. This fact can be seen by comparing Figs. 6 and 7 (Plate XXXVII),

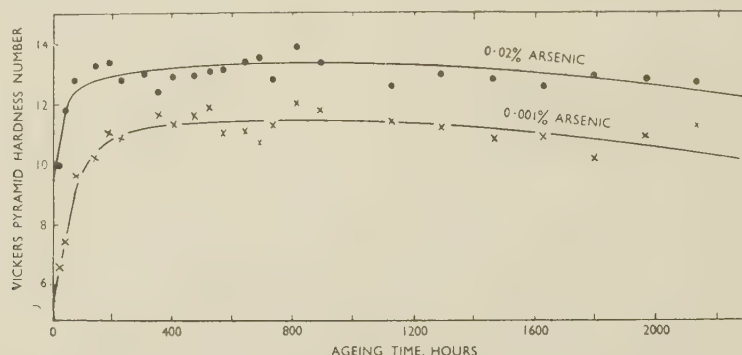


Fig. 3.—Age-Hardening Curves for Lead-0.85% Antimony Alloy Containing Various Amounts of Arsenic. Water-quenched from 300° C. and aged at 50° C.

slower than when the alloys were quenched from 300° C. The maximum hardness, approximately 9, was independent of arsenic content and was attained in 380 hr. from an initial value of 5.5-6.5.

V.—METALLOGRAPHIC EXAMINATION

The binary lead-0.85% antimony alloy extruded at any temperature was substantially homogeneous when examined immediately after extrusion, except for slight discontinuous precipitation which had occurred at grain boundaries during air cooling from the extrusion temperature (Fig. 4, Plate XXXVII).

Ageing the alloy extruded at all four temperatures for 12,000 hr. at 20° C. produced extensive continuous precipitation as fine globular particles and needles distributed throughout the grains (Fig. 5, Plate XXXVII). The width of the band of discontinuous precipitation had only slightly increased.

The alloy extruded at 300° C. and solution-treated for 24 hr. at 175° C. showed extensive continuous precipitation after subsequent ageing at both 50° and 100° C. A slight increase in the width of the discontinuous precipitation at grain boundaries occurred during the first few hours of ageing, but there was no further change. When the tests were abandoned, continuous precipitation was extensive. Discontinuous precipitation was no longer distinguishable at the grain boundaries, since the amount of antimony in solid solution within the grains had become similar to that in the new solid solution formed during the discontinuous precipitation.

which show, respectively, the binary alloy and ternary alloy containing 0.001% arsenic, both solution-treated for 1 hr. at 300° C. and aged for 120 hr. at 50° C.

VI.—DISCUSSION OF RESULTS

It has been shown that the binary lead-0.85% antimony alloy did not age-harden after solution-treatment at 175° C., or after air-cooling from higher extrusion temperatures. Only slight age-hardening occurred in the alloy after solution-treatment at 300° C., or after solution-treatment at 175° C. and prestraining in tension. Ternary alloys containing 0.01% copper or tin were similarly unresponsive to heat-treatment, but alloys containing 0.01% arsenic or silver age-hardened rapidly, the arsenic addition having the most marked effect. The rate of age-hardening of the ternary alloys containing arsenic was independent of the arsenic content, and 0.001% arsenic had almost as much effect as 0.02%.

The rate of age-hardening of the ternary alloys containing arsenic has been shown to be greater after heat-treatment at 300° C. than at 160° C. This difference can be attributed to the arsenic being in solid solution after solution-treatment at 300° C., but being probably nearly all rejected from solid solution during the treatment at 160° C. It is therefore probable that the slight age-hardening in the binary lead-0.85% antimony alloy, after solution-treatment at 300° C., was due to some minute quantity of impurity being in solid solution. When the impurity was rejected from solid solution, by heat-treatment

at 175° C., or by air-cooling from higher extrusion temperatures, no age-hardening took place.

It might be argued that the difference in the rate of hardening between the arsenic-bearing ternary alloys heat-treated at, and water-quenched from, 160° and 300° C. is due entirely to the difference between the resulting quenching strains. For example, Phillips and Brick⁸ have shown that, for aluminium alloys, the rate of age-hardening is markedly increased by the presence of quenching strains. Although quenching strains may have some effect in the present work, the observed results were not entirely due to this cause for two reasons. Firstly, hardening of the cast sticks occurred uniformly across their diameters; had there been a major effect of quenching strains the most rapid increase of hardness would have occurred near the outside circumference of the sticks, which must have been the most severely strained region during quenching. Secondly, a specimen of the ternary alloy, containing 0.001% arsenic, was cooled freely in air after solution-treatment at 300° C. Any cooling strains in this material must have been less than those in the quenched alloys, but the specimen age-hardened at 50° C. at the same rate as the material quenched from 160° C.

The literature records that a minor addition of copper accentuates the age-hardening of lead-antimony alloys, but the present work does not confirm this observation.

Any theory which is put forward to explain the observed phenomena recorded above must account for the following facts:

(i) The minor addition must be in solid solution in the lead-0.85% antimony alloy to be effective in causing age-hardening.

(ii) The minor addition of arsenic increases the dispersion, and probably the rate, of precipitation of the antimony-rich phase.

(iii) A small amount of tin, which is in solid solution, does not cause age-hardening.

(iv) The rate of age-hardening is increased markedly by 0.001% arsenic, which is in solid solution. Above 0.001% and up to 0.02% arsenic the rate of hardening is independent of the arsenic content.

A simple hypothesis in which the antimony-rich precipitate is nucleated by the prior precipitation of the minor addition is not tenable, since the insoluble arsenic rejected, at 160° C., from solid solution has only a small effect on the rate of age-hardening.

The theory put forward by Hardy⁹ to account for the effect of soluble minor additions on the age-hardening characteristics of an aluminium-4% copper-0.15% titanium alloy cannot be applied directly to explain the present phenomena. In the alloys investigated by Hardy, the chief alloying element, copper, and the minor additions had atomic diameters smaller and larger, respectively, than that of alumin-

ium. Hardy postulated that the small atoms of copper in solid solution form an "atmosphere" around the large atoms of the minor additions in such a way as to reduce the strain energy of the system to a minimum, such an arrangement being favourably placed for precipitation under suitable conditions. In the lead-0.85% antimony-arsenic alloys, however, both antimony and arsenic have atomic diameters less than that of lead, so that, providing that substitutional solid solutions are formed, the strain energy of the system will be a minimum when the atoms of antimony and arsenic tend to avoid each other and do not form an atmosphere of one type of atom around the other.

Although there seems to be no completely adequate theory to explain all the observed phenomena, the authors are indebted to Dr. W. Hume-Rothery for his suggestion as to the possible mechanism of the effect of the arsenic addition. He suggests that, although the diameter of the interstitial octahedral holes in the lead lattice are 0.41 times the diameter of the lead atom, assuming the atoms to be spheres, the high compressibility of lead atoms, might permit arsenic atoms, which have an atomic diameter 0.7 times that of lead, to take up interstitial positions. In the interstitial compounds of the transition elements, the limiting radius ratio for filling octahedral holes is about 0.6, so that an extension to 0.7 for lead would not seem unreasonable in view of the much higher compressibility. The arsenic atoms would, therefore, produce a local expansion of the lead lattice, so that under these conditions the strain energy of the system would be reduced when the substitutional antimony atoms, which cause local contraction of the lead lattice, form an atmosphere around the arsenic atoms. This arrangement, according to Hardy's theory, would be favourably placed for precipitation. Dr. Hume-Rothery points out that an arsenic atom in an interstitial hole would have six close neighbours, and that if some of these positions were occupied by antimony atoms, the bonds would be at right angles and might then provide a nucleus whose shape was favourable for the formation of the antimony structure which, although an (8-N) rule structure, is to a rough approximation nearly a simple cube. This effect might be expected for arsenic, which itself forms approximately right-angled bonds, but not for normal metals. Dr. Hume-Rothery, however, considers it unlikely that this theory can explain the effect of the silver addition, which is similar to that of the arsenic addition though less pronounced, since the atomic diameter of silver makes it unlikely that this element forms interstitial solid solutions in lead.

ACKNOWLEDGEMENTS

The authors wish to thank the Director and Council of the British Non-Ferrous Metals Research Association for permission to publish this paper.

REFERENCES

1. W. Hofmann, A. Schrader, and H. Hanemann, *Z. Metallkunde*, 1937, **29**, 39.
2. K. S. Seljesater, *Trans. Amer. Inst. Min. Met. Eng., Inst. Metals Div.*, **1929**, 573.
3. M. Bluth and H. Hanemann, *Z. Metallkunde*, 1937, **29**, 48.
4. E. E. Schumacher, G. M. Bouton, and L. Ferguson, *Indust. and Eng. Chem.*, 1929, **21**, 1042.
5. E. E. Schumacher, *Trans. Amer. Inst. Min. Met. Eng.*, 1950, **188**, 1097.
6. W. Hofmann and H. Hanemann, *Z. Metallkunde*, 1938, **30**, 416.
7. I. Obinata and E. Schmid, *Metallwirtschaft*, 1933, **12**, 101.
8. A. Phillips and R. M. Brick, *Trans. Amer. Inst. Min. Met. Eng.*, 1934, **111**, 94.
9. H. K. Hardy, *J. Inst. Metals*, 1950-51, **78**, 169.

THE EFFECT OF COLD WORK ON THE MICROSTRUCTURE AND CORROSION-RESISTANCE OF ALUMINIUM-5% MAGNESIUM ALLOYS CONTAINING 0-1% ZINC *

1441

By P. BRENNER,† Dr.Ing., MEMBER, and G. J. METCALFE,‡
M.Sc.Tech., MEMBER

SYNOPSIS

The effects of cold work, of prolonged ageing at 70° C., and of additions of up to 1% zinc on the microstructure, corrosion-resistance, and stress-corrosion-resistance of an aluminium alloy containing 5% magnesium, have been investigated.

The presence of zinc has little effect on the mechanical properties, but the alloy containing 1% zinc shows pronounced precipitation after ageing at 70° C., and corrosion attack is greater than in the case of the 0-0.5% zinc alloys, which show an incomplete grain-boundary network after ageing.

Small amounts of cold work reduce the corrosion-resistance of the alloys appreciably, but heavy cold work both of aged and unaged materials results in a corrosion-resistance as high as that of unworked material. The maximum corrosion attack, at about 30% cold work, is associated with the presence of continuous grain-boundary films formed on ageing. Comparable behaviour has been found in stress-corrosion tests, the maximum susceptibility to stress-corrosion occurring in material that has been given 30% cold work. Heavy cold work (50% reduction in thickness) produces material of high stress-corrosion-resistance. Explanations of the corrosion behaviour are given.

I.—INTRODUCTION

THE corrosion and stress-corrosion properties of aluminium-magnesium alloys have usually been investigated on alloys containing more than 5% magnesium. Wrought alloys containing 7-10% magnesium have been found particularly susceptible to intercrystalline corrosion and stress-corrosion in certain conditions of heat-treatment and cold working, and it has been shown that there is a correlation between microstructure and intercrystalline attack.^{1, 2, 3} Few published results relate to alloys with lower magnesium contents. Service failures in aluminium-5% magnesium alloys have been attributed to intercrystalline corrosion, probably accentuated by stress, by one of the present authors,⁴ who found that aluminium-5% magnesium alloy rivets failed as a result of severe intercrystalline corrosion, particularly at the junction of the shank and head. In this region the rivets had been very severely cold worked during driving, and heavy precipitation had occurred owing to exposure of the material to tropical temperatures. The corrosion attack was most severe in the regions of heaviest precipitation.

Since the aluminium-magnesium alloys are of great practical importance, it was considered advisable to obtain more information, particularly on their be-

haviour under tropical conditions. Siebel and Vosskühler⁵ have suggested that small additions of zinc have a pronounced influence on the corrosion-resistance of aluminium-magnesium alloys, and the investigation was therefore extended to cover aluminium-5% magnesium alloys with and without additions of zinc up to 1%. Subsequent work by Vosskühler⁶ has dealt with alloys of higher zinc content. In the present work the alloys were prepared in sheet form and were solution-treated and quenched from various temperatures. Subsequently the material was given up to 50% reduction in thickness by cold rolling and was tested both in the solution-treated condition and after ageing at 70° C. This temperature was chosen as being one likely to be reached in direct tropical sunshine.

II.—EXPERIMENTAL PROCEDURE

1. PREPARATION OF MATERIALS

The approximate chemical composition, treatment, and method of identification of the specimens were as follows:

(i) *Nominal Compositions*:—(1) Al-5% Mg; (2) Al-5% Mg-0.2% Zn; (3) Al-5% Mg-0.5% Zn; (4) Al-5% Mg-1% Zn.

Farnborough.

* Manuscript received 16 July 1952.

† Director of Research, Vereinigte Aluminiumwerke A.G. and Vereinigte Leichtmetallwerke G.m.b.H., Bonn (Rhein), Germany; formerly at the Royal Aircraft Establishment,

‡ Senior Research Metallurgist, Precious Metals Division, The Mond Nickel Co., Ltd., Acton; formerly at the Royal Aircraft Establishment, Farnborough.

(ii) *Treatments*:—*T*—2 hr. at 500° C., cooled to 300° C., held 1 hr., and cold-water quenched. *U*—2 hr. at 500° C., cooled to 280° C., held 1 hr., and cold-water quenched. *V*—2 hr. at 500° C., cooled to 260° C., held 1 hr., and cold-water quenched.

(iii) *Cold Work*:—0, 5, 10, 20, 30, 50% reduction by cold rolling.

(iv) *Ageing Treatments*:—*C*—14 days at 70° C.; *D*—28 days at 70° C.

Four alloys of the above nominal compositions were prepared, using metals of the following purity: aluminium 99.8%, magnesium 99.9%, and zinc 99.9%. Sufficient material to make two ingots, 5 in. in dia. and 16 in. long, in each alloy was melted and degassed with aluminium chloride at 680° C. The alloy was cast in water-cooled steel moulds, the water flow for each cast being maintained at 3 gal./min. The top 4 in. of each ingot was discarded, and the remainder machined to two portions each 4½ in. in dia. and 5¾ in. long.

The machined ingots were homogenized for 48 hr. at 450° C. before forging. The initial forging temperature was 380° C., but some cracking occurred, and subsequent operations were begun at 410° C. The cast alloy was forged to slabs approximately 5 in. wide and ¾ in. thick, and was machined after forging and before hot rolling.

Reduction of the material to 0.6 in. thick was carried out at 410° C., but subsequently the temperature was reduced to 390° C. and the material hot rolled to 0.072 in. thick at this temperature. Some of the material was further hot rolled at the same temperature to thicknesses of 0.050, 0.045, 0.040, and 0.038 in. All the four alloys rolled satisfactorily.

After hot rolling, all the material was annealed for 20 hr. at 380° C. and cooled in the furnace. The sheets were then cut into pieces which were given 1 hour's treatment at 390° C. to relieve stresses due to cutting.

The specimens *T*, *U*, and *V* were solution-treated for 2 hr. at 500° C. and transferred directly to ovens at 300°, 280°, and 260° C., respectively, held for 1 hr. and then cold-water quenched. These temperatures were chosen to cover both sides of the limit of solid solubility of 5% magnesium in aluminium.

Specimens of each alloy were given 50, 30, 20, 10, and 5% cold reductions in accordance with the following schedule, so that the finished material was all 0.036 in. thick.

Redn.	Passes
50%: 0.072 in. in 0.005 in. stages (8)	
30%: 0.050 in. in 0.005 in. stages (3)	
20%: 0.045 in. in 0.003 in. stages (3)	
10%: 0.040 in. in 0.002 in. stages (2)	
5%: 0.038 in. in 0.002 in. stage (1)	

The actual chemical compositions of the alloys used, as determined by chemical analysis, were:

Alloy	Mg, %	Zn, %	Fe, %	Si, %	Al
No. 1	4.98	Nil	0.1	0.07	Rest
No. 2	4.81	0.25	0.1	0.07	"
No. 3	5.02	0.45	0.1	0.09	"
No. 4	5.01	1.10	0.1	0.08	"

2. MICRO-EXAMINATION BEFORE CORROSION

All the specimens were electrolytically polished on sections parallel to the rolling direction and perpendicular to the rolled surface, etched after polishing, and then examined microscopically. The electro-polishing and etching techniques are described in the Appendix (p. 268).

The etching characteristics of the alloys change with their chemical composition and structure, the attack becoming greater with increasing zinc content. There was therefore a tendency for specimens of alloy 4 to be slightly over-etched, whereas alloy 1 was slightly under-etched.

The variations in zinc content, heat-treatment, and cold reduction had quite different effects on the microstructures. Some of these variables, such as small amounts of cold work or additions of zinc less than 0.5%, had only a slight effect on the microstructure, whereas other conditions, such as ageing at 70° C., the addition of 1% zinc, and large amounts of cold work, affected the microstructure considerably. The photomicrographs described are examples of typical structures produced by the different treatments.

3. MICROSTRUCTURES OF UNAGED SPECIMENS

The microstructures of alloys 1, 2, and 3 in the unaged condition were very similar, the grain boundaries usually being only very faintly revealed. One of the chief observations was the occurrence of etch-pits at the junctions of three grain boundaries, which tended to increase in number with decreasing zinc content. Occasionally, randomly distributed pits were also observed within the grains. These tended to increase in number with increasing zinc content, there being many more in alloy 4 than in the other three alloys. There was some indication that in alloy 4 the number of pits within the grains increased as the quenching temperature was raised. This was probably due to the reduced solubility of magnesium in aluminium in the presence of zinc and to the increased precipitation at temperatures below the solid-solubility line.⁷

After the specimens had been rolled to 5, 10, and 20% reduction in thickness, it was found that those in the worked but not aged condition had similar structures to those of the unworked specimens, except that there was probably a slight increase in the number of pits as the amount of rolling was increased. Heavier cold reductions resulted in an increase in the number of pits within the grains.

4. MICROSTRUCTURES OF SPECIMENS HEAT-TREATED AND AGED AT 70° C. (NOT COLD WORKED)

Ageing at 70° C. for 14 days affected the microstructures of the four alloys to different extents. Alloys 1, 2, and 3 were very similar, in that in specimens that had not been cold worked, an incomplete grain-boundary network was formed, as a result of precipitation occurring only on certain boundaries

between grains, as shown in Fig. 6 (Plate XXXVIII). In addition, pits were observed at grain-boundary junctions. There was no indication of any variations in microstructure due to the different heat-treatments *V*, *U*, and *T*. In alloy 4 a fine precipitate was observed at some parts of the grain boundaries, together with a few coarse plate-like particles.

In order to determine whether the incomplete network in the aged specimens was due to micro-segregations originating from the cast structure which may not have been completely removed by homogenization, specimens of alloy 1 were re-heat-treated at 460° C. for 16, 24, 40, and 64 hr., and water-quenched. No influence of the annealing temperature on the microstructure could be detected after subsequent ageing for 14 days at 70° C. The incompleteness of the grain-boundary network was very marked in all the specimens. Prolonging the time of etching caused stronger attack on the etched portions of the grain boundaries, which became more pronounced, but there was no tendency to form a complete network.

Examination of aged specimens that had been electrolytically polished and etched so as to produce etch pits,^{8,9} indicated that there was no preferred orientation of the grains, as judged by the changes in shape of the rectangular and triangular pits from grain to grain. It was also shown that quenching stresses played no part in the formation of the incomplete network, since structures identical with those previously described were observed after examination of specimens that had been aged at 70° C. after (a) cooling in air from 460° C. or (b) quenching in boiling water after soaking for 2 hr. at 460° C.

It is considered that the incomplete nature of the grain-boundary network is related to the difference in orientation between adjacent grains and possibly to the direction of the grain boundary.¹⁰ The distortion of the lattice in the grain-boundary zone, which varies appreciably with the difference in orientation of adjacent grains, influences the occurrence of precipitation.

5. MICROSTRUCTURES OF SPECIMENS COLD ROLLED AND AGED AT 70° C.

The effect of ageing the cold-worked material at an elevated temperature (i.e. 14 days at 70° C.) was very marked; 5, 10, and 20% cold reduction led to an increasing amount of precipitation in the grain boundaries and the gradual appearance of a more complete network with increased amounts of cold work. Specimens of alloy 1 that had been given 20% cold reduction had still an incomplete grain-boundary network of precipitation, as shown in Fig. 7 (Plate XXXVIII), and in a few grains there was very slight indication of precipitation on certain crystallographic planes (the slip planes). After 30% cold reduction the amounts of precipitation in the slip planes occurring after ageing gradually increased, but the distribution and density of the precipitate was not uniform

from grain to grain. Ageing after 50% cold reduction resulted in heavy precipitation, but again it was obvious that the degree of precipitation varied considerably from grain to grain.

In the zinc-containing alloys (2, 3, and 4) precipitation along slip lines was even more marked. Areas of heavy precipitation occurred in the middle of the grains as well as at the grain boundaries, at which the slip lines were frequently heavily distorted.

As might be expected, 50% cold reduction followed by ageing resulted in pronounced slip-plane precipitation in all four alloys. The grains in all the specimens were markedly elongated in the direction of rolling, and precipitation was heavier in some regions than in others. In fact, in some grains very little precipitation occurred. Fig. 8 (Plate XXXVIII) shows a typical example of the microstructures observed. Frequently a band of heavy precipitation in a series of slip lines crossed more than one grain without its direction being affected by the grain boundaries. Where this occurred there was severe distortion of the grain boundary, and marked steps were visible where the precipitation bands crossed the boundaries.

In specimens aged for 28 days at 70° C. structures were observed similar to those in specimens aged for 14 days at 70° C., but precipitation at the grain boundaries and along the slip lines was slightly heavier. Some specimens showed areas with steps in the grain boundaries caused by slip-plane movement (Fig. 9, Plate XXXVIII). Heavy precipitation also occurred on slip planes in the region of the grain boundary where the slip lines are bent at the boundary (Fig. 10, Plate XXXVIII). The neighbouring grain in Fig. 10 is free from any slip-plane precipitation.

In order to examine the development of precipitation and to determine the critical ageing time at which grain-boundary precipitation and precipitation along the crystallographic planes starts, specimens of alloys 1 and 4 were aged after treatments *V*, *U*, and *T* and 30% cold reduction for 2, 5, 8, 24, 80, 200, and 960 hr. at 70° C. No evidence of precipitation could be detected microscopically after periods up to 80 hr., but after 200 hr. precipitation started at the grain boundaries in all specimens, and faint slip lines appeared in some grains. The network, however, was incomplete. After 960 hr., alloy 1 showed an almost complete network and alloy 4 a complete network, and in both alloys many slip lines and bands were visible.

6. CORROSION TESTS

Specimens in the form of strips 4 in. long \times 0.75 in. wide \times 0.036 in. thick were suspended in a shed with one side (west) open and were sprayed with natural sea-water three times a day for five days a week. The tensile properties were determined before exposure and after 28 days' and 12 months' exposure, the test-pieces being cut from the corroded strips and tested in triplicate.

The results of tensile tests on unexposed materials in the aged and unaged conditions are shown graphically

in Fig. 1, plotted against the amount of cold reduction. Since no influence of the different heat-treatments *T*, *U*, and *V* was detected, each point on these graphs is the average figure for all three treatments. In the unaged condition, the tensile strength and, in

conditions appear to be less in alloys 3 and 4 than in alloys 1 and 2. Comparison of the properties in the unaged and aged conditions shows that age-hardening effects, if any, must be very small. The addition of zinc up to 1% has apparently no marked effect on the

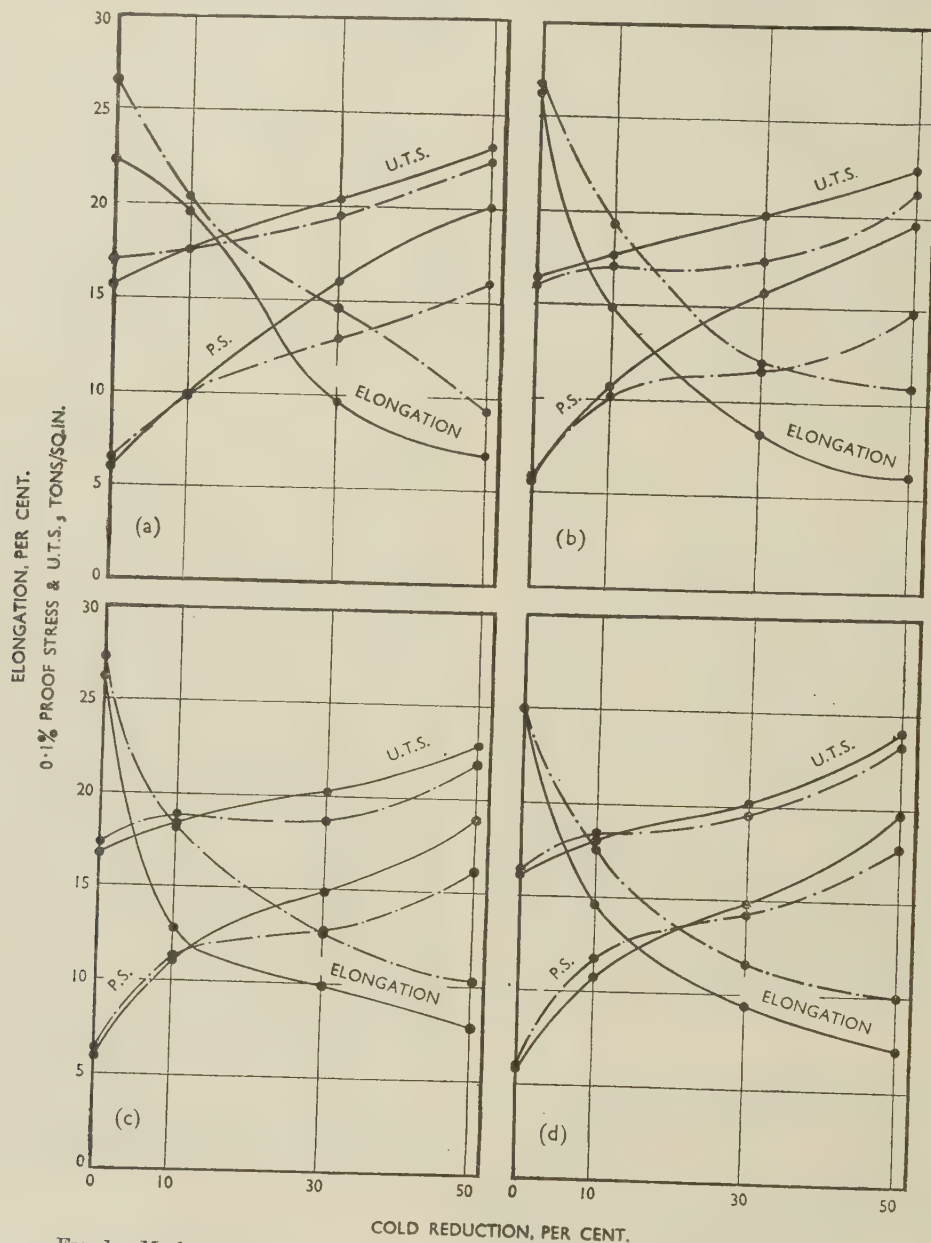


FIG. 1.—Mechanical Properties of (a) Alloy 1, (b) Alloy 2, (c) Alloy 3, and (d) Alloy 4.

— Before ageing.

- - - After ageing.

particular, the proof stress are considerably increased with increasing cold reduction, whilst the elongation decreases. After ageing for 28 days at 70° C., the ultimate tensile strength is not much affected, but in the cold-rolled condition the proof stress is clearly reduced and the elongation increased, as a consequence of recovery. The differences between the proof stress and elongation in the unaged and aged

tensile properties of an aluminium-5% magnesium alloy under the conditions used.

After 28 days' exposure, the specimens were only slightly attacked. On the surface of a number of specimens a few small pits were observed, which did not appear to be associated with a particular alloy or condition, but rather with inhomogeneities or local variations in the surface of the specimens (e.g.

rolled-in impurities) or local differences due to the cold work.

After 12 months' exposure corrosion was greater, but the attack was not uniform over the surface, and there were areas in most of the specimens that appeared almost unattacked. Numerous specimens showed local severe pits, which apparently increased with the zinc content. The pits sometimes formed striations in the rolling direction, particularly in alloy 4. The differences in the degree of attack of specimens of the same alloy and condition were frequently as great as the differences in the attack of different alloys and conditions. No difference between *V*-, *U*-, and *T*-treated specimens was detected, but the aged speci-

men appeared to be slightly more attacked than the unaged specimens. The 50% cold-rolled specimens, especially alloy 1 in the unaged condition, appeared to be less attacked than the other specimens.

The tensile strength and elongation were scarcely affected after 28 days' exposure, and only a few aged specimens of alloys 1, 2, and 3 with 5% and 30% cold reduction showed losses in elongation. The scatter in tensile strength and elongation was greater than before corrosion, however.

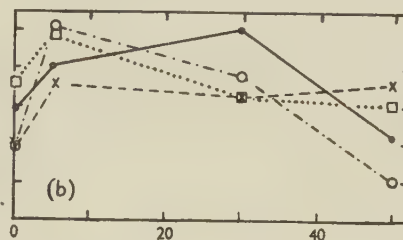
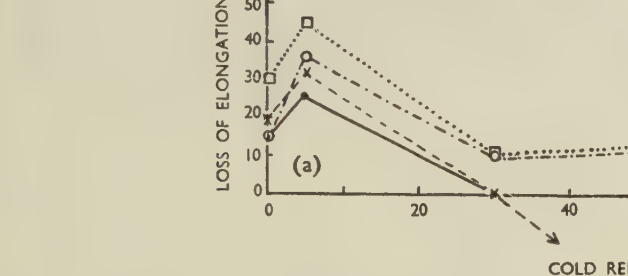


FIG. 2.—Percentage Loss of Elongation After 12 Months' Corrosion (a) Unaged and (b) Aged at 70° C.
KEY.

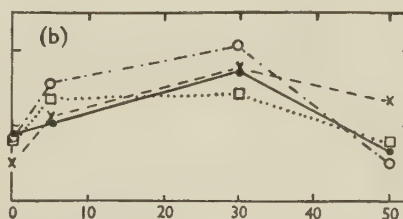
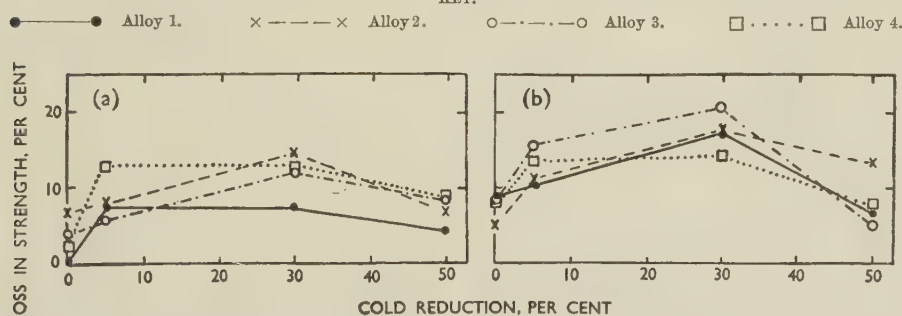


FIG. 3.—Percentage Loss of U.T.S. After 12 Months' Corrosion (a) Unaged and (b) Aged at 70° C.
Key as for Fig. 2.

mens appeared to be slightly more attacked than the unaged specimens. The 50% cold-rolled specimens, especially alloy 1 in the unaged condition, appeared to be less attacked than the other specimens.

The tensile strength and elongation were scarcely affected after 28 days' exposure, and only a few aged specimens of alloys 1, 2, and 3 with 5% and 30% cold reduction showed losses in elongation. The scatter in tensile strength and elongation was greater than before corrosion, however.

As would be expected, after 12 months' exposure the specimens had suffered greater corrosion attack, and the scatter range for the tensile strength was $\pm 20\%$ and for the elongation $\pm 40\%$. This high scatter may be due to the non-uniformity of the attack and possibly due also to segregation in some specimens causing severe local corrosion. The results are expressed graphically in Figs. 2 and 3. The superiority in tensile strength produced by high degrees of cold

reduction was maintained after 12 months' attack in both the unaged and aged conditions. It is clear, however, that there was a general tendency for loss of strength to increase with increasing cold reduction up to about 30%.

7. MICRO-EXAMINATION OF CORRODED SPECIMENS

The specimens for micro-examination were cut from the corroded samples before making the tensile test, in such a way that the polished surface was in the direction of rolling and perpendicular to the rolled surface. Though the surface corrosion was very slight after 28 days' exposure, in some specimens a little intercrystalline corrosion had occurred. After 12 months' exposure the attack had proceeded sufficiently for comparison to be made of the corrosion of the material in different conditions. In the unaged condition slight superficial corrosion with a tendency to intercrystalline attack was observed in the *V*-, *U*-, and *T*-treated specimens of alloy 1 (see Fig. 11, Plate XXXVIII). As a consequence of the elongation of the grains by cold reduction, the direction of the inter-

crystalline cracks formed small angles with the surface in specimens of high cold reduction. No intercrystalline corrosion was detected in alloy 4, but local heavy pits were observed (Fig. 12, Plate XXXVIII). The extent of pitting in alloys 2 and 3 was intermediate between that of alloys 1 and 4. The attack in alloy 2 resembled the intercrystalline attack of alloy 1, while alloy 3 showed a slight tendency to intercrystalline attack and local pits as in alloy 4.

In the aged condition, intercrystalline corrosion was very pronounced in alloy 1 without cold reduction, though only localized, as shown in Fig. 13 (Plate XXXVIII). Similar attack occurred in alloy 2 and to some extent in alloy 3, without cold reduction.

In alloy 4, aged for 28 days at 70° C., similar attack to that in the unaged condition, i.e. pitting without intercrystalline corrosion, was observed. Fig. 14 (Plate XXXVIII) shows severe local pitting in a specimen

stressed in bending and also in direct tension. The solution was not renewed during the test, but distilled water was added daily so that the volume remained constant. During the testing of alloys 1, 2, and 3 little change in the pH of the solution occurred, but during tests of alloy 4 there was a rise of pH. In the bending stress-corrosion test, the specimen, which was $\frac{3}{4}$ in. wide and about 4 in. long, was attached at the lower end to the bottom of a glass tank containing the corroding solution. The upper end of the specimen was attached to a lever at right-angles to the axis of the specimen. This lever was approximately 12 in. long and was so loaded that the desired bending stress could be produced by alteration of an adjustable weight or of the distance of the weight from the axis of the specimen, which was immersed for about two-thirds of its length in the corroding solution. The time for which a specimen resisted a specific

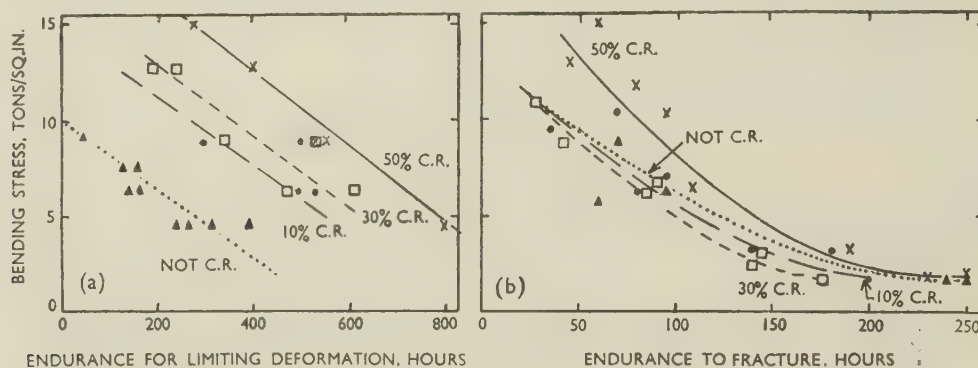


Fig. 4.—Bending Stress-Corrosion Tests on Alloy 1 (a) Unaged and (b) Aged at 70° C.

KEY.

▲ 0% cold work. ● — — — ● 10% cold work. □ — — — □ 30% cold work. × — — — × 50% cold work.

with 5% cold reduction. The type of attack appeared not to be influenced by 5% cold reduction in any of the alloys in the aged condition. After 30% cold reduction and ageing for 28 days at 70° C., intercrystalline corrosion was very pronounced in alloy 1 (Fig. 15, Plate XXXVIII), whereas alloy 4 in the same condition, showed only small pits. After 50% cold reduction and ageing, in addition to intercrystalline corrosion, attack along slip planes was detected in alloys 1, 2, and 3 (Fig. 16, Plate XXXVIII). Alloy 4, after 50% cold reduction and ageing, generally showed local pitting, with a slight tendency to intercrystalline attack in a few areas (Fig. 17, Plate XXXVIII), but no slip-plane attack was detected.

There was no indication of changes in the type or extent of corrosion attack that could be attributed to differences in the *V*, *U*, and *T* heat-treatments of any of the alloys in either the aged or unaged condition, either cold worked or as heat-treated.

8. STRESS-CORROSION TEST RESULTS

Some stress-corrosion tests were made in an accelerated corrosion-testing solution containing 3% sodium chloride and 1.2% hydrochloric acid by weight. The specimens were immersed in the solution and

bending stress was determined, the failure being assessed by fracture of the specimen or by its yielding a certain fixed amount. Yielding was determined by measurement of the deflection of the lever arm at a distance of 12 in. from the top end of the specimen.

For direct tension stress-corrosion tests, a special apparatus was designed in which the specimen was totally immersed in the corroding medium with the exception of the upper end, which was connected to a 20 : 1 lever. The lower end of the specimen was fixed in plastic wedge grips (Perspex) to a support in similar material, which was in turn fixed to the frame of the apparatus. The normal 4-in. strip tensile test-piece was used for the tests.

The results of the tests on specimens stressed in bending showed that the unaged specimens were very resistant to stress-corrosion failure, with the exception of those made from alloy 4, which failed after less than 100 hr. by yielding. Most of the specimens of alloys 1, 2, and 3 did not fail after more than 500 hr., and it was clear that the stress-corrosion properties of the cold-worked material were appreciably superior to those of the material that had been given no cold work in the case of all three alloys. The results of the tests on these three alloys were very

similar, and Fig. 4 (a), which shows graphically the results obtained on alloy 1, is typical. It should be noted that the points on the graph indicate the times at which a certain limit of deformation of the specimens had occurred corresponding to a drop of 100 mm. of the lever ends.

After ageing for 28 days at 70° C., the stress-corrosion properties of alloys 1, 2, and 3 decreased appreciably. In Fig. 4 (b) the results of tests on alloy 1 are shown, and these are typical of those obtained on alloys 2 and 3. The stress-corrosion properties of alloy 4 were scarcely affected by ageing at 70° C.

For alloys 1, 2, and 3 the stress-corrosion curves show that the lowest stress-corrosion-resistance occurred in aged specimens that had been given 30% cold reduction, and the highest stress-corrosion-resistance in specimens that had received 50% cold reduction. This was particularly noticeable in specimens stressed at high stresses.

The stress-corrosion tests in tension confirmed the bending stress-corrosion tests, but failure occurred

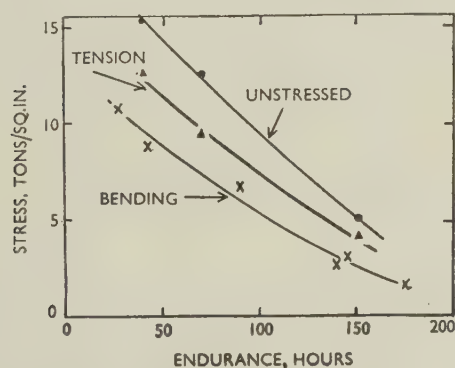


FIG. 5.—Bending and Tension Stress-Corrosion Tests on Alloy 1, Cold Rolled 30% and Aged at 70° C.

more slowly in the direct tension test. This is to be expected, since, as the test-piece cracks, the increase in stress is proportional to the square of the reduction in thickness in the bend test and to the reduction of thickness in the direct tension test. It may be expected, therefore, that bending stresses in service are much more dangerous than tension stresses if they are associated with corrosion attack.

The results of bending and tension stress-corrosion tests on alloy 1 in the aged condition after 30% cold reduction are shown graphically in Fig. 5, together with the results of residual strength tests on unstressed specimens exposed to the same corroding conditions and for the same time as the tension stress-corrosion test-pieces. The same relative positions of the three curves were obtained for all degrees of cold work of alloys 1 to 4 in both the aged and unaged conditions. Micro-examination confirmed that in both bending and tension stress-corrosion tests, specimens that had been given 30% cold reduction suffered much more severe intercrystalline attack in alloys 1, 2, and 3 than specimens that had been less severely cold worked. After 50% cold reduction the

attack occurred along slip planes as well as along grain boundaries, and since the boundaries were orientated parallel to the surface of the sheet, penetration across the section occurred less rapidly.

As regards the corrosion attack on alloy 4, microscopical examination showed that corrosion was in general of the pitting type and usually occurred in bands. This banded attack became less pronounced as the amount of cold work was increased, but even material that had been given 50% cold work was attacked much more rapidly than the alloys 1, 2, and 3.

III.—COMMENTS AND CONCLUSIONS

The results of the investigation have shown that additions of 0-1% zinc to aluminium alloys containing 5% magnesium have very little effect on the mechanical properties. The addition of up to 0.5% zinc has little effect on the corrosion properties, and the microstructure is only slightly affected, although after ageing at 70° C. there is a very slight increase in the amount of precipitate with increasing zinc content. Precipitation on ageing occurs at the grain boundaries and takes the form of an incomplete network. The alloy containing 1% zinc, however, shows pronounced precipitation after ageing at 70° C., and thus corrosion attack of the heat-treated material is increased.

The effect of cold work in general is to promote precipitation during ageing at 70° C. Two effects are evident in the microstructure as the amount of cold work is increased. There is an increased tendency to form a continuous network of precipitation at the grain boundaries with increasing amounts of cold work up to 30%, whilst precipitation along slip bands occurs at higher degrees of cold work.

The most interesting observation made in this investigation is, however, the effect of cold work on the corrosion-resistance of the alloys. Small amounts of cold work reduce the corrosion-resistance appreciably, but heavy cold work, both of aged and unaged material, results in a corrosion-resistance as high as that of material that has not been cold worked. The maximum corrosion attack at about 30% cold reduction can be correlated with continuous grain-boundary films formed on ageing. The increased corrosion-resistance at heavier reductions can probably be associated with a less localized attack due to the heavier and more general precipitation.

The reason for the corrosion behaviour of the unaged alloys is not very clear. It is known that cold work produces a surface in which there are couples at different electrolytic potentials, and it seems that smaller amounts of cold work, up to about 30%, cause increased local attack owing to non-uniformity of cold work. The effect of increasing the amount of cold work still further to 50%, however, results in a more uniformly cold-worked structure. The corrosion attack is therefore much more evenly distributed over the surface and the loss in tensile strength is smaller.

If this variation in degree of cold work were also associated with incipient precipitation of a second phase, the susceptibility to corrosion attack would be still further increased. No evidence for this assumption was found, however.

Comparable behaviour of the material has been found in stress-corrosion tests both in bending and in direct tension. The corroding medium used was very aggressive and bears no relation to the possible behaviour of the material in service conditions, though the results obtained indicate that ageing after 30% cold reduction produces a structure that is more susceptible to stress-corrosion attack than material that has had greater and smaller amounts of cold work.

ACKNOWLEDGEMENTS

This paper is published by kind permission of the Chief Scientist, Ministry of Supply. The authors would like to take this opportunity of thanking their colleagues of the Metallurgy Department of the Royal Aircraft Establishment, Farnborough, for their valuable assistance during the years 1945-47, when the laboratory work was completed. They are also indebted to Mr. E. A. G. Liddiard, M.A., of the Fulmer Research Institute, for helpful suggestions during preparation of the paper and for providing facilities for reproduction.

APPENDIX

Electropolishing and Etching Procedures

The method of electrolytic polishing adopted was a modification of that described by de Sy and Haemers¹¹ in which a perchloric acid-ethyl alcohol solution was used.

The electrolyte, which was placed in a 400-c.c. glass container, consisted of 200 c.c. of absolute alcohol and 40 c.c. of perchloric acid (75%). The cathode was a piece of aluminium sheet about 10 cm. long, bent to a radius of 5 cm., and immersed in the electrolyte to a depth of approximately 5 cm. The specimen formed the anode of the cell, and was placed about 5 cm. from the surface of the cathode. Current was supplied from the 230-V. D.C. mains, and the required voltage (12 V.) was obtained by means of a potentiometer.

Specimens of sheet, approximately 5 cm. long ×

0.5 cm. wide × 0.1 cm. thick, were polished on the cross-sectional surface with emery papers, the last paper used being 00, and the final scratches running longitudinally.

The specimen was immersed in the electrolyte to a depth of about 4 cm. in a vertical position, with the polished surface facing the cathode. The portion of the specimen that projected above the surface of the liquid acted as a contact. Stirring of the electrolyte was not satisfactory, as the edges of the specimen tended to become rounded owing to removal of material at a greater rate in this region. It was found, however, that excellent results were obtained if the specimen was subjected to slight vibration, which was produced by lightly tapping the specimen holder. As a result of the vibration a high and steady current passed through the cell and the potential was maintained at 12 V. by suitable adjustment of the potentiometer. It was necessary to keep the temperature of the electrolyte below 30° C. to ensure satisfactory results.

Normal methods of washing and etching failed to produce a uniformly etched surface, apparently owing to the presence of transparent films. It was found that satisfactory results could be achieved by washing with alcohol immediately after removal from the electrolyte, followed by washing with acetone and then with distilled water, after which the specimen was immediately immersed in the etching solution without having been allowed to dry at any of the intermediate stages.

The most satisfactory etching reagent proved to be one developed by Schulze and Wassermann¹² for etching aluminium-zinc-magnesium alloys. The solution contained 0.5 c.c. 60% HF, 100 c.c. water, 1 c.c. conc. HCl, 10 c.c. conc. HNO₃, 50 c.c. of a 10% solution of K₂Cr₂O₇. This solution deteriorated fairly rapidly when stored in a glass bottle. In order to overcome this difficulty two solutions were made up as follows:

Solution A	Solution B
500 c.c. Water	250 c.c. of 10% solution of
100 c.c. Conc. HNO ₃	K ₂ Cr ₂ O ₇
2.5 c.c. 60% HF	10 c.c. Conc. HCl

Solution A was stored in a suitable waxed bottle and was mixed with an equal volume of solution B as required. All the specimens examined were etched for 60 sec. in this reagent.

REFERENCES

1. P. Brenner and W. Roth, *J. Inst. Metals*, 1948, **74**, 159.
2. E. C. W. Perryman and G. B. Brook, *ibid.*, 1951, **79**, 19.
3. E. C. W. Perryman and S. E. Hadden, *ibid.*, 1950, **77**, 207.
4. G. J. Metcalfe, *ibid.*, 1946, **72**, 487.
5. G. Siebel and H. Vosskühler, *Z. Metallkunde*, 1940, **32**, 298.
6. H. Vosskühler, *Werkstoffe u. Korrosion*, 1950, **1**, 143, 179, 310, 357.
7. W. L. Fink and L. A. Willey, *Trans. Amer. Inst. Min. Met. Eng.*, 1937, **124**, 78.
8. C. S. Barrett and L. H. Levenson, *ibid.*, 1940, **137**, 76.
9. P. Lacombe and L. Beaujard, *Compt. rend.*, 1944, **219**, 66.
10. P. J. E. Forsyth, R. King, G. J. Metcalfe, and B. Chalmers, *Nature*, 1946, **158**, 875.
11. A. de Sy and H. Haemers, *Rev. Mét.*, 1941, **38**, 122.
12. E. Schulze and G. Wassermann, *Z. Metallkunde*, 1940, **32**, 415.

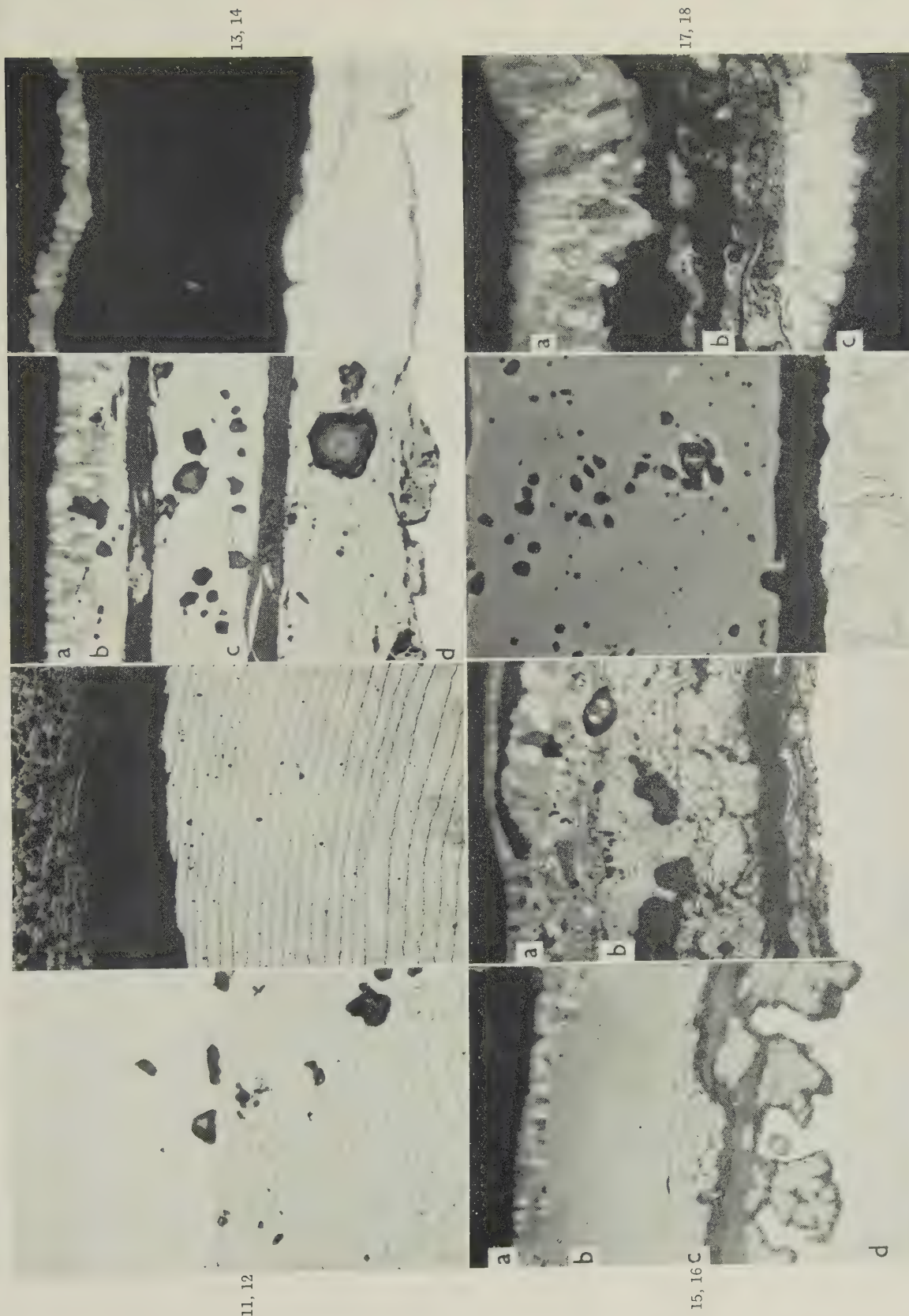


FIG. 13.—Scale on 1% Mg Alloy Oxidized at 800° C. *a*—cupric oxide; *b*—cuprous oxide; *c*—cuprous oxide + magnesia; *d*—metal. Unetched. $\times 300$.

FIG. 14.—Detached Cupric Oxide and Subscale on 2% Si Alloy Oxidized at 550° C. Unetched. $\times 500$.

FIG. 17.—Cuprous Oxide and Appearance of Second Phase in Underlying Metal on 2% Si Alloy Oxidized at 950° C. Unetched. $\times 200$.

FIG. 18.—Detached Scale on 3.5% Si Alloy Oxidized at 650° C. *a*—cupric oxide; *b*—cupric oxide + silica; *c*—cuprous oxide + silica. Unetched. $\times 1000$.

FIG. 11.—Junction Between Duplex Scale and Cuprous Oxide on a 2% Al Alloy Oxidized at 1000° C. Unetched. $\times 500$.

FIG. 12.—“Nessler Ring” Subscale on 1-2% Cr Alloy Oxidized at 1000° C. Etched in ammonia + hydrogen peroxide. $\times 30$.

FIG. 15.—Scale on 2% Si Alloy Oxidized at 750° C. *a*—cupric oxide; *b*—cuprous oxide; *c*—cuprous oxide + silica; *d*—metal. Unetched. $\times 300$.

FIG. 16.—Scale on 2% Si Alloy Oxidized at 800° C. *a*—cupric oxide; *b*—cuprous oxide + silica. Unetched. $\times 300$.

ETCH-PITS IN SUPER-PURITY ALUMINIUM. $\times 750$.

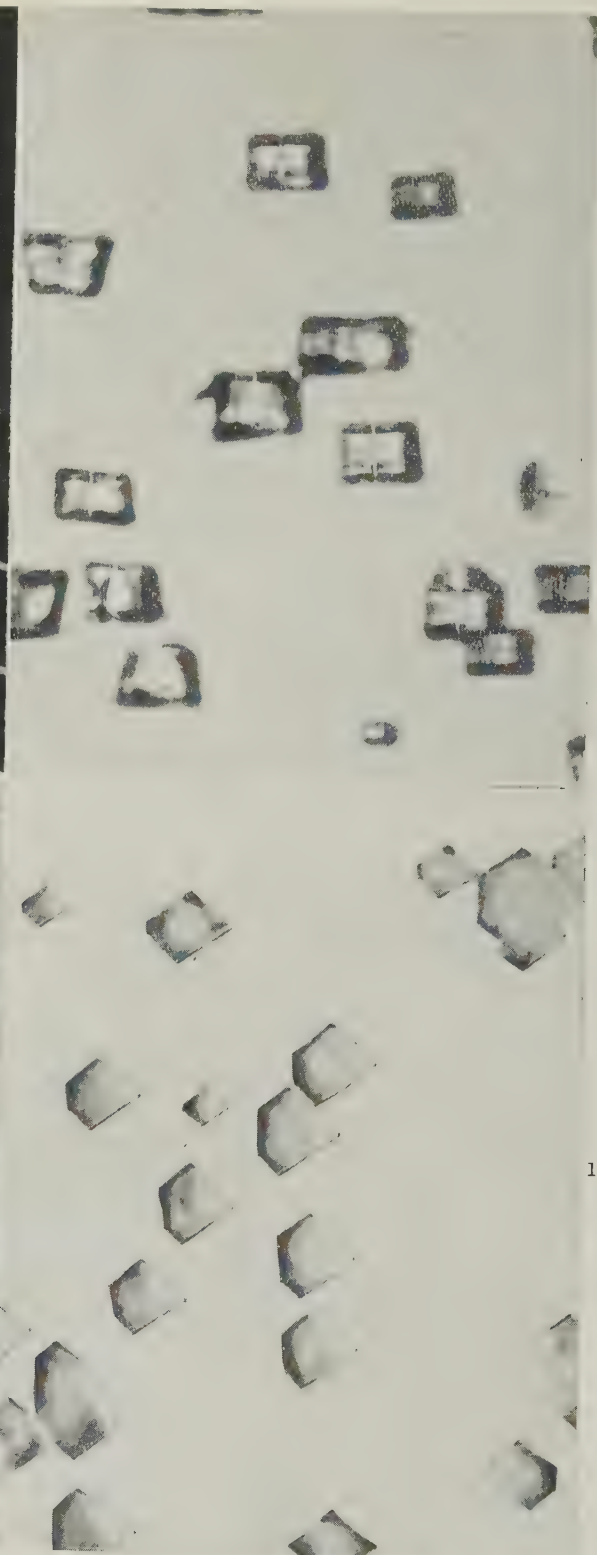
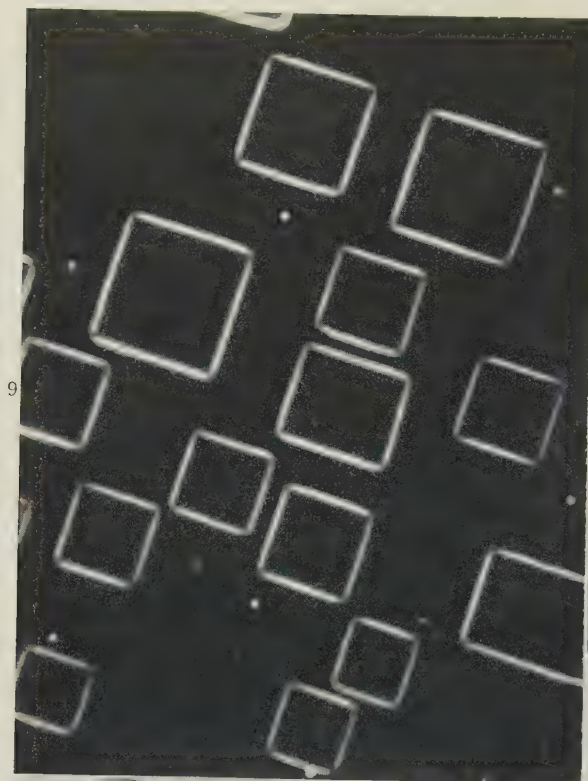
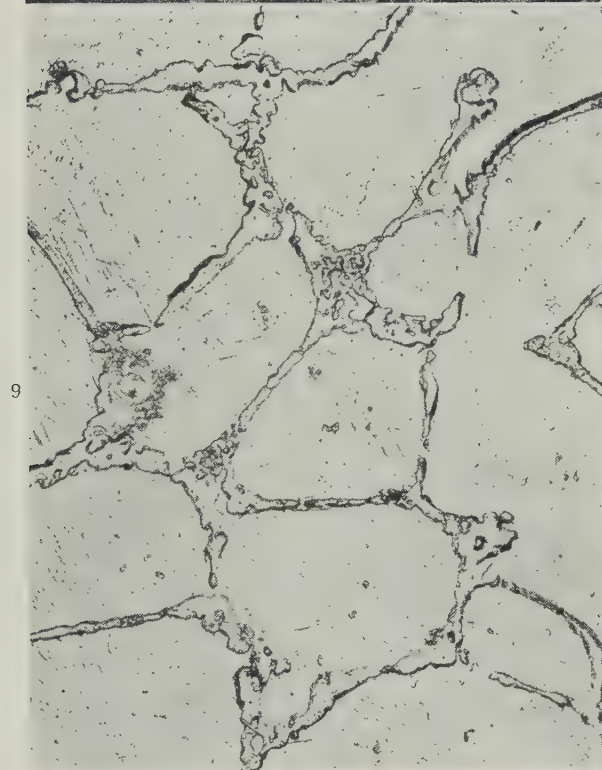
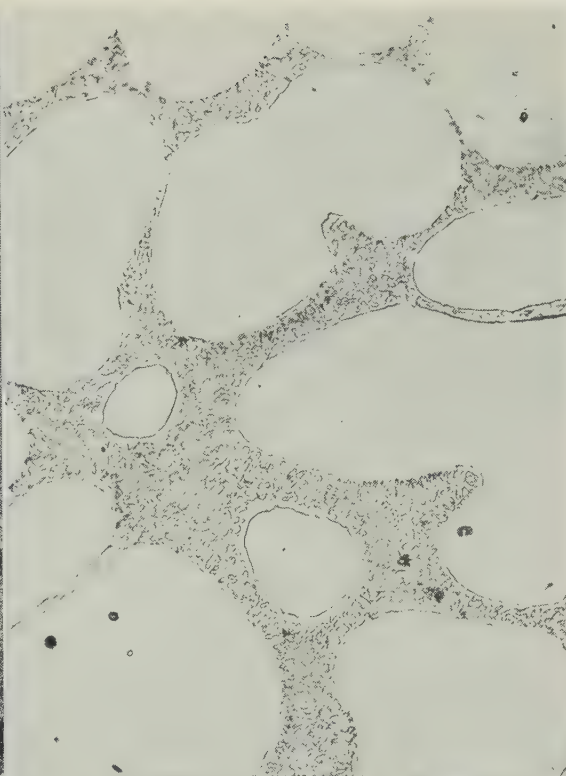
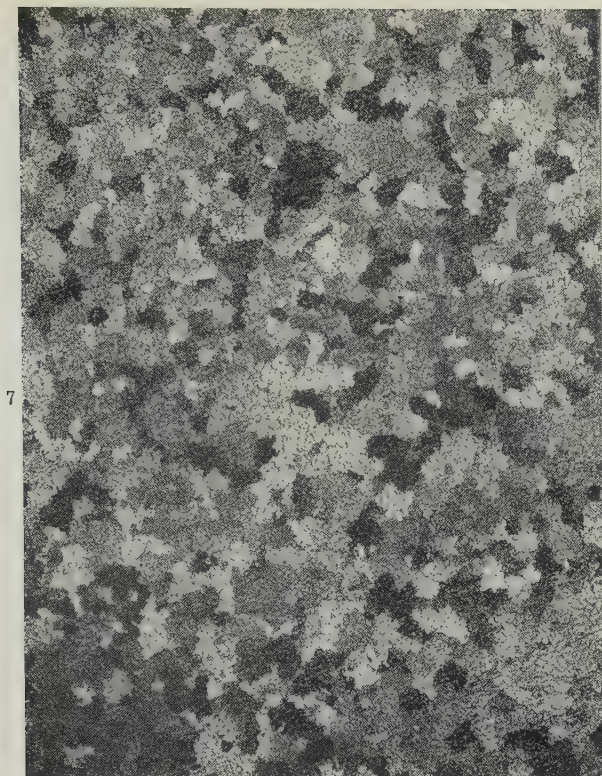


FIG. 9.—(001) Type. Dark-field illumination.
FIG. 11.—(111) Type.

FIG. 10.—(011) Type. Focused on bottom edges of pits.
FIG. 12.—Truncated Triangular Type.



FIGS. 7 and 8.—Alloy X38 (5.95% Cerium), As Cast. $\times 10$ (Fig. 7) and $\times 500$ (Fig. 8).
FIG. 9.—Alloy X32 (5.44% Rare Earths), As Cast. $\times 500$.
FIG. 10.—Alloy X109 (3.07% Rare Earths, 0.43% Zirconium), As Cast. $\times 750$.

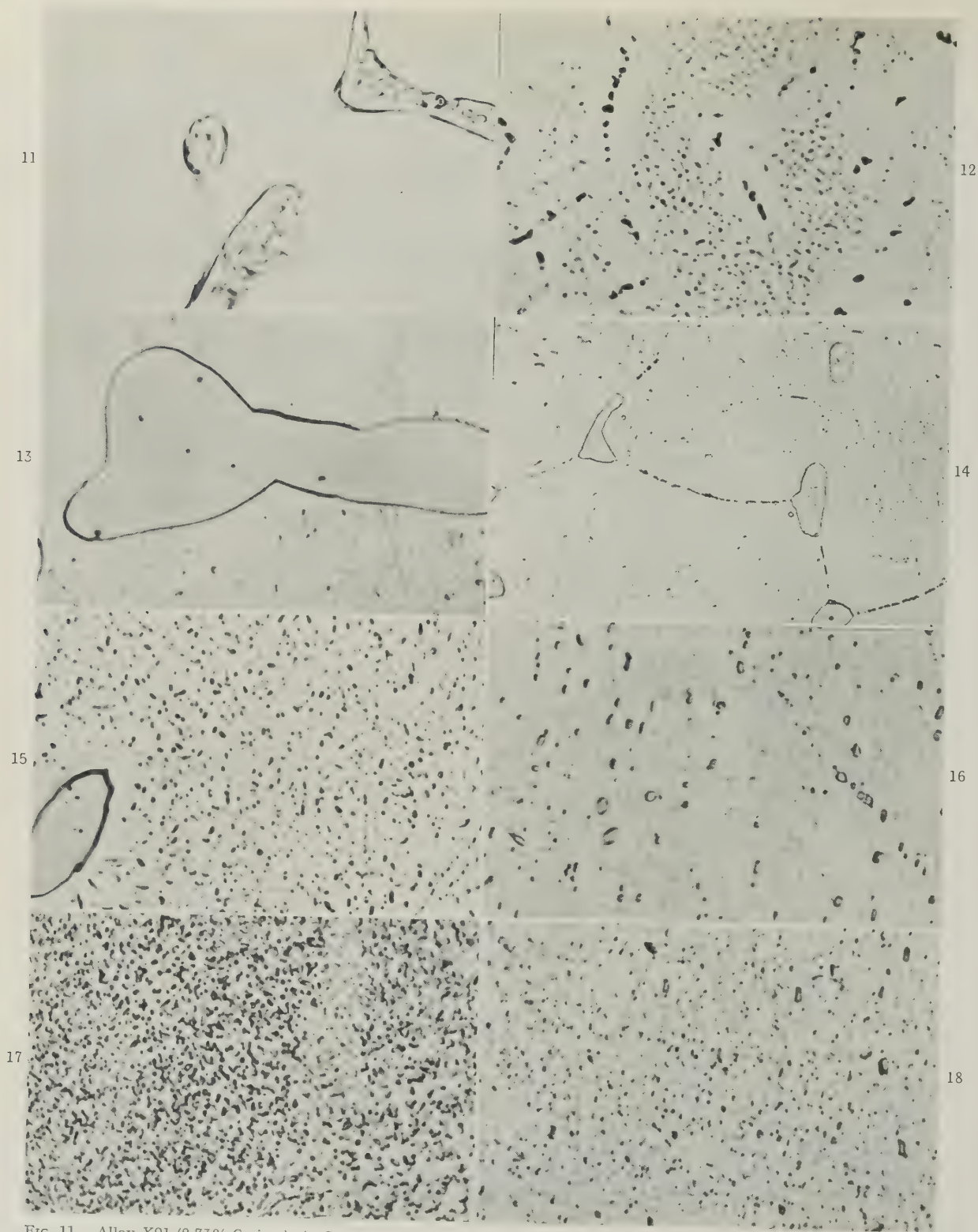


FIG. 11.—Alloy X91 (2.73% Cerium), As Cast. $\times 2000$.

FIGS. 12-14.—Alloy X101 (2.7% Cerium, 1.4% Manganese).

Fig. 12.—As Cast. $\times 2000$.

Fig. 13.—Cast, 24 Hr. at 580°C ., Water-Quenched. $\times 2000$.

Fig. 14.—As Fig. 13 and Aged 7 Days at 350°C . $\times 500$.

FIGS. 15 and 16.—Alloy X91 (2.73% Cerium), Cast, 24 Hr. at 580°C ., Water-Quenched. Aged 7 Days at 300°C . (Fig. 15) or at 350°C . (Fig. 16). $\times 2000$.

FIGS. 17 and 18.—Alloy X101 (2.7% Cerium, 1.4% Manganese), Cast, 24 Hr. at 580°C ., Water-Quenched. Aged 7 Days at 300°C . (Fig. 17) or at 350°C . (Fig. 18). $\times 2000$.

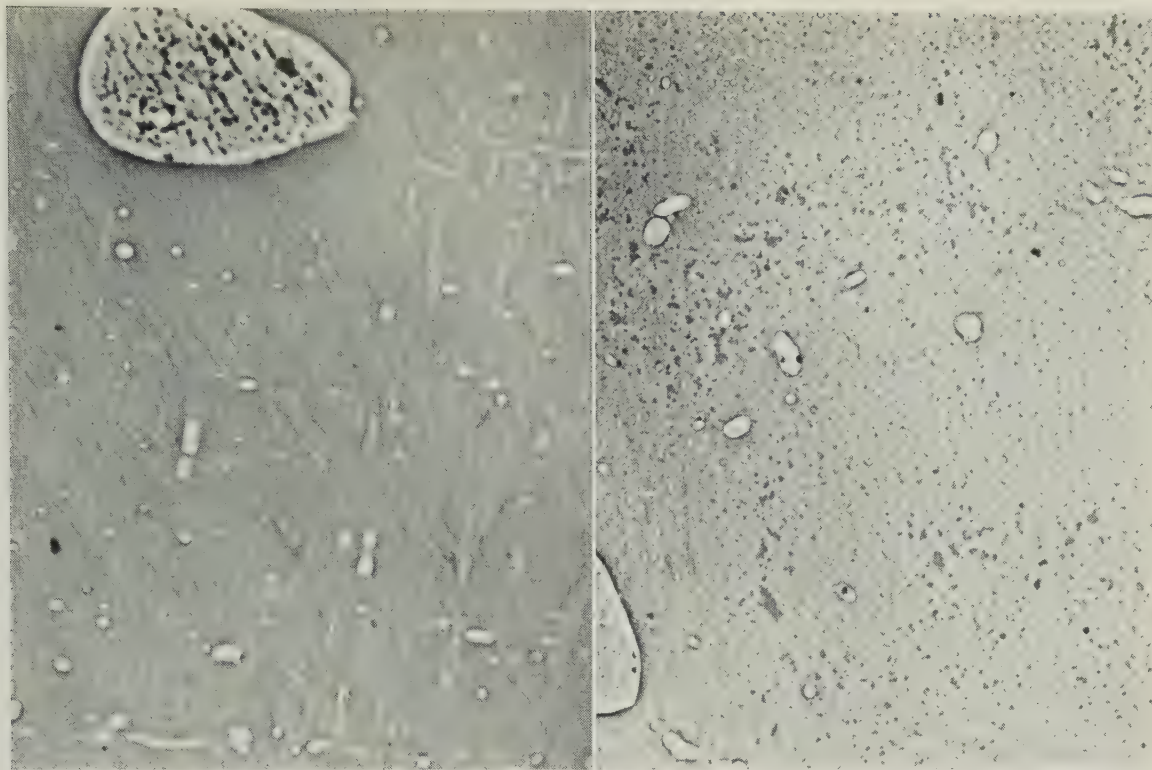


FIG. 19.—Electron Micrograph of Same Alloy as Fig. 16.
× 2500.

FIG. 20.—Electron Micrograph of Same Alloy as Fig. 18.
× 2500.



FIG. 21.—Alloy X64 (6.14% Rare Earths, 1.54% Manganese),
Rolled, 24 Hr. at 580° C., Water-Quenched. Tested at
300° C., 1 ton/in.² for 3660 hr. Centre of parallel portion.
× 2000.



FIG. 4.—Pb-0.85% Sb Alloy Air-Cooled after Extrusion at 300° C. Slight discontinuous precipitation at grain boundaries, although no continuous precipitation within the grains. $\times 300$.



FIG. 5.—Pb-0.85% Sb Alloy Air-Cooled after Extrusion at 160° C. and Aged at 20° C. for 12,000 Hr. Continuous precipitation within grains. $\times 300$.

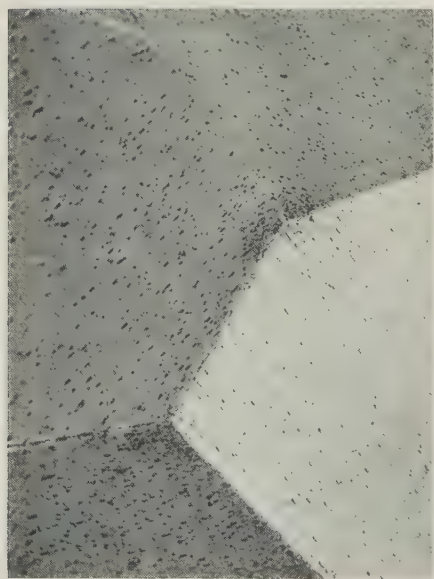


FIG. 6.—Pb-0.85% Sb Alloy Solution-Treated at 300° C., Water-Quenched and Aged 120 Hr. at 50° C. Slight continuous precipitation within grains; mainly in form of widely distributed needles. $\times 300$.

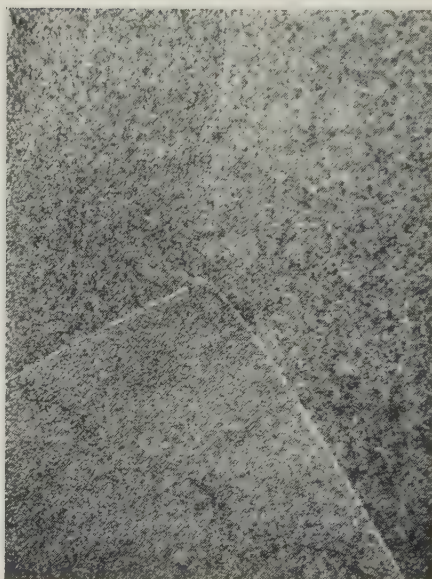


FIG. 7.—Pb-0.85% Sb-0.001% As Ternary Alloy Solution-Treated at 300° C., Water-Quenched and Aged 120 Hr. at 50° C. Extensive continuous precipitation within grains; precipitate is globular. $\times 300$.

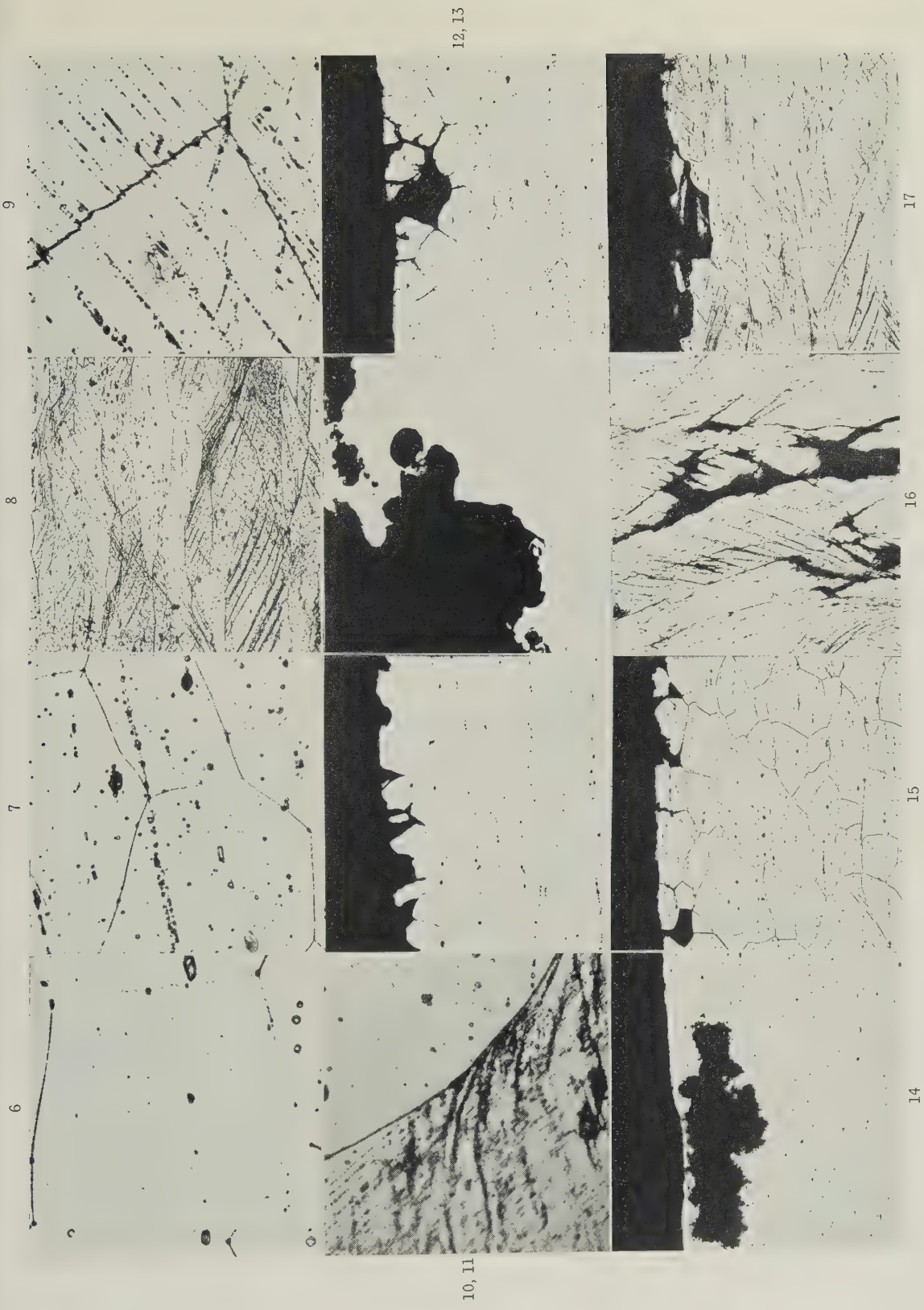


FIG. 6.—Alloy 1, Aged at 70° C., Showing Incomplete Grain-Boundary Network of Precipitate. $\times 1000$.
FIG. 7.—Alloy 1, Cold Rolled 20% and Aged at 70° C., Showing an Almost Complete Grain-Boundary Network of Precipitate. $\times 500$.
FIG. 10.—Alloy 4, Cold Rolled 30% and Aged at 70° C., Showing Precipitation and Distortion of Slip Planes near Grain Boundary. $\times 1000$.
FIG. 11.—Alloy 1, Not Aged, Exposed 12 Months, Showing Tendency to Inter-crystalline Corrosion. $\times 100$.
FIG. 14.—Alloy 4, Cold Rolled 5% and Aged at 70° C., Showing Severe Local Pitting. $\times 100$.
FIG. 15.—Alloy 1, Cold Rolled 30% and Aged at 70° C., Etched, Showing Inter-crystalline Corrosion. $\times 100$.
FIG. 8.—Alloy 4, Cold Rolled 50% and Aged at 70° C., Showing Heavy Precipitation Within Grains. $\times 100$.
FIG. 9.—Alloy 4, Cold Rolled 30% and Aged at 70° C., Showing Distortion of Grain Boundary Where Slip Planes Cross It. $\times 1000$.
FIG. 12.—Alloy 4, Not Aged, Exposed 12 Months, Showing Heavy Pitting. $\times 100$.
FIG. 13.—Alloy 1, Aged at 70° C., Exposed 12 Months, Showing Inter-crystalline Corrosion. $\times 100$.
FIG. 16.—Alloy 1, Cold Rolled 50% and Aged at 70° C., Showing Corrosion Attack Along Slip Planes. $\times 100$.
FIG. 17.—Alloy 4, Cold Rolled 50% and Aged at 70° C., Showing Local Pitting With Slight Tendency to Inter-crystalline Corrosion. $\times 100$.

ATMOSPHERIC CORROSION AND STRESS-CORROSION OF ALUMINIUM-COPPER-MAGNESIUM AND ALUMINIUM-MAGNESIUM-SILICON ALLOYS IN THE FULLY HEAT-TREATED CONDITION *

1442

By G. J. METCALFE,† M.Sc.Tech., MEMBER

SYNOPSIS

The corrosion behaviour of the aluminium alloys H10-WP and H15-WP in the extruded form has been determined in the stressed and unstressed condition by exposure to sea-water, river water, and various natural atmospheres. The corrosion attack was assessed by visual and microscopical examination and by tensile tests on the corroded material. The most severe attack of both alloys resulted from exposure to the industrial atmosphere of Sheffield, where the average loss of strength after 2 years' exposure was approximately 11%, which is equivalent to a loss of thickness of 0.012 in. There was no indication of stress-corrosion failure of either of the alloys at any of the exposure sites. The high stress-corrosion resistance of the H15-WP alloy is somewhat surprising, since in sheet form the alloy is known to be very susceptible to stress-corrosion failure. The absence of such failure is attributed to preferential attack ("foliation") occurring along grain boundaries and bands parallel to the direction of extrusion which redistributes the concentration of stress at corrosion pits. The rate of loss of strength of both alloys exposed at Sheffield, and of H15-WP alloy exposed to a marine atmosphere, was found to decrease with time, apparently exponentially. Scatter of the results from the remaining sites was appreciable, but it was clear that in general there was a decrease in the rate of corrosion with time.

I.—INTRODUCTION

IN order to assess the corrosion behaviour of the aluminium alloys H15-WP and H10-WP in the extruded form when exposed to atmospheric corrosion and to corrosion by salt water and river water, a series of field tests were begun at different stations throughout the country.

Most workers agree that in the early stages of film formation the corrosion/time curve is a logarithmic curve, the rate of corrosion decreasing with time. Early investigation was confined to work on aluminium of varying degrees of purity, using different indices of corrosion. Bryan¹ and Morris² determined the loss in weight during corrosion, and Champion³ measured the quantity of gas evolved. Vernon,⁴ on the other hand, determined the increase in weight in his study of films formed in air on aluminium. Guilhaudis,⁵ in very recent work, has determined the ultimate tensile strength and elongation of corroded aluminium-5% magnesium alloy and Duralumin exposed to marine conditions.

Champion,⁶ in considering the results of his work together with work by other investigators, has suggested that the corrosion/time curve is exponential. He further maintains that, in studying the results of field tests, the corrosion/time curves may be considered to follow an exponential relationship, although there may be an induction period during which no

corrosion is observed. This point is illustrated by drawing curves plotted from the average results obtained by other investigators who measured the corrosion effect by determining loss in weight, loss in ultimate tensile strength, loss in elongation, &c. These corrosion/time curves are asymptotic to a limiting value, so that any increase in metal thickness beyond a certain minimum, which corresponds to this limiting corrosion value, may be expected to ensure that the material will never fail by whatever parameter the corrosion is being measured, i.e. loss in strength, pitting, &c.

It is possible to calculate this minimum thickness, and Champion⁷ has shown, by taking as an example the corrosion of 17S-T alloy (exposed at La Jolla (California) in field tests of the American Society for Testing Materials⁸) that the residual strength of the material will not fall below that of the original 0.1% proof stress if the thickness is 0.055 in. If, therefore, a safety factor of 2 is adopted arbitrarily, the minimum thickness that should be used for structural purposes at La Jolla would be 0.11 in. Champion has, however, made no firm recommendations as to the safety factor that should be adopted to allow for variations in conditions and for scatter in results on individual specimens.

In the present investigation it was hoped that, by the examination of specimens at suitable intervals, enough information could be obtained in a com-

* Manuscript received 20 October 1952.

† Senior Research Metallurgist, Precious Metals Division,

The Mond Nickel Co., Ltd., Acton; formerly at the Fulmer Research Institute, Stoke Poges, Bucks.

paratively short time to allow a confident forecast to be made of the probable behaviour of H15-WP and H10-WP alloys in a variety of service conditions. The effect of stress acting in conjunction with corrosion by the exposure of specimens stressed by bending under constant strain in special jigs was also investigated. Most of the material used was similar, both as regards composition and heat-treatment, to that normally used in production.

In the present paper the average tensile-test results obtained at intervals during 2 years' exposure, are summarized graphically and in tables. Detailed results of the visual and microscopical examination and tensile testing have been deposited in the library of the Institute, and may be consulted there.

II.—EXPERIMENTAL DETAILS

1. MATERIAL

Channel-section extrusions were made from normal batches of H10-WP and H15-WP alloy billets. The sections were $1\frac{1}{4} \times 1 \times 1$ in. and were 0.1 in. thick. The extrusions were made by the normal production method, the H10-WP alloy extrusions being die-quenched and the H15-WP alloy extrusions being quenched after solution heat-treatment. After quenching the extrusions were straightened by stretching, the amount of stretching usually being of the order of 3%, although this figure may have varied between 1 and 8% in practice. Lengths were cut as required and were subjected to the appropriate ageing treatment. Chemical analysis of the extrusions gave the following results:

	Cu, %	Mg, %	Mn, %	Si, %	Fe, %	Ti, %
H10-WP . . .	0.04	0.68	0.04	0.98	0.27	...
	max.					
H15-WP . . .	3.81	0.74	0.54	0.95	0.25	0.02

The ageing treatments used for the field test-specimens were 8 hr. at 175° C. for H10-WP and 8 hr. at 170° C. for H15-WP.

2. EXPOSURE SITES AND METHOD OF EXPOSURE

Sites for the tests were chosen in different parts of the country, so that the behaviour of materials in different atmospheric environments could be assessed. Stressed, as well as unstressed specimens, were exposed in frames at each of these sites. The method of stressing was by 4-point loading, so that the middle 7 in. of the test-piece, which was $\frac{3}{4}$ in. wide and 12 in. long, was stressed in uniform bending at constant strain. Two stresses were used for each material. (i) An arbitrarily chosen design stress: 5.1 tons/in.² for H10-WP and 16 tons/in.² for H15-WP alloy, and (ii) the 0.1% proof stress: 15 tons/in.² for H10-WP and 24 tons/in.² for H15-WP alloy. Fig. 1 (Plate XXXIX) shows one of the frames with specimens in position.

Pieces of channel-section extrusion cut from the same lengths of extrusion as those from which the stressed specimens had been cut, were attached to the

stress-corrosion frames and were removed for examination and testing at the same time as the stressed test-pieces.

The nature and location of the sites and the visual appearance of the specimens were as follows:

Site No. I. Severe Industrial Atmosphere.—The British Iron and Steel Research Association's exposure site at the Brown-Firth Research Laboratories, Princess Street, Sheffield.

This site is by the side of a very busy railway siding, and the atmosphere is charged with soot and sulphurous fumes from burning coke, coal, and neighbouring steel-furnace plant. The frames were placed in a horizontal position on stands about 2 ft. 6 in. from the ground; the specimens rapidly became coated with soot and particles of solid matter from the steel-furnace smoke.

Site No. II. Normal Industrial Atmosphere.—The British Non-Ferrous Metals Research Association site on the roof of their building in Euston Street, London.

The frames were placed in a horizontal position on the flat roof of the building, which is only a short distance from Euston main-line railway station. The environment is typical of a normal industrial locality with smoke from factory and household chimneys polluting the atmosphere. The specimens gradually became coated with a fine deposit of soot.

Site No. III. Marine Atmosphere.—An Admiralty raft off Hayling Island in Chichester harbour (by arrangement with the Central Metallurgical Laboratory).

The specimens were exposed to the sea-water spray swept up to them by wind and, in heavy weather, to waves breaking over the raft on which the frames were fixed. The frames were in a vertical position attached to supports on the raft about 7 ft. above water level, and the raft was moored a short distance off-shore. The specimens soon became coated with a deposit of sea-salt and a certain amount of corrosion product.

Site No. IV. Rural Atmosphere.—Fulmer Research Institute, Stoke Poges, Bucks.

The site is in an open field in a rural district about 2½ miles north of Slough. The frames were supported in a horizontal position about 6 in. above the ground. The specimens showed little evidence of corrosion over a very long period, apart from a slight darkening in colour.

Site No. V. Total Immersion in Sea-Water.—Admiralty raft off Hayling Island in Chichester harbour (by arrangement with the Central Metallurgical Laboratory).

The frames were supported on jigs in a vertical position on the raft used at Site No. III. The raft was bottomless, and the frames were immersed in

sea-water to a depth of about 3 ft. The specimens became covered rapidly with fouling.

Site No. VI. Tidal Immersion in Sea-Water.—The Central Metallurgical Laboratory's site at Hayling Island.

This site is at half-tide level at Hayling Island. The frames were fixed in a vertical position and were completely immersed at high tide and completely free at low tide. Owing to the severe battering by waves in heavy weather the specimens were easily damaged.

Site No. VII. Total Immersion in Fresh Water.—River site at the Military Engineering Experimental Establishment, Christchurch, Hants.

The River Stour at Christchurch is tidal, and the frames of specimens were totally immersed in the river in a vertical position. Normally the frames were about 4 ft. below the surface, just clear of the river-bed, but owing to changes in current, &c., they were frequently buried in river mud. The specimens soon became coated with an organic film, possibly from sewage that is emptied into the river.

Site No. VIII. Tidal Immersion in Fresh Water.—River site at the Military Engineering Experimental Establishment, Christchurch, Hants.

By placing the frames in a horizontal position under a concrete pier, it was possible to subject the specimens to tidal immersion during normal and dry weather conditions. When flooding occurred, however, the frames were frequently totally immersed for several days at a time. The specimens became coated rapidly with a film of mud.

Site No. IX. Tidal Immersion in Sea-Water.—British Railways Docks, Southampton.

The frames were fixed at half-tide level under a concrete pier in one of the docks. The sea-water was contaminated with oil and bilge water from passing ships, and a greasy film soon formed on the specimens.

III.—RESULTS OF FIELD TESTS AFTER TWO YEARS' EXPOSURE

1. GENERAL DETAILS OF TESTS

Specimens were removed from the sites for examination at intervals, but, owing to heavy storms and possibly to removal by unauthorized persons, specimens exposed at the tidal site on Hayling Island (Site VI) were missing at the end of 2 years' exposure. No results are available, therefore, after 2 years' exposure at this site. The corroded specimens were visually examined and subjected to tensile tests, a 4-in. test-piece cut from mid-way between the centre supports being used for determining the residual strength of the material. The remainder of the stressed portion of the exposed specimen was subjected to microscopical examination.

Tensile tests were also made on test-pieces cut from

the web and flanges of pieces of unstressed channel-section which had been exposed to the same corroding conditions. Control tests were made on test-pieces cut from material from the same batch which had been stored in the laboratory and tested at the same time as the corroded test-pieces.

2. VISUAL EXAMINATION

After each period of exposure the specimens were visually examined. Detailed results are summarized for the different sites in Appendix I (p. 276). The conditions of exposure varied appreciably from one site to another, and it seemed that the heavy industrial atmosphere of Sheffield had an even more serious effect on the corrosion-resistance of the material than the marine atmosphere. The corrosion attack on totally immersed or intermittently immersed specimens was usually confined to isolated spots. This may have been due to local effects such as deposition of cathodic particles on the surface, or to local breakdown of a protective film. The high resistance of the material to immersion in sea-water seems to have been due to protection by marine growth, and, in the case of specimens exposed at Southampton Docks, also to the deposition of a thin film of oil.

3. MICROSCOPICAL EXAMINATION

From each corroded test-piece a specimen approximately $\frac{1}{2}$ in. long was removed and sectioned longitudinally for microscopical examination at a magnification of 100. The method of assessment and description of the corrosion damage are given in Appendix II (p. 277).

Microscopical examination has shown that the corrosion attack of the H10-WP alloy is usually of the intercrystalline type and varies in intensity to an appreciable extent from site to site. The most severe attack was at Sheffield (Site I), and after 2 years it was fairly general. Fig. 2 (Plate XXXIX) shows typical attack after this period. At Euston (Site II), which is semi-industrial, the corrosion was much less severe, as shown in Fig. 3 (Plate XXXIX), and at the marine-atmosphere site off Hayling Island (Site III), the attack was somewhere between that experienced at Sheffield and that at London. Fig. 4 (Plate XXXIX) shows typical attack on exposure to a marine atmosphere. The remaining atmospheric-exposure site, i.e. the rural atmosphere at Stoke Poges (Site IV), caused very slight intercrystalline corrosion at isolated spots, as shown in Fig. 5 (Plate XXXIX). In the total-immersion tests on the H10-WP alloy at Christchurch (Site VII) the attack (see Fig. 6, Plate XXXIX) was fairly severe at isolated spots and in some instances penetrated the thickness of the specimens. In spite of this, however, the results of tensile tests, which are described in the next section (p. 273), show that the residual strength after 2 years' exposure ranged from 13.4 to 18.9 tons/in.² and the average loss in strength was only 1.3 tons/in.². Total immersion in sea-water off Hayling Island (Site V)

caused much less severe attack. The results of tidal immersion at Christchurch (Site VIII) showed negligible attack after 2 years' exposure. At Southampton Docks (Site IX), where the specimens were exposed under a concrete pier at half-tide level, isolated spots of intercrystalline attack had occurred.

As judged by visual and microscopical examination, the corrosion of H15-WP alloy was more severe, in general, than that of H10-WP. The attack was frequently of the foliation type accompanied by intercrystalline corrosion which, however, was preferentially orientated longitudinally parallel to the direction of extrusion. Intercrystalline corrosion of the longitudinal type appeared to start first and was followed by foliation of the surface layers. In some cases where attack of the sub-grain boundaries started, the foliation was much more severe. Corrosion attack was most severe at Sheffield (Site I) as illustrated in Fig. 7 (Plate XL). Attack of the sub-grain network is shown in Fig. 8 (Plate XL). At Site II (Euston) the attack was of the same type, though much less severe (Fig. 9, Plate XL), and that at Hayling Island (Site III) (Fig. 10, Plate XL), was intermediate between that at Sheffield and at

TABLE I.—Average Tensile Strength and Loss in Strength of H10-WP Alloy Specimens Exposed at Various Sites.

Original U.T.S. = 18.8 tons/in.² (average of 9 tests).

Site	Property	Exposure Time, months				
		1	3	6	12	24
I	U.T.S., ton/in. ²	18.4	17.9	17.7	16.7	16.8
	Loss in strength, ton/in. ²	0.4	0.9	1.1	2.1	2.0
II	U.T.S., ton/in. ²	18.2	18.7	18.5	17.8	17.6
	Loss in strength, ton/in. ²	0.6	0.1	0.3	1.0	1.2
III	U.T.S., ton/in. ²	18.9	18.7	18.6	18.2	17.6
	Loss in strength, ton/in. ²	—0.1	0.1	0.2	0.6	1.2
IV	U.T.S., ton/in. ²	18.6	18.7	19.0	18.4	18.5
	Loss in strength, ton/in. ²	0.2	0.1	—0.2	0.4	0.3
V	U.T.S., ton/in. ²	18.6	18.9	18.2	18.3	17.4
	Loss in strength, ton/in. ²	0.2	—0.1	0.6	0.5	1.4
VI	U.T.S., ton/in. ²	18.6	19.1	18.6	18.4	} No results
	Loss in strength, ton/in. ²	0.2	—0.3	0.2	0.4	
VII	U.T.S., ton/in. ²	18.7	18.4	18.2	16.7	17.5
	Loss in strength, ton/in. ²	0.1	0.4	0.6	2.1	1.3
VIII	U.T.S., ton/in. ²	18.4	18.0	18.3	18.2	18.1
	Loss in strength, ton/in. ²	0.4	0.8	(8)* 0.5	0.6	0.7
IX	U.T.S., ton/in. ²	18.6	18.8	19.2	17.7	18.6 (8)*
	Loss in strength, ton/in. ²	0.2	0	—0.4	1.1	0.2

TABLE II.—Average Tensile Strength and Loss in Strength of H15-WP Alloy Specimens Exposed at Various Sites.

Original U.T.S. = 31.2 tons/in.² (average of 9 tests).

Site	Properties	Exposure Time, months				
		1	3	6	12	24
I	U.T.S., ton/in. ²	30.7	29.7	28.9	27.8	27.5
	Loss in strength, ton/in. ²	0.5	1.5	2.3	3.4	3.7
II	U.T.S., ton/in. ²	30.0	30.4	29.9	29.4	29.8
	Loss in strength, ton/in. ²	1.2	0.7	1.3	1.8	1.4
III	U.T.S., ton/in. ²	30.5	30.1	29.7	29.0	28.3 *
	Loss in strength, ton/in. ²	0.7	1.1	1.5	2.2	2.9
IV	U.T.S., ton/in. ²	31.2	31.3	31.5	30.2	30.0
	Loss in strength, ton/in. ²	0	—0.1	—0.3	1.0	1.2
V	U.T.S., ton/in. ²	30.4	30.7	30.4	30.7	30.3 (6) *
	Loss in strength, ton/in. ²	0.8	0.5	0.8	0.5	0.9
VI	U.T.S., ton/in. ²	29.9	30.0	29.3	29.5	} Specimens lost
	Loss in strength, ton/in. ²	1.3	1.2	1.9	1.7	
VII	U.T.S., ton/in. ²	30.6	30.6	30.3	29.3	30.0
	Loss in strength, ton/in. ²	0.6	0.6	0.9	1.9	1.2
VIII	U.T.S., ton/in. ²	30.4	29.5	29.5	29.2	30.5
	Loss in strength, ton/in. ²	0.8	1.7	1.7	2.0	0.7

* All U.T.S. values, except where indicated, are the average of 9 tensile tests, 3 of which were stressed at design stress, 3 at 0.1% proof stress, and 3 unstressed during exposure to various environments.

London. Fig. 11 (Plate XL) shows typical attack of the sub-grain network. The foliation type of attack on the H15-WP alloy was obvious by eye only after the specimens had been exposed for more than 1 year, and in some specimens it was marked at some points which would not necessarily form part of the tensile test-piece machined from the specimen. In one case an exceptionally low tensile-test result was obtained (20.3 tons/in.²), which was associated with foliation. No obvious attack was observed in the total-immersion tests at Hayling Island (Site V) and at Christchurch (Site VII) only isolated spots of longitudinal intercrystalline corrosion were present after 2 years' total immersion. The attack was even less severe in the intermittent-immersion tests at Christchurch (Site VIII), though at the isolated spots where attack occurred, cavities such as those shown in Fig. 12 (Plate XL) were observed.

The result of a much more severe form of foliation attack than that observed in any of the specimens examined is shown in Fig. 13 (Plate XL), which is a photomicrograph of a section of H15-WP alloy extrusion from part of an aluminium alloy frame that had been used for carrying a brine tank.

The high corrosion-resistance of the specimens exposed to tidal immersion at Christchurch (Site VIII) was surprising in view of the comparatively severe local attack at isolated spots on the specimens totally immersed in the river. This was the case with both alloys.

The results of total-immersion tests off Hayling Island (Site V) were also very satisfactory from the point of view of resistance to corrosion attack. This may again have been due to protection by marine growth which rapidly covered both specimens and frames. It is interesting to note that marine growths appear to protect aluminium rather than to accelerate attack.

At Southampton (Site IX), where only specimens of H10-WP alloy were exposed, there was frequently

of elongation was also unaffected by stress during corrosion.

The lack of susceptibility of the extruded specimens of H15-WP alloy to stress-corrosion is almost certainly due to structural inhomogeneities in this material, which give rise to planes of preferential corrosive attack parallel to the surfaces of the extrusion. Any corrosion pits and fissures which start from the surface fail to exert any stress-raising effect, since they are turned parallel to the surface and to the direction of stressing along these planes of inhomogeneity.

In practice, it is difficult to stress an extrusion in any direction which is not parallel to some of the planes of these inhomogeneities, so that in most cases these observations have an important practical significance in considering stress-corrosion susceptibility.

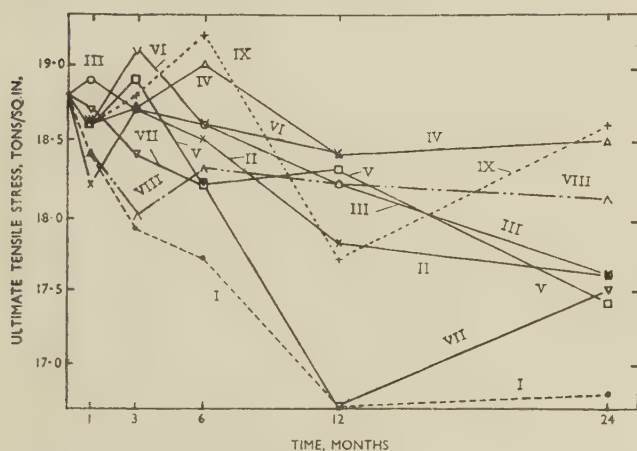


FIG. 14.—Average Tensile Strength of H10-WP Alloy Specimens Exposed at Various Sites.

- Site I. Atmosphere at Sheffield.
- × Site II. Atmosphere at London.
- Site III. Atmosphere at Hayling Island.
- △ Site IV. Atmosphere at Stoke Poges.
- Site V. Total Sea-Water Immersion at Hayling Island.

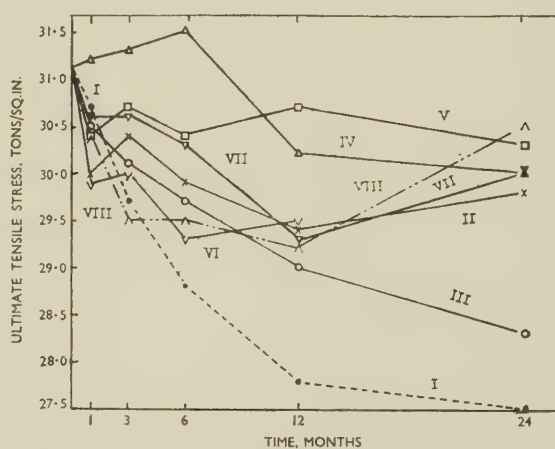


FIG. 15.—Average Tensile Strength of H15-WP Alloy Specimens Exposed at Various Sites.

KEY.

- ▽ Site VI. Tidal Sea-Water Immersion at Hayling Island.
- △ Site VII. Total Fresh-Water Immersion at Christchurch.
- ▽ Site VIII. Intermittent Fresh-Water Immersion at Christchurch.
- + Site IX. Tidal Sea-Water Immersion at Southampton.

a deposit of grease on the specimens which came from the oil effluent of passing ships. Such deposits appeared to protect the specimens, and although it is re-assuring to find that marine growths and oil deposits protect rather than accelerate attack, it would be wise to design on the assumption that such protective agents did not operate, since they may not invariably occur in practice.

4. TENSILE TESTS

Perhaps the most striking feature of the results of these tests was the absence of any effect of stress on the rate of corrosion damage on either of the materials. This is particularly surprising in the H15-WP material, which in sheet form is known to be susceptible to stress-corrosion. In general, the residual strength of the unstressed corroded material was similar to that of specimens stressed at the design stress or the 0.1% proof stress. The rate of loss

However, when extrusions are machined it may be possible to stress normal to these planes, in which case rapid failure as a result of stress and corrosion may occur. This aspect is being further investigated in the laboratory, together with the effects of heat-treatment.

Since it was clear from the results of these tests that stress had a negligible effect on corrosion damage, as judged by the residual strength of the corroded specimens, it was decided to determine the average residual strength of stressed and unstressed specimens and to use this average value (i.e. the average of 9 tests) when considering the corrosion behaviour of the material after different periods of exposure. These average values are summarized in Tables I and II, and are expressed graphically in Figs. 14 and 15. From these graphs it is clear that:

(i) The Sheffield atmosphere (Site I) caused the greatest deterioration in the properties of both alloys.

(ii) The percentage loss of strength is approximately the same for both alloys, i.e. about 12%, although, as shown graphically, the loss in tensile strength of H15-WP is usually greater than that of H10-WP.

(iii) In both alloys the atmospheric-exposure sites seem to have the greatest adverse effect apart from the rural site at the Fulmer Research Institute (Site IV) where the attack during 2 years had negligible effect on the mechanical properties.

(iv) The results of total-immersion tests at Hayling Island (Site V) show very little loss of strength, but at Christchurch (Site VII) the scatter is appreciable, owing apparently to more severe local attack.

(v) It seems that in the tidal-immersion tests at Southampton Docks (Site IX) a certain amount of protection was afforded by the oil effluent from ships.

(vi) The intermittent immersion tests at Christchurch (Site VIII) have given fairly satisfactory results,

times as much damage as another). The maximum damage of the H15-WP specimens was associated with severe local foliation which did not start until after 12 months' exposure and appeared to indicate a new type of attack, the incidence of which was much delayed and appeared to be progressing rapidly. In view of this it is not considered that the exponential type of curve can be applied directly to the design of structures exposed to atmospheric corrosion. From the test results on both materials from the remaining sites, smooth curves could not be drawn owing to scatter in the results, even taking average figures, but the corrosion damage was small and showed a tendency to occur at a decreasing rate with time. The scatter in the original ultimate tensile strength of uncorroded H15-WP alloy, in particular, was about ± 2.5 tons/in.², which would tend to mask the corrosion effect, particularly after short periods of exposure.

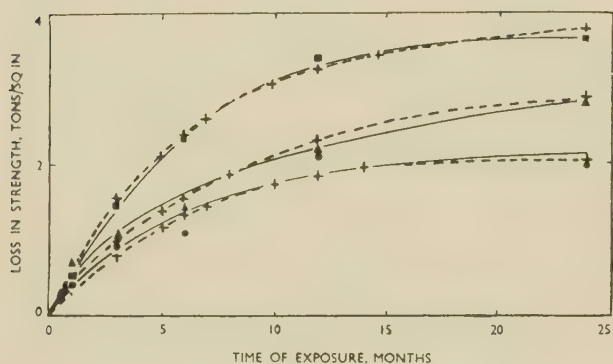


FIG. 16.—Variation of Loss in Strength with Increasing Exposure Period.

KEY.
 ---+--- Calculated Curve.
 ---■--- H15-WP Alloy at Sheffield (Site I).
 ---▲--- H15-WP Alloy at Hayling Island (Site III).
 ---●--- H10-WP Alloy at Sheffield (Site I).

which are appreciably superior to those of specimens totally immersed. There was a deposit of earthy material on these specimens which had been placed at approximately half-tide level under a concrete pier. Normally such deposits tend to promote attack on metals, but it seems that in this particular case, the deposit was protective, and it is possible that some other organic material, probably from sewage in the river, was also present in the deposit.

The loss in strength was plotted against the period of exposure for all sites and examined in the light of Champion's views⁶ regarding the decrease in rate of corrosion of aluminium alloys with time. It is possible to draw a curve of the type suggested by Champion to fit the experimental curves drawn through the average of 9 results for H15-WP and H10-WP alloy specimens exposed at Sheffield (Site I) and H15-WP at Hayling Island (Site III) (Fig. 16). There was, however, considerable scatter of the results of individual specimens (one specimen showing six

IV.—THE RESULTS OF TENSILE TESTS ON SPECIMENS STRETCHED 5% BEFORE EXPOSURE

When the specimens previously described had been exposed for some months, it was decided to test the effect of plastic deformation on material exposed to field tests. Specimens were therefore subjected to 5% stretch in a tensile-testing machine after solution heat-treatment and ageing, and immediately before exposure. Specimens were exposed at Sites I, III, and V in test frames identical with those used for the earlier tests. After 6 months' exposure the residual strength of both materials was quite high and superior to that of specimens that had not been stretched. The corrosion attack did not appear to be as severe. After 12 months' exposure, however, corrosion attack appeared to have increased in severity, and after 18 months the attack definitely appeared to be worse than that on the unstretched specimens.

The results of microscopical examination clearly indicated the increased severity of attack, particularly on the H10-WP alloy specimens which at Sheffield showed general intercrystalline corrosion attack occurring to a maximum depth of 0.022 in. after only 18 months' exposure. There is some indication also that specimens stressed at 0.1% proof stress are more heavily attacked than those stressed at the design stress. In the case of H15-WP specimens, however, the effect of cold work on the corrosion-resistance is not nearly so pronounced.

A similar effect is revealed by the results of tensile tests, from which there is a clear indication of a loss of approximately 2 tons/in.² in the last 12 months' exposure in the H10-WP specimens at Sheffield, whereas the loss in strength of H15-WP alloy exposed at Sheffield during the same period seems to be rather less than this. There was no evidence of rapid stress-corrosion failure of any of these specimens that had been given 5% stretch before exposure.

V.—COMMENTS AND CONCLUSIONS

The results of the field tests have shown that the most severe attack on H10-WP and H15-WP alloys occurs at Sheffield (Site I), where there is an average loss of strength of 2.0 and 3.7 tons/in.², respectively, after 2 years' exposure, representing a loss on original strength of 10.7 and 11.8%, respectively, or approximately 0.012 in. thickness. These values are greater than those reported in the A.S.T.M.⁸ tests at Altoona and New York City on 51S alloy after 3 years' exposure.

The maximum corrosion is much greater in the H15-WP specimens, being equivalent to the loss of approximately 33% or 0.033 in. thickness. This figure is based on one test specimen exposed for 2 years at Sheffield and is associated with foliation-type attack. In H10-WP specimens the maximum corrosion is equivalent to 15% or 0.015 in. thickness.

Although the average corrosion decreased with time in all specimens, severe foliation in H15-WP alloy becomes visually obvious only after 12 months' exposure to Sheffield or to marine atmospheres. This type of attack may be dangerous, since there is as yet no evidence that it will decrease with time. Protection of extrusions of this alloy by cladding, spraying, or painting seems to be advisable where exposed to severe industrial or marine atmospheres.

The present indications are that atmospheric attack on H10-WP alloy in all atmospheres decreases with time and that extrusions of 0.11 in. or more in thickness and not less than $\frac{1}{4}$ in. wide will retain a strength equivalent to the 0.1% proof stress for an indefinite period.

With regard to the application of Champion's exponential equation to the corrosion of these alloys, it seems that this might be fitted fairly well to the average corrosion/time curves in the severe industrial atmosphere, but that there is less agreement in marine and semi-industrial atmospheres, where the corrosion attack is comparatively small and may possibly be masked by the scatter in the original properties of the materials. Considering, however, the worst case, i.e. the Sheffield atmosphere, calculation on the basis of Champion's equations shows that the minimum thickness required for both H10-WP and H15-WP alloys to ensure that the residual strength of the material will never fall below the original 0.1% proof stress, is of the order of 0.058 and 0.055 in., respectively. These values are of the same order as those quoted by Champion⁷ in his calculations of the A.S.T.M. results on 17S-T.

At the same time it would be unwise to base any design directly on such a calculation for average loss. In many cases, failure of a structure may be caused by severe local attack. In other cases local penetration of a member with a large area may have no significant influence on strength. The actual test-pieces cut from the specimens after exposure to corrosion were only $\frac{1}{4}$ in. wide in the 2 in. gauge-length. One such specimen of H15-WP alloy that had a residual

strength of 20.3 tons/in.² had lost strength to the extent of 11.2 tons/in.², which is equivalent to three times the average (3.7 tons/in.²) for the 9 specimens exposed for 2 years at Sheffield. Hence it is possible that an H15-WP alloy extrusion, 0.10 in. thick, $\frac{1}{4}$ in. wide, and 18 in. long, may lose strength to such an extent that failure would occur when stressed to only five-sixths of the 0.1% proof stress after 2 years. In such case a factor of safety of 2 on the average corrosion rate would obviously be inadequate in calculating the thickness required for infinite life. The position with H10-WP alloy specimens exposed at Sheffield is not so serious, since the maximum loss in strength is only 15% higher than the average, and a factor of safety of 2 might be adequate for this alloy under these conditions.

The remaining sites at which there is total and intermittent immersion of the specimens in sea-water and fresh water, cause comparatively little attack on both alloys, but in some instances the attack is very local and rather severe. However, the effect of this attack on the overall strength after 2 years' exposure is small. In some instances the low rate of attack may be attributed to protective agents that are deposited on the aluminium-alloy surface, e.g. oil from ships at Southampton, dense marine growth at Hayling Island, and unidentified soiling of the specimens in the fresh water at Christchurch. Under conditions of total immersion in fresh water at Christchurch, complete penetration of a 0.10 in.-thick H10-WP alloy specimen was found locally after 2 years. The H15-WP alloy specimens totally immersed in fresh water showed no localized attack in these conditions. This is consistent with other workers'⁹ experience that under conditions of total immersion in relatively stagnant water the local pitting is much deeper and less widespread in alloys of higher purity. Apart from the localized pitting on total immersion in fresh water, visual examination of the specimens shows a marked superiority of H10-WP alloy over H15-WP alloy, particularly during the second year of exposure.

The corrosion attack of H10-WP alloy is usually of the intercrystalline type, and the effect of cold working the material by stretching is to increase the rate of attack. Although this causes no marked deterioration in properties compared with those of unstretched material after 18 months' exposure, it is expected that the higher rate of attack will result in the cold-worked material having a lower residual strength than material that has not been cold worked after a certain minimum period of exposure which may be of the order of 2 years at the Sheffield site. The effect of stretching the material before exposure seems to have very little effect on accelerating the corrosion attack of H15-WP alloy.

In neither of the alloys has there been any evidence of stress-corrosion occurring during the field tests. This is not unexpected in the case of the H10-WP alloy, in view of its comparatively high general corrosion-resistance. Judging by the results of tests on H15-WP alloy sheet, reported by many other in-

investigators, it was thought that some stress-corrosion failures of the extruded material might occur. This has not been the case, however, and the resistance to this type of failure is attributed to the longitudinal character of the corrosion attack, since a corrosion pit starting at the surface will tend to spread longitudinally rather than penetrate deeper into the material, and so will reduce the risk of high stress concentration.

ACKNOWLEDGEMENTS

This paper is published by kind permission of the Ministry of Supply and of Almin, Ltd., who were the joint sponsors of the work. The author wishes to thank his colleagues at the Fulmer Research Institute for their assistance, and in particular Mr. E. A. G. Liddiard for his personal interest and helpful comments.

The author is also indebted to the following associations, laboratories, and firms, for placing various exposure sites at his disposal: (1) The British Iron and Steel Research Association, and the Brown-Firth Research Laboratories, Sheffield; (2) The British Non-Ferrous Metals Research Association, Euston Street, London; (3) The Admiralty, Central Metallurgical Laboratory, Emsworth, Hants.; (4) The Military Engineering Experimental Establishment, Christchurch, Hants.; and (5) British Railways, Docks Department, Southampton.

APPENDIX I

RESULTS OF VISUAL EXAMINATION

Site I—Severe Industrial Atmosphere

Alloy H10-WP.

The specimens soon became coated with a thick deposit of soot and corrosion product. After 6 months' exposure the surface became roughened as a result of pitting, and after 12 months specimens were coated with a firmly adherent mixture of soot and corrosion product. There was little change in appearance after 2 years' exposure, except that the corrosion attack appeared to be rather more severe on the underside of the specimens.

Alloy H15-WP.

The specimens rapidly became coated with soot and a little corrosion product. The surface became roughened after 6 months' exposure, and after 12 months' exposure the attack had appreciably increased. After 2 years fairly severe general attack had occurred, particularly on the underside of the specimens. Unstressed channel-section specimens showed severe general foliation.

Site II—Normal Industrial Atmosphere

Alloy H10-WP.

A light sooty deposit formed on the specimens, but corrosion attack was only slight after 6 months.

Twelve months' exposure showed a heavier coating of soot and corrosion product, particularly on the tension side. There appeared to have been slight increase in corrosion attack after 2 years' exposure.

Alloy H15-WP.

The appearance of the specimens was very similar to that of H10-WP, corrosion attack being visible after 12 months and slight general pitting occurring after 2 years' exposure.

Site III—Marine Atmosphere

Alloy H10-WP.

The start of corrosion attack was comparatively slow, very slight general attack being visible after 3 months and developing into very slight general pitting after 6 months. An appreciable amount of sea-salt was mixed with the corrosion product. Little change in the appearance had occurred after 12 months' exposure, and after 2 years the specimens were covered with a thin uniform layer of corrosion product and a deposit of sea-salt. Underneath, however, only slight general pitting of the aluminium had occurred.

Alloy H15-WP.

The rate of attack was slightly greater than on the H10-WP alloy specimens, slight general pitting occurring after 6 months and some severe isolated patches of pitting occurring after 12 months' exposure. There was a fairly heavy deposit of corrosion product and sea-salt on the specimens after 2 years and some fairly deep isolated pits with indications of slight foliation, particularly on the underside of the unstressed specimens.

Site IV—Rural Atmosphere

Alloys H10-WP and H15-WP.

The attack on both materials at this site was very slight, even after 2 years, only slight darkening of the surfaces occurring, accompanied by very slight pitting.

Site V—Total Immersion in Sea-Water

Alloy H10-WP.

There was slight fouling of the specimens, and a few barnacles had attached themselves to the surface after only one month's exposure. After 3 months there was considerable fouling and marine growth on all the specimens, which were stained brown. The fouling increased, and it appeared that where barnacles became attached there was appreciable protection of the material. The corrosion attack of the aluminium, even after 2 years' exposure, was very slight, and it seemed that the marine growth served to protect the aluminium, since it was only in exposed places that very slight pitting had occurred.

Alloy H15-WP.

The behaviour was similar to that of the H10-WP alloy. Fouling occurred rapidly and seemed to afford appreciable protection. Corrosion attack was negligible.

*Site VI—Tidal Immersion in Sea-Water**Alloy H10-WP.*

The specimens rapidly became coated with a deposit of sea-salt and a little corrosion product; very slight pitting, however, was detected only after 6 months' exposure, and after 12 months little change had occurred.

Alloy H15-WP.

The attack was a little greater than in the H10-WP specimens, slight general attack being visible after 3 months' exposure and slight blistering on the tension surface had occurred after 6 months' exposure. This blistering became more general after 12 months and was possibly the beginning of foliation attack. These tests, however, were discontinued after 12 months, owing to severe damage by heavy seas and loss of specimens.

*Site VII—Total Immersion in Fresh Water**Alloy H10-WP.*

The specimens quickly became covered with a rust-like colouring which was probably an organic deposit from sewage that is emptied into the river. A deposit of mud and green algæ had formed after 3 months' exposure, but corrosion attack was very slight. Isolated spots of pitting were visible after 12 months' exposure, and this had increased in severity in some places after 2 years.

Alloy H15-WP.

The specimens behaved in a very similar manner to those of H10-WP alloy. They became covered fairly quickly with slight rust and a deposit of green algæ formed on the upper surface. The corrosion attack was very slight, but after 2 years' exposure isolated spots of foliation were observed on two of the specimens. The specimens were frequently covered with a thin film of mud.

*Site VIII—Tidal Immersion in Fresh Water**Alloy H10-WP.*

The specimens became covered rapidly with a deposit of mud, but corrosion attack was negligible. The mud became more adherent with time, but even after 2 years' exposure negligible corrosion had occurred.

Alloy H15-WP.

The deposition of mud was similar to that on the H10-WP alloy specimens, but fairly general corrosion attack of the tension surface had occurred after 6 months' exposure. This became rather more severe as time proceeded, and slight foliation was detected after 2 years' exposure.

*Site IX—Tidal Immersion in Sea-Water**Alloy H10-WP.*

There was considerable fouling by barnacles on the unstressed aluminium-alloy frame and specimens, but the deposition of barnacles was much slower on the stressed specimens. The frames and specimens became coated also with a thin film of oil, apparently from passing ships. It is not surprising, therefore, that negligible corrosion of the material occurred.

The specimens that had been stretched 5% before exposure at sites I, III, and V corroded rather more rapidly, but the general appearance was similar to that of specimens that had not been stretched.

APPENDIX II

METHOD OF ASSESSMENT OF CORROSION ATTACK

All specimens were cut from the corroded middle portion of the stressed test-pieces and from the unattached ends of the unstressed channel test-pieces. The section examined was parallel to the longitudinal axis and normal to the neutral plane of the test-piece. Examination was carried out at a magnification of 100, and the maximum depth of attack noted on each set of 3 specimens, the total length of the 3 microsections being approximately $1\frac{1}{2}$ in. The diameter of the field of view of the microscope was 0.060 in. approximately, and the grading of the degree of attack was as follows:

(a) *Negligible attack*.—No attack over at least 5 to 6 consecutive fields, i.e. 0.3 in.

(b) *Very slight attack*.—Attack only observed at intervals of 2 to 3 fields, i.e. 0.15 in. approx.

(c) *Slight attack*.—Spots of attack observed in consecutive fields, i.e. 0.050 in.

(d) *Slight general attack*.—Attack of the same depth occurring over 1 or 2 adjacent fields with gaps of 2 fields or more between these regions where no attack occurred.

(e) *General attack*.—Continuous attack of approximately the same depth for several fields.

(f) *Isolated spots*.—This term is self-explanatory and refers to isolated areas where attack to an abnormal extent has occurred.

(g) *Intercrystalline*.—This describes the type of corrosion where the grain boundary is attacked preferentially.

(h) *Longitudinal intercrystalline corrosion*.—Preferential attack along grain boundaries just below and parallel to the surface.

(j) *Pitting*.—Corrosion of the material where no preferential attack occurs.

(k) *Foliation*.—Where corrosion attack penetrates below the surface and then runs approximately parallel to the surface in the direction of the longitudinal plane of the specimen, the attack is termed foliation. Ultimately, formation of corrosion product causes the outer layer of material to lift and peel off ("foliate").

REFERENCES

1. J. M. Bryan, *Rep. Food Invest. Board, Dept. Sci. Indust. Research*, **1938**, 217.
2. J. M. Bryan and T. N. Morris, *J. Soc. Chem. Ind.*, 1940, **59**, 159.
3. F. A. Champion, *Trans. Faraday Soc.*, 1945, **41**, 593.
4. W. H. J. Vernon, *ibid.*, 1927, **23**, 150.
5. R. Guilhaudis, *Rev. Mét.*, 1952, **49**, (11), 791.
6. F. A. Champion, *Metal Ind.*, 1948, **72**, 440, 463.
7. F. A. Champion, *ibid.*, 1949, **74**, 7.
8. E. H. Dix, Jr., and R. B. Mears, *A.S.T.M. Symposium on Atmospheric-Exposure Tests on Non-Ferrous Metals*, **1946**, 57.
9. Unpublished work by the British Non-Ferrous Metal Research Association and Aluminium Laboratories Ltd., Canada.

THE MEASUREMENT OF THE RELATIVE HARDNESSES OF FINE POWDER PARTICLES *

1443

By J. B. MATTHEWS,† B.Sc., Ph.D., F.R.I.C.

SYNOPSIS

The experimental technique originally devised by Chalmers (*J. Inst. Metals*, 1941, **67**, 295) for the determination of the surface hardness of metallic strips, by their bombardment with a hard powder such as sand or carborundum, has been applied to the measurement of the relative hardnesses of different powder particles. The method depends on the decrease in specular reflectivity produced by the indentation of the reflecting surface by the bombarding powder particles, when the hardness of the surface is not far removed from that of the particles. Formal relationships have been derived connecting the decrease in reflectivity with the relative "hardness" of the particles.

I.—INTRODUCTION

THE standard methods of measuring the hardness of solids require test-pieces possessing a plane surface with an area of at least 5 mm.², and therefore they cannot be used to determine the hardness of fine powder particles. Similarly, the available micro-hardness techniques cannot be used for small powder particles. Mindt¹ has described a method for comparing the hardnesses of powder particles, in which the hardness is measured by the amount of abrasion produced by the particles under standardized conditions. This method, however, will not give results with a high degree of precision, and cannot discriminate between powders, the particle hardnesses of which are nearly equal. The method of measurement described in the present paper, on the other hand, can be applied to compare powders consisting of particles with relatively small differences in hardness. It was devised in order to determine the relative hardnesses of commercial grades of aluminium powder, but there is no fundamental reason why its application should not be extended to any powders, the particle hardnesses of which are covered by the range of substances capable of being strain-hardened by indentation.

II.—GENERAL PRINCIPLES OF THE METHOD

The principles on which the new method is based can be illustrated in the following way.

When a hard spherical body is allowed to fall on a softer metallic surface, the volume of the indentation formed in the latter is to a first approximation directly proportional to the kinetic energy lost during impact, and inversely proportional to the resistance to penetration, or hardness, of the surface. The

kinetic energy lost in impact is dissipated in various ways, one of which is the production of a state of strain in the metal surrounding the indentation, with a resultant increase in hardness, known as strain-hardening. If an identical body is now dropped from the same height, so that it hits the surface close to the first indentation, the volume of the indentation produced by the second falling body will be less than that produced by the first, because of the strain-hardened condition of the surface due to the first indentation.

If the receiving surface is chosen so that its original hardness is not very much less than that of the falling body, then it is possible that the second impact will not produce an indentation, because the strain-hardening produced by the initial impact may be sufficiently large to render the surface completely resistant to the second falling body. In fact, the second indentation will be equal in volume to the first only if it is produced outside the surface area affected by the strain-hardening resulting from the latter.

It is possible to extend this argument to the case of a stream of powder particles, falling in a uniform manner on a given surface, by treating this case as equivalent to a stream of identical spheres, which is permissible if the powder particles are neither needle-shaped nor flaked and are confined within narrow limits of size. The size of the average indentation produced by a given powder on a given surface can then be calculated from a knowledge of the disappearance of plane surface area as a function of the quantity of powder fallen, and a knowledge of the ratio of the plane-projected area of the average indentation to the corresponding area of plane surface rendered unresponsive to further indentation. Furthermore, from a comparison of the results obtained for different powders, using the same standard surface for each, values can be obtained

* Manuscript received 26 August 1952.

† Shell Petroleum Co., Ltd., Thornton Research Centre, Chester.

which give a measure of the relative hardnesses of the powder particles.

The disappearance of plane surface area as a function of the quantity of powder fallen, and the ratio of the plane-projected area of the average indentation to the corresponding area of plane surface rendered unresponsive to further indentation, can both be determined experimentally by measuring

standard surface was commercially pure aluminium (c. 98% purity). This was used in sheet form, of thickness $\frac{1}{32}$ in., and strips were given a high polish, using a polishing mop in conjunction with Canning's Peerless Polishing Powder, followed by annealing by heating to 280°C. for a few minutes. Surfaces prepared in this manner were found to be suitable for the purposes of the investigation, but, although

TABLE I.—*Densities and Analytical Data for the Powders.*

Powder	Density, g./c.c.	Cu, wt.-%	Mg, wt.-%	Si, wt.-%	Mn, wt.-%	Fe, wt.-%	Ni, wt.-%	Zn, wt.-%	Pb, wt.-%	Ti, wt.-%
Aluminium A . .	2.799	4.40	0.38	0.72	0.60	0.53	0.03	0.05	0.01	0.01
Aluminium B . .	2.795	4.53	0.98	0.70	0.60	0.54	0.03	0.06	0.01	0.01
Aluminium C . .	2.801	4.35	0.01	0.67	0.68	0.56	0.02	0.02	Tr.	0.02
Aluminium D . .	2.811	4.31	0.27	0.72	0.70	0.57	0.03	0.02	Tr.	0.01
Mg-Al alloy . .	2.147
Sand	2.662

the changes in specular reflectivity of the surface caused by the impact of the stream of powder particles.

III.—EXPERIMENTAL.

1. APPARATUS AND TECHNIQUE

The experimental technique used for following the changes in specular reflectivity, caused by the impact of a stream of powder particles, is the same as that described by Chalmers² for measuring the hardness of thin surface layers of metals and other materials. The apparatus consists essentially of two parts: a long tube for dropping known quantities of powder vertically on to a standard surface inclined at an angle of 45°, and a means of measuring the specular reflectivity of the surface during the course of the experiment. In the investigation described in the present paper the tube was 100 cm. in length and 0.74 cm. in dia., and the funnel for introducing the powder into the tube had an outlet 2 mm. in dia.

2. MATERIALS USED

The powders used in this investigation were four grades of blown aluminium powder, designated A, B, C, and D, a granulated alloy containing equal parts of aluminium and magnesium, and sand. All these powders were carefully sieved, and in each case only the fraction passing through the 120 B.S.S. mesh and retained by the 170 B.S.S. mesh was used. Thus, the limiting diameters of the particles could be taken as being 1.27×10^{-2} and 0.9×10^{-2} cm. The densities of the powder particles were determined pycnometrically, and the values obtained, together with analytical data for the aluminium powders, are given in Table I.

Since the softest powders were presumably the aluminium powders, the metal chosen to give the

there was no noticeable change in reflectivity on annealing and ageing, variations in reflectivity and hardness were apparent from one surface to another. It is desirable to eliminate such sources of error as

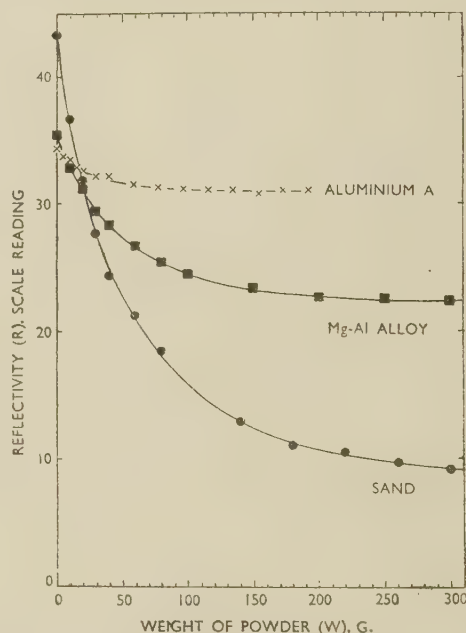


FIG. 1.—Variation of Reflectivity with Weight of Powder Dropped.

far as practicable, and it is possible that this could be achieved by preparing the standard surfaces by electropolishing.

3. RESULTS

A typical set of results obtained for the variation of specular reflectivity with the quantity of powder dropped is shown graphically in Fig. 1. Significant

data obtained for the whole series of experiments are given in Table II, in which R_0 is the initial re-

TABLE II.—Significant Reflectivity Values.

Powder	R_0	R_∞	$(R_0 - R_\infty)$	$\frac{R_0 - R_\infty}{R_0} \times 100$
Aluminium A	39.2, 40.3, 34.4, 32.5	35.0, 35.3, 31.3, 29.25	4.2, 5.0, 3.1, 3.25	10.7, 12.4, 9.0, 10.0
Aluminium B	31.15, 34.8	27.6, 31.15	3.55, 3.65	11.4, 10.5
Aluminium C	35.1, 34.65	29.5, 30.75	5.6, 3.9	15.7, 11.2
Aluminium D	38.4, 39.5	33.8, 34.6	4.6, 4.9	12.0, 12.4
Mg-Al alloy	35.5, 36.5	23.0, 25.5	12.5, 11.0	35.2, 30.2
Sand	43.3, 43.5, 35.0	9.0, 8.5, 7.5	34.3, 35.0, 27.5	79.1, 80.4, 78.6

fectivity of the surface and R_∞ the final reflectivity, expressed in units of the galvanometer scale reading. Since the reflectivity does not in practice reach a limiting value—the final portions of the graphs shown in Fig. 1 consisting of straight lines of finite slope—the value of R_∞ has been arbitrarily fixed as the value corresponding to the point at which the final linear portion of the curve is tangential to the initial curved portion.

IV.—INTERPRETATION OF RESULTS

In order to arrive at a formal relationship between the reflectivity data and the relative hardnesses of the powder particles, it is necessary to obtain information on, firstly, the relative average kinetic energies possessed by the particles just before hitting the standard surface (referred to subsequently as impact energies), and, secondly, the relationship between the energy of impact and the plane-projected area of the average indentation.

1. THE RELATIVE IMPACT ENERGIES OF THE POWDER PARTICLES

In view of the very large number of powder particles used to effect measurable changes in reflectivity, it is permissible to consider the powders as consisting of equal-sized spheres of 0.0109 cm. dia. (the average of the diameters of particles retained between B.S.S. Mesh Nos. 120 and 170). Now, the terminal velocity attained by a sphere falling freely through air is the velocity at which the frictional drag force is equal to mg , where m is the mass of the sphere and g is the acceleration due to gravity. The frictional drag force is some function of the velocity of the sphere, its radius, and the density and viscosity of air. The precise relationship is not known except over limited ranges of the variables, but it is possible to calculate the terminal velocities for the various powder particles, by the method of successive approximations, from the known empirical relationship between the Reynolds' number and the coefficient of drag for spheres.³ For the lightest and heaviest particles used (of density $\rho_s = 2.147$ and 2.811

g./c.c.) the terminal velocities falling through air at 20° C. ($\rho_a = 1.205 \times 10^{-3}$ g./c.c., and $\nu = 0.150$ cm.²/sec.) are found to be approximately 70 and 85 cm./sec., respectively. (ρ_a is the density of air and ν the kinematic viscosity of air.)

From the known experimental relationship³ between the Reynolds' number and the coefficient of drag, it can be assumed that, over the small range limited by the two terminal velocities given above, a linear relationship holds between the logarithms of these two parameters. With this assumption, and taking the frictional drag force corresponding to the terminal velocity to be equal to the weight of the particle, it may be shown that the limiting velocity of the particle (U_∞) is related to its density (ρ_s) by the expression :

$$U_\infty \propto \rho_s^{0.79} \quad (1)$$

These limiting velocities are lower than those which would be attained if Stokes' law were valid. Assuming the validity of Stokes' law, it is possible to calculate the terminal velocity, and also to obtain a close estimate of the distance which the particle must fall in order to attain it. In the case of the lightest and heaviest particles used, the Stokes' law terminal velocities become 76.9 and 100.7 cm./sec., respectively, and the corresponding distances fallen in order to reach 99% of these velocities are 22 and 37 cm.

Therefore, it may be safely assumed that in falling through the dropping tube, of length 100 cm., the velocities attained by the particles, which are their velocities just before impact, are their terminal velocities calculated from the relationship between their Reynolds' numbers and coefficients of drag.

2. THE RELATIONSHIP BETWEEN IMPACT ENERGY AND SIZE OF THE INDENTATION

Detailed investigations have been carried out by Martel^{4,5} into the conditions governing the size of the indentation produced in plane metallic surfaces by the impact of a rebounding hammer. Martel, using cone-shaped indenters, found that the ratio of the energy of impact to the volume of the indentation produced is constant for any given metal. Edwards and Willis,⁶ on the other hand, using spherical indenters, deduced the following relationship between the radius of the plane-projected circular area of the indentation (r) and the energy of impact (E) :

$$\frac{r}{4\sqrt{E}} = \text{constant} \quad (2)$$

In a subsequent paper, Edwards⁷ discusses both Martel's and his own work, and maintains the view that, generally speaking, his own experiments with different hemispheres indicate that the diameters of the indentations agree very closely with equation (2). But he admits that this expression is not absolutely accurate, and needs an additional correction factor

before it truly represents the resistance to penetration under impact. On the most simple picture of the physical process of indentation it can be assumed that the volume of the indentation is proportional to the energy absorbed during impact, but it does not immediately follow that the diameter of the indentation also obeys the same proportionality. If the final shape of the indentation is not spherical, and the divergence from the sphericity varies with the depth of penetration, then the ratios of volume and diameter of the indentation respectively to the energy of impact will not correspond, since a third factor is involved. Accepting the view that there is a fundamental difference between the Martel ratio and the Edwards and Willis ratio, it follows that in practice the choice of which to apply depends on the relationship being sought. In the present investigation, as will be seen later, the requirement is the relationship between the plane-projected area of the indentation and the energy of impact. Hence, the Edwards and Willis ratio will be adopted.

3. THE RELATIONSHIP BETWEEN REFLECTIVITY DATA AND RELATIVE HARDNESSES OF THE POWDER PARTICLES

A parallel beam of radiation incident on a plane reflecting surface will be reflected as a parallel beam, the angles of incidence and reflection being equal. If, however, the plane reflecting surface is indented by a sphere, all radiation incident within the area of the indentation, apart from the central ray, will be scattered from the main direction of the reflected beam. Therefore, if the intensity of the reflected beam is measured at a point which can be considered to be at infinity, the decrease in reflectivity produced by spherical indentations on the plane surface will be proportional to their total plane-projected area. Furthermore, the following conditions apply:

(a) The powder particles fall uniformly over the surface area subjected to impact.

(b) Subsequent impacts to the first do not affect the area of the indentation produced by the first impact; this has been shown to be the case experimentally by Edwards and Willis.⁶

(c) An indentation in the surface produces strain-hardening, not only below the indentation, but also for a certain distance along the plane surface outside its perimeter. Thus, Moore⁸ finds that for good reproducibility in the ball indentation test the indentations must not be formed at distances closer than five times their diameters.

From (b) and (c) it may be inferred that appreciable surface strain-hardening occurs in the immediate vicinity of an indentation, and it is probably true to say that the degree of this hardening falls off with distance from the perimeter of the indentation. If no hardening occurred, either in or around the indentation, the result of continual bombardment by the particles would be a continuous depression of the surface, the average appearance of which would

roughly correspond to a set of close-packed equal circular areas of indentation. On this basis the final reflectivity value of the surface would be the same in all cases and would be a fraction, equal to $\pi/2\sqrt{3}$, of the initial reflectivity.

Experimentally, it has been found (see Fig. 1) that the final reflectivities obtained cover a wide range of values, being greater for the softer powders. Hence, there is apparently an area surrounding each indentation which is unresponsive to further impact by the powder, and the softer the powder particles the greater is this area. Photomicrographical examination of the bombarded surfaces confirmed this conclusion.

Suppose the radius of the average spherical indentation is r , and the distance of closest approach of the perimeters of the circular areas of indentation in the limiting surface structure is $2D$. Then, from geometrical considerations, the ratio of the total plane-projected area of indentation to the original total surface area, in the limiting case, is given by:

$$\left\{ \frac{\text{Indented area}}{\text{Total area}} \right\}_{\infty} = \frac{\pi r^2}{2\sqrt{3}(r+D)^2} = 0.9067 \frac{r^2}{(r+D)^2} \quad (3)$$

Therefore, since the specular reflectivity is proportional to the plane surface area:

$$\frac{R_0 - R_{\infty}}{R_0} = 0.9067 \frac{r^2}{(r+D)^2} \quad (4)$$

in which R_0 and R_{∞} are the initial and final reflectivities, respectively.

From this is obtained the expression:

$$\frac{D}{r} = \sqrt{\frac{0.9067 R_0}{R_0 - R_{\infty}}} - 1 \quad (5)$$

Again, it follows on the premises (a), (b), and (c) that:

$$\frac{d(x+y)}{dW} = k\{A - (x+y)\} \quad (6)$$

in which k is a constant, x is the total plane-projected area of indentation, y is the total strain-hardened surface area unavailable for further indentation, when the total weight of dropped powder is W , and A is the initial area subjected to impact.

From equation (6) the following expression is derived:

$$\log_{10} \left(1 - \frac{x+y}{A} \right) = -\frac{kW}{2.303} \quad (7)$$

Now, x can be put equal to $A(R_0 - R_W)/R_0$ and also, from considerations of the limiting case, it follows that:

$$\frac{x}{x+y} = \left\{ \frac{\text{Indented area}}{\text{Total area}} \right\}_{\infty} = \frac{(R_0 - R_{\infty})A}{R_0 A} = \frac{R_0 - R_{\infty}}{R_0} \quad (8)$$

Hence,

$$(x + y) = \frac{R_0 \left\{ \frac{(R_0 - R_w)A}{R_0} \right\}}{R_0 - R_\infty} = A \times \frac{R_0 - R_w}{R_0 - R_\infty} \quad (9)$$

Substituting in equation (7):

$$\log_{10} \left(\frac{R_w - R_\infty}{R_0 - R_\infty} \right) = -\frac{kW}{2.303} \quad (10)$$

According to equation (10) a straight line should be obtained when $\log_{10} \left(\frac{R_w - R_\infty}{R_0 - R_\infty} \right)$ is plotted against W , the gradient of which is equal to $-k/2.303$. This is confirmed by the experimental data plotted in Fig. 2.

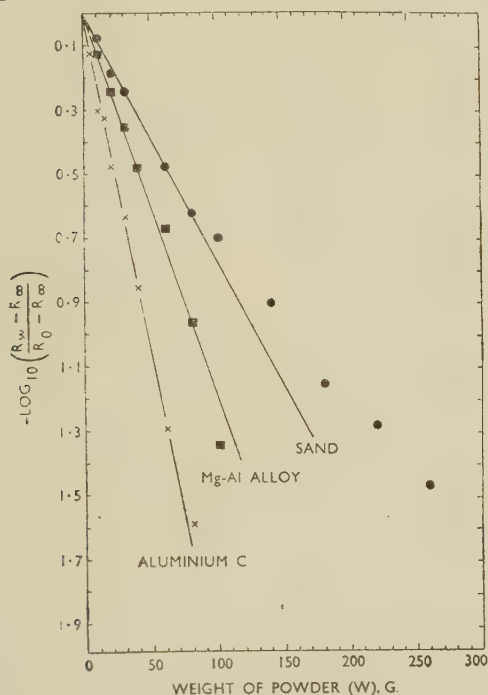


FIG. 2.—Logarithmic Relationship Between Decrease of Reflectivity and Weight of Powder Dropped.

Imagine that a quantity, W , of powder has fallen, rendering an area $(x + y)$ of the surface unresponsive to further impact, and at this stage suppose an additional small quantity, dW , of powder is allowed to fall. Then, the actual amount of powder in this small quantity dW which is effective in producing further indentation is given by:

$$\frac{dw}{dW} = \frac{A - (x + y)}{A} \quad (11)$$

in which dw is the weight of powder effective in producing indentation. It follows that the actual weight of powder which has been effective in producing indentation, when the total weight of powder dropped is W , is given by:

$$w = \int_w^0 dW \left(1 - \frac{x + y}{A} \right) \quad (12)$$

Substituting for dW from equation (6):

$$w = -\frac{1}{kA} \int_A^0 d(x + y) \quad (13)$$

Therefore, if $w_{0.5}$ is the weight of powder which has been effective in producing indentations when half the total change in the surface has been produced, then:

$$w_{0.5} = -\frac{1}{2k} \quad (14)$$

Also, from (10), the total weight of powder ($W_{0.5}$) which has been dropped in producing the half change is given by:

$$W_{0.5} = -\frac{2.303 \log_{10} 0.5}{k} \quad (15)$$

In the surface which has undergone half of the total change the number of indentations, $N_{0.5}$, is given by:

$$N_{0.5} = \frac{w_{0.5}}{\frac{1}{6}\pi(d)^3\rho_s} \quad (16)$$

in which (d) is the average particle diameter and ρ_s the density of the average particle.

Therefore, the ratio of indented area to original total area at the stage of half-change is given by:

$$\left\{ \frac{\text{Indented area}}{\text{Total area}} \right\}_{0.5} = \frac{x}{2(x + y)} = \frac{R_0 - R_\infty}{2R_0} = \frac{6w_{0.5}\pi r^2}{\pi(d)^3\rho_s A} \quad (17)$$

from which is obtained the following expression for r :

$$r = \sqrt{\frac{\rho_s(d)^3(R_0 - R_\infty)A}{12w_{0.5}R_0}} \quad (18)$$

Equation (18) can be put in the form:

$$r = \sqrt{\frac{k\rho_s(d)^3(R_0 - R_\infty)A}{6R_0}} \quad (19)$$

In columns 2 and 3 of Table III the observed values for k and $W_{0.5}$ are given, and in column 4 the values of $W_{0.5}$ calculated from equation (15). It will be seen that there is good agreement between the observed and calculated values for $W_{0.5}$ in the case of the aluminium powders, but that in the case of the magnesium-aluminium alloy powder the observed value is slightly less than the theoretical value, and in the case of sand the discrepancy is more pronounced. In other words, in the case of the harder powders, there is a departure from linearity in the relationship between $\log_{10} \{(R_w - R_\infty)/(R_0 - R_\infty)\}$ and W in the region of high values of W , which may be due to the number of simplifying assumptions which have been made. In this connection it should be stressed that the value of R_∞ used in evaluating equations (5) and (19) is that calculated from the slope of the linear portion of the curve relating $\log_{10} \{(R_w - R_\infty)/(R_0 - R_\infty)\}$ and W , and is not the arbitrarily chosen experimental value.

It is now necessary to assign some value to A . This value could be determined from direct measurement of the elliptical area subjected to impact. But, since the perimeter of this area is not clearly defined, it is more convenient to put A equal to the area of the ellipse formed by the intersection of a plane cutting at 45° to its axis a cylinder of diameter equal to the internal diameter of the dropping tube. Accordingly, A was found to be 0.608 cm.^2 .

All the data are now known from which to calculate r , using equation (19). The values obtained are given in column 6 of Table III. They are of the

obvious that the same degree of penetration is not achieved in all cases, the hardest powder, i.e. sand, penetrating further than the softer powders. The variation of the individual results, unfortunately, does not allow us to draw any definite conclusions with respect to the softer powders, but it appears that the magnesium-aluminium alloy produces a larger indentation than the aluminium powders, excluding aluminium powder D which apparently gives an equal indentation. Such results can be attributed to the mutual deformation of the particle and plane surface on impact. The softer the powder

TABLE III.—*Data Derived from Experimental Observations.*

Powder	$k, \text{g.}^{-1} \times 10^3$	$W_{0.5}, \text{g. (obs.)}$	$W_{0.5}, \text{g. (calc.)}$	$\frac{R_0 - R_\infty}{R_0} \text{ (calc.)}$	$r, \text{cm.} \times 10^4$	$r', \text{cm.} \times 10^4$	$\frac{D}{r}$
Aluminium <i>A</i>	6.63	11.0	10.5	0.102	0.50	0.50	1.98
	5.34	13.5	13.0	0.122	0.49	0.49	1.73
	4.42	16.2	15.7	0.090	0.38	0.38	2.17
	7.64	8.5	9.1	0.105	0.55	0.55	1.94
							(Av. = 1.955)
Aluminium <i>B</i>	5.11	13.8	13.6	0.114	0.46	0.46	1.82
	4.68	14.1	14.8	0.106	0.43	0.43	1.93
							(Av. = 1.875)
Aluminium <i>C</i>	3.91	17.4	17.7	0.163	0.49	0.49	1.36
	4.97	12.7	13.9	0.120	0.47	0.47	1.75
							(Av. = 1.555)
Aluminium <i>D</i>	6.27	11.0	11.1	0.120	0.53	0.53	1.75
	6.91	10.1	10.0	0.127	0.57	0.57	1.67
							(Av. = 1.710)
Mg-Al alloy	2.03	33.0	34.2	0.361	0.46	0.54	0.58
	2.58	25.5	26.9	0.313	0.48	0.54	0.70
							(Av. = 0.64)
Sand	1.68	35.0	41.2	0.861	0.71	0.74	0.026
	1.68	35.5	41.2	0.860	0.71	0.74	0.027
	1.73	36.5	40.1	0.828	0.71	0.74	0.047
							(Av. = 0.033)

same order of magnitude as the values obtained by Chalmers² for sand upon tin from direct microscopic and optical measurements, allowing for the difference in size of particles. Now, we know that the area of the indentation is a function of the kinetic energy of the particle just before impact (equation (2)) and also that this kinetic energy of the particle is a function of its density (equation (1)). Therefore, in order to make a true comparison between the powders, it is necessary to introduce a correction factor based on equations (1) and (2). If r' is the radius of the indentation corresponding to an energy of impact equal in all cases to the actual experimental energy of impact of, say, the average aluminium powder particle, then:

$$r' = r \left\{ \frac{2.799}{\rho_s} \right\}^{0.645} \quad (20)$$

where 2.799 (g./c.c.) is the density of aluminium A powder and ρ_s is the density of the powder in question.

Values obtained for r' are given in column 7 of Table III. From an examination of them it is

particle, the greater is the deformation it undergoes upon impact, and consequently the less energy is there available for deformation of the plane surface. When the hardness of the surface is such that no permanent deformation is produced in it on impact, then obviously the energy of impact is dissipated entirely in deforming the particle alone. This phenomenon, however, was not apparent on microscopic examination of the powder particles, because the amount of deformation is only a small fraction of the volume of the particle, the radius of the indentation formed by sand particles being only about one hundredth of the radius of the particle. It follows that the observed variation in r' provides a measure of the hardness of the powders, but the sensitivity of this comparison is low, and only large differences in hardness are detectable.

A much more sensitive measure of the relative hardnesses of the powder particles is given by the ratio D/r , in which D , it will be remembered, is half the width of the annulus surrounding the indentation which is strain-hardened to a sufficient degree to

resist deformation by the powder particle. It is probably true to say that this ratio is constant in the case of each powder over the whole of the observed range of values of r , and consequently it is not necessary to introduce any correction factor for the experimental differences in impact energy. Accepting the ratio D/r as a measure of the hardness of the powder particles, we see immediately that there is a marked difference in particle hardness between sand, magnesium-aluminium alloy powder, and the aluminium powders. The experimental errors forbid any definite conclusions to be drawn concerning the relative hardnesses of the four aluminium powders employed, but it would appear that A and B are softer than C and D .

V.—DISCUSSION

The measurement of the hardness of the particles in a powder has always presented a difficult problem, but the method described in the present paper provides a sensitive means of determining the relative particle hardnesses of a series of powders. If we take the size of the average indentation as the measure of hardness, the method is less sensitive than it is if we take the ratio D/r as the criterion. On the other hand, in the former case, the method then more closely resembles the conventional method for the determination of Brinell hardness, with the following difference. In the Brinell method a standard hard indenter is used, and the degree of penetration under specified conditions into the material under test is taken as the value of the hardness of the latter, making the assumption that the indenter suffers no deformation during the test. In the method described in this paper a standard soft surface is used, and the degree of penetration of a hard indenter, in the form of the powder particle, is taken as the measure of hardness. In this case the method depends on the fact that mutual deformation of the indenter and the surface occurs, and it is necessary in order to obtain any measurable results that their respective hardnesses should not be very different. Using the alternative criterion, the ratio D/r provides a more sensitive comparison between powders, and the method now utilizes the work-hardening which occurs when the standard soft surface is indented, in addition to the mutual deformation of the indenter and surface. The hardness of the particle is related to the ratio D/r in such a way that the harder the particle is, the smaller this ratio becomes.

The range of particle hardnesses which can be compared by this method is determined by the hardness of the standard surface. By choosing an appropriate series of standard surfaces, however, it should be possible to extend the range of particle hardnesses covered. Moreover, by suitable standardization it may be possible to establish a scale of hardness. This, unfortunately, would be an additional hardness scale with which to contend, but perhaps it would be possible to correlate it with existing hardness scales.

Because of the small diameters of the indentations, which are of the order of magnitude of the wavelength of light, diffraction phenomena will become more important as the indentation of the surface proceeds. A rigorous treatment of the problems which then arise would be difficult. However, if the indentations are considered to be completely light-absorbing areas, viewed along the direction which a specularly reflected beam from the non-indented surface would take, and the non-indented areas as constituting a diffraction mirror, the simple deduction follows that practically the whole intensity of the diffracted light is concentrated in the direction of the specularly reflected beam. This leads to approximately the same result as the assumption made in this paper.

ACKNOWLEDGEMENT

This work was carried out during the war years at the Armaments Research Department, Fort Halstead, Kent, and the author wishes to thank the Chief Scientist, Ministry of Supply, for permission to publish the results.

REFERENCES

1. W. Mindt, *Physikal. Ber.*, 1923, **4**, 1092.
2. B. Chalmers, *J. Inst. Metals*, 1941, **67**, 295.
3. S. Goldstein, "Modern Methods in Fluid Dynamics". Oxford: 1938 (Clarendon Press).
4. R. Martel, "Impact Testing of Hardness", *Commission des Méthodes d'Essai des Matériaux de Construction, Paris*, 1895, Vol. 3, Sec. A. (Métaux), p. 261.
5. D. Tabor, "The Hardness of Metals", Chapter 8. Oxford: 1951 (Oxford University Press).
6. C. A. Edwards and F. W. Willis, *Proc. Inst. Mech. Eng.*, 1918, **82**, 335.
7. C. A. Edwards, *J. Inst. Metals*, 1918, **20**, 61.
8. H. Moore, *Internat. Congr. Test. Mat., Copenhagen*, 1909, (II), 55, 57, 123, 252; cf. H. O'Neill, "The Hardness of Metals and Its Measurement", p. 252. London: 1934 (Chapman and Hall, Ltd.).

CRYSTAL FRAGMENTATION IN ALUMINIUM DURING CREEP*

1444

By D. McLEAN, B.Sc., MEMBER

(Communication from the National Physical Laboratory.)

SYNOPSIS

Seven specimens of super-pure aluminium having grain-sizes of $1-9\frac{1}{2}$ grains/mm., were made to creep at 200° C. under loads varying from about $\frac{1}{2}$ to $\frac{3}{4}$ ton/in.²; the extensions produced ranged up to 50%. Observations and measurements were made relating to the sub-crystals formed. These are consistent with a polygonization model for secondary creep and permit a quantitative check of this model to be made. Certain of the observations appear to be inconsistent with the theory of sub-crystal formation advanced by Wilms and Wood (*J. Inst. Metals*, 1948-49, 75, 693; 1951, 79, 159).

I.—INTRODUCTION

SEVERAL metals when made to creep by a few per cent. or more change their structure in a characteristic way, the original crystals fragmenting into sub-crystals. The first evidence for this was given by Jenkins and Mellor¹ in the case of iron. Detailed and explicit evidence for aluminium has been provided by Wood and his associates² and support has come from other workers.³⁻⁵ Subsequently, evidence for lead was advanced by Gifkins,⁶ for a tin-antimony alloy by Betteridge and Franklin,⁷ and for zinc by Cottrell and Aytakin.⁸ It thus seems that the phenomenon is a fairly general one.

One explanation is that this fragmentation is the outcome of polygonization. The latter process has been found to occur in certain metals when appropriately strained and subsequently heated,⁹ and it is natural to suggest that it also operates when strain and heat are applied simultaneously, as during creep testing. In a recent paper,¹⁰ dealing with aluminium, evidence was presented that under the conditions used, the fragmentation occurring was due to polygonization, which took place during second-stage creep and accounted for the deformation, with the exception of the small amount attributable to grain-boundary movement. A similar suggestion has been made by Greenough and Smith⁴ and by Mott.¹¹ The purpose of the present work was to extend the investigation over a range of grain-sizes and of stresses. Observations regarding slip bands and grain boundaries were also made on the specimens and are recorded elsewhere.^{12, 13} All the evidence obtained is consistent with the view expressed above.

An alternative theory of fragmentation, due to Wilms and Wood,² appears to envisage that the parent grains split along inner boundaries during deformation and that the sub-crystals so formed

then rotate relatively to each other. A direct experimental check of these two theories favours that of polygonization.

II.—EXPERIMENTAL

The seven specimens used were made from super-pure aluminium strip containing 0.002-0.003% iron, 0.003% silicon, and 0.003% copper. Details of preparation and technique have been given previously.^{10, 12} Briefly, the specimens were annealed to give grain-sizes of 1, $4\frac{1}{2}$, and $9\frac{1}{2}$ grains/mm. They were polished, so that micro-examination of the surfaces could be carried out during deformation, and were made to creep at 200° C. under loads ranging from $\frac{1}{2}$ to about $\frac{3}{4}$ ton/in.². A summary of the experimental work is given in Table I. The tapered specimens bore a stress that necessarily varied along the length of the specimen, and after test they were sectioned at positions corresponding to the stresses indicated in the table.

TABLE I.—*Summary of Experimental Work.*

(a) *Two Parallel-Sided Specimens*

Electropolished in orthophosphoric acid-carbitol solution.

Identification mark :	W	L
Grain-size :	Fine ($9\frac{1}{2}$ grains/mm.)	Coarse (1 grain/mm.)
Stress :	$\frac{1}{2}$ ton/in. ²	
During extension :	Removed from creep machine periodically for examination of surface and measurement of extension (slip-band and grain-boundary displacements also measured and reported separately).	
Extension continued to fracture at :	50.3%, 901 hr.	23.6%, 1145 hr.
After fracture :	Sections prepared, anodized, and subjected to micro-examination between crossed polaroids. No X-ray examination made.	


* Manuscript received 21 June 1952.

† Metallurgy Division, National Physical Laboratory, Teddington.
287

TABLE I.—*continued*.

(b) Five Tapered Specimens

Electropolished in perchloric acid-acetic acid solution.

Specimen no. :	I	II	III	IV	V
Grain-size :	Medium ($4\frac{1}{2}$ grains/mm.)				
Creep time, hr. :	1	5	25	118 $\frac{1}{2}$	696
Stress range due to taper :	About $\frac{1}{8}$ – $\frac{1}{2}$ ton/in. ²				About $\frac{1}{4}$ – $\frac{1}{2}$ ton/in. ²
After creep times given above :	Removed from creep machine. Examined and measured. Sectioned transversely at positions corresponding to stresses given below, and electropolished.				
Stress, ton/in. ²	Extension, %, at Position of Each Section				
	0.33	0.64	0.92	1.3	1.2
	0.86	2.1	3.4	5.4 *	3.6
	3.1	8.4 *	15.0 *	29.5 *	17.0 *
The sections were :	X-rayed. Anodized and subjected to micro-examination between crossed polaroids. Etched and subjected to micro-examination for sub-boundaries.				

* The disorientation between individual sub-crystals was large enough to be measured.

III.—OBSERVATIONS AND MEASUREMENTS

1. DETECTION OF SUB-CRYSTALS

The detection of sub-crystals is possible by X-ray examination, by micro-examination in polarized light of an anodized section, or by micro-examination of the deformed surface. On the deformed surface sub-crystals are revealed either by the appearance of surface tilts or by the "white line" made to appear at the junction between regions of different tilt by suitable adjustment of the microscope. These are the white lines first reported by Wilms and Wood.²

There is evidence that the junctions between regions of different surface tilt coincide with the sub-crystal junctions as seen by polarized light. For example, Fig. 1 (Plate XLI) shows an area of the deformed surface photographed with oblique lighting to reveal the bands, running approximately from top to bottom of the figure, of different surface tilt. (The horizontal black lines are slip bands.) The same field, after polishing flat and anodizing, is shown in Fig. 2 (Plate XLI), as it appeared between crossed polaroids. It resembles the X-ray micrographs, Fig. 6 (a) and (b) of Honeycombe's paper,¹⁴ taken after creep deformation. Corresponding sub-boundaries are identified by the same letter in Figs. 1 and 2; they have very similar shapes in both, a fairly certain indication that the same interfaces are delineated. Since Fig. 1 registers surface tilts and Fig. 2 lattice tilts, tilts in the surface and the lattice coincide. No direct evidence was obtained that the boundaries of the sub-crystals detected by X-rays coincided with those observed microscopically. However, as both methods showed sub-crystals in the same specimens (allowance being made for the greater sensitivity of the X-rays), it is reasonable to assume coincidence.

2. MEASUREMENT OF SUB-CRYSTAL DISORIENTATION AND DIAMETER

On the fine- and coarse-grained (parallel-sided) specimens the sub-crystal diameter and the mean component α of disorientation about the normal to the microscope stage, were measured in the manner previously described¹⁰ on three different sections, as indicated in Table II.

As before, the angle of disorientation proved to be similar for sections just under the surface and for the mid-section parallel to the surface, suggesting that the deformation did not vary much throughout the volume and that no special surface effect intruded seriously. On the transverse section, however, the angle was higher. The former values may be expected to be reduced by the general tendency towards preferred orientation during extension, while the latter should be unaffected; consequently, the angles measured on the transverse section are the true ones. This was not taken into account in the earlier paper, and hence the calculated extension is under-estimated there.

TABLE II.—*Values for Component α of Disorientation Between Sub-Crystals and for Sub-Crystal Diameter.*

Angle measurements: mean of 100 readings.

Diameter measurements: mean for 400–500 sub-crystals.

Position of Measurement	Fine-Grained Specimen (final extension 50.3%)		Coarse-Grained Specimen (final extension 23.6%)	
	α , degrees	Sub-Crystal Dia., cm. $\times 10^3$ *	α , degrees	Sub-Crystal Dia., cm. $\times 10^3$ *
Just under surface	5.3	2.73	4.2	2.53
Mid-section parallel to surface	6.5	2.42	3.6	2.81
Transverse section	11.8	2.00	6.2	2.40

* Measured in polarized light after anodizing.

TABLE III.—*Values of Sub-Crystal Disorientation θ and Diameter, and Dislocation Density ρ .*

Grain-Size of Specimen	Disorientation, θ		Sub-Crystal Dia., cm. $\times 10^3$	ρ , No. of Dislocations/ cm. ² $\times 10^{-4}$
	Degrees	Radian		
Fine ($9\frac{1}{2}$ grains/mm.) (final extension 50.3%)	16.6	0.29	2.28	8.9
Coarse (1 grain/mm.) (final extension 23.6%)	8.7	0.15	2.51	4.2

The mean component α is related to the mean total disorientation θ by the equation: ¹⁰

$$\cos \theta = \cos^2 \alpha \quad . \quad . \quad . \quad (1)$$

The values of θ obtained by means of equation (1) from the α values measured on a transverse section, are given in Table III.

The measured sub-crystal diameters should also be affected in a similar way by extension, but in this case

none of the measurements can be considered as unaffected. The best procedure seems to be to obtain from the first two rows of Table II a mean sub-crystal size as measured parallel to the surface, and then to form the mean between the resultant and the figure for the transverse section. The values so obtained are included in Table III.

For the measurements on the medium-grain-sized (tapered) specimens, the sub-crystal diameter as measured on a transverse section must be multiplied by the following empirical factor to obtain a more correct average diameter:

$$\begin{array}{ll} \text{50\% extension} & \text{factor} = \frac{2.28}{2.00} = 1.14 \\ \text{(fine-grained specimen)} & \\ \text{24\% extension} & \text{factor} = \frac{2.51}{2.40} = 1.04 \\ \text{(coarse-grained specimen)} & \end{array}$$

To a sufficiently close approximation this factor is $\left(1 + \frac{\epsilon}{4}\right)$, where ϵ is the fractional elongation.

Measurements in the case of the medium-grained specimens were made only on transverse sections.

increase and eventually become sufficiently large to be recorded. This view is supported by the fact that in the early stages of creep sub-boundaries existed which were not detected by the polarized-light method (cf. (a) and (b), Table IV).

Comment on these results is made in the next Section.

3. SUMMARY

During the primary stage of creep, sub-crystals could not be detected. X-ray examination showed disorientation of the crystals, increasing in amount as the extension became greater. The diffuse X-ray spots were eventually replaced by sharp discrete spots, by which time secondary creep had set in. The clusters of sharp spots indicate that the crystals had broken up into a limited number of relatively perfect areas of different orientation. Sub-crystals could be observed with the microscope some time after they had been detected by X-rays. They were first seen near grain boundaries, especially when the grain-size

TABLE IV.—Measurements of Sub-Crystal Disorientation, Diameter d , and Dislocation Density ρ on Medium-Grain-Sized Specimens.

Angle measurements: mean of 100 readings.

Diameter measurements: mean for 350–1000 sub-crystals.

Stress, ton/in. ²	$\frac{1}{2}$	$\frac{1}{2}$		$\frac{3}{4}$		
Creep time, hr.	696	118½	696	5	25	118½
Total elongation, %	3.65	5.4	17.0	8.4	15.0	29.5
Disorientation,* degrees $\begin{cases} \alpha & . & . & . \\ \theta & . & . & . \end{cases}$	$\begin{matrix} \dots \\ \dots \end{matrix}$	$\begin{matrix} 2.6 \\ 3.6 \end{matrix}$	$\begin{matrix} 9.9 \\ 14.0 \end{matrix}$	$\begin{matrix} 2.76 \\ 4.0 \end{matrix}$	$\begin{matrix} 3.49 \\ 4.7 \end{matrix}$	$\begin{matrix} 11.83 \\ 16.6 \end{matrix}$
Diameter † <i>d</i> , cm. × 10 ³ $\left\{ \begin{array}{l} \text{uncorrected} \\ \text{corrected} \end{array} \right.$	7.89 (<i>b</i>)	$\begin{matrix} 9.73 \text{ } (\alpha) \\ 6.85 \text{ } (b) \end{matrix}$	3.3 (<i>a</i>)	$\begin{matrix} 6.00 \text{ } (\alpha) \\ 3.65 \text{ } (b) \end{matrix}$	$\begin{matrix} 3.74 \text{ } (\alpha) \\ 3.58 \text{ } (b) \end{matrix}$	2.16 (<i>a</i>)
	7.98 (<i>b</i>)	$\begin{matrix} 9.85 \text{ } (\alpha) \\ 6.95 \text{ } (b) \end{matrix}$	3.44 (<i>a</i>)	$\begin{matrix} 6.10 \text{ } (\alpha) \\ 3.72 \text{ } (b) \end{matrix}$	$\begin{matrix} 3.89 \text{ } (\alpha) \\ 3.71 \text{ } (b) \end{matrix}$	2.21 (<i>a</i>)
Density ρ , no. of dislocations/cm. ² × 10 ⁻⁹	0.44	5.0	0.8	1.8	8.8

* α is the component of disorientation actually measured; θ is the total disorientation calculated from α , using equation (1).

† (a) Measured in polarized light after anodizing. (b) Measured using phase-contrast illumination after etching in Wyon and Crussard's reagent.⁵

The values obtained are given in Table IV. As indicated in Table I, in a proportion of the sections the disorientations were too small to be measured by the polarized-light technique, which has a sensitivity of $\frac{1}{2}^{\circ}$ – 1° ; with one exception, only those sections on which the disorientation could be measured are referred to in Table IV. The actual measured sub-crystal diameter and the diameter corrected by the factor mentioned above, are both given. The creep extensions are included in order to put the other measurements in their correct context.

It will be seen that the sub-crystal diameter apparently decreased with increasing extension under a given load. However, the whole of this apparent change may really have been a question of sensitivity of measurement. After a slight extension the lattice tilt at some sub-boundaries would be too small to detect, but with further extension the tilts would

was large (Fig. 4, Plate XLI). They were later found throughout the grains. The difference in orientation between adjacent sub-crystals increased progressively as creep proceeded.

At first no displacement along the sub-crystal boundaries was noted. After one or two hundred hours' creep, sub-boundary slip became perceptible (Fig. 5, Plate XLI, XX and YY). The lines along which the slip occurred coincided with the white-line network seen when the microscope was stopped down and the field thrown slightly out of focus (Fig. 6, Plate XLI). Eventually migration of the sub-boundaries was observed, and is the cause of the slight multiplicity of the sub-boundaries at XX (Fig. 5).

The size of the sub-crystals did not vary appreciably with grain-size (Table II). In coarse-grained specimens the sub-crystals were arranged in bands (Fig. 2, Plate XLI). These bands were less prominent in

medium-grained specimens and much less prominent in fine-grained specimens (Fig. 3, Plate XLI). They were most clearly marked in crystals in which one system of slip predominated and the direction of the bands then lay at right angles to the direction of the slip bands. When the bands were in two directions, one band lay parallel to the slip bands. This may be partly attributable to screw dislocations, as suggested previously, but seems also partly due simply to the concentration of dislocations in the prominent slip bands. The evidence for this is that bands of sub-crystals have been observed to follow bent slip bands (Figs. 36 and 37, Plate LXXIX, of ref. 10), whereas if due solely to screw dislocations, they would be parallel to crystallographic plates and therefore straight.

The sub-crystals grew smaller as the stress, and therefore the rate of strain, increased, as observed by Wood and Rachinger.¹⁵ The rate at which they

the sub-boundary can, however, be seen, although the microscope sensitivity is such that a displacement of 250 Å. can be detected. In the later stages of creep, when movements could be detected at the sub-boundaries, the amount of movement was less than one fifteenth of that which would be expected from the orientation differences between adjacent sub-crystals. For example, in the fine-grained specimen after 901 hours' creep, the average sub-boundary displacement was less than 0.2×10^{-4} cm.; since the average sub-crystal diameter was 2.3×10^{-3} cm., this would lead to an average disorientation of the sub-crystals of less than 1° . The measured disorientation was 16.6° . In a second case the measured average disorientation was 8.7° , whereas that calculated from the average sub-boundary displacement was less than $\frac{1}{2}^\circ$.

Nevertheless, it is confirmed that sub-boundary slip does occur. Although under the present conditions these displacements were small, it is probable

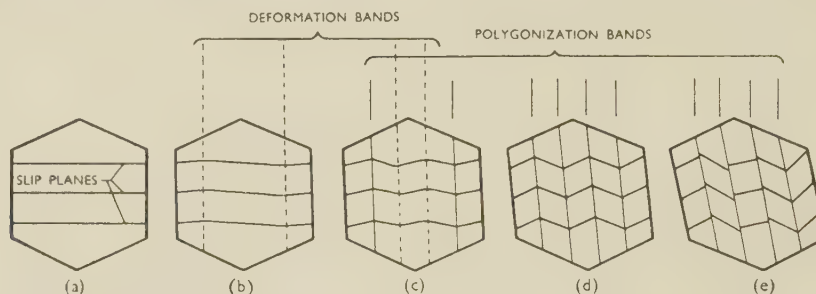


FIG. 8.—Model for Lattice Deformation During Creep. (a) Initial condition of crystal; (b) 1st-stage creep; (c) 1st-2nd-stage creep; (d) 2nd-stage creep; (e) late 2nd-stage creep. Changes shown for one operative slip direction only.

formed increased as the stress increased. At a stress of $\frac{3}{4}$ ton/in.² sub-crystals were detected by X-rays after 5 hr., but were not visible after 118½ hr. at $\frac{1}{3}$ ton/in.².

Some difficulty may be experienced in realizing how dislocation walls can produce the equiaxed sub-crystals observed, since ideally these are straight,⁹ but if it is considered that in general there are several slip directions, and that associated with each direction of slip there exist both edge and screw dislocations which polygonize in different planes, it will be seen that complex shapes and complex rotations of the sub-crystals can readily arise.

Polygonization, of course, produces a relative rotation of the sub-crystals by kinking of the lattice, as shown diagrammatically in Fig. 8, discussed in Section IV. Wood and Wilms have put forward the alternative view that this rotation occurs primarily by relative displacement at the sub-boundaries. Fig. 7 (Plate XLII) is a typical interference micrograph of a sub-boundary (PP) in a specimen that had crept 11.9% in 180 hr. at $\frac{1}{2}$ ton/in.². The difference in orientation between the crystals on the two sides of the boundary was about 3° and the sub-crystal diameter was about 0.005 cm. If the difference in orientation had been produced by the crystals sliding past each other, the displacement at the sub-boundary would have been about 12,500 Å. No displacement at

that at higher temperatures they would be relatively larger. They may be highly significant and are referred to again in the discussion (Section VI).

IV.—MODEL FOR CRYSTAL DEFORMATION DURING CREEP

1. BASIS

A model representing crystal deformation during creep has been built up on three bases: (1) The well-established fact that sub-crystals form during creep. (2) The dislocation theory of sub-crystal formation. (3) The deduction¹² that during transient creep many dislocations travel to the grain boundaries. No effect of grain boundaries is considered.

The model is illustrated diagrammatically in Fig. 8, where, for clarity, the changes for one operative slip direction only are shown. Other operative slip directions would produce an additional similar effect, as already mentioned. The stages shown separately would, of course, overlap in practice. Initially, stage (a), the lattice planes are flat. During primary creep some dislocations approach the boundary to produce deformation bands (b), and others form deformation bands in the crystal interior (c). During secondary creep polygonization develops, first near the crystal boundaries (c), and then in the whole crystal (d).

The structure depicted in (d) and the process leading up to it appear to characterize secondary creep, as far as deformation of each crystal is concerned. Subsequently displacement occurs at the sub-boundaries (e).

2. TEST OF MODEL

The measurements of θ were used to check the model in Fig. 8, employing the relation:¹⁰

$$E\% \cong 100\theta \quad (2)$$

which is based essentially on this model. To avoid confusion it may be desirable before proceeding further to consider just what part of the total extension is involved in equation (2). In the earlier paper interest centred on estimating the "missing creep". This was compared with the extension calculated from equation (2), which should include both the creep due to "fine" slip and that due to slip on easily visible slip bands. In the present paper, the important point to decide is what part of primary and secondary creep

probably nearer the truth for the coarse-grained specimen, and case (ii) for the others; the difference in practice is not very large, and for simplicity case (ii) has been assumed throughout.

The data are given in Table V for all the conditions available. The two quantities to be compared are printed in heavy type.

The agreement between calculated and measured creep ($A-B$) is fairly close, not being more in error than 2:1 in any instance. The scatter in the calculated creep, as compared with the measured values, is probably due mainly to the wide variations between individual disorientations, so that to get a good mean in every case, a very large number of readings would have to be taken. However, the degree of agreement in Table V provides further quantitative support for stage (d) of the model in Fig. 8.

It should be emphasized that the creep calculated here relies not on measurements made on the specimen surface, but on sections cut through the interior, and

TABLE V.—Comparison Between Calculated and Measured Secondary Creep.

Grain-size of specimen . . .	Fine ($9\frac{1}{2}$ grains/mm.)	Coarse (1 grain/mm.)	Medium ($4\frac{1}{2}$ grains/mm.)					
Load, ton/in. ² . . .	$\frac{1}{2}$	$\frac{1}{2}$	$\frac{1}{2}$		$\frac{3}{4}$			
Creep time, hr. . . .	901	1145	118 $\frac{1}{2}$	696	5	25	118 $\frac{1}{2}$	
Total creep (A), % . . .	50.3	23.6	5.4	17.0	8.4	15.0	29.5	
G.b. creep* (B), % . . .	7.5	0.4	0.5	1.5	0.4	0.7	1.4	
($A-B$), %	42.8	23.2	4.9	15.5	8.0	14.3	28.1	
Calculated creep,† % . . .	29.0	15.0	6.2	24.4	7.0	8.0	27.9	

* Extension due to grain-boundary displacement.

† Calculated from equation (2).

is to be included. It is clear that extension due to grain-boundary movement is to be excluded. To go further, it may help to consider two extreme cases which are modifications of Fig. 8. In case (i) all the primary creep is due to dislocations which travel to the grain boundary, where they eventually polygonize to cause tilts of θ_1 near the boundary, and the extension is $100\theta_1$. During secondary creep, when sub-boundaries have formed throughout the crystal interior, we have the case treated previously; the tilt is θ_2 and the extension $100\theta_2$. Neglecting the intermediate condition, when only a few sub-boundaries have formed, or when they are too weak to be certain of capturing dislocations, the total extension is $100(\theta_1 + \theta_2)$. In case (ii) even during primary creep, dislocations do not travel a distance greater than the sub-crystal diameter, owing to internal obstructions such as solute atoms, and polygonize to cause sub-boundaries throughout the crystal interior at which the mean tilt is θ_3 , giving a total extension of primary plus secondary creep of $100\theta_3$. Case (i) is probably approached by large-grained specimens of pure metal, and case (ii) by fine-grained metals and particularly by alloys. In the present investigation case (i) is

is therefore representative of the whole specimen volume.

V.—DISLOCATION DENSITIES *

Since few estimates of the dislocation density based on fairly direct theoretical interpretation have been made, it seems of interest to report values here, as these can be calculated from the simply derived equation¹⁰:

$$\rho = \frac{2\theta}{d\lambda} \quad (3)$$

where ρ is the dislocation density (i.e. the number of dislocations intersecting a surface 1 cm.² in area), λ is the unit slip distance, and d and θ , as before, are the sub-crystal diameter and disorientation, respectively. The qualification should be made that equation (3) counts only the dislocations in sub-boundaries. As, in the later stages of creep, the sub-boundaries appeared fairly undistorted when subjected to both micro- and X-ray examination, it is probable that the values relating to the later stages do include practically the whole dislocation density. It is equally probable that

* Counting only dislocations in the sub-boundaries.

the values relating to the early stages under-estimate the total density. The densities are included in Tables III and IV (pp. 288 and 289). The value taken for the sub-crystal diameter d was that found by the polarized-light method, i.e. the same method as that used for determining the disorientation. The densities are within the range of previous estimates, namely, that an annealed metal contains about 10^8 dislocations/cm.² and a heavily cold-worked metal about 10^{12} /cm.²

VI.—DISCUSSION

It is interesting to compare the sub-boundaries with the main grain boundaries in the same specimen. The displacement at the latter has been measured and is compared with that at the sub-boundaries in two specimens in Table VI.

TABLE VI.—Comparison of Displacement θ at Sub-Boundaries and Main Boundaries.

Grain-Size of Specimen	Sub-Boundaries		Main Boundaries
	Displacement, μ	Disorientation θ , degrees	Displacement, μ
Fine ($9\frac{1}{2}$ grains/mm.), after 901 hours' creep . . .	≥ 0.2	16.6	11.0
Coarse (1 grain/mm.), after 1145 hours' creep . . .	≥ 0.1	8.7	6.3

The main grain boundaries therefore underwent more than 50 times as much displacement as the sub-boundaries. The mean orientation tilt across the main boundaries was doubtless larger than that across the sub-boundaries* but could clearly be larger only by a few times. As there is no evidence that the rate of sub-boundary displacement increases rapidly with increasing disorientation, it appears as though a difference in kind exists between sub-boundaries and main boundaries. According to the dislocation theory of polygonization, the former consist initially of rows of dislocations. An alternative structure is that of a random arrangement of atoms, and presumably the main boundaries are so composed.

Another approach leads to the same conclusion. The polygonized array of dislocations forms because it has less energy than a more or less random arrangement of dislocations. It does not follow that the polygonized array is the most stable arrangement of atoms that can accommodate the orientation differences across the sub-boundary. In fact, since there

are innumerable alternative arrangements of atomic misfit, this is most unlikely. The polygonized array of dislocations is simply the arrangement first formed by migration from the initial random arrangement. The main grain boundaries, however, are formed in a different way during recrystallization and usually have more opportunity of approaching the arrangement of lowest energy. They are therefore likely to comprise some arrangement of general atomic misfit.

Given that an arrangement of general atomic misfit of lower energy than that due to polygonization exists, this will in time be attained by sub-boundaries initially polygonized; these will then have become ordinary grain boundaries and will display their properties, such as grain-boundary displacement and grain growth. The material will then have recrystallized.

The suggestion is therefore made that the sub-boundaries observed in the present work gradually underwent this transformation during creep, but that it was not complete before the tests ended. The observed results would then be produced if displacement occurred only along transformed parts of the sub-boundaries, and was there restricted by the anchoring effect of the untransformed parts.

ACKNOWLEDGEMENTS

The author desires to acknowledge the assistance given by Mr. M. H. Farmer. The work described was carried out as part of the general research programme of the National Physical Laboratory and the paper is published by permission of the Director of the Laboratory.

REFERENCES

1. C. H. M. Jenkins and G. A. Mellor, *J. Iron Steel Inst.*, 1935, **132**, 179p.
2. G. R. Wilms and W. A. Wood, *J. Inst. Metals*, 1948–49, **75**, 693.
W. A. Wood, G. R. Wilms, and W. A. Rachinger, *ibid.*, 1951, **79**, 159.
3. E. A. Calnan and B. D. Burns, *ibid.*, 1950, **77**, 445.
4. G. B. Greenough and E. M. Smith, *ibid.*, 1950, **77**, 435.
5. G. Wyon and C. Crussard, *Rev. Mét.*, 1951, **48**, 121.
6. R. C. Gifkins, *J. Inst. Metals*, 1951, **79**, 233.
7. W. Betteridge and A. W. Franklin, *ibid.*, 1951–52, **80**, 147.
8. A. H. Cottrell and V. Aytekin, *ibid.*, 1950, **77**, 389.
9. R. W. Cahn, *ibid.*, 1949–50, **76**, 121.
10. D. McLean, *ibid.*, 1951–52, **80**, 507.
11. N. F. Mott, *Proc. Phys. Soc.*, 1951, [B], **64**, 729.
12. D. McLean, *J. Inst. Metals*, 1952–53, **81**, (3), 133.
13. D. McLean, *ibid.*, 1952–53, **81**, (6), 293.
14. R. W. K. Honeycombe, *ibid.*, 1951–52, **80**, 39.
15. W. A. Wood and W. A. Rachinger, *ibid.*, 1949–50, **76**, 237.

* Some measurements with the polarized-light technique on an annealed specimen gave $\alpha = 29.4^\circ$, equivalent to a total mean tilt $\theta = 40.6^\circ$.

GRAIN-BOUNDARY SLIP DURING CREEP OF ALUMINIUM*

1445

By D. McLEAN,† B.Sc., MEMBER

(Communication from the National Physical Laboratory.)

SYNOPSIS

Grain-boundary displacements during creep at 200° C. have been measured in seven super-pure aluminium specimens. The tests covered a range of grain-size from 1 to 9½ grains/mm. and of stress from about ½ to about ¾ ton/in.². The curves of grain-boundary displacement plotted against time resemble the corresponding extension/time curves. The fraction of the total extension due to the grain-boundary displacements was calculated. At a constant load of ½ ton/in.² this increased with decrease in grain-size from about one-fiftieth for 1 grain/mm. to about one-sixth for a grain-size of 9½ grains/mm. At constant grain-size (4½ grains/mm.) it increased with decrease in load, from about one-fiftieth for a load of 1 ton/in.² to about one-fifth for a load of ¼ ton/in.². A plot of grain-boundary displacement against extension due to crystal deformation is linear for all specimens, suggesting a linear interaction between these two quantities. A model for this interaction is proposed, and calculation shows it to agree with experiment within 2 : 1.

I.—INTRODUCTION AND MAIN RESULTS

IN work previously reported¹ the average grain-boundary displacement in an aluminium specimen undergoing creep extension was measured and the extension due to these movements calculated. An improved technique² has now been used to measure the influence of grain-size and applied stress on such grain-boundary displacements.

Earlier work had shown that the ratio of grain-boundary movement to slip-band movement is higher the lower the stress^{3,4} and that there is a tendency for fine-grained material to creep faster than coarse-grained.⁵⁻⁸ These effects have been confirmed. In particular, a fine-grained specimen crept about twice as fast as a coarse-grained one. However, the grain-boundary displacements were responsible for not more than about one-sixth of the total extension, even in the fine-grained specimen, so that the more numerous grain boundaries in the latter cannot be an important cause of the greater creep rate. Although the grain-boundary slip was faster in the fine-grained specimen, the crystals themselves must also have deformed more rapidly.

The explanation of this fact may be assisted by a new observation. For all specimens, covering a range of creep rates of 30 : 1, a linear relation is found between the grain-boundary displacement and the crystal-lattice slip. From this it is inferred that an interaction occurs between the two. A model for this interaction is proposed that accords with qualitative observation and provides about the correct quantitative relation. According to this model the grain-boundary movement is linked to the process of crystal recovery.

Grain-boundary movements have been measured

previously by Kê,⁹ using a different method from that now employed. Since it is of interest to compare the results given by the two different methods, Section VII (p. 299) is devoted to such a comparison.

II.—EXPERIMENTAL

The preparation of the specimens and technique of measurement have been described fully in a paper² giving the results of measurements of slip bands in the same specimens as were used in the present experiments. Briefly, these were all of super-pure aluminium of about 99.98% purity (0.002–0.003% iron, 0.003% copper, 0.003% silicon), electropolished to avoid work effects. Different grain-sizes were obtained by annealing at different temperatures. As a precautionary measure all specimens were furnace-cooled from the various annealing temperatures to the test temperature of 200° C. in order to develop the equilibrium condition, e.g. as regards distribution of impurities between grain interior and grain boundary, pertaining to 200° C.

Seven specimens were employed. Two of these, one having 1 grain/mm. and the other 9½ grains/mm.† were used to explore the influence of grain-size. They were stressed at ½ ton/in.² and removed periodically for examination and measurement. The other five specimens were used to determine the influence of applied stress. They had a grain-size of 4½ grains/mm., and were tapered in width, a convenient way of obtaining a range of load extending from about ½ to about ¾ ton/in.². Each was loaded for a given time (1, 5, 25, 118½, or 696 hr.), removed from the machine, examined, and measured. From these measurements, curves against time for different loads from ½ to ¾ ton/in.² could be constructed. Whereas

* Manuscript received 21 June 1952.

† Metallurgy Division, National Physical Laboratory, Teddington.

‡ A duplicate fine-grained specimen was also prepared and measurements made on it after 6 hours' creep. The result is included in Fig. 2 (b) and shows satisfactory agreement.

the first two specimens were subjected to intermittent loading with opportunities for recovery, the latter five were continuously loaded, so that the results from the two sets of specimens are not strictly comparable.

The grain-boundary displacements are given as the average total displacement, \bar{p} , rather than as the actual measured vertical component. The former is obtained from the latter by a simple averaging procedure.²

III.—MEASUREMENTS OF GRAIN-BOUNDARY DISPLACEMENT

The influence of stress on grain-boundary displacement is shown in Fig. 1, where displacement is plotted

influence of stress on displacement and extension is similar; so, too, is the effect of difference in grain-size. The primary grain-boundary displacement and extension both increase with increase in grain-size, while the secondary rates decrease, with the result that the curves for different grain-sizes eventually cross. In this connection it should be borne in mind that the quantity plotted as grain-boundary displacement is the mean displacement at a single grain boundary, so that the smaller number of grain boundaries in the coarse-grained specimen is not responsible for the slower rate of displacement during secondary creep shown for this specimen in Fig. 2 (a). Two further points of resemblance between the displacement and the extension curves

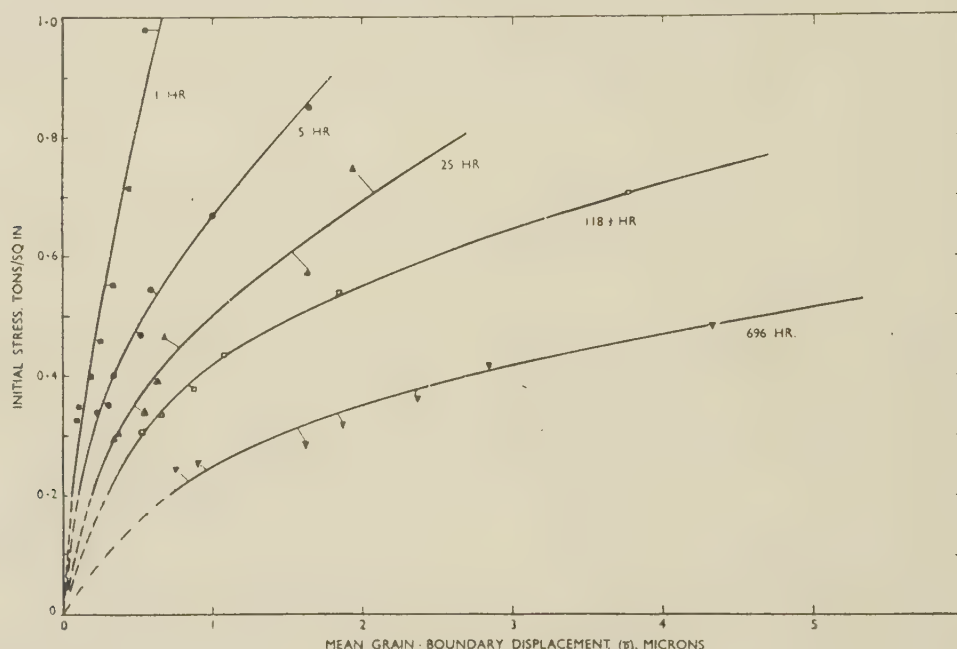


FIG. 1.—Influence of Initial Stress on Grain-Boundary Displacement for Medium-Grain-Sized Specimens. The tests were made at constant load, so that the actual stress increased with extension.

against initial stress for the five medium-grain-sized (tapered) specimens. Each curve therefore relates to a particular duration of creep. It is clear that the grain-boundary displacement increased with load faster than linearly.

From Fig. 1 were derived grain-boundary displacement/time curves for the three initial stresses of $\frac{1}{3}$, $\frac{1}{2}$, and $\frac{3}{4}$ ton/in.², and these are given in Fig. 2 (a), together with the corresponding curves for the fine- and coarse-grained specimens for $\frac{1}{2}$ ton/in.². The initial portions of these curves are shown on an enlarged time scale in Fig. 2 (b).

The curves closely resemble a typical creep curve, exhibiting the primary and secondary stages typical of creep extension/time curves, as may be seen by comparing Fig. 2 (a) with the extension/time curves for these specimens given in Fig. 3. The corresponding curves show the change from primary to secondary creep at about the same time; the

are that for the fine-grained specimen both show the tertiary stage of creep, and for the coarse-grained specimen both show, on the other hand, a fall in creep rate between the last two measurements. The latter behaviour seems anomalous, and the reason for it is uncertain, but that it occurred both in the grain-boundary displacement curve and the elongation curve provides additional evidence that the two quantities are connected.

The curves in Figs. 4 and 5 show how the rate of grain-boundary displacement $d\bar{p}/dt$, plotted logarithmically, changes as the displacement increases. Fig. 4 includes the curves for the fine- and coarse-grained specimens and shows the influence of grain-size for a given load; Fig. 5 reproduces the curves for the medium-grain-sized (tapered) specimens and illustrates the effect of stress for a given grain-size. The general trend is for $d\bar{p}/dt$ to fall steeply at first and then to level off; the curve for the fine-grained

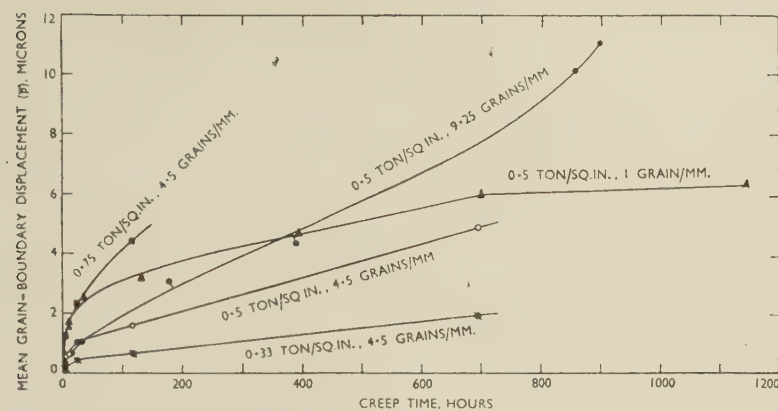


FIG. 2 (a).—Grain-Boundary Displacement During Creep Tests.

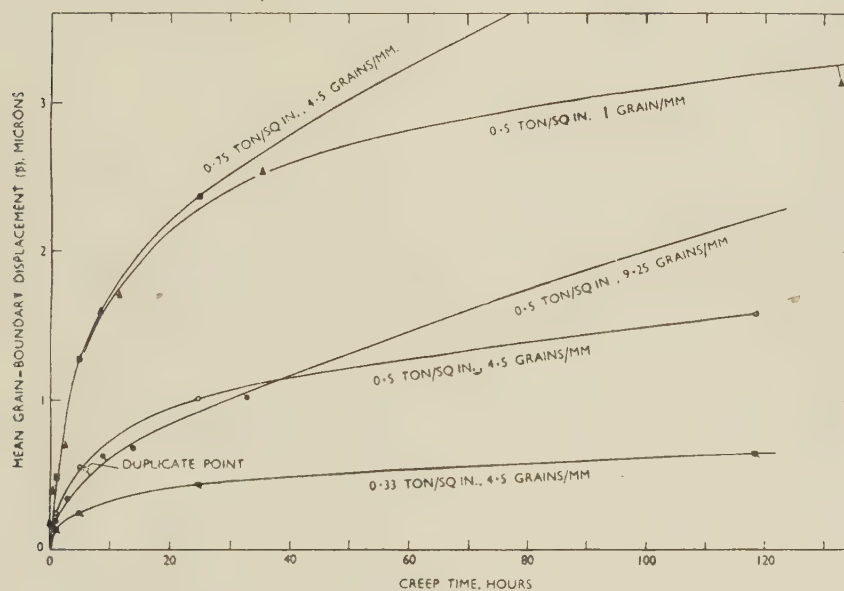


FIG. 2 (b).—As Fig. 2 (a) (on enlarged scale).

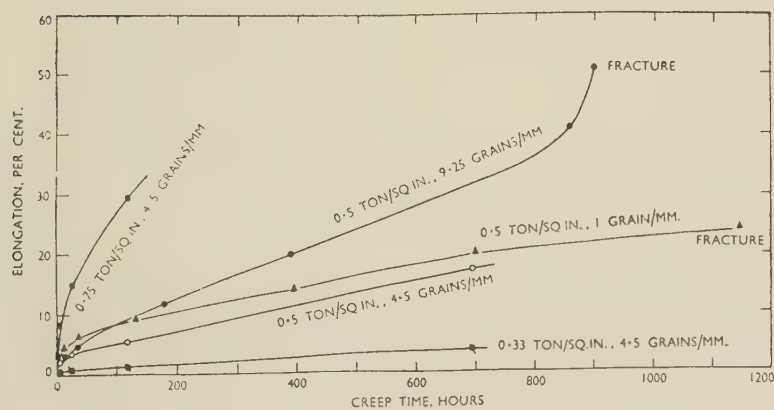


FIG. 3.—Creep Time/Elongation Curves.

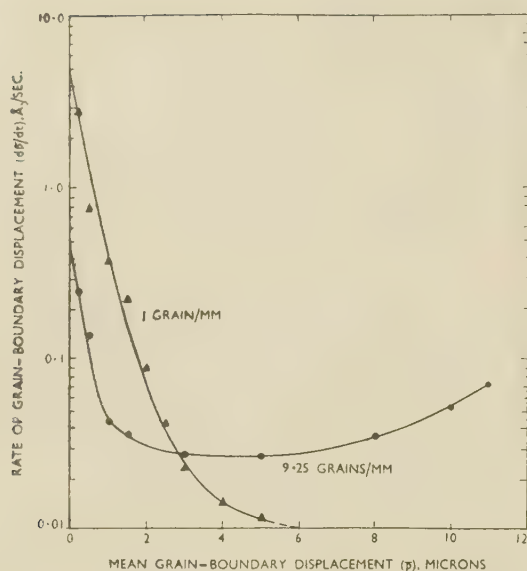


FIG. 4.—Influence of Grain-Size on Rate of Grain-Boundary Displacement Plotted Against Mean Displacement.

specimen (Fig. 4) exhibits also the final rise corresponding to tertiary creep. The initial rate of grain-boundary displacement for the fine-grained specimen was 0.45 Å./sec. and for the coarse-grained specimen 4.7 Å./sec. The ratio of these rates ($10.4:1$) is nearly equal to the ratio of the grain-sizes of the specimens ($9\frac{1}{4}:1$). This near equality may be significant. The minimum rates were 0.027 Å./sec. for the fine-grained and about 0.01 Å./sec. for the coarse-grained material. The ratio of $1:2.7$ presumably has no direct connection with grain-size.

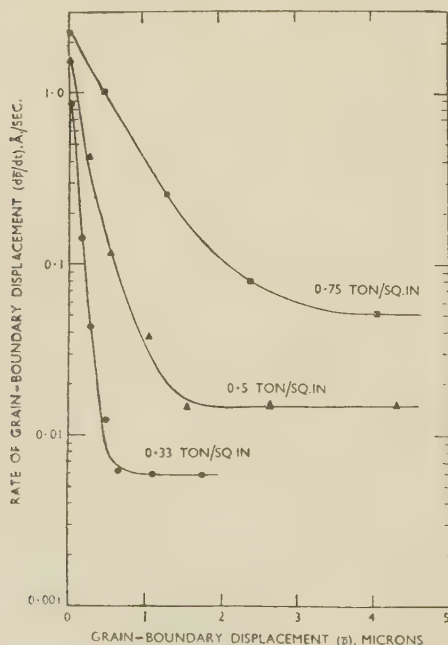


FIG. 5.—Influence of Stress on Rate of Grain-Boundary Displacement Plotted Against Grain-Boundary Displacement for Medium-Grain-Sized Specimens.

The initial rates of grain-boundary displacement for loads of $\frac{1}{3}$, $\frac{1}{2}$, and $\frac{3}{4}$ ton/in.² (Fig. 5) were respectively 0.85 , 1.55 , and 2.2 Å./sec. The minimum creep rates were 0.0058 , 0.014 , and 0.05 Å./sec. for the same loads.

The initial drop in rate of grain-boundary displacement implies that the resistance to movement at the grain boundaries increases as movement continues. Part, at least, of this effect is presumably due to obstruction at grain corners and protuberances. There are fewer of these the larger the grain-size, and their numbers should vary inversely as the grain-size; the initial rates of grain-boundary displacement might, therefore, be expected to vary in proportion to grain-size, as observed for the fine- and coarse-grained specimens. Beyond this, the mechanics of grain-boundary movement are unclear. However, one possibility is that, as crystal slip occurs concomitantly with grain-boundary displacement, the boundaries may become roughened, and this may be an additional factor impeding grain-boundary slip and one that increases in intensity as deformation progresses.

IV.—EXTENSION DUE TO GRAIN-BOUNDARY DISPLACEMENT COMPARED WITH MEASURED EXTENSION

From the grain-boundary displacements and the grain-sizes of the different specimens, the extension due to the grain-boundary displacements was calculated, using the formula:¹

$$E\%_{\text{g.b.}} = 100[\sqrt{(1 + \sqrt{2}n\bar{p} + n^2\bar{p}^2)} - 1]$$

where n is the number of grains/cm. as measured by the linear-intercept method. As $n\bar{p}$ in most cases is small compared with unity, this formula reduces fairly accurately to:

$$E\%_{\text{g.b.}} = \frac{100n\bar{p}}{\sqrt{2}}$$

which is linear in \bar{p} . Consequently, the curves of $E\%_{\text{g.b.}}$ plotted against time have the same shape as those of \bar{p} against time, and therefore the same as those of total elongation against time. This means that the ratio $E\%_{\text{g.b.}}/E\%_{\text{total}}$ does not vary much during extension. It does vary considerably, however, with stress and grain-size. The ratio is plotted logarithmically against initial stress in Fig. 6 for the medium-grain-sized specimens, and points are also plotted for the fine- and coarse-grained specimens.

It is clear that for a given initial stress the ratio increased in about the same proportion as the grain-size decreased, from 0.0186 for a grain-size of 1 grain/mm. to 0.148 for $9\frac{1}{4} \text{ grains/mm.}$ This sense of change is the same as that found by previous workers. It is usually considered to be due to the larger number of grain boundaries in fine-grained material. However, the fine-grained specimen crept twice as fast as the coarse-grained specimen during secondary creep, whereas the additive effect of the grain boundaries could give an increase only in the ratio of $5:4$. The faster creep rate of the fine-

grained specimen in this case is therefore not due simply to the larger number of grain boundaries. Nor is it due to the formation of grain-boundary fissures, for none were seen.

For the medium-grain-sized specimen the plot against initial stress confirms that at constant grain-size the grain-boundary movements contribute a smaller amount to the total extension the higher the load. The ratio ranges from about one-fiftieth at 1 ton/in.² to about one-fifth at $\frac{1}{4}$ ton/in.². If an

evidence of a linear interaction between the two quantities.

In another paper¹⁰ a model is proposed for the crystal deformation during second-stage creep. It is found that for a small extension this gives an interaction between grain-boundary displacement and

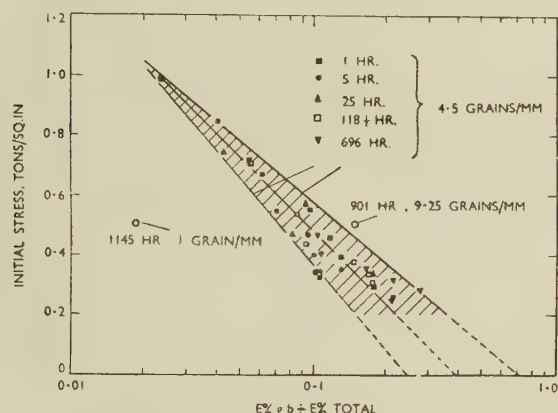


FIG. 6.—Influence of Grain-Size and Stress on Fraction of Total Creep Extension due to Grain-Boundary Displacement.

extrapolation to zero stress be risked, it indicates that about half the total extension is due to grain-boundary movements at zero stress.

V.—INTERACTION BETWEEN GRAIN-BOUNDARY DISPLACEMENT AND CRYSTAL SLIP

The close similarity of the curves of total elongation and of grain-boundary displacement against time suggested plotting these values against each other. It subsequently appeared more relevant to plot that part of the total elongation not due to grain-boundary displacement (and presumably due to crystal slip) against the grain-boundary displacement. The two curves in Figs. 7 (a) and (b) relate to the fine- and coarse-grained specimens and the three in Fig. 8 to the medium-grain-sized specimens at different stresses.

All the curves are straight lines within experimental error, except near the origin. Since the range of creep rates covered was about 30:1 and different grain-sizes and stresses were used, this can hardly be accidental, but suggests rather a linear interaction between grain-boundary displacement and crystal slip. The slopes increase with decrease in stress, but do not alter appreciably for a difference in grain-size of nearly 10:1, as shown by the curves for the fine- and coarse-grained specimens in Fig. 7 (a). This requires that the interaction be virtually independent of grain-size. The actual creep rates for these two specimens differed, so that the rates of crystal slip and of grain-boundary displacement must have changed in the same ratio. This provides further

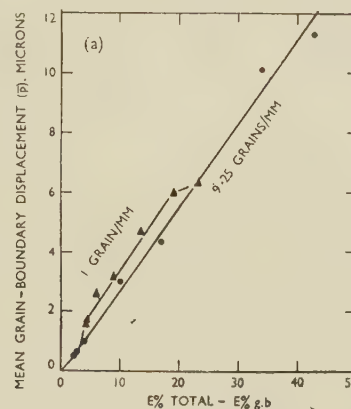


FIG. 7 (a).—Grain-Boundary Displacement Plotted Against Extension due to Crystal Slip (i.e. Total Extension—Extension due to Grain-Boundaries), for Large- and Fine-Grained Specimens.

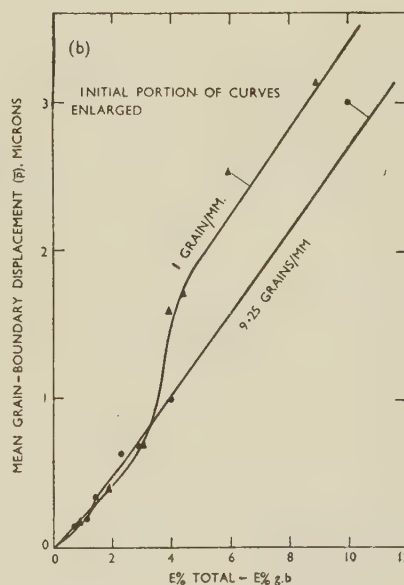


FIG. 7 (b).—As Fig. 7 (a) (on enlarged scale).

crystal slip independent of grain-size and with about the right numerical factor.

The essential feature of the model is depicted in Fig. 9, which shows a particular crystal in an aggregate before and after creep. Slip occurs on the glide planes *SS*, and the dislocations generated polygonize into rows arranged approximately at right angles to the slip planes, causing the lattice to be tilted alternately clockwise and anti-clockwise through an angle θ . The original crystal therefore splits up into sub-crystals bounded by rows of dislocations. For clarity, Fig. 9 shows the deformation caused by slip

in one direction only, but the same process is presumed to happen for each operative slip direction. For one operative slip direction the crystal splits up into sub-crystals of lamellar shape, as shown in Fig. 9, but for three operative directions the resultant sub-crystals are fairly equiaxed.

It has been shown¹ that polygonization can sometimes have been responsible for grain-boundary displacement, i.e. a displacement such as that marked

(The factor $\frac{1}{2}$ enters because one direction only of slip is under consideration.) This equation has the correct form, since it gives a linear relation between grain-boundary displacement and extension which is independent of grain-size. According to this equation the measured value of \bar{d} , the average sub-crystal size, should be equal to the value of \bar{p}/E given by the slopes of the curves in Figs. 7 and 8. Table I shows that this is so.

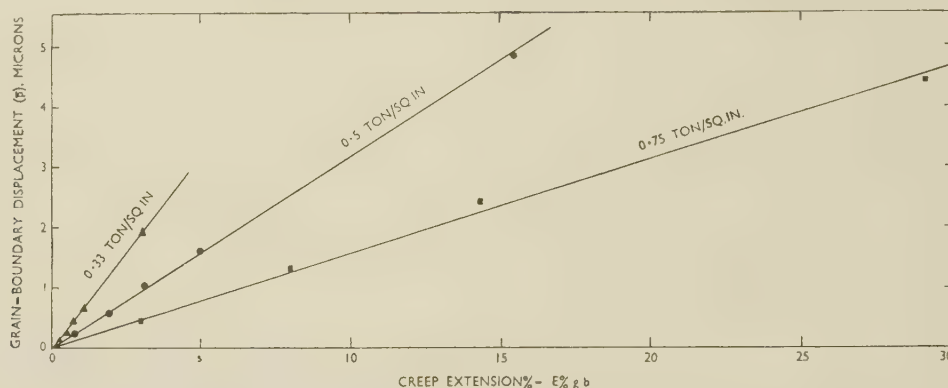


FIG. 8.—Grain-Boundary Displacement Plotted Against Extension due to Crystal Slip (i.e. Total Extension—Extension due to Grain Boundaries), for Medium-Grain-Sized Specimens at Different Stresses.

\bar{p} in Fig. 9 can be caused by the rotation of the lattice. Let us suppose this to be generally true and that the whole grain-boundary displacement arises in this way. It is an easy matter to deduce approximately the relation that should then hold between displacement and extension. The grain-boundary displacement associated with polygonization (see Fig. 9) is:

$$\bar{p} = d\bar{\theta}/2 \quad (1)$$

where \bar{p} and $\bar{\theta}$ both refer to average values and d is the spacing between polygonization bands, i.e. the width of the lamellae for one operative slip direction or the mean sub-crystal diameter for two or more operative slip directions. (In the general case a multiplying factor should be introduced to take into account the fact that polygonization bands are not necessarily parallel to grain boundaries. The average value of the factor should, however, be close to unity, and it has accordingly been omitted.) The observed \bar{p} is the difference between the movements of two crystals, both of which may have moved. If they move in opposite directions, the measured \bar{p} would be twice that given by equation (1). If they move in the same direction, $\bar{p} = 0$. The average measured value, \bar{p} , is therefore given by equation (1), and this is true whatever the direction of movement, provided that the movements are random. Using the equation connecting extension due to crystal slip with disorientation at polygonized boundaries:¹

$$E \cong \bar{\theta}/2 \quad (2)$$

where E is the fractional extension due to crystal slip, we obtain, substituting for $\bar{\theta}$ in equation (1):

$$\bar{p} = dE \quad (3)$$

Details of the measurement of \bar{d} are given in another paper.¹⁰ The agreement is as close as can reasonably be expected. It seems, therefore, that the model in Fig. 9, on which equation (3) is based, is possibly correct, and that under the conditions of test used in this work practically all the grain-boundary displacement may have been associated with polygonization in the manner depicted in Fig. 9. The

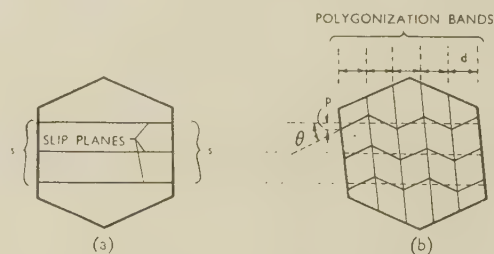


FIG. 9.—Model for Crystal Deformation and Grain-Boundary Movement During Creep. (a) Initial state of crystal; (b) State of crystal after creep.

existence of a relationship between the values of \bar{p} , which are measured on the surface of the specimen, and of E , which is a measurement of the extension of the material as a whole, suggests that the surface measurements do not seriously misrepresent the grain-boundary movements throughout the metal.

The model in Fig. 9 for the interaction between crystal slip and grain-boundary slip suggests the probability that one of these processes controls the other, and hence the total creep rate. It is a crucial matter to decide which process predominates, since methods of influencing it will influence the creep rate

TABLE I.—Comparison between Sub-Crystal Diameter (d) and \bar{p}/E

Specimen and Grain-Size	Initial Stress, ton/in. ²	d , cm. $\times 10^{-3}$	\bar{p}/E , cm./fractional extension $\times 10^{-3}$
Fine-grained (9½ grains/mm.)	½	2.3	2.8
Coarse-grained (1 grain/mm.)	½	2.5	2.9
Tapered, medium-grained (4½ grains/mm.)	⅓	8.0	6.6
	⅓½	3.4	3.2
	¼	2.2	1.55

to much the same degree. By a familiar principle, it should be that process which is the slower under the particular conditions. Before going further than this it is probably desirable to await the results of further experiments.

In Fig. 7 (*b*) are given on an enlarged scale the initial portions of the curves of grain-boundary displacement against crystal slip for the fine- and coarse-grained specimens. There is a fairly definite indication that both curves depart from linearity near the origin to follow the same shape. This suggests that the interaction between grain-boundary displacement and crystal slip does not operate right from the beginning of creep, and is consistent with the view that it characterizes the second stage of creep. Since, during the primary stage, the coarse-grained specimen extended much more than the fine-grained one, the fact that the departure from linearity extended to a larger elongation for the coarse-grained specimen is understandable on this hypothesis.

VI.—GRAIN GROWTH DURING CREEP

Besides the tangential slip at grain boundaries so far discussed, growth of one grain into another also occurred, as has been observed by Wyon and Crusaid¹¹ and by Chang and Grant.¹² This is illustrated in Figs. 11 and 12 (Plate XLII). Fig. 11 shows a boundary that has moved about 20 μ into the neighbouring grain. Fig. 12 is of the same field at a later stage and makes clear that growth of the left-hand grain into the right-hand one is actually occurring. Attention may be drawn to the "tide marks" parallel to the boundary, which are presumably due either to the grain growth or to the boundary slip, or both, being intermittent; and also to the tendency of the tide marks to anchor to etch pits, which is suggestive of a surface-tension effect.

Grain growth was considerably more marked the finer the grain-size. A possible reason for this is that the higher temperature of anneal used to produce a coarser-grained structure gives the grain-boundary atoms more opportunity of reaching positions of a good fit, i.e. of low energy, before test, than those in finer-grained specimens. If so, this difference must have persisted throughout the 700–1000 hr. of creep of the specimens to cause the observed difference in grain growth during creep. Taking the amount of grain growth occurring during any heating period as

a measure of the effectiveness of the heating in promoting grain-boundary equilibrium, this seems reasonable, because the amount of grain growth that occurred during the 1000 hr. of creep was much less than the amount that must have occurred during the annealing treatments to produce the stated grain-sizes.

VII.—COMPARISON OF PRESENT VALUES OF GRAIN-BOUNDARY DISPLACEMENT WITH KÊ'S MEASUREMENTS

Kê made measurements of creep which he has interpreted in terms of grain-boundary displacement.⁹ The experiment consisted of suddenly applying a very small twisting couple to a wire at elevated temperature and observing the torsional creep by the deflection of a spot of light. The creep was considered to be due to slip at grain boundaries, which were thought to behave in a viscous way, and a good deal of evidence is given to support this view. The slip was eventually brought to a halt owing, it was thought, to the resistance set up at grain corners. It was considered that such resistance was purely elastic at the low strains involved, an assumption supported by the facts that on removing the applied couple almost the entire twist was ultimately recovered and that the relation between stress and limiting creep deflection was linear for the very small stresses used. However, for large grain-boundary displacements the elastic resistance must clearly break down. Those in the present work must have been large enough for this to happen, so that, if the assumptions involved are correct, a suitable comparison with Kê's results should show at what grain-boundary displacement the breakdown occurs. A suitable comparison is between the curves of grain-boundary velocity plotted against displacement. To obtain these quantities some manipulation of Kê's published data is necessary; this, can, however, be done without introducing any serious assumption other than those which he himself made.

Kê gives the creep deflection as a fraction of the instantaneous deflection. It seems required by his results that the latter should be due to elastic shear. For a grain-size of a cm. the elastic-shear displacement across each grain, produced by a shear stress of S per unit area, would be Sa/G , where G is the rigidity modulus. The limiting creep deflection was observed to be 50% of the instantaneous deflection, and hence:

$$\text{grain-boundary displacement} = \frac{1}{2} \frac{Sa}{G} \sqrt{2}. \quad (4)$$

the factor $\sqrt{2}$ being due to the grain boundaries making, on an average, an angle of 45° with the applied shear stress. The grain-size of the wires used by Kê was 0.03 cm., and the rigidity modulus of aluminium is 2.7×10^{11} dynes/cm.². For an applied shear stress of ¼ ton/in.² (0.4×10^8 dynes/cm.²), a value used in the present work, the limiting grain-boundary displacement therefore works out at 320 Å., and this:

is the displacement that would have been reached had elastic resistance at the grain corners been maintained. Since the overall shear measured by the observed deflections must be in simple proportionality to the grain-boundary displacements—there being, according to Kê's assumptions, no other process contributing to creep—the displacements at intermediate stages can be worked out from the published deflections by simple arithmetic. Results are given in Table II for observa-

to the former curves is consistent with the idea that the elastic resistance at grain corners and protuberances breaks down at a certain grain-boundary displacement, since they lie well to the right of the curves derived from Kê's results. Corresponding pairs of curves can be joined up in a variety of ways, but if this is done without violent curvature, as indicated by the broken lines in Fig. 10 (a) and (b), they signify that the elastic resistance breaks down

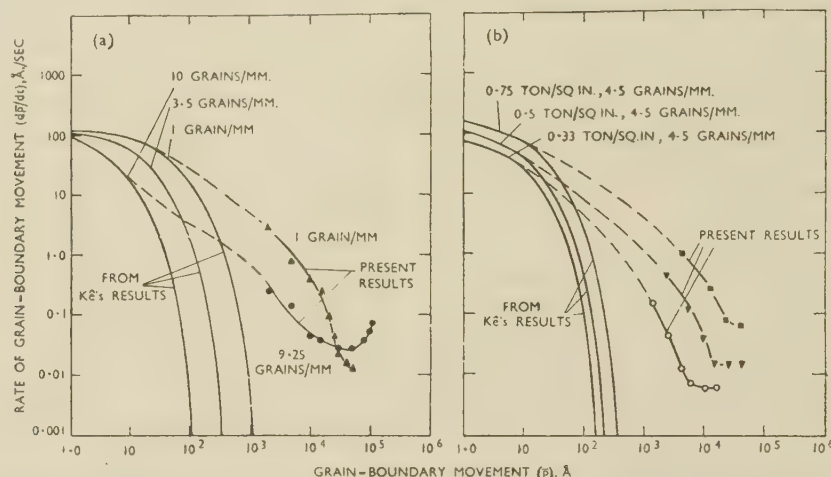


FIG. 10.—Comparison Between Results for Grain-Boundary Velocity Obtained by Kê⁹ and in Present Work. (a) Specimens of various grain-sizes. (b) Medium-grain-sized specimens at different stresses.

tions at 200° C. The grain-boundary velocities can be obtained from a plot of displacement against time on a linear scale, and these are also included in Table II.

TABLE II.—Grain-Boundary Displacements and Velocities for Aluminium at 200° C. from Kê's Measurements.⁹

Time, sec.	0	0.1	1.0	10	100	1000	3000
Displacement, Å.	0	13	38	73	190	280	320
Velocity, Å./sec.	120	54	11.6	1.6	0.4	0.04	0

The curve of velocity against displacement given by these results is presented in Fig. 10 (a) with logarithmic ordinate and abscissa. Two other curves have been drawn for grain-sizes of 0.1 and 1.0 mm. to compare with the fine- and coarse-grained specimens used in the present work. In Fig. 10 (b) three curves are drawn for a constant grain-size of $4\frac{1}{2}$ grains/mm. and relating to stresses of $\frac{1}{3}$, $\frac{1}{2}$, and $\frac{3}{4}$ ton/in.², again plotted logarithmically, to compare with the other conditions used in the present work. The initial portions of the derived curves have been drawn according to Kê's model, which gives the initial velocity as independent of grain-size, but proportional to stress. The curves with plotted points in the two figures, show the relation found in the present work for the five different combinations of grain-size and stress, and it is clear that their position in relation

at about 100 Å. mean displacement in the coarse-grained specimen and at about 10 Å. mean displacement in the other specimens. The former value seems reasonable, but the latter value appears to be too low to be consistent with the linearity that Kê has reported.

ACKNOWLEDGEMENTS

The author desires to acknowledge the helpful assistance given by Mr. M. H. Farmer. The work described above was carried out as part of the general research programme of the National Physical Laboratory, and the paper is published by permission of the Director of the Laboratory.

REFERENCES

1. D. McLean, *J. Inst. Metals*, 1951–52, **80**, (9), 507.
2. D. McLean, *ibid.*, 1952–53, **81**, (3), 133.
3. W. Rosenhain and J. C. W. Humphrey, *J. Iron Steel Inst.*, 1913, **87**, 219p.
4. W. A. Wood, G. R. Wilms, and W. A. Rachinger, *J. Inst. Metals*, 1951, **79**, 159.
5. D. Hanson and M. A. Wheeler, *ibid.*, 1931, **45**, 229.
6. C. L. Clark and A. E. White, *Proc. Amer. Soc. Test. Mat.*, 1932, **32**, (II), 492.
7. J. McKeown, *J. Inst. Metals*, 1937, **60**, 201.
8. K. von Hanffstengel and H. Hanemann, *Z. Metallkunde*, 1938, **30**, 41.
9. T. S. Kê, *Phys. Rev.*, 1947, [ii], **71**, 533.
10. D. McLean, *J. Inst. Metals*, 1952–53, **81**, (6), 287.
11. G. Wyon and C. Crussard, *Rev. Mét.*, 1951, **48**, 121.
12. H. C. Chang and N. J. Grant, *Trans. Amer. Inst. Min. Met. Eng.*, 1952, **194**, 619 (in *J. Metals*, 1952, **4**, (6)).

INTERCRYSTALLINE CORROSION IN CAST ZINC-ALUMINIUM ALLOYS*

1446

By C. W. ROBERTS,† B.Sc., A.I.M., MEMBER

SYNOPSIS

To determine the susceptibility of zinc-aluminium alloys to intercrystalline corrosion in an air/water-vapour atmosphere at 95° C. and to examine the effect of the presence of other elements on the incidence of this form of corrosion, alloys of various compositions within the range aluminium 0-22%, copper 0-1.5%, magnesium 0-0.09%, lead, tin, and cadmium 0-0.030%, bismuth 0-0.016%, and manganese 0-0.050% were prepared and tested in the as-cast condition.

The main conclusions drawn from the work are that: (1) intercrystalline corrosion is confined to the α (zinc-rich) phase, although attack is more severe when the β (aluminium-rich) phase is also present, as a result of the larger surface area of the α grains in the two-phase alloys; (2) the severity of attack is greatly increased by the presence of small percentages of lead, tin, cadmium, and bismuth; (3) the addition of a small amount of magnesium greatly reduces the severity of the corrosion, whether impurities are present or not, provided conditions are such that intermetallic compounds of magnesium with the impurity elements are not formed; and (4) the presence of copper increases the resistance of two-phase alloys to intercrystalline attack.

The results of the present investigation and those published by other investigators are discussed, and tentative theories are put forward to explain certain aspects of the phenomenon.

I.—INTRODUCTION

ZINC alloys have been used for pressure die-castings since the early years of the century, the alloying elements originally used being copper and tin, with smaller amounts of aluminium to prevent contamination of the alloy by iron during melting. It was later discovered that by increasing the aluminium content, the fluidity of these alloys was increased to such an extent that tin could be dispensed with altogether. By 1918 alloys containing up to 10% aluminium as the major alloying constituent had been widely adopted in the pressure die-casting industry, and large numbers of castings went into service. Serious corrosion trouble was soon encountered, however, particularly when the castings were used in humid conditions, and various cases were reported of castings distorting, swelling, and even disintegrating completely.

At that time any available grade of zinc, and even scrap metal, was used in the production of the alloys. Research showed that such failures were due to intercrystalline corrosion and that the severity of the attack was closely associated with the presence in the alloys of small quantities of certain impurities, in particular of lead. Subsequently, only the highest-purity metal then available (99.94%) was used in the manufacture of these alloys, and this resulted in a marked decrease in the number of failures of die-castings attributable to intercrystalline corrosion, although the scope of application of such castings was very limited.

About 1923 it was found that the presence of approximately 0.10% magnesium and up to 3.0%

copper reduced still further the susceptibility of zinc-aluminium alloys to intercrystalline attack and when, a year or so later, zinc of purity 99.99% became available commercially and was used in the manufacture of the alloys, the number of failures of die-castings due to intercrystalline corrosion decreased to very small proportions.

With the use of high-purity metal it was found that about 0.04% magnesium was sufficient to confer on the alloys immunity from intercrystalline attack and that the presence of copper in alloying proportions was no longer necessary. Consequently, the zinc die-casting alloy most commonly used in this country became standardized at 4.1% aluminium and 0.04% magnesium (Mazak 3), with impurities limited to very small percentages. An alloy of similar composition, but containing in addition about 1.0% copper (Mazak 5), is also used to some extent, both materials being covered by British Standard No. 1004.

Castings made from these materials are very resistant to both surface and intercrystalline corrosion when exposed in normal atmospheric conditions, but if, through contamination during processing, the percentage of harmful impurities reaches a figure much in excess of the limits stated in the relevant specification, the castings may become susceptible to corrosion of the intercrystalline type, particularly if they are used in warm, humid conditions.

A considerable amount of work has been done in the past with a view to elucidating the various phenomena associated with intercrystalline corrosion in these alloys, but the results reported are to some extent conflicting. The work described below was carried out in an attempt to clarify the problem.

* Manuscript received 30 July 1952.

† Research Department, Imperial Smelting Corporation, Ltd., Avonmouth.

II.—PREVIOUS WORK

Brauer and Peirce,¹ in 1923, made a very comprehensive study of the subject, using gravity-die-cast test-pieces prepared from various grades of zinc (one of which was of 99.98% purity). They used an air/water-vapour atmosphere at 95° C. as the corroding medium and from the results obtained came to the following conclusions: (1) Intercrystalline attack is confined to the α phase (zinc-rich), the γ phase (aluminium-rich—now described as β) remaining unaffected. (2) The decomposed γ phase is severely attacked as a result of the very large number of grain boundaries produced by the eutectoid decomposition. (3) The grain-size of zinc-aluminium alloys decreases with increasing aluminium content, and in coarse-grained alloys (below 2% aluminium) the depth of penetration is greater, although expansion may be slight. (4) The severity of attack, as affecting the physical characteristics of a specimen, depends upon the grain-size and the presence or absence of impurities or other metals added to the alloy. (5) As for the effect of the normal impurities present on the rate and severity of attack, lead is a powerful accelerator, cadmium and tin almost as detrimental, iron is less so, and nickel and manganese are only moderately detrimental. Copper to the extent of 0.5% is a powerful retarding agent and in amounts up to 5.0% is more or less beneficial.

Seven years later, Anderson² carried out similar steam-ageing tests on nine zinc die-casting alloys of various compositions and found that one only was free from intercrystalline corrosion. This particular alloy had the composition: aluminium 4.0%, copper 3.0%, magnesium 0.13%, and iron 0.023%, the manganese, lead, cadmium, and tin each being below 0.01%.

Using two grades of metal, described respectively as electrolytic zinc (99.98% purity) and refined zinc (98.86% purity), Guertler and his co-workers³ in 1935 carried out steam-ageing experiments with zinc alloys of the following range of compositions: (a) aluminium 0.4%, copper 2.0–8.0%, and (b) aluminium 2.0%, copper 4.0%, manganese 1.0%.

It was found that all alloys showed poor resistance to corrosion by salt solution and that all underwent deterioration when tested in steam at 95°–100° C., those made from “refined zinc” being most seriously affected in both series of tests.

In 1940 Petrich and Wolf⁴ published results obtained from tests on two series of zinc alloys (one containing 9.0% aluminium and 0.009–0.31% lead, the other 0.09% lead and 0.28–9.95% aluminium), which were examined after exposure for six days to water vapour at 95° C. Both series were exposed in the unstrained and compressed conditions, corrosion being more pronounced in the latter case. Even in the alloy with the lowest lead content, hairline cracks were visible after six days' steam-ageing, and it was observed that, in general, corrosion followed the grain boundaries with (presumably electrolytic) solution of the aluminium-rich phase.

Between 1941 and 1947 Löhberg published the results of his researches on the question in six papers.^{5–10} The purity of the zinc used in preparing the alloys was not always quoted, but in the first series of experiments there was present, in addition to the alloying elements, 0.02% lead, 0.002% cadmium, and 0.03% iron. The alloys tested were within the range 1.1–21.6% aluminium, 0.65–1.1% copper, 0.03–0.2% magnesium, and 0.02%–0.70% lead, but some of them presumably also contained small quantities of cadmium, thallium, tin, calcium, and sodium.

The standard steam-ageing testing procedure was used, and the conclusions reached may be summarized as follows: (1) The depth of penetration of the corrosion was found to be dependent upon the structure, being greatest with those of coarse grain. (2) Corrosion takes place only when the aluminium-rich (β) phase is present; it affects only this phase, and is intercrystalline only when this phase is concentrated along the grain boundary. (3) The degree of corrosion increases with increasing aluminium content, the maximum increase in weight and length as a result of corrosion being shown by alloys of eutectoid composition. (4) Corrosion is increased by the presence of lead, cadmium, thallium, and particularly tin, and is decreased by copper, calcium, sodium, and magnesium. The adverse effect of the first group of impurities is alleviated to some extent by the addition of magnesium.

Experimenting later with alloys of eutectoid composition containing in addition 0.4 and 0.7% lead, with and without 0.2% magnesium, Löhberg found that the material of higher lead content was completely disintegrated after two days' steam-ageing, whereas the material with 0.4% lead took three or four days to reach a similar state. He stated that the corrosion-resistance of the magnesium-containing alloy was greater than that of the magnesium-free alloy and suggested that this was due to the conversion of the lead to the compound Mg_2Pb , which, although intercrystalline, was more finely dispersed and evenly distributed. He also concluded that the decrease in grain-size produced by the magnesium additions contributed to the improvement in corrosion-resisting properties of these alloys.

Löhberg's fifth paper,⁹ which is on the subject of hydrogen evolution during the process of corrosion, throws little further light on the subject, except for a remark to the effect that if magnesium is present in the alloy it has an inhibiting effect due to the formation of a protective layer on the zinc.

The last paper in the series¹⁰ concerns the effect of temperature on the rate of corrosion both by water and by water vapour. The results obtained showed that the rate of corrosion increases (1) with increasing aluminium content of the alloy, (2) with increase in temperature—at 95° C. it is 100–200 times that at room temperature, and (3) with increasing grain-size.

In a more recent paper,¹¹ Löhberg has reported on the action of steam and water on compounds of

aluminium with antimony, copper, and magnesium and of magnesium with lead, tin, silicon, bismuth, antimony, cadmium, zinc, and copper, some of which compounds may occur in Mazak alloys. Magnesium plumbide (Mg_2Pb), which was found to be much more rapidly attacked than the other magnesium compounds, was completely decomposed in 4 hr. by steam at 95°C ., while in air at 20°C . it was completely oxidized in 49 days. The compound MgZn_2 showed no change in weight when exposed to air for 287 days.

It was concluded that an intermetallic compound is attacked by water or steam only if the components have widely different electrochemical potentials and that the attack can be halted by a protective oxide layer or by a protective layer of the nobler metal left after selective removal of the other component from the surface.

A number of other papers on the intercrystalline corrosion of zinc die-casting alloys have been examined, but the information contained in them was not found to be very relevant to the present investigation.

III.—EXPERIMENTAL WORK

The materials used in the present investigation were: Special high-purity zinc (99.999+ % pure); Crown Special zinc (B.S. 1003) (99.99+ % pure, the impurities being lead 0.0015%, cadmium 0.001%, iron 0.001%, and copper a trace); and aluminium of 99.98% purity. The other metals were the purest available.

The object of the research was to investigate generally the occurrence of intercrystalline corrosion in zinc-aluminium alloys. The scope of the investigation may be summarized thus: (a) to determine whether single-phase zinc-rich alloys are susceptible to intercrystalline corrosion; (b) to determine the extent to which two-phase alloys are attacked; (c) to examine the effect of other elements in alloying proportions on the susceptibility of these alloys to intercrystalline attack; (d) to examine the effect of impurity elements on the rate and intensity of intercrystalline attack; and (e) to assess the efficiency of magnesium in suppressing the intercrystalline attack in such alloys.

Preliminary experiments made in these laboratories¹² indicated that some intercrystalline corrosion occurs with single-phase zinc-rich alloys when there are no impurities present to act as cathode (assuming that the phenomenon is electrochemical in character), and that no corrosion takes place when the single-phase aluminium-rich alloy is tested under similar conditions.

To confirm these findings, and to extend the investigation, alloys numbered 1 to 10, of composition shown in Table I, were prepared and gravity die-cast in an iron mould to produce bars $\frac{3}{8}$ in. square. The test-pieces thus prepared were subjected to the standard steam test, i.e. ten days in an air/water-

vapour atmosphere maintained at $95^\circ \pm 2^\circ\text{C}$. When this treatment was completed, the test-pieces were withdrawn and the surface condition noted. Two complete cross-sections were cut from each sample, prepared in the normal manner, and examined at high magnification. The observations made on them are reported in column 3 of Table I.

In the light of the information obtained from this examination, alloys numbered 11-26 and 32-101, of composition shown in Table I, were prepared and subjected to the same steam-ageing treatment. Several commercial pressure die-castings in Mazak 3 were also included (27-31 of Table I). The information obtained from the subsequent metallographic examination of sections cut from all these test specimens also appears in Table I, column 3.

Figs. 1-9 (Plates XLIII and XLIV) show the effects of impurities and alloy composition on the character and extent of the corrosion. Fig. 1 depicts a typical field at the edge of alloy 2 (0.075% aluminium), the path of the corrosion round the grains being comparatively narrow. Alloy 6 contained 0.003% lead, the aluminium content being similar to that of alloy 2. The path of the corrosion in this case was somewhat wider, as shown in Fig. 2, but the depth of penetration was very little greater.

The corrosion at the edge of alloy 9 (0.04% magnesium, 0.013% lead) is shown in Fig. 3; attack appears to have been very intense and the path of the corrosion comparatively wide.

The type of intercrystalline corrosion observed in alloy 26 (4.44% aluminium, 0.048% magnesium), shown in Fig. 4, is very similar in appearance to that which can be induced in the standard pressure-die-cast Mazak 3 (Fig. 5).

Figs. 6 and 7 illustrate the effects of copper and copper with magnesium on the extent of the intercrystalline attack. The former is of a field in a specimen of alloy 52, containing 4.0% aluminium and 0.3% copper; the latter shows a field in a specimen of alloy of similar composition but containing in addition 0.05% magnesium (alloy 57).

The effect on the intercrystalline attack of adding 0.01% cadmium to an alloy consisting of 4% aluminium in high-purity zinc (alloy 68) is shown in Fig. 8. This should be compared with Fig. 9, which is of a similar alloy free of cadmium (alloy 38).

The photomicrographs also illustrate the degree and mode of occurrence of the intercrystalline attack in the various samples, as indicated in column 3 of Table I. The terms "severe" and "intense" indicate the type of attack illustrated in Figs. 3 and 5. Fig. 5 also illustrates intercrystalline corrosion occurring as a continuous layer, as opposed to individual patches as shown in Fig. 4. Fig. 6 shows corrosion of average intensity, and in Fig. 9 the corrosion is about midway between average and severe. The term "spine" is used to describe corrosion running along a single grain-boundary path; the beginning of a prominent example is shown in the lower centre of Fig. 2.

TABLE I.—Summary of Experimental Results.

Alloy No.	Composition, %	Occurrence, Severity, and Depth of Penetration of Intercrystalline Corrosion	Alloy No.	Composition, %	Occurrence, Severity, and Depth of Penetration of Intercrystalline Corrosion
1	Zinc (99.999%)	Nil.	35	S.P. Zn + 0.04 Al + 0.0015 Mg	Somewhat less frequent spines to 0.006 in.; no deeper penetration observed.
2	0.075 Al	General attack to 0.008 in.; individual spines to 0.024 in.	36	S.P. Zn + 0.02 Al	Occasional spines to 0.002 in.; a few to 0.005 in.
3	0.15 Al	General attack to 0.016 in.; individual spines to 0.040 in.	37	S.P. Zn + 0.005 Al	Nil.
4	0.27 Al	General attack to 0.040 in.	38	S.P. Zn + 4 Al	Layer to 0.015 in. max.; average 0.007 in.
5	0.003 Pb	Nil.	39	S.P. Zn + 4 Al + 0.001 Mg	Layer to 0.009 in. max.; average 0.005 in.
6	0.075 Al, 0.003 Pb	To a general depth of 0.013 in.; individual spines to 0.040 in. } The corrosion in these samples was of a more intense nature than that observed in the corresponding lead-free samples 2, 3, and 4.	40	S.P. Zn + 4 Al + 0.009 Mg	Layer to an average depth of 0.001 in.; moderately frequent patches to 0.005 in.
7	0.165 Al, 0.011 Pb		41	S.P. Zn + 4 Al + 0.026 Mg	Moderately frequent patches to 0.005 in. Much of the surface unattacked.
8	0.27 Al, 0.0075 Pb		42	S.P. Zn + 4 Al + 0.047 Mg	Moderately frequent patches to 0.005 in. Much of the surface unattacked.
9	0.04 Mg, 0.013 Pb	Very intense to 0.040 in.; less intense to 0.20 in.	43	S.P. Zn + 4 Al + 0.057 Mg	As No. 41.
10	0.038 Mg	Very occasional spines to 0.002 in.	44	S.P. Zn + 4 Al + 0.081 Mg	Moderately frequent patches to a depth of 0.003 in.
11	96.8 Al, 3.2 Zn	Nil.	45	S.P. Zn + 4 Al + 0.090 Mg	Moderately frequent patches to a max. depth of 0.004 in.
12	79.97 Al, 20.03 Zn	Nil.	46	S.P. Zn + 4 Al + 0.05 Mn	Intense to 0.005 in. Frequent spines to 0.050 in.
13	80.27 Al, 19.73 Zn, 0.001 Pb	Nil.	47	S.P. Zn + 4 Al + 0.05 Mn + 0.05 Mg	Comparatively infrequent patches to 0.003 in.
14	0.24 Al, 0.046 Mg	Occasional patches to 0.004 in.	48	C.S. Zn + 4 Al	Intense to 0.026 in.
15	0.28 Al, 0.044 Mg, 0.0063 Pb	To a general depth of 0.10 in.; less intense than that observed in No. 9.	49	C.S. Zn + 4 Al + 0.05 Mg	Fairly frequent patches to 0.003–0.004 in.
16	2.00 Al, 0.051 Mg, 0.006 Pb	General attack to 0.002 in.	50	C.S. Zn + 4 Al + 0.05 Cu	Intense to 0.040 in.
17	0.96 Al, 0.045 Mg, 0.0064 Pb	General to 0.004 in.; individual spines to 0.024 in.	51	C.S. Zn + 4 Al + 0.10 Cu	Very frequent (almost continuous) patches to 0.010 in.
18	0.095 Al, 0.047 Mg	Little or no corrosion observed.	52	C.S. Zn + 4 Al + 0.30 Cu	Very frequent (almost continuous) patches to 0.005–0.006 in.
19	0.046 Al	General to 0.012 in.	53	C.S. Zn + 4 Al + 0.80 Cu	Very frequent (almost continuous) patches to 0.008 in.
20	22.26 Al, 0.0063 Pb	General to 0.008 in.; patches to 0.10 in.; hairline cracks visible on surface of test-piece.	54	C.S. Zn + 4 Al + 1.5 Cu	Very frequent patches to 0.006–0.008 in.
21	0.61 Al	Attack to 0.007 in.; to 0.020 in. in places.	55	C.S. Zn + 4 Al + 0.05 Mg + 0.05 Cu	Comparatively frequent patches to 0.003 in. Fits to the same depth also observed.
22	1.83 Al	More intense to 0.010 in.; up to 0.016 in. in places.	56	C.S. Zn + 4 Al + 0.05 Mg + 0.10 Cu	Fairly frequent pits and patches to 0.001 in.; a few to 0.003–0.004 in.
23	4.48 Al	Fairly intense to 0.010 in.; to 0.028 in. in places.	57	C.S. Zn + 4 Al + 0.05 Mg + 0.30 Cu	Fairly frequent pits and patches to 0.001 in.; a few to 0.003–0.004 in.
24	22.40 Al	Intense to 0.010 in.; one patch to 0.080 in.	58	C.S. Zn + 4 Al + 0.05 Mg + 0.80 Cu	Fairly frequent pits and patches to 0.001 in.; a few to 0.003–0.004 in.
25	22.52 Al, 0.045 Mg	Intense to 0.005 in.; one patch to 0.100 in.	59	C.S. Zn + 4 Al + 0.05 Mg + 1.5 Cu	Fairly frequent pits and patches to 0.001 in.; a few to 0.003–0.004 in.
26	4.44 Al, 0.048 Mg	Patches of fairly intense intercrystalline corrosion to 0.003 in. Certain areas of the surface unattacked.	60	C.S. Zn + 0.004 Pb + 0.05 Mg	Intense throughout the sample.
27	Gravity die-cast Mazak 3	Very occasional patches to 0.003 in.	61	C.S. Zn + 0.005 Sn + 0.05 Mg	Attack of considerably less intensity to 0.10 in.
28	Pressure die-cast Mazak 3, stored one year	Very frequent patches to 0.004 in.	62	C.S. Zn + 0.005 Cd + 0.05 Mg	Attack to a depth of 0.025 in.; intensity as No. 61.
29	Pressure die-cast Mazak 3, stored six months	Less frequent patches to 0.004 in.	63	S.P. Zn + 4 Al + 0.05 Mg + 0.002 Cd	Occasional patches to 0.001 in.
30	Die-casting in Mazak 3	Fairly general to 0.003 in.	64	S.P. Zn + 4 Al + 0.05 Mg + 0.005 Cd	Frequent pits and patches to 0.002 in.
31	Die-casting in Mazak 3	Patches to 0.003 in.; somewhat more intense than No. 30.	65	S.P. Zn + 4 Al + 0.05 Mg + 0.008 Cd	Frequent patches to 0.005 in. max.
32	S.P. Zn + 0.08 Al + 0.021 Mg	Fairly frequent spines to 0.001 in.; occasional spines to 0.004 in.	66	S.P. Zn + 4 Al + 0.05 Mg + 0.014 Cd	A layer to 0.003 in.
33	S.P. Zn + 0.08 Al + 0.010 Mg	Fairly frequent spines to 0.005 in.; a few to 0.020 in.			
34	S.P. Zn + 0.04 Al + 0.003 Mg	Somewhat less frequent spines to 0.006 in.; a few to 0.012 in.			

TABLE I.—continued.

Alloy No.	Composition, %	Occurrence, Severity, and Depth of Penetration of Intercrystalline Corrosion	Alloy No.	Composition, %	Occurrence, Severity, and Depth of Penetration of Intercrystalline Corrosion
67	S.P. Zn + 4 Al + 0.05 Mg + 0.025 Cd	A layer to 0.006 in.	87	S.P. Zn + 4 Al + 0.05 Mg + 0.005 Sn + 0.005 Bi	Comparatively infrequent patches to 0.003–0.004 in.
68	S.P. Zn + 4 Al + 0.010 Cd	Attack to 0.012 in.	88	S.P. Zn + 4 Al + 0.05 Mg + 0.004 Pb + 0.005 Cd	Occasional patches to 0.003 in.
69	S.P. Zn + 4 Al + 0.05 Mg + 0.001 Sn	Patches to 0.002 in. average.	89	S.P. Zn + 4 Al + 0.05 Mg + 0.004 Pb + 0.005 Bi	Very frequent patches to 0.001–0.002 in.; occasional patches to 0.005 in.
70	S.P. Zn + 4 Al + 0.05 Mg + 0.002 Sn	Patches to 0.002 in. average.	90	S.P. Zn + 4 Al + 0.05 Mg + 0.005 Cd + 0.005 Bi	Fairly frequent patches to 0.001–0.002 in.; occasionally to 0.005 in.
71	S.P. Zn + 4 Al + 0.05 Mg + 0.005 Sn	Patches to 0.003 in. average.	91	S.P. Zn + 4 Al + 0.05 Mg + 0.004 Sn + 0.003 Pb + 0.004 Cd	Somewhat less frequent patches to 0.003–0.004 in.
72	S.P. Zn + 4 Al + 0.05 Mg + 0.008 Sn	Patches to 0.003 in. average.	92	S.P. Zn + 4 Al + 0.05 Mg + 0.004 Sn + 0.003 Pb + 0.003 Bi	Fairly infrequent patches to 0.003 in.
73	S.P. Zn + 4 Al + 0.05 Mg + 0.014 Sn	Frequent patches to 0.007 in.; more severe than Nos. 70–72.	93	S.P. Zn + 4 Al + 0.05 Mg + 0.004 Sn + 0.004 Cd + 0.003 Bi	Very frequent patches to 0.006 in.
74	S.P. Zn + 4 Al + 0.05 Mg + 0.025 Sn	A layer to 0.007 in. max.; more severe than Nos. 70–72.	94	S.P. Zn + 4 Al + 0.05 Mg + 0.003 Pb + 0.004 Cd + 0.003 Bi	Very frequent patches to 0.001–0.002 in.; one large patch 0.050 in. deep.
75	S.P. Zn + 4 Al + 0.010 Sn	Intense to 0.050 in.	95	S.P. Zn + 4 Al + 0.05 Mg + 0.004 Sn + 0.004 Pb + 0.004 Cd + 0.004 Bi	Frequent patches to 0.005–0.006 in.
76	S.P. Zn + 4 Al + 0.05 Mg + 0.0015 Pb	Patches to 0.004 in.	96	S.P. Zn + 4 Al + 0.05 Mg + 0.002 Bi	Comparatively infrequent patches to 0.004 in. max.
77	S.P. Zn + 4 Al + 0.05 Mg + 0.003 Pb	Patches to 0.004 in.	97	S.P. Zn + 4 Al + 0.05 Mg + 0.004 Bi	Comparatively infrequent patches to 0.004 in. max.
78	S.P. Zn + 4 Al + 0.05 Mg + 0.005 Pb	More frequent patches to 0.004 in.	98	S.P. Zn + 4 Al + 0.05 Mg + 0.005 Bi	Comparatively infrequent patches to 0.004 in. max.; one patch 0.010 in. deep.
79	S.P. Zn + 4 Al + 0.05 Mg + 0.030 Pb	Frequent patches to 0.006 in.; more severe than Nos. 76–78.	99	S.P. Zn + 4 Al + 0.05 Mg + 0.010 Bi + 0.020 Pb	Patches decidedly more frequent and intense than No. 96. Depth of penetration not much greater.
80	S.P. Zn + 4 Al + 0.05 Mg + 0.020 Pb	Patches to 0.004 in.; considerably less frequent than No. 79 but more severe than Nos. 76–78.	100	S.P. Zn + 4 Al + 0.05 Mg + 0.012 Bi	Attack somewhat less intense than that found in No. 99.
81	S.P. Zn + 4 Al + 0.008 Pb	Intense to 0.040 in.	101	S.P. Zn + 4 Al + 0.05 Mg + 0.016 Bi	Attack somewhat less intense than that found in No. 99.
82	S.P. Zn + 0.020 Cd	Nil.			
83	S.P. Zn + 0.020 Sn	Nil.			
84	S.P. Zn + 0.5 Cd	Nil.			
85	S.P. Zn + 4 Al + 0.05 Mg + 0.005 Sn + 0.004 Pb	Fairly general to 0.001 in.; comparatively frequent patches to 0.006 in.			
86	S.P. Zn + 4 Al + 0.05 Mg + 0.005 Sn + 0.005 Cd	Fairly general to 0.001 in.; less frequent patches to 0.004 in.			

In view of the suggestion made by Löhberg⁸ that the action of magnesium is to “fix” the lead as the intermetallic compound Mg_2Pb and because the alloy (No. 9 in the present series), which probably contained this compound as an intercrystalline constituent, was found to offer poor resistance to corrosion, a lead-magnesium alloy of composition corresponding to the compound was prepared and cast. It was found that the material was extremely brittle and disintegrated rapidly when exposed to moist air at room temperature.

IV—SUMMARY OF RESULTS

From a consideration of the results obtained in this series of experiments the following points emerge:

(1) Single-phase zinc-aluminium alloys of aluminium content between 0.08 and 0.02% are susceptible to intercrystalline corrosion when exposed to the air/water-vapour atmosphere at 95° C. The depth of penetration of the attack decreases with decreasing aluminium content, and it appears that no

attack occurs when the aluminium present is much below about 0.01%. The corrosion becomes much more severe when lead is present. In the absence of aluminium, zinc, either pure or contaminated with lead, is immune from intercrystalline attack. (Alloys 2, 5, 6, 19, 36, and 37.)

(2) The intercrystalline attack in these single-phase zinc-aluminium alloys appears to be almost completely suppressed by the addition of about 0.05% magnesium, but some attack takes place if the amount of magnesium present is much less than 0.03%. (Alloys 18 and 32–35.)

(3) The aluminium-rich (β) solid solution is not susceptible to intercrystalline attack by water vapour at 95° C. (Alloys 11, 12, and 13.)

(4) In two-phase zinc-aluminium alloys free from magnesium, it appears that the depth of penetration of the intercrystalline attack does not increase greatly with increasing aluminium content, but the intensity of attack is greater in the alloys of higher aluminium content. The presence of small percentages of lead (0.006–0.013%) in these alloys increases the severity

of the intercrystalline corrosion, but the simultaneous presence of about 0.05% magnesium causes a considerable reduction in the severity of the attack. The behaviour of alloy 15 was, however, anomalous. (Alloys 3, 4, 7, 8, 15, 16, 17, 20, 21, 22, 23, 24, and 25.)

(5) The resistance to intercrystalline attack of two-phase zinc-aluminium alloys is improved slightly by the addition of as little as 0.001% magnesium. Maximum resistance is obtained by the addition of 0.02–0.03% magnesium, but further additions of this element up to 0.09% appear to confer no significantly greater benefit. (Alloys 14, 25, 26, and 38–45.)

(6) Although Mazak die-castings of composition within the limits prescribed by British Standard 1004 show intercrystalline corrosion when subjected to steam-ageing treatment as defined in that specification, the depth of penetration is very small and is not likely to be greater than 0.004 in. This, though quite detectable, is inappreciable from a practical standpoint, since the conditions to which die-castings are normally exposed in service are far less severe than those in the steam tank. (Alloys 27–31.)

(7) The addition of up to 0.30% copper to zinc–4% aluminium alloys is beneficial with regard to resistance to intercrystalline corrosion. No further improvement is obtained with increasing percentages up to 1.5%. (Alloys 48 and 50–54.)

(8) When 0.05% magnesium is also present in these alloys, the addition of 0.10–1.5% copper slightly improves the resistance to intercrystalline corrosion, but in no case is the attack completely suppressed. (Alloys 49 and 55–59.)

(9) No intercrystalline corrosion occurs when small quantities of magnesium, lead, tin, or cadmium are present alone in pure zinc. When, however, a small percentage of magnesium is present, together with a small percentage of lead, tin, or cadmium, severe intercrystalline corrosion occurs, the severity of the attack being greatest with lead and least with cadmium. (Alloys 5, 9, 10, 60, 61, 62, 82, 83, and 84.)

(10) The presence in alloys of Mazak 3 composition of up to about 0.005% lead, tin, cadmium, or bismuth does not appear to modify greatly the susceptibility of these alloys to intercrystalline attack. The severity of the attack increases somewhat with increasing amounts of these impurities up to about 0.025%, the maximum figure used in the present series of experiments.

In the absence of magnesium the presence of small amounts of lead or tin greatly increases the severity and depth of penetration of the attack, whereas with a similar amount of cadmium present alone the severity of the attack is increased to a much lesser extent. (Alloys 63–81 and 96–101.)

(11) In the same respect, the presence (in alloys containing 4% aluminium + 0.05% magnesium) of small percentages of lead, tin, cadmium, and bismuth in various combinations has an effect similar in magnitude to that of the most potent element when present in amounts equal to the total of the impurity elements. (Alloys 85–95.)

(12) When manganese is present in the alloy as an impurity element, its effect on the incidence of intercrystalline corrosion is deleterious, but less so than that of lead or tin. The evidence is incomplete however. (Alloys 46–47.)

(13) The intermetallic compound Mg_2Pb is unstable in moist air at room temperature.

In the group of alloys 32–35 (single-phase zinc-aluminium alloys with decreasing amounts of magnesium), the aluminium content of the first two alloys was 0.08%, whereas in the latter two it was 0.04%. The results obtained from this series, therefore, are not directly comparable. Alloys 48–62 were prepared from “Crown Special” zinc; the remainder from special high-purity metal (99.999%). Alloy 50 contained 0.0005% tin; in the remainder of the alloys in that group tin was not detected.

V.—DISCUSSION OF RESULTS

An air/water-vapour atmosphere maintained at $95^{\circ} \pm 2^{\circ}C.$ has been used for some thirty years as a medium for testing the susceptibility of zinc die-casting alloys to intercrystalline corrosion. The results obtained should, however, be viewed in proper perspective, since the conditions involved are far more searching than those to which commercial die-castings are exposed in normal use. Nevertheless, apart from the intergranular attack, the general corrosive action of steam and boiling water on zinc and zinc-aluminium alloys is comparatively mild, the surface appearance of many of the test-pieces that suffered from intercrystalline corrosion being reasonably good.

Intercrystalline corrosion of a single-phase, or ostensibly single-phase, alloy is usually explained as an electrochemical phenomenon. Briefly and simply, the small amounts of insoluble impurities present segregate at the grain boundaries, and, if widely separated from the base metal or solid solution in electrochemical characteristics, they are liable to become poles of a galvanic couple.

In mildly corrosive conditions (insufficient to attack rapidly, if at all, the base metal or solid solution), the galvanic couples become active and, depending on the polarity, the intercrystalline film of impurities or the outer layer of the adjacent crystal is dissolved, with the formation of a void between neighbouring crystals.

The evidence obtained from the present investigations conflicts with the view that this mechanism is the primary cause of intercrystalline corrosion in zinc-aluminium alloys. Zinc free from aluminium but containing appreciable amounts of impurities does not suffer intercrystalline attack, whereas when aluminium is present in solid solution and the total impurity content is less than 0.001% the incidence of intercrystalline corrosion is considerable. Furthermore, the small amount of aluminium present in the zinc does not endow it with an electrode potential very different from that of pure zinc.

It appears, therefore, that the susceptibility of the single-phase alloy to intercrystalline attack is associated with the presence of aluminium in solution. The solubility of aluminium in zinc at normal temperature is low; it decreases from about 0.62% at 250° C. to 0.12% at 95° C. and 0.03% at 25° C. The solid solution that first forms on freezing is not stable, and the excess aluminium is precipitated at room temperature, rapidly in the initial stages and then at a decreasing rate, so that after about two years' ageing the aluminium content of the zinc-rich phase is reduced to about 0.03%, irrespective of the original aluminium content of this phase. The fact that precipitation takes place at room temperature suggests that the aluminium atoms within the zinc lattice possess considerable mobility, and since under ideal conditions precipitation takes place at grain boundaries, it seems probable that a tendency exists for the aluminium atoms to diffuse in the direction of grain boundaries.

Aluminium as an element has a high affinity for oxygen, but when exposed in bulk in an oxidizing environment, the strongly adherent film of oxide which forms immediately on the surface protects the remainder of the metal from further attack. In the case of dilute solutions of aluminium in zinc, the aluminium atoms near the surface are susceptible to attack by oxygen, though they are too widely spaced to allow of the formation of a protective oxide film. Further, such a film, if formed, would be mechanically weak, since the cubic Al_2O_3 would not fit closely on to the exposed faces of the hexagonal zinc crystals. It appears possible, therefore, that these highly reactive atoms near the grain surface catalyse the oxidation of zinc to ZnO by virtue of their high affinity for oxygen and their inability to form a stable oxide film.

If the "grain-boundary-seeking tendency" of the aluminium atoms is assumed, the atoms within the grain will diffuse to the surface (to maintain even distribution), and the process of oxidation will continue until the grains near the specimen surface are surrounded by a continuous envelope of oxide. There is, however, little direct experimental evidence available in support of such a theory, and it is put forward with some reserve to explain the striking influence on the behaviour of zinc of a small proportion of aluminium in solid solution.

It having been established that intercrystalline corrosion takes place in single-phase alloys, little further need be said on the subject of the phenomenon in two-phase alloys. The increase in the intensity of the attack is probably due to the fact that the second (β) phase appears at the grain boundaries of the primary crystals as a eutectoid with the α phase. This fine-grained lamellar eutectoid increases greatly the effective area of the α -phase boundaries and consequently the intensity of the attack. It is clear, however, that the view expressed by Löhberg that "corrosion takes place only when the aluminium-rich phase is present; it affects only this phase and is intercrystalline only when this phase is concentrated along the grain boundary", is

incorrect. Intercrystalline corrosion takes place in single-phase (α) alloys; the intensity of the attack is increased, but the attack is not initiated by the presence at the grain boundaries of the aluminium-rich (β) phase.

Regarding the action of the impurity elements lead, tin, cadmium, and bismuth, it was found that, with magnesium present also, the intensity of the intercrystalline attack was increased considerably but the depth of penetration only slightly. In the absence of magnesium the effect of lead and tin was very marked; cadmium appeared to be comparatively innocuous, however.

The action of these impurities is usually explained in terms of the electrochemical theory of corrosion, the impurities acting as cathode with the resulting dissolution of adjacent areas of zinc or zinc-rich phase in the presence of a mildly corrosive medium. Since the impurities segregate at the grain boundaries, the corrosion is of the intercrystalline type.

The standard electrode potentials of the four metals zinc, lead, tin, and cadmium are as follows (hydrogen = 0.000): lead 0.126, tin 0.136, cadmium 0.402, zinc 0.762 V.¹³ The comparative accelerating effect of these elements on corrosion was in the order to be expected from these figures, though the conditions are not comparable in all cases, since lead and tin are present as intercrystalline constituents whereas cadmium is in solution in the zinc. The fact that the least harmful impurity is in solution is, however, noteworthy.

Zinc itself is immune from intercrystalline corrosion even in the presence of metals such as lead which could act as cathode. When some aluminium is in solid solution, however, zinc is susceptible to intercrystalline corrosion, though when no impurities are present the rate of attack is less. The presence of lead or tin at the grain boundaries greatly accelerates the rate of attack in solid solutions of aluminium in zinc, presumably because these metals act as cathodes. In this electrochemical process, therefore, it appears that solid solutions of aluminium in zinc can act as the anode, but pure zinc cannot.

It is possible that the action of these impurity elements is also mechanical in that their presence, in eutectic form, at the grain boundaries of the α solid solution increases the effective area of the surface of this phase, and thus favours the progress of the intercrystalline attack. Since cadmium is in solid solution, it is ineffective in this respect.

It has been shown that the addition of 0.03–0.05% magnesium to zinc-aluminium alloys suppresses almost completely intercrystalline corrosion in single-phase alloys. The action of magnesium in preventing or minimizing intercrystalline corrosion in these alloys is difficult to explain. Löhberg, who assumed that lead was the primary instigator of the corrosion, suggested in one of his papers that the lead was converted to the intermetallic compound Mg_2Pb , which, although still intercrystalline, was apparently innocuous. He also stated that the reduction in grain-size caused by the magnesium addition contributed to the improved

resistance to corrosion of these alloys. In a later paper⁹ he states that when magnesium is present in these (zinc-aluminium) alloys it has an inhibiting effect owing to the formation of a protective layer on the zinc.

The first suggestion has been shown to be incorrect. The intermetallic compound Mg_2Pb was found to be unstable in moist air at room temperature (a fact since confirmed by Löhberg), and a specimen of high-purity zinc in which magnesium and lead were present together was severely corroded after ten days' exposure to steam.

The improved resistance to corrosion produced by a smaller grain-size is possibly due to there being available near the surface of the specimen a much larger area of grain surface. This would reduce the chances of the corrosion following a "grain-boundary path" continuously normal to the specimen surface, and consequently the corrosion would tend to occur as patches adjacent to the surface rather than as isolated spines of greater depth.

Regarding Löhberg's third suggestion, the solubility of magnesium in zinc at $360^\circ C.$ is 0.11%, whereas at room temperature it decreases to about 0.002% and it is probable that the solubility of this element in the α phase at corresponding temperatures is very little higher. When the single-phase alloy cools, the excess magnesium is precipitated at the grain boundaries, probably as the intermetallic compound $MgZn_5$, and may form a fairly continuous network enclosing the grains of the zinc-rich phase. The water vapour is thus prevented from coming into contact with this phase, and it has been shown that this intermetallic compound $MgZn_5$ is itself virtually unattacked by water vapour. Magnesium is more soluble in the aluminium-rich solution, and when this phase is present the magnesium content of the α phase may be so reduced that insufficient magnesium is precipitated to form a continuous envelope. Under these conditions the α phase is susceptible to some extent to attack by water vapour, but sufficient $MgZn_5$ is available to hinder progress of the attack.

The effect of the presence of copper on the resistance of zinc-aluminium alloys to intercrystalline corrosion is quite marked. In the alloy prepared from Crown Special zinc and free of magnesium and copper, the intercrystalline attack penetrated to a depth of 0.026 in. The presence of 0.30% copper reduced the depth of penetration to 0.006 in., but no improvement was obtained by increasing further the copper content.

When the standard amount of magnesium (0.05%) was present in addition, the presence of copper up to 0.30% also improved somewhat the resistance to corrosion of these alloys, but in this case the margin available for improvement was more restricted, since in the copper-free alloy the attack penetrated only 0.003 in.

Both copper and magnesium are corrosion inhibitors, therefore, though their modes of action are probably very dissimilar. Magnesium is only slightly

soluble in the α phase and is strongly electronegative, whereas copper has a substantial solubility in this phase at about $100^\circ C.$ (0.7% approximately) and is electropositive to zinc. Thus, when copper is present in the zinc-rich solid solution, the potential of this phase is moved towards the positive side (i.e. nearer to that of lead and tin) and, in addition, its presence appears to increase the solubility of aluminium. The action of copper may therefore be to reduce the electrode potential between the α phase and the intercrystalline impurities—if, indeed, this circumstance is relevant—and to stabilize the phase, thus decreasing the tendency of the aluminium atoms to diffuse towards the grain boundaries.

There is one further relevant point in this connection. The presence of magnesium and copper in zinc-aluminium alloys is known to delay the eutectoid transformation, which normally takes place at $270^\circ C.$ On cooling, therefore, this transformation takes place at lower temperatures and consequently the hexagonal (zinc-rich) phase separates from the β phase in granular form rather than in the normal lamellar form. These granules of the hexagonal phase are surrounded by the β phase, and are thus protected to a much greater extent from the action of the corrosive medium. The β phase (aluminium-rich) is not attacked by steam, and hence the decrease in the degree of the intercrystalline attack when either or both of these elements are present in the alloys.

The severe intercrystalline attack that takes place in pure zinc when a small amount of magnesium together with small amounts of lead or tin are present is not difficult to understand. All these elements have low solubilities in zinc and are precipitated at the grain boundaries, probably in the form of the intermetallic compounds Mg_2Pb and Mg_2Sn . The compound Mg_2Pb has been shown to be unstable in moist air, and Löhberg¹¹ has reported that Mg_2Sn is rapidly attacked by steam.

Cadmium, however, has considerable solubility in zinc, though the equilibrium between zinc, cadmium, and magnesium is not well known. Cadmium and magnesium are reported to form an intermetallic compound, $MgCd_3$, which if present at the grain boundaries would probably be susceptible to attack by steam. Löhberg¹¹ concluded that the intensity of the attack by steam on intermetallic compounds of this type varies with the difference between the electrochemical potentials of the components. The results obtained in the present experiments tend to confirm this conclusion, since the relevant data for the three alloys are as follows:

Compound Assumed to be Present	Electrode Potential Difference, V.	Depth of Penetration of Intercrystalline Corrosion, in.
Mg_2Pb	2.249	0.187
Mg_2Sn	2.239	0.100
$MgCd_3$	1.973	0.025
$MgZn_5$	1.613	Nil

This effect of magnesium is also of considerable interest from a practical point of view, since the

accidental contamination by magnesium of commercial grades of zinc which contain small amounts of lead would probably result in rapid disintegration of the material if stored or used in damp conditions. The contingency is, however, remote, since magnesium is rarely, if ever, used alone as an alloying element in zinc.

ACKNOWLEDGEMENTS

The author wishes to express his thanks to the Directors of The Imperial Smelting Corporation, Ltd., for permission to publish the paper, and to colleagues in the Research Department for helpful advice and discussion. The analysis of the samples was carried out by Mr. G. Ludwell and Mr. R. Starr.

REFERENCES

1. H. E. Brauer and W. M. Peirce, *Trans. Amer. Inst. Min. Met. Eng.*, 1923, **68**, 796.
2. H. A. Anderson, *Proc. Amer. Soc. Test. Mat.*, 1930, **30**, (I), 318.
3. W. Guertler, F. Kleweta, W. Claus, and E. Rickertsen, *Z. Metallkunde*, 1935, **27**, 1.
4. G. Petrich and W. Wolf, *ibid.*, 1940, **32**, 412.
5. E. Andres and K. Löhberg, *ibid.*, 1941, **33**, 208.
6. K. Löhberg, *ibid.*, 1941, **33**, 213.
7. K. Löhberg, *ibid.*, 1942, **34**, 73.
8. K. Löhberg, *Metallforschung*, 1946, **1**, 65.
9. K. Löhberg, *ibid.*, 1946, **1**, 66.
10. K. Löhberg, *ibid.*, 1947, **2**, 230.
11. K. Löhberg, *Z. Metallkunde*, 1950, **41**, 56.
12. K. P. Scott, Private communication.
13. H. H. Uhlig, "The Corrosion Handbook." 1948: New York (John Wiley and Sons, Inc.); London (Chapman and Hall, Ltd.).

NOTICE TO AUTHORS OF PAPERS FOR THE "JOURNAL" AND CONTRIBUTORS TO DISCUSSIONS

1. **Papers will be considered for publication from non-members as well as members of the Institute.** They are accepted for publication in the *Journal* and not necessarily for presentation at any meeting of the Institute. MSS. should be addressed to The Editor of Publications, The Institute of Metals, 4 Grosvenor Gardens, London, S.W.1.

2. **Papers suitable for publication may be classified as:**

(a) Papers recording the results of original research.

(b) First-class reviews of, or accounts of progress in, a particular field.

(c) Papers descriptive of works methods, or recent developments in metallurgical plant and practice.

(d) Papers in classes (a), (b), and (c) above, previously published in languages other than English, French, German, or Italian, if of sufficient merit.

3. **Manuscripts and illustrations** should be submitted in duplicate. MSS. must be typewritten (*double-line spacing*) on one side of the paper only, and authors are requested to sign a declaration that neither the paper nor a substantial part thereof has been published elsewhere. Exceptions may be made in certain cases where a paper has been published in a language other than English, French, German, or Italian (see 2(d) above). MSS. not accepted are normally returned within 6 months of receipt.

In the interests of economy, all papers must be written as concisely as possible; in general, internal research reports are not in suitable form for publication as papers in the *Journal*. All but the simplest mathematical expressions should be written by hand, with capital and small letters clearly distinguished. Superscript and subscript letters should also be plainly indicated. Greek letters and special signs should be identified in the margin. For style, spelling, and abbreviations used, any recent issue of the *Journal* may be consulted.

4. **Synopsis.** Every paper must have a synopsis (not exceeding 250 words in length) which, in the case of a paper reporting original research, should state its objects, the ground covered, and the nature of the results. The synopsis will appear at the beginning of the paper, and should be in a form suitable for use by abstracting organizations. Extracts from a "Guide for the Preparation of Synopses" drawn up by the Abstracting Services Consultative Committee are reproduced below.

5. **References** must be collected at the end of the paper and must be numbered in the order in which they occur in the MS. Initials of authors must be given, and the Institute's official abbreviations for periodical titles (as used in *Metallurgical Abstracts*) should be employed, where known. References to papers should be set out in the style:

A. L. Dighton and H. A. Miley, *Trans. Electrochem. Soc.*, 1942, 81, 321 (i.e. year, volume, page).

References to books should be in the following style:

C. Zener, "Elasticity and Anelasticity of Metals". Chicago: 1948 (University of Chicago Press).

6. **Illustrations.** Each illustration must have a number and description; only one set of numbers must be used in one paper, and it is desirable to number the half-tone illustrations consecutively, rather than to intersperse them with the line figures. The captions should be typed on a separate sheet.

The set of line figures sent for reproduction must be drawn (about twice the size to appear in the *Journal*) in Indian ink on smooth white Bristol board, good-quality drawing paper, co-ordinate paper, or tracing cloth, which are preferred in the order given. Co-ordinate paper, if used, must be blue-lined, with the co-ordinates to be reproduced finely drawn in Indian ink. Curves should be drawn boldly (i.e. at least twice the thickness of the frame). Experimental points should be indicated by open or closed circles, triangles, squares, &c. (preferably not crosses). Curves should be broken on each side of such symbols and plenty of allowance should be made for closing up in blockmaking. All lettering and numerals, &c., should preferably be in pencil, so that the Institute's standard lettering may be affixed, and ample margins must be left outside the framework of the figures to enable this to be done. The second set of line illustrations may be photostat copies.

Photographs must be restricted in number, owing to the expense of reproduction, and photomicrographs should be trimmed to the smallest possible of the following sizes consistent with adequate representation of the subject: 4 in. deep by 3 in. wide: 2 in. deep by 3 in. wide: 2 in. square. Magnifications of photomicrographs must be given in each case. Photographs for reproduction should be loose, not pasted down (and not fastened together with a clip, which damages them), and the figure number and author's name should be written on the back of each. Captions should be given to the photomicrographs, but these should be kept as brief as possible.

Because of the present high cost of printing and paper it is imperative that authors restrict illustrations (particularly photographs) to the absolute minimum deemed necessary to support their argument. Only in exceptional cases will illustrations be reproduced if already printed and readily available elsewhere.

7. **Tables or Diagrams.** Results of experiments, &c., may be given in the form of tables or figures, but (unless there are exceptional reasons) not both. Tables should bear Roman numbers, and each should have a heading that will make the data intelligible without reference to the text.

8. **Corrections.** A certain number of corrections in proof are inevitable, but any modification of the original text is to be avoided. Since corrections are very expensive, the Institute reserves the right to require authors to contribute towards their cost if the Editor deems them to be excessive. The Institute also reserves the right to require a contribution to the cost of remaking any block where this is necessitated by an error on the author's part.

9. **Reprints.** Individual authors are presented with a maximum of 25, and two or more authors with a maximum of 50 reprints from the *Journal*, without covers. Limited numbers of additional reprints can be supplied at the author's expense, if ordered before proofs are passed for press. (Orders should preferably be placed when submitting MSS.)

10. **Discussion.** Except in the case of special symposia, shorthand records of discussions are not taken at meetings. Written discussion may be submitted on any paper, preferably typewritten (*double-line spacing*). References should be given in the form of footnotes. Paragraphs 6 and 7 above are also applicable to such contributions. Reprints of discussion cannot be supplied to contributors.

GUIDE FOR THE PREPARATION OF SYNOPSSES

(As recommended by the Abstracting Services Consultative Committee)

1. **Purpose.** The synopsis is not part of the paper; it is intended to convey briefly the content of the paper, to draw attention to all new information, and to the main conclusions. It should be factual.

2. **Style of writing.** The synopsis should be written concisely and in normal rather than abbreviated English. It is preferable to use the third person. Where possible use standard rather than proprietary terms, and avoid unnecessary contracting.

It should be presumed that the reader has some knowledge of the subject, but has not read the paper. The synopsis should therefore be intelligible in itself without reference to the paper; for example, it should not cite sections or illustrations by their numerical references in the text.

3. **Content.** The title of the paper is usually read as part of the synopsis. The opening sentence should be framed accordingly and repetition of the title avoided. If the title is insufficiently comprehensive, the opening should indicate the subjects covered. Usually the beginning of a synopsis should state the objective of the investigation.

It is sometimes valuable to indicate the treatment of the subject by such words as: brief, exhaustive, theoretical, &c.

The synopsis should indicate newly observed facts, conclusions of an

experiment or argument and, if possible, the essential parts of any new theory, treatment, apparatus, technique, &c.

It should contain the names of any new compound, mineral species, &c., and any new numerical data, such as physical constants; if this is not possible, it should draw attention to them. It is important to refer to new items and observations, even though some are incidental to the main purpose of the paper; such information may otherwise be hidden, though it is often very useful.

When giving experimental results the synopsis should indicate the methods used; for new methods the basic principle, range of operation, and degree of accuracy should be given.

4. **References.** If it is necessary to refer to earlier work in the summary, the reference should always be given in full and not by number. Otherwise references should be left out.

When a synopsis is completed, the author is urged to revise it carefully, removing redundant words, clarifying obscurities, and rectifying errors in copying from the paper. Particular attention should be paid by him to scientific and proper names, numerical data, and chemical and mathematical formulae.

THE CONSTITUTION OF CHROMIUM-MANGANESE ALLOYS BELOW 1000° C.*

1447

By W. B. PEARSON,† D.F.C., M.A., D.Phil., MEMBER, and
W. HUME-ROTHERY,‡ O.B.E., F.R.S., MEMBER

SYNOPSIS

The constitution of chromium-manganese alloys between 1000° and 525° C. has been studied by microscopical and X-ray methods. The σ phase undergoes a transformation at 980°–1005° C. (according to composition), and high-temperature X-ray photographs show that both the high-temperature, σ' , and low temperature, σ , modifications have characteristic " σ " structures resembling that of the σ -iron-chromium phase. The phase appears to be stable down to 523° C., and no signs of a eutectoid decomposition could be found. The solid solubility of manganese in chromium diminishes markedly below 1000° C., the temperature of the $\sigma \rightleftharpoons \sigma'$ transformation. In the range 1000°–800° C. normal two-phase (α -Cr + σ) alloys are formed when the solubility limit is exceeded. Between 800° and 600° C., three-phase alloys are found consisting of α -Cr, σ , and small amounts of a phase denoted α' -Mn, whose crystal structure appears to be similar to that of α -manganese; the amount of this last phase diminishes gradually on prolonged annealing, and the stable equilibrium almost certainly involves two-phase (α -Cr + σ) alloys. Below 600° C., the solubility of manganese in chromium diminishes even more markedly, and three-phase (α -Cr + α' -Mn + small amounts σ) alloys are formed. With annealing periods of the order of 1–2 months at 600°–500° C., equilibrium conditions are not obtained, but it is thought that the α' -Mn phase has a composition in the region of Mn_2Cr . The lattice spacings of the solid solution of manganese in α -Cr have been determined.

I.—INTRODUCTION

THE equilibrium diagram of the system chromium-manganese was determined in 1949 by Carlile, Christian, and Hume-Rothery¹, and was shown to contain a wide solid solution of manganese in chromium followed by a phase denoted θ , which was shown later² to possess the same crystal structure as the σ phase in the system chromium-iron, and is therefore called σ in the present paper. The σ phase was shown to be formed by a peritectic reaction, and this was confirmed by Zwicker,³ although in an earlier paper⁴ this author had regarded the σ phase as involving a eutectic. The diagram of Carlile, Christian, and Hume-Rothery in the region 0–70 at.-% manganese was determined § only above 1000° C., although these authors noted that changes occurred on annealing at low temperatures, and this was confirmed by Zwicker,³ who showed the solubility of manganese in chromium to diminish greatly below 1000° C. The two investigations were not, however, in exact agreement where they overlapped, and as the purity and exact composition of Zwicker's alloys were not indicated,|| a further study of the system has been made, and has shown that non-equilibrium structures are produced when previously homogenized alloys are re-annealed at low temperatures. It is probable that conditions

of true equilibrium will require annealing treatments of several years, and the present paper is submitted to describe the structures obtained after annealing periods of the order of 5–71 days.

II.—EXPERIMENTAL TECHNIQUE

The manganese and chromium used were high-purity, electrolytic, hydrogen-reduced metals, and were melted in thoria-lined alumina crucibles in an H.F. induction furnace, using slight modifications of the methods described by Carlile, Christian, and Hume-Rothery, and by Pearson and Hume-Rothery.⁶ The ingots were homogenized by heating in hydrogen for more than 2 hr. at 15°–20° C. below the solidus. Subsequent annealing treatments were carried out by standard methods^{1,6} in sealed evacuated tubes. Powder X-ray-diffraction films were used to determine lattice spacings by standard methods. Phases were identified by drawing a file across the actual surface examined under a microscope, and where the specimen had been annealed and quenched from a high temperature, the filings were not annealed, because this resulted in loss of manganese. At lower temperatures filings were annealed in the ordinary way. Seventeen alloys in lump form, and eleven batches of annealed filings were analysed by Johnson, Matthey and

* Manuscript received 15 October 1952.

† Low-Temperature Solid-State Physics Department, National Research Council, Ottawa, Canada; formerly Inorganic Chemistry Laboratory, Oxford.

‡ Royal Society Warren Research Fellow, and University Lecturer in Metallurgical Chemistry, Oxford.

§ As pointed out later,⁵ owing to a mistake in drawing, the phase boundaries in one diagram were extended to low temperatures where they had not been determined.

|| The alloys do not seem to have been analysed, although loss of manganese is known to occur on melting and on annealing.

Co., Ltd., and no evidence of contamination was found.*

III.—LATTICE-SPACING DATA

The lattice spacing of pure chromium, containing 0.003% oxygen, was determined as 2.8786–2.8787 kX at 18° C., in good agreement with the value 2.8789 kX

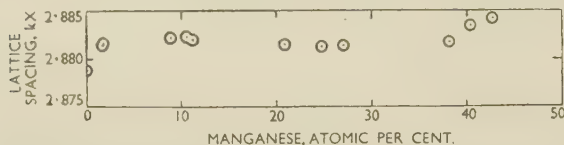


FIG. 1.—The Lattice Spacings of the Homogeneous Solid Solution of Manganese in Chromium. Alloy compositions were obtained by chemical analysis.

obtained by Carlile⁷ for pure Hilger chromium in lump form. The lattice spacings of the α -Cr solid solution are given in Fig. 1, which shows the change of

1000° C. the solubility of manganese in α -chromium is 69 at.-%, in agreement with the value of Carlile, Christian, and Hume-Rothery, but in contradiction to the value 65 at.-% given by Zwicker,³ although the latter's microstructures could be reconciled with the present results.

Below 1000° C. the solubility of manganese in chromium diminishes markedly, owing to a transformation in the σ phase with which the α -Cr phase is in equilibrium. The transformation gives rise to well-defined thermal arrests, and the temperature horizontals on the chromium-rich and manganese-rich sides of the σ phase were determined as 998° and 981° C., respectively, the transformation rising to a maximum temperature of 1005° C. in the middle of the σ field. Photographs obtained by a high-temperature X-ray camera showed that both the σ' (high-temperature) and σ (low-temperature) phases possess typical " σ " structures, but the nearly equal

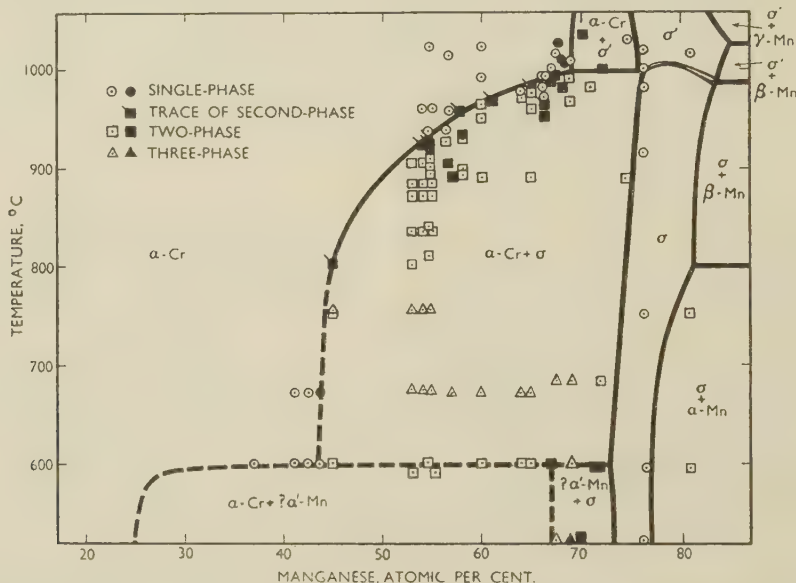


FIG. 2.—The Constitution of Chromium-Manganese Alloys. The full points refer to alloys which were analysed after the final annealing treatment. The open points refer to alloys which were not analysed, and are included only to show that the whole field was systematically examined. The compositions of these points are probably accurate to within ± 1 at.-%, but they should not be used for critical comparison, because occasional larger variations were found.

lattice spacing to be too small for the solubility curve to be determined by lattice-spacing methods. The abnormality at low concentrations is not understood, but is probably connected with the effect of traces of impurity. It is to be noted that Poole and Axon⁸ have shown that a rather similar abnormality in aluminium-rich aluminium-magnesium alloys is connected with the presence of only 0.01% silicon as impurity.

IV.—EXPERIMENTAL RESULTS

The results obtained in the present work by the microscopical method are shown in Fig. 2. At

scattering powers of chromium and manganese prevented any interpretation of the change.

From 1000° to 800° C. the solubility of manganese in chromium diminishes markedly, and when the solubility limit is exceeded, normal two-phase alloys of the (α -Cr + σ) type are formed. In this region of the diagram, X-ray powder photographs of 23 alloys were taken, and the results confirmed those shown in Fig. 2. From 800° to 600° C., the solubility of manganese in chromium continues to diminish, but the polyphase alloys, with very few exceptions, consisted of α -Cr, σ , and a third phase whose crystal structure was either identical with, or

* Both chromium and manganese were determined, and the analytical totals exceeded 99.90%, except for two batches of

filings where the total was only 99.80%, owing to the accidental inclusion of particles of silica from the annealing tubes.

very closely similar to, that of α -manganese, and which is therefore referred to as the α' -Mn phase. Fig. 3 (Plate XLV) shows the structure of a normal two-phase (α -Cr + σ) alloy, and Fig. 4 (Plate XLV) that of a three-phase (α -Cr + σ + α' -Mn) alloy; the etching methods used to distinguish between the σ and α' -Mn alloys are described in the Appendix (p. 314). In the region of the diagram from 800° to 600° C., X-ray powder photographs were taken of 18 alloys, and the results confirmed the microscopical work, and permitted the identification of the α' -Mn phase. In this range of temperature, the relative proportion of the α' -Mn phase diminished on prolonged annealing, and there is little doubt that above 600° C., conditions of true equilibrium involve two-phase (α -Cr + σ) alloys. In the X-ray films, the α' -Mn phase gave rise to a set of characteristic lines which could readily be recognized, and which were identified as due to a structure of the α -manganese type. Thus in alloy 64* the X-ray-diffraction film showed 3 lines due to the α -Cr phase, and 11 lines whose intensities and interplanar spacings agreed with the known values for α -manganese; the symbol α' -Mn is used to emphasize this resemblance.

Below 600° C., the solubility of manganese in chromium diminishes more rapidly, and in the region of the diagram between 523° and 600° C., powder X-ray photographs of 22 alloys were taken. In general, the microscopical and X-ray methods were in good agreement, although, in a few cases, alloys which had been described as two-phase on the basis of microscopical examination were found to contain traces of a third phase by the X-ray method. After annealing at 523° C. for 71 days, alloy 24.4 was homogeneous, whereas alloy 30.7 was of the two-phase (α -Cr + α' -Mn) type, and the solubility curve in Fig. 2 is drawn to agree with the X-ray data. In the composition range 30–65 at.-% manganese, alloys on annealing in the range 523°–600° C. were usually three-phase. The effect of increasing the annealing period was erratic, the proportion of the σ phase diminishing in some alloys, but remaining unchanged in others. When, however, alloys which had been annealed below 600° C., with the production of a three-phase (α -Cr + α' -Mn + σ) structure, were annealed above 600° C., the proportion of the α' -Mn phase diminished, and there seems no doubt that the equilibrium diagram contains a horizontal line at about 600° C. The proportion of the α' -Mn phase in the polyphase alloys increased with increasing manganese content up to 65 at.-%, but beyond this a change in the general structure of the alloys occurred, and they consisted of the σ phase, together with a fine structure in which both α -Cr and α' -Mn phases could be detected. This fine structure might be taken to indicate that the state of true equilibrium involves a eutectoidal decomposition of the σ phase into α -Cr and α' -Mn solid solutions, but this seems improbable for the following reasons:

(1) No combination of heat-treatment and deformation has yet caused a homogeneous σ alloy to decompose on annealing below 600° C.

(2) In this work, and in that of Carlile, Christian, and Hume-Rothery, alloys on the manganese-rich side of the σ phase showed (σ + α -Mn) structures after annealing at low temperatures. Most of these alloys were homogenized in the two-phase (σ + γ -Mn) region, and for those a low-temperature annealing treatment might perhaps transform the γ -manganese into α -manganese, and leave the σ phase unchanged owing to a sluggish transformation. The diagram of Carlile, Christian, and Hume-Rothery, however, shows one alloy homogenized in the σ region and one homogenized in the γ -Mn region, both of which consisted of (σ + α -Mn) on annealing at low temperatures, and it seems improbable that this should happen unless the σ phase persisted as a stable phase at low temperatures.

(3) In some alloys lying just outside the chromium-rich boundary of the σ phase, prolonged annealing below 600° C. gave structures which were essentially of the (σ + α' -Mn) type, the amounts of the α -Cr phase being relatively small, as though they were a remnant resulting from a failure to obtain complete equilibrium. This fact, together with the change in the nature of the alloys with more than 65 at.-% manganese, and the persistence of the homogeneous σ phase alloys at low temperatures, suggest that, under conditions of true equilibrium, the α' -Mn phase is formed by a peritectoid reaction at 600° C., and the dotted line in Fig. 2 indicates a possible composition for the α' -Mn phase. Annealing treatments have been extended up to 42 days at 600° C. and 71 days at 523° C., and under these conditions it has not been possible to obtain a homogeneous α' -Mn alloy, whilst no satisfactory correlation has been traced between the compositions of the alloys and the relative proportions of the different phases, so that the possibility that conditions of true equilibrium involve a eutectoidal decomposition of the σ phase cannot be excluded.

V—CONCLUSIONS

The diagram shown in Fig. 2 is an equilibrium diagram above 800° C. Below 800° C. it shows the limits of the chromium-base solid solution under conditions of annealing of the order of 1–2 months, and above 600° C. the solubility curve is not likely to be seriously in error. In the range 800°–600° C. when the solubility limit is exceeded three-phase alloys of the (α -Cr + σ + α' -Mn) type are produced on annealing previously homogenized specimens, and from these the α' -Mn phase gradually disappears on prolonged annealing. A horizontal almost certainly exists at 600° C., and below this temperature, three-phase alloys are again produced on annealing previously homogenized specimens, and it seems almost certain that, under conditions of true equilibrium, the

* Alloys are referred to by their atomic percentage of manganese.

α -Cr phase is in equilibrium with the α' -Mn phase, but the transformations are so sluggish that the composition of the latter cannot yet be determined. Thermodynamic considerations show that, as the alloys are so far from equilibrium after annealing for 42–71 days in the range 523°–600° C., it is probable that true equilibrium will be reached only after annealing treatments of some years, and the present paper is submitted to help the understanding of these difficult alloys.

ACKNOWLEDGEMENTS

The authors must express their thanks to Professor Sir Cyril Hinshelwood, F.R.S., for laboratory accommodation, and to Dr. F. M. Brewer for many other facilities which have encouraged their research.

APPENDIX

Etching Methods Used for Chromium-Manganese Alloys After Annealing at Low Temperatures

The two following reagents enable the different phases to be distinguished:

(i) *N/10 Hydrochloric Acid*.—In two-phase (Cr + σ) and (Cr + α' -Mn) alloys the σ or α' -Mn phase is

attacked when present in a chromium matrix. In three-phase (Cr + σ + α' -Mn) alloys, the α' -Mn phase etches very readily, much more so than the σ phase. When present in a σ matrix, particles of the α' -Mn phase remain clear and white, and the σ matrix is attacked.

(ii) *Alcoholic Nitric Acid* (10–15%).—The α' -Mn phase is etched very distinctly, whether it occurs in a σ or a chromium matrix. The reagent does not, however, etch particles of the σ phase when present in a chromium matrix.

REFERENCES

1. S. J. Carlile, J. W. Christian, and W. Hume-Rothery, *J. Inst. Metals*, 1949–50, **76**, 169.
2. W. B. Pearson, J. W. Christian, and W. Hume-Rothery, *Nature*, 1951, **167**, 110.
3. U. Zwicker, *Z. Metallkunde*, 1951, **42**, 277.
4. U. Zwicker, *ibid.*, 1949, **40**, 337.
5. W. Hume-Rothery and J. W. Christian, *Monthly J. Inst. Metals (News Section)*, **1950**, (May), 152.
6. W. B. Pearson and W. Hume-Rothery, *J. Inst. Metals*, 1952, **80**, 641.
7. S. J. Carlile, D.Phil. Thesis, Oxford: **1949**.
8. D. M. Poole and H. J. Axon, *J. Inst. Metals*, 1952, **80**, 599.

REPORT OF COUNCIL

FOR THE YEAR ENDED 31 DECEMBER 1952

THE Council is pleased to be able to report that the year 1952 was a very active and successful one for the Institute. Meetings were attended by larger numbers of members than for many years and, thanks to the generosity of the contributors to the Industrial Donations Fund, it was possible not only to maintain the standard of the Institute's publications—which have a world-wide reputation—but also to overcome the arrears of printing of MSS. of papers accepted for publication.

The Council's thanks are particularly due to the Chairman, Committee, and members of the Oxford Local Section for their invitation to hold the 1952 Autumn Meeting in Oxford. The arrangements made were excellent, the attendance was very good, and the generous hospitality offered to the members and their ladies was much appreciated.

MEMBERSHIP

The steady increase in the Institute's membership has been maintained, as will be seen from the table below. There is, however, still considerable scope for development both in the British Isles and in other countries throughout the world. The Council therefore again appeals to members to take all appropriate steps to increase the Institute's membership within their own industries and circle of acquaintances. Copies of a pamphlet on "The Institute of Metals: Particulars of its Objects, Work, and Membership" are available, on application, to all who can use them for membership development purposes.

It is particularly hoped that members resident outside the British Isles will be prepared to endeavour to increase the Institute's membership in their respective countries and branches of industry. To assist them, the Secretary will be glad not only to send them as many copies as are required of the pamphlet referred to above, but also to supply copies of lists of members in their respective countries for distribution with the pamphlets to possible members. Specimen copies of the (monthly) *Journal* and *Metallurgical Abstracts* can



Active Membership at 31 December 1908-1952.

also be sent by the Secretary to persons likely to be interested.

OBITUARY

The Council deeply regrets to record the death of Sir William Griffiths, Past-President.

It also much regrets to record the deaths of the following members, which were notified during the year: Mr. H. B. Barnard, Mr. J. S. Bowden, Professor L. C. F. de Brouckère, Mr. C. H. Carder, Colonel W. C. Devereux (Member of Council 1939-43), Dr. H. D. H. Drane, Mr. I. J. Espir, Mr. G. H. Field, Mr. W. R. Franklin, Dr. F. Johnson, Sir James Lithgow, Dr. A. Morris, Mr. E. H. Munnik, Mr. E. J. Overton, Mr. F. Powell, Mr. E. W. Pritchard, Mr. M. Schrero, and Dr. G. Vanzetti.

At 31 December	1945	1946	1947	1948	1949	1950	1951	1952
Honorary Members	6	6	9	9	11	11	11	11
Fellows	6	6	7	6	9	10	8	8
Ordinary Members	2213	2414	2491	2546	2685	2815	2941	3144
Junior Members	291	305	362
Associate Members	12	25	17	19	18
Student Members	361	529	655	746	783	452	462	423
Active List	2598	2980	3179	3326	3506	3579	3727	3948
Suspense List	179	58	36	55	67	97	124	95
Total	2777	3038	3215	3381	3573	3676	3851	4043

OFFICERS OF THE INSTITUTE

The following members were declared elected to fill vacancies as honorary officers of the Institute with effect from the 1952 Annual General Meeting :

President :

C. J. SMITHELLS, M.C., D.Sc.

Vice-Presidents :

G. L. BAILEY, C.B.E., M.Sc.
S. F. DOREY, C.B.E., D.Sc., F.R.S.

Honorary Treasurer :

E. H. JONES

Ordinary Members of Council :

ALFRED BAER, B.A.
N. I. BOND-WILLIAMS, B.Sc.
N. P. INGLIS, Ph.D., M.Eng.
IVOR JENKINS, D.Sc.
A. G. RAMSAY, B.Sc., Ph.D.
H. SUTTON, D.Sc.
Major P. LITHERLAND TEED, A.R.S.M.
W. J. THOMAS

In accordance with Article 42, the Council elected Professor F. C. THOMPSON, D.Met., M.Sc., as Senior Vice-President for the year 1952-53.

HONORARY CORRESPONDING MEMBERS TO THE COUNCIL

The Council desires to express to all Honorary Corresponding Members its appreciation for their help and advice during the past year.

The Honorary Corresponding Members to the Council are as follows : *Australia* : Professor H. K. Worner, D.Sc.; *Belgium* : H. P. A. Féron; *Canada* : Professor B. Chalmers, Ph.D., D.Sc., and Professor G. Letendre, B.A., Ph.D.; *France* : Professor P. A. J. Chevenard and Jean Matter; *India* : N. P. Gandhi, M.A., B.Sc., A.R.S.M., D.I.C.; *Italy* : Leno Matteoli, Dott.chim.; *Netherlands* : M. Hamburger; *South Africa* : G. H. Stanley, D.Sc., A.R.S.M., and Professor L. Taverner, A.R.S.M., D.I.C.; *Spain* : Professor J. Orland, M.Sc., M.A., Ph.D., D.D.; *Sweden* : Professor Carl A. F. Benedicks, Fil.Dr., D.Ing.e.h., Dr.Techn.h.c., and Professor Axel Hultgren; *Switzerland* : Professor A. von Zeerleder, Dr.Ing.; *United States of America* : Professor R. F. Mehl, Ph.D., Hon.Eng.D., Hon.Sc.D., Professor C. S. Smith, Sc.D., and Dr. R. A. Wilkins.

INSTITUTE OF METALS MEDAL

The Institute of Metals (Platinum) Medal for 1952 was awarded to Mr. WILLIAM SYDNEY ROBINSON, until recently President of the Consolidated Zinc Corporation, Ltd., in recognition of his outstanding services to the non-ferrous metal industries in developing the Australian zinc-lead industry and the British zinc industry.

As Mr. Robinson was unable to come to England to receive his medal from the President, the Governor-General of Australia kindly presented the medal on behalf of the Council at a private ceremony.

W. H. A. ROBERTSON MEDAL

The W. H. A. Robertson Medal for 1951 was awarded to Mr. CYRIL ERNEST DAVIES, for his paper on "The Cold Rolling of Non-Ferrous Metals in Sheet and Strip Form", published in the *Journal*, 1950-51, vol. 78, pp. 501-536.

ROSENHAIN MEDAL

The Rosenhain Medal for 1952 was awarded to Professor ANDRÉ GUINIER, of the Conservatoire National des Arts et Métiers, Paris, in recognition of his outstanding contributions in the field of physical metallurgy, particularly in connection with precipitation phenomena.

CAPPER PASS AWARDS

The Adjudicating Committee made no award for the year 1951 as, in its opinion, the quality and numbers of papers submitted for publication by the Institution of Mining and Metallurgy and the Institute of Metals, on the subjects for which the Capper Pass Awards are made, failed to reach a suitable standard.

It has been decided to include assaying within the fields for which the awards are made.

STUDENTS' ESSAY PRIZE

The first Students' Essay Prize of twenty guineas was awarded to Mr. J. C. WRIGHT (Student Member), Laboratory Assistant, Development and Research Department, The Mond Nickel Co., Ltd., Birmingham, for an essay on "The Metallographic Investigation of Failed High-Temperature Components". The essay was published in the *Bulletin*, 1952, vol. 1, pp. 112-115.

This competition is open to all Student Members of the Institute and to all Associate Members of Local Sections who are eligible for Student Membership, provided that both are within the normal age-limits for Student Membership, viz. 17 to 25 years.

PRESIDENTIAL BADGE OF OFFICE

The Council has gratefully accepted a generous offer by the Directors of Johnson, Matthey and Co., Ltd., to present to the Institute a suitable badge of office for the President.

PUBLICATIONS

In view of the generous response to the appeal to industry for regular financial support of the Institute's work, the Council was able, during the year, to approve a plan submitted by the Publication Committee to overcome the arrears of printing of papers accepted by the Institute. As a result, 81 papers and lectures were published in the *Journal* in the

calendar year 1952, as compared with 57 in 1951 and 61 in 1950 (the comparable figures for the financial year 1951-52 were 75 against 52 in the previous year, as mentioned in the Honorary Treasurer's Report), in addition to 13 papers published for a Symposium on "Properties of Metallic Surfaces". By December 1952 the delay in publication of acceptable MSS. of papers had been reduced to 4 months, which is the minimum period necessary for the processes of refereeing, editing, printing, and despatch.

During the year certain economies were authorized in the production of the *Journal* and *Metallurgical Abstracts* and, in particular, the experiment has been tried of inserting plates at one place in each issue, which has effected an appreciable saving in money.

A full list of papers and lectures published during the calendar year 1952 is given in Appendix I to this Report (p. 320).

Metallurgical Abstracts has continued to maintain its high standard. Publication of abstracts of the literature is more prompt than for many years, and the number of periodicals searched has been increased.

Annual Indexes. The delays in publication of the annual indexes to *Metallurgical Abstracts*, caused by staff changes, have been overcome. The index to the volume which ended with the August 1952 issue is in the press, and should be ready for despatch to members in January 1953.

10-Year Index. The production of the two volumes (names and subjects) of the index to Volumes 1-10 (1934-1943) of *Metallurgical Abstracts*, which had also been delayed by staff changes, is now well advanced. The "Names" volume of the index (516 pp.) has already been printed and is being bound, and the "Subjects" volume is now going through the press. It is confidently hoped that this index will be ready for distribution by the middle of 1953. The MS. of the index to Volumes 11-20 (1944-1953) has been prepared up to Vol. 19 (1951-52), and it is intended to proceed with its publication after the completion of Volume 20, which is the current volume.

In the *Monograph and Report Series* there were published during the calendar year No. 11: "Thermodynamics of Alloys", by Mr. J. Lumsden; No. 12: "The Cold-Working of Non-Ferrous Metals and Alloys"; No. 14: "Equipment for the Thermal Treatment of Non-Ferrous Metals and Alloys", and a second revised, edition of No. 3: "Atomic Theory for Students of Metallurgy", by Dr. W. Hume-Rothery, F.R.S. In addition, advance copies were published of the 13 papers to be included in No. 13: "Properties of Metallic Surfaces", the bound volume of which, containing a report of the discussion at a symposium on this subject, should be ready for publication early in 1953.

Discussions took place during the year regarding the possibility of co-operation between the British metallurgical societies in the publication of one comprehensive series of metallurgical abstracts, in lieu of the individual and independent abstracts

published by three of the societies, and of reports of progress in metallurgy. Though the publication of one comprehensive series of abstracts was agreed to be attractive in principle, the Council was informed that there were special circumstances which necessitated the continuation of the abstracts of one of the Institutes in their present form. As the proposed scheme would be financially unsound if there were duplicate publication, the Council regretfully reached the conclusion that no further action on this matter is desirable at the present time.

It appeared that no agreement could be reached by the four British metallurgical societies on the joint publication of periodical reports of progress in metallurgy. The Council is, however, exploring the possibility of publishing such reports with the exclusion of subjects directly relating to extraction and ferrous metallurgy, and has appointed a sub-committee to prepare a detailed plan and estimates of cost.

GENERAL MEETINGS

On Thursday, 3 January 1952 a General Meeting of the Institute was held in Birmingham, when there was an Informal Discussion, arranged by the Metallurgical Engineering Committee, on "Tool and Die Materials for the Extrusion of Non-Ferrous Metals and Alloys". There was a large attendance, and a valuable result of the meeting was the bringing closer together of the users and the die-steel manufacturers.

The Forty-Fourth Annual General Meeting was held in London from 24 to 27 March 1952, when Dr. C. J. SMITHELLS, M.C., was inducted into the Chair. The Forty-Second May Lecture was delivered on Monday, 24 March, at the Royal Institution, Albemarle Street, London, W.1, by Dr. J. J. P. STAUDINGER on "The Place of Plastics in the Order of Matter". One day of the meeting was devoted to a Symposium on "Equipment for the Thermal Treatment of Non-Ferrous Metals and Alloys", arranged by the Metallurgical Engineering Committee. An innovation was the holding of simultaneous scientific and technical sessions on widely differing subjects. The experiment was most successful, a large attendance being maintained at each session throughout the meeting. The procedure was repeated at the Autumn Meeting, when its success was confirmed. It may be assumed, therefore, that—whenever appropriate—simultaneous sessions on widely differing subjects will be arranged in connection with future General Meetings; they have enabled the maximum number of papers to be discussed, within the time available, by members of differing, and often specialist, interests.

The Forty-Fourth Annual Autumn Meeting was held in Oxford from 15 to 19 September 1952, by invitation of the Oxford Local Section. The meeting was most successful, and about 400 members, delegates, and ladies took part. The Twenty-Third Autumn Lecture was delivered in the Sheldonian Theatre on Monday, 15 September, by Professor H. W. SWIFT,

M.A., D.Sc., whose subject was "On the Foot-Hills of the Plastic Range". During the meeting there was an Informal Discussion on "Grain Boundaries", arranged, as an experiment, by the Metal Physics Committee.

On Wednesday, 19 November 1952, an all-day Symposium, arranged by the Metal Physics Committee, was held at the Royal Institution, Albemarle Street, London, W.1., on "Properties of Metallic Surfaces". Over 450 members and visitors were present, many of them from overseas. The large attendance and full discussion would appear to confirm the need for a meeting on this subject. The papers, and a report of the discussion, will be published at an early date as Monograph No. 13.

STUDENTS' EDUCATIONAL TOUR

An Easter Vacation Educational Tour for Junior and Student members was held in South Lancashire from 31 March to 4 April 1952, inclusive. It was attended by 31 Junior and Student Members, and 7 works were visited. The Council records its gratitude to the Directors of the works visited for their co-operation in making the tour a success.

As these tours appear to meet a real need, especially in the case of young men in industry and students at technical schools, another—to be held in the Birmingham area—is being arranged for the 1953 Easter Vacation.

LOCAL SECTIONS AND ASSOCIATED SOCIETIES

The six Local Sections (Birmingham, London, Oxford, Scottish, Sheffield, and South Wales) had good programmes of meetings during the winter session. The newly formed Oxford Local Section is to be particularly congratulated on its growth and keenness. Though it had only been in existence for one session, it acted as host to the Institute at one of the most successful of provincial Autumn Meetings of the Institute.

Members continued to enjoy the privilege of free membership of three Associated Societies (Leeds Metallurgical Society, Liverpool Metallurgical Society, and Manchester Metallurgical Society), and during the year arrangements were made for similar facilities to be granted to members by the North East Metallurgical Society, which became an Associated Society.

On 2 October 1952 a joint meeting of members of the Institute with local members of the Chemical Society, Royal Institute of Chemistry, and Society of Chemical Industry took place in Bristol, when Major P. L. TEED, A.R.S.M., read a paper on "Some Metallurgical Problems Imposed by Stratospheric Flight".

SPECIAL COMMITTEES

The Metal Physics Committee met three times during the year and arranged a scientific session at the Annual General Meeting, an Informal Discussion on "Grain Boundaries" at the Autumn Meeting,

and an all-day Symposium on "Properties of Metallic Surfaces" on 19 November. It also made arrangements for the presentation of papers on metal physics to Local Sections and Associated Societies.

The Metallurgical Engineering Committee met four times. It arranged an Informal Discussion on "Tool and Die Materials for Non-Ferrous Metals and Alloys" in Birmingham on 3 January and an all-day Symposium on "Equipment for the Thermal Treatment of Non-Ferrous Metals and Alloys" in connection with the Annual General Meeting. The Council has also approved a proposal by the Committee that, in connection with the 1953, 1954, and 1955 Annual General Meetings, there shall be a series of three all-day Symposia on "The Control of Quality in the Production of Wrought Non-Ferrous Metals" covering, respectively, the subjects of melting and casting (1953), working (1954), and heat-treatment and finishing (1955). The Committee has arranged an Informal Discussion on "Rolls and their Maintenance in the Non-Ferrous Metals Industry", to be held in Birmingham on 8 January 1953.

An *ad hoc* Committee is studying the question of the publication of reviews of progress in non-ferrous metallurgy.

A list of members of the main Committees of the Institute is given in Appendix III.

INDUSTRIAL DONATIONS FUND

The Council desires to record its warm appreciation of the continuing generous response to its appeal for regular financial support of the Institute's work by industry. A list of the contributions to the fund during the financial year ended 30 June 1952 is attached as Appendix II to this Report (p. 322).

Without this financial support, the Institute's work would have had to be severely restricted; with its aid, however, the Council has been able to expedite the publication of acceptable scientific and technical papers and to consider the provision of new services for science and industry.

STAFF

There were no changes among the senior members of the staff during the year.

JOINT ACTIVITIES

JOINT LIBRARY AND INFORMATION DEPARTMENT

Members, Government Departments, Research Laboratories, Universities, and other teaching establishments have continued to make great use of the facilities offered by the Library and Information Department. During 1952 13,448 publications were borrowed; in 1951 the figure was 11,617. The number of text-books acquired was 475, and the Council offers its thanks to the donors who presented copies of their works to the Library.

Use of the Lending Library is a valuable privilege

of membership. Books and periodicals can be borrowed, both from the Joint Library and also, on application through the Librarian, from the Science Library and the National Central Library. Under certain conditions photocopies of documents can be obtained for members, both at home and abroad; in 1952 130 photostat copies and 27 microfilms were supplied to members.

The Information Department, an important part of the service, is prepared to answer scientific and technical enquiries from members, but it is not its function to give the type of advice which comes within the field of the metallurgical consultant.

JOINT COMMITTEE FOR NATIONAL CERTIFICATES IN METALLURGY

The Joint Committee has approved five new schemes for National Certificates in Metallurgy during 1952; other schemes have been revised, and schemes are also being organized in districts not yet covered, with a view to suitable courses being started as soon as possible.

During 1952 the number of courses in operation has been:

Ordinary Certificate Courses	30
Contributory Centres with First- or First- and Second-year Courses	6
Higher Certificate Courses	18

Final examinations for the Ordinary National Certificate have been held at 28 Technical Colleges and for the Higher Certificate at 16 Technical Colleges.

The lists of those who have qualified for Certificates and for receipt of prizes are published in the Joint Committee's annual report. This report also contains reports on the final examinations held during the year.

JOINT COMMITTEE ON METALLURGICAL EDUCATION

The Joint Committee has published a report on "The Education and Training of Metallurgists". The following is a summary of the recommendations:

(1) The universities are at present, are likely to be, and should continue to be, the chief source of high-grade technologists. Universities should expand their output of technologists to the greatest extent they can achieve.

(2) Employers should finance the attendance of suitable employees at post-graduate courses in universities.

(3) Formally established methods should be adopted for training graduates immediately they enter industry.

(4) Since more technologists are needed than the universities can supply, the remainder coming from colleges of technology, a few colleges of technology should be upgraded and equipped for the education of high-grade technologists.

(5) In high-grade, technical teaching institutions, instruction in technical and elementary subjects

should be physically separated from that in higher technological subjects.

(6) The present standard of staffing in technical colleges and colleges of technology should be raised.

(7) There should be active collaboration in various fields between colleges of technology and employers.

(8) The whole of the present examinations in metallurgy for non-university students should be considered with a view to their co-ordination and rationalization and the establishment of the Associateship of the Institution of Metallurgists as the normal goal for almost all such students.

(9) Further provision for sandwich courses should be made.

(10) Since it appears that operatives in the metallurgical industries are insufficiently responsive to the opportunities offered for education and training, the greater use of incentives should be examined; employers should take into account any examination successes by their employees when considering promotion and the filling of vacancies in operational departments.

(11) To achieve a balance in the education of metallurgists, all teaching establishments—including the universities—and employers are recommended to instruct students and employees in the new humanities.

The Committee welcomes comments on the recommendations made in the report, and these will be given careful attention. Copies of the report can be obtained on application to the Secretary to the Joint Committee for Metallurgical Education at 4 Grosvenor Gardens, London, S.W.1.

MOND NICKEL FELLOWSHIPS COMMITTEE

During 1952 Mr. E. H. JONES replaced Mr. W. A. C. NEWMAN as representative of the Institute of Metals on the Committee.

The following awards were made for 1952:

A. G. DUCE (Joseph Lucas (Gas Turbine Equipment), Ltd.) to study in the United Kingdom, the Continent, the U.S.A., and Canada, the metallurgy and testing of materials, especially in sheet form, developed for high-temperature service, and the techniques employed in the manufacture of the combustion systems of gas-turbine engines.

F. G. HORTON (National Foundry College, Wolverhampton) to study casting production methods in the United Kingdom and on the Continent, with special reference to shell moulding, centrifugal casting, and sand-cement moulding.

G. P. KEMPSON (Henry Wiggin and Co., Ltd.) to study the development, application, and control of ferrous and non-ferrous melting and ingot-casting processes in the United Kingdom, on the Continent, the U.S.A., and Canada.

H. A. LONGDEN (Steel, Peech, and Tozer) to study metallurgical control methods in the United Kingdom, on the Continent, the U.S.A., and Canada, with special reference to open-hearth slag and temperature control.

APPENDIX I

LIST OF PAPERS PUBLISHED

The following is a complete list of the papers and lectures published by the Institute during the calendar year 1952 :

1342. The Production and Properties of Oxide-Reduced Copper Powder. By E. C. Ellwood, Ph.D., A.I.M., and W. A. Weddle, B.Sc.
1343. Unrelated Simultaneous Interdiffusion and Sintering in Copper-Nickel Compacts. By J. M. Butler, M.A., Ph.D., and T. P. Hoar, M.A., Ph.D., F.I.M.
1344. Heat-Treatment of Titanium-Rich Titanium-Iron Alloys. By H. W. Worner, M.Sc.
1345. The Solid Solutions of Zinc in Aluminium. By E. C. Ellwood, Ph.D., A.I.M.
1346. Metal Economics. I.—Primary Resources of Ferrous and Non-Ferrous Metals :
Introduction. By Professor A. J. Murphy, M.Sc., F.I.M.
The World Supply of Non-Ferrous Metals, Including the Light Metals. By R. Lewis Stubbs.
Metals as Natural Resources. By Professor S. Zuckerman, C.B., F.R.S.
World Demand and Resources of Iron Ore. By T. P. Colclough, C.B.E., D.Sc.
- Metal Economics. II.—Scrap Reclamation, Secondary Metals, and Substitute Metals :
The Scope for Conservation of Metals, Ferrous and Non-Ferrous. By C. A. Bristow, B.Sc., A.R.S.M., F.I.M., A. J. Sidery, Assoc.Met., and H. Sutton, D.Sc., F.I.M.
Economy by Standardization of Alloys and of the Method of Reclamation of Scrap Metals. By C. Dinsdale, M.Sc., F.I.M.
The Influence of Specifications on Productivity and the Economic Utilization of Ferrous and Non-Ferrous Metals. By F. Hudson, F.I.M.
Secondary Heavy Metals. By E. H. Jones, F.I.M.
Secondary Aluminium and Magnesium. By Colonel W. C. Devereux, C.B.E.
1347. Electric Furnaces for the Thermal Treatment of Non-Ferrous Metals and Alloys. By C. J. Evans, A.M.I.E.E., P. F. Hancock, B.A., F.I.M., F. W. Haywood, Ph.D., B.Sc., F.R.I.C., F.I.M., and J. McMullen, A.I.M.
1348. Gas Equipment for the Thermal Treatment of Non-Ferrous Metals and Alloys. By J. F. Waight, B.Sc.(Eng.), M.Inst.Gas E.
1349. Batch and Continuous Annealing of Copper and Copper Alloys. By Edwin Davis, M.Sc., F.I.M., and S. G. Temple, M.Sc., A.I.M.
1350. Bright Annealing of Nickel and Its Alloys. By H. J. Hartley, M.Sc., F.I.M., and E. J. Bradbury, M.Eng., A.M.I.Mech.E., A.I.M.
1351. Batch Thermal Treatment of Light Alloys. By C. P. Paton, B.Eng.
1352. Flash Annealing of Light Alloys. By R. T. Staples.
1353. Continuous Heat-Treatment of Aluminium Alloys of the Duralumin Type. By Marcel Lamouredieu.
1354. The Sintering of Copper-Zinc Powder Compacts. By D. D. Howat, B.Sc., Ph.D., F.R.I.C., R. L. Craik, B.Sc., A.R.T.C., and J. P. Cranston, B.Sc., Ph.D., A.R.T.C.
1355. The Effect of the Elements of the First Long Period on the $\alpha \rightleftharpoons \beta$ Transformation in Titanium. By A. D. McQuillan, Ph.D., B.Sc.
1356. Determination of Elastic Constants and Stress/Strain Relationship to Fracture of Sintered Tungsten Carbide-Cobalt Alloys. By E. Lardner, B.Sc., A.I.M., and N. B. McGregor.
1357. The Constitution of the Copper-Rich Copper-Zinc-Germanium Alloys. By P. Greenfield, Ph.D., B.Sc., and Professor G. V. Raynor, M.A., D.Sc.
1358. Micrographic Aspects of the Diffusion of Zinc and Aluminium in Copper. By H. Bückle, Dr.-Ing., and J. Blin.
1359. Note on Sub-Crystal Structure in Cold-Rolled Aluminium. By A. E. L. Tate, A.I.M., and D. McLean, B.Sc.
1360. Fundamental Reactions in the Vacuum-Fusion Method and Its Application to the Determination of O_2 , N_2 , and H_2 in Mo, Th, U, V, and Zr. By H. A. Sloman, M.A., F.R.I.C., F.I.M., and C. A. Harvey. With an Appendix by O. Kubaschewski, Dr. phil. nat. habil.
1361. The Opaque-Stop Microscope as a Means of Studying Surface Relief. By W. M. Lomer, M.Sc., B.A., and P. L. Pratt, B.Sc.
1362. A Modified Dew-Point Method for Vapour-Pressure Measurements of Lead-Mercury Alloys. By B. R. Burgan, R. C. Hall, and R. F. Hehemann.
1363. The Effect of Grain-Size on the Structural Changes Produced in Aluminium by Slow Deformation. By W. A. Rachinger, M.Sc.
1364. Observations on the Structure and Properties of Wrought Copper-Aluminium-Nickel-Iron Alloys. By Maurice Cook, D.Sc., Ph.D., F.I.M., W. P. Fentiman, B.Sc., A.I.M., and Edwin Davis, M.Sc., F.I.M.
1365. The Solid Solubilities of Cadmium, Indium, and Tin in Aluminium. By H. K. Hardy, Ph.D., M.Sc., A.R.S.M., A.I.M.
1366. The Constitution of the Aluminium-Chromium-Zinc Alloys at Low Chromium Contents. By A. R. Harding, B.Sc., Ph.D., and Professor G. V. Raynor, M.A., D.Sc.
1367. The Aluminium-Rich Alloys of the System Aluminium-Chromium-Iron. By J. N. Pratt, B.Sc., Ph.D., and Professor G. V. Raynor, M.A., D.Sc.
1368. The Equilibrium Diagram of the System Copper-Gallium in the Region 30-100 At.-% Gallium. By J. O. Betterton, Jr., D.Phil., B.S., and William Hume-Rothery, O.B.E., F.R.S.
1369. Presidential Address. By C. J. Smithells, M.C., D.Sc., F.I.M.
1370. A Study of Some Factors Influencing the Young's Modulus of Solid Solutions. By A. D. N. Smith, B.A.
1371. The Ageing Characteristics of Ternary Aluminium-Copper Alloys with Cadmium, Indium, or Tin. By H. K. Hardy, Ph.D., M.Sc., A.R.S.M., A.I.M.
1372. Residual Stresses in Chill-Cast and Continuously Cast Aluminium Alloy Billets. By R. A. Dodd, M.Sc., Ph.D., A.I.M., A.R.I.C.
1373. Stress-Recovery in Aluminium. By W. A. Wood, D.Sc., and J. W. Suiter, B.Sc.
1374. Creep Processes in Coarse-Grained Aluminium. By D. McLean, B.Sc.
1375. Electron-Microscopic Studies of Slip in Aluminium During Creep. By J. Trotter.
1376. Allotropic Transformation in Titanium-Zirconium Alloys. By Professor Pol Duwez, D.Sc.
1377. The Place of Plastics in the Order of Matter. Forty-Second May Lecture. By J. J. P. Staudinger, Dr.-Ing.
1378. Boundary Slip in Bicrystals of Tin. By K. E. Puttick, B.Sc., and Ronald King, B.Sc.
1379. X-Ray Diffraction Studies in Relation to Creep. By G. B. Greenough, Ph.D., (Mrs.) Catherine M. Bate-man, B.Sc., and (Mrs.) Edna M. Smith, B.A.
1380. The Formation of the Ni_3Al Phase in Nickel-Aluminium Alloys. By R. W. Floyd, B.Sc., A.I.M.
1381. The Effect of Metal/Mould Reaction on 85:5:5:5 Leaded Gun-Metal Sand Castings. By N. B. Rutherford, B.Sc., A.I.M.

1382. Segregation of Iron and Phosphorus at the Grain Boundaries in 70:30 Brass During Grain Growth. By H. M. Miekkoja, Sc.D.
1383. The Constitution of Nickel-Rich Alloys of the Nickel-Chromium-Titanium System. By A. Taylor, Ph.D., F.I.M., F.Inst.P., and R. W. Floyd, B.Sc., A.I.M.
1384. The Constitutional Diagram of the Chromium-Tungsten System. By H. T. Greenaway, B.Met.E.
1385. The Effect of Zirconium on the Properties and Structure of Superduralumin, with Particular Reference to Forgings. By M. Tournaire and M. Renouard.
1386. Lattice-Spacing Relationships in Aluminium-Rich Solid Solutions of the Aluminium-Magnesium and Aluminium-Magnesium-Copper Systems. By D. M. Poole, B.Sc., and H. J. Axon, D.Phil.
1387. Factors Affecting Equilibrium in Certain Aluminium Alloys. By E. C. Ellwood, Ph.D., F.I.M.
1388. The Factors Affecting the Formation of 21/13 Electron Compounds in Alloys of Copper and of Silver. By W. Hume-Rothery, O.B.E., F.R.S., J. O. Betterton, Jr., D.Phil., B.S., and J. Reynolds, B.A.
1389. The Lattice Spacings and Densities of Gold-Nickel Alloys at 25° C. By E. C. Ellwood, Ph.D., F.I.M., and K. Q. Bagley, Ph.D.
1390. The Metallography of Uranium. By B. W. Mott, M.A., and H. R. Haines.
1391. The Application of Polarized Light to the Examination of Various Anisotropic Metals and Intermetallic Phases. By B. W. Mott, M.A., and H. R. Haines.
1392. The Equilibrium Diagram of the System Copper-Indium in the Region 25-35 At.-% Indium. By J. Reynolds, B.A., W. A. Wiseman, and W. Hume-Rothery, O.B.E., F.R.S.
1393. The Constitution and Structure of Nickel-Vanadium Alloys in the Region 0-60 At.-% Vanadium. By W. B. Pearson, D.F.C., M.A., and W. Hume-Rothery, O.B.E., F.R.S.
1394. Twin Accommodation in Zinc. By P. L. Pratt, B.Sc., Ph.D., and S. F. Pugh, M.A., A.I.M.
1395. The Cubic-Tetragonal Transformation in Manganese-Copper Alloys. By Z. S. Basinski, B.A., and J. W. Christian, M.A., D.Phil.
1396. Specialized Microscopical Techniques in Metallurgy. By Professor S. Tolansky, D.Sc., F.R.S.
1397. Radioisotopes in the Study of Metal Surface Reactions in Solutions. By Massoud T. Simnad, Ph.D.
1398. The Influence of Machining and Grinding Methods on the Mechanical and Physical Condition of Metal Surfaces. By Peter Spear, B.Eng., Ian R. Robinson, B.Sc., and K. J. B. Wolfe, M.Sc.
1399. The Effect of Lubrication and Nature of Superficial Layer After Prolonged Periods of Running. By F. T. Barwell, Ph.D., D.I.C., B.Sc.(Eng.), Wh.Sch., M.I.Mech.E., A.M.I.E.E.
1400. The Crystalline Character of Abraded Surfaces. By P. Gay, M.A., Ph.D., and P. B. Hirsch, M.A., Ph.D.
1401. The Effect of Surface Conditions on the Mechanical Properties of Metals, Mainly Single Crystals. By Professor E. N. da C. Andrade, F.R.S.
1402. The Effect of Surface Condition on the Strength of Brittle Materials. By Professor C. Gurney, M.A., D.Sc., F.Inst.P.
1403. The Influence of Surface Condition on the Fatigue Strength of Steel. By R. J. Love, Wh.Sch., A.M.I.Mech.E.
1404. The Influence of Surface Films on the Friction and Deformation of Surfaces. By F. P. Bowden, Sc.D., F.R.S., and D. Tabor, Ph.D.
1405. Diffusion Coatings. By D. M. Dovey, M.A., A.R.I.C., A.I.M., I. Jenkins, D.Sc., F.I.M., and K. C. Randall, B.Sc.
1406. The Nature and Properties of the Anodic Film on Aluminium and Its Alloys. By H. W. L. Phillips, M.A., F.R.I.C., F.Inst.P., F.I.M.
1407. Chemical Behaviour as Influenced by Surface Condition. By U. R. Evans, Sc.D., M.A., F.R.S.
1408. The Effect of Method of Preparation on the High-Frequency Surface Resistance of Metals. By R. G. Chambers, M.A., Ph.D., and A. B. Pippard, M.A., Ph.D.
1409. Some Friction Effects in Wire Drawing. By G. D. S. MacLellan, M.A., Ph.D.
1410. The Viscosity of Molten Tin, Lead, Zinc, Aluminium, and Some of Their Alloys. By T. P. Yao, B.Sc., Ph.D., and V. Kondic, B.Sc., Ph.D.
1411. The Constitution of Nickel-Rich Alloys of the Nickel-Titanium-Aluminium System. By A. Taylor, Ph.D., F.Inst.P., and R. W. Floyd, B.Sc., A.I.M.
1412. Relative Grain Translations in the Plastic Flow of Aluminium. By W. A. Rachinger, M.Sc.
1413. The Influence of Primary Particles on the Grain-Size of Cast Magnesium-Aluminium Alloys. By W. A. Baker, B.Sc., F.I.M., Myriam D. Eborall, B.A., and A. Cibula, M.A., A.I.M.
1414. The Young's Modulus, Poisson's Ratio, and Rigidity Modulus of Some Aluminium Alloys. By N. Dudzinski, Dipl.Ing.(Chem.).
1415. Distribution Equilibria in Some Ternary Systems Me_1-Me_2-B and the Relative Strength of the Transition-Metal-Boron Bond. By Professor G. Hägg, Ph.D., and R. Kiessling, Ph.D.
1416. The Recovery of Polycrystalline Aluminium. By J. A. Ramsey, M.Sc.
1417. The Solid Solubility of Silver in Aluminium. By L. Rotherham, M.Sc., F.Inst.P., F.I.M., and L. W. Larke, A.F.R.Ae.S., L.I.M.
1418. The Constitution of Tantalum-Titanium Alloys. By D. Summers-Smith, B.Sc., A.R.T.C.
1419. Residual Stresses in Aluminium Alloy Sand Castings. By R. A. Dodd, M.Sc., Ph.D., A.I.M., A.R.I.C.
1420. The Creep/Time Relationship Under Constant Tensile Stress. By S. Bhattacharya, B.Sc., Ph.D., W. K. A. Congreve, B.A.Sc., Ph.D., and Professor F. C. Thompson, D.Met.
1421. The Temperature Dependence of Transient and Secondary Creep of an Aluminium Alloy to British Standard 2L42 at Temperatures Between 20° and 250° C. and at Constant Stress. By A. E. Johnson, D.Sc., M.Sc.Tech., M.I.Mech.E., and N. E. Frost, B.Sc., A.M.I.Mech.E.
1422. On the Foot-Hills of the Plastic Range. Twenty-third Autumn Lecture. By Professor H. W. Swift, M.A., D.Sc., M.I.Mech.E.
1423. The Embrittlement of Copper-Antimony Alloys at Low Temperatures. By D. McLean, B.Sc.
1424. The Gold-Platinum System. By A. S. Darling, B.Sc.Eng., A.M.I.Mech.E., R. A. Mintern, and J. C. Chaston, Ph.D., A.R.S.M., F.I.M.
1425. Crystal Slip in Aluminium During Creep. By D. McLean, B.Sc.
1426. The Viscosity of Aluminium and Binary Aluminium Alloys. By Professor W. R. D. Jones, D.Sc., and W. L. Bartlett, B.Sc., Ph.D.
1427. Plastic Deformation of Coarse-Grained Aluminium. By (Mrs.) V. M. Urie, B.Sc., and H. L. Wain, B.Met.E.
1428. Direct Examination of Solid Surfaces Using a Commercial Electron Microscope in Reflection. By J. W. Menter, M.A., Ph.D., A.Inst.P.
1429. A Study of Order-Disorder and Precipitation Phenomena in Nickel-Chromium Alloys. By A. Taylor, Ph.D., F.Inst.P., and K. G. Hinton, B.Sc.
1430. Deformation of Magnesium at Various Rates and Temperatures. By J. W. Suiter, B.Sc., and W. A. Wood, D.Sc.
1431. The Effect of Certain Solute Elements on the Recrystallization of Copper. By V. A. Phillips, A.R.S.M., B.Sc., D.Eng., A.I.M., and Professor Arthur Phillips, D.Eng.
1432. Equilibrium Relations at 460° C. in Aluminium-Rich Alloys Containing 0-7% Copper, 0-7% Magnesium, and 1-2% Silicon. By H. J. Axon, B.Met., D.Phil.
1433. An Example of Strain-Relief in Powder Specimens. By J. Gordon Parr, B.Sc.
1434. The Sub-Grain Structure in Aluminium Deformed at Elevated Temperatures. By J. A. Ramsey, M.Sc.
1435. The High-Temperature Oxidation of Some Cobalt-Base and Nickel-Base Alloys. By Professor A. Preece, M.Sc., F.I.M., and G. Lucas, Ph.D.

APPENDIX II

CONTRIBUTORS TO THE INDUSTRIAL DONATIONS FUND IN THE FINANCIAL YEAR ENDED 30 JUNE 1952

Donor	Gross, after Recovery of Tax by the Institute	Donor	Gross, after Recovery of Tax by the Institute
	£ s. d.		£ s. d.
United States Copper and Brass Industry : individual subscriptions totalling \$1950, by the following nine companies :		Booth (James) and Co., Ltd. (incl. John Wilkes, Sons and Mapplebeck, Ltd.)	100 0 0
American Brass Co., The		Copper Pass and Son, Ltd. (incl. George Pizey and Co., Ltd.; The Tyne Solder Co., Ltd.; and Victor G. Stevens, Ltd.)	100 0 0
Bridgeport Brass Co.		Colvilles, Ltd.	100 0 0
Bristol Brass Corp., The		Davy and United Engineering Co., Ltd.	100 0 0
Chase Brass and Copper Co.		Johnson, Matthey and Co., Ltd.	100 0 0
Chicago Extruded Metals Co.		*Manganese Bronze and Brass Co., Ltd., The	†100 0 0
New Haven Copper Co., The	692 9 9	Rylands Brothers, Ltd., and The Whitecross Co., Ltd.	100 0 0
Revere Copper and Brass, Inc.		*Consolidated Tin Smelters, Ltd. (incl. The Cornish Tin Smelting Co., Ltd.; Eastern Smelting Co., Ltd.; The Penpoll Tin Smelting Co., Ltd.; and Williams, Harvey and Co., Ltd.)	95 4 9
Scovill Manufacturing Co.		*Enthoven (H. J.) and Sons, Ltd.	95 4 9
Wolverine Tube Division, Calumet and Hecla Consolidated Copper Co., Inc.		*High Duty Alloys, Ltd.	95 4 9
*Enfield Rolling Mills, Ltd. (incl. Enfield Copper Refining Co., Ltd.; Enfield Rolling Mills (Aluminium), Ltd.; Holloway Metal Roofs, Ltd.; and London Zinc Mills, Ltd.)	523 16 1	*Stone (J.) and Co. (Charlton), Ltd.	†95 4 9
*Mond Nickel Co., Ltd., The (incl. Birlec, Ltd.; Henry Wiggin and Co., Ltd., and associated companies in the United States and Canada)	523 16 1	*Venesta, Ltd.	95 4 9
*Consolidated Zinc Corporation, Ltd., The (incl. The Broken Hill Corporation, Ltd.; Imperial Smelting Corporation, Ltd.; The National Smelting Co., Ltd.; New Broken Hill Consolidated, Ltd.; Northern Smelting and Chemical Co., Ltd.; Sulphide Corporation Ltd.; and The Zinc Corporation, Ltd.)	476 3 9	*Whiley (Geo. M.), Ltd.	95 4 9
*Goodlass Wall and Lead Industries, Ltd.: Associated Lead Industries, Ltd.	£190 9 6	Rubery, Owen and Co., Ltd.	75 6 6
Fry's Metal Foundries, Ltd. (incl. Antifriction Bearing Co., Ltd., The; Atlas Metal and Alloys, Ltd.; and The Eyre Smelting Co., Ltd.)	£95 4 9	Mallory Metallurgical Products, Ltd.	52 10 0
*Mufulira Copper Mines, Ltd.	285 14 3	Pyrotex, Ltd.	52 10 0
*Roan Antelope Copper Mines, Ltd.	285 14 3	*Murex, Ltd. (incl. Murex Welding Processes, Ltd.)	52 7 8
*Imperial Chemical Industries, Ltd., and its subsidiary companies	†250 0 0	*Associated Electrical Industries, Ltd., on behalf of the A.E.I. Group of Companies	50 0 0
Aluminium Laboratories, Ltd. (incl. Aluminium Union, Ltd.; Northern Aluminium Co., Ltd.; and Stand, Ltd.)	200 0 0	Birmingham Battery and Metal Co., Ltd., The Birmingham Small Arms Company, Ltd., on behalf of the B.S.A. Group of Companies	50 0 0
General Motors, Ltd. (incl. A.C. Sphinx Spark Plug Co., Ltd.; Delco-Remy-Hyatt, Ltd.; and Frigidaire, Ltd.)	200 0 0	*Brown (David) and Sons (Huddersfield), Ltd.	†50 0 0
Tube Investments, Ltd. (incl. The Chesterfield Tube Co., Ltd.; Mersey Cable Works, Ltd.; Reynolds Light Alloys, Ltd.; Reynolds Rolling Mills, Ltd.; Simplex Electric Co., Ltd.; South Wales Aluminium Co., Ltd.; and T.I. Aluminium, Ltd.)	200 0 0	Dale (John), Ltd.	50 0 0
*British Aluminium Co., Ltd., The (incl. Aluminium Corporation, Ltd.; William Mills, Ltd.; and North British Aluminium Co., Ltd.)	190 9 6	Danks (Edwin) and Co. (Oldbury), Ltd.	50 0 0
*McKechnie Brothers, Ltd.	190 9 6	Fairey Aviation Co., Ltd., The	50 0 0
*Magnesium Elektron, Ltd. (incl. F. A. Hughes and Co., Ltd.)	190 9 6	G.K.N. Group	50 0 0
*Metallo-Chemical Refining Co., Ltd.	150 0 0	Lucas (Joseph), Ltd. (inc. Rotax, Ltd.)	50 0 0
Nchanga Consolidated Copper Mines, Ltd.	150 0 0	*Morgan Crucible Co., Ltd.	50 0 0
Rhodesia Broken Hill Development Co., Ltd., The	150 0 0	Rolls-Royce, Ltd.	50 0 0
Rhokana Corporation, Ltd.	150 0 0	*Simon-Carves, Ltd.	50 0 0
Allen (W. H.) and Sons, Ltd.	105 0 0	*Tennant (C.), Sons and Co., Ltd.	†50 0 0
Vickers-Armstrongs, Ltd., and Vickers, Ltd. (incl. A.B.C. Motors, Ltd.; Robert Boby, Ltd.; Cooke, Troughton and Simms, Ltd.; Ioco, Ltd.; George Mann and Co., Ltd.; Palmers Hebburn Co., Ltd.; G. J. Worssam and Son, Ltd.; and Powers-Samas Accounting Machines, Ltd.)	105 0 0	Weir (G. and J.), Ltd. (incl. Argus Foundry, Ltd.)	50 0 0
		*Hopkinsons, Ltd.	49 11 5
		*A.P.V. Co., Ltd.	47 12 5
		*Birmetals, Ltd.	47 12 5
		*Birmingham Aluminium Casting (1903) Co., Ltd.	47 12 5
		*Bristol Aeroplane Co., Ltd., The	47 12 5
		*British Metal Corporation, Ltd., The	47 12 5
		*Chloride Electrical Storage Co., Ltd., The	47 12 5
		*Essex Aero, Ltd.	47 12 5
		*London and Scandinavian Metallurgical Co., Ltd.	47 12 5
		*Rotol, Ltd.	47 12 5
		*Star Aluminium Co., Ltd. (incl. Anglo-Swiss Aluminium Co., Ltd.)	47 12 5
		*Sterling Metals, Ltd.	47 12 5
		*Wolverhampton Metal Co., Ltd., The (incl. James Bridge Copper Works, Ltd.)	47 12 5
		Wednesbury Tube Co., Ltd., The	42 0 0
		*Hughes-Johnson Stampings, Ltd., The	40 0 0
		*Light Metal Forgings, Ltd.	40 0 0
		*Ferranti, Ltd.	38 1 11
		*Gibbons Brothers, Ltd. (incl. The Thermic Equipment and Engineering Co., Ltd.)	38 1 11
		*Parkinson Stove Co., Ltd., The	†38 1 11
		Aluminum Company of America (\$100)	35 14 10
		*British Tin Investment Corporation, Ltd.	30 0 0
		*Derby and Co., Ltd.	30 0 0
		*London Electric Wire Company and Smiths, Ltd., The (incl. Liverpool Electric Cable Co., Ltd.)	†30 0 0

Donor	Gross, after Recovery of Tax by the Institute	Donor	Gross, after Recovery of Tax by the Institute
	£ s. d.		£ s. d.
*Barker and Allen, Ltd.	28 11 5	Metal Products Co. (Willenhall), Ltd., The	10 10 0
*Bolton (Thomas) and Sons, Ltd.	28 11 5	New Metals and Chemicals, Ltd.	10 10 0
*British Lead Mills, Ltd.	28 11 5	Newey and Tayler, Ltd. (incl. Newey Brothers, Ltd., and D. F. Tayler and Co., Ltd.)	10 10 0
English Electric Co., Ltd., The (incl. D. Napier and Son, Ltd.)	26 5 0	North Thames Gas Board	10 10 0
Eso Petroleum Co., Ltd.	26 5 0	Platers and Stampers, Ltd.	10 10 0
Head, Wrightson and Co., Ltd.	26 5 0	Rover Co., Ltd., The	10 10 0
*Holroyd (John) and Co., Ltd.	26 3 9	Vauxhall Motors, Ltd.	10 10 0
Arkinstall Brothers, Ltd.	25 0 0	Wright, Bindley and Gell, Ltd.	10 10 0
Braby (Frederick) and Co., Ltd.	25 0 0	*Central Marine Engine Works (William Gray and Co., Ltd.)	10 0 0
British Timken, Ltd. (incl. Fischer Bearings Co., Ltd.)	25 0 0	Crittall Manufacturing Co., Ltd., The	10 0 0
British United Shoe Machinery Co., Ltd., The	25 0 0	Electric Furnace Co., Ltd. (incl. Electro Chemical Engineering Co., Ltd.)	10 0 0
Copper and Alloys, Ltd.	25 0 0	Electric Resistance Furnace Co., Ltd.	10 0 0
Gardner (Henry) and Co., Ltd.	25 0 0	Elliott Brothers (London), Ltd.	10 0 0
Messina (Transvaal) Development Co., Ltd., The	25 0 0	*Harland Engineering Co., Ltd., The	10 0 0
Plessey Co., Ltd., The	25 0 0	Newton, Chambers and Co., Ltd.	10 0 0
Pressed Steel Co., Ltd.	25 0 0	Rothschild (N. M.) and Sons	10 0 0
Roe (A. V.) and Co., Ltd.	25 0 0	Strebor Diecasting Co., Ltd.	10 0 0
Thompson (John) (Wolverhampton), Ltd.	25 0 0	West Yorkshire Foundries, Ltd. (Subsidiary of Leyland Motors, Ltd.)	10 0 0
Metal Box Co., Ltd., The	22 1 0	*Wild-Barfield Electric Furnaces, Ltd.	10 0 0
Almin, Ltd.	21 0 0	*Winfields Rolling Mills, Ltd.	10 0 0
Bull's Metal and Melloid Co., Ltd.	21 0 0	*Bound Brook Bearings (G.B.), Ltd.	9 10 6
Delta Metal Co., Ltd., The (incl. Heaton and Dugard, Ltd.)	21 0 0	*Hoyt Metal Company of Great Britain, Ltd., The	9 10 6
Leigh and Sillavan, Ltd.	21 0 0	*Hunt and Mitton, Ltd.	9 10 6
Monotype Corporation, Ltd., The	21 0 0	*Jenkinson (W. G.), Ltd.	9 10 6
Philips Electrical, Ltd.	21 0 0	*Shaw, Son and Greenhalgh, Ltd.	9 10 6
*International Alloys, Ltd.	20 19 0	*Stein (John G.) and Co., Ltd.	9 10 6
*Allen (Edgar) and Co., Ltd.	20 0 0	*Betts and Co., Ltd.	8 0 0
Brightside Foundry and Engineering Co., Ltd., The	20 0 0	*Glenfield and Kennedy, Ltd.	8 0 0
*British Tin Smelting Co., Ltd., The	20 0 0	United Wire Works (Birmingham), Ltd.	6 6 0
Deloro Stellite, Ltd.	20 0 0	Acton Bolt, Ltd.	5 5 0
*General Electric Co., Ltd., The	20 0 0	Barnard (H. B.) and Sons, Ltd.	5 5 0
Hall and Pickles, Ltd.	20 0 0	Bawn (W. B.) and Co., Ltd.	5 5 0
Hard Metal Tools, Ltd.	20 0 0	Blackwells Metallurgical Works, Ltd.	5 5 0
Park Gate Iron and Steel Co., Ltd., The	20 0 0	Cheswick and Wright, Ltd.	5 5 0
*Phosphor Bronze Co., Ltd., The	20 0 0	Cohen (Leonard), Ltd.	5 5 0
Renfrew Foundries, Ltd.	20 0 0	Corfield-Sigg, Ltd.	5 5 0
*Saunders-Roe, Ltd.	20 0 0	Dennison Watch Case Co., Ltd.	5 5 0
Société Anonyme pour l'Industrie de l'Alu- minium (Lausanne, Switzerland)	20 0 0	Easdale (R. M.) and Co.	5 5 0
Wickman, Ltd.	20 0 0	Electro-Alloys, Ltd.	5 5 0
*Chase Non-Ferrous Metal Co., Ltd.	19 0 6	Electroflo Meters Co., Ltd.	5 5 0
*Curran (Edward) Engineering, Ltd.	19 0 6	Headley, Birch and Co., Ltd.	5 5 0
*Rollet (H.) and Co., Ltd.	19 0 6	Jacks (William) and Co., Ltd.	5 5 0
*Wolverhampton Die-Casting Co., Ltd., The	19 0 6	Kemp (A.) and Son, Ltd.	5 5 0
Marconi's Wireless Telegraph Co., Ltd.	15 15 0	Lead Wool Co., Ltd., The	5 5 0
Perry Barr Metal Co., Ltd.	15 0 0	Metal Supplies, Ltd.	5 5 0
*Scottish Non-Ferrous Tube Industries, Ltd.	15 0 0	Miles (John) and Partners (London), Ltd.	5 5 0
*Loewy Engineering Co., Ltd., The	14 5 9	Oakland Metal Co., Ltd.	5 5 0
Brotherhood (Peter), Ltd.	12 12 0	Ratcliffs (Great Bridge), Ltd.	5 5 0
Bridge Foundry Co., Ltd., The	10 10 0	Rigby (John) and Sons, Ltd.	5 5 0
Carborundum Co., Ltd., The	10 10 0	Templewood Engineering Co., Ltd.	5 5 0
Clifford (Charles) and Son, Ltd.	10 10 0	Vincent Engineering Co., Ltd.	5 5 0
Crabtree (J. A.) and Co., Ltd.	10 10 0	Wilkinson (John) and Sons (Saltley), Ltd.	5 5 0
Fry's Diecastings, Ltd.	10 10 0	Cambridge Instrument Co., Ltd.	5 0 0
G. W. B. Electric Furnaces, Ltd.	10 10 0	Langley Alloys, Ltd.	5 0 0
Glynn Brothers, Ltd.	10 10 0	Blakeborough (J.) and Sons, Ltd.	4 4 0
Harrison (Birmingham), Ltd.	10 10 0	Kincaid (John G.) and Co., Ltd.	4 4 0
Highton and Son, Ltd.	10 10 0	*Acorn Anodising Co., Ltd.	† 3 16 2
Hills (West Bromwich), Ltd.	10 10 0	*Platt Metals, Ltd.	3 16 2
Hoover, Ltd.	10 10 0	Mining and Chemical Products, Ltd.	3 3 0
Incandescent Heat Co., Ltd., The (incl. Con- trolled Heat and Air, Ltd.; Metal Porcelains, Ltd.; Metalelectric Furnaces, Ltd.; and Selas Gas and Engineering Co., Ltd.)	10 10 0	Walterisation Co., Ltd., The	3 3 0
Johnson (Richard), Clapham and Morris, Ltd.	10 10 0	Beryllium and Copper Alloys, Ltd.	2 2 0
Lawley (Thomas), Ltd., and Jones and Rooke (1948), Ltd.	10 10 0	Carobronze, Ltd.	2 2 0
Maudslay Motor Co., Ltd., The	10 10 0	Follisain-Wycliffe Foundries, Ltd.	2 2 0
Metal Information Bureau, Ltd.	10 10 0	Gascoignes Non-Ferrous Foundries, Ltd.	2 2 0
		Premier Cooler and Engineering Co., Ltd., The	2 2 0
		Sheffield Testing Works, Ltd., The	2 2 0
		Tungum Sales Co., Ltd.	2 2 0
		Jenks (E. P.), Ltd.	1 1 0

* Annual Donation, Under Covenant, for Not Less Than 7 Years.

† Tax recoverable, but not actually recovered in the financial year 1951-52.

APPENDIX III

COMMITTEES

The main committees of the Institute which have served during the year were constituted as follows at 31 December 1952 :

FINANCE AND GENERAL PURPOSES COMMITTEE

BAER, Mr. Alfred (*Chairman*).
BAILEY, Mr. G. L.
BOLTON, Mr. E. A.
DOREY, Dr. S. F.
GRAHAM, Mr. A. B.
MURPHY, Professor A. J.
SMOUT, Sir Arthur.
TASKER, Mr. H. S.

Ex-officio :

SMITHELLS, Dr. C. J. (*President*).
THOMPSON, Professor F. C.
(*Senior Vice-President*).
JONES, Mr. E. H. (*Honorary Treasurer*).
SMITH, Mr. Christopher (*Chairman, Publication Committee*).

HIGNETT, Mr. H. W. G.
HUME-ROTHERY, Dr. W.
KING, Mr. Ronald.
LOMER, Mr. W. M.
MCLEAN, Mr. D.
NABARRO, Mr. F. R. N.
NUTTING, Dr. J.
OLIVER, Mr. D. A. (representing the Iron and Steel Institute and the British Iron and Steel Research Association).

RAYNOR, Professor G. V.
RICHARDS, Dr. T. Ll.
ROTHERHAM, Mr. L.

Ex-officio :

SMITHELLS, Dr. C. J. (*President*).
SMITH, Mr. Christopher (*Chairman, Publication Committee*).

LOCAL SECTIONS COMMITTEE

BOLTON, Mr. E. A. (*Chairman*).
ASHTON, Mr. A. B.
GARSIDE, Dr. J. E.
KENNETT, Dr. S. J.
WALTON, Mr. J. S.

RHODES, Dr. E. C. (*Honorary Secretary, London Local Section*).
FINNISTON, Dr. H. M. (*Chairman, Oxford Local Section*).
FROST, Dr. B. R. T. (*Honorary Secretary, Oxford Local Section*).
FOWLER, Mr. E. A. (*Chairman, Scottish Local Section*).
HAY, Mr. Matthew (*Honorary Secretary, Scottish Local Section*).
HALLETT, Mr. M. M. (*Chairman, Sheffield Local Section*).
MACDOUGALL, Mr. A. J. (*Honorary Secretary, Sheffield Local Section*).
SPRING, Mr. K. M. (*Chairman, South Wales Local Section*).
GRENFELL, Mr. W. H. (*Honorary Secretary, South Wales Local Section*).

Ex-officio :

SMITHELLS, Dr. C. J. (*President*).
THOMPSON, Professor F. C. (*Senior Vice-President*).
JONES, Mr. E. H. (*Honorary Treasurer*).
SYMONDS, Mr. H. H. (*Chairman, Birmingham Local Section*).
MATTHEWS, Mr. A. W. (*Honorary Secretary, Birmingham Local Section*).
RANSLEY, Dr. C. E. (*Chairman, London Local Section*).

MEDAL COMMITTEE

PRESIDENT (*Chairman*).
SENIOR VICE-PRESIDENT.

and

Not more than four Institute of Metals (Platinum) Medal-

lists who are, or have been, Members of Council (to be selected by the President), with power to the President to co-opt not more than two other persons.

METAL PHYSICS COMMITTEE

QUARRELL, Professor A. G. (*Chairman*).
BOWDEN, Dr. F. P.

COTTRELL, Professor A. H.
FINNISTON, Dr. H. M.
FRANK, Dr. F. C.

METALLURGICAL ENGINEERING COMMITTEE

THOMAS, Mr. W. J. (*Chairman*).
BAKER, Mr. W. A.
BOLTON, Mr. E. A.
BOWMAN, Mr. W. H.
CAMPBELL, Mr. D. F.
DAVIES, Mr. C. E.
FORD, Professor H.
MILLER, Mr. H. J.
PATON, Mr. Charles.
SALTER, Mr. J.

SINGER, Dr. A. R. E.
SWINDELLS, Dr. N.
WALTON, Mr. J. S.
WILKINSON, Mr. R. G.

Ex-officio :

SMITHELLS, Dr. C. J. (*President*).
SMITH, Mr. Christopher (*Chairman, Publication Committee*).

NOMINATIONS COMMITTEE

SMITHELLS, Dr. C. J. (*President*).
MURPHY, Professor A. J. (*Past-President*).

TASKER, Mr. H. S. (*Past-President*).
THOMPSON, Professor F. C. (*Senior Vice-President*).

PUBLICATION COMMITTEE

SMITH, Mr. Christopher (*Chairman*).
BAKER, Mr. W. A.
BOLTON, Mr. E. A. (representing the Local Sections Committee).
FORD, Professor H.
FOX, Dr. F. A.
GADD, Mr. E. R.
INGLIS, Dr. N. P.
JENKINS, Dr. Ivor.
PARKER, Dr. R. T.
PHILLIPS, Mr. H. W. L.
POWELL, Mr. A. R.
RAYNOR, Professor G. V.
THOMPSON, Professor F. C.

TURNER, Mr. T. H.

Ex-officio :

SMITHELLS, Dr. C. J. (*President*).
BAER, Mr. Alfred (*Chairman, Finance and General Purposes Committee*).
JONES, Mr. E. H. (*Honorary Treasurer*).
QUARRELL, Professor A. G. (*Chairman, Metal Physics Committee*).
THOMAS, Mr. W. J. (*Chairman, Metallurgical Engineering Committee*).

REPORT OF THE HONORARY TREASURER

FOR THE YEAR ENDED 30 JUNE 1952

THE accounts for the year show the continued growth of the Institute and its activities.

It will be seen that excess of expenditure over normal income increased from £2406 in 1950-51 to £6917 in 1951-52. This is some £1000 less than was forecast in the official estimates for the year under review; a direct comparison of the estimates with the accounts shows this figure as £2039, but the estimates provided for the printing of two books, at a cost of £975, which were delayed. The excess expenditure has been met by transfer from the Industrial Donations Fund. Costs of meetings and miscellaneous activities rose by £1941, while direct expenditure on publications (excluding salaries and overheads) increased by £7066. Printing trade charges for composition, machining, and binding were $17\frac{1}{2}$ per cent. higher than in the previous year. The printing order rose from 54,000 to 57,000 copies for the financial year 1951-52 and the *Journal* was enlarged to allow the printing of the *Bulletin*, a more ambitious form of the old News and Announcements Section. The change of format cost an estimated £800 in the year, but this sum was much more than recovered in increased revenue arising from the change.

Some £3000 of the increase in expenditure was due to the cost of a campaign to publish an accumulation of accepted papers, which was causing delay unfair to the authors. This operation has gone according to plan, the number of papers printed in the financial year 1951-52 being 75, compared with 52 in the financial year 1950-51, but it will take about half the present financial year to complete the scheme. The current year will show a further increase in general expenses; the salaries of the staff have been raised to make them more comparable with equivalent

positions in other London offices; on the other hand, paper has fallen in price to some extent offsetting this. Analysis of the expenditure with the assistance of an outside accountant has confirmed the estimate of the permanent officers of the Institute that approximately 85 per cent. is attributable to costs of publication.

Income has increased by £4496. Of this amount, subscriptions and meeting receipts accounted for £1722 and publication sales and advertisements for £2737; the remainder, £37, came from higher investment yield. The chief sources of revenue continue to show increases up to the present date. The change in format of the *Journal* has been justified; membership has not fallen, and the anticipated increase from sales and advertising revenue is growing.

Apart from the Capper Pass and Mond Nickel Fellowships Funds, the total resources and current surplus, including the Endowment Fund and the Industrial Donations Fund, amount to £51,095, against £46,155 in the previous year. However, the raising of the bank rate lowered the market value of investments by some £7600, but as the intention is to keep these until redemption, the loss will not be realized and any investment of new money will yield more than before the change.

The Industrial Donations Fund, so successfully launched during the presidency of Mr. Tasker, is producing about £10,000 per year at present. It is likely that this generous contribution of industry will somewhat diminish over the next six years, at which time donations are due to cease. However, the Institute may hope to achieve, with reasonable prudence, very nearly if not quite a balanced budget by then.

THE INSTITUTE OF METALS BALANCE SHEET AS AT 30 JUNE 1952

£	30.6.51	£	£	£	FIXED ASSETS
RESERVES AND ACCUMULATED FUND					
10,000	750				Office Furniture and Equipment:
1,000					Nominal Value as at 30 June 1947
4,478					Additions since, at cost
16,228					
Accumulated Fund:					
2,526	516				Less Depreciation to date
	1,850				
2,406					Library Books, etc.:
4,932					Nominal value as at 30 June 1947
2,276	2,406				INVESTMENTS
18,504	250				General Fund:
Less Excess of Expenditure over Income for the Year					
					Securities at cost or otherwise, as per schedule
					(Market value £15,183)
					Publications at nominal value
					Stock of stationery at valuation
					Due from War-Time Emergency Fund
					Debtors:
					Subscriptions
					Less Provision for doubtful subscriptions
					Sundry debtors and payments in advance
					W. H. A. Robertson Fund
					Lloyds Bank, Ltd.
					Cash in hand
					ENDOWMENT FUND
					Securities at cost, per schedule
					(Market value £16,361)
					Lloyds Bank, Ltd., Deposit Account
					Less Due to General Fund
					INDUSTRIAL DONATIONS FUND
					Due from General Fund
					Securities at cost, per schedule
					(Market value £1,746)
					Lloyds Bank, Ltd.
					Post Office Savings Bank
					Payments in advance for publications
					MOND NICKEL FELLOWSHIPS FUND
					Securities at cost, per schedule
					Post Office Savings Bank
					London Trustee Savings Bank
					Lloyds Bank, Ltd., Deposit Account
					Lloyds Bank, Ltd., Current Account
					Interest accrued due
					Less Creditor outstanding
					CAPPER PASS FUND
					Post Office Savings Bank
					Interest accrued due

We have audited the above Balance Sheet dated 30 June 1952, and the annual Income and Expenditure Account for the year ended 30 June 1952, and in our opinion proper books of account have been kept by the Institute, so far as appears from our examination of those books. The above mentioned Balance Sheet and annexed Income and Expenditure Account are in agreement with the books of Account. In our opinion, and to the best of our information, and according to the explanations given us, the case of the Income and Expenditure Account, of the excess of Expenditure over Income for the year ended 30 June 1952.

Approved on behalf of the Council: C. J. SMITHS, President.
E. H. JONES, Honorary Treasurer.
A. BAER, Chairman, Finance and General Purposes Committee.
S. C. GUILLAN, Secretary.

THE INSTITUTE OF METALS
INCOME AND EXPENDITURE ACCOUNT FOR THE YEAR ENDED 30 JUNE 1952

[illegible]

THE INSTITUTE OF METALS
FUNDS ACCOUNTS FOR THE YEAR ENDED 30 JUNE 1952
ENDOWMENT FUND

30.6.51		£	30.6.51
£		£	
769	To Transfer to General Fund—Investment Interest	769	By Balance at 30 June 1951
21,295	" Balance at 30 June 1952	769	" Interest on Investments and Bank Interest
<u>£22,064</u>		<u>£22,064</u>	

INDUSTRIAL DONATIONS FUND

£		£	
220	To Cost of Appeals, Administration and Stamp Duty	354	By Balance at 30 June 1951
—	" 10-Year Index to Metallurgical Abstracts	21	" Donations Received (including Tax recovered)
516	" Amount transferred to General Fund, being Excess of Expenditure over Income for the year ended 30 June 1952	6,917	" Income Tax Recovered (previous year)
6,356	" Balance at 30 June 1952	11,297	" Interest on Investments
<u>£7,092</u>		<u>£7,092</u>	

MOND NICKEL FELLOWSHIPS FUND

£		£	
3,723	To Grants to Fellows, including travelling	4,398	By Balance at 30 June 1951
34	" Printing, Stationery, Postages, and Publicity	124	" Donations Received
4	" Bank Charges	3	" Interest on Investments and Bank Interest
27	" Professional Charges	—	
250	" Secretarial Expenses	250	
23,827	" Balance at 30 June 1952	26,527	
<u>£27,875</u>		<u>£27,875</u>	

CAPPER PASS FUND

£		£	
200	To Grants	316	By Balance at 30 June 1951
325	" Balance at 30 June 1952	200	" Donations Received
<u>£525</u>		9	" Bank Interest
		<u>£525</u>	

W. H. A. ROBERTSON FUND

£		£	
30	To Balance at 30 June 1951 due to The Institute of Metals	32	By Donations received
2	" Expenditure during year	32	" Balance at 30 June 1951 due to The Institute of Metals
<u>£32</u>		<u>£32</u>	

SCHEDULE OF SECURITIES, 30 JUNE 1952

£	£	£	£
5,500	General Fund:	17,792	brought forward
1,070	3% Savings Bonds, at cost	525	Endowment Fund:
4,734	24% Treasury Stock, at cost	1,285	24% Defence Bonds, at cost
5,957	4% Consolidated Stock, at cost	£1,285	3% Savings Bonds, at cost
500	24% National War Bonds, at cost	19,483	4% Consolidated Loan, at cost
162	24% Defence Bonds, at cost	21,293	
829	£1 War Savings (see Note 1)		Industrial Donations Fund:
	4% Consolidated Loan (see Note 2)	950	3% Funding Stock, at cost
		—	4% Funding Stock 1960/90, at cost
17,792		950	
	Note 1. At cost plus accrued interest to 22.11.50.		Mond Nickel Fellowships Fund:
	Note 2. Transferred at Market Value on 22.11.50 from the War-Time Emergency Fund to the General Fund.	6,900	Woolwich Equitable Building Society
		1,250	Co-operative Permanent Building Society
		3,500	Hatfield Building Society
		5,000	Abbey National Building Society
		16,650	
		<u>£56,685</u>	
			Carried forward 17,792

17,792 carried forward

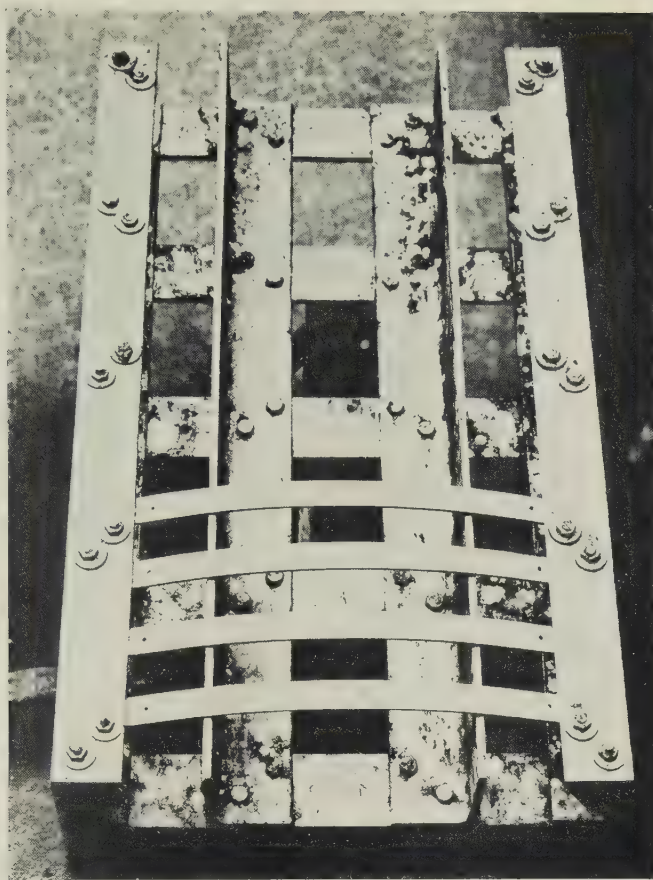


FIG. 1.—Stress-Corrosion Testing Frame for Field Tests.

MICROSECTIONS OF H10-WP ALLOY
SPECIMENS AFTER 2 YEARS'
EXPOSURE. $\times 100$.



FIG. 2.—Site I. Industrial atmosphere at Sheffield.

FIG. 3.—Site II. Semi-industrial atmosphere at London.

MICROSECTIONS OF H10-WP ALLOY SPECIMENS AFTER 2 YEARS' EXPOSURE. $\times 100$.

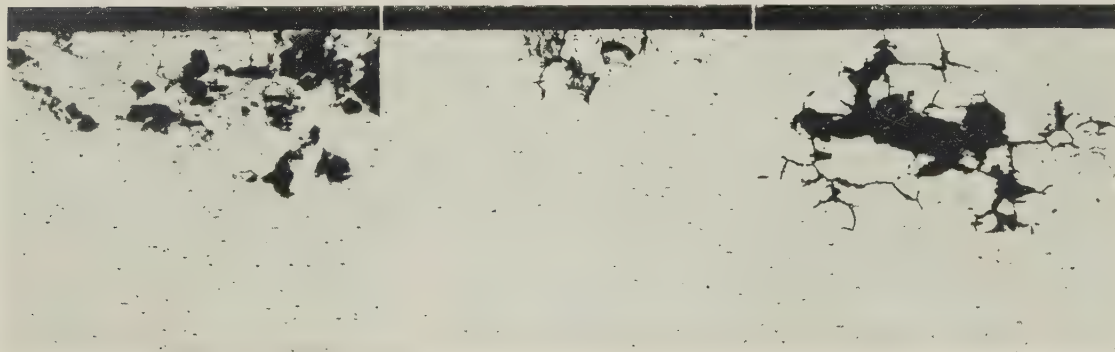
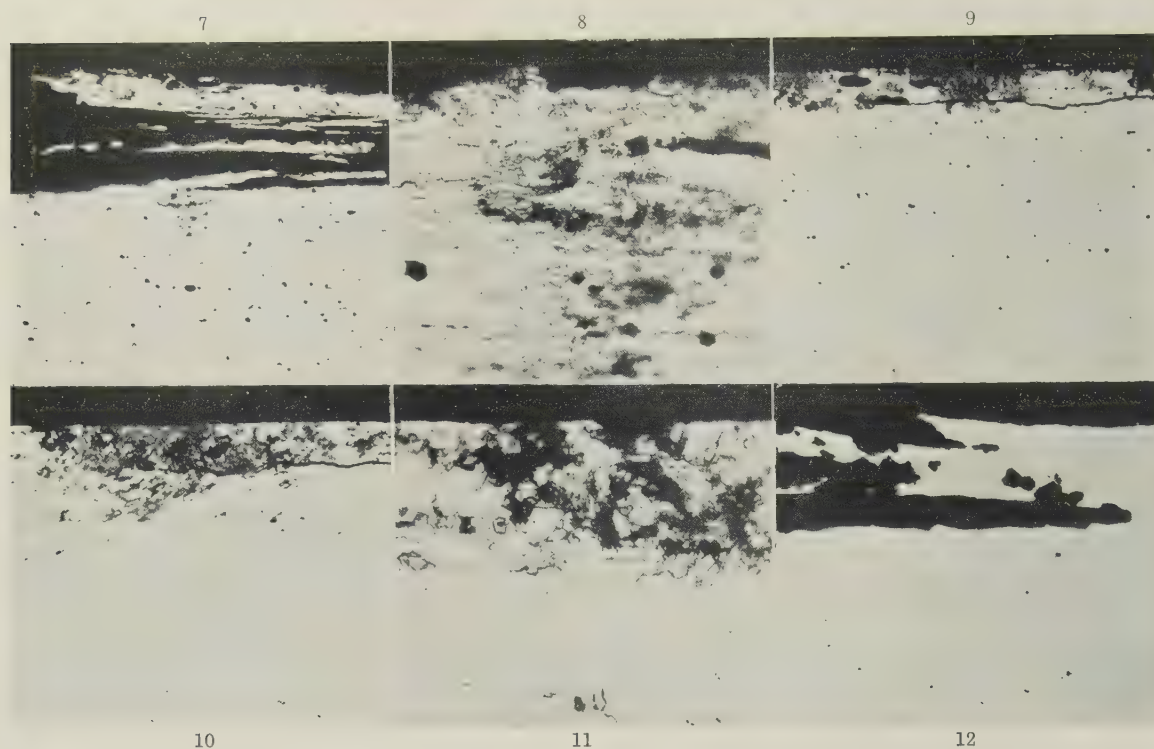
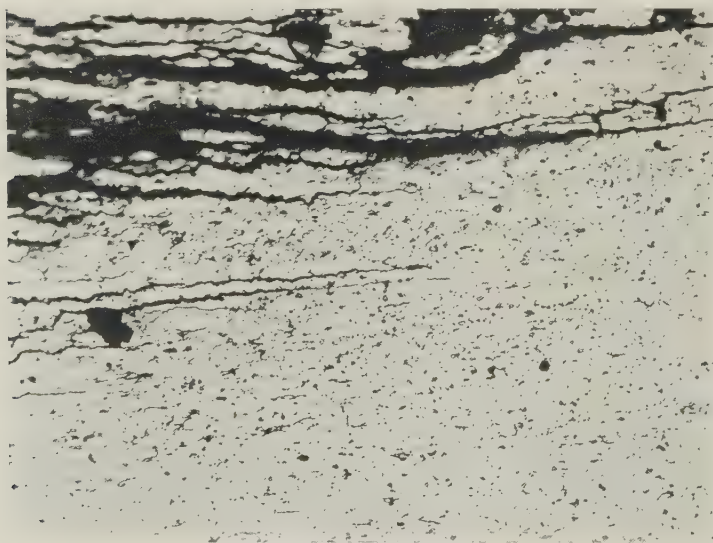


FIG. 4.—Site III. Marine atmosphere at Hayling Island.

FIG. 5.—Site IV. Rural atmosphere at Stoke Poges.

FIG. 6.—Site VII. Total immersion in fresh water at Christchurch.

MICROSECTIONS OF H15-WP ALLOY SPECIMENS AFTER 2 YEARS' EXPOSURE.

FIG. 7.—Site I. Industrial atmosphere at Sheffield. $\times 100$.FIG. 8.—As Fig. 7. Showing attack of sub-grain network. $\times 500$.FIG. 9.—Site II. Semi-industrial atmosphere at London. $\times 100$.FIG. 10.—Site III. Marine atmosphere at Hayling Island. $\times 100$.FIG. 11.—As Fig. 10. Showing attack of sub-grain network. $\times 500$.FIG. 12.—Site VIII. Intermittent immersion in fresh water at Christchurch. $\times 100$.FIG. 13.—Foliation of an H15-WP Extrusion Specimen Taken from a Brine-Tank Frame. $\times 250$.

CRYSTAL FRAGMENTATION IN ALUMINIUM DURING CREEP.



FIG. 1.—Banded Structure on Surface of Coarse-Grained Specimen Extended 13.8%. Photographed in focus, oblique lighting. $\times 50$.



FIG. 2.—Same Field After Polishing Flat and Anodizing. Specimen now extended 23.6%. Photographed between crossed polaroids. $\times 50$.

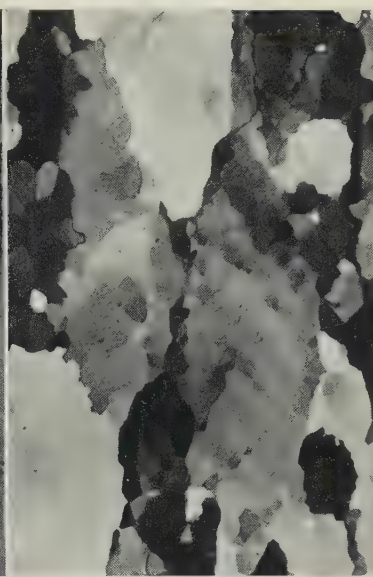


FIG. 3.—Relatively Unbanded Structure in Fine-Grained Specimen Extended 50%. $\times 100$.

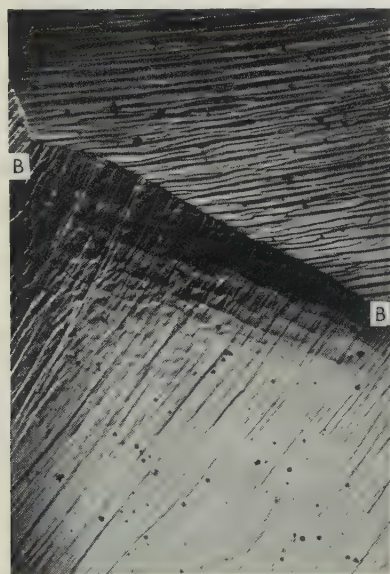


FIG. 4.—Polygonization in Coarse-Grained Specimen, Beginning First Near Grain-Boundary *BB*. The polygonized boundaries are those nearly parallel to *BB*; the other lines are slip bands. Specimen extended 4.02%. $\times 50$.

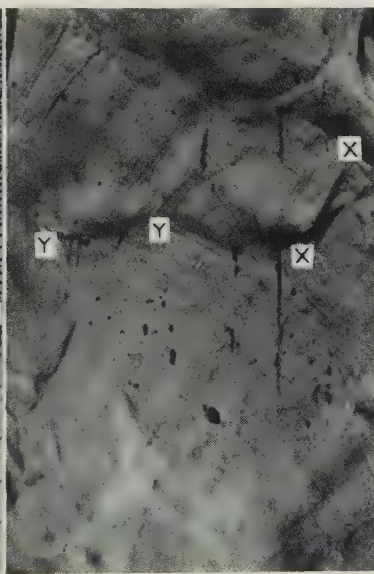


FIG. 5.—Displacement *XX* and *YY* at Sub-Crystal Boundaries in Fine-Grained Specimen Extended 69%. Photographed in focus. $\times 750$.

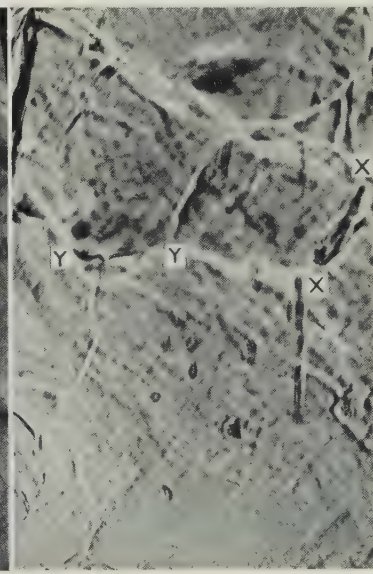


FIG. 6.—Same Field as Fig. 5, Stopped Down and Photographed Inside Focus to Show Polygonized Boundaries (Network of White Lines). $\times 750$.



FIG. 7.—Surface Tilt at Sub-Boundary *PP* in a Fine-Grained Specimen Extended 11.9%. Interference micrograph. $\times 310$.

GRAIN-BOUNDARY MIGRATION DURING CREEP OF ALUMINIUM.

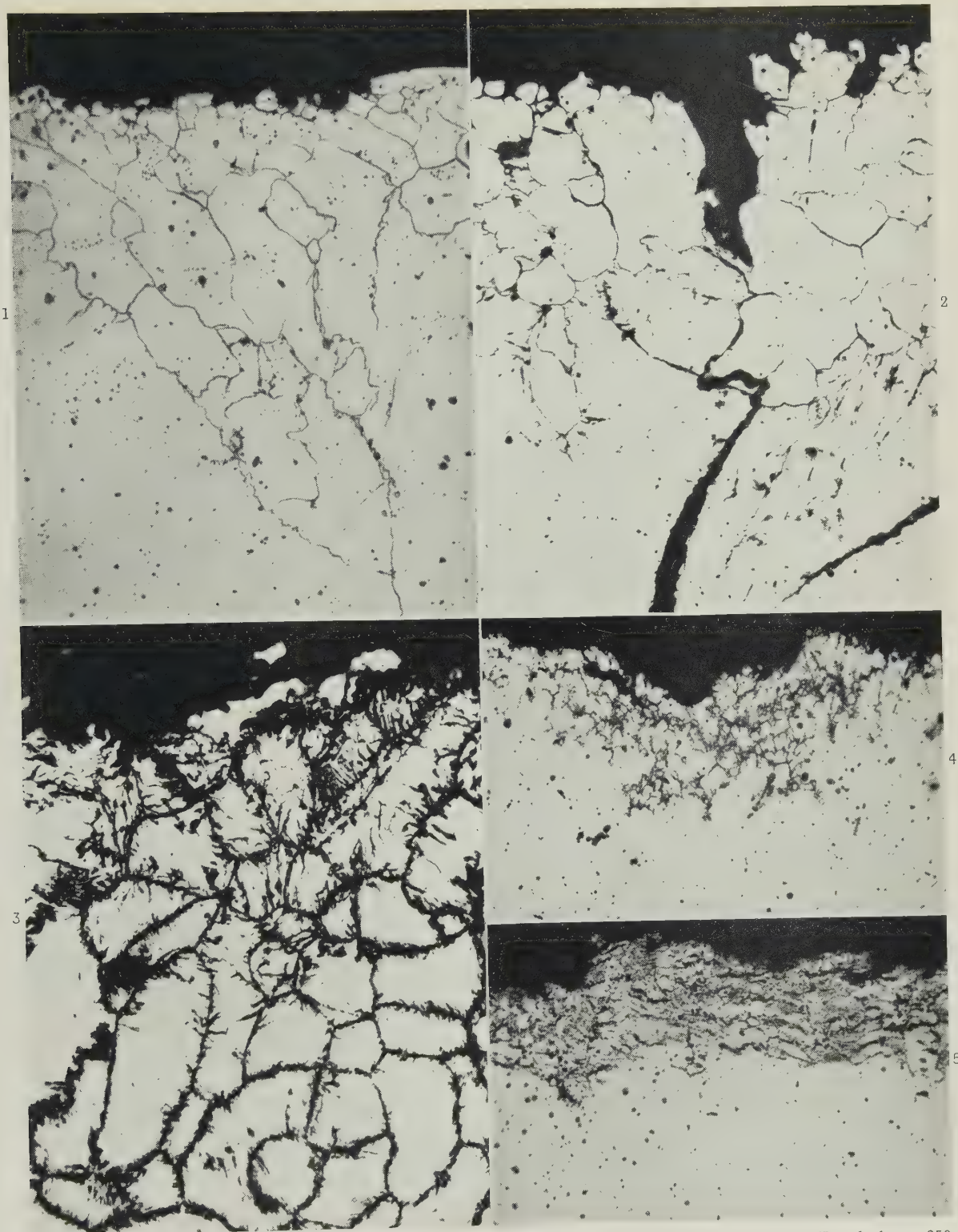


FIG. 11.—Grain Growth During Creep of Fine-Grained Specimen Extended 11.9%. The etch pits show that the left-hand grain has grown into the right-hand one. $\times 1250$.



FIG. 12.—Same Field After 19.8% Extension. $\times 1250$.

EXAMPLES OF INTERCRYSTALLINE CORROSION IN ZINC-ALUMINIUM ALLOYS.



FIGS. 1-5.—Cast Specimens After Exposure for 10 Days to an Air/Water-Vapour Atmosphere at 95° C. Unetched. $\times 250$

FIG. 1.—Alloy 2. S.H.P. Zinc with 0.075% Aluminium.

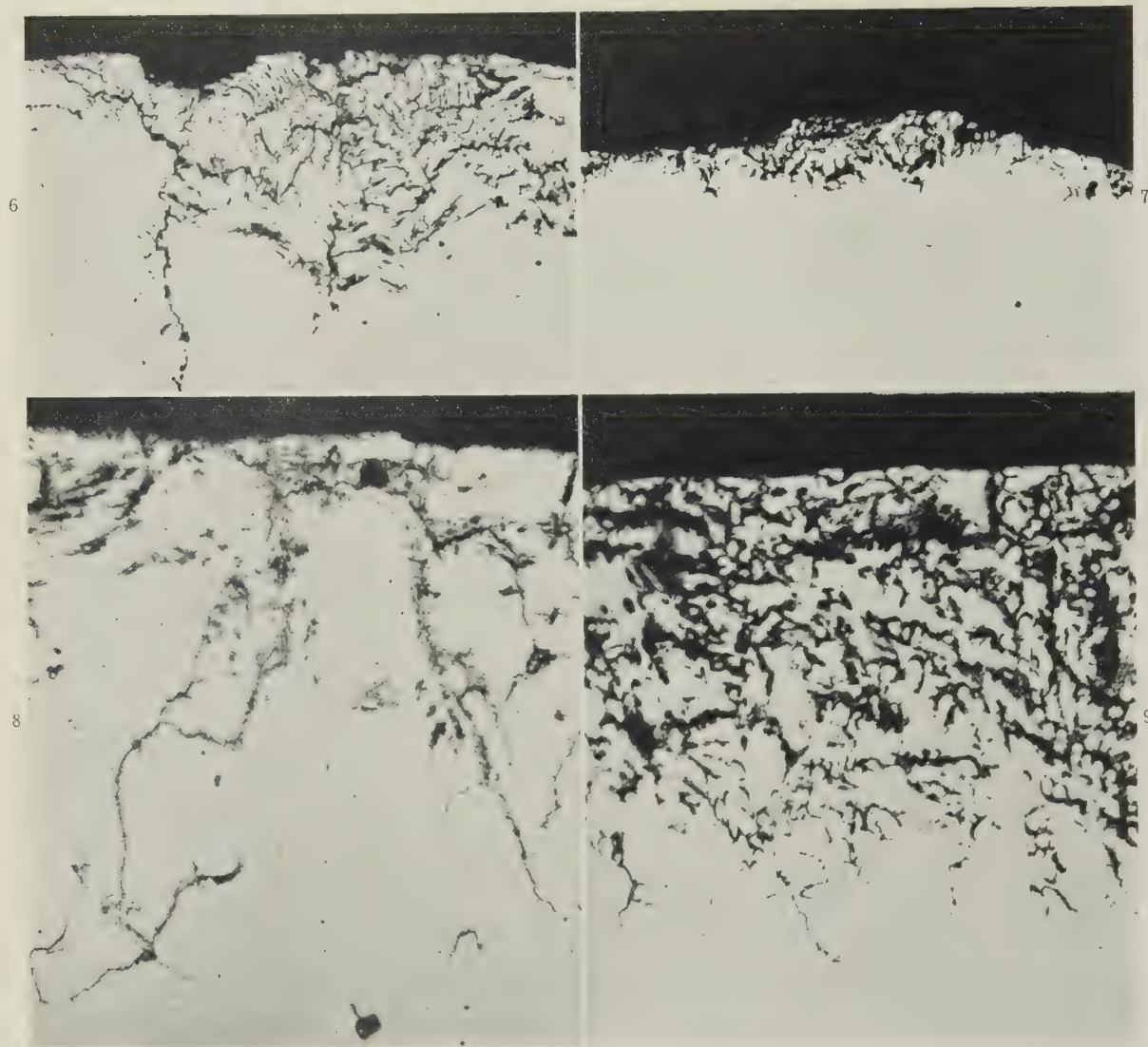
FIG. 2.—Alloy 6. S.H.P. Zinc with 0.075% Aluminium and 0.003% Lead.

FIG. 3.—Alloy 9. S.H.P. Zinc with 0.013% Lead and 0.04% Magnesium.

FIG. 4.—Alloy 26. S.H.P. Zinc with 4.44% Aluminium and 0.048% Magnesium.

FIG. 5.—Alloy 30. C.S. Zinc with 4.0% Aluminium and 0.04% Magnesium. (Pressure-die-cast Mazak.)

EXAMPLES OF INTERCRYSTALLINE CORROSION IN ZINC-ALUMINIUM ALLOYS.



FIGS. 6-9.—Cast Specimens After Exposure for 10 Days to an Air/Water-Vapour Atmosphere at 95° C. Unetched. $\times 250$.

- FIG. 6.—Alloy 52. C.S. Zinc with 4% Aluminium and 0.3% Copper.
FIG. 7.—Alloy 57. C.S. Zinc with 4% Aluminium, 0.3% Copper, and 0.05% Magnesium.
FIG. 8.—Alloy 68. S.H.P. Zinc with 4% Aluminium and 0.01% Cadmium.
FIG. 9.—Alloy 38. S.H.P. Zinc with 4% Aluminium.

MICROSTRUCTURES OF CHROMIUM-MANGANESE ALLOYS.



FIG. 3.—Alloy 60 After Annealing for 403 Hr. at 690° C. and Quenching. Particles of σ in a matrix of α -Cr solid solution. $\times 300$.

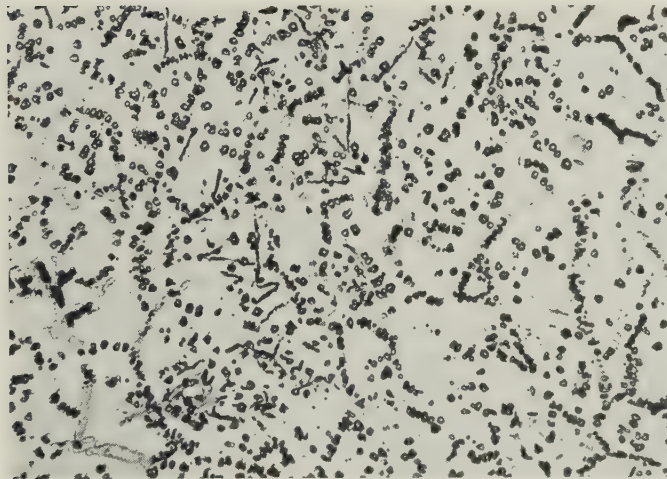


FIG. 4.—Alloy 53 After Annealing for 1018 Hr. at 675° C. and Quenching. A matrix of α -Cr, dark-etching crystals of α' -Mn, and light-etching crystals of σ . The distribution of α' -Mn particles in this alloy was uneven, and this photograph shows the region in which their relative number was greatest. $\times 200$.

THE PRINCIPLES OF TECHNICAL CONTROL IN METALLURGICAL MANUFACTURE *

1448

By A. R. E. SINGER,† B.Sc., Ph.D., MEMBER

SYNOPSIS

The effects of economic and technical factors on the quality of manufactured products are examined, and the characteristics of controlled processes analysed in terms of basic principles. Some aspects of statistical control of plant are considered in relation to present practice and probable future developments.

I.—INTRODUCTION

THE science of technical control of quality in manufacture has an underlying unity that is revealed only by careful analysis. Its applications are widespread, for it embraces the control of raw materials, processes, and manufactured products in the factory, as well as the methods whereby control is effected. Despite this wide coverage, there is a coherent body of knowledge dealing with the subject, and a number of important principles can be seen to run throughout. Whenever the subject of technical control of quality is mentioned, the techniques of control used in the factory immediately spring to mind. Inevitably, a greater attention is paid to them than to the fundamental principles, which are often assumed to be self-evident and scarcely worth enunciating. It is appropriate, therefore, at the beginning of this series of papers on technical control of quality, to examine on a broad basis the main factors affecting control. This is particularly desirable because the subject is one on which a great deal of research and development work is being done. Much of the work is concerned with only a small part of the total field, yet the same basic factors are operating throughout, and the accumulated experience from one part may be of great help in another. It is necessary in these circumstances to take an overall view of the situation, put the various pieces of research and development work into a correct perspective, and to formulate a plan of action in conformity with the whole rather than with the individual parts.

The science of control of quality is developing rapidly, and at no time is the situation static. The pattern will not repeat itself exactly in the future, yet it is with the near future that a progressive scientist or industrialist is primarily concerned. A mere

accumulation of experiences from the past is of little use for planning action in a changed future, and the only way to resolve the difficulty is to extract principles from present and past experience and use them as a guide for the further development of processes and techniques. Experience has shown that principles are more persistent in time than practice, and a good deal more reliable. The purpose of this paper, therefore, is to outline some of the underlying factors operative in the technical control of quality and where possible to deduce from them promising lines for future research and development.

The technical control of processes is not an end in itself. It should always be carried out for a specific purpose in order to achieve certain desired results, and it is very revealing to examine more closely what these results are. It would be generally accepted that high quality in a product is desirable and the higher the better. Unfortunately, the attainment of quality is directly related to cost, either because of higher cost of the materials, machines, and labour, or because of additional charges required for accumulating knowledge and carrying out research and development necessary for the manufacture of the product. In addition, the mere setting up of a system of control inevitably causes additional expenditure of money, and this again must be put on the debit side of the account. Under the heading "The Economic Aspect" (Section III), the problem will be examined in greater detail, but it soon becomes apparent that at any one time within a concern there is an optimum standard of quality for a product, and control of quality in the region of this standard is economically desirable.

The economic aspect cannot be left out of any comprehensive picture of control. In fact, it becomes an essential function of management to measure the success or failure of a system of control by relating the

* Manuscript received 3 November 1952. Contribution to a Symposium on "The Control of Quality in the Production of Wrought Non-Ferrous Metals and Alloys. I.—Melting

and Casting", to be held in London on 25 March 1953.

† Lecturer in Industrial Metallurgy, University of Birmingham.

results achieved to the new total cost of the product. Whilst this view would generally be conceded when the point is emphasized, it is not always kept clearly in mind. Frequently it happens in industry that schemes of instrumentation or recording are embarked upon, apparently for their own sake, with only a vague and rather hopeful picture of how the quality of the product or the economy of production will be affected. Such a state of affairs cannot be described as control, and any steps taken to define accurately the purpose of control in relation to quality and the reasons for its installation would be invaluable.

II.—QUALITY AND ITS MEASUREMENT

The word quality is a simple one describing a complex state that is difficult to interpret. There are two concepts of quality, not incompatible, but often leading to a confusion of thought. In the first place quality may be thought of as being measured on a scale leading to an objective perfection without relation to uses or applications. Secondly, the quality of a product may be linked with its ultimate use, in which case the criterion is fitness for purpose. If either of these definitions is adhered to rigidly, then difficulties of interpretation may occur. But the two concepts are not contradictory, and when it is realized that in the case of metallurgical manufacture an ideal standard is set by the purpose for which the product is intended, then the difficulty is resolved. Thus the standard might be complete freedom from porosity, which in the case of a casting would be unattainable. Alternatively, the standard might be a particular thickness for strip material, which in practice would never be attained exactly.

This leads directly to the question of how quality can be measured. In a great many cases no simple method of physical measurement is available, and in its absence the best that can be done is to set up certain standard examples and use them for making comparisons, classifying the products on the basis of the unaided judgment of the inspector. Such methods are unsatisfactory from a scientific point of view, but have to be applied at least in part with such features as surface finish, defects and blemishes of all kinds, porosity, segregation, and internal cleanliness of castings. Gradually more and more of these features are becoming amenable to physical measurement, and part of the answer to the problem may be a closer analysis of the situation, so that, for example, in the case of porosity and segregation, its location and dispersion are taken into account as well as effects of density or chemical composition.

Where it is possible to make physical measurements relating to quality, much more can be done by way of interpretation, and it is on this basis that it is now proposed to deal with the concept of quality. Suppose we take a simple example of strip metal being produced for subsequent deep drawing. The quality of the strip will then be a function of its chemical composition, metallurgical structure and properties, its

surface condition, and its dimensions, especially its thickness. All these quantities, except surface quality, can be measured with precision, but for the present purpose only the thickness need be considered, as a similar state of affairs pertains with the others. This aspect of quality is important because of the clearances between the tool and die. It will be a maximum at one particular thickness or ideal dimension, X_i , and in the ideal case strip would be produced at this size. However, this is a counsel of perfection not attainable in practice, and this is recognized by manufacturing to certain tolerances, say, $X_i \pm 0.003$ in. This means that quality falls as the thickness departs from X_i , and at any point beyond $X_i + 0.003$ or $X_i - 0.003$ in. is no longer acceptable. The best index of quality for an individual article is then the nearness of the strip to the standard expressed as a number. Similar criteria can, of course, be used for all the other quantities involved, except surface finish. In the case of a group of such strips the best measure of this aspect of quality would be the arithmetic mean \bar{X} of the dimensions or quality characteristics of the individuals taken in conjunction with their standard deviation σ . Such objective standards of quality are an immense aid to everyone in the factory, as they enable operators and inspectors to detect any deterioration with the maximum speed and certainty, and permit corrective action to be taken at the earliest moment. This is the essence of control of quality, and it greatly simplifies the work of the technical officer in charge if numerical values and limits can be provided to which he can work.

III.—THE ECONOMIC ASPECT

It has already been shown that for any given process, quality of product and cost of production tend to be mutually opposed, so that in practice some compromise solution must be sought. The question immediately arising is that of choosing how much of each to aim for. The situation is necessarily tied to the overall economy of the process and may be clarified by considering in diagrammatic form the cost of manufacture of a product as compared with its value to the consumer in terms of its usefulness. Here we are not concerned with the other aspects of value related to cost, esteem, or exchange.

If it is assumed that quality can be measured on a physical scale—in this example as an approach to an ideal dimension—then a value/quality diagram might take on a form such as that shown in Fig. 1. The curve V will usually flatten out as the ideal dimension is reached at X_i and will be zero at some point B , where the maximum acceptance tolerance for the article is reached. Such a value curve would refer to individual items of product at the exact dimensions indicated in the diagram. When applied to a productive process, the situation becomes more complex because it is not possible to manufacture at specific dimensions, and tolerances must be allowed. If the manufacturing process is considered alone and there is

no subsequent inspection of the product, then the frequency with which each quality of product occurs will in the general case follow a binomial distribution. In any process some defective items of product will

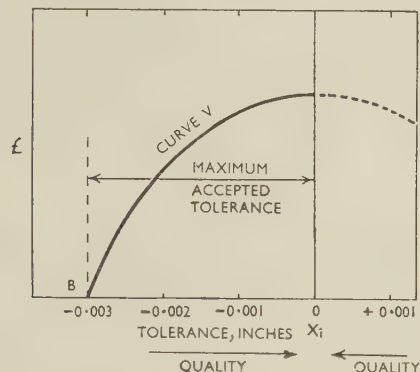


Fig. 1.—Value/Quality Relationship for Individual Items Produced.

always be made, and the manufacturing limits that can be held will depend on the proportion of defective items that can be tolerated in the output. With a normal frequency distribution, as shown in Fig. 2, and a proportion of defectives of, say, 1%, the tolerances will be $\pm 2.6\sigma$, where σ is the standard deviation for the process. On this assumption it is possible to draw both value and cost-of-production curves for manufacturing processes of varying degrees of precision, i.e. of varying σ . The curves may now take on the form shown in Fig. 3, where curve *V* is the value in pounds sterling of an individual item of those exact dimensions, as in Fig. 1. Curve *A* will then give the value of a product in which 1% of the output is defective or outside the manufacturing tolerances $\pm 2.6\sigma$. The curve will again flatten out at the ideal dimension and will be steep where it cuts the axis at *D*. At this point the value will be zero because of the large proportion of unacceptable material it contains—in this case about 2.3% or 3%.

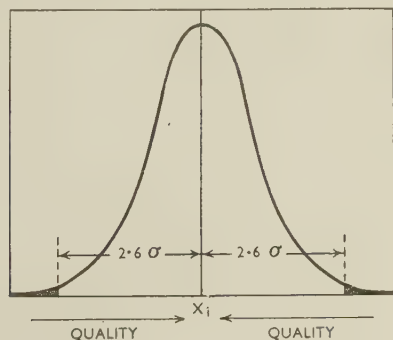


Fig. 2.—Frequency Distribution Curve for Varying Tolerances.

A further curve *C*, showing the cost of production by the process such that only 1% of defectives are produced at any particular tolerance, can now be inserted. Such a cost-of-production curve will always rise steeply as the ideal dimension is approached and

tolerances are narrowed, and will tend to a definite value in pounds sterling as tolerances are widened. It should be noted that curves *V* and *A* are hypothetical, in the sense that in practice it is possible to make only rough estimates of value at various qualities, but curve *C* can sometimes be drawn with fair accuracy. Furthermore, all the curves are drawn for one given state of technical knowledge and skill. As this improves with time, so curve *C* moves downwards and closer to the vertical axis at X_i , but at the same time, owing to competition in the industrial field, curves *V* and *A* tend to move in the same direction, so that the general pattern remains similar.

On the basis of the curves in Fig. 3, the point at which it is most profitable to manufacture is at X_p , where the value/cost-of-production loop is deepest. In other words, there is an optimum quality having tolerances of $\pm X_p$ where production should be held, and any departure from these tolerances with a rejection rate of 1% would lead to a decrease in profitability. If the two curves *A* and *C* did not intersect, then of course all production would be made at a loss.

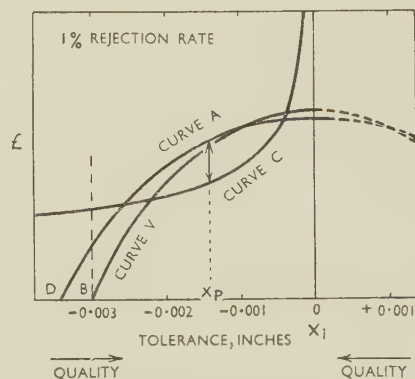


Fig. 3.—Value/Quality Relationship for Products Containing 1% of Defective Items.

Thus the curves, even though hypothetical in character, do succeed in illustrating the important point that ultimate economy dictates that at any one time in a manufacturing process the quality of the product should be controlled at one particular value, and that any divergence from this value will carry with it economic penalties. Here is a basic reason for the control of manufacturing processes.

It can be shown in a similar manner that for any process that is operating to fixed tolerances there is an optimum rate of rejection at which the cost of production per unit of acceptable product is a minimum. Such a curve might take the form shown in Fig. 4. The curves in Figs. 2 and 3 were, of course, drawn for a fixed rejection rate of 1%, but similar curves would have been obtained at any other rate. In any instance in practice there is a best rejection rate, or range of rates for a process, and efforts should be made to reach this rate rather than merely to reduce rejections to a minimum.

Mention has already been made of the fact that

improvement in quality of a product can be made in two principal ways. In the first place it can be achieved by raising the quality of raw materials, reducing tolerances by employing more skilled labour and supervision or machines of higher accuracy, and by more rigorous inspection methods. The other way of achieving higher quality in a product is to utilize scientific investigation with the object of finding better methods of manufacture. Both methods carry with them financial penalties, but there are important distinctions to be made between them.

The first method has as its principal advantage that of simplicity and the small time-factor involved. In response to an alteration in demand, it is usually possible to raise quality by this means within a short period, and the increase in cost of manufacture is then given by curve *C* in Fig. 3. The situation, however, is a static one, and the increase in cost is payable on every item of product made, however long pro-

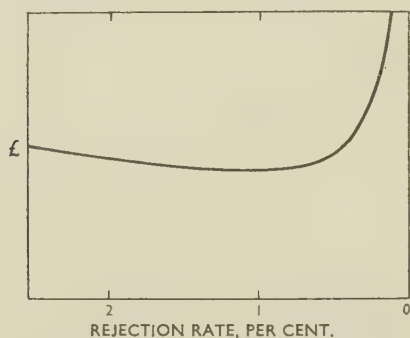


FIG. 4.—Cost of Production/Rejection Rate Relationship per Item of Acceptable Product.

duction continues and, as a first approximation, however many are made. In contrast, the method of scientific investigation achieves more lasting benefits. It is true that again a price has to be paid for quality in terms of costly research, development, and design, but once the work is done it is applicable to all the items of product manufactured, and the cost of investigation can be borne by indefinitely large numbers of the product. In addition, such work is cumulative, and one research worker starts building at the point at which another has left off. The situation is thus essentially a dynamic one, and a continual advancement in quality is the result.

The immediate disadvantages attached to such a method of improving quality are twofold. There is the time element to be considered, for research and development work is necessarily a lengthy process, and there is the need for the cost of the work to be spread over a large output. An additional point, of local significance only, is that the results of research are rapidly disseminated, and competitors soon use them to their own advantage. However, there is a constant interchange of such knowledge and, taking the broad view, the process is undoubtedly of benefit to the world at large.

The two ways of improving quality always proceed simultaneously, and it is virtually impossible to operate one without some intrusion by the other. The important thing is the emphasis given to each. The experience of the last two decades has brought out clearly the big advantages of the research method, and all indications are that in the future this will increase still further in importance. The present series of papers dealing with the control of quality in metallurgical manufacture is a significant step in this direction.

IV.—CONTROL AND ITS IMPLICATIONS

A definition of a controlled system given by Shewhart¹ can be used as a basis for further development. Shewhart's definition is as follows: "A phenomenon will be said to be controlled when, through the use of past experience, we can predict, at least within limits, how the phenomenon may be expected to vary in the future. Here it is understood that prediction within limits means that we can state, at least approximately, the probability that the observed phenomenon will fall within the given limits."

It is characteristic of machines and processes not subject to control, either automatically or by a human operator, that they will not continue of themselves to give a product of constant quality. After a time a discrepancy between the required and the actual quality value makes an appearance and can be called the "error". In any manufacturing process many variables will be operating at any one time, but to simplify the analysis we can suppose that each variable, with the error derived from it, is being considered by itself. The reason for the appearance of an error will then be twofold. One part of the error will have a recognizable pattern and will be attributable to a maladjustment of a known factor in the process. This cause of error can be termed an "assignable" cause, and action can be taken to correct the error by adjusting the cause of it. In many cases a correction can be made even though the cause is unknown, provided that the error has a recognizable orderly pattern and a means of correcting it is known. The other part of the error will not have a recognizable pattern, and will presumably be brought about by unknown factors operating in what is apparently an irregular manner. These causes of error can be termed "non-assignable", and although they may be treated by the statistical laws governing chance variations, no action can be taken to correct them.

The main problem confronting the control engineer is how to ensure, when an error not due to non-assignable causes is detected, that action is taken to reduce it. The recognition of errors having a regular pattern due to assignable causes, as opposed to those due to chance fluctuations (non-assignable causes) is not easy. In the first instance, therefore, it is best to consider the simple case where a succession of articles is being produced and the error indicated is an

integrated effect such that chance fluctuations do not make a significant contribution.

The way in which control is effected is by arranging for the error to set in action a mechanism that will lead to a reduction of the error. In other words, a compensating system is set up that is error-actuated, and this may be done wholly automatically or through a human operator. There is thus a clear distinction between a cycle of operations that is predetermined and rigid, and one that is error-actuated and not predetermined in its action. However complicated the first may be (e.g. the mechanism of an automatic gramophone-record changer), it is not a controlled cycle. For true control it is essential to have a closed-loop or feed-back system, as in the second case, and a way of correcting the error must be known and the necessary action taken before control can be effective.

Turning to the practical aspect of process control, it is convenient to take as an example the case of a product already in manufacture, on which technical control of quality has hitherto been a haphazard and arbitrary affair. The various steps to be taken to ensure adequate control can then be clearly brought out. The first step is to find out the major factors affecting the quality of the product in order to determine how, and to what extent, they affect it. This investigational stage is one of the biggest jobs in technical control, and may consume a large proportion of the time of trained scientific staff. The work, although lengthy and expensive, would employ normal scientific procedure for investigation, and should reveal assignable causes of variation in the quality of the product. But in every instance there are bound to be variations in manufacture that at any given state of knowledge cannot be tied to a particular cause. Some of these may show a regular and persistent pattern of behaviour, and can usually be related to some aspect of the process, in which case they can be placed in the category of assignable causes. The remainder can be termed non-assignable causes of variation. These variations are then best treated as random events following the statistical laws governing chance fluctuations. If these laws are not closely followed, then evidence is immediately provided by means of which the operating cause may be recognized and placed in the assignable category.

The investigation of causes of variation, their separation into assignable and non-assignable classes, and the relating of effect to cause is absolutely essential, and must be carried out before process control is established. Failure to do this is bound to lead to disappointment in the results of process control, and if the analysis of the process is unsatisfactory in this respect it is best to recognize immediately the grave limitations it will place on the effectiveness of control. In the metallurgical field this is generally realized, and a large proportion of the applied research effort is expended on obtaining a fuller understanding of manufacturing processes, and in particular the effect of manufacturing variables on the properties of the

product. Such effort is well directed, but it should be recalled that the research is not an end in itself and is only of value and can be justified only when it is used for effectively controlling the manufacturing processes.

The next stage in controlling the quality of a product during manufacture is to set up standards by defining the tolerances or limits within which the product may vary and yet remain acceptable. At the same time it is advisable to assign the corresponding limits to the factors causing or correcting the variations in quality. Whenever possible, such limits should be subject to physical measurement and expressed numerically. This stage is an important one for management because, as stated earlier, it involves a critical analysis of data on costs, yield, &c. The standards may be arrived at on a statistical basis or, more frequently, by a common-sense assessment of the position. The essential part of the process, however, is the setting up of standards and the defining of tolerances; once this is done control can be established. At this stage the method of control to be used has to be considered, and a number of different ones are available, each with its own characteristics. Four main methods, automatic control, control by human operator, statistical control, and operational research, will be considered here.

V.—AUTOMATIC CONTROL

It is simplest in the first instance to consider control systems involving mechanisms only, and then later to extend the general principles to cover the more complex case of a control system involving a human operator. A definition of control was given earlier, from which it appeared that an essential part was the indication of an error between the expected and the actual performance, followed by action to reduce the error. In the case of automatic control this is performed by a mechanism, and it is necessarily implied that some physical indication or measurement of the controlled variable is available. The field of application of automatic control is therefore limited at the moment to systems in which physical measurement of the variables can be made. However, within this field automatic mechanisms have revolutionized the outlook for process control, and complex problems involving the analysis of data relating to several variables can be solved quickly and reliably.

It might at first be thought that if the measurement of error was sufficiently sensitive, the construction of a system giving control within the required limits would be a simple affair. Yet when considered in detail it becomes clear that a stable and accurate system of control is dependent on a number of factors such as time, capacity, and transfer lags. It is not appropriate here to enter into the technicalities of automatic control, and indeed the published literature on the subject is immense,²⁻⁴ but a brief note of some of the problems associated with automatic mechanisms is useful, especially as many of them apply equally to human operators.

1. AUTOMATIC CONTROL OF PLANT AND PROCESSES

In all automatic control mechanisms a measuring or indicating unit is required for each variable being controlled. If we limit consideration to the control

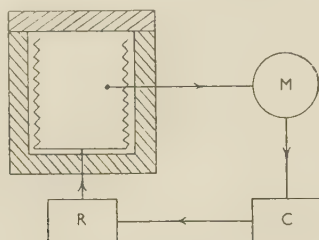


FIG. 5.—Annealing Furnace with Closed-Loop Automatic Control.

of a single variable, then we shall require in addition a regulating unit capable of effecting a change in the controlled variable and, connecting the two, a controlling unit that operates the regulating unit in response to the signal given by the measuring unit. The system is thus a closed loop of the type shown in Fig. 5. It is interesting to note that, although this type of control is accepted nowadays with scarcely a thought, it is of fairly recent origin, and until a short while ago metering of plant was used solely for performance and accounting purposes.

The signal from the meter (*M*), and therefore the input to the controller (*C*), is usually a weak one, and will need amplification and modification before it can be used satisfactorily for operating the regulating unit (*R*). The way in which this is done determines the performance of the controlled system, and is the chief problem in the design of automatic control

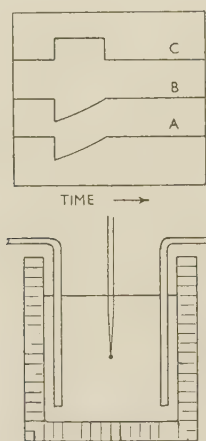


FIG. 6.—Temperature-Controlled Salt Bath, Showing Capacity Lag.

A = Temperature of bath.
B = Input to controller.
C = Output of regulator.

mechanisms. The application of automatic control to production processes in metallurgical industry differs from the more usual engineering applications in that the time element is much more extended. For

instance, an automatic pilot of an aeroplane is designed to correct errors of flight in short periods of time, whereas in many process-control applications the correction of an error may occupy many minutes or even many hours. The chief reasons for this difference lie in the magnitude and importance of transfer lags and capacity lags associated with production processes. The time lags occurring between the metering of the controlled variable and the operation of the regulator are relatively small and unimportant, as this connection is usually made electrically.

The effect of a capacity lag on a control system is clearly brought out in diagrammatic form in Fig. 6, where a step change in the controlled variable is caused by the addition of a metal charge to a temperature-controlled salt bath. It is assumed that the system is provided with an "ideal" two-position

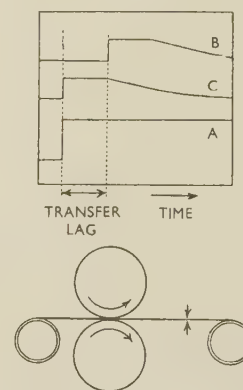


FIG. 7.—Rolling Mill Fitted with Gauge Control, Showing Transfer Lag.

A = Ingoing thickness.
B = Meter reading.
C = Outgoing thickness.

controller and that the heating elements immersed in the salt have a small thermal capacity. Because of the thermal capacity of the salt, a fall in temperature, although followed immediately by heat input from the immersed heaters, will not be corrected for an appreciable period of time, and control will be deficient to this extent.

A transfer lag is illustrated in Fig. 7 by a rolling mill whose screw-down gear is automatically operated through a proportional controller by a gauge measuring the thickness of the rolled strip. In this case the gauge is separated from the rolls by a short distance, so that there is a time interval between the rolling and the measuring of any particular part of the strip. A step change in the thickness of the ingoing strip will cause an increase in the outgoing thickness because of the elasticity of the rolls and housings, but the change will not register on the meter, and corrective action will not begin for a finite period of time because of the transfer lag. Then, provided that the lag is not too great compared with the rate of operation of the screw-down motor, the thickness of the strip will gradually be rectified. The transfer lag, together with its deleterious effects on quality, may

of course be reduced by decreasing the distance between the rolls and the thickness gauge, or it may be eliminated altogether by the method of Hessenberg

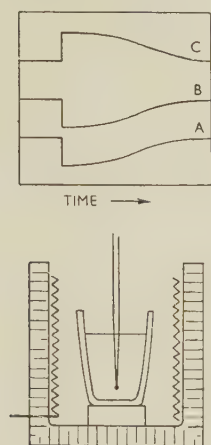


FIG. 8.—Controlled System with Capacity Lag and Thermal Resistance.

A = Temperature of metal.
B = Input to controller.
C = Output of regulator.

and Sims,⁵ using the rolling load at a constant roll setting as a measure of outgoing thickness.

The third example (Fig. 8) shows the effect of a step change in the temperature of a crucible of molten

motor. Similarly, cumulative oscillations, as in Fig. 9 (e), would occur in the system shown in Fig. 8, if the heat input to the elements were too high and the heat capacity of the furnace appreciable. At all cost, oscillations of this type must be eliminated from a system of control.

The type of controlling and regulating unit has to be chosen carefully so as to give the most effective control of the system. If the output from the regulating unit could be made instantaneously equal and opposite to the error, then the error would vanish and control would be ideal. As we have seen, various lags make this impossible, and the best that can be done is to correct the error as quickly and effectively as possible. By further amplification of the signal received from the meter, the output of the regulator, and therefore the rate of correction of the error, can be increased. But for a given set of lags the amplification that can be used is limited, because beyond a certain point over-correction exceeds the original error and an unstable condition is set up in which cumulative oscillations occur. The system is then wholly out of control and the amplitude of the oscillations will increase until limited by some other factor in the process.

The types and characteristics of automatic control units used for ensuring the best result in any given situation are not pertinent to this paper, although they form the hard core of control engineering. Suffice

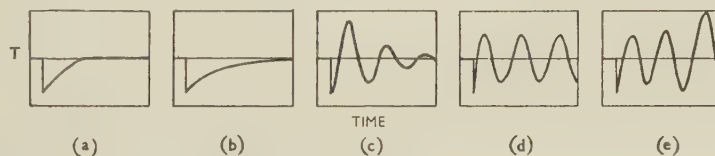


FIG. 9.—Responses of Controlled Systems to a Step Change in the Controlled Variable.

metal on a system having a single capacity lag and a thermal resistance. Here it is assumed that the furnace has a negligible heat capacity and that the system is fitted with a proportional controller. The step change in temperature causes an immediate input of current into the heating elements, but because of the thermal resistance of the crucible and the thermal capacity of the metal, there is a perceptible lag in the rise in temperature of the thermocouple. After a time, provided that the heat input is not too great, the temperature will once more attain the original level.

Fig. 9 illustrates some characteristic responses of controlled systems to a step change in the controlled variable. The fully damped response in (a) approaches the ideal and bears some similarity to that of Fig. 6, but the same system fitted with a proportional controller would give the characteristics of (b). The damped oscillations of (c) are a common effect, and are permissible for many industrial purposes. The hunting response of (d) would be given by the system shown in Fig. 7, if the transfer lag was too large in relation to the rate of operation of the screw-down

it to say that nowadays types of control unit are available to serve most of the needs of metallurgical processes. The limiting factor is usually in some other part of the control system. The conclusion is, therefore, that the characteristics of a process and of a control unit have to be considered together and must be carefully matched to give a product of good and consistent quality. Neither, considered separately, is likely to yield good results and, as we have seen, it frequently happens that the characteristics of a piece of plant are such that no control unit can give it a satisfactory performance.

2. CONTROL OF PRIMARY AND SECONDARY VARIABLES

One important factor applying forcibly to metallurgical process control is rarely given sufficient attention in the technical literature. It concerns what may be called the primary and secondary variables in a control system. Suppose we take the case of a continuous annealing furnace used for the annealing of metal strip, the temperature of the furnace being controlled automatically by an efficient controller. We can then

assume that the temperature of the strip is raised to a prearranged value and is allowed to remain there for a known period of time. It follows that if the original strip was of the correct composition, structure, and condition before annealing, it will possess the expected properties afterwards. The important point here is that the ultimate requirement is annealed strip with a certain structure and properties, whereas the variable being controlled is temperature. Putting the situation in diagrammatic form, as in Fig. 10, it is apparent

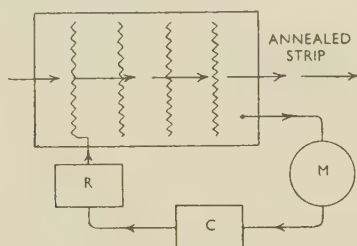


FIG. 10.—Control of Secondary Variable During Continuous Annealing of Strip.

that the primary variable—the structure and properties of the strip—does not form part of the closed loop and is not controlled directly. This state of affairs can clearly be distinguished from the true control of a primary variable, as in the control of thickness of metal strip during rolling by altering the front tension applied.⁵ Here the strip thickness is measured directly and forms part of the control loop.

The control of a primary variable is a much more satisfactory procedure, because if it is fully operative, then variations in the ingoing material are possible without seriously affecting the product. Thus, in the rolling-mill example in Fig. 11, within certain

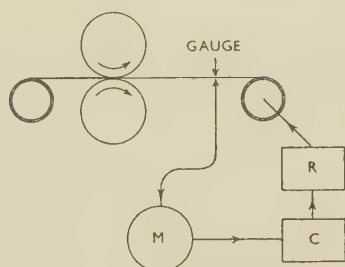


FIG. 11.—Control of Primary Variable During Continuous Rolling of Strip.

limits the gauge of the product is controlled irrespective of the variations of the ingoing strip, provided these are not too great. In the case of the annealing treatment under consideration we have an entirely different picture, for here it is essential to the formation of a uniform product that the ingoing strip be standardized. In other words, the structure and properties of the ingoing strip itself must be maintained within fine limits. This process may have to be pushed back still further in the sequence of processes, and eventually we may have to manufacture to fine limits throughout—a very costly and

time-consuming business. The control of a secondary variable does tend to have this effect in manufacture, so that whenever possible it is best to introduce the variable which it is wished to control into the control loop. A further consequence is that when controlling a secondary variable there is no direct indication that the primary variable is being maintained at the required value, and some additional independent measurement is necessary. Even more important is the fact that for success with this type of control it is imperative that there should be a fixed and definite relationship between the secondary variable, temperature in this case, and the primary variable, structure, because the controller is unable to make a correction for any change in the relationship. The relationship need not be linear, but it must be known with certainty, and auxiliary variables may also have to be controlled within fine limits to prevent undesirable disturbances being carried into the main control system. Later it will be shown that in spite of the obvious advantages of controlling primary variables, little progress in this direction has been made in metallurgical industry. This is both a challenge to and an opportunity for metallurgists.

VI.—CONTROL INVOLVING A HUMAN OPERATOR

Many of the principles of automatic control apply equally to control by a human operator. Where the work is purely mechanical, it is desirable from both an ethical and a material viewpoint to replace the human operator by a control mechanism. Automatic mechanisms come into their own when speeds of operation are high and time intervals short, but in a great number of process-control applications the time intervals involved are long and the situations complex. In many of these instances, ranging from the technical control of a small manufacturing variable to the managerial control of a works, it becomes advisable to employ a human operator. This is always true when the quantities are not measurable by physical means, or when the number of variables concerned is too great and their inter-relation too complex for automatic control, as in the last case. It is in connection with the simultaneous operation of a number of variables that the frailty of human judgement is brought out most clearly, and later we shall see that statistical methods of analysis and operational research methods may help us to make wiser decisions.

A good deal of light is thrown on the behaviour of a human operator when the characteristics of automatic control systems are extrapolated and applied to a closed-loop system of which he forms part. We can illustrate such a system by the independent process inspection of the quality of sheets produced by a simple two-high non-reversing rolling mill, as shown in Fig. 12. Several equivalences immediately appear. The transfer and metering lags correspond to the delay between the rolling of the sheets and their

inspection, and to the time taken by the inspector to arrive at a decision, respectively. Any persistent errors occurring during this period will lead to a quantity of bad product proportional to the lag, which must therefore be kept to a minimum, as with automatic systems. Where inspection is carried out in a haphazard manner, the lag is likely to be extended and may involve a prolonged post-mortem of many subsequent manufacturing processes before the trouble can be diagnosed and corrected.

Very frequently the inspection or measurement of an item of product can be used only for the correction of error on subsequent ones. This follows either from the time lags mentioned above or from the destruction of the article during inspection. During batch production the facts have to be faced that the maximum amount of information for control purposes is not being obtained and that the results of poor control are more serious numerically than with continuous production. For these reasons alone continuous production is more amenable to control and will generally give a higher yield of uniformly good product. Any delay between the discovery of a persistent error by the inspector and action being taken by the mill operator to reduce the error, will correspond to a time lag in the control and regulating part of an automatic system. Unless the organization is such that the transmission of information to the foreman and of an order to the mill operator can be effected quickly, then an appreciable output of bad work will occur.

If we now consider the overall characteristics of controlled systems we again find a number of parallels. It is essential for the process operator to know exactly how, and how much, to correct for a given error detected by the inspector. Such a correction will generally be of a step type, and two difficulties are

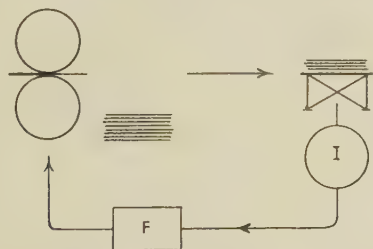


FIG. 12.—Control of Quality of Rolled Sheet by Human Operator.

I = Inspector. F = Foreman.

likely to arise, the first due to a faulty correction and the second due to chance fluctuations. Under-correction may continue to yield a poor product, but over-correction may be worse, for the initial cycles of the unstable system illustrated in Fig. 9 (e) (p. 335) may appear. Chance fluctuations always play some part in industrial processes, and due allowance must be made for them if control is to be effective. A situation where the normal run of product varies in a random manner is illustrated in Fig. 13. If the tolerances are set at the low value of $\pm 2\sigma$, then we

must expect approximately 1 in 20 of the products to be outside the tolerances. No special significance is to be attached to A , and no control action should be taken on such an isolated example. If a correction were made on the evidence of A , then point B would be out of tolerance, together with many subsequent ones. There are two ways of treating the problem. The more usual one is the common-sense way of waiting for an arbitrary number of readings to confirm a change in the process, but the problem may be



FIG. 13.—Random Distribution of Quality Values.

tackled on a statistical basis with considerably more confidence and accuracy.

The example first given related to a simple manufacturing process, but the principle is equally applicable to the control of a department or works. Lack of knowledge of how to correct errors, or delay in detecting and correcting them because of poor supervision or procrastination, allows a situation to get out of control. When action is taken, it is often a desperate measure leading to heavy over-correction as shown in Fig. 9 (d) and (e). Unfortunately, examples of this are familiar to everyone in industry, when affairs proceed from one crisis to another with monotonous regularity and lead to a general deterioration of morale and lowering of output. Such a situation is essentially related to that described above, and the cure for it is similar.

VII.—STATISTICAL CONTROL OF QUALITY

The particular feature of statistical control of quality is the recognition of the part played by chance fluctuations in manufacturing operations. It contains a procedure for dealing with them and reaching definite conclusions on action despite their occurrence. The fact that the statistical method makes allowance for chance happenings enables it to extract the maximum amount of legitimate information from data supplied by the meter in a control system. Consequently, it leads to the most efficient form of control, provided that the time interval allowable between metering and the necessary action is sufficiently long for the data to be studied. The admission of chance has another effect, namely that of eliminating the illusion of certainty and making it possible to predict only the best probable course of action. This apparent loss of certainty is unimportant, as uncertainty is inherent in the nature of the data supplied. It merely shows up clearly in a statistical analysis and is not derived from it. Moreover, the degree of uncertainty can be reduced at will by taking a greater number of observations, and in

each case the probability of error can be estimated. From a technical point of view statistical control of quality is evidently desirable wherever it can be operated. There is, however, the total economy of the process to be considered, for the installation of a system of statistical quality control means an initial increase in overheads, at least during the change-over period. This aspect cannot appropriately be dealt with here, except to note that it is an important managerial responsibility to decide whether or not the benefits derived from the more efficient control are sufficient to justify its installation.

The quality-control chart is now a familiar sight in metallurgical industry, and a few words about its limitations and significance will not be out of place. As in every other case, it is essential to know how to reduce a persistent error once it is detected in a system, for quality-control charts will indicate only when to take action and not what action to take. Similarly, it is necessary to distinguish the assignable causes of variation in quality so that they may be used for control purposes. The non-assignable causes of random variation are then treated in a statistical manner, and action is predicted on this basis.

Suppose we take a simple case where one variable is being controlled by individual meter readings and chance fluctuations are occurring. Then, for a given state of control at a value X_i , assuming a normal distribution, we can draw a diagram of the type shown in Fig. 2 (p. 331), giving the frequency with which each value of X occurs owing to chance causes. The diagram immediately shows the proportion of product falling within any given tolerances, as in Table I,

TABLE I.—*Rejection Rates at Given Values in Terms of Standard Deviation σ .*

Values	Rejections, %
σ	32
2σ	4.6
2.6σ	1.0
3σ	0.27
4σ	0.006

so that the value of A in Fig. 13 is not surprising even though the system is under full control. The effectiveness of control is shown by a value of \bar{X} as near as possible to X_i and a constant value of σ . This criterion holds for the great majority of practical cases, even though the distribution is appreciably skew or irregular.

The usual quality-control chart consists of quality data plotted chronologically in graphical form, and it is best to insert both action and warning lines, as in Fig. 14, so as to help in securing good control. If the two pairs of lines are calculated in terms of σ , then the probability of an individual exceeding these values is given by Table I, and too high a frequency of points outside the 2σ -band would serve as a warning that the process may be moving out of control. A close watch can then be kept on the process to see

whether the departure is a significant one. If it is, action to correct a persistent error can be taken with confidence when the action line is reached, and the amount of rejected product so kept to a minimum. Quality-control charts also show any evidence of drift in a process. This will be evident from a gradual widening of the difference between the \bar{X} and X_i values, and in magnified form gives the pattern shown in Fig. 15. The re-setting of the process at D is the

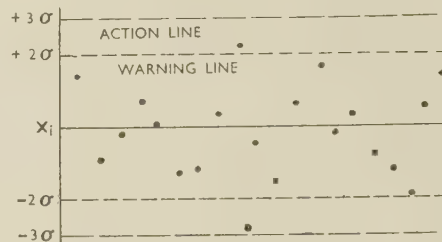


FIG. 14.—Quality Control Chart, Showing Good Control.

obvious action to take and, if drift is inherent in the process, appropriate new action and warning lines can be drawn.

Some instances occur in industry where the only satisfactory measure of the quality of a product is its performance in service. Little difficulty is caused by this when the number of items concerned is large, but when the number is small, and when some guidance is urgently needed for control purposes because the consequences of any decision are far-reaching, then operational research methods may be used. The object of operational research is to collect and analyse

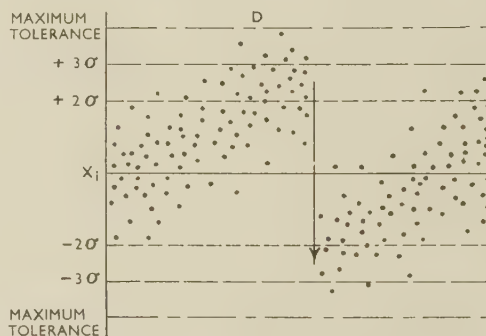


FIG. 15.—Quality Control Chart, Showing Drift of Process.

data obtained during normal manufacturing operations or usage, and to present the results as a basis for executive action. It is best separated from normal research activities, and is usually conducted by a group reporting directly to an executive, who, in this instance, would be responsible for controlling some essential technical factors in production. Statistical methods of analysis are invariably selected for dealing with the collected data, and a few results can be treated as effectively as large numbers. The only consideration when dealing with a few individuals is that the decisions to be made should be of sufficient importance to justify the higher cost of analysis of the data. These were, of course, precisely the reasons

prompting the widespread use of operational research during the latter stages of the Second World War. The method has great flexibility and uses all the available data for deciding the action to take at any given time and the standard at which to operate a control. It seeks to obtain the best answer from data that are necessarily limited and inadequate, and as such it should not be ignored.

VIII.—THE TECHNICAL CONTROL OF PROCESS VARIABLES IN INDUSTRIAL PRACTICE

After surveying the principles of control of quality it is instructive to see to what extent they have been

applied in practice. A review of all the metallurgical manufacturing processes would be far too lengthy, and it is intended to give here as an example only the melting and casting operations for producing non-ferrous ingots. Table II summarizes the situation, but is intended to be typical rather than comprehensive, although it represents the present state of technical advancement in the foundry. The principal purpose of the table is not so much to show present practice as to bring out ways in which technical advances may be made in the future.

We have already seen that in any manufacturing process there are variables whose control is essential for the output of a high-quality product. When such a variable was fundamental in relation to the process,

TABLE II.—*The Measurement and Control of Process Variables During the Melting and Casting of Non-Ferrous Metals.*

Operation	Variable	Type	Method of Measurement or Inspection	Type of Adjustment or Control
Melting	(1) Temperature of melt	Primary	Pyrometer or visual estimation	Manually controlled to required temperature by adjustment of fuel or power
	(2) Chemical composition of melt	„	Analysis of samples	Usually fixed by heat weighing. Occasionally controlled in accordance with rapid spectrographic analysis. With copper the oxygen content is controlled in accordance with the "set" of cast samples
	(3) Heat input to furnace	Secondary	Metering of fuel or power	Manually adjusted for the control of (1)
	(4) Composition of furnace atmosphere	„	Not generally measured	Rough adjustment made by means of air and fuel supplies, see (5)
Degassing and fluxing of melt	(5) Gas content of melt	Primary	Pfeiffer method, or visual observation of cast samples; density measurements	Sometimes controlled manually by adjustment of degassing agent or furnace atmosphere
	(6) Structural potentialities of melt (aluminium-silicon alloys and magnesium)	„	Examination of fracture of cast sample	Sometimes controlled manually by adjustment of sodium, flux, or other additions
	(7) Gas flow (chlorine, nitrogen, &c.)	Secondary	Metering of flow and quantity	Gas flow either fixed or manually adjusted for the control of (5)
	(8) Flux additions	„	Weighing	Flux additions either fixed or adjusted for the control of (5) or (6)
Casting	(9) Structure of ingot	Primary	Visual examination or measurement of grain-size, segregation, structure, and inclusions	No short-term control. Structure determined by (12), (13), (14), and (15)
	(10) Properties of ingot	„	Measurement of mechanical properties, density, porosity, hot and cold deformation; examination for internal defects by X-ray or ultrasonic methods	No short-term control. Properties determined by (9), (12), (13), (14), and (15)
	(11) External characteristics of ingot	„	Examination for surface defects, piping, and cracks	Partially controlled by adjustment of temperature and rate of pouring
	(12) Rate of pouring	Secondary	Visual estimation or fixed by tundish	Adjusted for control of (11) within certain limits fixed by (9) and (10)
	(13) Temperature of pouring	„	Pyrometer or visual estimation	Usually fixed; occasionally adjusted for control of (11) within certain limits fixed by (9) and (10)
	(14) Mould temperature	„	Pyrometer or unaided judgment	Fixed
	(15) Rate of withdrawal of ingot and flow of water in continuous-casting process	„	Metering of withdrawal rate and flow of water	Adjusted for control of (11)

we termed it primary, and when a variable was introduced only because it affected a primary variable, we termed it secondary. To take an example from Table II, in the melting operation the desired end-product is a bath of metal of a particular composition and temperature. The two latter quantities are then the primary variables. The heat input to the furnace is a variable not of value in itself and is used only for controlling the bath temperature. It is therefore a secondary variable. On the other hand, the temperature of the metal is a secondary variable during the casting operation, because it is useful only in that it helps to determine the structure and properties of the ingot. In Table II the words "controlled", "adjusted", and "fixed" are used frequently. In every case control is given the precise and restricted meaning of error-actuated control, as defined in Section IV (p. 332). Control is thus dynamic, and can be clearly distinguished from adjusting or fixing, which are essentially static.

An examination of Table II reveals that the only primary variable always controlled is the temperature of the metal in the melting operation. In view of the remarks made earlier as to the advantages arising from the control of a primary variable, this is a depressing state of affairs. It is true that in some instances other primary variables numbered (2), (5), (6), and (11) are controlled, but this is by no means universal. The reasons for the relative absence of control are, of course, the associated practical problems, which are undoubtedly of considerable magnitude. It is significant that the variables numbered (2) and (5) are quite recent additions, and in particular the rapid analysis of the metal bath is becoming more and more attractive to manufacturers. The practical problems

of controlling other primary variables will gradually be solved and bring a corresponding increase in the quality of the product. The control of secondary variables is less necessary when primary variables are controlled, and in any case they present an easier problem. Similar situations occur in other sections of non-ferrous metal manufacture, such as rolling, forging, drawing, annealing, heat-treatment, and welding. The general picture is, in fact, that big opportunities are offered for improving quality by the extension of control to other primary variables in manufacture.

IX.—CONCLUSIONS

(1) Physical measurements of quality characteristics should be made wherever possible in order to control production with certainty at economic tolerances and rejection rates.

(2) It is expected that an extension of automatic control to many metallurgical operations will occur in the near future. A better understanding of all industrial processes involving a human operator will result from applying the principles derived from the study of automatic control mechanisms.

(3) The use of continuous manufacturing processes will increase, together with the application of statistical quality control for achieving high and consistent quality at low cost. A greater use of statistical methods in industrial problems involving small numbers of products may be forecast.

(4) From a sample survey it is concluded that advances in the control of quality will be made by extending technical control to cover more of the primary variables in manufacture.

REFERENCES

1. W. A. Shewhart, "Economic Control of Quality of Manufactured Product". 1931: New York (D. Van Nostrand Co., Inc.).
2. D. P. Eckman, "Principles of Industrial Process Control". 1945: New York (John Wiley and Sons, Inc.).
3. J. W. Ashley, *Mech. World*, 1949, **125**, 29, 76, 133, 160, and 218.
4. G. S. Brown and D. P. Campbell, *Mech. Eng.*, 1950, **72**, 124.
5. W. C. F. Hesselberg and R. B. Sims, *Proc. Inst. Mech. Eng.*, 1952, [A], **166**, 75.

THE CONTROL OF QUALITY IN THE PRODUCTION OF BRASS INGOTS AND BILLETS*

1449

By MAURICE COOK,† D.Sc., Ph.D., F.I.M., MEMBER, and
C. L. M. COWLEY,‡ B.Sc., A.I.M., MEMBER

SYNOPSIS

After reference to relevant general considerations important in the formulation of quality-control procedures, the paper is mainly concerned with the application of basic principles and practical knowledge to eliminate or minimize the incidence of defects and so ensure the regular production of high-quality brass castings for the manufacture of alloys of this type in wrought forms.

The control of raw materials used in their production is dealt with, and the various factors involved in melting processes are considered with particular reference to low-frequency electric-furnace practice. Following some general observations on casting which include data concerning casting temperatures for different alloys and comments on cast structures, the significant factors relating to moulds and mould materials are reviewed. Pouring and the subsequent operation of feeding, which together constitute the process of casting, are in turn considered, and finally brief reference is made to inspection of cast products.

I.—INTRODUCTION

ALTHOUGH this paper is primarily concerned with the technological factors involved in controlling the quality of brass castings for the production of wrought products, there are other associated elements and functions of no less significance, since they feature importantly in the formulation of quality-control procedures and their successful application. A detailed consideration of these is, however, outside the scope of the paper, and therefore it is not possible to make more than brief mention of them.

Little more than a generation ago brass casting was carried out with practically none of the technical control which is so extensively exercised today. During the last three or four decades a wealth of knowledge has been accumulated regarding the effects which various factors have on the quality of castings, and it is now possible to specify with a high degree of precision the procedures that should be followed. It is indeed the effective implementation of this knowledge regularly in manufacturing processes which is the essence of control of quality.

The acquisition and application of information of this kind is continually increasing, and involves several important functions of an organization, such as production, research, laboratory control, inspection, engineering, work study, &c. The responsibility for maintenance of quality would seem fairly and logically to reside with production management, but the closest co-operation at all levels between production and the functions named is essential, if the maximum benefit is to be realized. From this

effective co-operation sound manufacturing procedures are born and established.

It does not suffice for details of techniques to be known to those immediately concerned and passed on by word of mouth, for therein lies the danger of inaccuracies arising and unauthorized changes being introduced which so often are the cause of quality falling below the standard that can otherwise be attained. They should take the form of written records in which the procedures to be followed and conditions to be observed are set out with clarity and precision. Such records or process manuals, which should be accessible to all connected with the supervision of the operations, provide the basis not only for control, but also for training and other schemes. While strict adherence to laid-down procedures is essential, it is also clearly important that these should be kept under constant and responsible review, in order that they may be immediately and appropriately modified in the light of new knowledge or as a consequence of plant or process alterations.

Successful control of quality depends vitally on the adequacy of supervision, the task of which is essentially to ensure that agreed and defined procedures are, in fact, meticulously carried out. Whilst, to this end, use is made of analytical and other technical services, instrumentation, and other aids, these are not to be regarded in any way as substitutes for the vigilance and skilled observation in the shops, which are so necessary to prevent deviations in detail from approved techniques.

As quality is affected by the way, and extent to which, the practised skill of operatives is utilized,

* Manuscript received 4 November 1952. Contribution to a Symposium on "The Control of Quality in the Production of Wrought Non-Ferrous Metals. I.—Melting and Casting", to be held in London on 25 March 1953.

† Joint Managing Director, Imperial Chemical Industries, Ltd., Metals Division, Birmingham.

‡ Technical Officer, Imperial Chemical Industries, Ltd., Metals Division, Birmingham.

it is essential for them to be fully instructed in the processes on which they are employed. Explanations of the why and wherefore of processes and of the cause and nature of defects of different types, as well as of their consequences at later stages of production or in the finished product, promotes an appreciation of the importance of quality and stimulates interest in working to techniques which have been devised to yield the best results.

Although melting and casting, by their very nature, are dirtier than many other metallurgical operations, the importance of effort directed to improving the standard of cleanliness cannot be gainsaid, not only with the object of minimizing contamination but for many other reasons also, including such obvious ones as increased efficiency, safety, and the like. That much can be achieved in this direction is abundantly demonstrated by the transformations brought about in some casting shops in recent years.

The whole subject of brass casting has been admirably surveyed by Hull.¹ The basic principles governing the production of good-quality non-ferrous metal ingots and billets for working have been dealt with by Bailey and Baker,² and the most important features of brass-melting practice, especially those of metallurgical interest, have been reviewed by Cook and Fletcher.³ The latter pointed out that many thousands of tons of chill-cast brass shapes are produced every week, and a high standard of quality is reached and maintained as a normal, everyday matter. Where defects do occur it is not because of serious technical difficulties in processes, or unsolved major metallurgical problems, but owing to ignorance, or lack of application, of the knowledge derived from long practical experience and specific investigations.

The purpose of the present paper is to indicate the manner in which basic principles and practical knowledge are applied and controlled to ensure the regular production of brass castings of high quality for the manufacture of substantial tonnages of these products for subsequent fabrication into sheet, strip, tube, rod, section, and wire. The alloys dealt with are the straight copper-zinc alloys containing 3-43% zinc, the more important of the copper-zinc alloys having relatively small additions of lead, tin, aluminium, &c., and the nickel silvers.

The quality of a metal casting for processing into wrought products such as sheet, strip, section, rod, tube, and wire, is determined by its composition, surface condition, internal soundness, and structure. The casting should be of uniform composition and alloying elements and impurities within specified limits. The surface must be substantially free from defects, such as cold shuts, pits, folds, porosity, entrapped oxides, or foreign matter, and even when such operations as scalping or milling are used to remove the cast surface either before or during fabrication, cast surface quality is still of importance in order to keep the scrap resulting from this operation at a minimum. A high degree of internal soundness

is required, and castings should be as free as possible from shrinkage cavities, blow-holes, gas pores, and other discontinuities. Finally, the structure of the cast product should be that most suitable for the particular method of working, or operation, to be used in processing the casting.

The maintenance of a high standard of quality in brass castings is essential, not only in order that the end product may have certain required properties and characteristics and be free from defects originating in the melting and casting operations, but also so that fabrication can be carried out in the most economic manner on the plant available. The total cost of fabrication is closely related to the amount of good saleable material that can be obtained from the cast product, and, in an endeavour to keep this cost as low as possible, scrap must at all stages be reduced to a minimum. Most avoidable scrap during fabrication can arise from faulty melting and casting techniques, and defects due to this cause may not become apparent until a late stage in fabrication has been reached and substantial expenditure incurred.

II.—RAW MATERIALS

The main raw materials used for the production of brass castings are virgin metals—copper, zinc, lead, tin, aluminium, nickel, &c.—temper alloys such as copper-iron, phosphor-copper, and cupro-manganese, and scrap brass. Rigid control over the quality of these raw materials and also over the relative proportions used for each particular alloy is necessary in order to ensure that the cast product is within the desired limits of composition. These limits may be those imposed by normal commercial specifications, by users' special requirements, or by the method of working to be employed. The importance of the latter consideration can be illustrated by the effect of small amounts of lead on the working properties of α -brasses. Whereas these alloys can be successfully cold rolled from the cast condition when containing lead up to the maximum of approximately 0.07% permitted in normal commercial specifications, for satisfactory hot rolling the lead content must not exceed 0.02%. Control over the quality of raw materials is effected by inspection, sampling, and analysis, supplemented by hand-sorting, magnetting, &c., where such treatments are required. The particular form and extent of control applied to the various raw materials depends on their origin and on knowledge and experience of their quality and reliability.

Virgin metals are today of such uniform quality and purity that it suffices to take representative samples from each delivery for the determination of impurities by suitable analytical methods. Temper alloys, although used in relatively small proportions, can be the cause of variable composition and a source of excessive impurities in the cast product, and they are, therefore, carefully sampled and analysed both for their main alloying elements and for impurities.

The raw material most likely to give rise to compositional variation and excessive impurities in the cast product is scrap brass, which is extensively used. The types of scrap commonly available can be classified into three broad groups:

- (i) Scrap arising during the normal course of fabrication of the casting into the finished or semi-finished product.
- (ii) Webbing scrap, trimmings, &c., returned from users.
- (iii) Miscellaneous scrap.

Process scrap arising during the normal course of fabrication is unlikely adversely to affect the quality of castings if due regard is paid to the proper segregation of alloys during manufacture. It is relevant in this connection to note that one of the commonest causes of mixing of scrap is an inadequate supply of suitable transportable containers in the processing plants and inadequate heat-room facilities. Sorting of mixed scrap not only throws increased responsibility on the casting-shop supervision, but involves substantial expenditure, despite which metal may have to be disposed of for low-grade usage.

Purchased scrap is the least reliable of all raw materials, and consequently requires the closest measure of control. Alloys may be mixed, there may be contamination by other metals such as iron, solder, metals used in plating, &c., and considerable amounts of non-metallic materials such as dirt and oil may be present. It is necessary, therefore, for all incoming scrap to be inspected, sorted where necessary, sampled, and analysed for major alloying elements and impurities.

The removal of particles of iron from brass swarf, turnings, and small scrap can readily be effected by use of the conventional belt-type magnetting machine. Baled scrap, however, because of its tightly packed form, cannot be dealt with in this manner, but may be checked for iron inclusions by passing the bales through a coil carrying a D.C. current. An indication of the amount of iron present in the bale can be obtained by measurement of the induced e.m.f. set up in a second coil wound concentric with the first. Bales found by this method to be contaminated may need to be broken down for further treatment on the magnetting machine. When the composition of scrap or swarf is unacceptably variable for use directly in making-up heats, it is separately melted—and so homogenized—and cast into the form of remelting ingots or pigs, the composition of which is then checked before the material is passed out for use.

The proportions in which virgin metals, scrap, and temper alloys are used in making up any particular alloy are determined to some extent by the nature of the alloy itself and also by the availability and purity of these alloying ingredients. It is clearly one of those matters which does not admit of generalizations. The make-up of each heat or furnace charge should be the responsibility of a qualified member of the supervisory staff, and written instruc-

tions should be given to those responsible for carrying out the actual heat preparation. Of the weighing operations themselves, it is necessary only to point out the obvious but sometimes overlooked importance of accurate weighing equipment. Because of the heavy duty to which this is subjected, checking must be frequent and, where it can be arranged, check weighing of charges on duplicate scales is a worthwhile additional control. Containers must be kept clean and tare weights frequently checked. Where charges contain alloying additions in such small quantity that they are liable to be overlooked if added to the main charge, and possibly introduced into the furnace at the wrong time, it is usually more satisfactory to make a separate issue of these materials in packets direct to the melting furnace.

III.—MELTING

The important defects in brass castings which can have their origin wholly or partly in the melting operations are incorrect or variable composition, the presence of undesirable metallic and non-metallic impurities, and, in the case of certain alloys, unsoundness due to gas absorption. Control over the melting operation should be such as to avoid, as far as possible, the incidence of these and also to ensure that the metal is raised to the requisite pouring temperature in the minimum time.

Today most of the brass produced for manufacture into wrought forms is melted in low-frequency furnaces. Units with melting capacities of 600–2400 lb./hr. are in common use, and recently furnaces of 10,000 lb./hr. capacity have been built.⁴ Crucible furnaces, both pit-fired up to approximately 200 lb. capacity and larger tilting units of up to approximately 1000 lb. capacity, are also extensively used, but more particularly in the melting of special alloys or relatively small tonnages, where the low-frequency furnace is unsuitable or uneconomic. Limited use is made of the arc furnace for certain alloys, particularly where a non-oxidizing atmosphere is advantageous. When considerable quantities of molten metal are required at a given time, as in the production of large plates, reverberatory furnaces are still employed to some extent.

While the economic advantages which the low-frequency furnace possesses over other methods of melting may have been the main reason for its introduction as a melting unit for brass, its adoption by the industry has itself been a major contribution to the maintaining of a high quality of casting. This is not to suggest that high-quality cast products cannot be obtained by the other methods of melting, for indeed everyday experience shows that they can, but it is to emphasize the comparative ease with which a high standard of quality can be achieved and maintained by low-frequency melting.

Compositional variations can arise in the melting operation from two causes: incomplete mixing of the constituents of the melt and excessive loss of one or more constituents by oxidation or volatilization

due to incorrect order of charging, overheating, or prolonged heating. In low-frequency melting the "motor" effect results in a very thorough mixing of the melt, even when elements of widely differing density are present, as in leady brass, but even so it is advisable to stir well immediately before skimming to ensure that any alloying additions that may have become entrapped in the oxide dross are completely dissolved in the melt. With other methods of melting, where the bath of metal is relatively quiescent, great care is necessary to ensure thorough mixing of the melt. In pit-fired crucibles a double stirring is advisable, one immediately before removing the crucible from the pit and the other immediately before pouring. With larger crucibles the stirring operation becomes more difficult owing to the buoyancy effect exerted on the stirrer, and particular attention to this operation is therefore required when furnaces of this type are used, if compositional variations are to be avoided.

Some loss of metal due to oxidation and volatilization is unavoidable during the melting of brass on a commercial scale, and it is customary to make allowance for this when weighing the furnace charge. Control of this loss is not only of considerable economic concern, but is of importance in maintaining a correct composition, since excessive loss of one or more elements from a melt will result in the cast product failing to meet specification requirements. Excessive loss is indicative of faulty melting technique, and loss figures provide an overall reflection of the standard to which the melting operation is being conducted.

The order and manner in which a furnace is charged have an important bearing on the amount of metal loss that occurs during melting. It is usual when melting in low-frequency furnaces to make an initial charge of medium scrap, followed by copper and light scrap and later by heavier scrap. Zinc, because of its high rate of loss at the temperature of molten brass, is added towards the end of the melting cycle. It is important that each addition should be completely immersed as quickly as possible, the effective introduction of light scrap and swarf being facilitated if it is in the form of bales or briquettes.

The form in which minor alloying elements are added, and the stage of the melting cycle at which they are introduced, depends on the amount of these additions and on such factors as their rate of solution, susceptibility to oxidation, volatilization, &c. Nickel, tin, and aluminium can conveniently be added as virgin metals, and it is usual to add these elements about three-quarters of the way through the melting cycle to allow time for complete solution and mixing. Lead is added as virgin metal or as a 50 : 50 copper-lead alloy, and it has been shown that in low-frequency furnaces the addition of this element can be made at any stage of the melting cycle without its distribution in the solidified ingot or billet being adversely affected.⁵ Although iron can be added in the form of thin sheet, this, because of its relatively slow rate

of solution, involves the risk of segregates of iron-rich constituents in the cast product, and, therefore, the addition of this element as a copper-iron or zinc-iron alloy containing 5–10% iron is the procedure normally followed. Manganese, phosphorus, and silicon, usually in the form of alloys with copper containing, respectively, 30% manganese, 5–15% phosphorus, and 10% silicon, are added at the end of the melting cycle. Additions of arsenic and antimony can conveniently be made as virgin metals in the finely divided form immediately before pouring.

It has been shown by one of the present authors⁶ that a substantial reduction in metal losses during the melting of brasses in low-frequency furnaces can be obtained by maintaining a protective cover over the melt and by adding a suitable flux before pouring. Although various carbonaceous materials such as coal, anthracite, and charcoal are effective as covers, charcoal in stick form is the most convenient to use. Sufficient should be added to the residual metal in the furnace before beginning the charging to provide a layer approximately 2 in. thick, and this should be maintained by further additions, if necessary, during the melting cycle. During melting, a dross cover consisting of a mixture of unburnt charcoal, metallic oxides (mainly that of zinc), together with particles of untrapped metal, builds up on the surface of the melt. By fluxing it is possible to lower considerably the metallic content of this dross, and although several materials such as salt, borax, ground glass, &c., are effective, it is usual to employ only salt because of its relative inertness to furnace linings. The quantity of salt used depends on the amount of dross formation. Where this is small, as in alloys of relatively low zinc content, approximately 1 lb. of salt/1000 lb. of melt suffices, but for alloys of high zinc content, or where a substantial proportion of swarf or light scrap has been melted, it may be necessary to increase the amount of salt to approximately 4 lb./1000 lb. of melt.

The heavy dross build-up which occurs during the melting of most of the brasses must be removed by skimming before pouring, to prevent its being carried into the tundish and possibly into the mould, where it might become entrapped in the casting. An exception to this procedure is common in the case of gilding metals, where the rate of build-up is much less and the dross layer can therefore be allowed to remain for a number of melts before removal. The insertion of a small piece of wood or plumbago in the furnace or crucible spout during pouring assists in preventing carry-over of residual dross into the tundish or mould.

In the majority of brass alloys of the type under consideration defects arising from the inclusion of oxides in the molten metal are not of common occurrence. Alloys containing additions of elements such as aluminium and silicon are, however, exceptions, and care is necessary at all stages to avoid turbulence or other conditions liable to result in the formation of the oxides of these metals and their inclusion in the molten bath.

Since metal loss is related to the time of melting, as well as to the temperature attained by the molten metal, it is desirable to standardize the melting cycle as closely as possible. This can more readily be effected in low-frequency furnaces, where heat input can be easily regulated, than in crucible furnaces, where the heat input is dependent on factors such as method of firing, quality of fuel, condition of crucible, &c. With the object of enabling a closer control over the melting cycle to be exercised, an instrument has been designed for use in conjunction with low-frequency furnaces which provides a record, shown diagrammatically in Fig. 1, of the time that a furnace is on full input, on standby input, and the time during which it is tilted for pouring. Such information provides those responsible for supervision with a means of detecting faulty melting technique and an opportunity for taking the necessary remedial action at the earliest moment.

Contamination of the melt can arise either from iron and other associated metals dissolved from the

if necessary. The walls and channels of the furnace must be thoroughly scraped, and it is advisable, too, for the volume of the wash charges to be larger than usual in order to cleanse as thoroughly as possible the area of furnace brickwork just above the normal metal level. Additionally, all tools used on the furnace should be thoroughly cleaned to remove any adherent metal.

Because of the high vapour pressure of zinc at the temperature of molten brass, gas absorption by these alloys is so small under normal conditions as to have no significant effect on the soundness of the casting and consequently no degassing treatment is called for. Nickel silver alloys, however, are liable to this type of defect, thus necessitating a modification to the general melting procedure to allow for the well-known oxidation-reduction treatment for the removal of dissolved gases to be carried out. Approximately 15 min. before pouring the charcoal cover is completely removed and the melt allowed to oxidize for about 10 min., after which a fresh charcoal cover

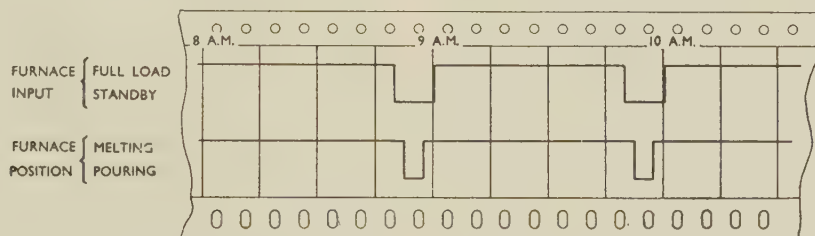


FIG. 1.—Record Chart Showing Electrical Input to Melting Furnace and Time Occupied on Melting and Casting.

tools used for stirring, or from the alloy previously melted, where a furnace has been changed from melting one alloy to another. To guard against contamination from stirrers, &c., it is usual for these to be fitted with plumbago or similar refractory sheaths of adequate length to ensure that the steel does not come in contact with the molten metal. The provision of suitable racks adjacent to furnaces to hold tools used in melting reduces the risk of impurities being introduced by pick-up from the floor of the shop. Contamination due to changing from one type of alloy to another is less likely to occur when small crucibles are used for melting, since it is generally convenient to use one crucible for one type of alloy. As far as possible the same procedure is adopted when low-frequency furnaces are used, or an endeavour is made so to arrange the sequence of alloys melted during the life of a furnace that the composition of each is not likely to be adversely affected by that preceding it. Frequently, however, changes of alloy have to be made which do not fall into this convenient sequence, and these can satisfactorily be carried out either by completely emptying the furnace or by reducing the molten heel in the furnace to a very low level, and in both cases melting two "wash-out" charges which are cast, analysed, and cut up for scrap

is added to the furnace. Immediately before pouring, a deoxidant in the form of cupro-manganese is added and stirred in. The charcoal cover is left in position during pouring, to avoid re-oxidation.

The analysis of a sample taken at the time of casting provides the final control of composition. When casting large rolling slabs and extrusion billets, a sample approximately $3 \times 1 \times \frac{3}{4}$ in. is taken from the pouring stream during the actual pouring operation; rolling slabs up to approximately 2 in. in thickness, such as are commonly used for cold rolling, can conveniently be sampled at the gating operation. Correlation between sample and casting is effected by a system of numbering or lettering, and castings are segregated until the results of analysis are available.

Although discussion of the analytical methods employed is outside the scope of this paper, it is necessary to refer to the frequency and type of analyses required for the proper control of composition. Frequency is determined by consideration of such factors as the specified limits of composition, the quantity and reliability of the various raw materials, particularly scrap, used in the preparation of the charge, and the significance of small amounts of impurities in relation to the working properties of the alloy,

Statistical analysis has shown that it is advisable, for the large majority of alloys, to determine copper on each cast. Alloying additions such as aluminium, nickel, tin, and lead, can, for most purposes, be appropriately determined on alternate casts, and intermediate casts submitted for analysis in the event of material falling outside specification limits. Impurities are determined, usually spectrographically, on every cast of alloys such as α -brasses and nickel silvers when these are to be fabricated by hot rolling, and on all alloys, whatever the method of fabrication, where close limits of impurity are specified. For fabrication by extrusion, cold rolling, &c., the impurity content is generally not so critical, and it suffices that impurities are determined on every third or fourth cast.

Speed of analysis is an important factor in effective control of composition, and aluminium and steel production is being aided in this respect by the use of the direct-reading spectrometer, which enables eleven or more elements to be determined in a matter of a few minutes. Considerable interest is being shown by the brass industry in the possible application of this type of instrument for the determination not only of impurities but also of major alloying elements. If this can be satisfactorily achieved, it will represent a most important advance in control of quality, since it will enable adjustment to be made to the composition of a furnace charge before pouring. This technique of holding furnaces until the results of analyses are available, with the object of adjusting the composition when necessary, is used to a limited extent and is a valuable form of control when furnace charges contain large percentages of scrap of uncertain composition. In order to avoid excessive delay, the analysis is usually confined to the determination of copper, which can be effected within approximately 10–15 min.

IV.—CASTING

Surface quality, structure, and, to a large extent, internal soundness of a casting are determined by the conditions which exist before, during, and immediately after the casting operation. These conditions, such as pouring temperature, type and condition of moulds, mould dressing, rate of pouring, and method of feeding, are determined for each alloy by metallurgical considerations and by the form and size of the castings.

1. TEMPERATURE

Control of temperature throughout the melting cycle is essential to the production of castings of high quality, and the regular measurement of temperature is even today not practised as completely as it should be. Too often it is left to the caster, by observation of various physical phenomena such as zinc burning, oxide-film formation, &c., to judge the pouring temperature. Whilst it may be that experience does allow some degree of skill to be attained in assessing the temperature of molten alloys, visual

judgment is, nevertheless, an undesirable practice, for it is neither sufficiently accurate nor reliable because it cannot adequately assess the influence which various factors, such as lighting conditions, emissivity, &c., can have on the appearance of the melt.

The various types of temperature-measuring equipment suitable for use in brass-melting shops are well known, and it suffices to say that the most desirable from the control aspect is one that gives a continuous record of temperature. As mentioned earlier, such a record is of value in controlling other features of the melting cycle. A record of this type (see Fig. 2, Plate XLVI) requires the use of a continuously immersed couple, and the problem arises of finding a sheath of adequate mechanical properties and ability to withstand, without rapid deterioration, continuous immersion in molten brass. Up to the present time the most satisfactory material for this purpose has been an iron-chromium alloy containing approximately 28% chromium. Even when using this alloy, lives of couple sheaths are relatively short and variable, and an improvement in this respect is necessary before continuous recording of temperatures can be generally adopted. Where the standard type of immersion pyrometer is employed, the temperature of each melt should be checked before casting. The rough usage to which casting-shop equipment is so commonly subject makes frequent checking of pyrometric equipment imperative for achieving a satisfactory degree of accuracy in temperature measurement.

The pouring temperature for a given alloy and type of mould is usually a compromise between that which will result in the greatest internal soundness and that which will produce the best surface condition and cast structure. A temperature below the optimum is liable to give rise to cold shuts, entrapped splashings, and oxides on the surface, although the casting will be of finer crystal structure and less prone to central unsoundness. A temperature above the optimum, while enabling an improved surface to be obtained, is likely to cause central unsoundness due to shrinkage, and a coarser structure. The optimum temperature for each alloy varies with the size and form of casting and the type of mould employed. In Table I are listed suitable casting temperatures for a number of brasses for casting into the form of rolling slabs and extrusion billets in cast-iron and water-cooled moulds. It will be seen that temperatures are specified to limits of $\pm 10^\circ \text{C}$., although it is not suggested that such close limits are necessary in many cases. For some alloys, however, control of temperature to within $\pm 10^\circ \text{C}$. is essential to obtain the necessary structural condition in the casting. This applies especially to the 66–67% copper alloy of the copper-zinc series, which falls within a critical range of composition inasmuch as at optimum hot-rolling temperatures a small proportion of the β phase is present. If the ingot is cast under conditions which cause it to have a coarse and mainly columnar type of structure, the β phase tends to segregate at

the boundaries of these large crystals, and severe cracking occurs in hot rolling. On the other hand, if the casting conditions are controlled so as to yield ingots composed mostly of small equiaxed crystals, the β phase is not segregated but distributed in the form of much smaller particles, a dispersal essential

TABLE I.—Casting Temperatures for Brasses.

Alloy Composition, %			Pouring Temperature, $\pm 10^\circ$ C.		
			Rolling Slabs		Billets
			Water-Cooled Moulds	Cast-Iron Moulds	Cast-Iron Moulds
Cu	Zn		Size of Casting $24\frac{1}{2} \times 3\frac{1}{2} \times 40$ in.	Size of Casting 4 to 16 \times $1\frac{1}{2}$ \times 39 to 24 in.	Size of Casting 5 to 7 in. dia. \times 60 to 70 in.
97	3		1180	1210	...
95	5		1170	1200	...
90	10		1150	1180	...
85	15		1130	1160	...
80	20		1110	1140	...
70	30		1070	1100	1080
67	33		1000	1050	...
65	35		1030	1060	...
64	36		1020	1050	...
63	37		1030	1060	...
76	22	Al 2	1110	...	1190 *
70	29	Sn 1	1080
62	36	Pb 2	1060
58	39	3	1010
58	40	2	1000	...	1010
		Ni		Size of Casting 8 to 12 \times $1\frac{1}{2}$ \times 34 in.	
60	32	8	...	1170	...
60	30	10	...	1180	...
60	28	12	...	1190	...
60	25	15	...	1200	...
60	22	18	...	1220	...
54	28	18	...	1220	...

* Durville casting. Billet size 4 to 7 in. dia. \times 42 to 24 in.

to the successful hot rolling of this alloy. Fig. 3 (a), (b), and (c) (Plate XLVII) show the structures obtained when this alloy is cast in a water-cooled mould at temperatures of 980° , 1000° , and 1020° C., respectively. As cast at 980° C., the ingots possess a fine equiaxed structure, whereas at 1020° C. the structure is mainly columnar, but the former is too low a temperature in respect of other considerations such as surface condition, and the optimum is 990° – 1010° C.

2. MOULDS

Both cast-iron and water-cooled moulds are extensively used for the production of brass castings, cast iron mainly for rolling slabs of relatively small section such as are required for cold rolling and for extrusion billets, while water-cooled copper-faced moulds are utilized mainly for slabs of relatively large section for hot rolling, although increasing interest is being shown in their use for billet casting.

Cast-iron moulds were introduced for brass casting during the last century, and it was usual until about 25 years ago for ingot moulds to be inclined at an angle of about 30° to the vertical; as a result metal as it entered the mould impinged on the lower face, causing severe local attack and overheating of the mould and consequent defects in the casting. With moulds so positioned there was additionally a tendency for oxide and other impurities to become entrapped on the upper face of the casting during solidification. These difficulties were overcome by the introduction of vertical moulds and pouring tundishes such as are now commonly used in brass casting.

Because of the severe thermal variations to which cast-iron moulds are subjected during a full casting cycle, they develop surface cracks which become progressively worse, and frequent and regular routine inspection of all moulds is necessary to ensure that they are withdrawn from service as soon as they have deteriorated to an extent that affects the quality of the casting. If allowed to remain too long in service severely cracked moulds give rise to blow-holes or internal porosity in castings through mould dressing or cooling water being entrapped in the cracks and vaporizing during the solidification of the metal. In extreme cases, this mould condition can interfere with contraction of the casting during solidification to such an extent that hot tears are caused on the ingot surface. The incidence of cracking is more acute when using this type of mould for alloys such as cupro-nickels and nickel silvers, where the pouring temperature is relatively high. To use two sets of moulds per furnace and to allow them to cool in air instead of cooling by water results in a significant improvement in mould life.

A substantial tonnage of brass rolling slabs and extrusion billets is today cast in copper-faced water-cooled moulds, which, in addition to providing more uniform mould conditions and greater chilling effect than are obtainable with the cast-iron mould, have the important advantage of not developing surface cracks during use. The successful operation of moulds of this type, however, requires careful attention to the quantity of water circulated through the mould during casting, the temperature at which the cooling water is delivered to the mould, and the manner in which it is distributed over the mould surfaces.

It has been found that cooling conditions suitable for the casting of brass rolling slabs weighing 1000 lb. in Junker-type moulds can be obtained by circulating water through the mould at the rate of approximately 100 gal./min. The temperature of the water delivered to the mould is maintained at approximately 70° F. (21° C.), which, under normal atmospheric conditions, is sufficiently high to prevent condensation occurring on the mould surfaces. Unless the cooling water is evenly distributed over the mould plates, castings having asymmetric structures may be produced, and the mould plates may become severely distorted. Uneven distribution of the cooling water may be due to faults in mould design or construction,

or to local blockages caused by waste products carried into the mould by the circulating water. Faults in mould design can be traced by a survey of the water temperatures in various parts of the mould, while blockage due to waste products is best prevented by providing adequate screens in the cooling system and by routine inspection of moulds after removal of face plates.

Owing to the expansion and contraction of the copper plates which occur during the casting cycle, moulds of the Junker type are prone to develop water leaks, particularly round the bolts holding the plates to the mould body, and routine maintenance is necessary if defective castings due to the presence of water in the moulds are to be avoided. Water leakage can be minimized by the choice of a suitable jointing material between the copper plate and water-jacket. Of the various materials used, such as lead wire, lead sheet, composite asbestos/lead packings, &c., the most satisfactory results have been obtained with a thin woven asbestos strip coated with white lead. The stresses set up in the mould during casting also result in progressive distortion of the mould plates, and a check on the extent to which this has developed should be carried out so that plates may be removed for re flattening or replacement when the distortion exceeds approximately $\frac{1}{16}$ in. These stresses are also liable to cause cracks to develop from the bolt holes, and it has been found that plates made from non-arsenical deoxidized copper are less liable to develop this type of defect than plates made from other varieties of copper.

3. MOULD DRESSINGS

Care in the selection of suitable mould dressings for different alloys and different casting conditions is essential to the production of satisfactory castings. The functions of a mould dressing have been summarized by Bailey and Baker² as:

- (i) To reduce the initial surface chill on the molten metal.
- (ii) To protect the mould face and prevent adherence of the molten metal to the mould.
- (iii) To provide, when desirable, an atmosphere of reducing gas within the mould and around the stream of metal.

These functions can be satisfied for the majority of brasses by the use of a mixture of mineral oil and powdered charcoal, with the addition of small amounts of tallow for alloys such as gilding metals which are poured at higher temperatures. Exceptions to this general practice are adopted for the casting of brass and gilding-metal rolling slabs in cast-iron moulds, when dressings of resin for brass and a mixture of tallow and charcoal for gilding metals are preferred. Nickel silvers, which are liable to absorb gas from normal oily dressings, are cast with mould coatings of lard oil and black lead thinly applied and thoroughly rubbed into the surface. When aluminium brasses

are cast by the Durville process, it is unnecessary to use a mould dressing of any type. In Table II are itemized the dressings used on water-cooled and cast-iron moulds for the more important commercial brasses.

To ensure consistency in quality and make-up, the preparation of mould dressings should be carried out in bulk under controlled conditions. Charcoal powder with a degree of fineness such that 95% will pass a 200-mesh sieve and a mineral oil having a Redwood No. 1 viscosity of 100 sec. at 200° F. (93° C.) and a flash point of 420° F. (215° C.) yield, when mixed in the proportions of 7 lb. charcoal to 1½ gal. oil, a mixture of suitable working consistency. The dressing must be well boiled before use to remove traces of moisture which, if allowed to remain, would impair the quality of the casting.

TABLE II.—*Mould Dressings for Commercial Brasses.*

Alloy Composition	Form of Casting	Type of Mould	Composition of Dressing
Cu 58–75%, balance Zn	Rolling slab	Water-cooled	Mineral oil and charcoal
" "		Cast-iron	Resin
Cu 76–97%, balance Zn		Water-cooled	Mineral oil, tallow, and charcoal
" "		Cast-iron	Tallow and charcoal
Nickel Silvers		"	Lard oil and black lead
Cu 76, Zn 22, Al 2%	Billets	Water-cooled	Mineral oil and charcoal
Cu 70%, balance Zn		Cast-iron	Mineral oil and charcoal
Cu 70, Zn 29, Sn 1%		"	" "
Cu 58, Zn 39, Pb 3%		"	" "
Cu 76, Zn 22, Al 2%		Cast-iron (Durville)	No dressing

The correct quantity of dressing to be applied to a mould is largely a matter of experience and does not lend itself to precise definition. Even distribution is essential and is facilitated by applying the dressing while hot to slab moulds by brush and to billet moulds by mop. The latter must fit closely in the mould and frequent replacement of mop coverings is necessary. The thickness of coating applied is varied for different alloys. Brasses containing 58–63% copper, for example, require, when cast in a water-cooled mould, a lighter application of dressing than alloys containing 64–75% copper, whereas for gilding metals a thicker coating is needed and is obtained by the addition of tallow to the oil-charcoal mixture. The rough areas liable to occur at the bottom corners of slabs and over the lower few inches of billet surfaces can be reduced or eliminated by dusting a little charcoal powder into the corners of slab moulds and by pouring a small quantity of liquid dressing into the bottom of billet moulds after the surface-dressing operation has been completed. The effects of faulty technique in the choice and application of mould dressings readily reveal themselves on the cast product. Too little dressing results in the casting sticking to the mould, while an excess gives rise to dirty

castings, sub-surface porosity, or, in extreme cases, blow-holes and gas inclusions.

Burnt mould dressing must be completely removed by scraping and brushing after each cast and, in addition, it is necessary to eliminate at frequent intervals the hard encrustation, consisting mainly of a mixture of zinc and zinc oxide, which builds up locally on the walls of cast-iron moulds. Unless removed, these encrustations tend to hold excessive quantities of mould dressing and thus give rise to surface imperfections.

4. POURING

The transfer of metal from crucible to mould at a rate and in a manner which would produce a sound casting was at one time a most important part of the art of casting. Distribution of the metal stream and the rate at which the mould was filled were dependent entirely on the caster's judgment. Today these are matters of accurate control, the introduction of the tundish for brass casting having provided a method both for ensuring constant rate of pouring and an even entry and distribution of the liquid in the mould.

Tundishes, usually of cast iron, are provided with a number of holes of a size to permit a rate of rise of metal in the mould of approximately $1-1\frac{1}{4}$ in./sec. For slab casting, the holes, approximately $\frac{3}{8}$ in. in dia., are evenly spaced along the centre line of the tundish. For billets, a single central hole of $\frac{3}{4}-1$ in. dia., depending on the size of billet, is used. The depth and positioning of the holes must be such as to ensure that the stream of metal falls cleanly down the centre of the mould and does not at any point impinge on the mould walls. In order to avoid progressive diminution in the rate of pouring or uneven distribution of metal in the mould, these holes must be carefully cleaned out by reamer after each cast to free them from the deposit of oxides and other matter with which they become coated.

Tundishes should be kept full during the whole of the pouring operation to ensure a steady supply of metal to the mould and also to reduce the risk of dross entering the mould with the metal stream. The initial filling of the tundish is important, and a sufficient volume of metal must be poured into it to cause a steady flow to begin almost immediately from each of the holes. This is achieved by inserting a plug in the spout of the furnace or crucible to hold back the metal until a sufficient degree of tilt has been attained. The steady flow of metal from furnace or crucible to tundish is also dependent on the spout being kept clear of dross and other material and on the correct shape being maintained by careful re-shaping to repair wear or damage.

Because of the impingement of molten metal, often on a constant and restricted area, tundishes are liable to severe erosion which, in addition to shortening their useful life, may lead also to iron contamination of castings. A dressing with tar provides a sufficient protective treatment for most purposes, although

when high-temperature alloys are being cast the additional provision of a small patch of refractory on the impingement area is a further safeguard.

Although brasses containing up to 2% aluminium can, under carefully controlled conditions, be successfully cast in vertical moulds with flaming dressings, the less convenient and more expensive Durville process is still employed for alloys of this type. The Durville machine, if it is in good mechanical condition and carefully operated, is capable of producing castings of exceptionally high quality, both as regards surface condition and internal soundness, although the rather coarse structure of brass ingots cast by this method may not be acceptable in all circumstances. Because of difficulties associated with adequate feeding, it is usual to confine the use of the process to the production of relatively short castings. As with all casting equipment, a high standard of cleanliness must be maintained, and the Durville machine, being somewhat less accessible than the normal mould and being fitted with a refractory-lined container from which particles of refractory readily become detached, requires particular attention in this respect. As stated earlier, mould dressings are not necessary when using this equipment for casting aluminium brasses, but the mould should be preheated to a temperature of approximately 100°C . before use to prevent the formation of cold shuts on the surface of the ingot or billet. Metal is usually transferred by ladle from the melting furnace to the container, and dross and oxide carefully removed by skimming before tilting. The tilting operation, which may be performed mechanically or manually, must proceed slowly, steadily, and smoothly, and this requires machines to be maintained in good mechanical order, for any jerkiness in movement as the assembly is turned about its point of balance gives rise to serious folds on the surface of the casting.

5. FEEDING

The purpose of feeding, which is a continuation of the pouring process, is to prevent unsoundness from two volume changes which occur during solidification, the initial contraction of the liquid as it cools to the point of solidification, and the further contraction during the actual solidification process. Good feeding practice demands an ample and as far as possible uninterrupted supply of metal at a suitable temperature to the top of the casting during the whole of the solidification process. The supply may be either direct from the furnace or crucible or via a hand ladle, depending on the operating conditions. Where a number of small castings or one large casting is being produced, direct feeding from the furnace is practised, but where a number of relatively large castings is being produced from one furnace it may be more convenient to feed one casting by hand ladle while the next is being poured. Even distribution of feed metal is facilitated by allowing it to pass through the runner box or tundish.

The temperature of the feed metal should approximate to that at which the casting was initially poured. In practice some drop in temperature does occur, but this is usually so slight as not to interfere with satisfactory feeding of castings of most brasses. For such alloys as gilding metals and nickel silvers, which solidify at relatively high temperatures, some provision for reducing heat losses of the feed metal and preventing premature solidification of the casting is to be recommended, and this can best be effected by the addition of a small quantity of charcoal to both the tundish and the top of the casting.

"Self" feeding by the use of "hot tops" is not normally practised for the production of brass castings for further fabrication, except indirectly in the continuous-casting processes where feeding proceeds continuously from the liquid metal lying above the solidified casting. A reduced rate of heat extraction in the upper part of the mould may, however, in some instances, provide a means of improved feeding. The reduction in wall thickness of billet moulds for the top few inches, and the provision in this area of an insulating material such as sand, have been found to improve the efficiency of the feeding operation; while for the casting of nickel silver in cast-iron moulds it is advantageous to apply an insulating coating of bone ash over the upper part of the mould before adding the normal mould dressing.

V.—INSPECTION

A routine system of inspection of all castings is essential for the proper control of quality, and, by enabling withdrawal of defective material at the first stage of processing, ensures that wasteful expenditure is kept to a minimum. The type of sampling and analysis necessary for checking composition has already been dealt with, and reference has been made to the main types of surface defects that may occur in brass castings. Trained personnel are required for the visual examination of cast products, and it is important that the inspection is carried out as soon after the casting operation as possible in order that the earliest opportunity can be taken of correcting any operational faults.

By experienced visual inspection the presence can be detected of certain impurities which impart a

distinctive colour to the casting, even in small quantities. Aluminium, for example, when present in amounts as low as 0.05% causes castings to have a golden colour, while small amounts of manganese and iron give rise to a reddish tinge and silicon to a silvery appearance.

Information regarding internal soundness is provided by examination of the sawn or sheared face after removal of the gate or top end, and before being passed out for processing castings are cut back until there is no evidence of unsoundness on the cut or sheared surface. To the practised and discerning eye other features, as well as unsoundness, which have a bearing on quality are revealed. The critical examination of cropped billets or ingots is not only an important but an essential part of the process of quality assessment, and calls for experience, knowledge, and meticulous care. Provided the melting and casting processes have been carried through all stages in accordance with well-established practice based on the results of experience and careful experiment, and all the necessary precautions observed, the amount which it is necessary to cut from an ingot to remove top-end unsoundness is but a small fraction of the length of the casting. The actual extent of the discard varies with the size and shape of the ingot, but if this is not only small, but consistently small, and the appearance of the sheared surface satisfactory in other respects, it provides adequate testimony of the success and effectiveness of quality control of many of the operations involved in the production of castings.

ACKNOWLEDGEMENTS

The authors wish to acknowledge their indebtedness to many of their colleagues for helpful discussions in connection with the preparation of this paper.

REFERENCES

1. D. R. Hull, "Casting of Brass and Bronze", 1950: Cleveland, O. (American Society for Metals).
2. G. L. Bailey and W. A. Baker, *J. Inst. Metals*, 1948-49, **75**, 285.
3. M. Cook and N. F. Fletcher, *ibid.*, 1948-49, **75**, 353.
4. J. J. Hoben and J. F. Mulvey, *ibid.*, 1950, **77**, 357.
5. M. Cook and E. Davis, *ibid.*, 1939, **65**, 65.
6. M. Cook, *ibid.*, 1935, **57**, 53.

THE CONTROL OF QUALITY IN MELTING AND CASTING COPPER AND HIGH-CONDUCTIVITY COPPER-BASE ALLOYS*

1450

By J. SYKES,† F.I.M., MEMBER

SYNOPSIS

Control is necessary at all stages during the production of high-conductivity copper shapes for subsequent working. The selection of raw materials and their blending into suitable furnace charges are discussed in relation to the type of furnace to be used. The fire-refining process for the production of high-conductivity copper wire-bars is outlined, and control methods are described in detail. Photographs show the changes occurring in the structure of button and tube samples during the course of oxidation and the later stages of the reduction process. The removal of arsenic by soda ash-lime fluxing is described, and a method is given for its control by conductivity testing.

Desirable qualities required for mould dressings are indicated, and reference is made to the influence of pouring speed and the oxygen content of the copper on the set of the final casting. Typical pouring temperatures and speeds are given.

Methods used in the production of phosphorus-deoxidized copper, tellurium copper, cadmium copper, and silver copper are outlined, with reference to the time of alloy addition and the control of oxygen content in the bath.

Typical casting defects and their causes are listed, and inspection and analytical methods outlined.

I.—INTRODUCTION

IN dealing with the control of quality in the melting and casting of copper and its alloys, it is inevitable that some reference be made to well-known processes and practices, since technique varies with the type of equipment and its function. The method of control will depend on the technique, and therefore it is impossible to avoid a certain amount of repetition of common knowledge.

The scope of the paper is confined to methods of control employed in melting and casting fire-refined copper, electrolytic copper, phosphorus-deoxidized copper, cadmium copper, tellurium copper, and silver-bearing copper. Some of the methods used to produce a sound casting are fairly general and applicable to other copper alloys not specifically mentioned. The selection of raw materials and charge make-up are considered in relation to the type of furnace and the metal or alloy to be produced. The control of contamination from fuels, furnace launders, ladle linings, and from charge materials is considered.

This is followed by a more detailed description of control methods employed during the fire-refining of copper in a large oil-fired reverberatory furnace, and its subsequent casting into horizontal wire-bars.

The production of vertically cast billets and rolling slabs is described, and mention is made of the effects of pouring speed, funnel shape and size, oxygen con-

tent of the metal, mould temperature and size, on the quality of the final casting.

The final section covers the testing and inspection of the cast shapes.

II.—RAW MATERIALS FOR MELTING AND REFINING

The materials available to fire-refiners and melters of copper include blister copper, process scrap, virgin electrolytic copper, and secondary electrolytic copper. The character and chemical composition of such metal varies very considerably, as can be judged from typical analyses given below, and careful attention must be paid to the make-up of individual charges. It will be appreciated later that there are limitations to the normal fire-refining process, and individual impurities in the charge must be kept below certain limits if economical furnace operation is to be ensured. In particular, bismuth, nickel, selenium, tellurium, cobalt, silver, and gold are not normally removed. Antimony and arsenic can be more or less entirely eliminated by special fluxing techniques. Tin and lead can be reduced to reasonable limits by excessive slagging, with a consequent increase in copper losses and reduction in refractory life. Iron, sulphur, zinc, cadmium, and aluminium are fairly readily removed.

Blister copper supplies to the United Kingdom come almost entirely from the copper belt of Northern

* Manuscript received 29 October 1952. Contribution to a Symposium on "The Control of Quality in the Production of Wrought Non-Ferrous Metals. I.—Melting and Casting",

to be held in London on 25 March 1953.

† Director, Enfield Copper Refining Co., Ltd., Brimsdown, Enfield, Middlesex.

Rhodesia. They arrive in the form of 350-lb., horizontally cast cakes, and the following analysis is typical of blister obtained from the Mufulira mines ¹:

	Per Cent.		Per Cent.
Cu . . .	99.5	Sb . . .	0.0003
Pb . . .	0.0012	Ni . . .	0.0062
Fe . . .	0.011	Co . . .	Trace
S . . .	0.066	Se . . .	0.0017
Bi . . .	0.0018	Te . . .	0.0001
As . . .	0.0012		

Each consignment of blister is stock-piled separately. Cakes are taken for drilling and the drillings mixed, quartered, and sent to the chemical laboratory for complete analysis.

With large consignments of scrap wire, sufficient samples are taken to make up a 3000-lb. melt. This melt is cast into ingots which are drilled and a truly representative analysis of the parcel obtained. The analyses obtained from various batches are used for blending satisfactory furnace charges.

Domestic scrap arisings, having already been refined, present no difficulties in usage, provided that efficient segregation is maintained in the mills. Too great an emphasis cannot be placed on the necessity for efficient scrap segregation. All scrap should be clearly identified and baled without delay. The advantages of baling are not confined to facilitating storage, as time is saved in furnace charging and oxidation losses are kept to a minimum.

Merchant scrap is normally the worst type of material to be handled, calling for rigorous inspection by trained scrap sorters and rapid analytical checks, normally by spectrographic means. Clean bright copper and clean burnt paper-covered wire present no great difficulties from the point of view of contamination. Heavy copper, burnt tinned wire, lead-splashed wire, and brazier copper present greater difficulties, as they contain higher amounts of tin, lead, or arsenic. They are not used in the production of high-conductivity copper, and are generally disposed of in special low-grade charges or as anodes for electrolytic refining. Alloys such as chromium copper and cadmium copper are undesirable, and use should be made of magnets to remove tramp iron and copper-clad steel.

Electrolytic copper cathodes are normally run down separately in special small oil-fired tilting furnaces, or in electric furnaces of the direct-arc type with atmosphere control. A typical analysis of primary electrolytic copper is: Cu 99.98, S 0.0003, Fe 0.0009, Bi 0.0001, Ni 0.0005, Se 0.0006, Te 0.0001, Sb 0.0001%. Secondary electrolytic copper usually conforms to British Standard No. 1035, but when it originates from pickling-acid regeneration plants it is often undesirably high in lead and occluded sulphate. However, compared with other materials available, the output of cathodes from acid-regeneration plants is almost negligible.

Small quantities of mill scale may also be added to a refining charge, but only if it is of very high grade. Scale with a high iron content is added to

anode casting furnaces for ultimate electrolytic refining.

Control in the selection of raw material is dependent on the accurate analysis of representative samples. Such analysis may be made chemically or spectrographically. With the exception of selenium and sulphur, for which the quartz spectrograph is unsuitable, all other elements of interest can be determined more rapidly by spectrographic analysis. The introduction of the direct-reading spectrograph for the analysis of non-ferrous metals has increased the speed at which results can be obtained. One of the minor disadvantages of this instrument, however, is its dependence on a minimum sample mass for accurate quantitative estimations. This means that the casting of standard-size test-pieces is desirable.

Inspection and segregation of alloy scrap follows similar lines, though this is even more important in that no refining occurs during remelting. Any undesirable elements present in the scrap will inevitably be reflected in the analysis of the final cast billet.

III.—CHARGE MAKE-UP AND BLENDING

In making up furnace charges consideration must be given to the method of melting to be employed, and to the extent to which the material can be refined. Where no refining is possible, charges must be blended so that a satisfactory analysis is achieved in the final casting.

Light scrap is usually charged in the larger refining furnaces to form a cushion on to which the heavier scrap and blister can be loaded. Small scrap should be baled tightly, and the charge arranged carefully in the furnace so that high melting rates are obtained. It must not be stacked in such a way that the flame is deflected on to the furnace roof or side walls, as incomplete combustion of the fuel may result. In the case of crucible furnaces, a dense charge in good contact with the crucible will result in maximum melting rates and minimum losses by oxidation.

IV.—TYPES OF FURNACE USED IN GREAT BRITAIN

1. OIL- OR FUEL-FIRED FURNACES

Within a particular metallurgical industry a considerable diversity of furnace construction and operation will usually be found. Some of these differences are due to local conditions, others to differences of opinion. Every good furnace operator or designer is continually testing his views by making minor changes in furnace operation or construction. Thereby progress is achieved.

The bulk of the high-conductivity shapes cast in the United Kingdom is produced from blister copper and high-grade copper scrap. Melting, followed by fire-refining, is carried out in reverberatory furnaces fired either by pulverized fuel or by fuel oil. Furnace capacities may vary from 50 to 180 tons, but the

charging, melting, refining, and casting sequence almost always covers a 24-hr. cycle.

The time during which tough-pitch copper can be maintained at pitch is limited, and casting must be arranged so that the furnace is emptied as rapidly as possible. When the charge is cast into horizontal wire-bars, or vertical-cast cakes on the casting wheel, little difficulty should be experienced in holding the metal at the correct pitch. However, in a plant which has to cast mixed shapes daily, e.g. vertically cast cakes, billets, and horizontal wire-bars, it is the practice to make use of 5-ton portable furnaces.

Metal is run down side launders to 5-ton portable furnaces before casting on the wheel is begun, and also at intervals while casting is proceeding. These furnaces are provided with oil burners so that the metal can be kept hot for long periods, thus making operations more flexible. If the copper has to be held for prolonged periods, the oxygen content of the metal is maintained at slightly less than 0.07% in order to get a minimum sulphur pick-up from the furnace gases. The bath is finally poled to the correct

of the reverberatory tilting type has been installed in the works of the Enfield Copper Refining Co. Melting in this furnace is rapid, and by careful control of combustion conditions the copper is nearly blown at the end of this operation; 45–50 tons/day are being cast from this furnace into 1000-lb. vertically cast cakes. Fuel consumption is very good. Charging times are eliminated in the normal sense, as the furnaces melt at the same time as they are being charged.

Special charges of electrolytic copper cathodes are melted in reverberatory furnaces, and in some cases only a limited refining process need be employed. Depending on the degree of purity and physical character of the cathodes, the oxidation period may be stopped when the bath contains 0.6% oxygen. At this stage sulphur, which is usually the principal impurity, will have been removed and poling operations can be begun.

2. FURNACES FOR DIRECT MELTING

Furnaces in which high-conductivity copper can be melted without the need of the oxidation–reduction cycle are of the electric type utilizing a form of atmosphere control.² The material making up the charge is invariably electrolytically refined copper in the form of cathodes.

Copper alloys containing the more refractory metals, such as chromium, are generally produced in rocking-arc furnaces of up to $\frac{1}{2}$ -ton capacity. The Durville method of casting is preferable for this type of alloy. Adequate chilling of the mould is necessary to reduce the possibility of segregation within the final casting. Chromium coppers can be produced in crucible furnaces provided that sufficient superheat is obtained in the copper before the chromium additions are made. Temperatures of the order of 2750° F. (1510° C.) are required, and thus the arc furnace is often considered more suitable.

Crucible furnaces of the oil- or gas-fired type are used for the production of alloys such as tellurium copper. Phosphorus-deoxidized copper cakes may also be produced from crucible furnaces, though more generally they are cast from the 5-ton portable furnaces mentioned above.

V.—THE INFLUENCE OF FUELS AND FURNACE ATMOSPHERE

In electric-arc furnace melting the risk of serious contamination of the charge is slight. The ash content of graphite or amorphous carbon electrodes is normally 0.5%, and the iron content of electrodes should be less than 0.1%.

Solid-fuel-fired furnaces of the grate type may be quickly dismissed, as they have been almost wholly superseded by furnaces fired with pulverized fuel or oil. Solid fuels should have a very low ash content and a high volatile content, particularly in the case of pulverized fuel where the whole of it is introduced into the furnace chamber. The sulphur content should be

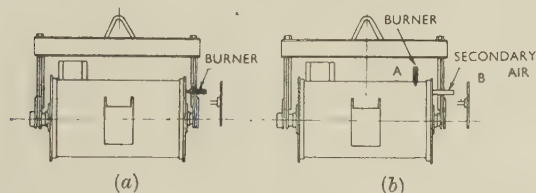


FIG. 1.—Sketch of 5-Ton Portable Furnace, Showing Burner Positions for (a) Horizontal and (b) Vertical Firing.

pitch when required for producing side-cast shapes on a wheel or in racks. Sulphur pick-up is also minimized if vertical firing is used on the portable furnaces when they are being brought up to temperature to receive molten copper, and also for the period during which the metal is being held. Horizontal firing is reverted to when the copper is being brought to pitch and during casting operations.

Fig. 1 shows a 5-ton portable furnace with the two burner positions indicated. When fired vertically the oil is atomized by high-pressure primary air, and enters the furnace as shown by the arrow (A). Secondary air enters the furnace through a second port in the end of the furnace (see arrow B). When horizontal firing is used, the oil- and primary-air burner is moved from position (A) to position (B). In this case the burner becomes more conventional in design, in that the oil, the primary air for atomization, and the secondary air, all enter the combustion zone in approximately the same direction.

Control of the operations in oil-fired or pulverized-fuel-fired rotary furnaces and tilting furnaces of up to 20 tons is similar to that practised on the larger reverberatory furnaces, though the whole refining cycle may be completed in as little as 6–8 hr. Rotary furnaces of the Thomas or Gottschalk type have been in use in Europe for copper refining for the past 15 years or so. Recently a 6-ton oil-fired furnace

as low as possible, and the degree of combustion as high as is practicable, to prevent its absorption into the bath.

In the case of oil-fired reverberatory furnaces two types of oil are often employed. During melting down, when a high heat input is required, and during part of the oxidation period in the refining process, heavy fuel oil is used. This may contain as much as 2.75% sulphur, but provided that oxidizing conditions and efficient combustion are maintained, no serious sulphur pick-up occurs. When the oxidation process has reached the stage where about 0.6% oxygen is present in the molten copper, the heavy oil burners are replaced by burners using a light gas oil. This oil is employed during the rest of the refining cycle, and it is desirable that it should have a sulphur content of less than 0.2%. In actual practice oils with sulphur contents up to 0.5% have been used successfully.

Satisfactory combustion is essential for economic furnace operation, and control of the fuel burners must

TABLE I.—*Flue-Gas Figures During a Complete Refining Cycle of a 175-Ton-Capacity Oil-Fired Furnace.*

Process	Time, hr.	Mean Flue-Gas Temperature		Oil Consumption, gal./hr.	Mean CO ₂ Content, %
		°F.	°C.		
Charging .	6	1770	966	Rises from 50 to 300 in 1st hour, then constant.	15
Melting .	6	1900	1038	300	15
Oxidizing .	4	1850	1010	180	10
Poling .	3	1850-1900	1010-1038	50	8
Casting .	5	1090	588	30-40	5

be very flexible. Oil burners capable of efficient combustion over a range of fuel flow from 15 to 170 gal./hr. are not uncommon.

To assist in obtaining the desired atmosphere during the refining process, draught gauges and carbon-dioxide recorders are installed in the furnace stack and uptake. Maximum fuel efficiencies are generally obtained when the flue gases contain 10-14% carbon dioxide, and during melting a maximum content is required, indicating complete combustion. Flame intensity and furnace temperature are increased with the aid of secondary air during melting. An oxidizing flame is necessary when blowing, and the excess air introduced to the furnace causes a reduction in the carbon dioxide content of the flue gases. During poling operations a neutral or slightly reducing flame is maintained, and the furnace is put under slight pressure with the object of drawing in as little oxygen as possible. Table I shows the mean carbon dioxide content of the flue gases from a 175-ton oil-fired refining furnace, during a complete refining cycle. Mean flue-gas temperatures and oil consumption are included for the sake of completeness. The charging time is longer than usual, as the charge in question had a rather high scrap content.

VI.—CONTROL OF THE FIRE-REFINING PROCESS

1. GENERAL PRACTICE

The process of fire-refining is well established in principle and has been described in considerable detail recently by Miller.³ In a straightforward charge in which no specialized processes are necessary for the removal of arsenic or antimony, four skimmings are usually made. The first skim is made when the bath is flat, and this is followed by taking the first button sample with a bone-ash-dressed "say-ladle". The first few buttons from a new ladle are usually unsatisfactory, and the ladle is burnt by dipping in the molten copper five or six times.

The appearance of the sample during and after solidification gives an indication of the length of time which the oxidation period is likely to take. Some brands of blister copper are highly oxidized and usually show a flat or sunken set in the button; others, low in oxygen, may contain from 0.05 to 0.10% sulphur, and buttons from these coppers will show a spew and will take longer to oxidize. The appearance of the set surface also shows the presence or absence of tin, lead, or phosphorus. When any of these impurities are present, steps can be taken to eliminate them in the refining furnace if the quantities are not too high.

Oxidation of the bath is begun when the charge is "off-bottom", low-pressure air at 20 lb./in.² being introduced below the surface of the bath through $\frac{3}{4}$ -in.-dia. steel pipes. Subsequent button samples change in appearance from a dirty brick red to a coarse-grain fracture. As the blow progresses, types of structure are obtained which are known as fine-grain, small-block, and big-block. The fine stringy grain structure contains 0.4% oxygen, corresponding to the eutectic point, and the big-block structure contains 0.9% oxygen. The oxygen content of "low-set" buttons (rising to 0.9%) may be estimated microscopically. The button is sectioned, polished, etched with nitric acid, and finally polished on dry Selvyt cloth before examination (see Fig. 4, Plate XLVIII, for photomicrographs of typical sections, and Appendix I, p. 362, for details of the etching reagents employed).

The second and third skims are usually taken at the fine-grain and small-block stages, respectively. When the big-block structure has been obtained, the furnace is skimmed perfectly clean for the last time, using silica sand and charcoal to thicken up the slag. The furnace is then covered with approximately 1 ton of low-sulphur coke, the dampers on the furnace are set, the flame adjusted to a neutral or slightly reducing condition, and poling begun.

After poling has been in progress for some time the taking of samples in the say-ladle is resumed. The ladle is coated with charcoal by rubbing it on a burnt poling tree, and the set obtained corresponds to a slightly lower oxygen content than that existing in the bath. The furnace operator is thus provided

with a small safety factor when estimating the condition of his melt.

In the early stages, immediately before the final solidification of the button sample, the "nigger" appears. This is actually a shrinkage cavity, and its presence is due to the low solubility of gases (hydrogen and carbon monoxide) in copper of high oxygen content⁴; the solubility is very low at about 0.07% oxygen, from which point it increases as the oxygen content decreases. The presence of gases in the copper diminishes the shrinkage of the metal on solidification. Thus, as poling continues, the shrinkage cavity decreases in size until it disappears entirely.⁵ When the copper is almost at pitch, as judged from the button samples, $9 \times 4 \times 4$ in. block castings are taken.

Once the oxygen content of the bath is judged to be down to 0.07%, no further additions of coke are made. Charcoal, being sulphur-free, is used from this stage of poling until casting is completed. If sulphur has been picked up during the later stages of poling, button samples tend to spew, giving a similar effect to that obtained from an over-poled bath. The relation of sulphur to the over-poling of copper has been discussed by Skowronski.⁶

When block samples show a "crown" set, casting is begun. The set of the wire-bars will be slightly lower, owing to oxygen picked up during pouring. A slightly low pitch can be detected by the appearance of groups of small black spots at either end of the bar almost as soon as the copper begins to solidify.

Just before, and during casting, $\frac{3}{4}$ -in.-dia. tube samples are taken from the stream of metal tapped from the furnace and checked for oxygen optically, being compared against standard photomicrographs of known oxygen content (see Fig. 5, Plate XLIX, for photomicrographs of typical tube-sample structures, and Appendix I, p. 362, for details of the etching reagents employed).

2. PROCESSES TO REDUCE IMPURITIES

After a charge is flat, the first button sample sometimes shows a dirty area just under the set on fracturing. This usually denotes the presence of arsenic or antimony. These elements can be almost completely eliminated by the use of soda ash and lime slagging.⁷ A method for arsenic removal and its control is described below.

Once the charge is off-bottom blowing begins. When the melt contains about 0.75% oxygen and has attained a temperature of about 2200° F. (1200° C.), the bath is skimmed clean. Soda ash and lime are blown under the surface of the bath from a special tank, using a 1-in.-bore steel pipe, which is passed through a port in one of the side doors near the uptake end of the furnace. Sometimes a pole is put in at the same time to keep the bath stirred. Details of the construction of the blow tank are shown in Fig. 2.

The arsenic slag is quite thick and floats on the surface of the bath, from which it can easily be skimmed as it accumulates.

A sample is taken from the furnace after each tank has been blown, transferred to a graphite pot in a pre-heated coke-fired furnace, poled up to pitch, and cast into a $\frac{1}{2}$ -in. square slug about 9 in. long. This slug is then rolled to $\frac{1}{4}$ -in.-dia. rod on a small sample mill, annealed, pickled, and drawn down to 0.0808-in.-dia. wire, annealed, cleaned, cut to length, and tested for conductivity. Details of the method of testing, using

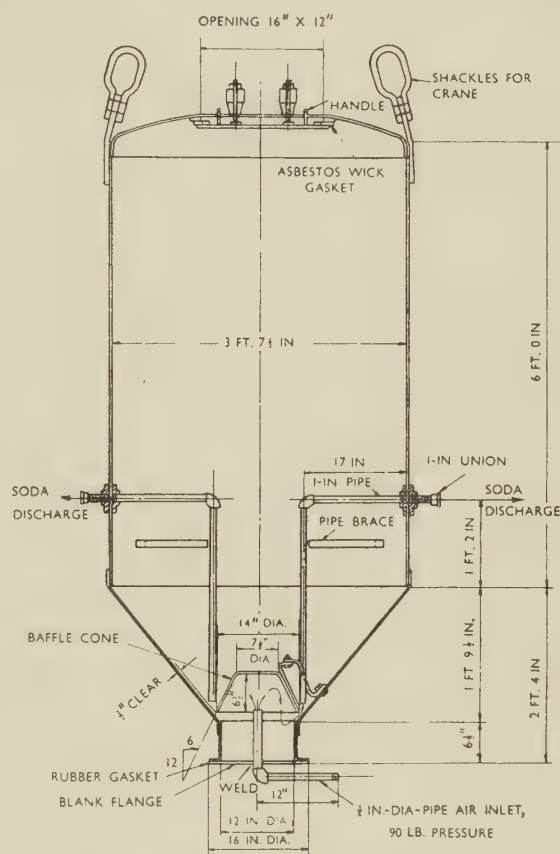


FIG. 2—Details of Construction of Blow Tank.

a Leeds and Northrup instrument, are given in Section XI (p. 361). If the result is less than 100% I.A.C.S.,* more soda ash and lime are blown into the furnace until a test gives the correct conductivity. The bath is kept skimmed clean until the result is available, and a pole is put into the metal between blows. When 100+ % conductivity has been obtained, the furnace is covered with coke and poled up to pitch.

It is possible to eliminate nearly all the arsenic, but generally it is reduced only to less than 0.0015%. Spectrographic tests can also be carried out for arsenic determination, and to some extent these remove the need for running conductivity tests during the blow.

* International Annealed Copper Standard.

Only the final one is necessary, once the spectrograph result has shown the arsenic content to be less than 0.002%. The quantities of soda ash and lime used depend upon the amount of arsenic present in the melt, but generally they approximate to 10–15 lb./ton of metal in the furnace. Soda slags are deleterious to the refractories, and a basic brick lining is desirable when this treatment has to be carried out. Rapid skimming of the furnace helps to minimize the destructive effect of the slag on the refractories.

Nielsen⁸ has suggested the use of a soda ash–lime–coal flux for the partial removal of selenium and tellurium. The process has to be carried out under reducing conditions, and considerable practical difficulties arise. As far as is known, it has not been adopted as a production routine in refineries.

An experimental charge which was refined using a double oxidation–reduction cycle and a soda ash–charcoal flux, resulted in a 70–80% removal of selenium. The charge consisted of 180 tons of blister copper with a selenium content varying between 0.07 and 0.10%. The bath was oxidized, skimmed, and poled in the usual way until the small-block stage had been reached in the reduction process. A mixture consisting of 1450 lb. of soda ash and 425 lb. of charcoal was then added to the bath, via a blow tank. All openings were tightly closed except for the skimming door, and poling and skimming continued during the addition and for 45 min. afterwards. White silica sand was thrown on to the bath, which was then skimmed perfectly clean. The brickwork temperature was kept high, so that very little soda slag remained on the walls after skimming. The bath was finally blown to 0.75% oxygen and reduced in the usual manner by low-sulphur coke, charcoal, and by poling. Most of the selenium was eliminated in the soda slag; this contained up to 5% selenium, half of which was water-soluble.

Removal of tin occurs late in the oxidation period, and is facilitated by using a basic slag containing soda ash and sodium nitrate. The resulting slags are, however, very corrosive to the furnace lining.

Lead is removed to some extent during the normal refining operations, though prolonged slagging with silica sand is necessary if a very low lead content is to be obtained from a charge high in lead. The slags removed may run as high as 30% copper, and it is obviously desirable to keep the volume of slag produced to a minimum.

3. CONTROL OF TEMPERATURE DURING REFINING AND CASTING

During melting, the maximum heat input to the furnace is maintained, consistent with the high-temperature properties of the furnace refractories. As the oxidation stage proceeds, heat is generated as a result of the exothermic reactions occurring in the bath, and this more than offsets the cooling effect of the air being blown in to achieve oxidation. The oil flow to the burners has therefore to be cut back

progressively, so that a fairly constant, high bath temperature is maintained.

High temperatures favour the absorption of oxygen, thus assisting the blowing operation. Experienced furnace operators can judge the metal temperature quite accurately from the solidification of the normal ladle button samples, but the use of pyrometers is more satisfactory. A Leeds and Northrup potentiometric optical pyrometer of the disappearing-filament type is often used for measuring molten metal temperatures. It is calibrated directly in degrees Fahrenheit, and measures temperatures with a high accuracy. It is light in weight, rugged in construction, and easily and rapidly operated.

Temperatures can be taken in crucibles and in induction and arc furnaces by sighting down a closed-end tube to give black-body conditions. If the temperature is to be taken just before pouring, a silica tube may conveniently be used, as the time lag for such a measurement is only about 45 sec.

Sighting the pyrometer on to the surface of the bath is not to be recommended, owing to the differences in thickness and composition of the oxide cover on the metal. Dip-type thermocouples are also used, with the platinum/platinum–rhodium couple protected by a primary silica sheath and a graphite secondary sheath.⁹ Continuous bath-temperature readings are not taken owing to the danger of mechanical damage to the protective sheath during furnace operations.

It is important during poling that the temperature be maintained as uniform as possible, and not allowed to fall or rise suddenly. If the metal temperature falls near the end of poling, and is then suddenly raised again, over-poled metal or a coarse-set bar will result, owing to absorption of sulphur from the fuel. Careful control of temperature as well as of the atmosphere in the furnace is, therefore, necessary to ensure the production of good-quality metal.

Typical temperatures taken at intervals during the refining process¹⁰ are given in Table II.

TABLE II.—*Typical Temperatures Taken During a Refining Cycle.*¹⁰

Stage During Process	Temperature	
	°F.	°C.
Off bottom or "afloat"	2150	1176
Coking	2175–2200	1191–1204
Poling: 1 hr. after coking	2125	1163
2 hr. " " " " "	2100	1149
Ready to cast	2070	1132
Casting	2060	1126

Before casting on the wheel begins, a 5-ton portable furnace is filled and the temperature finally checked by sighting an optical pyrometer on to the molten stream.

The usual pouring temperatures for horizontally cast wire-bars are :

135-lb. Bar	2050°–2060° F. (1121°–1126° C.)	Ladle to mould.
250-lb. Bar	2030°–2050° F. (1110°–1121° C.)	" "

4. CONTAMINATION FROM REFRACTORIES

Contamination of the metal from the magnesite-brick lining of the furnace hearth is negligible, as the impurity content of the refractories is very low. Some trouble is experienced with sulphur pick-up during the first few charges after the walls and roof have been rebricked with chemically bonded chrome magnesite, as the binders employed contain certain quantities of barium and sodium sulphate which are decomposed progressively.

The launder and ladle refractory must resist erosion by the hot metal, for otherwise non-metallic inclusions will be found in the final castings. The linings must also have a low heat capacity and a low thermal conductivity, so that no severe chilling of the metal occurs. A mixture found suitable consists of 49% washed sand, 49% Portland cement, and 2% fireclay (37% alumina). The ladle pouring lip is washed with a highly refractory cement (high alumina content), which sets extremely hard and withstands the chipping carried out to keep the lips free from skull.

5. CONTROL OF PITCH IN THE POURING LADLE

The use of charcoal in the ladle should be kept to a minimum, as its effect is not lasting and control to the desired pitch is made difficult. Whenever possible, the pitch should be regulated by poling and only sufficient charcoal briquettes or wood charcoal kept on the surface of the metal in the ladle to prevent atmospheric oxidation. When various sizes of castings are being produced, particularly if they vary in width, charcoal has to be used, as it offers the only method of rapidly changing the pitch to the desired level. Wider castings in general require less poling or charcoal to obtain a flat set, though pouring speed also has an influence, a fast pour tending to give a lower set, and vice versa.

Charcoal briquettes are normally preferred for ladle work, as wood charcoal tends to be small and dirty and dust blows into the moulds, affecting the quality of the castings. Wood charcoal is not so satisfactory for regulating the pitch of the metal in the ladle, but if the metal temperature tends to be low, less heat will be removed than if briquettes are used.

A wooden rabble is used to skim and stir the charcoal cover, thus eliminating iron contamination in the copper.

VII.—CONTROL IN THE CASTING OF HORIZONTAL WIRE-BARS

1. POURING

The tilting of the ladle and the speed of rotation of the wheel are controlled by the operator seated in the control box at the centre of the wheel. Pouring is a highly skilled job, but can be made easier by the use of a Vickers V.S.G. drive to the wheel. This makes possible a very fine and steady control over the acceleration and speed of rotation, necessary to pre-

vent movement of the copper in the mould, so forming rolled edges as the mould moves away from the pouring position. The temperature of the moulds at the time of casting has also to be controlled, and is usually held at about 160° F. (71° C.). A small pocket, 2 in. deep, is cast into the mould block so that a thermometer can be inserted as required.

The shape of the pouring lips of the ladle plays an important part in the production of sound castings free from splash marks. The channel is 2 in. square, and the lower corners are cut back and rounded with a $\frac{1}{4}$ -in.-dia. rat-tail file. The bottom surface of the lip is smoothed off into the edges of the file cuts. Lips of this shape have been found very successful in drawing the molten copper into a single stream without splashing. The channel must be kept quite clean and free of skulls by chipping. A pouring ladle is shown in Fig. 6 (Plate L), and three pouring lips can be seen. The refractory used is that given in Section VI, 4.

2. BONE ASH FOR MOULD DRESSING

Bone ash is sprayed on to the warm mould after the mould pockets have been cleaned with high-pressure water jets. The moulds must be sufficiently warm for the slurry to dry out completely before the mould reaches the pouring position, or blow-holes will be found in the surface of the wire-bars.

The following methods are suggested for testing the suitability of the bone ash :

(a) Loss on Ignition

Weigh a 10-g. sample into a porcelain crucible which has been previously ignited, and maintain it at 1700° F. (926° C.) in a muffle furnace for 30 min. Remove the crucible, cool it in a desiccator, and reweigh. Express the loss on ignition as a percentage. (Recommended limits 0.32–0.84%.)

(b) Titration Value

Transfer a 5-g. sample to a 250-c.c. beaker, add 200 c.c. distilled water, heat to boiling, and then cool. Add 10 drops phenolphthalein indicator and titrate with 0.5N-HCl, stirring rapidly until the pink colour disappears. The reappearance of colour is disregarded, as this will take place until the phosphate is all converted to the dibasic salt. The result is reported in c.c. of 0.5N-HCl used/5-g. sample. (Recommended limit ≥ 1.2 c.c.)

(c) Screen Test

Transfer 100 g. of sample to a 300-mesh screen and apply water with a soft camel-hair brush until the water runs clear. Wash the remaining residue from the screen on to a filter-paper in a Buchner funnel and filter, dry, and weigh. Express the result as percentage passing through 300-mesh screen wet. (Recommended percentage 95%.)

(d) Settling Test

A glass measuring cylinder of $1\frac{3}{4}$ -in. inside dia., and 12 in. high between the 0 and 500 c.c. graduation is required. The temperature of the water should be 25° C. Measure 400 c.c. of water in the graduated cylinder and add 100 g. of bone ash. Shake until the bone ash is thoroughly wet, then invert five times and allow to settle. The time required for 1 in. of clear water to appear on top is recorded by a stop watch, and the average of several readings taken. If the bone ash has been packed very hard, it should be passed through a coarse screen before making the test, as it is then easier to get the sample thoroughly wetted. The result is expressed as the number of seconds required for 1 in. of clear liquor to appear at the top of the cylinder. (Recommended limits 200–550 sec.)

3. MOULD MANUFACTURE AND LIFE

A three-pocket wire-bar mould usually has a life of 50–60 tons of casting. Then fine cracks can be seen developing in the radii, and if left these would absorb moisture from the mould dressing and cause blow-holes in the wire-bars. In the case of a wheel carrying 14 mould blocks, one or two would normally be replaced each day, depending on their condition, and the old ones recharged to the furnace.

In the production of a new mould very great care must be exercised to obtain metal at the correct pitch and temperature. The copper is tapped from the furnace down a side launder into the mother mould. The surface of the molten metal in the latter is carefully skimmed, and then a warm core which has previously been sprayed with 28° Bé. bone ash, is lowered into the copper. The design of the cores and their water-cooling channels is of great importance. After manufacture the mould pockets are very carefully examined for surface defects before being put into service.

4. CASTING DEFECTS IN HORIZONTAL CASTINGS,
AND THEIR CAUSES*(a) Moisture Holes*

Moisture holes are caused by steam generation from damp moulds, and are generally found if old moulds are in use. Small cracks in the mould surface hold moisture from the dressing. The holes are irregular in shape, and may occur at any position on the bar; they are larger than, but not so deep as, heat holes.

(b) Oil Holes

These are caused by spots of oil on the mould, which may have originated from an overhead crane or from the compressed-air line of the bone-ash spray-gun. The area of the bar affected is usually small, but may be in any position. The reducing gases evolved penetrate the outer skin of the casting, and cause holes which are often too deep to remove by chipping.

(c) Bone-Ash Inclusions

Inclusions of this type are caused by the application of too heavy a coating of bone ash, and its consequent flaking away. Too high a mould temperature will give the same effect.

(d) Cracks

The cracks are usually transverse, and can be brought about by cracked or uneven mould surfaces which tend to grip the solidifying bar. They are also found if the temperature of the copper is too high or if the moulds have been badly dressed.

(e) Sand Inclusions

These originate from the casting ladle or pouring lips, and can be more or less completely eliminated by use of correct refractories.

(f) High Set

A high set is due to over-poling or too much residual sulphur in the bar.

(g) Dimensional Defects

The length and width of a cast bar are governed by the mould condition. The weight of the bar is controlled by the depth to which the wheel-man fills the mould pockets.

(h) Laps

These are caused by splashes or cold sets which have not been turned in by the fisher.

(i) Heat Holes

This type of defect is normally found when the metal temperature is too high. The holes are small, uniform in shape, and occur grouped together in comparatively small areas, generally in the area where the stream first strikes the bottom of the mould.

(j) Rolled or Sloppy Edges

These may be due to too rapid pouring, to vibration from the wheel, or to a bad finish up at the end of the pour.

VIII.—THE CASTING OF VERTICAL
SHAPES

1. THE USE OF PORTABLE FURNACES

Vertically cast shapes may be cast on the main wheel or side-cast on racks. When cast on the main wheel, copper is tapped from the furnace to either one or two pouring ladles. In rack-casting the metal is poured from 5-ton portable oil-fired holding furnaces.

The portable holding furnaces are filled with copper from the main furnace and placed in a convenient position near the pouring site. The metal is then skimmed and a sample block taken to ascertain the pitch and temperature. The experienced furnace-man can estimate temperature fairly accurately by watching the metal flow from the ladle, the formation of skulls in the ladle, and also the colour of the molten copper. Accurate temperature measurements are taken by pouring a small quantity of the metal from

the furnace and using a disappearing-filament pyrometer. If the copper is not up to pitch, poling is carried out in the holding furnace. Alloying with silver or tellurium is also done in the furnace just before casting. Neither charcoal nor coke is used on holding furnaces.

2. MOULDS FOR VERTICAL CASTING

The moulds used in the production of rolling slabs and extrusion billets in various alloys are made from solid tough-pitch copper castings. The castings are machined-out to form the desired shape, with a slight taper to allow easy dropping of the final shapes. Water-cooling channels are also drilled through the blocks to ensure satisfactory chilling of the casting. In the case of a 1000-lb. cake mould, the rate of water circulation is 150 gal./min. at 60 lb./in.² pressure. The water temperature is usually in the range 190°–205° F. (88°–96° C.).

After a time the tops of slab moulds tend to bow outwards and the lower sections to draw in, and in extreme cases this could result in the cake being jammed in the mould. Before serious jamming can occur, however, the mould pockets are re-machined.

3. MOULD FUNNELS AND PELICAN LADLES

When billets and vertically cast wire-bars are being cast, it is essential that the stream of metal does not splash against the side of the moulds. They are therefore poured through a refractory-lined funnel, the size of the orifice being determined by the size of casting being made. For a 4-in.-square vertically cast bar, $\frac{9}{16}$ in. dia. is normally used, and $\frac{5}{8}$ in. dia. for $4\frac{1}{2}$ -in.-dia. billets. A typical funnel is shown in Fig. 7 (Plate L). The shape of the refractory lining counteracts any tendency for a vortex to form, and an unbroken stream of metal flows into the mould. The funnel must be accurately positioned and aligned for satisfactory results.

Pelican ladles are used for "floating" vertically cast cakes over 3 in. in thickness, with the object of avoiding defects at the bottom of the casting such as cold shuts, oxide, and bone-ash inclusions. They serve an additional purpose in providing a more even distribution of heat, and tend to eliminate the hot zone in the middle of the bottom of the casting. Such a hot zone constitutes a weak area, incapable of withstanding the strains set up on cooling, and results in "shadow cracks".

Fig. 8 (Plate L) shows the simultaneous casting of two 1000-lb. rolling slabs from a 5-ton portable furnace, and Fig. 9 (Plate L) illustrates a pelican ladle. Fig. 10 (Plate LI) shows a 3000-lb. high conductivity copper cake being cast into a one-piece water-cooled copper mould.

4. MOULD DRESSING FOR VERTICAL SHAPES IN REFINED COPPER

For casting refined copper the bone ash used as a mould paint must possess certain properties. It

should adhere to the mould and form a smooth surface which will not react with molten copper. High magnesium content should be avoided, or adherence will be poor, and no volatile substances should be present.

When pouring vertically cast cakes into a freshly machined mould, the first few cakes have areas of "sweat" towards the top edge of the cake. If these areas are ground off, the sheets eventually produced will show corresponding discoloured areas due to the high copper oxide content of the metal. This defect is usually eliminated by spraying high-Bé. bone ash round the top inside surface of the mould cavity.

Bone ash contains 75% Ca_3PO_4 , other constituents being sulphates, chlorides, carbonates, and oxides of calcium, magnesium, and potassium. Sodium and potassium hydroxides and some silica are also present. One per cent. of Na_2CO_3 and 1% NaOH cause pitting, but excess alkalinity can be reduced to 0.3% NaOH with sulphuric acid and pitting thus obviated. The presence of 3% silica will cause severe pitting. Up to 4% CaCO_3 in the bone ash does no harm, and little trouble is experienced in this respect, as bone ash usually contains only 2%. A fairly slow-settling bone ash is preferable.

5. POURING SPEED AND TEMPERATURE

Pouring speed is governed to some extent by the pitch of the metal being cast and the size and shape of the casting. As in the case of horizontal casting, a faster pour tends to give a lower set, and the speed at which a particular shape is cast is controlled in relation to the set obtained on the previous one. Approximate pouring speeds are as follows:

Cakes (1000-lb.)	:	:	:	400 lb./min.
Billets ($4\frac{1}{2}$ -in.-dia.)	:	:	:	72–90 sec.

Pouring temperatures in general use are as given below:

Ingots	2080°–2095° F. (1138°–1146° C.)	Ladle to mould.
Billets	2085°–2090° F. (1140°–1143° C.)	Holding furnace to funnel.
V.C. Bars	2090°–2100° F. (1143°–1149° C.)	Holding furnace to funnel.
V.C. Cakes (wheel)	2010°–2030° F. (1099°–1110° C.)	Ladle to mould.
V.C. Cakes (rack)	2030°–2050° F. (1110°–1121° C.)	Holding furnace to mould.

6. DEFECTS IN VERTICAL CASTINGS

(a) Shadow Cracks

Shadow cracks always occur towards the centre and within 4 in. of the bottom. If this portion is free from cracks, it may be taken that the cake as a whole is free. Unless the cracking is severe, these fine hair cracks can be detected only by removing the surface with a pneumatic chisel. The more nearly the cross-section of the mould approaches a square, the less likely is the occurrence of shadow cracks.

(b) *Cold Sets*

Cold sets or splashes are generally due to off-centre pouring or too rapid pouring which has caused turbulence in the mould.

(c) *Pitting*

This is caused by off-centre pouring which has washed dressing from the side of the mould, or is due to bone ash or cement inclusions.

IX.—HIGH-CONDUCTIVITY COPPER ALLOYS

1. PHOSPHORUS-DEOXIDIZED COPPER

In the production of phosphorus-deoxidized non-arsenical copper, the metal in the holding furnace is superheated to 2200° F. (1204° C.), skimmed, and poled to 0.040–0.045% oxygen. Copper–15% phosphorus alloy is then added to the bath to the extent of 1.1 g./lb. of metal in the furnace. A small tree is used to mix the addition and to stir the bath. The metal is poured after standing for 5 min. The range of phosphorus content is 0.015–0.030%.

Phosphorus-deoxidized copper is also produced in low-frequency induction furnaces of the Ajax–Wyatt type. Alumino-silicate linings can be used if the charges contain at least 80% deoxidized copper scrap. Oxygen-bearing scrap gives trouble by excessive attack on the refractories.

Moulds for use with phosphorus-deoxidized copper are oil-dressed with a mixture of machine mineral oil and lamp black, applied with a lambskin mop. The moulds should be as cool as possible, the colder the better. The metal is poured through funnels in the case of billets and through multiple-hole tundishes for cakes. Water is run into the mould through two $\frac{1}{8}$ -in.-dia. pipes once the bottom is covered with molten metal. Sufficient water is added to stop the dressing from flaming, approximately 500 c.c. being necessary on a 600-lb. cake. This helps to reduce the amount of phosphide slag which may be trapped in the sides and edges of the cakes. However, the danger of using water in the mould if the phosphorus content is very low or absent cannot be stressed too strongly.

2. 0.05% SILVER-BEARING COPPER

This alloy is also produced in 5-ton holding furnaces. The copper is poled to 0.05% oxygen and the alloying addition made in the form of pure silver. The melt is then stirred with a pole and the oxygen brought down to 0.04%. Casting proceeds into water-cooled moulds, as with refined copper shapes, using a bone-ash mould dressing.

3. TELLURIUM COPPER

Alloying is carried out using metallic tellurium or a 50:50 master alloy of copper and tellurium. The master alloy is made by melting copper swarf and

tellurium metal powder in a small crucible furnace, and no great difficulties are involved.

In the manufacture of the 0.5% tellurium high-speed machining alloy in a crucible furnace, the master alloy is added at an early stage. Melting is carried out under charcoal, and the metal poled until button samples give a slightly crowned set. The metal is then cast into water-cooled copper moulds, dressed with bone ash.

When large quantities are required, the alloy may be prepared in portable furnaces, using a similar procedure to that employed for silver-bearing copper.

4. CADMIUM COPPER

Cadmium copper castings for fabrication into trolley wire, line wire, and resistance-welding electrodes, are cast from a variety of melting furnaces, oil-fired tilting crucible furnaces, low-frequency induction furnaces, rocking-arc furnaces, and rocking-resistor furnaces, all being used successfully. The large refineries, however, usually side-cast cadmium copper into water-cooled copper moulds from portable holding furnaces. It has been found necessary in the past few years to use such moulds, as inverse segregation and subcutaneous porosity are thus minimized or completely eliminated. Cracking of the alloys during hot rolling has been found to be associated with these two defects.

Good high-grade material, such as electrolytic cathodes or ingots, must be used and impurities kept to a minimum; in particular the bismuth content must be less than 0.001% or trouble will be experienced in the rolling operations.

The production of this alloy in a large refining plant is carried out by the following technique. Two 5-ton holding furnaces are employed, one of which is superheated for a few hours before use. The second furnace, also superheated, is filled with tough-pitch copper from the wire-bar furnace, and a weighed quantity poured into the superheated furnace. The metal is then skimmed clean, poled up to a high "crown set," and covered with clean stick charcoal. Such a quantity of 15% phosphor copper is then added as to leave a residual phosphorus content of 0.008–0.010% in the metal. Copper–cadmium master alloy wrapped in copper foil is added and stirred with a pole. Casting follows immediately through a pouring funnel into oil-dressed water-cooled copper moulds. (The same oil dressing is used as with phosphorus-deoxidized copper.) The moulds should be kept as cool as possible. An improvement in the surface of the billet can be brought about if, just before casting, the inside surface of the mould is sprayed with finely atomized water. Cadmium copper should be poured hot, and the master alloy is not added until the bath temperature is up to 2300° F. (1260° C.).

About 0.10% loss of cadmium is allowed for when making 0.80% cadmium copper. A 35 or 50% cadmium alloy is used, and this is made by melting copper shot and metallic cadmium in a graphite crucible at as low a temperature as possible.

X.—INSPECTION AND TESTING OF REFINED COPPER SHAPES

1. SPECIFICATION REQUIREMENTS

The wire-bars, billets, or slabs must be free from non-metallic inclusions, fissures, and blow-holes. The porosity present to give a level set must be extremely fine and confined to the region immediately below the set. All surfaces must be free of holes, laps, cold sets, and inclusions, and the set surface should be of minimum area. Variations in the size of castings should be small, so that subsequent working operations will be facilitated.

The analysis of the copper should be well within the limits of the appropriate specification, and the electrical conductivity of the final rolled or drawn product in the annealed condition must be greater than 100% I.A.C.S.

2. PHYSICAL INSPECTION

All surfaces of the casting are carefully examined for laps, cracks, blemishes, and non-metallic inclusions. If any cracking is found, the material is automatically rejected and sent for remelting. The mould used is examined to find whether there are any irregularities in the mould surfaces that are liable to cause the hot tearing or cracking. Superficial cold sets and defects are chipped out and the casting re-examined for sub-surface defects in the locality which has been chipped clean. If further cracks or holes are revealed, the shape is rejected.

The cropping of cakes and billets is not begun until the results of the chemical and spectrographic analyses have proved satisfactory. The shapes are re-examined after sectioning to see whether any unsoundness has been revealed, and if any is discovered the material is remelted. Cast numbers are restamped on the sections cut from each billet, to allow of identification during subsequent working operations.

Density measurements are regularly carried out on the high-conductivity shapes by weighing them first in air and then in water, while they are suspended by a special stirrup attached to a steelyard-type weighing machine.

3. LABORATORY SERVICES

Samples are taken from furnace melts and from the cast shapes according to the requirements of the appropriate specifications. These samples may be drilled for chemical analysis or machined to a standard-size test-piece for spectrographic examination, depending on the elements to be determined.

The laboratory of the Enfield Copper Refining Co. is equipped with the conventional apparatus for volumetric and gravimetric estimations, and also with a Hilger medium quartz spectrograph, a polarograph, and Spekker photoelectric absorptiometers; a more recent addition is a direct-reading spectrograph.

Appendix II (p. 363) gives an outline of the methods of analysis employed for particular elements.

XI.—CONDUCTIVITY TESTING IN CONTROL OF REFINING

Conductivity testing plays an important part in the production of refined copper. Wire samples are produced from slug samples cast from the furnace bath. The following stages are involved in the measurement of conductivity:

- (i) Drawing the sample to wire—preferably 12 gauge.
- (ii) Annealing the wire to bring the conductivity to a maximum.
- (iii) Cleaning the wire to remove oxide and superficial blemishes.
- (iv) Cutting the wire to exact length.
- (v) Weighing the wire to ascertain the correction factor required to compensate for any deviation in diameter from the standard.
- (vi) Measuring the conductivity in a bridge.

The wire, 0.0808 in. in dia., is submitted to the laboratory in the form of a coil about 20 in. in dia. with a tag giving its identification. Six ft. of wire are required for each test.

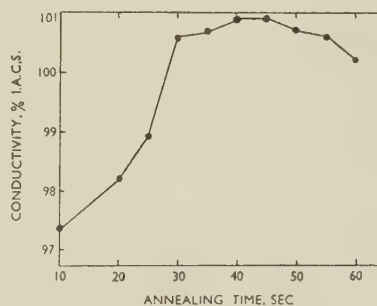


FIG. 3.—Effect of Annealing Time on the Conductivity of Copper.

The wire is annealed by passing a heavy current through it while it is suspended horizontally in the air between two brass clamps, supported on frames about 12 in. above the floor. These clamps are about 6 ft. apart, and form the terminals of a circuit from a special rotary converter producing a high amperage at low voltage. There are rheostats for adjusting the current flowing through the wire.

The wire to be tested is so fastened in the clamps as to be fairly taut. When the generator is up to speed, a switch is thrown and an initial current of about 155 amp. is passed through the wire. As the temperature of the wire increases, its resistance becomes greater and the current drops, so that in about 30 sec. it is down to 140 amp. The temperature of the wire increases during the first 50 sec., by which time it has levelled out at about 850°–900° C. The optimum duration of the annealing treatment for the particular kind of copper is established by tests, and each wire is subjected to the current for that time. Fig. 3 shows the effect of annealing time on the conductivity of the wire. At the end of the chosen time, the

current is interrupted, and the wire immediately cut about 4 in. from each clamp and allowed to fall into a V-shaped water trough extending from clamp to clamp.

During annealing the wire is superficially oxidized, and the oxide coating, and incidentally any small projecting imperfections, have to be removed. The wet wire is fastened at one end, wiped dry, scoured with fine emery cloth, and finally wiped clean. Care must be taken not to pull too hard on the wire and not to bend the wire with the fingers as the emery cloth passes along it, or re-hardening will occur. The wire is cut back 4 in. from the fastened end, and is then ready for cutting to length.

The special cutter employed consists essentially of a grooved bar with an adjustable plate on one end and a steel shearing knife on the other. The knife cuts the wire so that the end is flat and normal to the length. The wire is laid in the groove and about 4 in. cut from one end. The wire is then reversed in the groove with the square-cut end pushed against the back plate, and again cut, giving the 38-in. length required for weighing and testing.

A special balance is used for weighing, which has one stirrup extending below the balance and ending in a double hook, on which the wire to be tested can be laid horizontally. The balance is calibrated to give directly the percentage correction required to compensate for the deviation from the standard in cross-sectional area, assuming that the test sample and the standard have the same density. The difference in density of the standard and the sample wire is usually negligible, but corrections may be applied should the need arise.

A counterweight is furnished with the balance for each gauge of wire to be tested. For 12-gauge wire this is equivalent to 28.4 g. for wire 1 m. in length. The compensation for over- or under-weight is obtained by a rider sliding on a beam. The latter is so divided that when the counterpoise plus (or minus) the rider balances the wire, the reading equals the percentage correction to be applied by turning the compensator drum of the Hoopes bridge to the required number (with proper sign positive or negative); the bridge will then give the true reading directly.

The Hoopes conductivity bridge used was made by the Leeds and Northrup Co. The wire to be tested is clamped taut in the bridge, the sliding contact put in position on the wire, and the cover closed. As temperature affects the conductivity, it is necessary to have the wire tested at the same temperature as the standard. The wire is therefore left in the bridge until the temperature approximates that of the standard, as shown by the checking of two consecutive readings a minute apart. The sliding contact for balancing the bridge moves along a steel scale calibrated in conductivity per cent. Tenths are determined by a vernier scale attached to the contact. The bridge has an accuracy of 0.2%.

It is advisable to reverse the wire and repeat the test.

ACKNOWLEDGEMENTS

The author wishes to thank the Directors of the Enfield Rolling Mills, Ltd., for permission to publish this paper, and Mr. W. W. Kee and Mr. A. G. Adlington for their very valuable assistance in its preparation.

APPENDIX I

Etching Solutions for Sample Buttons Taken During Refining

For "Low-Set" Buttons (O_2 up to 0.9%)

75 c.c. conc. nitric acid.

25 c.c. distilled water.

Polish on dry Selvyt cloth after etching.

For Tube or Bar Samples

70 c.c. 10–12% ammonium persulphate solution.

15 c.c. ammonia.

15 c.c. distilled water.

For Structure Samples

10 g. ferric chloride.

75 c.c. hydrochloric acid.

25 c.c. distilled water.

For Phosphorus-Deoxidized Copper

50 c.c. nitric acid.

50 c.c. distilled water.

APPENDIX II

Methods of Analysis for Specific Elements

Material	Shape	Elements Determined	Outline of Analytical Method Employed
H.C. Copper	Wire-bars and V.C. Cakes	Sulphur	Reduction in hydrogen stream at 900° C. Subsequent estimation of cadmium sulphide using iodine.
		Oxygen	Reduction in hydrogen at 900° C., and absorption of H ₂ O evolved in magnesium perchlorate anhydrous.
		Iron	Visual colorimetric estimation using ferric thiocyanate.
		Bismuth	Visual colorimetric estimation using thiourea.
		Selenium	Distillation in hydrobromic acid, followed by sodium thiosulphate titration. ¹¹
Phosphorus-Deoxidized Copper	V.C. Cakes	Phosphorus	Spekker colorimetric estimation. Reduction of phosphomolybdate with stannous chloride. ¹²
Tellurium Copper	Billets	Tellurium	Spekker colorimetric estimation by reduction with stannous chloride, after addition of thiourea. ¹³
		Oxygen	As for H.C. copper.
		Iron	As for H.C. copper.
0.05% Silver-Bearing Copper	V.C. Cakes and Billets	Silver	Separation as silver chloride, and volumetric estimation using ammonium thiocyanate.
		Oxygen	As for H.C. copper.
Chromium Copper	Billets	Chromium	Spekker colorimetric estimation using diphenylcarbazide.
All Types of Copper-Base Alloys		General impurity content	Spectrographic estimation using the Hilger medium quartz instrument or direct-reading spectrograph.

REFERENCES

1. F. E. Buch, *A.I.M.M.E. Tech. Publ. No. 2248* (in *Metals Technology*, 1947, **14**, (8)).
2. R. H. Waddington and J. C. Bischoff, *Trans. Canad. Inst. Min. Met.*, 1946, **49**, 199.
3. H. J. Miller, "The Refining of Non-Ferrous Metals", p. 145. 1950: London (Institution of Mining and Metallurgy).
4. N. P. Allen and T. Hewitt, *J. Inst. Metals*, 1933, **51**, 257.
5. A. J. Phillips, *Trans. Amer. Inst. Min. Met. Eng.*, 1947, **171**, 17.
6. S. Skowronski, *ibid.*, 1919, **60**, 354.
7. W. J. Hillebrand, R. K. Poull, and H. C. Kenny, *ibid.*, 1933, **106**, 483.
8. O. Nielsen, British Patent Specification No. **449,471**, 1936.
9. P. H. Dike and M. J. Bradley, "Measurement and Control of Temperatures During the Smelting, Refining, and Melting of Non-Ferrous Metals", p. 1. 1946: New York (American Institute of Mining and Metallurgical Engineers).
10. —, *Canad. Min. J.*, 1937, **58**, 690.
11. J. S. McNulty, E. J. Center, and R. M. MacIntosh, *Analyt. Chem.*, 1951, **23**, 123.
12. F. W. Haywood and A. A. R. Wood, "Metallurgical Analysis by Means of the Spekker Photo-Electric Absorptiometer", p. 87. 1944: London (Adam Hilger, Ltd.).
13. P. B. Crossley, *Analyst*, 1944, **69**, 206.



THE CONTROL OF QUALITY IN THE CASTING OF ZINC AND ZINC ALLOY ROLLING SLABS AND EXTRUSION BILLETS *

By C. W. ROBERTS,† B.Sc., A.I.M., MEMBER, and B. WALTERS,‡
M.A., MEMBER

SYNOPSIS

The various techniques and procedures adopted commercially for the production of rolling slabs and extrusion billets in zinc and zinc alloys are briefly described, and the metallurgical principles involved are examined. The origins of the defects normally encountered in the castings are indicated, and the means adopted to minimize the incidence of such defects are discussed. The importance of control of chemical composition both in raw materials and in the final products is emphasized, and it is concluded that, although certain defects can be associated with particular methods of casting, several methods are available whereby satisfactory slabs or billets can be produced provided that supervision of the operations is adequate.

I.—INTRODUCTION

THE control of quality in metallurgical manufacturing processes has become increasingly important in recent years and is likely to receive even greater attention in the future. The reasons for this modification of emphasis in the organization of production are many and various, but among the more important may be mentioned :

- (1) The increasing scarcity and cost of raw materials.
- (2) The increasing cost of labour.
- (3) The high cost and complexity of modern metallurgical plant.
- (4) The higher consistency in properties required in semi-finished products, particularly where finishing operations involve a high degree of mechanization.
- (5) The general higher standard of finish and performance required of metal articles and components.

In the production of zinc rolling slabs and extrusion billets, two separate aspects of quality are involved. Firstly, the quality of the castings must be sufficiently high to allow them to be rolled or extruded in the conventional machinery by normal methods. In other words, quality in a particular instance cannot be allowed to deteriorate to such an extent that special methods have to be adopted to work a particular casting or group of castings. Secondly, the castings must be of such quality that the sheet, strip, or extrusions produced from them by conventional

methods possess the required properties and are suitable for use in this state or are suitable to receive such further work or treatment as is desired. In certain cases the two points of view are complementary, but in others a certain degree of conflict occurs, and consequently the most suitable degree of compromise has to be adopted.

In the present paper the subject is treated on general lines. The various procedures adopted for melting and casting are briefly described, the metallurgical principles involved are examined, the origins of the various defects encountered in the castings are indicated, and the means whereby the incidence of the defects can be minimized are discussed. Rolling slabs and extrusion billets are treated separately, the latter in less detail, since the tonnage of zinc and zinc alloys extruded in this country (and indeed throughout the world) is small and the products are of less metallurgical interest.

II.—PRODUCTION OF ROLLING SLABS

1. RANGE AND REQUIREMENTS OF PRODUCTS

The applications of zinc and zinc alloy sheet and strip are, in normal circumstances, somewhat limited and specialized, a fact which is reflected, to some extent, in the comparatively small range of alloy compositions normally employed. Many of the alloys commonly used are, in fact, refined grades of zinc with the naturally occurring impurities, lead and cadmium, held within specified limits, though other elements are sometimes added in alloying proportions. They are usually referred to as rolling mixes. Some

* Manuscript received 4 November 1952. Contribution to a Symposium on "The Control of Quality in the Production of Wrought Non-Ferrous Metals and Alloys. I.—Melting and Casting", to be held in London on 25 March 1953.

† Research Department, Imperial Smelting Corporation, Ltd., Avonmouth.

‡ Production Department, Imperial Smelting Corporation, Ltd., Avonmouth.

typical compositions in this category are shown in Table I.

True zinc alloys are used to a much lesser extent, those in general use in Great Britain being of the Kayem or Kirksite type, the compositions of which are also shown in Table I. A wide range of zinc alloys were developed in Germany during the war

Slabs of higher quality are required for strip rolling than for sheet production, the main reason for this being that in many cases the subsequent treatment of strip involves machinery working continuously and automatically. Certain defects in the strip may thus cause serious delays in the production lines and even extensive damage to costly machinery.

TABLE I.—*Compositions of Zinc Alloys for Sheet and Strip.*

Description of Alloy	Composition				
	Pb, %	Cd, %	Mg, %	Cu, %	Al, %
Ductile sheet	0.3–0.4
Engraving sheet *	0.3–0.4	0.15–0.25	0.006–0.010
Commercial sheet	0.8–1.3
Strip for Battery Cans {	0.8–1.0	0.04–0.07
	0.2–0.3	0.22–0.28
	0.15–0.25	0.06–0.10
Zilloy 40 (American)	0.10 max.	0.005 max.	...	0.85–1.25	...
Zilloy 15 (American)	0.15 max.	0.04 max.	0.006–0.016	0.85–1.25	...
Kayem	0.003 max.	0.003 max.	0.03–0.06	3.0	4.0
Kirksite		Similar in composition to Kayem			

* Nickel or iron, in amounts up to 0.01%, may also be present.

and were used in large quantities as substitutes for copper alloys. The main compositions are shown in Table II.¹

TABLE II.—*Compositions of Zinc Alloys for Sheet and Strip Developed in Germany.*¹

Description of Alloy	Composition					
	Al, %	Cu, %	Pb, %	Mg, %	Mn, %	Cd, %
Z410	4.0	1.0	...	0.04
Z010	1.2	0.2	...
Z020 { (a)	0.6	2.0	...	0.03
(b)	2.0	...	0.03	0.6	...
Z100	1.0	0.4
Z1010	10.0	0.8	...	0.05
Z1000	10.0	0.3
Z040	0.2	4.0
Z001 Mn	0.2	0.3	1.0	...	0.5	0.1

The properties and general quality required in sheet and strip vary greatly and depend upon the type and degree of subsequent treatment necessary, and on the ultimate application. Roofing sheet, for example, must be free from those impurities that decrease resistance to corrosion and must be reasonably ductile, whereas strip for use in the production of battery cans by deep drawing or impact extrusion must possess a much higher degree of ductility and be of the chemical composition that will ensure maximum battery storage life. Surface quality is highly important in sheet for the production of engraving plates, and this sheet must also possess a considerable degree of rigidity.

Irrespective of the final use, however, rolling slabs should be free from all defects that are likely to cause trouble during rolling, e.g. the presence of surface cracks and impurities that promote hot shortness.

It is probably true to say that by no method of production can perfect slabs be made and that even to approach this standard would involve prohibitive cost. All the methods normally available have certain virtues and certain shortcomings, and the procedures adopted in industry are a compromise between what is desirable and what is practicable. The various points involved are discussed in later sections, but it is convenient to summarize here the ideal requirements of rolling slabs. They are:

(a) The composition of the slab must be uniform throughout.

(b) The composition must be such that the required properties can be obtained in the final products.

(c) Other considerations apart, the composition must be such that mechanical working can be carried out with maximum efficiency, i.e. at maximum speed with minimum energy absorption.

(d) Since efficient working is generally associated with a high working temperature, the slab must be free from those impurities that cause high-temperature embrittlement.

(e) The grain-size and degree of randomness in grain orientation must be such that an adequate number of slip planes are available to allow substantial deformation during the early stages of working.

(f) If a fine-grained structure cannot be secured in the casting and preferred orientation cannot be avoided, the grain orientation must be such that the planes of easy slip lie in the direction most favourable for deformation.

(g) The slabs must be free from dissolved gas

and internal defects such as gas cavities, shrinkage cavities, oxide inclusions, &c.

(h) The slab surfaces must be continuous and free from such defects as laps, cold shuts, sinks, &c.

It may be stated that, although difficulties occur from time to time in the casting of zinc and zinc alloy slabs, a number of methods of casting are available whereby satisfactory products are obtained at low cost and with low rejection figures.

The defects that normally occur in rolling slabs fall naturally into two categories: (i) those that originate in the raw materials and in melting, and (ii) those that are due to faults in casting. These are discussed separately in the following sections.

2. CHARGE MIXING AND MELTING

A substantial tonnage of the zinc rolled to sheet comprises metal in various degrees of commercial purity with total impurities ranging from 0.01 to 1.3%, the actual composition, apart from maxima for individual impurities, not being accurately defined. To obtain a reasonable degree of consistency in composition, it is normal practice to mix several grades or consignments of commercial metal when making up each charge. Apart from scrap derived from the manufacturers' own processes, little zinc scrap is available in a form suitable for remelting, and its inclusion is undesirable because of the danger of contamination of the melt with deleterious impurities.

For the large-scale production of commercial-quality sheet, the metal is normally melted in gas- or oil-fired reverberatory furnaces of up to 100 tons capacity. Melting on such a large scale helps to even out variations in composition throughout a consignment, since the analytical figures supplied by the smelters are average values and do not represent each ingot in a particular consignment. By maintaining the temperature of the bath as low as possible, a certain amount of refining is effected, since lead in excess of the solubility limit at such a temperature separates and settles at the bottom of the furnace and can be removed from time to time. The solubility of lead in zinc at 460° C., for example, is about 1.15%.² A certain amount of iron in the form of the compound FeZn₇ may also be removed in this manner. This method of open-hearth melting is perfectly satisfactory in the case of zinc, since the solubility of the common gases in the metal is very low, and consequently the problems associated with the liberation of dissolved gases during solidification do not occur to any appreciable extent. Precautions must, however, be taken to prevent excessive volatilization and oxidation of the metal by local overheating.

When producing slabs for the manufacture of high-quality sheet or strip, the metal is often melted in low-frequency furnaces of the Ajax-Wyatt type. By using furnaces of this type cleaner melting conditions can be maintained, alloying elements in the form of

hardener alloys or pure metals can be added directly to the bath, the constant stirring action in the melt ensures homogeneity of composition, and the metal can be cast directly from the furnace to the mould, since these furnaces are normally designed for tilting.

When manufacturing certain zinc alloy rolling slabs, particularly those with high aluminium and copper contents, gas- or oil-fired crucible furnaces are sometimes used. This method is very convenient where small tonnages are involved, particularly when the alloy composition and impurity limits are critical (as for zinc-aluminium alloys), since accurate control of melting conditions, bath temperature, and alloying additions can be maintained.

When slab casting is carried out at the works of the zinc refiners, remelting is often dispensed with altogether, the metal being taken directly from the holding furnace. This system can be recommended only when the refining process can be relied upon to produce metal of constant composition; otherwise the expense involved in remelting off-grade slabs would be excessive. Fortunately, modern methods of zinc refining, such as the refluxing system, produce high-purity metal of remarkably constant composition, but it is important, nevertheless, that the system of identification whereby slabs are correlated with sample analysis be unambiguous.

It is probably true that as far as control of mechanical and physical defects are concerned, melting conditions are less critical in the case of zinc and zinc alloys than with most of the other non-ferrous metals owing largely to the low solubility of the common gases in the metal. However, like some other non-ferrous metals and alloys, zinc is very adversely affected by the presence of certain impurities, and at this stage of production the main emphasis in the control of quality is on chemical composition.

3. CONTROL OF CHEMICAL COMPOSITION

(a) *Effect of Chemical Composition on Properties*

Broadly speaking, the chemical composition of zinc and zinc alloy rolling slabs is governed by the purity of the original metal, the accuracy with which alloying is carried out (where necessary), the extent of loss by volatilization or preferential oxidation, and by the degree of contamination that occurs during melting and casting. The purity of the grades of zinc normally available varies greatly and, depending on the concentrates used, the method of smelting, and the degree of refining, may contain up to 1.3% lead, 0.20% cadmium, and 0.08% iron, with much smaller quantities of copper, arsenic, and sometimes tin and bismuth. It may be added that several commercial grades of zinc are of a very high degree of purity, the metal produced by the electrolytic process reaching a purity of 99.9%+, while metal refined by the refluxing system is normally of a purity greater than 99.99%. The quality of metal selected for the production of rolling slabs is determined only partly by the properties required in the finished sheet, for the amount

of certain impurities that can be tolerated is limited largely by the effect such impurities have on the working properties of the metal, and this precludes the more impure grades from consideration.

Regarding the impurities normally present, lead has little effect on the rolling properties of zinc at normal hot-working temperatures, and up to 1.3% can be tolerated. In fact, up to 1% is sometimes added as an alloying element but, whether present by design or as an impurity, it is liable to segregate when the concentration is greater than 0.9%.

The solubility of lead in liquid zinc at temperatures near the freezing point is 0.9% and, consequently, when more than this amount is present in the melt, a second, lead-rich, liquid is formed which, being of greater density, segregates downwards. Obviously such alloys require adequate mixing and, in melting, considerable advantage is derived from the use of the low-frequency induction furnace.

Iron is considerably more objectionable as an impurity in zinc. The solid solubility of this element is about 0.002%,³ and quantities much in excess of this figure form an intermetallic compound, FeZn_7 , which, being finely dispersed, increases the hardness and reduces the ductility. This leads to excessive edge-cracking during hot rolling, and the concentration of this element is therefore kept as low as possible; 0.02% is the normal maximum for commercial-quality sheet, but, because of its effect on mechanical properties, it is limited to about 0.006% in sheet and strip for deep drawing, &c.

The presence of iron adds further complications in alloys of zinc and aluminium. In this alloy system equilibrium conditions in the melt are such that an intermetallic phase FeAl_3 or Fe_2Al_5 is precipitated at a very low concentration of iron. The density of this phase is about half that of the liquid alloy (with aluminium of the order of 3-5%) and, consequently, it separates rapidly at the surface of the melt. If the alloy is held quiescent in the pouring ladle for any length of time, the total iron content will be concentrated in the first few slabs poured (or in the last when a ladle with a bottom outlet is used) and the aluminium content of the slabs would also be increased somewhat. The trouble can be eliminated by using a grade of zinc with a negligible iron content when making such alloys, and by incorporating a mechanical stirrer in the pouring ladle.

The tin content of zinc and zinc alloy rolling slabs must be of a very low order; the element should preferably be absent altogether. The metal crumbles during hot working when 0.004% tin or more is present, and even 0.002% causes an undesirable amount of edge-cracking. The solubility of tin in zinc is very low, and it is probable that with certain other impurities present, it forms an intercrystalline envelope of a eutectic, the melting point of which is near the temperature of hot working. The effect of the presence of tin on the corrosion-resistance of certain zinc alloys is discussed below.

The effect of arsenic and bismuth on the rolling

properties of zinc is similar to that of iron, and consequently these elements should be excluded, as far as possible, from metal that is to be hot worked.

Cadmium has a considerable solubility in zinc, and is known to exert a pronounced influence on the work-hardening properties of the sheet. If a dead-soft material is required, the cadmium content is limited to about 0.020%. The influence of the metal as an impurity on the corrosion-resistance of zinc alloys is also discussed later below.

Because of its effect on the work-hardening properties of zinc, cadmium is sometimes added in alloying proportions, particularly where a stiff, resilient sheet is required. Sheet for the manufacture of engraving plates has already been quoted as an example, but material for the production of certain types of battery cans also contains this element; its presence in sheet for this application is reported to prolong the storage life of the battery. Cadmium may be added to the melt as pure metal or as a cadmium-zinc alloy. It promotes the formation of a tenacious oxide film on the surface of the melt, which may be carried into the casting under conditions of turbulent pouring. The point is referred to in Section 4 (b).

Magnesium is not a naturally occurring impurity in zinc, but small quantities may be introduced by contamination during melting, e.g. by the inclusion of zinc alloy scrap containing magnesium. The presence of this element in any grade of zinc other than the highest-purity metal is very objectionable, since, with the lead that is normally present as an impurity, it forms the intermetallic compound Mg_2Pb , which segregates at the grain boundaries. This compound is rapidly decomposed by moist air at room temperature, and consequently its presence might bring about embrittlement or disintegration of the sheet if stored or used in damp conditions. Practical experience indicates, however, that this trouble is unlikely to occur unless both lead and magnesium are present in amounts exceeding about 0.02%.

Apart from consideration of their effect on rolling properties, the percentages of lead, tin, cadmium, and bismuth must be of a very low order in alloys of zinc containing aluminium, since the presence of these impurities promotes intercrystalline corrosion, which takes the form of exfoliation of the surface of the sheet with general embrittlement. When preparing these alloys, therefore, only the highest-purity metal must be used, and the impurity elements must be limited to lead 0.005% max., cadmium 0.005% max., bismuth 0.005% max., and tin 0.002% max.

Although small amounts of copper are sometimes found in zinc as an impurity, its main importance to the present subject is as an alloying element. Certain binary zinc-copper alloys are of limited commercial importance, but copper is more commonly used as an alloying element in zinc-aluminium-copper alloys. These possess considerable strength and hardness, their main use, in the form of rolled plate, being for the manufacture of blanking dies and forming tools for sheet-metal work.

(b) Means of Control of Chemical Composition

Virgin zinc is normally obtained from established smelters in standard grades, the chemical compositions of which are reasonably constant. When several grades of metal are obtained for subsequent blending, storage should be systematic and particular consignments should not be issued for melting until the smelters' analytical figures are known. Samples from a percentage of consignments are normally sent for check analysis, the actual percentage varying with the consistency of the metal normally obtained. The system whereby rolling slabs of constant composition are obtained by blending several grades of zinc has already been mentioned.

The return of process scrap to the melting shop must be supervised with care, and every precaution must be taken to prevent contamination of the charges with other metals. Iron and steel can conveniently be separated by means of magnets, and copper-rich material is easily identified by the characteristic colour. No satisfactory means are available for the removal of such a material as solder, and consequently it is necessary to ensure that no possibility exists of the inclusion of solder-containing scrap. The point is of particular importance because of the sensitivity of zinc to a very small degree of contamination by tin and of the fact that large quantities of zinc sheet are used in the manufacture of battery cans, some of which are fabricated by soldering. Where this and other methods of fabrication are employed, it is usual to segregate the soldering activities as far away as possible from other operations and to use the scrap metal for the manufacture of such products as zinc chloride.

Sheet scrap is normally formed into bundles of convenient size by means of a power press. This makes handling and charging considerably easier, although, from the point of view of quality control, the main advantage is that oxidation during melting is greatly reduced.

Scrap from external sources is not often used for the production of rolling slabs, but when this is necessary the material should, after sorting, be melted, cast into ingots, and analysed. Metal slightly off-grade can be added to charges in very small quantities, provided that the dangers of such a procedure are realized.

Because of the trouble associated with the pick-up of impurities, it is desirable that zinc-sheet production, and certainly casting operations, be carried out in a separate section of the works. This is normal practice with the larger manufacturers, but is not always possible with firms engaged in the rolling of a number of non-ferrous metals or alloys, particularly where zinc rolling comprises a minor proportion of the total activities. Fortunately, the effects of contamination are widely known and often become apparent at an early stage.

In the melting stage it is important to keep the bath temperature as low as possible to reduce oxidation and volatilization. A flux cover is not normally used during melting, but a cleaning flux is sometimes

added to the ladle (or to the bath in the case of small furnaces casting directly into the moulds) and skimmed before pouring begins. Fluxes consisting mainly of ammonium chloride and zinc chloride are quite satisfactory; a number of proprietary fluxes are also available. The main purpose of the flux is to facilitate the separation of oxide and dross from the metal and to clean the surface generally.

The treatment of certain zinc alloys with chloride-containing fluxes is undesirable, since such materials tend to remove magnesium and aluminium.

The importance of adequate and continuous stirring, particularly of charges containing a high percentage of lead or aluminium and iron, has been discussed in the previous section (p. 368).

The procedure adopted for the sampling of melts varies considerably with local conditions. With large furnaces melting commercial-quality metal on a continuous system, a sample is taken to represent a weight of metal charged, and, since such a sample does not represent a specific mass of metal, the frequency with which such samples must be taken to ensure adequate control can be decided only by experience. Naturally, samples are taken at more frequent intervals when impurity contents approach limiting values. When small furnaces are used for the production of zinc alloys a sample is usually taken to represent one charge, but, when working with raw materials from reliable sources, a proportion only of the samples is actually analysed. All melts of zinc alloys containing aluminium are analysed because of the critical effect of impurities on the resistance of such alloys to intercrystalline corrosion. Apparatus capable of producing results rapidly, such as the spectrograph, is particularly useful for the control of composition in zinc melting, since, if necessary, the charge can be held while samples are analysed or, if casting proceeds, the results should certainly be available by the time the slabs are required for rolling.

4. CASTING

It appears that a greater variety of methods are used for the production of rolling slabs in zinc than in any other metal; no particular method can be used universally, however, and the actual procedure adopted is governed by the following considerations:

- (i) Standard of excellence required.
- (ii) Type of metal or alloy involved.
- (iii) Size of slab required.
- (iv) Whether the slab is for sheet or for strip production.
- (v) Output required.
- (vi) Cost of equipment.

The standard of excellence is, of course, always a factor of primary importance, but it does not follow that the methods of casting used commercially are those that will produce the most perfect slab. The choice finally rests with the method that will produce a slab of sufficiently high quality for a particular purpose

at the lowest cost, and since a considerable quantity of zinc sheet is used as "commercial ironmongery", an approach to perfection in such cases is not practicable.

In this section "control of quality" is treated by outlining the methods of casting used commercially, considering the principles involved, indicating the limitations and inherent deficiencies in the methods, and describing the means adopted to minimize the slab defects occasioned by these deficiencies.

(a) *Slab Casting in Horizontal Moulds*

The method of casting most commonly employed in the zinc-rolling industry is that involving the open-top horizontal mould. These moulds, which are normally constructed of cast iron, are mounted horizontally on a revolving table and filled by means of a hand ladle in the case of small slabs or from a pouring ladle slung from a gantry crane when larger slabs are required. The size of slab produced is governed by the dimensions required in the finished sheet and by the power of the mill; when necessary, variations in dimensions can be made by inserting liners to reduce the length and width of the standard mould or by varying the height of metal poured. Means of cooling the mould are normally provided; these take the form of water sprays directed upwards against the bottom or cooling fins extending downwards from the base into running water. By these means the mould temperature can be controlled fairly accurately, figures within the range 100°–160° C. normally giving satisfactory results.

Under these conditions of casting solidification takes place mainly from the bottom upwards, and to a lesser extent from the sides inwards, and, since the characteristic feature of the solidification of zinc is strong columnar crystal growth, the final structure of a slab cast in this way comprises large columnar crystals extending from the base almost to the free surface, with shorter crystals extending from the sides, parallel to the free surface. The effect of crystal structure on rolling properties is discussed in a later section.

In slabs cast by this method, the shrinkage that takes place on solidification causes the formation of a depression or sink in the upper surface of the slab or, if this surface solidifies before the interior, a shrinkage cavity is formed below the surface. These features become more marked with increasing slab thickness, and both are undesirable, particularly the latter. Owing to the fact that the upper surface is rarely continuous, the surfaces of the cavity become oxidized, and consequently will not weld together on rolling. This normally results in blistering of the sheet surface or the formation of a series of cracks below the surface. A certain degree of sinking can be tolerated, since it often becomes "ironed out" during the first few passes, but it sometimes happens that a considerable amount of "sponginess" occurs at the centre of the sink (caused by oxidation and shrinkage) which may persist as an area of poor surface in the finished sheet.

Sinking of the free surface can be minimized to some

extent by placing a sheet of asbestos on top of the mould immediately after casting (the oxide film having first been skimmed from the surface), but better results are obtained by using a hot top. This consists of a steel cover, lined with refractory material, dimensioned to fit over the top of the mould and furnished with electrically heated elements concentrated near the sides. The power is turned on some time before the metal is cast, and when pouring is complete the cover is placed in position. By keeping the surface liquid for a longer period, freezing is more likely to take place uniformly from the bottom upwards, and the possibility of a surface sink occurring is correspondingly minimized.

A second method of avoiding surface sinks is illustrated by the Erichsen mould. This, in its original form, comprises a water-cooled copper base and a rectangular detachable frame, fitted with heating elements, which forms the sides of the mould. The sides are brought to a suitable temperature before pouring, and it is not necessary to cover the top during solidification. The metal freezes progressively from the bottom upwards, the edge-chilling being negligible, and consequently there is little tendency for sinks to form in the top surface. Zinc-aluminium-copper alloys were cast in this way in Germany during the war, and the quality of the products was reported to be very good, the surface being absolutely smooth and free from shrinkage. There are, however, difficulties associated with the casting of unalloyed zinc slabs in the Erichsen mould. Because of the severe chilling action of the water-cooled copper base, the formation of cold shuts at this surface is difficult to avoid and, in addition, the steep temperature gradient within the solidifying slab promotes the formation of long columnar crystals. Increasing the metal pouring temperature to minimize the occurrence of cold shuts (which can be done when casting zinc-aluminium-copper alloys) increases the size of the columnar crystals with attendant complications in the breaking-down stage of rolling, but the incidence of both defects can be reduced by substituting cast iron for copper in the base-plate.

This method of casting is not often used for the production of rolling slabs, but it would appear to offer some advantage when large slabs, substantially thicker than those normally cast in horizontal moulds, are required.

The formation of a surface sink is promoted by the existence of a steep temperature gradient within the solidifying slab, and consequently a pouring temperature as near as practicable to the freezing point of the metal or alloy and a mould temperature sufficiently high to prevent rapid edge-chilling are desirable. For fairly pure grades of zinc a metal temperature of about 460° C. and a mould temperature of 120°–140° C. would be satisfactory, provided that the rate of pouring is adequate. Pouring at too low a metal and/or mould temperature, particularly with slabs of large superficial area, frequently results in the formation of surface laps. This danger can be minimized

by tilting the mould slightly at the beginning, so that the edge remote from the ladle is raised an inch or two. The mould is returned gradually to the horizontal position as pouring continues, and thus a metal front of some depth gradually moves across the mould bottom. Water cooling is delayed until pouring is complete. Unfortunately, this method of casting tends to favour the formation of edge laps at the two corners nearest the point of pouring.

The main advantages of the horizontal mould are the low cost, the simplicity of the design, the ease with which slabs can be ejected, and the small restraint to linear shrinkage that is imposed upon the cooling slab. Regarding the last point, the large columnar crystals that form in zinc on solidification are so oriented that the basal plane of the crystal is at right angles to the surface of the casting, and it is known that the tensile strength of zinc crystals is lowest in the direction normal to the basal plane. It is evident therefore that unless the slab is free to contract away from the mould surface and to shrink evenly in all directions, the formation of surface cracks is highly probable. Maximum facility for such movement is afforded in the open-top horizontal mould, provided that the mould surfaces are maintained in a smooth condition. The use of a mould coating also assists; graphite or a suspension of one of the refractory metal oxides is often used.

(b) Slab Casting in Vertical Moulds

Provided that supervision of the casting operation is adequate and that means of minimizing surface shrinkage are adopted, sound rolling slabs can be produced by the horizontal casting method, but rigorous inspection of slabs is nevertheless necessary, as high consistency in quality cannot be expected owing to the considerable human factor involved. Other methods of casting, such as those involving a vertical mould, allow of a higher degree of control in the casting operations, and consequently such methods are adopted when consistency in slab quality is of major importance; e.g. in strip rolling, where the mill is working to a strict production schedule. Serious loss of production would result if a large percentage of slabs were found to be defective in batches cast in quick succession, particularly when it is inconvenient to maintain a large stock of slabs. Further, in modern strip mills, 10–20 slabs are rough rolled simultaneously, and, if one or more slabs in a particular batch gives trouble during rolling, the time schedule may be seriously upset and the result may well be the scrapping of a complete batch of slabs in an intermediate stage of breaking down owing to loss of heat.

The principles underlying vertical casting are comparatively straightforward. A section through a typical mould is shown in Fig. 1, where the ideal state is that molten metal is introduced into the mould at such a speed and temperature, and heat is extracted from the metal at such a rate, that the solidification front is maintained just below the molten metal surface. Under these conditions the temperature

gradient within the system is low, the tendency to form large columnar crystals is at a minimum, segregation is unlikely to occur, and a supply of molten metal is readily available to fill the shrinkage voids formed on solidification. Unfortunately, such conditions are difficult to attain in practice, and methods of casting embodying various degrees of compromise are adopted.

The most direct arrangement is that in which the mould is held vertically and the metal poured through a tundish into the mould. A modification is sometimes introduced in the form of a distributing tundish which results in several streams of metal falling into the mould in place of one large stream. There are various objections to this method: (i) a considerable amount of splashing occurs, with the result that beads of metal solidify on the mould walls and may persist in the slab as shallow cold shuts; (ii) owing to turbulence, oxide films and air may be carried deep

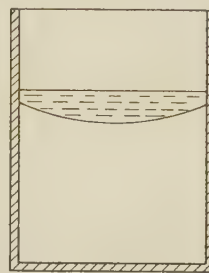


FIG. 1.—Ideal Conditions of Solidification in Vertical Moulds.

into the metal and may be entrapped between the growing dendrites; such inclusions would cause blisters or other defects in the finished sheet; and (iii) the weight of the stream carries hot metal well below the advancing liquid surface, and consequently freezing will proceed in a very irregular manner. The sides may freeze well ahead of the central portions, and bridging may occur across the upper area, while the lower centre is still molten. Feeding then becomes impossible, and shrinkage voids are formed within the slab or, if the shell is thin, the sides may collapse inwards, forming a surface sink. It may be added that, provided the walls of shrinkage cavities are clean and free from oxide or other films, they may weld up during rolling, but their presence is a considerable source of weakness, possibly causing trouble during the breaking-down stage, and is generally objectionable. Further, a central vertical column of molten metal is undesirable, since this allows segregation in a vertical direction to take place more easily. This is not very important, of course, when high-purity zinc is being cast. This method of casting is not often used for the production of zinc rolling slabs at the present time.

Some improvement is obtained when the mould is mounted on trunnions and tilted at the start of pouring so that the metal runs down the narrow side. Splash is negligible, the degree of turbulence is greatly decreased, and the influx of hot metal disturbs a smaller

volume of cooling metal. The contour of the solidifying front of metal synchronizes more closely with the rising liquid surface, and the tendency to bridging and the formation of central shrinkage cavities is hence less. Two additional complications are, however, introduced by this method of casting. First the mould is brought to the vertical position during pouring and, unless this is done continuously and smoothly,

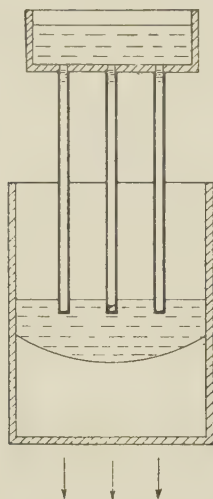


FIG. 2.—Method of Casting Designed to Minimize Turbulence. Contour of solidification front has been idealized.

surface laps may be formed at the short side remote from the metal stream or across the main surfaces of the slab. The rate of tilt should be so synchronized with the rate of pouring that a "tidemark" is not formed on the rising sides of the mould. Secondly, this system of pouring results in the side of the mould down which the metal is poured being considerably hotter than the corresponding opposite side, and consequently the metal solidifies preferentially on one side. This results in an unsymmetrical crystal structure and the concentration of the more fusible impurities near the hotter side, neither of which is particularly desirable. When pouring in this manner, metal may freeze in thin sheets on the mould surface adjacent to the stream, and these sheets may be washed into the mould later. Oxide films are thus introduced into the metal or, if the sheets are of considerable thickness and not remelted by contact with the molten metal, they form a defect akin to a cold shut.

A method used in Germany for the casting of zinc alloys and reported to produce good-quality rolling slabs appears to approach ideal casting conditions and will therefore be described briefly. The mould is of the conventional vertical type, either of "book" design or with a hinged bottom, and is mounted on a platform that can move in a vertical plane. The metal is poured through a tundish having three outlet tubes which extend almost to the bottom of the mould, the exit ports being at the lowest point of the tube wall, not at the bottom, and the mould is lowered con-

tinuously during the pour to maintain the port just below the liquid surface (Fig. 2). This method of casting appears to have several distinct advantages:

(i) The metal stream has minimum contact with the atmosphere, and consequently the possibility of oxide formation is reduced.

(ii) Provided that the tundish is kept full of metal, the possibility of introducing air or dross by turbulence is at a minimum.

(iii) Since the liquid metal enters the mould in a direction roughly parallel to the mould bottom, the solidifying areas below are disturbed to a lesser extent.

(iv) The rate of pouring can be accurately controlled by selecting stems of suitable diameter and, provided that the metal temperature and the rate of heat extraction from the mould are accurately adjusted, solidification should proceed along a front only slightly below the liquid surface.

Such conditions will minimize segregation and facilitate feeding and, since the possibility of introducing air and oxide is small, sound slabs should result. The main objection to this method of casting appears to be the provision of the moving platforms which, where large numbers of slabs are required, would add considerably to the capital outlay.

In this country, when slabs of the highest quality are required for the production of strip, Durville casting or a method akin to it is used. The Durville system of casting has been adequately described elsewhere, and when working with zinc of electrolytic purity, slabs of excellent quality of the approximate dimensions $30 \times 14 \times 2$ in. are produced with a very low rejection figure. The slab requires feeding from a hand ladle while solidification is in progress, and, if carried out effectively, only the top inch or two of the slab requires cropping.

The mould used in a method of casting that is somewhat similar to the Durville system is illustrated in Fig. 3. The mould is mounted on a horizontal axis,



FIG. 3.—Position of Mould During the Pouring Operation by the Method Similar to the Durville System.

and during the pouring operation it is inclined a few degrees from the horizontal, the open end being the higher. A few minutes after the end of pouring, the mould is brought to the vertical position and remains thus until solidification is complete. The top 25% or so of the slab is removed by cropping. The quality of slabs produced by this method is also extremely good.

In both these systems of casting the metal enters the mould in a comparatively tranquil state, and consequently the complications that result from turbulent pouring are virtually eliminated. However, even with the best combination of mould and metal temperature, a substantial volume of the metal is in the liquid state when the mould reaches the

vertical position, and there is, therefore, some risk of segregation occurring. This is not important when casting zinc of fairly high purity or the conventional rolling mixes, but it is doubtful whether either method would be particularly satisfactory for casting some of the zinc-aluminium-copper alloys, where one of the phases that may separate on solidification is of appreciably lower density than the liquid.

5. GENERAL REMARKS

(a) *Surface Cracks*

Contrary to the view sometimes expressed, it appears that surface cracks are comparatively uncommon in zinc slabs cast in vertical moulds. This may well be due to the care taken to ensure that the mould surfaces are maintained in a smooth state, as a roughened surface inhibits movement during cooling and thus promotes the formation of cracks. In addition, a shallow layer of equiaxial crystals, oriented somewhat favourably for slip to occur parallel to the mould walls, normally exists at the surface of the slabs and is, consequently, considerably more ductile than a structure comprising columnar crystals oriented with basal planes normal to the slab surface. This skin will deform when subjected to the stresses imposed by restraint to shrinkage, although cracks may occur in the underlying columnar crystals. Provided that this outer skin remains unbroken, thus preventing the entry of oxygen and other reactive gases, the fissures in the columnar crystals are comparatively innocuous, since they weld up during rolling.

(b) *Structure of Rolling Slabs*

Crystal structure is a point of primary importance in assessing the quality of rolling slabs, and considerable attention is normally directed to controlling grain-size, grain orientation, &c. The structure must be such that substantial deformation can be obtained at each pass in the breaking-down stage without the risk of excessive cracking, and this can normally best be accomplished when the structure consists of small equiaxial grains oriented at random, but under no conditions of casting that are commercially practicable can such a structure be obtained in zinc. Under normal conditions of casting the structure obtained comprises large columnar crystals, often extending from a plane near the surface to the centre of the slab, with a shallow layer of equiaxial crystals at the surface. The columnar crystals are so oriented that the basal plane is approximately normal to the surface,^{4,5} and it appears probable that, in the shallow outer layer, the orientation is such that the basal plane is parallel to the surface or within $\pm 15^\circ$ of this position.⁴ Much of the data necessary to analyse the mechanism of deformation in the hot rolling of zinc is lacking (such an analysis is in any case outside the scope of this paper), and consequently it is not possible to define with any degree of accuracy the most desirable structure in rolling slabs or to assess how far this

columnar structure is removed from the ideal. There is little doubt, however, that a coarse columnar structure in the slabs adds appreciably to the difficulties in the breaking-down stage of zinc rolling, and consequently attempts are made to decrease the size of the columnar crystals. Rapid chilling and inoculation with zinc dust⁶ bring about some improvement, and certain proprietary grain refiners are also used. The addition of small amounts of titanium brings about a considerable degree of grain refinement,⁷ but the presence of titanium has a marked effect on the mechanical properties of the finished sheet, and there is no evidence to indicate that this procedure has been adopted commercially.

(c) *Slab Surface Quality*

A higher quality of surface is required in zinc rolling slabs than in slabs of most other non-ferrous metals, since the former are not normally scalped. This operation is omitted partly to reduce cost, but mainly because the cutting action of the tool tends to tear the zinc crystals and thus form cracks. Alternatively, the removal of the outer surface of the slab by scalping may merely expose fissures that were already present in the underlying crystals.

(d) *Inspection of Rolling Slabs*

The most important point in the control of quality is to select methods of production that are fundamentally sound and capable of producing satisfactory slabs; the operations must be adequately supervised to ensure that the selected system is strictly followed. Inspection should include intelligent observation at the melting and casting stages, and any abnormalities such as excessive drossing, interrupted pouring, &c., noted; the castings involved should be treated as suspect.

The control of chemical composition has been discussed in an earlier section (p. 369). It is important that the system of identification whereby slabs are correlated with chemical composition be unambiguous, as otherwise the value of this aspect of control is lost.

Visual examination of slabs is invariably carried out, and products containing defects such as excessive sinks, surface cracks, laps, surface oxide inclusions, &c., can be segregated in this way. When cropping is carried out by sawing, examination of the exposed surface may be used to assess the probable degree of internal soundness. Radiographic examination of a proportion of slabs as a means of quality control is not common practice, but is to be recommended particularly where the castings are transported over a considerable distance between foundry and rolling mill.

Sectioning slabs to assess internal soundness is normal practice when the casting procedure is being developed or modified, and is frequently used for routine inspection when trouble from this source is encountered. Behaviour during rolling as a means of routine inspection can be very costly, since a "suspect" slab may damage equipment by its erratic

behaviour. However, the presence of a serious defect usually becomes evident during the first few passes, and the particular slab can be rejected before any serious trouble occurs.

Examples of internal defects in a vertically cast rolling slab of 2 in. thickness are shown in Figs. 4-8 (Plates LII and LIII). Fig. 4 is a reproduction of a radiograph taken through an area of the slab in which interdendritic shrinkage has occurred, and Fig. 5 is a photograph of a vertical section through this area. It will be observed that the interdendritic shrinkage has affected a considerable volume of metal.

A defect in a rolling slab caused by entrapped gas, secondary piping, or a combination of both is shown in Figs. 6 and 7, the former being a print from a radiograph and the latter a photograph of a horizontal section through the affected area.

The macrostructure of a vertically cast slab is shown in Fig. 8; the crystals are predominantly of the columnar type and the dendritic structure is very evident. Interdendritic shrinkage can be seen in the area at the left-hand end of the photograph which corresponds approximately to the centre of the rolling slab.

III.—EXTRUSION BILLETS

1. RANGE AND REQUIREMENTS OF PRODUCTS

Virtually all the extrusion billets cast in this country are used for the production of rod that is subsequently drawn to wire for use in the zinc-spraying process or, in finer gauges, for the production of woven brake linings. In the former application the main requirements are high resistance to corrosion, combined with sufficient strength and ductility to withstand the stresses encountered during the drawing operation. Wire produced from metal of purity greater than 99.99% (B.S. 1003) fulfils these requirements.

The finer wire, normally 32 S.W.G., for the production of woven brake linings, must also possess high resistance to corrosion and, apart from the additional stress encountered in drawing to this gauge, must be sufficiently strong to withstand the not inconsiderable shock loading that is imposed in the weaving process. The high-purity metal can be used for this application also, but because of the danger of grain growth after excessive cold work, small proportions of other metals are sometimes added as grain-growth inhibitors. The problem is similar to that encountered in the rolling of foil in high-purity zinc, where excessive grain growth may cause severe embrittlement. This is because the temperature of recrystallization in zinc is a little above room temperature and decreases with increasing degrees of cold work. As in the case of foil, the addition of small quantities of manganese inhibits crystal growth; the presence of other metals in small proportions has a similar effect, but complications may be introduced by the effect of such metals on hot-working properties and resistance to corrosion.

Apart from correct chemical composition, the main requirements of these extrusion billets are freedom from internal unsoundness, such as piping or shrinkage, and freedom from gross surface defects; shallow surface defects are not particularly important, since the outer shell of the billet is left in the extrusion press. The crystal structure, and hence the mechanical strength of the billet, is of less importance, since, unlike rolling slabs, the casting is supported on all sides during the hot-working process.

2. MELTING

At the authors' works, high-purity zinc extrusion billets are cast in metal taken from the holding bath of the "refluxer" (which produces high-purity zinc by fractional distillation). This method of refining produces metal to specification B.S. 1003 with remarkable consistency, and the routine system of sampling and analysis (spectrographic) is adequate to ensure that all billets conform to specification requirements, typical analytical figures for the metal being lead 0.002%, iron 0.002%, cadmium 0.001%, and other impurities present in traces only. All billets are stamped with a serial number so that they can be correlated with the relevant sample and are segregated until the results of analysis are known.

The metal for billets from which the fine wire is made is melted in crucible furnaces of approximately 1 ton capacity, and the required amount of manganese added as a zinc-5% manganese hardener. A sample from each melt is analysed, but this is not a particularly arduous system of control, since the alloying constituents and the impurities can be determined by means of the spectrograph.

3. CASTING

To a large extent the problems associated with the casting of extrusion billets are similar to those already discussed in connection with the casting of rolling slabs in vertical moulds, but three additional points must be taken into consideration: (i) The ratio of height to cross-sectional area is normally somewhat greater in the case of extrusion billets, and greater precautions must therefore be taken to prevent internal unsoundness, since the problem of ensuring adequate feeding is considerably more complex with castings of such shape. (ii) For reasons already stated, less importance attaches to surface quality provided that the defects present are comparatively shallow. Methods of casting can therefore be selected primarily to ensure internal soundness even when this involves some sacrifice of surface quality. (iii) The presence of large columnar crystals is less objectionable in billets than in rolling slabs, the reasons for this having already been indicated. Billets may therefore be allowed to cool more slowly and, if cooling is controlled so that the upper portion remains liquid while the bottom solidifies, feeding is facilitated.

It may be mentioned here that from the point of view of control of quality, the main problem in billet

casting is to prevent the occurrence of secondary piping, i.e. piping in the lower portions of the billet; primary piping can usually be prevented by feeding from a hand ladle, an operation that requires some degree of skill.

The mould used for casting extrusion billets consists of a cylinder of length 36 in. and internal dia. 5 in., the material of construction being good-quality grey cast iron; the bottom is detachable and the bore is tapered slightly to facilitate ejection of the billet. The upper half of the mould is lagged with asbestos sheet to ensure slower cooling of the metal in this area both by retaining heat in the mould walls between casts and by reducing the rate of heat loss when the mould is full and the metal solidifying. No dressing is used, but the mould walls are brushed between casts.

In the actual casting operation the mould is vertical and the metal poured through a tundish; pouring is completed in approximately 1 min., and feeding from a hand ladle is continued for approximately 10 min. Satisfactory results are obtained with a metal temperature of 450°–460° C. and an average mould temperature of 80°–100° C.

It is essential that the tundish be located accurately, since, if it is off-centre, the metal will impinge on the mould wall, causing a relatively deep defect in the billet surface. The tundishes inevitably receive rather rough treatment during service and, to ensure uniformity of casting conditions, they must be well maintained and replaced when necessary.

Although it departs from the theoretical ideal in several respects, this method of casting produces very satisfactory billets, and the percentage rejection is low. The large metal fall is undesirable in that it causes considerable splash, produces turbulence, and disturbs the progress of solidification at the lower areas. The surface defects that result from splashing are comparatively shallow, and are rarely sufficient to justify rejection of the billet. By keeping the tundish full, the entry of oxide and dross is largely prevented, but air is undoubtedly introduced by turbulence. However, it appears probable that pouring is complete before solidification has proceeded very far, and consequently the included air can coalesce and escape to the surface. Undoubtedly the lagging of the upper half of the mould reduces the rate of solidification in this area, and thus facilitates feeding of the lower centre. This method of casting is perfectly satisfactory for the production of billets in pure zinc or single-phase alloys, but an undesirable amount of segregation would probably occur if it were used with some of the more complex alloys.

The macrostructure of a billet of high-purity zinc cast in this manner is shown in Fig. 9 (Plate LIII). The working properties of such a billet are quite satisfactory, although the structure is obviously coarse and strongly columnar.

When casting billets in zinc alloys, a more satisfactory method is one similar to that described previously for the casting of slabs (Section II, 4 (b)), where the tundish has an extended stem and the mould is lowered continuously during pouring. This system was used in Germany during the war.

The system known as chill casting may also be used. The moulds are constructed of steel sheet of about 14 S.W.G. and are placed in tanks fitted with a water inlet at the bottom and an exit near the top. The moulds are filled and the water turned on so that the level rises slowly in the tank to a point about 6 in. below the top of the mould. Solidification takes place progressively and rapidly from the bottom, thus decreasing the possibility of segregation and facilitating feeding.

4. INSPECTION OF BILLETS

The high-purity zinc and zinc-manganese alloy billets are cropped to 30 in. before despatch, the cropped ends being remelted. Most of the billets are despatched without further treatment, but since they are cut into 15-in. lengths before extrusion, one in ten is cut in half before despatch and the exposed surfaces examined to assess internal soundness. Should a pipe be revealed on cropping or halving, the billet is rejected and a number on either side of it are rigorously examined for piping so that the extent of the trouble can be ascertained. The surface of the billets is also carefully inspected, and billets containing gross surface defects are rejected. The number of billets rejected owing to piping or surface defects is normally very low.

ACKNOWLEDGEMENTS

The authors acknowledge with gratitude the assistance received from the following firms in compiling this paper: The Hall Street Metal Rolling Co., Ltd., The Ever Ready Co. (Great Britain), Ltd., and Enfield Rolling Mills, Ltd. Their thanks are also due to the Directors of Imperial Smelting Corporation Ltd., for permission to publish the paper. The photographs and radiographs were taken by Mr. D. Challen and Mr. G. Ludwell.

REFERENCES

1. —, *B.I.O.S. Final Report No. 1159*, 1947.
2. —, *Metals Handbook (Amer. Soc. Metals)*, 1948, 1239.
3. E. C. Truesdale, R. L. Wilcox, and J. L. Rodda, *Trans. Amer. Inst. Min. Met. Eng.*, 1936, 122, 192.
4. G. Edmunds, *ibid.*, 1941, 143, 183.
5. L. Northcott, *J. Inst. Metals*, 1937, 60, 229.
6. J. A. Reynolds and C. R. Tottle, *ibid.*, 1951–52, 80, 93.
7. E. A. Anderson, E. J. Boyle, and P. W. Ramsey, *Trans. Amer. Inst. Min. Met. Eng.*, 1944, 156, 278.

THE CONTROL OF QUALITY IN THE MELTING AND CASTING OF ALUMINIUM ALLOYS FOR WORKING *

1452

By R. T. STAPLES,† MEMBER, and H. J. HURST †

SYNOPSIS

The special problems arising in the melting and casting of aluminium alloys and the best methods of quality control are considered in relation to nine standard groups of alloys intended for use in wrought forms.

The effects of the alloying additions and of impurities and incidental contaminants on foundry practice, on the setting up of standards of quality, and on the ultimate properties of the material, are treated under the specific alloy groups.

The limitations of the melting and casting processes available, and in particular of the direct-chill casting method, are outlined, and the degree of control which it is possible to exercise through routine physical and chemical inspection at the various stages is indicated.

I.—INTRODUCTION

THE preparation of cast blanks for extrusion, rolling, or forging entails problems which do not arise in the metallurgically simpler case of shaped castings, e.g. gravity die-castings, since the material must combine the requisites—seldom similar—for both casting and working. Foundries producing cast forms for working are called upon to supply these in alloys developed not primarily for their casting characteristics, but rather for their hot- and cold-working properties and for their good mechanical properties in the as-produced or heat-treated condition. Moreover, the requirement that the wrought material, both in the intermediate processes and in its final form, should approximate as closely as possible to the ideal elastic-plastic state imposes a restriction on the use of alloying additions which often detracts from the casting qualities. In the absence of an ideal casting process, standards of control must, therefore, be limited by the scope of the methods available, the use for which the material is intended, and economic considerations.

Since the war, a series of specifications has been drawn up by the British Standards Institution, in collaboration with the industry, to cover wrought aluminium alloy products for general engineering and Service requirements. Typical alloy compositions are set out in nine groups in Table I. Many of the variations in alloy content are very slight.

The problems of successful manufacture are increased by the fact that these nine alloy types are required in a wide diversity of cast forms, namely:

- (i) rolling slabs;
- (ii) extrusion billets;
- (iii) cast forging uses;

- (iv) wire-bars;
- (v) hollow billets for tube manufacture;
- (vi) slugs for impact extrusion;
- (vii) stock for rolled sections.

To meet specific demands it is usual to select a particular form and type of alloy, rather than to adopt the alternative of varying the quality of any one alloy or form at the casting stage. The aim of the foundry must be to produce consistently the best quality in every case, since the overriding requirement is that the material should meet the needs of the working process. Some scope as regards control of quality lies in the choice of melting and casting methods, and where more than one method will produce workable material, economic considerations will be decisive.

As the complexity of the alloy system increases, the limitations imposed by the fact that insufficient eutectic is available to ensure soundness tend to disappear,¹ but the higher alloying additions may be associated with segregation or gross intermetallic forms which give trouble in working. In some cases, owing to the solution-age-hardening effect typical of these alloys, hot or cold stress-cracking may result if the direct-chill-casting method is used. Of the wrought materials at present being produced, the aluminium-zinc-magnesium-copper group is the most prone to this type of failure.

The relation between the tendency to crack during freezing and alloy composition has been well demonstrated by the work of the Aluminium Development Association's Welding Research Team at Birmingham University.² The behaviour of the materials studied by these investigators under critical welding conditions has been found to be a reliable guide to the behaviour of similar material when cast in large sections under

* Manuscript received 5 December 1952. Contribution to a Symposium on "The Control of Quality in the Production of Wrought Non-Ferrous Metals and Alloys. I.—Melting and

Casting", to be held in London on 25 March 1953.

† T.I. Aluminium, Ltd., Birmingham.

conditions of accelerated freezing. The employment of high freezing rates is peculiar to the casting of wrought alloys, being necessitated in part by the large products involved, up to 500 in.² cross-section, and in part by the need to minimize segregation and suppress the formation of large constituent particles.

The following examples illustrate these points: (a) The simple binary aluminium-magnesium alloy is of the solid-solution type, exhibiting nearly ideal properties in the wrought state in all forms, but as a casting alloy it has an insufficiently long freezing range to permit large-section castings to be made free from shrinkage. In the preparation of large

avoidance of oxide in any form. Oxide in the grosser state can lead to failure during working, in a finer state to rejection of the semi-finished product, and in the most highly dispersed forms may result in premature failure of the final product. There is some evidence³ to suggest that oxide films, even of molecular thickness, strongly influence recrystallization, and so play a vital part in determining metallurgical properties. Therefore, if high quality is to be ensured, oxide formation in melting and casting must be strictly controlled.

The charge may prove a major source of oxide. With reverberatory furnaces, the melting loss may be

TABLE I.—Typical Compositions of Main Groups of Wrought Aluminium Alloys.

Group No.	Alloy Type	Alloying Additions or Impurities *									British Standard Designation
		Mg, wt.-%	Cu, wt.-%	Zn, wt.-%	Si, wt.-%	Fe, wt.-%	Mn, wt.-%	Ni, wt.-%	Ti, wt.-%†	Cr, wt.-%	
1	Commercially pure Al	0.05	0.10	...	0.12	0.25	0.05	1
2	Al-Mn	0.05	0.10	0.10	0.25	0.60	1.0-1.3	N3
3	Al-Mg	1.8-2.3	0.10	0.10	0.20	0.40	0.15-0.35	N4
		3.0-3.5	0.07	0.10	0.20	0.40	0.35-0.55	N5
		4.0-4.5	0.05	0.10	0.20	0.30	0.35-0.55
		4.6-5.3	0.05	0.10	0.20	0.20	0.15-0.35	N6
		6.5-7.0	0.05	0.05	0.20	0.20	0.15-0.35	N7
4	Al-Mg-Si	0.50-0.70	0.10	0.10	0.4-0.7	0.50	H9
		0.80-1.0	0.10	0.10	0.7-0.95	0.40	0.15-0.25	H10
5	Al-Cu-Mg	0.7-1.0	4.0-4.8	0.10	0.4-0.7	0.4-0.7	0.5-0.9	0.10	H14
6	Al-Cu-Mg-Si	0.55-0.85	4.2-4.6	0.10	0.65-0.9	0.3-0.6	0.65-0.85	0.10	H15
7	Al-Zn-Mg-Cu	2.2-2.7	1.2-1.5	5.5-6.0	0.15	0.40	0.25-0.30
		1.8-2.2	1.5-2.0	6.6-7.4	0.25	0.40	0.1-0.30	0.10	...	0.05-0.15	...
8	Al-Cu-Ni-Fe-Si	0.7-1.1	1.9-2.2	...	0.9-1.1	0.9-1.1	0.10	0.9-1.3	0.15	...	H12
9	Al-Si-Cu-Ni-Fe	0.8-1.2	0.7-1.0	...	11.0-11.5	0.4	0.10	0.7-1.3	0.10

* Alloying additions are printed in heavy type; other figures represent maximum permissible contents of impurities.

† Grain-refining agent; may be present in 0.01% content range.

rolling slabs, shrinkage may occur either at the mid-section or at the surface, depending upon the precise freezing conditions. To avoid both these faults calls for closely controlled foundry techniques. (b) Similar difficulties are encountered in the ternary group based on aluminium-magnesium-silicon, which are particularly versatile in the wrought state. The disparity between the requirements for working and those for casting is shown by the fact that the wrought forms have compositions approximating to aluminium-1% magnesium-1% silicon, whereas the cast material contains 2½% silicon or more.

II.—MELTING

1. BASIC PRINCIPLES

(a) Inclusions

The mechanical and chemical cleanliness of the metal can be controlled only in the liquid state, and in this respect the outstanding requirement is the

as much as 10% when fines are charged, as against 2.5% when melting pig and heavy process scrap.⁴ Such losses may be affected by the surface condition of the stock. If corrosion products are present on the solid charge, then a significantly higher melting loss due to oxides will occur; moreover, owing to the particularly objectionable form the oxide films can take, more difficulty will be found in removing them from suspension in the melt.

Another main cause of oxide formation is the reaction of the products of combustion of reverberatory furnaces with the surface of the melt, though this may be minimized by maintaining, as far as practicable, a non-oxidizing atmosphere over the hearth. The present authors' experience with a wide range of furnaces, variously fired, suggests an overall loss of about 2.5%, as practical considerations limit the degree of control that can successfully be exercised. Covering fluxes, which are discussed in more detail in Section II, 3, may be used to protect the melt from oxidation.

If a serious attempt is to be made to suppress oxide formation during melting, induction-heating methods must be employed. Although considerably lower figures for metal loss can be obtained by this means, the expected improvement in quality does not necessarily result, as the marked degree of turbulence caused by convection currents tends to retain the oxide entrapped in the melt. A separate settling operation in a radiant-heated holding bath is therefore needed to produce metal of adequate cleanliness.

With reverberatory melters, either of the batch or continuous type, the same necessity for holding arises, but in general a holding time is inherent in the process. In the present authors' opinion the value of holding is unquestionable. This view, however, is not fully supported by other producers, owing no doubt to the subtle variations in the form of oxide inclusions that may occur with different techniques.

Common inclusions, other than simple oxide films, which may be present, are :

	Density, g./c.c.
Al ₂ O ₃ (corundum)	3.95-4.10
Al ₂ O ₃ .MgO (spinel)	3.50
SiO ₂ (quartz)	2.65

In reverberatory melting these conglomerates of compound oxides are formed on the surface of the melt by thermit reaction; hence the first operation in removing them is surface fluxing and skimming. The accumulation of residues at the bottom of the bath indicates that, as might be expected from their densities, some of the conglomerates leave the surface and settle, at a rate determined by their form and composition.

The tapping method selected—either decanting or bottom tapping—depends on whether experience confirms that the undesirable oxides are retained at the surface, or penetrate the skin and enter the melt. The practice favoured in the authors' works consists of bottom tapping to discharge the metal, coupled with the use of low temperatures and adequate surface fluxing. The exigencies of production have not always permitted a detailed study of these inclusions, and their composition and origin may be other than those suggested above, as is demonstrated by the fact that considerable difficulties have been encountered from time to time with the products of low-frequency furnaces.

An outstanding variation which has been noted is the presence of manganese carbide in a manganese-rich alloy, the carbide originating in the manganese metal, which was produced by a thermal-reduction process. Because of the physical characteristics of the carbide, its presence gives rise to all the undesirable features commonly associated with inclusions of the spinel or corundum type.

The preparation of metal free from inclusions has been dealt with at some length because no single in-line technique for controlling quality is known, and use must therefore be made of basic production methods for the successful elimination of these harmful constituents.

(b) Control of Gas Content

A review of experience covering melting in furnaces of the crucible, electric-resistance and electric-induction, coal-fired, coke-fired, oil-fired, town-gas, and producer-gas-fired reverberatory types, indicates that metal with a low gas content can be produced independently of the heating medium employed, the governing factor being the attainment of metal/gas equilibrium at the casting temperature. As in general the melting temperature must be significantly higher than the casting temperature, an adequate holding period at the latter temperature is essential, 1-1½ hr. being normally sufficient.

Here again, control is not aided by any laboratory test, once the melting and holding practice has been established, such methods as the Straube-Pfeiffer test being insufficiently critical to discriminate between metal which in its ultimate form will give rise to troubles associated with gas content, and a cast metal that will be trouble-free. In view of the known accuracy of such tests, it is probable that many of the defects, particularly of the final product, commonly attributed to gas, are not to be related to the gas content of the molten metal. If suitable holding conditions are provided, equilibrium gas contents can to a large extent be assured, and if the direct-chill-casting process is adopted, then the content will be further reduced by the automatic rejection of excess gas required to fulfil equilibrium conditions at the freezing temperature. In the direct-chill process, using open moulds, the molten pool above the near-horizontal freezing plane is so shallow that little resistance is offered to the escaping gas. In view of these easily applied controls, there is no necessity to carry out degassing, which offers little advantage when large volumes of metal, up to 20 tons, are being handled. On the contrary, turbulence resulting from degassing would have the undesirable effect of entrapping all types of oxide particles.

(c) Alloying

When alloying aluminium with a metal of high melting point, special techniques are necessary, if troubles due to high-temperature oxidation are to be avoided. Further, the fact that the alloying metals tend to have densities markedly different from that of aluminium leads to practical difficulties which must be solved if uniform quality of the product is to be ensured. The alloying elements can be divided into two groups: (i) those having densities lower than that of aluminium, viz. magnesium and silicon; and (ii) those having higher densities, the chief of which are copper, manganese, nickel, iron, zinc, and chromium. With the exception of magnesium, which is added in the pure state, these elements are pre-alloyed with aluminium in a separate operation to form binary or ternary alloys of sufficiently low melting point to allow of their introduction into aluminium at a temperature of approximately 750° C. As this pre-alloying must be carried out at a high temperature,

special furnaces must be used, in which the melts are adequately protected by surface flux.

Since no true refining process to eliminate impurities can readily be introduced in aluminium smelting, the purity of the original ingredients is of the utmost importance, if the purity and cleanliness of the final product is to be maintained. In discussing general alloying practice it should be pointed out that, while the introduction of a high percentage of clean scrap and/or secondary ingot is also determined by economic considerations, it is a common observation that furnace charges on this basis produce material which in casting and working gives a more consistent performance than that produced from melts made up of virgin aluminium and hardeners. This holds good despite the fact that no chemical or metallographic controls indicate any imperfections in the alloying and melting techniques employed for material from virgin melts.

2. FURNACES

(a) Induction Furnaces

Success in alloying, even with the most diverse additions, can be assured by using induction furnaces for melting. For bulk production of aluminium the low-frequency loop-type furnace is generally used. For alloys this type of furnace is unsurpassed, and when used in conjunction with resistance-heated holding furnaces, is capable of providing material of the highest possible quality. Its use does not, however, necessarily solve many of the fundamental problems confronting the fabricator; hence the decision to install such equipment is normally based either on economic or general practical considerations, e.g. under the latter head, cast sections and process scrap may be of such large dimensions that direct introduction into the melting unit is physically impossible. The logical use for these furnaces in the wrought alloy industry is for the recovery, with low melting loss, of light scrap and fines, i.e. sawing, scaling, and milling swarf, scrap foil, &c.

(b) Duplex Reverberatory Furnaces

Present-day fabricating plant and techniques call for large cast blocks, which can be produced economically only by using furnaces capable of melting up to 2 tons/hr. and with a hearth capacity of 10–15 tons. With such a quantity of metal melting and alloying become major physical and mechanical operations. Rabbling, necessary to achieve alloying, and fluxing, necessary to minimize oxidation, must be carried out at temperatures higher than those required for casting; the preparation of the melt should therefore be divided into two stages, alloying and holding, the latter being regarded as the refining process. A double-hearth furnace makes it possible to combine continuous melting at a steady rate with an alternate holding and casting cycle.

3. MELTING TECHNIQUES FOR THE PRINCIPAL ALLOYS

(a) Group 1: Commercially Pure Aluminium

The influences exercised by impurities on the properties of any pure metal are experienced to the full with aluminium. In order to satisfy the wide diversity of applications to which the material known as "commercially pure aluminium" is put, it is therefore necessary to select the raw material carefully, or to alloy on a scale that is significant in the pure metal range.

Material of 99.99% purity is prepared by a special process, and if the standard is to be maintained, furnaces with suitable linings must be used for melting and processing. Lower grades (99.8, 99.7, and 99.6% purity) are not the product of any electrolytic refining process, but are prepared by the remelter selecting pig of appropriate composition. Furnaces with clean hearths, if necessary washed out with aluminium of lower purity, are essential; and during melting the unnecessary introduction of furnace tools must be avoided, owing to the rapid solution of iron that takes place despite protective wash coatings. Pick-up from refractories is not normally serious, as a lining of aluminium oxide forms on the hearth during working. If metal of such purities is melted in solid-fuel-fired reverberatory furnaces, the silica contained in the ash may be carried over in the products of combustion and contaminate the melt. No such effects have been noted with oil-fired or washed producer-gas-fired furnaces.

A random melting of Canadian pig with process scrap will yield a purity of the order of 99.5%. The preparation of metal of this grade calls for the minimum control in the melting operation, other than the general precautions already stated. However, the change-over from 100% pig to a mixture containing pig and scrap demands plant control for the segregation of process scrap, and an analytical checking of the molten metal to confirm the absence of contaminants, or their presence within acceptable limits. In a foundry handling the full range of aluminium alloys for working, contamination by a number of elements may be expected. If virgin metals only are involved, these are likely to be confined to magnesium, copper, zinc, silicon, iron, manganese, nickel, titanium, and chromium, all of which are standard alloying elements. If secondary ingot or dealers' scrap is concerned, then a check must also be made for such elements as lead, tin, and antimony.

Aluminium of purity lower than 99.6%, although commonly known as "pure aluminium", should more accurately be described as aluminium-iron-silicon ternary alloys, since iron and silicon are deliberately added to achieve specific properties. The system falls into two subdivisions: (i) alloys intended for tube manufacture, in which the purity is held at an average of 99.2% to obtain a fine grain-size and an adequate strength; and (ii) alloys used

for sheet manufacture, where in order to avoid the formation of needle-like crystals of AlFe_3 , the iron and silicon are deliberately added in a ratio of 4:1, so that a complex is formed which will spheroidize at 570°C . In the preparation of all grades of pure aluminium, especially when casting the larger sections, addition of a grain refiner is desirable, if not essential. The most suitable refining agent is a proprietary one, based on boron and titanium salts, plus a percentage of hexachlorethane which provides nascent carbon as an end product of decomposition. Its high reactivity enables adequate grain refinement to be effected with trace quantities only of boron and titanium, which do not affect the general purity.

(b) Group 2: Al-Mn Alloys

As already stated, the first step to ensure satisfactory final quality in this material is care in selecting the manganese metal, as any carbide contained in it cannot be removed. Freedom from carbide is essential, as drawing operations can be adversely affected by the presence of these hard insoluble particles.

Melting is complicated by the fact that even when a 5 or 10% hardener is used, the rate of solution in aluminium is relatively slow at the normal melting temperature. It is therefore usual to increase the working temperature by 50°C ., to approximately 780°C ., unless the holding time can be prolonged. Solution of the manganese can be aided by gentle rabbling.

When first introduced, this alloy was probably regarded as binary. Casting by the direct-chill method revealed a proneness to hairline cracking, difficult to avoid owing to the limits of operational control. It was therefore decided to alter the composition of the alloy and to improve its fluidity by increasing the iron content from the variable amount present in virgin aluminium, typically 0.2%, to a controlled amount of 0.4%. The addition of a grain refiner is essential, as the alloy shows a pronounced tendency to form large grains during casting.

(c) Group 3: Al-Mg Alloys

The aluminium-magnesium group, with its wide solid-solution range, permits the preparation of a series of alloys having satisfactory mechanical properties combined with high corrosion-resistance and good workability.

Their melting gives rise to a problem not so far discussed, namely, that of loss of the alloying constituent through preferential oxidation. Although it becomes more marked with larger amounts, the effect is not strictly related to the magnesium content, the extent of loss being determined more by the type of material charged and the method of working the bath. Preferential oxidation results in the formation of thin oxide films which are extremely difficult to remove from the liquid metal, and an attempt is

generally made to suppress its occurrence as far as possible. Of the many liquid covering fluxes used, that based on magnesium chloride and free from sodium salts has proved the most effective. To prevent flux particles being carried over, the last operation before casting is the careful removal by skimming of the contaminated flux.

The preferential formation, during the direct-chill casting operation, of magnesium nitride results in an irregular cast surface which must be completely removed before rolling. The introduction of 0.001% beryllium into the melt suppresses this effect completely and, incidentally, appears to improve the hot workability of the alloys.

When melting metal for direct-chill casting some attention must be paid to the iron content, as there is a tendency for the iron-rich fraction to be rejected from the magnesium-rich solution at the moment of freezing. As a consequence, the surface where exudation occurs, becomes enriched by particles of iron aluminide. These act as stress-raisers in the cast edges, themselves highly stressed in the rolling operation, and lead to failure by cracking. The alloy in which this has most significance is the 4% magnesium alloy used for ships' plates, and the iron content is here controlled to a maximum of 0.2%.

A phenomenon observed by the present authors more than once, which has defied explanation, is the exhibition by the 3 and 5% magnesium alloys of hot-shortness at normal rolling temperatures, if the copper content exceeds 0.07%. On the first occasion in which this was noted, a content of 0.07% appeared to be critical; the material with 0.06% rolled satisfactorily, whereas that containing 0.08–0.10% consistently failed by surface shattering. As the observation was made during actual production, adequate samples of other casts were available to confirm that casting and preheating techniques were not at fault.

Because of the high annealed strength of the 5 and 7% magnesium alloys, these are used where strong welded joints are required. It has been demonstrated⁵ that the gas content of the parent metal plays a significant part in determining behaviour during welding, and in consequence it is usual to degas these materials to a degree not normally necessary in preparing a sound casting. In order to achieve this low gas content various techniques, both preventative and curative, have been explored. On the preventative side the present authors have established by experiment that the magnesium itself is the main source of gas. This can be explained by the high solubility of hydrogen in pure magnesium, and further by the presence on the surface of present-day magnesium ingots of considerable amounts of corrosion product. The need to treat corroded ingot is not unusual, but whereas in the case of aluminium alloys the adverse effects can be minimized by preheating on a forehearth to 400°C ., this is not practicable in the case of magnesium. The industry would no doubt be glad to see a re-introduction of the pre-war method of packing used by the Japanese, in

which the ingots were wrapped in waterproof paper and sealed in metal containers.

The high gas content introduced by the magnesium means that at the beginning of melting the metal is supersaturated and thorough degassing is necessary. The best method is the use of a magnesium-chloride-base, liquid flux, which permits the free escape of gas; this is accelerated by maintaining an inert atmosphere over the melt, and by gentle rabbling to facilitate diffusion within the molten metal. By this means it has been possible to prepare casts which seem to be perfectly sound under the Straube-Pfeiffer test.

It is fortunate that the limitation of iron and copper content which has to be imposed in order to ensure good hot-working properties, is consistent with the high corrosion-resistance required in the finished product. Specifications call for the control of zinc, but there appears to be little justification for this, except in the broadest terms, as evidence favours, rather than condemns, the presence of a certain amount of this element.⁶ At various times the desirability of controlling the alkali-metal content of these alloys has been discussed, trace quantities of these metals being absorbed from the covering fluxes used. Further evidence as to the necessity or otherwise of controlling these impurities would be welcome.

Manganese is normally added, in order that the iron-manganese compound may be formed in preference to the iron-aluminium compound. Its introduction does not, however, present any problems in the percentages used.

(d) *Group 4: Al-Mg-Si Alloys*

If the compositions in this group are studied, it will be seen that only minor differences exist between one alloy and another. This is because the alloys are assessed on the basis of their characteristics in the wrought and heat-treated condition, when small changes in content of individual elements, or in the element ratios, play a major part in determining the ultimate behaviour. These variations are, however, of interest only to the fabricator, and at the melting stage few problems exist, other than that of maintaining precise control of composition.

(e) *Group 5: Al-Cu-Mg Alloys, and Group 6: Al-Cu-Mg-Si Alloys*

For these alloys to fulfil their functions in carefully designed, highly stressed structures, such as aircraft frames, a consistent performance must be assured. To achieve this, each of the elements in the quaternary alloy must be controlled within very precise limits indeed, and it is the usual practice to use a charge make-up into which a high percentage of secondary ingot of known analysis is introduced, or alternatively, clean scrap of definite composition. This practice also meets the economic necessity of re-introducing the high percentage of fabrication scrap, but quite apart from that aspect, the technique is preferable to

the handling of virgin charges, if reverberatory furnaces are employed. The existence of an enormous amount of scrap in these alloys has made it possible to demonstrate on the largest scale that metal, correctly handled, can be remelted many times without impairing any of its specific qualities.

The fact that this material is finally employed in thin, highly stressed sections means that metal cleanliness must be impeccable. The first control designed to this end is to ensure that no component of the charge is metallurgically unsatisfactory. Therefore no swarf is charged directly into these alloys; light scrap is baled and checked for freedom from moisture, oil, and other foreign matter; if secondary ingot is used, then its production from scrap is carried out under close supervision, utilizing flux-washing processes. The introduction of hardeners does not present a very serious problem, because the quantity introduced at any one time is limited by the high percentage of pre-alloyed material that it is possible to use in preparing a charge. Nevertheless, it has been found desirable to raise the temperature of the melting bath to ensure the complete solution of the hardener elements, aided by rabbling; the bath is then held at this higher temperature to facilitate the settling of non-metallic impurities in accordance with Stokes' law. At the end of this operation the melt is dressed with a cryolite-base flux and all floating drosses carefully removed. In the case of a single-hearth furnace, the metal is allowed to reach its correct tapping temperature and is then covered with a fresh liquid protective flux. With duplex furnaces, the metal is tapped into the second hearth after the first skimming treatment, and reskimmed to remove any oxide film formed during transfer. The clean metal is allowed to stand under a low flame and falling temperature for 1½ hr., while degassing takes place. Successful degassing depends entirely upon a correct initial temperature, for if the holding bath has to be reheated, the metal again becomes supersaturated with gas. As in practice it is almost impossible to observe these conditions, the ideal holding bath would incorporate muffle arches or resistance heating. Holding in the second hearth serves a dual purpose, as it not only degasses the metal but also permits further settling of non-metallics.

(f) *Group 7: Al-Zn-Mg-Cu Alloys*

Although the attractive properties of this group of alloys have long been known, successful production has had to await the development of suitable melting and casting techniques which allow of the preparation of cast blocks, sound and free from segregation. Because of the close relation of mechanical properties and of freedom from stress-corrosion to composition, emphasis at the melting stage will be upon uniform alloying. Using furnaces other than those of the induction type, zinc must be introduced as a 25% hardener; melts of uniform analysis can thus be prepared without excessive rabbling or a prolonged mixing time.

The strength of these alloys in their final form is one-third greater than that of the alloys of Groups 5 and 6, and in addition there seems to be some increase in notch sensitivity. In utilizing these alloys designers must be fully confident that premature failure will not occur, as a result either of mechanical fault associated with lack of cleanliness of the metal, or of stress-corrosion arising from segregation effects. Cleanliness must be carefully watched, as the alloys in the semi-fabricated state are prone to superficial corrosion; hence process scrap should be re-used immediately, or, if this is not possible, stored under good conditions or ingotted. In the melting operation proper, covering fluxes are used to prevent the preferential oxidation of magnesium and of zinc. The technique adopted is that already outlined for the aluminium-magnesium alloys of Group 3.

The fact that in these alloys requirements for working and those for casting probably diverge to the greatest extent, has led to a very detailed exploration of the influence on casting behaviour which the composition can exercise, while at the same time remaining within the prescribed limits. This problem has been very fully discussed by Cook, Chadwick, and Muir,⁷ and in more general terms by Pumphrey and Moore.⁸

(g) Group 8: *Al-Cu-Ni-Fe-Si Alloys*

These alloys are chiefly used for forging into components working at elevated temperatures in internal-combustion engines. Although complex, their melting presents no serious problems, if normal procedures are carefully used. To ensure uniform properties and ease of working, grain-refining treatment is standard practice. Titanium was formerly introduced as an alloying addition for this purpose, but better results are now obtained by using the proprietary agents based on titanium and boron which are added to the melt some 10–15 min. before tapping.

(h) Group 9: *Al-Si-Cu-Ni-Fe Alloys*

Metallurgically, this system is of considerable interest, because it has a eutectic and, further, because the production of material suitable for working depends upon its correct modification by super-cooling in the presence of sodium, which suppresses the formation of primary silicon. For this purpose the melt must be raised considerably above the normal temperature; in practice 780° C. is found desirable. At this high temperature there is a natural tendency for gas to be picked up, and some degassing treatment should therefore follow. Immediately before casting, sodium metal, wrapped for convenience in aluminium foil, is added, and the metal is allowed to stand for a critical time which depends on the production conditions obtaining. Casting must then be carried out as speedily as possible. In selecting the composition of this alloy, the absence of primary silicon will most readily be ensured if the silicon content is reduced to the minimum compatible with meeting all other requirements.

III.—METAL TRANSFER

Control in the melting process is concerned with the elimination of oxides introduced from the stock and with avoiding the formation of hard inclusions arising from thermit reactions on the surface of the melt. However, preventative measures during melting can be completely nullified if adequate care is not taken in tapping the furnace and transferring the metal to the casting mould.

The method of metal transfer will depend on the unit volume and rate of production. For small quantities hand ladling is favoured, as this has generally given better results than decanting from the furnace or bottom tapping, when comparative production trials have been conducted. This technique has proved satisfactory for castings up to 300 lb., although to counter the fall in temperature occurring in this slow process, it is necessary to raise the bath temperature higher than would be considered ideal. Its success appears to depend on the avoidance of turbulence created by bottom tapping of the bath, and of the splashing effects inevitable with any method of filling the crucible by means of a continuous discharge of metal from the furnace. However, the undesirable effects of a continuous stream can be reduced by tilting the crucible back towards the furnace. As throughput rates increase, more complicated methods, such as siphoning, can be employed, but in the absence of outstanding advantages the simpler methods are best for routine production.

Following this argument, it will be seen that in single-hearth melting the ideal would be a short launder, linking the furnace spout to a lip-axis tilting mould. It is not, however, possible to employ a transfer launder of this simple channel construction, as some oxide formation is inevitable, and a reservoir to reduce the velocity must be incorporated. The aim of the whole transfer operation is to preserve an absolutely steady flow of metal, so that the initial protective oxide film formed on the metal surface remains intact. Failure to do this leads to fresh oxide being formed and to broken particles of oxide film being entrained in the metal stream.

With static furnaces and fixed moulds such as are used in direct-chill casting, a permanent launder installation can be employed. However well the launder may be designed, two points of weakness remain: these are the point of entry of the metal into the launder from the holding bath and the efflux from the launder to the mould. Successful tapping of a bath is a problem that still awaits an ideal working solution. Because of this, every foundry is continuously engaged on minor modifications to equipment and the introduction of remedial measures, such as filtering with porous refractories and glass-wool compacts inserted in the launder. No general recommendation can be made, as the measures which give success vary according to the rate of flow and the heat loss that can be tolerated in the launder. Because of the impossibility, for the reasons already

stated, of employing sharp gradients in the launder, low gradients and slow rates of flow have to be adopted, but as these are associated with unacceptable heat loss, heating or insulation of the launder becomes essential. Whether good pre-heating or continuous heating during casting is chosen, some undesirable temperature variations are inevitable. The importance of this must be examined in relation to the high chilling rates employed in the direct-chill process, and the critical heat balance which must be maintained if the selected freezing conditions are to be ensured.

The mechanical construction of the launder and its ancillary equipment merits some attention. Three aspects in particular must be watched, the most important being to avoid the inclusion of refractory particles arising from spalling or from collapse of the lining. If internal gas heating of the launder is employed, moisture pick-up from the products of combustion may cause gassing of the metal. The varied contours normal to launder design make uniform heating a matter of considerable technical difficulty. A complete solution must be found, since the temperature of the initial flow of metal in the continuous-casting method can determine success or failure in obtaining a sound casting. Few more pertinent controls can be exercised than those of good original design and good maintenance during use of the metal-transfer system.

In analysing the requirements of any laundering system consideration must be given to the statement, already made, that the freezing equilibrium must be maintained within very close limits. A major factor influencing the rate of chill is the amount of metal in the mould. Therefore, if the metal level must not fluctuate, a constant rate of flow from the launder is necessary. In securing such a flow, allowance must be made for the density of aluminium, which renders the significance of the head of metal in the launder greater than would at first appear. The problem may be approached in two ways, either by direct control of the level in the launder by regulation of the flow from the furnace, or by automatic control of the level in the mould by float-valve distributors. In either case, whether running from the furnace to the launder or from the launder to the mould, the ideal is to discharge the metal through the bottom of the furnace and launder so that the formation of oxide skin is prevented. Such principles are not generally applicable to pouring into tilting moulds, unless heavy castings are being considered. In the continuous process, downward discharge from the launder can be accomplished if sufficient attention is paid to nozzle design. If a vortex is created in the reservoir, or if suction effects arise owing to the bore of the vertical tube being larger than is required for the rate of flow, thus permitting air induction, then bubbling will occur and will give rise to the continuous formation of oxide with disastrous results.

Bottom vertical tapping from large-capacity, stationary furnaces has not been adopted, primarily because of the practical problems involved. These

difficulties are resolved in the design of the fully continuous Junghans-Rossi casting machine, where the metal-dispensing system is reduced to one vertical tube fixed in the bottom of a tilting furnace. The base of the furnace is of a shallow V form and the discharge tube is inserted normal to the plane of one half of it. This construction permits the metal to be withdrawn from above the discharge tube, in the event of a failure in the control system. The stopping and starting of the flow, as well as the regulation of the rate, are accomplished by the insertion of a cone valve into the top of the tube. Undesirable suction effects are avoided because the high speed of casting permits the maintenance of an adequate fluid head in the mould, thus ensuring that the lower end of the tube is completely submerged at all times.

IV.—CASTING

1. GENERAL CONSIDERATIONS

The methods of casting now employed are the outcome of years of empirical work in evolving reliable techniques to permit the production on a large scale of castings having a wide diversity of freezing characteristics and of varying liability to segregation, stress-cracking, and other effects. Very precise determination of the ideal conditions has been necessary, because only the highest-quality material is satisfactory in the working processes.

In the preparation either of cylindrical extrusion billets or of rectangular slabs for rolling, by the older methods employing complete moulds, much of the success is dependent upon the skill of the operative, who has to vary the rate of flow in such a way that constant freezing conditions are maintained, since constant pouring gives rise to variations in freezing rates greater than are compatible with the preparation of completely sound castings. When casting alloys of Groups 1 and 2, satisfactory results can be obtained only if a hot mould is used. As this precludes water-cooling, the production technique for these materials is to work a number of moulds consecutively, the rhythm of production thus ensuring that the mould starting temperature is that required. The obvious drawbacks of such methods have encouraged the development of many casting procedures having as their objective the extraction of heat across the minimum section. The nearest approach to success has been achieved in the direct-chill or continuous-casting process, which has also the advantage of enabling large sections to be prepared in any desired length.

At the risk of over-simplification, the principle relating freezing range to cooling rate may be stated as follows: as the freezing range increases, from pure metals and eutectic alloys to more complex systems having a progressively greater difference between the liquidus and solidus temperatures, so the temperature of the mould must be reduced.

The initial approach to solving this problem was to

reduce the size of the casting and, where necessary, to use a heavier mould with a greater capacity for heat absorption. The limits of these possibilities were soon reached, and higher rates of heat extraction had to be employed. This led to the development of, first, the water-cooled cast-iron mould, then the water-cooled copper mould, and finally the direct-chill process, in which the metal is cast into a shallow water-cooled mould or form of the required cross-section, and quenched by water sprays impinging on the solidified shell of metal as it is withdrawn from the mould by mechanical means at controlled casting speeds.

The direct-chill process, in any of its modifications, is sufficiently versatile to permit satisfactory castings to be made in any of the alloys of the groups mentioned, whatever their freezing characteristics. As might be expected, however, the process has problems peculiar to itself. These problems, and the controls necessary to overcome them, are discussed below for the various groups of alloys, the older processes still in use being also examined. Freezing ranges for typical compositions in each of the groups of wrought aluminium alloys are as follows:

Alloy Group	No.	Representative Freezing Range, °C.
C.P. Al	1	30
Al-Mn	2	20
Al-Mg	3	35
Al-Mg-Si	4	40
Al-Cu-Mg	5	130
Al-Cu-Mg-Si	6	130
Al-Zn-Cu-Mg	7	170
Al-Cu-Ni-Fe-Si	8	90
Al-Si-Cu-Ni-Fe	9	20

2. CASTING TECHNIQUES FOR THE MAIN ALLOY GROUPS

(a) Group 1: Commercially Pure Al, and Group 2: Al-Mn Alloys

The metallographic structures obtained by the older methods of casting these alloys are so satisfactory that a change-over to the direct-chill method has been delayed until it can be adapted to produce equally good results.

Figs. 1 and 2 (Plate LIV) are photomicrographs typical, respectively, of materials of Groups 1 and 2, cast in hot solid cast-iron book moulds. In neither case was a grain refiner used, and the structure is that resulting from the casting conditions adopted. Longitudinal sections (not shown) confirm the general freedom from preferred orientation. Figs. 3 and 4 (Plate LIV) and Figs. 5 and 6 (Plate LV) illustrate transverse and longitudinal sections of continuously cast rolling slabs. In this case a grain-refiner has been used for the Group 2 alloy (Figs. 4 and 6). The longitudinal sections show that, despite the generally fine grain in the cross-section, there is a pronounced tendency for the grains to be columnar in form, thus imparting undesirable directionality to the material. Figs. 7-10 (Plate LV) are photomicrographs of the

same materials. The coarser precipitates occurring in the hot-mould castings are seldom of practical significance. The precipitates within the grain parameter, seen in the direct-chilled material, occasion more concern owing to the directionality thereby perpetuated.

In actual casting the only method of controlling the quality of the final product lies in the choice of the casting method. With rolling slabs, some opportunity to exercise control arises at the scalping operation, where cold shuts, dross inclusions, hot tears, and surface cracks are revealed. For this reason scalping may be regarded as one of the main inspection methods operating in the foundry. The attribution of the causes of such defects is in some degree a matter of experience, but as they are generally traceable to shortcomings either in equipment or personnel, cause and effect can be rapidly correlated. The 100% inspection at the scalping stage may, however, be later proved to have been ineffective by failure of material at the hot mill, due to unexpected shrinkage effects, or at the final sheet-inspection stage, where heavy rejections due to blisters may occur with annealed sheet produced from stock which would otherwise have been regarded as normal.

Casting of slabs in solid moulds is liable to produce central weakness, if there is any slight departure from standard practice. In order to detect the occurrence of such defects at an early stage, the product of each mould is sampled in turn by taking sections from the centre of the slab, which are fine machined and etched. This type of defect is, however, more often related to the control of temperature and pouring speed in casting than to the condition of the mould. The life of solid cast-iron moulds is limited by the onset of heat-crazing of the surface and by graphitization, with consequent loss of heat conductivity. When serious cracks and non-uniform chilling become evident, the mould faces are reconditioned by planing.

As a result of the low alloying contents of these materials, few segregation effects arise which can be regarded as controllable. In the case of direct-chilled pure aluminium, bands rich in iron and silicon occur at regular intervals across the face of the slab. A similar general enrichment occurs in the slabs from solid moulds, but the enriched layer is not so thick. Figs. 11 and 12 (Plate LV) show microsections through the surface layers on material produced by the two methods, and the iron and silicon contents are given below:

	Fe, %	Si, %
Produced in cast-iron book mould (Fig. 12):		
Surface	1.20	0.15
Interior	0.29	0.12
Direct-chill-cast (Fig. 11):		
Surface	3.45	0.92
Interior	0.25	0.12

As this banding persists and can be detected in the partly processed sheet, and even in the finished sheet, if a sufficiently critical survey is made, scalping has to be applied more generally than would be the case

if soundness and cleanliness of appearance were the sole criteria of quality in slabs.

The casting of pure aluminium rolling slabs, even in the largest sections, by the direct-chill process has not proved unduly difficult in practice. In the casting of other solid sections, such as wire-bars and extrusion billets, serious trouble is encountered owing to the enormous shrinkage that takes place on freezing. In the case of wire-bar of approximately 4-in. Gothic section, the intensity of chill is so great that

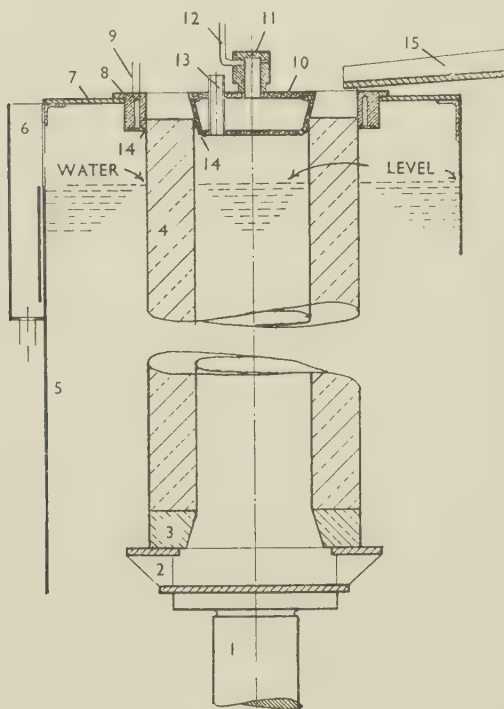


FIG. 17.—Equipment for Direct-Chill-Casting a Hollow Billet 20 in. in Outside Dia. \times 10 $\frac{3}{4}$ in. dia. Bore.

KEY.

- | | |
|-----------------------------|----------------------------|
| 1. Ram for lowering billet. | 9. Water pipe to die. |
| 2. Stool plate. | 10. Mandrel. |
| 3. Stool. | 11. Water box on mandrel. |
| 4. Hollow billet. | 12. Water pipe to mandrel. |
| 5. Water casing. | 13. Steam escape pipe. |
| 6. Weir to drain. | 14. Cooling-water jets. |
| 7. Top-hinged plate. | 15. Launder from furnace. |
| 8. Die. | |

star-cracking due to shrinkage is present to a high degree (Fig. 13, Plate LVI). The intermediate sizes, approximating to 6-, 9-, and 12-in.-dia. extrusion billets, call for freezing rates which can readily be provided within the limits of the method. Large cross-sections tend to show unsound centres at the finish of casting, unless precautions are taken to prevent severe piping and possible cracking. The obvious remedy of casting more slowly is not always a practical one, owing to the probable occurrence of cold shutting.

Whilst the casting of large solid sections presents a problem, hollow billets for the manufacture of tube blooms can be cast fairly easily, owing to the absence of a focal point for shrinkage effects. Fig. 14 (Plate

LVI) illustrates the largest hollow billet so far cast, viz. 20-in. outside dia. \times 10 $\frac{3}{4}$ -in. bore. Fig. 17 shows schematically the casting arrangement for this billet; while the casting conditions can be noted from the Standard Practice Sheet shown in Fig. 18. Inspec-

Standard Practice Part II—Foundry		Index No. : Date :	
Alloy : PA	Product Size : 20 in. outside dia. \times 10 $\frac{3}{4}$ in.-dia. bore	Furnaces Concerned : No. 6	
Product Type : C.C.P. Hollow			
Melting Bath		Holding Bath/Pot	
Fluxing : Flux No. 5—6 lb.		Fluxing :	
Melting Procedure : Bring Melt up to 730° C. Rabble for 5 min. Add Flux No. 5—Dry off Skim Clean—Allow Temperature to rise to 740°–745° C.			
Furnace Temp. : 740°–745° C.			
Melting Part Charges	Weight of Metal : 500 lb.	Bath Temp. : 740°–745° C.	
Fluxing : Flux No. 5—6 lb. per Shift		Holding Time of Bath : 20 min.	
Part Charge Procedure : After addition of part charge rabble for 2 min. At end of shift add Flux No. 5. Dry off—skim clean		No. of Operators : Firemen : 1 Casting : 2	
Recharging : 500 lb. after each drop		Tapping Temp. : 740°–745° C.	
Plant		Casting	
Type of Unit : C.C.P.	Baffles : Nil	Casting Temp. : 690°–695° C.	No. Cast/Drop : 1
Die Type : C, 20 in.; B, 3 $\frac{1}{2}$ in.	Mandrel Type : K	Length of Cast : 44 in.	Casting Speed : 3–3 $\frac{1}{2}$ in./min.
Launder Type :	Launder Cap :	Die Water : 16 gal./min.	Mandrel Water : 9 gal./min.
Stool Shape : Concave		Height of Pit Water : 5 in. below die skirt	Height of Metal in Die : 1 $\frac{1}{2}$ in. from top
Basic Output/Shift :		Weight of Product/in. : 20–18 lb.	
Other Plant Remarks :		Other Remarks on Casting Technique :	

FIG. 18.—Specimen Standard Practice Sheet.

tion control for such castings is concerned with bore finish, chemical composition, and accuracy of dimensions. As the casting conditions are critical, little deliberate modification of the macrostructure is possible.

(b) Group 3 : Al-Mg Alloys

Of the non-heat-treatable range of alloys the aluminium-magnesium group offers those having the greatest strength in the wrought state. These alloys are therefore of considerable value, and are likely to assume still greater importance as production techniques overcome the problems set by their manufacture.

The relative difficulty of casting can be illustrated by the fact that while solid-mould techniques have been developed which permit 2% magnesium alloy

to be cast into slabs up to 250 lb. in weight, the 3% alloy cannot be cast into slabs weighing more than 1 cwt., and pre-extrusion has to be employed in the preparation of rolling blanks in the 5 and 7% magnesium alloys. Even with modern direct chilling, no satisfactory technique is available in the United Kingdom for the casting in 7% magnesium alloy of a slab capable of being directly rolled, though it is understood that this is being done on the Continent.

If the equilibrium diagram is considered, it will be seen that of the four commercial alloys produced, only the 2% alloy is single-phase. The presence of the second phase is of no practical significance in the 3% alloy, but considerable attention must be paid to its control in the 5 and 7% alloys. For successful rolling, with freedom from crocodiling, edge-cracking, and surface crazing, an increasing rate of chill in relation to the alloying addition must be employed in casting. If this rate changes significantly, from such a cause as variation in the level of the metal in the mould, shrinkage or a coarse β phase will result and lead to surface breaking when rolling. The occurrence of a dross-film inclusion at the slab face can similarly upset the rate of heat extraction at the instant of solidification, and occasion notable departures from the ideal cast state.

The lack of sufficient eutectic in the 2% magnesium alloy shows itself by a tendency to fail by hot tearing, if slight stresses are set up as a result of the mould face being imperfectly dressed, or owing to the mould becoming slightly distorted. Cracks of this nature are in the horizontal sense, and tend to occur at the slab edges. Another indication of the same tendency is the formation of vertical surface cracks due to irregular cooling, such as might result from a blocked spray hole.

It has already been mentioned, when dealing with melting and alloying, that a trace addition of beryllium is made to alloys containing 3% or more of magnesium. Using the direct-chill process, the observed effect of this addition is to produce slabs and billets having cast skins freer from exudation effects than if no beryllium is added. The reduction of exudation to a minimum makes casting easier, in that the metal/mould-face relationship is kept more nearly constant. The economy effected by the addition of this costly element is, however, to be found less in the improvement of the cast face, than in the avoidance of the small surface imperfections that appear in the scalped face of hot-rolled metal not so treated. In certain cases, also, the addition of beryllium will obviate the milling of slab edges, the necessity for which arises from the fact that exudations break off during hot rolling and are rolled into the main faces of the plate, with consequent damage to the surface.

Emphasis has been placed upon the preparation of these alloys in slab form, because the hot-rolling operation is more sensitive to faults in material than is the extrusion process. Unquestionably the preparation of cast blanks for forging and pressing also calls for material of the highest quality; forging is,

however, such a limited field that it is not sufficiently familiar to serve as a general illustration.

Extrusion billets can be satisfactorily and economically prepared in a completely water-jacketed mould, in which case control will be concerned almost entirely with the production of billets free from central weakness. This is ensured by careful selection of method and by seeing that it is scrupulously followed, particularly as regards casting temperature, speed, and the topping operation. If the direct-chill process is adopted perfect soundness can be obtained, but the difficulties inherent in the alloy system, already discussed in connection with the casting of rolling slabs, are again encountered.

A sufficient demand for tubing exists to justify the casting of special hollow billets in the 2% magnesium alloy, a typical size being 9-in. outside dia. \times 2-in. bore. Defects met with are those associated with the difficulty of starting to cast successfully, and with maintaining the metal at a constant level, so that hot-tearing effects are avoided. It has not been found possible to suppress exudation either in the bore or on the outer surface, and the bores are machined to a depth of $\frac{1}{8}$ in. on the radius before extrusion into bloom. The preparation of hollow billets in the 3, 5, and 7% magnesium alloys has not yet been attempted.

(c) Group 4: Al-Mg-Si Alloys

Owing to the great difficulties of casting this group of alloys by the direct-chill process, it is not employed except for some major economic or other reason. Consideration of the alloy system will show that little is to be expected metallurgically of the direct-chill method in suppressing segregation effects or in giving greater soundness. In fact, because of the tendency towards preferentially orientated structures, the use of cast blank so prepared can prove an embarrassment.

All sizes of extrusion billets can be satisfactorily produced, using either solid iron or water-cooled moulds. Rolling slabs up to $30 \times 25 \times 5\frac{1}{2}$ in. can also be made in solid cast-iron moulds. No points arise regarding the technical control of these methods of production which have not already been discussed. In using the direct-chill method, however, control of casting practice becomes more critical, as the alloys are extremely prone to shrinkage, which can be exaggerated by stress arising from the heat-treatment effect to which they are subject. Successful casting, therefore, depends upon obtaining the nearest possible approximation to the ideal of vertical heat extraction from a horizontal cooling face. Cooling in this manner is initiated by using a stool cooled by internal sprays. The general direction of chilling is further established by immersing the solid cast section in water almost immediately below the mould. To minimize the inevitable side-chilling effects through the walls of the box mould, the flow of water is reduced to a volume sufficient only to prevent the mould from over-heating. In addition, the water passing through the mould is discharged to waste,

instead of being directed on to the casting by suitably inclined jets. To encourage the formation of a horizontal freezing plane, distributors can be used which direct the incoming hot metal to the extremities of the mould, thus countering to some extent the adverse effects of side chilling. It follows, from the well-known fact that the depth of the freezing cusp is directly determined by the speed of casting, that these alloys must run at a slow rate.

Correct indication of the speed selected and its steady maintenance throughout the entire casting operation are therefore factors of major importance in maintaining control. Instruments of sufficient accuracy for this and other control purposes in the chill-casting process are not readily available. Given efficient equipment, which enables precise standard practices to be observed, the present authors are of the opinion, contrary to that expressed by Thomas and Fowler,⁹ that good castings can be produced consistently in these and any other alloys, and that it is shortcomings in this direction, rather than undefined variation in metal quality, that cause failure.

From the foregoing it will be seen that in the casting of these alloys quality control is concerned less with the metallurgical characteristics than with the mechanical means necessary to produce sound castings. Of some metallurgical interest is a feature observed very noticeably in the alloy containing 0.7% manganese, but also seen in the 1¼% manganese alloy of Group 2, namely the profound effect which the direct-chill process has on the subsequent recrystallization behaviour of the material in the wrought state. This is of considerable importance economically, as extensive homogenization has to be undertaken before the material will respond freely and uniformly to annealing treatments.

(d) *Group 5: Al-Cu-Mg; Group 6: Al-Cu-Mg-Si; Group 7: Al-Zn-Cu-Mg; and Group 8: Al-Cu-Ni-Fe-Si Alloys*

The successful casting of slabs for direct rolling in most of the alloys of Groups 5-8 has been made possible only by the direct-chill process. The general difficulty of casting these complex alloys in such a way as to refine their structure sufficiently to make them acceptable for direct working, is enhanced by the fact that all the alloys are heat-treatable and that complicated stress systems are set up as a result of the solution effects of direct chilling. Precise control of every stage of the operation is therefore essential. Severe exudation, which is a result of the complexity of the systems, necessitates deep scalping in the case of rolling slabs and machining in the case of extrusion billets.

Segregation, other than that associated with surface exudation, is not a matter for routine control, and defects are confined to cracking in its various forms. Types encountered include: central delayed-stress cracking in the low-copper alloys of Groups 5 and 6;

vertical cracking in the same groups, associated generally with too slow a casting speed; and "trouser-leg" splitting in Group 7, which is the resultant of the high heat-treatment response of this alloy system in conjunction with the low hot strength. Most of these defects are self-evident, but 100% macro-inspection or examination by ultrasonic means is carried out to ensure that no material is processed which is unsound in any degree. Fig. 16 (Plate LVII) is a photograph of a 6-in.-dia. billet cast in one of the alloys of Group 6; perfectly sound as cast, it cracked in the manner shown during preheating for extrusion.

(e) *Group 9: Al-Si-Cu-Ni-Fe Alloys*

Whilst this billet alloy presents no serious problems during casting by any method, the following experience may be of interest. The successful production of 12-in.-dia. billets by the direct-chill process could at one stage not be reproduced in the authors' works owing to failure eventually traced to the type of mould lubricant used. Based on evidence gained from comparative trials, a general change had been made in the foundry from simple mineral oils and greases to a proprietary silicone-bearing mixture. While this was successful with all the company's other alloys, and has been retained for use with them, it proved to be reactive with the alloy of high silicon content and gave rise to intense shutting effects which rendered the billets useless. A return to ordinary mineral oil produced the smooth surface commonly obtained with this alloy.

V.—APPLIED CONTROLS

1. CHEMICAL COMPOSITION

The techniques outlined above should yield cast blocks having the minimum variation in composition due to segregation. Some variation associated with these effects must be accepted, but successful production will depend upon the attainment of the desired mean composition.

The preparation of casts to give a correct target composition, involving in many cases four or five alloying elements and three or more impurities, calls for comprehensive sampling schemes and adequate analytical facilities. Most of the material to be examined is in the molten state, and liquid samples may be taken and cast into the most convenient form. Considerable care must be used in selecting the precise method to be adopted if misleading values are not to be obtained. If tapping is protracted, samples should be taken at least from the beginning and the end of the run, and more samples should always be cast than are normally required, so that the existence of faults may be confirmed and the seat of any trouble located.

The methods of analysis vary considerably, but any control laboratory has available bench equipment for gravimetric determinations, and some type of colorimeter, polarograph, and spectrograph. This diversity

of equipment has been necessary in the past owing to the difficulty of analysing aluminium alloys, which made it essential, if results were to be obtained in the minimum time, to adopt the method of determination most appropriate to each element. Fortunately, the direct-reading spectrograph now gives results for the majority of the elements in a few minutes, and permits a high order of control checks and release analyses to be made while melting is in progress.

2. MELTING

In earlier sections an attempt has been made to summarize the main sources of trouble and causes of defects in each of the groups of material commonly handled, and to indicate the principles to be observed if a consistently satisfactory quality is to be attained. In practice, a specific interpretation of these principles must be applied to each individual class of product. For the purpose of shop control, all the information relevant to a certain type, based on experimental work in the foundry culminating in trial production runs, is assembled on one or more sheets known as "Standard Practice Sheets." Part, or the whole, of these data are then passed to the key personnel. A typical form is shown in Fig. 18 (p. 386). The quality of the material produced in the trial runs is subjected to close laboratory control, both at the foundry and at the fabricating plant. Moreover, no standard is accepted as final until normal or improved yields are obtained.

On the Standard Practice Sheet temperatures are specified for each stage of the operation. This calls for suitable pyrometric equipment. As the typical furnace unit is large, and the cycles in consequence protracted, continuously recording instruments are favoured. Instruments of robust design, and possessing open scales that can be read with ease, should be employed, and each one should be installed, if possible, adjacent to the charging station, where the furnaceman may have it under constant observation. The industry finds difficulty in obtaining a suitable material for thermocouple sheaths, capable of withstanding immersion in molten aluminium for long periods. No refractory sheath has been found entirely satisfactory, failures being due to mechanical or thermal weakness. Sheaths of heat-resistant cast iron are therefore used, but a reasonable life can be assured only if they are given a refractory wash after each shift. Whilst the accuracy of modern instruments leaves little to be desired, a false confidence will be gained unless due consideration is given to the many factors determining the actual temperature recorded. Amongst these are the heavy nature of the sheaths and the fact that the couple is normally protected from mechanical damage by being located in the furnace lining. Both these factors cause considerable lag. The position of the hot junction of the thermocouple needs to be carefully selected in relation to the depth of the melt, as with reverberatory furnaces a 40° C. gradient between the melt

surface and the hearth floor has been observed in baths of 18-in. working depth. This accounts for the apparently anomalous fact that rabbling causes a rise in the temperature indicated. The siting of the thermocouples in the bath is decided when the original design is completed. The site, or sites, selected can seldom be related to the points of thermal significance, as other considerations prevail and the thermal behaviour is thus to some degree a matter of conjecture. This is nowhere more obvious than at the beginning of melting; until a completely molten pool is obtained the pyrometric installation is useless, and the avoidance of overheating becomes a matter for personal control by the operative.

In casting, there are also considerable limiting factors in determining temperature. If casting direct from the holding bath is practicable, the minimum temperature at which tapping can successfully be undertaken becomes *ipso facto* the general tapping temperature. The temperature of the metal at the time of tapping can be widely altered. Excessive preheating of the launder may cause over-heating of the initial stream; more frequently, however, the low temperature of the launder results in the metal being too cool. In the case of transfer of metal by ladle some heat loss is inevitable, and allowance must be made for this.

For a battery of small reverberatory furnaces working on the continuous-melting principle with ladle transfer of the metal, a multiple-station temperature-indicating system has been found satisfactory. The system is so devised that the operator has only a thermocouple to handle. When this is lifted from its hook the circuit peculiar to the furnace is isolated, and without any further action on his part, the temperature of a thermocouple permanently immersed in the bath is indicated on a 24-in.-dia. illuminated dial (Fig. 15, Plate LVI). Meanwhile, if the operative so wishes, he can immerse the hand-thermocouple in the melt in the ladle and this temperature will be indicated 10 sec. after lifting the couple from its hook. A permanent record of all temperature measurements from this battery of furnaces is made on a master recorder installed in the Superintendent's office.

Where the melting unit is large enough, efficient combustion of fuels will be aided by installing flue gas CO₂ recorders and by fitting pressure indicators to the heat-exchange chamber. In all cases, however, the necessity of opening doors for charging, fluxing, skimming, &c., renders any continuous record of little use.

3. CASTING

If casting is to be reliably executed, the following controls are necessary in addition to those regulating metal temperature. The temperature of the cooling water must be kept constant within 1° or 2° C., and suitable mercury-in-steel indicating thermometers should be fitted. Provision of a means of adjusting

the cooling-water temperature is, of course, assumed. Of equal importance is the rate-of-flow indicator, which ideally should be provided for regulating the supply of water to each mould. Control of speed of casting is of vital importance, both as regards correct indication of speed from the instant when initial movement begins, and sensitivity to changes in speed. The ideal may be a combination of good instrumentation and mechanical regulation.

A non-standard requirement is the automatic control of the height of the metal in the mould, which becomes progressively more desirable as the number of feed points increases beyond the possibility of manual control. This can be achieved within very close limits by means of a float-operated valve distributor in the mould.¹⁰

In the case of castings of smaller cross-section, where the introduction of a float is not feasible, constant orifices fed from a fixed head provide a simple means of control.

4. INSPECTION AND TESTING

(a) *Physical Inspection*

An adequate method of identification must be operated, if location of faults is to be made easy. Although an onerous task, it is well worth while to preserve the identity of the material in batches related to the basic production-process unit, throughout all the various operations.

The general dimensions of the cast product are determined by those of the moulds and dies employed, and the successful attainment of correct dimensions depends on adequate allowance being made for shrinkage and contraction effects. If scalping and turning are required, the size of the finished product should be checked, to ensure that the full amount of material to comply with metallurgical requirements has been cut away.

(b) *Visual Inspection*

Most of the defects to which rolling slabs and extrusion billets are prone can be detected by systematic visual inspection. This operates at several levels, the operative and foundry supervisors carrying out a general check on their own work, and a final inspection being made by a special staff. Typical defects are cold shuts, hot tears, surface-oxide inclusions, longitudinal, transverse, and central cracks. If machining is carried out, these defects will be revealed more clearly, although in some cases the machining operations eliminate the more superficial examples.

(c) *Non-Destructive Testing*

Whatever method may be employed, visual inspection cannot concern itself with more than the immediate surface layer of the material. Inspection is not complete unless some assurance of central soundness is also obtained. An important aid in

this respect is the ultrasonic flaw detector, which enables a check to be made for relative freedom from shrinkage, central cracks, or random inclusions. Depending upon the use for which the material is intended, this inspection may be applied at various rates up to 100%. It is particularly suited to the examination of extrusion billets, as defects arising from this processing method are not self-revealing in the early stages as are those occurring in the rolling of slabs.

(d) *Destructive Testing*

Whatever the method of casting, the bases and tops of billets and slabs are non-uniform with the bulk of the material. When any critical application is involved, therefore, it is common practice for an appreciable discard to be made from each end, at the most convenient stage in processing. The consistency of the macrostructure of the most critical alloys, cast as extrusion billets, is checked by inspection of a slice cut for this purpose from each cast length, and prepared for examination by fine machining and etching. This type of inspection is not so extensively used for rolling slabs, because scalping serves as a general inspection, and few major defects pass through the hot mill unnoticed.

VI.—ORGANIZATION OF CONTROL

In reviewing the factors significant in the melting and casting of aluminium alloys for working, the conclusion must be reached that quality can be maintained only by the simultaneous operation of a multiplicity of indirect controls. Departures from standard practice can accordingly take place without the cause being obvious. To ensure that information concerning cases of failure is made widely known and that adequate remedial action is promptly taken, presents a considerable problem in organization. In the authors' works, in addition to the direct supervision exercised by the production staff, an inspection staff operates during the whole of the twenty-four hours. Members of this staff report major defects as soon as found and summarize their findings at the end of each working shift. Each morning the findings on the material inspected during the preceding twenty-four hours are summarized and placed before the Foundry Superintendent. Similarly, summaries are prepared covering each week's work on one furnace for any one product, and in this case a sub-analysis against shifts is shown. This analysis is kept as far as possible up to date, and is available for scrutiny by the production staff.

In order to arrange suitable and co-ordinated action, a weekly meeting is held, attended by representatives of the production, inspection, and metallurgical staffs. At these meetings the inspection department table their findings, summarized for the week, and the metallurgical department present any complaints regarding material which have arisen in the main or sub-plants. The Standard Practice

Sheets already mentioned, are based on this information, and the committee decides when a Standard Practice has been established. The yield values obtained in producing any particular run of material provide a means of assessing both its quality and the efficiency of the controls applied, thus providing target values for action.

The general success of the control measures outlined in the present paper is considered to be proved by the fact that, although the works handles a wide diversity of materials, 90% or more of the gross production weight cast is forwarded to the rolling and extrusion mills.

Confirmation of the success of the foundry techniques has, however, to await the processing of the material to its final stage in the fabricating plants, where the more subtle variations in quality of the material tend to be revealed.

ACKNOWLEDGEMENTS

The authors wish to thank the Directors of T.I. Aluminium, Ltd., for permission to publish this paper and to incorporate in it all available information.

A review paper of this nature is based on experience in all branches of the process, and the co-operation of the authors' colleagues is gratefully acknowledged.

REFERENCES

1. D. C. G. Lees, *J. Inst. Metals*, 1946, **72**, 350.
2. A. R. E. Singer and S. A. Cottrell, *ibid.*, 1947, **73**, 33.
A. R. E. Singer and P. H. Jennings, *ibid.*, 1947, **73**, 197, 273.
P. H. Jennings, A. R. E. Singer, and W. I. Pumphrey, *ibid.*, 1948, **74**, 227.
P. H. Jennings and W. I. Pumphrey, *ibid.*, 1948, **74**, 249.
W. I. Pumphrey and D. C. Moore, *ibid.*, 1948, **74**, 425; 1948-49, **75**, 257, 727.
W. I. Pumphrey and J. V. Lyons, *ibid.*, 1948, **74**, 439.
W. I. Pumphrey and P. H. Jennings, *ibid.*, 1948-49, **75**, 203, 235.
W. I. Pumphrey and D. C. Moore, *Trans. Inst. Weld.*, 1949, **12**, 116.
3. R. Irmann, *Techn. Rundschau*, 1951, (19), 1.
F. Rohner, *J. Inst. Metals*, 1947, **73**, 285.
4. A. v. Zeerleder, "Technology of Light Metals", p. 115, Table 19. 1949: New York (Elsevier Publishing Co., Inc.); London (Cleaver-Hume Press).
5. —, "The Gas Welding of Aluminium" (Aluminium Development Association Information Bulletin No. 5), p. 11. 1952: London (The Association).
6. P. Brenner and W. Roth, *J. Inst. Metals*, 1948, **74**, 159.
7. M. Cook, R. Chadwick, and N. B. Muir, *ibid.*, 1951, **79**, 293.
8. W. I. Pumphrey and D. C. Moore, *ibid.*, 1948, **74**, 425.
9. W. I. Thomas and W. A. Fowler, *ibid.*, 1948-49, **75**, 921.
10. P. Brenner, *Aluminium*, 1951, **27**, 14 (Fig. 3).

THE CONTROL OF QUALITY IN MELTING AND CASTING MAGNESIUM ALLOYS FOR HOT WORKING *

1453

By R. G. WILKINSON,† B.Sc., MEMBER, and S. B. HIRST,† B.Sc.Tech.

SYNOPSIS

A description is given of present practices in the control of quality and inspection in the melting and casting of the three principal types of magnesium alloy used for wrought purposes, viz. magnesium-manganese, magnesium-aluminium-zinc-manganese, and magnesium-zirconium-zinc. The zirconium-containing alloys are considered separately, not only because special procedures are involved in their melting, but also because they are always cast by the semi-continuous direct-chill process.

Except on a laboratory scale, rolling, extrusion, and forging are not carried out in the authors' works, and thus the use of commercial-scale hot working as a running routine "inspection" method is not possible. The inspection processes applied before the cast stock is sent out to other works are therefore crucial.

I.—INTRODUCTION

BEFORE the commercial introduction of the new high-strength magnesium-zirconium-zinc alloys some years ago, the wrought alloys produced in Great Britain were restricted to the "classical" magnesium-manganese and magnesium-aluminium-zinc-manganese types. These alloys were—and in general still are—melted and alloyed in holding crucibles of 2 tons capacity, before being decanted into 300-lb. crucibles and chill cast into extrusion billets and rolling slabs in "book" moulds. When operated by reasonably skilled labour, this procedure gives cast stock of a quality acceptable for most purposes and, since operating costs are not unreasonable and because production volume has not justified the capital outlay for more modern plant, the installation still remains in use for the bulk of the output in the older alloys.

When the zirconium-containing alloys were being commercially introduced, the semi-continuous direct-chill (D.C.) casting process was being developed, and, after this had been thoroughly proved on all types of alloy, the D.C. casting machine was devoted to the production of the new materials and of certain especially critical items, e.g. forging stock, in the older alloys.

Although a small rolling mill and extrusion press are available for research and test purposes, no rolling, extrusion, or forging on a commercial scale is carried out at the authors' works, and therefore any defects in the cast stock are not disclosed on a day-to-day, or even week-to-week, basis in full-size hot-working operations. In these circumstances control of quality and the application of rigorous inspection processes

before the stock is sent out to other companies are matters of prime importance. In practice the steps described in the present paper have proved over a long period of years to be successful in maintaining rejections at the very satisfactorily low level of considerably less than 1%.

II.—THE CLASSICAL ALLOYS: Mg-Mn (AM503) AND Mg-AL-ZN-MN (AZM AND AZ855)

1. MELTING AND CASTING PROCEDURE

These alloys, the nominal and specified compositions of which are given in Table I, are produced in cast-steel melting and holding crucibles of 2 tons capacity, heated in pit-type producer-gas-fired furnaces. The charge normally consists of large "cheeses" of virgin magnesium (crudely cast directly from the output of the electrolytic cells), together with process scrap, but in certain cases small additions of secondary ingot are also made. Alloying constituents, aluminium, zinc, and/or manganese (the latter introduced in the form of manganese chloride), are added by an alloying bucket and the melt is plunged thoroughly. Throughout the melting and alloying operations a fluid ("Z") flux rich in magnesium chloride is used to protect the metal from oxidation, and at subsequent stages of the operations an inspissated flux ("E"), producing a stiff protective cover, is also applied.

When alloying has been completed, the crucible is transferred to a tilting furnace which will maintain a metal temperature of about 750°C. The crucible is then used as a reservoir of molten metal for filling a series of fabricated mild-steel crucibles of 300 lb. capacity. These crucibles, after filling, are taken to

* Manuscript received 11 December 1952. Contribution to a Symposium on "The Control of Quality in the Production of Wrought Non-Ferrous Metals and Alloys. I.—Melting and

Casting", to be held in London on 25 March 1953.

† Magnesium Elektron, Ltd., Clifton Junction, nr. Manchester.

producer-gas-fired furnaces, and the melts are there refined by stirring-in the inspissated "E" flux whilst the temperature is brought up to about 800° C. The melts are then ready to be taken to the billet- or slab-pouring points, each crucible being transported by crane to the gas-heated holder of the pouring machine.

The moulds are installed in wheeled carriages, and can therefore be brought up on rails in succession to a

essentially upon accurate weighing. Thus, control of this factor is vested almost wholly in the reliability of the operator.

A sample in the form of a "Churchill block" (Fig. 1, Plate LVIII) is taken from each 2-ton melt by a ladle, precautions being taken against contamination (see Appendix, p. 400), and this is analysed¹ for the elements covered in the particular specification, some

TABLE I.—Designations and Compositions of Magnesium-Base Wrought Alloys.

Elektron Alloy Designation	Wrought Form	D.T.D. Specification No.	Nominal Composition and Normal Manufacturing Limits				D.T.D. Specification Requirements								
			Al, %	Zn, %	Mn, %	Zr, %	Al, %	Zn, %	Mn, %	Zr, %	Cu, % max.	Si, % max.	Fe, % max.	Ni, % max.	Ca, % max.
AM503	Sheet Extrusions Tubes	118A 142A 737	} (0.7-1.2)	1.5 (1.0-2.0)	...	0.05 max.	0.03 max.	1.0-2.0	...	0.02	0.02	0.03	0.005	0.02
AZM	Extrusions " Tubes Forgings	259A 749 348A 88C					6.0 (5.5-6.5)	0.3 (0.2-0.4)	5.5- 8.5 5.5- 6.5	1.5 max. 0.5-1.5	0.2- 0.4	...	0.03	0.05	0.03
AZ855	Press forgings	88C	8.0 (7.5-8.5)	0.4 (0.3-0.5)	0.3 (0.2-0.4)	...	7.5-8.5	1.0 max.	0.2-0.4	...	0.03	0.05	0.03	0.005	...
AZ31 * (High Purity)	All wrought forms	Specifications under consideration	3.0 (2.5-3.5)	1.0 (0.7-1.2)	0.3 (0.2-0.4)	...	2.5-3.5	0.6-1.4	0.2 min.	...	0.05	0.3	0.005	0.005	0.3
			Total of Other Elements 0.3 max.												
ZW3 †	Sheet Extrusions Press forgings Impact forgings	626 622 619 729	} ...	3.0 (2.7-3.3)	...	0.7 (0.5-0.9)	0.02 max.	2.5-4.0	0.15 max.	0.5-1.0	0.03	0.01	0.01	0.005	...
ZW1 *	Fully argon-arc-weldable sheet, extrusions, and tubes	Specifications under consideration					...	1.5 (1.2-1.7)	...	0.7 (0.5-0.9)	0.02 max.	1.0-2.5	0.15 max.	0.5-1.0	0.03

* The specification requirements quoted are those under consideration.

† The D.T.D. specification details and requirements quoted are those under consideration for revised issues.

position in which the runner of each mould is aligned with the lip of the crucible.

The crucible holder is fitted with lip-axis tilting gear, and pouring is controlled by hand winding. At the start the mould is tilted at an angle of approximately 15° to the horizontal, the axis of tilt being through the mouth of the runner, and is allowed to come back to the vertical position as it is filled with metal. When the mould is full, a red-hot cast-steel "top-hat", heated in a muffle furnace, is placed on the top. The crucible is then lifted a few inches in a vertical direction and the casting is fed through the open top of the heated ring.

Finally, when the billet or slab has solidified and cooled for a short time, the mould is opened and the casting removed, melt and cast identification numbers being marked on it with crayon.

2. CONTROL OF COMPOSITION

Control of composition presents few difficulties. For each melt a Melt Control Card is issued which specifies the charge in terms of the weights of the various constituents and serves as the record of all other essential details. Given raw magnesium of constant impurity content from the electrolytic cells, reliable segregation of process scrap, and the known analysis of any secondary ingot used, the ensurance of correct composition of the melt depends

of which are determined spectrographically and others by wet methods. Internal and A.I.D. inspection procedures are normal and need not be detailed.

3. CONTROL OF VOIDS

Although it cannot be claimed that book moulds are capable of producing castings of the same density as those made by the D.C. process, they do give billets and slabs of acceptable quality when proper attention is paid to the control of the pouring operation. The moulds (see Fig. 2, Plate LVIII) are designed to have a varying section giving a heavier chill at the base and, with a side runner and slot gate, they give a good degree of directional solidification.

The moulds are heated by gas torches before being brought into operation, and, in most cases, the first one or two billets or slabs cast in each are scrapped. However, the moulds quickly develop a favourable temperature gradient from top to bottom, the magnitude of which varies with the diameter, but which is always at least 50° C. and may in some cases reach 150° C. A typical range is 200-300° C. For the AM503 alloy, which has a great tendency to piping, both the moulds and the "top-hats" are fitted with gas-ring heaters for use during the actual casting operation. In all cases special attention must be paid to adequate feeding of the solidifying metal, and it is usually necessary to feed more than once.

Careful observance of correct pouring temperatures and speeds is all-important for the production of sound stock. Details of these are given in Table II.

TABLE II.—*Pouring Temperatures and Times for Billets and Slabs Cast in Book Moulds.*

Billet Size, mm.	Pouring Temperature, °C.		Pouring Time, min.
	AM503	AZM and AZ855	
73	790	760	1
106	770	750	1½
112	770	750	1½
133	760	740	2
175	750	730	2½
246	750	730	3½
295	750	730	5
Slab 16 × 24 × 3 in. . . .	780	...	3

Throughout all alloying, refining, and casting operations mild-steel-sheathed pyrometers are used in the molten metal and are coupled to a system of 6-point potentiometric recorders. In D.C. casting a pyrometer may also be used in the metal reservoir. The thermocouples are of Chromel/Alumel, insulated by means of porcelain beads.

The AM503 alloy is distinctly prone to the formation of internal shrinkage, or "bridging", cavities (Fig. 4, Plate LIX), which are totally enclosed by metal and do not outcrop to the surface. Every care is taken to minimize the frequency of their occurrence, but in practice it seems that they weld up satisfactorily in the extrusion or rolling operation. This alloy never contains micro-porosity.

The AZM and AZ855 alloys are susceptible to both macro- and micro-porosity (Fig. 5, Plate LIX), and control of casting conditions is very important in minimizing these defects. Rolling slabs are not made in these alloys because they are not normally used in sheet form. Inspection for internal cavities in billets by means of routine "cut-up" tests is automatically supplemented by periodic reports from the various mills where the billets are normally cut into lengths before extrusion.

4. CONTROL OF NON-METALLIC INCLUSIONS

Cleanliness of the castings depends upon proper treatment of the melt and good pouring practice. The standard fluxing procedures, which have been fully described as to both practice and function by Emley,^{2,3} can always be relied upon to ensure that clean metal is available for casting, and then only tranquil pouring in a sulphur atmosphere is required.

In melting and alloying, protective "Z" flux (dyed pink) is used to prevent burning of the charge, and a small quantity is sprinkled on the bottom and around the inside of the crucible before the solid metal is added. The operators then add the flux as required, so that when the metal is fully molten there is a fluid protective cover over the whole surface.

It will be recalled that 2-ton crucibles are used as

reservoirs for the filling of 300-lb. crucibles in which the refining is carried out and from which the metal is poured. Before each 2-ton crucible is taken from the melting furnace to the tilter, the melt is given a good cover of inspissated "E" flux (grey) to form a stiff crust from beneath which the metal can be poured into the smaller refining crucibles. This cover is repaired after each tilt.

When refining the alloy, "E" flux is sprinkled on to the surface of the melt and allowed to fuse. At a temperature of about 760° C. this flux is then stirred through the metal until the surface appears bright and silvery. This constitutes the refining operation, after which the melt is given a stiff cover of "E" flux before heating up to 800° C. as a preliminary to taking the crucible to the casting machine. At the casting machine the flux cover is repaired and the crucible tilted in its lip-axis container to the pouring position, the cover again being repaired if necessary.

Now that clean metal is available at the mould, the vital factor in avoiding oxide inclusions is the prevention of contact between the molten metal and the atmosphere during the pouring operation by ensuring that there is continuous chemical or physical protection of the metal, and by minimizing turbulence. The flux cover is very carefully drawn back from the crucible lip, which is itself scraped clean, and at the same time a sprinkling of sulphur is applied so that the small area of exposed metal is protected from oxidation. The interior of the mould is dusted with sulphur (from a muslin bag) before pouring begins, and it is important that throughout the casting operation the exposed metal surface in the crucible and the pouring stream are both dusted with sulphur continuously.

In pouring, the crucible and mould lifting and tilting gear must be operated very smoothly, so that the initial protective oxide skin formed as a "tube" around the metal stream remains unbroken from start to finish. With the mould tilted at 15° to the horizontal, pouring is started by tilting the crucible until the rate of pour in the early stages is such that the metal stream flows gently down the runner of the mould in a straight line and strikes the bottom with the minimum turbulence. The runner is separated from the main cavity of the mould by a narrow ($\frac{1}{4}$ – $\frac{1}{2}$ in.) slot which prevents oxide skins formed during pouring from entering the billet. Pouring is continued at this rate until the metal reaches within $\frac{1}{2}$ in. of the top of the mould, when lowering of the mould is begun. The latter operation must be carried out as gently as possible to prevent breakage of the protective oxide skin.

When the mould is full, a red-hot "top-hat" is placed in position, the crucible raised vertically, the metal surface skimmed, and the feeding operation carried out with due care. Finally, the surface is dusted with sulphur and a plate placed over the "top-hat" to exclude air during the final stage of solidification.

Flux inclusions in the billets or slabs occur very

rarely, but if careless operation does result in this trouble it is readily evident in the machining operation and the stock is scrapped (see Fig. 6, Plate LIX).

5. CONTROL OF GRAIN-SIZE

(a) *Magnesium-Manganese Alloy (AM503)*

Alloy AM503 is notorious for possessing an extremely pronounced tendency to develop a very coarse and columnar grain structure which, in rolling, can give rise to severe surface and edge cracking at worst, and, at best, a noticeable, but not serious "orange peel" effect on the blank in the breaking-down operation. (In the U.S.A. it is normal practice to add 0.1-0.2% calcium to the alloy to produce a reasonably fine equi-axed structure in the slab, but in Great Britain calcium is strictly controlled as a trace impurity in the interests of good gas-weldability.) The grain-size of AM503 is indeed one of the most difficult quality factors to control, and it must be said that to obtain a reasonably uniform and not excessively coarse-grain structure is more of an art than a science; however, adherence to the pouring temperatures and speeds (Table II, p. 395) established from experience gives acceptable slabs and billets (see Fig. 4, Plate LIX). It is of interest to note that the "diagonal" mode of growth of columnar crystals in D.C. cast AM503 slabs was found in early tests to be associated with poor rolling properties.

(b) *Magnesium-Aluminium-Zinc-Manganese Alloys (AZM and AZ855)*

As has been remarked previously, only extrusion billets are book-mould-cast in these alloys, and no special care is needed to control the grain-size, because this is not critical, and it is in any case reasonably fine (Fig. 7, Plate LX).

6. CONTROL OF GAS CONTENT, CRACKING, AND SEGREGATION

Magnesium melts do not readily absorb hydrogen from the melting atmosphere, but strict precautions are necessary in the avoidance of contact with moisture, as, for example, in corroded scrap or wet flux. It is also essential that clean, dry crucibles are used and that mould dressings* are dried very thoroughly.

Only AM503 alloy is sensitive to contraction cracking. The avoidance of this defect rests solely on a suitable design of the mould to eliminate "holding". On rare occasions when such cracks have appeared—always when new moulds have been put into use—they have proved extremely troublesome to detect before the rolling or extrusion operation. The cracks are very fine, and it is difficult, even after machining and macro-etching, to differentiate between them and the grain boundaries and other purely structural markings.

In both Mg-Mn and Mg-Al-Zn-Mn alloys there is no serious tendency to either normal or inverse segregation when cast in book moulds.

7. CONTROL OF SURFACE QUALITY

All magnesium alloy extrusion billets are supplied to the mills fully machined, and the AM503 alloy rolling slabs are scalped on the two major surfaces. Control of surface quality therefore lies in the hands of the machining operator, who normally works to depths of skim of $\frac{1}{8}$ – $\frac{3}{16}$ in., only increasing these in cases where surface defects such as "cold shuts" are encountered.

III.—MAGNESIUM-ZIRCONIUM-ZINC ALLOYS (ZW3 AND ZW1)

1. DEVELOPMENT OF THE ALLOYS

The compositions of these alloys are given in Table I (p. 394). In the early stages of development of the wrought magnesium-zirconium-zinc alloys, rolling slabs and extrusion billets were cast in the normal chill moulds which have been described, and with certain exceptions the results were reasonably satisfactory. However, there were some serious troubles, for example the incidence of outcropping micro-porosity resulting in internal oxidation and nitride formation at the high pre-heating temperatures (450°–520° C.) used for rolling slabs. This was especially deleterious to the rolling properties, and could naturally be expected to result in unreliable sheet. Another major trouble which arose was segregation of zirconium-rich particles during the solidification of the largest sizes of billet. In 1944 Magnesium Elektron, Ltd., designed and constructed a small plant for D.C. casting, and there followed a period of intensive development to work out suitable conditions for the casting of slabs and billets in all types of alloy. The magnesium-manganese alloy AM503 and the magnesium-aluminium-zinc-manganese alloys AZM and AZ855, particularly the former, were quickly found to present few problems, and once the right casting conditions had been firmly established it was decided to concentrate the use of the machine on the zirconium-containing alloys both for development and production.

With the commercial launching of ZW3 alloy, the outstanding feature of which is its remarkable hot workability combined with high strength,⁴ the Company was naturally anxious to send out to the rolling and extrusion mills, and to the forging shops, cast stock representing the very highest quality possible. The policy of especially rigorous control and inspection has been justified by results and, although the production tonnages of the alloy have so far been substantially lower than for the old-established alloys, rejections over the period have been very much lower than 1%.

* The mould dressing consists of 80% French chalk and 20% boric acid, well mixed in water to give a paste sufficiently thin for use in a spray gun.

2. CASTING BY THE D.C. MACHINE

The D.C. machine (Fig. 3, Plate LVIII) consists essentially of three units for pouring, controlling, and casting the metal, respectively. There is a heated, lip-axis, tilting container for a 300-lb. crucible, the inside being fitted with a refractory lining incorporating a gas burner of sufficient capacity to maintain the metal at any desired temperature up to 780° C.

The metal is poured from the crucible into the mould either via a reservoir, for rolling slabs and the larger size of billet, or down a simple launder for the smaller billets. The reservoir is held in a gas-heated refractory-lined container, the heat applied being sufficient to maintain a metal temperature of up to 720° C. The metal enters the reservoir down a very short launder and leaves at the other end through a valve which controls the flow of metal into the mould.

From the reservoir outlet, the metal flows through a funnel into a "tundish", or distribution vessel, of similar shape to, but of smaller cross-section than, the billet or slab being cast, this tundish being supported centrally at the top of the mould. The metal leaves this vessel through a number of narrow slots in its sides. The level of the metal in the mould is maintained at such a height as just to cover the tops of the slots, and the funnel mouth is always kept submerged. The purpose of this tundish is to act as a combined metal distributor and oxide trap.

For smaller-diameter billets (6 in. and less), the reservoir is replaced by a simple straight launder with a pouring funnel attached. The launder is heated by gas burners in order to prevent freezing of the flowing metal. No tundish has been found necessary for these smaller billets, the metal entering the mould through the mouth of the funnel itself, the tip of which is kept immersed.

Multiple casting of the smaller billets has been developed, but is not normally used in production.

The moulds are of the "collar" type, cooled by external spray rings, one or two in number, according to the depth of the mould. An additional lower spray is used for cooling the emerging billet.

The ram of the D.C. casting machine is hydraulically operated, and is of the double-acting type giving a positive downward pull during casting. The flow of oil also drives an electric tachometer indicating the speed in in./min. Frequent checks are made on the calibration of this instrument by actual timing of the casting operation.

The ram is fitted with a tray surrounding the head to collect water which will act as a douche in the event of a "run-out" of molten metal. Although there should be no danger from such a "run-out", provided that sufficient water is present, it is deemed an essential safety precaution for the operating platform to be sealed off from the cooling chamber in which the emerging billet comes into contact with water.

Melting on a 2-ton scale is not carried out in the D.C. foundry, and the 300-lb. charges generally

consist of refined magnesium ingot (rather than crude cell metal), process scrap, and zinc, with the addition of a zirconium "master salt". The scrap and ingot are melted using a special "HE" flux (dyed blue) to prevent burning. When all the metal has been charged, the requisite quantity of master salt is added and the whole mass melted and brought up to a temperature of 700°–750° C. After the zinc addition has been made, the temperature is raised to and held at 800° C. The melt is then puddled with a preheated plunger in such a way that the master salt at the bottom of the crucible is brought into thorough contact with the metal. During this operation, "HE" flux is used to prevent burning.

A sample of the melt is then taken in a clean, red-hot ladle and poured into a small die-mould. This sample bar is fractured and the zirconium content is assessed from the grain-size. If this is satisfactory, a Churchill block sample (Fig. 1, Plate LVIII), is taken, again with a clean, red-hot ladle. If, however, the zirconium content is judged to be low, the melt is puddled again and the sampling procedure repeated.

The sides of the crucible above the metal level are then scraped clean and the flux cover is renewed. It is generally unnecessary to refine the melt after the puddling operation, but this may be done if any burning has been seen.

The crucible is taken by crane from the producer-gas-fired furnace and placed in the preheated tilting container of the D.C. machine, where it is allowed to settle for 10–20 min., during which period it is brought to the correct pouring temperature of 750°–780° C., depending upon the type and size of the product (see Table III).

TABLE III.—*Essential D.C. Casting Conditions for ZW3 and ZW1 Alloys.*

Billet Size, mm.	Ram Speed, in./min.	Water Flow, gal./min.			Crucible Temp., °C.
		Top	Middle	Bottom	
73	6.3	20	780
92	6.2	30	...	5	775
106	4.5	20	...	20	770
133	4.2	40	...	20	770
175	4.0	40	...	20	770
220	3.8	40	...	40	760
246	3.5	40	30	15	760
295	2 → 3.5 → 2	40	30	15	760
Slab 14½ × 4½ in. section	3.5	40	20	10	750

Immediately before pouring, the flux round the wall of the crucible near the pouring lip is cut away with a clean spoon and the surface of the metal dusted with sulphur. The sulphur bag is used continuously from now until the casting is complete. Pouring is begun, either into the reservoir or, for the smaller billets, into the long launder. Protection of the molten metal throughout the pouring system is effected by means of powdered sulphur or jets of sulphur dioxide.

3. CONTROL OF COMPOSITION

The nominal and specified compositions of ZW3 and ZW1 alloys are given in Table I (p. 394). Control of the zinc content presents little difficulty, since process scrap is carefully segregated and any zinc additions required are weighed out accurately. Greater care is, however, required in controlling the effective "soluble" zirconium content^{5,6} at the required level of 0.5–0.9%. The critical test for this is the examination of the fractured die-bar sample, and an experienced observer can readily estimate the success of the alloying operation by visual observation of the fracture grain-size in the centre of the bar. (Reference standards are, of course, available in cases of doubt.) If the fracture is not satisfactory, the puddling operation is repeated, or in very rare cases a further addition of master salt may be required. When the zirconium content is judged satisfactory—and in practice one puddling usually suffices—a Churchill block sample is taken and analysed for zirconium, zinc, and the specified impurities (Table I).

4. CONTROL OF FLUX INCLUSIONS

It is now well known that many years of research were required to develop a process for the introduction of zirconium via a reducible salt, while avoiding the presence in the alloy of corrosive flux inclusions.⁵⁻⁷ The master salt, which has been in commercial use since 1946, is in fact foolproof from this point of view when used with a proper technique in conjunction with the special "HE" flux. This flux is "weighted" with barium chloride and is a dual-purpose flux combining the functions of protecting against burning in melting and alloying and providing an efficient cover for the melt. In practice, it has been found that there is no danger of flux inclusions being present in the main bulk of the billet or slab, and it is only necessary to be vigilant against this defect at the end of the pouring operation when, with a careless operator, there is a possibility of some of the residual fluid alloying mixture at the bottom of the crucible passing into the mould with the last metal poured.

When the billet or slab has been removed from the machine and has cooled, it is taken to the machine shop and short "discards" are cut off at the base and top. As a matter of routine, the top discard (which varies in length according to the diameter of the stock) is subjected to exposure in a "humidity chamber" as a routine inspection for flux inclusions. A 1-in. section is cut from the lower surface of this discard, i.e. that surface which coincides with the top surface of the billet proper, and, after milling, it is exposed for 48 hr. in an atmosphere of 80% relative humidity,* care being taken to protect the newly machined surface from finger marking, dust, or other contamination in transit to the test chamber. After this period, any flux inclusions, even those of a

very minor character, will be clearly visible. If the test section is of a satisfactory standard, it can be confidently assumed that the whole of the billet or slab is free from flux inclusions, or, for the smaller sizes, in which a number of billets are successively cast from the one melt, that all are clean. If, however, there are significant signs of flux in the section from the discard, further test samples are cut and exposed until the defect has been eliminated.

5. CONTROL OF OXIDE AND NITRIDE INCLUSIONS

Assuming that the fluxing has been properly carried out in the melting and alloying operations, and that clean metal is brought to the reservoir of the casting machine, freedom of the cast stock from oxide and nitride inclusions naturally depends on minimizing turbulence in the pouring system and on the effectiveness of the protection provided by the sulphur and sulphur dioxide atmospheres. It is also vital that all components of the system should be free from moisture.

Both top and basal discards of each casting are acid pickled and examined for oxide inclusions (Fig. 8, Plate LX). It is the unavoidable turbulence which takes place at the beginning of each pour that makes it necessary for a basal discard to be taken. However, this discard is small because at the beginning of the pour the mould "stool" at the head of the ram is brought to within 2 in. of the top of the mould.

It should be mentioned that routine examination (for cracking) of the billets and slabs by the ultrasonic flaw detector also gives a reliable indication of freedom from oxide inclusions.

6. CONTROL OF VOIDS AND CRACKS

The D.C. casting process normally provides an almost completely automatic insurance against the occurrence of voids. Throughout the authors' experience the worst defect of this nature has been the presence of extremely light, distributed, and quite insignificant micro-porosity. The castings are not, therefore, inspected for voids.

D.C. casting does not, however, provide an insurance against cracking. Although there is now a substantial body of theoretical knowledge of the D.C. process, it is not possible to lay down, in advance of *ad hoc* trials, precise casting conditions for the avoidance of cracking. In practice reliance is placed upon the strict observance of casting temperatures, speeds, water-flow figures, water-distribution characteristics, &c., established in trials. The basic conditions for the zirconium-containing alloys are given in Table III (p. 397).

Inspection for cracking is straightforward. Any outcropping cracks are easily discernible during machining and/or pickling, and the supersonic flaw detector is used as a matter of routine for the internal cracks.

* The atmosphere in a closed chamber containing a saturated solution of sodium thiosulphate.

7. CONTROL OF SURFACE CONDITION

All D.C. cast billets and slabs are machined on all surfaces, with normal depths of skin of $\frac{1}{4}$ – $\frac{3}{8}$ in., to remove all traces of inverse segregation and surface folds. After machining, rolling slabs (for which surface condition is critical) are acid pickled and examined by an experienced inspector to ensure that no traces of surface defects remain. In certain cases where residual portions of any particularly deep folds are evident, these may be removed by local dressing.

Whereas the magnesium-manganese (AM503) and magnesium-aluminium-zinc-manganese (AZM, AZ855, &c.) alloys—especially the former, which has a very narrow freezing range—invariably give little surface trouble in D.C. casting, ZW3 and ZW1 alloys are prone to the occurrence of surface folds. In practice these defects are kept to the minimum by strict observance of standard casting conditions; maintenance of a uniform metal level in the mould is especially important. A mould vibrator has been tried experimentally, but was found to result in an interesting, but highly deleterious, side effect of “banded” zirconium precipitation and associated β -phase formation (see Fig. 9, Plate LX).

8. CONTROL OF METALLOGRAPHIC STRUCTURE

Reference has already been made to the die-bar fracture test applied after the alloying operation to check that the melt contains a fully effective zirconium content giving a correspondingly fine grain-size. Final reliance is not, however, placed on this, and every billet and slab is metallographically examined on samples taken from the top discard (last metal poured) as a check on the effective zirconium content, as evidenced not only by the grain-size, but more particularly in this case, by freedom from undue quantities of β phase. (It is to be noted that one of the primary effects of the zirconium addition to a magnesium-zinc binary alloy lies in its power to inhibit the formation of magnesium-zinc compound which—the binary eutectic temperature being 341° C.—would ruin hot workability at the much higher temperatures used. With a “full” zirconium content, the solidus temperature of ZW3 is about 590° C.).

These factors are naturally of fundamental importance in rolling, which is normally carried out at 480°–500° C. In extrusion, at lower temperatures, it is equally essential to have a fully effective zirconium content to achieve maximum mechanical properties.

Fig. 10 (a), (b), and (c) (Plate LXI) shows the standards of metallographic structure which have been established from experience. It can be seen that the “good” structure, with an average grain-size of 0.055 mm., shows straight boundaries enclosing grains with pronounced zirconium coring. The “weak” structure has a grain-size of 0.10 mm., shows “wandering” grain boundaries with little or no sign of an effective zirconium content in the crystals, and contains significant quantities of β phase. The “satisfactory” structure, with a grain-size of 0.065

mm., represents the border-line case, and is intermediate in characteristics.

It is of interest to note that although normal (as opposed to inverse) segregation effects are rare in D.C. casting, one interesting example has been encountered in ZW3 alloy. This is illustrated in Fig. 11 (Plate LXI), and takes the form of a continuous concentration of β phase which has been found to result from mal-positioning of the tundish.

9. CONTROL OF HOT-ROLLING AND MECHANICAL PROPERTIES

Small sections are taken from the top discard of every slab and, after preheating to the normal temperature of 500° C., they are broken-down under careful observation for cracking tendencies or surface defects such as oxide skins.

It has been noted that the mechanical properties of ZW3 and ZW1 extrusions depend very largely upon the effective zirconium content, and therefore in any doubtful cases short, 3-in.-dia. extrusion billets may be cut from the top or the bottom of the casting and extruded under standard conditions on the laboratory 400-ton extrusion press. Using a standard billet temperature of 300°–320° C. and a speed of 1 ft./min., ZW3 billets are rejected unless tensile properties exceeding 18.5 tons/in.² 0.1% proof stress, and 23.0 tons/in.² ultimate stress are obtained from standard $\frac{3}{4}$ -in.-dia. bar. Slightly lower properties are acceptable in the case of ZW1 alloy.

IV.—OTHER D.C. CAST PRODUCTS

Brief mention must be made of some products in the older alloys which are D.C. cast to obtain maximum soundness and structural homogeneity for critical hot-working operations.

1. AZM ALLOY BILLETS FOR FORGING

Whereas billets in the magnesium-aluminium-zinc-manganese alloy (AZM) cast in book moulds possess very poor forgeability as a result of the existence of some micro-porosity and large pools of β phase, billets cast by the D.C. process may be satisfactorily forged after a homogenization heat-treatment. In addition to being extremely sound, the D.C. billets show excellent β -phase dispersion.⁴

The billets are cast by the same D.C. casting equipment as that employed for the zirconium-containing alloys, the metal being melted in 300-lb. crucibles by a technique similar to that already described for AZM alloy (Section II, 1). One essential difference in casting procedure is that whereas the zirconium-containing alloys are cast at comparatively high temperatures, AZM alloy is poured at the lowest possible temperature consistent with satisfactory flow of metal into the mould (approximately 690° C.). This is necessary to avoid “sticking” of the metal to the mould wall, with consequent tearing of the billet, a tendency to which AZM alloy is somewhat prone. Special care must be taken with this alloy to ensure that no water or steam enters the gap between the

emerging billet and the mould, since this has been found to be a source of oxide inclusions in the stock.

The inspection procedure for AZM alloy forging billets consists in examination for cracks and oxide inclusions by means of the ultrasonic flaw detector, and in fracturing a section cut from the top of the billet. This latter procedure provides a useful method of checking the presence of skins resulting from incursion of water into the mould; if present they show as brown or black markings in the fracture. The sections are also metallographically examined before and after homogenization.

2. ROLLING SLABS IN HIGH-PURITY AZ31 ALLOY

Since this alloy, the composition of which is given in Table I (p. 394), is normally required to a high standard of purity, with a maximum iron content of 0.005%, a special melting procedure is necessary. The metal in the crucible is not allowed to exceed a temperature of 760° C., the melting process is carried out as quickly as possible, and the holding period after alloying and refining is strictly curtailed in order to minimize pick-up of iron from the crucible.

Casting and inspection procedures closely follow those employed for AZM alloy.

V.—CONCLUSION

It will be evident from this paper that, as in many other industries, control of quality of magnesium-alloy cast stock rests very largely upon the employment of experienced and conscientious operatives, and that the retention of key foremen and chargehands and the maintenance of good labour relations are correspondingly important. All operatives concerned are paid on time rates only.

It has already been emphasized that, since the cast stock is worked elsewhere, control and inspection are especially rigorous and exhaustive, and this applies particularly to the relatively new zirconium-containing alloys. Naturally the procedures are subject to continuous review in the light of experience and in relation to production costs.

The functions of control and inspection are the responsibility of the Metallurgical Research Department, which maintains a special team of melting and casting observers and inspectors who work in close collaboration with foundry personnel. This system, in addition to other merits, is essential for successful production development of new alloys.

ACKNOWLEDGEMENTS

The authors are indebted to the Chairman and Directors of Magnesium Elektron, Ltd., for permission to publish this paper, and to many of their past and present colleagues who have helped to develop the procedures described. Special thanks are due to Mr. L. Lasch and Mr. J. H. T. Petch for assistance in the preparation of the tables and figures.

Acknowledgements are also due to the various companies who have collaborated in the establish-

ment of standards in extrusion, rolling, and forging behaviour of the cast stock.

APPENDIX

NOTES ON SAMPLING THE MELT AND ON THE SPECTROGRAPHIC TEST-PIECE MOULD

(a) Sampling

A clean iron ladle, holding about 1 kg. of metal, and kept for the sampling of one particular alloy type alone, is first "washed" in the melt for not less than 30 sec. The ladle is then half filled with metal, care being taken that no part of the flux cap is swept into it, and this is quickly poured into the spectrographic test-piece mould (see Fig. 1, Plate LVIII). The cast test-piece is stamped on the side with the alloy type and melt number. It is then placed in a wooden sample container in the foundry, with other samples to await analysis.

The metal sampler is required to observe the following points:

1. The ladles used for sampling must be kept free from adhering metal scraps of the previous melt.
2. The copper baseplate of the mould should be previously heated, and kept in a thoroughly clean condition.
3. The "washing" of the ladle in the melt must be strictly adhered to.
4. The test block must be free from flux, oxide inclusions, and gas holes.
5. The test block must be correctly marked with the steel punch stamps by the person who cast it.

(b) Details of the Mould

The spectrographic test-piece mould (see Fig. 1, Plate LVIII) is a metal frame fitted with asbestos-covered handles and hinged at one side to facilitate removal of the test block after solidification. The lining of the mould consists of two hard amorphous carbon sections, which when placed together form a cylinder about 2 in. in dia. and 3½ in. in height, and have a tapered cavity in the centre into which the molten metal is poured. It should be noted particularly that the carbon sections protrude below the metal framework of the mould, so that good contact is made with the copper plate, and therefore no metal leaks out during casting.

The copper plates used are approximately 12 × 8 × ½ in. and are fitted with handles for carrying.

REFERENCES

1. —, "Methods of Analysis of Magnesium and Its Alloys", 1946: London (F. A. Hughes and Co., Ltd.).
2. E. F. Emley, *Symposium on the Refining of Non-Ferrous Metals (Inst. Min. Met.)*, 1950, 407.
3. E. F. Emley, *J. Inst. Metals*, 1948-49, 75, 431.
4. R. G. Wilkinson and F. A. Fox, *ibid.*, 1949-50, 76, 473.
5. C. J. P. Ball, *Metallurgia*, 1947, 35, 125, 211.
6. C. J. P. Ball, *Chem. and Ind.*, 1948, (34), 531.
7. E. F. Emley, *J. Inst. Metals*, 1948-49, 75, 481.

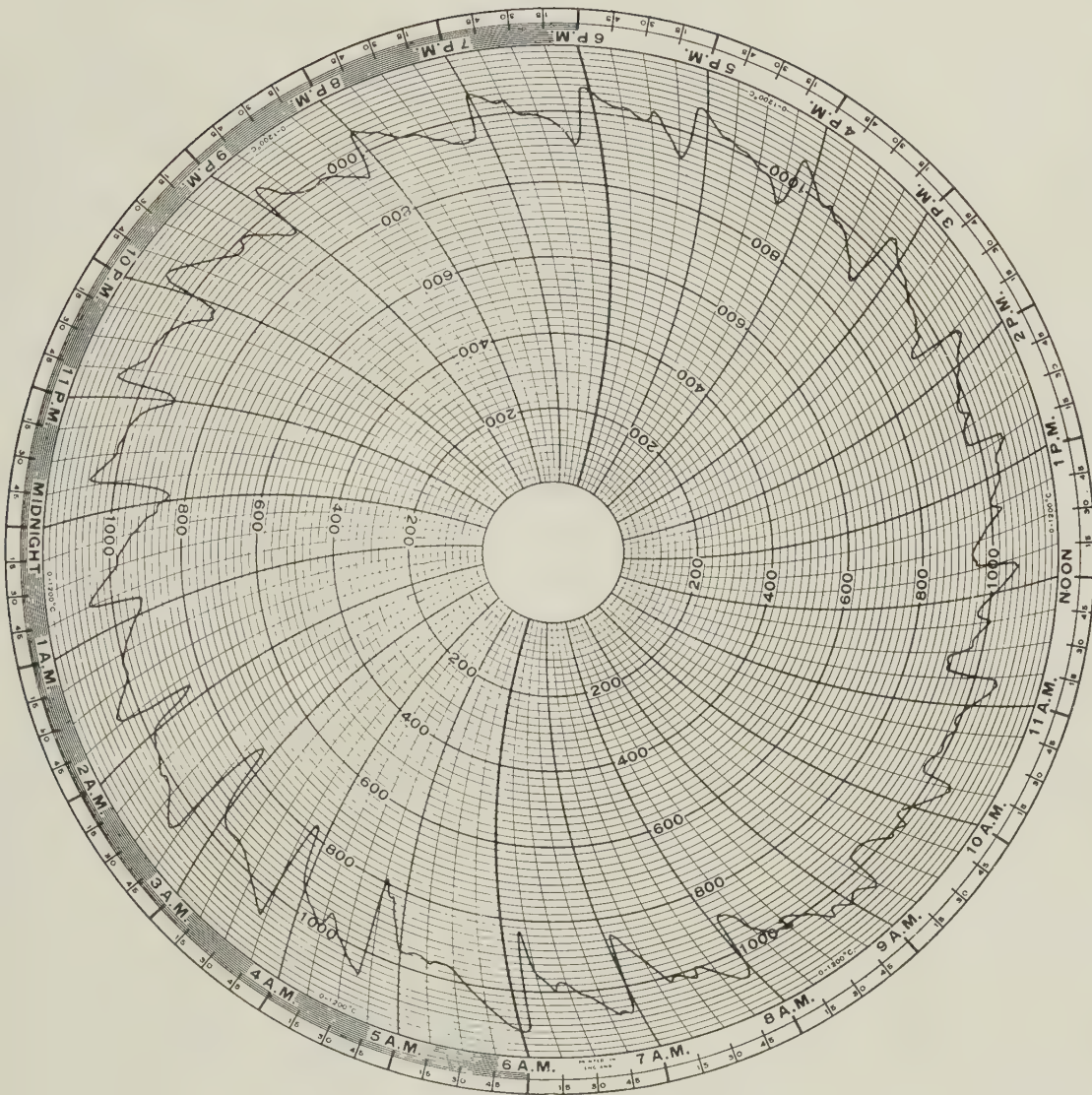


FIG. 2.—Chart Showing Record of Pouring Temperature.

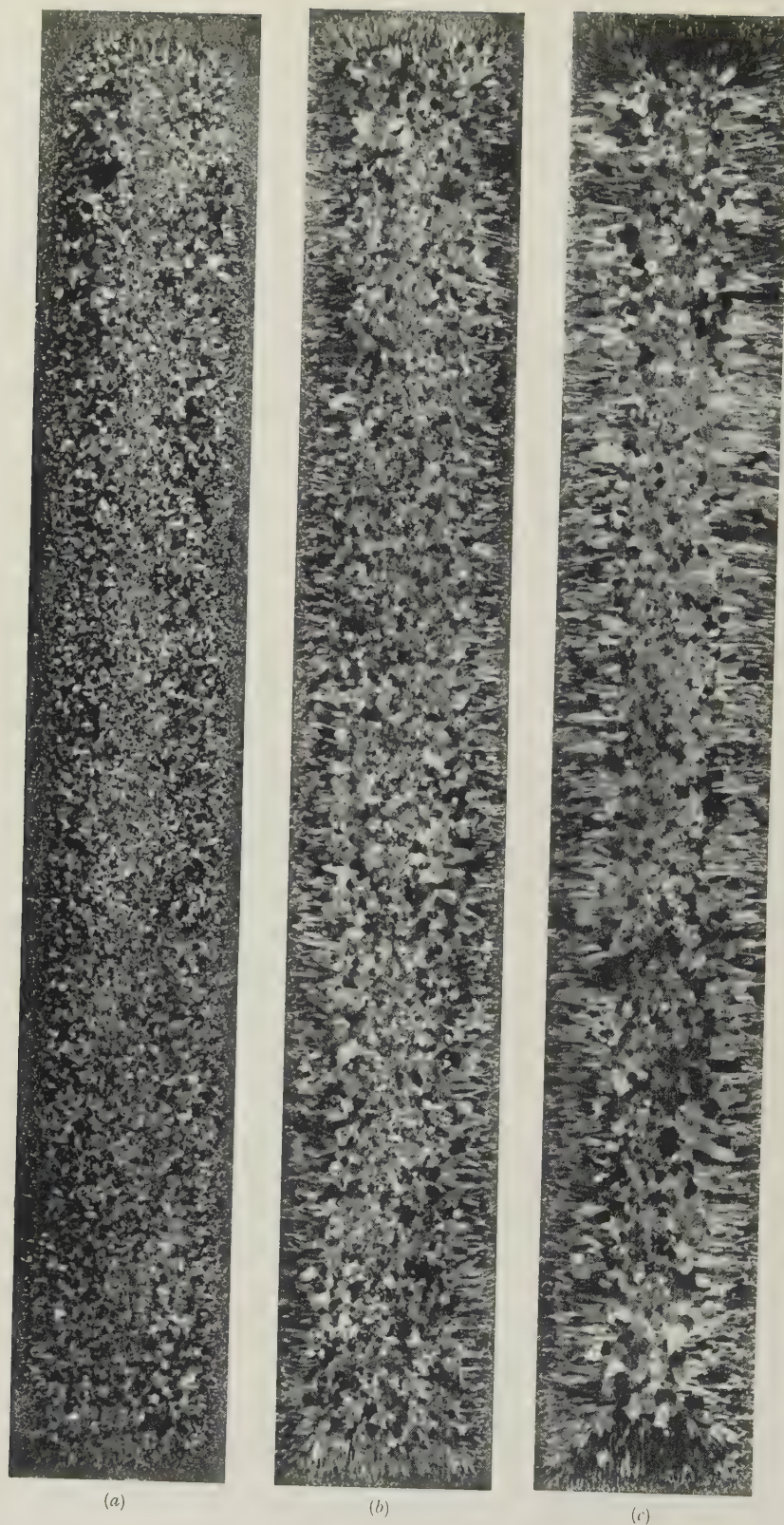


FIG. 3.—Transverse Medial Cross-Sections of 67 : 33 Brass Rolling Slabs Cast in Water-Cooled Moulds. $\times \frac{1}{3}$. Casting temperatures: (a) 980°, (b) 1000°, and (c) 1020° C.

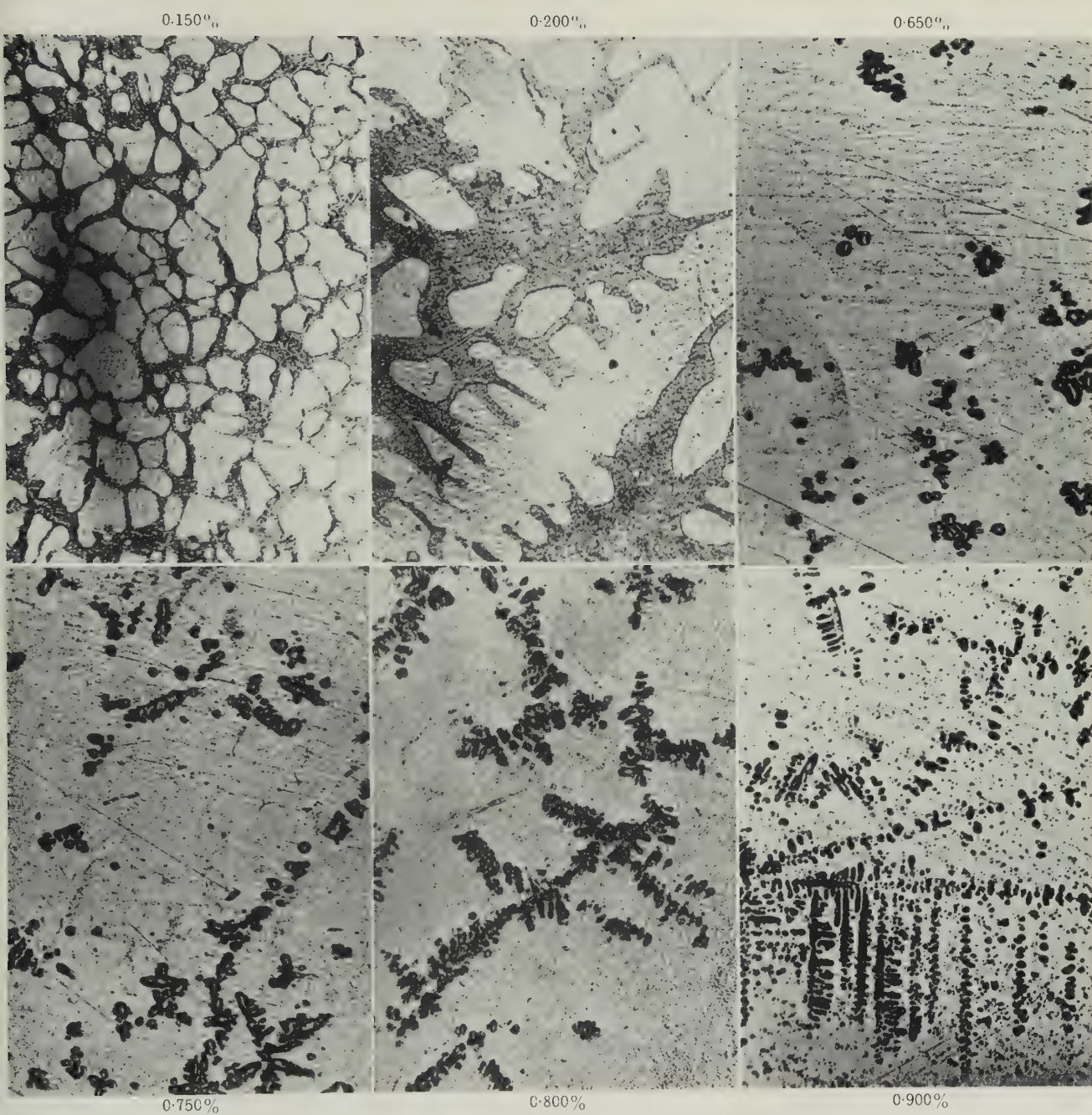


FIG. 4.—Structures of "Low-Set" Copper Buttons Containing Various Percentages of Oxygen. $\times 100$.

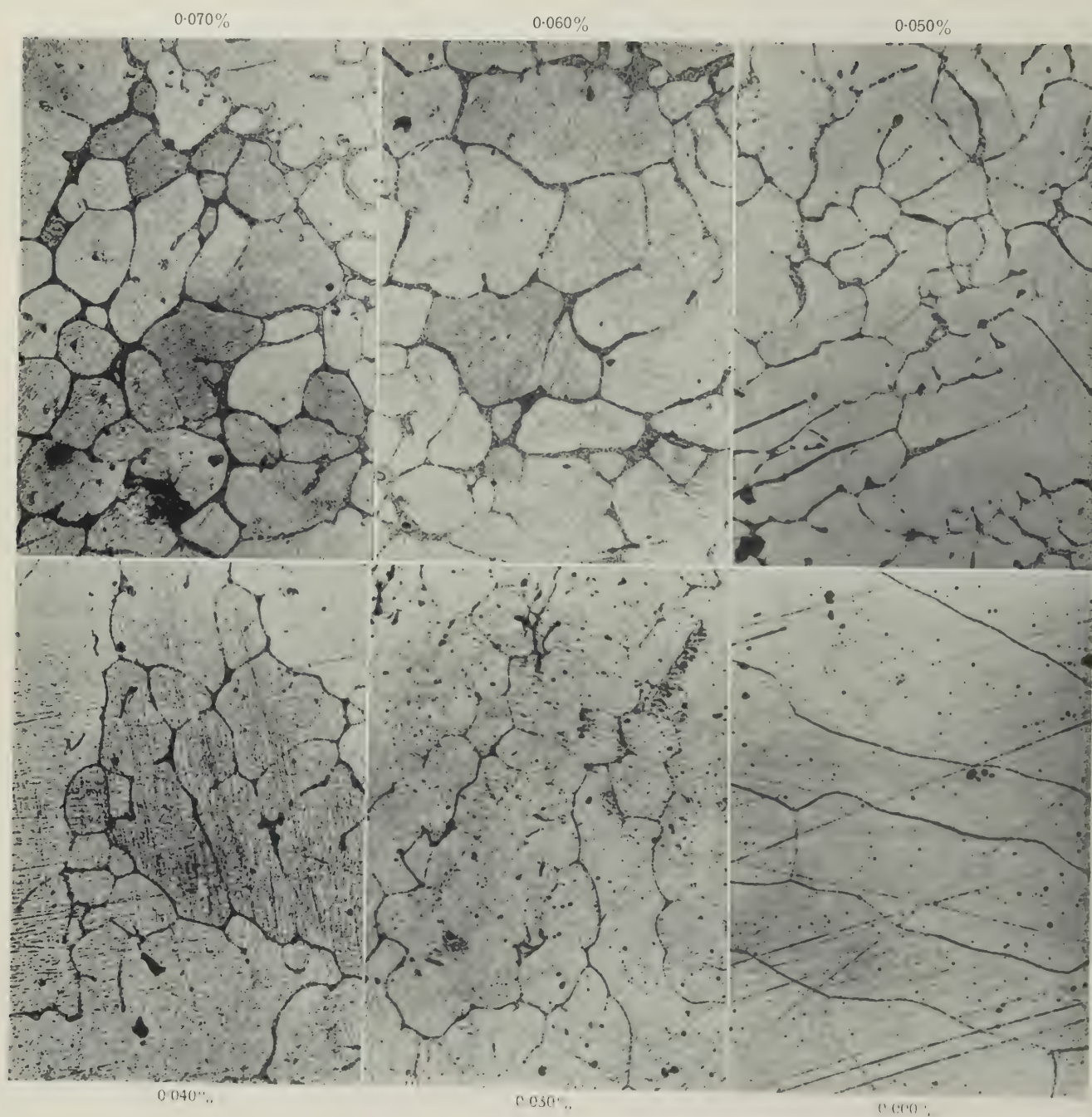


FIG. 5. Structures of Tube Samples of Copper Containing Various Percentages of Oxygen. $\times 100$.

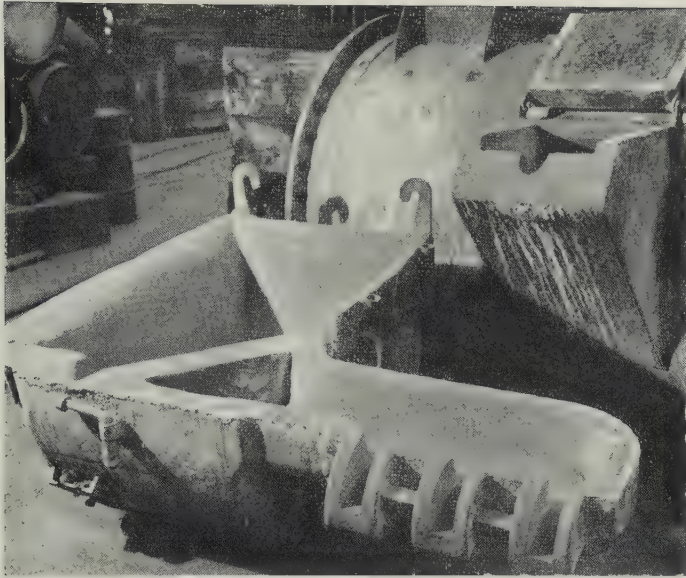


FIG. 6.—A Pouring Ladle Used in the Production of Horizontally Cast Wire-Bars.



FIG. 7.—A Funnel Used to Pour Vertically Cast Billets.

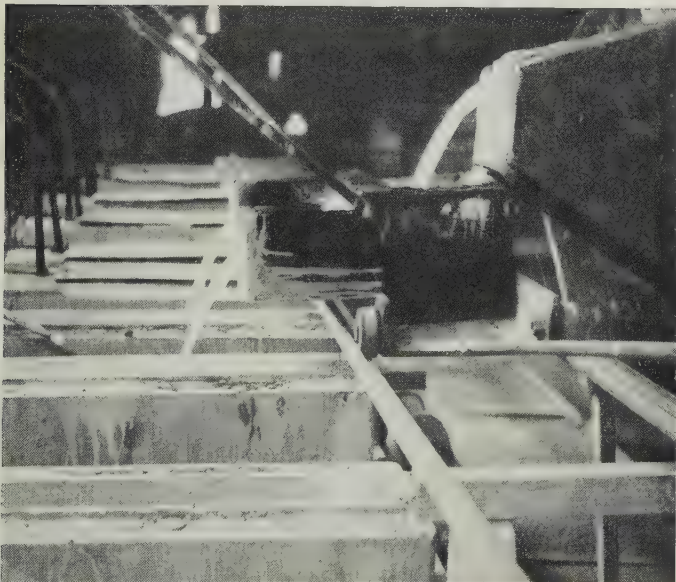


FIG. 8.—The Simultaneous Casting of Two 1000-Lb. Rolling Slabs from a 5-Ton Portable Furnace.



FIG. 9.—A Pelican Ladle Used for "Floating" Vertically Cast Cakes.



FIG. 10.—A 3000-Lb. High-Conductivity Copper Cake Being Vertically Cast into a Water-Cooled Copper Mould.

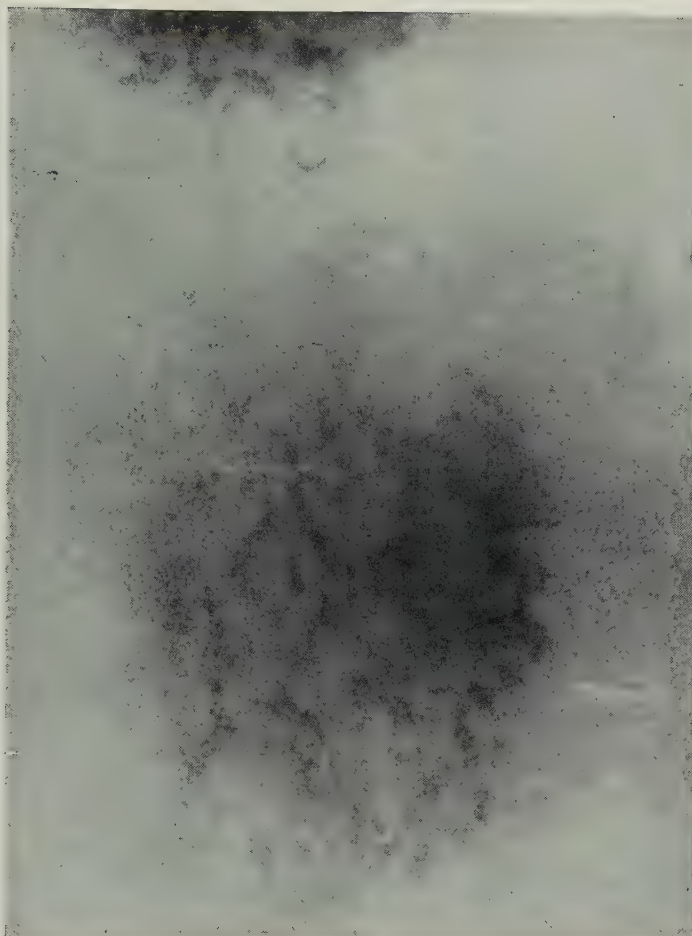


FIG. 4.—Radiograph of Zinc Rolling Slab Containing Interdendritic Shrinkage. $\times 1$.

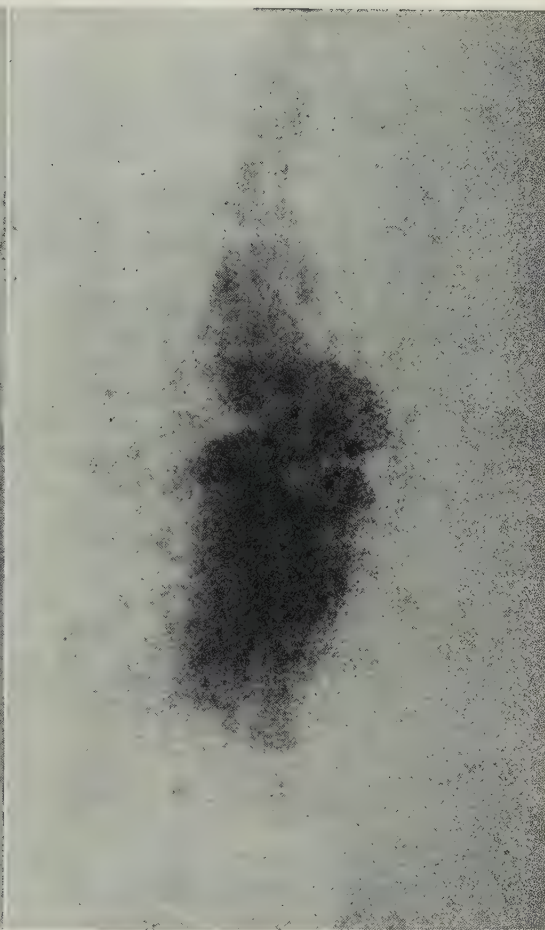


FIG. 6.—Radiograph Showing Large Gas Cavity in Zinc Rolling Slab. $\times 1$.

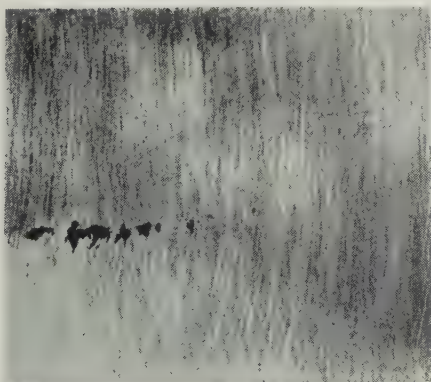


FIG. 5.—Photograph of Vertical Section through Area Covered by Fig. 4. $\times 1$ approx.

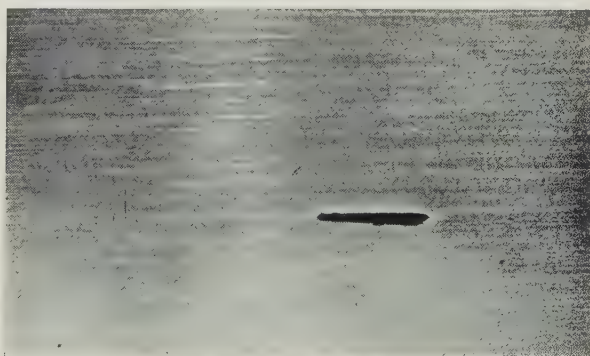


FIG. 7.—Photograph of Horizontal Section through Gas Cavity Shown in Fig. 6. $\times 1$ approx.

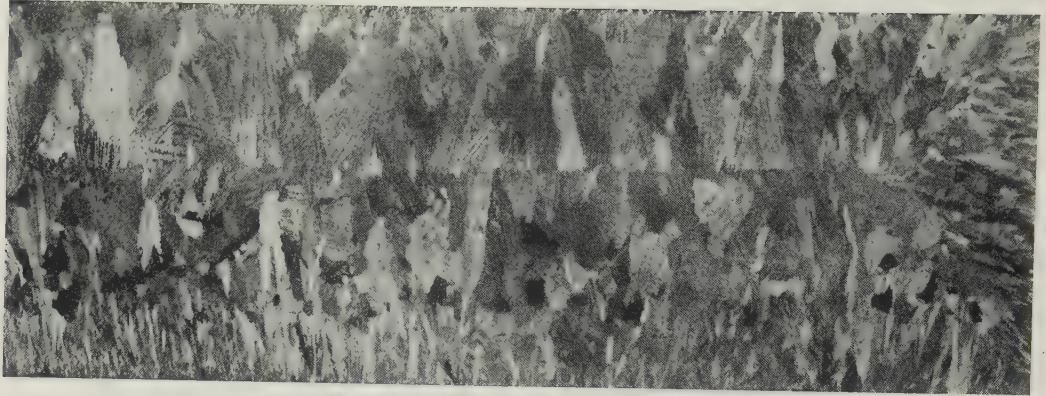


FIG. 8.—Macrostructure of Vertically Cast Zinc Rolling Slab. $\times 1$ approx.

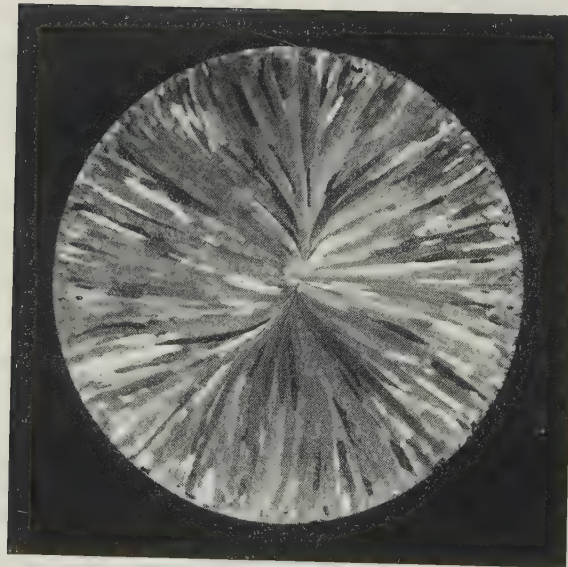


FIG. 9.—Macrostructure of Vertically Cast Zinc Extrusion Billet. $\times \frac{1}{2}$ approx.



FIG. 1.—Transverse Section of Commercially Pure Aluminium Rolling Slab, Cast in Solid Cast-Iron Book Mould. Etched. $\times \frac{1}{2}$ (reduced by $\frac{1}{5}$ in reproduction).



FIG. 2.—Transverse Section of Aluminium-Manganese Alloy Cast in Solid Cast-Iron Book Mould. Etched. $\times \frac{1}{2}$ (reduced by $\frac{1}{5}$ in reproduction).

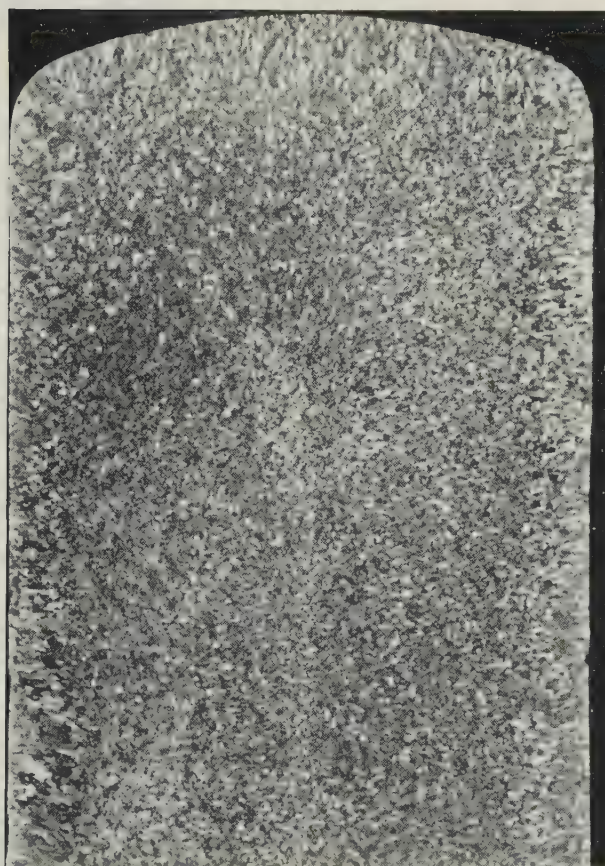


FIG. 3.—Transverse Section of Commercially Pure Aluminium, Direct-Chill-Cast. Etched. $\times \frac{1}{2}$ (reduced by $\frac{1}{4}$ in reproduction).



FIG. 4.—Transverse Section of Aluminium-Manganese Alloy, Direct-Chill-Cast. Etched. $\times \frac{1}{2}$ (reduced by $\frac{1}{4}$ in reproduction).

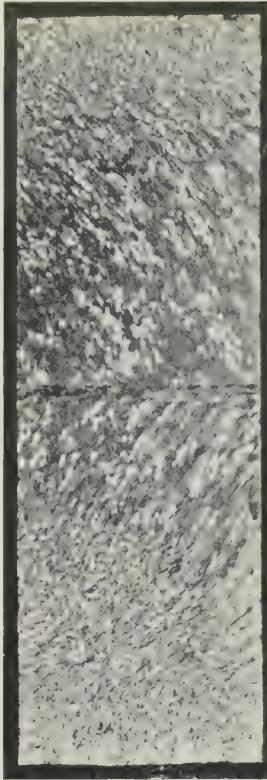


FIG. 5.—Longitudinal Section of Commercially Pure Aluminium, Direct-Chill-Cast. Etched. $\times \frac{1}{2}$.

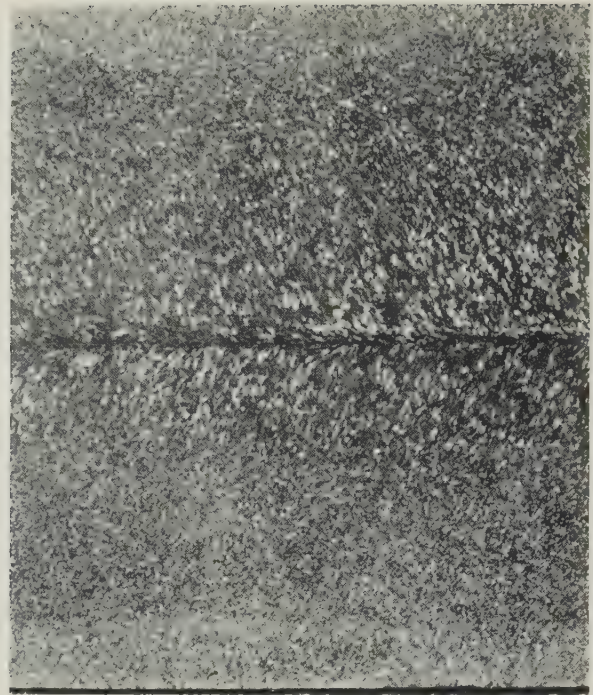


FIG. 6.—Longitudinal Section of Aluminium-Manganese Alloy, Direct-Chill-Cast. Etched. $\times \frac{1}{2}$.

FIG. 7.—Commercially Pure Aluminium Cast in Solid Cast-Iron Book Mould.

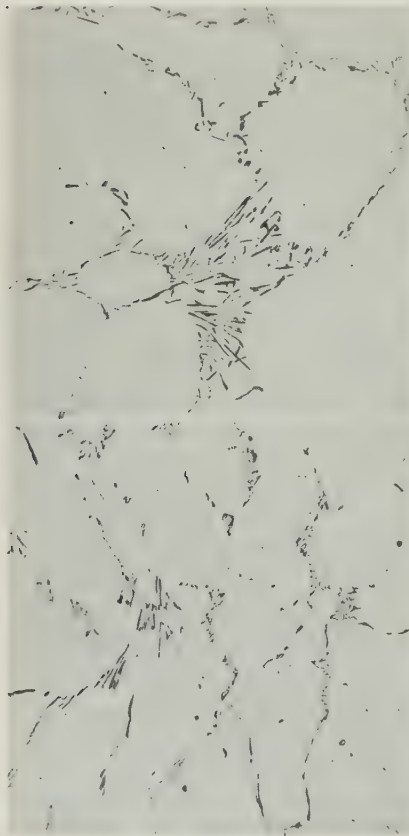


FIG. 10.—Aluminium-Manganese Alloy, Direct-Chill-Cast.

FIG. 8.—Aluminium-Manganese Alloy Cast in Solid Cast-Iron Book Mould.

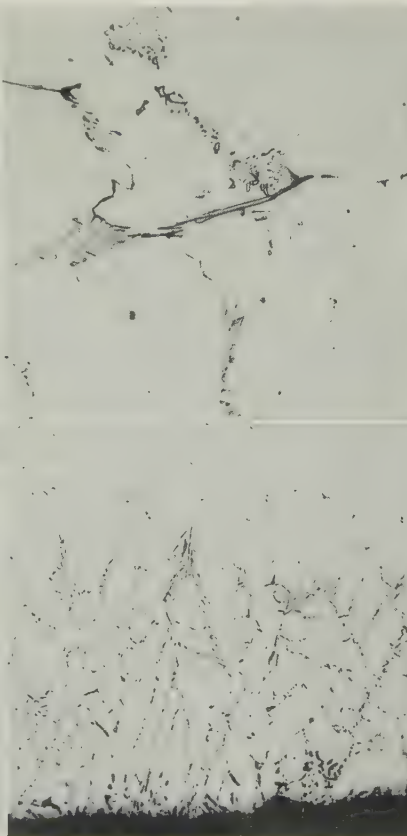


FIG. 11.—Structure at Surface of Commercially Pure Aluminium, Direct-Chill-Cast.

FIG. 9.—Commercially Pure Aluminium, Direct-Chill-Cast.

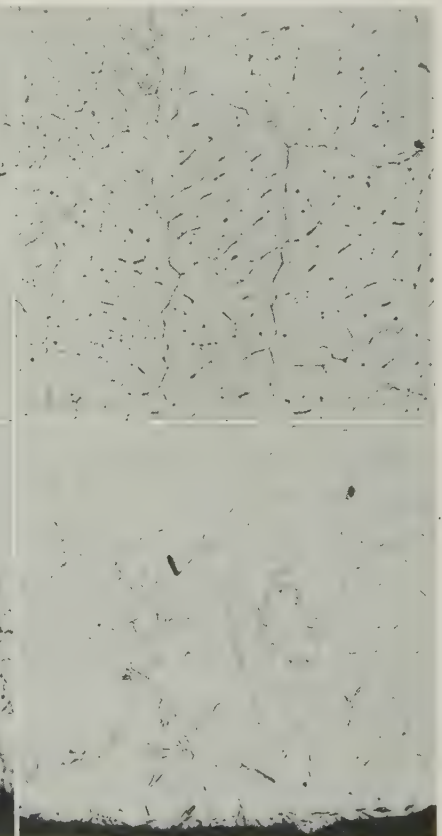


FIG. 12.—Structure at Surface of Commercially Pure Aluminium Cast in Solid Cast-Iron Book Mould.

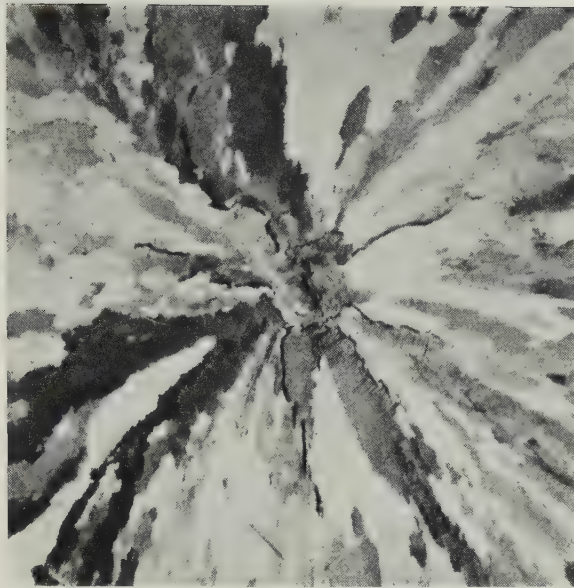


FIG. 13.—Structure at Centre of Transverse Section of 4 × 4-in. Gothic Wire Bar, in Commercially Pure Aluminium Direct-Chill-Cast. Etched. × 2.

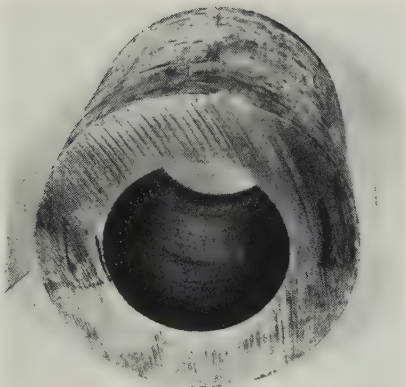


FIG. 14.—Hollow Billet, 20-In. Outside Dia. × 10 $\frac{3}{4}$ -In. Bore, in Commercially Pure Aluminium, Direct-Chill-Cast.

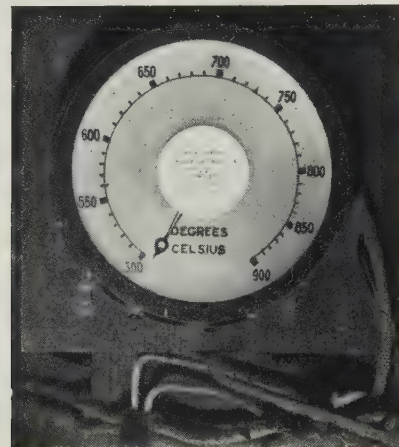


FIG. 15.—20-In.-Dia. Illuminated Dial of Temperature-Indicating Apparatus.

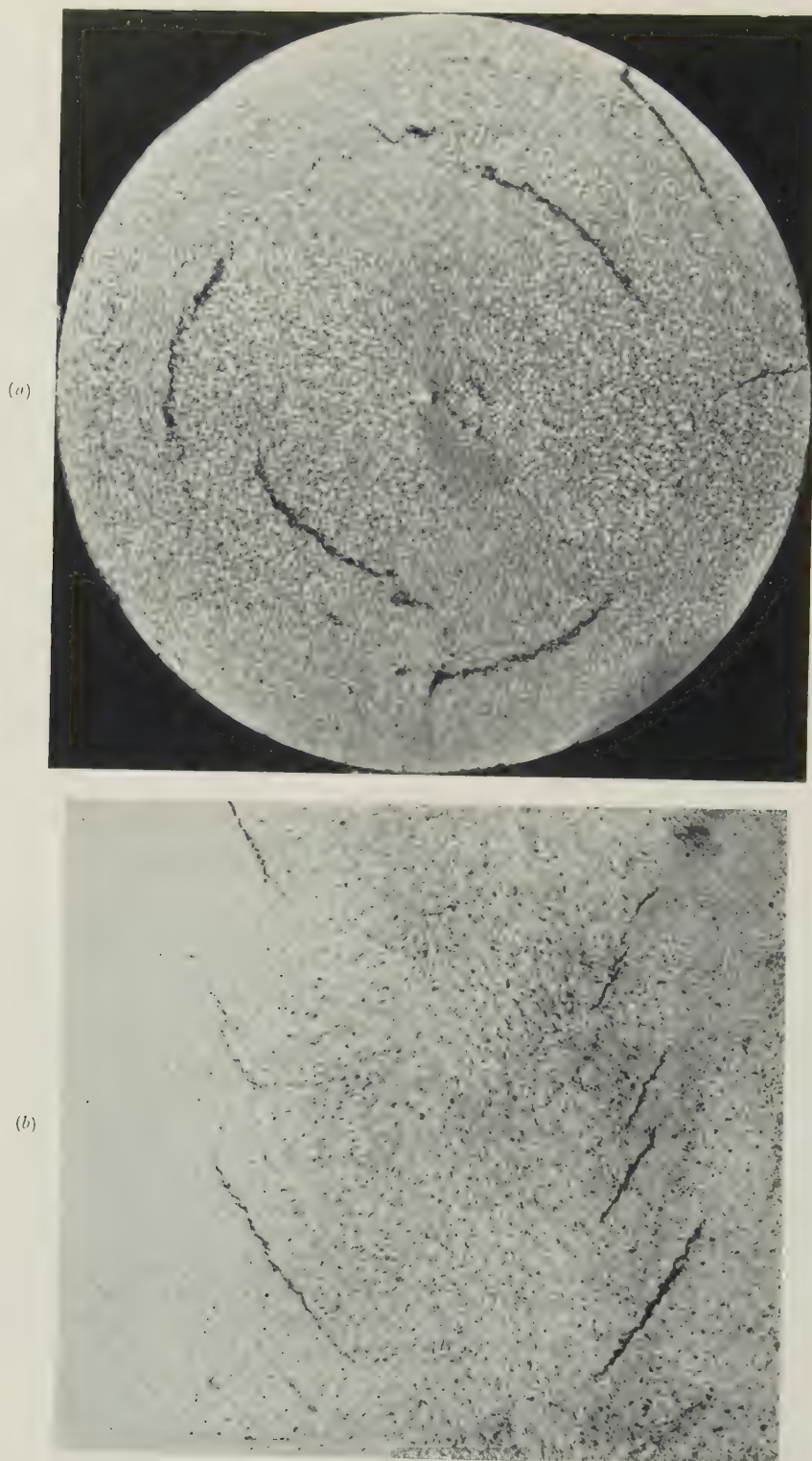


FIG. 16.—(a) Transverse and (b) Longitudinal Section of 6-In.-Dia. Billet in Material of Group 6 (Al-Cu-Mg-Si), Direct-Chill-Cast, Showing Cracks Developed During Homogenizing. Etched. $\times \frac{2}{3}$.

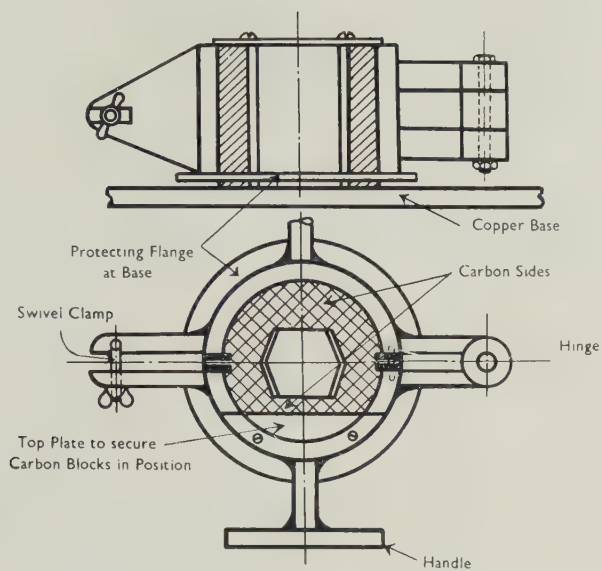


FIG. 1.—Spectrographic Test-Piece Mould for Casting a "Churchill Block". Size of test-piece $3\frac{1}{2}$ in. high, $1\frac{1}{2}$ in. wide, and $2\frac{1}{2}$ in. broad.

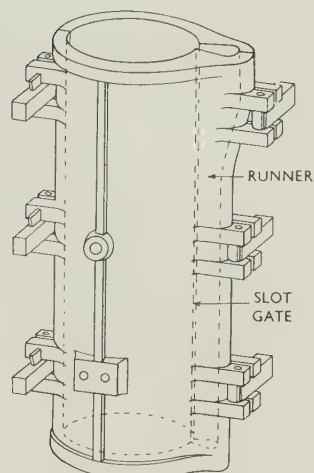


FIG. 2.—Typical Book Mould for Extrusion Billets in the "Classical" Alloys.

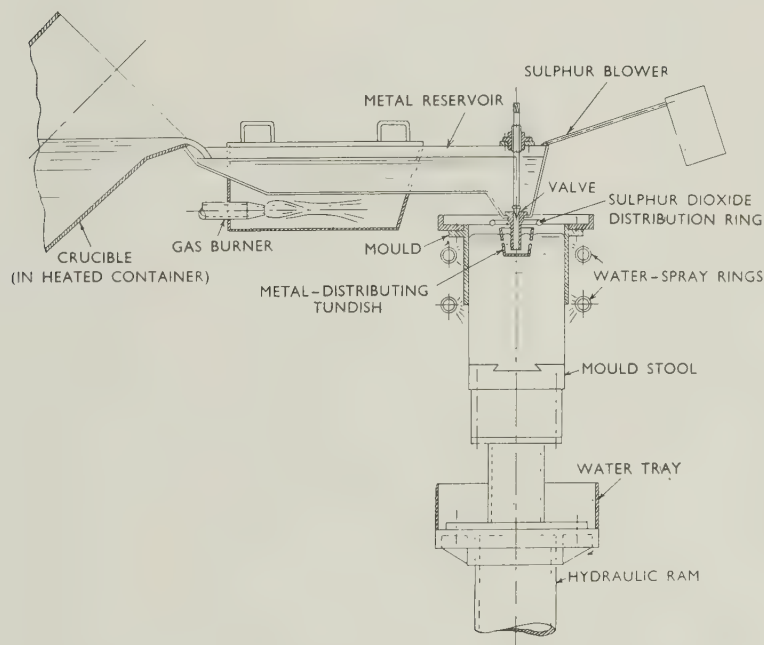


FIG. 3.—The Essential Components of the D.C. Casting Machine.

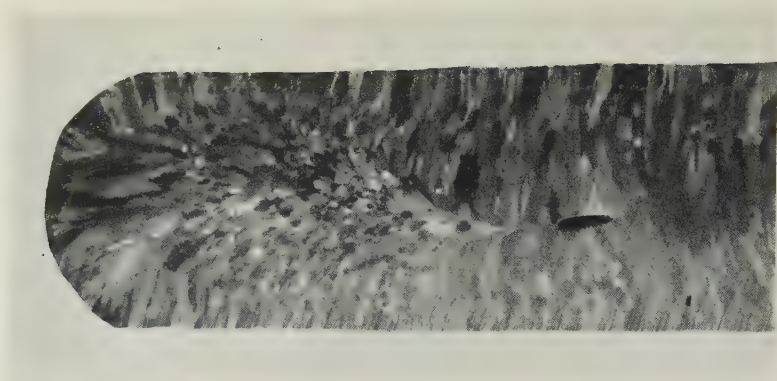


FIG. 4.—Part of a Macro-Etched Transverse Section of an AM503 Alloy Rolling Slab Cast in a Book Mould Showing "Bridging" Cavity and Normal Grain-Size. Approx. $\frac{1}{2}$ size.

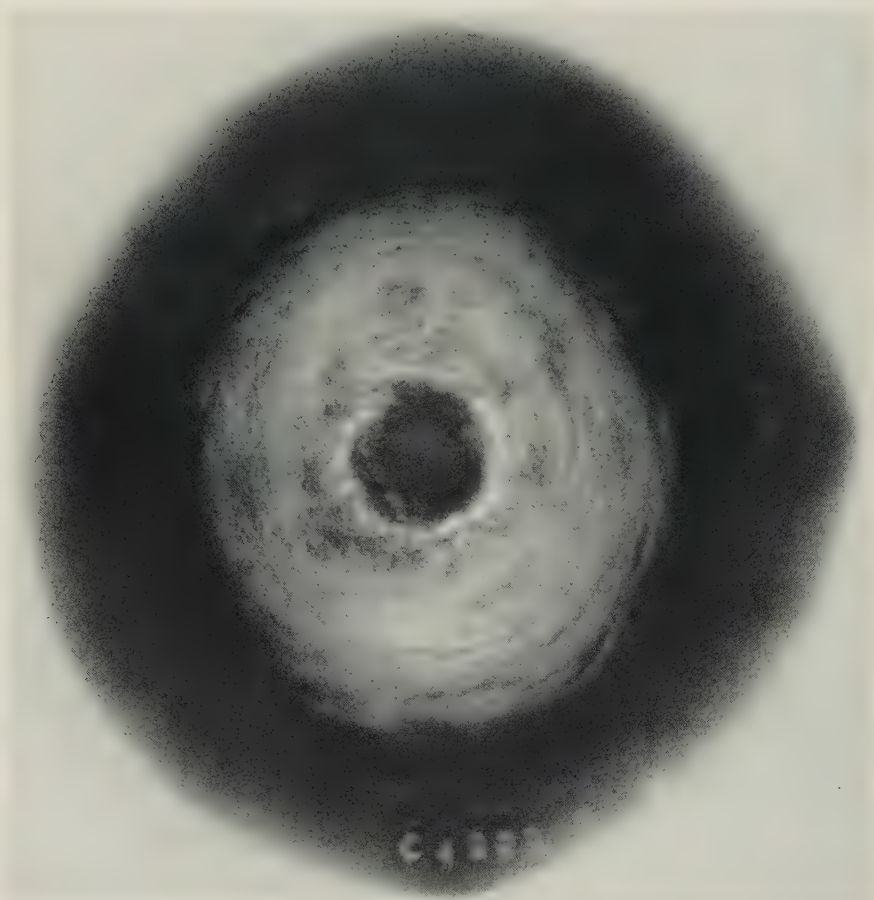


FIG. 5.—Radiograph of Section from AZM Alloy Billet Showing Macro- and Micro-porosity.

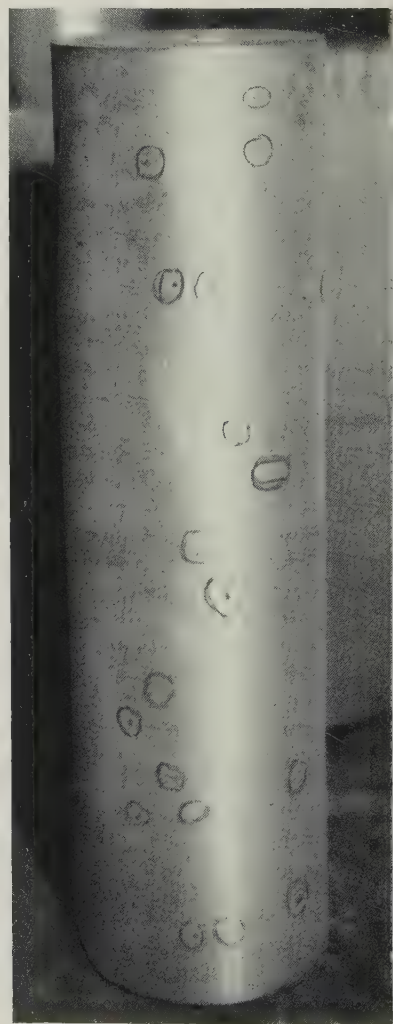
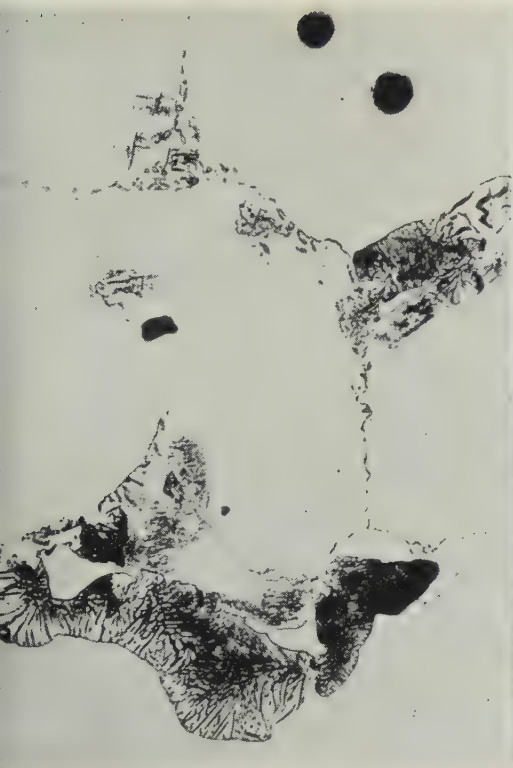


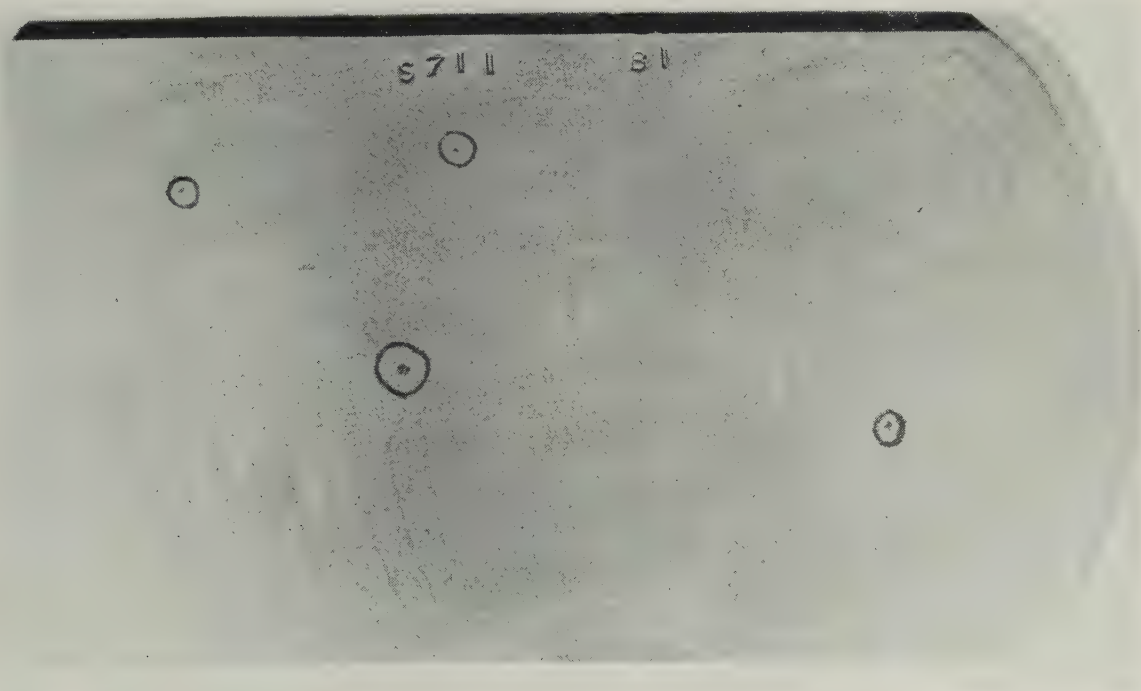
FIG. 6.—Flux Inclusions in a Billet of AZ855 Alloy Disclosed in Machining.



7.—Typical Microstructure of AZM Billet Cast in a Book Mould. As cast. $\times 250$.



9.—Sectioned ZW3 Alloy Billet Showing Banded Zirconium Precipitation and Associated β Phase Resulting from the Use of a Mould Vibrator.



8.—Etched Section from Direct-Chill-Cast Slab Showing Oxide Inclusions.



FIG. 10.—Microstructures of ZW3 Alloy Direct-Chill-Cast Billets and Slab. $\times 500$.

(a) Good structure. Grain-size : 0.055 mm. (b) Satisfactory structure. Grain-size : 0.065 mm. (c) Weak structure. Grain-size : 0.10 mm.



FIG. 11.—ZW3 Alloy Direct-Chill-Cast Slab, Sectioned Vertically, Showing Massive Concentration of β Phase Resulting from Mal-Positioning of the Tundish.

By PROFESSOR F. C. THOMPSON,† D.Met., M.Sc.

SYNOPSIS

A survey is made of the state of metallographic knowledge when the Institute of Metals was formed in 1908.

ELECTION to the Presidency of the Institute of Metals is an honour which any metallurgist must highly appreciate. The responsibilities of the office are, however, heavy, and it is in a spirit of some trepidation that I have taken them over.

The Institute came into existence at a time when the foundations of scientific metallography had been well and truly laid. The advances which have been made since then have in no inconsiderable degree been the result of the work of our own Members, and much of this work is recorded in our *Journal*. The Institute may take a legitimate pride in the part which it has played in fostering knowledge in its own field of science. It seems worth while, therefore, to look back and spend a few minutes in considering the state that metallography had reached when the Institute came into existence in 1908.

The metallographic techniques then available were the microscopic examination of metals and alloys, the construction and interpretation of thermal-equilibrium diagrams, and their correlation with a wide range of chemical, physical, and mechanical properties. These techniques are still employed, though now enriched by others which have since been developed.

Although modern microscopic techniques, such as phase-contrast or the use of polarized light, had not then been applied to metallic systems, the results obtained by the older metallographer were of a high standard, being little, if at all, inferior to those obtained to-day. In no instance is the swing of the pendulum of scientific fashion more evident than in the return to favour of the microscope, with its new accessories, after a period of semi-eclipse, during which some people believed that other, and more modern, techniques had rendered it obsolescent and perhaps even obsolete. After Sorby's disappointment at the earlier neglect of his work, it can readily be imagined with what pleasure he would have welcomed these further developments of the microscope for the examination of metals.

In 1908 most of the methods now employed for the development of microstructures had already been introduced. Heat-tinting had been used with success by Martens, and methods for etching both at high temperature and in vacuum had been employed. A

technique then common, but which has since tended to fade out, was the simultaneous polishing and etching, known as "polish-attack", but, in some forms of electrolytic preparation, something not very different from this has again come to the front.

Not only was it *known* from evidence drawn from a wide variety of sources that the grains in a metal or alloy were crystalline, but the occurrence of sub-crystalline structures had been observed by Andrews as early as 1895. Howe, too, had recognized grains of the "first and second orders"; what, in the case of iron, we should now call α -veining, the smaller grains being regarded by him as "irregular fragments into which the larger grains had been broken". That this sub-granular structure consists of fragments of almost identical orientation was supported by the already well-known fact that slip bands passed from one cell to another without appreciable deviation, unlike the marked change of direction which normally occurs at the crystal boundaries.

Work on the thermal-equilibrium diagrams of metals will always be connected with the names of Roozeboom and especially of Heycock and Neville, and it is of interest that in his recent book on thermodynamics of alloys Lumsden¹ deliberately employed some of their data as being, for his purpose, the best even yet available. Nor was the early work by any means confined to alloy systems of low melting point, for Carpenter and Keeling's iron-carbon diagram was published in 1904. Although such diagrams were essentially regarded as being expressions of experimental fact, the surfaces depicting the heat contents of alloys had already received consideration, a point of view which a little later was discussed by Tammann, and which clearly bears some relationship to the more modern concept of "free energy".

The preparation of pure metals by electrodeposition was an already established technique, and work on the properties of iron, using electrolytic material, which even to-day would be regarded as of high purity, had been done by many people. It was also appreciated that the properties of such iron as deposited differed greatly from those of the same metal in the normal condition, and further that this difference might be due on the one hand to some unknown change of structure, or on the other to the occlusion

* Delivered at the Annual General Meeting, London, 24 March 1953.

† Professor of Metallurgy, University of Manchester.

of hydrogen, the effect of which on iron, and particularly on palladium, had been extensively studied.

The sub-division of metallic alloys into eutectics, solid solutions, and intermetallic compounds had long been understood, and the work of Matthiessen had correlated such metallographic structures with physical properties such as electrical conductivity. Although the arbitrary separation of metallography into the ferrous and non-ferrous fields is of long standing, it is, in fact, one indivisible branch of knowledge. This is well exemplified by Arnold's paper of 1895 on "The Influence of Carbon on Iron".² Shocked to the core as he himself would have been to be told so, this paper is of importance in that it represents one of the earliest attempts to examine in detail the breakdown of a solid solution into a eutectoid.

At the time which we are considering, the idea of the superlattice had not, so far as I am aware, been enunciated, but the evidence again was there. When Roberts-Austen published his liquidus curves for the copper-zinc system in 1897, a horizontal line at a temperature of about 470° C. was introduced over the range in which the β -phase exists. I believe that Le Chatelier had also observed an abnormality in the cooling curve at this point, and I may perhaps be permitted to digress somewhat to remind you of the fact that it was Tammann who, in 1918, first suggested, in the words of Desch: "That a kind of isomerism was possible in alloys consisting of a solid solution; that is, there might be two alloys of the same composition, each consisting of a single phase and having the same crystalline form but differing in properties. The differences would arise from the different distribution of the several kinds of atoms on the points of the space lattice." This work of Tammann is not as generally known as it deserves to be, and it is a pleasure to pay tribute to a master of our science.

The first attempt to elucidate the relationship between atomic volume and the mechanical properties of alloys seems to have been due to Roberts-Austen. His work, coupled with that of Arnold and Jefferson on gold, and of Arnold himself on iron, had demonstrated that, so long as the added element passed into solid solution, the relationship of the atomic volumes of the solvent and solute atoms was a potent factor in controlling the strength (or in other words the structure) of the alloy. Looking back on this work in the light of present knowledge, it is clear, although the fact was then but dimly perceived, that the whole evidence required for an appreciation of the influence of the "size-factor" was already there. The Second Report to the Alloys Research Committee³ in 1893 concludes that: "In all probability, therefore, the introduction of free molecules of an added element must create a disturbance, the nature and magnitude of which will bear some relation to the volume of the disturbing atom." The other factors determining solid solubility were still unknown until they were later revealed by the work of Hume-Rothery. It is of interest, too, that the possibility of interstitial as well as of substitutional solid solutions was thoroughly

well appreciated, and the necessity of the solute atom in the former case being small compared with that of the solvent was fully realized.

With the aid of the recording pyrometer which he had designed, Roberts-Austen investigated, amongst other things, the surfusion of metals and alloys. He showed, for instance, that in those alloys of lead and tin which were slightly richer in lead than the eutectic, considerable surfusion could occur, a fact which was later to assume great significance in connection with the process of "modification".

Lacking modern resources such as X-ray methods of investigation, these earlier workers were at times compelled to rely on specially devised techniques, some of which were of considerable ingenuity. As an example may be quoted the proof by Benedicks that the bars in the austenite-martensite structure were, in fact, magnetic. This he did by placing the polished and etched specimen between the poles of a powerful electromagnet in a bath of colloidal iron in acetone, the iron being attracted to the magnetic "needles" and thus producing a structure similar to that obtained by normal etching. It may be that, with the wider range of techniques at the disposal of the present-day worker, this spirit of ingenuity is now less evident, and, if this be so, metallography has suffered a serious loss.

The classical work of Benedicks on the marked effect which might be exerted by stress, both internal and external, on changes in metallurgical systems had just appeared when this Institute was founded. It was already well known that if a high-carbon steel is quenched from a high temperature, a partial retention of the austenite can be effected. This austenite, however, instead of occurring at the surface as would be expected, since the rate of cooling there is a maximum, is, in fact, found in the centre of the bar. Benedicks's demonstration that austenite could be retained, even in plain carbon steels, right up to the surface by the imposition of compressional stress is one of the most ingenious experimental results of early metallography. He did this by fusing the surface of the steel in a carbonaceous container, thus obtaining a shell of the white-iron eutectic, the rigidity of which during the subsequent heat-treatment of the composite bar inhibited the expansion which results when austenite transforms to martensite, and so prevented the change. This was not by any means, however, the first attempt which had been made to correlate the condition of strain with the transformations in steel, and Roberts-Austen, as far back as 1893, had shown that the change points in steel could be depressed by the application of pressure, and had studied the corresponding effects on Newton's alloy, the ternary eutectic of bismuth, lead, and tin.

Diffusion in solid metals had been the subject of much work both in the ferrous and non-ferrous fields, by Roberts-Austen amongst others, and that such diffusion followed the normal Fick law was known. The diffusion of carbon in iron at very high temperatures had been investigated in detail by Arnold,

and his results have not, so far as I am aware, been examined from the theoretical point of view even to-day. It was realized by some, although this was probably never published, that such solid diffusion involved a distortion of the crystal structure of the metal, and I well remember as a student a most satisfying explanation of the changes of structure brought about by normalizing an overheated steel, based on such lattice imperfections. The day of the "dislocation" had not yet dawned, but that the metallic crystals were, in most cases at any rate, far from perfect was well understood.

Although Wilm had not yet published his pioneer work on age-hardening, there were already, if eyes had been available to see it, clear indications of some such effect. In particular may be mentioned the fact, already well known, that the electrical and magnetic characteristics of soft-iron transformer cores changed in the course of time.

This "ageing"—and the term was already in use—was known to bring about a slow deterioration, resulting in reduced permeability and increased hysteresis. It was further known that these effects were not due to mechanical fatigue, but were the result of some change in the iron resulting from long-continued low-temperature treatment. The effect of both time and temperature on the hysteresis was examined by Roget, whose death was but recently reported, in 1898, and results were obtained identical with those of the classical researches on age-hardening. At as low a temperature as 65° C. and in a period of only 27 days, an increase of the hysteresis loss of over 53% was observed. As the temperature was raised, the rate of increase became greater, then a maximum was shown, and later a falling off, which became more and more rapid, whilst the maximum in the curve fell progressively, until at 700° C. the effect was almost non-existent.

It was the same situation that we have come across repeatedly. The facts were there, but the explanation of the facts awaited more mature consideration, and further accumulation of knowledge drawn from a wide variety of sources.

The first experiments in powder metallurgy had been conducted long before the period with which we are here concerned, and with such experiments the name of Spring of the University of Liège must always be associated. Not only did he succeed in producing compacts even of brittle metals such as bismuth, but he showed that eutectics could be synthesized by pressure, producing the quaternary eutectic of bismuth, lead, tin, and cadmium with a melting point corresponding to that of the eutectic itself, although the most fusible of the constituents of which the powders were made did not commence to melt till a temperature some 130° C. higher had been reached. When such compacts were heated, Tammann, amongst others, obtained the clearest evidence of diffusion, a fact of which some recent workers seem to have been unaware.

The metallography with which we are concerned

was in the main linked with physical chemistry; it might almost be defined as the physical chemistry of the metallic state; and the re-orientation with the formation of a metallurgical-physical bond was still in the future. The revolution which resulted from the introduction of X-ray techniques, for instance, can perhaps be best appreciated by reading a text-book of metallography written before 1914, when Bragg worked out the structure of copper. It may be argued, however, that metallography as a whole has lost substantially in this divorce from physical chemistry, and it is for this, amongst other reasons, that we welcome so whole-heartedly the magnificent text-book of metallography recently published by Professor Masing,⁴ whom the Institute is honouring to-day.

Passing on now to the metallographic effects of cold work, the general outlines of the mechanism of plastic deformation, both by twinning and slipping, were common knowledge. So far as the former was concerned, and despite the fact that the day of X-ray investigation had not yet dawned, it was *known*, as a result, for instance, of the work of Osmond and Cartaud, that the twinning of iron took place on the {112} planes, and the crystallography of the Neumann lamella and of the Widmanstätten pattern in meteorites had been worked out by classical crystallographic methods. It was further known that the space lattice in which α -iron crystallizes was body-centred cubic. That the mechanical properties were a function of crystalline orientation was equally clearly appreciated. That metals and their alloys deform, in general, by a process of slip had been proved conclusively by Ewing and Rosenhain. This work was of fundamental importance not only in demonstrating the mode of deformation, but also in providing some of the most substantial evidence in support of the view that the grains in a metallic aggregate are truly crystalline. Although the process as they envisaged it is now known to be over-simplified, it was not long before the realization came that on the planes of slip fragmentation of the crystal must occur. Further, although the belief was unpublished, there were those who envisaged the slip not as a single, more or less catastrophic fault, but as a series of smaller movements extending only over atomic distances but on a correspondingly large number of planes.

No account of the state of metallographic knowledge in 1908 regarding the deformation of metallic crystals would be complete without some mention of the work of Beilby. As a result of simple, but ingenious experimental techniques, fortified by a keen and inquiring mind, he had shown the effect of polish on a metallic surface and demonstrated that the surface layer was non-crystalline or amorphous. Later electron-diffraction experiments probably did no more than confirm what Beilby had already demonstrated. His attempt to extend this idea to the slip planes of a metal when deformed was more hypothetical, but one aspect of this explanation, namely the temporary, so-called "mobile", condition affords

an explanation, at any rate no less convincing than some which have been subsequently proposed, of the effect of deformation on the elastic limit. That when plastic flow takes place the structure of the crystals is in a highly unstable state is beyond doubt, and it would be no surprise to me if some ingenious experimenter, sooner or later, demonstrates that Beilby was in fact right in his supposition, and that the *immediate* effect of cold work, so far from hardening the metal, is to soften it.

That most articles made from metals and alloys were a seat of internal stresses had long been known, and methods were already available for their measurement, in which field it would appear that Kalakoutsky may claim priority. The originator of the suggestion that the mechanical properties of metals could be improved by pre-stressing is uncertain, but the application of the process to gun tubes was suggested by Jacob in 1907, and probably to him the name "autofrettage" is due. Clearly, then, not only were the bad effects of internal stress only too well appreciated, but also the fact that these might, in suitable cases, be turned to good use, was not novel.

That such internal stresses were unstable even at ordinary temperatures was a matter of common knowledge. The "weathering" of castings before machining was frequently resorted to to minimize distortion during the machining operation, and I remember well a Sheffield firm that "weathered" their nickel-silver ingot for 12 months before cold-rolling, in the belief that the treatment diminished edge-cracking and similar difficulties.

The absorption of energy by a metal due to cold working had been inferred by Osmond and Werth from their calorimetric studies, in which they found that cold-forged steel when dissolved in copper ammonium chloride solution gives out more heat than does the same material in the annealed state. In the case of cold-worked copper, on the other hand, they were unable to find a corresponding difference; this is not surprising in view of the fact that the measured rise of temperature was only about 0.1°C ., whilst their experimental error was roughly one-third of this. In discussing these results, Howe says: "Such minute differences in heat evolution are less naturally ascribed to allotropism (as Osmond and Werth had suggested) than to unnoted differences in condition." "The shattering, stretching, or crumpling of resilient crystals, the creation of stress, macro- or micro-, are possible causes." So wrote Howe in 1891, and these words are even more justified in the light of work which has been done on cold-worked structures since then. O'Neill had shown that cold hammering lowered the density of copper, as far back as 1861, and that a similar effect was to be observed with other materials was already known. "In short", says Howe, "the probabilities seem strongly against Osmond's theory [of allotropy], and in favour of the belief that cold work produces a special kind of change . . . roughly alike in the different malleable metals. What the nature of this change is I will not

attempt to say, beyond surmising that it is essentially physical." Howe then dismisses the idea that the cold-worked material differs from the annealed only in the presence of stress, believing, as has already been mentioned, that some definite physical change has been produced in the crystals themselves. He was aware of the phenomenon which we should now call strain-ageing, and says that gentle heating, which should relieve the stress, may actually intensify the effect of cold working.

Although the term "preferred orientation" was not introduced until much later, the effect was already well known. The first published account of the phenomenon appears to have been due to Stead, who showed that after certain types of mechanical and thermal treatment, the crystals in soft iron assumed a specific orientation such that the cube faces lay in the surface and at 45° to the direction of rolling. He published, in diagrammatic form, a typical example of a uniform crystalline orientation associated with a definite form of brittleness, still known as "Stead's brittleness". In his own words "just as light produces a latent invisible picture on the photographic plate, so the act of rolling steel sets up a latent disposition to crystallize in definite directions". Surely as clear a definition of preferred orientation as, in the absence of that term, could be expected.

I am assured by Dr. Maurice Cook that the effect must also have been known in the non-ferrous alloys ever since cups were first made by pressing (by the ears which it causes), although it was not associated until many years later with a definite crystalline structure.

The excessive crystal growth which results from small amounts of strain followed by an appropriate annealing treatment had also been observed by Stead in the case of iron. It is almost certain that a similar effect must have been equally well known, by those in the industry, to occur with non-ferrous metals and alloys; and single metallic crystals had been cleaved from such coarsely crystalline samples and their properties examined. It was left to Carpenter and Elam, however, to devise, on the basis of such knowledge, their strain-anneal technique for the routine production of single crystals.

I may perhaps be pardoned for mentioning the property now known as damping capacity, a tool increasingly useful in metallographic research. Although that designation was not used until the nineteen-thirties, the ability of a solid to dissipate mechanical vibrational energy had been appreciated for a long time. Weber, in 1837, described work on the elasticity of silk fibres, in which he stated that the decay of amplitude of a vibrating system is not due entirely to air friction, but is partly the result of mechanisms operating within the elastic parts of the system. He further stated that a relationship must exist between the logarithmic decrement and the elastic after-effect which is observed, for example, in galvanometer suspension wires.

In 1865 Lord Kelvin published results of the meas-

urement of the viscosity of solid metals, derived from the fall of amplitude of a system in torsional vibration; he noted the high rate of decay for zinc, compared, for example, with that for copper, silver, and aluminium. Previous analysis of the thermo-elastic effect allowed him to state from fundamental considerations that here was a mechanism which must of necessity, under certain conditions, endow even a perfect isotropic crystal with what we now call damping capacity. Another important conclusion drawn from his experiments was that the variation of damping with frequency differed from that to be expected if the damping forces obeyed the same law as that which holds for a classical viscous fluid.

There is one field in which factual knowledge was almost as complete fifty years ago as to-day. This is the inter-relation between magnetic characteristics and mechanical deformation. The remarkable, and often extremely complex effects of both elastic and plastic deformation on magnetic properties had been examined by a large number of workers. As an example may be cited the transitory circular magnetization produced when a longitudinally magnetized wire is suddenly twisted, or when a longitudinal magnetizing force is suddenly applied to a rod in a state of torsion, and it is of interest that it was in connection with these tests, in which the magnetization lagged behind the twist, that the word "hysteresis" seems first to have been used. This is connected with the Wiedemann effect, and has subsequently been re-examined and related to damping characteristics. There is here an almost inexhaustible mine of information which still awaits detailed

examination in the light of modern magnetic and deformational theory. During the last forty years or so, explanations based on the "domain" theory of magnetism have clarified considerably our understanding of these phenomena, but much still waits to be done.

Such, then, was the broad state of metallographic knowledge when this Institute was formed. The foundations were built on rock and have withstood the storms of time. Is the superstructure equally sound?

Whole sections of the science, i.e. the chemical aspects, have perforce been left out, and many names of illustrious workers are omitted.

Well may it be said of such as these :

"Let us now praise famous men, and our fathers that begat us. . . .

"All these were honoured in their generations, and were the glory of their times."

Have I overpainted the picture? Well, read the first edition of Dr. Desch's "Metallography", published early in 1910, and I think, like the Queen of Sheba, you will agree "Lo! The half was not told me!"

REFERENCES

1. J. Lumsden, "Thermodynamics of Alloys". London : 1951 (Institute of Metals).
2. J. O. Arnold, *Proc. Inst. Civil Eng.*, 1895-96, **123**, 127.
3. W. C. Roberts-Austen, *Proc. Inst. Mech. Eng.*, **1893**, 102.
4. G. Masing, "Lehrbuch der allgemeinen Metallkunde". Berlin : 1950 (Springer-Verlag).

THE KINETICS OF THE EUTECTOID TRANSFORMATION IN ZINC-ALUMINIUM ALLOYS *

1455

By R. D. GARWOOD,† M.Sc., MEMBER, and A. D. HOPKINS,‡ M.Sc.

SYNOPSIS

Time/temperature/transformation diagrams have been constructed for a zinc alloy containing 22.5% aluminium from data obtained in dilatometric, metallographic, and hardness studies. The methods agree as to the times for the start of transformation, yielding a C-shaped curve, with the transformation taking place most rapidly at 150° C. Discrepancies occur, however, in the times for the completion of the transformation; these are discussed and related, on X-ray evidence, to the slow change in composition of the α constituent in the decomposition product.

Age-hardening studies on isothermally transformed specimens are included to explain peculiarities in the hardness results observed at the nose of the C curve. A four-stage mechanism is postulated for the transformation at low temperatures. The reaction rate becomes controlled by diffusion at a lower temperature than is expected from the theoretical "spinodal" line calculated by Borelius and Larsson (*Arkiv Mat., Astron. Fysik*, 1948, [A], 35, (13)).

I.—INTRODUCTION

ALTHOUGH eutectoid transformations occur in a number of binary alloy systems, only the decomposition of austenite in iron-carbon alloys has been extensively investigated. The most effective method of research has proved to be that used by Davenport and Bain,¹ of allowing austenite to transform isothermally at sub-critical temperatures. Besides yielding information on the morphology of the transformation product, this technique enables the course of the transformation to be recorded quantitatively in the form of a time/temperature/transformation (*TTT*) diagram which, for plain carbon steels, has a characteristic C shape. Until recently, structurally analogous transformations in other systems had been neglected, with the notable exception of Smith and Lindlie's research into the decomposition of the β phase in the copper-aluminium system.² However, since 1948 the method has been applied to eutectoid transformations in the copper-aluminium,^{3,4} iron-nitrogen,⁵ copper-silicon,⁶ and copper-beryllium⁷ systems.

In the zinc-aluminium system the eutectoid transformation involves the decomposition of the α' face-centred cubic phase containing 78% zinc into the face-centred cubic, aluminium-rich α solid solution and the close-packed hexagonal, zinc-rich β solid solution.⁸ Although this offers the advantage that the precipitated phases should be primary solid solutions, no comprehensive study using the isothermal-transformation technique has been reported. This may be due to the experimental difficulties arising from the speed of decomposition of the quenched alloy at room temperature.

The rapid decomposition of quenched zinc-alumin-

ium alloys containing between 40 and 80% zinc was first investigated by Hanson and Gayler.⁹ Alloys so treated spontaneously evolved sufficient heat to raise the temperature of the specimen approximately 50° C. within a few minutes. The progress of transformation in a 77% zinc alloy at 0° C. was observed microscopically by quenching previously polished specimens in iced water and etching them after fixed intervals. Decomposition was reported to proceed by the appearance and growth of fine dark fragments within the grains of the α' phase, the conversion being complete within 10 min. of quenching. Age-hardening studies showed that the hardness rose to a maximum within a few minutes and then decreased rapidly, reaching a low constant value after 3 hr.

Later investigations showed that the transformation is accompanied by a contraction in volume of 0.28%¹⁰⁻¹² and that the electrical resistivity varies in a similar way to the hardness.¹³ However, Bugakov¹⁴ reported that the alloy continues to soften slightly over a period of months after the change in resistivity is complete. The period of induction preceding rapid transformation at 0° C. may be prolonged by raising the quenching temperature;¹² alloying elements, notably copper and magnesium, also retard the transformation.^{15, 16}

X-ray studies of the decomposition of the quenched alloy at room temperature have been possible only when the reaction was delayed by the addition of a small amount of magnesium. The face-centred cubic α' lines in the spectra gradually fade on standing, as the hexagonal β lines become visible.¹⁷ The lines of the aluminium-rich α phase appear only later, possibly owing to the lower reflecting power of the aluminium lattice.¹⁸ There is no evidence of any intermediate structure being formed during the

* Manuscript received 11 August 1952.

† Lecturer in Metallurgy, University College, Cardiff.

‡ G.K.N. Group Research Laboratory, Wolverhampton; formerly at University College, Cardiff.

transformation,¹⁶ the final products being the α and β primary solid solutions in equilibrium concentrations.¹⁹

Recently, Borelius and Larsson²⁰ have redetermined certain features of the zinc-aluminium equilibrium diagram, and from their revised data have estimated the points at which the second derivative of the free energy (F) with respect to the concentration (C) is zero ($d^2F/dC^2 = 0$), for the undercooled range of α - α' solid solutions. Kinetic studies on a series of alloys containing 9-82% zinc were carried out to confirm that decomposition is most rapid at these "spinodal" temperatures, the change in resistivity that occurs when the quenched alloy transforms isothermally in an oil bath being used to follow the course of decomposition. Agreement with the theoretical curve

forging. Finally, the rolled strip was normalized by cooling in air after a 1-hr. treatment at 350° C. The alloy contained 77.5% zinc and 22.5% aluminium (by difference).

2. DILATOMETER EXPERIMENTS

A quenching-type dilatometer was designed to take a strip test-piece 9 cm. long \times 1 cm. wide \times 0.113 cm. (0.045 in.) thick. This was maintained in tension between hooked silica rods by means of a weighted lever, as shown in Fig. 1. The soaking furnace and the isothermal-transformation liquid bath stood side by side so that the dilatometer could be quickly transferred to the liquid. The specimens were heated for 30 min. at 375° C. before transformation, and these

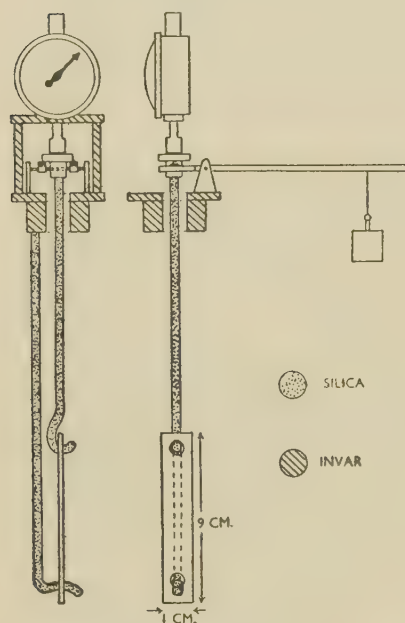


FIG. 1.—Dilatometer for Use with Thin Strip Specimens.

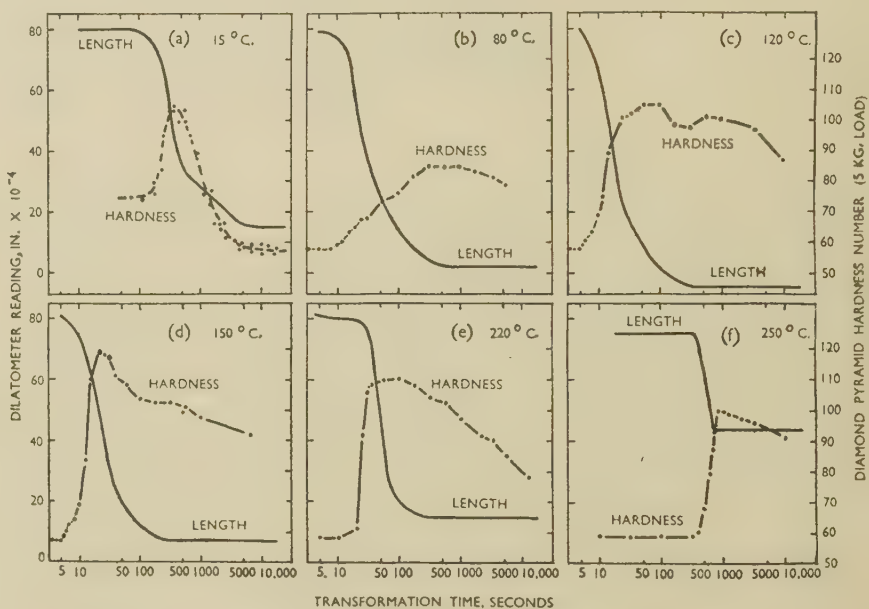


FIG. 2.—The Variation in Length and Hardness of a Zinc-22.5% Aluminium Alloy During Isothermal Transformation at Various Temperatures.

was good, but the complex shape of the resistivity/time curves at the higher zinc concentrations made the analysis uncertain.

II.—EXPERIMENTAL WORK

In the experimental work to be described, the decomposition of a near-eutectoid zinc-aluminium alloy has been studied throughout the temperature range 0°–270° C., and changes in length, microstructure, hardness, and X-ray-diffraction patterns have been correlated at the various temperatures.

1. PREPARATION OF THE ALLOY

The alloy was made from super-purity aluminium (99.99%) and "Crown Special" zinc (99.99%), melted in a Salamander crucible previously coated with an alumina cement wash. The 1-in.-dia. chill-cast bars were annealed for 48 hr. at 350° C. and then hot rolled into strip 0.045 in. thick after flattening by

conditions were rigidly maintained in all tests, since a variation in either time or temperature has been shown to alter the speed of transformation in similar investigations.^{3, 14} The transformation bath was thermostatically controlled to within $\pm 1^\circ$ C. and the liquid mechanically stirred.

The liquids used in the isothermal-transformation bath varied with the transformation temperature; they were low-vapour-pressure oil (270°–220° C.), glycerol-water mixtures (220°–100° C.), water (100°–10° C.), and iced water (0° C.). To test their quenching efficiency, trials were carried out with pure zinc specimens in the dilatometer. These showed that the specimen attained the bath temperature within 5 sec. in water, within 10 sec. in glycerol-water mixtures, and within 20 sec. in oil. The relatively inefficient quench at the higher temperatures was unavoidable because of the limited choice of suitable liquids.

Isothermal-transformation studies with the dilatometer were conducted at intervals of 20° C. through-

out the temperature range 0°–270° C. Typical length/log time curves are plotted in Fig. 2. These and similar curves have been used to construct the time/temperature/transformation diagram shown in Fig. 3. In the range 80°–200° C. it proved impossible to fix accurately the time at which transformation begins; so that within these limits the lines for partial transformation are uncertain. To obtain the points shown, the length change within this range of temperature was estimated from a graph of percentage contraction against transformation temperature.

The *TTT* curve has the C shape characteristic of other eutectoid transformations. The rate of transformation is low just below the equilibrium eutectoid temperature, increases to a maximum at approximately 150° C.—the “nose” of the curve—and then decreases progressively as the temperature falls.

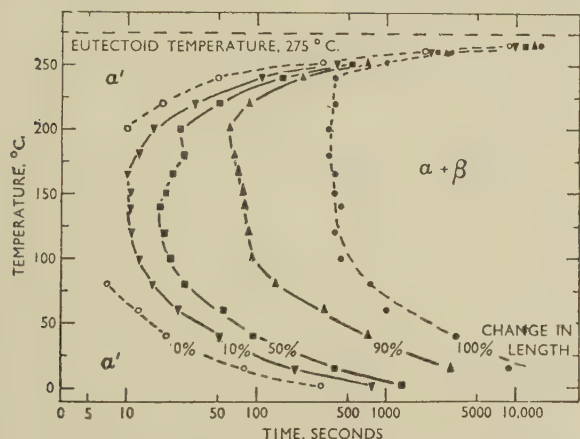


Fig. 3.—Time/Temperature/Transformation (*TTT*) Diagram for Zinc-22.5% Aluminium Alloy, Constructed from Dilatometer Curves.

Below 240° C., the later stages of contraction are prolonged, giving rise to a marked discontinuity in the line representing 100% volume change.

3. MICROSTRUCTURE

For the metallographic studies small specimens of the strip, 0.5 in. long \times 0.25 in. wide, were isothermally transformed in the liquid baths for appropriate time intervals. Transformation was arrested by water-quenching to room temperature, the specimens being left in the quenching water for 24 hr. before sectioning and preparation. This ensured the complete transformation of any residual α' solid solution without the specimen being affected by the accompanying evolution of heat.

The microstructures of typical specimens are shown in Figs. 4–7 (Plate LXII), the high-temperature decomposition product being light in colour, whereas the room-temperature product, corresponding to the untransformed α' , is dark and granular. The mechanism of transformation at these higher temperatures closely resembles the formation of pearlite. At 265° C. transformation begins at a few scattered points which

develop as typical pearlite-group nodules²¹ encompassing parent α' grains (Fig. 4). The newly formed product consists of regular, parallel lamellæ (Fig. 10, Plate LXII) but on prolonged treatment at this temperature the structure coarsens and takes on the appearance of irregular whorls. This process takes place slowly and is not complete (i.e. relatively straight, parallel lamellæ are still present in some areas) after 2 weeks at temperature. At lower temperatures the interlamellar spacing of the initial product decreases (Fig. 11, Plate LXII), the subsequent coarsening and whorling of the structure still being observed. It is not possible to resolve the lamellæ in decomposition products formed below 200° C.

As the transformation temperature falls, the number of centres of growth increases. Nucleation occurs chiefly at the parent α' grain boundaries, but some centres of growth are distributed at random within the grains. The surface of the specimens also nucleates transformation. This can be seen in Fig. 6 (Plate LXII) at the junction between the specimens held, respectively, for 20 and 25 sec. at 220° C. In partially transformed specimens at 180° C. (Fig. 7, Plate LXII), it is difficult to identify the individual centres of growth along the grain boundaries, and the extent of transformation varies from one boundary to another. At 150° C. (Fig. 8, Plate LXII), the contrast between the etching characteristics of the high-temperature and room-temperature transformation products becomes so poor that it is impossible to judge the progress of the decomposition with accuracy, particularly when the reaction is nearing completion.

To overcome this difficulty, the progress of the transformation at lower temperatures was observed in specimens polished before heat-treatment and etched soon after water-quenching. A light repolish was found necessary before etching, but both operations could be completed within 30 sec. This is considerably shorter than the 80 seconds' induction period shown by the dilatation experiments to precede decomposition of α' at room temperature. In this way, the transformation product is obtained in a matrix of the untransformed α' grains. In the captions to the photomicrographs (Plate LXII) the two metallographic procedures are referred to as Method I and Method II, respectively. The clarity with which the course of the transformation can be followed by using the improved technique may be gauged by comparing Figs. 8 and 9 (Plate LXII), which are both of specimens held for 10 sec. at 150° C. The disadvantage of Method II is that the field examined is not truly representative, since the surface nucleates transformation. Stronger etching reagents were necessary to give short etching times, and the dark, mottled appearance of the α' grains in Fig. 9 is due to the severe attack of the 5% caustic soda solution used for etching. An aqueous nitric acid solution gives a less severe attack and a colour reversal of the constituents similar to that reported by Greaves and Wrigton for zinc alloys.²²

The morphology of the transformation product does

not materially alter below the nose of the *TTT* curve. The α' grains are primarily consumed by the development of isolated spherulites in the grains, although transformation starts at the grain boundaries. This can be seen in Figs. 12–15 (Plate LXII), representing various stages of decomposition at 80° C. In Fig. 15, when transformation is just complete, the position of the α' grain boundaries can still be discerned. However, on repolishing and etching a day later, the boundaries were no longer visible.

For studies at room temperature and 0° C., the time when etching was complete was taken as the transformation time. The precipitates formed were similar to those shown for 80° C., although the centres of growth distributed at random within the α' grains were more numerous. The structure of the decomposition product formed at room temperature could not be resolved with an oil-immersion objective, but

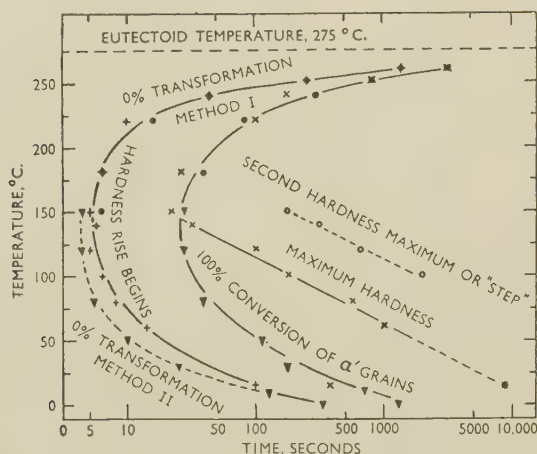


FIG. 18.—Time/Temperature/Transformation Diagram Constructed from Results of Metallographic and Hardness Tests.

- KEY.
- Microstructure (Method I).
 - ▼ " (" II).
 - + Hardness change begins.
 - x Maximum hardness.
 - o Second hardness maximum or "step".
 - * Hardness change complete at room temperature.

it appeared to be granular rather than lamellar. On re-examination some months later, a considerable coarsening of the structure had occurred (Fig. 16, Plate LXIII). The disappearance of all traces of the original α' grain boundaries from the newly formed transformation product, noted at 80° C., was also observed at room temperature.

The times for the beginning and end of transformation obtained from these metallographic studies have been plotted in the form of a *TTT* curve in Fig. 18. At 150° C., where slightly different times for the beginning of transformation were obtained with the different experimental techniques, both points are shown. For this reason the curves corresponding to 0% transformation, as determined by the two experimental methods, have not been joined up.

4. HARDNESS

The hardness changes during room-temperature decomposition reported by previous workers were confirmed by a series of determinations on a specimen quenched from 375° C. The test-piece was left on the anvil of the hardness machine during transformation, the mass of steel preventing an excessive temperature rise. The variation in hardness is shown in Fig. 2 (a) (p. 408) for transformation at 15° C. The hardness rises rapidly to a maximum value 400 sec. after quenching, then falls at a decreasing rate, and finally becomes constant after approximately 90 min. This value was unchanged a week later, but over a period of months there was a further slight decrease of 4 hardness numbers. These results indicate that sufficient time must be allowed for the residual, untransformed α' to decompose, before making hardness determinations to follow the progress of transformation at elevated temperatures. To ensure this, the isothermally transformed specimens were left in the quenching water for 24 hr. before testing. Typical results are recorded in Fig. 2 (b)–(f).

At all temperatures the beginning of transformation is characterized by an increase in hardness which continues until a maximum has been reached. Afterwards the alloy softens, but in no instance is the extent of softening so great as at room temperature (Fig. 2 (a)). The difference between the hardness/log time curves constructed for room temperature and those for all higher transformation temperatures must be emphasized. In Fig. 2 (a), the hardness recorded is that obtaining during the actual decomposition of the metastable α' phase, whereas the other curves show the hardness of mixtures of the high- and room-temperature decomposition products. Hardness/time curves of the latter type could not be plotted below 60° C. because of the small difference in hardness between the two transformation products.

Two maxima appear on the curve for transformation at 120° C. (Fig. 2 (c)), and a similar effect was obtained at 100° C. Evidence of this secondary rise in hardness is also present at 150° C. (Fig. 2 (d)), where a retardation in the rate of softening occurs after 100 sec. A rather larger "step" was observed at 140° C., developing into the second maximum at 120° C. At this temperature, the hardness value obtained during the second rise is slightly lower than the first, but at 100° C., the reverse is true. No secondary rise could be detected at 60° or 80° C.

The times at which the hardness change begins and those corresponding to maximum hardness have been included on the metallographic *TTT* curve (Fig. 18). Below 150° C., where there is a marked discontinuity, the maximum hardness points fall away linearly on the log time scale. The point for room temperature (15° C.) transformation, lying on the dotted extrapolation of this line, represents the time at which softening ceased. The maximum hardness observed during room-temperature decomposition occurs much earlier and is shown as an isolated point.

5. X-RAY EXAMINATION

By using fast film, unfiltered cobalt radiation, and a specimen-film distance of 3 cm., it was possible to obtain satisfactory back-reflection photographs with exposure times of less than 15 min., operating at 50 kV. and 20 m.amp. Under these conditions a series of photographs was taken during the decomposition at room temperature (18° C.) of the water-quenched alloy. Cobalt radiation was chosen because its K_{α} components give the (331) α (aluminium) spectra at an approximate Bragg angle of 74°, well clear of the nearest β -phase (zinc) rings, the (203) and (105), which occur at approximate Bragg angles of 71° and 80°, respectively. The first exposure, made between 2 and 15 min. after quenching, is reproduced in Fig. 17 (a) (Plate LXIII). This shows a spotted (331) ring of the comparatively coarse-grained, parent α' solid solution and also weak, diffuse but continuous rings corresponding to the fine-grained α and β phases in the decomposition product. The lattice parameter of the parent α' calculated from this spectra is 3.986 ± 0.001 kX. Subsequent exposures showed no trace of this spotted ring, thus supporting the microscopic evidence that the α' grains transformed within 11–12 min. of quenching.

The continuous (331) halo of the α phase in the decomposition product extends over a much wider angle than the diffuse (203) ring of the β phase. Although this broad (331) α halo was present in the second exposure of the series (19–35 min. after quenching), it had intensified at its outer extremity. In later photographs this intensified region became a diffuse ring which sharpened with the passage of time, but at a lower rate than the corresponding β spectra. There was also a further slight increase in the diameter of this α ring. No equivalent shifts in the position of the β rings could be detected during ageing. The lattice-parameter changes corresponding to the increase in (331) α ring diameter are given in Table I, together with the equivalent percentages of zinc in solid solution, taken from Ellwood's lattice parameter/composition data.²³ The gradual sharpening of the spectra is also noted in the table, a process which is only finally complete some months after quenching (Fig. 17 (b), Plate LXIII).

The extent of the (331) α halo in the first exposure can be gauged by comparing Fig. 17 (a) and (b). The broad weak halo extends from a diameter just greater than that of the spotted (331) α' rings to the final position of the sharp (331) α rings, attained 3 months later. From this it is concluded that the face-centred cubic constituent in the newly formed decomposition product is of intermediate composition, the equilibrium composition being slowly approached over a period of not more than 4 hr.

Precision lattice-parameter measurements of the final decomposition products were obtained by means of a 19-cm. powder camera, the filings being taken from the specimen used in the back-reflection series. The values obtained were $a = 4.0401(7)$ kX for the

α phase, and $a = 2.6584$, $c = 4.9387$ kX for the β phase at 18° C. On the basis of Ellwood's data for the aluminium-rich solid solution and Burkhardt's²⁴ values for the zinc-rich phase, these correspond to 4.25 wt.-% zinc and 0.05 wt.-% aluminium in solid solution, temperature corrections being made where necessary.

No comprehensive X-ray study of specimens partially transformed at elevated temperatures was attempted, owing to the rapidity with which the residual α' transforms on water-quenching. Back-reflection photographs were taken of specimens transformed at selected temperatures either to the completion of the volume change or to the microscopically observed conversion of the α' grains, where these times differed. In all cases the exposures were made as soon as possible after heat-treatment.

TABLE I.—*Lattice-Parameter Measurements of α Phase in Zn-22.5% Al Alloy Observed During Decomposition at Room Temperature (18° C.).*

Ageing Time	Lattice Parameters			Remarks
	α' , kX	a , kX	Zinc, in Solid Solution, at.-%	
2–15 min.	3.986	4.023	23	Corresponds to mean diffraction angle of broad (331) α halo.
19–35 min.	...	4.031	12	Calculated from intensified outer edge of (331) α halo.
45–60 min.	...	4.033	10	Broad halo replaced by diffuse ring.
2–2½ hr.	...	4.035	8	...
4–4½ hr.	...	4.039	3	K_{α_1} , K_{α_2} just resolvable in Zn lines.
1 day	...	4.040	2	K_{α_1} , K_{α_2} just resolvable in Al lines.
7 days
2 months	...			Separation of K_{α} doublets complete.

At 260° and 240° C., specimens in which the volume change had ended gave sharp spectra, although the specimens were relatively hard when photographed (87 and 103 D.P.N., respectively). Both the α and β rings were shifted to correspond to the higher percentage of alloying elements in solid solution. At 260° C. the rings exhibited regions of locally enhanced intensity, indicating the existence of a definite crystallographic relationship with the lattice of the parent α' solid solution. The effect was not observed at 240° C. nor at lower temperatures.

At 150° C., a specimen held to the completion of the microstructural transformation (40 sec.) gave very diffuse zinc and aluminium rings. However, the broad (331) α halo observed during decomposition at room temperature could not be detected. A specimen transformed to the completion of the volume change (500 sec.) resulted in sharper spectra, particularly for the zinc-rich β phase. All the specimens were re-photographed after standing for several months at room temperature. In this interval both the α and β

phases had altered in composition to the equilibrium value for room temperature, and in the case of the 150° C. specimens there was a noticeable improvement in sharpness. In this interval the hardness of the 40-sec. specimen had decreased from 113 to 88 D.P.N., whereas the 500-sec. specimen was unchanged at 101 D.P.N.

III.—ANALYSIS OF RESULTS

1. CORRELATION OF KINETIC DATA

A comparison of the *TTT* diagrams obtained by the various experimental methods shows that the times at which transformation begins are substantially identical. The metallographic and hardness methods enabled the times for the beginning of transformation at the nose of the *C* curve to be determined, where the dilatometric data were inconclusive. The only significant discrepancy between results occurs when the start of transformation is judged by the microstructure of a surface polished before heat-treatment (Method II). Where this modified technique was necessary, the induction period appears shorter.

Above approximately 240° C. the times for the end of transformation, as determined by the dilatometer and metallographic methods, coincide, but at lower temperatures the contraction continues long after the conversion of the α' grains is complete. The onset of this deviation is marked by a discontinuity on the 100% length-change line of the *TTT* curve (Fig. 3). This continued contraction below 240° C. cannot be correlated with the observed coarsening of the lamellae in the product. Both grain growth and softening continue after the volume change is complete.

Above the nose of the *TTT* curve, maximum hardness is attained slightly before the microstructural changes cease. This rise in hardness is due to the greater hardness of the newly formed high-temperature decomposition product compared with that formed at room temperature. Below 150° C., the times for maximum hardness recede from those corresponding to the conversion of the α' grains until, at 60° C. approximately, they coincide with the end of the volume change. Within this temperature range the "step" or second maximum is observed on the hardness/log time isotherms.

At room temperature, where the hardness/log time curve has a different physical significance, the contraction and softening end simultaneously. Maximum hardness at this temperature again occurs slightly before the α' grains have completely transformed. It is significant that there is a definite change of slope on the contraction/log time curve (Fig. 2 (a)) at this instant. A subsequent, prolonged contraction equivalent to 0.09% of the original gauge-length takes place during the softening stage. The X-ray results indicate that this contraction is due to the slow approach to the equilibrium concentration of the α phase in the newly formed transformation product. The simultaneous softening is associated with the sharpening of the X-ray spectra, but neither

of these processes ceases entirely when the volume change is complete. Both continue over a period of months, accompanied by the gradual coarsening of the microstructure. However, the disappearance of all traces of the α' grain boundaries indicates that a definite structural alteration takes place within the first 24 hr.

The length/time curves for 0° and 40° C. also show abrupt changes in slope at points corresponding to the complete disappearance of the α' phase. The absence of similar discontinuities at 60° C. and higher temperatures is due to a more rapid reaction in the final stages of the contraction. This is also the reason for the absence of a broad (331) α halo in the back-reflection photograph of the specimen held at 150° C. until the conversion of the α' grains is complete. Certainly the contraction continues long after this and is accompanied by a sharpening of the X-ray spectra. At the higher temperatures, e.g. 260° C., where the end of the volume change coincides with the microstructural transformation, the X-ray rings are well defined.

2. AGE-HARDENING STUDIES ON ISOTHERMALLY TRANSFORMED SPECIMENS

The close coincidence of maximum hardness with the 100% transformation line obtained from the metallographic studies, both above 150° C. and during decomposition at room temperature, suggests that a similar coincidence would be found at intermediate temperatures if it were possible to measure the hardness during isothermal transformation. The observed disappearance of the first hardness maximum between 150° and 60° C. may be due to the ability of the newly formed transformation product to soften at room temperature after quenching. On the other hand, the products formed at temperatures above the nose of the *TTT* curve are relatively stable on quenching, and the hardness maxima are retained on the hardness/time curves.

This possibility was investigated by determining the hardness at intervals after water-quenching of specimens held in the isothermal liquid bath for various times. Transformation temperatures of 220° and 80° C. were employed to represent behaviour above and below the nose of the *TTT* curve, respectively. The results of these studies, plotted in Fig. 19, show that:

(a) Quenching before appreciable decomposition of the α' has taken place, does not alter the course of subsequent decomposition at room temperature.

(b) For temperatures above and below the nose of the *TTT* curve, the newly formed transformation product is very hard on quenching. Whereas the 220° C. product undergoes a further slight increase of hardness on standing, the 80° C. specimen softens rapidly, but at a lower rate and to a higher final hardness than a specimen allowed to transform completely at room temperature.

(c) Prolonged holding, i.e. to the completion of the volume change, results in both cases in a reduction in hardness of the alloy. However, the softening is much greater at 80° than at 220° C. This treatment has also stabilized the 80° C. specimen, which undergoes little change on standing at room temperature. The 220° C. specimen again shows a small increase of hardness after quenching.

These studies have confirmed the hypothesis advanced concerning the relative stabilities of the initial transformation products formed at temperatures

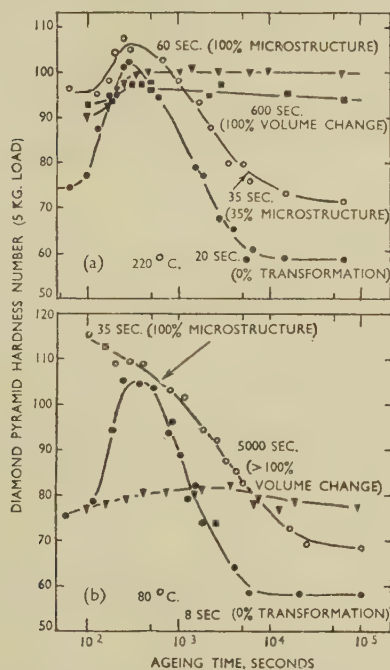


FIG. 19.—Age-Hardening at Room Temperature of Specimens Isothermally Treated at (a) 220° C., (b) 80° C. for the Times Indicated.

above and below the nose of the *TTT* curve. The rate and extent of softening of the product formed below the nose, after quenching to room temperature, are determined by: (i) the isothermal transformation temperature, and (ii) the time the specimen is held at temperature after the conversion of the α' grains is complete. The lower the transformation temperature, the more marked is the softening, leading to the gradual elimination of the first hardness peak. The stabilizing effect that results from prolonged holding at the isothermal bath temperature gives rise to the "step" or second maximum on the hardness/time curves in this temperature range.

3. CALCULATION OF THE THEORETICAL VOLUME CHANGE

The lattice-parameter values obtained during the X-ray investigation at room temperature (18° C.) permit the calculation of the theoretical volume

change. The values used, together with the mean atomic volumes of each phase, are given in Table II. The theoretical decrease in volume obtained from these data is 0.91%, equivalent to a linear shrinkage of 0.31%. This is in good agreement with the experimental value of 0.28% reported by Fraenkel and Wachsmuth.¹²

TABLE II.—Mean Atomic Volumes of Phases in the Zn-Al System at 18° C.

Phase	Lattice Parameter, kX		Zinc Content		Mean Atomic Volume, kX ³
	<i>a</i>	<i>c</i>	Wt.-%	At.-%	
α (Al)	4.0402	...	4.25	1.8	16.485
α'	3.986	...	77.50	58.75	15.833
β (Zn)	2.6584	4.9387	99.95	99.85	15.113

Partial confirmation of the presence of a face-centred cubic constituent of intermediate composition in the newly formed room-temperature decomposition product, was obtained by an estimate of the volume change during transformation. This was based on the assumption that the composition of this material corresponded to a lattice parameter of 4.023 kX, the value derived from the mean diameter of the broad (331) α halo in Fig. 17 (a) (Plate LXIII). On this basis, the theoretical linear contraction during the conversion of the α' grains should be 0.21%. This leaves a residual contraction of 0.10% in the final stage, compared with the observed value of 0.09%.

IV.—DISCUSSION

The eutectoid transformation in zinc-aluminium alloys has been found to be very similar to that of austenite in iron-carbon alloys, the time/temperature/transformation diagram having a simple C shape. The morphology of the transformation product is such that quantitative nucleation and growth studies similar to those of Hull, Colton, and Mehl on pearlite²⁵ could be readily carried out. However, it would be difficult to extend these below a transformation temperature of 180° C. without using specimens polished before heat-treatment. These would give an erroneously high value for *N*, the rate of appearance of nuclei, owing to the disturbed state of the structure at the surface.

There is little obvious change in morphology below the nose of the C curve. The low-temperature product is certainly not bainitic, but closely resembles the anomalous structures obtained by Greninger and Troiano²⁶ in hyper-eutectoid steels. Similar structures have been obtained in iron-nitrogen alloys by isothermal transformation below the nose of the C curve.⁵

A study of the quenched alloy at room temperature indicates that decomposition proceeds in four distinct stages:

- (1) A well-defined incubation period during which no change in physical properties or microstructure is observed.

(2) The growth of the transformation product from the grain boundaries of the parent α' phase and as spherulites from random centres within the grains. This stage is accompanied by a marked rise in hardness and electrical resistivity¹³ and a decrease in volume. The particle size of the phases in the product is sub-microscopic, and the diffuse nature of the X-ray spectra indicates a high degree of lattice strain. The β (zinc-rich) phase in the newly formed precipitate is of approximately equilibrium concentration, but the α (aluminium-rich) constituent is of intermediate composition.

(3) Relief of the highly localized stresses in the newly formed product by recrystallization, resulting in a marked reduction of hardness and electrical resistivity. This is accompanied by further precipitation of zinc from the non-equilibrium face-centred cubic regions. The two processes are related, for when the equilibrium concentration is reached and contraction ceases, the rapid softening also stops.

(4) A slow increase in particle size over a period of months in which the driving force for grain growth is provided by surface tension. During this time, the resolution of the doublets in the X-ray spectra is improved, and there is a further slight decrease in hardness.

The mechanism of decomposition at elevated temperatures is similar, except that stages (2) and (3) overlap to a greater extent as the transformation temperature is raised. Above 240° C. the end of the volume change coincides with the disappearance of the α' grains in the microstructure. It may be inferred that above this temperature the phases in the newly formed product are of equilibrium concentration. The greater hardness of specimens transformed to the completion of the volume change (i.e. to stage (3)), at elevated temperatures is unexpected, but may, in part, be due to further precipitation from the primary solid solutions in the eutectoid mixture after quenching. If this is the case, the hardening must occur very rapidly, for little change in hardness of either the 80° or 220° C. specimens was detected on standing at room temperature (Fig. 19). This rise of hardness does not continue indefinitely with higher transformation temperatures; the wider spacing of the lamellae in the pearlitic product leads to reduced values above the nose of the curve.

The discontinuity on the maximum-hardness line on the *TTT* diagram (Fig. 18) arises because of the ability of the newly formed transformation product to soften on ageing at room temperature. That this softening occurs only when the transformation temperature is below 150° C., is a clear indication of some fundamental change in the nature of the product at this temperature. Similar views have been expressed for other eutectoid transformations.⁵ The relative stability of the product formed at high temperatures may be attributed to a retarding effect which the

higher percentages of alloying elements in solid solution exert on diffusion. However, this will not explain why the differences in behaviour set in so markedly at 150° C., the temperature of most rapid reaction. It is more probable that the size and shape of the sub-microscopic particles in the transformation product are the controlling factors.

In Fig. 20, results from the kinetic studies have been re-plotted in the form of a reciprocal-rate graph. Below 65° C. the curves representing the incubation period, the conversion of the α' grains, and the completion of the volume change, respectively, become linear and are approximately parallel. The activation energy derived from the slope of these lines gives the relatively low value of 9000 cal./g.-atom. This may

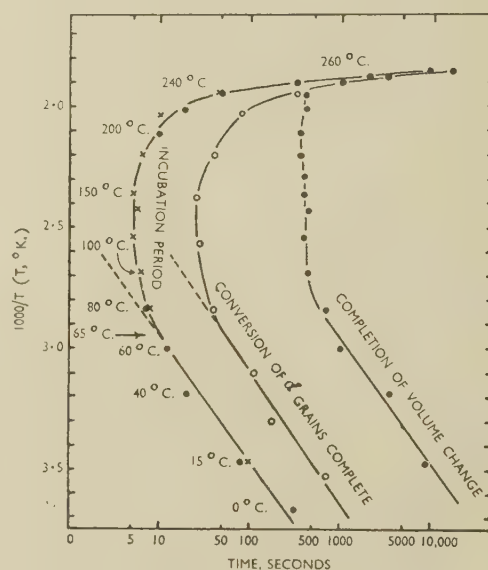


FIG. 20.—Reciprocal-Rate Plot of Kinetic Data.

KEY TO EXPERIMENTAL METHODS.

● Dilation, ○ Microstructure, × Hardness.

occur because concentration gradients formed in the solid solution ahead of the advancing interface are largely dispersed by diffusion through the phases in the newly formed transformation product. In this respect there is some evidence²³ of the existence of vacant lattice sites in the metastable α solid solution.

The temperature at which the reaction appears to become diffusion-controlled (65° C.) is rather lower than the calculated "spinodal" of Borelius and Larsen,²⁰ where $d^2F/dC^2 = 0$ at 100° C. for a 77.5% zinc alloy. However, this is not unexpected in view of the microscopic and X-ray evidence that transformation proceeds by the growth of an ($\alpha + \beta$) agglomerate. In the light of Fisher's analysis of the formation of pearlite from austenite,²⁷ the nucleation of the transformation product involves the nucleation of both the α and the β phases. Below the "spinodal", α segregates can form without an activation energy for nucleation, but this is not the case for the β phase.

Nucleation of the two-phase product is thus most likely at the grain boundaries, where the high degree of lattice strain aids the nucleation of the β . This is true for all temperatures investigated, although the number of centres of growth scattered at random within the grains increases as the transformation temperature is depressed.

The broad (331) α halo in the X-ray back-reflection photograph (Fig. 17 (a)), taken during decomposition at room temperature, has been attributed to the formation of α precipitates of intermediate composition. This is quite possible from free-energy considerations, where the first stage in decomposition is the formation of segregates. These can form without an activation energy for nucleation, provided that d^2F/dC^2 is negative. They may also form at higher temperatures and appear to do so up to approximately 240° C., although an addition of free energy, i.e. an activation energy, is now necessary.

V.—CONCLUSION

Although there are many similarities between the eutectoid transformation in zinc-aluminium alloys and those in other systems, there are also certain differences. The most notable is the formation of a non-equilibrium face-centred cubic constituent in the decomposition product at low temperatures. This is possible theoretically because of the continuous free-energy/composition curve for the undercooled (α - α') range of solid solutions. The subsequent slow approach to equilibrium results in property/time isotherms of complex shape.

ACKNOWLEDGEMENT

The authors wish to thank Professor W. R. D. Jones, Department of Metallurgy, University College, Cardiff, for the provision of research facilities and for his constant interest and encouragement.

REFERENCES

1. E. S. Davenport and E. C. Bain, *Trans. Amer. Inst. Min. Met. Eng., Iron Steel Div.*, **1930**, 117.
2. C. S. Smith and W. E. Lindlief, *Trans. Amer. Inst. Min. Met. Eng.*, **1933**, **104**, 69.
3. D. J. Mack, *ibid.*, **1948**, **175**, 240.
4. E. P. Klier and S. M. Grymko, *ibid.*, **1949**, **185**, 611.
5. B. N. Bose and M. F. Hawkes, *ibid.*, **1950**, **188**, 307.
6. W. R. Hibbard, Jr., G. H. Eichelman, Jr., and W. P. Saunders, *ibid.*, **1949**, **180**, 92.
7. R. H. Fillnow and D. J. Mack, *ibid.*, **1950**, **188**, 1229.
8. G. V. Raynor, *Inst. Metals Annotated Equilib. Diagr. Series*, No. 1, 1943.
9. D. Hanson and M. L. V. Gayler, *J. Inst. Metals*, **1922**, **27**, 267.
10. T. Ishihara, *Sci. Rep. Tôhoku Imp. Univ.*, **1926**, [i], **15**, 209.
11. T. Tanabe, *J. Inst. Metals*, **1924**, **32**, 415.
12. W. Fraenkel and E. Wachsmuth, *Z. Metallkunde*, **1930**, **22**, 162.
13. H. Meyer, *Z. Physik*, **1932**, **76**, 268.
14. V. Bugakov, *Physikal. Z. Sowjetunion*, **1933**, **3**, 632.
15. W. Fraenkel and J. Spanner, *Z. Metallkunde*, **1927**, **19**, 58.
16. E. Gebhardt, *ibid.*, **1941**, **33**, 328.
17. M. v. Schwarz and O. Summa, *Metallwirtschaft*, **1932**, **11**, 369.
18. M. L. Fuller and R. L. Wilcox, *Trans. Amer. Inst. Min. Met. Eng.*, **1935**, **117**, 338.
19. I. Obinata, M. Hagiya, and S. Itimura, *Tetsu to Hagane*, **1936**, **22**, 622.
20. G. Borelius and L. E. Larsson, *Arkiv Mat., Astron. Fysik*, **1948**, [A], **35**, (13).
21. F. C. Hull and R. F. Mehl, *Trans. Amer. Soc. Metals*, **1942**, **30**, 381.
22. R. H. Greaves and H. Wrighton, "Practical Microscopical Metallography", 2nd edn., p. 242. **1933**: London (Chapman and Hall, Ltd.).
23. E. C. Ellwood, *J. Inst. Metals*, **1951-52**, **80**, 217.
24. A. Burkhardt, *Z. Metallkunde*, **1936**, **28**, 299.
25. F. C. Hull, R. A. Colton, and R. F. Mehl, *Trans. Amer. Inst. Min. Met. Eng.*, **1942**, **150**, 185.
26. A. B. Greninger and A. R. Troiano, Jr., *ibid.*, **1940**, **140**, 307.
27. J. C. Fisher, "Thermodynamics in Physical Metallurgy", p. 201. **1950**: Cleveland, O. (American Society for Metals).

The Liquid Immiscibility Region in the Aluminium-Lead-Tin System at 650°, 730°, and 800° C.*

1456

By MORGAN H. DAVIES,† B.Sc., JUNIOR MEMBER

SYNOPSIS

The analyses of successive pairs of congruent solutions, obtained by adding tin to liquid aluminium-lead or aluminium-lead-tin alloys, have been used to plot the miscibility gaps in the liquid alloys at 650°, 730°, and 800° C.

PREVIOUS work at the Fulmer Research Institute, under the sponsorship of the Tin Research Institute, has included a redetermination of the aluminium-tin phase diagram¹ and has shown that aluminium-tin alloys possess interesting potentialities as bearing

materials.² The possibility that lead might replace part of the tin in aluminium-tin alloys has prompted a determination of the miscibility gap in the liquid alloys.

The materials used were Analar-grade lead

* Manuscript received 18 December 1952.

† Fulmer Research Institute, Ltd., Stoke Poges, Bucks.

(99.97+%), super-purity aluminium (99.99%), and Chempur tin (99.99%).

The alloys were melted in alumina crucibles about 10 cm. high with a total volume of 20–25 ml. For the 730° and 800° C. isotherms, aluminium and lead, or aluminium, lead, and tin, were melted in such proportions as to give approximately equal volumes of the two immiscible liquids. Tin was added and the two liquids sampled after holding times of up to 16 hr. In general, 4 hr. (with intermittent stirring with graphite or alumina rods) was sufficient to establish near-equilibrium conditions; 16-hr. holding times relate to overnight standing.

A monotectic reaction takes place in the aluminium-lead binary system at 658° C.;³ the primary aluminium-lead-tin alloys for the 650° C. isotherm were therefore made by adding tin to the aluminium-lead liquids in equilibrium at about 675° C. The temperature was then allowed to fall to 650° C. and sampling proceeded in the usual way.

Samples were obtained from the less-dense liquid by dipping 1-mm.-bore silica quills into it, and creating a partial vacuum by means of a controlled leak to a vacuum reservoir. After the quill had been dipped into the denser liquid, argon under pressure was allowed to trickle for a short time through the tube to force out all the liquid. The pressure was then reduced, and a partial vacuum again created, so that only liquid appropriate to the depth of immersion was sampled.

A sample about 8 in. long was obtained. At the lower tin concentrations no appreciable errors were introduced by analysing only small sections of this sample, but for the higher tin concentrations the total sample was dissolved and aliquot parts were taken for the triple determination, thus avoiding errors due to segregation. Some silica contamination was encountered at 800° C., but this was reduced to a minimum by preheating the quills above the melt, thus reducing the time of immersion required to regain stable conditions. The method is similar to that used by Campbell *et al.*, in investigating the aluminium-indium-tin system.⁴

Tin was determined by titration of a chloride solution (to which CaCO_3 and KI were added) against chloramine-*T*. Lead was determined as PbO_2 deposited on the anode during electrolysis. The presence of copper ions in the solution prevented the deposition of lead on the cathode. Aluminium was precipitated as $\text{Al}(\text{OH})_3$, and estimated as Al_2O_3 . At high tin concentrations the error in individual determinations was estimated to be 0.5–1%. Analysis for lead and

tin in aluminium-rich liquids (>75%), and for aluminium and tin in lead-rich liquids, was probably accurate to 0.1%.

Some 150 analyses were carried out, and the results were used to draw the three isothermal curves shown in Fig. 1. For the sake of clarity the tie-lines are included on the 800° C. isotherm only. The measured

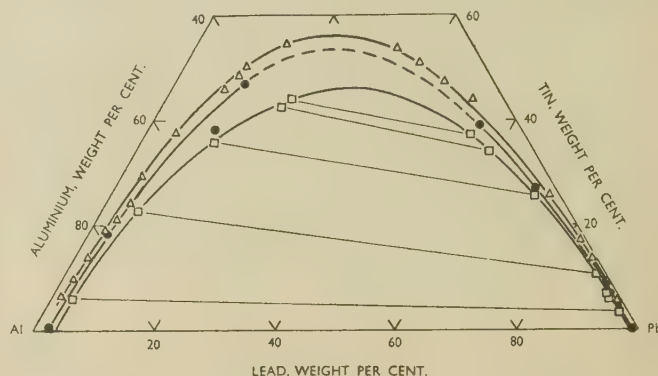


FIG. 1.—The Liquid Immiscibility Region in the Aluminium-Lead-Tin System at 650° (Δ), 730° (\bullet), and 800° C. (\square).

values of the solubilities in the aluminium-lead binary system at 730° C., and the extrapolated values at 800° C. are in fair agreement with the published work.³

It is clear that only a small percentage of lead can be added to aluminium-tin alloys containing up to 30% tin, before the composition enters the miscibility gap. Additions of lead would therefore have to be closely limited and controlled.

ACKNOWLEDGEMENTS

The author and the Fulmer Research Institute wish to thank the International Tin Research Council for permission to publish this note. The author's thanks are due to Miss P. Cutler, who performed the chemical analyses, and to Dr. H. K. Hardy, for helpful criticism.

REFERENCES

1. A. H. Sully, H. K. Hardy, and T. J. Heal, *J. Inst. Metals*, 1949–50, **76**, 269.
2. H. K. Hardy, E. A. G. Liddiard, J. Y. Higgs, and J. W. Cuthbertson, *Proc. First World Met. Congress (Amer. Soc. Metals)*, 1951, 457; also *Metal Progress*, 1951, **60**, (4), 97.
3. W. L. Fink and L. A. Willey, *Metals Handbook (Amer. Soc. Metals)*, 1948, p. 1165.
4. A. N. Campbell, L. B. Buchanan, J. M. Kuzmak, and R. H. Tuxworth, *J. Amer. Chem. Soc.*, 1952, **74**, (8), 1962.

THE INFLUENCE OF THALLIUM ON THE CREEP OF LEAD*

1457

By R. C. GIFKINS,† B.Sc., A.I.M., MEMBER

SYNOPSIS

Extruded specimens of high-purity alloys of lead with additions of thallium in the solid-solution range have been tested at room temperature, under constant load, after a standard annealing treatment. At a stress of 500 lb./in.², progressive additions of thallium produced first a decrease in minimum creep rate, then with more than 0.5% thallium a marked increase, and above about 8% a decrease again. Finally, at 40% thallium, the creep rate increased and corrosion and cracking occurred. Tests at lower stresses revealed similar but less marked changes. The extension on loading decreased regularly, but the complex variations in extension were present after one day's creep. The average creep rate and time to rupture showed variations similar to those of the minimum creep rate. The elongation at rupture was a maximum at any given stress for alloys containing about 8% thallium, and this elongation was greater the lower the stress; the largest extension recorded was 372%.

The variation in creep characteristics is explained in terms of the relative proportions of slip and grain-boundary movement, which depend on the grain-size, particularly in alloys containing less than 8% thallium. This has been confirmed by tests on specimens of one alloy prepared in a range of grain-sizes; the creep rate varied in a manner similar to that of a range of alloys of comparable grain-size. In alloys containing more than 8% thallium, although the grain-size continued to diminish, the reduced creep rate was apparently due to strengthening of the grain boundaries, since grain-boundary flow still appeared to be the major mechanism of deformation. It is suggested that this change in creep-resistance at about 8–10% thallium may be connected with the rate of change of lattice spacing, as Tang and Pauling (*Acta Cryst.*, 1952, 5, 39) have recently shown that only a slight decrease in lattice spacing takes place up to 10% thallium, but that it subsequently decreases more rapidly.

I.—INTRODUCTION

DURING a preliminary survey of the effect of solute atoms on the creep of lead, it was found that the progressive addition of thallium changed the creep characteristics in a complex manner, even though the maximum addition was well below the limit of solid solubility. A more detailed examination of the effect of thallium additions thus seemed desirable, both to make a general comparison of various additions of an element in solid solution and to make a systematic study of the creep of a series of alloys containing increasing amounts of an added element in solid solution. Although there are other elements which have a high solid solubility in lead, thallium was chosen because of the preliminary indications of complex behaviour, and also because it was known that the alloys could be polished and retained in the polished condition for sufficient time for microscopical observations to be made during creep. Such observations, with related X-ray back-reflection photographs for one of the lead-thallium alloys, have been published already.¹

Previous workers have paid considerable attention to the effect on creep of specific additions of various elements to various metals, but they have been concerned mainly with comparing one addition with another and with the addition of amounts exceeding the solid solubility limit. Extensive reference to such investigations has been made by Sully² and by Smith.³

Hanson and Sandford^{4, 5} recognized the importance of grain-size as a factor governing creep; Greenwood and Worner⁶ made standard small additions of a number of elements to lead and found some to produce marked changes in creep. These latter workers⁷ and Russell⁸ also showed that the influence of an element could be greatly affected by the purity of the basis lead. Phillips⁹ found evidence that solid-solution alloying decreased the creep of lead, the effect of standard additions of elements being probably proportional to their maximum solid solubilities. Most of the above tests were made after standard treatments, so that variations in grain-size were present. Recently, Robinson, Tietz, and Dorn,¹⁰ investigating the effect of solute atoms on the creep of aluminium, kept the grain-size constant, although this introduced the possibility of other changes dependent on the differing heat-treatments. Thus the present author, in uncompleted work, has found that the time of annealing at a given temperature greatly affects the creep of high-purity lead, although the grain-size is little altered.

The present paper describes experiments designed to examine the influence of a particular solute atom, thallium, on the creep of high-purity lead. The results given consist of creep data together with microscopical and X-ray observations which illustrate the variations in creep characteristics.

* Manuscript received 5 June 1952.

† Baillieu Laboratory, University of Melbourne, Australia.

II.—MATERIALS AND EXPERIMENTAL TECHNIQUE

The alloys used were made from lead containing 0.0008% total impurities and thallium containing traces of calcium and cadmium as determined spectroscopically. Full details of the experimental techniques of making the alloys and specimens, and of the testing procedure, have been given previously.¹ Briefly, the procedure consisted of vacuum casting, working and annealing to homogenize the alloys, and then extrusion at room temperature to form specimens $5 \times \frac{1}{2} \times \frac{1}{8}$ in. These were annealed for $2\frac{1}{2}$ hr. at 100°C . (except where otherwise stated) and chemically polished in a 70 : 30 mixture of acetic acid and hydrogen peroxide. Creep was induced by direct loading, axially arranged, at room temperature, namely $70^\circ \pm 2^\circ\text{F}$. ($21^\circ \pm 1.5^\circ\text{C}$). Although for short periods during some of the tests the temperature rose to 80°F . (26.7°C) when the weather was very hot, it was not possible to detect any change in steady-state creep which could be attributed to such temperature changes. Extension was measured on a 2-in. gauge-length by a travelling microscope, reading to the nearest hundredth of a millimetre; the distance between the specimen grips was 3 in.

III.—EXPERIMENTAL RESULTS

1. CHEMICAL ANALYSIS

Chemical analyses were made by a straightforward gravimetric method for all except the two most dilute alloys, for which a colorimetric method was used.

TABLE I.—*Grain-Size and Hardness of Lead-Thallium Alloys, Extruded and Annealed for $2\frac{1}{2}$ hr. at 100°C .*

Thallium, wt.-%	Grains in Standard Area ($3\frac{1}{2} \times 2\frac{1}{2}$ in.) at $\times 150$	Mean Grain Dia., μ , mm.	Reciprocal of Grain Dia., $1/\mu$, cm^{-1}	Diamond Pyramid Hardness No.
0	1.6	0.40	25	3.2
0.01	4.5	0.24	42	3.7
0.25	12	0.15	69	3.8
0.47	43	0.08	131	3.7
1.25	52	0.07	144	3.9
2.45	70	0.06	166	4.3
3.92	122	0.05	220	4.2
4.35	140	0.04	238	4.4
4.81	134	0.04	230	4.5
7.87	137	0.04	233	5.0
13.45	192	0.03	276	5.5
26.58	492	0.02	445	6.8
40.50	650	0.02	510	6.9

The results of these analyses are given in the first column of Table I. The alloys were well within the δ terminal solid-solution field, which extends to 87.5 at.-%* according to Tang and Pauling.¹¹

2. GRAIN-SIZE and HARDNESS

The grain-size of all the extruded and annealed alloys was measured by counting the grains on

polished specimens in a number of random, standard areas. The mean grain diameters are given in Table I. The incidence of annealing twins became progressively greater with increasing thallium content; thus the number of twinned grains in the 2.45% alloy was about one in eight, whereas in the 13.45% alloy about half the grains were twinned. Table I also shows that the hardness increases fairly regularly with thallium content.

3. CONSTANT-LOAD CREEP TESTS

Annealed specimens of all the alloys and of the pure lead were loaded at initial stresses of 500 and 300 lb./in.²; most of the alloys were also loaded at 200

TABLE II.—*Creep of Lead-Thallium Alloys at 500 lb./in.².*

Thallium, wt.-%	Initial Extension, %	Extension after 1 Day, %	Extension at Rupture, %	Time to Rupture, days	Minimum Creep Rate, mm./mm./day $\times 10^{-4}$	Duration of Minimum Creep, days
0	0.93	1.55	34	26	32.5	2
0.01	0.69	1.51	50	46	27.5	10
0.25	0.45	1.35	45	151	14.7	11
0.47	0.65	1.17	60	390	7.0	85
1.25	0.47	1.30	100	220	17.1	42
2.45	0.48	1.60	208	99	48.0	25
3.92	0.28	1.60	159	48	93.0	7
4.35	0.32	1.56	180	55	86.0	9
4.81	0.27	1.57	122	68	66.0	7
7.87	0.10	1.38	228	50	100.0	5
13.45	0.08	1.15	101	89	53.0	23
26.58	0.08	0.30	67	299	7.6	50
40.50	0.03	0.30	(48)*	(88)*	(24.0)	(5)

* Specimens unloaded before fracture.

TABLE III.—*Creep of Lead-Thallium Alloys at 300 lb./in.².*

Thallium, wt.-%	Initial Extension, %	Extension at Rupture, %	Time to Rupture, days	Minimum Creep Rate, mm./mm./day $\times 10^{-4}$	Duration of Minimum Creep, days
0	0.39	(9.6)*	(717)*	14.5	190
0.01	0.25	(4.0)*	(400)*	8.0	(380)*
0.25	0.20	(4.4)*	(350)*	11.4	(330)*
0.47	0.20	(11.2)*	(724)*	15.0	(700)*
1.25	0.16	(3.1)*	(350)*	40.0	(330)*
2.45	0.12	191	538	127.0	186
3.92	0.22	273	267	290.0	38
4.35	0.02	175	188	316.0	20
4.81	0.08	205	241	230.0	30
7.87	0.10	372	221	310.0	19
13.45	0.02	325	321	120.0	48
26.58	0.00	(35.5)*	(740)*	27.6	148

* Test and minimum creep still in progress.

lb./in.², and some at higher stresses. All the tests at 200 lb./in.² and a few at other stresses are still in progress, but the rest were carried through to rupture. Certain numerical features of the tests are given in Tables II, III, and IV.

* For lead-thallium alloys, wt.-% and at.-% may be interchanged without appreciable error.

Duplicate tests were made with the pure lead and several alloys; these showed, however, sufficient consistency for the properties to be assessed from single tests, except sometimes for the time and strain at rupture of specimens that recrystallized during creep. A

TABLE IV.—*Creep of Lead-Thallium Alloys at 200, 400, and 600 lb./in.².*

Thallium, wt.-%	200 lb./in. ²		400 lb./in. ²		600 lb./in. ²	
	Min. Creep Rate, mm./day $\times 10^{-3}$	Duration of Min. Creep, days	Min. Creep Rate, mm./day $\times 10^{-3}$	Duration of Min. Creep, days	Min. Creep Rate, mm./day $\times 10^{-4}$	Duration of Min. Creep, days
0	46	(300) *	35.5	25
0.01	27	(336) *	34.5	29	60	2
0.25	43	(350) *	25.0	60
0.47	48	(600) *	25.0	286	14	15
1.25	150	(300) *
2.45	477	480	250	40	140	12
3.92	1100	235
4.81	850	200	400	15
7.87	895	175
13.45	682	175

* Test and minimum creep still in progress.

test in which the "creep yield" curve¹² was plotted against strain on a logarithmic scale was devised. This served as a check on the self-consistency of tests at various stresses for any one alloy, because the logarithmic plot yielded a straight line, and unreliable tests were readily seen as those which did not lie on such straight lines.

The addition of thallium produced marked changes in the creep of lead at 500 lb./in.² stress; these can be summarized as follows:

(a) Up to 0.47% thallium there was a decrease in minimum creep rate and a marked increase in total life, while the total extension increased slightly.

(b) From 0.47 to 7.8% thallium there was a marked increase in minimum creep rate with a corresponding diminution in the duration of minimum creep and of the total life, but the total extension increased markedly.

(c) From 7.8 to 26.6% thallium there was a decrease in minimum creep rate, back to values comparable with those in group (a), and at the same time a marked increase in total life and a decrease in total extension.

(d) The 40.5% thallium alloy gave a curve similar to group (b), but no minimum creep rate, since the creep rate was found to increase continuously throughout the test. (The tests on this alloy were discontinued after 90 days because corrosion took place.)

These trends were repeated at lower stresses, although the alloys in group (a) showed progressively smaller changes with decreasing stress; at 200 lb./in.² stress the change from group (b) to (c) occurred at a lower thallium concentration. Recrystallization

during creep occurred at an increasingly high strain in tests with the alloys of group (a) only.

4. THE EFFECT OF GRAIN-SIZE ON THE CREEP OF 4.35% AND 26.58% THALLIUM ALLOYS

Two specimens of the 26.58% thallium alloy were annealed at 250° C. instead of at 100° C., and this resulted in a larger grain-size; the creep rates of the coarse-grained specimens both at 500 and 300 lb./in.² were found to be much lower than those for the fine-grained ones. Details of these tests are given in Table V.

TABLE V.—*Effect of Grain-Size on the Creep of the 26.58% Thallium Alloy.*

Annealing Temp., °C.	Mean Grain Dia., d, mm.	500 lb./in. ²			300 lb./in. ²		
		Extension, %	Duration of Creep, days	Min. Creep Rate, mm./day $\times 10^{-4}$	Extension, %	Duration of Creep, days	Min. Creep Rate, mm./day $\times 10^{-5}$
100	0.02	67 *	300	7.6	28	650	27.6
250	0.24	1.5	650	0.23	0.5	650	0.77

* Fractured; the other tests still in progress.

TABLE VI.—*Grain-Size, Hardness, and Creep at 300 lb./in.² of the 4.35% Thallium Alloy.*

Annealing Temp., °C.	Grains in Standard Area at $\times 150$	Reciprocal of Grain Dia., $1/d$, cm. ⁻¹	Diamond Pyramid Hardness No.	Initial Extension, %	Min. Creep Rate, mm./day $\times 10^{-3}$
100	140	240	4.3	0.02	316
114	96	190	4.1	0.10	141
126	63	155	3.9	0.20	56
136	43	130	3.9	0.22	30
146	29	110	3.8	0.22	18
175	12	69	3.7	0.28	6

All the tests still in progress (200 days).

Because of these striking differences, specimens of the 4.35% thallium alloy were annealed at various temperatures to provide a range of grain-sizes, and these specimens were tested at an initial stress of 300 lb./in.². Details of the tests are given in Table VI. They show a marked and regular decrease in creep rate with increasing grain-size, and the minimum creep period was well defined.

5. METALLOGRAPHIC AND X-RAY-DIFFRACTION OBSERVATIONS

Detailed examination of many specimens was carried out during creep, using both optical and X-ray-diffraction techniques. Those relevant to the changes in creep characteristics brought about by thallium additions are reported below. It is hoped to present more general observations elsewhere.

The polishing and X-ray techniques used have been described previously.¹ For optical or X-ray examination specimens were removed on a flat plate to the appropriate camera, but no systematic differences,

such as those observed by Chaston,¹³ were found between the creep curves for these specimens and others which were continuously under load. The alloys are considered in the groups used in the previous subsection.

(a) *Alloys Containing Up to 0.5% Thallium*

For pure lead and alloys containing less than 0.5% thallium, slip appeared progressively in all grains at the higher stresses, although there was evidence of grain-boundary flow, for boundaries broadened and migrated, as shown in Fig. 1 (Plate LXIV) on a specimen after 4.5% extension in 8 days. Fig. 12 (Plate LXV) shows, by the displacement of marker lines, that there was some rotation of grains at this stage. As the thallium content increased, slip became less complex and less marked. At low stresses the slip traces were fewer and more widely spaced; boundary migration was considerable, as Fig. 2 (Plate LXIV) shows, on a specimen of pure lead after 5% extension in 270 days. Recrystallization during creep occurred in the pure lead at 3–5% extension and at progressively higher extensions in the alloys; the new grains were large and usually very irregular in shape. Coarse slip appeared in the new grains, crossing the old grain boundaries; there was some migration at the new boundaries.

The X-ray back-reflection observations showed parallel changes; before recrystallization during creep, arcs occurred along the Debye circles of the initially sharp reflections at all stresses. Fig. 14 (Plate LXV), which is an X-ray back-reflection photograph of pure lead, illustrates this. After recrystallization, new large reflections were observed, and these subsequently became arcs and often tended to show a spotty sub-structure, particularly at the lower stresses. This type of reflection, which has been observed previously by Hirst¹⁴ in large and single crystals of lead, will be considered in detail in a future paper.

(b) *Alloys Containing 0.5–8% Thallium*

With thallium additions between 0.5 and 8%, the tendency for the amount of slip to decrease continued. Thus, the only slip seen with normal illumination in the 7.87% alloy stressed at 200 lb./in.² consisted of isolated groups of widely spaced traces. There was evidence, however, of a significant amount of very fine slip in this and similar specimens, but since this did not appear to vary markedly with thallium concentration, it will not be considered further in the present paper. The changes for this group of alloys are illustrated by Figs. 3–6 (Plate LXIV). In Fig. 3, which shows the microstructure of a specimen of the 1.25% thallium alloy after 10% extension in 50 days, the amount and type of slip is in contrast to that shown in Fig. 1. In Fig. 4, which is a multiple-beam interferogram corresponding to Fig. 3, the tilting of the grains and the nature of the slip traces are clearly shown by the fringe pattern. A similar extension was attained by the 7.87% thallium alloy in 11 days at the

same stress, and the structure at this stage is shown in Fig. 5; multiple-beam fringes denoted a greater amount of tilting of the grains than that shown in Fig. 4. At the lowest stress of 200 lb./in.², marked slip traces were infrequent, especially with alloys containing 2.45% or more thallium. Fig. 6 shows an area typical of this, on the 2.45% alloy after 10% extension in 190 days.

Despite the comparative absence of slip, arcs occurred in the X-ray reflections to some extent with all specimens of this group, even during the first 10% extension; for example, Fig. 15 (Plate LXV) shows the X-ray pattern corresponding to Fig. 6. However, even at large extensions of over 100%, complete arcing to form a circle was not found at the lower stresses, as can be seen in Fig. 16 (Plate LXV), which shows the X-ray pattern from the 4.81% thallium alloy after 169% extension in 930 days. No subdivision of the reflections appeared to take place, and no new sharp reflections were observed at any stage of these experiments. The absence of recrystallization during creep for specimens of this group was indicated by the absence of new sharp reflections, of slip traces crossing the original boundaries, and of the characteristic acceleration of creep rate.

When specimens which, from these criteria, had not recrystallized during creep were repolished after fracture—some of them after considerable extensions—the grain-sizes were found to be essentially the same as before creep. There were detailed differences of structure,¹⁵ however, which may be significant in the general elucidation of the mode of deformation in lead and its alloys.

It was found that the changes in microstructure obtained with alloys containing progressive additions of thallium up to about 8% were very similar to those associated with a decrease in strain rate for the 2.45% thallium alloy previously reported,¹ and to those of the specimens of the 4.35% thallium alloy which had been heat-treated to yield a similar range of grain-sizes.

(c) *Alloys Containing Over 8% Thallium*

Above 8% thallium the previous trends were continued, but a new tendency for marked broadening of the transverse boundaries was noted, particularly at lower stresses. Fig. 7 (Plate LXIV) shows the microstructure of the 13.45% thallium specimen after 10% extension in 24 days, stressed at 500 lb./in.²; this should be compared with those shown in Figs. 1, 3, and 5. Fig. 8 (Plate LXIV) is the interferogram corresponding to Fig. 7; it illustrates the general absence of slip and the broadened, transverse boundaries which have formed with relatively little tilting of the grains (cf. Fig. 4). At lower stresses and higher extensions, the broadening of transverse boundaries was more evident, as Fig. 9 (Plate LXV) shows on a specimen which had extended 45% in 475 days. The absence of slip and surface rumpling at this stage was clearly shown by the phase-contrast microscope. Fig. 10 (Plate LXV) shows part of a large grain with negative phase-contrast illumination; it was necessary to

select a large grain for this illustration, in order to adjust the illumination correctly for phase-contrast. However, since it was invariably found that large grains showed slip at an earlier stage than small grains, this served to emphasize the absence of surface changes within grains.

With the 26.58% thallium alloy, particularly at 300 lb./in.², grains or groups of grains tended to move apart or subside below the general level, with very few superficial markings. Fig. 11 (Plate LXV) shows this after 50% extension in 875 days, when the broadened transverse boundaries were very marked. This specimen had been very lightly repolished at 20% extension, when the very small amount of slip present was polished away. Despite the appearance of the transverse boundaries, no cracks were found on repolishing specimens of this group after fracture. The X-ray results confirmed that there was very little distortion within the grains below about 10% extension, for the reflections remained relatively sharp. An example is given in Fig. 17 (Plate LXV), which was obtained from the 13.45% thallium alloy at 4.5% extension in 65 days.

(d) Alloy Containing 40.5% Thallium

On specimens of the 40.5% thallium alloy superficial transverse cracks developed in association with scab-like areas of corrosion product; observation of detail was not possible because of rapid tarnishing. Since corrosion represented an obvious departure from the standard creep conditions, experiments with this alloy were discontinued, and no alloys containing higher proportions of thallium were made.

(e) General Observations

All the fractures were of the ductile knife-edge type, although those of the 26.58% thallium alloy showed a tendency towards the granular type of fracture. Specimens extended uniformly, necking often taking place only after considerable extension during tertiary creep, especially in alloys containing between 1.25 and 13.45% thallium. For example, a specimen of the 13.45% alloy, initially stressed at 300 lb./in.², showed a variation in width of 1 part in 25 along its length when the extension was 164% and therefore after about 100% extension during tertiary creep; it subsequently fractured after a further 160% extension, when the actual stress was many times that initially imposed upon it. The majority of fractures were located within the gauge-length, presumably because the high ductility of these alloys permitted the formation of shoulders at the grips. Fig. 13 (Plate LXV) shows the specimen of the 7.87% thallium alloy which has so far given the greatest extension before fracture; it is shown with a specimen before creep for comparison.

In general, although these observations followed trends which it was possible to correlate with the creep characteristics, they did not appear to be sufficient to predict or explain them completely.

IV.—ANALYSIS OF CREEP CURVES AND DISCUSSION

The information summarized in Tables I-IV has been used to construct a number of curves which illustrate the variation of creep characteristics with thallium concentration.

The effect of thallium concentration on the creep rate is brought out most clearly by Fig. 18, in which

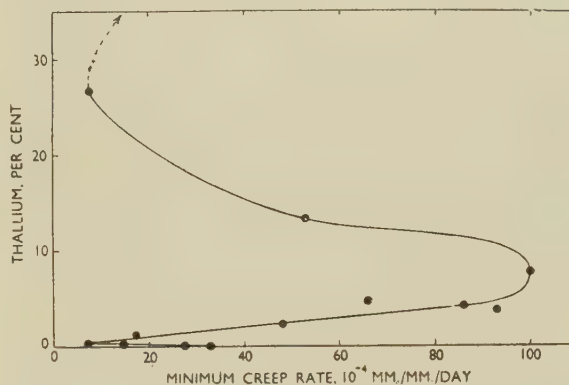


FIG. 18.—Variation of Minimum Creep Rate with Thallium Content at 500 lb./in.².

thallium content has been plotted against minimum creep rate at 500 lb./in.². It shows the grouping described in Section III, 3, there being turning points in the curve at about 0.5, 8, and 26% thallium, with fairly regular changes between these points.

The changes at stresses of 300 and 200 lb./in.² were similar to those at 500 lb./in.², but the inversion at the dilute alloy part of the curve became less pronounced as the stress decreased. It appeared from the scatter

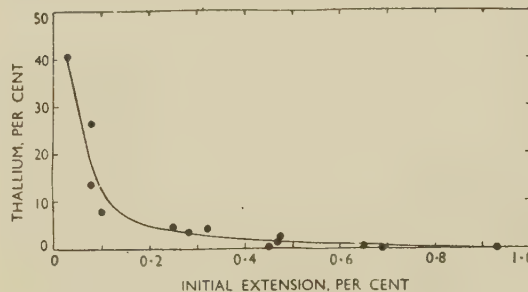


FIG. 19.—Variation of Initial Extension with Thallium Content at 500 lb./in.².

obtained that in the vicinity of 5% thallium the creep of the alloys may be very sensitive to some factor not controlled in these tests.

The thallium concentration which produced least resistance to creep diminished as the stress decreased.

At a stress of 400 lb./in.², tests were made with fewer of the alloys, but the concentration/minimum creep rate curves were intermediate between those obtained at 500 and 300 lb./in.²

In Fig. 19 thallium content has been plotted against

the extension obtained on loading at 500 lb./in.². The initial extension decreases as the thallium concentration is increased, and is the kind of variation which would be expected in the tensile extension of alloys having hardnesses as shown in Table I. At 300 lb./in.² the initial extension decreased in a similar manner, but at 200 lb./in.² the extensions were of the same order as the experimental error in reading them, and there was therefore considerable scatter. Thus the variations in creep rate obtained with increasing thallium concentration appear to be a consequence of deformation at low rates.

The spreading of creep rates to a complex distribution appears, moreover, to be an immediate consequence of deformation at low rates of strain, even before a minimum creep rate has been obtained. Fig. 20 shows the thallium content plotted against the extension after 1 day at 500 lb./in.², and although the positions of the turning points are slightly different from those in Fig. 18, the general form of the curve is

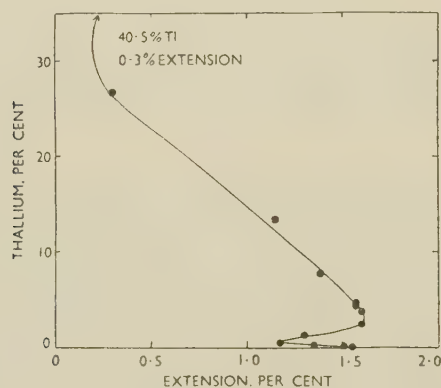


Fig. 20.—Variation of Extension After 1 Day with Thallium Content at 500 lb./in.².

remarkably similar. The curve is in fact, intermediate between those of Figs. 18 and 19. Similar curves have been obtained by plotting thallium content against the time to reach given small extensions.

In analysing creep results in the manner shown in Fig. 18, there is a danger of misrepresenting the fundamental variations in creep which have occurred because of the arbitrary choice of the characteristic—minimum creep rate in this instance—selected to represent the creep. In many of the tests in the present paper, the duration of minimum creep rate was short, especially when recrystallization during creep took place or when there was an extended tertiary stage. Thus, although it is common practice to select minimum creep rate as an index of creep behaviour, it is worth examining some other features.

Tests at 500 lb./in.² have all been carried through to rupture, and Figs. 21 and 22 show the thallium content plotted against average creep rate and time to rupture, respectively. Even though some scatter may have been introduced by such factors as premature rupture, owing to the influence of the grips or other

stress concentrators, these curves exhibit similar turning points and the same general character as Fig. 18.

It seems reasonable to conclude, therefore, that the minimum creep rate is a representative quantity to use

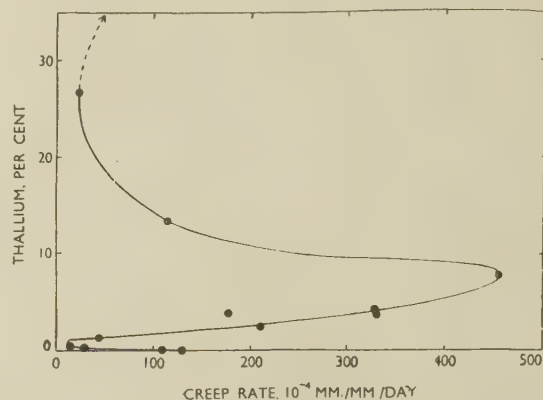


Fig. 21.—Variation of Average Creep Rate with Thallium Content at 500 lb./in.².

in discussing the effects of additions of thallium on the creep of lead. This is supported by a further relation between minimum creep rate and time to rupture which has been plotted on a log-log scale in Fig. 23. The points fall fairly close to a pair of straight lines intersecting at about the point representing the 0.47% thallium alloy. Results for alloys containing 0.047% thallium are on one straight line, those for alloys containing 0.47–7.87% thallium are on another, and those for alloys containing 7.87–26.58% thallium move back along the latter. Thus there appears to be a close relationship between minimum creep rate and time to rupture, which also divides the alloys into the groups previously noted in Section III, 3. This linear relation between minimum creep rate and time

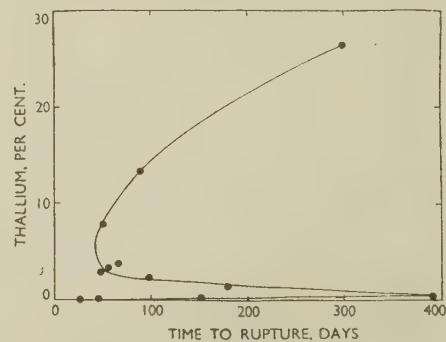


Fig. 22.—Variation of Time to Rupture with Thallium Content at 500 lb./in.².

to rupture has been noted by Servi and Grant¹⁶ in tests with aluminium in which temperature and not composition was the variable; the creep curves for aluminium were such that a large proportion of the creep had been at the minimum rate, whereas in the present experiments with lead–thallium alloys this was only true for the tests represented by points near the intersection in Fig. 23.

In Fig. 24 the reciprocal grain diameter ($1/d$) has been plotted against minimum creep rate for the alloys at 500 lb./in.²; such a curve will be referred to as a " $1/d$ " curve in subsequent discussion. It will be seen that the general form of the curve is similar to that of Fig. 18, in which thallium content replaces $1/d$, and there is a linear portion between the points representing the 0.47 and 7.87% thallium alloys. A similar linear portion has been found on the $1/d$ curves for stresses of 400, 300, and 200 lb./in.², between the point representing the 0.47% thallium alloy and a value of $1/d$ of about 240.

As suggested by Sully,² the linearity found in the $1/d$ curves, typified by Fig. 24, indicates that the variation in grain-size may be a major factor in determining creep rate, at least over a range of thallium concentration, provided that the deformation takes place by grain-boundary flow. This is demonstrated more clearly by Fig. 25, which shows part of the $1/d$ curve

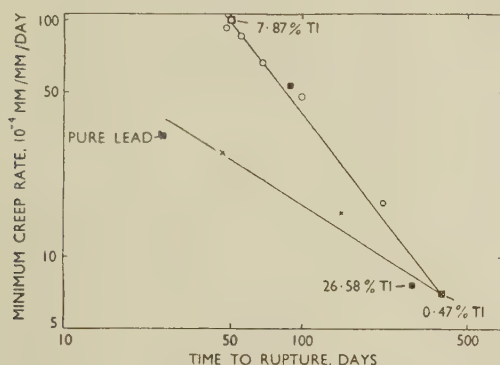


Fig. 23.—Relation Between Minimum Creep Rate and Time to Rupture at 500 lb./in.².

KEY.
 × 0.47% TI. ○ 0.47-7.87% TI. ■ 7.87-26.58% TI.

for the tests at 300 lb./in.², and the $1/d$ curve for the various grain-sizes of the 4.35% thallium alloy. The changes in creep rate brought about by altering the grain-size of one alloy are thus seen to be very similar indeed to those brought about by varying the grain-size by additions of thallium. It should also be noted that the 4.81% thallium alloy appears to behave anomalously, as in other diagrams, falling away from the most likely curve.

Hanson¹⁷ has suggested that the number of grains in the cross-sectional area is a fundamental way of denoting grain-size in creep relations, but using this quantity instead of $1/d$ in the present work did not give curves which differed greatly from those in Fig. 25.

There is thus evidence that the observed variations in alloys containing up to 7.8% at 500 lb./in.² and alloys containing up to about 5% at 200 lb./in.² are mainly the result of grain refinement. This is in agreement with the results of Tang and Pauling,¹¹ who have found that the lattice spacing of lead-thallium alloys decreases very slightly up to 10% thallium and then decreases at an increasing rate up to

about 75%. From calculations of atomic radii, based on these results, they suggest that thallium replaces lead isomorphously and assumes the valency of lead (2.14) up to 10%; thereafter, the valency of

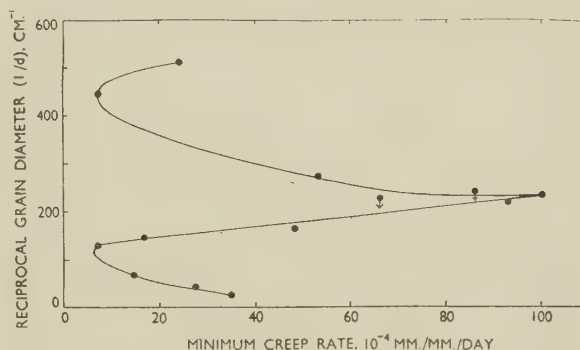


Fig. 24.—Relation Between the Reciprocal of the Grain Diameter ($1/d$) and the Minimum Creep Rate at 500 lb./in.².

dissolved thallium gradually rises to its calculated value of 2.5. It might be expected, therefore, that alloys containing thallium up to 10% would show little change in plastic properties, except through the influence of grain-size. The observed changes in creep due to the initial thallium additions up to 0.47% appear to be associated with the elimination of slip, because the changes are less marked at the lowest stress, when the amount of slip is small even in pure lead. It is possible that the proportion of slip in these coarse-grained alloys depends, in turn, on the relation of grain-size to the cross-sectional area of the specimen.

The lead-thallium alloys containing up to 10% thallium thus differ from the solid-solution alloys investigated by Robinson, Tietz, and Dorn,¹⁰ who attributed the increased resistance to creep to the "Cottrell effect" and the resistance to recovery induced

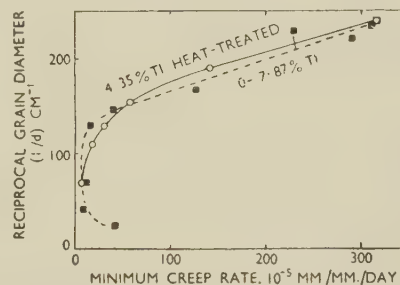


Fig. 25.—Effect of Variation of Grain-Size on Minimum Creep Rate at 300 lb./in.².

by small solute additions. With the lead-thallium alloys, it might be expected that there would be very little difference in the creep rates of these alloys if tests were made on specimens of the same grain-size.

The change to a decreasing creep rate at about 8% thallium does not appear to be associated with any major property of the alloys, such as hardness or electrical resistivity,¹⁸ and since the grain-size continues to diminish with thallium additions, some other

factor must be sought. The X-ray and microscopical observations indicated a continuance of the earlier trends, although there was an increasing tendency for transverse boundaries to broaden, which led to cracking in the 40.5% thallium alloy. Thus, these alloys appeared to deform, even more than the earlier ones, by grain-boundary flow, but the actual "strength" of the boundary appeared to increase, as demonstrated by the 26% thallium alloy, which developed low creep rates that were comparable with the 0.47% thallium alloy, despite the very much smaller grain-size of the former.

Another factor which could affect the creep of alloys containing above 8% thallium, was the presence of an increased number of annealing twins. The orientation change between a twin and a neighbouring grain will be different from that of the parent grain and the same neighbour, and hence the presence of twins might inhibit boundary flow because of abrupt changes of energy in boundaries intersected by twins; alternatively, the presence of twins might prevent readjustment when interlocking at irregularities occurred in boundary flow.

The fact that recrystallization during creep occurs only in the alloys containing up to 0.47% thallium may be connected with the changes in the mechanism of deformation. It is probable that recrystallization during creep occurs after internal changes, such as slip, have increased the stored energy to a sufficiently high level, and when most of the movement is at the grain boundary the energy necessary to activate recrystallization is not built up.

It was found that there was a systematic variation with stress of the slope and position of the linear portions of the $1/d$ curves. The slope increased as the stress diminished in such a manner that a plot of the stress against the logarithm of the slope was a straight line. This was similar to an effect which has been noted by other observers, e.g. Gohn, Arnold, and Bouton,¹⁹ who found that the change in creep rate due to grain refinement was less marked at lower stresses. With the lead-thallium alloys this can be seen by comparing the ratios of the minimum creep rates at 500 and 200 lb./in.² for the 0.47 and 3.92% thallium alloys, which are 14.5 and 8.4, respectively.

The change may be associated with stress in the following way. At high stresses, slip is readily activated when interlocking of grains has blocked relative movement, and so the high creep rate of the fine-grained alloys results from the combination of increased boundary area and ability to slip. With low applied stresses, however, considerable time may be necessary to build up local stresses large enough to activate slip when boundary flow is blocked, and thus it is only the change in grain-boundary area which operates. It follows that the change in creep rate is then less than at high stresses, for the same change in grain-size. The logarithmic relation between stress and slope of the $1/d$ lines is probably an indication of the time factor involved in the above process.

Besides resulting in the relatively small change in

creep rate at lower stresses, this effect may be the explanation of the high extensions at fracture of fine-grained specimens and of the increase in such extensions with lower stresses. Dollins²⁰ has recently found some alloys of lead to give first a decrease and then an increase in extension at rupture, as the stress is decreased, although the changes are much less marked than with the thallium alloys. He associates the original high ductility with slip and explains the other changes in a similar manner to that outlined above.

V.—SUMMARY

The investigations described have shown that the additions to lead of thallium in solid solution cause complex changes in the creep characteristics of extruded and annealed specimens of the alloys, and that these characteristics are modified as the testing stress is decreased. The diagram in Fig. 26, and points

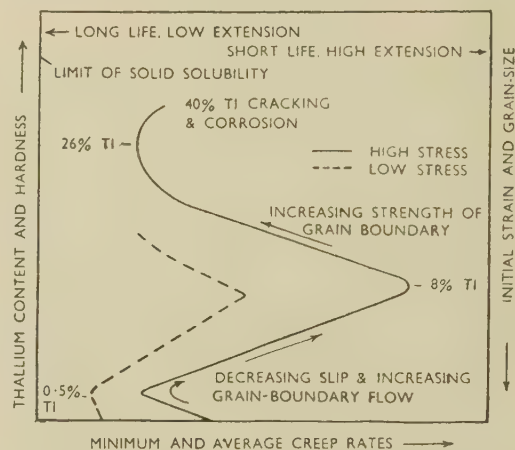


Fig. 26.—Schematic Summary, Illustrating the Effect of Thallium Concentration on the Creep of Lead.

1-6 below, attempt to summarize these; in Fig. 26, the full line is for tests at 500 lb./in.², and the dotted line for lower stresses.

1. The initial extension obtained on loading the alloys shows a regular decrease with additions of thallium. This confirms the observations of Robinson, Tietz, and Dorn¹⁰ on aluminium.

2. After even the small amount of creep that takes place in one day, a complex relation between thallium content and creep extension is established.

3. A major effect of thallium additions is to decrease the grain-size obtained after a standard treatment. Consequently, the creep-resistance decreases at all stresses, and very markedly at high stresses, up to about 8% thallium; this is approximately the range in which there is very little change in lattice spacing. The creep rates and structural changes of alloys in this range at 300 lb./in.² are very similar to those of specimens

of an alloy which have been heat-treated to yield a similar range of grain-sizes.

4. Above 8% thallium, the creep rate decreases markedly, despite continued grain refinement, and there is an increasing tendency to cracking, although grain-boundary flow is still predominant.

5. Thallium increases the extension at rupture of lead during creep and the maximum extension (nearly 400%) occurs at about 8% thallium; at compositions between 2 and 13% thallium there is a marked increase in the extension at rupture of any alloy with decreasing stress.

6. Grain movement and rotation have been found to replace visible slip progressively as the thallium content increases. With more than about 8% thallium there is, in addition, an increasing tendency to form superficial shallow

fissures along boundaries transverse to the stress. Cracks, however, have only been observed in the 40.5% thallium alloy, which corroded rapidly.

ACKNOWLEDGEMENTS

The work described in this paper formed part of a programme of research by the Physical Metallurgy Section of The Commonwealth Scientific and Industrial Research Organization and was carried out at the Baillieu Laboratory, University of Melbourne, under the general direction of Professor J. Neill Greenwood, whose encouragement and advice in the course of many discussions are gratefully acknowledged. The author also wishes to thank Mr. J. A. Corbett for carrying out the chemical analyses, and his colleagues for the help they have given during discussions in the course of the investigations.

REFERENCES

1. R. C. Gifkins, *J. Inst. Metals*, 1951, **79**, 233.
2. A. H. Sully, "Metallic Creep and Creep-Resistant Alloys", London: 1949 (Butterworths Scientific Publications).
3. G. V. Smith, "The Properties of Metals at Elevated Temperatures", London and New York: 1950 (McGraw-Hill).
4. D. Hanson and E. J. Sandford, *J. Inst. Metals*, 1936, **59**, 159.
5. D. Hanson and E. J. Sandford, *ibid.*, 1938, **62**, 215.
6. J. N. Greenwood and H. K. Worner, *ibid.*, 1939, **64**, 135.
7. J. N. Greenwood and H. K. Worner, *Proc. Australasian Inst. Min. Met.*, 1936, (**104**), 385.
8. R. S. Russell, *ibid.*, 1936, (**101**), 33.
9. A. J. Phillips, *Proc. Amer. Soc. Test. Mat.*, 1936, **36**, (II), 171.
10. A. T. Robinson, T. E. Tietz, and J. E. Dorn, *Trans. Amer. Soc. Metals*, 1952, **44**, 689.
11. Y. Tang and L. Pauling, *Acta Cryst.*, 1952, **5**, (1), 39.
12. J. N. Greenwood and J. H. Cole, *Metallurgia*, 1948, **37**, 285.
13. J. C. Chaston, *J. Inst. Metals*, 1935, **57**, 109.
14. H. Hirst, *Proc. Australasian Inst. Min. Met.*, 1941, (**121**), 11, 29.
15. R. C. Gifkins, *Nature*, 1952, **169**, 238.
16. I. S. Servi and N. J. Grant, *Trans. Amer. Inst. Min. Met. Eng.*, 1951, **191**, 909.
17. D. Hanson, *ibid.*, 1939, **133**, 15.
18. G. Tammann and H. Rüdiger, *Z. anorg. Chem.*, 1930, **192**, 35.
19. G. R. Gohn, S. M. Arnold, and G. M. Bouton, *Proc. Amer. Soc. Test. Mat.*, 1946, **46**, 990.
20. C. W. Dollins, *Univ. Illinois Bull.*, 1950, **43**, (17).

The Constitution of Tantalum-Titanium Alloys

By D. SUMMERS-SMITH

(Journal, this vol., p. 73.)

Mr. D. J. MAYKUTH*: We have recently concluded work on the constitution of titanium-tantalum alloys† and are pleased to report that our work is in substantial agreement with that of Mr. Summers-Smith on all but one of the principal features of the constitutional diagram.

We have confirmed the complete solid solubility of tantalum and β -titanium and have also shown that the solidus line for the system rises as a smooth curve, without a maximum or minimum, from the melting point of titanium to that of tantalum. The approximate melting points given by the author all fell within a 50° C. spread of the solidus curve which we established by optical observation on induction-melted alloys and by incipient-melting techniques.

We also observed that the solid solution in alloys containing 79.1 at.-% titanium or less was retained upon quenching from the β field; quenching of β alloys containing 85.0 at.-% titanium or more resulted in martensitic transformation structures. Comparable work by the author bracketed the limit of the stable β composition between 82.2 and 86.1 at.-% titanium.

Comparison of the $(\alpha + \beta)/\beta$ boundary curves from the two diagrams shows that both have essentially the same shape and slope. The curve obtained by Mr. Summers-Smith is, however, displaced to slightly higher temperatures in alloys containing above 8.1 at.-% tantalum.

The only point of major discrepancy between the two investigations is concerned with the range of solubility of tantalum in α -titanium. The author places the limit of tantalum solubility at less than 0.5 at.-% at 700° C., whereas the results of our investigation show that the solubility of tantalum increases with decreasing temperature to a maximum of about 3.64 at.-% at 550° C. Our data, based largely on metallographic work, show that, at 700° C., about 3.07 at.-% tantalum is soluble in the α -phase. In addition, some X-ray-diffraction data were obtained which show that, at 530° C., the α solubility extends beyond 1.49 at.-% tantalum. These data, given in Table A, show that increasing additions of tantalum in amounts up to 1.49 at.-% produce a linear expansion of the α -titanium lattice in the c direction, while having no significant effect on the a parameter.

TABLE A.—Lattice Parameters of α -Titanium Solid-Solution Alloys Annealed at 530° C.

Tantalum, at.-%	Lattice Parameter, Å.		c/a Ratio
	a	c	
0	2.9503 \pm 0.0001	4.6834 \pm 0.0001	1.587
0.26	2.9512 \pm 0.0001	4.6845 \pm 0.0001	1.587
1.01	2.9506 \pm 0.0003	4.6858 \pm 0.0002	1.588
1.49	2.9502 \pm 0.0003	4.6873 \pm 0.0002	1.589

We note that, in the metallographic procedures described by Mr. Summers-Smith, all the samples used to investigate the extent of the $(\alpha + \beta)$ field were initially treated by heating within the β -phase field. As he observed, such treatment of alloys containing above 86.1 at.-% titanium produces transformed β structures in which the degree of α acicularity is

dependent upon the cooling rate from temperature. These transformation structures are very tenacious in that subsequent treatment below the $(\alpha + \beta)$ boundary does not modify the gross microstructure to any appreciable extent, i.e. the acicular or plate-like character of the initial α precipitate is not removed. As illustrated in Figs. 3 and 4 (Plate XI) of the paper, this offers no serious metallographic problems in phase differentiation when a relatively large volume of equilibrium β phase has been obtained in subsequent treatment. However, our experience with titanium-rich alloys shows that metallographic identification of trace quantities of β in an acicular α structure is exceedingly tenuous. For this reason, our metallographic studies on the α solubility were carried out by bringing cold-worked alloy samples into equilibrium. The combination of cold work and heat-treatment produces an equi-axed, α grain structure in which small quantities of β phase may be readily recognized.

The AUTHOR (in reply): It is gratifying to see that the work at the Battelle Memorial Institute substantially confirms the diagram proposed in my paper. In an attempt to remove the discrepancy regarding the solubility of tantalum in α -titanium, four alloys containing 4.5, 2.4, 1.0, and 0.6 at.-% tantalum were cold worked to 50% reduction and separate samples of each alloy were annealed at 800° and 700° C. for 24 hr. and water-quenched. Metallographic examination showed the structures given in Table B.

TABLE B.—Structure of Alloys Containing up to 4.5 At.-% Tantalum.

Tantalum, at.-%	Structure	
	At 800° C.	At 700° C.
4.5	$\alpha + \beta$	$\alpha + \beta$
2.4	$\alpha + \beta$	$\alpha + \beta$
1.0	$\alpha + \beta$	α
0.6	α	α

As Mr. Maykuth states, the acicular decomposition product is very stable and, even after this treatment, traces of it could still be seen in the 4.5 and 2.4% tantalum alloys. To remove these and ensure that equilibrium had been obtained, the cold-working and heat-treatment cycle was repeated for all the samples. The alloys now had equi-axed grain structures, but no change in the proportions of the two constituents could be detected in the two-phase alloys. A considerable amount of β was present in the 2.4% alloy quenched from 700° C., suggesting that at this temperature the solubility limit lies closer to 1% than 2.4% tantalum.

While this shows that the solubility of tantalum in α -titanium is greater than that proposed in the paper, it seems most unlikely, as a result of the present experiments, that the solubility at 700° C. is as great as 3%, the value given by Mr. Maykuth and his co-workers; more probably it lies at about 1.5%. The present results no longer conflict with the X-ray data given by Mr. Maykuth.

* Battelle Memorial Institute, Columbus, O., U.S.A.

† H. R. Ogden, R. I. Jaffee, and D. J. Maykuth, *J. Metals*, 1953, in the press.

SOME METALLOGRAPHIC OBSERVATIONS ON AGED ALUMINIUM-COPPER ALLOYS*

1458

By I. J. POLMEAR,† B.Met.E., JUNIOR MEMBER, and
H. K. HARDY,‡ M.Sc., Ph.D., A.R.S.M., A.I.M., MEMBER

SYNOPSIS

The occurrence of Gayler's "light phenomenon" in aluminium-copper alloys has been studied in detail. It has been concluded that it is not formed as an integral part of the ageing process, but that it originates as a grain-boundary recrystallization process to relieve strains induced by cold-water quenching and subsequent precipitation on ageing.

The effect of very small additions of indium or tin on the ageing of aluminium-copper alloys has been investigated by optical and electron microscopy. The particles of θ' are smaller, more numerous, and occur at an earlier stage in the ageing of the ternary alloy. This supports the previous conclusion that the ternary additions facilitate the nucleation process in the ageing of aluminium-copper alloys.

I.—INTRODUCTION

SYSTEMS undergoing precipitation have frequently been studied by microscopic methods, and notable contributions have been made by Gayler^{1,2} to our knowledge of the structures of aged aluminium-copper alloys. During intensive metallographic studies of the binary aluminium-4% copper alloy, Gayler has been able to distinguish three precipitates under the microscope, viz. copper-rich regions, θ' , and θ . The copper-rich regions occur before the peak on the ageing curve at 130° C. Gayler concludes that age-hardening is primarily due to the precipitation of these copper or copper-rich aggregates, together with the accompanying formation of crystallites of the aluminium solid solution stable at the temperature of ageing. These crystallites are better known as the "light phenomenon". The structure is clearly evident in the grain boundaries after ageing for 50 days at 130° C., and is said to be visible within the grains during the second rise to peak hardness (5-40 days at 130° C.).

More recent theories³ also postulate that the ageing of binary aluminium-copper alloys involves a series of precipitates designated as G.P. (Guinier-Preston) zones [1] and [2], θ' , and θ . The G.P. zones [2] are Gayler's copper-rich regions, but the "light phenomenon" does not form an essential part of the current theories of the ageing process. Thus it was thought that a wider metallographic investigation would help to determine the conditions under which the "light phenomenon" is formed.

The work described in the second part of this paper arose out of recent investigations by Hardy,⁴ who has shown that small quantities—of the order of 0.05-0.1 wt.-%—of cadmium, indium, or tin,

exert a pronounced influence on the response of aluminium-copper alloys to artificial ageing. The rate of artificial ageing is greatly enhanced, and the tensile properties, notably the proof stress, are considerably increased. It was thought that a metallographic comparison between the binary and ternary alloys might yield some information about the ageing mechanism involved in the latter series.

In carrying out the investigation it was found that the structures of the aged alloys were frequently finer than the limit of resolution of the optical microscope. Resort was therefore made to the technique of electron microscopy.

II.—THE "LIGHT PHENOMENON" IN AGED ALUMINIUM-COPPER ALLOYS

Most of the investigation was confined to the binary aluminium-copper alloys, though a limited comparative survey was made of the ternary series of aluminium-4% copper alloys with 0.05% indium or tin. In all cases the microspecimens were prepared from the hardness test-pieces used by Hardy^{3,4} in obtaining his hardness/ageing curves. In order that the work can be referred to, the hardness/time curves (Fig. 1) have been reproduced from previous papers;^{3,4} they show the ageing curves for aluminium-4% copper and aluminium-4% copper-0.05% indium alloys at 130° and 190° C.

1. EXPERIMENTAL METHOD

Binary aluminium-copper alloys with copper contents of 2, 3, 4, and 4.5% were examined after ageing for various times at 130°, 165°, and 190° C. Ternary alloys containing 4% copper were investigated after ageing at 130° and 190° C. Details of the

* Manuscript received 28 October 1952.

† Aeronautical Research Laboratories, Melbourne, Australia; attached to Fulmer Research Institute, Ltd., Stoke

Poges, Bucks.

‡ Senior Metallurgist, Fulmer Research Institute, Ltd., Stoke Poges, Bucks.

preparation of the hardness specimens have been given earlier.³ Briefly, it consisted of cold forging the chill-cast alloys, which were subsequently solution-treated and water-quenched before ageing.

Microsections were cut from the hardness specimens, which had been stored after ageing, and were rubbed down on a series of emery papers finishing with 000 grade. They were then electropolished for 4–8 min. in De Sy and Haemers's solution⁵ consisting of 4 parts absolute alcohol and 1 part 60% perchloric acid, with a potential difference of 10–12 V. In general, etching was carried out for 10–15 sec. in a solution of 0.5 g. NaF, 1 c.c. HNO₃, 2 c.c. HCl in 97 c.c. H₂O, which is very similar to Keller's etch. This reagent gave excellent contrast between the "light phenomenon" and the matrix.

2. METALLOGRAPHIC APPEARANCE

The distinctive characteristics of the "light phenomenon" made recognition simple, and, as

4 and 4.5% copper alloys. This is much less than the time required to the completion of the initial rise of the hardness/time curve (see Fig. 1). Growth of the crystallites continued up to a time somewhat beyond that corresponding to the peak hardness (50 days), after which their size remained constant, while the hardness continued to decrease (examples are shown in Figs. 2 and 3 (Plate LXVI)). The number of sites did not change appreciably once the "light phenomenon" was clearly visible. The final size and, to a lesser extent, the frequency was greater in the alloys of higher copper content.

(b) Specimens Aged at 165° C.

The "light phenomenon" was again absent in the 2% copper alloy; traces or "threads" could be observed in the other alloys after short ageing times, e.g. 8 hr. in the 3% copper specimens and 4 hr. in the 4–4.5% copper alloys. The number and maximum size after peak hardness (3½ days for the 4%

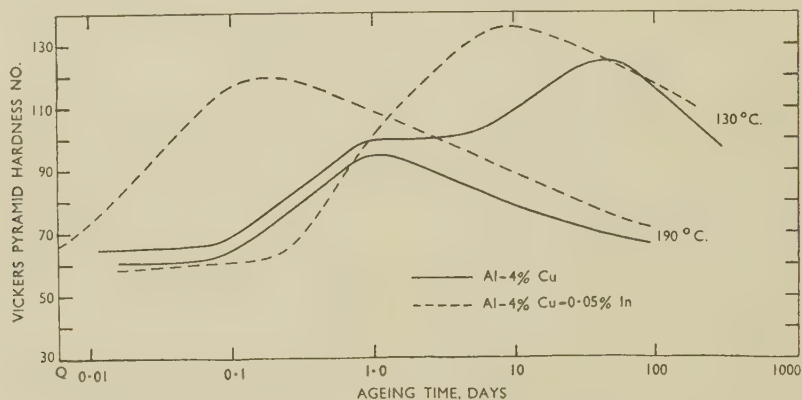


FIG. 1.—Hardness Curves for Aluminium-4% Copper and Aluminium-4% Copper-0.05% Indium Alloys Aged at 130° and 190° C. (After Hardy.^{3,4})

shown in Figs. 2 and 3 (Plate LXVI), the structure possessed a straight boundary with one grain and a more clearly defined serrated boundary with the adjoining grain. The structure was in relief both in the unetched and etched condition and was thus easily distinguished from simple grain-boundary depletion of the solute. Etching caused some pitting in the region constituting the "light phenomenon", but otherwise it was unaffected. Contrary to Gayler's observation, the "light phenomenon" was seen only in the grain boundaries.

3. OCCURRENCE OF THE "LIGHT PHENOMENON" IN BINARY ALUMINIUM-COPPER ALLOYS

(a) Specimens Aged at 130° C.

No traces of the structure were observed in the 2% copper alloy. However, with higher copper contents varying amounts of the "light phenomenon" were present in specimens which had been aged from several hours to 800 days or longer. Traces were found in the 3% copper alloy after 16 hours' ageing, whilst the effect was noted after 8 hr. in both the

copper alloy) was less than that found at 130° C. As before, the distribution remained more or less constant from just beyond peak hardness up to at least one hundred days.

(c) Specimens Aged at 190° C.

The "light phenomenon" was not found in either the 2 or 3% copper alloys, and only minor traces were found in the alloys of higher copper content.

4. OCCURRENCE OF THE "LIGHT PHENOMENON" IN THE TERNARY ALLOYS

The restricted survey indicated that in general the "light phenomenon" was present to a similar extent in the ternary alloys.

5. DISCUSSION OF RESULTS

As indicated previously, Gayler considered the "light phenomenon" to be an integral part of the ageing process of binary aluminium-copper alloys. She suggested that the flat on the ageing curve resulted from a balance between the formation of

sub-microscopic copper-rich areas and the relief of strain by recrystallization to form sub-microscopic particles of the "light phenomenon". Gayler reported that the crystallites did not grow, but visible formation of the new particles continued during the rise to peak hardness and possibly for much longer ageing times.

The present observations gave no evidence of the "light phenomenon" within the grains, and the discussion will be limited to its occurrence in the grain boundaries. Perryman and Blade⁶ have also observed the "light phenomenon" in the grain boundaries of aluminium-zinc alloys, and their results lend weight to the following remarks.

It has been revealed that the "light phenomenon" originates at a very early stage in the ageing process—certainly before the time corresponding to the flat on the two-stage ageing curve. Growth continues until the ageing has advanced just beyond the peak hardness, but the number of sites remains relatively constant. The "light phenomenon" also occurs at a very early stage in the ageing of the ternary alloys.

It would appear to originate as a recrystallization process, probably resulting from strains arising from the cold-water quench and precipitation on ageing. The observation that the amount of "light phenomenon" increases with increasing copper content is in accordance with this view, as the higher the solute concentration the greater is each of these two strain factors. The fact that growth ceases when over-ageing, or softening, occurs would indicate that the presence of the "light phenomenon" is closely associated with the precipitation process, since the continued precipitation of θ' and θ within the grains reduces lattice strain. The smaller amounts of the "light phenomenon" found after ageing at 165° and 190° C. may be due to relief of strain by grain-boundary flow, whereas recrystallization provides a more rapid means of relief at the lower temperature of 130° C. The smaller hardening on ageing at the higher temperature would also indicate less lattice strain than at 130° C. and account for a decreased tendency to form the "light phenomenon".

The intermediate precipitate, θ' , is probably formed in the grain boundaries at an early stage in the ageing process, and, as suggested by Gayler, the "light phenomenon" may well have a composition close to that of the equilibrium solid solution at the ageing temperature. As described by Hardy,³ the formation of a more stable phase must be accompanied by re-solution of the less-stable precipitate. Diffusion is more rapid in the grain boundaries than within the grains, and migration of the interface across a small volume of the metal will provide a path for easy diffusion and hence rapid precipitation. Particles of precipitate can also be formed at the new interface and may anchor the movement leading to the typical serrated edge.

Gayler has observed the "light phenomenon" in an air-cooled aluminium-4% copper specimen,

in which the quenching strains would be considerably less. The build-up of strains here is to be associated with volume changes in the region of the grain boundaries brought about by precipitation in the boundaries during air cooling.

III.—COMPARISON OF THE STRUCTURES OF AGED ALUMINIUM-4% COPPER AND ALUMINIUM-4% COPPER-0.05% INDIUM (OR TIN) ALLOYS BY OPTICAL AND ELECTRON MICROSCOPY

The microspecimens were obtained from the hardness test-pieces of Hardy^{3,4} in a manner similar to that indicated in Section II, 1 (p. 428), but the work was limited to the binary and ternary alloys with 4% copper. Preliminary observation of the two ternary alloys showed negligible differences in structure, and so it was considered necessary to compare only one of these with the corresponding binary alloy.

1. COMPARISON BY OPTICAL MICROSCOPY

A number of etching procedures were examined, but the most satisfactory one was to increase the HCl content of the etching reagent used in seeking the "light phenomenon". This was necessary because the more dilute mixture did not provide a satisfactory result on the ternary alloys. The maximum magnification attainable was 2000 diameters.

The alloys were compared after ageing at 30°, 130°, 190°, and 350° C. for varying times. With the exception of the specimens aged at 350° C., the structures were generally too fine to provide much useful information. Nevertheless, the following observations were made:

(i) Neither the binary nor ternary alloys showed evidence of visible precipitation within the grains or in the grain boundaries after ageing at 30° C. for times up to 800 days. However, the binary alloy exhibited greater preferential staining of the grains, which suggested that ageing, by segregation of copper atoms in preferred planes, was further advanced in this alloy. This would be in accordance with Hardy's findings that the rate of natural ageing was depressed by very small amounts of indium or tin.⁴

(ii) Specimens aged at 130° and 190° C. had structures which were incompletely resolved, and the only conclusion which could be drawn was that the precipitate in the ternary alloys appeared to be finer.

(iii) Any effects due to ternary additions that were shown up at lower ageing temperatures were not observed on ageing at 350° C., as the structures of both alloys were virtually identical.

2. COMPARISON BY ELECTRON MICROSCOPY

Hardness measurements have shown that it is in alloys aged in the range 100°–200° C. that the ternary

additions have their greatest effect (Fig. 1, p. 428). As the structures were too fine for optical comparison, it was decided to take some electron micrographs. It was hoped to compare the particle sizes determined by this means with previously published results on the binary alloy and with those obtained from X-ray analysis.

(a) Previous Work

Several authors have taken electron micrographs of age-hardened alloys: Castaing and Guinier⁷⁻¹¹ have investigated aluminium-copper and aluminium-magnesium-silicon alloys, and Keller and Geisler¹²⁻¹⁴ have given results on aluminium alloys of commercial interest. Nishimura and Murakami,¹⁵ Buinov and Lerinman,¹⁶ and Saulnier and Syre,¹⁷ have also taken electron micrographs of a series of age-hardened aluminium alloys. The relation between the structure of the alloy and the appearance of the replica has been discussed by Keller¹² and by Castaing.¹⁰

(b) Experimental Technique

Most workers on aluminium alloys have obtained replicas of the surface by depositing and stripping an oxide film. This technique has been followed, but a new method of stripping has been employed.

The microspecimens were first electropolished in De Sy and Haemers's solution,⁵ and, after a quick wash in running water, they were then anodized in a bath consisting of 12% $\text{Na}_2\text{HPO}_4 \cdot 12\text{H}_2\text{O}$ and 0.4% H_2SO_4 in distilled water, using a lead cathode. The thickness of the film depends primarily on the applied voltage and only to a small extent on the anodizing time. A potential difference of 20 V. for 2 min. proved satisfactory.

The conventional method of stripping involves immersion in a solution of mercuric chloride and results in total loss of the specimen. In addition, the films require careful washing before they are clean enough to be used as replicas. An alternative scheme was therefore adopted.¹⁸ The specimen was removed from the anodizing bath and washed; cuts with a razor blade were then made $\frac{1}{8}$ in. apart, and the specimen was transferred to the Jacquet¹⁹⁻²¹ electropolishing bath (65% acetic anhydride and 35% perchloric acid). The usual cooling jacket was discarded and a beam of light focused on the specimen to allow careful observation of the surface. An initial potential difference of 10 V. was slowly increased to 20 V. over a period of 2 min. and then maintained at this value until the films could be seen to be lifting from the surface. The specimen was then carefully placed in a beaker of distilled water and gently agitated until the squares of the anodic film became detached from the surface. A suitable replica was collected on a fine copper grid, dried, and placed in the electron microscope for examination.

In most cases the microspecimens were not etched before anodizing. Further replicas could readily be obtained once the film had been stripped completely, if the above procedure was repeated.

(c) Experimental Results

Examples of the structures observed are shown in Figs. 4-7 (Plate LXVI), and those shown in Figs. 8 and 9 (Plate LXVI) compare the results obtained by optical and electron microscopy on an aluminium-4% copper alloy aged for 96 days at 190° C. The platelets in Figs. 4-7 are both dark and light, but this is due chiefly to the particle size in relation to the replica thickness and not to a difference in alloy composition. After fairly short ageing times the platelets in the ternary alloys have a dotted appearance (Fig. 5), which is absent from the binary alloys (Fig. 4). No such difference was detected after longer ageing times when the particles were larger. Castaing and Guinier⁸ have reported an appreciable variation in thickness along the diameter of individual θ' platelets in the aluminium-4% copper alloy aged at temperatures below 250° C. In the present work, the effect was much more noticeable in the ternary than in the binary alloy. The micrographs (Figs. 4-7) show that the particles were more numerous in the ternary than in the binary alloys.

The platelets visible in the micrographs can be identified as θ' from previous²² and parallel^{23, 24} X-ray work. A few small dots were noted in the aluminium-4% copper alloy which had been aged to peak hardness at 130° C. Here, X-ray analysis indicates the presence of G.P. zones [2] with a small

TABLE I.—Sizes of θ' Particles.

Ageing Time	Alloy	Diameter, Å.	Thickness, Å.
<i>Ageing Temperature 130° C.</i>			
50 days (peak hardness)	Al-4% Cu	Dots approx. 100	...
6 days (peak hardness)	Al-4% Cu- 0.05% Sn	<700	<100
200 days	Al-4% Cu	1000-5000	200
200 days	Al-4% Cu- 0.05% Sn	<1500	100
<i>Ageing Temperature 190° C.</i>			
1 day (peak hardness)	Al-4% Cu	900-5500	100
7 hr. (peak hardness)	Al-4% Cu- 0.05% Sn	<1000	<100
3 days	Al-4% Cu	1000-10,000	<300
3 days	Al-4% Cu- 0.05% In	500-3500	<300
96 days	Al-4% Cu	1000-9000	100-500
96 days	Al-4% Cu- 0.05% In	900-7500	200-500
300 days	Al-4% Cu- 0.05% In	1500-7500	500-600

quantity of θ' . No structures were observed in this alloy at times shorter than the time to reach peak hardness (50 days) at 130° C., although Castaing¹⁰ has recorded a mottling effect, at magnifications of 33,000 in the 4% copper alloy aged 12 hr. at 150° C., due to G.P. zones [2]. Contrary to the results of Buinov and Lerinman¹⁶ and of Saulnier and Syre,¹⁷

small white dots were not observed in the micrographs of the aluminium-4% copper alloy aged for very short times.

The ternary alloy aged to peak hardness at 130° C. (6 days) showed the θ' precipitate already present to an appreciable size, and the same effect was noted in both the binary and ternary alloys aged to their peak hardnesses at 190° C. (1 day and 7 hr., respectively). The particle sizes are given in Table I, in which the values quoted for the thickness of the smaller plates are less reliable than those given for their diameters. This is because the resolving limit of the electron microscope employed was in the range 100–200 Å. It will be seen from Table I that, except in the specimens aged to peak hardness at 130° C., the θ' particles were larger in the binary than in the ternary alloy. This applied even though the θ' particles had been formed much earlier in the ternary alloys. For example, after 200 days at 130° C. the θ' particles have been present for at least 195 days in the ternary alloy, but only for about 150 days in the binary alloy, and yet the particles were appreciably larger in the latter. A similar effect occurred after 3 days at 190° C., although the sizes were more equal after 96 days at this temperature. The particle sizes reported previously are for rather scattered ageing conditions which do not allow a direct comparison with the present work. The

available results indicate size ranges fairly similar to those of the binary alloy in Table I.

(d) Discussion of Results

It is not possible to deduce the ageing mechanism of the ternary alloys, because no structures were visible before the formation of θ' . However, the results clearly indicate the formation of θ' before the peak hardness is attained in the ternary alloy at 130° C., whereas θ' is formed only at ageing times close to the peak hardness in the binary alloy at the same temperature. For equal ageing times, and for similar relative positions on the ageing curves, the formation of the platelets of θ' is much more advanced in the ternary alloy, although the particles are smaller and much more numerous. The results support the general conclusion⁴ that the ternary addition (cadmium, indium, or tin) accelerates the nucleation process in the ageing of aluminium-copper alloys, but a discussion of the mechanism must await the results of X-ray analysis.

ACKNOWLEDGEMENTS

The authors' thanks are due to their colleagues at the Fulmer Research Institute who contributed to the experimental work, and particularly to Mrs. E. M. Smith, B.A., for her assistance in obtaining the electron micrographs.

REFERENCES

1. M. L. V. Gayler, *J. Inst. Metals*, 1940, **66**, 72.
2. M. L. V. Gayler, *ibid.*, 1946, **72**, 243.
3. H. K. Hardy, *ibid.*, 1951, **79**, 321.
4. H. K. Hardy, *ibid.*, 1951–52, **80**, 483.
5. A. De Sy and H. Haemers, *Aluminium*, 1942, **24**, 96.
6. E. C. W. Perryman and J. C. Blade, *J. Inst. Metals*, 1950, **77**, 263.
7. R. Castaing, *Compt. rend.*, 1949, **228**, 1341.
8. R. Castaing and A. Guinier, *ibid.*, 1949, **228**, 2033.
9. R. Castaing and A. Guinier, *ibid.*, 1949, **229**, 1146.
10. R. Castaing, *Recherche Aéronaut.*, 1950, (13), 3.
11. R. Castaing, "Metallurgical Applications of the Electron Microscope". (*Inst. Metals Monograph and Rep. Series No. 8*), 1950, 156 (discussion).
12. F. Keller, *ibid.*, 85.
13. F. Keller and A. H. Geisler, *Trans. Amer. Inst. Min. Met. Eng.*, 1944, **156**, 82.
14. A. H. Geisler and F. Keller, *ibid.*, 1947, **171**, 192.
15. H. Nishimura and V. Murakami, *Mem. Fac. Eng. Kyoto Univ.*, 1950, **12**, (4), 47.
16. N. N. Buinov and R. M. Lerinman, *Doklady Akad. Nauk S.S.S.R.*, 1950, **74**, 707, 929.
17. A. Saulnier and R. Syre, *Rev. Mét.*, 1952, **49**, 1.
18. D. Whitwham, private communication.
19. P. Jacquet, *Métaux, Corrosion-Usure*, 1943, **18**, 198.
20. P. Jacquet, *Metal Finishing*, 1949, **47**, (11), 62.
21. P. Lacombe and L. Beaujard, *J. Inst. Metals*, 1948, **74**, 1.
22. A. Guinier, *J. Phys. Radium*, 1942, [viii], **3**, 124; *Bull. Lab. d'Essais*, 1946, (21).
23. J. M. Silcock, T. J. Heal, and H. K. Hardy, to be published.
24. J. M. Silcock and T. J. Heal, unpublished work.

1459 The Log-Log Plot of Solubility Data in Ternary Metallic Systems*

By H. K. HARDY,† M.Sc., Ph.D., A.R.S.M., A.I.M., MEMBER

SYNOPSIS

The slope of the solubility curve of an ideal ternary solution plotted on log-log co-ordinates has been analysed for the case when the phase in equilibrium is a ternary compound. A straight line is not predicted, but the slope will be equal to the ratio of the solute components in the compound when the same ratio exists between the solute components in the solution in equilibrium. The curvature will be slight for very dilute solutions, whose solubility data will give a straight-line plot as though in equilibrium with a binary compound.

HUME-ROTHERY¹ has deduced from mass-action principles that the isothermal solubility curve of a ternary solution should give a straight line when the atomic fractions of the solute elements are plotted on logarithmic co-ordinates, provided that (a) the solution is in equilibrium with an intermetallic compound composed of the two solute elements, and (b) the solution is thermodynamically ideal, so that the activities are equal to the atomic fractions. In addition, the straight line is expected to have a negative slope of the same value as the ratio of the constituents in the intermetallic compound. Hume-Rothery¹ showed that the principle applied to the liquidus isothermals of the aluminium-magnesium-silicon liquid in equilibrium with Mg_2Si , a case which has been further examined by Phillips.² Similar behaviour has been found experimentally when the solution is in equilibrium with a ternary compound, e.g. the $\alpha/(\alpha + Al_2CuMg)$ boundary of the aluminium-copper-magnesium system,³ and the $\alpha/(\alpha + Al_2Mg_3Zn_3)$ boundary of the aluminium-zinc-magnesium system,⁴ give straight-line log-log plots of the isothermal solubility curves.

The case in which the solution is in equilibrium with a ternary compound has not been examined theoretically. Let the equilibrium be represented by the equation:



The sum of the chemical potentials is equal to zero at equilibrium and

$$n_X \cdot \mu_X + n_Y \cdot \mu_Y + n_Z \cdot \mu_Z = \mu_{XYZ}$$

Putting $\mu_i = \mu_i^0 + RT \ln a_i$, where a is the activity, leads to:

$$\ln a_{XYZ} - n_X \cdot \ln a_X - n_Y \cdot \ln a_Y - n_Z \cdot \ln a_Z = - \left(\frac{\mu_{XYZ}^0 - n_X \mu_X^0 - n_Y \mu_Y^0 - n_Z \mu_Z^0}{RT} \right) = - \frac{\Delta F^0}{RT} = \ln K.$$

For homogeneous equilibrium all the reactants and products are gases or are in solution. For heterogeneous equilibrium it is conventional to give the activity of the condensed phase a constant value,

which here applies along the equilibrium solubility curve, and we have:

$$\phi \equiv n_X \cdot \ln a_X + n_Y \cdot \ln a_Y + n_Z \cdot \ln a_Z - C = 0$$

where $C = \ln a_{XYZ} - \ln K$.

For an ideal solution the activities may be replaced by the atomic fractions and differentiation then gives:

$$\frac{d \ln y}{d \ln z} = - \frac{\partial \phi / \partial \ln z}{\partial \phi / \partial \ln y} = - \frac{n_Z}{n_Y} \left(\frac{1 - \frac{n_X}{n_Z} \cdot \frac{z}{x}}{1 - \frac{n_X}{n_Y} \cdot \frac{y}{x}} \right)$$

since $\partial x / \partial y = \partial x / \partial z = -1$ is obtained from the subsidiary condition $x + y + z = 1$.

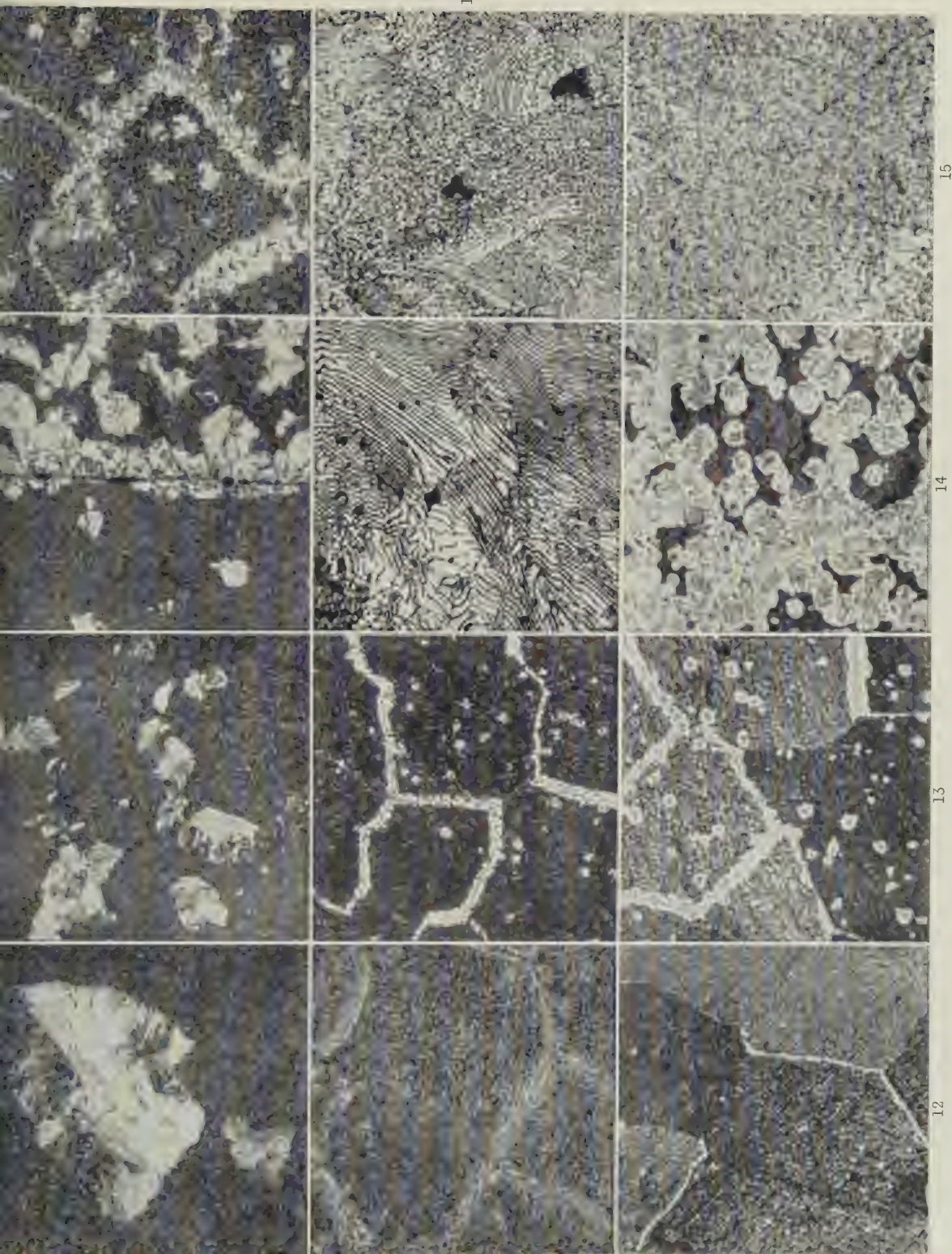
We need to consider only the range of composition in which $x/z > n_X/n_Z$ and $x/y > n_X/n_Y$. For a binary compound $n_X = 0$ and the slope reduces to the value given by Hume-Rothery.¹ On the other hand, the term in brackets is unity for a ternary compound only when $z/y = n_Z/n_Y$ and the slope of $-n_Z/n_Y$ is limited to one point on the solubility curve. When $z/y < n_Z/n_Y$, the slope will become more negative (tending towards $-\infty$). When $z/y > n_Z/n_Y$ the slope will become less negative (tending towards zero), and this effect is to be seen in the results of Brommelle and Phillips for the liquidus curves of the Al_2CuMg phase.⁵ If the solution is very dilute, the fractions z/x and y/x will be very small, and the slope will be close to $-n_Z/n_Y$. This probably accounts for the pseudo-binary behaviour of the $\alpha/(\alpha + Al_2CuMg)$ and $\alpha/(\alpha + Al_2Mg_3Zn_3)$ boundaries, although other compensating factors may also be present.

REFERENCES

1. W. Hume-Rothery, *Phil. Mag.*, 1936, [vii], **22**, 1013.
2. H. W. L. Phillips, *J. Inst. Metals*, 1946, **72**, 229.
3. A. T. Little, W. Hume-Rothery, and G. V. Raynor, *ibid.*, 1944, **70**, 491.
4. A. T. Little, G. V. Raynor, and W. Hume-Rothery, *ibid.*, 1943, **69**, 423, 467.
5. N. S. Brommelle and H. W. L. Phillips, *ibid.*, 1948-49, **75**, 529.

* Manuscript received 29 December 1952.

† Senior Metallurgist, Fulmer Research Institute, Ltd., Stoke Poges, Bucks.



FIGS. 4-8.—Transformation Products at Various Temperatures. Prepared by Method I. $\times 200$.

FIG. 4.—10,000 sec. at 255°C .; typical pearlite group nodule.

FIG. 5.—70 sec. at 240°C .

FIG. 6.—20 (a) and 25 (b) sec. at 220°C .; troostitic nodules.

FIG. 7.—16 sec. at 180°C .

FIG. 8.—10 sec. at 150°C .

FIG. 9.—As Fig. 8, but Prepared by Method II. $\times 200$.

FIG. 10.—Coarse Lamellar Product Obtained After 3200 sec. at 260°C . Whorling beginning in top left hand corner. $\times 606$.

FIG. 11.—Similar to Fig. 10, but Showing Decrease of Interlamellar Spacing at Lower Temperature. 400 sec. at 240°C . $\times 1000$.

FIGS. 12-15.—Stages of Decomposition at 80°C . Prepared by Method II. $\times 200$.
FIG. 12.—6 sec. FIG. 13.—10 sec. FIG. 14.—22 sec. FIG. 15.—100 sec.

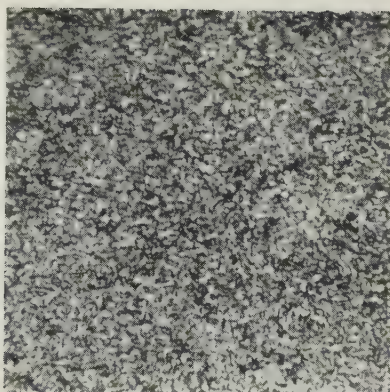
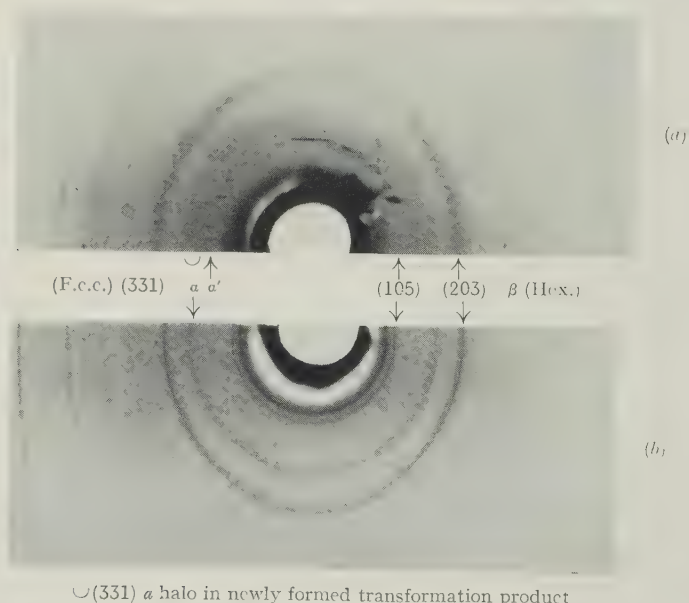


FIG. 16.—Granular Nature of Decomposition Product After 3 Months at Room Temperature, $\times 1300$.



$\cup(331) \alpha$ halo in newly formed transformation product

FIG. 17.—X-Ray Back-Reflection Photographs Taken During Decomposition of Zinc-22.5% Aluminium Alloy at Room Temperature (18°C.). (a) Between 2 and 15 min. after quenching; (b) 3 months later.

← Direction of Applied Stress →

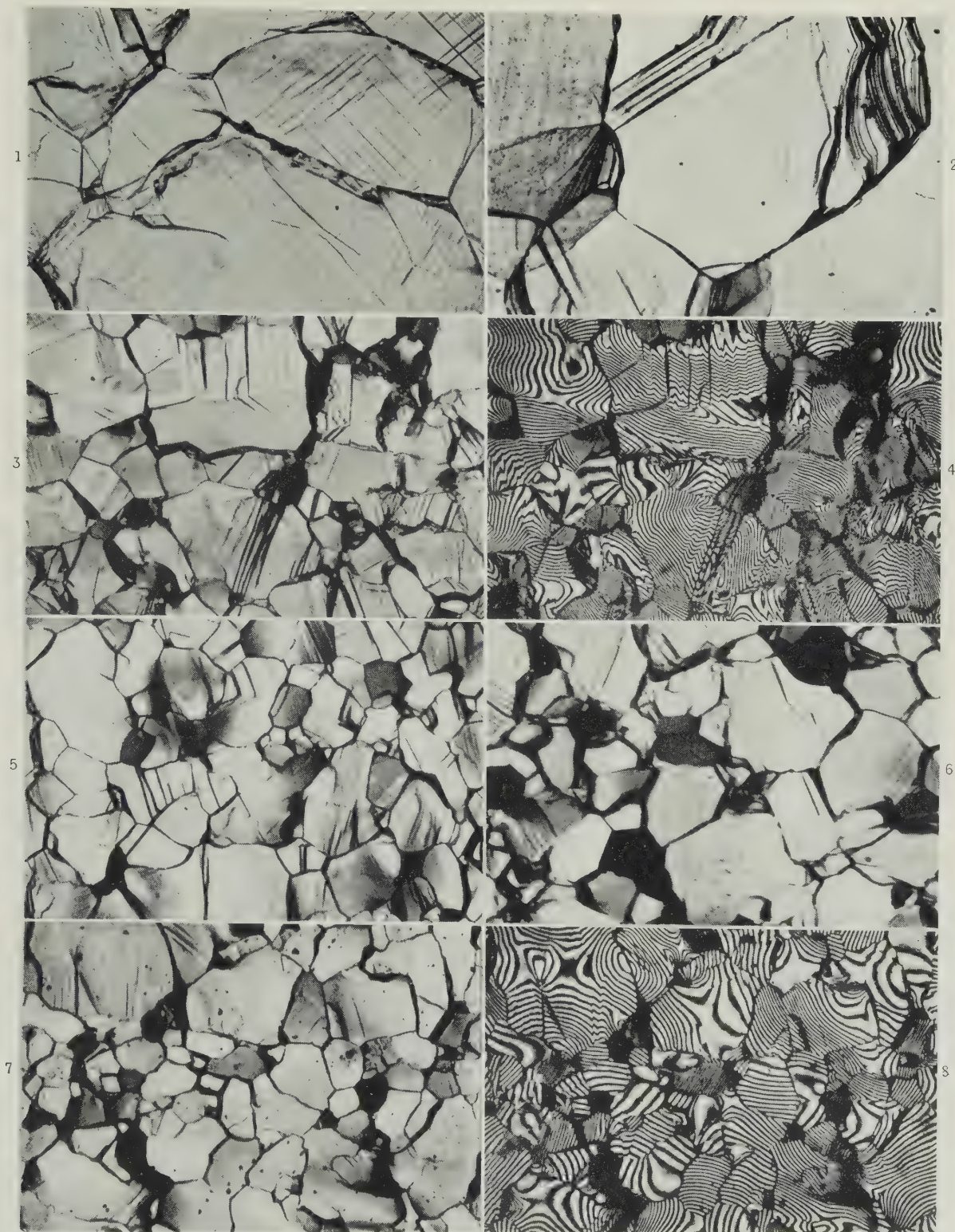


FIG. 1.—Pure Lead; 500 lb./in.²; 4.5% Extension in 8 days.
 FIG. 2.—Pure Lead; 300 lb./in.²; 5% Extension in 270 days.
 FIG. 3.—1.25% Thallium; 500 lb./in.²; 10% Extension in 50 days.
 FIG. 4.—Multiple-Beam Interferogram of same Area as Fig. 3.
 FIG. 5.—7.87% Thallium; 500 lb./in.²; 10% Extension in 11 days.
 FIG. 6.—2.45% Thallium; 200 lb./in.²; 10% Extension in 190 days.
 FIG. 7.—13.45% Thallium; 500 lb./in.²; 10% Extension in 24 days.
 FIG. 8.—Multiple-Beam Interferogram of same Area as Fig. 7.

LEAD-THALLIUM ALLOYS.

← Direction of Applied Stress →

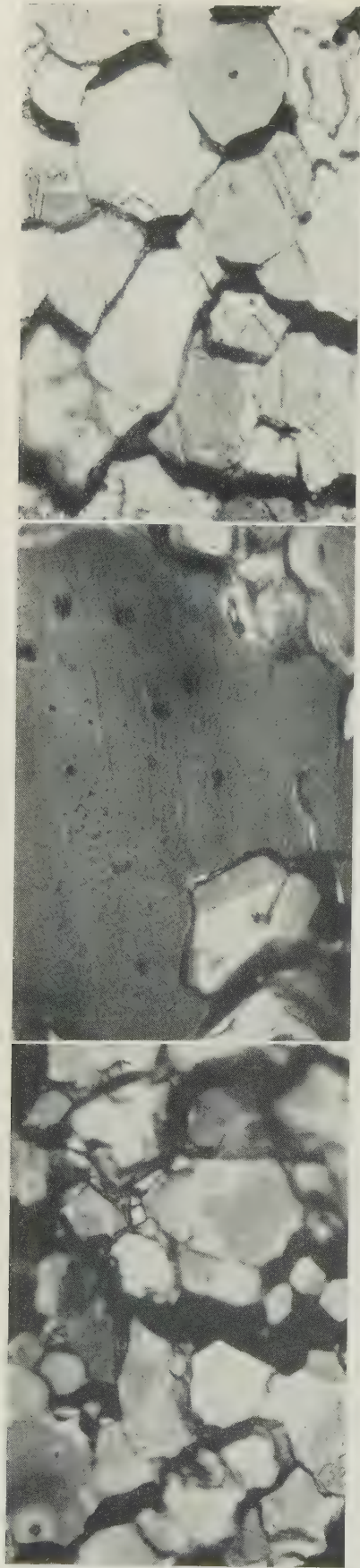
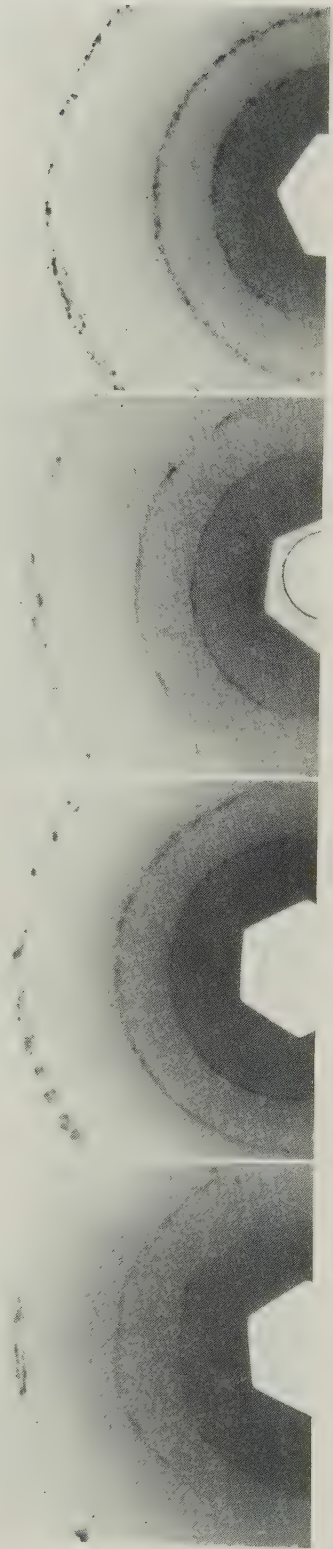
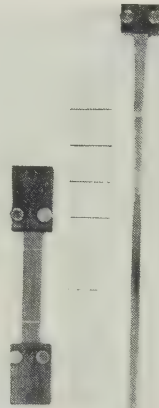


FIG. 9.—13.45% Thallium; 200 lb./in.²; 45% Extension in 475 days. $\times 400$.
FIG. 10.—As Fig. 9, Another area, with negative phase-contrast illumination. $\times 600$.
FIG. 11.—26.58% Thallium; 300 lb./in.²; 50% Extension in 875 days. $\times 400$.



FIG. 12.—Pure Lead; 500 lb./in.²; 5% Extension in 9 days; Unpolished. $\times 150$.

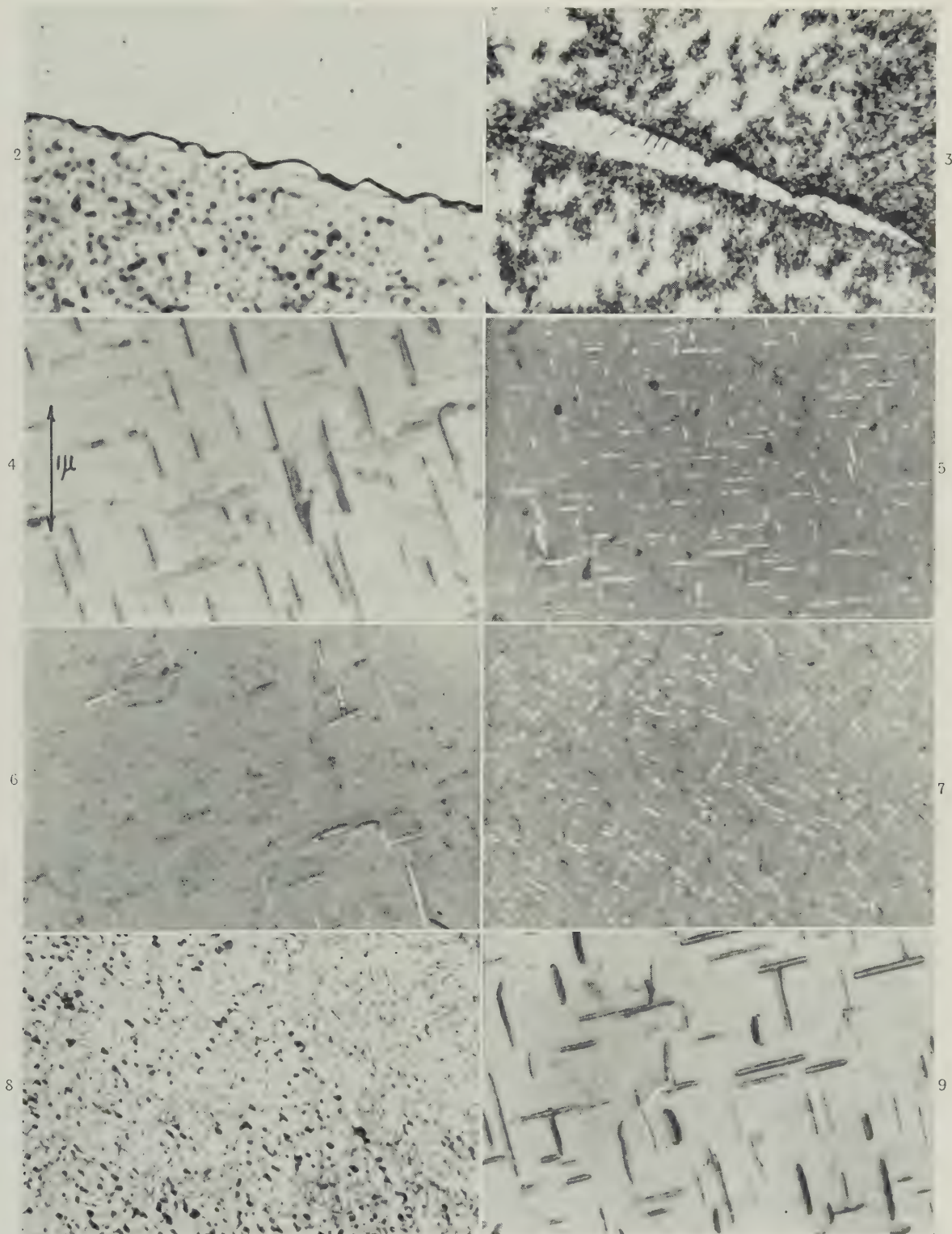
FIG. 13.—Fractured Test-Piece of 7.87% Thallium Alloy after Testing at 300 lb./in.², Showing 372% Extension in 221 days, Compared with an Untested Specimen. Approx. $\times \frac{1}{2}$.



FIGS. 14-17.—X-Ray Back-Reflection Photographs.

FIG. 14.—Pure lead; 500 lb./in.²; 4.5% Extension in 9 days; Unpolished. $\times 150$.
FIG. 15.—2.45% Thallium; 200 lb./in.²; 4.81% Extension in 221 days. $\times 400$.
FIG. 16.—4.81% Thallium; 200 lb./in.²; 13.45% Extension in 875 days. $\times 400$.
FIG. 17.—13.45% Thallium; 300 lb./in.²; 50% Extension in 875 days. $\times 400$.

STRUCTURES OF AGE-HARDENED ALUMINIUM ALLOYS.

FIG. 2.—Al-4% Cu. Aged 16 hr. at 130° C. Optical microscope. $\times 2500$.FIG. 3.—Al-4% Cu. Aged 200 days at 130° C. Optical microscope. $\times 1600$.FIG. 4.—Al-4% Cu. Aged 3 days at 190° C. Electron microscope. $\times 20,000$.FIG. 5.—Al-4% Cu-0.05% In. Aged 3 days at 190° C. Electron microscope. $\times 20,000$.FIG. 6.—Al-4% Cu. Aged 200 days at 130° C. Electron microscope. $\times 20,000$.FIG. 7.—Al-4% Cu-0.05% Sn. Aged 200 days at 130° C. Electron microscope. $\times 20,000$.FIG. 8.—Al-4% Cu. Aged 96 days at 190° C. Optical microscope. Black plates in lower grain are approximately parallel to the plane of polish. $\times 1600$.FIG. 9.—Al-4% Cu. Aged 96 days at 190° C. Electron microscope. $\times 20,000$.

MECHANICAL ANISOTROPY IN SOME DUCTILE METALS*

1460

By PROFESSOR W. A. BACKOFEN,† S.B., Sc.D., and
B. B. HUNDY,‡ B.Sc., Ph.D., MEMBER

SYNOPSIS

Fracturing test-specimens in tension after prestraining in torsion has shown that a fibrous crack-like structure, causing a considerable degree of mechanical anisotropy, exists in 70 : 30 brass, nickel, Monel metal, and Armco iron. The same programme of testing has also revealed the presence of such a structure in high-purity aluminium, but, for reasons that are not clear, the tensile behaviour of torsionally prestrained commercially pure (2S) aluminium gives no indication of its presence.

I.—INTRODUCTION

MANY investigations¹⁻¹⁰ have shown that wrought metals are highly anisotropic and that the anisotropy is not eliminated by annealing. The fracture properties, in particular, have been found to be affected by the direction of testing. The majority of these investigations were carried out on steels or high-strength non-ferrous alloys in which the mechanical anisotropy is usually attributed to alignment in the direction of metal flow of regions of segregation, of cavities, or of various phases in the microstructure. Anisotropy may also be the result of preferred orientation of the grains, and there are examples of directionality of mechanical properties being caused by a combination of both "fibring" and preferred orientation.

Recent work by the present authors¹¹ has shown that mechanical anisotropy is developed in pure copper by severe hot working or by cold working and annealing. The presence of anisotropy in the metal was demonstrated by fracturing in tension, specimens previously twisted to various degrees of prestrain.§

The tensile fracture stress, ductility, and type of fracture were not affected by small amounts of twisting, but when the specimens were twisted more severely, fracture occurred by abrupt separation across a helical surface rather than in the usual ductile manner. The change in the appearance of the fracture was accompanied by a fall in the fracture stress and ductility. If a specimen was twisted severely and then untwisted, subsequent tension testing showed that prestraining had not significantly altered either the fracture stress or the ductility, and the ductile mode of fracture reappeared. These results seemed to indicate that the material was highly anisotropic before twisting; this conclusion was confirmed by tests on specimens cut in different directions from the original material.

The copper used in these experiments was of high purity, and therefore the results could not be explained by alignment of secondary phases or impurities in the direction of metal flow. An examination of the torsion texture of copper¹³ showed that preferred orientation of the grains could not account for the anisotropy, and it was therefore suggested that it resulted from a highly oriented structure of flaws.

These flaws behave very much like cracks, and in the present paper they will be described as micro-cracks, even though they are apparently too small to be visible under normal microscopical examination. It is thought that some micro-cracks originate during solidification of the ingot, and some perhaps are formed during plastic working when they all, regardless of origin, become aligned in the direction of metal flow. They weaken the metal in the transverse direction, but do not affect the longitudinal mechanical properties. Torsional prestraining of a specimen containing micro-cracks aligned in the longitudinal direction causes them to follow a helical path, and in subsequent tension fracture takes place across this path.

Apart from the experiments on copper described above, there is very little published information on mechanical anisotropy in pure ductile metals or in single-phase alloys. The work reported in the present paper arose from a desire to determine whether plastic working of such metals could give rise to mechanical anisotropy and whether such an anisotropy, if found, could be explained by means of the micro-crack hypothesis outlined above.

As in the previous research, the mechanical anisotropy was studied by fracturing in tension, specimens that had been previously twisted to various strains. The experiments show that mechanical anisotropy exists in most of the metals considered and that the anisotropy can be explained by an oriented micro-crack structure.

* Manuscript received 3 November 1952.

† Massachusetts Institute of Technology, Cambridge, Mass., U.S.A.

‡ British Iron and Steel Research Association, Sheffield.

§ This method was suggested by the work of Swift¹² on the effect of torsional prestrain on the tensile properties of mild steel.

II.—EXPERIMENTAL PROCEDURES

1. MATERIALS

Table I summarizes many of the experimental details, and Fig. 1 gives the dimensions of the torsion specimens and of the tension specimens prepared from them after twisting. All materials were obtained as wrought bars in which the principal direction of metal flow during processing coincided with the axis of the bar. The torsion specimens were machined from these materials in the cold-worked, as-received condition. They were then annealed at the temper-

processing history. The material of the series-A specimens was obtained from a commercial source, whereas that of the series-B specimens was specially prepared with a final cold reduction in area of 87% by forging.

2. PRESTRAINING AND TENSILE TESTING

Both twisting and untwisting were done at a rate of $120^\circ/\text{min}$. The strain gradient in a twisted round bar is linear; shear strain, γ , increases from zero at the centre to a maximum value at the surface which is given by $\gamma = r\theta/l$, where r is the radius of the bar,

TABLE I.—Summary of Experimental Details.

Material	Processing History	Annealing Treatment of Torsion Specimens after Machining	Testing Procedure
70 : 30 Brass	$\frac{5}{8}$ -in.-dia. cold-drawn rod prepared from an ingot of high-purity components.	30 min. at 950°F . (510°C .)	Torsion—Tension.
Commercially Pure ("A") Nickel	$\frac{3}{4}$ -in.-dia. cold-finished rod obtained from a commercial source.	30 min. at 1350°F . (732°C .)	Torsion—Tension.
Monel Metal		30 min. at 1400°F . (760°C .)	Series A : Torsion—Tension. Series B : Torsion—Annealed 30 min. at 1400°F .—Tension.
Armco Iron		20 min. at 1500°F . (816°C .)	Series A : Torsion—Tension. Series B : Torsion—Annealed 20 min. at 1500°F .—Tension.
Commercially Pure (2S) Aluminium : Series A : Series B :	$\frac{3}{4}$ -in.-dia. cold finished rod obtained from a commercial source. 1-in.-dia. rod prepared by forging; 87% final cold reduction in cross-sectional area.	60 min. at 600°F . (316°C .)	Torsion—Tension.
High-Purity Aluminium (99.99%)	$\frac{3}{4}$ -in.-dia. rod prepared by forging; 75% final cold reduction in cross-sectional area.		

atures shown in the table. Both torsion and tension specimens were polished down to 0000 emery paper after machining and annealing, and before any mechanical testing was carried out.

Table I shows that two series of Monel metal, Armco iron, and 2S aluminium specimens were prepared. The B series of Monel metal and of Armco

iron is the total amount of twist in radians, and l is the length over which twisting takes place. This makes it a simple matter to calculate the shear strain in the surface of the smaller-diameter tension specimen.

An hydraulic machine was used for tensile testing. An average true stress/true strain curve was plotted for each test, and from these curves the tensile fracture stress and the strain to fracture (expressed as a percentage reduction in area) were obtained. Generally, diameter measurements at intervals throughout the test were adequate for calculating strain. But when the specimens became elliptical in cross-section, as did those of unstrained and only slightly prestrained aluminium, the instantaneous area of cross-section required for the strain calculation was determined from measurements of both major and minor axes.

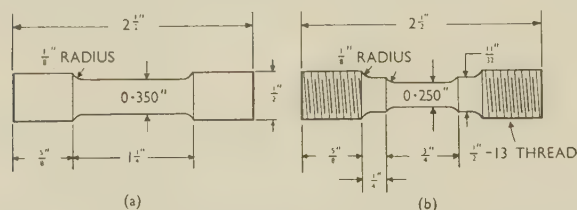


FIG. 1.—Dimensions of the (a) Torsion and (b) Tension Test Specimen.

iron differed from the A series in the anneal given after twisting and before tensile testing. Both the A and B series of 2S aluminium were tested in tension directly after prestraining, but they differed in

III.—EXPERIMENTAL RESULTS

The relationship between tensile fracturing characteristics and the amount of prestraining for the brass, nickel, Monel metal, and iron specimens, tested

directly after prestraining, is presented in Fig. 2. These curves show that the fracture stress and the ductility were not much affected until the shear strain introduced by unidirectional twisting exceeded a value of about 1, after which both, with the exception

nounced for all metals except Armco iron. But it was only in this respect that iron differed; the other effects of prestraining on ductility and mode of fracture were very much the same for all these metals.

After prestraining in excess of the critical amount,

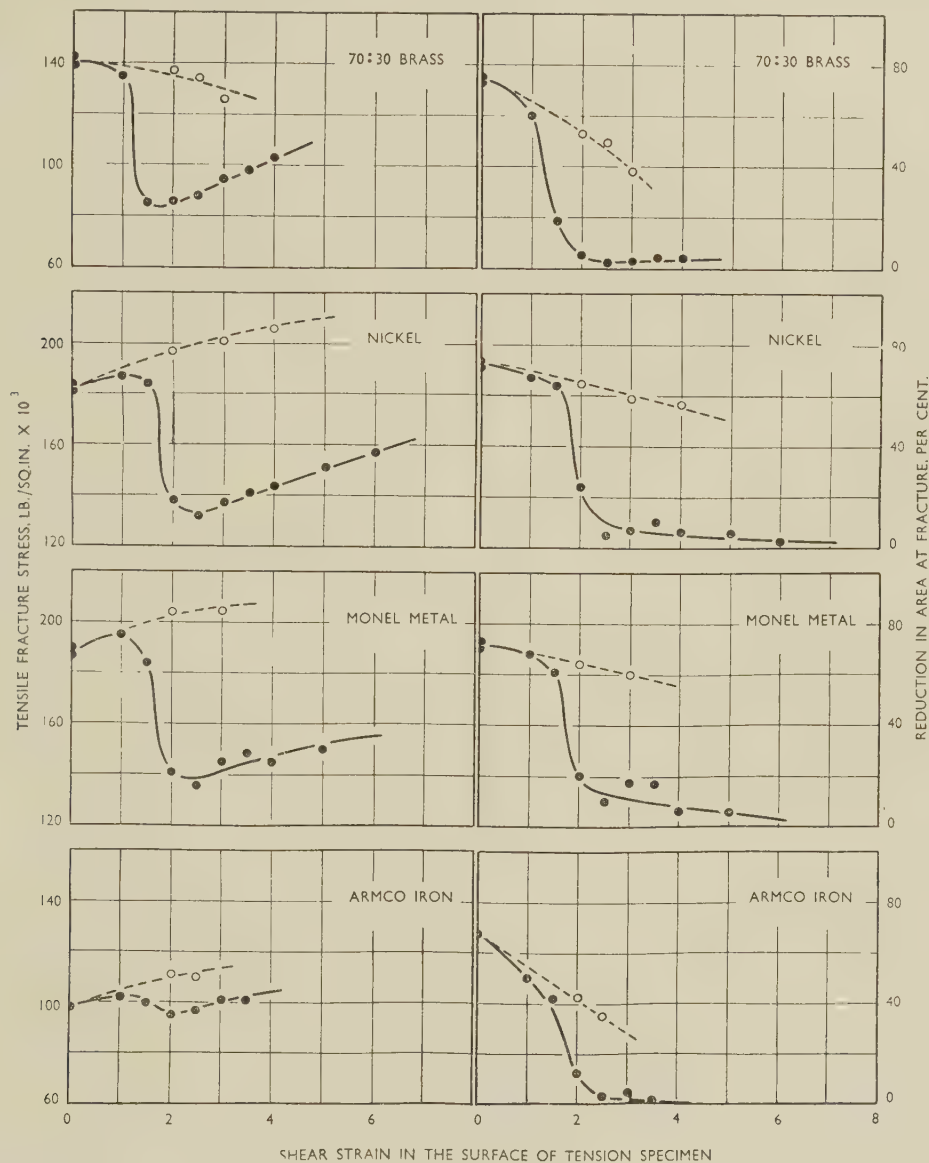


FIG. 2.—The Effect of Torsional Prestrain on the Tensile Fracture Stress and Ductility of Specimens Tested Directly after Prestraining.

KEY.

- Specimens twisted to the indicated strain and then tested in tension.
- Specimens twisted to the indicated strain, then completely untwisted, and tested in tension.

of the Armco iron fracture stress, underwent an abrupt decrease. The strain at which this marked change in fracturing characteristics begins will be referred to as the critical shear strain. With increasing prestrain, the fracture stress reached a minimum and then rose, whereas the ductility continued to fall.

The trend in the fracture stress data was very pro-

the usual ductile type of tensile fracture was replaced by a helical separation such as had previously been observed in copper. Fig. 6 (Plate LXVII) illustrates the fracture transition by means of typical fractures occurring in the series of nickel specimens. It is apparent from a study of these photographs that the angle α , included between the helical path of fracture in the specimen surface and a reference mark per-

pendicular to the specimen axis, became smaller with increasing prestrain. The measurements plotted in Fig. 3 were made from photographs similar to these.

On the other hand, when prestraining consisted of equal amounts of twisting and untwisting, the tensile fracturing characteristics and fracture appearance

Monel metal and of Armco iron. Measurements of the fracture angle, α , in Monel metal specimens are plotted in Fig. 3. Comparison of Figs. 2 and 4 shows that an intermediate anneal brought about a general increase in ductility, a continuous decrease in the fracture stress with increasing prestrain, and a higher value of

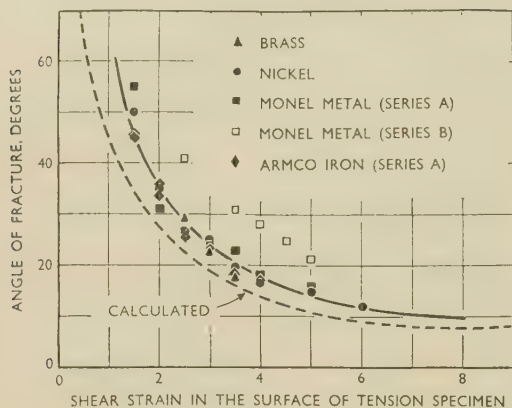


FIG. 3.—The Variation of the Fracture Angle, α , with Prestrain for Various Metals.

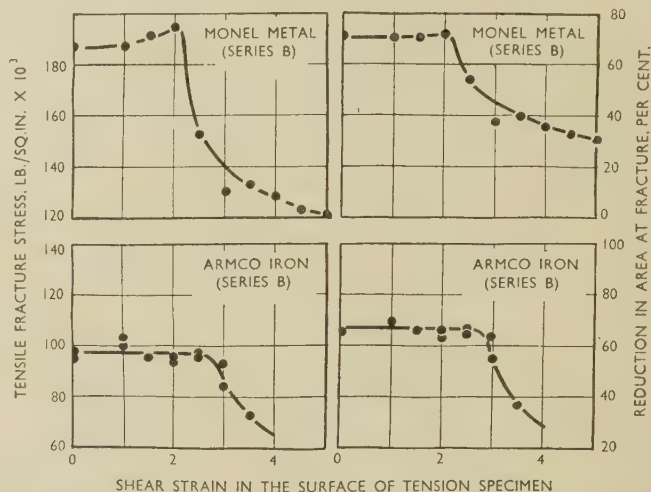


FIG. 4.—The Effect of Torsional Prestrain on the Tensile Fracture Stress and Ductility of Monel Metal and Armco Iron Specimens Annealed Before Tension Testing. All specimens were prestrained by twisting in one direction only.

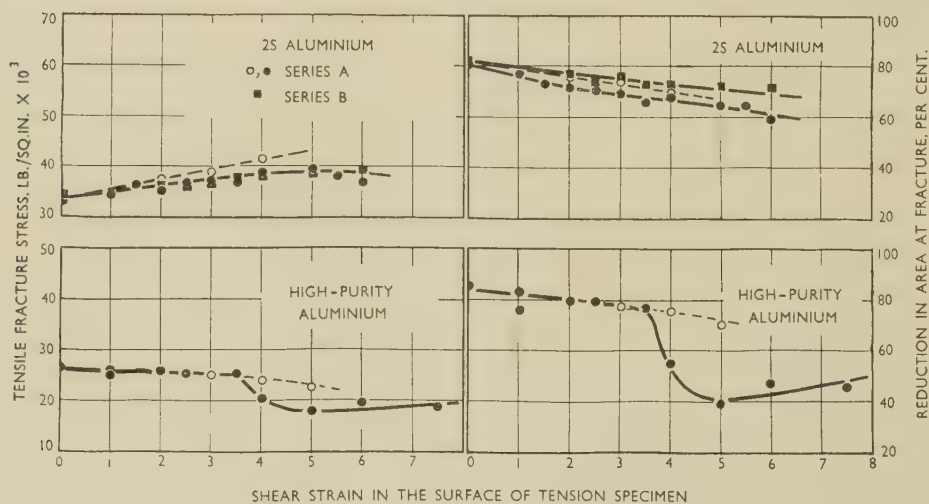


FIG. 5.—The Effect of Torsional Prestrain on the Tensile Fracture Stress and Ductility of Commercially Pure (2S) and High-Purity Aluminium Tested Directly after Prestraining.

KEY.

- Specimens twisted to the indicated strain and then tested in tension.
- Specimens twisted to the indicated strain, then completely untwisted, and tested in tension.

were much more like those of specimens not prestrained at all. The values of fracture stress and ductility for specimens prestrained in this way are plotted in Fig. 2 at the maximum shear strain which preceded untwisting. Photographs of the fractures in such specimens are also included in Fig. 6 (Plate LXVII).

The effect of annealing after prestraining on the relationship between fracturing characteristics and prestrain is illustrated in Fig. 4 for the B series of

the critical shear strain; there was also an enlargement of the fracture angle of the Monel metal specimens. The variation of fracture stress in the B series of Armco iron specimens showed the most noticeable effect of annealing. The difference between that metal and the others (Fig. 2) was eliminated by removing the cold work due to prestraining. Armco iron specimens could not be twisted to strains much greater than the critical value of series B, however, so that the helical fractures were not sharply defined,

and angular measurements could not be obtained for plotting in Fig. 3. The important conclusion to be drawn from these experiments is that annealing does not eliminate the condition created by prestraining which is responsible for the helical fracture and for the reduced fracture stress and ductility.

The experiments with commercially pure (2S) aluminium gave completely unexpected results. Although specimens were prestrained over the widest possible range, the tensile fracturing characteristics remained substantially unaltered. As is shown in Fig. 5, the fracture stress rose and the ductility fell slightly with increasing prestrain. But there was no sudden change in either after any amount of prestraining. In addition, the tensile fracture of severely twisted 2S aluminium specimens, two of which are shown in Fig. 7 (Plate LXVII), was not of the distinct helical type observed in similarly prestrained specimens of other metals. After these results had been obtained, the experiments with series-B specimens were carried out. The processing of the specially prepared rod for this series differed considerably from usual commercial practice. But the fracturing characteristics, which are also included in Fig. 5, were still essentially the same as those of the series-A specimens, as was the appearance of the fractures.

The results of the experiments with high-purity (99.99%) aluminium were equally surprising. Because of its purity, of the near absence of inclusions, and of the results of the preceding work with 2S aluminium, the fracturing characteristics were not expected to be sensitive to prestrain. Yet curves in Fig. 5 show that they did undergo a fairly marked change, although only after a rather large torsional strain. The tensile fracture of such a specimen prestrained in excess of the critical amount, like the one shown in Fig. 8 (Plate LXVII), was closer to being helical than the fracture of any 2S specimen. When prestraining was accomplished by equal amounts of forward and reverse torsion, both fracturing characteristics and fracture appearance were more nearly like those of the unstrained specimen. Thus the response of high-purity aluminium to prestraining resembled that of the other metals more closely than it did that of 2S aluminium.

IV.—DISCUSSION OF RESULTS

A fibrous micro-crack structure, creating a mechanical anisotropy, again provides, as in the previous experiments with copper, an explanation of many of the experimental results. The orientation of such a crack structure in an unstrained specimen is simply represented by a straight line in the surface and parallel to the axis of the specimen. During twisting, this line follows a helical path which may be described by an angle α' , similar to the angle α plotted in Fig. 3 (p. 436). After introducing a shear strain, γ , into the specimen surface, α' is equal to $(90^\circ - \tan^{-1}\gamma)$. The agreement in Fig. 3 between the broken curve, describing the calculated variation of the fracture

angle with prestrain, and the experimental curve implies, as before, that the helical tensile fracture occurs by separation over a surface of cracks whose directions are governed by the twisting. Only the re-orientation of a crack structure by untwisting satisfactorily explains the different tensile behaviour of specimens prestrained by equal amounts of forward and reverse torsion.

The experiments with high-purity aluminium also suggest the presence of a fibrous crack structure. The less-marked effects of torsional prestrain on this metal may mean a less highly developed structure. They might also be attributed to the metal's inherently greater ductility; the flow preceding the tensile fracture, which is a function of the ductility, causing the helical crack structure to straighten slightly, thus tending to enlarge the fracture angle, α . Such reasoning also explains the greater critical shear strain observed after annealing prestrained specimens of Monel metal and Armco iron.

The results obtained with high-purity aluminium make it difficult to understand the tensile behaviour of prestrained 2S aluminium. Although less pure and containing more inclusions, it is relatively insensitive to torsional prestrain. Apparently inclusions are not a dominant cause of mechanical anisotropy in these materials, and, for unknown reasons, the small-scale crack structure is either absent or not sufficiently developed in 2S aluminium to be revealed by the torsion-tension testing procedure. It does not seem that a complete absence of the crack structure is a satisfactory explanation, however, for Jacquesson and Laurent,¹⁴ by studying the dependence of fatigue strength on direction in rolled sheet of a commercially pure aluminium, found indications of a fibrous structure.

The suggestion has been made in the previous work with copper that the holes seen in the fracture surface of ductile metals broken directly in tension, as well as the holes and fibrous markings which are frequently observed in the helical type of fracture, may result from the enlargement of the micro-cracks to visible dimensions by the stresses associated with fracture. Similar patterns of holes and markings were also observed in varying degrees, in the fracture surfaces of the metals tested in this investigation. They were particularly noticeable in specimens of high-purity aluminium, but they were not at all conspicuous in 2S aluminium, as the photographs in Figs. 9 and 10 (Plate LXVII) show. Of course, this is only one difference between the two metals, yet it may reflect the relative intensity of the crack structure and thus help to explain the different tensile behaviour of these highly prestrained specimens.

V.—SUMMARY AND CONCLUSIONS

Fracturing test specimens in tension after prestraining in torsion has shown that a fibrous structure of flaws, which behave like cracks more than anything else, exists in 70 : 30 brass, nickel, Monel metal,

and Armco iron. Before the presence of the crack structure in these materials becomes apparent, however, the maximum shear strain introduced by twisting must exceed a critical value that varies from about 1 to 2.5, depending upon the metal and on whether or not prestraining is followed by annealing. If the critical prestrain is exceeded, the fracture strength and ductility decrease with increasing prestrain, and the fracture occurs by separation across a helical surface which defines the position in the twisted specimen of an array of cracks originally aligned parallel to the specimen axis. After prestraining by equal amounts of forward and reverse torsion, the original orientation of the crack structure is unchanged, and this explains why the fracturing characteristics and fracture appearance are not greatly different from those encountered when there is no prestraining. Observations similar to these resulted from the same programme of testing with high-purity

(99.99%) aluminium; a crack structure apparently exists in this metal as well as in the others. But for reasons that are not clear, the tensile behaviour of prestrained commercially pure (2S) aluminium gave no indication of the presence of such a structure.

Finding this condition in a number of relatively pure metals and single-phase alloys suggests that there is a definite limit to what can be accomplished in controlling the directionality of wrought materials through the quantity, size, shape, and distribution of extra phases in the microstructure.

ACKNOWLEDGEMENTS

The authors are indebted to the Office of Naval Research for sponsoring this research, and to Mr. R. S. Templin of the Aluminum Company of America for kindly providing the specially prepared rods of commercial and high-purity aluminium.

REFERENCES

1. A. W. Brearley and H. Brearley, "Ingots and Ingot Moulds", London: 1918 (Longmans, Green and Co.).
2. G. Charpy, *J. Iron Steel Inst.*, 1918, **98**, 7.
3. H. Unkel, *Z. Metallkunde*, 1939, **31**, 104.
4. G. Sachs, *J. Inst. Metals*, 1939, **64**, 261.
5. L. J. Klingler and G. Sachs, *J. Aeronaut. Sci.*, 1948, **15**, 731.
6. L. J. Klingler, C. C. Chow, and G. Sachs, *Trans. Amer. Inst. Min. Met. Eng.*, 1949, **185**, 927.
7. C. Wells and R. F. Mehl, *Trans. Amer. Soc. Metals*, 1949, **41**, 715.
8. W. F. Brown, H. Schwartzbart, and M. H. Jones, [*U.S.*] *Nat. Advis. Cttee. Aeronautics, Research Memo.*, 1951, (**E.50L28**).
9. D. M. McElhinney, *Aircraft Eng.*, 1951, **23**, 62.
10. H. Kostron, *Metall*, 1951, **5**, 58.
11. W. A. Backofen, A. J. Shaler, and B. B. Hundy, *Trans. Amer. Soc. Metals*, in the press.
12. H. W. Swift, *J. Iron Steel Inst.*, 1939, **140**, 181.
13. W. A. Backofen, *Trans. Amer. Inst. Min. Met. Eng.*, 1950, **188**, 1454.
14. R. Jacquesson and P. Laurent, *Rev. Mét.*, 1949, **46**, 89.

THE FORMATION OF INTRACRYSTALLINE VOIDS IN SOLUTION-TREATED MAGNESIUM- ALUMINIUM ALLOYS*

1461

By E. LARDNER,† B.Sc., A.I.M., MEMBER

SYNOPSIS

It has been observed that occasionally the solution-treatment of cast magnesium-aluminium alloys results in the formation of small hexagonal voids in the centre of many grains. These voids have been shown to be orientated with their hexagonal axes parallel to the hexagonal axes of the crystals in which they occur. No explanation has been found for their formation, but it has been shown that in a sample of an alloy that does form cavities, the cavity formation increases to a maximum and then eventually vanishes with increasing homogenization. It has also been shown that the cavities are probably produced on cooling after solution-treatment rather than during the progress of the heat-treatment.

I.—INTRODUCTION

DURING the war years a considerable amount of research was undertaken with the object of reducing the scatter in the mechanical properties of magnesium-base castings. This work involved the examination of very many microsections of alloys that were then commonly used. It was observed that the alloy Elektron AZ91 (aluminium 9.5, zinc 0.5, manganese 0.3%) in the solution-treated condition often showed well-defined cavities in the central regions of many of the grains. The position of these cavities within the grains, and their well-marked geometric form, clearly distinguished them from other cavities, such as those due to microporosity.

These cavities, which were observed only in alloys that had been solution-treated, were found to be in the form of hexagonal-faced, parallel-sided voids with average dimensions of about 0.015 mm. across the flats of the hexagon and 0.008 mm. in height between the hexagonal faces. The dimensions, especially the height, varied considerably, and cavities up to twice the size mentioned have been observed. In the microsection the cavities were usually seen as rectangles, with occasional triangles, and more occasionally still, perfect hexagons. These shapes were consistent with random sectioning of the hexagonal prism shape already described. In many cases several cavities were observed within a single grain (Fig. 1, Plate LXVIII), and in such cases it was evident that the cavities had a common orientation. By giving specimens a precipitation-treatment at a relatively high temperature, thereby inducing a coarse precipitation in known crystallographic planes, it was possible to establish that the hexagonal voids and the hexagonal lattice of the crystal in which they were situated had the same orientation.¹

Fig. 2 (Plate LXVIII) shows the appearance of one of these cavities in a sample of Elektron AZ91 which had been solution-treated and then precipitation-treated at 250°C. From the appearance of the precipitate, it can be seen that the section had been cut very nearly parallel to the basal planes.

Cavities were never observed in any material that had not been solution-treated. They were observed most commonly in Elektron AZ91, less commonly in Elektron A8 (aluminium 8, zinc 0.5, manganese 0.3%), and in no other commercial alloy. With various experimental alloys such cavities were observed only when a substantial amount of aluminium was present and never in alloys free from aluminium.

Various attempts have been made to account for the formation of these cavities, but no satisfactory explanation has been found. However, in view of the recent observations of similar cavities in other alloy systems, the details of the occurrence of such cavities in magnesium-base alloys assume fresh interest. Thus, Bückle and Blin² have described similar cavities produced by the diffusion of aluminium and zinc in copper. Barnes³ has described cavities produced by the diffusion of nickel in copper, and Brasunas⁴ has reported sub-surface cavities in Inconel and 80 : 20 nickel-chromium alloy associated with the loss of chromium from the surface.

II.—EXPERIMENTAL WORK

As the production of these cavities was obviously connected in some way with the solution-treatment, it was decided to investigate the way in which cavity formation was connected with the two main variables in the solution-treatment, viz. time and temperature.

Since cavities were found in only a comparatively

* Manuscript received 25 November 1952.

† Metallurgist, Hard Metal Tools, Ltd., Coventry; formerly

with Magnesium Elektron, Ltd., Clifton Junction, near Manchester.

small number of batches of AZ91, it was first necessary to obtain a stock of metal in the "as-cast" condition which was known to produce cavities on normal solution-treatment.

A batch of sand-cast test-bars from a single melt of AZ91 was prepared, and a small test-piece from each bar checked for cavity formation, until a suitable batch was obtained. This batch was of normal commercial purity. Typical impurity contents would be:

Si	< 0.014%	Pb	< 0.05%	Cd	< 0.01%
Cu	< 0.006%	Sn	< 0.03%	Ag	< 0.005%
Fe	< 0.014%	Ca	< 0.005%	Ni	< 0.005%

1. EFFECT OF SOLUTION-TREATMENT TIME

When a suitably checked supply of material had been obtained, the following solution-treatments were carried out in a small air-circulating heat-treatment furnace: 5 hr. at 385° C., followed by heating at 420° C. for 5, 10, 15, 20, 25, 30, 40, 48, and 72 hr. The samples were allowed to cool freely in air. The preliminary treatment for 5 hr. at 385° C. was given in order to prevent any possible formation of liquid phase due to the presence of traces of the ternary eutectic.

On examination of the solution-treated samples, cavities were detected in all except one, which was heat-treated at 385° C. only. The cavities formed showed characteristics that varied with the time of treatment. At short times the cavities were less sharply defined and rather smaller, especially in height, than those seen after the normal 24-hr. treatment. In the samples solution-treated for short times, it was commonly observed that one or both of the hexagonal faces of the void was convex. This was at first thought to be due to distortion effects during polishing, but it was later found to be the true shape of the void, and to be characteristic of cavities formed after a short solution-treatment.

Between 15 and 40 hr. no difference in cavity formation could be detected. However, after 48 hours' treatment a decrease in the number of cavities produced was observed, and after 72 hours' treatment only a few cavities could be detected.

2. EFFECT OF SOLUTION-TREATMENT TEMPERATURE

Using the same "as-cast" material, the following solution treatments were carried out: 24 hr. at 360°, 380°, 400°, 420° C.; 3 hr. at 420° C. + 21 hr. at 440° C.; and 3 hr. at 420° C. + 21 hr. at 450° C.

When these samples were examined, the effect of increasing temperature was found to be very similar to that of increasing time. The sample that had been solution-treated at 360° C. was completely free from cavities, but much undissolved Mg_4Al_3 remained. That treated at 380° C. showed a few small narrow cavities, but solution was still far from complete. At 400°, 420°, and 440° C., a normal cavity formation was obtained. At 450° C. the cavities had decreased

considerably in number, but the ones that were observed were rather larger than usual, most of the size increase being in the distance between the hexagonal faces.

These tests gave a plain indication that cavity formation diminished with increase in time or temperature of solution-treatment. Accordingly, combinations of increased time and temperature were tried, and it was found that cavities were completely absent after a treatment of 5 hr. at 385° C. + 16 hr. at 420° C. + 16 hr. at 450° C. This stepped treatment was used in order to prevent any incipient fusion at the higher solution-treatment temperature.

These results indicated that the tendency to produce cavities progressively increased with the degree of solution, and then gradually decreased until eventually no cavities at all were formed.

In view of these results, several tests were made to determine whether cavities already existing in solution-treated AZ91 could be removed by further heat-treatment. It was then discovered that cavities already existing could not be removed by either very long additional solution-treatments, or by solution-treatments at higher temperatures. This rather surprising result suggested that the cavities could not be produced progressively during solution-treatment and then closed up again with further heat-treatment. Instead it seemed most probable that the cavities were not produced at all during the heat-treatment, but were formed during cooling from the solution-treatment temperature, and were due to some condition set up in the metal by the heat-treatment.

3. EFFECT OF COOLING RATE AFTER SOLUTION-TREATMENT

If this supposition were true, cavity formation might be influenced by the rate of cooling from the solution-treatment temperature.

A number of samples of the "as-cast" AZ91 specimens were solution-treated for 8 hr. at 385° C. and 16 hr. at 420° C. and cooled from the solution-treatment temperature at different rates. The various rates of cooling were obtained by water-quenching, oil-quenching, air-cooling, air-cooling in a crucible packed with scrap metal, cooling in a laboratory tube-furnace, and cooling in a large industrial-type air-circulating furnace. In the two latter cases the specimens were allowed to cool in the furnace in which the solution-treatment had been carried out. The times to cool from 420° to 100° C. varied from a few seconds for the quenched samples to about 1 hr. for the large crucible packed with scrap, 6 hr. for the tube furnace, and 20 hr. for the large heat-treatment furnace. All the test-pieces, except those that were furnace-cooled, showed normal cavity formation. The two samples that were furnace-cooled were similar to each other, despite the big difference in their respective rates of cooling, and both showed only a very few cavities.

These were not of the characteristic appearance. They lacked the normal sharp straight outlines and showed rounded corners.

4. EFFECT OF GRAIN-SIZE

Using a batch of AZ91 ingots which were known to give sand-cast test-bars that produced many cavities on normal solution-treatment, several chill-cast spectrographic pencils (4 mm. in dia.) and D.T.D. sand-cast test-bars were made. The grain-size of the spectrograph pencil castings was very fine, and that of the material in the heads of the sand-cast test-bars quite coarse. Samples cut from the spectrograph pencils, the test-bars, and the test-bar heads gave a fairly wide range of grain-sizes.

A number of solution-treatments were given to these pieces. In the spectrograph pencils, the solution of the Mg_4Al_3 occurred rapidly, solution being complete in about 6 hr. at 420° C. Samples from these pencils were solution-treated for 4, 6, 8, 16, and 24 hr. at 420° C. No cavities were found in any of these, although test-pieces cut from the sand-cast test-bars showed normal cavity formation after 24 hr. at 420° C.

The coarse-grained pieces cut from the feeder heads contained no cavities after 24 or 48 hr. at 420° C., but showed many abnormally large cavities after being heat-treated for 48 hr. at 440° C.

In addition to these experiments on the effect of grain-size, tests were also carried out on a block cast into a water-cooled mould, similar to that described by Northcott.⁵ The walls were of thin steel sheet, and the base was a water-cooled copper plate. Solidification was almost perfectly uni-directional, and the rate of cooling varied over a wide range from bottom to top of the cast block. The structure also varied considerably. At the base of the block of AZ91 cast in this mould, the structure was of a fine-grained solid-solution type, almost free from any Mg_4Al_3 . The grain-size gradually coarsened, and the quantities of massive Mg_4Al_3 increased towards the top portion of the block, where there was a structure very similar to that of a normal sand-cast test-bar. Complete vertical sections, approximately $3\frac{1}{2}$ in. long, were cut from these blocks and solution-treated for 8 hr. at 385° C. + 16 hr. at 420° C. Cavities were found only in the top $\frac{3}{4}$ in. of these strips.

5. EFFECT OF VOLUME CHANGE DURING SOLUTION-TREATMENT

A number of tests in connection with other work had been carried out to determine the volume changes that occurred during the heat-treatment of magnesium-base casting alloys. These tests were made by measuring the dimensions of a rod 5 in. long by $\frac{3}{4}$ in. dia. machined from a sand-cast test-bar, before and after heat-treatment.

AZ91 would be expected to show a slight contraction on solution-treatment, but the results

obtained were erratic; expansions occurring as often as contractions. When microspecimens were cut from the solution-treated test-pieces, it was found that the bars that had expanded showed considerable cavity formation, whereas the bars that had contracted were free from cavities. So far as it was possible to judge from the examination of micro-sections, the amount of expansion was roughly proportional to the extent of the cavity formation.

In view of these results several volume-change test-pieces were prepared from the reference batch of AZ91, and solution-treated for 8 hr. at 385° C. + 16 hr. at 420° C. + 24 hr. at 450° C. After this treatment no cavities were present, and the test-bars showed a consistent contraction.

III.—CAVITIES IN ALLOYS OTHER THAN AZ91

During the work, cavities were produced in AZ91, A8, and some experimental alloys containing 10 and 12% aluminium. It was not found possible to produce cavities in AZG (aluminium 5, zinc 3, manganese 0.3%) or AZM (aluminium 6, zinc 0.5, manganese 0.3%), although an old test-piece of AZG was found that showed a small number of cavities. In any alloy the cavity formation was found to vary from melt to melt, even if the structure and analysis were almost identical.

Numbers of scrap castings in solution-treated AZ91 were examined, and it seemed that cavities were produced more frequently in castings made under commercial conditions than in samples of the same alloy prepared under laboratory conditions.

A number of experimental alloys were made under laboratory conditions and attempts made to produce cavities by solution-treatments. The alloys and their solution-treatments were as follows:

Mg-8% Al-2% Zn	} Solution-treated 24, 48, and 72 hr. at 350° C.
Mg-6% Al-4% Zn	
Mg-4% Al-6% Zn	
Mg-6% Al-2% Zn	} Solution-treated 8, 16, and 24 hr. at 420° C.
Mg-6% Al	
Mg-4% Al	} Solution-treated 24, 48, 72, and 96 hr. at 300° C.
Mg-4% Zn	
Mg-6% Zn	
Mg-8% Zn	
Mg-10% Zn	
Mg-12% Zn	

None of these alloys formed cavities.

In general, it seems that cavity formation is associated with high aluminium contents. The effect is reduced by the replacement of aluminium with zinc, and binary magnesium-zinc alloys do not form cavities.

IV.—SUMMARY AND CONCLUSIONS

The work that has been described indicates that there is some relationship between the degree of solution and cavity formation. It is also very probable that the cavities are formed during cooling

from solution-treatment rather than during the treatment. It is, however, evident that other factors are involved in the formation of cavities, and no explanation for the wide variation in cavity formation from one batch to another of the same alloy can be offered.

It is suggested that the cavity formation is in some way connected with the aluminium concentration gradient existing in any particular grain at the time that it is cooled from the solution-treatment temperature.

A sand casting in AZ91 contains an appreciable amount of massive Mg_4Al_3 and the average aluminium content of the α -phase crystals will probably be of the order of 4%. A considerable difference in aluminium content must exist in any grain between its centre and a boundary in contact with the massive Mg_4Al_3 . Owing to the slow rate of diffusion, this gradient possibly builds up during the early stages of solution-treatment and exists to quite a marked extent after all the massive Mg_4Al_3 has been absorbed. Considerable further time at solution-treatment temperature is required to produce a uniform aluminium content throughout all the α grains.

That such a gradient does exist can be seen readily by precipitating to equilibrium a sample which has been solution-treated just sufficiently to remove the massive Mg_4Al_3 . The precipitated Mg_4Al_3 will be seen to be greater in quantity near the grain boundaries, and the centre of the grains will be quite free. This effect can be seen in Fig. 2 (Plate LXVIII). The cavity formation always occurs in these zones which are obviously low in aluminium.

The fact that after solution-treatment for a long time or at a high temperature cavities are not formed will, on this hypothesis, be explained as being due to the reduction or elimination of the concentration gradient by the heat-treatment. This concentration gradient may set up internal stresses within the crystal, which on cooling after solution-treatment, and when some other condition is satisfied, gives rise to cavity formation. There has been no evidence to indicate the nature of this unknown factor, but it may be associated with melting conditions, and the

gas content of the metal is an aspect of the problem worth further attention. However, it is unlikely, from the sharply defined geometrical shape of the cavities, that they could be associated with a high internal gas pressure.

A recent paper by Bückle and Blin² describes the production of cavities of a very similar nature in brass which had been given a diffusion treatment when in intimate contact with pure copper. The crystallographic relationship of the cavities in the brass to the brass grain, and that of the cavities in the magnesium to the magnesium grain suggest very strongly that a similar mechanism is responsible in both cases.

In the instances described in the present paper the cavities are associated with the diffusion of aluminium *into* magnesium, but in the case of Bückle and Blin's phenomenon it is a case of the diffusion of zinc *out of* brass. It will be noted that both cases have in common the production of a concentration gradient of the solute element, but whereas the solution of aluminium in magnesium causes a contraction of the parent lattice, solution of zinc in copper has the opposite effect.

It is hoped that this description of cavities produced in magnesium-aluminium alloys may help in obtaining a satisfactory explanation of the phenomenon.

ACKNOWLEDGEMENTS

The author is indebted to the Directors of Magnesium Elektron, Ltd., and to Captain A. C. Jessup, Chief Metallurgist, for permission to publish this paper. The work described was carried out several years ago under the general supervision of Dr. F. A. Fox.

REFERENCES

1. F. A. Fox and E. Lardner, *J. Inst. Metals*, 1943, **69**, 373.
2. H. Bückle and J. Blin, *ibid.*, 1951-52, **80**, 385.
3. R. S. Barnes, *Proc. Phys. Soc.*, 1952, [B], **65**, 512.
4. A. de S. Brasunas, *Metal Progress*, 1952, **62**, (6), 88.
5. L. Northcott, *J. Inst. Metals*, 1939, **65**, 173.

A NOTE ON THE MATHEMATICAL ANALYSIS OF CREEP CURVES*

1462

By L. M. T. HOPKIN,† B.Sc., A.R.S.M., A.I.M., MEMBER

(Communication from the British Non-Ferrous Metals Research Association.)

SYNOPSIS

The Andrade equation $L_t = L_0(1 + \beta t^{1/3})\exp Kt$ and an equation containing a logarithmic term have been found to give good, but not perfect, fits of creep curves, obtained from constant-stress tests on a high-purity lead and a lead-1% tin alloy, for times up to 300 hr., although the Andrade equation was the better for longer times up to 5000 hr.

An attempt to correlate the values of the constants in the Andrade equation with the effects of grain-size and stress on creep behaviour was not possible for the high-purity lead owing to relatively large errors involved in the calculation of the constants. For the lead-1% tin alloy, however, it was found that the $\sqrt[3]{K}$ was linearly related to stress and relative grain-boundary areas, although no simple relationship existed between these variables and the β constant.

I.—INTRODUCTION

ANDRADE,¹ in his classical work on the flow of metals in 1910, derived a mathematical equation for creep curves obtained under conditions of constant stress. The constants in this equation are generally believed to have some physical significance,^{2,3} one of them has been associated with transient creep, and another is thought to represent flow of a viscous nature. Since Andrade's early work, many alternative creep equations have been proposed; that most frequently suggested contains a logarithmic function which has been associated, also, with transient creep.⁴⁻⁶

At the beginning of a recent and detailed investigation of the effect of constitutional factors on the creep properties of lead and lead alloys,⁷ it was considered that mathematical analysis of the creep curves might facilitate interpretation of the results. In consequence, the creep tests were made under conditions of constant stress, instead of at constant load as in most investigations, to enable the creep curves to be so analysed.

In the present paper a comparison is made between the Andrade and the logarithmic equations to determine their relative accuracies in fitting the experimental results from tests of relatively long duration. An attempt is also made to correlate the effect of grain-size and stress on creep behaviour with the numerical values of the constants obtained by analysing the creep curves by the Andrade equation.

II.—EXPERIMENTAL PROCEDURE

The analysis of the high-purity lead (99.999% pure) and an alloy of this basis material with 1% tin, together with the experimental technique, have

been reported elsewhere.⁷⁻⁹ Both materials were extruded at various temperatures, in a laboratory extrusion press, to obtain a range of grain-sizes, the values of which were determined by a comparison method and by the statistical method due to Johnson.¹⁰ The statistical method gives a spatial grain-size number which is inversely proportional to the actual grain-size.

III.—RESULTS OF EXPERIMENTS

1. COMPARISON OF THE ANDRADE AND LOGARITHMIC EQUATIONS

In the Andrade equation $L_t = L_0(1 + \beta t^{1/3})\exp Kt$, where L_t represents the length of the specimen at any time t , and L_0 , β , and K are constants; L_0 is similar to the length of the specimen immediately after loading. Andrade himself suggests that the equation is only an approximation and fits a creep curve only for short times; his own tests lasted less than a working day. The present author, however, has shown previously that the equation is a good representation of the experimental results for times at least up to 1000 hr.⁹

The logarithmic equation may be written in a form similar to that due to Andrade, i.e. $L_t = A(1 + B \log t)\exp Ct$, where L_t represents the length of the specimen at any time t , and A , B , and C are constants.

The constants in both equations were calculated for a creep curve by solving three simultaneous equations obtained by substituting in the general equation the length of the specimen at three times separated by equal intervals. The elongation of a specimen at any time was determined to $\pm 0.01\%$, and this limit of

* Manuscript received 28 November 1952. The work described in this paper was made available to members of the British Non-Ferrous Metals Research Association in a confidential research report issued in November 1952.

† Metallurgy Division, National Physical Laboratory, Teddington; formerly Investigator, British Non-Ferrous Metals Research Association, London.

accuracy produced an error in the constants of the equations the maximum possible value of which was estimated by a method set out in the Appendix

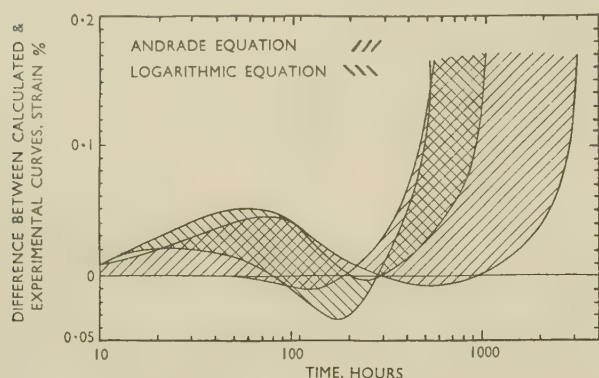


FIG. 1.—Comparison of the Andrade and Logarithmic Equations at Short Times for High-Purity Lead Extruded at 250° C. and Tested at 300 lb./in.². The constants in both equations were calculated from the values of the strains determined experimentally at 7, 143, and 279 hr. Strain at 1000 hr. was 1.85%.

(p. 447). In comparing the curves calculated from the two equations with the experimentally determined creep curves in Figs. 1, 2, and 3, the shaded areas for each equation cover a range of values which are possible owing to the errors involved in the determination of the constants.

For short times of test (Fig. 1), both equations are a good, but not perfect, representation of the experimental results for the high-purity lead. However, for longer times of test (Figs. 2 and 3), where the strains involved are approximately 3% for the high-purity lead and 20% for the 1% tin alloy, the Andrade equation is better than the logarithmic equation. In consequence, further work was limited to the Andrade equation.

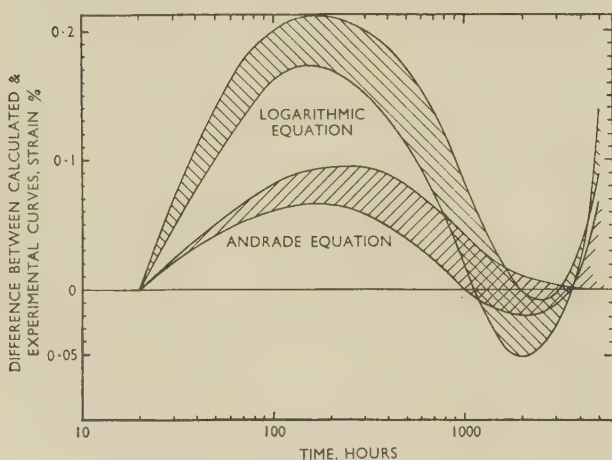


FIG. 2.—Comparison of the Andrade and Logarithmic Equations at Long Times for High-Purity Lead Extruded at 250° C. and Tested at 300 lb./in.². The constants in both equations were calculated from the values of the strains determined experimentally at 20, 1600, and 3180 hr. Strain at 5000 hr. was 3.25%.

2. VARIATION OF THE CONSTANTS IN THE ANDRADE EQUATION WITH DATA FROM WHICH THE CONSTANTS ARE CALCULATED

As the Andrade equation does not fit an experimental curve perfectly, the values of the constants in the equation depend on the data which are

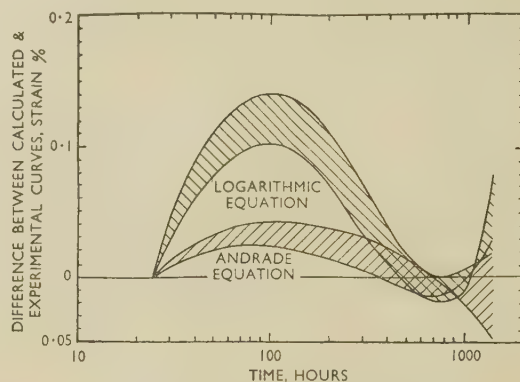


FIG. 3.—Comparison of the Andrade and Logarithmic Equations for Lead-1% Tin Alloy Extruded at 100° C. and Tested at 500 lb./in.². The constants in both equations were calculated from the values of the strains determined experimentally at 25, 550, and 1075 hr. Strain at 1400 hr. was 19.66%.

arbitrarily selected from the creep curve at three times, t_1 , t_2 , and t_3 . This is shown in Table I, the effect on both constants being large for the high-purity lead. Table I also shows that the maximum

TABLE I.—Variation of Constants in the Andrade Equation, for One Creep Curve, with Data from Which the Constants are Calculated.

Material	Constants in the Andrade Equation Calculated from Experimental Data at the Following Times, hr.	Value of β , $\text{hr.}^{-1/3} \times 10^4$	Maximum Error in Value of β , $\text{hr.}^{-1/3} \times 10^4$	Value of K , $\text{hr.}^{-1} \times 10^4$	Maximum Error in Value of K , $\text{hr.}^{-1} \times 10^4$
High-purity lead extruded at 250° C. and tested at 300 lb./in. ²	$t_1 = 7$ $t_2 = 143$ $t_3 = 279$	10.5	± 2.0	5.9	∓ 3.4
	$t_1 = 7$ $t_2 = 300$ $t_3 = 593$	11.7	± 1.3	3.00	∓ 1.4
	$t_1 = 7$ $t_2 = 603$ $t_3 = 1200$	11.9	± 0.9	2.68	∓ 0.67
	$t_1 = 20$ $t_2 = 1600$ $t_3 = 3180$	15.2	± 0.7	0.79	∓ 0.25
Lead-1% tin alloy extruded at 100° C. and tested at 500 lb./in. ²	$t_1 = 25$ $t_2 = 120$ $t_3 = 215$	27.5	± 4.2	109	∓ 6.7
	$t_1 = 25$ $t_2 = 250$ $t_3 = 475$	23.6	± 2.1	114	∓ 2.3
	$t_1 = 25$ $t_2 = 400$ $t_3 = 775$	31.4	± 1.5	106	∓ 1.2
	$t_1 = 25$ $t_2 = 550$ $t_3 = 1075$	31.9	± 1.2	107	∓ 0.9

possible error in the calculation of the constants decreases as t_1 , t_2 , and t_3 are selected farther apart.

To minimize this effect of t_1 , t_2 , and t_3 in the correlations between the values of the constants and the factors influencing creep-resistance, the constants for different curves were calculated, as far as possible, from the same values of t_1 , t_2 , and t_3 .

specimens of all grain-sizes tested at one stress, it indicates that the curves of all these specimens have been fitted from the same values of t_1 , t_2 , and t_3 . The magnitude of these errors for the high-purity lead makes it impossible to attach any significance to the values of the constants for this material. The errors are large owing to the small values of t_1 , t_2 ,

TABLE II.—Variation of β and K with Grain-Size and Stress.

Material	Stress, lb./in. ²	Temp. of Extrusion, °C.	Mean Grain- Size by Comparison Method, mm. ²	Grain-Size No. Johnson Method	β , hr. ^{-1/3} $\times 10^4$	Approx. Error in β , hr. ^{-1/3} $\times 10^4$	K , hr. ⁻¹ $\times 10^6$	Approx. Error in K , hr. ⁻¹ $\times 10^6$
High-purity lead	300	100	0.15	—0.4	6.74	± 2.0	6.61	± 3.4
		150	0.38	—2.0	8.94		4.4	
		200	0.86	—2.9	10.5		2.2	
		250	1.8	—3.4	10.5		15.3	
	500	100	As for stress of 300 lb./in. ²		34.7	± 15	0.00	± 230
		150			34.7		0.00	
		200			30.9		36.0	
		250			40.3		26.8	
	750	100	As for stress of 300 lb./in. ²		62.8	± 38	1220	± 1700
		150			71.3		533	
		200			69.4		448	
		250			86.3		534	
	1000	100	As for stress of 300 lb./in. ²		101	± 24	5040	± 4500
		150			125		2780	
		200			131		2090	
		250			168		3870	
Lead-1% alloy tin	300	100	0.0024	5.6	11.7	± 0.92	29.7	± 0.67
		150	0.013	4.1	5.28		8.85	
		200	0.023	2.8	3.21		2.84	
		250	0.11	0.2	2.07		1.17	
	500	300	0.39	—0.17	2.75		5.03	
		100	As for stress of 300 lb./in. ²		30.3	± 1.2	107	± 0.86
		150			19.6		30.4	
		200			14.6		11.2	
		250			16.8		5.04	
	750	300			23.1		6.69	
		100	As for stress of 300 lb./in. ²		65.9	± 2.0	350	± 3.8
		150			53.2		113	
		200			51.7		47.0	
		250			57.3		21.8	
	1000	300			73.6		39.0	
		100	As for stress of 300 lb./in. ²		114	± 3.0	1010	± 13.0
		150			130		251	
		200			117		119	
		250			121		30.2	
		300			165		156	

To minimize the errors involved in the calculation of the constants, t_1 , t_2 , and t_3 were selected as far apart as possible on the curves before the inflection which is now generally considered to be due to recrystallization.

3. EFFECT OF GRAIN-SIZE AND STRESS ON THE CONSTANTS IN THE ANDRADE EQUATION

Table II shows the effect of grain-size and stress on the values of the constants β and K for the high-purity lead and the 1% tin alloy. Where the errors in the calculations of a constant are the same for

and t_3 which had to be taken owing to the early recrystallization at all stresses. The errors for the 1% tin alloy were, however, comparatively small.

Table II shows that at each stress the values of the constants for the 1% tin alloy extruded at 300° C. were anomalous, since the values were larger than would be expected from those corresponding to the alloy extruded at lower temperatures. Although the value of β for the 1% tin alloy decreased as the stress was lowered, there was no obvious relationship between the two variables for material of constant grain-size. At a given stress there was no consistent

effect of grain-size on the value of β , except, perhaps, at the lowest stress, where the value increased as the grain-size diminished.

Fig. 4 shows that a relationship approximating to a straight line is obtained when $\sqrt[3]{K}$ is plotted against stress for specimens of the 1% tin alloy of constant grain-size. No straight line was obtained, however, for specimens with the largest grain-size.

mined by the Johnson method, which is more reliable than the comparison method.

III.—DISCUSSION OF RESULTS

In view of the effect of the arbitrary selection of t_1 , t_2 , and t_3 on the values of the constants in the Andrade equation, and the errors involved in their calculation

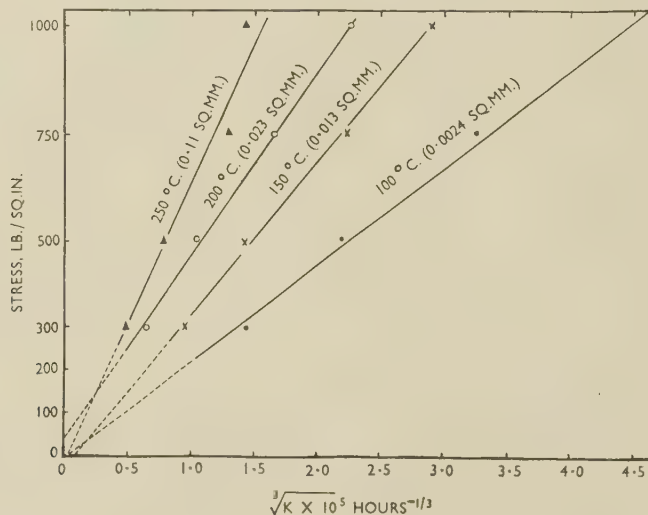


FIG. 4.—Relationship Between $\sqrt[3]{K}$ and Stress for the Lead-1% Tin Alloy Extruded at Different Temperatures. The average grain-sizes of the materials are shown in parentheses.

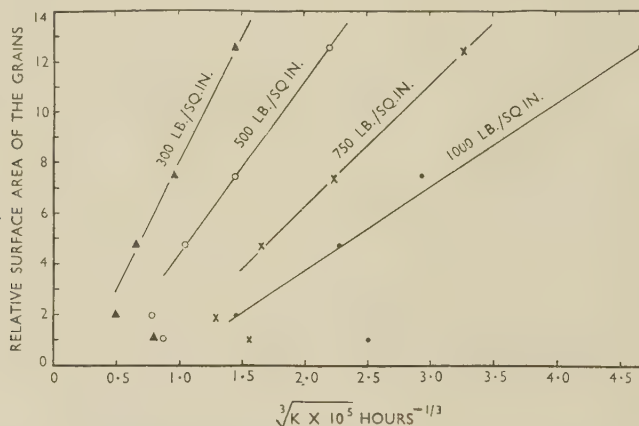


FIG. 5.—Relationship Between $\sqrt[3]{K}$ and the Relative Grain-Boundary Areas of the Lead-1% Tin Alloy Tested at Different Stresses.

In Fig. 5 a straight-line relationship is obtained by plotting $\sqrt[3]{K}$ against the relative grain-boundary areas of the grains per unit volume for the 1% tin alloy tested at a given stress. The values of K corresponding to the specimens with the largest grain-size do not fall on the straight lines, probably because of the anomalous behaviour of these specimens. The relative grain-boundary areas per unit volume were calculated from the grain-sizes deter-

mined by the Johnson method, which is more reliable than the comparison method.

Extrapolation of the straight-line relation between $\sqrt[3]{K}$ and stress in Fig. 4 suggests that K becomes zero at zero stress. This supports the general view that K is associated with flow which is of a viscous nature, although K is not linearly related to stress.

However, in Fig. 4 the values of K for specimens of constant grain-size tested at different stresses were not obtained from the same values of t_1 , t_2 , and t_3 . Thus, the straight-line relationship between $\sqrt[3]{K}$ and stress may be in error, which would explain why this result differs from that found by Cottrell and Aytakin¹¹ and by Andrade and Jolliffe,¹² who showed $\log K$ to be directly proportional to stress.

The marked dependence of K on the relative grain-boundary area of the grains per unit volume suggests that K is associated with flow at the grain boundaries. On the other hand, the straight line relating $\sqrt[3]{K}$ and relative grain-boundary area in Fig. 5 also indicates that K is inversely proportional to the volume of the grains, since the grain-boundary area per unit volume is inversely proportional to the diameter of the grains. The straight lines in Fig. 5 cut the abscissa at positive values of K when the relative grain-boundary area of the grains per unit volume is zero, i.e. when the specimens are single crystals. This suggests that K flow can occur within the grains as well as, possibly, at grain boundaries. Cottrell and Aytakin¹¹ have shown that K flow occurs in single crystals of zinc.

IV.—SUMMARY AND CONCLUSIONS

1. The Andrade and logarithmic equations were found to be a good representation of the experimentally determined creep curve for short times up to about 300 hr. The Andrade equation, however, was the better of the two for longer times up to 5000 hr.

2. As the Andrade equation does not represent the experimental results perfectly for tests of long duration, the values of the constants in the equation depend on the arbitrarily selected experimental data. For this reason and because of the errors involved in the calculation of the values of the constants, the significance of the correlations between the values of the constants with grain-size and stress must be accepted with reserve.

3. The errors involved in the determination of the constants, β and K , in the Andrade equation for the high-purity lead, due to the ease with which this material recrystallizes under test, made it impossible to correlate the calculated values with either grain-size or stress.

4. For the lead-1% tin alloy, β decreased as the stress was reduced, though not in any simple way. There was no consistent effect of grain-size on β . For specimens of constant grain-size, $\sqrt[3]{K}$ was linearly related to stress and, for constant stress, to relative grain-boundary areas of the grains per unit volume.

ACKNOWLEDGEMENTS

The author wishes to thank The Director and Council of the British Non-Ferrous Metals Research Association for permission to publish this paper.

APPENDIX

ESTIMATION OF THE ERRORS IN THE CALCULATION OF THE CONSTANTS IN THE ANDRADE EQUATION

Error in β .

The Andrade equation $L_t = L_0(1 + \beta t^{1/3}) \exp Kt$ is fitted to the creep curves by the quadratic method. Solving three simultaneous equations, obtained by substituting in the general equation the length of the specimen at three times (t_1 , t_2 , t_3), separated by equal intervals, results in the following quadratic in β :

$$\frac{L_2^2}{L_1 L_3} = \frac{(1 + \beta t_2^{1/3})^2}{(1 + \beta t_1^{1/3})(1 + \beta t_3^{1/3})}$$

If γ is the strain at time t , then:

$$\frac{(1 + \gamma_2)^2}{(1 + \gamma_1)(1 + \gamma_3)} = \frac{(1 + \beta t_2^{1/3})^2}{(1 + \beta t_1^{1/3})(1 + \beta t_3^{1/3})} \quad (1)$$

If γ is small then the left-hand side of (1)

$$\simeq \exp(2\gamma_2 - \gamma_1 - \gamma_3)$$

The approximate form of the Andrade equation is:

$$\gamma = \beta t^{1/3} + Kt$$

so that

$$\gamma \geq \beta t^{1/3}$$

\therefore The right-hand side of (1) can be written $\exp \beta(2t_2^{1/3} - t_1^{1/3} - t_3^{1/3})$

$$\therefore 2\gamma_2 - \gamma_1 - \gamma_3 \simeq \beta(2t_2^{1/3} - t_1^{1/3} - t_3^{1/3})$$

Let ϵ be the error in γ at any time t and ϵ_β be the error in β resulting from that in γ . Then the maximum value of ϵ_β is given by:

$$2(\gamma_2 + \epsilon) - (\gamma_1 - \epsilon) - (\gamma_3 - \epsilon) \simeq (\beta + \epsilon_\beta)(2t_2^{1/3} - t_1^{1/3} - t_3^{1/3})$$

$$\text{Then } 4\epsilon \simeq \pm \epsilon_\beta(2t_2^{1/3} - t_1^{1/3} - t_3^{1/3}).$$

Error in K .

To find K , the equation $\frac{L_2}{L_1} = \frac{1 + \beta t_2^{1/3}}{1 + \beta t_1^{1/3}} \exp K(t_2 - t_1)$ is solved.

By reasoning as above,

$$\gamma_2 - \gamma_1 \simeq \beta(t_2^{1/3} - t_1^{1/3}) + K(t_2 - t_1).$$

Let ϵ_K be the error in K resulting from the error in γ and β .

Then ϵ_K is a maximum when

$$\gamma_2 - \gamma_1 + 2\epsilon \simeq (\beta + \epsilon_\beta)(t_2^{1/3} - t_1^{1/3}) + (K + \epsilon_K)(t_2 - t_1)$$

$$\text{Then } 2\epsilon \simeq \epsilon_\beta(t_2^{1/3} - t_1^{1/3}) + \epsilon_K(t_2 - t_1)$$

$$\epsilon_K \simeq \mp \frac{2\epsilon - \epsilon_\beta(t_2^{1/3} - t_1^{1/3})}{(t_2 - t_1)}$$

REFERENCES

1. E. N. da C. Andrade, *Proc. Roy. Soc.*, 1910-11, [A], **84**, 1.
2. A. H. Sully, "Metallic Creep and Creep-Resistant Alloys". London: **1949** (Butterworths Scientific Publications).
3. L. Rotherham, "Creep of Metals". London: **1951** (Institute of Physics).
4. P. Chevenard, *Rev. Mét.*, 1934, **31**, 473.
5. H. J. Tapsell and L. E. Prosser, *Engineering*, 1934, **137**, 262.
6. C. L. Smith, *Proc. Phys. Soc.*, 1948, **61**, 201.
7. L. M. T. Hopkin and C. J. Thwaites, *J. Inst. Metals*, 1952-53, **81**, (5), 255.
8. J. McKeown, *Metallurgia*, 1950, **42**, 189.
9. L. M. T. Hopkin, *Proc. Phys. Soc.*, 1950, [B], **63**, 346.
10. W. A. Johnson, *Metal Progress*, 1946, **49**, 87.
11. A. H. Cottrell and V. Aytakin, *J. Inst. Metals*, 1950, **77**, 389.
12. E. N. da C. Andrade and K. H. Jolliffe, *Proc. Roy. Soc.*, 1952, [A], **213**, 3.

EQUILIBRIUM RELATIONS AT 460° C. IN ALUMINIUM-RICH ALLOYS CONTAINING 0-7% COPPER, 0-7% MAGNESIUM, AND 0.6% SILICON*

1463

By H. J. AXON,† B.Met., D.Phil., JUNIOR MEMBER

SYNOPSIS

The equilibrium isothermal at 460° C. is given for quaternary alloys rich in aluminium and containing 0-7 wt.-% magnesium, 0-7 wt.-% copper, and constant (0.6 wt.-%) silicon. The phases encountered are the aluminium-rich solid solution, CuAl_2 , Mg_2Si , Si , the ternary phase Al_2CuMg (S), and the quaternary phase $\text{Al}_5\text{Cu}_2\text{Mg}_3\text{Si}_6$ (Q). The general form of the isothermal containing 0.6% silicon is similar to that previously reported for alloys containing 1.2% silicon (*J. Inst. Metals*, 1952-53, **81**, 209), but the phase fields are all translated towards the aluminium-rich corner.

I.—INTRODUCTION

THE present paper contains the results of an investigation into the equilibrium constitution at 460° C. of aluminium-rich alloys which contain copper in the range 0-7%, magnesium 0-7%, and with constant (0.6%) silicon, all compositions being by weight. The results of previous workers, and the experimental methods used in the present work, have been described in a previous paper.¹ The chemical analyses were again conducted by Messrs. Johnson, Matthey and Co., Ltd., and the author's thanks are due to Mr. A. R. Powell for his care and attention to this aspect of the work.

II.—EXPERIMENTAL RESULTS

Fig. 1 shows the phase fields which occur on annealing aluminium-rich alloys containing 0.6% silicon for four weeks at 460° C. In Fig. 1 the point X on the vertical axis is taken from the ternary aluminium-copper-silicon system and corresponds to the $(\alpha + \text{Si})/(\alpha + \text{Si} + \theta)$ phase boundary for alloys containing 0.6% silicon. Points Y and Z on the horizontal axis are taken from the ternary aluminium-magnesium-silicon system, and correspond respectively to the $(\alpha + \text{Si})/(\alpha + \text{Si} + \text{Mg}_2\text{Si})$ and the $(\alpha + \text{Si} + \text{Mg}_2\text{Si})/(\alpha + \text{Mg}_2\text{Si})$ phase boundaries for alloys containing 0.6% silicon.

As in the previous work, the critical alloys were analysed for magnesium and silicon only, since work on this type of system has shown that the synthetic composition with respect to copper may be readily obtained. The points in Fig. 1 which correspond to analysed alloys are denoted by the letter A placed above the points. The limits of accuracy of Fig. 1

are: as regards temperature $460^\circ \pm 2^\circ \text{C.}$, and as regards composition silicon $0.6 \pm 0.03\%$ with 0.016% iron.

If Fig. 1 is compared with the corresponding isothermal for alloys containing 1.2% silicon,¹ it will be seen that in both isothermals the number and general disposition of the phase fields are similar. The chief differences are that the $(\alpha + \text{Si} + \theta + Q)$, $(\alpha + \text{Mg}_2\text{Si} + \theta + Q)$, $(\alpha + \text{Si} + Q)$, $(\alpha + \text{Mg}_2\text{Si} + Q)$, $(\alpha + \text{Mg}_2\text{Si} + \text{Si} + Q)$, and $(\alpha + \text{Si} + \text{Mg}_2\text{Si})$ phase fields are narrower in the 0.6% silicon isothermal than in the 1.2% silicon isothermal, and are also displaced to a lower magnesium composition. The phase boundaries of Fig. 1 have been drawn to agree with the amounts of the various phases present, and the symbols used in Fig. 1 are the same as those used in Fig. 4 of the previous paper.¹

It is convenient to designate the individual points in Fig. 1 by the notation: (x, y) , meaning an alloy containing 0.6% silicon with x wt.-% copper and y wt.-% magnesium (synthetic compositions); and $(x, y)A$, meaning that the alloy was analysed for magnesium and the analytical result is used in designating the alloy. Point $(1.0, 4.31)A$ is important in fixing the $(\alpha + \text{Mg}_2\text{Si})/(\alpha + \text{Mg}_2\text{Si} + S)$ phase boundary, since it contains α , Mg_2Si , and a very small amount of the ternary S phase. The straight boundaries of the four-phase field $(\alpha + \text{Mg}_2\text{Si} + \theta + S)$ appear to be satisfactorily determined by the alloys: $(6.0, 2.00)A$, which contains a minute trace of S existing as very small crystals; $(4.0, 2.11)A$, which contains a trace of S existing as occasional large crystals; $(6.0, 3.03)A$, which contains a trace of θ uniformly distributed throughout the alloy; and $(4.0, 2.65)A$, which contains a trace of θ distributed around the edge of the specimen only. This is

* Manuscript received 19 November 1952.

† Lecturer in Electrometallurgy, The University of Manchester.

probably because the surface of the specimen loses magnesium by volatilization during annealing. The surface layers of all specimens are removed before analysis; hence point (4.0, 2.65)A has been plotted as an $(\alpha + \text{Mg}_2\text{Si} + S)$ alloy near to the $(\alpha + \text{Mg}_2\text{Si} + \theta + S)$ boundary. The boundaries of the four-phase field $(\alpha + \text{Mg}_2\text{Si} + \theta + S)$ shown in Fig. 1 appear to interpolate well between the corresponding

The boundaries of the $(\alpha + Q)$ phase field have been drawn to coincide in size and shape (but not position) with the $(\alpha + Q)$ phase field of the 1.2% silicon section, and it is satisfactory to note how well the boundaries so drawn agree with the experimental results. No experimental evidence has been obtained for the existence of the $(\alpha + \text{Mg}_2\text{Si} + \text{Si} + Q)$ phase field, which is very small but which must exist

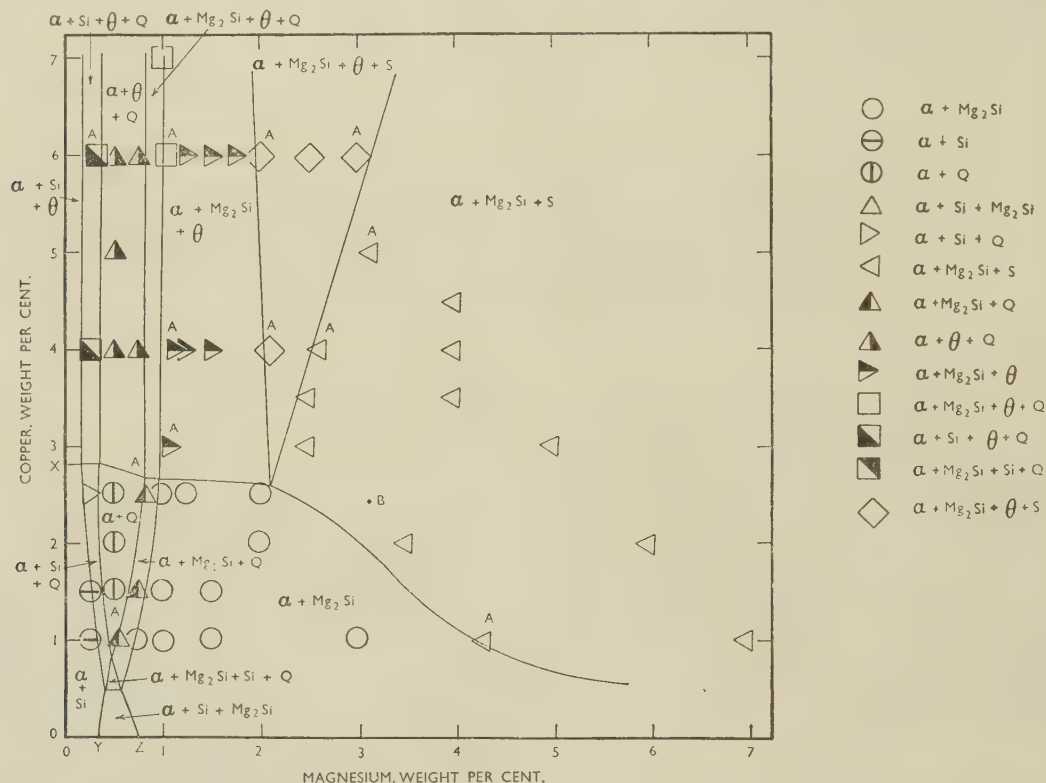


FIG. 1.—The 460° C. Isothermal for Aluminium-Rich Alloys Containing Magnesium, Copper, and Silicon. All alloys in this isothermal contain 0.6 wt.-% silicon. The point B indicates the apex of the $(\alpha + \text{Mg}_2\text{Si} + \theta + S)$ phase field for alloys containing 1.2 wt.-% silicon. Note added in proof.—The attention of the reader is drawn to the fact that the scale of this figure is slightly different from that used for the figures in the earlier paper.¹ This arose from factors outside the control of the author, who hopes inconvenience will be minimized by this note.

boundaries in the 1.2% silicon section and the $(\alpha + \text{Mg}_2\text{Si} + S)$ boundaries of the ternary aluminium-magnesium-copper system at 460° C. Evidence for the existence of the narrow $(\alpha + \text{Si} + \theta + Q)$ and $(\alpha + \text{Mg}_2\text{Si} + \theta + Q)$ phase fields is given by alloys (6.0, 0.31)A and (4.0, 0.25), both of which contain minute amounts of silicon, and alloys (7.0, 1.0), (6.0, 1.09)A, and (3.0, 1.07)A, of which the first two contain minute traces of Q distributed throughout the alloy, whilst the third contains small crystals of Q at the rim of the specimen only.

in the 0.6% silicon section in order to satisfy the geometrical requirements of the previous work.

ACKNOWLEDGEMENTS

The author thanks Professor F. C. Thompson for research facilities and continued encouragement, and The Royal Society for a grant in aid of the research.

REFERENCE

1. H. J. Axon, *J. Inst. Metals*, 1952-53, **81**, 209.

THE CONSTITUTION OF NICKEL-RICH ALLOYS OF 1464 THE NICKEL-CHROMIUM-ALUMINIUM SYSTEM*

By A. TAYLOR,† Ph.D., F.Inst.P., MEMBER, and
R. W. FLOYD,‡ B.Sc., A.I.M., MEMBER

SYNOPSIS

The equilibrium relationships in nickel-chromium-aluminium alloys containing more than 50 at.-% nickel have been studied over the temperature range 750°–1150° C. It has been shown that the phase fields of the nickel primary solid solution, γ , and of the β solid solution based on NiAl both contract as the temperature falls, whereas that of the γ' phase based on Ni_3Al extends. The equilibrium between the γ and β phases which exists from the solidus breaks down at about 1000° C., giving rise to equilibrium between γ' and α -chromium by a four-phase reaction: $\beta + \gamma \rightleftharpoons \alpha + \gamma'$. The ordering of the γ phase is enhanced by the presence of aluminium atoms, and for alloys with more than 10 at.-% aluminium the ordering temperature is over 1150° C. The equilibrium between the γ and γ' phases is such that over a range of compositions the lattice parameters of the phases are almost identical.

I.—INTRODUCTION

THIS investigation of the nickel-chromium-aluminium system was undertaken as part of a more extensive survey of nickel-base alloys containing chromium, titanium, and aluminium. Accounts have already been given of the nickel-chromium-titanium¹ and nickel-titanium-aluminium² systems, with which the nickel-chromium-aluminium system links to form the boundaries of the nickel corner of the quaternary nickel-chromium-titanium-aluminium system. Revisions of the binary nickel-chromium and nickel-aluminium systems which have been described in these papers have been incorporated in the present work.

Nickel and chromium form a simple eutectiferous system with primary solid solutions which are extensive at the eutectic temperature of 1345° C. (Fig. 1). As the temperature falls, so the solubility of chromium in the nickel decreases steadily from 50 at.-% at the solidus to 38 at.-% at 750° C. In the neighbourhood of Ni_3Cr the face-centred cubic nickel solid solution, γ , is ordered below 540° C.³ The solubility of nickel in body-centred cubic α -chromium decreases rapidly from 32 at.-% at the solidus to 2 at.-% at 750° C. The modifications to the phase diagram proposed by Bloom and Grant⁴ have not been substantiated by observations made by the present authors.

The binary nickel-aluminium phase diagram is shown in Fig. 2. The solubility of aluminium in the nickel solid solution falls from 21 at.-% at 1385° C. to 11.9 at.-% at 750° C. The ordered face-centred cubic Ni_3Al phase, γ' , forms via a peritectic reaction,^{5,6} and its phase field widens to 23.3–27.3 at.-% aluminium at 750° C. The phase field of the ordered

body-centred cubic NiAl phase (β) which has a wide range at 1400° C. becomes restricted at lower temperatures. The boundary with the ($\beta + \gamma'$) region lies at 30 at.-% aluminium at 1350° C. and 38 at.-%

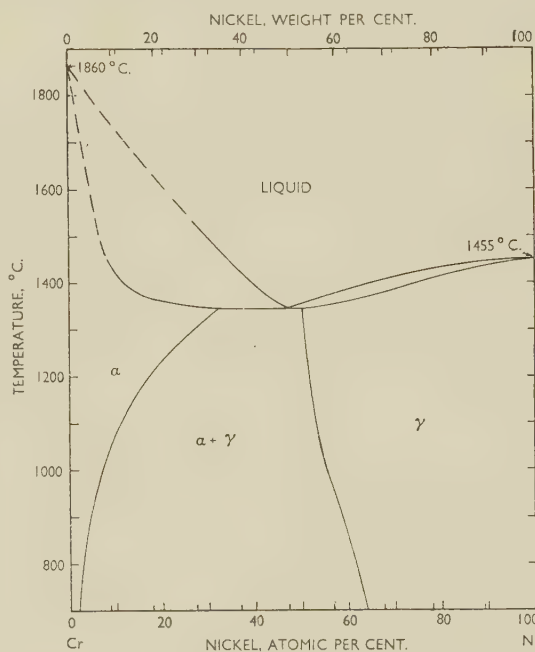


FIG. 1.—The Nickel-Chromium Phase Diagram.

aluminium at 850° C.⁷ The other phases occurring in the system have no bearing on the part of the nickel-chromium-aluminium system which is described here.

The only phase of the chromium-aluminium system

* Manuscript received 8 November 1952.

† Horizons Inc., Cleveland, O., U.S.A.; formerly with

The Mond Nickel Co., Ltd., Birmingham.

‡ The Mond Nickel Co., Ltd., Birmingham.

which is involved in the present work is the chromium solid solution (α). Bradley and Lu⁸ have shown

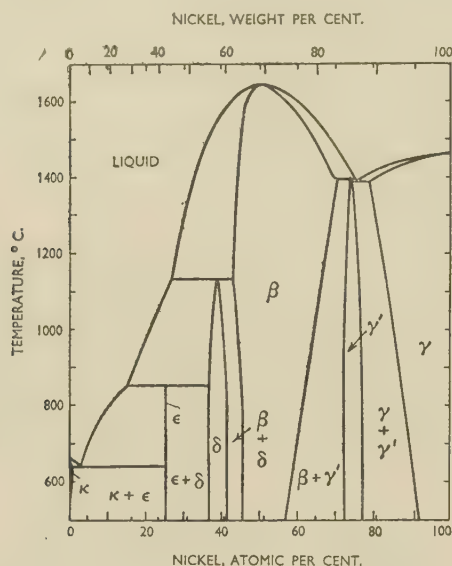


FIG. 2.—The Nickel-Aluminium Phase Diagram.

that the solubility of aluminium in chromium is about 45 at.-% above 900° C. and 28 at.-% below 800° C.

II.—EXPERIMENTAL WORK

As in the case of the other systems referred to in the previous section, all the alloys were synthesized by melting together the component metals in charges of about 50 g. The raw materials used were Mond nickel pellet, chromium from Murex, Ltd., and high-purity aluminium from The British Aluminium Co., Ltd. Melting was carried out in alumina-lined crucibles in a 4-kVA. induction furnace in a low pressure of hydrogen, the alloys being allowed to solidify in the crucibles at a pressure of about 10^{-3} mm. "As-cast" microspecimens were taken from

the ingots, and then the remainder of each ingot was annealed at 1150°–1250° C. for 4 days to promote homogeneity. The majority of the alloys were analysed chemically for the main elements, and a few were checked for minor impurities, which could in all cases be accounted for by those present in the initial charge. With few exceptions good agreement was obtained between actual and nominal compositions.

The system was first explored by a study of the X-ray-diffraction patterns of powder samples slowly cooled from 900° C. over 2 weeks. Subsequently X-ray and microscopic techniques were employed on specimens isothermally heat-treated as follows:

	Temp., °C.	Time
X-ray samples	750	3 weeks
"	850	3 weeks
Microspecimens	850	3 weeks
"	1000	4 days
"	1150	2 days

The X-ray-diffraction patterns were obtained in a 9-cm. Debye-Scherrer camera, using manganese $K\alpha$ radiation, and accurate lattice parameters were obtained by the usual extrapolation method.⁹ Microspecimens were prepared by grinding to 600 grit, followed by polishing on γ -alumina or diamond dust. After trying out a number of etching reagents, it was found that a 5% hydrofluoric acid and 10% glycerine aqueous solution, used electrolytically, satisfactorily revealed the phases in alloys over a wide range of composition without staining or pitting the surfaces of the specimens.

For studying the system at the lower temperatures the X-ray and microscopic methods of examination were used together. In the first place the arrangement of the phase fields was mapped out from a qualitative estimate of the X-ray evidence. Examination of the microspecimens was of particular value in elucidating the structure of the alloys consisting of the two face-centred cubic phases, γ and γ' , which could not in all cases be differentiated by visual examination of

TABLE I.—Composition and Structure of Nickel-Chromium-Aluminium Alloys.

Alloy No.	Composition, at.-%			Observed Structure					
	Ni	Cr	Al	As-Cast	Quenching Temperature				Slowly Cooled
					1150° C.	1000° C.	850° C.	750° C.	
10	90.0	4.9	5.1	γ	γ	γ
34	85.1	12.2	2.7	γ	γ	γ
11	84.9	9.9	5.2	γ	γ	γ
98	84.3	5.2	10.5	γ	$\gamma + \gamma'$	$\gamma + \gamma'$	$\gamma + \gamma'$
99	82.8	9.6	7.6	γ	γ	γ	γ
100	79.9	14.8	5.3	γ	γ	γ
101	79.4	12.8	7.8	γ	$\gamma + \gamma'$	$\gamma + \gamma'$	$\gamma + \gamma'$
12	79.3	9.9	10.8	$\gamma + \gamma'$	$\gamma + \gamma'$	$\gamma + \gamma'$
102	76.6	9.9	13.4	...	γ	$\gamma + \gamma'$	$\gamma + \gamma'$	$\gamma + \gamma'$	$\gamma + \gamma'$
103	76.6	5.2	18.2	$(\beta +) \gamma + \gamma'$	γ	$\gamma + \gamma'$	$\gamma + \gamma'$	$\gamma + \gamma'$	$\gamma + \gamma'$
35	74.6	22.4	3.0	γ	γ
13	74.9	19.8	5.2	γ	γ	γ
74	75.0	17.2	7.8	γ	$\gamma + \gamma'$	$\gamma + \gamma'$	$\gamma + \gamma'$
146	73.9	18.2	7.9	$\gamma + \gamma'$	$\gamma + \gamma'$	$\gamma + \gamma'$
73	74.9	14.8	10.3	γ	$\gamma + \gamma'$	$\gamma + \gamma'$	$\gamma + \gamma'$

TABLE I.—continued.

Alloy No.	Composition, at.-%			Observed Structure					
	Ni	Cr	Al	As-Cast	Quenching Temperature				Slowly Cooled
					1150° C.	1000° C.	850° C.	750° C.	
72	74.5	12.2	13.3	...	γ	$\gamma + \gamma'$	$\gamma + \gamma'$	$\gamma + \gamma'$	$\gamma + \gamma'$
71	74.6	9.8	15.6	$\gamma + \gamma'$	$\gamma + \gamma'$	$\gamma + \gamma'$	$\gamma + \gamma'$
36	73.9	7.5	18.6	...	γ	$\gamma + \gamma'$	γ	γ	γ
14	74.8	4.9	20.3	...	$\gamma + \gamma'$	γ	γ	γ	γ
219	75.1	2.8	22.1	$\beta + \gamma + \gamma'$	$(\gamma + \gamma') \gamma'$	$\gamma + \gamma'$
218	74.5	2.7	22.8	$\beta + \gamma + \gamma'$	γ'	γ'
209	73.6	5.0	21.4	...	γ'	γ'
37	73.8	2.8	23.4	γ'	γ'	γ'	γ'
251	71.7	17.3	11.0	$\gamma + \gamma'$	$\gamma + \gamma'$	$\gamma + \gamma'$...
250	72.1	15.0	12.9	...	γ	$\gamma + \gamma'$	$\gamma + \gamma'$	$\gamma + \gamma'$...
38	71.9	9.4	18.7	...	γ	$\gamma + \gamma'$	γ'	γ'	γ'
294 *	72.5	7.5	20.0	$\beta + \gamma + \gamma'$	$\gamma + \gamma'$	γ
210	71.8	4.9	23.4	...	γ	γ
217	72.1	2.4	25.5	...	$(\beta + \gamma) \gamma'$	γ'
39	69.9	27.4	2.7	γ	γ	γ
15	69.9	24.7	5.4	γ	γ	γ
108	69.7	21.7	8.6	...	γ	γ	$\gamma + \gamma'$	$\gamma + \gamma'$	$\gamma + \gamma'$
149	68.4	22.0	9.6	$\gamma + \gamma'$	$\gamma + \gamma'$	$\gamma + \gamma'$
107	69.0	20.3	10.7	...	γ	γ	$\gamma + \gamma'$	$\gamma + \gamma'$	$\gamma + \gamma'$
40	68.6	17.5	13.9	...	γ	$\gamma + \gamma'$	$\gamma + \gamma'$	$\gamma + \gamma'$	$\gamma + \gamma'$
106	68.9	15.1	16.0	...	γ	$\gamma + \gamma'$	γ'	γ'	γ'
147	69.8	12.6	17.6	...	γ	$\gamma + \gamma'$	γ'	γ'	γ'
299 *	70.0	10.0	20.0	$\beta + \gamma$	$(\beta + \gamma) \gamma + \gamma'$	$(\beta + \gamma) \gamma + \gamma'$
105	68.8	10.2	21.0	...	$\gamma + \gamma'$	$\gamma + \gamma'$	γ'	γ'	γ'
295 *	70.0	7.5	22.5	$\beta + \gamma + \gamma'$	$\gamma + \gamma'$	$\gamma + \gamma'$
211	71.2	5.1	23.7	$\beta + \gamma'$	γ'	γ'
298 *	70.0	5.0	25.0	$\beta + \gamma + \gamma'$	$\beta + \gamma'$	$\beta + \gamma'$
216	70.9	2.5	26.6	$\beta + \gamma + \gamma'$	$\beta + \gamma'$	$\beta + \gamma'$
300 *	67.5	12.5	20.0	$\beta + \gamma$	$\beta + \gamma + \gamma'$	$\beta + \gamma + \gamma'$
296 *	67.5	7.5	25.0	$\beta + \gamma + \gamma'$	$\beta + \gamma + \gamma'$	$\beta + \gamma + \gamma'$
16	68.5	4.9	26.6	$\beta + \gamma'$	$\beta + \gamma'$	$\beta + \gamma'$
41	64.7	32.5	2.8	γ	γ	γ
17	64.9	29.3	5.8	γ	γ	γ
113	65.1	27.2	7.7	...	γ	γ	$\gamma + \gamma'$	$\gamma + \gamma'$	$\gamma + \gamma'$
145	65.5	24.0	10.5	...	γ	$(\alpha + \gamma) \gamma$	$\gamma + \gamma'$	$\gamma + \gamma'$	$\gamma + \gamma'$
112	64.3	24.9	10.8	$(\alpha + \gamma) \gamma$	$(\alpha + \gamma) \gamma + \gamma'$	$\gamma + \gamma'$	$\gamma + \gamma'$
111	65.0	22.6	12.4	...	γ	$(\alpha + \gamma) \gamma$	$(\alpha + \gamma) \gamma + \gamma'$	$\gamma + \gamma'$	$\gamma + \gamma'$
110	64.6	20.2	15.2	$\beta + \gamma$	γ	$(\alpha + \gamma) \gamma + \gamma'$	$(\alpha + \gamma) \gamma + \gamma'$	$\gamma + \gamma'$	$\gamma + \gamma'$
302 *	65.0	17.5	17.5	$\beta + \gamma$	$\beta + \gamma$	$\beta + \gamma + \gamma'$
109	64.3	16.7	19.0	$\beta + \gamma$	$(\alpha + \gamma) \beta + \gamma$	$(\alpha + \gamma) \beta + \gamma + \gamma'$	$\alpha + \gamma'$	γ'	γ'
301 *	65.0	15.0	20.0	$\beta + \gamma$	$\beta + \gamma$	$\beta + \gamma + \gamma'$
42	64.9	9.9	25.2	$(\alpha + \gamma) \beta + \gamma + \gamma'$	$\beta + \gamma'$	$\beta + \gamma'$	$\beta + \gamma'$
43	60.1	34.8	5.1	γ	...	$(\alpha + \gamma) \gamma$	$\alpha + \gamma$	$\alpha + \gamma$	$\alpha + \gamma$
117	60.1	31.7	8.2	...	γ	$(\alpha + \gamma) \gamma$	$(\alpha + \gamma) \gamma + \gamma'$	$\alpha + \gamma + \gamma'$	$\alpha + \gamma + \gamma'$
148	61.5	29.0	9.5	...	$(\alpha + \gamma) \gamma$	$(\alpha + \gamma) \gamma$	$(\alpha + \gamma) \gamma + \gamma'$	$\alpha + \gamma + \gamma'$	$\alpha + \gamma + \gamma'$
116	60.6	29.0	10.4	γ	$(\alpha + \gamma) \gamma$	$(\alpha + \gamma) \gamma$	$(\alpha + \gamma) \gamma + \gamma'$	$\alpha + \gamma + \gamma'$	$\alpha + \gamma + \gamma'$
115	59.8	24.9	15.3	$\beta + \gamma$	$\alpha + \gamma + \gamma'$	$\alpha + \gamma + \gamma'$	$\alpha + \gamma + \gamma'$
303 *	60.0	25.0	15.0	$\beta + \gamma$	$(\alpha + \gamma) \beta + \gamma$	$\alpha + \beta + \gamma + \gamma'$
44	62.6	16.1	21.3	...	$(\alpha + \gamma) \beta + \gamma$	$\alpha + \beta + \gamma + \gamma'$	$(\alpha + \gamma) \gamma + \gamma'$	γ'	γ
297 *	62.5	7.5	30.0	$\beta + \gamma'$	$\beta + \gamma'$	$(\alpha + \gamma) \beta + \gamma'$
88	59.1	19.7	21.2	$\beta + \gamma$	$\beta + \gamma$	$\beta + \gamma$	$\alpha + \beta + \gamma'$	$\alpha + \gamma'$	$\alpha + \gamma'$
114	58.2	10.8	31.0	β	$(\alpha + \gamma) \beta$	$(\alpha + \gamma) \beta + \gamma'$	$\alpha + \beta + \gamma'$	$\alpha + \beta + \gamma'$	$\alpha + \beta + \gamma'$
118	55.5	34.2	10.3	$\alpha + \gamma + \gamma'$	$\alpha + \gamma + \gamma'$	$\alpha + \gamma + \gamma'$
151	55.0	34.8	10.2	$\alpha + \gamma$...	$\alpha + \gamma$	$\alpha + \gamma + \gamma'$	$\alpha + \gamma + \gamma'$	$\alpha + \gamma + \gamma'$
304 *	55.0	30.0	15.0	$\beta + \gamma$	$\alpha + \beta + \gamma$	$\alpha + \beta + \gamma$
305 *	52.5	37.5	10.0	$\alpha + \gamma$	$\alpha + \beta + \gamma$	$\alpha + \beta + \gamma$
119	50.3	25.6	24.1	$\alpha + \beta + \gamma$	$\alpha + \beta + \gamma$	$\alpha + \beta + \gamma + \gamma'$	$\alpha + \beta + \gamma'$	$\alpha + \beta + \gamma'$	$\alpha + \beta + \gamma'$
223 *	45.0	40.0	15.0	$\alpha + \beta + \gamma$
174	34.0	34.2	31.8	$\alpha + \beta$	$\alpha + \beta$	$\alpha + \beta$...
175	25.4	54.6	20.0	$\alpha + \beta$	$\alpha + \beta$	$\alpha + \beta$...
176	16.2	69.1	14.7	$\alpha + \beta$	$\alpha + \beta$	$\alpha + \beta$...

* Composition nominal.

the diffraction patterns. Similarly, microscopical examination provided a ready means of identifying the body-centred cubic α and β phases, especially in alloys in which they were present in such small amounts that the superlattice lines characterizing the β phase would be below the visibility limit. The accurate location of the boundaries of the γ and γ' phase fields was obtained from lattice-parameter

TABLE II.—Lattice-Parameter Data.

(a) Alloys in the γ Phase Field at 750° C.

Alloy No.	Composition, at.-%			Heat-Treat-ment	Lattice Parameter, kX
	Ni	Cr	Al		
...	100	3.5168
1	90.2	9.8	...	SC *	3.5273
10	90.0	4.9	5.1	750° C.	3.5270
2	84.8	15.2	...	SC	3.5302
34	85.1	12.2	2.7	750° C.	3.5302
11	84.9	9.9	5.2	SC	3.5315
99	82.8	9.6	7.6	750° C.	3.5317
3	80.2	19.8	...	SC	3.5314
100	79.9	14.8	5.3	750° C.	3.5342
4	75.1	24.9	...	SC	3.5352
35	74.6	22.4	3.0	750° C.	3.5388
13	74.9	19.8	5.3	SC	3.5396
5	70.2	29.8	...	750° C.	3.5374
39	69.9	27.4	2.7	SC	3.5380
15	69.9	24.7	5.4	750° C.	3.5412
6	65.2	34.8	...	SC	3.5419
41	64.7	32.5	2.8	750° C.	3.5441
17	64.9	29.3	5.8	SC	3.5437
				750° C.	3.5442
				SC	3.5471
				750° C.	3.5483
				SC	3.5509
				750° C.	3.5518
				SC	3.5519
				750° C.	3.5533
				SC	3.5543
				750° C.	3.5582
				SC	3.5591
				750° C.	3.5569
				SC	3.5582
				750° C.	3.5610

(b) Alloys in the ($\gamma + \gamma'$) Phase Field at 750° C.

Alloy No.	Composition, at.-%			Heat-Treat-ment	Lattice Parameter, kX	
	Ni	Cr	Al		γ	γ'
98	84.3	5.2	10.5	SC	3.5362	3.545
101	79.4	12.8	7.8	750° C.	3.5382	3.547
12	79.3	9.9	10.8	SC	3.5411	3.547
102	76.7	9.9	13.4	750° C.	3.5423	...
103	76.6	5.2	18.2	SC	3.5399	3.549
74	75.0	17.2	7.8	750° C.	3.5406	3.553
146	73.9	18.2	7.9	SC	3.5428	3.5506
73	74.9	14.8	10.3	750° C.	...	3.5510
72	74.5	12.2	13.3	SC	...	3.5514
71	74.6	9.8	15.6	750° C.	...	3.5518
251	71.7	17.3	11.0	SC	3.5497	...
250	72.1	15.0	12.9	750° C.	3.5486	...
108	69.7	21.7	8.6	SC	3.5497	...
149	68.4	22.0	9.6	750° C.	3.5478	3.5517
107	69.0	20.3	10.7	SC	...	3.5521
113	65.1	27.2	7.7	750° C.	...	3.5515
145	65.5	24.0	10.5	SC	3.5516	...
112	64.3	24.9	10.8	750° C.	3.5532	...
111	65.0	22.6	12.4	SC	3.5527	...
110	64.6	20.2	15.2	750° C.	3.5546	...
				SC	3.5555	...
				750° C.	3.5558	...
				SC	3.5558	...
				750° C.	3.5604	3.553
				SC	3.5644	3.555
				750° C.	3.5611	3.5549
				SC	3.5627	3.5561
				750° C.	3.5657	3.5560
				SC	3.5620	3.5552
				750° C.	3.5656	3.5568
				SC	3.5613	3.5544
				750° C.	...	3.5534

(c) Alloys in the γ' Phase Field at 750° C.

Alloy No.	Composition, at.-%			Heat-Treat-ment	Lattice Parameter, kX
	Ni	Cr	Al		
36	73.9	7.5	18.6	SC	3.5519
14	74.8	4.9	20.3	750° C.	3.5532
37	73.8	2.8	23.4	SC	3.5537
22	74.0	...	26.0	SC	3.5579
38	71.9	9.4	18.7	SC	3.5600
40	68.6	17.5	13.9	SC	3.5515
106	68.9	15.1	16.0	750° C.	3.5537
147	69.8	12.6	17.6	SC	3.5556
105	68.8	10.2	21.0	SC	3.5559
109	64.3	16.7	19.0	750° C.	3.5564
44	62.6	16.1	21.3	SC	3.5593
				750° C.	3.5570
				SC	3.5569
				750° C.	3.5585

(d) Alloys Containing α or β Phase at 750° C.

Alloy No.	Composition, at.-%			Heat-Treat-ment	Structure	Lattice Parameter, kX		
	Ni	Cr	Al			γ	γ'	α
16	68.5	4.9	26.6	SC	$\beta + \gamma'$...	3.5639	...
42	64.9	9.9	25.2	750° C.	$\beta + \gamma'$...	3.5653	...
7	60.7	39.3	...	SC	$\beta + \gamma'$...	3.5659	...
43	60.1	34.8	5.1	750° C.	$\alpha + \gamma$	3.5657
117	60.1	31.7	8.2	SC	$\alpha + \gamma$	3.5646
148	61.5	29.0	9.5	750° C.	$\alpha + \gamma + \gamma'$	3.5620
116	60.6	29.0	10.4	SC	$\alpha + \gamma + \gamma'$	3.5604	3.554	2.8752
115	59.8	24.9	15.3	750° C.	$\alpha + \gamma + \gamma'$	3.5645	3.5570	...
88	59.1	19.7	21.2	SC	$\alpha + \gamma + \gamma'$	3.5615	3.5545	2.8762
8	55.5	44.5	...	750° C.	$\alpha + \gamma$	3.559	3.5535	2.878
118	55.5	34.2	10.3	SC	$\alpha + \gamma + \gamma'$...	3.5604	2.876
				750° C.	$\alpha + \gamma$	3.5656
				SC	$\alpha + \gamma$	3.5646
				750° C.	$\alpha + \gamma + \gamma'$	3.5607	3.5539	2.8764
					β			
114	58.2	10.8	31.0	SC	$\alpha + \beta + \gamma'$	2.5634	3.5660	2.877
119	50.3	25.6	24.1	SC	$\alpha + \beta + \gamma'$	2.8616	3.5651	2.877

* SC = Slowly cooled from 900° C. in 2 weeks.

data which also enabled the corners of the three-phase triangles to be located.

The form of the phase diagram at higher temperatures was determined from micro-examination alone, as the characteristics of the constituents had already been established and difficulty was anticipated in satisfactorily heat-treating filings at the higher temperatures for X-ray examination.

The chemical composition of the alloys examined and their structures are given in Table I. Table II details the lattice-parameter data from which the 750° C. isothermal was determined.

III.—THE EQUILIBRIUM AT 750° AND 850° C.

The greater part of the investigation was devoted to establishing the 750° C. isothermal for alloys containing more than 50 at.-% nickel, with an accuracy of about $\pm \frac{1}{2}\%$, and in particular the relationship between the γ and γ' phases. The diagram, shown in Fig. 3, is based on the findings on alloys annealed at 750° C. and on those slowly cooled from 900° C. to room temperature in 14 days, which were very similar. The region denoted by γ consists of the primary solid solution of chromium and aluminium in nickel and has a face-centred cubic structure which can become ordered in the neighbourhood of Ni_3Cr .³ The γ' phase is based on the structure of Ni_3Al , which has an ordered face-centred cubic

lattice in which nickel atoms occupy cube faces and aluminium and chromium atoms occupy cube corners. The γ' phase field is quite extensive, and the structure will absorb 19 at.-% chromium in place of aluminium and nickel.

Between these single-phase fields lies the two-phase ($\gamma + \gamma'$) region, in which the tie-lines link together the phase structures which are in equilibrium

phase regions linked with it lay outside the scope of the present investigation.

A more extended region covering the triangle Ni-Cr-NiAl is shown in Fig. 4 to display the general relationship of the nickel-rich alloys with the main body of the system.

Observations on alloys quenched at 850° C. show small changes in the equilibrium relationships from

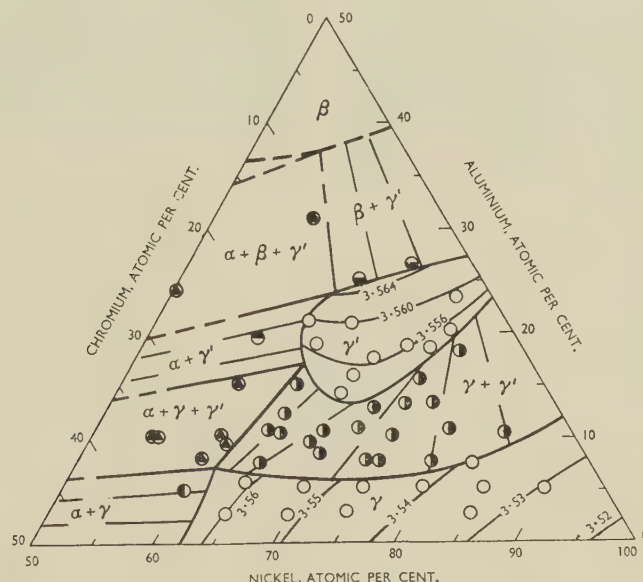


FIG. 3.—The Nickel-Chromium-Aluminium Phase Diagram: Isothermal Section for 750° C.

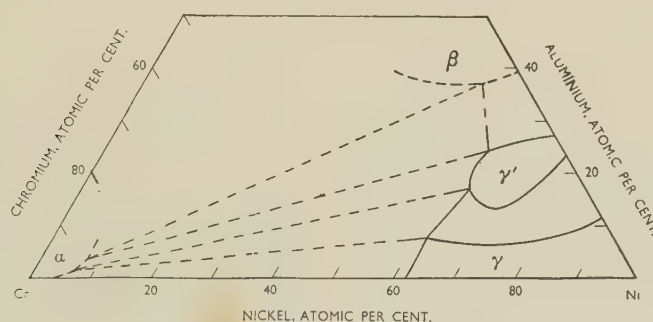


FIG. 4.—The Nickel-Chromium-Aluminium Phase Diagram: Isothermal Section for 750° C., Showing Relationship Between Nickel-Rich Alloys and the α Phase.

with each other at 750° C. A two-phase equilibrium also exists between the γ phase and the body-centred cubic α phase based upon chromium. A three-phase ($\alpha + \gamma + \gamma'$) region links the three structures together, followed by the two-phase ($\alpha + \gamma'$) region. The γ' phase also co-exists in equilibrium with the body-centred cubic β phase, based upon NiAl, which has a CsCl-type superlattice. The two-phase ($\beta + \gamma'$) region is indicated in the diagram in addition to the ($\alpha + \beta + \gamma'$) region, but an accurate determination of the β phase boundary and of the two- and three-

those obtaining at 750° C. As shown in Fig. 5, the γ phase takes into solution approximately 0.5% more aluminium and 2% more chromium than alloys slowly cooled or quenched from 750° C. The boundary at the chromium-rich end of the γ' phase recedes towards the composition Ni₃Al, narrowing the ($\alpha + \gamma'$) two-phase region and widening the ($\gamma + \gamma'$) region.

It has been shown by previous workers^{5, 10, 11} that in the binary nickel-aluminium system the phase field of the γ solid solution is separated from that of

the γ' solid solution by a two-phase ($\gamma + \gamma'$) region. The lattice parameters of the co-existing structures in alloys isothermally treated at 750° C. ($a = 3.54$ kX for γ and $a = 3.56$ kX for γ') are sufficiently different to produce complete resolution of the two sets of high-angle (311) $K\alpha$ doublets in Debye-Scherrer photographs taken with manganese radiation (Fig. 13 (a), Plate LXIX). However, if the aluminium level is maintained in the region of 12.5 at.-% and then nickel is replaced by chromium, the lattice parameter of the γ phase in the duplex structures increases quite rapidly, while that of the γ' phase changes but little. In consequence, it is observed that the (311) $K\alpha$ doublets of the γ phase move to a lower Bragg angle, reducing their angle of separation from

region is bounded by a side of the ($\alpha + \gamma + \gamma'$) three-phase triangle. An alternative explanation of the sequence of diffraction patterns described above would be that γ and γ' form two quite distinct phase fields separated by a ($\gamma + \gamma'$) two-phase region in which the lattice parameters of the co-existing phase structures become equal over a restricted range of composition. Of these alternatives the second can be shown to be correct from a consideration of the lattice-parameter data computed from the diffraction patterns of single-phase γ and γ' alloys, and from duplex alloys in the ($\gamma + \gamma'$) phase field.

Lattice-parameter data for a series of slowly cooled γ -phase alloys, are plotted in Fig. 6. It will be seen that there is a steady increase in parameter

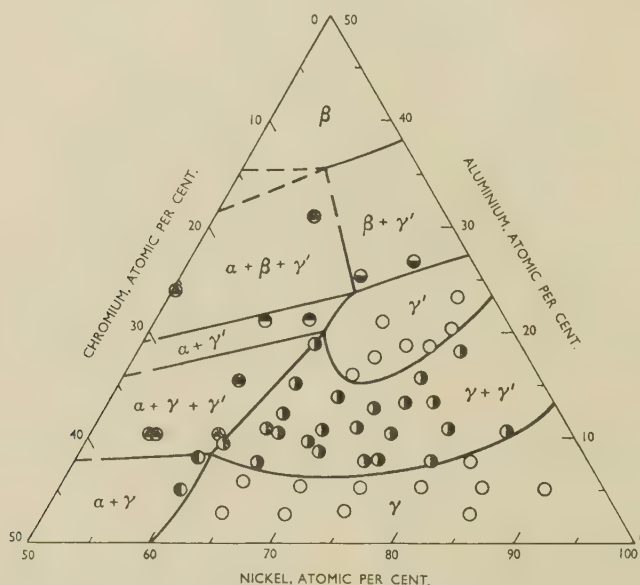


FIG. 5.—The Nickel-Chromium-Aluminium Phase Diagram: Isothermal Section for 850° C.

those of γ' (Fig. 13 (b), Plate LXIX), until ultimately the doublets appear to overlap exactly and the diffraction patterns give the appearance of belonging to single-phase alloys, as illustrated by Fig. 13 (c) and (d) (Plate LXIX). In other words, the ($\gamma + \gamma'$) gap of the nickel-aluminium binary system appears to be enclosed by a binodal curve, and the γ phase of the nickel-chromium system seems to stretch across the composition triangle as far as Ni_3Al . Thus γ' would appear to be merely the ordered portion of the γ phase field, as it appeared to be in the nickel-iron-aluminium system¹² until it was re-examined by classical metallographic methods.⁷

At still higher chromium contents, the group of end-doublets again breaks up into two pairs having progressively increased separation as the chromium content increases (Fig. 13 (e), Plate LXIX). This would seem to indicate the existence of a second ($\gamma + \gamma'$) two-phase field, in which it is the γ' constituent that has the lower lattice parameter, and this two-phase

with increase in both the chromium and aluminium contents, the values rising continuously along the 5 at.-% aluminium line from 3.525 kX at zero chromium to 3.56 kX at approximately 30 at.-% chromium. The smoothness of the curves is consistent with the single-phase character of the region. Sections across the diagram from Ni_3Cr to Ni_3Al and along a parallel direction at the 70 at.-% nickel level (Fig. 7) show that the lattice parameter of the ordered face-centred cubic γ' phase based on Ni_3Al , decreases steadily as aluminium is replaced by chromium, but, in each case, there are two well-defined discontinuities before the portion relating to the γ phase field is reached. These discontinuities clearly mark the boundaries of the γ and γ' phase fields. The fact that the diffraction pattern of alloy No. 108 (Fig. 13 (d), Plate LXIX) has a single-phase appearance yet gives a parameter which does not lie on either the γ or γ' branch of the curve is evidence that this alloy is, in fact, two-phase ($\gamma + \gamma'$), but

with the co-existing structures having closely similar lattice parameters.

Further evidence of the complete separation of the γ and γ' phase fields by a $(\gamma + \gamma')$ field is to be found in the isoparametric contours drawn in Fig. 3. The intersection of these contours with the phase boundaries gives the lattice parameters of the ends of the tie-lines linking the co-existing phase-structures. It is evident from the diagram that the lattice parameters increase much more rapidly along the boundary of the γ phase than they do along the γ' boundary as the chromium content is increased. This makes the tie-line directions principally dependent on the parameter of the γ constituent, which can be obtained

A feature of a number of the diffraction patterns, which adds complications to their interpretation by visual inspection alone, is the fact that slowly cooled alloys lying well within the γ single-phase field all show faint but well-defined superlattice lines based on a highly ordered Ni_3Cr structure, though with a few chromium atoms replaced by aluminium. These superlattice lines overlap those of the γ' phase, so that their presence on a powder photograph is no evidence of the alloy being duplex, as is the case in the $(\beta + \beta')$ two-phase field of the iron-nickel-aluminium system,¹² or in the $(\alpha + \alpha_1)$ field of the copper-nickel-aluminium system,¹³ both of which display the phenomenon of two similar structures in

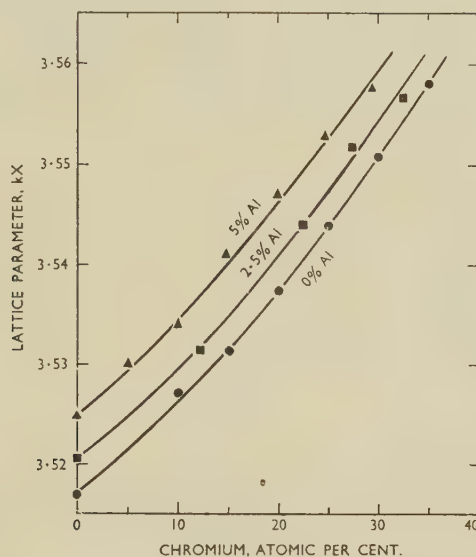


FIG. 6.—Lattice Parameters of Slowly-Cooled γ -Phase Alloys.

quite satisfactorily for a large proportion of the alloys in the two-phase field. The few additional tie-lines whose directions depend mainly on the parameter of the γ' phase field, fit into the scheme in a self-consistent manner. The parameter data show that the tie-lines start parallel to the nickel-aluminium side of the system and pivot round Ni_3Al until they lie askew across the $(\gamma + \gamma')$ field. The alloys of these skew tie-lines are the ones which are apparently single-phase, and it is found that their lattice parameters are a weighted mean of the parameters of the two co-existing phases at their extremities. The differences between the γ and γ' parameters are of the order of one part in 1000, so that resolution of their individual reflections is impossible; but the two-phase structure of these alloys is confirmed beyond doubt by their microstructures (Fig. 16, Plate LXIX). Careful inspection of the line shapes indicates a slight degree of unsharpness which does not normally occur with homogeneous, well-annealed, single-phase alloys. Beyond this region, the tie-lines close up fan-wise about the low-nickel end of the $\gamma/(\gamma + \gamma')$ boundary.

equilibrium with each other having equal lattice parameters.

The micrographic work places the phase boundaries in practically the same positions as those determined from the X-ray parameter data, provided that due attention is given to the changes taking place between the melting point and the temperature of annealing. This is particularly necessary in the case of alloys at the chromium-rich end of the region in which are to be found small amounts of α phase persisting either from the melt or from the breakdown of $(\beta + \gamma)$ eutectic (discussed below).

The microstructures of alloys in the $(\gamma + \gamma')$ region, annealed at 850°C ., vary considerably with composition. In all cases the one phase appears as a precipitate within the other, but the form and distribution of the precipitate differ from alloy to alloy. The γ' phase appears to be formed by precipitation from the γ matrix in all the two-phase alloys examined.

Examples of the types of structure observed in the $(\gamma + \gamma')$ phase field are shown in Figs. 14–17, (Plate LXIX). The dispersed globular precipitation of

γ' in γ represented in Fig. 14 is the most common structure. In some of the alloys the dispersed precipitate lies in regular rows along crystallographic planes of the matrix and may also be present in the form of needles (Fig. 15). The fine precipitate in the structure shown appears to lie on the octahedral (111) planes of the matrix, a relatively massive form occurring at the grain boundaries. An unusual appearance is presented by alloys at the middle of the $(\gamma + \gamma')$ field (Fig. 16), in which the precipitate assumes a rectangular shape and appears to form on the cube faces (100) of the matrix structure. There are only a few alloys in which this type of structure has been observed at this temperature, and in no case is the difference in spacings of the two phases sufficient to distinguish the diffraction pattern from

about 9%. That the α phase precipitates from β on cooling in the same way as does γ' is shown in Fig. 19 (Plate LXX), where it can be seen as small round particles unaffected by the etching reagent, while the γ' phase appears as a middle tone. At higher chromium contents, lakes of α phase formed from the melt can be seen in addition to α globules precipitated from the β phase (Fig. 20, Plate LXX).

Adjacent to the $(\alpha + \beta + \gamma')$ phase field lies a two-phase $(\alpha + \gamma')$ region which should include alloy No. 88, according to the X-ray evidence. The microstructure of this alloy (Fig. 21, Plate LXX) obviously contains more than two phases, the dark pools consisting of β phase which has not completely transformed. This is not unexpected, for, as discussed later, this alloy solidifies as primary dendrites

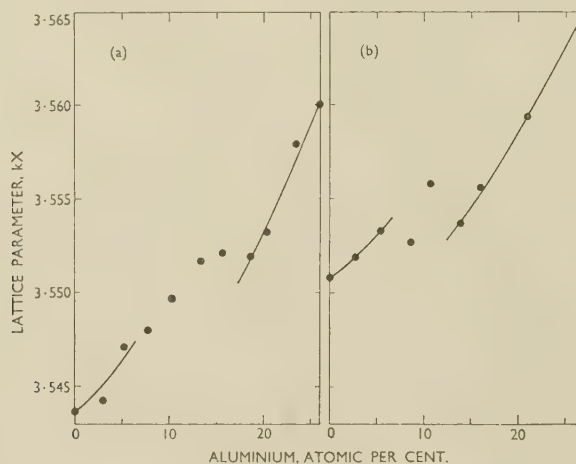


Fig. 7.—Lattice Parameters of Slowly-Cooled Alloys Containing (a) 75 at.-% Nickel and (b) 70 at.-% Nickel.

that of a single phase. The growth of one face-centred cubic phase on the (100) planes of another is rather unexpected, since precipitation normally occurs on the (111) planes.

A further variation in the $(\gamma + \gamma')$ structures is exhibited by alloy No. 103 (Fig. 17). From the positions of the boundaries and tie-lines of this two-phase field, the predominating phase must be γ' , and what appears to be the infilling between the grains is really the primary solid solution from which the γ' has precipitated.

On the aluminium side of the γ' phase lies the two-phase $(\beta + \gamma')$ region. From microscopical examination, it is evident that the β phase extends over a much greater range of composition at temperatures near the solidus than at the lower temperatures. The β phase in an alloy such as No. 16 has a striated structure in the "as-cast" state and, on annealing at lower temperatures, the γ' phase separates out as plates lying parallel to each other within the darker-etching pools of β phase (Fig. 18, Plate LXX). The $(\beta + \gamma')$ region is limited by the appearance of the α phase when the chromium content is more than

of β with $(\beta + \gamma)$ eutectic (Fig. 26, Plate LXXI), both phases transforming at lower temperatures. The proportion of β phase remaining after annealing at 850° C. is less than might be judged at first sight, as the pools of β contain large amounts of α and γ' . It would appear that on further annealing the β disappears entirely, as no trace can be detected in the X-ray-diffraction pattern, presumably because filings for X-ray examination attain equilibrium more rapidly than solid microspecimens on account of the heavy cold work imparted to them, and in this particular case the X-ray data are more reliable.

The $(\alpha + \gamma')$ region is separated from the $(\alpha + \gamma)$ region by an area in which the alloys consist of three phases: $\alpha + \gamma + \gamma'$. Microstructures of two alloys in this region, Nos. 115 and 151 (Figs. 22 and 23, Plate LXX), show distinct differences in the appearance of the constituents. In both structures the α phase appears white, but in the one alloy its boundaries are clearly defined, whereas in the other they are quite indistinct. The appearance of the γ and γ' phases also shows marked differences. To explain these structures, it is necessary to refer to the original

"as-cast" structure of the alloys. Alloy No. 115 solidified as primary γ dendrites with an infilling of $(\beta + \gamma)$ eutectic (Fig. 24, Plate LXXI), and the pattern of the structure was not changed on annealing at 1150° C. Because of this, annealing at 850° C. resulted in the β phase breaking down to the α and γ' phases, as in alloy No. 88 (Fig. 21, Plate LXX), while the greater part of the γ phase transformed to γ' . The $(\gamma + \gamma')$ pattern obtained is similar to that exhibited by alloy No. 103 (Fig. 17, Plate LXIX), the finely divided constituent resembling a "precipitate" being in fact the remnants of the original γ phase. On the other hand, alloy No. 151 in the "as-cast" state consisted mainly of $(\alpha + \gamma)$ eutectic with excess primary γ . Annealing this at 850° C. did not change the amount of α to a great extent, but the γ split up into the γ and γ' phases in approximately equal proportions. Much of the γ' phase occurs as well-formed particles, but the appearance of parts of the

At 750° C. both α and β phase fields extended well into the diagram, and lattice-parameter measurements indicate that in the two-phase $(\alpha + \beta)$ alloy No. 175 the parameters of the two phases do not differ by more than one part in 400, which is much less than in alloys in the three-phase $(\alpha + \beta + \gamma')$ region.

IV.—THE SOLIDIFICATION DIAGRAM

From the foregoing observations on the structures of alloys at 750° and 850° C., it will be seen that to interpret the microstructures of alloys annealed at 850° C. it was necessary from time to time to refer to the structures of the "as-cast" alloys. This led to a fairly extensive examination of alloys in the cast state, from which it was possible to map out tentatively the fields of primary crystallization within the composition range Ni-Cr-NiAl as shown in Fig. 8.

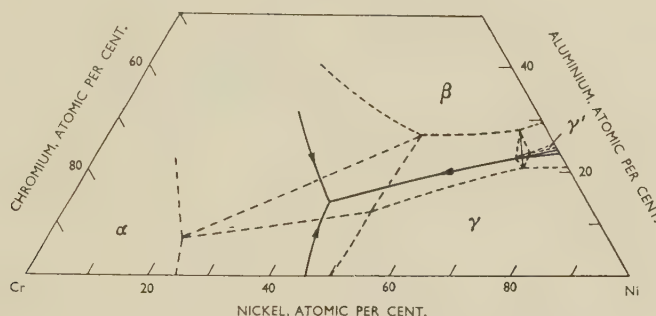


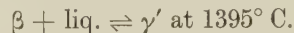
FIG. 8.—Tentative Diagram of Fields of Primary Crystallization.

matrix suggests that some is there in a very finely divided form, probably accompanied by some α phase. Consideration of these two structures, along with a number of others, has indicated that, in the presence of α phase, the γ phase may sometimes be differentiated from γ' by the lack of definition of the α/γ interface, as compared with α/γ' interface.

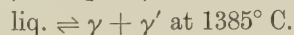
In the iron-nickel-aluminium system^{7, 12} a single-phase field extends across the composition triangle to link the β -iron phase with the ordered β -NiAl phase. This suggested that in the nickel-chromium-aluminium system the α -chromium phase would likewise link with β -NiAl to give a single-phase field which would form a natural limit to investigations of the system starting from the nickel corner. Consequently, a brief survey was made along the line Cr-NiAl, and it was found that the microstructures of the cast alloys (Fig. 29, Plate LXXI) corresponded to those of a eutectiferous binary system with the eutectic point lying near 30 : 40 : 30 at.-% Ni-Cr-Al and that the duplex structures persisted in alloys annealed at temperatures down to 750° C. This result indicated that the half of the ternary system defined by the corners Ni, Cr, and NiAl could be regarded from a practical viewpoint as self-contained.

Subsequently the equilibria at 1150° and 1000° C. were determined in order to relate the phase relationships at the solidus with those at 750° C.

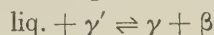
Reference has already been made to alloys which in the cast state consist of either γ or β phase with an infilling of a $(\beta + \gamma)$ eutectic. No two-phase equilibrium exists between the γ and β phase in the binary nickel-aluminium system, although it has been observed in the copper-nickel-aluminium¹⁴ and iron-nickel-aluminium⁷ systems. In the nickel-aluminium system there occur two three-phase reactions,



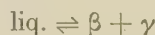
and



involving liquid of almost the same composition.⁵ As chromium is added to the nickel-aluminium alloys, the temperatures of the above reactions fall and at the same time approach each other, as do also the compositions of the participating liquids, until both become identical at about 8 at.-% chromium. At this temperature ($1340^\circ \pm 10^\circ \text{ C.}$) there is a four-phase invariant plane in which the following reaction takes place :



Below this plane there are the three-phase equilibria ($\beta + \gamma + \gamma'$) and ($\text{liq.} + \beta + \gamma$), which give rise to the eutectic reaction:



Although the four-phase reaction given above is in accord with the findings of Bradley⁷ on the iron-nickel-aluminium system, Alexander¹⁴ regards the reaction as untenable, since he considers it improbable that the liquid and the γ' phases would react to form β in view of the peritectic reaction of the binary

Ni-Cr-NiAl triangle (Fig. 30, Plate LXXI). The composition of the ternary eutectic point is in the neighbourhood of 45:40:15 at.-% Ni-Cr-Al at $1320^\circ \pm 10^\circ \text{C}$.

From Fig. 8 (p. 459) it will be seen that most of the nickel-rich alloys solidify as γ or β or as a mixture of the two phases and that the composition range within which the γ' phase occurs is quite small. When the γ' phase does appear in the structures it is usually in the form of envelopes separating the β phase from γ (Fig. 27, Plate LXXI). The α phase

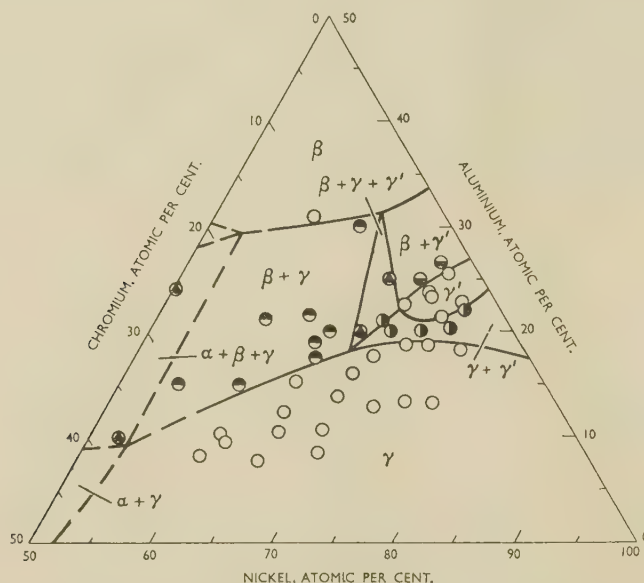
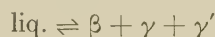


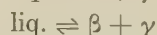
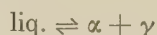
FIG. 9.—The Nickel-Chromium-Aluminium Phase Diagram: Isothermal Section for 1150°C .

system by which γ' is formed from liquid and β . However, his proposed reaction

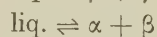


is even more improbable, as it represents a ternary eutectic.

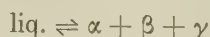
It was at first thought that the ($\beta + \gamma$) eutectic might run into the ($\alpha + \gamma$) eutectic, forming a trough in the liquidus surface across the nickel corner. However, when it was found that the α and β phases existed separately from the melt, it was realized that this construction was impossible. The existence of the three binary eutectics,



and



suggested that they might run together to form a ternary eutectic,



That this was in fact the case was confirmed by the structures of alloys lying near the centre of the

appears in cast alloys only if the nickel content is below about 52 at.-% (Fig. 28, Plate LXXI).

V.—THE 1150°C . ISOTHERMAL SECTION

Apart from changes in the positions of the phase boundaries, the phase relationships remain the same as the temperature falls from the solidus to 1150°C . (Fig. 9). The γ and β phase fields contract towards the nickel corner and NiAl, respectively, and the γ' phase field extends slightly, moving the ($\beta + \gamma + \gamma'$) three-phase triangle away from the nickel-aluminium edge of the composition triangle. Alloys within the ($\beta + \gamma$) phase field remain little changed in appearance, apart from the spheroidizing of the eutectic and the occurrence of small globules of α -chromium associated with the β phase (Fig. 32, Plate LXXII). The ($\gamma + \gamma'$) phase field is very narrow, the γ and γ' phase fields being separated by a gap of less than 2 at.-% aluminium at one point. Alloys containing 70–80 at.-% nickel and lying in the γ phase field between the 10 at.-% aluminium line and the $\gamma/(\gamma + \gamma')$ boundary are highly ordered, and at the boundary have practically the same

lattice parameter as the γ' alloys, on the $\gamma'/(\gamma + \gamma')$ boundary. In consequence the X-ray-diffraction patterns of γ , $(\gamma + \gamma')$, and γ' alloys are almost indistinguishable from each other. It has been mentioned earlier that, in some $(\gamma + \gamma')$ alloys in which the parameters of the two phases were nearly identical after annealing at 750° C., the γ' precipitate assumed a cubic form instead of the more usual rounded shape. Similar cubic precipitates were also observed in alloys annealed at 1150° and 1000° C. (Figs. 31 and 35, Plate LXXII). This seems to con-

alloy in the γ phase field at 1150° C. may be in the γ' phase field at 750° C. and have precisely the same structure as at the higher temperature. At intermediate temperatures it consists of a mixture of the two phases of which γ' is always ordered while the γ is probably disordered at the lower temperatures. Although it has not been confirmed experimentally, on account of the difficulty in obtaining satisfactory parameter measurements on alloys quenched from very high temperatures, the run of the isoparametric contours determined for the γ and γ' phase fields at

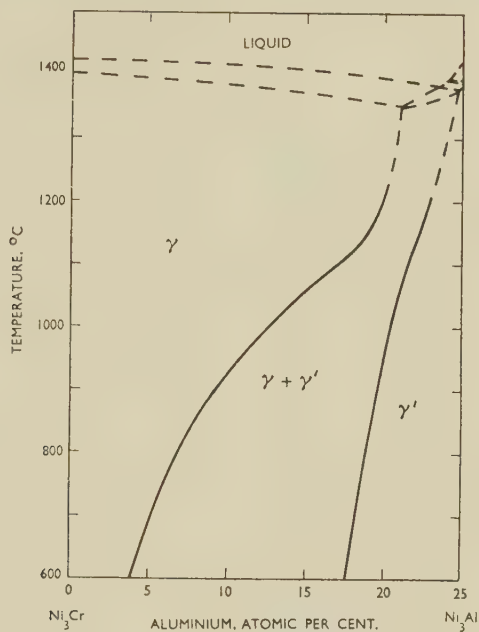


FIG. 10.—Vertical Section at 75 at.-% Nickel.

firm the idea that this type of precipitate occurs in preference to the spherical type whenever the lattice parameters are, within close limits, the same. Similar structures have been shown by Bradley¹⁵ in alloys within the $(\beta + \beta')$ phase field of the iron-nickel-aluminium system, where two body-centred cubic phases with equal lattice parameters co-exist in equilibrium.

By comparison of the 1150° and 750° C. isothermals (Figs. 9 and 3) and reference to the vertical section (Fig. 10) it will be seen that alloys within a range of composition at the aluminium-rich side of the γ phase field at 1150° C. transform to γ' on cooling to 750° C. The γ' phase is ordered throughout its whole range with aluminium atoms preferentially occupying the cube-corner positions. The γ phase is ordered around the Ni_3Cr composition at low temperatures, with chromium atoms at the cube corner sites, and as the solubility of aluminium in γ increases with temperature, so the aluminium atoms tend to replace the chromium atoms and the ordering temperature rises rapidly. As a result of this an

750° C. suggests that the lattice parameter of such an alloy in the γ' state is higher than in the γ state.

VI.—THE 1000° C. ISOTHERMAL SECTION

The structures of alloys annealed at 1000° C. reveal a distinct change in phase relationships from those existing at higher temperatures. The phase diagram for the nickel-rich alloys is shown in Fig. 11. The γ and β phase fields are both smaller and the γ' field larger than at 1150° C. The $(\beta + \gamma')$ and $(\gamma + \gamma')$ two-phase regions persist and become considerably more extensive. Many of the alloys which at 1150° C. lay in the $(\beta + \gamma)$ and $(\beta + \gamma + \gamma')$ phase fields contain appreciable amounts of α phase at 1000° C. and γ' phase appears in alloys previously in the $(\alpha + \beta + \gamma)$ field. This evidence points to the existence of a four-phase invariant plane at or near 1000° C. in which α , β , γ , and γ' are in equilibrium together. Consideration of the phase fields at temperatures above and below 1000° C. shows that such a four-phase plane must exist. At 1150° C.

the four single-phase fields are linked by the two three-phase triangles ($\alpha + \beta + \gamma$) and ($\beta + \gamma + \gamma'$) and the two-phase region ($\beta + \gamma$) (Fig. 12 (a)). The two-phase fields ($\alpha + \gamma$), ($\alpha + \beta$), ($\beta + \gamma'$), and ($\gamma + \gamma'$) persist throughout the temperature range from the solidus to 750° C. and are not involved in the transition. At 750° and 850° C. the single-phase fields are linked by the two three-phase triangles ($\alpha + \beta + \gamma'$) and ($\alpha + \gamma + \gamma'$) and the two-phase field ($\alpha + \gamma'$) (Fig. 12 (c)). The disappearance of the ($\beta + \gamma$) phase field and formation of the ($\alpha + \gamma'$) phase field can be achieved only by an invariant four-phase transition plane on which they

the microstructures is that of alloy No. 88, which contains very little α phase at 1000° C. and apparently no γ' . At 850° C. some β remains in the microstructure, although the X-ray diffraction pattern of a filed sample annealed at 750° C. shows only α and γ' . The reason for this may be associated with the fact that the composition of the alloy lies very near the β - γ diagonal of the four-phase plane, so that the equilibrium between the β and γ phases is more stable than in alloys with more or less chromium. This has been taken into consideration in placing the boundaries in the 1000° C. diagram.

Mention has been made in earlier sections of the

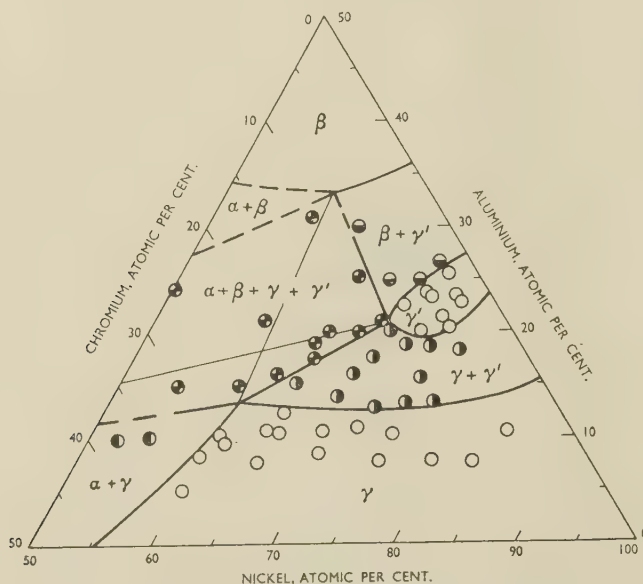
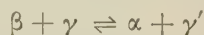


FIG. 11.—The Nickel-Chromium-Aluminium Phase Diagram: Isothermal Section for 1000° C.

are represented by the diagonals (Fig. 12 (b)). The transition may be expressed in the form:



This reaction bears some resemblance to both a eutectoid and a peritectoid, but since all four phases persist through the four-phase plane, the only terms by which it is adequately described are "four-phase transition" and "2/2 inversion". As far as the authors are aware, no similar instance of such a transition involving four solid phases in an actual alloy system has been recorded in the literature.

The microstructures of alloys within the four-phase plane vary considerably, as would be expected from the various changes in structure taking place on cooling to 1000° C. (Figs. 36 and 37, Plate LXXII). The amount of α phase visible in the structures is small, but is in accord with the low solubility of nickel in chromium at this temperature, which places the α corner of the phase field near the chromium corner of the composition triangle. An exception among

presence of small amounts of α phase in the microstructures of some of the annealed alloys in which it would not be expected. It has been found that in almost every alloy examined in which the β phase crystallizes from the melt, angular globules of α phase form on annealing either in or adjacent to the β phase. These are readily recognized microscopically since they are a brilliant bluish white, whereas the β phase is light brown (Fig. 32, Plate LXXII). Even when the original β has disappeared as a result of structural changes such as the formation of γ' , the α remains and cannot be accounted for by the phase diagram. Similarly, where α occurs in the cast structure, β is to be found in the same parts of the structure on annealing. In the case of an alloy such as No. 305 (Figs. 28, Plate LXXI, 33, and 38, Plate LXXII) there is no evidence to indicate that the β phase should not be present at 1150° C., but the run of the boundaries at 1000° C., based on the evidence from other alloys, places the alloy in the ($\alpha + \gamma$) field, although the β persists in the structure. These

structures may well be caused by lack of homogeneity in the alloys, for, while an alloy consisting of a single phase at temperatures near the solidus can be made homogeneous provided sufficient time of annealing is allowed, an alloy with a polyphase structure at the solidus will consist of more than one phase, however long it is annealed. Hence, on annealing at lower temperatures, the phases transform independently of each other, except at their interfaces. Because of this, traces of eutectic are to be found around the primary dendrites in many of the alloys, and it is in these regions that the anomalous α - β changes occur. It may be inferred from the readiness with which the one phase forms from the other that there is a very marked reduction of solubility of β in α and of α in β as the temperature

position of the last-formed γ' , depositing γ' of a composition intermediate between those of β and γ . Whereas the β/γ' and γ'/γ interfaces in the structures resulting from the peritectic reaction are normally strongly dissimilar in appearance under the microscope, owing to the fact that the γ phase was liquid,⁶ there is no marked difference between them in structures produced by annealing the solid alloys in which the peritectoid reaction takes place. This is attributable to the long time during which diffusion can take place and to the approximately equal rates of diffusion in the solid alloys.

VII.—SUMMARY

The part of the nickel-chromium-aluminium system defined by the composition triangle Ni-Cr-NiAl is in essence a self-contained ternary eutectic system in which the participating solid phases are the solid solution based on nickel (γ), NiAl (β), and chromium (α). The temperature of the ternary eutectic is $1320^\circ \pm 10^\circ \text{C}$. The solidification of low-chromium alloys containing 20–30 at.-% aluminium is complicated by the formation of the γ' phase, based on Ni_3Al , via a peritectic reaction.

As the temperature falls, the γ and β phase fields, which are extensive at the solidus, contract towards the nickel corner and NiAl, respectively. At the same time, the γ' phase field extends in the direction of the nickel-chromium edge of the composition triangle, chromium atoms replacing both nickel and aluminium in the Ni_3Al structure. From the solidus to a temperature in the neighbourhood of 1000°C , the γ and β phases are in equilibrium with each other, the two-phase field diminishing in extent until it disappears in a four-phase plane representing the isothermal reaction:



The two-phase ($\alpha + \gamma'$) field which is formed as a result of this reaction widens as the temperature falls.

The face-centred cubic γ and γ' phases have separate identities throughout the temperature range explored. The equilibrium between them is such that their lattice parameters in some of the ($\gamma + \gamma'$) alloys are almost identical, giving rise to microstructures in which the precipitated γ' assumes a cubic form.

Although specific-heat and resistivity measurements have shown that the γ phase is ordered below 540°C . at the Ni_3Cr composition, superlattice lines cannot be seen in Debye-Scherrer photographs of this alloy. However, they show clearly in diffraction patterns of similar alloys containing 5 at.-% aluminium after slow cooling to room temperature. Diffraction patterns of alloys quenched from 1150°C . show that ordering persists to this temperature when the aluminium content is more than 10 at.-%.

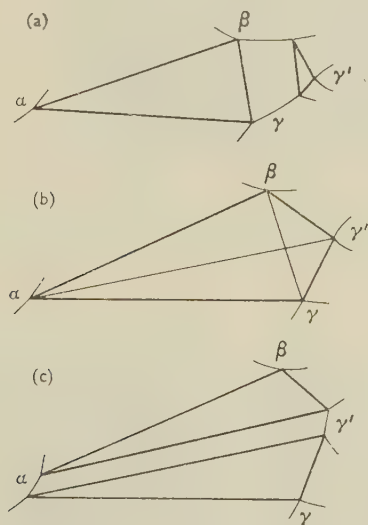


FIG. 12.—The Transition from β - γ to α - γ' Equilibrium.

falls, particularly along the side of the ($\alpha + \beta$) region nearest the nickel-chromium edge of the composition triangle. In order to derive a phase diagram which represents the probable equilibrium relationships, small amounts of α or β in the structures of some of the alloys have had to be ignored.

Some of the alloys which lie in the ($\beta + \gamma + \gamma'$) three-phase region at temperatures above 1000°C . present a structural feature which is worth noting. The microstructure of an alloy such as No. 300 at 1150°C . (Fig. 34, Plate LXXII) shows γ' precipitated within the γ phase and envelopes of γ' surrounding the β phase, reminiscent of the γ' formed by the peritectic reaction between the liquid and β (Fig. 27, Plate LXXI). Since the alloy solidified from the melt as ($\beta + \gamma$) another explanation has to be sought. In fact, the formation of these γ' envelopes at temperatures below the solidus is due to an interaction between β and γ which might be described as a peritectoid, for, as the temperature falls, the ($\beta + \gamma + \gamma'$) triangle moves away from the com-

ACKNOWLEDGEMENTS

The authors wish to thank The Mond Nickel Co., Ltd., for permission to publish this paper and Mr. H. W. G. Hignett and Mr. E. H. Bucknall for their interest and helpful discussions.

REFERENCES

1. A. Taylor and R. W. Floyd, *J. Inst. Metals*, 1951-52, **80**, 577.
2. A. Taylor and R. W. Floyd, *ibid.*, 1952-53, **81**, (1), 25.
3. A. Taylor and K. G. Hinton, *ibid.*, 1952-53, **81**, (3), 169.
4. D. S. Bloom and N. J. Grant, *Trans. Amer. Inst. Min. Met. Eng.*, 1951, **191**, 1009.
5. W. O. Alexander and N. B. Vaughan, *J. Inst. Metals*, 1937, **61**, 247.
6. R. W. Floyd, *ibid.*, 1951-52, **80**, 551.
7. A. J. Bradley, *J. Iron Steel Inst.*, 1949, **163**, 19.
8. A. J. Bradley and S. S. Lu, *J. Inst. Metals*, 1937, **60**, 319.
9. A. Taylor and H. Sinclair, *Proc. Phys. Soc.*, 1945, **57**, 108.
10. A. J. Bradley and A. Taylor, *Proc. Roy. Soc.*, 1937, [A], **159**, 56.
11. J. Schramm, *Z. Metallkunde*, 1941, **33**, 347.
12. A. J. Bradley and A. Taylor, *Proc. Roy. Soc.*, 1938, [A], **166**, 353.
13. A. J. Bradley and H. Lipson, *ibid.*, 1938, [A], **167**, 421.
14. W. O. Alexander, *J. Inst. Metals*, 1938, **63**, 163.
15. A. J. Bradley, *J. Iron Steel Inst.*, 1951, **168**, 233.

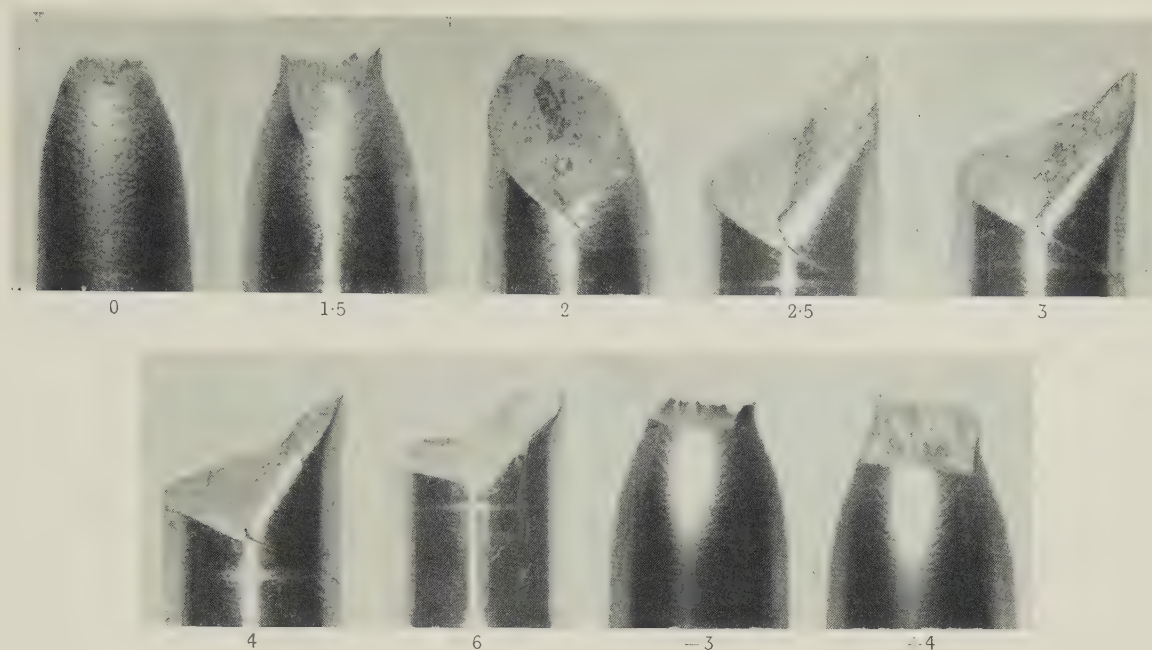


FIG. 6.—Tensile Fractures in Prestrained Nickel Specimens. The shear strain in the surface of each specimen is indicated below the photograph. The photographs labelled with numbers preceded by \pm show tensile fractures after twisting to the indicated strain and then completely untwisting. Approx. $\times 4$.

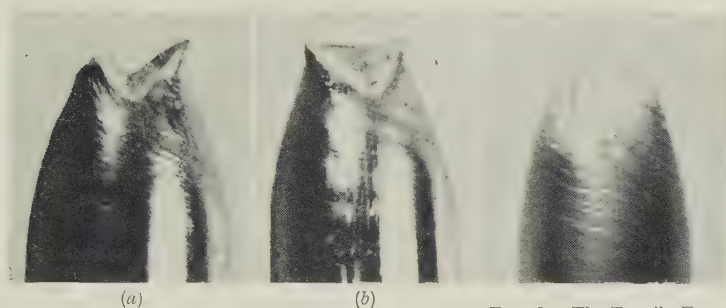


FIG. 7.—Tensile Fractures in Commercially Pure (2S) Aluminium Specimens Twisted to Shear Strains of (a) 4 and (b) 5. Approx. $\times 4$.

FIG. 8.—The Tensile Fracture in a High-Purity Aluminium Specimen Twisted to a Shear Strain of 6. Approx. $\times 4$.

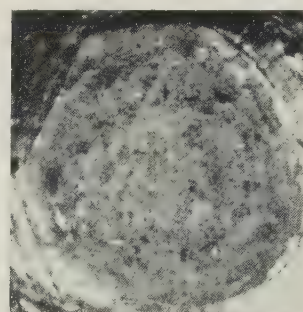


FIG. 9.—The Tensile Fracture in a Commercially Pure Aluminium Specimen Tested Without Prestraining. Approx. $\times 16$.

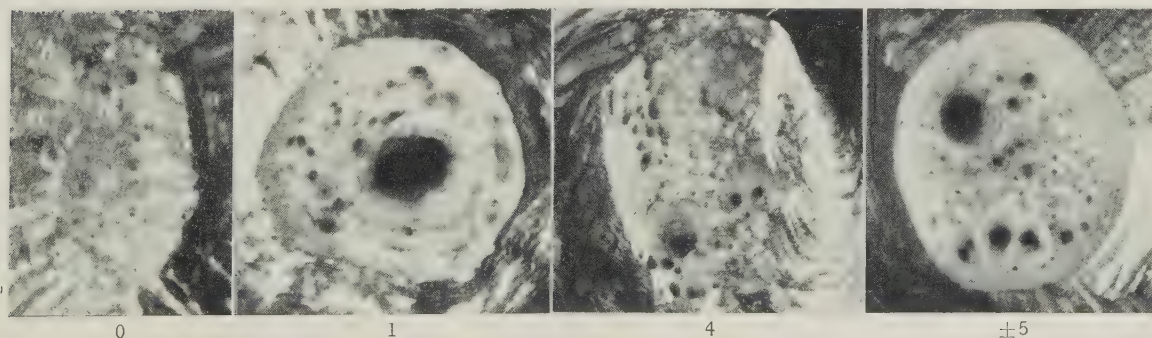
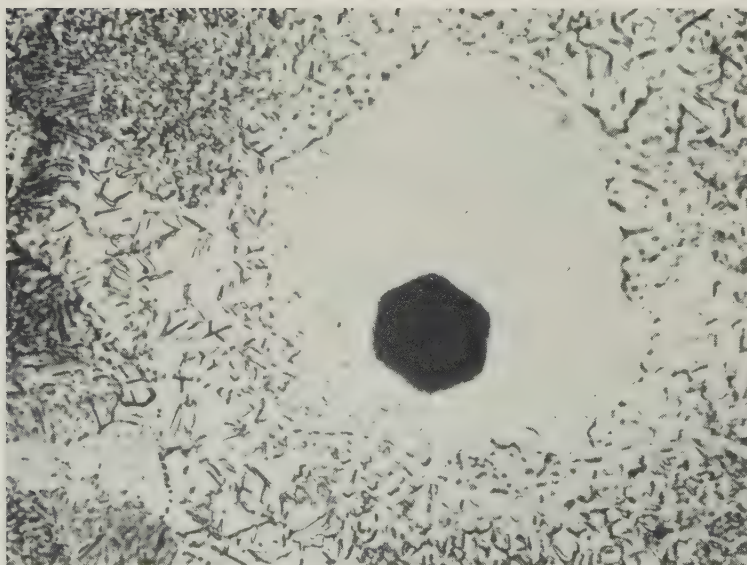


FIG. 10.—Tensile Fractures in High-Purity Aluminium. The shear strain in the surface of each specimen is indicated below the photograph. The \pm sign has the meaning indicated in the caption to Fig. 6. Approx. $\times 16$.

MAGNESIUM-ALUMINIUM ALLOYS.

FIG. 1.—Several Cavities Within One Large Grain. $\times 750$.FIG. 2.—Cavity in a Grain Sectioned Nearly Parallel to the Basal Planes. $\times 750$.

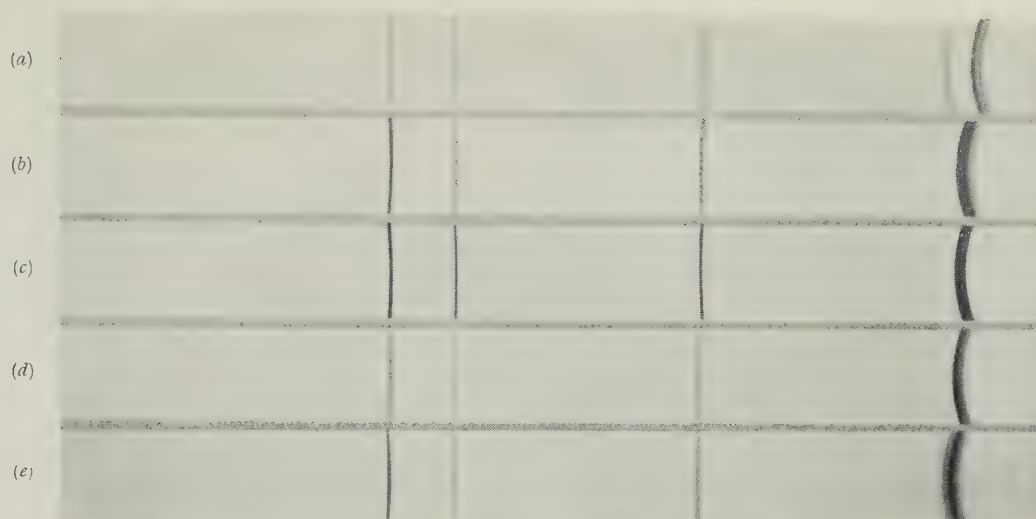


FIG. 13.—X-Ray-Diffraction Patterns of Alloys in the $(\gamma + \gamma')$ Phase Field at 750° C. (Mn $K\alpha$ Radiation).

(a) 83.9/16.1 at.-% Ni-Al.

(b) 76.7/9.9/13.4 at.-% Ni-Cr-Al.

(c) 72.1/15.0/12.9 at.-% Ni-Cr-Al.

(d) 69.7/21.7/8.6 at.-% Ni-Cr-Al.

(e) 65.0/22.6/12.4 at.-% Ni-Cr-Al.

MICROSTRUCTURES OF NICKEL-CHROMIUM-ALUMINIUM ALLOYS ANNEALED AT 850° C.

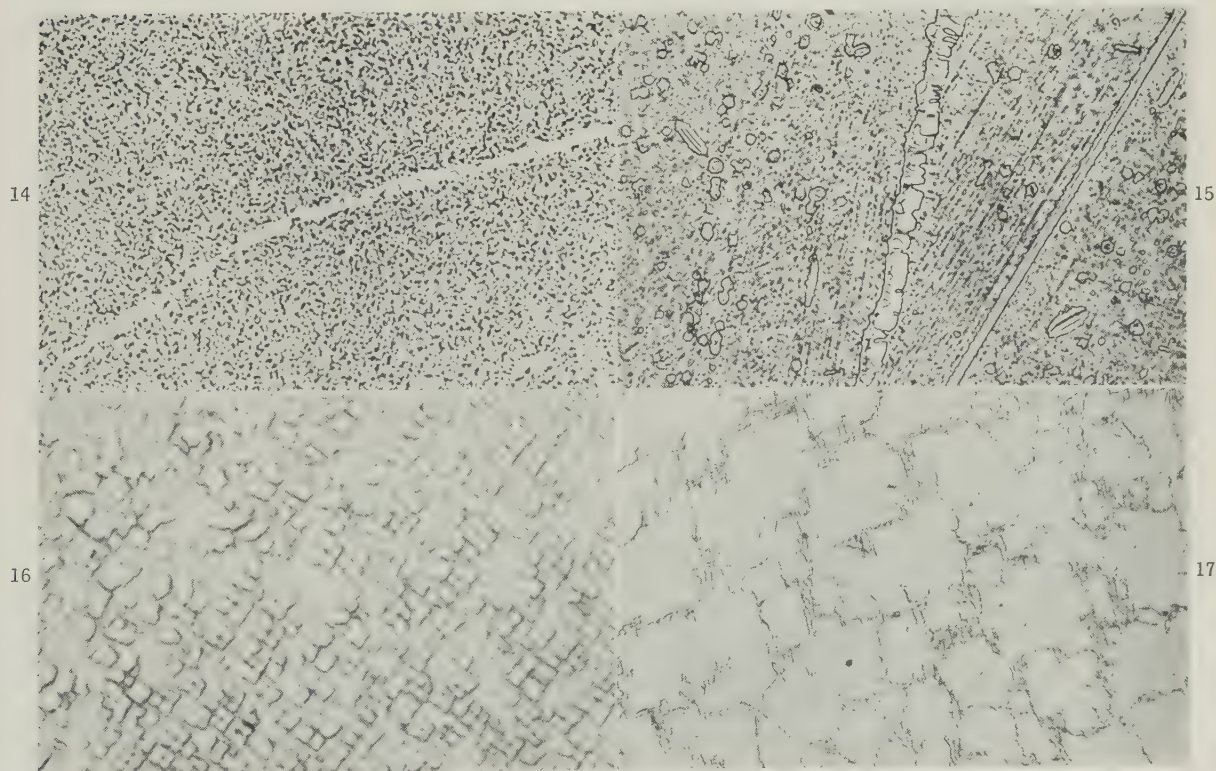


FIG. 14.—Alloy No. 71. 74.6/9.8/15.6 at.-%. $\gamma + \gamma'$. $\times 500$.

FIG. 15.—Alloy No. 107. 69.0/20.3/10.7 at.-%. $\gamma + \gamma'$. $\times 500$.

FIG. 16.—Alloy No. 251. 71.7/17.3/11.0 at.-%. $\gamma + \gamma'$. $\times 1500$.

FIG. 17.—Alloy No. 103. 76.6/5.2/18.2 at.-%. $\gamma + \gamma'$. $\times 500$.

MICROSTRUCTURES OF NICKEL-CHROMIUM-ALUMINIUM ALLOYS ANNEALED AT 850° C.

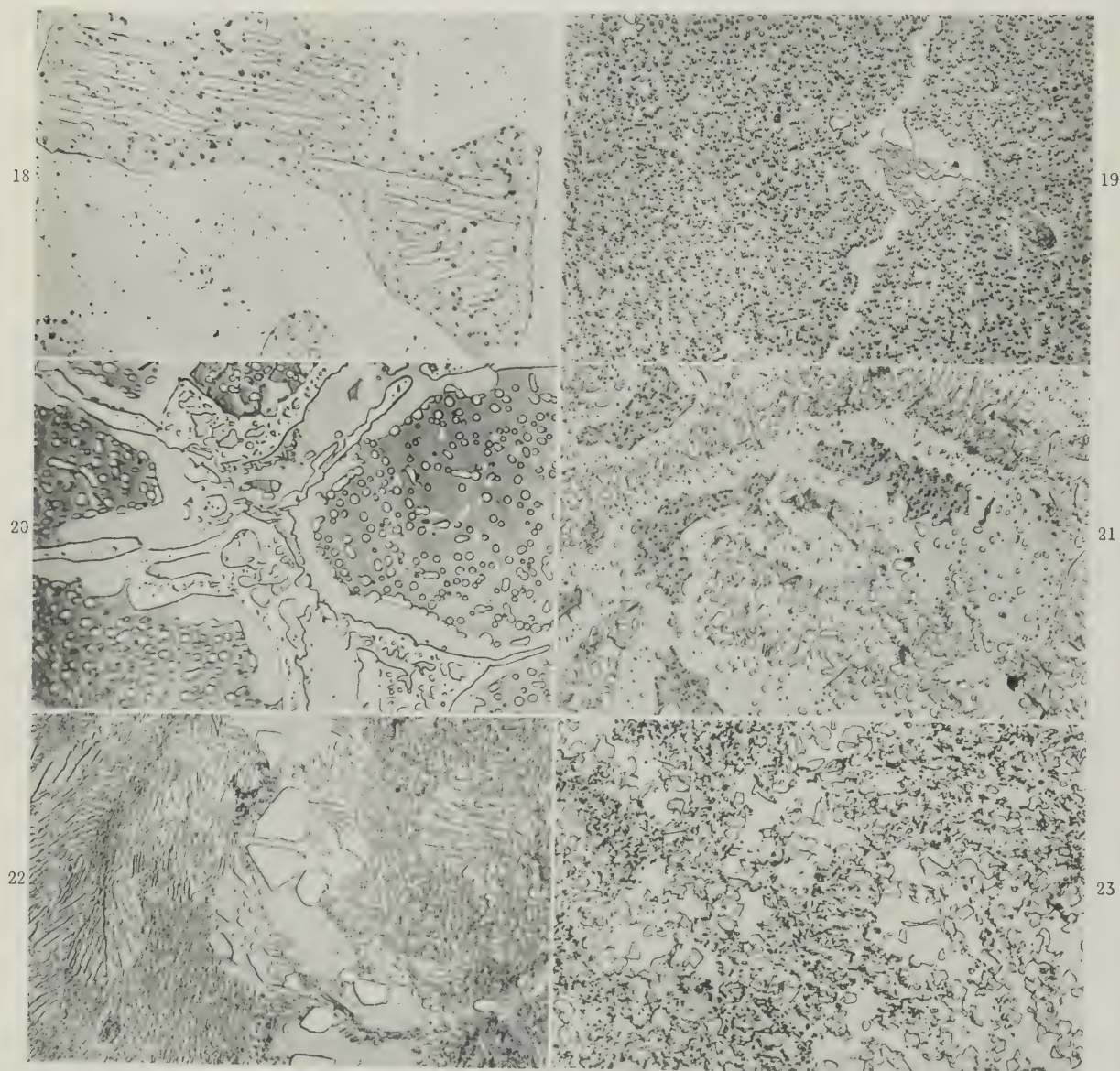
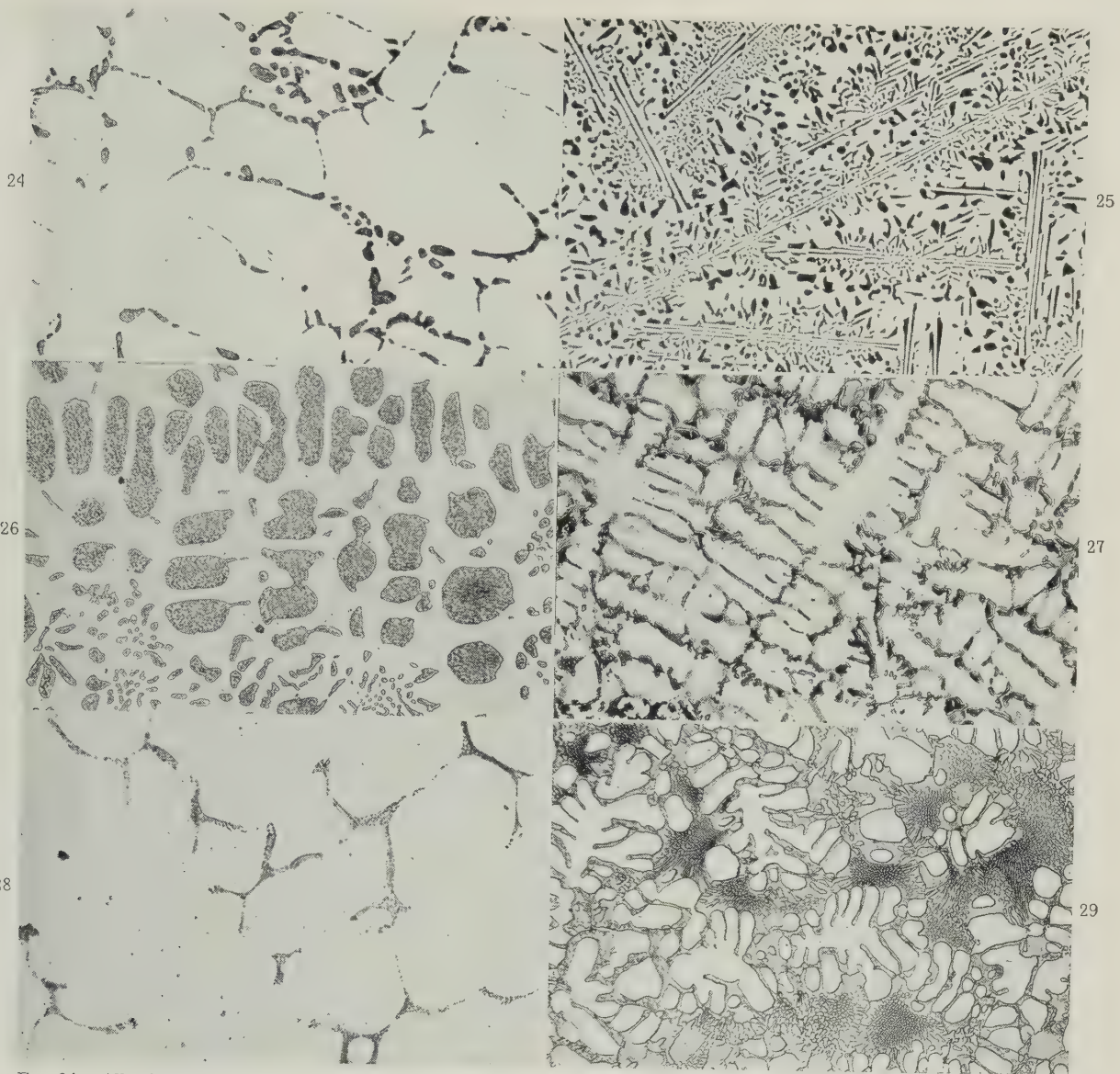
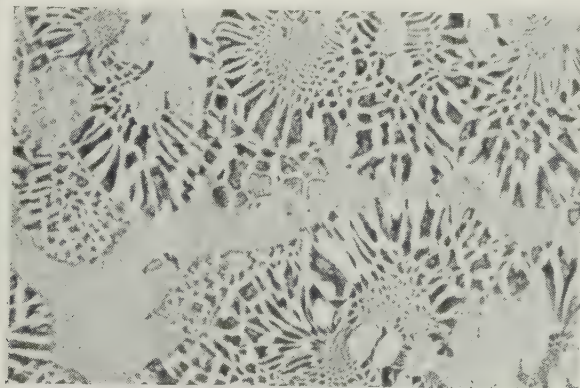
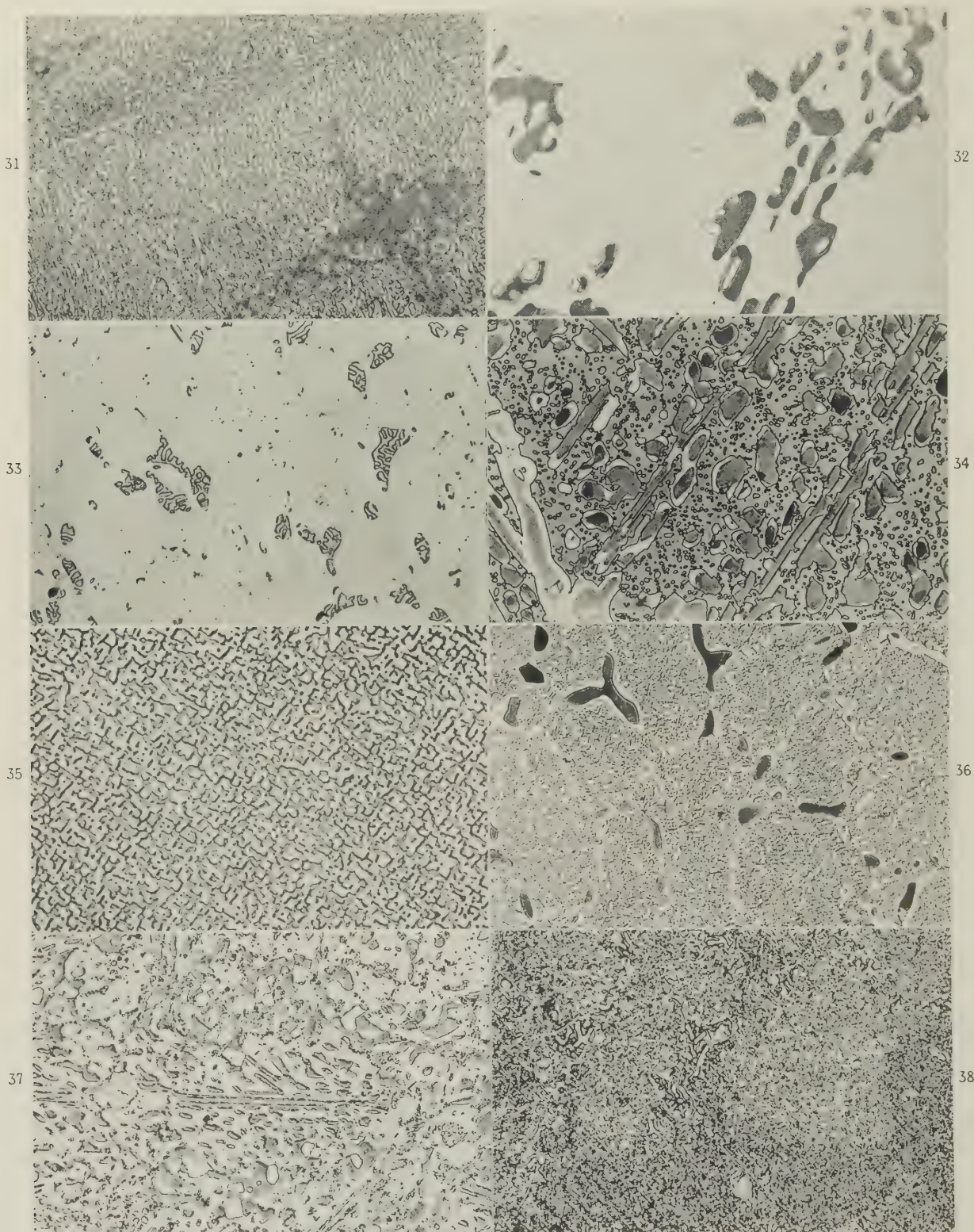


FIG. 18.—Alloy No. 16. 68.5/4.9/26.6 at.-%. $\beta + \gamma'$. $\times 500$.
 FIG. 19.—Alloy No. 114. 58.2/10.8/31.0 at.-%. $\alpha + \beta + \gamma'$. $\times 500$.
 FIG. 20.—Alloy No. 119. 50.3/25.6/24.1 at.-%. $\alpha + \beta + \gamma'$. $\times 1000$.
 FIG. 21.—Alloy No. 88. 59.1/19.7/21.2 at.-%. $\alpha + \beta + \gamma'$. $\times 500$.
 FIG. 22.—Alloy No. 115. 59.8/24.9/15.3 at.-%. $\alpha + \gamma + \gamma'$. $\times 500$.
 FIG. 23.—Alloy No. 151. 55.0/34.8/10.2 at.-%. $\alpha + \gamma + \gamma'$. $\times 500$.

MICROSTRUCTURES OF AS-CAST NICKEL-CHROMIUM-ALUMINIUM ALLOYS.

FIG. 24.—Alloy No. 115. 59.8/24.9/15.3 at.-%. $\beta + \gamma$. $\times 150$.FIG. 26.—Alloy No. 88. 59.1/19.7/21.2 at.-%. $\beta + \gamma$. $\times 200$.FIG. 28.—Alloy No. 305. 52.5/37.5/10 at.-%. $\alpha + \gamma$. $\times 200$.FIG. 25.—Alloy No. 300. 67.5/12.5/20 at.-%. $\beta + \gamma$. $\times 200$.FIG. 27.—Alloy No. 295. 70/7.5/22.5 at.-%. $\beta + \gamma + \gamma'$. $\times 200$.FIG. 29.—Alloy No. 175. 25.4/54.6/20 at.-%. $\alpha + \beta$. $\times 200$.FIG. 30.—Alloy No. 223. 45/40/15 at.-%. $\alpha + \beta + \gamma$. $\times 200$.
Unetched; phase contrast.

MICROSTRUCTURES OF NICKEL-CHROMIUM-ALUMINIUM ALLOYS.



FIGS. 31-34. Annealed at 1150° C.

FIG. 31.—Alloy No. 14. 74.8/4.9/20.3. $\gamma + \gamma'$. $\times 200$. FIG. 32.—Alloy No. 109. 64.3/16.7/19.0. $\alpha + \beta + \gamma$. $\times 200$.
 FIG. 33.—Alloy No. 305. 52.5/37.5/10. $\alpha + \beta + \gamma$. $\times 200$. FIG. 34.—Alloy No. 300. 67.5/12.5/20. $\beta + \gamma + \gamma'$. $\times 200$.

FIGS. 35-38.—Annealed at 1000° C.

FIG. 35.—Alloy No. 147. 69.8/12.6/17.6. $\gamma + \gamma'$. $\times 500$. FIG. 36.—Alloy No. 109. 64.3/16.7/19.0. $\alpha + \beta + \gamma + \gamma'$. $\times 200$.
 FIG. 37.—Alloy No. 303. 60/25/15. $\alpha + \beta + \gamma + \gamma'$. $\times 200$. FIG. 38.—Alloy No. 305. 52.5/37.5/10. $\alpha + \beta + \gamma$. $\times 200$.

THE PRESENT AND FUTURE METALLURGICAL REQUIREMENTS OF THE CHEMICAL ENGINEER *

By SIR CHRISTOPHER HINTON,† M.A., M.I.C.E., M.I.Mech.E.

SYNOPSIS

Up till about 1925 the designer of chemical plant made use only of the range of constructional materials that had been developed for other purposes. In the last twenty-five years, however, the chemical engineer has made increasing demands on the metallurgist for new materials to meet his special requirements. In particular, the plant needed for operations in connection with the exploitation of atomic energy has presented a number of metallurgical problems. A brief survey of some of these is given.

It is suggested that a better range of halide-resistant materials is necessary, and that greater attention should be paid to methods of fabricating new materials.

I.—INTRODUCTION

ENGINEERING, like metallurgy, is not an exact science; indeed, engineering design is best thought of as an art with a scientific basis, and therefore the final solution to a design problem is a compromise between the conflicting advantages and disadvantages of many alternative solutions which present themselves. It follows that, although in all design work there are certain fundamental rules of soundness and purity which must normally be respected, the application of those rules and the finished form of the design will depend on the taste and training of the designer. There are usually alternative solutions to every design problem, all equally acceptable; which of these is adopted depends on the background against which the designers work; some of this background is peculiar to the individual, but much of it is common to all those engaged within a particular field. Because of this, we should be wise, before we survey the materials of construction which the chemical-plant designer needs or will need, to consider the tradition of design which forms the background against which he works.

The foundations of the modern heavy-chemical industry lie in the second half of the 18th century, when the manufacture of sulphuric acid, bleaching powder, and black ash began on an industrial scale. Throughout the Industrial Revolution there was a steady expansion. The manufacture of heavy alkalies was put on its present basis by the introduction of the ammonia soda process in 1873 and the invention of the electrolytic soda process in 1890; the contact process for the manufacture of sulphuric acid was made practicable in about 1870. Meanwhile similar developments were taking place in the industries centred around coal tar. By 1802 Boulton and Watt were

lighting their factory at Birmingham by coal gas, and from the growth of the coal-distillation industry arose the developments of synthetic dyestuffs which continued throughout the 19th century, though the initiative was largely lost to Germany before the First World War.

That war called for an expansion of the chemical industry on a scale which was without precedent; later, it will be noted that the last war stimulated the beginnings of atomic energy in a similar way. There had been great developments in the explosives industry under Nobel, but in 1914 T.N.T. had only just been approved as a high explosive, and the demand for it and for cordite led to a great programme of factory building which was carried out by the Government under Lord Moulton and Quinan. At the end of the war Britain, having learned the seriousness of lacking supplies of ammonium nitrate and the danger of not having a well-developed coal-tar industry, started the fixation of atmospheric nitrogen and encouraged the growth of the dyestuffs industry. The formation of great combines of chemical manufacturers, which followed in the late 1920's, left the business organization of the industry roughly in the form in which we know it today.

II.—MATERIALS IN USE UP TO 1925

Until 1925 the chemical engineer had never demanded from the metallurgical industry the materials which he preferred or required for the manufacture of his plants; he had taken the materials which had been developed for other industries, and had devised processes which could be worked in vessels made of the available materials. The foundry industry had developed rapidly during the Napoleonic wars to

* Delivered at the Annual General Meeting, London, 23 March 1953.

† Deputy Controller of Atomic Energy (Production), Ministry of Supply.

supply the Navy and Army with guns and shot, and it had grown still further to meet the requirements of the engineering industry in the Industrial Revolution. The steel industry had grown largely to meet the needs of transport—the railways and shipping companies; the lead industry largely to meet the needs of the building industry; and the copper industry those of the domestic user, the builder, and the shipwright.

The chemical engineer seized on these and on ceramic materials, all of which had been intended for other industries, and used them skilfully to build his plants. He did little to demand that materials should be invented to meet his requirements, and so his vessels were made of cast iron or mild steel, lined with blue brick if necessary; they were of timber lined with lead, or of copper. The chemical processes had to be so devised that they could be worked in these vessels. The engineering and metallurgy of chemical plants followed the growth of technique in the general engineering industry—it did not lead it.

III.—PRESENT POSITION REGARDING MATERIALS FOR THE CHEMICAL ENGINEER

The late 1920's marked a turning point, and from then onwards chemical engineers began to demand the materials which they require for the construction of their plants. It is interesting to speculate on how the change came about; perhaps it was due to the general development and growth of the chemical industry which was then taking place in Great Britain, the construction of dyestuffs plants, plants for cellulose chemistry, and plants for high-pressure reactions; perhaps the formation of the large combines placed chemical firms in a stronger position to state their needs. Possibly the new outlook did not arise entirely from changed conditions in this country; in the late 1920's the American oil industry was expanding rapidly, it was young and energetic, the efficiency of many of its processes could be improved by using higher pressures and temperatures, and it could afford to take risks. It did not hesitate to specify its metallurgical requirements and to demand improvements, and the line it adopted may have influenced us.

Perhaps all these factors and others acted together to bring about the change, but in the metallurgical industry the conditions were favourable. Most of the demands of the chemical industry are for materials which are corrosion- and erosion-resistant, and in 1913 Brearley had invented stainless steel. The original material, containing 12–14% chromium and 0.3% carbon, could be hardened by heat-treatment and was suitable for the cutlery industry; it was of little use to the chemical engineer, however, as the range of chemicals to which it was resistant was limited and it was not easily fabricated. Development was retarded by the First World War, but in 1923 it was found that the corrosion-resistance could be increased by higher chromium contents, and in 1925 the 18% chromium, 2% nickel steel, now covered by British Standard S80, was evolved. This martensitic steel

was still of only limited interest to the chemical engineer, but the later development of the austenitic, and to a lesser extent the ferritic, stainless steels went far to meet his requirements.

Simultaneously with these advances in ferrous metallurgy there had been a corresponding widening in the range of non-ferrous alloys available for chemical plant construction. The manufacture of nickel had been put on an industrial basis at the beginning of the century, and at the end of the 1914–18 war it was important as an alloying material in ferrous metallurgy and as a plating material. In the period of which we are now talking its merits and the merits of non-ferrous nickel alloys as corrosion- and heat-resisting materials were realized. To complete our outline picture of the second quarter of the century, we should call to mind the progress which took place in the non-metallic protection of plant by rubber and glass covering, and in the use of plastics.

It is reasonable to ask ourselves what the chemical engineer has succeeded in doing with these great new facilities. It is doubtful whether he can claim correspondingly to have broadened the number of generic varieties of chemical products which are marketed, though, within a rather wider generic field, he can claim considerably to have increased the number of species. But he can certainly claim that he has made good use of the new materials to evolve more elegant and more economical plants. Possibly the best single example of this is in the manufacture of nitric acid. In our first period it was made in large quantities from Chile nitrate in plants built mainly of cast iron and acid-resisting brick; but in the second period the use of the cheaper ammonia-oxidation process was made possible only by developments in the austenitic stainless steels.

IV.—PROBLEMS IN FABRICATING CHEMICAL PLANT

1. CONDITIONS OF OXIDIZING CORROSION

With this background we can ask ourselves what further developments may reasonably be asked for by the chemical engineer. In answer we can say that not only must he have satisfactory materials but he must also have the techniques necessary for their use; too often these techniques are not immediately available and have to be developed with some loss of time, to meet specific problems. The austenitic steels provide an example.

Modern austenitic stainless steels give very good resistance to corrosion under oxidizing conditions, but the chemical engineer is not concerned with the properties of the plate so much as with the properties of the vessels and plants which he can fabricate from it, and it is not possible to have the same confidence in the welded joint of a stainless-steel vessel as in the parent metal. Under conditions which are not too rigorous it is normal to use a steel containing 18% chromium and 8% nickel, with a stabilizer chosen to suit the conditions; although this steel is commonly

called austenitic, it has in reality a duplex structure containing both austenite and ferrite. Under severe corrosion conditions, such a steel is often found to be more readily attacked than one free from ferrite. To eliminate the duplex structure and to secure a completely austenitic matrix, the nickel content must be increased and on an average the safe minimum nickel content for a fully austenitic steel is 13%. To avoid the weld-decay type of corrosion, additions of strong carbide-forming elements are necessary, and where a great deal of cross-welding is expected niobium is generally preferred to titanium. A steel of this type containing 19% chromium, 13% nickel, and 1% niobium can have many uses in chemical engineering; in the form of plate it also has a high resistance to nitric-acid corrosion, but the conditions in welded joints require further consideration. If the electrode deposit is fully austenitic, there is grave danger of producing fine cracks in the weld. In the adjoining zone the liability to cracking in the plate owing to faulty welding technique is accentuated.

Faced with this problem in our plants, we have adopted the compromise solution of using an 18 : 8 : 1 welding electrode which gives a certain amount of ferrite in the weld metal, though this is not a solution about which one can feel entirely happy. In the chemical plants associated with atomic-energy processes it often happens that, because of the radioactivity of the chemicals handled, it is impossible to approach vessels to carry out examinations or repairs, and in these conditions we have been particularly alive to problems of fabrication. We should feel safer if we could guarantee both freedom from cracks and freedom from ferrite.

We have met similar problems in making welded joints in stainless-steel pipe lines. In plants where conditions are not too severe and where repairs are possible, it is satisfactory to make such joints by metallic-arc welding, but this gives rise to dangers, either of incomplete penetration or of too large and irregular an internal bead; both conditions can encourage corrosion. We have evolved a reasonable solution by making the first run of weld metal by the argon-arc process. The ends of the pipes are machined to a modified J-end having a fairly thin root face. This enables a small weld pool to be maintained during the argon-arc run, making possible adequate control of penetration, and the edges are fused together giving a fully austenitic weld on the inside of the pipe. The remainder of the weld is filled by metallic-arc welding with metal with a low ferrite content. Thus the weld metal exposed to the corrosive liquors is of the same composition as the body of the pipe. To prevent the under side of the weld from becoming heavily oxidized, it is necessary to provide argon backing inside the tube during welding. This is done by inserting removable sponge-rubber plugs in the pipe on each side of the weld and admitting argon into the space between them. For closing welds when sponge-rubber plugs cannot be withdrawn, balloons are inserted on either side of the joint and in-

flated to provide the seal; these balloons can be withdrawn when welding is complete.

The welded seams on all vessels which have to contain highly radioactive material are X-rayed, and all welded joints in pipes which work under similar conditions are either internally examined with an Introscope or, where this is not possible, are X-rayed.

A major difficulty has been to define the standard of acceptance; X-ray examination of welds has been developed mainly for the examination of Class A pressure vessels, and the standard of acceptance is based not on any absolute or scientific level of perfection but on a comparison of X-ray plates with similar photographs of welds which have or have not proved satisfactory. It did not follow that the same criteria would be applicable to our requirements, and a great deal of experimental work was necessary to determine which characteristics on an X-ray plate should lead to rejection and which were tolerable. For the development of such new techniques as these, we were mainly dependent on our own resources, though we had most willing and sympathetic collaboration from the fabricators.

But the picture that I want to present is that, when faced with a new problem in chemical-plant design and construction, it is comparatively easy to select a material which will reasonably meet our requirements, but it is much more difficult to devise fabrication techniques for this material. It seems to me that this is a common difficulty in the development of chemical plant, and it has certainly been met with in the history of stainless steel since the early days of its use in the chemical industry. The problem is not confined to stainless steels, and one can think of a number of cases of materials which in billet or plate form exhibit most valuable properties of corrosion-resistance, but where the technique of fabrication still presents serious difficulties and limitations.

This forms the basis of the first plea that I should like to make on behalf of the chemical engineer—that methods of fabrication should keep pace with developments in basic materials of construction. I suggest that there is too great a tendency to carry out laboratory corrosion tests on plate or billet samples when, in fact, the important tests are those on welded joints or on samples cut from castings. It is wrong and uneconomical that the cure for weld decay should be found only after extensive trouble has been experienced on full-scale plant.

The difficulty is not an easy one to solve, since collaborative effort is necessary. Some responsibility must unquestionably rest with the user, who, I think, must state his requirements more clearly, not merely in respect of the properties that he requires in his materials of construction, but also in respect of the sort of plant into which he expects to fabricate these materials. But I think that the main responsibility must inevitably fall on the metal manufacturer and that he ought to develop a greater consciousness of the problems of fabrication. Many of the large metal-

lurgical firms have contracting engineering workshops of their own. I suggest that these workshops might be encouraged to take an interest in fabrication problems of new materials that are being developed. Where the metallurgical manufacturer does not possess such facilities, he might make a collaborative arrangement with one of the manufacturers of chemical-plant vessels to achieve the same advantages.

2. CONDITIONS OF HALIDE ATTACK

We have said that, provided suitable fabrication techniques are worked out, the austenic steels meet most of the reasonable requirements of the chemical engineer in oxidizing corrosion conditions. But there are limitations to their use; firstly, their resistance results from the formation of a protective surface film, and for this reason they are not fully satisfactory where there is erosion; and secondly, their resistance to corrosion is destroyed in the presence of halides. In regard to the first of these limitations, almost all the corrosion-resistant materials owe that property to the formation of a protective film, and the film on stainless steels and on nickel and its alloys is so thin, tough, and adherent that it would, in my opinion, be unrealistic to expect much improvement in its mechanical properties. I think that the engineer must expect to have to deal with the erosion element of the erosion-corrosion problem by skilful design, rather than look to the metallurgist to provide a solution.

The position in the field of halide attack is far less satisfactory than in the field of oxidizing attack. In the case of dry halides, mild steel can be satisfactorily used provided the temperature is not too high; even fluorine can be handled in the dry state in mild-steel plant, provided the temperature is below 200° C. Above this temperature violent attack can take place. The temperature limitation can be raised by using nickel or Monel, but even these are not safe above 500° C.

Where hydroxyl ions are present, the problem becomes very much more difficult. In the case of hydrochloric acid and its corrosive compounds chemical engineers usually take refuge in the use of glass- or rubber-lined vessels. Glass-lined vessels have limitations in size and complexity, while rubber-lining cannot be employed at temperatures much above 90° C. if it is to give a reasonable life. The only metals which give good corrosion-resisting properties in this field are the nickel-molybdenum alloys in the Hastelloy group, but these are extremely difficult to fabricate.

The position in regard to bromine is still less satisfactory, since rubber can be less readily utilized, but one meets the greatest difficulty in dealing with the fluorine compounds. Here not only rubber-lining but also glass-lining and ceramics are normally excluded. Mild steel, nickel and nickel alloys, copper, and aluminium can be used with suitable temperature limitations and in "dry" conditions, but these are very severe limitations to place on the

plant designer. Thus the second reasonable request that the chemical engineer may make to the metallurgist is, for a better range of materials to resist halogen action, and within this field I stress the need for materials to withstand fluorine attack. I believe that this is of peculiar importance, as there is likely to be great growth in the status of fluorine chemistry in the next ten years. The only substance that can at present be recommended for use under severe conditions of fluorine attack is graphite, and even with modern developments there are limitations to the plants and vessels which can be built of this material. I think that the chemical industry itself has not sufficiently realized its responsibility in regard to developments in this field; for the construction of chemical plants one needs not only metals or other materials of which to build plant vessels, but also such auxiliaries as jointing material, gland packing, and gland seals. The efforts made to produce such materials have not been sufficiently determined, and unless steps are taken to provide better materials for the construction of plants subject to fluorine corrosion, I think that this country may find that it is left behind in a new and important field of development.

3. OTHER PROBLEMS

We have now examined the position in two broad generic groups which we have called the oxidizing-corrosion problem and the problem of halide attack. There remain two other groups: those of high-temperature and of high-pressure. In the first of these I include processes where the type of corrosion of which we have already spoken does not occur, but where the temperature is beyond that normal in chemical-plant practice and the creep of metals becomes a dominant design feature. I would suggest that in this field the requirements of the chemical engineer are likely to be covered by those of the gas-turbine industry. If that is the case, the chemical engineer does not need to formulate his own demands, but can follow in the wake of the developments being made for the aircraft-engine and power-plant industries, watching only the problem of fabrication to ensure that a reasonable number of the heat-resisting alloys produced can be formed into the shapes in which he needs to use them. The problem of high-pressure chemical plant is very specialized, and it is not a field in which I have experience.

Before we leave orthodox chemical engineering there is one other problem which we ought to consider. A great deal of corrosion-resistant material is used for chemical-plant construction where conditions are not strictly corrosive. Stainless steel, nickel, and nickel alloys, are extensively used in plants for the food and pharmaceutical industries to ensure the biological cleanliness necessary there; in yet other processes the chemical industry is no longer content with the dark and dirty plants so common twenty years ago, and is rightly aiming at a far higher standard of amenity. The plant designer has found it perhaps too easy to provide the higher standard demanded of

him by using expensive corrosion-resisting alloys merely to secure cleanliness. This is a question to which the metallurgical industry might wisely give attention. Unless they are able to provide a cheaper means of providing materials which give cleanliness, there may be a swing towards the use of inexpensive plastic materials in these conditions. There is already some indication that this is taking place in the food industries.

With this question of cleanliness and ease of maintenance of plant one ought to associate the problem of building maintenance which is often so heavy in the chemical industry. In a great many cases the chemical engineer should eliminate this problem, as has been done in the oil industry, by centralizing the controls and instruments and placing the plant in the open. But there are plants where this is not possible and where corrosion of the building is severe. Reinforced concrete construction is not a satisfactory solution, because of the fear that corrosive liquids may penetrate to the reinforcing rods and for other reasons. In these cases a structural steel which could be kept in good condition at reasonable cost would be very helpful.

V.—MATERIAL REQUIREMENTS FOR ATOMIC ENERGY

I should like now to speak of some of the metallurgical problems which arise in connection with atomic-energy development. These can be divided into two groups: those associated with the atomic piles and those associated with the ancillary chemical plants. The chain of processes involved in the manufacture of fissile material starts with the extraction of uranium from its ore, followed by its purification and reduction to the metallic form. In this form it is made into rods which are enclosed in aluminium cans. The canned uranium rods are placed in the atomic-energy pile, where part of the uranium is converted into plutonium. The irradiated rods containing this plutonium and the associated fission products are discharged from the pile; they are then extremely radioactive and can only be handled remotely. The irradiated rods go to the chemical-separation plant, where they are dissolved in nitric acid and processed to separate an impure plutonium, impure uranium, and the fission products. The plutonium goes through a purification process and is reduced to metallic form; the fission-products solution, which contains most of the radioactivity, is stored indefinitely.

It is not widely realized that in these early days of atomic energy, more than half the industrial effort and technical difficulty lies, not in the piles but in the chemical plants, and these problems are engineering, chemical, and metallurgical in nature. This will probably not always be the case and, as the use of atomic energy for power production develops, the volume of effort will probably swing in the other

direction, but we shall consider first of all the present and future metallurgical requirements of the chemical plants. The processes for the manufacture of uranium from ore are fairly conventional; they involve corrosion problems throughout, but these are well covered by the suggestions already put forward in connection with the development of materials to withstand oxidizing corrosion and halide attack.

The chemical plants in which the separation of the plutonium and fission products is carried out, after the uranium has been irradiated, are unconventional in that they are handling materials of such high radioactivity that the plants must be remotely controlled, and many of these plants cannot be approached for repair when they have once operated. Basically, therefore, the problem of materials of construction is the same as for other chemical plants which are subject to oxidizing corrosion, but the problem is made more difficult and interesting by the consideration that repairs cannot be carried out, and failure must therefore be avoided. Very careful consideration of methods of fabrication has therefore been necessary. We believe that the solution to many of our problems can be found with fairly conventional materials, providing use is made of the very finest techniques in design and fabrication.

The metallurgical problems in connection with the atomic piles are quite different and have nothing in common with those of the chemical plants. Piles (or as they are now more often called reactors) can be divided into two broad classes, thermal reactors and fast reactors. The thermal reactor uses as its fuel either natural uranium which contains 0.7% of the fissionable U_{235} isotope, or uranium which has been slightly enriched in this isotope by a physical process of isotope separation. Fission of a U_{235} atom produces, on an average, rather more than two neutrons; we require that approximately one of these should be captured by an atom of U_{238} to form U_{239} , which breaks down first to neptunium and then to plutonium, while one other neutron is used to cause fission of a further atom of U_{235} which will release more neutrons to continue the chain of reaction. Since our uranium contains 140 atoms of U_{238} for every atom of fissionable U_{235} , it is obvious that our neutrons are much more likely to strike atoms of U_{238} and to be absorbed than they are to strike atoms of U_{235} and cause fission; if this happens, we stop the further release of neutrons and our chain of reaction dies out.

We must therefore increase the probability that our neutrons will cause fissions of U_{235} ; this is done by slowing them down in a moderator to energies which correspond with the temperature of that moderator; they are then called thermal neutrons. A neutron is a valuable article; we need all we have got in the pile, either to form plutonium or to cause further fissions of U_{235} ; we cannot afford to waste them by having them uselessly absorbed by other materials. Our problem therefore in a thermal reactor is to select metals for use in the reacting core which will absorb the minimum number of neutrons and yet will meet

our other requirements; those most readily available are aluminium and magnesium.

Until now aluminium has been used, particularly for the manufacture of the cans in which the uranium is enclosed. And here we have met the problem, so common in atomic-energy experience, that for the conditions which have to be met the material has defects. Commercial aluminium is most satisfactory for the uses to which it is currently put, but it contains non-metallic inclusions, and to obtain cans free from defects we had to do quite a lot of development in collaboration with the manufacturers. But if we are to use our reactor to generate industrial power we must release the heat at a high temperature; aluminium and magnesium, with their comparatively low softening and melting points, set a limit on the permissible temperature, and there is reason for interest in beryllium and zirconium which also have low neutron-capture cross-sections and which have higher melting points.

The position in the fast reactor is different; here the fuel element contains a high proportion of fissile material; there is no need to maintain a balance between the neutrons which are captured to form plutonium and those which cause further fissions because the quantity of U_{238} in the fuel element is small enough to take care of this. It is therefore unnecessary to slow our neutrons down by using a moderator and we make use of the fast neutrons. They are less likely than thermal neutrons to be captured by metals used in the construction of the reacting core, and in the design of a fast reactor nuclear physics gives us a greater choice of materials. But we run into many other difficulties. Because our fissile material is less diluted than it was in the thermal reactor, the volume and therefore the surface area of our fuel elements is far less, and for this reason we are faced with very high rates of heat transfer and very high temperature gradients. Heat can be removed at the necessary rate only by using liquid-metal coolants, such as mercury, sodium, potassium, lead, bismuth, or alloys of these materials, each having its own advantages and disadvantages. The heat flow from the fuel element is so great as to cause heavy temperature stresses in the container, and in selecting a material for this, the problem is to choose a material which has high heat conductivity, so as to keep these stresses to a minimum, and high creep strength, and which is not corroded either by the liquid-metal coolant or by the fuel, which may be either uranium or plutonium. The problem is further complicated by the fact that the material is subjected to intense neutron bombardment; this bombardment is liable to knock atoms out of their normal position in the crystal-lattice structure, and it may therefore alter the physical and chemical properties of the material. The effect is likely to be least marked on pure metals and

on alloys which are simple solid solutions; more complicated alloys may be materially changed.

There is one other metal which I should mention as being of interest in atomic-energy work. Uranium is our only source in nature of fissionable atoms; we can use neutrons from these fissionable atoms to convert part of our uranium into plutonium which is also fissionable. But we can also use the neutrons which are produced from fission of U_{235} to bombard atoms of thorium and so produce another isotope of uranium with atomic mass 233 which is fissionable and which has many desirable properties. It is from this that our interest in the metallurgy of thorium arises.

VI.—CONCLUSION

We have now briefly surveyed the present and future metallurgical requirements of the engineer in the atomic-energy field; neither time nor security considerations would allow us to go into them in much greater detail. We have looked at the shortcomings of the metals of construction available to the more orthodox chemical engineer, and I asked that greater attention should be paid to problems of fabrication when new metals were being developed and proposed that there should be closer collaboration between the metal manufacturers, the plant fabricator, and the user at all stages of development. I also suggested that the range of materials available for the construction of plants that are subject to halide (and particularly fluorine) attack is unsatisfactory.

Even without these additional materials the chemical engineer has at his disposal today far more, far better, and far more expensive materials of construction than were available to him twenty-five years ago, and I would like to conclude with a plea for moderation in their use.

In the old days research chemists in devising new processes paid very close attention to the metallurgical problems which would arise. Some of the solutions provided have great simplicity and cheapness; for instance, in the ammonia soda process, soda ash of high commercial purity can be produced in cast-iron and mild-steel plant, not because these materials are inherently resistant to the chemicals used, but because suitable chemical conditions have been devised for the formation of protective scales. Chemists ought still to be alive to such possibilities and to avoid assuming that the metallurgist can and should solve for him the problems of plant materials to which his processes give rise. I hold that chemical engineers should be discriminating in their choice of materials and avoid "getting the stainless-steel habit"; perhaps lastly I might even venture to suggest that the metal manufacturer should avoid overselling his corrosion-resisting materials; it is neither in his own interest nor in the interest of the chemical industry to do so.

THE USE OF DIAMOND ABRASIVES FOR A UNIVERSAL SYSTEM OF METALLOGRAPHIC POLISHING *

1466

By L. E. SAMUELS,† B.Met.E., MEMBER

SYNOPSIS

An investigation has been carried out to determine the most efficient and economical methods of using diamond abrasives for metallographic polishing. It has been found that the abrasive is most efficiently used when dispersed in a carrier paste, the polishing rate then being 4–5 times that of dry application, and that it can be used economically only in the finer grades (0–10 μ particle-size range). The polishing rates are then extremely high; even with hand polishing, the rates are frequently higher than that of electrolytic polishing.

The results of the work are applied to the development of a system of metallographic polishing, the costs of abrasive for which are sufficiently low to permit its use for general, and even routine, polishing. To bridge the gap over which diamond abrasives cannot be used economically, a cast wax-abrasive lap has been developed, the characteristics of which are such as utilize the full potential of the subsequent diamond stages. Consideration has also been given to final polishing treatments necessary to give truly scratch-free surfaces. The system finally developed is very rapid and produces a polish of very high quality, with a surface free from objectionable deformation.

I.—INTRODUCTION

THE advantages of the use of diamond abrasives for metallographic polishing have been discussed in a number of recent papers, but in most cases the authors have concentrated upon the preparation of samples that are difficult, or impossible, to prepare by classical methods. Woodside and Blackett¹ described processes for refractory materials, such as molybdenum carbide and arc-cast molybdenum, and for other difficult specimens, such as grey cast iron and specimens of large surface area. Tarasov and Lundberg² developed a system for polishing harder materials and specimens containing constituents likely to polish in relief. Perryman's³ process was also intended primarily for non-ferrous specimens containing constituents or areas differing greatly in polishing characteristics; Davies and Hoare⁴ and Greenfield and Davies⁵ have applied Perryman's³ methods to tin-coated materials. Tottle²⁶ has recently described a modification of Perryman's system.

The above processes are of two general types: first, those in which the diamond abrasive is added to the polishing pad as a dry powder^{2–5} and, secondly, those in which it is added by means of an impregnated carrier paste.¹ Impregnated carrier pastes would appear to have considerable advantages both in ease of handling of the diamond dust and in ensuring a more even distribution of the abrasive particles on the polishing pad. All processes so far described are based on rotating pads, and in that employed by Perryman³ the specimen was also made

to rotate and to traverse the pad simultaneously. In most processes a napped cloth is recommended for the polishing pad, although Tarasov and Lundberg² recommend silk. Water,² carbon tetrachloride,¹ and white spirits (light paraffin oil)^{3–5} have been suggested as suitable lubricants. The preliminary polishing stages recommended for general specimens also differ appreciably in detail, but are essentially of the following basic types:

(a) Grade 000 or 0000 emery paper,^{3–5} immediately preceding the fine diamond stage.

(b) A coarse diamond pad, (10–35) μ grade, is used between the abrasive papers and the fine diamond finishing stages.⁶

(c) A fixed abrasive lap is used as an intermediate stage between the abrasive papers and the diamond pads. Lead laps, lead-foil laps,⁴ diamond grinding wheels, and a vitrified diamond hand hone² have been suggested for this purpose.

Although the emphasis has been on the use of diamond abrasives for special purposes, all authors recognize that the process is very rapid and would give very high-quality results with the more usual types of metallographic specimen. The application of diamond abrasives to general metallographic polishing, however, must depend essentially on economic considerations of abrasive costs. The purpose of the present investigation, therefore, was to establish the most efficient methods of using diamond abrasives with a view to developing an economically feasible system of routine polishing.

* Manuscript received 15 December 1952.

† Senior Scientific Officer, Defence Research Laboratories, New South Wales Branch, Sydney, Australia.

Furthermore, the high polishing rates obtained with diamond abrasives suggest that the abrasive would be suitable for hand-polishing processes, and attention was particularly directed to this end.

II—INVESTIGATION OF CHARACTERISTICS OF DIAMOND ABRASIVES

A systematic investigation has been made of the relative merits of the various methods of using the abrasive by determining the polishing rates of pads charged under a range of conditions, by different methods, and with different grades and weights of abrasive. Since this included an assessment of the value of impregnated carrier pastes, it was first necessary to develop a suitable paste of this type.

1. DIAMOND-IMPREGNATED CARRIER PASTE

The essential requirement of a carrier paste is that it should be a permanent emulsion prepared from liquids. The abrasive may then be suspended in one of the liquids before mixing and obtained in uniform dispersion throughout the final paste. It is desirable that the paste should be miscible with water to permit water-washing of the specimens if desired, and that it should be readily absorbed by all types of polishing pads. Grodzinski⁷ has published the formula of a patented paste, and several types are available commercially.

A simple stearic acid-triethanolamine soap emulsion has been developed and found to be quite satisfactory for metallographic purposes. The components of a batch of paste of convenient size are as follows:

Stearic acid.	.	.	.	12.5 g.
Triethanolamine	.	.	.	6.0 ml.
Water	.	.	.	25 ml.
Diamond abrasive *	.	.	.	0.5 g.

* Ex Triefus and Co., Ltd.

The stearic acid is melted and heated to 80°–90° C. The triethanolamine and most of the water are mixed and heated to the same temperature range, a small amount of wetting agent and the diamond dust are added, and the abrasive shaken into a uniform suspension. The molten stearic acid is stirred vigorously with a mechanical stirrer and the abrasive suspension introduced rapidly; the water not used in the original suspension can then be used to wash in any abrasive remaining in the container. The mixture emulsifies immediately, but stirring should be continued until the emulsion cools and thickens. The paste can be conveniently stored in, and dispensed from, tin-lined lead collapsible tubes.

In normal use, a 3–4-in. ribbon of paste (containing 15–20 mg. of diamond) is rubbed well into the polishing pad. Almost any napped polishing cloth, including "Selvyt" cloth, is suitable, but a proprietary synthetic suede cloth ("Microcloth") has been found particularly satisfactory because of its high wear-resistance. For reasons discussed below, kerosene (light paraffin oil) has been adopted as the most suitable lubricant.

2. POLISHING-RATE TESTS

(a) *Method of Determining Polishing Rate*

The polishing rates (μ /min.) were calculated from the loss of weight of a clean unmounted specimen during a definite polishing period. It is difficult to standardize completely the numerous variables of a polishing process, and no attempt was made to substitute mechanical devices for the normal hand-polishing procedure, particularly as it was found that the condition of the pad was a major variable. Furthermore, it was desired to obtain some indication of the polishing rates to be expected in normal usage. All polishing was done by two experienced operators, polishing alternately for 1-min. periods, and the loss in weight was measured after a total polishing time of 5 min. Except in the first series of tests (see Section II, 2 (b)), the results of 4–6 such polishing periods were averaged. The results are thought to be comparative and reproducible in any one series to within approximately $\pm 5\%$. The synthetic suede polishing cloth and kerosene lubricant were used in all these tests.

(b) *Method of Adding Abrasive*

A comparison was made between two pads, the first charged with diamond dust shaken into a suspension in carbon tetrachloride, and the second charged by means of the impregnated carrier paste. In the former case an effort was made to distribute the abrasive particles as uniformly as possible. Both pads were charged with a total weight of 20 mg. of an (8–20) μ grade of abrasive, and the polishing rate of an annealed copper specimen (hardness 45 D.P.N.) was determined for a succession of 5-min. polishing periods.

The polishing rate of the suspension-charged pad remained substantially constant at 0.8 μ /min. The polishing rate of the paste-charged pad, however, increased rapidly with time until, after approximately 30 minutes' total polishing time, the polishing rate reached a stable value of 4.0 μ /min.—five times that of the suspension-charged pad (see Fig. 1, Plate LXXIII).

The paste-charged pads retained a high polishing rate for long periods. For example, a record was kept of the polishing rate of the paste-charged (4–8) μ -grade pad used for the tests described in Sections II, 2 (c) and II, 2 (d). It was found that the maximum polishing rate (6–7 μ /min.) was maintained on the standard annealed copper specimen for approximately 350 minutes' total polishing time; thereafter, the polishing rate decreased slowly, eventually reaching 2–3 μ /min. after a total pad life of 700 min. The fall in polishing rate is presumably due to drag-off losses of abrasive. Paste-charged pads, therefore, do not have to be regularly cleaned and recharged, as in normal practice. Provided precautions are taken against gross contamination, the pads in the author's laboratory can be used continuously without attention for several weeks, in which period several hundred specimens are polished.

The higher polishing rate of the paste-charged pads is thought to result primarily from a more even distribution of the abrasive particles. When the abrasive is added dry, or as a liquid suspension, groups of abrasive particles settle into that part of the pad which they strike first and do not appear to spread during subsequent use of the pad. With the paste the individual abrasive particles must spread with the paste; the abrasive distribution of a paste-charged pad can therefore be expected to be initially more uniform and to improve as the paste is spread during use.

In any event, it was apparent that the abrasive is most efficiently used when applied by means of a carrier paste, and all further attention was confined to such pastes. The results also indicated that it is necessary to work a polishing pad to a stable condition before any reliable polishing-rate tests can be made.

(c) Weight of Abrasive on Polishing Pad

The polishing rates of two samples, an annealed copper (hardness 45 D.P.N.) and a fully heat-treated aluminium-magnesium-chromium alloy (hardness 105 D.P.N.), were determined on pads charged with progressively increasing amounts of paste such that the weight of added abrasive increased from 10 to 120 mg. Three grades of abrasive were tested, namely (0-1) μ , (4-8) μ , and (20-30) μ particle size. The results of these tests are shown in Fig. 2 (Plate LXXIII).

The polishing rates of the (0-1) μ and (4-8) μ grades were, in the range tested, independent of the weight of abrasive. As expected, the polishing rate of the (4-8) μ grade was greater than that of the (0-1) μ grade. At low abrasive weights the polishing rate of the (20-30) μ grade was considerably less than either of the other two grades, but the polishing rate gradually increased as further abrasive was added. These observations can be interpreted by assuming that the maximum polishing rate is attained when the number of abrasive particles per unit area is not less than a certain critical value, and that the critical value is substantially independent of particle size. For the pad area used in these tests, the critical number is apparently contained in less than 10 mg. of the (0-1) μ and (4-8) μ grades, but more than 120 mg. would be required to attain the critical number in the (20-30) μ grade. It is to be noted that the number of particles per unit weight decreases as the third power of particle size.

(d) Grade of Abrasive

The results of the tests described in the preceding section indicated that, if the weight of abrasive added to the polishing pad was to be kept within reasonably economic limits (say 10-40 mg.), only the finer grades of abrasive could be used effectively. Further quantitative information as to the most suitable grades was obtained from comparative polishing-rate tests made with the annealed copper

and the heat-treated aluminium alloy specimens referred to previously, and with a B.S.970:En 9 steel heat-treated to a hardness of 250 D.P.N. The following particle-size grades were tested: (0- $\frac{1}{2}$) μ , (0-1) μ , (4-8) μ , (20-30) μ , and 300 mesh. With all grades 40 mg. of abrasive was added to the polishing pad by means of an impregnated paste. In Fig. 3 (Plate LXXIII) the polishing rates have been plotted against the maximum particle size of each abrasive grade.

It will be noted that the copper and aluminium alloy showed a maximum polishing rate at approximately the (4-8) μ grade, and steel a small maximum at the (0-1) μ grade. This information indicates that only grades in the (0-10) μ particle-size range can be used effectively in general polishing. Since the polishing rates of the finer grades of diamond abrasive do not differ greatly, it is for consideration whether the diamond abrasive pads should not be confined to one of the finer grades, say (0-1) μ . Two diamond stages are considered desirable, however, even if only to ensure that the final pad is protected from contamination. For the first or roughing pad, a coarser grade (e.g. (4-8) μ) is the most suitable in order to take advantage of the maximum polishing rate that some metals show in this range. As for the second or finishing pad, it has been found that the quality of finish obtained with (0- $\frac{1}{2}$) μ and (0-1) μ grades of abrasive is substantially the same. In both cases the maximum scratch depth appears to be largely determined by the type and condition of the polishing cloth, and it is thought, therefore, that no advantage would result from the use of even finer grades of abrasive. The (0-1) μ grade is clearly to be preferred for the finishing pad because of its higher polishing rate.

The results so far discussed were obtained with hand polishing; some consideration was also given to the use of mechanical wheels for the diamond abrasive pads. A number of tests indicated that, under otherwise similar conditions, the polishing rate of a mechanical pad rotating at 250 r.p.m. was of the order of 2-3 times that of a stationary hand pad. Although hand-operated (4-8) μ -grade diamond pads can readily cope with the surfaces produced on the wax lap described in Section III, the use of a mechanical wheel for this roughing pad greatly speeds the operation and ensures a more thorough treatment on the pad.

(e) Lubricant

No systematic survey has been made of polishing lubricants. It has been repeatedly found, however, that the pads must be maintained in a reasonably moist condition in order to achieve the maximum polishing rate. For example, the polishing rate of the aluminium alloy on a (4-8) μ -grade pad falls as low as 2-3 μ /min. when the pad is excessively dry; the addition of a small amount of kerosene restores the polishing rate to the normal value of 7-8 μ /min. Volatile lubricants, such as carbon tetrachloride, are therefore considered unsuitable, since it is virtually

impossible to maintain the polishing pad in a satisfactorily moist condition.

(f) *Material of Specimen*

It will be noted that the polishing rate of the aluminium-alloy specimen in the tests reported in Section II, 2 (d) was consistently higher than that of the copper specimen, although the hardness was over twice that of the copper. On the other hand, the polishing rate of the steel specimen of approximately twice the hardness again was only a fraction of that of the aluminium alloy. These features are in conformity with the theory advanced by Bowden and Hughes⁸ that the process of polishing is greatly influenced by the relative melting point of the abrasive and the material being polished and that the relative hardness is comparatively unimportant. To obtain

metals polish to slightly but noticeably different levels on these pads; the grain relief shown under phase-contrast illumination in the super-purity aluminium specimen of Fig. 9 (Plate LXXIV) entirely originated on the diamond abrasive pads. The effect is most noticeable in coarse-grained and non-cubic metals. It is suggested, therefore, that polishing rate is an anisotropic property. There is clearly no relationship between polishing rate and hardness.

In the last column of Table I previously published values of the electrolytic polishing rate of similar metals are also given. It will be noted that the polishing rate of metals of low and intermediate melting point on the diamond pad is usually at least of the same order as, and in most cases considerably greater than, the rate of the standard electrolytic polishing process. If, as suggested, polishing rate is

TABLE I.—*Polishing Rates of Metals in Relation to Melting Point.*

Specimen				Polishing Rate, μ /min.		
Alloy	Condition	Melting Range, $^{\circ}$ C.	Hardness, D.P.N.	Alumina Wax Lap, (10-30) μ Grade	Diamond Pad, (4-8) μ Grade	Electrolytic Polishing
Bismuth-tin-lead eutectic	As-Cast	95	11	50	16.8	...
Tin	As-Cast	231	9	30	5.9	5 ⁹
Cadmium	Annealed	321	22	25	8.8	...
Lead	Annealed	327	5	...	4.7	...
Zinc-0.25% cadmium alloy	Annealed	420	50	17	7.5	0.2 ⁹
D.T.D. 289 cast magnesium alloy	Heat-Treated	455-610	65	16	10.5	...
Aluminium alloy	Heat-Treated	580-650	105	15	8.4	0.25 ¹⁰
Aluminium alloy	Annealed	580-610	40	...	5.3	...
Aluminium	Annealed	660	25	22	5.7	3 ¹⁰
Brass (40% Zn)	Extruded	900-905	155	17	9.7	...
Brass (30% Zn)	Annealed	915-955	95	13	9.4	...
Silver	Annealed	960	30	...	7.6	...
Copper (Tough-pitch)	Annealed	1083	45	10	7.0	0.9 ⁹
Austenitic 18 : 8 stainless steel	Annealed	1400-1425	170	5	2.2	0.6 ⁹
B.S. 970 : En 9 steel	Heat-Treated	1425-1450	250	...	0.8	0.75 ¹¹
B.S. 970 : En 9 steel	As-Hardened	1425-1450	800	...	0.7	...
B.S. 970 : En 2A steel	Annealed	1450-1500	150	8	0.8	1.0 ⁹
Nickel	Annealed	1452	125	8	0.2	60 ⁹
Titanium	Annealed	1725	275	...	0.1	...

further information on this point, polishing-rate tests were carried out on a series of samples representing a range of melting points and hardness values. The specimens were tested in groups of similar melting point, and each group was compared with the annealed copper specimen, so that, by correcting the results to a polishing rate for copper of 7.0 μ /min., the effect of variation in the condition of the polishing pad could be eliminated. The results are set out in Table I, the materials being arranged in order of increasing melting point.

The results suggest there is a general relationship between the polishing rate of the diamond abrasive pad and melting point of the specimen being polished, although, when specific comparisons are made, there are a number of departures from a strict relationship. It would appear, therefore, that the polishing rate is partly dependent on features other than the melting point. Further support for this conclusion is found in the observation that the individual grains of many

related inversely to melting point, the electrolytic polishing rate of high-melting-point metals can be expected to exceed that of diamond polishing, since the former is unrelated to the melting point of the specimen.

3. SUMMARY OF OPTIMUM CONDITIONS OF USE OF DIAMOND ABRASIVES

The important features of the above experiments, so far as the practical use of diamond abrasives in general metallographic polishing is concerned, may be summarized as follows:

(a) Diamond abrasives are most efficiently used when dispersed in a carrier paste which ensures even distribution of the abrasive on the polishing pad.

(b) If the amount of abrasive added to the polishing pad is to be kept within reasonably economic limits, abrasive grades must be restricted to the (0-10) μ particle-size range. The most suitable

abrasive grades in this range are a grade of approximately $(5-10) \mu$ particle size for a roughing pad and a $(0-1) \mu$ grade for a finishing pad. An addition of 10-20 mg. of these grades is sufficient to attain the maximum polishing rate.

(c) Polishing pads charged as above do not require constant cleaning and recharging, as in normal practice, but can be used continuously over considerable periods. Abrasive costs are, therefore, nominal.

(d) The polishing rates even of hand-operated diamond abrasive pads used in this manner are very high. The polishing rate would appear to depend partly on the melting point of the specimen and partly on other factors, as yet unidentified.

III.—DEVELOPMENT OF A PRACTICAL POLISHING SYSTEM

The most serious limitation of diamond abrasives for general metallographic polishing is the restriction, on economic grounds, to relatively fine grades. There is also a limitation to the fineness of finish obtainable both because of the limited range of grades at present available and because of the influence of the polishing cloth itself on the finish. It would therefore seem that, although diamond abrasives are eminently suitable as the basis of a polishing procedure, it may be necessary to develop auxiliary stages to cover the ranges over which diamond abrasives are not suitable. The development of such stages is considered in this section of the paper.

1. PRELIMINARY PREPARATION

(a) Requirements

In spite of their high polishing rates, the coarsest practicable diamond abrasive pads cannot remove in a conveniently short period of hand polishing the scratches produced by the usual preliminary abrasive papers; even more difficulty would be experienced in ensuring removal of the deformed layer associated with such surfaces. Although it would be possible to follow the abrasive papers with a relatively long machine operation, experience has shown that it is much more satisfactory to introduce an intermediate stage of polishing, using commoner abrasives, such as alumina, between the abrasive papers and diamond pads. These remarks apply particularly to silicon carbide waterproof papers, which are available only in relatively coarse grades, but which are nevertheless preferred to the finer emery papers as being more uniform and consistent in use.

It was first recognized by Vilella,^{12, 13} Morrogh,¹⁴ and Amberg¹⁵ that an intermediate stage of the type contemplated must be of the fixed-abrasive lap type if non-metallic inclusions are to be retained, edges preserved, and excessive relief between constituents avoided. A lap of this type is essential to

ensure that the full potential of the diamond pads can be utilized.

(b) Development of Intermediate Lap

A large number of different types of fixed-abrasive laps has been developed in recent years. The earlier types consisted of a surfaced block of cast iron, lead, or paraffin wax which was charged by rolling abrasive into the surface. Laps of this type, which have been described by Amberg,¹⁵ Ellinger and Acken,¹⁶ Jarrett,¹⁷ and Ferguson,¹⁸ are satisfactory only when freshly surfaced and, consequently, are uncertain in use and require constant attention. To overcome these difficulties, Cohen and Maker¹⁹ developed a process in which the abrasive was rubbed into the surface of a strip of lead foil. The foil can be used for a short period only, and must then be discarded. Vilella¹³ has described a wax-impregnated cloth lap which is charged by rubbing abrasive into the surface; this lap can be easily cleaned and recharged. Similar pads have been in use in the author's laboratory for a number of years, and are known to operate satisfactorily when correctly prepared. The charging of such laps is, however, very critical and somewhat uncertain, and they require frequent cleaning and recharging.

An entirely different type of lap has been suggested by Dowdell and Wahl²⁰ and by Dauber,²¹ in which a mixture of molten wax and abrasive is cast on to a polishing head to form a wax-abrasive slab. This type is considered to be the most satisfactory of all tried, but the type of wax and the proportions of wax to abrasive previously suggested^{20, 21} have been found unsuitable for hand polishing. For this purpose, the wax must have a high melting point, so that it will not "pick up" during polishing, but it must also be sufficiently ductile to withstand the casting contraction stresses. A compounded wax with a melting range of 70° - 85° C. has been found to be suitable. The abrasive:wax ratio is also somewhat critical. Although, in general, this ratio should be as high as possible, an excessive abrasive concentration results in a hard lap which does not cut freely and evenly. Once the optimum ratio has been established for a particular wax and abrasive grade, the laps are quite reproducible. For the wax and abrasive used in the present work, the optimum concentration is 150 g. abrasive: 50 g. wax; this charge size being suitable for a 20-cm.-dia. lap.

The method of preparing a lap is as follows: A network of saw cuts is made in the face of a standard metal polishing head, a paper dam is fixed around the periphery of the head, and the head is mildly preheated. The wax is melted and the abrasive added and stirred in well to a uniform mixture. The mixture is then cast on to the head and allowed to cool slowly in still air. Finally, the working face is dressed flat in a lathe.

It has been found absolutely essential to use an elutriated grade of abrasive in the lap. If the finer particles of the usual bulk abrasive are not removed,

the lap clogs very rapidly and does not cut freely. The elimination of the very coarse particles is also desirable in order to obtain the maximum uniformity of finish. The most suitable grade of alumina for a lap to follow silicon carbide waterproof papers is an elutriated "20 sec." grade ($(10-30) \mu$ nominal particle size), as prepared by the method described by Rodda.²²

(c) Operation of the Intermediate Lap

The laps must be used dry, since lubricants, even water, loosen the surface abrasive and the fixed-abrasive characteristic is lost. The working surface consequently clogs with debris and must be cleaned after being used for several specimens. The cleaning is normally carried out simply by rubbing the surface with cotton wool moistened with alcohol. This treatment also removes the superficial layer of worn abrasive, and the cleaned lap is ready for immediate use in the optimum cutting condition. After extensive use the simple treatment may fail to clean the surface effectively; in addition, it may become excessively undulating. The surface should then be flooded with benzol, the surface layers softened by rubbing with the fingers and scraped off with a straight-edge, thus forming a new flat working surface. The main advantage of the lap is that it can be kept in the optimum cutting condition by these simple cleaning treatments, without the need for re-charging.

This lap is intended for hand operation while stationary; it is not suitable for use as a rotating wheel. The cutting rate by hand, however, is very high, being of the order of that attained with abrasive papers. The lap can readily deal with the finish produced on 400-mesh silicon carbide waterproof paper. For comparison with the diamond pads, the results of a number of polishing-rate tests are included in Table I; these rates were determined from the loss of weight for several 15-sec. polishing periods on freshly cleaned laps, and thus represent the maximum polishing rates. It will be noted that this series is in good agreement with Bowden and Hughes's theory of polishing.⁸ The finish produced by the lap is fine, uniform, and clean, and is a marked improvement on that produced by the finest emery papers (see Fig. 5, Plate LXXIV); the lap scratches can usually be removed in less than 1 min. of hand polishing on a $(4-8) \mu$ -grade diamond abrasive pad. This, combined with the retention of inclusions and the high degree of flatness of the surface produced, makes the lap an ideal preparation for the subsequent diamond stages.

On the basis of the correlation between polishing rate and the relative melting points of abrasive and specimen, an alumina-abrasive lap can be expected to have some limitations. It has been found in practice that materials with melting points much above 1500°C. , such as titanium, molybdenum, and tungsten, cannot be satisfactorily polished with this lap; for such materials an intermediate stage using an abrasive of higher melting point is probably

necessary. The present lap is intended, therefore, only for the more usual lower-melting-point metals.

2. FINAL POLISHING

The finish produced by the finer diamond abrasive pads has been reported to be satisfactory as a final polish for many ferrous materials.^{2,6} As noted by Perryman,³ however, the finest diamond finish on the usual non-ferrous materials shows noticeable scratches, and a further final polishing stage is desirable for photomicrography. A Selvyt cloth pad charged with a fine grade of alumina is usually recommended for this purpose.³⁻⁵ The author's preference is for calcined magnesium oxide for the final polishing stage; it has been found, moreover, that this treatment also results in an appreciable improvement in the finish of many ferrous materials.

It is doubtful, however, whether surfaces finished by either of these methods are truly scratch-free. The as-polished surface may appear to be satisfactory when examined in normal bright-field illumination, but more critical examination under oblique illumination or, more particularly, under phase-contrast illumination usually reveals a maze of fine background scratches. For example, the specimen of as-cast super-purity aluminium shown under phase-contrast illumination in Fig. 8 (Plate LXXIV) was finished by the usual technique on a hand-operated magnesium oxide pad and appeared to be substantially free from scratches under bright-field illumination, as does the matrix of Fig. 7 (Plate LXXIV). Whether or not an etched specimen appears to be scratched depends on the characteristics of both the etching reagent and the material of the specimen. When the etch is light and the matrix still highly reflecting, the surface will appear unscratched in bright-field illumination; if, however, the etch removes little material and is of the colouring or staining type, the scratches may be made quite obvious. A heavy etch frequently removes completely the scratched surface layer.

It is thought that the major scratches produced on a magnesium-oxide pad result from the polishing cloth rather than the abrasive. On this basis, the following final polishing technique was evolved. The magnesium oxide is mixed into a very thick paste with water and pushed through a fine-mesh sieve on to the polishing pad; the sieving treatment serves both to remove extraneous grit and to break up the paste into a smooth thick cream. The paste is spread over the surface of the polishing cloth and the pad operated with a light pressure so that the specimen skids over a packed bed of paste without touching the nap of the cloth. This technique is capable of producing surfaces which, even in the softest low-melting-point metals, appear scratch-free under phase-contrast illumination. The super-purity aluminium specimen finished by the "skidding" technique is shown in Fig. 9 (Plate LXXIV) for comparison with Fig. 8 (Plate LXXIV); some shallow undulations are present in the surface, apparently

because the major grooves produced on the (0-1) μ -grade diamond pad are partly reproduced even after extensive periods of polishing, but there is no evidence of scratches as such. The specimens of tin and zinc shown in Figs. 10 and 11 (Plate LXXIV) were prepared by this method, and apparently are also completely free from scratches.

The polishing rate of such a pad is of the same order as that of normal magnesium-oxide pads and, if the pad is operated on a low-speed mechanical wheel, the polishing is quite adequate for finishing the lower-melting-point non-ferrous metals; this applies to metals with a melting point at least as high as that of aluminium. It is usually even possible to remove (0-1) μ diamond scratches on higher-melting-point metals in a reasonable time (less than 5 min.), but it may not be practicable to remove completely the deformation beneath these scratches. In such cases, it has been found necessary to increase the polishing rate by the use of a "polish-attack" technique. It is possible to control such a technique to a high degree in the present process by using a definite concentration of the required etching reagent in the solution used for mixing the magnesium-oxide paste.

Among the commoner alloys only copper and copper alloys, in the author's experience, require a polish-attack technique. The usual etching reagents for these alloys seem to be particularly sensitive in revealing the deformation zones associated with the previous system of diamond scratches. Ammonium persulphate has been found to be the most suitable reagent, the concentration required in the paste solution differing somewhat for the various alloys and final etching methods; a concentration of the order of 10-15 g./l. is suitable for copper and 15-30 g./l. for alloys such as high-zinc α -brasses.

One further precaution is necessary when this technique is used with metals, such as aluminium and zinc, which are strongly electropositive with respect to the copper alloys normally used for polishing heads. Severe etch-pitting may develop in these cases as a result of electrolytic effects between the specimen and the polishing head. The effect can be completely prevented, however, by fitting a thin disc of an insulating material between the polishing cloth and head. This precaution was taken during the final polishing of the aluminium and zinc specimens shown in Figs. 9 and 11 (Plate LXXIV), respectively.

IV.—SUMMARY AND DISCUSSION

The main results of the investigation have been, first, that the methods of obtaining the maximum polishing rates with diamond abrasives have been established and, secondly, that it has been possible to evolve a system of metallographic polishing based on diamond abrasives, the abrasive costs for which are so low as to permit its use for general, and even routine, polishing. The stages of this system are summarized below:

(1) *Abrasive Papers.*

Silicon carbide waterproof papers used with flowing water lubricant.

(a) 220-mesh grade.

(b) 400-mesh grade.

(2) *Intermediate Lap.*

Cast wax-abrasive lap charged with (10-30) μ -grade elutriated alumina. Used dry; hand-operated.

(3) *Diamond Abrasive Pads.*

Impregnated paste on napped cloth. Kerosene lubricant; hand or preferably machine operation.

(a) Roughing stage; (4-8) μ grade (optional).

(b) Finishing stage; (0-1) μ grade.

(4) *Finish Polishing.*

Magnesium oxide used on Selyvt cloth in one of the following manners. Hand or machine operation.

(a) As a slurry.

(b) As a thick paste with water, so that the specimen skids over a bed of paste.

(c) As in (b); paste made with a dilute solution of a suitable etching reagent.

The treatment of all the usual specimens is the same up to the finish-polishing stage; the most suitable method of finish polishing for a particular type of specimen must be determined by trial. The major portion of the polishing takes place on diamond pads, so that the overall process is extremely rapid. The average preparation time to the end of the diamond stages never exceeds 5 min.; the time required for final polishing depends on the specimen, but, even with the skidding techniques, it rarely exceeds 5 min., and is usually of the order of 1-2 min.

As a typical example, the surface condition of an unmodified aluminium-13% silicon alloy at the major stages of the process is illustrated in Figs. 4-7 (Plate LXXIV); the specimen was finished by Method (4a) above. This series illustrates particularly the uniform clean finish, free from relief, obtained on the wax lap, the improvement resulting from the magnesium-oxide final polish, and the high quality of the final result.

Although the rapidity of the process is an important advantage, an even more important feature associated with the use of diamond abrasives is the marked improvement in the quality of the polish produced. This results from low relief between constituents and dissimilar zones, the high degree of flatness of the surface, the sharp retention of edges, and the complete retention of non-metallic inclusions—features which have been fully discussed by previous authors.^{1, 3, 4, 5} Furthermore, considerably less skill is required on the part of the operator to obtain such results. It is considered that in these respects the use of diamond abrasives represents a major advance in metallographic technique.

It has also been noted that surfaces produced by this process are invariably free from polishing arti-

facts, i.e. deformation of the surface during polishing which is detectable during the microscopic examination. Two metals that are notoriously difficult to prepare to a truly representative surface by mechanical polishing have been selected as examples, namely, tin and zinc. Mechanically polished specimens of tin frequently contain artifacts in the form of a fine-grained recrystallized layer or mechanical twins,^{5, 23} which, in previous polishing systems, required removal by a laborious series of alternate polishing and etching treatments.⁵ Tin specimens prepared by the present method are invariably free from such defects on the first etch (see Fig. 10, Plate LXXIV); if present, the depth of the deformed layer on the as-polished surface must therefore be less than the thickness removed by etching.

Specimens of zinc when polished by the present method show no evidence of the mechanical twins that are so characteristic of specimens prepared by earlier polishing methods.^{23, 24} The specimen shown in Fig. 11 (Plate LXXIV) was photographed in the unetched condition in polarized light; in this case, therefore, the as-polished surface itself is established to be true. The high polarization contrast in Fig. 11 is also of interest, as it has previously been suggested that it is not possible to obtain optimum grain contrast under polarized light on mechanically polished surfaces of zinc.^{23, 25} It is to be emphasized that both

these specimens were polished by the standard method and were not etched between stages; the tin specimen was given only the one final etch after polishing, whereas the zinc specimen was not etched at any stage.

It has been noted that the only precaution necessary to produce artifact-free surfaces in such sensitive specimens is to ensure that the specimen is given a thorough treatment on the (4–8) μ -grade diamond pad. It is thought that the artifacts normally found on mechanically polished surfaces largely originate in the early abrasion stages. The high cutting rate of the diamond abrasive pad apparently effects the complete removal of the deformed layer produced in these stages without itself seriously deforming the surface. It is clear, however, that this aspect requires further investigation, and such an investigation is in hand.

ACKNOWLEDGEMENTS

The author wishes to acknowledge the assistance received from Mr. G. J. Wright in the development of the carrier paste and from Mr. P. G. McDougall and Mr. A. S. Malin, who carried out the polishing-rate tests. He is indebted to the Chief Scientist, Department of Supply (Australia), for permission to publish this paper.

REFERENCES

1. G. C. Woodside and H. H. Blackett, *Metal Progress*, 1947, **51**, 945.
2. L. P. Tarasov and C. O. Lundberg, *ibid.*, 1949, **55**, 183.
3. E. C. W. Perryman, *J. Inst. Metals*, 1950, **77**, 61.
4. J. E. Davies and W. E. Hoare, *J. Iron Steel Inst.*, 1951, **168**, 134.
5. L. T. Greenfield and J. E. Davies, "The Preparation of Tin and Tin Alloys for Microscopical Examination". Greenford: 1951 (Tin Research Institute).
6. D. J. Blickwede, M. Cohen, and G. A. Roberts, *Trans. Amer. Soc. Metals*, 1950, **42**, 1161.
7. P. Grodzinski, *Indust. Diamond Rev.*, 1950, **10**, 122.
8. F. P. Bowden and T. P. Hughes, *Proc. Roy. Soc.*, 1937, [A], **160**, 575.
9. P. A. Jacquet, *Métaux, Corrosion-Usure*, 1943, **18**, 1.
10. P. A. Jacquet, "Le Polissage Electrolytique des Surfaces Métalliques et Ses Applications". Tome I. Paris: 1948 (Editions Métaux).
11. H. J. Merchant, *J. Iron Steel Inst.*, 1947, **155**, 179.
12. J. R. Vilella, *Metals and Alloys*, 1932, **3**, 205.
13. J. R. Vilella, "Metallographic Technique for Steels". Cleveland: 1937 (American Society for Metals).
14. H. Morrogh, *J. Iron Steel Inst.*, 1941, **143**, 195.
15. K. Amberg, *Metal Progress*, 1940, **37**, 146.
16. G. A. Ellinger and J. S. Acken, *Trans. Amer. Soc. Metals*, 1939, **27**, 382.
17. T. C. Jarrett, *ibid.*, 1939, **27**, 758.
18. M. Ferguson, *Metal Progress*, 1943, **43**, 743.
19. J. B. Cohen and J. H. Maker, *ibid.*, 1945, **47**, 509.
20. R. L. Dowdell and M. J. Wahll, *Metals and Alloys*, 1933, **4**, 181.
21. C. J. Dauber, *Metal Progress*, 1946, **49**, 347.
22. J. L. Rodda, *Trans. Amer. Inst. Min. Met. Eng.*, 1932, **99**, 149.
23. B. W. Mott and H. R. Haines, *J. Inst. Metals*, 1951–52, **80**, 629.
24. L. Capdecombe and M. Orliac, *Compt. rend.*, 1941, **213**, 383.
25. E. C. W. Perryman, "Polarized Light in Metallography" (Edited by G. K. T. Conn and F. J. Bradshaw), p. 70. London: 1952 (Butterworths Scientific Publications).
26. L. G. Tottle, *Bull. Inst. Metals*, 1953, **1**, (18), 146.

By PROFESSOR E. A. OWEN,† M.A., D.Sc., MEMBER, and
E. A. O'DONNELL ROBERTS,‡ M.Sc., Ph.D.

SYNOPSIS

The X-ray measurements that have been made to determine the solubility of indium in copper, and thus the α -phase boundary of the copper-indium system over the range of temperature from 710° to 470° C., are recorded. The maximum solubility of indium in copper is found to be 10.9₀ at.-% at 575° C.; the solubility at the peritectic temperature (710° C.) is 10.0₅ and at 500° C., 8.1₀ at.-%.

I.—INTRODUCTION

IN a recent paper by Owen and Morris¹ some unpublished results on the solubility of indium in copper in the temperature range between about 470° and 710° C., were quoted in support of the view that X-ray measurements are capable of yielding results which fix the positions of phase boundaries in equilibrium diagrams of alloy systems as accurately at high as at low temperatures. The purpose of the present paper is to place on record the measurements made in arriving at the solubility values quoted in the earlier paper.

The technique developed to produce ingots of alloys in a state of equilibrium, homogeneous and of known composition, has been described in some detail in a paper by the present authors on the solubility of certain metals in gold,² and has been further explained and amplified in the discussion³ on the paper by Owen and Morris. There is therefore no need to go into further detail here, and only the briefest account of essential experimental procedure will be given.

II.—EXPERIMENTAL TECHNIQUE

The alloys were prepared from copper and indium of purities 99.95 and 99.98%, respectively, in $\frac{1}{2}$ -g. ingots, by fusion in quartz tubes. A preliminary investigation was carried out to find how quenching in oil compared with quenching in water as far as the production of homogeneous alloys was concerned. It was definitely demonstrated that for these alloys quenching in water was by far the more satisfactory method. Several alloys were prepared and quenched in water from 20°–50° C. above the liquidus temperatures. Weight losses in the alloys after annealing amounted to less than 1 part in 3000 in five of the alloys, and to 1 part in 2000 in two. Before examination, alloys containing 2.55, 5.08, 9.12, and 10.84 at.-% indium were lump-annealed at 600° C. for 19 days and alloys containing 1.38, 3.78, and 5.83 at.-% indium at 700° C. for 14 days.

III.—RELATION BETWEEN LATTICE
PARAMETER AND COMPOSITION

The lattice-parameter measurements showed that the alloys, prepared in the form of small cylinders, were fairly free from segregation. The figures given

TABLE I.— α -Phase Lattice Parameters of Copper-Indium Alloys at 18° C.

Indium Content, at.-%	Specimen and Lattice Parameter, kX					Estimated Lattice Parameter, kX
	A	B	C	D	E	
1.38	3.6204	3.6202 ₅	3.6201	3.6198	3.6206	3.6201
2.55	3.6316	3.6311	3.6310	3.6313	3.6310	3.6310
3.78	3.6428	3.6426 ₅	3.6427 ₅	3.6432	3.6432	3.6427 ₅
5.08	3.6546	3.6547	3.6550	3.6547	3.6550	3.6550
5.83	3.6615	3.6618	3.6620	3.6620	3.6623	3.6620
9.12	3.6927	3.6926	3.6922 ₅	3.6917	3.6922 ₅	3.6922 ₅
10.84	3.7074	3.7072	3.7072 ₄	3.7069	3.7072	3.7072 ₄

in Table I show the variation in lattice parameter observed in samples taken from different parts of the ingot. Samples A, C, and B were taken respectively from the outside surface, central longitudinal section, and a longitudinal section at a distance about half the radius of the ingot from the central section; samples D and E were taken from the two ends of the ingot. It will be observed that the greatest difference between the lattice-parameter values is found in the end samples of alloy containing 1.38 at.-% indium; this amounts to 0.0008 kX, which corresponds to less than 0.1 at.-% in composition.

The values shown in the last column, which are the same as those in column C, were considered to be the most representative and were used to draw the curve showing the relation between lattice parameter and composition across the α -phase region. These are included in Fig. 1 with those of Weibke and Eggers,⁴ who were the first to investigate this system of alloys. On the whole there is fair agreement between the two results. Most of the points obtained in the present

* Manuscript received 13 February 1953.

† Physics Department, University College of North Wales, Bangor.

‡ Formerly of University College of North Wales, Bangor; now Chief Development Engineer, Mullard Radio Valve Co., Ltd., Mitcham, Surrey.

investigation lie within 0.0002 kX of the curve drawn in the diagram.

IV.— α -PHASE BOUNDARY BETWEEN 710° AND 470° C.

Several ingots of composition within the adjacent two-phase regions were prepared, from which powder specimens were taken, annealed at different temperatures, and quenched in cold water. Nickel radiation was used to obtain the photographs. Table II

occurs at this temperature. The temperature of the reaction agrees closely with the value 574° C. found by Weibke and Eggers.

Since most of the experimental values of the α -phase lattice parameters are within 0.0002 kX of the parameter/composition curve, there is justification in assuming the lattice parameter of the α -phase alloys read from the parameter/composition curve to be correct to within ± 0.0002 kX.

At temperatures above 575° C. it is considered that the solubility values are correct to within ± 0.05 at.-%

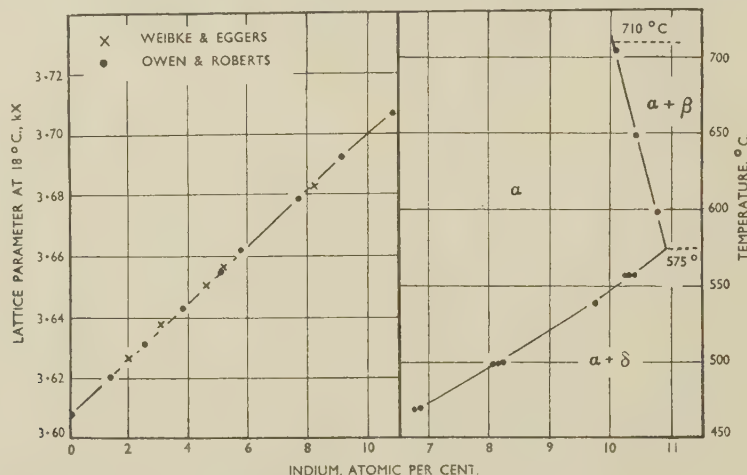


Fig. 1.—Lattice Parameter/Composition Curve for Copper-Indium α -Phase Alloys.

Fig. 2.— α -Phase Boundary of Copper-Indium Alloy System Between 715° and 470° C.

contains the results of measurements made on samples of alloys annealed between 704° and 469° C., alloys which were considered to have reached the equilibrium

TABLE II.—Data to Determine the α -Phase Boundary.

Annealing Treatment		Lattice Parameters at 18° C., kX				Boundary Point, at.-% In
		Indium Content, at.-%				
Time, hr.	Temp., °C.	7.66	9.12	10.84	11.89	
0.25	704	3.7011 ₅	3.7011	10.1 ₁
1	649	3.7040	3.7041 ₅	10.4 ₃
0.75	599	3.7069		} 10.7 ₅
2.5	599	3.7069 ₅		
2	598	3.7070	10.7 ₆
2	557	3.7036	...	10.3 ₈
2	557	3.7025	10.2 ₆
2.5	558	3.7030	10.3 ₂
2.5	538	3.6979	9.7 ₅
2	500	...	3.6837 ₅	8.2 ₀
4	499	3.6830	...	8.1 ₂
4	499	3.6825	8.0 ₆
5	469	3.6705 ₅	6.7 ₇
5	469	...	3.6713	3.6713	...	6.8 ₅

state. The temperature range is that shown in Fig. 6 (p. 160) of the paper by Owen and Morris.¹

The results are shown in Fig. 2. The α -phase boundary shows a sharp discontinuity at 575° C. corresponding to the eutectoid transformation $\beta \rightarrow (\alpha + \delta)$; maximum solution, 10.9 at.-% indium,

after allowing ± 0.0002 kX for errors in the two-phase parameter values. Below 575° C. errors are introduced not so much through errors in parameter, as through errors in temperature measurement, since an error of 1° C. is equivalent to 0.04 at.-% in composition.

The accuracy of the final figures given for the position of the boundary at temperatures below 575° C., can be placed at about ± 0.2 at.-%, which includes errors in pure and in mixed lattice-parameter values.

It will be necessary to conduct a further investigation with even purer metals to check this boundary, especially since at temperatures below 575° C. the solubility is found to exceed that determined by metallurgical methods, which is contrary to the usual findings. It would be desirable also to extend the boundary to still lower temperatures. Such an investigation is now nearing completion, so that the results will shortly be available.

REFERENCES

1. E. A. Owen and D. P. Morris, *J. Inst. Metals*, 1949-50, **76**, 145.
2. E. A. Owen and E. A. O'D. Roberts, *ibid.*, 1945, **71**, 213.
3. E. A. Owen and D. P. Morris, *ibid.*, 1949-50, **76**, 677 (discussion).
4. F. Weibke and H. Eggers, *Z. anorg. Chem.*, 1934, **220**, 273.

By J. G. RIGG,† Ph.D., and E. W. SKERREY,‡ B.Sc., A.I.M.

(Joint contribution from the Research Laboratories of The British Aluminium Company, Ltd., Chalfont Park, Gerrards Cross, Bucks., and the Imperial Smelting Corporation, Ltd., Widnes, Lancs.)

SYNOPSIS

The results obtained from the exposure of light alloy specimens for 6 months in rural, industrial, and marine atmospheres, with various primers under aluminium top coats, have been published previously, and the present paper gives the further information obtained on continuation of the tests for 3½ years.

The results confirmed earlier indications. Zinc chromate and zinc tetroxychromate primers were superior in protective value to iron oxide primer, although the latter provided satisfactory protection, especially to aluminium in the less severe environments. Red lead primer was definitely harmful on light alloys, and especially on magnesium in corrosive environments. In these tests both types of chromate primer were found to be slightly preferable to red lead on mild steel. Zinc chromate and zinc tetroxychromate pigments are preferred for primers for composite structures of steel and light alloys in severe exposure conditions, while iron oxide is adequate for milder conditions.

I.—INTRODUCTION

THIS paper records the final results obtained, after 3½ years, from tests comparing the protective behaviour of various paint primers on aluminium and magnesium alloys and mild steel in rural, industrial, and marine atmospheres. The tests were designed primarily to determine the relative protection given by certain priming pigments when applied to light alloys, and the comparison was simplified by the use of single pigments. The four pigments selected were zinc chromate, zinc tetroxychromate, iron oxide, and red lead. Priming coats

No attempt to clean or maintain the test panels has been made during the tests. Representative singleton withdrawals of all the paint-metal systems have been made periodically for detailed laboratory examination, and all specimens have been examined *in situ* at intervals of approximately 6 months. The specimens have been examined by the methods previously used.¹

II.—RESULTS OF EXPOSURE TESTS

The results obtained at the completion of the tests, after exposure for up to 3½ years, are summarized

TABLE I.—Analysis of Metals Included in Tests.

Material	C, %	Si, %	Fe, %	Cu, %	Mn, %	Zn, %	Mg, %	Al, %	S, %	P, %
Aluminium	0.24	0.31	0.008	0.008	0.010	...	*
B.S.S. 5L3	0.54	0.40	3.95	0.59	0.018	0.60	*
D.T.D. 120A, high-purity base	0.006	0.0005	0.006	0.42	0.93	*	6.10
D.T.D. 118, normal-purity base	0.005	0.021	0.004	1.54	0.005	*
D.T.D. 59A, normal-purity base	0.010	0.022	0.002	0.28	0.59	*	7.70
D.T.D. 59A, high-purity base	0.010	0.0010	0.002	0.18	0.58	*	7.83
Steel	0.16	<0.01	*	...	0.26	0.040	0.027

* Remainder.

based on these four pigments, in a phenolic-linseed stand oil-oiticica oil varnish medium, were tested both alone and under two coats of aluminium in (i) medium-length linseed-oil-modified alkyd resin (D.T.D. 260A) and (ii) nitrocellulose non-drying alkyd resin media (D.T.D. 63A). Full details of the design of the tests and the results obtained after exposure for about 6 months have been given in a previous paper.¹ The chemical analyses of the metals tested are reproduced in Table I.

below and in Tables II–VI. The results for the whole investigation are summarized in Table VI by quoting the approximate times required for the various panels to suffer slight corrosion. In assessing these values, all types of corrosion, including scratch-line effects, have been considered. Typical photographs of specimens withdrawn from the marine site are given in Figs. 1–3 (Plates LXXXV–LXXXVII).

The severity of the exposure conditions decreased in the order: marine (Dungeness, Kent), accelerated

* Manuscript received 2 December 1952.

† Research Department, Imperial Smelting Corporation, Ltd., Widnes, Lancs.

‡ Research Laboratories of The British Aluminium Co., Ltd., Chalfont Park, Gerrards Cross, Bucks.

TABLE II.—Summary of Results for Dungeness (Marine Tests) Specimens after 3½ Years' Exposure.

Paint System	Main Paint Failures and Corrosion						
	Aluminium (99.5%)	B.S.S. 5L3	D.T.D. 120A, high purity	D.T.D. 118, normal purity	D.T.D. 59A, high purity	D.T.D. 59A, normal purity	Steel
Zinc chromate primer (c).	Trace of flaking.	Trace of flaking.	Very slight flaking, very slight local corrosion, and trace of cor- rosion at scratch.	*Considerable local corrosion, con- siderable pitting, and very slight corrosion at scratch.	Slight flaking, very slight local cor- rosion, very slight pitting, and trace of cor- rosion at scratch.	*Moderate flaking, moderate local corrosion, moder- ate pitting, and moderate cor- rosion at scratch.	*Moderate local corrosion and very slight cor- rosion at scratch.
Zinc chromate primer + D.T.D. 63A top coat (g).	Slight flaking.	Moderate flaking, slight local cor- rosion, very slight pitting, and trace of corrosion at scratch.	Considerable flak- ing, very slight local corrosion, very slight pit- ting, and trace of corrosion at scratch.	Severe flaking, con- siderable local corrosion, con- siderable pitting, and very slight corrosion at scratch.	Considerable flak- ing, very slight local corrosion, and trace of pit- ting, and trace of corrosion at scratch.	Moderate flaking, moderate local corrosion, moder- ate pitting, and considerable cor- rosion at scratch.	*Moderate local corrosion and slight corrosion at scratch.
Zinc chromate primer + D.T.D. 260A top coat (i).	Very slight flaking.	Moderate flaking.	Severe flaking, trace of pitting, and trace of cor- rosion at scratch.	Very severe flak- ing, slight local corrosion, moder- ate pitting, and trace of corrosion at scratch.	Trace of flaking, trace of pitting, and trace of cor- rosion at scratch.	Moderate flaking, moderate local corrosion, con- siderable pitting, and considerable corrosion at scratch.	*Slight local cor- rosion and slight corrosion at scratch.
Zinc tetroxy- chromate primer (d).	Moderate erosion.	Slight erosion and trace of pitting.	Very slight erosion and flaking, very slight local cor- rosion, trace of pitting, very slight corrosion at scratch.	Slight erosion and flaking, consider- able local cor- rosion, moderate pitting, and slight corrosion at scratch.	Slight erosion and flaking, slight local corrosion, very slight pit- ting, and slight corrosion at scratch.	*Severe erosion and flaking, consider- able local cor- rosion, and severe corrosion at scratch.	*Moderate local corrosion and moderate cor- rosion at scratch.
Zinc tetroxy- chromate primer + D.T.D. 63A top coat (h).	Slight flaking.	Slight flaking.	Moderate flaking, very slight local corrosion, trace of pitting, and very slight cor- rosion at scratch.	Considerable flak- ing, moderate local corrosion, moderate pitting, and very slight corrosion at scratch.	Moderate flaking, very slight local corrosion, slight pitting, and very slight corrosion at scratch.	Very slight flaking, considerable local corrosion, con- siderable pitting, and severe cor- rosion at scratch.	*Moderate local corrosion and very severe cor- rosion at scratch.
Zinc tetroxy- chromate primer + D.T.D. 260A top coat (m).	Very slight flaking.	Considerable flak- ing.	Very severe flak- ing, very slight local corrosion, trace of pitting, and trace of cor- rosion at scratch.	Severe flaking, moderate local corrosion, moder- ate pitting, and very slight cor- rosion at scratch.	Slight flaking, very slight local cor- rosion, trace of pit- ting, and trace of corrosion at scratch.	Very slight flaking, considerable local corrosion, con- siderable pitting, and considerable corrosion at scratch.	*Slight local cor- rosion and moder- ate corrosion at scratch.
Red lead primer (e).	Considerable chalk- ing, moderate local corrosion, moderate pitting, and moderate cor- rosion at scratch.	Considerable chalk- ing, considerable local corrosion, moderate pitting, and severe cor- rosion at scratch.	All specimens with- drawn after 4 months (Table VI).	All specimens with- drawn after 4 months (Table VI).	All specimens with- drawn after 4 months (Table VI).	All specimens with- drawn after 4 months (Table VI).	*Moderate local corrosion and slight corrosion at scratch.
Red lead primer + D.T.D. 63A top coat (f).	Trace of crumbling, moderate local corrosion, moder- ate pitting, and considerable cor- rosion at scratch.	Trace of crumbling, considerable local corrosion, moder- ate pitting, and very severe cor- rosion at scratch.	All specimens with- drawn after 1½ years (Table VI).	All specimens with- drawn after 1½ years (Table VI).	Very severe crum- bling, consider- able local cor- rosion, considerable pitting, and very severe corrosion at scratch.	*Very severe crum- bling, moderate local corrosion, considerable pit- ting, and very severe corrosion at scratch.	*Moderate local corrosion and severe corrosion at scratch.
Red lead primer + D.T.D. 260A top coat (n).	Trace of crumbling, slight local cor- rosion, moderate pitting, and con- siderable cor- rosion at scratch.	Trace of crumbling, considerable local corrosion, moder- ate pitting, and very severe cor- rosion at scratch.	All specimens with- drawn after 1½ years (Table VI).	All specimens with- drawn after 1½ years (Table VI).	Very severe crum- bling, consider- able local cor- rosion, considerable pitting, and very severe corrosion at scratch.	*Very severe crum- bling, severe local corrosion, con- siderable pitting, and very severe corrosion at scratch.	*Moderate local corrosion and severe corrosion at scratch.
Iron oxide primer (f).	Slight chalking, very slight local corrosion, and very slight cor- rosion at scratch.	Moderate chalking, slight local cor- rosion, trace of pit- ting, and very slight corrosion at scratch.	Very slight chalk- ing, very slight local corrosion, moderate pitting, and trace of cor- rosion at scratch.	*Slight chalking, moderate local corrosion, and very slight cor- rosion at scratch.	Slight chalking, slight local cor- rosion, very slight pitting, and trace of corrosion at scratch.	*Very severe flak- ing, considerable local corrosion, moderate pitting, and very severe corrosion at scratch.	*Moderate local corrosion and very severe cor- rosion at scratch.
Iron oxide primer + D.T.D. 63A top coat (k).	Slight flaking, very slight local cor- rosion, and very slight corrosion at scratch.	Considerable flak- ing, slight local corrosion, trace of pitting, and very slight corrosion at scratch.	Slight flaking, very slight local cor- rosion, moderate pitting, and slight corrosion at scratch.	Very severe flak- ing, severe local corrosion, severe pitting, and slight corrosion at scratch.	Severe flaking, slight local cor- rosion, slight pit- ting, and trace of corrosion at scratch.	Severe flaking, severe local cor- rosion, consider- able pitting, and severe corrosion at scratch.	*Moderate local corrosion and very severe cor- rosion at scratch.
Iron oxide primer + D.T.D. 260A top coat (o).	Slight flaking, very slight local cor- rosion, and trace of corrosion at scratch.	Considerable flak- ing, very slight local corrosion, trace of pitting, and very slight corrosion at scratch.	Severe flaking, very slight local corrosion, slight pitting, and very slight corrosion at scratch.	Very severe flak- ing, severe local corrosion, con- siderable pitting, and slight cor- rosion at scratch.	Considerable flak- ing, slight local corrosion, very slight pitting, and trace of corrosion at scratch.	Severe flaking, severe local cor- rosion, consider- able pitting, and severe corrosion at scratch.	*Slight local cor- rosion and very severe corrosion at scratch.
Plain metal (untreated) (a).	Slight to moderate general corrosion, and trace of pit- ting.	Moderate general corrosion and trace of pitting.	Slight general cor- rosion and moder- ate pitting.	*Severe general corrosion and moderate pitting.	Slight general cor- rosion and moder- ate pitting.	Considerable gen- eral corrosion and moderate pitting.	All specimens with- drawn after 1½ years (Table VI).
Plain metal (chromated or pickled) (b).	Slight to moderate general corrosion and trace of pit- ting.	Moderate general corrosion and trace of pitting.	Slight general cor- rosion and slight pitting.	*Severe general corrosion and moderate pitting.	Slight general cor- rosion and moder- ate pitting.	Considerable gen- eral corrosion and moderate pitting.	*Very severe gen- eral corrosion.

* All material withdrawn after 2½ years (results given after 2½ years).

TABLE III.—Summary of Results for Widnes (Industrial) Specimens after 3½ Years' Exposure.

Paint System	Main Paint Failures and Corrosion				
	Aluminium (99.5%)	B.S.S. 5L3	D.T.D. 118, normal purity	D.T.D. 59A, normal purity	Steel
Zinc chromate primer (c).	Slight pitting on back only and trace of corrosion at scratch.	Slight local corrosion on back only, very slight pitting on front only, and very slight corrosion at scratch.	*Trace of flaking and slight to moderate pitting on back only.	*Trace of flaking, slight local corrosion, and slight corrosion at scratch.	*Moderate local corrosion on front only, moderate general corrosion on back only, and severe corrosion at scratch.
Zinc chromate primer + D.T.D. 63A top coat (g).	Considerable flaking at scratch and very slight corrosion at scratch.	Very slight corrosion at scratch.	Slight flaking on front, very severe flaking on back, moderate local corrosion on back only, slight pitting on front only, and trace of corrosion at scratch.	*Very slight flaking.	Considerable flaking at scratch only, moderate local corrosion, and considerable corrosion at scratch.
Zinc chromate primer + D.T.D. 260A top coat (l).	Trace of corrosion at scratch.	Trace of corrosion at scratch.	Severe flaking, moderate local corrosion, and trace of corrosion at scratch.	*None.	Severe flaking at scratch only, very slight local corrosion on front only, and considerable corrosion at scratch.
Zinc tetroxychromate primer (d).	Considerable erosion, slight local corrosion on front only, slight pitting on back only, and trace of corrosion at scratch.	Severe erosion, moderate local corrosion on front only, slight pitting on back only, and very slight corrosion at scratch.	Severe erosion, moderate local corrosion, and very slight corrosion at scratch.	*Trace of flaking, slight local corrosion, and slight corrosion at scratch.	*Moderate local corrosion and severe corrosion at scratch.
Zinc tetroxychromate primer + D.T.D. 63A top coat (h).	Trace of corrosion at scratch.	Very slight corrosion at scratch.	Considerable flaking at scratch only and trace of corrosion at scratch.	*Trace of flaking.	Severe flaking at scratch only, slight to moderate local corrosion, and very severe corrosion at scratch.
Zinc tetroxychromate primer + D.T.D. 260A top coat (m).	Trace of corrosion at scratch.	Trace of corrosion at scratch.	Slight flaking at scratch only and trace of corrosion at scratch.	*None.	Severe flaking at scratch only and very severe corrosion at scratch.
Red lead primer (e).	Moderate chalking, severe general corrosion on back only, moderate pitting on front only, and slight corrosion at scratch.	Moderate chalking, considerable local corrosion on front only, severe general corrosion on back only, and slight corrosion at scratch.	All specimens withdrawn after 8 months (Table VI).	All specimens withdrawn after 8 months (Table VI).	All specimens withdrawn after 1½ years (Table VI).
Red lead primer + D.T.D. 63A top coat (j).	Moderate local corrosion, slight pitting, and very slight corrosion at scratch.	Considerable local corrosion, moderate pitting, and slight corrosion at scratch.	Very severe flaking, considerable general corrosion, and very slight corrosion at scratch.	*Severe flaking at scratch and moderate corrosion at scratch.	Severe corrosion at scratch.
Red lead primer + D.T.D. 260A top coat (n).	Slight corrosion at scratch.	Slight pitting on back only and very slight corrosion at scratch.	Moderate flaking on back only, considerable local corrosion on front only, and considerable corrosion at scratch.	*Severe flaking at scratch, moderate local corrosion, and slight corrosion at scratch.	Very slight local corrosion and severe corrosion at scratch.
Iron oxide primer (f).	Severe chalking, slight local corrosion, slight pitting, and very slight corrosion at scratch.	Severe chalking, considerable local corrosion, moderate pitting, and slight corrosion at scratch.	Very severe flaking and considerable general corrosion.	*Moderate chalking and slight flaking, considerable flaking at scratch, moderate local corrosion, and very slight corrosion at scratch.	All specimens withdrawn after 1½ years (Table VI).
Iron oxide primer + D.T.D. 63A top coat (k).	Slight flaking on back only, slight local corrosion, and slight corrosion at scratch.	Slight corrosion at scratch.	Very severe flaking, moderate local corrosion, and very slight corrosion at scratch.	*Considerable flaking and trace of pitting.	Considerable flaking at scratch only, moderate to considerable local corrosion, slight pitting, and very severe corrosion at scratch.
Iron oxide primer + D.T.D. 260A top coat (o).	Trace of pitting, and very slight corrosion at scratch.	Trace of corrosion at scratch.	Very severe flaking and considerable local corrosion.	*Slight flaking and slight local corrosion.	Slight flaking at scratch only, slight local corrosion on back only, and very severe corrosion at scratch.
Plain metal (untreated) (a).	Slight to moderate general corrosion.	Moderate general corrosion.	Considerable general corrosion and slight pitting.	*Moderate general corrosion and slight to moderate pitting.	Very severe general corrosion.
Plain metal (chromated or pickled) (b).	Slight to moderate general corrosion.	Moderate general corrosion.	Moderate general corrosion and moderate pitting.	*Moderate general corrosion and slight to moderate pitting.	Very severe general corrosion.

* All material withdrawn after 2½ years (results given after 2½ years).

TABLE IV.—Summary of Results for Frodsham (Rural) Specimens after 3½ Years' Exposure.

Paint System	Main Paint Failures and Corrosion				
	Aluminium (99.5%)	B.S.S. 5L3	D.T.D. 118, normal purity	D.T.D. 59A, normal purity	Steel
Zinc chromate primer (c).	None.	None.	Moderate pitting on back only and very slight corrosion at scratch.	*Very slight flaking and very slight pitting.	Slight to moderate local corrosion on front only, severe general corrosion on back only, and moderate corrosion at scratch.
Zinc chromate primer + D.T.D. 63A top coat (g).	Moderate flaking at scratch.	Moderate flaking at scratch.	Very slight flaking, slight pitting on back only, and slight corrosion at scratch.	Moderate flaking, and very slight local corrosion.	Severe flaking at scratch, slight pitting on front only, and slight corrosion at scratch.
Zinc chromate primer + D.T.D. 260A top coat (f).	None.	None.	Slight flaking at scratch and very slight corrosion at scratch.	Slight flaking, very slight pitting, and trace of corrosion at scratch.	Very slight corrosion at scratch.
Zinc tetroxychromate primer (d).	Severe erosion.	Severe erosion.	Severe erosion, moderate local corrosion on front only, and slight pitting on back only.	*Trace of flaking, slight local corrosion, very slight pitting, and very slight corrosion at scratch.	Moderate erosion, moderate to considerable local corrosion, and considerable corrosion at scratch.
Zinc tetroxychromate primer + D.T.D. 63A top coat (h).	Moderate flaking at scratch.	None.	Considerable flaking at scratch and trace of corrosion at scratch.	Very slight flaking and trace of corrosion at scratch.	Considerable flaking at scratch and considerable corrosion at scratch.
Zinc tetroxychromate primer + D.T.D. 260A top coat (m).	None.	None.	Severe flaking at scratch and trace of corrosion at scratch.	Trace of flaking and trace of corrosion at scratch.	Very slight corrosion at scratch.
Red lead primer (e).	Moderate chalking and crumbling, considerable erosion, and considerable local corrosion on back only.	Moderate chalking and crumbling, considerable erosion, and moderate to considerable local corrosion.	All specimens withdrawn after 8 months (Table VI).	All specimens withdrawn after 1½ years (Table VI).	Moderate chalking and erosion, severe local corrosion, and considerable corrosion at scratch.
Red lead primer + D.T.D. 63A top coat (j).	Trace of corrosion at scratch.	Slight pitting on back only and trace of corrosion at scratch.	Trace of flaking at scratch and considerable corrosion at scratch.	Considerable flaking at scratch and slight corrosion at scratch.	Very slight pitting on back only and considerable corrosion at scratch.
Red lead primer + D.T.D. 260A top coat (n).	Slight corrosion at scratch.	None.	Slight pitting on front only and considerable corrosion at scratch.	Considerable flaking and slight corrosion at scratch.	Slight corrosion at scratch.
Iron oxide primer (f).	Severe chalking.	Severe chalking.	Considerable chalking, trace of flaking, considerable local corrosion, and moderate corrosion at scratch.	*Moderate chalking and very severe flaking.	Very severe flaking and severe general corrosion.
Iron oxide primer + D.T.D. 63A top coat (k).	None.	None.	Very severe flaking, slight pitting, and very slight corrosion at scratch.	Very severe flaking at scratch, slight pitting, and trace of corrosion at scratch.	Considerable flaking at scratch, moderate local corrosion on front only, very slight pitting on back only, and severe corrosion at scratch.
Iron oxide primer + D.T.D. 260A top coat (o).	None.	None.	Considerable erosion on front only, severe flaking, and slight pitting.	Moderate flaking and very slight corrosion at scratch.	Moderate flaking, very slight pitting on back only, and moderate corrosion at scratch.
Plain metal (untreated) (a).	Slight general corrosion.	Moderate general corrosion and slight pitting.	Considerable general corrosion and moderate pitting.	Slight general corrosion and slight pitting.	Severe general corrosion.
Plain metal (chromated or pickled) (b).	Slight general corrosion.	Moderate general corrosion and slight pitting.	Considerable general corrosion and moderate pitting.	Slight general corrosion and slight pitting.	Severe general corrosion.

* All material withdrawn after 2½ years (results given after 2½ years).

test (sea-water spray), industrial (Widnes, Lancashire), and rural (Frodsham, Cheshire).

Apart from much greater exposure to wind at the marine station, which encouraged flaking of the top coats, more especially from the scratch line, the specimens at this station behaved in a similar manner to those in the accelerated test, where specimens exposed outdoors were sprayed twice daily with sea water, and the relative merits and disadvantages of

the various materials were the same for the two sites. Further comments on the accelerated test are therefore omitted.

At each site the primers are considered in the order red lead, iron oxide, and the two chromates. Results for the panels which were primed only are given first in each case, followed by results for the full paint system with respect to each of the primer types.

1. MARINE STATION

The red lead primer suffered considerably by chalking and erosion in the absence of a top coat; this was apparent on both light alloys and steel. With top coats there was considerable failure owing to crumbling of the whole paint film. The red lead primer accelerated the corrosion of the light alloys and especially the magnesium alloys, which were severely corroded after about 6 weeks' exposure even with the full paint system. The rapid deterioration caused by red lead primers on magnesium alloys and, to a lesser extent, on aluminium alloys is illustrated by the values given in Tables V and VI and the specimens shown in Figs. 1 and 2 (Plates LXXV and LXXVI). The adverse effect of the red lead primer, noted with the primer alone,¹ was thus delayed but not prevented by the completion of the full paint system.

The iron oxide primer maintained its colour in the absence of a top coat, although it suffered by rather marked chalking. This was prevented by the application of the top coat. The iron oxide primer, with or without top coats, still provided appreciable protection to aluminium alloys, but protection of magnesium alloys had practically ceased after 3½ years' exposure (Figs. 1 and 2). There was only one case suggesting that the iron oxide primer might have a slightly adverse effect on the magnesium alloys. This was the normal-purity magnesium alloy, D.T.D. 59A, primed with iron oxide and without top coat, which showed more severe corrosion at the scratch than the unpainted control specimen that had been similarly chromate treated (Table II). This may possibly have been due to scratching through the

chromate film on the former specimen, whereas the control specimen was not scratched.

The zinc chromate and zinc tetroxychromate primers afforded more protection than iron oxide to the light metals. This was clearly shown by those specimens where the iron oxide primer had failed, i.e. mainly on the magnesium alloys (Figs. 1 and 3, Plates LXXV and LXXVII). There was little evidence to distinguish between the two chromate primers in the full paint systems, although where no top coat had been applied the zinc tetroxychromate had suffered a moderate amount of erosion. The zinc chromate primer appeared to be slightly preferable on the less corrosion-resistant metal (B.S.S. 5L3, D.T.D. 118, and D.T.D. 59A of normal purity), whereas the zinc tetroxychromate primer appeared to be slightly preferable on the more resistant metal (99.5% purity aluminium, D.T.D. 120A, and D.T.D. 59A of high purity).

Some serious flaking of the top coats occurred on all panels exposed with chromate or iron oxide primers, although the oil-medium (D.T.D. 260A) top coat had a tendency to give better adhesion than the cellulose-medium (D.T.D. 63A) top coat. The cellulose top coat suffered considerably by erosion (Fig. 1). The serious flaking and erosion at the marine station were attributed partly to the very exposed conditions. The specimens were exposed to the full forces of prevailing cross-winds and in stormy weather to actual sea-spray. Flaking occurred almost entirely between the various paint coats rather than between paint and metal.

Chromate treatment of magnesium alloys without painting, and especially those of high-purity base, improved the corrosion-resistance markedly. After

TABLE V.—Losses in Weight for D.T.D. 118 (Normal Purity) and Steel Specimens after 2½ Years' Exposure at the Marine Site and in the Accelerated Tests.

Paint System	Weight Loss, g./m.*			
	Marine Site (Dungeness)		Accelerated Test (Chalfont Park)	
	D.T.D. 118, normal purity	Steel	D.T.D. 118 normal purity	Steel
Zinc chromate primer (c)	33	251	9	241
Zinc chromate primer + D.T.D. 63A top coat (g)	9	414	3	1560
Zinc chromate primer + D.T.D. 260A top coat (l)	4	17	1	48
Zinc tetroxychromate primer (d)	32	469	21	1530
Zinc tetroxychromate primer + D.T.D. 63A top coat (h)	3	173	4	1050
Zinc tetroxychromate primer + D.T.D. 260A top coat (m)	0	46	3	508
Red lead primer (e)	177 *	448	214 †	2330
Red lead primer + D.T.D. 63A top coat (j)	371 †	173	345 †	1920
Red lead primer + D.T.D. 260A top coat (n)	263 †	197	398 †	1480
Iron oxide primer (f)	37	711	66	3150
Iron oxide primer + D.T.D. 63A top coat (k)	16	756	23	2180
Iron oxide primer + D.T.D. 260A top coat (o)	17	336	38	1020
Plain metal (untreated) (a)	90	905 ‡	342	4390 ‡
Plain metal (chromated or pickled) (b)	77	1560	139	4860

All material withdrawn after * 4 months (results given after 4 months), † 9 months (results given after 9 months), and ‡ 1½ years (results given after 1½ years).

TABLE VI.—Summary Table: the Approximate Time in Years Required for the Panels to Suffer Slight Corrosion.

Paint System	Marine Site (Dungeness)							Accelerated Tests (Chalfont Park)						
	Aluminium (99.5%)	B.S.S. 5L3	D.T.D. 120A, high purity	D.T.D. 118, normal purity	D.T.D. 59A, high purity	D.T.D. 59A, normal purity	Steel	Aluminium (99.5%)	B.S.S. 5L3	D.T.D. 120A, high purity	D.T.D. 118, normal purity	D.T.D. 59A, high purity	D.T.D. 59A, normal purity	Steel
Zinc chromate primer (c)	> 3½	> 3½	> 3½	1	> 3½	1	½	> 3½	> 3½	> 3½	1½	> 3½	1	½
Zinc chromate primer + D.T.D. 63A top coat (g)	> 3½	> 3½	> 3½	1½	> 3½	1	1½	> 3½	> 3½	> 3½	1½	> 3½	1½	1½
Zinc chromate primer + D.T.D. 260A top coat (l)	> 3½	> 3½	> 3½	1½	> 3½	1	2	> 3½	> 3½	> 3½	2½	> 3½	1½	1½
Zinc tetroxychromate primer (d)	> 3½	> 3½	> 3½	1	3½	1	½	> 3½	> 3½	> 3½	1½	> 3½	1	½
Zinc tetroxychromate primer + D.T.D. 63A top coat (h)	> 3½	> 3½	> 3½	1½	3½	1	1½	> 3½	> 3½	> 3½	1½	> 3½	1	1
Zinc tetroxychromate primer + D.T.D. 260A top coat (m)	> 3½	> 3½	> 3½	1½	> 3½	1	1½	> 3½	> 3½	> 3½	1½	> 3½	1½	1½
Red lead primer (e)	¼	¼	< ¼	< ¼	< ¼	< ¼	½	¼	¼	< ¼	< ¼	< ¼	< ¼	½
Red lead primer + D.T.D. 63A top coat (j)	1	1	< ¼	< ¼	< ¼	< ¼	1½	1	½	< ¼	< ¼	< ¼	< ¼	1
Red lead primer + D.T.D. 260A top coat (n)	1	1	< ¼	< ¼	< ¼	< ¼	1½	1	½	< ¼	< ¼	< ¼	< ¼	1½
Iron oxide primer (f)	> 3½	3½	1½	½	3½	1	¼	3½	2½	1	1	> 3½	½	½
Iron oxide primer + D.T.D. 63A top coat (k)	> 3½	3½	2½	1	3½	1	1	3½	2½	> 3½	1½	3½	1	1
Iron oxide primer + D.T.D. 260A top coat (o)	> 3½	> 3½	3½	1	3½	1	1	> 3½	2½	1½	1	3½	1	1
Plain metal (untreated) (a)	1½	½	1½	½	1½	¼	¼	1½	1	...	¼	1½	½	¼
Plain metal (chromated or pickled) (b)	1½	½	1½	½	2	¼	¼	1½	1	1½	½	1½	½	¼

Paint System	Industrial Site (Widnes)					Rural Site (Frodsham)				
	Aluminium (99.5%)	B.S.S. 5L3	D.T.D. 118, normal purity	D.T.D. 59A, normal purity	Steel	Aluminium (99.5%)	B.S.S. 5L3	D.T.D. 118, normal purity	D.T.D. 59A, normal purity	Steel
Zinc chromate primer (c)	3½	3½	2½	1	½	> 3½	> 3½	1½	> 2½ *	½
Zinc chromate primer + D.T.D. 63A top coat (g)	> 3½	> 3½	1½	> 2½ *	1½	> 3½	> 3½	1½	> 3½	2
Zinc chromate primer + D.T.D. 260A top coat (l)	> 3½	> 3½	3	> 2½ *	1½	> 3½	> 3½	> 3½	> 3½	> 3½
Zinc tetroxychromate primer (d)	3½	3	1½	1½	1	> 3½	> 3½	3	2½	1½
Zinc tetroxychromate primer + D.T.D. 63A top coat (h)	> 3½	> 3½	> 3½	> 2½ *	1½	> 3½	> 3½	> 3½	> 3½	2
Zinc tetroxychromate primer + D.T.D. 260A top coat (m)	> 3½	> 3½	> 3½	> 2½ *	1½	> 3½	> 3½	> 3½	> 3½	> 3½
Red lead primer (e)	2	½	< ¼	< ¼	¼	1	½	< ¼	< 1	1½
Red lead primer + D.T.D. 63A top coat (j)	2½	2½	2	1½	1	> 3½	> 3½	1	3½	1½
Red lead primer + D.T.D. 260A top coat (n)	3½	3½	1½	1½	1	> 3½	> 3½	1	3½	3½
Iron oxide primer (f)	3	1½	1	½	¼	> 3½	> 3½	1	< 1	½
Iron oxide primer + D.T.D. 63A top coat (k)	3½	3½	2	2½	1	> 3½	> 3½	1½	3½	1½
Iron oxide primer + D.T.D. 260A top coat (o)	> 3½	> 3½	2	> 2½ *	1	> 3½	> 3½	1½	> 3½	2½
Plain metal (untreated) (a)	1	1	½	½	< ¼	1½	½	½	½	< ¼
Plain metal (chromated or pickled) (b)	1	1	½	½	< ¼	1½	½	½	½	< ¼

* Specimens withdrawn after 2½ years before showing slight corrosion.

prolonged exposure, however, pitting of the chromated metal was evident, and this pitting was deeper than on the untreated and unprotected aluminium and B.S.S. 5L3.

The results showed that except for the systems using red lead primer, all the light alloys tested were markedly superior to mild steel. For example, the worst of the light alloys is compared with steel in Table V (p. 485). Paint failure on the mild-steel specimens was due partly to flaking of the paint film and partly to rusting of the metal causing blisters which subsequently dislodged the paint films.

2. INDUSTRIAL STATION

In the case of magnesium alloys (D.T.D. 59A) records ceased after 2½ years, since many of these specimens were either lost or heavily damaged during a severe storm. No high-purity-base magnesium alloys were exposed at the industrial station.

Red lead primer unprotected by top coats failed by chalking, leading to crumbling of the paint film. Definite acceleration of corrosion occurred on the light metals before failure of the paint film as a whole, especially on normal-purity magnesium alloys, and severe corrosion developed on these latter alloys within 6 weeks in the absence of top coats. On the aluminium alloys some acceleration of corrosion was noted in the absence of top coats, particularly on the backs of the specimens, where there was a higher moisture retention. Red lead primer without a top coat ceased to give adequate protection to mild steel after 12 months. A very marked improvement in the behaviour of red lead primer resulted from the application of top coats, and, although corrosion occurred, no acceleration was observed on any metal. The complete paint systems based on red lead primers were on the whole inferior to the corresponding ones based on iron oxide primers for the protection of light alloys (Table III, p. 483). It seemed probable from the behaviour of specimens primed but without top coats, that acceleration of the corrosion of light alloys would occur in time with lead primers if the top coats were not adequately maintained. In general, the oil top coat (D.T.D. 260A) proved somewhat superior to the cellulose top coat (D.T.D. 63A).

Iron oxide primers also failed by chalking when unprotected by top coats, but failure developed more slowly than with red lead. Colour and gloss were maintained for about 12 months. As a rule, iron oxide in the absence of top coats gave quite good protection to all metals while the paint film was intact, but as paint failure developed protection ceased to become effective. This was attributed to lack of the chemical corrosion-inhibitive properties possessed by the chromates on all metals and by red lead on steel. With mild steel, protection by the iron oxide primer alone was poor, and rusting became severe after about 12 months. On normal-purity magnesium alloy D.T.D. 118, severe flaking of the

primer with considerable corrosion occurred after about 3 years. The addition of top coats gave considerable improvement to the performance of iron oxide primers, that with D.T.D. 260A again proving the more effective, particularly on magnesium alloys and mild steel. A tendency was noted for the two primer coats on the top-coated systems to flake apart, especially on the magnesium alloy D.T.D. 118, thereby reducing the effective life of the systems.

The behaviour of the two zinc chromate primers was definitely better than that of either iron oxide or red lead. In the absence of top coats, both pigments gave good protection to the light metals for 3 years (except perhaps with the normal-purity magnesium) and on mild steel the protection was considerably better than with red lead. After 3 years, the single coat of zinc tetroxochromate failed by progressive erosion, the primer continuing to inhibit corrosion until, after 3½ years, the paint film became too thin to prevent corrosion on the least resistant metals. Zinc tetroxochromate gave rather better results than the normal chromate on mild steel.

With the top-coated systems there was little difference in performance between the two chromate pigments. The tetroxochromate appeared rather better on normal-purity magnesium alloy D.T.D. 118 and on mild steel, but the zinc chromate was more effective in preventing scratch-line corrosion on mild steel. Apart from flaking, described below, both top-coated systems gave very satisfactory results with both chromates.

There was a serious, though erratic, tendency for flaking to occur on top-coated systems based on the two zinc chromate and iron oxide primers, particularly at the scratch lines. On most metals this took place between the two primer coats, the second primer coat and the top coats flaking away together from the first primer coat. On the normal-purity magnesium alloy D.T.D. 59A, the flaking tended to occur down to the bare metal. The relative freedom from flaking with the red lead primer was attributed to the more matt surface obtained with this formulation. Undoubtedly the oil medium (D.T.D. 260A) gave better adhesion than the cellulose medium (D.T.D. 63A) over the primers tested.

The cellulose top coats (D.T.D. 63A) failed after about 3 years by erosion. The industrial site was in a very exposed situation, and this tended to accentuate the degree of erosion, particularly on the panel fronts which faced partly in the direction of the prevailing winds.

Chromate treatment of the magnesium alloys gave a definite improvement in corrosion-resistance in the case of D.T.D. 118 and, initially at least, with D.T.D. 59A.

The light alloy specimens suffered very much less corrosion than the corresponding mild-steel specimens, whether painted or not. Even the magnesium alloys (which were the most susceptible of the light alloys to corrosion) when primed with red lead (the worst

exposure condition) have not shown the same depth of corrosion encountered on the best mild-steel specimens. The latter suffered particularly at the scratch lines.

3. RURAL STATION

No high-purity magnesium alloys were exposed at the rural station.

The red lead primer, when not protected by top coats, failed by chalking, which led to crumbling of the paint film, and considerable erosion developed on the specimens which were exposed for more than 2½ years. In the absence of top coats, definite acceleration of corrosion by this primer was evident on light metals before complete failure of the paint film; on the aluminium alloys this was restricted to the panel backs; the performance on mild steel, as at the industrial site, was not good, and marked corrosion developed. Red lead primer protected by top coats gave comparatively good results even on magnesium alloys, corrosion being mainly restricted to scratch lines (Table IV, p. 484).

The iron oxide primer unprotected by top coats suffered progressive chalking comparable with that at the industrial site. No acceleration of corrosion was noted, and useful protection was afforded to aluminium alloys while the paint film remained intact. With the magnesium alloy D.T.D. 118, moderate local corrosion developed after about 18 months and on the magnesium alloy D.T.D. 59A severe flaking occurred. Generally, however, the areas attacked were less than at the industrial and marine sites. On mild steel, corrosion was severe after 12 months.

The top-coated systems using iron oxide primer gave excellent protection to aluminium alloys for the full period of exposure, but protection of the magnesium alloys was handicapped by severe flaking. There was little to choose between the two top coats. On mild steel the D.T.D. 260A top coat gave quite good protection even after 3½ years, but on this metal the D.T.D. 63A top coat was not quite as satisfactory.

As might be expected from the milder corrosive conditions prevailing at Frodsham, the specimens primed with single coats of zinc chromate and tetroxychromate withstood corrosion even better than at the other sites. There was little to choose between the two primers until erosion seriously reduced the thickness of the tetroxychromate film after about 3 years' exposure. In spite of this erosion, no corrosion occurred on aluminium alloys after 3½ years. The tetroxychromate gave rather better protection to mild steel than the ordinary chromate. Very good protection was maintained with full paint systems incorporating chromate primers for all metals after 3½ years.

As at the other sites, erratic flaking was noted with the complete paint systems based on iron oxide, zinc chromate, and zinc tetroxychromate primers. Here again adhesion tended to fail between the two primer coats. In spite of this tendency towards

flaking, no appreciable corrosion occurred with the chromate primers. The flaking was generally rather worse with the systems using the cellulose top-coat (D.T.D. 63A) than with the oil (D.T.D. 260A) and usually commenced at the scratch lines. With the magnesium alloy D.T.D. 59A flaking occurred down to the metal surface. Erosion of the cellulose top coats was perhaps even more severe at Frodsham than at the other sites, despite the comparatively sheltered situation.

A slight improvement in the performance of both the unpainted magnesium alloys resulted from chromate treatment.

As at the other sites, corrosion of unpainted light alloys was generally considerably less than with corresponding mild-steel panels. Under these comparatively mild conditions the corrosion of light alloys was prevented, and the corrosion of mild steel was only very slight with the best of the complete paint systems.

III.—DISCUSSION OF RESULTS

The first paper describing this investigation¹ summarized the provisional results obtained after about 6 months' exposure at the four stations. After exposure for 3½ years, breakdown has reached the stage where a reasonably complete assessment can be made for all the systems tested.

The exposure to sea-water spray was intended to give acceleration of corrosion as compared with the marine site at Dungeness, and although this acceleration was not achieved, the term is retained for convenience. The marine site was in a very exposed situation, with prevailing winds blowing across the fronts of the specimens. This gave a much greater degree of flaking on the fronts of the specimens, especially at the scratch lines and edges, at the marine site than in the accelerated tests, which were carried out in a fairly sheltered location. The lack of acceleration on specimens subject to sea-water spray tests is attributed partly to this factor and partly to under-estimation of the severity of conditions at Dungeness. The accelerated tests served a useful purpose, however, in providing severe marine conditions on specimens under continuous observation.

The light alloys in general suffered rather less attack at the industrial site than at the marine or accelerated test sites. The industrial and marine sites were comparable in exposure to prevailing winds, and the consequent flaking on the front surfaces of the specimens.

At the rural site the light metals were comparatively mildly corroded, but there was marked attack on mild steel. The site had relatively long periods of sunshine unfiltered by smoke layers in the atmosphere, and moisture deposition was of a high order owing to frequent night mists. Chalking was consequently heavier than at the other sites. Winds and dust storms from nearby arable land were sufficiently frequent to produce erosion and flaking.

Corrosion was frequently more severe on the panel backs than on the front surfaces, probably owing to the sheltering from direct solar radiation and wind causing slower evaporation of condensed moisture and to a much smaller removal of corrosive deposits by rain.

At all the sites definite evidence of acceleration of corrosion of light metals was observed with single coats of red lead primer, and this was particularly marked on magnesium alloys. At the marine and accelerated exposure sites red lead primer accelerated corrosion of all the light metals even when complete paint systems were applied. No such acceleration was observed at the industrial and rural sites with the complete paint systems exposed for $3\frac{1}{2}$ years, but these did not give as efficient protection to light alloys as the systems free from lead pigments, and in time might give acceleration even in these atmospheres, especially if maintenance were poor. Red lead primer gave fairly effective protection to mild steel at the marine, accelerated, and rural sites, but it was less satisfactory at the industrial site.

Iron oxide primer generally gave a good measure of protection to light metals at all of the sites, the longest life being obtained at the less corrosive sites (rural and industrial) or with the more corrosion-resistant metals (aluminium alloys and high-purity magnesium alloys). Iron oxide on mild steel was in general inferior to red lead, zinc chromate, and zinc tetroxychromate. It was apparent from the type of failure that iron oxide conferred protection by physical rather than chemical means, and once film breakdown occurred corrosion proceeded owing to the absence of inhibiting properties in the pigment. These results confirm the suitability of iron oxide as a diluent for inhibiting pigments and the greater importance of maintenance when iron oxide is used without additions of inhibiting pigments.

The zinc chromate and zinc tetroxychromate primers were outstandingly successful at all the sites, and for practical purposes these two primers are considered to have comparable protective properties on light metals and mild steel. The good performance of zinc tetroxychromate was achieved with a much lower pigmentation of the non-volatile portion of the paint than with any of the other priming pigments. The pigment volume concentrations (on the total non-volatiles) for zinc tetroxychromate, zinc chromate, red lead, and turkey red oxide were 24, 36, 50, and 38% respectively. One of the authors (J. G. R.) has found from other recent work that the pigment volume concentrations of zinc tetroxychromate can with advantage be increased without loss of good brushing properties. This has a tendency to harden the primer film, which consequently suffers less from erosion in the absence of top coats, and to decrease

the gloss, thus giving better adhesion between paint coats.

Adhesion between the various paint coats in the complete paint systems was generally rather unsatisfactory, except in the case of the red lead primer (which had a matt surface). The possibility of this type of failure (due to the unusual formulation of the primer) was foreseen when the tests were designed, but it was considered that the primers should be formulated from single pigments, rather than from mixed pigments and extenders, in order to simplify direct comparison of the individual priming pigments. In designing formulations for commercial use, these considerations do not apply, and mixed pigments can be employed.

In general, the cellulose top coat (D.T.D. 63A) tended to suffer erosion and to give rather more flaking between the priming coats and top coats of the full systems than the corresponding oil top coat (D.T.D. 260A). Possibly this difference was partly due to the use of a single primer medium for both systems and the better leafing characteristics of aluminium paste in oil varnish media than in cellulose media.

IV.—CONCLUSIONS

The general conclusions with respect to materials are:

(1) Red lead primers should be avoided on light metals, especially in marine atmospheres. This effect is much more marked on magnesium and its alloys than on aluminium and its alloys.

(2) Iron oxide primers with appropriate top coats are satisfactory for light and ferrous metals where corrosive conditions are not too severe.

(3) Zinc chromate or zinc tetroxychromate primers with appropriate top coats should be used on light metals for the most severe corrosive conditions. They are very suitable for ferrous metals, and are particularly appropriate for composite structures of steel and light alloys.

(4) Alkyd-linseed stand oil varnish (D.T.D. 260A) is preferred to cellulose (D.T.D. 63A) as a medium for aluminium finishing paints.

ACKNOWLEDGEMENTS

The authors wish to express their appreciation of the advice and assistance received from Messrs. Cellon's, Ltd., who made up the paints. They also thank the Magnesium Metal Corporation for the preparation of the magnesium alloy specimens.

REFERENCE

1. J. G. Rigg and E. W. Skerrey, *J. Inst. Metals*, 1948-49, **75**, 69; discussion, p. 1015.

Discussion

The Effect of Grain-Size on the Structural Changes Produced in Aluminium by Slow Deformation

By W. A. RACHINGER

(*Journal*, this vol., p. 415.)

Dr. I. S. SERVI,* S.M. (Member): The excellent experimental evidence of structural changes produced in aluminium by slow deformation at elevated temperatures is a substantial contribution to the understanding of the phenomenon of sub-grain formation, because it helps to unify, at least partially, the rather contrasting theories that have been suggested on this subject. The most important experimental observations, including the effect of grain-size on structural changes at elevated temperatures, are in good agreement with the observations made, quite independently, by Servi and Grant.†

A comparison of as-deformed and repolished and etched structures (Figs. 3, 4, 14, 15, and 20, Plates LXI and LXII) reveals that the grain boundaries undergo marked migration during deformation. The sub-boundaries of the as-deformed structures do not coincide exactly with the sub-boundaries of the repolished and etched structures. The discontinuous dotted lines along old-grain (Fig. 15) and dendrite (Fig. 20) boundaries may be due to segregated impurities (probably oxides) that do not diffuse away at the temperature of testing. A statement concerning the etching reagent used by the author would be appreciated. It would also be interesting to know whether he has ever observed a sub-structure in cast "very large-grained aggregates" before deformation.

The results of Mr. Rachinger's investigation show that there is no physical difference between grain boundaries and sub-boundaries. Rather, there is indication that the only difference lies in the mechanism of formation, since the sub-boundary formation does not involve nucleation and growth.

The report on experimental observations of sub-grain formation by Servi, Norton, and Grant‡ may give further explanation of the "banded appearance" of the sub-structure of Fig. 11 (Plate LXII).

The AUTHOR (*in reply*): As Dr. Servi intimates, a unification of the diverse views on the mechanism of sub-grain

formation may be near at hand. The work of Cahn,§ Honeycombe,|| and McLean** indicates that the banded sub-structures arise from "polygonization under stress" of deformation bands formed by inhomogeneous straining of the grains. The mode of formation of the "polygonal" type of sub-structure at higher temperatures is more difficult to ascertain, both because of the high mobility of the sub-boundaries†† and of the relatively small number of cells contained within each grain. One promising suggestion is that the sub-grains are, in all cases, formed from deformation bands, the width of the bands, and hence the size of the sub-grains, increasing with an increase in temperature or decrease in strain rate.

A coincidence of the deformation markings and the etched sub-boundaries is not to be expected if the sub-boundaries are mobile. The surface markings may have formed at any stage of the deformation, whereas the etched structures show only the final boundary positions. The pits visible in Fig. 14 or 15 are probably formed by gas bubbles adhering to the surface during electropolishing. It is agreed that the etching of the dendrite boundaries (Fig. 20) is probably due to segregated impurities.

The only structure observed metallographically in the cast crystals was the dendritic structure. The X-ray diffraction patterns from these crystals indicate a structure of slightly disoriented crystalline blocks. Whether this is in fact identical with the dendritic structure is not known. However, since the size of the sub-grains varies systematically with the rate and temperature of deformation, it seems unlikely that these sub-grains can be identified with any sub-structure present in the undeformed metal.

The appearance of sub-boundaries etched in a mixture of 25% HNO₃, 2% HF, and 73% water has invariably been similar to that of grain boundaries. However, the work of Wyon and Crussard‡‡ suggests that when the angle between contiguous sub-crystals is sufficiently small the boundary will etch differently from a normal grain boundary.

* Research Metallurgist, Union Carbide and Carbon Research Laboratories, Inc., Niagara Falls, N.Y., U.S.A.

† I. S. Servi and N. J. Grant, *Trans. Amer. Inst. Min. Met. Eng.*, 1951, **191**, 917.

‡ I. S. Servi, J. T. Norton, and N. J. Grant, *Trans. Amer. Inst. Min. Met. Eng.*, 1952, **194**, 965.

§ R. W. Cahn, *J. Inst. Metals*, 1951, **79**, 129.

|| R. W. K. Honeycombe, *ibid.*, 1951-52, **80**, 45.

** D. McLean, *ibid.*, 1951-52, **80**, 507.

†† R. C. Gifkins and J. Kelly (Baillieu Laboratory, University of Melbourne), private communication.

‡‡ P. G. Wyon and C. Crussard, *Rev. Mét.*, 1951, **48**, 121.

THE CONTINUITY OF SLIP LINES ACROSS A GRAIN BOUNDARY*

1469

By G. J. OGILVIE,† Ph.D., JUNIOR MEMBER

SYNOPSIS

Slip lines on the surfaces of polished and subsequently strained specimens of aluminium and 70 : 30 brass are sometimes continuous across a grain boundary. Investigation of the interior of the brass specimens shows that this is not merely a surface effect, but that the intersection of the slip planes does in fact lie in the grain boundary. It is shown that this intersection lies at an angle of less than 2° from one of the $\langle 110 \rangle$, $\langle 112 \rangle$, or $\langle 123 \rangle$ directions in both the slip planes concerned. When the duration of annealing, before the final deformation, is increased, there is, within a given surface area, an increase in the number of grain-boundary sections where slip lines cross. It is therefore suggested that the boundary configuration favourable to slip-line crossing has a low interfacial free energy.

It is shown that approximately half the adjacent crystal pairs in a random aggregate are favourably oriented for slip-line crossing to occur.

I.—INTRODUCTION

In the course of a metallographic study of deformation in metals, occasional cases were seen where sets of slip lines crossed a boundary between two crystals with, in general, a change in direction. Lacombe and Beaujard¹ had also noted a similar phenomenon. The present study was undertaken to determine whether the coincidence of slip planes at the surface of the specimen was accidental or whether the effect had some crystallographic significance.

II.—EXPERIMENTAL PROCEDURE

Tensile specimens were prepared from cold-rolled $\frac{3}{32}$ -in. aluminium sheet ($>99.98\%$ pure) and from commercial $\frac{3}{16}$ -in. brass sheet (zinc 31.72, iron 0.04, lead 0.02%, trace of tin, balance copper). The aluminium specimens were annealed at 600°C . for 2 hr. and then electropolished, using a perchloric acid-acetic anhydride bath.² The brass specimens, after preliminary annealing at 600°C . *in vacuo* for 8 hr., were given a tensile strain of 3%. These specimens were then re-annealed at 600°C . *in vacuo* for periods of 1, 5, 25, 48, and 100 hr. and electropolished in orthophosphoric acid (900 g./l.). After electropolishing, the specimens were elongated 10% to produce slip lines. In all cases numerous examples were found of slip lines crossing grain boundaries (Figs. 1 and 2, Plate LXXVIII).

As slip lines in brass can be revealed by etching,^{3,4} the brass specimens were used to determine whether the phenomenon was restricted to the surface. Selected areas of the specimen, which had been annealed for 48 hr., were re-examined at levels 10, 40, and 110 microns below the original surface, the latter being removed by electropolishing.

The other brass specimens were used to study the effect of annealing time on the frequency of occurrence of boundary sections with crossing slip lines by counting the number of cases within a standard area.

III.—RESULTS

The following observations were made during the metallographic survey:

(1) The *same* slip planes meet at the boundary at different levels. This is shown by Figs. 3–5 (Plate LXXVIII), where some of the etched lines can be identified with the original slip lines. Identification of individual slip zones was effected by comparing slip-line spacings. Cut photographs were superposed to allow a direct comparison of the spacings.

(2) The portion of a grain boundary across which slip lines are continuous is always nearly straight. A boundary may have more than one such straight section, but in this case different sets of slip lines are, in general, continuous across the different sections. Fig. 2 illustrates this point: one boundary between two crystals is divided into three sections, and different sets of slip lines cross the different straight sections.

(3) Slip lines usually change direction as they cross the boundary. The frequency histogram (Fig. 6) shows that the maximum observed change in direction is 65° , while the peak of the distribution occurs at zero direction change.

It follows from (1) and (2) that the boundary is plane where slip lines are continuous across it and the intersecting slip planes meet it in parallel straight lines.

For each pair of crystals the orientation of this direction of intersection relative to both crystals was determined from measurements on the slip lines in the crystals.⁵ It was found that this direction

* Manuscript received 12 November 1952.

† Division of Tribophysics, Commonwealth Scientific and

Industrial Research Organization, University of Melbourne, Australia.

was $\langle 110 \rangle$, $\langle 112 \rangle$, or $\langle 123 \rangle$ in both crystals (but not necessarily the same direction in each crystal) with a maximum error of 2° . However, the boundary plane was not found to have a simple orientation in either crystal. Although slip occasionally occurred on planes other than $\{111\}$, it was found that those slip lines which crossed a boundary were always the traces of $\{111\}$ planes.

It can be seen from the figures given in Table I that the number of boundary sections where slip lines cross increases with annealing time. This is so, in spite of the increase in grain-size and the corresponding decrease in the number of grain-

critical shear stress is exceeded on the relevant slip system in each crystal. The favourable boundary configuration may not be possible for certain ranges of relative orientations of the crystal pair. Therefore, it becomes necessary to enquire what proportion of the total number of crystal pairs in a random aggregate will have the necessary relative orientations, so that this boundary condition may be established.

For this problem it is convenient to consider a method of obtaining an arbitrary orientation from a reference orientation in a cubic crystal. Two perpendicular rotation axes are chosen, one lying in the $[111]$ direction and the other in the (111)

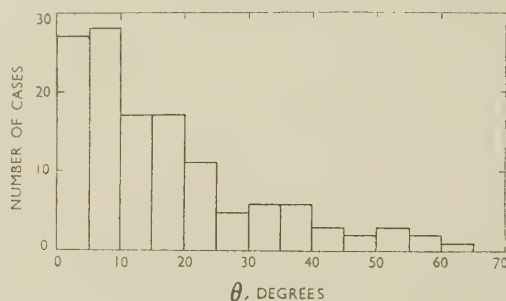


Fig. 6.—Histogram of the Deviation of Slip Lines After Crossing a Grain Boundary.

boundary sections in the standard area. If the increase in grain-size is taken into account, increasing the annealing time from 1 to 100 hr. increases the

TABLE I.—The Variation with Annealing Time of the Number of Boundaries at Which Slip-Line Crossing Occurs.

Annealing Time, hr.	Average Linear Grain-Size, mm.	Number of Cases of Sets of Slip Lines Crossing a Boundary in an Area 18.57×4.82 mm.	Number of Grains in Standard Area, $\times 10^3$
1	0.15	27	4
5	0.20	63	2.2
25	0.25	97	1.4
100	0.25	125	1.4

proportion of boundary sections with crossing slip lines by a factor of 14 instead of the factor 5 indicated in Table I.

IV.—DISCUSSION

Since grain boundaries will tend to assume their most stable position during annealing and since the proportion of boundary sections with crossing slip lines increases strikingly with annealing time, it follows that plane boundaries containing a $\langle 110 \rangle$, $\langle 112 \rangle$, or $\langle 123 \rangle$ direction in each crystal are more stable than other configurations. Probably the interfacial free energy of this type of boundary is relatively small. For slip lines to cross a given boundary the following conditions must be satisfied. The relative orientation of the two crystals and of the boundary with respect to those crystals must be suitable, and the deformation must be such that the

plane at an angle α to (say) the $[\bar{1}01]$ direction. If the lattice is then rotated in turn about the fixed axis through an angle β , and about the movable axis through an angle γ , the desired orientation may be attained. One orientation may then be expressed relative to another in terms of the three parameters α , β , and γ . If α and β are restricted to a range of 60° and γ varies from 0° to 360° , then all possible orientations are described once only. A three-dimensional diagram may therefore be constructed with α , β , and γ plotted on orthogonal axes, and all orientations which could have a boundary containing, within a given maximum divergence, a $\langle 110 \rangle$, $\langle 112 \rangle$, or $\langle 123 \rangle$ direction in each crystal bounded by contour surfaces. Since the maximum divergence observed was 2° , the corresponding contours will be studied. Consideration of the $\langle 110 \rangle$, $\langle 112 \rangle$, and $\langle 123 \rangle$ directions lying only in the (111) plane of each lattice gives contours which have the form of right prisms based on parallelograms. Fig. 7 shows a section perpendicular to the γ axis of the $\alpha/\beta/\gamma$ diagram giving the form and location of these prisms. The total volume enclosed by them is 7.11% of the total. All other coincidences between $\langle 110 \rangle$, $\langle 112 \rangle$, and $\langle 123 \rangle$ directions will give tubular 2° contour surfaces inclined at some angle to the base of the diagram and having a variable cross-section. The average cross-section of these contours is approximately 8 deg.² and the length is at least 60° . There are 1116 such contours passing through the $\alpha/\beta/\gamma$ diagram, and therefore the volume contained in the 2° limit (approximately 5×10^6 deg.²) is approximately half the total volume (1.296×10^6 deg.²).

To check this qualitative conclusion, direct measurements have been made along two lines through A and B (Fig. 7) perpendicular to the base plane. For fixed γ and each of the 16 intersections between the $\{111\}$ planes in the two lattices, the two angles between an intersection and the nearest $\langle 110 \rangle$, $\langle 112 \rangle$, or $\langle 123 \rangle$ direction were determined by using a large (50-cm.) Wulff net. The larger of these two angles was taken and the minimum, δ , of the 16 angles selected in this way is plotted as a function of γ in Fig. 8 A and B. Along the line through A, 40.6%

preferred orientation. Thus, the fact that the fraction of boundaries where crossing takes place increases with the time of annealing must be attributed to changes in the orientation of boundaries relative to the crystals.

Attention should be drawn to a possible implication of these conclusions. Since slip lines may cross a boundary under certain conditions, it seems likely that the effect of this boundary configuration on the plastic properties will not be as great as that of a random boundary. That is, the stiffening effect of

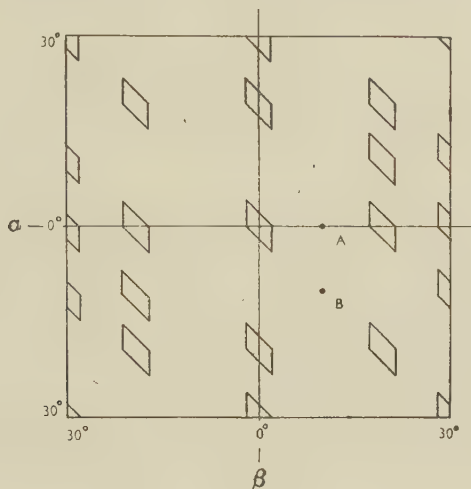


FIG. 7.—Section of the $\alpha/\beta/\gamma$ Diagram Perpendicular to the γ Axis.

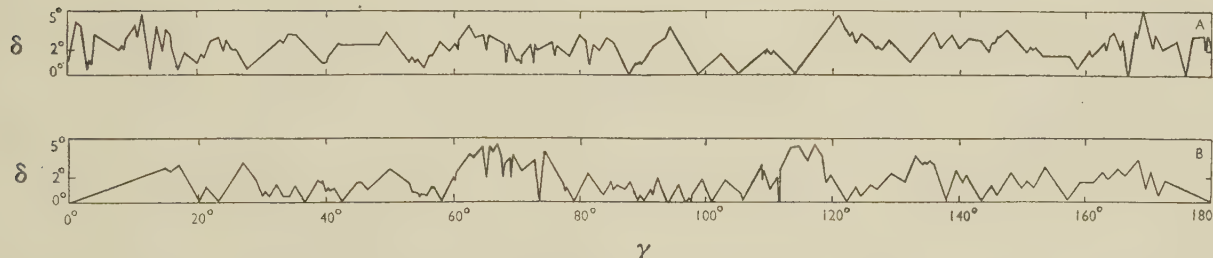


FIG. 8 A and B.—Variation of δ along the Two Lines Marked A and B in Fig. 7, Parallel to the γ Axis. The diagram is symmetrical about $\gamma = 180^\circ$.

of the total orientation range was within a 2° contour and along the one through B, 78.5% was included. Details of this calculation are given in an Appendix.

It seems probable, therefore, that more than half of the crystal pairs in a random aggregate are oriented with respect to each other so that at least one range of positions of their common boundary will be favourable to slip-line crossing. These positions are defined by the set of planes which have a common direction, which is the direction of intersection of the slip planes crossing the grain boundary. It is observed that the proportion of grain boundaries with crossing slip lines is small compared with the proportion of crystal pairs having a favourable relative orientation. In these experiments the effect of the deformation condition is constant, as the extension is the same in all specimens and there is no appreciable

the grain boundary will be less since dislocations can apparently pass through the boundary. Thus, for example, the elastic limit of a polycrystalline aggregate, which has boundaries only of this special type, should be less than the elastic limit of an aggregate of the same grain-size with boundaries in general positions. This point has not been studied, but it is felt that it may be worth investigation.

REFERENCES

1. P. Lacombe and L. Beaujard, *J. Inst. Metals*, 1948, **74**, 1.
2. P. A. Jacquet, *Métaux, Corrosion-Usure*, 1943, **18**, 198.
3. D. McLean, *J. Inst. Metals*, 1948, **74**, 95.
4. P. A. Jacquet, *Rev. Mét.*, 1950, **47**, 355.
5. C. S. Barrett, "Structure of Metals", p. 40. New York: 1943 (McGraw-Hill).

APPENDIX

The Graphical Determination of δ

For the determination of δ it is necessary to have a large Wulff net on which two transparent sheets are

placed at 90° to the centre of the projection, as on the lower sheet. The movable rotation axis is placed at 90° to the centre of the net and, as implied in the second paragraph of Section IV, it must lie at 90° to the $[111]_U$ pole. The two $[111]$ poles (one on each sheet) are now superposed, and the $[\bar{1}01]_U$ pole

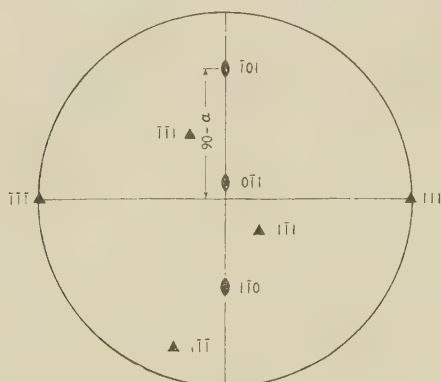


FIG. 9.—Positions of Some Low-Index Poles on the Lower Sheet.

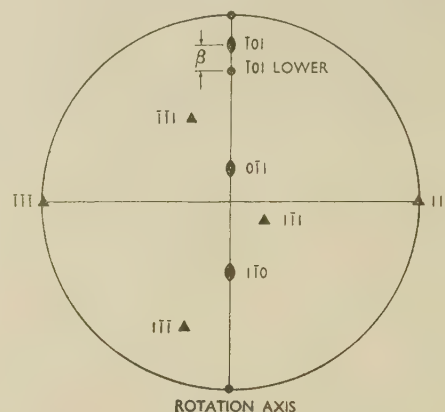


FIG. 10.—Positions of the Same Poles on the Upper Sheet.

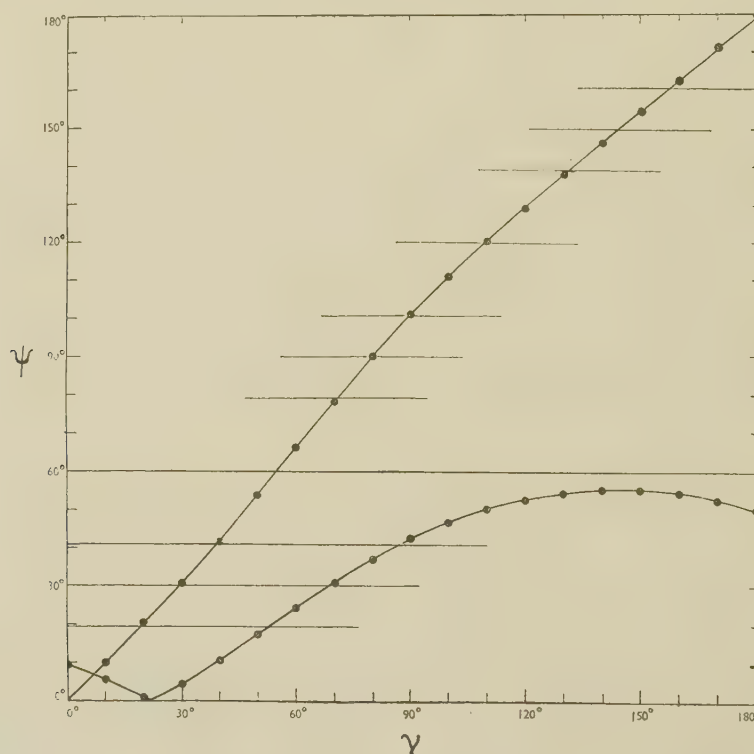


FIG. 11.— ψ/γ Curves for the Intersection Between the $(\bar{1}11)_L$ and the $(\bar{1}11)_U$ Planes for the Orientation Range Represented by the Line Through B in the $\alpha/\beta/\gamma$ Diagram (Fig. 7).

placed. On each of these are marked the poles of low indices of one of the crystals. On the lower sheet (lattice L) the poles are placed so that the $[111]_L$ pole is at 90° to the centre of the projection and the $[\bar{1}01]_L$ pole is placed at $(90^\circ - \alpha)$ from the centre, as shown in Fig. 9.

On the upper sheet (lattice U) the $[111]_U$ pole is

is placed at the required angle β from the $[\bar{1}01]_L$ pole to give the array of poles shown in Fig. 10.

For each value of γ (10° intervals were chosen) the array of poles on the upper sheet must be rotated 10° about the movable rotation axis. In the calculation it is necessary to follow only the position of the $\langle 110 \rangle_U$ and $\langle \bar{1}11 \rangle_U$ poles for reasons that will

emerge subsequently. The rotation axis for this manipulation is placed coincident with the poles of the Wulff net, and the sequence of positions of each pole may be rapidly plotted by marking each 10° interval along the latitude line on which that pole is found.

If a pair of $\{111\}$ planes, say the $(1\bar{1}1)_L$ and the $(11\bar{1})_U$, are chosen and their intersection plotted for each position of the $(11\bar{1})_U$ plane, the nearest $\langle 110 \rangle$, $\langle 112 \rangle$, or $\langle 123 \rangle$ direction to that intersection in lattice L and lattice U must always lie in the $(1\bar{1}1)_L$ plane and the $(11\bar{1})_U$ plane, respectively. It

$\langle 123 \rangle$ direction in each lattice may be rapidly read from the two curves. The larger of these two angles, μ , is used to determine the value of δ , and the values of γ for which μ has a maximum or minimum can be rapidly determined by sliding a vertical straight-edge across the diagram and noting the positions where each curve is at the same distance from a horizontal line. Between these points the curve is very nearly straight and is, except in exceptional circumstances, as when both curves are very nearly horizontal, sufficiently closely approximated

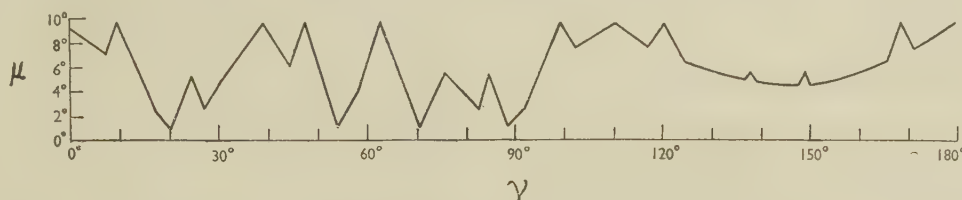


FIG. 12.— μ/γ Curve Derived from the ψ/γ Curves of Fig. 11.

is necessary to measure only the angle ψ that the intersection makes with a given direction in each plane to specify its position and to obtain the values of δ in a convenient manner. A typical ψ/γ curve is shown in Fig. 11. The positions of the relevant directions can be inserted into the diagram as shown. Thus, for a given value of γ , the angle that the intersection makes with the nearest $\langle 110 \rangle$, $\langle 112 \rangle$, or

to by a straight line. Fig. 12 gives the μ/γ plot corresponding to Fig. 11.

If, for the other 15 possible intersections, the μ/γ curve is obtained in the same way and all the μ/γ curves superposed, then the smallest value of μ of any of the curves for given γ is the value of δ . Thus the envelope given by the minimum values is the δ/γ curve.

NOTICE TO AUTHORS OF PAPERS FOR THE "JOURNAL" AND CONTRIBUTORS TO DISCUSSIONS

1. Papers will be considered for publication from non-members as well as members of the Institute. They are accepted for publication in the *Journal* and not necessarily for presentation at any meeting of the Institute. MSS. should be addressed to The Editor of Publications, The Institute of Metals, 4 Grosvenor Gardens, London, S.W.1.

2. Papers suitable for publication may be classified as:

(a) Papers recording the results of original research.
(b) First-class reviews of, or accounts of progress in, a particular field.

(c) Papers descriptive of works methods, or recent developments in metallurgical plant and practice.

(d) Papers in classes (a), (b), and (c) above, previously published in languages other than English, French, German, or Italian, if of sufficient merit.

3. Manuscripts and illustrations should be submitted in duplicate. MSS. must be typewritten (double-line spacing) on one side of the paper only, and authors are requested to sign a declaration that neither the paper nor a substantial part thereof has been published elsewhere. Exceptions may be made in certain cases where a paper has been published in a language other than English, French, German, or Italian (see 2(d) above). MSS. not accepted are normally returned within 6 months of receipt.

In the interests of economy, all papers must be written as concisely as possible; in general, internal research reports are not in suitable form for publication as papers in the *Journal*. All but the simplest mathematical expressions should be written by hand, with capital and small letters clearly distinguished. Superscript and subscript letters should also be plainly indicated. Greek letters and special signs should be identified in the margin. For style, spelling, and abbreviations used, any recent issue of the *Journal* may be consulted.

4. Synopsis. Every paper must have a synopsis (not exceeding 250 words in length) which, in the case of a paper reporting original research, should state its objects, the ground covered, and the nature of the results. The synopsis will appear at the beginning of the paper, and should be in a form suitable for use by abstracting organizations. Extracts from a "Guide for the Preparation of Synopses" drawn up by the Abstracting Services Consultative Committee are reproduced below.

5. References must be collected at the end of the paper and must be numbered in the order in which they occur in the MS. Initials of authors must be given, and the Institute's official abbreviations for periodical titles (as used in *Metallurgical Abstracts*) should be employed, where known. References to papers should be set out in the style:

A. L. Dighton and H. A. Miley, *Trans. Electrochem. Soc.*, 1942, 81, 321 (i.e. year, volume, page).

References to books should be in the following style:

C. Zener, "Elasticity and Anelasticity of Metals". Chicago: 1948 (University of Chicago Press).

6. Illustrations. Each illustration must have a number and description; only one set of numbers must be used in one paper, and it is desirable to number the half-tone illustrations consecutively, rather than to intersperse them with the line figures. The captions should be typed on a separate sheet.

The set of line figures sent for reproduction must be drawn (about twice the size to appear in the *Journal*) in Indian ink on smooth white Bristol board, good-quality drawing paper, co-ordinate paper, or tracing cloth, which are preferred in the order given. Co-ordinate paper, if used, must be blue-lined, with the co-ordinates to be reproduced finely drawn in Indian ink. Curves should be drawn boldly (i.e. at least twice the thickness of the frame). Experimental points should be indicated by open or closed circles, triangles, squares, &c. (preferably not crosses). Curves should be broken on each side of such symbols and plenty of allowance should be made for closing up in blockmaking. All lettering and numerals, &c., should preferably be in pencil, so that the Institute's standard lettering may be affixed, and ample margins must be left outside the framework of the figures to enable this to be done. The second set of line illustrations may be photostat copies.

Photographs must be restricted in number, owing to the expense of reproduction, and photomicrographs should be trimmed to the smallest possible of the following sizes consistent with adequate representation of the subject: 4 in. deep by 3 in. wide: 2 in. deep by 3 in. wide: 2 in. square. Magnifications of photomicrographs must be given in each case. Photographs for reproduction should be loose, not pasted down (and not fastened together with a clip, which damages them), and the figure number and author's name should be written on the back of each. Captions should be given to the photomicrographs, but these should be kept as brief as possible.

Because of the present high cost of printing and paper it is imperative that authors restrict illustrations (particularly photographs) to the absolute minimum deemed necessary to support their argument. Only in exceptional cases will illustrations be reproduced if already printed and readily available elsewhere.

7. Tables or Diagrams. Results of experiments, &c., may be given in the form of tables or figures, but (unless there are exceptional reasons) not both. Tables should bear Roman numbers, and each should have a heading that will make the data intelligible without reference to the text.

8. Corrections. A certain number of corrections in proof are inevitable, but any modification of the original text is to be avoided. Since corrections are very expensive, the Institute reserves the right to require authors to contribute towards their cost if the Editor deems them to be excessive. The Institute also reserves the right to require a contribution to the cost of remaking any block where this is necessitated by an error on the author's part.

9. Reprints. Individual authors are presented with a maximum of 25, and two or more authors with a maximum of 50 reprints from the *Journal*, without covers. Limited numbers of additional reprints can be supplied at the author's expense, if ordered before proofs are passed for press. (Orders should preferably be placed when submitting MSS.)

10. Discussion. Except in the case of special symposia, shorthand records of discussions are not taken at meetings. Written discussion may be submitted on any paper, preferably typewritten (double-line spacing). References should be given in the form of footnotes. Paragraphs 6 and 7 above are also applicable to such contributions. Reprints of discussion cannot be supplied to contributors.

GUIDE FOR THE PREPARATION OF SYNOPSES

(As recommended by the Abstracting Services Consultative Committee)

1. Purpose. The synopsis is not part of the paper; it is intended to convey briefly the content of the paper, to draw attention to all new information, and to the main conclusions. It should be factual.

2. Style of writing. The synopsis should be written concisely and in normal rather than abbreviated English. It is preferable to use the third person. Where possible use standard rather than proprietary terms, and avoid unnecessary contracting.

It should be presumed that the reader has some knowledge of the subject, but has not read the paper. The synopsis should therefore be intelligible in itself without reference to the paper; for example, it should not cite sections or illustrations by their numerical references in the text.

3. Content. The title of the paper is usually read as part of the synopsis. The opening sentence should be framed accordingly and repetition of the title avoided. If the title is insufficiently comprehensive, the opening should indicate the subjects covered. Usually the beginning of a synopsis should state the objective of the investigation.

It is sometimes valuable to indicate the treatment of the subject by such words as: brief, exhaustive, theoretical, &c.

The synopsis should indicate newly observed facts, conclusions of an

experiment or argument and, if possible, the essential parts of any new theory, treatment, apparatus, technique, &c.

It should contain the names of any new compound, mineral species, &c., and any new numerical data, such as physical constants; if this is not possible, it should draw attention to them. It is important to refer to new items and observations, even though some are incidental to the main purpose of the paper; such information may otherwise be hidden, though it is often very useful.

When giving experimental results the synopsis should indicate the methods used; for new methods the basic principle, range of operation, and degree of accuracy should be given.

4. References. If it is necessary to refer to earlier work in the summary, the reference should always be given in full and not by number. Otherwise references should be left out.

When a synopsis is completed, the author is urged to revise it carefully, removing redundant words, clarifying obscurities, and rectifying errors in copying from the paper. Particular attention should be paid by him to scientific and proper names, numerical data, and chemical and mathematical formulae.

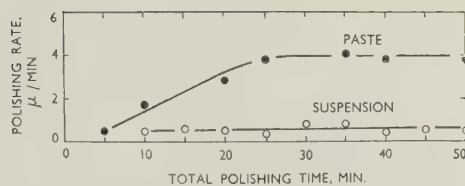


FIG. 1.—Comparative Polishing Rates for Paste-Charged and Suspension-Charged Pads. Specimen: annealed copper; diamond abrasive: (8–20) μ grade.

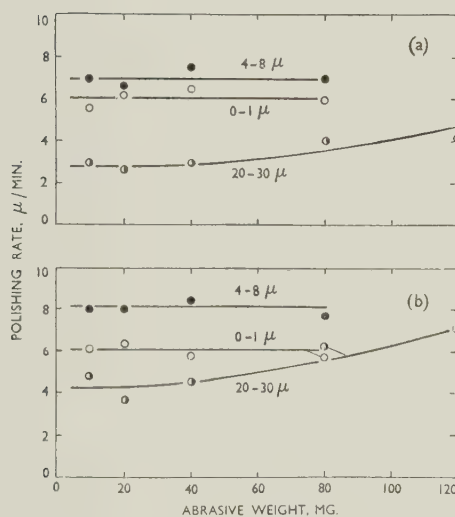


FIG. 2.—Variation in Polishing Rate with Weight of Added Abrasive. (a) Annealed copper; (b) heat-treated aluminium alloy. Abrasive added as impregnated paste.

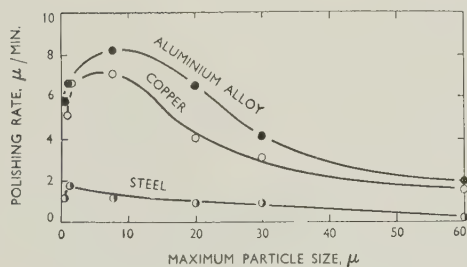
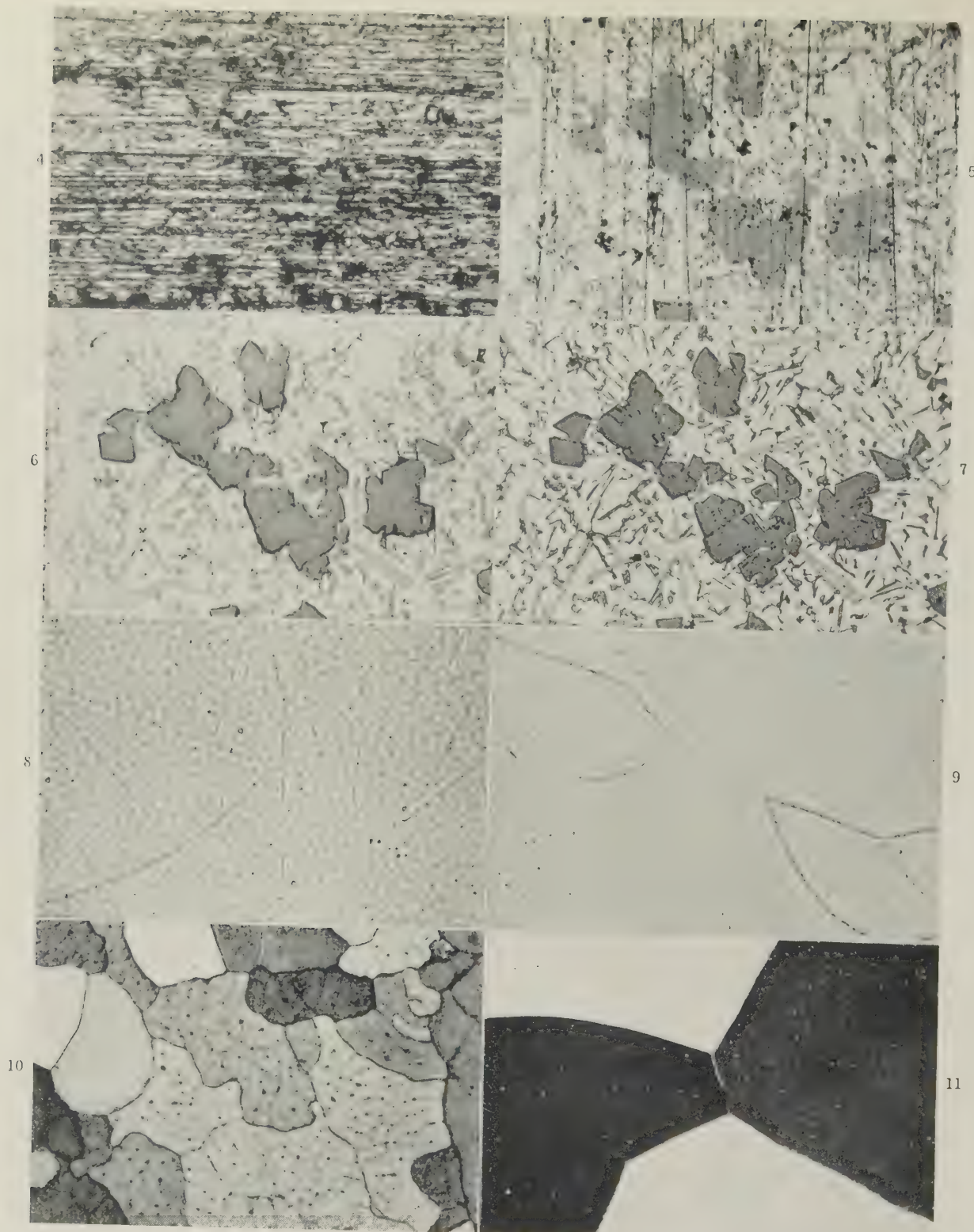


FIG. 3.—Variation in Polishing Rate with Abrasive Particle Size. Abrasive added as impregnated paste; abrasive weight 40 mg.



FIGS. 4-7.—Aluminium-13% Silicon Alloy at Major Stages of Polishing Process. $\times 250$.

FIG. 4.—400-Grade silicon carbide paper.

FIG. 5.—Alumina wax lap.

FIG. 6.—(0-1) μ -grade diamond pad.

FIG. 7.—Magnesium oxide pad, etched 0.5% HF solution.

FIG. 8.—Super-Purity Aluminium. Normal magnesium-oxide pad. Phase-contrast illumination. $\times 100$.

FIG. 9.—As for Fig. 8. Finish-polished by skidding technique.

FIG. 10.—Tin, Etched in 5% Ammonium Persulphate. $\times 250$.

FIG. 11.—Annealed Zinc, under Polarized Light. $\times 100$.




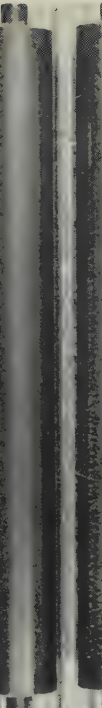

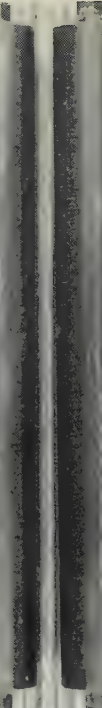

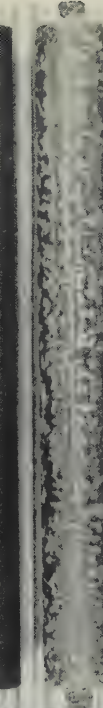
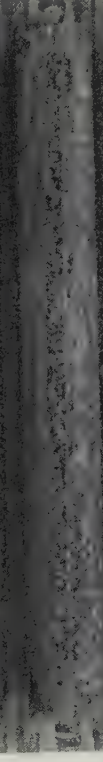
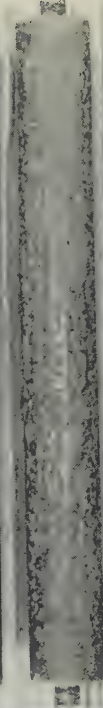




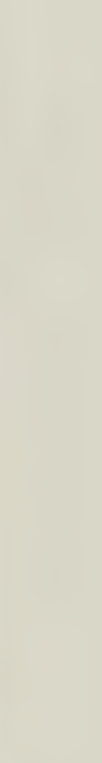
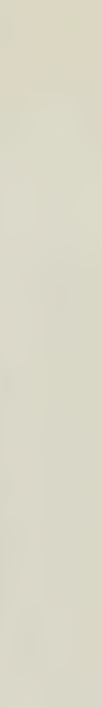
Mark	Primer	Top Coat	Before Cleaning	After Cleaning
<i>g</i>	Zinc chromate	D.T.D. 63A		
<i>i</i>	Zinc chromate	D.T.D. 260A		
<i>h</i>	Zinc tetroxy-chromate	D.T.D. 63A		
<i>m</i>	Zinc tetroxy-chromate	D.T.D. 260A		
<i>j</i>	Red lead	D.T.D. 63A		
<i>n</i>	Red lead	D.T.D. 260A		
<i>k</i>	Iron oxide	D.T.D. 63A		
<i>o</i>	Iron oxide	D.T.D. 260A		

FIG. 1.—Cast Bars of High-Purity Magnesium Alloy (D.T.D. 59A) after 3½ Years' Exposure at the Marine Site.

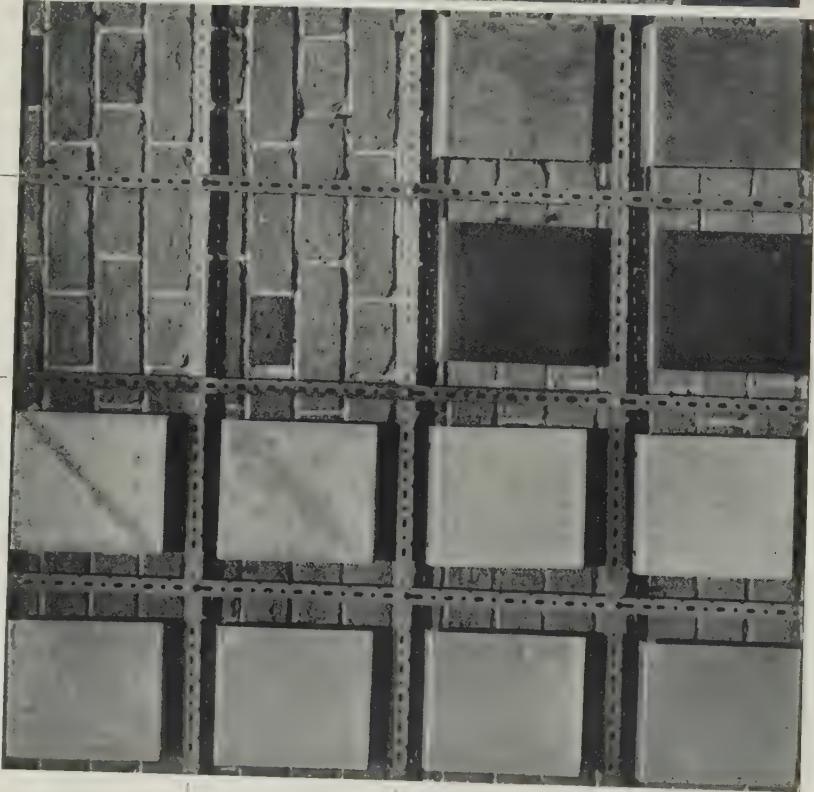
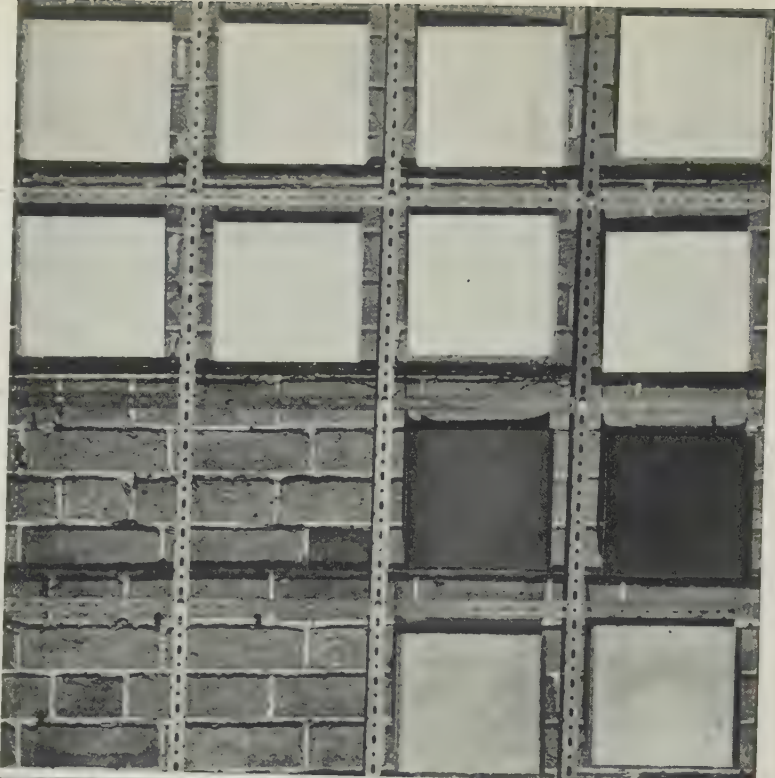
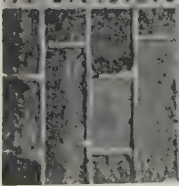
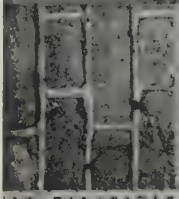
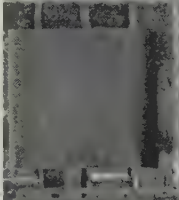

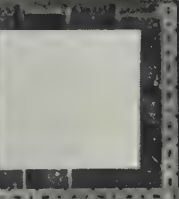

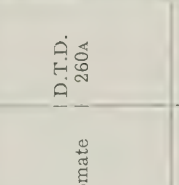
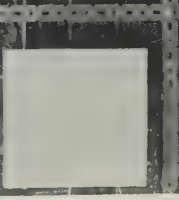
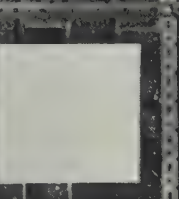


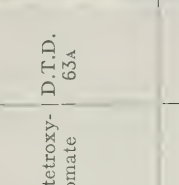
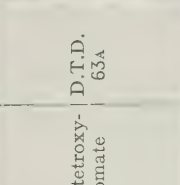




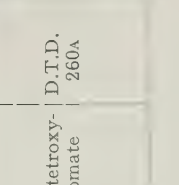




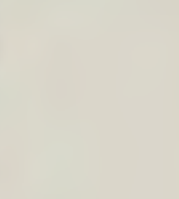
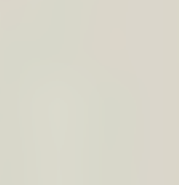
Mark	Primer	Top Coat	Aluminium (Alloys)		Magnesium Alloys		Magnesium Alloys		Aluminium (Alloys)	
			Pure Aluminium	Alloy B.S.S. 5L3	High Purity D.T.D. 120A	Normal Purity D.T.D. 118	Normal Purity D.T.D. 118	High Purity D.T.D. 120A	Alloy B.S.S. 5L3	Pure Aluminium
j	Red lead	D.T.D. 63A								
n	Red lead	D.T.D. 260A								
k	Iron oxide	D.T.D. 63A								
o	Iron oxide	D.T.D. 260A								
										

FIG. 2.—Cleaned Panels after 3½ Years' Exposure at the Marine Site.

Mark	Primer	Top Coat	Aluminium (Alloys)		Magnesium Alloys		Aluminium (Alloys)	
			Pure Aluminium	Alloy B.S.S. 5L3	High Purity D.T.D. 120A	Normal Purity D.T.D. 118	Alloy B.S.S. 5L3	Pure Aluminium
<i>g</i>	Zinc chromate	D.T.D. 63A						
<i>l</i>	Zinc chromate	D.T.D. 260A						
<i>h</i>	Zinc tetroxy-chromate	D.T.D. 63A						
<i>m</i>	Zinc tetroxy-chromate	D.T.D. 260A						

Fronts

Backs

FIG. 3.—Cleaned Panels after 3½ Years' Exposure at the Marine Site.

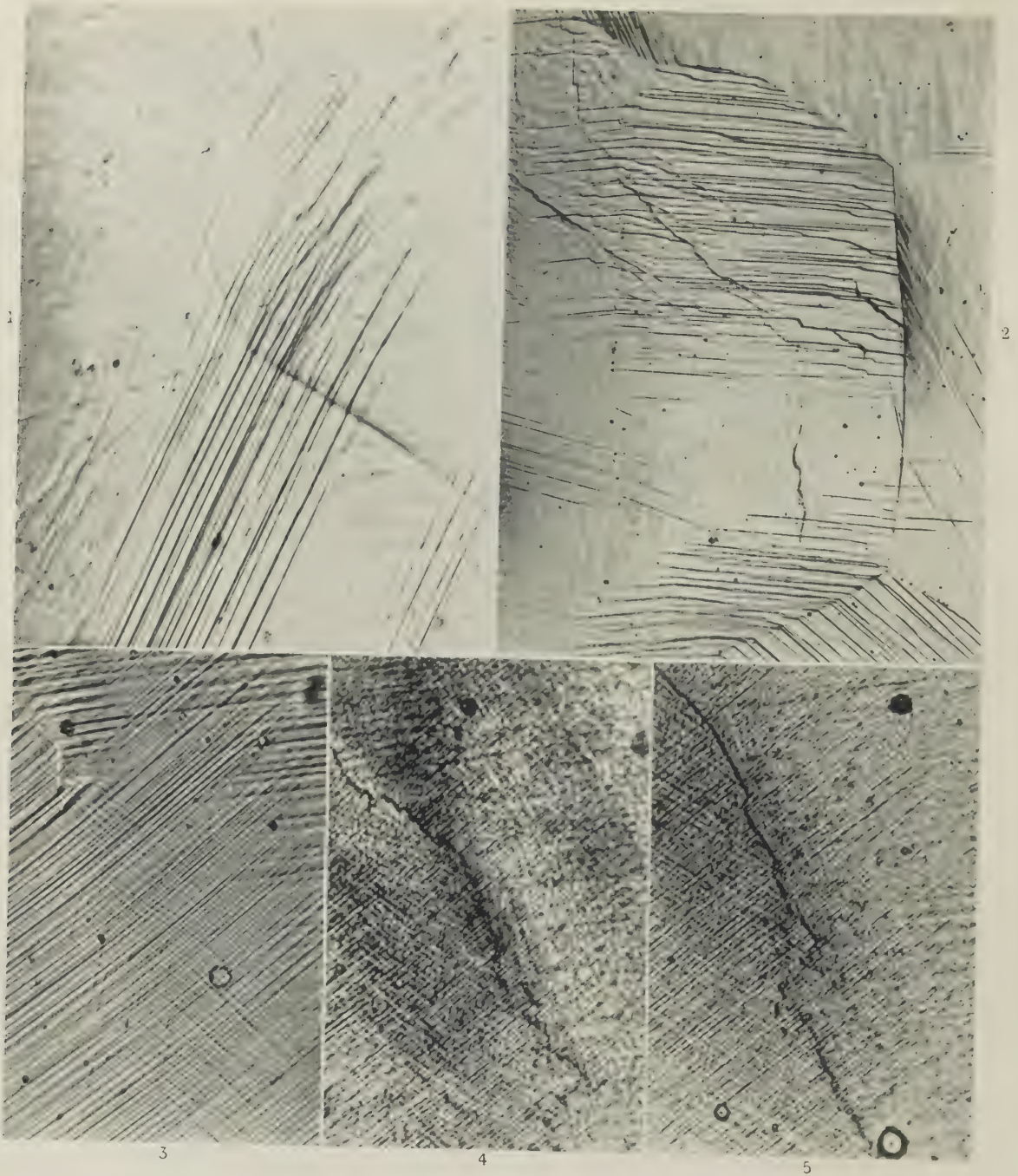


FIG. 1.—Slip Lines Crossing Grain Boundaries in Pure Aluminium. $\times 200$.

FIG. 2.—Grain of Pure Aluminium with Its Boundary Divided into a Number of Nearly Straight Sections. $\times 150$.

FIGS. 3-5.—Grain-Boundary Region in α -Brass. $\times 600$.

FIG. 3.—Original surface.

FIG. 4.—Same field after electropolishing 10 microns from surface and then anodic etching in dilute $\text{Na}_2\text{S}_2\text{O}_3$.

FIG. 5.—Same field after polishing 40 microns from the surface.

HYDROGEN BLISTERS IN BRASS SHEET*

1470

By R. EBORALL,† M.A., MEMBER, and A. J. SWAIN,‡ M.A.,
MEMBER

(Communication from the British Non-Ferrous Metals Research Association.)

SYNOPSIS

Blisters appearing near the centre plane of brass sheet were attributed to hydrogen collecting and persisting in central voids of the cast slab, so that these voids did not weld up during rolling; expansion of the compressed hydrogen on annealing the brass after it had been reduced to thin sheet and so was unable to withstand the stresses produced, caused the appearance of blisters. It was found that hydrogen was lost during annealing, and an effective remedy was developed based on this observation and on a proposed mechanism of blistering. Approximate measurements of the solubility of hydrogen in solid 2:1 brass gave values somewhat lower than the published values for copper.

I.—INTRODUCTION

THE work described in the present paper was undertaken to ascertain the causes of a very severe and persistent case of blistering in 2:1 and 70:30 brass sheet. The sheet was made from chill-cast ingots by breaking down hot and subsequently rolling cold, after surfacing, with intermediate anneals. Considerable amounts of cross-rolling were involved. The blisters first appeared after annealing when the sheets were from about $\frac{1}{8}$ in. thick to about 18 gauge, depending on the thickness of the original ingot, and were all on or near the centre plane of the sheet.

Preliminary experiments, in which blisters were drilled *in vacuo* and the released gas measured and analysed, showed the gas to consist entirely of hydrogen. The calculated volume of one blister was approximately 30 mm.³, and the quantity of hydrogen obtained from it was 15.6 mm.³ at N.T.P. Thus the hydrogen exerted a pressure of approximately $\frac{1}{2}$ atmosphere in the blister at room temperature, or about $1\frac{1}{2}$ atmospheres at the annealing temperature (550°C.). The surface of the metal inside the blisters was completely clean.

The fact that the gas extracted from the blisters was pure hydrogen indicated that the blisters did not arise from mechanically entrapped bubbles of gas injected into the solidifying ingot during pouring—a generally accepted and well-established cause of surface blistering in cross-rolled brass sheet¹—and experiments were accordingly planned to determine whether the blisters were formed by another mechanism, which is generally accepted for some other metals. A brief outline of this mechanism is given and the experimental work and remedial measures and their successful application in practice are described.

II.—MECHANISM OF BLISTER FORMATION

The established mechanism of blister formation in metals as a result of the presence of dissolved gas (see, for instance, Edwards² on pickling steel) may be summarized briefly as follows. A dissolved gas exists in solution in a metal in the atomic or ionic state, and is frequently present in excess of the equilibrium solid solubility at atmospheric pressure and at the temperature of heat-treatment. This dissolved gas may be present in the ingot as cast, and in some circumstances the quantity may be increased by surface reactions, e.g. during pickling or during heat-treatment in an unsuitable atmosphere. In many cases the dissolved gas atoms are practically immobile at room temperature, but at elevated temperatures they become free to diffuse through the metal; this would be expected in the case of copper-base alloys. When they are sufficiently mobile, the dissolved gas atoms associate to form molecules at the free surface of the metal, these are evolved into the atmosphere, and the concentration of dissolved gas just below the surface tends towards the value in equilibrium with the partial pressure of the particular gas in the atmosphere. At any internal cavity or discontinuity, gas atoms similarly associate and are released into the cavity; here, however, the gas is not free to escape, and so a gas pressure is built up in the cavity, until equilibrium is reached with the dissolved gas which is present around the cavity. Since the solubility of a diatomic gas such as hydrogen is proportional to the square root of the pressure, it is evident that large pressures may be developed in the cavity; for instance, if the gas is present at a concentration of 10 times the equilibrium value at atmospheric pressure (a not unusual occurrence), a pressure of 100 atmospheres may be developed.

* Manuscript received 19 February 1953. The work described in this paper was made available to members of the B.N.F.M.R.A. in a confidential Technical Memorandum issued in November 1949.

† Head of the General Metallurgy Section, British Non-Ferrous Metals Research Association, London.

‡ Aluminium Wire and Cable Co., Ltd., Swansea; formerly Investigator, British Non-Ferrous Metals Research Association.

Heating the metal to sufficiently high temperatures will result in diffusion over longer distances, and the concentration of dissolved gas throughout the metal will tend towards the value in equilibrium with the external atmosphere; this value may be greater or less than the original concentration. Although large pressures may frequently be developed, it is unlikely that a blister will form unless either the metal is very weak, e.g. partially molten, or the cavity is particularly suitable. It is evident that an extensive flat discontinuity parallel to the surface and only a short distance below it is the most conducive to blister formation, while a small spherical hole at a great depth can only be enlarged by a very great pressure.

The prerequisites for the formation of gas blisters, therefore, are: (a) The presence of gas in the metal in quantities substantially exceeding the solubility at the temperature concerned and at atmospheric pressure. (b) The presence of suitable discontinuities, the most favourable to blistering being discontinuities of large length and breadth in a plane parallel to the surface and lying a little below it.

In the present instance the cavities concerned were near the central plane of the sheet, and it can readily be seen that the disposition of the cavities becomes more favourable to blistering as the sheet becomes thinner, for the lateral dimensions of any cavities initially present are progressively enlarged and the distance below the surface is reduced. It is evident, too, that strip rolling should give a product less liable to this type of trouble, for by this method the cavities are simply extended in one direction and the bridge of metal over them is therefore short and well supported.

To understand the blistering occurring in this instance, it is necessary to know (a) the source of hydrogen and the way in which the hydrogen content varies in processing, and (b) the origin of the cavities.

III.—GAS CONTENT OF CAST AND WROUGHT BRASSES

1. OCCURRENCE OF CAVITIES

The ingots, which were normally about 3 ft. long and $1\frac{1}{4}$ in. thick, were chill cast in vertical cast-iron moulds which were coated with a mixture of lard oil and resin that volatilized during pouring and burned at the mouth of the mould. Pouring was done through a tundish with a number of holes and was completed in 10–15 sec.

Examination of an ingot showed it to be substantially sound apart from some centre-line shrinkage. It is improbable that a much sounder product could be obtained by altering the casting conditions, unless the thickness of the ingot were increased. The amount of central shrinkage, although not large, appeared to be sufficient to explain the occurrence of centre-line blisters during fabrication, provided that sufficient hydrogen was present.

2. HYDROGEN CONTENT OF THE METAL

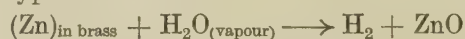
The hydrogen present in the metal might have come from one or more of several sources. The most obvious possibilities were:

(i) Raw materials and scrap used for the furnace charge. These might introduce hydrogen into the molten metal.

(ii) Melting furnace atmosphere. Hydrogen might be absorbed from moisture and/or other hydrogen-containing gases, although the high vapour pressure of zinc in the molten brass would minimize such absorption.

(iii) Mould atmosphere. Hydrogen might be introduced during casting from the cracking of hydrocarbons from the volatile dressing or from the decomposition of steam by the zinc.

(iv) Preheating furnace atmosphere. The ingots were preheated for rolling in a coal-fired furnace in which the flue gases formed the furnace atmosphere. There appeared to be a possibility that a reaction of the type



could occur and that some of this hydrogen might be forced into the metal, as it is when the analogous reaction occurs with aluminium-magnesium alloys. It is unlikely that hydrogen itself would be present in the atmosphere in any large quantity.

(v) Annealing furnace atmosphere. Intermediate anneals during cold rolling were done in air in an electric muffle furnace, and it was thought unlikely that gas was absorbed at this stage.

Accordingly, samples were taken from typical products and examined for hydrogen content with the results shown in Table I.

TABLE I.—*Hydrogen Contents of 2:1 Brass Samples Taken at Random at Various Stages of Production.*

Stage in Production	Hydrogen Content, c.c. at N.T.P./100 g.
Ingot	0.36, 0.34
(a) <i>Normal Hot- and Cold-Rolling Schedule:</i>	
Hot-rolled plate ($\frac{3}{8}$ or $\frac{7}{16}$ in.) . .	0.24
0.068 in. sheet	0.06 *
0.041 in. sheet	0.06 *
(b) <i>Cold-Rolled from Ingot:</i>	
$\frac{3}{16}$ in. plate (annealed at $\frac{7}{16}$ in.) . .	0.12
$\frac{1}{8}$ in. sheet (annealed again at $\frac{3}{16}$ in.)	0.02 †
20 S.W.G. sheet (0.036 in.)	0.04 †
" " " (annealed)	0.08 †

* From sound parts of sheets.

† There is a blank error (not allowed for) probably associated with the surface of the sample, and this will be proportionately greater for thin samples. The higher figures obtained on 20-S.W.G. sheet compared with $\frac{1}{8}$ -in. sheet may, therefore, not represent a real increase in hydrogen content.

In a further experiment a 2:1 brass ingot was cut in half and one half hot rolled. Samples taken from the ingot and from the equivalent position in the hot-rolled plate gave gas contents of 0.29 and 0.14 c.c./100 g., respectively.

A small sample of a 70 : 30 brass melt was poured on to a copper block free from mould coating, and another sample was taken from an ingot cast from this melt in the usual way. The corresponding gas contents were 0.13 and 0.44 c.c./100 g., which may indicate absorption of gas during casting, although some gas may have escaped from the thin sample poured on to the copper block.

The results show that the metal as cast has a considerable hydrogen content, and that hydrogen is lost in both the preheating and the annealing furnaces.

The mechanism postulated for the blistering in this case is, therefore, that during preheating for hot rolling some of the hydrogen present in the ingot diffuses to the shrinkage cavities and develops a large pressure of gaseous hydrogen in them. On hot rolling the cavities are closed up to some extent, but complete welding up is prevented by the compressed hydrogen. These flattened-out cavities remain in existence during the subsequent cold rolling until the sheet becomes thin enough to allow the gas pressure to expand the cavities to a visible extent when the metal softens during annealing.

IV.—REMEDIAL MEASURES AND THEIR PRACTICAL APPLICATION

The foregoing measurements show that hydrogen is removed by annealing. Experiments were done to see how rapidly this removal occurred and to what extent it was limited by atmospheric conditions.

Samples approximately $1 \times \frac{3}{4} \times \frac{1}{4}$ in., from the ingot and hot-rolled plate ((a) of Table I) were heated to 800° C. for 1 hr. in a silica-tube furnace in dry air and in a steam/air mixture (very roughly equal quantities of each). The hydrogen contents after treatment were as shown in Table II.

TABLE II.—Effect of Annealing Atmosphere on Gas Content of 2 : 1 Brass.

Sample	Hydrogen Content, c.c. at N.T.P./100 g.		
	Initially	After Heating to 800° C. for 1 Hr.	
		In Dry Air	In Steam/Air
Ingot	0.29	0.01	0.01
Hot-rolled plate. . .	0.14	0.02	0.02

A subsequent test on samples from which the gas had been extracted *in vacuo* showed that the blank was of this order of magnitude, so that the true hydrogen content after treatment was effectively zero.

Samples of the same size, taken from the hot-rolled plate, were given shorter treatments in dry air at 600° and 800° C. and the loss of hydrogen followed, with the results shown in Table III.

The hydrogen content of a $\frac{1}{4}$ -in.-thick piece is thus reduced to a very low value after $\frac{1}{4}$ hr. at 800° C. or

1 hr. at 600° C. Corresponding times for other thicknesses may be obtained by multiplying by the square of the thickness ratio; thus for x in. thick at 600° C. the time would be $16x^2$ hr., and at 800° C. it would be $4x^2$ hr.

TABLE III.—Removal of Hydrogen by Annealing.

Time, hr.	Hydrogen Content, c.c. at N.T.P./100 g.	
	800° C.	600° C.
$\frac{1}{4}$	0.01	0.12
$\frac{1}{2}$	0.01	0.04
1	0.01	0.02
$1\frac{1}{2}$...	0.02

These results suggest a possible remedy for blistering. The hydrogen can be almost completely removed by annealing at such a stage that: (a) the cavities are substantially flattened out at the start of annealing, so as not to provide a reservoir for the gas, (b) the metal is thick enough to withstand the very large pressures developed in the flattened cavities at the start of annealing, and (c) the metal is not so thick that the required combination of time and temperature is impracticable.

On this basis a remedy was proposed, consisting of returning the hot-rolled plates (7/16 in. thick) to the preheating furnace (700°–800° C.) for 2 hr.

Samples were taken of the products at different stages from two ingots of the same batch, one of which was given the normal processing and the other given the extra furnace treatment. The hot-rolled plate had a hydrogen content of 0.39 c.c. at N.T.P./100 g. compared with 0.02 c.c. at N.T.P./100 g. for the similar plate after the extra furnace treatment.

Production trials showed that the remedy was completely effective. A large-scale test was carried out in which a batch of 100 ingots, cast four per melt, was halved, two ingots per melt being in each half-batch. One half-batch was processed by the usual hot- and cold-rolling schedule, and the sheet produced proved to be even more severely blistered than usual, 90% of the sheets being rejected because of this defect. The other half-batch was given the extra heat-treatment of 2 hr. in the preheating furnace at about 800° C., and none of the sheets produced was rejected for blistering.

V.—SOLUBILITY OF HYDROGEN IN 2 : 1 BRASS

1. EXPERIMENTAL METHODS

The method used was to soak sound, gas-free metal in hydrogen, quench it, and subsequently measure the gas content in the usual way. The hot-rolled plate (with initially 0.14 c.c. hydrogen at N.T.P./100 g.) described above was used for all experiments. Pieces of the plate were degassed by heating in dry air at 800° C. for $\frac{1}{2}$ hr. The oxide scale was removed

by filing. The pieces were then hammered to close any internal discontinuities, the thickness being reduced by about 25% in this operation. Samples of the plate so prepared were heated in dry hydrogen at various temperatures, in most cases for more than one period in order to check the degree of saturation, and were quenched into molten lead and then into iced water. After removal of the zinc-impoverished layer (about 1 mm. was removed from each surface after soaking at the highest temperature), the hydrogen content was estimated by vacuum extraction in the usual way.

2. RESULTS

The results of the solubility measurements are given in Table IV, and values derived from these are

TABLE IV.—Results of Solubility Measurements on 2 : 1 Brass.

Temperature, °C.	Duration of H ₂ Soak, hr.	H ₂ Content, c.c. at N.T.P./100 g.	Mean H ₂ Content, c.c. at N.T.P./100 g.
875	2½	{ 0.385	{ 0.347
850	3	{ 0.310	{ 0.088
		{ 0.081	
800	2	{ 0.080	{ 0.087
	4	{ 0.091	
		{ 0.095	
750	3½	{ 0.083	{ 0.063
	4	{ 0.062	
		{ 0.065	
700	5½	{ 0.063	{ 0.049
	6½	{ 0.050	
		{ 0.052	
650	7	{ 0.045	{ 0.019
		{ 0.049	
	8	{ 0.021	
		{ 0.021	
600	4	{ 0.018	{ 0.032
	7½	{ 0.017	
		{ 0.015 *	
		{ 0.025	
		{ 0.040	

* Ignored, since saturation may not have been reached.

plotted logarithmically against the reciprocal of the temperature in Fig. 1. The line drawn represents the best straight line for the points relating to alloys free from β phase (i.e. excluding the highest temperature).

Values for the solubility at 100° C. intervals in the range 500°–800° C., obtained from the best straight line of Fig. 1 are given in Table V. No great accuracy

TABLE V.—Solubility of Hydrogen in 2 : 1 Brass.

Temperature, °C.	Solubility, c.c. at N.T.P./100 g.
800	0.076
700	0.044
600	0.023
500	0.010

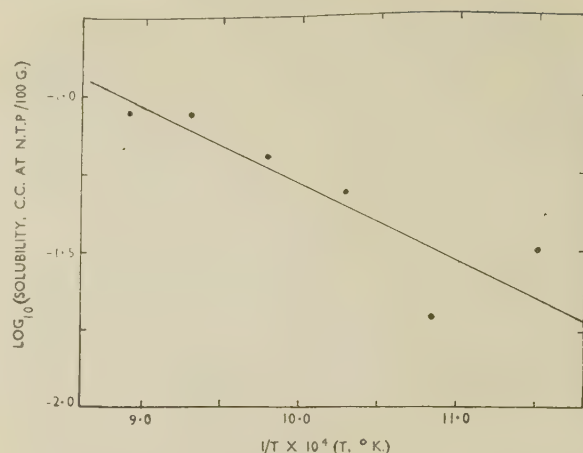


FIG. 1.—Solubility of Hydrogen in 2 : 1 Brass.

is claimed for these values, which are certainly liable to errors of up to ± 0.01 c.c./100 g. at the higher temperatures. They suffice, however, to indicate that the explanation of blistering put forward above is not based upon false assumptions. The results are substantially lower than those given by Sieverts and Krumbhaar³ and by Röntgen and Möller for copper.⁴

The two measurements at 875° C., at which temperature some β phase is present, appear to indicate that the solubility in the β phase may be considerably higher.

VI.—CONCLUSIONS

1. A form of centre-plane blistering in α -brass sheet has been shown to be due to hydrogen.

2. The hydrogen is present in the cast billet and is to some extent reduced at every anneal, even in a burnt-coal atmosphere.

3. The blistering can be eliminated by allowing the hydrogen to diffuse away under suitable conditions.

4. Hydrogen has a fair solubility in α -brass, though it is somewhat less than the published values for copper.

5. Hydrogen diffuses fairly rapidly in α -brass at 600° C. and above.

ACKNOWLEDGEMENTS

The authors are indebted to the Director and Council of The British Non-Ferrous Metals Research Association for permission to publish this paper.

REFERENCES

1. R. Genders and G. L. Bailey, "The Casting of Brass Ingots" (B.N.F.M.R.A. Research Monograph No. 3). London: 1934.
2. C. A. Edwards, *J. Iron Steel Inst.*, 1924, **110**, 9.
3. A. Sieverts and W. Krumbhaar, *Z. physikal. Chem.*, 1910, **74**, 277.
4. P. Röntgen and F. Möller, *Metallwirtschaft*, 1934, **13**, 81, 97.

CRITICAL-STRAIN EFFECTS IN COLD-WORKED WROUGHT ALUMINIUM AND ITS ALLOYS *

1471

By W. M. WILLIAMS,† B.Sc., and R. EBORALL,‡ M.A., MEMBER
(Communication from the British Non-Ferrous Metals Research Association.)

SYNOPSIS

Straining and annealing treatments have been applied to super-purity and commercial-purity aluminium and to four aluminium alloys, to test their behaviour against a set of empirical rules describing the effects of strain, annealing temperature, and initial grain-size on the critical strains and final grain-sizes. The final grain-size of the recrystallized material was found, for a given composition, to depend strongly on the strain and in most cases comparatively little on the annealing temperature and initial grain-size, although the latter had a definite effect, especially in super-purity aluminium. Owing to the strength of this effect in super-purity aluminium, the maximum grain-size which could be produced by annealing at a given temperature was generally increased by coarsening the initial grain-size, although for other materials the reverse was normally true.

I.—INTRODUCTION

THE experiments described in the present paper were designed to test the recrystallization behaviour of aluminium and some of its commercial alloys, with particular reference to critical strains and the coarse grain-sizes associated with them and to the effect of original grain-size. Published literature on this subject indicates that the grain-sizes produced by recrystallization during annealing can be described to a fair approximation in terms of the following general empirical rules:

(a) When a metal is cold worked and then annealed, the as-recrystallized grain-size decreases as the amount of deformation before annealing is increased, and is substantially independent of the annealing temperature.

(b) With a given annealing treatment, there is a critical strain below which complete recrystallization does not occur. This critical strain gives rise to the largest grains after annealing.

(c) The critical strain is higher, the lower the annealing temperature.

(d) For a given annealing temperature, the critical strain is higher, the larger the initial grain-size of the material and, because the recrystallized grain-size is mainly dependent on the strain, the maximum grain-size which can be produced by the given annealing treatment is smaller for initially coarse material than for fine-grained material.

The first three rules, and particularly (b) and (c), have been widely appreciated, and are derived from very early work, especially that of Chappell¹ and of

Carpenter and Elam.² Rule (d) is not so well known, but reference may be made to the work of Matthaes and Schroeder on Duralumin-type alloys³ and that of Gries and Esser on iron.⁴ Anderson and Mehl⁵ found that coarse-grained aluminium had both a slower rate of nucleation for new grains and a slower rate of grain growth under given conditions, than had a fine-grained material, and this would lead to a similar result.

The validity of these rules, as applied to aluminium and several of its alloys, has been tested, and the quantitative results are reported in the following sections. The rules take no account of any changes, such as coalescence and secondary recrystallization, which may in some metals take place after recrystallization during prolonged annealing or annealing at a high temperature.

II.—MATERIALS

The materials were all supplied by the courtesy of a member firm in the form of cold-rolled sheet of various tempers, and 0.064 in. thick. The analyses of these materials are given in Table I.

III.—EXPERIMENTAL PROCEDURE

1. PRODUCTION OF MATERIALS WITH VARIOUS INITIAL GRAIN-SIZES

For all the materials, except super-purity aluminium, a range of initial grain-sizes was obtained by annealing batches of different tempers at suitable temperatures. In several cases where the as-received materials did not yield a sufficient range of grain-sizes on annealing,

* Manuscript received 10 September 1952. The work described in this paper was made available to members of the B.N.F.M.R.A. in a confidential research report issued in January 1951.

† Investigator, British Non-Ferrous Metals Research Association, London.

‡ Head of the General Metallurgy Section, British Non-Ferrous Metals Research Association, London.

TABLE I.—Analyses of Alloys Examined.

Material	Fe, %	Si, %	Cu, %	Mn, %	Ti, %	Zn, %	Mg, %	Ni, %	Pb, %
S.p. Al	0.004 *	<0.002 *	<0.001 *	<0.001	<0.002 †	≤0.01 †	<0.01	<0.01 †	<0.002 †
C.p. Al	0.45	0.16	0.02	0.01	0.01	≤0.01 †	<0.01	<0.01 †	<0.002 †
2% Mg alloy . .	0.34	0.22	0.02	0.49	~0.01	0.01	2.1 *	<0.01 †	<0.002 †
1% Mg, 1% Si alloy .	0.4	0.98 *	~0.01	~0.02	<0.01	≤0.01 †	0.90 *	<0.01 †	<0.002 †
Duralumin-type alloy .	0.35	0.73 *	4.78 *	0.73 *	<0.01	≤0.01 †	0.43 *	<0.01 †	<0.002 †
1½% Mn alloy . .	0.59	0.21	0.12	1.14 *	<0.01	≤0.01 †	0.008	<0.01 †	~0.002

* Chemically determined, remainder spectrographically.

† Not detected.

they were annealed, rolled to a suitable reduction, or stretched by a suitable amount in a tensile machine, and then re-annealed to obtain the desired grain-size. As far as possible, the same annealing temperature was used throughout for any one alloy. Details of these treatments are given later.

In super-purity aluminium coalescence occurs readily at temperatures above 300° C., and specimens of the as-received material were accordingly annealed at various temperatures from 300° to 500° C. to produce various degrees of coalescence.

Using such methods, fully-annealed specimens of various initial grain-sizes were obtained with each material. For each different working and annealing treatment, an X-ray back-reflection photograph was taken to confirm that recrystallization was complete. This was followed by a metallographic examination of the grain structure. Except in the case of the Duralumin-type alloy (which was hand-polished at the final stage), the micro-specimens were electrolytically polished after a preliminary hand-polish and then anodically or chemically etched.

Grain counts were made with a Vickers projection microscope fitted with a moving stage and two vernier scales. The distance traversed when 50 grains passed the cross-wires was measured and used to give the number of grains/cm. traversed. Between five and ten separate counts were made in random directions on the surface of each specimen, and the reciprocal of the average count was taken as the grain dia. All grain-sizes were measured on the etched surface of the sheet.

2. RECRYSTALLIZATION EXPERIMENTS

The recrystallization behaviour of super-purity aluminium, commercial-purity aluminium, 2% magnesium alloy, and the 1% magnesium, 1% silicon alloy was conveniently studied by using tapered tensile specimens. Specimens were machined from the supplied sheet with their length parallel to the rolling direction, with a gauge-length of 20 cm., and a width decreasing from 1 in. at one end to ½ in. at the other. These gave a suitable range of strains when stretched or broken in tension.

Before being annealed to produce a range of initial grain-sizes, the gauge-length of each specimen was marked out at intervals of approximately 1 cm., the actual intervals being measured to 0.01 mm. with

a travelling microscope. Batches of the specimens were then annealed at a temperature appropriate to the particular alloy to produce several different starting grain-sizes. These annealing treatments were carried out in air in a muffle furnace, and details are given later.

The specimens were stretched in an Avery tensile-testing machine and each one remeasured with the travelling microscope to determine the exact strain at each point along the gauge-length. They were introduced into a salt bath to recrystallize as soon after deformation as possible (within a few hours) in order to minimize any effects on the recrystallization characteristics due to prior recovery at room temperature. The temperature of the salt bath was constant to $\pm 1^\circ$ C., and the annealing time in all cases was 30 min. Several recrystallization temperatures were used for each alloy with each initial grain-size. On removal from the salt bath, the specimens were macro-etched in a solution of one part water, one part conc. HNO_3 , one part conc. HCl , and one-sixth part conc. HF by volume.

The grain-size was measured at various points along the recrystallized portion of the gauge-length and related to the strain values before recrystallization. The critical strain was taken to be the strain at the junction between the recrystallized and unrecrystallized parts of the gauge-length, the exact point being that beyond which none of the original structure was retained.

A modification to the above sequence of operations had to be made for the Duralumin-type and the 1½% manganese alloys. The critical strains were too large to be studied by using tensile specimens, and the specimens were therefore deformed by rolling, as follows. Rectangular strips approximately 8 in. long and 1 in. wide were annealed to obtain the required initial grain-size, and then "wedge-rolled", i.e. the rolls were screwed down more one side than the other and the strip was fed with its length parallel to the axes of the rolls to give a range of deformation along the length of the strip. A micrometer measurement of the reduced thickness at any point gave a direct value of the reduction at that point. The lateral spread ($\sim 1\%$) was negligible. In this way a range of strain of 10–75% could be produced on a single specimen; the typical range necessary was about 15–50%. Subsequent procedure was then

similar to that for the tapered tensile specimens, the rolled pieces being recrystallized at various temperatures for $\frac{1}{2}$ hr.

The Duralumin-type and $1\frac{1}{4}\%$ manganese alloys

such a series of pictures it was possible to gauge the point of critical strain with reasonable accuracy (see X-ray patterns Figs. 13 (a) and (b), Plate LXXIX). The surface of that part of the specimen where the

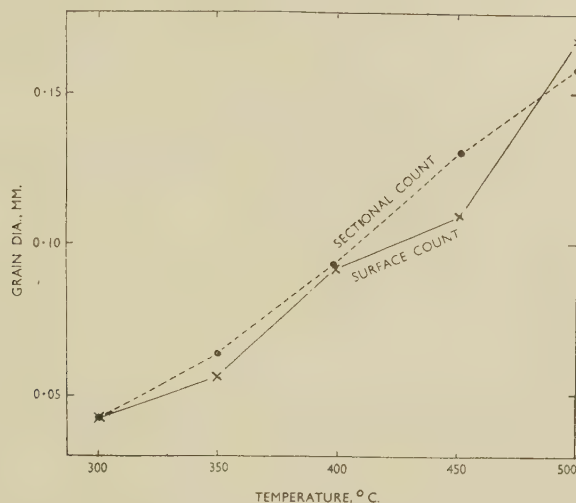


FIG. 1.—Grain-Size/Heat-Treatment Curve for Super-Purity Aluminium Annealed $2\frac{1}{2}$ hr. at $298^{\circ}\text{C.} + 1$ hr. at Various Temperatures.

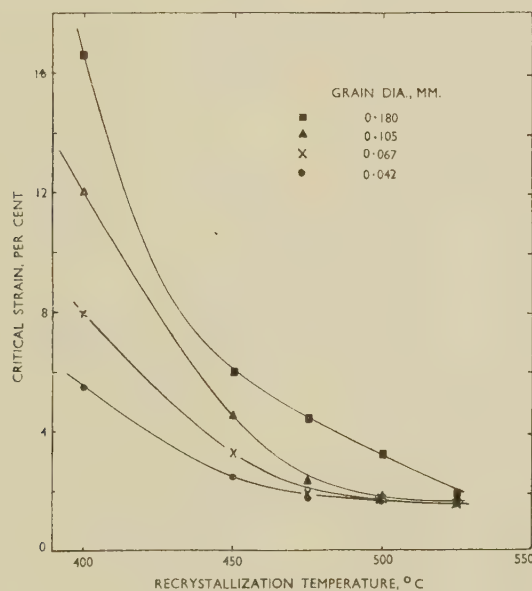


FIG. 2.—Critical-Strain/Recrystallization-Temperature Curves for Super-Purity Aluminium with Various Initial Grain-Sizes. Annealing time 30 min.

presented a new difficulty in that a macro-etch in mixed acids was suitable only for the highest temperature of recrystallization used. At other temperatures a micro-etch was necessary in order to reveal the grain-sizes after recrystallization. The boundary between the recrystallized and the unrecrystallized parts of the gauge-length was not readily detected by micro-examination and, to determine the point of critical strain, a series of X-ray back-reflection patterns was taken along the length of the rolled and partly recrystallized specimen. From

critical strain had occurred was then polished and etched to reveal the grain-size.

IV.—EXPERIMENTAL RESULTS

1. SUPER-PURITY ALUMINIUM

The results obtained with high-purity aluminium are reported in detail, since they are typical of the behaviour of all the materials tested. The results presented later for each individual alloy differ only

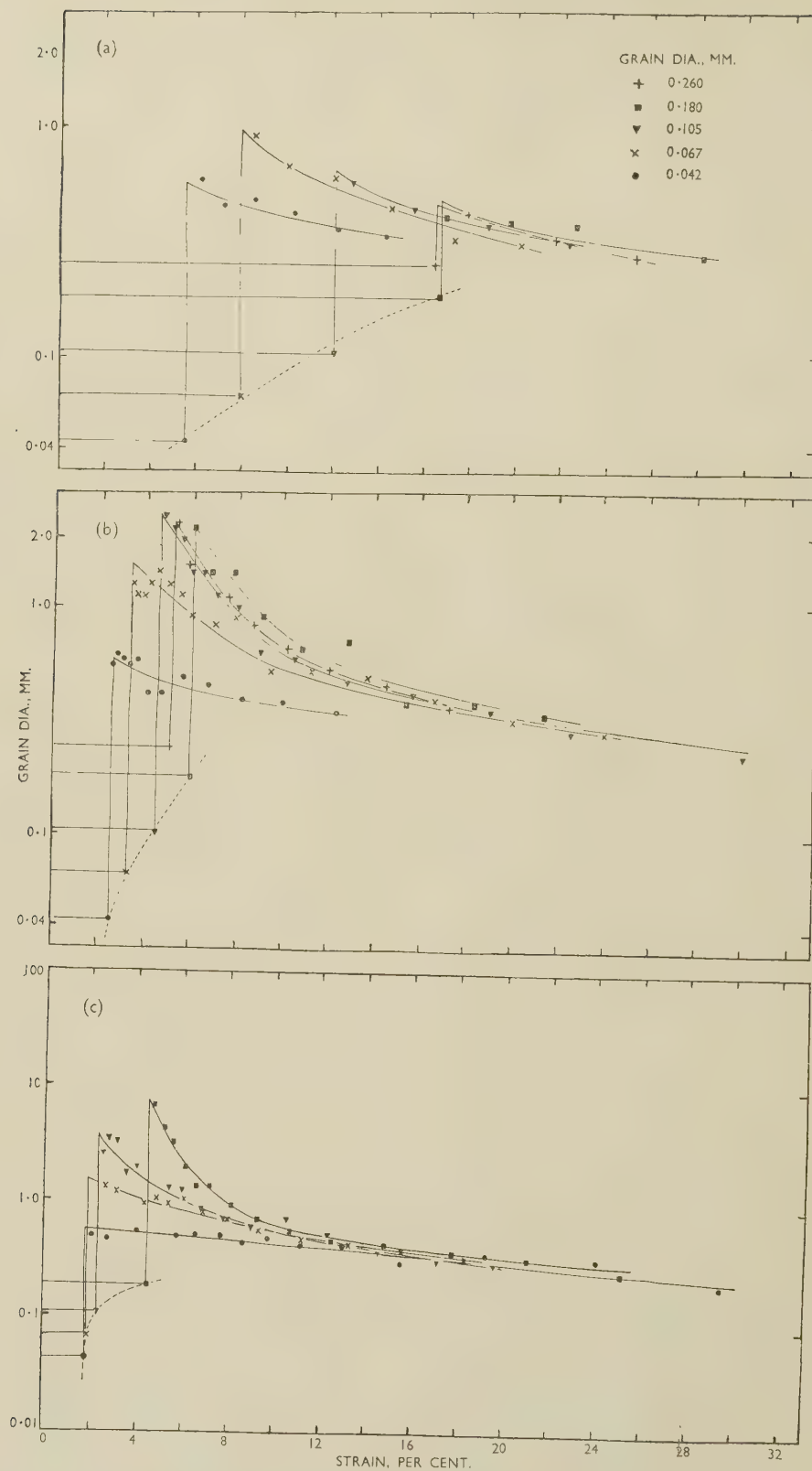


FIG. 3.
(For caption see opposite page.)

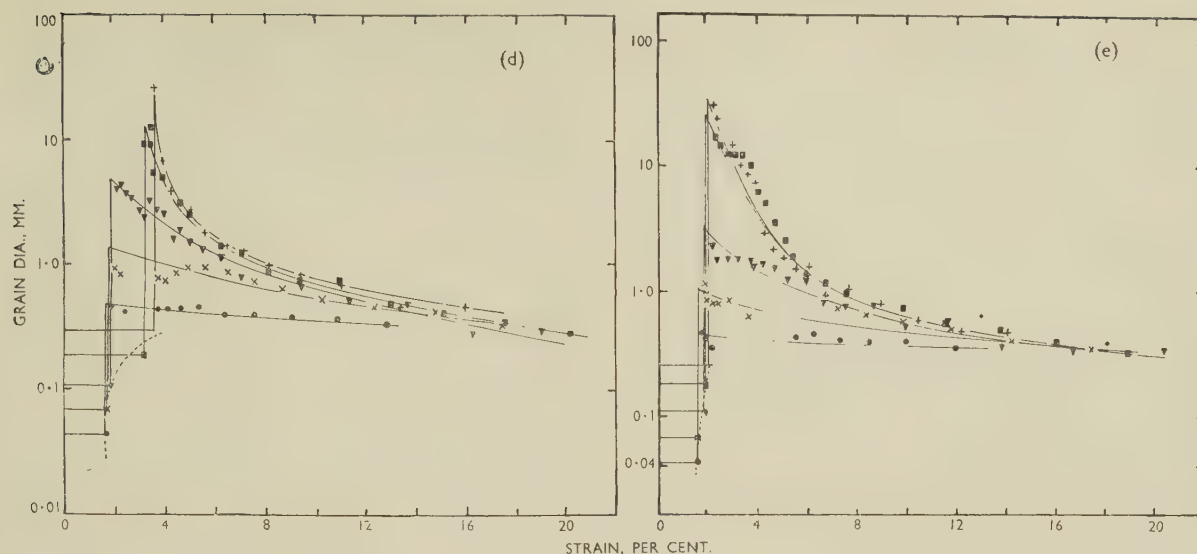


FIG. 3.—Recrystallization Diagrams for Super-Purity Aluminium with Various Grain-Sizes. Heat-treatment was 30 min. at (a) 400° C., (b) 450° C., (c) 475° C., (d) 500° C., and (e) 525° C.

numerically from those given for super-purity aluminium.

As mentioned previously, various initial grain-sizes were obtained by annealing as-received material in air at temperatures ranging from 298° to 500° C. (Fig. 1). Specimens with initial grain-sizes from 0.042 to 0.26 mm. were used in the tests.

Curves relating critical strain with temperature for various initial grain-sizes are given in Fig. 2. It will be seen that at the lower temperatures the critical strain is greatly dependent on the original grain-size, increasing with increasing grain-size. The dependence on initial grain-size rapidly diminishes, however, at higher recrystallization temperatures. For the initially fine-grained specimens the critical strain is relatively insensitive to the annealing temperature, so that at these higher temperatures it is almost independent both of the temperature and of the initial grain-size for the grain-size range studied.

Curves relating original grain-size with final grain-size for various strains are given in Fig. 3 (a)–(e) for the five temperatures used, viz. 400°, 450°, 475°, 500°, and 525° C. To gauge the effect of any coalescence occurring after recrystallization on the final grain-sizes initially shown in these curves, a short series of experiments was made. These consisted of measuring the grain-size of specimens with initial grain-sizes of 0.28 and 0.5 mm., before and after heat-treatments of 30 min. at temperatures up to 525° C. The results showed that the effect of coalescence is negligible for the grain-sizes and temperatures occurring in the present experiments, and the results given in Fig. 3 (a)–(e) should therefore be the true as-recrystallized values.

Each set of curves shows similar characteristics, and the following generalizations can be made:

(i) For a particular initial grain-size and temperature, coarse grain is developed at the

critical strain, the grain-size then rapidly decreasing with greater deformations to a less rapidly varying value.

(ii) Comparison of the curves in Fig. 3 (a)–(e), for specimens with a given initial grain-size shows that the final grain-size is mainly determined by the strain before annealing and is little affected by the temperature of the anneal, except near the points of critical strain (see also Fig. 11, Plate LXXIX).

These observations are in accordance with the general rules set out in Section I. There are other features of note, however, which are not predicted by these empirical rules.

(iii) For a constant strain, the resultant grain-size is finer, the finer the original grain-size; this effect is particularly noticeable with initially fine-grained material at small strains. So marked is this effect in super-pure aluminium when the initial grain-size is small and when the annealing temperature is high, that the empirical rule (d) does not in general apply to this material, the grain-size after critical straining and annealing in many conditions being larger, the greater the initial grain-size. However, the rule does apply when the initial grain-size is large and the annealing temperature is low (Fig. 3), and, as will be seen later, it applies to the other materials examined (Fig. 12, Plate LXXIX) in almost all the conditions studied.

(iv) For fine-grained super-pure aluminium (0.042 mm. grain-size), the dependence of the final grain-size on the amount of strain is small, and the grain-size after critical straining and annealing is not very much coarser than the final grain-size resulting from a relatively high deformation, e.g. 12%.

2. COMMERCIAL-PURITY ALUMINIUM AND ALUMINIUM ALLOYS

The curves relating grain-size with overstrain for the other materials (except for the Duralumin-type alloy, for which the information was insufficient to allow complete curves to be drawn) were all of similar type to those shown in Fig. 3 (a)–(e). In view of this similarity, the curves themselves are not reproduced; instead the chief features are given in the form of tables and figures below.

(a) Commercial-Purity Aluminium

Table II shows the preliminary heat-treatments for the sheets of different tempers in order to get a suitable range of initial grain-sizes. The treatments were carried out in air, in an electric muffle furnace, and were followed by air cooling.

TABLE II.—Preliminary Treatments for Commercial-Purity Aluminium.

Previous Deformation, %	Annealing Treatment	Resultant Grain-Size, mm.
15	24 hr. at 450° C. 1½ hr. at 400° C.	0.6
29		0.045
45		0.031
55		0.023

Fig. 4 shows the curves relating critical overstrain with temperature for commercial-purity aluminium of each of the four initial grain-sizes. Though the

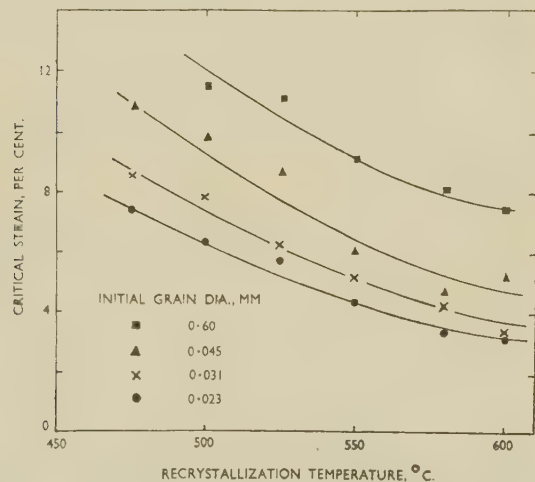


Fig. 4.—Critical-Strain/Recrystallization-Temperature Curves for Commercial-Purity Aluminium with Various Initial Grain-Sizes. Annealing time 30 min.

form of the curves is approximately the same as that for super-purity aluminium, the critical strains for comparable initial grain-sizes and the same temperature are much higher (cf. Fig. 2, p. 503).

Table III shows, for material with various initial grain-sizes, the grain-size developed at the critical strain after annealing at different temperatures.

Comparing the behaviour of commercial-purity aluminium having an initial grain-size of 0.045 mm.

with that of super-pure aluminium having an initial grain-size of 0.042 mm., it is seen that for the same annealing temperature it is the former which develops

TABLE III.—Grain-Sizes of Commercial-Purity Aluminium after Critical Strain and Annealing.

Initial Grain-Size, mm.	Final Grain-Sizes after Annealing at Various Temperatures, mm.					
	475° C.	500° C.	525° C.	550° C.	575° C.	600° C.
0.6	...	1.0	1.0	1.0	1.4	1.4
0.045	1.8	2.0	2.3	2.2	5.5	9.4
0.031	2.4	3.2	5.0	2.2	4.8	18.0
0.023	3.8	4.8	4.4	3.0	6.8	6.0

the coarser grain-size after critical straining and annealing. With larger initial grain-sizes (over about 0.1 mm.) it is not possible to make a strict comparison, but the indications are that the super-pure material may develop very much larger grains after critical straining and annealing, the difference between the two materials appearing to increase as the initial grain-size increases above this figure.

TABLE IV.—Grain-Sizes of Commercial-Purity Aluminium Recrystallized after Various Extensions.

Initial Grain-Size, mm.	Temp., °C.	Grain-Size after Various Extensions, mm.		
		5%	10%	20%
0.6	500	0.56
	550	...	0.83	0.51
	600	...	0.90	0.52
0.045	500	...	1.8	0.29
	550	...	0.78	0.31
	600	(10)	1.2	0.36
0.031	500	...	1.1	0.29
	550	(2.2)	0.65	0.26
	600	2.0	0.53	0.23
0.023	500	...	0.88	0.24
	550	2.0	0.59	0.23
	600	1.9	0.66	0.31

When the critical strain is exceeded in this material, the grain-size becomes progressively finer, as in super-purity aluminium, falling to about 0.2 mm. at about 25% strain. Some values for various fixed strains are given in Table IV.

(b) 2% Magnesium Alloy (Containing Manganese)

The preliminary treatments for the production of a range of initial grain-sizes are given in Table V.

TABLE V.—Preliminary Treatments for 2% Magnesium Alloy.

Previous Deformation, %	Annealing Treatment *	Resultant Grain-Size, mm.
15	3 hr. at 500° C. 1 hr. at 400° C.	0.30
30		0.042
45		0.024
60		0.018

* In air, as for commercial aluminium.

The curves relating critical strain with temperature, shown in Fig. 5, follow the usual pattern, the critical strain decreasing with temperature and becoming

TABLE VI.—*Grain-Sizes of 2% Magnesium Alloy after Critical Strain and Annealing.*

Initial Grain-Size, mm.	Final Grain-Sizes after Annealing at Various Temperatures, mm.			
	400° C.	450° C.	500° C.	575° C.
0.3	0.33	0.41
0.042	0.12	0.26	1.20	1.30
0.024	0.27	0.55	2.40	8.00
0.018	0.34	1.00	4.00	5.20

smaller, the finer the original grain-size. The numerical values of the critical strain are not very

given in Table VI, a grain structure can be developed in this alloy quite as coarse as some of those in commercial-purity aluminium at comparable temperatures (Table III).

At the higher strains (25% and more) the grain-sizes gradually decrease to values of about 0.1 mm. dia. and smaller (Table VII).

(c) 1% Magnesium, 1% Silicon Alloy

The age-hardening properties of the 1% magnesium, 1% silicon alloy made it necessary to anneal the specimens, to obtain a variety of initial grain-sizes, only just before they were needed. Table VIII gives the annealing treatment necessary to produce the grain-sizes shown. After this anneal, the specimens were quenched in water, stretched in the tensile

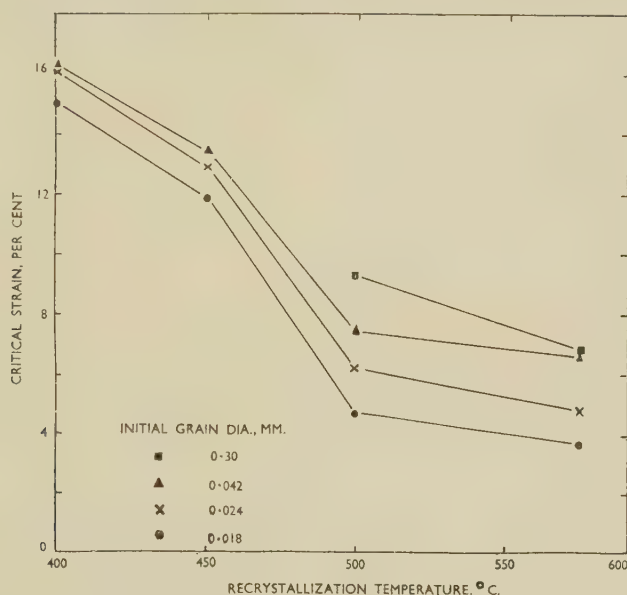


FIG. 5.—Critical-Strain/Recrystallization-Temperature Curves for 2% Magnesium Alloy with Various Initial Grain-Sizes. Annealing time 30 min.

different from those of commercial-purity aluminium at comparable initial grain-sizes and at the same temperature. Moreover, as is clear from the data

TABLE VII.—*Grain-Sizes of 2% Magnesium Alloy Recrystallized after Various Extensions.*

Initial Grain-Size, mm.	Temp., °C.	Grain-Size after Various Extensions, mm.		
		5%	10%	20%
0.30 {	500	...	0.33	...
	575	...	0.38	...
0.042 {	500	...	0.50	...
	575	...	0.37	...
0.024 {	500	...	0.53	...
	575	5.8	0.42	0.16
0.018 {	500	3.2	0.31	...
	575	1.7	0.29	...

machine, measured, and recrystallized for 30 min. at the appropriate temperature as soon as possible. These operations were completed within an hour or two of quenching.

TABLE VIII.—*Preliminary Treatments for 1% Magnesium, 1% Silicon Alloy.*

Previous Deformation, %	Annealing Treatment *	Resultant Grain-Size, mm.
15	1 hr. at 420° C. {	0.33
50		0.038
70		0.028

* In air, as for commercial aluminium, but water-quenched.

The critical-strain/temperature curves for the three initial grain-sizes are given in Fig. 6, and the effects of temperature and initial grain-size follow the usual trend. The critical strains necessary to produce

coarse grain are relatively low, lower than for commercial-purity aluminium under comparable con-

TABLE IX.—*Grain-Sizes of 1% Magnesium, 1% Silicon Alloy after Critical Straining and Annealing.*

Initial Grain-Size, mm.	Final Grain-Sizes after Annealing at Various Temperatures, mm.				
	380° C.	415° C.	465° C.	515° C.	550° C.
0.33	0.5	0.68	1.3	2.4	3.0
0.038	0.6	0.82	4.5	9.0	13
0.028	1.2	1.5	10	14	11

ditions. Table IX gives the grain-sizes developed at the critical strains and shows that grain-sizes can be produced as coarse as those developed in super-pure aluminium under the same conditions. At about

(d) Duralumin-Type Alloy

As in the 1% magnesium, 1% silicon alloy, the age-hardening characteristics of Duralumin-type alloy necessitated a continuous sequence of annealing for grain-size, quenching in water, rolling (instead of stretching), and recrystallizing with as little delay as possible. To test the effect of different amounts of alloying elements in solution, two batches of specimens were quenched in water from two different temperatures after annealing to obtain suitable initial grain-sizes. Two initial grain-sizes were used, and the annealing treatments for their production are given in Table XI.

The critical-strain/temperature curves for the two initial grain-sizes and for the two quenching treatments are given in Fig. 7. As for the previous materials, the critical strains are higher for the coarser-grained specimens, but the effect of different

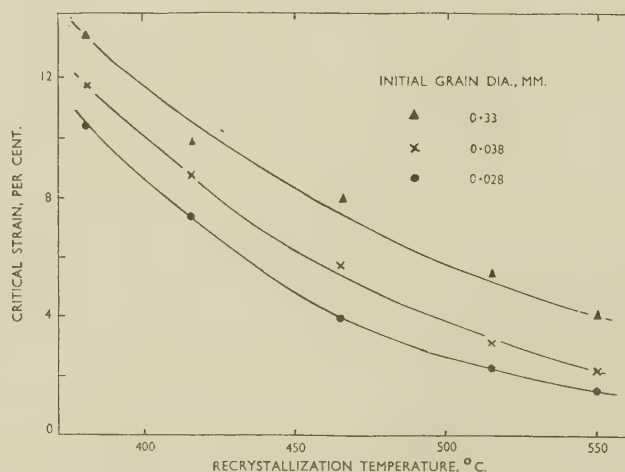


FIG. 6.—Critical-Strain/Recrystallization-Temperature Curves for 1% Magnesium, 1% Silicon Alloy with Various Initial Grain-Sizes. Annealing time 30 min.

25% overstrain the recrystallized grain-sizes are of the order of 0.1 mm. dia. (see Table X).

TABLE X.—*Grain-Sizes of 1% Magnesium, 1% Silicon Alloy Recrystallized after Various Extensions.*

Initial Grain-Size, mm.	Temp., °C.	Grain-Size after Various Extensions, mm.		
		5%	10%	20%
0.33	415	...	0.75	...
	465	...	0.58	0.27
	515	...	0.52	0.20
	550	...	0.56	0.26
0.038	415	...	0.50	...
	465	...	0.45	0.15
	515	1.8	0.43	0.14
	550	0.96	0.35	...
0.028	415	...	0.51	...
	465	3.9	0.35	0.14
	515	1.4	0.33	0.13
	550	0.76	0.31	...

amounts of alloying elements in solution is a much greater one, especially at the lower temperatures.

The grain-sizes developed after the critical straining and annealing are given in Table XII.

TABLE XI.—*Preliminary Treatments for Duralumin-Type Alloy.*

Previous Deformation, %	Annealing Treatment	Resultant Grain-Size, mm.
15	(i) 6 hr. at 500° C. and quenched. (ii) 6 hr. at 500° C., furnace-cooled to 425° C., held 1 hr. at temp., and quenched.	0.17
70	(i) 1 hr. at 500° C. and quenched. (ii) 1 hr. at 425° C. and quenched.	0.035

The variation of these grain-sizes with temperature is the usual one, viz. the lower the temperature, the finer the grain-size after critical straining and anneal-

ing. In the case of material quenched from 425° C., the effect of initial grain-size on the grain-size after critical straining and annealing is in accordance with rule (d) (p. 501). From Table XII (a), however, it will be seen that the opposite is the case for material quenched from 500° C. This behaviour is reminiscent of that of super-pure aluminium.

The effect of the quenching treatment on the values of the grain-size after critical straining and annealing is very marked, as would be expected from the substantial difference in the critical-strain values

TABLE XIII.—Preliminary Treatments for 1½% Manganese Alloy.

Previous Treatment	Annealing Treatment *	Resultant Grain-Size, mm.
Homogenized, cold rolled 25% .	8 hr. at 500° C.	0.34
Unhomogenized, cold rolled 25% .	128 hr. at 500° C.	0.36
Homogenized, cold rolled 85% .	5 hr. at 500° C.	0.026
Unhomogenized, cold rolled 85% .	5 hr. at 500° C.	0.027

* In air, as for commercial aluminium (air-cooled).

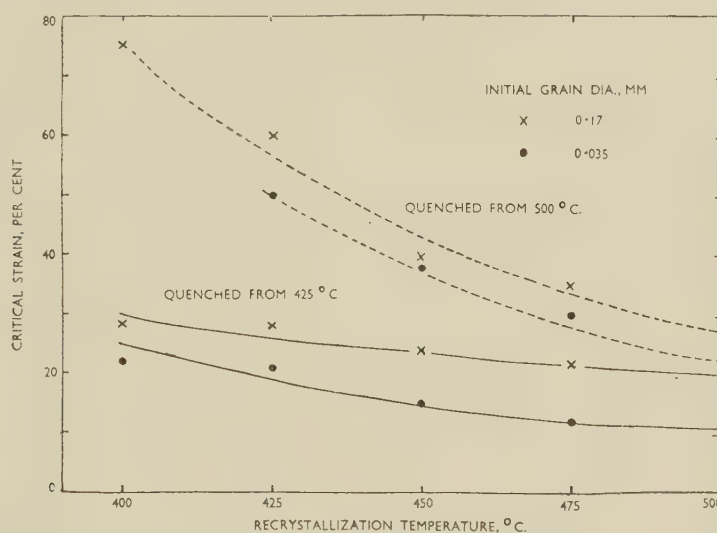


Fig. 7.—Critical-Strain/Recrystallization-Temperature Curves for Duralumin-Type Alloy with Various Initial Grain-Sizes. Annealing time 30 min.

already noted. In short, for Duralumin-type alloys the greater the amounts of alloying elements in solution, the higher is the critical strain, and hence the

TABLE XII.—Grain-Sizes of Duralumin-Type Alloy after Critical Straining and Annealing.

Initial Grain-Size, mm.	Final Grain-Sizes after Annealing at Various Temperatures, mm.				
	400° C.	425° C.	450° C.	475° C.	500° C.
(a) Material Quenched from 500° C.					
0.035	0.025	0.028	0.032
0.17	...	0.026	0.030	0.033	0.050
(b) Material Quenched from 425° C.					
0.035	0.075	0.085	0.2	0.5	0.55
0.17	0.037	0.038	0.05	0.067	0.059

finer is the largest grain-size which can be obtained by annealing at a given temperature.

(e) 1½% Manganese Alloy

The 1½% manganese alloy was supplied in two batches: (i) homogenized before hot rolling and (ii) unhomogenized. The homogenization treatment

consisted of a 27-hr. anneal of the cast billet, finishing at 600° C.

Table XIII shows the preliminary heat-treatments for the production of two initial grain-sizes (0.35 and 0.026 mm.) in both homogenized and unhomogenized materials.

Curves are plotted in Fig. 8 of critical strain versus temperature for both homogenized and unhomogenized materials. In either material the critical

TABLE XIV.—Grain-Sizes of 1½% Manganese Alloy after Critical Straining and Annealing.

	Initial Grain-Size, mm.	Final Grain-Sizes after Annealing at Various Temperatures, mm.			
		425° C.	450° C.	500° C.	550° C.
Homogenized {	0.35	0.12	0.15	0.17	0.21
	0.026	0.13	0.17	0.33	1.40
Unhomogenized {	0.35	...	0.038	0.095	0.10
	0.026	0.032	0.034	0.10	0.17

strain decreases with rise in temperature, and fine-grained material makes for lower critical strains. It will be seen too that the critical strains are lower for material homogenized before hot rolling, though the

distinction becomes less important at the higher temperatures.

Table XIV gives the value of the recrystallized grain-size after critical straining and annealing. These grain-sizes are finer for the material not homogenized before hot rolling (in accordance with

super-pure aluminium are qualitatively in agreement with those of Anderson and Mehl.⁵

No departure at all has been found from rules (b) and (c), but (d) now needs some qualification, as it has been found that the recrystallized grain-size may, for a given deformation and annealing temperature,

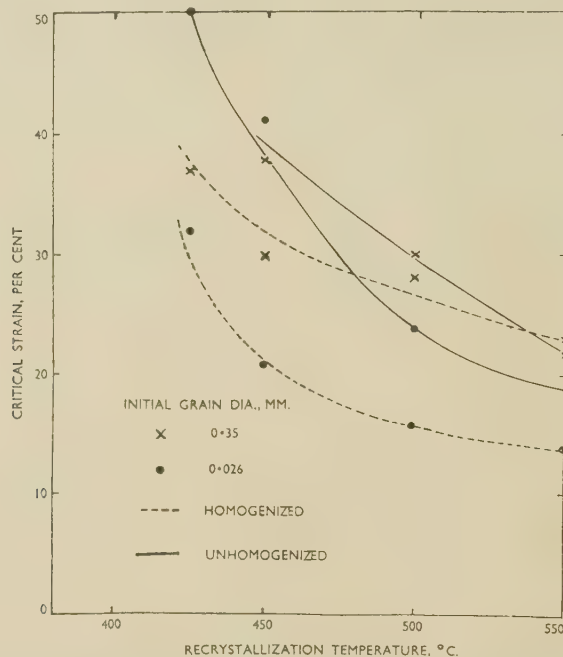


FIG. 8.—Critical-Strain/Recrystallization-Temperature Curves for Homogenized and Unhomogenized 1 1/4% Manganese Alloy with Various Initial Grain-Sizes. Annealing time 30 min.

the higher critical strain) and are comparable with those found in the Duralumin-type alloy.

V.—DISCUSSION

The experiments reported show the effects of some of the controlling factors, viz. amount of cold deformation, temperature, and original grain-size, on the recrystallization of several alloys; other variables, including time at temperature and rate of heating, have not been investigated. Apart from some additional effects of the initial grain-size, discussed below, the results substantiate the empirical rules set out in the introduction (p. 501). Rule (a), that the grain-size in a particular material is primarily determined by deformation before annealing and is substantially independent of the annealing temperature, can be roughly checked by comparison of the recrystallization diagrams for any particular material at different temperatures. The temperature of recrystallization has, however, a slight effect on the final grain-size, the final grain-size being in general finer, the higher the temperature. Fig. 9 gives two examples. Super-purity aluminium (Fig. 9 (a)) appears to show the effect most strongly of the materials for which adequate data are available, and in all cases the largest effect is at low strains. These results for

depend more or less strongly on the initial grain-size. This effect is especially noticeable in super-purity aluminium and for small deformations, with the result that for this material at high temperatures the maximum grain-size obtainable by critical strain increases with the initial grain-size, instead of decreasing as predicted. The first part of the rule, however, that the critical strain increases with the initial grain-size (as in Fig. 12, Plate LXXIX), remains true in practically all cases.

The dependence of the final grain-size on the initial grain-size presumably arises from the fact that during recrystallization after low strains nuclei form preferentially at structural discontinuities, especially grain boundaries; in fine-grained material the grain-boundary area is larger and more nuclei will be formed in any given conditions than in coarse-grained. For higher strains, nucleation takes place also within the grains, so that the difference in grain-boundary area has a less-marked effect and the final grain-size becomes progressively less dependent on the initial grain-size as now observed. The strong dependence observed in super-purity aluminium, compared with that in other alloys, is no doubt largely due to the comparatively very low critical strains, for a given grain-size, which make observations possible in a strain range which does not occur in other materials;

but the difference does not appear to be completely accounted for in this way, and there may be other factors operative, such as the possible effect of minor constituents or dissolved elements in promoting nucleation within the grains relative to nucleation at the grain boundary.

There is little in the literature on the effect of alloying on recrystallization. However, experiments

manganese, but not magnesium, had a large effect in increasing the critical strain. On the other hand, the grain-size on recrystallization after a given large strain (in the range above about 20% extension) was considerably larger for a 1½% manganese alloy than for commercial-purity aluminium or a 1% magnesium alloy, while in ternary alloys magnesium tended to offset the coarsening effect of manganese.

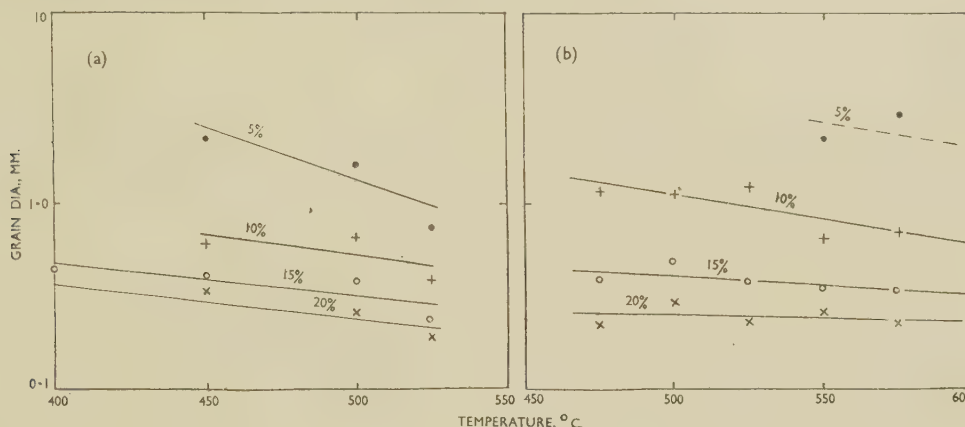


FIG. 9.—Effect of Recrystallization Temperature on Final Grain-Size for Various Amounts of Cold Deformation.

(a) Super-purity aluminium with initial grain-size 0.105 mm.

(b) Commercial-purity aluminium with initial grain-size 0.031 mm.

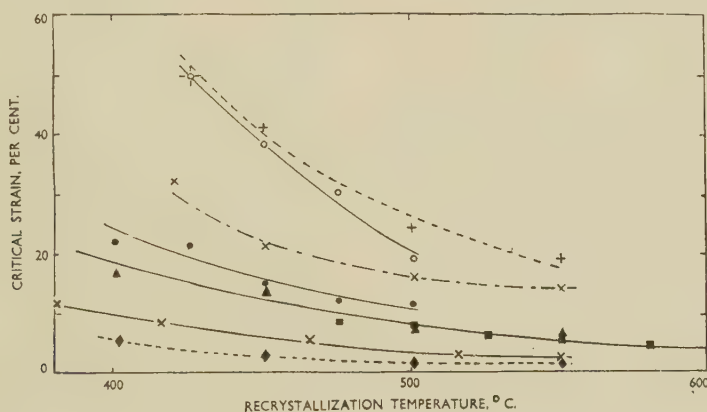


FIG. 10.—Relationship Between Critical Strain and Recrystallization Temperature for All Alloys Tested.

--- + --- Al-1½% Mn alloy. Unhomogenized. Initial grain-size 0.026 mm.
 --- x --- Al-1½% Mn alloy. Homogenized. Initial grain-size 0.026 mm.
 --- o --- Duralumin-type alloy. Quenched from 500° C. Initial grain-size 0.035 mm.

KEY.

--- ● --- Duralumin-type alloy. Quenched from 425° C. Initial grain-size 0.035 mm.
 --- ■ --- Commercial-purity aluminium. Initial grain-size 0.031 mm.
 --- ▲ --- Al-2% Mg alloy. Initial grain-size 0.042 mm.
 --- x --- Al-1% Mg-1% Si alloy. Initial grain-size 0.038 mm.
 --- ♦ --- Super-purity aluminium. Initial grain-size 0.042 mm.

of a type similar to those described in the present paper have been reported by Chadwick, Richards, and others^{6,7} both for an alloy of the Duralumin type and for a series of alloys with small quantities of magnesium and manganese. These authors concluded that the critical strain for recrystallization at 500° C. in the Duralumin-type alloy increased with the amount of alloying elements in solution, and that in the aluminium-magnesium-manganese series

If the entire results of the present investigation are plotted in the form of a graph of recrystallized grain-size against previous deformation, the points lie within a band, the width of which corresponds to a variation of grain-size of the order of 30:1 for any given deformation; but it has not been found possible to generalize in any useful way on the effects of alloying on the grain-size produced on recrystallization.

The most striking effect of composition observed is

that on the critical strain. Curves illustrating the variation of critical strain with temperature for materials of comparable grain-size are given in Fig. 10. There are very wide differences, e.g. between 3 and 40% at 450° C. As might be expected, super-pure aluminium has the lowest critical strain, and alloying elements and impurities have in general the effect of raising the critical strain. The element most effective in this way appears to be manganese, and the least effective magnesium. The critical strain for the manganese alloy was much reduced by an homogenizing treatment before hot rolling, while for the Duralumin-type alloy the values were much larger for the material quenched from 500° C. than those given by material quenched from 425° C., presumably owing to the greater amount of the alloying elements in solution.

VI.—CONCLUSION

With one exception, the results confirm the empirical rules set out in the Introduction (p. 501). This exception is that, especially in super-purity aluminium recrystallized after given small strains, the final grain-size varies to some extent with the initial grain-size. The effect is not large in most of the materials. The most striking effect of composition is the large effect of some elements on the critical strain.

ACKNOWLEDGEMENTS

The authors are indebted to the Director and Council of The British Non-Ferrous Metals Research Association for permission to publish this paper.

REFERENCES

1. C. Chappell, *J. Iron Steel Inst.*, 1914, **89**, 460.
2. H. C. H. Carpenter and C. F. Elam, *J. Inst. Metals*, 1920, **24**, 83.
3. K. Matthaes and A. Schroeder, *Aluminium*, 1941, **23**, 599.
4. H. Gries and H. Esser, *Arch. Eisenhüttenwesen*, 1929, **2**, 749.
5. W. A. Anderson and R. F. Mehl, *Trans. Amer. Inst. Min. Met. Eng.*, 1945, **161**, 140.
6. R. Chadwick and W. H. L. Hooper, *J. Inst. Metals*, 1948-49, **75**, 609.
7. R. Chadwick, T. Ll. Richards, and K. G. Sumner, *ibid.* p. 627.

THE APPLICATION OF GRAIN REFINEMENT TO CAST COPPER-ALUMINIUM ALLOYS CONTAINING THE BETA PHASE *

1472

By J. P. DENNISON,† B.Sc., Ph.D., JUNIOR MEMBER, and
E. V. TULL,‡ B.Sc., A.I.M., JUNIOR MEMBER

SYNOPSIS

A consideration of previous work pointed to the nucleation method as offering the greatest chance of success in refining the grain-size of cast duplex ($\alpha + \beta$) copper-aluminium alloys. Accordingly, melts were treated with a range of additions likely to form nucleating compounds. The selection of possible compounds was based on their having a lattice structure and dimensions similar (within certain limits) to those of either the α or the β phase of the copper-aluminium system. Good confirmation of the nucleation theory was obtained, particularly with additions of boron, which is thought to produce nucleation when present as boron carbide. It has been found that in the presence of boron the mechanism of solidification of the 90:10 copper-aluminium alloy involves the initial solidification of the β phase. Results obtained on the laboratory scale were entirely confirmed by tests on a commercial scale with 500-lb. billets. With the latter, comparative mechanical tests showed that the tensile strength had increased by 13% and the elongation by 46%, when refinement was at a maximum.

I.—INTRODUCTION

THE literature on the mechanism of grain refinement in castings provides a preponderance of evidence in favour of the nucleation theory. When investigating the possibilities of reducing the as-cast grain-size of copper-aluminium alloys, it was therefore decided to make first an attempt to produce grain-refining nuclei in the molten alloy. As the mode of solidification of the duplex copper-aluminium alloy containing 10% aluminium was in some doubt, the initial work aimed at producing nuclei favourable to the crystallization of either the α or the β phase. It was found that in the presence of certain nuclei, thought to be boron carbide, which would be expected to nucleate the β phase, this alloy solidified with the initial deposition of β crystals. Considerable grain refinement was obtained.

The commercial alloy containing 14% aluminium and 5% iron, which initially deposits β crystals, showed grain refinement of the same order as that of the copper-12% aluminium alloy cast in the laboratory, which consists entirely of the β phase.

The effect was studied of reductions in grain-size on the mechanical properties of the duplex 10% aluminium alloy. Previous work ¹ had indicated that little improvement was to be expected for two-phase material, but the present results show considerable increases in both tensile strength and elongation.

II.—PREVIOUS WORK

1. MECHANISM OF GRAIN REFINEMENT

The fact that a reduction in pouring temperature tends to increase the proportion of equi-axial grains in castings of certain alloys has been explained by Genders and Bailey,² who outline two methods of formation of such grains:

(i) *Growth Restriction*.—The growth of the initial columnar crystals sets up such concentration gradients within the still-liquid alloy that there is an excess of the low-melting-point constituent in the immediate vicinity of the columnar crystals, and hence on further cooling, independent crystallization begins in the main bulk of the liquid alloy beyond this low-melting-point region. This process is further aided by the latent heat of solidification of the columnar crystals, which causes a slight increase in the temperature of the liquid alloy in their immediate vicinity. The tendency towards independent crystallization becomes greater with decrease in temperature gradient from the outside of the ingot to the centre, i.e. it increases with decrease in pouring temperature. A similar theory was put forward by Northcott^{3,4} to account for the periodic crystallization of steel and certain non-ferrous alloys.

* Manuscript received 12 December 1952.

‡ Research Student, University College, Swansea.

† Lecturer in Metallurgy, University College, Swansea.

(ii) *Nucleation by Solid Particles in the Molten Alloy*.—Solid particles may be present in the liquid zone as a result of the injection by the pouring stream of solid from the ingot top. Similar effects are observed when turbulence is produced in other ways, e.g. by the use of volatile mould dressings.⁵

Subsequent theories have been based on these two main concepts.

An interesting adaptation of the nucleation theory was introduced by Scheil,⁶ who found that the grain-size of cast ingots could be refined appreciably by inserting wires of the metal in the mould before casting. The resulting grain-size was a function of the number and diameter of the wires used. It was assumed that the wires acted as artificial nuclei.

In 1936, Iwasé, Asato, and Nasu⁷ investigated the grain refinement produced in some binary copper alloys by the addition of iron or cobalt. They concluded that the grain refinement resulted from the break-up of primary crystals during a peritectic reaction caused by these additions, thus providing a large number of nuclei for the formation of secondary crystals.

Mitsche,⁸ in the same year, published details of his work on the effect of non-metallic inclusions on the grain-size of aluminium, cast iron, and steel. He considered that two kinds of nuclei existed: "kindred nuclei", which were fragments of metallic lattices and refined the grain-size by inoculation; and "foreign nuclei", which were non-metallic inclusions, and could either refine or coarsen the grain-size depending on their size and concentration in the melt.

Further evidence in support of the concentration-gradient theory was provided in 1937 by the work of Hanemann and Hofmann⁹ on the effect of various additions on the grain-size of magnesium alloys.

In 1938, Northcott⁴ made a systematic study of the effect of small additions (0.01–2%) of 35 elements on the grain-size of copper. He considered grain-refinement to be due to growth restriction, which could arise from two causes: (a) the existence of concentration gradients, as postulated by Genders and Bailey;² or (b) the adsorption of a very thin layer of the alloying element on the surface of the crystallites, thus preventing further growth. Northcott believed the latter to be the main factor in determining the refinement achieved, and thought that the effect was a periodic one, dependent on the structure of the outer electron shells of the element adsorbed.

This work was extended to cover the effect of larger additions of several of these elements on the grain-size of copper.¹⁰ An attempt was made to correlate the results obtained with constitutional diagrams, and in doing so the effect of an additional, or "second-phase", factor had to be considered. The concentration-gradient effect increased with increase in freezing range, whilst the adsorption effect reached a maximum at a very low percentage of alloying

element, and thereafter remained constant or even decreased. The "second-phase" effect could either refine or coarsen grain-size, depending on the nature of the second phase. If the latter was a eutectic, refinement generally occurred, whereas if it was a peritectic the reverse was true, in opposition to the peritectic theory of Iwasé, Asato, and Nasu⁷ previously described.

Since 1939, a great deal of work has been done upon the grain refinement of magnesium-¹¹⁻¹⁸ and aluminium-base¹⁹⁻²⁴ alloys, resulting in a theory of grain refinement due to Cibula, which is applicable to alloys in general.²² Cibula states that there are two ways in which grain refinement can be achieved:

(i) *Concentration Gradients*.—This is a growth-restriction process, and is associated with increased undercooling at the surface of castings, and, more particularly, with the spread of undercooling into the interior of the casting, the latter condition producing an equi-axial structure. This type of grain refinement is relatively slight, until a large proportion of the alloying element is present, and is never very marked.

(ii) *Nucleation*.—The formation of nuclei upon which the alloy crystallizes easily; this effect being associated with the virtual suppression of undercooling. This mechanism in itself will only refine a coarse columnar structure to a much finer but still columnar one, and will not give rise to the equi-axial structures characteristic of marked grain refinement. The combination of these two effects, however, produces grain refinement to a high degree. In cases where the grain-refining element is sufficiently soluble in the parent alloy, it may provide both nuclei and concentration gradients; where the solubility of the grain-refining element in the parent alloy is too small to permit the formation of concentration gradients, the latter must be produced by the addition of another element.

According to Cibula the conditions to be satisfied by a foreign particle to produce nucleation of the alloy are as follows: (1) Attractive forces should exist between the atoms of the solid metal and of the foreign particle; and (2) there should be an absence of strain in the metal lattice at the nucleus/metal interface.

The first condition is also that which results in the formation of stable solutions or intermetallic compounds, i.e. it would lead to solution of the foreign particle. If solution is not to occur, the stability of the compound forming the foreign nuclei must be very high.

The second factor requires a fairly close structural relation between the lattice of the solid metal and that of the foreign particle. In this respect, van der Merwe²⁵ states that a limiting lattice misfit exists which allows the formation of an oriented nucleus on a substrate. He estimated the limiting difference to

be 9%, or somewhat greater if there are strong attractive forces between the deposited atoms and the substrate. Thus Royer²⁶ has proved that differences in lattice dimensions of up to 16% can be tolerated in the case of halides deposited from solution on to crystals of lead sulphide, potassium chloride, sodium chloride, and mica.

Cibula found that the quantities of the combining elements necessary to produce satisfactory nucleation and refinement are extremely small, of the order of 0.001–0.1%, and that the number of nuclei present was several hundred times the number of grain centres on solidification. Formation of the nucleating compounds within the molten metal was more efficient from the point of view of nucleation than the direct addition of the compounds to the melt, the difference being attributed to the difficulty in obtaining satisfactory wetting in the latter case.

The above theory offers a satisfactory explanation of most of the phenomena associated with grain refinement, and has been used as the basis of the present work. Crossley and Mondolfo²⁷ have offered an alternative explanation of the grain refinement of aluminium alloys involving a peritectic-reaction theory, but the evidence in support of their theory is inconclusive.

2. GRAIN REFINEMENT OF COPPER-BASE ALLOYS

Apart from the work of Northcott,^{4,10} very little has been published on the grain refinement of copper and copper-base alloys. Northcott found that in additions from 0.1 to 2% the most effective grain refiners were lead, thallium, platinum, oxygen, tin, selenium, arsenic, and indium, in that order. He then investigated the grain-size of a series of binary alloys of copper over a wide range of compositions. Copper-aluminium alloys were characterized by very large crystal size, having longer and much wider columnar crystals than those found in the other binary alloys examined. Northcott showed that aluminium is capable of conferring the property of wide columnar growth upon other alloys to which it is added. Curves of crystal length against composition were plotted for these binary alloys. For copper-aluminium alloys of the eutectic composition (8.5% aluminium) the structure is wholly columnar. Further increase in aluminium content results in a slight reduction in columnar crystal length, to a minimum at 10% aluminium and 40% reduction in crystal length, the curve then rising again until at 12% aluminium the structure is again wholly columnar (the all- β region).

Hermann and Sisco²⁸ in 1931 studied the effect of 1% and 5% additions of iron, nickel, manganese, cobalt, and silicon on the structure and hardness of 8%, 10%, and 12% aluminium bronzes. Iron gave the greatest refinement in grain-size, and manganese also produced some refinement. Nickel and cobalt had no effect, and silicon produced grain coarsening.

These results were confirmed by Iwasé, Asato, and Nasu in 1936.⁷

The complex aluminium bronzes containing nickel and iron (e.g. Cu 80, Al 10, Fe 5, Ni 5%) have an equi-axial grain structure throughout the ingot even when relatively high pouring temperatures are employed. Murphy and Callis²⁹ suggest the possibility that the primary crystals of iron-bearing constituent found in these alloys are the nuclei responsible for grain refinement.

Additions of several other elements to aluminium bronze have been made by various workers, but the effect upon the grain-size has not been considered in most cases. Landolt and Pyne,³⁰ however, report that lithium additions of the order of 0.005–0.02% produce some grain refinement in high-conductivity copper, gun-metal, and nickel bronze.

Colton and Margolis³¹ studied the effect of nickel additions (0–5%) upon the cast macrostructure of an 85:5:5:5 copper-tin-zinc-lead alloy, and concluded that the element responsible for the small grain-size (as compared with that of pure copper) was lead, nickel additions having no effect on grain-size.

3. EFFECT OF GRAIN-SIZE ON THE MECHANICAL PROPERTIES OF CAST ALLOYS

It has long been recognized that the grain-size of cast alloys may have an important influence upon their tensile properties, the precise effect in each case being the resultant of several factors. The most obvious factor is, of course, the resistance offered by grain boundaries to the simple type of deformation undergone by a single crystal, the effect of which is to increase tensile strength as the grain-size decreases.

In cubic alloys, however, other indirect effects of grain-size variation may far outweigh the grain-boundary factor; e.g. Cibula and Ruddle²¹ found that in certain aluminium alloys the distribution and shape of the intergranular shrinkage voids, as influenced by grain-size, was the dominant factor in determining the tensile properties. In this case, the type of void associated with small grain-size was the least detrimental, but this is not always the case, as was shown by the work of Ames and Kahn³² on tin bronzes, in which maximum tensile properties were associated with a coarse-grained structure.

Northcott¹ has studied the influence of crystal size and orientation upon the mechanical properties of several copper-base alloys in the cast condition. He found that single-phase alloy test-pieces composed of columnar crystals disposed longitudinally showed low values for maximum stress but high elongation; transverse columnar crystals exhibited a higher maximum stress but low elongation; and small equi-axial crystal samples showed the highest maximum stress, but low to intermediate elongation. The tensile properties of two-phase alloys were found to be much less affected by crystal size, a fact Northcott

attributed to the presence within each crystal of phase boundaries which behaved like ordinary crystal boundaries in their resistance to slip.

III.—SELECTION OF POSSIBLE INOCULANTS

At the beginning of the present work, the mode of solidification of a binary copper-base alloy containing 10% aluminium was in doubt. The constitutional diagram indicates that the β phase is the first to solidify, but Ruddle and Mincher³³ suggest that under non-equilibrium conditions eutectic crystallization may occur, initiated by nuclei of the α phase. Inoculants were therefore selected to cover both possibilities and particulars of these are given in Table I. Lattice misfit up to $\pm 16\%$, the highest

TABLE I.—Possible Inoculants for Copper-10% Aluminium Alloy.

Compound	Structure	Lattice Dimensions, Å.*	Lattice Misfit, % *
<i>A—Suitable for α-Phase Nucleation</i>			
α -Cu-Al (7.5% Al)	F.c.c.	$a_0 = 3.657$ (ref. 35)	...
CaB ₂	Cubic	$a_0 = 4.15$	+13.3
CeB ₂	"	$a_0 = 4.13$	+12.9
CoB	Orthorhombic	$a_0 = 3.95$, * $b_0 = 5.24$, $c_0 = 3.04$	+ 7.9
Co ₂ B	?	$a_0 = 5.00$, $c_0 = 4.21$ *	+15.0
TiB ₂	Hex. c.p.	$a_0 = 3.03$, $c_0 = 3.23$ *	-11.8
ZrB ₂	"	$a_0 = 3.15$, * $c_0 = 3.53$ *	-14, -3.6
ZrO	Cubic	$a_0 = 3.81$	- 9.6
CeO ₂	Tetragonal	$a_0 = 3.87$, * $c_0 = 6.48$	+ 5.8
AlB ₂	Hex. c.p.	$a_0 = 3.00$, $c_0 = 3.25$ *	-11.3
<i>B—Suitable for β-Phase Nucleation</i>			
β -Cu-Al (10.0% Al)	B.c.c.	$a_0 = 5.887$ (ref. 33)	...
CeO ₂	Tetragonal	$a_0 = 3.87$, $c_0 = 6.48$ *	+10.0
CaO ₂	"	$a_0 = 5.48$, * $c_0 = 6.37$ *	-6.8, +8.1
CaS	Cubic (NaCl-type)	$a_0 = 5.67$	-3.8
Li ₂ S	Cubic (CaF ₂ -type)	$a_0 = 5.70$	-3.3
B ₄ O	Rhombohedral	$a_0 = 5.62$, * $c_0 = 12.12$	-4.5

* Where more than one lattice parameter is given, misfit is calculated only for the parameter marked with an asterisk.

value at which nucleation has been reported,²⁶ was tolerated, although the limiting misfit is generally taken as about 9–10%.^{25,34}

IV.—LABORATORY TESTS

1. EXPERIMENTAL PROCEDURE

The melts were prepared from copper-aluminium alloy containing Al 12.27, Fe 0.07, Si 0.04, Zn 0.02%, balance Cu, and high-purity copper (B.S.S. MC3) containing Cu 99.96, Ni 0.01, O 0.019, Bi 0.0003%, and a trace of As. A straight copper-10% aluminium alloy prepared from these materials showed no difference in macrostructure from a similar alloy prepared from the same copper and super-purity aluminium (99.99%). It was therefore assumed that the 0.07% iron in the copper-12% aluminium alloy had no grain-refining effect.

The various elements intended to produce grain refinement were added either in elemental form, or as alloys with copper or aluminium, with the exception

of cerium (added as Mischmetall, a 50% alloy with rare earth metals). Additions of the pure metals and the Mischmetall were wrapped in copper foil; in the case of carbon, acetylene was bubbled through the molten metal in the casting-machine reservoir via a thin silica tube. All additions were made to the melt in the furnace, with the exception of the Mischmetall, lithium, and copper sulphide, which were added in the reservoir of the casting machine.

Cerium Mischmetall was used instead of pure cerium for economic reasons. For comparison, a melt was cast using pure cerium. The macrostructure of the two ingots showed no significant difference.

Analyses of the various alloys used are given below:

Boron (as copper-base alloy):

B 4.75, Cu 93.7, Si 0.6, Fe 0.06, Mg 0.20%, traces of Mn and Pb.

Cerium (as Mischmetall):

Typical analysis: Ce 51–53, Nd 15–17, Pr 3–4, La 22–25, Sm 2–3, Y + Tb 3, Fe 5, C approx. 0.054, CaC₂ approx. 0.022, Ca approx. 0.014%, traces of Al and Si.

Cobalt (as copper-base alloy):

Co 12.0, Ni 0.20%, balance Cu.

Titanium (as aluminium-base alloy):

Ti 10.3, Fe 0.47, Si 0.33, Cu 0.08%, balance Al.

Zirconium (as aluminium-base alloy):

Zr 8.2, Ti 0.20, Fe 0.50, Si 0.35, Cu 0.10%, balance Al.

Calcium and Lithium: added as pure metals.

Copper sulphide: added as powder (Analar purity).

All melts were made in a high-frequency electric furnace, employing a Sillimanite crucible, and a proprietary flux was used to clean the metal before casting. The ingots were Durville-cast into steel moulds. The melt temperature was checked by immersing a thermocouple in the reservoir of the casting machine (consisting of a Salamander crucible) immediately before pouring. Exothermic feeding compound was applied to the ingot top to prevent the formation of shrinkage cavities, and a constant pouring temperature (1150° C.) and pouring rate were employed for all casts. This temperature proved sufficiently high to ensure that untreated ingots would have a coarse-grained macrostructure consisting entirely of columnar crystals.

The ingots were cylindrical, 3 in. dia. \times 8 in. long. For macro-examination they were sectioned halfway between the bottom of the pipe and the base of the ingot, parallel to the base. The surface so exposed was machined and then etched in a warm saturated solution of ammonium bichromate containing 10% conc. H₂SO₄ and 1% HCl, with continuous swabbing for about 10 min.

2. RESULTS ON GRAIN REFINEMENT

It will be seen from the results given in Table II that marked grain refinement was obtained in all the ingots containing boron. Since boron additions produced refinement when used alone, the part played by calcium, cerium, cobalt, titanium, and zirconium in ingots 2–6 inclusive may not have been important, i.e. the nucleating compound may have been a compound of boron with some other element

already present in the copper-aluminium alloy. External addition of carbon was not essential to grain refinement by boron, as shown by ingot 13. This does not, however, rule out the possibility that the nucleating compound was boron carbide, since

TABLE II.—Effect of Various Additions on the Grain-Size of Copper-10% Aluminium Alloy.

Ingot No.	Desired Compound	Lattice Misfit, %	Addition, % (nominal)	Degree of Grain Refinement	Average Grain-Size of Equi-Axial Crystals, mm.
1	...	Standard ingot		...	Entirely columnar.
A—Suitable for α -Phase Nucleation					
2	CaB ₂	+13.3	0.04 Ca,* 0.01 B	Marked	0.5
3	CeB ₂	+12.9	0.04 Ce,* 0.01 B	"	0.5
4	CoB	+ 7.9	0.01 Co, 0.01 B	"	0.5
5	Co ₂ B	+15.0	0.01 Ti, 0.01 B	"	0.5
	TiB ₂	-11.8		"	
	ZrB ₂	-14, -3.6		"	
6		+ 5.8(α)	0.01 Zr, 0.01 B	"	0.5
7	CeC ₂	+10.0(β)	0.04 Ce * + C	Slight	{ Entirely columnar.
B—Suitable for β -Phase Nucleation					
9	CaC ₂	-6.8, +8.1	0.04 Ca * + C	Moderate	2.0
10	CaS	-3.8	0.04 Ca,* 0.01 S	Nil	Entirely columnar.
11	Li ₂ S	-3.3	0.04 Li,* 0.01 S	"	0.5
12	B ₄ C	-4.5	0.01 B + C	Marked	0.5
13	B ₄ C	-4.5	0.01 B	"	0.5

* Nominal addition increased to allow for high oxidation loss of these elements during addition.

Cibula²² has shown that even super-purity aluminium (99.99%) contains enough carbon to combine with added titanium to form the nucleating compound titanium carbide. If the nucleating compound was in fact boron carbide, this would imply that the β phase is the first to solidify, since the boron-carbide lattice is favourable to β -phase nucleation only. On

TABLE III.—Macrostructure and Grain-Size of Laboratory Ingots.

Ingot dimensions; 3 in. dia. \times 8 in. long.

Ingot No.	Addition, % (nominal)	Average Grain-Size, mm.		Structure
		Columnar (width)	Equi-Axial	
1 *	Standard	2.0	...	Entirely columnar to centre (1.5 in. long).
7	0.04 Ce + C	1.5	...	Columnar crystals $\frac{7}{8}$ in. long. Equi-axial central zone.
9	0.04 Ca + C	1.5	2.0	
13 †	0.01 B	1.0	0.5	Columnar crystals $\frac{5}{8}$ in. long. Equi-axial central zone.

* 10 and 11 similar.

† 2, 3, 4, 5, 6, and 12 similar.

the other hand, the nucleating compound may have been aluminium boride, which is an α -phase nucleator, in which case the α -phase must be the first to solidify.

Calcium additions, in conjunction with acetylene bubbling, also produced some refinement, but this was not nearly so marked as with boron additions, although producing an equi-axed zone. Cerium in conjunction with acetylene gave slight indications

of grain refinement by diminishing the width of columnar crystals.

The macrostructure of copper-10% aluminium alloy, without and with boron additions, is illustrated in Figs. 1 and 2 (Plate LXXX), respectively. In the untreated alloy, the structure consists of coarse columnar crystals extending to the centre of the ingot, whereas in the boron-treated alloy these columnar crystals are much smaller, and the whole of the centre of the ingot consists of fine equi-axial crystals.

A more detailed description of the macrostructure and grain-size of the ingots is given in Table III.

3. MODE OF SOLIDIFICATION OF COPPER-10% ALUMINIUM ALLOY.

A means of refining the grain-size of the duplex copper-10% aluminium alloy having been found, the solidifying phase in this alloy was next determined. Three ingots containing 7.5%, 10%, and 12.5% aluminium, respectively, were cast, representing the all- α , duplex ($\alpha + \beta$), and all- β structures. A further series of three ingots was then cast of the same aluminium contents, but with 0.01% boron added to each alloy before casting. Comparison of the macrostructures of the six ingots showed that boron additions refined the grain-size of the ($\alpha + \beta$) (Figs. 1 and 2) and all- β alloys (Figs. 3 and 4, Plate LXXX), but not that of the all- α alloys. In the presence of boron the solidifying phase in the duplex copper-10% aluminium alloys must therefore be β . This finding does not, however, entirely rule out the theory of Ruddle and Mincher³³ that, under non-equilibrium conditions, the α phase is the first to solidify and initiates eutectic-type solidification, since in the absence of suitable nuclei undercooling may occur to such an extent that this mechanism becomes possible. In the presence of suitable nuclei, such as are provided by boron additions, undercooling is prevented, and solidification conditions approach much more closely to those indicated by the equilibrium diagram, i.e. the β phase is the first to solidify. Further, since the aluminium boride structure is suitable only for nucleating the α -phase, it can be ruled out as an inoculant, thus lending further support to the view that boron carbide is the nucleating compound. Similarly, the nucleating compounds in ingots 2-6 cannot be the metal borides listed in column 2 of Table II, since these compounds are also suitable only for nucleating the α phase.

The macrostructure of the boron-treated copper-12.5% aluminium ingot showed a $\frac{1}{4}$ -in.-deep zone of equi-axial crystals round the periphery of the ingot. These crystals were largest at the immediate edge of the ingot, and decreased in size towards the inner edge of the zone, the finest crystals being comparable in size with those in the centre of the ingot. It is difficult to account for the presence of the columnar zone between these two zones of equi-axial crystals. It may represent a form of periodic crystallization, as outlined by Northcott,³ which would imply that

The results obtained are given in Table VI. Macro-examination of ingots containing 0.02 and 0.03% boron revealed a completely equi-axial structure, with no outer band of columnar crystals (see Table V). Data on the macrostructure of the 0.0025% boron

TABLE V.—*Macrostructure and Grain-Size of Commercial Ingots.*

Ingot dimensions : 7 in. dia. \times 45 in. long.

Addition, nominal)	Average Grain-Size, mm.		Structure
	Columnar (width)	Equi-axial	
Standard	2.5	...	Entirely columnar to centre (3.5 in. long).
0.04% Ca	1.2	2.0	Columnar crystals 1.75 in. long. Equi-axial central zone.
0.0025% B	1.5	2.2	Columnar crystals 1.5 in. long. Equi-axial central zone.
0.01% B	4.0	1.0	Columnar crystals 0.5 in. long. Equi-axial central zone.
0.02% B	...	0.7	Entirely equi-axial.
0.03% B	...	0.5	" "

TABLE VI.—*Effect of Varying Boron Additions on the Mechanical Properties of Copper-10% Aluminium Alloy.*

Nominal Boron Content, %	Position of Test-Piece *	Tensile Strength, tons/in. ²	Elongation, % on 1-in. Gauge-Length
0	Transverse (top)	{ 22.0	12.5
0		{ 23.0	17.0
0.01		{ 22.9	14.5
0.02		{ 24.0	16.0
0.02		{ 25.6	25.0
0.03		{ 26.2	26.0
		{ 25.9	22.0
		{ 26.9	22.0
0	Longitudinal	{ 22.4	18.5
0		{ 23.2	24.0
0.02		{ 24.3	22.0
0.02		{ 22.7	15.0
0.02		{ 26.5	25.0
0.03		{ 26.4	24.5
		{ 27.0	31.5
		{ 26.2	29.5
0	Transverse (centre) †	{ 24.1	19.0
0		{ 23.2	20.0
0.02		{ 24.5	22.0
0.02		{ 24.3	20.0
0.02		{ 26.5	28.0
0.03		{ 26.4	28.0
		{ 26.4	26.0
		{ 26.7	30.5

* The test-pieces were machined according to B.S. No. 18 (1938).

† From the end of the 9-in. length nearest to the centre of the ingot (i.e. the lower end).

and 0.04% calcium ingots cast during the previous commercial tests (Section V, 1) are included in Table V.

Table V indicates that an addition of 0.02% boron to commercial ingots of copper-10% aluminium

completely eliminates columnar crystal growth, and that further increase in boron reduces the size of the equi-axial crystal slightly.

Table VI indicates that boron additions increase both the tensile strength and ductility of copper-10% aluminium by virtue of their grain-refining effect.

The average of the results given in Table VI for each individual boron addition, together with the percentage increase in tensile strength and elongation relative to the untreated alloy, are set out in Table VII. Analyses for aluminium content were made on samples from the ingots, and the results are included in the table.

TABLE VII.—*Percentage Increase in Tensile Strength and Elongation Produced by Boron Additions in Copper-10% Aluminium Alloy.*

Nominal Boron Content, %	Aluminium Content, %	Tensile Strength, tons/in. ²	Increase in Tensile Strength over Untreated Alloy, %	Elongation, % on 1-in. Gauge-Length	Increase in Percentage Elongation over Untreated Alloy, %
0	9.50	23.4	...	18.4	...
0.01	9.39	25.6	9.4	25.0	35.9
0.02	9.49	26.4	12.8	26.3	42.9
0.03	9.42	26.5	13.2	26.9	46.2

Micro-examination of specimens from the untreated and boron-treated ingots revealed no differences in constitution. No foreign nuclei were visible, even under a magnification of 1500 \times , in the boron-treated ingots.

3. OTHER COMMERCIAL APPLICATIONS

Experiments on commercial castings have shown that boron additions may be used to advantage in obtaining grain-refinement of the hard 14% aluminium, 5% iron alloys used in the manufacture of die-blocks, which have an all- β phase structure. A cast hollow cylinder, 14 in. outside dia. \times 8 in. inside dia. \times 6 in. high, which was normally entirely columnar on solidification, exhibited a completely equi-axial structure when 0.01% boron was added to the melt, other conditions being maintained constant. The average diameter of the equi-axial crystals was 2 mm.

VI.—SUMMARY AND CONCLUSIONS

It has been found that additions of boron of between 0.0025 and 0.03% to molten copper-aluminium alloy containing 10% aluminium produce grain refinement of the alloy on solidification, the degree of refinement increasing with the quantity of boron added up to about 0.02%, when a completely equi-axial structure is obtained in contrast to the entirely columnar structure of the untreated alloy. This grain refinement is associated with increased tensile strength and percentage elongation.

It has been shown that in the presence of these

boron additions, the copper-10% aluminium alloy solidifies initially as the β phase, which is nucleated by some compound formed as a result of the boron additions. This compound is thought, from lattice-structure considerations, to be boron carbide, B_4C .

Additions of calcium in conjunction with carbon (as acetylene gas bubbled through the molten alloy) also resulted in grain refinement, but this was associated with micro-porosity and cracking.

The grain refinement produced by boron additions was found to be practically unaffected by repeated

remelting and casting, indicating that loss of boron on remelting was negligible.

The use of high pouring temperatures tended to decrease the degree of grain refinement in cases where the boron addition was not sufficient to produce a completely equi-axial structure.

Boron additions also refined the grain-size of the copper-14% aluminium alloys used in the manufacture of die-blocks, which consist entirely of the β phase on solidification.

REFERENCES

1. L. Northcott, *J. Inst. Metals*, 1942, **68**, 189.
2. R. Genders and G. L. Bailey, "The Casting of Brass Ingots" (B.N.F.M.R.A. Research Monograph No. 3), p. 59. London: 1934.
3. L. Northcott, *J. Iron Steel Inst.*, 1934, **129**, 171.
4. L. Northcott, *J. Inst. Metals*, 1938, **62**, 101.
5. G. L. Bailey and W. A. Baker, *ibid.*, 1948-49, **75**, 285.
6. E. Scheil, *Z. Metallkunde*, 1936, **28**, 228.
7. K. Iwasé, J. Asato, and N. Nasu, *Sci. Rep. Tôhoku Imp. Univ.*, 1936, [i], (Honda Anniv. Vol.), 652.
8. R. Mitsche, *Carnegie Schol. Mem., Iron Steel Inst.*, 1934, **23**, 65; 1936, **25**, 41.
9. H. Hanemann and W. Hofmann, *Z. Metallkunde*, 1937, **29**, 149.
10. L. Northcott, *J. Inst. Metals*, 1939, **65**, 173.
11. K. Achenbach, H. A. Nipper, and E. Piwowarsky, *Giesserei*, 1939, **26**, 597.
12. F. A. Fox and E. Lardner, *J. Inst. Metals*, 1945, **71**, 1.
13. W. A. Baker and M. D. Smith, *B.N.F.M.R.A. Research Rep.*, 1945, (A.694).
14. J. A. Davis, L. W. Eastwood, and J. De Haven, *Amer. Foundryman*, 1945, **8**, (1), 34.
15. C. H. Mahoney, A. L. Tarr, and P. E. Le Grand, *Trans. Amer. Inst. Min. Met. Eng.*, 1945, **161**, 328.
16. N. Tiner, *ibid.*, 1946, **166**, 242.
17. C. E. Nelson, *Trans. Amer. Found. Soc.*, 1948, **56**, 1.
18. W. A. Baker, M. D. Eborall, and A. Cibula, *J. Inst. Metals*, 1952-53, **81**, (1), 43.
19. A. Dumas, *Rev. Mét.*, 1944, **41**, 273.
20. M. D. Eborall, *J. Inst. Metals*, 1949-50, **76**, 295.
21. A. Cibula and R. W. Ruddle, *ibid.*, 1949-50, **76**, 361.
22. A. Cibula, *ibid.*, 1949-50, **76**, 321.
23. V. Kondic and D. Shutt, *ibid.*, 1950-51, **78**, 105.
24. A. Cibula, *ibid.*, 1951-52, **80**, 1.
25. J. H. van der Merwe, *Discussions Faraday Soc.*, 1949, (5), 201.
26. L. Royer, *Compt. rend.*, 1925, **180**, 2050.
27. F. A. Crossley and L. F. Mondolfo, *Trans. Amer. Inst. Min. Met. Eng.*, 1952, **195**, 1190.
28. S. F. Hermann and F. T. Sisco, *Trans. Amer. Inst. Min. Met. Eng., Inst. Metals Div.*, 1931, 262.
29. A. J. Murphy and G. T. Callis, *J. Inst. Metals*, 1948-49, **75**, 325.
30. P. E. Landolt and F. R. Pyne, *Foundry*, 1949, **77**, 90, 262.
31. R. A. Colton and M. Margolis, *Trans. Amer. Found. Soc.*, 1951, **59**, 360.
32. B. N. Ames and N. A. Kahn, *ibid.*, 1950, **58**, 229.
33. R. W. Ruddle and A. L. Mincher, *J. Inst. Metals*, 1950-51, **78**, 229.
34. J. A. Reynolds and C. R. Tottle, *ibid.*, 1951-52, **80**, 93.
35. A. J. Bradley and P. Jones, *ibid.*, 1933, **51**, 131.

THE STRUCTURE OF TITANIUM-TIN ALLOYS IN THE RANGE 0-25 AT.-% TIN *

1473

By H. W. WORNER,† M.Sc., MEMBER

SYNOPSIS

Titanium-tin alloys in the range 0-25 at.-% tin have been investigated by metallographic and Debye-Scherrer X-ray-diffraction methods, and a partial phase diagram has been established. Detailed results for two groups of alloys are given; one group was based on a commercial grade of titanium, the other on titanium refined by the iodide process. Tin depresses the freezing point of titanium, and there appears to be a eutectic point in the vicinity of 17 at.-% tin at 1550° C. approximately, the solid constituents involved in the eutectic transformation being a solid solution of tin in β -titanium and a phase, designated γ , based on Ti_3Sn . The solid solubility of tin in α -titanium is just over 10 at.-%, and it varies only slightly in the range 700°-880° C. The solubility of tin in β -titanium increases from 7.5 at.-% at 885° C. to approximately 10 at.-% at 1100° C. Addition of tin to titanium depresses the $\alpha \rightleftharpoons \beta$ transformation region to a minimum of 845° C. at 5 at.-% tin; above 5 at.-% the ($\alpha + \beta$) range rises to meet a peritectoid horizontal at 885° C. The peritectoid composition is 10.5 at.-% tin, and the peritectoid reaction is: α (10.5 at.-% Sn) $\rightleftharpoons \beta$ (7.5 at.-% Sn) + γ (22 at.-% Sn). The γ phase has an ordered structure (DO_{19} -type) based on the hexagonal close-packed structure. Tin hardens α -titanium considerably, but the hardness of the alloys cannot be appreciably varied by heat-treatment.

I.—INTRODUCTION

THE investigation to be described formed part of a research programme concerned with titanium-base alloy systems in which the alloying elements have atomic sizes similar to that of titanium itself. Very little information about titanium-tin alloys has been published. Craighead, Simmons, and Eastwood¹ have shown that 0.7 at.-% tin can be held in solid solution in both α - and β -titanium. Pietrokowsky and Duwez² have determined the crystal structure of Ti_5Sn_3 , and Pietrokowsky³ has reported the structure of Ti_3Sn .

The present work covered the range 0-25 at.-% tin. Alloys made with a commercial grade of titanium were first studied in an exploratory investigation, then alloys based on refined titanium were examined. The exploratory investigation was designed partly to yield results of practical value, but chiefly to provide some general information about the system so that the number of purer alloys made in the subsequent work could be kept to a minimum in the interests of economy. Both stages of the research involved metallographic and X-ray-diffraction studies of heat-treated specimens. Particular attention was paid to the effect of tin on the $\alpha \rightleftharpoons \beta$ transformation in titanium and to the limits of solubility of tin in the two forms of titanium. The freezing ranges of the alloys were estimated only very approximately.

II.—MATERIALS USED

Titanium prepared by the Kroll process was used in the exploratory work. This metal, which was

made by the United States Bureau of Mines, will be referred to as commercial titanium. Metal refined by the iodide process in the Philips Laboratories, Holland, was used in more critical experiments aimed at establishing phase boundaries. Impurities found in these two grades of titanium are listed in Table I.

TABLE I.—Concentrations of Impurities in Commercial and Refined Titanium after Melting in an Argon-Arc Furnace.

Impurity	Commercial Ti, at.-%	Refined Ti, at.-%
Oxygen	0.6	0.15
Nitrogen	0.2	0.03
Carbon	0.1	...
Iron	0.15	0.02
Magnesium	0.1-0.2	Faint trace *
Silicon	Trace *	Strong trace *
Antimony	Not detected *	Strong trace *
Tin	Trace *	Strong trace *
Copper	Trace *	Trace *
Na, K, Ca, Sr, Ba, Be, Al, Ag, Zn, Cd, Pb, Bi, As, Co, Ni, Cr, Mo, W, V, Nb, Ta, Zr	Not detected *	Not detected *

* Result of spectrographic test.

The oxygen concentrations reported in the table were determined by the chlorination method, as described by Corbett.⁴

The $\alpha \rightleftharpoons \beta$ transformation range for each grade of titanium was determined by observing the microstructures of specimens quenched from various temperatures. For the commercial metal, the range was 870°-960° C. and for the refined grade, 885°-895° C.

* Manuscript received 12 January 1953.

† Physical Metallurgy Section, Commonwealth Scientific

and Industrial Research Organization, Baillieu Laboratory, University of Melbourne, Australia.

The tin, which was supplied by the Bureau of Analysed Samples, Ltd., England, contained the following impurities: iron, 0.015; antimony, 0.0035; lead, 0.0025; copper, 0.001; and bismuth, 0.0003 at.-%.

III.—EXPERIMENTAL

The alloys were made by melting together weighed amounts of titanium and tin in an argon-arc furnace of the type developed by Kroll.⁵ Both metals were initially in lump form. The commercial titanium had been previously melted in the arc furnace; pieces of refined titanium were taken direct from the "as-deposited" bars.

The metals mixed readily during melting, and losses due to spitting and fuming were small. Most of the alloys were analysed, and a comparison of the analytical results with the nominal compositions showed that losses during melting comprised a little tin and practically no titanium. For practical purposes, the composition of an alloy could be calculated from the mass of titanium used and the mass of the final ingot, assuming the difference to be the mass of tin in the ingot. This calculated value will be termed the synthetic composition.

In the text of this paper all alloy compositions will be reported in at.-% tin, and the analytical results rather than synthetic compositions will be used for alloys which were analysed.

The "ingots" were limited in weight to about 2 g. Such small specimens cooled rapidly after the arc was switched off, and the sudden chilling minimized macro-segregation during solidification. After the first melting operation, the ingots were allowed to solidify and were then inverted and remelted. This was repeated two or three times to ensure thorough mixing of the component metals in the liquid state. A cross-section through each ingot was examined to ascertain the as-cast structure and to check its uniformity.

Alloys containing not more than 13.5 at.-% tin could be mechanically worked at about 700°–800° C. They were hammered in this temperature range in order to facilitate the attainment of equilibrium in subsequent heat-treatments. The superficial oxide layer formed during hot working was removed by first grinding the surface and then pickling in a mixture of concentrated nitric acid (80% by volume) and concentrated hydrofluoric acid (20%).

Specimens for heat-treatment were sealed in small, clear silica bulbs in which the pressure had been reduced to approximately 5×10^{-3} mm. mercury. Each bulb had a volume of only 0.1–0.2 c.c., so that residual gases after evacuation would cause little or no contamination of the specimen during subsequent heating. To minimize diffusion of atmospheric gases through the silica envelopes during heat-treatments, the bulbs were placed inside a continuously evacuated silica tube in which the pressure was kept below 10^{-2} mm. mercury. The temperature of the furnace could be maintained within $\pm 2^\circ$ C. of the required

value. For treatments above 950° C. the minimum period of heating necessary to produce a practically stable structure was found to be of the order of 2–3 hr. At temperatures in the range 700°–900° C. the duration of heating had to be increased to at least 5 hr. Most of the heat-treatments consisted in heating the specimens up to the required temperature, maintaining them at that temperature for the necessary time, and then quenching into water. Some of the treatments involved first heating the specimens to 100°–200° C. above the quenching temperature, then cooling to the latter, holding at that temperature, and finally quenching. Quenching was effected by rapidly withdrawing the tube enclosing the specimens from the furnace and tipping the specimen bulbs into a shallow dish of water. After entering the water the bulbs were broken by a light blow from a hammer.

During the heating and subsequent water quenching, slight superficial contamination of the alloys occurred. Care was taken in removing the contaminated layer, especially from specimens intended for Debye-Scherrer X-ray-diffraction experiments. For practically all the X-ray-diffraction work, small, solid specimens were used. These were initially prepared in the form of small prisms, approximately 1.5 mm. square by 8 mm. long. After heat-treatment, the prisms were pickled in the nitric acid-hydrofluoric acid mixture described above until the cross-sectional width was reduced to 0.5–0.8 mm. This ensured removal of the contaminated surface as well as producing specimens with dimensions convenient for Debye-Scherrer experiments. Microscopical examination of two-phase alloys prepared as outlined above revealed no significant evidence of preferential dissolution of one phase.

Cobalt $K\alpha$ radiation was employed in all the X-ray experiments, photographic records being made with an 11.46-cm.-dia. powder camera which had been calibrated by means of 99.986% silver and spectroscopically pure copper. All calculations of lattice parameters were carried out by Cohen's method of least squares.

Specimens for metallographic examination were pickled to remove the contaminated surface layers, roughly polished by means of waterproof carborundum papers, and finally polished by hand on fine linen laps furnished with diamond dust. An aqueous solution containing 2 wt.-% nitric acid and 1 wt.-% hydrofluoric acid was used to etch most of the alloys. A similar etchant, but containing a higher concentration of hydrofluoric acid (up to 3 wt.-%) was used in some cases to reveal more markedly the fine, acicular structure which results from a rapid $\beta \rightarrow \alpha$ transformation occurring during a quench.

The effect of tin on the freezing point of titanium was ascertained by following the cooling of the alloys, after melting in the arc furnace, with the aid of a disappearing-filament optical pyrometer. On account of the rapidity of cooling in the arc furnace, considerable undercooling is likely to occur. Moreover, the

effect of tin on the emissivity of titanium is not known. The freezing ranges of the alloys could thus be estimated only very approximately.

IV.—ALLOYS MADE WITH COMMERCIAL TITANIUM

1. ALLOYS USED

The alloys made in the course of the exploratory investigation are listed in Table II. Losses during

TABLE II.—Alloys Made with Commercial Titanium.

Synthetic Composition, at.-% tin	Analytical Result	
	Tin, at.-%	Tin, wt.-%
3.3	3.4	8.0
5.3	5.4	12.0
7.5	7.7	16.9
10.0	9.9	21.6
11.1	11.2	23.8
11.5	11.4	24.2
15.3
17.0
18.6	18.7	36.3
21.9	22.0	41.1
23.2	23.5	43.0

the melting of the 15.3 and 17.0 at.-% tin alloys were only very slight, and therefore these alloys were not analysed.

2. FREEZING RANGES AND AS-CAST STRUCTURES

Addition of tin lowered the freezing point of titanium, the greatest depression, of the order of 150°-200° C., being noted at 17.0 at.-% tin. There seemed to be comparatively little difference between the freezing ranges of the 18.7, 22.0, and 23.5 at.-% tin alloys; all these alloys appeared to start solidifying only 50°-100° C. below the freezing point of titanium.

In the as-cast condition, alloys containing from 3.4-11.4 at.-% tin exhibited a columnar macro-structure. On a microscopic scale there was a fine, acicular structure, similar to that shown in Fig. 7 (Plate LXXXI), resulting from the $\beta \rightarrow \alpha$ transformation during rapid cooling. Hence it would appear that alloys containing up to 11.4 at.-% tin crystallized as columnar grains of β solid solution which subsequently transformed rapidly to α solid solution during cooling to normal temperatures. The alloy with 15.3 at.-% tin consisted partly of a constituent having the fine acicular structure represented in Fig. 7, the remainder being a fine mixture of phases arranged in lamellar form. The 17.0 at.-% tin alloy consisted wholly of this fine, lamellar mixture. As-cast alloys containing 18.7, 22.0, and 23.5 at.-% tin consisted largely of a slightly cored, dendritic constituent surrounded by a matrix with a fine, duplex structure. The dendritic constituent, which had obviously crystallized before the matrix, was found to be an intermediate phase, which will be termed the γ phase.

The evidence presented above suggests that there is probably a eutectic point close to 17 at.-% tin, the solid constituents involved in the eutectic transformation being the γ phase and β solid solution with a tin content between 11.4 and 15.3 at.-% tin.

3. MICROSTRUCTURES OF HEAT-TREATED ALLOYS

The microstructures of alloys quenched from temperatures in the range 650°-1100° C. are represented graphically in Fig. 1. These results indicate that the solid solubility of tin in the α form of the commercial titanium lies between 7.7 and 9.9 at.-% in the range 650°-860° C. From 1020° to 1100° C. the solubility of tin in the β modification of the metal also appears to lie in the region 7.7-9.9 at.-%. Fine

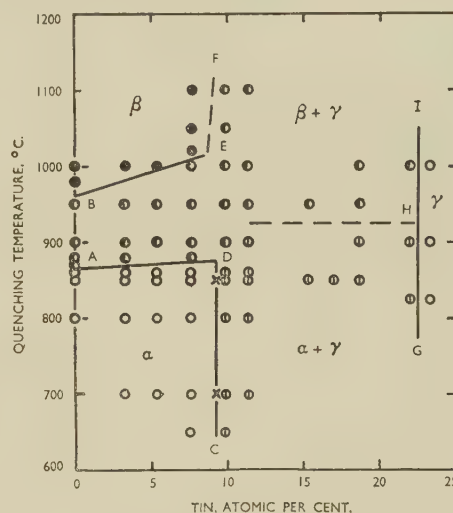


FIG. 1.—Results of Quenching Experiments on Alloys Made with Commercial Titanium.

KEY.

- Constituent with fine, acicular structure, as shown in Fig. 7 (Plate LXXXI).
- Single phase (bright etching).
- ⊙ Mixture of bright-etching phase and constituent with fine, acicular structure.
- ⊖ Mixture of two bright-etching constituents.
- x Determined from X-ray diffraction results.

acicular structures like that shown in Fig. 7 (Plate LXXXI) and represented by the symbol ● in Fig. 1 are taken as evidence of a rapid $\beta \rightarrow \alpha$ transformation having occurred during water-quenching. Hence the area above the boundary BE in Fig. 1 is marked β .

Only the low-tin boundary (GHI) of the γ phase field was determined. It was found that the etching characteristics of the γ phase were similar to those of the 7.7 at.-% tin α solid solution.

The ($\alpha + \gamma$) structures were very fine, and all exhibited a Widmanstätten pattern like that shown in Fig. 8 (Plate LXXXI). The microstructures of alloys quenched from the ($\beta + \gamma$) field (FEDHI in Fig. 1) were similar to the ($\alpha + \gamma$) structures, except that some regions possessed the fine, acicular structure which results from the rapid $\beta \rightarrow \alpha$ change. This fine, acicular structure was not well developed in the fine-grained $\gamma +$ acicular α mixtures, and it could be clearly revealed only by relatively deep etching.

The structures of alloys quenched from the area *ABED* in Fig. 1, i.e. between the α and β fields, were very much coarser than those of alloys quenched from the $(\beta + \gamma)$ and $(\alpha + \gamma)$ fields (cf. Figs. 8 and 9, Plate LXXXI). Because of the similarity in etching characteristics of the α solid solutions and the γ phase, it was impossible to identify, with certainty, the bright-etching constituents in the alloys quenched from the field *ABED*. Attempts to distinguish between the saturated α solid solutions and the γ phase by microhardness tests were unsuccessful because the microhardnesses of these phases proved to be similar.

4. DEBYE-SCHERRER X-RAY-DIFFRACTION OBSERVATIONS

The X-ray-diffraction results are summarized, together with pertinent metallographic results, in Table III. By combining the two sorts of evidence for each quenching experiment, the structure at the quenching temperature can be deduced in each instance. The deductions are included in Table III.

TABLE III.—X-Ray-Diffraction Results and Metallographic Observations for Alloys Made with Commercial Titanium.

Tin Content, at.-%	Quenching Temp., °C.	Microstructure *	Phases Identified by X-Ray Diffraction	Structure at Quenching Temp., Deduced from Microstructure and X-Ray Results
3.4	1000	All A.C.	Strained α	β
	850	All B.E.C.	α	α
5.4	1000	All A.C.	Strained α	β
	950	A.C. + B.E.C.	Strained α	$\alpha + \beta$
	850	All B.E.C.	α	α
7.7	1020	All A.C.	Strained α	β
	950	A.C. + B.E.C.	Strained α	$\alpha + \beta$
	850	All B.E.C.	α	α
9.9	1050	A.C. + B.E.C.	Strained	$\beta + \gamma$
	850	2 B.E.C.'s	$\alpha (+ \gamma?)$	$\alpha + \gamma$
	700	2 B.E.C.'s	$\alpha (+ \gamma?)$	$\alpha + \gamma$
11.2	1000	A.C. + B.E.C.	γ	$\beta + \gamma$
	850	2 B.E.C.'s	$\alpha + \gamma$	$\alpha + \gamma$
	1100	A.C. + B.E.C.	γ	$\beta + \gamma$
11.4	950	A.C. + B.E.C.	γ	$\beta + \gamma$
	850	2 B.E.C.'s	$\alpha + \gamma$	$\alpha + \gamma$
	700	2 B.E.C.'s	$\alpha + \gamma$	$\alpha + \gamma$
18.7	1000	B.E.C. + A.C.	γ	$\beta + \gamma$
	850	2 B.E.C.'s	$\alpha + \gamma$	$\alpha + \gamma$
22.0	1000	B.E.C. + A.C.	γ	$\gamma + \beta$
	825	2 B.E.C.'s	γ	$\gamma + \alpha$
23.5	1000	All B.E.C.	γ	γ
	825	All B.E.C.	γ	γ

* A.C. = Constituent with fine, acicular structure.
B.E.C. = Bright-etching constituent.
Heavy type denotes the preponderant phase.

It will be noted that the diffraction experiments confirmed the existence of an α solid solution field extending to a limit between 7.7 and 9.9 at.-% tin. Fig. 2 shows the lattice-parameter/tin-concentration relationship for α phase in alloys containing up to 11.4 at.-% tin. These data indicate that the limit

of solubility of tin in the α form of the commercial titanium is 9.3 at.-% at both 850° and 700° C.

Alloys consisting entirely of the constituent with the fine, acicular structure (cf. Fig. 7, Plate LXXXI) were shown to possess a strained hexagonal close-packed lattice structure like that found in the commercial titanium after quenching from the β range. Diffraction lines at Bragg angles in excess of 60° were broad and the α_1, α_2 doublets were not resolved in the highest-angle reflections. The broadening of the lines was greater, the higher the tin content. The high-angle reflections from the 7.7 at.-% tin alloy quenched from 1020° C. were so broad that they were not easy to detect.

The patterns from the 23.5 at.-% tin alloy were the same for both quenching temperatures (1000° and

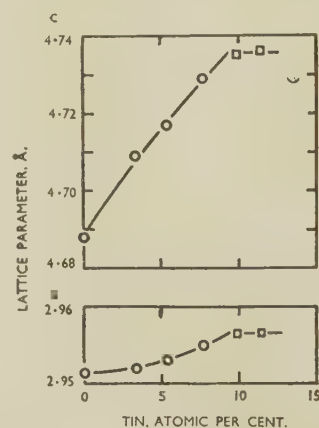


Fig. 2.—Lattice Parameters of α Phase in Alloys Made with Commercial Titanium.

KEY.

○ Single-phase alloys water-quenched from 850° C.
□ Duplex alloys water-quenched from 850° and 700° C.

825° C.) and were found to comprise a set of lines practically identical with the spectrum of the high-tin α solid solutions together with a set of weaker lines. All the reflections could be indexed on the basis of a hexagonal lattice with $c/a = 0.80$ approximately, and it was apparent that the phase designated γ in Fig. 1 possessed an ordered structure based on the hexagonal close-packed structure. In Table IV are listed the indices assigned to the reflections, together with the observed values of $(1/d)^2$ and line intensities. The calculated values of $(1/d)^2$ included in Table IV were derived from the expression $(1/d)^2 = 0.03810(h^2 + k^2 + l^2) + 0.04406 l^2$. It will be noted that the calculated and observed values of $(1/d)^2$ agree reasonably well. The parameters of the structure cell calculated by the method of least squares from the (40.3), (30.4), (42.1), and (22.4) reflections were: $c = 4.768 \pm 0.004$ Å, $a = 5.922 \pm 0.005$ Å, $c/a = 0.805$. It will be noted that (hkl) reflections were absent when $l \neq 2n$; this indicates space group D_{6h}^{4h} , $C6/mmc$ or a sub-group thereof.

The diffraction data in Table IV were compared with Pietrokowsky's³ results for the "compound"

Ti_3Sn , and it becomes apparent that the lattice structure of the 23.5 at.-% tin alloy was practically identical with that of Ti_3Sn . Hence it can be considered that the γ phase is based on Ti_3Sn , which,

TABLE IV.—X-Ray Diffraction (Debye-Scherrer) Data for 23.5 at.-% Tin Alloy, Water-Quenched from 825° C. (γ phase).

hkl	Relative Intensity Observed	$(1/d)^2, \text{\AA}^{-2}$	
		Observed	Calculated
10-1	M	0.0829	0.0822
11-0	W	0.1146	0.1143
20-0	M	0.1529	0.1524
00-2	S	0.1764	0.1763
20-1	VS	0.1968	0.1965
10-2	VW	0.2140	0.2144
11-2	W	0.2912	0.2906
21-1	W	0.3112	0.3108
20-2	M	0.3289	0.3287
22-0	M	0.4579	0.4572
20-3	S	0.5493	0.5490
22-2	M	0.6336	0.6334
40-1	M	0.6544	0.6536
00-4	M	0.7045	0.7050
40-2	W	0.7867	0.7858
11-4	VW	0.8190	0.8193
20-4	M	0.8575	0.8574
32-2	W	0.8982	0.9001
21-4	} W	0.9758	0.9717
41-2			0.9763
50-1	VW	0.9971	0.9965
40-3	M	1.0070	1.0061
30-4	W	1.0500	1.0479
42-0	W	1.0668	1.0667
00-5	W	1.1006	1.1015
42-1	M	1.1101	1.1108
10-5	W	1.1403	1.1396
22-4	S	1.1614	1.1622

V.S = Very strong. S = Strong. M = Medium. W = Weak. VW = Very weak.

as reported by Pietrokowsky, possesses the DO_{19} -type structure.

Examination of the diffraction patterns for the 11.2, 11.4, and 18.7 at.-% tin alloys quenched from the $(\alpha + \gamma)$ field in Fig. 1 (p. 523) revealed that almost the whole spectrum of the γ phase was present. The only definite evidence of the presence of α phase was the (11.4) reflection which was sufficiently distant from the (22.4) reflection of the γ phase to be distinguished and measured accurately. All the other reflections from the α phase were apparently so close to the corresponding reflections from the γ phase as to be indistinguishable therefrom. This introduced some uncertainty into the calculation of lattice parameters for the phases in $(\alpha + \gamma)$ mixtures. However, since there was a preponderance of α phase in the 9.9, 11.2, and 11.4 at.-% tin alloys quenched from 860° C. or lower, diffraction patterns from these could be used to estimate the lattice parameters of α solutions saturated with tin.

The 22.0 at.-% tin alloy quenched from the $(\alpha + \gamma)$ range contained such a high proportion of γ phase that the (11.4) reflection from the α constituent could not be detected. Therefore the lattice

parameters of γ phase saturated with titanium could be calculated from the diffraction patterns for the 22.0 at.-% tin specimens. The actual values were: $c = 4.762 \pm 0.004 \text{ \AA}$, $a = 5.916 \pm 0.005 \text{ \AA}$, $c/a = 0.805$. These values pertain to a specimen quenched from 825° C.

Diffraction patterns for the 11.2, 11.4, and 18.7 at.-% tin alloys quenched from the $(\beta + \gamma)$ field in Fig. 1 (p. 523) all showed evidence of the presence of the γ phase. The patterns from the 9.9, 11.2, and 11.4 at.-% tin specimens seemed to contain weak, broad (11.4) reflections from strained α phase, but in this respect the evidence was not conclusive, except perhaps for the 9.9 at.-% alloy.

The diffraction patterns of alloys quenched from the field $ABED$ in Fig. 1 (p. 523) were all rather similar to those of alloys quenched from the β field. There were no indications of the presence of γ phase. These results suggest that the area $ABED$ can be correctly described as the $(\alpha + \beta)$ field. An alloy quenched after being brought to equilibrium as an $(\alpha + \beta)$ mixture would contain strained α phase, formed from β during quenching, together with comparatively strain-free α . Broad reflections from the strained α would naturally tend to mask sharp reflections from strain-free α .

5. SUMMARY

The exploratory investigation has shown that tin depresses the freezing point of titanium. There seems to be a eutectic point at about 17 at.-% tin, the temperature being of the order of 200° C. below the freezing point of the commercial titanium. Constituents of the eutectic mixture are a solid solution of tin in β -titanium and an intermediate phase designated γ .

It has been revealed that tin dissolves to the extent of approximately 9 at.-% in both forms of the commercial titanium. It has also been shown that tin causes a slight elevation of the $\alpha \rightleftharpoons \beta$ transformation range in the titanium. This suggests a peritectoid system. However, the experiments on the commercial-purity alloys did not yield any conclusive evidence of an $\alpha \rightleftharpoons \beta + \gamma$ reaction. Probably the chief reason for this is the broad transformation range (870°-960° C.) in the commercial titanium. The impurities which produce this effect would almost certainly cause a peritectoid type of transformation to occur over a considerable temperature range.

The effect of tin on the lattice parameters of α -titanium is worthy of note; the c parameter is appreciably increased by addition of tin, whereas a is only slightly expanded. The c/a ratio for the saturated α solid solution is 1.600 as compared with 1.588 for the commercial titanium.

Quenching in water does not cause solid solutions of tin in the β -form of the commercial titanium to be retained with their high-temperature crystal structure. During the quench, a rapid $\beta \rightarrow \alpha$ change occurs with the production of a constituent which, on etching, exhibits a characteristic, fine acicular microstructure.

The intermediate phase γ has an ordered hexagonal crystal structure. It can be considered as based on Ti_3Sn , which, as shown by Pietrokowsky,³ has the DO_{19} -type structure. The interatomic distances in the γ phase are close to those of tin-saturated α solutions.

V.—ALLOYS MADE WITH REFINED TITANIUM

1. ALLOYS USED

Compositions of alloys used are listed in Table V. There was satisfactory agreement between the analytical results and the synthetic compositions up

TABLE V.—Alloys Made with Refined Titanium.

Synthetic Composition, at.-% tin	Analytical Results	
	Tin, at.-%	Tin, wt.-%
3.4	3.5	8.2
6.35	6.5	14.4
8.5	8.5	18.9
11.1	11.0	23.6
13.15	13.3	27.6
21.2
24.0

to 13.3 at.-% tin. The 21.2 and 24.0 at.-% tin alloys were not analysed, because the losses during the melting of these alloys were very slight and it was considered safe to use the synthetic compositions.

2. FREEZING RANGES AND AS-CAST STRUCTURES

In general, the observations were in agreement with those reported for the commercial-purity alloys. Addition of tin up to 13.3 at.-% tin depressed the freezing point of the refined titanium. The depression was of the order of 150°C . at 13.3 at.-% tin. The 21.2 and 24.0 at.-% tin alloys started to solidify at temperatures only about 50°C . below the freezing point of the titanium.

The structures of as-cast alloys containing 3.5-13.3 at.-% tin were very similar to those already reported for the commercial-purity alloys with 3.4-11.4 at.-% tin. The structure of the 21.2 at.-% tin alloy as cast resembled that of the 18.7, 22.0, and 23.5 at.-% tin commercial-purity alloys in the same condition, and the 24.0 at.-% tin alloy consisted entirely of slightly cored, dendritic grains of γ phase.

3. MICROSTRUCTURES OF HEAT-TREATED ALLOYS

The results of experiments covering the range 600°C – 1120°C . are set out in Fig. 3. There is a general similarity between these results and those presented in Fig. 1 (p. 523) for alloys made with the commercial titanium. However, the quenching experiments on the purer alloys have given a much clearer picture of the phase relationships in the range 850°C – 900°C ., especially in respect to the $\alpha \rightleftharpoons \beta$ transformation range. Results for this range are presented in

greater detail in Fig. 4, from which it is apparent that the boundaries of the $(\alpha + \beta)$ field are depressed by the addition of 3.5 at.-% tin; with further additions of tin, the $(\alpha + \beta)$ range is elevated up to about 880°C .

Two types of heat-treatment were used to locate the boundaries of the $(\alpha + \beta)$ field: (a) Simply heating

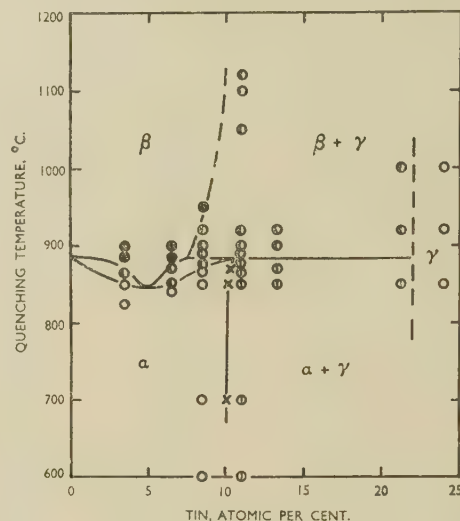


FIG. 3.—Results of Quenching Experiments on Alloys Made with Refined Titanium. Key as in Fig. 1 (p. 523).

the specimen to the quenching temperature and maintaining it at that temperature for at least 5 hr. before quenching (see Fig. 4 (a)). (b) First heating the specimen at 1000°C ., i.e. in the β field, for 1-2 hr., then cooling it in the furnace to the desired tem-

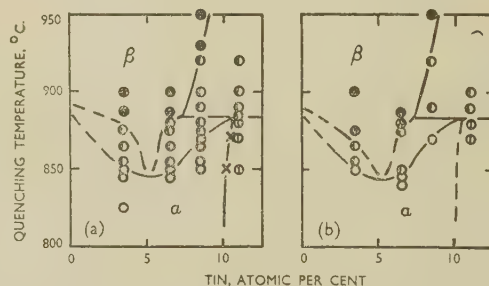


FIG. 4.—Results of Quenching Experiments on Alloys Made with Refined Titanium. (a) Alloys heated to desired temperature and water-quenched. (b) Alloys heated to 1000°C ., cooled to desired temperature, and quenched. Key as in Fig. 1 (p. 523).

perature, at which it is maintained for at least 5 hr. and finally quenching it (see Fig. 4 (b)).

There was good agreement between the results in respect of the $\alpha/(\alpha + \beta)$ boundary, but the $\beta/(\alpha + \beta)$ boundary determined by heat-treatments of type (a) was a little higher than that deduced from experiments of type (b). This discrepancy indicates that the times of heating at the quenching temperatures were not quite sufficient to permit equilibrium to be attained. However, it can be assumed that the

equilibrium $\beta/(\alpha + \beta)$ boundary lies between the two $\beta/(\alpha + \beta)$ boundaries shown in Fig. 4.

The results presented in Figs. 3 and 4 indicate that there is a peritectoid horizontal at about 885° C. The most interesting metallographic evidence relating to the peritectoid transformation is shown in Figs. 10 and 11 (Plate LXXXI), which represent the structures found in the 11.0 at.-% tin alloy after quenching from 880° and 890° C., respectively. Heating from 880° to 890° C. caused a change from a relatively coarse-grained, almost single-phase (α) structure to a very fine, duplex structure. This fine structure was observed even when the rate of heating through the range 880°-890° C. had been as low as 0.2° C./min. Further, the structure could be coarsened only slightly by heating at temperatures in the range 1000°-1100° C. for 2 hr. As shown in Fig. 11, the quenched peritectoid mixture consisted of roughly equiaxed particles in a matrix with an acicular structure. Apparently the continuous phase had been β solid solution which had transformed to α during the quench. X-ray-diffraction experiments, the results of which will be discussed in the next section, proved the existence of γ phase in the 11.0 at.-% tin alloy quenched from 900° C. or higher; hence it can be taken that the fine particles in the peritectoid mixture were γ constituent.

4. DEBYE-SCHERRER X-RAY-DIFFRACTION OBSERVATIONS

The X-ray-diffraction results for the purer alloys are presented, together with the corresponding metallographic results, in Table VI. The table also

TABLE VI.—X-Ray-Diffraction Results and Metallographic Observations for Alloys Made with Refined Titanium.

Tin Content, at.-%	Quenching Temp., °C.	Microstructure *	Phases Identified by X-Ray Diffraction	Structure at Quenching Temp., Deduced from Microstructure and X-Ray Results
3.5	887	All A.C.	Strained α	β
	850	All B.E.C.	α	α
6.5	887	All A.C.	Strained α	β
	865	A.C. + B.E.C.	Strained α	$\alpha + \beta$
	845	All B.E.C.	α	α
8.5	950	All A.C.	Strained α	β
	890	A.C. + B.E.C.	γ	$\beta + \gamma$
	875	A.C. + B.E.C.	Strained α	$\alpha + \beta$
	865	All B.E.C.	α	α
11.0	1120	A.C. + B.E.C.	γ	$\beta + \gamma$
	900	A.C. + B.E.C.	γ	$\beta + \gamma$
	870	2 B.E.C.'s	α	$\alpha + \gamma$
13.3	850	2 B.E.C.'s	α	$\alpha + \gamma$
	700	2 B.E.C.'s	α	$\alpha + \gamma$
	900	A.C. + B.E.C.	γ	$\beta + \gamma$
21.2	875	2 B.E.C.'s	$\alpha + \gamma$	$\alpha + \gamma$
	1000	B.E.C. + A.C.	γ	$\gamma + \beta$
24.0	850	2 B.E.C.'s	γ	$\gamma + \alpha$
	1000	All B.E.C.	γ	γ
24.0	850	All B.E.C.	γ	γ

* A.C. = Constituent with fine, acicular structure.
B.E.C. = Bright-etching constituent.
Heavy type denotes the preponderant phase.

includes deductions based on the results. These deductions are in general concordance with those given in Table III (p. 524) for alloys based on the commercial titanium.

The lattice-parameter/composition relationship for the α phase (Fig. 5) revealed that the limit of solubility of tin in the α -form of the refined titanium was 10.5 at.-% at 870° C. and just over 10 at.-% at 850° and 700° C. These values are higher than those already reported for alloys based on the commercial-purity titanium, viz. 9.3 at.-% tin at 850° and 700° C.

The lattice parameters of the titanium-saturated γ phase were determined by experiments on 21.2 at.-% tin specimens quenched from 850° and 1000° C.

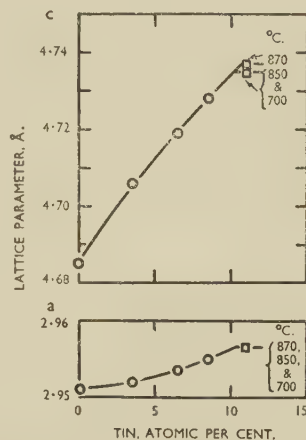


FIG. 5.—Lattice Parameters of α Phase in Alloys Made with Refined Titanium.

KEY.
○ Single-phase alloys water-quenched from 840°-850° C.
□ Duplex alloys water-quenched from temperatures shown.

For both quenching temperatures, the cell dimensions were: $c = 4.758 \pm 0.004$ Å., $a = 5.915 \pm 0.005$ Å., $c/a = 0.805$. The parameters of the 24.0 at.-% tin alloy quenched from 850° C. were $c = 4.766 \pm 0.004$ Å., $a = 5.920 \pm 0.005$ Å., $c/a = 0.805$. These data may be compared with the values reported by Pietrokowsky³ for Ti_3Sn made with refined titanium, viz., $c = 4.764 \pm 0.004$ Å., $a = 5.916 \pm 0.004$ Å., $c/a = 0.805$.

X-ray reflections for the γ constituent of quenched peritectoid mixtures in the 11.0 at.-% tin alloy were broad, and this was attributed partly to the fineness of the γ phase in these mixtures. The breadth of the diffraction lines could be reduced only a little by heating the peritectoid mixture for 1 hr. at 1120° C. This result is in conformity with the metallographic observation, already mentioned, that the peritectoid structures could be coarsened only slightly by heating to temperatures as high as 1100° C.

5. DISCUSSION

Perhaps the most interesting feature of the system is the comparatively small effect of tin on the temperature of the $\alpha \rightleftharpoons \beta$ transformation in titanium. All the $\alpha \rightleftharpoons \beta$ changes occur in the range 845°-890° C.

Another point of interest is that the solid solubility of tin in α titanium at 700° C. is only a little less than it is at 870° C.

Most of the metals which have atomic sizes close to that of titanium form more or less extensive β solid-solution series, but only very restricted α solution ranges. However, tin must be classed as a member of a very small group of metals which have atomic sizes similar to that of titanium and which dissolve to an appreciable extent in both forms of titanium. The other metals in this group are zirconium and aluminium. Unfortunately, it does not seem possible at present to offer any satisfactory theoretical explanation of these facts.

Recently McPherson and Hansen⁶ reported that tin elevates the $\alpha \rightleftharpoons \beta$ range of zirconium, there being a peritectoid point at about 8 at.-% tin and 980° C. In respect to some general features, the titanium-rich portion of the titanium-tin system is similar to the corresponding part of the zirconium-tin system. This, of course, is not surprising in view of the physical and chemical similarities of titanium and zirconium.

VI.—HARDNESS OF HEAT-TREATED ALLOYS

The effects of tin content and heat-treatment on hardness were determined for both groups of alloys, and the results are given in Fig. 6. It was found that tin hardened α -titanium appreciably, the effect being greater in alloys in which the α phase had the acicular structure produced by quenching from the β field. However, the effects of heat-treatment were small, except perhaps for the 7.7 at.-% tin alloy made with commercial titanium.

The hardness of the γ phase was about 100 D.P.N. lower than that of the high-tin α solid solutions. This explains why the maxima in the hardness/composition curves occur at, or near to, the α solid-solution limits.

Despite its comparatively low hardness, the γ phase could not be forged either at normal temperature or

in the range 600°–800° C. The brittleness of this constituent was in marked contrast to the ductility of the harder, high-tin α solid solutions. The latter could be distorted to a very considerable extent at

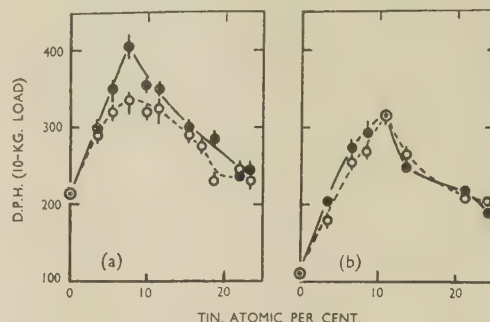


Fig. 6.—Diamond Pyramid Hardness of Heat-Treated Alloys Made with (a) Commercial Titanium and (b) Refined Titanium.

KEY.

- Water-quenched from β and $(\beta + \gamma)$ fields. (a) 950°–1000° C., (b) 900°–950° C.
- Water-quenched from α and $(\alpha + \gamma)$ fields. (a) 850° C., (b) 845°–870° C.

about 700° C., and they would withstand an appreciable amount of cold forging before starting to crack.

ACKNOWLEDGEMENTS

The investigation formed part of the programme of the Physical Metallurgy Section of the Commonwealth Scientific and Industrial Research Organization, Australia. The work was carried out in the Baillieu Laboratory, University of Melbourne, under the general direction of Professor J. Neill Greenwood, to whom the author expresses his thanks. Other members of staff of the Baillieu Laboratory are also thanked for their assistance. Mr. J. A. Corbett performed all the chemical analyses required, and Mr. A. White helped in the preparation of specimens.

Spectrographic analyses were done by the Defence Research Laboratories, Maribyrnong.

The United States Bureau of Mines kindly supplied the commercial titanium used in making the alloys.

REFERENCES

1. C. M. Craighead, O. W. Simmons, and L. W. Eastwood, *Trans. Amer. Inst. Min. Met. Eng.*, 1950, **188**, 485.
2. P. Pietrokowsky and P. Duwez, *ibid.*, 1951, **191**, 772.
3. P. Pietrokowsky, *ibid.*, 1952, **194**, 211.
4. J. A. Corbett, *Analyst*, 1951, **76**, 652.
5. W. J. Kroll, *Trans. Electrochem. Soc.*, 1940, **78**, 35.
6. D. J. McPherson and M. Hansen, *Trans. Amer. Soc. Metals*, 1953, **45**, 915.

SOME OBSERVATIONS ON CREEP AND FRACTURE 1474

FROM INVESTIGATIONS ON LEAD

CABLE-SHEATH ALLOYS *

By A. LATIN,† Ph.D., M.Eng., F.I.M., MEMBER

SYNOPSIS

Tests have been conducted, both at constant internal pressure and at constant hoop stress, on lead and lead alloys chiefly in the form of pipe as extruded for cable sheathing. The results have given some indication of the effects of alloy additions, of grain-size, and of prior deformation (coiling over a drum) upon fracture and general ductility under creep. Some alloy additions, notably antimony (e.g. 0.35%) and tellurium (0.01%), appear to promote considerable embrittlement at slow creep rates, and to some extent their effects have been related to time-dependent (ageing) changes. In several cases, however, poor ductility at slow creep rates does not appear to have any connection with such ageing changes.

Some theoretical concepts are offered, based on the view that intercrystalline cracking in creep results from the occurrence of elastic strain fields at certain grain-boundary localities, as a result of structural and flow heterogeneities. Particularly poor ductility, it is considered, arises from augmentation of such elastic strains by effects due to the alloy additions concerned and to other factors.

I.—INTRODUCTION

THE fractures resulting from the creep of lead and lead alloys as extruded for cable sheathing change from ductile types at moderate creep rates, or more rapid strain rates, to intercrystalline forms at slow creep rates. This has also been observed in other metals and alloys. The ductility, as measured by the general extensions reached at the time of fracture, can also vary notably with the creep conditions. For some alloys at least, very low ductility values are obtained at small creep rates. The chief object of the present paper is to record some observations and views on these matters, based on investigations connected with the development of sound sheathing for types of electricity-supply cables operating under pressure of gas or oil.

II.—METHODS OF INVESTIGATION

Investigations were carried out chiefly on materials extruded in the form of pipe (approximate range of sizes 2–3 in. dia., 0.1–0.13 in. wall thickness) on cable-sheathing presses of both the ram type (including an experimental press and a factory press fitted with liquid-lead seal¹) and the Pirelli continuous (screw) type.² The lead used was of Tadanac or Broken Hill grades of high purity (better than 99.95%) and lead of similar quality was used for the alloys.

Samples (each of 3 or 4 yards length) of the extruded pipe were submitted to internal pressures

calculated to give a suitable range of fracture times from a few hours to several thousand hours. Details of procedure have been described previously.^{3,4} In one series of tests the pressure was maintained constant in each sample; in another series the hoop (circumferential) stress in the pipe wall was kept constant by suitably decreasing the pressure as creep progressed. The majority of these latter tests were conducted at a temperature thermostatically controlled at 27° C. ($\pm 2^\circ$ C. maximum variation); the former tests were conducted at room temperature. The constant-stress tests were carried out on samples kept straight during and after extrusion so as to be as strain-free as possible initially. The constant-pressure tests were carried out both on similar samples and on samples taken from coils on cable drums. These will be referred to as “straight lengths” and “drum lengths”, respectively. Samples of pipe were also tested for changes resulting from prolonged standing (“ageing”) for times up to several thousand hours after extrusion, the creep and fracture characteristics being compared with those of samples tested shortly after extrusion.

Some creep tests at constant uniaxial stress were conducted on samples of strip (4 in. gauge-length, $\frac{1}{2}$ in. width) taken from pipe or extruded as strip. A “hyperbolic pulley” method due to Pearson⁵ was used, constancy of stress being achieved within 2% maximum error, as judged by calibration. Tests have also been made with a new apparatus⁶ designed to eliminate friction. The temperature was thermostatically controlled at $28^\circ \pm 1^\circ$ C.

* Manuscript received 22 April 1952; in revised form 5 November 1952.

† Head of the Department of Metallurgy and Chemistry,

National Coal Board, Central Research Department II, Isleworth, Middlesex; formerly at the Research Department, British Insulated Callender's Cables, Ltd., London.

TABLE I.—*Results of Tests of Pipe Samples at Constant Pressure.*

Nominal Composition	Type of Press	Mean Grain Dia., mm.	Initial Hoop Stress, lb./in. ²	Time to Failure, hr.	General Diametral Expansion, %	Mean Creep Rate, %/hr.	Type of Fracture *	Remarks
Pure Lead	Ram	0.75	830 600 450	27.5 518 11,600	11.7 11.3 9.6	0.43 0.022 0.0008	KE KE IC	Wide scatter of extension (6 to 12%). Straight lengths.
0.2% Sn	Ram	0.35	800 600 500	491 3,338 11,384	13.0 14.8 15.8	0.027 0.0044 0.0014	KE KE SI	Analysis gave 0.21% Sn. Straight lengths.
	Screw	0.5	800 600 500	213 1,518 9,381	10.1 12.6 13.4	0.048 0.0084 0.0014	KE KE IC	Analysis gave 0.21% Sn. Straight lengths.
0.075% Cd	Ram	0.25	800 700 600	479 1,455 4,235	14.1 18.3 17.9	0.03 0.013 0.004	KE KE KE	Analysis gave 0.06% Cd. Straight lengths.
	Screw	0.45	800 700 600	946 1,903 7,697	20.5 17.0 12.6	0.021 0.0089 0.0016	KE IC IC	Analysis gave 0.05% Cd. Straight lengths.
0.2% Sn, 0.075% Cd	Ram	0.25	1,180 800 650	297 3,860 5,380	15.5 16.5 11.6	0.063 0.0045 0.0022	KE IC IC	Analysis gave 0.23% Sn, 0.066% Cd. Straight lengths.
	Screw	0.5	1,250 800	39 2,500	14.0 5.8	0.36 0.002	KE IC	Analysis gave 0.18% Sn, 0.064% Cd. Straight lengths.
0.4% Sn, 0.15% Cd	Ram	0.2	1,300 1,200 1,000 800	180 263 1,490 3,466	19.4 23 19.9 12.9	0.108 0.087 0.013 0.0038	KE SI IC IC	Alloy C to B.S. 801. Straight lengths.
	Screw	0.4	1,400 1,300 1,200 800	94 120 489 3,283	12.1 13.2 10.2 3.2	0.128 0.11 0.021 0.00096	KE SI IC IC	Straight lengths.
	Screw	0.4	1,400 1,300 800	361 542 5,583	8.3 6.8 1.7	0.023 0.013 0.00029	IC IC IC	Drum lengths.
0.4% Sn, 0.2% Sb	Ram	0.25	1,400 1,000 800	89 3,990 6,318	18.5 9.3 5.4	0.21 0.0023 0.0008	IC IC IC	Alloy E to B.S. 801. Analysis gave 0.34% Sn, 0.21% Sb. Straight lengths.
Pure Lead	Screw	0.7	650 550 460	1,065 2,882 31,106	7.7 9.9 12.1	0.0072 0.0034 0.00032	KE KE IC	Drum lengths.
0.4% Sn, 0.2% Sb	Screw	0.3	1,400 1,000 800 500	66 1,129 8,280 44,600	16.0 7.5 4.0 1.95	0.24 0.0066 0.00048 0.000044	IC IC IC IC	Knife-edge fracture at higher strain rates. Drum lengths.
0.35% Sb	Screw	0.3	1,400 1,100 500	21 728 31,530	17.3 9.1 3.7	0.82 0.048 0.00012	SI IC IC	Knife-edge fracture at higher strain rates. Drum lengths.
0.009% Te	Screw	0.5	1,125 1,000 500	43 238 37,188	21.1 16.0 2.3	0.49 0.011 0.000062	SI IC IC	Knife-edge fracture at higher strain rates. Drum lengths.
0.015% Te	Screw	0.7	1,100 1,000 500	52 186 26,400	16.3 10.3 2.2	0.31 0.055 0.000083	IC IC IC	Knife-edge fracture at higher strain rates. Drum lengths.
0.1% Sn, 0.005% Ag	Screw	0.5	1,250 1,100 650	87 288 3,120	9.4 6.1 1.5	0.11 0.021 0.00049	IC IC IC	Knife-edge fracture at higher strain rates. Drum lengths.

* KE represents knife-edge splits, IC represents intercrystalline fracture, and SI (semi-intercrystalline) represents intermediate types.

III.—RESULTS OF TESTS ON PIPE SAMPLES AT CONSTANT PRESSURE

Several results have been published previously.^{3,4} Some further results are summarized in Table I. In this table the third column represents mean values of the grain diameter as obtained from counts taken radially across the pipe wall, the sixth column represents the mean percentage increase in diameter away from the fracture location at time of fracture, and the next column shows the value obtained by dividing this percentage extension by the number of hours before failure occurred.

The chief results of significance as regards fracture, from these and the previous tests, can be summarized as follows:

(1) The change in type of fracture, from knife-edge splits to intercrystalline cracks occurred roughly at a hoop stress of 500 lb./in.² and a mean creep rate of about 0.001%/hr. for the lead, and most of the alloy additions increased this value. In general, the change in type of fracture took place over a range of conditions rather than at a single well-defined hoop stress or mean creep rate, intermediate forms of fracture being observed in several tests.

(2) The materials tested fell broadly into two groups as regards ductility (as measured by diametral extension) at long times to fracture. (a) There was no marked extension decrease (although there was usually considerable scatter of values) even if intercrystalline fracture occurred. The unalloyed lead and some dilute solid-solution alloys, e.g. those containing 0.1% tin or 0.1% antimony, appeared to belong to this group. Addition of copper (up to about 0.06%) also appeared to have no deleterious effects upon ductility at slow creep in pipe free from undesirable extrusion defects which sometimes result from copper additions. (b) Alloys containing higher percentages of antimony, in particular those above the equilibrium solid-solubility limit (e.g. one containing 0.35% antimony), alloy E (0.4% tin and 0.2% antimony, conforming to B.S. 801), alloys containing small percentages of tellurium (about 0.01%), and some alloys containing silver (e.g. 0.1% tin and 0.005% silver, tested in drum lengths only) exhibited a marked decrease in ductility (extensibility) at slow creep rates. All the alloys tested gave knife-edge fractures when tested at sufficiently large rates of strain.

(3) In general, ductility at slow creep rates of a given alloy improved with decrease of grain-size. This can be seen from the results on some of the alloys containing tin and cadmium extruded on the ram press. Similar alloys extruded on the screw press had a larger grain-size as a result of the use of higher die temperatures. The effect of grain-size has been confirmed by some tests on extruded strip of fine grain-size (e.g. alloy E of 0.05 mm. grain dia.), which exhibited particularly good ductility at slow creep rates.

(4) Tests on drum lengths showed that the "pre-

strain" involved in coiling had very complex effects which appeared usually to result in a decrease of extensibility and in some cases to promote intercrystalline fracture. In the case of some alloys, only drum lengths were available for test, and the precise behaviour of these alloys when free from prestrain is not known. There can be little doubt, however, that alloy additions had a marked influence *per se* (see, e.g., the results in Table I for straight lengths of alloy E).

IV.—RESULTS OF TESTS AT CONSTANT STRESS

The well-known equation of Andrade⁷ for creep at constant applied stress can be expressed sufficiently accurately for application to the tests here described, in the approximate form:

$$\epsilon - \epsilon_0 = \beta t^{\frac{1}{2}} + \kappa t,$$

where ϵ = strain at time t and ϵ_0 , β , and κ are constants. Considerable significance is usually attached to the values of β and κ , the former corresponding to a "transient" creep term, the rate of which decreases with time, and the latter to a steady creep of constant rate or, more exactly, of constant "logarithmic strain" rate.

The equation can also be written:

$$(\epsilon - \epsilon_0)t^{-\frac{1}{2}} = \beta + \kappa t^{\frac{1}{2}}.$$

A straight line should be obtained on plotting corresponding values of the left-hand side against $t^{\frac{1}{2}}$ if the approximate form of the Andrade equation is obeyed. The slope of this line gives κ , and the value of β is given by the intercept at $t = 0$ on the strain co-ordinate axis. A suitable value of ϵ_0 (a type of "adjustment" constant) must be chosen; it was usually small for the tests here described, and could be identified more or less with a small initial "instantaneous" extension. This method of analysis is a slightly modified version of that due to Nabarro.⁸

Constancy of stress in the tests on pipe specimens was checked by measurements of the final wall thickness away from the actual fracture locality. Some results are shown in Table II.

TABLE II.—Original and Final Calculated Hoop Stresses in Pipe Samples Tested at Constant Stress.

Material	Original		Final		Original Hoop Stress, lb./in. ²	Final Hoop Stress, lb./in. ²
	Outside Dia., in.	Wall, in.	Outside Dia., in.	Wall, in.		
Pure Lead.	2.713	0.107	2.985	0.098	450	445
0.1% Sn .	3.307	0.130	3.582	0.119	550	551.5
0.1% Sb .	2.724	0.109	3.100	0.097	650	640
0.06% Cu .	3.270	0.131	3.670	0.119	950	957

The results of some tests at constant stress on unalloyed lead and on alloy E have been published previously.³ Creep curves for times up to 800 hr., obtained for the dilute solid-solution alloys containing

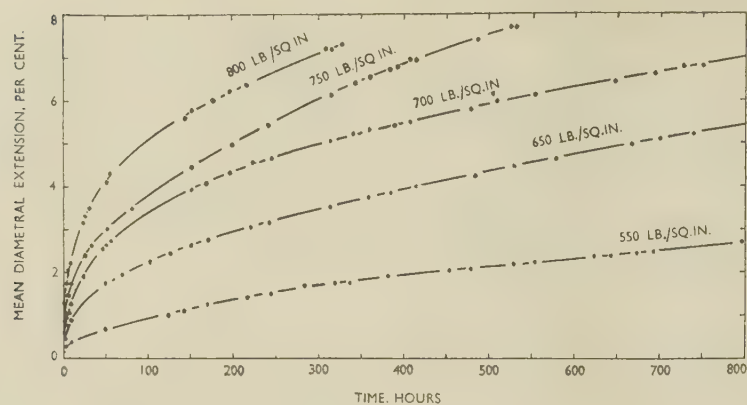


FIG. 1.—Constant-Stress Creep Curves for 0.1% Tin Alloy Pipe (20° C.).

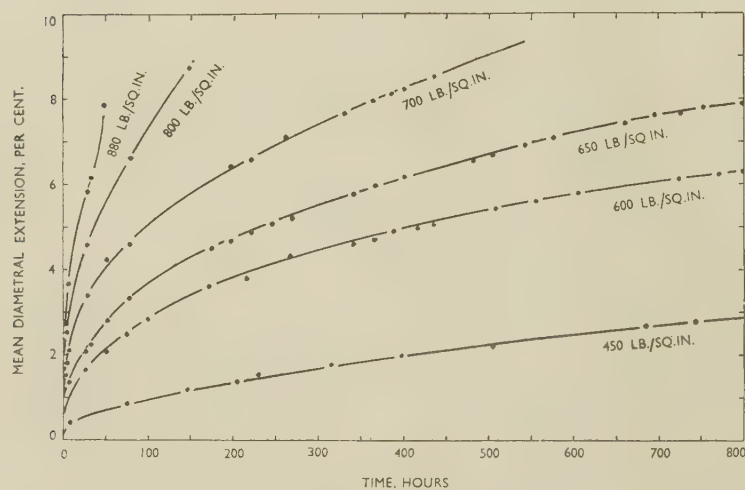


FIG. 2.—Constant-Stress Creep Curves for 0.1% Antimony Alloy Pipe (28° C.).

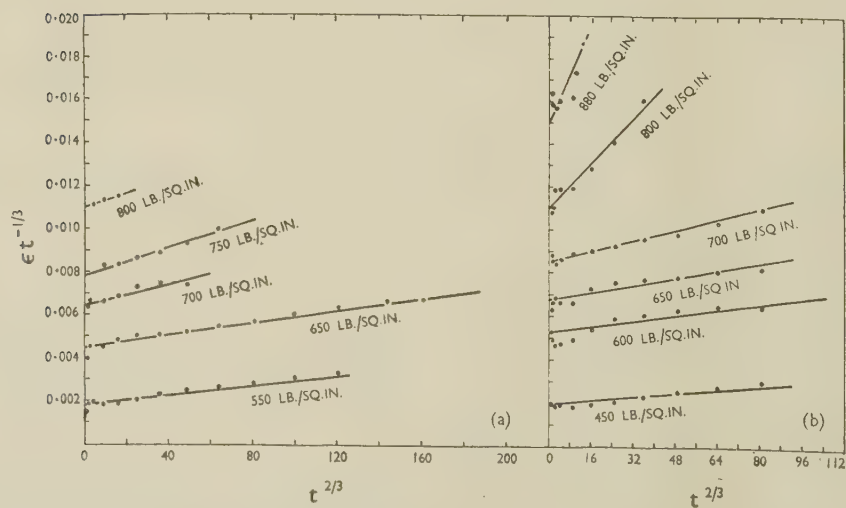


FIG. 3.—Nabarro Analysis Graphs for (a) 0.1% Tin Alloy Pipe, and (b) 0.1% Antimony Alloy Pipe.

FIG. 4.—Constant-Stress Creep Curves for 0.1% Tin Alloy Strip.

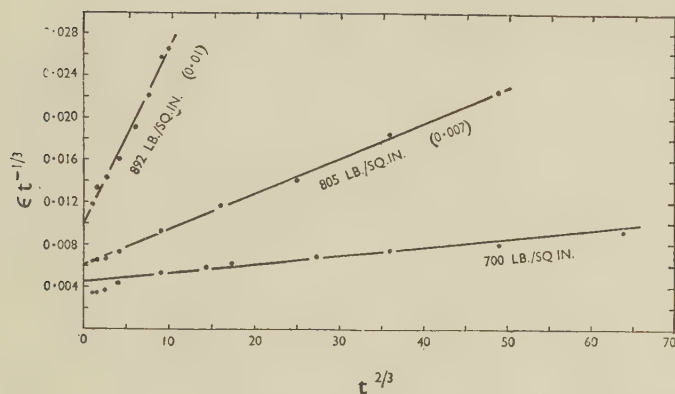
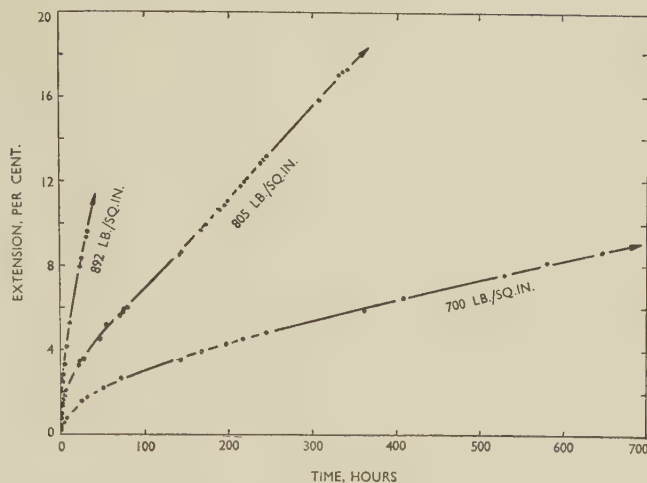


FIG. 5.—Nabarro Analysis Graphs of 0.1% Tin Alloy Strip.

TABLE III.—Results of Constant-Stress Tests (Pipe Samples) Taken to Fracture.

Composition	Type of Press	Stress, lb./in. ²	β , hr. ^{-1/3}	$\kappa \times 10^3$, hr. ⁻¹	Time to Fracture, hr.	Mean General Extension, %	Type of Fracture *
Unalloyed Lead	Ram	725	0.0108	0.204	82.5	7.2	KE
		650	0.0089	0.0066(?)	1,080	10.0	KE
		450	0.002	0.0050	11,600	9.7	IC
0.06% Cu	Ram	750	0.006	0.134	2,025	16.6	KE
		550	0.007	0.0154	20,000	...	Not failed
		450	0.0002	0.0028	Over 20,000	...	" "
0.21% Sn	Ram	1,000	0.0057	0.056	278	13.5	KE
		600	0.0018	0.025	11,560	22.1	IC
0.06% Cd	Ram	1,000	0.012	0.19(?)	281	14.75	KE
		600	0.0016	0.039	Over 10,000	...	Not failed
0.05% Cd	Screw	1,000	0.017	0.035	784	19.4	SI
		600	0.0012	0.021	Over 10,000	...	Not failed
0.23% Sn, 0.07% Cd	Ram	1,250	0.021	0.074	425	20.7	KE
		1,000	0.012	0.039	1,016	17.1	IC
		760	0.0035	0.04(?)	4,903	17.0	IC
0.18% Sn, 0.06% Cd	Screw	1,250	0.027	0.10	87	13.9	SI
		1,000	0.013	0.046	417	11.6	IC
		750	0.004	0.020	2,173	8.0	IC
0.4% Sn, 0.15% Cd	Ram	1,200	0.0057	0.048	1,504	13.7	IC
		1,000	0.0033	0.060	2,630	10.8	IC
	Screw	1,200	0.0050	0.045	616	7.0	IC
0.004% Ag	Ram	975	0.016	0.045	600	17.4	KE
		875	0.012	0.011	1,280	16.0	IC

* Key as in Table I.

0.1% tin and 0.1% antimony, are shown in Figs. 1 and 2, respectively. The corresponding "Nabarro graphs" are given in Fig. 3 (a) and (b). The agreement with the Andrade equation is seen to be moderately good. Fig. 4 shows some curves for strip of the 0.1% tin alloy, and Fig. 5 the corresponding analysis graphs. In general, the values of the Andrade constants obtained for strip differed from those for pipe samples.

Values of β and κ , together with some values for pure lead also, are shown plotted on a logarithmic scale against stress in Fig. 6. The variation with

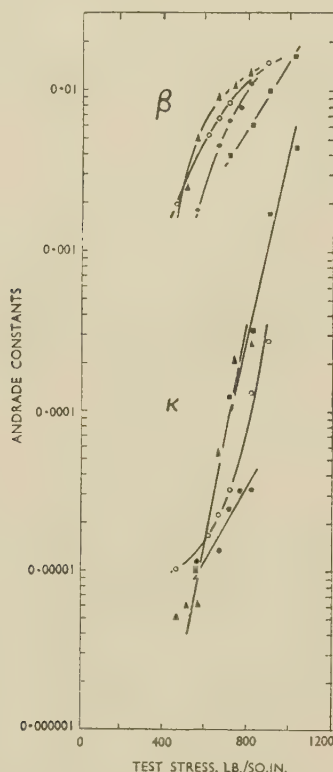


FIG. 6.—Variation of Andrade Constants with Stress for Lead Alloy Pipe and Strip Samples.

KEY.
 ▲ Pure Lead Pipe. ● 0.1% Tin Alloy Pipe.
 ○ 0.1% Antimony Alloy Pipe. ■ 0.1% Tin Alloy Strip.

stress within the range here concerned is seen to be approximately of the exponential form found, more particularly for the κ value, by Andrade and other investigators.⁹

In Table III are collected some further results, with data concerning fracture.

The results of principal significance can be summarized as follows:

(1) The value of κ corresponding to change of fracture type (about $0.005 \times 10^{-3} \text{ hr.}^{-1}$ for unalloyed lead) was in general increased by addition of alloying elements; the corresponding β values were less affected.

(2) Increase of grain-size appeared to result in an

increase of the value of κ corresponding to the beginning of intercrystalline types of fracture in place of ductile (knife-edge split) types.

(3) No obvious fundamental difference in the creep process corresponding to the two different types of fracture could be observed, as judged in particular from the form of the creep curves.

(4) No clear effects due to recrystallization, such as, for example, that observed by Andrade with highly pure lead,¹⁰ were apparent. Metallographic examination confirmed that recrystallization had not occurred as readily as might have been expected, little or no change being observed usually in general grain-size during test. This may in part have been due to the somewhat large grain-size compared with the wall thickness of the specimens.

(5) The values of κ at a given stress appeared to be somewhat greater for strip than for pipe of corresponding quality. General extensions for strip were difficult to compare with those for pipe, but they appeared to be greater. The "tertiary creep" period (the final accelerated creep preceding ultimate rupture) was usually more in evidence in the tests on strip, owing to the fact that total extensions were measured. The use of constant stress did not prevent tertiary creep occurring in those tests which were taken to fracture, although its incidence was delayed.

It should be noted that the values of constants given here were usually determined from the first 800 hr. of test. Several tests were carried on for many thousands of hours. Deviations from the initial curve occurred, but it is not known how far this may have been due to cumulative error.

V.—INFLUENCE OF STANDING ("AGEING") BEFORE TEST

Various results on samples of pipe are shown in Table IV. Comparisons of tests to fracture at moderately rapid rates of extension (short-time tests) with similar tests on the freshly extruded material are given, and also with some results from the slow creep tests (long-time tests).

From these results it would appear to be possible to group the materials tested as follows:

(1) Those in which no decrease of ductility resulted from prolonged standing, the substances concerned showing also no marked decrease at slow creep rates. Pure lead, the dilute solid-solution alloys mentioned above, and the alloy containing 0.06% copper belonged to this group.

(2) Those in which a marked decrease of ductility (diametral extension at time of fracture) was observed for the short-time test after prolonged standing, of a similar order to that observed in long-time creep tests. An example is the alloy containing 0.35% antimony. The marked decrease of creep rate at the test stress as a result of ageing will also be noted.

(3) Those in which ageing resulted in a considerable decrease of ductility, though of a smaller order than

that observed in the slow creep tests. Alloy E and the tellurium lead behaved in this manner.

(4) Those in which no decrease of ductility was observed as a result of prolonged standing before the short-time test, though the ordinary long-time creep test showed a marked decrease of extension at fracture. The alloy containing 0.005% silver and 0.1% tin is an example. The series of alloys containing both tin and cadmium also showed little or no signs of the "simple ageing" effect.

The effect of ageing upon the ductility of the alloys containing antimony and tellurium appears to be connected with the precipitation of antimony and of

creep tests. There is much evidence from the fracture characteristics of other metals¹²⁻¹⁴ in creep to support this view. It remains possible that deformation during creep could affect, for example, the distribution of alloying elements or impurities as between grains and grain boundaries, and this could in turn affect the fracture characteristics; strain-induced changes of other kinds might also occur.

VI.—THEORETICAL CONSIDERATIONS

Although it is not proposed to deal here with all the factors concerned with fracture behaviour in

TABLE IV.—Effect of Standing Upon the Ductility of Pipe Samples Under Creep.

Composition of Alloy	Type of Press	Time of Ageing, hr.	Rapid Creep Test Hoop Stress, lb./in. ²	Slow Creep Test		Mean Creep Rate, %/hr.	General Diametral Expansion, %	Type of Fracture*	Remarks
				Hoop Stress, lb./in. ²	Time to Failure, hr.				
Unalloyed Lead	Ram	...	1,100	0.22	6.0	KE	Initial short-time test. Similar test after straining.
		24,800	1,040	1.0	7.0	KE	
	Screw	...	1,010	0.16	6.2	KE	
		24,600	1,010	0.67	7.5	KE	
0.4% Sn, 0.2% Sb (Alloy E)	Ram	...	1,448	0.45	11.9	SI	
		50,000	1,448	0.014	3.1	IC	
	Screw	...	1,400	0.32	16.7	IC	Rapid creep test on original pipe. Slow creep test on original pipe.
		800	4,896	0.0007	2.8	IC	
		7,100	1,400	0.034	9.2	IC	
0.35% Sb	Screw	...	1,280	0.28	17.0	SI	
		600	25,000	0.0001	2.5	IC	
		19,000	1,280	0.0016	1.6	IC	
		28,600	1,280	0.0014	1.0	IC	
0.23% Sn, 0.06% Cd	Ram	...	1,245	0.12	15.7	KE	
		17,800	1,250	0.11	18.2	KE	
0.18% Sn, 0.06% Cd	Screw	...	1,250	0.36	14.1	KE	
		17,800	1,250	0.39	16.4	KE	
0.009% Te	Screw	...	1,125	0.46	17.9	SI	
		650	19,200	0.0007	1.4	IC	
		23,000	1,125	0.068	7.8	IC	
0.1% Sn, 0.005% Ag	Screw	...	1,250	0.52	9.7	KE	Samples from different pipe from that shown in Table I.
		500	14,000	0.00025	3.4	IC	
		10,150	1,250	0.61	9.2	KE	

* Key as in Table I.

a tellurium-rich phase, respectively, at the grain boundaries and within the grains, some degree of precipitation-hardening resulting.^{4, 11}

That such changes need not in themselves lead to intercrystalline fracture in creep was indicated for some results on the alloy E of fine grain mentioned above. As illustrated by Fig. 7 (Plate LXXXII), extensive changes could occur at grain boundaries during creep deformation, but these did not lead to intercrystalline fracture.

In general, it can be concluded that effects due to creep *per se* were for several alloys of more moment than any due to purely time-dependent ageing changes upon the fracture characteristics in prolonged

creep, but rather to offer more general theoretical considerations, it may be of value to summarize some of the chief factors concerned.

(1) The mechanism of flow or deformation with particular regard to differences between grain interiors and grain-boundary regions. Associated with this is the relationship between the imposed stresses and the stress/strain system at any point within the substance.

(2) The effect of impurities or addition elements and their distribution between grain interiors and grain-boundary regions; atomic size-factors, &c.

(3) Grain-boundary structure in relation to the presence or development of defects or discontinuities which could aid micro-crack formation.

(4) The effects of addition elements upon cohesive bond strengths or upon the free energy of crack surfaces resulting from bond disruption.

(5) The effects of grain-size and other structural factors such as second phases or precipitates.

(6) The possibility of purely time-dependent changes (ageing) and the effects of stress and strain upon such changes.

(7) The previous history (prestrain, work-hardness, &c.) of the substance.

(8) Factors influencing crack propagation rate.

(9) Surface and environmental conditions.

(10) The effect of temperature.

It is usually accepted, particularly for local fractures of brittle nature, that disruption must be preceded by the development of elastic strains sufficiently large to break interatomic bonds in at least some small region of the material. It is probable also that a minimal size of elastically strained region is usually necessary for the inception of fracture, i.e. there is a "nucleation effect".

Various criteria for the incidence of the different types of fracture have been proposed; on general theoretical grounds that most applicable to the present case would seem to be one of a critical elastic strain energy. Freudenthal,¹⁵ for example, has advanced a general mathematical analysis of fracture inception based on this criterion, his treatment including consideration of the energy of volumetric expansion as an important contribution. It would seem acceptable also that the effect of inelastic strain components as such can either be inhibitory to fracture, for example by superseding local elastic strains, or contributory to fracture, by intensification of strains on adjacent maintained interatomic bonds (i.e. bonds between atoms not taking active part in the inelastic strain processes).

The mechanism of creep in metals is complex in nature. Many theories are extant (see, e.g., Sully¹²) and there have been considerable recent developments both in theoretical concepts and in experimental studies of the mechanism. Questions particularly appropriate to the problems discussed in the present paper are: (i) to what extent glide-plane slip processes occur, such as are involved in ordinary plastic deformation; (ii) to what extent motion of dislocations, now widely accepted as being involved in glide-plane slip, occurs both along and, possibly, out of glide planes; (iii) to what extent, if any, motion of lattice vacancies (Schottky defects) may occur; and (iv) to what extent grain-boundary slip and other possible occurrences at grain boundaries take place.

(i) Dislocation-slip theory has been applied with some success to transient creep and more particularly to "exhaustion creep,"¹⁶ but with less success to explanations of the mechanism of steady creep, which plays a major part in tests such as those concerned in the present work. It is common observation that glide-plane slip is not so readily discernible in steady creep as in other types of deformation, and it would

seem therefore that such creep involves mechanisms dissimilar from those involved in ordinary plastic deformation.

(ii) A possible clue to the mechanism of steady creep would appear to have been obtained from studies (by Wood and Scrutton¹⁷ &c.) of the cellular "sub-structures" which develop during the creep of some metals. These suggest, apart from other possible explanations, motion of or collection of dislocations outside the ordinary slip systems, and would in fact appear to be allied, in some respects at least, to the effect known as "polygonization".¹⁸

(iii) Nabarro¹⁹ has pointed out that, in theory, creep could result from motion of lattice vacancies (self-diffusion), though his calculations indicated the unlikelihood of such action contributing in practicable measure to creep deformation. Mott,²⁰ however, has since shown that glide-plane motion of dislocations combined with effects due to associated lattice vacancies, allowing dislocations to move out of their glide-planes as a result also of stress concentrations, would appear to involve activation energies of the right order for steady creep.

(iv) Many investigations have indicated relative movements of adjacent grains during steady creep. In connection with "anelastic" effects in general, Zener²¹ has proposed the possibility of viscous movements at grain boundaries, resulting in local stress relaxations, and his theories would appear to be supported by several experimental studies of Kê.^{22, 23} King *et al.*²⁴ have confirmed the occurrence of Zener-type slip at grain boundaries under shear stress. Such slip would appear to involve Newtonian flow when of small amount. Some results of Kê²³ suggest that the mechanism is one of self-diffusion. This is in agreement with theoretical calculations of Read and Shockley²⁵ based on a "dislocation-array" model of grain boundaries. When the orientation difference between adjacent grains is not small, this model amounts to the more readily acceptable one of a "transition zone" between the lattices. Aust and Chalmers²⁶ have obtained experimental evidence supporting this transition zone concept.

Since movements of dislocations and, for edge-dislocations,²⁰ probably also associated lattice vacancies are likely to be concerned in creep, the mechanism of intercrystalline cracking may well include the collection or agglomeration of such discontinuities at grain boundaries. The basic mechanism of fracture, however, still involves the presence of elastic strain fields of sufficient magnitude for the development of, or propagation of, any micro-cracks concerned.

Zener²¹ (pp. 126 *et seq.*, 158) has proposed a mechanism of intercrystalline cracking in creep based upon effects resulting from viscous slip at grain boundaries. Fracture stresses are postulated as produced where a boundary on which slip occurs meets another across which stress relaxation does not occur, i.e. on which there is absence of shear components. A somewhat similar mechanism has been

propounded by Mott,²⁷ involving mutual blockage at grain-boundary junctions (triple points). Mott has also explained poor ductility under conditions of slow creep as being the result of relative ease of viscous slip at grain boundaries as compared with resistance to deformation of the grains themselves at small stresses. Difficulties arise, however, in any attempt at quantitative development of such theories. This is because intercrystalline cracking may be associated with strains of some magnitude, and initial grain-boundary slip is presumably blocked at very small strains if it is to be blocked at all. It would seem, therefore, that the development of elastic strain energies of critical magnitude must involve processes not dependent upon such slip alone. An application of Mott's theories of creep to the problem of fracture mechanism has been made by Servi and Grant.^{13, 28} Mott's theories²⁹ have indicated that (at a given stress) grain-boundary slip does not occur below a certain "critical" temperature. The type of creep which then takes place is that which he has called "exhaustion creep", in which the strain produced remains limited. Servi and Grant have connected this with change of fracture characteristics in aluminum. However, the prolonged period of definite steady creep in the tests on lead with which the present paper is concerned, do not indicate that exhaustion creep as such, or for that matter any radical change in creep type, is concerned.

A concept leading to a visualization of the intercrystalline fracture process of attractive simplicity, is that of creep as a flow process which can be represented for an ideally homogeneous substance by a vector point function \mathbf{u} , the velocity of flow of each elementary particle. It is usually accepted that density changes do not occur in creep, though actually slight decreases have been noted (e.g. by Hanson and Wheeler³⁰). For the "ideal" substance, however, it can be stated that at every point $\text{div } \mathbf{u} = 0$. This statement is based on the "equation of continuity" which connects volume changes (divergence of \mathbf{u}) with density changes:

$$\text{div } \mathbf{u} = -\dot{\rho}/\rho$$

where ρ = density at the locality concerned and $\dot{\rho}$ = the "substantial" time rate of density change (see e.g. Brand³¹ p. 259).

Real substances are not ideally homogeneous, nor is creep flow ideally uniform, certainly not on the atomic or even microscopic scale. In particular, in polycrystalline materials structural inhomogeneities and flow complications occur at grain boundaries. The hypothesis is offered that, as a result, at certain localities at grain boundaries in a substance undergoing creep, $\text{div } \mathbf{u}$ is positive, i.e. $\dot{\rho}$ is negative and dilatation occurs; associated with such volumetric expansion there must be elastic strains. It is arguable that at localities of structural discontinuity, such as grain boundaries, the equation of continuity cannot be applied rigorously. The transition-zone theory indicates, however, that, as an approximation

at least, the function \mathbf{u} and its derivatives can be regarded as continuous at grain boundaries, although possibly changing suddenly with both position and time.

The relationship between \mathbf{u} and the externally imposed constraints on a specimen undergoing creep is obviously not susceptible to exact determination in general. The relationship between $\text{div } \mathbf{u}$ and the local extensile components of the rate of strain tensor can, however, be expressed very simply:

$$\text{div } \mathbf{u} = e_{11} + e_{22} + e_{33}$$

e_{11} , &c., being the three (orthogonal) strain rates concerned.

In applying the equation of continuity, consideration is given to volumetric expansion alone, and it remains possible that other elastic distortion terms (e.g. elastic shear components) may contribute to the total local elastic strain energy. However, the tensors of stress, strain, and strain-rate can always be expressed in terms of the three "principal" components which do not contain shears. Furthermore, combination of the concepts offered here with the Zener theory of fracture, described above, indicates the probable absence of shear components along the actual surface of fracture inception at a suitable grain boundary.

Some further justification for this simplification arises from the observation that intercrystalline fracture often begins in boundaries more or less transverse to the applied stress (or hoop stress in pipe samples). This suggests that the maximum local elastic strain is approximately parallel to the principal stress direction. In addition, it seems likely that in the most probable region of fracture inception there is complete restriction of transverse flow, i.e. taking e_{11} as the rate parallel to the stress axis, fracture has maximum likelihood where $e_{22} = e_{33} = 0$. This corresponds to local triaxial tension, the region concerned expanding elastically in a direction parallel to the stress and not contracting in the orthogonal directions. No dilatation or elastic strain occurs, it should be noted, where $e_{22} = e_{33} = -\frac{1}{2}e_{11}$; this expresses the general conditions of inelastic strain away from the actual locality of fracture inception.

If λ represents the current length, parallel to the stress axis, of the elastically expanding region of fracture initiation visualized, then:

$$-\dot{\rho}/\rho = \text{div } \mathbf{u} = e_{11} = \dot{\lambda}/\lambda$$

In such a region, the critical strain energy for fracture corresponds to a critical value of the local elastic strain. It follows that the general extension of the specimen reached at the time of fracture depends upon the relationship between $\dot{\lambda}/\lambda$ and the general creep rate of the specimen. Simple proportionality of the one to the other leads to an independence of the general extension (reached at beginning of fracture) from the creep rate, and this could at once explain the results for unalloyed lead and for some of the alloys. It is of interest to note

further that, as Orowan³² has pointed out, the order of theoretical strain for the breakage of atom-pair bonds is about 10–20%. This is of the same order as the general extensions reached for the substances here concerned, and suggests that the local elastic strain eventually responsible for fracture may be commensurate with the general inelastic creep strain. Logical interpretation of this would lead to the conclusion that the local stress concentration involved (at least on the atomic scale) would result in a maximum stress of the same order as the theoretical strength of the substance. This is not impossible, but it is arguable that it is improbable, and that the maximum value of the local stress likely to be attained is that corresponding to the so-called "brittle-fracture" stress. However, this must be of quite large value (since the substances concerned do not show notch-brittleness) and furthermore the fracture conditions in creep probably differ considerably from those concerned in ordinary brittle fracture or in notch sensitivity. In any case there is some support for the proposal of a simple relationship between the local elastic strain and the general creep strain for approximate calculation.

On the other hand, it must be quite clearly realized that the simplifications involved in such a calculation are extreme. Elastic distortion terms, or at least the effects of local elastic shear components, in all probability cannot be neglected. The final values of extension experimentally determined must be affected also by the rate of fracture propagation, and this in itself probably depends on quite complex factors. The "tertiary creep" period appeared to follow actual fracture inception in the tests above described, and, in those on pipe, appeared also to be very local. The difference between the total extension at the fracture locality and the general extension of the specimen was sometimes quite large, but usually smaller at slow creep rates than for the more rapid tests.

Notwithstanding possible complications, the simplified concepts above are suggested as being acceptable as first approximations, or as in a sense representing "semi-ideal" but possible conditions. An important consequence is the recognition of the good ductility (extensibility) of lead, even under conditions of creep leading to intercrystalline fracture, as the possible outcome of an expected independence of the extension at fracture from the creep rate.

On the basis of this theory the poor ductility at slow creep of various alloys can be explained as the result of occurrences leading to augmentations of the elastic strain fields at grain boundaries. Elastic strains around foreign atoms could be concerned, or strains resulting from precipitation of antimonial or tellurium-rich constituents, for example, in the lead alloys described above. Work-hardening by deformation before, or even during, primary creep could be another cause of elastic strain augmentation. Stress concentration at discontinuities (or micro-cracks) could also be concerned.

The marked increase of ductility, at slow creep, resulting from decrease of grain-size for a given alloy must, on the same basis, result from a decrease in the intensity or likelihood of elastic strains in boundary localities. The simplest explanation is that this is due to increased ease of recrystallization or grain-boundary migration; this view is supported by some results on the fine-grained samples of alloy E mentioned above, which recrystallized at large strains. Recrystallization was, however, less obvious in some of the other alloys and cannot afford a complete explanation. Increased ease of grain-boundary slip without stoppage can be suggested as one possible contributory cause of good ductility in fine-grained alloys.

The change in type of fracture with the creep conditions must result basically from differences in the mechanism of creep and ordinary plastic deformation. There is much evidence that the detailed mechanism of creep alters notably with applied stress and with temperature.^{17, 28, 33, 34} The change in type of fracture for the substance studied must result from the absence of processes (multiple slip, localized deformations at boundaries, &c.) which limit the development of elastic strains at grain boundaries in ordinary plastic deformation. It would seem quite possible that there is a difference in distribution of associated elastic strains in slow creep and in plastic deformation. At slow creep rates such elastic strains, it is suggested, can become concentrated at localities of structural heterogeneity (providing these are suitably orientated with respect to the imposed stress system) and in plastic deformation they are more uniformly spread. The difference in behaviour in this respect is, it is further suggested, greater the slower the creep rate and the less the finer the grain-size.

VII.—SUMMARY AND CONCLUSIONS

(1) Creep tests to fracture have been conducted on samples of lead and lead alloys as used for cable sheathing, the samples being chiefly in the form of pipe extruded under similar conditions to those used for cable sheathing. The diametral extension produced by internal pressure has been found to be more or less independent of the time to fracture, within wide limits, for pure lead, some dilute solid-solution lead alloys, and some other lead alloys not of the solid-solution type, e.g. one containing 0.06% copper as an alloying addition. Alloys containing antimony in excess of the solid solubility limit (e.g. 0.35% antimony), alloy E (0.4% tin and 0.2% antimony), and some leads containing very small amounts of tellurium (about 0.01%) showed very poor ductility at slow creep rates.

All the substances tested were ductile at sufficiently rapid rates of strain (pipe samples under internal pressure failing with knife-edge longitudinal splits), but showed increasing liability to fracture of the intercrystalline type at slow creep rates.

(2) Tests on samples of pipe with the hoop stress

maintained constant indicated that the Andrade equation was at least approximately obeyed. The value of κ (the steady creep constant) corresponding to supervision of intercrystalline fracture was greater for the alloys than for unalloyed lead; the value of β (the transient creep constant) was less affected. Tests on samples in strip form at constant stress have also shown fair agreement with the Andrade equation. The value of κ at given stress was in general greater for strip than for pipe of the same alloy of similar grain-size.

(3) The creep conditions corresponding to change in type of fracture were notably affected by grain-size, decrease of which, for a given alloy, resulted in improvement in ductility. The results were also affected by degree of deformation of the samples before test, samples taken from coils on drums being in general less ductile under creep than those kept straight before testing.

(4) Some of the alloys, notably those containing antimony and those containing tellurium, showed marked influence of ageing upon the behaviour under

subsequent creep; the ductility being greatly decreased. Other alloys having poor ductility under slow creep conditions did not appear to exhibit any purely time-dependent effects due to ageing.

(5) Some theoretical concepts have been advanced in connection with the fracture behaviour observed. It is indicated that under slow creep, elastic strain fields are likely to occur at grain boundaries as a result of structural and flow heterogeneities. Application of the "equation of continuity", together with some simplifying assumptions, has led to an explanation of the difference in behaviour of unalloyed lead and the dilute solid-solution alloys studied, from the alloys exhibiting very poor ductility at slow creep. Elastic strain "augmenting" effects, it is considered, must account for the behaviour of the latter group of alloys.

ACKNOWLEDGEMENT

Acknowledgement is due to Dr. L. G. Brazier, Director of Research, British Insulated Callender's Cables, Ltd., for permission to publish these results.

REFERENCES

1. C. J. Beaver, *Elect. Rev.*, 1945, **136**, 468.
2. —, *Engineering*, 1949, **167**, 319.
3. A. Latin, *J. Inst. Metals*, 1948, **74**, 259.
4. A. Latin, *Engineering*, 1950, **170**, 121.
5. C. E. Pearson, *J. Inst. Metals*, 1934, **54**, 111.
6. A. Latin, *J. Sci. Instruments*, 1952, **29**, (3), 98.
7. E. N. da C. Andrade, *Proc. Roy. Soc.*, 1911, [A], **84**, 1; 1914, [A], **90**, 329.
8. F. R. N. Nabarro, *J. Inst. Metals*, 1948, **74**, 678 (discussion).
9. A. H. Cottrell and V. Aytakin, *ibid.*, 1950, **77**, 389.
10. E. N. da C. Andrade, *Nature*, 1948, **162**, 410.
11. J. McKeown and L. M. T. Hopkin, *Metallurgia*, 1950, **41**, 135, 219.
12. A. H. Sully, "Metallic Creep and Creep-Resistant Alloys". London: 1949 (Butterworths Scientific Publications).
13. I. S. Servi and N. J. Grant, *Trans. Amer. Inst. Min. Met. Eng.*, 1951, **191**, 909.
14. W. D. Jenkins and T. G. Digges, *J. Research Nat. Bur. Stand.*, 1950, **45**, 153.
15. A. M. Freudenthal, "Inelastic Behaviour of Engineering Materials", pp. 156 *et seq.* New York: 1950 (John Wiley and Sons, Inc.).
16. N. F. Mott and F. R. N. Nabarro, *Phys. Soc. : Rep. Conf. on Strength of Solids, Bristol*, 1948, 1.
17. W. A. Wood and R. F. Scrutton, *J. Inst. Metals*, 1950, **77**, 423.
18. R. W. Cahn, "Progress in Metal Physics" (Edited by B. Chalmers), Vol. 2, pp. 151 *et seq.* London: 1950 (Butterworths Scientific Publications).
19. F. R. N. Nabarro, *Phys. Soc. : Rep. Conf. on Strength of Solids, Bristol*, 1948, 75.
20. N. F. Mott, *Proc. Phys. Soc.*, 1951, [B], **64**, 729.
21. C. Zener, "Elasticity and Anelasticity of Metals", pp. 147 *et seq.* Chicago: 1948 (University of Chicago Press).
22. T. S. Kê, *Phys. Rev.*, 1947, [ii], **71**, 533.
23. T. S. Kê, *J. Appl. Physics*, 1949, **20**, 274.
24. R. King, R. W. Cahn, and B. Chalmers, *Nature*, 1948, **161**, 682.
25. W. T. Read, Jr., and W. Shockley, *Symposium on Plastic Deformation of Crystalline Solids (Pittsburgh)*, 1950, 124.
26. K. T. Aust and B. Chalmers, *Proc. Roy. Soc.*, 1950, [A], **201**, 210.
27. N. F. Mott, *Research*, 1949, **2**, 162.
28. I. S. Servi and N. J. Grant, *J. Inst. Metals*, 1951-52, **80**, 33.
29. N. F. Mott, *Proc. Phys. Soc.*, 1948, **60**, 391.
30. D. Hanson and M. A. Wheeler, *J. Inst. Metals*, 1931, **45**, 229.
31. L. Brand, "Vector and Tensor Analysis". New York: 1947 (John Wiley and Sons, Inc.).
32. E. Orowan, *Trans. Inst. Eng. Ship. Scotland*, 1946, **89**, 165.
33. D. McLean, *J. Inst. Metals*, 1951-52, **80**, 507.
34. W. A. Rachinger, *ibid.*, 1952-53, **81**, (1), 33.

NOTICE TO AUTHORS OF PAPERS FOR THE "JOURNAL" AND CONTRIBUTORS TO DISCUSSIONS

1. **Papers will be considered for publication from non-members as well as members of the Institute.** They are accepted for publication in the *Journal* and not necessarily for presentation at any meeting of the Institute. MSS. should be addressed to The Editor of Publications, The Institute of Metals, 4 Grosvenor Gardens, London, S.W.1.

2. **Papers suitable for publication** may be classified as:

(a) Papers recording the results of original research.
(b) First-class reviews of, or accounts of progress in, a particular field.

(c) Papers descriptive of works methods, or recent developments in metallurgical plant and practice.

(d) Papers in classes (a), (b), and (c) above, previously published in languages other than English, French, German, or Italian, if of sufficient merit.

3. **Manuscripts and illustrations** should be submitted in duplicate. MSS. must be typewritten (*double-line spacing*) on one side of the paper only, and authors are requested to sign a declaration that neither the paper nor a substantial part thereof has been published elsewhere. Exceptions may be made in certain cases where a paper has been published in a language other than English, French, German, or Italian (see 2(d) above). MSS. not accepted are normally returned within 6 months of receipt.

In the interests of economy, all papers must be written as concisely as possible; in general, internal research reports are not in suitable form for publication as papers in the *Journal*. All but the simplest mathematical expressions should be written by hand, with capital and small letters clearly distinguished. Superscript and subscript letters should also be plainly indicated. Greek letters and special signs should be identified in the margin. For style, spelling, and abbreviations used, any recent issue of the *Journal* may be consulted.

4. **Synopsis.** Every paper must have a synopsis (not exceeding 250 words in length) which, in the case of a paper reporting original research, should state its objects, the ground covered, and the nature of the results. The synopsis will appear at the beginning of the paper, and should be in a form suitable for use by abstracting organizations. Extracts from a "Guide for the Preparation of Synopses" drawn up by the Abstracting Services Consultative Committee are reproduced below.

5. **References** must be collected at the end of the paper and must be numbered in the order in which they occur in the MS. Initials of authors must be given, and the Institute's official abbreviations for periodical titles (as used in *Metallurgical Abstracts*) should be employed, where known. References to papers should be set out in the style:

A. L. Dighton and H. A. Miley, *Trans. Electrochem. Soc.*, 1942, 81, 321 (i.e. year, volume, page).

References to books should be in the following style:

C. Zener, "Elasticity and Anelasticity of Metals". Chicago: 1948 (University of Chicago Press).

6. **Illustrations.** Each illustration must have a number and description; only one set of numbers must be used in one paper, and it is desirable to number the half-tone illustrations consecutively, rather than to intersperse them with the line figures. The captions should be typed on a separate sheet.

The set of line figures sent for reproduction must be drawn (about twice the size to appear in the *Journal*) in Indian ink on smooth white Bristol board, good-quality drawing paper, co-ordinate paper, or tracing cloth, which are preferred in the order given. Co-ordinate paper, if used, must be blue-lined, with the co-ordinates to be reproduced finely drawn in Indian ink. Curves should be drawn boldly (i.e. at least twice the thickness of the frame). Experimental points should be indicated by open or closed circles, triangles, squares, &c. (preferably not crosses). Curves should be broken on each side of such symbols and plenty of allowance should be made for closing up in blockmaking. All lettering and numerals, &c., should preferably be in pencil, so that the Institute's standard lettering may be affixed, and ample margins must be left outside the framework of the figures to enable this to be done. The second set of line illustrations may be photostat copies.

Photographs must be restricted in number, owing to the expense of reproduction, and photomicrographs should be trimmed to the smallest possible of the following sizes consistent with adequate representation of the subject: 4 in. deep by 3 in. wide: 2 in. deep by 3 in. wide: 2 in. square. Magnifications of photomicrographs must be given in each case. Photographs for reproduction should be loose, not pasted down (and not fastened together with a clip, which damages them), and the figure number and author's name should be written on the back of each. Captions should be given to the photomicrographs, but these should be kept as brief as possible.

Because of the present high cost of printing and paper it is imperative that authors restrict illustrations (particularly photographs) to the absolute minimum deemed necessary to support their argument. Only in exceptional cases will illustrations be reproduced if already printed and readily available elsewhere.

7. **Tables or Diagrams.** Results of experiments, &c., may be given in the form of tables or figures, but (unless there are exceptional reasons) not both. Tables should bear Roman numbers, and each should have a heading that will make the data intelligible without reference to the text.

8. **Corrections.** A certain number of corrections in proof are inevitable, but any modification of the original text is to be avoided. Since corrections are very expensive, the Institute reserves the right to require authors to contribute towards their cost if the Editor deems them to be excessive. The Institute also reserves the right to require a contribution to the cost of remaking any block where this is necessitated by an error on the author's part.

9. **Reprints.** Individual authors are presented with a maximum of 25, and two or more authors with a maximum of 50 reprints from the *Journal*, without covers. Limited numbers of additional reprints can be supplied at the author's expense, if ordered before proofs are passed for press. (Orders should preferably be placed when submitting MSS.)

10. **Discussion.** Except in the case of special symposia, shorthand records of discussions are not taken at meetings. Written discussion may be submitted on any paper, preferably typewritten (*double-line spacing*). References should be given in the form of footnotes. Paragraphs 6 and 7 above are also applicable to such contributions. Reprints of discussion cannot be supplied to contributors.

GUIDE FOR THE PREPARATION OF SYNOPSES

(As recommended by the Abstracting Services Consultative Committee)

1. **Purpose.** The synopsis is not part of the paper; it is intended to convey briefly the content of the paper, to draw attention to all new information, and to the main conclusions. It should be factual.

2. **Style of writing.** The synopsis should be written concisely and in normal rather than abbreviated English. It is preferable to use the third person. Where possible use standard rather than proprietary terms, and avoid unnecessary contracting.

It should be presumed that the reader has some knowledge of the subject, but has not read the paper. The synopsis should therefore be intelligible in itself without reference to the paper; for example, it should not cite sections or illustrations by their numerical references in the text.

3. **Content.** The title of the paper is usually read as part of the synopsis. The opening sentence should be framed accordingly and repetition of the title avoided. If the title is insufficiently comprehensive, the opening should indicate the subjects covered. Usually the beginning of a synopsis should state the objective of the investigation.

It is sometimes valuable to indicate the treatment of the subject by such words as: brief, exhaustive, theoretical, &c.

The synopsis should indicate newly observed facts, conclusions of an

experiment or argument and, if possible, the essential parts of any new theory, treatment, apparatus, technique, &c.

It should contain the names of any new compound, mineral species, &c., and any new numerical data, such as physical constants; if this is not possible, it should draw attention to them. It is important to refer to new items and observations, even though some are incidental to the main purpose of the paper; such information may otherwise be hidden, though it is often very useful.

When giving experimental results the synopsis should indicate the methods used; for new methods the basic principle, range of operation, and degree of accuracy should be given.

4. **References.** If it is necessary to refer to earlier work in the summary, the reference should always be given in full and not by number. Otherwise references should be left out.

When a synopsis is completed, the author is urged to revise it carefully, removing redundant words, clarifying obscurities, and rectifying errors in copying from the paper. Particular attention should be paid by him to scientific and proper names, numerical data, and chemical and mathematical formulae.

SIMULTANEOUS DETERMINATION OF THE SURFACE TENSION OF TIN AND ITS CONTACT ANGLE WITH SILICA BY THE USE OF CONICAL CAPILLARIES*

1475

By D. V. ATTERTON,† M.A., Ph.D., JUNIOR MEMBER, and
T. P. HOAR,‡ M.A., Ph.D., F.I.M., MEMBER

SYNOPSIS

The surface tension of a liquid and its contact angle with a solid that it does not wet may be determined by measuring the pressures required to force the liquid into two capillaries of the solid, at least one of which is conical. Experimental and mathematical details of the method, especially as applied to molten metals, are described.

The surface tension of molten tin between 400° and 800° C. in a hydrogen atmosphere, determined by the method, is $(700 \pm 25) - (0.17 \pm 0.015)T$ dynes/cm., where T is the temperature in °K. The contact angle of tin with fused or polished silica surfaces, determined by the same experiments, is $145^\circ \pm 10^\circ$, independent of temperature but sensitive to the degree of roughness of the surface.

I.—INTRODUCTION

THE reliable determination of surface tension and contact angles of molten metals and alloys has both fundamental and practical interest. Considerable insight into fundamental matters such as the mechanism of solidification, the adsorption of solutes or of gas molecules at molten metal surfaces, and the theory of metallic binding forces could be obtained from appropriate surface-tension measurements. In practical matters such as joining with molten metals, the production by "atomizing" of metal powders, the many kinds of metal casting, and the holding of molten metals in porous refractories, surface-tension phenomena play a critical part: we have previously shown¹ how the penetration of a range of metals into compacted moulding sands is governed by metallostatic pressure, surface tension, and contact angle, and we have indicated² the similar state of affairs prevailing in blast-furnace hearths carrying molten iron. All these studies will be greatly facilitated when more reliable values of surface tension, for a range of metals and alloys and for a range of temperatures, become available.

The experimental determination of the surface tension of molten metals and alloys presents several difficulties: the relatively high temperatures involved, the high contact angles between molten metals and refractory solids, and the ease with which metals become contaminated owing to oxidation or adsorption. These difficulties are emphasized by the large discrepancy between the published values of surface

tension of molten metals; Fig. 1 shows the more reliable results that have been obtained for tin. The highest precision has been attempted in these determinations, and the scatter of each observer's results

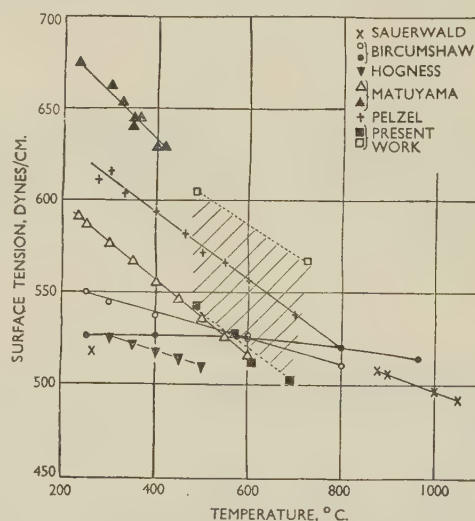


FIG. 1.—The Surface Tension of Molten Tin Between 232° and 1000° C., According to Several Authors.

is only a few dynes/cm.; yet the differences between the various sets of results are as high as 30%. Unfortunately, full details of experimental technique have not always been published, so that assessment of the results is difficult.

Most determinations of metal surface tension have

* Manuscript received 4 December 1952.

† Formerly, Research Student, Department of Metallurgy, Cambridge University; now Research and Development

Manager, Foundry Services, Ltd., Birmingham.

‡ Lecturer, Department of Metallurgy, Cambridge University.

been made using the method of maximum bubble pressure,³⁻⁶ but the drop-weight,^{7,8} sessile-drop,⁹⁻¹² sessile-bubble,¹³ hanging-drop,¹⁴ and capillary-height¹⁵ methods have also been used. Such quantitative determinations of the contact angles of molten metals with solids as have been made have usually been incidental to the determination of surface tension by the sessile-drop or capillary-height¹⁶ methods; large values, 130°–180°, have been estimated. In previous work,¹ we have observed contact angles of *c.* 130° for sessile drops of several molten metals on silica.

The present paper gives details of a new method¹⁷ for the simultaneous determination of surface tension of molten metals and their contact angles with silica or other refractory solids up to at least 1200° C., under conditions whereby surface contamination can be minimized. The method has so far been used to determine the surface tension of molten tin and its contact angle with silica between 400° and 800° C. Although the method is not at present capable of extreme precision, we believe that the results are reliable.

The principle of the method¹⁷ is to force molten metal into conical silica capillaries to predetermined depths and to measure the pressure differences across the resulting molten metal surfaces. If the metal is forced by a pressure, P dynes/cm.², into a conical capillary of apical angle 2ϕ , then evidently

$$P = - \frac{2\sigma \cos(\theta - \phi)}{r} \quad (1)$$

where σ dynes/cm. is the surface tension of the molten metal, θ is the contact angle, and r cm. is the radius of the capillary at the depth where the liquid leaves contact with it. Alternatively, it can be shown* that if s cm. is the capillary radius at the depth of the liquid tip, then

$$P = - \frac{2\sigma}{s} \left(\frac{\cos \theta}{\cos \phi} + \tan \phi \right) \quad (2)$$

Thus, measurement of P and either r or s for two capillaries of different ϕ (one of which may be cylindrical with $\phi = 0$) provides simultaneous equations from which σ and θ can be separately evaluated.

The metal is melted in a silica crucible having a silica tube carrying several capillary bores, at least one of them conical, fused into its bottom. The gas pressure required to force the molten metal to a depth predetermined by means of a metal contacting wire is then measured for each conical capillary, and that required to effect metal entry into each cylindrical capillary is similarly found. The total pressure across the metal surface in a capillary is the sum of the applied gas pressure and the metallostatic pressure of the molten metal in the crucible. The metallostatic pressure cannot be measured

directly with any degree of accuracy; consequently, for a single determination of surface tension and contact angle, measurements are made simultaneously on three capillaries, at least one of which is conical, so that three equations containing the three unknowns σ , θ , and the metallostatic pressure are available for their determination.

Several determinations of $\sigma \cos \theta$ for tin and silica, made with cylindrical capillaries only, are also described below. Measurement of the pressure required to force molten metal into a cylindrical capillary of radius r' cm. enables the product $\sigma \cos \theta$ to be determined by means of the usual formula

$$P = - \frac{2\sigma \cos \theta}{r'} \quad (3)$$

II.—EXPERIMENTAL TECHNIQUE

1. MATERIALS AND APPARATUS

(a) Tin

The tin was of 99.998% purity, the only detectable impurity being 0.002% lead.

(b) Silica Capillaries

Conical capillaries were prepared by grinding and polishing from quadruple-bore transparent silica capillary tubing supplied by The Thermal Syndicate,

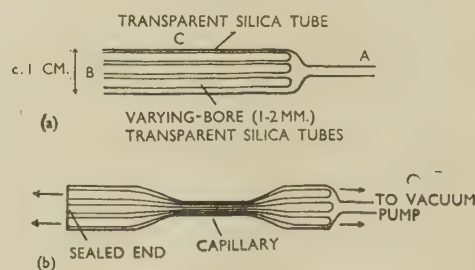


FIG. 2.—Preparation of Multibore Cylindrical Capillary Silica Tubing.

Ltd. Five-cm. lengths of the tubing having one bore of which the major and minor axes differed by less than 0.5% were selected microscopically; such a capillary was used as the cylindrical in those determinations in which two conical and one cylindrical capillaries were used. Grinding tools were prepared by grinding cones, *c.* 2 cm. long, on the ends of 0.3–0.4-cm.-dia. silver-steel rods. A grinding tool, coated with a water slurry of 600-mesh carborundum, was inserted in the capillary and steadily rotated by hand; a conical shape, *c.* 0.4–0.5 cm. long, could be produced in about 1 hr. The final stages of the grinding were followed on a projection microscope to ensure that there was good radial symmetry of the conical portion about the longitudinal axis of the capillary. After grinding, the capillary was thoroughly

* See Appendix I (p. 548).

cleaned with water. A polishing tool was prepared by coating the tip of the grinding tool with molten picien wax, softened by the addition of a little white spirit; while the wax was still soft, it was pressed into the ground portion of the capillary, which had been moistened with water. This produced a sharp wax replica of the ground cone. When the wax had set hard, it was coated with a slurry of very fine rouge and the tool was steadily rotated in the conical portion, the slurry being renewed at intervals. One conical capillary could be polished in *c.* 4–8 hr. to complete transparency. After polishing, the capil-

then drawn down to an external diameter of *c.* 0.4 cm. (Fig. 2 (b)).

(c) General

The apparatus (Fig. 3) consisted of a vertical tube furnace suitable for melting small amounts of metal in vacuum or in purified gas atmospheres, by means of high-frequency current obtained from a 35-kVA. spark-gap generator. The vacuum pump was a Speedivac capable of producing a vacuum of 10^{-5} cm. of mercury.

The silica crucible for holding molten metal had

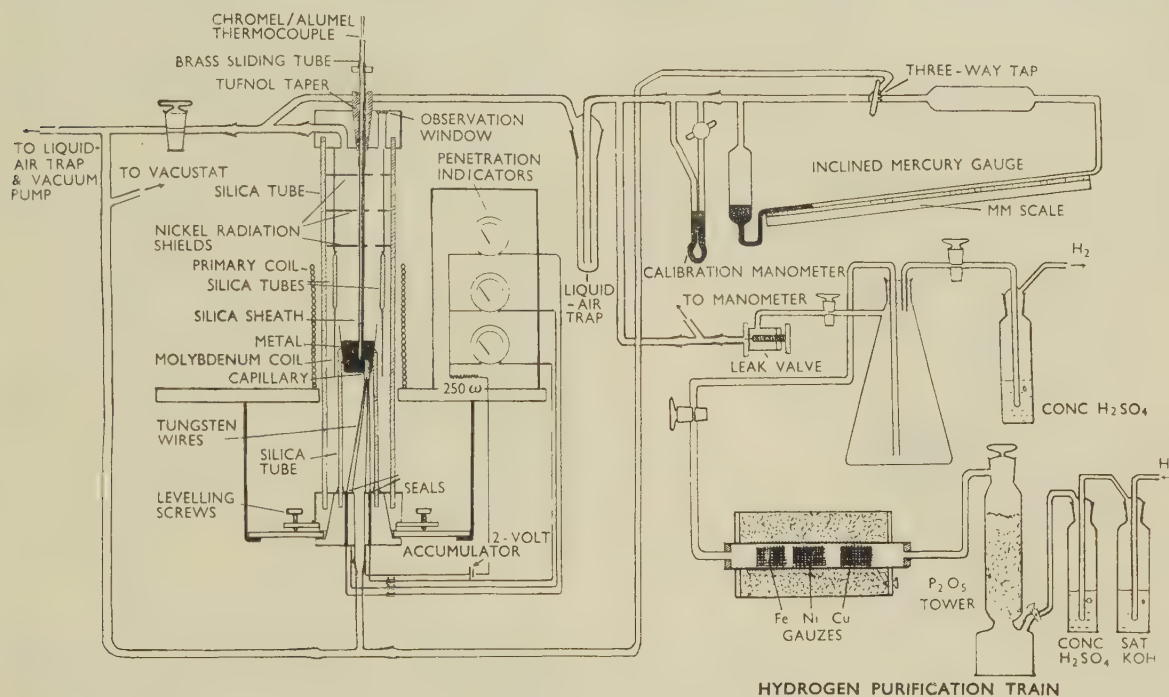


FIG. 3.—General Arrangement of Apparatus.

laries were thoroughly cleaned by boiling successively in hydrochloric and nitric acids.

Multibore cylindrical capillaries for the determination of $\sigma \cos \theta$ were prepared as follows. Silica tubes were drawn down to have similar external diameter but varying bore (0.1–0.2 cm.); several of such tubes, sealed at one end, were then packed into a larger transparent silica tube (Fig. 2 (a)). The outer tube was heated for *c.* 5 min. and then end *B* was sealed, the open ends of the smaller tubes being sealed by allowing them to touch the viscous silica at *B*. The end *A* was connected to a vacuum pump and the outer tube was vigorously heated, whereupon it collapsed on to the smaller tubes and the interstices between them sealed up; collapse of the smaller tubes was prevented by the gas pressure inside them. The tube was then strongly heated at point *C* and steadily rotated, until the silica became sufficiently plastic for the gas pressure in the capillaries to make them become cylindrical. The fabricated tube was

the multibore silica capillary fused vertically into a point approximately one-third along the diameter of the crucible base; the length of the capillary in the crucible was 1–1.5 cm. The crucible was fused into the end of a silica tube (Figs. 3 and 4) and the tube was then sealed with picien wax into a recess machined into the bottom brass furnace end (Fig. 3). Temperature gradients in the metal were minimized by surrounding the crucible with an auxiliary heater prepared by close-winding 0.04-cm.-dia. molybdenum wire on a former covered with paper, coating the wire with a thin layer of alumina cement, drying out the coil packed in charcoal at 600° C. in a muffle furnace, and baking it at 1000° C. in vacuum in the high-frequency furnace. The temperature of the molten metal was measured by means of a Chromel/Alumel thermocouple, of which the hot junction was carried in a silica sheath fixed in a brass tube with picien wax. The brass tube passed through a Tufnol taper, fitted into the top furnace end, with a push fit,

so that the position of the hot junction could be adjusted. The e.m.f. of the thermocouple was measured with a millivoltmeter calibrated against standard metals up to $1100^{\circ}\text{C}.$; readings were accurate to $\pm 1^{\circ}\text{C}.$, spatial and temporal fluctuations were probably $\pm 3^{\circ}\text{C}.$, and thus estimated temperatures are probably accurate to $\pm 4^{\circ}\text{C}.$

The furnace atmosphere and the gas used for pressure application was hydrogen, purified by passing through saturated potassium hydroxide solution, concentrated sulphuric acid, phosphorus pentoxide, copper, nickel, and iron gauzes (these metals being heated to $650^{\circ}\text{C}.$), and a trap cooled in liquid oxygen. It was admitted to the system through a leak valve. The use of hydrogen, in the present experiments with tin at $400^{\circ}\text{--}800^{\circ}\text{C}.$, ensured the removal of tin oxides present on the metal before melting.

Gas pressure could be applied above the molten metal to force it into the capillaries. The difference of pressure above and below the molten metal was measured by means of an inclined mercury manometer covering a range of 4 cm. of mercury; this

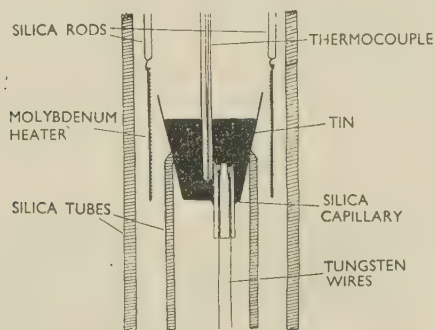


Fig. 4.—Detail of Silica Crucible and Capillaries.

was calibrated with a vertical mercury manometer on which pressure differences were measured cathetometrically, so that measurements could be made to ± 0.0005 cm. of mercury. To minimize sticking of the mercury in the inclined manometer, its stand was continually tapped with an electric buzzer during calibration and use. Rectilinear calibration curves were obtained for two inclined manometers *A* and *B*. *A* was used for vacuum determinations of $\sigma \cos \theta$ and *B* for all other determinations. In *A*, the space above the mercury in the inclined arm was evacuated to $c. 10^{-4}$ cm. of mercury and was then sealed; consequently, the manometer was suitable for use only for pressures between 0 and 4 cm. of mercury. In *B*, the space above the mercury in the inclined arm was connected directly to the underside of the capillaries, and thus this manometer was suitable for measuring any pressure difference of up to 4 cm. of mercury.

A fixed point in each capillary was located by means of a tungsten wire. As the molten metal penetrated into the capillary, the instant of contact with the tungsten wire tip was indicated by means of an

electrical circuit. The manometer reading at the time of contact was recorded photographically.

2. PROCEDURE

(a) Determination of Capillary Dimensions

Before fusion of the capillaries into the silica crucible, the diameters at various depths in the conical capillaries were measured. Wax replicas of the conical portions were prepared in the same way as for the polishing tools; the wax was allowed to cool completely in the conical portion under the continuous application of pressure. The diameter of a replica at different distances along its length was measured on a projection microscope with a magnification of $\times 100$. The plot of diameter against distance along a replica was always rectilinear; from it the apical angle of a capillary could be calculated, and from a single microscopic measurement of the diameter of the mouth of the capillary, the diameter of the cone at any depth below the mouth could be found. Several replicas were examined for each capillary.

The diameters of the cylindrical capillaries were determined to the nearest 10^{-4} cm. by means of a projection microscope with magnification from 75 to 150, depending on the capillary size; each diameter was determined by a dozen measurements taken radially in 30° steps. The difference between the major and minor axes of all cylindrical capillaries used in the experiments was always less than 1.0% and usually less than 0.5%.

(b) General

The capillaries were fused into a silica crucible, with heating from the underside of the crucible to avoid excessive heating of the conical portions and the capillary mouths; the crucible was then fused into a silica tube. Tungsten wires, $c. 0.025$ cm. in dia., for electrical contacts in the capillaries were heated in air to redness in order to coat the surface of the wire with oxide; this oxide is not wetted by molten metal and thus acts as a barrier to further molten-metal penetration into a capillary after contact has been made with the wire. The tips of the oxidized wires were then snipped off and the wires adjusted until their tips were at approximately the desired depths below the capillary mouths; the wires were then sealed through silica tubes in the bottom end of the furnace with picien wax. The depths of the wire tips below the capillary mouths were measured with a travelling microscope; six separate determinations of each depth were made.

Locating wires were arranged in each conical capillary; a contact wire was also put into the cylindrical capillaries, when these were used, and a further wire in a larger "dummy" capillary provided the necessary first contact with the molten metal.

Small pellets of tin were packed in the crucible, and the apparatus was assembled as shown in Fig. 3.

It was evacuated to a pressure of $1-2 \times 10^{-4}$ cm. of mercury; purified hydrogen was then passed in and the apparatus re-evacuated. This cycle was repeated several times. Power was switched on to the furnace and, when a temperature of 350°C. was reached, the thermocouple junction was pushed into the melt to a depth calculated so that it was adjacent to the capillary mouths. By running the high-frequency generator at fixed values between 3 and 7 kVA., it was found that the temperature reached a constant value after 5-10 min. and remained constant to within $\pm 1-2^\circ\text{C.}$ over a period of several minutes. At *c.* 400°C. , purified hydrogen was admitted into the system until a pressure of *c.* 40 cm. of mercury was reached. After the temperature had remained constant for 1-2 min., differential pressure was applied by admitting hydrogen to the upper part of the system only, at a rate controlled by the leak valve. The metal thus forced into the capillaries, coming from the bulk of the metal, was as free from surface contamination as possible; if necessary, preliminary passage of hydrogen upwards through the metal could provide still better conditions of cleanliness. The three pressure readings at which contact between the penetrating molten metal and the tungsten wires occurred were recorded photographically on the same photographic plate. Super-speed ortho-chromatic plates were used; they were slightly under-exposed, and developed for three times the normal time in fine-grain developer. This procedure greatly increased contrast and enabled the manometer scale to be read to an accuracy of ± 0.005 cm., the photographic record being enlarged to about 2.5 times actual size.

(c) Determination of Expansion of Indicating Wires

The tungsten wires used for locating fixed points in the conical capillaries were heated by conduction through the silica, by conduction along the wire, and by radiation from the crucible. Consequently, the wires expanded and their tips were nearer to the mouths of the capillaries than had been determined in the cold with the travelling microscope. The expansion of the wire consists of two parts: y_1 cm., the expansion of the small length, l_1 cm., in the capillary surrounded by molten tin at a temperature $T_m^\circ\text{C.}$, and y_2 cm., the expansion of the length, l_2 cm., between the point where the capillary leaves the constant temperature zone and the point where the wire is fixed at the bottom end of the furnace, which is substantially at room temperature.

y_1 is equal to $l_1\alpha(T_m - T_r)$, where α is the coefficient of expansion of tungsten, 5×10^{-6} cm./cm./ $^\circ\text{C.}$, and $T_r^\circ\text{C.}$ is room temperature.

y_2 may be determined from the temperature variation along the length l_2 of the wire. This variation was determined experimentally for a tungsten wire having molybdenum wires spot-welded at various points along its length, so as to make a series of tungsten/molybdenum thermocouples. This wire was inserted as usual into a capillary crucible in which the

normally used weight of tin was melted and allowed to reach a constant temperature. During this period, the e.m.f.s of the series of tungsten/molybdenum thermocouples were measured at intervals. Fig. 5 shows the variation of temperature down the length of the wire. After 10 min., a logarithmic relation between temperature and distance was experimentally found,

$$\log_e(T - T_r) = \log_e(T_m - T_r) - bl$$

or

$$T - T_r = (T_m - T_r)e^{-bl},$$

where $T^\circ\text{C.}$ is the temperature of the wire at a distance l cm. from the point where the capillary leaves the uniform temperature zone of the crucible

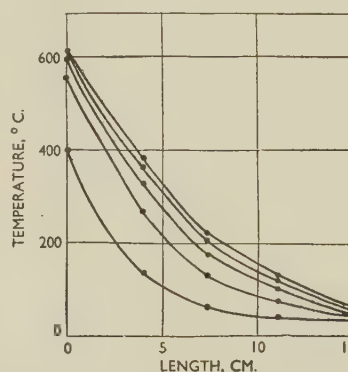


FIG. 5.—Variation of Temperature Along Length of Indicating Wire.

and b is a constant. Thus the expansion of the small length of wire dl at temperature T is

$$\alpha(T - T_r)dl = \alpha(T_m - T_r)e^{-bl} \cdot dl,$$

and the total expansion y_2 of the length l_2 of the wire is

$$\begin{aligned} & \alpha \int_0^{l_2} (T_m - T_r)e^{-bl} \cdot dl \\ &= -\frac{\alpha}{b} [(T_m - T_r)e^{-bl}]_0^{l_2} \\ &= -\frac{\alpha}{b} [T - T_r]_0^{l_2}. \end{aligned}$$

Taking $T = T_m$ when $l = 0$ and $T = T_r$ when $l = l_2$ (the latter a near approximation), we have:

$$y_2 = \frac{\alpha}{b} (T_m - T_r).$$

Thus, the experimental determination of b by the above method enables us to estimate y_2 for any values of T_m and T_r .

III.—RESULTS AND INTERPRETATION

1. SURFACE-TENSION DETERMINATION

The relevant data of these determinations are given in Table I. An atmosphere of carefully purified hydrogen was used for these experiments, since

preliminary work (described later in this Section) had shown that results obtained for $\sigma \cos \theta$ in hydrogen had better reproducibility than those obtained in vacuum. Fig. 1 shows the surface-tension results

discussed later in this Section. The results of experiment 2 (Table I), evidently due to experimental error, have been ignored; they serve to illustrate that any small error in the experimental measure-

TABLE I.—Data and Results of σ and θ Determinations with Conical Capillaries.

Expt. No.	Temp., °C.	Density of Tin, g./c.c.	Angle, ϕ	Depth of Wires below Capillary Mouths, cm.	Expansion Correction, ($l_1 + l_2$), cm.	Radius, s , cm.	Applied Gas Pressure, p_g , cm. Hg.	Pressure Correction for Depths of Wires and for Menisci, p_c , cm. Hg.	σ , dynes/cm.	θ , deg.	$\sigma \cos \theta$, dynes/cm.
1	489	6.77	7° 36' 4° 30' 0°	0.176(5) 0.337(5) ...	0.016(0) 0.015(7) ...	0.0610 0.0403 0.0246(5)	0.482 1.038 2.512	0.068 0.151 ...	543	155	492
2	408	6.83	6° 50' 4° 50' 0°	0.438 0.350 ...	0.013(2) 0.013(4) ...	0.0628(3) 0.0532 0.0255	0.418 0.716 2.629	0.205 0.162 ...	768	132	514
3	609	6.71	6° 50' 4° 50' 0°	0.426 0.377 ...	0.017(2) 0.017(4) ...	0.0647(5) 0.0510(8) 0.0255	0.348 0.680 2.377	0.187 0.164 ...	512	159	478
4	572	6.73	7° 38' 4° 32' 0°	0.410 0.419 ...	0.018(1) 0.018(1) ...	0.0592 0.0436 0.0248	0.307 0.755 2.302	0.181 0.188 ...	528	152	466
5	692	6.64	7° 38' 4° 32' 0°	0.398 0.439 ...	0.020(1) 0.020(0) ...	0.0610 0.0420 0.0248	0.197 0.669 2.061	0.174 0.196 ...	503	148	426
6	727	6.63	7° 50' 5° 29' 4° 55'	0.200 0.244 0.309(5)	0.022(1) 0.021(9) 0.021(7)	0.0653(3) 0.0467(5) 0.0398(7)	0.490 0.880 1.090	... 0.023 0.055	567	142	448
7	489	6.77	7° 50' 5° 29' 4° 55'	0.215 0.196 0.299	0.016(0) 0.016(0) 0.015(7)	0.0623 0.0507 0.0401	0.664 0.962 1.265	0.008 ... 0.052	604	143	482

TABLE II.—Data and Results of $\sigma \cos \theta$ Determinations with Cylindrical Capillaries.

Expt. No.	Atmosphere	Temperature, °C.	Radii, cm.			Pressures, cm. Hg.			$\sigma \cos \theta$, dynes/cm.
			r_1	r_2	r_3	p_1	p_2	p_3	
1	Vacuum *	723	0.0528	0.456	...	0.590	0.750	...	354
2	"	468	0.0674	0.0482	...	0.695	1.074	...	423
3	"	525	0.0674	0.0482	...	0.657	1.008	...	392
4	"	567	0.0674	0.0482	...	0.520	0.902	...	426
5	"	629	0.0674	0.0580	0.0482	0.583	0.725	0.926	384 †
6	"	580	0.0528	0.0456	...	0.530	0.710	...	398
7	Hydrogen ‡	460	0.0528	0.0456	...	0.645	0.834	...	418
8	"	608	0.0674	0.0580	0.0482	0.592	0.735	0.938	387 †
9	"	539	0.0652	0.0416	...	0.683	1.201	...	393
10	"	672	0.0652	0.0416	...	0.640	1.153	...	389
11	"	756	0.0652	0.0416	...	0.572	1.055	...	366
12	"	789	0.0547	0.0412	...	0.523	0.847	...	356

* Hydrogen at $1-5 \times 10^{-4}$ cm. Hg.

† Mean of three values (calculated from the radius and pressure results taken in pairs), all within $\pm 2\%$ of the mean.

‡ At 40–50 cm. Hg.

obtained over a temperature range of 400°–800° C. The solid squares in the figure represent the variation of surface tension with temperature as determined with two conical and one cylindrical capillary experiments. The two open squares represent results obtained by the use of three conical capillaries; they are significantly higher than the other values, a matter

ments may produce a large error in σ , as discussed in Appendix II (p. 550).

2. CONTACT-ANGLE DETERMINATION

The relevant data and results are given in Table I. With the exception of the value from experiment 2, the contact-angle values from experiments with two

conical and one cylindrical capillaries are all substantially the same. The two experiments with three conical capillaries gave a somewhat lower result.

3. $\sigma \cos \theta$ DETERMINATION

Preliminary experiments were made with cylindrical capillaries to determine values of $\sigma \cos \theta$ for tin and silica in a vacuum (hydrogen at $1-5 \times 10^{-4}$ cm. of mercury). The relevant data are given in Table II, and the results are shown in Fig. 6. The reproducibility was not very good, possibly on account of a slow rate of approach of the contact angle to its equilibrium value, or on account of surface contamination. To minimize contamination, further experiments were carried out in purified hydrogen at 40–50 cm. of mercury; the results, also shown in Fig. 6, were more reproducible. The regression curves for $\sigma \cos \theta$ on temperature for vacuum and hydrogen conditions are not significantly different,

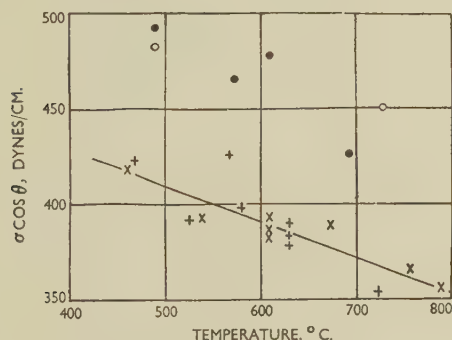


FIG. 6.— $\sigma \cos \theta$ Determinations for Molten Tin Between 400° and 800° C.

KEY.

- + Vacuum: $\sigma \cos \theta$.
- × Hydrogen: $\sigma \cos \theta$.
- Two conical, one cylindrical capillaries: $\sigma \times \cos \theta$.
- Three conical capillaries: $\sigma \times \cos \theta$.

and the straight line of best fit for the joint data is given.

When the products of the surface tension and cosines of contact angles, obtained from the conical-capillary experiments, are plotted against temperature (Fig. 6), the results are significantly higher (by about 50–80 dynes/cm.) than the $\sigma \cos \theta$ values obtained using cylindrical capillaries. These higher values can only be explained by a different contact angle of tin on the two different silica surfaces, the conical capillaries having a ground and polished surface and the cylindrical having a fused surface. Consequently, since the silica surfaces of the three conical capillaries are essentially the same, we think that the values of surface tension and contact angle obtained with these may be more reliable than the other values. From these surface tension values and the data of the cylindrical capillary experiments, the contact angle of tin with the fused-surface cylindrical capillaries prepared in the laboratory may be calculated as c. 132° at 489° and 727° C.

When the contact angle determined in the experiments with three conical capillaries, viz. 142°, is used for a re-calculation of the experiments with two (polished) conical and one (fused, Thermal Syndicate) cylindrical capillaries, the contact angle for the cylindrical capillary may be calculated to be very close to the same figure. This arises from the form and parameters of the simultaneous equations, which, although they allow a perfect separation of σ and $\cos \theta$ in principle, are very sensitive to small errors. Further mathematical investigation is required to determine the best values of capillary angles and radii for providing the most significant separation of σ and $\cos \theta$ by solution of the simultaneous equations, and further experimental work is necessary to determine the precise influence of surface preparation on contact angle. Meanwhile, the present experimental results are consistent with the following expressions for the surface tension of tin, σ_{Sn} , and its contact angle, $\sigma_{\text{Sn-SiO}_2}$, with fused or polished silica in the range 400°–800° C.:

$$\sigma_{\text{Sn}} = (700 \pm 25) - (0.17 \pm 0.015)T \text{ dynes/cm.}$$

$$\theta_{\text{Sn-SiO}_2} = 145^\circ \pm 10^\circ, \text{ independent of temperature.}$$

The limits of the expression for σ_{Sn} , in which T is the temperature in °K., are indicated in Fig. 1. The expression leads, by extrapolation, to a value of 614 dynes/cm. for the surface tension of tin at the melting point (232° C.), in close agreement with the value of 610 dynes/cm. recently reported for this temperature by Smirnova and Ormont,¹⁴ who used an improved hanging-drop technique.

IV.—DISCUSSION

The values obtained for the surface tension of tin are of the same order of magnitude as previous results (Fig. 1), although the scatter is somewhat greater. The large discrepancy between the results of various workers may be due partly to contamination of the tin caused by insufficient degassing of the apparatus and by incomplete purification of furnace atmosphere, and partly to differing degrees of purity of the tin. That used in the present experiments was of high purity, which may possibly explain the slightly higher values of surface tension obtained as compared with those of the majority of previous workers. A small percentage of impurity, e.g. lead, in the tin probably has a considerable influence on the surface tension; lead is selectively absorbed at the surface of the tin with consequent reduction of surface energy, as shown experimentally by Bircumshaw.³ Another possible source of discrepancy is that the theory underlying most methods is insufficiently exact and leads to errors in calculation as well as in experiment.

The variation of surface tension with temperature is similar to that obtained by several other workers, notably Pelzel,⁶ Matuyama,⁸ and, to a lesser degree,

Sauerwald and Drath.⁴ Substitution of the best results from the present work in the thermodynamic relation $E_s = \sigma - T \frac{d\sigma}{dT}$, where E_s is the total surface energy necessary to form 1 cm.² of new surface, σ is the surface tension, equivalent to the work done in forming 1 cm.² of surface, and T is the temperature in °K., gives a value of *c.* 700 ergs/cm.² for the total surface energy of liquid tin, independent of temperature, and *c.* 0.17 erg/cm.²/°K. for the surface entropy. If we make the common assumption that surface energy and entropy concern the first atomic layer only, these values correspond to a total surface energy of 9400 cal./g.-atom and a surface entropy of 2.3 cal./g.-atom/°K. These values may be compared with the approximately known latent heat of evaporation, 79,000 cal./g.-atom, and the standard entropy of evaporation, 29.5 cal./g.-atom/°K.; it may be noted that the transfer of a tin atom from the bulk to the surface of liquid tin is associated with only small fractions of the energy and entropy changes occurring during the transfer of an atom from the bulk of the liquid to the vapour phase.

The high values of contact angle between tin and silica are not unexpected, being due to the high cohesion of the metal and its relatively low adhesion to the non-metal, a matter readily understood in terms of the accepted theories of metallic and non-metallic bonding.

The lower values of contact angle found on the surface of the fused capillaries as compared with the values obtained on the ground and polished capillaries may well be due to the greater smoothness of the fused silica surface. Since the true contact angle of tin on perfectly smooth silica is certainly greater than 90°, the tin does not penetrate into micro-crevices on a rough silica surface and there is no adhesion over these crevices; consequently, the average work of adhesion is less than on a smooth surface, which results in a higher contact angle.

In the early work of Smith¹⁵ on liquid-metal surface tensions, calculations were based upon a contact angle of 180° between the metals and graphite; later, Libmann¹⁶ observed very high contact angles between metals and alumina, and, in some cases, calculations were based upon $\cos \theta = -1$. Although a contact angle of 180° cannot be physically possible, it is quite likely that the relatively rough graphite and alumina surfaces used by Smith and by Libmann led to contact angles of greater than 170°, so that the error in taking $\cos \theta = -1$ may well have been small. Extension of the present work using deliberately roughened conical and cylindrical capillary surfaces might well show that, for many metals in contact with roughened silica, $\cos \theta = -1$ is a near approximation, and that consequently surface tensions could conveniently be measured by determinations of $\sigma \cos \theta$ with roughened cylindrical capillaries only. Such a method would greatly simplify both experiment and calculation, as well as minimizing errors in both.

V.—SUMMARY

(1) A method for the simultaneous determination of the surface tension of a molten metal and its contact angle with a refractory solid by the use of conical capillaries is described in experimental and theoretical detail.

(2) The surface tension of tin between 400° and 800° C. in a hydrogen atmosphere, determined by the method, is $(700 \pm 25) - (0.17 \pm 0.015)T$ dynes/cm., where T is the temperature in °K. The contact angle of tin with fused or polished silica over the same temperature range is $145^\circ \pm 10^\circ$, independent of temperature.

(3) Theoretical and practical implications of the method and of the results are discussed.

ACKNOWLEDGEMENTS

This work was carried out in the Department of Metallurgy, University of Cambridge. We thank Dr. A. G. Metcalfe, lately of the Department, for a calibration curve of the tungsten/molybdenum thermocouple, and Dr. E. S. Hedges, Director of Research of the Tin Research Institute, for kindly providing the pure tin.

Our thanks are also due to the Department of Scientific and Industrial Research for a Maintenance Allowance to one of us (D. V. A.), during the tenure of which the work was carried out.

APPENDIX I

Theory of Conical Capillaries

Fig. 7 represents the meniscus zone of a liquid, e.g. a molten metal, in a capillary of a solid that it

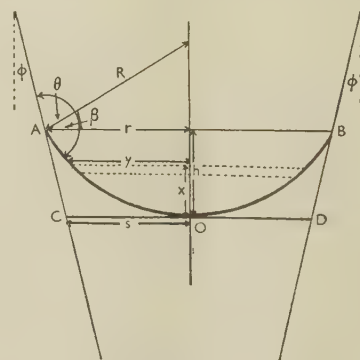


FIG. 7.—Geometry of Non-Wetting Liquid in Conical Capillary.

does not wet. O is the point located by means of a central contacting wire.

If P dynes is the total pressure difference across the liquid surface, r cm. the radius of the capillary at the level AB where the liquid leaves the surface, σ dynes/cm. the surface tension of the liquid, θ the

contact angle, and 2ϕ the apical angle of the capillary, then by resolving forces vertically

$$P \cdot \pi r^2 = \sigma \cdot 2\pi r \cos \{180 - (\theta - \phi)\}$$

and

$$P = -\frac{2\sigma \cos (\theta - \phi)}{r} \quad (1)$$

The experimental location of the point O enables the radius s cm. of the capillary in the plane CD to be determined. Thus if R cm. is the radius of curvature of the liquid meniscus, assumed spherical, then from Fig. 7

$$\begin{aligned} r &= s + h \tan \phi \\ &= s + R(1 - \sin \beta) \tan \phi \\ &= s + \frac{r}{\cos \beta} (1 - \sin \beta) \tan \phi \end{aligned}$$

$$\text{or} \quad r = \frac{s \cos \beta}{\cos \beta - (1 - \sin \beta) \tan \phi};$$

and since $\beta = 180 - (\theta - \phi)$,

$$r = \frac{s \cos (\theta - \phi)}{\frac{\cos \theta}{\cos \phi} + \tan \phi} \quad (4)$$

Substitution in (1) gives

$$P = -\frac{2\sigma}{s} \left(\frac{\cos \theta}{\cos \phi} + \tan \phi \right) \quad (2)$$

The total pressure P for a conical capillary is made up of several parts—the measured applied gas pressure p_g , the head of liquid above the capillary, and the pressure due to the weight of mercury within the capillary. The head of liquid above the capillary is treated as an unknown and is determined by the use of an extra capillary; the correction for the liquid in the capillary is calculated from the experimentally determined dimensions of the capillary.

When determinations are made with two conical and one cylindrical capillaries, it is convenient to define as p_m the depth of liquid from the surface to the level of the capillary mouths, plus that due to the weight of liquid in the cylindrical capillary when its meniscus is just about to enter and run down to its contacting wire. p_m thus includes the meniscus correction H_1 for the cylindrical capillary (Fig. 8), H_1 being the height of a cylinder of liquid of radius equal to that of the capillary and weight equal to that of the liquid meniscus. The meniscus corrections for conical capillaries are H_2 , &c. The correction to be added to $p_g + p_m$ for a conical capillary to take account of the depth of liquid in it below the level XY is thus (Fig. 8)

$$\begin{aligned} p_c &= l \frac{\rho_{\text{Sn}}}{\rho_{\text{Hg}}} \\ &= \{k - H_1 - (h - H_2)\} \frac{\rho_{\text{Sn}}}{\rho_{\text{Hg}}} \text{ cm. of mercury} \quad (5) \end{aligned}$$

where k is the depth of the contacting wire below the capillary mouth, and the ρ 's are the metal densities.

The values of h and H for various capillary apical angles and values of the radius s are found as follows. From Fig. 7,

$$\begin{aligned} h &= \frac{r}{\cos \beta} (1 - \sin \beta) \quad (6) \\ &= \frac{r(1 - \sin \{180 - (\theta - \phi)\})}{\cos \{180 - (\theta - \phi)\}}, \end{aligned}$$

and substituting for r by means of (4) and simplifying, we have

$$\frac{h}{s} = \frac{\sin (\theta - \phi) - 1}{\frac{\cos \phi}{\cos \theta} + \tan \phi} \quad (7)$$

Consider now a circular section of the meniscus shown in Fig. 7, with radius y cm., height x cm.

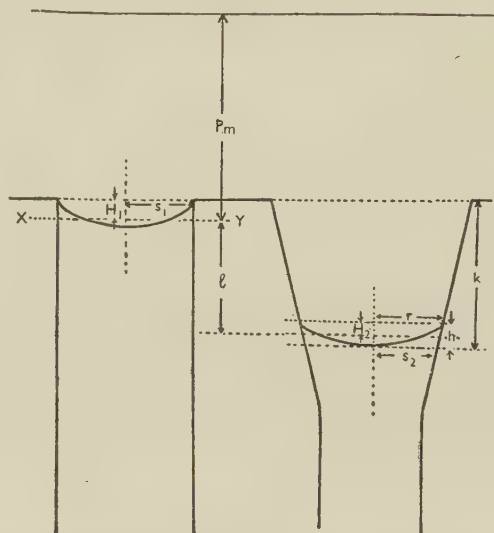


FIG. 8.—Corrections for Head of Metal, Metal in Capillaries, and Menisci.

above the point O and thickness dx cm. Its volume is $\pi y^2 dx$, and hence the total volume of the meniscus is

$$\begin{aligned} \int_0^h \pi y^2 dx &= \pi \int_0^h \{R^2 - (R - x)^2\} dx \\ &= \pi \left(Rh^2 - \frac{h^3}{3} \right) \end{aligned}$$

Thus the height of the cylinder radius r having the same volume is

$$\begin{aligned} H &= \frac{\pi \left(Rh^2 - \frac{h^3}{3} \right)}{\pi r^2} \\ &= \frac{h^2}{r^2} \left(R - \frac{h}{3} \right) \end{aligned}$$

Substituting $R = r/\cos \beta$ and for h by means of (6) we obtain

$$H = \frac{r(1 - \sin \beta)^2(2 + \sin \beta)}{3 \cos^3 \beta},$$

and finally substituting for r by means of (4)

$$\frac{H}{s} = \frac{(1 - \sin \beta)(2 + \sin \beta)}{3(1 + \sin \beta)\{\cos \beta - (1 - \sin \beta) \tan \phi\}}$$

$$= - \frac{\{1 - \sin(\theta - \phi)\}\{2 + \sin(\theta - \phi)\}}{3(1 + \sin(\theta - \phi))\left\{\frac{\cos \theta}{\cos \phi} + \tan \phi\right\}} \quad (8)$$

Table III gives values for $\frac{H}{s}$ and $\frac{(h-H)}{s}$ computed by means of (7) and (8) for different values of θ and ϕ . By its use (with suitable interpolation), the heights H_1 for a cylindrical capillary ($\phi = 0$) and $(h - H_2)$ for a conical may be found for any measured values of the radii s_1 , s_2 , and substitution of these values in (5) gives the correction p_c for the conical capillary.

TABLE III.—Computed Values of H/s and $(h-H)/s$ for Meniscus Corrections.

θ	H/s for $\phi = 0^\circ$	$(h-H)/s$ for	
		$\phi = 4^\circ 30'$	$\phi = 8^\circ$
130°	0.190	0.159	0.145
140°	0.250	0.204	0.193
145°	0.285	0.226	0.217
150°	0.321	0.249	0.241
160°	0.407	0.292	0.289

When three conical capillaries are used, the pressure p_m is defined to take in that due to the height of metal in the least deeply penetrated capillary, including that equivalent to its meniscus zone. The calculation of the corrections p_c is otherwise similar to that given above.

APPENDIX II

Typical Calculation of σ and θ from Experimental Data

Experiment 1.—For data see Table I.

$$- \frac{2\sigma}{13.56 \times 981} \left\{ \frac{\cos \theta}{0.0610 \cos 7^\circ 36'} + \frac{\tan 7^\circ 36'}{0.0610} \right\}$$

$$= 0.482 + p_m + p_{c_1} \quad (9)$$

$$- \frac{2\sigma}{13.56 \times 981} \left\{ \frac{\cos \theta}{0.0403 \cos 4^\circ 30'} + \frac{\tan 4^\circ 30'}{0.0403} \right\}$$

$$= 1.038 + p_m + p_{c_2} \quad (10)$$

$$- \frac{2\sigma}{13.56 \times 981} \left\{ \frac{\cos \theta}{0.0246(5)} \right\} = 2.512 + p_m \quad (11)$$

p_m and p_{c_1} , p_{c_2} are the pressure corrections for the head of metal in the crucible and for the metal in the conical capillaries (as shown in Appendix I).

Assume $\theta = 150^\circ$; then from (5) and Table III (Appendix I):

$$p_{c_1} = 0.176(5) - 0.016 - 0.008 - 0.015$$

$$= 0.137(5) \text{ cm. Sn} = 0.069 \text{ cm. Hg.}$$

$$p_{c_2} = 0.337(5) - 0.016 - 0.008 - 0.010$$

$$= 0.303(5) \text{ cm. Sn} = 0.152 \text{ cm. Hg.}$$

Subtracting (9) from (11), we have

$$- \frac{2\sigma}{13.56 \times 981} \{40.56795 \cos \theta - 16.53865 \cos \theta - 2.18738\} = 2.512 - 0.482 - 0.069 \quad (12)$$

and subtracting (10) from (11)

$$- \frac{2\sigma}{13.56 \times 981} \{40.56795 \cos \theta - 24.89055 \cos \theta - 1.95285\} = 2.512 - 1.038 - 0.152 \quad (13)$$

Dividing (12) by (13), we have

$$\frac{24.02930 \cos \theta - 2.18738}{15.67740 \cos \theta - 1.95285} = \frac{1.961}{1.322} = 1.4833585$$

$$24.0293 \cos \theta - 2.18738 = 23.2552 \cos \theta - 2.89678$$

$$0.7741 \cos \theta = -0.70940$$

$$\cos \theta = -0.9164$$

$$\theta = 156^\circ 30'.$$

We now recalculate p_{c_1} and p_{c_2} for the contact angle of $156^\circ 30'$, obtaining as before from (5) and Table III in Appendix I:

$$p_{c_1} = 0.176(5) - 0.016 - 0.009 - 0.016$$

$$= 0.135(5) \text{ cm. Sn} = 0.068 \text{ cm. Hg.}$$

$$p_{c_2} = 0.337(5) - 0.016 - 0.009 - 0.011$$

$$= 0.301(5) \text{ cm. Sn} = 0.151 \text{ cm. Hg.}$$

Whence

$$24.0293 \cos \theta - 2.18738$$

$$15.6774 \cos \theta - 1.95285$$

$$= \frac{2.512 - 0.482 - 0.068}{2.512 - 1.038 - 0.151} = \frac{1.962}{1.323}$$

$$24.0293 \cos \theta - 2.18738 = 23.2495 \cos \theta - 2.89607$$

$$0.7798 \cos \theta = -0.70869$$

$$\cos \theta = -0.90881$$

$$\theta = 155^\circ$$

and from (12)

$$-2\sigma(24.0293 \cos \theta - 2.18738) = 1.962 \times 13.56 \times 981$$

$$2\sigma(24.02547) = 26099.23$$

$$\sigma = 543 \text{ dynes/cm.}$$

APPENDIX III

ESTIMATION OF ERRORS

(1) Determination of Surface Tension and Contact Angle

The errors in the values of σ and θ obtained depend on the experimental errors in ϕ , s , and p_c . Although the fundamental equation (2) is an approximation, the error involved is considerably less than these experimental errors.

Error in Capillary Angle, ϕ .

The semi-apical angle of the conical capillary was determined from a plot of diameter of a wax replica

against its length. It may be estimated from the graphs obtained that the error is probably only $\pm 1'$.

Error in Radius, s cm.

(a) The travelling microscope, used for determining the depth of a wire tip below a capillary tip, had a depth of focus of just less than 0.001 cm. It was found experimentally that the readings, on the wire tip and on the capillary tip, could be obtained consistent to 0.001 cm., i.e. the depth could be estimated to ± 0.0005 cm. An error of ± 0.0005 cm. in the depth corresponds to an error of $\pm 0.0005 \tan \phi$ cm. in the radius; thus, since $\tan \phi$ is c. 0.1, the error in the radius is c. ± 0.00005 cm.

(b) There is an additional error in the radius associated with the error in the estimation of the expansion of the indicating tungsten wire. The magnitude of this second-order error is not known, but the reproducibility of surface tension and contact angle values suggest that it is small.

(c) An error due to the expansion of silica is also present, but it is so small that it may be ignored.

Error in Pressure, p_g cm. Hg

The solution of the simultaneous equations for σ and θ involves pressure differences and not absolute pressures; consequently, any possible errors in gauge calibration, or any systematic errors in reading the gauge, are largely eliminated. The photograph of the gauge, enlarged approximately to 2.5 times the actual gauge size, enabled the readings to be obtained to ± 0.005 cm.; thus, since the gauge had a magnification factor of over 5, the error in the absolute pressure is probably less than ± 0.001 cm. of mercury.

Table IV records the influence of these errors on

the values of surface tension and contact angle, as calculated by the use of equation (2).

TABLE IV.

Error in	Error in θ	Error in σ
Capillary angle: $\pm 1'$.	$\pm 0.6\%$	$\mp 0.75\%$
Radius: ± 0.00005 cm. .	$\pm 1.0\%$	$\mp 1.25\%$
Pressure: ± 0.001 cm. Hg. .	$\pm 1.25\%$	$\mp 1.45\%$
Total error: . . .	$\pm 3.0\%$	$\mp 3.5\%$

(2) Determination of $\sigma \cos \theta$

For a single determination of $\sigma \cos \theta$, the gas pressure, p_g , needed to force the molten metal into a cylindrical capillary of known radius, r' cm., was measured for two capillaries. The values obtained were substituted in equation (3), and the value of $\sigma \cos \theta$ was calculated by solving the resultant simultaneous equations.

Error in Radius, r' cm.

The radii of the capillaries were measured to ± 0.00005 cm., using a projection technique.

Error in Pressure, p_g cm. Hg

This is the same as for conical capillaries, viz. ± 0.001 cm. of mercury.

Consideration of these errors in the radius and pressure shows that the $\sigma \cos \theta$ values should be accurate to $\pm 1.2\%$. However, this is an underestimate, since the difference between the major and minor axes of the capillary bores (usually, however, less than 0.5% and always less than 1.0%) has not been considered.

REFERENCES

1. T. P. Hoar and D. V. Atterton, *J. Iron Steel Inst.*, 1950, **166**, 1.
2. T. P. Hoar and D. V. Atterton, *ibid.*, 1952, **170**, 145.
3. L. L. Bircumshaw, *Phil. Mag.*, 1926, [vii], **2**, 341.
4. F. Sauerwald and G. Drath, *Z. anorg. Chem.*, 1926, **154**, 79; 1927, **162**, 301.
5. T. R. Hogness, *J. Amer. Chem. Soc.*, 1921, **43**, 1621.
6. E. Pelzel, *Berg- u. hüttenmänn. Monatsh. montan. Hochschule Leoben*, 1948, **93**, 248.
7. P. Quincke, *Ann. Chem.*, 1859, **55**, 227.
8. Y. Matuyama, *Sci. Rep. Tōhoku Imp. Univ.*, 1927, [i], **16**, 555.
9. H. Siedentopf, *Ann. Physik u. Chem.*, 1897, **61**, 235.
10. R. Herzfeld, *ibid.*, 1897, **62**, 450.
11. C. Kemball, *Trans. Faraday Soc.*, 1946, **42**, 246.
12. H. H. Kellogg, private communication, 1951.
13. A. Portevin and P. Bastien, *Proc. Inst. Brit. Found.*, 1935-36, **29**, 88; and *Found. Trade J.*, 1936, **55**, 28.
14. Y. I. Smirnova and B. F. Ormont, *Doklady Akad. Nauk S.S.S.R.*, 1952, **82**, 751.
15. S. W. Smith, *J. Inst. Metals*, 1914, **12**, 168.
16. E. E. Libmann, *Univ. Illinois Eng. Exper. Sta. Bull.*, 1928, (173).
17. T. P. Hoar and D. V. Atterton, *Research*, 1951, **4**, 42.

A THEORETICAL INVESTIGATION OF THE DEFORMATION TEXTURES OF TITANIUM*

1476

By D. N. WILLIAMS,† Ph.D., MEMBER, and PROFESSOR D. S. EPPELSHEIMER,‡ D.Sc., MEMBER

SYNOPSIS

The deformation process in titanium was examined by applying the Calnan and Clews method of texture analysis (*Phil. Mag.*, 1950, [vii], **41**, 1085; 1951, [vii], **42**, 616, 919; 1952, [vii], **43**, 93) to the experimentally determined textures. It proved possible to develop a theoretical deformation process which would result in the formation of the observed deformation textures. This deformation process required the interaction of three slip systems, $\{0001\}\langle 11\bar{2}0 \rangle$, $\{10\bar{1}1\}\langle 11\bar{2}0 \rangle$, and $\{10\bar{1}0\}\langle 11\bar{2}0 \rangle$, and two types of twinning, $\{10\bar{1}2\}$ and $\{11\bar{2}2\}$. Each of these modes of deformation was examined separately, and then they were combined to give the observed deformation textures. The critical shear stresses for slip (C_s) and for twinning (C_t) were found to be related in the following manner: $C_{s0001} = 1.1 C_{s10\bar{1}1} = 1.02 C_{s10\bar{1}0} = C_{t10\bar{1}2} = C_{t11\bar{2}2}$.

I.—INTRODUCTION

THE cold-rolled textures of several hexagonal metals have been found to be predominantly $(0001)[11\bar{2}0]$. This texture is the result of $\{0001\}\langle 11\bar{2}0 \rangle$ slip and $\{10\bar{1}2\}$ twinning.¹ Recent investigations of the metals titanium,² zirconium,³ and beryllium⁴ have indicated that these hexagonal metals do not deform by this simple mechanism, since their cold-rolled textures deviate considerably from the ideal $(0001)[11\bar{2}0]$ texture.

Titanium showed the greatest deviation from the ideal hexagonal texture; it showed a $(0001)[10\bar{1}0]$ texture rotated 30° toward the transverse direction. The textures of titanium after compression⁵ and cold rolling⁶ were re-determined, using a semi-quantitative Geiger-counter pole-figure technique. The results of these experimental texture studies were examined by the method of texture analysis developed by Calnan and Clews,⁷⁻¹⁰ which had been successful in predicting the texture of both zinc and magnesium.

By use of the Calnan and Clews method of texture analysis, it was possible to postulate a theoretical deformation process which would result in the formation of the experimentally observed deformation textures of titanium.

II.—THE DEFORMATION TEXTURES OF TITANIUM

No texture studies of the tension texture of titanium have been reported in the literature. The wire texture has been examined by Yen¹¹ and found to be $[10\bar{1}0]$. The tension texture is generally similar to the wire texture in hexagonal metals. The tension

texture of titanium has therefore been assumed to be $[10\bar{1}0]$ in the following discussions.

The compression texture of iodide titanium has been described as a rotated $[0001]$ texture.⁵ As the amount of reduction in compression increased, the angle of rotation of the $[0001]$ texture decreased, varying from 32.5° at low reductions to 17.5° at 98.9% reduction. The relative intensity of the 0001 maximum was practically constant regardless of the amount of reduction, suggesting that the compression texture was an equilibrium texture existing between two opposing end textures. A slight indication that the $[0001]$ rotation occurred about a $\langle 10\bar{1}0 \rangle$ axis was noticed in the $10\bar{1}0$ and $10\bar{1}1$ pole figures.

The texture of cold-rolled iodide titanium was found to be $(0001)[10\bar{1}0]$, rotated 30° in the transverse direction⁶ as previously reported. A very strong maximum was found in the rolling direction of the $10\bar{1}0$ pole figure. This maximum was seven times stronger than the second maximum in the $10\bar{1}0$ pole figure. The 0001 pole figure showed a spread of orientations from the transverse direction to the rolling plane normal along the transverse axis. An 0001 maximum was measured at an angle of 30° from the rolling plane normal with a minimum occurring at the rolling plane normal. At lower reductions a weak 0001 maximum was noticed in the transverse direction. This maximum disappeared as the reduction increased.

III.—THE CALNAN AND CLEWS METHOD OF TEXTURE ANALYSIS

The Calnan and Clews method of texture analysis, referred to below as the Calnan and Clews method, is

* Manuscript received 28 November 1952.

† Research Engineer, Kaiser Aluminium and Chemical Corporation, Spokane, Washington; formerly National Lead Research Fellow, Missouri School of Mines and Metallurgy,

Rolla, Missouri, U.S.A.

‡ Professor of Metallurgical Engineering, Missouri School of Mines and Metallurgy, Rolla, Missouri, U.S.A.

a method of averaging the slip-rotation tendencies of grains with all possible orientations for the determination of the main rotation tendency leading toward the formation of the deformation texture.

The Calnan and Clews method is based on the following assumptions:

1. Only the slip or twinning system which has the maximum resolved shear-stress ratio will be active. The resolved shear-stress ratio is defined as the ratio of the resolved shear stress to the critical shear stress. When the value of this ratio is greater than unity, slip or twinning should occur. For double slip to occur, two slip systems must have equal resolved shear-stress ratios. Multiple slip occurs whenever three or more slip systems have equal resolved shear-stress ratios.

2. Slip and twinning are equally probable when the resolved shear-stress ratio for slip equals the resolved shear-stress ratio for twinning. If the resolved shear-stress ratio for twinning exceeds the resolved shear-stress ratio for slip, twinning will occur.

3. The value of the resolved shear stress is calculated from the position of the effective stress, T_e , rather than from that of the applied stress, T_a . It is possible for T_e to be some distance from T_a . By the use of the concept of effective stress, it is possible to explain why a single grain can deform by multiple slip when the applied stress position is such that only single slip should occur. Thus it is possible for single, double, and multiple slip to occur in the same grain owing to differences in the positions of the effective stress in various parts of the grain. The movements of T_e from T_a can be visualized as the result of grain-boundary influences.

To determine the general rotation tendencies, the resolved shear-stress contour diagram for the slip system having the highest resolved shear-stress ratio is plotted in the unit triangle. If two or more slip systems are active within the unit triangle, the resolved shear-stress diagram for each system is plotted in the portion of the unit triangle in which it is active.⁸

The rotation tendencies for single slip and double slip are determined for each position of T_a within the unit triangle. In single slip, the slip plane normal rotates toward the stress axis in compression and the slip direction rotates toward the stress axis in tension. In double slip, the great circle joining the two active slip plane normals rotates toward the stress axis in compression and the great circle joining the two active slip directions rotates toward the stress axis in tension. In multiple slip no rotation occurs if the stress axis is located symmetrically. If the stress axis is unsymmetrically located, rotation occurs towards a symmetrical position. These rotations are shown by appropriate movements of the stress axis in the unit stereographic triangle, since the slip direction and slip plane normal are fixed.

For simplicity, the movement of T_e is restricted to a contour gradient, that is, T_e is allowed to move only along the most direct route from one resolved shear-stress contour line to the next lower line. Whenever

the resolved shear stress exceeds the critical stress necessary for slip to take place, slip may occur or T_e may move to a position of lower resolved shear stress such that the resolved shear stress is no longer greater than the critical shear stress. The movement of T_e and its effect on texture formation is discussed fully by Calnan and Clews.⁷⁻⁹

The Calnan and Clews method has been successful in explaining the deformation textures of the hexagonal metals magnesium and zinc⁹ and also metals in the face-centred cubic,⁷ body-centred cubic,⁸ and orthorhombic¹⁰ systems.

IV.—THE CALCULATION OF RESOLVED SHEAR-STRESS VALUES

The resolved shear stress for any slip system is equal to $T_a \cos x \cos \lambda$, where x is the angle between the stress axis and the slip plane normal, λ is the angle between the stress axis and the slip direction, and T_a is the applied stress.

The resolved shear stress for any twinning system is equal to $T_a \cos \gamma \cos \delta$, where γ is the angle between the stress axis and the twin plane normal, δ is the angle between the stress axis and the twinning shear direction, and T_a is the applied stress.

The resolved shear-stress values for all the slip planes in the slip system being considered were calculated, and the resolved shear-stress contour diagram plotted for the slip plane having the maximum value. A similar calculation was made for each twin plane in the twinning systems considered.

Values of x , λ , γ , and δ were determined by direct measurement over a 7-in. Wulff net graduated in 2° intervals. Measurements were made by estimating to the nearest 0.2° and the results of the cosine function plotted. Shear-stress contour diagrams were obtained by making sufficient measurements to locate the approximate position of each contour line. These diagrams are probably accurate to about 2°. Boundary lines between two slip systems or between slip and twinning systems were located by plotting the positions of T_a and measuring the values of the appropriate angles until the following equations were solved:

$$\text{for slip: } \cos x_1 \cos \lambda_1 / C_s = \cos x_2 \cos \lambda_2 / C_s \quad (1)$$

$$\text{for twinning: } \cos x \cos \lambda / C_s = \cos \gamma \cos \delta / C_t \quad (2)$$

where C_s is the critical shear stress for slip and C_t is the critical shear stress for twinning.

A mathematical analysis⁸ has shown that this boundary may have two possible forms. At least three points were located on each boundary to determine its position and its form.

Values of the ratios between the critical shear stresses had to be assumed. In some cases there was justification for the assumptions made, but in most cases there was a considerable range of possible values.

V.—DEFORMATION BY SLIP

The hexagonal metals subjected to critical study have been found to slip in the $\{0001\}\langle 11\bar{2}0 \rangle$ system.¹ This system will tend to give a tension texture of the type $[11\bar{2}0]$. Examination of the wire texture of titanium¹¹ showed titanium to have a strong $[10\bar{1}0]$ texture. A preliminary report on the plastic flow of titanium¹² showed slip in titanium to occur on both the $\{10\bar{1}0\}$ and $\{10\bar{1}1\}$ planes. These results have not yet led to a determination of the slip direction. Since the slip direction is usually retained in other metals which exhibit slip on several planes, a $\langle 11\bar{2}0 \rangle$ slip direction was assumed. The results showed no evidence of $\{0001\}$ slip, but at the low reduction necessary for location of slip elements by the trace method, this mode of slip may be relatively inactive. As will be shown later, $\{0001\}$ slip was essential in the explanation of the compression and rolling textures. The resolved shear-stress contour diagram for each of these three slip systems was developed, and the resulting tension and compression textures were examined. Finally, the three slip systems were combined to give a tension and compression texture that agreed as much as possible with the observed textures.

1. $\{0001\}\langle 11\bar{2}0 \rangle$ SLIP

Slip on the base plane is simplified by the existence of only one active slip plane. The resolved shear-

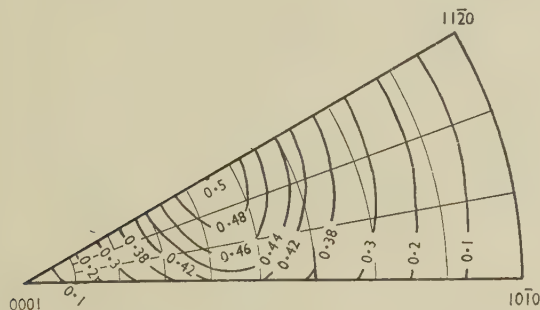


FIG. 1.—Resolved Shear Stress Contours for $\{0001\}\langle 11\bar{2}0 \rangle$ Slip.

stress contour diagram is shown in Fig. 1. At both the $[0001]$ point and the $[10\bar{1}0]$ – $[11\bar{2}0]$ edge the resolved shear stress is zero and no slip can occur. Within the unit triangle slip occurs on the $\{0001\}\langle 11\bar{2}0 \rangle$ system. Double slip occurs along the $[0001]$ – $[10\bar{1}0]$ edge on the $\{0001\}\langle 11\bar{2}0 \rangle$ and $\{0001\}\langle 2\bar{1}\bar{1}0 \rangle$ systems.

Single-slip rotations in tension are toward $[11\bar{2}0]$. Double-slip rotations in tension are toward $[10\bar{1}0]$. The tension texture will therefore consist of a moderate $[11\bar{2}0]$ component with a spread of orientations along the $[10\bar{1}0]$ – $[11\bar{2}0]$ edge.

In compression both single and double slip rotations lead to a $[0001]$ position, resulting in a strong $[0001]$ compression texture.

Slip on the $\{0001\}\langle 11\bar{2}0 \rangle$ system has been examined by Calnan and Clews, and a complete

discussion of the rotation tendencies may be found in their treatment.⁹

2. $\{10\bar{1}1\}\langle 11\bar{2}0 \rangle$ SLIP

The $\{10\bar{1}1\}\langle 11\bar{2}0 \rangle$ system contains six slip planes, each of which has two possible slip directions. The

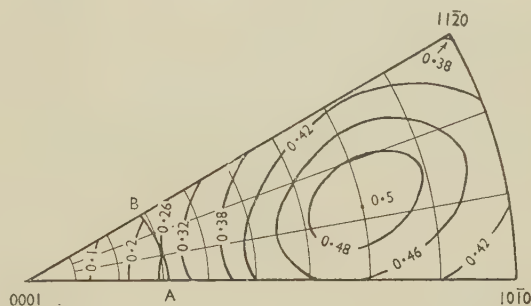


FIG. 2.—Resolved Shear Stress Contours for $\{10\bar{1}1\}\langle 11\bar{2}0 \rangle$ Slip.

resolved shear-stress diagram for this system is shown in Fig. 2. This diagram is more complicated than that for $\{0001\}$ slip, since two different slip systems are active within the unit stereographic triangle. In addition, points B , $[11\bar{2}0]$, and $[10\bar{1}0]$ each support multiple slip on four slip systems. In

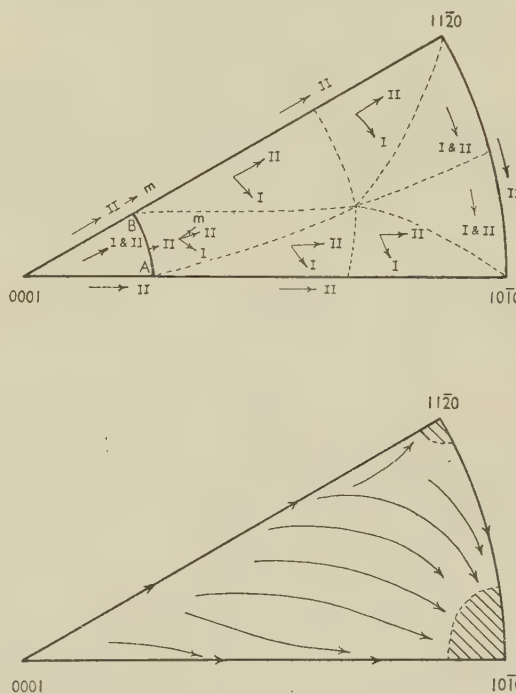


FIG. 3.—Tension Slip Rotations and Tension Texture Resulting from $\{10\bar{1}1\}\langle 11\bar{2}0 \rangle$ Slip.

the region A – B – $[11\bar{2}0]$ – $[10\bar{1}0]$ slip occurs on the $\{01\bar{1}1\}\langle 2\bar{1}\bar{1}0 \rangle$ slip system. In the region $[0001]$ – A – B slip occurs on the $\{1\bar{1}01\}\langle 11\bar{2}0 \rangle$ slip system. Double slip occurs along the boundaries $[0001]$ – $[10\bar{1}0]$, $[10\bar{1}0]$ – $[11\bar{2}0]$, $[11\bar{2}0]$ – B , B – $[0001]$, and A – B .

The tension rotations and the resulting tension texture for $\{10\bar{1}1\}$ slip are given in Fig. 3. Owing to the unsymmetrical position of the slip planes at point *B*, multiple slip occurs. Single slip rotations are shown by an arrow marked I, double slip rotations by an arrow marked II, and multiple slip rotations by an arrow marked *m*. Areas within which the rotation tendencies are similar are enclosed by dashed lines. Examination of the tension rotations shows a strong $[10\bar{1}0]$ texture plus a weak $[11\bar{2}0]$ texture. Those orientations along the $[11\bar{2}0]$ - $[0001]$ edge have a strong probability of rotating by double slip to the $[11\bar{2}0]$ point, where they will be stable.

In the compression rotations (Fig. 4) there exist a number of possible end positions. Double slip along the $[11\bar{2}0]$ -*B* edge causes rotation of the stress axis toward the great circle joining the two active slip-plane normals. This will give a strong preferred orientation at approximately 32° from the $[11\bar{2}0]$ point. Since single slip rotates most of the orientations within the *A*-*B*- $[11\bar{2}0]$ - $[10\bar{1}0]$ region to the $[11\bar{2}0]$ -*B* edge, the concentration at 32° should be the

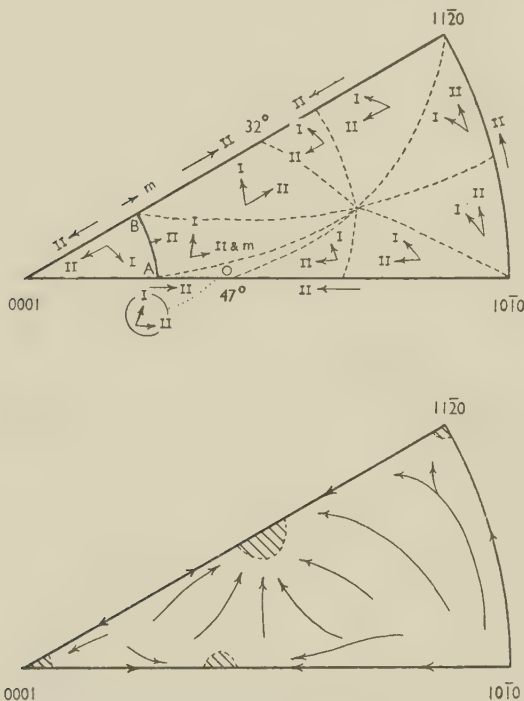


FIG. 4.—Compression Slip Rotations and Compression Texture Resulting from $\{10\bar{1}1\}\langle 11\bar{2}0 \rangle$ Slip.

main texture in the $\{10\bar{1}1\}$ slip system. Subsidiary textures are probable at the points indicated in Fig. 4.

3. $\{10\bar{1}0\}\langle 11\bar{2}0 \rangle$ SLIP

This slip system is symmetrical about the midpoint between the $[10\bar{1}0]$ and $[11\bar{2}0]$ points, as is shown in Fig. 5. Within the unit triangle slip occurs on the $(01\bar{1}0)[2\bar{1}\bar{1}0]$ system. Double slip occurs along the $[0001]$ - $[10\bar{1}0]$ and $[0001]$ - $[11\bar{2}0]$ edges.

The single-slip tension rotations are toward $[2\bar{1}\bar{1}0]$, while double-slip rotations are toward $[11\bar{2}0]$ along the $[0001]$ - $[11\bar{2}0]$ edge and toward $[10\bar{1}0]$ along the $[0001]$ - $[10\bar{1}0]$ edge. This will result in the formation

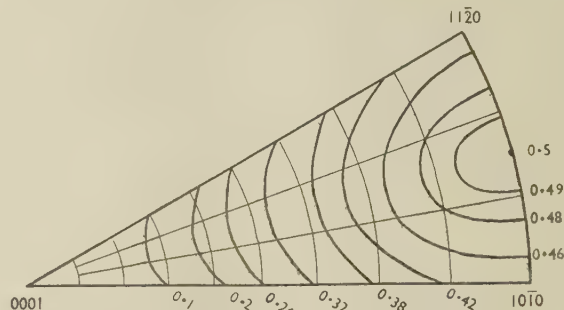


FIG. 5.—Resolved Shear Stress Contours for $\{10\bar{1}0\}\langle 11\bar{2}0 \rangle$ Slip.

of a strong $[10\bar{1}0]$ component plus a weak $[11\bar{2}0]$ component in the tension texture.

The single-slip compression rotations are toward $[01\bar{1}0]$, while the double-slip rotations remain the same as in tension. A strong $[11\bar{2}0]$ component plus a weak $[10\bar{1}0]$ component will occur in the compression texture.

4. COMBINED SLIP SYSTEM

Before the three slip systems are combined it is necessary to consider the experimental data. The tension texture of titanium has been shown to be primarily $[10\bar{1}0]$.¹¹ Thus either $\{10\bar{1}0\}$ or $\{10\bar{1}1\}$ slip must predominate near the $[10\bar{1}0]$ - $[11\bar{2}0]$ edge. The compression texture has been shown⁵ to have a maximum in the 0001 pole figure 30° from the axis of compression. The angle between this maximum and the compression axis decreased with increased reduction. A slight tendency for the compression axis to be on the $[0001]$ - $[11\bar{2}0]$ edge was also noticed. Since $\{10\bar{1}0\}$ slip cannot produce rotation toward $[0001]$ in compression and since $\{10\bar{1}1\}$ slip tends to produce a 0001 maximum 58° from the axis of compression (see Fig. 4), $\{0001\}$ slip must be active at least to a point within 32° of the $[11\bar{2}0]$ point along the $[0001]$ - $[11\bar{2}0]$ edge.

The determination of slip elements of titanium¹² indicated that $\{0001\}$ slip was absent and $\{10\bar{1}0\}$ slip was the primary mechanism of slip. Because of these results the $\{0001\}$ - $\{10\bar{1}1\}$ slip boundary was adjusted so that the critical shear stress for $\{0001\}$ slip was as large with respect to the critical shear stress for $\{10\bar{1}1\}$ slip as possible without allowing $\{10\bar{1}1\}$ slip to form the maximum along the $[0001]$ - $[11\bar{2}0]$ edge 32° from $[11\bar{2}0]$. This was accomplished by placing the boundary between the two systems 30° from $[11\bar{2}0]$. Equation (1) was used for this calculation, and the following ratio of the critical shear stresses was obtained,

$$C_{s0001} = 1.1 C_{s10\bar{1}1} \quad (3)$$

Although the results of the above-mentioned determination of slip elements in titanium indicated that $\{10\bar{1}0\}$ slip predominates at low reductions, the lack of appreciable $[11\bar{2}0]$ compression texture at higher reductions⁵ indicates that it is relatively unimportant or possibly completely absent at high reductions. For the purpose of this development the $\{10\bar{1}0\}$ - $\{10\bar{1}1\}$ slip boundary was calculated on the assumption that it crossed the $[0001]$ - $[11\bar{2}0]$ edge 5° from $[11\bar{2}0]$. This resulted in a ratio of critical shear stresses of:

$$C_{s10\bar{1}0} = 1.078 C_{s10\bar{1}1} \quad (4)$$

The assumption that $\{10\bar{1}0\}$ slip is occurring is unnecessary at high reductions, but it is included so that its effect at lower reductions may be considered.

Combining equations (3) and (4) gives the following relationship between the critical shear stresses for slip on the three slip systems:

$$C_{s0001} = 1.1 C_{s10\bar{1}1} = 1.02 C_{s10\bar{1}0} \quad (5)$$

The tension and compression textures resulting from the assumption that the above ratios of critical shear stress were correct are shown in Figs. 6 and 7. The slip systems active in the combined slip system are given in Table I.

Examination of the tension rotations and the resulting tension texture given in Fig. 6 shows that the

texture plus a weak secondary $[11\bar{2}0]$ texture. Also of interest is the noticeable increase in density along the $[0001]$ - $[11\bar{2}0]$ edge which is the preferred route

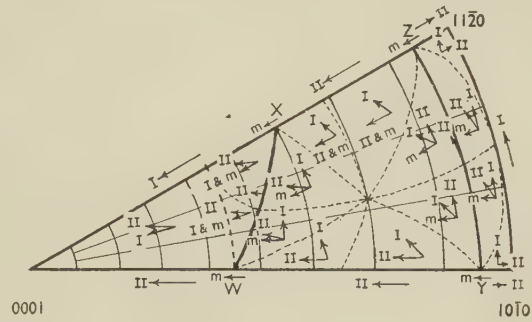
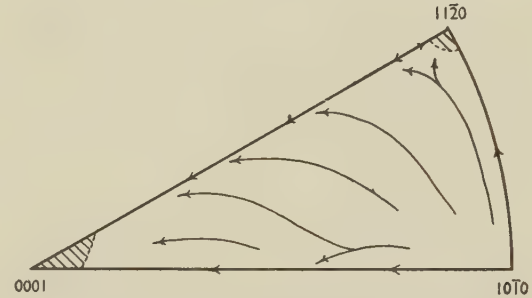


Fig. 6.—Tension Slip Rotations and Tension Texture Resulting from Combined Slip System.



of rotation to the $[0001]$ position. Although the slip system developed here gives the desired rotation tendency for the observed compression texture, the maximum 30° from $[0001]$ is not developed and must be a result of mechanical twinning.

TABLE I.—Active Slip Elements in the Combined Slip Systems.

Position	Active Slip System
$[0001]$	None—Fracture
$[10\bar{1}0]$	$(01\bar{1}0)[2\bar{1}10]$; $(1\bar{1}00)[11\bar{2}0]$
$[11\bar{2}0]$	$(01\bar{1}0)[2\bar{1}10]$; $(10\bar{1}0)[12\bar{1}0]$
W	$(0001)[11\bar{2}0]$; $(0001)[2\bar{1}10]$; $(01\bar{1}1)[2\bar{1}10]$; $(1\bar{1}01)[11\bar{2}0]$
X	$(0001)[11\bar{2}0]$; $(01\bar{1}1)[2\bar{1}10]$; $(10\bar{1}1)[12\bar{1}0]$
Y	$(01\bar{1}1)[2\bar{1}10]$; $(1\bar{1}01)[11\bar{2}0]$; $(01\bar{1}0)[2\bar{1}10]$; $(1\bar{1}00)[11\bar{2}0]$
Z	$(01\bar{1}1)[2\bar{1}10]$; $(10\bar{1}1)[12\bar{1}0]$; $(01\bar{1}0)[2\bar{1}10]$; $(10\bar{1}0)[12\bar{1}0]$
$[0001]$ -W	$(0001)[11\bar{2}0]$; $(0001)[2\bar{1}10]$
$[0001]$ -X	$(0001)[11\bar{2}0]$
W-X	$(0001)[11\bar{2}0]$; $(01\bar{1}1)[2\bar{1}10]$
W-Y	$(01\bar{1}1)[2\bar{1}10]$; $(1\bar{1}01)[11\bar{2}0]$
X-Z	$(01\bar{1}1)[2\bar{1}10]$; $(10\bar{1}1)[12\bar{1}0]$
Y-Z	$(01\bar{1}1)[2\bar{1}10]$; $(01\bar{1}0)[2\bar{1}10]$
$[10\bar{1}0]$ -Y	$(01\bar{1}0)[2\bar{1}10]$; $(1\bar{1}00)[11\bar{2}0]$
$[11\bar{2}0]$ -Z	$(01\bar{1}0)[2\bar{1}10]$; $(10\bar{1}0)[12\bar{1}0]$
$[10\bar{1}0]$ - $[11\bar{2}0]$	$(01\bar{1}0)[2\bar{1}10]$
$[0001]$ -W-X	$(0001)[11\bar{2}0]$
W-X-Z-Y	$(01\bar{1}1)[2\bar{1}10]$
Y-Z- $[11\bar{2}0]$ - $[10\bar{1}0]$	$(01\bar{1}0)[2\bar{1}10]$

texture will be predominantly $[10\bar{1}0]$. A weak $[11\bar{2}0]$ texture is also evident.

The compression rotations and the compression texture as given in Fig. 7 show a predominant $[0001]$

VI.—DEFORMATION BY TWINNING

Hexagonal close-packed metals twin most easily on the $\{10\bar{1}2\}$ planes. It has been shown¹³ that metals with a c/a ratio of less than 1.732 will not

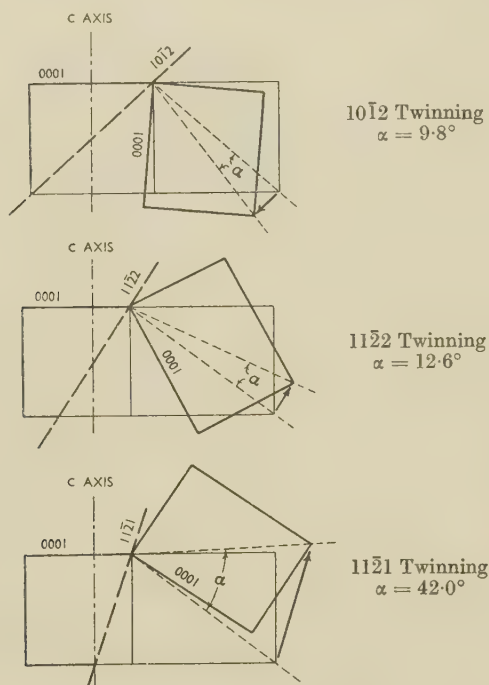


FIG. 8.—Twinning Shear Direction of Twinning on $\{10\bar{1}2\}$, $\{11\bar{2}2\}$, and $\{11\bar{2}1\}$ Planes of Titanium.

twin by $\{10\bar{1}2\}$ twinning when the axis of compression is along the c -axis of the unit cell. Thus the minimum near $[0001]$ apparent from the 0001 pole figure for compressed and for cold-rolled titanium cannot be the result of twinning on the $\{10\bar{1}2\}$ planes.

To explain the minimum evident in the compression texture, a new type of twinning must be assumed which can occur in compression from the $[0001]$ position. Several types of twinning can be visualized which will take place from this position. The $\{10\bar{1}1\}$ twinning reported in magnesium¹⁴ would be an example. Similarly, both the $\{11\bar{2}1\}$ and $\{11\bar{2}2\}$ twinning reported in titanium¹² have the ability to occur from a $[0001]$ position in compression.

A comparison of the twinning shear angles, the angle between the diagonals of the twinned and untwinned unit cell, of $\{10\bar{1}2\}$, $\{11\bar{2}1\}$, and $\{11\bar{2}2\}$ twinning is given in Fig. 8. It seems likely from inspection of this figure that $\{11\bar{2}2\}$ twinning should occur much more readily than $\{11\bar{2}1\}$ twinning. Attempts to develop a satisfactory picture of the atom movements in $\{11\bar{2}1\}$ and $\{11\bar{2}2\}$ twinning such as has been done for $\{10\bar{1}2\}$ twinning¹³ were unsuccessful.

For the purpose of this development of the twinning effects, the following assumptions were made:

(1) $\{10\bar{1}2\}$ and $\{11\bar{2}2\}$ twinning are of about equal frequency and $\{11\bar{2}1\}$ twinning is relatively rare.

(2) The twinning shear stress for $\{11\bar{2}2\}$ twinning is in the direction shown in Fig. 8, and the c -axis, twin plane normal, and twinning shear direction are in the same plane.

(3) The critical shear stresses for $\{10\bar{1}2\}$ twinning and $\{11\bar{2}2\}$ twinning are equal to the critical shear stress for $\{0001\}$ slip.

The method of twinning analysis shown to give satisfactory results for magnesium and zinc⁹ was used.

1. $\{10\bar{1}2\}$ TWINNING

For the purpose of calculation the assumption was made that the critical shear stress for twinning on the $\{10\bar{1}2\}$ planes was equal to the critical shear stress for slip on the $\{0001\}$ planes. Thus, from equation (5):

$$C_{t10\bar{1}2} = C_{s0001} = 1.1 C_{s10\bar{1}1} = 1.02 C_{s10\bar{1}0} \quad (6)$$

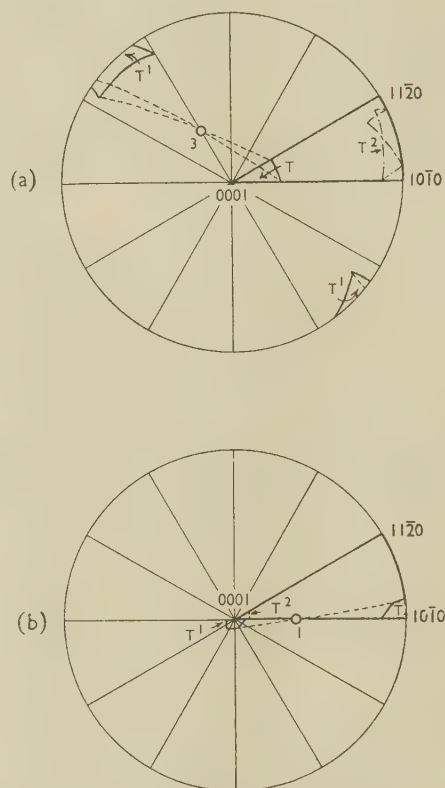


FIG. 9.—Reorientation Resulting from $\{10\bar{1}2\}$ Twinning from the Combined Slip System.

- (a) $\{10\bar{1}2\}$ twinning in tension.
(b) $\{10\bar{1}2\}$ twinning in compression.

The boundary between the slip and twinning areas was determined by use of the formulæ:

$$\cos \gamma \cos \delta = n \cos x \cos \lambda \quad \text{in tension} \quad (7)$$

$$\cos \gamma \cos \delta = -n \cos x \cos \lambda \quad \text{in compression} \quad (8)$$

where $n = C_t/C_s$.

The boundaries for twinning in both tension and compression based on the combined slip system shown in Figs. 6 and 7 were calculated for all six of the possible $\{10\bar{1}2\}$ twinning systems. The most favourable system was assumed to be that which included the greatest area of the unit stereographic triangle.

Each point in the twinning area will move to the same angle beyond the twin plane normal as its initial angle from the twin plane normal. The twinning area, T , the active twin plane normal, marked by number, the new twinned orientation, T^1 , and the new twinned orientation placed in the unit stereographic triangle, T^2 , are shown in Fig. 9.

It is seen that $\{10\bar{1}2\}$ twinning assists slip rotations by twinning toward the $[0001]$ in compression and toward the $[10\bar{1}0]$ – $[11\bar{2}0]$ edge in tension.

2. $\{11\bar{2}2\}$ TWINNING

The boundary conditions for $\{11\bar{2}2\}$ twinning were determined in the same manner as those for $\{10\bar{1}2\}$ twinning. In this case, however, the signs of the two equations, (7) and (8), were reversed because of

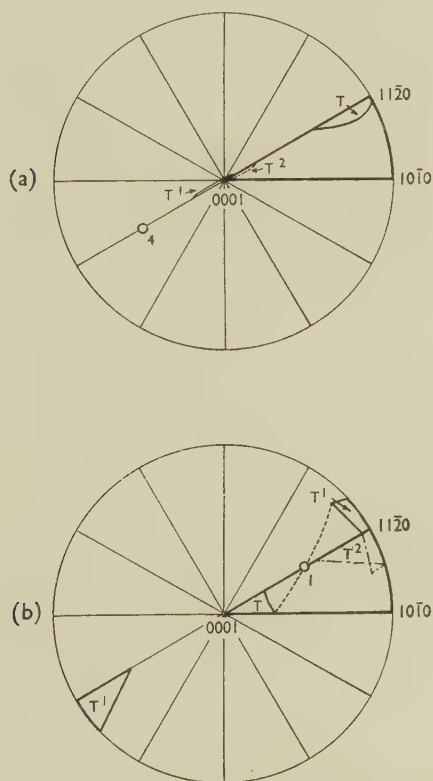


FIG. 10.—Reorientation Resulting from $\{11\bar{2}2\}$ Twinning from the Combined Slip System.

- (a) $\{11\bar{2}2\}$ twinning in tension.
(b) $\{11\bar{2}2\}$ twinning in compression.

the change in the twinning shear direction (see Fig. 8). The shear stress ratios were assumed to be

$$C_{11\bar{2}2} = C_{0001} = 1.1 C_{10\bar{1}1} = 1.02 C_{10\bar{1}0} \quad (9)$$

The most favourable twinning system was determined in the same manner as in the case of $\{10\bar{1}2\}$ twinning. The results of the twinning re-orientations

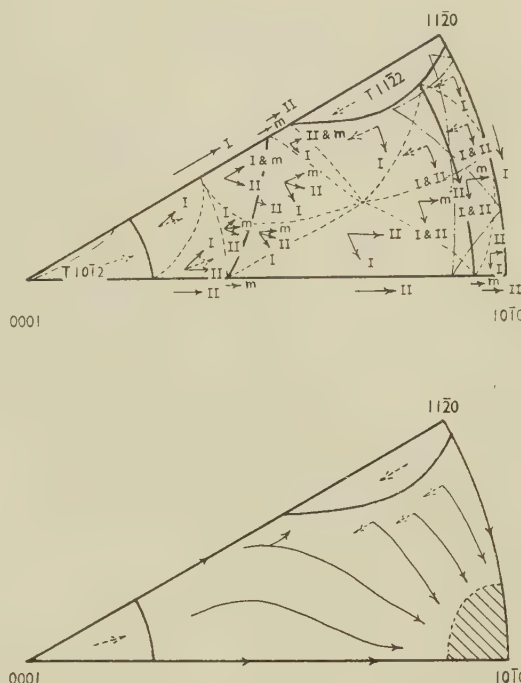


FIG. 11.—Tension Texture Resulting from Combined Slip on the $\{0001\}\langle 11\bar{2}0\rangle$, $\{10\bar{1}1\}\langle 11\bar{2}0\rangle$, and $\{10\bar{1}0\}\langle 11\bar{2}0\rangle$ Slip Planes and Twinning from the $\{10\bar{1}2\}$ and $\{11\bar{2}2\}$ Planes.

are given in Fig. 10. $\{11\bar{2}2\}$ twinning opposes slip rotation in compression, but in tension its only effect is to remove those poles in the subsidiary $[11\bar{2}0]$ texture.

Since, from the geometry of twinning shown in Fig. 8, $\{11\bar{2}1\}$ twinning appeared much less likely to occur than $\{11\bar{2}2\}$ twinning, no calculations were made for this twinning system. The general effects of $\{11\bar{2}1\}$ twinning would be the same as for $\{11\bar{2}2\}$ twinning.

VII.—THE TENSION TEXTURE OF TITANIUM

The results plotted in Figs. 6, 9, and 10 for tension are combined in Fig. 11. In this figure it is seen that $\{10\bar{1}2\}$ twinning aids in developing the $[10\bar{1}0]$ texture, while $\{11\bar{2}2\}$ twinning prevents the formation of the subsidiary $[11\bar{2}0]$ texture. The net result of slip on three systems and twinning on two is a strong $[10\bar{1}0]$ tension texture. This texture should be developed early. As the critical shear stress on the $\{10\bar{1}0\}$ slip planes increases, the boundary between $\{10\bar{1}1\}$ and $\{10\bar{1}0\}$ slip moves toward the $[10\bar{1}0]$ – $[11\bar{2}0]$ edge. When the critical shear stress has increased until the two systems are equally favoured at $[10\bar{1}0]$, when $C_{10\bar{1}1} = 0.878 C_{10\bar{1}0}$, there are six active and stable slip systems at $[10\bar{1}0]$. The $[10\bar{1}0]$ tension texture

would therefore be expected to remain unchanged until the material failed.

VIII.—THE COMPRESSION TEXTURE OF TITANIUM

The data from Figs. 7, 9, and 10 are combined in Fig. 12. In this case $\{11\bar{2}2\}$ twinning is active in preventing the slip rotation from reaching the stable

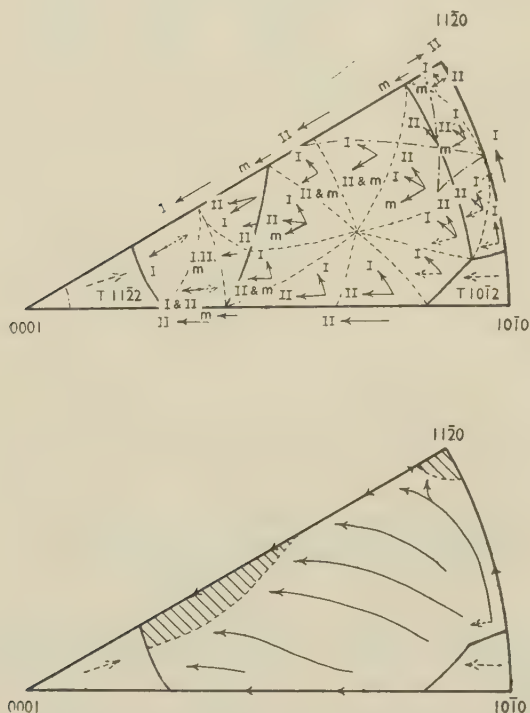


FIG. 12.—Compression Texture Resulting from Combined Slip on the $\{0001\}\langle 11\bar{2}0\rangle$, $\{10\bar{1}1\}\langle 11\bar{2}0\rangle$, and $\{10\bar{1}0\}\langle 11\bar{2}0\rangle$ Slip Planes and Twinning from the $\{10\bar{1}2\}$ and $\{11\bar{2}2\}$ Planes.

end position. $\{10\bar{1}2\}$ twinning is of little importance in compression. As the slip rotations lead to the twinning region, the grains are twinned to a position near the $[11\bar{2}0]$ point. Thus, as deformation increases, the slip rotations tend to be concentrated more completely along the $[11\bar{2}0]$ – $[0001]$ edge of the unit triangle. This accounts for the preferred orientation noticed in the $10\bar{1}0$ and $10\bar{1}1$ pole figures of compressed titanium.⁵

As the slip rotations lead toward the $[0001]$ position and the twinning re-orientation leads away from this position, a spread of orientations from the slip-twinning boundary to the $[11\bar{2}0]$ position will occur. An equilibrium texture will arise near the slip-twinning boundary. The decrease of the angle between the compression axis and the $[0001]$ position with increased reduction may be attributed to a relative change in the ratio of the critical shear stress for $\{0001\}$ slip and $\{11\bar{2}2\}$ twinning such that the boundary between slip and twinning moves toward $[0001]$.

The absence of any appreciable $[11\bar{2}0]$ compression texture indicates that $\{10\bar{1}0\}$ slip is probably completely absent at high reductions. The ability of the $\{10\bar{1}1\}$ slip system to trap the stress axis in the minimum occurring in the resolved shear-stress diagram at $[11\bar{2}0]$ (see Fig. 4) would be sufficient to account for the slight $[11\bar{2}0]$ texture apparent at high reductions.

IX.—THE COLD-ROLLED TEXTURE OF TITANIUM

Cold rolling can be considered as tension in the rolling direction and compression on the rolling plane.¹⁵ The observed cold-rolling texture of titanium, $(0001)[10\bar{1}0]$ rotated 30° in the transverse direction, can therefore be visualized as a combination of the $[10\bar{1}0]$ tension texture and the rotated $[0001]$ compression texture. Since the $[0001]$ rotation occurs preferentially about a $\langle 10\bar{1}0\rangle$ axis, both the tension and the compression textures may be satisfied simultaneously in cold rolling.

In Fig. 13 the compression and tension rotations and the twinning re-orientation are shown in a 0001 pole figure. If random initial orientation is assumed, the following tendencies are apparent. Since tension rotation tends to move a $\langle 10\bar{1}0\rangle$ direction into the rolling direction, the 0001 poles should move to the transverse axis along the line of most rapid descent, a great circle passing through the rolling direction and the 0001 pole being considered. Compression rotations tend to move the 0001 poles toward the rolling plane normal. The tension and compression rotations are marked T and C in Fig. 13. The

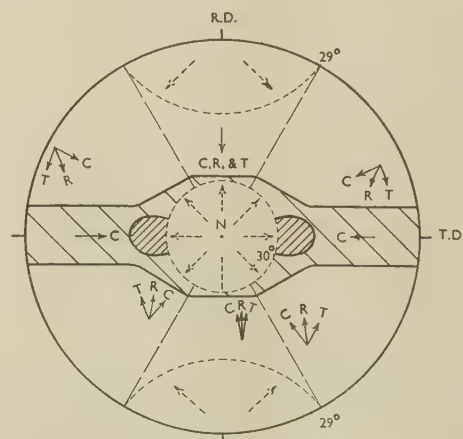


FIG. 13.—Form of the (0001) Pole Figure of Titanium Resulting from Tension in the Rolling Direction and Compression Along the Rolling Plane Normal.

resultant 0001 pole rotation is shown by an arrow marked R . Tension twinning on the $\{10\bar{1}2\}$ planes (Fig. 9) will tend to remove all 0001 poles within approximately 29° of the rolling direction to a

position near the transverse direction. Compression twinning on the $\{11\bar{2}2\}$ planes will twin the 0001 poles from a region within 30° of the rolling plane normal to a region near the circumference of the pole figure (Fig. 10). Twinning re-orientations are indicated by dashed arrows in Fig. 13. Those poles falling within the $\{10\bar{1}2\}$ tension twinning area near the rolling direction will be twinned to the transverse direction, depleting the area enclosed by the long dashes. As the resultant slip rotations tend to move the 0001 poles toward the transverse axis, and from there toward the rolling plane normal, an equilibrium state will gradually be established in which the 0001 poles rotate by compression toward the rolling plane normal and by twinning are removed to the transverse direction to rotate again toward the rolling plane normal. The resulting 0001 pole figure will have a shape similar to that indicated by shading in Fig. 13.

X.—DISCUSSION

By application of the Calnan and Clews method it has been possible to develop a theoretical deformation process based on the experimentally determined deformation textures of titanium. It should be emphasized that the agreement of the theoretically developed textures with those actually observed is the result of the choice of assumptions and does not indicate that the assumptions are correct. The validity of the assumptions made cannot be determined until more complete information is available on the actual modes of slip and twinning in titanium.

The method developed by Calnan and Clews is seen to be quite versatile, allowing not only the prediction of the deformation textures when the modes of deformation are known but also the prediction of the modes of deformation when the deformation textures are known. The ability of their method to give an indication of the ratio of critical shear stresses among various systems may also prove of value as more accurate deformation textures are determined.

The change in the critical shear-stress ratio between two types of slip or between slip and twinning allows changes in the deformation texture with increased reduction to be considered. The assumption that the actual boundary may be located exactly by the methods of texture analysis requires the consideration of an additional factor. In the analysis of the compression texture, for example, the slip-twinning boundary is placed 30° from the $[0001]$ point to agree with experimental results. The ability of T_c to move away from T_a is not considered. If it is assumed that the actual boundary is 10° from $[0001]$ in Fig. 12, the decrease in intensity from 30° to 10° in the measured compression texture can be attributed to the variation in movement of T_c from T_a . That is, if T_c is assumed to have a probability of further movement rather than slip decreasing with increased distance from T_a and equal to zero when T_c has moved 20° from T_a , both the maximum at 30° and

the variation between 30° and 10° would be explained. It should be remembered that movement of T_c does not imply movement of T_a . A crystallite oriented so that T_a was at 30° could conceivably twin from this position even though the slip-twinning boundary was at 10° if T_c was allowed sufficient freedom of movement. This will introduce the effect of freedom of movement of T_c to the already discussed change of ratio of the critical shear stresses which should be considered in placing boundaries. Since there is at present no provision for considering the maximum movement of T_c or the effect of increased deformation on the maximum movement in the method of analysis developed by Calnan and Clews, this factor has been neglected. As more critical studies of the deformation textures of metals are conducted, the movement of T_c may be found to give an explanation of the differences in the deformation textures among metals of the same crystal structure.⁷

The existence of an equilibrium type of cold-rolled texture may account for the large amount of deformation by cold rolling which titanium can absorb without failure. The slip planes which support the major portion of the slip are continually changing during the deformation process, so that there is no rapid work-hardening on any one set of slip planes. The absence of any point of zero resolved shear stress is also of interest.

This analysis of the deformation textures of titanium would also be expected to explain satisfactorily the deformation textures of zirconium and beryllium with slight modifications of the critical shear-stress ratios.

XI.—CONCLUSIONS

By suitable choice of slip and twinning elements and their relative critical shear stresses, it was possible to develop a satisfactory explanation of the tension, compression, and cold-rolling textures of titanium, using the theoretical method of texture analysis developed by Calnan and Clews. Slip was assumed to occur on the $\{0001\}\langle 11\bar{2}0 \rangle$, $\{10\bar{1}0\}\langle 11\bar{2}0 \rangle$, and $\{10\bar{1}1\}\langle 11\bar{2}0 \rangle$ slip systems, with $\{10\bar{1}1\}\langle 11\bar{2}0 \rangle$ slip being most prominent. $\{11\bar{2}2\}$ twinning was shown to be a possible cause of the minimum near the centre of the 0001 pole figure in the cold-rolled texture of titanium. An equilibrium-type texture existing between the stable end-points for slip and twinning was found to be probable in compression. A stable $[10\bar{1}0]$ texture was developed in tension. The rolling texture consisted of a combination of the tension and compression textures such that tension in the rolling direction kept one set of opposing $\langle 10\bar{1}0 \rangle$ poles in position in the rolling direction while the remaining poles were free to rotate in the transverse direction about this axis, according to the compression tendency for the 0001 pole to move continually between positions 30° and 90° from the rolling plane normal. The experimentally determined compression and cold-rolling textures made it possible

for the ratio of the critical shear stresses for slip (C_s) and for twinning (C_t) to be calculated. The critical shear stresses were found to be related according to the following approximate equation,

$$C_{s0001} = 1.1 C_{s10\bar{1}1} = 1.02 C_{s10\bar{1}0} = C_{t10\bar{1}2} = C_{t11\bar{2}2}$$

ACKNOWLEDGEMENT

The authors wish to take this opportunity to thank the Titanium Alloy Manufacturing Division of the National Lead Company for support of the fellowship under which this work was conducted.

REFERENCES

1. C. S. Barrett, "Structure of Metals", p. 289. New York: 1943 (McGraw-Hill).
2. H. T. Clark, Jr., *Trans. Amer. Inst. Min. Met. Eng.*, 1950, **188**, 1154.
3. R. K. McGeary and B. Lustman, *ibid.*, 1951, **191**, 994.
4. A. Smigelskas and C. S. Barrett, *ibid.*, 1949, **185**, 145.
5. D. N. Williams and D. S. Eppelsheimer, *ibid.*, 1952, **194**, 615.
6. D. N. Williams and D. S. Eppelsheimer, to be published.
7. E. A. Calnan and C. J. B. Clews, *Phil. Mag.*, 1950, [vii], **41**, 1085.
8. E. A. Calnan and C. J. B. Clews, *ibid.*, 1951, [vii], **42**, 616.
9. E. A. Calnan and C. J. B. Clews, *ibid.*, 919.
10. E. A. Calnan and C. J. B. Clews, *ibid.*, 1952, [vii], **43**, 93.
11. M. K. Yen, *Interim Rep. to Watertown Arsenal*, 1950, (WHL 401/14-4).
12. F. D. Rosi, C. A. Dube, and B. H. Alexander, *J. Metals*, 1952, **4**, 145.
13. C. S. Barrett, *The Cold Working of Metals* (Amer. Soc. Metals), 1949, 84.
14. E. Schiebold and G. Siebel, *Z. Physik*, 1931, **69**, 458.
15. F. Wever, *Trans. Amer. Inst. Min. Met. Eng., Inst. Metals Div.*, 1931, 51.

THE INFLUENCE OF COMPOSITION ON THE INCIDENCE OF STRAIN MARKINGS IN ALUMINIUM ALLOYS *

1477

By W. H. L. HOOPER,† B.Sc., A.I.M., MEMBER

SYNOPSIS

Using the surface-measuring technique previously described (*J. Inst. Metals*, 1951-52, **80**, 17), the form and intensity of stretcher-strain markings in relation to composition and thermal treatment have been investigated. It has been established that, in aluminium-magnesium alloys of commercial and high purity, magnesium itself, rather than impurities or grain-refining additions, is responsible for stretcher-strain effects, which are absent with less than about 1% magnesium, and severe only with more than about 2% of this element. Low-intensity markings are developed in aluminium-copper-magnesium alloys after quenching to retain the alloying constituents in solid solution. It is concluded that, as in mild steel, strain markings are associated with atomic re-arrangement in an unstable, supersaturated solid solution.

I.—INTRODUCTION

OF the aluminium alloys used commercially in sheet-metal work, those containing magnesium as the principal alloying addition appear to be particularly prone to stretcher-strain effects. Strain markings in these materials have been studied and described in some detail,^{1,2} since they are of significantly greater magnitude than similar effects observed in some other aluminium alloys.^{3,4}

A method of approach to the investigation of yield-point phenomena to which considerable attention has been paid is the study of stress/strain curves, the occurrence of discontinuities on which is frequently associated with the incidence of stretcher-strain markings on the specimen under test. For example, MacReynolds⁵ has shown that the presence either of small quantities of impurities or of deliberate additions of copper in 99.996% aluminium causes steps to appear in the originally smooth stress/strain curve, indicating a change in the manner of deformation from a process of uniform extension to one involving a series of sudden yields in rapid succession.

The most detailed studies of strain markings in relation to composition have been made on mild steel,⁶⁻⁸ and it has been established that the sharp yield point which accompanies the formation of strain bands is not an inherent property of pure iron, but depends on the presence of small traces of carbon and is intensified by the presence of nitrogen. Thus Snoek⁶ found that pure iron with less than 0.0001% carbon showed no such sharp yield point, but that the addition of 0.003% carbon was sufficient to produce a clear discontinuity in the stress/strain curve. Mild steel, in which these discontinuous straining effects are evident, also exhibits strain-

ageing effects, i.e. light straining at room temperature is followed by age-hardening, but no such effect is apparent in pure iron. Edwards, Phillips, and Jones⁹ have found that elements such as titanium, which have a strong affinity for carbon, and form carbides in steel, reduce this strain-ageing effect. There is thus strong evidence for the presumption that strain-band formation in steel is associated with the presence of a supersaturated phase.

Existing data referring to aluminium alloys point to the analogy between the behaviour in strain of mild steel and that of industrial aluminium-magnesium alloys in which the magnesium content exceeds the equilibrium α solid-solution limit at room temperature—the magnesium-rich β phase in these alloys can, in fact, be precipitated at temperatures as low as 50° C. However, the possible influence of other elements generally present, such as iron, silicon, and manganese, must be recognized.

II.—SCOPE OF INVESTIGATION

Straining experiments were carried out on alloys in the form of sheet in the soft recrystallized condition resulting from appropriate annealing or heat-treatment. Since it had been established in the earlier published investigation,² and amply confirmed in subsequent experiments, that stretcher-strain effects were developed only in sheet with a mean grain-size of less than 0.05 mm., each material was subjected to appropriate processing to obtain the required fine grain. It was necessary to make grain-refining additions to high-purity alloys, which could not otherwise be prepared with a suitably fine-grain structure, and since it was found that small proportions of chromium, manganese, and titanium had

* Manuscript received 11 February 1953.

† Research Technical Officer, Imperial Chemical Industries, Ltd., Metals Division, Birmingham.

no significant effect on the stretching characteristics of pure aluminium, these elements were used for the purpose.

Because of the apparent significance of magnesium in relation to strain markings, both high-purity and commercial-grade alloys were prepared over a range of magnesium contents from 0 to 6%, the object being to separate the effect of impurities normally present in industrial alloys, and to determine the relationship between intensity of marking and magnesium content. Additional information was obtained from other representative alloys in the standard industrial range covered by British Standard No. 1470.

III.—PREPARATION OF MATERIAL

In the case of the aluminium-magnesium alloys with less than 1% magnesium made from either pure

TABLE I.—*Composition of Non-Heat-Treatable Alloys.*

Alloy Number	Cu, %	Mn, %	Mg, %	Si, %	Fe, %	Ti, %	Cr, %	Zn, %
<i>Experimental Alloys</i>								
1	<0.01	0.24	0.12	0.02	0.04	0.11	...	<0.005
2	0.014	0.23	0.27	0.01	0.04	0.12	...	<0.005
3	<0.01	0.23	0.56	0.02	0.04	0.11	...	<0.005
4	0.01	0.30	0.58	0.16	0.20	0.10	...	<0.005
5	<0.01	0.29	0.87	0.03	0.03	0.14	...	<0.005
6	0.01	0.30	0.9	0.10	0.18	0.10	...	<0.005
7	<0.01	0.22	1.11	0.01	0.04	0.002	...	<0.005
8	<0.01	0.27	2.33	0.01	0.035	0.002	...	<0.005
9	<0.01	0.02	3.11	0.017	0.04	0.12	...	<0.005
10	0.02	...	2.59	0.11	0.27	0.01	0.44	<0.005
<i>Industrial Alloys (B.S. 1470)</i>								
NS3	0.02	1.21	0.01	0.16	0.32	0.07	...	<0.005
NS5	0.08	0.22	3.87	0.18	0.27	0.02	...	<0.005
NS6	0.12	0.21	5.13	0.09	0.21	0.02	...	0.01
NS7	0.01	0.14	6.03	0.12	0.28	0.02	...	<0.005
S1B	0.02	<0.01	<0.01	0.03	0.05	<0.01	<0.01	<0.005
S1C	0.02	<0.01	0.01	0.15	0.3	0.06	...	<0.005

or commercial aluminium, it was not possible by any combination of rolling and annealing to obtain a suitably fine grain-size. The necessary grain-refining

was effected by additions of manganese and titanium, or of chromium, since experiments with high-purity binary alloys had indicated that these elements were not in any way responsible for strain markings. The compositions of the alloys are recorded in Table I.

Alloys 1-10, containing up to about 3% magnesium, were prepared under laboratory conditions, from the purest available virgin-metal constituents, in cast slabs of 20 lb. weight. All the remaining alloys, including the higher members of the aluminium-magnesium series, were taken from hot-rolled commercial stock. Heavy cold-rolling reductions, of the order of at least 70-75%, were applied before the final anneal, in order to obtain the necessary fine grain.

The annealing of aluminium-magnesium alloys with up to 1.1% magnesium was carried out at 300° C., grain growth being rapid at higher annealing temperatures. Alloys of greater magnesium content were subjected to a standard annealing treatment of 2 hr. at 400°-430° C. The aluminium-manganese alloy (NS3) was flash-annealed in a salt bath at 500° C.

The three heat-treatable alloys (see Table IV) were obtained in a fully softened condition by annealing at the appropriate temperature and slowly cooling in the furnace. Other specimens of these alloys were prepared in different conditions involving solution-treatment and ageing, as detailed in the table.

The method of preparation of the 8 × 2-in. specimens for stretching has been described previously.² In brief, surface treatments involving electropolishing or a chemical bright dip were supplemented where necessary by hand-polishing. Grain-sizes were estimated on etched portions of each specimen by comparison with standard photomicrographs, and values are recorded in Tables II, III, and IV.

IV.—STRETCHING EXPERIMENTS

Strains in the critical range 0-1% with which random-type stretcher-strain markings are associated, were measured with a Lamb roller extensometer of

TABLE II.—*Stretching Characteristics of Experimental Non-Heat-Treatable Alloys.*

Alloy Number	Principal Alloying Additions			Annealing Treatment	Grain-Size, mm.	Appearance of Specimens during Stretching			
						Extension 0-2%	Maximum Talysurf Deviation, 10 ⁻³ in.	At 5% Extension	Maximum Talysurf Deviation, 10 ⁻³ in.
1	0.12	0.11	0.24	4 hr. at 300° C.	0.040	No markings	<0.1	No markings	<0.1
2	0.27	0.12	0.23		0.040	"	<0.1	"	<0.1
3	0.56	0.11	0.23		0.040	"	<0.1	"	<0.1
4	0.58	0.10	0.30		0.035	"	<0.1	"	<0.1
5	0.87	0.14	0.29		0.035-0.040	Slight random markings	0.5	Slight parallel bands	0.15
6	0.90	0.10	0.30		0.030	Very slight random markings	0.2	"	0.12
7	1.11	...	0.22		0.026	Severe random markings	1.5	Parallel bands	0.20
8	2.33	...	0.27	2 hr. at 400° C.	0.01-0.03	"	1.8	"	0.14
9	3.11	0.12	...		0.015	"	2.0	"	0.18
10	2.59	...	Cr, % 0.44		0.01	"	1.8	"	0.18

TABLE III.—*Stretching Characteristics of Industrial Non-Heat-Treatable Alloys.*

Code Number (B.S. 1470)	Principal Alloying Additions			Annealing Treatment	Grain-Size, mm.	Appearance of Specimens during Stretching			
	Mg, %	Ti, %	Mn, %			Extension 0-2%	Maximum Talysurf Deviation, 10 ⁻³ in.	At 5% Extension	Maximum Talysurf Deviation, 10 ⁻³ in.
NS3	...	0.07	1.21	½ hr. at 500° C. in salt bath	0.030	No markings	<0.1	No markings	0.1
NS5	3.87	0.02	0.22	2 hr. at 400° C.	0.015	Severe random markings	2.2	Parallel bands	0.18
NS6	5.13	0.02	0.21	2 hr. at 430° C.	0.025	" " "	1.7	" "	0.20
NS7	6.03	0.02	0.14	" "	0.02	" " "	1.9	" "	0.17
S1B	99.5% Al			4 hr. at 300° C.	0.035-0.040	No markings	<0.1	No markings	0.1
S1C	99.0% Al				0.035	"	<0.1	"	0.1

TABLE IV.—*Stretching Characteristics of Heat-Treatable Alloys.*

Code Number (B.S. 1470)	Heat-Treatment	Grain-Size, mm.	Appearance of Specimens during Stretching			
			Extension 0-2%	Maximum Talysurf Deviation, 10 ⁻³ in.	At 5% Extension	Maximum Talysurf Deviation, 10 ⁻³ in.
HS10 (Cu 0.03, Mn 0.66, Mg 0.75, Si 0.96, Fe 0.28, Ti 0.01%)	2 hr. at 375° C.; furnace-cooled	0.035	No markings	0.1	No markings	0.1
	½ hr. at 540° C.; quenched	0.02	Slight parallel bands at 2% extension	0.1	Slight parallel bands	0.13
	½ hr. at 450° C.; quenched	0.02	" " "	0.1	" " "	0.11
HS14 (Cu 4.07, Mn 0.56, Mg 0.76, Si 0.46, Fe 0.44, Ti 0.02%)	½ hr. at 540° C.; quenched; aged 18 hr. at 160° C.	0.02	No markings	<0.1	Fractured at less than 5% extension	...
	2 hr. at 375° C.; furnace-cooled	0.01	No markings	<0.1	Parallel bands	0.2
	½ hr. at 495° C.; quenched at 20° C.	0.02	Random markings	0.5	" "	0.22
	½ hr. at 495° C.; quenched at 100° C.	0.02	" "	0.5	" "	0.21
	½ hr. at 450° C.; quenched at 20° C.	0.02	" "	0.5	" "	0.22
	½ hr. at 450° C.; quenched at 100° C.	0.02	" "	0.6	" "	0.20
	½ hr. at 450° C.; quenched in oil at 20° C.	0.02	" "	0.7	" "	0.21
	½ hr. at 400° C.; quenched at 100° C.	0.015	" "	0.5	" "	0.18
	½ hr. at 400° C.; quenched in oil at 20° C.	0.015	" "	0.6	" "	0.18
	½ hr. at 495° C.; quenched; aged 8 hr. at 165° C.	0.02	No markings	<0.1	Fractured at less than 5% extension	...
	½ hr. at 495° C.; quenched; aged 7 days at room temperature	0.02	Slight random markings	0.4	No markings	0.1
D.T.D. 363A (Cu 1.31, Mn 0.49, Mg 2.86, Si 0.14, Fe 0.34, Ti 0.11, Cr 0.34, Zn 5.90%)	2 hr. at 375° C.; furnace-cooled	0.025	No markings	<0.1	No markings	0.1
	½ hr. at 460° C.; quenched at 20° C.	0.02	"	<0.1	Slight parallel bands	0.12
	½ hr. at 460° C.; quenched; aged 18 hr. at 125° C.	0.02	"	<0.1	Fractured at less than 5% extension	...

the mirror-and-scale type, the stretching operation being interrupted at appropriate extensions for Talysurf traces to be made of the rolled surface. The larger extensions associated with parallel bands were measured with dividers. Relevant data on the stretching characteristics of high-purity and commercial aluminium-magnesium alloys, and the standard B.S. alloys are summarized in Tables II-IV.

1. NON-HEAT-TREATABLE ALLOYS (TABLES II AND III)

(a) Aluminium-Magnesium

No markings were detected on alloys 1 to 4, containing 0.1-0.58% magnesium. A specimen of alloy 4 after stretching to 1% elongation is illustrated in Fig. 1 (Plate LXXXIII).

Among alloys based on high-purity aluminium, the lowest magnesium content, 0.87%, at which random markings occurred was in alloy 5, and very faint markings, less than one-third of the depth of similar markings observed previously in the 3% magnesium alloy,² were detected at $\frac{1}{2}$ % elongation (Fig. 2, Plate LXXXIII). Alloy 6, made from commercially pure metal with 0.90% magnesium, was subject to very slight markings at $\frac{1}{2}$ % extension, the deepest being 0.0002 in. It is probable that in commercially pure material, part of the magnesium is combined with silicon, and the amount in solid solution is thus reduced.

Severe markings, of a depth and distribution comparable to that observed in the commercial 3% magnesium alloy described in the earlier paper,² occurred at $\frac{1}{2}$ % extension in alloy 7 (1.11% magnesium), and a similar intensity was obtained with alloys 8 and 9 (2.33 and 3.11% magnesium, respectively), the former containing manganese and the latter titanium as grain-refining agent. The markings obtained with $\frac{1}{2}$ % extension in the latter alloy are shown in Fig. 3 (Plate LXXXIII). Alloys with 3.8, 5.0, and 6.0% magnesium (NS5-7) were also subject to severe random markings, the intensity and distribution of which were not significantly different from those observed in the higher-purity series.

All alloys which were sensitive to random markings with strains of up to 2% were also subject to parallel bands at higher extensions, and the mechanism by which the bands deepened and subsequently caused failure of the sheet was similar to that observed in the previous investigations on the 3% magnesium alloy. Alloys free from random markings showed no parallel bands. Summarized data on the stretching characteristics of the materials described above are included in Tables II and III.

(b) *Aluminium and Aluminium-1 $\frac{1}{4}$ % Manganese*

High-purity aluminium (S1B), commercial-grade aluminium (S1C), and aluminium-1 $\frac{1}{4}$ % manganese alloy (NS3) were free from markings at all stages of stretching up to the point of fracture.

2. HEAT-TREATABLE ALLOYS (TABLE IV)

(a) *Aluminium-Magnesium-Silicon (HS10)*

(i) *Fully Annealed.*

No markings of any type were detected, either in the first stage of stretching to 2% elongation, or in the second stage from 2% up to fracture.

(ii) *Solution-Treated.*

Solution-treatment was carried out at temperatures of 540° and 450° C., followed in each instance by quenching. No random markings were detected in the critical range of strain, 0-2%, but slight parallel bands occurred at an angle of about 69° to the tension axis at higher strains.

(iii) *Fully Heat-Treated.*

Specimens aged for 18 hr. at 160° C. after solution-treatment fractured at right angles to the tension axis at about 2% extension, the low ductility being probably attributable to the difficulty in getting accurate alignment of the wide specimen. No markings were detected either during stretching or on the fractured halves on subsequent examination.

(b) *Aluminium-Copper-Magnesium (HS14)*

(i) *Fully Annealed.*

In fully annealed aluminium-copper-magnesium alloy no random markings were observed on stretching to extensions of 0-2%, but at about 4% elongation parallel bands appeared comparable in depth to those observed in the aluminium-magnesium alloys at 5% extension. With further stretching, failure eventually occurred by necking through a pair of bands.

(ii) *Solution-Treated.*

Slight random markings occurred in sheet specimens of the aluminium-copper-magnesium alloy, solution-treated for $\frac{1}{2}$ hr. at 495° C. and quenched in cold water. The markings occurred in a strain range of 0.05-0.5%, which is narrower than the range of extensions (0.015-2.0%) with which markings are associated in aluminium-3% magnesium alloy sheet.

Previous experience has shown that when aluminium-3% magnesium sheet is quenched from a suitably high temperature, quenching stresses are set up which prevent the formation of random markings. Relief of quenching stresses by some method, such as, for example, low-temperature annealing, causes a return to the condition in which intense random markings occur on stretching. Attempts were therefore made to produce markings of greater intensity in the heat-treatable aluminium-copper-magnesium alloy by reducing quenching stresses. The procedure adopted involved solution-treatment at different temperatures and quenching in cold water, boiling water, or oil. Some results of stretching tests on specimens quenched at 495°, 450°, and 400° C. are given in Table IV.

The markings were most intense in specimens freshly quenched from 450° C., and were most clearly defined after oil-quenching. The intensity was slightly reduced when stretching was carried out after ageing at room temperature for 7 days. A typical example of random markings in solution-treated aluminium-copper-magnesium alloy is illustrated in Fig. 4 (Plate LXXXIV). As stretching continued, random markings in freshly quenched specimens were replaced by parallel bands, which were deeper than bands observed in 3% magnesium alloy sheet stretched the same amount; room-temperature-aged strips, on the other hand, after the disappearance of random markings, stretched smoothly to failure without any further markings occurring. A typical

example of parallel bands in aluminium-copper-magnesium alloy sheet is illustrated in Fig. 5 (Plate LXXXIV), which shows a solution-treated specimen stretched 9%, the maximum depth of marking being 0.0003 in.

(iii) *Fully Heat-Treated.*

Solution-treated specimens of aluminium-copper-magnesium alloy, aged for 8 hr. at 165° C., fractured at right angles to the stretching direction at extensions of less than 5%, and no strain markings of any type were detected either during stretching or on the pieces of strip after failure.

(c) *Clad Aluminium-Copper-Magnesium*

Experiments similar to those described above were carried out on specimens of aluminium-copper-magnesium alloy sheet clad on both surfaces with a skin of pure aluminium 5% of the total thickness of the material. Fully annealed specimens developed only parallel bands at extensions of about 5% and over; on the other hand, solution-treated and oil-quenched sheet exhibited random markings at strains between 0.1 and 0.5%, but, as might be expected, the intensity was less than that observed in the corresponding unclad sheet owing to the masking effect of the aluminium skin. A typical area of random markings in clad sheet is illustrated in Fig. 6 (Plate LXXXIV).

(d) *Aluminium-Zinc-Copper-Magnesium*
(D.T.D. 363A)

(i) *Fully Annealed.*

Specimens annealed at 375° C. and furnace-cooled extended, without developing any strain markings, until fracture was imminent, when several distinct parallel bands appeared at an angle of about 64° to the tension axis, necking through one pair of bands eventually leading to failure.

(ii) *Solution-Treated.*

Sheet, solution-treated for $\frac{1}{2}$ hr. at 460° C. and quenched, developed slight parallel bands at about 5% extension. Further bands appeared as stretching was continued to failure, but did not reach measurable depth at any stage of straining.

(iii) *Fully Heat-Treated.*

Specimens aged for 18 hr. at 125° C. after solution-treatment fractured at about 2% extension, no markings being detected. Fracture occurred at right angles to the axis of tension.

V.—DISCUSSION

The experiments described have established that random markings occur in aluminium-magnesium alloys over a wide range of magnesium contents, the lower limit being between 0.6 and 0.9%, and the upper

limit greater than 6%. Maximum intensity of markings, measured on Talysurf tracings, has been plotted against magnesium content in Fig. 7, in which the curve reaches a maximum at a little over 1% and continues without significant variation to the maximum of 6% investigated.

Unalloyed aluminium, aluminium-manganese alloy, and aluminium-magnesium alloys containing 0.6% magnesium and less, were free from any type of marking at all extensions. The relatively coarse grain-size (0.04 mm.) of these low-magnesium alloys cannot account for their freedom from random markings, since material which, in the fine-grained condition, is subject to random markings always exhibits parallel bands in both fine- and coarse-grained states. However, no parallel bands were observed in these alloys when stretching was continued to the point of fracture. On the other hand,

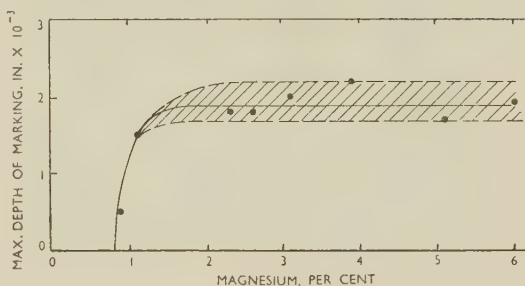


FIG. 7.—Maximum Depth of Random Markings in Aluminium-Magnesium Alloys.

the heat-treatable aluminium-magnesium-silicon and aluminium-zinc-copper-magnesium alloys, although without detectable random markings in all conditions of heat-treatment, developed parallel bands when stretched in the solution-treated condition.

Random markings in aluminium-copper-magnesium-type alloy sheet have not previously been reported, yet solution-treated material of this type is often subjected to stretching operations, for example, in flattening after quenching and in the stretch-forming of aircraft panels. The alloys are, of course, generally coated with pure aluminium, which, as already indicated, renders the markings less conspicuous. Moreover, the markings are less severe than those on aluminium-magnesium alloys, and since they occur with very small extensions and disappear at an elongation of 0.5%, they are probably pulled out in most flattening or forming operations. The occurrence of random markings in solution-treated and quenched aluminium-copper-magnesium alloy sheet appears, upon first consideration, to be anomalous, since in aluminium-magnesium alloys random markings can be avoided by quenching from comparable temperatures. The conclusion that this effect is associated with internal stresses receives some support from the observation that the markings were more intense with less drastic quenching. Ageing at 165° C. completely removed any tendency to strain

marking, a result which might be related to the removal of magnesium from solid solution by the precipitation of a magnesium-rich phase.

Both aluminium-magnesium and aluminium-copper-magnesium alloys, in the physical condition in which strain marking is developed on stretching, are supersaturated in respect of solute elements or compounds. In both types of alloy, moreover, some decomposition of the solid solution is known to be induced by straining. The analogy with mild steel, therefore, appears to be close, and current theories,

associating strain markings with atomic movements in the lattice analogous to those experienced in precipitation-hardening processes, receive further support.

ACKNOWLEDGEMENT

The encouragement and advice accorded to the author by Mr. R. Chadwick in discussions during the course of the investigation and in preparing the paper for publication is gratefully acknowledged.

REFERENCES

1. G. A. Knight and G. Murray, *Sheet Metal Ind.*, 1946, **23**, 1741.
2. R. Chadwick and W. H. L. Hooper, *J. Inst. Metals*, 1951-52, **80**, 17.
3. J. C. Arrowsmith, K. J. B. Wolfe, and G. Murray, *ibid.*, 1942, **68**, 109.
4. E. W. Fell, *Carnegie Schol. Mem.*, *Iron Steel Inst.*, 1937, **26**, 123.
5. A. W. MacReynolds, *Trans. Amer. Inst. Min. Met. Eng.*, 1949, **185**, 32.
6. J. L. Snoek, *Physica*, 1941, **8**, 711.
7. J. R. Low, Jr., and M. Gensamer, *Trans. Amer. Inst. Min. Met. Eng.*, 1944, **158**, 207.
8. L. B. Pfeil, *J. Iron Steel Inst.*, 1928, **118**, 167.
9. C. A. Edwards, D. L. Phillips, and H. N. Jones, *ibid.*, 1940, **142**, 199P.

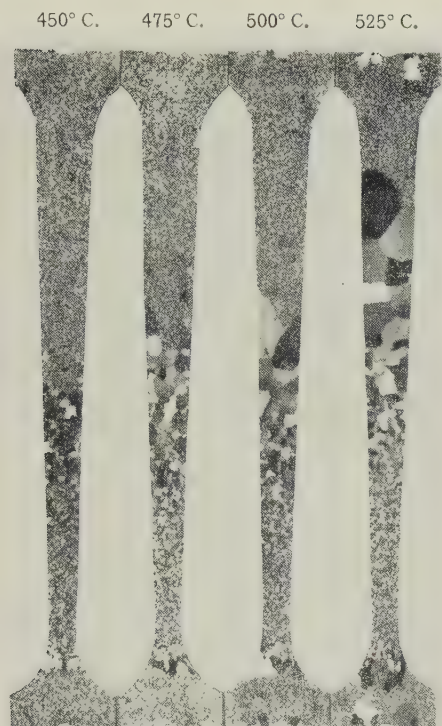


FIG. 11.—Effect of Temperature on Final Grain-Size. Super-purity aluminium pulled 2–20% and recrystallized for 30 min. at various temperatures. Initial grain-size 0.3 mm. $\times \frac{1}{2}$.

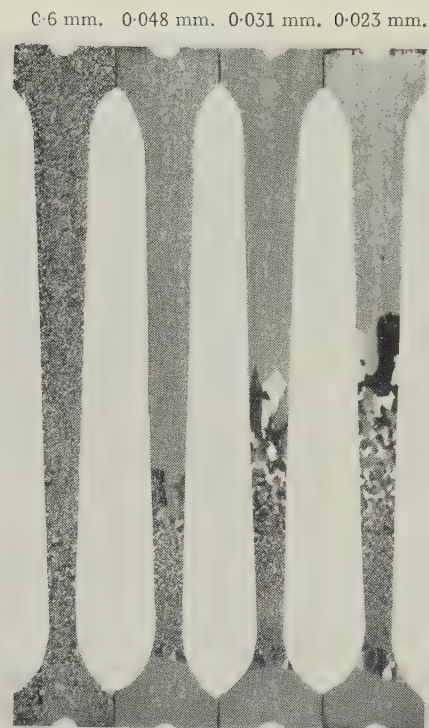


FIG. 12.—Effect of Initial Grain-Size on Final Grain-Size. Commercial-purity aluminium pulled 1–18% and recrystallized for 30 min. at 600° C. from various initial grain-sizes. $\times \frac{1}{2}$.

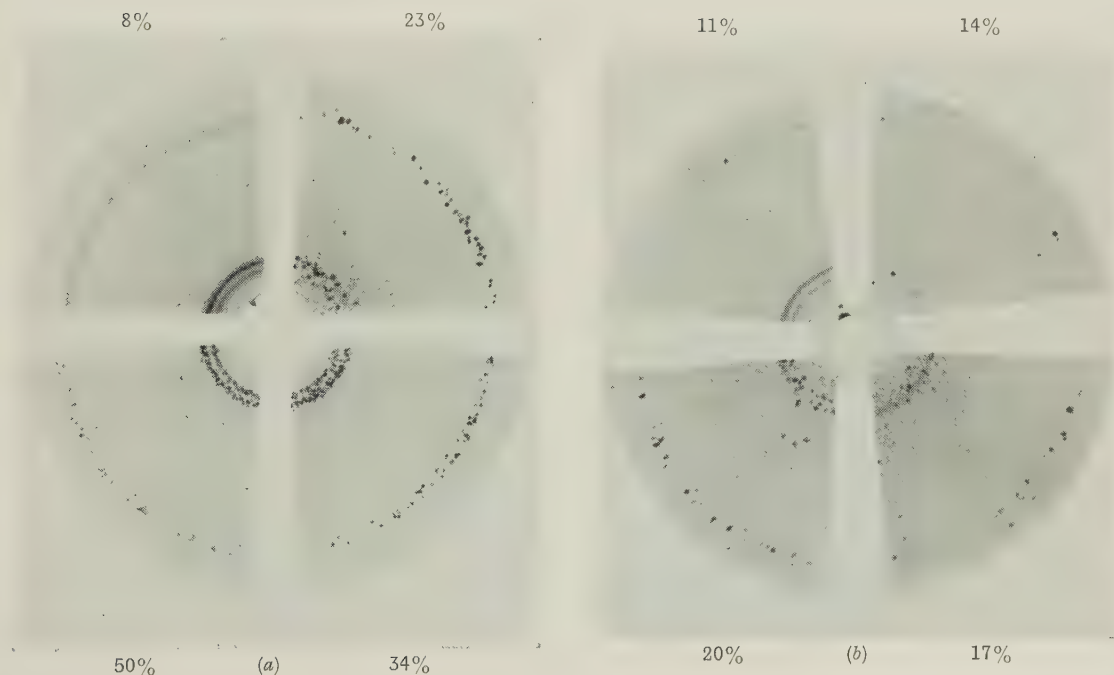


FIG. 13.—X-Ray Back-Reflection Photographs Taken at Various Points along a Wedge-Rolled Specimen. Critical reduction = 21%.

GRAIN REFINEMENT OF COPPER-ALUMINIUM ALLOYS.

Figs. 1-4.—Transverse Sections of Laboratory Ingots, $\times \frac{2}{3}$.

FIG. 1.—10% Al.

FIG. 2.—10% Al with 0.01% B.

FIG. 3.—12.5% Al.

FIG. 4.—12.5% Al with 0.01% B.

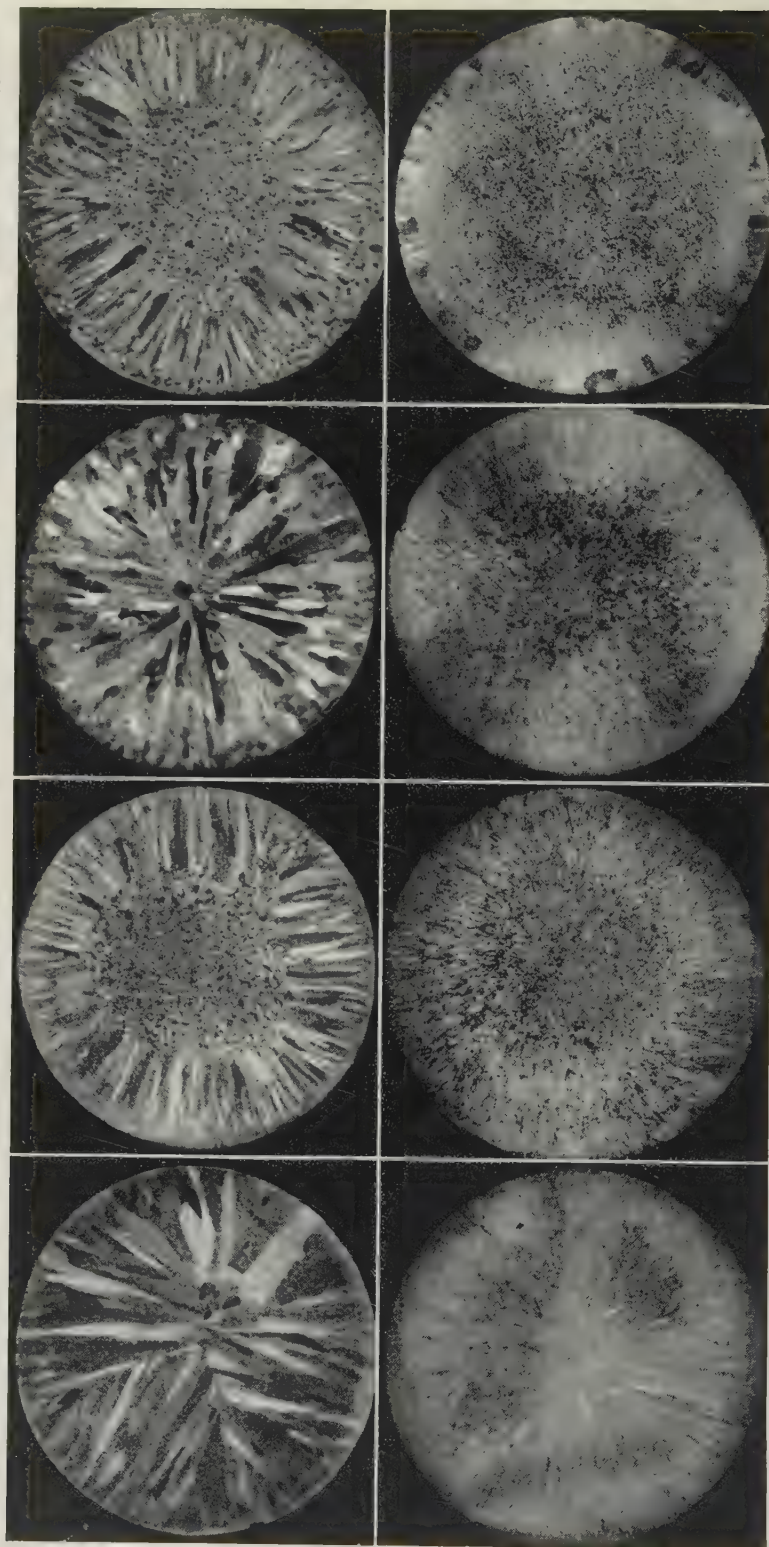


FIG. 5.—Standard Ingot.

FIG. 6.—0.04% Ca Addition.

FIG. 7.—0.0025% B Addition.

FIG. 8.—0.01% B Addition.

Figs. 5-8.—Transverse Sections of Commercial Ingots of Copper-10% Aluminium Alloy.

Approx. $\frac{1}{3}$.

MICROSTRUCTURES OF TITANIUM-TIN ALLOYS.

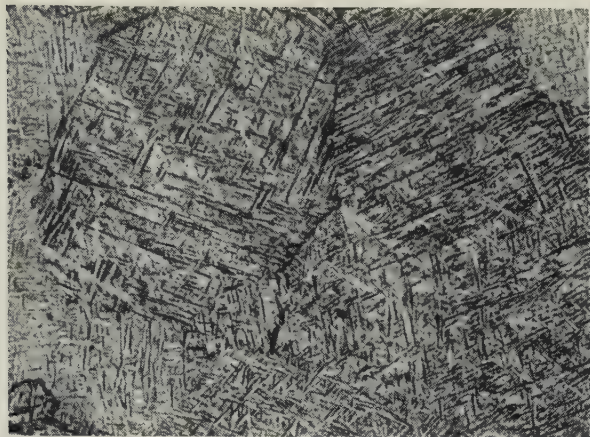


FIG. 7.—7.7 at.-% Tin Alloy (Commercial Titanium), Quenched from 1020° C. α in acicular form due to rapid $\beta \rightarrow \alpha$ change. $\times 200$.

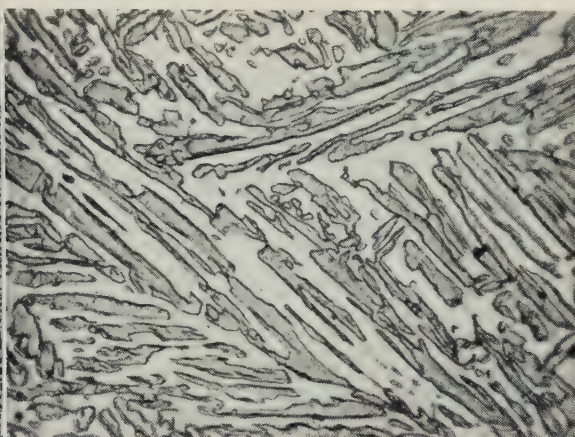


FIG. 8.—15.3 at.-% Tin Alloy (Commercial Titanium), Quenched from 850° C. $\alpha + \gamma$. $\times 1500$.



FIG. 9.—7.7 at.-% Tin Alloy (Commercial Titanium), Quenched from 950° C. Equilibrium α in matrix of acicular α . $\times 200$.

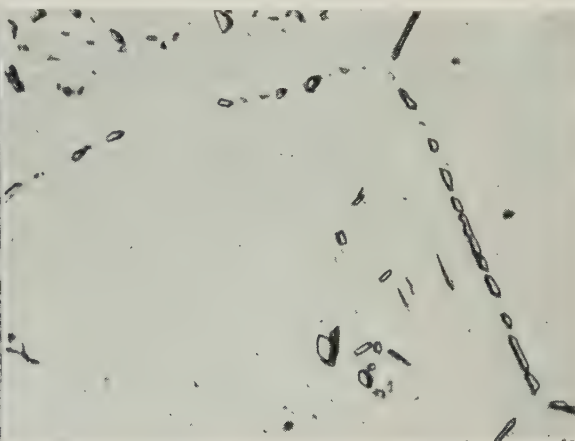


FIG. 10.—11.0 at.-% Tin Alloy (Refined Titanium), Quenched from 880° C. α with a little γ . $\times 1000$.

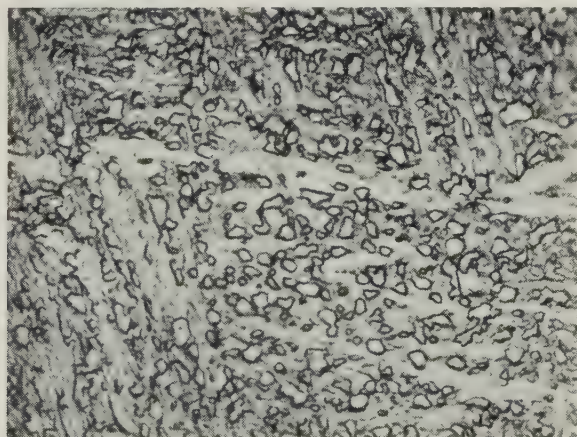


FIG. 11.—11.0 at.-% Tin Alloy (Refined Titanium), Quenched from 890° C. γ in matrix of acicular α . $\times 1500$.

All specimens were etched in 2 wt.-% $\text{HNO}_3 + 1$ wt.-% HF in water.

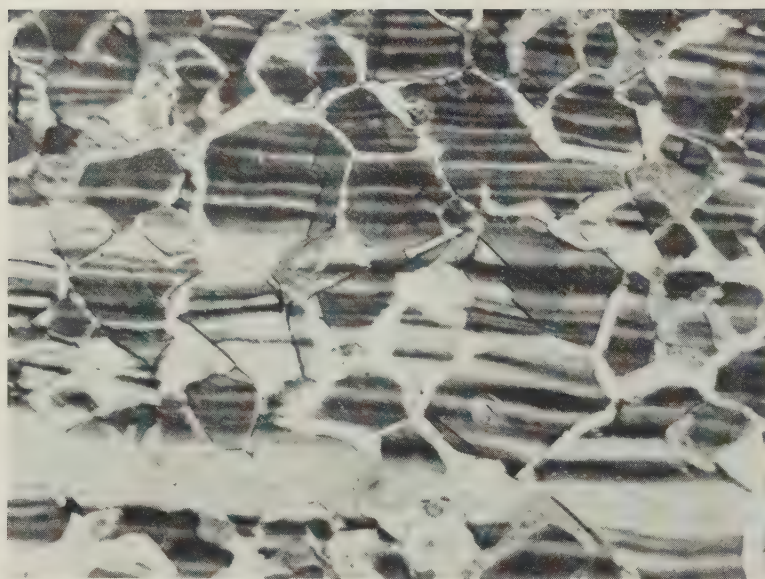


FIG. 7.—Structure of Fine-Grained Alloy E after 144 hr. at 860 lb./in.² Stress (12% extension). $\times 270$.

STRETCHER-STRAIN MARKINGS IN ALUMINIUM ALLOYS AND CORRESPONDING TALYSURF TRACES.

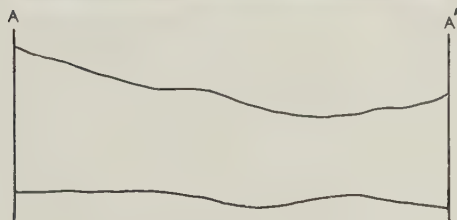


FIG. 1.—Aluminium-0.58% Magnesium Alloy.
Annealed 4 hr. at 300° C. Permanent
extension 1%.

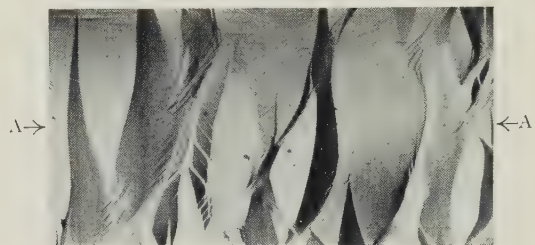


FIG. 3.—Aluminium-3.11% Magnesium Alloy.
Annealed 2 hr. at 400° C. Permanent
extension $\frac{1}{2}$ %.

↑
× 500
→
× 1

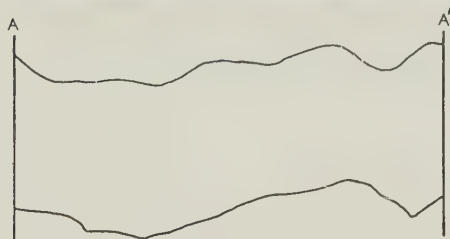
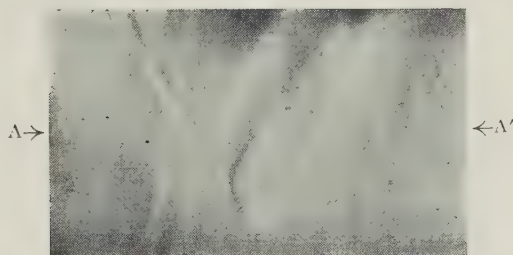


FIG. 2.—Aluminium-0.87% Magnesium Alloy.
Annealed 4 hr. at 300° C. Permanent
extension $\frac{1}{2}$ %.

STRETCHER-STRAIN MARKINGS IN ALUMINIUM ALLOYS AND CORRESPONDING TALYSURF TRACES.

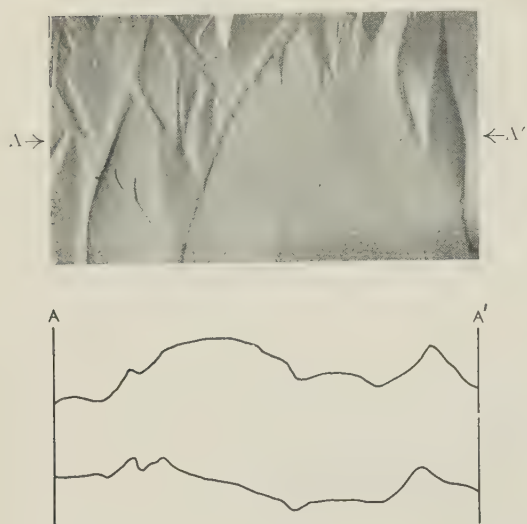


FIG. 4.—Aluminium-Copper-Magnesium Alloy. Solution-treated $\frac{1}{2}$ hr. at 450° C. and quenched in oil. Permanent extension 0.3%.

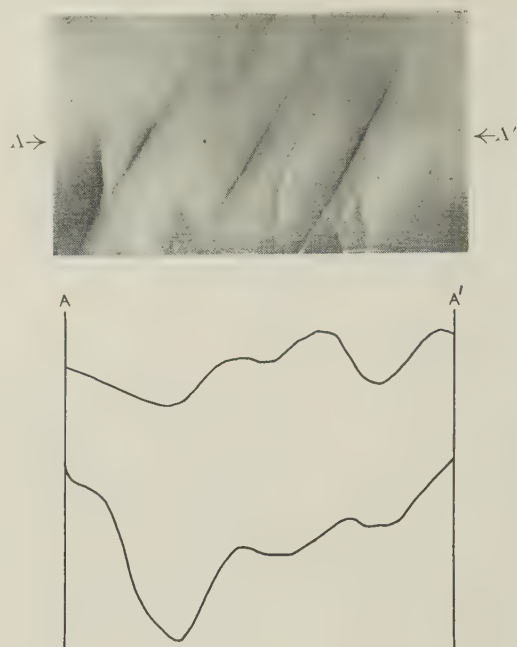


FIG. 6.—Aluminium-Copper-Magnesium Alloy, Clad with Pure Aluminium. Solution-treated $\frac{1}{2}$ hr. at 450° C. and quenched in oil. Permanent extension 0.3%.

$\times 500$
 $\times 1$

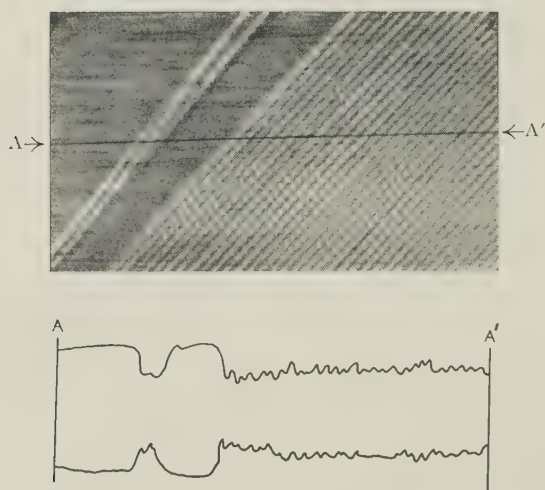


FIG. 5.—As Fig. 4. Permanent extension 9%.

THE PROPERTIES OF CAST CHROMIUM ALLOYS AT ELEVATED TEMPERATURES *

1478

I.—The Melting and Casting of Chromium-Rich Alloys

By A. H. SULLY,† M.Sc., Ph.D., F.Inst.P., F.I.M., MEMBER,
E. A. BRANDES,‡ B.Sc., A.R.C.S., F.I.M., MEMBER, and
A. G. PROVAN,§ B.Sc., A.R.T.C., A.R.I.C.

SYNOPSIS

A furnace is described in which chromium and its alloys may be melted and cast in a vacuum or in an inert or reducing atmosphere. Refractory problems in crucibles and in investments for casting are considered. The estimation of the oxygen content of chromium is described, and methods for reducing the content of this element to a low level during melting and casting are discussed. Treatment of the molten alloys with hydrogen is not recommended, the best results being achieved either by carbon reduction of the chromic oxide present in the melt or by melting, in a good vacuum, chromium purified by prior treatment in the solid state with pure dry hydrogen.

I.—INTRODUCTION

THE work described in this paper is part of a more general investigation of the properties of chromium and chromium-rich alloys. Melting and casting offers one method of making these alloys, the alternative being the use of powder-metallurgical methods. The melting and casting of chromium and its alloys presents, however, many points of special difficulty, and the complexity of the techniques involved is, undoubtedly, the major reason why the properties of chromium-rich alloys have only recently received detailed examination. In the first place chromium has a high melting point (1860° C. according to the most recent and reliable measurement¹). This introduces problems in the selection of suitable refractory materials for melting and casting operations. Secondly, chromium has a very high affinity for carbon, nitrogen, and oxygen, and melting and casting must be conducted under conditions which result in a low content of these elements, all of which can have an important effect on the properties of chromium-rich alloys. Thirdly, chromium at temperatures approaching its melting point has an appreciable vapour pressure, and the volatilization of chromium during melting constitutes a considerable inconvenience.

A furnace for melting chromium and its alloys has been described by Parke and Bens,² in which melting and casting are both carried out in a vacuum. The furnace and techniques described in the present paper differ in several important particulars from those described by Parke and Bens, and bottom-

pouring and vacuum centrifugal-casting techniques, which were used by these authors, are both avoided.

II.—THE OXYGEN CONTENT OF ELECTROLYTIC CHROMIUM

The purest commercially available form of chromium is electrolytic flake. A typical analysis of such material is: Fe 0.06, Si <0.01, S 0.026, N 0.01%. Although the content of these elements is low, the material also contains oxygen in appreciable quantities. The determination of this oxygen content presents several points of interest. It was first demonstrated by Adcock³ that the oxygen could be estimated as chromic oxide, Cr₂O₃, if the chromium was first heated to 800° C. in a vacuum and then dissolved in dilute hydrochloric acid, the oxide being left behind as an insoluble residue. If, however, the chromium was not previously heated to 800° C., it was completely soluble in acid. The precise form of occurrence of the oxygen in electrodeposited chromium is of considerable interest, but is not within the scope of the present paper. Since Adcock in his paper does not give specific details of the period of heating at 800° C. and the dilution of acid used for the extraction of the insoluble oxide, an examination has been made of the reliability of this method for the determination of the oxygen content of electrolytic chromium. The results of a somewhat similar investigation have been reported by Short.⁴

The chromium used was taken from a single batch of electrolytic chromium flake. In the first series of experiments the insoluble content was determined by

* Manuscript received 18 February 1953.

† Principal Physicist, Fulmer Research Institute, Stoke Poges, Bucks.

‡ Head of Experimental Casting Section, Fulmer Research

Institute, Stoke Poges, Bucks.

§ Metallurgist, Fulmer Research Institute, Stoke Poges, Bucks.

solution in approximately 50% hydrochloric acid (209 g. HCl/l.) after previous heating in a vacuum in sealed-off silica tubes for various times at temperatures from 800° to 1150° C., the results being given in Table I.

TABLE I.—Variation of Insoluble Oxide Content with Time and Temperature of Prior Heat-Treatment.

Conditions of Heat-Treatment		Insoluble Oxide Content, in a Solution containing 209 g. HCl/l., %
Temp., °C.	Time, hr.	
As-received		0.012
800	3	0.12
800	24	0.21
800	48	0.17
1000	48	0.89
1150	36	2.08

These results show that in chromium in the "as-received" condition the insoluble content was very small, though it increased progressively to 2.08% on

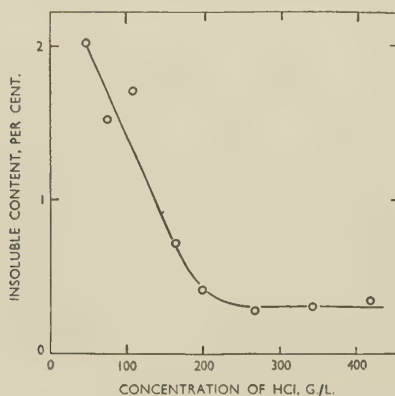


FIG. 1.—Relationship Between Acid Dilution and Insoluble Content for Electrolytic Chromium Heated in a Vacuum for 50 Hr. at 800° C.

heating in a vacuum at temperatures of 800°, 1000°, and 1150° C. The nature of the insoluble matter was checked by X-ray-diffraction examination and, in all cases, was confirmed to be Cr_2O_3 . Corresponding to these estimations the microstructure of the samples was examined, and it was found that the size of the oxide particles increased as the temperature of prior heating was increased. The solubility of the oxide particles in the acid used is probably a function both of the particle size and of the temperature to which the chromium is heated. The latter is in accordance with published information on the chemical properties of Cr_2O_3 .⁵

In order to study the variation of solubility with acid strength, another series of experiments was made on chromium from the same batch as that used in the first series, which was heated in a vacuum for 50 hr. at 800° C. Samples of this material were dissolved in hydrochloric acid of increasing dilution. The results are shown in Fig. 1, in which the acid-insoluble content is plotted against the acid dilution. Although

the results show a certain amount of scatter, which is probably related to the fact that the estimations were carried out on rather small samples of 200 mg., it will be seen that there is a sharp rise of insoluble content as the acid dilution is reduced below 200 g. HCl/l. At 42 g. HCl/l., which is about the lower limit of dilution at which solution of the chromium can be accomplished in a reasonable time, the insoluble content is 2.04%, a figure which agrees with the specimen heated to 1150° C. and dissolved in more concentrated acid (Table I).

As a more searching test of the accuracy of this method of determining the oxygen content, a comparison has been made of the results obtained by this method and by vacuum fusion. Estimations were made by both methods at the National Physical Laboratory, Teddington, and by the acid-insoluble method by the authors on identical samples with low and with fairly high oxygen contents. The results are set out in Table II.

TABLE II.—Comparison of Vacuum-Fusion and Acid-Insoluble Methods of Oxygen Determination.

Sample	Oxygen Content, %		
	N.P.L. Results		Authors' Results *
	From Acid-Insoluble Content after 1½ hr. in a Vacuum at 850° C.	By Vacuum Fusion	
A	0.23	0.18	0.25
B	0.025	0.02	0.027

* Oxygen content is calculated from the insoluble residue on the assumption that the residue consists wholly of Cr_2O_3 .

It will be seen that the agreement between the two methods both at low and relatively high oxygen contents is reasonably satisfactory, and consequently estimations of oxygen content have been made by the simple method of acid-insoluble determination throughout the work described in this paper. As a safeguard, X-ray checks have been made in many cases to ensure that the insoluble residue is predominantly Cr_2O_3 .

III.—THE VACUUM-MELTING FURNACE

The furnace developed for this work, which enables both melting and casting to be carried out in a vacuum or in a reducing or inert atmosphere has been described elsewhere.⁶ The internal construction is shown in Fig. 2. The silica furnace tube is lined with insulating brick, and the base is of recrystallized pure alumina, on which stands a heater sleeve of molybdenum wire⁷ that provides linkage to the coil of a H.F. generator. The crucible has attached over it by alumina cement a throat of commercial bonded alumina. The mould is held inverted over the throat, which rests in the pouring basin of the mould,

which is of copper-chromium alloy or of refractory investment. A suitable investment mixture consists of fused alumina bonded with ethyl silicate, and a pattern spray of 4 parts of zircon flour to 3 parts of calcined alumina bonded with sodium silicate has proved sufficiently refractory.

The melt can be viewed and temperature measurements made through the glass cap to the furnace and a $\frac{3}{16}$ -in.-dia. cylindrical prolongation of the mould cavity, which is closed by means of a gravity-operated shutter when the furnace is rotated on trunnions for casting. The furnace can be evacuated by large-capacity rotary oil and diffusion pumps, and measurements of the pressure in the furnace are made by a McLeod gauge.

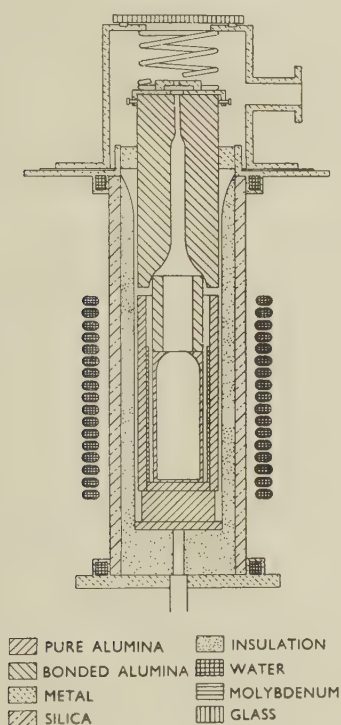


FIG. 2.—Internal Construction of the Vacuum-Melting Furnace.

Slip-cast recrystallized pure alumina crucibles are fairly satisfactory for melting alloys of chromium with metals of lower melting point, but because alumina softens at 2050° C.⁸ pure chromium cannot be superheated much above its melting point in alumina crucibles. They are also unsatisfactory for melting alloys containing as little as 5% titanium and zirconium which react with alumina; beryllia, too, is unsuitable. The most satisfactory material is thoria, which is not wetted by molten chromium.

Vacuum casting into metal or refractory moulds was not successful owing to the porosity produced by gas given off by the mould when first in contact with the hot metal. This trouble was cured by changing the atmosphere from a vacuum to one of argon at atmospheric pressure immediately before casting. Investment casting gave more satisfactory ingots than chill

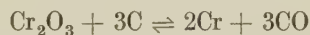
casting, since directional solidification in chill moulds produced a columnar crystallization which resulted in planes of weakness parallel to the direction of the columnar structure. Investment-cast alloys had a fine-grained, equiaxed structure.

IV.—MELTING AND PURIFICATION TECHNIQUE

Chromium-rich alloys oxidize when melted in a vacuum as low as 0.005 mm. mercury. A 90:10 chromium-cobalt alloy made from chromium containing 2.1% Cr_2O_3 by straightforward melting in a vacuum contained 2.61% Cr_2O_3 when cast.

In order to attain a low oxygen content in the alloys, steps must be taken to reduce the oxide to metallic chromium. One method by which this may be accomplished is by treatment of the melt with purified hydrogen. Experiments have shown, however, that the speed of this reaction is too slow for the method to be adopted as a standard procedure. This is illustrated by the case of a 90:10 chromium-cobalt alloy that was melted under a stream of purified hydrogen, the flow of which was continued for $\frac{1}{2}$ hr. when the alloy was in a molten condition. The content of Cr_2O_3 in this alloy when cast was 1.6%. Although some reduction of the oxide content was achieved, it was obvious that a much longer period would be required substantially to eliminate the oxide content. Such long periods with the alloy in the molten condition are undesirable because of damage to refractories and because a large proportion of the chromium in the charge volatilizes and condenses in other parts of the furnace.

An alternative method for the removal of oxygen from chromium is the technique of carbon deoxidation described by Parke and Bens.² In this method an addition of carbon is made to the charge which is slightly more than that required to combine with the oxide content according to the reaction:



For temperatures above 1250° C. this reaction moves towards the right. At the temperature of liquid chromium alloys, the reaction is very strong and this, together with the pumping away of the carbon monoxide, causes the reduction to proceed almost to completion. The progress of the reaction may be followed by taking pressure readings in the furnace. A typical pressure/time curve for the purification of a 90:10 chromium-cobalt alloy is shown in Fig. 3. The first pressure peak, after about 20 min., is due to the evolution of hydrogen from the electrolytic chromium of the charge. After 60 min. the cobalt begins to melt, taking some chromium into solution, and the reduction reaction starts, accompanied by a sharp rise of pressure. The pressure may fall and rise again, as shown in Fig. 3, owing to local solidification and melting in the charge as the higher-melting-point constituents dissolve in the first-melting constituents. Often several subsidiary pressure peaks

occur in this region. Eventually, however, when the charge is all molten, a sharp drop of pressure occurs, indicating that the reduction reaction is approaching completion. The moment of casting must be chosen with some care, since, if it is too soon, excess carbon will be present, whereas, if it is too late, some re-oxidation of the chromium may occur. By the choice of a suitable pressure at which to cast, a carbon content of 0.02–0.03% can be combined with a Cr_2O_3 content of 0.2% or less (0.06% oxygen or less). Figs. 16–19 (Plate LXXXV) illustrate the deoxidation techniques applied to a 90:10 chromium–cobalt alloy. Fig. 16 shows the structure of an alloy melted and cast in a vacuum without purification. The Cr_2O_3 content of this alloy was 2.61% and the nitrogen content 0.043%. Fig. 17 shows the reduction of oxide content obtained by hydrogen treatment of the melt for 30 min. The Cr_2O_3 content is 1.6% and the

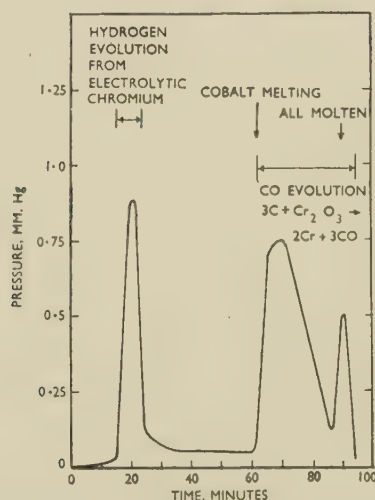


Fig. 3.—Pressure/Time Changes During the Melting of a 90:10 Chromium–Cobalt Alloy, Using the Carbon Purification Technique.

nitrogen content 0.011%. Fig. 18 shows the structure of an alloy to which 0.6% carbon was added and the melt cast at 0.1 mm. Hg pressure before the deoxidation reaction was complete. The carbon content was 0.097%, and the structure shows a carbide network around the grains. The Cr_2O_3 content was 0.44% and the nitrogen content 0.016%. Fig. 19 is typical of an alloy cast at about the optimum end-point of the reaction. The residual carbon content was 0.02%, the Cr_2O_3 content 0.16% (0.05% oxygen), and the nitrogen content 0.01%.

The carbon-reduction technique has been used successfully for alloys of chromium containing iron, cobalt, nickel, molybdenum, tungsten, tantalum, niobium, palladium, and vanadium. It has not, however, proved successful for alloys containing titanium or zirconium. In such alloys typical pressure/time readings during melting are not obtained and there is no clear end-point to the reaction. Such melts were found to have a slag on the surface and a high content of matter insoluble in dilute acid.

This behaviour is probably attributable to the formation of highly stable carbides of titanium and zirconium.

Some attempts were also made to deoxidize chromium melts with aluminium and with titanium. Aluminium proved quite effective in reducing Cr_2O_3 , and the acid-insoluble portion of a melt treated with aluminium was shown by X-ray examination to consist entirely of Al_2O_3 . The objection to this form of deoxidation, however, is that it only replaces a dispersion of one form of non-metallic inclusion in the metal by another.

For alloys which cannot be purified by the carbon-reduction method or in which it may be desirable to maintain a particularly low carbon content, the expedient may be adopted of remelting chromium in which the oxide content is reduced by prior reduction in the solid state with dry purified hydrogen. Such reduction may be accomplished at a reasonable speed at a temperature of 1450°–1500° C., the time required being dependent on the size of chromium particles being treated. For electrolytic chromium with a particle size of 22–30 mesh to 72–100 mesh, satisfactory reduction of oxygen content to a value which may be less than 0.01% can be achieved in 3 hr. at 1450° C. with a hydrogen flow-rate of about 5 l./min. Electrolytic chromium flakes of thickness about 1 mm. or less are also suitable for reduction by this method, but samples of thickness greater than about 1.2 mm. will still contain some residual oxide at the centre after the above treatment, and longer times would be required for adequate elimination of the oxide.

A certain increase in oxide content on remelting this chromium in vacuum must be accepted. For example, an 80:20 chromium–cobalt alloy made by remelting chromium purified by this method contained 0.28% insoluble Cr_2O_3 in the cast condition. The carbon content was 0.01%.

ACKNOWLEDGEMENTS

The authors are indebted to Mr. W. H. Mayes for many useful suggestions in the construction of the apparatus which is described, to Mr. H. H. Smith for the chemical analysis, and to Mr. C. S. Campbell, M.A., for assistance and advice on the reduction of chromic oxide by hydrogen.

REFERENCES

1. S. J. Carlile, J. W. Christian, and W. Hume-Rothery, *J. Inst. Metals*, 1949–50, **76**, 169.
2. R. M. Parke and F. P. Bens, *Symposium on Materials for Gas Turbines* (Amer. Soc. Test. Mat.), 1946, p. 80.
3. F. Adcock, *J. Iron Steel Inst.*, 1927, **115**, 369.
4. H. G. Short, *Analyst*, 1950, **75**, 335.
5. H. Gernert, *Zhur. Priklad. Khim.*, 1931, [B], **4**, 429.
6. W. Hume-Rothery, J. W. Christian, and W. B. Pearson, "Metallurgical Equilibrium Diagrams", London: 1952 (Institute of Physics).
7. E. A. Brandes, *Research*, 1948, **1**, 382.
8. E. Ryschkewitsch, "Oxydkeramik der Einstoffsysteme vom Standpunkt der physikalischen Chemie", Berlin: 1948 (Julius Springer).

II.—Some Properties of Certain Binary Chromium-Rich Alloys

By A. H. SULLY, M.Sc., Ph.D., F.Inst.P., F.I.M., MEMBER and
E. A. BRANDES, B.Sc., A.R.C.S., F.I.M., MEMBER

SYNOPSIS

A comparative study has been made of the resistance to creep at 900° C. of cast chromium-rich binary alloys with iron, nickel, cobalt, and palladium. The highest creep-resistance is found in chromium-iron alloys containing 5–15% iron. These alloys are homogeneous solid solutions, and constitute a promising base for further alloying to obtain enhanced resistance to deformation at high temperatures.

The effect of heat-treatment on the creep properties has been studied for some of the alloys. In general, a high-temperature solution-treatment, even when followed by a stabilizing heat-treatment at the test temperature, reduces the creep-resistance in comparison with the "as-cast" condition. The resistance to oxidation of all the alloys tested is adequate at 900° C., but the alloys are brittle at room temperature.

I.—INTRODUCTION

THE work to be described constitutes the first part of a survey of the resistance to deformation at high temperatures of certain chromium-rich alloys, and is concerned primarily with those alloys of chromium with other elements which are common constituents of high-temperature alloys and which melt at temperatures lower than the melting point of chromium. These are iron, cobalt, nickel, and aluminium. In addition, one chromium-palladium alloy has been examined. In order to provide a uniform basis of comparison, the resistance to deformation has been assessed by the behaviour in compression creep tests carried out at a stress of 3 tons/in.² and a temperature of 900° C. Most of the alloys have been tested in the "as-cast" condition, but the effect of heat-treatment on the creep properties has also been studied in some cases. In addition, some observations have been made on the hardness at room temperature and the structure of these alloys.

II.—EXPERIMENTAL PROCEDURE

The alloys were made by high-frequency melting in the vacuum furnace described in Part I. The materials used were of the highest available purity, viz. electrolytic chromium and cobalt, carbonyl nickel, Krupps W.W. iron, and refined palladium sponge.

Melting was carried out in recrystallized alumina crucibles, and in most cases the oxygen content of the melt was reduced by treatment with carbon as previously described. A few alloys were made by remelting chromium of which the oxide content had been reduced by prior treatment with purified dry hydrogen for 4 hr. at 1450° C. Most of the alloys were cast in argon into refractory investment moulds. The castings were X-rayed, and creep-test specimens were ground from portions of the ingots which the radiographs showed to be free from casting defects.

All the alloys were analysed for major constituents and for carbon and oxide, the latter by the method previously described (p. 570). The extracted insoluble matter was, in most cases, examined by X-rays to confirm that it was mainly Cr₂O₃. The reported insoluble content often includes a small proportion of alumina, due to pick-up from the crucible. The nitrogen content was usually substantially less than 0.02%.

Small compression creep-test specimens with a gauge portion of length 0.25 in. and 0.125 in. dia. with shoulders at each end of 0.25 in. dia. and 0.125 in. long were prepared by grinding from sound portions of the cast ingots. These were tested in compression creep machines of the type previously described.¹ Earlier work has shown a good correlation between tensile and compressive creep properties, and the accuracy and reproducibility of compression creep tests is considered to be sufficiently high to justify the distinctions in creep performance which are made between different alloys. Whenever creep results are discussed in the present paper they are the results of these compressive creep tests. Tensile time-to-rupture tests are discussed separately in Part III (p. 581).

The test temperature was in most cases 900° C., and for purposes of sorting more promising from less promising alloys a stress of 3 tons/in.² proved sufficient to differentiate between the binary alloys, which, in general, do not possess a high level of creep properties. Specimens were in all cases maintained at temperature in the testing machines for 16–20 hr. before loading.

A metallographic examination was made of all alloys in the as-cast condition and, in some cases, after various heat-treatments. No X-ray crystallographic investigation was made of the alloys, since the metallographic examination revealed no points significantly at variance with published equilibrium diagrams.

III.—EXPERIMENTAL RESULTS

1. CHROMIUM-IRON ALLOYS

The analysed compositions of the alloys which were tested are given in Table III. The alloys comprise a series containing from 0 to 30% iron. Two alloys containing approximately 10% iron are included. In

TABLE III.—Analysed Compositions and Hardness of the Chromium-Iron Alloys.

Nominal Iron Content, %	Melt Number	Analysed Composition, %			Vickers Hardness Number (5 kg. load)
		Iron	Carbon	Oxygen *	
0	H73	Remelted hydrogen-reduced chromium			126
5	H165	8.00	0.06	0.08	...
10	H42	10.14	0.13	0.20	347
10	H55	9.50	0.04	0.21	303
15	H60	15.06	0.02	0.17	377
20	H41	20.35	0.06	0.07	423
30	H40	31.24	0.06	0.04	393

* Calculated on the assumption that the acid-insoluble content is entirely Cr_2O_3 .

one of these (H42) the carbon content was higher than usual (0.13%). A second alloy with a lower carbon content (0.04%) was therefore tested in order to determine whether the carbon content had a significant effect on the creep properties.

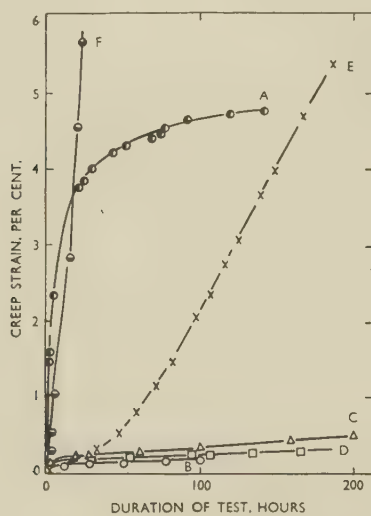


FIG. 4.—Compression Creep Curves of As-Cast Chromium-Iron Alloys at 3 Tons/in.² and 900° C.

KEY.

Test A : Chromium.
 Test B : H42 (10.14% Fe, 0.13% C).
 Test C : H55 (9.5% Fe, 0.04% C).
 Test D : H60 (15.06% Fe).
 Test E : H41 (20.35% Fe).
 Test F : H40 (31.24% Fe).

The creep properties of these alloys at a stress of 3 tons/in.² at 900° C. are illustrated by Fig. 4. A large variation of creep properties with iron content is apparent. Chromium, itself, showed a very rapid

initial creep, the strain being 3.5% in the first 20 hr. of test. Subsequently, however, it settled down to quite a low rate of creep, which suggests that even at 900° C., it has considerable capacity for work-

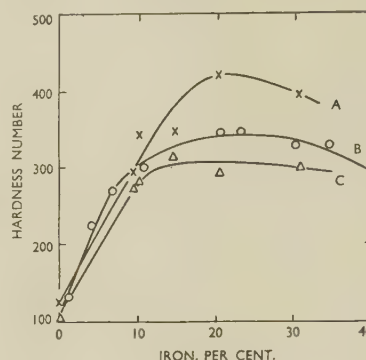


FIG. 5.—Hardness of Chromium-Iron Alloys at Room Temperature.

KEY.

Test A : Vickers Pyramidal Diamond, 5-kg. load.
 Test B : Brinell, 2-mm. ball, 40-kg. load (Adcock).
 Test C : Brinell, 2-mm. ball, 40-kg. load (Present work).

hardening. Alloys with 8–15% iron showed very much smaller creep strains in the primary stage of creep and very low secondary creep rates (less than 0.001%/hr.). The tertiary, accelerating, stage of creep did not occur within the duration of the tests. There was no significant difference in secondary creep rate between the two 10% iron alloys containing 0.13% and 0.04% carbon, respectively. The 20% iron alloy entered a stage of tertiary creep after only 25 hr., and the 30% iron alloy crept very rapidly from the start of the test, the creep strain being 4.5% in the first 20 hr. It appears, therefore, that for creep-resistance there is an optimum iron content of about 5–15%, the creep properties deteriorating outside this range. The existence of an optimum iron content is at first sight unexpected, as the chromium-iron alloys over the range of composition investigated are single-phase solid solutions. This was confirmed by metallographic examination, the microstructure consisting of a solid-solution matrix with some oxide dispersed throughout the grains and some particles of carbide at the grain boundaries.

It appears, however, that iron causes marked solid-solution hardening of chromium. This is illustrated by Fig. 5, in which curve A gives the results of Vickers pyramidal diamond hardness measurements at 5 kg. load on the alloys which underwent creep tests. Previous measurements of the hardness of chromium-iron alloys have been made by Adcock,² whose results are given in curve B of Fig. 5. For pure chromium and for the alloys containing 10–30% iron the hardness values given by Adcock are less than the measurements corresponding to curve A. Adcock, however, measured Brinell hardness values with a 2-mm. ball and a 40-kg. load. The hardness of the alloys used in the present work was therefore remeasured under the same conditions as those used by Adcock, and the

results are shown in curve *C*. The values are in general less than those reported by Adcock. It is interesting to note the difference between the Vickers and Brinell hardness values, which increases more or less progressively as the iron content is increased; from about 20 for chromium to 100 or more for the alloys with 20–30% iron. The optimum creep properties are associated with the rising portion of the hardness curve, and the creep properties deteriorate when the hardness becomes relatively constant. The difference in hardness as determined by pyramidal diamond and ball impressions could not be investigated satisfactorily by variation of P/D^2 in the Brinell test, as loads greater than 40 kg. produced irregular impressions, accompanied, in some cases, by cracking. The Brinell impressions at 40 kg. and the Vickers diamond impressions were quite satisfactory.

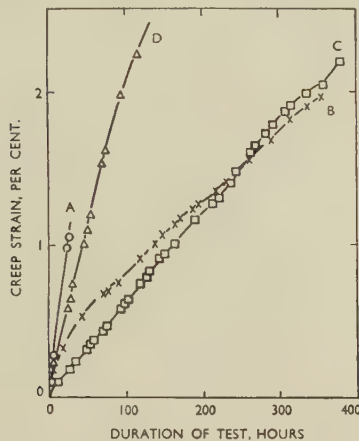


FIG. 6.—Effect of Recrystallization and Grain Growth on the Creep Properties of Chromium–10% Iron Alloy.

KEY.

- Test A : As cast. Tested at 5 tons/in.² and 900° C.
 Test B : Specimen for Test A cooled to room temperature, heated to 1000° C. in 2 hr. unstressed, held for ½ hr., cooled to 900° C., and retested at 5 tons/in.².
 Test C : As for test B, but heated to 950° C. for 8 hr. under a stress of 6 tons/in.². Retested at 5 tons/in.² at 900° C.
 Test D : As for test B, but tested at 6 tons/in.² at 900° C.

The creep properties of the alloy containing 10% iron were further investigated at higher stresses at 900° C. It was found that the creep properties of the alloy were influenced to a considerable extent by the effects of recrystallization and grain growth. In the as-cast condition under 5 tons/in.² at 900° C., the initial creep rate was high (curve *A*, Fig. 6), the strain being about 1% in 20 hr. If, however, the specimen after this strain was heated to 950°–1000° C. for a short period, either unstressed or under an applied stress, and subsequently tested at 900° C. the creep was appreciably less; and in this condition tests were continued to 360 hr. at 5 and 6 tons/in.² without the onset of tertiary creep (curves *B* and *C*, in Fig. 6). This strain-annealing treatment produced recrystallization and grain growth in the gauge portion of the specimen. Figs. 20 and 21 (Plate LXXXV) show the structure of the shoulders of the specimen (which are not significantly strained) and of the gauge-

length of the specimen the creep curve of which is *B* of Fig. 6. The appreciably larger grain-size inferred from the distribution of grain-boundary constituents in the gauge portion will be noted. It will also be noted that the curves *B* and *C* of Fig. 6 show small variations of creep rate during the course of the test. This phenomenon was encountered several times during the testing of materials the grain-size of which was of the same order as the gauge dia. or materials which undergo recrystallization and grain growth during the course of the test.

The effect of a high-temperature homogenizing heat-treatment was also studied for the 10% iron alloy. The creep at 3 tons/in.² at 900° C. for an as-cast sample was compared with that of a sample of the same alloy heat-treated for 24 hr. at 1250° C. in argon. The heat-treatment resulted in a definite decrease in resistance to creep. It may be noted that Parke and Bens,³ in an investigation of chromium–iron–molybdenum alloys, concluded that no heat-treatment of these alloys produced creep properties superior to those which the alloys possessed in the cast and stabilized condition. The hardness of none of the chromium–iron alloys was significantly altered by a heat-treatment of 24 hr. at 1250° C. This is in accordance with the single-phase nature of the alloys.

2. CHROMIUM–COBALT ALLOYS

Three alloys containing approximately 10, 20, and 30% cobalt were tested. Analysed compositions and hardness measurements are given in Table IV.

TABLE IV.—Analysed Compositions and Hardness of Chromium–Cobalt Alloys.

Nominal Cobalt Content, %	Melt No.	Analysed Composition, %			Vickers Hardness No. (5 kg.)			
					As Cast	After 24 hr. at 1250° C.	After 24 hr. at 1250° C. + 2 hr. at 900° C.	After 24 hr. at 1250° C. + 16 hr. at 900° C.
		Cobalt	Carbon	Oxygen				
10	H33	11.84	0.08	0.05	459	---	---	---
20	H34	18.50	0.06	0.07	547	563	577	534
30	H36	27.90	0.05	0.04	595	580	883	933

Alloys containing 40% cobalt were also made, but could not be tested owing to their extreme brittleness. In the as-cast condition, the 11.8 and 18.5% cobalt alloy contained particles of a second phase, attributable to the decomposition of the solid solution on cooling. According to the most recent equilibrium diagram for this system, due to Elsea, Westerman, and Manning,⁴ all the alloys tested should be homogeneous solid solutions above 1200° C., but at 900° C. the alloys with more than 10% cobalt lie in a two-phase region. The potentialities for precipitation-hardening of these alloys at 900° C. were therefore investigated. The alloys were solution-treated in argon for 24 hr. at 1250° C., and hardness measurements were made after rapid cooling from 1250° C. and after ageing for

successive periods at 900° C., with the results given in Table IV.

The microstructure of the alloys containing 18.5 and 27.9% cobalt after solution-treatment and ageing at 900° C. for 16 hr. are shown in Figs. 22 and 23

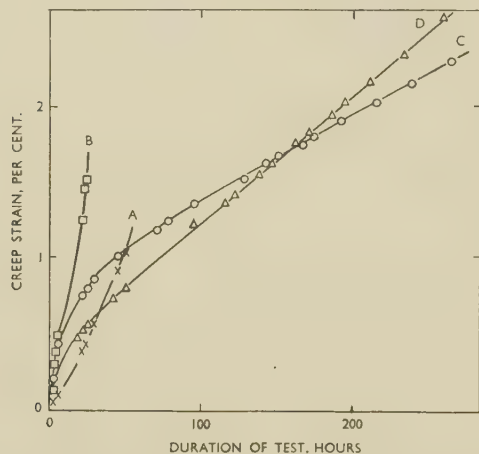


FIG. 7.—Compression Creep Curves of Chromium-Cobalt Alloys at 3 Tons/in.² and 900° C.

KEY.

Test A : H33 (11.8% Co) }
 Test B : H34 (18.5% Co) } As cast.
 Test C : H36 (27.9% Co) }
 Test D : H36 (27.9% Co). Heat-treated for 24 hr. at
 1250° C. followed by 16 hr. at 900° C.

(Plate LXXXV). The 18.5% cobalt alloy shows only a very small amount of second phase present after this heat-treatment, and the precipitation is not accompanied by significant hardening. The 27.9% cobalt alloy, on the other hand, precipitation-hardens appreciably, and the microstructure (Fig. 23) shows large quantities of precipitate in a Widmanstätten relationship to the matrix.

Creep curves for the alloys in the as-cast condition and for the 27.9% cobalt alloy in the solution-treated and precipitation-hardened condition are shown in Fig. 7. The alloy containing 11.8% cobalt showed an accelerating creep rate from early stages of the test (curve A). That containing 18.5% cobalt crept 1.5% in 30 hr. when the test was discontinued. The 27.9% cobalt alloy had a high secondary creep rate of 0.0055%/hr. after a primary creep deformation approaching 1%. The creep-resistance therefore increases with the cobalt content up to at least 28% cobalt. The level of creep properties of the 27.9% cobalt alloy is, however, appreciably inferior to that of the solid-solution chromium-10-15% iron alloys referred to above.

The effect of heat-treatment on the 27.9% cobalt alloy was to reduce the extent of primary creep, but to increase the secondary creep rate, so that, although initially superior to the as-cast alloy, the heat-treated alloy shows greater creep after about 150 hr.

An interesting feature of the creep curves which may be pointed out is their regularity compared with those of the chromium-iron alloys, which showed fluctuations in creep rate during the test. This is associated

with the much finer structure of the 27.9% cobalt alloy, the irregular curves being typical of alloys with a large crystal size.

3. CHROMIUM-NICKEL ALLOYS

Three alloys, containing approximately 5, 10, and 20% nickel respectively, were tested, the compositions and hardness measurements being given in Table V.

TABLE V.—Analysed Composition and Hardness of Chromium-Nickel Alloys.

Nominal Nickel Content, %	Melt No.	Analysed Composition, %			Vickers Hardness No. (5 kg.)			
					As Cast	After 24 hr. at 1250° C.	After 24 hr. at 1250° C. + 2 hr. at 900° C.	After 24 hr. at 1250° C. + 16 hr. at 900° C.
		Nickel	Carbon	Oxygen				
5	H70	4.77	0.01	n.d.
10	H69	8.84	0.04	n.d.	604
20	H37	18.94	0.04	0.05	945	859	480	411

n.d. = not determined.

The equilibrium diagram for this system, due to Jette, Nordstrom, Queneau, and Foote,⁵ shows the solubility of nickel in chromium at 900° C. as approximately 4%. In the as-cast condition all the alloys were duplex, the structure of the 18.94% nickel alloy being shown in Fig. 24 (Plate LXXXVI). The effect of heat-treatment was followed on the alloy containing 18.9% nickel. A treatment of 24 hr. at 1250° C.,

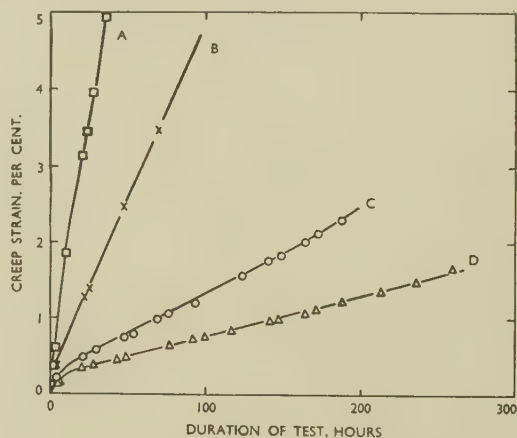


FIG. 8.—Compression Creep Curves of Cast Chromium-Nickel Alloys at 3 Tons/in.² and 900° C.

KEY.

Test A : H70 (4.8% Ni) }
 Test B : H69 (8.8% Ni) } As cast.
 Test C : H37 (18.9% Ni) }
 Test D : H37 (18.9% Ni). Heat-treated for 24 hr. at
 1250° C. followed by 16 hr. at 900° C.

followed by air-cooling, produced a reduction in hardness only from 945 to 859 V.P.N. The microstructure (Fig. 25, Plate LXXXVI) suggests that the solution created at 1250° C. had decomposed on cooling from the solution-treatment temperature. This was confirmed by ageing tests at 900° C. on the air-cooled alloy,

the hardness values being reduced after 2 and 16 hr. at 900° C. to 480 and 411 V.P.N., respectively. The reduction of hardness was associated with the appearance of finely dispersed precipitation in the alloy (Fig. 26, Plate LXXXVI).

The results of creep tests on the as-cast alloys and on the homogenized and stabilized 18.9% nickel alloy are given in Fig. 8. The creep-resistance increases with the nickel content of the alloys. Unlike the 27.9% cobalt alloy, the creep-resistance of the 18.9% nickel alloy is improved by homogenizing and stabilizing, the secondary creep rate of the as-cast alloy being approximately halved by homogenizing at 1250° C. and stabilizing for 16 hr. at 900° C. Even in this condition, however, the duplex 18.9% nickel alloy is appreciably inferior in creep properties to the solid-solution chromium-10-15% iron alloys.

It was not possible to investigate the properties of alloys containing higher nickel contents, as these proved to be excessively brittle at room temperature, and test-pieces could not be ground from them.

4. CHROMIUM-PALLADIUM ALLOYS

Only one alloy containing palladium was tested. This contained 6.77% palladium, 0.06% carbon, and

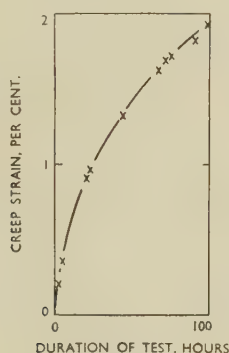


Fig. 9.—Compression Creep Curve of Cast Chromium-6.8% Palladium Alloy at 3 Tons/in.² and 900° C.

0.18% oxygen. The palladium addition was chosen as a value in excess of the estimated solid solubility in chromium at 900°-1000° C. The microstructure of the as-cast alloy showed the presence of a second phase in small amounts.

The creep curve for this alloy at 3 tons/in.² at 900° C. in the cast condition is shown in Fig. 9. The initial creep rate was high, and although it decreased continuously during the course of the test, the deformation at 100 hr. was 1.8%. In view of the high cost of palladium and the superiority in creep of the cheaper chromium-iron alloys, it was not considered that the chromium-palladium alloys merited further investigation.

5. CHROMIUM-ALUMINIUM ALLOYS

Attempts to investigate the properties of these alloys were unsuccessful. Several alloys containing up to 15% aluminium were melted and cast, but they

were so intensely brittle that specimens could not be ground from the ingots. Work on these alloys was therefore abandoned.

6. RESISTANCE TO OXIDATION

The resistance to atmospheric exposure at 900° C. of all the alloys that were tested appeared to be adequate. In exposures of up to several hundred hours at 900° C., no serious oxidation was noticed, the oxide scale being thin, adherent, and protective. Heat-treatments at about 1250° C. in air were accompanied by some nitride and oxide contamination at, and slightly below, the surface of the specimen, but this may be avoided by the use of a protective atmosphere of hydrogen or argon during heat-treatment.

VI. DISCUSSION OF RESULTS

The object of this work was to survey some of the binary chromium-rich alloys in order to discover the most promising base for further alloying to produce increased resistance to deformation at high temperatures. It has been found that a high level of creep-resistance at 900° C. is not encountered in chromium-rich alloys of the systems chromium-cobalt, chromium-nickel, and chromium-palladium. Simple binary solid-solution alloys containing 10-15% iron are, however, themselves fairly resistant to creep at 900° C. and moreover, being solid solutions, offer considerable promise for further alloying with other high-melting-point metals to improve the creep properties.

A point which must be mentioned is the low ductility of these alloys at room temperature. Chromium itself, of the purity attained in the present investigation, has a Brinell hardness of 106 and may be filed or sawn. It has, however, little ductility at room temperature, and may be fractured easily by impact. The same is true of all the alloys that have been tested, although there are considerable variations in strength from one alloy system to another. Chromium-aluminium alloys, for example, were too brittle to handle, and some chromium-nickel alloys could not be ground to test-pieces. Chromium-cobalt and chromium-iron alloys were noticeably less brittle, and no difficulty was experienced in grinding specimens from these alloys.

ACKNOWLEDGEMENTS

The authors' thanks are due to their former colleagues Mr. G. N. Cale and Mr. G. Willoughby for assistance with the experimental work.

REFERENCES

1. A. H. Sully, *Metal Ind.*, 1949, **75**, 491.
2. F. Adcock, *J. Iron Steel Inst.*, 1931, **124**, 99.
3. R. M. Parke and F. P. Bens, *Symposium on Materials for Gas Turbines (Amer. Soc. Test. Mat.)*, 1946, p. 80.
4. A. R. Elsea, A. B. Westerman, and G. K. Manning, *Trans. Amer. Inst. Min. Met. Eng.*, 1949, **180**, 579.
5. E. R. Jette, V. H. Nordstrom, B. Queneau, and F. Foote, *ibid.*, 1934, **111**, 361.

III.—The Creep Properties of Ternary and More Complex Chromium-Base Alloys

By A. H. SULLY, M.Sc., Ph.D., F.Inst.P., F.I.M., MEMBER, and
E. A. BRANDES, B.Sc., A.R.C.S., F.I.M., MEMBER

SYNOPSIS

The creep-resistance of cast ternary alloys consisting of chromium and iron alloyed with tantalum, niobium, tungsten, molybdenum, or vanadium has been measured in compression tests at 900° and 1000° C. Tensile time-to-rupture tests on the most promising alloys, chromium-iron-tantalum, have shown a large scatter of properties which is attributed to the effect of casting defects in a material very sensitive to notch effects. The resistance to thermal shock of cast chromium alloys is not of a high order. It does not appear to be possible to hot work chromium-iron or chromium-iron-tantalum alloys. The conclusion is drawn that it is unlikely that chromium-rich alloys can combine high creep-resistance with a sufficient degree of ductility to permit their use with confidence in engineering applications.

I.—INTRODUCTION

WORK described in Part II has shown that the binary chromium-iron alloys containing 5–15% iron have a very high degree of creep-resistance at 900° C. In addition, these alloys are single-phase solid solutions, and consequently constitute a promising base for further alloying in an attempt to improve the creep properties. In the investigation described in the present Part the creep properties have been examined of ternary and some quaternary alloys of chromium and iron with tantalum, niobium, tungsten, molybdenum, and vanadium.

II.—CREEP-RESISTANCE AT 900° C.

The compositions of the alloys investigated are given in Table VI. The alloys were all prepared by the technique described in Part I, the metals, in the purest commercially available form, being melted by high-frequency induction in vacuum in recrystallized alumina crucibles. The oxygen content of the melt, which arose from the electrolytic chromium, was reduced by treatment of the melt with carbon, the carbon monoxide resulting from the reduction of chromic oxide being pumped off until a sudden reduction of pressure in the furnace indicated substantial completion of the reduction process. The melts were cast in an atmosphere of argon into either a copper chill mould or as 0.5-in.-dia. bars in a refractory mould. Specimens for compression creep tests, having a gauge portion 0.25 in. long and 0.125 in. dia., were ground from these castings and tested at 900° C.

1. CHROMIUM-IRON-TANTALUM ALLOYS

Fig. 10 gives a typical series of compression creep curves for chromium-iron-tantalum alloys at a stress of 9 tons/in.² at 900° C. The iron content was either 10 or 20% (nominal), and the tantalum content was

varied from 2.5 to 28%. In the first place it is to be noted that the optimum tantalum content appears to be about 5–10%, the creep properties falling off with increasing or decreasing tantalum content. A

TABLE VI.—*Compositions of Alloys Investigated.*

Melt No.	Composition, % by weight							
	Fe	V	W	Ta	Nb	Mo	C	Si
H62	10.72	6.97
H64	10.05	2.57
H68	11.37	5.07	0.06	0.46
H76	10.1	10.75	<0.04	0.03
H77	10.7	18.63	<0.04	0.19
H78	21.4	5.69	<0.04	0.10
H79	21.3	9.22	<0.04	0.18
H80	21.5	17.49	<0.04	0.27
H81	28.5	19.8	0.31	0.18
H82	15.35	9.72	0.16
H83	9.94	14.94	<0.04	...
H87	9.35	27.5	0.10	...
H86	18.6	16.05	0.28	...
H91	(17.0)	(27.5)
H94	10.35	1.42	7.55	...	0.04	...
H95	11.07	3.52	18.52	...	0.13	...
H96	20.3	1.5	8.0	...	0.07	...
H97	19.09	3.19	16.7	...	0.18	...
H101	20.2	...	19.3	0.05	...
H102	10.7	...	12.7	0.04	...
H99	(8.5)	...	(28.1)
H127	9.55	9.46	<0.04	...
H128	9.69	14.17	<0.04	...
H131	11.01	27.30	<0.04	...
H132	18.75	10.45	0.05	...
H135	20.7	15.7	0.04	...
H110	11.38	5.9	7.63	0.04	...
H117	9.88	3.28	12.59	<0.04	...
H109	12.6	...	12.3	6.63	<0.04	...
H122	10.5	...	9.6	10.48	<0.04	...
H112	10.95	...	5.8	6.03	<0.04	...
H116	(10.0)	(5.0)	(5.0)	(5.0)	<0.04	...
H120	(5.0)	(5.0)	(5.0)	(10.0)	<0.04	...
H113	(5.0)	(5.0)	(5.0)	(5.0)	<0.04	...

Figures in parentheses = nominal analyses only.

10% iron-15% tantalum alloy was superior to a 20% iron alloy with the same tantalum content, indicating that, as in the binary chromium-iron alloys, the optimum iron content is of the order of 10%. The 10% iron-7% tantalum alloy under a stress of 9 tons/in.² at 900° C. suffered a total deformation of about 0.25% in 100 hr. and had a steady-state creep

rate of about 0.0003%/hr. This represents a high degree of creep-resistance.

The creep behaviour of these alloys can be correlated with their microstructure. Typical microstructures

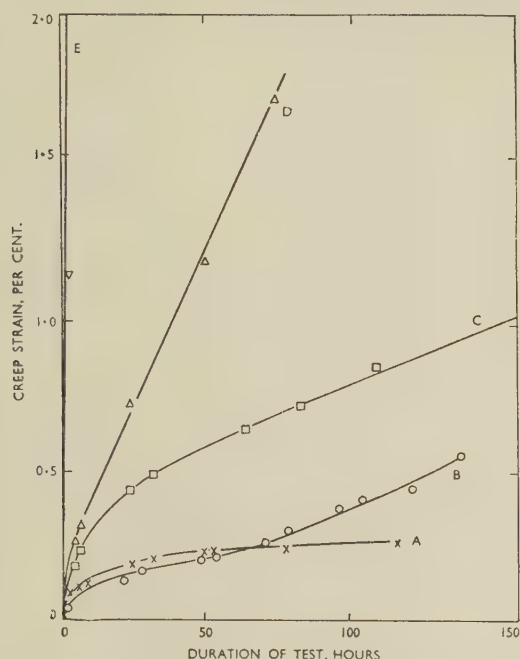


FIG. 10.—Compression Creep Curves of Cast Chromium-Iron-Tantalum Alloys at 9 Tons/in.² and 900° C.

KEY.

Test A: H62 (10.72% Fe, 6.97% Ta).
 Test B: H64 (10.05% Fe, 2.57% Ta).
 Test C: H83 (9.94% Fe, 14.94% Ta).
 Test D: H86 (18.6% Fe, 16.05% Ta).
 Test E: H87 (9.35% Fe, 27.5% Ta).
 Test F: H91 (17.0% Fe, 27.5% Ta).

are shown in Figs. 27–30 (Plate LXXXVI). Alloys containing up to 10% tantalum consisted of a solid-solution matrix containing a fine pearlitic type of eutectic (Figs. 27 and 28), the amount of eutectic increasing with the tantalum content. As the tantalum content is increased, the scale of the structure alters and consists primarily of a coarse degenerate eutectic. In addition, a structure appears which etches dark and is believed to be a ternary eutectic (Figs. 29 and 30). The creep properties deteriorate as the amount of ternary eutectic increases.

2. CHROMIUM-IRON-NIOBIUM ALLOYS

The niobium-containing alloys covered the same range of composition as the tantalum alloys. These alloys, however, proved to be extremely brittle and, in most cases, it was impossible to produce test-pieces for creep tests from the cast ingots. The creep curve of one alloy containing 10.3% iron and 7.5% niobium is shown in Fig. 11 (curve A). The creep-resistance of the alloy was inferior to that of the corresponding tantalum alloy. Because of this inferiority and the greater brittleness of the niobium alloys, no further work was carried out on the alloys containing niobium.

The structures of the niobium alloys (Figs. 31–34, Plate LXXXVII) are similar to those of the corresponding tantalum alloys. At 8–10% niobium (Figs. 31 and 32) with 10 and 20% iron the structure consists mainly of solid-solution matrix, degenerate eutectic, and small patches of dark-etching ternary eutectic. At higher niobium contents (Figs. 33 and 34) the structure changes to primary dendrites in a background of binary eutectic with ternary eutectic pools.

3. CHROMIUM-IRON-MOLYBDENUM ALLOYS

The alloys tested covered the range 10–20% iron and 10–25% molybdenum. Creep curves for alloys containing up to 15% molybdenum are given in Fig. 11. The optimum creep-resistance was again associated with alloying additions of 10%, decreasing with additions of both iron and molybdenum. The creep behaviour of the best alloy was, however, markedly inferior to that of the chromium–10% iron–10% tantalum alloy, the deformation in 100 hr. being 1.6%, compared with 0.25% for the latter. In addition, the creep rate of the molybdenum alloy continuously increased during the course of the test after the completion of the primary stage of creep.

No satisfactory compression creep tests were carried out on alloys with molybdenum contents greater than 15%. Under the conditions of the test, these alloys suffered a very severe form of oxidation attack which resulted in the complete destruction of the test-

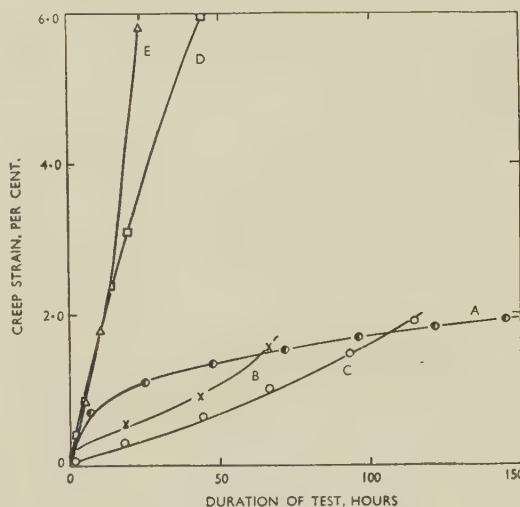


FIG. 11.—Compression Creep Curves of Chromium-Iron-Niobium and Chromium-Iron-Molybdenum Alloys at 9 Tons/in.² and 900° C.

KEY.

Test A: H94 (10.35% Fe, 7.55% Nb).
 Test B: H128 (9.69% Fe, 14.17% Mo).
 Test C: H127 (9.55% Fe, 9.46% Mo).
 Test D: H135 (20.7% Fe, 15.7% Mo).
 Test E: H132 (18.75% Fe, 10.45% Mo).

piece after a few hours at 900° C. This behaviour is abnormal in that it does not occur when the alloys are held at the same temperature under conditions in which air circulates freely over the specimen. It

appears to be a form of "catastrophic oxidation" similar to that noted with other molybdenum-containing alloys.¹ This subject will be discussed more fully later (p. 583). Because the apparatus could not easily be modified to allow free circulation of air over the specimen, it was not possible to carry out compression creep tests on alloys of the type developed by Parke and Bens,² containing 15–25% iron and 15–25% molybdenum.

In the as-cast condition the alloys consisted of single-phase solid solutions containing small quantities of dispersed oxide not removed by treatment of the melt with carbon. The single-phase nature of these alloys agrees with the finding of Goldschmidt.³

4. CHROMIUM-IRON-TUNGSTEN ALLOYS

The chromium-iron-tungsten alloys were very similar to the molybdenum-containing alloys in creep behaviour at 900° C. (Fig. 12). The optimum creep-resistance was associated with a 10% iron and 10% tungsten content and decreased with increasing content of iron or tungsten. The deformation rate for the 10% iron-10% tungsten alloy was of the same order as that for the 10% iron-10% molybdenum alloy and markedly greater than that for the 10% iron-10% tantalum alloy. The resistance to oxida-

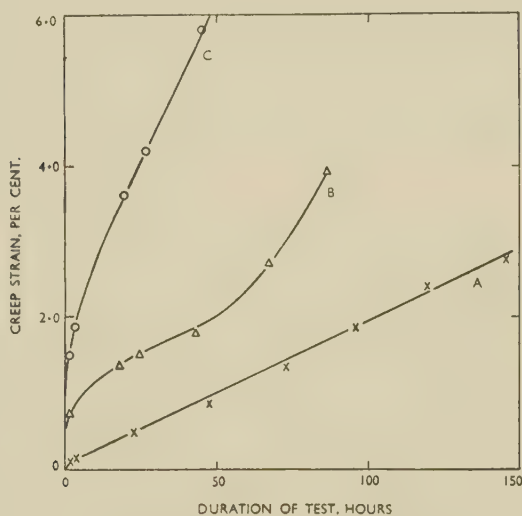


FIG. 12.—Compression Creep Curves of Chromium-Iron-Tungsten Alloys at 9 Tons/in.² and 900° C.

KEY.
Test A: H102 (10.7% Fe, 12.7% W).
Test B: H99 (8.5% Fe, 23.1% W).
Test C: H101 (20.2% Fe, 19.3% W).

tion at 900° C. of all the alloys tested appeared to be adequate.

Like the molybdenum alloys, the tungsten alloys in the cast condition were single-phase solid solutions.

5. CHROMIUM-IRON-VANADIUM ALLOYS

Chromium-iron-vanadium alloys were investigated over the ranges of composition 10–20% iron and 5–20% vanadium. Creep curves at 9 tons/in.² at

900° C. are shown in Fig. 13. The interpretation of the results of the creep tests is complicated by the fact that additions of vanadium seriously impair the

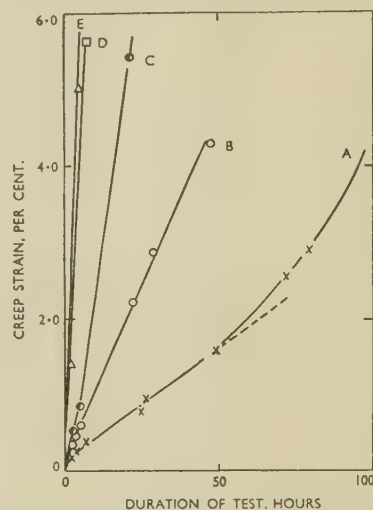


FIG. 13.—Compression Creep Curves of Chromium-Iron-Vanadium Alloys at 9 Tons/in.² and 900° C.

KEY.
Test A: H76 (10.1% Fe, 10.75% V).
Test B: H68 (11.37% Fe, 5.07% V).
Test C: H77 (10.7% Fe, 18.63% V).
Test D: H79 (21.3% Fe, 9.22% V).
Test E: H78 (21.4% Fe, 5.69% V).

oxidation-resistance of chromium-iron alloys. An enhanced rate of scaling at 900° C. is apparent with an addition of only 5% vanadium and at vanadium contents of 10% or more the rate of oxidation is so high that it is doubtful whether the creep curves given in Fig. 13 truly represent the creep-resistance of these alloys. As far as may be judged, the optimum creep-resistance occurs with 10% iron and 10% vanadium, but the creep properties of this alloy are poor compared with those of the chromium-10% iron-10% tantalum alloy.

The alloys were all predominantly single-phase solid solutions, but all contained substantial quantities of oxide, the amount of which increased with the vanadium content. The oxide took a different form from that normally present in cast chromium alloys free from vanadium, and was usually present as flakes in both crystals and crystal boundaries, having some resemblance to graphite flakes in cast iron (Fig. 35, Plate LXXXVII).

6. QUATERNARY ALLOYS

The most creep-resistant ternary alloy disclosed by the above tests was the chromium-10% iron-10% tantalum alloy. The most creep-resistant and stable alloy that was single-phase in the cast condition was the chromium-10% iron-10% tungsten alloy. A few alloys were made to see whether tantalum additions to the ternary chromium-iron-tungsten solid solution resulted in a higher degree of creep-resistance than tantalum additions to the binary

chromium-iron solid solution. The results of compression creep tests on some of these alloys are given in Fig. 14. Although the alloys containing 10% iron

at 1000° C. Creep curves are given in Fig. 15. Under these conditions, the best alloy was the chromium-10% iron-10% tungsten-10% tantalum alloys which had a steady-state creep rate of 0.0013%/hr. and had not entered the tertiary stage of creep after 300 hr.

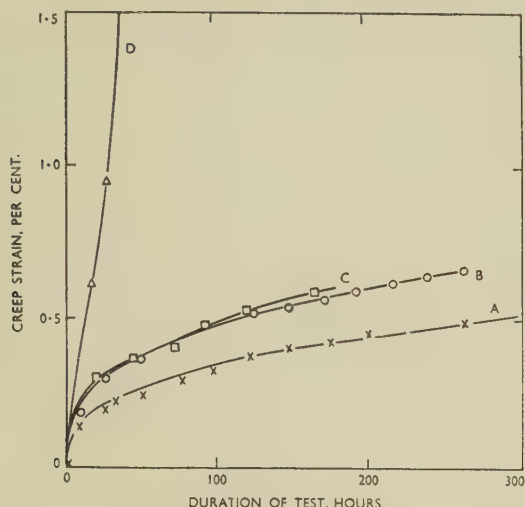


Fig. 14.—Compression Creep Curves of Quaternary Chromium Alloys at 9 Tons/in.² and 900° C.

KEY.

Test A : H122 (10.5% Fe, 9.6% W, 10.48% Ta).
Test B : H112 (10.95% Fe, 5.8% W, 6.03% Ta).
Test C : H109 (12.6% Fe, 12.3% W, 6.63% Ta).
Test D : H110 (11.38% Fe, 7.63% W, 5.9% V).

with 5-10% tungsten and 5-10% tantalum showed a relatively high resistance to creep at 900° C., none was superior to the ternary chromium-10% iron-10% tantalum alloy tested earlier.

III.—CREEP-RESISTANCE AT 1000° C.

A few alloys only, mainly the quaternary alloys mentioned above, were tested at a stress of 5 tons/in.²

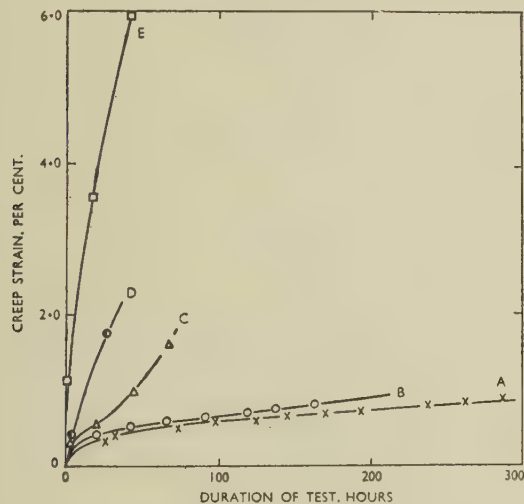


Fig. 15.—Compression Creep Curves of Some Chromium-Base Alloys at 5 Tons/in.² and 1000° C.

KEY.

Test A : H122 (10.5% Fe, 9.6% W, 10.48% Ta).
Test B : H109 (12.6% Fe, 12.3% W, 6.63% Ta).
Test C : H128 (9.69% Fe, 14.17% Mo).
Test D : H127 (9.55% Fe, 9.46% Mo).
Test E : H110 (11.38% Fe, 7.63% W, 5.9% V).

IV.—TENSILE TIME-TO-RUPTURE TESTS

The survey of creep characteristics made in compression indicated that, of the alloys investigated, the chromium-iron-tantalum alloys possessed the highest resistance to deformation at 900° C., and further effort was largely concentrated on alloys of this type. Time-to-rupture tests at 900° C. on these alloys were made in 5-ton creep machines, using Nimonic 80A adaptors. The specimens had a gauge portion 1 in. long and 0.179 in. dia. and at each end shoulders of 0.43 in. dia. The specimens were ground from cast 0.5-in.-dia. bars. The results obtained from time-to-rupture tests are set out in Table VII. The tests were usually made at stresses of 12 or 15 tons/in.². In addition to the tests listed in Table VII, a number of other tests were carried out, in which the test-pieces broke during loading to the test stress.

TABLE VII.—Results of Tensile Time-To-Rupture Tests at 900° C.

Melt No.	Nominal Composition, %	Stress, tons/in. ²	Time-to-Rupture, hr.	Elongation at Rupture, %	Remarks
H145	Cr-10 Fe-10 Ta	12.0	55.3	1.2	Broke in head of specimen. High carbon content. Not purified.
H152		12.0	232.3	2	
H171		12.0	23.7	...	
H194		12.0	19.7	2	
H196	Cr-10 Fe	12.0	32.5	3.3	Twin bars from same melt.
H153		15.0	19.1	0.7	
H155		15.0	31.0	5	
H155		15.0	32.4	9	
H158	Cr-10 Fe-10 W	15.0	33.0	2.2	
H163		15.0	22.6	2.2	
H188		12.0	58	1.5	
H162		9.0	5	0.7	
H149	Cr-15 Fe-25 Mo	15.0	0.3	1	
H167		15.0	45	4.5	

In contrast to the results obtained in compression, the tensile time-to-rupture results showed a large scatter of properties. In many tests fracture appeared to be determined more by defects of the cast test-pieces than by the intrinsic creep behaviour of the alloy. This is suggested by the relatively small difference in time-to-rupture between tests at 12 tons/in.² and tests at 15 tons/in.², except for one test-piece (H152). Microscopic examination of longitudinal sections of broken test-bars indicated in most cases that the fracture was associated with regions of porosity or interdendritic shrinkage. These regions were, however, generally no more frequent or more severe than in most cast materials. An exaggerated example is shown in Fig. 36 (Plate LXXXVII), which shows the structure at and near the fracture of a cast specimen that failed in the head during loading. Another observation tending to suggest variability in

the cast structure of the alloys is the scatter in values of elongation at rupture which varied from 0 to as much as 9%. It is possible that flaws were present in some specimens as a result of cracks formed during the grinding operation.

Attempts were made to eliminate casting defects by modifications to the shape of the casting. In order to obtain improved feeding to the gauge portion of the test-piece a change was made from a cylindrical casting to a dumb-bell-shaped casting approximating to the shape of the finished test-piece. This unfortunately did not eliminate the scatter of results, and small regions of porosity were still present in the test-pieces. It appears that fracture is normally initiated in regions of interdendritic porosity, and the crack which leads to fracture at the test temperature is propagated through the degenerate eutectic present in the chromium-10% iron-10% tantalum alloy. The typical appearance adjacent to the fracture at 900° C. of a test-piece of this alloy is shown in Fig. 37 (Plate LXXXVII).

The problem of producing castings in chromium alloys which are so consistently free from defects as to ensure reproducibility in subsequent creep testing has not been solved. The difficulties involved in handling molten chromium alloys are considerable. It is possible to work with only a small amount of superheat owing to the limitations of available refractories for crucibles and to the high volatility of chromium at high temperatures. As much as 25% of the chromium may be volatilized during the melting procedure as normally practised. Although it is possible that the quality of the castings could be improved by pouring into preheated moulds or by centrifugal casting, neither of these techniques is easy to apply in a vacuum or in a controlled atmosphere, and they have not been attempted.

It should be emphasized that the poor behaviour of chromium alloy castings is not due to the fact that the castings contain more defects than castings in other alloys, but that these minor defects have an exaggerated importance in materials of such limited ductility. In a material having normal ductility, it is possible that the stress-raising effect of minor casting defects would be relatively unimportant.

V.—THERMAL-SHOCK TESTS

Thermal-shock tests have been carried out by Messrs. Rolls-Royce, Ltd., on three chromium-base alloys: Cr-10% Fe-10% Ta, Cr-15% Fe-25% Mo, and Cr-30% Fe. The tests were carried out on cast wedge-shaped test-pieces $3\frac{1}{4}$ in. long, $\frac{7}{16}$ in. thick at the base of the triangular section and $1\frac{1}{16}$ in. wide. The test involved repeated rapid heating in a compressed-air-paraffin flame to 900°–930° C. and quenching in water mist. The test is intended to assess the suitability of alloys for use as nozzle guide vanes. The alloy H.R. Crown Max stands about 30 cycles on this test. The performance of the chromium alloys was as follows:

(i) *Cr-10% Fe-10% Ta Alloy*.—Major crack on first cycle and broke at crack during examination.

(ii) *Cr-15% Fe-25% Mo Alloy*.—Developed 12 major cracks after 5 cycles and showed large areas of minor cracking. After a further 5 cycles the test-piece came apart during removal from its holder.

(iii) *Cr-30% Fe Alloy*.—Developed a major crack near the root at the end of 5 cycles and exhibited local areas of continuous minor cracking. The test-piece was run for a further 25 cycles with inspection at 5-cycle intervals. Propagation was slow but at 30 cycles 3 major cracks had developed at the thin edge.

The behaviour in these thermal-shock tests varied roughly inversely with the creep behaviour at high temperatures. The highly creep-resistant alloy containing iron and tantalum suffered early failure owing to thermal shock, and the best behaviour was shown by the chromium-30% iron solid-solution alloy which, however, suffered appreciable creep deformation at 900° C. under stresses as low as 3 tons/in.². The chromium-iron-molybdenum alloy was intermediate in resistance to both creep and thermal shock. A microscopical examination of the samples subjected to thermal-shock tests showed both major and minor cracks to be primarily transcrystalline in character (Fig. 38, Plate LXXXVII).

VI.—SWAGING EXPERIMENTS

In view of the deficiencies of the cast structure revealed by creep and thermal-shock tests, some attempts have been made to modify the structure of these alloys by mechanical working in the hope that this might improve the consistency of the creep behaviour.

With the collaboration of the Research Department of the General Electric Co., Ltd., attempts were made to hot-swage chromium alloys in rotary swages of the type used for swaging tungsten. The alloys chosen for these experiments were the chromium-10% iron-10% tantalum alloy and the solid-solution chromium-10% iron alloy. Bars approximately 6–7 in. long and 0.25 in. in dia. were ground from castings of these alloys. These were swaged both directly and inside closely fitting sheaths of mild steel. The bars were preheated to 1450° C. in a hydrogen atmosphere and swaged at approximately 1300° C. No success was achieved with either alloy. In direct swaging, the bars suffered multiple transverse fractures after only a very small reduction of area. Sheath-swaging was equally unsuccessful. The chromium alloys proved to be so much more resistant to deformation than the mild steel that all the deformation took place in the latter, the chromium alloy being unreduced in area and often cracked inside the sheath.

VII.—RESISTANCE TO OXIDATION

With two exceptions, the various types of chromium alloy which have been investigated during this work have possessed a high degree of resistance to oxidation

in air at 900° C. The two exceptions were certain chromium-iron-molybdenum and chromium-iron-vanadium alloys.

Difficulties were first encountered during the compression creep testing of alloys containing more than about 15% molybdenum. These alloys were so badly oxidized after a very short exposure at 900° C. that creep tests could not be carried out satisfactorily. Fig. 39 (Plate LXXXVIII) shows the initial and final appearance of a chromium-15% iron-25% molybdenum alloy before and after heating to 900° C. in the compressive creep machine for 40 hr. This result was entirely unexpected, as this alloy composition had been extensively investigated by Parke and Bens,² who described it as having a high degree of surface stability at 875° C. It is, however, well known that certain molybdenum alloys can suffer an enormously accelerated form of oxidation attack in conditions in which air does not circulate freely over the surface of the specimen. This phenomenon has been called "catastrophic oxidation", and its occurrence has been attributed either to the dissociation of molybdic trioxide at the surface of the specimen with the release of nascent oxygen (Leslie and Fontana¹) or to the formation of low-melting-point oxide eutectics (Meijering and Rathenau⁴). In the compression creep machines used in this work the specimen was enclosed inside a hollow cylindrical steatite guide and compressed between recrystallized alumina rods which were a close fit inside the guide. The atmosphere around the specimen was therefore stagnant, and conditions were favourable for "catastrophic oxidation" to occur. Confirmation of this was provided by heating a sample of the same alloy in an open-ended furnace tube at 900° C. The amount of oxidation in periods as long as several hundred hours was very slight indeed. Attempts were therefore made to synthesize the conditions leading to the aggravated form of oxidation. This proved to be much more difficult than had been expected, and it was necessary to achieve a high degree of stagnancy in the atmosphere before the desired result could be produced. The method which was found most successful and reproducible was to enclose the specimen inside a closed-ended transparent silica tube a little longer than the specimen. The silica tube was then drawn down at the open end to a fine capillary open to the atmosphere. Under these conditions "catastrophic oxidation" occurred quite readily. Figs. 40 and 41 (Plate LXXXVIII) show the appearance of two pieces of the chromium-15% iron-25% molybdenum alloy initially almost identical in size, after heating for 216 hr. at 900° C. in free air and inside a capillary-ended silica tube, respectively. The specimen heated in free air was only very lightly oxidized, whereas that heated in stagnant air was very heavily attacked. In Fig. 41 the large encrustations of oxide have been broken away from the specimen to show the residual core of unattacked metal.

Chromium alloys containing appreciable quantities of vanadium, on the other hand, were very severely

oxidized in air at 900° C., and the attack was not much influenced by the condition of stagnancy of the atmosphere. The effect was seen at vanadium concentrations as low as 5% when a heavy scale formed in periods of the order of 100 hr. at 900° C. At vanadium contents of 10% and above the oxidation was extremely rapid. Fig. 42 (Plate LXXXVIII) shows a compression creep-test specimen of an alloy containing 20% vanadium after 117 hr. in air at 900° C., which had been completely converted to a mass of spongy oxide. It is obvious that substantial vanadium concentrations have no merit in chromium-base alloys for high-temperature service.

VIII.—GENERAL DISCUSSION

Although this investigation has confirmed that certain chromium alloys have a very high degree of resistance to deformation and to oxidation at high temperatures, it has also disclosed a major disadvantage of these alloys for engineering applications. This is their extreme brittleness, which is shown by the ease with which cracks are formed in them and, once formed, are easily propagated, causing failure with very low ductility. This has been manifested in the work described above by the sporadic incidence of failure in cast alloys in creep tests or during loading to the test stress, by the early incidence of cracking in thermal-shock tests, and by the behaviour in swaging tests. At room temperature the brittleness is particularly marked and is shown in greater or lesser degree by pure chromium and all the alloys consisting predominantly of chromium which have been investigated.

The general brittleness of chromium-rich alloys is thus bound up to a very considerable extent with the brittleness of elemental chromium. It was first demonstrated by Marden and Rich,⁵ and it has since been adequately confirmed, that although chromium is brittle at room temperature it possesses appreciable ductility at elevated temperatures. Marden and Rich have reported the successful hot swaging to wire of chromium compacts prepared by sintering chromium powder of fairly high purity. The factors which influence the ductility of metallic chromium have been the subject of investigation by the present authors, and will be discussed in a further communication. It has been found that chromium shows a sharp transition from ductility to brittleness over a narrow range of temperature and that the value of this transition temperature is influenced by the purity of the chromium. With the means at the authors' disposal, however, it has not been possible to produce chromium which has any significant ductility under tensile stress at room temperature, and unfortunately those elements which must be added to chromium to enhance the resistance to creep at elevated temperatures also have the effect of raising to considerably higher values the temperature of transition from brittleness to ductility. The conclusion is therefore regretfully drawn from this work that it is unlikely that

any chromium-base alloy will have a high degree of resistance to deformation at high temperatures and to thermal shock combined with ductility adequate to enable it to be successfully and reliably applied in engineering practice.

ACKNOWLEDGEMENTS

The authors thank Mr. E. A. G. Liddiard, Director of Research, Fulmer Research Institute, for his encouragement and interest in this investigation. They also thank their colleague Mr. T. J. Heal and their former colleagues Mr. G. N. Cale and Mr. G. Willoughby for valuable contributions to the experimental work, and Mr. H. E. Gresham of Rolls-

Royce, Ltd., and Dr. I. Jenkins of The General Electric Co., Ltd., for providing facilities for thermal-shock tests and swaging trials respectively.

REFERENCES

1. W. C. Leslie and M. G. Fontana, *Trans. Amer. Soc. Metals*, 1949, **41**, 1213.
2. R. M. Parke and F. P. Bens, *Symposium on Materials for Gas Turbines (Amer. Soc. Test. Mat.)*, 1946, p. 80.
3. H. J. Goldschmidt, *Iron Steel Inst. Special Rep.* 1952, (43), 249.
4. J. L. Meijering and G. W. Rathenau, *Nature*, 1950, **165**, 240; *Metallurgia*, 1950, **42**, 167.
5. J. W. Marden and M. N. Rich, U.S. Patent No. **1,760,367**, 1930.

THE EFFECT OF TEMPERATURE AND PURITY ON THE DUCTILITY AND OTHER PROPERTIES OF CHROMIUM*

1479

By A. H. SULLY,† Ph.D., M.Sc., F.Inst.P., F.I.M., MEMBER,
E. A. BRANDES,‡ B.Sc., A.R.C.S., F.I.M., MEMBER, and
K. W. MITCHELL,§ B.Sc.(Eng.), Wh.Sch., A.M.I.Mech.E.

SYNOPSIS

Chromium shows a sharp transition from ductile to brittle behaviour over a small range of temperature. The effect of impurities and of strain rate on this transition temperature have been investigated. Oxygen in quantities greater than 0.002% has comparatively little effect, but additions of other elements substantially raise the transition temperature, the effect being in general dependent upon the solid-solution hardening produced by the addition. The lowest temperature at which a chromium sample showed ductile behaviour in bend tests was 50° C.

The effect of impurities in chromium is compared with their influence on iron. The transition temperature varies with the strain rate according to an exponential relationship. It has been confirmed that under compressive stress chromium may show ductile behaviour at temperatures at which it is brittle under tensile stress, and deformation at room temperature has been accomplished in this way.

Electrical-resistance measurements on pure chromium confirm the existence of a transition reported by earlier workers at about 37° C., but this is not considered to have any significant influence on the plastic behaviour.

I.—INTRODUCTION

ALLOYS consisting predominantly of chromium have been shown to have a high degree of resistance to oxidation and to deformation at elevated temperatures.^{1,2} Such alloys have, moreover, the advantage that they can be made from materials in fairly ready supply, which is an important consideration in the economy of the use of strategically important metals. Unfortunately, however, chromium-rich alloys produced by melting and casting are extremely brittle at room temperature, and are extremely sensitive to the effect of notches even at elevated temperatures, a crack once formed being propagated with great ease. The resistance to thermal shock of such alloys is very low. For these reasons, chromium-rich alloys are unlikely to have any large-scale use in the engineering industries unless some means can be found to improve their ductility with a consequent gain in the reproducibility of their properties and their resistance to impact and to thermal shock. Since the same disadvantages which the alloys possess are possessed also by chromium in its commercially pure form, it was logical to investigate the factors which affect the ductility of pure chromium in order to determine the feasibility of the development of a ductile chromium base for further alloying with other

elements to produce alloys having the required strength characteristics.

The question to which an answer was most urgently required was whether the brittleness of commercial chromium was intrinsic or whether it was due to the presence of a certain specific impurity. If the latter, it was of importance to discover whether the impurity level could be fairly readily reduced to a value which resulted in reasonable ductility or whether some element could be added to chromium which counteracted the deleterious effect. The present investigation provides a partial answer to these questions.

II.—PREVIOUS WORK ON THE DUCTILITY OF CHROMIUM

A number of other workers have reported earlier—some while the present work was in progress—that chromium is ductile at elevated temperatures, though brittle at room temperature. Hunter and Jones³ have shown that small pellets of chromium produced by the reduction of chromium chloride with sodium can be hot worked; Marden and Rich⁴ claim to have worked compacts made from chromium powder in the range 600°–1100° C.; and Kroll⁵ has reported that chromium is ductile and can be hot worked at 1250° C. During later work, Kroll, Hergert, and Yerkes⁶ have shown that chromium in which the

* Manuscript received 2 April 1953.

† Principal Physicist, Fulmer Research Institute, Stoke Poges, Bucks.

‡ Head of Experimental Foundry Section, Fulmer Research Institute, Stoke Poges, Bucks.

§ Head of Engineering Section, Fulmer Research Institute, Stoke Poges, Bucks.

oxygen content is reduced by lengthy heat-treatment in hydrogen can be compacted and sintered at 1300° C. in a vacuum to produce material which can be pressed at 800° C. and subsequently rolled to sheet at this temperature. They state that this worked chromium is quite ductile above 500° C., but very brittle at room temperature. As well as these investigators, Adcock⁷ and Brenner, Burkhead, and Jennings,⁸ who studied methods of producing chromium of low impurity content, have reported that pure chromium is brittle at room temperature.

A recent investigation of the working of chromium has been made by Gilbert, Johansen, and Nelson.⁹ These workers arc-melted in an inert atmosphere electrolytic chromium powder previously purified by hydrogen treatment. The purity of their ingot metal is given as iron 0.001, silicon 0.05, oxygen 0.003, nitrogen 0.002, and hydrogen 0.005%. They found that such ingots could be forged at 800°–850° C. and that, after the cast structure had been broken down, further working could be accomplished at 500° C. They state, however, that this material was brittle at room temperature.

Other workers have reported a limited degree of ductility in chromium at room temperature. Greiner¹⁰ found slip markings on chromium compacts, made by sintering in hydrogen and helium at 1300° C., when these were compressed between hardened steel blocks. Cross¹¹ states that single crystals of chromium made by thermal decomposition of chromium tetraiodide are brittle when struck with a hammer, but can be reduced in compression by about 40% in thickness without cracking. The same result can be obtained after the crystals are arc-melted in an inert atmosphere. These results have recently been described in detail by Goodwin, Gilbert, Schwartz and Greenidge.²⁶

III.—THE PREPARATION OF PURE CHROMIUM

A necessary starting point for an investigation of the effect of impurities on the ductility of chromium is a supply of chromium in a state of high purity. In previous work on chromium alloys reported by the present authors,² cast alloys were used in which the oxygen content was reduced by treatment of the melt with carbon. However, this method is not entirely suitable for the production of pure chromium because it is extremely difficult to gauge the end-point of the carbon reduction sufficiently accurately to ensure that both carbon and oxygen are at a low content (less than about 0.02–0.04%). In addition, the melting point of chromium (1860° C.) is appreciably higher than the melting points of most of the alloys which were investigated, and it was found that with alumina crucibles, which were most generally used, reaction between the crucible and the molten chromium at temperatures of about 1900° C. resulted in contamination of the chromium by aluminium to the undesirably high extent of about 0.3%.

The purest chromium available commercially is the electrolytic metal. That used for the present investigation contained iron 0.06, nitrogen 0.007, sulphur 0.026, and less than 0.01% silicon. In addition, this metal contained appreciable quantities of oxygen. The method of determining the oxygen content has been described previously;² it consists in heating the chromium in vacuum at 800° C. and determining the quantity of oxide by solution of the chromium in dilute hydrochloric acid. It has been shown by the present investigators, by Short,¹² and by Brenner, Burkhead, and Jennings⁸ that determinations by this method agree well with the results of vacuum-fusion gas analysis. The oxygen content of electrolytically deposited chromium is normally about 0.6%, although Brenner and his colleagues⁸ have shown that this is dependent upon the temperature of the plating bath, being lower the higher the bath temperature.

Rohn¹³ and Adcock⁷ showed that the oxygen content may be reduced by treatment in pure dry hydrogen which reduces the chromic oxide to metallic chromium. Adcock recirculated pure dry hydrogen over electrolytic chromium at 1500°–1600° C. and reduced the content of oxide insoluble in dilute acid from 1.31% to zero. Kroll, Hergert, and Yerkes⁶ have also used this method of purification, though they generated their supply of pure hydrogen by heating zirconium hydride. They carried out their treatment at 1000° C., achieving a reduction of the oxide content from 1.0% (0.32% oxygen) to 0.2% (0.07% oxygen) in 3 days at this temperature. Kroll and his colleagues point out, however, that a higher temperature of reduction is to be preferred, since a higher content of water vapour can be tolerated in the hydrogen, the higher the reduction temperature. The following values from Grube and Flad¹⁴ and Wartenberg and Aoyama¹⁵ may be taken for the partial pressures of water vapour in the $\text{Cr}_2\text{O}_3/\text{H}_2$ equilibrium as a function of temperature:

Temp., °C.	$p_{\text{H}_2\text{O}}$, mm.
1022	0.29
1210	1.33
1300	2.02
1500	6.0 (extrapolated)

Kroll, however, chose a fairly low reduction temperature in order to avoid silicon contamination of the chromium which occurs as a consequence of the reduction by hydrogen of silica in the furnace refractories to volatile silicon monoxide, the silicon monoxide then reacting with the chromium to form Cr_2O_3 and chromium silicide, CrSi . As shown by Tombs and Welch,¹⁶ this reduction is known to take place rather rapidly above 1300° C. In the present work, contamination by silicon has been avoided by lining the furnace tube, which was of mullite, with pure sintered alumina, the chromium to be reduced being held in boats of the same material. In this way it has been possible to carry out the reduction at 1500° C. with a considerable economy in time, greater tolerance for water vapour in the hydrogen,

and a silicon content in the reduced chromium which rarely exceeded 0.02%.

Most of the present work has been carried out on compacts prepared by the methods of powder metallurgy and sintered in pure, dry hydrogen for 4 hr. at 1450° C. The chromium used was pure electrolytic granules of the analysis given above. In the first place, a lengthy ball milling was required in order to break the chromium down to a fine state of subdivision. This was usually carried out for 10 days in a steel mill with steel balls. Although it resulted in some contamination of the chromium powder with iron, this method was preferable to milling with refractory mills and balls, since contamination by refractory constituents could not easily be eliminated, whereas iron contamination could, although by a lengthy operation involving simmering the powder for 10 days in 50% nitric acid at the boiling point. As a consequence of this treatment, the iron content was reduced to a value as low as, and in some cases inexplicably lower than, that of the original chromium before milling, the iron content in some specimens being less than 0.02%. The ball-milled and simmered chromium was pressed into specimens usually of dimensions $2\frac{1}{2} \times \frac{1}{2} \times 0.1$ – 0.2 in. in a die at a pressure of 20 tons/in.². The pressing was aided by the use of a temporary wax bond, "Ceremul R", which was removed from the specimens after pressing by heating to and holding at 300° C. They were then sintered at 1450° C. in pure dry hydrogen, as described above. The lowest oxygen content achieved by this method was 0.003%, corresponding to a content of 0.01% chromic oxide. This, however, was with thin electrolytic chromium flakes, and with powder compacts the average oxygen content was somewhat higher, being of the order of 0.01–0.02% (0.03–0.06% chromic oxide). The silicon content was usually less than 0.02% and the nitrogen content of the same order. The carbon content rarely exceeded 0.01%. The overall purity was, therefore, about 99.85–99.90%.

For some of the work, use was made of chromium produced by the decomposition of chromium hydride. This was of lower purity than the electrolytic chromium and contained iron 0.54, nitrogen 0.22, silicon 0.14, sulphur 0.014, and oxygen 0.65%. When this chromium was sintered in hydrogen, the oxygen content was reduced to a level as low as that obtained with the electrolytic chromium; the nitrogen content was also very considerably reduced to 0.02–0.04% or less. The content of the other impurities, except sulphur, was not affected by this treatment. This form of chromium had certain experimental conveniences connected with its use, since it was in an extremely fine state of subdivision and could be pressed directly without the use of a temporary bond and did not require the lengthy pre-treatment involving milling and acid simmering.

Specimens prepared in this way had a very fine grain-size, but exhibited considerable porosity. The porosity varied from batch to batch, but was usually

in the range 6–15%. Fig. 12 (Plate LXXXIX) shows a typical microsection. The pores are apparently disconnected and are not much affected by refiring at a higher temperature after the initial sintering.

IV.—EXPERIMENTAL METHODS OF MECHANICAL TESTING

1. BEND TESTS

Three-point bend tests provide a convenient means of studying the variation of the ductility of chromium with temperature. The test-piece was of the size given above, viz. a rectangular block of dimensions approximately $2\frac{1}{2} \times \frac{1}{2} \times 0.15$ in. This rested inside a furnace on two cylindrical rods of recrystallized alumina, lying in grooves in a block of magnesia. The distance between the points of support was 1.75 in. The load was applied by means of a lever with a 10:1 loading ratio to an alumina rod which had a V-shaped lower end applying the load at the centre of the specimen along a line at right angles to the major axis of the specimen. The rod was guided to move vertically. Deflection readings were taken during loading by a dial gauge in contact with the loading lever.

Two types of test were carried out in this equipment. In one, loading was carried out in incremental steps until a stress was applied which caused the specimen to break, or alternatively to bend to the full extent permitted by the apparatus, corresponding to a deflection of about 0.2 in. at the centre of the span. Sometimes several tests were carried out on a single specimen which was first loaded to its yield point at a temperature at which it was ductile and then unloaded, the temperature reduced, and the loading repeated. This process could be repeated until a temperature was reached at which the specimen broke in the elastic range.

In the second type of test, bend tests were made at a constant rate of strain. The modification to the apparatus to allow this to be done is shown diagrammatically in Fig. 1. The loading beam was made to deflect at a constant and known rate by driving it by means of an electric motor working through reduction gearing. A weigh-bar, consisting of a light alloy sheet tensile specimen carrying an electrical-resistance strain-gauge, was inserted between the motorized drive and the loading beam. The strain-gauge reading gave a measure of the applied load, and was calibrated by static loading of the weigh-bar. A check on the accuracy of measurement was made by bend tests at room temperature on an HE 10 WP aluminium alloy specimen of known elastic constants. This gave a relationship between load and deflection of 1.165×10^{-4} in./lb., compared with a theoretical value of 1.155×10^{-4} in./lb., an error of less than 1%. By variation of the reduction gearing, tests were carried out at three rates of strain on the specimen, viz. 0.00297, 0.0696, and 0.77 in./min., an overall variation of 260:1.

Tests were made both on unnotched specimens and

on specimens carrying a notch 0.5 mm. deep, with 60° included angle, and a radius at the base of the notch of approximately 0.25 mm.

2. IMPACT TESTS

Impact tests were carried out on standard Charpy-type unnotched specimens 10 mm. square and 60 mm. long, ground to size from sintered chromium compacts 0.45 in. square and 2½ in. long, prepared by exactly the same procedure as that used in the preparation of specimens for bend test. The specimens were all tested normal to the direction of pressing of the original compacts. Since the impact value of chromium is low, even at temperatures at which it is ductile in bend tests, a standard impact-testing machine was found to be insufficiently sensitive, and

exhibits some plastic deformation. In practice this distinction was quite clear cut, since yield, when it occurred, was quite well marked and, in general, specimens which showed yield had appreciable ductility, often deforming without failure to the full extent permitted by the apparatus.

The first important conclusion from the bend tests was that chromium shows a very sharp transition from brittleness to ductility over a range of only a few degrees of temperature. Although there was, from batch to batch of specimens, a considerable variation in the transition temperature, the temperature for one batch, with identical impurity contents and processed in exactly the same way, could usually be defined within 5°–10° C. if the number of specimens permitted such a close investigation. A typical family of stress/strain curves, in this case

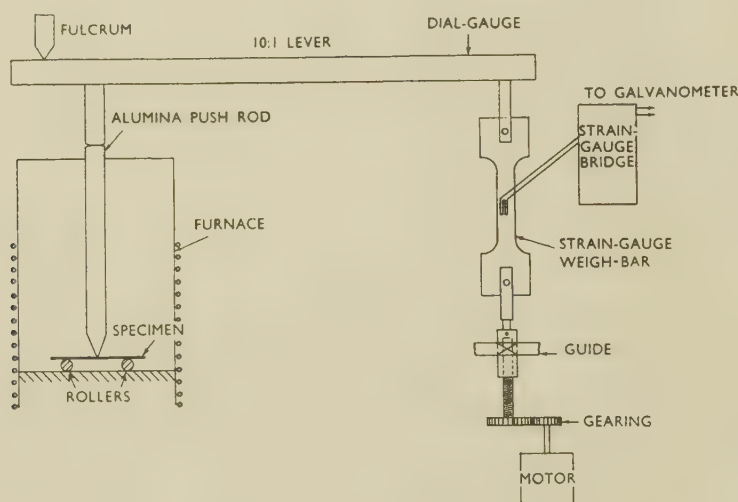


Fig. 1.—Diagrammatic Arrangement of Apparatus for Bend Tests at Constant Strain Rate.

a small pendulum-type Charpy machine of 10 ft.-lb. capacity was constructed. The specimens were brought up to temperature in a furnace, alongside the machine, in approximately ½ hr. and then held at temperature for 15 min. before the test. The velocity of impact in this machine was 16.38 ft./sec. (11,794 in./min.).

3. TENSILE TESTS

Small tensile specimens, of 0.179 in. gauge dia., were ground from the centre of chromium compacts, 0.45 in. square and 2½ in. long, and tested at temperatures up to 900° C. in a Hounsfield Tensometer testing machine.

V.—MECHANICAL TEST RESULTS

1. BEND TESTS

The distinction drawn between brittleness and ductility depends upon whether the specimen, in the bend test, fractures in the elastic range or whether it

for a series of samples of electrolytic chromium containing 0.05% aluminium, is shown in Fig. 2. It will be seen that the onset of yield is defined quite precisely between 190° C., at which temperature fracture occurred in the elastic range, and 195° C., at which temperature a sharp onset of yield occurred and the specimen showed a large plastic deformation.

Fig. 3 shows the variation of amount of bend with temperature for a large batch of hydride chromium specimens. Although, in this series, the transition temperature is not closely defined, owing to the fact that the specimens were not all sintered at the same time and under the same conditions, it will be seen that, with two exceptions, the specimens either broke in the elastic range or were so ductile that they deformed without fracture to the full extent permitted by the apparatus.

Table I lists some results, which will be considered more fully below. The temperatures are, for each batch of specimens, the highest at which a specimen was brittle and the lowest at which a specimen was ductile.

It will be noted that the transition temperature, defined within the limits given previously, varies very considerably from batch to batch of specimens.

TABLE I.—Transition Temperatures in Bend Tests with Incremental Loading for Electrolytic and Hydride Chromium Samples Containing No Deliberate Additions of Other Elements.

Batch No.	Preparation		Ductility		Analysis, %				Hardness, V.P.N. (1 kg.)
	Mill- ing, hr.	Sim- mering, hr.	Brittle at and below, °C.	Ductile at and above, °C.					
					O ₂	Si	Fe	N ₂	
<i>Electrolytic Chromium</i>									
S42	240	240	80	90	0.019	≤ 0.05	Trace	n.d.	71
S44			25	50	0.012	≤ 0.05	0.05	0.04	48.5
S47			...	70	0.10	0.02	0.06	n.d.	44.6
S56 *			50	55	0.87	0.02	0.02	n.d.	72
<i>Hydride Chromium</i>									
S14	Nil	Nil	300	350	0.05	n.d.	n.d.	n.d.	n.d.
S15			350	400	n.d.	n.d.	n.d.	0.04	n.d.
S16			...	240	0.041	0.34	0.61	0.02	133.4
S26			390	400	n.d.	n.d.	n.d.	n.d.	144
S66 *			350	365	(0.9)	n.d.	n.d.	n.d.	n.d.

n.d. = not determined.

* Sintered in argon; no reduction of oxide.

The lowest temperature at which a specimen was ductile was 50° C., and the highest temperature at which a specimen was brittle was 390° C. These differences cannot be correlated with any microstructural difference between the specimens, as the grain-size was much the same for all the specimens examined, being usually in the range 0.001–0.003 in.,

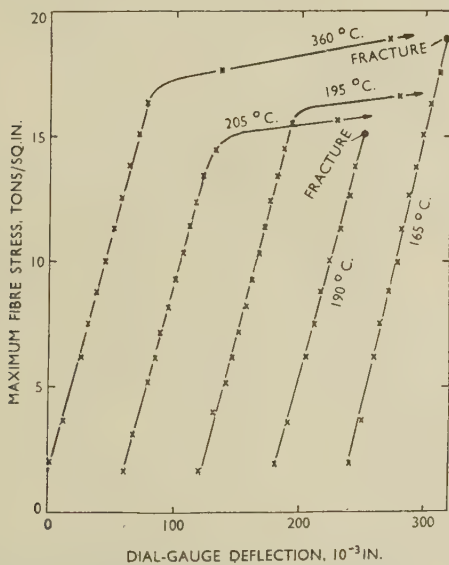


FIG. 2.—Stress/Strain Curves at Various Temperatures for Electrolytic Chromium Containing 0.05% Aluminium.

and no other differences were detected. Although the porosity varied from specimen to specimen and from batch to batch, there was no correlation between porosity and transition temperature.

Table I discloses a consistent difference in transition

temperature between compacts made from electrolytic and hydride chromium, respectively. The lower purity of the latter material, which gives compacts with a high transition temperature, has

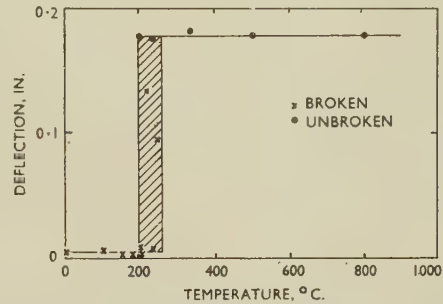


FIG. 3.—Variation of Ductility with Temperature for a Batch of Specimens Prepared from Hydride Chromium.

already been mentioned, and the effect of specific impurities on the transition temperature must be considered.

(a) Effects of Oxygen and Nitrogen

The most common impurity in chromium is oxygen, and by analogy with other pure metals such as molybdenum and iron, it is this element more than any other which has been suspected of being responsible for the lack of ductility of chromium. The results of the present investigation do not support this view. Probably the purest chromium made in the course of the present work, taking into account the three elements oxygen, silicon, and iron, is Batch S44 (Table I), which contained 0.012% oxygen, 0.05% iron, and much less than 0.05% silicon. This batch was ductile at 50° C., but brittle at room temperature (25° C.). Batch S42, with slightly more oxygen, less iron, and 0.05% silicon, had a transition temperature between 80° and 90° C.

In contrast to these batches of low oxygen content, Batch S56 was prepared in exactly the same way and contained 0.02% iron and 0.02% silicon, but was sintered in argon instead of in hydrogen, so that no reduction of the oxide content was achieved and the samples contained 0.87% oxygen. The transition temperature for this batch was between 50° and 55° C., the second lowest recorded in the present series of tests. It is clear, therefore, that a variation in oxygen content from 0.87 to 0.012% has no significant effect on the temperature of transition from brittleness to ductility.

It may, of course, be argued that even 0.012% oxygen may be sufficient to produce any deleterious effect for which this element is responsible. The authors were, however, able to secure, by the courtesy of Dr. N. P. Allen of the Metallurgy Division, National Physical Laboratory, a sample of highly purified electrolytic chromium flake, prepared in that laboratory by Mr. J. H. Rendall. The oxygen content of this, as determined by vacuum fusion, was 0.002%

and the nitrogen content 0.001%. The sample was not, unfortunately, large enough to enable its transition temperature to be determined accurately, but it, too, was brittle at ambient temperature. Since Batch S44, containing 0.012% oxygen, had a transition temperature between 25° and 50° C., it is obvious that the further reduction of the oxygen content to 0.002% had not caused any large reduction of the transition temperature, and if oxygen is held to be in any way responsible for the brittleness of chromium at ambient temperature its effects must be produced by contents of less than 0.002% and are not aggravated by a further increase up to at least 0.87%, an increase by a factor of over 400.

Similar effects have been noted in the case of specimens made from hydride chromium. Thus Batch S66, which was not reduced and probably contained about 0.8–0.9% oxygen, had a transition temperature of 350°–365° C., which is of the same order as that of other batches made from the same chromium in which the oxygen content was reduced to a low level by sintering in hydrogen.

What has been said of oxygen also appears to be true of nitrogen. Although the nitrogen content of hydride chromium is high, this is largely eliminated during the sintering operation and, in the sintered bars, is only slightly higher than in bars made from electrolytic chromium. The nitrogen content cannot, therefore, be held to be responsible for the difference between hydride and electrolytic chromium, and since the sample of chromium from the N.P.L. had a nitrogen content of 0.001%, while Batch S42, which was ductile at 50° C., contained 0.04% nitrogen, this element, like oxygen, must produce its effects at very low contents if it is responsible for the brittleness of chromium below the transition temperature.

(b) *Effects of Other Elements*

It is clear from the above that the difference in transition temperature between specimens made from electrolytic and hydride chromium, respectively, cannot be accounted for by any differences in oxygen and nitrogen content in the sintered aggregates. The difference, if due to an impurity, must be ascribed to other elements present in one but not in the other. In order to investigate this point more fully, batches of specimens of chromium to which deliberate additions of other elements had been made before sintering were examined.

Iron (0.54%) and silicon (0.14%) are present in appreciably greater quantities in hydride chromium than in electrolytic chromium, and spectrographic analysis showed that a strong trace of aluminium, estimated at 0.05%, was also present in the former though absent in the latter. Experiments were therefore made in which these elements were added separately to electrolytic chromium and the effect on the transition temperature measured. In iron, according to Rees, Hopkins, and Tipler,¹⁷ manganese has a marked effect in lowering the transition from ductility to brittleness in notched-bar impact tests.

In order to discover whether similar effects occurred in chromium, additions of manganese (0.5–3%), cobalt, nickel, tungsten, and copper (1% each) were made and the effect on the transition temperature determined. The additions were made by milling the mixed powders of chromium and these elements together before pressing and sintering in the normal manner.

The results are summarized in Table II and plotted in Fig. 4. Table II also gives the "strain factors", i.e. the ratio $\frac{d_A - d_{Cr}}{d_{Cr}}$, where d_{Cr} and d_A are the atomic diameters of chromium and the addition element, respectively. This factor thus gives an estimate of the local strain introduced into the lattice by the substitution of the addition atom for the chromium atom. It will be seen that all the additions increased the transition temperature, although an inconsistency will be noted for aluminium, in which the nominally smaller addition produced a greater effect than the larger. Fig. 4 shows that there is no satisfactory correlation between the "strain factor" and the rate of increase of the transition temperature with content

TABLE II.—*Effect of Added Elements on the Transition Temperature of Chromium in Bend Tests with Incremental Loading.*

Batch No.	Added Element, wt.-%	Transition Temperature, °C.	Hardness, V.P.N., (1 kg.)	"Strain Factor" $\left(\frac{d_A - d_{Cr}}{d_{Cr}}\right) 100$,
S44	None ($\ll 0.05\%$ Si and 0.05% Fe present)	< 50	48.5	...
S42	None (0.05% Si and trace Fe present)	80–99	71	...
S48	0.30 Fe	120–140	76	} –1.94
S50	0.50 Fe	120–140	103	
S52	0.50 Si	130–140	94.6	...
S62	0.05 * Al	190–195	130	} +8.9
S65	0.10 * Al	150–155	...	
S67	0.44 Mn	210–220	126	} +3.9 †
S68	2.10 Mn	300	136	
S69	3.40 Mn	340–345	...	
S70	0.98 Co	275–280	155	–2.72
S71	1.0 Ni	> 430	184	–3.1
S72	0.93 W	190–200	96.6	+9.7
S73	0.5 Cu	280–290	88.8	–0.78

* Nominal analysis.

† Value subject to some uncertainty in the value to be taken for d_{Mn} .

of the added element. Although iron, cobalt, and nickel have progressively larger effects in accordance with the increasingly negative strain factors, the effect of copper is very much greater than is to be expected from consideration of size-factors alone, and it is probable that electronic effects are also involved. This is supported by the small solubility of copper in chromium. Similarly, tungsten, manganese, and aluminium do not form a logical pattern, although the calculation of the "strain factor" for

manganese is complicated by the uncertainty in the atomic diameter of this element.

These results suggest that the observed difference in transition temperature between hydride chromium and electrolytic chromium can be accounted for by the cumulative raising of the transition temperature by the greater amounts of iron, silicon, and aluminium present in the former.

(c) Effect of Simmering

In the course of these experiments another effect was observed which is worthy of note. This is the effect of the simmering in acid which is normally

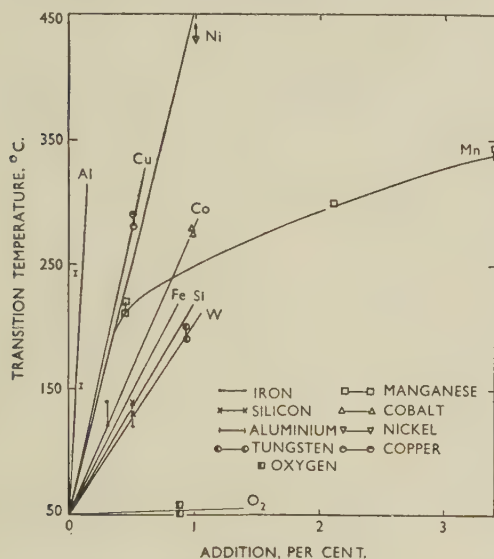


FIG. 4.—Effect of Addition Elements on the Ductile-Brittle Transition Temperature.

carried out on the electrolytic chromium after ball milling with the object of removing iron contamination from the mill. Results are given in Table III.

TABLE III.—Effect of Simmering in 50% Nitric Acid on Transition Temperature.

Batch No.	Type of Chromium	Time of Milling, hr.	Time of Simmering, hr.	Transition Temperature, °C.
S57	Electrolytic {	257	Nil	325–335
S57		257	168	120–150
S55	Hydride {	Nil	Nil	>385
S55		Nil	240	270–300

S57 was prepared from electrolytic chromium after ball milling for 257 hr. One set of bars was made from the resulting powder without simmering, while another set was made from the same powder after simmering in acid for 168 hr. In order to eliminate any sintering variations, both sets of bars were sintered at the same time for 3 hr. at 1500° C. in hydrogen. The transition temperature was 325°–335° C. for the bars from the unsimmered chromium

and 120°–150° C. for those made from simmered chromium. At first sight it appears that this difference might be due to the considerable pick-up of iron which is known to result from the milling operation but is removed by simmering in acid. Spectrographic examination showed, however, that the iron content of this set of bars was only 0.5%, and when a deliberate addition of this amount of iron was made to electrolytic chromium, the transition temperature was raised by less than 100° C. (Table II, p. 590). The same experiment was repeated with hydride chromium, bars made from unsimmered hydride chromium being compared with bars made from simmered hydride chromium, all sintered together. Whereas the bars made from unsimmered chromium had a transition temperature higher than 385° C., those made from the simmered chromium had their transition between 270° and 300° C. This effect is puzzling and suggests that, in addition to removing any surface contamination by iron which may be present, the simmering treatment also removes surface concentrations of some other impurity which has a marked effect on the transition temperature. Nitrogen estimations on bars of the same batch made from simmered and unsimmered chromium, respectively, reveal the same nitrogen content in both cases, so that this element cannot be held to be responsible.

After sintering, specimens are cooled in hydrogen, and to determine whether residual hydrogen in the compacts could have any effect on the transition temperature, tests have been made on specimens from the same batch of specimens, with and without a vacuum heat-treatment at 1000° C. to remove residual hydrogen. The transition temperature was not significantly affected by the vacuum treatment. This accords with the work of Martin,¹⁸ who found that hydrogen absorbed by chromium at high temperatures is almost completely evolved on cooling.

It will be noted from the analysis given earlier that the electrolytic chromium used for this investigation contained 0.026% sulphur, and it is pertinent to enquire whether this element exercises any influence on the fracture behaviour. Analysis shows, however, that the sintering treatment in hydrogen effects a considerable reduction in the sulphur content. Thus the analysed sulphur contents of batches S42 and S47 of sintered specimens (Table I) were, in both cases, less than 0.002%. Since the sulphur content was at such a very low level in the samples on which mechanical tests were made, it is unlikely to play any large part in determining the plastic behaviour.

(d) Correlation of Transition Temperature and Hardness

Hardness measurements have been made on batches of sintered chromium bars on which bend tests had been made. Pyramidal diamond impressions at a load of 1 kg. were made in order to produce small impressions which were relatively unaffected by the porosity of the bars. The hardness is plotted against

the transition temperature in Fig. 5. It will be seen that there is at least a rough correlation between hardness and transition temperature, the transition temperature rising with increase in hardness. The lowest hardness recorded was 45 V.P.N. Samples made from hydride chromium with transition tem-

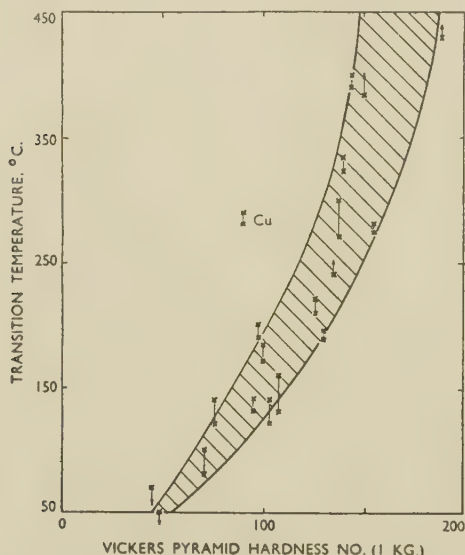


FIG. 5.—Relation Between Transition Temperature and Hardness.

peratures of the order of 300° C. and above usually had a hardness in the range 130–150 V.P.N. There is thus a relationship between the transition temperature and the solid-solution hardening produced in the chromium by impurity contents or contents of added elements. It will be noted that the effect of copper is anomalous in that the addition of this element produced an effect on the transition temperature which was very much larger than would be predicted from its effect on the hardness.

(e) Bend Tests at Constant Strain Rates

A large number of specimens (about 40) were prepared in several batches, the processing conditions being kept, as far as possible, identical for all batches. The specimens were divided into three lots by random

TABLE IV.—Results of Bend Tests at Different Rates of Strain.

Average Strain Rate, in./min.	Transition Temperature, °C.
0.00297	60–70
0.0696	70–80
0.77	110–120

selection, and bend tests were made at various temperatures at three rates of strain, viz. 0.00297, 0.0696, and 0.77 in./min., to determine the transition temperatures. The results are summarized in Table IV.

The results indicate a dependence of transition temperature on strain rate—a point discussed more fully below in consideration of the results of impact tests.

The effect of notching the specimens was also examined for the two slower rates of bend. Consistent values of the transition temperature were found, the values being approximately 40° C. higher than for the corresponding unnotched bars, i.e. 100°–110° C. and 110°–120° C.

2. IMPACT TESTS

Specimens prepared and processed in exactly the same way as for the bend tests at different strain rates were tested in the small Charpy machine described earlier (p. 587).

The impact values of unnotched specimens at temperatures up to 700° C. are plotted in Fig. 6. Although there is some scatter at the higher temperatures, the results can be interpreted as lying on two straight lines with an intersection at 325° C. Whereas the impact values below this temperature do not exceed 0.5 ft.-lb. and are indicative of the extreme brittleness of the material, the impact values at higher temperatures rise steeply with increasing temperature. Even at 600°–700° C., however, the impact value is only 8 ft.-lb., so that chromium does not possess any considerable “toughness” even at temperatures well above the transition temperature.

This value of the transition temperature may be correlated with a particular strain rate if the assumption is made—and it appears to be justified—that the energy

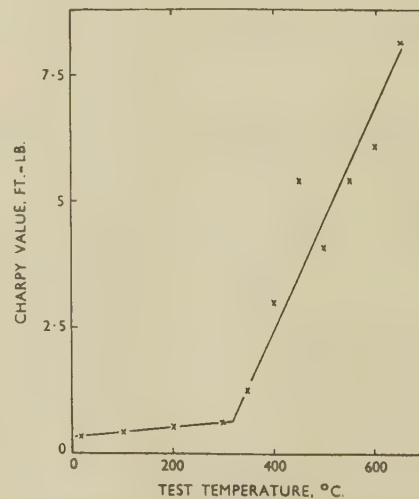


FIG. 6.—Variation of Impact Values of Chromium with Temperature.

absorption on impact is so small that the velocity of the pendulum on striking the specimen is the same as the strain rate. This velocity is 11,794 in./min.

Zener and Hollomon¹⁹ have postulated that the mechanical properties of a metal depend upon a dimensionless quantity and therefore upon the ratio

of the strain rate and some rate characteristic of the metal itself. Most rates characteristic of metals, e.g. diffusion rate, relaxation rate, &c., have an activation energy, and if it is assumed that only one type of rate affects the mechanical properties, the isothermal stress/strain relationship, \bar{S} , can be related to the strain ϵ and the strain rate $d\epsilon/dt$ by a single parameter P :

$$S = S(P\epsilon)$$

and that this parameter has the form $P = \frac{d\epsilon}{dt} \cdot e^{Q/RT}$

This expression has been used by Shepler²⁰ to correlate the brittle ductile transition temperature in iron and steels with the temperature. Fig. 7 shows the plot of log strain-rate against the inverse of the absolute temperature for the bend and impact tests reported here for chromium. The results conform fairly well to a straight-line relationship, the calculated value of the activation energy Q being 26.8

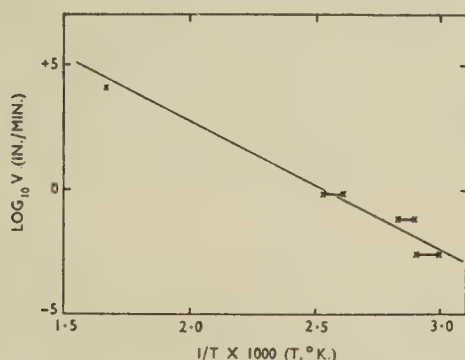


FIG. 7.—Plot of Log Strain Rate Against the Inverse of the Transition Temperature ($^{\circ}\text{K}.$).

kg.cal./g.-mol. The value for mild steel, according to Shepler, is 19.6 kg.cal./g.-mol.

3. TENSILE TESTS

The results of Tensometer tensile tests at a few temperatures up to $900^{\circ}\text{C}.$ are given in Table V.

The results show that chromium has no measurable ductility at room temperature, but that at $500^{\circ}\text{C}.$

TABLE V.—Results of Tensile Tests.

Temp., $^{\circ}\text{C}.$	Max. Stress, tons/in. ²	Elongation on $4\sqrt{A}$, %	Reduction of Area, %
20	6.76	0	0
500	6.22	1	0
900	5.44	4	2
900	5.18	3	2
900 *	5.12	5	2

* Time-to-rupture test.

and above some ductility can be measured, albeit small. The elongation at fracture was slightly increased by raising the stress to a value a little

below the stress for immediate fracture and allowing it to remain until fracture occurred. In the case of the test marked with an asterisk in Table V, failure occurred after $9\frac{1}{4}$ min. The elongation values obtained in these tests may be adversely affected by the porosity of the sintered specimens on which the tests were made, and it would be unwise to infer that the values for sound metallic chromium would be equally low.

VI.—FRACTURE AND DEFORMATION CHARACTERISTICS

The fracture of chromium below its transition temperature occurs by cleavage. The cleavage plane has not been determined during the course of the present work, but other body-centred metals cleave along (100) planes and the same is probably true of chromium. As far as can be judged, fracture is almost entirely transcrystalline. Rees, Hopkins, and Tipler¹⁷ have found that for pure iron, below its transition temperature, the fracture habit is also transcrystalline, but that, when the transition temperature is raised by the presence of oxygen, the fracture becomes partly intercrystalline. They suggest that the oxygen introduces intercrystalline weakness and the initial fracture nucleus is intercrystalline, although it may spread, at least partly, by transcrystalline propagation. The grain-size of the sintered compacts used in the present work has been too small in most cases to permit a thorough investigation of the fracture to be made, but such evidence as has been obtained suggests that intercrystalline weakness plays no significant part in determining the fracture habit of chromium. The appearance of a typical fracture crack in chromium is illustrated for a sample of fairly large crystal size by Figs. 13 and 14 (Plate LXXXIX) taken by normal and oblique illumination respectively. This sample was prepared by melting, in an arc furnace on a water-cooled copper hearth in a purified argon atmosphere, some sintered specimens of chromium which, in bend tests, had a transition temperature of 130° – $160^{\circ}\text{C}.$ Specimens ground from the as-cast arc-melted ingot had a transition temperature of 340° – $395^{\circ}\text{C}.$ Spectrographic analysis indicated that during arc-melting the chromium had become contaminated with traces of copper, nickel, and vanadium. The marked increase of transition temperature may have been partly attributable to these impurities or others not detected in the analysis. Melting was associated with a rise in hardness from 108 to 178 V.P.N. (1 kg.), suggesting some increase in impurity content. The microstructure was relatively free from oxide, and there was no indication of any significant amount of grain-boundary constituent. A careful examination of the fracture showed it to be almost entirely of the transcrystalline type, with no indication that it had originated from an intercrystalline nucleus. Intercrystalline portions of the fracture occurred only

when the grain boundary was favourably oriented with respect to the exit direction from a particular grain. Thick cracks traverse the grain boundary for only a small distance and then cut across a grain. In the middle of Fig. 13 is an interesting example of a crack which runs parallel and very close to a grain boundary, but does not enter it. An enlarged view of this is shown in Fig. 15 (Plate LXXXIX).

Some interesting observations were made on a sample of arc-melted chromium corresponding to the material shown in Figs. 13 and 14, in which large diamond indentations were made at various temperatures. It was thought that a study of the deformation adjacent to the impressions made below and above the transition temperature might show differences in the deformation behaviour. The specimen was polished and etched before testing in a modified Rockwell machine at temperatures up to 500° C. The deformation around the indentation showed no significant variation with temperature. The appearance at the edge of an indentation made at room temperature is shown in Fig. 16 (Plate LXXXIX). There is no indication of cracking around the impression, but a very considerable rumpling of the surface occurs in what appear to be deformation bands. The localized plastic behaviour at a temperature much below the transition temperature revealed by this observation is in accordance with the observations of Greiner¹⁰ already mentioned and supports his conclusion that chromium can show plastic behaviour when subjected to compression in the presence of a superimposed biaxial stress system preventing deformation at right angles to the applied stress.

Further information on this point has been obtained from experiments in which samples of chromium cast in an atmosphere of purified argon in an arc furnace were compressed between mild-steel plates at room temperature in an 80-ton press. These experiments are illustrated by Fig. 17 (Plate LXXXIX). A typical arc-melted specimen is shown as No. 3. Small specimens of about 8 mm. cube were sawn from such specimens and compressed in the way described. The samples tested were as follows:

No. 1. Hydrogen-purified electrolytic chromium. Oxygen content approximately 0.02%.

No. 2. Unpurified electrolytic chromium. Oxygen content approximately 0.9%.

No. 4. Remelted specimens corresponding to sintered batch S71 (Table II, p. 590), containing 1% nickel. Transition temperature in bend tests of sintered bars above 430° C.

No. 5. Aluminothermic chromium containing 0.12% aluminium, 0.16% silicon, and 0.21% iron. Transition temperature unknown, but probably at least 300° C.

The results were as follows:

Nos. 1 and 2. Could be compressed to about 20% of their original thickness before further deformation was prevented by contact between

the steel plates which occurred because the compressed chromium had caused local deformation of the soft steel.

No. 4. Fragmented under pressure with only very slight deformation.

No. 5. Compressed to about 50% of its original thickness, but was heavily cracked.

Specimens (1) and (2) after compression were free from cracks except around the edges, where some cracking occurred under the tensile hoop stress developed during the deformation. The compressed specimens were quite brittle in bending at room temperature.

These results provide an interesting confirmation of the fact that under a stress system in which there is a hydrostatic compressive stress component, chromium can show ductile behaviour. Under these conditions the transition temperature is depressed below room temperature.

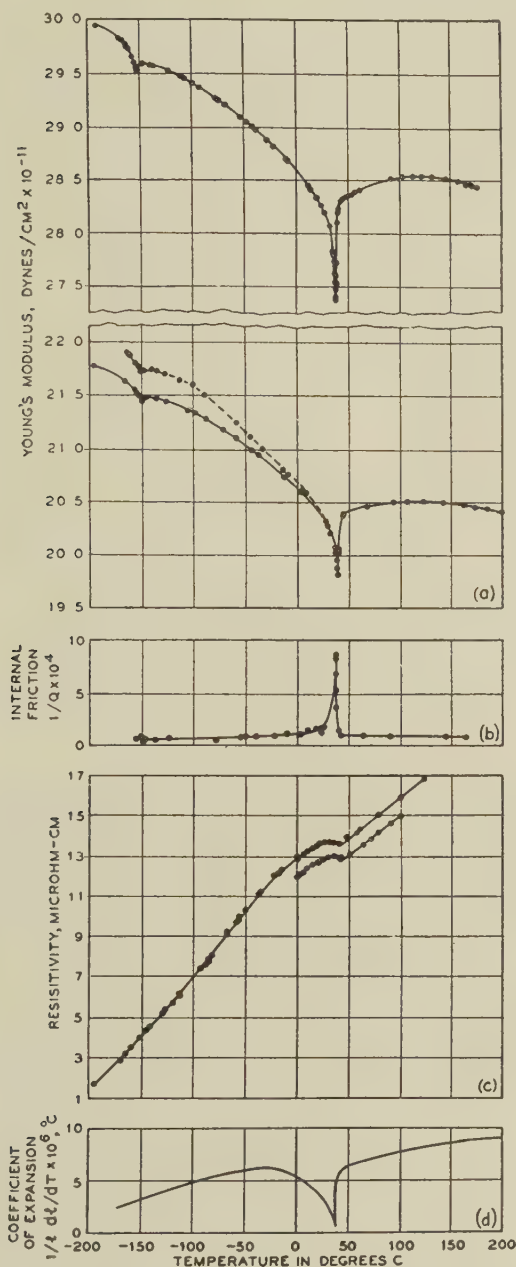
The results also show that, as demonstrated by the bend tests described earlier, the oxygen content has relatively little effect on the ductile behaviour, but that the ductility is markedly affected by elements in solid solution which raise the transition temperature, e.g. nickel in specimen No. 4 and small amounts of aluminium, silicon, and iron in the aluminothermic chromium.

VII.—OTHER PHYSICAL MEASUREMENTS

While the present work was in progress, a paper appeared by Fine, Greiner, and Ellis,²¹ who made careful measurements of the variation with temperature of Young's modulus, internal friction, coefficient of expansion, electrical resistivity, thermoelectric power, and lattice parameter of two samples of chromium, one sintered from electrolytic powder and the other prepared by electrodeposition. The results of their measurements of Young's modulus, internal friction, electrical resistivity, and coefficient of expansion are reproduced in Fig. 8. All these properties showed discontinuous changes, from which the authors deduced that a transformation takes place in chromium at a temperature of about 37° C. They did not discuss the significance of their findings in any detail in relation to the purity of their chromium, but they noted that similar results in measurements of electrical resistivity had been observed by Söchtig,²² who found a minimum at 41° C., and in measurements of thermal expansion by Erling,²³ who reported an inflection at 36° C. The anomaly in Young's modulus has also been observed by Pursey.²⁴

No inflection was found by Fine, Greiner, and Ellis in the plot of lattice parameter against temperature, although the bulk coefficient of expansion showed an inflection. The difference was considered to imply some departure from the ideal body-centred cubic lattice in passing through the transition temperature,

the structure being somewhat more close-packed above than below, either by some atoms assuming interstitial positions or by the disappearance of vacant lattice sites.



[Courtesy American Institute of Mining and Metallurgical Engineers.]

FIG. 8.—Thermal Dependence of Some Properties of Chromium.

- (a) Young's modulus ($1 \text{ dyne/cm}^2 = 1.4504 \times 10^{-5} \text{ lb./in.}^2$).
 Upper curve: Wrought electrolytic chromium.
 Lower curve: Electroformed chromium.
 Broken curve: Electroformed chromium before heating to 207°C .
 (b) Internal friction of wrought electrolytic chromium.
 (c) Electrical resistivity.
 Upper curve: Wrought electrolytic chromium.
 Lower curve: Electroformed chromium.
 (d) Coefficient of expansion of wrought electrolytic chromium.

[After Fine, Greiner, and Ellis.²¹]

Measurements of electrical resistance and lattice parameter have been made on some of the materials used in the present investigation.

1. MEASUREMENTS OF ELECTRICAL RESISTANCE

The variation of electrical resistance with temperature was measured for several specimens, the temperature range covered being from -75° to 700°C . Measurements were made on sintered specimens of the same size or half the size of those used for bend tests. The resistance was measured potentiometrically, the specimen having two current leads and two potential leads made of stainless steel screwed into it along its length. The current was measured by the potential drop across a standard resistance in series with the specimen. The apparatus was so

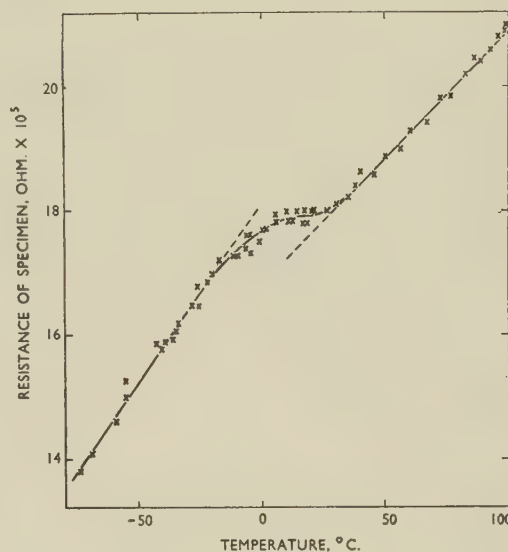


FIG. 9.—Variation of Electrical Resistance of Sintered Hydride Chromium with Temperature.

arranged that measurements could be made on four specimens at the same time. For temperatures lower than room temperature the specimen assembly was placed in a lagged tank containing acetone and solid CO_2 and the temperature equalized throughout the bath by stirring with air blown through a perforated lead tube coiled at the bottom of the bath. For temperatures above room temperature the specimen assembly was placed in a furnace controlled by hand with a Variac transformer. Temperature measurements were made on individual specimens by thermocouples in contact with them. Results were discarded if the temperature of the specimen altered by more than 1°C during the course of the measurement.

The variation of resistance with temperature for a sample prepared from hydride chromium is shown from -75° to $+100^\circ \text{C}$ in Fig. 9. This clearly shows the existence of an anomaly which is very similar to that noted by Fine, Greiner, and Ellis. The results

were completely reversible, Fig. 9 being built up from several experiments in which measurements were taken on heating and, in others, on cooling. A specimen of pure tin on which simultaneous measurements were made in the same apparatus showed no anomalies. The resistance/temperature curve is made up of two straight-line portions with an inflection between them. Deviation from linearity occurs between -20° and $+35^{\circ}$ C. The latter figure is in close agreement with the value of 37° C. reported by Fine, Greiner, and Ellis. The ratio of the temperature coefficients of resistance above 35° C. and below -20° C. is 1 : 1.41.

Measurements were extended to higher temperatures in order to discover whether there were any other anomalies in the resistance/temperature relationship corresponding to the temperature of transition from brittleness to ductility. Specimens were used which in bend tests had transitions from 120° to 390° C. and measurements were made from room temperature to 600° – 700° C. Typical resistance/temperature curves are plotted in Fig. 10. Except when specimens had previously been deformed but not broken in bend tests, the resistance/temperature curves were smooth and did not indicate any anomaly that might be related to the temperature at which the transition from brittleness to ductility occurred in bend tests. When specimens which had previously

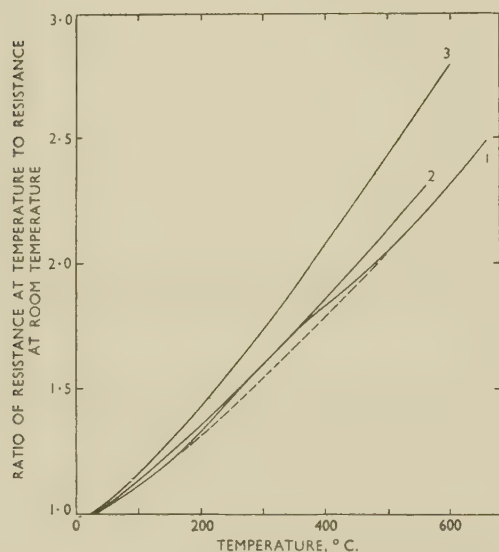


FIG. 10.—Resistance/Temperature Curves for Chromium.

Curve 1: Hydride chromium (transition temperature 390° – 400° C.).

Curve 2: Same specimen annealed 40 hr. at 700° C.

Curve 3: Electrolytic chromium (transition temperature below 130° C.) after annealing for 26 hr. at 700° C.

been bent but not broken in bend tests were used for resistance measurements, the resistance/temperature curve often showed a change of slope, usually at a temperature of about 400° C. It was found, however, that this effect was eliminated by a preliminary

anneal at 700° C. (cf. curves 1 and 2, Fig. 10), and the effect is, therefore, due to the strain introduced during the bend test.

2. MEASUREMENTS OF LATTICE SPACING

A sample of electrolytic chromium, purified by hydrogen reduction at 1450° C., was crushed in an

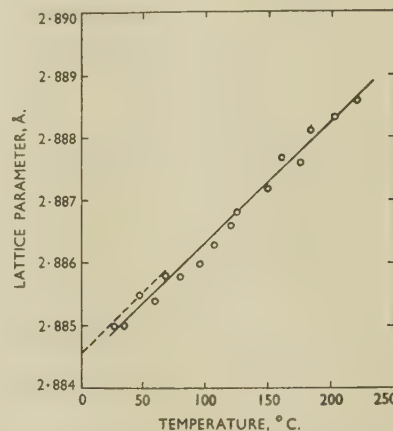


FIG. 11.—Variation with Temperature of Lattice Parameter of Purified Electrolytic Chromium.

— Present work.
 - - - Results of Fine, Greiner, and Ellis.²¹

agate mortar and powder finer than 200 mesh used for lattice-parameter measurements at temperatures from room temperature to 220° C. The parameters were calculated from films taken with chromium radiation in a Unicam 19-cm. high-temperature camera, the temperature being controlled to within $\pm 1^{\circ}$ C. The results are plotted in Fig. 11 and are compared with the results of Fine, Greiner, and Ellis. The experimental points can be represented by a straight line, the maximum divergence of any of the points from this line being approximately 1 in 15,000, which is about the same as the experimental accuracy of the measurements. The values of Fine, Greiner, and Ellis are represented by the dotted line in Fig. 11. The slope of the straight line given by them is slightly less than that representing the present series of measurements. There was no indication of any irregularity of the lattice-spacing/temperature plot at about 37° C.

VIII.—DISCUSSION OF RESULTS

The present investigation shows clearly that chromium exhibits a sharp transition from plastic deformation with measurable ductility to brittle cleavage failure in the elastic range over a range of a few degrees in temperature. In this respect, the behaviour of chromium is closely similar to the

behaviour of iron, which shows a similar transition in notched-bar impact tests. Similar behaviour has been noted for the other body-centred cubic metals tungsten and molybdenum. In iron, however, the transition is below room temperature, and although the temperature at which it occurs is raised by certain elements, it is possible, by the avoidance of these elements in dangerous quantities, to develop strong alloys of iron which are above their transition temperature at their normal operating temperatures and which consequently exhibit adequate ductility for use in engineering applications.

In iron and in molybdenum, oxygen has a marked effect in raising the transition temperature. Rees, Hopkins, and Tipler¹⁷ have shown that, for the purest iron they examined, the transition temperature in notched-bar impact tests was -15°C ., but that this was raised to $+16^{\circ}$ and $+64^{\circ}\text{C}$. by additions of 0.0037 and 0.016% oxygen, respectively. Manganese, on the other hand, depressed the transition temperature of pure iron, 2% of this element lowering it to -50°C .

The present investigation shows that chromium behaves quite differently from iron. Thus, oxygen appears to have relatively little influence on the transition temperature, at least in quantities greater than 0.001%. It is possible, however, that although oxygen has little influence on the transition temperature, it may nevertheless reduce the ductility at temperatures above the transition temperature at which chromium shows plastic behaviour. The low oxygen content may, for example, have contributed to the good hot-working characteristics of the chromium investigated by Gilbert, Johansen, and Nelson,⁹ although having relatively little effect on the transition temperature. On the other hand, it is a matter of elementary observation that electrolytic chromium flakes, without reduction of the oxygen content, which is about 0.6%, may be bent over quite small radii when heated to dull red heat in a welding torch.

Unlike the case of iron, also, no other element has been found which depresses the transition temperature of chromium when alloyed with it. All the elements which have been investigated raise this temperature, and the extent to which it is raised seems to correspond at least approximately to the amount of solid-solution hardening produced by the added element. For this reason, the alloying of chromium by other elements results in a substantial extension of the temperature range in which the alloys are brittle, and Sully and Brandes² have demonstrated in previous work that the brittleness and notch sensitivity of creep-resistant chromium-

rich alloys is so marked that these alloys have little promise for practical applications, although their resistance to deformation at high temperatures is outstandingly good. For this reason it is considered that although it may be found, in later work, that a higher degree of purification than that achieved in the present work may depress the transition temperature by the further small interval required to take it below normal atmospheric temperature, so that it may be deformed at room temperature, this will not contribute materially to the possibility of the development of strong chromium alloys having any important degree of ductility at room temperature.

The transition which occurs in several physical properties of chromium at about 37°C . is not associated with a change of cohesive forces in the chromium lattice which affects the transition from brittleness to ductility. There appeared to be a possibility that this might not be so, since 37°C . lies very close to the minimum temperature of 50°C . at which chromium showed ductility in bend tests. Pursey,²⁵ however, has demonstrated that the addition of iron depresses the temperature at which the anomaly in the elastic moduli occurs, whereas the present work shows that iron has a marked effect in raising the transition temperature from brittleness to ductility.

The conclusion reached from this work is that the brittleness of chromium is an aspect of the more general phenomenon of the large temperature dependence of ductility in body-centred cubic metals. The fundamental reason for this phenomenon is still obscure, and it remains to be discovered whether it is intrinsic to the body-centred lattice or whether it is due to the small content of impurity still present in these metals when purified to the utmost extent possible by existing techniques. It is trebly unfortunate that for chromium, unlike iron, the transition from ductile to brittle fracture occurs at a temperature above room temperature, that it occurs at very slow strain rates, and that the temperature at which it occurs is raised by all the elements which could be added to chromium to increase its strength at high temperatures.

ACKNOWLEDGEMENTS

The authors are grateful to Mr. E. A. G. Liddiard, Director of Research, Fulmer Research Institute, for his interest in the investigation. They also thank their colleague Mr. C. S. Campbell and their former colleague Mr. D. S. Box for assistance in the experimental work.

REFERENCES

1. R. M. Parke and F. P. Bens, *Symposium on Materials for Gas Turbines* (Amer. Soc. Test. Mat.), **1946**, p. 80.
2. A. H. Sully, E. A. Brandes, and (in part) A. G. Provan, *J. Inst. Metals*, 1952-53, **81**, 569.
3. M. A. Hunter and A. Jones, *Trans. Amer. Electrochem. Soc.*, 1923, **44**, 23.
4. J. W. Marden and M. N. Rich, U.S. Patent No. **1,760,367**, 1930.
5. W. J. Kroll, *Z. anorg. Chem.*, 1935, **226**, 23.
6. W. J. Kroll, W. F. Hergert, and L. A. Yerkes, *J. Electrochem. Soc.*, 1950, **97**, 258.
7. F. Adcock, *J. Iron Steel Inst.*, 1927, **115**, 369.
8. A. Brenner, P. Burkhead, and C. W. Jennings, *J. Research Nat. Bur. Stand.*, 1948, **40**, 31.
9. H. L. Gilbert, H. A. Johansen, and R. G. Nelson, *Trans. Amer. Inst. Min. Met. Eng.*, 1953, **197**, 63.
10. E. S. Greiner, *ibid.*, 1950, **188**, 891.
11. H. Cross, *Iron Steel Inst. Special Rep.*, 1952, (**43**), 346 (discussion).
12. H. G. Short, *Analyst*, 1950, **75**, 335.
13. W. Rohn, *Z. Metallkunde*, 1924, **16**, 275.
14. G. Grube and M. Flad, *Z. Electrochem.*, 1939, **45**, 835; 1942, **48**, 377.
15. H. Wartenberg and S. Aoyama, *ibid.*, 1927, **33**, 144.
16. N. C. Tombs and A. J. E. Welch, *J. Iron Steel Inst.*, 1952, **172**, 69.
17. W. P. Rees, B. E. Hopkins, and H. R. Tipler, *ibid.*, 1951, **169**, 157.
18. E. Martin, *Arch. Eisenhüttenwesen*, 1929-30, **3**, 407.
19. C. Zener and J. H. Hollomon, *J. Appl. Physics*, 1944, **15**, 22.
20. P. R. Shepler, *Weld. J.*, 1946, **25**, 321s.
21. M. E. Fine, E. S. Greiner, and W. C. Ellis, *Trans. Amer. Inst. Min. Met. Eng.*, 1951, **191**, 56.
22. H. Söchtig, *Ann. Physik*, 1940, [v], **38**, 97.
23. H. D. Erfling, *ibid.*, 1938-39, [v], **34**, 139.
24. H. Pursey, *Nature*, 1952, **169**, 150.
25. H. Pursey, Private communication.
26. H. B. Goodwin, R. A. Gilbert, C. M. Schwartz, and C. T. Greenidge, *J. Electrochem. Soc.*, 1953, **100**, (4), 152.

Discussion

The Gold-Platinum System

By A. S. DARLING, R. A. MINTERN, and J. C. CHASTON

(*Journal*, this vol., p. 125.)

Dr. H. K. HARDY * M.Sc., A.R.S.M., A.I.M. (Member): It is pleasant to have an authoritative account of the gold-platinum phase diagram to replace the confusing picture gained by studying all the previous publications. The authors' diagrams are admirably sized and scaled to allow numerical values to be read easily from the phase boundaries.

The gold-platinum system offers several points of thermodynamic interest. Analysis shows that a wide difference in concentration between the liquidus and solidus curves results from free energy/compositional curves which are relatively flat.†‡ and are to be associated with positive heats of solution of approximately equal magnitude in both the liquid and solid phases.‡§ The solidus between zero and 30% gold may well have an inflected form. Scatchard and Hamer § applied the regular solution model (with allowance for the latent heat of fusion) to the liquidus and solidus curves and found the heats of solution (A in equation (1)) in the liquid and solid phases to be respectively 5290 and 5330 cal./g.-atom.

The regular solution model sets the excess free energy of solution as ‡||

$$\Delta F = Axy + RT(x \ln x + y \ln y). \quad (1)$$

where x and y are the atomic fractions, T the absolute temperature, and Axy is the integral molar heat of solution. I have recently examined the properties of a "sub-regular" solution model in which A is made linearly dependent on composition so that**

$$\Delta F = A_1x^2y + A_2xy^2 + RT(x \ln x + y \ln y) \quad (2)$$

It is a property of this expression that the solubility curve can be represented by the following equation

$$\phi \equiv (x_1 + x_2) RT \ln x_1/x_2 + (y_1 + y_2) RT \ln y_1/y_2 = -(A_1 - A_2)(x_1 - x_2)^3 \quad (3)$$

where x_1 and x_2 , y_1 and y_2 are the compositions in equilibrium along the solubility boundaries of phases with the same lattice structure. When the left-hand side of equation 3, conveniently called ϕ , is plotted against $(x_1 - x_2)^3$ a straight line passing through the origin will be obtained as long as $(A_1 - A_2)$ is independent of temperature, so that the solubility data can be fitted by the sub-regular solution model. The solubility curves of Wictorin †† and the authors are plotted in this manner in Fig. A. Wictorin's results show a very gentle curve which can reasonably be represented by the straight line and approximate to the sub-regular solution behaviour. The authors' solubility data (corrected to atomic

per cent. from their Fig. 5) exhibit a more pronounced curvature and deviate appreciably from the straight line below 950° C. The reason is that the solubility curve in their Fig. 5 has been drawn symmetrically about the 40 wt.-% gold ordinate, thus forcing a higher degree of asymmetry ($(A_1 - A_2)$ greater) at the lower temperatures. My plot of Wictorin's solubility curve agrees much better with the authors' own results at the platinum-rich side between 900°–1100° C. than the curve they have drawn in Fig. 5. At the gold-rich side, Wictorin's curve is at higher gold contents than the authors'.

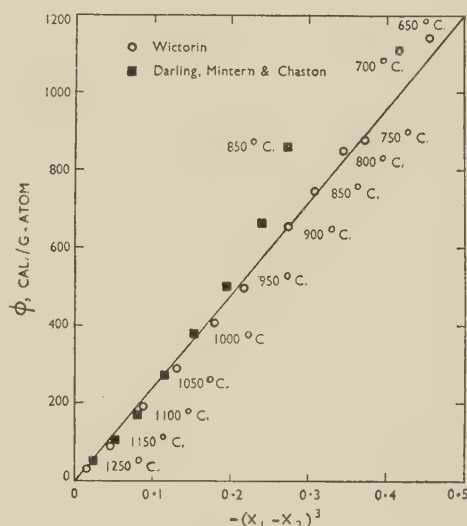


FIG. A.

His results are not symmetrical about the 40 wt.-% gold ordinate and consequently fall closer to the straight line in Fig. A. The calculated values $A_1x^2y + A_2xy^2$ give the integral molar free energy of solution (excluding the positional entropy) at $x = 0.5$ and 1250° C. as 1435 cal./g.-atom (from Wictorin's curve) and 1450 cal./g.-atom (from the authors' curve) compared with 1430 cal./g.-atom of Scatchard and Hamer (the last figure is also the integral molar heat of solution, as it is completely independent of temperature).

The analysis cannot pretend to decide between the experi-

* Senior Metallurgist, Fulmer Research Institute, Stoke Poges, Bucks.

† H. W. Bakuis Roozeboom, *Z. physikal. Chem.*, 1899, **30**, 385.

‡ J. H. Hildebrand and R. L. Scott, "The Solubility of Non-Electrolytes", 3rd edn. New York: 1950 (Reinhold Publishing Corp.).

§ G. Scatchard and W. J. Hamer, *J. Amer. Chem. Soc.*, 1935, **57**, 1809.

|| J. H. Hildebrand, *Proc. Nat. Acad. Sci.*, 1927, **13**, 267.

¶ J. H. Hildebrand, *J. Amer. Chem. Soc.*, 1929, **51**, 66.

** H. K. Hardy, *Acta Met.*, 1953, **1**, (2), 202.

†† C.-G. Wictorin, "Studies in Gold-Platinum Alloys". Stockholm: 1947 (Ivar Høggström).

C.-G. Wictorin, *Arkiv. Mat., Astron. Fysik*, 1949, [B], **36**, (9).

mental results, and below 1200° C. there is substantial agreement between the solubility curves of Victorin and the authors. However, the calculations show that the phase diagram they have put forward leads to self-consistent energy values from all the data it contains, i.e. the liquidus, solidus, and solubility curves are in accordance with a positive heat of solution in both the liquid and solid phases.

The AUTHORS (*in reply*): In thanking Dr. Hardy for his

able analysis of our experimental data, we should like to take this opportunity of pointing out that the concentrations in Fig. 5 of our paper are plotted in terms of *weight* per cent. and not *atomic* per cent. as designated. The misprint, which was unfortunately missed in proof-reading, has been privately pointed out to Dr. Hardy, who has kindly drawn his curve accordingly.

It is gratifying to learn that the phase boundaries we have determined are self-consistent on thermodynamic grounds.

THE STEPPED STRESS/STRAIN CURVE OF SOME ALUMINIUM ALLOYS*

1480

By N. KRUPNIK,† D.I.C., and PROFESSOR HUGH FORD,‡
D.Sc., Ph.D., MEMBER

SYNOPSIS

With a view to establishing basic yield-stress curves, tensile tests were made with four aluminium alloys pulled at constant rates of either loading or straining.

It was found that alloys which showed stepped yielding over the whole stress/strain curve under normal testing conditions could be made to give a smooth stress/strain relation only under special test conditions, viz. (1) very low rates of stress, and (2) constant rates of strain. The smooth curve, where it was obtained, appeared to agree well with the envelope of the stepped curves for the same material, the steps being deviations below the basic curve. In these tests, the large initial type-*A* yield did not occur, and in this case the type-*B* steps show a gradually increasing size from the first perceptible plastic deformation until final fracture.

It was found that any sudden disturbance of the testing machine caused an otherwise smooth yield curve to break down into steps, and this may explain some of the irregularities observed in tensile tests on these alloys with normal testing methods.

I.—INTRODUCTION

It is well established that steel is not the only material to exhibit a sudden yield at the end of its elastic range. Various investigators¹⁻⁶ have found that many metallic alloys show one or more of such sudden yields at room temperature under certain test conditions. Thus, Fell² and McReynolds⁵ found that Duralumin underwent a number of sharp yields with progressive loading, and certain brasses show the same phenomenon, though only in the annealed state, and then only after a strain of a few per cent. Sutoki⁶ has reported the same phenomenon in a nickel alloy at 300° C.

II.—PREVIOUS WORK

Fell² investigated the yielding of steel and Duralumin under stress and described the stress/strain curve of Duralumin as showing a number of sudden large yields, thus giving the yield-stress curve the form of a stair-stepped curve. He observed many similarities in the distortion patterns of steel and Duralumin and pointed out that both materials have lattices of the cubic type.

A more extensive investigation into the steps was made by McReynolds,⁵ using various commercial-purity aluminium alloys and some high-purity aluminium-copper alloys, and strains of not more than 2.5%. He found that pure aluminium (99.996%) did not show any steps and that its stress/strain curve was smooth. An alloying element, even in very small quantities, was necessary to produce the steps in the curve. Magnesium and copper, which are elements that cause strain-ageing, were found to

be the alloying elements necessary to produce steps. The steps disappeared when the temperature was lowered below a certain value or raised above a certain upper critical value, the limits depending on the alloy. The size of the steps grew as the content of the alloying element was increased, and was always roughly proportional to the instantaneous value of the stress. McReynolds noticed almost no effect of heat-treatment on the occurrence of the steps.

The phenomenon of sudden yield has been closely studied in connection with the yield point of steel. Recent papers by Cottrell⁷ and Cottrell and Bilby⁸ have proposed a theory that accounts for the yield point in steel—qualitatively and to some extent even quantitatively.

Both Fell and McReynolds point to many similarities in the yielding of aluminium alloys and of steel, and a theory, on the general lines of Cottrell's, was suggested by McReynolds, although he considered that the then-existing experimental evidence was not sufficient or satisfactory enough to allow definite conclusions to be reached. Eborall, Lack, and Phillips⁹ have shown that there are two types of yielding in aluminium alloys, one similar to that in steel, and a second (the stair-stepped type) which has been investigated in the present tests.

III.—SCOPE OF THE PRESENT WORK

In previous researches, no systematic investigation appears to have been made into the effect of rate of straining or rate of loading. These aspects are important in plasticity, where basic yield-stress curves are needed, for example in mechanical-working processes, such as cold rolling, extrusion, &c.; if,

and Technology, London.

* Manuscript received 24 April 1953.

† Haifa, Israel; formerly at Imperial College of Science

‡ Imperial College of Science and Technology, London.

under the straining rates usual in such processes, a stepped yield curve is obtained, then the resulting flow patterns may be modified. It is also important to determine for such processes the yield-stress curve for much larger strains than are available at present.

Four aluminium alloys were used. One was examined for the effect of ageing at room temperature for a long period, and the other alloys were tested in the as-extruded and heat-treated conditions.

The general characteristics of the yield-stress curve were studied under constant rate of stress and constant rate of strain. These tests were not intended to throw light on the fundamental or metallurgical aspects of step formation, but only on their possible influence on flow patterns in plasticity.

IV.—MATERIALS AND APPARATUS

Table I shows the composition and heat-treatment of the alloys tested. The test-pieces were turned from round (extruded) bars of each alloy to the

and the steady-loading pan was replaced by a 40-gallon container hung on the end of the beam.

Water could be run into the container from a constant-level head tank which had an orifice plate in the bottom. By changing the orifice size, the rate of loading could be varied between 0.02 and 8.5 tons/in.²/min.

The test-pieces are shown at Fig. 1, the effective area being 0.025 in.². They have theoretically no exactly defined gauge-length but are machined to very close tolerances so that comparisons can be made, and diagrams have been plotted on a basis of extension rather than of strain.

The actual rate of flow in a test was checked by weighing the amount of water that flowed into the container in a given time. In preliminary tests, the constancy of flow through the orifice was confirmed.

The extensometer designed for the creep machine was used (1 $\frac{5}{32}$ in. gauge-length, see Fig. 1), and an elongation of about 10% was possible. The indicator is a dial-gauge, and readings were taken every 5 or

TABLE I.—*Composition and Heat-Treatment of Alloys Tested.*

Material	Mark	Composition, %					Conditions Tested	
		Cu	Mg	Mn	Si	Fe	1	2
Duralumin	A	4.00	0.55	0.60	0.40	0.40	About 400 days' ageing at room temperature.	
Special Al-Cu alloy	B	1.35	...	nil	0.02	0.02	Solution-treated: soaked 40 min. in air furnace as temperature rose from 507°–512° C., then water-quenched.	As-extruded.
Special Al-Cu alloy	C	3.83	...	nil	0.025	0.02		As-extruded.
3.5% Mg-type alloy	D	0.03	3.63	0.29	0.18	0.22		As-extruded.

dimensions given in Fig. 1. The important dimensions were machined to very close tolerances.

The 1 $\frac{1}{2}$ % and 4% copper alloys were specially prepared from high-purity aluminium and were supplied either as-extruded or in the solution-treated condition.*

All the material showed normal microstructures, with equi-axed grains and no coarse-grained outer band. The average grain diameters were: Alloy B, solution-treated 770 μ ; as-extruded 460 μ ; Alloy C, solution-treated 440 μ ; as-extruded 400 μ .

The "static" tensile tests were carried out on a standard round specimen of 2-in. gauge-length, the diameter being 0.5625 in. A 10-ton Buckton single-lever-type machine and a Lindley extensometer were used. This extensometer limited the strains to 4 $\frac{1}{2}$ %.

The constant-rate-of-loading tests were all made on a Denison miniature creep-testing machine,¹⁰ consisting of a single-lever loading device to which steady loads could be applied. The lever was extended to give a 20 : 1 leverage (this is twice the design leverage),

10 sec., depending on the rate of loading. In the very rapid loading tests, a cine-camera was used to photograph continuously the readings of both the dial-gauge and the stop-clock. The camera was run at 6 frames/sec., giving a large number of readings from which a true picture of the load/extension curve could be obtained. With this technique, the number of readings is so great that the individual points are not generally shown on the graphs; where points are shown, they correspond to every fifth or tenth frame.

For the constant-rate-of-strain tests, a special apparatus was constructed. The framework of a Dalby torsion-testing machine was used as the straining unit, the worm gearing of which was coupled to a geared motor so that the final spindle made 1.275 rev./hr. This drove the square-thread nut of the test-head shown in Fig. 2 and gave a rate of straining of 0.1595 in./hr. (i.e. just over 0.0025 in./in./hr.).

The load was measured by a mild-steel weigh-bar, 0.75 in. long \times 0.4 in. dia., one end of which was screwed to the specimen. Spherical seatings at both

* The authors are very grateful to Aluminium Laboratories, Ltd., and particularly to Mr. G. Forrest, for the care taken in preparing these alloys. They also wish to thank Dr. E. G.

West, of the Aluminium Development Association, for his kindness in supplying the aluminium-magnesium alloy.

ends eliminated bending, and strain gauges were cemented on the weigh-bar to measure the load. A Savage and Parsons high-sensitivity strain indicator, R.A.E. type II, was used to measure the strain, the weigh-bar having been carefully calibrated beforehand. An accuracy of $\pm 1\%$ was obtained.

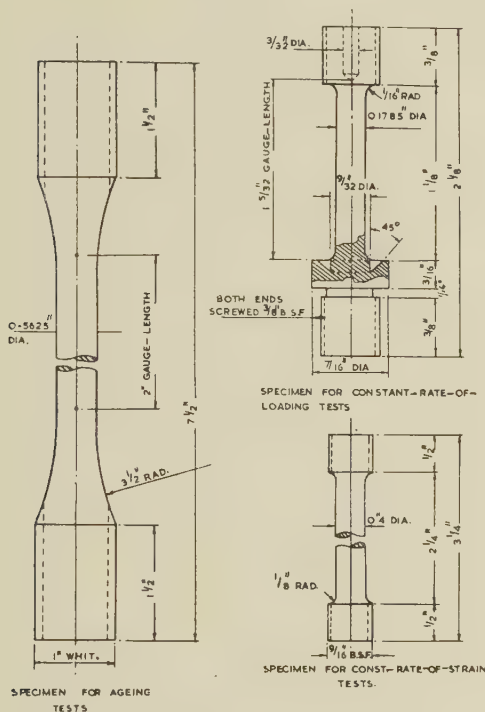


FIG. 1.—Test Specimens.

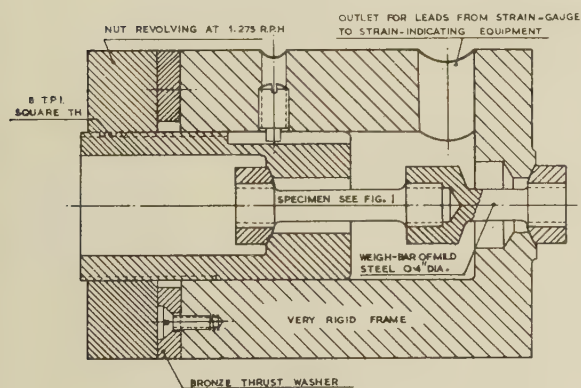


FIG. 2.—Device for Tensile Tests at Constant Strain Rate.

The design of the test-head was such that there was very little stress in any part of the head, and therefore the elastic strains were very small. The extension of the weigh-bar was only 0.00067 in. at the maximum load of 1.5 tons, and was negligible compared with a total extension of 0.2 in. on the specimen. The object in making a rigid frame was that, if the specimen yielded suddenly, it would be at once evident whether

the material lost strength on yielding. With mild steel, the sudden yield is usually masked so far as the stress/strain relation is concerned, because, as the normal testing machine cannot follow the extension sufficiently quickly, the load is lost until strain-hardening has taken place to the point where equilibrium with the load is again established. Tests had shown a slightly different mechanism in aluminium alloys, and it was therefore decided to use an extremely slow, steady straining rate, and the most rigid strain device possible, so that, if steps tended to form, they would be at once detected. Readings of strain were taken every 30 sec.

V.—TEST PROCEDURES AND RESULTS

1. AGEING TESTS

The first evidence of the stepped yield-stress curve had been obtained in the course of some tests to establish the stress/strain curve for a Duralumin (A, Table I) in a normal tensile test, carried out some weeks after receipt of the material from the manufacturer.

The early results had established clearly defined steps in both the as-received and the annealed conditions. It was found that the steps could be most sharply delineated by applying very small increments of load at $\frac{1}{2}$ -min. intervals, and when sudden yield occurred, an interval of 5 min. was allowed, values of the extension being noted against time during this period. Usually by that time the "creep" had essentially stopped. The time/extension curve at each step was, in fact, very close to the typical creep curve in shape. Table II gives details of four typical tests.*

TABLE II.—*Tensile Tests on Material A.*
(Duralumin).

Ref. Mark	Heat-Treatment	Load Increments, tons	Time Intervals
C	...	0.02	5 min. between each load increment.
F	...	0.05	30 sec. after loads, unless yield occurred, when 5 min. was allowed before increase of load.
R	Annealed	0.05	
S	"	0.05	

Steps were clearly found in these tests (Fig. 3), both before and after annealing. The same material was retested after a long time (about 400 days) at room temperature. The same procedure was used as before, some results being given in Fig. 4. The steps have almost completely disappeared. In one case three very faint steps appeared, but after the third step, a smooth curve was resumed.

* These tests were carried out by Mr. E. F. Hart, to whom the authors' thanks are due.

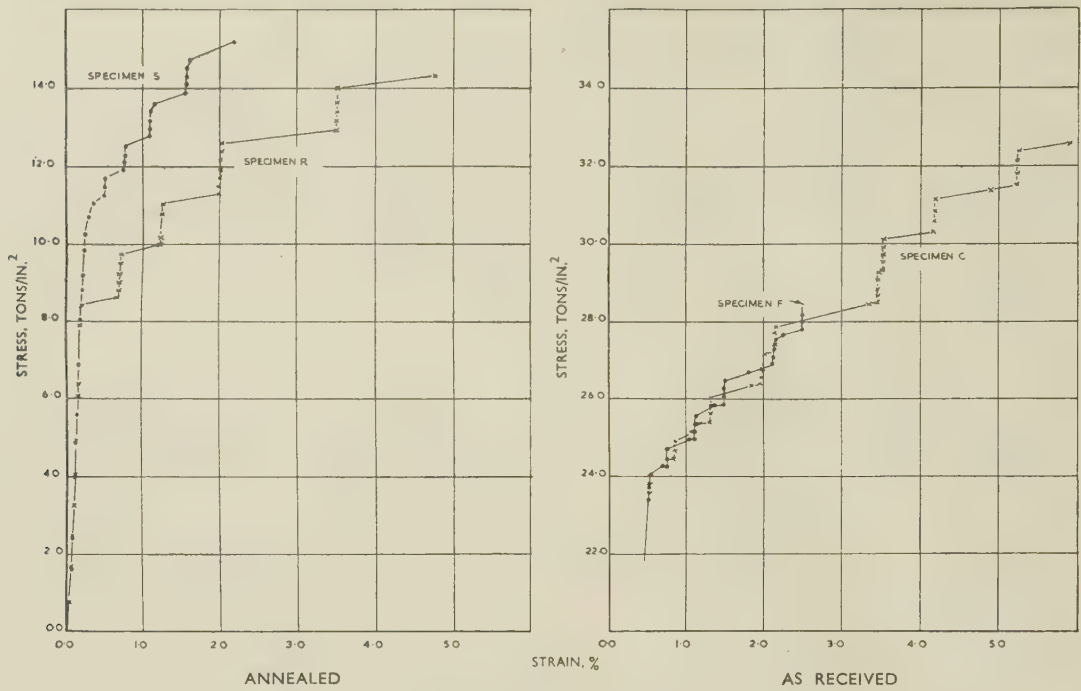


FIG. 3.—Stress/Strain Curves of Duralumin (A).

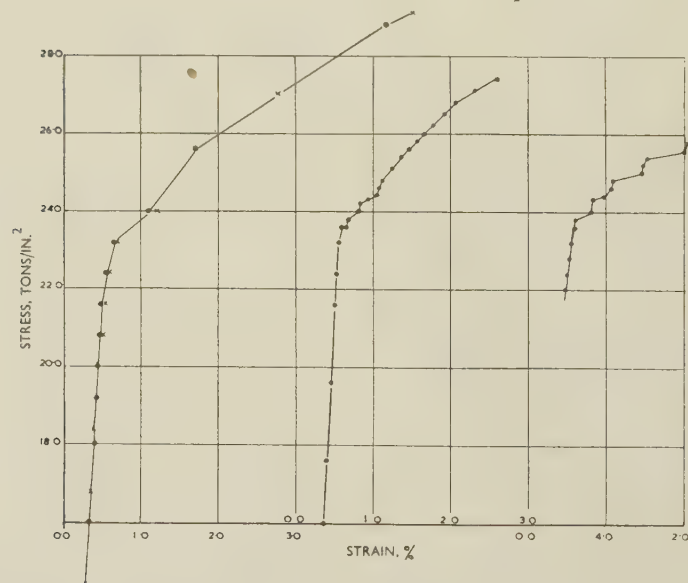


FIG. 4.—Stress/Strain Curves of Duralumin (A) After Ageing for 400 Days at Room Temperature.

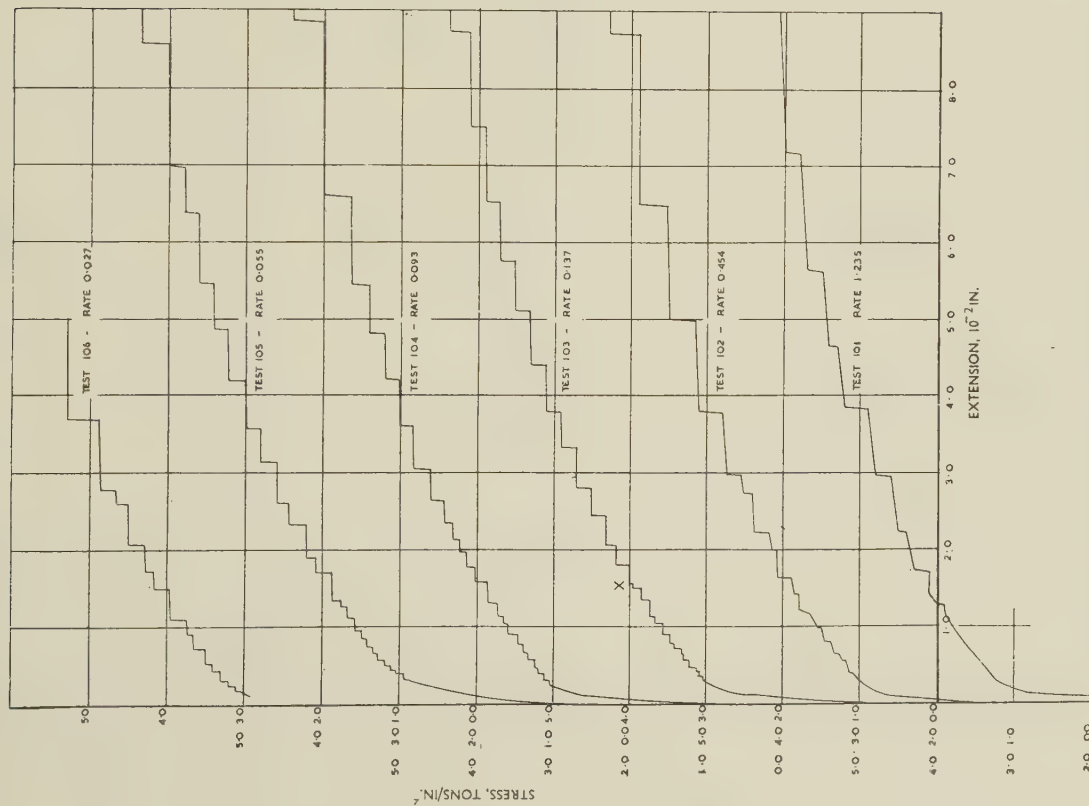


Fig. 5.—Stress/Strain Curves of Solution-Treated 1.35% Copper Alloy (B) at Constant Rate of Stress. All rates of loading in tons/in.²/min.

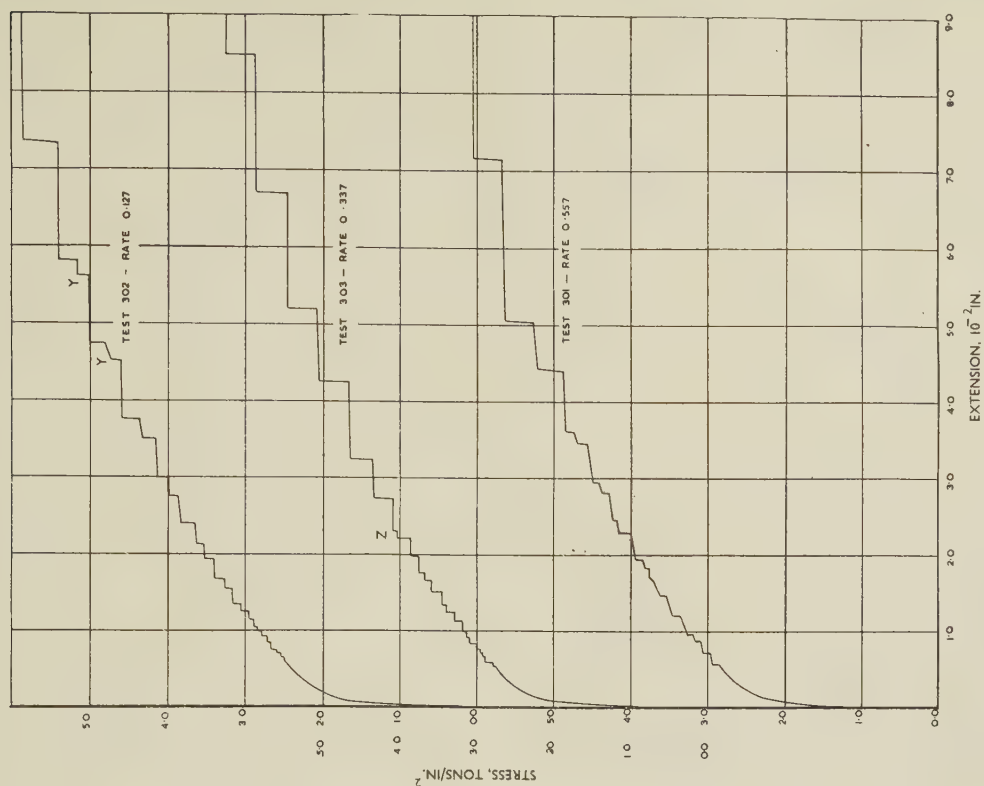


Fig. 6.—Stress/Strain Curves of As-Extruded 1.35% Copper Alloy (B) at Constant Rate of Stress. All rates of loading in tons/in.²/min.

2. CONSTANT-RATE-OF-LOADING TESTS WITH ALUMINIUM-1.35% COPPER ALLOY

Numerous test-pieces were made from material B (see Table I) and tested in both the as-extruded and the solution-treated conditions, using the modified creep machine already described. Some of the test results are listed in Table III. All the curves exhibited clear, sharply defined steps, beginning at the end of

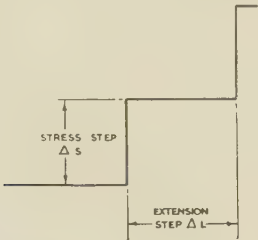


FIG. 7.—Alternative Ways of Defining Step Size.

the elastic range, but these were so small (in some cases as small as 0.00005 in.) that they could not be shown in the plotted curves (Figs. 5 and 6). The steps grew larger as the stress increased, and although the total extension was limited to 0.1 in., the steps continued right up to fracture in all cases.

The rate of loading had no effect on the formation of steps, and the steps had the same character in both the as-extruded and solution-treated states.

In some cases, otherwise regular steps show a tendency to break up into double steps (e.g. at X in

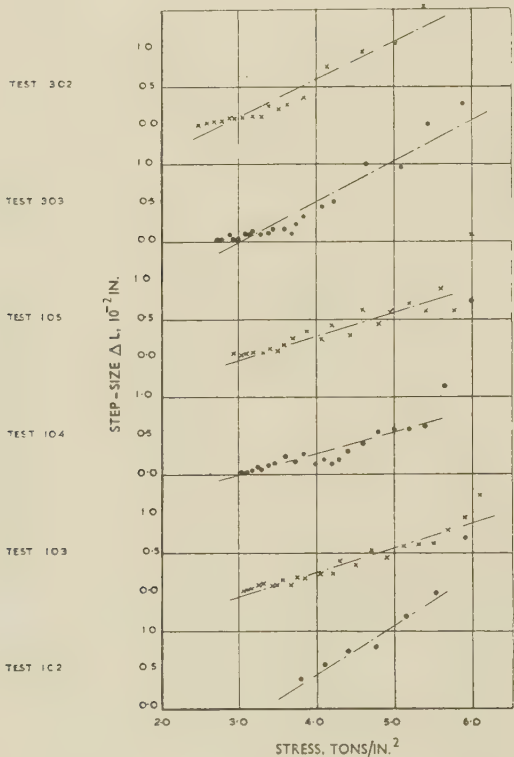


FIG. 8.—Step-Size Analysis (ΔL) for 1.35% Copper Alloy (B).

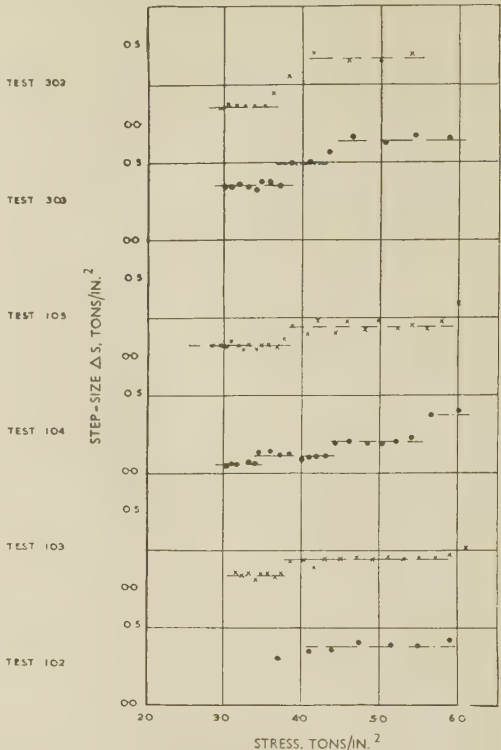


FIG. 9.—Step-Size Analysis (ΔS) for 1.35% Copper Alloy (B).

test 103, Y in test 302, Z in test 303). There seemed to be no cause for this, the steps settling down again immediately afterwards.

Although high rates of loading did not suppress the step formation, the steps at the beginning were very

TABLE III.—Constant-Rate-of-Loading Tests with 1.35% Copper Alloy (B).

Test No.	Condition	Rate of Loading, tons/in. ² /min.	Curve Shown in Fig. No.	Step-Size Analysis in Fig. No.
101	Solution-treated	1.235	5	...
102	"	0.454	5	8, 9
103	"	0.137	5	8, 9
104	"	0.093	5	8, 9
105	"	0.055	5	8, 9
106	"	0.027	5	...
301	As-extruded	0.557	6	8, 9
302	"	0.127	6	8, 9
303	"	0.337	6	8, 9

small, becoming large and distinct after a certain extension (see tests 101, 301). There was also a tendency for the yielding to become progressively more sloping as the rate of loading increased.

The size of the steps can be defined in two possible ways. One way is to measure the amount of extension, ΔL , of each step (McReynolds⁵); the second way is to define the size of step as the amount of stress increment, ΔS , which has to be applied to cause the next step (Fig. 7). Using the first definition, the

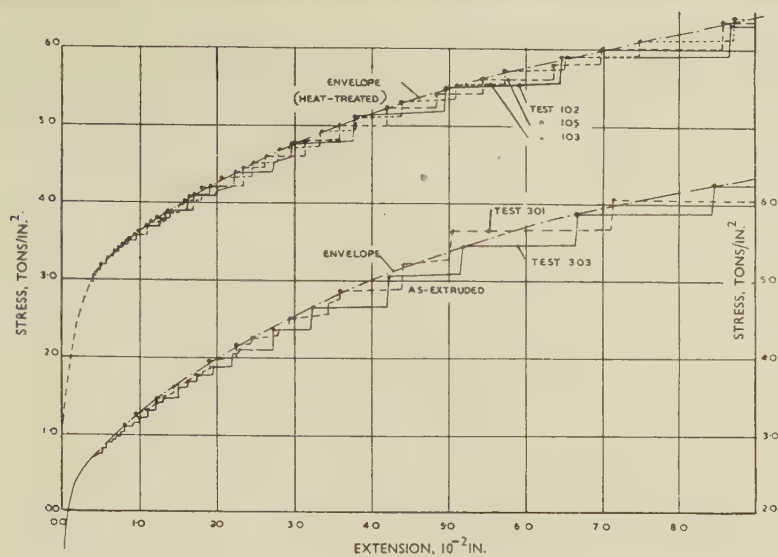


FIG. 10.—Comparison of Stress/Strain Curves for 1.35% Copper Alloy (B) in the Heat-Treated and As-Extruded Conditions.

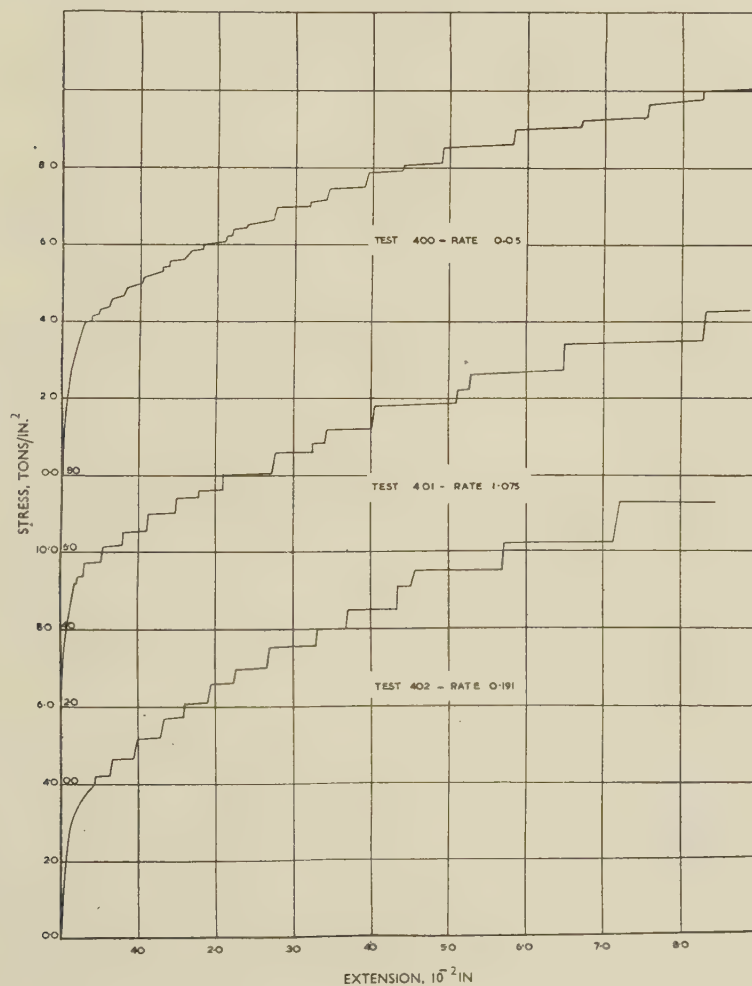


FIG. 11.—Stress/Strain Curves for As-Extruded 3.8% Copper Alloy (C). All rates of loading in tons/in.²/min.

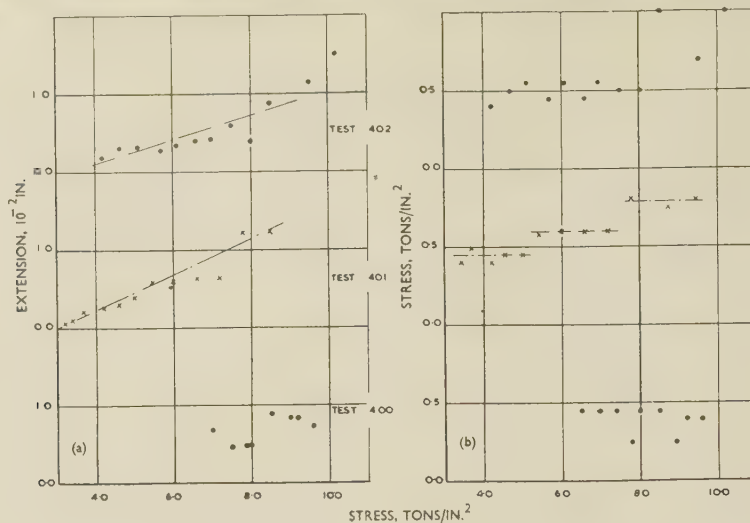


FIG. 12.—Step-Size Analysis for 3.8% Copper Alloy (C). (a) ΔL , (b) ΔS .

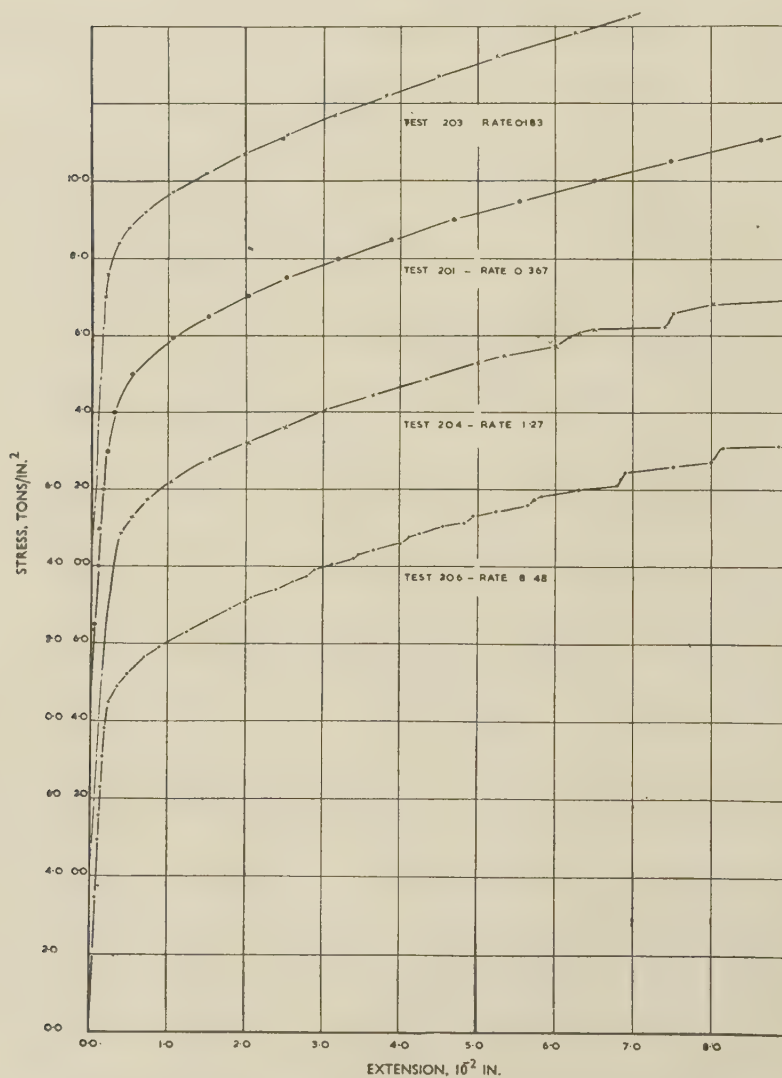


FIG. 13.—Stress/Strain Curves for Heat-Treated 3.8% Copper Alloy (C). All rates of loading in tons/in.²/min.

steps increase roughly proportionately to the stress (Fig. 8). In Fig. 9 the corresponding stress increments ΔS are shown for the tests; the increments tend to fall on horizontal lines, except for sudden jumps at irregular intervals in some cases.

took place, the steps disappearing completely in the slow-loading tests (e.g. Nos. 201, 203, Fig. 13) even up to 10% strain. (Some very small steps—about 0.2×10^{-4} in. long—occurred just beyond the elastic limit, but these were so small that they do not appear

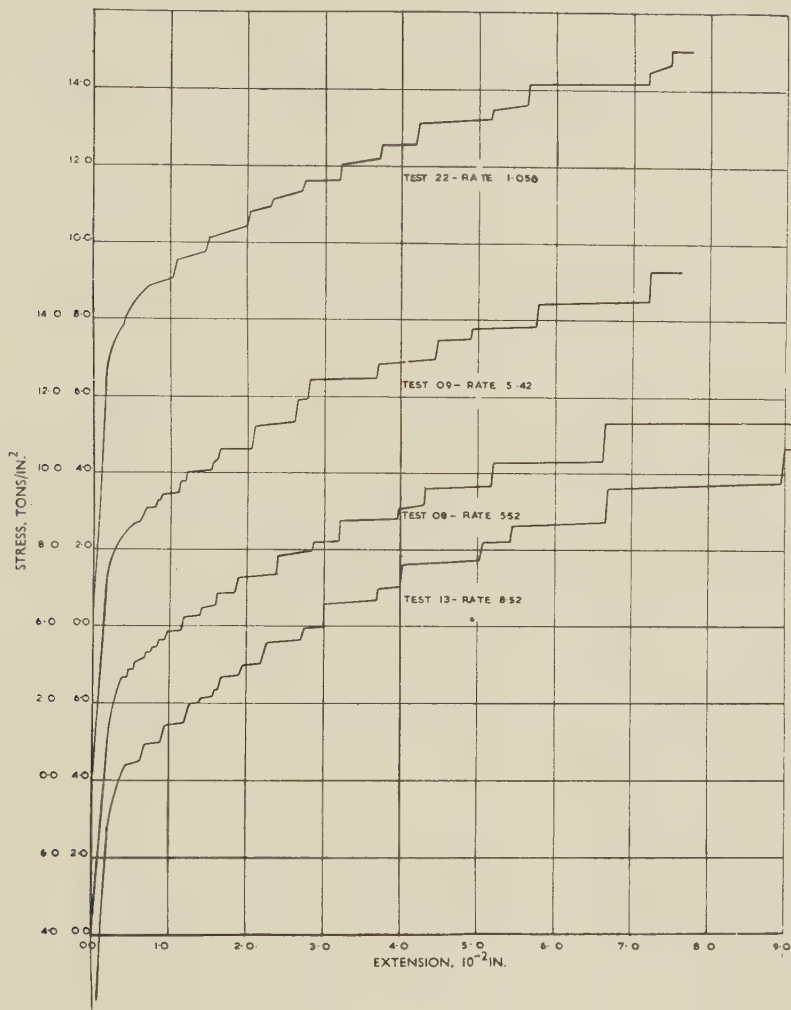


FIG. 14.—Stress/Strain Curves for 3.6% Magnesium Alloy (D) at High Rates of Stress. All rates of loading in tons/in.²/min.

Fig. 10 shows that, when all the curves are superimposed, the upper corners of the steps fall on a smooth envelope.

3. CONSTANT-RATE-OF-LOADING TESTS WITH ALUMINIUM-3.8% COPPER ALLOY

Similar tests (see Table IV) were made on the 3.83% copper alloy, to investigate the effect of copper content. In the as-extruded condition (Fig. 11), no appreciable changes were noticed, except that at the beginning of the curve with higher rates of loading, the steps tended to be larger. The steps were clearly defined throughout all the curves. The results were not quite so consistent as in material B, but the steps show the same characteristics (Fig. 12).

In the heat-treated material, noticeable changes

on Fig. 13, and nothing further was found over the rest of the curve.) At rates of loading above 1 ton/in.²/min., however, the steps reappeared after about 4% straining, and were ill-defined at first. Even

TABLE IV.—Constant-Rate-of-Loading Tests with 3.8% Copper Alloy (C).

Test No.	Condition	Rate of Loading, tons/in. ² /min.	Curve Shown in Fig. No.	Step-Size Analysis in Fig. No.
201	Heat-treated	0.367	13	...
203	"	0.183	13	...
204	"	1.272	13	...
206	"	8.48	13	...
400	As-extruded	0.05	11	12
401	"	1.075	11	12
402	"	0.191	11	12

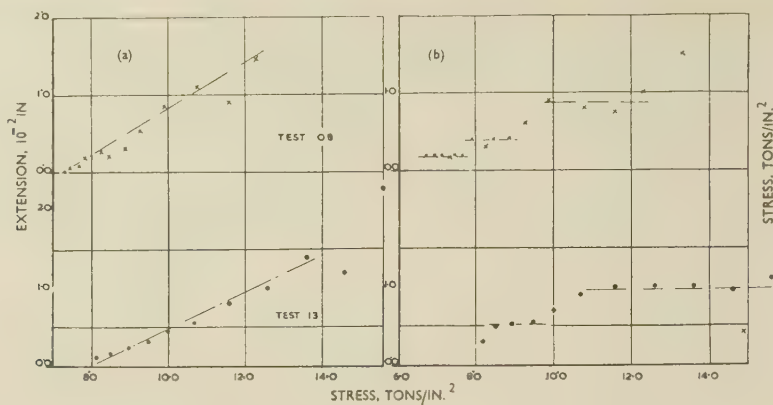


FIG. 15.—Step-Size Analysis for 3.6% Magnesium Alloy (D) at High Rates of Stress. (a) ΔL , (b) ΔS

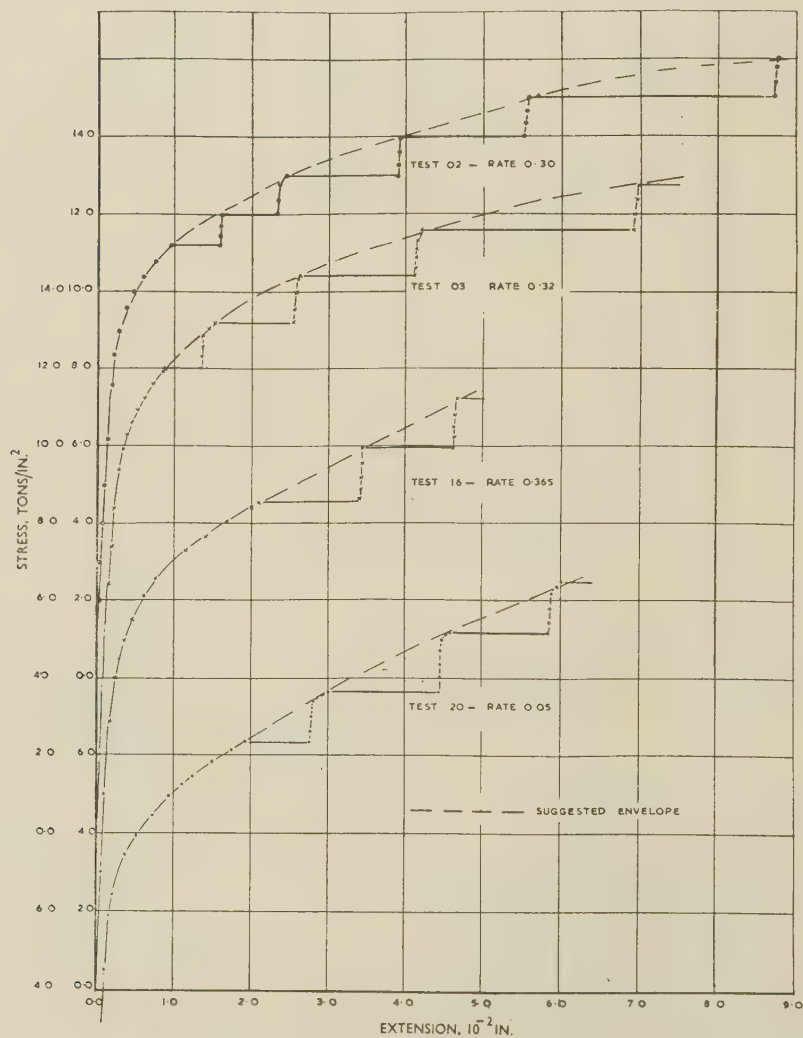


FIG. 16.—Stress/Strain Curves for 3.6% Magnesium Alloy (D) at Medium Rates of Stress. All rates of loading in tons/in.²/min.

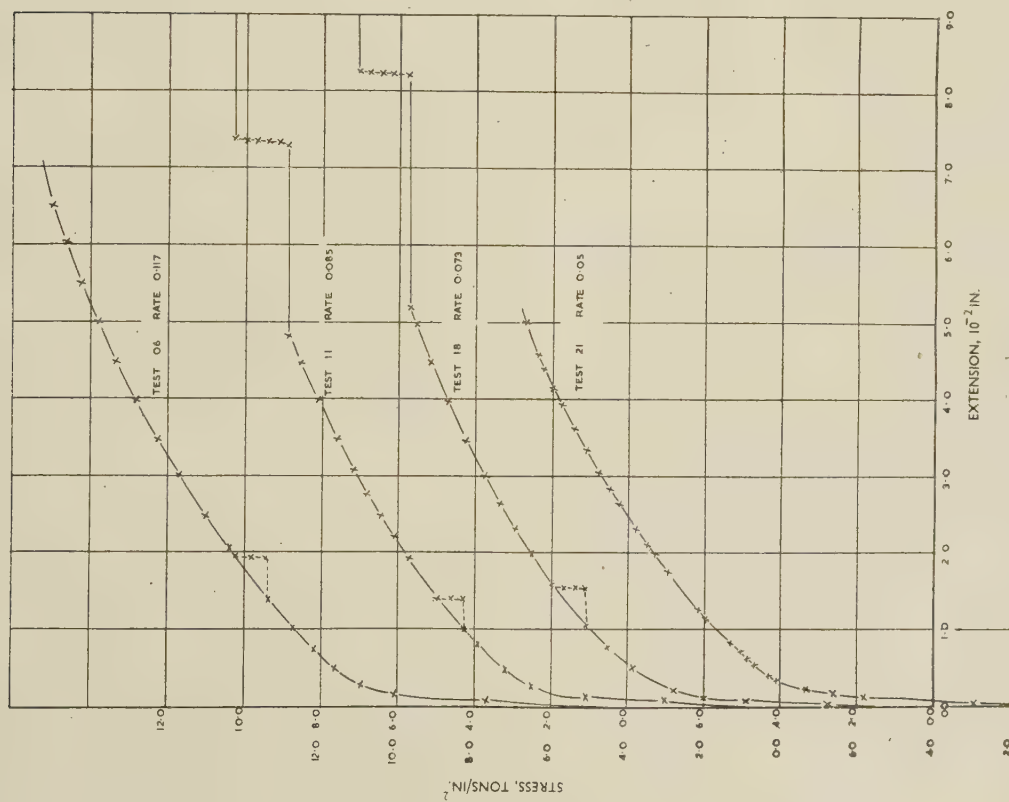


FIG. 17 (a).—Stress/Strain Curves for 3.6% Magnesium Alloy (D) at Slow Rates of Loading. All rates of loading in tons/in.²/min.

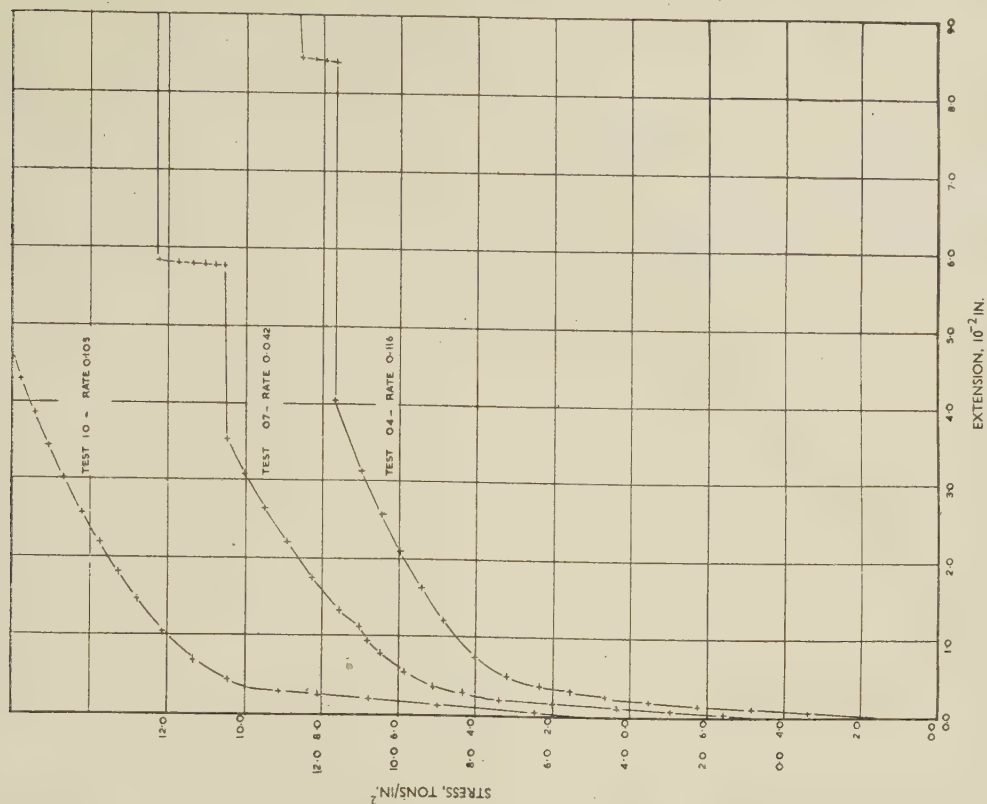


FIG. 17 (b).—Stress/Strain Curves for 3.6% Magnesium Alloy (D) at Slow Rates of Loading. All rates of loading in tons/in.²/min.

after large strains, the steps had rounded corners and were rather wavy in form so that it was difficult to specify their size.

The correlation among the curves is not very good, for although the deviations are not larger than 4% of the absolute stress, these cannot be attributed to inaccuracies in testing or procedure.

These results contradict the theory that the steps arise through rapid ageing during the test, since in that case the slow tests would show steps, the rapid-

the further strain from 1 to 10%. They were all of equal stress height on any one curve, from $\Delta S \approx 1.0$ to ≈ 1.6 tons/in.², ΔL being as large as 3.2×10^{-2} in. in some cases. At very low rates of

TABLE V.—Constant-Rate-of-Loading Tests with 3.6% Magnesium Alloy (D) in As-Received Condition.

Test No.	Curve Shown in Fig.	Step-Size Analysis in Fig. No.	Rate of Loading tons/in. ² /min.
13	14	...	8.52
08	14	15	5.52
09	14	...	5.42
22	14	15	1.058
16	16	...	0.365
03	16	...	0.321
02	16	...	0.30
05	18	...	0.12
06	17 (a)	...	0.117
04	17 (b)	...	0.116
10	17 (b)	...	0.105
11	17 (a)	...	0.085
18	17 (a)	...	0.073
20	16	...	0.05
21	17 (a)	...	0.05
07	17 (b)	...	0.042

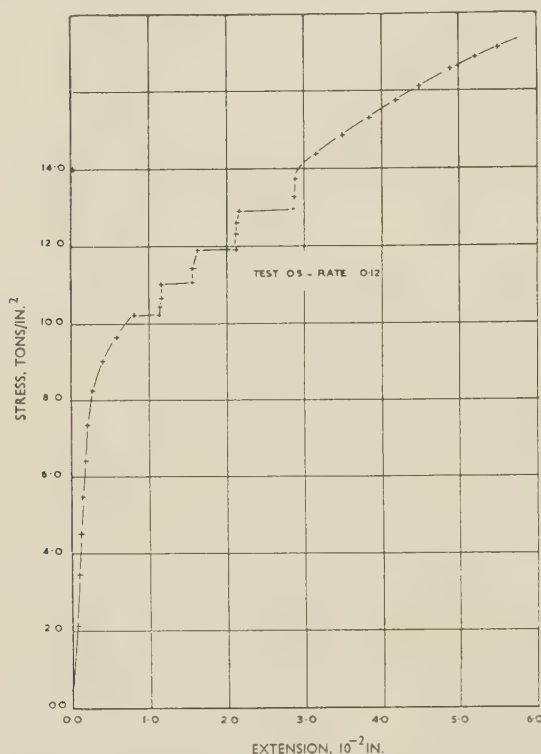


FIG. 18.—Stress/Strain Curve for 3.6% Magnesium Alloy (D) Obtained in Test No. 05. All rates of loading in tons/in.²/min.

loading tests being more likely to provide insufficient time for ageing to occur.

4. CONSTANT-RATE-OF-LOADING TESTS ON THE ALUMINIUM-3.6% MAGNESIUM ALLOY (D)

This alloy was made from commercial-purity aluminium (Table I), and was subjected to a wide range of loading rates. Details are given in Table V.

At high rates of loading, clear, well-defined, and sharp-cornered steps were obtained throughout (Figs. 14 and 15). The steps were very small at first (0.0002 in. was measured, but is not shown in the graph), and grew in size with increasing load. Many of the steps broke down into double steps, but their lengths are roughly proportional to stress (Fig. 15).

At medium loading rates (Fig. 16) no steps appeared until 1% strain, after which very sharp steps were found, of very large size, covering, in 3 to 6 steps,

strain, these effects became even more marked, no steps appearing until about 4–7% strain (Fig. 17), and then one or two very large steps brought the strain to the limit of the experiment. In some cases, no steps appeared within the range of the test, and in others a small step occurred near the start; this was found to arise from any disturbance, such as a slight tap on the testing-machine frame. In one exceptional case, at 0.12 ton/in.²/min., steps began at 0.8% elongation, continuing for four steps before returning to a smooth yield curve up to 6% elongation when the test was stopped (Fig. 18).

A remarkably close correlation was found in some cases between the stepped curves at high rates and the smooth curves at low rates, the top corners of the steps coinciding with the smooth curve. Some of these are shown in Fig. 19, although it is obvious that not all the curves will superimpose.

In these tests, the rise of the step has the slope of the elastic line, and it is to be noted that the smooth curve, when it appeared, formed the envelope of the top corners of the stepped curves, not the bottom corners as has been suggested elsewhere.

5. CONSTANT-RATE-OF-STRAIN TESTS ON MATERIALS B, C, AND D

Tests were made in the special rig (Fig. 2) on the three alloys which produced steps. The results are given in Fig. 20 to a time base, which is also a strain base, since the total strain is directly proportional to time. The load is formed as a result of the elastic strain in the weigh-bar. Even at the maximum load of 1.5 tons, the extension of the weigh-bar was less than 0.0001 in., while the steps formed in the materials were roughly 0.015 in.

All curves obtained were smooth and continuous;

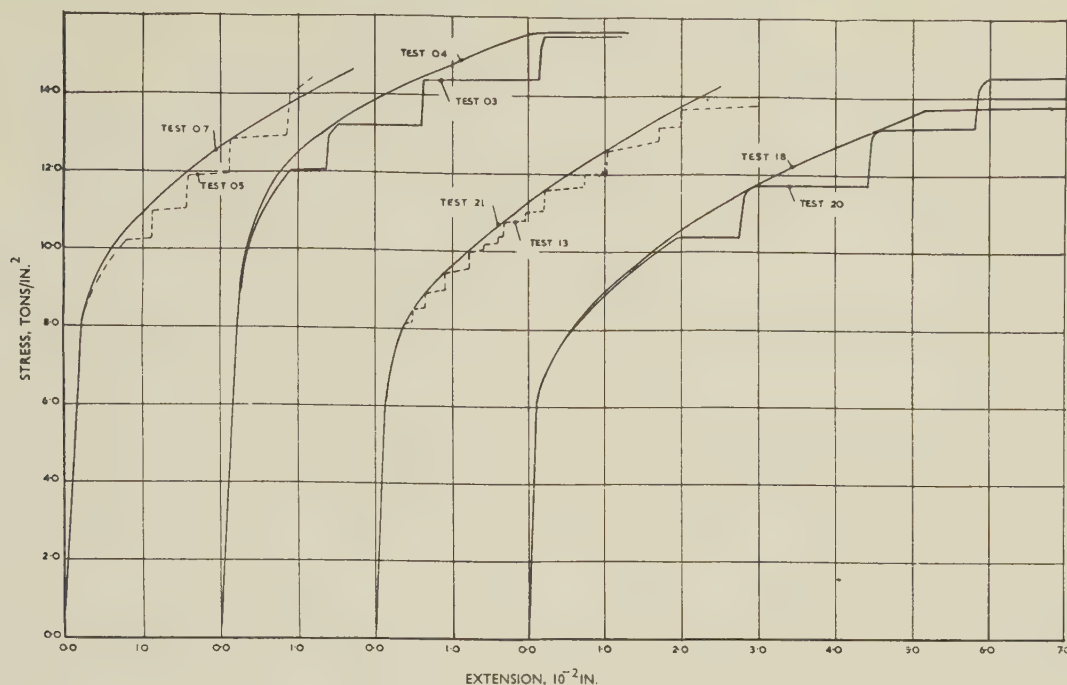


FIG. 19.—Comparison of Stress/Strain Curves for 3.6% Magnesium Alloy (D).

no sudden yields were observed, and although the indicating instrument was watched continuously during the test, the load was never seen to fall, but rose steadily at all times.

The tests confirm that the presence of copper or magnesium is necessary if steps are to be formed.

Eborall, Lack, and Phillips⁹ define two kinds of sudden yield in aluminium alloys, which they designate type *A* and type *B*. Type *A*, the large initial yield similar to that in annealed mild steel, was not obtained in these tests; it requires a fine-grained structure, which was not realized in any of the present materials. The type-*B* yield (referred to in the present paper as stair-stepped yielding), occurring over the whole range of strain up to 10% or more, has been described in a number of papers, but there is still a lack of unanimity as to its character.

Steps, whenever they appear, are well-defined and usually sharp-cornered, consisting of a sudden yield at constant load and a straight, apparently elastic, rise in stress up to the next yield. In high-rate loading tests, yield seems to take place at a slightly rising load, possibly because, although the time taken for the yield to exhaust itself is very short, it is nevertheless sufficient for the stress to have risen appreciably.

In the as-extruded condition, all the alloys showed steps whose size was independent of the amount of alloying element. This seems to be in contradiction to McReynolds' finding that the steps grew smaller with diminishing alloy content, but it is more likely that other factors, such as grain-size, are more important than merely the amount of alloying element.

It is already established that stepped curves exist only within a certain temperature range, and that

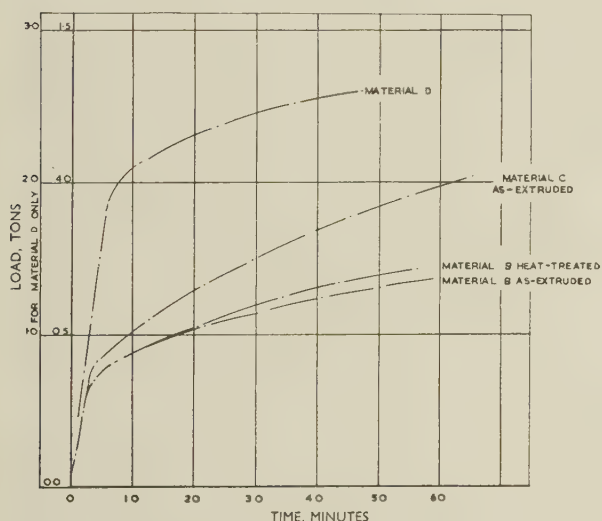


FIG. 20.—Stress/Strain Curves for Materials B, C, and D in Constant-Rate-of-Strain Tests.

VI.—DISCUSSION

All the experiments were carried out at room temperature, and they show that a stair-stepped stress/strain curve is a common occurrence in aluminium alloys containing copper or magnesium.

above and below these limits smooth, continuous curves are obtained.

Three approaches were used in trying to realize a continuous curve at room temperature. First, a Duralumin was allowed to age for a very long time at room temperature, and, though no comparison can be drawn between the partly aged and fully aged yield-stress curves, it is clear that the steps have almost completely disappeared after ageing. Secondly, specimens were tested at very slow rates of loading. With material C (3.8% copper), smooth curves were obtained even at a rate of 0.367 tons/in.²/min.; with material D (3.6% magnesium), smooth curves were obtained up to 5% and even 7% strain at rates up to 0.1 ton/in.²/min. Comparison of these curves with the stepped curves obtained at higher rates showed satisfactory agreement when the smooth curve was superimposed as the envelope of the stepped curves.

The constant-strain-rate tests represent a third attempt at obtaining a continuous yield-stress curve. The idea behind the experiments was as follows: the load on the stretched specimen is not a weight or a hydraulic pressure which cannot be unloaded immediately yield occurs. The load arises from the very small elastic strain in the weigh-bar, and, therefore, if a sudden yield occurs, with a loss of strength as suggested by Cottrell, the specimen will elongate, the load will fall off until equilibrium is again reached, and yield will stop. If this happens, the record of stress against time should be a "saw tooth" curve. In reality, continuous smooth curves were always obtained and a sudden drop in load was not observed.

Returning to the constant-loading-rate tests, there was a marked tendency for steps to break down into double steps of smaller size. This may be attributable to the extrusion process, in view of the fact that this and other irregularities disappeared when the material was heat-treated, though it is more likely to be due to outside disturbances.

In the heat-treated condition, the aluminium-copper alloys showed an effect of the amount of alloying element; with 1.35% copper, the steps were of the usual form and size, but with the 3.8% copper alloy, the steps were not so sharp in outline, and as the rate of loading was progressively reduced, the steps disappeared altogether.

In all cases, the step size grew with increasing stress. If the extension of each step, ΔL , is taken as a criterion of the step size, there is a direct proportionality with stress, except for the last step, which is almost always much larger. This has also been noted by previous investigators.

A better agreement with test results is achieved if the height of the step, ΔS , is the criterion. It was found that the step size remained constant over a wide range, and when the rate of loading was slow enough, all the steps were the same height throughout the experiment; this was particularly so with material D (3.6% magnesium). Where the step does change in size, this occurs as a sudden jump, and the new value of ΔS again becomes steady (Figs. 9, 12).

The yield-point mechanism proposed by Cottrell,⁴ as extended by Nabarro,¹¹ could probably account for this behaviour.

It has been shown that, in many cases and particularly for material B (1.35% copper), the stepped curves can be superimposed and that the top corners of the steps touch a common envelope. Where a yield-stress curve starts off as a smooth continuous curve (e.g. Fig. 18) and then suddenly yields to give a stepped curve, the continuation of the smooth curve would pass through the top corners of the steps, not the bottom corners. This is illustrated further in Figs. 16 and 17, where smooth curves were obtained at low rates of loading as against stepped curves at higher rates. In only one case (Test 402, Fig. 11) was there any tendency for a vertical rise to occur before yielding, and the general behaviour of a sudden yield followed by recovery is further demonstrated in Fig. 17 (Tests 06, 11, and 18), where smooth curves were obtained up to large strains, except where an accidental shock or vibration disturbed the testing machine and a step suddenly appeared; these steps lie below the smooth curve.

These tests suggest strongly that the stepped yield-stress curve depends for its form and (to some extent) for its occurrence on the method of test. The method of loading in the present case involved no increments of load, as in the normal beam-and-weight testing machine, the water flow being continuous and of constant amount. The hydraulic-type testing machine is not entirely free from pulsations, even when set for a constant rate of strain; any adjustments of the controls can cause an impulse. While it is obvious that the steps are closely dependent upon previous history and metallurgical treatment of the material, it is possible that some of the inconsistencies among previous experimental findings may have arisen from slight shocks, caused either by the method of test or by extraneous sources.

The initial large yield found in certain alloys heat-treated to give a fine grain structure and called by Eborall, Lack, and Phillips type-*A*, is similar to the yield-point phenomenon in annealed mild steel, and was not investigated in these tests. Clearly, it can be interpreted in terms of Cottrell's mechanism. Type-*B* yield is that illustrated in the present paper, steps being formed successively, starting as very small steps and gradually increasing to very large increments of extension. By the steady-loading-rate technique used, it was possible to establish that, in materials where type-*B* yielding is well-defined, the steps start the moment the elastic limit is passed; they are so small at first as not to be discernible in the normal way, being masked by extraneous effects, unless great care is taken to avoid disturbing their natural development.

Although no type-*A* yielding was observed, it is quite clear that Eborall, Lack, and Phillips are fully justified in differentiating it from the continuous-step mechanism such as that described here. Although Cottrell's theory explains the type-*A* yield, it would

not appear to explain all the effects observed with type-*B* yield. For example, if the recovery represented by the vertical face of the steps is the result of ageing, then it is necessary to suppose that the ageing can take place very rapidly, since the steps are large and clearly defined at high rates of loading. Yet it has been shown that at very slow rates of loading the steps disappear, although far more time is available for the ageing process to be completed. Moreover, the present tests suggest that the sudden yield is a departure *below* the smooth yield envelope, the recovery merely bringing the strength back to the envelope value.

The first tests on the Duralumin sample also show that, where specimens are allowed to age at room temperature for a considerable time, there is a marked tendency for the steps to disappear, although the strength is increased by this treatment (Fig. 4). While the enhanced strength is consistent with Cottrell's theory, it also requires that once the dislocations are again torn from their atmospheres, the sudden yield should once more manifest itself. Some modification or extension of the theory would therefore seem necessary to cover these facts relating to the type-*B* yield.

The constant-rate-of-strain tests also require explanation. They definitely establish that when the test-piece is pulled very slowly and without jerks, the material yields smoothly. The apparatus was deliberately made as rigid as possible, and any sudden extension would have been at once observed as a

drop in load. That this was not evident calls for further investigation.

In these tests, when a sudden yield has begun, the specimen extends rapidly and the load should fall off or remain steady, and stop any further yield. In actual fact there was no falling off in load, nor was the load momentarily constant at any time. This means that the steps do not appear to have occurred at all in these constant-rate-of-strain tests.

Tests of unloading in the middle of the yield wave with reloading at various strain rates should show whether the curve resumes a smooth form or whether, the moment the load has reached that at which the step occurred originally, the sudden yield is resumed.

It would seem that aluminium alloys exhibiting type-*B* yield are difficult to use in plasticity research. Either a material having a smooth, steady work-hardening curve or a perfectly plastic material showing no work-hardening is required. In checking theoretical results, tests have shown that the strain distribution in a rapidly work-hardening material is radically different from that in a perfectly plastic material, the latter being approached by fully hardened metals.

On the other hand, alloys showing a strong type-*A* first yield might prove very satisfactory for plasticity tests, since the yield must presumably be at constant stress, as in the type-*B* yield. There is a sharp yield point also, and such a material would presumably behave like the perfect plastic mass of theory.

REFERENCES

1. P. Tury and S. Krausz, *Nature*, 1936, **138**, 331.
2. E. W. Fell, *Carnegie Schol. Mem., Iron Steel Inst.*, 1937, **26**, 139.
3. C. A. Edwards, D. L. Phillips, and Y. H. Liu, *J. Iron Steel Inst.*, 1943, **147**, 145.
4. A. H. Cottrell and D. F. Gibbons, *Nature*, 1948, **162**, 488.
5. A. W. McReynolds, *Trans. Amer. Inst. Min. Met. Eng.*, 1949, **185**, 32.
6. T. Sutoki, *Sci. Rep. Tôhoku Imp. Univ.*, 1941, [i], **29**, 673.
7. A. H. Cottrell, *Phys. Soc.: Rep. Conf. on Strength of Solids*, 1948, 30.
8. A. H. Cottrell and B. A. Bilby, *Proc. Phys. Soc.*, 1949, [A], **62**, 49.
9. R. Eborall, M. Lack, and V. A. Phillips, *Bull. Inst. Metals*, 1952, **1**, (7), 58.
10. G. T. Harris, *Metallurgia*, 1946, **34**, 129.
11. F. R. N. Nabarro, *Phys. Soc.: Rep. Conf. on Strength of Solids*, 1948, 38.

DISCONTINUOUS FLOW AND STRAIN-AGEING IN A 6% TIN PHOSPHOR-BRONZE *

1481

By N. H. POLAKOWSKI,† Dipl.Eng., Ph.D., MEMBER

SYNOPSIS

Tension tests were carried out on 0.2-in.-dia. α -bronze rods after various initial treatments. The effects of the following factors on deformation properties were investigated: grain-size, strain rate, slow and rapid cooling from the annealing temperature, kind and amount of prestrain, state of residual stress in the metal, ageing treatment, and testing temperature. It was found that the mechanical behaviour of this material was almost identical with that of low-carbon steel under comparable conditions. However, in contrast to steel, quenching or strain-ageing (even repeated) did not produce any extra embrittlement of the bronze beyond the normal exhaustion of ductility caused by plastic strain alone.

The mode of propagation of Lüders deformation along the strain-aged rods was followed by direct diameter measurements, of which representative results are given. The yield-point discontinuity increased in size with total strain, and reached about 7% in samples which were prestretched to a sufficient extent and aged afterwards. The fronts of the Lüders deformation waves were sharp in the fine-grained material, but very diffuse in the coarse-grained one.

The observations are discussed on a phenomenological basis, and their bearing on the problem of strain markings on non-ferrous sheet-metal products is emphasized. By analogy with steel, these results are felt to support the idea that "flamboyant" and "parallel-band" markings are caused by fundamentally identical mechanisms. It appears that the stress distribution in the metal being deformed and the variable rate of strain-ageing are the factors which control the form and mode of propagation of the surface markings.

I.—INTRODUCTION

THE discontinuous character of plastic flow at the yield point is a notable property of annealed or strain-aged low-carbon steel. Its occurrence gives rise to certain well-known defects during forming operations on steel sheets (Lüders lines or stretcher-strains). As far as non-ferrous metals are concerned, discontinuous yielding was recorded over 30 years ago by Bach and Baumann¹ on two copper-base alloys. In the following years relevant observations were made on several other metals and alloys.²⁻¹¹ Sometimes the unstrained metals showed smooth stress/strain curves, though abrupt yield points appeared after straining and ageing; in other cases the whole extension records were serrated, the distance between the consecutive serrations roughly increasing with progressive deformation. This behaviour was reminiscent of that encountered in iron-carbon alloys at blue-heat temperatures. It was also accompanied by formation of specific surface markings, which have been described in detail by Jevons¹² and others.^{8, 11}

Suggestions have been put forward from time to time that all these effects are essentially caused by a single mechanism,^{7, 9, 12, 13} which is operative in metals that contain small quantities of certain impurities, such as, for example, carbon or nitrogen. Nitrogen, in particular, was found to be responsible for strain-ageing phenomena in several metals, both in mono- and polycrystalline form.

The purpose of the present work was to investigate in some detail the deformation and strain-ageing behaviour of a cubic, face-centred α -bronze, and to compare it with that exhibited by ordinary mild steel in similar circumstances. In order that a reasonably detailed and systematic comparison might be drawn, an attempt was made to take into account as many variables as possible.

II.—YIELD-POINT EFFECTS IN IRON, AND FACTORS AFFECTING THEIR OCCURRENCE AND MAGNITUDE

Before describing the experiments, it may be useful to recapitulate the more important features of discontinuous yielding and ageing in iron and steel, to facilitate subsequent analysis of the results obtained. In originally unstrained, i.e. annealed or normalized, iron-carbon alloys, the following points are of significance:

(i) When the initial yield stress is exceeded, a relatively large plastic deformation occurs at a virtually constant tensile load. A distinct, approximately horizontal line is in effect traced on the extensometer record.

(ii) Separate "upper" and "lower" yield points are frequently observed.

(iii) In a given material, the value of the initial (lower) yield stress and the length of the yield horizontal are directly related to one another.

* Manuscript received 19 March 1953.

† I.C.I. Research Fellow, Metallurgical Department, University College, Swansea.

(iv) The two parameters under (iii) are grain-size-dependent, and the finer the grain, the more pronounced and extensive are the yield-point effects.

(v) An increase of the rate of straining also causes the yield effects to increase.

(vi) A discontinuous yield point is associated with non-uniform deformation of the material. If straining is interrupted before the end of the horizontal portion of the extension diagram is reached, it will be found that only a part of the metal yielded plastically, the remainder being left substantially in the original condition.

(vii) Quenching of carbon-containing iron from elevated temperatures (above 400° C.) causes the yield phenomenon to become fainter or even to disappear entirely.

(viii) The discontinuous yield can be eliminated by giving the metal a small reduction by rolling (skin pass) or by bending it over an ample radius in alternate directions. The magnitude of the initial yield stress is thereby reduced.^{14, 15}

If the metal was initially in the overstrained condition, for example by prestretching, the following additional points are to be noted:

(ix) When plastic stretching is resumed immediately after the first prestraining operation, abrupt yielding is absent and the second curve represents virtually a smooth continuation of the first one.

(x) Ageing of the prestrained metal, for example by heating it for some time at a slightly elevated temperature, causes the return of a sharp yield. The new yield point appears at a higher stress than that reached at the end of the prestraining operation.

(xi) Such ageing treatment results in a substantial fall in the residual elongation value as compared with the prestrained but unaged condition.

(xii) Inducing sufficiently high residual stresses in the metal by inhomogeneous plastic deformation (drawing, torsion, and the like) retards or even suppresses the recurrence of a sharp yield point upon ageing.¹⁵

(xiii) The extension curve becomes serrated when the test temperature is between 100° and 250° C., irrespective of whether the steel was initially prestrained or not. In this range the U.T.S. increases and the elongation falls considerably as compared with the room-temperature properties ("blue-heat phenomenon"¹⁸).

The above points were accepted as a basis for the present experimental work and, in spite of certain limitations of the available equipment, none of the points was neglected.

III.—EXPERIMENTAL TECHNIQUE

1. MATERIAL

The work was carried out on commercial-quality, nominally 5% tin, phosphor-bronze rods, which were cold drawn 27.6% from the annealed condition to 0.200 in. dia. Their percentage composition was as follows: Sn 5.9, P 0.15, As 0.02 (by chemical

analysis); Pb 0.10 (max.), Fe 0.03, Bi 0.002, Ni 0.01, Sb 0.005, Zn 0.03, Mn trace (determined spectrographically); Cu 93.75 (by difference). The U.T.S. of the as-drawn rod was 31.5 tons/in.² and the elongation on 4 in. was 17.3%.

2. TENSION TESTS

With one exception, the tests were performed on a weight-pendulum motor-driven Amsler machine, and a 1-ton scale was used. Two head-travel speeds were available, 0.5 and 1.5 in./min.; unless otherwise stated, the lower speed was employed. An ordinary 4-in. extensometer was used, and the record was obtained autographically in a 2:1 magnification.

Two tensile tests at elevated temperatures were carried out at the B.I.S.R.A. Laboratory at Swansea on a similar tensile machine, equipped with a hand-drive only. In this case the extension diagram was obtained by driving the drum from the moving head of the machine, the distance between the grip faces being 7 in. at the beginning of the test.

3. AGEING TREATMENT

The prestrained specimens were usually aged by boiling them in water. A thermostatically controlled oven was used for heating up to 250° C.

IV.—EXPERIMENTAL RESULTS

1. EFFECTS OF GRAIN-SIZE AND STRAIN RATE

Different grain-sizes were produced by annealing three of the rods at 500°, 675°, and 850° C. for 2, 1, and 1 hr., respectively. After cooling in air, the

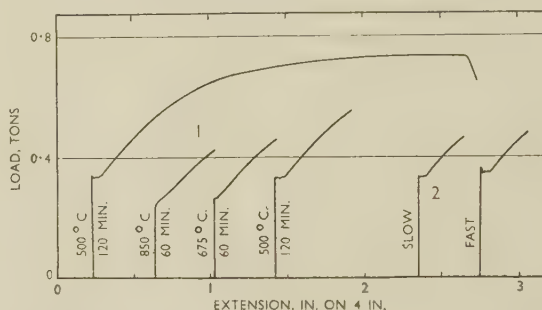


FIG. 1.—Effects of (1) Annealing Temperature (Grain-Size) and (2) Strain Rate on the Yield Point of Bronze. The range of speed in (2) was 1:3.

grain diameter was approximately 0.02 mm. in the first rod, 0.05 in the second, and 0.1 in the third. The initial portions of the corresponding extension curves, together with a complete curve of the fine-grained material, are shown in Fig. 1. The specimen with the coarsest grain did not exhibit an abrupt yield point at all, whereas the other two did, the magnitude of the phenomenon increasing as the grains became finer (cf. Section II (iv)).

The last two curves in Fig. 1 indicate the effects of strain rate on the yield point. In view of the small range of speeds available (1:3), the effect was not

likely to be marked. Nevertheless, the yield platform in the faster test was on a distinctly higher stress level, as might reasonably be expected (Section II (v)). The pronounced "upper" yield point on the last curve was presumably due to the inertia of the pendulum rather than to any intrinsic quality of the specimen under test.

2. EFFECT OF REVERSED FLEXURE ON THE YIELD POINT

Curves (a) of Fig. 2 show the effect of a single reversed bend over the diameters indicated on the respective curves, followed by straightening out, on the yielding behaviour of a normalized 0.22% carbon steel rod of 0.2 in. dia. The results of tension tests on bronze rods annealed for 2 hr. at 500° C. and afterwards subjected to similar treatment, are depicted in curves (b); the similarity between the two sets of curves is clearly apparent. Naturally, the fall of the yield-point stress after bending is less pronounced in the non-ferrous alloy because its yield platform is much shorter than in the case of steel. If an identical experiment were carried out on a coarser-grained steel

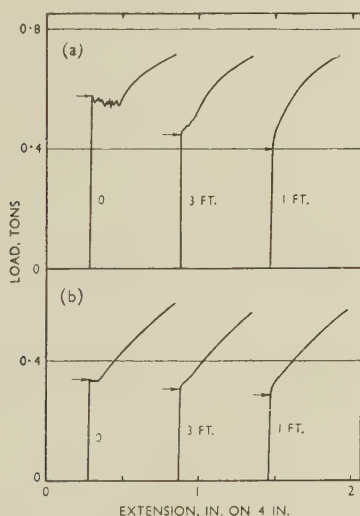


FIG. 2.—Effects of a Single Reversed Bend over the Diameters Indicated on the Yield Point of (a) Normalized 0.22% Carbon Steel and (b) Annealed Bronze. All rods 0.2 in. in dia.

than that used, the attendant depression of the yield point would be also much less conspicuous.

3. RETURN OF AN ABRUPT YIELD AFTER STRAIN-AGEING

A number of typical results are shown in Fig. 3. Specimens 1, 3, and 5 were fine-grained, whereas 2 and 4 had a coarse grain (50 and 10 grains/mm., respectively). In each case it was sufficient to heat a pre-stretched test-piece for 1 hr. at 100° C. in order to cause a yield phenomenon to develop. In fact, a much shorter period was enough for this purpose,

but the above treatment was taken arbitrarily as a standard.

Curves 3 and 4 indicate that, as the total strain received by the specimen increases, the yield hori-

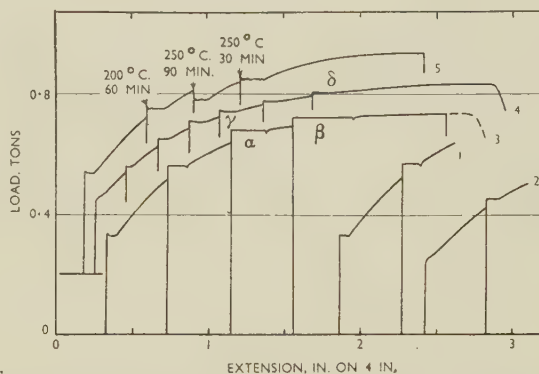


FIG. 3.—Tension Tests with Intermediate Ageing Treatments on (1, 3, 5) Fine-Grained and (2, 4) Coarse-Grained Bronze with 50 and 10 Grains/mm., Respectively. All ageing was carried out at 100° C. for 1 hr., except in the case of specimen (5), which was as indicated.

zontal becomes longer. This point will be referred to later on, when the numerical values of the yield discontinuities marked by Greek letters will be quoted and discussed (p. 621). It is also noticeable that specimens 2 and 4, which do not exhibit abrupt yield points in the as-annealed condition, show well-developed discontinuities after strain-ageing. There is a distinct difference between the shapes of the yield "platforms" in each case: in the fine-grained specimen these are perfectly straight and horizontal, and they end suddenly with an accompanying slight drop of the load pointer; in the coarse-grained bronze, the "horizontals" are slightly dished, and they merge smoothly into the uniform-flow curve.

The effect of raising the ageing temperature (curve 5) consists in producing a somewhat irregular, wavy form of yield platform. A temperature of 250° C. results in a slight but distinct softening, due presumably to partial recovery.

Although specimens 3 and 5 broke outside the gauge portion, it can be confidently said that no matter how many consecutive ageing treatments were employed, these did not result in a fall of ductility. If the steps caused by ageing are disregarded, curve 3 proves to be an almost perfect duplicate of that given in Fig. 1. This statement is supported not only by direct measurements of the diameters of the broken rods, but also by further results to be shown below under (4).

4. AGEING BEHAVIOUR OF QUENCHED SPECIMENS

By analogy with low-carbon steel, it is to be expected that any precipitate responsible for the sharp yield point after slow (or relatively slow) cooling after annealing, will remain in solution after quenching. Consequently, a smooth extension diagram should be obtained when this procedure is employed.

Curves 1 and 2 of Fig. 4 show indeed that after quenching the bronze rods in water from 550°C. the yield discontinuity was absent. Nevertheless, ageing for a short time at 100°C. after plastic deformation produces the usual effects, exactly as in the case of initially annealed specimens.

Direct ageing after quenching tended to restore the yield-point phenomenon, but the rate at which the latter returned was extremely slow, as can be

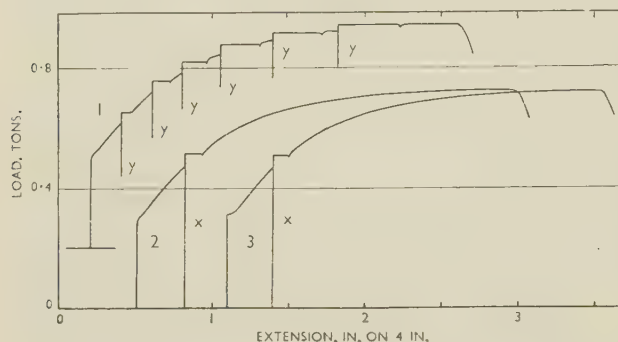


FIG. 4.—Tension Tests on Bronze Rods Initially (1, 2) Quenched in Water from 550°C., and (3) Quenched as Above and Aged at 250°C. for 18 hr. Intermediate ageing at 100°C. for $\frac{1}{2}$ hr. (y), or 1 hr. (x).

seen from the initial portion of curve 3, which was obtained after heating a quenched sample for 18 hr. at 250°C. This behaviour is again not unlike that found in steel, where the yield point returns very sluggishly after quench-ageing.^{15, 16}

A comparison of the three curves in Fig. 4 with the one shown in Fig. 1 proves that no embrittlement was induced by the quench- and strain-ageing treatments, the elongations being almost exactly equal in all cases.

5. DISCONTINUOUS PLASTIC FLOW AFTER STRAIN-AGEING

McReynolds⁶ has described experiments designed to determine the mode of propagation of plastic flow in commercially pure aluminium which showed stair-step yielding. In his tests, a number of resistance strain-gauges were affixed at close intervals along the specimen, each gauge being connected to a quick-response, multi-channel recorder. It was found that the gauges responded to plastic strain in succession, thereby indicating that the deformation traversed the specimen in the form of a wave arising at one of the ends. In some cases the waves were stopped by structural barriers of undetermined nature before they had passed through the entire length.

Sylwestrowicz and Hall¹⁹ made careful visual observations of a similar nature on mild-steel strips by using a special illumination. In their case, too, the plastic flow spread from a point of stress concentration at one of the grips or fillets, and the front of the wave was easily discernible.

Because of the convenient shape and size of the specimens used in the present work, not only was it

possible to follow the propagation of plastic deformation with ease, but in addition the Lüders strain could be directly measured. This was done by interrupting the test at an intermediate stage of discontinuous yielding and then measuring the variation of diameter along the gauge portion by means of a micrometer. The procedure and findings are illustrated diagrammatically in Fig. 5.

The specimen was first prestretched till it had a uniform diameter d_1 . It was then removed from the testing machine, aged, and again reloaded along *a* until the stress level of the yield platform *b* was reached. Further extension along *b* took place at a constant load, and, upon interrupting the test midway on *b*, it was found that a part of the test rod still retained the initial diameter d_1 , whereas the remainder was reduced to d_2 . The ratio of the cross-sectional areas of the "unyielded" and "yielded" portions ($(d_1/d_2)^2$) determined the value of the discontinuous Lüders strain. As could be expected, the sudden thinning from d_1 to d_2 began at one of the grips and moved gradually forward, until the Lüders strain covered the whole length of the specimen. In some cases, a second front began to move after a time from the other grip towards the centre portion of the sample, where the two eventually met. Fig. 5 shows a case of this kind. At the moment at which the discontinuous elongation had just ended, a slight drop of the load pointer of the machine was invariably

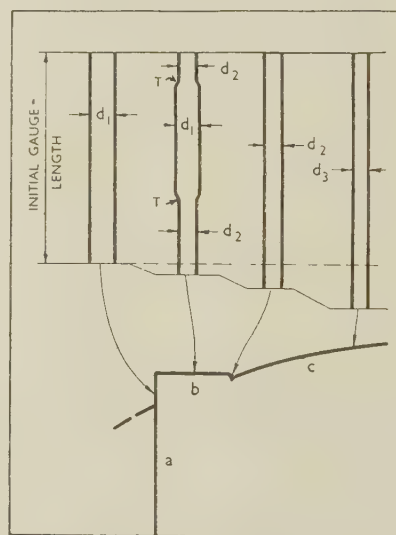


FIG. 5.—Propagation of Lüders Strain along a Strain-Aged Bronze Rod (Schematic). Diagram *a-b-c* is the as-aged stress/strain curve; *T* is a taper-shaped front of a Lüders deformation wave.

noticed in the experiments with fine-grained material. Upon further stretching beyond this point, the flow was homogeneous, and the transition from d_2 to a smaller diameter, d_3 , took place in a perfectly uniform manner all along the rod.

As has already been mentioned under (3), the change from discontinuous to homogeneous deformation in

the coarse samples was gradual, and no load drop was observed. This difference is apparently associated with the form of the taper, T , which connects the already deformed and the still undeformed portions of the specimen. Although it was not possible to establish the exact dimensions (profiles) of these conical transitions in each case, it was quite clear that in the coarsest-grained rods the cone generators were several times longer than in the fine-grained ones. At the same time, the d_1/d_2 ratios behaved in an opposite manner, in view of the smaller Lüders strain in the coarser metal. It is easy to see that in these conditions the change of deformation pattern from discontinuous to uniform was bound to be almost instantaneous in the fine-grained material, whilst being very gradual in the other. Incidentally, the above difference in the geometry of T also accounts for the front of the "Lüders wave" being sharp and well defined in the first case, but diffuse in the second.¹⁹

The values of d_1 and d_2 were measured on many rods. Typical figures, referring to the positions marked by α , β , γ , and δ in Fig. 3, are given below. A metric micrometer was used, and the dimensions are quoted in millimetres:

Position:	α	β	γ	δ
d_1	4.63	4.46	4.63	4.37
d_2	4.53	4.31	4.57	4.30

From these figures it was possible to compute the Lüders deformation $(d_1/d_2)^2$ in each case. For α and β the values obtained in that way were 4.3 and 6.8%, respectively, whereas direct measurements of the yield platforms from the diagram gave 3.9 and 7.15%. This discrepancy was considered reasonable, being due mainly to the error in calculating the mean diameter, which showed slight variations along and across the test rod. The error gradually decreases as the d_1/d_2 ratio becomes larger. For the same reason, it was not possible to determine with sufficient accuracy the small yield strain in the annealed metal from diameter measurements.

For the coarse-grained specimens, γ and δ , these ratios were much smaller than in the first two. Moreover, since there was no drop of the load pointer when the two diffuse fronts met, it was not possible to determine the precise length of the yield horizontal (or rather "dish") from the records. Hence a comparison of the resulting figures in the same manner as was made above with α and β could not be undertaken.

6. EFFECT OF RESIDUAL STRESSES ON DISCONTINUOUS YIELDING

The effect of residual stresses on the yielding behaviour of carbon steel has been described by the author previously,¹⁵ and the results reproduced in Fig. 6 show that they affect phosphor-bronze in the same manner. That is, whenever the method of deformation used was other than by tension, the return of the yield discontinuity upon ageing was considerably retarded. No trace of a yield point in

tension appeared on ageing after previous torsion (curves 1 and 2). A single reversed bend over a 5-in. diameter was sufficient to prevent the return of an abrupt yield in subsequent tension in spite of an intermediate ageing treatment (curves 3, 4). However, reversed bending is not a very effective means of suppressing the yield phenomenon, presumably because of the low magnitude of the residual stresses it leaves behind.¹⁵ Consequently, although this treatment was sufficient for the coarse-grained specimen 3, it was not quite so satisfactory with the fine-grained material 4, in which an incipient recurrence of the discontinuity after ageing may be noticed.

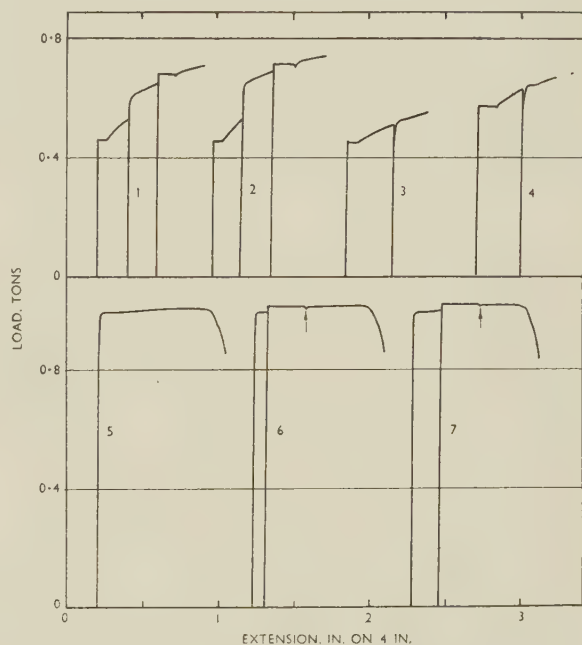


FIG. 6.—Effect of Residual Stresses on the Discontinuous Yielding of Bronze. (1) Twisted over 30°/in. and aged at 100° C. for 2 hr.; (2) twisted over 60°/in. and aged as above; (3) and (4) bent over 5 in. dia., straightened out, and aged as above; (5) cold-drawn 27.0% to 0.2 in. dia. and aged as above; (6) and (7) drawn as above, slightly stretched afterwards, and aged at 100° C. for $\frac{1}{2}$ hr. Specimen (3) was coarse-, all others fine-grained.

This is again in line with the experience gained from the use of roller-levellers for preventing stretcher-strains on alternatively fine- and coarse-grained steel sheet.

Curves 5–7 relate to rods in the as-cold-drawn condition (see Section III, 1). Curve 5 applies to a rod that was boiled for 2 hr. before being pulled. Boiling did not result in any changes in the mechanical behaviour, and did not alter the shape of the original as-drawn rod. It should be pointed out that the very slight fall of the curve beyond the macroscopic "yield point", has nothing to do with a true yield discontinuity. This type of deformation curve is common in both steel and various ductile non-ferrous metals after moderate reductions by cold drawing, but it is not accompanied by non-uniform yielding.

This point is made because the author knows of instances where the feature has been referred to as "discontinuous yielding". However, it was sufficient to give the drawn rods only a slight additional stretch in order to develop a real and very strong yield phenomenon. This is displayed in curves 6 and 7, in which the ends of the yield platforms are marked with small arrows, but which are otherwise self-explanatory.

7. SERRATED OR "STEPPED" EXTENSION DIAGRAMS

This type of extension curve is quite general in various aluminium-base alloys, particularly those containing magnesium as the main alloying element. These steps may be regarded as a series of yield discontinuities following one another at close intervals. It is noticeable that the spacing (pitch) of these steps gradually increases towards the higher total strains, as may be seen on the specimen curve 3 (Fig. 7) and

increased. In effect, each spot of the specimen had a different strain and ageing history. Both test-pieces broke near the upper grips and hence away from the furnace, which was mounted on the lower machine head. When the fractured rod was removed from the machine, it was found that the diameter of the portion which had been in the hot zone till the end of the experiment was exactly the same as that in tests at room temperature (4.10 mm. = 0.1615 in.). From this the tentative conclusion was drawn that, in contrast to low-carbon steel, whether rimming or killed, the bronze did not suffer from a loss of ductility at 250°–300° C.

It may be added that the violent load fluctuations seen on curves 1 and 2 in Fig. 7, were due partly to the absence of an oil damper on this particular machine.

IV.—DISCUSSION

The results presented strongly support the belief that the mechanisms of discontinuous yielding in iron

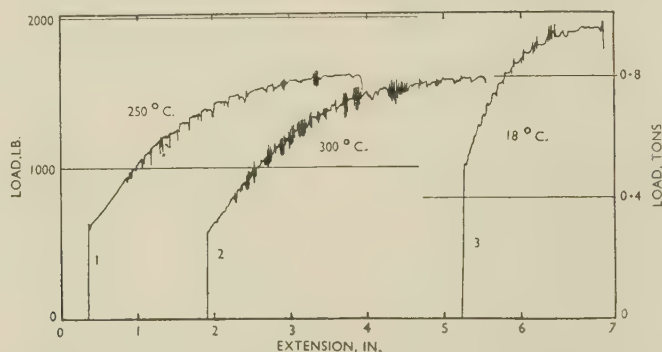


FIG. 7.—Tension Tests on (1, 2) Annealed, Fine-Grained Bronze and (3) Annealed Aluminium-5% Magnesium Alloy, at the Temperatures Indicated. The extension scale must be halved for (3), and should refer to in. on 4 in.

even more clearly elsewhere.^{6, 8, 17} This feature indicates a connection with the type of curves 3 and 4 in Fig. 3, and 1 in Fig. 4, where a similar effect was obtained as a result of successive strain-ageing treatments.

The above similarity supports the opinions ascribing the stair-step yielding to rapid ageing of the newly deformed metal during the test.^{9, 18} Indeed, two tension tests performed at 250° and 300° C., respectively, on specimens annealed at 500° C. gave the same kind of curves as that obtained at room temperature on the aluminium-5% magnesium alloy (curves 1, 2, Fig. 7).

Because of the primitive equipment available for the last two experiments, it was not possible to establish with certainty whether or not the bronze used was subject to the "blue-heat phenomenon" (Section II (xiii)). The heating furnace was only 4 in. high, and it was unlikely that a length of more than 3 in. along the rod actually reached the temperatures indicated. The conditions were further complicated by the fact that as the metal stretched, the ratio (cold length:hot length) continually

containing certain impurities and in some non-ferrous metals are very similar. It has been shown that almost all the factors influencing the yield behaviour of carbon steel in a specific manner may affect certain face-centred non-ferrous metals in a virtually identical way. This applies to variables such as grain-size, deformation rate, rate of cooling after annealing, state of residual stresses in the metal, &c. Broadly speaking, of the thirteen points listed in Section II, (i)–(x), (xii), and in part (xiii) hold both for steel and for the bronze investigated.

Notwithstanding these striking similarities between the behaviour of iron and that of bronze, an important difference was also observed. The bronze studied was free from embrittlement after quenching or strain-ageing, except for the gradual exhaustion of ductility caused by plastic deformation. As is well known, either treatment would have induced extra embrittlement in iron-carbon alloys, quite apart from that associated with work-hardening by itself. A low-carbon steel showing 40% elongation in a continuous tension test at room temperature may have this figure almost halved if the test is interrupted twice

and the specimen aged each time. In other words, the effects of strain-ageing on the mechanical behaviour of the copper alloy are of a transient nature and, contrary to what occurs in iron, they do not lead to any permanent changes whatsoever. The platform-like step appearing on the stress/strain curve after each successive ageing treatment represents merely a superstructure on the basic stress/strain curve, which remains practically unaffected.

A qualitative picture of the mechanism by which a discontinuous yield point is produced in a polycrystalline metal is provided by the concept of a grain-boundary structure which strengthens the parent metal.^{13, 14, 19} This structure is assumed to collapse during straining and to re-form upon subsequent ageing. The dislocation theory offers, in addition, a fairly detailed description of the sudden yield mechanism on an atomic scale. However, neither seems to account for the permanent embrittlement caused in iron by ageing.¹⁹ This difficulty does not arise with the material used in the present work, since the yield effect it exhibits is a "pure" one, unaccompanied by complicating secondary effects, such as, for example, fall of ductility.

If a copper alloy is capable of producing a yield phenomenon in its pure form (as just defined), it may be asked whether the ageing behaviour of common iron-carbon alloys is not the sum of two separate processes. One of them may be responsible for the gradual return of the yield horizontal, and the other for the loss of ductility. It remains to be seen whether this is so or not, and it would be premature to enlarge on this question here.

As is well known, discontinuous flow is associated with the formation of certain surface markings on the strained metal. Since their formation and nature cannot be followed conveniently on round rods, no attempt was made to make observations of this kind in the course of the present work. Nevertheless, it is felt that the results reported have a definite bearing on this question.

Jevons¹² has classified strain markings into two categories: "flamboyant" and "criss-cross". The first term covers the kind of surface blemishes referred to commonly as stretcher-strain markings, which occur frequently on annealed mild-steel sheets. In non-ferrous metals stretcher-strain markings are rare, but Eborall⁸ and Chadwick and Hooper¹¹ have described cases where they were found on aluminium alloy sheets. Their basic similarity to those observed in steel is supported by the fact that they appear only during the early stages of deformation (up to 2% extension),^{8, 11} they are more pronounced in fine-grained metal,¹¹ and they can be eliminated by temper rolling.¹¹ Chadwick and Hooper¹¹ do not

say so, but it is not unreasonable to expect that processing in a roller-leveller would also have removed or at least reduced the "random type" markings from their aluminium-3% magnesium sheets, as in Fig. 6, curves 3 and 4.

The second type of marking does not necessarily lead to a commercially objectionable surface appearance. It is noteworthy, however, that Chadwick and Hooper's measurements of surface roughness associated with these markings indicated that the degree of roughening increased progressively with total strain. This observation links up with the general features of serrated stress/strain curves which were described in Section III, 7. It thus seems reasonable to consider curves 3 and 4 (Fig. 3) and curve 1 (Fig. 4) as "slow-motion" equivalents of those portrayed in Fig. 7. Reference may also be made to the work of Rosi and Perkins,¹⁰ who noticed a progressive increase of the yield phenomenon after successive strain-ageing treatments of titanium. Such similarity of behaviour in metals with markedly different lattice structures is very striking indeed.

In annealed mild steel, the strain markings appearing at the initial yield may assume either the first or the second form, depending on the rigidity of the test-piece and on the constraints imposed by the grips.^{19, 20} Apparently, it is the heterogeneous stress distribution across and along the strained metal that causes the markings to acquire an irregular, flamboyant pattern, and one may reasonably expect the same to apply to metals other than iron. Conclusive proof of this could best be obtained on sheet specimens of a non-ferrous metal which is prone to stretcher-straining; by varying the size and shape of the samples, alternative types of surface markings should arise.* As soon as local stress concentrations are relieved by a certain amount of plastic flow, the markings which appear later on (for instance, after intermediate ageing) are of the regular, parallel-band type in both ferrous and non-ferrous sheet.

When the rate of strain-ageing of a specific metal is only a small fraction of the rate at which the metal is being deformed in the course of testing or fabrication, then only one family of strain markings will appear, immediately after the initial yield. This is obviously the case with mild steel or with the tin bronze used in the present investigation, and it is much more so with "non-ageing" steel or commercially pure titanium.¹⁰ On the other hand, if ageing follows plastic strains very rapidly, differential hardness levels are almost certain to arise in the material as soon as the first Lüders wave traverses its entire length. In such a case, the portions which were deformed first had relatively ample time to age, whereas the one deformed last had none. Indeed,

3.5% yield elongation was obtained on straight, 0.75-in.-wide tension specimens. Initial yielding was accompanied by the formation of extensive *parallel-band-type markings*. At the time of writing this note, flamboyant markings could not yet be produced.

* Note added in proof.—When this work had already been completed, a quantity of 95:5 bronze strip of 0.1 × 1.5 in. section was obtained from another source. This material displayed precisely the same deformation and ageing features as the 0.2-in. rod described above. After rolling to 0.040–0.025 in. thickness and then annealing at 475°–500° C., up to

the front of the following deformation wave may well be stopped at a barrier represented by some critical hardness level, and it may take some time before the stress in the metal just deformed is built up sufficiently to overcome this barrier. Zonal or local differences of grain-size are likely either to alleviate or to accentuate these obstructions. Such a process is visualized by the author as taking place during progressive stretching of alloys which give serrated stress/strain diagrams. The fact that the parallel-band (or "criss-cross" or "ripple") type of marking is propagated by jumps, or runs alternately up and down the sheet or specimen^{11, 12} seems to be consistent with the above idea.

The author believes that the suggestion that both kinds of surface marking just discussed are caused by essentially the same factors¹¹⁻¹³ is well supported by the results now presented and by relevant observa-

tions. The evidence presented is primarily phenomenological in nature, and certain of the findings call for further inquiry. In particular, this applies to the absence of embrittlement caused by ageing the α -bronze after straining, and to the gradual increase of the Lüders strain after successive strain-ageing treatments.

ACKNOWLEDGEMENTS

The author wishes to thank Professor H. O'Neill for facilities in his Department; Mr. N. F. Fletcher (Imperial Chemical Industries, Ltd., Metals Division, Landore, Swansea) for arranging for the analysis of the material; Mr. D. L. Phillips (B.I.S.R.A., Swansea) for permission to use some of his equipment; and Mr. P. Roderick (University College, Swansea) for making the grain counts. An I.C.I. Research Fellowship is gratefully acknowledged.

REFERENCES

1. C. Bach and R. Baumann, "Festigkeitseigenschaften und Gefügebilder der Konstruktionsmaterialien", Figs. 733 and 760. Berlin: 1921 (Julius Springer Verlag).
2. W. Köster, *Z. Metallkunde*, 1927, **19**, 309.
3. P. Túry and S. Krausz, *Nature*, 1936, **138**, 331; 1937, **139**, 30.
4. C. A. Edwards, D. L. Phillips, and Y. H. Liu, *J. Iron Steel Inst.*, 1943, **147**, 145.
5. G. A. Knight and G. Murray, *Sheet Metal Ind.*, 1946, **23**, 1741.
6. A. W. McReynolds, *Trans. Amer. Inst. Min. Met. Eng.*, 1949, **185**, 32.
7. H. L. Wain and A. H. Cottrell, *Proc. Phys. Soc.*, 1950, [B], **63**, 339.
8. R. Eborall, *J. Inst. Metals*, 1950-51, **78**, 703 (discussion).
9. J. D. Lubahn, *Trans. Amer. Soc. Metals*, 1952, **44**, 643.
10. F. D. Rosi and F. C. Perkins, *ibid.*, 1953, **45**, 972.
11. R. Chadwick and W. H. L. Hooper, *J. Inst. Metals*, 1951-52, **80**, 17.
12. J. D. Jevons, *J. Inst. Metals*, 1950-51, **78**, 563.
13. M. Kuroda, *Sci. Papers Inst. Phys. Chem. Research (Tokyo)*, 1938, **34**, 1528.
14. N. H. Polakowski, *Proc. First World Met. Congr. (Amer. Soc. Metals)*, 1952, p. 553.
15. N. H. Polakowski, *J. Iron Steel Inst.*, 1952, **172**, 369.
16. W. Köster, *Inst. Hierro Acero*, 1952, **5**, 221.
17. N. H. Polakowski, *J. Inst. Metals*, 1950-51, **78**, 692 (discussion).
18. F. Fettweis, *Stahl u. Eisen*, 1919, **39**, 1, 34.
19. W. Sylwestrowicz and E. O. Hall, *Proc. Phys. Soc.*, 1951, [B], **64**, 495; also E. O. Hall, *ibid.*, p. 742.
20. W. M. Lomer, *J. Mechanics Physics Solids*, 1952, **1**, 64.

YIELD-POINT PHENOMENA AND STRETCHER-STRAIN MARKINGS IN ALUMINIUM-MAGNESIUM ALLOYS*

By V. A. PHILLIPS,† A.R.S.M., D.Eng., B.Sc., A.I.M., MEMBER,
A. J. SWAIN,‡ M.A., MEMBER, and R. EBORALL,§ M.A., MEMBER

(Communication from the British Non-Ferrous Metals Research Association.)

SYNOPSIS

The formation of stretcher-strain markings in aluminium-magnesium alloys has been correlated with the stress/strain diagram. There is an initial yield, similar to that of steel, and the deformation associated with this, which is a shear, produces markings resembling Lüders markings in steel. In pressing, markings of this type (type *A*) occur in lightly strained regions, and constitute a serious defect. This type-*A* yield is characteristic of the fine-grained, recrystallized alloy. It is absent in coarse-grained materials, and is also absent in materials which have been worked, even if subsequently aged.

In a tensile test at room temperature, there are many subsequent yields. These (type-*B*) yields are shown to be due to strain-ageing during the test. The associated deformation is confirmed to be a symmetrical thinning without shear, and the markings do not become conspicuous unless a heavy stretch is applied. The yields produced by strain-ageing are hardly sensitive at all to changes in grain-size, and still occur in material which does not show type-*A* yielding.

The type-*A* yield point is attributed to the blocking of the propagation of slip from grain to grain, owing to the presence of a high concentration of magnesium in solution at the grain boundary. Strain-ageing and the type-*B* yielding are attributed to a simple Cottrell mechanism, with magnesium as the most important solute element.

I.—INTRODUCTION

At the present time aluminium alloys, especially those of the aluminium-magnesium type, are coming into increasing use for pressings. Strain markings, sometimes of considerable severity, have occurred with a number of alloys in such applications. In their most objectionable form, these markings¹ are similar in appearance to the stretcher-strain or Lüders markings produced in pressing annealed mild steel, and they occur on lightly strained regions. Their visibility is often enhanced by the wide expanse and slightness of curvature of the parts of the pressings in which they occur. Markings may also appear as a system of parallel shallow ripples in the surface, generally in more severely deformed parts, where they are less conspicuous. Although Knight and Murray² have shown that aluminium-3% magnesium alloy sheet rolled to only 20% reduction before the final anneal, and so having a relatively large grain-size, may be practically free from strain markings on pressing, the causes of the phenomenon have not been fully understood, and further investigation appeared desirable.

While the present work was in progress, Chadwick and Hooper,³ in a study of the aluminium-3% magnesium alloy, showed that two types of surface marking developed during the stretching of annealed recrystallized sheet. Random markings, consisting of a series of kinks, reached maximum intensity at about 1% extension and decayed with a 2% extension. They were found only in material with a grain-size below about 0.05 mm. Parallel bands, caused by local thinning or necking, occurred in all material irrespective of grain-size, but where this exceeded 1.0 mm. they were completely masked by the orange-peel effect.

As in mild steel,|| the markings appear to be a yield-point effect,⁴ and the present work includes the correlation of the markings with features of the stress/strain curve (including the steps or serrations which are a common feature of the curves of these and other aluminium alloys⁸⁻¹⁵) and a more detailed examination of the markings themselves. A study has been made of the effects of composition and of mechanical and thermal treatments, and the results are interpreted in terms of the blocking of slip movements by the magnesium atoms of the solid solution at the grain boundaries and elsewhere.

* Manuscript received 16 April 1953. The work described in this paper was made available to members of the B.N.F.M.R.A. in a series of confidential research reports issued over the period August 1950 to February 1953.

† Investigator, British Non-Ferrous Metals Research Association, London.

‡ Formerly Investigator, British Non-Ferrous Metals Research Association, London; now with Aluminium Wire and Cable Co., Ltd., Swansea.

§ Head of General Metallurgy Section, British Non-Ferrous Metals Research Association, London.

|| See, for instance, the general discussion of markings by Jevons⁵ and the reviews of yield-point effects by Kenyon and Burns⁶ and by Bilby.⁷

II.—CORRELATION BETWEEN DEVELOPMENT OF MARKINGS AND OCCURRENCE OF STEPS ON THE STRESS/STRAIN CURVE

1. FEATURES OF THE STRESS/STRAIN DIAGRAM IN RELATION TO APPEARANCE OF MARKINGS ON PRESSING AND CUPPING

Tensile tests made with an Avery weight-and-lever machine on a number of soft-temper commercial sheet materials, in the as-received condition and with magnesium contents covering the range 2–7% Mg, gave curves of which the three shown in Fig. 1 are typical. In every case there was a relatively large yield at or soon after the start of plastic deformation followed by a series of smaller steps. These later steps tended to become longer as the strain increased.

The suppliers of the materials referred to in Fig. 1, all of which contained about 3½% magnesium, commented on their liability to develop strain markings on stretching or pressing in the way indicated in the penultimate column of Table I. It is clear from this table that the severity of the markings may be

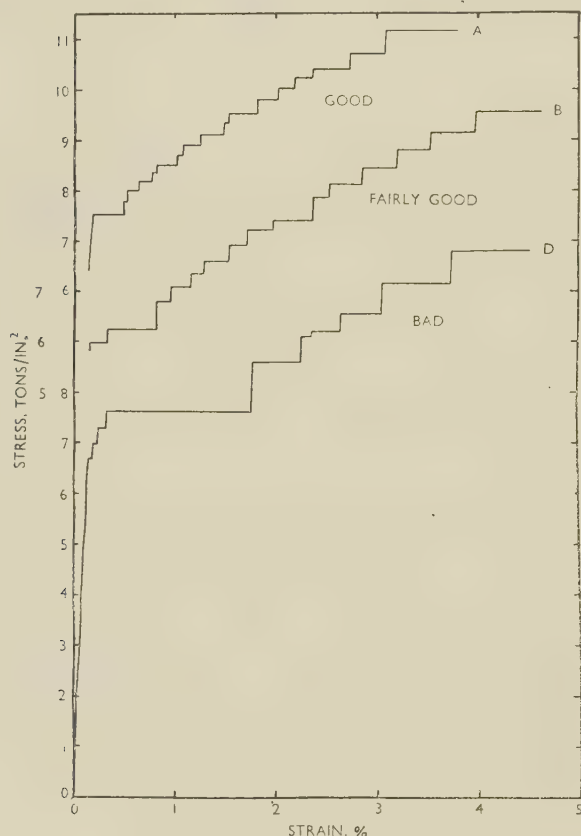


FIG. 1.—Stress/Strain Curves Typical of Good (A), Fairly Good (B), and Bad (D) Material (see Table I).

correlated with the size of the large early yield, measured from the stress/strain diagram.

The correlation is confirmed by observations of the markings formed on the flange of 2½-in.-square

Erichsen test specimens (the test being carried to approximately 80% of the cup depth at failure), and it was found for the other materials examined in this

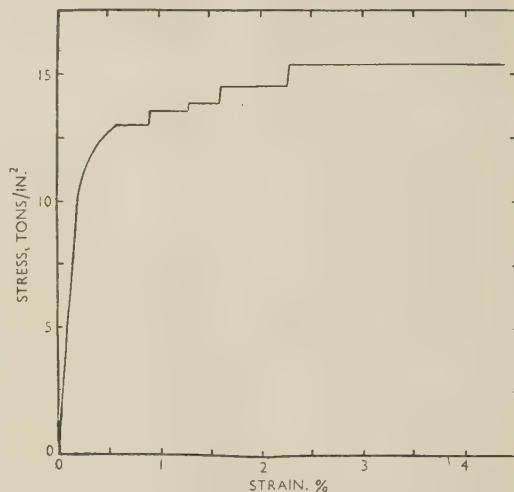


FIG. 2.—Stress/Strain Curve for Commercial Aluminium-3½% Magnesium Alloy, Half-Hard.

way that markings were apparent on the flange only when the first large yield elongation exceeded 0.5%.

Tensile tests of half- and fully-hard materials gave a stepped stress/strain curve from which the first

TABLE I.—Behaviour of Four Commercial Aluminium-3½% Magnesium Alloy Sheets.

Alloy	Gauge of Sheet, S.W.G.	Elongation at Large Yield, % *		Suppliers' Remarks	Markings in Erichsen Test
		During Yield	Total Plastic Strain at End		
A	16	0.35	0.35	Slight evidence of markings on stretching.	None.
B	18	0.56	0.65	No markings on normal pressing operation.	Very slight.
C	22	1.07	1.18	Showed severe markings on pressing.	Severe.
D	18	1.29	1.58	Severely marked on stretching.	Severe.

* Average of two test results.

large yield was absent (Fig. 2), and these materials showed no markings in the Erichsen test.

2. DEVELOPMENT OF STRAIN MARKINGS IN SIMPLE STRETCHING

Observations were made on the development of markings in soft, unflattened, commercial 3½% magnesium alloy (OZX), during the stretching on an Amsler hydraulic machine of polished rectangular strips 7–8 in. long × 1¼–1½ in. wide. At the same time an autographic record was made of the load

and the cross-head movement. Markings at different stages of development were photographed either on a Vickers microscope or by a modified Schlieren method due to Loro.¹⁶ Fig. 3 (Plate XC) shows the appearance of strips of the commercial 3½% magnesium alloy OZX, after stretching part way through the initial large yield, and the two photographs illustrate a characteristic difference between specimens with sheared edges and ones which have been annealed after shearing to relieve strains at the edges. In the first, yielding has been initiated at numerous points along the sheared edges, while in the second it has begun at relatively few points and the wedge markings are less complex, usually with nearly straight boundaries. The yielded wedges grow by approximately parallel movement of the boundaries. Occasionally, in the second type of specimen, only one yield wedge forms and spreads until the whole specimen has yielded.

The faint ripples left behind and parallel to the moving boundary (see Figs. 3 (b) and 4, Plate XC) are characteristic of samples pulled in the Amsler machine at room temperature at slow strain rates. Yielding proceeds in a series of jumps; the boundary moves rapidly forward into the unyielded material, the load drops, yielding stops, the machine reloads, rapid yielding again starts, the load drops and so on, and at each place where the boundary pauses a ripple is left when it moves on. In this respect the Amsler machine differs from the Avery lever machine in which the load remains applied during a sudden extension, provided that the beam is kept floating.

In general, the first appearance of markings was found to correspond to the beginning of the large initial yield shown on the autographic record, and the end of the yield, marked by a rise in stress, occurred when the surface was almost completely covered by the yielded areas. When yielded areas joined, the boundaries frequently vanished, but this was not always so, and the surface was not left completely smooth when yielding was complete. When pulling was continued beyond the completion of the first large yield, a second set of markings appeared, superimposed on the residual markings of the first type and locally effacing them. These had the form of ripples or bands inclined at about 58° to the stress axis. Fig. 5 (a) (Plate XCI) shows the appearance of the second set of markings in a strip pulled to 8% extension. On an occasional specimen, the bands formed in two conjugate directions at an early stage of stretching as in Fig. 5 (b), but more usually the conjugate direction appeared shortly before fracture. The condition of the edges did not appear to affect the markings of the second type, as similar results were obtained whether the strips were annealed after shearing or not.

The markings observed on polished tensile test specimens, which had milled edges, were in general similar to those found on the strips, except that the first markings were never of the striking complex type shown in Fig. 3 (a).

It will be convenient in what follows to distinguish between the markings associated with the first, large, yield and those formed at larger strains. These are subsequently referred to as type-A and type-B markings, respectively.

3. CORRELATION BETWEEN DEVELOPMENT OF STRAIN MARKINGS AND STEPS IN STRESS/STRAIN DIAGRAM

The development of the markings was followed during tensile tests on polished test-pieces to permit a more detailed correlation between the development of markings and the course of the stress/strain curve.

Fig. 10 shows a typical stress/strain curve for the commercial 3½% magnesium alloy, which on a stretched strip gave pronounced type-A markings. The curve was obtained on the Avery machine, the

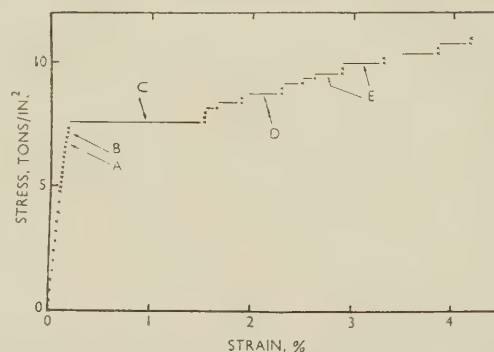


FIG. 10.—Stress/Strain Curve for Commercial Aluminium-3½% Magnesium Alloy (OZX2) as Annealed. Grain-size 0.018 mm.

KEY.

- A. Small wedge at one extensometer pip.
- B. Wedge spread a little.
- C. Inclined sharp boundary ran down gauge-length and one ran up to meet it, leaving slight confused markings behind.
- D. Ripple (type-B marking) ran part way along gauge-length, through slight irregularities left from large yield.
- E. Several new ripples moved.

load being applied by fixed increments. In this specimen the first visible sign of yielding was the appearance of a small type-A yielded wedge at one of the extensometer pips, extending from one edge of the specimen to the pip. This coincided with a departure of the stress/strain curve from linearity. On increasing the stress, the wedge spread a little, and finally the boundary broke free at the beginning of the large yield shown on the curve, running down the specimen to meet the boundary of a similar yielded area which had formed and spread from the other end of the gauge-length. At the end of this initial yield, the whole active gauge-length had undergone yielding, and the two boundaries of the single type-A yielded area were at the shoulders of the specimen.

The further yield steps which occurred were mostly seen to coincide with the appearance within the yielded area of one or more regions in which further yielding had apparently occurred. Each such region had straight parallel boundaries, inclined to the stress axis at a constant angle, and during a yield step it was observed to spread by the rapid movement of

one or both of its boundaries. The boundaries were not sharply defined like the type-*A* boundaries, but had the appearance of a ripple in the surface, showing up as a bright or dark band of some width. Those regions of additional yielding did not usually spread to cover the whole gauge-length, and the boundary ripples at their rest position formed the characteristic type-*B* ripple markings, which thus gradually accumulated on the surface. The original type-*A* boundary markings meanwhile moved slowly into the shoulders of the test-piece, and remained there as a pair of clearly defined rings (illustrated for another specimen of the same material in Fig. 6, Plate XCI).

Many examples of this general behaviour were found, in commercial materials and in high-purity material prepared in the laboratory. Frequently a distinct, small, premature yield due to the formation

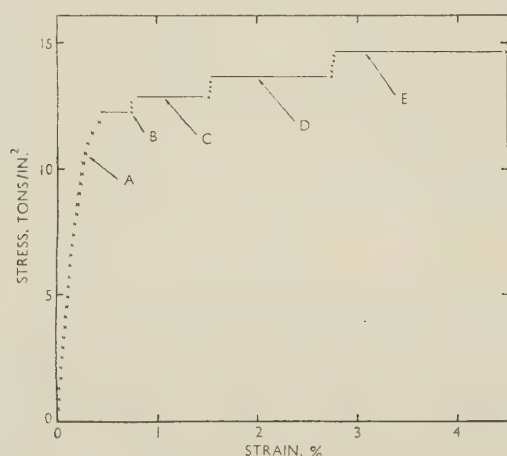


FIG. 11.—Stress/Strain Curve for Commercial Aluminium-3½% Magnesium Alloy (OZX3) Cold-Rolled to 10% Reduction. Grain-size 0.018 mm.

KEY.

- A. Slight creep observed.
- B. No creep beyond this point.
- C. Ripple marking ran up gauge-length.
- D. Several ripple markings ran up gauge-length.
- E. Several ran part way.

of a type-*A* wedge at the extensometer attachment was noted, and occasional “split” yields were obtained in which the boundary of a type-*A* yield became arrested at a nick in the edge of the specimen, and the yield was completed at a slightly higher stress by movement of a boundary from the other end of the specimen.

In contrast, and in agreement with Chadwick and Hooper, a specimen of commercial 3½% magnesium alloy which showed type-*A* markings when stretched in the soft condition showed no such markings when pulled after receiving a 10% reduction by rolling. The cold-rolled sheet showed no markings in the Erichsen test. An annotated stress/strain diagram is given in Fig. 11. Fig. 7 (Plate XCI) shows the type-*B* markings formed by stretching approximately 4% in the Amsler machine, and it will be noted that there are no prominent ring markings in the shoulders (cf. Fig. 6). These in fact appear to be characteristic of the type-*A* yield.

At this stage, therefore, it is reasonable to conclude that in annealed aluminium alloys containing 2–7% magnesium there are two types of discontinuous yielding: (1) a large, single initial yield which may account for a strain increment of as much as 1.5% and (2) a succession of smaller subsequent yields. These have been called type-*A* and type-*B* yields, respectively. Type-*A* yielding is characterized by “flamboyant” or wedge-type Lüders markings and by the ultimate formation of a sharply defined ring marking at the shoulders of tensile test-pieces. If a large type-*A* yield is present, markings are produced in the flange of Erichsen test-pieces. The remarks of sheet suppliers indicate that when a large type-*A* yield is present the sheet is liable to show severe stretcher-strains on pressing. Type-*A* yielding is absent in sheet which has been rolled after annealing.

Type-*B* multiple yielding at room temperature is characterized by the appearance of parallel ripple markings on severe stretching. Unlike the type-*A* yield, it does not give rise to a sharp ring marking in the shoulders of a tensile test-piece, and it is not revealed in the Erichsen test. It is apparently not usually a cause of practical difficulty. It is not suppressed in cold-rolled material.

III.—TOPOGRAPHY OF THE TWO TYPES OF MARKING

The different characteristics of the initial and subsequent yields, particularly the difference in appearance between the two corresponding types of strain marking, suggest that it may be instructive to examine the topography of the markings in greater detail.

Chadwick and Hooper³ had already studied the markings with a profilometer and found the two types of marking to be different, but their observations on the type-*A* markings were apparently inconsistent with those given in the previous section, since they found no thinning of the sheet as a result of the formation of the markings.

In the first instance parallel observations were made by microscopic focusing and by multiple-beam interferometry¹⁷ at corresponding points upon both sides of a polished strip specimen of a commercial 3½% magnesium alloy (OZX, grain-size 0.018–0.020 mm.), which had been pulled part way through the large yield, producing complex type-*A* markings. These confirmed that the strip had deformed in such a way that the surface became divided into alternate yielded and undeformed nearly plane areas sharply tilted with respect to one another, the width of the sharply curved region between the yielded and unyielded areas being approximately 0.1 mm. The values of the tilt angle obtained by interferometry and from focusing measurements agreed well, and there was in general close agreement between the angle at a point on one side of the sheet and at the corresponding point on the opposite side. The mean angle of tilt, derived from interferometric observations at 16 pairs

of points at the boundaries of four yield wedges was 26.5 min. (range 22–33 min.). This is very much greater than the angle derived in Chadwick and Hooper's experiments on a similar material (order of 1 min.).

More detailed observations were made upon a single type-*A* wedge produced upon a strip of the commercial 3½% magnesium alloy annealed for 1 hr. at 350° C. and furnace-cooled to stress-relieve the sheared edges.

Two holes were drilled through the strip in the unyielded material, one on either side of the wedge on a line parallel to the stress axis, as seen in Fig. 8 (Plate XCII). Assuming that the boundary surfaces between yielded and unyielded areas are plane, the angles between these planes and the stress axis may be calculated from a knowledge of the angles θ and ϕ , Fig. 8. The angles ϕ were measured directly from photographs, and angles θ were calculated from measurements of the distances of *A*, *B*, *A'*, and *B'* from *X* and *Y*.

The values of angles θ were found to be $40^\circ \pm 2^\circ$ and those of angles ϕ , $71.5^\circ \pm 0.5^\circ$. The corresponding angle between the two boundary planes and the stress axis is calculated as 48° . This is probably accurate to about $\pm 3^\circ$.

The angles α (Fig. 8) were found to be 25.5 ± 2 min. These were determined as follows. A series of slightly overlapping photographs was taken along each of three parallel traverses across the wedge, the middle traverse being in line with the drilled holes. The photographs were trimmed and mounted in registry to provide a composite pattern of fringes across the wedge. The result, greatly reduced in size, is shown in Fig. 9 (Plate XCII) for one side of the strip.

The fringes mark contour lines of the surface, so that the area shown in Fig. 9 is made up of three nearly plane areas inclined to each other. The angles of tilt, calculated from the fringe spacing perpendicular to the boundary at corresponding points on the two surfaces (*A*, *A'*, *B*, *B'*, *F*, *F'*, &c., in Figs. 8 and 9), were found to be 27 ± 2 min. (six pairs of measurements). The surface profiles along the line *XY* joining the two holes are plotted in Fig. 12, in which each dot represents a fringe.

The angles α (Fig. 8) are readily determined from the mean angle ϕ to be $25\frac{1}{2} \pm 2$ min.

From the measurements described above, it is evident that the deformation involved in the yield is a shear parallel to a plane near the one of maximum shear stress. The thinning of the specimen due to this shear may be calculated from the initial thickness (0.043 in.) and the known angles θ (40°) and α ($25\frac{1}{2}$ min.), and is 3×10^{-4} in. From the curvature of one of the plots in Fig. 12, it is apparent that there is some 2×10^{-4} in. thinning towards the middle of the yielded area, which is additional to the shear deformation. The total observed thinning is thus 5×10^{-4} in. From Fig. 10, the yield-point extension for this sheet (OZX2) is about 1.4%, which corresponds to a thinning

of 6×10^{-4} in., so agreement between the two types of measurement is good.

The greater visibility of the type-*A* markings, compared with those of type-*B*, may be readily understood, since the former correspond to very sharp angular surface changes, giving sharply defined boundaries, and the yielded areas are tilted so that when the surface is highly reflective they are likely to reflect light into the eyes when the rest of the surface does not.

The type-*B* markings have neither the tilt nor the very sharp boundary.

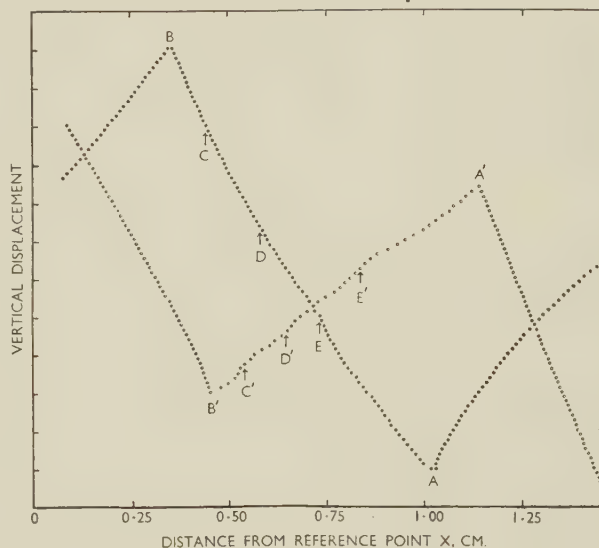


FIG. 12.—Surface Profile Across Yield Wedge in Commercial Aluminium-3½% Magnesium Strip (OZX2) of 0.018 mm. Grain-Size, Determined from the Multiple Interference Pattern. Open circles (curve *B'A'*) represent one surface, filled-in circles (curve *BA*), the opposite surface, both shown in Fig. 8 (Plate XCII). Ordinate axis marked at 4λ intervals, where $\lambda = 5461 \text{ \AA}$.

IV.—EXPERIMENTAL STUDY OF THE TWO TYPES OF YIELDING

1. HYPOTHESIS TO ACCOUNT FOR THE TWO TYPES OF YIELD

The differences in form of the two types of strain marking are such as to suggest that different mechanisms are involved in their formation. Moreover, in preliminary experiments, the type-*A* yield appeared to have a strong grain-size dependence, whereas the type-*B* yields did not.

It is apparent from the foregoing experiments that the type-*A* yield is a true initial yield; the small departures from elastic deformation which frequently take place before the type-*A* yield, when a stress/strain curve is recorded, have been shown to be due simply to premature local yielding at points of high stress concentration. As it is further apparent that the type-*A* yield does not occur in cold-worked materials, it is reasonable to suppose that it corresponds to the first spread of yielding into undeformed grains. It is proposed that under these conditions

slip in an undeformed grain starts from the grain boundary at points where slip in a neighbouring grain impinges upon it. Magnesium atoms tend to collect in the grain boundary, because, being large, they are more readily accommodated there, and stabilize the grain-boundary structure so that it is more difficult to break away dislocations from the boundary to start the slip in the undeformed grain. A picture of this kind leads naturally to a strong dependence of the yield stress on grain-size,¹⁸ and it may further be deduced (i) that high-temperature treatments followed by quenching would tend to disperse the concentration of magnesium atoms at the boundary and so to eliminate the yield point, and (ii) that the type-A yield would not return once the material had been deformed unless the metal was recrystallized or made to recover so completely that it was almost in its original condition.

0.028-in thick material being 81 and 89%, respectively, and the final annealing temperature 285°–300° C. The commercial materials were obtained as annealed sheet and, except for NFO, had received no flattening treatment. It will be noted that some were extremely fine-grained. The grain-sizes given in the table were measured in a plane parallel to the surface of the sheet, by the intercept method. A number of checks on sections through the sheets showed that in these recrystallized materials the grains were approximately equiaxed.

X-ray examination with a Wooster goniometer showed that the materials had no strong preferred orientation.

(b) Tensile Test Procedures

For most of the tests, an Avery weight-and-lever machine was used, in conjunction with a Lindley

TABLE II.—Composition and Grain-Size of Materials.

Mark	Nominal Sheet Thickness, in.	Analysis, %								Grain-Size § mm.	Condition of Sheet	
		Mg	Cu	Fe	Si	Mn	Ti	Na ‡	Zn, ‡			
High-Purity Alloys												
PHT 1a	0.048	} 3.06	0.003	0.011	0.003	n.d.	<0.001	n.d.	n.d.	{ 0.033-0.036 0.023-0.025	Annealed, not flattened. "	
PHT 1b	0.028											
PHT 2a	0.048	} 3.65	0.002	0.008	0.006	n.d.	<0.001	n.d.	n.d.	{ 0.033-0.035 0.023-0.025		
PHT 2b	0.028											
Commercial Alloys												
NFO	0.048	6.84	0.013	0.18 ‡	0.15 ‡	0.25 ‡	Tr. ‡ (< 0.01)	...	Tr.	0.067	Soft, not known whether flattened. "	
OLZ1	0.064	3.5 †	0.033	0.18 †	0.13 †	0.24 †	"	"	"	0.039		
OMA1	0.028	3.5 †	0.024	0.25 †	0.16 †	0.28 †	"	"	"	0.015		
OZX1 *	0.048	3.24	0.010	0.20 †	0.12 †	0.35 †	"	~0.003	"	0.018-0.020		
OZX2		3.21	0.011	0.19 †	0.12 †	0.34 †	"	"	"		Annealed, not flattened.	
OZX3		3.44	0.014	0.28 †	0.13 †	0.38 †	"	"	"			
OZX4		3.45	0.014	0.27 †	0.13 †	0.39 †	"	"	"			

* All from same batch, sheets analysed separately.

† Nominal content.

‡ Spectrographic, remainder chemical.

§ Intercept method.

n.d. = not detected.

Ni, Cr, Sn, B, not detected in any sample.

Limits of detection: Ni . . . 0.01% B . . . 0.005%
 Cr . . . 0.01% Na . . . 0.001%
 Sn . . . 0.01% Zn . . . 0.01%
 Be . . . 0.0005%

The type-B or subsequent yields are attributed to strain-ageing during room-temperature deformation; each yield is followed by strain-ageing, which produces a new yield point and so on. It was considered that magnesium in solid solution was probably also responsible for this strain-ageing effect, by a mechanism of the Cottrell type.¹⁹⁻²⁰ These conclusions were examined in further experiments described below.

2. MATERIALS AND PROCEDURES FOR TENSILE TESTING

(a) Materials

The compositions of the principal materials used are set out in Table II. The high-purity materials were melted in the laboratory, degassed with chlorine, and chill cast. They were cold rolled with interstage annealing, the final reductions for the 0.048-in. and

extensometer having a sensitivity of 2.5×10^{-5} . Unless otherwise indicated, standard (B.S. No. 485) sheet tensile test-pieces were employed, with a 2-in. gauge-length $\times \frac{1}{2}$ in. width. Some use was also made of an Amsler hydraulic machine, as indicated in the text.

In using the Avery machine, alternative procedures were followed:

(i) *Continuous Loading*.—The load was smoothly increased by suitable increments, with measurement of the strain, until the extensometer indicated a sudden extension. The load and strain were then recorded, and the load was again increased smoothly until a further sudden extension was observed. The curves obtained by this method are indicated throughout by lines without points.

(ii) *Stepped Loading*.—As procedure (i) was inadequate for some purposes, the following procedure

was later adopted. The load was increased by fixed increments of 20 lb. (715 lb./in.² on the usual 18-S.W.G. specimen) in the elastic region and later of 10 lb. In general, the movements indicated by the Lindley extensometer were completed within 1-3 sec. of increasing the load. When movement continued for a much longer period, the load was increased

with boiling water, melting ice, melting chloroform ($-63.3^{\circ}\text{C}.$), and solid carbon dioxide ($-78.5^{\circ}\text{C}.$) as fixed points. A mixture of trichlorethylene and solid carbon dioxide was used to maintain a constant (measured) temperature of $-76^{\circ}\text{C}.$ For tests at temperatures between 0° and $-76^{\circ}\text{C}.$ the bath temperature was controlled quite readily within $1^{\circ}\text{C}.$

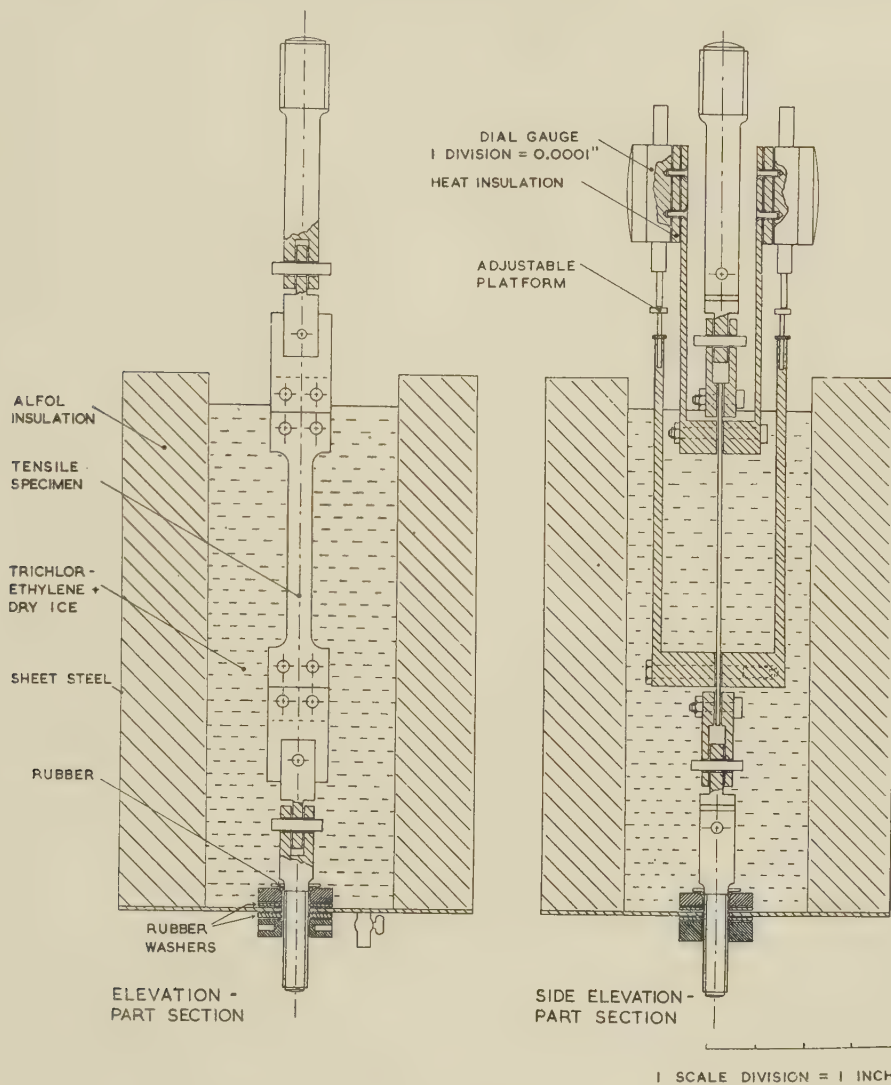


FIG. 13.—Low-Temperature Tensile-Testing Apparatus.

at intervals of 1 min., strain readings being taken just before each load increment was applied.

In both procedures, the beam was kept floating throughout the test, and the time occupied in completing a test was about 15 min. (rather longer if creep occurred).

For tests at low temperatures, the apparatus shown in Fig. 13 was used. The temperature was measured potentiometrically with a Chromel/Alumel thermocouple, tied on so that the tip was near the middle of the gauge-length, with the cold junction immersed in melting ice. The couple was calibrated

by adding pieces of solid carbon dioxide as necessary. A melting-ice bath was used for tests at $0^{\circ}\text{C}.$

With this arrangement, the specimen length was standardized at 4.00 ± 0.03 in. between the shoulders, so that the results of different tests are directly comparable, though the effective gauge-length was uncertain. To obtain an estimate of this, eight commercial-alloy specimens with scribe marks 3 in. apart were stretched, and after unloading the average extension was found to be 3.3% on the 3-in. length, while the average plastic extension as measured on the gauges was 14.63×10^{-2} in. The corresponding effective

gauge-length of 4.43 in. has been used when required to calculate approximately the percentage extensions.

The stepped-loading procedure was used throughout the low-temperature tests. When the limit of the dial gauges (approx. 17×10^{-2} in. ($\sim 4\%$) extension)

3. THE INFLUENCE OF TEMPERATURE OF TEST ON YIELDING BEHAVIOUR

If the multiple type-*B* yielding observed at room temperature is due to rapid strain-ageing during the

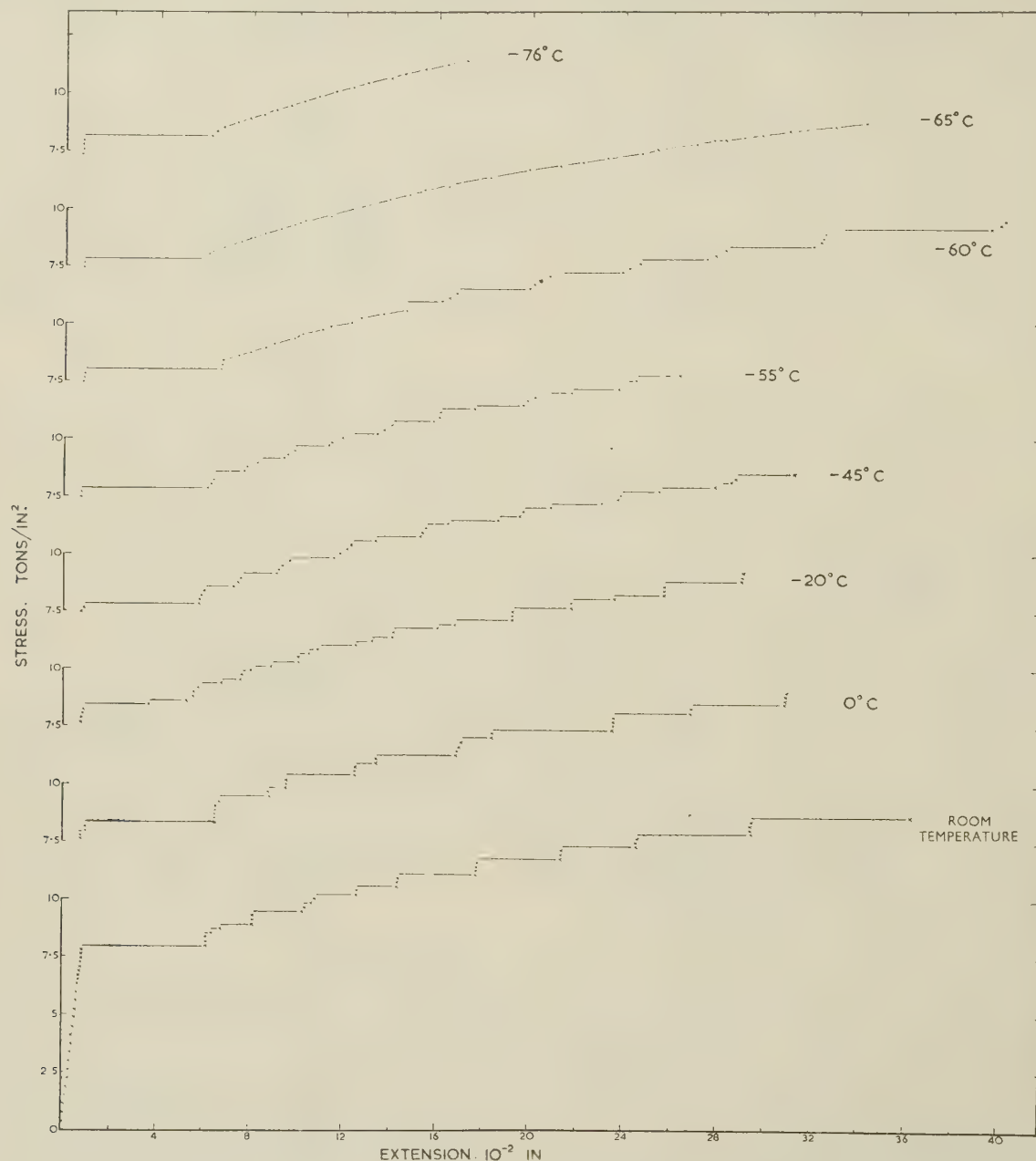


FIG. 14.—Effect of Testing Temperature on the Stress/Strain Curve of Annealed Commercial Aluminium-3½% Magnesium Alloy (OZX3). Grain-size 0.018 mm.

was approached, the load was reduced by 40 lb. to stop creep, and the gauges were reset to zero, an operation which took approximately $1\frac{1}{2}$ min., the load was raised 10 lb. above its former maximum value, and after 1 min. the first strain reading was taken. Specimens were pulled in this way to about 10% extension.

test, it should disappear on testing at some lower temperature. The type-*A* yield, however, is supposed to be characteristic of the initial condition of the material, and should not disappear.

Specimens of the soft commercial alloy (grain-size 0.018 mm.) were pulled at temperatures ranging from room temperature to -76°C . The stress/extension

curves obtained (Fig. 14) show that with the exception of the initial large yield, which is present at all temperatures, there is a gradual transition from a stepped curve at room temperature to a smooth curve at -76°C .

At room temperature the deformation caused by each load increment, including the first yield, was

less than the scatter of results on duplicate specimens from the same sheet.

The specimens whose curves are given in Fig. 14 were examined after the test, and all showed ring markings at the shoulder, characteristic of the type-A yield. In addition, those pulled at room temperature, 0° , -20° , and -45°C . showed type-B markings

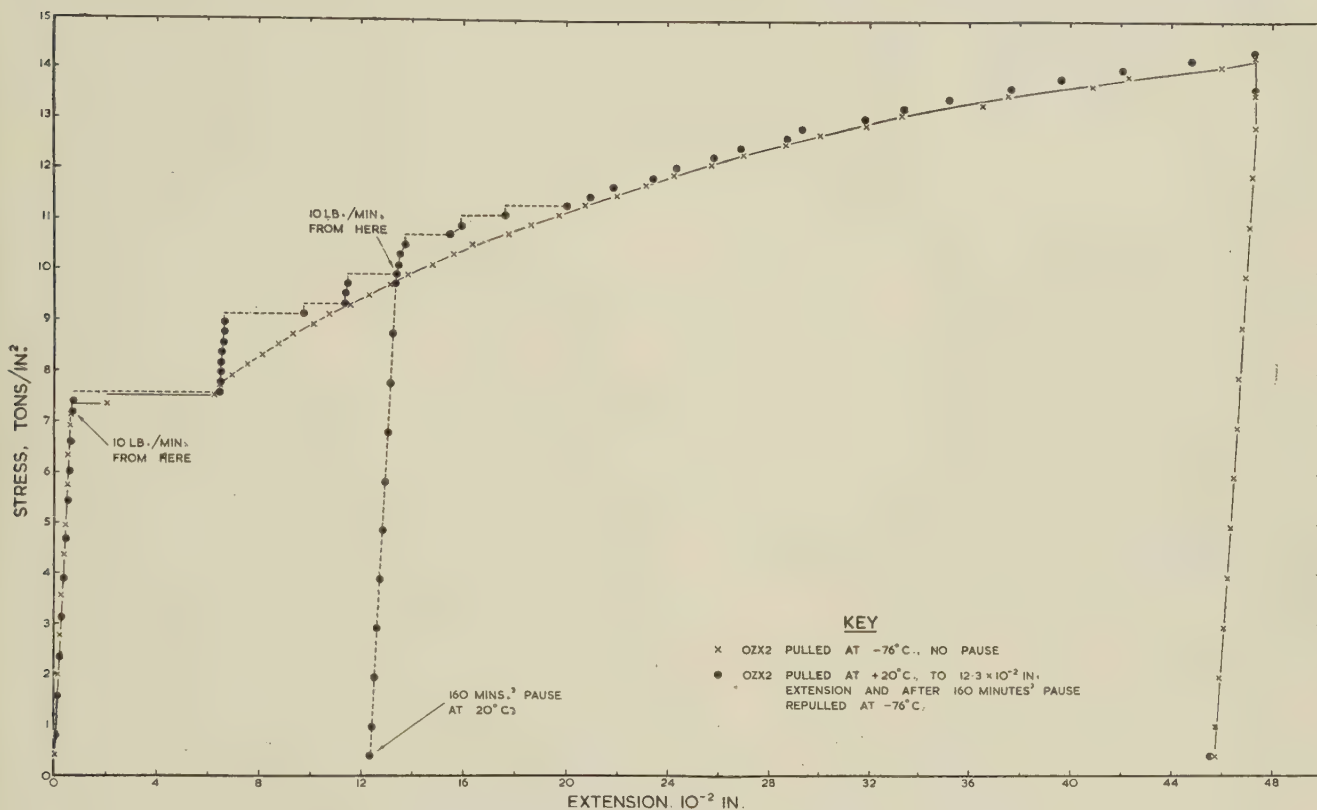


FIG. 15.—Effect of Pulling to Approximately 2.8% Extension at Room Temperature on the Subsequent Curve at -76°C . for Commercial Aluminium-3½% Magnesium Sheet (OZX2) of 0.018 mm. Grain-Size in the Soft Condition.

complete within 1–3 sec. From the slope of the curve, deformation between the steps appeared to be mainly elastic at room temperature. As the temperature was lowered, deformation occurred more slowly, and deformation between the discontinuous yields included progressively more plastic strain. At -76°C ., in marked contrast to room temperature, the extension during the initial yield occurred fairly slowly and steadily, often taking nearly a minute for completion. Occasionally it took longer, and a “split” yield would then be recorded, since the load was increased at 1-min. intervals. After the initial yield had occurred, the extension following each load increase had always practically ceased before the next was applied. The extension was perfectly smooth.

The average values of stress and extension during the initial large yield for the tests shown in Fig. 14 and a number of others are given in Table III. There appears to be no significant temperature effect on either stress or extension, the change, if any, being

(inclined bands or ripples) on the surface, although they were very faint on the last of these.

TABLE III.—Effect of Temperature on the Initial Yield Point in Aluminium-3½% Magnesium Alloy.

Commercial-purity sheet OZX3; grain-size 0.018 mm.

Number of Tests Results Averaged	Testing Temperature, $^{\circ}\text{C}$.	Initial (Type-A) Yield		
		Stress, tons/in. ²	Extension Between Shoulders	
			Actual, $\times 10^{-2}$ in.	Nominal * Elongation, %
4	Room temp.	8.4	5.32	1.20
2	0	8.4	5.94	1.34
1	-20	8.5	4.39	0.99
1	-45	7.9	5.06	1.14
1	-55	7.8	5.37	1.21
1	-60	8.1	5.80	1.31
4	-65	8.1	5.41	1.22
5	-76	8.2	5.21	1.18

* Assuming 1% elongation $\equiv 4.43 \times 10^{-2}$ in. extension between shoulders.

The gradual transition of the stepped curve to a smooth curve as the testing temperature was lowered strongly supports the view that the multiple type-*B* yielding is due to strain-ageing, which is extremely rapid at room temperature, but becomes very slow compared with the time occupied in testing at -76°C .

In confirmation, a specimen of OZX2 was pulled at room temperature to approximately 2.8% extension, unloaded, and after 160 minutes' pause, cooled to -76°C , and pulled again. As shown in Fig. 15, after a short period of discontinuous yielding, the stress/strain curve again became smooth. The ends

A single type-*B* yield may be produced by stretching at -76°C , ageing at room temperature, and pulling again at -76°C . (see Fig. 16), and the transience of the increase in flow stress which produces the type-*B* yield point is again apparent.

4. THE INFLUENCE OF GRAIN-SIZE ON THE TWO TYPES OF YIELD

The effect of grain-size was investigated in two series of $3\frac{1}{2}\%$ magnesium alloy sheet samples, each series being made from the same sheet by further

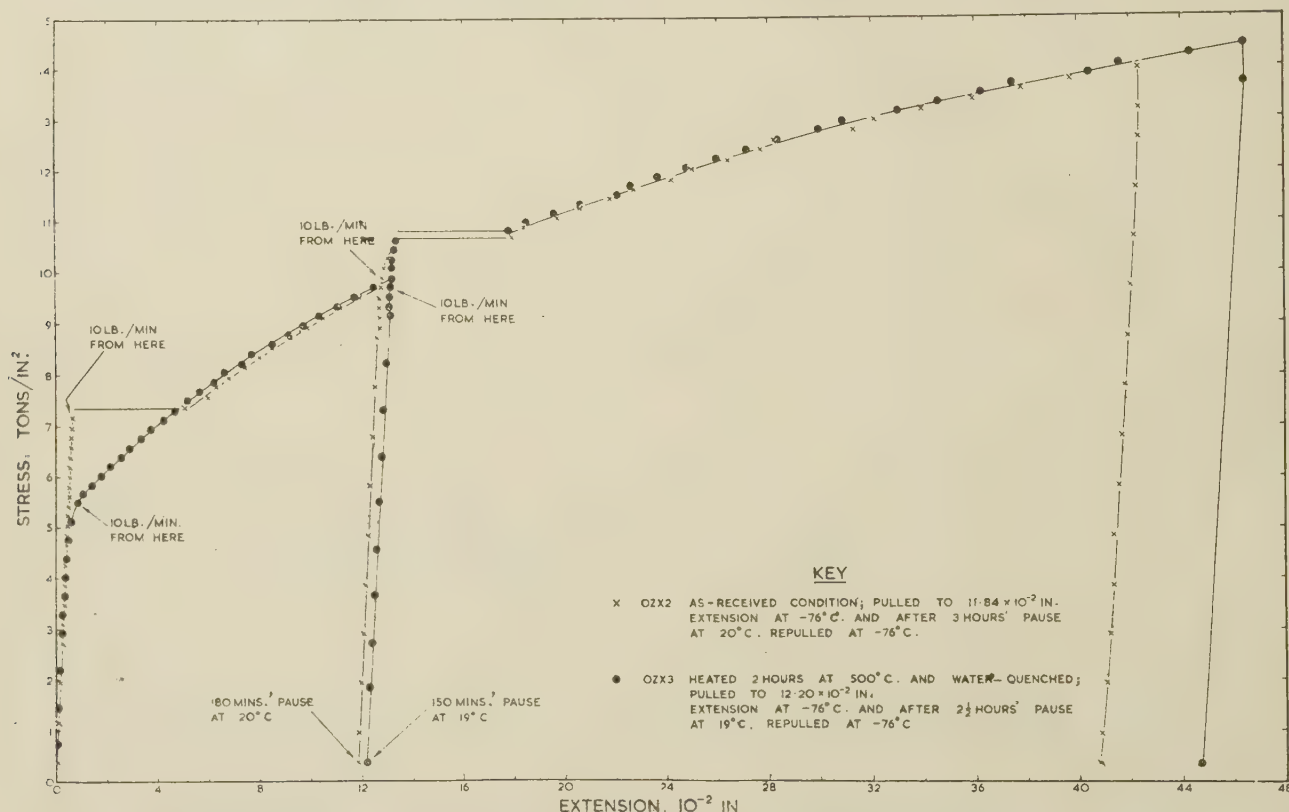


FIG. 16.—Interrupted Stress/Strain Curves at -76°C , Showing Single Type-*B* Yields Produced by Strain-Ageing. Soft commercial aluminium- $3\frac{1}{2}\%$ magnesium alloy sheet of 0.018 mm. grain-size, (1) as received, with initial (type-*A*) yield, and (2) after quenching from 500°C , with no initial yield.

of the steps at 20°C . and the smooth curve at -76°C . after the pause coincide fairly closely with the smooth curve obtained by pulling a similar specimen at -76°C . without pausing. Thus the strain-ageing during pulling and pausing at 20°C . did not appear substantially to displace the subsequent smooth curve upwards, as would be expected if any real precipitation or age-hardening occurred. It appears therefore that type-*B* yielding is a transient phenomenon. This behaviour might well be expected if the type-*B* yield is due to the formation of atmospheres of solute atoms round the dislocations and their subsequent break away at higher stress, according to the Cottrell mechanism.¹⁹

rolling and annealing treatments. For the first series the material used (OLZ1) had a small initial yield in the as-received condition, and for the second, the starting material (OMA1) had a large initial yield. Different grain-sizes were obtained by cold rolling or stretching the material by different amounts and annealing for 7 hr. at 450°C , followed by air-cooling. Details are given in Table IV.

The stress/strain curves obtained from both sets of samples showed the same general features. With large initial grain-size (0.5 mm., OMA11) there was no large initial step. For smaller grain-sizes the large initial step was present* and increased in size as the grain-size was reduced (Fig. 17).

* As explained on p. 628, the very small preliminary yields found on some curves, including two in Fig. 17, are regarded as part of the main large initial yield.

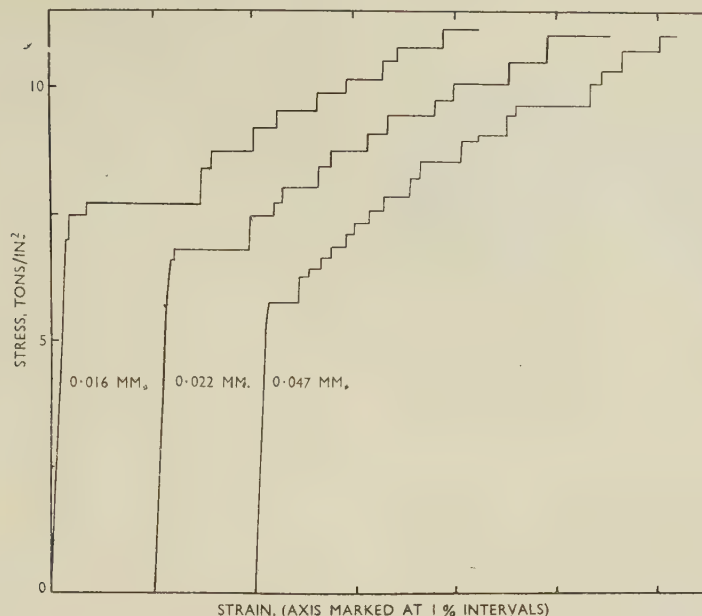


FIG. 17.—Dependence of Initial Yield on Grain-Size of Aluminium-3½% Magnesium Alloy (OLZ1), Recrystallized.

The yield stress and yield-point elongation (total plastic strain at end of yield), for all the curves obtained, are plotted in Fig. 18 as a function of grain-size. It is clear that in these tests the yield-point elongation increases with the yield stress. In fact, the curves in each set (except for the coarse-grained OMA11) can be approximately superimposed after the initial yield, differing only in the details of the steps, so that the initial yield appears as a departure from a basic curve, the magnitude of the departure being determined by the yield stress.

Erichsen tests on 2½-in.-square specimens of the same two series of samples showed clear markings when the yield elongation exceeded 0.5–0.6%, i.e. when the grain-size was less than about 0.03–0.04 mm. Coarsening the grain-size of a similar material (OZX4) from 0.019 mm. approx. to 0.039 mm. (by

min., corresponding to the reduced yield-point extension and reduced visibility of the markings.

Changing the grain-size had a much slighter effect, if any, on the later (type-B) yields, and all the tensile

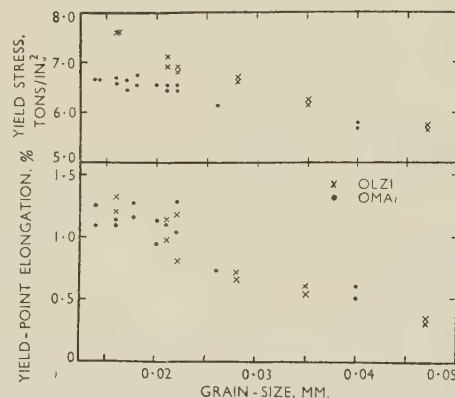


FIG. 18.—Effect of Grain-Size on Initial Yield Stress and Yield-Point Elongation in Recrystallized Aluminium-3½% Magnesium Alloy (OLZ1 and OMA1).

TABLE IV.—Preparation of Samples with Different Grain-Sizes.

Material OLZ1 (originally with small initial yield)			Material OMA1 (originally with large initial yield)		
Mark	Rolling Reduction, %	Final Grain-Size, mm.	Mark	Rolling Reduction, %	Final Grain-Size, mm.
OLZ12	18.7	0.047	OMA11	7.5 †	0.55
OLZ13	28.9	0.035	OMA12	23.2	0.040
OLZ14	40.7	0.028	OMA13	34.0	0.021–0.026
OLZ15	50.9	0.022	OMA14	39.3	0.020–0.022
OLZ16	61.2	0.021	OMA15	51.9	0.017–0.018
OLZ162 *	61.2	0.016	OMA16	55.4	0.014–0.016

* Annealed for 4 hr. at 350° C.

† Stretched.

cold rolling 20% and annealing for 1 hr. at 400° C.) caused a reduction in the mean tilt angle at the markings on a stretched strip from 27 ± 2 to $11\frac{1}{2} \pm 2$

specimens showed the characteristic type-B markings after test, except when the orange-peel effect was strong (OMA11).

To investigate this point further, pieces of sheet were prepared (from OZX3) with coarse grain-sizes as follows :

(a) Cold rolled to approx. 11% reduction, annealed for 2 hr. at 550° C., and furnace cooled. Grain-size 0.13 mm.

(b) As (a) but quenched. Grain-size 0.18 mm.

(c) Stretched approx. 5%, heated from 200° to 550° C. in about 6 hr., held for 2 hr., and quenched. Grain-size 2.6 mm.

None of these materials showed a type-*A* yield, as the grain-sizes were too large.

Tensile specimens machined from these strips were pulled at -76°C . with a pause at room temperature to allow strain-ageing to take place, as described above. The increase in grain-size from 0.018/0.021 to 0.13/0.18 mm., which completely eliminated the initial yield, also had some effect on the yield produced by strain-ageing (see Fig. 19), the increase in flow stress at the new yield point being reduced from approx. 0.96 to 0.77 ton/in.² (specimens (a) and (b)

400°C .,* water-quenched, and tested again immediately.

Typical results for three ageing temperatures, showing the original stretching through the initial yield and the stress/strain curve after ageing, are given in Fig. 20. No significant variation of the results with time of ageing was found at any of these temperatures. It was evident that (a) at no time and temperature did the type-*A* yield return sufficiently, either to be distinguishable from the expected small, type-*B* yields, or to give rise to

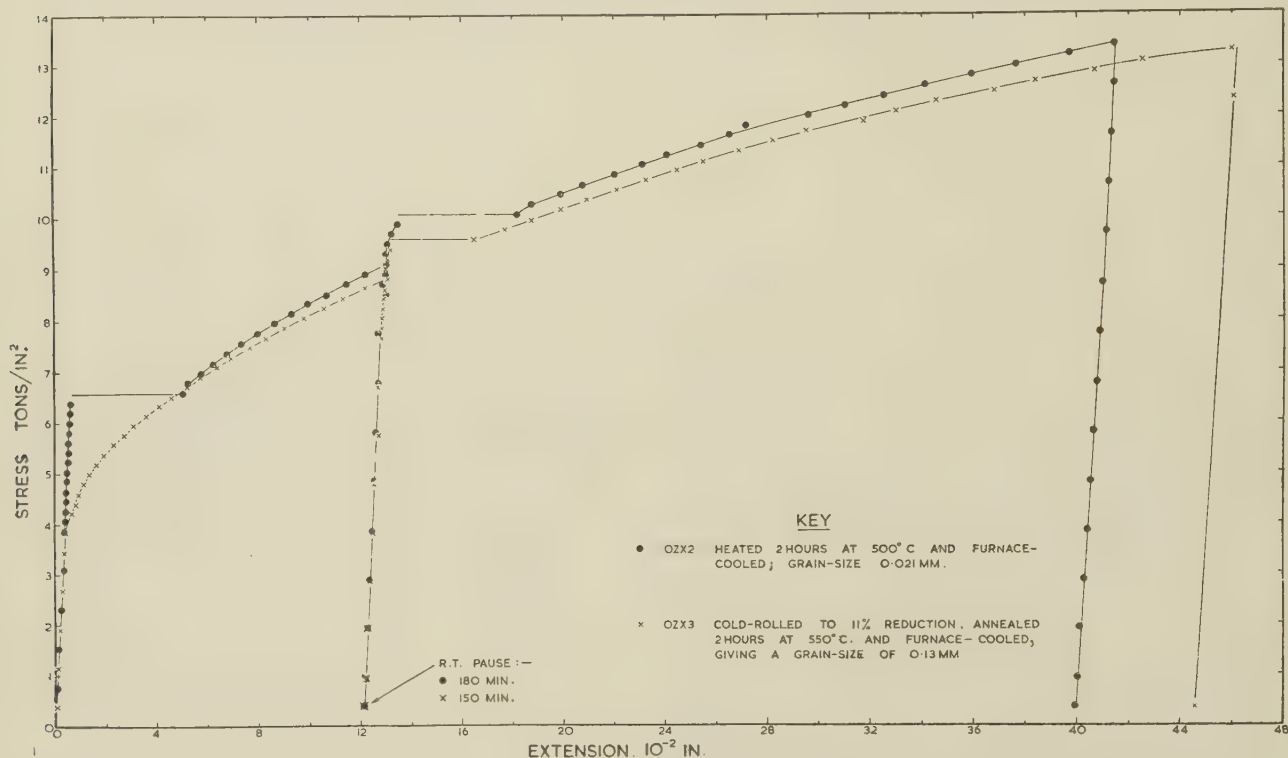


FIG. 19.—Effect of Grain-Size on Type *A* and *B* Yielding in Commercial Aluminium-3½% Magnesium Alloy Sheet (OZX) Pulled at -76°C . with Pause at Room Temperature.

above). However, the further increase in grain-size to 2.6 mm. produced little change, the increase in flow stress for specimen (c) being 0.74 ton/in.².

5. DEPENDENCE OF THE TYPE-*A* YIELD ON PRIOR DEFORMATION AND HEAT-TREATMENT

The results so far presented suggest that the large initial yield (type *A*) in the fine-grained, recrystallized alloys occurs only in unworked material. However, to determine whether it would return after deformation when sufficient ageing treatment was given, tensile specimens of the 3½% magnesium alloy (OZX) were stretched through the initial yield (i.e. approx. 1.5% plastic extension), immediately aged for times up to approx. 1000 hr. at seven temperatures up to

visible markings, and that (b) the high-temperature treatments caused recovery, with a marked fall in the general level of the curves. As might be expected, the recovery was accompanied by a reduction in the elongation at the type-*B* yield steps occurring during the first 1 or 2% strain.

The dependence of the type-*A* yield in unworked material on the heat-treatment previously received was examined as follows. Specimens of the 3½% magnesium alloy (OZX, grain-size 0.020 mm.) were heated for 2 hr. at various temperatures from 250°C . to 500°C ., and cooled at different rates. The outstanding result was that after water-quenching from 500°C . the large initial yield was absent (Fig. 21). Somewhat slower cooling (i.e. in air) allowed the alloy to revert to the condition giving a large yield, and

* After 130 hr. at 400°C ., lattice-parameter measurements showed no serious loss of magnesium by oxidation. Further, unstrained specimens treated at 350° and 400°C . showed no

significant variation in properties with time, up to the longest times.

so also did reheating for 3 days at 125° C. Slighter reductions of the initial yield were found after quenching from 400° and 450° C.

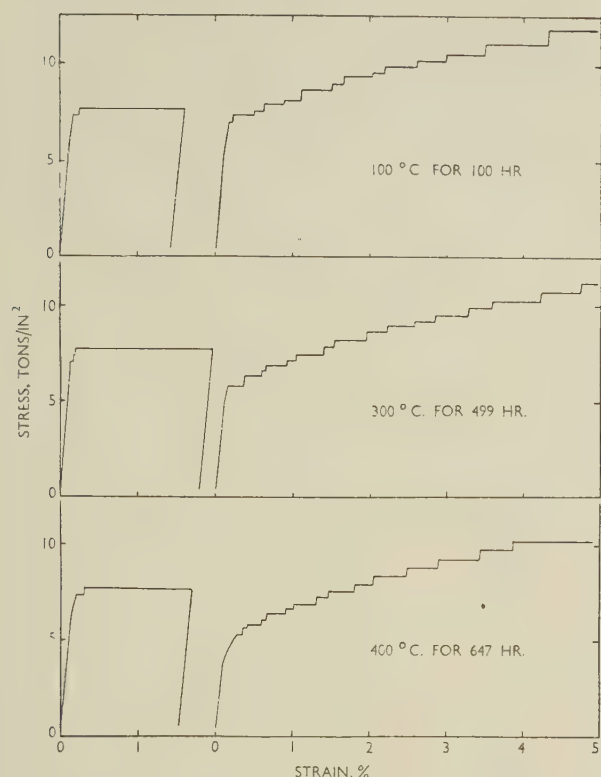


FIG. 20.—Effect of Ageing After Straining Aluminium-3½% Magnesium Alloy (OZX) Through Initial Yield. Specimens stretched through initial yield, as shown, and unloaded, then aged as indicated and tested in tension at room temperature.

The effect of heating to 500° C. for 2 hr., followed by furnace-cooling to various temperatures and quenching, either immediately or after holding for 2 hr., is seen in Fig. 22. Again the alloy reverts, on cooling, to the condition giving a yield point, the process being nearly complete at 350° C.

None of these treatments had any notable effect on the occurrence of the later steps in the stress/strain curves, and all the test-pieces after test showed characteristic type-B inclined ripple markings.

TABLE V.—Effect of Slow Cooling on Initial Yield Point.

3½% Mg Alloy (OZX) *			7% Mg Alloy (NFO) †		
Treatment	Yield Stress, tons/in. ²	Yield-Point Elong., %	Treatment	Yield Stress, tons/in. ²	Yield-Point Elong., %
Air-cooled from 400° C.	7.36 7.19	1.70 1.75	Air-cooled from 420° C.	10.00/10.79 10.38	1.59 † 1.54
Slowly cooled from 400° C. (4° C./hr.)	7.01 7.33	1.63 1.68	Slowly cooled from 420° C. (4° C./hr.)	8.09/8.41 8.13	0.44 † 0.43

* 0.020 mm. grain-size. Heated 2 hr. before cooling.

† 0.018 mm. grain-size after the 3-hr. treatments at 420° C. were given. (Previously cold-rolled 55% to produce recrystallization in this treatment.)

‡ Split yield assumed.

Although the 3½% magnesium alloy is super-saturated with magnesium at temperatures below about 220° C., even very slow cooling does not cause detectable precipitation. The 7% alloy, on the other hand, precipitates magnesium as the β phase on slow cooling. This difference is reflected in the yielding behaviour of specimens cooled at 4° C./hr. (Table V); for the 3½% alloy (no precipitation) air-cooled and slowly cooled specimens give similar results, whereas

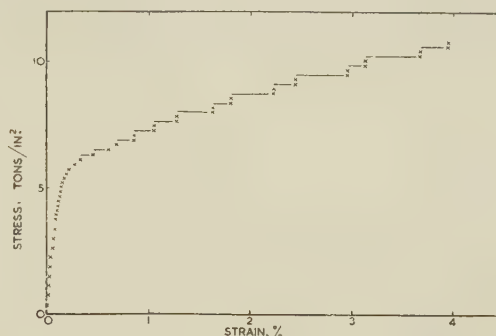


FIG. 21.—Stress/Strain Curve for Commercial Aluminium-3½% Magnesium Alloy, Heated for 2 Hr. at 500° C. and Water-Quenched.

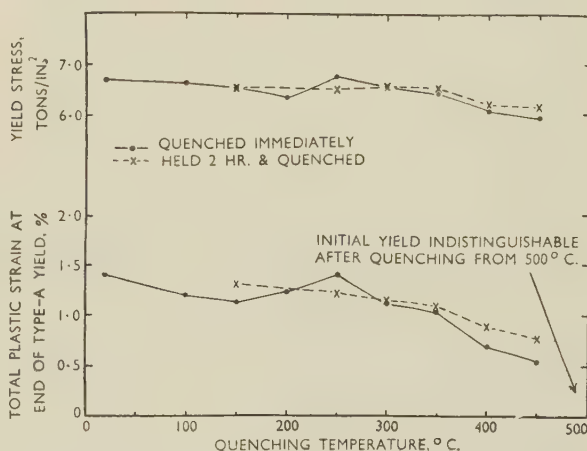


FIG. 22.—Variation of Yield Effects in Commercial Aluminium-3½% Magnesium Alloy (OZX), Annealed for 2 Hr. at 500° C., Furnace-Cooled to a Given Temperature and Either Immediately Quenched or Held for 2 Hr. Before Quenching.

for the 7% alloy slow cooling causes a marked fall in yield stress and elongation. The yield stress, for these cooling rates, is thus a function of the magnesium content of the solid solution. These results clearly indicate that it is chiefly magnesium in solid solution, rather than any adventitious impurity, which produces the yield point.

6. KINETICS OF THE FORMATION OF THE TYPE-A YIELD: QUENCH-AGEING EXPERIMENTS

It has been shown that the initial yield in an annealed material is suppressed by quenching from 500° C. By finding the rate at which the yield point is restored on reheating to lower temperatures, it

should be possible to determine the activation energy for the diffusion processes involved. This can then be compared with that expected for the diffusion of any particular element.

Tensile specimens of the commercial $3\frac{1}{2}\%$ magnesium alloy (OZX2) were heated for 2 hr. at 500°C . and water-quenched. This treatment was known to produce little if any change in grain-size. Immediately after quenching, the specimens were reheated for various lengths of time at 50° , 75° , 100° , 125° , and 150°C ., water-quenched, and tested

the yield returned on reheating, at a rate which increased with the temperature.

In all these tests at -76°C . the deformation at each load increment, above about 4 tons/in.², continued slowly for some time, and with the procedure used (loading by 10-lb. increments at 1-min. intervals), there was considerable rounding of the curve in the region of the yield point. It is thus difficult to assess the true yield stress and yield-point extension. The yield-point extensions for the curves of Fig. 23 have been taken as the sums of the extensions indicated by

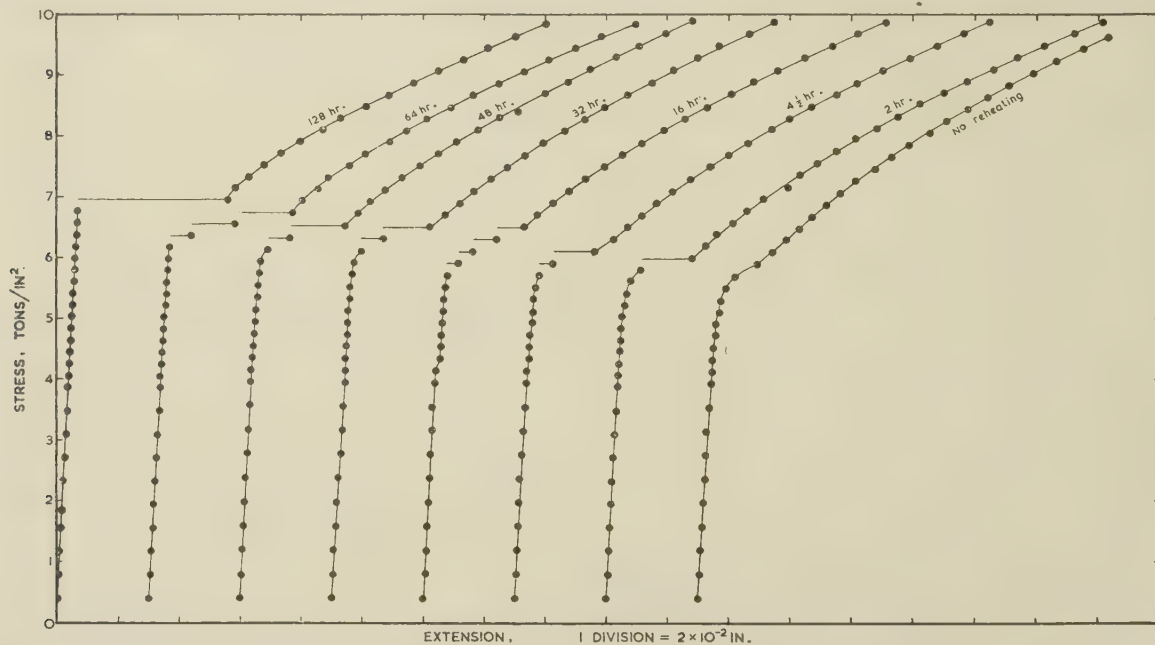


FIG. 23.—Return of Type-A Yield on Reheating Commercial Aluminium- $3\frac{1}{2}\%$ Magnesium Alloy (OZX2) Quenched from 500°C . Nominal grain-size 0.022 mm.; tests at -76°C .; reheating temperature 100°C .

at -76°C . This temperature of test permitted the initial yield point to be observed, uncomplicated by strain-ageing effects.

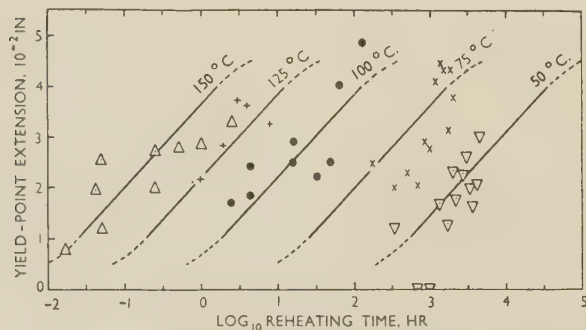


FIG. 24.—Return of the Initial Yield on Reheating at Temperatures Indicated after Quenching from 500°C . Spacing between the lines drawn corresponds to an activation energy of 27 k.cal./g.-atom.

Some of the stress/strain curves obtained are given in Fig. 23. In the absence of reheating, a smooth curve was obtained with hardly any yield step, and

horizontal lines, and similarly for other temperatures. For the present purpose only comparative values are required.

Fig. 24 shows the yield-point extension values for all temperatures plotted against log (time). If the process involved proceeds to the same degree at all temperatures and differs only in the rate, and if the rate is controlled by an activation energy, Q , then with this method of plotting the same curve must be obtained at each temperature, but the curve for a temperature T_2 is displaced along the \log_{10} (time) axis from that for a temperature T_1 by an amount $\delta(\log_{10}t)$,

$$\text{where } \delta(\log_{10}t) = \frac{1}{2.303} \cdot \frac{Q}{R} \cdot \left(\frac{1}{T_1} - \frac{1}{T_2} \right).$$

The curves are drawn at intervals corresponding to an activation energy of 27 k.cal./g.-atom, and this figure evidently gives a fairly good approximation to the results.

This treatment assumes that the equilibrium distribution of the diffusing element is unaltered by change of temperature in this range. Since lowering the temperature favours the formation of the yield

point, this is only approximately true, and the result above is slightly low. An estimate of the error may be made as follows. The element concerned is distributed between two types of position, in one of which it causes the appearance of a yield point, and the highest quenching temperature giving rise to a yield point is 450°C . It may be assumed for a rough approximation that the ratio of concentrations in the two sites is approximately $\exp(-V/RT)$, where $-V$ is the difference in energy for the two positions. Hence, to a first approximation, $-V = RT$, where $T = (450 + 273)^{\circ}\text{K}$. or $-V = 1.4 \text{ k.cal./g.-atom}$.

7. STRAIN-AGEING IN THE ABSENCE OF TYPE-A YIELD

It is clear that by quenching from 500°C . the type-*A* yield may be suppressed, and that when suppressed it is unlikely to return in a short time. The formation of a type-*B* yield can thus be studied in isolation.

Four specimens of the commercial alloy were annealed for 2 hr. at 500°C . and water-quenched to suppress the type-*A* yield. This treatment caused no detectable increase in the grain-size, which remained at 0.018 mm. Two of the specimens were

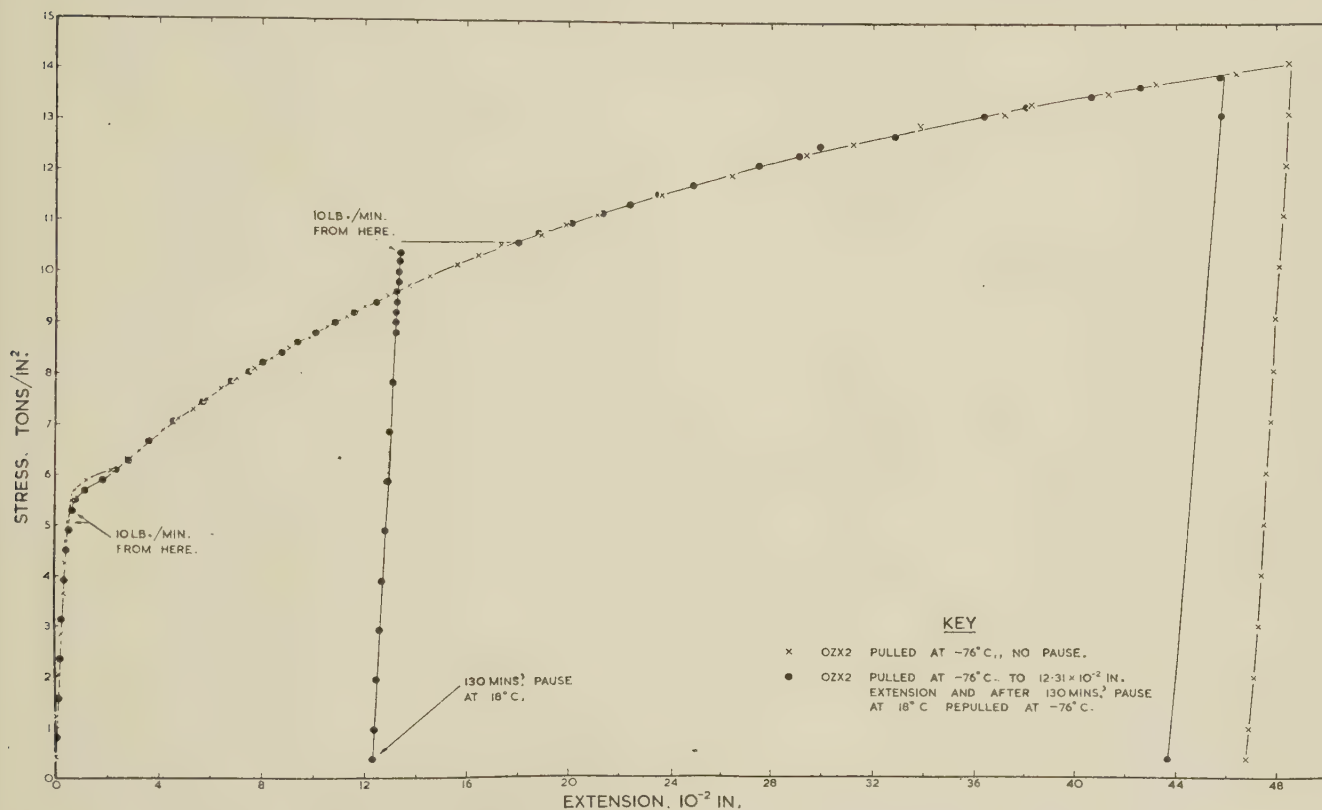


FIG. 25.—Effect of a Pause at 18°C . During Pulling at -76°C . on Commercial Aluminium- $3\frac{1}{2}\%$ Magnesium Alloy (OZX2) of 0.018 mm. Grain-Size, Annealed for 2 Hr. at 500°C . and Water-Quenched.

This energy is to be added to the figure given above for the measured activation energy, giving a corrected figure of about $28\frac{1}{2} \text{ k.cal./g.-atom}$. It must be emphasized, however, that this correction is subject to considerable uncertainties.

When this result is compared with the activation energy for diffusion of magnesium, as a test of the hypothesis that magnesium is responsible for the effects observed, it is found that the range of published values is very considerable, viz. $26.8\text{--}38.5 \text{ k.cal./g.-atom}$.²¹ The majority, however, are near the lower limit of this range, and it is suggestive that the Langmuir-Dushman relationship, which gives good agreement with experiment for other, better-established, aluminium-base solutions,²² predicts a value of $29 \text{ k.cal./g.-atom}$.

pulled at -76°C . with a pause at room temperature, as above, at approximately 2.8% extension, and two were pulled at -76°C . without pausing. In all four the initial yield was almost or completely absent. The pause at room temperature produced a single step when pulling was resumed at -76°C ., followed by a smooth curve. One curve obtained by pausing is shown in Fig. 16, with one obtained for the as-received alloy, and the other is shown in Fig. 25, with one of those obtained without pausing.

Strain-ageing thus caused the appearance of a new yield point and corresponding step in the curve, irrespective of the presence or absence of the initial type-*A* yield. The amount of strain-ageing produced by a similar pausing treatment at room temperature was nearly the same for the specimen showing the

type-*A* yield as for the specimen from the same sheet heat-treated to suppress the type-*A* yield.

Clearly, by suitable straining at -76°C . followed by ageing at room temperature, it is possible to produce a material which will then show a single initial yield in a test at -76°C . On the hypothesis advanced, this is a type-*B* yield point, whereas the initial yield point in an annealed material is of type *A*. To make a comparison

5.2×10^{-2} in. for the original sheet. It was examined after an extension of approx. 3%; the faint ring marking found at each shoulder, though similar in plan to that found for the untreated sheet, was diffuse and much less clearly visible. In section, it was found to correspond to parallel necking, as expected for a type-*B* yield, whereas the untreated sheet gave the shear deformation typical of type-*A*

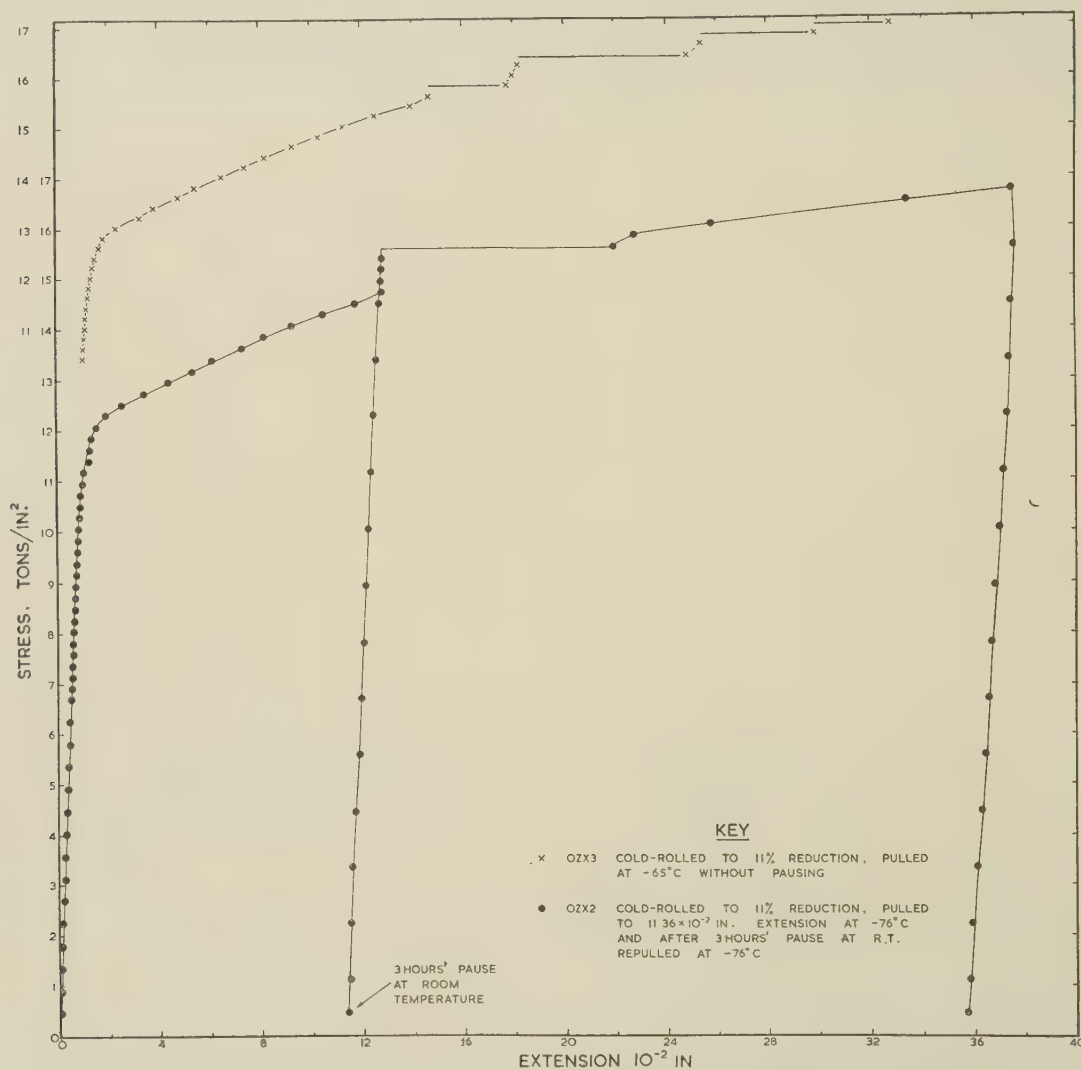


FIG. 26.—Effect of Light Cold-Rolling on Type *A* and *B* Yielding in Commercial Aluminium-3½% Magnesium Alloy (OZX) of 0.018 mm. Grain-Size.

of the type of deformation produced, under closely similar conditions, the following experiment was carried out. A rectangular strip (OZX3) was stretched approx. 5% in the Amsler machine while cooled in dry ice. The middle of the strip had then undergone the initial yield but had a smooth surface. From this piece a tensile specimen of the normal type was prepared and polished. On testing at -76°C . this specimen gave an initial yield, due to strain-ageing, with an extension of 4.2×10^{-2} in. (approx. 1%), compared with an average initial yield extension of

markings with the characteristic sharp boundary (Fig. 6, Plate XCI).

8. STRAIN-AGEING IN COLD-ROLLED MATERIAL

Pieces of the commercial alloy of 0.018 mm. grain-size were cold-rolled to reductions of the order of 10%, and tensile specimens cut from them transversely were pulled at -65° and -76°C . (Fig. 26).

A slightly increased rate of strain-ageing during pulling was noted (cf. curves for -60°C ., as-annealed,

Fig. 14, and $-65^{\circ}\text{C}.$, rolled, Fig. 26). Neither at -76° nor at $-65^{\circ}\text{C}.$ was any initial yield observed on the curve, in agreement with results of tests at room temperature (Figs. 2 and 11).

Similar results were obtained when the strips were cooled in liquid oxygen before rolling. Table VI shows that the increase in flow stress on pausing during the tensile test was nearly the same, whether rolling was done at room temperature or below, and that it was in fact little different from that found in the previous tests on annealed material.

Holden²³ has reported a similar absence of yield point in rolled and aged single crystals of carburized

9. EXPERIMENTS ON HIGH-PURITY MATERIALS

The effect of temperature on the stress/strain curves of high-purity materials was almost exactly similar to that found for the commercial alloy. Room-temperature stress/strain curves had the same general characteristics as those for the commercial material, and a curve for $-60^{\circ}\text{C}.$ is given, with one for $-76^{\circ}\text{C}.$ with a room-temperature pause, in Fig. 27.

The result of warming to room temperature after giving a small extension at $-76^{\circ}\text{C}.$ was to introduce a new yield point on continuing the test at $-76^{\circ}\text{C}.$

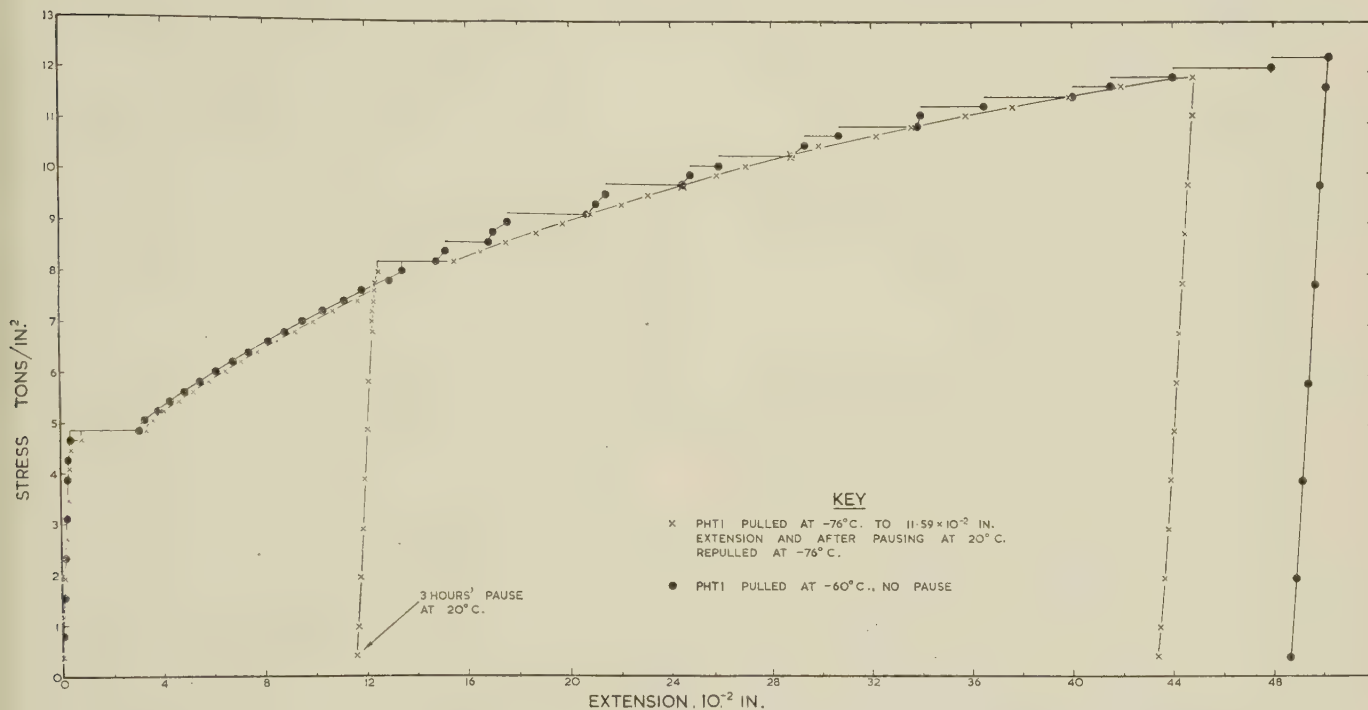


FIG. 27.—Test at $-76^{\circ}\text{C}.$ with Room-Temperature Pause, and Continuous Test at $-60^{\circ}\text{C}.$ on High-Purity Aluminium-3% Magnesium Alloy (PHT1a). Grain-size 0.033–0.036 mm.

iron, although stretching and ageing a similar crystal produced a yield point as expected.

TABLE VI.—Effect of Light Rolling on the Strain-Ageing of Commercial Aluminium-3½% Magnesium Sheet.

Sheet OZX2, 0.018 mm. grain-size. Transverse specimens pulled at $-76^{\circ}\text{C}.$, with a 3-hr. pause at room temperature after the stated straining treatment.

Rolling Procedure	Rolling Reduction, %	Pre-Stress, tons/in. ²	Plastic Pre-Stretch, 10^{-2} in.	Increase in Flow Stress, tons/in. ²
Dipped in liquid oxygen	9	15.03	11.67	0.87
" " "	7	14.67	11.67	0.85
Room temperature	11	14.73	11.36	0.89
" " "	16	17.39	11.49	0.94

(Fig. 27), as in the commercial alloy. The increase in flow stress (0.57 ton/in.²) produced by this strain-ageing treatment was somewhat lower than that for the commercial alloy.

The initial yield point in these materials occurred at a somewhat lower stress than in the commercial material, but the whole level of the stress/strain curve was lower, and the yield-point extension was very much what would have been expected for commercial material of similar grain-size. Fig. 28 shows that coarsening the grain-size removes the initial yield, but has little effect on the new yield point produced by strain-ageing.

Since heating to $500^{\circ}\text{C}.$ produced marked grain growth, it was impossible to examine the effect of quenching from that temperature on the initial yield, but it was expected from the results on the com-

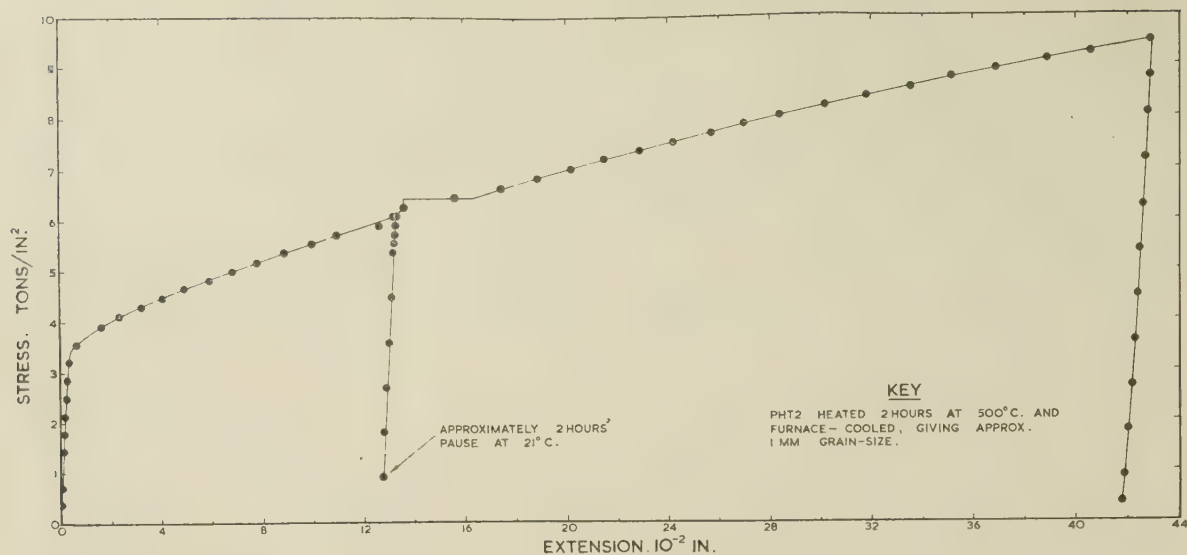


FIG. 28.—Stress/Extension Curve for High-Purity Aluminium-3.65% Magnesium Alloy Sheet (PHT2a) of Approx. 1 mm. Grain-Size, Pulled at -76°C . with Pause at 21°C . Initial yield absent.

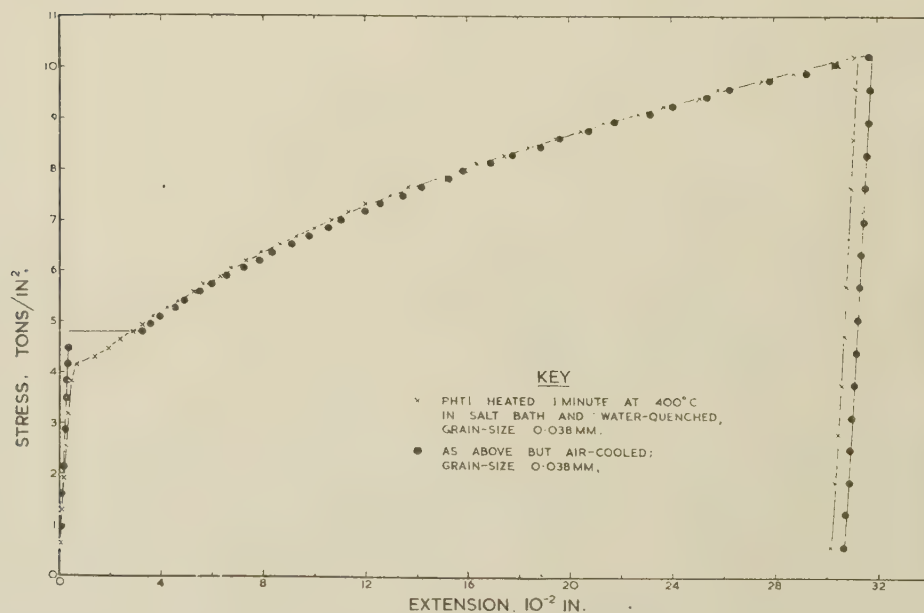


FIG. 29.—Showing Effect of Cooling Rate from 400°C . on Type-A Yield in High-Purity Aluminium-3% Magnesium Alloy Sheet (PHT1b) Pulled at -76°C .

mercial alloy that quenching from 400° C. would have an observable effect. Accordingly, two specimens were heated for 1 min. in a salt bath at 400° C., and one was quenched while the other was air-cooled. The stress/strain curves obtained at -76° C. are shown in Fig. 29.

All the strain-ageing results on these materials are

heating the unstrained specimens are similar in the two metals.^{32, 33}

The chief differences appear to be that both the initial yield point and the yield effects produced by strain-ageing are weaker in aluminium-magnesium alloys than in mild steel, and that strain-ageing is much more rapid in the aluminium-magnesium alloys,

TABLE VII.—Amount of Strain-Ageing in High-Purity Alloy Sheet Specimens Pulled at -76° C. with Room-Temperature Pause.

Material	Condition	Grain-Size, mm.	Pre-Stress, tons/in. ²	Plastic Pre-Stretch, 10 ⁻³ in.	Pausing Time, min.	Pausing Temp., °C.	Increase in Flow Stress, tons/in. ²	Elongation at Step, 10 ⁻³ in.
PHT1	As annealed.	0.033/0.036	7.58	11.59	180	20	0.57	2.97
"	Heated 1 min. at 400° C. in salt bath, water-quenched.	0.045	7.58	12.02	120	21	0.57	3.16
"	Heated 1 hr. at 400° C. in vacuo, furnace-cooled.	0.043 approx.	6.79	12.77	180	20	0.39/0.59 *	1.10 + 2.25 = 3.35
"	Heated 2 hr. at 500° C., water-quenched.	1 approx.	5.82	12.33	180	20	0.39/0.58 *	1.83 + 2.32 = 4.15
PHT2	" " "	1 approx.	6.42	12.51	52	22	0.35	1.78
"	Heated 2 hr. at 500° C., furnace-cooled.	1 approx.	6.06	12.65	175	21	0.36	1.97

* Split yield.

assembled in Table VII; increases in flow stress range from 0.35 to 0.59 ton/in.², in good agreement with the value found by Sherby, Anderson, and Dorn²⁴ (0.44 ton/in.²).

V.—DISCUSSION

1. COMPARISON WITH STEEL

Both the markings formed and the yield phenomena bear many resemblances to those found in mild steel. The complex type-*A* markings formed on pressings¹ are quite similar to those formed on pressing annealed mild steel,⁵ and in both cases the initial yield point is concerned. Markings similar in appearance to the type-*A* markings found here in strips have also been observed in steel; Nadai,²⁵ in experiments on steel strips containing stress-raisers, found markings very similar to those of Fig. 3 (*a*) (Plate XC), Miklowitz²⁶ has obtained markings on steel strip which bear some resemblance to Fig. 4 (Plate XC), and other similarities may be found in the work of Kuroda.²⁷ It has not been generally recognized, however, that this type of marking in steel might be formed by a shear deformation, as has been demonstrated for the present alloys. Nevertheless, such a shear has been observed in thin wire, strip, and bar specimens.²⁸⁻³⁰

In steel, as in the aluminium-magnesium alloys, there is a strong dependence of the initial yield point on grain-size, whereas the yield point produced by strain-ageing is much less grain-size dependent. In both metals strain-ageing effects may be produced in a coarse-grained material, even though the initial yield is absent.³¹ The effects of quenching and re-

so that multiple discontinuous yielding is observed at room temperature instead of at 100°-300° C.^{27, 31, 34-39}

2. DISSOLVED ELEMENTS RESPONSIBLE FOR THE YIELD-POINT EFFECTS

In steel the yield point has been shown to be due to the presence of small quantities of carbon or nitrogen in solution,⁴⁰ and the strain-ageing behaviour has been convincingly interpreted⁴¹ in terms of the diffusion of interstitially dissolved carbon or nitrogen atoms to the dislocations present, where they lock the dislocations in position and so prevent slip until the stress is raised, according to the theory of Cottrell.^{19, 20}

These small quantities of impurity are effective in producing a yield point in steel, because they can produce extreme distortion of the lattice, including both expansion and shear distortions, and so can interact strongly with both hydrostatic and shear components of the strains round the dislocations. In an aluminium alloy, however, owing to the different crystal structure, a hypothetical interstitial impurity could produce only a spherically symmetrical distortion, and in this respect it does not differ from the substitutionally dissolved metallic impurities or alloying elements.

It seems certain that in the alloys studied in the present work magnesium is the dissolved element principally involved in both the type-*A* and type-*B* yields, although the normal impurities appear to strengthen the latter. Both are formed in the high-purity aluminium-magnesium alloys, though absent in pure aluminium, and the quench-ageing experiments

indicate an activation energy consistent with the type-*A* yield being due to magnesium. Further proof that the type-*A* yield is due to magnesium is given by the behaviour of the 7% magnesium alloy, in which precipitation of the magnesium reduces the magnitude of the yield, while similar treatments applied to the 3½% magnesium alloy, in which precipitation of the magnesium-containing phase does not occur, produce no such effect.

The behaviour of some other aluminium alloys is discussed in another paper.⁴² Although there are evidently a number of dissolved elements which can give rise to type-*B* yielding, type-*A* yielding was practically absent in the other alloys, which did not contain large amounts of magnesium.

3. MECHANISM OF STRAIN-AGEING AND THE TYPE-*B* YIELD

Both types of yield are transient effects; the smooth stress/strain curve which is obtained after either kind of yield, at temperatures low enough to prevent strain-ageing, is the same as that obtained when the yield is absent (Figs. 16, 25, and 29). In other words, the feature responsible for the yield point blocks the initiation of slip until a certain stress is exceeded, but it does not hinder the continuation of slip in a region in which slip has started. In view of this observation, type-*B* yields cannot be attributed to strain-accelerated age-hardening; that would result in a raising of the whole level of the stress/strain curve. Of the mechanisms proposed to explain strain-ageing effects, that due to Cottrell is the only one which predicts this behaviour. There is no reason why a substitutional solute in a face-centred cubic metal should not produce a yield point by this mechanism, although it would be expected to be weaker than that produced in a system such as iron-carbon, in agreement with observation.

The rate at which the type-*B* yield is established on ageing after straining is more rapid than at first might be expected by comparison with steel, as magnesium diffuses more slowly in aluminium than does carbon in α -iron. Moreover, Sherby, Anderson, and Dorn,²⁴ studying strain-ageing in high-purity aluminium-3% magnesium, found activation energies which are well below that for diffusion of magnesium. They suggested that instead of the magnesium diffusing to the dislocations, the dislocation lines adjust themselves to pass through or near the magnesium atoms. Two objections may be raised to this

view: first, that it would involve increasing the length of each dislocation by a factor of the order of $1\frac{1}{2}$, and this would almost certainly need a larger amount of energy than would be available from the interaction energy between the magnesium atoms and the dislocations;* and secondly, that it would not allow "saturation" of the dislocation with magnesium atoms, but would only allow one magnesium atom to every three or four atoms' length of dislocation.

The rapidity of the strain-ageing process, however, does not appear incompatible with the diffusion of magnesium atoms when the concentration of the solid solution is considered. In the 3½% magnesium alloy, very roughly one atom in every cube of side three atoms, on average, is a magnesium atom, so that in many cases a movement of only one atomic distance would be required to bring a magnesium atom into the optimum position; as this distance lies within the region in which the stress due to the dislocation is strong, and as this stress in most cases tends to move the atom in the required direction, diffusion must be considerably assisted. In more detail, if to saturate the dislocation it is required to build up a chain of magnesium atoms, one in each (111) plane cut by the dislocation, roughly one-quarter of the total magnesium atoms have to diffuse one atomic distance, rather less than half of the total have to diffuse two atomic distances, and the remainder, three atomic distances. The atoms nearest to the dislocation will receive most assistance from the stress field, so that the activation energy would be expected to rise during the process of strain-ageing, as observed by Sherby, Anderson, and Dorn.²⁴ The calculated interaction energy again falls short of that required to account for the observed results, but only by a factor of about four. The calculation is approximate, and, further, the activation energy for diffusion will also be considerably reduced in the neighbourhood of the dislocation by the opening out of the structure on the "tension" side. Taking these points together, the normal process of diffusion of the solute atoms to the dislocation appears perfectly feasible.

4. MECHANISM OF THE INITIAL YIELD POINT (TYPE-*A* YIELD)

An outline has already been given (p. 629) of the proposed mechanism for the initial yield point, according to which the speed of yielding from grain to grain is hindered by "equilibrium segregation"

* The energy of a dislocation has been estimated⁴³ at 1–5 eV. ($0.6\text{--}3 \times 10^{-11}$ ergs) per atom plane. Hence, increasing the length by 50% would give an increase in energy of $0.2\text{--}1 \times 10^{-11}$ ergs per atomic distance of the new length. From the formula given by Cottrell,¹⁹ the interaction energy, for a magnesium atom in the stress field of an edge-dislocation in an aluminium solid solution, is $5 \times 10^{-13} r/R$ erg, when the magnesium atom lies directly over the dislocation, r being the radius of an aluminium atom and R the distance of the magnesium atom from the dislocation centre. The smallest

possible value of R is about equal to r , so that about 5×10^{-13} erg is available for every magnesium atom absorbed by the dislocation. As only about one in three or four atoms in its length can be a magnesium atom, the energy available falls short of the requirement by a factor of about twenty. The result is rough, as the energies are obtained by the use of approximate models, but it appears sufficient to cast considerable doubt on the mechanism proposed by Sherby, Anderson, and Dorn.²⁴

of magnesium atoms in solid solution to the grain boundary, and the observations have been consistent with this mechanism. A hindrance to the spread of initial yielding from grain to grain, like that now postulated, has been shown to occur in annealed steel⁴⁴ (but not in deformed, or strain-aged steel) by means of microhardness tests. The mechanism proposed is not the same as the cementite-film theory of Dalby,⁴⁵ Nadai,²⁵ and Kuroda,^{27, 46} who envisaged a film of a hard second phase at the boundary, but is of the general type proposed by Cottrell, in which dislocations are stabilized by solute atoms; the presence of many magnesium atoms at the boundary stabilizes the structure, and so makes it more difficult to break out a dislocation and start slip in the undeformed grain.

Hall¹⁸ has shown, following Eshelby, Frank, and Nabarro,⁴⁷ that when slip occurs in one grain, there is a large concentration of shear stress where the slip plane meets the boundary. The stress-concentration factor increases with the grain diameter, and it is shown that, if a fixed stress at the boundary is assumed necessary to propagate the yield, the applied external stress causing yielding varies as $d^{-1/2}$, where d is the mean grain diameter. Of the present results, those obtained for the material OLZ1 agree well with this relation, and those for OMA1 deviate slightly.

This view of the initial yield implies that the yield stress is that for propagating rather than initiating the yield, and the upper yield stress is simply the stress required to spread the yielded area beyond some critical point at which the required stress is a maximum. This is certainly true in the present experiments, in many of which small yielded areas were known to be present at a stress below the yield stress and spread down the gauge-length at the yield point. Experiments with the relatively "hard" Amsler machine showed that there was little fall of stress at the initial yield, the upper and lower yield stresses being almost coincident.

Hall's treatment shows that the shear-stress concentration in an undeformed grain, adjacent to one in which slip has occurred, falls off rapidly with distance from the grain boundary. Hence, we may suppose that in a recrystallized metal, in which dislocations are sparse, there will be little chance of a dislocation in the body of the grain lying within the highly stressed region. When the metal has been deformed, however, the dislocation density is higher, and some dislocations will usually lie in this region; these dislocations will move much more readily than those bound in the grain boundary, and hence there will be no effective barrier to the spread of yielding. Thus the type-*A* yield should be characteristic of the undeformed material, as observed, and should not return through strain-ageing.

Finally, it is possible to compare the observed rate of restoration of the initial yield, on reheating after quenching from 500°C., with that expected if the postulated mechanism holds. On quenching, the magnesium is supposed to be evenly distributed

between the grains and the grain boundaries. On reheating, the equilibrium changes to give a high concentration of magnesium at the boundaries.

For a calculation of the orders of magnitude, let it be assumed that the concentration of magnesium at the boundary is one atom in three and that the boundary is effectively two atoms thick. In the grains there is roughly one magnesium atom in thirty, so that the magnesium required to saturate the boundary is initially contained in a band ten atoms thick each side of the boundary. The diffusion layer will presumably not become completely denuded of magnesium, and may therefore be somewhat thicker than this; it might well be twice this thickness, i.e. 50 Å. thick.

Taking an average value of the diffusivity, from the data given by Smithells,²¹ to be 4×10^{-10} cm.²/sec. at 450°C., the limiting values quoted by him for the activation energy of diffusion lead to approximately 6×10^{-17} and 6×10^{-20} cm.²/sec., respectively, for the diffusivity, D , at 125°C. At this temperature the yield point is fully established after a time, t , of about 10^4 sec., so that the approximate thickness, \sqrt{Dt} , of the diffusion layer which can be established in this time lies between 80 and 2.5 Å. As indicated earlier, we prefer the higher value, corresponding to the lower activation energy. The figure of 50 Å. quoted above lies in this range.

Thus, the present observations on the rate of restoration of the yield point are broadly in agreement with the view that magnesium is the solute element producing the type-*A* yield and that it acts by "equilibrium segregation" at the grain boundaries. Unfortunately, the diffusion data available are not consistent enough to provide a rigorous test.

5. METHODS OF AVOIDING STRETCHER-STRAIN MARKINGS

As the type-*B* (ripple) markings are not conspicuous in the annealed material after small strains, the important thing is to control the formation of type-*A* or "flamboyant" markings in pressing. This may be done in a number of ways. Control of the grain-size^{2, 3} is effective up to a point. As shown in Section IV, by increasing the grain-size to about 0.04 mm., the yield-point elongation is reduced so that markings would be barely noticeable. A further increase to about 0.15 mm. would remove the yield point altogether, but the orange-peel effects would then be obtrusive, and, for optimum results, the limits need to be fairly close, say, 0.04–0.06 mm. This remedy has been applied in practice, but involves an extra anneal to give a reduction of about 20% to finished thickness, and exact control of the grain-size may be troublesome.

Type-*A* yield is removed by overstraining in tension, and this removal appears to be permanent for practical purposes. This is not in itself a practical method of avoiding markings, for a stretched sheet will show residual markings from the type-*A* yield. It suggests,

however, that other methods of overstraining, such as roller-levelling, would be effective, provided that it could be ensured that all the material was given some overstrain. Any such treatment must, to some extent, raise the proof stress and increase the liability to type-*B* markings, but the experiments reported in Section IV show that the material can be softened by a non-recrystallizing anneal without the type-*A* yield returning. In these experiments the material was quenched after treatment. In a further experiment it was found that a specimen stretched through the initial yield and annealed at 400° C. showed no initial yield point if quenched or air-cooled, but did develop a small initial yield (0.4%) if furnace-cooled; this, however, was insufficient to produce detectable markings, and it appears that it is unnecessary in practice to quench.

No rolled material has shown a type-*A* yield, and "temper rolling" is clearly a method of avoiding markings. Again, the lightly rolled material can be softened by a non-recrystallizing anneal without causing a return of the markings in a stretched strip.³

A further possibility is quenching from a high temperature, e.g. 500° C. To be effective, the quenching evidently must be prompt, since the feature responsible for the yield is partly restored at 450° C., and rapid. The improvement effected by this treatment would not be permanent; some return of the yield would be expected in the 3½% magnesium alloy on ageing for a period of the order of 6 weeks at 50° C., or, by extrapolation, some 5–10 years at 20° C. It would be undesirable to apply a treatment of this type to an alloy of the 7% magnesium type, since it would result in taking precipitated β phase into solution, and this would promote subsequent grain-boundary precipitation with attendant stress-corrosion susceptibility if the alloy was warmed for long periods in service. With 5% or less magnesium, however, the alloys as normally supplied do not contain free β phase, and so no deterioration could be caused.

The following treatments were tried out on a commercial scale, all except the first being applied to fine-grained material:

- (1) Controlling the grain-size to 0.04–0.06 mm.
- (2) Overstraining by light or moderate roller-levelling.
- (3) Overstraining by heavy roller-levelling or light rolling (about 5% reduction) followed by a non-recrystallizing anneal.
- (4) Quenching from 500° C., followed by flattening.

Four firms co-operated in supplying materials. The sheets were examined in the laboratory and a large number of pressings were made in a shape known to be liable to give rise to conspicuous markings. The results are fully described in another paper.⁴⁸ It was found that the grain-size control treatment was effective, provided that the specified grain-size was obtained. Orange-peel effects were serious at 0.10 mm. grain-size. Overstraining by roller-levelling was effective only if a moderately severe treatment was applied; with light roller-levelling the material was evidently not deformed throughout and gave a characteristic transverse ripple marking on a lightly stretched strip. The treatments described under (3) were designed to decrease the susceptibility to type-*B* markings in heavily overstrained material, but in fact no type-*B* markings were found in any pressing. It is probable that with soft material they would be found only in a pressing in which a free surface received a heavy unidirectional stretch. The quenching treatments were effective except in one case; presumably in this case the quench was delayed or too slow.

It was found that there was a complete correlation between the results of stretching strips in the laboratory and the markings formed on the pressing, and moreover, by simple visual examination of the stretched strips and by determinations of grain-size, it was possible to deduce very easily where the treatments which failed were at fault.

Of the treatments described, temper-rolling is possibly the most certain in application, since it is possible to ensure that all the metal is deformed, but it requires very close control of the sheet thickness both before and after the temper-rolling. Moreover, it cannot readily be applied to finished sheet. The heavy roller-levelling treatment, however, can be applied to finished sheet, as the thickness is not materially altered, and it does not involve alteration of the normal production methods. The treatments entailing a non-recrystallizing anneal after overstraining, or quenching followed by light flattening, are particularly recommended where maximum ductility is required, as in severe drawing operations.

ACKNOWLEDGEMENTS

The authors wish to express their thanks to Mr. A. Loro, who carried out most of the interferometric measurements, and to the many with whom they have had fruitful discussion, particularly Professor A. H. Cottrell, Mr. G. Murray, and Mr. J. R. Handforth.

The authors are indebted to the Director and Council of The British Non-Ferrous Metals Research Association for permission to publish this paper.

REFERENCES

1. J. D. Jevons, *J. Inst. Metals*, 1950-51, **78**, 563.
2. G. A. Knight and G. Murray, *Sheet Metal Ind.*, 1946, **23**, 1741.
3. R. Chadwick and W. H. L. Hooper, *J. Inst. Metals*, 1951-52, **80**, 17.
4. R. Eborall, *ibid.*, 1950-51, **78**, 703 (discussion).
5. J. D. Jevons, "The Metallurgy of Deep Drawing and Pressing, p. 220. 2nd edn. London: 1941 (Chapman and Hall).
6. R. L. Kenyon and R. S. Burns, *Age-Hardening of Metals (Amer. Soc. Metals)*, 1940, 262.
7. B. A. Bilby, *Sheet Metal Ind.*, 1950, **27**, 707.
8. W. Rosenhain and S. L. Archbutt, 10th Rep. *Alloys Research Cttee. (Inst. Mech. Eng.)*, 1912, 319.
9. A. Portevin and F. Le Chatelier, *Compt. rend.*, 1923, **176**, 507.
10. R. J. Anderson, *Proc. Amer. Soc. Test. Mat.*, 1926, **26**, (II), 349.
11. E. W. Fell, *Iron Steel Inst., Carnegie Schol. Mem.*, 1937, **26**, 123.
12. C. F. Elam, *Proc. Roy. Soc.*, 1938, [A], **165**, 568.
13. A. W. McReynolds, *Trans. Amer. Inst. Min. Met. Eng.*, 1949, **185**, 32.
14. J. D. Lubahn, *ibid.*, 1949, **185**, 702.
15. H. Chossat, *Rev. Mét.*, 1950, **47**, 167, 306, and 343.
16. A. Loro, unpublished work.
17. S. Tolansky, "Multiple-Beam Interferometry of Surfaces and Films". Oxford: 1948 (Clarendon Press).
18. E. O. Hall, *Proc. Phys. Soc.*, 1951, [B], **64**, 747.
19. A. H. Cottrell, *Phys. Soc.: Rep. Conf. on Strength of Solids*, 1948, 30.
20. A. H. Cottrell and B. A. Bilby, *Proc. Phys. Soc.*, 1949, [A], **62**, 49.
21. C. J. Smithells, "Metals Reference Book". London: 1949 (Butterworths).
22. R. M. Barrer, "Diffusion in and through Solids". Cambridge: 1941 (University Press).
23. A. N. Holden, *Trans. Amer. Inst. Min. Met. Eng.*, 1952, **194**, 182.
24. O. D. Sherby, R. A. Anderson, and J. E. Dorn, *ibid.*, 1951, **191**, 643.
25. A. Nadai, *Z. techn. Physik.*, 1924, **5**, 369.
26. J. Miklowitz, *J. Appl. Mechanics*, 1947, **14**, A21.
27. M. Kuroda, *Sci. Papers Inst. Phys. Chem. Research (Tokyo)*, 1938, **34**, 1528.
28. E. Orowan and W. Chitruk, quoted by W. Sylvestrowicz and E. O. Hall, *Proc. Phys. Soc.*, 1951, [B], **64**, 495.
29. E. O. Hall, *ibid.*, 1951, [B], **64**, 1085.
30. W. M. Lomer, *J. Mechanics Physics Solids*, 1952, **1**, 66.
31. C. Boulanger, *Compt. rend.*, 1949, **228**, 2026.
32. W. Köster, *Arch. Eisenhüttenwesen*, 1928-29, **2**, 503; 1929-30, **3**, 637.
33. M. Kuroda, *Sci. Papers Inst. Phys. Chem. Research (Tokyo)*, 1932, **20**, 29.
34. A. le Chatelier, *Rev. Mét.*, 1909, **6**, 914.
35. E. Körber and A. Pomp, *Mitt. K.W. Inst. Eisenforschung*, 1927, **9**, 339.
36. R. L. Kenyon and R. S. Burns, *Proc. Amer. Soc. Test. Mat.*, 1934, **34**, (II), 48.
37. N. J. Manjoine, *J. Appl. Mechanics*, 1944, **11**, A211.
38. S. Epstein, H. J. Cutler, and J. W. Frame, *Trans. Amer. Inst. Min. Met. Eng.*, 1950, **188**, 830.
39. E. O. Hall, *J. Iron Steel Inst.*, 1952, **170**, 331.
40. J. L. Snoek, *Physica*, 1941, **8**, 734.
41. F. R. N. Nabarro, *Phys. Soc.: Rep. Conf. on Strength of Solids*, 1948, 38.
42. V. A. Phillips, *J. Inst. Metals*, 1952-53, **81**, 649.
43. N. F. Mott, *Research*, 1949, **2**, 162.
44. R. Eborall, M. Lack, and V. A. Phillips, *Bull. Inst. Metals*, 1952, **1**, (7), 58.
45. W. E. Dalby, *Proc. Roy. Soc.*, 1913, [A], **88**, 281.
46. M. Kuroda, *Sci. Papers Inst. Phys. Chem. Research (Tokyo)*, 1931, **17**, 111.
47. J. D. Eshelby, F. C. Frank, and F. R. N. Nabarro, *Phil. Mag.*, 1951, [vii], **42**, 351.
48. V. A. Phillips, unpublished work.

1483 SOME METHODS OF MEASURING SURFACE TOPOGRAPHY AS APPLIED TO STRETCHER-STRAIN MARKINGS ON METAL SHEET*

By W. H. L. HOOPER,† B.Sc., A.I.M., MEMBER, and J. HOLDEN,‡ Ph.D.

Two techniques for measuring the surface topography of sheet metal showing stretcher-strain markings are described, the first using the Talysurf surface-measuring instrument and the second, light-interference effects.

The Talysurf consists essentially of a stylus tipped with a diamond of 0.0001 in. radius, which makes contact with the surface under examination. The rise and fall of the stylus as it travels over the surface are magnified electronically, and these magnified displacements are traced by a high-speed autographic recorder, the magnification chosen for stretcher-strain measurements being $\times 1000$ vertically and $\times 2$ horizontally. Traces are taken from both surfaces of the specimen between two fixed points.

The interferometry method involves covering the area of specimen under examination with a small thin piece of optical glass, and illuminating the covered area by a parallel beam of monochromatic light. The specimen is viewed through a metallurgical microscope, modified by placing an extra iris diaphragm in the illumination arm; the usual 16-mm. objective is satisfactory. Interference fringes are produced, and their changes in separation and direction indicate the topography of the surface in the field of view.

The methods are illustrated by reference to stretched parallel-sided strip specimens of dead-soft mild steel and aluminium-3% magnesium alloy, both of which develop strain markings of similar superficial appearance, as soon as the yield point is reached.

In mild steel two effects are distinguished by Talysurf traces, one consisting of coincident depressions in opposite sides of the sheet, so that a neck associated with appreciable local thinning is formed, and the other taking the form of kinking, which occurs without perceptible thinning of the material.

Interference patterns indicate that the first type of marking consists in its most typical form of a groove with a narrow flat bed and flat sides inclined at equal small angles of between 20' and 30' to the undisturbed surface. The groove walls recede from each other as stretching progresses, fresh markings appearing between about $\frac{1}{2}$ and 2% elongation, but with further extension they merge, and the surface becomes comparatively smooth again.

Similar measurements made on stretched annealed strips of aluminium-3% magnesium alloy sheet indicate that strain markings on this material reach their greatest intensity when first formed at the start of plastic deformation; at this stage they consist of kinks, the peak on one surface being represented on the other by a valley, so that no thinning occurs. As stretching proceeds, fresh groups form, and spread either by a smooth movement or by a more rapid shooting and branching, until at between 1 and 2% extension they merge and thereafter rapidly diminish in intensity. Measurements indicate that adjacent areas of plane surface are inclined to each other at a slight angle, less than 1' relative to the undisturbed reference surface. The maximum depths of markings are approximately the same in both steel and aluminium, i.e. about 3/1000 in.

The two experimental methods are complementary. Thus the Talysurf is particularly suitable for examining both surfaces of a sheet specimen, but on the other hand, measurement of an area is a lengthy operation involving taking a number of closely spaced, parallel traces. By means of interferometric techniques, the contours of small areas are clearly indicated. Used in conjunction, therefore, the two methods have a scope and versatility which are adequate for most problems involving surface-profile measurements in the laboratory.

* Summary of a paper contributed to a Symposium on "New Techniques of Metallurgical Research" organized by the Birmingham Local Section of the Institute and held on 29 February 1952. The full paper with illustrations was published in the *Bulletin* of the Institute of Metals, 1953, 1,

(18), 161-165.

† Research Technical Officer, Imperial Chemical Industries, Ltd., Metals Division, Birmingham.

‡ I.C.I. Research Fellow, Royal Holloway College, London University.

EFFECT OF COMPOSITION AND HEAT-TREATMENT 1484 ON YIELD-POINT PHENOMENA IN ALUMINIUM ALLOYS*

By V. A. PHILLIPS,† A.R.S.M., D.Eng., B.Sc., A.I.M., MEMBER
(Communication from the British Non-Ferrous Metals Research Association.)

SYNOPSIS

Discontinuous yielding has been studied in commercial aluminium and some common alloys not containing large amounts of magnesium. The initial yield found in fine-grained aluminium-magnesium alloys was weak or absent in the present materials, even when the grain-size was fine, but strain-ageing effects were present, the strength of which depended on the composition and heat-treatment. These effects gave rise to stepped stress/strain curves at room temperature. The increase in flow stress produced by ageing after straining at a low temperature can be separated into two parts, σ_t , a transient increase which disappears as soon as further deformation takes place, and σ_p , a permanent increase which raises the level of the whole subsequent stress/strain curve. σ_t is attributed to locking of dislocations by a Cottrell mechanism, σ_p to normal age-hardening, which in some cases is accelerated by the prior strain.

I.—INTRODUCTION

IN another paper,¹ it is shown that stress/strain curves of aluminium-magnesium alloys, when determined at room temperature on a "soft" machine, are liable to show discontinuous yield effects, namely: (a) a single sudden yield, occurring at the start of plastic flow, the magnitude of which increases sharply with decreasing grain-size, and (b) a series of steps, in which elastic extension alternates with sudden yielding (Fig. 1, curve A).

In fine-grained annealed materials (grain-sizes of the order of 0.02 mm.) the initial yield, *A*, gives 1% or more elongation. Such materials show severe stretcher-strain markings on stretching part way through the initial yield. The multiple yields, *B*, occurred in all the materials investigated, irrespective of whether the initial yield, *A*, was present or not. They are associated with the formation of inclined band or ripple markings on stretching.

Pronounced differences in the form of the markings and the response to various treatments suggest that a distinction may be drawn between the two yield effects, and they are referred to as type-*A* and type-*B* yields, respectively. Type *A* has been shown by low-temperature tests to be a true initial yield (Fig. 1, curve B), and in fact shows many resemblances to the initial yield point in annealed mild steel. Type-*B* yields are the result of strain-ageing during the test.

Multiple yielding, with associated ripple markings, has been observed in many aluminium alloys; McReynolds² found it absent in 99.996% aluminium,

but present in a commercial aluminium sample containing 0.14% copper and in high-purity aluminium-copper alloys with 0.025, 0.1, and 0.5% copper, and

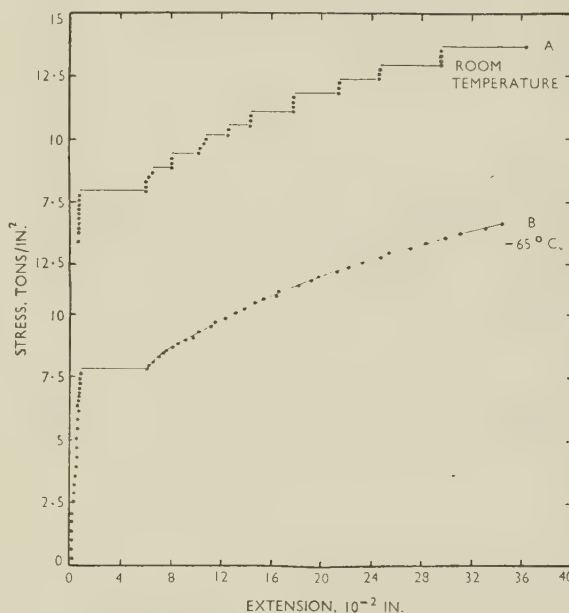


Fig. 1.—Stress/Extension Curves for a Commercial-Purity Aluminium-3½% Magnesium Alloy at Room Temperature and -65°C. Grain-size 0.018 mm.

there are many observations of its occurrence in age-hardening alloys, including aluminium-zinc,^{3,4} aluminium-copper-manganese and Duralumin types,⁵⁻⁸ aluminium-copper-chromium,⁹ and aluminium-mag-

* Manuscript received 17 April 1953. The work described in this paper was made available to members of the B.N.F.M.R.A. in a confidential research report issued in

September, 1952.

† Investigator, British Non-Ferrous Metals Research Association, London.

nesium-silicon alloys.¹⁰ Except in the aluminium-magnesium alloys, however, the initial type-*A* yield and characteristic markings have not been observed.

Failure to observe any type-*A* yield in these materials might have been due to the use of samples which were not in the appropriate condition. It therefore appeared of interest to explore the yielding behaviour of some typical aluminium-base materials when they were in the fine-grained, recrystallized condition (grain-size <0.05 mm.) which in aluminium-magnesium alloys gives rise to an initial type-*A* yield. Tests have been carried out at low temperatures, as well as at room temperature, in order to effect a clear separation of the initial yield, if any, and yields due to strain-ageing.¹ At a sufficiently low temperature strain-ageing is suppressed, so that the stress/strain curve is smooth, except for the initial yield if one is present. By interrupting the test and ageing under controlled conditions, e.g. by warming to room temperature for a fixed time, the amount of strain-ageing can be conveniently assessed.

III.—APPARATUS AND TESTING PROCEDURE

All specimens were pulled on an Avery beam-type dead-weight loading machine, and the beam was kept floating throughout. For most room-temperature tests, standard sheet tensile specimens were used (B.S. No. 485), with a Lindley extensometer and 2-in. gauge-length. For all tests below room temperature, the specimen and apparatus described previously were used.¹ In these tests the specimen was immersed in a low-temperature bath whose temperature was maintained within $\pm 1^\circ$ C., and the extension between the shoulders was measured to 0.0001 in.; 4.43×10^{-2} in. extension was approximately equivalent to 1% elongation.

The load was raised in increments of 10 lb. on the thicker specimens and 5 lb. on the commercial aluminium and on all specimens 0.032 in. thick or thinner, except the solution-treated and the aged Duralumin specimens, and the strain was read after

TABLE I.—Analyses of Materials.

Material	Mg, %	Cu, %	Si, %	Mn, %	Fe, %	Ti, %	Zn, %	Ni, %
Commercial-purity aluminium	<0.01	0.02	0.16	0.01	0.45	0.01	≤ 0.01 (n.d.)	<0.01 (n.d.)
Duralumin-type alloy	0.43 *	4.78 *	0.73 *	0.73 *	0.35	<0.01	"	"
Aluminium-magnesium-silicide alloy	0.90 *	~ 0.01	0.98 *	~ 0.02	0.4	"	"	"
Aluminium-1½% manganese alloy	0.008	0.12	0.21	1.14 *	0.59	"	"	"

* Chemical determination, rest spectrographic.

n.d. = not detected.

The discontinuous yielding and other strain-ageing effects in age-hardening alloys have frequently been ascribed to simultaneous deformation and age-hardening^{2, 5, 8, 10}; on the other hand, similar effects in aluminium-magnesium alloys have been shown to be transient, in the sense that after the yield is completed there is no permanent hardening, and they have been attributed to locking of dislocations by the Cottrell mechanism.¹ The present experiments on age-hardening alloys have been extended to separate these effects.

II.—MATERIALS

The materials studied were: (a) commercial aluminium, (b) aluminium-1½% manganese alloy, (c) an aluminium-magnesium-silicide-type alloy, and (d) a Duralumin-type alloy. All were sheet materials of commercial purity, and their analyses are given in Table I. The commercial aluminium and 1½% manganese alloy were examined in the annealed condition, and the age-hardening alloys were examined as annealed and after solution-treatment and various ageing treatments. The treatments given to produce recrystallized structures of the required grain-size are detailed in Tables II and III or in the text with the results. The grain-sizes were obtained by the intercept method.

each increase. Where creep occurred, that is when deformation continued for some time after applying each load increment, a standard loading rate of 10 lb./min. (or 5 lb./30 sec.) was adopted, the strain being read immediately before each load increment was applied.

At the beginning of each test and during pauses which were introduced to allow controlled strain-ageing, a load of 20 lb. was kept on the specimen in all cases except that of the aluminium-manganese alloy specimen heated at 99° C., which was removed from the apparatus for this treatment. The extensometer was reset to zero after the pauses.

IV.—EXPERIMENTAL RESULTS

1. COMMERCIAL ALUMINIUM

Commercial aluminium, hot rolled to 0.20 in. and then cold rolled (68% reduction) to 0.064 in., was annealed at various temperatures from 375° to 600° C. and water-quenched or furnace-cooled. After the anneal at the lower temperatures, the grain-size was very fine, e.g. 0.026 mm. after annealing at 425° C., but increased somewhat at higher temperatures.

Although smaller stress increments (160 lb./in.²) were used in loading this material than for the others, little tendency to discontinuous yielding could be

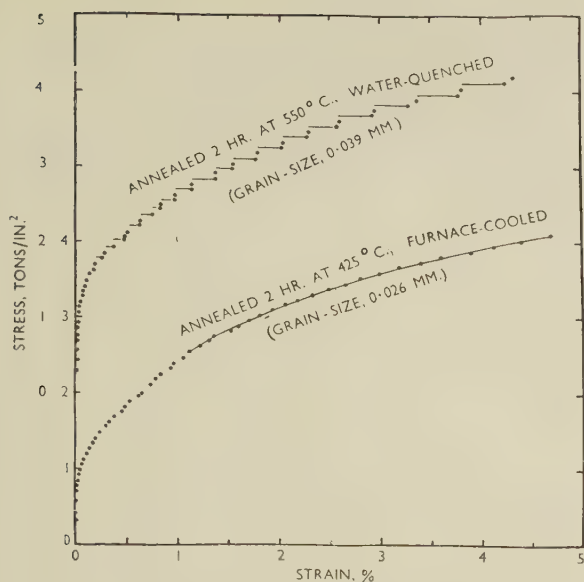


FIG. 2.—Stress/Strain Curves for Commercial-Purity Aluminium Tested at Room Temperature.

detected in stress/strain curves at room temperature, except for specimens annealed at a high temperature. Slow cooling (5°C./hr.) from 500°C. removed the tendency to discontinuous yielding observed in speci-

mens quenched or furnace-cooled from this temperature. Typical stress/strain curves are given in Fig. 2.

2. ALUMINIUM-1 $\frac{1}{4}$ % MANGANESE ALLOY

The stress/strain curves obtained at room temperature were fairly smooth, and reflected only a slight tendency to strain-age, as indicated by some irregularity in the spacing of the points and two or three definite steps in one of the curves (Fig. 3). The curves were practically identical whether, after the final reduction of 77.5% to 0.032 in. thickness, the alloy was annealed for 2 hr. at 400°C. and air-cooled, re-annealed for a further 46 hr. at 400°C. and air-cooled, or re-annealed for 1 hr. at 500°C. and water-quenched. In all three cases back-reflection X-ray photographs taken on the centre sections of the annealed specimens showed only sharp spots, indicating that recrystallization was substantially complete.

On testing at -76°C. , a smooth curve was obtained with no initial (type-A) yield (Fig. 4). A pause of 3 hr. at 20°C. , after pulling to about 2.9% elongation and unloading, produced a slight drop in the stress level of the curve obtained on reloading at -76°C. (Fig. 4). A similar test with a pause of 1 hr. at 99°C. showed a considerable drop in the level of the curve, suggesting that recovery was responsible

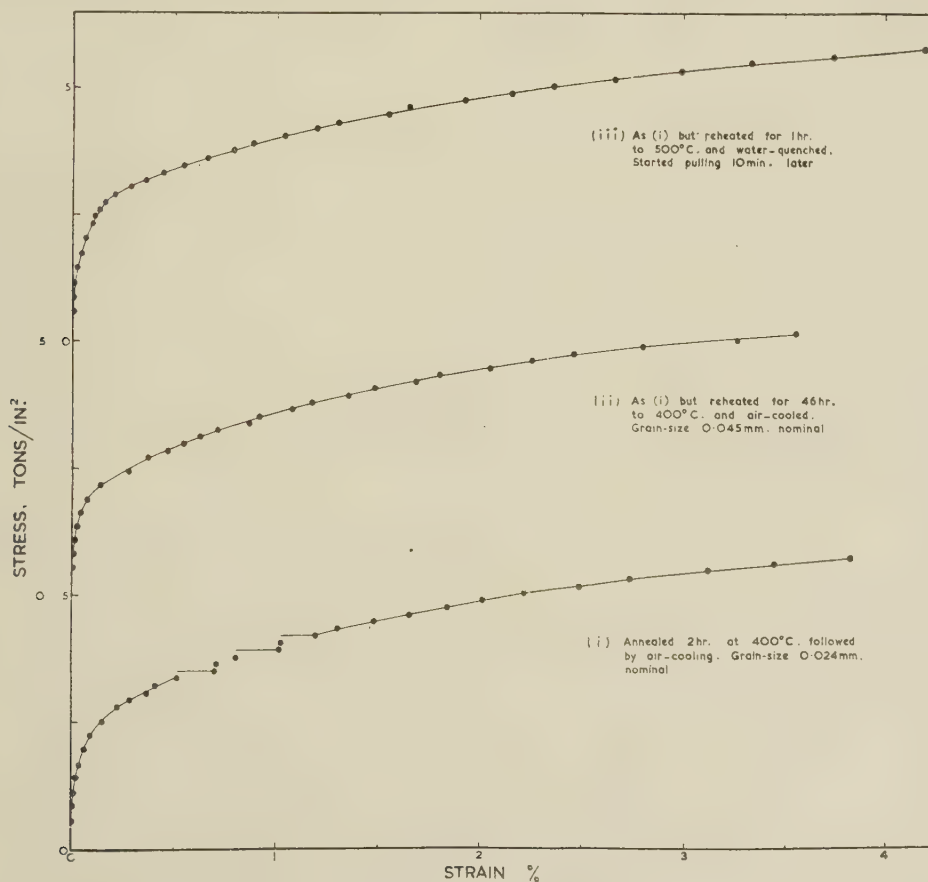


FIG. 3.—Stress/Strain Curves for an Aluminium-1 $\frac{1}{4}$ % Manganese Alloy Tested at Room Temperature.

for the lowering of the curve in both cases and that this was greater than any strain-ageing effect which might be present (Fig. 4). In a further test at -76°C . with a pause of 15 min. at -30°C . (Fig. 4), no strain-ageing was evident after the pause, although the lowering of the curve was now barely perceptible. Thus it seems that the strain-ageing tendency

the annealed material is seen in Fig. 6. As would be expected, strain-ageing becomes less marked as the temperature is reduced, and at -40°C . and below the curves are completely smooth.

Stress/extension curves at -76°C ., with a pause at 20°C . to allow strain-ageing to take place after approximately 2.7% strain, are given in Fig. 7.

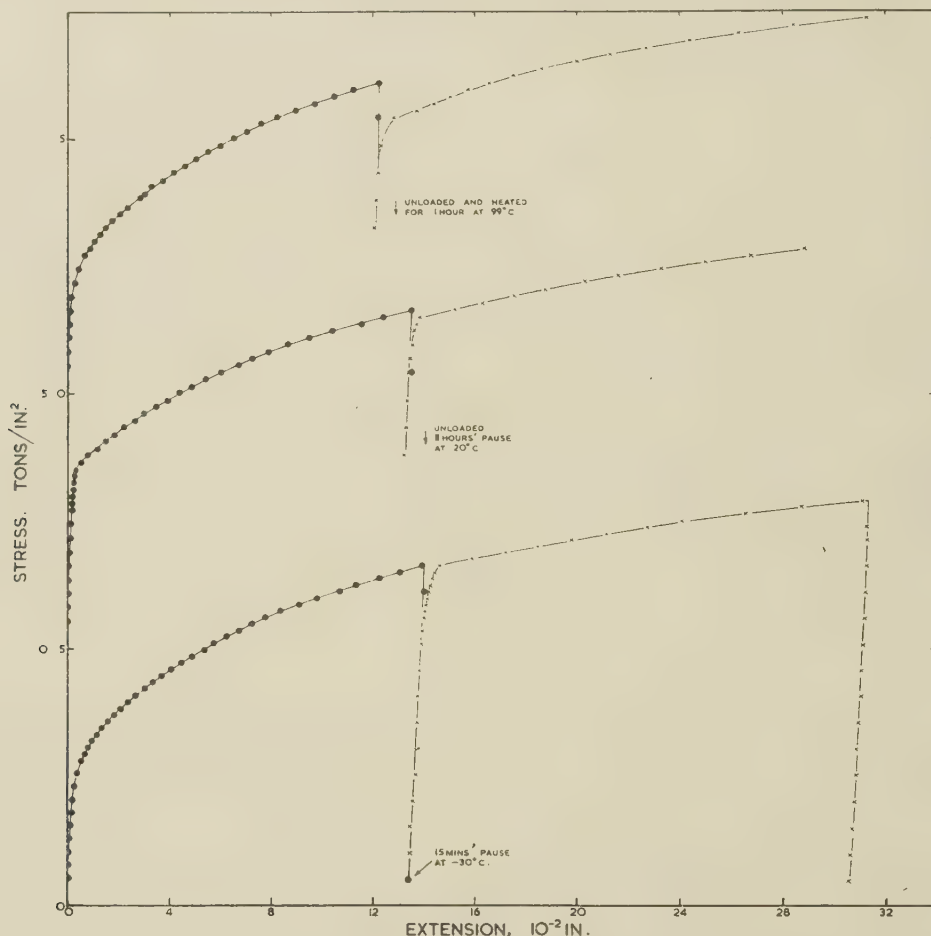


FIG. 4.—Effect of Pausing Temperature and Time on the Stress/Extension Curve of an Aluminium-1½% Manganese Alloy Annealed for 2 Hr. at 400°C . and Air-Cooled, Grain-Size 0.024 mm., Pulled at -76°C .

of this alloy is small. No initial yield point was found in any test.

3. ALUMINIUM-MAGNESIUM-SILICIDE ALLOY

The stress/strain curves obtained for this alloy in various conditions at room temperature are shown in Fig. 5. The annealed and solution-treated materials both show multiple steps, but ageing at room temperature causes the strain-ageing to become sluggish, and after ageing at 170°C . a smooth curve is obtained. There is no large initial yield, and, where the curves are stepped, some continuous plastic strain occurs before the first small steps. The effect of reducing the temperature of testing for

In the annealed material, strain-ageing produced a transient yield, beyond which the original smooth curve was continued. The solution-treated alloy gave a much larger increase of flow stress after the strain-ageing treatment, and the whole level of the stress/strain curve was raised after the yield.

By extrapolating the subsequent curve back to intercept the elastic part of the reloading curve in the manner employed by Lubahn,¹¹ the total increase in flow stress can be analysed into the two parts, σ_p , corresponding to the increase in level of the curve, and σ_s , a transient increase in flow stress corresponding to the yield. Values of these quantities are shown in Table II, and may be compared with the corresponding values for the annealed material.

σ_p may be regarded as a permanent strengthening due to age-hardening, in contrast to σ_s , which may be viewed as a transient increase in flow stress due to strain-ageing according to the Cottrell mechanism, giving rise to a yield point. Lubahn, however, appears to regard these two quantities differently.

showed that, by choosing a suitable time and (reduced) temperature of ageing, σ_p could be reduced to zero, whereas σ_s was only slightly reduced below the value resulting from a 3-hr. pause at 20° C. Thus the transient strain-ageing effect can be physically separated from the permanent hardening effect

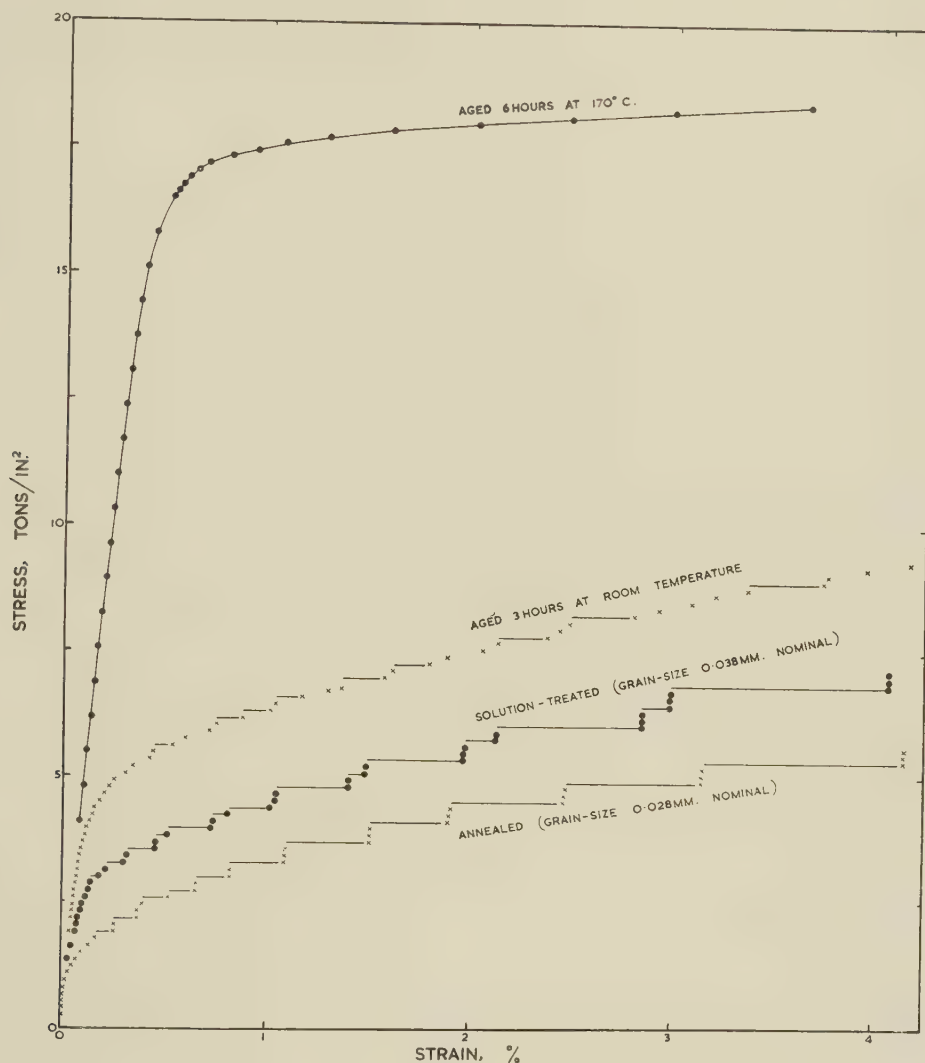


FIG. 5.—Effect of Heat-Treatment on the Stress/Strain Curve of an Aluminium-Magnesium-Silicide-Type Alloy Tested at Room Temperature.

The finding that σ_s for the solution-treated material is larger than for the annealed material (see Table II) is to be expected on the Cottrell theory, since more solute atoms will be available to anchor dislocations in the former, while, similarly, in the fully aged material the solution is effectively depleted in solute by ageing and no strain-ageing is found.

A series of solution-treated specimens were pulled at -76°C . to about 2.8% permanent strain, unloaded, warmed up, and, after ageing at chosen temperatures, retested at -76°C . The results (Table II and Fig. 8)

and this separation justifies the analysis of the increase in flow stress into the two parts, σ_s and σ_p .

The low-temperature tests show that no detectable initial yield is present in any condition.

4. DURALUMIN-TYPE ALLOY

The results obtained were somewhat similar to those for the magnesium-silicide alloy. The room-temperature stress/strain curves (Fig. 9) are stepped for the annealed and solution-treated materials, and,

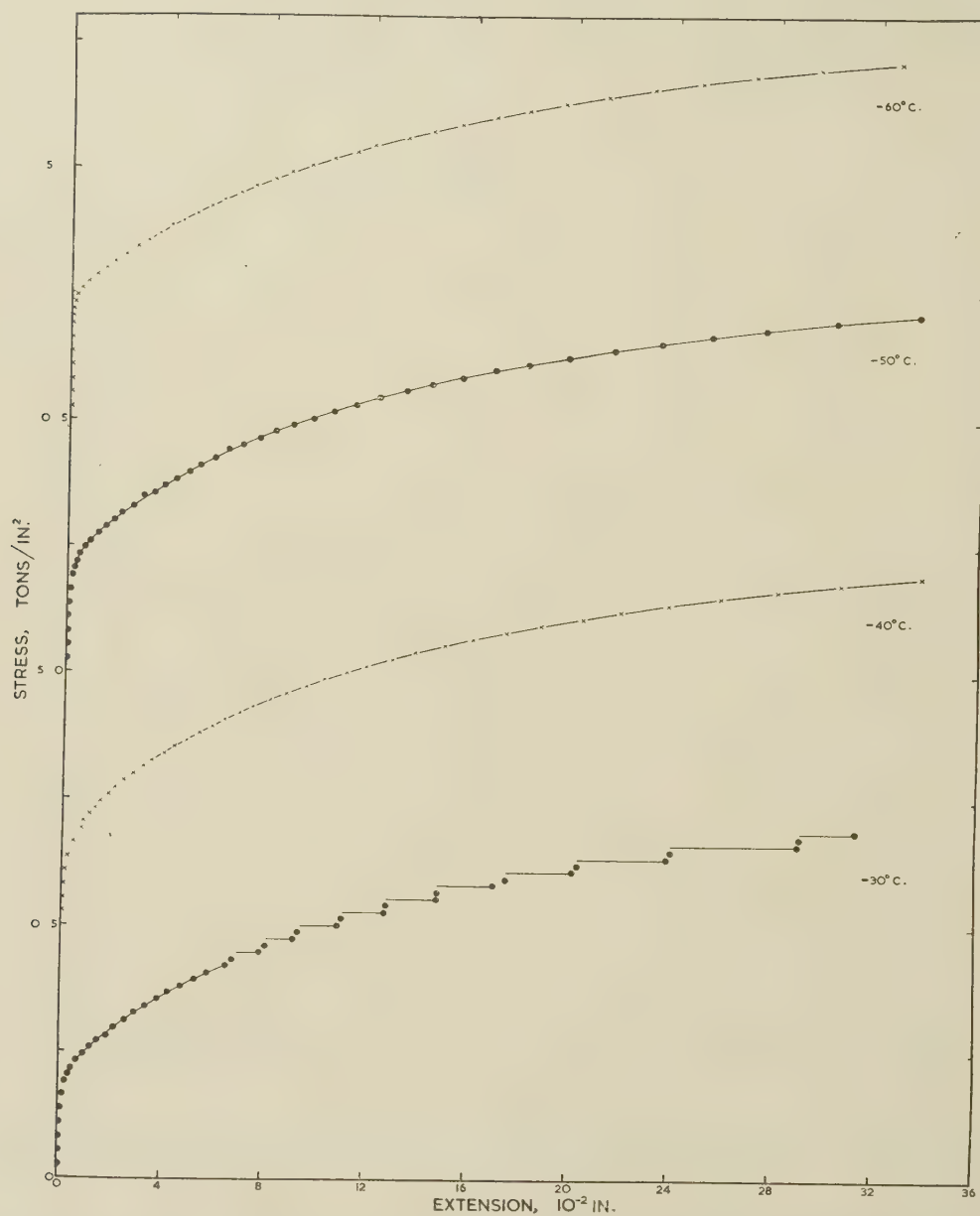


FIG. 6.—Effect of Temperature on the Stress/Extension Curve of an Annealed Aluminium-Magnesium-Silicide-Type Alloy of 0.028 mm. Grain-Size.

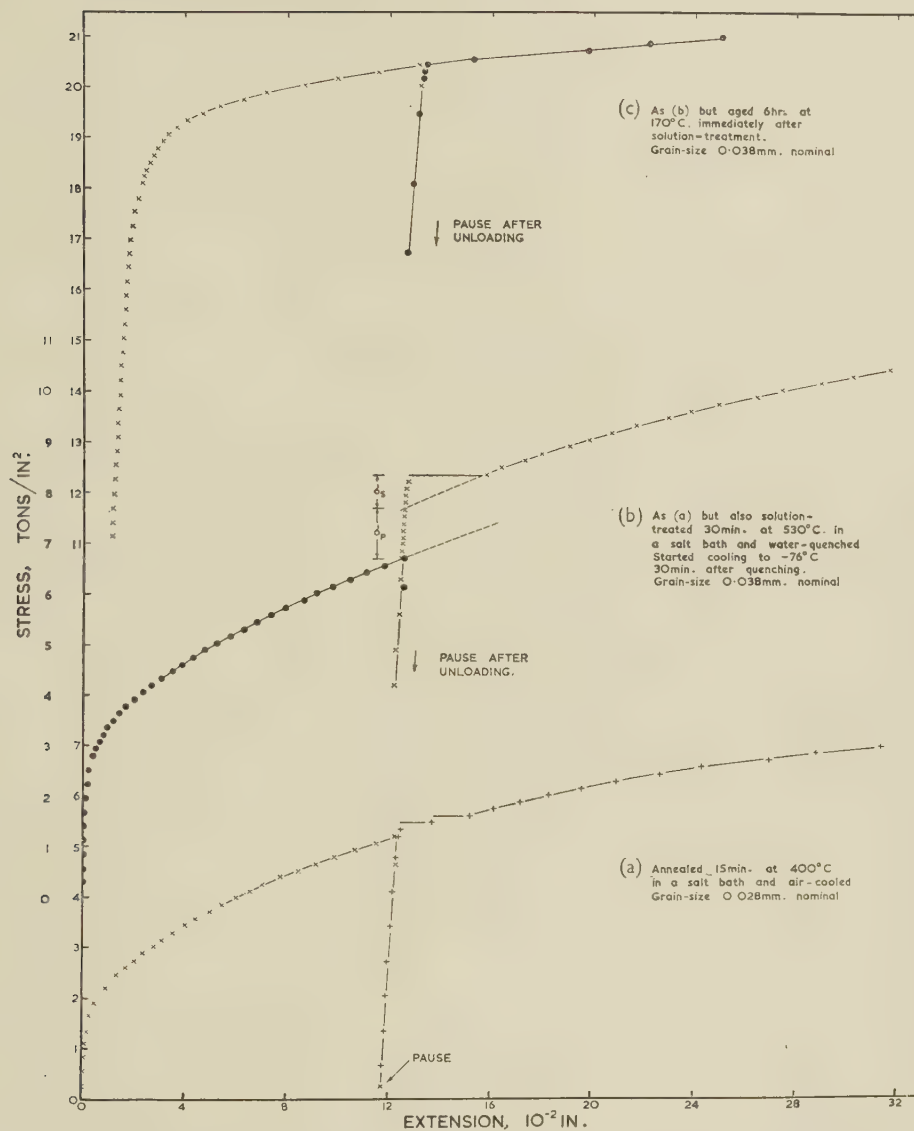


FIG. 7.—Effect of Prior Heat-Treatment on the Ageing After Strain of an Aluminium-Magnesium-Silicide-Type Alloy. Specimens pulled at -76°C . and, after a 3-hr. pause at 20°C ., repulled at -76°C .

TABLE II.—Summarized Results of Tests on an Aluminium-Magnesium-Silicide-Type Alloy.

Final Cold Reduction, %	Thick-ness as Tested, in.	Heat-Treatment						Grain-Size, mm.	Testing Temp., °C.	0.1% Proof Stress, tons/in. ²	Pre-stress, tons/in. ²	Plastic Pre-stretch		Pause (un-loaded)		Yield			
		Annealing		Solution-Treatment		Ageing						Increase in Flow Stress, tons/in. ²		Extension at Step					
		hr.	°C.	hr.	°C.	hr.	°C.					Total	σ_s	σ_p	10 ⁻² in.	%			
		10 ⁻² in.	%																
51	0.064	0.25	400 ° A.C.					0.028	-76	2.10	5.44	12.08	~2.72	3	20	0.28	0	1.91	~0.43
"	"	"	"					"	"	2.00	5.21	11.72	~2.65	3	"	0.27/0.41	0	1.26 + 1.46 = 2.72	~0.61
"	"	"	"					"	-60	2.64	"	"	"	"	"	"	"	"	"
"	"	"	"					"	-50	2.45	"	"	"	"	"	"	"	"	"
"	"	"	"					"	-40	1.92	"	"	"	"	"	"	"	"	"
"	"	"	"					"	-30	2.25	"	"	"	"	"	"	"	"	"
"	"	"	"					"	r.t.	1.72	"	"	"	"	"	"	"	"	"
"	"	"	"					"	"	1.64	"	"	"	"	"	"	"	"	"
51	0.064	0.25	400 ° A.C.	0.50	530 ° W.Q.	0.33	r.t.	0.038	-76	2.98	6.42	11.77	~2.66	3	20	1.67	0.57	1.10	2.82
82	0.024	"	"	"	"	0.50	"	"	"	3.12	6.70	11.79	~2.66	"	"	1.67	0.67	1.00	3.09
"	"	"	"	"	"	0.45	"	0.035	"	3.43	7.17	12.51	~2.82	3.1	0	1.10/1.28	0.55/0.73	0.55	1.65 + 2.19 = 3.84
"	"	"	"	"	"	"	"	"	"	3.57	6.98	12.11	~2.73	0.17	"	0.74	0.59	0.15	"
"	"	"	"	"	"	0.27	"	"	"	3.53	7.17	12.63	~2.85	0.75	"	0.55	0.55	0	3.17
"	"	"	"	"	"	0.39	"	"	"	3.70	7.37	13.29	~3.00	0.17	"	0.37	0.37	0	2.96
"	"	"	"	"	"	0.42	"	"	"	3.12	6.99	12.03	~2.72	0.25	"	0.38	0.38	0	2.48
51	0.064	0.25	400 ° A.C.	"	"	0.07	"	0.038	r.t.	3.05	"	"	"	"	"	"	"	"	1.84
"	"	"	"	"	"	3	"	"	"	4.69	"	"	"	"	"	"	"	"	"
51	0.064	0.25	400 ° A.C.	0.50	530 ° W.Q.	6	170 A.C.	0.038	-76	18.26	20.46	10.66	~2.41	3	20	0	"	"	"
"	"	"	"	"	"	"	"	"	"	18.23	20.46	10.89	~2.45	"	"	0	"	"	"
"	"	"	"	"	"	"	"	"	"	16.45	"	"	"	"	"	"	"	"	"
"	"	"	"	"	"	"	"	"	"	16.30	"	"	"	"	"	"	"	"	"

TABLE III.—Summarized Results of Tests on a Duralumin-Type Alloy.

Final Cold Reduction, %	Thick-ness as Tested, in.	Heat-Treatment						Grain-Size, mm.	Testing Temp., °C.	0.1% Proof Stress, tons/in. ²	Pre-stress, tons/in. ²	Plastic Pre-stretch		Pause (un-loaded)		Yield						
		Annealing		Solution-Treatment		Ageing						10 ⁻² in.	%	hr.	°C.	Total	σ _s	σ _p	Increase in Flow Stress, tons/in. ²		Extension at Step	
		hr.	°C.	hr.	°C.	hr.	°C.												10 ⁻² in.	%		
		hr.	°C.	hr.	°C.	hr.	°C.					10 ⁻² in.	%	hr.	°C.	Total	σ _s	σ _p	10 ⁻² in.	%		
78	0.026	1.5	350 A.C.					0.024	-76	5.16 5.00 5.14 5.35 5.15 5.22 B 4.82 4.80	10.62 10.64	12.25 11.59	2.76 2.61	2.08 3	20	0.49 0.49	0	2.57 1.68	0.58 0.38			
78	0.026	1.5	350 A.C.	0.25	510 * W.Q.	0.33 0.30 0.33 3 0.08 0.23 0.50 8 24	r.t. " " " " " " " "	0.022	-76 " " " r.t. " " " " "	7.73 7.75 7.62 7.90 9.20 7.53 B B B 9.42 ~15.60 15.55	13.42 12.91 13.57	11.47 10.99 12.38	2.59 2.48 2.79	3 " 3.08	20 " -76	4.59 4.96 0.99	1.0 1.2 0.99	3.6 3.8 0	2.84 3.82 3.55	0.64 0.86 0.80		
78	0.026	1.5	350 A.C.	0.25	510 * W.Q.	7 " " " " " " "	180 A.C. " " " " " "		-76 " r.t.	26.65 26.30 23.40	29.41 28.48	9.64 5.81	2.17 1.31	3 " "	20 " "	Broke "						
46	0.064	0.25	510 * W.Q.	24 +16	180 A.C. 220 A.C.		-76	23.97 14.37	20.23	10.45	2.36	3	20	0						

B = 1st yield below this stress. * Salt bath. A.C. = Air-cooled. W.Q. = Water-quenched. r.t. = Room temperature.

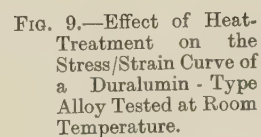
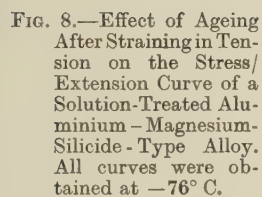
B = 1st yield below this stress.

* Salt bath.

A.C. = Air-cooled.

W.Q. = Water-quenched.

r.t. = Room temperature.



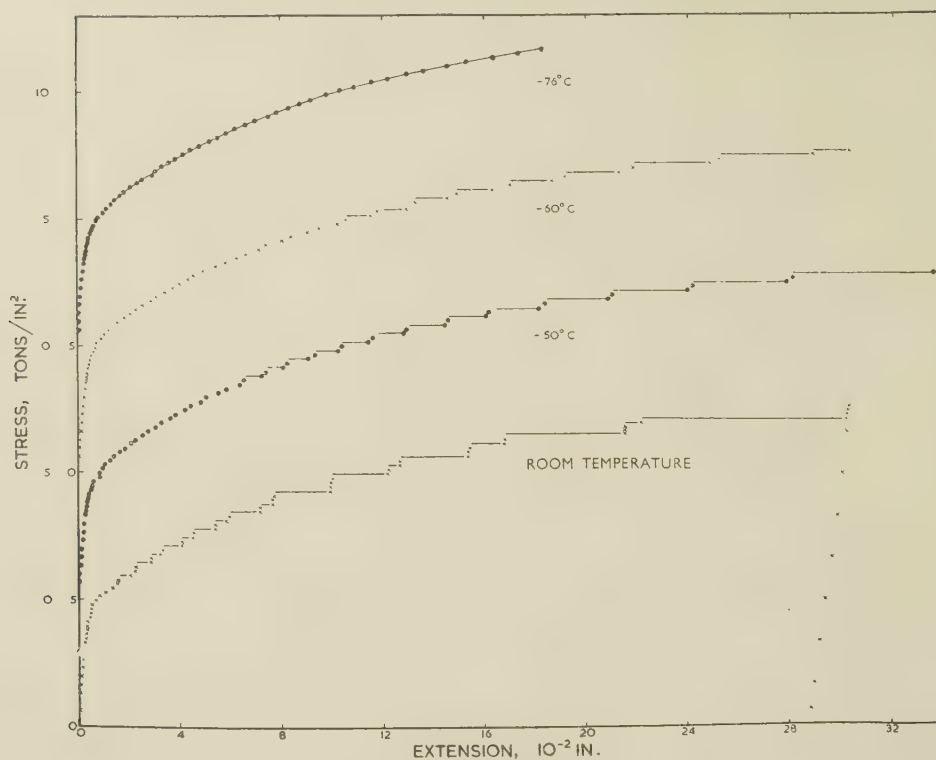


FIG. 10.—Effect of Testing Temperature on the Stress/Extension Curve of an Annealed Duralumin-Type Alloy of 0.024 mm. Grain-Size.

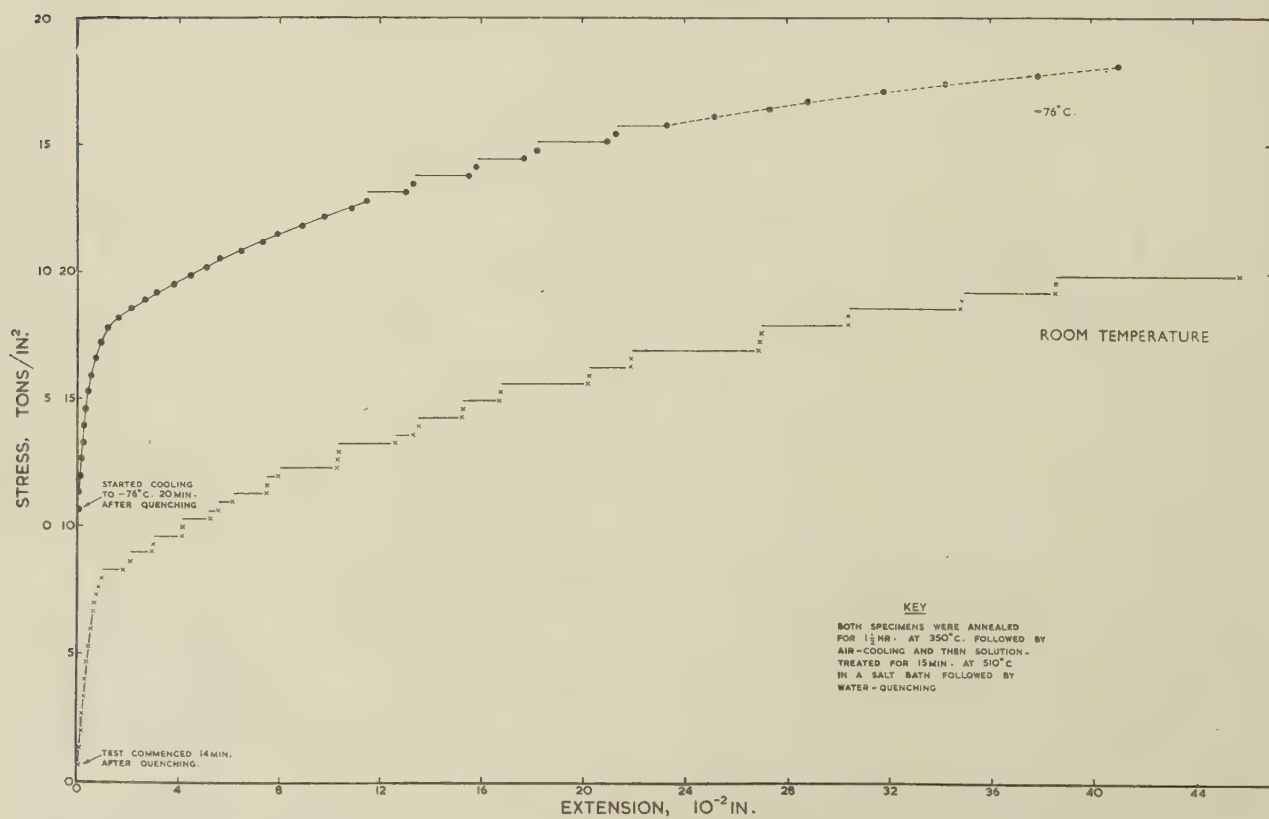


FIG. 11.—Effect of Testing Temperature on the Stress/Extension Curve of a Solution-Treated Duralumin-Type Alloy of 0.022 mm. Nominal Grain-Size.

as in the other alloy, the steps tend to disappear on ageing. After 7 hours' ageing at 180°C ., however, there is still a slight tendency to strain-age, indicated by the irregularity of the points on the curve, and on

is reduced, but persists to a lower temperature than it does in the magnesium-silicide alloy, the behaviour in this respect being more like that of the $3\frac{1}{2}\%$ magnesium alloy.¹ In the solution-treated alloy, some

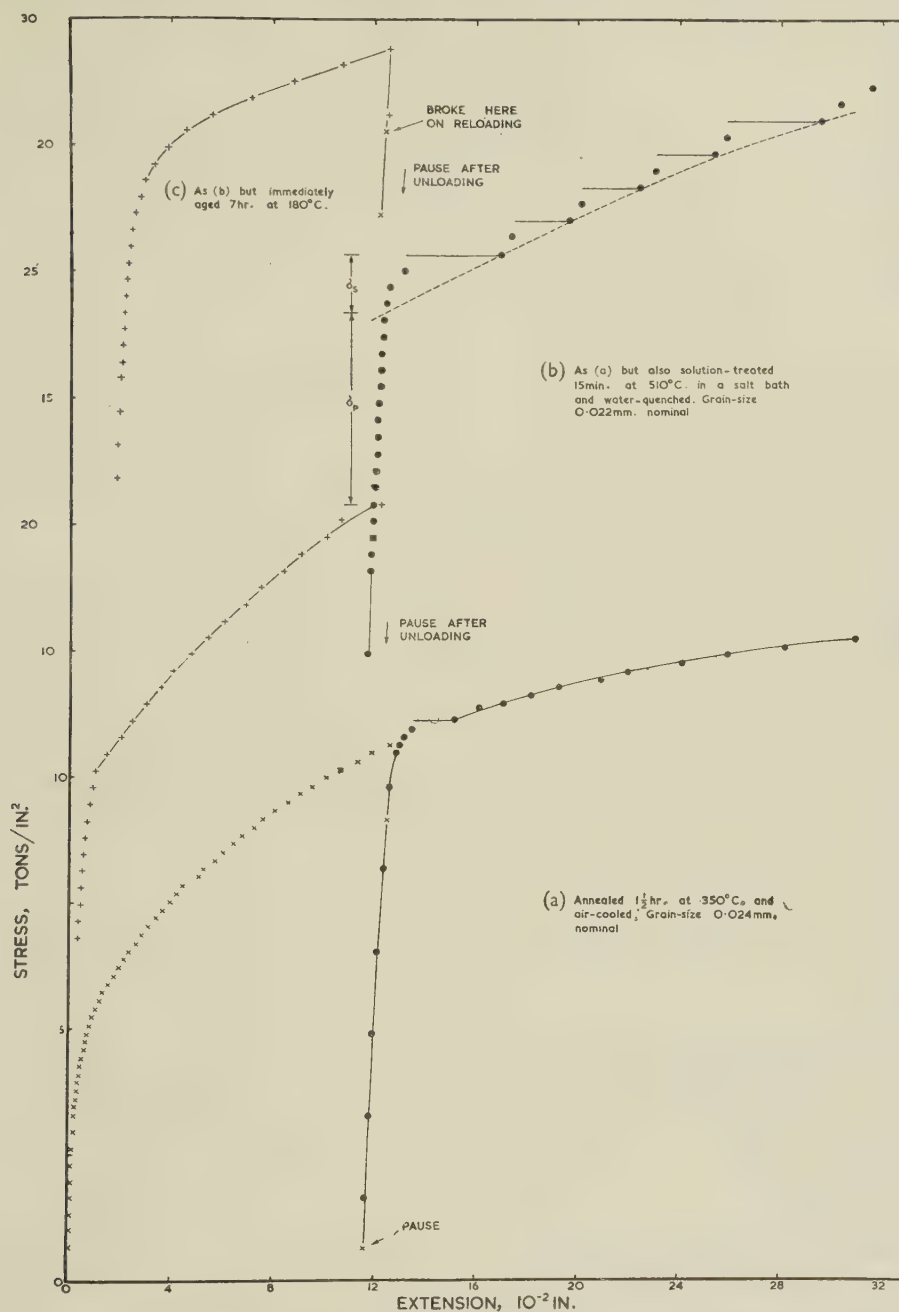


FIG. 12.—Effect of Prior Heat-Treatment on the Ageing After Strain of a Duralumin-Type Alloy. Specimens pulled at -76°C . and, after a 3-hr. pause at 20°C ., repulled at -76°C .

pulling to fracture the characteristic type-B markings (ripple markings) appeared on the surface indicating definite discontinuous yielding at higher strains.

The effect of reducing the testing temperature for the annealed material is seen in Fig. 10. Strain-ageing is progressively suppressed as the temperature

strain-ageing occurs after about $2\frac{1}{2}$ –3% strain, even at -76°C . (Fig. 11).

Stress/extension curves at -76°C ., with a pause at 20°C ., are shown in Fig. 12. The increase in flow stress brought about by strain-ageing is much greater for the solution-treated than for the annealed material

(see also Table III). The artificially aged material persistently broke on reloading before the original stress was reached. As in the uninterrupted tests at -76°C ., the solution-treated alloy gave steps at the higher strains, i.e. after the pause.

By the same treatment as before, the increase in flow stress on strain-ageing can be separated into parts, σ_s and σ_p , although less exactly because of the subsequent steps in the curve. For this purpose the curve after the yield step is clearly to be taken as that passing through the ends of the later steps, since these are upward departures from the basic

temperature for 3 hr. there does appear to be a small initial yield step (Fig. 13) which was absent after artificial ageing. This initial yield point is very much smaller than those found for aluminium-magnesium alloys of comparable grain-size.

V.—DISCUSSION

None of the materials tested showed a pronounced initial yield point, although they were in the grain-size range in which a large initial yield (order of 1% elongation) is found in annealed aluminium-mag-

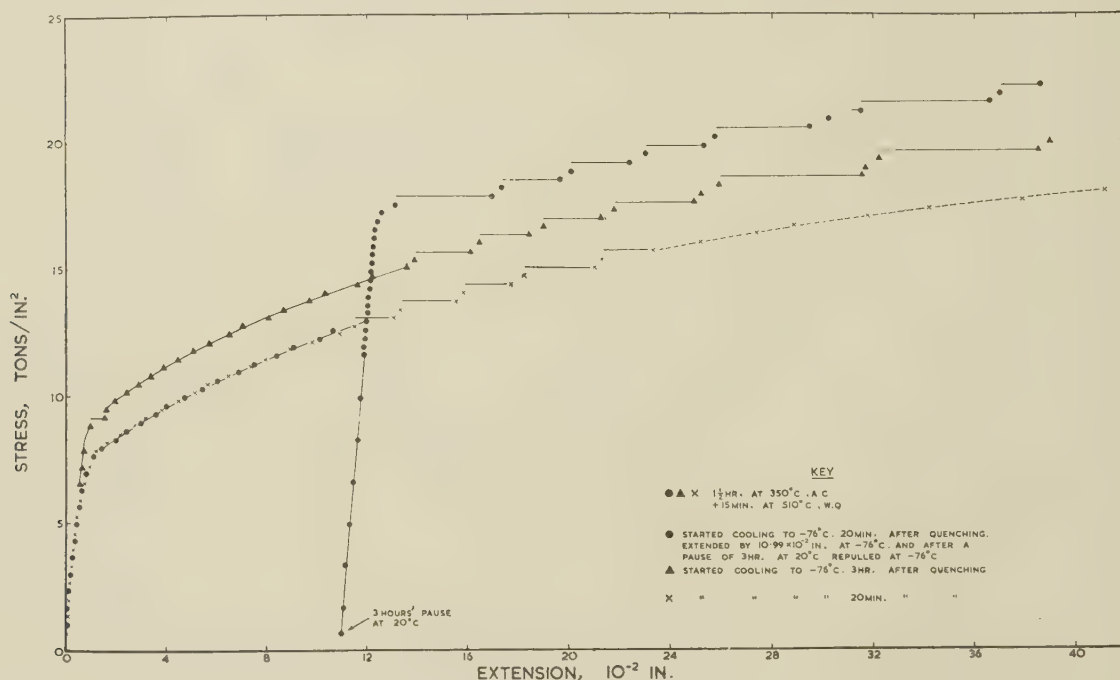


Fig. 13.—The Effect of Strain on the Ageing of a Duralumin-Type Alloy After Solution-Treatment. Nominal grain-size 0.022 mm. Specimens tested at -76°C .

curve. As in the other alloy, σ_s was higher for the solution-treated than for the annealed alloy, the average values of the results given in Table III being 1.1 and 0.49 tons/in.², respectively, for similar strain-ageing treatments, in accord with the fact that a large number of solute atoms would be available to anchor dislocations in the former material.

It was found that previous tensile straining at -76°C . accelerated the age-hardening of the alloy at room temperature. Thus, in tests at -76°C ., the increase in the general stress level of the curve produced by a pause (unloaded) of 3 hr. at 20°C . after a plastic strain of about 2.5% was approximately double that produced by the same ageing treatment before any strain was applied (Fig. 13).

It will be noted that in most of these tests at -76°C . on the Duralumin-type alloy, the stress/strain curve is initially completely smooth, i.e. there is no detectable initial yield, but in the materials aged at room

temperature for 3 hr. there does appear to be a small initial yield step (Fig. 13) which was absent after artificial ageing. This initial yield point is very much smaller than those found for aluminium-magnesium alloys of comparable grain-size.¹ It seems probable therefore that strong effects of this kind are peculiar to the solute magnesium. A trace of an initial yield is found in the Duralumin-type alloy aged for a short time (3 hr.) at room temperature. If this is analogous to the initial yield in aluminium-magnesium alloys, which is believed to be due to an increase in the concentration of magnesium atoms in solid solution at the grain boundary ("equilibrium segregation"), the occurrence of the effect after this particular heat-treatment is readily understandable; the largest possible amount of copper is then in solution and time has been allowed for some diffusion to the grain boundaries to take place. Further ageing would effectively remove copper from solution, so removing the yield point.

All the materials showed marked multiple yielding at room temperature due to strain-ageing during the test, except the commercial aluminium and the aluminium-1½% manganese alloy, in which the effects

were very slight, and the aluminium-magnesium-silicide and Duralumin-type alloys after considerable ageing. In the latter two alloys, the greater the degree of ageing the higher was the strain at which the curves first became stepped. The Duralumin-type alloy showed slight discontinuous yielding even after ageing at 180° C., but the aluminium-magnesium-silicide alloy showed no evidence whatever of discontinuous yielding in the artificially aged condition.

The slight effects observed in the aluminium-manganese alloy could be attributed to the copper content (0.15%) in view of the observations of McReynolds.² The commercial aluminium, which contained only 0.02% copper, also showed very slight effects, but these were more marked after high-temperature treatments, and may well be due mainly to dissolved silicon or iron.

In the aluminium-magnesium alloys the increase in flow stress due to strain-ageing is entirely transient, there being no increase in the general level of the stress/strain curve after the yield,¹ and it is concluded that the mechanism of strain-ageing must be of the Cottrell type. In the age-hardening alloys studied here, strain-ageing effects such as multiple yielding have hitherto been attributed to simultaneous straining and age-hardening. The experiments on ageing after straining at low temperatures show that age-hardening does indeed account for a part, σ_p , of the increase in flow stress on ageing after straining, and that the ageing may be accelerated by straining. There remains, however, an increase in the flow stress, σ_s , which is purely transient and cannot be accounted for in this way. This transient hardening is more rapid than the permanent hardening and can be made to occur under conditions in which no permanent hardening takes place. It cannot therefore be due to normal ageing, whether strain-accelerated or not, because normal ageing would raise the whole level of the curve, and it seems reasonable to attribute the transient hardening, σ_s , to true strain-ageing according to the Cottrell mechanism. The transient hardening is the feature associated with the discontinuous yield on strain-ageing, and is thus responsible for the multiple discontinuous yielding in tests at room temperature.

VI.—CONCLUSIONS

(1) An initial yield point (type *A*), such as occurs in testing the annealed commercial aluminium-3½% magnesium alloy, was not found in alloys in which magnesium was not the major alloying constituent, even when the alloys were fine-grained. A possible exception was a Duralumin-type alloy, aged for 3 hr. at room temperature, which showed a small initial yield point; this was absent, however, after artificial ageing.

(2) All the alloys examined showed multiple discontinuous yielding at room temperature, except an aluminium-magnesium-silicide alloy fully aged at 170° C. and the aluminium-1¼% manganese alloy. In the latter, faint indications of a similar effect were obtained, and slight effects were also obtained in commercial aluminium after heating to a high temperature. Where marked discontinuous yielding was found, it was confirmed to be a strain-ageing effect.

(3) The materials which showed this effect could be separated into two groups. In the first group, the increase in flow stress produced by ageing after strain was a purely transitory effect, the stress/strain curve after the new yield point being a continuation of the original curve, while in the second there was also a transitory effect but the whole level of the curve was raised. The second group comprised only the age-hardenable alloys in the solution-treated condition. The behaviour of this group is attributed to ordinary age-hardening (which can be accelerated by the prior strain) proceeding concurrently with true strain-ageing of the Cottrell type. The contributions of the two effects could be separated.

(4) For the age-hardening alloys, the true strain-ageing is greater for the solution-treated condition than for the annealed condition, and much reduced or absent in the fully age-hardened alloys. These effects can be attributed to variations in the amount of alloying elements in true solution.

ACKNOWLEDGEMENT

The author is indebted to the Director and Council of the British Non-Ferrous Metals Research Association for permission to publish this paper.

REFERENCES

1. V. A. Phillips, A. J. Swain, and R. Eborall, *J. Inst. Metals*, 1952-53, **81**, 625.
2. A. W. McReynolds, *Trans. Amer. Inst. Min. Met. Eng.*, 1949, **185**, 32.
3. W. Rosenhain and S. L. Archbutt, 10th Report to the Alloys Research Committee (*Inst. Mech. Eng.*), 1912, p. 319.
4. H. Chossat, *Rev. Mét.*, 1950, **47**, 167.
5. A. Portevin and F. Le Chatelier, *Compt. rend.*, 1923, **176**, 507.
6. C. F. Elam, *Proc. Roy. Soc.*, 1938, [A], **165**, 568.
7. E. W. Fell, *Iron Steel Inst., Carnegie Schol. Mem.*, 1937, **26**, 123.
8. R. J. Anderson, *Trans. Amer. Soc. Test. Mat.*, 1926, **26**, (II), 349.
9. M. Kuroda, *Sci. Papers Inst. Phys. Chem. Research (Tokyo)*, 1938, **34**, 1528.
10. J. D. Lubahn, *Trans. Amer. Inst. Min. Met. Eng.*, 1949, **185**, 702.
11. J. D. Lubahn, *Trans. Amer. Soc. Metals*, 1952, **44**, 643.

Discussion

The Effects of Certain Solute Elements on the Recrystallization of Copper

By V. A. PHILLIPS and ARTHUR PHILLIPS

(*Journal*, this vol., p. 185.)

Dr. MAURICE COOK * (Member) and Dr. T. LL. RICHARDS † (Member): We welcome this paper, since it is a natural extension of our own theory. The authors are to be congratulated on the wide scope of their research and on the wealth of useful results they have obtained. While not disagreeing with their main conclusions, we should, however, like to sound a note of warning, and in particular, draw attention to a number of pitfalls which lie in the path of those engaged in this type of work.

To this end, it is necessary to outline the steps in the development of the theory. It goes without saying that in measurement of isothermal recrystallization rate, the fraction of metal recrystallized at any stage must be determined. It may be possible to make a direct determination of the fraction recrystallized, but it is generally more convenient to observe changes in a secondary property such as hardness, provided the relation between the property and fraction recrystallized can be established, it being still more convenient if the relationship is linear.

As in our own work, the authors have chosen hardness as the secondary property for observation of annealing rate. While hardness determination is very convenient, it suffers from one rather serious drawback arising from the localized nature of the tests and the inhomogeneity of partly recrystallized metal. This drawback is reflected very noticeably in the scatter of the experimental results in the calibration of hardness against percentage recrystallization in Fig. 23 (p. 193) of the paper. We should point out also that the calibration in Fig. 23 refers specifically to recrystallization of copper or its alloys to cube texture on annealing and does not necessarily apply to alloys which do not recrystallize in the same manner.

Having acquired the data, we must next consider how to carry out the analysis. The obvious first step is to examine whether rate of recrystallization follows that of a simple first-order process typical of unimolecular reaction. It was readily apparent, from the results we obtained on isothermal annealing rates of heavily rolled copper, that the process was not of the first-order type. That is, $\ln \frac{1}{1-x}$ did not conform to the

relation $\ln \frac{1}{1-x} = kt + c$, where k and c are constants and x and t represent fraction recrystallized and time of annealing, respectively. We noticed, however, that the relation $\ln \frac{1}{1-x} = kt^2 + c$ fitted our results fairly well. This suggested that a second process was involved. Since there was no structural evidence in support of this view, we postulated an initial recovery process of slow exponential rate. It should be emphasized that our method was developed on the basis that recovery was slow, and it is probably not legitimate to extend the treatment as Thorley ‡ has done to the case where recovery is rapid and proceeds to completion before recrystallization.

As the authors of the present paper point out, Thorley's treatment leads to a linear relation, equation (4), p. 186. In the example which the authors have chosen for illustration (Fig. 27, p. 199), the last two points are well off the straight line. The question therefore arises as to whether this deviation is real or only experimental error. The hardness data in the present investigation are not sufficiently accurate to enable us to come to any definite conclusion. Smoother annealing curves are obtained by thermoelectric measurement, and these exhibit a deviation similar to that in Fig. 27. This suggests

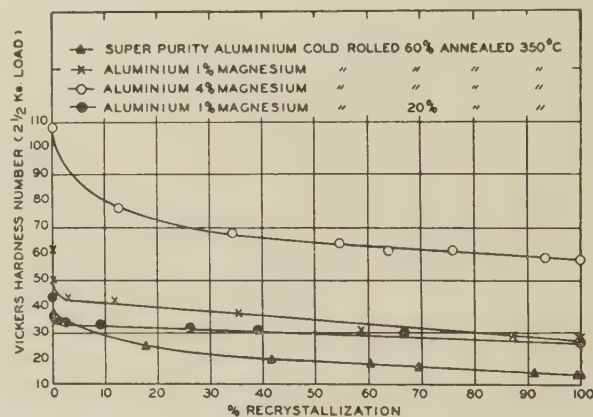


FIG. A

that successive processes are involved for which standard methods of analysis are available.

Mr. E. C. W. PERRYMAN, § M.A., A.I.M. (Member): I would like to ask the authors whether they are quite satisfied that the softening on annealing is proportional to the percentage recrystallization for all the materials tested, and furthermore does this hold for other copper-base alloys? With super-purity aluminium and super-purity-base aluminium-magnesium alloys, the relationship between hardness and percentage recrystallization is by no means so simple. Fig. A. shows the Vickers hardness number plotted against percentage recrystallization for super-purity aluminium and two alloys containing 1% and 4% magnesium, respectively. To determine the percentage recrystallization, specimens were electropolished and anodized, five photographs were taken for each annealing time, and the recrystallized areas measured by means of a planimeter. The five areas were averaged and the percentage recrystallization obtained. It is clear from the curves shown in Fig. A that it would be a dangerous procedure to determine

* Joint Managing Director, Imperial Chemical Industries, Ltd., Metals Division, Birmingham.

† Research Physicist, Imperial Chemical Industries, Ltd. Metals Division, Birmingham.

‡ N. Thorley, *J. Inst. Metals*, 1950, 77, 141.

§ Aluminium Laboratories Limited, Kingston, Ontario, Canada.

the percentage recrystallization from softening curves of aluminium and its alloys.

In super-purity aluminium and in alloys containing 0.5 and 1.0% magnesium, cold rolled from 20 to 80% and annealed at 250°, 375°, and 400° C., I have observed that recrystallization and recovery proceed together. Moreover, recrystallization nuclei have been observed only in unrecovered or partially recovered areas, and have never been observed in fully recovered areas, that is in areas showing a polygonized structure. These have been shown to be fully recovered by micro-hardness tests. It seems, therefore, that the assumption made in the theory of Cook and Richards that recrystallization does not proceed until recovery is completed, cannot be applied to aluminium and its alloys. Have the authors any direct experimental evidence that this occurs in copper? The fact that the authors' results can be fitted to the equation derived from the theory of Cook and Richards is no proof that recovery must be completed before recrystallization can begin, because an equation of exactly the same form has been derived by Avrami from considerations of N and G which does not necessitate the above-mentioned assumption.

From the authors' photographs it would appear that the new recrystallized grains are far from spherical. Could they say whether they measured the longest or shortest direction for determining G ? In measurements I have recently carried out, the new grains have been elongated, and for super-purity aluminium rolled 60% and annealed at 350° C., G has been found to be 18.0×10^{-4} and 3.3×10^{-4} cm./sec. in the longitudinal and transverse directions, respectively. This difference decreases for smaller amounts of cold work and appears to be connected with the texture.

The authors give only the as-recrystallized grain-size of a few of the alloys that they have investigated. From these results it would appear that the grain-size is almost entirely controlled by the rate of nucleation, which agrees with my findings on super-purity aluminium and aluminium-magnesium alloys. In view of this, could the authors tell us what effect the addition of 0.0271 at.-% silver and 0.0025 at.-% phosphorus had on the as-recrystallized grain-size? From the authors' results, one would expect phosphorus to have a much smaller effect than silver.

Could the authors suggest any mechanism whereby such small amounts of solute can cause such large changes in N and G ? G would probably be decreased if the solute concentrated at the boundary between the new grain and the unrecrystallized matrix, but until we know more about the nucleation process it is difficult to understand how such solute additions can affect N so markedly.

The AUTHORS (*in reply*): Before replying to the numerous points raised, we should like to make good a number of omissions in Figs. 13 and 14. In Fig. 13 (Plate XXVII) the glancing-angle photographs Nos. M101 and 141 correspond to 7½ min., M149 to 15 min., M225, 138, and 147 to 16 hr. annealing time, respectively. In Fig. 14 (Plate XXVIII) photographs Nos. M115 and 123 correspond to annealing times of 30 min. and 16 hr., respectively.

We regret that, owing to the difficulty of etching to distinguish non-cubically-aligned grains from the worked matrix at high magnifications, it was not possible to estimate the percentage recrystallization micrographically, except in materials giving the cube texture. Nevertheless, the linear relation between hardness and percentage recrystallization was found to be valid both for pure copper and for alloys with silver additions, which produced enormous changes in the rate of recrystallization and in the rates of nucleation and growth, and we know of no reason why it should not be valid in the case of the other materials.

Dr. Cook and Dr. Richards have suggested that the scatter of the experimental results in the calibration of hardness against percentage recrystallization in Fig. 23 is due to scatter in the hardness determinations. We would like to point out

that the scatter in Fig. 23 arises mainly from difficulties in estimating the percentage recrystallization micrographically owing to the inhomogeneity of recrystallization in the materials giving the cube texture. This difficulty would not have been overcome if some property other than hardness had been selected for correlation with the percentage recrystallization. Each hardness value in our paper is the average of four or more tests, and these average values gave smooth hardness/annealing-time curves in almost every case, indicating that the average values were satisfactory. In reply to Mr. Perryman, we know of no work on other copper-base alloys in which hardness has been correlated with percentage recrystallization.

The results obtained by Mr. Perryman and shown in his Fig. 4 are of considerable interest and indicate that there are important differences in behaviour between copper- and aluminium-base materials. This is not unexpected, since Tammann* has pointed out that, although in the case of copper, silver, and gold all the properties change in the same temperature interval and in copper, for example, microscopic changes can be observed at the same time, in the case of aluminium, iron, and nickel, the different properties change in different temperature regions. The observation by Mr. Perryman that under his experimental conditions recrystallization and polygonization are competitive processes throws light on these results and emphasizes that it is essential to include detailed micrographic observations in all recrystallization studies.

In determining growth rates, the largest dimension of the largest grain in a section was measured, as stated on pp. 195 and 197. Deviations from a round shape were great only in the case of recrystallized grains having the cube orientation and then only in longitudinal and rolling-plane sections and not in transverse sections. In most cases the growth-rate values were obtained by averaging measurements on both cross and longitudinal sections, as shown in Tables IX and X (p. 197). Owing to the grain shape in materials recrystallizing to the cube texture, the growth rate was sometimes greater when measured on a longitudinal section than when measured on a cross-section. It was never more than twice as great, however.

Mr. Perryman suggests that the as-recrystallized grain-size is almost entirely controlled by the rate of nucleation. If this were so, then alloys P-L(5) and As-H(17), which had rates of nucleation at 215.8° C. more than ten times greater than alloys P-M(6) and P-H(20), should have had much finer grain-sizes than the latter. In fact, the grain-sizes were very similar. Furthermore, one would expect a big change of grain-size with annealing temperature, but this was not observed. In answer to Mr. Perryman's question, the grain-size of the 0.0025 at.-% phosphorus alloy annealed at 215.8° C. was 0.007 mm., as stated in Table III (p. 192). The grain-size of the 0.0271 at.-% silver alloy annealed at 215.8° C. was not measured precisely, but was of the order of 0.025 mm., and this alloy was thus considerably finer-grained than the other cubically aligned materials, which had grain-sizes of the order of 0.1 mm. Our results suggest that the recrystallized grain-size is qualitatively controlled by the ratio G/N , as Anderson and Mehl† found to be the case in rolled aluminium.

It is difficult to suggest a mechanism whereby small amounts of solute can cause large changes in N and G , since no data appear to be available on the diffusion rates of the solutes in severely deformed copper. It is possible, as Mr. Perryman suggests, that the solute atoms are concentrated in special positions, for example, at the boundaries of the growing grains, and in this connection radioisotopes would provide a most useful research tool.

Our paper shows that recrystallization in a range of copper alloys can be accurately described in terms of a two-stage process with separate activation energies, as proposed by Cook

* G. Tammann, *Z. Metallkunde*, 1934, **26**, 97.

† W. A. Anderson and R. F. Mehl, *Trans. Amer. Inst. Min. Met. Eng.*, 1945, **161**, 140.

and Richards, but cannot be viewed as a single-stage process governed by a constant activation energy, except as an approximation when the activation energies for the two stages are nearly equal. There is at present no structural evidence that the two stages correspond to recovery and recrystallization or that recovery is completed before recrystallization begins. It is hoped that our paper will stimulate further investigation of such changes, and copper containing 0.005–0.01 wt.-% arsenic appears to be the most suitable material for such work. If a generally valid relation for the variation of N with annealing time had been obtained, a reaction-rate equation could have been derived in terms of N and G . One would expect this to be similar in form to that derived from the theory of Cook and Richards, which has been shown to fit all the results obtained.

Dr. Cook and Dr. Richards have questioned the validity of Thorley's extension of their treatment to the case where recovery is rapid and proceeds to completion before recrystallization, but without providing any convincing evidence for their change of view. They have drawn attention to the

fact that the last two points in Fig. 27 (p. 199) deviate from the linear relation expected from Thorley's treatment. These deviations were observed in general when recrystallization was over 90% complete, and here the uncertainty in hardness measurement becomes large in relation to the value of $H_h - H_i$ in equation (13) (p. 199), so that it is difficult to say how far the deviation is significant. The interpretation of thermoelectric data is somewhat speculative, since, as far as we know, no one has correlated thermoelectric measurements with the percentage recrystallization determined micrographically. Complications may arise in the later stages of recrystallization owing to impingement of the growing grains.

We agree with Dr. Cook and Dr. Richards that caution is necessary in interpreting reaction-rate data. In particular, we should like to point out that different grains recrystallize at different rates, whereas the rate observations represent an overall picture. For this reason, we think that further advances in recrystallization theory will be achieved by clarification of the structural changes rather than from further analysis of the existing reaction rate data.

By T. P. HOAR,† M.A., Ph.D., F.I.M., MEMBER, and
A. J. P. TUCKER,‡ M.A., Ph.D.

SYNOPSIS

Investigations into the growth and structure of sulphide films on copper, produced under simple conditions in liquid media, are described.

The reaction of copper with sulphur dissolved in benzene produces "cuprous sulphide" of composition between $\text{Cu}_{1.66}\text{S}$ and $\text{Cu}_{1.80}\text{S}$. The attack is not uniform; those parts of the sulphide layer that form the most rapidly have the lowest copper content. The rate of attack increases with sulphur concentration.

The reaction of copper with dilute aqueous ammonium polysulphide solutions for a few minutes produces films showing interference colours, which have been used to estimate the rate of film growth. The rate is initially approximately constant with time ("rectilinear" growth), proportional to the total polysulphide concentration, and increased by increase of the illumination of the tarnishing surface; during the later stages of growth, the rate becomes inversely proportional to film thickness ("parabolic" growth), and much less dependent upon polysulphide concentration and upon intensity of illumination. The rate is increased by increase of $p\text{H}$ of the attacking solution. The results are explained by an extension of the electrochemical theory of film thickening by lattice transport; in the early stages of film growth the major rate-determining process is the arrival by diffusion of active polysulphide ions at the film surface, while in the later stages the rate-determining process is the migration of cuprous ions through the film. The results are compared with those for iodide films on copper and silver, and a general scheme is suggested.

When electrolytically polished copper is tarnished with polysulphide solutions, films of different colours are obtained on each grain. On annealed material, the film on any one grain is of uniform colour, and is monocrystalline. Although grains of many different orientations are present, only relatively few differently coloured films are formed. Many minute polarization figures on each grain are sometimes visible when the specimen is viewed in convergent plane-polarized light, indicating that growth resulting in a monocrystalline film begins from many nuclei. Sulphide films grown on plastically deformed copper are more complicated; heavily worked material shows uneven films, and slightly deformed material gives films showing optical peculiarities at the metal slip bands. The results are compared with similar observations on films of cuprous iodide and oxide on copper and brass and of silver iodide and sulphide on silver.

I.—INTRODUCTION

THE sulphidation of copper is a process as practically important and as theoretically interesting as the oxidation, but has received relatively little fundamental study. Examples of technically undesirable sulphidation reactions are those that occur when copper and its alloys are exposed to hot sulphur-bearing gases, to sulphur-polluted atmospheres, and to sulphur-bearing liquors. On the other hand, the deliberate production of sulphide films on copper is practised for decorative purposes in "oxidized" copper, and has also been used as a metallographic technique in the examination of copper-manganese alloys,¹ of internal oxidation and strains in copper alloys,² of dezincification in brass,³ and of the interdiffusion of nickel and copper.⁴ Furthermore, a widely used process for the bonding of rubber to metal depends upon the interaction of sulphur in the rubber mix with a brass layer previously deposited on the metal.⁵ From the theoretical standpoint, sulphida-

tion reactions afford important parallels and contrasts with the corresponding oxidations, and, along with the similar reactions of metals with the other non-metals wherein films of solid reaction product are formed on the metal surface, constitute a field of study still far from completely explored.

The present investigation was undertaken to gain fundamental knowledge of the growth and structure of sulphide films on copper that might have value from both the practical and theoretical points of view. In the time at our disposal, it has not been possible to make anything like an exhaustive study, and it will be seen that the work reported in each of the three parts of this paper is capable of being greatly amplified, especially from the quantitative point of view; it is hoped to proceed with such work in due course. Nevertheless, it has been possible to obtain new information on the interaction of copper both with sulphur dissolved in benzene and with aqueous polysulphide solutions, and to study the latter reaction microscopically.

* Manuscript received 2 March 1953.

† Lecturer, Department of Metallurgy, Cambridge University.

‡ Formerly Research Student, Department of Metallurgy, Cambridge University; since 1948, with Imperial Chemical Industries, Ltd., Billingham Division, Billingham, Co. Durham.

II.—THE INTERACTION OF COPPER WITH SULPHUR IN BENZENE SOLUTION

1. EXPERIMENTAL TECHNIQUE

(a) *Preparation of Metal Specimens*

The copper used was commercially pure hard-rolled sheet (22 S.W.G.). It was cut into specimens 4×4 cm. and prepared by abrasion with glass paper or by electrolytic polishing, generally followed by an ageing period in a calcium chloride desiccator to allow a reproducible oxide film to grow on the surface. In some experiments the specimens were cathodically cleaned, either before or after the ageing period, in sodium carbonate solution.

(i) *Abrasion*.—The abraded specimens were first degreased by swabbing with acetone, and then abraded with fresh fine glass paper, along the rolling direction, until all original surface imperfections were obliterated. They were then degreased again with acetone, and placed in a desiccator.

(ii) *Electrolytic Polishing*.—The electrolytically polished specimens were first ground on one side as far as 000 Durex emery paper, and then the back, edges, and a soldered-on wire connection were coated with celluloid applied from acetone solution. The specimen was made the anode in a 40 : 60 v/v syrupy phosphoric acid/water bath,⁶ being disposed horizontally with a horizontal cathode 3 cm. above; an e.m.f. of 1.9 V. was applied from an accumulator for 2–4 min. The specimens were cleaned by a jet of distilled water followed by a jet of pure dry benzene, which also dried them; they were then placed in the desiccator.

(iii) *Cathodic Cleaning*.—For cathodic cleaning, the specimen to be cleaned was made the cathode in 5% sodium carbonate solution, a stainless steel anode being used: an e.m.f. of 12 V. was applied for 1 min.; hydrogen was vigorously evolved during the cleaning process. The cleaned specimen was washed with a strong jet of tap water, and then with benzene, or, where no celluloid was present, with acetone. It was placed directly in the corrosive solution, or in the desiccator for ageing.

(b) *Conditions of Reaction*

Definite volumes of various solutions of pure sulphur in dry, redistilled benzene were placed in 600-ml., tall, straight-sided, lipless beakers. The specimens were then inserted, either lying horizontally on the bottom, or standing nearly vertically against the side; clock glasses were placed over the beakers, and they were left in a room kept at $25 \pm 0.5^\circ \text{C}$. Visual observations were made during and at the end of a period of 24 hr., and the specimen was finally also examined microscopically.

(c) *Analysis of Corrosion Product*

In a number of experiments the corrosion product was analysed. Enough material—it was usually flaky and loose when quite dry—was brushed from the specimen, weighed, and dissolved in concentrated

hydrochloric acid saturated with bromine. Sulphate was precipitated and weighed as barium sulphate with the usual precautions, and copper was determined iodometrically in the filtrate.

2. RESULTS AND INTERPRETATION

The results of a number of experiments, selected from many more to show the influence of various factors, are summarized in Table I.

The salient features of the results are as follows. The corrosion product in every case consisted of a black or nearly black, usually fairly thick, but by no means continuous, layer distributed as described below. Beneath the layer the metal was dulled and pitted.

(a) *Influence of Concentration of Sulphur*

The rate of attack during the first few hours was visibly much increased by increase of sulphur concentration in the benzene. After 24 hr., the total amount of attack was in some cases sufficient to remove nearly all the sulphur from the solution; thus, a "vertical" specimen immersed in 250 ml. of solution containing 0.001% w/v sulphur was after 24 hr. only faintly speckled with tiny black spots, whereas one in a 0.005% solution was considerably more attacked (weight gain 0.011 g.) and one in 0.01% solution was completely covered with a thick black layer (weight gain 0.020 g.). It is probable that the rate of attack is, in fact, proportional to the sulphur concentration, as found by Bradley⁷ for the similar reaction of copper with sulphur in carbon tetrachloride solution, but further accurate quantitative experiments are necessary to establish this.

(b) *Distribution of Attack*

The corrosion product first appeared as small black, blue-black, or grey spots. These grew to a considerable thickness—of the order of 100,000 Å., as determined by microscopic focusing—while the surrounding metal remained quite bright. The spots appeared at a large number of places and, on abraded specimens, tended to spread along the abrasion lines rather than across them, so that the corrosion product eventually consisted of a number of mounds elongated in the direction of the abrasion lines (Fig. 8, Plate XCIII). On electrolytically polished specimens, the spots were random and asterisk-shaped, not elongated in any particular direction. Abraded specimens initially aged in air at 25°C . showed in general less attack than similar specimens aged at *c.* 15°C ., on which the air-formed oxide film was presumably thinner and less complete.

In the more concentrated sulphur solutions, the spots grew sufficiently to link up and form an apparently continuous layer. However, if this layer, which with abraded specimens was usually quite loose when dry, was allowed to flake off, it could be seen to be perforated by a number of tiny holes; and the underlying metal, although generally dulled, was covered with a corresponding number of spots of bright, unattacked metal.

TABLE I.—*Summarized Visual Results of Reaction of Sheet Copper Specimens with Sulphur in Benzene Solution.*

Temperature : 25° C.

Time of Attack : 24 hr.

Abrasion along rolling direction of metal, which is "vertical" in "vertical" specimens; except where otherwise stated. For influence of the following factors, compare experiments numbered as shown :

Preparation of Surface (abraded or electrolytically polished) : 3, 4; 5, 6.

Ageing and/or Cathodic Cleaning of Surface : 1, 2; 9, 11; 3, 10, 12; 5, 13, 15; 14, 16; and see footnote *.

Concentration of Sulphur : 6, 7; 9-12, 13-16, 17-20.

Volume of Solution : 13, 21; 14, 22.

Attitude of Specimen : 7, 8; 9, 10; 11, 12; 13, 14; 15, 16; 17, 18; 19, 20; 21, 22

Direction of Rolling and/or Abrasion : 14, 23, 24, 25.

Run	Abraded (A) or Electrolytically polished (E)	Aged for 24 hr. (AG)	Temperature of Ageing, °C.	Cathodically Cleaned (C)	Specimen Attitude : Horizontal (H) or Vertical (V)	Concentration of Solution : % w/v of Sulphur	Vol. of Solution, ml.	Appearance after 24 Hr.	Remarks
1	E	AG	15	...	H	0.001	250	Generally filmed to yellow (1100 Å.). Random black spots.	No change visible after 24 hr. Results given after 48 hr.
2	E	C	H	0.001	250	Fairly evenly filmed to red (1200 Å.). No black spots.	As 1.
3	A	C	V	0.01	250	Blackened; black spots following abrasion lines and thickest at top. Adherent product.	
4	E	C	V	0.01	250	Blackened layer, starting and thickest at top. Adherent product.	Edges of specimen and back surface masked by celluloid.
5	A	C	H	0.005	250	Blackened by spots following abrasion lines, closest at edges of specimen. Partly loose product.	
6	E	C	H	0.005	250	Mostly covered with adherent, random black spots.	As 4.
7	E	C	H	0.001	250	Number of adherent, random black spots; surface generally unfilmed.	As 4.
8	E	C	V	0.001	250	As 7, but spots closest towards top of specimen.	As 4.
9	A	AG	15	...	H	0.01	250	Completely covered with adherent black layer.	
10	A	AG	15	...	V	0.01	250	Completely covered along top and bottom edges; fewer spots across middle.	
11	A	AG	15	C	H	0.01	250	Almost identical with 9. Trace of loose product.	Cathodic treatment before ageing.
12	A	AG	15	C	V	0.01	250	Almost identical with 10. Some loose product, especially across middle.	As 11.
13	A	AG	15	...	H	0.005	250	Continuous grey film around edges; black spots following abrasion lines elsewhere. Adherent product.	
14	A	AG	15	...	V	0.005	250	Grey film across top and bottom of specimen; black spots following abrasion lines across middle.	
15	A	AG	15	C	H	0.005	250	Extremely loose grey layer over surface.	Cathodic treatment before ageing.
16	A	AG	15	C	V	0.005	250	Almost identical with 14, but product very loose.	As 15.

* Experiments 9-20 were repeated with specimens aged at 25° instead of 15° C. The results were similar, except that in each case there were fewer spots and less total attack, and the reaction product was less adherent.

TABLE I—continued.

Run	Abraded (A) or Electrolytically polished (E)	Aged for 24 hr. (AG)	Temperature of Ageing, °C.	Cathodically Cleaned (C)	Specimen Attitude: Horizontal (H) or Vertical (V)	Concentration of Solution: % w/v of Sulphur	Vol. of Solution, ml.	Appearance after 24 Hr.	Remarks
17	A	AG	15	...	H	0.001	250	Slightly tarnished to purple (450 Å.) around edges, generally bright elsewhere. Large number of tiny black spots following abrasion lines.	
18	A	AG	15	...	V	0.001	250	Almost unchanged. One or two spots on each side near top.	Spots probably where specimen held by tongs when placed in position.
19	A	AG	15	C	H	0.001	250	Elongated black spots following abrasion lines and at point where specimen gripped by tongs. Adherent product. Rest of surface bright.	Cathodic treatment before ageing.
20	A	AG	15	C	V	0.001	250	Very such smaller spots closest in narrow band along top edge, following lines of abrasion and mark made by tongs. Loose product, especially across centre.	As 19.
21	A	AG	25	...	H	0.005	500	Similar to 13, but rather more attack. Adherent product.	
22	A	AG	25	...	V	0.005	500	Wide continuous black band across top and bottom edges; black spots along abrasion lines across middle. More attack than in 14. Fairly adherent product.	
23	A	AG	25	...	V	0.005	250	Distribution identical with 14.	Rolling direction vertical, abrasion horizontal.
24	A	AG	25	...	V	0.005	250	Distribution identical with 14.	Abrasion direction vertical, rolling horizontal.
25	A	AG	25	...	V	0.005	250	Distribution identical with 14.	Abrasion and rolling directions horizontal.

These results show clearly that the inception and growth of the sulphide corrosion product is greatly influenced by the state of the original oxide film on the metal surface. It is likely that the initial points of attack are at thin or cracked parts of the oxide film.

The sulphide layer curled up when it flaked off the metal, into rolls of which the axis was parallel to the original abrasion lines; the outside of the layer was the outside of the roll. Thus the upper parts of the layer as it formed must have been in greater compression than the lower. The curling up of separated films that have grown on abraded metal has been observed in many other cases, notably with oxide films on iron⁸ and nickel.⁹ We think that no really satisfactory explanation has yet been given, and that further work—for example on vacuum-annealed abraded metal, and on stressed and strained electrolytically polished metal—is needed to disentangle the possible influences of stress and/or strain in the metal⁹⁻¹¹ and of the geometry of the surface.

Apart from the appearance of individual spots, and the distribution along the abrasion lines, another effect was apparent on all specimens placed nearly vertically in the solutions, i.e. standing on the bottom of the beaker, leaning against the side. This was the production of bands of generally enhanced attack, some 1 cm. wide, near to the top and bottom of the specimen (Fig. 1), and occurred indifferently on specimens with the rolling direction and/or the abrasion direction placed vertically or horizontally. It appears to be due to a more rapid supply of sulphur to the more attacked zones, due to convection currents set up by concentration differences. This explanation receives support from a special series of experiments with 0.01% sulphur solutions, in which specimens disposed as shown in Fig. 1 gave the various distributions of attack illustrated. Such patterns must arise through the initiation of the attack, probably at the top and bottom edges, followed by its spreading out to zones best supplied with fresh sulphur by complicated convection currents.

(c) Composition of Corrosion Product

Films flaked off from the top, middle, and bottom zones of specimens placed "vertically" in a 0.01% w/v solution in benzene gave the analytical results shown in Table II. It will be seen that all the films

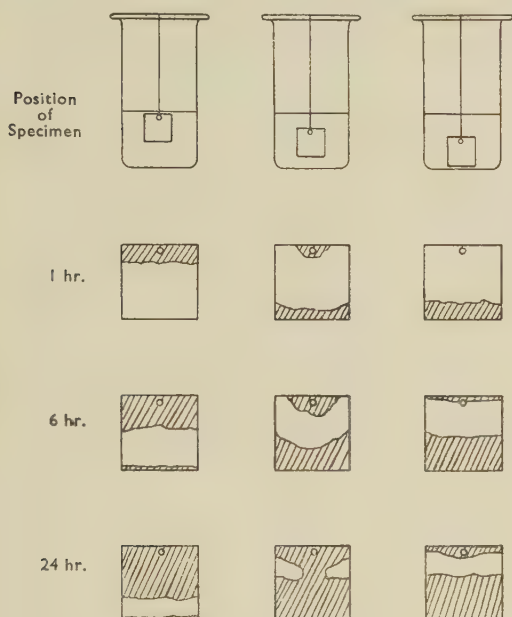


FIG. 1.—Influence of Position of Specimen on Distribution of Attack.

had the composition of non-stoichiometric cuprous sulphide, deficient in copper, the deficiency being the greater for the faster-formed films removed from the top and bottom zones of the specimens.

TABLE II.—Composition of Corrosion Product

Films formed on "vertical" abraded specimens after 24 hr. in 0.01% w/v sulphur in benzene.

Position of Film on Specimen	Copper Found, wt.-%	Sulphur Found, wt.-%	Total Found, wt.-%	Mean Formula
Top	76.7	23.3	100.0	$\text{Cu}_{1.66}\text{S}$
	76.4	23.4	99.8	
	76.8	23.2	100.0	
Middle	78.1	22.2	100.3	$\text{Cu}_{1.80}\text{S}$
	78.0	21.6	99.6	
Bottom	77.4	22.3	99.7	$\text{Cu}_{1.77}\text{S}$
	77.6	21.8	99.4	
Values for stoichiometric cuprous sulphide	79.86	20.14	100.0	Cu_2S

3. DISCUSSION

The above experiments show clearly that the reaction between copper and elementary sulphur dissolved in an organic solvent is influenced in a rather complex way by the initial state of the surface and by the detailed geometry of the experimental arrange-

ment. The second factor, which decides the form of the complicated movements of the liquid that must occur in the absence of deliberate stirring, makes a study of the reaction kinetics difficult without complicated apparatus, and must militate against the precise use of the reaction for the study by simple techniques of tarnish-inhibiting agents for copper, as attempted by Blow and Hopkins.¹² Further, the considerable but incomplete flaking of the sulphide product makes determinations of weight gain or weight loss too approximate for detailed interpretation, besides leading to lack of reproducibility. Nevertheless, the experiments here reported, besides illustrating the known influence of oxide films in partly inhibiting sulphidation,¹³ demonstrate qualitatively the marked dependence of the rate of sulphidation on the sulphur concentration, and show that the reaction product is cuprous sulphide deficient in copper, the deficiency increasing with increase of rate of reaction, and thus presumably with increase of local sulphur concentration.

The marked dependence of the rate of sulphidation on sulphur concentration shows that the rate-determining step in the process is the arrival of sulphur at the copper surface by diffusion or convection, as pointed out by Bradley⁷ for the similar reaction using carbon tetrachloride solutions, and that neither diffusion processes within the sulphide film nor electron-transfer processes are rate-determining. The fact that the sulphide product appears as a relatively loose, rapidly forming layer of highly copper-deficient cuprous sulphide is in harmony with this hypothesis. The growth of the solid sulphide must occur by the lattice-transport mechanism given by Wagner¹⁴ and interpreted electrochemically by Hoar and Price;¹⁵ and for rapid, non-rate-determining, lattice transport at room temperatures a highly defective lattice having high electrical conductivity is essential. We may note that while the conductivity of stoichiometric cuprous sulphide is low, it is increased many thousandfold by a 1% increase of sulphur content,¹⁶ so that films having the compositions indicated in Table II will have the high conductivity required for a rapid sulphidation reaction not limited by diffusion through the sulphide film.

Bradley⁷ assumed his reaction product to be cupric sulphide; Fischbeck and Dorner,¹⁷ in a study of the reaction of copper powder with sulphur in carbon disulphide solution, concluded that cuprous sulphide forms first, and is then partly converted into cupric; and Satake,¹⁸ in a study of the reaction of copper with sulphur-bearing rubber mixes, found that the product could be represented as five parts of cuprous sulphide with three of cupric (i.e. $\text{Cu}_{1.625}\text{S}$). It is likely that all these products are best described as non-stoichiometric cuprous sulphide highly deficient in copper, with its composition varying with the conditions, and especially the rate, of its formation; a rapidly forming product, produced with the greatest supply of sulphur, will be the more copper-deficient, as found in the present work.

We shall consider the mechanism of cuprous-sulphide film growth in more detail after reporting quantitative growth curves obtained for thin interference-colour films formed in aqueous polysulphide solutions in Section III of this paper, and again in the light of the microscopic investigations reported in Section IV.

III.—THE INTERACTION OF COPPER WITH AQUEOUS AMMONIUM POLYSULPHIDE

Copper is rapidly attacked by polysulphide solutions, giving adherent films showing a range of interference colours and eventually a relatively loose black deposit very similar to that produced by the attack of sulphur dissolved in organic solvents (*vide supra*). Fischbeck¹⁹ showed that the rate of film growth often approximately obeys the so-called "parabolic" law. Dyess and Miley²⁰ determined the thickness of sulphide films on copper corresponding to the various interference colours, up to the second order, by the coulometric method developed by Miley;²¹ their results, given in Table III, provide a convenient visual method of estimating film thickness in the interesting region of the earlier stages of attack.

TABLE III.—*Thickness of Sulphide Films on Copper (Dyess and Miley²⁰)*

Colour	Thickness, Å.	Colour	Thickness, Å.
First Order :		Second Order :	
Dark brown . .	340	Yellow . . .	970
Red brown . .	390	Orange . . .	1,100
Purple . . .	440	Red . . .	1,230
Violet . . .	470	Purple-violet .	1,450
Blue . . .	510	Blue . . .	1,540
Silvery green .	815		

Since the reaction is very rapid except in very dilute ammonium polysulphide solutions, its quantitative study is difficult unless very small copper surfaces, that do not exhaust the polysulphide available in reasonable volumes of very dilute solutions, are used. With such small specimens, the visual method is the only one capable of giving consistent and reasonably accurate results, and it has the further advantage over the possible gravimetric, coulometric, and other analytical methods of providing, if desired, continuous indication of the progress of film formation over the few minutes required for the first two orders of interference colours to be traversed; consequently, it has been used in the present investigation, and although we realize that the thicknesses estimated may not be absolute, we consider that any error is likely to be systematic, and thus unimportant in affecting the general form of the thickness/time curves obtained.

1. EXPERIMENTAL TECHNIQUE

(a) Materials

Commercially pure bright copper wire, 18 S.W.G., was cut into specimens 1 cm. long and degreased with acetone.

Two stock solutions of ammonium polysulphide were prepared. Solution A was made by diluting 1 volume of 0.880 s.g. ammonia with 3 volumes of water, saturating the dilute ammonia with hydrogen sulphide, and allowing the product to stand in air; it is the ordinary reagent "yellow ammonium sulphide". Solution B was made by diluting 1 volume of 0.880 s.g. ammonia with 1 volume of water, and dividing the dilute ammonia into two equal volumes; the first was saturated with hydrogen sulphide and allowed to stand in a warm room for some time; the second was then added, and the whole allowed to stand over finely ground sulphur in the dark, out of contact with air. These stock solutions were greatly diluted as required with a 2% solution of A.R. sodium carbonate in distilled water, or with similar inert solutions of different pH values.

(b) Conditions of Reaction

The apparatus shown in Fig. 2 was used. The degreased specimen, *A*, was mounted in a rubber bung at the end of the glass tube, *B*, through which electrical

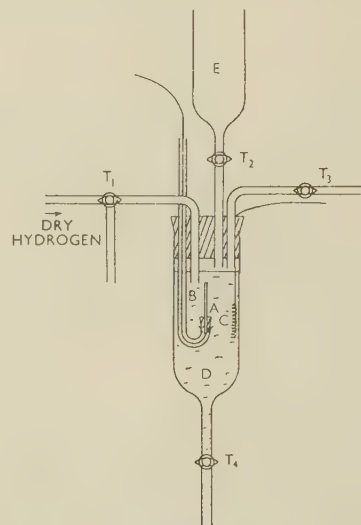


FIG. 2.—Apparatus for Tarnishing Experiments on Wire Specimens.

KEY.			
A	Degreased specimen.	D	Reaction vessel.
B	Glass tube.	E	Liquid reservoir.
C	Platinum coil.	T ₁ , T ₂ , T ₃ , T ₄	Taps.

connection to the specimen could be made for cathodic cleaning purposes; the platinum coil, *C*, served as anode. The reaction vessel, *D*, and the liquid reservoir, *E*, could be swept out with dry hydrogen delivered from tap *T*₁ by manipulation of taps *T*₂, *T*₃, and *T*₄.

In early experiments, the copper was first cleaned with a mixture of acetone and hydrochloric acid, and then cathodically cleaned in 2% sodium carbonate solution; this was then run out of *D* under hydrogen and replaced by the polysulphide-containing solution, through which hydrogen had been bubbling. It was later found that still more consistent results could be

obtained by the simpler means of cathodic cleaning in the tarnishing solution itself; this was run in with the specimen and the platinum anode already connected to the battery, and when the current was switched off after the cathodic cleaning, tarnishing began.

The experimental conditions were modified by varying

(a) Type of polysulphide (stock solutions A and B).

(b) Concentration of polysulphide.

(c) pH (by modifying the supporting 2% sodium carbonate solution with bicarbonate or hydrochloric acid).

(d) Illumination—after it had been discovered to be a considerable factor influencing the rate of tarnishing.

The temperature of all experiments was *c.* 15°–18° C.; no difference in rate could be detected in duplicate experiments within this range.

2. RESULTS AND INTERPRETATION

(a) Polysulphide Solution A

The results of typical experiments using polysulphide stock solution A diluted with 2% sodium carbonate solution are shown in Figs. 3 (a) and

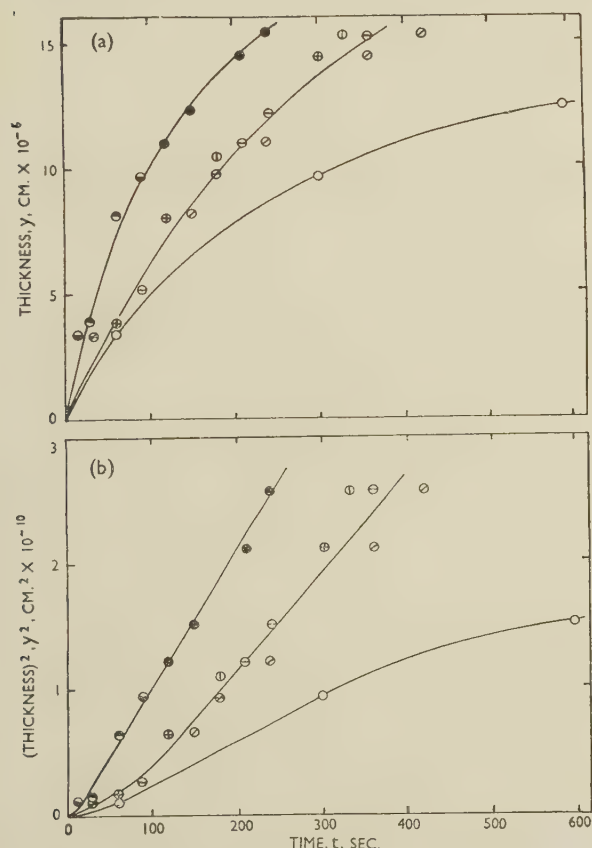


FIG. 3.—Relationship Between Film Thickness and Time. Polysulphide stock solution A, diluted with 2% sodium carbonate solution. Very subdued daylight.

KEY: ●, ○ 1:1000 dilution; ⊙, ⊙ 1:2000 dilution; ○ *c.* 1:3000 dilution.

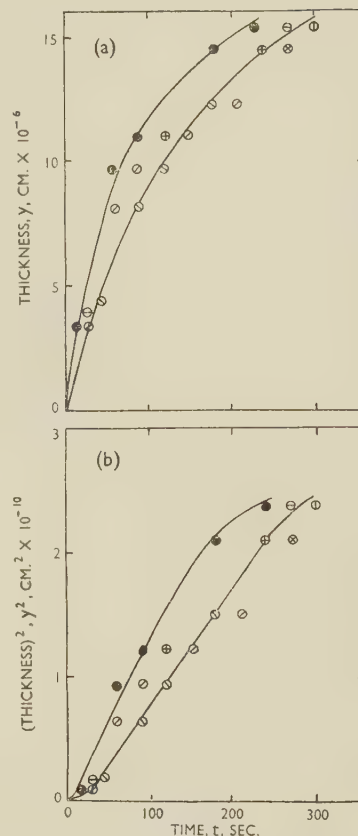


FIG. 4.—Relationship Between Film Thickness and Time. Polysulphide stock solution A, diluted with 2% sodium carbonate solution. Bright daylight.

KEY: ● 1:1000 dilution; ⊙, ⊙, ○ 1:2000 dilution.

4 (a) as plots of film thickness, y cm., against time, t sec., and in Figs. 3 (b) and 4 (b) as plots of (thickness)² against time. In several cases results of replicated experiments are plotted, to indicate the very reasonable degree of reproducibility obtained. The results of Fig. 3 were obtained in experiments conducted in very subdued daylight, those of Fig. 4 in experiments conducted in bright diffuse daylight.

It will be seen that:

(1) During the early stages of film growth, the rate of thickening is approximately constant with time, and is approximately doubled by a doubling of the concentration of polysulphide in the attacking reagent. It is also considerably increased by increase of intensity of illumination.

(2) During the later stages of film growth, the rate of thickening falls off with time, the thickness/time relationship being parabolic, of the form $y^2 = At + B$; it is now very much less dependent upon polysulphide concentration and also upon the intensity of illumination.

These results show that the rate of thickening in the early stages of film growth is limited mainly by the rate at which active polysulphide ions can reach the film surface through a diffusion layer in the liquid,

while in the later stages it is limited mainly by the rate at which copper (and/or sulphide) ions can move through the growing sulphide film. The accelerating influence of light in the early stages of film growth may be explained by supposing that there are certain polysulphide species (e.g. S_4^{--}) that react only very slowly in the dark but that are activated in the presence of light, so that a greater rate of arrival of active polysulphide ions at the film surface is possible. The lesser accelerating influence of light in the later stages of film growth may well be caused by photochemical assistance of the polysulphide-reduction reaction (see below) or of the diffusion process within the solid sulphide film.

A detailed model of the film thickening can be given by an extension of the electrochemical interpretation of the lattice-transport theory of film growth.^{14, 15} Here the growing film comprises both the electrolyte and the metallic connection of a short-circuited galvanic cell, the metal/film interface being the anode and the film surface an inert basis for the cathodic reduction of the attacking agent. If Faraday's and Ohm's laws* are applied to the cell, we obtain for the rate of film thickening:

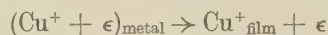
$$\frac{dy}{dt} = \frac{\kappa n_e(n_a + n_c)JE}{\rho \mathcal{F}} \cdot \frac{1}{y} \quad (1)$$

where κ mhos cm^{-1} is the film specific conductivity, n_e , n_a , and n_c are the transport numbers of electrons, anions, and cations, respectively, J is the gram-equivalent weight and ρ g./ cm^3 the density of the film substance, \mathcal{F} coulombs is the Faraday, and E V. is the working e.m.f. of the film cell. Then if E is taken as constant (i.e. no polarization, or polarization constant with change of film thickness),

$$y^2 = \frac{2\kappa n_e(n_a + n_c)JE}{\rho \mathcal{F}} \cdot t + \text{const.} \quad (2)$$

the familiar "parabolic law" of film thickening. If E is not constant with y , equation (1) is still valid, but equation (2) is not.

In the present case, the electrolytic conduction is probably mainly by copper ions moving through the defective cation lattice of the non-stoichiometric cuprous-sulphide film; the electronic conduction is provided by the cupric ions in the film acting as impurity centres for "defect" semi-conduction; while the anodic reaction at the metal/film interface is



and the cathodic reaction at the film surface is the reduction of polysulphide, e.g.



where S_n^{--} represents any active polysulphide ion or ions present. It is reasonable to assume that the anodic polarization is negligible, that cathodic activation polarization is appreciable, and that concentration polarization also is set up at the cathode when film thickening is the most rapid, i.e. at the outset. Fig. 5 shows the type of polarization curves to be expected on such a scheme. The anodic curve, A , is a straight line parallel to the current axis, indicating no polarization; it is convenient to take the anode single potential as an arbitrary potential zero. The two cathodic curves C , C' shown, for two different polysulphide concentrations (one double the other), have the form of polarograms, with limiting "diffusion" currents i , i' , proportional to the polysulphide con-

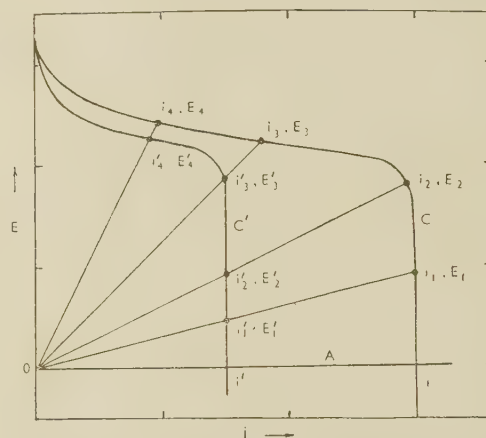


FIG. 5.—Relationship Between Cathode Potential E and Current i in Film Cell, for Two Concentrations of Polysulphide. (Schematic.)

centration. We consider first the case of the larger polysulphide concentration, giving cathodic curve C . In the early stages of film growth, the film is thin and its electrical resistance (per unit area) small; here a relatively large current in the film-cell, i_1 , equivalent to a high rate of film growth, is obtained from a relatively small working e.m.f., E_1 . When the film thickness, and hence its resistance, has doubled, the current i_2 , almost as great as i_1 , is obtained, because the working e.m.f. has increased to E_2 , almost double E_1 ; this is a consequence of the nearly infinite gradient of curve C under these conditions where the current is limited by the rate of arrival of polysulphide ions at the film surface. Over this range of film thickness, then, the rate of film growth dy/dt , equivalent to the current, is nearly constant. After a further doubling of the film thickness, however, the current is reduced to i_3 , only a little over one-half of i_2 ; this is a consequence of the small gradient of curve C and

* Ohm's law is valid up to field strengths of $c. 10^6$ V./cm.; at greater field strengths, the relation between current and p.d. is a hyperbolic sine.²² In the present case, the p.d. across the growing film can never exceed $c. 0.4$ V., corresponding to the free-energy change of the sulphidation reaction,

and thus Ohm's law is applicable to films thicker than about 50 \AA. ; for thinner films, the current for a given p.d. is greater than that corresponding to Ohm's law. We are here concerned mainly with the rates of thickening of films of thickness greater than 100 \AA. , where Ohm's law applies.

the small change in E from E_2 to E_3 . After yet another doubling of the film thickness, the rate of thickening is similarly approximately halved to the equivalent of i_4 . Thus over this latter range of film thickness, the rate of thickening is approximately inversely proportional to thickness. Both these "growth laws" are, of course, implicit in equation (1); rectilinear growth occurs when dy/dt is held constant by the limiting rate of arrival of cathodic reactant and here $E \propto y$; while parabolic growth occurs when E is substantially constant and $dy/dt \propto 1/y$. In the case

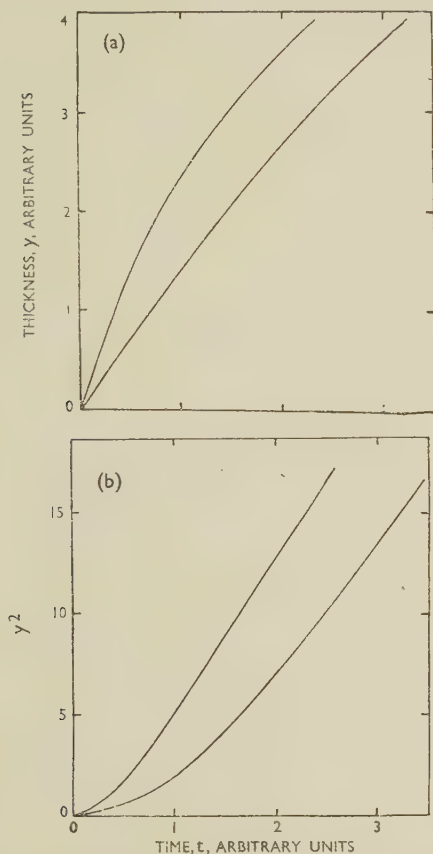


FIG. 6.—Relationship Between Film Thickness and Time. (Schematic.) y against t and y^2 against t curves derived from E against i curves of Fig. 5, with $y \propto E/i$ and $dy/dt \propto i$ for each point.

of the smaller (one-half) polysulphide concentration, curve C' , the same considerations apply, but rectilinear growth now continues until a film thickness corresponding to i_3' , E_3' is reached; thereafter parabolic growth at nearly the same rate as for the larger polysulphide concentration proceeds, i_3' being nearly equal to i_3 and i_4' to i_4 . The initial rectilinear growth is, of course, at approximately half the rate of that for the larger polysulphide concentration, i_1' and i_2' being half of i_1 and i_2 , respectively. Schematic y/t and y^2/t curves corresponding to the two polysulphide concentrations, as deduced from the schematic curves of Fig. 5, are shown in Fig. 6 (a) and (b); they agree

in detailed form with the experimental curves of Figs. 3 and 4.

It is, of course, possible in principle to reverse the procedure just described and, instead of constructing schematic growth curves from the hypothetical cathodic polarization curves of Fig. 5, to use experimental growth curves such as those of Figs. 3 and 4 to deduce "real" polarization curves: the resistance of the film cell may be taken as proportional to the thickness y and the current density to dy/dt , whence one may determine in arbitrary units the film-cell e.m.f., $y \cdot dy/dt$, and (assuming zero or constant anodic polarization) the cathodic potential for a series of values of the current density. However, dy/dt cannot be determined from the present y/t curves with any degree of precision (such gradient determinations require very precise data), and the film-growth mechanism is better demonstrated by the method used above.

The foregoing analysis does not take account of the variation of the specific conductivity of the cuprous-sulphide film across its thickness, consequent upon the variation of the concentration of lattice defects: the film nearest the metal will be less defective in copper than that nearest the attacking polysulphide. Wagner¹⁴ and Hoar and Price¹⁵ showed that a "parabolic" thickening equation is still obtained when this effect is allowed for; the parameters, of course, differ from those of the simpler equation. In the absence of any satisfactory data on the specific conductivity and transport numbers of cuprous sulphide of varying copper deficiency, quantitative calculations using the parameters of either equation are of little value; thus a qualitative analysis based on the simpler assumption of constant specific conductivity is all that can be given.

(b) Polysulphide Solution B

Typical results of experiments using polysulphide stock solution B diluted with 2% sodium carbonate solution are shown in Fig. 7 (a) and (b). These experiments were carried out in total darkness, and each point on the curves is a result of a separate timed experiment; the smoothness of the curves is noteworthy, and gives confidence in the reproducibility of conditions achieved. The form of the curves is again precisely paralleled by that of the theoretical curves of Fig. 6 (a) and (b). Comparison of Fig. 7 with Figs. 3 and 4 shows, however, that although qualitatively similar results were obtained whether stock polysulphide solution A or B was used for preparing the attacking reagent, a much greater concentration of B was required to give a similar initial rate of film growth (this was also true for experiments with stock solution B when light was not excluded). Evidently B contained fewer "active" polysulphide ions. Since A was prepared by air oxidation of monosulphide, and B by the reaction of sulphur with monosulphide, it is likely that A contained largely S_2^{--} and perhaps S_3^{--} ions, while B contained largely S_4^{--} and S_5^{--} with few S_2^{--} .²³ On general grounds we should expect the

simpler polysulphide ions to react much the more readily at the film cathode, with much less activation polarization, since there are fewer covalent bonds to be broken; thus the greater concentration of stock polysulphide B as compared with A required to give the same initial rate of film thickening probably reflects its much smaller S_2^{--} content. This point deserves fuller investigation with various completely

diminishes with lowering of pH . This is probably due to the tendency of the polysulphide ions to become more highly polymerized as the pH is lowered,²⁴ so that there are fewer active S_2^{--} ions; indeed, the solution at pH 7 showed a distinct Tyndall effect, indicating that polymerization far beyond S_5^{--} had occurred, sulphur itself being formed.

3. DISCUSSION

We have shown that the form of the growth curves of the sulphide films formed on copper by dilute polysulphide solutions, with subsidiary supporting evidence, leads to the conclusion that the reaction is limited in the earliest stages by the rate of arrival of active polysulphide ions at the surface, and later (at least for thicknesses up to some 1600 Å.) by lattice transport of copper (and possibly sulphide) ions through the growing film. It is interesting to compare this conclusion with those reached by other workers for the cases of other similar films formed at room temperature.

Evans and Bannister²⁶ showed that the form of the thickness/time curves for iodide films on silver reacting with iodine dissolved in organic solvents is at first approximately rectilinear and then parabolic, the rate throughout being dependent upon iodine concentration; they therefore concluded that the rate-determining process is at first the arrival of iodine at the film surface and later the diffusion of iodine molecules through the growing film. Bircumshaw and Everdell²⁷ obtained similar results for the corresponding reaction of copper, and gave additional evidence, based on the formation of duplex iodide films, that iodine diffuses through the film first formed. The same authors²⁸ showed that cuprous-iodide films, whether formed from iodine dissolved in organic solvents or from aqueous tri-iodide solutions, do not limit the rate of further iodide formation from aqueous tri-iodide solutions, which is constant with time and proportional to tri-iodide concentration, and therefore solely controlled by the rate of arrival of tri-iodide ions at the film surface. They noted that the cuprous-iodide films are wetted by water but not by organic solvents; this may well indicate a very easy capillary penetration along pores by aqueous solutions containing tri-iodide ions, although the diffusion over pore surfaces of iodine molecules evaporating from organic solvents may be relatively sluggish. They also showed that cuprous-iodide films can be made much more protective by mechanical buffing, which would be expected to heat the films sufficiently to allow plastic deformation to occur and partly to close the pores.

These results for silver- and cuprous-iodide films contrast with the present ones for cuprous-sulphide films grown in aqueous polysulphide solutions in that they can be explained only by the assumption of diffusion of the attacking reagent through pores in the film. In the cuprous-sulphide case such diffusion—of polysulphide ion—is most unlikely, since the rate of

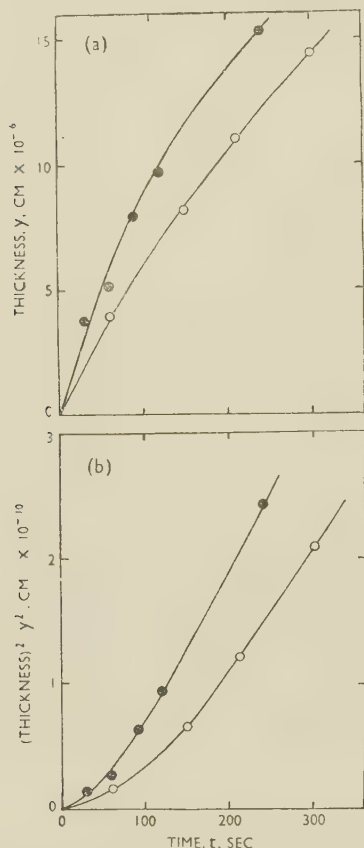


FIG. 7.—Relation Between Film Thickness and Time. Polysulphide stock solution B, diluted with 2% sodium carbonate solution. In darkness.

KEY: ● 1:100 dilution; ○ 1:200 dilution.

defined polysulphide solutions analysed by the chemical and electrochemical methods used by Valensi²⁴ and Peschanski²⁵ in their study of polysulphide equilibria and oxidation-reduction potentials.

TABLE IV.—Influence of pH on Rate of Film Thickening

pH	Colour of Film after 5 min.	Thickness, Å.
7.0	Nil	<100
7.5	1st order brown	340
8.4	1st order purple	440
9.3	2nd order purple	1450

Some results showing the influence of the pH of the supporting carbonate solution are given in Table IV. It will be seen that the rate of film thickening

growth in the "parabolic" period is nearly independent of polysulphide concentration. Here, lattice transport of ions that are the *products* of the reaction, Cu^+ and S^{--} , by the Wagner mechanism, seems to be the mode by which the film grows. Of course, it is likely, indeed necessary, that sub-microscopic crystallites of the iodide films themselves grow by lattice transport of Cu^+ , Ag^+ , and/or I^- ; but the seat of such growth must be the near neighbourhood of the metal/film interface, whither iodine molecules have diffused through the pores in the bulk of the film. It is alternatively possible that next to the metal there is a very thin film, substantially impermeable to I_3^- and I_2 , that grows by the Wagner mechanism, does not limit the total rate of film growth, and continuously breaks down mechanically at its outer surface producing in time a relatively thick, porous layer that is freely permeable to I_3^- and moderately so to I_2 .

This latter hypothesis is attractive in that it brings the iodide films into a general scheme that can be applied, with quantitative modifications depending on the electrical and mechanical properties of the reaction products, to a large number of sulphide, iodide, and indeed oxide films. It is proposed to discuss this in detail elsewhere; here it may be briefly stated as follows:

When bare metal is exposed to a film-forming reagent, the rate of attack is at first limited either by energy-hump considerations or by the rate of arrival of attacking reagent through the liquid (or gaseous) phase. The first film forms by lattice transport of its own ions (it may often be pseudomorphic with the underlying metal, and monocrystalline over any one metal grain (see below, Section IV)) and grows until its internal stresses cause it to disintegrate at its outer surface into a relatively porous, polycrystalline layer. This may occur (a) when the initial film is very thin (as in the iodide films just discussed, and probably in cuprous-sulphide films grown from sulphur in organic solvents); (b) when it has shown several orders of interference colours (cuprous-sulphide films grown from aqueous polysulphide); or (c) not until it is a relatively thick scale (oxide and other films formed at high temperatures, which are much more plastic and therefore, as pointed out by Evans,²⁹ do not break down easily). Thus, in general, the rate of attack may be determined by either:

(1) diffusion of the attacking reagent in the liquid (or gaseous) phase ("rectilinear" thickening, rate proportional to concentration of attacking reagent);

(2) lattice transport of the products of reaction in a growing, non-porous, but lattice-defective, film ("parabolic" thickening, rate nearly independent of concentration of attacking reagent); or

(3) diffusion of the attacking reagent in a growing porous film ("parabolic" thickening, rate proportional to concentration of attacking reagent).

This analysis does not include the case of "logarithmic" thickening, which has been admirably explained by Evans²⁹ in terms of breakdown of the first compact film by the formation of rifts ("cavity barriers") parallel to the metal surface; such rifts, if wide enough, would be expected to spoil the optical homogeneity of the film and prevent the production of interference colours, which are often, in fact, not observed in cases of "logarithmic" thickening. The present suggestion of breakdown by the formation of pores roughly *perpendicular* to the metal surface also implies a loss of optical homogeneity, but to a less extent from the point of view of approximately normally reflected light;²⁹ thus such porous films may be expected sometimes to show reasonably bright interference colours, as the iodide films often do. It is notable, however, that the non-porous (though lattice-defective) sulphide films here reported give very much brighter colours, until they finally disintegrate to a relatively loose, black top layer.

IV.—THE MICROSCOPIC STRUCTURE OF CUPROUS-SULPHIDE AND RELATED FILMS

The production of sulphide films of even colour on abraded or drawn copper is a matter of some difficulty, but can be readily achieved with careful cleaning technique. Electrolytically polished copper, however, gives films of distinctly different colour on the different grains. This effect has often been observed for many films on metals, and has been used by Jacquet² in a metallographic study of internal oxidation of copper alloys. In the present work, a number of cuprous-sulphide and similar films, produced under various conditions on electrolytically polished metal, have been examined in ordinary and in plane-polarized light.

1. EXPERIMENTAL TECHNIQUE

Commercially pure electrolytic copper, and for comparative experiments, ordinary α -brass sheet and high-purity electrolytic silver strip, were used. Different structures were produced as follows:

Annealed Metal with Randomly Oriented Equi-axed Grains.—Specimens $2 \times 2 \times 1$ cm. cut from a block of electrolytic copper were hammered gently on all sides, and annealed for 1 hr. at 700°C . under charcoal in an electric furnace.

Annealed Metal with Preferred Orientation.—Electrolytic copper was cold-reduced by about 80%, cut into strips, and annealed as above.

Partially Annealed Metal.—Hammered or rolled copper was annealed for 10 min. at 700°C .

Unannealed Metal.—The cold-reduced electrolytic copper was used.

Silver was annealed in the same way as copper; α -brass, by heating for 3 hr. at 500°C .

All the metals were electrolytically polished, copper

and brass by the method described in Section II of this paper, with rather longer polishing times of 5–10 min. Silver was much more difficult to polish, but after numerous baths had been tried unsuccessfully, reasonable results were obtained in the cyanide/ferrocyanide bath cited by Hogaboom,³⁰ if *vertical* anodes kept in *vigorous motion* were used, with about 1.2–2 V. across the cell.

The main tarnishing reagent was sodium polysulphide solution. A stock solution was prepared by dissolving 40 g. of pure crystalline sodium sulphide in 1 l. of distilled water and allowing the solution to stand over excess pure sulphur. This solution was much diluted for use; it is more stable and generally more convenient than ammonium polysulphide solutions. For the production of cuprous-iodide films a very dilute chloroform solution of iodine was used, the specimen being previously wetted with chloroform. Oxide films were produced by heating the metal in air.

After removal from the electrolytic polishing bath, the metal was washed successively in an unused bath of the same composition, tap-water, and distilled water, and immediately dried by a jet of air carrying some ether vapour, which causes the water to gather into drops and be blown off. This rapid washing and drying procedure eliminates dangers of staining. The clean electrolytically polished metal was at once placed in diluted polysulphide reagent. Copper tarnished suitably in a few seconds; in some experiments, it was made cathodic as it was inserted (to reduce any oxide film), and tarnishing began when the current was switched off, but no difference in the optical nature of the film was apparent when this refinement was used. Silver required up to 30 min. even in a relatively concentrated reagent, and brass had to be dipped successively into the reagent and back into the polishing bath, if films of suitable thickness were to be formed; these effects were probably due to tenacious compact oxide or other films remaining on the metal after electrolytic polishing, a matter discussed elsewhere.^{31, 32} The films were all washed, and dried by the air–ether jet, as described above. The iodide films were washed in pure chloroform and allowed to dry; the oxide films did not, of course, require washing and drying.

The optical system of the Bausch and Lomb microscope used allows surfaces to be examined by reflected light, which on incidence is either circularly polarized (giving normal bright-field illumination) or plane-polarized. The rotating stage of the microscope provides means of turning the specimen relative to the plane of polarization.

2. RESULTS AND INTERPRETATION

(a) *Annealed Metal*

When a sulphide film of mean thickness in the region of 100–1500 Å. (corresponding to the first- and second-order interference colours) was grown on annealed

electrolytically polished copper, a multi-coloured patchwork corresponding to the grain structure of the metal was produced; the film was of uniform colour over any one grain (Fig. 9, Plate XCIII). The colours found of different grains might be due to films of different thickness or refractive index or both; and although, as shown later, the film crystals are anisotropic and therefore have different refractive indices, depending on their orientation with respect to the light path, it is clear from the gravimetric measurements of Bénard and Talbot³³ that certain copper crystallographic planes *oxidize* more rapidly than others, and it is thus likely that variation in film thickness from grain to grain is the major cause of the colour differences after sulphidation.

The patchwork showed only a limited number of colours, corresponding to a limited number of film thicknesses (and/or refractive indices), and since there must be an infinite number of grain orientations with respect to the surface (at least in randomly oriented material), it is clear that grains having orientations *near to* a limited number of special orientations give rise to the same films as grains having *exactly* these special orientations; a rather similar phenomenon has been observed by Leidheiser and Gwathmey³⁴ in the oxidation of spherical single crystals of copper. If the electrolytically polished macroscopic surface makes a small angle with, say, a (111) crystallographic plane, it consists of many very small steps, of which the “risers” are probably one atom (at most two or three atoms) high and the longer “treads” are (111) planes. From such a surface it is not unreasonable to suppose that the film crystal grows at the same rate as it does from an exactly (111) macroscopic surface. Similarly, grains whose surfaces make only a small angle with a (110) plane behave towards the tarnishing reagent as “exact” (110) planes. Thus the colours produced on the specimen correspond to the relatively limited number of major close-packed planes. The patchwork on specimens that had been heavily cold-rolled before annealing showed rows of grains of the same colour, lying along the rolling direction (Fig. 10, Plate CIII); this is a result of preferred orientation in the metal, many grains having the same, or nearly the same, orientation, and so giving similar film colours.

The films grown on twinned grains were sometimes of the same, but more often of different, colour (Fig. 9); evidently, if the twinning plane makes an angle with the macroscopic surface near to one of the several special angles (90° being one of them), then the surfaces of the twins are sufficiently nearly identical to give the same rate of film growth, whereas if the twinning plane makes (as is more likely) some other angle with the surface, then the surfaces of the twins are considerably different and give different rates of film growth.

When the electrolytically polished, sulphide-filmed surfaces described above were illuminated with plane-polarized white light and viewed through an analyser crossed with the polarizer, a similar patchwork corre-

sponding to the grain structure of the metal could be seen, but with quite different and much more varied colours (Fig. 11, Plate XCIII); in particular, twins showed much greater differences in colour. The intensity and tint of the colours on the great majority of the grains altered when the specimen was rotated relative to the plane of polarization of the incident light; for any one grain, the intensity of reflected light showed a minimum every 90° , and each tint was repeated every 180° , the complementary colour appearing at 90° . This confirms that the film over each grain is monocrystalline and shows that the film substance is anisotropic (as might be expected for the orthorhombic form of cuprous sulphide stable below $90^\circ\text{C}.$). The colours arise because the incident plane-polarized light becomes elliptically polarized on reflection from the film-covered surface;³⁵⁻³⁷ the degree of ellipticity produced depends on the film thickness, on the wave-length of light, and (for anisotropic films) on the orientation of the film crystal with respect to the plane of polarization of the incident light. There is thus a component of the reflected light transmitted by the analyser, and this component varies in intensity and tint from grain to grain, and also varies for any one grain as the specimen is rotated. Twins are more readily distinguishable in polarized than in ordinary light, because those twinned grains that, as explained above, give rise to film crystals of the same thickness nevertheless have them in different orientations with respect to the plane of polarization. The few grains where the colour does not change on rotation of the specimen must be those having films so oriented that the optic axis is vertical.

Annealed, electrolytically polished 70:30 α -brass gave results (Fig. 12, Plate XCIII) similar to those of copper, except that, as noted above, the rate of formation of the sulphide film was very much slower. Oxide films grown on electrolytically polished copper heated in air, sulphide films on annealed electrolytically polished silver exposed to polysulphide solution, and iodide films on copper exposed to iodine in chloroform solution, also showed differently coloured films on different grains: in silver-sulphide films the area near the boundary of a grain usually showed a colour indicating a film slightly thicker than that on the body of the grain. When cuprous-oxide and silver-sulphide films were viewed in plane-polarized light, the majority of the grains showed some variation in intensity and tint of colour as the specimen was rotated, although the effect was less marked than with cuprous-sulphide films. Now cuprous oxide and silver sulphide are normally cubic and isotropic; thus the optical anisotropy shown by the films must be due either to the formation of special anisotropic modifications dictated by the structure of the underlying metal, or (we think more probably) to compressional stresses set up in the films during growth. Bright areas, due to very strong birefringence, could sometimes be seen in polarized light at and near the grain boundaries in silver-sulphide films (and in oxide films on α -brass). It might be expected that compressional

stresses would produce the greatest strains at grain boundaries; the effect is apparently analogous to the birefringence at and near the grain boundaries of polycrystalline silver-chloride strips elastically strained in tension, observed by Nye.³⁸

Another effect, first observed on very slightly sulphidized silver viewed in polarized light, is the appearance of minute diffraction figures recalling the polarization figures produced by anisotropic crystals in convergent plane-polarized light, in that they consist of a black cross surrounded by one or two coloured rings. These figures could be observed before there was any sign of a visible coloured film; they appeared at scattered points on each grain and, during sulphidation, multiplied in number without growing in size until the whole grain surface was covered. The figures on any one grain were geometrically similar. Figures of the same kind, though less distinct, could sometimes be seen on sulphidized copper. It appears likely that the figures are caused by thin patches of film beginning to grow at many similar nuclei on each grain—probably the “steps” in the surface, already mentioned. This explanation is supported by the facts that: (a) figures cannot be seen on clean electrolytically polished copper or silver, or on the same surfaces after etching (without staining) with ferric chloride—but an etched surface that is tarnished or stained may show them; and (b) figures can be seen on electrolytically polished, sulphidized copper and silver only on grains that change colour on rotation when viewed in plane-polarized light, never on grains that do not change colour. Thus it is clear that the figures are caused by a film that is anisotropic and of which the optic axis is not perpendicular to the metal surface; they cannot be caused by other diffraction effects due to etched surfaces.

It is likely that lateral growth from the film nuclei links them up and results in the formation of the visible films already described, monocrystalline over any one grain, since the many nuclei are similarly oriented. In some specimens where an imperfect electrolytic polish had resulted in the formation of very minute etch figures, polycrystalline films showing a very small-scale patchwork upon each metal grain were produced; here it is likely that differently orientated film nuclei were formed on different facets of the etch figures.

Some mechanically polished annealed copper specimens were also examined. Those with an ordinary metallographic finish gave sulphide films of overall uniform tint, provided they were completely cleaned before sulphidation; clearly the “amorphous” metal in the polish layer gives rise to a submicrocrystalline film of random orientation. It was found, however, that very light hand polishing can lead to a surface in which the polish layer is so thin that the patchwork structure in the sulphide film is produced almost as well as with an electrolytically polished surface; Fig. 13 (Plate XCIII) shows such a film formed on a surface delicately polished by hand over a period of many hours.

(b) *Non-Annealed Metal*

The imperfect crystals of cold-rolled or partially annealed copper, and of slightly deformed annealed metal, were found to give rise to film structures of greater complexity. Cold-rolled material gave films clearly showing the shattered nature of the grains, and furthermore the film over any one grain was very unevenly coloured (Fig. 14, Plate XCIII). It is likely that the "steps" on an electrolytically polished cold-rolled grain are anything but parallel, owing to the great distortion of the lattice, and thus the film nuclei cannot grow into a monocrystalline film. Partially annealed (10 min. at 700° C.) copper also gave unevenly coloured films (Fig. 15, Plate XCIII), perhaps because recrystallized grains inherit some distortion or stress from the original grains.

Slightly deformed annealed copper, when sulphidized or iodized and viewed in plane-polarized light, showed bright areas of high birefringence at grain boundaries and sometimes near slip bands (Fig. 16, Plate XCIII). The effect is not due directly to surface irregularities on the metal, for it was much less noticeable on annealed specimens deformed *after* sulphidation or iodidation. It seems rather to be caused by stress or distortion in the film material, suggested above as the cause of the similar effect found with sulphide films on *annealed* silver, but in this latter case inherited from the distorted metal from which it has formed. The formation of distorted films from distorted metal may be one reason why relatively thick sulphide films grown on abraded metal flake off more readily than those grown on electrolytically polished metal, as reported in Section II of this paper.

3. DISCUSSION

If it be accepted that the different colours of the films on different grains arise mainly from differences in thickness rather than in refractive index, then evidently the rate of film growth is different on different grains with differently oriented films. Since it is clear from the results of Section III of this paper that the rate of sulphide-film growth from polysulphide solutions is determined by the film itself, at least over the thickness range that gives rise to first- and second-order interference colours, the variation in rate of growth with orientation implies anisotropy in

the electrical conductivity (and/or transport numbers) as well as in the optical properties of the film. This is a reasonable conclusion, for it is to be expected that the mobility of ions and electrons in an anisotropic lattice will vary with direction, and many cases are known, of both semi-conductors and metals, where the conductivity is in fact anisotropic.

The detailed examination of the optical properties of thin films on metal surfaces generally has in the past yielded important information, and is capable with the newer techniques of yielding much more. The use of polarized light in the present preliminary work on cuprous-sulphide and related films has already shown numerous effects qualitatively. Hone and Pearson,³⁹ in work published after most of the above experiments were conducted, illustrate in colour the very similar optical results given by anodized electrolytically polished pure aluminium when this is viewed in polarized light. Their films were about 100 times thicker than the present, and far too thick to show interference colours in ordinary light, but being of high transparency, well adapted to produce the colour phenomena due to the reflection of plane-polarized light. (The anisotropy of the alumina film was previously demonstrated by Lacombe and Beaujard⁴⁰ and by Huber and Gaugler⁴¹.) We hope to pursue studies of films in polarized light with the aid of an elliptical compensator on the microscope, so that the change of ellipticity produced by reflection at the filmed surface can be measured quantitatively and used to determine film orientation. Colour photography for recording purposes has been successfully used by Jacquet² and by Hone and Pearson.³⁹ We have ourselves found it possible to make Dufay-colour transparencies of high fidelity to the original colours; Stuart⁴² is now making colour kine-films of the progress of sulphidation, which besides having visual interest will provide quantitative data of the kinetics of film formation even under conditions of very rapid filming.

ACKNOWLEDGEMENT

Our thanks are due to the Department of Scientific and Industrial Research for the award of a Maintenance Allowance to one of us (A. J. P. T.), during the tenure of which (1946-48) the work was carried out.

REFERENCES

1. S. Wologdine, *Rev. Mét.*, 1907, **4**, 25.
2. P. A. Jacquet, *ibid.*, 1945, **42**, 133.
3. T. P. Hoar and G. C. Smith, 1945, unpublished work.
4. J. M. Butler and T. P. Hoar, *J. Inst. Metals*, 1951-52, **80**, 207.
5. C. Buchan, "Rubber to Metal Bonding", p. 136 *et seq.* London : 1948 (Crosby Lockwood).
6. P. A. Jacquet, *Bull. Soc. chim. France*, 1936, [v], **3**, 705.
7. R. S. Bradley, *Trans. Faraday Soc.*, 1938, **34**, 278.
8. U. R. Evans, *Nature*, 1930, **126**, 130.
9. U. R. Evans, "Symposium on Internal Stresses in Metals and Alloys" (*Institute of Metals Monograph No. 5*), 1947, pp. 291, 467.
10. R. F. Mehl, E. L. McCandless, and F. N. Rhines, *Nature*, 1934, **134**, 1009.
11. R. F. Mehl and E. L. McCandless, *ibid.*, 1936, **137**, 702.
12. C. M. Blow and G. Hopkins, *J. Soc. Chem. Ind.*, 1945, **64**, 316.
13. W. H. J. Vernon, *Trans. Faraday Soc.*, 1927, **23**, 113.
14. C. Wagner, *Z. physikal. Chem.*, 1933, [B], **21**, 25.
15. T. P. Hoar and L. E. Price, *Trans. Faraday Soc.*, 1938, **34**, 867.
16. G. G. Urazov, *Zhur. Russ. Fiziko-Khim. Obshch.*, 1919, **51**, 311; see *C. Abs.*, 1923, **17**, 3446.
17. K. Fischbeck and O. Dorner, *Z. anorg. Chem.*, 1929, **182**, 228; 1929, **184**, 167.
18. S. Satake, *J. Soc. Rubber Ind. Japan*, 1935, **8**, 461; *Rubber Chem. Technol.*, 1936, **9**, 301.
19. K. Fischbeck, *Z. anorg. Chem.*, 1931, **201**, 177.
20. J. B. Dyess and H. A. Miley, *Trans. Amer. Inst. Min. Met. Eng.*, 1939, **133**, 239.
21. H. A. Miley, *Carnegie Schol. Mem., Iron Steel Inst.*, 1936, **25**, 197.
22. J. Frenkel, "Kinetic Theory of Liquids", pp. 43-44. Oxford : 1946 (Oxford University Press).
23. D. Peschanski and G. Valensi, *Compt. rend.*, 1948, **227**, 845.
24. G. Valensi, *Bull. Soc. chim. France*, 1945, [v], **12**, 642.
25. D. Peschanski, *Compt. rend.*, 1948, **227**, 770.
26. U. R. Evans and L. C. Bannister, *Proc. Roy. Soc.*, 1929, [A], **125**, 370.
27. L. L. Bircumshaw and M. H. Everdell, *J. Chem. Soc.*, 1947, **1119**.
28. L. L. Bircumshaw and M. H. Everdell, *ibid.*, 1942, 598.
29. U. R. Evans, *Trans. Electrochem. Soc.*, 1947, **91**, 547.
30. G. B. Hogaboom, *ibid.*, 1942, **81**, 210 (discussion).
31. T. P. Hoar and J. A. S. Mowat, *Nature*, 1950, **165**, 64; *J. Electrodepositors' Tech. Soc.*, 1950, **26**, 7.
32. T. P. Hoar and T. W. Farthing, *Nature*, 1952, **169**, 324.
33. J. Bénard and J. Talbot, *Compt. rend.*, 1947, **225**, 411; 1948, **226**, 912.
34. H. Leidheiser and A. T. Gwathmey, *Trans. Electrochem. Soc.*, 1947, **91**, 95.
35. P. Drude, *Wied. Ann.*, 1889, **36**, 532, 865; 1890, **39**, 481.
36. L. Tronstad, *Trans. Faraday Soc.*, 1933, **29**, 502; 1935, **31**, 1151.
37. A. B. Winterbottom, *Nature*, 1937, **140**, 364.
38. J. F. Nye, *Proc. Roy. Soc.*, 1949, [A], **200**, 47.
39. A. Hone and E. C. Pearson, *Metal Progress*, 1948, **53**, 363.
40. P. Lacombe and L. Beaujard, *Journées des Etats de Surface (Paris)*, 1945, 44.
41. K. Huber and A. Gaugler, *Helv. Chim. Acta*, 1945, **28**, 1416; *Experientia*, 1947, **3**, 277.
42. N. Stuart and T. P. Hoar, work in progress.

Intercrystalline Corrosion in Cast Zinc-Aluminium Alloys

By C. W. ROBERTS

(*Journal*, this vol., p. 301.)

Dr. habil. K. LÖHBERG*: I was very interested in this paper, but regret I cannot agree with some of Mr. Roberts' conclusions. In the first place there is a misunderstanding. Mr. Roberts writes on p. 307: "It is clear, however, that the view expressed by Löhberg that 'corrosion takes place only when the aluminium-rich phase is present; it affects *only* this phase and is intercrystalline only when this phase is concentrated along the grain boundary' is incorrect." What I stated in my paper† was that the corrosion attacks *first* the aluminium-rich phase and *then* the zinc-rich phase. If I understand him correctly, Mr. Roberts means just the same in saying, on p. 307: "Aluminium as an element has a high affinity for oxygen . . . and their inability to form a stable oxide film." It may, however, be possible that single-phase zinc-aluminium alloys of aluminium content between 0.08 and 0.02% aluminium are susceptible to intercrystalline corrosion; but I am not sure that the solubility of aluminium in solid zinc between 20° and 100° C. is known exactly. With regard to my investigation on the corrodibility of intermetallic compounds, I think it possible that a single-phase alloy may be attacked if the solvent metal has a more noble electrochemical potential than the solute atoms, as is the case in single-phase zinc-aluminium alloys. But in any case corrosion affects first the aluminium or the aluminium-rich phase.

Mr. Roberts writes on p. 307: "Löhberg, who assumed that lead was the primary instigator of the corrosion, suggested in one of his papers that the lead was converted to the intermetallic compound Mg_2Pb , which, although still intercrystalline, was apparently innocuous." What I concluded in my paper‡ was that "magnesium is able to offset to a certain extent the ill effects of the contaminating metals" and that "magnesium compensates the ill effects of lead to a lesser degree than those of bismuth." I think it possible that Mg_2Pb , although unstable, affects the corrodibility of the zinc-aluminium alloys less than the lead, which has a more noble electrochemical potential than the intermetallic compound. But this does not mean that Mg_2Pb may be "innocuous". I would emphasize the fact that I investigated zinc-aluminium alloys only. The behaviour of the alloy No. 9 of the list given by Mr. Roberts is very interesting and seems to confirm what Dr. W. Wolf told me several years ago. He found that zinc-magnesium alloys corrode in the same manner as the zinc-aluminium alloys contaminated by lead or the like.

Mr. Roberts' statement on the solubility of magnesium in the solid zinc crystals and the conclusions therefrom seem to be of importance. In work so far unpublished, we have found the solubility of magnesium in solid zinc to be as follows:

Temp., °C.	Wt.-%
(eutectic) 364	0.16-0.17 (extrapolated)
350	0.12
325	0.05
300	0.02
200	0.008

The agreement with the results given by Mr. Roberts is as good as can be expected. The ternary solid solutions of zinc with aluminium and magnesium contain:

Temp., °C.	Al, %	Mg, %
(eutectic) 350	0.9-0.95	0.22-0.25
330	0.75	0.2
290	0.60	0.15

These figures confirm Mr. Roberts' statement that "it is probable that the solubility of this element (i.e. magnesium) in the α phase (i.e. single-phase zinc-rich alloys) at corresponding temperatures is very little higher."

The AUTHOR (*in reply*): The information Dr. Löhberg has supplied is most valuable, particularly the figures for the combined solubility of aluminium and magnesium in zinc, which, as far as I know, have not previously been published. I regret having misconstrued his conclusions regarding the order in which the zinc-rich and aluminium-rich phases are attacked, but, nevertheless, disagree with the corrected version also. I found that no intercrystalline corrosion occurred in single-phase aluminium-rich alloys, but that a considerable degree of intercrystalline attack occurred in single-phase zinc-rich alloys, and consequently I found it difficult to accept the view that in duplex alloys the aluminium-rich phase is attacked first. My remarks on p. 307 quoted by Dr. Löhberg to the effect that "aluminium as an element has a high affinity for oxygen . . . stable oxide film", referred to the aluminium atoms in the zinc lattice and not to precipitated particles of the aluminium-rich phase, which, in a single-phase alloy, would not be present.

Regarding the effect of lead and the intermetallic compound Mg_2Pb on the intercrystalline attack, I do not think that the difference in the electrochemical potentials of these two impurities is very relevant, since their modes of action are dissimilar. The action of lead (if its action is, in fact, electrochemical) would be to accelerate the attack on the zinc-rich phase because of its "more noble" potential (the element itself remaining unattacked), whereas Mg_2Pb is rapidly attacked by water vapour and the corrosion is intercrystalline only because the compound occurs as an intercrystalline constituent in the alloy.

* Metallgesellschaft A.G., Frankfurt-am-Main, Germany.

† *Z. Metallkunde*, 1942, 34, 78.

‡ *Ibid.*, p. 73.

THE OXIDATION OF COPPER IN THE TEMPERATURE 1486 RANGE 200°–800° C.*

By R. F. TYLECOTE,† M.A., M.Sc., Ph.D., F.I.M., MEMBER

SYNOPSIS

By means of a continuously recording balance, the changes in weight during oxidation of high-purity copper sheet have been measured over periods up to 100 hr. The effect of different oxidizing atmospheres, such as air, oxygen, "oxygen-free" nitrogen, and air containing water vapour, has been determined. Other factors investigated were: the effects of specimen shape, of an oxide film formed in air before high-temperature oxidation, and of recrystallization on the growth of the oxide on work-hardened copper.

The sudden weight changes that take place under a wide range of conditions are ascribed to the relief of internal stress in the growing film, and the mode of stress-relief has been correlated with the previously determined physical properties of the film at various temperatures. In particular, limited periods of parabolic oxidation followed by discontinuous oxidation occur in the range 200°–365° C. At higher temperatures (520°–700° C.) oxidation frequently obeys initially the cube law: $w^3 = K_3 t + c$, and then generally approximates to the parabolic law, with sudden weight increases occurring at the same time.

Addition of moisture reduces the oxidation rate at 370° C., and increases it between 420° and 700° C. Oxygen decreases the oxidation rate as compared with air, between 200° and 420° C.; at 520° C. and above there is a slight increase. At 420° C., the initial oxidation rate of wire is considerably less than that of sheet.

Cold-worked sheet has initially a lower oxidation rate than annealed sheet. Annealing during oxidation, however, results in a final weight gain similar to that of annealed copper. This is explained on the basis of preferred orientations.

The activation energy for parabolic oxidation in the range 200°–600° C. is between 16,000 and 17,000 cal. mole, and that for cubic oxidation 28,000 cal. mole. Both are substantially independent of the oxidizing conditions.

I.—INTRODUCTION

PREVIOUS work on the oxidation of copper has shown that at high temperatures the oxide films formed are comparatively ductile, whereas those formed at low temperatures are hard and brittle. The information available on the oxidation rates of copper suggests that there may be a change in mechanism at 600°–700° C.

The present work was designed to find how far the change in ductility of the film was connected with the supposed change in mechanism, and to determine the effect of various atmospheres and other variables on the properties of the film.

Compressive stresses are set up during the formation of oxide films on copper, since the volume of the oxide is larger than that of the metal from which it is formed. Since this stress, if unrelieved, could assume an impossibly high value, it was considered of some interest to investigate the manner of stress-relief at different temperatures in the light of the change in film properties.

II.—PREVIOUS WORK

The author has already reviewed the information on the oxidation of copper published up to December

1949.¹ The present summary, therefore, will be confined to work published since that date, and to earlier work that has particular reference to the aspects of the oxidation of copper dealt with in this paper.

In 1923, Pilling and Bedworth² investigated the oxidation of copper sheet and wire in oxygen at 400°–1000° C. and in air at 800°–1000° C. The results obtained between 400° and 700° C. showed wide scatter, which was attributed to the brittle nature of the film formed, and to its being under compressive stress. At 500° C., oxidation seemed to start by obeying the parabolic law, but after about 25 min. spasmodic increases in weight occurred, which were ascribed to local cracking of the film. The original film formed in air at room temperature was not removed before testing.

Hudson and his colleagues³ carried out oxidation experiments in air on arsenical copper (0.12% oxygen, 0.47% arsenic) between 300° and 600° C. Here again, the initial film was not removed, and parabolic oxidation was assumed on the basis of results of separate oxidation experiments for 1, 2, 4, and 6 hr.

Valensi⁴ made a few tests on the oxidation of degassed copper in air in the range 369°–580° C., with and without an initial room-temperature film.

* Manuscript received 28 January 1953.

† Department of Metallurgy, King's College, University of

Durham, Newcastle-on-Tyne; formerly I.C.I. Research Fellow, Royal School of Mines, London.

In intermittent tests he found that specimens with a pre-existing film did not oxidize in accordance with the parabolic law, whereas those first reduced in hydrogen did so up to the maximum period of the experiment, i.e. 6 hr.

Recent work by Rhodin,⁵ Lustman and Mehl,⁶ and Campbell and Thomas,⁷ has contributed to the following picture of the oxidation of copper between –195° and 256° C. Oxidation obeys the logarithmic law:

$$w = K_2 \log (t/a + 1) \quad . \quad . \quad . \quad (1)$$

from –195° to about 20° C. At about 50° C. there is a transition from the logarithmic law to a cube law of the type:

$$w^3 = K_3 t + c \quad . \quad . \quad . \quad (2)$$

Campbell and Thomas also found that moisture reduced by about 10% the oxidation rate in the range 100°–160° C. These results seem to support the theory of Cabrera and Mott⁸ that the rate-determining process in the formation of the oxide films is the transfer of metal ions through a strong electric field to the reaction zone on the oxide/oxygen interface, as a result of space-charge effects.

The film thickness at which the space-charge effect becomes important with copper is equivalent to that caused by oxidation at 50° C. for about 30 min., i.e. a thickness of 40 Å. according to Rhodin.⁵ This is in full agreement with calculations of Cabrera. The oxidation rate in the range of temperatures where the logarithmic law operates would be expected to be independent of oxygen pressure. According to Cabrera and Mott, the conditions for the transition from the cubic to the parabolic law of oxidation are satisfied when the thickness reaches 2×10^{-4} cm. in a few hours. They concluded from the results then available, which showed fair obedience to the parabolic law above 700° C., that diffusion of ions and electrons must occur in such a way that the space-charge effect is no longer important.

The present author has already investigated the physical properties of the films produced on copper between 300° and 900° C.⁹ and has shown that these films do not become ductile below 600°–700° C., and that, on specimens with a pre-existing air-formed film, the parabolic law is not obeyed at short times below about 500°–600° C.,¹⁰ i.e. until the film has become sufficiently plastic. From the results to be described, the parabolic stage, which appeared to occur after long times at low temperatures (300°–500° C.), is now considered to be merely a later stage of a “crack-heal” type of oxidation.

III.—EXPERIMENTAL TECHNIQUE

1. MATERIAL

High-purity vacuum-melted copper was used, having the composition reported in the earlier work.⁹ The copper was cold-rolled to strip 0.010 and 0.040 in. thick, and annealed in a high vacuum at 700° C.

2. THE BALANCE

Oxidation was followed by means of a continuous gravimetric technique, using a thermo-balance, similar to that used by Dumez¹¹ and Chevenard,¹² and shown in Fig. 1 (Plate XCIV).

The basis of the apparatus was a semi-micro-chemical balance, specially modified so that the specimen was supported on a quartz fibre above the left-hand end of the beam. A mirror was fixed to the centre of the beam so that considerable increase in sensitivity could be obtained by means of an optical lever.

The furnace was supported over the left-hand end of the beam and was free to slide vertically. A reaction chamber, closed at the top, was placed over the quartz fibre and specimen. The gas was introduced into the reaction chamber from the bottom by a quartz tube, which terminated 0.5 in. from the top of the chamber.

Temperature was measured by a Chromel/Alumel thermocouple, the junction of which was about $\frac{1}{2}$ in. above the specimen. A temperature calibration was made between this couple and one placed temporarily at the mid-point of the specimen.

The light spot from the optical system was about 1 mm. in dia. and was projected on to a drum camera, which had two speeds, viz.: one revolution in 24 hr. and one revolution in 24 min., giving horizontal scales of 0.66 in./hr., and 0.66 in./min., respectively. The vertical scale could be adjusted, that normally used being 0.16 mg./in. At high temperatures this was found to be too sensitive, and the scale was altered to 0.70 mg./in. for oxidation above 500° C.

The effect of vibrations and of changes in balance temperature ($\pm 5^\circ$ C.), was such that a variation of ± 0.10 in. was the greatest likely to be obtained, according to checks made with a gold specimen at 500° C. over a period of 24 hr. This corresponds to an accuracy of measurement of ± 0.016 mg. (high-sensitivity scale).

3. THE SPECIMENS

The specimens consisted of small pieces of copper strip 0.010 or 0.040 in. thick, with a hole about 0.03 in. in dia. made near the top, through which a small hook of platinum was passed to attach the specimen to the hook on the quartz fibre. Since the thin material would have been completely oxidized at higher temperatures, the thicker material was used for experiments above 520° C. The specimens were prepared by electropolishing in diluted phosphoric acid (sp. gr. = 1.3–1.4).

The specimen area was varied to obtain an oxidation curve which made use of the full movement of the balance in a period of 100 hr. at each temperature.

4. TEMPERATURE VARIATION OF SPECIMEN

The furnace was not wound to compensate for end-losses, since it was particularly necessary to keep the lower end cool. There was thus a tempera-

ture gradient, which meant that the specimen was cooling in the course of an experiment at a rate of 4.8° C. during 100 hr. Oxidation was always started 2.4° C. above the nominal temperature, so that the maximum variation was about $\pm 3.0^\circ$ C. It must be noted, however, that a single movement of the rider through 1.0 mg. to maintain the light spot on the chart would result in a sudden increase of temperature of 4.8° C., but as far as can be ascertained by comparison of different experiments this seems to have had no measurable effect on the rate of oxidation.

5. OXIDIZING ATMOSPHERES AND PREVIOUS REDUCTION

The standard oxidizing atmosphere was purified air at atmospheric pressure, provided by a small reciprocating pump at a rate of 14 l./hr. Air was drawn from the room atmosphere via a filter. It was then passed through a small regulating valve, through a drying train, and finally through a filter and flow-meter, before being injected into the furnace via the quartz tube mentioned above.

In previous work¹⁰ the specimens were heated to the oxidation temperature in purified nitrogen, thus maintaining the pre-existing air-formed oxide film. In this investigation the technique normally adopted was to heat the specimen in a mixture of "oxygen-free" nitrogen and dry hydrogen in the proportions 2 l./hr. of hydrogen to 14 l./hr. of nitrogen. This mixture was non-explosive on admission of air at oxidation temperatures, and sufficiently reducing to remove the air-formed film in a matter of seconds at 500° C. By this means the film formed in laboratory air after polishing was removed, and an accurate point for the start of oxidation, i.e. the time of admission of air or oxygen, was obtained.

There was one possible disadvantage in this reduction technique—the probable increase in the surface roughness ratio, due to reduction of the initial room-formed film. However, recent work by Rhodin¹³ has shown that whereas the reduction of thin oxide films (10–300 Å.) may increase the surface roughness by factors up to 2.46, the addition of a film only 100 Å. thick during oxidation reduces the roughness ratio to unity again. Therefore, any increase in surface roughness due to reduction will be eliminated in the first 10 sec. of oxidation at 200° C., and in shorter times at higher temperatures.

In the few experiments made by heating in air to establish the effect of a preformed oxide film, "buoyancy" corrections had to be made. Since reduction and oxidation were carried out at constant temperature, "buoyancy" corrections were not normally necessary.

When oxygen was used as the oxidizing medium, it was admitted before the drying train. Commercial oxygen containing about 2% nitrogen was used.

For the experiments with moist air, the drying train was replaced by a moisture saturator, consisting of a horizontal glass cylinder containing distilled

water. The air stream was baffled with cotton-wool kept moist by the water. The difference in weight before and after an oxidation experiment corresponded to a moisture content of 13.1 g./m.³, which is the amount of moisture contained in saturated air at 15° C.

6. PROCEDURE

The procedure generally adopted was as follows:

A specimen of copper was electrolytically polished, washed, dried, and attached to the quartz fibre. The reaction chamber was placed in position, the nitrogen-hydrogen mixture passed at a rate of 16 l./hr., the recording camera started, and the furnace heated to about 550° C. in the raised position and then lowered; the temperature in the reaction chamber reached 500° C. in about 5 min. When the specimen was to be oxidized at 500° C. or below, it was reduced for 10 min. and allowed to cool in the nitrogen-hydrogen mixture to the oxidation temperature; the reducing atmosphere was then cut off and air admitted, this being the zero of oxidation.

If the oxidation temperature was above 500° C., the heating time was considered sufficient for reduction, and the air was admitted after the steady temperature had been reached.

After oxidation had been carried out for 100 hr. the camera was removed and the specimen allowed to cool in air. During cooling some of the scale exfoliated and the rest remained loosely attached to the specimen. Above 600° C., there was a tendency for all scale to remain firmly attached to the specimen. Measurements of weight increases were made from the photographic records at time intervals appropriate to a logarithmic scale. These were, 0.25, 0.5, 0.75, 1, and 1.5 hr., then every hour up to 10, 12, 15, 24, 30 hr. and then every 10 hr. up to 100 hr.

IV.—EXPERIMENTAL RESULTS

1. THE EARLY STAGES OF OXIDATION OF ANNEALED COPPER IN DRY AIR

The first stage in the oxidation of copper is the formation of a solid solution of oxygen in the surface layers of the copper, and subsequent supersaturation in which nuclei of oxide appear. The nuclei grow laterally to form a continuous film of oxide. This lateral spread, together with growth in thickness, seems to produce a sigmoid curl, when weight is plotted against time,^{14, 15} rather than the straight line which would be expected for the pure chemical reaction between copper and oxygen.

Since this initial reaction is very rapid and of short duration in the temperature range under investigation, a faster time base and larger specimens than for the normal 100-hr. oxidations had to be used to observe it. The camera speed was therefore increased to 0.66 in./min. The high-sensitivity range of the balance was used throughout. The minimum temperature at which the initial stages could be adequately observed was 370° C.

Fig. 2 shows a typical record of the first 10 min. of oxidation at 670° C. The specimen was heated to temperature in the hydrogen-nitrogen mixture, the hydrogen turned off, and 1 min. after this the nitrogen

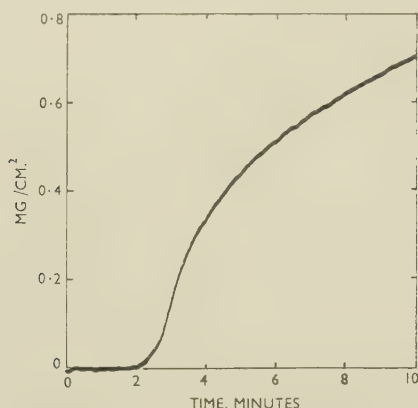


FIG. 2.—Weight/Time Curve for the Early Stages of Oxidation of Annealed Copper in Dry Air at 670° C.

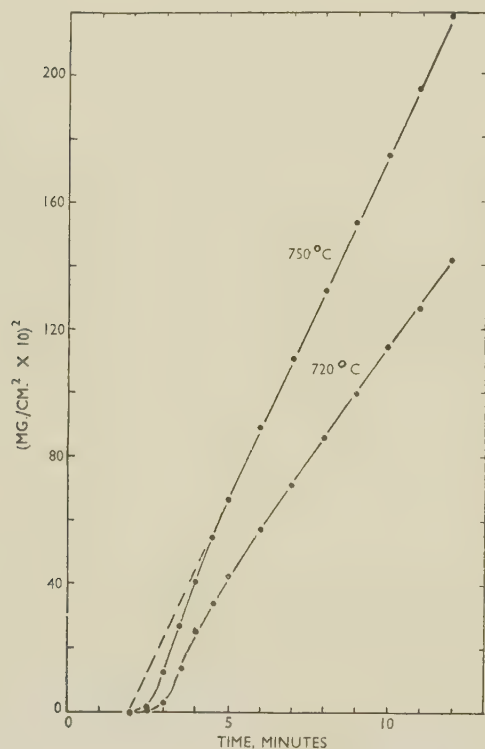


FIG. 3.—“Parabolic” Plot of Oxidation of Annealed Copper in Dry Air.

turned off and the air turned on. The origin of all curves reproduced in this paper occurs at this point. The horizontal induction period of about 2 min. is probably the time required to displace the nitrogen and produce a sufficiently oxidizing mixture to cause measurable oxidation.

At 520° C., the duration of the induction period decreased from 2.6 to 1.2 min. as the air flow was increased from 6 to 24 l./hr. During this period

solution of oxygen in the oxygen-free copper would occur, but with no measurable weight increase.

The photographic records obtained during the first 15–20 min. have been re-plotted in the conventional manner $((\text{mg./cm.}^2)^2 \text{ against time})$, in order to observe the transition from the initial sigmoid curl to the expected parabolic curve for diffusion through the completely formed oxide film. In the resulting curves (Figs. 3–6), oxidation according to the parabolic law

$$w^2 = K_1 t + B \quad (3)$$

would be shown by a straight line.

Only at 750° C. is the initial sigmoid curl followed by parabolic oxidation, although oxidation at some of the other temperatures seems to approximate to the parabolic law. The results which follow for long-term oxidation show, however, that the curves depart more and more from the parabolic with increasing time at low temperatures.

As would be expected, there is no sharp change in curvature where the sigmoid curl ends, but a very gradual merging into the near-parabolic curve (see Fig. 3); this stage is identified with the lateral

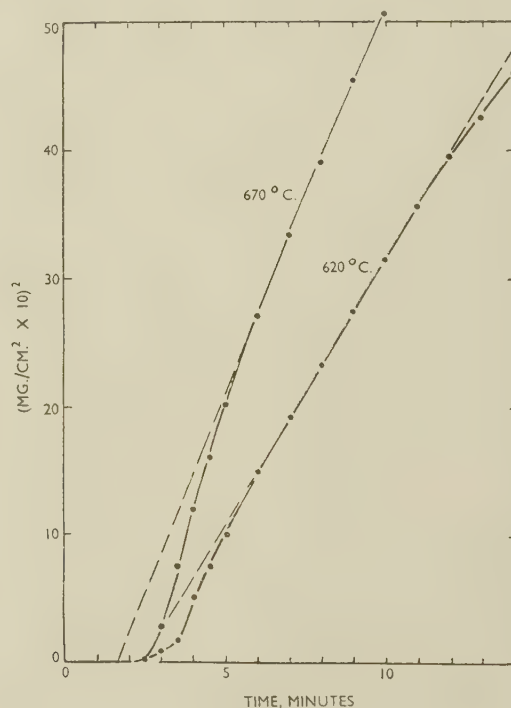


FIG. 4.—“Parabolic” Plot of Oxidation of Annealed Copper in Dry Air.

spread of oxide nuclei until complete coverage is obtained, which should follow the parabolic or some other law applicable to a diffusion process.

The extrapolation of the parabolic portion in Figs. 3–6 passes through the point where sigmoidal oxidation starts, showing that, if the induction period is ignored, i.e. if the start of oxidation is taken as 2 min. after the introduction of air, the constant B of the parabolic equation may be assumed to be zero.

2. OXIDATION OF ANNEALED COPPER SHEET IN DRY AIR

In the preceding section it has been shown that, after the first few minutes' oxidation, diffusion conditions prevail, which would be expected to give rise to a power law of the type:

$$w^n = K_1 t + B \quad (4)$$

where w is the weight gain (mg./cm.²), K is a constant, t is the time (hr.), and B is a constant (probably zero when $n = 2$).

In experiments designed to last for 100 hr., the accuracy of measurement of weight-gains at times of less than 1 hr. was not good, and hence not much importance must be attached to figures obtained from 100-hour oxidation curves during the first hour.

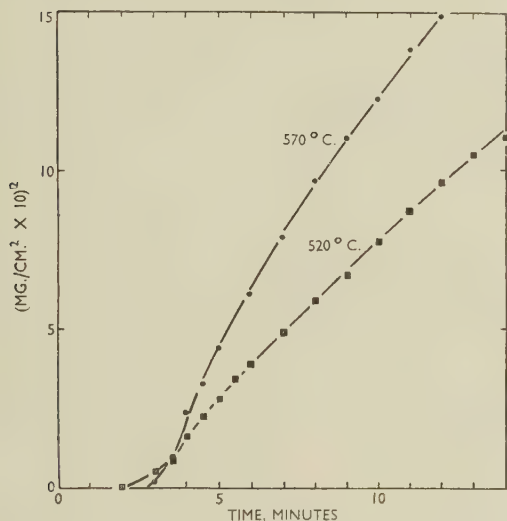


FIG. 5.—“Parabolic” Plot of Oxidation of Annealed Copper in Dry Air.

Weight-gains were measured from the curves and plotted logarithmically on vertical weight and horizontal time scales. This method of plotting permitted different stages of oxidation, e.g. parabolic or cubic, to be recognized from the slopes of the straight portions of the curves. For example, if oxidation was of a type $w^n = K_1 t$, the factor n can be derived from the slope of the log/log plot.

The actual records of oxidation experiments at 200°, 265°, and 315° C., appear to indicate an approximate parabolic type of oxidation in this range (see, for example, Fig. 7). When plotted, however, on a log/log scale, it is seen that no single oxidation law is obeyed at any one temperature (Fig. 8). At 200° C., the slope of the curve between 0.75 and 5 hr. is 0.51, indicating parabolic oxidation. Between 5 and 110 hr., there is a slight scatter of points around a straight line with a slope of 0.35. It is possible that this corresponds to a period of oxidation of the cubic type. This view is reinforced by an examination of the log/log plot for 265° C. (Fig. 8), where

there is a similar transition from a line with a slope of 0.50 (parabolic) to one with a slope of 0.37. The weight-gain at which this transition takes place is, however, not the same at both temperatures.

At 315° C., there is again an initial parabolic stage with a slope of 0.48. After about 4 hr. the rate of oxidation gradually decreases along a curve up to the limit of oxidation time of 100 hr. The final slope is of a very small order, about 0.15 (Fig. 8).

Since it was possible that this might be a logarithmic stage, the curve was re-plotted to show weight-gain in mg./cm.² against log time. The results showed a reasonably straight line from 3 to 100 hr., but the earlier stage, 0–3 hr., could not be considered to be part of the same logarithmic curve.

Log/log plots (Fig. 8) show that the initial parabolic stage disappears entirely between 365° and 465° C.,

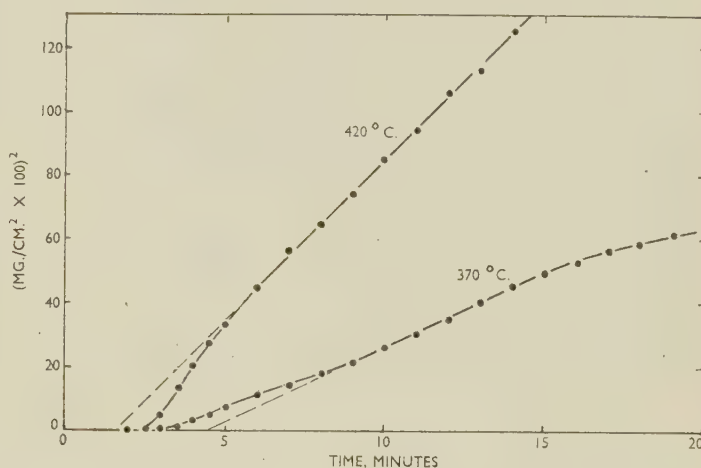


FIG. 6.—“Parabolic” Plot of Oxidation of Annealed Copper in Dry Air.

with very great deviations from slopes of the order of 0.5. The type of oxidation in this range is characterized by periods of very low oxidation rate followed

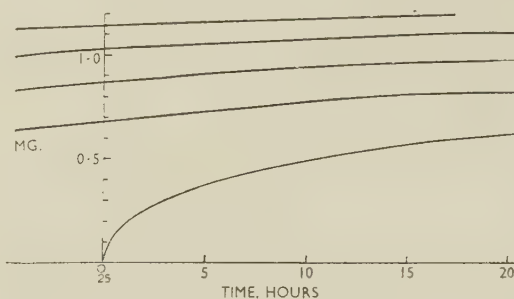


FIG. 7.—Weight/Time Curve for Annealed Copper Sheet Oxidized in Dry Air at 265° C. Area = 2.32 cm.².

by sudden increases. At 420° and 465° C., the original weight/time curves show less marked, but quite definite, increases in rate.

Weight/time records at 520°, 570°, 625°, and 670° C. showed the absence of obvious sudden increases in weight. It appeared that the ductility of the film was now becoming sufficient to permit gradual relief of stress. More gradual changes in weight can be seen on the log/log plots for this temperature range (Fig. 8). However, the weight/time curves obtained at 725° C. showed sudden increases in weight. This behaviour was unexpected, since previous work on the properties of films by the author⁹ had shown them to possess considerable ductility at 700° C.

Generally, between 200° and 365° C., there seems to be an initial period of parabolic oxidation lasting from 1 to 4 hr. and resulting in weight gains given in Table II.

Expressed in weight per unit area, the initial parabolic period and the weight-gain for departure from it are not constant but increase with temperature. This is probably due to either increasing film ductility or improved adhesion with rise in temperature. Oxidation in the range 365°–465° C. seems to belong to the blister-crack-heal type with blistering occurring

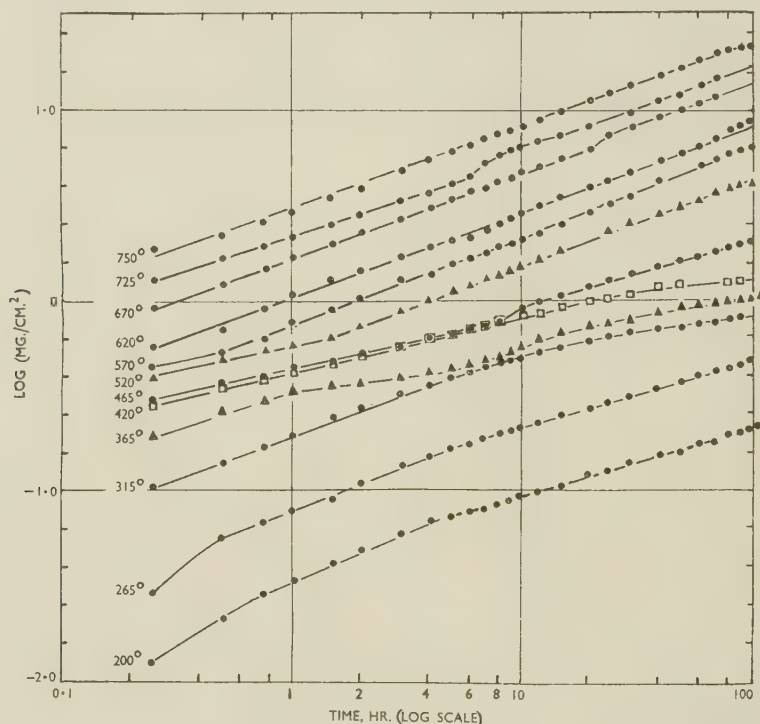


FIG. 8.—Log/Log Plot for Annealed Copper Sheet Oxidized in Dry Air at Various Temperatures (°C.).

One obvious difference between the high-temperature weight changes and those at lower temperatures (365°–465° C.) is that the former are not preceded by a slowing down of the weight increase below that required for the parabolic type of oxidation. This suggests that the high-temperature changes have no connection with loss of adhesion and buckling of the films.

The results obtained at 520°–750° C. plotted on a log/log scale (Fig. 8) show a general tendency to approximate to straight lines with a slope of 0.46. At 520° C., there is an initial period of oxidation up to 1½ hr. with a slope of considerably less than 0.46. At 620° C., there is a slight scatter about a line with a slope of 0.46. The sudden increases already mentioned are clearly visible at 725° and 670° C.

A summary of information obtained from the oxidation of annealed copper sheet in dry air, is given in Table I. Where definite straight-line periods are obtained in the log/log plots, the slopes are given in columns 6 and 8.

during the first 20 min. at about 370° C., as shown by the results obtained during the early stages of oxidation (Fig. 9). It is probable that sudden discontinuities caused by cracking, are visible on

TABLE I.—Oxidation of Annealed Copper Sheet in Dry Air (After Hydrogen Reduction).

Temp., °C.	Increase in Weight (mg./cm. ²) after :			Log/Log Plot			
	1 hr.	10 hr.	100 hr.	Period, hr.	Slope	Period, hr.	Slope
200	0.034	0.095	0.208	0.5–4.0	0.51	4.0–110	0.35
265	0.079	0.213	0.49	0.5–3.0	0.50	3.0–110	0.37
315	0.195	0.505	0.84	0.4–0	0.48	4.0–100	Non-linear
365	0.325	0.57	1.12	0.1–0	0.49	1.5–0	0.25
						5–100	Non-linear
420	0.412	0.83	1.30	0–20	0.32	20–100	0.33
465	0.45	0.92	2.06	0–8.0	0.25	10–100	0.33
520	0.59	1.50	4.07	0–1.5	0.25	1.5–70	0.46
570	0.80	2.11	6.40	0–100	0.46
625	1.04	2.85	8.70	0–100	0.47
670	1.68	4.70	13.8*	0–20	0.46	50–70	0.46
725	2.16	6.4	18.5*	0.5–6.0	0.40	20–70	0.50
750	3.20	8.6	22.0	0–90	0.43

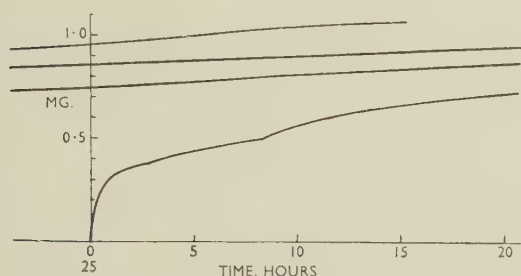
* Extrapolated from 70-hr. values.

TABLE II.—Oxidation of Annealed Copper Sheet:
Periods of Parabolic Oxidation (mg./cm.²).

Temp., °C.	Range of Weight- Gains, mg./cm. ²	Remarks
200	0–0.067	Later, cubic (?)
265	0–0.137	„
315	0–0.36	Later, non-linear or logarithmic
365	0–0.325	Later, discontinuous
520	0.66 upwards	
570	Whole range	
625	„	
670	„	
725	„	
750	„	

the weight/time curves only when large areas of the film crack over short periods of time.

At temperatures above 470° C., the blistering

FIG. 9.—Weight/Time Curve for Annealed Copper Sheet
Oxidized in Dry Air at 365° C. Area = 0.98 cm.².

period appears to start and cease within the first 15 min., since any abrupt increases that take place later are not preceded by periods of reduced weight

increase. Such weight increases as do occur must be ascribed to other causes and are discussed later.

The slopes of the log/log plots in the range 570°–750° C. all fall between 0.40 and 0.50 (Table I), showing that oxidation is approximately parabolic.

3. OXIDATION OF HARD-ROLLED COPPER SHEET IN DRY AIR

The object of this part of the investigation was to determine the possible effect of annealing of the basis metal on the type of oxidation. It was realized that a certain amount of recrystallization might occur during the removal of the pre-existing film in hydrogen-nitrogen mixtures at elevated temperatures. To minimize this, the specimens were reduced at 400° C., and cooled as rapidly as possible. The time taken to cool the specimen from 400° C. to the oxidizing temperature varied from 45 min. for the specimen oxidized at 210° C., to 2 min. for that oxidized at 365° C. Two effects which occur during recrystallization might influence the oxidation process, viz. change in the direction of preferred orientation during recrystallization and subsequent grain growth. According to Barrett,¹⁶ one would expect cold rolling of copper to produce a preferred orientation with the (110) plane parallel to the surface of the metal. It has been found that, after recrystallization, the (100) cube face is preferred. According to Cook and Richards,¹⁷ the percentage of the structure with the (100) plane preferred, on annealing for 1 hr. after cold reductions of 90%, increases with temperature from 50% at 100° C. to 93% at 900° C.; hence changes in orientation are not likely to be

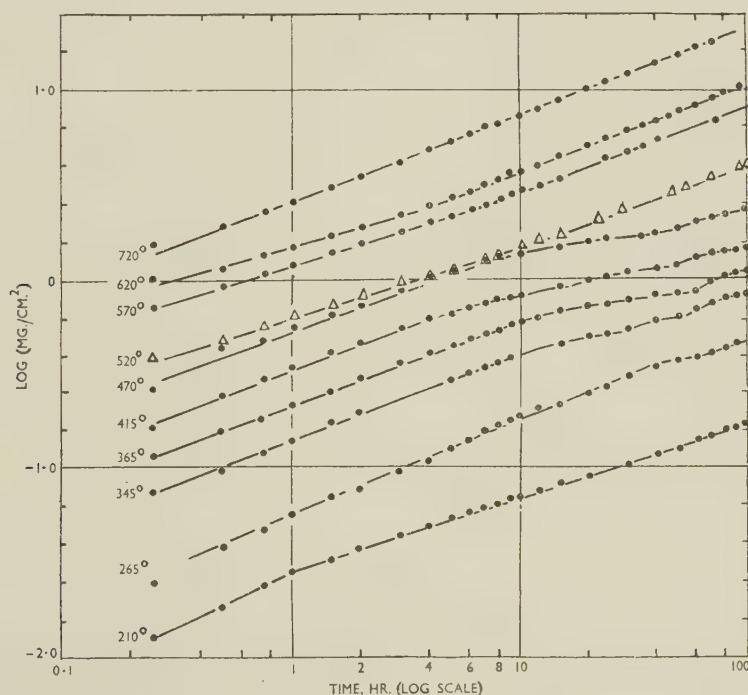


FIG. 10.—Log/Log Plot for Hard Copper Oxidized in Dry Air at Various Temperatures (°C.).

complete at the start of oxidation. Moreover, grain growth of the copper would continue at the higher temperatures after the start of oxidation, and might have some influence on the relief of internal stress in the oxide or on its adhesion to the basis metal.

The log/log plot for oxidation at 210° C. (see Fig. 10), consists almost completely of a single straight line of slope 0.35. It appears that here the conditions are suitable for oxidation of the cubic type, as found by Campbell and Thomas⁷ at temperatures between 100° and 256° C.

Comparison of the log/log plots at 265° C. (Figs. 8 and 10), shows that the parabolic range has been lengthened from 2 hr. for soft copper to 50 hr. for hard copper. Between 345° and 470° C., the parabolic law is more accurately obeyed, and this stage lasts considerably longer than for the soft copper, suggesting that recrystallization of the basis metal in this range has improved the adherence. Discontinuities occur after long times, as with oxidation

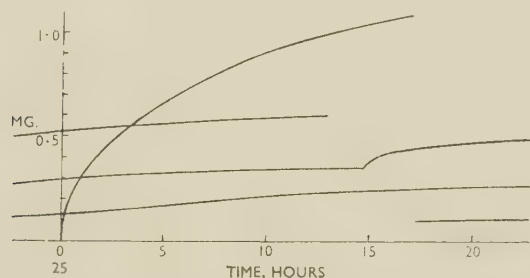


FIG. 11.—Weight/Time Curve for Hard Copper Oxidized in Dry Air at 365° C. Area = 1.52 cm.².

at 365° C. (Fig. 11). As was to be expected there is no noticeable difference in the type of oxidation of hard and soft copper between 520° and 720° C.

The increase in weight at 1, 10, and 100 hr. for the whole range of oxidation temperatures is given in Table III, together with details of the slope of log/log plots.

TABLE III.—*Oxidation of Hard-Rolled Copper Sheet in Dry Air (After Hydrogen Reduction).*

Temp., °C.	Increase in Weight (mg./cm. ²) after:			Log/Log Plot			
	1 hr.	10 hr.	100 hr.	Period, hr.	Slope	Period, hr.	Slope
210	0.0285	0.069	0.162	0.75–100	0.38
265	0.057	0.182	0.500*	1.0–50	0.50	50–100	Non-linear
345	0.136	0.38	0.83*	0–10	0.47	10–100	"
365	0.209	0.597	1.06	0–10	0.47	10–100	"
415	0.329	0.82	1.44	0–5	0.47	5–100	"
470	0.534	1.33	2.31	0–5	0.46	5–100	"
520	0.63	1.44	3.95	0–7	0.37	7–100	0.45
570	1.20	2.86	7.95*	0–10	0.37	10–100	0.45
625	1.45	3.75	10.4	0–4	0.35	4–100	0.46
720	2.52	7.20	13.2*	0–100	0.46

* Extrapolated from 70 hr.

The general picture of oxidation of hard-rolled copper is much the same as that of soft copper, except that the initial parabolic stage at low temperatures is prolonged to greater film thicknesses

and to higher temperatures. The limiting values of weight-gain for parabolic oxidation, given in Table IV, are considerably in excess of those given in Table II for the same temperatures.

TABLE IV.—*Oxidation of Hard-Rolled Copper Sheet: Periods of Parabolic Oxidation (mg./cm.²).*

Temp., °C.	Range of Weight-Gains, mg./cm. ²	Remarks
265	0–0.358	Later, discontinuous
345	0–0.452	" "
365	0–0.597	" "
415	0–0.603	" "
470	0–1.2	" "
520	1.23 upwards	Earlier, cubic
570	2.86	" "
625	2.42	" "
720	4.90	All parabolic

Some effect caused by recrystallization appears therefore, to be responsible for extending the thickness range for parabolic oxidation. This is probably the change of preferred orientation which has occurred during oxidation. The plane parallel to the surface of the hard-rolled metal would be the (110) plane before oxidation, and the (100) cube face after.¹⁶ Since the (100) planes have double the rate of oxidation of the (110) and (111) planes,^{5,18} it would be expected that the oxidation rate of hard copper would be less than that of annealed copper. During the recrystallization of the cold-worked metal, the rate of oxidation would increase, until the recrystallization process was completed. These conclusions were confirmed by the present experiments (Table V). The difference is less noticeable at high temperatures, owing to more complete recrystallization during the hydrogen-reduction period; it ceases to be marked at about 465° C.

TABLE V.—*Differences in Oxidation Weight-Gains of Hard and Soft Copper Due to Recrystallization of Hard Copper.*

Temp., °C.	Weight-Gains, mg./cm. ²			
	After 1 hr.		After 10 hr.	
	Hard	Soft	Hard	Soft
200–210	0.029	0.034	0.069	0.095
265	0.057	0.079	0.182	0.213
365	0.209	0.325	0.597	0.57
415–420	0.329	0.412	0.820	0.83
465–470	0.534	0.45	1.33	0.92

After 10 hours' oxidation, at 365° C. and above, recrystallization appears to be complete, so that there is little difference between hard and soft copper.

4. THE EFFECT OF MOISTURE ON THE OXIDATION OF ANNEALED COPPER SHEET IN AIR

Oxidation tests were made between 370° and 750° C. The weight/time curves for temperatures from 370°

to 625° C. show no sign of sudden weight increases. Such discontinuities were, however, present in the curves at 725° and 750° C.

The log/log plots (Fig. 12) show that at 370° and 420° C. there is a gradual reduction of slope after a certain time, which is the main feature of previous log/log plots in this temperature range. Again there is a period of approximately parabolic oxidation, followed by oxidation at a reduced rate. This latter is not marked by sudden increases in rate as formerly, which suggests that the film substance has been strengthened by the presence of moisture, but that its adherence to the basis metal has not been improved. This strengthening probably explains the absence of sudden increases in the weight/time curves. At 520° C. and above, oxidation starts

A summary of data for oxidation in moist air is given in Table VII.

TABLE VII.—*Oxidation of Annealed Copper Sheet in Moist Air.*

Temp., °C.	Increase in Weight (mg./cm. ²) after:			Log/Log Plot			
	1 hr.	10 hr.	100 hr.	Period, hr.	Slope	Period, hr.	Slope
370	0.123	0.377	0.737	0–15	0.50	15–100	Non-linear
420	0.23	0.78	1.45	0–10	0.54	10–100	"
520	0.93	2.06	5.4	0–5	0.34	5–100	0.45
625	1.10	3.2	9.6	0–3	0.38	3–100	0.49
725	2.69	7.2	20.5	0–1.5	0.36	1.5–100	0.46
750	2.9	8.5	22.2	0–0.75	0.39	0.75–100	0.46

During the parabolic ranges of oxidation, the weight-gain at 370° C. in moist air is about half that

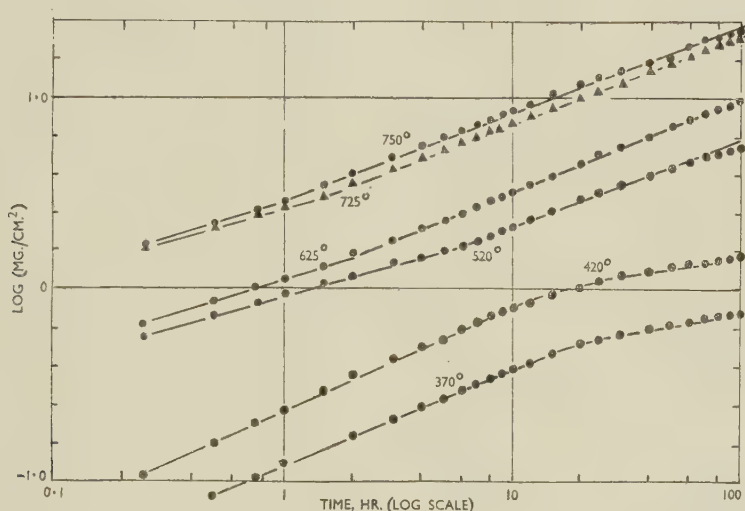


FIG. 12.—Log/Log Plot for Annealed Copper Oxidized in Moist Air at Various Temperatures (°C.).

with a slope of about 0.35, and after times varying from 5 hr. at 520° to 1½ hr. at 725° C., goes over to the parabolic oxidation curve with a slope of 0.5 approximately. This high-temperature parabolic period is again characterized by sudden changes in rate.

The initial period of oxidation in the range 520°–750° C. seems to obey a power law of the type $w^n = K_1t + c$, n ranging from 2.6 to 2.9. The limit-

in dry air, as shown in Table VIII. However, at 520° C., the position is reversed, and oxidation in moist air is about 50% more rapid than in dry air.

TABLE VIII.—*Comparison of Oxidation Weight Gains (mg./cm.²) for Moist and Dry Air (Parabolic Range).*

Temp., °C.	Time, hr.	Air	
		Dry	Moist
370	1.0	0.325	0.123
520	10	1.5	2.06
620–625	10	2.85	3.2
725	10	6.4	7.2
750	10	8.6	8.5

TABLE VI.—*Oxidation in Moist Air: Periods of Parabolic Oxidation.*

Temp., °C.	Weight-Gain, mg./cm. ²
520	Above 1.57
625	" 1.75
725	" 3.05
750	" 2.49

ing weight-gain for conformity to this law is about 1.5–3.0 mg./cm.², above which the oxidation approximates to the parabolic law (Table VI).

The difference in rate decreases with increase in temperature, so that at 750° C. the rates are identical, in agreement with Pilling and Bedworth's finding at 800° C.

5. OXIDATION OF ANNEALED COPPER SHEET IN DRY OXYGEN

The results so far reported suggested that the sudden changes in oxidation rate, visible in some of the weight/

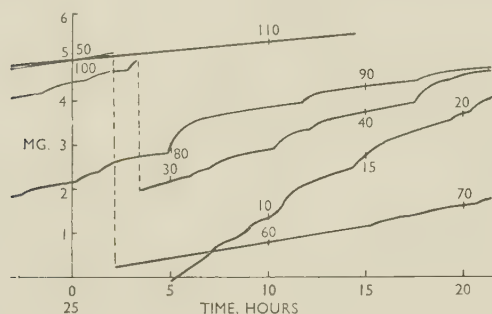


FIG. 13.—Weight/Time Curve for Annealed Copper Oxidized in Oxygen at 725° C. Area = 0.80 cm.².

time records, were connected with a complex blister-crack-heal process. It was necessary to find whether

change from near-parabolic to non-parabolic oxidation between 200° and 420° C. Comparison with results in moist air (Fig. 12) for oxidation at 370° and 420° C. shows that the weight increments and slopes of the curves are almost identical, indicating that the effect of removing nitrogen is almost the same as that of adding moisture in this temperature range.

At 625° C. the log/log plot has the same features as for dry air at 620° C., i.e. intermittent cracking and a general obedience to the parabolic law. Log/log plots for oxidation in oxygen at 520°, 625°, and 725° C. do not show an initial period of lower slope (0.35–0.40), as do the results for moist air in this temperature range (see Fig. 12).

The vertical scale of Fig. 13 at 725° C. was magnified by using a comparatively large specimen, which required movement of the rider several times during oxidation. This curve shows a feature of some interest, namely periods of intense cracking activity followed by periods of less activity. Sudden changes in slope are apparent during oxidation in the period between 5 and 50 hr. Between 50 and 70 hr. there

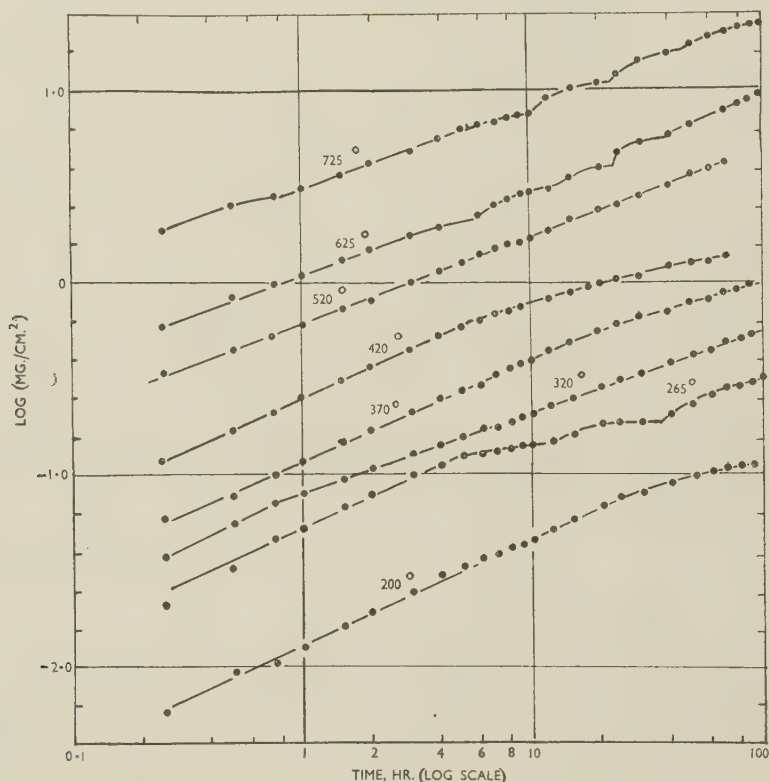


FIG. 14.—Log/Log Plot for Annealed Copper Oxidized in Oxygen at Various Temperatures (°C.).

this mechanism was in any way influenced by the presence of inert nitrogen in the blister found during oxidation in air.

In dry oxygen at 370°, 420°, and 520° C., there were no sudden changes in rate, but at 625° and 725° C. (Fig. 13) such changes occurred. The log/log plots (Fig. 14) show the usual reduction in slope, i.e.

is a period of almost straight-line oxidation, followed by a period of activity between 70 and 95 hr. Again, between 95 and 115 hr. there is a period in which no cracking occurs.

A summary of the weight increments at each temperature after 1, 10, and 100 hr. is given in Table IX, with details of the slopes of the log/log plots.

Weight increments for periods of parabolic growth are given in Table X.

TABLE IX.—Oxidation of Annealed Copper Sheet in Dry Oxygen.

Temp., °C.	Increase in Weight (mg./cm. ²) after:			Log/Log Plot			
	1 hr.	10 hr.	100 hr.	Period, hr.	Slope	Period, hr.	Slope
200	0.0128	0.046	0.118	0–24	0.55	24–100	Non-linear
265	0.051	0.142	0.315	0.75–5	0.52	5–100	0.33
320	0.080	0.210	0.560	0–100	0.43
370	0.118	0.39	1.0	0–15	0.53	15–100	Non-linear
420	0.25	0.77	1.48 *	0–7	0.55	7–70	"
520	0.61	1.71	5.0	0–70	0.46
625	1.07	3.0	11.3	0–3	0.45	3–100	0.50
725	2.24 *	6.6	21.0	0–100	0.48

* Extrapolated.

TABLE X.—Oxidation in Dry Oxygen: Periods of Parabolic Oxidation.

Temp., °C.	Weight-Gain, mg./cm. ²	Temp., °C.	Weight-Gain, mg./cm. ²
200	0–0.077	420	0–0.69
265	0–0.112	520	Whole range
320	0–0.080	625	"
370	0–0.48	725	"

Comparison of weight gains of annealed copper in dry oxygen with those for annealed copper in dry air, shows that between 520° and 725° C. the oxidation rates are slightly greater in oxygen. Between 200° and 370° C. they are considerably less (Table XI).

TABLE XI.—Effect of Oxygen Pressure on Oxidation of Annealed Copper Sheet (Parabolic Oxidation).

Temp., °C.	Time, hr.	Weight-Gain, mg./cm. ²	
		Air (155 mm. Hg)	Oxygen (760 mm. Hg)
200	1.0	0.034	0.0128
265	1.0	0.079	0.051
315–320	1.0	0.195	0.080
365–370	1.0	0.325	0.118
420	1.0	(0.412) *	0.250
520	10	1.50	1.71
620–625	10	2.85	3.00
725	10	6.40	6.60

* Oxidation not parabolic.

It seems that the result of using oxygen instead of air has merely been to strengthen the film, and this has resulted in less cracking and therefore in a lower oxidation rate.

6. OXIDATION OF ANNEALED COPPER SHEET IN "OXYGEN-FREE" NITROGEN

It was not possible to carry out experiments at sub-normal pressures in this apparatus, but the use of "oxygen-free" nitrogen, which has a partial oxygen pressure of about 8×10^{-3} mm. Hg, provided a useful means of studying the effect of low pressures.

Experiments were carried out at 370°–725° C. There were no sudden weight changes, but clear evidence of non-parabolic oxidation, particularly at low temperatures. The results, plotted in logarithmic form in Fig. 15, show that the effect of oxidation in "oxygen-free" nitrogen has been to retard the early sigmoid stage, so that, at 375° C., it lasts for the total period of oxidation, i.e. 100 hr. The logarithmic plot at this temperature can be resolved into two components, a straight line of slope = 0.23, probably representing the nucleation period, and a line of slope 0.79, representing lateral growth and growth in thickness.

At higher temperatures, the nucleation period is not shown, but the near-linear portion of the sigmoid curve is present, with a slope of 0.83–0.86. This is followed by a parabolic portion at 525° C. and above, but at 420° C., there is a very rapid transition to a line with a slope of 0.30. A change from nitrogen to air at 50 hr. made no difference to the slope of the curve for oxidation at 420° C.

The most important point arising from these results is the short-time range of conformity with the parabolic law at 420°, 625°, and 725° C. The final law obeyed is of the cubic type, with slopes of the order of 0.30–0.38. For some reason, the parabolic law (slope 0.51) has been obeyed up to 100 hr. at 525° C. This exception seems to illustrate the extreme sensitivity of oxidation to experimental conditions in the early stages. An alternative explanation of the portion with a slope of the order of 0.5 at 420°, 625°, and 725° C., is that it is part of the sigmoid curl, which later gives way to the cubic relationship.

Comparison of the weight-gains obtained during oxidation in "oxygen-free" nitrogen with those obtained in air, shows that the period of steep slope (c. 0.80) lasts up to a gain of about 0.4 mg./cm.² in "oxygen-free" nitrogen. In air, however, this period is over by the time a gain of 0.01 mg./cm.² is reached. This seems to indicate that in "oxygen-free" nitrogen, oxide nuclei grow more in depth and reach full surface coverage much later than in air. Probably some of the extra weight of oxygen absorbed is accounted for by the greater amount of internal oxidation in such low-pressure atmospheres.

The absence of sudden weight changes in "oxygen-free" nitrogen suggests less porous films, although weight-gains of the order of those obtained in air at 725° C. were never attained. The close conformity with the cubic law after 3 hr. at 420°, 625°, and 725° C. is probably due to the simultaneous existence of thin films and good ductility at the higher temperatures. The weight range for obedience to the cubic law is from 0.35 to at least 6.0 mg./cm.² in "oxygen-free" nitrogen, compared with a range of 0.4–3.0 mg./cm.² for hard copper in air.

It would be expected that the lower dissociation temperature of CuO in this atmosphere would lead to lower CuO contents in the film formed in "oxygen-free" nitrogen, compared with those formed in air.

It is hoped that the whole question of film composition will be the subject of a further report.

7. THE EFFECT OF A PRE-EXISTING FILM

In previous work carried out by the author,¹⁰ no effort was made to remove the original air-formed film before high-temperature oxidation. In other respects, the oxidation technique was similar and

reduced copper at 210° C. Oxidation curves at 510° and 550° C. are seen to be near-parabolic (slopes 0.44), whereas for reduced copper in the present work, the initial slope for oxidation at 520° and 570° C. is 0.37. At the lower temperatures, 350°–450° C. (Fig. 16), the discontinuous type of oxidation is apparent, as for reduced copper. A summary of the results obtained is given in Table XII.

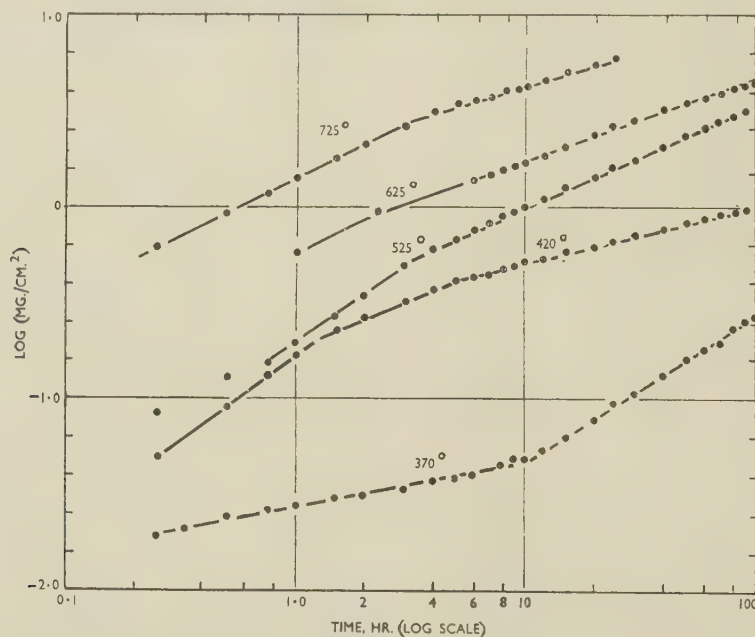


FIG. 15.—Log/Log Plot for Annealed Copper Oxidized in "Oxygen-Free" Nitrogen at Various Temperatures (°C.).

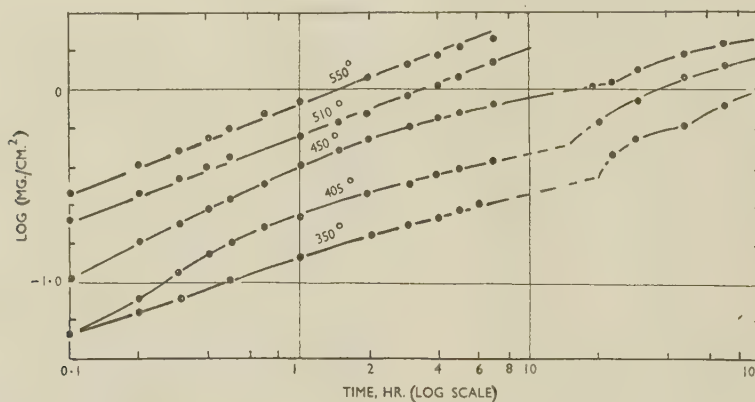


FIG. 16.—Log/Log Plot for Hard-Drawn Copper Bar Oxidized in Dry Air Without Previous Reduction.

results are comparable. Since the previous results were obtained on cold-drawn rod after light pickling, they will be compared with those obtained on hard-rolled copper in the present work; Fig. 16 shows those obtained between 550° and 350° C. after replotting on a log/log scale. It will be seen that the initial parabolic portion (slope 0.5) is not present at 350°–450° C. The initial part of the curve for 350° C. approximates to a straight line of slope 0.38, i.e. this may be a period of cubic oxidation as found for

Comparison with Table III shows that the rates are not substantially different. The main difference is that the oxidation of surfaces with a pre-existing film is not initially parabolic between 350° and 450° C. At 510° and 550° C., oxidation seems to start parabolically and continue so (slopes = 0.44 in Fig. 16).

Some oxidation experiments were made without previous reduction, at 435°, 485°, and 570° C., on the electrolytically polished surfaces used in this investigation. At 435° and 485° C., the oxidation curve is

initially parabolic (slope 0.50), and then goes over to the discontinuous type, apparently because of cracking. At 570° C., oxidation seems to be wholly

TABLE XII.—*Results Previously Obtained on the Oxidation of Pure, Cold-Worked Copper Bar in Dry Air.*

Heating-up in nitrogen; no pre-reduction; surface, as-rolled and pickled.

Temp., °C.	Weight-Gain, mg./cm. ² after :			Log/Log Plot	
	1 hr.	10 hr.	100 hr.	Period, hr.	Slope
350	0.14	0.35 *	0.98	0–100	Discontinuous
405	0.22	0.46 *	1.60	0–100	"
450	0.40	0.87 *	1.78	0–100	"
510	0.57	1.58 *	...	0–7	0.44
550	0.88	2.35 *	...	0–7	0.44

* Interpolated or extrapolated.

parabolic (slope = 0.53). A summary is given in Table XIII.

The film on electropolished surfaces has caused a very large reduction in oxidation rate. For example, at 570° C., the electropolished surface with no hydrogen reduction has a weight-gain of 1.82 mg./cm.² after 10 hr., whereas the reduced surface has a gain of 2.86 mg./cm.² (Table III). At 435° C., the weight-gain after 10 hr. is 0.57 mg./cm.² for air-formed films on an electropolished surface, and 0.82 mg./cm.², at 415° C., for a reduced surface.

TABLE XIII.—*Results Obtained during Oxidation of Hard Copper Sheet in Dry Air.*

No previous reduction. Surfaces electropolished.

Temp., °C.	Weight-Gain (mg./cm. ²) after :			Log/Log Plot			
	1 hr.	10 hr.	100 hr.	Period, hr.	Slope	Period, hr.	Slope
435	0.114	0.57	1.00 *	0–1.5	0.50	1.5–100	Non-linear
485	0.184	0.53	2.85	0–5	0.50	5–100	"
570	0.52	1.82 *	5.78	0–100	0.53	...	"

* Interpolated.

This cannot be due to any difference between an ordinary air-formed film and a reduced surface, since a comparison of Tables III and XII shows no such difference. It can be due only to the presence of an oxide film on the electropolished surface, either considerably thicker or more oxidation-resistant than that formed in atmospheric air.

8. EFFECT OF SPECIMEN SHAPE

The conditions under which the oxide film grows vary with the shape of the specimen. With wires undergoing oxidation, the area available for the growing oxide film will increase with film thickness, and it would be expected that the internal compression stress would decrease in the outer layers as growth proceeds.

With an infinite plate (i.e. with no edges) there can theoretically be no stress between the oxide and the

metal in a direction normal to the surface. However, in a finite plate, edge conditions must modify the stress conditions, causing stresses to appear perpendicular to the surface, which may initiate separation.

These normal or radial stresses are likely to be very much greater in a wire, owing to the tendency of the oxide to break away from the metal and form a cylinder of equilibrium diameter greater than that when in contact with the metal. It would be expected, therefore, that at any given temperature there would be a greater tendency for cavities to form between the oxide and the metal in wire than in sheet.

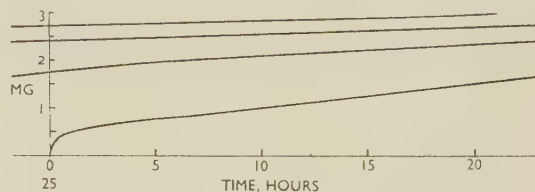


FIG. 17.—Weight/Time Curve for Annealed Copper Wire Oxidized in Dry Air at 420° C. Area = 3.43 cm.².

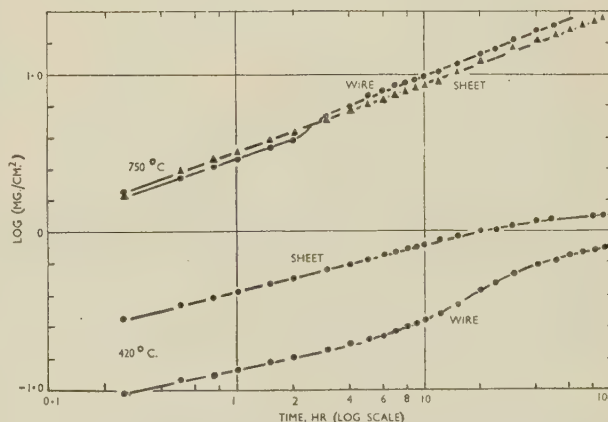


FIG. 18.—Log/Log Plot for Annealed Copper Wire and Sheet Oxidized in Dry Air at 420° and 750° C.

Owing to the high sensitivity of the balance a very small specimen area had to be used at high temperatures, where the weight-gains were large. At 750° C. this meant that the behaviour of a sheet specimen 0.040 in. thick, and only 0.10 in. wide, was being compared with that of a wire specimen 0.034 in. in dia. It is to be expected that under such conditions there would be very little difference in behaviour, since the growing oxide film would soon start to assume a rounded form on the "sheet" specimen.

Oxidation tests were made at 420° and 750° C. Fig. 17 shows the weight/time curve for annealed copper wire at 420° C. No abrupt weight changes are visible, in agreement with the curve obtained for annealed sheet. However, a change in slope is apparent at about 6 hr.; this is also shown on the log/log plot (Fig. 18). The curve is non-parabolic,

the initial part up to 6 hr. having a slope of 0.26, which is approximately the same as that of the early part of the curve for annealed sheet at the same temperature.

At 750° C., the early part of the weight/time curve for annealed wire shows many marked changes in slope (Fig. 19), whereas the corresponding curve for annealed sheet is reasonably smooth. Fig. 18 shows that the log/log plot for annealed sheet at 750° C. is a straight line with a slope of 0.44, indicating approximately parabolic oxidation. The curve for annealed wire is initially parallel, but has a slightly slower rate up to 2 hr., when fractures occur. The final rate is slightly greater than that for sheet, with a slope of 0.46. In both types of specimen, fractures of the oxide take place in the later stages, e.g. in annealed sheet at 19 and 48 hr., and in wire at 12, 32,

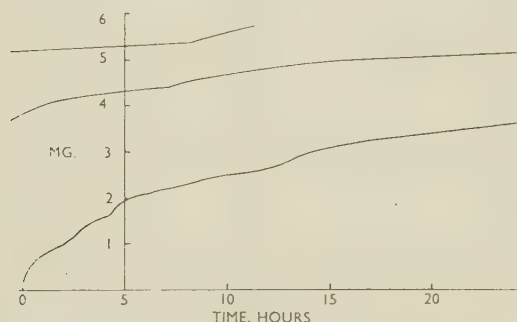


FIG. 19.—Weight/Time Curve for Annealed Copper Wire Oxidized in Dry Air at 750° C. Area = 0.26 cm.².

and 57 hr. A summary of the figures is given in Table XIV, together with figures obtained on annealed sheet at the same temperatures.

TABLE XIV.—*Effect of Specimen Shape on the Oxidation of Annealed Copper in Dry Air.*

Shape	Temp., °C.	Weight Gain, mg./cm. ² , after :		
		1 hr.	10 hr.	100 hr.
Wire	750	2.90	9.6	...
Sheet	750	3.20	8.6	22.0
Wire	420	0.132	0.268	0.82
Sheet	420	0.412	0.832	1.30

The results for wire show the following characteristics: (1) At 420° C., a lower oxidation rate; increasing slope of the log/log plot followed by reduction of slope; and (2) at 750° C., earlier and more frequent "cracking" than on the sheet.

The lower oxidation rate at 420° C. is most likely due to the formation of cavities between the wire and oxide, the cracking of which is delayed until after 6 hours' oxidation. Fig. 18 shows that there is a tendency for the curves for sheet and wire to converge at some time after 100 hr. At 750° C., there is no significant difference after the first 12 hr. During the early stages, considerable stress-relief appears to occur.

It seems that the main difference between sheet and wire results from the increased size of the cavity barriers that arise in the initial stages of oxidation of the wire. This is probably due to the radial stress, caused by the oxide jacket trying to form a cylinder of inside diameter greater than that of the wire itself. At low temperatures, as the oxide film on the wire thickens, the compressive stresses can be withstood without further buckling of the film, owing to its inherent stability.

V.—THE TEMPERATURE DEPENDENCE OF THE OXIDATION RATE

At high temperatures it has been assumed that oxidation is controlled by a diffusion process due to a concentration gradient. With copper, the rate-controlling mechanism has usually been considered to be that of outward migration of copper ions to react with oxygen at the oxide/gas interface. In fact, there must also be an inward movement of oxygen, since during the oxidation of copper wire it was found by the author⁹ that when the wire was completely oxidized, it formed a filament of solid oxide rather than a tube. The latter would be expected if the mechanism were one of outward movement of copper only.

It is difficult to postulate any mechanism for inward diffusion of oxygen at 900° C., other than vacancy or interstitial diffusion. As the oxide is plastic and under compression, it is unlikely that rifts are formed through which the oxygen molecules could diffuse inwards, as would be possible at low temperatures. Outward or inward diffusion through a compact film either by vacant sites or interstitial movement would be expected to obey the parabolic law.

Other workers have shown that laws other than the parabolic are valid over wide ranges of temperatures. Whatever the oxidation law, if it is assumed that the properties of the oxide film are characteristic of the thickness, and that the only effect of temperature is to accelerate a single process of oxidation, then for a normal activated process, we can expect:

$$K = Ae^{-Q/RT} \quad \dots \quad (5)$$

where A is a constant, T the absolute temperature (°K.), Q the activation energy (cal./mole), R the gas constant, and K the oxidation-rate constant.

Previous investigators plotted the log of the rate constants obtained from parabolic oxidation at high temperatures against the reciprocal of the absolute temperature, and obtained a straight line representing a constant activation energy Q . When the results of low-temperature work (20°–600° C.) were plotted in the same manner (i.e. where parabolic oxidation was found, or assumed), another straight line was also obtained.¹ For high-temperature oxidation, Q is about 40,000 cal., and for low-temperature about 20,000 cal. The two lines intersect in the range 500°–700° C.

If it is assumed that the oxidation curve is parabolic for copper at all temperatures, the change in activation energy at 500° C. can be explained only if there is no fundamental change in mechanism, but a change in values, i.e. a slowing down in the decrease of vacant sites or a change in the relative importance of lattice diffusion and grain-boundary diffusion.

The preceding sections have shown that there is a fairly general obedience to the parabolic law at 520° C. and above, but between 200° and 475° C. this law is generally not obeyed except for short initial periods.

1. TEMPERATURE DEPENDENCE OF PARABOLIC RATE CONSTANT

If it is assumed that the parabolic law typifies a single process of oxidation, we can proceed to examine the temperature dependence of the parabolic rate constant obtained from the equation :

$$K_1 = \frac{w^2 - B}{t},$$

where w is the weight gain (g./cm.²), t the time (hr.), B a constant, and K_1 will be in (g./cm.²)²/hr., or g.²cm.⁻⁴ hr.⁻¹.

At the beginning of oxidation there is a period

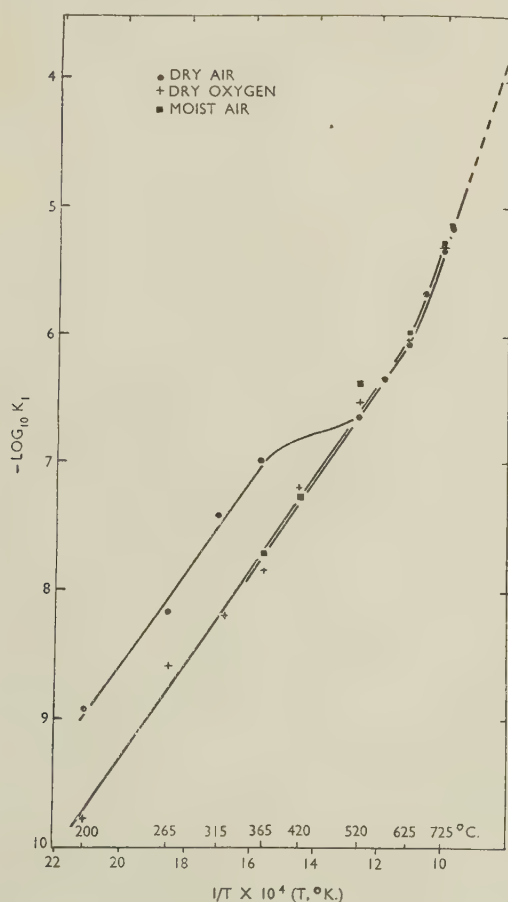


FIG. 20.—Plot of Log of Parabolic Rate Constant, K_1 , against the Reciprocal of Absolute Temperature for Annealed Copper Oxidized in Various Atmospheres.

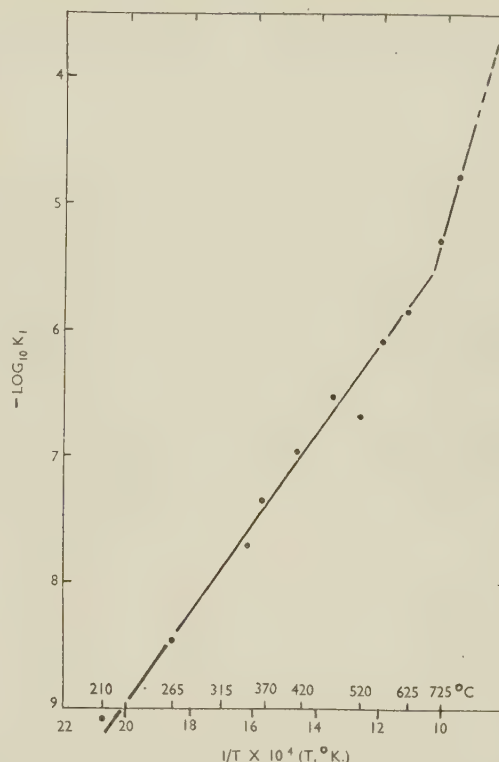


FIG. 21.—Plot of Log of Parabolic Rate Constant, K_1 , against the Reciprocal of Absolute Temperature for Hard Copper Oxidized in Dry Air.

in which growth of nuclei takes place, resulting in a sigmoid increase in weight, until the whole surface is covered by an oxide film. Only then can oxidation take place by diffusion leading to the general parabolic law (equation (3)). Since the slopes of the log/log plots are based on times longer than 1 hr., the sigmoid period of oxidation has been neglected, and the constant B is assumed to be zero.

The logarithms of the parabolic rate constants ($\log_{10} K_1$) have been plotted against $1/T$ in Figs. 20 and 21. Fig. 20 shows the effect of the variation of the atmosphere on the oxidation of annealed copper sheet. At temperatures above 620° C., all points tend to lie on a single curve which becomes asymptotic to a straight line representing an activation energy of the order of 38,000 cal. This is of the same order as the value obtained by previous workers for the high-temperature oxidation of copper.

At lower temperatures, all points between 520° and 620° C. and those below 520° C. for moist air and oxygen, tend to lie on a straight line representing an activation energy of 17,200 cal. The values for dry air at low temperatures, however, lie on a straight line with a slope corresponding approximately to the same activation energy (16,400 cal.), but removed to the left, i.e. having a different constant, A . This curve appears to go over to the general curve at a temperature between 365° and 520° C.

The figures for the oxidation of hard copper in dry air, plotted in Fig. 21, appear to lie on two

straight lines with activation energies of 43,000 and 16,200 cal. at high and low temperatures, respectively. The position of the point at 520° C., which

TABLE XV.—Activation Energies (Q) and Constants (A).

Copper and Atmosphere	High-Temperature		Low-Temperature	
	Q , cal./mole	A , g. ³ cm. ⁻⁴ hr. ⁻¹	Q , cal./mole	A , g. ³ cm. ⁻⁴ hr. ⁻¹
Annealed dry air	38,000 *	79.5	16,400	4.5×10^{-2}
Annealed, moist air and oxygen	38,000 *	100	17,200	0.112
Hard, dry air	43,000 *	1410	16,200	1.26×10^{-2}

* Two temperatures only.

falls off the general curve, is presumably due to complex blistering and cracking conditions in the

reasonably close to a single straight line, suggesting that at both high and low temperatures, obedience to this law results from the same mechanism. The constants in the equation (5) are :

$$A_3 = 0.025 \text{ g.}^3 \text{ cm.}^{-6} \text{ hr.}^{-1}$$

$$Q = 28,300 \text{ cal./mole.}$$

In this case the value of Q is higher than that for the parabolic process at low temperatures. The atmospheric conditions under which the experiment is carried out appear to have little effect on the rate constants.

VI.—PHYSICAL CHARACTERISTICS OF OXIDE FILMS

Visual examination of the specimens after cooling shows that at 200° C. and below, the stresses imposed

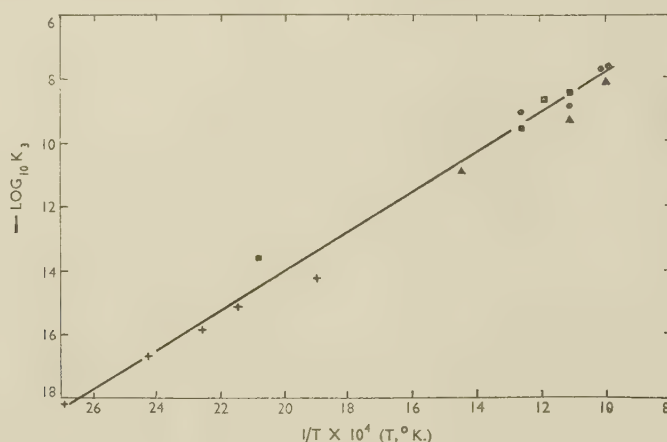


FIG. 22.—Plot of Log of Cubic Rate Constant, K_3 , against the Reciprocal of Absolute Temperature.

KEY.

▲ Annealed copper, "oxygen-free" nitrogen.
● " " " " moist air.
■ Hard copper, dry air.
+ " " " " (Campbell.)

film. It will be noted that it occurs in the same range of temperature as the change in Fig. 20. A summary of the activation energies, Q , and constants, A , is given in Table XV.

2. TEMPERATURE DEPENDENCE OF THE CUBIC RATE CONSTANT

It has been pointed out that for considerable periods of oxidation at both high and low temperatures, equation (2) seems to be obeyed. This has been explained by space-charge effects,⁸ where it occurs before parabolic oxidation at any given temperature. As far as is known, any adherence to this law after periods of parabolic oxidation is completely fortuitous and has no theoretical explanation.

The cubic rate constants, K_1 (g.³ cm.⁻⁶ hr.⁻¹), obtained in the course of this work and those calculated from Campbell and Thomas's work⁷ for oxidation times of 1 hr. at 100°–250° C. are plotted in Fig. 22 against $1/T$ °K. It will be seen that all points lie

on the film due to differential contraction are not sufficient to cause much exfoliation. As the temperature rises to 300°–350° C., exfoliation becomes complete; at 400°–450° C., the film again becomes more adherent, but in dry air and in oxygen at 520° C. and in moist air at 625° C. it becomes considerably less adherent.

At 670° C. and above, films formed under all conditions are uniformly adherent. It seems that at this temperature the natural adhesion of oxide to metal is sufficient to withstand the stresses imposed on cooling. It is suggested that the conditions governing exfoliation are the reduction in plasticity as the temperature is reduced from 600° C., and decreasing adherence with decrease in oxidation temperature. The adhesion decreases steadily with decreasing temperature of oxidation, while the plasticity begins to fall off only in the vicinity of 600° C., and therefore the stress imposed on the cooling film due to differential contraction is constant above this temperature.

The exfoliated scale was usually black on both sides, suggesting that it was mainly CuO . Some of the specimens from which scale was exfoliated had a mauve appearance indicative of the presence of Cu_2O . It is possible, however, that this Cu_2O was formed at low temperatures after the exfoliation of the CuO , since previous work⁹ has shown that scales formed at 500° C., after 4 hr., tend to exfoliate at about 300° C.

The surfaces of the scales and the underlying copper surface were examined with a low-power microscope. This had to be done after cooling, and during this process some additional strain had been imparted to the scale, which may have been responsible for some of the effects noted. Frequently, the grain structure was clearly visible, as has been shown by Bouillon.¹⁹

The main defects noticed in the scales were: (1) formation of micro-blisters or fine pimples, (2) grain-boundary blistering, (3) isolated large blisters, and (4) growth of "whiskers" of CuO .

Micro-blisters were found after oxidation at all temperatures in dry air, whether on soft or hard copper. In moist air or dry oxygen, they were found only after oxidation at temperatures above 520° C. (Fig. 23, Plate XCIV).

Grain-boundary blistering was found only after oxidation in dry air in the range 265°–625° C. (Fig. 24, Plate XCIV). Where exfoliation had taken place, the areas where there had been contact between metal and oxide were deeply etched, while those coinciding with the blisters stood out in relief (Fig. 25, Plate XCIV). It seems that during oxidation, the bulk of the scale remained adherent, permitting outward movement of copper ions. However, in the vicinity of the oxide grain boundaries, blisters formed owing to relief of internal stress along lines of weakness. The blisters prevented the outward movement of metal ions immediately beneath them, and therefore the metal below them was left above the general surface level when oxidation was complete.

Isolated large blisters appear to be confined to oxidation in dry air. They occur in soft copper in the ranges 200°–265° and 520°–625° C., and in hard copper in the range 200°–370° C. The formation and cracking of these blisters may have occurred during cooling (Fig. 23, Plate XCIV).

The growth of "whiskers", which appear to consist of fine filaments of CuO , occurs mainly during oxidation in dry oxygen in the range 370°–420° C., and in moist air at 725°–750° C. (Fig. 26, Plate XCIV). It seems to occur when gross blistering is absent, indicating that it is connected with the presence of a dense film.

The general conclusions are that films are stronger and denser when formed in dry oxygen and moist air and undergo little stress-relief in the form of large blisters. Films formed in dry air appear to be far weaker and more porous, stress-relief occurring by the formation of micro-blisters and certain forms of gross blistering at all temperatures. In presence of

moisture, the film formed is so strong that hardly any gross blistering takes place.

VII.—DISCUSSION OF RESULTS

The work reported here has shown that the oxidation of copper in the intermediate temperature range is a complex process.

Since the natural volumes of both cuprous and cupric oxides are 1.7 times the volume of metal from which they are formed, the oxide film grows under the influence of compressive stresses. Dankov and Churaev²⁰ have recently shown that, even at room temperature, partial stress-relief must occur, since it is quite impossible for oxide films to withstand the theoretical stress indicated by a volume change of this order; their experiments indicated that the residual internal stresses were of the order of 10–25 tons/in.².

Previously the author⁹ had shown that the oxide films formed on copper became reasonably plastic at about 600°–700° C., above which temperature they could stand considerable externally applied stress without breaking away from the metal.

Since the object of the present work was to investigate the effect of the transition from brittle to plastic films on the kinetics and the mechanism of oxidation, this discussion is mainly devoted to elucidating from the results presented the reasons for:

- (1) The sudden weight changes noted in many of the oxidation curves at all temperatures above about 370° C.

- (2) The re-appearance of the cubic oxidation law at high temperatures after a period of parabolic oxidation at moderate temperatures. Purely theoretical considerations would suggest a transition from the logarithmic law at low temperatures, through the cubic, to the parabolic law at higher temperatures.

- (3) The change in rate and type of oxidation caused by variation of the atmosphere.

- (4) The change in activation energy at about 600° C.

In the range 200°–370° C., any departure from the law obeyed at the start (here 0.25 hr.) involves the slowing down of oxidation below the rate required for the law to continue. As Evans²¹ has pointed out, it is possible to derive the parabolic law on the basis of the existence of cavities, but, in doing so, one must suppose that as each new layer is laid down, the cavities form on top of the ones in the layer below. In fact, their only effect is to cut down the nett surface area available for outward metal transport. It seems possible for the parabolic law to hold even if the cavities are formed at random, so long as the ratio of cavities to oxide in each layer is constant. Any reduction in slope of the log/log plot would mean that the proportion of cavities had increased.

But it appears that whatever the theoretical explanation of the parabolic law below 470° C., this law requires the presence of some defect, i.e. cavity or crack. The transition from parabolic to a slower rate (200°–265° C. in soft copper) might be attributed to failure of the uppermost cavities to crack. It is probable that if oxidation were prolonged in these cases beyond 100 hr., further periods of parabolic oxidation might occur as a result of further cracking. Macroscopic examination of scales formed by oxidation at 200°–265° C. does show evidence of gross blistering, but the fine blistering which manifests itself as superficial pimples seems to be present in all scales formed in the range 200°–750° C., and would be quite sufficient to account for the reduced rate.

At slightly higher temperatures (265°–470° C.), grain-boundary and other gross forms of blistering are observed. These would be quite sufficient to cause the very marked changes in weight in this temperature range (Fig. 9, p. 687). This effect does not seem to be connected with any lack of adhesion at the grain boundaries of the copper—the two sets of grain boundaries do not necessarily correspond.

One feature is common to the log/log plots (Figs. 8, 10, 12, and 14), namely that below 420° C. the slopes tend to decrease with increasing oxidation time, whereas above 520° C. they tend to increase. The transition in type occurs at about 470° C., indicating that the weight changes above 470° C. are associated with the more frequent fracture of the micro-blisters, while those below 470° C. are connected with less frequent formation and fracture of the grosser types of blister.

The reappearance of the cubic law at 520° C., in certain instances, suggests that in close contact with the metal is a layer of cuprous oxide where space-charge conditions operate. Between 210° and 520° C., the formation of blisters and subsequent cracking seriously interferes with this layer, so that cubic oxidation is replaced by other forms of oxidation, in some cases approaching the parabolic.

At low temperatures, cubic oxidation sometimes follows parabolic oxidation. Since this case is not covered by the explanation of the cubic law, it is probable that adherence to it is fortuitous. If it is a fact that cubic oxidation occurs at both high and low temperatures, as suggested by Campbell and Thomas's results⁷ for the range 100°–256° C., and by the results of the present work for 525°–700° C., then can the parabolic law at intermediate temperatures be explained otherwise than by the formation of blisters?

In moist air, at 370° and 420° C., where the parabolic law holds from zero to 10–15 hr., there was no evidence of pimples or superficial blisters. But later oxidation took place with reduced slope (Fig. 12), suggesting that cracks previously developed were then being healed. At 520° C. and above, the cubic law holds for hard copper up to weight-gains varying from 1.2 mg./cm.² at 520° C., to 2.42 mg./cm.² at 625° C. This corresponds to a thickness of about

1.3×10^{-3} cm., if the film is assumed to contain 50% CuO and has a density of 6.0 g./c.c. This thickness is greater than that predicted by Cabrera and Mott⁸ for the limit of cubic oxidation (2×10^{-4} cm.).

In the parabolic ranges of growth at 520° C. and above, it has been shown that sudden weight changes occur (Fig. 13). Previous work indicates that scales formed at temperatures as high as 900° C. are porous, and it may be assumed that stress-relief in the plastic range still takes place by a blistering process. Presumably the blisters develop cracks at certain stages, which are responsible for the sudden weight changes. Macroscopic examination of the surface in this temperature range generally shows little evidence of gross blistering, and the weight changes are mainly connected with cracking of the micro-blisters.

It therefore seems that at moderate temperatures (200°–470° C.), the parabolic law is operative at the same time as blistering occurs. However, at higher temperatures (520°–700° C.), it is possible for thin films to be compact and not porous, owing to the natural plasticity of the oxide at these temperatures, giving the cubic law. As the films grow in thickness there is a return to the parabolic type of oxidation.

We must now consider the reasons for the marked effect of the oxidizing atmosphere at low temperatures. The weight/time curves show that discontinuous growth is more pronounced in dry air than in either moist air or oxygen. It is suggested that when a blister forms in dry air, the oxygen diffusing into the blister is used up rapidly by oxidizing the metal surface within the blister and converting the internal surfaces of the blister to the higher oxide CuO. The nitrogen, however, remains within the blister and seems to prevent its early collapse, which presumably takes place in dry oxygen. For this mechanism to operate, the inward diffusion of oxygen and nitrogen must be assumed, and moreover this must take place in such a way that the channels are afterwards closed so as to prevent further inward diffusion of air or outward diffusion of nitrogen.

It has generally been thought that at high temperatures the rate-determining mechanism in the oxidation of copper is the outward diffusion of metal ions through the cuprous oxide layer by means of vacant sites in the cation lattice. However, for the reasons already stated, some oxygen must diffuse inwards. This cannot readily take place by interstitial diffusion of oxygen ions, since their radius is too great. It is possible that there may be vacant sites in the anion (oxygen) lattice, but it is more likely that inward diffusion occurs through rifts caused by the cracking of blisters, or a type of "shear cracking" put forward by Evans.²¹ Such channels will gradually tend to fill up and seal themselves by oxidation, provided that metal-ion transport outward is not completely prevented. Evidence that such transport still takes place at low temperatures (370° C.) is given by the change of level of the metal surface in the vicinity of a blister.

Since sudden changes in rate are relatively absent at low temperatures during oxidation in pure oxygen, it must be assumed that the cracking of blisters is more frequent and less catastrophic. In moist air, also, sudden weight changes are not much in evidence at low temperatures, a fact that can be explained by the increased strength of the film. The reduction in slope of the log/log curves after long periods of oxidation can be accounted for only by the occurrence of blistering in the lower layers of the film.

The change in activation energy as shown by the change in slope in the plot of log rate constant versus reciprocal temperature must now be considered. Early workers such as Wilkins and Rideal²² have explained this by a change from bulk diffusion at high temperatures, necessitating a high activation energy, to grain-boundary diffusion at low temperatures, requiring a lower activation energy. In cuprous oxide, the high-temperature oxidation rate would be expected to be directly proportional to the conductivity. A plot of log conductivity versus the reciprocal of absolute temperature, for a wire composed of Cu_2O shows a single straight line down to about 500° C.,¹⁰ indicating that a single mechanism is rate-determining down to this temperature. It is usually considered that this mechanism is the outward movement of cations.

However, in Fig. 21 and to a less noticeable extent in Fig. 20, a change in slope occurs at about 700° C., suggesting that below this temperature, some other mechanism is becoming important, which is presumably not associated with cationic migration.

It is known that, as the oxidation temperature is lowered, the proportion of CuO increases, and the author⁹ has shown that at 700° C. it is about 35%. According to experimental and theoretical work by Valensi,⁴ the proportion of CuO is 20–30% at 700° C. Macroscopic observation on scales formed at 625° C., in the course of 100 hours' oxidation, showed that they contained about 50% CuO . Both Murison²³ and Miyake²⁴ report that a considerable proportion of CuO is formed during oxidation at 300°–500° C. According to Valensi,⁴ at low temperatures CuO should form nearly 100% of the oxide. In practice, at 300° C. it has been found to form 95%, and it would, therefore, be expected that at low temperatures the oxidation rate would be controlled largely by the cupric oxide. There would be a gradual transition at some intermediate temperature from one mechanism to another.

The results of work recently reported by Hauffe and Grunewald²⁵ confirm the earlier theory of Dünwald and Wagner²⁶ that CuO is a "transition-conductor", i.e. one having stoichiometric composition. This is in contrast to Cu_2O , which has excess oxygen by virtue of vacant sites in the cation lattice. The type of ionic disorder in "transition-conductors" is not clear, but it may be that some of the ions, either metal or oxygen, leave their sites in the lattice and take interstitial positions.

Allen and Lauder²⁷ have recently provided

evidence for the diffusion of oxygen in CuO by showing that at 600° C. 25% of the oxygen in the CuO had changed places with oxygen in the surrounding atmosphere in 4 hr.

It should be remembered that the parabolic law $w^2 = K_1 t + B$, where w is weight of oxygen absorbed, can be said to be equivalent to the ideal law $y^2 = K_1 t + B$, where y is film thickness, only when $w \propto y$. This is not the case when the composition of the film is changing with time, and when the density of the film is changing through the growth of pores, as pointed out by Evans.²¹

On a theoretical basis supported by a limited series of measurements made on films formed at 860° C., Valensi⁴ supposed that the composition of the film is constant at any given temperature. This has recently been disproved by Dravnieks²⁸ for low pressures at 500° C., and by Dankov and Ignatov²⁹ for air at 200° C. Further, Dravnieks showed that with an oxygen pressure of 760 mm. Hg, the composition of the film formed at 500° C. reaches 95% CuO in a very short time.

It would appear, therefore, that at 300°–600° C. oxidation of copper is controlled by diffusion through CuO , which forms a large proportion of the film. Both outward diffusion of metal ions and inward diffusion of oxygen ions probably take place by means of lattice defects or interstitially. As the temperature increases above 650° C., the thickness of the CuO film becomes very small, and outward diffusion of metal ions in Cu_2O becomes the rate-determining mechanism.

It would be expected that the formation of fresh oxide on the $\text{Cu}_2\text{O}/\text{CuO}$ interface would have a detrimental effect on the adherence of Cu_2O to CuO , either during oxidation or on cooling. In fact, this action could be responsible for a considerable amount of the porosity present in the low-temperature films. The fact that the oxidation reaction can take place below the upper surface of the CuO may explain the absence of gross porosity, in some cases, on superficial examination.

It should be noted that there is no significant variation of the activation energy, Q , with atmosphere or hardness of copper in the low-temperature range (Figs. 20 and 21), showing that the oxidation mechanism is in all cases the same. It is merely the constant A that alters; and this is believed to imply a change in the degree of blistering and cracking.

VIII.—SUMMARY AND CONCLUSIONS

The principal results determined in this work may be summarized as follows:

(1) Oxidation of annealed copper sheet in dry air at 200°–365° C. is initially parabolic, going over to discontinuous oxidation after 1–4 hr. owing to increasing gross porosity and later cracking.

(2) At 420° and 465° C. there is no parabolic period in air, oxidation being discontinuous.

(3) At 520° C. and above oxidation is parabolic,

the index n in the equation $w^n = K_1 t + B$ varying from 2.0 to 2.2.

(4) Addition of moisture (saturating the air at room temperature) strengthens the film, and reduces the oxidation rate by 50% at 370° C., but increases it by 50% at 520° C. At 750° C., the effect of moisture on the oxidation rate is negligible.

(5) The use of oxygen rather than air decreases the intensity of blistering and cracking. The oxidation rate at 370° C. is about one-third and at 420° C. about one-half of that in air, but at 520° C. and above it is slightly greater than that in air.

(6) The presence of a pre-existing film maintained by heating in nitrogen, inhibits the initial parabolic oxidation at low temperatures, but does not significantly affect the weight increments. The film formed on electropolished specimens produces a large reduction in oxidation rate.

(7) The rate of oxidation of wire is much less than that of sheet at 420° C.

(8) The initial oxidation rate of cold-rolled copper is less than that of annealed copper in the range 200°–420° C.

(9) The variation of the parabolic rate constant K with temperature indicates that between 200° and 600° C. the activation energy is 16,000 cal./mole, and is substantially independent of the oxidizing conditions.

(10) With hard-rolled copper oxidized in dry air and annealed copper oxidized in moist air there is an early period of oxidation which appears to conform approximately to the cubic law, as found by Campbell and Thomas.⁷ Adherence to this law is found only

at 210° C. and in the range 520°–750° C., the upper limit of obedience in terms of oxygen absorbed being about 1–3.0 mg./cm.², which corresponds to a film thickness of $1-3 \times 10^{-3}$ cm. The activation energy required for cubic oxidation is of the order of 28,000 cal./mole.

(11) Scales formed at 300°–550° C. tend to exfoliate on cooling, while those formed above 650° C. and at 200° C. are adherent.

These results are felt to justify the conclusions that the rate-determining process at high temperatures is the outward movement of metal ions through a film consisting substantially of Cu₂O, but at low temperatures it is the diffusion of metal and oxygen in the CuO layer.

ACKNOWLEDGEMENTS

The author wishes to thank Professor C. W. Dannatt for the use of the facilities of the Department of Metallurgy of the Royal School of Mines, in which this work was done. Thanks are also due to Dr. M. S. Fisher for helpful advice.

This work has been carried out during the author's tenure of an I.C.I. Research Fellowship in the University of London, for which grateful acknowledgement is made.

Thanks are also due to Imperial Chemical Industries, Ltd., and to the Central Research Fund of the University of London for additional grants towards the cost of the apparatus, and to The British Non-Ferrous Metals Research Association for the supply of high-purity copper.

REFERENCES

1. R. F. Tylecote, *J. Inst. Metals*, 1950–51, **78**, 259.
2. N. B. Pilling and R. E. Bedworth, *ibid.*, 1923, **29**, 529.
3. O. F. Hudson, T. M. Herbert, F. E. Ball, and E. H. Bucknall, *ibid.*, 1929, **42**, 221.
4. G. Valensi, [*Proc.*] *Pittsburgh Internat. Conf. on Surface Reactions*, 1948, 156.
5. T. N. Rhodin, Jr., *J. Amer. Chem. Soc.*, 1950, **72**, 5102.
6. B. Lustman and R. F. Mehl, *Trans. Amer. Inst. Min. Met. Eng.*, 1941, **143**, 246.
7. W. E. Campbell and U. B. Thomas, *Trans. Electrochem. Soc.*, 1947, **91**, 623.
8. N. Cabrera and N. F. Mott, *Rep. Progress Physics*, 1948–49, **12**, 163.
N. Cabrera, *Phil. Mag.*, 1949, [vii], **40**, 175.
9. R. F. Tylecote, *J. Inst. Metals*, 1950–51, **78**, 301.
10. R. F. Tylecote, *ibid.*, 1950–51, **78**, 327.
11. A. M. Dumez, *Métaux, Corrosion, Usure*, 1943, **18**, 50, 68, 97.
12. P. Chevenard, X. Waché, and R. de la Tullaye, *ibid.*, 1943, **18**, 121.
13. T. N. Rhodin, Jr., *J. Amer. Chem. Soc.*, 1950, **72**, 4343.
14. C. Wagner and K. Grunewald, *Z. physikal. Chem.*, 1938, [B], **40**, 455.
15. D. H. Bangham (reporting results of V. Bloomer), *J. Sci. Instruments*, 1945, **22**, 230.
16. C. S. Barrett, "The Structure of Metals", p. 407, 426. New York: 1943 (McGraw-Hill).
17. M. Cook and T. Ll. Richards, *J. Inst. Metals*, 1947, **73**, 1.
18. A. T. Gwathmey and A. F. Benton, *J. Chem. Physics*, 1940, **8**, 431.
19. F. Bouillon, *Bull. Soc. Chim. Belge*, 1951, **60**, 337.
20. P. D. Dankov and P. V. Churaev, *Doklady Akad. Nauk S.S.S.R.*, 1950, **73**, 1221.
21. U. R. Evans, *Trans. Electrochem. Soc.*, 1947, **91**, 547.
22. F. J. Wilkins and E. K. Rideal, *Proc. Roy. Soc.*, 1930, [A], **128**, 394.
23. C. A. Murison, *Phil. Mag.*, 1934, [vii], **17**, 96.
24. S. Miyake, *Sci. Papers Inst. Phys. Chem. Research (Tokyo)*, 1936, **29**, 167.
25. K. Hauffe and H. Grunewald, *Z. physikal. Chem.*, 1951, **198**, 248.
26. H. Dünwald and C. Wagner, *ibid.*, 1933, [B], **22**, 212.
27. J. A. Allen and I. Lauder, *Nature*, 1949, **164**, 142.
28. A. Dravnieks, *J. Amer. Chem. Soc.*, 1950, **72**, 3761.
29. P. D. Dankov and D. V. Ignatov, *Izvest. Akad. Nauk S.S.S.R.*, 1949, [Khim.], (3), 234.

The Control of Quality in the Production of Wrought Non-Ferrous Metals and Alloys. I.—The Control of Quality in Melting and Casting*

Mr. N. I. BOND-WILLIAMS,† B.Sc., A.I.M. (Member of Council): No one in industry today can overrate the importance of the control of quality in manufacturing operations. Regardless of other attributes, no product can be sold unless the consumer is satisfied that its quality is suitable to his need. Subsequently he will consider price and availability, but above all the quality must be right. There is a growing tendency to relate cost and quality, and is some circumstances it may suit both consumer and producer to define, as an ideal measure of quality, not maximum performance but a level less than the maximum suitable not only for the ultimate use but also for low-cost production.

In his paper Dr. Singer deals in detail with these overriding considerations of quality control. Having established that such control can be effective only when the elements of quality have been standardized and rendered capable of numerical measurement, he shows that the fixing of tolerances has a most important bearing on the economics of the manufacturing process, a concept stated concisely in British Standard, No. 600, which defines the level of control in this way: "The level of control specifies quantitatively the nature of a statistically uniform variation to which the quality of the material or manufactured article is subject. In a manufactured article it is dependent on the producer's mastery over technical processes of manufacture and the economic factors governing their exercise."

From this point, the basis of inspection being in existence, Dr. Singer goes on to show how this is first used to investigate the stability of a manufacturing operation and to improve it to a point where the desired level of control is economically possible and some form of process control is practicable. During this stage the intention is to reduce the width of the histogram typically shown in Fig. 2 (p. 331) of his paper. Dr. Singer emphasizes that it is in this state of the development of a process that there is the greatest expenditure of effort on investigation and research. When a suitable degree of stability has been achieved, it is then possible to apply various forms of automatic control, error-actuated and based on either primary or secondary variables.

Throughout, Dr. Singer emphasizes the difference between adjustment or fixing, and control. "Control" is always used to describe a deliberate change in the process initiated by a measured error, whether the change is made automatically or by a combination of meter and human operator. The work done in investigating an unstable process and modifying it to become a stable one, in which the number of variables is not too great to be controlled automatically or by a human operator, is regarded by Dr. Singer not as control but as process investigation.

With this point of view the other five authors disagree, as the main content of their papers is an account of the results of a great deal of process investigation directed towards the stabilization of quality in the cast product. Nevertheless, there are many threads of similarity running through the papers which relate to Dr. Singer's main points.

Each deals with a material to meet a different demand and, therefore, with an individual concept of quality. This, together with the varying manufacturing techniques of these branches of the metal industry, causes the quality emphasis to shift in each case.

Dr. Cook and Mr. Cowley attach importance to the control of composition, inclusions, gas absorption, temperature, metal losses during melting, mould dressing, and the method of feeding during casting. Mr. Sykes highlights the control of furnace atmospheres, both as regards analysis and temperature, of oxygen content of the molten metal and the timing of additions in melting, quality control of mould-dressing material, regulation of the liquid stream and the avoidance of turbulence in casting, and the details of the final quality test—conductivity measurements under standardized conditions. Mr. Roberts and Mr. Walters emphasize crystal orientation as a major quality factor, allied with freedom from porosity and accurate shape, with smooth surfaces. They suggest that control is essential to reduce turbulence in feeding, to prevent shrinkage, and to regulate the direction and rate of heat flow in the mould. Mr. Staples and Mr. Hurst apply all the usual controls, such as those for composition and temperature, but pay most attention to that of gas absorption in the furnace, turbulence, and the pick-up of oxide and other non-metallic inclusions. Mr. Wilkinson and Mr. Hirst are almost equally interested in the control of turbulence, but concentrate even more on the control of fluxes and protective gases during melting, and describe an unusual method of producing and controlling the zirconium content of magnesium-zinc-zirconium alloys.

Reference to Table II in Dr. Singer's paper (p. 339) may help us in comparing the extent to which the other authors agree or differ in regard to the types of control which they deliberately exercise over their melting and casting procedures. The "variable" headings provide a very useful basis of comparison, and in making it I shall adhere as closely as possible to Dr. Singer's definition of control.

Temperature of Melt.—All five papers state or imply control over melting temperature by automatic or manual control.

Chemical Composition of Melt.—The most complete control is that of Staples and Hurst, who refer to analysis by direct-reading spectrograph, stated to take only a few minutes while the heat is held in the melting zone of the duplex furnace; the composition may thus readily be adjusted before transfer to the holding bath. Sykes has a control almost as rapid in effect by examining fractured test castings, and a similar method is used by Wilkinson and Hirst to determine zirconium.

Cook and Cowley also refer to the direct-reading spectrograph, but do not state whether it is employed to correct molten charges. Roberts and Walters make no use of control of composition of the molten metal. They refer to its composition, but not to control in the sense in which Dr. Singer defines it.

Heat Input to Furnace.—Cook and Cowley, Sykes, and Staples and Hurst all have a control of this factor.

Composition of Furnace Atmosphere.—Sykes controls the

* Joint discussion on Papers Nos. 1448–1453 (*Journal*, this vol., pp. 329–400) held in London on 25 March 1953.

† Managing Director, Aston Chain and Hook Co., Ltd., Birmingham.

atmosphere by alteration of burner situation and adjustment. Staples and Hurst endorse the use of CO₂ recorders and the consequent adjustment of burners.

Gas Content of Melt.—Sykes examines samples, and Staples and Hurst refer to the Straube-Pfeiffer method as occasionally used.

Structure Potentialities of Melt.—Roberts and Walters alone refer to the adjustment of grain-size by nucleation after examination of set samples.

Gas Flow.—Sykes alone controls gas flow during the oxidation of the melt.

Flux Additions.—Sykes alone controls flux additions by reference to the results of method (6) of Singer's Table II, the fracture of the sample.

Casting.—Control, in the sense in which Dr. Singer uses the word, appears to be applicable to casting only when the continuous or semi-continuous or direct-chill method is being used. Roberts and Walters use the term "chill casting" to describe an alternative method of casting which may be confused with the term "direct chill" used both by Staples and Hurst and by Wilkinson and Hirst. In each case, however, all the controllable factors (11)–(15) in Table II, are being covered; but even these controls are unable to eliminate the difficulties, and, in particular, the internal cracking suffered by some of the more difficult light alloys.

Among modern methods of non-destructive inspection, ultrasonic flaw detection is mentioned by Staples and Hurst and by Wilkinson and Hirst as a useful tool in discovering internal cracks in large billets.

From this brief summary it appears that most of the primary factors in Table II of Dr. Singer's paper are being controlled, though in some cases the controls may be either insufficiently critical or insufficiently rapid in counteracting errors to satisfy him. Nevertheless, the impression which I gain from reading these papers is that all the processes described have been brought to a stage of development where they are sufficiently stable and capable of repetition without wandering outside the appropriate quality limits demanded by the product.

There is one point on which all the authors are agreed, namely, the effect of the skilled man's activities on the success or failure of the processes. Although more of a management subject than a metallurgical one, it is interesting to see that detailed attention is being paid to process manuals, operator's instructions, the organization and control of people as well as equipment, and to education and training. I do not think that too much emphasis can be laid on the stimulation of interest in the caster and the furnaceman in the quality of the product and the effect which their work can have, not only on the casting but also on the subsequent processes.

The control of quality within exact limits, both high and low, is a technique which is advancing rapidly, and if the available knowledge on this subject were to be applied rapidly throughout all the factories in this industry, I have no doubt that a very great improvement in products and productivity would follow.

Mr. CHRISTOPHER SMITH,* F.I.M. (Member of Council), said that he agreed with Dr. Singer that we could not afford to ignore the importance of statistical analysis, but that he doubted whether it was possible to apply to a range of manufacturing operations involving the human factor a system that worked satisfactorily in a purely mechanical process such as the production of turned parts in a capstan lathe. He felt that the cost of assembling the relevant facts would be prohibitive.

He did not think that it would ever be possible to conduct manufacturing processes entirely by control of primary variables, but that inevitably secondary variables must be utilized. In the case of the strip-annealing furnace shown in Fig. 10 (p. 336) of Dr. Singer's paper, the strip was being heated for a specific time and at a specific temperature. A good control of secondary variables would in the majority of cases result in strip of the desired grain-size, but he did not see how it was

possible to devise a process which would turn off the heat when the growing grains reached the required diameter.

Dr. Singer's observations on the various lags which arose in controlling mechanisms were very much to the point, as these frequently cost industry dear in wastage of time and material.

He would like to ask Dr. Cook and Mr. Cowley whether, in their view, it would be possible to effect a more precise control by using the continuous-casting process. On p. 346 of their paper reference was made to a 67:33 copper-zinc alloy, which was notoriously difficult to hot roll. In the conditions described, control of the structure in the ingot had to be achieved within a temperature range of 20° C., which, bearing in mind the possible effects of spout and tundish temperatures, was a very critical matter. The continuous-casting machine presented no such problem.

Mr. Sykes had referred (p. 360) to the difficulties arising from segregation in the casting of cadmium copper, which he had said must be poured from superheated furnaces. He (Mr. Smith) thought that this would accentuate the degree of segregation and that the lowest practicable temperature would be preferable. He would appreciate more details from the author on this point.

The methods of casting and problems involved in the paper by Mr. Roberts and Mr. Walters on zinc and its alloys reminded him strongly of those which had faced the aluminium industry about 25 years ago. At that date the horizontal-casting technique, the Erichsen mould, and the sheet-metal mould referred to on p. 375, had all been applied to aluminium alloys. He had also seen the apparatus illustrated in Fig. 2 (p. 372) in use and had been appalled by the degree of turbulence occurring and the amount of oxide formed. Had the authors had any actual experience of this device? It seemed to him that in the case of zinc and its alloys much better quality would result from the application of the semi-continuous methods currently in use in aluminium alloy foundries. Was there some fundamental reason why they could not be introduced? As far as directional solidification was concerned, these methods seemed to offer an ideal method of control, and with pure zinc, at least, immaculate cast surfaces should be obtainable. Was the reason economic? In the aluminium industry increased control over the cooling of the ingots had eliminated scrap, except with certain difficult alloys, with an accompanying rise in the output per man-hour.

To all workers in aluminium foundries control of gas content and of oxides or other non-metallic impurities was of prime importance. He himself believed in the need for a specific degassing treatment and was reluctant to accept the theory that retaining the metal for a prescribed period in a holding furnace would make it possible to produce castings entirely free from porosity. In his experience minute traces of gas were not always completely rejected from the liquid pool during casting, and with some alloys they might be entrapped in the solid-liquid mass. This was particularly true of castings of the rolling-slab type, in which cross-sections were small. He would like to ask whether anyone had had experience of the use of porous refractories for promoting a stream of minute quiescent bubbles of collector-gas in a melt.

Mr. Smith said that he wondered whether level pouring was to be preferred to siphoning or piping systems. Laundering had a number of advantages, but the problem of getting the metal into and out of the launders was a difficult one. Piping overcame this but in general the pipe had to be of cast iron and apart from iron pick-up, insulation had to be provided and there was a danger of the metal freezing-up. Tests carried out with glass tubes some years ago had been quite successful as long as the molten metal was flowing through them, but they proved so fragile that they had to be abandoned.

The comments of Mr. Staples and Mr. Hurst regarding the effect of alkali metals on the hot-working properties of aluminium-magnesium alloys were amply confirmed by his own experience. He was of the opinion that sodium was chiefly responsible.

* Works Superintendent, James Booth and Co., Ltd., Birmingham.

Mr. D. W. BROWN* said that Mr. Smith had questioned the possibility of using porous refractories for gas-flushing distributors. Experiments still in progress had not so far been very encouraging. There was a tendency for the bubbles of gas to recombine after leaving the porous distributor, and it seemed necessary for the distributor to be fairly large in area to prove effective.

Mr. G. L. BAILEY,† C.B.E., M.Sc. (Vice-President), said that the problem with which they were particularly concerned was to control the variables governing quality. That involved two questions: how did one measure ingot quality, and having measured it, how could it be put right if it was going wrong?

It was very difficult in the casting operation to suggest an aspect of ingot quality that was capable of direct measurement and direct control as one went along. Properties of rolled strip, such as thickness, were much easier to gauge, and control could be based on direct measurement. He would appreciate from Dr. Singer some elucidation of his definition of primary and secondary variables. His own conception of a primary variable was as one of the measures of ingot quality that could be controlled directly in some way or other.

The aim was to produce an ingot of the right composition, sound and free from shrinkage, from gas, cracks, and other causes of unsoundness, having a good surface and the desired grain-size. In his view, the only one of these qualities that could be directly measured and corrected was composition. Mr. Staples and Mr. Hurst had shown how the direct-reading spectrograph was being used in the aluminium foundry, and there was every prospect in the near future of the same type of instrument, suitably modified, being introduced in the copper industry. A large output and melts of considerable size, were, however, necessary to justify the expense of such an instrument, which costs something like \$30,000.

The soundness of an ingot, however, could not be measured and could be controlled only to a very limited extent during the casting process. He thought that Dr. Singer's challenge to metallurgists could best be met by making inspection at the ingot stage as rigid as possible and reducing as far as practicable the chances of defects showing and leading to rejection at the stage of subsequent working.

Dr. W. G. HISCOCK,‡ B.Sc., F.R.I.C., F.I.I.A. (Member), stressed the importance in the interests of final quality of maintaining the exact limits of composition of the various materials used in making up an alloy. His own company produced zinc of 99.99+ % purity by using a refluxing technique which took advantage of the difference in boiling point between zinc and its impurities. The plant, developed by the New Jersey Zinc Co. of America, was novel in design, and consisted, in principle, of columns of carborundum trays mounted one above the other, one or more columns separating out the higher-boiling-point materials, such as lead and iron, and the others distilling off the lower-boiling-point impurities, mainly cadmium. The control of these refluxing operations had to be exact to yield metal of the purity required for the Mazak alloys, which were very sensitive to impurities. The grade of zinc known as "Crown Special" had to meet British Standard No. 1003, which permitted no more than 0.003% lead and 0.003% cadmium. Control would be extremely difficult were it not possible to test for uniformity so rapidly by means of the spectrograph. This could detect even trace impurities, such as indium and thallium, which were present in some ores and must not be allowed to appear in the final metal.

Mr. F. KASZ§ B.Sc., A.R.Ae.S. (Member): I shall devote attention principally to the paper by Mr. Staples and Mr. Hurst, and, to restrict the discussion, it may be permissible to reduce the aims in any casting shop to two. The first is the

production of a homogenous liquid of required composition (and in "composition", I include all impurities whether solid, liquid, or gaseous, elementary or compound); and having transferred the liquid, without change, to a container or mould, the second aim is to effect a heat exchange such that components are distributed as desired in the resulting solid.

In respect of composition, an impressive feature of all the papers is the fine limits to which impurities are controlled on an industrial scale. But the observation on p. 380, that scrap and secondary-ingot charges give more consistent results than virgin charges, suggests that such control must be extended. This experience does not exactly match our own. In the early 1930s, it was certainly the case that reduction-furnace metal, on first solidification, showed very variable casting behaviour, associated with widely varying alkali metal, gas, and oxide contents, and that, on remelting, the casting behaviour and associated characteristics were much more consistent. Since the compositional factors have been recognized and controlled, however, quite a wide variety of charges are made to yield equally consistent results. In the absence of such control, the mere "shuffling effect" of melting together scrap from various sources may contribute to the effect observed by the authors.

Mr. Staples and Mr. Hurst enquire whether alkali-metal content should be controlled. In pre-war days, chill-cast (cast-iron moulds) $22 \times 17 \times 2\frac{1}{2}$ in. slabs of 99.4% purity used to give periodic epidemics of supra-solidus cracking. With a small but detectable sodium content, rejects due to cracking amounted to only 1% or less; but with a three- or four-fold increase, rejections would increase to 50% and more. A modified form of Norton hot-shortness test showed that metal of normal purity and sodium content would, when sand cast, lift a weight of 168 lb. without cracking; very small increases in sodium content and purity would reduce that load to 135 lb. and even to 41 lb. At a later date, it was shown that deliberate sodium additions to certain alloys could cause semi-continuously cast blocks to explode with dangerous violence. The adverse effect of sodium on the hot-rolling behaviour of certain alloys is no less readily demonstrable. There is no doubt, therefore, that alkali-metal content must be controlled in any up-to-date works.

I would agree that oxide inclusions in light-alloy blocks can be disastrous. But when the authors refer (p. 378) to the more finely divided forms, I wonder whether they are offering us evidence or pure speculation. Our own experience shows that gross oxide, visible to the naked eye or under the microscope and caused by turbulent metal transfer, is associated with processing difficulties and defects in the finished sheet. If a quiescent transfer is ensured, the lumps of oxide and their associated defects disappear. If turbulence at some stage is unavoidable, the evidence suggests that a matter of a few seconds' settling, rather than the $1\frac{1}{2}$ hr. mentioned on p. 379, is adequate for the oxide lumps to settle out. But if turbulence occurs, our work has shown clearly that a two-slot distributor in the mould serves only to form inclusions in two lines down the block, instead of one. We do not therefore regard the distributor as an effective oxide trap, as Mr. Wilkinson and Mr. Hirst suggest on p. 397.

I am puzzled by Mr. Staples' and Mr. Hurst's advocacy and condemnation on p. 379, of the induction furnace, to avoid oxide; and I question the wisdom of the authors' favoured method of bottom tapping (p. 379), in view of the thick deposits that are to be seen on most furnace hearths after quite short campaigns. It is also rather surprising, in view of the importance of temperature, to find no mention of thermostatic control, commonly practised in the light-alloy industry.

Turning now to chill casting, the authors tell us nothing about the kind of control they exercise over the mould and ancillary variables, and some of their statements suggest that certain outdated misconceptions still persist. The heat

* The Morgan Crucible Co., Ltd., London.

† Director, British Non-Ferrous Metals Research Association, London.

‡ Director of Operations, Imperial Smelting Corporation, Ltd., London.

§ Head, Experimental Department, The British Aluminium Co., Ltd., Falkirk.

exchange in a chill mould represents a case of unsteady flow; and in the important early stages of solidification, the characteristics of the mould material determining the heat-extraction rate are its temperature and thermal diffusivity. The total mass is irrelevant, and it is therefore not at all surprising that heavier moulds, and even water-cooled copper moulds, soon reached the limits of their possibilities, as the authors put it (p. 385).

The temperature gradient through the mould wall, rising to and falling from a maximum value, causes mould distortion (usually irregular) which has important effects on heat extraction and certain defects. For example, as the temperature gradient begins to diminish, the mould wall starts to move outwards away from the slab shell, causing a recalescence in the slab surface temperature and, of course, reducing the heat-extraction rate. This movement has an important effect on exudations, or blebs, amongst other things, and by applying a thermally insulating mould dressing the extent and duration of the inward movement can be controlled to suppress blebs—a procedure exactly paralleled by Mr. Sykes' application of bone ash to suppress "sweat" on vertically-cast copper cakes (p. 359).

The quality of the casting can be influenced very materially, therefore, by the behaviour of the mould, so that it would be interesting to know just what sort of control Mr. Staples and Mr. Hurst do in fact exercise over it, and also to learn the order of change in thermal diffusivity they have established as due to graphitization in older moulds (p. 385).

Semi-continuous casting presents its own problems, but offers a nearer approach to unidirectional solidification. Coarse grain is sometimes a disadvantage, and grain refinement may be profitable to avoid as-cast cracking. Although we would not say that grain refinement is essential, have the authors tried it to avoid the radial cracking shown in Fig. 13 (Plate LVI)? Experimental blocks with crystals up to 12 in. in dia. have often been rolled by us to quite satisfactory sheet. And if the cast structure must be refined, the addition of titanium and boron salts is often an unnecessarily expensive way of achieving this end. The shallow solidification front of the semi-continuously cast block is one of its advantages, tending to minimize shrinkage and gas porosity; but in respect of the latter, I should be surprised if the benefits occurred through automatic ejection of the gas, as the authors suggest (p. 379).

The major difficulties of direct-chill casting arise from cracking, from the fact that a hot-short, thin shell is being moved past a stationary mould, and from marked inverse segregation. Mr. Staples and Mr. Hurst seem to believe that cracking is due to hot-shortness, or to stresses caused by ageing. I agree that supra-solidus cracking does occur, and that the work of the Aluminium Development Association's Welding Research Team at Birmingham University can be profitably applied. But, though allowing that ageing stresses can influence a block after casting, I cannot agree that they are the primary cause of sub-solidus cracking while casting proceeds. Under otherwise constant casting conditions, cracks can be caused, or avoided, merely by moving the pouring point or by changing the block section. By choice of suitable conditions, the failures common to heat-treatable alloys can be simulated in alloys which, to the best of my knowledge, do not age at all; and at least one alloy that does age-harden is not at all prone to crack. How do the authors explain these facts on an ageing-stress hypothesis?

Our evidence leads us to believe that the primary cause of sub-solidus cracking is thermal stressing, and that the stress systems may be of two kinds and of differing magnitudes, as outlined by my colleague, Mr. Phillips.*

The movement of the thin block shell past the stationary mould does cause trouble with tears and run-outs. In this connection, the authors tell us of trouble with the 2-3% magnesium alloy (p. 386), but do not say how they overcome it. I suggest that alloys of this kind contract away from the mould

wall less than others, owing to a low thermal diffusivity. If the authors base their action on that point, I believe the difficulty will be reduced to manageable proportions.

Mr. Staples and Mr. Hurst mention casting difficulties with alloys of the 14% manganese and H10 type (pp. 381 and 387), but these have not arisen in our experience. The H10 composition is on the fringe of a hot-short range, and appropriate action based on this fact should remove the difficulty.

The authors mention the necessity for controlling the cooling-water temperature to within 1° or 2° C. (p. 389). I find it difficult to understand why this temperature should be so critical, when the importance of latent heat to water's quenching efficiency is borne in mind. Some years ago, when testing the flooded-pit arrangement shown in Fig. 17 (p. 386), we found erratic temperature gradients in the water of 20°–50° C./in. I find it difficult therefore to envisage how the control is exercised effectively. Could the authors tell us more about this, and also the sort of trouble encountered if the water temperature does vary by more than 2° C.?

Mr. J. E. NEWSON,† M.Met., F.I.M. (Member), said that he was surprised at Dr. Singer's statement "that the only primary variable always controlled is the temperature of the metal in the melting operation . . . this is a depressing state of affairs". In his own experience, extending over about thirty years, he had found that an endeavour had always been made, he thought with a fair measure of success, to control not only the temperature of the melt, but also its chemical composition, and the structure of the ingot, its properties and external characteristics, although these were not defined as primary or secondary variables. Considerable attention was paid to such details as rate of pouring, temperature of pouring, and mould dressing, to secure the result desired. He thought that Dr. Singer was rather pessimistic in assuming that the primary variables numbered 2, 5, 6, and 11, in Table II (p. 339) of his paper were not generally controlled in producing brass billets. In his (Mr. Newson's) opinion, to apply automatic control mechanisms to most of the problems involved in melting and casting would be extremely difficult, but in other processes such as rolling, annealing, and forging there were great opportunities for applying scientific control of quality.

In connection with the paper by Dr. Cook and Mr. Cowley, he disagreed with the suggestion that a small quantity of liquid dressing should be poured into the bottom of billet moulds after the surface-dressing operation had been completed, to reduce or eliminate roughness on the lower few inches of the billet. Unfortunately, in his experience, this led to cold shuts and unsoundness, and to avoid accumulation of surface dressing at the end of the mould, it was best to apply it at as short an interval as possible before casting. He would like to know whether the authors had found any serious contamination of the melt from the use of a continuously immersed thermocouple with an iron-28% chromium alloy sheath, in view of the relatively short life mentioned. For billets, his firm had gone over entirely to water-cooled, copper-lined moulds, with a marked improvement in the billet quality.

Mr. C. L. M. COWLEY,‡ B.Sc., A.I.M. (Member): Mr. Newson's experience that the practice, mentioned in our paper, of pouring a small quantity of liquid dressing into the bottom of billet moulds after the surface-dressing operation has been completed results in the production of dirty castings, is quite contrary to our own. It seems probable that this difference is associated with factors such as consistency and types of mould dressing used, mould temperature, and with the period of time which elapses between applying the mould dressing and casting.

Mr. Newson also asks whether there is any serious iron contamination of the melt when a continuously immersed thermocouple with an iron-chromium sheath is used. We have found no significant contamination, since the general attack on the couple is relatively small and failure is usually due to local penetration.

* H. W. L. Phillips, *J. Inst. Metals*, 1948–49, **75**, 1059.

† Vickers-Armstrongs, Ltd., Newcastle-upon-Tyne.

‡ Technical Officer, Imperial Chemical Industries, Ltd., Metals Division, Birmingham.

Dr. G. L. D'OMBRAIN,* Ph.D., B.Sc.(Eng.), M.I.E.E.: I speak with an interest in the subject of automatic control of industrial processes, but without any specific knowledge of the metallurgical industry. Consequently Dr. Singer's paper is the one to which I shall devote most of my remarks.

The first matter on which I should like to comment is an unfortunate departure in the paper from standard terminology. Control engineers have a glossary of standard terms.† I would particularly ask Dr. Singer to adopt these terms, as it will be most regrettable if separate terms are developed within, and peculiar to, the metallurgical industry. I would draw attention in particular to Dr. Singer's use of the term "transfer lag," where we should say "distance velocity lag", and to the use of "capacity lag" where we should say "transfer lag". In control, in general, "distance velocity lag" signifies a measurement of a variable which is a correct measurement, but made at some time later. A precise example occurs in Fig. 7 (p. 334) of the paper. The term "capacity lag" employed in the paper is in itself unfortunate, because a lag does not exist by virtue of capacity alone, but because of a capacitance and an associated resistance, the combination forming the time constant.

On p. 335 Dr. Singer states that "if the output from the regulating unit could be made instantaneously equal and opposite to the error, then the error would vanish and control would be ideal". This is incorrect. The output of a regulating unit fitted with a suitable valve positioner is immediately responsive to the output of the controller. The controller output is immediately responsive to the input error function. Nevertheless, even assuming an ideal measuring element with no lag, the process will still show an error on changing loads, due to the transfer lags associated with the process itself.

Mr. Sykes, on p. 354 of his paper, states that draught gauges and carbon-dioxide recorders are installed and that various adjustments are made in accordance with these readings. Have controllers been tried? What is the time factor in making the measurement of electrical conductivity described on p. 361, and would a reduction improve the quality of the product?

Mr. Staples and Mr. Hurst on p. 388 say: "Correct indication of the speed selected and its steady maintenance throughout the entire casting operation are therefore factors of major importance in maintaining control. Instruments of sufficient accuracy for this and other control purposes in the chill-casting process are not readily available." Could they enlarge on this statement a little and state what controls are required and their interrelationship?

On p. 389 these authors raise the question of the siting of a particular thermocouple or thermocouples. There is, they say, a 40° C. gradient between the melt surface and the hearth floor. Should I be correct in assuming that the actual reading of this thermocouple is immaterial, i.e. that its reading is not necessarily related to any average temperature through the melt, and therefore for a different furnace there would in fact be a different reading, so that the question of accuracy, so frequently brought up when the measurement of temperatures is discussed, is replaced by one of reproducibility?

On the same page, the authors say: "The temperature of the cooling water must be kept constant within 1° or 2° C., and suitable mercury-in-steel indicating thermometers should be fitted." Is not this rather a case of maintaining the rate of heat extraction at some constant or programmed value? That has a bearing on control, because it would be possible to devise automatic control which would maintain the rate of heat extraction according to some law.

The science of control is now developing rapidly, having received a considerable impetus from the developments in the servo-mechanism field during the last war. Great potentialities exist, though at the present time control is mainly confined to single-loop control owing to the limitation of apparatus

commercially available. The future is likely to see rapid advances in multi-loop control in which information of divers kinds will be fed into computing mechanisms which, acting on this information, will provide inter-related output signals to regulate the various parts of the plant.

Dr. A. R. E. SINGER,‡ B.Sc. (Member): First of all, I should like to explain that my paper essentially looks to the future. The data put forward and the suggestions made are not necessarily applicable straightaway to metallurgical industry, but after some development work there is a possibility that different methods of control might be introduced that would in many instances lead to a marked improvement in the quality of product.

To take up a point raised by Mr. Christopher Smith, it should be possible in a strip-annealing furnace to control the primary variable—the structure and properties of the metal strip—by means of a supersonic-detector mechanism employing very high frequencies to estimate the grain-size of the material leaving the furnace. Some work has been published recently showing that, by using such high frequencies, supersonic detectors can determine the number of grain boundaries through the thickness of a piece of strip.§ Thus there exists the possibility of feeding-back measurements from the detector to the heating elements of the furnace and so perhaps achieving control over the grain-size. The material would, of course, have to be cooled as it left the furnace before it entered the detecting or metering unit.

An alternative method would be to instal an X-ray crystallographic set at the exit point. By means of a counter mechanism—which would, however, cost many thousands of pounds and be quite a complicated piece of equipment—it should be possible to determine the grain-size of material leaving the furnace, or even while it is in the furnace, and again by means of a feed-back mechanism, to control the grain-size. In this case temperature does not enter into the problem, and measurements could be made on the hot material. This may represent the type of control of the future, though similar considerations apply to other processes of metallurgical manufacture, including melting and casting. Already there is in operation in the U.S.A. an automatic liquid-metal-level control on the continuous casting of steel by the Junghans process, in which X-rays are passed through the top liquid portion of the ingot and a counter unit is used to control the reciprocation of the mould. Similar mechanisms may well be applied to the non-ferrous foundry.

Finally, I wish to emphasize that the word "control" can be used in two senses: firstly, in the loose, everyday sense and, secondly, as I have used it in this paper, in the strict sense of feed-back control. These two meanings of the word should be clearly differentiated if confusion of thought is to be avoided.

Mr. P. F. HANCOCK,|| B.A., F.I.M. (Member), pointed out that one of the primary variables was the temperature of the melt, and that the desirability of regulating this variable, preferably by full automatic control, had been emphasized in several of the papers. In no type of furnace was temperature regulation more readily effected than in the low-frequency induction furnace, and for this reason, as well as others both technical and economic, its extended use seemed likely. The Ajax-Wyatt furnace, for example, had for many years been regarded as standard for zinc alloys, but it had certain limitations when used for other classes of alloy. Developments in recent years to overcome these limitations had been principally concerned first with devising modified forms of inductor loop for the easy cleaning of channels without emptying the furnace, and secondly with improvements in refractory lining.

As a result of these developments, the low-frequency furnace had been applied to an increasing extent in the light-alloy fields, where channel blockage had formerly been the difficulty,

* Electrical Engineering Department, Battersea Polytechnic, London.

† "Glossary of Terms Used in Automatic Control and Regulating Systems", British Standard No. 1523: 1949.

‡ Lecturer in Industrial Metallurgy, University of Birmingham.

§ R. Wilson, *Sheet Metal Ind.*, 1953, 30, (310), 146.

|| Chief Metallurgist, Birlec, Ltd., Birmingham.

and also to the higher-melting-point copper-base alloys. Recent trials on a small furnace had been directed towards the possibility of melting aluminium bronze in the type of low-frequency furnace developed primarily for light alloys. Though the trials were still in their early stages, results were promising, the known difficulties of channel blockage having been readily overcome by a rodding operation between channels at 24-hr. intervals.

On these trials, both with aluminium bronze and with straight copper, a continuously immersed thermocouple had been employed having a heavy outer sheath of silicon carbide and an inner sheath of pure silica or alumina, to prevent contact of the precious-metal couple with the silicon carbide and contamination resulting therefrom. This arrangement had worked well, and the continuous control of temperature had been quite satisfactory.

Dr. C. J. SMITHELLS,* M.C., F.I.M. (Past-President), said that he would like to emphasize the point that before trying to control quality it was essential to understand the exact nature of the factor that it was desired to control. For example, for many years trouble had been experienced with blister in certain qualities of aluminium, and attempts had been made to find a cure for it without understanding the real phenomena involved.

Fundamental experiments were eventually put in hand in the laboratory to determine accurately the solubility of hydrogen in solid and liquid aluminium and the mechanism of diffusion, and it then became possible to work out methods for the avoidance of blister so that it no longer represented a problem.

There were still many other factors about which not enough was known for control mechanisms to be applied. It would not be possible to gain the necessary information by means of innumerable factory trials followed by statistical analysis of the results; it could be achieved only by fundamental work in the laboratory based on a proper understanding of the phenomena involved. A great deal remained to be done to determine the cause of quality defects before any methods could be applied to the control of quality.

Dr. BØRGE LUNN † (Member) mentioned the requirement laid down in British Standard No. 1464 (Aluminium Brass Tubes) regarding microscopic examination, namely that the material ". . . shall show *reasonable freedom from inclusion of dirt, slag and . . .*". This gave no indication of the limits to which the control of the quality of the melt had to be carried out. International regulation seems to be needed to avoid such lack of precision in standard specifications.

When an improved method of casting was introduced, it was essential to examine it in relation to all the other processes which the material had to undergo. For example, the continuous or semi-continuous casting of aluminium 2S would yield a much improved ingot, but difficulties as regards preferred orientation might be experienced in circles made from strip material.

Dr. K. W. J. BOWEN ‡ (Member) expressed the view that in the present state of knowledge of quality control, there were several directions in which more benefit could be derived than at present from the application of metallurgical principles. One example was the use of the existing knowledge of gases in metals to detect internal unsoundness in castings, so that these might be rejected before further expensive operations were carried out on them. Another example was the development of dependable spot tests for various alloys, particularly those which formed tenacious oxide films; this was important at a time when maximum utilization of scrap was urged, necessitating careful segregation of alloys.

Much had been said about temperature indication and

control, and it was clear that continuous indication and recording of temperature were limited throughout industry by the want of a refractory material sufficiently resistant to erosion and thermal shock under conditions of continuous immersion. At the present time, generally speaking, a continuous-reading instrument was always suspect owing to thermocouple attack and subsequent deterioration. Surely such an important factor as temperature measurement was in all probability better controlled by spot readings taken by a responsible person. Under such an arrangement frequent checking of the instrument was possible.

One of the most important elements in quality control, he said, was the human factor, and even the most carefully prepared and technically sound scheme was useless if it was not implemented thoroughly on the shop floor. Had any of those present facilities available in their works for instructing furnacemen and other operatives, and were handbooks, illustrating in general terms the important points in processes, issued to foremen?

Mr. C. P. PATON,§ B.Eng. (Member): I heartily endorse Dr. Singer's statement that the optimum quality is not always the best. We must think of the end use and consider the overall cost of the finished product. No one will question the wonderful reputation which Great Britain has built up abroad for quality. However, I have had some experience in American, British, and Canadian plants and have gained the impression that in this country there is apt to be more emphasis on the control of quality at intermediate stages. I am not convinced that in some cases we do not overdo this. One point that must be established is just what items it is necessary to control in order to ensure the desired final quality.

Probably the principal problem in a melting shop is to control blisters and inclusions. I was interested in Dr. Smithells's statement that blisters are no longer a serious problem with his Company, and I should like to question him a little further on this. In my experience, although this matter has been brought under better control, occasional blister epidemics still occur.

It has always seemed to me that for eleven months in the year metal can be thrown carelessly into the furnace and cascaded down launders without serious trouble arising. Then in the twelfth month everything seems to go wrong. Our metallurgists used to say that our sins were catching up with us, that the works pipe-line was full of dross, and that until it was cleaned out we should never get rid of blisters. In my opinion that never proved to be the whole story. During such epidemics equal troubles would arise with melts of virgin ingot, and this usually led the melting-shop people to try to cast the blame on the smelter. Perhaps Dr. Smithells will comment on the effect of possible variations in incoming ingot on blister rejections.

As regards the significance of moisture in the air above the furnace, an associate of mine once carried out a test of unusual severity which seems to rule out this factor. Steam was fed by means of a hose pipe, under the furnace grate, over the grate, and finally directly into a small batch of the metal. The only batch suffering abnormal blister trouble was that into which steam was introduced directly.

One cannot experience these occasional troubles without wondering whether some trace element is not responsible. Reference was made earlier to the effects of sodium on cracking. Can sodium or any similar trace element have an influence on hydrogen content?

Many controls which before the war were considered important for the sake of quality have now been dropped. It was once customary to dry the coke, to break down the harder alloys before scalping, and sometimes even to plate them before breaking down and scalping. Very careful control was also maintained on the surface finish of the scalped ingot. In North

* Director of Research, The British Aluminium Co., Ltd., Gerrards Cross, Bucks.

† Nordiske Kabel- og Traadfabriker (Northern Cable & Wire Works), Copenhagen.

‡ Technical Manager, Imperial Chemical Industries, Ltd., Metals Division, Landore Works, Swansea.

§ Northern Aluminium Co., Ltd., London.

America these practices have generally been discontinued because there is less tendency for a well-made semi-continuous cast ingot to suffer surface cracking. Certainly practices are in use today which would have proved impossible before the war, and seem to result in good and in most cases in cheaper products, indicating that we should review our controls and practices frequently to see whether advancing techniques have not rendered some of them unnecessary.

Nearly all the papers under consideration report very favourably upon the induction furnace for melting. Our experience with a range of sizes has shown that lining problems are roughly proportional to the capacity, and some trouble has been experienced with the larger units. The induction furnace offers definite metallurgical advantages, but with the run-of-the-mill alloys of the aluminium and aluminium-manganese types the improvement is so slight that it can almost be disregarded. Maintenance is generally higher, charging big pieces is difficult, and electric power is usually expensive enough to rule the furnace out for anything but the melting of dirty scrap or swarf. I believe that oil is now about the cheapest fuel for melting aluminium, but some furnace builders may disagree with this view. Metallurgically, it seems to be satisfactory.

There is considerable mention in the papers of the dangers of furnace contamination, but not much suggestion as to how to overcome it. In the aluminium industry there is an increasing interest in non-wetting fire bricks. It might be of interest to have some comments on the practice of coating furnace linings with salts. Our Company adopted this method two years ago in an experimental furnace, following the German practice. The lining was taken out recently, and we were amazed to see how clean the furnace was and how little penetration had taken place. I wonder why the practice is not more frequently adopted.

I was surprised, on reading the paper by Mr. Staples and Mr. Hurst, to observe the large number of alloys being cast in book-type moulds. It was our impression that while there may still be metallurgical advantages in casting by this process alloys that are intended for deep drawing, economics usually favour the semi-continuous method. The latter is now used for practically all alloys in our group of companies.

An aspect of interest is the effect of charging methods on quality. Most plants, I believe, still charge much of their material by hand, although in some cases bales are pushed in mechanically. Some firms stress the importance of flashing-off oil on a forehearth, while others feel that the practice is of doubtful value. Unfortunately, our experience is that making up the bale costs almost as much as pushing the loose material through the door, and we wonder whether there is not an efficient and cheap method of introducing loose scrap. Pusher mechanisms have been used to introduce loose scrap through the door, which has the advantage of distributing the charge fairly well. Other producers have arranged for sections of the furnace walls to hinge out, so that the material can be dumped over the top. The ideal way would appear to be to charge the material through the roof, providing the fall did not damage the furnace bottom.

Mr. Staples and Mr. Hurst also mention the advantage of including a certain amount of scrap or reclaimed ingot in the melt to facilitate casting and further fabrication. Our experience would not lead us to substantiate this statement.

Frequent reference is made in the papers to the Straube-Pfeiffer instrument for the control of gas content. It is our impression that no simple relationship exists between gas in the metal and blistering. Gas and oxide must be present simultaneously. If there is gas, but no oxide to form nuclei upon which it can settle, or flaws in the ingot towards which it can diffuse, no trouble will occur. In our experience the Straube-Pfeiffer instrument is not a bad measure of the gas in the metal, but does not necessarily indicate whether the sheet will ultimately show blisters. We should be interested in comments on this or any other instrument for gas determination, and on whether or not qualitative or quantitative measurements of gas provide a useful tool for controlling blistering.

Some reference has been made to the possibility of straining

metal through porous filters or glass cloth. We have experimented with this a little and have found that a very large percentage of the inclusions can be thus removed. We have never been able to prove, however, that there was any marked improvement in the quality of the finished sheet, particularly in regard to blisters. In the same connection, I question whether the expense can be justified for any but the most complicated alloys, such as those of the Al-Zn-Mg-Cu type, or perhaps where very high metallurgical quality is required, for example, for jet-engine parts.

Mr. Staples and Mr. Hurst mention favourable results obtained with silicone greases. We have made a fairly exhaustive study of these greases, and have not experienced sufficiently beneficial results to recommend them for moulds in our melting department.

While control of melting procedure is very important, careless pouring can undo all the good previously done. I do not think, however, that holding periods of $1\frac{1}{2}$ hr. are necessary before casting. If we are not in the "twelfth month" to which I have referred, a very limited holding period, perhaps 15 min., seems adequate. If the metal quality is such that $1\frac{1}{2}$ -2 hr. is needed to clear it up, it is probably better to flux it with chlorine or aluminium chloride. However, when high-quality metal has reached the pouring spout, it is important to assure quiescent transfer to the casting machine. The importance of this increases with the weight of the cast. If quantities in the region of 10,000 lb. are being dropped in one pour, the transfer becomes very critical, and emphasis should be laid on large troughs, a certain settling area, and screens of some type to hold back the large dross.

After working abroad and then in England, I have observed some interesting inconsistencies in the theories of my associates. For example, many North American works pride themselves on the rather complex but very tidy dip-tube system of pouring ingots, whereby the metal is brought out in a launder, preferably almost level with the bath, and let down through a tube which discharges past a valve below the surface of the molten metal in the ingot. This is said to minimize the vortex effect and assure quiescent transfer. Most European companies seem to run the metal down a relatively simple launder into the mould. Similarly, one plant will favour a high-level quenching procedure, keeping the casting pit filled with water, while another will prefer to keep the pit dry and allow the water to run down the surface of the ingot. I have never seen figures favouring any one of these methods.

Some mention is made of the grain refinement of the aluminium-manganese alloys by the use of proprietary fluxes. It has always been our experience that there is little relationship between the grain-size in the ingot and that in the finished sheet. Some of the boron-containing fluxes will give a very fine grain in the ingot, but a very coarse grain may occur in the finished sheet, unless proper inter-annealing and cold-rolling practices are observed. The control of grain is more a matter of the distribution and form of the manganese constituent, and this can be better effected by control of casting methods and preheating, than by fluxing.

Dr. C. J. SMITHELLS said that Dr. Ransley, in his detailed contribution, would cover Mr. Paton's questions regarding the effect of gases. Mr. Paton, by his mention of a "twelfth month" in which everything went wrong, had given an excellent illustration of the function of the research department. It was depressing to a director of research to find a team, after five years' hard work, coming to the conclusion that the factory was doing exactly the right thing. That often proved to be the case, but the difference was that when the "twelfth month" occurred, it was possible to identify the cause of the trouble, which could not often be done merely on the basis of statistics from factory experience. That was why it was well worth while carrying out a long-period research to establish the fundamentals involved.

Before anything could be done about controlling the effect of gas in metals, and blister, an accurate method of measurement had to be developed, which required a great deal of work. The Straube-Pfeiffer instrument was very crude. What

would really be desirable would be to be able to carry out a continuous gas analysis, so that gas content could be measured in the same way that a thermocouple indicated temperature.

Professor A. J. MURPHY,* M.Sc., F.I.M. (Past-President), said that on reading the five papers it was surprising, even making allowance for the different characteristics of the metals, to see how much variation there was in methods of casting ingots. He hoped that one result of the symposium would be to counteract any tendency for cleavages to spring up in practice between the various sections of the non-ferrous metals industry. Dr. Singer's paper was invaluable in showing how important it was to investigate the factors underlying the control of quality in melting and casting and to establish some unifying principle.

From the paper by Dr. Cook and Mr. Cowley, it was possible to pick out the different operations and to assess to what extent they were relatively under control. As regards batch casting—the ordinary, conventional casting of a few years ago—control was pretty good in the selection of raw materials, in melting—especially if low-frequency induction furnaces could be employed—and to some extent in temperature regulation. Here, however, he would confirm what other speakers had said, namely that poor results were too often achieved in the measurement of the temperature of the molten metal by pyrometers. This was bad from all points of view, and not least in that failures of pyrometric equipment destroyed the confidence of the operative in measures of technical control and caused him to fall back on the old empirical methods of judgement on which he, or a previous generation, had been brought up.

At some of the other stages in the production of the ingot or billet, control was far from being in a satisfactory state. For example, specifications for mould dressings, as instanced by those given in Table II (p. 348) of Cook and Cowley's paper, could not by any stretch of the imagination be related to a pure function. The viscosity of the oil probably did not matter at all and its inclusion was only a rather desperate means of trying to ensure that something which had been found empirically to be satisfactory in the past would be obtained in further purchases. This uncertainty as to the function of the various constituents of mould dressings represented a corresponding uncertainty as to the condition of the mould surfaces which had at varying times been subjected to the action of these poorly controlled dressings, with successive heatings and coolings.

Feeding was another operation about which there was still a surprising difference of view and of practice. When adding feed metal to a large ingot, for example, was it better to add it in small quantities, maintaining its temperature, or to make two or three large additions; or was it preferable not to add any feed metal at all, but to employ the hot-top device to make the ingot self-feeding?

All these ill-controlled variables assumed a new significance in the light of the advance in continuous casting, and a number of them ceased to present any difficulty at all. The question of mould dressing was practically settled without much debate or anxiety, the mould surface became a more stable and less troublesome factor, and the problem of feeding was almost completely and automatically resolved.

Professor Murphy said that, as a result of these considerations, he had come to the conclusion—so well expressed by Dr. Smithells—that control became the less precarious and the more reliable as the true understanding of processes advanced. An important stage in this progress was the ability to isolate, and then to measure, the significant factors. While awaiting this development, which might take some time, it must be realized that control was rendered unduly onerous by measuring an unnecessary number of data, many of which were ultimately shown to be irrelevant. This struck at the root of one of the problems of today, which was the provision of sufficient numbers of suitably trained men in industry. With the

elaboration of processes it was not surprising that the demand for men with technical training and capable of taking positions of responsibility increased rapidly, but it would make for the more effective use of these men if processes could be so analysed as to reduce the number of stages at which close control had to be achieved, by a true understanding of the function of each of the variables involved.

Dr. C. E. RANSLEY,† M.Sc., F.I.M. (Member): I propose to confine my remarks to the paper by Mr. Staples and Mr. Hurst, and to deal mainly with their remarks on the "Control of Gas Content" on p. 379. We attach a good deal of importance to this aspect of quality control, and find that science needs to come to the aid of nature rather more vigorously than the authors suggest.

The first point which I would emphasize is that gas content is not now a somewhat mysterious factor to be judged by *ad hoc* methods such as the Straube-Pfeiffer test, but can be measured with considerable precision by vacuum-extraction technique. We have ourselves carried out many hundreds of these measurements for both research and production purposes and believe that we now have a good quantitative background in this field.

In the absence of proper data on gas contents, it is possible to draw wrong conclusions on several aspects of the behaviour of aluminium and aluminium alloys. It is very often assumed that the undoubted advantage which the direct-chill-casting method has over the chilled-mould method as far as gas content is concerned, results from the fact that the mode of freezing allows an appreciable amount of the gas to escape from the casting. This is not true. In fact, when pure aluminium or aluminium alloys containing normal amounts of gas are direct-chill cast at the speeds usual in production (2–6 in./min.) there is little or no significant loss of gas from the metal and, in addition, the average gas content across the solidified block is the same at the top of the casting as at the bottom.

In the case of hydrogen in aluminium, and probably with other metals as well, it is incorrect to assume that because the solubility in the solid is a good deal less than in the liquid, hydrogen is automatically rejected to the liquid in freezing. It is, in fact, initially retained by the solid, and whether or not it then passes to the liquid, and so leads to porosity formation, depends on the rate of diffusion of the gas in the solid in relation to the rate of advance of the solid face.

We have found that high-purity aluminium, when direct-chill cast, develops a negligible amount of porosity, even when the gas content is as high as 0.6 c.c./100 g.; the solubility of hydrogen in aluminium at the freezing point is of the order of 0.7 c.c./100 g., so that in the absence of a freezing range a gas content representing near saturation of the liquid can be almost completely retained in solid solution on casting at the normal direct-chill casting speeds. The presence of an appreciable freezing range, however, greatly modifies this situation. The conditions existing during the casting of such an alloy can be represented somewhat as shown in Fig. A (Plate XCV). The solid is within short-range distance of liquid for a relatively long period, and the hydrogen dissolved in it thus has time to diffuse into the interdendritic liquid. Bubbles are formed when the liquid becomes saturated, and since this normally occurs towards the solidus, e.g. at X in Fig. A, these are nearly all trapped in position.

It can be seen, therefore, that porosity development depends on the initial gas content of the liquid metal, the freezing range of the alloy, the solubility in the eutectic liquids, and the speed of casting. The effect of freezing range is illustrated in Fig. B (Plate XCV), which shows the amount of porosity in various types of direct-chill-cast blocks as a function of the gas content. High-purity metal (S.P.) shows virtually no porosity, even at high gas contents, but an appreciable amount develops in the 99.8% pure metal under the same conditions and more still in the 99.2% pure metal. Alloys with an even longer

* Professor of Industrial Metallurgy, Birmingham University.

† Research Laboratories, The British Aluminium Co., Ltd., Gerrards Cross, Bucks.

freezing range, such as Duralumin-type alloys, develop porosity at a much lower gas level; the dotted curve in Fig. B is characteristic of one of these alloys, and it will be noted that in this case porosity formation becomes appreciable at about 0.16 c.c./100 g. The other dotted curve shows the porosity/gas content relationship for small sand-cast bars of 99.2% pure metal, and comparison with the direct-chill-casting curve for this alloy illustrates the very marked effect of freezing rate on the release of gas from solution. The final slope of these curves is about the same, and indicates that the porosity is formed at just over atmospheric pressure at the solidification temperature.

It is clear from these results that the advantage of the direct-chill process over normal chill-mould casting is due not to the expulsion of gas, but solely to the more rapid rate of solidification.

Porosity development in rolling blocks, though technically undesirable (and also capable of leading to indirect effects), need not necessarily result in blister formation in the final rolled sheet. A blister occurs only when there exist, in combination with a high gas content, flaws in the rolled sheet comparable in length with the thickness of the overlying metal. Flaws occurring near the surface of the sheet are thus important, and it is very desirable to avoid porosity near the surface of the cast blocks. The distribution of porosity across direct-chill-cast blocks is not uniform and has some features of direct interest in quality control. Fig. C (Plate XCV) shows the characteristic distribution of copper, hydrogen, and porosity across a large (38×8 in.) rolling block of D.T.D. 603B alloy with a rather high gas content (>0.30 c.c./100 g.). We are now in a position to explain the main features of the segregation indicated by these curves. The feeding-through of eutectic from the liquidus to the solidus isothermals, together with the effects of remelting and blebbing at the point where the shell leaves the mould wall (indicated at Y in Fig. A), leads to a transference of gas to the outer layers of the block. A porous zone is formed there which is deleterious and can lead to serious blister trouble. Although the wasteful and expensive procedure of deep scalping can be adopted as a palliative, the real remedy is to reduce the gas content of the metal entering the casting to a safe level.

The porosity disappears almost entirely at a quite well-marked gas level, and it is possible for us to define, for this alloy and for others of commercial importance, the threshold value below which gas, under normal conditions, ceases to be an important factor in metal quality. This, as I mentioned just now, is about 0.16 c.c./100 g. for Duralumin-type alloys.

This is a very useful step forward. The next point is: How is the desired level of gas to be attained in practice?

The gas content of a bath of freshly melted metal, whether pure or alloy, is a rather variable quantity and is usually too high for the metal to be cast without any treatment. The first question which arises is whether the type of furnace used is important? We do not think so and agree with the authors that electric and fuel-fired furnaces of widely different types can all be used successfully for aluminium production, providing certain factors are recognized. The most important of these is temperature control. High temperatures are particularly deleterious, and furnaces must be so designed that overheating of the surface of the bath does not occur; for example, by flame impingement directly on the metal. Automatic temperature control is very desirable for this reason, as well as for other considerations.

Pure aluminium, if held at temperatures less than 750°C ., tends to lose gas by diffusion, and metal of a quality suitable for direct-chill casting can be obtained without much difficulty.

Alloying elements, however, can exert a potent effect on the gas behaviour of a melt. Magnesium, in particular, leads to marked gas pick-up by the molten metal, so that holding by itself is not effective for alloys containing this element. In the case of the Duralumin-type alloys (Staples and Hurst's

Group 5) the level of gas that can be tolerated if a sound block is to result is lower than is normally obtained in melting, and a decisive degassing treatment is thus required for this class of alloy if good-quality rolled metal is to be obtained.

There does not appear to be a great deal of difference between the efficacy of the various commonly used degassing agents, providing that they are used in comparable amounts, i.e. the volume of degasser actually bubbled through the metal is the same in each case. Once again, however, temperature is an important variable, and the best results are obtained only if the metal temperature is kept as low as possible during the degassing process. Degassing is a slow and inefficient process, however, and large weights of metal require very substantial additions of degassing agents. Since gas pick-up occurs if the melt is allowed to stand subsequent to degassing, casting should take place soon after the degassing treatment has been carried out.

Finally, what can be done about the routine control of quality as far as gas is concerned? Vacuum-extraction determinations are useful only for inquest purposes, and there is no casting-shop test which meets the case; the vacuum-solidification test has its uses, but is not sensitive enough for this type of work. As I have just remarked, the gas content of a freshly melted bath is a very variable quantity, and at the moment all we can do to ensure adequate quality is to specify a degassing treatment which can cope with the worst conditions that arise. This procedure is wasteful of both time and material, and the ideal solution would be to read the hydrogen content of the metal accurately on the spot, so that each melt can be degassed individually to the desired level. This is a difficult but not impossible goal.

M. W. VINAVER* said that he would like to discuss the effect of iron content on the structure of zinc ingots for rolling. In ingots cast by the conventional open-top method there was a marked difference between the top and bottom of the ingot, and consequently between the upper and lower sides of the sheet. It was customary in French rolling mills to speak of the "good" and "bad" sides of the sheet. The variation in properties might be attributed to crystal structure, to chemical composition, and to blisters which occurred on the upper surface. In some cases, however, it had been found that the good and bad qualities were reversed, and that in bend tests the sheet sometimes cracked on the "good" side.

In nearly all these abnormal cases crystals of zinc-iron intermetallic compound could be detected near the surface of the under side of the sheet. The phenomenon occurred with an iron content as low as 0.025–0.030%. The zinc-iron diagram established by Schramm† indicated a eutectic at approximately 0.09% iron, and if this were correct, segregation of an intermetallic compound would be impossible at iron contents as low as those mentioned. On the other hand, it was well known that in the zinc melt there was downward segregation of hard zinc, and that when zinc of commercial quality was melted at about 450°C . the iron content of the bath, after deposition of the hard zinc on the bottom of the furnace, was about 0.025%. It was clear therefore that Schramm's diagram was not quite correct.

A further investigation of the liquidus in the region of low-iron content had accordingly been undertaken. A zinc-1% iron alloy had been melted in a plumbago crucible and cooled very slowly in a furnace, the temperature of the metal being measured by means of a Chromel/Alumel thermocouple connected to a potentiometer. Samples of liquid metal were taken from the top portion of the melt at various temperatures by means of a Pyrex glass pipette, after dross had been cautiously removed from the surface. The iron content of the samples was then determined colorimetrically. After complete solidification, drillings were also taken from the upper portion of the solid metal. A liquidus curve was established which differed considerably from that of Schramm (see

* Compagnie Royale Asturienne des Mines, Auby-Lez-Douai (Nord), France.

† J. Schramm, *Z. Metallkunde*, 1936, 28, 203.

Fig. D). The iron content of the solidified metal was 0.012%, instead of 0.09%, as indicated by Schramm. At 450° C., the iron content was 0.025%, and at 500° C. it was 0.075%. This explained why, when casting zinc of commercial grade in a horizontal mould, a certain downward segregation of zinc could be expected if the iron content exceeded 0.012%, which was often the case (see Fig. E, Plate XCV). In this particular case, said M. Vinaver, careful bath-temperature control at the casting stage could eliminate the segregation in the ingot of a layer of hard zinc-iron crystals, which would lead to embrittlement of the sheet.

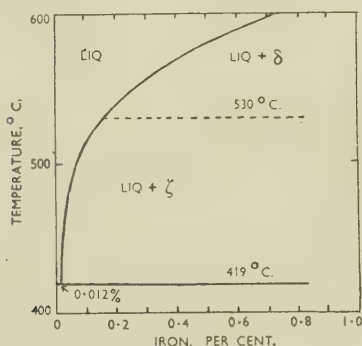


FIG. D.—Solubility of Iron in Zinc.

Mr. Christopher Smith had expressed surprise that continuous or semi-continuous casting methods were not applied to zinc. In his (M. Vinaver's) opinion the benefits to be expected from such methods were much less than for other metals, very coarse columnar structure resulting even when they were applied. The influence of rate of cooling on the grain of the metal was very slight, while the rapid cooling of the ingot involved in the continuous-casting process set up internal stresses which might later result in cracks during rolling.

Mr. C. W. ROBERTS,* B.Sc., A.I.M. (Member): Regarding Mr. Christopher Smith's question as to the casting method (described on p. 372 of our paper) in which the mould is lowered continuously during the pour, we have had no direct experience with this system of casting and, to the best of our knowledge, it is not used in this country for the production of zinc rolling slabs. It is reported to have been employed in Germany for the production of zinc alloy rolling slabs, and was mentioned because it appeared to represent, in principle at least, a method whereby turbulence can be minimized provided the rate of metal flow is accurately adjusted.

Mr. Smith also enquired about the semi-continuous casting of zinc rolling slabs. This method is not used in this country because outputs are not sufficiently high to justify the cost of the plant and there is no evidence to suggest that the quality of the products would be higher. Zinc alloy rolling slabs were cast by a semi-continuous method in Germany during the war, but are reported to have been more troublesome during rolling than those cast by more conventional methods.

It may be relevant to add that the zinc sheet produced by the Hazelett mill, which involves the continuous casting of the metal between slowly revolving rolls, has been found to be unsatisfactory for most purposes because of the marked directional properties of the material.

In reply to Mr. Bond-Williams's question regarding specification in the zinc industry, British Standard No. 1003 defines the metal of 99.99% purity, and metal for the production of alloys such as Kayem is ordered to this specification. Zinc of lower purity is covered by British Standards Nos. 220, 221,

and 222, which define the various grades in terms of maxima for impurities, but since most rollers require metal with certain elements (e.g. cadmium) held within definite limits, these specifications are not of very much value in ordering metal for rolling.

M. Vinaver's remarks on the effect of the iron content on the rolling properties of zinc are very interesting, and the figures he quotes indicate that the solubility of iron in liquid zinc may be lower than is generally accepted at present. The limits adopted in practice are in conformity with his figures, since, while 0.020% iron is acceptable in sheet for general purposes, a maximum of 0.006% is set for sheet to be used for deep drawing, which is below the solubility figure at the freezing point quoted by M. Vinaver (0.012% iron at 419° C.).

Dr. R. T. PARKER,† B.Sc., A.R.S.M., F.R.I.C., F.I.M. (Members), said that, owing to the necessity of directing control with the ultimate use of the material in mind, the paper by Mr. Roberts and Mr. Walters must be commended for its clear statement of the important factors. Items (a) to (h), listed on p. 366, showed that the authors appreciated that the material they were preparing in the foundry had to go forward to be used in other departments where it had to meet certain limitations. None of the other authors had defined the necessary properties of the cast material in terms of further use and final properties quite so plainly. In this respect, Dr. Singer's paper on statistical control did not go far enough, and he too should relate the control of quality of the cast material to the properties expected from the material subsequently. If his paper was one intended to cover the principles of technical control in subsequent portions of this symposium, it should have been much wider in its thinking. Interest would be centred not only on first-order but also on second- and third-order effects. For this reason it would seem beneficial for the casting process to be regulated by a control of quality in subsequent products and not necessarily by immediate control in the foundry. This, of course, was not always desirable and had the disadvantage, stated by Dr. Singer, of lack of immediate control due to the time lag that must occur.

Dr. A. E. R. SINGER: I was surprised to hear Dr. Parker advocating remote control in preference to close control, and I would draw his attention to Table II (p. 339) of my paper, in the fourth column of which appears: "Measurement of mechanical properties, density, porosity, hot and cold deformation." I think that wherever possible we should try to use the final qualities and properties of the material to control the ingots being produced. In this respect the paper by Mr. Sykes is commendable, for he casts small samples of copper, draws them down to wire, and makes conductivity tests. It is an instance of utilizing the time interval during which the bath of copper is molten, to carry out a test for control purposes. It is a practical example answering Dr. Parker's criticism.

There has been much talk about primary and secondary variables, yet there is no fundamental difference between them, for a primary variable in one process may be a secondary variable in another. All depends on the process. Taking a particular instance such as the melting operation, the primary variable is the quantity that has an immediate and direct effect upon the product and the quantity that we value and use in the final product. In the case of an ingot, it is obviously the structure and properties of the ingot that we require, and with a bath of metal it is the temperature and composition of the metal.

I am completely unrepentant about Table II. In the third section of that table, for instance, under "Casting", it is stated that there is no short-term control of the structure of the ingot. I know of no way in which such short-term control is effected at present. It is effected in a long-term sense, because when we have carried out many hundreds of experiments we

* Research Department, Imperial Smelting Corporation, Ltd., Avonmouth.

† Director of Research, Aluminium Laboratories Limited, Banbury, Oxon.

know from our experience that a particular combination of techniques will produce a certain structure or certain properties, and it therefore represents a form of long-term control.

It is important that in the metallurgical industry we should not try to justify our prejudices with regard to control, and it is all too easy to assume that the present situation is satisfactory. In certain cases primary variables are measured and used for control purposes by the more advanced firms in a particular field, but the vast majority of material processed is not subject to such control. The quality of the product may be very much enhanced by introducing the control of primary variables, and that is the main point that I would emphasize. There are enormous opportunities before us. They may seem difficult of achievement at the moment, but they will eventually be achieved, and if we direct our efforts towards them we shall increase the quality of our product much more rapidly than would otherwise be the case.

Mr. L. C. BATCHELOR,* A.I.M. (Member): Statistical control has been referred to by Dr. Singer. This is likely to be developed to a much greater extent in the sections of the symposium to be held later, dealing with the fabrication and working of the materials. It is very difficult to be sure that a casting is a good one, although it is often possible to reject the really bad ones. I think that there are two main methods of statistical control which can probably be inserted between casting and the final product. One involves the recording of the results of examination of samples. In this there is a risk that the samples, however they are taken, may not represent the bulk. The second method is to have 100% inspection to ensure entire freedom from defects. This in my experience has never been, and I think cannot be, entirely satisfactory, because some of the defects will escape detection. However, a combination of these two methods on a statistical basis would go a long way towards improving quality and showing a trend on which action would be taken.

I am particularly interested in the paper by Mr. Sykes, and I have one or two questions to put to him. In dealing with types of furnace, does he not think that it would be better to use smaller units with a shorter cycle of operations for the feeding of holding units for the casting of vertical shapes? For chromium copper he mentions a temperature of 1510° C. What sort of mould is used for that temperature and what is the surface condition of the casting? I know that chromium losses in copper-chromium alloys are very considerable, and I think that it is quite satisfactory if the chromium can be controlled within 0.2%. My experience is that with high temperature there is better absorption of the chromium but also a very high loss from oxidation.

The say-ladle tests are very important in the refining and preparation of oxygen-bearing copper, and I was interested in the treatment of the ladle with charcoal. I should have thought that a bone ash dressing would be more satisfactory.

I am surprised at the pouring temperatures mentioned, limits of 1140°–1143° C. on billets and 1099°–1110° C. on vertical-cast cakes. I have found it very difficult to get a pyrometer or any control to work to such a fine degree as that. Mr. Sykes also mentions the occurrence of shadow cracks in vertical castings. Can he suggest any methods to control or eliminate these defects?

On the practical side of the control of quality, I think that in brass and copper-alloy production it is very important to employ individual operators with the required skill. They should work on medium-size furnaces and should have responsibility for mould preparation. It is also preferable, in my opinion, for a caster to produce fairly large batches in one quality, which can then be followed through the later stages of production, and to specialize in a particular shape, whether a billet or a slab, and a particular material, e.g. one operative

working on 60 : 40 and one on 70 : 30 brass, or whatever the alloy may be.

Mr. J. SYKES,† F.I.M. (Member): In reply to Mr. Batchelor, the use of a number of small furnaces rather than one large one is a question of economics, plant design, and the variety of shapes to be produced. It is not possible to discuss this question without first knowing what capacity is needed, the range of sizes to be produced, and how quickly they are required.

Mr. Batchelor and Mr. Bond-Williams both suggest that difficulty might be experienced in controlling the chromium content of chromium copper. As stated in the paper, we can control the content within 0.2%, but a temperature must be attained in the furnace high enough to ensure complete solution of the chromium, and that is why we emphasized the high temperature to which the melt must be superheated. A cast-iron mould with an inert dressing is used for this material.

In preparing oxygen-bearing copper, the say-ladle is coated with charcoal in order to give a slightly lower oxygen content than in the bath, thus providing a small factor of safety.

Professor d'Ombain asks about carbon dioxide recorders and whether we have tried automatic control. We have not done so, but it has been attempted in the U.S.A. It has been found impracticable to fit automatic recorders to the large refining furnaces.

The conductivity test takes about 30 min. The final test is now made by spectrograph, and there is ample time for the conductivity test to be carried out.

Mr. S. B. HIRST,‡ B.Sc. Tech.: The only question which I have to answer concerns the effectiveness of the metal distributor shown in the diagram of our direct-chill casting machine (Fig. 3, Plate LVIII). We find this quite effective, not so much in trapping the oxide as in directing it to the side of the billet. The metal enters down a funnel which feeds into a distributing cup with side slots, and the metal flow is then directed through the slots to the side of the billet. Any oxide skins which may come through the slots are diverted to the side of the billet and subsequently machined off in the machining operation.

I should like to refer to a point mentioned in the paper by Mr. Staples and Mr. Hurst (p. 381) concerning the effect of corrosion products on magnesium ingots in introducing gas into aluminium-magnesium alloys. As mentioned in our paper, in the magnesium industry we have very little trouble from gas, as such, and we are not convinced that a normal pure-magnesium ingot in reasonable condition could lead to serious gas trouble in aluminium alloys. I think that the ingot concerned must have been part of old stock, of which there were considerable quantities available in the years following the war. This was imported metal kept over a long period, probably not under ideal storage conditions. We cannot see any reason for special wrappings for ingots produced in this country and stored under normal conditions. Ingots shipped abroad are, of course, protected by such wrappings.

Mr. R. T. STAPLES § (Member): The problem which we hoped would provoke discussion has undoubtedly done so, and that is the question of gas control. I am going to take up the challenge by saying that, using the techniques outlined in our paper, gas determinations on hot-rolled blank show a hydrogen content as low as 0.17, and are commonly less than 0.2 c.c./100 g., below which level subsequent trouble with blisters should not be experienced.

Another point arising is the very significant effect of porosity near the edge, where scalping is still needed. We can confirm that, as we get porosity in the outer $\frac{1}{2}$ in. There would seem to be direct confirmation of the gas distribution

* Imperial Chemical Industries, Ltd., Metals Division, Birmingham.

† Director, Enfield Copper Refining Co., Ltd., Brimsdown, Enfield, Middlesex.

‡ Magnesium Elektron, Ltd., Clifton Junction, nr. Manchester.

§ T.I. Aluminium Ltd., Birmingham.

already indicated in the discussion, but below that level we look for other factors for the suppression of blisters in Duralumin-type alloys.

In discussing blister, it is important to note that different problems arise with the Duralumin-type alloys from those arising with pure aluminium and the near-pure types. We have not experienced any serious trouble with the last two types, and in discussing blister we invariably think in terms of Duralumin-type alloys. We can produce a Duralumin sheet with only a few per cent. (varying from batch to batch) of blister. We have such confidence in our technique that we carry out no degassing at all in the duplex furnace.

In using the Straube-Pfeiffer test, we have followed the B.N.F. technique, but we have never looked on it as anything more than a signpost to the way we are going.

We seem to have created a wrong impression in the paper with regard to the use of what are commonly known as book moulds, either solid cast-iron or water-jacketed moulds. In common with other producers, we do not employ these, and where they have been mentioned in the text it is to illustrate a point, not to suggest that they provide an ideal method of production, though we did hope to bring out the fact that the direct-chill method does not provide by any means a complete answer. I had expected to hear more about the problem of directionality, which arises with pure aluminium when the block is cast by the direct-chill method; the preparation of sheet with random orientation becomes much more difficult and quality has to be sacrificed to some extent—if random orientation is the test of quality—on changing from the old solid-mould slab to the chill-cast method.

We should like to thank Mr. Kasz and Mr. C. Smith for their most useful information on the effect of sodium. Mr. Kasz asked what evidence we had for the occurrence of fine particles of oxide and for their suppression by standing. The evidence of occurrence is mainly of a direct nature, in the preparation of thin-walled cable sheathing. This is made in very long lengths and is then pressure-tested. In 18 gauge, anything in the nature of an inclusion remaining in it is revealed in the pressure test. It was when we started to manufacture this material that we had to revise our melting techniques. Another effect observed more than once, and connected with the same phenomenon, is that in making sheets with a random orientation, if the casting is carried out in the old type of solid mould, then holding apparently has a beneficial effect. As that has been associated with the production of cleaner material, we thought that the two might be in some way related.

On the question of bottom tapping, we adopt that, perhaps, as an expedient. We are interested to obtain confirmation of the fact that particles of residue do collect on the bottom of the bath, but we avoid that by draining the bath once a week only and discarding the residue.

Mr. Kasz asks how we overcome hot-tearing with the 2-3% magnesium alloy and the trouble with the H10-type alloy which is very prone to central cracking. The answer is fairly simple; we cast at lower speeds. That is not altogether a satisfactory solution, since the production manager wants as much metal produced as possible, and we should like to know how we can cast faster and still get a solid block. We have standard techniques for producing these materials.

With regard to the control of water temperature, in print, 1°-2° C. may look alarming, but a definite effort is made to achieve this, the control being taken from the feed-water to the pit. We find that any considerable departure from this temperature in the pit water leads to trouble. While we refute any inference from our paper that 1°-2° C. control is essential, we would make the point that, if a standard practice is to be consistently observed, water-temperature control is necessary.

Professor d'Ombrain spoke about instrumentation. We

feel that there is a very real need for speed indicators and flow meters for the continuous-casting process, in that, with aluminium, the casting speed is critical to within very fine limits. We are not aware of instruments adequate for that purpose being available.

CORRESPONDENCE

Mr. D. M. LEWIS,* B.Sc., A.I.M. (Member): A feature present in Figs. 5 and 6 (Plate LV) of the paper by Mr. Staples and Mr. Hurst may be of some importance in the continuous or direct-chill casting of light alloys. These two illustrations exhibit in both the longitudinal sections distinct periodicity of structure, shown by a wavy boundary below the billet surface. The two outline diagrams reproduced in Figs. F and G make the effect clearer, if compared with Figs. 5

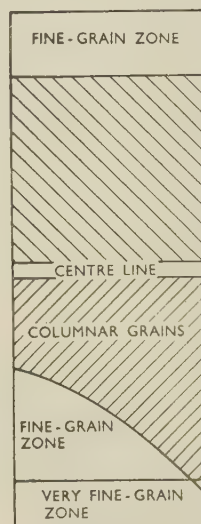


FIG. F.

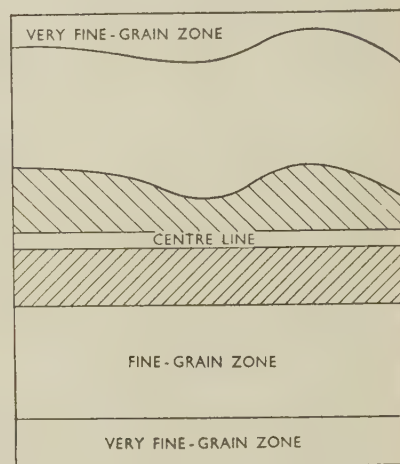


FIG. G.

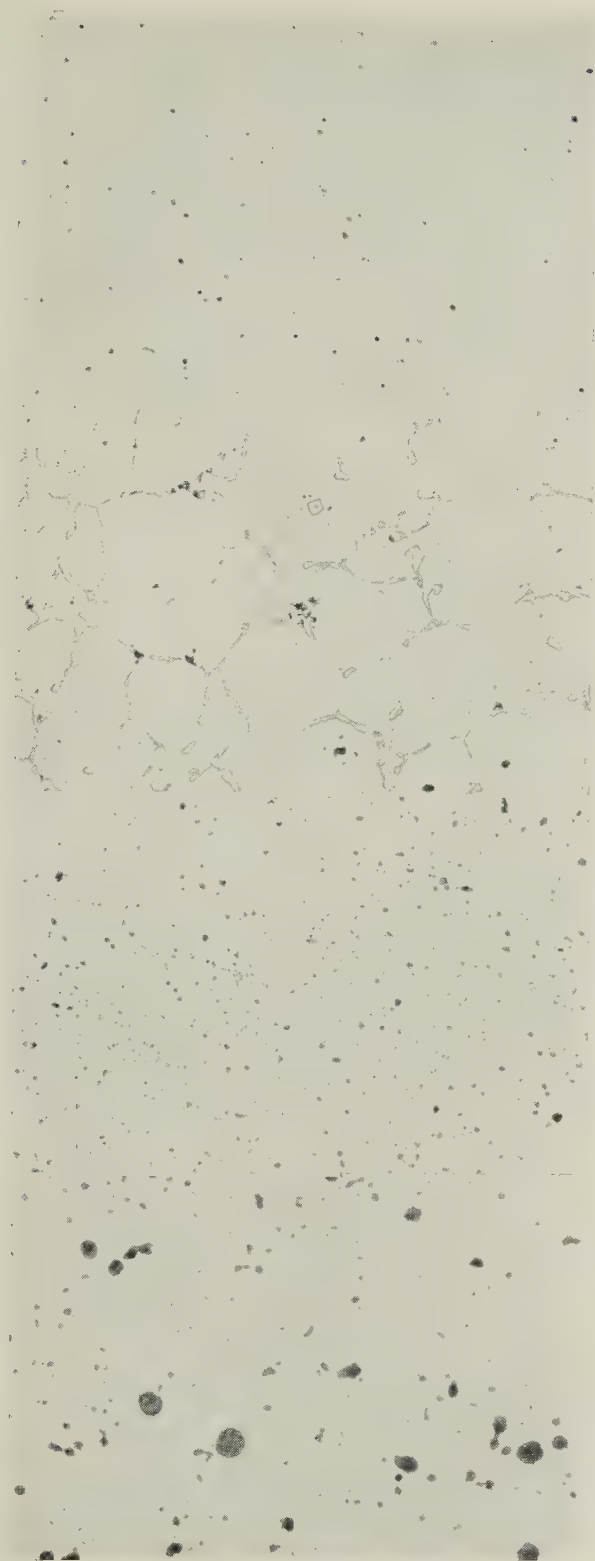
and 6. In Fig. 5 the length of the section is too small for the full wave to be shown.

This effect confirms some observations made at Aluminium Laboratories, on the frequent anisotropy of continuously cast materials. Fig. H (Plate XCVI) shows a typical etched longitudinal section of a 5½-in.-dia. billet in 11% silicon alloy cast at 6 in./min. A well-defined staggered effect is noticeable in the position of the zone troughs and crests of the wave pattern, indicating a spiral layout when considered in three dimensions. Measurements made on this cross-section indicate that the pitch of the spiral is about 4.3 in. That the effect is associated with non-uniformity in the macrostructure of a transverse section is shown by Fig. J (Plate XCVI).

It is of interest to link up the internal structure with the normal variations in the surface profile of the billet. As illustrated in Fig. K (Plate XCVI) the billet described above has a profile showing distinct hollows which are displaced in a definite helix whose pitch works out at about 4.6 in., in reasonable agreement with the 4.3 in. measurement from the macrostructure.

The usual explanation for this lack of symmetry of structure, when seen in transverse cross-sections, is non-uniformity of mould cooling, but the fact that the effect spirals up through the billet proves that this cannot really be the case.

* Aluminium Laboratories, Limited, Banbury, Oxon.



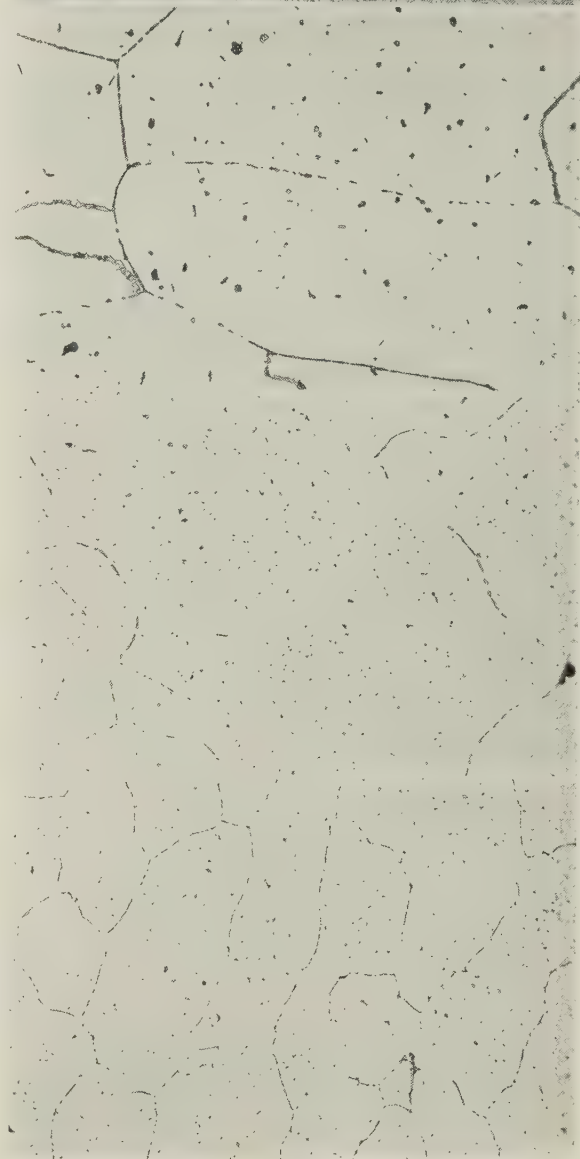
Figs. 16-19.—Microstructures of a 90:10 Chromium-Cobalt Alloy. $\times 250$.

FIG. 16.—Melted and cast in a vacuum without purification.

FIG. 17.—After hydrogen reduction of the melt for 30 min.

FIG. 18.—Treated with 0.6% carbon and cast at 0.1 mm. mercury pressure.

FIG. 19.—Cast at the optimum end-point of the carbon-reduction reaction.



Figs. 20-21.—Creep-Test Specimen of Chromium-10% Iron Alloy after Test B (Fig. 6, p. 575). $\times 100$.

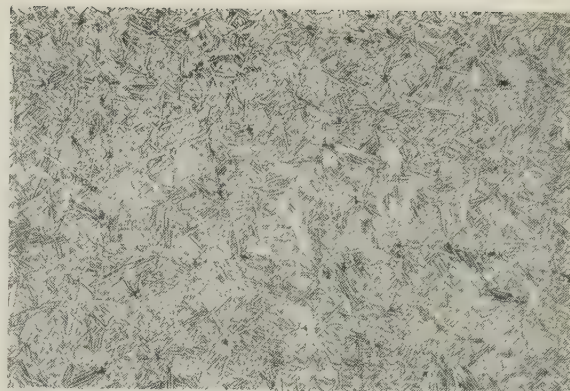
FIG. 20.—Unstrained shoulder.

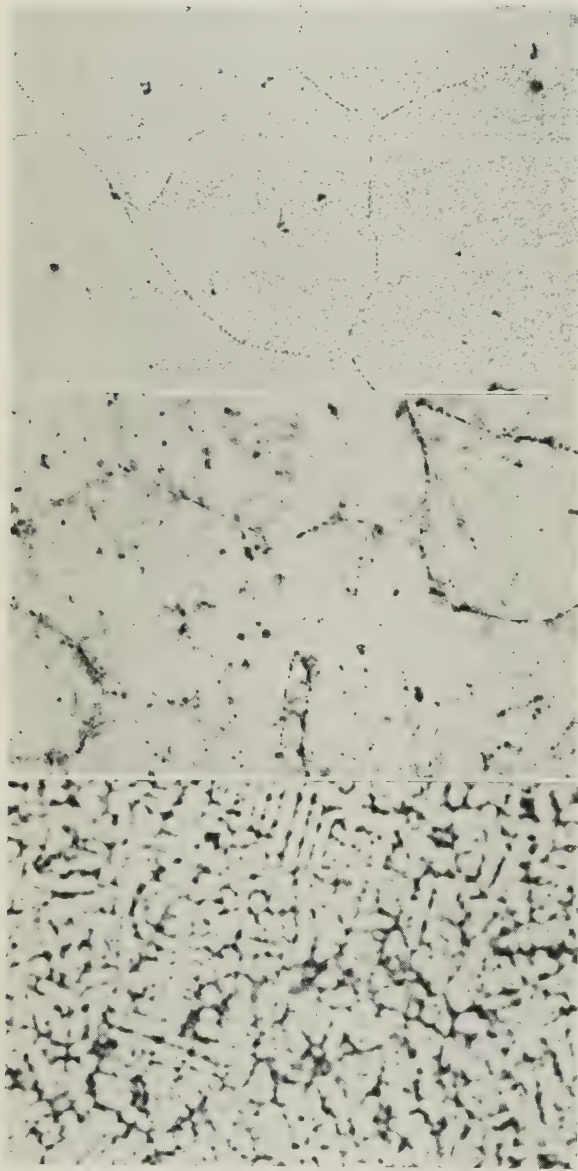
FIG. 21.—Strained gauge-portion.

FIG. 22.—18.5% Cobalt.

at 900°C . $\times 250$.

FIG. 23.—27.9% Cobalt.



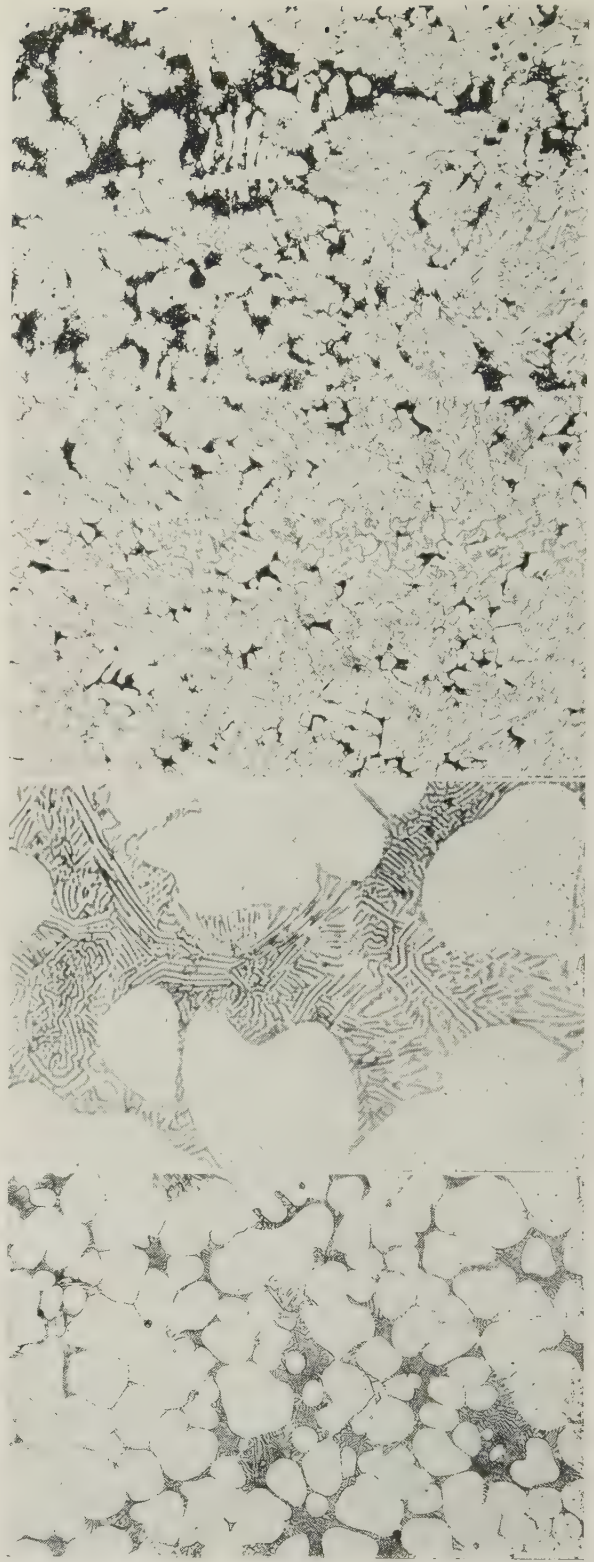


Figs. 24-26.—Microstructures of Chromium-18.94% Nickel Alloys. $\times 250$.

Fig. 24.—As cast.

Fig. 25.—After 24 hr. at 1250° C. followed

Fig. 26.—After 24 hr. at 1250° C., air-cooling, and heating at 900° C. for 16 hr.



Figs. 27-30.—Microstructures of Cast Chromium-Iron-Tantalum Alloys.

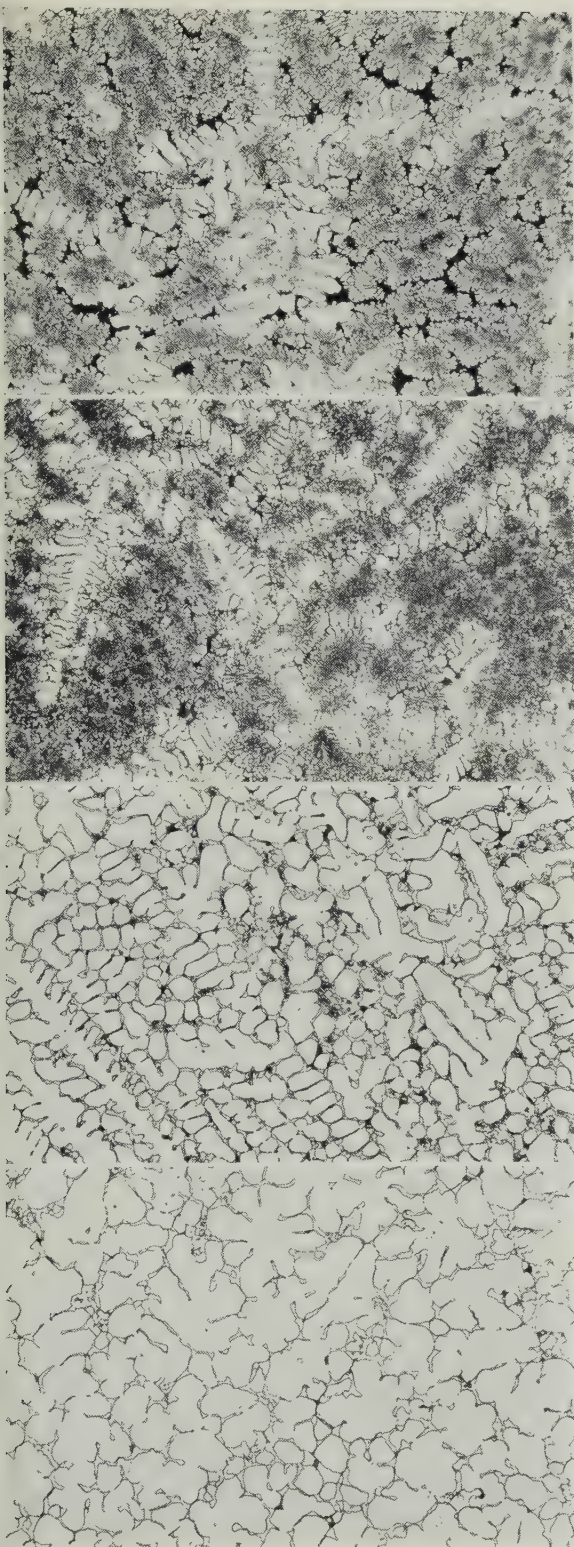
Fig. 27.—Alloy H171 (10% Fe, 10% Ta). $\times 250$.

Fig. 28.—Alloy H171 (10% Fe, 10% Ta). $\times 1000$.

Fig. 29.—Alloy H91 (17.0% Fe, 27.5% Ta). $\times 250$.

Fig. 30.—Alloy H87 (9.4% Fe, 27.5% Ta). $\times 250$.

Electrolytically etched in a solution of *aqua regia* in glycerine.



Figs. 31-34.—Microstructures of Cast Chromium-Iron-Niobium Alloys. $\times 250$.

FIG. 31.—Alloy H94 (10.4% Fe, 7.6% Nb).

FIG. 32.—Alloy H96 (20.3% Fe, 8.0% Nb).

FIG. 34.—Alloy H97 (19.1% Fe, 16.7% Nb).

Electrolytically etched in a solution of *aqua regia* in glycerine.

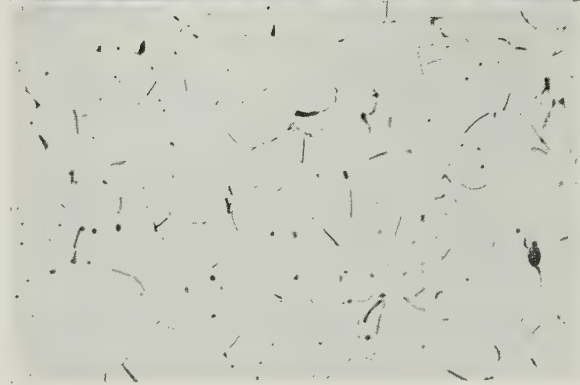


FIG. 35.—Alloy H80 (21.5% Fe, 17.5% V). As cast. $\times 250$.



FIG. 36.—Structure of Tensile Creep Test-Piece Containing 10% Fe and 10% Ta Which Fractured in the Head During Loading. Showing Interdendritic Porosity at End near the Fracture. $\times 40$.

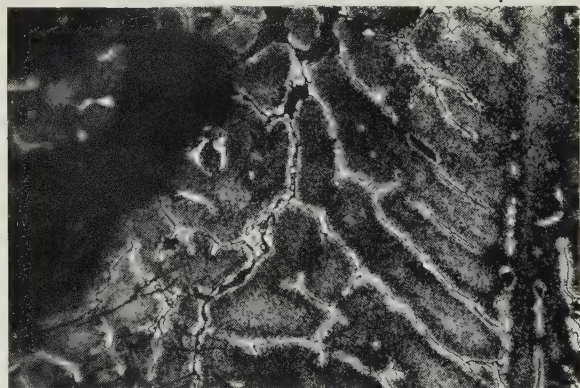


FIG. 37.—Alloy H171 (10% Fe, 10% Ta), Showing Cracks Associated with Fracture in Tensile Creep-Test at 900° C. $\times 250$.

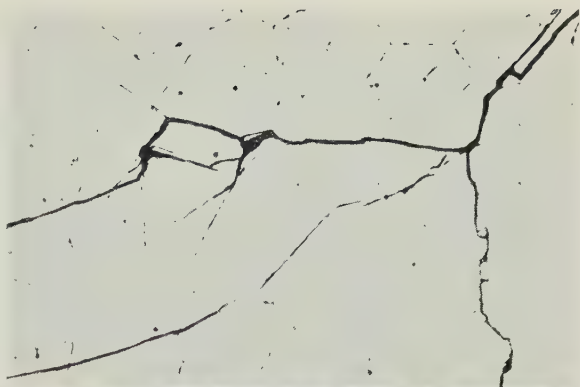


FIG. 38.—Cracking, Mainly Transcrystalline, in Cr-15% Fe-25% Mo Alloy Subjected to Thermal-Shock Test. $\times 150$.

FIG. 39. Compression Creep-Test Specimen of Cr 15% Fe-25% Mo Alloy Before and After Test for 40 Hr. at 900° C. $\times 5$ approx.



FIG. 40.—Cr-15% Fe-25% Mo Alloy After 216 Hr. at 900° C. in Free Air. $\times 3$.

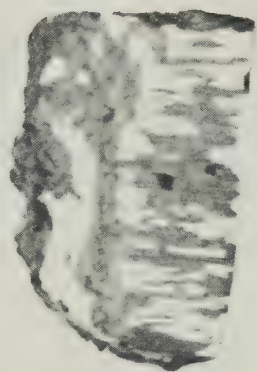
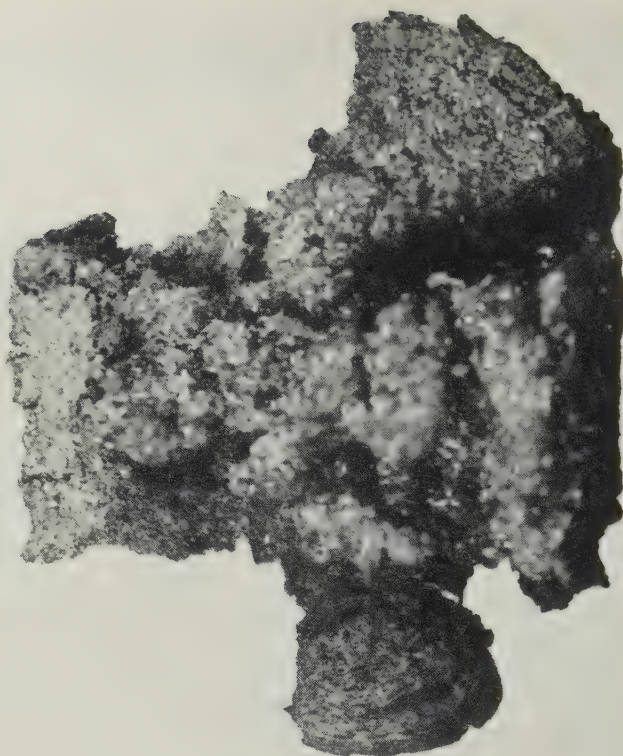


FIG. 41.—Cr-15% Fe-25% Mo Alloy After 216 Hr. at 900° C. in Stagnant Air. $\times 3$.



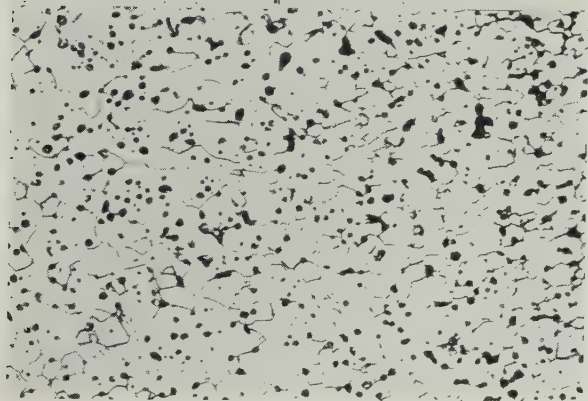
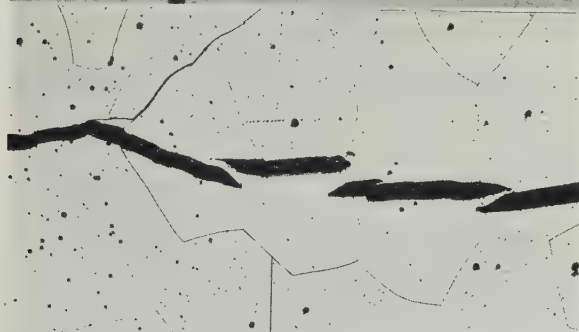


FIG. 12.—Structure of Sintered Hydride Chromium. The black spots are pores. Etched electrolytically in 10% oxalic acid. $\times 150$.



FIGS. 13-14.—Transcrystalline Cracks in Arc-Melted Chromium. Etched electrolytically in 10% oxalic acid. $\times 50$.

FIG. 13.—Normal illumination.

FIG. 14.—Oblique illumination.



FIG. 15.—Crack Shown in Fig. 13 at Higher Magnification. $\times 250$.

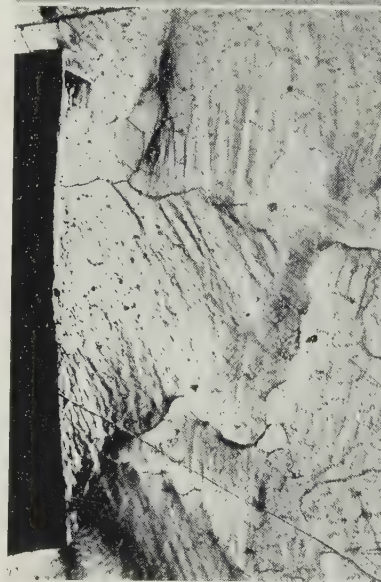


FIG. 16.—Deformation Around Edge of Diamond Impression made in Polished and Etched Arc-Melted Chromium at Room Temperature. Load, 60 kg. Time of application, 15 sec. $\times 100$.

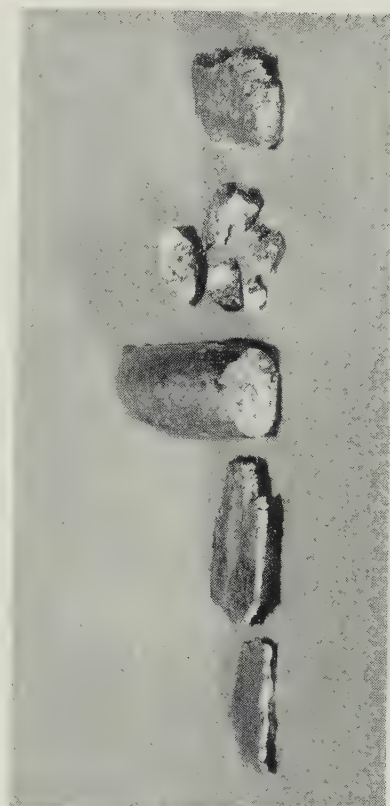


FIG. 17.—Samples of Chromium Compressed at Room Temperature. $\times 1$.

1. Hydrogen-purified electrolytic chromium.
2. Unpurified electrolytic chromium.
3. Arc-melted chromium.
4. Remelted chromium containing 1% Ni. Cf. Batch S71 (Table II, p. 590).
5. Aluminothermic chromium.



FIG. 3.—Type-A Markings in Commercial Aluminium-3½% Magnesium Alloy Strips (OZX) Stretched Part Way Through the Initial Yield. $\times 1$.

(a) Complex markings in strip with sheared edges. Approx. 1% extension.

(b) Simple markings in similar strip annealed for 1 hr. at 350° C. after shearing. Approx. $\frac{3}{4}$ % extension.

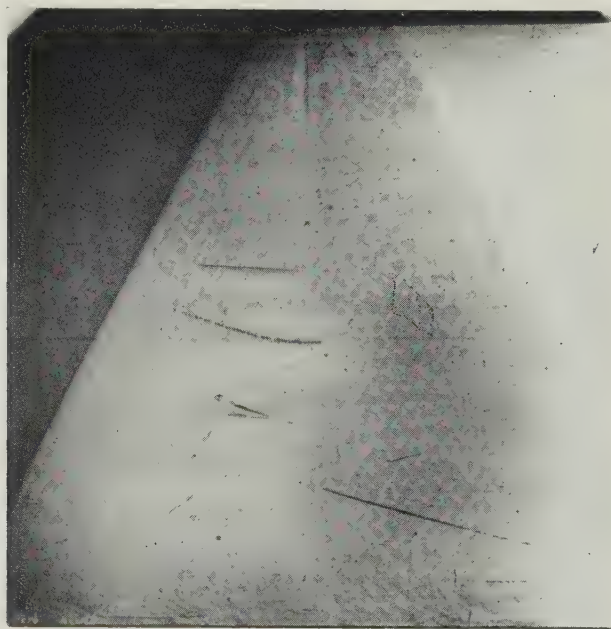


FIG. 4.—Single Yield Wedge, Produced by Stretching a Strip of Commercial Aluminium-3½% Magnesium Alloy, Annealed for 1 hr. at 450° C. and Air-Cooled, Approx. $\frac{1}{2}$ % in an Amsler Testing Machine, Showing Faint Ripples Parallel to Boundaries. $\times 2$.

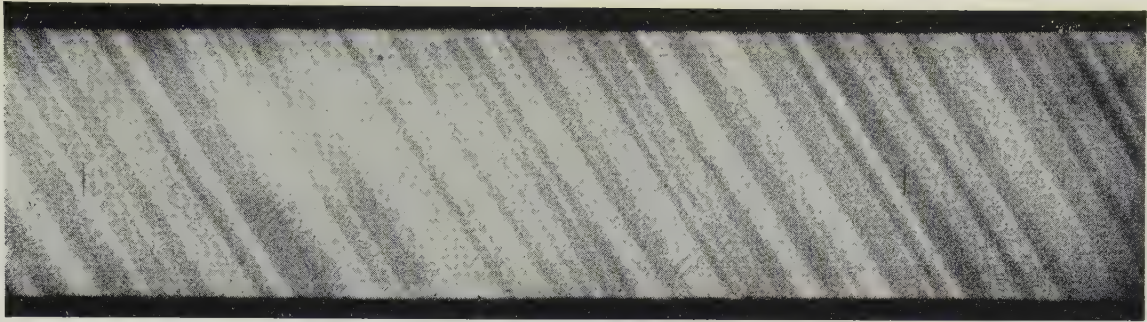


FIG. 5 (a).—Type-*B* Markings in a Strip of Commercial Aluminium-3½% Magnesium Alloy, Annealed for 1 Hr. at 450° C. and Air-Cooled after Shearing the Edges. Pulled to approx. 8% extension. × 1.

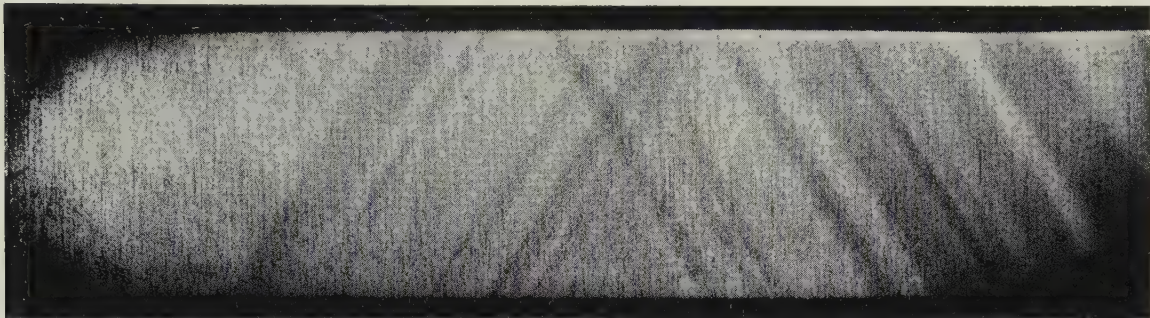


FIG. 5 (b).—Type-*B* Markings in Two Conjugate Directions. Commercial aluminium-3½% magnesium alloy, cold-rolled 10% and pulled to approx. 3% extension. × 1.

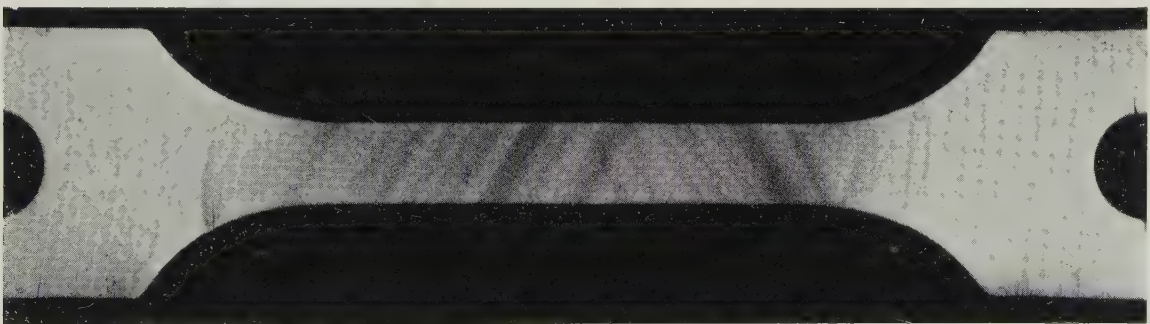


FIG. 6.—Showing Ring and Type-*B* Markings in Specimen of Commercial Aluminium-3½% Magnesium Alloy Pulled to Approx. 4% Extension on Amsler Machine. × 1.

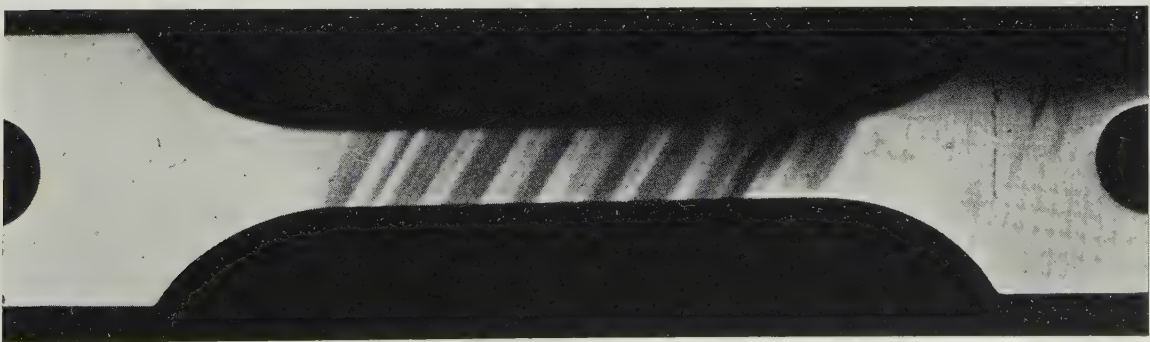


FIG. 7.—Type-*B* Markings in Specimen Machined from Commercial Aluminium-3½% Magnesium Alloy Cold-Rolled 10% to Suppress Type-*A* Markings and Pulled to Approx. 4% Extension on Amsler Machine. No ring markings. × 1.

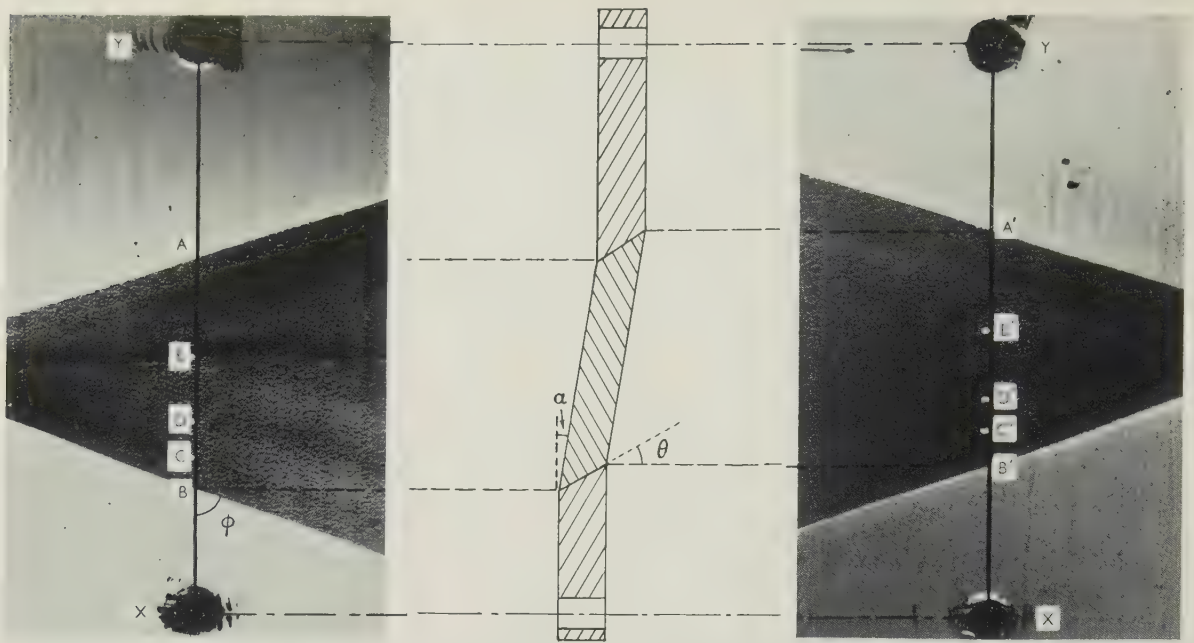
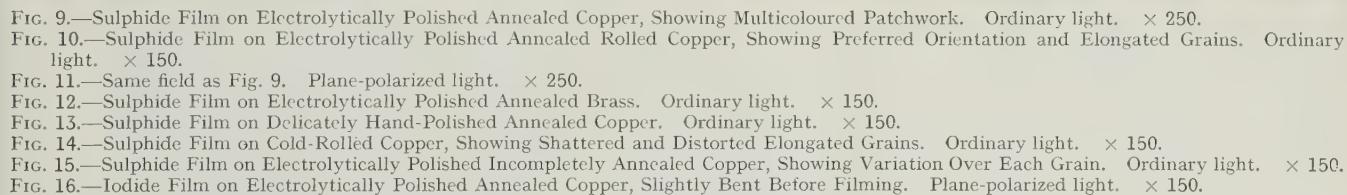
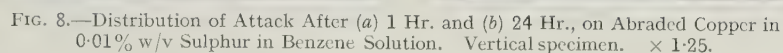


FIG. 8.—Schematic Section Through Type-A Yield Wedge in a Strip of Aluminium-3½% Magnesium Alloy (OZX), Illustrating Mode of Formation of Markings. Grain-size 0.018 mm. $XY (= 1.63 \text{ cm.})$ is parallel to the tensile axis.



FIG. 9.—Multiple Interference Pattern for One Face of Specimen Shown in Fig. 8. $XY = 1.63 \text{ cm.}$



FIGS. 9-16 are black-and-white prints from panchromatic negatives. All reduced by $\frac{1}{8}$ in reproduction.



FIG. 1.—General View of Autographic Thermo-Balance and Auxiliary Apparatus.



FIG. 23.—Surface of Scale Formed by Oxidation at 200° C. in Dry Air, Showing Small Pimples and Large Blisters. $\times 63$.



FIG. 25.—Surface of Copper after Exfoliation of Scale Resulting from Oxidation in Dry Air at 420° C. $\times 63$.

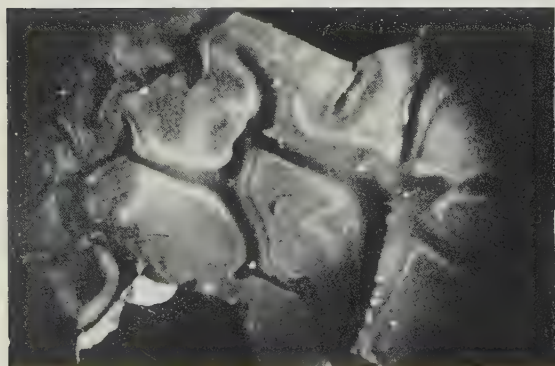


FIG. 24.—Piece of Scale Resulting from Oxidation in Dry Air at 465° C., Showing Grain-Boundary Blistering. $\times 30$.

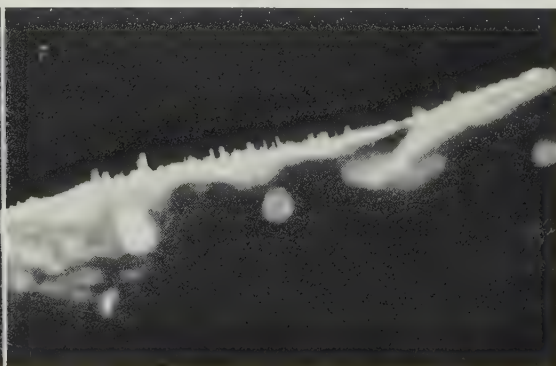


FIG. 26.—“Whiskers” Growing from Film Formed by Oxidation in Dry Oxygen at 420° C. $\times 63$.

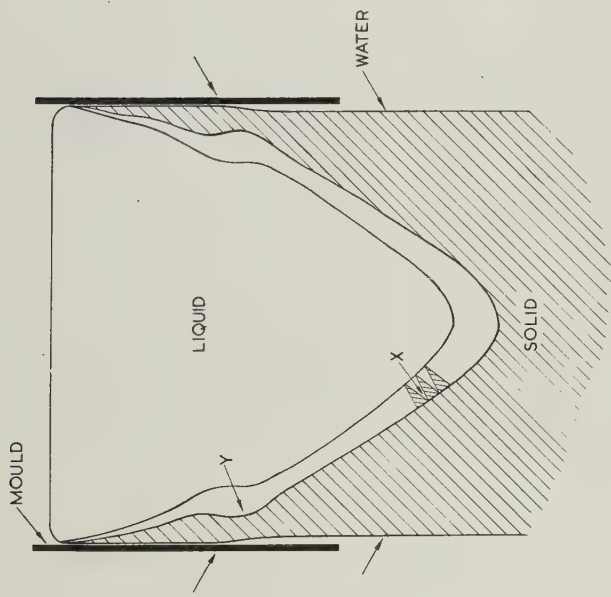


FIG. A.—Liquidus-Solidus Configuration in Direct-Chill Casting (Schematic). (Ransley.)

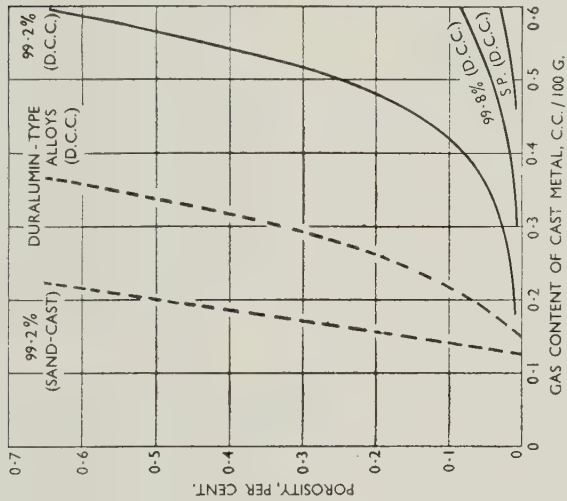


FIG. B.—Effect of Freezing Range and Rate of Solidification on Porosity Formation in Rolling Blocks. (Ransley.)

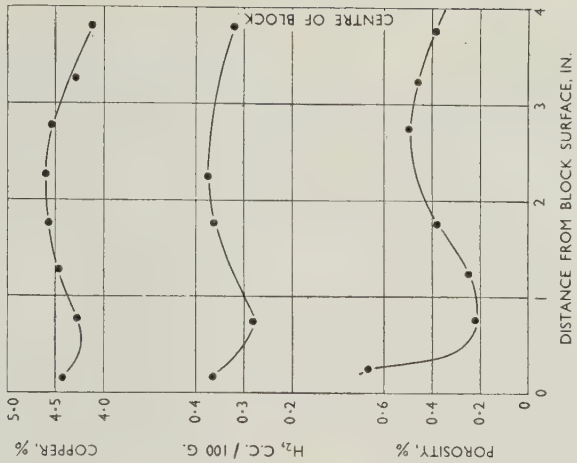


FIG. C.—Distribution of Copper, Hydrogen, and Porosity Across an 8-In.-Thick D.T.D. 603B Rolling Block Cast by the Direct-Chill Process. (Ransley.)

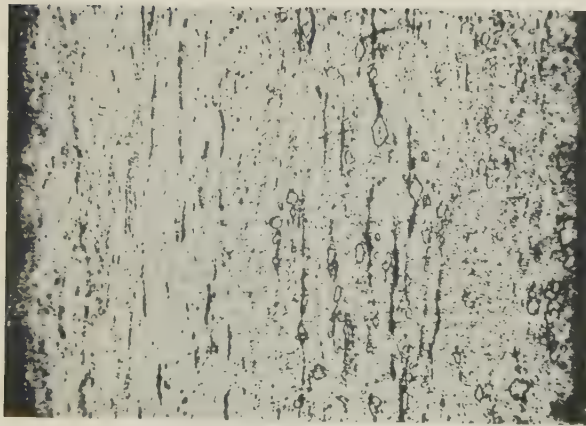


FIG. E.—Cast Slab of Commercial Zinc Showing Segregation of Iron, $\times 100$. (Vinauer.)

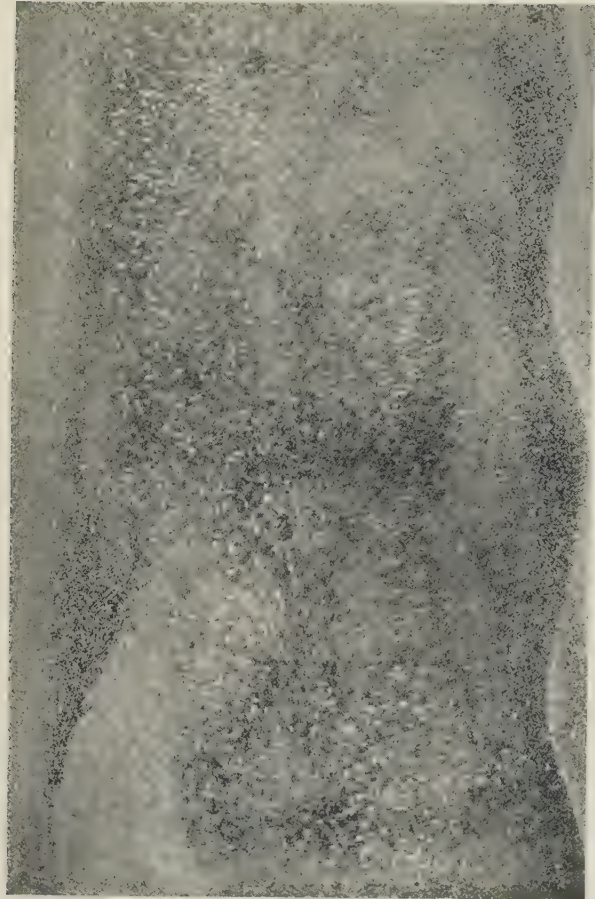


FIG. H.—Longitudinal Section through Continuously Cast $5\frac{1}{2}$ -in.-dia. Billet of Aluminum-11% Silicon Alloy. (Lewis.)

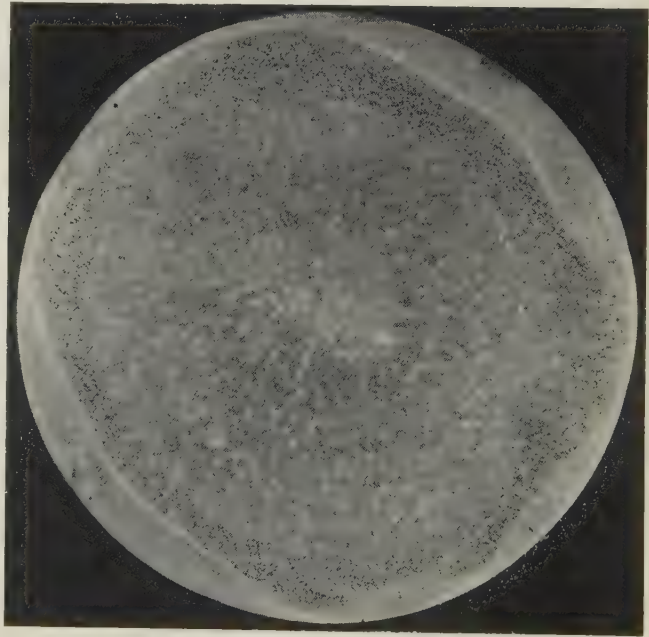


FIG. J.—Transverse Section through Billet Shown in Fig. H.

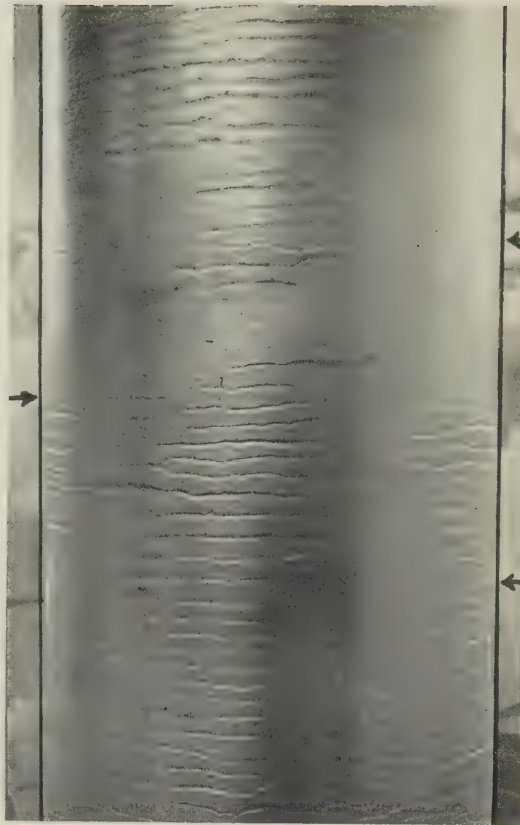


FIG. K.—Surface Appearance of Billet Shown in Fig. H. (Lewis.)

Some Friction Effects in Wire Drawing

By G. D. S. MACLELLAN

(Journal, this vol., p. 1.)

Mr. H. G. BARON,* M.Sc., L.I.M. (Member): Dr. MacLellan maintains that the variation of the coefficient of friction with interfacial pressure can be neglected. No doubt this is frequently true, but I feel that it is not a safe generalization. Some recent experiments by Lueg and Treptow† provide further evidence on this point. The graph shown in Fig. A is based on data from their Table III for the drawing of

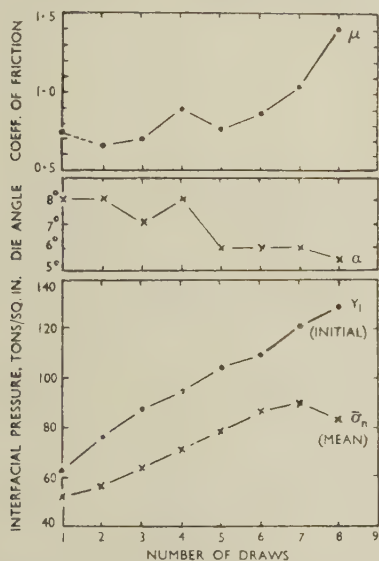


FIG. A.—The Effect of the Interfacial Pressure and Die Angle on the Coefficient of Friction. (Based on data by Lueg and Treptow.)

patented medium-carbon steel wire through tungsten carbide dies, using a soap lubricant and pulverized soap "lubricant-carrier". The wire was drawn down in successive reductions of about 30% until it finally broke. In this graph the coefficient of friction has been calculated from Sachs's equation, and the mean interfacial pressure $\bar{\sigma}_n$ was calculated from Lewis's basic equation as given by MacLellan.‡ The initial pressure Y_1 is the interfacial pressure when plastic flow begins, and is taken to equal the yield stress.

Mr. K. H. Treptow has informed me that the length of the parallel in these dies was one-fifth of the wire diameter or less. The effect of this parallel length has been neglected, but in spite of this and other possible sources of error, certain trends are clear. It will be seen that the coefficient of friction increases with increasing die angle and increasing initial pressure. The effect of pressure is masked in the first five draws by variations in the die angle, and the slight fall in the coefficient of friction between the first and second draw is probably due to an improvement in the surface finish of the wire. It was suggested in the paper by Baron

and Thompson§ that the initial pressure, rather than the mean pressure, together with other factors govern the depth of the lubricating film, and hence the coefficient of friction, and these curves support this view.

Dr. MacLellan's explanation of the intercept at zero reduction of area in reduction-of-area/drawing-tension curves, is very convincing. Some time ago I was interested in the rather academic question of elastic drawing, as a possible method of measuring the coefficient of friction. This idea was quickly dropped, but some calculations made at the time may be of interest. The drawing force under elastic conditions was estimated by an analysis which followed the usual lines except that the elastic strain condition:

$$\left(1 - \frac{D}{D_1}\right) = \sigma_n \left(\frac{m-1}{mE}\right) + \sigma_z \left(\frac{1}{mE}\right)$$

was introduced instead of a plastic stress condition. The reduction and expansion zones of the die may conveniently be neglected, since the work of elastic deformation, some of which can be recovered in the expansion zone, is extremely small. The drawing load is then due to friction in the parallel extension, and is given by:

$$P_{0.1}(r=0) = A_2 m E \left(1 - \frac{D_2}{D_1}\right) \left(1 - e^{-\frac{4\mu l}{m-1}}\right),$$

where $1/m$ is Poisson's ratio, E is Young's modulus, D_1 is the initial and final diameter of the wire, and D_2 is the diameter in the parallel zone. The other symbols follow the author's notation.

It is evident that the phrase "effective die angle", used by Baron and Thompson, should have been explained more fully. The method of measurement is illustrated in Fig. B,

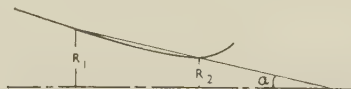


FIG. B.—Illustrating the Method Used to Measure the Effective Die Angle α .

in which R_1 and R_2 are the initial and final radii of the wire and α is the effective die angle. With most of the dies the approximation was appreciably better than that shown in the diagram, and little would have been gained by using the more accurate method suggested by Dr. MacLellan.

He has found that our experimental values§ of the additional drag caused by parallel extensions is less than the theoretical value. Consideration of various possible reasons for this difference has led me to the unfortunate conclusion that the operative length of parallel in these experiments may have been somewhat smaller than the apparent lengths shown in our Figs. 8 and 9 (pp. 425 and 427 of our paper). In view of the method of polishing dies, it seems possible that the apparently parallel extensions may in fact have been slightly double-concave in profile. At the exit side, an increase in diameter of the order of 0.00005 in. would allow the wire to break contact with the die. This change in diameter would

* Armament Research Establishment, Woolwich.

† W. Lueg and K. H. Treptow, *Stahl u. Eisen*, 1952, 72, 399.

‡ G. D. S. MacLellan, *J. Iron Steel Inst.*, 1948, 158, 347.

§ 3 C

§ H. G. Baron and F. C. Thompson, *J. Inst. Metals*, 1950-51, 78, 415.

be too small to be measured by our impression technique, in fact it is even too small to be measured by the profilometer described by Withers.* After considerable wear one may be certain that the full "parallel" length is operative, but the dies we used were in new condition. This possible source of error in new dies having parallel extensions will not affect our experimental results or have other repercussions, but it is clearly a matter that should be borne in mind in any future work.

In the paper by Baron and Thompson the values of μ for castor oil obtained from back-pull experiments were not given, because of some lack of reproducibility, which perhaps amounts to ± 0.015 in the derived coefficient. However, these results acquire an added interest in view of Dr. MacLellan's work with this lubricant. The coefficients of friction which were considered to be the most reliable range from 0.067 to 0.107, the smallest figure being obtained with a 3.0° die angle. The mean value was 0.084, and I prefer this to the value 0.12 given for these experiments in Dr. MacLellan's Table III (p. 11). The other results in which the reduction of area was small or the die angle large gave values of μ

between 0.11 and 0.18. It was pointed out that under these conditions the derived coefficients of friction are probably inaccurate owing to the complicating effect of redundant strains. In addition, there was some difficulty in estimating the effective die angle with the smallest reduction of area.

The AUTHOR (*in reply*): The recently published data quoted by Mr. Baron provide strong support for the view that in some circumstances interfacial pressure does have a considerable influence on the magnitude of μ , but the fact that the results he quotes lead to values of μ of an order of magnitude larger than those hitherto considered from published work, puts them in a new category.

The value of 0.12 which I gave in my Table III (p. 11) for the coefficient of friction with castor oil was derived from Fig. 16 (p. 443) of Baron and Thompson's paper, and represents a mean value for the three larger reductions, for which the die angle was nearly constant. The corresponding values for μ which I derive from curves 1 and 2 of their Fig. 18 (p. 444) are 0.071 and 0.084, that for curve 3 being somewhat higher and not accurately determinable from the data.

Discussion

The Viscosity of Metals and Alloys†

Dr. E. W. FELL,‡ M.Sc., F.R.I.C., F.I.M. (Member): With regard to the different methods used by the authors of these two papers, the outer-rotating-cylinder method is much to be preferred to the oscillating-pendulum method on theoretical grounds, for the determination of the true viscosity of the liquid metal. In this connection, it is well to recall the definition of the true viscosity of a liquid, which may be expressed in mathematical language approximately as follows: For a liquid in motion, the shear stress S at any point of a plane situated between two layers of liquid moving in the same direction though with different velocities (as in laminar motion), is equal to the product of the viscosity of the liquid η and the velocity gradient at the point taken in a direction normal to the plane, or:

$$S = \eta \cdot \frac{\partial u}{\partial y} \cdot \dots \dots \dots (a)$$

My preference for the outer-rotating-cylinder method is based on the fact that equation (1) of the paper by Professor Jones and Dr. Bartlett, from which these authors determine the viscosity η , is based on equation (a) above. In the oscillating-pendulum method, on the other hand, there is no such exact mathematical equation representing the flow of the liquid, and containing explicitly its viscosity η , and that is due to the complicated, and mathematically intractable, motion of the liquid resulting from the reversals of the pendulum.

There is a further point of importance in support of the outer-rotating-cylinder method, which becomes evident from a study of the position of the experimental points plotted on the graphs reproduced in the two papers. The values plotted to represent viscosity at specific temperatures, e.g. in Fig. 3 (p. 19) (pure tin), Fig. 4 (p. 20) ("Crown" pure zinc), Fig. 6 (p. 21) (aluminium), of the paper by Dr. Yao and Dr. Kondic, show considerable "scattering", or deviation from the assumed position of the smooth curve. Occasionally, for the zinc and the aluminium, the difference between two points plotted for the same temperature amounts to as much as a third of a centipoise according to the ordinate axis. In comparison, there is very little "scattering" of the values for the viscosity of high-purity aluminium, plotted as a mean

value in Fig. 3 (p. 147) of the paper by Professor Jones and Dr. Bartlett. Moreover, the viscosity is plotted to a scale twice as large as that in the paper by Dr. Yao and Dr. Kondic.

With reference to Fig. 2 (p. 147) of the paper by Professor Jones and Dr. Bartlett, illustrating the relation between angular displacement θ and speed expressed by $1/t$ for conditions described by them as non-slip and slip, I am of the opinion that the non-linear character of the broken-line curve for water, attributed by the authors to slip, may be due rather to an alteration of conditions at the solid/liquid interface as a result of the application of wax to the surface of the graphite cylinder, thereby affecting the motion of the water. I think it very desirable to draw attention to the generally acknowledged assumption that slip of a liquid past the surface of a solid occurs only with "perfect" liquids, i.e. those having zero viscosity. In practice, the liquid metal in immediate contact with the surface of the outer rotating solid cylinder would have no velocity relative to the surface of that cylinder (i.e. the liquid metal does not slip) by the boundary-layer theory of fluid dynamics. In consequence, I am unable to accept the authors' conclusion, on p. 147, that the complete form of the curve "can be of use in determining whether or not there is slip between molten aluminium and the graphite-cylinder wall".

Professor JONES and Dr. BARTLETT (*in reply*): We agree with Dr. Fell that the non-linear character of the broken-line curve in Fig. 2 (p. 147) of our paper is due to an alteration of the conditions at the solid/liquid interface, such as would establish surface tension or "wettability". If the liquid wets the surface of the solid container, then there will be no motion of the liquid relative to the solid, i.e., a condition of non-slip. However, when the liquid does not wet the surface of the solid, slip between them may occur. It is upon this basis that we carried out the experiment upon a waxed (i.e. non-wetted) surface and, in our opinion, the broken-line curve shows definitely that there was a small amount of slip with the waxed surface. Whichever point of view is accepted, non-slip between the molten aluminium and graphite container prevailed, a condition essential for accurate operation of the viscometer.

* R. M. J. Withers, *J. Iron Steel Inst.*, 1950, **164**, 63.

† Joint discussion on the papers by T. P. Yao and V. Kondic (*J. Inst. Metals*, this vol., p. 17) and W. R. D. Jones

and W. L. Bartlett (this vol., p. 145).

‡ Lecturer in Metallurgy, Technical College, Bradford.

Discussion

Creep and Plastic Deformation*

Dr. N. P. ALLEN,† M.Met., F.I.M. (Member): Several of the papers under discussion originate in the observation made at the National Physical Laboratory, and reported in the names of Wood and Tapsell,‡ that deformation taking place by creep at high temperature results in less general disturbance of the lattice structure than equal deformation taking place rapidly, or at low temperature.

Of the two explanations, that which attributes the final structure to slip by the process of migration of dislocations, followed by polygonization, appears to be gaining ground. The work of Mr. McLean, showing how little of the deformation is to be attributed to grain-boundary movement, and how much may be attributable to very minute slip, is of great importance. Dr. Wood and his collaborators have demonstrated very completely how the sub-grain size is affected by temperature and rate of deformation, and their work is a permanent addition to knowledge of the mechanism of deformation at high temperature, but they have apparently been misled into assuming that where slip cannot be seen it does not exist.

The sub-crystal formation is largely the consequence of the inhomogeneity of the deformation of an aggregate of crystals. Sir Geoffrey Taylor's view that each crystal undergoes the deformation of the mass as a whole by the use of five modes of slip is clearly incorrect.§ The crystals acquire the necessary degree of freedom to accommodate themselves to their neighbours by using different modes of slip in different parts, as Calnan and Burns|| showed, and Mrs. Urie and Mr. Wain have now confirmed. It follows that different parts rotate during deformation in different directions, and these varying rotations lead ultimately to the sub-structure. Calnan and Clews¶ have also shown how these rotations lead to deformation textures.

The stresses are also unevenly distributed about the sample, and must be higher in those parts where complex modes of deformation or excessive local deformation are called for. Slip, grain rotation, and grain-boundary movement all occur, and if the specimen is not to crack, the stresses must be so distributed that the metal can move harmoniously as a whole. One of the interesting aspects of Mr. McLean's papers is the demonstration that each of the processes is dependent upon the rest. A yield in one place is followed by associated movements elsewhere, and it would not be unreasonable to think that the whole pace is set by the rate of stress relaxation in the most highly stressed parts; using dislocation theory, one might say that it is controlled by the rate of diffusion away of dislocations from the points at which they are most closely crowded together.

These considerations are important to investigators who try to derive fundamental laws from the study of creep curves. The division of the creep process into a primary stage (slip), followed by a second stage (grain-boundary movement), obviously has to go overboard and with it such equations as the Andrade equation which assume a sharp distinction between the processes occurring in these stages. The Andrade equation appears just as one of a number of moderately

successful equations, and I incline to the view that for the purpose of predicting behaviour the simple equation $\sigma = AS^{2k}$ is probably as useful, and as full of pitfalls, as any. I have considerable sympathy with the exhaustion theory of the primary stage, inasmuch as there are undoubtedly places in the metal where the activation energy necessary to start plastic deformation is low, and these account for the rapid initial creep, but I prefer it in the form recently advocated by Cottrell,** in which the number of regions having a given activation energy is assumed to rise with the value of the activation energy. We have, however, no idea of the form of the N/E curve, and we might as well admit it.

As regards steady-rate creep, I have some liking for the Kauzmann theory, for we are undoubtedly concerned with the surmounting by thermal fluctuations of an energy barrier to movement, and this barrier is made less by the application of stress; but I look with a jaundiced eye upon any attempt to claim that the equation predicts behaviour over a wide range of stresses and temperature. The stress τ in the equation:

$$V = 2kT/h \exp(\Delta S/R) \exp(-Q/RT) \sinh(Al\tau/kT)$$

refers to stress acting at the point in the metal where the primary-creep process occurs, and this is different at every point of the metal. The activation energy Q is not independent of the temperature. It is primarily dependent on the inter-atomic forces, and these in most industrial metals are largely made up of ion-ion reactions which are strongly dependent upon the exact distance between the ions, and increase rapidly as the temperature falls. The effect of this is seen in the elastic constants, which fall considerably as the temperature rises, often quite rapidly in the temperature range in which creep begins to be important.

Dr. K. W. ANDREWS,†† B.Sc., F.I.M. (Member) and Mr. M. G. GEMMILL,‡‡ B.Sc., A.I.M.: We shall confine our remarks to the papers by Dr. Bhattacharya, Dr. Congreve, and Professor Thompson, and by Dr. Johnson and Mr. Frost. Although these deal either with pure metals or with non-ferrous alloys, and our own experience has been with ferrous materials, we are gratified to find ourselves in general agreement with the conclusions reached, especially in regard to the best way of representing the creep/time relationship at constant stress.

Some years ago the late Dr. Jay, working in this laboratory, concluded that the most satisfactory relationship for representing the variation of creep strain with time would be given by ϵ (strain) $\propto \sqrt{t}$. Andrade's law was certainly not found to apply in as many cases, whereas the \sqrt{t} relationship applied to a considerable number of creep curves obtained from commercial steels and alloys. It was later decided, however, that a more general power law should be used, and it was shown that this gave a satisfactory creep/time relationship, over at least part of the range for 107 out of 126 creep curves examined. The general power law $\epsilon = at^m$, where $m < 1$, does of course correspond to a creep rate which varies as a power of $(1/\epsilon)$

* Joint discussion on the following papers published in the *Journal*: S. Bhattacharya, W. K. A. Congreve, and F. C. Thompson (this vol., p. 83); G. B. Greenough, C. M. Bateman, and E. M. Smith (1951-52, 80, 545); A. E. Johnson and N. E. Frost (this vol., p. 93); D. McLean (1951-52, 80, 507; this vol., pp. 133, 287, 293); K. E. Puttick and R. King (1951-52, 80, 537); W. A. Rachinger (1951-52, 80, 415; this vol., p. 33); J. A. Ramsey (this vol., pp. 61, 215); J. Trotter (1951-52, 80, 521); V. M. Urie and H. L. Wain (this vol., p. 153); W. A. Wood and J. Suiter (1951-52, 80, 501; this vol., p. 181).

† Superintendent, Metallurgy Division, National Physical Laboratory, Teddington, Middlesex.

‡ W. A. Wood and H. J. Tapsell, *Nature*, 1946, 158, 415.

§ (Sir) G. I. Taylor, *J. Inst. Metals*, 1938, 62, 307.

|| E. A. Calnan and B. D. Burns, *ibid.*, 1950, 77, 445.

¶ E. A. Calnan and C. J. B. Clews, *Phil. Mag.*, 1950, [vii], 41, 1085.

** A. H. Cottrell, *J. Mechanics Physics Solids*, 1952, 1, 53.

†† Research and Development Department, The United Steel Companies, Ltd., Rotherham, Yorks.

and which is thus infinite initially, when $\epsilon = 0$ and $t = 0$. We have found this law to be quite generally applicable.

Several attempts have been made to represent the second and third stages of creep, and our attention was given for some time to a formula discussed by de Lacombe*:

$$\epsilon = \epsilon_0 + at^m + bt^n$$

where ϵ_0 = instantaneous extension on loading, a and b are constants, and $1 > m > 0$ and $n > 1$. This empirical formula has the advantage that it can be fitted to technical creep curves, which it can represent to a sufficient degree of accuracy. By means of the methods described by de Lacombe, it is possible to apply it to find, from the actual experimental results:

- (1) An exact value of ϵ_0 .
- (2) The four constants, a , b , m , and n .
- (3) The time to minimum creep rate (i.e. where the deceleration due to the second term is exactly balanced by the acceleration due to the third term)—a function of a , b , m , and n only.
- (4) The minimum creep rate itself.

If, however, the test has not been carried on for a sufficient length of time, the possible errors in b and m are likely to be

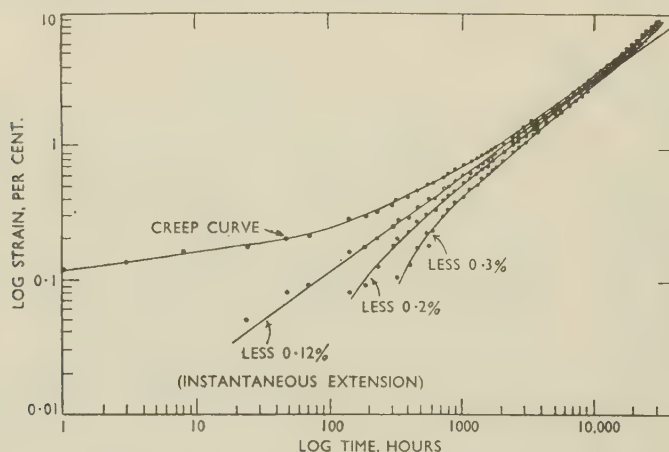


FIG. A.—Results for a Lead-1% Tin Alloy Extruded at 200° C. and Tested under Constant Stress Conditions at 300 lb./in.².

uncertain. Thus, we have recently obtained some accurate data from a series of tests on a widely used commercial steel. This gives exceedingly good plots on the simple power law for the greater part of the creep curve at lower stresses and temperatures, but at higher stresses and temperatures the second term becomes appreciable within the range of testing time.

These later results have enabled us to consider the effect of stress and temperature. The constants a and b can both be represented in terms of fractional powers of the stress, so that we support the views of Dr. Bhattacharya, Dr. Congreve, and Professor Thompson, that the stress is involved in a manner similar to that suggested by the Nutting and Scott-Blair relationship. The variation of the constant a , with temperature at constant stress appears to be adequately represented by an expression of the form:

$$a = \text{const.} \times \exp(-Q/RT)$$

Q , the activation energy, has values between 21,200 and 34,000 cal./g.-atom., varying somewhat with the stress. The values obtained appear to be of the right order. A similar variation has been described by Hazlett and Parker.†

We should like to emphasize the importance of these

attempts to represent the creep curves analytically, from the point of view of the manufacturer and user of commercial alloys, since it would be most valuable if some reliable formula were available for interpolation between stresses and temperatures for which creep curves had actually been determined. In certain cases extrapolation to longer times and/or lower stresses, could also be safely carried out.

We should also like to comment briefly on the suggestion by Dr. Bhattacharya, Dr. Congreve, and Professor Thompson on p. 89, that the mechanism of creep is not dissimilar in the primary and secondary stages. This may be true, particularly with the materials, stresses, and temperatures they employed, and perhaps generally with many other materials. Our experience would, however, lead us to support the view that if the total creep strain is separated into two parts by the use of some such formula as that given above, certain characteristic properties can sometimes be associated with one or other of these fractions of the total creep strain. Thus, in certain cases, if the terms ϵ_0 and at^m are subtracted from the total creep strain, there remains a residual creep strain which we call "quasi-viscous creep", the term at^m representing "transient creep". It is not necessary to postulate that either of these parts of the creep strain is definitely associated with a single type of slip process or movement along inter-

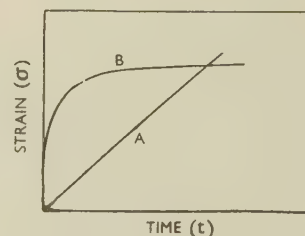


FIG. B.—Extreme Types of Creep Curve.

crystalline boundaries. It has, however, been found that either of these components derived in this way may show its own peculiar dependence upon, say, a particular alloying element or some other variable. Thus, it was noted in a study of the effect of phosphorus in a series of $\frac{1}{2}\%$ molybdenum steels under low deformation conditions, that the transient creep, but not the quasi-viscous creep, was directly influenced by the phosphorus content. In other types of steel both transient and quasi-viscous creep may depend on the relative proportions of transformed austenite and primary ferrite present in the specimen, after heat-treatment before testing.

Dr. L. M. T. HOPKIN,† B.Sc., A.R.S.M., A.I.M. (Member): Dr. Bhattacharya, Dr. Congreve, and Professor Thompson express the belief that the power equation is universally a good representation of experimentally determined creep curves. However, it can be seen in Fig. A that the power equation does not provide a good fit of creep curves for long periods of time. The results shown were obtained from a lead-1% tin alloy extruded at 200° C. and tested under constant stress conditions at 300 lb./in.². Tertiary creep was not reached at the longest time of test. The upper curve shows the creep curve plotted directly, which is far from a straight line. The

* J. de Lacombe, *Rev. Mét.*, 1939, **36**, 178; 1942, **39**, 105, 152, 171.

† T. H. Hazlett and E. R. Parker, *Trans. Amer. Inst. Min.*

Met. Eng. (in *J. Metals*), 1953, **197**, 318.

‡ Metallurgy Division, National Physical Laboratory, Teddington, Middlesex.

next curve shows the plot of the creep strains only, as suggested by Bhattacharya *et al.*, i.e. total strain minus instantaneous extension. A straight line is obtained for short times, but the creep strains for long times are greater than those predicted by the power equation. Subtracting from the total extension values greater than that of the instantaneous extension actually observed, does not produce better straight lines. The lower portions of the lines now curve downwards, while for long times they still curve upwards. Thus, even before tertiary creep begins, it would be dangerous to use the power equation for extrapolation purposes.

In many tests the period of secondary creep extends over a major portion of the creep curve. Two extreme types of creep curve fall within this category, as shown in Fig. B. Considering secondary creep as represented by the straight-line equation $\sigma = mt + c$, we have:

$$\log \sigma = \log \left(t + \frac{c}{m} \right) + \log m$$

In the curve of type A, c is small or zero and m is large, so that the logarithmic equation becomes a straight line of slope 45° . In a curve of type B, c is large and m is small, so that $\log \sigma$ is constant for small values of t , i.e. the plot is a horizontal line. As t increases, the horizontal line bends upwards and eventually approaches the straight line of slope 45° . Thus, although the usual creep curve lies somewhere between these two extremes it would seem that there is no modified relationship between strain and time for short times, as claimed by the authors in their Fig. 13 (p. 89). It seems more likely that the two intersecting straight lines in Fig. 13 are parts of smooth curves and in fact the figure could easily be so drawn.

Bhattacharya *et al.* consider that the parallelism of their plots of $\log \sigma$ and $\log \dot{\sigma}t$ against $\log t$ shows that the power equation is a true representation of creep curves. However, during secondary creep, these lines can be parallel only in special cases. During secondary creep the rate of creep is constant, so that a straight line of slope 45° is obtained, for all values of t , when $\log \dot{\sigma}t$ is plotted against $\log t$. This straight line can be parallel with the plot of $\log \sigma$ against $\log t$ only when t is large compared with c/m , as explained earlier. In the paper none of the plots of $\log \dot{\sigma}t$ against $\log t$ has a slope of 45° , showing that secondary creep was not reached in the authors' longest times of test. Thus, their straight lines must either abruptly change their slope when secondary creep begins, which is unlikely, or the lines are not straight but gentle curves.

Mr. R. C. GIFFKINS,* B.Sc., A.I.M. (Member), and Mr. J. W. KELLY,* B.Sc.: We consider Mr. McLean's paper on "Creep Processes in Coarse-Grained Aluminium" (Vol. 80, p. 507) a significant contribution to knowledge of creep. The discussion of some of the points raised is perhaps best postponed until our own work on this subject is completed. However, there are a few comments we should like to make now.

The white-line patterns brought out by stopping-down the illumination and de-focusing have interested us, since it was by this technique that Wilms† first obtained metallographic evidence of the cell sub-structure. We find that several distinct patterns may be obtained corresponding to focus above or below the Gaussian plane.

From multiple-beam interference fringes obtained with specimens showing the various patterns, we find that:

(i) Most white-line patterns obtained inside focus correspond to ridges of up to 2μ height and of about 0.05 mm. lateral extension.

(ii) White lines outside focus often correspond to comparable troughs.

(iii) Patterns white outside focus and black inside or vice versa occur; these correspond to ridges or troughs of about 0.15μ vertical extension or to the line of intersection of slightly inclined areas.

(iv) Sometimes black and white lines, similar to diffraction fringes, are seen; again black and white interchange on moving through focus. These correspond to a sinusoidal topography similar in size to (iii).

Patterns (iii) and (iv) show a greater degree of correspondence to cell boundaries revealed by deep etching or anodic filming than do (i) and (ii). The change in focus necessary to observe all the patterns is about $\pm 6.8\mu$, and they have been observed at as little as 2% extension.

The types of pattern are illustrated by Figs. C, E, and F (Plate XCVII). Figs. C and E show an area on a specimen deformed 14% at 200°C ., inside and outside focus, respectively; white lines of types (i) and (ii) and reversible lines of type (iii) can be seen. Fig. D (Plate XCVII) is the multiple-beam interferogram from the same area, and illustrates the surface features associated with the patterns. Fig. F shows examples of types (iii) and (iv) on a specimen deformed 12% at 325°C ., repolished and extended a further 3%.

We had ascribed all these patterns to diffraction effects similar to those observed by Griffin,‡ using the same microscopical technique, on beryl crystals, although his suggestion of systematic irregularities along the edges of small steps did not seem likely with aluminium. Recently our attention was drawn to work by Berek,§ who used diffraction theory to calculate the intensity distribution of the image of a line discontinuity adjacent to the true image plane, and it appears to us that at least some of the patterns observed with aluminium may be due to similar diffraction effects at changes in curvature. Although the patterns listed under (i) and (ii) above may be due to the geometrical effect suggested by Mr. Lomer (p. 511 of Mr. McLean's paper), this explanation is not so convincing when such large radii of curvature are involved.

The diffraction origin of the patterns is strongly indicated also by evidence obtained with zinc deformed at elevated temperature. The cell boundaries under narrow-pencil illumination and out-of-focus conditions are always of types (iii) or (iv); examples of these have been published.|| Usually at a given focal setting all those boundaries at the bottoms of valleys formed by cells appear white, whilst those at the crests appear black.

The fact that the out-of-focus markings can indicate either ridges or troughs would appear to strengthen the polygonization hypothesis of cell formation. This is also supported by further evidence of the banded nature of cells like those Mr. McLean noted, which we have found, using the anodic-film technique, on specimens deformed at various rates and temperatures up to 300°C . At 300°C . the banded nature of the cells is not apparent on deep etching, probably because of the rapid migration of cell boundaries which we find often occurs under stress. Our observations on cell boundaries suggest that they do not differ greatly from ordinary grain boundaries between grains of similar orientation.

Finally, we have been unable, using the phase-contrast microscope, to detect fine slip in specimens deformed 1.0% or more at 300°C . This confirms and extends to lower strains the electron-microscope observations of Garrod, Suiter, and Wood.¶ We have confirmed its presence, however, on a specimen deformed 2.7% at 200°C ., but find that soaking the specimen, unstressed, at 200°C . for 48 hr. causes a distinct diminution of the fine slip. It may be that this thermal polishing (or oxide film formation), explains, at least in part, Mr. McLean's failure to detect fine slip at later stages of the test and its apparent absence in tests at higher temperatures.

* Baillieu Laboratory, University of Melbourne, Australia.

† G. R. Wilms and W. A. Wood, *J. Inst. Metals*, 1949, **75**, 693.

‡ L. J. Griffin, *Phil. Mag.*, 1951, [vii], **42**, 775.

§ M. Berek, *Optik*, 1949, **5**, 1, 144, and 329.

|| J. A. Ramsey, *J. Inst. Metals*, 1951–52, **80**, 167.

R. C. Giffkins, *Australasian Eng.*, 1952, (May), 63.

¶ R. I. Garrod, J. W. Suiter, and W. A. Wood, *Phil. Mag.*, 1952, [vii], **43**, 677.

Mr. A. P. Miodownik,* B.Sc., L.I.M. (Student Member): The wealth of experimental data now available on creep marks a stage in the study of this subject which has already been passed in that of age-hardening. Bearing in mind the conflicting arguments which have raged and are still raging on the ultimate mechanism of age-hardening, it is instructive to compare certain aspects of the two fields of research, in order that unnecessary conflict as regards creep may be avoided.

Although at first sight not closely related, the two subjects exhibit several basic similarities. Changes on ageing consist essentially of the constraint of excess solute ions in enforced solid solution being relieved by clustering, rearrangement, and lattice change. The final equilibrium condition is not attained until a series of interdependent processes have taken place, there being a wide variation in the rates of reaction for the various stages, particularly in relation to temperature. It is generally admitted that precipitation of any kind, even under equilibrium conditions, is preceded by pre-precipitation phenomena, which become, however, progressively more transient as the conditions of precipitation approach equilibrium. The processes occurring during the creep of aluminium, as envisaged by Mr. McLean, show a striking resemblance to those occurring during ageing, if the term "solute atoms" is replaced by "dislocations". Thus, the restraint in the initial condition is thought to be due to an enforced excess of dislocations in the lattice, and relief is obtained by clustering of dislocations (the polygonization process), followed by a gradual rearrangement of the dislocation boundaries which leads to a type of boundary with the properties and characteristics of a conventional grain boundary.

The value of the comparison lies in the acceptance in the field of creep of the concept already enunciated for precipitates, namely that the equilibrium condition is always preceded by some transient stages, and that the temperature will largely control the rate of reaction of each stage. The controversy between the school of thought which adheres to direct fragmentation of grains into cells, and that which upholds the alternative theory of polygonization, can then be resolved simply into a question of the rate of polygonization.

While this concept is admittedly an oversimplification of the problem, it would be interesting and instructive to obtain some values of the rate of polygonization, although owing to the marked heterogeneity of such a process, the experimental difficulties are very great and, to the best of my knowledge, no such values are available at present in the literature.

Mr. E. C. W. PERRYMAN,† M.A., A.I.M. (Member): During a study of the recrystallization characteristics of super-purity aluminium and super-purity-base aluminium-magnesium alloys, I have also investigated the recovery process and found similar sub-grain structures to those shown by Mr. Ramsey in connection with his first paper. I have not observed any sub-structure in the as-cold-worked material, but find that there is a tendency for the sub-structure after annealing to become finer as the amount of cold work increases from 20 to 80%. For example, after annealing at 375° C. super-purity aluminium cold worked 20% gave sub-grains approximately 30 μ in size, whereas after 60% cold work the grains measured about 10 μ . Like the author, I found that these sub-structures, once formed, did not change in size or shape with longer annealing times, and, moreover, formed in certain grains and certain regions of grains more readily than in others (see Fig. G, Plate XCVII).

The equi-axed type of sub-structure, similar to that illustrated in Fig. 8 (Plate VIII) of the paper, forms in very short times; for example, with 50% cold work such sub-structures were observed in specimens annealed for only 10 sec. at 375° C. X-ray examination of these equi-axed sub-structures

by an oscillating-beam method similar to that used by Mr. Ramsey showed that after short annealing times discrete spots from the sub-grains are obtained, superimposed on an intense diffuse background. With longer annealing times the intensity of the background decreases. It would thus seem that the polygonized areas become more strain-free as the annealing time increases. Further support for this was obtained by carrying out micro-hardness tests on the polygonized areas. The hardness of areas showing an equi-axed sub-structure decreased slightly with annealing time, but they were always much harder (approx. 25 D.P.N.) than the fully recrystallized areas (18 D.P.N.). It thus appears that these sub-structures are not completely strain-free; further evidence for this is found in the observation that slip proceeds far more readily in the fully recrystallized grains than in the polygonized areas (see Fig. H, Plate XCVII).

Growth of new grains takes place within the recovered areas and, in view of the observations mentioned above, it appears that the driving force for this growth is the remaining strain energy. It is not necessary to assume, as Beck‡ has recently done, that the driving force for growth is the increased surface energy due to the small size of the sub-grains.

It has often been suggested that these sub-grains or polygons may act as the nuclei for recrystallization. In the specimens examined, I never observed recrystallization nuclei within these polygonized areas, but observed them within the unrecovered areas. Fig. G shows recrystallization nuclei within a grain which showed no signs of recovery, while the neighbouring grain had started to recover. Has Mr. Ramsey been able to identify recrystallization nuclei with the sub-grains in the recovered areas?

Is he convinced that the recovered structures of the equi-axed type are formed by a diffusion of dislocations such as that described by Cahn? It is possible that the much smaller sub-grains, approximately 2 μ in size, which have been observed in cold-worked materials by Heidenreich§ and by Hirsch and Kellar|| are unstable at higher temperatures and thus grow until an equilibrium size is reached? In view of this suggestion it would be instructive to investigate the recovery of material which had been cold worked at very low temperature.

Dr. W. A. RACHINGER,¶ M.Sc. (Junior Member): Dr. Greenough, Mrs. Bateman, and Mrs. Smith have shown that a solid-solution aluminium-silver alloy breaks down, during slow deformation at an elevated temperature, into a sub-structure of small, relatively perfect crystal blocks. This they attribute to a polygonization process activated by both stress and temperature, dislocation movement being unimpaired by the presence of the silver atoms, which are of approximately the same size as the aluminium atom. On the other hand, a two-phase alloy did not exhibit a sub-structure after deformation, the interpretation being that the dislocation movements necessary for polygonization are inhibited by the presence of precipitate particles.

It is of interest to compare these results with the findings of a similar investigation on aluminium-magnesium alloys carried out at the Baillieu Laboratory, University of Melbourne. The results and their interpretation followed the same general trends as those described by the authors, although some minor differences existed.

Solid-solution alloys (1% magnesium), deformed slowly at various temperatures, developed a sub-structure whose size was the same as that observed in high-purity aluminium deformed under similar conditions. The cells formed in the alloy had, however, not achieved the same degree of internal perfection as those formed in pure aluminium. This was evidenced by a slight blurring of the X-ray reflections from an internal section of the alloy test-piece. Apparently many

* Research Demonstrator, Battersea College of Technology, London.

† Aluminium Laboratories, Ltd., Kingston, Ont., Canada.

‡ P. A. Beck, *Trans. Amer. Inst. Min. Met. Eng.*, 1952, 194, 979.

§ R. D. Heidenreich, *Bell System Tech. J.*, 1951, 30, (4), 867.

|| P. B. Hirsch and J. N. Kellar, *Acta Cryst.*, 1952, 5, 162.

¶ Aeronautical Research Laboratories, Melbourne, Australia.

of the dislocations were unable to take part in the polygonization process and remained in the interior of the cells, thus causing minor disorientations. It seems likely that the large magnesium solute atoms inhibited dislocation movement.

The structure of the deformed two-phase alloys (10% magnesium) is also of interest. It was found that, for a given strain, the internal disorientations suffered by the grains decreased with increasing temperature of deformation. Cell formation was not observed, provided that the alloys were strain-free before the high-temperature deformation. Here the interpretation was the same as that of the authors, namely that the precipitate particles act as effective dislocation traps. If, however, the alloy was deformed at room temperature ($\sim 5\%$ elongation), a cell structure was developed during subsequent creep at an elevated temperature, and the size of these cells was found to be much smaller than those formed in pure aluminium deformed under the same conditions. It would appear that, of the large number of dislocations produced by the initial cold working, some are able to take part in a polygonization process whose extent is limited by the presence of precipitate particles.

Dr. Greenough and his collaborators also found that the deformation sub-structure of high-purity aluminium, as revealed by X-ray-diffraction methods, was the same at the surface as in the interior of test specimens. These results presumably apply to specimens whose final elongation was of the order of 10%. With heavier deformations ($\sim 50\%$ elongation) slight structural differences can be observed. The cells in the surface grains were found to be less perfect than those in the interior, as demonstrated by a slight blurring of their X-ray reflections. It is not surprising that such an effect exists, since recent work* has shown that during the slow deformation of aluminium at elevated temperatures the surface grains deform to a much greater extent than those in the interior.

The cells formed in the surface grains of aluminium-magnesium solid-solution alloys were found to be less perfect than those in the interior. Here the effect was more marked, being readily observable at 10% elongation. If more dislocations are produced in the surface grains and consequently more are trapped by the solute atoms, this feature may readily be explained.

In his paper on "Grain-Boundary Slip During Creep of Aluminium" (p. 293) Mr. McLean has shown that, during creep, the strain due to grain-boundary slip bears a linear relation to that due to crystal slip. He has furthermore derived a theoretical relationship between these two quantities (equation (3), p. 298) and has shown that this is numerically in agreement with his experimental results. However, in view of the assumptions made and the mode of derivation of equation (3), this agreement might appear fortuitous.

Briefly the assumptions are:

(a) Grain-boundary slip is due entirely to polygonization, i.e. lattice rotation in the neighbourhood of the grain boundary, as indicated in Fig. 9 (p. 298).

(b) The extension of the individual crystals arises wholly from polygonization movements. This means: (i) that all the dislocations remain within the crystal, ultimately forming a polygonized array and giving rise to the observed tilts between sub-crystals, and (ii) that the dislocations move only through distances of the order of d , the sub-grain size.

It is to be noted that in an earlier paper,† it was not the total extension due to crystal slip, but only the "missing creep" which was identified with polygonization. Mr. McLean found that this "missing creep" accounted for approximately one-half of the total extension. If this is the case for the present experiments, whose conditions were not widely different from the earlier ones, the values of \bar{p}/E shown in the last column of Table I (p. 299) should be increased by a factor of about two.

If, moreover, two slip directions are considered, as in Mr. McLean's earlier papers,‡ equation (2) (p. 298) would read $E \approx \theta$, whilst the mean value of p , as given by equation (1) (p. 298), would remain unchanged. Equation (3) would then be replaced by $d = 2\bar{p}/E$. Thus, for purposes of comparison with the values of d , the quantities in the last column of Table I should be increased by a factor of 3 or 4. The comparison still shows the quantities involved to be of the same order of magnitude, but their agreement can hardly be considered as evidence of the correctness of assumption (a).

Thus, although the linear relationship between the total elongation and the elongation due to grain-boundary slip is well founded, it is uncertain whether this feature is due to the physical processes which Mr. McLean envisages.

A further objection to the proposed mechanism of grain-boundary slip is that it does not necessarily imply a wholesale movement of one grain past another, but requires only localized movements at the boundary to accommodate shears in the neighbouring deformation band. Thus, marker lines drawn on the surface would be expected to show deflections near a grain boundary even in the absence of boundary migration. This is not generally the case.§

An obvious difficulty arises on consideration of the case in which no deformation banding occurs,|| the grains retaining their internal perfection throughout the deformation. On Mr. McLean's hypothesis, grain-boundary slip would necessitate large grain rotations of approximately 1° for each 1% elongation. X-ray diffraction evidence shows that the rotations are much smaller than this. It seems more likely that the grain-boundary slip arises from translatory movements. Systematic movements of this type are necessary if boundary slip is to contribute to the deformation. Observed differences in the lateral displacement of the longitudinal and transverse marker lines* would tend to suggest that this is the case.

The existence of a linear relationship between the grain-boundary displacements, as measured on the surface, and the total elongation, is said to suggest that "the surface measurements do not seriously misrepresent the grain-boundary movements throughout the metal" (p. 298). In view of the recent work on this subject* I feel that, although the amount of grain-boundary slip is linearly related to the total elongation, the factor of proportionality will be dependent on the distance below the surface. Considerations such as this suggest the vital need for new experimental techniques which will allow investigations of the interior of a plastically deforming metal.

Dr. JOHNSON and Mr. FROST (*in reply*): We entirely agree with Dr. Allen's remark that the division of the creep process into primary and secondary stages has to be abandoned, and with it any equation which assumes a sharp distinction between processes occurring in these stages. On the other hand, equations which indicate the simultaneous progress of a number of processes throughout the whole creep test are certainly rational in form. The writers and Mr. A. Graham, of the National Gas-Turbine Establishment, among others, are attempting to develop this type of equation on a sound experimental basis.

With regard to the view expressed by Dr. Allen that equations of the type $\sigma = AS^{\alpha}t^k$ are as likely as any reasonably to predict behaviour, we would point to the suggestion made on p. 106 of our paper that such an equation is valid for a limited temperature range. Further data in our possession indicate that at a specific temperature the creep strain may be well represented over considerable periods of time by a generalized version of the above equation, viz. $\sigma = \Sigma AS^{\alpha}t^k$. This equation, of course, fulfils the condition mentioned above of representing several co-existing processes throughout the whole creep period concerned. The constants in such an

* W. A. Rachinger, *J. Inst. Metals*, this vol., p. 33.

† *J. Inst. Metals*, 1951-52, 80, 507.

‡ *ibid.*, 1951-52, 80, 507; this vol., p. 287.

§ See e.g. W. A. Rachinger, *ibid.*, this vol., Plate V, Fig. 2.

|| W. A. Wood, G. R. Wilms, and W. A. Rachinger, *ibid.*, 1951, 79, 159.

equation can be determined from moderately short tests over a reasonably wide stress range.

However, the use of such equations must obviously be restricted on two counts. They give no information concerning actual fracture, and for very long life periods they give no account of thermal deterioration of the material. Nevertheless, as Dr. Andrews has emphasized, their usefulness in restricted fields should not be under-estimated.

In view of the remarks of Dr. Allen quoted above, we were somewhat surprised that he should express sympathy with the exhaustion theory of creep, although he does express a preference for it in the form advocated by Cottrell. Our paper has shown that, for the particular material tested, the exhaustion theory as expressed by Mott and Nabarro is very inadequate to represent the results obtained. Admittedly, as Dr. Allen points out, there are places in the metal where the activation energy is low, and accordingly some mechanism of the exhaustion type is likely to be operative, but it appears that this must be allied in the theory with some other co-existing mechanism. The modification of the Mott and Nabarro equation given by Cottrell involves the Orowan assumption of a work-hardening relation, the shortcomings of which were discussed in our paper (p. 97). We do not, therefore, regard it as a satisfactory means of relating the exhaustion theory to our experimental results.

Dr. Allen's preference for the Kauzmann theory of secondary flow, as against the Nowick and Feltham theories, is in a sense somewhat invidious, since all three theories are based on the Eyring rate-process theory, used in conjunction with an expression of statistical probability of occurrence of the basic-flow operation, and they virtually say the same thing in different words (whether the units of operation are termed units of flow or dislocations), and yield similar numerical results in any specific case.

Dr. Allen may be perfectly correct in his remark that the activation energy would be expected to vary in a manner not dissimilar from that of the elastic moduli with temperature. However, this consideration does not affect the validity of our interpretation of Fig. 6 (p. 100) of our paper. At 20°, 100°, 150°, 200°, and 250° C., 2L42 alloy has the approximate moduli 10.5, 10.1, 9.8, 9.4, and 8.9×10^9 lb./in.², respectively. Obviously in the range up to 200° C. these values cannot be said to be dropping at all rapidly, and accordingly, as indicated in Fig. 6, the Kauzmann equation (other things being equal) would, on Dr. Allen's criterion, be expected to apply reasonably within this range. This is not, however, to say that causes other than the deviation of the value of Q do not contribute to the failure of the equation to represent the results beyond 200° C.

With regard to the stress τ , it seems possible that while, as Dr. Allen suggests, τ varies from point to point in the metal, the Kauzmann relation might reasonably hold with an effective statistically averaged value of τ .

However, the above remarks should not be taken as advocacy on our part of the Kauzmann theory of secondary creep. Our general view is precisely that expressed in the opening paragraph of our reply.

Finally, we wish to emphasize a point which appears to have been largely overlooked by contributors to the discussion, i.e. the existence and quite appreciable magnitude of purely anelastic and recoverable creep strain. In the tests described in the paper, this anelastic strain represented the whole of the creep at 20° C. and was still of the order of 20–30% at 150° C. Accordingly, such anelastic strain cannot be neglected in framing any theoretically based equation to represent the creep field. Any such equations to be truly general must apply both to the loaded and unloaded state and must accordingly treat anelastic strain as a separate entity. In this connection the efforts of Yu. N. Rabotnov* are to be applauded.

In the majority of practical cases of creep, where strains are of a relatively low order and primary creep persists for long

periods, the recoverable portion may remain a comparatively large proportion of the total creep. The reason why this aspect of creep has been largely overlooked by physicists in framing their equations is probably that the majority of their tests have used stresses and temperatures giving large strains in short times (i.e. the opposite to practical requirements) and under these conditions the recoverable creep is relatively unimportant.

Dr. BHATTACHARYA, Dr. CONGREVE, and Professor THOMPSON (*in reply*): It is gratifying to find that Dr. Andrews and Mr. Gemmill are in general agreement with the conclusions which we have reached. It is implicit in our paper, however, that the power-law equation has been shown to apply specifically only to cases where phase changes are excluded. In the case of the steels, and in certain non-ferrous alloys as well, structural changes may go on simultaneously, and as a result creep relationships distinctly more complicated than that which we have proposed are required to express the results with any degree of exactitude. In the steels, for instance, spheroidization of the carbide and, not impossibly, even changes in the ferritic matrix may complicate matters considerably. It is possibly for this reason that Dr. Andrews and Mr. Gemmill prefer equations containing more terms than are required by the simple power law, and why in certain cases they find residual strains. We would emphasize that no equation can be other than merely empirical which does not satisfy ordinary dimensional requirements. On this ground, therefore, we should regard both the equation of de Lacombe, for instance, and their own equation for secondary creep as being merely empirical in nature and possessing no real physical meaning. As to Dr. Hopkin's remarks concerning the parallelism of the plots of $\log \sigma$ and $\log \dot{\sigma} t$ against $\log t$, we must point out that he has suggested an equation for secondary creep which we should not accept in the case of a pure metal. It is not surprising, therefore, that he reaches conclusions not altogether consistent with our own.

Mr. D. McLEAN (*in reply*): My experience with the white-line patterns is similar to that of Mr. Gifkins and Mr. Kelly, except that I have ascribed those listed under (i) and (ii) to the occurrence of large slip bands. Some examples in their Figs. C and E (Plate XCVII) seem to be due to this; certain of the white lines bordering the "prominent" slip bands running from bottom left to top right change from one side of the slip band to the other as the specimen is moved through focus. This is the effect that optical theory predicts at a step in the surface.

Another factor may affect the image of a stepped surface. I understand that all objectives give a small phase-contrast effect, at least when stopped-down, since the optical path along the axis may differ in length from one near the perimeter. This might sometimes complicate the interpretation of appearances such as are shown in Figs. C and E.

In reply to Dr. Rachinger, the extension associated with polygonization was not intended to be identified only with the "missing creep" in my earlier paper,[†] although this impression may have been given in the short résumé in the Introduction. According to a later definition[‡] the extension associated with polygonization is correctly explained as being the whole of that part of the extension due to deformation of the crystals, as distinct from that part due to sliding of the crystals over each other. If this is accepted, it eliminates Dr. Rachinger's first factor of 2.

Dr. Rachinger suggests that a second factor of 2 should be included when two slip directions operate, since the relation derived between extension and angle of disorientation is $E = \theta/2$ for one slip direction and $E = \theta$ for two directions, i.e. the extension is twice as large for the same disorientation in the latter case. The inclusion of this second factor leads, as Dr. Rachinger points out, to the relation between grain-boundary

* Yu. N. Rabotnov, *Vestn. Moskov. Univ.*, 1948, (10), 81.

† D. McLean, *J. Inst. Metals*, 1951–52, 80, 507.

‡ D. McLean, *ibid.*, this vol., p. 291 (1st column).

displacement and extension $\bar{p} = dE$ (d is the sub-crystal diameter) for one slip direction and $\bar{p} = dE/2$ for two slip directions, i.e. for a given extension the grain-boundary displacement is halved if there are two slip directions. This, however, seems a little questionable. Consider the two slip directions to operate, not simultaneously, but consecutively. Dr. Rachinger's formula then becomes equivalent to assuming that slip in a second direction produces an increment of extension but not of grain-boundary displacement. According to the model I depicted,* that is so only in the special case where the second slip direction is parallel to the grain boundary. In other cases Dr. Rachinger's factor will be less than 2. My formula makes the alternative assumption that slip in a second direction produces an increment of extension and a proportionate increment of grain-boundary displacement, thus maintaining the relation $\bar{p} = dE$. This in turn is true only when the two slip directions make the same angle with the boundary. The correct conclusion to be drawn from the model in Fig. 9* appears to be as stated in the same page, namely that a multiplying factor should be introduced to take into account the fact that slip bands are not necessarily normal to grain boundaries (consequently, that polygonization bands are not necessarily parallel to grain boundaries). In Dr. Rachinger's argument this factor is 2, in mine 1, but as its average value is in the region of unity, is it worth considering in detail before the $\bar{p} = dE$ relation has been tested much more widely?

I agree with Dr. Rachinger that, in so far as the results and the model in Fig. 9 of my paper imply that grain-boundary displacement other than that associated with polygonization does not occur, both are unexpected and difficult to account for. I also agree that in the case where the grains do not break down into sub-crystals this model predicts that relative grain rotation takes place. If the amount predicted is consistently greater than that found, this would be evidence that the model does not apply under such conditions.

Dr. Rachinger's last point about the degree to which the surface movements are typical of those occurring in the interior is a most important but difficult one. The difficulty lies in establishing a reliable standard. On the one hand, surface measurements are open to the objection that the surface may deform differently from the interior; while on the other hand the alternative procedure of deducing the amount of grain deformation from measurements of grain shapes as they appear on sections is open to the objection that grain-boundary migration occurs during creep and will produce some modification of shape apart from, or in addition to, that due to grain deformation. However, at 200° C., the temperature at which some of Dr. Rachinger's † and all my tests were made, there is good agreement between our results where the other conditions were similar. For an aluminium specimen containing 10 grains/mm. strained at a rate of 0.1%/hr., Dr. Rachinger found from measurements on a section that grain deformation contributed 88/100ths of the total extension, while under virtually identical conditions my result from surface measurements was that 86/100ths was contributed by grain deformation. Since under these conditions the two different methods of measurement agree, they probably measure the same thing. At higher temperatures and a similar rate of strain and grain-size, Dr. Rachinger found that the surface and interior appeared to behave differently. Pos-

sibly under these and other different conditions one or both of the tendencies referred to above become significant.

In connection with the discussion on finding formulae to fit creep curves, two types of formulae are involved. The controversy in some of the papers and contributions to the discussion is concerned with the type of formulae produced by fitting curves to experimental data. Such formulae cannot safely be extrapolated but enable interpolations to be made between experimental results. To be useful in this way they must be accurate, and making them accurate will probably limit their field of application. Consequently, to prove or disprove the applicability of such formulae to conditions other than those to which they were originally fitted is to assess their value for something which they were not designed to do. There is also the type of formula deduced by supposing a particular mechanism of creep. From such formulae one cannot as yet reasonably demand great accuracy, but one is entitled to expect them to be approximately substantiated whenever, or if ever, the supposed mechanism is dominant.

Mr. J. A. RAMSEY (*in reply*): As regards Mr. Perryman's first question, my own work on the subject began as an attempt to discover possible structural changes during recovery, and, if any such changes occurred, to determine whether they could be related to the predisposition of the deformed structure, at least in parts, to form recrystallization nuclei. Therefore, when the existence of the recovery effect was established, I went to some trouble to find out, both by X-ray diffraction and microscopically, whether individual sub-grains became active and grew rapidly at the expense of their neighbours, i.e. acted as recrystallization nuclei. As far as I could discover, this did not occur; generally the nucleus developed with an orientation quite different from the range of orientation occurring in the grains under observation.

The second question is rather more difficult to answer. Deformation occurs by slip on a variety of systems of planes, though a single system evidently predominates in a number of grains. One would not expect, therefore, to find the same straight boundaries, and the simple dislocation movements suggested, as are obtained with annealed bent single crystals. Further, I feel that the boundaries observed in deformed polycrystals after heating are, at least in part, delineated during the deformation at room temperature as more or less sharp curvatures in the lattice, similar to the main boundaries of deformation bands. It would certainly be of great interest, as Mr. Perryman suggests, to study the deformation structure produced at very low temperatures, in order to eliminate thermal effects as far as possible, and the subsequent recovery of such structures.

Lastly, I would like to comment on Mr. Perryman's interpretation of the results of his microhardness measurements and the effect of straining after recovery. It would seem that the higher hardness of the recovered zone might be due to the impression covering a number of sub-grains tilted with respect to each other.

It has been suggested ‡ that the absence of slip in the sub-structure might be due to the fact that the small diameter of the sub-grains forces the dislocations to behave non-dynamically, § thus producing widespread slip which may not be visible even with phase-contrast illumination at a magnification of 200 times.

* D. McLean, *J. Inst. Metals*, this vol., p. 298 (Fig. 9).

† W. A. Rachinger, *ibid.*, this vol., p. 33.

‡ R. C. Gifkins, private communication.

§ N. F. Mott, *Phil. Mag.*, 1953, [vii], 44, 742.

Discussion

Young's Modulus of Alloys*

Professor G. V. RAYNOR,† M.A., D.Sc. (Vice-President): It is perhaps appropriate that I should consider the paper by Mr. Dudzinski first, because I was to a slight extent associated with this investigation in its early days, and because of the interesting way in which the results can be related to the constitution of the alloys. When I first became aware of the work, the effects on Young's modulus of silicon, beryllium, cobalt, manganese, and nickel had been examined, and the question arose as to what further solute metals to try. It seemed, on the basis of results then available, that the effect of a given solute metal on the Young's modulus of aluminium could be interpreted in terms of two main factors: firstly, the magnitude of the modulus of the intermetallic compound or other hard particles in the alloy, and secondly, the percentage of aluminium in the compound. Thus, in comparing two alloys with the same amount of intermetallic compound present, the one with the higher modulus will be that for which the compound has the higher modulus. It is also fairly clear that if we are dealing with the effect of a compound *A* which contains a high proportion of aluminium, a given solute percentage will provide more intermetallic compound, and hence a higher Young's modulus, than in the case of a compound *B*, of equal Young's modulus to *A*, but of lower aluminium content. We know so little of the Young's modulus of compounds that it was necessary to consider the magnitude of the heat of formation of a compound as a rough indication of the magnitude of its modulus, on the general grounds that the stronger the bonding, the stiffer would be the structure. This takes no account of structure, and that of course, is the weakness of the concept. These general considerations were dealt with during the discussion of Mr. Dudzinski's earlier paper,‡ so I will not dwell on them here.

One of the most interesting features of the present paper is the work on the aluminium-manganese-chromium alloys. I believe that I am right in saying that this was undertaken as a result of my suggestion some years ago that if aluminium-manganese-chromium alloys containing a ratio of 4 manganese atoms to 1 chromium atom were to be annealed below 590° C., the increase in Young's modulus would exceed that expected from the additive effects of manganese and chromium, because of the precipitation of a phase of composition approximating to (CrMn)Al₁₃. Table II (p. 52) shows that this increase does in fact occur, under precisely the conditions laid down, and this is quite gratifying. I also committed myself to saying that no improvement over the additive effects of manganese and nickel was to be expected in the aluminium-manganese-nickel system, since the ternary compound formed, Ni₄Mn₁₁Al₆₀, contained a smaller proportion of aluminium than MnAl₆. Table IV (p. 53) confirms this in the main; the relatively low values of the modulus in alloys rich in manganese but poor in nickel may be due essentially to this reduction in the aluminium content of the compound. I think we can also give a reason for the relatively high values obtained at low manganese and high nickel, because it is just in this composition region that a metastable ternary phase appears, the aluminium content of which is unknown but probably relatively high. This phase does not belong to the equilibrium diagram, but is of remarkable persistence, and disappears only after very long annealing. It would almost certainly be present under the conditions employed. With regard to the aluminium-chromium-silicon alloys, no predictions were made, but I think it is possible to understand the effects referred to on p. 52. In this ternary system, according to the composition,

there may be deposited as primary crystals either α (AlCrSi), which has a ratio of aluminium atoms to solute atoms of approximately 3:2, or β (AlCrSi) which is very poor in aluminium. In either case the ternary compound contains much less aluminium than CrAl₇, and the decrease below the calculated additive value is to be expected.

Turning to the binary alloys, the observation that chromium is more effective than manganese, while copper is much less effective than nickel, again confirms earlier predictions, which were, however, incorrect with regard to iron. This is much more effective than it should be according to the composition and heat of formation of FeAl₃. I am afraid that I mistrust Mr. Dudzinski's explanation of this. The reported breakdown of FeAl₃ into Fe₂Al₇ and Fe₂Al₅ takes place below 600° C., so that I do not see how secondary crystals of Fe₂Al₇ can exist in the microstructure of Fig. 5 (Plate VII). I should add here that at Birmingham we have recently obtained diffraction patterns from crystals of FeAl₃ extracted from slowly cooled alloys, from alloys chill cast and annealed for long times above the suspected transformation, and from alloys chill cast and annealed for long times below the suspected transformation. These were all identical, and we doubt very much whether the reported decomposition does indeed take place under either our conditions or those of Mr. Dudzinski.

As the author states, the results for titanium, vanadium, molybdenum, and silver are relatively easy to understand in terms of the compounds formed, but it must be admitted that the low value of the increment for tungsten is a little surprising, in view of the high proportion of aluminium in WAl₁₂. This fact, and the fact that CaAl₄, in spite of its high heat of formation, depresses the Young's modulus of aluminium, definitely show that the early interpretation was seriously incomplete.

Where one general type of intermetallic compound of relatively complex crystal structure is under consideration, the correlation with heat of formation and alloy constitution is not unsatisfactory, but it is apparent that we cannot carry these considerations over to include all cases. What is now required, as a complementary research to this very valuable piece of work, is a full-scale investigation of the relationship of Young's modulus to heat of formation and to crystal structure for a wide range of intermediate phases. It might then be possible to develop a real theory, but in the meantime one must congratulate Mr. Dudzinski on having, as he says, provided enough information on which to base the development of a commercial alloy of considerably enhanced elastic properties.

The work described by Mr. Smith is of great interest in quite another way. Here we are concerned with the effect on Young's modulus of a foreign atom in solid solution, and Mr. Smith has set out clearly the factors which are likely to prove important, and proceeds to make a check by calculating the part of the variation which may be expected to be due to atomic-size differences, the remaining part being regarded as due to electronic factors. It appears to be a little indefinite as to whether the effect due to electronic factors is proportional to (solute valency)², or to the electron concentration. It is a pity that the accuracy attainable does not permit a choice between these alternatives; I do not criticize the author on this point, because he has probably squeezed the last ounce of accuracy out of this method. What I must criticize, however, is his choice of the apparent atomic diameters as a basis for the calculation of the atomic size effect. It is well known that the lattice distortion produced by metals of the B sub-groups

* Joint discussion on the papers by A. D. N. Smith (*J. Inst. Metals*, 1951-52, **80**, 477), and N. Dudzinski (this vol., p. 49).

† Professor of Metal Physics, Birmingham University.

‡ *J. Inst. Metals*, 1948, **74**, pp. 686, 697 (discussion).

in copper and silver depends intimately on the valency of the solute. An analysis of lattice spacings indicates very strongly that the distortion produced is the resultant of the atomic size-effect, which may lead to expansion or contraction according to whether the introduced atom is larger or smaller than that of the solvent, and a valency effect such that an expansion is produced if the solute has a valency higher than that of the solvent. It is for this reason that germanium expands the lattice of copper, in spite of its much smaller atomic size. Now, the apparent atomic diameter which Mr. Smith has used is obtained, essentially, by extrapolating the lattice-spacing/composition curve to 100% of solute, and therefore includes the whole of the distortion due to valency, and it may well be that part of the effect of valency on the Young's modulus has therefore been included in trying to make allowance for the size-effect. I feel that it would have been far better to take the closest distances of approach in the crystals of the elements for assessing the size-effect. Let us see what happens if we do this. If we consider the atomic diameters of zinc and cadmium to be the closest distances of approach in the respective crystals, and take, for the complex gallium structure and the partially ionized indium structure, the atomic diameters of 2.595 and 2.926 Å. deduced from other work, we find that Z in Table II (p. 480 of the paper) works out as follows (assuming the same proportionality factor in equation (3) as the author):

In Cu		In Ag	
Zn	Ga	Cd	In
10	1	6	1

Hence the quantity $X-Z$ becomes:

In Cu		In Ag	
Zn	Ga	Cd	In
27	81	21	64
or a ratio of 1 : 3		or again a ratio of 1 : 3	

This means that, when plotted in terms of electron:atom ratio, the curves of the valency contribution to the decrease in Young's modulus against electron concentration do not superimpose, as in Fig. 5 (p. 481), but lie apart, the curve for gallium in copper having twice the slope of that for zinc in copper, and that for indium in silver having twice the slope of that for cadmium in silver. This is a relationship of exactly the same type as that shown by the lattice distortion due to valency. I make no claim that this is a correct interpretation, but it indicates that there may be alternative interpretations. In particular, the use of apparent atomic diameters may be misleading. I must admit that tin and germanium do not work out nicely on the analysis I have suggested, and this may be connected with the marked shrinkage of the ion as we pass along each period from copper to germanium, or from silver to tin. This is a factor which has not been taken into account explicitly in the present paper, but which should be considered. We know that the elastic constants are intimately connected with the degree to which the ions overlap, and this factor may be important. In spite of the difficulties of interpretation, this paper has made a very useful contribution; and in view of these difficulties, I would heartily support the author's suggestion that further work should be carried out on single crystals, rather than on polycrystalline aggregates.

Mr. G. BRADFIELD*: At the National Physical Laboratory much information has been collected on elastic constants of alloys. The effect of preferred orientation, which is liable to cause serious errors in elasticity measurement, has been studied and details of means of correcting for or avoiding these errors

by measuring three elastic constants instead of one, have been published.†

I shall confine my remarks on the paper by Mr. Smith to comments concerning the techniques employed and the author's recommendation for future work of high accuracy.

The accuracy of the bending-mode-vibration method used in the above investigation is low. The longitudinal and torsional vibration methods which we employ can give errors five to ten times smaller, but it is the errors arising from the effect of preferred orientation which are most serious, since they can frequently amount to several per cent. for degrees of preferred orientation which are difficult to assess by X-rays.

It is to be noted that the values of dE/dC deduced for the Cu-Zn system from Fig. 1 (p. 479 of the paper) and given in Table II (p. 480) as 37 units, would be 55 units if the first four alloy points were used and the final one ignored. 55 units is much nearer to the Köster and Rauscher figure and much nearer the value measured at the N.P.L. Such a slope may therefore be in error by 50%, when obtained by these means.

It should be pointed out that the value of the modulus shown for silver is high by well over 1½%.

Finally, I feel that the statement (p. 481) that "the most profitable line of attack for work of high accuracy would seem to be to use single crystals" needs some qualification. A standard deviation of $\pm 1/5\%$, i.e. 0.2%, for a straight line representing a plot of $\Delta E/\Delta C$ for an alloy series can be achieved on polycrystalline materials carefully made and measured by existing techniques. Thus, although the single-crystal method is highly desirable for other reasons, e.g. because it gives all the elastic constants, it is not essential for reasons of accuracy, and it is dangerous to assume that the available techniques for making alloy single crystals will at present produce what is required.

Mr. J. LUMSDEN,‡ B.Sc., A.R.I.C. (Member): Mr. Smith has discussed the relation between the Young's modulus of alloys and their electron:atom ratio. I should like to make a plea for an alternative approach, through proximate rather than ultimate causes.

As has been shown by Druyvesteyn and Meijering,§ the entropy of an alloy can be calculated from its elastic constants. For solid solutions of zinc in copper they found poor agreement with the entropy calculated from other thermodynamic data then available. From later vapour-pressure measurements,|| I have calculated the partial molal entropy of the zinc,¶ and find it to be in excellent agreement with Mr. Smith's figures for Young's modulus. On many alloys it is difficult to measure the free energy over a sufficiently large temperature range to give an accurate value of the entropy; a knowledge of elastic constants should be useful for deriving the complete thermodynamic properties.

A free-energy equation contains two terms, heat content and entropy, which can be related, respectively, to the interatomic energies and the rates at which the interatomic forces vary with distance. I suggest that atomistic explanations should be directed at these interatomic energies and forces, rather than at particular equilibrium properties such as phase boundaries. For instance, from the thermodynamic viewpoint, the course of a solidus line has significance only in conjunction with the course of the corresponding liquidus. These two boundaries are determined by the condition that the thermodynamic potential of each component is the same in both phases; their initial courses are determined by the heat of fusion of the solvent and the ratio between the activity coefficients of the solute in the liquid and solid alloys. It is difficult to see how the slope of a solidus line, by itself, can have any fundamental theoretical significance.

In general, the variation with composition of thermodynamic

* Physics Division, National Physical Laboratory, Teddington, Middlesex.

† G. Bradfield and H. Pursey, *Phil. Mag.*, 1953, [vii], **44**, 437.

‡ Research Department, Imperial Smelting Corporation, Ltd., Avonmouth.

§ M. J. Druyvesteyn and J. L. Meijering, *Physica*, 1941, **8**, 1059.

|| A. W. Herbenar, C. A. Siebert, and O. S. Duffendack, *Trans. Amer. Inst. Min. Met. Eng.*, 1950, **188**, 323.

¶ J. Lumsden, "Thermodynamics of Alloys" (*Inst. Metals Monograph and Rep. Series*, No. 11), 1952, p. 257.

properties can be deduced only for dilute solutions. If, however, the atoms are of equal size and no directional forces are operative, simple statistical mechanics predicts that the deviation from linearity of the energy and compressibility should be represented by a symmetrical function, which, to a first approximation, is proportional to the product of the atomic fractions. This theoretical prediction is fulfilled for alloys of gold and silver, which have practically equal atomic volumes and also the same valency. The measurements on the gold-silver system prove it unjustifiable to assume that the variation with composition of the energy or elastic constants of alloys can be completely accounted for as the sum of effects attributable to differences between the atomic volumes and valencies of the components.

In liquids, the atomic arrangement is already so irregular that no special difficulty arises in accommodating an atom of different size. When the interatomic energies and forces are intrinsically the same in the solid and liquid states, the effect of relative atomic sizes should be represented by the extent to which the heat or entropy of formation of a solid alloy from its solid components exceeds that of the corresponding liquid alloy from its liquid components.*

The terminology customarily used in discussing the electron: atom ratio of alloys rather glosses over the fact that the solute is a different metal from the solvent. A satisfactory formulation for solid solutions of zinc in copper would include the properties of face-centred cubic zinc. It may be pointed out that the aluminium-zinc phase diagram clearly suggests a melting point for face-centred cubic zinc not much below 350° C.; analogy with the gold-platinum system supports this extrapolation. The molal free energy of transformation of the stable hexagonal zinc to the face-centred cubic form is therefore probably about 200 cal.

Dr. F. R. MORRAL,† B.Sc. (Member): The data presented by Mr. Dudzinski should make it possible to design new and useful aluminium alloys.

TABLE A.

Alloying Element					Second Phase	
Position in Table I (p. 51)	Symbol	Crystal Structure	Lattice Constant, Å.	Solid Solubility, % at 20° C.	Crystal Structure	Formula
1	Cr	Body-centred cubic	2.88	0.01	Monoclinic *	CrAl ₇
3	Mn	Complex (?)	...	0.05	Orthorhombic	MnAl ₆
4	V	Body-centred cubic	3.01	0.37	"	VAl ₇
5	Mo	" "	3.14	0.2	?	MoAl ₅
6	Fe	" "	2.86	0.03	Orthorhombic	FeAl ₃
10	W	" "	3.16	1.7	?	WAl ₁₃
2	Ti	Close-packed hexagonal	...	0.03	Tetragonal	TiAl ₃
7	Be	" "	...	0.05	Close-packed hexagonal	Be
8	Co	" "	...	0.02	Monoclinic	Co ₂ Al ₉
14	Mg	" "	...	1.1	Face-centred cubic (?)	Mg ₂ Al ₃
9	Ni	Face-centred cubic	3.51	0.05	Orthorhombic	NiAl ₃
12	Cu	" "	3.61	0.1	Tetragonal	CuAl ₃
13	Ag	" "	4.08	0.5	Hexagonal	Ag ₂ Al
15	Sr	" "	5.66	0.3	Body-centred tetragonal	SrAl ₄
16	Ca	" "	6.07	0.7	" "	CaAl ₄

* Some authors consider this phase to be orthorhombic.

The high elastic properties are explained in one case as being due to the presence of CrAl₇, which contains a large proportion of aluminium atoms. The effect of titanium is attributed to the high elastic modulus of TiAl₃, and the limited effect of CaAl₄ to the low modulus value of calcium itself.

The effect of the addition elements seems to show fairly good

correlation when other factors listed in Table A, are taken into consideration. The basic data, the order of effect of the alloying elements, are taken from Table I (p. 51) of the paper.

This correlation seems to indicate that the solid solubility of the alloying elements for a given crystal structure, as well as the crystal structure of the second phase, may be significant.

Mr. J. T. RICHARDS,‡ B.Sc. (Member): We have conducted tensile tests on aluminium-beryllium alloys containing 35-40% beryllium and have obtained *E*-modulus values ranging from 20 to 23 × 10⁶ lb./in.². These values compare favourably with a calculated value of 22 × 10⁶ lb./in.² for an alloy containing 37.5% beryllium, based upon *E*-moduli of 10 × 10⁶ lb./in.² for aluminium and 42 × 10⁶ lb./in.² for beryllium.

As a result, the increment in *E*-modulus for 1 wt.-% of added element becomes approximately 0.307 × 10⁶ lb./in.². Comparison of this value with the figures of 0.188 × 10⁶ lb./in.², listed by Mr. Dudzinski in Table I (p. 51), suggests either a non-linear relationship or a broken modulus/composition curve in the case of beryllium additions.

Dr. A. N. TURNER,§ B.Sc., A.R.S.M., A.I.M. (Member): I should like to discuss the practical utilization of the information contained in Mr. Dudzinski's paper. Mr. Dudzinski believes that it should be possible to develop an alloy having elastic properties approximately 20% higher than those aluminium alloys at present in use. We have, in fact, carried out work on the production by conventional means of alloys of high Young's modulus on a pilot-plant scale and have succeeded in producing 36-in.-wide sheet, 0.080 and 0.036 in. thick, which goes some way towards fulfilling this promise. I would like, however, to make a few observations on the difficulties encountered.

First, it may be said that, in general, the type of alloy suggested as a result of Mr. Dudzinski's work suffers from two disadvantages during casting by the semi-continuous process. These are segregation and axial cracking. Segregation is most pronounced and difficult to control in those alloys containing hypereutectic silicon. Primary silicon is lighter than the material from which it crystallizes, and consequently rises to the surface of the molten pool during casting, leading to the build-up of a silicon-rich semi-solid crust, which periodically breaks away, leading to gross inhomogeneity in the ingot. Other elements, e.g. manganese, may also segregate as primaries, but so long as they are more dense than the melt, they tend to sink and cause less difficulty during casting or subsequent working. Axial cracking tends to increase with the brittleness of the as-cast alloy, and it is necessary to balance carefully the operating conditions and the composition, in order to cast an alloy successfully at all.

The alloys are not easy to roll, hot rolling in particular causing some difficulty. Ingots must be scalped before breaking down and again after breaking down, before hot rolling is continued. The greatest difficulty is surface crazing, which may lead to the general break-up of the ingot. There are indications that this phenomenon is connected with the presence of coarse primary intermetallic constituents at the surface, and that a great improvement in rolling characteristics may be obtained by cladding the ingot with a thin layer of commercial-purity aluminium before rolling.

Another difficulty in the fabrication of these materials is that even if the alloy has been successfully cast and rolled, it does not follow that the properties obtained are those expected. For example, an alloy prepared to contain approximately silicon 10, manganese 2.4, nickel 2.35, cobalt 0.18, and copper 2.0%, which according to the results given in Mr. Dudzinski's paper should have given a modulus of a little over 12 × 10⁶ lb./in.², actually gave a value in the sheet form of about 10.6 × 10⁶ lb./in.², notwithstanding the fact that in the as-cast condition the modulus was very much that calculated. The reason for this discrepancy is not difficult to see when the micro-structure of the alloy is examined. Fig. A (Plate XCVIII)

* J. Lumsden, *loc. cit.*, p. 343.

† Kaiser Aluminum and Chemical Corporation, Spokane, Wash., U.S.A.

‡ Development Engineer, The Beryllium Corporation, Reading, Pa., U.S.A.

§ Aluminium Laboratories Ltd., Banbury.

for example, illustrates the presence of a large manganese-bearing primary particle in the rolled sheet. It may be seen that the particle has not been deformed nor reduced appreciably in size, but is surrounded by a series of cracks separating it completely from the matrix. The volume occupied by this constituent, therefore, acts as a void, and the modulus of the material, far from being increased by the presence of manganese, is actually decreased in proportion to the cross-sectional area of the constituent involved. This separation of the primary constituents from the matrix occurs during hot rolling. There appear to be two possible solutions to this difficulty; either to produce alloys in which the constituents do not appear as large brittle primaries, or alternatively to devise methods of deformation which do not lead to the separation of the constituent from the matrix. How practicable these two methods may be is largely a matter for conjecture. However, we have distinct hopes that it may be possible to evolve a method of producing an alloy with a Young's modulus of elasticity of at least 12×10^6 lb./in.² with acceptable other mechanical properties, by the normal methods of fabrication in general use today.

Mr. DUDZINSKI (*in reply*): Professor Raynor has discussed the effect of the heat of formation of intermetallic compounds on the elastic properties of alloys. It may be useful to say a few words about the detrimental effect of calcium. Expressing the heat of formation of the compound in cal./g. of the alloying element, it is found that the values increase in the following order: $\text{CuAl}_2 < \text{Co}_2\text{Al}_3 < \text{FeAl}_3 < \text{NiAl}_3 < \text{CaAl}_4$, and the corresponding increments of E referred to 1 wt. % of the alloying element are: Cu 0.08, Co 0.185, Fe 0.23, Ni 0.165, Ca 0.3 lb./in.² $\times 10^6$. The reason for the low value of E in aluminium-calcium alloys is obvious. CaAl_4 has a typical layer structure in which the elastic modulus along one crystallographic axis is relatively high, but in the plane perpendicular to it is low. As reported by the German workers, the compounds of magnesium with bismuth or antimony, which also have a layer structure, show a similar behaviour in spite of their heteropolar type of bonding.

It is also possible that the structure of the two outermost electron shells of the atom of the alloying element have an effect upon the elastic modulus of the alloy. If the increments in E are expressed per 1 at. %, and the elements are arranged according to their groups in the Periodic Table, the result is as follows:

Group	IIA Ca	IVA Ti	VA V	VIA Cr	VIIA Mn	VIIIA Fe	VIIIB Co	VIIIC Ni	IB Cu
ΔE	-0.4	0.6	0.55	0.82 Mo 0.97 W 0.75	0.62	0.44	0.37	0.32	0.18

In solid calcium the forces of cohesion are small. Its high compressibility and high atomic volume (26) indicate a weak atomic bonding. Metals of this type show a low value of E . Titanium, the next element after scandium (not investigated) in the First Long Period, has a strong cohesive force because, according to Pauling, the electrons derived from the (4s) and (3d) energy states of the free atoms are hybridized in the solid, giving a strong bond. Accordingly, the increment in E for aluminium-titanium alloys is large. This process develops further in Groups VA and VIA. The atomic diameters of vanadium and chromium, as defined by the closest approach of atoms in the crystals, decrease. The melting point of vanadium, however, decreases a little, and the increment in E for aluminium-vanadium alloys is of the order of 0.55. The elements of Group VI show the highest increase in E , and it is interesting to note that in this group the number of electrons taking part in the bond formation is, according to Pauling, 5.78 electrons/atom. Molybdenum, the element lying below chromium, shows the highest effect on E of the alloying additions, and its melting point is higher than that of chromium. One would expect, therefore, that ΔE for aluminium-tungsten alloys would be still higher, but or some unknown reason the increment is lower than for molybdenum-bearing alloys. In the elements beyond Group

VIA the Pauling theory does not hold; there is a decrease in the cohesive forces, and the beneficial effects of manganese, iron, cobalt, and nickel also decrease in the order named. This may perhaps explain why the values of E for aluminium-nickel alloys are lower than expected from the heat of formation of the compound. In copper the strength of bonding is further lowered by the fact that the third quantum shell has been completely filled and only the valency electrons of the (4s) shell take part in bonding, assisted by van der Waals forces; the value of ΔE for aluminium-copper alloys is therefore low.

I am grateful to Professor Raynor for clarifying the position regarding the transformation $\text{FeAl}_3 \rightarrow \text{Fe}_2\text{Al}_7$. The results given in Fig. 2 (p. 51) are correct, but it is apparent that their interpretation is wrong. The paragraph on p. 52 dealing with aluminium-iron alloys should therefore read: "Annealing at 530° C. below the temperature for the hypothetical transformation $\text{FeAl}_3 \rightarrow \text{Fe}_2\text{Al}_7$ and also, for comparison, just below the eutectic temperature, resulted, however, in only a slight improvement in E ." As there is no direct evidence that the above transformation occurs, it is possible that the recorded variation in E should be ascribed to some other unknown reasons. The Young's modulus of these alloys, when annealed and slowly cooled, returned to its previous values for the as-chill-cast condition.

Dr. Turner describes the difficulties encountered in connection with the development of an alloy of high elastic modulus for commercial application, and shows a photomicrograph in which a large constituent has separated from the matrix, resulting in the reduction of E . This is rather a gloomy picture. The composition of the alloy in which these "voids", as defined by Dr. Turner, occurred, was approximately silicon 10, copper 2, nickel 2, manganese 2.4, cobalt 0.2%. The manganese content in alloys of this type is critical, i.e. the MnAl_3 constituent separates in very large formations above certain concentrations of manganese. I have suggested a composition: silicon ~11, copper 4, nickel 2, manganese 0.5, magnesium 0.3, cobalt 0.2, titanium 0.1%. This alloy is very complex, and its microstructure is not very well known. It probably contains CuAl_2 , ternary Al-Cu-Ni complex, NiAl_3 , Mg_2Si , ternary Al-Co-Fe complex and quaternary Al-Fe-Si-Mn complex. I was aware that this type of alloy would not be easy to cast by a continuous process or to roll, and I am therefore grateful to the Aluminium Laboratories for their excellent work in overcoming the difficulties. An alloy of composition very similar to that given above was rolled to 14 and 20 S.W.G. sheet, and when examined by Mr. Meikle and his associates gave the following properties:

TABLE B.

Condition	20 S.W.G.			14 S.W.G.			Elongation, %
	0.1% P.S., tons/in. ²	U.T.S., tons/in. ²	E , lb./in. ² $\times 10^6$	0.1% P.S., tons/in. ²	U.T.S., tons/in. ²	E , lb./in. ² $\times 10^6$	
A	14.5	26.0	11.8	14.5	26.2	12.0	10
B	22.0	28.7	11.8	21.4	28.7	11.9	5½
"	21.3	27.9	11.8	21.6	28.4	11.9	5½

A = Solution-treated and aged at room temperature. B = Fully heat-treated

The results shown in the table are very close to the predicted values. One could increase the manganese content to about 1% by reducing the copper content to about 2% and keeping the other alloying additions at the same concentration, or even increase it to 2% by leaving the nickel out.

Returning to the photomicrograph (Fig. A, Plate XCVIII), I am not sure that the large manganese-bearing constituent has dissociated itself from the matrix, although it exhibits cracks which are detrimental to the properties. It looks rather as though some parts of it had been crushed out in the polishing operation. In some other regions one can distinguish small black areas associated with the silicon particles; these also may be considered as holes. I have encountered a similar tearing out of brittle constituents in polishing, as shown in Figs.

B and C (Plate XCVIII). These represent the structure of cast binary aluminium alloys containing, respectively, 6.37% chromium and 2.4% vanadium. The Young's modulus of these alloys was 11.9 and 10.4 lb./in.² $\times 10^6$, the values agreeing with calculation. To eliminate such large formations, I would suggest pre-forging or pre-extrusion, so that the constituent might be broken up before the rolling process, or a slight reduction of temperature in the first stage of rolling to facilitate the breaking up of the manganese-bearing phase.

With regard to Dr. Morral's contribution, various workers have shown the detrimental effect of elements which form solid solutions with copper or silver, and a similar effect might be anticipated with aluminium. The few experiments which I have carried out indicate that this is the case, but the fact that the solid solubility of other elements in aluminium is very low, limits its extent.

The crystal structure of the second phase is undoubtedly important, but unfortunately little is known about the structure of the intermetallic compounds formed in equilibrium with the aluminium solid solution. The CaAl_4 and SrAl_4 compounds display a typical layer structure similar to that of Mg_3Sb_2 or Mg_3Bi_2 . In this type of structure the binding in one crystallographic axis is smaller than in the plane perpendicular to it, and as mentioned above, the forces of cohesion in metallic calcium are low, with a corresponding reduction of the Young's modulus of aluminium-calcium and aluminium-strontium alloys. At a higher concentration of calcium the compound CaAl_2 makes its appearance. This belongs to the group of Laves phases characterized by a very high co-ordination number; this favourable condition to some extent offsets the effect of weak bonding, and the Young's modulus for CaAl_2 is accordingly higher than for CaAl_4 .

Mg_2Si is a typical valency compound, anti-isomorphic with CaF_2 . The elastic modulus of Mg_2Si is higher than that of magnesium, and therefore the detrimental effect of magnesium in aluminium alloys is counteracted by the addition of silicon.

The structure of the CuAl_2 compound may be regarded as being derived from two face-centred cubic copper units stacked vertically, in which the atoms at the centre of the vertical faces are each replaced by a pair of aluminium atoms; in addition such a structure has been elongated horizontally. Here, the size-factor is important and is reinforced by strong bonding. As a result the values of E for aluminium-copper alloys are above the line connecting the values for the two elements.

It is interesting to note that high values of E are shown by certain electron compounds, such as the Hume-Rothery phases (e.g. Cu_3Al , Cu_5Zn_8 , Cu_3Sn_6) with a constant electron : atom ratio of 21 : 13, and possessing a complex structure.

The binary compounds formed by aluminium with the transition metals in equilibrium with the primary solid solution are CrAl_7 , MnAl_6 , FeAl_3 , Co_3Al_9 , and NiAl_3 . According to Raynor,* an approximately constant electron : atom ratio of about 2.1 is maintained in these compounds, with the exception of FeAl_3 . They crystallize in a complex structure of low symmetry and having rather large unit cells. They are all effective in raising the value of E , their effect diminishing in the order named. It is interesting to note that Co_3Al_9 is isomorphic with the ternary FeNiAl_9 compound. In an examination of the elastic properties of aluminium-iron-nickel alloys, I found a marked improvement in E when the ratio of iron to nickel was about 1 : 1.

Mg_2Al_3 has a cubic structure, and the values of E for aluminium-magnesium alloys follows the rule of mixtures.

Mr. Richards suggests a non-linear relationship or a broken modulus/composition curve in the case of beryllium additions. It is difficult to comment on this suggestion, as we examined the elastic moduli of binary aluminium alloys only up to 5.6 wt.-% beryllium, very remote from the range of compositions studied by Mr. Richards. In correspondence previously

published,† it was shown by a mathematical calculation that the values of Young's modulus of the alloys assume a linear relationship with the vol.-% of the beryllium content.

The increment in the values of Young's modulus for binary alloys given in the present paper persisted also in ternary aluminium-cobalt-beryllium and aluminium-copper-beryllium alloys; in aluminium-silicon-beryllium alloys, however, an increment of 0.32 lb./in.² $\times 10^6$ was observed, which approaches the figure given by Mr. Richards.

Mr. SMITH (*in reply*): I am grateful to Professor Raynor for pointing out the error in my use of the "apparent atomic radii" as a measure of the atomic sizes of the solutes. He is quite correct in saying that by this means the effect of valency may twice be taken into account. In point of fact it is doubtful whether any useful result is to be obtained by separating out the contribution from the size-effect to the overall measured effect, since neither quantity is known with sufficient accuracy. On the other hand, if no account at all is taken of the size-effect, the measured values of dE/dC obtained in the paper for the B sub-group alloys vary quite closely as the square of the valency of the solutes. This is shown in Table C.

TABLE C

Element	In Copper				In Silver		
	Zn	Ga	Ge	As	Cd	In	Sn
Measured $(-dE/dC) =$ $X, \text{ kg./mm.}^2/\text{at.}\%$	3.7	8.2	15.0	24.0	2.7	6.5	9.2
$X (\text{valency of solute})^{-2}$	9.2	9.1	9.4	9.6	6.7	7.2	5.7

This result may well be fortuitous, and no particular significance should be attached to it at this stage.

I fully agree with Mr. Bradfield's point that accurate measurements may be made of the elastic constants of polycrystalline aggregates, using the technique developed at the National Physical Laboratory to which he refers. It is certainly to be preferred to measurements on single crystals, having regard to the difficulties of their production.

With regard to the slope of the line for the copper-zinc system, I agree that if the last point is ignored the value increases from 37 to 55 units. The fact that the latter figure is in agreement with measurements at the National Physical Laboratory argues that this should be done. On the other hand, one expects that the lines for different copper alloys should intersect the pure copper axis at the same point. On this basis it is difficult to draw any other line for the copper-zinc system than that shown in Fig. 1 (p. 479) of the paper, whether the last point is ignored or not.

In reply to Mr. Lumsden, my object in comparing the slopes of the modulus and solidus lines was to demonstrate that both appear to vary together. Hence, factors which influence one probably also influence the other, and Jones' theory‡ indicates that the atomic size and valency are the most important factors in determining the solidus line. I agree that other factors also affect the modulus, as pointed out by both Professor Raynor and Mr. Lumsden, but for the particular alloys considered here it seems likely that the valency effect is the most important. Although it appears probable that the relationship between the slopes of the solidus and modulus lines, shown in Figs. 2 and 3 (p. 479) of the paper, is largely coincidental, it is of interest to see what happens when the points are plotted non-dimensionally. This is done by dividing the abscissæ by the modulus, and the ordinates by the absolute melting temperature, of the pure metal. The slopes of the lines (shown dotted in the figures) then become nearly equal for the copper and silver alloys, having values of 1.38 and 1.31, respectively. This fact suggests that there may be some rational basis for the comparison.

* G. V. Raynor, "Progress in Metal Physics", Vol. I, p. 49. 1949: London (Butterworths Scientific Publications).

† *J. Inst. Metals*, 1948, **74**, 706 (correspondence).

‡ H. Jones, *Proc. Phys. Soc.*, 1937, **49**, 243.

Discussion

High-Temperature Oxidation of Alloys*

Dr. O. KUBASCHEWSKI,† (Member): The oxidation of copper alloys has been widely studied, but very little information has been available on alloys of cobalt, and this part of the present work is therefore particularly welcome.

There are two ways of approaching the problem of finding oxidation-resistant alloys: one may either explore systematically simple gas-metal systems and try to determine the fundamental mechanisms, or one may work empirically and copy exactly the conditions that occur in practice. Professor Preece and his co-workers have chosen a middle way, and the research worker interested in the fundamental side of the problem would have liked to see parallel experiments carried out in pure dry oxygen, not only with pure cobalt and pure nickel, and also further experiments with much smaller percentages of the alloying elements, which might have included monovalent metals. On the other hand, engineers might ask for some sodium sulphate and vanadium pentoxide to be present in the fuel gas. In view of the formation of generally badly adhering oxidation layers, they might also ask for parallel oxidation tests under temperature changes.

I am more interested in the conclusions of a general nature that can be drawn from the present results. I note that the oxidation rates found for pure nickel agree with those observed by Pilling and Bedworth. As nickel of "commercial purity" was used, it is not surprising to find that the authors' oxidation rates are somewhat higher than the bulk of the data obtained with high-purity nickel.‡§ This is in agreement with the diffusion mechanism in NiO, as I have described elsewhere.‡||

The peak in the oxidation/temperature curve for cobalt is somewhat puzzling. It was not observed by Johns and Baldwin,¶ and I wonder whether the authors have any explanation for this discrepancy. True, thermochemical data show that Co_3O_4 decomposes in air at about 950°C ., as was confirmed by the authors experimentally, but this does not explain the peak unless mechanical imperfections are developed in the layers. The formation of two distinct layers of CoO structure is interesting. The authors' interpretation of this implies that CoO is an amphoteric conductor, i.e. stable with an excess as well as with a deficit of metal. One could imagine the inner layer to possess vacant anion sites, the outer layer vacant cation sites. This would account for the diffusion mechanism propounded by the authors. The difficulty that such a mechanism would create a space between the two CoO layers could be overcome by the assumption that the interface energy pulls the two surfaces continuously together as the vacancies are formed. The interface thus does not correspond to a change in phase, but is simply a mechanical boundary. I doubt whether this interpretation is correct, but it may be that the authors have hit upon an important idea in interpreting certain oxidation phenomena. Previous interpretations of the diffusion mechanism in CoO have been divided, some workers favouring the mechanism of an oxygen diffusion inwards, others that of a diffusion of Co^{++} ions outward. It

would be welcome if the present authors could strengthen their point by oxidizing cobalt in the presence of inert markers, which should be found after oxidation at the mechanical interface within the CoO layer. The platinum wires used for suspending the specimens may have provided this information, as they did in the case of the oxidation of titanium.**

There is no reason why a true diffusion of oxygen should not frequently occur in oxide layers. When Pfeil's now well-known experiments with inert markers on iron surfaces showed for the first time that the cations, rather than oxygen, provide the exchange of matter in oxidation layers, this came as such a surprise that public opinion accepted this mechanism as being of quite a general nature. Another authority in this field, C. Wagner, also favoured the idea of cationic diffusion in oxides, on the basis of considerations of ion sizes. This should be no deterrent, however, to assuming a diffusion of oxygen ions, for instance over vacant anion sites, whenever justified by experimental evidence. The conclusions concerning the oxidation of iron at low temperatures drawn by Vernon, Calnan, Clews, and Nurse †† may be mentioned as an example. Dr. Dennison and Professor Preece have assumed oxygen diffusion also in cupric oxide and, since this is a transition conductor,‡‡ I should say that such a mechanism is possibly applicable. I should like to ask them, however, how they explain the difference between their curve for the composition of the oxide layer on copper (Fig. 4, p. 231) and the corresponding one determined by Valensi,§§ which does not show the inflection that they found. Is it attributable to the difference in the gaseous atmosphere, which was dry oxygen in Valensi's experiments? Or is it somehow due to the change in the oxidation mechanism of copper generally assumed to occur between 500° and 600°C .? An explanation of this point would be quite important, as Valensi has based his theory of multilayer formation on his experimental results.

With regard to the oxidation of alloys, I have already mentioned that it would be useful to know the effects of small percentages of the additions on the oxidation rate, as this would help to elucidate the mechanism of diffusion.¶¶ As long as no second oxide layer is formed, one would expect, on the basis of the Wagner mechanism of oxidation, that high-valency metals should increase, monovalent metals decrease, the oxidation rates of copper, nickel, and possibly cobalt. This applies, for instance, to the copper-chromium alloys. The authors explain why there is not sufficient chromium to produce a protective Cr_2O_3 layer; they do not explain the increase in oxidation actually observed. This, I suggest, is due to the creation of additional cation holes in Cu_2O , which is a cation-deficit conductor, by replacement of monovalent Cu^+ by trivalent Cr^{+++} . It is also possible that the relatively high oxidation rates of the cobalt-10% chromium alloy observed by the authors are due to an increase of the number of vacant lattice sites in the CoO lattice, corresponding to similar observations with nickel-chromium alloys discussed by Wagner and Zimens||| and by ourselves.¶¶ This would require, however, that

* Joint discussion on the papers by A. Preece and G. Lucas (*J. Inst. Metals*, this vol., p. 219) and J. P. Dennison and A. Preece (this vol., p. 229).

† Metallurgy Division, National Physical Laboratory, Teddington.

‡ O. Kubaschewski and O. v. Goldbeck, *Z. Metallkunde*, 1948, **39**, 158.

§ W. J. Moore and J. K. Lee, *Trans. Faraday Soc.*, 1952, **48**, 916.

|| O. Kubaschewski and B. E. Hopkins, "Oxidation of Metals and Alloys". 1953: London (Butterworths Scientific

Publications).

¶ C. R. Johns and W. M. Baldwin, Jr., *Trans. Amer. Inst. Min. Met. Eng.*, 1949, **185**, 720.

** M. H. Davies and C. E. Birchenall, *ibid.*, 1951, **191**, 877.

†† W. H. J. Vernon, E. A. Calnan, C. J. B. Clews, and T. J. Nurse, *Proc. Roy. Soc.*, 1953, [A], **216**, 375.

‡‡ K. Hauffe and H. Grunewald, *Z. physikal. Chem.*, 1951, **198**, 248.

§§ See O. Kubaschewski and B. E. Hopkins, *loc. cit.*, p. 139.

||| C. Wagner and K. E. Zimens, *Acta Chem. Scand.*, 1947, **1**, 547.

CoO, like NiO, be a cation-hole conductor, contrary to the suggestions made earlier. At least, I feel, one should be very careful in generalizing from a few empirical observations. The authors hold the view that the formation of spinel structures on alloys is undesirable for oxidation-resistance. Arkharov* has expressed just the opposite view. The obvious answer to this difference of opinion is that the spinel structure, as such is neither a typical inhibitor nor accelerator of oxidation, any more than any other structure, for instance the NaCl-type. The diffusion mechanism in an oxidation layer depends on the concentration and type of defects in the lattice, and the spinels must be treated individually from this point of view. With this in mind, Hauffe and Pschera† have investigated the diffusion rates in the NiO.Cr₂O₃ spinel. The results indicate that this particular spinel should, in fact, offer quite a good protection to oxidation. Since pure chromium oxide is not particularly protective, the high oxidation-resistance of 80:20 nickel-chromium must be due either to the spinel or to a chromium oxide that contains nickel ions in solid solution. Corresponding considerations may apply to cobalt-chromium alloys.

The results obtained with the copper-aluminium alloys are interesting. If diffusion in the alloys were infinitely rapid, only alumina should be formed on oxidation, owing to its high free energy of formation. Diffusion rates are, however, not infinite, and the effect that this would have on the type of oxidation layers formed was recently discussed by Wagner.‡ From the work of da Silva and Mehl§ it follows that the individual diffusion rate of aluminium in aluminium-copper alloys increases with temperature, relative to that of copper. This is in qualitative agreement with the authors' observation that coherent, protective Al₂O₃ layers are formed only at high temperatures, while at low temperatures insufficient aluminium diffuses to the surface to form more than clusters of alumina in the Cu₂O. It follows that selective oxidation at very low oxygen pressures (i.e. in H₂O/H₂ mixtures) should produce protective films on alloys of, for instance, aluminium with copper or cobalt.

Finally, I should like to ask Professor Preece and Dr. Lucas to state the time of oxidation in Tables I-VI (pp. 221-223); and, although there appears to be little difference in the rates of attack by air and air/fuel gas mixtures, it would be useful to know which of the atmospheres had actually been used to obtain the figures in the tables.

Mr. E. LL. EVANS,|| B.Sc. (Member): Dr. Kubaschewski has mentioned the care needed in drawing general conclusions on the protective or non-protective properties of a group of oxides such as the spinels. I wish to underline this point, because these substances have often been the subject of broad generalizations based on observations on one or two particular spinels. Quarrell in 1940¶ identified the protective oxide on a 13% Cr, 13% Ni steel as a spinel, and suggested that spinels in general should afford good protection against continued oxidation owing to their flexibility in composition and their stability. (The exceptional behaviour of magnetite was related to the ease with which it would break down to form ferrous oxide.) In an electron-diffraction study of oxide films on alloys of iron, cobalt, nickel, and chromium, Hickman and Gulbransen** identified spinels in a number of films, both protective and non-protective. In the summarized conclusions at the end of their paper, they remarked only upon those spinels which appeared protective, and a number of superficial readers have been led to believe that this work confirms the view once advanced by Quarrell. The converse may easily happen as a result of a hurried perusal of the paper by Professor Preece and Dr. Lucas. Of the four spinels encountered, two are detrimental (Co₃O₄ and CoO.Cr₂O₃), one seems not

particularly detrimental (CoO.Al₂O₃), and the fourth is described by the authors as not appearing to have any serious effect on the rate of oxidation (NiO.Al₂O₃). Despite these mixed observations, the authors state without qualification in their conclusions (p. 227) that "this type of structure greatly accelerated the oxidation process", and in their synopsis (p. 219) that "spinel formation is shown to be detrimental to the formation of a protective oxide layer". This kind of statement is to be regretted, if only because abstractors, particularly those reading a foreign language, may tend to be guided to some extent by authors' own summaries.

The spinel structure is very stable, and can accommodate a number of species of metallic ions. There has appeared no reason *inherent in the structure*, however, why any particular spinel should not form a protective or a non-protective oxide layer in any given circumstances. Rather, it might even prove possible, as a result of this flexibility in composition, and in view of the variety of oxidation-resistant properties so far observed, to produce spinels of any desired resistance to continued oxidation. It is certainly undesirable and unnecessary to speak in this connection of the properties of spinels as a class.

I should have welcomed the inclusion of fuller details of experimental methods, in both papers, if only by suitable references where the methods have been described previously. For many years Professor Preece has been associated with work on scaling, and he and his various colleagues have given us a series of excellent and valuable papers. It is just possible that, the various techniques they have developed and applied having become so familiar and commonplace to them, they may overlook the fact that the methods may be of great interest to other people. I refer particularly to methods of mounting and polishing samples for the microscopical examination of scale and adjacent metal. There are very few accounts of such methods in metallurgical literature, and it is evident from the photomicrographs in the present papers that Professor Preece and his collaborators have much to teach us.

Mr. M. H. DAVIES,†† B.Sc. (Junior Member): These papers form a useful addition to the literature on the practical aspect of the oxidation-resistance of materials for possible use at high temperatures. The underlying fundamental reasons for the oxidation behaviour should, however, not be neglected, since only a full understanding of the oxidation process in both pure metals and alloys will lead ultimately to the best practical solution of the problems associated with high-temperature service.

During protective scale formation, and in the absence of transformations occurring in the metal or major changes in the nature of the products of oxidation, it is to be expected that the rate of oxidation will be a smooth function of temperature. That is, the standard Arrhenius plot of the logarithm of *k*, the rate constant, against the reciprocal of the absolute temperature will yield: (1) a straight line, or (2) a smooth curve. The smooth curve will be produced if the composition limits of the phase, diffusion in which is the rate-controlling step, alter with temperature so that there will be an additional change in concentration gradient and thus an added contribution to the rate of growth of the phase. This is implied in the formal diffusion equations.

The discontinuity in the rate of oxidation/temperature curve plotted for cobalt in Fig. 2 (p. 220) is attributed by Professor Preece and Dr. Lucas to the disappearance from the reaction products of the thin outermost layer of Co₃O₄. From the general oxidation behaviour of cobalt it appears more likely that cobalt-ion diffusion through the principal oxide CoO will be the rate-determining step, and thus the presence or absence of a small amount of Co₃O₄ should not

* V. I. Arkharov, *Izvest. Akad. Nauk. S.S.S.R.*, 1946, [Khim.], 127.

† K. Hauffe and K. Pschera, *Z. anorg. Chem.*, 1951, 264, 217.

‡ C. Wagner, *J. Electrochem. Soc.*, 1952, 99, 369.

§ L. C. C. da Silva and R. F. Mehl, *Trans. Amer. Inst.*

Min. Met. Eng., 1951, 191, 155.

|| Chemical Research Laboratory, D.S.I.R., Teddington.

¶ A. G. Quarrell, *Nature*, 1940, 145, 821.

** J. W. Hickman and E. A. Gulbransen, *Trans. Amer. Inst. Min. Met. Eng.*, 1947, 171, 344.

†† Fulmer Research Institute, Ltd., Stoge Poges, Bucks.

markedly affect the oxidation rate. It is suggested in the paper that the presence of this oxide at the outer surface of the scale increases the rate of oxygen transfer to the underlying CoO. This contention implies strong oxygen-pressure-dependence of the rate of scaling, and it would be of value to know whether or not a variation of scaling rate with partial oxygen pressure has been found.

In most other cases of protective scale formation where a parabolic rate law is obeyed, the rate-controlling step is the diffusion of ions (or vacancies which result in a net ion transfer) through the scale. On considering the oxidation of iron* under conditions which allow formation of Fe_2O_3 in one case (oxidation in O_2) and which prevent it in another (oxidation in water vapour), one finds no material difference in the overall scaling rate. Diffusion through "FeO" is the rate-determining step, and different rates of oxidation are obtained at the same temperature only by controlling the atmosphere to such an extent that the composition gradient in "FeO" is limited (no Fe_2O_3 or Fe_3O_4 is formed) and considerably less than the maximum allowed by the width of the equilibrium phase field.† Thus, it is hard to ascribe the vast change in oxidation behaviour of cobalt at 950°C . merely to the disappearance of a scale constituent which occupies only a small volume fraction of the total scale, unless there is an extremely strong oxygen-pressure dependence.

The figures for the oxidation of cobalt for 50 hr. at temperatures between 800° and 1200°C . (taken from Tables I–IV, pp. 221–222) show that the temperature increment of the rate constant decreases in the region 900° – 1000°C ., but the sharp inflection of Fig. 2 (p. 220) (for 24-hr. oxidation times) is not indicated. Although only a few results are given, it appears that the plots for the oxidation of cobalt for varying times do not conform to the parabolic relationships found by other workers.‡§ Additional results in the range 900° – 1000°C . would assist in showing whether there is a marked difference in the shape of the rate/temperature curves obtained for different times of oxidation. Such a difference should not exist, and reasons for any apparent difference must be sought in the experimental methods.

Fischbeck and Salzer|| observed discontinuities in the rate/temperature plot for the oxidation of iron in various atmospheres, and attributed it to the transformation in the metal. Later work,* however, showed that such apparent discontinuities were due to the experimental conditions, i.e. to the non-isothermal oxidation in the initial stages. Fischbeck and Salzer allowed their specimens to heat from room temperature to the operating temperature in the oxidizing atmosphere. An oxide film was formed during the initial heating, and on passing through the ferrite/austenite transformation the volume change occurring led to partial rupture at the oxide/metal interface. This resulted in a lower apparent oxidation rate referred to the original surface area, due to the decreased supply of iron ions across the reduced coherent interfacial area. It also resulted in an alteration of the proportions of higher oxides found.¶ Strict isothermal oxidation of iron results in a smooth variation of the oxidation rate with temperature.

Other investigations on the oxidation of cobalt have not indicated any inflection in the rate/temperature plot. Thus it may be pertinent to ask: (1) whether the present experiments were carried out isothermally, (2) whether oxygen in solution in the metal could raise the transformation temperature, thus producing the mechanical effect which might

manifest itself in an apparent reduction of oxidation rate. This transformation might be restricted to a very thin zone in the neighbourhood of the metal/oxide interface since there will be an oxygen-concentration gradient in the metal.

Mechanical effects such as that described, or the development of "diffusion holes", or the stresses associated with the mass/volume relationships of oxide and metal, are frequently responsible for inconsistency in the results of oxidation experiments. Experimental conditions should therefore be held under the strictest possible control, if the maximum benefit and accuracy of information is to be obtained.

Dr. U. R. EVANS,** M.A., Sc.D., F.I.M., F.R.S. (Member): The paper by Dr. Dennison and Professor Preece is most interesting, and its interest is increased if the results are considered in connection with other work not mentioned by the authors. It is perhaps a pity that they confine themselves so closely to the contents of Dr. Tylecote's admirable review, which of necessity contains no references to work published since it was written and no reference to metals other than copper, although progress in our understanding of the oxidation of one metal must help us to understand the behaviour of another. The recent tendency to confine literature surveys up to the date of publication of some text-book or review is a disquieting feature of the times, which deserves the attention of the Publication Committee.

An interesting question discussed in the paper is whether oxide scale grows by outward passage of metal or by inward passage of oxygen. It is of great practical importance to settle this matter in any particular case, for outward passage results in holes below the scale which, being left unsupported, can break down even though the scale material is intrinsically protective. This is well illustrated in the recent work on iron at 1090°C . of Dunnington, Beck, and Fontana,†† who showed, how, by diffusion of vacancies in the metal, the numerous holes of atomic size left below the scale can combine to give a few large holes; then the scale covering the holes becomes leaky, a new scale forms at the bottom of each hole, and the process repeats itself, leading to the formation of a number of scales separated by cavities. Caplan and Cohen‡‡ studying high-chromium steel, showed that these break-downs are accompanied by sudden rises in oxidation rates; in favourable cases, they found a relation between the number of scales and the number of sudden rises in the oxidation/time curves.

Applying these ideas to copper alloys, it is helpful to study the three papers by de Brouckère and Hubrecht§§ on copper-beryllium alloys; their results agree broadly with those recorded by Dr. Dennison and Professor Preece but, since they concentrated on one class of alloys, they naturally provide greater detail. It appears that once a layer of beryllia has appeared between the cuprous oxide film and the metal, it prevents passage of either copper or oxygen through it, and the only change which can then occur is the conversion of the cuprous oxide to cupric oxide; in some cases this conversion becomes complete. Does it occur by passage of copper cations outwards (as in the formation of cuprous oxide films on metallic copper) or by the passage of oxygen inwards? If the latter, how does oxygen move inwards? It should be noted that the driving force is the same in both cases; adsorbed oxygen atoms attract electrons, becoming oxygen ions, and the electric field thus set up can either draw cations outwards or force anions inwards; the decision between the two

* M. H. Davies, M. T. Simnad, and C. E. Birchenall, *Trans. Amer. Inst. Min. Met. Eng.*, 1951, **191**, 889.

† L. Himmel, unpublished work, Metals Research Laboratory, Carnegie Institute of Technology.

‡ C. R. Johns and W. M. Baldwin, Jr., *Trans. Amer. Inst. Min. Met. Eng.*, 1949, **185**, 720.

§ J. S. Dunn, quoted by J. S. Dunn and F. J. Wilkins in "Review of Oxidation and Scaling of Heated Solid Metals" (Department of Scientific and Industrial Research). 1935: London (H.M. Stationery Office).

|| K. Fischbeck and F. Salzer, *Metallwirtschaft*, 1935, **14**,

733, 753.

¶ J. Bénard and O. Coquelle, *Rev. Mét.*, 1946, **43**, 113.

** Reader in the Science of Metallic Corrosion, Cambridge University.

†† B. W. Dunnington, F. H. Beck, and M. G. Fontana, *Corrosion*, 1952, **8**, 2.

‡‡ D. Caplan and M. Cohen, *Trans. Amer. Inst. Min. Met. Eng.*, 1952, **194**, 1057.

§§ L. Hubrecht, *Bull. Soc. Chim. Belges*, 1951, **60**, 311; **61**, 205.

L. de Brouckère and L. Hubrecht, *ibid.*, 1951, **61**, 101.

alternatives is likely to be determined by the presence of holes which will permit the movement of ions or other particles, and also facilitate the atomic rearrangement involved when cuprous oxide disappears and cupric oxide is formed.

At the outset, there is little doubt that cuprous ions move outwards through the cuprous oxide, taking up positions between the adsorbed oxygen ions and starting to build up cupric oxide at certain favoured points; for vacant cation sites exist in cuprous oxide, whilst, so far as is known, there are no vacant anion sites. When once cupric oxide has formed at a point on the outer surface, it can still spread sideways, but the mechanism of growth in depth requires consideration. Cupric oxide (unlike cuprous oxide, which contains less metal than the formula Cu_2O would suggest, and thus possesses vacant cation sites) is believed to possess a composition represented fairly accurately by CuO , and to be almost free from vacant ionic sites. The electronic conductivity is due to electrons being out of place; cupric oxide is an *Eigenhalbleiter*, as the Germans call it; its electrical behaviour is discussed by Hauffe and Grunewald.* It is difficult to see how either ion can pass readily through cupric oxide, which should theoretically be protective, although most investigators, from Pilling and Bedworth† onwards, seem to regard it as being, in practice, non-protective. A possible reason may be the fact (for which evidence has long existed) that the nucleation rate of cupric oxide is low, so that it is formed at a limited number of points, growing sideways and outwards; this doubtless accounts for the somewhat columnar structure of the cupric oxide seen in the authors' photomicrographs (Plate XXXII) which is very different from that of the cuprous oxide layer below it. Until the cupric oxide crystals starting at different points have grown laterally into contact, some outward passage of cuprous ions to join the adsorbed oxygen is still possible; but if the crystals meet one another, sealing the whole surface, the outward movement must cease, and it might be thought that conversion would be at an end. It seems likely that the crystals do not grow into contact at all points, and that pores remain, perhaps along the lines where three crystals approach one another; such a pore would permit oxygen to pass inwards as molecules (not ions) and to convert cuprous oxide to cupric oxide at the base of the pore. In some circumstances, it might be expected that the pores would become blocked, and possibly the Pilling-Bedworth ratio may be determinative in deciding whether blockage occurs, although there is in recent years a tendency to regard lattice parameters as the determining factor. This matter cannot be discussed here, but it is significant that 1 g.-mol. of Cu_2O occupies 23.86 c.c., whereas 2 g.-mol. of CuO (containing the same amount of copper) occupy 24.87 c.c.—perhaps an insufficient volume increase to press the crystals into lateral contact at all points. Such an explanation, however, is put forward tentatively; the argument has several doubtful features.

"Outward movement" does not involve the dissociation of cuprous oxide into cupric oxide and metallic copper, but the dissociation of two Cu^+ ions into two Cu^{++} ions and two electrons; an oxygen atom adsorbed at the outer face of the cupric oxide layer will take up two electrons, becoming an ion, and the electric field set up will cause a Cu^{++} ion to move into place alongside it at the outer surface of the cupric oxide layer. In effect, two new molecules of CuO are formed, one at each interface. The e.m.f. available for the outward movement of Cu^{++} ions is the same as that available for inward passage of O^{--} ions. The question will be decided by the resistance to the two forms of motion. It seems, however, a little doubtful whether either Cu^{++} or O^{--} could readily move through a cupric oxide film, if it is true that there is no deviation from the composition CuO . Thus, the possibility of O_2 molecules moving inwards along pores between the crystals at least deserves consideration.

Dr. K. SACHS,‡ M.Sc., A.I.M. (Junior Member): It is known that the presence of molybdenum in heat-resistant alloys containing chromium may cause a very rapid type of oxidation which has been dramatized by the adjective "catastrophic". It is attributed to the accumulation of volatile MoO_3 near the surface, and is closely related to the accelerated scaling produced by the presence of vanadium pentoxide, which Professor Preece and Dr. Lucas observed in the oxidation of the cobalt-32% chromium alloy with 0.64% vanadium.

It is surprising, therefore, that in binary cobalt-molybdenum and nickel-molybdenum alloys the formation of a molybdate was capable of suppressing the liberation of free MoO_3 . The fact that MoO_3 was found above 1200°C ., and that oxidation became very rapid at that temperature, suggests that MoO_3 vapour is in equilibrium with the molybdate and that the rate of flow of the gases past the specimens, reported to have been "well above the critical speed", was sufficient to sweep away the MoO_3 volatilized at lower temperatures, but could not cope with the quantity of vapour present at 1200°C . To explore the effect of varying molybdenum contents on the oxidation of the cobalt-32% chromium alloy would have been of great interest because a number of creep-resistant alloys, particularly those of American manufacture, are based on cobalt and contain both molybdenum and chromium, though usually rather less than 30% of the latter; it would have been helpful to know to what extent the higher chromium content protects this type of alloy against the influence of volatile MoO_3 derived from the molybdenum content.

Professor Preece and Dr. Lucas express disappointment that none of the elements added to the cobalt-32% chromium alloy increased the adhesion of the scale. One factor which favours the adhesion of oxide layers is the presence of metallic particles in the scale, which help to key the brittle oxide to the surface; such metallic particles tend to make their appearance in the presence of an element less readily oxidized than the base metal. In the case of a cobalt alloy, one would suggest copper or the precious metals. However, experiment may show that the additions required to give the effect are higher than the alloy can support, either from an economic point of view or because other properties will be affected.

In the paper by Dr. Dennison and Professor Preece on the oxidation of copper alloys, information is given regarding the peculiar behaviour of silicon. Apparently, no silica is found in scales formed above about 850°C ., contrary to thermodynamic requirements, which insist that silicon oxidizes more readily than copper at all temperatures. It requires little ingenuity to devise a mechanism to account for the observation, but in the absence of any experimental evidence this is perhaps a more suitable place than the paper itself to discuss the matter.

It is possible that silicon goes into solution in the scale at the lower temperatures and, as it diffuses outwards, is oxidized to silica; at the higher temperatures silicon is prevented from entering the scale and is completely protected against oxidation because it cannot diffuse through the oxide layer. The main effect of the temperature on the scale appears to be to determine the proportion of cupric oxide present. Cupric oxide and silica both disappear from the scale at temperatures above 850°C .

It cannot be said that silicon is capable of dissolving in cupric oxide but not in cuprous oxide, because even when the former is present it is on the outside of the scale layer, so that silicon would have to enter the Cu_2O lattice. The latter is known to contain bivalent copper ions, balanced by lattice vacancies, and it is possible that temperatures which make cupric oxide unstable may have the same effect on cupric ions in the CuO lattice. It may be this effect of rising temperature which accounts for the failure of silicon to enter the lattice.

Whatever the mechanism, the results indicate that silicon

* K. Hauffe and H. Grunewald, *Z. physikal. Chem.*, 1951, 198, 248.

† N. B. Pilling and R. E. Bedworth, *J. Inst. Metals*, 1923,

29, 529.

‡ G.K.N. Research Laboratory, Wolverhampton.

accumulates at the metal surface, so that in effect an alloy of higher silicon content is being oxidized. Increase in silicon content from 2 to 3.5% increases the rate of oxidation above 800° C. (Figs. 8 and 9, p. 233). However, since silicon does not enter the oxide, oxidation depends on the rapid diffusion of copper through the silicon-enriched layer at the surface.

When the silicon-rich phase covers most of the surface, it may form a barrier to the entry of copper into the scale, and one can perhaps predict that a further rise in the silicon content beyond 3.5% would have the effect of decreasing oxidation, provided that melting is avoided. The increase in silicon content of the surface layer should have a similar effect in all copper-silicon alloys oxidized. At 850° C. oxidation will be very rapid at first, but will slow down when a continuous silicon-rich phase has been built up on the surface of the metal; this will occur earlier, the higher the silicon content of the alloy. Above 850° C. a liquid phase will be present as soon as about 5% silicon has accumulated in the surface layer.

Mr. J. CANTRELL* (Member): The results presented by Professor Preece and Dr. Lucas are of great interest. One point, however, causes some uncertainty, since some of the alloys tested were prepared by sintering, followed by working.

We have observed a tendency, particularly in mixtures containing two metals of widely differing melting points, for the sintered body to retain a very fine, continuous porosity, even when high density values are obtained. Although cold working may remove all evidence of this porosity and yield theoretical densities, a subsequent heat-treatment may cause certain of the original discontinuities to reappear. This effect can be seen in worked compacts of certain iron powders which, after heating in a protective atmosphere, are left in moist conditions. A network of internal corrosion can often be detected.

In the processing of molybdenum, heavy drafting of the sintered ingot during swaging may cause "lap-over" of the square section. This fin will apparently become a part of the body of the material and cannot be detected after a little further reduction in diameter. Often, however, the weakness will reveal itself during the annealing of the finished wire, even at diameters as small as 0.002 in., the reheating apparently causing "springing out" of the sealed fin.

We can visualize the possibility of such a mechanism in the experiments covered by the paper. Is it possible that the heating during oxidation testing may have caused partial reopening of the pores from the initial porosity of the sintered material? If, in Fig. 9 (Plate XXXI), the microsection has been cut at right angles to the direction of rolling, the nature of the internal oxidation may be a result of the mechanism which we have suggested. Difficulties experienced with residual porosity in our own work have been eliminated by hot pressing the powder mixtures to 100% density before working.

I should like to ask the authors if any tests were made on the sintered alloys, before working, to ensure that there was no trace of continuous porosity networks.

Professor PREECE and Dr. LUCAS (*in reply*): We must first apologize for the omission of the time factor from the Tables. This should be 50 hr.

With regard to the point raised by Dr. Kubaschewski concerning the two types of CoO layer, there is little doubt that the junction is coincident with the original metal surface. This was shown both by measurements and by markers in the form of the platinum supporting wires.

The pronounced peak in the oxidation/temperature curve for pure cobalt certainly raises several interesting questions and appears to have been missed by other investigators. We first noticed that the results obtained in the 60:1 turbine atmosphere at 900° and 1000° C. were almost identical. This suggested some alteration in the mechanism of oxidation in the region of the $\text{Co}_3\text{O}_4 \rightarrow \text{CoO}$ transformation, and it was decided to investigate this point by further tests, using pure

dry oxygen at much closer temperature intervals. The furnace was purged with nitrogen during the heating period. The reproducibility of the results is indicated in Fig. 2 (p. 220) either by the size of the point on the graph, or, at temperatures close to the peak where greater scatter occurred, by the small arrows.

In considering this temperature range, it seems relevant to mention Mme. Chaunevet's work† on the $\text{Co}_3\text{O}_4 \rightarrow \text{CoO}$ transformation, in which it is shown that the oxygen content of Co_3O_4 falls below stoichiometric requirements at approximately 800° C., gradually changing to CoO with an increased oxygen content before finally reaching the stoichiometric composition of CoO at about 1075° C. This result strongly suggests that, in our experiments, the complex transition was greatly influencing the mechanism of oxidation.

With regard to Mr. Davies' remarks on the oxidation curve for cobalt, we did find a difference between the results obtained in air and in oxygen, the former being much lower at 900° and 1000° C., but approximately the same at 800° or 1100° C. The results obtained after 24 hr. in the 60:1 atmosphere were:

°C.	Wt. increase g./cm. ²	°C.	Wt. increase g./cm. ²
800	0.013	900	0.029
1000	0.031	1100	0.103

and these may be compared with the values shown in Fig. 2.

His further statement that the sharp inflection in Fig. 2 is not indicated in the results obtained in the 60:1 atmosphere is surprising in view of the fact that the values at 900° C. (0.042 g./cm.²) and 1000° C. (0.045 g./cm.²) are almost identical, as is also the case in Fig. 2. Results in the intervening temperature range were not included in the Tables, since the peak had already been indicated in a detailed manner in Fig. 2. The oxidation of cobalt obeys the parabolic law irrespective of temperature, and Mr. Davies is incorrect in comparing results for 24 hr. in oxygen with those for 50 hr. in the 60:1 atmosphere. The experimental method used in this work has been shown to be satisfactory, since the shape of the rate/temperature curve in the 60:1 atmosphere was the same for times ranging from 24 to 120 hr. The fact that the layer of Co_3O_4 occupies only a small volume fraction of the total scale does not necessarily imply that this constituent may be ignored, since the rate of oxidation is controlled by the properties of the oxide rather than by its relative thickness.

It does not appear that the diffusion of cobalt ions through CoO is the rate-determining factor, as suggested by Mr. Davies, since, if this were true, one would not expect the oxidation rate at 1000° C. to be much lower than at 950° C., as is found to be the case, since at that temperature the scale also consists very largely of CoO.

Consequently, it seems feasible to us that of all the factors involved the most influential is that governing the transfer of oxygen into the CoO lattice. In the presence of a Co_3O_4 layer, the energy barrier for this movement might be replaced by a combination of a low barrier between the gas and the Co_3O_4 and a low transfer barrier between Co_3O_4 and CoO.

The question of the effect of spinel formation on the oxidation process is discussed by Mr. E. Ll. Evans. We would point out that the influence of a spinel is certain to be governed by the presence of other oxide layers. In the cobalt-chromium alloys, it is found in direct contact with the metal surface in association with CoO, whereas in the nickel-aluminium system a layer of aluminium oxide is interposed between the spinel and the metal, and this would be expected to provide a strong rate-influencing effect, as indeed is the case. The same reasoning may be appropriate to the cobalt-aluminium alloys, although no alumina layer was actually detected.

We would further draw Mr. Evans' attention to the fact that the paper by Hickman and Gulbransen to which he refers was published in 1947, whereas the statement of these authors that: "Our results do not indicate that the marked non-

* The Carborundum Co., Ltd., Trafford Park, Manchester.

† G. Valensi, *Métaux et Corrosion*, 1950, 25, 283 (reporting

results obtained by Mme. G. Chaunevet, *Dr. Thesis, Université de Caen*).

oxidizing property of the 80:20 nickel-chromium series of alloys may be explained on the basis of the formation of $\text{NiO} \cdot \text{Cr}_2\text{O}_3$, as postulated by Iitaka and Myake, but rather that long lifetime may be associated with the occurrence of Cr_2O_3 and the absence of $\text{NiO} \cdot \text{Cr}_2\text{O}_3$, was made by them in 1949.* In the best nickel-chromium-iron alloys, although Hickman and Gulbransen observed the presence of a small amount of spinel, the alloys formed Cr_2O_3 primarily.

While we would hesitate to make a general statement on the protective properties of spinels, no spinel has ever been shown to be more protective than a pure oxide film; furthermore, their flexibility in composition should not be quoted as a favorable property for confirming oxidation-resistance, since this may actually promote diffusion rather than prevent it.

With reference to Mr. Evans' request for further experimental details concerning the procedure for mounting scaled specimens, this is as follows: A metal cylinder, approximately 1 in. in dia. \times 1 in. high, is glued to a glass plate and the specimen placed inside in the required position. The cylinder is filled with N.P.A. Bakelite Cement, a thermosetting liquid. The mount is treated for about 1 hr. in a vacuum desiccator attached to a water-suction pump. This removes the occluded air in the scale and, on releasing the vacuum, the cement is forced into the pores of the scale. Heating to 80° C. overnight, followed by a final hardening at 120° C. for 1 hr., completes the mounting process. The specimen is then carefully polished by the usual methods.

Dr. Sachs' remarks on the cobalt-molybdenum and nickel-molybdenum alloys may be supplemented by noting that the molybdate is surrounded by an excess of cobalt oxide which may suppress the action of any free MoO_3 . As the temperature is increased, the molybdate will undoubtedly become more unstable, and the amount of free MoO_3 formed is such that coherent scale formation is impossible. We do not think that free MoO_3 was swept away by the air stream at the lower temperatures, since, had this been the case, it would have been found on the cooler parts of the apparatus, as at the higher temperatures.

Mr. Cantrell's contribution is very interesting. However, we feel certain that the relatively shallow zone of internal oxidation which we observed was not due to an effect similar to that which he mentions; the particles of oxide did not constitute a network at grain boundaries, nor was any weakness noticed in the remaining section of the alloy. The variation of the thickness of the internal oxide region was in accordance with theoretical considerations.

Dr. DENNISON and Professor PREECE (*in reply*): Dr. Kubaschewski points out that Valensi† has stated that in the reaction between copper and pure oxygen to form Cu_2O and CuO the relative thickness of the two oxide layers is independent of time. This observation is not in agreement with our experimental results. In either ordinary air or the simulated gas-turbine atmosphere, the percentage of cupric oxide in the scale increased with time, as shown in Fig. 4 (p. 231) of the paper under discussion. Moreover, during oxidation of copper in air at 650° C., the proportion of cupric oxide in the scale formed increased with time, as indicated in Fig. A.

In our opinion it is necessary to assume a change in the oxidation mechanism with temperature to account for the variation in the proportions of Cu_2O and CuO after different periods of oxidation. We found that from 850° to 600° C. an outer layer of CuO formed an increasing percentage of the scale with decrease in temperature. Consideration of the results obtained on the 2% aluminium and 2% silicon alloys (pp. 232 and 234) shows that oxygen must in some way diffuse inwards to cause an originally Cu_2O layer to be converted to CuO . The mechanism for this inward diffusion may be either the existence of anion vacancies in the CuO lattice or, as Dr.

U. R. Evans suggests, by way of gaps in the crystal structure of the CuO layer formed under these conditions.

Fig. B shows a distinct change in the relationship between rate constant and temperature for the high-conductivity copper oxidized in air. As a straight-line relationship exists from 1000° C. to between 550° and 600° C., presumably the mechanism of oxidation remains the same within this range. Above 900° C. no CuO exists in the scales, and therefore the

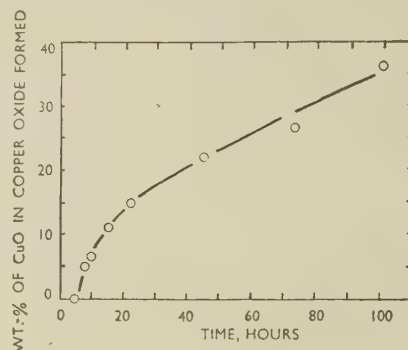


FIG. A

ruling factor will be the rate of outward diffusion of copper through Cu_2O . This mechanism presumably controls the overall rate of oxidation down to 500°–600° C. As shown in Fig. A., for a temperature within this range, the percentage of CuO in the scale increases with time. This may perhaps be explained by a dual process of film growth comprising outward diffusion of copper through Cu_2O and inward diffusion of oxygen through CuO . The relative rates of growth of

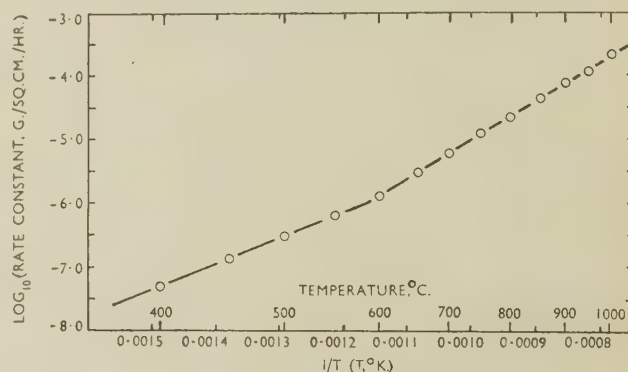


FIG. B

the films may be determined by the concentrations of copper and oxygen at the interface between the two oxide layers. Cu_2O alone will be formed until the concentration of copper at the scale surface falls below a limiting value, when the higher oxide will begin to form.

At 550°–600° C. there is a sudden decrease in the percentage of CuO formed in a given time, corresponding with the break in the relationship between oxidation rate constant and temperature. Zhuze and Kurchatov‡ suggest that there is a corresponding increase in the conductivity of the scale formed on copper at temperatures below 600° C.

This may be taken to indicate that below this temperature range the relative diffusion rates of copper through Cu_2O and of oxygen through CuO will be affected, with the result that

* J. W. Hickman and E. A. Gulbransen, *Trans. Amer. Inst. Min. Met. Eng.*, 1949, **180**, 519.

† G. Valensi, [*Proc.*] *Pittsburgh Internat. Conf. on Surface Reactions*, 1948, 156

‡ V. P. Zhuze and B. V. Kurchatov, *J. Eksper. Teoret. Fiziki*, 1932, **2**, 309; also *Physikal. Z. Sowjetunion*, 1933, **2**, 453.

greater proportions of Cu_2O will be found in the scales at temperatures immediately below this break than at those just above it. It may be that at these lower temperatures the rate of diffusion of oxygen inwards through the CuO layer is the controlling factor in overall oxidation rate, once the latter oxide has begun to form. Analysis of the scales formed after various periods of oxidation at 400° and 500°C . seems to suggest that a CuO outer layer is formed almost immediately on entering this temperature range, an observation which is supported by the work of Cruzan and Miley,* who detected CuO in films of the order of 100°A . thick at temperatures within this lower range.

It is obvious that further work is necessary on the composition of oxides formed on copper, particularly with regard to the effect of varying atmospheres.

In reply to Dr. U. R. Evans, we would point out that the investigations recorded in the paper were carried out in the period 1947-49 and have been available as a report of the British Non-Ferrous Metals Research Association since early in 1950. In this report a more detailed review of the literature was given. We believe that to enter upon a comprehensive review of the oxidation of metals for each new publication is impossible in view of the ground to be covered and the space available. A great many comparisons from previous work

could have been quoted with equal, if not greater, justification than those which Dr. Evans has brought forward.

Dr. Evans does not appear to have noticed that the ideas involved in the work of Hubrecht and de Brouckère on copper-beryllium alloys are very similar to those outlined in the present paper for the behaviour of the copper-aluminium series of alloys, but not repeated in detail for the copper-beryllium alloys. He does, however, provide an interesting alternative for the diffusion of oxygen inwards through CuO , but at first sight this does not appear to account for the conversion of a layer initially consisting of Cu_2O to one entirely of CuO .

The explanation offered by Dr. Sachs for the behaviour of the copper-silicon series unfortunately does not take into account all the experimental evidence. His assumption of solution of silicon in the scale in the lower temperature ranges is incompatible with the formation of pronounced subscale layers consisting of precipitated SiO_2 at temperatures below 750°C . (p. 233 of the paper). In addition, scale analysis shows that the silicon, when present in the scale, invariably exists as SiO_2 .

It appears that, contrary to Dr. Sachs' opinion, an explanation taking into account all the experimental evidence available will require some considerable degree of ingenuity.

Discussion

A Method of Determining Orientations in Aluminium Single Crystals and Polycrystalline Aggregates

By G. E. G. TUCKER and P. C. MURPHY

(*Journal*, this vol., p. 235.)

Dr. J. HÉRENGUEL † (Member) and M. P. LELONG ‡: We consider this method of determining orientations in aluminium and certain of its alloys very interesting, and to demonstrate its value would recall the applications of the etch-pit technique made by one of us (J. H.) with various co-workers during the last ten years.

As the authors point out, it is necessary to take into consideration the complications that may arise through simple or multiple truncations of the pits caused by impurities or deliberate additions to the aluminium. We have studied these etch-pits extensively on high-purity and commercial-purity aluminium (containing iron and silicon)§ and have identified the fundamental forms shown in Fig. A. We have



FIG. A.—Possible Truncations of an Etch-Pit.

confirmed, by taking sections perpendicular to the etched surface, that the centre of the elementary cube forming the hollow depression is always considerably above the surface being examined. Therefore, observation of the three edges of the basic trihedron is easy and accurate, thus removing all uncertainty arising from the use of truncated pits. Such observation is facilitated by utilizing certain characteristics of the microscope, e.g. a variable angle of incidence of the beam and a revolving stage.

The nature of the etching reagent and the conditions of

attack also have a marked effect on the degree of complexity of the pits. Moreover, the treatment undergone by the specimen before etching plays a part in modifying the number, size, and form of the pits. We are thus led to believe, in agreement with Mahl and Stranski, that the surface oxide layer plays a part in the attack. In particular, we have observed that washing in 10% caustic soda at 50°C . for several seconds after electrolytic polishing and before etching proper, generally has a beneficial effect. Of course, it cannot be considered valid to study crystal orientations by means of etch-pits on a sample polished only mechanically, as the cold-worked surface layer introduces a very considerable disturbing effect.

It is essential to use a microscope with a graduated rotating stage and a vernier. Precision is unlikely to be better than $\frac{1}{2}^\circ$. Most metallurgical microscopes, because of their construction, give with direct examination, with projection on a ground-glass screen, or with photography, a "left" image symmetrical with the object actually seen "right". It is essential to take this into consideration in the interpretation in order to obtain the correct orientation.

Use may be made of the measurement of the angles of the basic triangle in several ways:

(a) It is possible, as shown by Tucker and Murphy and by Kostron, to pass directly by calculation, by diagrams, or by tables, to the conventional Miller indices.

(b) The pole of the observed plane may be plotted on a stereographic projection. This is accomplished either by calculation of the angles made by the plane being studied

* C. G. Cruzan and H. A. Miley, *J. Appl. Physics*, 1940, **11**, 631.

† Director of Research to the Société des Tréfileries et Laminoirs du Havre and to the Compagnie Française des

Métaux, Centre de Recherches d'Antony (Seine), France.

‡ Research Assistant, Centre de Recherches d'Antony (Seine), France.

§ J. Héringuel, *Rev. Mét.*, 1949, **46**, 309.

with the three {100} planes, or by direct construction. Mr. Tucker and Mr. Murphy have established a particularly convenient double-entry table for such calculations.

(c) Simple models allow a rapid appreciation of the orientation being studied; we have used for this purpose a cut-out triangle (identical with the etch-pit), which is fitted into a hollow trihedron of Plexiglas.* It is even easier to construct the measured angles using a jointed triangle, in which is placed a trirectangular trihedron or a cube; this indicates immediately the required orientation (Fig. D, Plate XCIX). These methods are particularly useful for the study of progressive disorientations of a lattice. The law which this disorientation obeys is found unambiguously; this, as is well known, is not always the case with X-ray diagrams or stereographic representations.

We give below some examples of investigations which it has been possible to carry out satisfactorily by the use of etch-pits, and for which the classical methods employing X-rays could be used only with difficulty. The reagent was, basically, that of Lacombe, mentioned by the authors, modified only in respect of the concentrations of HCl and HNO₃. The temperature of etching was kept between 0° and 10° C., depending on the purity of the metal or the composition of the alloy.

(1) Twinned Structures Obtained in Semi-Continuous Casting.†

By this casting process a crystalline structure with a very high degree of order throughout the entire ingot is usually obtained in aluminium of about 99.5% purity. This is made up as follows:

(a) An outer zone, e.g. 5–15 mm. in thickness, with the ordinary columnar structure having a [100] fibre axis.

(b) The interior, which has a texture in which the basic unit is a flat plate composed of twin elements in contact on a (111) plane. A large number of plates are associated with one another, the twin plane of each being almost vertical, the [112] axis frequently containing the principal vector of the heat flow. In these units a progressive disorientation from

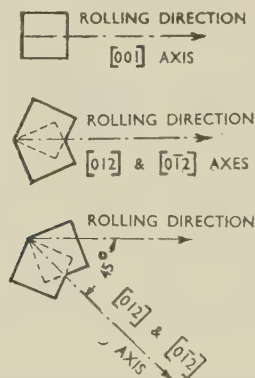


FIG. B.—Principal Orientations Shown by a Sheet of 99.5% Aluminium with a Very Strong Cube Texture.

plate to plate is often seen. At the junction of two such units, which are fairly strongly disorientated relative to one another, interpenetration of the type known as "felting" can be seen (Fig. H, Plate C). The constituents forming a separate phase are regularly distributed either at the junction of the plates (never on the twinning plane or in its immediate vicinity), or regularly spaced on the {100} planes. In section this structure has the appearance of a fish-bone, each bone being attached to a plate boundary. Fig. E (Plate C) shows a typical example.

Since the time of this investigation, a twin texture has been

found in aluminium ingots solidified in a permanent mould (Fig. F, Plate XCIX) and in ingots of very complex alloys (e.g. Al-Zn-Mg-Cu).

(2) Preferred Orientation After Annealing.

Products rolled from semi-continuously cast ingots tend to exhibit, on annealing, textures with a high proportion of

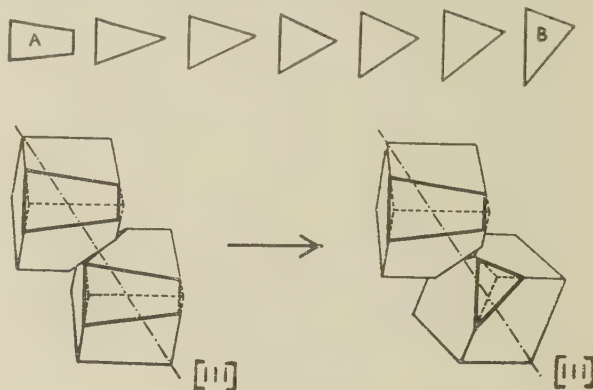


FIG. C.—Diagram of the Etch-Pits Shown on the Test-Piece Illustrated in Fig. K (Plate C).

A. Initial position in single crystal.

B. Final position, perceptibly twinned.

the cube texture. This has been studied in aluminium of 99.5% purity by means of etch-pits;* the orientations illustrated diagrammatically in Fig. B are based on statistical considerations. By this method it is also easy to estimate quantitatively the amount of cube texture and to determine its distribution on various scales (Fig. J, Plate C). This identification of the units on a large scale (whether in the cube texture or other relationship) is significant in connection with the surface markings which develop after deformation of the test-piece (orange-peel effect).‡

(3) Internal Disorientation of Grains Produced by Plastic Deformation.

Anomalies observed in the anodic oxidation of homogenized and cold-worked high-purity aluminium-magnesium alloys led to a study of the effects of plastic deformation on a single crystal.§ The disorientations were determined and measured by various micrographic methods used in combination: etch-pits, examination of oxide films in normal and polarized light, chemical "engraving", and observation of slip lines after deformation. The growth of deformation bands by progressive curvature has been clearly revealed, measurements of the relative orientations and dimensions of the bands and of the zones of curvature being carried out without difficulty. We have observed, as a result of increasing cold work, the appearance of multiple systems of alternating bands made up of short, strictly regular units, finally affecting the whole of the initial lattice. Fig. K (Plate C) shows a zone of curvature revealed by etch-pits. Fig. C illustrates diagrammatically, by means of some of the etch-pits observed, the transition from the initial orientation of the lattice to that of the band itself, by a plane curvature having a [111] axis of rotation common to the whole structure. The (110) plane containing this [111] axis forms the interface between the band and the initial lattice.

(4) Rate of Anodic Oxidation as a Function of Orientation.

In this investigation the orientations were again established rapidly and accurately by means of etch-pits.|| A marked

* J. Hérenghuel, *Rev. Mét.*, 1948, **45**, 505.

† J. Hérenghuel, *ibid.*, 1949, **46**, 309.

‡ J. Hérenghuel and G. Scheidecker, *ibid.*, 1949, **46**, 537.

§ J. Hérenghuel and P. Lelong, *ibid.*, 1951, **48**, 875; 1952, **49**, 374.

|| J. Hérenghuel and P. Lelong, *ibid.*, 1952, **49**, 374.

anisotropy has been established and measured. For the aluminium-3% magnesium alloy studied, the planes of maximum oxidation were around [111], those of minimum oxidation around [100]. For a c.d. of 27 amp./dm.² the relative difference was about 33%. More recent determinations have shown that this figure varies with current density. Fig. G (Plate XCIX) shows two neighbouring grains of different orientation carrying etch-pits and having, respectively, oxide films 50 μ and 57 μ thick. A transition zone can be seen extending over about 180 μ . Finally, etch-pits can be equally useful for indicating the variations in composition of a solid solution, for instance in the region of phases which have separated out in the cast structure.* By precipitation, or conversely, by homogenization, the distribution and density of the etch-pits can be changed, making it possible to follow the evolution of the structure. It may be noted that, in a cast alloy, the groupings of the pits follow, and thus delineate, preferred crystallographic directions which are traces of the {100} planes on which the phases precipitate, there being a composition gradient around each. These traces of the {100} planes, after etching, can be examined at low magnification in order to determine the grain orientation. Fig. L (Plate C) provides a good illustration of this in 99.5% aluminium.

These examples show the use which can be made of the etch-pit technique in the study of aluminium alloys in general. It would be valuable to extend its applications by finding etching reagents suitable for ferrous metals and alloys based on copper, &c.

The AUTHORS (*in reply*): The examples of possible applications of etch-pit methods cited by Dr. Hérenghuel and M. Lelong will be of great value to everyone interested in textural relationships in aluminium alloys, and it is to be hoped that their contribution will stimulate the wider use of such techniques.

It is interesting to note that mechanical methods of specimen preparation are regarded as unsuitable; although it is obvious that a very heavily worked surface layer could have a disturbing effect, we have observed perfectly formed etch-pits on pure aluminium samples polished mechanically. In our experience, moreover, the validity of the angular measurements is unaltered by such factors as surface strain, though it is undoubtedly true that ease of measurement and the perfection of the etch-pits can be affected.

Although desirable, it is not essential for the measuring microscope to be fitted with a graduated revolving stage; in fact, we prefer in some cases to lock the stage and instead to turn the eye-piece and cross-hair, the angular rotation being measured by an arm attached to the eye-piece and rotating around a co-axial graduated scale.

We agree that care must be taken to ascertain the relation between the observed image and the actual surface being examined, not only because of possible lateral inversion, but also because of possible rotation of the image. The microscope we used produced no lateral inversion, but a 90° rotation of the image.

We have recognized in the past the value of models in allowing a rapid appreciation of orientation, and the apparatus described by Dr. Hérenghuel and M. Lelong appears to be very convenient. It will be realized, however, that such methods are of qualitative rather than quantitative value and cannot be used for recording the results of investigations.

Professor P. LACOMBE,† Dr.ès Sci. (Member): The authors are to be congratulated, not only on their systematic study of

the effect on the shape of etch-pits of the composition of the etching reagent and of the metal itself, but on their method of deriving crystal orientation mathematically from the measured angles of the etch-pits on the surface. Thus modern micrography, profiting by Jacquet's development of the electropolishing technique, is getting nearer and nearer to orientation micrography, leading eventually to three-dimensional micrography. Classical micrography, which was limited to identifying the different phases of an alloy or to determining the crystal boundaries of a polycrystalline aggregate, retained the qualitative characteristics of a descriptive or morphological method. The growing use of etch-pits has greatly increased the interest of micrography, by conferring upon it the status of a quantitative method. Following on our first study,‡ a number of workers have made use of reagents producing etch-pits and have suggested variations in the composition of the reagent for study in

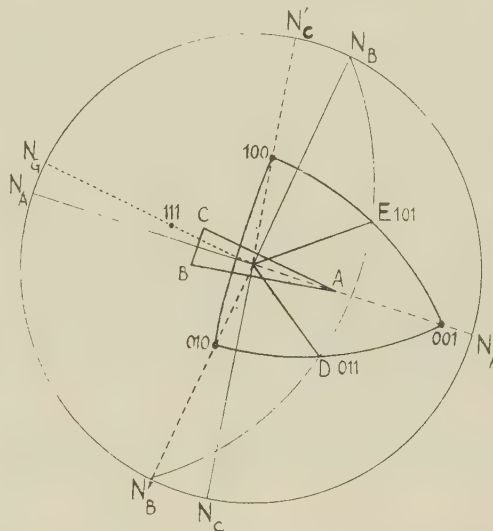


FIG. P.—Stereographic Projection for the Determination of the Orientation from the Direction $N_B N'_B$ of a System of Slip Lines. The great circle passing through the (101) and (011) poles (points E and D) must cut the basic circle at the same points as the direction $N_B N'_B$ of the slip lines.

various fields: investigations on commercial-purity aluminium and industrial alloys,§ electron microscopy,|| creep,¶ &c.

Great interest attaches to the authors' calculations, which are simpler than those of Kostron; ** in particular Table I, which gives values of the angles α , β , and γ , between the cube planes and the plane of micrographic section, as a function of the angles A, B, and C of a triangular pit, is extremely useful. These angles can then easily be plotted on the stereographic projection along the normals to the sides of the etch-pits, thus giving directly the (100), (010), and (001) poles.

In this connection I should like to recall that Beaujard †† and I have suggested a purely graphical method, an example of the application of which was given ‡‡ in relation to Fig. 17 of our earlier paper.§§ Fig. M (Plate C) shows the triangular pits, and Fig. P the corresponding stereographic projection. The procedure is as follows, using the attacked micrographic surface as the plane of stereographic projection.

(i) From the centre of the stereographic diagram are traced the directions parallel to the three sides of the etch-pit, and then the normals N_A , N_B , and N_C to these directions, which

156, 157 (discussion).

A. F. Brown, *ibid.*, p. 103.

¶ G. Wyon and C. Crussard, *Rev. Mét.*, 1951, **48**, 121.

** H. Kostron, *Z. Metallkunde*, 1950, **41**, 370.

†† L. Beaujard, *Thèse*, Paris: 1949.

‡‡ P. Lacombe, *Métalurgie, Corrosion-Ind.*, 1951, **26**, 392.

§§ P. Lacombe and L. Beaujard, *loc. cit.*, Plate V.

* J. Hérenghuel, *Rev. Mét.*, 1950, **47**, 29.

† Director, Centre de Recherches Métallurgiques de l'Ecole des Mines de Paris.

‡ P. Lacombe and L. Beaujard, *J. Inst. Metals*, 1947, **74**, 1.

§ J. Hérenghuel, *Rev. Mét.*, 1948, **45**, 505.

|| R. Castaing and A. Guinier, *Inst. Metals: Symposium on Metallurgical Applications of the Electron Microscope*, 1950,

are the loci of the poles of all planes which could produce surface traces parallel to the three sides of the pit. It is also possible, as Tucker and Murphy suggest, to draw the actual shape of the etch-pit, suitably orientated with respect to a reference direction.

(ii) There is superimposed on the stereographic diagram a standard projection of the {100} cube poles, with one such pole at the centre of the projection. By means of the small concentric circles of a Wulff net, this standard projection may be rotated in such a way as to cause the various {100} poles to lie on the three normals to the etch-pit sides. The crystal orientation is then determined.

This construction is similar to that employed to determine the orientation of a crystal from the traces of slip planes, or of orientated needles of a precipitated phase in a solid solution (Widmanstätten structure). An identical method has been used for the case of crystals containing twinned crystals developed on at least three different {111} planes of the matrix crystal.*

The only difficulty of the graphical method lies in the choice of the axis of rotation which will bring the poles of the standard projection to lie on the normals to the sides of the etch-pit. This amounts to defining the relative initial position of the standard projection with respect to the stereogram of the crystal. Three solutions leading to the same result are possible, according as to whether in rotating the standard projection, the (100) pole originally at the centre is moved along the normal N_A , N_B , or N_C . To increase the accuracy of the graphical method it is desirable to choose the position which requires the least angular rotation (case (d) of Fig. Q, which represents a typical construction).

Several other points must be taken into consideration in order to get the best results and to avoid complete dependence on the angles A , B , and C , values for which may be inaccurate if the sides of the etch-pit are not strictly linear.

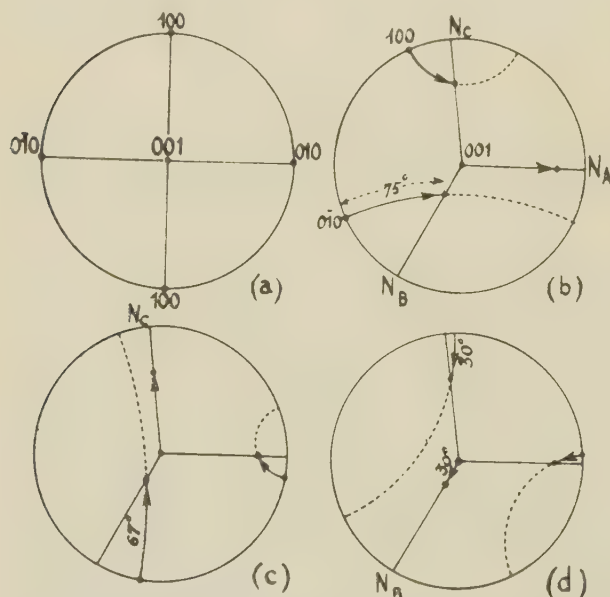


FIG. Q.—General Method of Determining Orientation by Rotation of the Standard Projection of the {100} Poles (Fig. Q (a)) to Bring the Three {100} Poles into Coincidence with the Three Normals N_A , N_B , and N_C to the Sides of the Etch-Pit.

In practice, accuracy in determining the (100), (010), and (001) poles depends largely on the size of the three angles A , B , and C , being greatest when these are of the same order of magnitude. If one of them approaches 0° or 90° , a con-

siderable error can be introduced in estimating the position of two poles.

The example given in Fig. P has been specially chosen to make this point clear. The angle A (14°) can be measured with great accuracy and reproducibility on several neighbouring etch-pits, but a more difficult problem is presented by

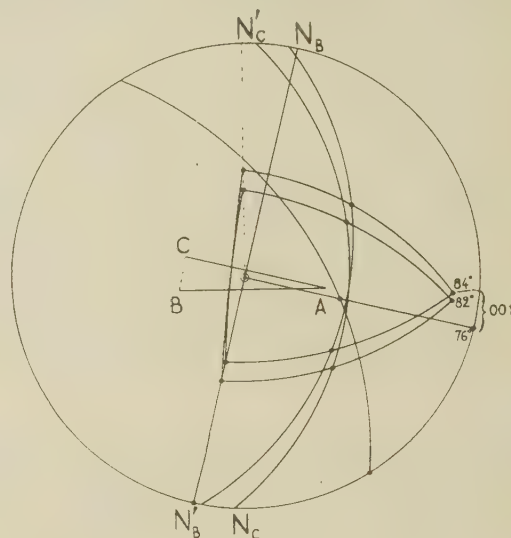


FIG. R.—Illustrating the Large Displacement of the (100) and (010) Poles, in Comparison to the (001) Pole, Resulting from Inaccuracy in the Values of the Angles B and C of the Etch-Pit. Angle A is assumed to be constant and $= 14^\circ$.

angles B and C , which are both in the neighbourhood of 90° . The shortness of BC , and above all the curvature of sides AB and AC make accurate measurement difficult. Thus, the value of angle B measured on several etch-pits varies from 76° to 84° . Fig. R shows the stereographic plot for the three values, 76° , 82° , and 84° , of angle B . While the (001) pole suffers a relatively small displacement, it is far otherwise for the (100) and (010) poles.

In these difficult cases useful verification can be obtained either from the slip-band directions or from the [100], [010], and [001] directions of the three edges of the cubic pit. These can be derived from the three lines of intersection of each pair of etch-pit faces. This is one of the reasons for trying to produce etch-pits of sufficient size to be observed with a low-power lens of great depth of focus. It is then possible to focus at the same time on the unattacked surface and on the bottom of the etch-pit.

It can be clearly seen in Fig. P that one of the $\langle 100 \rangle$ lines of intersection almost bisects angle A . Therefore angles B and C should be approximately equal to $\frac{180^\circ - 14^\circ}{2} = 83^\circ$.

Another graphical verification is based on the direction of the slip lines, which are traces of the {111} octahedral planes. In Fig. M (Plate C) the slip lines are almost perpendicular to the side AC of the etch-pits. This direction is plotted on the stereographic diagram, where in this particular case it falls on the straight line $N_B N'_B$. It is then necessary to construct the (111) plane, which gives the trace $N_B N'_B$. This plane is represented by a great circle, on which it is sufficient to know two points. If the (100), (010), and (001) poles are joined two by two by arcs of great circles, one of the poles (110), (101), or (011) can be fixed on each arc. The (111) plane is determined by a great circle passing through two of its {110} poles, such as D and E , situated at 45° from (100), (001), or (010) (Fig. P). If the position of the (100) poles is correct, the great circle representing the (111) plane must cut the basic circle of the stereographic projection at the same

* D. Whitwham, M. Moufflard, and P. Lacombe, *Trans. Amer. Inst. Min. Met. Eng.*, 1951, **191**, 1070 (discussion).

points $N_B N'_B$. By trial and error it is thus possible to determine with very great accuracy the exact position of the {100} poles, even in a case as unfavourable as this.

It is preferable to plot the (100), (010), and (001) poles on extensions of the N_A , N_B , and N_C normals drawn from the centre O of the projection on the three sides of the etch-pits. In this way the spherical triangle formed by joining the (100), (010), and (001) poles by arcs of a great circle, is orientated in a similar manner to the etch-pit. Moreover, the [100], [010], and [001] directions and also the [110] direction are parallel to the various intersections of the etch-pit faces among themselves or with a slip plane. This similarity of shape and orientation makes the interpretation of the stereographic diagram much easier, especially when trying to determine the relative orientation of two adjoining crystals.

It is in this last case that the use of etch-pits presents most interest, because the orientation can be determined even when the size of the adjoining crystals is extremely small. X-ray methods would necessitate special techniques, such as the microbeam used by Fournier* and by Hirsch and Kellar,† or lengthy exposure times. As an example, mention may be made of the study of so-called "insular crystals",‡ small crystals enclosed within a very large crystal developed either during recrystallization after critical cold working, or by secondary recrystallization. Such small crystals have an orientation closely approaching that of the enveloping crystal, or are exact twins of it.

A characteristic example of these two types of crystal is given in Fig. 5 of the paper by Lacombe and Berghézan.‡ A

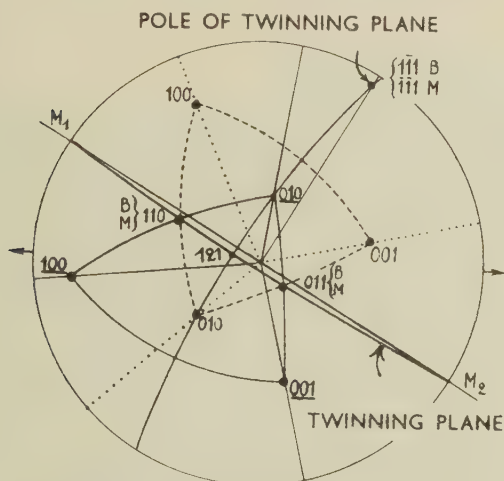


FIG. 5.—Stereographic Projection for the Determination of the Orientation of an Insular Twinned Crystal M in Relation to a Large Crystal B .

Full-line spherical triangle: {100} poles of crystal B .
Dotted-line spherical triangle: {100} poles of crystal M .

large crystal B contains both an insular crystal A of closely similar orientation and an insular crystal M twinned with respect to B (Fig. N, Plate C). It will be noticed that the etch-pits on crystals B and M are almost symmetrical with respect to the rectilinear portion of the grain boundary separating M from B , which is in fact the (111) twinning plane common to both.

As before, it is easy to construct from the etch-pit angles the stereographic projection of the three {100} poles of the two crystals M and B (Fig. S). Also in marking on this projection the direction M_1M_2 of the rectilinear boundary of

crystal M , considered as the twin boundary between B and M , the twin relationship between B and M is clearly confirmed. Indeed, the normal N to the direction M_1M_2 passes through a pole P common to the stereographic projection of M and B and having the same (111) indices. The great circle situated at 90° from P can be held to represent the twin plane of B and M , since it passes through three poles common to B and M and having the same (110) indices. This is adequate to define unambiguously the twin relationship. Finally, it may be noted that in this case the twinning plane is at about 4° from the perpendicular to the micrographic surface; this is in agreement with the relatively symmetrical shape of the etch-pits with respect to the rectilinear boundary of the twin.

These examples show the importance of the information that may be obtained from etch-pits when stereographic methods are applied to the interpretation of X-ray diagrams. One further very promising development of the etch-pit technique may be mentioned. This is its use to reveal macromosaic or polygonization boundaries in crystals of pure aluminium§ or of its solid solutions. In general the etch-pits do not concentrate on boundaries between two crystals of differing orientation. Rather do they group themselves preferentially at the "intragranular" boundaries associated with polygonization, where it has been suggested by Orowan and by Cahn|| that dislocations collect. Thus, it might be visualized that each etch-pit originates at the site of a dislocation. This led Read and Shockley¶ to suggest that the minimum distance between two etch-pits on a polygonization boundary could be used to determine the very small difference of orientation between adjacent sub-grains. Fig. O (Plate C) shows a crystal of pure aluminium whose surface is parallel to the (111) plane, divided by polygonization boundaries into several sub-grains, the degree of disorientation between which can be precisely determined from the very distinct etch-pits. To conclude, in this last case also the micrographic method has distinct advantages over X-ray methods. It is possible, indeed, to determine the disorientation between two selected sub-grains and to make a systematic study of the distribution of such disorientation between the several sub-grains of a large crystal.

The AUTHORS (*in reply*): Professor Lacombe's remarks are of great interest, especially in defining the uses and limitations of etch-pit techniques.

We agree that the accuracy of positioning of the poles plotted from measurements made on triangular etch-pits is, to a large extent, governed by the shape of the triangle, and we have carried out some calculations which are relevant to this point.

The partial differential coefficients of α , β , and γ may be calculated with respect to angles A , B , and C from equations (5) (p. 239) of our paper. These derivatives are of two general forms, such as:

$$\frac{\partial \alpha}{\partial B} \Big|_C = \frac{\sec^2 B}{2 \tan B \tan \alpha} \dots \dots (1)$$

and

$$\frac{\partial \alpha}{\partial B} \Big|_A = \frac{\partial \alpha}{\partial B} \Big|_C - \frac{\partial \alpha}{\partial C} \Big|_A \dots \dots (2)$$

It can be shown that when $C \geq B \geq A$ (the case considered in the paper) the largest of the eighteen possible derivatives, arithmetically, is:

$$\frac{\partial \gamma}{\partial B} \Big|_A = \frac{\sec^2 B}{2 \tan B \tan \gamma} \dots \dots (3)$$

This expression tends to infinity as C tends to 90° , and has a minimum value of $\frac{\sqrt{3}}{2\sqrt{2}}$ when $A = B = C = 60^\circ$. If these

calculations are applied to the example cited by Professor

* F. Fournier, *Rev. Mét.*, 1949, **46**, 360.

† P. B. Hirsch and J. N. Kellar, *Proc. Phys. Soc.*, 1951, [B], **64**, 369.

‡ P. Lacombe and A. Berghézan, *Métaux et Corrosion*, 1949, **24**, 1.

§ P. Lacombe and L. Beaujard, *loc. cit.*

|| R. W. Cahn, *J. Inst. Metals*, 1949–50, **76**, 121.

¶ W. T. Read and W. Shockley, *Phys. Rev.*, 1950, [ii], **78**, 275.

Lacombe in Figs. P and R, it is found that if $A = 14^\circ$, $B = C = 83^\circ$, then

$$\left. \begin{aligned} \frac{\partial \gamma}{\partial B}_A &= 4.01 \\ \frac{\partial \alpha}{\partial B}_A &= 0 \\ \frac{\partial \beta}{\partial B}_A &= -4.01 \end{aligned} \right\} \dots \dots (4)$$

Thus, neglecting errors in the positions of the radii (which, in any case, affect only the (001) pole), the errors in the (100) and (010) poles are approximately four times the error of measurement of angle B , while the (001) pole is not affected by the error of angle B .

The development of straight-sided etch-pits is, of course, one of the greatest practical difficulties in any method involving angular measurements. The only solution appears to lie in the development of reagents which give a "clean" crystallographic attack. If this is impracticable in any particular instance, then the specimen may have to be regarded as outside the scope of the method; it is in such doubtful cases that useful information can be obtained from observations of the positions of the cube edges. It can be shown that the bottom edges should appear perpendicular

to the opposite etch-pit sides, and this property may enable the true direction of a curved side to be determined with greater accuracy. This relationship has, of course, been assumed by Professor Lacombe in calculating angles B and C .

As Professor Lacombe says, slip lines can in certain circumstances provide valuable data for correcting slightly inaccurate measurement or plotting. This is especially true when slip lines which are almost parallel with the shortest side of the etch-pit are present on the specimen. If, however, the only slip lines available are almost perpendicular to the shortest etch-pit side, they are of little value, as alteration of the basal angles (B and C) of the etch-pit will merely cause the {111} pole to move along the radius normal to the slip lines (or across it at a very shallow angle). In this case no accurate estimate of angles B and C corresponding to a "best" fit of the {111} pole can be obtained.

This limitation in the use of slip lines may thus be particularly inconvenient if only one family of slip lines has been developed on the specimen; if, however, three or four families of slip lines are present, then at least one of these will serve as a check. Ideally, all four families of slip planes should be developed, but the practical difficulties involved may be very great, especially in sheet, unless the orientation is such that all the slip lines can be made to appear without undue working of the specimen.

Discussion

Corrosion of Aluminium Alloys*

Dr. U. R. EVANS,† M.A., Sc.D., F.I.M., F.R.S. (Member): I am particularly interested in the fact that Mr. Metcalfe attributes the absence of failure in H15-WP to the attack turning in a direction parallel to the specimen face. Mr. Farmery, working with me on aluminium-magnesium alloys in a state more sensitive than would occur in practice, finds that occasionally a specimen may have an abnormally long life (perhaps 1000 times the normal value), and this also seems to be due to the attack spreading sideways, instead of across the specimen. But the phenomenon should not necessarily be regarded as desirable. If the crack turns along a plane parallel and close to the surface, and if the voluminous corrosion product is formed within the crack, the expansion may dislodge the outer layer. Such cracking off of flakes from the surface was, I believe, often met with at a time when wrought iron was an important structural material, since here corrosion tends to follow zones parallel to the surface. The cause of the difference between the behaviours of the Q (quickly corroding), R (resistant), and V (very resistant) zones found in wrought iron is being studied in my laboratory by Mr. Chilton.

Mr. Metcalfe uses his results to test a view, now held in certain quarters, that it is possible, by observations made during relatively short-time experiments, to calculate a thickness which will ensure that the specimens will last for ever. He makes some salutary observations which should be pondered by anyone inclined to adopt this "hope of eternal life" for aluminium alloys. He notes after 12 months' exposure "severe local foliation," constituting "a new type of attack, the incidence of which was much delayed and appeared to be progressing rapidly." This evidently could not have been foreseen from observations at the outset, and it will be recollected that Dr. Vernon,‡ in his early work on aluminium, also noted sudden and unpredicted acceleration in the oxidation after all action appeared to have ceased.

However, quite apart from these special cases, conclusions

based on interpolation should always be regarded as dangerous. A set of experimental points offered on the early part of a time/strength study may fall, within experimental error, upon a curve which becomes asymptotic to a horizontal line, and may seem to indicate a strength-loss which will never be exceeded even after an infinitely long exposure. However, the same set of points will probably fall equally close to another curve which becomes asymptotic to a *sloping* line, which would seem to indicate that the loss of strength will never cease. In general, the expression defining the slope of an asymptotic curve will contain transient and time-independent terms. The former are dominant in the early stages, and the latter in the later stages. Measurements made in early stages will furnish no idea of the value of the time-independent term, since it will be swamped by the effect of the transient terms. Thus, it is impossible to say whether the time-dependent term is negligibly small or large enough to become important in the later stages when the transient terms have lost their importance. In the latter case, a slow weakening will continue indefinitely.

In a matter where great expense, and even loss of life, may result from structural failure, it would be altogether wrong to conceal the opinion that the "eternal life" belief is a dangerous one. It is satisfactory to note that Mr. Metcalfe seems to hold very much the same opinion.

Mr. R. CHADWICK,§ M.A., F.I.M. (Member): Dr. Brenner and Mr. Metcalfe have adopted somewhat unusual conditions for stress-corrosion testing. In carrying out such a test the use of a highly aggressive corroding medium is undesirable because, if the medium is one causing severe attack on the unstressed specimens, the effective area of cross-section will change during testing, and stress per unit area will thus be far from constant. It is therefore preferable to employ neutral salt solution, or even distilled water, as the corroding medium.

When, in the plotted results of stress-corrosion tests in

* Joint discussion on the papers by P. Brenner and G. J. Metcalfe (*Journal*, this vol., p. 261) and by G. J. Metcalfe (this vol., p. 269).

† Reader in the Science of Metallic Corrosion, Cambridge

University.

‡ W. H. J. Vernon, *Trans. Faraday Soc.*, 1927, **23**, 154.

§ Assistant Research Manager, Imperial Chemical Industries, Ltd., Metals Division, Birmingham.

acidified salt solution (Fig. 5, p. 267) the curve for stress-corrosion in tension is compared with that for unstressed specimens subjected to a similar corrosive environment, the difference is found to be about 20% in terms of stress. Having regard to the authors' statement (p. 265) on the large observed differences in degree of attack on any one alloy, and their figure of $\pm 20\%$ for the scatter range in determinations of residual tensile stress on corroded specimens, it is doubtful whether Fig. 5 can be regarded as providing any really conclusive evidence that the applied stress significantly affects the rate of corrosion, and indeed the authors do not specifically make any claim that there is such an effect. However, they subsequently discuss the behaviour of the alloys in stress-corrosion as if a real effect were in fact established, and in both the synopsis and the final conclusions a relationship is defined between susceptibility to stress-corrosion and the degree of cold work. The indirect recognition of a stress-corrosion effect is contrary to the evidence of the experimental work, and is likely to be very misleading when the synopsis, or the comments and conclusions, are read without a detailed study of the whole paper.

In regard to the description of the test itself, it is not clear what is meant by "1.2% hydrochloric acid by weight". Is this the content of HCl or of a concentrated solution of HCl? In addition, the volume of corroding medium relative to the surface area of specimens immersed should preferably be stated.

Since even very small amounts of copper may significantly affect corrosion, it would have been most desirable to have determined this element in chemical analysis of the alloys.

Dr. F. A. CHAMPION,* A.R.C.S., F.I.M. (Member): Undoubtedly the most reliable method of assessing the behaviour and life of a metal under given corrosion conditions is direct assessment under the natural conditions, but this is often impractical, since the natural lives required are usually far in excess of the time that can be allowed for obtaining the information. We are therefore faced with the alternatives of accelerating the corrosion process or making observations over relatively short periods and extrapolating from them. Evidently, extreme use of either method is likely to invalidate the conclusions reached, and it seems more appropriate to combine the two methods, each in moderation. Extrapolation is commonly used for rectilinear corrosion/time curves and, in view of the experimental evidence† of the applicability of the exponential equation to aluminium and its alloys under a considerable range of conditions, it seems reasonable to employ extrapolation in assessing the parameters of this equation. These parameters are particularly useful in comparing alloys or conditions in the laboratory, where reasonably accurate assessment under controlled conditions can be made. With natural exposure, uncontrolled variation of the conditions occurs, and the steps in Dr. Vernon's curve to which Dr. Evans (p. 738) referred were evidently due to this cause,‡ the effect decreasing as film formation on the metal proceeded. Where mechanical properties are to be assessed, relatively thin specimens are required to attain the accuracy desirable for assessing the parameters of corrosion/time curves. Mr. Metcalfe's paper is particularly valuable in giving results of direct interest to the structural engineer, since his metal was just thick enough to be within the engineer's common range, while natural exposure in a wide variety of conditions was employed. Unfortunately, these factors, and the rather wide scatter in the initial mechanical properties, rendered most of the results too insensitive for use in testing the applicability of the exponential equation. Assuming the equation to hold, however, the results from the conditions giving the most severe corrosion did permit the calculation of the parameters. It is encouraging to note that Mr. Metcalfe's calculations on this basis gave for the worst alloy the same theoretical minimum thickness (0.060 in.) as my own.

I feel that the application of the data obtained on this basis to service problems should have the object not only of achieving economy of material by avoiding unnecessary allowances for corrosion, but also of demonstrating the false economy of using metal which is too thin. Taking as an example the thickness of 0.06 in. mentioned above, it is evident that metal 0.072 in. thick will have far more than twice the life of metal 0.036 in. thick. More precise application of these results to design requires the inclusion of an appropriate safety factor, the assessment of which can come only from experience, as with other metals. The fact that one specimen at Sheffield suffered a loss of strength three times the average cannot be taken as representative of scatter liable to occur in service, where the greater cross-sectional area of structural members will have a somewhat similar effect to the averaging of results from these $\frac{1}{2}$ -in.-wide specimens. I feel, therefore, that Dr. Evans need not fear that an increased risk will result from the application of the exponential equation, provided that the application is made intelligently, including recognition of the fact that under some conditions the exponential equation does not hold. In the latter cases other measures are desirable. Thus, the few aluminium alloys which are susceptible to stress-corrosion or exfoliation should be protected under severe exposure conditions by cladding or spraying, to which Mr. Metcalfe has referred.

The second paragraph of Mr. Metcalfe's introduction (p. 269) is liable to be misleading. As far as I am aware, the only useful quantitative data on the initial logarithmic phase of film formation (on film-free metal) was obtained by Steinheil.‡ The work quoted in that paragraph is concerned with the later exponential phase. I should also like to have Mr. Metcalfe's views as to whether the surprisingly greater attack at Christchurch by total as compared with partial immersion was due to contamination of the water in the former case, for example with heavy metals.

The paper by Dr. Brenner and Mr. Metcalfe gives valuable new information on the effect of zinc on the microstructure of the aluminium-5% magnesium alloy, and I should like to ask whether the incomplete boundary observed on ageing homogenized specimens (p. 263) was due to inadequate ageing time. It is much more difficult, however, to extract useful information from the results of their corrosion tests. Thus, Fig. 12 (Plate XXXVIII) of the unaged alloy 4 shows pitting at least 15 mils deep, which is described as "heavy", whereas Fig. 14 (Plate XXXVIII) of aged alloy 4 shows pitting 5 mils deep, which is described as "severe". On p. 266 reference is made to intercrystalline attack in Fig. 17 (Plate XXXVIII), but not in Fig. 14, whereas the photomicrographs tend to show the reverse, though there is very little in either case.

There is doubt as to whether the aluminium-5% magnesium alloy is susceptible to stress-corrosion in the practical sense (e.g. the absence of stress-corrosion failures in extensive Naval use), and it is unfortunate that this paper should describe tests which I feel, for the reasons given below, do little more than confuse the issue.

(i) The corrosion medium has a pH below 1, and is, therefore, too far removed from natural exposure conditions to give useful quantitative data.

(ii) A specimen suffering uniform corrosion without any type of selective attack would bend under load owing to the reduction in cross-sectional area, and therefore "endurance for limiting deformation" gives no information on stress-corrosion susceptibility.

(iii) It is not clear whether all the aged alloys failed by fracture or whether some failed by bending.

It would be useful if the authors could give information or comment on the following points:

(1) What were the copper contents of the alloys?

(2) It is concluded (p. 265) that increasing zinc content produced no improvement in corrosion-resistance of the aged and unaged alloys. Figs. 2 and 3 (p. 265) suggest that

* Research Laboratories of The British Aluminium Co., Ltd., Gerrards Cross, Bucks.

† F. A. Champion, *Metal Ind.*, 1948, 72, 440, 463.

‡ A. Steinheil, *Ann. Physik*, 1934, [v], 19, 465.

increasing zinc content reduced the effect of ageing on the loss of mechanical properties.

(3) A reference to experimental work on the relation between "electrolytic potentials" and cold work on these alloys (as mentioned on p. 267) would be useful.

Mr. E. A. G. LIDDIARD,* M.A., F.I.M. (Member): The most important fact emerging from the papers by Dr. Brenner and Mr. Metcalfe is the influence of structure on the corrosion and stress-corrosion behaviour of aluminium alloys. It is quite clear from Mr. Metcalfe's paper that the relatively good behaviour of the HE15 material compared to that of HE10, is due to the structure of the former, which has caused the corrosion to take place along planes parallel to the surfaces of the original extrusion. This layer type of corrosion ensures that the effect on mechanical properties is at a minimum. More recent results, obtained from work which Miss W. A. Bell has been carrying out at Fulmer, confirm that once this layer corrosion has reached a certain depth it then proceeds at a much increased rate, and there is no real doubt that the HE10 material is superior to the HE15 when exposed to severe industrial atmospheres. I am not at all sure that the results given in the paper by Dr. Brenner and Mr. Metcalfe can be ascribed to the effect of cold work on structural directionalities. If Figs. 8 and 17 (Plate XXXVIII) are examined, it will be seen that there is a marked tendency for the grain boundaries to be elongated in a direction parallel with the surface, and this probably influences the spread of corrosion crevices so that they are relatively less harmful to the mechanical properties of the test-piece. This effect of cold work in reducing the rate of corrosion damage may therefore have nothing to do with precipitation at grain boundaries. The statement on p. 267 that "bending stresses in service are much more dangerous than tension stresses if they are associated with corrosion attack", needs qualification in view of the results of some experiments started by Mr. Metcalfe when he was at Fulmer, and which are described in greater detail in a paper by Miss Bell and myself.† Typical results are shown in Table A. Some of these were on sheet material,

TABLE A.—Influence of Structure on Stress-Corrosion Behaviour of H15 Aluminium Alloy, Using Different Methods of Testing.

Specimens sprayed daily with 3% NaCl solution.

Type of Test	Average Time to Fail Under Stress of 20 tons/in. ² , days					
	Extrusions			Sheet		
	Direction of Stressing	Mn-free	Mn-contg.	Mn-free	Mn-contg.	Thickness, in.
Direct-Tension	Longitudinal to extrusion direction	46	60	2 3	2 5	0.2 0.1 0.05
	Transverse to extrusion direction	5	4	2	2	
Four-Point-Load Bend Test	Longitudinal to extrusion direction	>320	>320	9 7 10	97 13 5	0.2 0.1 0.05
		12 *	38 *	0.1
				

* Sheet rolled from extruded bar.

and some on extrusions. In the experiments on sheet the bending was by four-point loading, and the top surface of the specimen was in tension and the bottom in compression. The specimens were in a covered unheated hut and were sprayed daily with a 3% NaCl solution. The times to failure of the H15 sheet, with and without manganese, were very much shorter in direct tension than in bending. I cannot explain why this should be so, unless it is that the directional

effects become more marked in bending than in direct tension, and it may be significant that the alloy containing manganese shows a greater disparity between direct tension and bending than the manganese-free alloy.

Turning to the behaviour of extrusions, no failure by stress-corrosion occurred in either alloy in a bend test in which the specimens were cut longitudinal to the direction of extrusion. In direct tension, however, even longitudinal specimens failed in 46–60 days, but specimens cut transverse to the direction of extrusion failed in 4–5 days. It is only fair to state, however, that there is a fundamental difference in the

TABLE B.—Stress-Corrosion Tests on Coated H15 Aluminium Alloy Sheet 0.036 In. Thick.

Specimens sprayed daily with 3% NaCl solution.

Type of Coating	Stress, tons/in. ²	No. of Days to Fracture
Sprayed: Commercial Al (99.7% purity) Al-1% Zn Zinc	18	>300 not broken
	15	>219 not broken
	18	>300 not broken
	15	>219 not broken
	18	129
Zinc paint	15	132
	18	56
Not protected Shot-blasted surface	15	84
	18	14
	15	38

specimens, the bend specimens were, of course, flat with rectangular cross-section, whereas the direct-tension specimens were circular, and penetration by corrosion at two of the sides would not be delayed by the structural inhomogeneity. In case the layer corrosion and stress-corrosion of the H15 aluminium alloy present too depressing a picture, I should like to quote some recent results (Table B) which show that the provision of a sprayed anodic coating on H15 sheet appears to be completely effective in preventing stress-corrosion, and so far as I know there have been no cases of stress-corrosion failures of clad Duralumin-type sheet. The spraying in this case was done with a powder pistol. It will be seen that zinc spraying, which in this case was only 0.002 in. thick, increased the life by some four to nine times. A metallic zinc paint was rather less effective, but still showed an improvement. These particular tests were carried out using cantilever bending, and not the four-point-loading specimens referred to previously. I should again like to emphasize that these results were obtained on laboratory tests using salt spray, and probably do not represent the behaviour of the material in practice. However, it is clear that anodic protection is effective in preventing stress-corrosion of this type of alloy, and may therefore be highly desirable in certain structural work.

Mr. J. C. TUCKER,‡ B.Sc., A.I.M. (Junior Member): The bending stress-corrosion tests on the unaged and aged 5% magnesium alloy without zinc are illustrated graphically in Figs. 4 (a) and (b) (p. 266) of the paper by Dr. Brenner and Mr. Metcalfe, the initial bending stress being plotted against the time to failure. If we imagine two alloys of widely different tensile properties stressed at the same value under the same conditions of corrosion, and these alloys are attacked at the same rate, then the stronger material will have the greater endurance, since stress-corrosion cracks will have to progress further before the cross-sectional area has been reduced sufficiently for the tensile strength of the material to be exceeded. The alloys in Fig. 4 have been given between

* Director, Fulmer Research Institute, Stoke Poges, Bucks.

† E. A. G. Liddiard and (Miss) W. A. Bell, *J. Inst. Metals*,

1953–54, 82, (9), 426.

‡ Aluminium Laboratories Ltd., Banbury.

0 and 50% cold reduction, and exhibit widely different tensile properties, as shown in Fig. 1 (a) (p. 264); the curves in Fig. 4 might be of greater interest, therefore, if instead of plotting the actual stress against endurance, this stress was represented as a percentage of the 0.1% proof stress. If this is done for Fig. 4 (b), illustrating the aged alloy, the relative positions of the graphs are altered as shown in Fig. A. The alloy with 30% cold reduction would still remain of lowest resistance but that with no cold reduction would show the greatest resistance, and the graphs for alloys with 10% and 50% reduction with approximately equal resistance would fall between the graphs for 30% and 0% reduction. Similarly, in Fig. 4 (a), the differences between the alloys would be not nearly so marked as is shown. Referring still to Fig. 4 (a), we have, at Banbury, carried out bending stress-corrosion tests in a similar manner to that described by the authors. Specimens yielded throughout the tests without, however, showing a marked decrease in tensile properties over unstressed specimens after one year's exposure. Fig. 4 (a) indicates that the alloys possess widely different stress-corrosion properties, and we should be interested to know,

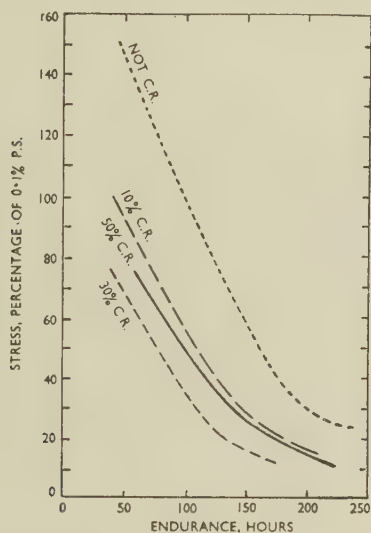


Fig. A.—Bending Stress-Corrosion Tests on 5% Magnesium Alloy Aged at 70°C. (Replotted curves of Fig. 4 (b) of Brenner and Metcalfe's paper.)

therefore, whether these specimens were tensile tested after stress-corrosion testing, to determine whether any marked loss of properties was observed as compared with unstressed specimens.

The influence of cold reduction on the corrosion-resistance of the cold-worked and aged alloy without zinc is of interest. The 5% magnesium alloy has useful tensile properties after cold reduction of the order of 30%. However, this alloy had the poorest resistance of the alloys tested by the authors. They have shown that sheet tested in the aged condition after 50% cold reduction has a superior resistance to stress-corrosion as compared with sheet tested in the aged condition after 30% cold reduction, and have correlated this behaviour with the distribution of the precipitate, there being more general precipitation in the alloy cold-reduced 50%. This indicates the desirability of obtaining a property level corresponding to a cold reduction of the order of 30%, by a low-temperature heat-treatment after heavy cold reduction, i.e. by temper-annealing rather than by temper-rolling. I can amplify this by referring to some work carried out at our Kingston Laboratories on a 5.5% magnesium alloy in the half-hard condition. The material was produced by both temper-rolling and temper-annealing, and all material was given a low-temperature

ageing treatment of 3 days at 100° C. to simulate exposure under tropical conditions. The stress-corrosion tests were then carried out in a NaCl/H₂O₂ solution under direct tension at 75% of the 0.2% proof stress. In the temper-rolled condition the endurance of the specimens varied between 1 and 36 hr., and in the temper-annealed condition between 25 and 60 days, some specimens remaining unbroken at 60 days. The superiority of temper-annealing over temper-rolling is well demonstrated.

The AUTHORS (*in reply*): As suggested by Dr. Evans, it would indeed be wrong to conceal the danger of expecting aluminium alloys to have eternal life, and an effort was made in the paper to emphasize the wisdom of preventive measures when serious corrosion attack, particularly of the foliation type, is observed. One is, however, inclined to favour the view of Dr. Champion that, used intelligently, the exponential equation can be applied, provided that precautions are taken to give suitable protection to alloys susceptible to stress-corrosion or to foliation under severe exposure conditions.

In reply to Dr. Champion's enquiry, the specimens totally immersed in the river at Christchurch frequently became completely buried in river mud owing to variations in the rate of flow of the river causing deposition of silt, and it would not be surprising if under these conditions contamination of the specimens with heavy metals occurred. The examples of the beneficial effects of sacrificial protective coatings given by Mr. Liddiard are particularly encouraging, since the possibilities of using alloys of much higher strength, which are susceptible to stress-corrosion, may be envisaged.

It has been suggested by Dr. Champion that the presence of an incomplete grain-boundary network in the homogenized material described in the paper on the corrosion of aluminium-5% magnesium alloys might be due to inadequate ageing. No information in support of this view was found, and little change in structure was observed after ageing for 28 days at 70° C. as compared with the normal 14 days at 70° C. The copper content of the alloys was, unfortunately, not determined, but as very high-purity materials were used, it is unlikely that the figure exceeded about 0.04%. In reply to Dr. Champion's and Mr. Tucker's criticisms of the use of the accelerated corrosion medium (i.e. a solution of 3% sodium chloride containing 1.2% hydrogen chloride by weight), while it is agreed that the quantitative data obtained should not be compared with service conditions, we believe that such accelerated tests may be valuable in the fundamental investigation of stress-corrosion behaviour, especially in the case of highly corrosion-resistant materials such as the aluminium-5% magnesium alloys.

The plotted results of stress-corrosion tests obtained under these conditions show a real effect of stressing in both tension and bending compared with unstressed specimens exposed for the same period, as the scatter in the accelerated test is smaller than the difference between the three curves. The figure of $\pm 20\%$ for the scatter range, mentioned on p. 265, refers to the non-uniform attack of the spray test, and not, as Mr. Chadwick erroneously infers, to the more uniform attack in the accelerated stress-corrosion test.

It is not true that bending under load ("yielding") occurs only when the attack is uniform and non-selective as it may also occur when corrosion attack penetrates at a uniform rate along all grain boundaries. This type of attack accounts for the fact that not all the specimens fractured in the accelerated test but some failed by yielding.

Considering the high range of scatter in the results after twelve months' exposure, we should not like to conclude from Figs. 2 and 3 (p. 265) that increasing the zinc content reduces the effect of ageing on the mechanical properties, as Dr. Champion suggests.

The relation between electrolytic potentials and cold work on metals and alloys is a well-known phenomenon described by Heyn and Bauer.* It seems, as a result of the later work referred to by Mr. Liddiard, that although theoretically when

* E. Heyn and O. Bauer, *Mitt. deut. Materialprüfanst.*, 1911, 29, 2.

stress concentration occurs in service, bending stresses are more dangerous than tensile stresses, this requires modification when further corrosion leads to release of stress owing to the attack progressing along planes perpendicular to the application of the load.

Our thanks are due to Mr. Tucker for drawing attention to the beneficial effects of temper-annealing as opposed to temper-rolling. Presumably the improvement in properties is due to relief of stress and possibly to break up of any continuous network of the precipitated phase.

Discussion

The Kinetics of the Eutectoid Transformation in Zinc-Aluminium Alloys

By R. D. GARWOOD and A. D. HOPKINS

(*Journal*, this vol., p. 407)

Mr. A. R. BAILEY,* M.Sc., A.I.M. (Member): I should like to raise a small point regarding the terminology used in this paper. Is it justifiable to refer to the isothermal reaction at 275° C. in the zinc-aluminium system as a eutectoid transformation? The relevant region of the equilibrium diagram is identical with that involving a monotectic reaction. I suggest, therefore, that the reaction in question should strictly be regarded as a monotectoid, even though eutectoid-type microstructures may result.

The AUTHORS (*in reply*): We agree with Mr. Bailey that the α/α' phase boundary in the accepted zinc-aluminium equilibrium diagram is similar to the liquidus/liquid-solubility curves in binary systems of the monotectic type. It would thus be terminologically more correct to describe the transformation as a monotectoid. However, in view of the limited

use of such terms as "liquidoid" and "solidoid", we do not feel justified in departing from the precedent set by previous workers in describing the transformation as an eutectoid. Adoption of the suggested term would also presuppose that the present diagram is correct, although the cause of the point of inflection on the solidus near 60% zinc is still in doubt. In this respect a recent study by Russian workers † on the variation of electrical resistivity with composition at 360°–422° C. indicates a discontinuity between 66 and 69% zinc. This effect, and a corresponding anomaly in the lattice-parameter/composition curves, are attributed to the ordering of the solid solution in this composition range. Should these findings be confirmed, a revision of the diagram may be necessary, since it is the contention of Rhines and Newkirk ‡ that the order-disorder changes are normal Gibbsian phase changes. In this event the suggested term would no longer be necessary.

Discussion

Diffusion and the Kirkendall Effect §

Dr. BÜCKLE: I should like to illustrate some work which has been done since my paper was published, and which helps to confirm my conclusions.

Fig. A (Plate CI) indicates the general distribution of the holes in a copper/copper-7% aluminium couple after heating at 800° C. for 25 days. However, the Kirkendall effect is much more pronounced when several phases are involved in the diffusion process. Fig. B (Plate CI) shows, in the centre, the polished section of a copper/zinc couple after 1 hr. at 380° C. The Hume-Rothery phases ϵ , γ , and β (very thin) have been formed. A series of microhardness impressions along the length of the specimen serve as markers. After a further 1 hr. at 380° C. the impressions were examined under a microscope having a calibrated micrometer ocular, and their position compared with those before the additional treatment. The results, illustrated by diagram and photograph in the lower half of Fig. B, show a marked

contraction on the zinc side (loss of zinc) and an expansion on the copper side (i.e. an expansion of the newly formed γ phase). This represents a displacement of the whole specimen relative to a fixed point of reference. Fig. C (Plate CII) shows the distortion of the microhardness impressions due to the expansion. As the displacement of the diffusion couples takes the form of a relative movement, some means are required of demonstrating its occurrence. Fig. D (Plate CII) shows two copper/zinc couples arranged in such a way that their movements should take place in opposite directions and thus become visible (see diagram (a)); experiment confirms that this is so (see photograph (b)).

The remaining illustrations show the growth of the various phases, during diffusion at 380° C., in multilayer specimens consisting of about ten thin sheets of copper and zinc placed alternately. In Fig. E (Plate CIII) the thickness of the copper is 140 μ and of the zinc 120 μ , corresponding to the

* Lecturer in Metallurgy, Constantine Technical College, Middlesbrough.

† D. A. Petrov and T. A. Badaeva, *Zhur. Fiz. Khim.*, 1947, **21**, 785.

‡ F. N. Rhines and J. B. Newkirk, *Trans. Amer. Soc.*

Metals, 1953, **45**, 1029.

§ Joint discussion on the papers by H. Bückle and J. Blin (*J. Inst. Metals*, 1951–52, **80**, 385), and by E. Lardner (this vol., p. 439).

composition of saturated α -brass. After $5\frac{1}{2}$ hr. (Fig. E (a)) the zinc has disappeared and broad bands of the γ and β phases have been formed; lines of porosity are to be seen in the region where the zinc originally was. At the end of 120 hr. (Fig. E (b)) the γ phase has been replaced by β and the copper takes a more active part in the diffusion process, being converted into α . The second specimen (Fig. F, Plate CIII) (copper 80 μ , zinc 300 μ) corresponds in composition to the ϵ phase. The development of the phases is markedly different from that of the first specimen. After 30 min. (Fig. F (a)) broad bands of γ have already formed, with narrower bands of ϵ on the zinc side. At the end of 27 hr. (Fig. F (b)) the copper and zinc have completely disappeared, giving place to ϵ , which has also absorbed a large part of the γ phase. As diffusion is governed by the interaction between γ and ϵ , its rate is much faster and the porosity more pronounced than in the case of the first specimen, in which the interaction between β and α was the dominant factor.

Mr. R. S. BARNES,* B.Sc. (Member): The observations described in the paper by Dr. Bückle and M. Blin are in complete agreement with my own observations on copper/ α -brass and copper/nickel couples, first mentioned in the discussion on the paper by da Silva and Mehl† and later described more fully.‡ I should like to mention one point from this latter paper in order to confound those critics who may think that the voids observed after interdiffusion are merely due to some polishing effect. That the voids were really present *inside* the metal after diffusion was proved by taking a microradiograph of the diffusion zone. Fig. G (Plate CIII) is such a microradiograph of the voids in a copper/nickel sandwich and shows, not only that the voids do not result from the polishing process, but also that their polyhedral shape is intrinsic.

While there is no doubt that voids form as a result of interdiffusion, the exact mechanism of their formation may be open to some conjecture. It may be suggested that the voids are formed either by gas coming out of solution or as a result of a gas reaction. The crystallographic shape of the voids is against such an explanation. Also, as the increase in the volume of the couples is independent of the purity of the metals, their previous treatment, and the annealing atmosphere, this explanation is very unlikely to be the correct one. The experimental results all suggest that the voids form as a direct result of the diffusion mechanism itself.

To explain the results, the authors invoke a mechanism involving the simultaneous diffusion of vacancies and interstitial atoms. As theoretical values for the activation energies of formation of vacancies and interstitial atoms favour a simple vacancy mechanism in face-centred cubic metals, it seems unnecessary to invoke such an involved idea, especially as all the results can be adequately explained, much more simply, by considering the migration of vacancies alone.

The results of the experiments can be summarized by Fig. H, which represents a diffusion couple consisting of two metals A and B, with three reference lines, denoted x , y , and z ; line y represents the marked interface between the two metals and lines x and z marked positions in the metals A and B, respectively. As a result of diffusion, the reference lines shift relative to one another, line y moving towards the reference line z and away from the reference line x (this movement is usually referred to as the Kirkendall shift). In addition to this movement, the two outer reference lines x and z move apart as a result of a volume increase of the couple, caused by the formation of voids in metal B near to the original interface. It is found that the interface y always moves towards the metal with the lower melting point and also that the voids appear in this metal.

If we use a simple vacancy mechanism, i.e. a mechanism whereby an atom can diffuse only by exchanging positions with a neighbouring vacancy, all these results can be explained

quite simply. The preferential flow of atoms in the positive direction in Fig. H will be accompanied by an equal flow of vacancies in the opposite, negative, direction. Such a flow of vacancies across the interface will disturb the equilibrium conditions in the diffusion zone; the number of vacancies in the region above y (in Fig. H) will be depleted, and vacancies will be generated here in an attempt to maintain equilibrium; in the region below y , vacancies will accumulate and exceed the equilibrium number, when they will tend to precipitate out of the lattice. The vacancies necessary for this preferential flow can be generated (above y) at lattice defects such as grain boundaries, polygon boundaries, and edge dislocations, and precipitated (below y) on similar defects; but if the supersaturation of vacancies here is high enough, then some of the vacancies will coalesce and form microscopic voids. The generation of vacancies above y and the precipitation of vacancies below y would cause an expansion and contraction, respectively, and the formation of voids (below y) would in addition result in an increase in the total volume of the couple.

Only if all the vacancies eventually go to form voids, i.e. none are annihilated at lattice discontinuities, will the distance

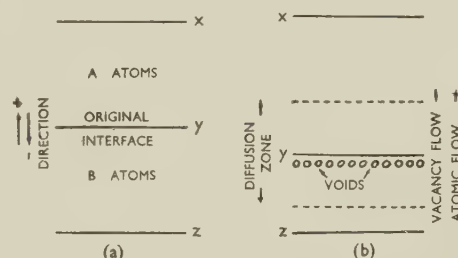


FIG. H.—Diagram to Illustrate Proposed Vacancy Mechanism.

yz (which contains the voids) remain constant. If the above explanation is the correct one, then the distance yz must decrease and can never increase. Observations show that this is the case; moreover, the reproducibility of this decrease would be very difficult to explain if the voids were the result of some process, e.g. a gas reaction, not *directly* connected with the diffusion process.

For this mechanism of void formation to be valid, the energy necessary to form the voids must come from the diffusion process. Rough calculations reveal that the energy released by the metals interdiffusing is about 10^4 times the total surface energy of the voids, so that this mechanism is quite feasible from an energy point of view.

With regard to the paper by Mr. Lardner, I should like to propose that the results he obtained can be accounted for in terms of the ideas I have outlined. The cast alloys used contained concentration gradients, and the solution-treatment of these alloys permitted the individual atoms of the alloys to diffuse and the concentration gradients to be reduced. As the melting point of magnesium is less than that of aluminium, it is to be expected that the magnesium atoms would diffuse the faster, or, in terms of vacancies, that the vacancies would flow from the aluminium-rich regions to the magnesium-rich regions. The accumulation of vacancies in the magnesium-rich regions could cause voids to form in this region. The crystallographic shape of the voids which Mr. Lardner observed suggests that these voids are formed in a way similar to those in diffusion couples, and their appearance in the magnesium-rich regions fits in well with this point of view.

After one of the high-temperature solution-treatments (5 hr. at 385° C. + 16 hr. at 420° C. + 16 hr. at 450° C.) (p. 440), it was found that cavities were completely absent. I should like to ask the author whether, in this particular

* Atomic Energy Research Establishment, Harwell, Berkshire.

† A. D. Le Claire and R. S. Barnes, *Trans. Amer. Inst. Min.*

Met. Eng., 1951, **191**, 1060 (discussion).

‡ R. S. Barnes, *Proc. Phys. Soc.*, 1952, [B], **65**, 512.

case, the absence of cavities might not be due to incipient melting of the alloy? After all other solution-treatments cavities were found, although an increase of time or temperature resulted very often in fewer but larger cavities; this might be expected if large cavities grow at the expense of the small ones.

Mr. Lardner's results suggest that the rate of cooling had no effect on the formation of voids, and if the absence of cavities in this one particular case could be accounted for by incipient melting, then the inability to remove already existing cavities would not be unexpected, and there would no longer be any need to look to the cooling of the samples for an explanation of their formation.

These experiments suggest that the voids result from the smoothing out of the concentration gradients, i.e. as a result of the diffusion process. Although other interpretations may be put upon these experiments, it is perhaps significant that the crystallographic nature of the voids is similar to that observed after the interdiffusion of two metals, and also that the position of the voids is in accord with their position in diffusion couples.

Dr. J. C. CHASTON,* A.R.S.M., A.Inst.P., F.I.M. (Member): These two papers deal with one aspect of what has come to be called the Kirkendall effect. As Dr. Bückle and M. Blin explain, this was first observed by Smigelskas and Kirkendall in America when studying the interdiffusion of copper and zinc, using brass samples electroplated with copper. They found by means of molybdenum wire markers that the original interface was displaced towards the brass side, and interpreted this to mean that the zinc diffused out of brass into copper faster than copper diffused into brass. These observations were confirmed in 1951 by da Silva and Mehl.

Dr. Bückle and M. Blin report that in these circumstances holes appear in the diffusion zone on the alloy side. It is perhaps proper to point out that, since these observations were made, Hersch† has found holes under the surface of 70:30 brass from which zinc had been distilled in a vacuum, and in a more detailed paper Balluffi and Alexander‡ have described many instances of cavity formation in diffusion couples (and sometimes in the couples before diffusion).

The explanation suggested by all these workers for the appearance of cavities has been well expressed by Balluffi and Alexander: "Porosity appears in α -brass when zinc is removed either by evaporation into vacuum or diffusion into copper. No matter where the zinc goes, it apparently moves out of the alloy by diffusion and leaves voids behind. One is tempted to say that this is a direct result of the unequal diffusion rates of copper and zinc in α -brass and that zinc atoms which diffuse outwards are replaced, not by copper atoms but by vacancies which may precipitate to form microscopic voids. The voids may subsequently be removed by a sintering process, but presumably the sintering process is slower than the diffusional process of forming voids."

In considering these phenomena, I suggest that three questions arise:

(1) Are the observations really consistent with the proposed explanation? As I understand it, the explanation suggests that the copper surface has such an attraction for zinc atoms that they diffuse into it faster than they can be replaced either by copper atoms or by zinc atoms coming from the brass immediately beneath the surface. This surely implies that we should expect to find holes collected immediately beneath the surface, becoming more and more sparsely distributed as we proceed farther from the interface. The distribution shown in Fig. 3 (Plate LVIII) of Bückle and Blin's paper gives no evidence at all, however, of any bunching near the interface. The holes are distributed quite uniformly in a wide zone extending about 0.2 in. below the

surface and then abruptly vanish. To me, such a distribution is quite inexplicable on the proposed theory. It should be pointed out, incidentally, that although the authors describe the region containing cavities as the diffusion zone, no evidence is actually given as to the extent of diffusion.

(2) Do cavities actually exist in other circumstances to which the same argument can be applied? I am surprised that none of the investigators of this problem has hitherto extended observations to cored structures. The use of welded sandwiches or electroplated specimens must always raise questions of local entrapment of gases. On the other hand, a sound brass or bronze casting would provide concentration gradients in an ideal form for diffusion studies. As far as I know, cavity formation has never been recorded when a cored brass casting is homogenized.

(3) Can the cavities be explained on established rational grounds without introducing new theoretical ideas? One possibility for the cavities observed by Bückle and Blin is that they may be due to inclusions pulled out during polishing, to leave pits subsequently enlarged by etching. It is significant that these workers polish on felt and velvet, which is particularly likely to drag out inclusions. I would suggest that for studies such as this, the use of diamond-powder polishing techniques is essential.

A second possibility is that gas reactions may be involved. Some of the cavities, such as those on the right of Fig. 4 (Plate LVIII), are undoubtedly due to gas reactions in copper. Admittedly, gas reactions are not normally encountered in brass, but experience has shown that they can occur in unexpected circumstances when catalysed by the presence of impurities or third elements.

On the whole I think that none of the work so far reported can be accepted as incontrovertible evidence for the view that cavities can be formed directly as a result of intermetallic diffusion. That the cavities may be due to side reactions has never yet been completely ruled out.

In this discussion reference has been made only to the paper by Bückle and Blin. It seems difficult to fit Lardner's observations into the general picture, but as the cavities which he observed were formed only during cooling, I suggest that they represent gas cavities produced by a reaction around centres nucleated during the preliminary heat-treatment.

Dr. T. P. HOAR,§ M.A., F.R.I.C., F.I.M. (Member): Strong evidence for the production of voids when two metals interdiffuse is provided by the net increase in volume often observed, for example, in the early stages of the heat-treatment of copper-nickel powder compacts.|| This fact seems to confirm the metallographic evidence that Dr. Chaston doubts.

The separate diffusion of two metal species in an alloy has received general notice only within the last few years. This is astonishing: the separate diffusion of different species in gaseous and liquid systems has been recognized for a century or so, while the phenomenon was treated theoretically by Wagner for solids generally, and demonstrated by him and by Pfeil for a number of metallic compounds, about 25 years ago. The balance between knowledge of diffusion in metallic and non-metallic solids has now been handsomely redressed by those interested in atom movements in alloy systems; but, much as one may approve the opening up of the metallic field by the paper of Smigelskas and Kirkendall, may one suggest that the "effect" that they demonstrated for a single pair of metals has been somewhat inappropriately named?

Mr. M. C. INMAN,¶ B.Sc.: Dr. Chaston has emphasized the importance of accurate measurement of concentration/distance curves for the understanding of diffusion phenomena. At Leeds a group of investigators, under the direction of Dr. R. Shuttleworth, is using radioactive tracers to measure

* Manager, Research Laboratories, Johnson, Matthey and Co., Ltd., Wembley.

† H. N. Hersch, *J. Appl. Physics*, 1952, **23**, 1055.

‡ R. W. Balluffi and B. H. Alexander, *ibid.*, 1952, **23**, 1237.

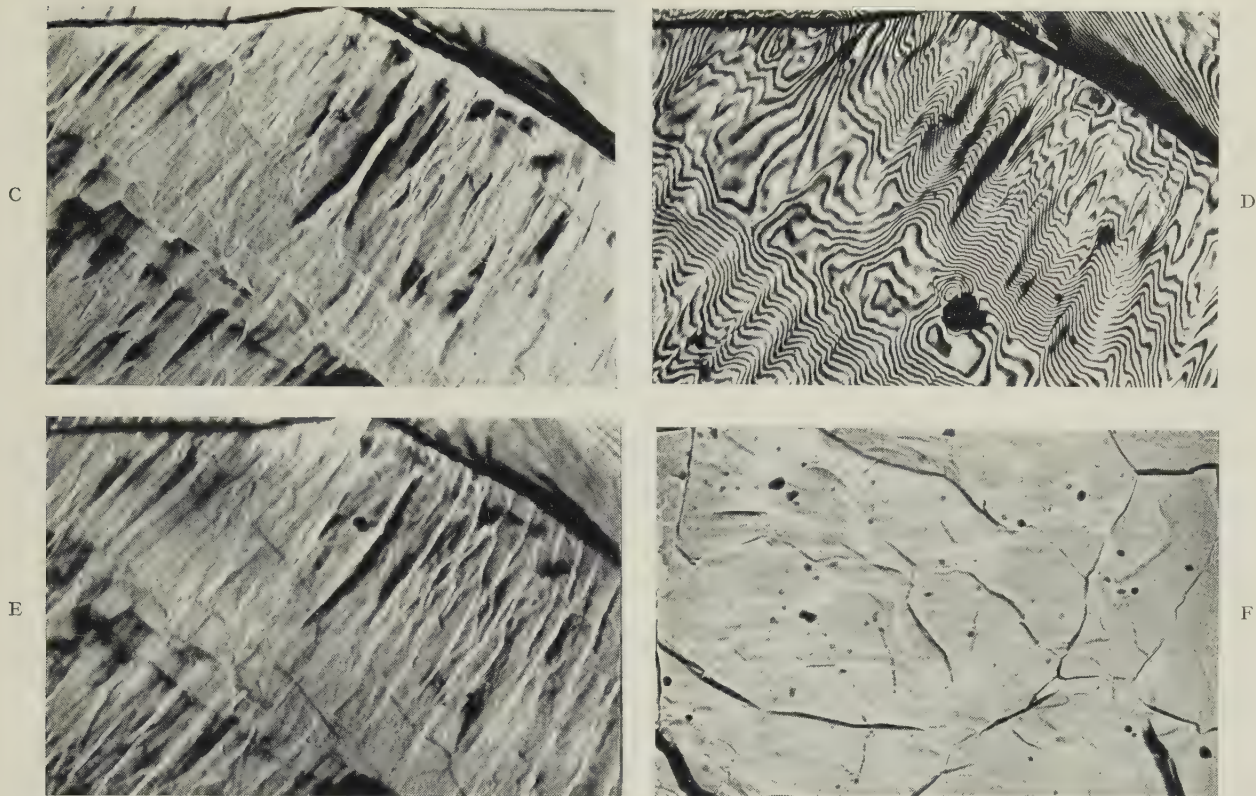
§ Lecturer, Department of Metallurgy, Cambridge

University.

|| J. M. Butler and T. P. Hoar, *J. Inst. Metals*, 1951-52, **80**, 207.

¶ Yorkshire Copper Works Fellow, Metallurgy Department, University of Leeds.

CREEP AND PLASTIC DEFORMATION.



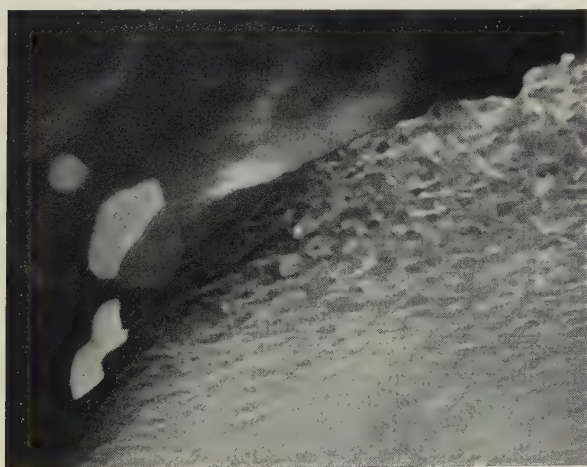
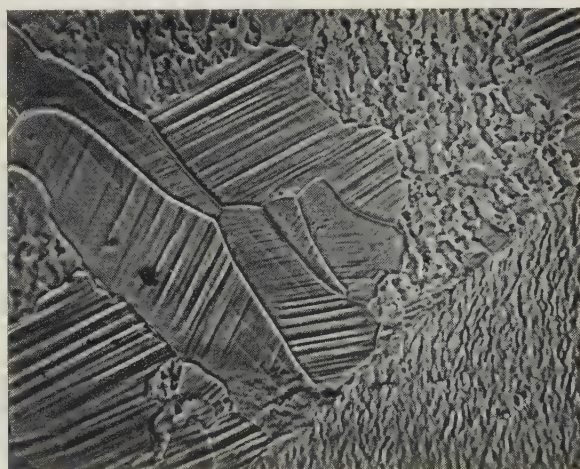
FIGS. C-E.—Area on Pure Aluminium Deformed 14% in 75 Hr. at 200° C.

FIG. C.—Inside focus.
FIG. E.—Outside focus.

FIG. D.—Multiple-beam interferogram.

FIGS. C and E.—Narrow-pencil illumination. $\times 140$.FIG. F.—Aluminium Deformed 12% at 325° C. in 8 Hr., Repolished Flat, Further Strained 3% at 300° C. Outside focus. Narrow-pencil illumination. $\times 150$.

(Gifkins and Kelly.)

FIG. G.—Super-Purity Aluminium Cold-Rolled 20% and Annealed 1 min. at 375° C. Anodized. Photographed under polarized light. $\times 200$. (Perryman.)FIG. H.—Super-Purity Aluminium Cold-Rolled 50% and Annealed 10 sec. at 375° C. Etched in 25 HNO₃, 73 H₂O, 2 HF at 50° C. Bent slightly after etching. Photographed under phase contrast. $\times 200$. (Perryman.)

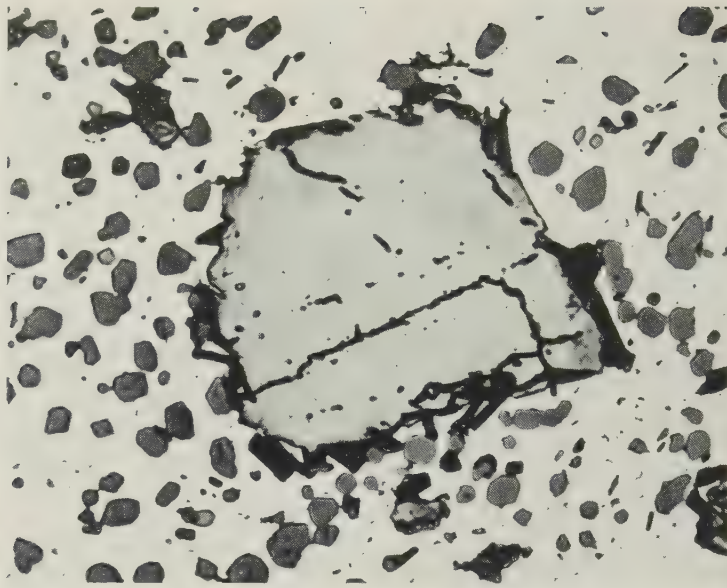


FIG. A.—Primary Manganese-Bearing Constituent in a Eutectic Aluminium-Silicon Alloy. (*Turner on Dudzinski.*)

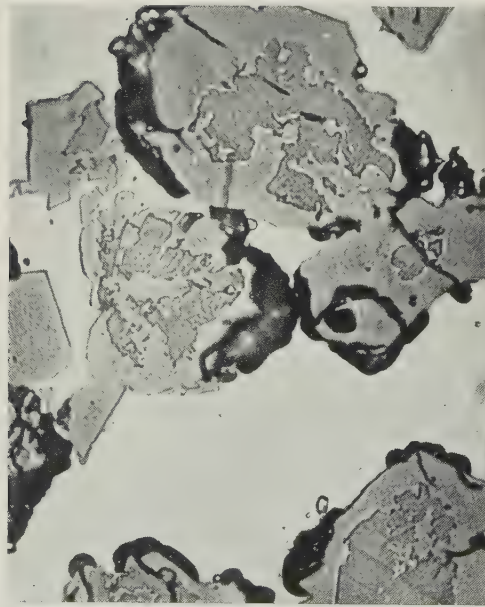


FIG. B.—Aluminium-6.37% Chromium Alloy, Chill-Cast and Annealed. $\times 750$. (*Dudzinski's reply.*)

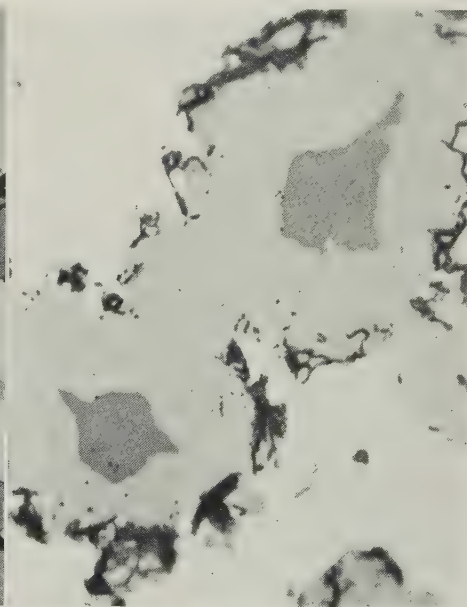


FIG. C.—Aluminium-2.4% Vanadium Alloy, Chill-Cast and Annealed. $\times 1000$. (*Dudzinski's reply.*)

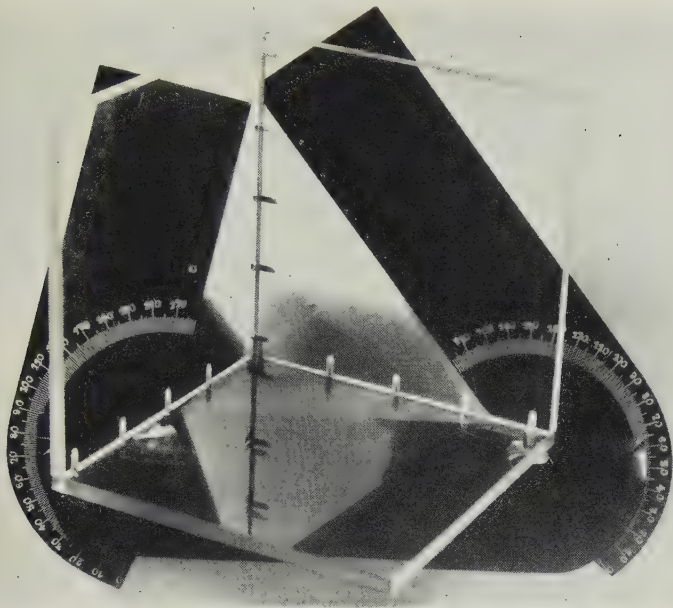


FIG. D.—Jointed Triangle for the Direct Interpretation of Etch-Pits. (Plan.)

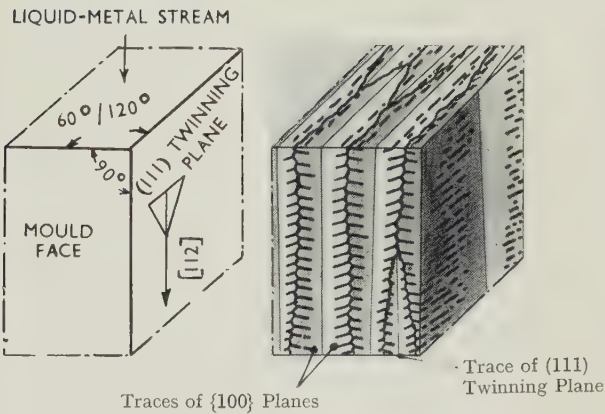


FIG. E.—Twin Texture in 99.5% Aluminium, Semi-Continuously Cast.

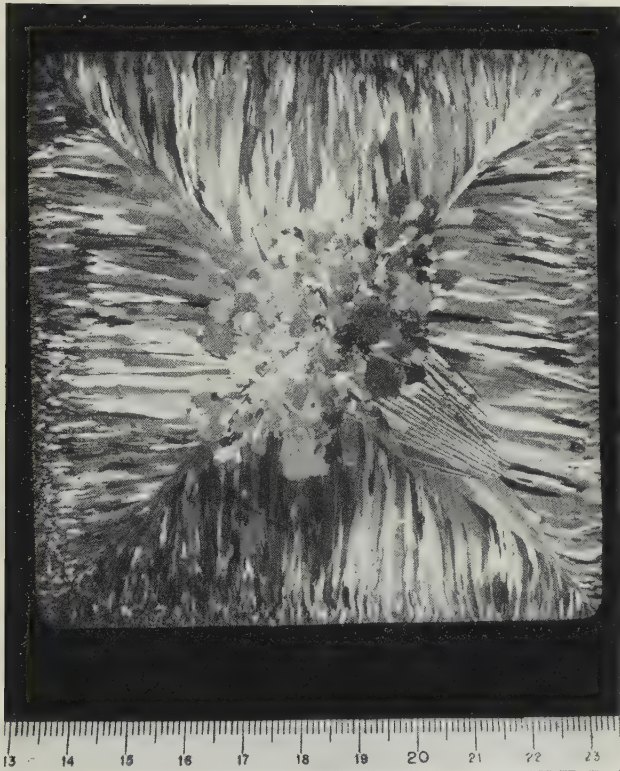


FIG. F.—Fan-like Twinned Structure in a 99.5% Aluminium Wire Bar, Cast in a Permanent Mould.

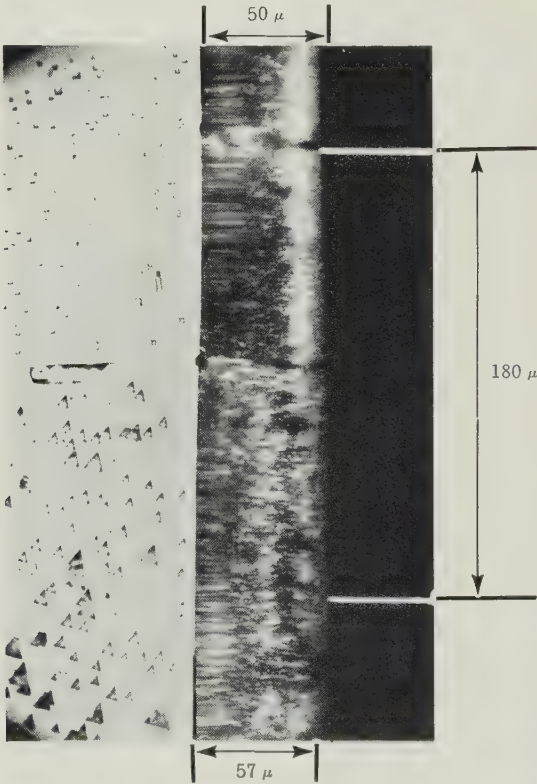


FIG. G.—Illustrating Use of Etch-Pits in Determining the Orientation of Two Neighbouring Grains of an Aluminium-3% Magnesium Alloy, Carrying Anodic Oxide Layers of Different Thickness. $\times 300$.

(Hérensuel and Lelong on Tucker and Murphy.)

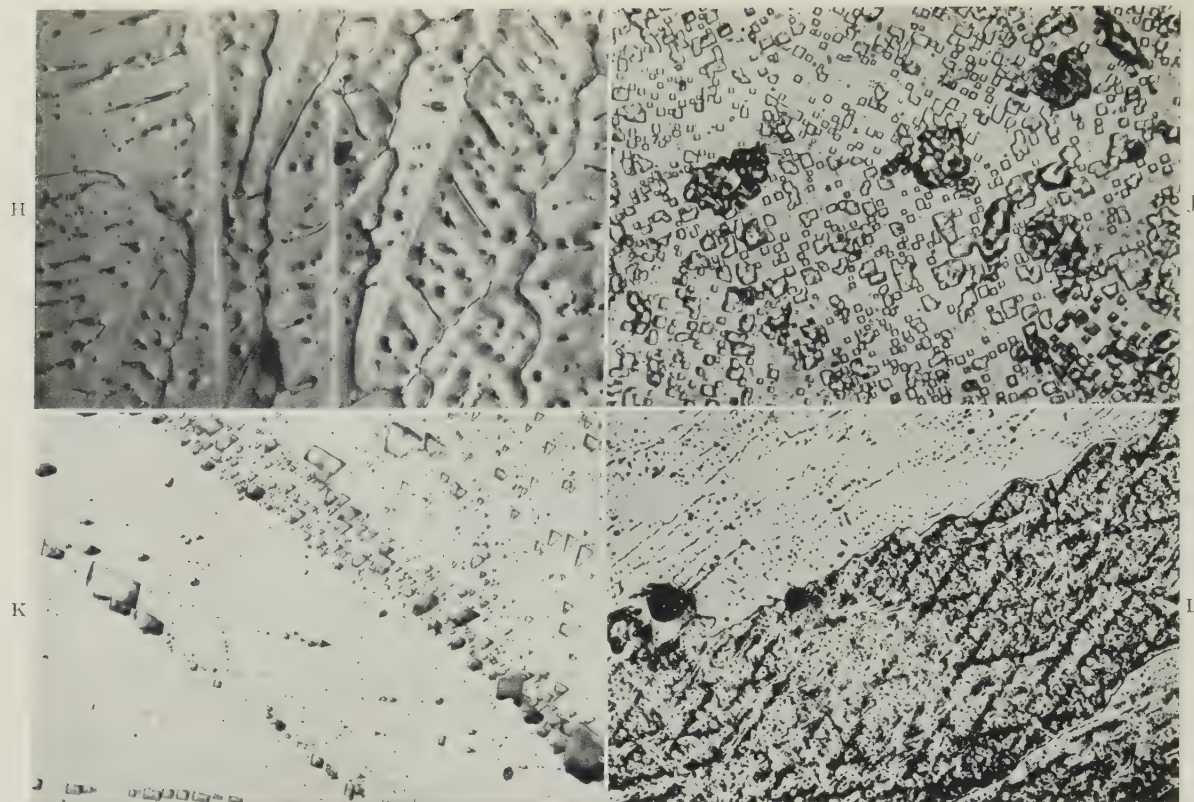


FIG. H.—Junction of Two Twin Elements with a Strong Relative Disorientation. $\times 120$.

FIG. J.—Cube Texture Revealed by Etch-Pits. $\times 350$.

FIG. K.—Zone of Progressive Curvature at the Boundary of a Deformation Band in a Cold-Worked Single Crystal of Aluminium-3% Magnesium Alloy, as Revealed by Etch-Pits. $\times 600$.

FIG. L.—Distribution of Etch-Pits in Alignment Parallel to $\{100\}$ Traces on As-Cast 99.5% Aluminium. $\times 25$.

(Hérénguel and Lelong on Tucker and Murphy.)

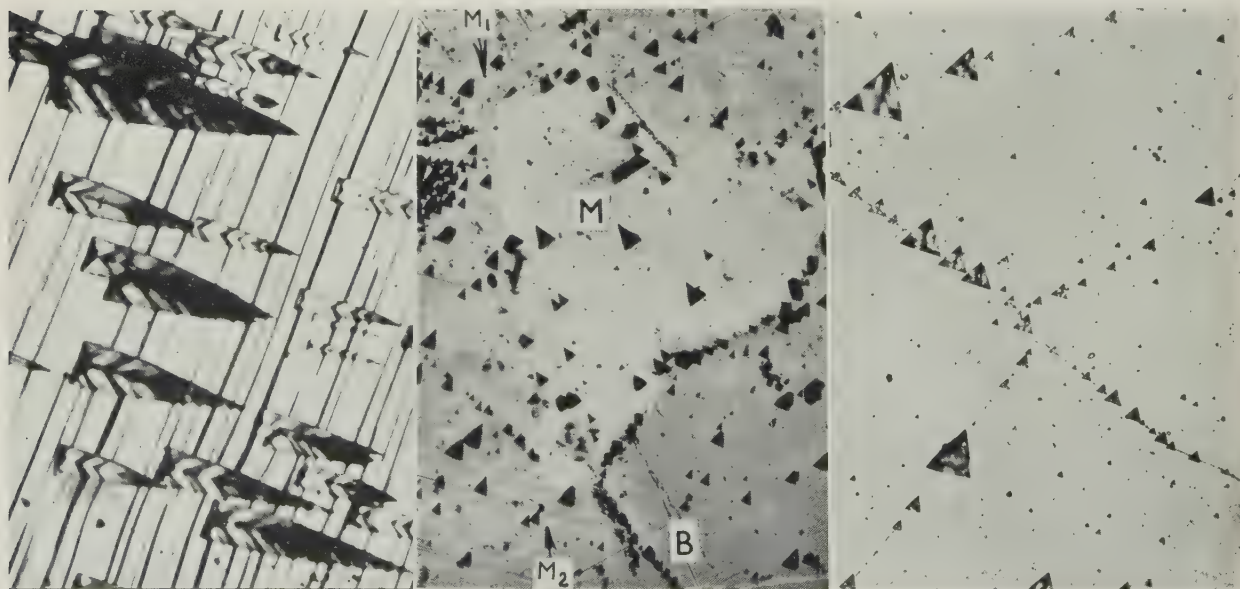


FIG. M.—Etch-Pits and Slip Lines on a Pure Aluminium Single Crystal. $\times 350$.

FIG. N.—Insular Crystal M Enclosed in a Large Crystal B in a Relatively Twinned Position (M, M_2 linear boundary represents trace of the $\{111\}$ twinning plane). $\times 100$.

(Lacombe on Tucker and Murphy.)

FIG. O.—Intragranular Polygonization Boundary, Marked by a Series of Etch-Pits, in an Aluminium Crystal with Orientation Approximately Parallel to the $\{111\}$ Plane. $\times 500$.

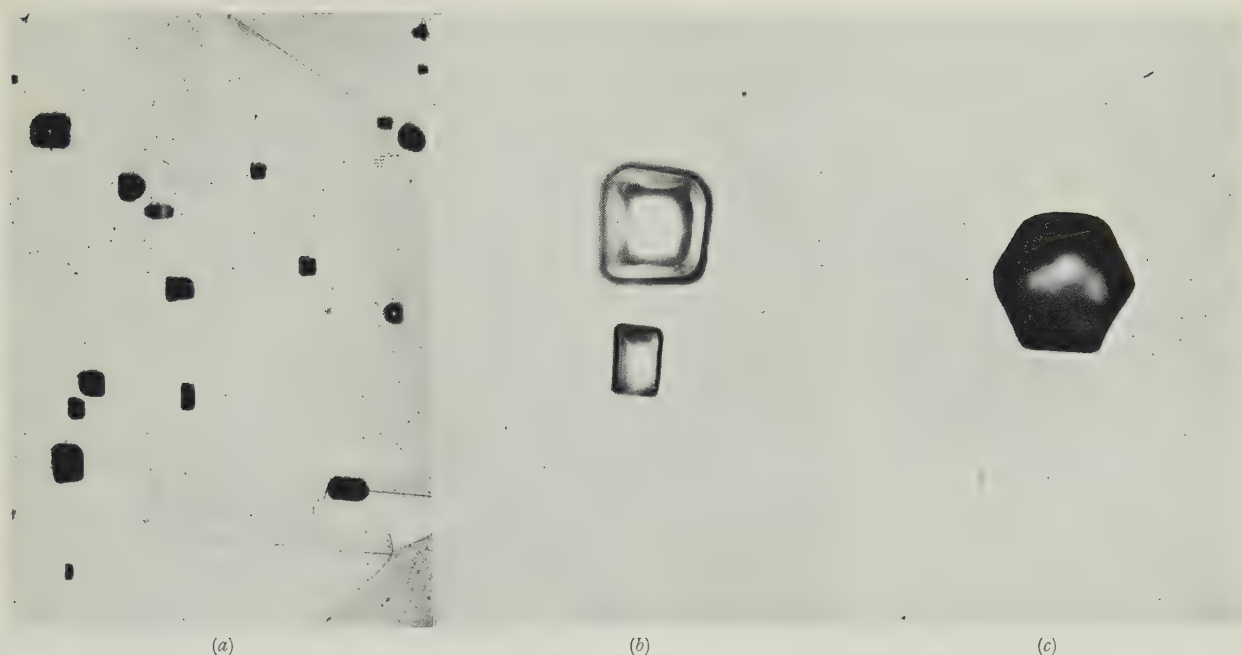


FIG. A.—Size and Distribution of Holes in a Copper/Copper-7% Aluminium Alloy Couple after Diffusion for 25 Days at 800° C. (a) $\times 100$. (b) and (c) $\times 350$. (Buckle.)

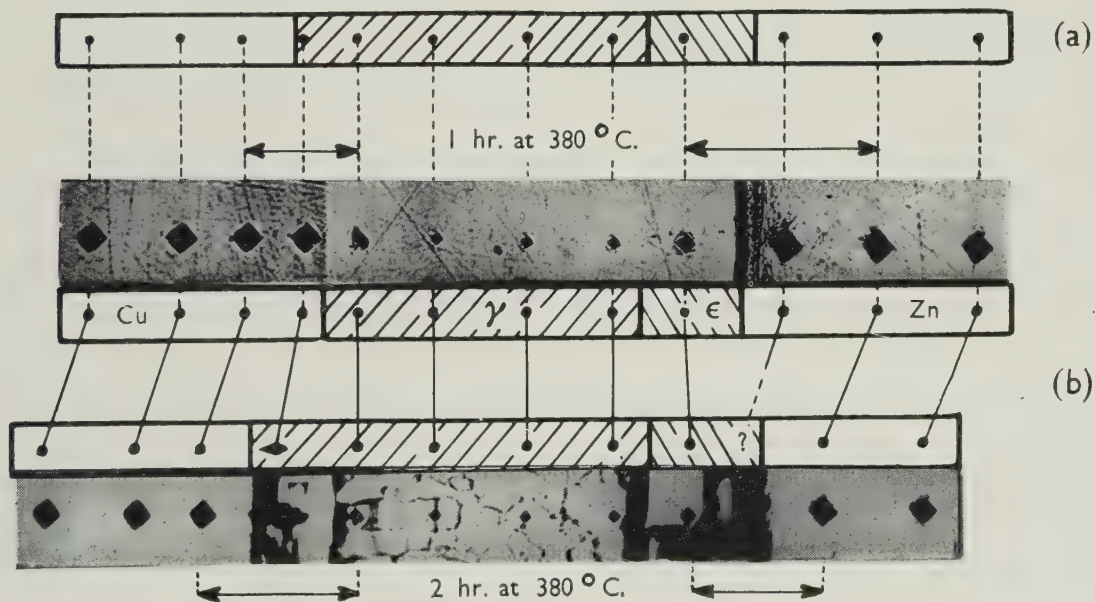


FIG. B.—Multiple-Phase Diffusion in a Copper/Zinc Couple, Showing Anomalous Expansion on the Copper Side (left) and Contraction (Kirkendall Effect) on the Zinc Side (right). (a) According to classical theory. (b) Actually observed. $\times 450$. (Buckle.)

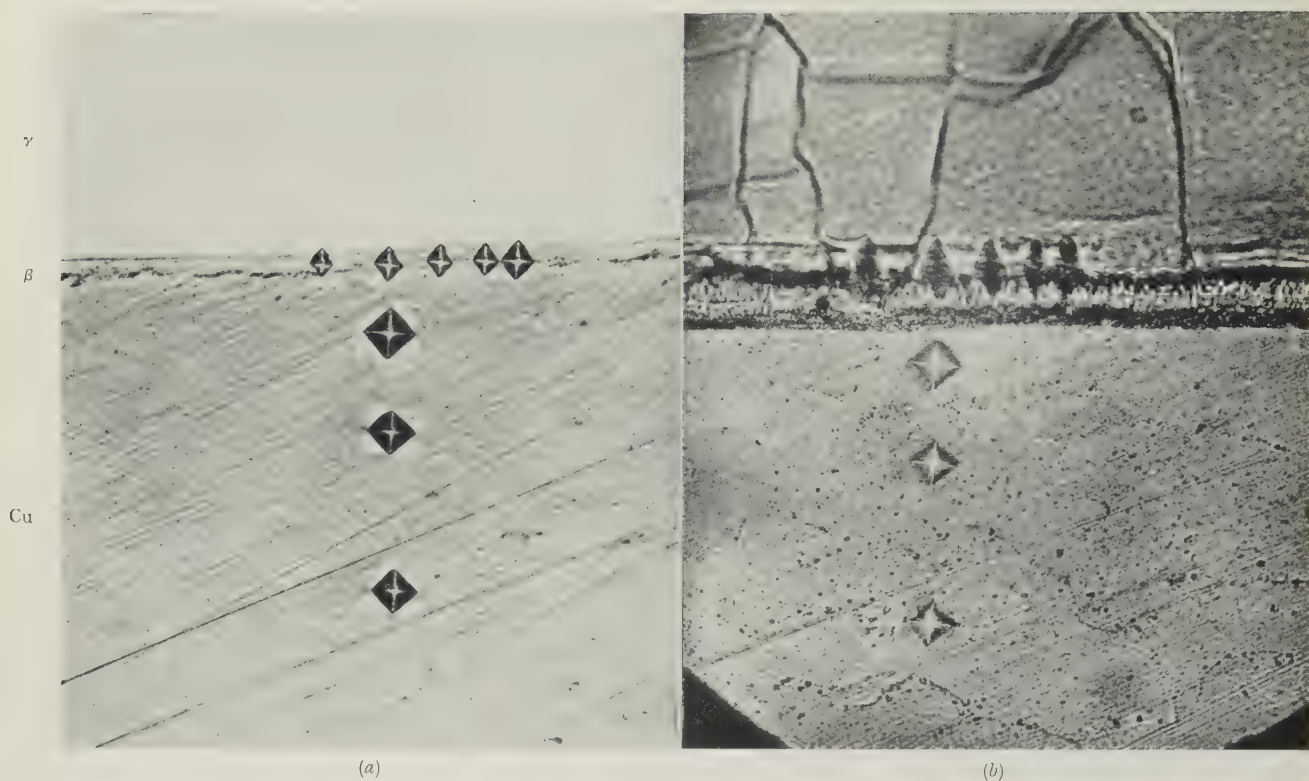


FIG. C.—Anomalous Swelling Revealed by Deformation of Micro-hardness Impressions. (a) Before. (b) After the second treatment. $\times 650$. (Bückle.)

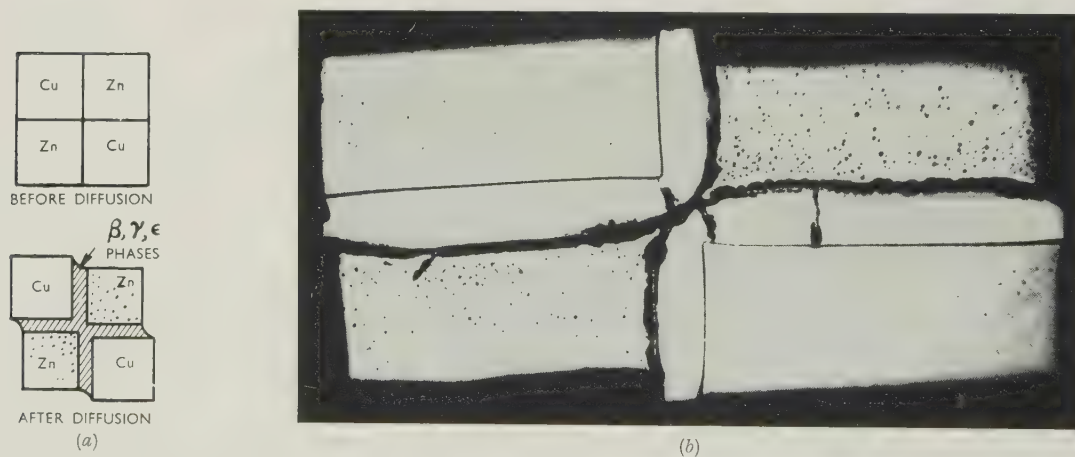


FIG. D.—Displacement of Copper/Zinc Couples After Diffusion for 27 hr. at 380°C . (a) Diagrammatic. (b) Experimental observation. $\times 10$. (Bückle.)

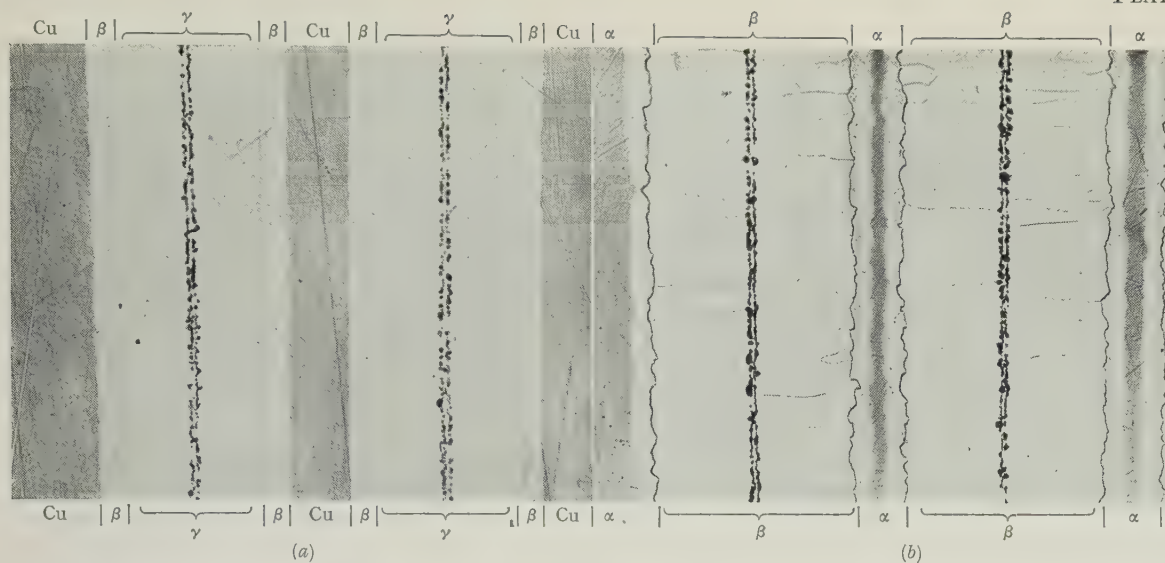


FIG. E.—Copper 140 μ thick, zinc 120 μ thick. (a) After 5½ hr. (b) After 120 hr. $\times 200$.

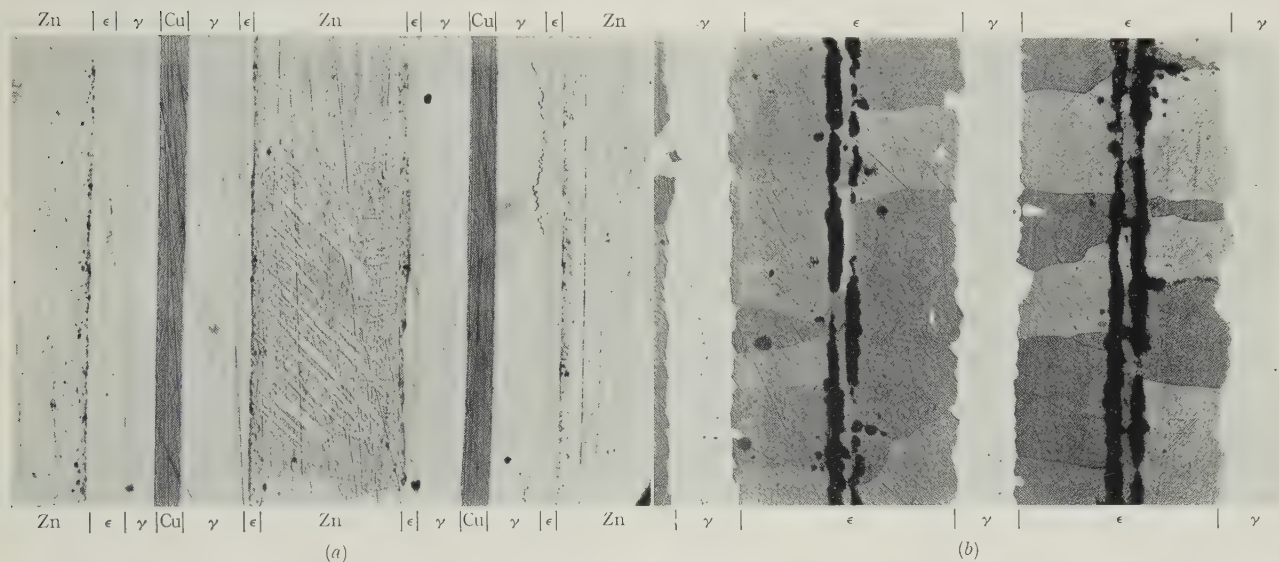


FIG. F.—Copper 80 μ thick, zinc 300 μ thick. (a) After 30 min. (b) After 27 hr. $\times 150$.

FIGS. E and F.—Showing Evolution of Various Phases Formed During Diffusion at 380° C. in Multi-Layer Specimens of Alternate Copper and Zinc Sheets. (Buckle.)

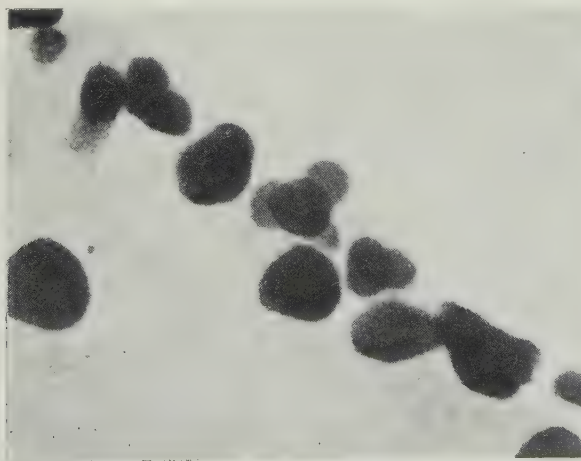


FIG. G.—Microradiograph of Voids in a Copper/Nickel Sandwich, Showing That They do Not Result from the Polishing Process and That Their Polyhedral Shape is Intrinsic. (Barnes.)

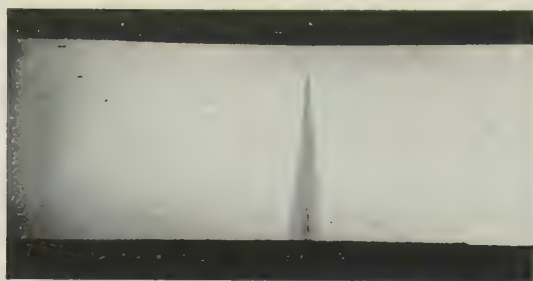


FIG. A.—Standard Tensile Test-Piece of Narrow Central Gauge-Length, Showing Normal Markings First Formed. $\times 1$. (*Chadwick and Hooper.*)

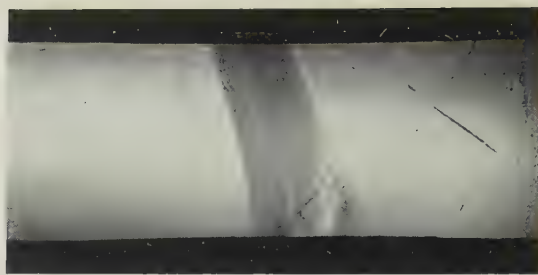


FIG. B.—Illustrating Formation of Tongue-Shaped Markings on Further Stretching of Test-Piece. $\times 1$. (*Chadwick and Hooper.*)



FIG. D.—Stretcher-Strain Markings on a Steel Pressing. $\times 1$. (*Hundy.*)

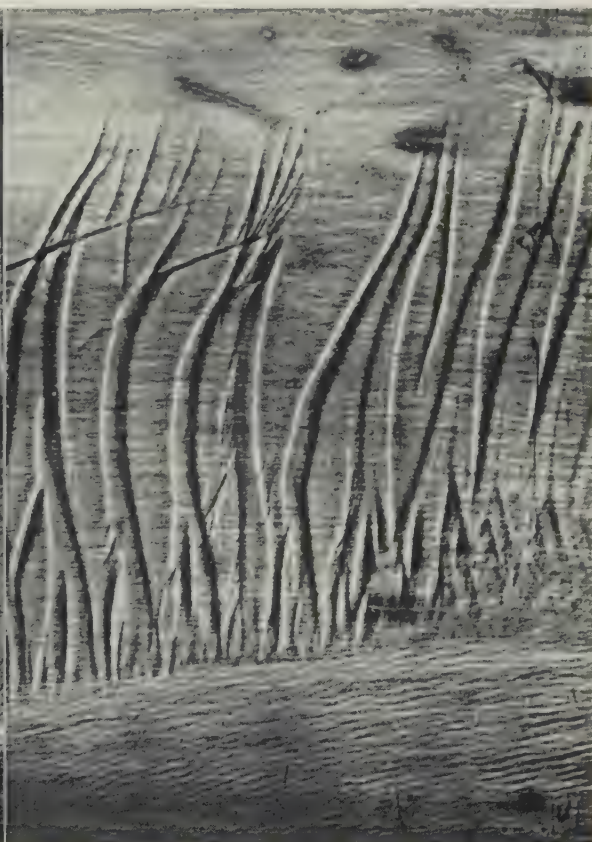


FIG. E.—Stretcher-Strain Markings on an Aluminium-Magnesium Alloy Pressing. $\times 1$. (*Hundy.*)

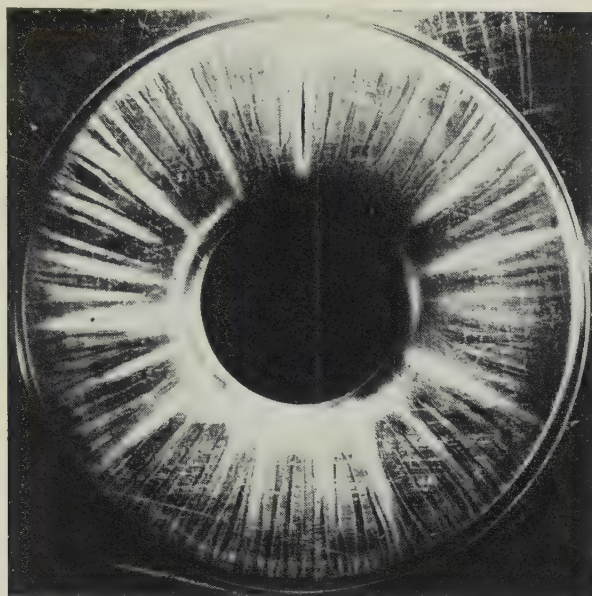


FIG. F.—Steel Pressing Showing Stretcher-Strains, Localized Necks, and Fracture. $\times 1$. (Hundy.)

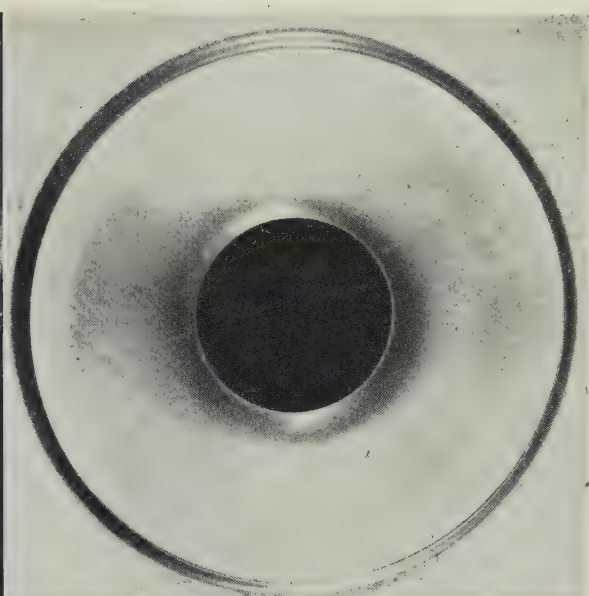


FIG. G.—Similar Pressing to Fig. F but the Steel Was Temper-Rolled Before Pressing to Remove All the Defects. $\times 1$. (Hundy.)

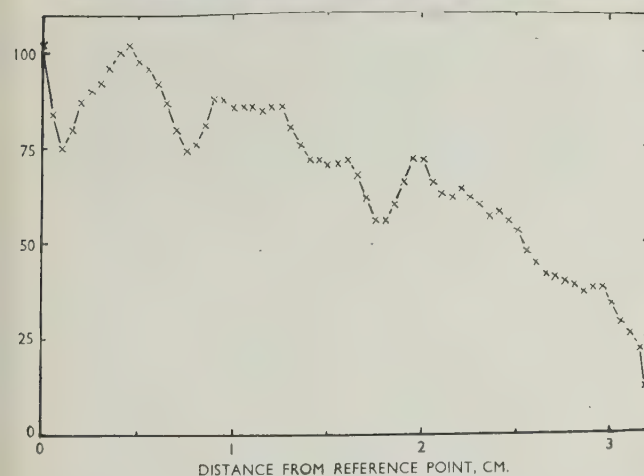
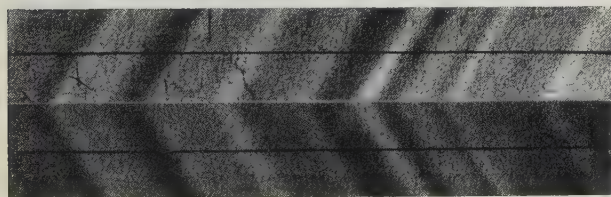
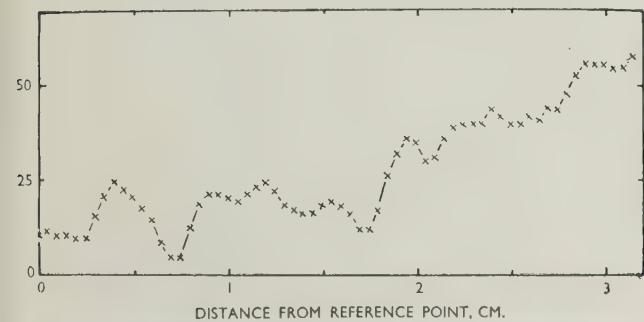


FIG. O.—Relation Between Profile and Type-B Markings on Strip of Commercial Aluminium- $3\frac{1}{2}\%$ Magnesium Alloy, Grain-Size 0.018 mm., Rolled to 0.044 in. Thick ($\sim 10\%$ Reduction) and Stretched to Fracture. (Phillips.)

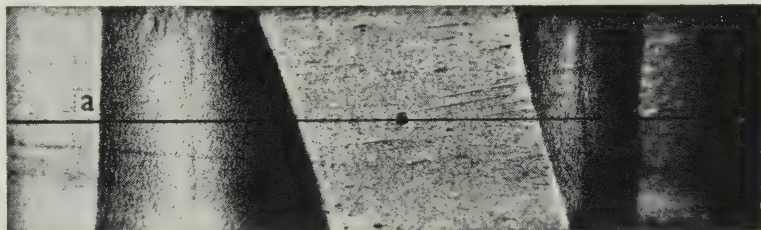


FIG. P.—Two Type-A Wedge Markings Formed on Annealed Mild Steel Strip of 0.023 mm. Grain-Size, Stretched Part Way Through the Yield-Point Elongation of 4%. $\times 2.6$. (Phillips.)

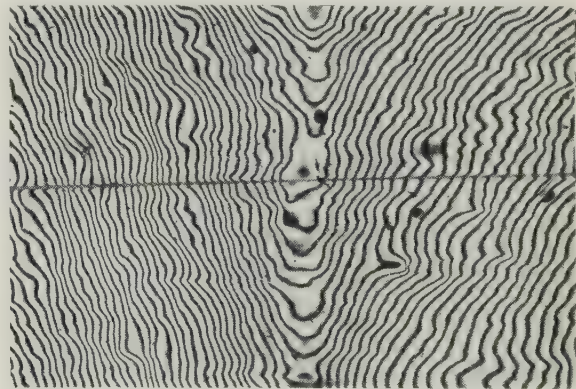


FIG. Q.—Multiple-Beam Interference Pattern Showing Sharp Tilt at Boundary *a* of Fig. P Between Yielded and Unyielded Material. A reference scratch runs across the field. $\times 41$. (Phillips.)



FIG. R.—Illustrating Type-B Ripple Markings Formed on Strip of Same Steel as Fig. P, Stretched to Fracture at $170^{\circ} \pm 5^{\circ} \text{C}$. $\times 2.6$. (Phillips.)

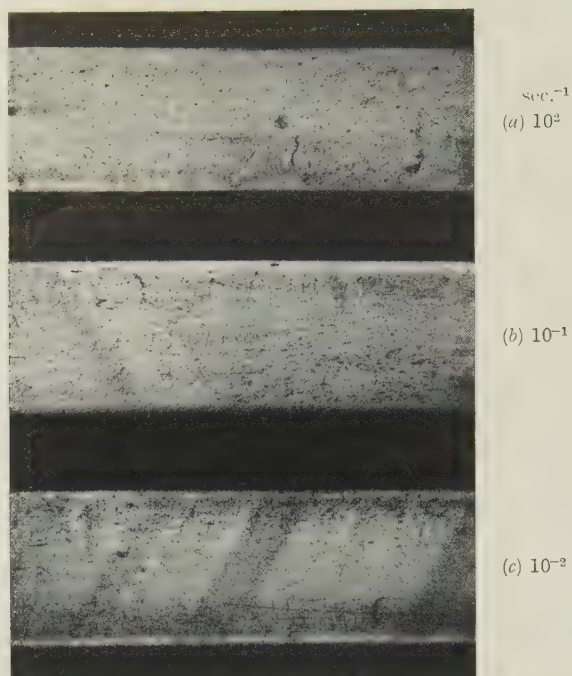


FIG. S.—Effect of Rapid Straining at Room Temperature on the Occurrence of Type-B Ripple Markings in Commercial Aluminium-3½% Magnesium Alloy Strip (OZN), Rolled to Approx. 0.012 in. Thick and Annealed. Approximate strain rates (in sec.^{-1}) as indicated. $\times 2.5$. (*Eborall and Phillips.*)



FIG. T.

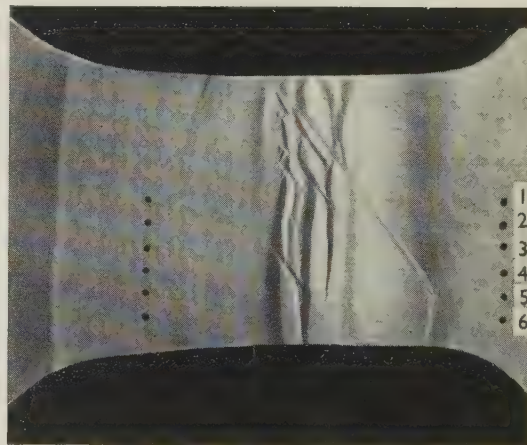


FIG. U.

FIGS. T and U.—Type-A and Type-B Markings Present Together in Mild Steel. (*Chadwick and Hooper.*)

these curves in copper-zinc alloys. I am studying the self-diffusion of copper and zinc in β -brass, whilst Mr. L. W. Mercer and Mr. D. Johnston are studying two α -brasses containing 1 and 30% of zinc, respectively.

The appearance of pores in the chemical-diffusion experiments of Dr. Bückle and M. Blin and of Mr. Lardner shows that in these systems atom movement occurs by interchange with vacancies. The pores are formed because the preferential interchange of one component with vacancies causes vacancies to be pumped from one side of the couple to the other, and thus produces a vacancy supersaturation so great that some of the vacancies combine to form pores. If the vacancy supersaturation had been less, the vacancies would have been annihilated at dislocations.

Whilst the occurrence of pores and of Kirkendall displacements during chemical diffusion proves that atom movements occur by interchange with vacancies, experiments on the diffusion of isotopes in a chemically homogeneous system have a more immediate interpretation in terms of the interaction of the vacancies with the two kinds of atom in an alloy. For

anneal sections parallel to the weld are turned off in the lathe and collected in weighing bottles. The γ activities of these sections are measured by a ring of six Geiger counters, connected in parallel to a single scaler. Since the half-lives of radioactive copper and zinc are 12.9 hr. and 250 days respectively, separate activity/penetration curves for copper and zinc are easily obtained without the need for a chemical separation, for the activity of a section immediately after diffusion is due to both copper and zinc, whilst after ten days the copper has decayed and the remaining activity is due solely to the zinc.

The activity per unit volume c , at a distance x from the origin, is given by :

$$c/c_0'' = (4\pi Dt)^{-1/2} \exp[-x^2/4Dt] \quad (2)$$

where c_0'' is the initial activity per unit area at the origin and t is the diffusion time. In Fig. J are shown the activity/penetration curves for copper and zinc in β -brass after diffusion for 15.7 hr. at 732° C. Especially to be noticed is the large diffusion distance, comparable to that of interstitial carbon in iron at the same temperature. Values of D_{Cu} and D_{Zn} were calculated by equation (2) from the activity/penetration curves and these are given for various temperatures in Table A.

TABLE A.

Temp. (°C.)	D_{Zn} , cm. ² /sec.	D_{Cu} , cm. ² /sec.	D_{Zn}/D_{Cu}
678	1.35×10^{-7}	0.65×10^{-7}	2.08
732	2.67×10^{-7}	1.37×10^{-7}	1.95
777	4.26×10^{-7}	2.26×10^{-7}	1.88
831	7.27×10^{-7}	4.04×10^{-7}	1.80
870	1.07×10^{-6}	6.14×10^{-7}	1.75

It should also be noted that since the values of D_{Cu} and D_{Zn} are measured simultaneously, the ratio D_{Zn}/D_{Cu} should be free from systematic errors. This ratio is important because, by equation (1), it equals n_{Zn}/n_{Cu} , the relative frequency of interchange of the two kinds of atom with the vacancies. The temperature-dependence of the diffusion coefficients is given by the equations :

$$D_{Cu} = 0.038 \exp[24,900/RT] \quad D_{Zn} = 0.024 \exp[22,800/RT] \quad (3)$$

The experimentally determined activation energy is the sum of the energy necessary to create a vacancy and the energy required for an adjacent atom to interchange with this vacancy. In 50:50 β -brass the energy needed to create a vacancy will be about the same for all sites, and so the difference in activation energy for copper and zinc (2.1 kg.cal.) can be identified as the difference between the energy required for a copper and a zinc atom to exchange with a neighbouring vacancy.

Preliminary measurements by Mr. Johnston on a 70:30 brass show that at 830° C. :

$$D_{Cu} = 1.50 \times 10^{-9} \text{ cm.}^2/\text{sec.} \quad D_{Zn} = 4.83 \times 10^{-9} \text{ cm.}^2/\text{sec.}$$

Dr. F. ROHNER* (Member): The similarity of the phenomena described in these two extremely interesting papers leaves little doubt that they must derive from the same origin.

The observation by Dr. Bückle and M. Blin that formation of porosity is connected with the Kirkendall effect in copper/zinc and copper/aluminium diffusion couples has been substantiated and shown to be true for other diffusion systems.† Those authors who embark upon a detailed discussion of the possible mechanisms involved agree that the pores must be looked upon as agglomerations or precipitates of vacancies, and that some source of vacancies must be operating in the diffusion zone. The concentration of vacancies in metals due to thermal excitation is much too small to account for the

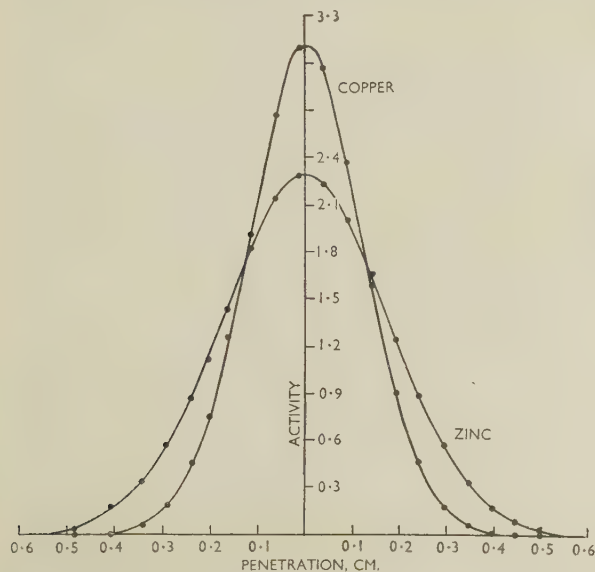


Fig. J.—Normalized Activity/Penetration Curve for Self-Diffusion of Copper and Zinc in β -Brass for 15.7 hr. at 732° C.

$$\begin{aligned} c/c_0'' &= (4\pi Dt)^{-1/2} \exp[-x^2/4Dt] \\ D_{Cu} &= 1.37 \times 10^{-7} \text{ cm.}^2/\text{sec.} \\ D_{Zn} &= 2.67 \times 10^{-7} \text{ cm.}^2/\text{sec.} \\ D_{Zn}/D_{Cu} &= 1.95. \end{aligned}$$

the self-diffusion coefficient of a component is simply related to n , the frequency with which an atom of that component jumps to adjacent lattice sites, by the equations :

$$D_A = \alpha n_A a^2 \quad D_B = \alpha n_B a^2 \quad (1)$$

where D_A and D_B are the self-diffusion coefficients of the two components, a is the cubic lattice constant, and α is a numerical constant (1/8 for body-centred cubic and 1/12 for face-centred cubic crystals).

A technique has been devised to measure simultaneously the self-diffusion coefficients of copper and zinc in brass. A foil of the brass, 0.005 in. thick, is irradiated in a pile so that it contains both copper and zinc radioactive atoms. This foil is then welded between two discs of brass of the same chemical composition and the sandwich annealed for about a day at the diffusion temperature. After this the diffusion-

* Research Laboratories, Aluminium Industrie, A.G., Neuhausen, Switzerland.

† L. C. C. da Silva and R. F. Mehl, *Trans. Amer. Inst. Min. Met. Eng.*, 1951, **191**, 155.

H. N. Hersch, *J. Appl. Physics*, 1952, **23**, 1055.

R. W. Balluffi and B. H. Alexander, *ibid.*, 1952, **23**, 1237.

W. Seith and A. Kottmann, *Angew. Chem.*, 1952, **64**, 379.

development of the pores. Smoluchowski* estimates the normal concentration of vacancies attributable to this cause at a small fraction of 1%. Seitz† has suggested that the vacancies in the case of the Kirkendall effect might be created at the specimen surfaces. This possibility has been disproved by several investigators, notably by Bückle and Blin; their experiments with specimens Nos. 2 and 5 show the Kirkendall effect to operate whether the outer surface is of copper or of brass.

The mere existence of the Kirkendall effect rules out any direct place-exchange or ring-diffusion mechanism.‡ The fact that porosity is associated with the Kirkendall effect is a strong point in favour of a defect mechanism of diffusion, either of an interstitial type, based on the existence of Frenkel defects, or of a vacancy type, based on the existence of Schottky defects. Either mechanism must upset the thermodynamic defect equilibria locally, if two species of atoms with different diffusion rates are involved. This would result in a super-concentration of vacancies on the side with the higher content of the faster-diffusing species. The formation of pores with crystallographic faces can therefore be explained on both hypotheses. Seitz§ holds that the experimental facts do not allow any choice to be made between the two mechanisms. Bückle and Blin favour the interstitial type, rightly I think; this mechanism gives a simpler picture, the surplus vacancies being created on the side on which they are actually found as pores.

Porosity has been proved to occur not only in solid diffusion couples and sandwich specimens, but also in gas-phase/solid diffusion systems.|| Mr. Lardner has now shown that the same type of porosity may develop in diffusion connected with the rejection of solutes from supersaturated substitutional solid solutions. In this type of diffusion only one species of atom is involved. The solvent atoms have no incentive to diffuse in any definite direction, because they cannot relieve the supersaturation. This can only be effected by a diffusion of the solvent atoms to spots suitable for their rejection. Formally, it may be said that the difference in the diffusion rates of the two species of atom involved is at a maximum, because the diffusion rate of one species—the solvent atoms—is zero; actually this is not so, but the diffusion of the solvent atoms is not co-ordinated with the diffusion of the solute atoms. There can, of course, be no displacement of an interface here; but Lardner's observation of pores with crystallographic faces shows that the diffusion is again coupled with the creation of vacancies. This is an argument in favour of the interstitial diffusion mechanism, because to explain the creation of vacancies by the vacancy mechanism would lead to difficulties in this case.

In 1947 I postulated the creation of vacancies as a mechanism for the rejection of copper from supersaturated aluminium-copper solid solutions,¶ thereby explaining experimental data obtained bearing on the kinetics of age-hardening. In the aluminium-copper system no pores with crystallographic faces have so far been observed. It seems probable that the vacancies do not agglomerate in this system as readily as in the magnesium-aluminium system. The more pronounced age-hardening effect found with aluminium-copper alloys may be due to this difference. My views concerning the hardening effect of vacancies have gained support from the observations of Billington and Siegel** and of Dugdale.†† Further developments of my ideas regarding the dependence of mechanical properties on the free path of slip have been published more recently.‡‡

Dr. H. BÜCKLE (*in reply*): The main object in publishing this work was to provide additional experimental data, which

might serve to settle certain points hitherto in doubt. I am glad to find that the experimental results are completely confirmed by Mr. Barnes and by those contained in a number of other papers cited elsewhere in the discussion.

There is still considerable difference of opinion, however, regarding the mechanism responsible for the formation of the voids observed in the diffusion zone. It would seem that the concept of an interstitial mechanism is generally rejected as being heretical, although Balluffi and Alexander considered such a mechanism quite independently. I put forward this concept, which avoids certain of the difficulties involved in the idea of a vacancy mechanism alone, rather with a view to its further examination by experts, than as a complete solution of the problem. I agree with Mr. Barnes that a calculation of the activation energies appears to favour a vacancy mechanism. I think, however, that the force of this argument is greatly weakened by two facts: (i) The calculation is valid for a pure metal under ideal conditions, whereas disorder of the Frenkel type, suggested in the paper, might well be associated with the presence of impurity atoms and might be a special function of the concentration of such atoms. The fact that, in certain couples, the holes are strictly confined to a narrow concentration band favours this view. (ii) As the phenomena observed could be accounted for by assuming a very small interstitial flow, the number of atoms in a disordered state might represent a very small proportion of the vacancies in equilibrium, which are responsible for the classical balanced-flow mechanism. There is, of course, no reason why such a complex phenomenon should be due to the action of a single mechanism; Shirn, Wajda, and Huntington §§ have recently demonstrated, in the case of the self-diffusion of zinc, the simultaneous occurrence of two mechanisms, both probably vacancy mechanisms, though this has not been conclusively proved.

The concept advanced by Mr. Barnes is certainly simple and ingenious, but it seems to me to contain a fundamental weakness. The mechanism proposed requires the continuous generation of a considerable number of vacancies, to ensure the supplementary flow postulated. To explain why the source of vacancies does not become exhausted, it is necessary to introduce such factors as the formation of stresses and their interaction with dislocations. Thus, although, once initiated, such a cycle would continue, there seems to be no reason why it should begin. In other words, the setting up of a preferential and oriented flow of vacancies and its source (of necessity on the side opposite to the holes) is based merely on a postulate, whereas the initiation of an interstitial flow and the formation of holes would arise inevitably from the equilibrium structure of the component in which the holes are formed; that the mechanism has its origin in this component is supported by the fact that the holes stop abruptly at the original interface. It does not, however, seem unreasonable to suppose that the two mechanisms may operate concurrently.

It may be noted that the mechanism proposed by Mr. Barnes does not necessarily require different intrinsic diffusion coefficients. In this respect the experiment described by Mr. Inman is of particular interest, because it proves that, at least in the case of self-diffusion of brass, copper and zinc have distinct diffusion coefficients. The mechanism proposed by Mr. Barnes cannot explain the experimental result in this instance, but the assumption of interstitial flow fits the facts very well. The hypothesis proposed by Mr. Inman requires only that the two metals shall have different activation energies, and this can as well be so with an interstitial flow mechanism, partial or total, as with a pure vacancy mechanism. To decide between the two alternatives, therefore, additional factors must be sought. On the basis of the vacancy mech-

* R. Smoluchowski and H. Burgess, *Phys. Rev.*, 1949, [ii], 76, 309.

† F. Seitz, *ibid.*, 1948, [ii], 74, 1513.

‡ C. Zener, *Acta Cryst.*, 1950, 3, 346.

§ F. Seitz, *Acta Met.*, 1953, 1, 355.

|| H. N. Hersch, *loc. cit.*

R. W. Balluffi and B. H. Alexander, *loc. cit.*

¶ F. Rohner, *J. Inst. Metals*, 1947, 73, 285.

** D. S. Billington and S. Siegel, *Metal Progress*, 1950, 58, 847.

†† R. A. Dugdale, *Phil. Mag.*, 1952, [vii], 43, 912.

‡‡ F. Rohner, *Z. angew. Math. u. Physik*, 1952, 3, 383.

§§ G. A. Shirn, E. S. Wajda, and H. B. Huntington, *Acta Met.*, 1953, 1, 513.

anism it is the more difficult to explain a net flow of zinc, the smaller is the concentration of zinc and the greater is the degree of order of the phase; in an ordered phase a net increase in one of the components could be explained only on the basis of the interstitial mechanism. The expansion of the β phase in the case of the multilayer specimens heated to 380° C. which I described (Fig. C, Plate CII), would appear to provide evidence in favour of this mechanism, though without furnishing absolute proof.

In replying to Dr. Chaston's three questions, I shall refer largely to the preceding discussion.

(i) The explanations advanced merely require that the holes should be confined to the diffusion zone. This has in fact been observed in all instances. In the case of the copper/brass couple, the holes are scattered throughout the entire diffusion zone on the brass side, being most numerous near the interface; their distribution along the zones of equal concentration is statistical, although the section shown in Fig. 3 (Plate LVIII) of the paper is too small to bring out this fact. The extent of the diffusion zones is implicit in the data accompanying the illustrations; Fig. 2 (p. 387), however gives a definite example.

(ii) It is indeed surprising that cored structures have not been investigated more extensively. I would point out, however, that such cases do not lead to unequivocal conclusions, since the grains of a polycrystalline structure do not represent a mechanically free system. Zones in which holes are likely to form alternate with zones liable to expand, in such a way that the holes may easily be closed up, the plasticity of the material at the homogenization temperature being very great.

(iii) The microradiograph reproduced by Mr. Barnes (Fig. G, Plate CIII), removes any doubt as to the existence of the holes. I would emphasize moreover, that the holes which we observed were certainly not due to inclusions having been pulled out. Polishing with diamond powder is undoubtedly of assistance in certain metallographic work, particularly in automatic polishing, but skill and experience are nevertheless much more important than details of technique in arriving at a correct interpretation, and there is no likelihood of an experienced investigator confusing polishing imperfections with a true effect. It would, moreover, be hard to believe that inclusions would be torn out exclusively in the diffusion zone and always on the same side of the interface, regardless of the purity of the alloys, and in a manner perfectly reproducible in the dozens of specimens examined. Neither are the cavities shown in Fig. 4 (Plate LVIII) due to a gas reaction, for they are unmistakably characteristic of micro-fissures. They occur only in the corners formed by the copper and the zinc on one side, and by the protective layer of copper enveloping certain of the specimens, on the other. It is obvious that the expansion of the copper and the contraction of the brass set up mechanical disturbances in such areas.

I entirely agree with Dr. Chaston that, in considering this new aspect of the problem of porosity, the classic causes of hole formation should not be overlooked, since in the case of the majority of commercial alloys these are of far greater importance than holes due to diffusion. I also share his opinion that the holes observed by Mr. Lardner cannot be explained on the basis of the Kirkendall effect. Mr. Lardner, by numerous careful experiments, has established the following points:

(1) The holes occurred only in those specimens which originally contained residual Mg_2Al_3 (β) (Section II, 4 of Mr. Lardner's paper).

(2) Time and temperature operated in the same sense; holes appeared only within certain limits of time and temperature; they were no longer found if the time and/or temperature were raised beyond those limits (Section II, 1, 2).

(3) Holes already formed on cooling did not disappear on prolonged heat-treatment (Section II, 2).

(4) Hole formation was associated with a fairly rapid cooling rate. Very slow cooling diminished their number and produced rounded shapes (Section II, 3).

(5) The number and size of the holes increased with increase in grain-size of the specimens (Section II, 4).

(6) Holes were consistently formed at the centre of the grains, in the region poorest in aluminium (Sections I, IV, Fig. 2, Plate LXVIII).

An analysis of these facts does not furnish a single argument in favour of the Kirkendall effect. As regards point (1), this is undoubtedly a question of multi-phase diffusion, a schematic diagram for which is presented in Fig. H. From this, the following conclusions may be drawn:

(a) The maximum gradient is always at the original α/β interface.

(b) The width of the zone possessing the steepest gradients first increases, passes through a maximum, and then diminishes again.

(c) Steep gradients are associated with the presence of residual β .

(d) The holes observed are generally situated outside the diffusion zone, at any rate in the region of minimum gradients.

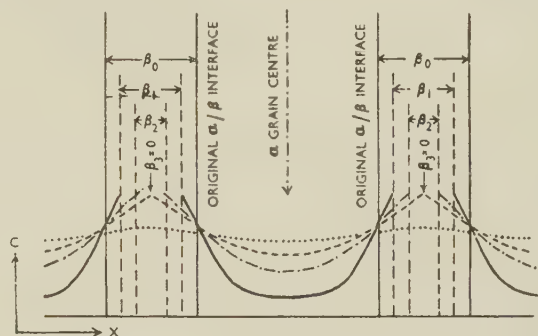


Fig. H.—Showing Evolution of the Concentration (C)/Distance (x) Curves in the α Grain and Width of the β Phase After Various Solution-Treatment Times.

$t = 0: \beta = \beta_0$
 ————— $t_1 > 0$ - - - - - $t_3 > t_2$ (β has just disappeared)
 - · - · - $t_2 > t_1$ $t_4 > t_3$

Without going into details, it is evident that points (3) (considered together with (2)) and (4), taken in conjunction with points (a) and (d), exclude any explanation based on the Kirkendall effect. But all the facts point to a simple explanation. The dissolution of β causes a contraction of the lattice which is, at first, confined to the grain boundaries. This results in a high tensile stress at the centre of the grain, liable to give rise either to micro-fissures, when the stresses are released by the mechanical operation of polishing, or to corrosion figures, which might be described as due to local stress-corrosion, polishing being in fact a mechanical-chemical process. The regular shape of the holes is not surprising in a hexagonal phase; similar phenomena are in certain cases observed with zinc, especially in twinned areas. It is obvious that the wider the zone of steep gradients and the steeper the gradients, the higher are the stresses, in complete agreement with the facts (points (1) and (c), (2) and (b), (5)). The explanation of point (3) now becomes clear, as well as the influence of cooling; only on extremely slow cooling do the stresses become levelled out. It would be interesting to test this hypothesis by means of specially designed experiments.

Dr. Hoar draws attention to the volume changes in sintered compacts. Similar observations have been made in the case of sintered copper/tin and copper/zinc. Fig. D (Plate CII) represents a kind of large-scale model of a sintered specimen, illustrating this phenomenon.

I should like to emphasize the importance of the demonstration first made by Smigelskas and Kirkendall. The earlier demonstration of distinct diffusion coefficients in certain compounds did not make it possible, *a priori*, to draw the same conclusions with regard to substitutional structures having metallic bonding. It was therefore only because this unexpected phenomenon had not been sought, that it was not revealed sooner in metallic structures.

As regards the first part of Dr. Rohner's contribution, I

would refer him to the preceding discussion. I do not think, however, that, if I understand him correctly, I entirely share his views on the mechanism of precipitation. I do not see why in this case only one kind of atom should be involved. Once past the complex stage of nucleus formation, the growth of the nucleus entails diffusion in the surrounding matrix, where the gradients are essentially determined by the equilibrium concentration and the degree of supersaturation. The picture then closely resembles that of Fig. H, but reversed and reduced to the scale of precipitates. That is not to say that the Kirkendall effect will not appear, given the necessary conditions; but it will be much less pronounced, since the volumes involved are very small. These arguments are not applicable to the phenomenon described by Mr. Lardner, since the holes were not observed after precipitation-treatment, but on the contrary after homogenization treatment (see preceding discussion). Age-hardening at room temperature (as in Duralumin) must also be excluded, because here diffusion undoubtedly plays a very small part. Thus, Laves and Jagodzinski* have even put forward strong arguments in favour of a mechanism which does not involve diffusion at all.

Mr. LARDNER (*in reply*): Dr. Rohner and Mr. Barnes have both decided that the cavities that I described in solution-treated magnesium-aluminium alloys are a manifestation of the Kirkendall effect, whilst Dr. Chaston thinks it most unlikely and suggests that they are some form of gas cavities.

On the one hand the formation of these voids as a result of the accumulation of vacancies in the magnesium-rich solid solution fits in well with the observations of Dr. Bückle and Mr. Blin, and, as explained by Mr. Barnes, the formation of voids might well be predicted in such a system. Moreover, the characteristic geometric form and orientation of the

cavities, their position, and their obvious connection with the diffusion of aluminium into the grains of the magnesium-rich solid solution, indicate that these voids are closely related to those observed as being associated with diffusion in artificially produced metallic sandwiches.

On the other hand, the magnesium-aluminium system is not unique, and such void formation might equally well be expected in many other common alloy systems, though apparently none has so far been observed. The production of such voids would also be expected to depend upon the concentration gradients existing in the as-cast structure, and as these depend mainly upon casting conditions, such cavities would be expected always to result when castings in the same alloy were solution-treated. In fact, however, the formation of these cavities is comparatively uncommon and is found to be peculiar to occasional casts of alloy. This strongly suggests that some other condition besides the necessary diffusion is required if cavities are to be produced. Dr. Chaston's suggestion of gas cavities is very attractive here, but surely sharp hexagonal-shaped cavities with a well-defined crystallographic orientation are a strange form for cavities due solely to gas to assume.

Evidently the question cannot be decided upon the evidence at present available. The fact that the cavities appeared to form on cooling now seems open to doubt, and Mr. Barnes' suggestion of incipient fusion during the high-temperature solution-treatment obviously needs close attention.

Dr. Rohner's statement that "it has now been shown that the same type of porosity may develop in diffusion connected with the rejection of solutes from supersaturated substitutional solid solutions" indicates a misreading of the paper. What has been demonstrated is that the formation of the same type of porosity is associated with the homogenization of the cast structure.

Discussion

Priming Paints for Light Alloys

By J. G. RIGG and E. W. SKERREY

(*Journal*, this vol., p. 481)

Mr. E. A. G. LIDDIARD,† M.A., F.I.M. (Member): A pellet of magnesium powder containing 20 wt.-% ferric oxide will react violently in a 3% solution of sodium chloride, and, in fact, produces the stoichiometric quantity of hydrogen from the reaction, assuming that all the magnesium reacts in about 3-5 minutes, while there is a very marked heat evolution. Pellets compressed from magnesium powder without additions, and pellets containing 20 wt.-% magnesia, show only a slight reaction, which tends to decrease with time, and there is no rise in temperature. Such pellets will retain their general form in the NaCl solution over a period of several days.

In view of this fact I cannot believe that iron oxide is a suitable material to bring into contact with magnesium, despite the authors' conclusions. Incidentally, mixtures of magnesium metal and metallic iron powder were used during the war for hydrogen generation in sea-water. The process was worked out at the British Non-Ferrous Metals Research Association and is patented.‡ It was subsequently found that ferric oxide was much more effective in stimulating the reaction than metallic iron. This emphasizes the danger in using an easily reducible metal oxide in contact with aluminium or magnesium under conditions in which the hydrogen-evolution type of corrosion attack can take place.

It is very clear from the results reported in the paper that

the suitability of the various oxides as primers decreases as the metal of the oxide become more noble. The fact that reasonably good results have been obtained by the authors in their experiments on paints can, I think, mean only that the pigment vehicle is the protecting agent and that it will protect light alloys in spite of the presence of an accelerating oxide. There is no significant difference in the rate of corrosion of a pellet made up with 20% magnesia and one without any admixed oxide, so that the increased rate of corrosion in the magnesium-iron oxide pellet is not due to the greater separation of the individual particles of magnesium metal by the oxide, particularly since the volume of magnesia is, of course, greater than the volume of iron oxide used.

This brings me to my main point. Why do we use a primer at all on aluminium, and if we do so, why do we employ an easily reducible oxide of a more noble metal as a filler? Would it not be so much more sensible to use a primer in which the filler was the oxide of the metal to be painted, or a highly stable oxide, as, for example, titania? It seems to me thoroughly regrettable that nobody has attacked this problem of developing a paint especially suitable for light metals, but that instead priming paints developed for the painting of iron, steel, and wood have been adopted. I was surprised to find that in the earlier paper by these authors,§

* H. Jagodzinski and F. Laves, *Z. Metallkunde*, 1949, **40**, 296.

† Director, Fulmer Research Institute, Stoke Poges, Bucks.

‡ British Patent No. 579,246, 1946.

§ J. G. Rigg and E. W. Skerrey, *J. Inst. Metals*, 1948-49, **75**, 69.

in which the results of the six months' tests are described, they report the use of cobalt naphthenate as a drier for all the paints and for the D.T.D. 260A top coat. I suppose one can be thankful that they didn't use a mercury compound! It may be argued that since the results of their exposure tests are quite good, there is really nothing to worry about, but I do not subscribe to that view. If the results are good it is, I suggest, in spite of the filler and driers used in the paint scheme, and we should be able to do a great deal better if we used primers which were logically suitable for aluminium and magnesium.

In all normal circumstances it is unnecessary to protect aluminium and aluminium-magnesium alloys, and it is only with the high-strength materials, particularly those containing copper, that some form of protection is necessary if they are to operate in an industrial or marine atmosphere. I therefore should have liked to see more work done by the authors on fully heat-treated aluminium-copper-magnesium alloys. The B.S. 5L3 alloy is, of course, only room-temperature aged, and in this condition is not particularly susceptible to intercrystalline corrosion. The alloy more likely to be used for structural work is B.S. 1476 HE15-WP. It is with this alloy that there is serious danger of stress-corrosion or layer-corrosion, and judging from recent experience, the latter form of attack does not seem to have been prevented by painting, even when zinc oxide and chromate primers were used. We do know, however, that the most satisfactory method of preventing attack on these high-strength alloys is by cladding. Less information is available on the effect of anodic sprayed coatings, but such work as has been done is very promising. It has been suggested that a sprayed coating may be even more effective than a clad coating, because of the tendency of inert corrosion products to form in the pores of the sprayed coatings. This appears to be another argument in favour of considering alumina as the ideal inert substance for covering aluminium.

The use of zinc, in the form either of metallic paint or a sprayed coating, to protect aluminium has something to be said for it in that zinc is usually anodic to aluminium under normal exposure conditions, despite the fact that it is some distance away from aluminium in the electrochemical series. My experience has been that zinc coatings on aluminium-copper alloys are less effective than aluminium coatings in delaying stress-corrosion failure, and I think there can be no doubt that zinc is not to be compared with aluminium in its general corrosion-resistance.

I would therefore suggest that the best means of protecting high-strength aluminium alloys against corrosion is to provide an anodic coating, preferably of pure aluminium, either by cladding or spraying, and to use paints which contain no compounds of the more noble metals. More attention should be given to the possible use of alumina in the formulation of paints for aluminium and of magnesia in paints for magnesium.

Mr. A. W. BRACE,* A.I.M. (Member): The authors indicate that the medium used might not be regarded as a usual one, and it is perhaps unfortunate that they did not employ more conventional paint vehicles in conjunction with the pigments chosen. In particular, the inclusion of oiticica oil in the medium can be associated with a tendency to embrittlement of the paint film, with consequent flaking during subsequent weathering. It is well established that red lead does not develop its full anti-corrosive properties in the protection of steel with this type of medium; that required by B.S. 1011, however, gives an outstanding performance not excelled by any other vehicle. In tests being carried out by Goodlass

Wall and Lead Industries, Ltd., in collaboration with the Aluminium Development Association, the known merit of a B.S. 1011 red lead primer is being exemplified. After 18 months' exposure in marine and industrial atmospheres, one coat of this primer is still in good condition on both steel and aluminium panels. One coat of a red lead primer in a linseed vehicle with a synthetic quick-drying addition has not shown the same good results on steel, although on aluminium the coat is still in fairly good condition. The authors' conclusions, therefore, would appear to be valid only for the particular medium employed.

The use of iron oxide as a major constituent in primers for aluminium should not be dismissed lightly, for although in itself it has no outstanding properties, the addition of a percentage of zinc chromate substantially improves its performance, and in some applications a red oxide primer containing zinc chromate is to be preferred to a straight zinc chromate primer.

An important point not fully studied by the authors is the effect of surface preparation of the metal before painting. Results have been published in this country† and in the United States‡ and elsewhere, which show that a much longer paint life can be obtained on steel which has been pickled either in a phosphoric-acid or phosphate-base solution, than on steel which has been only weathered and wire-brushed. For aluminium several distinct forms of pretreatment are available, suitable for shop or site use. Had such methods of preparation been employed, the results on paint life quoted by the authors might have been quite different.

It is something of a challenge to learn that B.I.S.R.A. tests show that a paint life of up to 15 years can be obtained with a two-coat system on steel, and that even under industrial conditions a life of 7 years is not unusual. Unfortunately, no comparable test data seem to be available for aluminium.

The phenomenon of the accelerated corrosion of the aluminium and magnesium panels induced by lead pigments is one of some complexity. Tests made by Goodlass Wall and Lead Industries, Ltd., have shown that immersion of aluminium panels in suspensions of lead pigments (red lead, white lead, basic lead sulphate) in water does not produce any rapid attack on their surface. On the other hand, panels immersed in a dilute solution of soluble lead soaps containing 0.15 wt.-% of both lead and organic acids were rapidly attacked, especially if the water contained 0.5–3.0% of sodium chloride. Similar behaviour was observed with a zinc soap solution containing 0.4% zinc and 1.6% of aromatic organic acids. Work carried out by Whitby,§ using potential/time curves, showed that there was a tendency for red lead paints to attack in this way painted aluminium panels immersed in sea-water, distilled water, or a 0.001-N sulphuric acid solution. White lead paints showed no such tendency.

It is not easy to find a simple explanation, but it may be that the acids formed by the breakdown of the linseed oil vehicle|| release soluble lead soaps from the pigments, which, in conjunction with chloride, produce rapid attack on the aluminium. In observations which I have made on a few examples of the phenomenon it has been noticeable that only when the paint film has suffered decided deterioration does the marked attack on the aluminium begin. There is some indication that it may not be general to all lead pigments. Further studies are in progress.

Zinc chromate primers are fairly widely used on aluminium, but their efficiency obviously depends on the inhibition due to the release of soluble chromate ions produced by the controlled entry of moisture into the paint vehicle. It is not unusual, however, to apply over the chromate primer further

* Metallurgist, Aluminium Development Association, London.

† 2nd Interim Rep. of Joint Technical Panel JP/1 on "Painting of Structural Steelwork". 1949: London (B.I.S.R.A.).

J. C. Hudson and T. A. Banfield, *J. Iron Steel Inst.*, 1948, 158, 99.

J. C. Hudson, *ibid.*, 1951, 169, 153.

‡ *Official Digest New England Paint and Varnish Club*, 1949 (Nov.), 792.

J. S. Pettibone, *Amer. Soc. Test. Mat. Special Tech. Publ.*, 1952, (147).

§ L. Whitby, *Paint Research Sta. Tech. Paper*, 1939, (125).

|| L. A. O'Neill, *ibid.*, 1949, (159).

coats which act essentially either as ion barriers or as a continuous protective layer such as that afforded by leafing aluminium, which aims at the exclusion of corrosive agents. It may well be that this combination is not one which gives optimum efficiency. Furthermore, it may be found that the type of paint system which effectively protects the more corrosion-resistant materials, such as the aluminium-magnesium alloys, is less satisfactory on the Duralumin-type alloy. The special chemical properties of aluminium alloys demand paint formulations somewhat different from those commonly employed on steel, and still further adjustments in the protective system used may be necessary for the various groups of aluminium alloys.

Work on the effects of pretreatment and alloy composition on paint life on aluminium-base materials has been undertaken as part of an A.D.A. investigation, but a more fundamental study of the behaviour of different types of pigment and paint vehicles would be welcome. As compared with steel, there is a relative lack of published information of a systematic nature on this subject. Joint action between the metallurgist and the paint technologist is to be encouraged, in view of the growing use of aluminium for structural purposes and in a wide variety of other fields where techniques suitable for site application have to be developed, as opposed to the rather more refined methods used on small assemblies in the shop.

Mr. R. J. BROWN,* F.I.M. (Member): It is unfortunate that the authors did not include in their series of paints the modern etch primers, which are very widely used in industry and extend greatly the service life of the paint coating; nor did they investigate pretreatment with phosphoric acid, which is a common alternative to etching in chromic-sulphuric acid solutions. Although their purpose was to evaluate the primers in general use, the performance of any priming coat is very considerably affected both by the pretreatment of the metal and by the coatings subsequently applied over the priming-paint.

In Table VI (p. 486) it is indicated that uncoated steel panels suffered only slight corrosion during a period of 3 months' exposure at the marine site, and in the accelerated tests. This is fantastic, as uncoated degreased steel will rust overnight in most atmospheres, even under cover. Reference is made in the paper to the more severe corrosion experienced on the panel backs. This is hardly surprising, as careful examination of exposed panels during atmospheric tests will show not only that evaporation on the upper surface is more rapid, but that condensation on the under surface is more severe. The effect of direct solar radiation is to promote the breakdown of the vehicle of the paint coating, the degree of breakdown being related to the intensity of corrosion resulting from prolonged exposure. The severity of the corrosion on the panel backs should be attributed directly to the effect of moisture, and not to sheltering from solar radiation.

Dr. F. A. CHAMPION,† B.Sc., A.R.C.S., F.I.M. (Member): Theoretical considerations lead one to expect that lead pigments would be liable to stimulate the corrosion of aluminium, and even more so that of magnesium, and that this would be most marked in environments providing a strong electrolyte, e.g. marine and industrial atmospheres. The work of Dr. Rigg and Mr. Skerrey has confirmed these expectations and provides a valuable assessment of the practical importance of the effects in different types of exposure conditions. It is rather surprising to note signs that they were operative even in the rural atmosphere, as shown, for example, by the greater corrosion at scratch lines with systems using lead primer as compared with those using iron oxide primer (see Table IV, p. 484). Some mechanical damage is usually inevitable

before maintenance is justified in service, and it therefore seems desirable to avoid lead pigments for light alloys in all conditions where protective paints are called for.

The authors have pointed out that iron oxide or preferably zinc chromate or tetroxychromate should be used all over composite structures of aluminium and steel, and it should be added that they are also required for aluminium-coated steel (e.g. sprayed coatings). In spite of Mr. Liddiard's purist objections, the results confirm the suitability of iron oxide as a diluent for chromate pigments in primers for aluminium and its alloys.

Mr. A. J. FIELD,‡ M.C., B.Sc., F.I.M. (Member): It is not clear whether, in the priming paint, as the conditions are intentionally of a non-electrolytic character, the pigment has effect on the durability of the medium or of the underlying metal. This suggests that it might be of interest to test the three interactions separately, namely, pigment on metal, medium on metal, and pigment on medium.

Mr. H. SILMAN,§ B.Sc., F.R.I.C., M.I.Chem.E., F.I.M. (Member): The problem of formulating a suitable priming paint for aluminium cannot be reduced to the simple one of combining an aluminium-base pigment with a drying oil. Many other factors enter into the matter, including in the first place the compatibility of the pigment with the medium, not only from the point of view of the protective value of the finish but also of the stability of the paint itself. Other aspects include covering power and corrosion-inhibiting properties.

Mr. Liddiard tends rather to over-simplify the economic and technical considerations of paint manufacture in the suggestions he makes for the formulation of a satisfactory priming paint for aluminium.

The AUTHORS (*in reply*): We note that Mr. Liddiard considers that we are lacking in caution in advocating the use of iron oxide pigments on light alloys, while Mr. Brace holds that we are too cautious in our objection to the use of red lead. We therefore feel that the discussion, on balance, supports the moderate view we have taken.

The iron oxide pigment was selected as being a non-inhibitive priming pigment in common use. Despite the observation that iron oxide will catalyse the dissolution of magnesium in sodium chloride solution, it did, nevertheless, provide a useful degree of protection in our tests, with no indication of acceleration of corrosion. The inference is not, however, as Mr. Liddiard suggests, that the medium is making up for the shortcomings of the pigment. No medium of this type without pigment could be expected to give such a long period of protection. As has been pointed out, the iron oxide increases the durability of the film.

Mr. Brace does not see any advantage in the use of zinc chromate primers under relatively impervious top coats. Even leafing aluminium top coats are, however, still slightly pervious,|| and the exclusion of moisture will rarely be 100% efficient. The primer is, therefore, necessary to provide maximum protection under these conditions and above all to take care of accidental damage, since the chromates continue to protect even where the priming film has been rendered discontinuous in places. We agree with Mr. Brace that mixed chromate-iron oxide films give priming paints suitable for most purposes.

Mr. Liddiard's objections to the use of cobalt driers are of a theoretical nature. Unfortunately, efficient drying can be achieved only in the presence of certain metallic salts or soaps and, of the metals available, cobalt is the most active drier and is therefore used in the smallest concentration possible.

We sympathize with Mr. Brace's remarks about red lead giving the best protection to steel in a medium of the type

* Chief Chemist and Metallurgist, Nuffield Central Research Laboratories, Morris Motors, Ltd., Coventry.

† Research Laboratories, The British Aluminium Co., Ltd., Gerrards Cross, Bucks.

‡ Works Manager, The British Aluminium Co., Ltd., Falkirk.

§ Research Manager, Ford Motor Co., Ltd., Birmingham.

|| V. J. Hill, *Paint, Oil and Colour J.*, 1952, 122, 137.

specified in B.S.1011, and for that reason did not lay stress in the paper on the comparatively poor results obtained with the oiticica oil medium on this metal. Better media could have been chosen for all the other three priming pigments. Since the emphasis was on priming pigments for light metals and the number of panels had to be kept within reasonable bounds, a single priming medium was selected which gave a reasonable degree of adhesion on all these metals, and was at the same time compatible with both types of aluminium top coat. The manufacturer who so kindly formulated the paints drew on a medium in common commercial use at the time—a time moreover when paint oils and resins were in short supply.

The results from tests by Goodlass Wall and Lead Industries, Ltd., which Mr. Brace quotes, in which aluminium specimens were immersed in suspensions of lead pigments or soaps, appear to be in accord with our own results, namely that an electrolyte (e.g. 0.5–3.0% NaCl) is necessary to give the ill effects. In the exposure tests, the serious effects of lead pigment were, similarly, noted only in industrial and marine conditions where the necessary electrolyte was provided for the galvanic cell.

Several contributors have drawn attention to omissions from the paper. We agree with these contributors, and with Mr. Field, that there is scope for further work in all these directions, and we endorse the statement by Mr. Silman that the problems are complex and should not be considered to be as simple as Mr. Liddiard might suppose. Our results (and especially comparison of the high- and low-purity magnesium-base alloys) confirm Mr. Brace's expectation that a paint system which is satisfactory on the more resistant metals gives a shorter life on the less resistant. Since no paint film is completely impervious, the corrosion characteristics of the underlying metal must be added into the sum of the total corrosion-resistance of the entire system. We do not believe that there is a call for special formulation for particular aluminium

alloys, other than adjustment of the protective value of the paint film. This can be done by varying its total thickness or the content of inhibiting pigment to the requirements of the underlying metal, in the same way that it is adjusted to the severity of the exposure conditions.

We would emphasize that we have not attempted a general discussion on the painting of light alloys, but have simply recorded an investigation with a limited objective, namely, the comparison of various single primer pigments on light alloys, although a few incidental observations have been included in the paper. The tests were designed to eliminate as far as possible factors irrelevant to this investigation, in order to obtain reliable results as quickly as possible. For example, the inclusion of "etch primers" (not then available in this country) would have delayed information on the primary objective. We entirely agree that there should be no difficulty in designing procedure and paint systems which would provide better and more enduring protection than the best of the range employed for this particular investigation. Choice of different media and mixed-pigment formulation would be two possible steps in this direction.

As a matter of interest, however, a few of the panels have remained on test, and the best systems have continued to give good protection to the more resistant light metals after exposure for seven years at the most severe sites.

We agree that sheltering from direct solar radiation would extend the time for which the backs of the panels remain wet and so contribute to the effect of moisture, as indicated by Mr. Brown, and would also avoid breakdown of the medium by ultra-violet absorption. Mr. Brown finds it difficult to accept our assessment of the attack on plain steel panels after three months' exposure. We wonder whether he has appreciated that our terms of assessment bear a definite relation to numerical values,* e.g. slight attack included infrequent pitting up to 10 mils deep and general attack up to 0.6 mils deep.

Discussion

Stretcher-Strain Markings†

Dr. W. A. BAKER,‡ F.I.M. (Member of Council): In reading the several papers on stretcher-strain markings and discontinuous flow, it seems rather remarkable that these phenomena, so long familiar in steel, should previously have received so little attention in non-ferrous metals. The occurrence of the particularly objectionable types of marking in lightly strained aluminium-magnesium alloys has stimulated a good deal of the current work on the subject, and the close analogy between the behaviour of steel and non-ferrous metals is becoming more and more apparent. The authors are to be congratulated on the careful way in which they have studied the nature and mode of occurrence of these markings, because, although we by no means understand the subject as fully as we would like, they have at least shown how the appearance of the markings depends on various factors, and their observations have gone a long way towards dispelling some misconceptions about stretcher-strains not only in non-ferrous metals but also in steel.

There seems to be little doubt that the initial yield occurring in an annealed material is to be distinguished from the yields that succeed it, and from the yield that occurs in a strain-aged steel. Not only are the two types of yielding dependent

on different factors, but they give rise to distinctively different types of marking. In the case of steel, this distinction seems to have been obscured in the past, for the observer has frequently failed to distinguish between stretcher-strains in fully annealed material and those which develop in strained and aged material, and even in one of the present papers Dr. Polakowski suggests that the irregular flamboyant or random markings, now clearly shown to be associated with the first yield in a fully annealed material, arise only from heterogeneous stress distribution in the specimen during straining. This author suggests that whenever these local stress concentrations are relieved by a certain amount of plastic flow, the markings revert to the regular parallel-band type. However, Dr. Phillips, Mr. Swain, and Mr. Eborall state that if care is taken to avoid notches in the specimen, the shear deformation involved in the initial yielding will spread continuously through the test-piece and no major strain marking will be visible. Thus, although they show that the highly irregular flamboyant markings, so objectionable in practice, are caused by local stress concentrations which propagate this deformation from a number of points at one time, their observations seem to be inconsistent with Dr. Polakowski's

* J. G. Rigg and E. W. Skerrey, *J. Inst. Metals*, 1948–49, 75, 69.

F. A. Champion, *ibid.*, 1943, 69, 47.

† Joint discussion on the following papers published in the *Journal*: R. Chadwick and W. H. L. Hooper (1951–52, 80, 17); W. H. L. Hooper (this vol., p. 563); W. H. L. Hooper

and J. Holden (this vol., p. 648, and *Bulletin*, 1953, 1, 161); N. Krupnik and H. Ford (this vol., p. 601); N. H. Polakowski (this vol., p. 617); V. A. Phillips, A. J. Swain, and R. Eborall (this vol., p. 625); V. A. Phillips (this vol., p. 649).

‡ Research Manager, British Non-Ferrous Metals Research Association, London.

suggestion that only one type of deformation occurs and that the differences between the appearance of the markings is dependent only on the conditions of straining.

From the practical point of view it is comforting to find that Mr. Chadwick and Mr. Hooper, and Dr. Phillips, Mr. Eborall, and Mr. Swain, reach essentially the same conclusions about remedial measures for stretcher-strain markings in the aluminium-magnesium alloys. One of the remedies that involves rapid cooling from a high temperature is perhaps of more academic than practical interest. The two groups of investigators appear to interpret this result, and the effect of subsequent reheating of the quenched material to lower temperatures, in different ways. Thus, Mr. Hooper suggests that quenching from high temperatures introduces internal stresses, which in some unspecified way prevent the formation of the objectionable random markings. On his view the effect of subsequent heat-treatment at lower temperatures is to relieve these internal stresses and thereby make the material again susceptible to stretcher-strain marking. The other investigators make no reference to any possible effect of internal stresses but interpret the effects of quenching and reheating in terms of the distribution of magnesium atoms between the grain bodies and the grain-boundary regions. They hold that their observations are consistent with the view that the solute atoms diffuse to, and concentrate at, the grain boundaries during low-temperature heat-treatments, and thereby produce a grain-boundary barrier which impedes the propagation of slip from one grain to another and is thus responsible for the marked initial yield. Their data on the effects of various times and temperatures of heat-treatment seem to me to rule out the suggestion that the effects are due to internal stresses. If one refers to their Fig. 24 (p. 638) and considers, for example, the effects of reheating at 150° and 100° C., it will be found that to restore the yield point to an equivalent degree by heating at these two temperatures, the heating times at 100° C. would have to be roughly one hundred times as long as at 150° C. This fact seems to me to be incompatible with the idea that the relief of internal stress is responsible for the effects noted, because observations on the creep properties of a variety of aluminium alloys, including aluminium-magnesium alloys, show that the resistance of the materials to creep at the two temperatures I have quoted differs by a factor of only about 2, or at most 4. On this score it seems to me that the internal-stress effect, if any, might be disregarded, but I should be very interested to hear the authors' further observations on this point.

Turning to the less objectionable type of strain marking, the parallel ripples or Lüders bands (described by Dr. Phillips and his colleagues as type-B markings), there seems to be no doubt that these markings arise from yields, whether single or multiple, occurring in strain-aged material. Until one reads the paper by Mr. Krupnik and Professor Ford the picture seems to be fairly straightforward, in that all the investigators seem satisfied that these yields and their associated markings can be explained in terms of Cottrell's theory of strain-ageing. Krupnik and Ford, however, complicate the issue by showing that at slow, constant rates of loading, and more particularly by straining at constant rates in a very rigid machine, the discontinuous yielding and the associated ripple markings are suppressed. These authors consider that their findings throw doubt on the view that discontinuous yielding can be explained by current theories of strain-ageing phenomena. I do not propose to venture into that particular argument, but I should like the exponents of whatever theory is put forward to explain in a little more detail just how the deformation associated with type-B markings occurs. In the description of the behaviour of materials when yielding is observed, Lüders-band markings are described as running up and down the gauge-length of the specimen, although the description of the contours of the specimens after such yielding has occurred makes it clear that what really happens is that a great many small contiguous necks are formed in rapid succession. One

then has the picture that the load on the material is increased till the point is reached at which slip occurs in some region, presumably where there is a local stress concentration, and the slip gives rise to a small neck. Why does yielding stop in this region, to be followed immediately by yielding in a similar very small adjacent area? I do not see why, in the light of what is said in the several papers, the boundary of the first necked region does not spread continuously through the metal, and I cannot help wondering whether a more careful consideration of the macroscopic mode of deformation associated with type-B yielding might explain the observations of Krupnik and Ford on the effect of straining at slow and constant rates. Could it be, for example, that under their conditions of testing in a rigid machine the volume of metal affected in each of these small necked regions might be smaller still, so that the deformation process became one in which the boundaries of the initially necked region spread right through the material?

MR. R. CHADWICK,* M.A., F.I.M. (Member) and Mr. W. H. L. HOOPER,† B.Sc., A.I.M. (Member): Although we clearly stated in our first paper (p. 19) our belief that type-A or random markings are, when first formed, at right angles to the direction of stress, this important fact should be repeated and emphasized, because the issue has tended to be obscured for two reasons. First, the terminology suggested, i.e. "random" or "flamboyant", has emphasized the curvature which often develops as stretching progresses and the stress system becomes more complex. Secondly, the flamboyant character of the markings really arises from the employment of wide test specimens. Although such specimens are most desirable for obtaining good illustrations, uniform stressing is inherently difficult, while slight gauge variations cause irregularities even with accurate specimen alignment. On a standard tensile test-piece of narrow central gauge-length, the first-formed markings (Fig. A, Plate CIV) are normal, and diverge from this position only after continued stretching (Fig. B, Plate CIV), forming the tongue-shaped markings such as those illustrated in Fig. 2, Plate III (Chadwick and Hooper) and seen also in Fig. 3 (a), Plate XC (Phillips, Swain, and Eborall).

There appears to be no serious divergence in views as to the general form of metal surfaces affected by type-A markings, the model illustrated in our first paper (Chadwick and Hooper, Fig. 12, Plate VI) being generally accepted. Dr. Phillips, Mr. Swain, and Mr. Eborall made measurements of the angle of tilt between adjacent surfaces at a strain line produced at an early stage in the stretching of an aluminium-magnesium alloy. Using both optical interferometry and differential focusing, they obtained values ranging from 22' to 33'. We used the former method only and obtained angles in the same range, i.e. 20'–30' on both aluminium-magnesium and mild-steel specimens (Hooper and Holden). A somewhat different series of values was obtained from Talysurf measurements on specimens of aluminium-magnesium alloy subjected to a greater amount of stretching, so that type-A markings were numerous and fully developed. On these specimens the Talysurf traces show that surfaces generally have significant curvature. The geometry is indicated in Fig. C on the usual exaggerated vertical magnification of the Talysurf trace. The angle to a reference surface AA' is obtained from measurement of the tangent of the mean slope ZY/XY of the area between two strain lines X and Z . A typical measured angle, ϵ , is about 1'. The angle α between adjacent surfaces forming the cusp at Z is quite obviously larger than ϵ , but at this stage of stretching is smaller than at the earlier stage where the 20'–30' measurements were taken.

Again, on the subject of type-A markings, Phillips, Swain, and Eborall (p. 628), quote us as having found no thinning of sheet as a result of the formation of markings. This is incorrect, because no measurements of thickness were, in fact, made, but clearly if a specimen is stretched by 1% or so there

* Assistant Research Manager and † Research Technical Officer, Imperial Chemical Industries, Ltd., Metals Division, Birmingham.

must be some corresponding thinning, which is, however, an overall and not a local thinning. Possibly we were guilty of over-simplification in our synopsis (Chadwick and Hooper, p. 17), but the point we made was that random (type-A) markings were due to kinking, in contrast to the parallel bands (type-B), which are due to local thinning or necking.

The parallel bands or type-B markings have been characterized as occurring in aluminium alloys at a later stage in stretching than the type-A markings, and there is general agreement on their topography. We found that these markings first became apparent in Talysurf measurements after type-A markings had been largely dispersed and attenuated at about 2% extension. There is, however, a good deal of evidence that strong type-B markings appear at a much earlier stage. For example, in the picture by Phillips, Swain, and Eborall (Fig. 3 (a), Plate XC) of type-A markings, with a 1% extension, many of the finer markings are at angles of 52°–55° and must be regarded as of type B; similar but smaller markings are shown by Hooper (Fig. 3, Plate LXXXIII), after $\frac{1}{2}$ % extension. As yet very little work has been done on the topography of markings in mild steel, but the work of Mr. Hooper and Mr. Holden suggests that the two types of marking often occur together. Fig. 4 (*Bulletin*, 1953, 1, 162), for example, shows kinking and necking occurring simultaneously. The central marking is quite definitely a neck

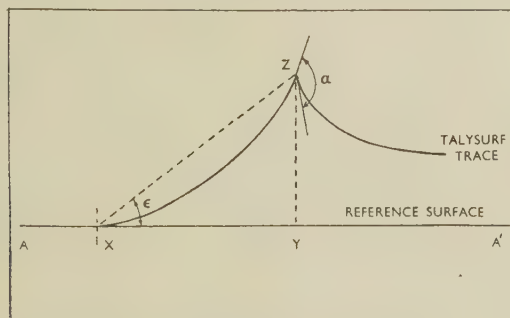


FIG. C.—Geometry of Talysurf Traces on Aluminium-Magnesium Alloys on Which Type-A Markings Were Fully Developed.

from the Talysurf traces. Angles measured on Figs 4 and 5 (*Bulletin*, p. 162) range between 50° and 55°.

There has unfortunately as yet been little attempt to correlate the results of topographical measurements with stress/strain curves. The obvious difficulty in trying to relate existing data is the small number of discontinuities in the stress/strain curve compared with the total number of strain markings. Thus Phillips, Swain, and Eborall generally show less than 20 discontinuities in a 5% extension, where there must be literally hundreds of separately identifiable strain lines. It is interesting in this connection to note the finding of Professor Ford that when specimens are stretched under special conditions at constant rate of strain, the discontinuities in the stress/strain curve do not appear, although there were no related topographical observations. It seems possible that the formation of a single strain line, whether it be a kink or a neck, is insufficient to show any effect on the stress/strain curve. Under normal testing methods with a non-rigid machine, however, the sudden yielding when a single strain line forms would cause a disturbance sufficient to trigger-off several more strain lines, which would in total give a visible break in the stress/strain curve. This would be repeated at intervals, and the magnitude of each step in the

curve would be largely fortuitous, depending upon the number of strain lines triggered-off, the controlling factors being the mechanical condition and degree of elastic recovery in the testing machine. This would account for the irregularity in size and spacing of steps characteristic of most published stress/strain curves.

Professor A. H. COTTRELL,* B.Sc., Ph.D. (Member): The results presented in this very interesting group of papers contribute substantially to the rapidly accumulating evidence †‡§|| that yield points can be produced in face-centred cubic metals when these contain substitutional solute atoms. Interpreted in terms of the dislocation theory, yield points are to be expected in such alloys because the dislocations responsible for slip exist in a form (i.e. as pairs of Shockley half-dislocations) in which they are capable of attracting to themselves substitutional solute atoms. However, this attraction is weaker than in the case of interstitially dissolved carbon and nitrogen in ferritic iron, where a notable yield point can be produced. For example, according to elasticity theory, the energy binding a zinc atom to a dislocation in copper is about 0.12 eV., whereas the corresponding value for carbon in iron is about 0.5 eV.|| This is important, because the concentration of dissolved atoms in equilibrium with a dislocation atmosphere of a given density rises exponentially as the binding energy is reduced. For an atmosphere that will give a strong yield point at room temperature, the amount of carbon or nitrogen in solution in iron need only be about 10^{-7} %. But for zinc in copper, the corresponding concentration has to be about 1%. This means that yield points in face-centred cubic metals are unlikely to be observed at ordinary temperatures unless fairly substantial alloy additions (e.g. up to a few per cent.) are made, and these additions are retained in solid solution. These conclusions agree with the observations that face-centred cubic metals do not normally show yield points unless they contain appreciable amounts of impurity or alloy additions, and that serrated yielding is observed most clearly in freshly cooled specimens, where most of the alloying elements are retained in solution.

Serrated yielding in these face-centred cubic metals has two interesting features. It often does not begin until a small amount of plastic deformation has taken place. Secondly, if we interpret the serrations as being caused by strain-ageing during the course of plastic deformation, as is known to be the case with carbon and nitrogen in iron, the necessary rate of ageing is far too fast to be accounted for by the diffusion coefficient of the solute atoms, as determined from high-temperature measurements. That this fast ageing does really occur is demonstrated in the paper by Dr. Phillips, Mr. Swain, and Mr. Eborall, as well as in some rather similar work in America.‡

Both these features can be explained ¶ on the bases (i) that the diffusion coefficient is too small, at the start of plastic deformation, to give appreciable strain-ageing during deformation, and (ii) that the diffusion coefficient increases during plastic deformation, through the creation of vacant atomic sites and related atomic defects,**†† and after a certain strain becomes large enough to cause strain-ageing during deformation. According to Mott** and to Seitz †† the concentration of vacancies created by plastic deformation is about $10^{-4} \epsilon$, where ϵ is the strain, and an estimate ¶ based on this formula gives the expected rate of substitutional diffusion in worked aluminium at room temperature as $10^{-13} \epsilon$ cm.²/sec., in order of magnitude. By analysing published data on serrated yielding in iron, one can show ¶ that it occurs when the rate of diffusion (of carbon or nitrogen) is about $10^{-9} \dot{\epsilon}$ cm.²/sec., where $\dot{\epsilon}$ is the rate of strain. Let us consider

* Professor of Physical Metallurgy, Birmingham University.

† C. A. Edwards, D. L. Phillips, and Y. H. Liu, *J. Iron Steel Inst.*, 1943, 147, 145.

‡ O. D. Sherby, R. A. Anderson, and J. E. Dorn, *Trans. Amer. Inst. Min. Met. Eng.*, 1951, 191, 643.

§ R. E. Smallman, G. K. Williamson, and G. Ardley, *Acta Met.*, 1953, 1, 126.

|| G. Ardley and A. H. Cottrell, *Proc. Roy. Soc.*, 1953, [A], 219, 328.

¶ A. H. Cottrell, *Phil. Mag.*, 1953, [vii], 44, 829.

** N. F. Mott, *ibid.*, 1952, [vii], 43, 1151; 1953, [vii], 44, 187, 742.

†† F. Seitz, *Advances in Physics*, 1952, 1, 43.

a typical experiment on an aluminium alloy at room temperature, where the rate of strain is, say, 10^{-5} /sec. Then the rate of diffusion at which serrated yielding occurs should, by analogy with iron, be about 10^{-16} cm.²/sec. Now the diffusion coefficient at room temperature, deduced from the high-temperature data, is of the order of 10^{-23} cm.²/sec.; it is thus far too small to give serrated yielding. But with plastic deformation the rate of diffusion increases, and according to the formula $10^{-13} \epsilon$, a strain of 10^{-3} should be sufficient to cause serrations to appear. A further development* of this theory suggests that the serrations disappear, and that the stress/strain curve becomes smooth again, if the rate of diffusion becomes too high, or the rate of strain too low. In this connection it would be most interesting to know if the smooth stress/strain curves obtained by Mr. Krupnik and Professor Ford at constant rates of strain persist at higher rates, or whether they break down into the serrated type. Are they smooth because the rate of strain is too small, or is there some other effect present?

Mr. A. J. FIELD,† M.C., B.Sc., F.I.M. (Member): These informative papers will be of assistance to the light-metal sheet-producing industry in dealing with the nuisance of stretcher-strain markings on certain alloys. They bring to mind similar phenomena encountered some 30 years ago in the production of binary aluminium-2.5% and 3% copper alloy sheets supplied in the annealed condition for such uses as camera cases. In some instances the formation of the parallel bands was then observed in the tensile-testing machine, always at an angle of approximately 60° to the direction of the applied force. These bands started with a clink-like noise and thereafter one edge of a band could be seen to run away from the other, which might have remained stationary. The distance travelled was sometimes quite considerable, sometimes less so, the breadth of the band depending on the distance of propagation of the molecular disturbance. After the first disturbance had ceased on a test-piece and following a further period of apparently elastic extension, another oblique band would originate and broaden by propagation of one edge. Sometimes this ran in an opposite direction, and the bands sloping in opposite directions sometimes ran opposite ways. The rate of propagation of the band boundary could be followed, and appeared to be of the order of 50 ft./min. In the case of these alloys, parallel bands did not always occur, there being no doubt some small differences in annealing conditions; there were no instances of flamboyant markings, which supports the observation of Dr. Phillips that these occur only on the aluminium-magnesium alloys. The adjective can be commended as more picturesquely descriptive than "type A", which some authors are beginning to adopt, with type B for the oblique parallel bands.

The binary wrought aluminium-magnesium alloys were little used in the early 1920s, although their virtues and possibilities had been clearly shown by Schirmeister's results.‡

It is of interest that the flamboyant markings are reported not to register a diminution of thickness, but only to exhibit a change of angle relative to the rest of the sheet. As extension has taken place and no change of density is reported, it is to be supposed that all extension has taken place at the joints between the flamboyant markings and the undistorted sheet.

Use is made in certain of the papers of the term "strain-ageing". The word "age" involves the factor of time, and information as to the relationship of hardness to time would be of interest. It is true that all events have to happen at intervals of time, and that all phenomena unavoidably cover a lapse of time, but unless there is a fairly definite

and particular relation of an effect to lapse of time, as in the precipitation-hardening of an aluminium alloy after quenching, and if strain is the causative factor and increase of hardness the effect, perhaps the factor of time is not specific and a more accurately descriptive term should be adopted.

The method of rectification, sometimes adopted in the case of steel pressings, of filling in such defects as flamboyant markings with lead solder would not be acceptable for light alloys. Methods of prevention or avoidance are indicated in some of the papers. One method is to quench the non-heat-treatable aluminium-magnesium alloys from 500° C., but this process has the disadvantage of a rather high cost. The use of material with a somewhat larger grain-size might be undesirable in some instances. Other suggestions made include the use of roller levelling, which was earlier recommended for restraining the "worming" (i.e. flamboyant marking) of steel sheets. Certainly a simple, cheap, and effective solution to the problem is much to be desired.

Professor H. FORD,§ D.Sc., Ph.D. (Member): A study of the various papers shows that the size and progression of the steps in the yield-stress curve, while following the same general characteristics, appear to depend upon whether the material shows both type-A and type-B yielding. In certain of the experiments made by Dr. Phillips, Mr. Swain, and Mr. Eborall, the materials exhibit both types of yielding, and it appears clear that the effect of type-A yield can return, if time is allowed for it to do so. In these circumstances, the steps do not show a gradually increasing size, as in materials in which only a type-B yield is present. It also appears that the type-A yielding exhibits all the attributes of a true yield, as in mild steel, and after appropriate ageing this large step returns, yielding at a value slightly above the normal yield-stress curve. This could explain the finding of Phillips, Swain, and Eborall, that the bottom corners of the steps appeared to touch a common curve, whereas in the tests of Krupnik and myself, the upper corner undoubtedly was the envelope of the curves and was also the smooth yield-stress curve, where this was obtained.

Mr. D. HUMPHREYS||: Manufacturers of sheet metal must have gained a great deal of practical information from the papers on stretcher-strain marking. As producers of aluminium-magnesium alloy sheet we have found that (i) control of grain-size, (ii) small amounts of cold working followed by a non-recrystallizing anneal, (iii) quenching from 500° C., all afford means of overcoming the type-A or flamboyant markings. The last method is attractive in that it gives a fully soft, fine-grained sheet.

However, in many plants in this country the only means of quenching from 500° C. is in quench tanks working in conjunction with sodium nitrate salt baths. References in the literature¶ stress the possible hazards in treating magnesium alloys in salt baths, and afford evidence** of a violent reaction occurring at 450° C. in the case of the 7% magnesium alloy. I should be glad to learn of the experience of members in this matter, and furthermore, what is likely to be the effect of this rapid quenching on the corrosion-resistance of the alloys.

Dr. B. B. HUNDY,†† B.Sc. (Member): At B.I.S.R.A. we are primarily concerned with stretcher-strains in mild steel, and at present we are working to improve the industrial methods of eliminating these markings. The close similarity of ferrous and certain non-ferrous alloys in respect of the yield-point phenomena and of stretcher-strain markings has been pointed out in a number of these papers, but I think that this similarity should be emphasized. A steel pulled in the

* A. H. Cottrell, Chapter in "The Relation of Properties to Structure" (American Society for Metals 1953 Seminar), in the press.

† Works Manager, The British Aluminium Co., Ltd., Falkirk.

‡ H. Schirmeister, *Stahl u. Eisen*, 1915, **35**, 650, 873, 996.

§ Imperial College of Science and Technology, London.

|| Northern Aluminium Co., Ltd., Banbury.

¶ — "The Treatment of Aluminium Alloys", *American Military Specification No. MIL/H/6088*, 1950.

** — "Precautions in the Use of Nitrate Salt Baths", *Factory Department Memo. No. 848*, 1950.

†† British Iron and Steel Research Association, Sheffield.

"blue brittle" range, behaves in a similar fashion to an aluminium-magnesium alloy tested at room temperature; the initial yield point gives rise to the flamboyant type-*A* markings, and the serrations in the later part of the stress/strain curve can be associated with the appearance of type-*B* markings. Measurements of these markings on photographs reproduced in the literature* show that they usually lie between 55° and 60° to the specimen axis. This agrees quite well with the quoted figure of 58° for the aluminium alloys. The fact that these markings all appear at this particular angle can be explained by consideration of Hill's theory of localized necking in thin sheets.† The theory predicts that localized necks should form at an angle of 55° to the specimen axis and as the type-*B* markings apparently have the characteristics of necks, one would expect them to form at this angle. The variation from this figure, which is observed, can probably be explained on the basis of anisotropy in the specimens.

Another point of similarity in the type-*B* markings in steel and the aluminium alloys is that the markings disappear when certain solute atoms are removed from solid solution in the base metal. The addition of aluminium or vanadium to steel stabilizes the nitrogen and prevents the formation of markings; whilst Mr. Krupnik and Professor Ford have shown here that the stepped stress/strain curve of freshly quenched Duralumin, which is associated with these markings, gradually smooths out as ageing proceeds.

The characteristics of the flamboyant type-*A* markings are also very similar in mild steel and in aluminium-magnesium alloys. Two identical box pressings were made in mild steel and in an aluminium-3% magnesium alloy and the appearance of the markings was remarkably alike in the two cases. Figs. D and E (Plate CIV) show the same part of each pressing for comparison. Talysurf tracings across some of these markings showed that the deformation occurred by kinking both in the aluminium alloy and in the mild-steel pressing. The angle of kinking for the aluminium-magnesium pressing was found to be about 31°, which is in reasonable agreement with the figure quoted by the B.N.F. workers but rather higher than that quoted by Mr. Chadwick and Mr. Hooper. The kinking angle for the mild steel was, as might be expected, considerably higher, and was found to be about 2° 30'. There seems to be little doubt that the flamboyant markings, or true stretcher-strains, occur by a kinking or shearing mechanism, rather than, as was thought at one time, by thinning without kinking. The actual amount of kinking is probably dependent on the metal and on factors such as grain-size. A hypothesis to explain why the deformation takes place by a kinking mechanism has been put forward by Lomer.‡

It seems that mild steel differs from non-ferrous alloys in two respects only. First, the type-*A* markings on the aluminium-magnesium alloys are permanently removed by cold rolling, whereas they return when mild steel is aged after rolling. Secondly, mild steel shows a pronounced rise in strength and fall in ductility on strain-ageing, which is not shown by the non-ferrous alloys. Have any of the authors an explanation for this?

I would now like to make one or two more specific comments on the papers presented here.

Have Mr. Krupnik and Professor Ford, or the B.N.F. workers, applied Professor Cottrell's recent theory of the type-*B* yielding in aluminium alloys§ to their own results? His theory seems to explain most of the effects associated with this particular type of stress/strain curve, and I should be interested in any comments on this.

I am rather surprised that Dr. Polakowski attributes the sharp yield point obtained after slow cooling from a high

temperature to the formation of a precipitate, and the absence of a yield point on quenching to the precipitate remaining in solution. I think that the dislocation theory of the yield point is now generally accepted, and on this theory we should expect quite the opposite effect; for instance, Cottrell and Leak|| have shown that ageing a quenched specimen, so as to precipitate the carbon out of solution, can reduce the rate of subsequent strain-ageing by a factor of 5. It is my opinion that the absence of a yield point after quenching is mainly due to its being masked by intergranular quenching stresses, in a manner similar to that suggested by Dr. Polakowski in another paper.¶ This mechanism might also explain why type-*A* markings can be eliminated in aluminium-magnesium alloys by quenching, though the theory put forward by Dr. Phillips, Mr. Swain, and Mr. Eborall is most attractive. Still referring to Dr. Polakowski's paper, I would suggest that the increase of the Lüders strain after each successive strain-ageing treatment is only a reflection of the shape of the stress/strain curve. If the rise in the yield stress after each ageing treatment is constant, then the Lüders strain will increase as the rate of work-hardening decreases.

Can any of the authors suggest why magnesium is the only element that will give rise to a yield point in aluminium? Is this due to the particular type of lattice distortion caused by a magnesium atom, or is it due to some other reason?

Finally, I would like to point out that stretcher-strains can lead not only to bad appearance, but also to failure during pressing. Fig. F (Plate CV) shows a mild-steel pressing where localized necking and fracture has occurred along the radial stretcher-strains. We believe that this will occur when the pressing speed is high enough to raise the yield point above the ultimate tensile strength. Temper-rolling removed the yield point, and Fig. G (Plate CV) shows that the pressing could then be made without failure occurring.

Dr. C. F. TIPPER,** M.A. (Member): Some years ago, I†† devised a means of independently recording load and extension against time, for use on the Quinney machine in the Engineering Department at Cambridge University.

The object was to determine the effect of the rigidity of the machine upon the shape of the load/extension curve, when discontinuous deformation occurred, and to investigate the effects of rate of loading, rate of straining, and ageing. The work was never completed, but the results have some bearing on the present series of papers.

The method of recording had the advantage that the rate of yielding was indicated. Moreover, by suitably marking and measuring the test-piece (in all cases round test-pieces were used) the location of the deformation was determined.

In the yielding of iron and steel a very rapid extension was followed by a gradual spread of the deformation, depending upon the rate of separation of the two heads of the machine. In a jump extension of the aluminium alloys, in which no yields of type *A* were recorded, the drop in load was immediately followed by a gradual rise to a slightly higher load, when another jump occurred. This observation is in accordance with the view that the increase in resistance to deformation is associated with the plastic yielding and that ageing is not necessarily involved, a conclusion supported by the curves in Fig. 19 (p. 613) of the paper by Mr. Krupnik and Professor Ford.

Although there is a general tendency for the size of the steps to increase with the stress, probably owing to the greater available strain energy in the machine, the strains are not by any means uniform in a round bar. In any of the spring- or pendulum-type machines, when a test is being made at a constant rate of extension, the time taken to bring the load

* M. Kuroda, *Sci. Papers Inst. Phys. Chem. Research (Tokyo)*, 1938, **34**, 1528.

E. O. Hall, *J. Iron Steel Inst.*, 1952, **170**, 331.

S. Epstein, H. J. Cutler, and J. W. Frame, *Trans. Amer. Inst. Min. Met. Eng.*, 1950, **188**, 830.

† R. Hill, *J. Mechanics Physics Solids*, 1952, **1**, 19.

‡ W. M. Lomer, *ibid.*, 1952, **1**, 64.

§ A. H. Cottrell, *Phil. Mag.*, 1953, [vii], **44**, 31.

|| A. H. Cottrell and G. M. Leak, *J. Iron Steel Inst.*, 1952, **172**, 301.

¶ N. H. Polakowski, *ibid.*, 1952 **172**, 369.

** Engineering Department, Cambridge University.

†† C. F. Elam, *Engineering*, 1940, **149**, 325.

back to the same, or a slightly higher, value increases as the strain associated with each jump increases, and here ageing may become important.

I suggest that the absence of steps in the slow tests carried out in the rigid machine of Krupnik and Ford can be attributed to its rigidity. Plastic deformation will presumably cease as soon as the load falls below a certain value, and in a very rigid machine the extension and drop in load, associated with each jump, would be too small to measure.

There seems no valid reason for attributing all discontinuous yielding to strain-ageing. The Cottrell mechanism can account for the onset of the yield without it. There are other examples, such as twin formation in crystals, which give similar stepped curves, where ageing does not enter into the picture.

Another matter of great interest in these papers is that of the inclination of the striations to the direction of loading. It is difficult to determine the slope in the direction perpendicular to the plane of the strip in this thin material. Dr. Phillips, Mr. Swain, and Mr. Eborall are to be congratulated on their method. The subject is discussed by Nadai,* and it would be interesting to know if the effect of the ratio of width to thickness was investigated in any of the alloys.

Mr. R. EBORALL: The observations of Mr. Krupnik and Professor Ford on the effect of the rate of stressing

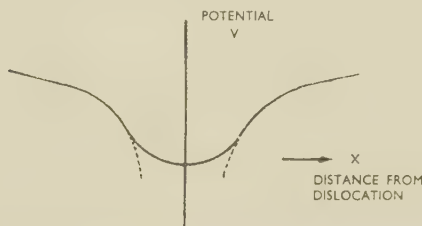


FIG. H.—Potential of a Solute Atom Near a Dislocation.

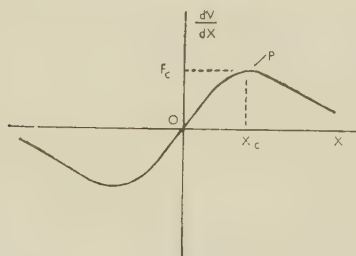


FIG. J.—Restoring Force on a Solute Atom.

might perhaps be explained in the following way. These authors find, in effect, that their stress/strain curves have a common envelope, and that by sufficiently slow, very smooth, stressing they can obtain a smooth curve coinciding with this envelope. Now a solute atom near a dislocation is sited in a sort of potential trough (Fig. H). The restoring force, if it is displaced, is thus given by a curve such as that of Fig. J. Thus, if the dislocation is moved slowly, the solute atom tends to follow, the force dragging it along increasing up to the point P. If the force F_c is sufficient to enable the atom to keep pace with the dislocation there will be no sudden yield, but the dislocation movement is hindered, so that the level of the stress/strain curve is raised.

Putting in some very rough figures, it appears from Mr. Krupnik and Professor Ford's results that at about 1% strain the critical rate of stressing approximates to 0.1 ton/in.²/min. From the stress/strain curve the rate of straining (for smooth straining) is then $\sim 10^{-5}$ strain/sec., and the corresponding dislocation velocity (assuming that there are $\sim 10^{10}$ active

dislocations/cm.²) is $\sim 10^{-7}$ cm./sec. To enable the solute atom to keep pace, when acted on by the restoring force available, the diffusion coefficient then has to be of the order of 10^{-15} – 10^{-16} cm.²/sec. This is much greater than the value expected by extrapolating the high-temperature values to

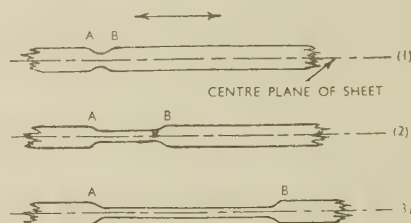


FIG. K.—Stages in the Formation of a Type-B Marking.

room temperature, but the metal is in a worked condition, and Professor Cottrell has already explained how high values of this order may be expected in these circumstances.

An essential feature of this situation is that any shock or disturbance will give rise to a momentarily increased rate of straining and so start off a sudden yield, as Mr. Krupnik and Professor Ford observe.

Replying to Mr. Chadwick and Dr. Baker, what is seen during the formation of type-B markings has been aptly described by Mr. Field. The mode of formation of the markings appears to be as indicated in Fig. K.

At the beginning of a type-B yield, localized yielding occurs as in sketch (1). When the metal within the neck has been stretched sufficiently to carry the applied load, the yielded area starts to spread, one, or sometimes both, of the half-necks A and B moving along the surface as a ripple. A type-B marking is left only if the yielding is halted when either A or B is still within the area under examination. If a strip is stretched in a machine which maintains the load during yielding, in the early stages of deformation the ripples usually travel through a substantial part of the specimen length, or even perhaps the whole of it, before becoming stuck. Later, movements are more restricted. The characteristic rippled appearance of a stretched strip arises when a great many half-necks have accumulated on the surface.

If a strip is stretched in a machine in which the applied load falls off progressively during yielding, the situation is a little different, because when the yielded area has spread a certain distance the load becomes insufficient to produce further yielding and there is a pause during which strain-ageing can take place. The type-B marking has no sharp boundary, so that, in Fig. L, all the material between P and Q

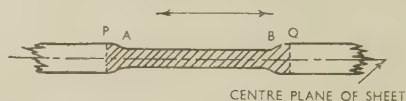


FIG. L.—Limits of Region Hardened by Straining and Ageing After Type-B Yield and Subsequent Pause.

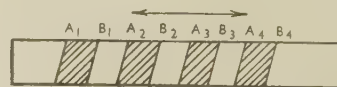


FIG. M.—Plan View of Yielded Regions in Strip Lightly Stretched by Semi-Hard Machine. (Schematic.)

has received some deformation and will consequently strain-age to some extent. When the load is later restored so that yielding again takes place, it would be expected to start outside the hardened region PQ.

As a result, the surface of the strip acquires a whole series

* A. Nadai, "Theory of Flow and Fracture of Solids", Vol. I. 2nd edn. 1950: London and New York (McGraw-Hill).

of separate yielded regions, as in Fig. M. Occasionally, on further increase of the applied load, the next set of yielded regions comes neatly in between the first.

Dr. PHILLIPS (*in reply*): With regard to Dr. Baker's comments, it seems clear that there is a distinct difference in topography between the two kinds of marking which we have called respectively, types *A* and *B*, formed in the annealed aluminium-3½% magnesium alloy of fine grain-size. As illustrated in Fig. 8 (Plate XCII) of our paper, the type-*A* markings form primarily by a shear mechanism, shear occurring parallel to a plane near one of maximum shear stress. Type-*B* markings, the parallel ripple markings formed at higher strains in the same alloy, as shown by Mr. Chadwick and Mr. Hooper, are in the form of incipient necks, and have neither the tilt nor the very sharp boundary associated with the type-*A* or flamboyant markings. This may also be seen in Fig. O (Plate CV), which illustrates rather clearly the relation between the ripple markings and the surface topography. The profile was determined by a microscope-focusing technique, and with oblique illumination it will be seen that the expected sequence of dark and light bands is formed.

With reference to Mr. Chadwick and Mr. Hooper's remarks, I am glad to see that they are now able to confirm that the surface angular change at boundaries between yielded and unyielded material in the case of annealed aluminium-magnesium sheet was in fact similar to our own results. I am also glad to learn that they now agree that thinning occurs within the type-*A* yielded regions, notwithstanding the statements in their papers,*† and in the synopsis‡ which I also read.

The analogy between the yield-point phenomenon in aluminium-magnesium alloys and in steel is so close that one would expect to find the same two types of marking in steel. Exploratory experiments which we have carried out confirm that this is the case. The steel examined was deep-drawing quality strip, which after cold rolling had been annealed just below the lower critical temperature and had received no subsequent working. By analysis it contained 0.059% carbon, and 0.04% nitrogen.§ This steel had a grain size of 0.023 mm. and a yield-point elongation of 4%. A tensile specimen was stretched part-way through the yield, forming two simple wedge markings (Fig. P, Plate CV). The profile was examined using the microscope-focusing technique and then after being lightly chromium-plated to increase the reflectivity, was examined by multiple-beam interferometry. The profile was that typical of the type-*A* markings formed in aluminium-magnesium alloys. Fig. Q (Plate CV) shows the sharp tilt at a boundary between yielded and unyielded material. The average tilt at a number of such boundaries was 64' as determined by the microscope-focusing method and 62' as determined by multiple-beam interferometry.

On stretching to fracture in the annealed condition at room temperature this steel exhibited no ripple markings. A similar specimen tested at $170^\circ \pm 5^\circ \text{C}$. was found to be covered with parallel ripple markings (Fig. R, Plate CV). Examination by the microscopic-focusing technique showed that the visible ripples corresponded to incipient necks in the material, and fracture occurred along one of them. These markings are quite similar to the type-*B* markings formed in aluminium-magnesium alloys at room temperature.

Mr. Hooper and Dr. Holden have observed, at the initial yield in annealed steel, the formation of a channel type of marking, as well as the shear type commonly observed at the initial yield in fine-grained annealed aluminium-magnesium alloys. Although in this channel type of marking (e.g. that denoted *a* in Fig. 4 || of their paper), a depression on one surface of the sheet corresponds to a depression on the opposite

surface, it is probable that this marking is of essentially the same form as type *A*, but is caused in this case by two superimposed shears instead of by a single shear (Fig. N). This would account both for the observed contour and for the fact, illustrated in Fig. 9 || of the paper, that the marking *a* consists of plane areas of surface tilted sharply with respect to each other. This would seem to be an essential characteristic of markings formed by the shear process, whereas the type-*B* markings which we have examined are rounded in outline. We have observed a marking which would appear to have been formed by double shear in a lightly stretched strip of aluminium-magnesium alloy.

As shown in our paper, by lowering the temperature so that appreciable ageing does not occur during a test, a basic curve can be determined which passes through the bottom corners of the steps formed at higher testing temperature. Mr. Krupnik and Professor Ford show in their constant-rate-of-loading tests that the top corners of the steps similarly fall on a smooth curve, which will presumably always be the case where the strain rate, total strain, temperature, &c., are such

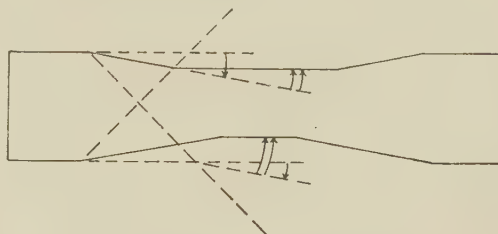


Fig. N.—Schematic Diagram Showing Suggested Double Shear Process for Producing a Type-*A* Channel Marking. Single arrows indicate the first shear and double arrows indicate the second shear.

that substantially complete ageing can occur at each step. Under these conditions the upper and lower envelope curves between them will determine the size of the steps, although inertia effects in the machine may produce overshooting of the basic curve.

Mr. Krupnik and Professor Ford observe that in the as-extruded condition the step size of the stress/strain curves was independent of the amount of alloying element, and they suggest that this contradicts McReynolds'¶ findings. The apparent contradiction disappears, however, if one takes into account the fact that only that part of the alloying element which is in solution is available for anchoring dislocations. The three copper alloys examined by Krupnik and Ford contained 4.0, 3.8, and 1.4% copper, respectively. The solubility of copper is approx. 1% at 370°C ., so that in the extruded air-cooled condition it is unlikely that the amount of copper in solution was very different in the three materials. McReynolds, on the other hand, compared high-purity alloys with 0.025, 0.1, and 0.5% copper, where the whole of the addition would be in solution.

Mr. EBORALL and Dr. PHILLIPS (*in further reply*): We were interested to read Dr. Tipper's contribution, and thank her for her compliment on technique. We believe that, in speaking of strain-ageing, we differ from her only in nomenclature. Some doubts have been raised in the discussion about the occasions on which type-*A* and type-*B* stretcher-strain markings occur. Dr. Polakowski has mentioned in his paper that the kind of marking produced at the initial yield point in an annealed material is influenced by the uniformity or otherwise of the stressing. We would agree with this but

* R. Chadwick and W. H. L. Hooper, *J. Inst. Metals*, 1951-52, 80, p. 19.

† W. H. L. Hooper and J. Holden, *Bull. Inst. Metals*, 1953, 1, p. 165; *J. Inst. Metals*, this vol., p. 648.

‡ R. Chadwick and W. H. L. Hooper, *J. Inst. Metals*, 1951-52, 80, p. 17.

§ An erroneous figure for nitrogen was previously given (*Bull. Inst. Metals*, 1952, 1, 59).

|| W. H. L. Hooper and J. Holden, *Bull. Inst. Metals*, 1953, 1, p. 162 (Fig. 4), p. 164 (Fig. 9).

¶ A. W. McReynolds, *Trans. Amer. Inst. Min. Met. Eng.*, 1949, 185, 32.

consider that the differences produced are in the complexity, not the type, of marking. Similarly, Mr. Chadwick, drawing attention to Fig. 4 of the paper by Mr. Hooper and Dr. Holden,* suggests that type-*A* and type-*B* markings can occur simultaneously at the initial yield point in mild steel and that the diagonal markings (particularly that denoted *a* in the figure) are of type *B*. The authors state, however, and Fig. 9 of their paper shows, that this marking is in the form of a channel, and Dr. Phillips and Dr. Hundy have indicated how such a marking can arise as the result of two superimposed shears; in other words, it is very probably a type-*A* marking. Diagonal markings at the initial yield also often occur in aluminium-magnesium alloy, as Mr. Chadwick and Mr. Hooper point out. Fig. 12 of Hooper and Holden's paper shows a striking example; here the diagonal markings are obviously branches of the main type-*A* marking and are tilted in the same sense. Mr. Chadwick and Mr. Hooper are in fact in error in assuming that markings such as these and the fine ones in our Fig. 3 (*a*) (Plate XC) are of type-*B* because they make angles of 52°–55° with the stress axis. We have examined the profile of many markings formed at the initial yield in annealed aluminium-magnesium alloys and have always found them to be of type *A*, whatever the angle made with the stress axis.

We are somewhat surprised at Dr. Hundy's statement that type-*A* markings can occur in a strain-aged steel. However, we have a good deal to learn of the exact reasons why markings should take particular forms, and there is obviously scope for further work here. It is possible that the apparent difference may be due to the stronger locking of dislocations which can develop in steel on prolonged strain-ageing, as compared with aluminium-magnesium. Certainly, the markings we have seen on a very limited number of lightly strain-aged steel specimens (including those tested at elevated temperatures) are of type *B*. If one considers the propagation of slip from grain to grain in a strain-aged specimen, it is obvious that as the dislocations become more strongly locked the spread of slip depends more and more strongly on the stress concentration near the boundary, and the first dislocations broken free in a newly slipping grain under the influence of the stress concentration then originate from a progressively narrower layer next to the boundary; from the geometrical point of view there is thus a progressive return to the situation in annealed material in which the dislocations, on our hypothesis, originate in the boundary itself.

Dr. Baker has given one good reason for preferring our own explanation of why quenching an aluminium-magnesium alloy from a high temperature removes the initial yield-point effects (viz. through dispersion of the magnesium concentrated in the boundaries) to Mr. Hooper's (viz. through masking by quenching stresses). It might also be mentioned that to produce a quenching stress the temperature gradients must have been severe enough to strain the metal plastically during cooling, whereas the behaviour of our quenched aluminium-magnesium alloy specimens on reheating differed fundamentally from that of the strained material (contrast our Fig. 20 (p. 637) with Fig. 23 (p. 638)). Moreover, from thermal considerations it is rather unlikely that stressed systems of the type considered by Polakowski, in which the skin is in compression with respect to the centre, or vice versa, could be set up in so thin a specimen of an aluminium alloy. Under our conditions, the temperature difference between surface and centre in quenching was probably not more than 5°.

Dr. Hundy asks why only magnesium produces an initial yield in aluminium alloys. There may well be other elements which do so; we have only investigated a few. Copper, in some conditions, can produce a small initial yield. Magnesium, however, is practically unique in that it produces a large lattice strain but is not rapidly removed from solution

by an age-hardening or other precipitation process. Considering copper again, a solution-treated and freshly quenched aluminium alloy containing copper would not show an initial yield point, because the copper would be uniformly distributed; on the other hand, when ageing was at all advanced, the effective copper content of the solution would be much reduced through the separation of copper at Guinier-Preston zones or in precipitate. Only at some intermediate stage can the conditions be at all favourable for the formation of an initial yield point, and even then there is competition for the available copper. One would expect zinc to behave similarly to copper. It is perhaps noteworthy that the copper-tin system is similar to the aluminium-magnesium system, in that the tin atom is much larger than the copper atom but considerable quantities of tin can readily be retained in solution.

The effect of rapid straining, at room temperature, on repeated discontinuous yielding is of practical importance because of the high speed of many industrial presses, and Professor Hill has suggested to us that in such presses there might not be time for strain-ageing to occur. This suggestion is in agreement with available data. No visible type-*B* markings were formed (p. 633) on specimens stretched 10% at about 3×10^{-5} strain/sec. at or below –55°C. From this result and an activation energy for strain-ageing it should be possible to devise a corresponding strain-rate at room temperature, at (or above) which no visible markings should be formed. Sherby, Anderson, and Dorn † found an activation energy initially of 8 kg.cal./g. atom, rising to 15 kg.cal./g. atom as strain-ageing progressed. This variation introduces some uncertainty, but if a value of 11 kg.cal./g. atom is taken as representative, no markings should be visible after straining at about 3×10^{-2} sec.⁻¹ at room temperature. The strain rate for a typical crank press would be of the order of 1 sec.⁻¹.

To investigate this point experimentally, three small strips of commercial aluminium-3½% magnesium alloy were stretched at approximately 10⁻², 10⁻¹, and 10² strain/sec., the first two in a Hounsfield tensometer and the third with an attachment to a standard Izod machine. The surfaces (rather rough, unfortunately) are illustrated in Fig. S (Plate CVI), and it can be seen that the markings are much less prominent at 10⁻¹ strain/sec. and are absent at 10² strain/sec.

Mr. CHADWICK and Mr. HOOPER (*in further reply*): In discussion of the effect of quenching on the incidence of type-*A* markings, Dr. Baker, and later Mr. Eborall and Dr. Phillips, have criticized our tentative explanation based on internal stresses and have brought forward further evidence to support their own theory, which supposes that the diffusion of magnesium atoms to and from grain boundaries is involved. Whilst neither theory can be regarded as proven, the further arguments appear to be unsoundly based, and after a critical examination of the evidence, and with additional support from a new and crucial experiment described below, our preference for the quenching-stress theory is maintained.

One of our critics, Dr. Baker, objects to our theory because he assumes that according to it the quenching stresses "in some unspecified way prevent the formation of objectionable markings." We therefore propose to elaborate somewhat on the mechanism, although we had regarded it as elementary, and indeed it has already been explained in some detail by Polakowski.‡ It is first of all necessary to affirm that quenching stresses can be present in thin sheet, a matter which Mr. Eborall and Dr. Phillips have doubted. Quenching of sheet at 500°C. does, in fact, lead to straining, and in industrial practice distortion of large sheets is considerable.

Reference to our original paper § shows that plastic strain before the formation of type-*A* markings, if it exists at all, is

* W. H. L. Hooper and J. Holden, *Bull. Inst. Metals*, 1953, 1, p. 162 (Fig. 4), p. 164 (Figs. 9 and 12).

† O. D. Sherby, R. A. Anderson, and J. E. Dorn, *Trans. Amer. Inst. Min. Met. Eng.*, 1951, 191, 643.

‡ N. H. Polakowski, *J. Iron Steel Inst.*, 1952, 172, 369.

§ R. Chadwick and W. H. L. Hooper, *J. Inst. Metals*, 1951–52, 80, Figs. 5 and 6 (Plate IV).

extremely small, and up to the point at which yielding first occurs, the straining is purely elastic. Now, any small portion of sheet will consist of a number of elements, some of which are under compressional and others under tensional stresses to varying extents, the sum of such stresses being zero. On the application of an externally applied tension, the elements under the highest internal tensional stress will first reach the elastic limit, and other will follow in succession, so that the condition under which a strain band can spread, i.e. by sudden yielding of a large area, will not be realized. However, after 2-3% extension, the whole of the material will have suffered appreciable plastic strain and the original inequalities will be smoothed out. The absence of any effect on type-B markings would therefore be predicted. Heat-treatment at 150° C., which restores the tendency to form type-A markings, is known to be effective in relieving internal stresses.

Turning now to the discussion of the atom-migration theory, we note with interest that Professor Cottrell applies it to the serrated or type-B yielding only, and quotes figures for atom diffusion rates in strained and unstrained material which indicate that in aluminium-magnesium alloy a plastic extension of at least 0.1% is necessary before this mechanism can operate. Our earlier experiments* showed that before the first large yield point associated with the formation of type-A markings, any plastic extension was not more than about 0.02%.

In order to provide fresh evidence on the possible effect of grain-boundary barrier films on the incidence of type-A markings, a new experiment has been devised. This was carried out on an aluminium-7% magnesium alloy in which it is readily possible, by thermal treatment, to form a continuous grain-boundary network of magnesium-rich phase, which, unlike that postulated by Eborall and his colleagues, is visible under the microscope. Sheet with such a grain-boundary film was heated in a salt bath at 500° C. for 1 min. and quenched in cold water. This period of heating was sufficient to bring the metal up to the temperature of the salt bath and allow a further time for it to reach a steady temperature condition throughout, but was insufficient to take the whole of the grain-boundary film into solution. Specimens so treated were stretched both in the as-quenched condition and after reheating for a short time at 150° C. The as-quenched specimens were free from random markings, whereas intense markings developed on the reheated specimens. Since, in this experiment, strain markings developed irrespective of the presence of grain-boundary films, it would seem that a barrier of this kind is not in any way a significant factor.

A further point on which discussion has centred is the differentiation between type-A and type-B markings in mild steel. We have suggested in the discussion that in the samples illustrated by Hooper and Holden,† which are reproduced in Figs. T and U (Plate CVI), both types are present together, as indeed they appear to be in some examples of strained aluminium-magnesium alloys. Dr. Phillips, and later Mr. Eborall and Dr. Phillips, argue that the channel-shaped markings in these figures are, in fact, extensions of type-A markings. It should, however, be pointed out that, besides being of the shape typical of type-B markings observed in aluminium alloys, i.e. they are necks and not kinks, they also invariably lie at the characteristic angle of type-B markings. The contour of the markings illustrated in Fig. 9‡ has been cited by Dr. Phillips in this connection, but this has little relevance, since no data are available on the contours of individual type-B markings. Our own measurements on specimens of aluminium alloys showing type-B markings were invariably carried out on specimens with many partially overlapping markings present. On the other hand, Dr. Phillips' attempt to explain mathematically the mechanism by which the type

of deformation found in type-A markings can give rise to the characteristic configuration of type-B markings, may well contain the germ of an idea which could lead to a rational explanation of the relation between the two types of markings, especially if it could be shown that the two are indeed manifestations of a single deformation mechanism.

Dr. POLAKOWSKI (*in reply*): With reference to Dr. Baker's comments, I do not think that it has yet been established beyond doubt whether the two types of yield (*A* and *B*) differ basically or are merely different manifestations of the same phenomenon. Information given in my paper§ appears to support the second possibility, although it is agreed that visual observation may not carry sufficient conviction. Dr. Hundy's mention of the occurrence of type-A markings on temper-rolled and subsequently aged steel sheet would also indicate that the difference between the two species may not after all prove to be fundamental. I am not convinced on this point, but believe that a definite proof to the contrary is still lacking.

In reply to Dr. Hundy, I agree that the term "precipitate" was not very fortunate. I should have used "segregation" or "grain-boundary segregation" instead.

As far as the reason for the absence of a yield platform in quenched bronze is concerned, I presume that again either of the two alternative explanations may apply. Suitable critical experiments should enable this question, too, to be decided. I should be only too glad if the explanation to which Dr. Hundy referred proved to be universally correct.

I wish to make one point in connection with the remedies for stretcher-straining advocated by Dr. Phillips, Mr. Swain, and Mr. Eborall. These authors recommend, among other treatments, "light rolling (about 5%) followed by a non-recrystallizing anneal".|| They thus suggest imparting to the sheet first some 5% cold reduction and then introducing an additional heat-treatment operation in order to eliminate the work-hardening caused by this very temper-pass.

In steel sheet or strip manufacture a 1 or 1.5% skin-pass reduction is sufficient to eliminate some 5% yield elongation. With aluminium alloys the *A*-yield varies between 0.5 and 1.5%, and 1% rolling should be ample for the purpose in view. So small a reduction should render any subsequent thermal softening treatment redundant. It is not clear from the paper whether the authors' reason for recommending the double treatment arose from the difficulties of obtaining and controlling a sufficiently light rolling reduction, or has some more fundamental origin.

Professor FORD (*in reply*): Several views have been expressed about the reason why Mr. Krupnik and I found a stepped yield-stress curve to be absent under steady loading or straining conditions. The views are somewhat contradictory, and it is clear that further experimental work is required before a definite explanation can be put forward. Mr. Chadwick and Mr. Hooper have pointed out that it is difficult to obtain uniform stressing of wide, flat specimens, and it should be remembered that our tests were carried out on round specimens in machines in which, as far as possible, the load was applied axially. Mr. Chadwick and Mr. Hooper comment, however, that we did not make topographical records with our type-B yielding or in our steady-strain tests. These authors and other contributors who raised this question may be interested to know that further experimental work is now in hand, using a larger straining apparatus, which will be equally rigid, but in which measurements of the stress/strain characteristics and topographical records can both be taken. It will also be possible to make tests at different strain rates, and these tests should allow the interesting point raised by Professor Cottrell to be decided. It is perhaps significant that the strain rate in our constant-rate-of-strain tests was less than 10⁻⁶ sec.⁻¹.

* R. Chadwick and W. H. L. Hooper, *loc. cit.*

† W. H. L. Hooper and J. Holden, *Bull. Inst. Metals*, 1953, 1, 162 (Figs. 4 and 5).

‡ W. H. L. Hooper and J. Holden, *loc. cit.*, p. 164.

§ N. H. Polakowski, *J. Inst. Metals*, this vol., p. 623 (foot-note).

|| V. A. Phillips, A. J. Swain, and R. Eborall, *ibid.*, this vol., p. 646.

Dr. Tipper's suggestion that the smooth curve we obtained can be accounted for by reason of the rigidity of the straining gear is unlikely to be correct, because in our apparatus the load was measured on the only non-rigid link in the equipment, i.e. on the small loading bar, which extended about 0.0007 in. at the maximum load. Any sudden yielding of the specimen, therefore, would definitely have been indicated by a fall in the load, or if yielding took place at constant stress, the

load would remain constant for a short time, and again this would have been observable. We agree, however, with the rest of her remarks.

Dr. Phillips has pointed out that we used much larger amounts of copper than McReynolds; this was done deliberately, but it clearly explains why McReynolds found that his results depended upon copper content, while ours did not.

Discussion

Properties of Chromium and its Alloys*

Dr. E. GREGORY,† M.Sc., F.R.I.C., F.I.M. (Member): In view of the very high melting points of chromium and the chromium-base alloys, one can quite appreciate the difficulties encountered in melting and casting and, in particular, in the selection of the refractory materials having the desired combination of properties to resist chemical attack and contain the molten metal. It should be stressed, too, that the melting problem and that of chemical reaction are both appreciably influenced by the "appetite" chromium has for carbon, oxygen, and nitrogen at the very high temperatures involved. The authors have made a most praiseworthy attempt to overcome these difficulties and to improve on past methods of vacuum melting and casting techniques.

In Part I of the first paper, they lay emphasis on the volatilization of chromium, due to its appreciable vapour pressure near to, and above, its melting point, and state (p. 582) that as much as 25% of the chromium may be lost by this means. This appears to be an extraordinarily high figure, and it would be of interest to have some indication of the vapour pressure of liquid chromium near its melting point. A reason for this request arises from our experiences in connection with the oxygen-lancing of electric-arc-furnace charges consisting of 100% stainless steel scrap, where the molten metal is under both oxidizing and reducing conditions in turn, and where practically 100% of the chromium in the initial charge is recovered, which means, of course, that no chromium is lost by volatilization.

Unfortunately, it is impossible to measure the temperature attained; optical and radiation pyrometers are quite out of the question in view of the amount of fume and flame generated. The temperatures reached are well above the upper limit for the platinum/platinum-rhodium immersion thermocouple, but my estimate is of the order of 2000° C.; even so, we do not lose any chromium by volatilization and, moreover, the chromium recovery is highest when the highest temperatures are used. This may sound paradoxical in view of the remarks regarding our inability to measure the final temperatures, but the answer is really quite simple. From experience it has been determined that a bath temperature of 1600° C., before using the oxygen-lance, gives the best chromium recovery; if the temperature is much below this value before lancing, the chromium recovery is not nearly so good, but even in these circumstances there is no volatilization loss, any chromium not recovered being retained in the slag covering the molten metal.

The method of analysis adopted by the authors for the chemical determination of the oxygen contents of the chromium used in their experiments, although simple, appears to yield reasonably accurate results, but I was glad to note that they took the precaution of making sure by X-ray-diffraction examination that the insoluble residue was indeed Cr_2O_3 .

It seems tolerably certain that the reason why the carbon-

reduction technique failed to function adequately with alloys containing titanium and zirconium, is connected not only with the high stability of the carbides of these two elements but also with the avidity with which they will search for oxygen and then cling to it in the form of oxides.

In view of the high order of creep-resistance of the binary chromium-iron alloys at temperatures in the region of 900° C. and above, the authors were perhaps justified in hoping that the examination of similar properties of a series of ternary and even more complex alloys having chromium and iron as base might lead to encouraging results.

It must have been with some disappointment, therefore, that their experimental efforts in this direction forced them to the conclusion that material defects, associated with casting difficulties, together with a pronounced sensitivity to shock effects and a relatively low resistance to thermal shock, rendered these alloys unsuitable for use at elevated temperatures even under compressive load conditions.

Observing that the chromium-rich alloys possessed certain undesirable characteristics both at elevated and normal temperatures, features apparently inherent in the chromium itself, the authors naturally desired to find whether these were caused by incidental impurities or were intrinsic in the chromium.

Unfortunately, whilst their investigations have indicated that oxygen (as determined by the simple method used), in amounts greater than 0.002%, has comparatively little influence on the sharp transition from brittle to ductile behaviour of "pure" chromium, the same cannot be claimed for the other incidental elements investigated. Alloying chromium with even small amounts of iron, silicon, aluminium, copper, nickel, cobalt, and tungsten, and varying quantities of manganese, all resulted in a substantial extension of the temperature range within which the alloys are brittle, and the lowest transition temperature for the chromium-rich alloys is still apparently somewhat above normal atmospheric temperatures. It seems most unfortunate that such a valuable technical contribution should have to conclude with the statement (p. 597) that, though a higher degree of purification than that achieved in the present work (if ultimately obtained) may depress the transition temperature below normal atmospheric temperature, it is unlikely that this will result in the production of strong chromium-rich alloys having significant ductility at room temperature.

In only one instance, I think, throughout these papers are the authors guilty of some degree of exaggeration, when they state, on p. 597, that: "the temperature at which it [the transition] occurs is raised by all the elements which could be added to chromium to increase its strength at high temperatures". I cannot find any reference to molybdenum additions, either in Table II (p. 590) or throughout that section of the contribution beginning on p. 573, regarding the properties of the binary chromium-rich alloys. Chromium

* Joint discussion on the papers by A. H. Sully, E. A. Brandes, and A. G. Provan (*J. Inst. Metals*, this vol., p. 569), and by A. H. Sully, E. A. Brandes, and K. W. Mitchell (p. 585).

† Director and Chief Metallurgist, Edgar Allen and Co., Ltd., Sheffield.

and molybdenum form a continuous series of solid solutions, and it would be interesting to have the authors' views regarding the properties of the chromium-molybdenum system.

With reference to the final paragraph on p. 597 regarding the respective parts played by structure and by impurities in inducing brittleness in body-centred cubic metals, I would point out (i) that ductile α -iron at normal temperatures is body-centred cubic, and (ii) that α -iron exhibits maximum ductility only when it is completely deoxidized. I suggest, therefore, that the difficulties experienced in producing ductile chromium at normal temperatures are due to impurity and not to its lattice structure. In an attempt to be constructive, I suggest to the authors a remelting of their chromium, with the addition of about 0.20% manganese, in an argon atmosphere. By this means, it may be possible to produce chromium having an exceedingly low oxygen content.

In neither paper is any reference made to spectrographic analysis, and it would be of interest to learn whether the authors contemplated this method of determining the amounts of other impurities likely to influence the results of their work. It is well known that, in some instances, very small additions of any element may exert a profound influence on the properties of metals, and I need only cite the really enormous effect of as little as 0.002% boron on the hardenability of manganese-molybdenum steels.

It is my earnest hope that the authors will continue their endeavours to produce ductile chromium at room temperatures, even though this may necessitate entirely different techniques. A careful study of Dr. Cook's Autumn Lecture to the Institute of Metals* may perhaps give them some ideas for the furtherance of their own particular investigations.

Mr. A. R. EDWARDS,† B.Met.E., Dr. H. L. WAIN † (Member), and Mr. H. T. GREENAWAY,† B.Met.E.: Work on chromium has been in progress for several years at the Aeronautical Research Laboratories, Melbourne. The suggestion on p. 574 of the paper on the properties of cast chromium alloys that chromium has a considerable capacity for work-hardening at 900° C., is supported by the results of rolling experiments at that temperature conducted at these Laboratories. Hardness values of chromium strip produced in this way approximated to 200 V.P.N., as compared with 110 V.P.N. after annealing.

Parts II and III of this paper indicate that a remarkably high level of creep-resistance is attainable in chromium alloys. Of particular interest is the general tendency, also found by Parke and Bens, for the alloys to exhibit better creep-resistance in the as-cast condition than after heat-treatment. As noted by the authors, this occurred (with respect to the secondary creep rate) even in the 27.9% cobalt alloy, which is a precipitation-hardening material. A relevant point in this connection is the recent statement by Pfeil‡ that, in commercially established alloys, optimum creep properties are associated with a fully heat-treated structure. Any comments which the authors may have on this divergence of behaviour would be appreciated.

The thermal-shock test results on the three alloys reported in Part III of the paper (p. 582) are not promising, but it seems possible that the test used was unduly severe. The alloy H.R. Crown Max, cited as a comparison material, is noted for its resistance to thermal shock, and it is felt that a test which causes cracking of this material after only 30 cycles may well be too demanding as an initial test for experimental alloys.

In the paper dealing with the ductility of chromium, it is stated (p. 586) that the use of alumina crucibles for melting chromium resulted in contamination by aluminium to as much as 0.3%. This is not in agreement with our experience that experiments involving contact between molten chromium and alumina ware caused aluminium contamination of less

than 0.01% as determined by chemical tests, and a trace by spectrographic methods.

In regard to the iron contamination due to ball milling (p. 587), this troublesome feature can be obviated by the use of chromium-plated steel balls in a chromium-plated mill. This method has proved quite successful at these Laboratories.

Specimens used in the authors' work consisted in the main of sintered compacts in which the final porosity varied from 6 to 15% (p. 587). This porosity may well account for the remarkably low hardness values quoted in several parts of the paper (e.g. 48.5 V.P.N. in Table I, p. 589), and for the low value of 6.76 tons/in.² (15,160 lb./in.²) given for the ultimate tensile strength of chromium at 20° C. (Table V, p. 593). This latter figure may be compared with a yield stress of 51,500 lb./in.² and an ultimate stress of 89,000 lb./in.² obtained at room temperature on rolled chromium strip produced in our Laboratories. Furthermore, it is perhaps not surprising that the authors failed to find any room-temperature ductility in their specimens, as it is well known that porosity has an exceedingly marked effect on the ductility of powder-metal-lurgy products. For example, work done at the Watertown Arsenal some years ago§ showed that the elongation of sintered iron specimens fell from 34 to 7% and the resistance to impact at room temperature fell from 50 to 7 ft.-lb. as the porosity of the material increased from 5 to 15%. Thus it is entirely possible, in our opinion, for sintered chromium to show significant room-temperature ductility, if the degree of sintering is high enough. Certainly our own experiments|| would support this view. We have shown that chromium strip, produced from arc-melted ingots by more or less conventional working methods, exhibits considerable ductility in a bend test and a certain degree of ductility in a tensile test at normal rates of strain and at normal temperatures, provided that absorption of certain impurities is prevented during fabrication. Furthermore, preliminary work has revealed a similar room-temperature ductility in a bend test for a chromium-1% tungsten alloy. In view of these facts we must record our disagreement with the authors' conclusions (p. 597) "that the transition from ductile to brittle fracture occurs (for chromium) at a temperature above room temperature, that it occurs at very slow strain rates, and that the temperature at which it occurs is raised by all the elements which could be added to chromium to increase its strength at high temperatures."

Finally, the authors' contention (p. 597) that "the brittleness and notch sensitivity of creep-resistant chromium-rich alloys is so marked that the alloys have little promise for practical applications" is perhaps an overstatement. Such materials may well be quite ductile at operating temperatures, and the fact that they may undergo a ductile-to-brittle transition between the operating temperature and room temperature would not seem to rule them out as useful high-temperature materials. Although room-temperature ductility is obviously desirable, it has not yet been shown to be mandatory. If a material can be produced in the required form, and if it is strong enough, the extent of room-temperature brittleness may possibly be of relatively minor importance.

Mr. J. H. RENDALL,¶ B.Sc., A.R.S.M., A.I.M. (Member): In the second paper, the question is raised as to whether the large effect of temperature on ductility is a property of body-centred cubic metals (p. 597). At the National Physical Laboratory we have carried out bend tests on tantalum at liquid-oxygen temperatures and find the metal to be ductile; in fact, $\frac{1}{8}$ -in.-dia. rods can be bent to 150° round a $\frac{1}{8}$ -in. radius. We have also hammered a piece of niobium immediately after removing it from liquid oxygen without any signs of cracking.

Now, if it is assumed that the transition from ductile to brittle behaviour is very approximately a constant fraction of the absolute melting temperature, one would expect the

* M. Cook, *J. Inst. Metals*, 1953-54, **82**, (3), 93.

† Aeronautical Research Laboratories, Department of Supply, Melbourne, Australia.

‡ L. B. Pfeil, *Materials and Methods*, 1953, **37**, (3), 79.

§ A. Squire, *Watertown Arsenal Lab. Rep.*, 1944, (671/16).

|| H. L. Wain and F. Henderson, *Proc. Phys. Soc.*, 1953, [B], **66**, 515.

¶ Metallurgy Division, National Physical Laboratory, Teddington.

transition temperature of tantalum to be higher than that of chromium or molybdenum, whereas it is about 200° C. lower. (The transition temperature of molybdenum is between about 30° and 100° C.)

If it is assumed that this low-temperature brittleness is due to small amounts of an interstitial impurity straining and thus weakening the lattice, an explanation for this difference is available. The tantalum lattice is larger than that of chromium, molybdenum, or iron, i.e. the nearest distance of approach of the atoms is 2.854 Å. between centres for tantalum and 2.493, 2.720, and 2.477 Å. for chromium, molybdenum, and iron, respectively. Thus, there may be larger holes for accommodation of interstitial impurities in the tantalum lattice.

Another point which might be mentioned is the difference between the effect of oxygen on chromium and its effect on iron or molybdenum. In both these latter metals as the oxygen content is increased the fracture changes from transcrystalline to intercrystalline; in molybdenum, for example, this occurs at about 0.0005 wt.-% oxygen (0.003 at.-%). The work of Sully and his colleagues suggests that this is not so for chromium, the fracture with high oxygen contents being always transcrystalline.

Now, if it is assumed, as suggested above, that the brittleness is due to interstitial impurities straining the lattice, one can imagine that, above a certain critical percentage, atoms of the impurity will concentrate strongly at the grain boundary and weaken it. If, on the other hand, the solubility of oxygen in chromium were very much lower than this, the critical percentage might never be reached. We have some slight evidence at the National Physical Laboratory that the solubility of oxygen in chromium is very low. The oxygen content of a piece of hydrogen-reduced chromium was determined by vacuum-fusion analysis and by weighing the chromic oxide residue after solution of the metal in 10% HCl. The results were as follows:

	Oxygen, wt.-%
Vacuum fusion	0.002
Oxygen in insoluble Cr ₂ O ₃	0.001

In other words, if the amount of chromic oxide not in solution in the metal is the same as that insoluble in HCl, the solubility of oxygen in chromium is about 0.001%. The solubility of oxygen in molybdenum is 0.004%* at 1000° C. There appear to be no reliable figures for the solubility of oxygen in α -iron, but there is some evidence for placing it at about 0.004%.† There is a third and last point which might be mentioned. One of my colleagues, Mr. Carrington, hammered a piece of arc-melted chromium and examined the fragments under a microscope. He obtained what we think are Neumann bands,‡ one of which apparently shifted by slip.

The AUTHORS (*in reply*): Dr. Gregory's observations are very interesting. Probably the difference in the amounts of chromium lost by volatilization in our experiments and in the oxygen-lancing of stainless steels can be accounted for by a combination of three factors: (i) the pressure of chromium vapour over stainless steel can be only one-fifth of the vapour pressure of pure chromium, assuming an ideal solution; (ii) whereas our experiments were made in vacuum, Dr. Gregory refers to operations at atmospheric pressure, which would limit the rate of volatilization; and (iii) our melting operation was comparatively lengthy. Our experience in the loss of chromium by vaporization was much the same as that recorded by Parke and Bens.§ The vapour pressure of chromium may be derived from measurements made by Speiser, Johnston, and Blackburn.|| At 2000° C. it is 22 mm.

We note Dr. Gregory's agreement with our general conclusions and regret that our statement that *all* the elements which might be added to chromium raise the brittle/ductile transition temperature is perhaps unjustifiably general, since we did not include the effect of molybdenum. In work not described in the paper, however, we found that these alloys are also brittle at room temperature.

Trace elements were extensively sought by spectrographic techniques, but none were found whose incidence could be related to the brittleness of the samples examined.

Mr. Edwards, Dr. Wain, and Mr. Greenaway and their colleagues have made a recent and valuable contribution to our knowledge of chromium, in demonstrating that chromium rolled under conditions in which the surface is not contaminated shows ductility at room temperature. We do not, however, agree with some of their comments on the present work. In the first place we cannot accept their suggestion that porosity alone is responsible for the lack of ductility shown by our compacts at room temperature. As explained in the paper, we could find no correlation between porosity and the transition temperature, and the fact that melting of powder compacts in an arc furnace in purified argon raised the transition temperature by about 200° C. (p. 593) does not confirm this hypothesis. The effect can scarcely be explained by the pick-up of impurities during arc melting, since uranium and zirconium could both be melted in this furnace without significant contamination. We are more inclined to the view that the crystalline texture has an effect on the transition temperature, and it appears that the structure resulting from hot working is associated with a lower transition temperature than a sintered or a cast structure of the same purity. What is important is the extent of this depression of the transition temperature and the effect of alloying. We still see no reason to modify our conclusion on p. 597 that although in later work "a higher degree of purification . . . may depress the transition temperature by the further small interval required to take it below normal atmospheric temperature . . . this will not contribute materially to the possibility of the development of strong chromium alloys having any important degree of ductility at room temperature". Before Mr. Edwards, Dr. Wain, and Mr. Greenaway can justifiably disagree with our statement that the transition temperature is raised by strengthening additions, they should first measure the transition temperatures of their alloys, which have not yet been reported. They cannot ignore the possibility that the transition temperature of their alloy with 1% tungsten may be higher than that of pure chromium, although still below room temperature. Certainly much more than 1% tungsten would be required to produce an alloy with good creep properties at high temperatures. It may be noted that Gilbert, Johansen, and Nelson¶ could not sheath-roll even at 800° C. chromium alloys containing 5–20% of aluminium, iron, molybdenum, or nickel, or 5–10% of copper, manganese, and silicon, and this is in line with our own experience.

We fully agree with the statement that: "Although room-temperature ductility is obviously desirable, it has not yet been shown to be mandatory." There are, of course, degrees of brittleness, and if chromium alloys could be handled as readily as, say, cast iron, they would have potentialities. They are, however, so shock-sensitive and so easily cracked (for example during grinding) that it would, in our opinion, be impossible to use them for a vitally important engineering component such as a turbine blade. The thermal-shock test, which is criticized as being too severe, is in fact intended to simulate conditions to which turbine blading may be subjected on occasions in service, and it is possible to set a minimum standard of performance, not met by the chromium alloys,

* W. K. Few and G. K. Manning, *Trans. Amer. Inst. Min. Met. Eng.*, 1952, **194**, 271.

† W. P. Rees and B. E. Hopkins, *J. Iron Steel Inst.*, 1952, **172**, 403.

‡ W. E. Carrington, *J. Inst. Metals*, 1953–54, **82**, (4), 170.

§ R. M. Parke and F. P. Bens, *Symposium on Materials for Gas Turbines (Amer. Soc. Test. Mat.)*, 1946, p. 80.

|| R. Speiser, H. L. Johnston, and P. Blackburn, *J. Amer. Chem. Soc.*, 1950, **72**, 4142.

¶ H. L. Gilbert, H. A. Johansen, and R. G. Nelson, *U.S. Bur. Mines, Rep. Invest.*, No. **4905**, 1952.

which must be attained in such a test before an alloy can be regarded as having any promise for this application.

About the pick-up of aluminium on melting chromium in alumina crucibles we can only agree to differ. The figure of 0.3% aluminium (p. 586) was derived by chemical analysis of an electrolytic chromium sample melted in alumina. Aluminium pick-up by the alloys described in the first paper was much less and of the order described by Edwards, Wain, and Greenaway. This was due to the lower melting point of the alloys. It is worth noting that Parke and Bens used beryllia and zirconia crucibles and that although Adcock used alumina crucibles for melting pure chromium, he lined them with thoria.

Discussion

Oxidation and Sulphidation of Copper*

Mr. E. C. WILLIAMS,† M.Sc., A.Inst.P.: It is clear from the observations of Dr. Tylecote on the oxidation, and of Dr. Hoar and Dr. Tucker on the sulphidation, of copper that there are other important controlling factors besides transport of ions across a growing film of reaction product. The most interesting results of the detailed series of experiments carried out by Dr. Tylecote cannot be explained solely by any theory of ionic transport such as the Wagner theory, and the inadequacy is apparent from Dr. Tylecote's own discussion. I am disappointed, however, in the very last sentence of his paper (p. 700), which suggests that the Wagner mechanism in particular, and the transport of ions in either direction across a film as a rate-determining factor, is still predominant in the author's mind. Something more is required to explain the notable difference reported between the oxidation rates in air and in oxygen, the low rate for electropolished specimens, the low rate for wire as compared with sheet, and the difference again between cold-worked and annealed metal. Too much emphasis has been placed in the past on Wagner's theory, and thought on this subject of oxidation may have been stultified in consequence.

Dr. Hoar and Dr. Tucker have invoked the well-known Hoar-Price electrochemical interpretation of film growth to explain qualitatively the kinetics of sulphidation of copper. While this approach was enlightening fifteen years ago, I feel that to-day there is no fresh understanding of the phenomena of film growth to be gained by unduly pressing the analogy between a galvanic cell and a system metal/oxide (or sulphide)/environment, as the authors have done in deriving the schematic growth curves of Fig. 6 (p. 673) from the hypothetical "polarization" curves of Fig. 5 (p. 672). I suggest in particular that the elaborate analogy of cathodic polarization adds nothing to the authors' principal deductions from the observed rates of growth, i.e. that in the initial stages growth is limited mainly by the rate at which polysulphide ions can reach the film surface through the liquid, and in the later stages by the rate at which copper (and/or sulphide) ions can move through the growing sulphide film. In the present stage of knowledge concerning these complicated phenomena of film growth it is most essential to discover more about the actual physical processes taking place, and in this respect the factual content of the paper by Dr. Hoar and Dr. Tucker is admirable and of great value. Their microscopic studies are particularly impressive.

An aspect of metal-surface reactions which seems to me to have been largely neglected is the effect of heterogeneity of

We do not hold very definite views on the effect of heat-treatment on the creep properties of the alloys and on the divergence between chromium alloys and commercial creep-resistant alloys in this respect. Possibly the difference is between the behaviour of cast and wrought alloys.

Mr. Rendall makes some very interesting speculations on the role of interstitial impurities in chromium and other body-centred cubic metals. He may well be right. Experimental verification must, however, await the purification of chromium to a higher degree than we could achieve. Mr. Carrington's interesting finding is another example of plasticity induced in chromium by a non-homogeneous stress system, imposed in this case by hammering.

solid surfaces. In wet corrosion heterogeneity is taken for granted, perhaps too much so. In the thinking of physical chemists, particularly with regard to catalytic reactions, it is very much to the fore. The microscopic observations of Dr. Hoar and Dr. Tucker confirm my belief that this factor is important. The polarizing microscope indicates, for example, that in an aqueous attacking medium copper sulphide starts to form at preferred localities, and it seems likely that a film becomes continuous by lateral growth from nuclei. Dr. Tylecote, on p. 683, states that the first stage in the oxidation of copper is the formation of a solid solution with oxygen in the surface layers, followed by the appearance of nuclei of oxide which grow laterally to form a continuous film. In only five lines a world of potentially important effects is suggested, and I would have liked to have read much more in this tenor. The sigmoidal curve of weight-gain against time which Dr. Tylecote has produced for the initial stage of oxidation at high temperatures (Fig. 2, p. 684) may be explained by a process of nucleation and growth. The form of the equation is available from theoretical considerations on recrystallization‡ and for two-dimensional growth we may write:

$$w = d\rho(1 - e^{-kt^2})$$

where w is the weight increase per unit area, d is the thickness, assumed constant, of the spreading oxide layer of density ρ , and k is a factor involving the rates of nucleation and growth. The fact that the sigmoidal curve has only been observed once or twice does not necessarily mean that nucleation and growth is not a general phenomenon in film formation. The shape of the curve is determined by the factor k , which may well be such that the variation approximates to simple relationships—linear, parabolic, &c. It is also possible that further thickening after an initial layer has completely, or even partly, covered the metal occurs by nucleation and lateral growth of a second layer. One cannot imagine the surface of an oxide film as being any more homogeneous than the solid surface on which it is formed.

In conclusion, I suggest that the driving force in surface reactions should now be more intimately considered in relation to surface free energy, or to the chemical potential of metallic atoms at a free metallic surface and at interfaces with another phase. This quantity will vary from point to point, and will be greatest at local patches of high structural disorder, where nucleation will probably occur. Once a nucleus is formed it may be expected to spread laterally rather than grow

* Joint discussion on the papers by R. F. Tylecote (*J. Inst. Metals*, this vol., p. 681) and by T. P. Hoar and A. J. P. Tucker (this vol., p. 665).

† Technical Officer, Imperial Chemical Industries, Ltd.,

Metals Division, Birmingham.

‡ J. E. Burke and D. Turnbull, "Progress in Metal Physics", Vol. 3, p. 220. 1952: London (Pergamon Press).

vertically, because the free energy of the metal at the edge of the nucleus may be increased by strain arising from cohesive interaction between the layer of reaction product and its substrate.

Dr. HOAR (*in reply*): Mr. Williams believes that the film-cell concept is past its usefulness and in particular that the "analogy" of cathodic polarization used in the paper by Dr. Tucker and myself adds nothing to our understanding of the phenomena. Now, the process by which polysulphide ions in solution produce sulphide ions in the cuprous sulphide film must be one in which they pick up electrons, and it is highly likely that it takes place on the surface of the growing film. That surface is thus an actual cathode, and the rate of the process may depend on the supply of reactant, on the removal of product, and on an energy-hump related to the electrical potential difference across the surface, i.e. the p.d. between the adsorbed layer of polysulphide reactant and the sulphide film just below its surface. Thus the change of this p.d. with process rate (i.e. current) is not "analogous" to cathodic polarization: it is cathodic polarization. Certainly we wish to discover more detail about the actual physical processes occurring during film formation; but I think we shall not do so by forgetting that a reaction between ions and electrons taking place at a conducting interphase is an electrode reaction, that the movement of ions and electrons under a potential gradient are respectively electrolytic and electronic conduction, and that these processes can be treated by simple electrochemical methods whether they take place in conventional "liquid" cells or in cells with solid electrolytes that are at the same time electronic conductors.

The simple film-growth theory given originally by Wagner and subsequently in electrochemical form by Jost and by Price and myself is, of course, an approximation and was explicitly so described by its originators. The usefulness of the "cell" model can, however, be much extended by including in it several refinements. In the simplest and most approximate model, the film cell is assumed to operate at constant e.m.f., with the film specific resistance constant in time and space, and with the field strength in the film small enough for Ohm's law to be valid. None of these assumptions is ever strictly true, and one or more of them may be very far from true in particular cases. The influence of polarization in giving rise to a variable e.m.f. is discussed qualitatively in my present paper with Tucker; Wagner, and Price and I, provided early discussions of the influence of variable specific conductivity. Many more recent papers, notably by Wagner, Mott, Hauffe, and their schools,* have extended the theory by adopting more complex models; the "physical" school have preferred to reason *ab initio* by

the methods of electrostatics, while the "chemical" workers have sometimes preferred to begin with the inexact "cell" model and to apply refinements such as may be visualized in terms of real current-producing cells and non-ohmic electrical networks. Either approach can lead to the same result if equivalent assumptions are made, and although the physical method is the more elegant, it is perhaps the less easily appreciated by chemists and metallurgists. Consequently, I do not agree with Mr. Williams that the original Wagner theory and the "cell" model are past their usefulness; all models, however abstract, are only "ideas" of truth, and there is often something to be said for the cruder "engineering" kind of model as a better aid to elementary understanding than are the more refined models springing from current fundamental physics.

In the case of Dr. Tylecote's results, it seems to me that one way to interpret the growth curves would be to consider them as deviations from the parabolic curves that can be derived from the ideal model. As well as the refinements for growth by lattice transport referred to above, mechanical factors such as cracking, shearing, and splitting of the film would, of course, have to be taken into account. The well-proved general method of investigating real results as deviations from those to be expected from a simple ideal model, which has been so fruitful in the thermodynamic field, seems to me to be more promising than the fitting of certain of the results by more complex models, such as that leading (in my view, by somewhat dubious reasoning) to a "cubic" growth law. The present results that are approximately fitted by the cubic law do not seem sufficiently clear-cut to lend experimental support to its theory, and appear to be capable of better explanation in terms of deviations from the "ideal" parabolic law.

Dr. TYLECOTE (*in reply*): I still believe that the Wagner mechanism is the driving force in high- and intermediate-temperature oxidation processes. I regard the mechanical processes that occur owing to internal stresses as complicating factors superimposed on the general Wagner mechanism, and not as a mechanism replacing it. That is the reason for the last sentence of my paper. I feel that such mechanical processes are sufficient to explain the departures from the parabolic law in the higher range of temperatures. I shall be surprised if the application of free-energy considerations gives a better working hypothesis than the Wagner mechanism.

In reply to Dr. Hoar, it appears to me that the deviation from the "ideal" parabolic law is sufficiently large to justify another explanation, such as that given by Mott† and by Cabrera,‡ resulting in the cubic growth law.

* A good summary and bibliography covering most of the field is provided by O. Kubaschewski and B. E. Hopkins, "Oxidation of Metals and Alloys". 1953: London (Butter-

worths Scientific Publications).

† N. F. Mott, *Trans. Faraday Soc.*, 1940, **36**, 472.

‡ N. Cabrera, *Phil. Mag.*, 1949, [vii], **40**, 175.

Discussion

Structure of Nickel Alloys*

Dr. G. BULLOCK,† M.Sc., A.M.C.T. (Junior Member): Dr. Taylor and Mr. Hinton are to be congratulated on having proved the occurrence of an order-disorder change in the nickel-base 25 at.-% chromium alloy, in spite of the difficulties encountered in X-ray analysis owing to the closeness of the atomic scattering factors for nickel and chromium and the rather unexpected resistivity/temperature relationship. They seem to have explained quite fully certain property changes which accompany this transformation. I would suggest, however, that it would have been worthwhile considering the very real advantages to be obtained by the use of quantitative thermal curves ‡ in place of the Sykes method. An advantage of thermal-curve values is that they may be compared directly with the heating and cooling resistivity values.

The authors' views would be appreciated with regard to the possible effect on the scatter of the experimental points and the shape of the curves shown in Fig. 3 (p. 173), of comparing the temperatures of the specimen and the enclosure at one point only in each.

In Fig. 4 (p. 177) it is possible to draw a curve through the points obtained when plotting resistivity ρ against degree of order S . Inspection shows that this curve obeys neither a linear nor a square-law relationship. It does, however, yield a resistivity value, at $S = 0$, of approximately 101 microhm-cm., which is in the region of that obtained using the relationship $\rho = f(S^2)$. This seems to account for the fairly close agreement at high temperatures between the equilibrium curve and the curve for complete disorder, where $\rho = f(S^2)$, as shown in Fig. 5 (p. 177). At values of S other than 0 or 1, Fig. 4 shows that the relationship $\rho = f(S^2)$ appears to be only a slightly better approximation than $\rho = f(S)$, and this understandably limits the general applicability of equation (9) (p. 178).

Dr. B. R. COLES,§ B.Sc. (Junior Member): The papers under discussion and others by Dr. Taylor and Mr. Floyd have added greatly to the information we possess on the phase equilibria of nickel alloys. With the aid of such work we should shortly be able to understand more clearly the alloying behaviour of nickel, much as the assembly of data on copper alloys made possible the theoretical advances that followed it. In particular, I should like to see more work being done on alloys of nickel with the B sub-Group elements and a comparison of the results with those on corresponding palladium alloys.

The results of Dr. Taylor and Mr. Hinton on the nickel-chromium system are of especial interest, since this system has always seemed peculiarly simple. The complete absence of intermediate phases contrasts strangely with the nickel-titanium, nickel-vanadium, and nickel-manganese systems. In all these systems, however, and in the simple solid-solution systems nickel-iron and nickel-cobalt, ordered structures are found at the composition Ni_3X . Ni_3Ti and Ni_3V are discrete phases, but it seems highly probable that in the other systems effects other than size-factor ones (which are small) lead to the formation of superlattices, and the profound changes in physical properties in the Ni_3Mn and Ni_3Cr structures support this suggestion. In neither of these structures does a fall in electrical resistance take place on ordering, but there

is the usual ferromagnetic decrease in resistance in ordered Ni_3Mn some 80° C. below the critical temperature.

The specific-heat curves for the two alloys correspond closely, and the large high-temperature excess specific heat suggests strongly that not all the nickel 3d-band holes have been filled in Ni_3Cr .

The results of the electrical-resistance investigations of this alloy are extremely interesting. I agree that the increase in resistivity observed is associated with an ordering process, but I find it difficult to believe that a simple Brillouin-zone restriction of the freedom of the s-band electrons is responsible. The change in the effective number of free electrons would have to be enormous to counteract the large decrease in the perturbation of the lattice by random solid solution. The strongest evidence we yet have for superlattice Brillouin zones is the work of Komar || on the magnetoresistance and Hall effect in Cu_3Au . The Hall coefficient even changes sign on ordering, but the resistance decreases in the usual way. I am inclined to attribute the increase to some change in the electronic configuration of the d-electrons in the alloy, with a consequent change in the transition probability for scattering, and I suspect that the possibility of such change in electronic structure may be partially responsible for the occurrence of order with such low size-factors. This still leaves unexplained, however, the large value of the residual resistance. There is no theoretical justification for the insertion, into a formal treatment, of ρ_ω "the residual resistance at absolute zero of a completely ordered alloy". No matter how large the transition probability, when the perturbation of the lattice tends to zero the resistance must also tend to zero. It would be very interesting to examine the Hall coefficient and magnetoresistance of this alloy, and I should also expect the magnetic susceptibility to exhibit strange effects.

Dr. A. TAYLOR (in reply): Regarding Mr. Bullock's suggestion, the method of Sykes for determining the specific heat was chosen in preference to others, since the technique is an absolute one and yields the specific heat directly. Its main disadvantages are that it cannot be used with falling temperature and that the accuracy decreases rapidly at temperatures above 1000° C. owing to electrical leakages. This latter difficulty could presumably be overcome with improved types of refractory materials. The thermal-curve method is not so direct as that of Sykes, and, according to Handford ¶ its accuracy is somewhat lower.

Many tests were carried out on the temperature variation from point to point on the specimen. On the whole this was less than 1° C., and since the specimen is enclosed in what is virtually a uniform-temperature enclosure at the same temperature, the errors due to the use of a single reference point on the specimen are negligible compared with those from other sources.

The resistivity is probably more accurately a function of S^2 than of S . Bragg and Williams' ** choice of the latter function was purely arbitrary. However, the S^2 function may be obtained by the application of a rigorous quantum-mechanical argument as shown by Dienes, †† and it is gratifying that the very simple reasoning employed in our paper leads to precisely the same result.

* Joint discussion on the papers by A. Taylor and R. W. Floyd (*J. Inst. Metals*, this vol., pp. 25 and 451) and by A. Taylor and K. G. Hinton (p. 169).

† Lecturer, Applied Chemistry Department, Manchester University.

‡ C. Handford, *Nature*, 1938, **141**, 368.

§ T. F. Russell, *J. Iron Steel Inst.*, 1939, **139**, 147p.

¶ W. S. Walker, Thesis for Ph.D. degree, University of Manchester, 1946.

|| R. J. Maitland, Thesis for M.Sc.Tech. degree, University

of Manchester, 1952.

§ Lecturer in Metal Physics, Imperial College of Science and Technology, London.

|| A. Komar, *J. Physics (U.S.S.R.)*, 1941, **4**, 547.

A. Komar and S. Sidorov, *ibid.*, 552.

¶ *Loc. cit.*

** W. L. Bragg and E. J. Williams, *Proc. Roy. Soc.*, 1934, [A], **145**, 699.

†† G. J. Dienes, *J. Appl. Physics*, 1951, **22**, 1020.

NAME INDEX

- Allen, N. P. Discussion on "Creep and Plastic Deformation", 715.
- Andrews, K. W., and M. G. Gemmill. Discussion on "Creep and Plastic Deformation", 715.
- Atterton, D. V., and T. P. Hoar. Paper: "Simultaneous Determination of the Surface Tension of Tin and Its Contact Angle with Silica Using Conical Capillaries", 541.
- Axon, H. J. Papers: "Equilibrium Relations at 460°C. in Aluminium-Rich Alloys Containing 0-7% Copper, 0-7% Magnesium, and 1-2% Silicon", 209; "Equilibrium Relations at 460°C. in Aluminium-Rich Alloys Containing 0-7% Copper, 0-7% Magnesium, and 0-6% Silicon", 449.
- Backofen, W. A., and B. B. Hundy. Paper: "Mechanical Anisotropy in Some Ductile Metals", 433.
- Bailey, A. R. Discussion on "The Kinetics of the Eutectoid Transformation in Zinc-Aluminium Alloys", 742.
- Bailey, G. L. Discussion on "The Control of Quality in Melting and Casting", 703.
- Baker, W. A. Discussion on "Stretcher-Strain Markings", 751.
- Myriam D. Eborall, and A. Cibula. Paper: "The Influence of Primary Particles on the Grain-Size of Cast Magnesium-Aluminium Alloys", 43.
- Barnes, R. S. Discussion on "Diffusion and the Kirkendall Effect", 743.
- Baron, H. G. Discussion on "Some Friction Effects in Wire Drawing", 713.
- Bartlett, W. L. See Jones, W. R. D.
- Batchelor, L. C. Discussion on "The Control of Quality in Melting and Casting", 711.
- Berghézan, A. See Lacombe, P.
- Bhattacharya, S., W. K. A. Congreve, and F. C. Thompson. Paper: "The Creep/Time Relationship Under Constant Tensile Stress", 83; reply to discussion, 720.
- Bond-Williams, N. I. Discussion on "The Control of Quality in Melting and Casting", 701.
- Bowen, K. W. J. Discussion on "The Control of Quality in Melting and Casting", 706.
- Brace, A. W. Discussion on "Priming Paints for Light Alloys", 749.
- Bradfield, G. Discussion on "Young's Modulus of Alloys", 723.
- Brandes, E. A. See Sully, A. H.
- Brenner, P., and G. J. Metcalfe. Paper: "The Effect of Cold Work on the Microstructure and Corrosion-Resistance of Aluminium-5% Magnesium Alloys Containing 0-1% Zinc", 261; reply to discussion, 741.
- Brook, G. B. See Perryman, E. C. W.
- Brown, D. W. Discussion on "The Control of Quality in Melting and Casting", 703.
- Brown, R. J. Discussion on "Priming Paints for Light Alloys", 750.
- Bückle, H. Reply to discussion on "Micrographic Aspects of the Diffusion of Zinc and Aluminium in Copper", 742, 746.
- Bullock, G. Discussion on "Structure of Nickel Alloys", 765.
- Cantrell, J. Discussion on "High-Temperature Oxidation of Alloys", 731.
- Chadwick, N. Discussion on "Corrosion of Aluminium Alloys", 738.
- and W. H. L. Hooper. Reply to discussion on "Some Observations on the Occurrence of Stretcher-Strain Markings in an Aluminium-Magnesium Alloy", 752, 758.
- Champion, F. A. Discussion on "Corrosion of Aluminium Alloys", 739; discussion on "Priming Paints for Light Alloys", 750.
- Chaston, J. C. Discussion on "Diffusion and the Kirkendall Effect", 744; see also Darling, A. S.
- Cibula, A. See Baker, W. A.
- Coles, B. R. Discussion on "Structure of Nickel Alloys", 765.
- Congreve, W. K. A. See Bhattacharya, S.
- Cook, Maurice, and C. L. M. Cowley. Paper: "The Control of Quality in the Production of Brass Ingots and Billets", 341; reply to discussion, 704.
- and T. L. Richards. Discussion on "The Effects of Certain Solute Elements on the Recrystallization of Copper", 662.
- Cottrell, A. H. Discussion on "Stretcher-Strain Markings", 753.
- Cowley, C. L. M. See Cook, Maurice.
- Darling, A. S., R. A. Mintern, and J. C. Chaston. Paper: "The Gold-Platinum System", 125; reply to discussion, 600.
- Davies, Morgan H. Discussion on "High-Temperature Oxidation of Alloys", 728; note: "The Liquid Immiscibility Region in the Aluminium-Lead-Tin System at 650°, 730°, and 800°C.", 415.
- Dennison, J. P., and A. Preece. Paper: "High-Temperature Oxidation Characteristics of a Group of Oxidation-Resistant Copper-Base Alloys", 229; reply to discussion, 732.
- and E. V. Tull. Paper: "The Application of Grain Refinement to Cast Copper-Aluminium Alloys Containing the Beta Phase", 513.
- Dodd, R. A. Paper: "Residual Stresses in Aluminium Alloy Sand Castings", 77.
- Dudzinski, N. Paper: "The Young's Modulus, Poisson's Ratio, and Rigidity Modulus of Some Aluminium Alloys", 49; reply to discussion, 725.
- Eborall, Myriam D. See Baker, W. A.
- Eborall, R. Discussion on "Stretcher-Strain Markings", 756; see also Phillips, V. A.; Williams, W. M.
- and A. J. Swain. Paper: "Hydrogen Blisters in Brass Sheet", 497.
- Edeleanu, C. Discussion on "Mechanism of Precipitation in Aluminium-Magnesium Alloys", 15.
- Edwards, A. R., H. L. Wain, and H. T. Greenaway. Discussion on "Properties of Chromium and Its Alloys", 761.
- Eppelsheimer, D. S. See Williams, D. N.
- Evans, E. L. Discussion on "High-Temperature Oxidation of Alloys", 728.
- Evans, U. R. Discussion on "Corrosion of Aluminium Alloys", 738; discussion on "High-Temperature Oxidation of Alloys", 729.
- Fell, E. W. Discussion on "The Viscosity of Metals and Alloys", 714.
- Field, A. J. Discussion on "Priming Paints for Light Alloys", 750; discussion on "Stretcher-Strain Markings", 754.
- Floyd, R. W. See Taylor, A.
- Ford, H. Discussion on "Stretcher-Strain Markings", 754; see also Krupnik, N.
- Forsyth, P. J. E. Reply to discussion on "Some Metallographic Observations on the Fatigue of Metals", 218.
- Frost, N. E. See Johnson, A. E.
- Garwood, R. D., and A. D. Hopkins. Paper: "The Kinetics of the Eutectoid Transformation in Zinc-Aluminium Alloys", 407; reply to discussion, 742.
- Gemmill, M. G. See Andrews, K. W.
- Giffins, R. C. Paper: "The Influence of Thallium on the Creep of Lead", 417.
- and J. W. Kelly. Discussion on "Creep and Plastic Deformation", 717.
- Greenaway, H. T. See Edwards, A. R.
- Gregory, E. Discussion on "Properties of Chromium and Its Alloys", 760.
- G. G., and R. Kiessling. Paper: "Distribution Equilibria in Some Ternary Systems Me₂-Me₃-B and the Relative Strength of the Transition-Metal-Boron Bond", 57.
- Hancock, P. F. Discussion on "The Control of Quality in Melting and Casting", 705.
- Hardy, H. K. Discussion on "The Gold-Platinum System", 599; note: "The Log-Log Plot of Solubility Data in Ternary Metallic Systems", 432; reply to discussion on "The Ageing Characteristics of Binary Aluminium-Copper Alloys", 162; see also Polmear, I. J.
- Haworth, J. B. Note: "New Values of the Coefficients of Equivalence for Manganese, Iron, Cobalt, and Nickel in Copper-Zinc Alloys", 254.
- Head, A. K. See Wood, W. A.
- Heal, T. J., and (Miss) J. M. Silcock. Discussion on "The Ageing Characteristics of Binary Aluminium-Copper Alloys", 160.
- Hérenghuel, J., and P. Lelong. Discussion on "A Method of Determining Orientations in Aluminium Single Crystals and Polycrystalline Aggregates", 733.
- Hinton, (Sir) Christopher. May Lecture: "The Present and Future Metallurgical Requirements of the Chemical Engineer", 465.
- Hinton, K. G. See Taylor, A.
- Hirst, S. B. See Wilkinson, R. G.
- Hiscock, W. G. Discussion on "The Control of Quality in Melting and Casting", 703.
- Hoar, T. P. Discussion on "Diffusion and the Kirkendall Effect", 744; see also Atterton, D. V.
- and A. J. P. Tucker. Paper: "Growth of Sulphide Films on Copper", 665; reply to discussion, 764.
- Holden, J. See Hooper, W. H. L.
- Hooper, W. H. L. Paper: "The Effect of Composition on the Incidence of Strain Markings in Aluminium Alloys", 563; reply to discussion, 752, 758; see also Chadwick, R.
- and J. Holden. Paper: "Some Methods of Measuring Surface Topography as Applied to Stretcher-Strain Markings on Metal Sheet", 648; reply to discussion, 752, 758.
- Hopkin, L. M. T. Discussion on "Creep and Plastic Deformation", 716; paper: "A Note on the Mathematical Analysis of Creep Curves", 443.
- and C. J. Thwaites. Paper: "The Effect of Minor Additions on the Age-Hardening Properties of a High-Purity Lead-Antimony Alloy", 255.
- Hopkins, A. D. See Garwood, R. D.
- Hume-Rothery, W. See Pearson, W. B.
- Humphreys, D. Discussion on "Stretcher-Strain Markings", 754.
- Hundy, B. B. Discussion on "Stretcher-Strain Markings", 754; see also Backofen, W. A.
- Hurst, H. J. See Staples, R. T.
- Inman, M. C. Discussion on "Diffusion and the Kirkendall Effect", 744.
- Johnson, A. E., and N. E. Frost. Paper: "The Temperature Dependence of Transient and Secondary Creep of an Aluminium Alloy to British Standard 2L42 at Temperatures Between 20° and 250°C. and at Constant Stress", 93; reply to discussion, 719.
- Johnston, T. L. Discussion on "The Ageing Characteristics of Binary Aluminium-Copper Alloys", 160.

- Jones, W. R. D., and W. L. Bartlett. Paper: "The Viscosity of Aluminium and Binary Aluminium Alloys", 145; reply to discussion, 714.
- Kasz, F. Discussion on "The Control of Quality in Melting and Casting", 703.
- Kelly, J. W. See Gifkins, R. C.
- Kiessling, R. See Hagg, G.
- Kondic, V. See Yao, T. P.
- Krupnik, N., and Hugh Ford. Paper: "The Stepped Stress/Strain Curve of Some Aluminium Alloys", 601; reply to discussion, 754, 759.
- Kubaschewski, O. Discussion on "High-Temperature Oxidation of Alloys", 727.
- Lacombe, P. Discussion on "A Method of Determining Orientations in Aluminium Single Crystals and Polycrystalline Aggregates", 735.
- and A. Berghézan. Discussion on "Mechanism of Precipitation in Aluminium-Magnesium Alloys", 15.
- Lardner, E. Paper: "The Formation of Intracrystalline Voids in Solution-Treated Magnesium-Aluminium Alloys", 439; reply to discussion, 748.
- Larke, L. W. See Rotherham, L.
- Latin, A. Paper: "Some Observations on Creep and Fracture from Investigations on Lead Cable-Sheath Alloys", 529.
- Lelong, P. See Hérenquiel, J.
- Lewis, D. M. Discussion on "The Control of Quality in Melting and Casting", 712.
- Liddiard, E. A. G. Discussion on "Corrosion of Aluminium Alloys", 740; discussion on "Priming Paints for Light Alloys", 748.
- Löhberg, K. Discussion on "Intercrystalline Corrosion in Cast Zinc-Aluminium Alloys", 680.
- Lucas, G. See Preece, A.
- Lumsden, J. Discussion on "Young's Modulus of Alloys", 723.
- Lunn, Børge. Discussion on "The Control of Quality in Melting and Casting", 706.
- McLean, D. Discussion on "Fatigue of Metals", 217; papers: "Crystal Fragmentation in Aluminium During Creep", 287; reply to discussion, 720; "Crystal Slip in Aluminium During Creep", 133; reply to discussion, 720; "Grain-Boundary Slip During Creep of Aluminium", 293; reply to discussion, 720; "The Embrittlement of Copper-Antimony Alloys at Low Temperatures", 121; reply to discussion on "Creep Processes in Coarse-Grained Aluminium", 720.
- MacLellan, G. D. S. Paper: "Some Friction Effects in Wire Drawing", 1; reply to discussion, 714.
- Matthews, J. B. Paper: "The Measurement of the Relative Hardnesses of Fine Powder Particles", 279.
- Maykuth, D. J. Discussion on "The Constitution of Tantalum-Titanium Alloys", 426.
- Meijering, J. L. Discussion on "The Ageing Characteristics of Binary Aluminium-Copper Alloys", 161.
- Mellor, G. A., and R. W. Ridley. Paper: "Creep at 250° and 300°C. of Some Magnesium Alloys Containing Cerium", 245.
- Menter, J. W. Paper: "Direct Examination of Solid Surfaces Using a Commercial Electron Microscope in Reflection", 163.
- Metcalfe, G. J. Paper: "Atmospheric Corrosion and Stress-Corrosion of Aluminium-Copper-Magnesium and Aluminium-Magnesium-Silicon Alloys in the Fully Heat-Treated Condition", 269; reply to discussion, 741; see also Brenner, P.
- Mintern, R. A. See Darling, A. S.
- Miodownik, A. P. Discussion on "Creep and Plastic Deformation", 718.
- Mitchell, K. W. See Sully, A. H.
- Morral, F. R. Discussion on "Young's Modulus of Alloys", 724.
- Murphy, A. J. Discussion on "The Control of Quality in Melting and Casting", 708.
- Murphy, P. C. See Tucker, G. E. G.
- Newson, J. E. Discussion on "The Control of Quality in Melting and Casting", 701.
- Ogilvie, G. J. Paper: "The Continuity of Slip Lines Across a Grain Boundary", 491.
- d'Ombain, G. L. Discussion on "The Control of Quality in Melting and Casting", 705.
- Owen, E. A., and E. A. O'Donnell Roberts. Paper: "The Solubility of Indium in Copper", 479.
- Parker, R. T. Discussion on "The Control of Quality in Melting and Casting", 710.
- Parr, J. Gordon. Note: "An Example of Strain-Relief in Powder Specimens", 214.
- Paton, C. P. Discussion on "The Control of Quality in Melting and Casting", 706.
- Pearson, W. B., and W. Hume-Rothery. Paper: "The Constitution of Chromium-Manganese Alloys Below 1000°C.", 311.
- Perryman, E. C. W. Discussion on "Creep and Plastic Deformation", 718; discussion on "The Ageing Characteristics of Binary Aluminium-Copper Alloys", 161; discussion on "The Effects of Certain Solute Elements on the Recrystallization of Copper", 662.
- and G. B. Brook. Reply to discussion on "Mechanism of Precipitation in Aluminium-Magnesium Alloys", 16.
- Phillips, Arthur. See Phillips, V. A.
- Phillips, V. A. Paper: "Effect of Composition and Heat-Treatment on Yield-Point Phenomena in Aluminium Alloys", 649; reply to discussion, 757.
- and Arthur Phillips. Paper: "The Effect of Certain Solute Elements on the Recrystallization of Copper", 185; reply to discussion, 663.
- A. J. Swain, and R. Eborall. Paper: "Yield-Point Phenomena and Stretcher-Strain Markings in Aluminium-Magnesium Alloys", 625; reply to discussion, 757.
- Polakowski, N. H. Discussion on "Fatigue of Metals", 217; paper: "Discontinuous Flow and Strain Ageing in a 6% Tin Phosphor-Bronze", 617; reply to discussion, 759.
- Polmear, I. J., and H. K. Hardy. Paper: "Some Metallographic Observations on Aged Aluminium-Copper Alloys", 427.
- Preece, A. See Dennison, J. P.
- and G. Lucas. Paper: "The High-Temperature Oxidation of Some Cobalt-Base and Nickel-Base Alloys", 219; reply to discussion, 731.
- Provan, A. G. See Sully, A. H.
- Rachinger, W. A. Discussion on "Creep and Plastic Deformation", 718; paper: "Relative Grain Translations in Plastic Flow of Aluminium", 33; reply to discussion on "The Effect of Grain-Size on the Structural Changes Produced in Aluminium by Slow Deformation", 490.
- Ramsey, J. A. Papers: "The Recovery of Polycrystalline Aluminium", 61; reply to discussion, 721; "The Sub-Grain Structure in Aluminium Deformed at Elevated Temperatures", 215; reply to discussion, 721.
- Ransley, C. E. Discussion on "The Control of Quality in Melting and Casting", 708.
- Raynor, G. V. Discussion on "Young's Modulus of Alloys", 722.
- Rendall, J. H. Discussion on "Properties of Chromium and Its Alloys", 761.
- Richards, J. T. Discussion on "Young's Modulus of Alloys", 724.
- Richards, T. Ll. See Cook, M.
- Ridley, R. W. See Mellor, G. A.
- Rigg, J. G., and E. W. Skerrey. Paper: "Priming Paints for Light Alloys", 481; reply to discussion, 750.
- Roberts, C. W. Paper: "Intercrystalline Corrosion in Cast Zinc-Aluminium Alloys", 301; reply to discussion, 680.
- and B. Walters. Paper: "The Control of Quality in the Casting of Zinc and Zinc Alloy Rolling Slabs and Extrusion Billets", 365; reply to discussion, 710.
- Roberts, E. A. O'Donnell. See Owen, E. A.
- Rohner, F. Discussion on "Diffusion and the Kirkendall Effect", 745.
- Rotherham, L., and L. W. Larke. Paper: "The Solid Solubility of Silver in Aluminium", 67.
- Samuels, L. E. Paper: "The Use of Diamond Abrasives for a Universal System of Metallographic Polishing", 471.
- Servi, I. S. Discussion on "The Effect of Grain-Size on the Structural Changes Produced in Aluminium by Slow Deformation", 490.
- Silcock, (Miss) J. M. See Heal, T. J.
- Silman, H. Discussion on "Priming Paints for Light Alloys", 750.
- Singer, A. R. E. Paper: "The Principles of Technical Control in Metallurgical Manufacture", 329; reply to discussion, 705, 710.
- Skerrey, E. W. See Rigg, J. G.
- Smith, A. D. N. Reply to discussion on "A Study of Some Factors Influencing the Young's Modulus of Solid Solutions", 726.
- Smith, Christopher. Discussion on "The Control of Quality in Melting and Casting", 702.
- Smithells, C. J. Discussion on "The Control of Quality in Melting and Casting", 706, 707.
- Staples, R. T., and H. J. Hurst. Paper: "The Control of Quality in the Melting and Casting of Aluminium Alloys for Working", 377; reply to discussion, 711.
- Suiter, J. W., and W. A. Wood. Paper: "Deformation of Magnesium at Various Rates and Temperatures", 181.
- Sully, A. H., and E. A. Brandes. Paper: "The Properties of Cast Chromium Alloys at Elevated Temperatures. II. Some Properties of Certain Binary Chromium-Rich Alloys", 573; "III. The Creep Properties of Ternary and More Complex Chromium-Base Alloys", 578; reply to discussion, 762.
- E. A. Brandes, and K. W. Mitchell. Paper: "The Effect of Temperature and Purity on the Ductility and Other Properties of Chromium", 585; reply to discussion, 762.
- E. A. Brandes, and A. G. Provan. Paper: "The Properties of Cast Chromium Alloys at Elevated Temperatures. I.—The Melting and Casting of Chromium-Rich Alloys", 569; reply to discussion, 762.
- Summers-Smith, D. Paper: "The Constitution of Tantalum-Titanium Alloys", 73; reply to discussion, 426.
- Swain, A. J. See Eborall, R.; Phillips, V. A.
- Swift, H. W. Autumn Lecture: "On the Foot-Hills of the Plastic Range", 109.
- Sykes, J. Paper: "The Control of Quality in Melting and Casting Copper and High-Conductivity Copper-Base Alloys", 351; reply to discussion, 711.
- Taylor, A., and R. W. Floyd. Papers: "The Constitution of Nickel-Rich Alloys of the Nickel-Chromium-Aluminium System", 451; reply to discussion, 765; "The Constitution of Nickel-Rich Alloys of the Nickel-Titanium-Aluminium System", 25; reply to discussion, 765.
- and K. G. Hinton. Paper: "A Study of Order-Disorder and Precipitation Phenomena in Nickel-Chromium Alloys", 169; reply to discussion, 765.
- Thompson, F. C. Presidential Address, 401; see also Bhattacharya, S.
- Thwaites, C. J. See Hopkin, L. M. T.
- Tipper, C. F. Discussion on "Stretcher-Strain Markings", 755.
- Tucker, A. J. P. See Hoar, T. P.
- Tucker, G. E. G., and P. C. Murphy. Paper: "A Method of Determining Orientations in Aluminium Single Crystals and Polycrystalline Aggregates", 235; reply to discussion, 735, 737.
- Tucker, J. C. Discussion on "Corrosion of Aluminium Alloys", 740.
- Tull, E. V. See Dennison, J. P.
- Turner, A. N. Discussion on "Young's Modulus of Alloys", 724.
- Tylecote, R. F. Paper: "The Oxidation of Copper in the Temperature Range 200°-800°C.", 681; reply to discussion, 764.

Urie, (Mrs.) V. M., and H. L. Wain. Paper: "Plastic Deformation of Coarse-Grained Aluminium", 153.

Vinaver, W. Discussion on "The Control of Quality in Melting and Casting", 709.

Wain, H. L. See Edwards, A. R.; Urie, (Mrs.) V. M.

Walters, B. See Roberts, C. W.

Wilkinson, R. G., and S. B. Hirst. Paper: "The Control of Quality in Melting and Casting Magnesium Alloys for Hot Working", 393; reply to discussion, 711.

Williams, D. N., and D. S. Eppelsheimer. Paper: "A Theoretical Investigation of the Deformation Textures of Titanium", 553.

Williams, E. C. Discussion on "Oxidation and Sulphidation of Copper", 763.

Williams, W. M., and R. Eborall. Paper: "Critical-Strain Effects in Cold-Worked Wrought Aluminium and Its Alloys", 501.

Wood, W. A. See Suiter, J. W.
— and A. K. Head. Reply to discussion on "Some New Observations on the Mechanism of Fatigue in Metals", 218.

Worner, H. W. Paper: "The Structure of Titanium-Tin Alloys in the Range 0-25 At.-% Tin", 521.

Yao, T. P., and V. Kondic. Paper: "The Viscosity of Molten Tin, Lead, Zinc, Aluminium, and Some of Their Alloys", 17.

UNIVERSITY OF ILLINOIS AT CHICAGO
3 8198 316 018 512

